Scientific and Technical Aerospace Reports

An Abstract Journal

Volume 31, Number 11
November 1993
N93-28464 to N93-31039

The NASA STI Program ... in Profile

Since its founding, NASA has been dedicated to the advancement of aeronautics and space science. The NASA Scientific and Technical Information (STI) Program plays a key part in helping NASA maintain this important role.

The NASA STI Program provides access to the NASA STI Database, the largest collection of aeronautical and space science STI in the world. The Program is also NASA's institutional mechanism for disseminating the results of its research and development activities.

Specialized services that help round out the Program's diverse offerings include creating custom thesauri, translating material to or from 34 foreign languages, building customized databases, organizing and publishing research results ... even providing videos.

For more information about the NASA STI Program, you can:

- **Phone** the NASA Access Help Desk at (301) 621-0390
- **Fax** your question to the NASA Access Help Desk at (301) 621-0134
- **E-mail** your question via the **Internet** to help@sti.nasa.gov
- **Write** to:

NASA Access Help Desk
NASA Center for AeroSpace Information
800 Elkridge Landing Road
Linthicum Heights, MD 21090-2934

Scientific and Technical Aerospace Reports

STAR

***Scientific and Technical Aerospace Reports* (*STAR*)**, is published each month as a major product of the International Aerospace Database, managed by the NASA Scientific and Technical Information (STI) Program.

Inside this issue you will find:

Front Matter
A typical citation and abstract sample explaining the standard format, which includes codes for ordering reports.

An Abstract Section
Citations and abstracts of reports and publications that provide comprehensive coverage of worldwide aerospace-related topics including aeronautics and space science technology. *STAR* lists published and publicly available reports entered into the NASA STI Database during the four weeks preceding publication of this issue. These citations and abstracts are listed by subject categories.

An Index Section
- Subject
- Personal author
- Corporate source
- Contract number
- Report number.

Appendix
A guide for ordering cited reports, registering with the NASA STI Program, and using the available products and services. Additionally, price schedules, phone numbers, and addresses are included in this information packed section.

NASA also sponsors companion journals, *International Aerospace Abstracts (IAA)*, and *NASA Open Volumes on Aerospace (NOVA)*. They list abstracts of the open literature on aerospace subjects available worldwide. IAA is available from the American Institute of Aeronautics and Astronautics (AIAA), and *NOVA* is for internal NASA use only, available from the NASA Center for AeroSpace Information (CASI).

Reports found in *STAR* are also available through the NASA online retrieval service, RECON, and the Aerospace Database through DIALOG.

The NASA STI Program gathers information through national and international agreements and exchanges and makes this information available to the NASA community and to the public in many forms through various outlets.

For additional information on the NASA STI Program, call the NASA Access Help Desk at (301) 621-0390, or write to:

NASA Center for AeroSpace Information
800 Elkridge Landing Road
Linthicum Heights, Maryland 21090-2934

US ISSN 0036-8741

This publication was prepared by the NASA Center for AeroSpace Information,
800 Elkridge Landing Road, Linthicum Heights, MD 21090-2934, (301) 621-0390.

Volume 31 Number 11 / November 1993

TABLE OF CONTENTS

AERONAUTICS For related information see also *Astronautics.*

01 AERONAUTICS (GENERAL) 3227

02 AERODYNAMICS 3238
Includes aerodynamics of bodies, combinations, wings, rotors, and control surfaces; and internal flow in ducts and turbomachinery. For related information see also *34 Fluid Mechanics and Heat Transfer.*

03 AIR TRANSPORTATION AND SAFETY 3243
Includes passenger and cargo air transport operations; and aircraft accidents. For related information see also *16 Space Transportation* and *85 Urban Technology and Transportation.*

04 AIRCRAFT COMMUNICATIONS AND NAVIGATION 3245
Includes digital and voice communication with aircraft; air navigation systems (satellite and ground based); and air traffic control. For related information see also *17 Space Communications, Spacecraft Communications, Command and Tracking* and *32 Communications and Radar.*

05 AIRCRAFT DESIGN, TESTING AND PERFORMANCE 3247
Includes aircraft simulation technology. For related information see also *18 Spacecraft Design, Testing and Performance* and *39 Structural Mechanics.* For land transportation vehicles see *85 Urban Technology and Transportation.*

06 AIRCRAFT INSTRUMENTATION 3250
Includes cockpit and cabin display devices; and flight instruments. For related information see also *19 Spacecraft Instrumentation* and *35 Instrumentation and Photography.*

07 AIRCRAFT PROPULSION AND POWER 3251
Includes prime propulsion systems and systems components, e.g., gas turbine engines and compressors; and onboard auxiliary power plants for aircraft. For related information see also *20 Spacecraft Propulsion and Power, 28 Propellants and Fuels,* and *44 Energy Production and Conversion.*

08 AIRCRAFT STABILITY AND CONTROL 3259
Includes aircraft handling qualities; piloting; flight controls; and autopilots. For related information see also *05 Aircraft Design, Testing and Performance.*

09 RESEARCH AND SUPPORT FACILITIES (AIR) 3260
Includes airports, hangars and runways; aircraft repair and overhaul facilities; wind tunnels; shock tubes; and aircraft engine test stands. For related information see also *14 Ground Support Systems and Facilities (Space).*

ASTRONAUTICS For related information see also *Aeronautics.*

12 ASTRONAUTICS (GENERAL) 3262
For extraterrestrial exploration see *91 Lunar and Planetary Exploration.*

13 ASTRODYNAMICS 3269
Includes powered and free-flight trajectories; and orbital and launching dynamics.

14 GROUND SUPPORT SYSTEMS AND FACILITIES (SPACE) 3270
Includes launch complexes, research and production facilities; ground support equipment, e.g., mobile transporters; and simulators. For related information see also *09 Research and Support Facilities (Air).*

15 LAUNCH VEHICLES AND SPACE VEHICLES 3270
Includes boosters; operating problems of launch/space vehicle systems; and reusable vehicles. For related information see also *20 Spacecraft Propulsion and Power.*

16 SPACE TRANSPORTATION 3271
Includes passenger and cargo space transportation, e.g., shuttle operations; and space rescue techniques. For related information see also *03 Air Transportation and Safety* and *18 Spacecraft Design, Testing and Performance.* For space suits see *54 Man/System Technology and Life Support.*

17 SPACE COMMUNICATIONS, SPACECRAFT COMMUNICATIONS, COMMAND AND TRACKING....3273
Includes telemetry; space communications networks; astronavigation and guidance; and radio blackout. For related information see also *04 Aircraft Communications and Navigation* and *32 Communications and Radar.*

N.A.—No abstracts were assigned to this category for this issue.

18 SPACECRAFT DESIGN, TESTING AND PERFORMANCE **3274**
Includes satellites; space platforms; space stations; spacecraft systems and components such as thermal and environmental controls; and attitude controls. For life support systems see *54 Man/System Technology and Life Support.* For related information see also *05 Aircraft Design, Testing and Performance, 39 Structural Mechanics*, and *16 Space Transportation.*

19 SPACECRAFT INSTRUMENTATION **3285**
For related information see also *06 Aircraft Instrumentation* and *35 Instrumentation and Photography.*

20 SPACECRAFT PROPULSION AND POWER **3286**
Includes main propulsion systems and components, e.g., rocket engines; and spacecraft auxiliary power sources. For related information see also *07 Aircraft Propulsion and Power, 28 Propellants and Fuels, 44 Energy Production and Conversion*, and *15 Launch Vehicles and Space Vehicles.*

CHEMISTRY AND MATERIALS

23 CHEMISTRY AND MATERIALS (GENERAL) **3290**

24 COMPOSITE MATERIALS **3294**
Includes physical, chemical, and mechanical properties of laminates and other composite materials. For ceramic materials see *27 Nonmetallic Materials.*

25 INORGANIC AND PHYSICAL CHEMISTRY **3309**
Includes chemical analysis, e.g., chromatography; combustion theory; electrochemistry; and photochemistry. For related information see also *77 Thermodynamics and Statistical Physics.*

26 METALLIC MATERIALS **3320**
Includes physical, chemical, and mechanical properties of metals, e.g., corrosion; and metallurgy.

27 NONMETALLIC MATERIALS **3329**
Includes physical, chemical, and mechanical properties of plastics, elastomers, lubricants, polymers, textiles, adhesives, and ceramic materials. For composite materials see *24 Composite Materials.*

28 PROPELLANTS AND FUELS **3341**
Includes rocket propellants, igniters and oxidizers; their storage and handling procedures; and aircraft fuels. For related information see also *07 Aircraft Propulsion and Power, 20 Spacecraft Propulsion and Power*, and *44 Energy Production and Conversion.*

29 MATERIALS PROCESSING **3352**
Includes space-based development of products and processes for commercial application. For biological materials see *55 Space Biology:*

ENGINEERING For related information see also *Physics.*

31 ENGINEERING (GENERAL) **3353**
Includes vacuum technology; control engineering; display engineering; cryogenics; and fire prevention.

32 COMMUNICATIONS AND RADAR **3379**
Includes radar; land and global communications; communications theory; and optical communications. For related information see also *04 Aircraft Communications and Navigation* and *17 Space Communications, Spacecraft Communications, Command and Tracking.* For search and rescue see *03 Air Transportation and Safety*, and *16 Space Transportation.*

33 ELECTRONICS AND ELECTRICAL ENGINEERING **3404**
Includes test equipment and maintainability; components, e.g., tunnel diodes and transistors; microminiaturization; and integrated circuitry. For related information see also *60 Computer Operations and Hardware* and *76 Solid-State Physics.*

34 FLUID MECHANICS AND HEAT TRANSFER **3415**
Includes boundary layers; hydrodynamics; fluidics; mass transfer and ablation cooling. For related information see also *02 Aerodynamics* and *77 Thermodynamics and Statistical Physics.*

35 INSTRUMENTATION AND PHOTOGRAPHY **3430**
Includes remote sensors; measuring instruments and gauges; detectors; cameras and photographic supplies; and holography. For aerial photography see *43 Earth Resources and Remote Sensing.* For related information see also *06 Aircraft Instrumentation* and *19 Spacecraft Instrumentation.*

36 LASERS AND MASERS **3435**
Includes parametric amplifiers. For related information see also *76 Solid-State Physics.*

37 MECHANICAL ENGINEERING 3442
Includes auxiliary systems (nonpower); machine elements and processes; and mechanical equipment.

38 QUALITY ASSURANCE AND RELIABILITY 3449
Includes product sampling procedures and techniques; and quality control.

39 STRUCTURAL MECHANICS 3450
Includes structural element design and weight analysis; fatigue; and thermal stress. For applications see *05 Aircraft Design, Testing and Performance* and *18 Spacecraft Design, Testing and Performance.*

GEOSCIENCES For related information see also *Space Sciences.*

42 GEOSCIENCES (GENERAL) 3456

43 EARTH RESOURCES AND REMOTE SENSING 3456
Includes remote sensing of earth resources by aircraft and spacecraft; photogrammetry; and aerial photography. For instrumentation see *35 Instrumentation and Photography.*

44 ENERGY PRODUCTION AND CONVERSION 3463
Includes specific energy conversion systems, e.g., fuel cells; global sources of energy; geophysical conversion; and windpower. For related information see also *07 Aircraft Propulsion and Power, 20 Spacecraft Propulsion and Power,* and *28 Propellants and Fuels.*

45 ENVIRONMENT POLLUTION 3467
Includes atmospheric, noise, thermal, and water pollution.

46 GEOPHYSICS 3475
Includes aeronomy; upper and lower atmosphere studies; ionospheric and magnetospheric physics; and geomagnetism. For space radiation see *93 Space Radiation.*

47 METEOROLOGY AND CLIMATOLOGY 3480
Includes weather forecasting and modification.

48 OCEANOGRAPHY 3486
Includes biological, dynamic, and physical oceanography; and marine resources. For related information see also *43 Earth Resources and Remote Sensing.*

LIFE SCIENCES

51 LIFE SCIENCES (GENERAL) 3490

52 AEROSPACE MEDICINE 3492
Includes physiological factors; biological effects of radiation; and effects of weightlessness on man and animals.

53 BEHAVIORAL SCIENCES 3498
Includes psychological factors; individual and group behavior; crew training and evaluation; and psychiatric research.

54 MAN/SYSTEM TECHNOLOGY AND LIFE SUPPORT 3500
Includes human engineering; biotechnology; and space suits and protective clothing. For related information see also *16 Space Transportation.*

55 SPACE BIOLOGY 3509
Includes exobiology; planetary biology; and extraterrestrial life.

MATHEMATICAL AND COMPUTER SCIENCES

59 MATHEMATICAL AND COMPUTER SCIENCES (GENERAL) 3509

60 COMPUTER OPERATIONS AND HARDWARE 3520
Includes hardware for computer graphics, firmware, and data processing. For components see *33 Electronics and Electrical Engineering.*

61 COMPUTER PROGRAMMING AND SOFTWARE 3522
Includes computer programs, routines, algorithms, and specific applications, e.g., CAD/CAM.

62 COMPUTER SYSTEMS 3537
Includes computer networks and special application computer systems.

63 CYBERNETICS 3540
Includes feedback and control theory, artificial intelligence, robotics and expert systems. For related information see also *54 Man/System Technology and Life Support.*

64 NUMERICAL ANALYSIS 3546
Includes iteration, difference equations, and numerical approximation.

65 STATISTICS AND PROBABILITY 3552
Includes data sampling and smoothing; Monte Carlo method; and stochastic processes.

66 SYSTEMS ANALYSIS 3556
Includes mathematical modeling; network analysis; and operations research.

67 THEORETICAL MATHEMATICS 3556
Includes topology and number theory.

PHYSICS For related information see also *Engineering.*

70 PHYSICS (GENERAL) 3560
For precision time and time interval (PTTI) see *35 Instrumentation and Photography*; for geophysics, astrophysics or solar physics see *46 Geophysics, 90 Astrophysics*, or *92 Solar Physics.*

71 ACOUSTICS 3561
Includes sound generation, transmission, and attenuation. For noise pollution see *45 Environment Pollution.*

72 ATOMIC AND MOLECULAR PHYSICS 3563
Includes atomic structure, electron properties, and molecular spectra.

73 NUCLEAR AND HIGH-ENERGY PHYSICS 3573
Includes elementary and nuclear particles; and reactor theory. For space radiation see *93 Space Radiation.*

74 OPTICS 3577
Includes light phenomena and optical devices. For lasers see *36 Lasers and Masers.*

75 PLASMA PHYSICS 3583
Includes magnetohydrodynamics and plasma fusion. For ionospheric plasmas see *46 Geophysics.* For space plasmas see *90 Astrophysics.*

76 SOLID-STATE PHYSICS 3591
Includes superconductivity. For related information see also *33 Electronics and Electrical Engineering* and *36 Lasers and Masers.*

77 THERMODYNAMICS AND STATISTICAL PHYSICS 3603
Includes quantum mechanics; theoretical physics; and Bose and Fermi statistics. For related information see also *25 Inorganic and Physical Chemistry* and *34 Fluid Mechanics and Heat Transfer.*

SOCIAL SCIENCES

80 SOCIAL SCIENCES (GENERAL) 3608
Includes educational matters.

81 ADMINISTRATION AND MANAGEMENT 3609
Includes management planning and research.

82 DOCUMENTATION AND INFORMATION SCIENCE 3611
Includes information management; information storage and retrieval technology; technical writing; graphic arts; and micrography. For computer documentation see *61 Computer Programming and Software.*

83 ECONOMICS AND COST ANALYSIS 3624
Includes cost effectiveness studies.

84 LAW, POLITICAL SCIENCE AND SPACE POLICY .... N.A.
Includes NASA appropriation hearings; aviation law; space law and policy; international law; international cooperation; and patent policy.

85 URBAN TECHNOLOGY AND TRANSPORTATION 3625
Includes applications of space technology to urban problems; technology transfer; technology assessment; and surface and mass transportation. For related information see *03 Air Transportation and Safety, 16 Space Transportation,* and *44 Energy Production and Conversion.*

SPACE SCIENCES For related information see also *Geosciences.*

88 SPACE SCIENCES (GENERAL) 3629

89 ASTRONOMY 3629
Includes radio, gamma-ray, and infrared astronomy; and astrometry.

90 ASTROPHYSICS 3632
Includes cosmology; celestial mechanics; space plasmas; and interstellar and interplanetary gases and dust. For related information see also *75 Plasma Physics.*

91 LUNAR AND PLANETARY EXPLORATION 3639
Includes planetology; and manned and unmanned flights. For spacecraft design or space stations see *18 Spacecraft Design, Testing and Performance.*

92 SOLAR PHYSICS 3652
Includes solar activity, solar flares, solar radiation and sunspots. For related information see also *93 Space Radiation.*

93 SPACE RADIATION 3653
Includes cosmic radiation; and inner and outer earth's radiation belts. For biological effects of radiation see *52 Aerospace Medicine.* For theory see *73 Nuclear and High-Energy Physics.*

GENERAL

Includes aeronautical, astronautical, and space science related histories, biographies, and pertinent reports too broad for categorization; histories or broad overviews of NASA programs.

99 GENERAL 3654

SUBJECT INDEX I-1

PERSONAL AUTHOR INDEX I-167

CORPORATE SOURCE INDEX I-187

CONTRACT NUMBER INDEX I-217

REPORT NUMBER INDEX I-223

APPENDIX A-1

TYPICAL CITATION AND ABSTRACT

NASA SPONSORED
ON MICROFICHE

ACCESSION NUMBER →	N93-10068*# Washington Univ., Seattle. Dept. of Atmospheric Sciences.	← **CORPORATE SOURCE**
TITLE →	**AIR-SEA INTERACTION AND REMOTE SENSING Status Report, 1 Dec. 1991 - 30 Nov. 1992**	
AUTHORS →	Kristina B. Katsaros and Serhad S. Ataktuerk 1992	← **PUBLICATION DATE**
	12 p Original contains color illustrations	
CONTRACT OR GRANT →	(Grant NAGw-1322)	
REPORT NUMBERS →	(NASA-CR-190913; NAS 1.26:190913) Avail: CASI HC A03/MF A01; 2 functional color pages	← **AVAILABILITY SOURCE AND PRICE CODE**

The first part of the proposed research was a joint effort between our group and the Applied Physics Laboratory (APL), University of Washington. Our own research goal is to investigate the relation between the air-sea exchange processes and the sea state over the open ocean and to compare these findings with our previous results obtained over a small body of water namely, Lake Washington. The goals of the APL researchers are to study (1) the infrared sea surface temperature (SST) signature of breaking waves and surface slicks, and (2) microwave and acoustic scattering from water surface. The task of our group in this joint effort is to conduct measurements of surface fluxes (of momentum, sensible heat, and water vapor) and atmospheric radiation (longwave and shortwave) to achieve our research goal as well as to provide crucial complementary data for the APL studies. The progress of the project is summarized. Author

VOLUME 31 NUMBER 11 / November 1993

Scientific and Technical Aerospace Reports

A Monthly Publication of the National Aeronautics and Space Administration

01 AERONAUTICS (GENERAL)

N93-28576# Air Force Systems Command, Wright-Patterson AFB, OH. Foreign Aerospace Science and Technology Center.
INTERNATIONAL AVIATION (SELECTED ARTICLES)
18 Mar. 1993 75 p Transl. into ENGLISH from Guoji Hangkong (China), no. 7, 1989 p 6-20 LIMITED REPRODUCIBILITY: More than 20% of this document may be affected by microfiche quality
(AD-A262566; FASTC-ID(RS)T-0625-92) Avail: Isssuing Activity (Defense Technical Information Center (DTIC))

China's Aerodynamics Research and Development Center (hereafter called 'Center') is China's largest aerodynamics research and testing organ. It is located within Mianyang City in Sichuan Province. The Center is subordinate to the State Commission of Science, Technology, and Industry for National Defense. Its primary missions are to conduct experimental research, theoretical research, and applied research of aircraft and spacecraft and wind engineering; provide the results of their research to aircraft design organs and other state economic agencies; and to undertake the research and design of aerodynamic test equipment. DTIC

N93-29712*# Universities Space Research Association, Houston, TX.
PROCEEDINGS OF THE SEVENTH ANNUAL SUMMER CONFERENCE. NASA/USRA: UNIVERSITY ADVANCED DESIGN PROGRAM
1991 325 p Conference held in Cocoa Beach, FL, 17-21 Jun. 1991
(Contract NASw-4435)
(NASA-CR-192962; NAS 1.26:192962) Avail: CASI HC A14/MF A03

The Advanced Design Program (ADP) is a unique program that brings together students and faculty from U.S. engineering schools with engineers from the NASA centers through integration of current and future NASA space and aeronautics projects into university engineering design curriculum. The Advanced Space Design Program study topics cover a broad range of projects that could be undertaken during a 20-30 year period beginning with the deployment of the Space Station Freedom. The Advanced Aeronautics Design Program study topics typically focus on nearer-term projects of interest to NASA, covering from small, slow-speed vehicles through large, supersonic passenger transports and on through hypersonic research vehicles. Student work accomplished during the 1990-91 academic year and reported at the 7th Annual Summer Conference is presented. For individual titles, see N93-29713 through N93-29761.

N93-29713*# California State Polytechnic Univ., Pomona.
HIGH-ALTITUDE RECONNAISSANCE AIRCRAFT **c05**
Renee Anna Yazdi *In* Universities Space Research Association, Houston, Proceedings of the Seventh Annual Summer Conference. NASA/USRA: University Advanced Design Program 1991 p 11-18 Previously announced in IAA as A91-54045 (For primary document see N93-29712 11-01)
Avail: CASI HC A02/MF A03

At the equator the ozone layer ranges from 65,000 to 130,000+ ft, which is beyond the capabilities of the ER-2, NASA's current high-altitude reconnaissance aircraft. This project is geared to designing an aircraft that can study the ozone layer. The aircraft must be able to satisfy four mission profiles. The first is a polar mission that ranges from Chile to the South Pole and back to Chile, a total range of 6000 n.m. at 100,000 ft with a 2500-lb payload. The second mission is also a polar mission with a decreased altitude and an increased payload. For the third mission, the aircraft will take off at NASA Ames, cruise at 100,000 ft, and land in Chile. The final mission requires the aircraft to make an excursion to 120,000 ft. All four missions require that a subsonic Mach number be maintained because of constraints imposed by the air sampling equipment. Three aircraft configurations were determined to be the most suitable for meeting the requirements. The performance of each is analyzed to investigate the feasibility of the mission requirements. Author (revised)

N93-29714*# California State Polytechnic Coll., San Luis Obispo.
PROJECT SUMMARY **c05**
In Universities Space Research Association, Houston, Proceedings of the Seventh Annual Summer Conference. NASA/USRA: University Advanced Design Program 1991 p 19-28 (For primary document see N93-29712 11-01)
Avail: CASI HC A02/MF A03

California Polytechnic State University's design project for the 1990-91 school year was the design of a close air support aircraft. There were eight design groups that participated and were given requests for proposals. These proposals contained mission specifications, particular performance and payload requirements, as well as the main design drivers. The mission specifications called for a single pilot weighing 225 lb with equipment. The design mission profile consisted of the following: (1) warm-up, taxi, take off, and accelerate to cruise speed; (2) dash at sea level at 500 knots to a point 250 nmi from take off; (3) combat phase, requiring two combat passes at 450 knots that each consist of a 360 deg turn and an energy increase of 4000 ft. - at each pass, half of air-to-surface ordnance is released; (4) dash at sea level at 500 knots 250 nmi back to base; and (5) land with 20 min of reserve fuel. The request for proposal also specified the following performance requirements with 50 percent internal fuel and standard stores: (1) the aircraft must be able to accelerate from Mach 0.3 to 0.5 at sea level in less than 20 sec; (2) required turn rates are 4.5 sustained g at 450 knots at sea level; (3) the aircraft must have a reattack time of 25 sec or less (reattack time was defined as the time between the first and second weapon drops); (4) the aircraft is allowed a maximum take off and landing ground roll of 2000 ft. The payload requirements were 20 Mk 82 general-purpose free-fall bombs and racks; 1 GAU-8A 30-mm cannon with 1350 rounds; and 2 AIM-9L Sidewinder missiles and racks. The main design drivers expressed in the request for proposal were that the aircraft should be survivable and maintainable. It must be able to operate in remote areas with little or no maintenance. Simplicity was considered the most important factor in achieving the former goal. In addition, the aircraft must be low cost both in acquisition and operation. The summaries of the aircraft configurations developed by the eight groups are presented. Author (revised)

N93-29715*# California State Univ., Northridge.
PROJECT ARES 2: HIGH-ALTITUDE BATTERY-POWERED AIRCRAFT **c05**
In Universities Space Research Association, Houston, Proceedings of the Seventh Annual Summer Conference. NASA/USRA: University Advanced Design Program 1991 p 29-33 (For primary document see N93-29712 11-01)
Avail: CASI HC A01/MF A03

A high-altitude, battery-powered, propeller-driven aircraft was designed and is being built by undergraduate students at California State University, Northridge. The aircraft will fly at an altitude of 104,000 ft at Mach 0.2 (190 ft/sec) and will be instrumented to record flight performance data, including low Reynolds number propeller and airfoil information. This project will demonstrate the feasibility of electric-powered flight in a low-density, low-temperature Earth environment that models the atmosphere of Mars. Data collected will be used to design a Mars aircraft to investigate the surface of Mars prior to manned missions. The instrumented payload and the mission profile for the high-altitude Earth flight were determined. Detailed aerodynamic and structural analyses were performed. Control, tracking, and data recording subsystems were developed. Materials were obtained and fabrication begun. The aircraft has a 32-ft wing span, a wing area of 105 sq ft, is 17.5 ft long, has a 12-in payload bay, and weighs 42 lb. It is composed primarily of lightweight materials, including Mylar, and composite materials, including graphite/epoxy and aramid core honeycomb sandwich. Low-altitude flight testing to check guidance and control systems and to calibrate data-gathering instruments will take place this summer, followed shortly by the 104,000-ft flight. Author

N93-29716*# Case Western Reserve Univ., Cleveland, OH.
CONCEPTUAL DESIGN OF A TWO-STAGE-TO-ORBIT VEHICLE c05
In Universities Space Research Association, Houston, Proceedings of the Seventh Annual Summer Conference. NASA/USRA: University Advanced Design Program 1991 p 35-43 (For primary document see N93-29712 11-01)
Avail: CASI HC A02/MF A03

A conceptual design study of a two-stage-to-orbit vehicle is presented. Three configurations were initially investigated with one configuration selected for further development. The major objective was to place a 20,000-lb payload into a low Earth orbit using a two-stage vehicle. The first stage used air-breathing engines and employed a horizontal takeoff, while the second stage used rocket engines to achieve a 250-n.m. orbit. A two-stage-to-orbit vehicle seems a viable option for the next-generation space shuttle. Author

N93-29717*# Kansas Univ., Lawrence.
PRELIMINARY DESIGN STUDIES OF AN ADVANCED GENERAL AVIATION AIRCRAFT c05
In Universities Space Research Association, Houston, Proceedings of the Seventh Annual Summer Conference. NASA/USRA: University Advanced Design Program 1991 p 45-56 (For primary document see N93-29712 11-01)
Avail: CASI HC A03/MF A03

Preliminary design studies are presented for an advanced general aviation aircraft. Advanced guidance and display concepts, laminar flow, smart structures, fuselage and wing structural design and manufacturing, and preliminary configuration design are discussed. This project was conducted as a graduate level design class under the auspices of the KU/NASA/USRA Advanced Design Program in Aeronautics. The results obtained during the fall semester of 1990 (Phase 1) and the spring semester of 1991 (Phase 2) are presented. Author (revised)

N93-29718*# Notre Dame Univ., IN.
DESIGN STUDY TO SIMULATE THE DEVELOPMENT OF A COMMERCIAL TRANSPORTATION SYSTEM c05
In Universities Space Research Association, Houston, Proceedings of the Seventh Annual Summer Conference. NASA/USRA: University Advanced Design Program 1991 p 57-64 (For primary document see N93-29712 11-01)
Avail: CASI HC A02/MF A03

Seven teams of senior-level Aerospace Engineering undergraduates were given a Request for Proposals (RFP) for a design concept of a remotely piloted vehicle (RPV). The RPV designs were intended to simulate commercial transport aircraft within the model of 'Aeroworld.' The Aeroworld model was developed so that the RPV designs would be subject to many of the engineering problems and tradeoffs that dominate real-world commercial air transport designs, such as profitability, fuel efficiency, range vs. payload capabilities, and ease of production and maintenance. As part of the proposal, each team was required to construct a prototype and validate its design with a flight demonstration. Author (revised)

N93-29719*# Ohio State Univ., Columbus.
THE DESIGN OF TWO-STAGE-TO-ORBIT VEHICLES c05
In Universities Space Research Association, Houston, Proceedings of the Seventh Annual Summer Conference. NASA/USRA: University Advanced Design Program 1991 p 65-75 (For primary document see N93-29712 11-01)
Avail: CASI HC A03/MF A03

Two separate student design groups developed conceptual designs for a two-stage-to-orbit vehicle, with each design group consisting of a carrier team and an orbiter team. A two-stage-to-orbit system is considered in the event that single-stage-to-orbit is deemed not feasible in the foreseeable future; the two-stage system would also be used as a complement to an already existing heavy lift vehicle. The design specifications given are to lift a 10,000-lb payload 27 ft long by 10 ft diameter, to low Earth orbit (300 n.m.) using an air breathing carrier configuration that will take off horizontally within 15,000 ft. The staging Mach number and altitude were to be determined by the design groups. One group designed a delta wing/body carrier with the orbiter nested within the fuselage of the carrier, and the other group produced a blended cranked-delta wing/body carrier with the orbiter in the more conventional piggyback configuration. Each carrier used liquid hydrogen-fueled turbofanramjet engines, with data provided by General Electric Aircraft Engine Group. While one orbiter used a full-scale Space Shuttle Main Engine (SSME), the other orbiter employed a half-scale SSME coupled with scramjet engines, with data again provided by General Electric. The two groups conceptual designs, along with the technical trade-offs, difficulties, and details that surfaced during the design process are presented. Author (revised)

N93-29720*# Ecole Polytechnique Feminine, Sceaux (France).
ASUR c05
In Universities Space Research Association, Houston, Proceedings of the Seventh Annual Summer Conference. NASA/USRA: University Advanced Design Program 1991 p 77-81 (For primary document see N93-29712 11-01)
Avail: CASI HC A01/MF A03

The Ecole Polytechnique Feminine (EPF) is a French engineering school for women. The students who presented the project at the Summer Conference are in the fourth year of a five year program. For the second time, the EPF worked on an aeronautical project with the Ohio State University. This year, the theme was to design a hypersonic carrier aimed to launch an orbiter at Mach 6, a range of 375 miles and an altitude of 95,000 ft. The plane was called ASUR which in French means the blue sky, the same sky that links our countries across the ocean. Moreover, ASUR is an anagram of USRA. This work benefits from work on reusable hypersonic aircraft in Europe, and especially on two of them: STAR-H and Sanger. STAR-H is a French project. This hypersonic aircraft would replace Ariane 5 in launching a shuttle smaller than Hermes. Sanger is a German project. Its objective is to launch a manned shuttle called HORUS, but Ariane 5 would be kept for heavy cargo launches. These two projects are in competition in Europe to be a launcher of the European Space Agency. Author (revised)

N93-29721*# Purdue Univ., West Lafayette, IN.
DESIGN OF A TURBOFAN POWERED REGIONAL TRANSPORT AIRCRAFT c05
In Universities Space Research Association, Houston, Proceedings of the Seventh Annual Summer Conference. NASA/USRA: University Advanced Design Program 1991 p 83-88 Previously announced as N92-20260 (For primary document see N93-29712 11-01)
Avail: CASI HC A02/MF A03

The majority of the market for small commercial transport aircraft is dominated by high-efficiency, propeller-driven aircraft of non-U.S. manufacture. During the past year senior student design teams at Purdue developed and then responded to a Request For Proposal (RFP) for a regional transport aircraft. The RFP development identified promising world markets and their needs. The students responded by designing aircraft with ranges of up to 1500 n.m. and passenger loads of 50 to 90. During the design project, special emphasis was placed upon keeping acquisition cost and direct operating costs at a low level while providing passengers with quality comfort levels. Twelve student teams worked for one semester developing their designs. Several of the more successful designs and those that placed a high premium on innovation are described. The depth of detail and analysis in these student efforts are also illustrated. Author (revised)

N93-29722*# Worcester Polytechnic Inst., MA.
SOLAR POWERED MULTIPURPOSE REMOTELY POWERED AIRCRAFT **c05**
In Universities Space Research Association, Houston, Proceedings of the Seventh Annual Summer Conference. NASA/USRA: University Advanced Design Program 1991 p 89-94 (For primary document see N93-29712 11-01)
Avail: CASI HC A02/MF A03

Environmental problems such as the depletion of the ozone layer and air pollution demand a change in traditional means of propulsion that is sensitive to the ecology. Solar-powered propulsion is a favorable alternative that is both ecologically harmless as well as cost effective. Integration of solar energy into designs ranging from futuristic vehicles to heating is, therefore, beneficial to society. The design and construction of a Multipurpose Remotely Piloted Vehicle (MPRPV) seeks to verify the feasibility of using solar propulsion as a primary fuel source. This task has been a year-long effort by a group of eight students, divided into four teams, each dealing with different aspects of the design. The aircraft was designed to take off, climb to the design altitude, fly in a sustained figure-eight flight path, and cruise for approximately one hour. This mission requires flight at Reynolds numbers between 150,000 and 200,000 and demands special considerations in the aerodynamic design to achieve flight in this regime. Optimal performance requires a lightweight configuration with both structural integrity and maximum power availability. The structural design and choice of solar cells for the propulsion were governed by weight, efficiency, and cost considerations. The final design is an MPRPV weighing 35 N that cruises at 7 m/s at the design altitude of 50 m. The configuration includes a wing composed of balsa and foam NACA 6409 airfoil sections and carbon fiber spars, a tail of similar construction, and a truss structure fuselage. The propulsion system consists of 98 12.5 percent-efficient solar cells donated by Mobil Solar, a NiCad battery for energy storage, and a folding propeller regulated by a lightweight and efficient control system. The airfoils and propeller chosen for the design were researched and tested during the design process. Author (revised)

N93-29723*# Alabama Univ., Huntsville.
A HIGH-TEMPERATURE FURNACE FOR APPLICATIONS IN MICROGRAVITY **c14**
In Universities Space Research Association, Houston, Proceedings of the Seventh Annual Summer Conference. NASA/USRA: University Advanced Design Program 1991 p 97-104 (For primary document see N93-29712 11-01)
Avail: CASI HC A02/MF A03

Technology in the area of material processing and crystal growth has been greatly furthered by research in microgravity environments. The role of efficient, lightweight furnaces with reliable performance is crucial in these experiments. A need exists for the development of a readily duplicated, high-temperature furnace satisfying stringent weight, volume, and power constraints. A furnace was designed and is referred to as the UAH SHIELD. Stringent physical and operating characteristics for the system were specified, including a maximum weight of 20 kg, a maximum power requirement of 60 W, and a volume of the furnace assembly, excluding the batteries, limited to half a Get-Away-Special canister. The UAH SHIELD furnace uses radiation shield and vacuum technology applied in the form of a series of concentric cylinders enclosed on either end with disks. Thermal testing of a furnace prototype was performed in addition to some thermal and structural analysis. Results indicate the need for spacing of the shields to accommodate the thermal expansion during furnace operation. In addition, a power dissipation of approximately 100 W and system weight of approximately 30 kg was found for the current design. Author (revised)

N93-29724*# Arizona Univ., Tucson.
ADVANCED DESIGN FOR ORBITAL DEBRIS REMOVAL IN SUPPORT OF SOLAR SYSTEM EXPLORATION **c18**
In Universities Space Research Association, Houston, Proceedings of the Seventh Annual Summer Conference. NASA/USRA: University Advanced Design Program 1991 p 105-111 (For primary document see N93-29712 11-01)
Avail: CASI HC A02/MF A03

The development of an Autonomous Space Processor for Orbital Debris (ASPOD) is the ultimate goal. The craft will process, in situ, orbital debris using resources available in low Earth orbit (LEO). The serious problem of orbital debris is briefly described and the nature of the large debris population is outlined. This year, focus was on development of a versatile robotic manipulator to augment an existing robotic arm; incorporation of remote operation of robotic arms; and formulation of optimal (time and energy) trajectory planning algorithms for coordinating robotic arms. The mechanical design of the new arm is described in detail. The versatile work envelope is explained showing the flexibility of the new design. Several telemetry communication systems are described which will enable the remote operation of the robotic arms. The trajectory planning algorithms are fully developed for both the time-optimal and energy-optimal problem. The optimal problem is solved using phase plane techniques while the energy optimal problem is solved using dynamics programming. Author

N93-29725*# California Univ., Los Angeles.
THE 1990/1991 PROJECT SUMMARIES **c12**
In Universities Space Research Association, Houston, Proceedings of the Seventh Annual Summer Conference. NASA/USRA: University Advanced Design Program 1991 p 113-116 (For primary document see N93-29712 11-01)
Avail: CASI HC A01/MF A03

Four projects carried out in 1990-9l at the University of California, Los Angeles, under NASA/USRA sponsorship are summarized. One of the projects described is a mission design, the three others include the design and construction of space-related hardware and testing. Topics researched include: manned voyage to Mars with periodic refueling from electrically propelled tankers; ground speed of balloons on Mars; tripod lunar landing structure; and grappling/docking device accommodating large lateral and angular misalignment. Author (revised)

N93-29726*# University of Central Florida, Orlando.
DESIGN, BUILDING, AND TESTING OF THE POSTLANDING SYSTEMS FOR THE ASSURED CREW RETURN VEHICLE **c16**
Kenneth C. Hosterman and Loren A. Anderson *In* Universities Space Research Association, Houston, Proceedings of the Seventh Annual Summer Conference. NASA/USRA: University Advanced Design Program 1991 p 117-121 (For primary document see N93-29712 11-01)
Avail: CASI HC A01/MF A03

The design, building, and testing of the postlanding support systems for a water-landing Assured Crew Return Vehicle (ACRV) are presented. One ACRV will be permanently docked to Space Station Freedom, fulfilling NASA's commitment to Assured Crew Return Capability in the event of an accident or illness. The configuration of the ACRV is based on an Apollo Command Module (ACM) derivative. The 1990-1991 effort concentrated on the design, building, and testing of a one-fifth scale model of the egress and stabilization systems. The objective was to determine the feasibility of (1) stabilizing the ACM out of the range of motions that cause seasickness and (2) the safe and rapid removal of a sick or injured crew member from the ACRV. The development of the ACRV postlanding systems model was performed at the University of Central Florida with guidance from the Kennedy Space Center ACRV program managers. Emphasis was placed on four major areas. First was design and construction of a one-fifth scale model of the ACM derivative to accommodate the egress and stabilization systems for testing. Second was the identification of a water test facility suitable for testing the model in all possible configurations. Third was the construction of the rapid egress mechanism designed in the previous academic year for incorporation into the ACRV model. The fourth area was construction and motion response testing of the attitude ring and underwater parachute systems. Author

N93-29727*# Colorado Univ., Boulder.
EARTH TO LUNAR CELSS EVOLUTION **c54**
In Universities Space Research Association, Houston, Proceedings of the Seventh Annual Summer Conference. NASA/USRA: University Advanced Design Program 1991 p 123-132 (For primary document see N93-29712 11-01)
Avail: CASI HC A02/MF A03

The comprehensive results of human activities on the environment, such as deforestation and ozone depletion, and the natural laws that govern the global environment have yet to be determined. Closed Ecological Life Support Systems (CELSS) research can play an instrumental role in dispelling these mysteries, as well as have the ability to support life in hostile environments, which the Earth one day may become. CELSS conclusions, such as the timescales in which plants fix carbon dioxide (CO2), will be the key to understanding each component and how it affects the ecological balance between plants and animals, the environment, and the biological engines that drive Earth's system. However, to understand how CELSS can be used as an investigative tool, the concept of a CELSS must be clearly defined. A definition of CELSS is given. The evolutionary establishment of a lunar base with a bioregenerative life support system in a Space Station Freedom (SSF) module to support a crew of four for two weeks duration was chosen as the design topic. Derived from text

N93-29728*# Florida Univ., Gainesville.
DESIGN OF BIOMASS MANAGEMENT SYSTEMS AND COMPONENTS FOR CLOSED LOOP LIFE SUPPORT SYSTEMS **c54**
In Universities Space Research Association, Houston, Proceedings of the Seventh Annual Summer Conference. NASA/USRA: University Advanced Design Program 1991 p 133-137 (For primary document see N93-29712 11-01)
Avail: CASI HC A01/MF A03

The goal of the EGM 4000/1 Design class was to investigate a Biomass Management System (BMS) and design, fabricate, and test components for biomass management in a closed-loop life support system (CLLSS). The designs explored were to contribute to the development of NASA's Controlled Ecological Life Support System (CELSS) at Kennedy Space Center. Designs included a sectored plant growth unit, a container and transfer mechanism, and an air curtain system for fugitive particle control. The work performed by the class members is summarized. Author

N93-29729*# Florida Agricultural and Mechanical Univ., Tallahassee.
LUNAR LANDER GROUND SUPPORT SYSTEM **c14**
In Universities Space Research Association, Houston, Proceedings of the Seventh Annual Summer Conference. NASA/USRA: University Advanced Design Program 1991 p 139-142 (For primary document see N93-29712 11-01)
Avail: CASI HC A01/MF A03

This year's project, like the previous Aerospace Group's project, involves a lunar transportation system. The basic time line will be the years 2010-2030 and will be referred to as a second generation system, as lunar bases would be present. The project design completed this year is referred to as the Lunar Lander Ground Support System (LLGSS). The area chosen for analysis encompasses a great number of vehicles and personnel. The design of certain elements of the overall lunar mission are complete projects in themselves. For this reason the project chosen for the Senior Aerospace Design is the design of specific servicing vehicles and additions or modifications to existing vehicles for the area of concern involving servicing and maintenance of the lunar lander while on the surface. Derived from text

N93-29730*# Georgia Inst. for Research, Atlanta.
THE 1990-1991 PROJECT SUMMARIES **c12**
In Universities Space Research Association, Houston, Proceedings of the Seventh Annual Summer Conference. NASA/USRA: University Advanced Design Program 1991 p 143-144 (For primary document see N93-29712 11-01)
Avail: CASI HC A01/MF A03

Project summaries for 1990-91 at the Georgia Institute of Technology are presented. The following research projects were studied: a lunar surface vehicle model; lunar loader/transporter; trenching and cable-laying device for the lunar surface; a lunar vehicle system for habitat transport and placement; and lunar storage facility. CASI

N93-29731*# Georgia Inst. for Research, Atlanta.
THE 1990-1991 PROJECT SUMMARIES **c12**
In Universities Space Research Association, Houston, Proceedings of the Seventh Annual Summer Conference. NASA/USRA: University Advanced Design Program 1991 p 145-148 (For primary document see N93-29712 11-01)
Avail: CASI HC A01/MF A03

Georgia Tech's School of Textile & Fiber Engineering and School of Mechanical Engineering participated in four cooperative design efforts this year. One group designed a thermal shield for a lunar telescope. The second group designed a selenotextile habitat shielding structure. The third group designed a pneumatically assisted elbow joint for the NASA zero-prebreathe suit (ZPS). The final group designed an electromechanical system to power an astronaut's finger joints. Summaries of these projects are presented. Author

N93-29732*# Houston Univ., TX.
SOLAR ENERGY EMPLACEMENT DEVELOPER **c44**
Michael Mortensen and Bob Sauls *In* Universities Space Research Association, Houston, Proceedings of the Seventh Annual Summer Conference. NASA/USRA: University Advanced Design Program 1991 p 149-154 (For primary document see N93-29712 11-01)
Avail: CASI HC A02/MF A03

A preliminary design was developed for a Lunar Power System (LPS) composed of photovoltaic arrays and microwave reflectors fabricated from lunar materials. The LPS will collect solar energy on the surface of the Moon, transform it into microwave energy, and beam it back to Earth where it will be converted into usable energy. The Solar Energy Emplacement Developer (SEED) proposed will use a similar sort of solar energy collection and dispersement to power the systems that will construct the LPS. Author (revised)

N93-29733*# Idaho Univ., Moscow.
EXERCISE/RECREATION FACILITY FOR A LUNAR OR MARS ANALOG **c54**
In Universities Space Research Association, Houston, Proceedings of the Seventh Annual Summer Conference. NASA/USRA: University Advanced Design Program 1991 p 155-158 (For primary document see N93-29712 11-01)
Avail: CASI HC A01/MF A03

The University of Idaho, NASA/USRA project for the 1990-91 school year is an exercise/recreation station for an Earth-based simulator of a lunar or martian habitat. Specifically, a stationary bicycle that will help people keep fit and prevent muscular atrophy while stationed in space was designed. To help with motivation and provide an element of recreation during the workout, the bicycle is to be enhanced by a virtual reality system. The system simulates various riding situations, including the choice of a mountain bike or a road bike. The bike employs a magnetic brake that provides continuously changing tension to simulate actual riding conditions. This braking system is interfaced directly with the virtual reality system. Also, integrated into the virtual reality display will be a monitoring system that regulates heart rate, work rate, and other functions during the course of the session. Author

N93-29734*# Kansas State Univ., Manhattan.
AUTOMATION OF CLOSED ENVIRONMENTS IN SPACE FOR HUMAN COMFORT AND SAFETY **c54**
In Universities Space Research Association, Houston, Proceedings of the Seventh Annual Summer Conference. NASA/USRA: University Advanced Design Program 1991 p 159-163 (For primary document see N93-29712 11-01)
Avail: CASI HC A01/MF A03

The development of Environmental Control and Life Support Systems (ECLSS) for Space Station Freedom, future colonization of the Moon, and Mars missions presents new challenges for present technologies. ECLSS that operate during long-duration missions must be semi-autonomous to allow crew members environmental control without constant supervision. A control system for the ECLSS must address these issues as well as being reliable. The Kansas State University Advanced Design Team is in the process of researching and designing controls for the automation of the ECLSS for Space Station Freedom and beyond. The ECLSS for Freedom is composed of six subsystems. The temperature and humidity control (THC) subsystem maintains the cabin temperature and humidity at a comfortable level. The atmosphere control and supply (ACS) subsystem insures proper cabin pressure and partial pressures of oxygen and nitrogen. To protect the space station from fire damage, the fire detection and suppression (FDS) subsystem provides fire-sensing alarms and extinguishers. The waste management (WM) subsystem compacts solid wastes for return to Earth, and collects urine for water recovery. The atmosphere revitalization (AR) subsystem removes CO2 and other dangerous contaminants from the air. The water recovery and management (WRM) subsystem collects and filters condensate from the cabin to replenish potable water supplies, and processes urine and other waste waters to replenish hygiene water supplies. These subsystems are not fully automated at this time. Furthermore, the control of these subsystems is not presently integrated; they are largely independent of one another. A fully integrated and automated ECLSS would increase astronauts' productivity and contribute to their safety and comfort. Author

N93-29735*# Maryland Univ., College Park.
DELTA ADVANCED REUSABLE TRANSPORT (DART): AN ALTERNATIVE MANNED SPACECRAFT c18
T. Lewerenz, M. Kosha, and H. Magazu *In* Universities Space Research Association, Houston, Proceedings of the Seventh Annual Summer Conference. NASA/USRA: University Advanced Design Program 1991 p 165-175 (For primary document see N93-29712 11-01)
Avail: CASI HC A03/MF A03

Although the current U.S. Space Transportation System (STS) has proven successful in many applications, the truth remains that the space shuttle is not as reliable or economical as was once hoped. In fact, the Augustine Commission on the future of the U.S. Space Program has recommended that the space shuttle only be used on missions directly requiring human capabilities on-orbit and that the shuttle program should eventually be phased out. This poses a great dilemma since the shuttle provides the only current or planned U.S. means for human access to space at the same time that NASA is building toward a permanent manned presence. As a possible solution to this dilemma, it is proposed that the U.S. begin development of an Alternative Manned Spacecraft (AMS). This spacecraft would not only provide follow-on capability for maintaining human space flight, but would also provide redundancy and enhanced capability in the near future. Design requirements for the AMS studied include: (1) capability of launching on one of the current or planned U.S. expendable launch vehicles (baseline McDonnell Douglas Delta II model 7920 expendable booster); (2) application to a wide variety of missions including autonomous operations, space station support, and access to orbits and inclinations beyond those of the space shuttle; (3) low enough costing to fly regularly in augmentation of space shuttle capabilities; (4) production surge capabilities to replace the shuttle if events require it; (5) intact abort capability in all flight regimes since the planned launch vehicles are not man-rated; (6) technology cut-off date of 1990; and (7) initial operational capability in 1995. In addition, the design of the AMS would take advantage of scientific advances made in the 20 years since the space shuttle was first conceived. These advances are in such technologies as composite materials, propulsion systems, avionics, and hypersonics. Author (revised)

N93-29736*# Maryland Univ., College Park.
TAURUS LIGHTWEIGHT MANNED SPACECRAFT EARTH ORBITING VEHICLE c18
M. Bosset *In* Universities Space Research Association, Houston, Proceedings of the Seventh Annual Summer Conference. NASA/USRA: University Advanced Design Program 1991 p 177-186 (For primary document see N93-29712 11-01)
Avail: CASI HC A02/MF A03

The Taurus Lightweight Manned Spacecraft (LMS) was developed by students of the University of Maryland's Aerospace Engineering course in Space Vehicle Design. That course required students to design an Alternative Manned Spacecraft (AMS) to augment or replace the Space Transportation System and meet the following design requirements: (1) launch on the Taurus Booster being developed by Orbital Sciences Corporation; (2) 99.9 percent assured crew survival rate; (3) technology cutoff date of 1 Jan. 1991; (4) compatibility with current space administration infrastructure; and (5) first flight by May 1995. The Taurus LMS design meets the above requirements and represents an initial step toward larger and more complex spacecraft. The Taurus LMS has a very limited application when compared to the space shuttle, but it demonstrates that the U.S. can have a safe, reliable, and low-cost space system. The Taurus LMS is a short mission duration spacecraft designed to place one man into low Earth orbit (LEO). The driving factor for this design was the low payload carrying capabilities of the Taurus Booster - 1300 kg to a 300-km orbit. The Taurus LMS design is divided into six major design sections. The Human Factors section deals with the problems of life support and spacecraft cooling. The Propulsion section contains the Abort System, the Orbital Maneuvering System (OMS), the Reaction Control System (RCS), and Power Generation. The thermal protection systems and spacecraft structure are contained in the Structures section. The Avionics section includes Navigation, Attitude Determination, Data Processing, Communication systems, and Sensors. The Mission Analysis section was responsible for ground processing and spacecraft astrodynamics. The Systems Integration Section pulled the above sections together into one spacecraft, and addressed costing and reliability. Author (revised)

N93-29737*# Maryland Univ., College Park. Mechanical Engineering.
WALKING ROBOT: A DESIGN PROJECT FOR UNDERGRADUATE STUDENTS c37
In Universities Space Research Association, Houston, Proceedings of the Seventh Annual Summer Conference. NASA/USRA: University Advanced Design Program 1991 p 187-190 (For primary document see N93-29712 11-01)
Avail: CASI HC A01/MF A03

The objective of the University of Maryland walking robot project was to design, analyze, assemble, and test an intelligent, mobile, and terrain-adaptive system. The robot incorporates existing technologies in novel ways. The legs emulate the walking path of a human by an innovative modification of a crank-and-rocker mechanism. The body consists of two tripod frames connected by a turning mechanism. The two sets of three legs are mounted so as to allow the robot to walk with stability in its own footsteps. The computer uses a modular hardware design and distributed processing. Dual-port RAM is used to allow communication between a supervisory personal computer and seven microcontrollers. The microcontrollers provide low-level control for the motors and relieve the processing burden on the PC. Author

N93-29738*# Massachusetts Inst. of Tech., Cambridge.
PROJECT COPERNICUS: AN EARTH OBSERVING SYSTEM c43
In Universities Space Research Association, Houston, Proceedings of the Seventh Annual Summer Conference. NASA/USRA: University Advanced Design Program 1991 p 191-196 (For primary document see N93-29712 11-01)
Avail: CASI HC A02/MF A03

Hunsaker Aerospace Corporation is presenting this proposal for Project Copernicus to fulfill the need for space-based remote sensing of Earth. Concentration is on data acquisition. Copernicus is designed to be a flexible system of spacecraft in a low near-polar orbit. The goal is to acquire data so that the scientists may begin to understand many Earth processes and interactions. The mission objective of Copernicus is to provide a space-based, remote-sensing measurement data acquisition and transfer system for 15 years. A description of the design project is presented. Derived from text

N93-29739*# Michigan Univ., Ann Arbor.
PROJECT MEDSAT c18
In Universities Space Research Association, Houston, Proceedings of the Seventh Annual Summer Conference. NASA/USRA: University Advanced Design Program 1991 p 197-203 (For primary document see N93-29712 11-01)
Avail: CASI HC A02/MF A03

During the winter term of 1991, two design courses at the University of Michigan worked on a joint project, MEDSAT. The two design teams consisted of the Atmospheric, Oceanic, and Spacite System Design and Aerospace Engineering 483 (Aero 483) Aerospace System Design. In collaboration, they worked to produce MEDSAT, a satellite and scientific payload whose purpose was to monitor environmental conditions over Chiapas, Mexico. Information gained from the sensing, combined with regional data, would be used to determine the potential for malaria occurrence in that area. The responsibilities of AOSS 605 consisted of determining the remote sensing techniques, the data processing, and the method to translate the information into a usable output. Aero 483 developed the satellite configuration and the subsystems required for the satellite to accomplish its task. The MEDSAT project is an outgrowth of work already being accomplished by NASA's Biospheric and Disease Monitoring Program and Ames Research Center. NASA's work has been to develop remote sensing techniques to determine the abundance of disease carriers and now this project will place the techniques aboard a satellite. MEDSAT will be unique in its use of both a Synthetic Aperture Radar and visual/IR sensor to obtain comprehensive monitoring of the site. In order to create a highly feasible system, low cost was a high priority. To obtain this goal, a light satellite configuration launched by the Pegasus launch vehicle was used. Author (revised)

N93-29740*# Michigan Univ., Ann Arbor.
PROJECT UM-HAUL: A SELF-UNLOADING REUSABLE LUNAR LANDER **c18**
In Universities Space Research Association, Houston, Proceedings of the Seventh Annual Summer Conference. NASA/USRA: University Advanced Design Program 1991 p 205-211 (For primary document see N93-29712 11-01)
Avail: CASI HC A02/MF A03

The establishment of a lunar base is technologically and financially challenging. Given the necessary resources and political support, it can be done. In addition to the geopolitical obstacles, however, there are logistical problems involved in establishing such bases that can only be overcome with the acquisition of a significant transportation and communications network in the Earth-Moon spatial region. Considering the significant number of payloads that will be required in this process, the mass-specific cost of launching these payloads, and the added risk and cost of human presence in space, it is clearly desirable to automate major parts of such an operation. One very costly and time-consuming factor in this picture is the delivery of payloads to the Moon. Foreseeable payloads would include atmospheric modules, inflatable habitat kits, energy and oxygen plant elements, ground vehicles, laboratory modules, crew supplies, etc. The duration of high-risk human presence on the Moon could be greatly reduced if all such payloads were delivered to the prospective base site in advance of crew arrival. In this view, the idea of a 'Self-Unloading Reusable Lunar Lander' (SURLL) arises naturally. The general scenario depicts the lander being brought to low lunar orbit (LLO) from Earth atop a generic Orbital Transfer Vehicle (OTV). From LLO, the lander shuttles payloads down to the lunar surface, where, by means of some resident, detachable unloading device, it deploys the payloads and returns to orbit. The general goal is for the system to perform with maximum payload capability, automation, and reliability, while also minimizing environmental hazards, servicing needs, and mission costs. Our response to this demand is UM-HAUL, or the UnManned Heavy pAyload Unloader and Lander. The complete study includes a system description, along with a preliminary cost analysis and a design status assessment.
Author (revised)

N93-29741*# Minnesota Univ., Minneapolis.
MARS INTEGRATED TRANSPORTATION SYSTEM MULTISTAGE MARS MISSION **c18**
In Universities Space Research Association, Houston, Proceedings of the Seventh Annual Summer Conference. NASA/USRA: University Advanced Design Program 1991 p 213-218 (For primary document see N93-29712 11-01)
Avail: CASI HC A02/MF A03

In accordance with the objective of the Mars Integrated Transport System (MITS) program, the Multistage Mars Mission (MSMM) design team developed a profile for a manned mission to Mars. The purpose of the multistage mission is to send a crew of five astronauts to the martian surface by the year 2019. The mission continues man's eternal quest for exploration of new frontiers. This mission has a scheduled duration of 426 days that includes experimentation en route as well as surface exploration and experimentation. The MSMM is also designed as a foundation for a continuing program leading to the colonization of the planet Mars. Author

N93-29742*# Minnesota Univ., Minneapolis.
SINGLE-STAGE MARS MISSION **c12**
In Universities Space Research Association, Houston, Proceedings of the Seventh Annual Summer Conference. NASA/USRA: University Advanced Design Program 1991 p 219-226 (For primary document see N93-29712 11-01)
Avail: CASI HC A02/MF A03

President Bush established a three phase Space Exploration Initiative for the future of space exploration. The first phase is the design and construction of Space Station Freedom. The second phase is permanent lunar base. The last phase of the Initiative is the construction of a Mars outpost. The design presented is the concept of a single-stage Mars mission developed by the University of Minnesota Aerospace Design Course. The mission will last approximately 500 days including a 30-60 day stay on Mars.
Author

N93-29743*# Naval Postgraduate School, Monterey, CA.
MULTIPURPOSE SATELLITE BUS (MPS) **c18**
In Universities Space Research Association, Houston, Proceedings of the Seventh Annual Summer Conference. NASA/USRA: University Advanced Design Program 1991 p 227-236 (For primary document see N93-29712 11-01)
Avail: CASI HC A02/MF A03

The Naval Postgraduate School Advanced Design Project sponsored by the Universities Space Research Association Advanced Design Program is a multipurpose satellite bus (MPS). The design was initiated from a Statement of Work (SOW) developed by the Defense Advanced Research Projects Agency (DARPA). The SOW called for a 'proposal to design a small, low-cost, lightweight, general purpose spacecraft bus capable of accommodating any of a variety of mission payloads. Typical payloads envisioned include those associated with meteorological, communication, surveillance and tracking, target location, and navigation mission areas.' The design project investigates two dissimilar missions, a meteorological payload and a communications payload, mated with a single spacecraft bus with minimal modifications. The MPS is designed for launch aboard the Pegasus Air Launched Vehicle (ALV) or the Taurus Standard Small Launch Vehicle (SSLV).
Author

N93-29744*# Ohio State Univ., Columbus.
PROJECT WISH: THE EMERALD CITY **c18**
In Universities Space Research Association, Houston, Proceedings of the Seventh Annual Summer Conference. NASA/USRA: University Advanced Design Program 1991 p 237-240 (For primary document see N93-29712 11-01)
Avail: CASI HC A01/MF A03

Project WISH (Wandering Interplanetary Space Harbor) is a three-year design effort currently being conducted at The Ohio State University. Its goal is the design of a space oasis to be used in the exploration of the solar system during the midtwenty-first century. This spacecraft, named Emerald City, is to conduct and provide support for missions to other planetary bodies with the purpose of exploration, scientific study, and colonization. It is to sustain a crew of between 500 and 1000 people at a time, and be capable of traveling from a nominal orbit to the planets in reasonably short flight times. Such a ship obviously presents many technical and design challenges, some of which were examined through the course of Project WISH. This year, Phase 2 (1990-1991) of Project WISH was carried out. The basic design of the Emerald City resulting from Phase 1 (1989-1990) was taken and improved upon through more detailed analysis and revision. At the core of this year's study were orbital mechanics, propulsion, attitude control, and human factors. Throughout the year, these areas were examined and information was compiled on their technologies, performances, and relationships. Then, using the data obtained through these studies, two specific missions were designed: an envelope mission from a nominal orbit of 4 AU to Saturn and a single point design for a specific mission from the Earth to Mars. The latter was designed in view of the special interest that Mars is attracting for near-future space exploration. The mission to Saturn has all the first six planets within its flight envelope in less than or equal to a 3-year flight time at any time upon demand, and it has Uranus in its flight envelope most of the time upon demand. These mission studies provided data on the approximate size, weight, number of engines, and other important design values that would be required for the Emerald City.
Author (revised)

N93-29745*# Old Dominion Univ., Norfolk, VA.
FROM ORBITAL DEBRIS CAPTURE SYSTEMS THROUGH INTERNAL COMBUSTION ENGINES ON MARS **c12**
In Universities Space Research Association, Houston, Proceedings of the Seventh Annual Summer Conference. NASA/USRA: University Advanced Design Program 1991 p 241-248 (For primary document see N93-29712 11-01)
Avail: CASI HC A02/MF A03

The investigation and conceptualization of an orbital debris collector was the primary area of design. In addition, an alternate structural design for Space Station Freedom and systems supporting resource utilization at Mars and the moon were studied. Hardware for production of oxygen from simulate Mars atmosphere was modified to permit more reliable operation at low pressures (down to 10 mb). An internal combustion engine was altered to study how Mars atmosphere could be used as a diluent to control combustion temperatures and avoid excess Mars propellant production requirements that would result from either methane-rich or oxygen-rich, methane-oxygen combustion. An elastic loop traction system that could be used for lunar construction vehicles was refined to permit testing. A parabolic heat rejection radiator system was designed and built to determine whether it was capable of increasing heat rejection rates during lunar daytime operation. In addition, an alternate space station truss design, utilizing a pre-integrated concept, was studied and found to reduce estimate extravehicular activity (EVA) time and increase the structural integrity when compared to the original Warren truss concept. An orbital-debris-capturing spacecraft design which could be mated with the Orbital Maneuvering Vehicle was studied. The design identified Soviet C-1B boosters as the best targets of opportunity in Earth orbits between an altitude of 900 km and 1100 km and at an inclination of 82.9 deg. A dual robot pallet, which could be spun to match the tumbling rate of the C-1B booster, was developed as the conceptual design. Author (revised)

N93-29746*# Pennsylvania State Univ., University Park.

MARS SAMPLE RETURN MISSION: TWO ALTERNATE SCENARIOS **c66**

In Universities Space Research Association, Houston, Proceedings of the Seventh Annual Summer Conference. NASA/USRA: University Advanced Design Program 1991 p 249-252 (For primary document see N93-29712 11-01)

Avail: CASI HC A01/MF A03

Two scenarios for accomplishing a Mars Sample Return mission are presented. Mission A is a low-cost, low-mass scenario, while Mission B is a high-technology, high-science alternative. Mission A begins with the launch of one Titan 4 rocket with a Centaur G' upper stage. The Centaur performs the trans-Mars injection burn and is then released. The payload consists of two lander packages and the orbital transfer vehicle, which is responsible for supporting the landers during launch and interplanetary cruise. Near Mars, the landers separate - one bound for a polar site and the other for an equatorial site. After descending to the surface, the landers deploy small, local rovers to collect samples. The rovers return these samples to the landers for loading on the direct return rockets, which return the samples directly to the Earth's surface. Mission B starts with four Titan 4 launches, used to place the components of the planetary transfer vehicle (PTV) into orbit. The fourth launch payload is able to move to assemble the entire vehicle by simple docking routines. Once complete, the PTV begins a low-thrust trajectory out from low Earth orbit, through interplanetary space, and into low Mars orbit. It deploys a communications satellite into a one half sol orbit and then releases the lander pad cage at 500 km altitude. The lander package contains the lander, the Mars ascent vehicle (MAV), two lighter-than-air rovers (called Aereons), and one conventional land rover. The entire package is contained within a biconic aeroshell. After release from the PTV the lander package descends to the surface, where all three rovers are released to collect samples and map the terrain. The Aereons attempt to circumnavigate Mars and collect samples from a wide variety of sites, while the land rover examines a local area more thoroughly. The Aereons are equipped with small sample return rockets that can return their samples to the lander in the event that an Aereon is incapable of returning to the lander itself. Once all samples have been collected they are loaded onto the MAV and launched into orbit. The PTV then collects the samples and returns them to Earth orbit for recovery. Author (revised)

N93-29747*# Prairie View Agricultural and Mechanical Coll., TX.

MARS HABITAT **c54**

In Universities Space Research Association, Houston, Proceedings of the Seventh Annual Summer Conference. NASA/USRA: University Advanced Design Program 1991 p 253-263 (For primary document see N93-29712 11-01)

Avail: CASI HC A03/MF A03

The College of Engineering & Architecture at Prairie View A&M University has been participating in the NASA/USRA Advanced Design Program since 1986. The interdisciplinary nature of the program allowed the involvement of students and faculty throughout the College of Engineering & Architecture for the last five years. The research goal for the 1990-1991 year is to design a human habitat on Mars that can be used as a permanent base for 20 crew members. The research is being conducted by undergraduate students from the Department of Architecture. Author

N93-29748*# Puerto Rico Univ., Rio Piedras.

SELENIA: A HABITABILITY STUDY FOR THE DEVELOPMENT OF A THIRD GENERATION LUNAR BASE **c54**

In Universities Space Research Association, Houston, Proceedings of the Seventh Annual Summer Conference. NASA/USRA: University Advanced Design Program 1991 p 265-273 (For primary document see N93-29712 11-01)

Avail: CASI HC A02/MF A03

When Apollo astronauts landed on the Moon, the first generation of lunar bases was established. They consisted essentially of a lunar module and related hardware capable of housing two astronauts for not more than several days. Second generation lunar bases are being developed, and further infrastructure, such as space station, orbital transfer, and reusable lander vehicles will be necessary, as prolonged stay on the Moon is required for exploration, research, and construction for the establishment of a permanent human settlement there. Human life in these habitats could be sustained for months, dependent on a continual flow of life-support supplies from Earth. Third-generation lunar bases will come into being as self sufficiency of human settlements becomes feasible. Regeneration of water, oxygen production, and development of indigenous construction materials from lunar resources will be necessary. Greenhouses will grow food supplies in engineered biospheres. Assured protection from solar flares and cosmic radiation must be provided, as well as provision for survival under meteor showers, or the threat of meteorite impact. All these seem to be possible within the second decade of the next century. Thus, the builders of Selenia, the first of the third-generation lunar bases are born today. During the last two years students from the School of Architecture of the University of Puerto Rico have studied the problems that relate to habitability for prolonged stay in extraterrestrial space. An orbital personnel transport to Mars developed originally by the Aerospace Engineering Department of the University of Michigan was investigated and habitability criteria for evaluation of human space habitats were proposed. An important finding from that study was that the necessary rotational diameter of the vessel has to be on the order of two kilometers to ensure comfort for humans under the artificial gravity conditions necessary to maintain physiological well being of passengers, beyond the level of mere survival. Author (revised)

N93-29749*# Rensselaer Polytechnic Inst., Troy, NY.

THE LIGHTCRAFT PROJECT **c16**

Don G. Messitt and Leik N. Myrabo *In* Universities Space Research Association, Houston, Proceedings of the Seventh Annual Summer Conference. NASA/USRA: University Advanced Design Program 1991 p 275-280 (For primary document see N93-29712 11-01)

Avail: CASI HC A02/MF A03

Rensselaer Polytechnic Institute has been developing a transatmospheric 'Lightcraft' technology which uses beamed laser energy to propel advanced shuttle craft to orbit. In the past several years, Rensselaer students have analyzed the unique combined-cycle Lightcraft engine, designed a small unmanned Lightcraft Technology Demonstrator, and conceptualized larger manned Lightcraft - to name just a few of the interrelated design projects. The 1990-91 class carried out preliminary and detailed design efforts for a one-person 'Mercury' Lightcraft, using computer-aided design and finite-element structural modeling techniques. In addition, they began construction of a 2.6 m-diameter, full-scale engineering prototype mockup. The mockup will be equipped with three robotic legs that 'kneel' for passenger entry and exit. More importantly, the articulated tripod gear is crucial for accurately pointing at, and tracking the laser relay mirrors, a maneuver that must be performed just prior to liftoff. Also accomplished were further design improvements on a 6-inch-diameter Lightcraft model (for testing in RPI's hypersonic tunnel), and new laser propulsion experiments. The resultant experimental data will be used to calibrate Computational Fluid Dynamic (CFD) codes and analytical laser propulsion models that can simulate vehicle/engine flight conditions along a transatmospheric boost trajectory. These efforts will enable the prediction of distributed aerodynamic and thruster loads over the entire full-scale spacecraft. Author (revised)

N93-29750*# Texas Univ., Austin.

ASPEC: SOLAR POWER SATELLITE **c18**

In Universities Space Research Association, Houston, Proceedings of the Seventh Annual Summer Conference. NASA/USRA: University Advanced

Design Program 1991 p 281-285 (For primary document see N93-29712 11-01)
Avail: CASI HC A01/MF A03

The solar power satellite (SPS) will provide a clean, reliable source of energy for large-scale consumption. The system will use satellites in geostationary orbits around the Earth to capture the Sun's energy. The intercepted sunlight will be converted to laser beam energy that can be transmitted to the Earth's surface. Ground systems on the Earth will convert the transmissions from space into electric power. The preliminary design for the SPS consists of one satellite in orbit around the Earth transmitting energy to a single ground station. The SPS design uses multilayer solar cell technology arranged on a 20 km squared planar array to intercept sunlight and convert it to an electric voltage. Power conditioning devices then send the electricity to a laser, which transmits the power to the surface of the Earth. A ground station will convert the beam into electricity. Typically, a single SPS will supply 5 GW of power to the ground station. Due to the large mass of the SPS, about 41 million kg, construction in space is needed in order to keep the structural mass low. The orbit configuration for this design is to operate a single satellite in geosynchronous orbit (GEO). The GEO allows the system to be positioned above a single receiving station and remain in sunlight 99 percent of the time. Construction will take place in low Earth orbit (LEO); array sections, 20 in total, will be sailed on solar wind out to the GEO location in 150 days. These individual transportation sections are referred to as solar sailing array panels (SSAP's). The primary truss elements used to support the array are composed of composite tubular members in a pentahedral arrangement. Smart segments consisting of passive and active damping devices will increase the control of dynamic SPS modes. Author (revised)

N93-29751*# Texas Univ., Austin.
B AND T: LUNAR LANDERS **c18**
In Universities Space Research Association, Houston, Proceedings of the Seventh Annual Summer Conference. NASA/USRA: University Advanced Design Program 1991 p 287-289 (For primary document see N93-29712 11-01)
Avail: CASI HC A01/MF A03

In the early twenty-first century, astronauts will return to the Moon and establish a permanent base. To achieve this goal safely and economically, B&T Engineering has designed an unmanned, reusable, self-unloading lunar lander. The lander is designed to deliver 15,000-kg payloads from an orbital transfer vehicle (OTV) in a low lunar polar orbit and at an altitude of 200 km to any location on the lunar surface. Author

N93-29752*# Texas Univ., Austin.
SPACELY'S ROCKETS: PERSONNEL LAUNCH SYSTEM/FAMILY OF HEAVY LIFT LAUNCH VEHICLES **c15**
In Universities Space Research Association, Houston, Proceedings of the Seventh Annual Summer Conference. NASA/USRA: University Advanced Design Program 1991 p 291-293 (For primary document see N93-29712 11-01)
Avail: CASI HC A01/MF A03

During 1990, numerous questions were raised regarding the ability of the current shuttle orbiter to provide reliable, on demand support of the planned space station. Besides being plagued by reliability problems, the shuttle lacks the ability to launch some of the heavy payloads required for future space exploration, and is too expensive to operate as a mere passenger ferry to orbit. Therefore, additional launch systems are required to complement the shuttle in a more robust and capable Space Transportation System. In December 1990, the Report of the Advisory Committee on the Future of the U.S. Space Program, advised NASA of the risks of becoming too dependent on the space shuttle as an all-purpose vehicle. Furthermore, the committee felt that reducing the number of shuttle missions would prolong the life of the existing fleet. In their suggestions, the board members strongly advocated the establishment of a fleet of unmanned, heavy lift launch vehicles (HLLV's) to support the space station and other payload-intensive enterprises. Another committee recommendation was that a space station crew rotation/rescue vehicle be developed as an alternative to the shuttle, or as a contingency if the shuttle is not available. The committee emphasized that this vehicle be designed for use as a personnel carrier, not a cargo carrier. This recommendation was made to avoid building another version of the existing shuttle, which is not ideally suited as a passenger vehicle only. The objective of this project was to design both a Personnel Launch System (PLS) and a family of HLLV's that provide low cost and efficient operation in missions not suited for the shuttle. Author (revised)

N93-29753*# Texas Univ., Austin.
RS LANDERS: LUNAR LANDER **c18**
In Universities Space Research Association, Houston, Proceedings of the Seventh Annual Summer Conference. NASA/USRA: University Advanced Design Program 1991 p 295-297 (For primary document see N93-29712 11-01)
Avail: CASI HC A01/MF A03

The future of the U.S. space program outlined by President Bush calls for a permanently manned lunar base. A payload delivery system will be required to support the buildup and operation of that lunar base. In response to this goal, RS Landers developed a conceptual design of a self-unloading, unmanned, reusable lunar lander. The lander will deliver a 7000-kg payload, with the same dimensions as a space station logistics module, from low lunar orbit (LLO) to any location on the surface of the Moon. Author

N93-29754*# Texas Univ., Austin.
SPECS: ORBITAL DEBRIS REMOVAL **c18**
In Universities Space Research Association, Houston, Proceedings of the Seventh Annual Summer Conference. NASA/USRA: University Advanced Design Program 1991 p 299-300 (For primary document see N93-29712 11-01)
Avail: CASI HC A01/MF A03

The debris problem has reached a stage at which the risk to satellites and spacecraft has become substantial in low Earth orbit (LEO). This research discovered that small particles posed little threat to spacecraft because shielding can effectively prevent these particles from damaging the spacecraft. The research also showed that, even though collision with a large piece of debris could destroy the spacecraft, the large pieces of debris pose little danger because they can be tracked and the spacecraft can be maneuvered away from these pieces. Additionally, there are many current designs to capture and remove large debris particles from the space environment. From this analysis, it was decided to concentrate on the removal of medium-sized orbital debris, that is, those pieces ranging from 1 cm to 50 cm in size. The current design incorporates a transfer vehicle and a netting vehicle to capture the medium-sized debris. The system is based near an operational space station located at 28.5 deg inclination and 400 km altitude. The system uses ground-based tracking to determine the location of a satellite breakup or debris cloud. These data are uploaded to the transfer vehicle, which proceeds to rendezvous with the debris at a lower altitude parking orbit. Next, the netting vehicle is deployed, tracks the targeted debris, and captures it. After expending the available nets, the netting vehicle returns to the transfer vehicle for a new netting module and continues to capture more debris in the target area. Once all the netting modules are expended, the transfer vehicle returns to the space station's orbit where it is resupplied with new netting modules from a space shuttle load. The new modules are launched by the shuttle from the ground and the expended modules are taken back to Earth for removal of the captured debris, refueling, and repacking of the nets. Once the netting modules are refurbished, they are taken back into orbit for reuse. In a typical mission, the system has the ability to capture 50 pieces of orbital debris. One mission will take approximately six months and the system is designed to allow for a 30 deg inclination change on the outgoing and incoming trips of the transfer vehicle. Author (revised)

N93-29755*# Texas Univ., Austin.
THE 1990-1991 PROJECT SUMMARIES **c12**
In Universities Space Research Association, Houston, Proceedings of the Seventh Annual Summer Conference. NASA/USRA: University Advanced Design Program 1991 p 301-303 (For primary document see N93-29712 11-01)
Avail: CASI HC A01/MF A03

The Mechanical Engineering Department at The University of Texas at Austin participated in the NASA/USRA University Advanced Design Program on both an undergraduate and a graduate level during the 1990-91 academic year. The focus of study was on four design projects that fall into one of the following areas: (1) the establishment of a lunar base and (2) mission planet Earth. The design projects were incorporated into already existing design courses and students worked together in groups of three to five. A background of each area of study is provided, along with synopses, conclusions, and recommendations for further study for each design project. Author

N93-29756*# Naval Academy, Annapolis, MD.
MARS AQUARIUS MISSION AND TITAN EXPLORER **c66**
Brian Dulla, Christina Glaser, Jason Lopez, Jeffrey Lucas, Michelle Reyes, James Rimrodt, Stephen Philpott, Paul Diedrich, Terry Ladau, and David Lagassa et al *In* Universities Space Research Association, Houston, Proceedings of the Seventh Annual Summer Conference. NASA/USRA: University Advanced Design Program 1991 p 305-308 (For primary document see N93-29712 11-01)
Avail: CASI HC A01/MF A03

The Mars Aquarius Mission is designed to carry out several scientific studies of the surface and subsurface of Mars with an emphasis on locating subterranean water. This mission is a precursor to a manned mission to Mars. A manned mission will require an extended stay on the planet's surface, and an accessible source of water will greatly simplify life support requirements. Using data from previous Mars observations, four sites were selected as possible locations of subsurface water. The Aquarius spacecraft carries one penetrator for each of these sites. Author

N93-29757*# Utah State Univ., Logan.
THERMION: VERIFICATION OF A THERMIONIC HEAT PIPE IN MICROGRAVITY **c34**
In Universities Space Research Association, Houston, Proceedings of the Seventh Annual Summer Conference. NASA/USRA: University Advanced Design Program 1991 p 309-312 (For primary document see N93-29712 11-01)
Avail: CASI HC A01/MF A03

The Idaho National Engineering Laboratory (INEL) is conducting intensive research in the design and development of a small excore heat-pipe-thermionic space nuclear reactor power system (SEHPTR). The SEHPTR spacecraft will be able to supply 40 kW of power in any given orbit. The key components in this reactor are the thermionic heat pipes. The heat pipes have two major functions: (1) to convert heat energy into electrical energy, and (2) to radiate the excess heat to space. Thermionic power conversion is the process of converting heat energy into electrical energy with no moving parts. Heat is applied to the cathode surface. This heat will boil off electrons that will jump across the gap to the cooler surface of the anode, which will cause a potential difference between the two plates and induce a current through the load. Thermionic power conversion is incorporated as part of the heat pipe. The heat pipe, which is being developed by Thermacore Inc., is actually two heat pipes. It uses a radial heat pipe, called the emitter, and an axial heat pipe collector. The emitter heat pipe will pass the heat from the nuclear core to the cathode surface. The collector heat pipe keeps the anode surface cooler by transferring the heat from the anode surface and radiating it to space. Author (revised)

N93-29758*# Virginia Polytechnic Inst. and State Univ., Blacksburg.
SOLAR ELECTRIC PROPULSION CARGO SPACECRAFT FOR MARS MISSIONS **c20**
In Universities Space Research Association, Houston, Proceedings of the Seventh Annual Summer Conference. NASA/USRA: University Advanced Design Program 1991 p 313-316 (For primary document see N93-29712 11-01)
Avail: CASI HC A01/MF A03

One of the topics available to the 1990-91 Aerospace Engineering senior class was the development of a preliminary design of an unmanned cargo ferry that would support the Mars mission by bringing equipment and supplies from a low Earth orbit (LEO) to a low Mars orbit (LMO). Several previous studies initiated by NASA have indicated that low-thrust transportation systems seem to offer the best performance for Mars missions. Such systems are characterized by long spiral times during escape and capture maneuvers, high payload mass fractions, and, typically, low propellant mass fractions. Of two main low-thrust candidates, nuclear electric propulsion (NEP) and solar electric propulsion (SEP), only the first one received extensive consideration because it seemed to represent the most promising concept for a manned mission to Mars. However, any sustained Mars initiative will have to include an unmanned cargo transportation system, for which an SEP concept deserves very careful consideration. The key assumptions and requirements established in cooperation with the Space Exploration Initiative office at the NASA Langley Research Center were (1) vehicle is assembled at the Space Station Freedom (SSF); (2) Earth-to-orbit delivery of the vehicle components, propellant, and payload is via shuttle-C; (3) vehicle's cargo mass is 61,000 kg; (4) vehicle delivers cargo to LMO at an altitude of 500 km and inclination of 70 deg; (5) vehicle returns (without cargo) to SSF; (6) vehicle should be reusable for at least three missions; and (7) vehicle is powered by ion argon thrusters. Two configurations were developed by two student teams, working mostly independently. Author (revised)

N93-29759*# Washington Univ., Seattle.
ANTARES: A LOW COST MODULAR LAUNCH VEHICLE FOR THE FUTURE **c15**
In Universities Space Research Association, Houston, Proceedings of the Seventh Annual Summer Conference. NASA/USRA: University Advanced Design Program 1991 p 317-328 (For primary document see N93-29712 11-01)
Avail: CASI HC A03/MF A03

The single-stage-to-orbit launch vehicle Antares is a revolutionary concept based on identical modular units, enabling the Antares to efficiently launch communications satellites, as well as heavy payloads, into Earth orbit and beyond. The basic unit of the modular system, a single Antares vehicle, is aimed at launching approximately 10,000 kg (22,000 lb) into low Earth orbit (LEO). When coupled with a standard Centaur upper stage, it is capable of placing 4000 kg (8800 lb) into geosynchronous Earth orbit (GE0). The Antares incorporates a reusable engine, the Dual Mixture Ratio Engine (DMRE), as its propulsive device. This enables Antares to compete and excel in the satellite launch market by dramatically reducing launch costs. Inherent in the design is the capability to attach several of these vehicles together to provide heavy lift capability. Any number of these vehicles can be attached depending on the payload and mission requirements. With a seven-vehicle configuration, the Antares' modular concept provides a heavy lift capability of approximately 70,000 kg (154,000 lb) to LEO. This expandability allows for a wide range of payload options, such as large Earth satellites, Space Station Freedom material, and interplanetary spacecraft, and also offers a significant cost savings over a mixed fleet based on different launch vehicles. Author (revised)

N93-29760*# Wisconsin Univ., Milwaukee.
GENESIS 2: ADVANCED LUNAR OUTPOST **c54**
Gary T. Moore *In* Universities Space Research Association, Houston, Proceedings of the Seventh Annual Summer Conference. NASA/USRA: University Advanced Design Program 1991 p 329-334 (For primary document see N93-29712 11-01)
(Contract NASw-4435)
Avail: CASI HC A02/MF A03

Advanced, second-generation lunar habitats for astronauts and mission specialists working on the Moon are investigated. The work was based on design constraints set forth in previous publications. Design recommendations are based on environmental response to the lunar environment, habitability, safety, near-term technology, replaceability and modularity, and suitability for NASA lunar research missions in the early 21st century. Scientists, engineers, and architects from NASA/JSC, Wisconsin aeronautical industry, and area universities gave technical input and offered critiques at design reviews throughout the process. The recommended design uses a lunar lava tube, with construction using a combination of Space Station Freedom-derived modules and lightweight Kevlar-laminate inflatables. The outpost includes research laboratories and biotron, crew quarters and support facility, mission control, health maintenance facility, and related areas for functional and psychological requirements. Furniture, specialized equipment, and lighting are included in the design analysis. Author

N93-29761*# Worcester Polytechnic Inst., MA.
ROTATIONAL FLUID FLOW EXPERIMENT **c34**
In Universities Space Research Association, Houston, Proceedings of the Seventh Annual Summer Conference. NASA/USRA: University Advanced Design Program 1991 p 335-338 (For primary document see N93-29712 11-01)
Avail: CASI HC A01/MF A03

This project which began in 1986 as part of the Worcester Polytechnic

Institute (WPI) Advanced Space Design Program focuses on the design and implementation of an electromechanical system for studying vortex behavior in a microgravity environment. Most of the existing equipment was revised and redesigned by this project team, as necessary. Emphasis was placed on documentation and integration of the electrical and mechanical subsystems. Project results include reconfiguration and thorough testing of all hardware subsystems, implementation of an infrared gas entrainment detector, new signal processing circuitry for the ultrasonic fluid circulation device, improved prototype interface circuits, and software for overall control of experiment operation. Author (revised)

N93-30673*# National Aeronautics and Space Administration. Ames Research Center, Moffett Field, CA.
NASA/FAA HELICOPTER SIMULATOR WORKSHOP
William E. Larsen, ed. (Federal Aviation Administration, Moffett Field, CA.), Robert J. Randle, Jr., ed. (Sverdrup Technology, Inc., Moffett Field, CA.), Richard S. Bray, ed. (Sverdrup Technology, Inc., Moffett Field, CA.), and John Zuk, ed. Apr. 1992 187 p Workshop held in Santa Clara, CA, 23-26 Apr. 1991
(Contract DTFA01-88-Z-02015)
(NASA-CP-3156; A-92020; NAS 1.55:3156; DOT/FAA/RD-92-2) Avail: CASI HC A09/MF A02

A workshop was convened by the FAA and NASA for the purpose of providing a forum at which leading designers, manufacturers, and users of helicopter simulators could initiate and participate in a development process that would facilitate the formulation of qualification standards by the regulatory agency. Formal papers were presented, special topics were discussed in breakout sessions, and a draft FAA advisory circular defining specifications for helicopter simulators was presented and discussed. A working group of volunteers was formed to work with the National Simulator Program Office to develop a final version of the circular. The workshop attracted 90 individuals from a constituency of simulator manufacturers, training organizations, the military, civil regulators, research scientists, and five foreign countries. For individual titles, see N93-30674 through N93-30691.

N93-30674*# National Aeronautics and Space Administration. Ames Research Center, Moffett Field, CA.
PART 1: EXECUTIVE SUMMARY
William E. Larsen (Federal Aviation Administration, Moffett Field, CA.), Robert J. Randle, Jr. (Sverdrup Technology, Inc., Moffett Field, CA.), Richard S. Bray (Sverdrup Technology, Inc., Moffett Field, CA.), and John Zuk *In its* NASA/FAA Helicopter Simulator Workshop Apr. 1992 p 1-11 (For primary document see N93-30673 11-01)
Avail: CASI HC A03/MF A02

A workshop was convened by the FAA and NASA for the purpose of providing a forum at which leading designers, manufacturers, and users of helicopter simulators could initiate and participate in a development process that would facilitate the formulation of qualification standards by the regulatory agency. Formal papers were presented, special topics were discussed in breakout sessions, and a draft FAA advisory circular defining specifications for helicopter simulators was presented and discussed. A working group of volunteers was formed to work with the National Simulator Program Office to develop a final version of the circular. The workshop attracted 90 individuals from a constituency of simulator manufacturers, training organizations, the military, civil regulators, research scientists, and five foreign countries. A great amount of information was generated and recorded verbatim. This information is presented herein within the limits of accuracy inherent in recording, transcribing, and editing spoken technical material. Author

N93-30675*# National Aeronautics and Space Administration. Ames Research Center, Moffett Field, CA.
HELICOPTER SIMULATOR STANDARDS **c09**
Edward M. Boothe *In its* NASA/FAA Helicopter Simulator Workshop Apr. 1992 p 31-33 (For primary document see N93-30673 11-01)
Avail: CASI HC A01/MF A02

The initial advisory circular was produced in 1984 (AC 120-XX). It was not finalized, however, because the FAR's for pilot certification did not recognize helicopter simulators and, therefore, permitted no credit for their use. That is being rectified, and, when the new rules are published, standards must be available for qualifying simulators. Because of the lack of a data base to support specification of these standards, the FAA must rely on the knowledge of experts in the simulator/training industry. A major aim of this workshop is to form a working group of these experts to produce a set of standards for helicopter training simulators. Author

N93-30676*# National Aeronautics and Space Administration. Ames Research Center, Moffett Field, CA.
HELICOPTER SIMULATION: AN AIRCREW TRAINING AND QUALIFICATION PERSPECTIVE **c53**
Richard A. Birnbach and Thomas M. Longridge *In its* NASA/FAA Helicopter Simulator Workshop Apr. 1992 p 35-38 (For primary document see N93-30673 11-01)
Avail: CASI HC A01/MF A02

This paper reviews some of the unique considerations that distinguish the commercial rotary wing domain from its fixed-wing counterpart. These considerations should give the FAA cause to proceed cautiously in drawing upon its fixed-wing experience. One major point to consider is the following: device qualification should be accomplished in a context of an overall training and qualification system. This approach would take as its starting point a detailed analysis of rotary-wing missions and tasks from which proficiency objectives can be systematically developed. Author (revised)

N93-30677*# National Aeronautics and Space Administration. Ames Research Center, Moffett Field, CA.
ROTORCRAFT MASTER PLAN
Peter V. Hwoschinsky *In its* NASA/FAA Helicopter Simulator Workshop Apr. 1992 p 39-44 (For primary document see N93-30673 11-01)
Avail: CASI HC A02/MF A02

The Rotorcraft Master Plan contains a comprehensive summary of active and planned FAA vertical flight research and development. Since the Master Plan is not sufficient for tracking project status and monitoring progress, the Vertical Flight Program Plan will provide that capability. It will be consistent with the Master Plan and, in conjunction with it, will serve to ensure a hospitable environment if the industry presents a practical vertical-flight initiative. Author

N93-30678*# National Aeronautics and Space Administration. Ames Research Center, Moffett Field, CA.
SIMULATORS FOR CORPORATE PILOT TRAINING AND EVALUATION **c09**
Curt Treichel *In its* NASA/FAA Helicopter Simulator Workshop Apr. 1992 p 45-47 (For primary document see N93-30673 11-01)
Avail: CASI HC A01/MF A02

Corporate aviation relies heavily on simulation to meet training and evaluation requirements. It appreciates the savings in fuel, money, noise, and time, and the added safety it provides. Also, simulation provides opportunities to experience many emergencies that cannot be safely practiced in the aircraft. There is a need to focus on the advantages of simulator training over aircraft training and to provide appropriate changes in the regulations to allow the community to make it possible for users to take full advantage of simulation. Author

N93-30679*# National Aeronautics and Space Administration. Ames Research Center, Moffett Field, CA.
TRAINING EFFECTIVENESS ASSESSMENT: WHERE ARE WE? **c53**
Greg McGowan *In its* NASA/FAA Helicopter Simulator Workshop Apr. 1992 p 49-54 (For primary document see N93-30673 11-01)
Avail: CASI HC A02/MF A02

Over 9,000 pilot training courses have been conducted at FSI using the Bell 222 and Sikorsky S-76 simulators. Through the use of FAA exemptions, these simulators can be used for certain training and checking credit. The history of the development and use of commercial helicopter simulators and the opportunities for their increased utilization and use were explored. Author

N93-30680*# National Aeronautics and Space Administration. Ames Research Center, Moffett Field, CA.
CURRENT TRAINING: WHERE ARE WE? **c53**
Gerald Golden *In its* NASA/FAA Helicopter Simulator Workshop Apr. 1992 p 55-59 (For primary document see N93-30673 11-01)
Avail: CASI HC A01/MF A02

Petroleum Helicopters, Inc. maintains a staff of 750 helicopter pilots.

The initial, transition, upgrade, and recurrent training for these pilots requires a significant financial outlay. Since a major portion of that training is done to satisfy the requirements of FAR 61.57, 'Recent Flight Experience, Pilot in Command' and 135.297, 'Pilot in Command: Instrument Proficiency Check Requirements', much could be accomplished using an approved simulator. However, it is imperative that credit be given for training time spent in the simulators and that the device be realistic, practical, and affordable.
Author

N93-30681*# National Aeronautics and Space Administration. Ames Research Center, Moffett Field, CA.
HELICOPTER SIMULATOR QUALIFICATION c09
Brian Hampson *In its* NASA/FAA Helicopter Simulator Workshop Apr. 1992 p 61-64 (For primary document see N93-30673 11-01)
Avail: CASI HC A01/MF A02

CAE has extensive experience in building helicopter simulators and has participated in group working sessions for fixed-wing advisory circulars. Against this background, issues that should be addressed in establishing helicopter approval criteria were highlighted. Some of these issues are not immediately obvious and may, indeed, be more important than the criteria a themselves. Author (revised)

N93-30682*# National Aeronautics and Space Administration. Ames Research Center, Moffett Field, CA.
HELICOPTER SIMULATION: MAKING IT WORK c09
Barry Payne *In its* NASA/FAA Helicopter Simulator Workshop Apr. 1992 p 65-68 (For primary document see N93-30673 11-01)
Avail: CASI HC A01/MF A02

The opportunities for improved training and checking by using helicopter simulators are greater than they are for airplane pilot training. Simulators permit the safe creation of training environments that are conducive to the development of pilot decision-making, situational awareness, and cockpit management. This paper defines specific attributes required in a simulator to meet a typical helicopter operator's training and checking objectives.
Author

N93-30683*# National Aeronautics and Space Administration. Ames Research Center, Moffett Field, CA.
HELICOPTER TRAINING SIMULATORS: KEY MARKET FACTORS c09
John McIntosh *In its* NASA/FAA Helicopter Simulator Workshop Apr. 1992 p 69-76 (For primary document see N93-30673 11-01)
Avail: CASI HC A02/MF A02

Simulators will gain an increasingly important role in training helicopter pilots only if the simulators are of sufficient fidelity to provide positive transfer of skills to the aircraft. This must be done within an economic model of return on investment. Although rotor pilot demand is still only a small percentage of overall pilot requirements, it will grow in significance. This presentation described the salient factors influencing the use of helicopter training simulators. Author (revised)

N93-30684*# National Aeronautics and Space Administration. Ames Research Center, Moffett Field, CA.
TRAINING EFFECTIVENESS ASSESSMENT: METHODOLOGICAL PROBLEMS AND ISSUES c53
Kenneth D. Cross *In its* NASA/FAA Helicopter Simulator Workshop Apr. 1992 p 77-90 (For primary document see N93-30673 11-01)
Avail: CASI HC A03/MF A02

The U.S. military uses a large number of simulators to train and sustain the flying skills of helicopter pilots. Despite the enormous resources required to purchase, maintain, and use those simulators, little effort has been expended in assessing their training effectiveness. One reason for this is the lack of an evaluation methodology that yields comprehensive and valid data at a practical cost. Some of these methodological problems and issues that arise in assessing simulator training effectiveness, as well as problems with the classical transfer-of-learning paradigm were discussed.
Author

N93-30685*# National Aeronautics and Space Administration. Ames Research Center, Moffett Field, CA.
DETERMINING THE TRANSFERABILITY OF FLIGHT SIMULATOR DATA c09
David Green *In its* NASA/FAA Helicopter Simulator Workshop Apr. 1992 p 91-108 (For primary document see N93-30673 11-01)
Avail: CASI HC A03/MF A02

This paper presented a method for collecting and graphically correlating subjective ratings and objective flight test data. The method enables flight-simulation engineers to enhance the simulator characterization of rotor craft flight in order to achieve maximum transferability of simulator experience. Author (revised)

N93-30686*# National Aeronautics and Space Administration. Ames Research Center, Moffett Field, CA.
PROGRESS THROUGH PRECEDENT: GOING WHERE NO HELICOPTER SIMULATOR HAS GONE BEFORE c09
Richard J. Adams *In its* NASA/FAA Helicopter Simulator Workshop Apr. 1992 p 109-114 (For primary document see N93-30673 11-01)
Avail: CASI HC A02/MF A02

Helicopter simulators have been approved by means of special exemption; there are no FAA standards for simulators used in training or airmen Certification checking. The fixed-wing industry provides a precedent which can be used for expediting implementation of helicopter simulators. The analysis in this paper is founded on the experience with that precedent and is driven by a clear definition of helicopter user needs for (1) improved training at lower cost, (2) more comprehensive emergency training at lower risk, (3) increased fidelity of transition and instrument training compared with low-cost aircraft alternatives, and (4) certification credit for improved simulator training. Author (revised)

N93-30687*# National Aeronautics and Space Administration. Ames Research Center, Moffett Field, CA.
TRANSFER OF TRAINING AND SIMULATOR QUALIFICATION OR MYTH AND FOLKLORE IN HELICOPTER SIMULATION c09
Jack Dohme *In its* NASA/FAA Helicopter Simulator Workshop Apr. 1992 p 115-121 (For primary document see N93-30673 11-01)
Avail: CASI HC A02/MF A02

Transfer of training studies at Fort Rucker using the backward-transfer paradigm have shown that existing flight simulators are not entirely adequate for meeting training requirements. Using an ab initio training research simulator, a simulation of the UH-1, training effectiveness ratios were developed. The data demonstrate it to be a cost-effective primary trainer. A simulator qualification method was suggested in which a combination of these transfer-of-training paradigms is used to determine overall simulator fidelity and training effectiveness. Author

N93-30688*# National Aeronautics and Space Administration. Ames Research Center, Moffett Field, CA.
VALIDATION AND UPGRADING OF PHYSICALLY BASED MATHEMATICAL MODELS c64
Ronald DuVal *In its* NASA/FAA Helicopter Simulator Workshop Apr. 1992 p 123-129 (For primary document see N93-30673 11-01)
Avail: CASI HC A02/MF A02

The validation of the results of physically-based mathematical models against experimental results was discussed. Systematic techniques are used for: (1) isolating subsets of the simulator mathematical model and comparing the response of each subset to its experimental response for the same input conditions; (2) evaluating the response error to determine whether it is the result of incorrect parameter values, incorrect structure of the model subset, or unmodeled external effects of cross coupling; and (3) modifying and upgrading the model and its parameter values to determine the most physically appropriate combination of changes. Derived from text

N93-30689*# National Aeronautics and Space Administration. Ames Research Center, Moffett Field, CA.
FREQUENCY-RESPONSE TECHNIQUES FOR DOCUMENTATION AND IMPROVEMENT OF ROTORCRAFT SIMULATORS c09
Mark B. Tischler *In its* NASA/FAA Helicopter Simulator Workshop Apr. 1992 p 131-146 (For primary document see N93-30673 11-01)
Avail: CASI HC A03/MF A02

Pilot-in-the-loop characterizations are most naturally formulated in terms of end-to-end frequency responses, so a frequency-response-based method is the natural approach to assessing simulator dynamic fidelity. A comprehensive frequency-response approach used heavily by Ames Research Center researchers was described, and results were presented

from a number of simulator fidelity assessment studies. Those studies included UH-60 mathematical model validation and upgrade, ASTOVL linear model extraction, and documentation of the Vertical Motion Simulator (at Ames Research Center) motion and visual system characteristics.
Derived from text

N93-30690*# National Aeronautics and Space Administration. Ames Research Center, Moffett Field, CA.
BANDWIDTH AND SIMDUCE AS SIMULATOR FIDELITY CRITERIA **c09**
David Key *In its* NASA/FAA Helicopter Simulator Workshop Apr. 1992 p 147-160 (For primary document see N93-30673 11-01)
Avail: CASI HC A03/MF A02

The potential application of two concepts from the new Handling Qualities Specification for Military Rotorcraft was discussed. The first concept is bandwidth, a measure of the dynamic response to control. The second is a qualitative technique developed for assessing the visual cue environment the pilot has in bad weather and at night. Simulated Day Usable Cue Environment (SIMDUCE) applies this concept to assessing the day cuing fidelity in the simulator. Derived from text

N93-30691*# National Aeronautics and Space Administration. Ames Research Center, Moffett Field, CA.
METHODOLOGY DEVELOPMENT FOR EVALUATION OF SELECTIVE-FIDELITY ROTORCRAFT SIMULATION **c09**
William D. Lewis, D. P. Schrage, J. V. R. Prasad, and Daniel Wolfe *In its* NASA/FAA Helicopter Simulator Workshop Apr. 1992 p 161-166 (For primary document see N93-30673 11-01)
Avail: CASI HC A02/MF A02

This paper addressed the initial step toward the goal of establishing performance and handling qualities acceptance criteria for realtime rotorcraft simulators through a planned research effort to quantify the system capabilities of 'selective fidelity' simulators. Within this framework the simulator is then classified based on the required task. The simulator is evaluated by separating the various subsystems (visual, motion, etc.) and applying corresponding fidelity constants based on the specific task. This methodology not only provides an assessment technique, but also provides a technique to determine the required levels of subsystem fidelity for a specific task. Derived from text

02 AERODYNAMICS

Includes aerodynamics of bodies, combinations, wings, rotors, and control surfaces; and internal flow in ducts and turbomachinery.

For related information see also *34 Fluid Mechanics and Heat Transfer.*

N93-28493# Air Force Systems Command, Wright-Patterson AFB, OH. Foreign Aerospace Science and Technology Center.
EFFECT OF CANARD WING POSITIONS ON AERODYNAMIC CHARACTERISTICS OF SWEPT-FORWARD WING
Zhang Binqian and B. Laschka 25 Feb. 1993 17 p Transl. into ENGLISH from Kongqidonglixue Xuebao (China), v. 8, no. 4, Dec. 1990 p 404-408
(AD-A262373; FASTC-ID(RS)T-0825-92) Avail: CASI HC A03/MF A01

Based on force measurements, oil flow observations, and eddy measurements in low air-speed wind tunnels, the paper studies the mechanism underlying the effect of canard wing positions on the aerodynamic characteristics of swept-forward canard wing configurations. As shown in studies, canard wing positions play the most significant role with respect to aerodynamic characteristics. Improvements in characteristics through a large incident angle in the swept-forward canard wing configuration depends on the relative position and the mutual control of the eddy at the leading edge of main wing. Based on the experimental results of an assembly with swept-forward and swept-back canard wing as well as the main wing, the paper presents the two- dimensional shapes of the canard and main wings, as well as their relative positions when adopting canard configuration. in addition, the authors express some of their views on the configuration of dual swept forward wings. DTIC

N93-28662# Pacific Northwest Lab., Richland, WA.
A DEMONSTRATION OF SIMPLE AIRFOILS: STRUCTURAL DESIGN AND MATERIALS CHOICES
L. Roy Bunnell and Steve W. Piippo (Richland School District, WA.) Jan. 1993 10 p Presented at the National Educator's Workshop, Oak Ridge, TN, 11-13 Nov. 1992
(Contract DE-AC06-76RL-01830)
(DE93-007882; PNL-SA-21578; CONF-9211178-3) Avail: CASI HC A02/MF A01

An educational unit is presented for building and evaluating simple wing structures, in order to learn about materials choice and lightweight construction. This unit is appropriate for a high school materials science class or lower-division college courses in structural engineering, materials science, or aeronautical engineering. DOE

N93-29005# Royal Inst. of Tech., Stockholm (Sweden). Dept. of Numerical Analysis and Computing Science.
THE NUMERICAL SOLUTION OF LOW MACH NUMBER FLOW IN CONFINED REGIONS BY RICHARDSON EXTRAPOLATION
B. Christer V. Johansson 25 Mar. 1992 40 p
(Contracts N00014-83-K-0422; NUTEK-726-91-01071; TFR-91-402)
(TRITA-NA-9207) Avail: CASI HC A03/MF A01

We use artificial compressibility together with Richardson extrapolation in the Mach number M as a method for solving the time dependent Navier-Stokes equation for very low Mach number flow and for incompressible flow. The question of what boundary conditions one should use for low Mach number flow, especially at inflow and outflow boundaries, is investigated theoretically, and boundary layer suppressing boundary conditions are derived. For the case of linearization around a constant flow we show that the low Mach number solution will converge with the rate O(M-squared) to the true incompressible solution, provided that we choose the boundary conditions correctly. However, if the boundary conditions are chosen incorrectly, it might happen that the low Mach number solution converges to an incompressible solution that looks physical, even though the difference between the true incompressible solution and the limit solution derived as M-squared approaches 0 is O(1). The reason is that the limit solution in this case does not satisfy the boundary conditions. The results of numerical calculations for the time dependent, nonlinear equations and for flow situations with time dependent inflow velocity profiles are presented. The convergence rate M-squared to incompressible solution is numerically confirmed. It is also shown that using Richardson extrapolation to M-squared = 0 in order to derive a solution with very small divergence can with good result be carried through with M-squared as large as 0.1 and 0.05. As the time step in numerical methods must be chosen approximately such that delta-t x (i/M delta-x + v/delta-x squared) is in the stability region of the time stepping method, and as M-squared = 0.05 is sufficiently small to yield good results, the restriction on the time step due to the Mach number is not serious. Therefore the equations can be integrated very fast by explicit time stepping methods. This method for solving very low Mach number flow and incompressible flow is well suited to parallel processing. Author (revised)

N93-29006# Deutsche Forschungsanstalt fuer Luft- und Raumfahrt, Goettingen (Germany). Abt. Stabilitaet und Antwort.
TRANSONIC FLOWS ON AN OSCILLATING AIRFOIL AND THEIR EFFECT ON THE FLUTTER-BOUNDARY Ph.D. Thesis - Technische Univ. Munich [TRANSSONISCHE STROEMUNGEN AN EINEM SCHWINGENDEN PROFIL UND DEREN EINFLUSS AUF DIE FLATTERGRENZE]
Lorenz Tichy May 1992 145 p In GERMAN
(DLR-FB-92-08; ETN-93-93733) Avail: CASI HC A07/MF A02; DLR, VB-PL-DO, Postfach 90 60 58, 5000 Cologne, Germany, HC

A mount system for experiments on a two dimensional airfoil in a transonic wind tunnel is described. The system permits the measurement of static and dynamic pressure distributions and forces as well as flutter experiments. The study is based on results for the NACA 0012 airfoil oscillating in plunging and pitching modes. Different types of pressure fluctuations for weak and strong shocks and for shock induced separation are detailed. Flutter calculations based on measured unsteady aerodynamic derivatives show the effect of these pressure fluctuations on the flutter boundary in transonic flow. ESA

N93-29035# Sandia National Labs., Albuquerque, NM.
THE DEVELOPMENT OF A PARACHUTE SYSTEM FOR AERIAL DELIVERY FROM HIGH SPEED CARGO AIRCRAFT
V. L. Behr 1992 11 p Presented at the 12th Royal Aeronautical Society/AIAA Aerodynamic Decelerator Systems Technical Conference, London, England, 10 May 1993
(Contract DE-AC04-76DP-00789)
(DE93-008339; SAND-92-1889C; CONF-930580-2) Avail: CASI HC A03/MF A01

Supply of military personnel on the ground with cargo has long been accomplished with parachute delivery systems from aircraft. Structural limits of aircraft have typically limited these operations to no more than 150 KCAS. A desire for increased survivability of cargo delivery aircraft has led to the development and fielding of aircraft capable of delivering cargo at substantially higher speeds. This paper describes efforts undertaken to design develop and test a cargo delivery system for use at speeds compatible with those high speed cargo aircraft. DOE

N93-29124 Virginia Polytechnic Inst. and State Univ., Blacksburg.
AN EXPERIMENTAL STUDY OF FLOW OVER A 6 TO 1 PROLATE SPHEROID AT INCIDENCE Ph.D. Thesis
Seungki Ahn 1992 307 p
Avail: Univ. Microfilms Order No. DA9306841

In two-dimensional flow, the point of flow separation from the surface coincides with the point at which the skin friction vanishes. However, in three-dimensional flow, the situation is much more complex and the flow separation is rarely associated with the vanishing of the wall shear stress except in a few special cases. Though the effects of cross-plane separation are substantial and have been recognized for some time, the phenomenon of flow separation over three-dimensional bodies is still far from being completely understood. The flow is so complex that no completely satisfactory analytical tools are available at the moment. In an attempt to logically identify the various effects and parametric dependence while simultaneously minimizing configuration dependent issue, the flow over a 6 to 1 prolate spheroid, which is a generic three dimensional body, is investigated. For the identification of the general flow pattern and better understanding of the flow field, surface-oil-flow visualization tests and force and moment tests were performed. The angle of attack effect and Reynolds number effect on the separation location are studied with natural transition. Forces and moments tests, surface pressure distribution measurements as well as the surface pressure fluctuations, and mini-tuft flow visualization tests were made to document the flow characteristics on the surface of the body with an artificial boundary layer trip. It was found that there exists a critical Reynolds number at which the flow characteristics of the after body changes. This critical Reynolds number was also confirmed by the force and moment tests. Above this Reynolds number, as the Reynolds number increases, the separation lines do not change their circumferential location but stretch to the upstream of the body. For the low super critical Reynolds number range, the angle of attack effect on the location of the primary separation is not as prominent as in the higher Reynolds number range where the crossflow component effect becomes dominant. Surface pressure fluctuation data and surface pressure spectra were measured and documented for the first time for this type of three-dimensional flow. For the extension of the study to unsteady transient motion effects, a new Dynamic-Plunge-Pitch-Roll (DyPPiR) model mount was designed and developed to generate required transient motions. The measurements carried out are to be used as reference data to identify the unsteady transient effect of the flow field undergoing unsteady transient maneuvers. Dissert. Abstr.

N93-29160*# National Aeronautics and Space Administration. Langley Research Center, Hampton, VA.
PERFORMANCE CHARACTERISTICS OF TWO MULTIAXIS THRUST-VECTORING NOZZLES AT MACH NUMBERS UP TO 1.28
David J. Wing and Francis J. Capone Washington May 1993 111 p
(RTOP 505-62-30-01)
(NASA-TP-3313; L-17151; NAS 1.60:3313) Avail: CASI HC A06/MF A02

The thrust-vectoring axisymmetric (VA) nozzle and a spherical convergent flap (SCF) thrust-vectoring nozzle were tested along with a baseline nonvectoring axisymmetric (NVA) nozzle in the Langley 16-Foot Transonic Tunnel at Mach numbers from 0 to 1.28 and nozzle pressure ratios from 1 to 8. Test parameters included geometric yaw vector angle and unvectored divergent flap length. No pitch vectoring was studied. Nozzle drag, thrust minus drag, yaw thrust vector angle, discharge coefficient, and static thrust performance were measured and analyzed, as well as external static pressure distributions. The NVA nozzle and the VA nozzle displayed higher static thrust performance than the SCF nozzle throughout the nozzle pressure ratio (NPR) range tested. The NVA nozzle had higher overall thrust minus drag than the other nozzles throughout the NPR and Mach number ranges tested. The SCF nozzle had the lowest jet-on nozzle drag of the three nozzles throughout the test conditions. The SCF nozzle provided yaw thrust angles that were equal to the geometric angle and constant with NPR. The VA nozzle achieved yaw thrust vector angles that were significantly higher than the geometric angle but not constant with NPR. Nozzle drag generally increased with increases in thrust vectoring for all the nozzles tested. Author (revised)

N93-29165*# National Aeronautics and Space Administration. Langley Research Center, Hampton, VA.
EVALUATION OF FOUR ADVANCED NOZZLE CONCEPTS FOR SHORT TAKEOFF AND LANDING PERFORMANCE
P. Frank Quinto, Guy T. Kemmerly, and John W. Paulson, Jr. Jun. 1993 98 p Sponsored by NASA, Washington
(RTOP 505-59-30-02)
(NASA-TP-3314; L-16998; NAS 1.60:3314) Avail: CASI HC A05/MF A02

Four advanced nozzle concepts were tested on a canard-wing fighter in the Langley 14- by 22-Foot Subsonic Tunnel. The four vectoring-nozzle concepts were as follows: (1) an axisymmetric nozzle (AXI); (2) an asymmetric, load balanced exhaust nozzle (ALBEN); (3) a low aspect ratio, single expansion ramp nozzle (LASERN); and (4) a high aspect ratio, single expansion ramp nozzle (HASERN). The investigation was conducted to determine the most suitable nozzle concept for short takeoff and landing (STOL) performance. The criterion for the best STOL performance was a takeoff ground roll of less than 1000 ft. At approach, the criteria were high lift and sufficient drag to maintain a glide slope of -3 to -6 deg with enough pitching-moment control from the canards. The test was performed at a dynamic pressure of 45 lb/sq ft and an angle-of-attack range of 0 to 20 deg. The nozzle pressure ratio was varied from 1.0 to 4.3 at both dry power and after burning nozzle configurations with nozzle vectoring to 60 deg. In addition, the model was tested in and out of ground effects. The ALBEN concept was the best of the four nozzle concepts tested for STOL performance. Author (revised)

N93-29166*# National Aeronautics and Space Administration. Langley Research Center, Hampton, VA.
HYPERSONIC LATERAL AND DIRECTIONAL STABILITY CHARACTERISTICS OF AEROASSIST FLIGHT EXPERIMENT CONFIGURATION IN AIR AND CF4
John R. Micol and William L. Wells Washington Jun. 1993 42 p
(RTOP 506-40-41-01)
(NASA-TM-4435; L-17154; NAS 1.15:4435) Avail: CASI HC A03/MF A01

Hypersonic lateral and directional stability characteristics measured on a 60 deg half-angle elliptical cone, which was raked at an angle of 73 deg from the cone centerline and with an ellipsoid nose (ellipticity equal to 2.0 in the symmetry plane), are presented for angles of attack from -10 to 10 deg. The high normal-shock density ratio of a real gas was simulated by tests at a Mach number of 6 in air and CF4 (density ratio equal to 5.25 and 12.0, respectively). Tests were conducted in air at Mach 6 and 10 and in CF4 at Mach 6 to examine the effects of Mach number, Reynolds number, and normal-shock density ratio. Changes in Mach number from 6 to 10 in air or in Reynolds number by a factor of 4 at Mach 6 had a negligible effect on lateral and directional stability characteristics. Variations in normal-shock density ratio had a measurable effect on lateral and directional aerodynamic coefficients, but no significant effect on lateral and directional stability characteristics. Tests in air and CF4 indicated that the configuration was laterally and directionally stable through the test range of angle of attack. Author (revised)

N93-29284# SRI International Corp., Menlo Park, CA. Molecular Physics Center.
KINETICS AND ENERGY TRANSFER IN NONEQUILIBRIUM FLUID FLOWS Final Report, 17 Jun. 1990 - 16 Sep. 1992
David R. Crosley 3 Feb. 1993 70 p
(Contract DAAL03-90-K-0001)
(AD-A263612; ARO-27864.3-EG-SDI) Avail: CASI HC A04/MF A01

Chemical kinetics and energy transfer have been investigated for nonequilibrium fluid flow. The particular process of interest is ultraviolet emission from the A2 sigma + excited electronic state of NO, which is generated under nonequilibrium conditions in the bow shock waves of ascending missiles at 50 to 100 km altitude. A literature survey of the pertinent rate constants and mechanism for use in computer models of the process has been undertaken. Emission from NO has been studied in shock tubes, using shock heated air and other gas mixtures. Collisional quenching of the A2 sigma + state is the reverse of heavy particle excitation of the emission. Its temperature dependence has been studied in a heated cell and a shock tube. An attempt was made to determine the final vibrational state distribution in the ground electronic state, concluding that the NO is transferred into high vibrational levels. DTIC

N93-29410 Wright Lab., Wright-Patterson AFB, OH.
MODAL SURVEY OF A FULL-SCALE F-18 WIND TUNNEL MODEL Interim Report, Mar. 1991 - Jul. 1992
Vincent J. Levraea, Douglas A. Henderson, Arnel P. Pacia, and Michael P. Banford Sep. 1992 63 p Limited Reproducibility: More than 20% of this document may be affected by microfiche quality
(AD-A262482; WL-TM-92-350-FIBG) Avail: CASI HC A04

The purpose of this investigation was to perform a ground vibration test (GVT) to determine the resonant frequencies, damping, and mode shapes for the F-18 vertical tail structure. This effort represents a subtask of the twin tail buffet work currently studying the buffet response of the F-18 vertical tails to forebody vortices generated at high angles of attack. The GVT was conducted on a full-scale F-18 airframe which had been significantly modified to enable it for use as a full-scale wind tunnel model in the NASA Ames 80 ft x 120 ft wind tunnel facility. Because the major emphasis of the test was to obtain the dynamic characteristics of the vertical tails under tunnel mounting conditions, the GVT was performed with the full-scale model mounted on the tunnel pedestals in the same configuration as would be used for the wind tunnel tests. The primary excitation frequencies of the vortical wake were expected to be below 100 hertz, thus the GVT only measured tail response frequencies below this value. The results give dynamic response information for the first bending, second bending, and first torsional modes of the vertical tails. DTIC

N93-29449*# National Aeronautics and Space Administration. Langley Research Center, Hampton, VA.
HIGH-REYNOLDS-NUMBER TEST OF A 5-PERCENT-THICK LOW-ASPECT-RATIO SEMISPAN WING IN THE LANGLEY 0.3-METER TRANSONIC CRYOGENIC TUNNEL: WING PRESSURE DISTRIBUTIONS
Julio Chu and Pierce L. Lawing Dec. 1990 201 p
(RTOP 505-61-01-01)
(NASA-TM-4227; L-16704; NAS 1.15:4227) Avail: CASI HC A10/MF A03

A high Reynolds number test of a 5 percent thick low aspect ratio semispan wing was conducted in the adaptive wall test section of the Langley 0.3 m Transonic Cryogenic Tunnel. The model tested had a planform and a NACA 64A-105 airfoil section that is similar to that of the pressure instrumented canard on the X-29 experimental aircraft. Chordwise pressure data for Mach numbers of 0.3, 0.7, and 0.9 were measured for an angle-of-attack range of -4 to 15 deg. The associated Reynolds numbers, based on the geometric mean chord, encompass most of the flight regime of the canard. This test was a free transition investigation. A summary of the wing pressures are presented without analysis as well as adapted test section top and bottom wall pressure signatures. However, the presented graphical data indicate Reynolds number dependent complex leading edge separation phenomena. This data set supplements the existing high Reynolds number database and are useful for computational codes comparison. Author

N93-29450*# National Aeronautics and Space Administration. Langley Research Center, Hampton, VA.
AERODYNAMIC CHARACTERISTICS OF A ROTORCRAFT AIRFOIL DESIGNED FOR THE TIP REGION OF A MAIN ROTOR BLADE
Kevin W. Noonan May 1991 79 p
(DA Proj. 1L1-62211-A-47-AA; RTOP 505-61-59-76)
(NASA-TM-4264; L-16855; NAS 1.15:4264; AVSCOM-TR-91-B-003; AD-B156202L) Avail: CASI HC A05/MF A01

A wind tunnel investigation was conducted to determine the 2-D aerodynamic characteristics of a new rotorcraft airfoil designed for application to the tip region (stations outboard of 85 pct. radius) of a helicopter main rotor blade. The new airfoil, the RC(6)-08, and a baseline airfoil, the RC(3)-08, were investigated in the Langley 6- by 28-inch transonic tunnel at Mach numbers from 0.37 to 0.90. The Reynolds number varied from 5.2 x 10(exp 6) at the lowest Mach number to 9.6 x 10(exp 6) at the highest Mach number. Some comparisons were made of the experimental data for the new airfoil and the predictions of a transonic, viscous analysis code. The results of the investigation indicate that the RC(6)-08 airfoil met the design goals of attaining higher maximum lift coefficients than the baseline airfoil while maintaining drag divergence characteristics at low lift and pitching moment characteristics nearly the same as those of the baseline airfoil. The maximum lift coefficients of the RC(6)-08 varied from 1.07 at M=0.37 to 0.94 at M=0.52 while those of the RC(3)-08 varied from 0.91 to 0.85 over the same Mach number range. At lift coefficients of -0.1 and 0, the drag divergence Mach number of both the RC(6)-08 and the RC(3)-08 was 0.86. The pitching moment coefficients of the RC(6)-08 were less negative than those of the RC(3)-08 for Mach numbers and lift coefficients typical of those that would occur on a main rotor blade tip at high forward speeds on the advancing side of the rotor disk. Author

N93-29512# Army Research Lab., Aberdeen Proving Ground, MD.
RECENT APPLICATIONS OF CFD TO THE AERODYNAMICS OF ARMY PROJECTILES Final Report, Jan. 1989 - Sep. 1992
Walter B. Sturek, Charles J. Nietubicz, Jubaraj Sahu, and Paul Weinacht Dec. 1992 64 p
(AD-A262953; ARL-TR-22) Avail: CASI HC A04/MF A01

The ability to predict the complete set of aerodynamic performance parameters for projectile configurations has been a stated goal of the Computational Aerodynamics Branch, U.S. Army Ballistic Research Laboratory. In order to achieve this goal, predictive capabilities which utilize Navier-Stokes computational techniques have been developed and applied to an extensive number of projectile configurations. A summary of code validation efforts and applications for both spin stabilized and fin stabilized projectile configurations are described. Significant progress in the predictive capability for projectile aerodynamics has been achieved through the availability of substantial supercomputer resources and modern computational techniques. Current and future research areas of interest are described and provide an indication of computer resources and code enhancements needed to continue the progress in projectile computational aerodynamics. DTIC

N93-29862# Air Force Inst. of Tech., Wright-Patterson AFB, OH. Foreign Aerospace Science and Technology Center.
SOLUTION OF EULER EQUATIONS FOR FOREBODY-INLET ENSEMBLE OF AIRCRAFT AT HIGH ANGLE OF ATTACK
Zheng Xiaoqing and Shen Huili 27 Apr. 1993 19 p Transl. into ENGLISH from unidentified Chinese language document p 161-168
(AD-A263905; FASTC-ID(RS)T-0870-92) Avail: CASI HC A03/MF A01

A computational procedure was developed to simulate inviscid flows over integrated forebody-inlet ensemble of an aircraft model. The analysis, which includes the effect of Mach number, angle of attack, and engine mass flow is based on the solution of three-dimensional Euler equations. A finite-volume spatial discretization and a Runge-Kutta time stepping scheme are employed in solving the equations. To achieve the required geometric flexibility, a multizone mesh is used. The entire computational domain is divided into three zones. The mesh of each zone is generated by interpolating the fluxes across the interface between adjacent zones during iterations. A new type of treatment of inlet exit boundary conditions was developed and tested. The procedure was applied to forebody-inlet analysis for a range of flight conditions including subsonic, transonic, and supersonic flight with various engine mass flows and angles of attack. In addition, the steady states of supersonic flight up to 15 degrees of angle of attack for the subcritical engine regime were obtained. The results are in good agreement with the experimental data. DTIC

N93-29891# Naval Surface Warfare Center, Bethesda, MD. Propulsion and Auxiliary Systems Dept.

UNSTEADY VORTEX LOOP/DIPOLE THEORY APPLIED TO THE WORK AND ACOUSTICS OF AN IDEAL LOW SPEED PROPELLER Progress Report

Earl Quandt Mar. 1993 28 p

(AD-A264057; CDNSWC/PAS-92/52) Avail: CASI HC A03/MF A01

The vortex loop/dipole singularities used to simulate blade lift and thickness in potential flow models of turbomachines are examined in an unsteady form. The three-dimensional potential fields created as these singularities rotate in the absolute frame are shown to provide the input forces, ideal work and wake energy for an incompressible fluid, as well as the tonal acoustics for slight compressibility. For typical low Mach number propellers, the sound field is dominated by the lift force and exhibits large cancellation effects with multiple blades. It is concluded that the unsteady formulation illustrates well the physics of a turbomachine, and in addition, highlights some basic principles of potential flow. DTIC

N93-29919# Air Force Inst. of Tech., Wright-Patterson AFB, OH. Foreign Aerospace Science and Technology Center.

THE APPLICATION OF CONCENTRIC VORTEX SIMULATION TO CALCULATING THE AERODYNAMIC CHARACTERISTICS OF BODIES OF REVOLUTION AT HIGH ANGLES OF ATTACK

Ban Xianlin and Tu Xing 27 Apr. 1993 16 p Transl. into ENGLISH from Kongqidonglixue Xuebao (China), v. 8, no. 2, 1990 p 161-167

(AD-A263879; FASTC-ID(RS)T-0869-92) Avail: CASI HC A03/MF A01

The aerodynamic characteristic of sharp nosed bodies of revolution is calculated by using concentric vortex simulation in this paper. Based on the experimental results, an appropriate set of free integration parameters is selected and an empirical relation between initial separation angle and the Reynolds number is established. Thus, the effect of the Reynolds number is reasonably considered in the calculation. The effect of the Mach number is corrected by using Gothert's rule. The differential equations of vortex motion are solved by using the fourth order Runge Kutta method with varying step size. Three different initial step sizes are used in different integration positions in order to increase the speed of calculation. Two models (F3Al6 and F3.5A7) were calculated in this paper. DTIC

N93-30020# Office National d'Etudes et de Recherches Aerospatiales, Paris (France).

SONIC BOOM PROBLEM FOR FUTURE HIGHSPEED AIRCRAFT [LE PROBLEME DU BANG SONIQUE POUR DE FUTURS AVIONS DE TRANSPORT A HAUTE VITESSE]

Andre Auriol, Claude Lecomte, and Christian Thery 1990 52 p In FRENCH

(ONERA-NT-1990-3; ETN-93-93723) Avail: CASI HC A04/MF A01

The various physical characteristics of sonic booms are recalled: origin, atmospheric propagation, and circumstances under which focusing takes place. The main effects on structures and living creatures are outlined. The only noticeable nuisance from the sonic boom is due to the fact that it startles people. This reaction increases in intensity with the severity of the boom and the steepness of the shock fronts. No acceptance threshold has been defined so far, but startle reactions become scarce for boom intensities less than 50 pascals, or for those booms having a shock front of weak intensity followed by a gradual compression. This milder reaction could, therefore, be attained by changing the aerodynamic geometry of the aircraft appropriately. It is, therefore, recommended that work continues, with the following: studies on startle reactions, to define bearable booms of unconventional shapes; and studies of the aerodynamic shapes of planes able to generate such booms. Ways also have to be found to reduce the effects of the unavoidable strengthening of the boom due to the transonic acceleration of the plane. ESA

N93-30119# Army Natick Labs., MA.

A COMPUTATIONAL MODEL THAT COUPLES AERODYNAMIC AND STRUCTURAL DYNAMIC BEHAVIOR OF PARACHUTES DURING THE OPENING PROCESS Final Report, Oct. 1991 - Jan. 1993

Keith R. Stein, Richard J. Benney, and Earl C. Steeves Apr. 1993 31 p

(AD-A264115; Natick/TR-93/029) Avail: CASI HC A03/MF A01

In parachute research, the canopy inflation process is the least understood and most complex to model. Unfortunately, it is during the opening process that the canopy often experiences the largest deformations and loadings. The complexity of modelling the opening process stems from the coupling between the structural dynamics of the canopy, lines and payload with the aerodynamics of the surrounding fluid medium. The addition of a computational capability to model the coupled opening behavior would greatly assist in the understanding of the canopy inflation process. Ongoing research at the U.S. Army Natick Research, Development and Engineering Center (Natick) focuses on this coupled problem. The solution to the coupled problem is expected to assist in the development of future U.S. Army airdrop systems which include the capability of deploying at low altitudes and high speeds. A computational fluid dynamics (CFD) code and structural dynamic mass spring damper (MSD) code are coupled with an explicit marching method. The CFD flow solver provides the differential pressure values at node points along a radial which are used as input in the MSD model. The MSD code integrates the equations of motion for the canopy and returns current nodal positions and velocities to the CFD code. The node points on the MSD model coincide with a unique set of adjacent CFD grid points for all time. This coupled model predicts behavior for a quarter-scale C-9 parachute which compares favorably with experimentally determined behavior. DTIC

N93-30151# Phillips Lab., Kirtland AFB, NM.

VORTEX SHEDDING BY BLUNT/BLUFF BODIES AT HIGH REYNOLDS NUMBERS. VOLUME 4: RECTANGLES Final Report, 17 Jun. 1991 - 31 Jul. 1992

B. R. Merrill Mar. 1993 204 p

(AD-A264154; PL-TR-92-1053-Vol-4) Avail: CASI HC A10/MF A03

This report documents the analysis of vortex shedding data collected by the Phillips Laboratory at the U.S. Air Force Academy Subsonic Wind Tunnel facility. The analysis is primarily of the power spectrum of the vortex shedding as seen in the force and moment coefficient power spectra. The shedding frequencies as seen in the power spectra are used to analyze for the Strouhal number. The analysis suggests that shape and orientation in the wind field have an effect on the shedding of vortices. DTIC

N93-30171# Phillips Lab., Kirtland AFB, NM.

VORTEX SHEDDING BY BLUNT/BLUFF BODIES AT HIGH REYNOLDS NUMBERS. VOLUME 1: DATA ANALYSIS Final Report, 17 Jun. 1991 - 31 Jul. 1992

B. R. Merrill Mar. 1993 52 p

(AD-A264151; PL-TR-92-1053-Vol-1) Avail: CASI HC A04/MF A01

This report documents the analysis of vortex shedding data collected by the Phillips Laboratory at the U.S. Air Force Academy Subsonic Wind Tunnel facility. The analysis is primarily of the power spectrum of the vortex shedding as seen in the force and moment coefficient power spectra. The shedding frequencies as seen in the power spectra are used to analyze for the Strouhal number. The analysis suggests that shape and orientation in the wind field have an effect on the shedding of vortices. DTIC

N93-30172# Phillips Lab., Kirtland AFB, NM.

VORTEX SHEDDING BY BLUNT/BLUFF BODIES AT HIGH REYNOLDS NUMBERS. VOLUME 2: CYLINDERS, OCTAGON, HEXAGON Final Report, 17 Jun. 1991 - 31 Jul. 1992

B. R. Merrill Mar. 1993 182 p

(AD-A264152; PL-TR-92-1053-Vol-2) Avail: CASI HC A09/MF A02

This report documents the analysis of vortex shedding data collected by the Phillips Laboratory at the U.S. Air Force Academy Subsonic Wind Tunnel facility. The analysis is primarily of the power spectrum of the vortex shedding as seen in the force and moment coefficient power spectra. The shedding frequencies as seen in the power spectra are used to analyze for the Strouhal number. The analysis suggests that shape and orientation in the wind field have an effect on the shedding of vortices. DTIC

N93-30173# Phillips Lab., Kirtland AFB, NM.
VORTEX SHEDDING BY BLUNT/BLUFF BODIES AT HIGH REYNOLDS NUMBERS. VOLUME 3. CUBES Final Report, 17 Jun. 1991 - 31 Jul. 1992
B. R. Merrill Mar. 1993 243 p
(AD-A264153; PL-TR-92-1053-Vol-3) Avail: CASI HC A11/MF A03

This report documents the analysis of vortex shedding data collected by the Phillips Laboratory at the U.S. Air Force Academy Subsonic Wind Tunnel facility. The analysis is primarily of the power spectrum of the vortex shedding as seen in the force and moment coefficient power spectra. The shedding frequencies as seen in the power spectra are used to analyze for the Strouhal number. The analysis suggests that shape and orientation in the wind field have an effect on the shedding of vortices.
DTIC

N93-30373*# Purdue Univ., West Lafayette, IN. School of Mechanical Engineering.
TURBULENCE CHARACTERISTICS OF AN AXISYMMETRIC REACTING FLOW Final Report
Richard D. Gould, Warren H. Stevenson, and H. Doyle Thompson Washington Feb. 1988 213 p
(Grant NAG3-502; RTOP 505-90-11)
(NASA-CR-4110; E-3813; NAS 1.26:4110) Avail: CASI HC A10/MF A03

Simultaneous two-componet laser velocimeter measurements were made in the turbulent flow field following an axisymmetric sudden expansion with and without combustion. The fuel (propane) and air were fully premixed to give a constant fuel-air ratio of 0.032 at the inlet (corresponding to an equivalence ratio of 0.5) for the combusting flow measurements. Reynolds number based on step height was 5.57 x 10 exp 4. The primary objective of the study was to obtain detailed measurements which would be of use to modelers. Quantities measured included mean axial and radial velocities, Reynolds stresses, and turbulent triple products. In addition, simultaneous time resolved temperature measurements were made in the reacting flow using high speed thermocouples. This permitted the computation of velocity-temperature correlations. Experimental results were compared to predictions from a widely used numerical code based on the k-epsilon turbulence model and the combustion model of Magnussen and Hjertager. Relatively good agreement was found for the cold flow case as in previous studies, but predicted values of temperature in the reacting flow case deviated substantially from the measurements. Sizable errors in the predictions for the velocity field also were found. Possible sources for the observed differences and suggestions for future model development are suggested.
Author (revised)

N93-30387# National Oceanic and Atmospheric Administration, Silver Spring, MD. Air Resources Lab.
VORTEX WAKE CHARACTERISTICS OF B757-200 AND B767-200 AIRCRAFT USING THE TOWER FLY-BY TECHNIQUE
L. J. Garodz and K. L. Clawson Jan. 1993 138 p See also PB92-114586 and Volume 2, PB93-180263
(PB93-180255; NOAA-TM-ERL-ARL-199-Vol-1) Avail: CASI HC A07/MF A02

The body of the report is a compilation of the reports and the conference proceedings cited above. It draws most heavily from the report by L.J. Garodz and K.L. Clawson, issued to NOAA in 1992. However, it also contains new evaluation methods, conclusions, and recommendations not previous reported in any form, most of which originated with K.L. Clawson. It is divided into two volumes: the first contains the body of the report, while the second contains the appendices. The document is Volume 1.
NTIS

N93-30388# National Oceanic and Atmospheric Administration, Silver Spring, MD. Air Resources Lab.
VORTEX WAKE CHARACTERISTICS OF B757-200 AND B767-200 AIRCRAFT USING THE TOWER FLY-BY TECHNIQUE
L. J. Garodz and K. L. Clawson Jan. 1993 570 p See also Volume 1, PB93-180255
(PB93-180263; NOAA-TM-ERL-ARL-199-Vol-2) Avail: CASI HC A24/MF A04

The body of the report is a compilation of the reports and the conference proceedings cited above. It draws most heavily from the report by L.J. Garodz and K.L. Clawson, issued to NOAA in 1992. However, it also contains new evaluation methods, conclusions, and recommendations not previous reported in any form, most of which originated with K.L. Clawson. It is divided into two volumes: the first contains the body of the report, while the second contains the appendices. The document is Volume 2.
NTIS

N93-30583 Virginia Polytechnic Inst. and State Univ., Blacksburg.
COMPRESSIBLE TURBULENCE IN A HIGH-SPEED HIGH REYNOLDS NUMBER MIXING LAYER Ph.D. Thesis
Rodney Dale Welch Bowersox 1992 257 p
Avail: Univ. Microfilms Order No. DA9302663

Compressible turbulence in a high-speed, high Reynolds number, supersonic free shear layer was studied. A two-dimensional free mixing layer was chosen to study turbulence rather than a wall bounded flow due to the experimental fact that the effects of compressibility become significant at lower Mach numbers. The overall flow structure was documented with the shadowgraph and conventional mean flow probes. Image processing techniques were developed in order to determine root-mean-square index of refraction (density) fluctuation levels from the shadowgraph plates. The research concentrated on the Reynolds averaged form of the Navier-Stokes equations, where the effects of compressibility are manifested through 'apparent mass' terms (i.e. p'u'(sub i)). These terms appear in all of the Reynolds averaged Navier-Stokes equations (continuity, momentum, and energy). A new turbulence transformation, coupled with innovative experimental methods, allowed the full compressible Reynolds shear stress to be directly measured. The full compressible heat flux and apparent mass terms were also estimated from cross-wire results. Profiles were obtained at four downstream stations which were strategically located to map different levels of development of the shear flow. It was found, experimentally, that the effects of compressibility on turbulence were more than significant accounting for about 75 percent of the total level of the Reynolds shear stress formulation. For the present mean adiabatic flow, the compressible turbulence accounted for 100 percent of the turbulent heat flux. The apparent mass in the continuity equation was, by definition, only due to compressibility. These results led to the development of a new Compressible Apparent Mass Mixing Length Extension (CAMMLE) model that accounts for compressible turbulence in all of the governing equations. A total of seven turbulence models were experimentally evaluated: the CAMMLE model, the Prandtl incompressible and the Situ-Schetz compressible mixing length models, the Prandtl and Bradshaw turbulent kinetic energy (TKE) formulations, and two compressible TKE extensions that are based upon a newly defined compressible TKE formulation. The measured turbulence data was used to assess the various models, where the measured mean flow profiles were used in the model formulations. The incompressible formulations were generally successful in representing the measured incompressible part of the Reynolds shear stress. However, this term only accounted for about 25 percent of the total shear stress level. All of the compressible extensions provided accurate estimates of the full compressible Reynolds shear stress.
Author (revised)

N93-30645 Stanford Univ., CA.
TURBULENT DRAG REDUCTION: STUDIES OF FEEDBACK CONTROL AND FLOW OVER RIBLETS Ph.D. Thesis
Haecheon Choi 1993 293 p
Avail: Univ. Microfilms Order No. DA9309581

The objective is to explore concepts for control of turbulent boundary layers leading to skin-friction reduction using the direct numerical simulation technique. Three different control methods are investigated; a passive control by longitudinal riblets, an active control by sensing and perturbing structures near the wall, and a feedback control procedure guided by control theory. In Part 1 significant drag reduction is achieved when the surface boundary condition is modified to suppress the dynamically significant coherent structures present in the wall region. The drag reduction is accompanied with significant reduction in the intensity of the wall layer structures and reductions in the magnitude of Reynolds shear stress throughout the flow. Two essential drag reduction mechanisms are presented. In Part 2 mathematical methods of control theory are applied to the problem of control of fluid flow. The procedure of how to cast the problem of controlling turbulence into a problem in optimal control theory is presented through the formalism and language of control theory. Then a suboptimal control and feedback procedure are presented using methods of calculus of variations through the adjoint state and gradient algorithms. This suboptimal feedback control procedure is applied to the distributed and boundary controls of the stochastic Burgers equation. Most cases considered show significant reductions of the costs. In Part 3 direct numerical simulation is performed to analyze turbulent flow over longitudinal riblets, and to reduce the mechanism of drag reduction by riblets. The computed drags on the riblet surfaces are in good agreement with the existing experimental data. Differences in the mean-velocity profile and turbulence quantities are found to be limited to the inner region of the boundary layer. Velocity and vorticity fluctuations as well as the Reynolds shear stresses above the riblets are reduced in drag-reducing configurations. Instantaneous flow fields near the riblets are investigated in detail and a physical explanation for the observed drag reduction is proposed. Dissert. Abstr.

N93-30892 California Inst. of Tech., Pasadena.
A THEORETICAL AND COMPUTATIONAL STUDY ON ACTIVE WAKE CONTROL Ph.D. Thesis
Luca Cortelezzi 1993 165 p
Avail: Univ. Microfilms Order No. DA9307031

A two-dimensional unsteady separated flow past a semi-infinite plate with transverse motion is considered. The flow is assumed incompressible and at high Reynolds number. The rolling-up of the separated shear-layer is modeled by a point vortex whose time dependent circulation is predicted by an unsteady Kutta condition. A power-law starting flow is assumed along with a power-law for the transverse motion. The effects of the motion of the plate on the starting vortex circulation and trajectory are presented. A suitable vortex shedding mechanism is introduced and a class of flows involving several vortices is presented. Subsequently, a control strategy able to maintain constant circulation when a vortex is present is derived. An exact solution for the non-linear controller is then obtained. Dynamical system analysis is used to explore the performance of the controlled system. Finally, the control strategy is applied to a class of flows and the results are discussed. The previous results are extended to the case of a two dimensional unsteady separated flow past a plate of variable length. Again the rolling-up of the separated shear layer is modeled by a vortex pair whose time dependent circulation is predicted by an unsteady Kutta condition. A power-law starting flow is assumed while the plate length is kept constant. The results of the simulations are presented and the model validated. A time dependent scaling which unveils the universality of the phenomenon is discussed. The previous vortex shedding mechanism is implemented and a vortex merging scheme is tested in a class of flows involving several vortices and is shown to be highly accurate. Subsequently, a control strategy able to maintain constant circulation when a vortex pair is present is derived. An exact solution for the non-linear controller is obtained in the form of an ordinary differential equation. Dynamical system analysis is used to explore the performance of the controlled system and the existence of a controllability region is discussed. Finally, the control strategy is applied to two classes of flows and the results are presented. Dissert. Abstr.

N93-30947 Stanford Univ., CA.
THE NUMERICAL SIMULATION OF CIRCULATION CONTROLLED AIRFOIL FLOWFIELDS Ph.D. Thesis
Samuel Witherspoon Linton 1993 173 p
Avail: Univ. Microfilms Order No. DA9309631

A Circulation Controlled Airfoil has a rounded trailing edge, so that the rearward stagnation point is not fixed, but is free to move along the surface. In addition, it uses upper surface blowing near the trailing edge to energize the boundary layer, thus increasing its resistance to separation. Since the jet flow rate is controlled, there is direct control of the separation point location, and thus of the circulation and lift of the airfoil. The delayed separation of the boundary layer near the trailing edge can result in a very high maximum lift coefficient. The present research is the numerical simulation of two- and three-dimensional flows over a Circulation Controlled geometry using a fully implicit Navier-Stokes code, and the comparison to experimental results. Mach numbers of 0.3 and 0.5 and jet total to freestream pressure ratios of 1.4 and 1.8 are investigated. The Baldwin-Lomax and k-epsilon turbulence models are used, each modified to include the effect of strong streamline curvature. A new numerical technique is presented for the implicit treatment of the nonlinear source terms in the k-epsilon equations. In addition to the steady-state unstalled solutions, the first known numerical solutions of jet stalled Circulation Controlled Airfoil fields are computed. In two-dimensions, the alternation between adverse pressure gradient and shock induced separation of the boundary layer on the airfoil trailing edge results in a highly repeatable periodic flow field. The first known three-dimensional computations about a Circulation Controlled Wing are also performed. The steady state solutions on the aspect ratio 4 semispan wing show locally two-dimensional behavior inboard of about the 70 percent span station, but strong roll up of the jet sheet into the tip vortex outboard. The post-stall three-dimensional computations show the same mechanism of stall as the corresponding two-dimensional results, but the oscillations are somewhat less regular. The outboard flow field is strongly influenced by the unsteady tip vortex, and the stream-lines there are highly three-dimensional. In some cases, three-dimensionality is important inboard as well, since the oscillations in lift are not in phase over the wing, but seem to travel inboard along it. Dissert. Abstr.

N93-31037*# Colorado Univ., Boulder.
THE HSCT MISSION ANALYSIS OF WAVERIDER DESIGNS Final Report, 15 May 1991 - 14 May 1993
1993 10 p
(Grant NAG1-1295)
(NASA-CR-193467; NAS 1.26:193467) Avail: CASI HC A02/MF A01

The grant provided partial support for an investigation of wave rider design and analysis with application to High-Speed Civil Transport (HSCT) vehicles. Proposed was the development of the necessary computational fluid dynamics (CFD) tools for the direct simulation of the waverider vehicles, the development of two new wave rider design methods that would provide computational speeds and design flexibilities never before achieved in wave rider design studies, and finally the selection of a candidate waverider-based vehicle and the evaluation of the chosen vehicle for a canonical HSCT mission scenario. This, the final report, reiterates the proposed project objectives in moderate detail, and it outlines the state of completion of each portion of the study, providing references to current and forthcoming publications that resulted from this work. Author (revised)

N93-29778*# Kansas Univ. Center for Research, Inc., Lawrence.
CONSTRUCTION, WIND TUNNEL TESTING AND DATA ANALYSIS FOR A 1/5 SCALE ULTRA-LIGHT WING MODEL
Michael D. James and Howard W. Smith *In its* The Ultra Light Aircraft Testing 1993 41 p (For primary document see N93-29774 11-05)
(Grant NAG1-345)
Avail: CASI HC A03/MF A02

N93-30979*# Battelle Pacific Northwest Labs., Richland, WA.
CONSTRUCTION AND TESTING OF SIMPLE AIRFOILS TO DEMONSTRATE STRUCTURAL DESIGN, MATERIALS CHOICE, AND COMPOSITE CONCEPTS
L. Roy Bunnell and Steven W. Piippo (Richland School District, WA.) *In* NASA. Langley Research Center, National Educators' Workshop. Update 92: Standard Experiments in Engineering Materials Science and Technology Jun. 1993 p 449-459 (For primary document see N93-30948 11-23)
Avail: CASI HC A02/MF A04

03 AIR TRANSPORTATION AND SAFETY

Includes passenger and cargo air transport operations; and aircraft accidents.

For related information see also *16 Space Transportation* and *85 Urban Technology and Transportation.*

N93-28571# Lawrence Livermore National Lab., CA.
WORLD COMMERCIAL AIRCRAFT ACCIDENTS
C. Y. Kimura Jan. 1993 517 p
(Contract W-7405-eng-48)
(DE93-010892; UCRL-ID-112905) Avail: CASI HC A22/MF A04

This report is a compilation of all accidents world-wide involving aircraft in commercial service which resulted in the loss of the airframe or one or more fatality, or both. This information has been gathered in order to present a complete inventory of commercial aircraft accidents. Events involving military action, sabotage, terrorist bombings, hijackings, suicides, and industrial ground accidents are included within this list. Included are the following topics: accidents involving world commercial jet aircraft, world commercial turboprop aircraft, world commercial pistonprop aircraft with four or more engines, and world commercial pistonprop aircraft with two or three engines from 1946 to 1992. Each accident is presented with information in the following categories: date of the accident, airline and its flight numbers, type of flight, type of aircraft, aircraft registration number, construction number/manufacturers serial number, aircraft damage, accident flight phase, accident location, number of fatalities, number of occupants, cause, remarks, or description (brief) of the accident, and finally references used. The sixth chapter presents a summary of the world commercial aircraft accidents by major aircraft class (e.g. jet, turboprop, and pistonprop) and by flight phase. The seventh chapter presents several special studies including a list of world commercial aircraft accidents for all aircraft types with 100 or more fatalities in order of decreasing number of fatalities, a list of collision accidents involving commercial aircrafts, and a list of world commercial aircraft accidents for all aircraft types involving military action, sabotage, terrorist bombings, and hijackings. DOE

N93-29152*# Massachusetts Inst. of Tech., Cambridge. Aeronautical Systems Lab.

A PASSIVE INFRARED ICE DETECTION TECHNIQUE FOR HELICOPTER APPLICATIONS

Adam L. Dershowitz and R. John Hansman, Jr. 20 Aug. 1991 54 p
(Grant NAG3-927)
(NASA-CR-193187; NAS 1.26:193187; ASL-91-4) Avail: CASI HC A04/MF A01

A technique has been developed, and successfully tested, to detect icing remotely on helicopter rotor blades. Using passive infrared (IR) thermometry it is possible to detect the warming caused by latent heat released as supercooled water freezes. During icing, the ice accretion region on the leading edge of the blade is found to be warmer than the uniced trailing edge resulting in a chordwise temperature profile characteristic of icing. Preliminary tests, using an IR Thermal video system, were conducted on a static model in the NASA Icing Research Tunnel (IRT) for a variety of wet (glaze) and dry (rime) ice conditions. A prototype detector system was built consisting of a single point IR pyrometer, and experiments were run on a small scale rotor model. Using this prototype detector, the characteristic chordwise temperature profiles were again observed for a range of icing conditions. Several signal processing methods were investigated, to allow automatic recognition of the icing signature. Additionally, several implementation issues were considered. Based on both the static and subscale rotor tests, where ice was successfully detected, the passive IR technique appears to be promising for rotor ice detection. Author (revised)

N93-29211 Virginia Polytechnic Inst. and State Univ., Blacksburg.

GENERATION OF CARBON MONOXIDE IN COMPARTMENT FIRES Ph.D. Thesis

Daniel T. Gottuk Dec. 1992 266 p
(Grant NANB-1-D1176)
(PB93-146702; NIST/GCR-92/619) Avail: Issuing Activity

A test compartment was used to investigate the burning of four fuels (hexane, PMMA, spruce, and flexible polyurethane foam) in compartment fires. Empirical correlations between the upper-layer yield of major species and the plume equivalence ratio were shown to exist. The results reveal that the production of CO is primarily dependent on the compartment flow dynamics and upper layer temperature. A chemical kinetic analysis indicated that increased compartment temperature affects upper-layer species yields in two ways: (1) the generation of species in the plume is changed, and (2) oxidation of post-flame gases in the layer is affected. The correlations developed in the compartment fires were qualitatively similar to those developed by Beyler for simplified upper-layer environments. The species yields downstream of hexane compartment fires were investigated and compared to upper-layer yields. Results showed that downstream CO yields can be correlated to the plume equivalence ratio when taking into account the occurrence of external burning. NTIS

N93-29286# Federal Aviation Administration, Washington, DC. Flight Standards Service.

FAA INTERNATIONAL CONFERENCE ON AIRPLANE GROUND DEICING

29 May 1992 317 p Conference held in Reston, VA, 28-29 May 1992
(AD-A263617) Avail: CASI HC A14/MF A03

On March 22, 1992 US Air Flight 405, departing from New York's La Guardia Airport, crashed on takeoff. The Federal Aviation Administration (FAA) is proceeding on the assumption that this tragedy was due to icing. In response, the FAA initiated a 6-month effort to improve the safety of winter flight operations. This effort will result in safety improvements that will be implemented before next winter. A better understanding of airplane ground deicing and anti-icing issues is a crucial prerequisite to the implementation of feasible and effective safety improvements. To achieve this goal, the FAA sponsored a conference at which the international aviation community could exchange thoughts and offer recommendation on a variety of issues concerning safe winter operations. On May 28 and 29, 1992, the FAA held the International Conference on Airplane Ground Deicing to develop a better understanding of airplane deicing and anti-icing issues. More than 750 participants discussed the problems posed by aircraft deicing and examined possible solutions. The conference produced suggestions for corrective actions the should be taken before this winter and possible long-term improvements to existing systems. The focus of the conference was carrier operated turbine-powered airplanes with more than 30 passenger seats. DTIC

N93-30194# Army War Coll., Carlisle Barracks, PA.

AIR PIRACY AND TERRORISM DIRECTED AGAINST U.S. AIR CARRIERS Study Project

Charles E. Martin 5 Apr. 1993 32 p
(AD-A264120) Avail: CASI HC A03/MF A01

Air piracy and terrorism have presented an increasing challenge to the air carriers of the United States and to the air carriers of the rest of the world. The air carriers of the United States represent a particularly lucrative target because airlines are symbols of nations. Airliners, which may be carrying as many as 350 hostages or victims, can be pirated and controlled by a small force. Or they can be blown up by a small explosive device placed in baggage or cargo. Terrorist groups and air pirates differ significantly in their goals, aims, means, capabilities as well as many other characteristics. They represent causes and ideals which cover the ideological spectrum. No matter their cause or ideal they cause confusion and fear in the government and population of their target country. This study will examine air piracy and terrorism historically and provide a survey of more recent highly publicized and political acts against U.S. air carriers. DTIC

N93-30274 Senstar Corp., Kanata (Ontario).

FUTURE DIRECTIONS IN AVIATION SECURITY

M. C. Maki *In* Engineering Inst. of Canada, Canadian Conference on Electrical and Computer Engineering, Volumes 1 and 2 1990 4 p (For primary document see N93-30215 11-31)
Avail: Engineering Inst. of Canada, 2050 rue Mansfield, Suite 700, Montreal, Quebec H3A 1Z2 Canada

N93-30275 American Science and Engineering, Inc., Cambridge, MA.

AUTOMATIC DETECTION OF EXPLOSIVES USING X RAY IMAGING

David Schafer and Martin Annis *In* Engineering Inst. of Canada, Canadian Conference on Electrical and Computer Engineering, Volumes 1 and 2 1990 4 p (For primary document see N93-30215 11-31)
Avail: Engineering Inst. of Canada, 2050 rue Mansfield, Suite 700, Montreal, Quebec H3A 1Z2 Canada

N93-30276 Scintrex Ltd., Concord (Ontario).

EXPLOSIVES DETECTION SYSTEMS FOR AIRPORT SECURITY GAS CHROMATOGRAPHIC BASED DEVICES

S. Nacson, C. Castledine, T. Siu, T. Lu, and O. Legrady *In* Engineering Inst. of Canada, Canadian Conference on Electrical and Computer Engineering, Volumes 1 and 2 1990 3 p (For primary document see N93-30215 11-31)
Avail: Engineering Inst. of Canada, 2050 rue Mansfield, Suite 700, Montreal, Quebec H3A 1Z2 Canada

04 AIRCRAFT COMMUNICATIONS AND NAVIGATION

Includes digital and voice communication with aircraft; air navigation systems (satellite and ground based); and air traffic control.

For related information see also *17 Space Communications, Spacecraft Communications, Command and Tracking* and *Communications and Radar.*

N93-28625# Federal Aviation Administration, Atlantic City, NJ.
RESULTS OF DATAS INVESTIGATION OF ATCRBS ENVIRONMENT AT THE LOS ANGELES INTERNATIONAL AIRPORT Final Report, 14 Dec. 1992 - 15 Jan. 1993
Leo Wapelhorst, Thomas Pagano, and John VanDongen Apr. 1993 37 p
(Contract FAA-T1101-F)
(DOT/FAA/CT-93/6) Avail: CASI HC A03/MF A01

The deployment of the Data Link Test and Analysis System (DATAS) as a Traffic Alert and Collision Avoidance System (TCAS) monitor at the Los Angeles International Airport (LAX) is documented. The purpose was to identify aircraft which were reporting illegal Mode Select ID's. Data were also taken on the downlink portion of the environment in order to characterize the environment after the implementation of TCAS. The project was conducted by the Airborne Collision and Data Link Systems branch of the Federal Aviation Administration (FAA) Technical Center. Author (revised)

N93-28936*# California Polytechnic State Univ., San Luis Obispo.
HELICOPTER APPROACH CAPABILITY USING THE DIFFERENTIAL GLOBAL POSITIONING SYSTEM M.S. Thesis
David N. Kaufmann Jun. 1993 56 p
(Contract NCC2-775)
(NASA-CR-193183; NAS 1.26:193183) Avail: CASI HC A04/MF A01

The results of flight tests to determine the feasibility of using the Global Positioning System (GPS) in the differential mode (DGPS) to provide high accuracy, precision navigation, and guidance for helicopter approaches to landing are presented. The airborne DGPS receiver and associated equipment is installed in a NASA UH-60 Black Hawk helicopter. The ground-based DGPS reference receiver is located at a surveyed test site and is equipped with a real-time VHF data link to transmit correction information to the airborne DGPS receiver. The corrected airborne DGPS information, together with the preset approach geometry, is used to calculate guidance commands which are sent to the aircraft's approach guidance instruments. The use of DGPS derived guidance for helicopter approaches to landing is evaluated by comparing the DGPS data with the laser tracker truth data. Both standard (3 deg) and steep (6 deg and 9 deg) glideslope straight-in approaches were flown. DGPS positioning accuracy based on a time history analysis of the entire approach was 0.2 m (mean) +/- 1.8 m (2 sigma) laterally and -2.0 m (mean) +/- 3.5 m (2 sigma) vertically for 3 deg glideslope approaches, -0.1 m (mean) +/- 1.5 m (2 sigma) laterally and -1.1 m (mean) +/- 3.5 m (2 sigma) vertically for 6 deg glideslope approaches and 0.2 m (mean) +/- 1.3 m (2 sigma) laterally and -1.0 m (mean) +/- 2.8 m (2 sigma) vertically for 9 deg glideslope approaches. DGPS positioning accuracy at the 200 ft decision height (DH) on a standard 3 deg slideslope approach was 0.3 m (mean) +/- 1.5 m (2 sigma) laterally and -2.3 m (mean) +/- 1.6 m (2 sigma) vertically. These errors indicate that the helicopter position based on DGPS guidance satisfies the International Civil Aviation Organization (ICAO) Category 1 (CAT 1) lateral and vertical navigational accuracy requirements. Author (revised)

N93-28990# Naval Command, Control and Ocean Surveillance Center, San Diego, CA.
ADVANCED UNMANNED SEARCH SYSTEM (AUSS) SUPERVISORY COMMAND, CONTROL AND NAVIGATION Final Report
H. B. McCracken Nov. 1992 85 p
(NR Proj. S03-97)
(AD-A263171; NRAD-TR-1533) Avail: CASI HC A05/MF A01

This document summarizes three major facets of Advanced Unmanned Search System (AUSS) vehicle operation. It describes the AUSS vehicle system's four command groups: the basic vehicle mode commands, which alter the vehicle's basic mode of operation; movement commands, which move the vehicle around; search commands, which control the vehicle's search sensors; and informational and miscellaneous commands, which provide information to surface operators. The document details the operation of individual basic vehicle mode, movement, and search commands. The document discusses the two types of AUSS vehicle navigation: dead reckoning and Doppler navigation. It describes the main computer system and the sensor computer group that comprise the AUSS vehicle's basic computer architecture, and it summarizes AUSS vehicle computer system components and their specific functions. DTIC

N93-29285# Army War Coll., Carlisle Barracks, PA.
USING TODAY'S TECHNOLOGY TO IMPROVE MOBILE C4I FOR THE OPERATIONAL COMMANDER
Robert D. Fox 15 Apr. 1993 45 p
(AD-A263613) Avail: CASI HC A03/MF A01

The rapid development of communications and computer technology in the commercial market provides the Army with a unique opportunity to relook the way we provide command, control, communications, computers, and intelligence (C4I) on the battlefield. Desert Shield/Storm experiences demonstrated the capability and reliability of off-the-shelf equipment and enhancements in battlefield awareness provided by new military systems. However, after action reviews also revealed significant problems for operational commanders during Desert Shield/Desert Storm with command and control 'on the move'. As a result, the Chairman, Joint Chiefs of Staff approved a program called 'C4I for the Warrior'. The thrust of the program is to provide a seamless C4I architecture to support the warfighter. The effort is phased over three periods; Quick Fix Phase (POM years), Mid-Term Phase (POM plus 10), and Objective Phase (beyond Mid-Term period). This study looks a leveraging current technology and new military systems in the Quick Fix and Mid-Term phases to provide a communications and computer workstation for an operational commander's command and control vehicle (C2V). DTIC

N93-29468# Trimble Navigation, Sunnyvale, CA.
SYSTEM ANALYSIS FOR A KINEMATIC POSITIONING SYSTEM BASED ON THE GLOBAL POSITIONING SYSTEM Final Report
G. J. Geier, Peter V. Loomis, and Alfred Kleusberg Dec. 1992 136 p
(Contract DACW72-89-C-0025)
(AD-A262830; TEC-DRP-92-8) Avail: CASI HC A07/MF A02

This report documents the findings of a study to design a kinematic positioning system to support U.S. Army Corps of Engineers dredging and hydrographic survey operations. Survey quality GPS receivers are considered, due to the accuracy constraints (10 cm vertical positioning). Use of auxiliary sensors (i.e., INS and high quality clocks) is considered to improve navigation performance when GPS is unavailable. Predicted navigation performance indicates that the accuracy requirements can be met, except at the extremes of the expected separation distances from the reference station. The integer ambiguities associated with the carrier phase measurements can generally be resolved within 7 minutes by processing all available satellites. Measurement gaps of roughly 60 seconds can be tolerated without losing the integers when using a high quality INS. DTIC

N93-29653*# National Aeronautics and Space Administration. Ames Research Center, Moffett Field, CA.
NEURAL NETWORKS APPLICATION TO DIVERGENCE-BASED PASSIVE RANGING
Yair Barniv Dec. 1992 26 p
(RTOP 505-64-52)
(NASA-TM-103981; A-92198; NAS 1.15:103981) Avail: CASI HC A03/MF A01

The purpose of this report is to summarize the state of knowledge and outline the planned work in divergence-based/neural networks approach to the problem of passive ranging derived from optical flow. Work in this and closely related areas is reviewed in order to provide the necessary background for further developments. New ideas about devising a monocular passive-ranging system are then introduced. It is shown that image-plan divergence is independent of image-plan location with respect to the focus of expansion and of camera maneuvers because it directly measures the object's expansion which, in turn, is related to the time-to-collision. Thus, a divergence-based method has the potential of providing a reliable range complementing other monocular passive-ranging methods which encounter difficulties in image areas close to the focus of expansion. Image-plan divergence can be thought of as some spatial/temporal pattern. A neural network realization was chosen for this task because neural networks have generally performed well in various other pattern recognition applications. The main goal of this work is to teach a neural network to derive the divergence from the imagery. Author (revised)

N93-29818# Coast Guard Research and Development Center, Groton, CT.

A COMPARISON OF SIMULATED PARALLAX AND SINGLE-STATION RANGE AIDS TO NAVIGATION

Kevin Laxar, S. M. Luria, and Marc B. Mandler Apr. 1993 59 p
(Contract MIPR-Z51100-9-0002)
(AD-A263460; USCG-D-03-93; NSMRL-1168) Avail: CASI HC A04/MF A01

An appropriately designed parallax (two-station) range allows a mariner to accurately determine a range line--the correct path on which to steer the vessel--at greater distances. Less expensive alternatives to parallax ranges are desirable, and many ideas, principally single-station ranges, have been proposed. However, the mariners' abilities to establish range lines with them have not been measured. The present work has quantified the navigational sensitivity afforded by parallax ranges and three different types of single-station range display systems. The single-station ranges used (1) temporal characteristics, (2) spatial representation, or (3) color changes of the signal to represent changes in lateral position. Range systems were simulated either opto-mechanically or on a high resolution computer display system. The mariners' ability to determine both lateral position in a channel and direction of motion across a channel was assessed psychophysically for each range system. DTIC

N93-30605 Stanford Univ., CA.

ATTITUDE DETERMINATION USING GPS: DEVELOPMENT OF AN ALL SOLID-STATE GUIDANCE, NAVIGATION, AND CONTROL SENSOR FOR AIR AND SPACE VEHICLES BASED ON THE GLOBAL POSITIONING SYSTEM Ph.D. Thesis

Clark Emerson Cohen 1993 203 p
Avail: Univ. Microfilms Order No. DA9309582

The Global Positioning System (GPS) is poised to revolutionize aerospace Guidance, Navigation, and Control. While traditionally thought of as a navigation system, GPS is demonstrated to be a formidable sensor for attitude determination as well. In fact, GPS may now be considered a 10 state sensor, providing continuous real-time Position, Velocity, Time, and Attitude (PVTA) for all axes. Attitude determination is derived from precise (5mm, 1sigma) differential range measurements among multiple GPS antennas mounted on a flight vehicle. Experimental testing on 3m baselines is demonstrated pointing accuracies below 0.1 deg (1sigma) with a usable bandwidth of several tens of Hz. The design and development of a new and unique GPS receiver with full PVTA capability is described. It chronicles the key innovations which made this technology possible and addresses the fundamentals and performance of GPS-based attitude determination. A prototype receiver base on antenna multiplexing is presented which offers prospects of significantly reducing the size, weight, power, and cost of the hardware. Other conceptual designs are presented for achieving the highest possible performance. Methods of resolving the cycle ambiguities of the GPS carrier based on motion are developed and tested in an effort to derive the robustness of attitude determination toward perfection. Maiden space flights of the new receiver are scheduled for launch into low Earth orbit. Test data is presented from extensive flights on a single-engine Piper Dakota to explore aircraft applications of attitude determination. Among these, attitude and precise position sensing using GPS can be applied to the estimation of the aircraft dynamic model in flight. The wealth of dynamic response data obtained through GPS can be used to estimate aircraft stability derivatives and, surprisingly, aeroelastic effects with millimeter-level clarity. This new capability is likely to enhance the overall safety and efficiency of aviation. Dissert. Abstr.

N93-30671# Technische Univ., Berlin (Germany). Fachgebiet Ortung und Navigation.

DESIGN AND IMPLEMENTATION OF A GLOBAL POSITIONING SYSTEM (GPS) SUPPORTED AREA NAVIGATION SYSTEM WITH ELECTRONIC AIRCRAFT [ENTWURF UND IMPLEMENTIERUNG EINES GPS-GESTUETZTEN FLAECHENNAVIGATIONSSYSTEMS MIT ELEKTRONISCHER LUFTFAHRTKARTE]

Detlef Stolze 14 Sep. 1992 192 p In GERMAN
(ILR-Mitt-275(1992); ETN-93-94175) Avail: CASI HC A09/MF A02

The development of an area navigation system with GPS (Global Positioning System) based position acquisition is described, with focus on low cost concepts and real time operation. A modular software solution was chosen which can be used on computers with Intel processors. An electronic airchart with a moving map display was selected as man machine interface. A course line computer was used for trajectory points management and for calculation of characteristic magnitudes of area navigation. A modified horizontal situation indicator was used for result representation. ESA

N93-31005 Princeton Univ., NJ.

AIRCRAFT GUIDANCE FOR WIND SHEAR AVOIDANCE: DECISION-MAKING UNDER UNCERTAINTY Ph.D. Thesis

Donald Alexander Stratton 1992 220 p
Avail: Univ. Microfilms Order No. DA9306544

Severe low-altitude wind shear poses a significant threat to air transportation safety. Concepts for assisting critical decision making under uncertainty are advanced to promote the avoidance of hazardous weather, particularly microburst wind shear. Computational strategies founded on probability and optimal estimation theories enable flight deck integration of diverse forecasting and detection systems, from airport weather information services to airborne forward-looking wind sensors. A decision-making policy for wind shear is developed from a comprehensive investigation of microburst phenomenology, its observed characteristics, and its effects on aircraft flight. Existing avoidance guidelines for wind shear are extended to exploit the latest available technology, such as Doppler weather radar and lidar. Theories for probability based decision making facilitate real-time computer reasoning with dynamic, conflicting data from a wide array of sources. Bayesian neural networks fused with multivariable estimators account for the limited precision, reliability, and timeliness of correlated sensor measurements. Monte Carlo analyses are conducted to refine a disturbance prediction Kalman filter for forward-looking sensors, with statistical results completing their incorporation into Bayesian reasoning. Symbolic and numerical processes for a Wind Shear Safety Advisor are implemented and evaluated. A risk assessment model based on empirical and analytical results is used to compare the relevance of available wind shear information sources. Simulations of the risk assessment model show its insensitivity to parameter variations. Validations of overall Wind Shear Safety Advisor logic illustrate how it conveys beneficial advance warnings in rapidly developing microburst encounter situations. These results prove that intelligently-integrated detection systems can warn pilots of threatening wind shear sooner, more frequently, and more effectively than isolated systems can. Dissert. Abstr.

N93-29588*# Jet Propulsion Lab., California Inst. of Tech., Pasadena.

THE EFFECT OF CLOCK, MEDIA, AND STATION LOCATION ERRORS ON DOPPLER MEASUREMENT ACCURACY

J. K. Miller *In its* The Telecommunications and Data Acquisition Report 15 May 1993 p 7-21 (For primary document see N93-29586 11-32)
(RTOP 310-10-63-84-02)
Avail: CASI HC A03/MF A03

N93-30299 McMaster Univ., Hamilton (Ontario). Communications Research Lab.

CLASSIFICATION OF RADAR CLUTTER IN AN AIR TRAFFIC CONTROL ENVIRONMENT

Simon Haykin, Wolfgang Stehwien (Litton Systems, Canada Ltd., Etobicoke, Ontario.), Cong Deng, Peter Weber, and Richard Mann *In* Engineering Inst. of Canada, Canadian Conference on Electrical and Computer Engineering, Volumes 1 and 2 1990 3 p (For primary document see N93-30215 11-31)
Avail: Engineering Inst. of Canada, 2050 rue Mansfield, Suite 700, Montreal, Quebec H3A 1Z2 Canada

N93-30323 Hughes Aircraft Co., Goleta, CA. Systems Div.

THE CANADIAN AUTOMATED AIR TRAFFIC SYSTEM

Don E. Ludwig *In* Engineering Inst. of Canada, Canadian Conference on Electrical and Computer Engineering, Volumes 1 and 2 1990 4 p (For primary document see N93-30215 11-31)
Avail: Engineering Inst. of Canada, 2050 rue Mansfield, Suite 700, Montreal, Quebec H3A 1Z2 Canada

N93-30324 Sony Corp. of America, San Diego, CA.
COMPUTER-CONTROLLED ALIGNMENT FOR A 2000-LINE COLOR MONITOR
David A. Eccles, Manabu Suzuki (Sony Corp., Tokyo, Japan.), Hiroshi Nakano (Sony Corp., Tokyo, Japan.), Yuki Okamoto (Sony Corp., Tokyo, Japan.), and Kazuo Kii (Sony Corp., Tokyo, Japan.) *In* Engineering Inst. of Canada, Canadian Conference on Electrical and Computer Engineering, Volumes 1 and 2 1990 4 p (For primary document see N93-30215 11-31)
Avail: Engineering Inst. of Canada, 2050 rue Mansfield, Suite 700, Montreal, Quebec H3A 1Z2 Canada

N93-30325 Centre d'Etudes de la Navigation Aerienne, Toulouse (France).
EVOLUTION OF RADAR DATA PROCESSING IN THE FRENCH AIR TRAFFIC CONTROL SYSTEM
D. Figarol and B. Kriner *In* Engineering Inst. of Canada, Canadian Conference on Electrical and Computer Engineering, Volumes 1 and 2 1990 4 p (For primary document see N93-30215 11-31)
Avail: Engineering Inst. of Canada, 2050 rue Mansfield, Suite 700, Montreal, Quebec H3A 1Z2 Canada

N93-30330 Canadian Marconi Co. Ltd., Kanata (Ontario).
EMBEDDED GPS: THE CANADIAN MARCONI APPROACH
James M. Brown and R. K. Tiedemann *In* Engineering Inst. of Canada, Canadian Conference on Electrical and Computer Engineering, Volumes 1 and 2 1990 4 p (For primary document see N93-30215 11-31)
Avail: Engineering Inst. of Canada, 2050 rue Mansfield, Suite 700, Montreal, Quebec H3A 1Z2 Canada

N93-30338 Transport Canada, Ottawa (Ontario).
ADAPTING SYSTEM ENGINEERING PRINCIPLES TO THE CANADIAN AIRSPACE SYSTEM
T. E. Thompson and R. G. Lewis (Martin Marietta Canada Ltd., Ottawa, Ontario.) *In* Engineering Inst. of Canada, Canadian Conference on Electrical and Computer Engineering, Volumes 1 and 2 1990 4 p (For primary document see N93-30215 11-31)
Avail: Engineering Inst. of Canada, 2050 rue Mansfield, Suite 700, Montreal, Quebec H3A 1Z2 Canada

N93-30339 MacDonald, Dettwiler and Associates Ltd., Ottawa (Ontario).
APPLICATION AND INTEGRATION OF DIVERSE TECHNOLOGY IN AN AVIATION SYSTEM: THE NATIONAL AERONAUTICAL INFORMATION PROCESSING SYSTEM
Karl Snider and Tim Daniel *In* Engineering Inst. of Canada, Canadian Conference on Electrical and Computer Engineering, Volumes 1 and 2 1990 4 p Prepared in cooperation with MacDonald, Dettwiler Proprietary Ltd., New South Wales, Australia (For primary document see N93-30215 11-31)
Avail: Engineering Inst. of Canada, 2050 rue Mansfield, Suite 700, Montreal, Quebec H3A 1Z2 Canada

N93-30350 CompEngServ Ltd., Ottawa (Ontario).
ISSUES OF ATC CONFLICT RESOLUTION UNDER REAL-TIME CONSTRAINTS
I. G. Smith and C. A. Crabb *In* Engineering Inst. of Canada, Canadian Conference on Electrical and Computer Engineering, Volumes 1 and 2 1990 4 p (For primary document see N93-30215 11-31)
Avail: Engineering Inst. of Canada, 2050 rue Mansfield, Suite 700, Montreal, Quebec H3A 1Z2 Canada

N93-30351 Mitre Corp., McLean, VA.
NATIONAL AIRSPACE SYSTEM PERFORMANCE ANALYSIS CAPABILITY (NASPAC) SIMULATION MODEL
Lynne Fellman *In* Engineering Inst. of Canada, Canadian Conference on Electrical and Computer Engineering, Volumes 1 and 2 1990 4 p (For primary document see N93-30215 11-31)
Avail: Engineering Inst. of Canada, 2050 rue Mansfield, Suite 700, Montreal, Quebec H3A 1Z2 Canada

N93-30352 Mitre Corp., McLean, VA.
PROCEDURAL DEVELOPMENT PROTOTYPE IN AUTOMATED EN ROUTE AIR TRAFFIC CONTROL
C. Vanessa Fong *In* Engineering Inst. of Canada, Canadian Conference on Electrical and Computer Engineering, Volumes 1 and 2 1990 3 p (For primary document see N93-30215 11-31)
Avail: Engineering Inst. of Canada, 2050 rue Mansfield, Suite 700, Montreal, Quebec H3A 1Z2 Canada

N93-30353 Mitre Corp., McLean, VA.
ENHANCING AVAILABILITY, PERFORMANCE, AND FLEXIBILITY OF AIR TRAFFIC CONTROL AIR-GROUND SERVICES
Gian P. Jain, Douglas L. Bamford, and Leone C. Monticone *In* Engineering Inst. of Canada, Canadian Conference on Electrical and Computer Engineering, Volumes 1 and 2 1990 5 p (For primary document see N93-30215 11-31)
Avail: Engineering Inst. of Canada, 2050 rue Mansfield, Suite 700, Montreal, Quebec H3A 1Z2 Canada

N93-30354 Mitre Corp., McLean, VA.
CHANGING ROLE OF TELECOMMUNICATIONS MANAGEMENT IN AIR TRAFFIC CONTROL IN THE FAA
Kikram Prabhu *In* Engineering Inst. of Canada, Canadian Conference on Electrical and Computer Engineering, Volumes 1 and 2 1990 4 p (For primary document see N93-30215 11-31)
Avail: Engineering Inst. of Canada, 2050 rue Mansfield, Suite 700, Montreal, Quebec H3A 1Z2 Canada

N93-30356 Mitre Corp., McLean, VA.
DEVELOPING AUTOMATION FOR TERMINAL AIR TRAFFIC CONTROL: CASE STUDY OF THE IMAGING AID
Anand D. Mundra and Kerry M. Levin *In* Engineering Inst. of Canada, Canadian Conference on Electrical and Computer Engineering, Volumes 1 and 2 1990 4 p (For primary document see N93-30215 11-31)
Avail: Engineering Inst. of Canada, 2050 rue Mansfield, Suite 700, Montreal, Quebec H3A 1Z2 Canada

N93-30357 Transport Canada, Ottawa (Ontario).
AIRSPACE DESIGN EXPERT SYSTEM (ADES), A 2D/3D MAPPING AND MODELLING TOOL INCORPORATING AN EXPERT SYSTEM FOR USE IN INSTRUMENT APPROACH DESIGN
J. C. Ainsworth, L. Lam (Virtual Prototypes, Inc., Montreal, Quebec.), B. Schoor (Virtual Prototypes, Inc., Montreal, Quebec.), and M. McQueen (Virtual Prototypes, Inc., Montreal, Quebec.) *In* Engineering Inst. of Canada, Canadian Conference on Electrical and Computer Engineering, Volumes 1 and 2 1990 4 p (For primary document see N93-30215 11-31)
Avail: Engineering Inst. of Canada, 2050 rue Mansfield, Suite 700, Montreal, Quebec H3A 1Z2 Canada

N93-30358 MiTech, Inc., Washington, DC.
EVALUATION OF CATEGORY 3 MLS DESIGNS
Rick Cassell, Kelly R. Markin (Mitre Corp., McLean, VA.), and Alex E. Smith *In* Engineering Inst. of Canada, Canadian Conference on Electrical and Computer Engineering, Volumes 1 and 2 1990 4 p (For primary document see N93-30215 11-31)
Avail: Engineering Inst. of Canada, 2050 rue Mansfield, Suite 700, Montreal, Quebec H3A 1Z2 Canada

05 AIRCRAFT DESIGN, TESTING AND PERFORMANCE

Includes aircraft simulation technology.

For related information see also *18 Spacecraft Design, Testing and Performance* and *39 Structural Mechanics.*For land transportation vehicles see *85 Urban Technology and Transportation.*

N93-28586# Aurora Flight Sciences Corp., Manassas, VA.
DEVELOPMENT AND TESTING OF THE PERSEUS PROOF-OF-CONCEPT AIRCRAFT
John S. Langford 26 Feb. 1993 68 p Prepared in cooperation with National Inst. for Global Environmental Change, Davis, CA

(Contract DE-FC03-90ER-61010)
(DE93-010121; DOE/ER-61010/002; AR-9301) Avail: CASI HC A04/MF A01

Many areas of global climate change research could benefit from a flexible, affordable, and near-term platform that could provide in situ measurements in the upper troposphere and lower stratosphere. To provide such a capability, the Perseus unmanned science research aircraft was proposed in 1989. As a first step toward the development of Perseus, a proof-of-concept (POC) demonstrator was constructed and tested during 1990 and 1991. The POC was a full scale Perseus airframe intended to validate the structural, aerodynamic, and flight control technologies for the Perseus within a total budget of about $1.5 million. Advanced propulsion systems needed for the operational Perseus were not covered in the POC program due to funding limitations. This report documents the design, development, and testing of the Perseus POC. DOE

N93-28693*# Texas A&M Univ., College Station. Aerospace Engineering Div.
PRELIMINARY DESIGN OF AN INTERMITTENT SMOKE FLOW VISUALIZATION SYSTEM
Donald T. Ward and James H. Myatt Jun. 1993 65 p
(Grant NAG2-651; RTOP 533-02-35)
(NASA-CR-186027; H-1917; NAS 1.26:186027; TEES-AERO-TR-91-1) Avail: CASI HC A04/MF A01

A prototype intermittent flow visualization system that was designed to study vortex flow field dynamics has been constructed and tested through its ground test phase. It produces discrete pulses of dense white smoke consisting of particles of terephthalic acid by the pulsing action of a fast-acting three-way valve. The trajectories of the smoke pulses can be tracked by a video imaging system without intruding in the flow around in flight. Two methods of pulsing the smoke were examined. The simplest and safest approach is to simply divert the smoke between the two outlet ports on the valve; this approach should be particularly effective if it were desired to inject smoke at two locations during the same test event. The second approach involves closing off one of the outlet ports to momentarily block the flow. The second approach requires careful control of valve dwell times to avoid excessive pressure buildup within the cartridge container. This method also increases the velocity of the smoke injected into the flow. The flow of the smoke has been blocked for periods ranging from 30 to 80 milliseconds, depending on the system volume and the length of time the valve is allowed to remain open between valve closings. Author (revised)

N93-29153*# Arizona State Univ., Tempe.
AN INTEGRATED OPTIMUM DESIGN APPROACH FOR HIGH SPEED PROP-ROTORS INCLUDING ACOUSTIC CONSTRAINTS Semiannual Progress Report, 1 Jan. - 30 Jun. 1993
Aditi Chattopadhyay, Valana Wells, Thomas McCarthy, and Arris Han 30 Jun. 1993 11 p
(Contract NCC2-795)
(NASA-CR-193222; NAS 1.26:193222) Avail: CASI HC A03/MF A01

The objective of this research is to develop optimization procedures to provide design trends in high speed prop-rotors. The necessary disciplinary couplings are all considered within a closed loop multilevel decomposition optimization process. The procedures involve the consideration of blade-aeroelastic aerodynamic performance, structural-dynamic design requirements, and acoustics. Further, since the design involves consideration of several different objective functions, multiobjective function formulation techniques are developed. Derived from text

N93-29268# Technische Univ., Eindhoven (Netherlands).
QUIET BY DESIGN: NUMERICAL ACOUSTO-ELASTIC ANALYSIS OF AIRCRAFT STRUCTURES Ph.D. Thesis
Nicolaas Bernardus Roozen 1992 158 p Sponsored by Fokker B.V. Original contains color illustrations
(ISBN-90-386-0042-9; ETN-93-93578) Avail: CASI HC A08/MF A02

The development of feasible analysis methods and models to calculate the dynamic behavior of fuselage and the so called acousto-elastic interaction with its enclosed acoustic cavity, is reported. These methods are to be used in the design optimization of aircraft resulting in considerable noise reduction. The so called structural detuning concept, in which the fuselage structure and propulsion system are designed in such a way that the aircraft resistant frequencies and the propulsion system excitation frequencies are well separated, was applied. The two analysis methods investigated were the continuous analysis (analytical) models and discrete analysis (finite element method) models. ESA

N93-29409# Wright Lab., Wright-Patterson AFB, OH.
A REAL-TIME, HARDWARE-IN-THE-LOOP SIMULATION OF AN UNMANNED AERIAL RESEARCH VEHICLE Final Report, 1 May 1991 - 28 Aug. 1992
Scott D. Robertson Aug. 1992 65 p
(AF Proj. 2403)
(AD-A262477; WL-TR-93-3005) Avail: CASI HC A04/MF A01

Simulation is a valuable tool for rapidly and cost effectively developing and verifying new systems. This report describes the design and development of a system which simulates an unmanned aircraft and verifies the proper operation of its flight computer. Flight computers, being time critical devices, must execute at a certain rate in order to safely and accurately control an aircraft. In order to verify the proper operation of the flight computer, the simulation must execute in 'real-time', which is a rate of 100 Hz for this flight computer. The flight computer's inputs and outputs are connected to the simulation so that the flight computer thinks it is flying. The simulation architecture is a VME-based computer system, consisting of an input board (designed for this project) which demodulates 13 channels of pulse-width modulated signals, a processor board which executes the simulation software, and a digital-to-analog output board. The existing simulation software was ported to the C language and re-hosted on a 68030 processor board. Additional software was written to handle all the I/O and data conversions. The system accurately simulates the unmanned aircraft, runs in real-time, and verifies the proper operation of the flight computer. DTIC

N93-29464# European Space Agency, Paris (France).
FLIGHT MECHANICAL MODEL FOR PERFORMANCE CALCULATIONS AND INTERACTIONS BETWEEN FLIGHT VEHICLE AND RAMJET IN REGARD TO THE FLIGHT ORBIT
Frans G. J. Kremer (Deutsche Forschungsanstalt fuer Luft- und Raumfahrt, Cologne, Germany.) Oct. 1992 93 p Transl. into ENGLISH of Flugmechanikmodel fuer Leistungsrechnungen und Wechselwirkungen zwischen Flugkoerper und Staustrahltriebwerk mit Unterschallverbrennung in bezung zur Flugbahn (Cologne, Germany, DLR), Feb. 1991 p 1-95 Original language document was announced as N91-32131
(ESA-TT-1267; DLR-FB-91-03; ETN-93-93714) Avail: CASI HC A05/MF A02; Original German version available from DLR, Wissenschaftliches Berichtswesen, VB-PL-DO, Postfach 90 60 58, 5000 Cologne, Germany, HC

A flight mechanics model for performance calculations and relationships between flight vehicle and ramjet engine with subsonic combustion relative to the flight path is described. Performance calculation for a ramjet engine initially required determination of the burst demand throughout the flight path. This is the objective of a flight mechanics computer model. The computer model described is based on the assumption of equilibrium of forces at the center of gravity of the flight vehicle. A further input is an aerodynamic model of the flight vehicle. The flight path is input with a statement of the flight profile, acceleration on flight direction and turning acceleration. The interaction between flight vehicles and ramjet engines in conjunction with the flight path is considered. The influencing variables in the consumption relating to mission phases are described. The role of the angle of incidence and the significance of the design are explained. Interactions are described on the basis of modification of parameters for flight path data (ram pressure, acceleration in flight direction and turning acceleration). ESA

N93-29498*# Boeing Commercial Airplane Co., Seattle, WA. Technology and Product Development Div.
ADVANCED TECHNOLOGY COMPOSITE AIRCRAFT STRUCTURES Monthly Technical Progress Report No. 25, 1-31 May 1991
Larry B. Ilcewicz and Thomas H. Walker 14 Jun. 1991 133 p
(Contract NAS1-18889)
(NASA-CR-190420; NAS 1.26:190420) Avail: CASI HC A07/MF A02

Work performed during the 25th month on NAS1-18889, Advanced Technology Composite Aircraft Structures, is summarized. The main objective of this program is to develop an integrated technology and demonstrate a

confidence level that permits the cost- and weight-effective use of advanced composite materials in primary structures of future aircraft with the emphasis on pressurized fuselages. The period from 1-31 May 1991 is covered.
Author

N93-29774*# Kansas Univ. Center for Research, Inc., Lawrence. Dept. of Aerospace Engineering.
THE ULTRA LIGHT AIRCRAFT TESTING Final Report
Howard W. Smith 1993 172 p
(Grant NAG1-345)
(NASA-CR-193043; NAS 1.26:193043) Avail: CASI HC A08/MF A02

The final report for grant NAG1-345 is presented. Recently, the bulk of the work that the grant has supported has been in the areas of ride quality and the structural analysis and testing of ultralight aircraft. The ride quality work ended in May 1989. Hence, the papers presented in this final report are concerned with ultralight aircraft. For individual titles, see N93-29775 through N93-29779.

N93-29775*# Kansas Univ. Center for Research, Inc., Lawrence. Dept. of Aerospace Engineering.
REPORT ON THE TEST SET-UP FOR THE STRUCTURAL TESTING OF THE AIRMASS SUNBURST ULTRALIGHT AIRCRAFT
William Zimmerman and Howard W. Smith *In its* The Ultra Light Aircraft Testing 1993 5 p (For primary document see N93-29774 11-05)
(Grant NAG1-345)
Avail: CASI HC A01/MF A02

This report reviews the test set-up and procedure for the structural testing of the Airmass Sunburst Ultralight Aircraft. In general aviation today, there is a growing need for more stringent design criteria for ultralight aircraft. Unlike most general aviation aircraft, the ultralight lacks sufficient design criteria and more importantly it lacks sufficient certification enforcement. The Airmass Sunburst ultralight that is currently being tested is responsible for over a dozen deaths. It is believed that had there been a more stringent criteria and certification process, this might have been prevented. Our attempt is to show that the failing loads of the aircraft in question are so far below that of the current design criteria, that the laws need to be changed. Author (revised)

N93-29776*# Kansas Univ. Center for Research, Inc., Lawrence. Dept. of Aerospace Engineering.
LOAD TEST SET-UP FOR THE AIRMASS SUNBURST ULTRA-LIGHT AIRCRAFT
Daniel W. Krug and Howard W. Smith *In its* The Ultra Light Aircraft Testing 1993 41 p (For primary document see N93-29774 11-05)
(Grant NAG1-345)
Avail: CASI HC A03/MF A02

The purpose of this project was to set up, instrument, and test a Sunburst Ultra-Light aircraft. The intentions of the project were that the aircraft would need to be suspended from the test stand, leveled in the stand, the strain gauges tested and wired to the test equipment, and finally, the aircraft would be destroyed to obtain the failing loads. All jobs were completed, except for the destruction of the aircraft. This notebook shows the group's progress as these tasks were completed, and the following section attempts to explain the photographs in the notebook.
Author (revised)

N93-29777*# Kansas Univ. Center for Research, Inc., Lawrence. Dept. of Aerospace Engineering.
NASTRAN ANALYSIS FOR THE AIRMASS SUNBURST MODEL 'C' ULTRALIGHT AIRCRAFT c39
John Verbestel and Howard W. Smith *In its* The Ultra Light Aircraft Testing 1993 32 p (For primary document see N93-29774 11-05)
(Grant NAG1-345)
Avail: CASI HC A03/MF A02

The purpose of this project was to create a three dimensional NASTRAN model of the Airmass Sunburst Ultralight comparable to one made for finite element analysis. A two dimensional sample problem will be calculated by hand and by NASTRAN to make sure that NASTRAN finds similar results. A three dimensional model, similar to the one analyzed by the finite element program, will be run on NASTRAN. A comparison will be done between the NASTRAN results and the finite element program results. This study will deal mainly with the aerodynamic loads on the wing and surrounding support structure at an attack angle of 10 degrees.
Author (revised)

N93-29778*# Kansas Univ. Center for Research, Inc., Lawrence.
CONSTRUCTION, WIND TUNNEL TESTING AND DATA ANALYSIS FOR A 1/5 SCALE ULTRA-LIGHT WING MODEL c02
Michael D. James and Howard W. Smith *In its* The Ultra Light Aircraft Testing 1993 41 p (For primary document see N93-29774 11-05)
(Grant NAG1-345)
Avail: CASI HC A03/MF A02

This report documents the construction, wind tunnel testing, and data analysis of a 1/5 scale ultra-light wing section. Wind tunnel testing provided accurate and meaningful lift, drag, and pitching moment data. This data was processed and graphically presented as follows: C(sub L) vs. gamma; C(sub D) vs. gamma; C(sub M) vs. gamma; and C(sub L) vs. C(sub D). The wing fabric flexure was found to be significant and its possible effects on aerodynamic data was discussed. The fabric flexure is directly related to wing angle of attack and airspeed. Different wing section shapes created by fabric flexure are presented with explanations of the types of pressures that act upon the wing surface. This report provides conclusive aerodynamic data for ultra-light wings. Author (revised)

N93-29779*# Kansas Univ. Center for Research, Inc., Lawrence. Dept. of Aerospace Engineering.
SELECTION AND STATIC CALIBRATION OF THE MARSH J1678 PRESSURE GAUGE c35
Charles R. Oxendine and Howard W. Smith *In its* The Ultra Light Aircraft Testing 1993 32 p (For primary document see N93-29774 11-05)
(Grant NAG1-345)
Avail: CASI HC A03/MF A02

During the experimental testing of the ultralight, it was determined that a pressure gauge would be required to monitor the simulated flight loads. After analyzing several factors, which are indicated in the discussion section of this report, the Marsh J1678 pressure gauge appeared to be the prominent candidate for the task. However, prior to the final selection, the Marsh pressure gauge was calibrated twice by two different techniques. As a result of the calibration, the Marsh gauge was selected as the appropriate measuring device during the structural testing of the ultralight. Although, there are commerical pressure gauges available on the market that would have proven to be more efficient and accurate. However, in order to obtain these characteristics in a gauge, one has to pay the price on the price tag, and this value is an exponential function of the degree of accuracy efficiency, precision, and many other features that may be designed into the gauge. After analyzing the extent of precision and accuracy that would be required, a more expensive gauge wouldn't have proven to be a financial benefit towards the outcome of the experiment. Author (revised)

N93-29885*# University of South Florida, Tampa. Dept. of Civil Engineering and Mechanics.
EFFECT OF DESIGN SELECTION ON RESPONSE SURFACE PERFORMANCE
William C. Carpenter Washington Jun. 1993 181 p
(Grant NAG1-1378; RTOP 505-63-50)
(NASA-CR-4520; NAS 1.26:4520) Avail: CASI HC A09/MF A02

Artificial neural nets and polynomial approximations were used to develop response surfaces for several test problems. Based on the number of functional evaluations required to build the approximations and the number of undetermined parameters associated with the approximations, the performance of the two types of approximations was found to be comparable. A rule of thumb is developed for determining the number of nodes to be used on a hidden layer of an artificial neural net and the number of designs needed to train an approximation is discussed. Author (revised)

N93-29713*# California State Polytechnic Univ., Pomona.
HIGH-ALTITUDE RECONNAISSANCE AIRCRAFT
Renee Anna Yazdi *In* Universities Space Research Association, Houston, Proceedings of the Seventh Annual Summer Conference. NASA/USRA: University Advanced Design Program 1991 p 11-18 Previously announced in IAA as A91-54045 (For primary document see N93-29712

11-01)
Avail: CASI HC A02/MF A03

N93-29714*# California State Polytechnic Coll., San Luis Obispo.
PROJECT SUMMARY
In Universities Space Research Association, Houston, Proceedings of the Seventh Annual Summer Conference. NASA/USRA: University Advanced Design Program 1991 p 19-28 (For primary document see N93-29712 11-01)
Avail: CASI HC A02/MF A03

N93-29715*# California State Univ., Northridge.
PROJECT ARES 2: HIGH-ALTITUDE BATTERY-POWERED AIRCRAFT
In Universities Space Research Association, Houston, Proceedings of the Seventh Annual Summer Conference. NASA/USRA: University Advanced Design Program 1991 p 29-33 (For primary document see N93-29712 11-01)
Avail: CASI HC A01/MF A03

N93-29716*# Case Western Reserve Univ., Cleveland, OH.
CONCEPTUAL DESIGN OF A TWO-STAGE-TO-ORBIT VEHICLE
In Universities Space Research Association, Houston, Proceedings of the Seventh Annual Summer Conference. NASA/USRA: University Advanced Design Program 1991 p 35-43 (For primary document see N93-29712 11-01)
Avail: CASI HC A02/MF A03

N93-29717*# Kansas Univ., Lawrence.
PRELIMINARY DESIGN STUDIES OF AN ADVANCED GENERAL AVIATION AIRCRAFT
In Universities Space Research Association, Houston, Proceedings of the Seventh Annual Summer Conference. NASA/USRA: University Advanced Design Program 1991 p 45-56 (For primary document see N93-29712 11-01)
Avail: CASI HC A03/MF A03

N93-29718*# Notre Dame Univ., IN.
DESIGN STUDY TO SIMULATE THE DEVELOPMENT OF A COMMERCIAL TRANSPORTATION SYSTEM
In Universities Space Research Association, Houston, Proceedings of the Seventh Annual Summer Conference. NASA/USRA: University Advanced Design Program 1991 p 57-64 (For primary document see N93-29712 11-01)
Avail: CASI HC A02/MF A03

N93-29719*# Ohio State Univ., Columbus.
THE DESIGN OF TWO-STAGE-TO-ORBIT VEHICLES
In Universities Space Research Association, Houston, Proceedings of the Seventh Annual Summer Conference. NASA/USRA: University Advanced Design Program 1991 p 65-75 (For primary document see N93-29712 11-01)
Avail: CASI HC A03/MF A03

N93-29720*# Ecole Polytechnique Feminine, Sceaux (France).
ASUR
In Universities Space Research Association, Houston, Proceedings of the Seventh Annual Summer Conference. NASA/USRA: University Advanced Design Program 1991 p 77-81 (For primary document see N93-29712 11-01)
Avail: CASI HC A01/MF A03

N93-29721*# Purdue Univ., West Lafayette, IN.
DESIGN OF A TURBOFAN POWERED REGIONAL TRANSPORT AIRCRAFT
In Universities Space Research Association, Houston, Proceedings of the Seventh Annual Summer Conference. NASA/USRA: University Advanced Design Program 1991 p 83-88 Previously announced as N92-20280 (For primary document see N93-29712 11-01)
Avail: CASI HC A02/MF A03

N93-29722*# Worcester Polytechnic Inst., MA.
SOLAR POWERED MULTIPURPOSE REMOTELY POWERED AIRCRAFT
In Universities Space Research Association, Houston, Proceedings of the Seventh Annual Summer Conference. NASA/USRA: University Advanced Design Program 1991 p 89-94 (For primary document see N93-29712 11-01)
Avail: CASI HC A02/MF A03

06 AIRCRAFT INSTRUMENTATION

Includes cockpit and cabin display devices; and flight instruments.

For related information see also *19 Spacecraft Instrumentation* and *35 Instrumentation and Photography.*

N93-28621*# Computer Sciences Corp., Hampton, VA.
ADVANCED TRANSPORT OPERATING SYSTEM (ATOPS) FLIGHT MANAGEMENT/FLIGHT CONTROLS (FM/FC) SOFTWARE DESCRIPTION Report, Jan. 1989 - Feb. 1991
David A. Wolverton, Richard W. Dickson, Winston C. Clinedinst, and Christopher J. Slominski Apr. 1993 370 p
(Contract NAS1-19038; RTOP 505-64-13)
(NASA-CR-191457; NAS 1.26:191457) Avail: CASI HC A16/MF A03

The flight software developed for the Flight Management/Flight Controls (FM/FC) MicroVAX computer used on the Transport Systems Research Vehicle for Advanced Transport Operating Systems (ATOPS) research is described. The FM/FC software computes navigation position estimates, guidance commands, and those commands issued to the control surfaces to direct the aircraft in flight. Various modes of flight are provided for, ranging from computer assisted manual modes to fully automatic modes including automatic landing. A high-level system overview as well as a description of each software module comprising the system is provided. Digital systems diagrams are included for each major flight control component and selected flight management functions. Author (revised)

N93-29004# Industrial Coll. of the Armed Forces, Washington, DC.
STANDARDIZATION OF AUTOMATIC TEST EQUIPMENT IN THE US AIR FORCE Research Report, Aug. 1991 - Apr. 1992
Arthur J. Rooney, Jr. Apr. 1992 31 p
(AD-A262076; NDU-ICAF-92-S79) Avail: CASI HC A03/MF A01

The USAF has failed to standardize automatic test equipment (ATE) used to support aircraft avionics systems. Although the savings from standardization are difficult to estimate, studies indicate the Air Force could save over $200M through standardization of ATE. Aside from the monetary savings, other benefits such as reduced training requirements and provisioning fewer items could be realized through standardization. This paper will focus on three areas. First, we will look at standardization from definition through highlighting the importance of standard ATE. Next, a review of the impediments to achieving commonality of ATE within the Air Force. Finally, an actual example of acquiring common ATE for the Special Operations Forces will be examined. The paper concludes with recommendations to achieve greater commonality of ATE within the Air Force. DTIC

N93-29971# Naval Postgraduate School, Monterey, CA.
A CONCLUDING STUDY OF THE ALTITUDE DETERMINATION DEFICIENCIES OF THE SERVICE AIRCRAFT INSTRUMENTATION PACKAGE (SAIP) M.S. Thesis
Daniel G. Sergent 25 Mar. 1993 64 p
(AD-A263515) Avail: CASI HC A04/MF A01

Previous research at the Naval Postgraduate School addressed the aerodynamic effects that caused the altitude determination errors in the Service Aircraft Instrumentation Package (SAIP). This thesis builds on the previous work and focused on establishing a correction for the SAIP using both aerodynamic and atmospheric corrections to the Extended Area Test System (EATS) system evaluator program. By using a quadratic function of Mach number to estimate the Cp, the aerodynamic errors can be reduced to enable the SAIP to measure altitude correctly to within 100 ft for velocities up to Mach 0.8. This correction is used to modify the static pressure read by the SAIP. Further flight tests will have to be accomplished to determine the correction for a range of altitudes and aircrafts. The atmospheric errors can be corrected by analyzing the sounding data generated by the Geophysics Department at Pt. Mugu and substituting

actual lapse rate information into the standard altitude equation. This model is shown to predict altitudes to within 200 feet up through 60,000 feet.
DTIC

N93-30416*# National Aeronautics and Space Administration. Pasadena Office, CA.
VIRTUAL REALITY FLIGHT CONTROL DISPLAY WITH SIX-DEGREE-OF-FREEDOM CONTROLLER AND SPHERICAL ORIENTATION OVERLAY Patent Application
Brian C. Beckman, inventor (to NASA) (Jet Propulsion Lab., California Inst. of Tech., Pasadena.) 23 Apr. 1993 31 p
(Contract NAS7-918)
(NASA-Case-NPO-18733-1-CU; NAS 1.71:NPO-18733-1-CU; US-Patent-Appl-SN-056503) Avail: CASI HC A03/MF A01

A virtual reality flight control system displays to the pilot the image of a scene surrounding a vehicle or pod having six degrees of freedom of acceleration or velocity control by the pilot and traveling through inertial space, the image itself including a superimposed figure providing the pilot an instant reference of orientation consisting of superimposed sets of geometric figures whose relative orientations provide the pilot an instantaneous feel or sense of orientation changes with respect to some fixed coordinate system. They include a first set of geometric figures whose orientations are fixed to the pilot's vehicle and a second set of geometric figures whose orientations are fixed with respect to a fixed or interstellar coordinate system. The first set of figures is a first set of orthogonal great circles about the three orthogonal axes of the flight vehicle or pod and centered at and surrounding the pilot's head, while the second set of figures is a second set of orthogonal great circles about the three orthogonal axes of a fixed or interstellar coordinate system, also centered at and surrounding the pilot's head.
NASA

N93-28871# Westinghouse Electric Corp., Baltimore, MD. Electro-Optical Systems Dept.
DESIGN CONSIDERATIONS FOR A NIGHT, AIR-TO-SURFACE ATTACK CAPABILITY ON A DUAL ROLE FIGHTER
Robert A. Hale, John J. Chino, L. Larkin Niemyer, John R. Jadik, and Barry E. Lightner *In* AGARD, Combat Automation for Airborne Weapon Systems: Man/Machine Interface Trends and Technologies Apr. 1993 8 p Prepared in cooperation with Westinghouse Electric Corp., Orlando, FL (For primary document see N93-28850 11-54)
Copyright Avail: CASI HC A02/MF A03

07 AIRCRAFT PROPULSION AND POWER

Includes prime propulsion systems and systems components, e.g., gas turbine engines and compressors; and onboard auxilliary power plants for aircraft.

For related information see also *20 Spacecraft Propulsion and Power, 28 Propellants and Fuels,* and *44 Energy Production and Conversion.*

N93-28609*# Ohio Aerospace Inst., Brook Park.
NAVIER-STOKES ANALYSIS OF RADIAL TURBINE ROTOR PERFORMANCE
L. M. Larosiliere Jun. 1993 20 p Presented at the 29th Joint Propulsion Conference and Exhibit, Monterey, CA, 28-30 Jun. 1993; sponsored by AIAA, SAE, ASME, and ASEE
(Contract NCC3-208; RTOP 505-62-10)
(NASA-CR-191153; E-7937; NAS 1.26:191153; AIAA Paper 93-2555)
Avail: CASI HC A03/MF A01

An analysis of flow through a radial turbine rotor using the three-dimensional, thin-layer Navier-Stokes code RVC3D is described. The rotor is a solid version of an air-cooled metallic radial turbine having thick trailing edges, shroud clearance, and scalloped-backface clearance. Results are presented at the nominal operating condition using both a zero-clearance model and a model simulating the effects of the shroud and scalloped-backface clearance flows. A comparison with the available test data is made and details of the internal flow physics are discussed, allowing a better understanding of the complex flow distribution within the rotor.
Author

N93-28617*# Ohio Aerospace Inst., Brook Park.
ANALYSIS OF UNSTEADY WAVE PROCESSES IN A ROTATING CHANNEL
L. M. Larosiliere and M. Mawid (Illinois Univ., Chicago.) Jun. 1993 22 p Presented at the 29th Joint Propulsion Conference and Exhibit, Monterey, CA, 28-30 Jun. 1993; sponsored by AIAA, SAE, ASME, and ASEE
(Contract NCC3-208; RTOP 505-62-10)
(NASA-CR-191154; E-7939; NAS 1.26:191154; AIAA Paper 93-2527)
Avail: CASI HC A03/MF A01

The impact of passage rotation on the gas dynamic wave processes is analyzed through a numerical simulation of ideal shock-tube flow in a closed rotating-channel. Initial conditions are prescribed by assuming homentropic solid-body rotation. Relevant parameters of the problem such as wheel Mach number, hub-to-tip radius ratio, length-to-tip radius ratio, diaphragm temperature ratio, and diaphragm pressure ratio are varied. The results suggest possible criteria for assessing the consequences of passage rotation on the wave processes, and they may therefore be applicable to pressure-exchange wave rotors. It is shown that for a fixed geometry and initial conditions, the contact interface acquires a distorted three-dimensional time-dependent orientation at non-zero wheel Mach numbers. At a fixed wheel Mach number, the level of distortion depends primarily on the density ratio across the interface as well as the hub-to-tip radius ratio. Rarefaction fronts, shocks, and contact interfaces are observed to propagate faster with increasing wheel Mach number.
Author

N93-28697*# National Aeronautics and Space Administration. Lewis Research Center, Cleveland, OH.
EXPERIMENTAL EVALUATION OF A COOLED RADIAL-INFLOW TURBINE
Lizet Tirres (Sverdrup Technology, Inc., Brook Park, OH.), L. Danielle DiCicco, and Brent C. Nowlin Jun. 1993 18 p Presented at the 29th AIAA Joint Propulsion Conference and Exhibit, Monterey, CA, 28-30 Jun. 1993; cosponsored by SAE, ASME, and ASEE
(RTOP 535-05-10)
(NASA-TM-106230; E-7948; NAS 1.15:106230; AIAA Paper 93-1795)
Avail: CASI HC A03/MF A01

Two 14.4 inch tip diameter rotors were installed and tested in the Small Engines Component Turbine Facility (SECTF) at NASA Lewis Research Center. The rotors, a solid and a cooled version of a radial-inflow turbine, were tested with a 15 vane stat or over a set of rotational speeds ranging from 80 to 120 percent design speed (17,500 to 21,500 rpm). The total-to-total stage pressure ratios ranged from 2.5 to 5.5. The data obtained at the equivalent conditions using the solid version of the rotor are presented with the cooled rotor data. A Reynolds number of 381,000 was maintained for both rotors, whose stages had a design mass flow of 4.0 lbm/sec, a design work level of 59.61 Btu/lbm, and a design efficiency of 87 percent. The results include mass flow data, turbine torque, turbine exit flow angles, stage efficiency, and rotor inlet and exit surveys.
Author

N93-28984# Naval Postgraduate School, Monterey, CA.
AN ANALYSIS OF THE CORRELATION BETWEEN THE J52 ENGINE COMPONENT IMPROVEMENT PROGRAM AND IMPROVED MAINTENANCE PARAMETERS M.S. Thesis
Leonard B. Gordon Dec. 1992 81 p
(AD-A262062) Avail: CASI HC A05/MF A01

This thesis is a study of the J52 Engine Component Improvement Program (CIP). The objective of the thesis was to determine if the correlation between J52 CIP expenditures and improved maintenance parameters at the component level could be quantified. The major focus of the study revolved around developing a methodology to accomplish the objective using existing databases and open dialogue between the J52 engine manufacturer (Pratt and Whitney), NAVAIRSYSCOM Engine Program Manager, and various NADEP engineers. The methodology evolved using the Fuel Nozzle Support Assembly and was validated using the Fuel Pump. The thesis reached the conclusion that observed improvements in maintenance parameters can be linked to CIP expenditures at the component level.
DTIC

N93-29065*# National Aeronautics and Space Administration. Lewis Research Center, Cleveland, OH.

EFFECTS OF FLOW-PATH VARIATIONS ON INTERNAL REVERSING FLOW IN A TAILPIPE OFFTAKE CONFIGURATION FOR ASTOVL AIRCRAFT

Jack G. McArdle and Barbara S. Esker Jun. 1993 23 p Presented at the 29th Joint Propulsion Conference and Exhibit, Monterey, CA, 28-30 Jun. 1993; cosponsored by AIAA, SAE, ASME, and ASEE
(RTOP 505-68-32)
(NASA-TM-106149; E-7643; NAS 1.15:106149; AIAA Paper 93-2438)
Avail: CASI HC A03/MF A01

A one-third-scale model of a generic tailpipe offtake system for an advanced short takeoff, vertical landing (ASTOVL) aircraft was tested at the NASA Lewis Research Center Powered Lift Facility. The basic model consisted of a tailpipe with a center body to form an annulus simulating turbine outflow with no swirl; twin offtake ducts with elbows at the ends to turn the flow to a downward direction; flow control nozzles at the ends of the elbows; and a blind flange at the end of the tailpipe to simulate a closed cruise nozzle. The offtake duct-to-tailpipe diameter ratio was 0.74. Modifications of a generic nature were then made to this basic configuration to measure the effects of flow-path changes on the flow and pressure-loss characteristics. The modifications included adding rounded entrances at the forward edges of the offtake openings, blocking the tailpipe just aft the openings instead of at the cruise nozzle, changing the location of the openings along the tailpipe, removing the center body, and varying the Mach number (flow rate) over a wide range in the tailpipe ahead of the openings by changing the size of the flow control nozzles. The tests were made with unheated air at tailpipe-to-ambient pressure ratios from 1.4 to 5. Results are presented and compared with performance graphs, total-pressure contour plots, paint streak flow visualization photographs, and a flow-angle probe traverse at the offtake entrance.
Derived from text

N93-29072*# Ohio Aerospace Inst., Brook Park.

THREE-DIMENSIONAL NUMERICAL SIMULATION OF GRADUAL OPENING IN A WAVE ROTOR PASSAGE

Louis M. Larosiliere Jun. 1993 23 p Presented at the 29th Joint Propulsion Conference and Exhibit, Monterey, CA, 28-30 Jun. 1993; sponsored by AIAA, SAE, ASME, and ASEE Original contains color illustrations
(Contract NCC3-208; RTOP 505-62-10)
(NASA-CR-191157; E-7957; NAS 1.26:191157; AIAA Paper 93-2526)
Avail: CASI HC A03/MF A01; 10 functional color pages

The evolution of the contact interface and the propagation of compression waves inside a single wave rotor passage gradually opening to and traversing an inlet port is studied numerically using an inviscid formulation of the governing equations. Insights into the response of the interface and kinematics of the flow field to various opening times are given. Since the opening time is inversely proportional to the rotational speed of the rotor, the effects of passage rotation such as centripetal and Coriolis accelerations are intrinsically coupled to the gradual opening process. Certain three-dimensional features associated with the gradual opening process as a result of centripetal and Coriolis accelerations are illustrated. For the range of opening times or rotational speeds considered, a portion of the interface behaves like a vortex sheet that can degenerate into a complex interfacial structure. The vortices produced along the interface can serve as a stirring mechanism to promote local mixing. Coriolis and centripetal accelerations can introduce three dimensional effects such as interfacial distortions in meridional planes and spanwise migration of fluid elements.
Author

N93-29162*# National Aeronautics and Space Administration. Lewis Research Center, Cleveland, OH.

THE 3-D VISCOUS FLOW CFD ANALYSIS OF THE PROPELLER EFFECT ON AN ADVANCED DUCTED PROPELLER SUBSONIC INLET

Chanthy Iek, Donald R. Boldman, and Mounir Ibrahim (Cleveland State Univ., OH.) Jun. 1993 41 p Presented at the 29th Joint Propulsion Conference and Exhibit, Monterey, CA, 28-30 Jun. 1993; sponsored by AIAA, SAE, ASME, and ASEE Original contains color illustrations
(RTOP 505-03-10)
(NASA-TM-106240; E-7958; NAS 1.15:106240; AIAA Paper 93-1847)
Avail: CASI HC A03/MF A01; 14 functional color pages

A time marching Navier-Stokes code called PARC3D was used to study the 3-D viscous flow associated with an advanced ducted propeller (ADP) subsonic inlet at take-off operating conditions. At a free stream Mach number of 0.2, experimental data for the inlet-with-propeller test model indicated that the airflow was attached on the cowl windward lip at an angle of attack of 25 degrees became unstable at 29 degrees, and separated at 30 degrees. An experimental study with a similar inlet and with no propeller (through-flow) indicated that flow separation occurred at an angle of attack a few degrees below the value observed when the inlet was tested with the propeller. This tends to indicate that the propeller exerts a favorable effect on the inlet performance. During the through-flow experiment a stationary blockage device was used to successfully simulate the propeller effect on the inlet flow field at angles of attack. In the present numerical study, this flow blockage was modeled via a PARC3D computational boundary condition (BC) called the screen BC. The principle formulation of this BC was based on the one-and-half dimension actuator disk theory. This screen BC was applied at the inlet propeller face station of the computational grid. Numerical results were obtained with and without the screen BC. The application of the screen BC in this numerical study provided results which are similar to the results of past experimental efforts in which either the blockage device or the propeller was used.
Author (revised)

N93-29926# Advisory Group for Aerospace Research and Development, Neuilly-Sur-Seine (France). Propulsion and Energetics Panel.

HEAT TRANSFER AND COOLING IN GAS TURBINES [LE TRANSFERT THERMIQUE ET LE REFROIDISSEMENT DANS LES TURBINES A GAZ]

Feb. 1993 492 p 80th Symposium held in Antalya, Turkey, 12-16 Oct. 1992
(AGARD-CP-527; ISBN-92-835-0701-0) Copyright Avail: CASI HC A21/MF A04

The symposium was arranged in the following sessions: turbine blades--external heat transfer; turbine blades--internal heat transfer; measurement techniques; rotating disks, labyrinth seals, and shafts; combustors; design, interactions; and prediction methods. Heat transfer and cooling in gas turbines are still key factors for achieving high performance, increased life, and improved reliability. Any progress in this field will lead to a reduction of maintenance cost and fuel consumption. The purpose of the symposium was to bring together experts from industry, research establishments, and universities to discuss fundamental and applied heat transfer problems relevant to gas turbines, to exchange practical experience gained, and to review the state of the art. For individual titles, see N93-29927 through N93-29964.

N93-29927# Rensselaer Polytechnic Inst., Troy, NY.

KEYNOTE ADDRESS: UNSTEADY, MULTIMODE TRANSITION IN GAS TURBINE ENGINES

Robert E. Mayle *In* AGARD, Heat Transfer and Cooling in Gas Turbines Feb. 1993 7 p (For primary document see N93-29926 11-07)
Copyright Avail: CASI HC A02/MF A04

A theory for unsteady, multimode transition on gas turbine airfoils is presented. The theory, which provides a correction to the Mayle-Dullenkopf multimode model, considers a more physically correct viewpoint by taking into account the periodic disturbance caused by both the wake-induced turbulent strips and the 'becalmed' flow following them. In addition, a comparison of the theory with data is provided, which shows excellent agreement, and results illustrating the effects of transition onset distance and wake-passing Strouhal number on multimode transition are presented.
Derived from text

N93-29928# Defence Research Agency, Farnborough (England). Aerodynamics and Propulsion Dept.

HEAT TRANSFER AND AERODYNAMICS OF A 3D DESIGN NOZZLE GUIDE VANE TESTED IN THE PYESTOCK ISENTROPIC LIGHT PISTON FACILITY

K. S. Chana *In* AGARD, Heat Transfer and Cooling in Gas Turbines Feb. 1993 11 p (For primary document see N93-29926 11-07)
Copyright Avail: CASI HC A03/MF A04

In HP turbines, predictions of the heat transfer to the blade and endwalls is particularly important for an accurate assessment of turbine component life. On the endwalls, there are often complex 3D (secondary) flows present which make predictions of heat transfer particularly difficult. A detailed investigation of this area has been carried out on a fully annular cascade of highly 3D nozzle guide vanes. Measurements were made on the vane and endwalls to determine heat transfer and aerodynamic characteristics. Testing was conducted in a short duration Isentropic Light Piston Test Facility, at engine representative Reynolds number, Mach number, and gas-to-wall temperature ratio. Interpreted test data are compared with computations obtained at test conditions. Author (revised)

N93-29929# Minnesota Univ., Minneapolis. Dept. of Mechanical Engineering.

VORTEX STRUCTURE AND MASS TRANSFER NEAR THE BASE OF A CYLINDER AND A TURBINE BLADE

M. Y. Jabbari and R. J. Goldstein *In* AGARD, Heat Transfer and Cooling in Gas Turbines Feb. 1993 14 p Sponsored in part by AFOSR (For primary document see N93-29926 11-07)

Copyright Avail: CASI HC A03/MF A04

Results of naphthalene sublimation measurements and flow visualization studies near the base of round and a square cylinder mounted on a flat plate are compared with similar measurements in the endwall region of a turbine blade. Differences and similarities of the flow and mass transfer are discussed. Samples of mass transfer distribution and visualization results in the region are provided. Supported by the sublimation and the flow visualization results models for the vortex structure in the flow are suggested. Derived from text

N93-29930# Von Karman Inst. for Fluid Dynamics, Rhode-Saint-Genese (Belgium).

THERMAL EFFECTS OF A COOLANT FILM ALONG THE SUCTION SIDE OF A HIGH PRESSURE TURBINE NOZZLE GUIDE VANE

T. Arts and I. Lapidus (Societe Nationale d'Etude et de Construction de Moteurs d'Aviation, Villaroche, France.) *In* AGARD, Heat Transfer and Cooling in Gas Turbines Feb. 1993 8 p Sponsored in part by SNECMA (For primary document see N93-29926 11-07)

Copyright Avail: CASI HC A02/MF A04

The purpose is to try to describe some of the influences on external convective heat transfer of a coolant film whose position varies along the suction side of a high pressure turbine nozzle guide vane. The measurements were performed in the short duration Isentropic Light Piston Compression Tube Facility CT-2 of the von Karman Institute. The effects of external and internal flow are considered in terms of Mach number, Reynolds number, freestream turbulence intensity, blowing rate, and coolant to freestream temperature ratio. The way to evaluate those results in terms of heat transfer coefficient is finally discussed. Author (revised)

N93-29931# Poitiers Univ. (France). Lab. d'Etudes Aerodynamiques.

EXPERIMENTAL STUDY OF HEAT TRANSFER CLOSE TO A PLANE WALL HEATED IN THE PRESENCE OF MULTIPLE INJECTIONS (SUBSONIC FLOW) [ETUDE EXPERIMENTALE DU TRANSFERT DE CHALEUR PRES D'UNE PAROI PLANE CHAUFFEE EN PRESENCE D'INJECTIONS MULTIPLES (ECOULEMENT SUBSONIQUE)]

E. Foucault, P. Deniboire, J.-L. Bousgarbies, J.-J. Vullierme, and E. Dorignac *In* AGARD, Heat Transfer and Cooling in Gas Turbines Feb. 1993 10 p In FRENCH (For primary document see N93-29926 11-07)

Copyright Avail: CASI HC A02/MF A04

The results of a detailed experimental study of the aerodynamic and thermic fields within the boundary layer of a plane wall heated in the presence of localized injections of hot air are presented. For two values of the ratio of jet speed/main flow (0.6 and 1.6) the three components of the flight path vector and the local temperature of the flow are measured in many positions, respectively by Doppler laser anemometry using a cold probe wire. A map of the temperature of the plane wall is obtained by means of an infrared camera. The results show the strongly 3D aspect of the flow downstream from the jet which is dominated by the presence of swirling structures. These last areas generate strong rates of turbulence and have a great influence on the temperature field in the wake of the jets. For the largest of the two speed ratios considered, the cross-flow penetrates under the jets downstream from the injection openings and thus, is in opposition to the heat transfer. Author (revised)

N93-29932# Massachusetts Inst. of Tech., Cambridge. Gas Turbine Lab.

THE INFLUENCE OF NON-UNIFORM SPANWISE INLET TEMPERATURE ON TURBINE ROTOR HEAT TRANSFER

G. R. Guenette, G. Pappas, and A. H. Epstein *In* AGARD, Heat Transfer and Cooling in Gas Turbines Feb. 1993 10 p Sponsored in part by Rolls-Royce, Inc. (For primary document see N93-29926 11-07)

Copyright Avail: CASI HC A02/MF A04

The influence of a spanwise varying, circumferentially uniform inlet total temperature distortion was measured on a transonic turbine stage in a short duration turbine test facility. Large levels of distortion were found to increase rotor blade heat transfer, especially on the pressure surface. A three-dimensional, steady, multi-blade row, Euler code and a streamline curvature calculation were used to interpret the data but did not account for all of the heat transfer increase observed. Author (revised)

N93-29933# Naval Air Warfare Center, Trenton, NJ. Aircraft Div.

DETERMINATION OF SURFACE HEAT TRANSFER AND FILM COOLING EFFECTIVENESS IN UNSTEADY WAKE FLOW CONDITIONS

M. Sautner, S. Clouser, and J. C. Han (Texas A&M Univ., College Station.) *In* AGARD, Heat Transfer and Cooling in Gas Turbines Feb. 1993 12 p (For primary document see N93-29926 11-07)

Copyright Avail: CASI HC A03/MF A04

The effect of unsteady wake flows on blade heat transfer and film cooling effectiveness was experimentally determined by using a spoked-wheel type wake generator. The experiments were performed with a five airfoil linear cascade at the Texas A&M University low speed wind tunnel facility. The mainstream Reynolds number based on airfoil chord length was about 3 x 10 exp 5. The wake Strouhal number was varied between 0 and 0.4 by changing the rotating wake passing frequency. A hot wire anemometer system was located at the cascade inlet to detect the instantaneous velocity, phase-averaged mean velocity, and turbulence intensity induced by the passing wake. A pressure tap instrumented blade was used to measure the surface static pressure distributions and compared well with predicted velocity distributions in the cascade. An instrumented blade without film holes equipped with a thin foil thermocouple was used to determine the surface heat transfer coefficient distributions. The results show that the periodically passing wake promotes earlier boundary layer transition, causing much higher heat transfer on the suction surface. The passing wake also significantly enhances the heat transfer on the pressure surface. The other thin foil thermocouple instrumented blade contained several rows of film cooling holes at the stagnation region and on both the suction and pressure surfaces, and was employed to determine the film cooling effectiveness distributions. The results show that the strong passing wake interacts with the film layer and causes a relatively lower film effectiveness on both the suction and pressure surfaces for all three blowing ratios studied (M = 0.4, 0.8, and 1.2). Derived from text

N93-29934# Oxford Univ. (England). Dept. of Engineering Science.

MEASUREMENT OF TURBULENT SPOTS AND INTERMITTENCY MODELLING AT GAS-TURBINE CONDITIONS

J. P. Clark, J. E. LaGraff (Syracuse Univ., NY.), P. J. Magari, and T. V. Jones *In* AGARD, Heat Transfer and Cooling in Gas Turbines Feb. 1993 14 p (For primary document see N93-29926 11-07)

(Contract F49620-92-J-0079; AF-AFOSR-0427-89)

Copyright Avail: CASI HC A03/MF A04

Measurements have been made of instantaneous heat-transfer rates to a flat-plate surface under a transitional boundary layer. The thin-film surface instrumentation used in the study was capable of time-resolving the effects of changes in the heat-transfer rate within an accuracy of 10 microseconds. The tests were conducted in the Oxford University 6 inch Isentropic Light-Piston Tunnel (ILPT) under simulated gas turbine Reynolds numbers, Mach numbers, gas-to-wall temperature ratios, and pressure gradients. The ability to observe and track the end stage of the transition process (i.e., turbulent spots) in a laminar boundary layer undergoing transition allowed turbulent-spot convection speeds and spreading angles to be estimated. In these tests, the important fluid-dynamic parameters of Mach number, Reynolds number, and streamwise pressure gradient were varied independently over a wide range of values characteristic of those encountered in the turbine environment. Using quantitative values of the measured turbulent-spot characteristics, a simple time-marching code was developed based on Emmons' turbulent-spot theory to estimate the intermittency. Derived from text

N93-29935# Wright Lab., Wright-Patterson AFB, OH. Aero Propulsion and Power Directorate.

HEAT TRANSFER IN HIGH TURBULENCE FLOWS: A 2-D PLANAR WALL JET **c34**

R. B. Rivir, W. T. Troha, W. A. Eckerle (Cummins Engine Co., Inc., Columbus, IN.), and W. J. Schmoll (Dayton Univ. Research Inst., OH.) *In* AGARD, Heat Transfer and Cooling in Gas Turbines Feb. 1993 12 p (For primary document see N93-29926 11-07)

Copyright Avail: CASI HC A03/MF A04

The accurate prediction of turbine heat transfer remains beyond our current capabilities. To investigate this condition, nonconventional turbulence generation techniques have been employed to explore the impact of high turbulence or unsteadiness on heat transfer. The heat transfer from a 2D planar wall jet is compared with an axisymmetric wall jet with twice the turbulence scale and more turbulent kinetic energy - with an increased heat transfer shown by the planar configuration. The resulting comparisons of wall jet augmented heat transfer to engine turbine blade heat transfer is quite favorable. Derived from text

N93-29936# Purdue Univ., West Lafayette, IN. School of Mechanical Engineering.

HEAT TRANSFER WITH MODERATE FREE STREAM TURBULENCE **c34**

S. N. B. Murthy *In* AGARD, Heat Transfer and Cooling in Gas Turbines Feb. 1993 33 p (For primary document see N93-29926 11-07)
(Contract F49620-87-K-0008)

Copyright Avail: CASI HC A03/MF A04

Turbulence in turbine flows of gas turbine engines is generally inhomogeneous and is also characterized by wide ranges of intensity and scale. The interaction between Free Stream Turbulence (FST) and boundary layer turbulence (BLT) is complicated in all but the case of low values of both intensity and scale. In a recent investigation, an attempt was made to establish the effect of homogeneous FST on wall friction (when there is no heat transfer) in the relatively simple case of a flat plate, zero pressure gradient boundary layer. In the current paper, the method was extended for the prediction of heat transfer in the same flow field. In any problem involving heat and momentum transport, it is common to introduce some type of similarity between the two transport processes. The current method is based on the application of a similarity rule governing the spectra of turbulence intensity and temperature variance. The principal outcome is a method of establishing heat transfer in a given flow field for which experimental data are available under cold flow conditions and have been verified with the model prediction scheme. Author (revised)

N93-29937# University Coll. of Swansea (Wales). Dept. of Mechanical Engineering.

THE EFFECT OF ORTHOGONAL-MODE ROTATION ON FORCED CONVECTION IN A CIRCULAR-SECTIONED TUBE FITTED WITH FULL CIRCUMFERENTIAL TRANSVERSE RIBS **c34**

W. D. Morris and R. Salemi *In* AGARD, Heat Transfer and Cooling in Gas Turbines Feb. 1993 11 p Sponsored in part by Science Research Council and Rolls-Royce Ltd. (For primary document see N93-29926 11-07)

Copyright Avail: CASI HC A03/MF A04

This paper presents the results of an experimental program aimed at investigating the effect of Coriolis forces and centripetal buoyancy on forced convection in an internally finned circular tube which rotates about an axis orthogonal to the tube's central axis. This geometric arrangement typifies the internal coolant channels of gas turbine rotor blades. It is demonstrated that, as with smooth-walled tubes, Coriolis-driven secondary flows give rise to relatively better heat transfer on the trailing edge of the tube compared with that on the leading edge. Leading edge heat transfer is shown to be significantly impaired in relation to that which occurs under non-rotating conditions. Centripetal buoyancy is shown to improve local heat transfer on the leading and trailing edges for a given value of the through flow Reynolds number and the Rossby number. Although duct rotation tends to improve heat transfer on the trailing edge in comparison with normal stationary duct forced convection, serious overprediction of heat transfer results from ignoring rotational effects on the leading edge. This is an important observation in the context of the design of turbine rotor blade cooling systems. Author (revised)

N93-29938# Manchester Coll. of Science and Technology (England).

TURBULENT FLOW AND HEAT TRANSFER IN IDEALIZED BLADE COOLING PASSAGES

T. Bo and B. E. Launder *In* AGARD, Heat Transfer and Cooling in Gas Turbines Feb. 1993 16 p Sponsored in part by Ministry of Defence and Rolls-Royce Ltd. (For primary document see N93-29926 11-07)

Copyright Avail: CASI HC A03/MF A04

The paper brings together recent research at UMIST directed at the prediction of flow through tight, square sectioned U-bends rotating in orthogonal mode. The cases of flow through rotating straight ducts and stationary U-bends are considered first to allow comparison with experimental data; finally, having demonstrated the level of accord achieved with experiment, predictions for the rotating U-bend are provided. A fairly simple turbulence model was adopted with the usual high Reynolds number k-epsilon model being interfaced with a 1-equation near-wall model. To achieve, in the case of the U-bend, grid independent behavior with the available computer core, a bounded third-order discretization of convective transport had to be applied to all dependent variables. The agreement with the available experimental data is broadly satisfactory in the case of the rotating straight duct (the substantial modifications to the Nusselt number on the pressure and suction faces of the duct due to Coriolis and buoyant forces being well reproduced. Agreement is less complete in the case of the U-bend but even so, the predicted levels of Nusselt number and the distribution of velocity downstream of the bend are broadly in line with experiment. The results point to the desirability of incorporating second-moment closure into the bend-flow calculations as models of this type have a track record of capturing the sensitivity of the turbulent stresses to complex strains better than the eddy viscosity model adopted here. Author (revised)

N93-29939# Fiat Aviazione S.p.A., Turin (Italy).

COOLING GEOMETRY OPTIMIZATION USING LIQUID CRYSTAL TECHNIQUE

G. Lodigiani, A. Trovati, L. Paci, and P. Pirrelli (Elasis S.C.p.A., Brindisi, Italy.) *In* AGARD, Heat Transfer and Cooling in Gas Turbines Feb. 1993 12 p (For primary document see N93-29926 11-07)

Copyright Avail: CASI HC A03/MF A04

Experimental results concerning the cooling performance of jet engine blading internal passages are presented. Use was made of the Liquid Crystal Transient Technique in order to obtain detailed information about heat transfer coefficients on the internal blade surfaces in presence of turbulence promoters. A peculiar behavior of the cooling channels with turbulators was detected, which reduces the expected heat transfer effectiveness. Heat transfer experimental results, reproducing actual engine operating conditions, were employed to predict the blade metal temperature: cooling flow parameters and internal channel characteristics were therefore tuned in order to attain a suitable metal temperature distribution, and to optimize the cooling effectiveness. The outcome of experimental and calculation work was then compared to the engine test blade surface temperature distribution, obtained by means of thermal paints. The comparison showed fairly good agreement, demonstrating once more the usefulness of the Liquid Crystal Transient Technique in allowing designers to improve present blade cooling devices. Author (revised)

N93-29940# Oxford Univ. (England). Dept. of Engineering Science.

FUNDAMENTAL STUDIES OF IMPINGEMENT COOLING THERMAL BOUNDARY CONDITIONS **c34**

M. G. Lucas, P. T. Ireland, Z. Wang, T. V. Jones, and W. J. Pearce (Rolls-Royce Ltd., Bristol, England.) *In* AGARD, Heat Transfer and Cooling in Gas Turbines Feb. 1993 10 p Sponsored in part by Ministry of Defence; Science Research Council; and Rolls-Royce Ltd. (For primary document see N93-29926 11-07)

Copyright Avail: CASI HC A02/MF A04

Measurements were made of the local heat transfer at the surface of a flat plate underneath a confined impinging jet. Thermochromic liquid crystals were used to measure the surface temperature of a uniformly heated plate cooled by an impinging jet. The temperature of the wall through which the jet passes was controlled, and experiments were performed to measure the two heat transfer coefficients which arise from this three temperature problem. The effect of Reynolds number and plate to jet spacing on heat transfer was investigated. The heat transfer results are discussed in terms of the interpreted flow field. Author (revised)

N93-29941# Pratt and Whitney Aircraft of Canada Ltd., Longueuil (Quebec).
PREDICTION OF JET IMPINGEMENT COOLING SCHEME CHARACTERISTICS (AIRFOIL LEADING EDGE APPLICATION) **c34**
A. Riahi, H. J. Saabas, and W. Abdel Messeh *In* AGARD, Heat Transfer and Cooling in Gas Turbines Feb. 1993 14 p (For primary document see N93-29926 11-07)
Copyright Avail: CASI HC A03/MF A04

A control volume, finite difference method based on the work of Rhie in conjunction with a high Reynolds k-epsilon model and a two layer turbulence model was used to predict the heat transfer coefficients underneath an impinging circular jet in the absence of cross flow. The numerical results are compared to experimental measurements for two different impingement height to jet diameter ratios: H/D = 2, and H/D = 10. The comparisons indicate that, although both the k-epsilon and the two layer turbulence models are adequate in the prediction of the flow field, the two layer model resulted in heat transfer predictions that were closer to experimental observations. It was also observed that the predicted heat transfer coefficients for the case of H/D = 2 were sensitive to the assumed jet exit turbulence levels, whereas they were not for H/D = 10. This information is useful to the designer of cooled turbine components. Author (revised)

N93-29942# Deutsche Forschungsanstalt fuer Luft- und Raumfahrt, Cologne (Germany). Inst. for Propulsion Technology.
AN L2F-MEASUREMENT DEVICE WITH IMAGE ROTATOR PRISM FOR FLOW VELOCITY ANALYSIS IN ROTATING COOLANT CHANNELS **c35**
M. Beversdorff, O. Hein, and R. Schodl *In* AGARD, Heat Transfer and Cooling in Gas Turbines Feb. 1993 7 p (For primary document see N93-29926 11-07)
Copyright Avail: CASI HC A02/MF A04

For further improvement of the turbine blade cooling process, the knowledge concerning the heat transfer in radial coolant channels has to be deepened. Due to rotation, the velocity distribution, as well as the turbulence structure and therefore the heat transfer, will be influenced. To carry out experimental data of the flow field within a rotating duct a non-intrusive continuous measuring system (Laser-Two-Focus) with an image rotator prism is presented. The design of the system is explained in detail. Problems of application are discussed and results of the first successful measurements compared with numerical results are presented. Author (revised)

N93-29943*# Arizona State Univ., Tempe. Dept. of Mechanical and Aerospace Engineering.
LOCAL HEAT TRANSFER MEASUREMENT WITH LIQUID CRYSTALS ON ROTATING SURFACES INCLUDING NON-AXISYMMETRIC CASES
D. E. Metzger and Y. K. Kim *In* AGARD, Heat Transfer and Cooling in Gas Turbines Feb. 1993 11 p Sponsored by NASA. Marshall Space Flight Center and Rockwell International Corp. (For primary document see N93-29926 11-07)
Copyright Avail: CASI HC A03/MF A04

An overview and summary of test methods and results are given for the problem of measuring local heat transfer on rotating surfaces that model gas turbine engine disks. Disk cavity situations generically similar to those encountered in the high pressure stage disk cooling are considered, with cooling air supplied both at or near the wheel centerline as well as through single or multiple jets impinging outboard on the wheel near the blade attachment region. In some situations provision has been made for ingestion into the disk-cavity from the gas path region radially outboard of the disk. Local heat transfer rates in all cases are determined from the color display from a thin coating of encapsulated liquid crystals sprayed onto the disk, in conjunction with use of a video camera and computer vision system. For cases with axisymmetric disk surfaces, the coated surfaces are illuminated and viewed continuously, and detailed radial distributions of local Nusselt number are obtained. For non-axisymmetric disk surfaces, such as encountered in the vicinity of bolt heads, the disk is illuminated with stroboscopic light, and a method has been developed and used to synchronize the computer frame grabber with the illumination. Author (revised)

N93-29944# Nottingham Univ. (England). Dept. of Mechanical Engineering.
THE SWOLLEN POLYMER TECHNIQUE AND ITS USE FOR HEAT TRANSFER INVESTIGATIONS ON FILM COOLED SURFACES **c34**
N. Hay, D. Lampard, and N. MacLeod (Edinburgh Univ., Scotland.) *In* AGARD, Heat Transfer and Cooling in Gas Turbines Feb. 1993 21 p (For primary document see N93-29926 11-07)
Copyright Avail: CASI HC A03/MF A04

The Swollen Polymer Technique is a mass transfer analogy method for obtaining heat transfer data. It is similar in principle to the naphthalene method, but it has an advantage in that it can be combined with interferometric measuring methods giving a panoramic view of the distribution of the transfer coefficient over the working surface. Additionally, the mass transfer process is reversible, and the working surface can be used repeatedly. Changes in thickness of a polymer coating on the working surface, initially swollen with an ester, are measured, using holographic interferometry to yield a fringe pattern depicting loci of equal transfer coefficient over the surface. The paper describes the basis of the method, the equipment required to implement it, the precautions necessary for its successful use, its advantages, its limitations, and its future potential. The technique yields data useful in the design process. Examples of its application to film cooled surfaces are given, including the effects of geometry, density ratio, and acceleration of the mainstream flow on the heat transfer coefficient. Extension of the technique for the simultaneous measurement of effectiveness and heat transfer coefficient is described, and its further extension for use with curved surfaces is outlined. A recent development to the technique itself by the use of a thermoplastic plate for recording the holograms opens up the possibility of further advancement using electronic image processing. Author (revised)

N93-29945# Calspan Advanced Technology Center, Buffalo, NY.
THE USAF ADVANCED TURBINE AEROTHERMAL RESEARCH RIG (ATARR) **c09**
C. W. Haldeman, Jr., M. G. Dunn, C. D. MacArthur (Wright Lab., Wright-Patterson AFB, OH.), and C. G. Murawski (Wright Lab., Wright-Patterson AFB, OH.) *In* AGARD, Heat Transfer and Cooling in Gas Turbines Feb. 1993 14 p (For primary document see N93-29926 11-07)
Copyright Avail: CASI HC A03/MF A04

The Advanced Turbine Aerothermal Research Rig (ATARR) has been under development and construction at Wright-Patterson Air Force Base for the past three years. Construction of the facility is now complete and demonstration experiments are underway. These demonstration experiments involve use of an instrumented turbine stage (both surface pressure and surface heat flux instrumentation) to obtain measurements for comparison with predictions, flow path measurement of total pressure, total temperature, and static pressure to determine flow path uniformity, as well as instrumentation to ascertain proper operation of all facility components. At the time of this writing, the experiments designed to obtain the data just mentioned are underway but results are not available. Therefore, the written paper will be confined to a description of: (1) the facility and its design capabilities, (2) a description of the operation of the major components with limited supporting data, e.g., main valve opening and closing times, and (3) a brief description of an uncertainty analysis that has been completed for the instrumentation and aero-performance measurements. Author

N93-29946# Motoren- und Turbinen-Union Muenchen G.m.b.H. (Germany).
TRANSIENT THERMAL BEHAVIOUR OF A COMPRESSOR ROTOR WITH AXIAL COOLING AIR FLOW AND CO-ROTATING OR CONTRA-ROTATING SHAFT
C. Burkhardt, A. Mayer, and E. Reile *In* AGARD, Heat Transfer and Cooling in Gas Turbines Feb. 1993 9 p (For primary document see N93-29926 11-07)
Copyright Avail: CASI HC A02/MF A04

Heat transfer measurements were made in a five-cavity compressor drum rig, in which cooling air passed axially through the center of the discs. The rig also contained a central drive shaft which could be either co- or contrarotated. Tests were conducted for different mass flow rates, rotational speeds and air temperatures. Typical engine conditions for steady state and transient operating conditions were simulated. Local Nusselt numbers were obtained for the discs of one cavity and compared with other published results. Furthermore an investigation into the effect of co- and contrarotating shaft on the surface temperatures of the discs and on the Nusselt number distribution was also carried out. It was found that the direction of rotation and speed of the shaft influenced the disc temperatures as well as the Nusselt numbers. Author

N93-29947# Office National d'Etudes et de Recherches Aerospatiales, Bagneux (France). Direction de l'Energetique.

AEROTHERMIC CALCULATIONS OF FLOWS IN INTERDISC CAVITIES OF TURBINES [CALCULS AEROTHERMIQUES D'ECOULEMENTS DANS DES CAVITES INTERDISQUES DE TURBINES]

D. Dutoya and P. PoncelindeRaucourt (Societe Nationale d'Etude et de Construction de Moteurs d'Aviation, Moissy-Cramayel, France.) *In* AGARD, Heat Transfer and Cooling in Gas Turbines Feb. 1993 9 p In FRENCH (For primary document see N93-29926 11-07)

Copyright Avail: CASI HC A02/MF A04

The operating temperatures of turboshaft engines oblige the manufacturers to cool the parts of the engine located downstream from the combustion chamber and in particular the turbines. Knowledge of the air flow in the air ventilation paths is essential to optimize the cooling of the engines. In order to precisely determine the phenomena of heat exchanges and the aerodynamic forces on the walls of complex cavities, SNECMA uses the MATHILDA code developed with ONERA. The MATHILDA code solves the three dimensional Navier-Stokes equations for flows of compressible fluid. The equations are treated using a finite volume method accomplished on a mesh structure. The resolution scheme is decentered by the order of 2. An implicit method of the ADI type makes it possible to stabilize and accelerate the calculation. This article presents the work of the validation of the MATHILDA code for applications to the flows in interdisc cavities. The cases presented were studied by the implementation of the axisymmetric two-dimensional version. Two types of experimental cavities served as the validations, rotor/stator cavities and rotor/rotor cavities. The solutions obtained, compared with the experimental measurements, are satisfactory, from an aerodynamic point of view and a thermal point of view. The last calculation, on a real configuration of the internal cavity of the engine, makes it possible to apprehend the difficulties encountered in the implementation of this type of modeling, and to measure the contribution of the code solving the Navier-Stokes equations to the description of the cooling flows. Transl. by FLS

N93-29948# Institut de Mecanique des Fluides de Marseille (France).

STUDY OF FLOW STRUCTURE IN ROTATING CAVITIES: NUMERICAL PREDICTIONS OF LAMINAR AND TURBULENT, STEADY, AND UNSTEADY FLOWS c34

P. Maubert, R. Schiestel, L. Elena, A. Randriamampianina, A. M. Chaouche, E. CrespodelArco, and P. Bontoux *In* AGARD, Heat Transfer and Cooling in Gas Turbines Feb. 1993 23 p Sponsored in part by CCVR; CNRS; IMT; Conseil Regional PACA; Defence Research Establishment Toronto; International Exchange Program; and Ministere des Affaires Etrangeres (For primary document see N93-29926 11-07)

Copyright Avail: CASI HC A03/MF A04

The flow regimes in rotating cavities (modelling corotating disks or rotor-stator systems), with or without through flow, are studied by numerical approach using different techniques: spectral and finite volume methods. Comparisons between these techniques have been carried out for a typical test case. The solutions have been also compared satisfactorily to asymptotical approximations and to experimental results. The computations with spectral methods have been carried out until the onset of unsteady instabilities and transition to turbulence. The turbulent regimes have been treated with the finite volume method based on modelling derived from a k-epsilon or algebraic model of second order. Author (revised)

N93-29949# Rolls-Royce Ltd., Derby (England).

MODELLING THERMAL BEHAVIOUR OF TURBOMACHINERY DISCS AND CASINGS

R. D. Monico and J. W. Chew *In* AGARD, Heat Transfer and Cooling in Gas Turbines Feb. 1993 10 p (For primary document see N93-29926 11-07)

Copyright Avail: CASI HC A02/MF A04

The thermal behavior of discs and casings in gas turbine engines has important effects on engine performance and integrity and theoretical or computer modelling of these effects is an essential part of the design process. In this paper the current status of thermal modelling is reviewed, problem areas are identified, examples of where application of the latest numerical and modelling techniques have led to improvements are given, and prospects for further developments are discussed. It is concluded that, although recent research and computing advances are improving the predictive capability, considerable scope for further improvement remains. Author

N93-29950# Bath Univ. (England). School of Mechanical Engineering.

FLOW AND HEAT TRANSFER BETWEEN GAS-TURBINE DISCS

X. Gan, M. Kilic, and J. M. Owen *In* AGARD, Heat Transfer and Cooling in Gas Turbines Feb. 1993 11 p Sponsored in part by Ministry of Defence and Science Research Council (For primary document see N93-29926 11-07)

Copyright Avail: CASI HC A03/MF A04

The paper provides both a brief review of some recent research into the flow and heat transfer associated with the turbine and compressor discs of gas turbine engines and some new results for flow between contra-rotating turbine discs. Elliptic solvers, parabolic solvers and integral methods have all been applied successfully to some important axisymmetric boundary-layer-dominated flows, and multigrid elliptic solvers used in conjunction with parallel computers offer great promise for the future computation of nonaxisymmetric flows. LDA velocity measurements and computations have given fresh insight into the flow between contra-rotating turbine discs. Batchelor-type flow, in which there are boundary layers on the discs and a shear layer in the midplane, has been computed for laminar flow but has not been observed in practice, even at local rotational Reynolds numbers as low as 2.2 x 10(exp 4). The actual flow structure comprised radial outflow in boundary layers on the discs and a central core of radial inflow in which rotational effects were weak. Although the flow in the core was always turbulent, the flow in the boundary layers was laminar for rotational Reynolds numbers up to at least 1.2 x 10(exp 5). Agreement between the computed turbulent velocities and the measured values was good for Reynolds numbers above 4.5 x 10(exp 5). Author (revised)

N93-29951# Karlsruhe Univ. (Germany). Lehrstuhl und Inst. fuer Thermische Stroemungsmaschinen.

HEAT TRANSFER AND LEAKAGE IN HIGH-SPEED ROTATING STEPPED LABYRINTH SEALS

W. Waschka, S. Wittig, S. Kim, and T. Scherer *In* AGARD, Heat Transfer and Cooling in Gas Turbines Feb. 1993 10 p (For primary document see N93-29926 11-07)

Copyright Avail: CASI HC A02/MF A04

A new experimental and numerical research program was conducted to determine the effects of rotation on the leakage loss and the heat transfer coefficients of compressible flows in modern high performance labyrinth seals. In this study, the interest is focused on divergent shaped stepped labyrinth seals. That type of labyrinth seal is the last one within a row of different labyrinth seals, investigated at the University of Karlsruhe: straight-through, staggered labyrinth seals and convergent shaped stepped labyrinth seals have been the other geometries. For heat transfer and leakage loss measurements our high temperature test facility was used, providing realistic conditions of gas temperatures, pressure ratios as well as a wide range of axial and peripheral Reynolds numbers. In addition, numerical codes have been verified by experimentally obtained data. Heat transfer coefficients for the stator and the rotor are derived utilizing the well-known standard k-epsilon model and the Stanton-analogy. This report discusses some new rotational effects, which are significant for the divergent shaped seal. In addition, these results are compared with those obtained from our other seal geometries studied. Author (revised)

N93-29952# Technische Univ., Darmstadt (Germany). Inst. fuer Technische Thermodynamik.

FLUID FLOW AND HEAT TRANSFER IN THE ENTRANCE REGION OF AN ANNULUS BETWEEN INDEPENDENTLY ROTATING TUBES WITH A TURBULENT AXIAL FLOW c34

H. Pfitzer, T. Rothe, and H. Beer *In* AGARD, Heat Transfer and Cooling in Gas Turbines Feb. 1993 11 p (For primary document see N93-29926 11-07)
Copyright Avail: CASI HC A03/MF A04

Experimental and numerical investigations of turbulent flow and heat transfer have been performed in the entrance region of a concentric annulus between independently rotating tubes. The horizontally mounted test section has an electrically heated outer wall and an adiabatic inner wall. The mean heat transfer rate in the hydrodynamic and thermal entrance region as well as the local Nusselt number at the axial position z/db(sub h) approx. = 60, which is the end of the rotating annular channel, were determined experimentally. Hotwire and thermocouple probes allowed for measurement of velocity and temperature distributions at the end of the annulus. Numerical predictions, applying a k-epsilon eddy viscosity model with a modification by the flux Richardson number, are compared with the experimental results. The comparison shows that general effects of the rotation can be predicted quite well with the aid of a simple turbulence model. Due to stabilizing or destabilizing effects of centrifugal forces in the fluid and due to the additional shear stress, the rotation of the inner and the outer tube influences remarkably fluid flow and heat transfer in the annulus. Author (revised)

N93-29953# Technische Univ., Darmstadt (Germany).
THE EFFECT OF MAIN STREAM FLOW ANGLE ON FLAME TUBE FILM COOLING c34
H. Klinger and D. K. Hennecke *In* AGARD, Heat Transfer and Cooling in Gas Turbines Feb. 1993 12 p Sponsored in part by BMFT (For primary document see N93-29926 11-07)
Copyright Avail: CASI HC A03/MF A04

Generally film cooling configurations are positioned such that they are oriented perpendicular to the main stream flow direction. However in many cases, in particular combustor applications, different flow angles may occur. Then, due to the interaction between the main stream and the cooling film, a complex three-dimensional flow field with a vortex is formed. An experimental study was done to study the basic effects. The cooling configuration was a vertical slot which could be turned by up to about 60 degrees from the position perpendicular to the main stream. Velocity distributions were measured and the adiabatic film cooling effectiveness was determined using the liquid crystal technique. The results show that, along lines parallel to the slot, the film cooling effectiveness varies strongly, even with small slot turning angles. This would lead to hot and cold spots in a combustor application. A simple semi-empirical correlation for the average cooling effectiveness is derived using the main stream velocity component perpendicular to the slot. Author

N93-29954# Leeds Univ. (England). Dept. of Fuel and Energy.
IMPINGEMENT/EFFUSION COOLING c34
G. E. Andrews, A. M. AlDabagh, A. A. Asere, F. Bazdidi-Tehrani, M. C. Mkpadi, and A. Nazari *In* AGARD, Heat Transfer and Cooling in Gas Turbines Feb. 1993 10 p (For primary document see N93-29926 11-07)
(Contract SRC-GR/D/53029)
Copyright Avail: CASI HC A02/MF A04

Impingement/effusion cooling offers one of the most effective ways of cooling gas turbine combustor walls and turbine blades. The design principles are reviewed and cooling effectiveness data presented for a range of typical geometries with holes at 90 degrees to the surface. The main variable studied was the number of impingement/effusion holes. Comparison was made with the effusion cooling effectiveness. Optimum configurations were demonstrated with a 0.7 overall cooling effectiveness at a mass flow per unit surface area of 0.2 kg/sm(exp 2)bar. This was equivalent to 10 percent of the combustor air flow for a typical gas turbine combustor. Data is also presented for the overall wall heat transfer coefficient. The mechanism of the enhanced heat transfer within the impingement/effusion double skin wall was investigated using a CFD code. This predicted the complex aerodynamics in the impingement gap and also gave good agreement with the measured overall heat transfer data. Author (revised)

N93-29955# Middle East Technical Univ., Ankara (Turkey). Dept. of Chemical Engineering.
EVALUATION OF MULTI-DIMENSIONAL FLUX MODELS FOR RADIATIVE TRANSFER IN CYLINDRICAL COMBUSTION CHAMBERS c34
Nevin Selcuk *In* AGARD, Heat Transfer and Cooling in Gas Turbines Feb. 1993 6 p (For primary document see N93-29926 11-07)
Copyright Avail: CASI HC A02/MF A04

Four flux-type models for radiative heat transfer in cylindrical configurations were applied to the prediction of radiative flux density and source term of a cylindrical enclosure problem based on data reported previously on a pilot-scale experimental combustor with steep temperature gradients. The models, which are Schuster-Hamaker type four-flux model derived by Lockwood and Spalding, two Schuster-Schwarzschild type four-flux models derived by Siddall and Selcuk and Richter and Quack and spherical harmonics approximation, were evaluated from the viewpoint of predictive accuracy by comparing their predictions with exact solutions produced previously. The comparisons showed that spherical harmonics approximation produces more accurate results than the other models with respect to the radiative energy source term and that the four-flux models of Lockwood and Spalding and Siddall and Selcuk for isotropic radiation field are more accurate with respect to the prediction of radiative flux density to the side wall. Author

N93-29956# Office National d'Etudes et de Recherches Aerospatiales, Paris (France).
CALCULATIONS OF REACTIVE TURBULENT FLOWS IN AERONAUTICAL CHAMBERS [CALCULS D'ECOULEMENTS TURBULENTS REACTIFS DANS LES FOYERS AERONAUTIQUES] c34
P. Caillau and F. Dupoirieux *In* AGARD, Heat Transfer and Cooling in Gas Turbines Feb. 1993 13 p In FRENCH (For primary document see N93-29926 11-07)
Copyright Avail: CASI HC A03/MF A04

The progress which was recently achieved in the modeling of turbulent combustion for applications to propulsion are described. The averaged equations of reactive turbulent flows are given, then the Probabilist EUlerian Langrangian model (PEUL) intended for the calculation of the average source terms of categories and of enthalpy are presented. The possibility of taking into account by this model the reactional mechanisms to several categories is applied to the prediction of the pollutants and in particular to the calculation of thermal NO. In order to obtain the best possible prediction of the chemical composition and the temperature, three total mechanisms of oxidation of methane are successively coupled with the PEUL model and their results compared. Two applications are then studied. The first application is a premixed flame stabilized by a hot gas flow. The computation results are compared with the experimental results obtained with ONERA and present a suitable agreement, in particular with regard to the profiles of thermal NO. The second concerns a portion of an annular aeronautical chamber. The comparison of the average production rates obtained with a model of turbulent combustion with rapid chemistry and with the PEUL model highlights, in this case, the importance of not making the hypothesis of rapid chemistry. Author (revised)

N93-29957# Alfa Romeo S.p.A., Naples (Italy). Research and Development.
AERO-THERMAL DESIGN OF A COOLED TRANSONIC NGV AND COMPARISON WITH EXPERIMENTAL RESULTS
S. Colantuoni, A. Colella, L. DiNola, D. Carbone, and D. Marotta *In* AGARD, Heat Transfer and Cooling in Gas Turbines Feb. 1993 25 p (For primary document see N93-29926 11-07)
Copyright Avail: CASI HC A03/MF A04

The aerothermal design process applied to a Nozzle Guide Vane of a gas-generator axial-flow turbine for a compact advanced technology core engine is described. The principal characteristics of the NGV are: Overall Tip Radius, 108.8 mm; Blade height, 19.7 mm; Blade aspect ratio, 0.53; Solidity, 1.37; Mean Exit isentropic Mach Number, 0.95; Inlet Temperature, 1450K. The NGV is cooled by a combination of different solutions, like impingement cooling and film-cooling on the front side, and forced convection on the rear side, followed by a cooling ejection at pressure side near the trailing edge. Representative results of the computational fluid-dynamics and of the thermal analysis of the NGV blade, together with some experimental data obtained from component test rig and engine demonstrator are presented and discussed. Author (revised)

N93-29958# ABB Power Generation, Inc., Baden (Switzerland).

THE AERODYNAMIC EFFECT OF COOLANT EJECTION IN THE LEADING EDGE REGION OF A FILM-COOLED TURBINE BLADE

A. Beeck, L. Fottner (Munich FAF Univ., Neubiberg, Germany.), E. Benz (Karlsruhe Univ., Germany.), and S. Wittig (Karlsruhe Univ., Germany.) *In* AGARD, Heat Transfer and Cooling in Gas Turbines Feb. 1993 10 p Sponsored in part by Bundesministerium der Verteidigung (For primary document see N93-29926 11-07)

Copyright Avail: CASI HC A02/MF A04

Air ejection for film-cooling affects the aerodynamic behavior of the blading by the mixing of the coolant with the mainstream as well as by the interaction between the jet and the boundary layer. The main objective is to receive more information on the flow field in the leading edge region. The focus is the aerodynamic behavior of ejection in the stagnation region. A Navier-Stokes code was used to evaluate the flow field considering the ejection. The calculated results are compared with experimental investigations. Cold gas experiments were conducted in a cascade wind tunnel on three large scaled turbine blades with slotted leading edges. The mass flux ratio was varied from 0.0 to 2.5 to simulate film cooling effects. A high resolution of the flow field especially close to the wall (nearest distance: 50 microns) was achieved by Laser-2-Focus measurements. The pressure distributions on the blade surface and in the wake were measured in order to determine the overall behavior of the blades quantitatively while oil flow patterns and Schlieren pictures provide qualitative results. The experimental results show that the strong pressure gradient near the stagnation point affects the velocity distribution of the jets. This non-uniformity produces additional aerodynamic losses. To take these effects into account for the Navier-Stokes calculation a multi-block grid was used to model the flow field in the ejection holes and in the mainstream. Thus, the experimental and numerical results show a good agreement. Author (revised)

N93-29959# Von Karman Inst. for Fluid Dynamics, Rhode-Saint-Genese (Belgium).

ON THE DEVELOPMENT OF A FILM COOLING LAYER c34

F. Lopez Pena and T. Arts *In* AGARD, Heat Transfer and Cooling in Gas Turbines Feb. 1993 12 p Sponsored by Commission of the European Communities (For primary document see N93-29926 11-07)

Copyright Avail: CASI HC A03/MF A04

Different aerodynamic aspects of the flow field generated when a single jet or a row of jets are ejected into a mainstream are experimentally investigated. The similarity parameters are taken such as to match those of the three-dimensional film cooling. The objective is to deepen the understanding of the complex phenomena associated with these flows, and to provide a comprehensible and detailed data base for validation of numerical codes. To be able to obtain high resolution measurements, the study is made on large scale models. The scale enlargement obliges to use moderate velocities, so that the Reynolds number can be kept within realistic limits and the similarity preserved. The use of low air speeds prevents the analysis of compressibility effects. This restriction is not as severe as one can think because, according to the related bibliography, these effects start to be noticeable at Mach numbers higher than 0.8, while the designers avoid to inject the coolant in the vicinity of shock waves to avoid boundary layer separation. The study is made on three different models installed in a low speed wind tunnel. A first model consists of a flat plate with a single inclined circular hole. The isolated jet/mainstream interaction is investigated by means of this first test plate. The other two models present the same configuration as the first but having now a row of holes with different pitch to diameter ratios in each case. These models are useful to understand the interaction between jets and to analyze the formation and development of the coolant layer. Author (revised)

N93-29960# Centre National de la Recherche Scientifique, Ecully (France). Lab. de Mecanique des Fluides et d'Acoustique.

MODELING OF A TURBULENT FLOW IN THE PRESENCE OF DISCRETE PARIETAL COOLING JETS [MODELISATION D'UN ECOULEMENT TURBULENT EN PRESENCE DE JETS PARIETAUX DISCRETS DE REFROIDISSEMENT]

J. M. Maurice, F. Leboeuf, and P. Kulisa *In* AGARD, Heat Transfer and Cooling in Gas Turbines Feb. 1993 13 p In FRENCH (For primary document see N93-29926 11-07)

Copyright Avail: CASI HC A03/MF A04

The high temperature level reached in the first turbine stages requires efficient blade cooling. Film cooling has proved its ability to protect the wall from the hot upstream flow. However, the jets strongly disturb the aerodynamic flow characteristics. As a consequence, the main objective of the designers is to get the best compromise between thermal strains and aerodynamic losses. A two-dimensional viscous flow model, with discrete jets and based on a boundary layer concept, was developed at Ecole Centrale de Lyon. The turbulence closure was first performed by a mixing length model. A low Reynolds number version of a k-epsilon model is presented. A space averaging method in the transverse direction is used; thereby the two-dimensional character of the computation is preserved, while the specific effects of the discrete jets are taking into account in the model. Comparisons with experimental results are given in the case of a row of jets, as injected through a turbulent boundary layer on a flat plate, near the injection orifice. Author (revised)

N93-29961# Deutsche Forschungsanstalt fuer Luft- und Raumfahrt, Cologne (Germany). Inst. fuer Antriebstechnik.

COUPLING OF 3D-NAVIER-STOKES EXTERNAL FLOW CALCULATIONS AND INTERNAL 3D-HEAT CONDUCTION CALCULATIONS FOR COOLED TURBINE BLADES

A. Heselhaus, D. T. Vogel, and H. Krain *In* AGARD, Heat Transfer and Cooling in Gas Turbines Feb. 1993 9 p (For primary document see N93-29926 11-07)

Copyright Avail: CASI HC A02/MF A04

The problem of cooled gas turbine blades is theoretically investigated. The presented code solves the 3D-Reynolds averaged-Navier-Stokes equations for the external passage flow and the 3D-heat conduction equation for the interior of the blade. Both calculation schemes are coupled without any modeling of the heat transfer boundary conditions at the blade surface. Calculations are presented for a thin hollow flat plate and a typical guide vane blade with a simple cooling channel configuration. Both geometries are cooled by prescribing fixed heat transfer boundary conditions at the inner boundaries. Additionally numerical results are compared to analytical data. The agreement is quite satisfactory. Author (revised)

N93-29962# Politecnico di Milano (Italy). Dipt. di Energetica.

A NAVIER-STOKES SOLVER WITH DIFFERENT TURBULENCE MODELS APPLIED TO FILM-COOLED TURBINE CASCADES

F. Bassi, S. Rebay, M. Savini (National Center for Energetics and Propulsion, Peschiera Borromeo, Italy.), S. Colantuoni (Alfa Romeo S.p.A., Naples, Italy.), and G. Santoriello (Alfa Romeo S.p.A., Naples, Italy.) *In* AGARD, Heat Transfer and Cooling in Gas Turbines Feb. 1993 16 p (For primary document see N93-29926 11-07)

Copyright Avail: CASI HC A03/MF A04

The numerical simulation of transonic flows through film-cooled turbine cascades is described. The modelization of coolant injection was implemented in a computational code which solves either the laminar or the Reynolds-averaged Navier-Stokes equations in cascades. Turbulence effects are accounted for by means of the eddy viscosity concept. Two turbulence models were implemented in the code. The first is the Baldwin-Lomax algebraic model and the second is the two-equation k-omega model proposed by Wilcox. Both models were coupled with a Navier-Stokes solver in a simple, robust, and efficient way. The numerical solution of both the flow and the turbulence model equations is based on a cell centered finite volume scheme and on an explicit Runge-Kutta method for time integration. The code was applied to compute the transonic flow in a cascade of nozzle guide vanes (NGV's) developed by Alfa Romeo Avio S.p.A. The computations were performed both for a cascade of 'solid' vane profiles and for a cascade of 'cutted' vane profiles that allow coolant flow ejection through a slot on the pressure side near the trailing edge. The NGV cascade is still under testing and at present only the experimental data for the 'solid' NGV cascade are available for code validation. The computational results presented show that the proposed coupling of the k-omega model with the explicit Navier-Stokes solver does not seem to suffer from the stiffness problems often characterizing other two-equation turbulence models. Author (revised)

N93-29963*# National Aeronautics and Space Administration. Lewis Research Center, Cleveland, OH.
NAVIER-STOKES ANALYSIS OF THREE-DIMENSIONAL FLOW AND HEAT TRANSFER INSIDE TURBINE BLADE ROWS
C. Hah *In* AGARD, Heat Transfer and Cooling in Gas Turbines Feb. 1993 11 p (For primary document see N93-29926 11-07)
Copyright Avail: CASI HC A03/MF A04

A numerical method for solving the three-dimensional, Navier-Stokes equations for unsteady, viscous flow and heat transfer through multiple turbomachinery blade rows is presented. The method solves the fully three-dimensional Navier-Stokes equations with an implicit scheme which is based on a control volume approach. A two-equation turbulence model with a low Reynolds number modification is employed. A third-order accurate upwinding scheme is used to approximate convection terms while a second order accurate central difference scheme is used for the discretization of viscous terms. A second-order accurate scheme is employed for the temporal discretization. The numerical method is applied to study the unsteady flow and heat transfer field of the High Pressure Fuel side Turbo-Pump (HPFTP) of the Space Shuttle Main Engine (SSME). The stage calculation is performed by coupling the stator and the rotor flow fields at each time step through an over-laid grid. Numerical results for the complete geometry with the vane trailing edge cutback are presented and compared with the available experimental data. Author (revised)

N93-29964# Sener Ingenieria y Sistemas S.A., Madrid (Spain).
COOLING PREDICTIONS IN TURBOFAN ENGINE COMPONENTS
A. Matesanz, R. Rebolo, A. Viedma (Universidad Politecnica de Madrid, Spain.), and M. Rodriguez (Universidad Politecnica de Madrid, Spain.) *In* AGARD, Heat Transfer and Cooling in Gas Turbines Feb. 1993 7 p (For primary document see N93-29926 11-07)
Copyright Avail: CASI HC A02/MF A04

How the metal temperature measured in a convergent divergent nozzle and in a turbine exhaust diffuser of a turbofan engine can be predicted with reasonable approximation using the data available in the open literature is shown. It is shown how the simplified fluid dynamic equations with the appropriate experimental correlation allow the prediction of these results in other flight conditions than those tested. Author (revised)

N93-29999# ABB Kraftwerke A.G., Manheim (Germany). Abt. Gasturbinenentwicklung.
OPTICAL BLADE VIBRATION MEASUREMENT Final Report [OPTISCHE SCHAUFELSCHWINGUNGSMESSUNG. SCHLUSSBERICHT]
Christian Wuethrich, Ernst-Michael Zuefle, and Lars Hillstroem Jun. 1992 85 p In GERMAN
(Contract BMFT-0326800D)
(ETN-93-93454) Avail: CASI HC A05/MF A01

A theoretical analysis of the optical method for blade vibration measurements with special emphasis on multiprobe systems (more than two probes) was performed. On the basis of a theoretical model, guidelines for the optimization of the experimental setup and for the analysis of experimental errors are given. Test calculations show that the blade vibrations can be reliably detected even in the presence of disturbances. In multiprobe systems, equidistant arrangements of the probes on the circumference of the rotor are preferred. For this case, robust evaluation algorithms are presented. It is shown that blade vibrations can be analyzed not only for static but also for fast transient excitations using the optical system. ESA

N93-30168# Oak Ridge National Lab., TN.
CHARACTERIZATION OF CERAMIC COMPOSITE MATERIALS FOR GAS TURBINE APPLICATIONS
K. Reifsnider (Virginia Polytechnic Inst. and State Univ., Blacksburg.), W. Stinchcomb (Virginia Polytechnic Inst. and State Univ., Blacksburg.), K. Liao (Virginia Polytechnic Inst. and State Univ., Blacksburg.), L. Oleksuk (Virginia Polytechnic Inst. and State Univ., Blacksburg.), and D. Stinton 1993 7 p Presented at the 38th ASME International Gas Turbine and Aeroengine Congress and Exhibition, Cincinnati, OH, 24-27 May 1993
(Contract DE-AC05-84OR-21400)
(DE93-009719; CONF-930502-6) Avail: CASI HC A02/MF A01

Ceramic composite materials have the capability to sustain high stress in the presence of high temperatures and aggressive atmospheres. Such materials are being considered for application as combustors, burner cubes, heat exchangers, headers. hot-gas filters, and even rotors of stationary gas turbine engines. In the present program, Nicalon preforms of tubular geometry were fabricated with different fiber architectures (filament winding, 3D braiding, or cloth winding) to tailor the mechanical properties for specific applications. However, these applications require that candidate materials be carefully characterized. Mechanical characterization must establish the properties and performance that are essential for structural design of the turbine components. For this purpose, a full complement of properties is needed, i.e., the stiffness and strengths of the composite material at a range of temperatures, and the fatigue and creep behavior of the materials under the stress states anticipated by the user. This mechanical characterization requires specialized equipment and methodologies, which are now under development by the authors. This paper will present a description of the methodologies required for ceramic composite characterization, and will describe initial results for ceramic composite tubes, a representative geometry for gas turbine components. Future needs and opportunities will also be discussed. DOE

N93-30877# M-DOT, Inc., Phoenix, AZ.
THRUST AUGMENTATION SYSTEM FOR LOW-COST-EXPENDABLE TURBOJET ENGINE Final Report, 26 Jun. 1992 - 31 Mar. 1993
Bryan J. Seegers and David G. Shreiner 31 Mar. 1993 65 p
(Contract DAAH01-92-C-R359)
(AD-A263727) Avail: CASI HC A04/MF A01

During the performance period, a dump-combustor afterburner and water/methanol injection system were designed, fabricated, and tested on a Sundstrand TJ-90 expendable-turbojet engine. Maximum thrust measured was 150 lbs. This yields an augmentation ratio of 1.57. Also evaluated were silicone based and alumina based lining materials for the afterburner combustion tube and coated-graphite and alumina based materials for the exit nozzle. Water/methanol injection was tested at four engine stations: 8 inches upstream of the compressor face, directly upstream of the compressor deswirl vanes, directly into the combustor dilution region and downstream of the turbine exit. Maximum predicted water/methanol flow rates could not be achieved due to combustor flame out. Performance was measured in the following ways: dry, with water/methanol only, with afterburner only, and with afterburner and water/methanol injection. DTIC

08 AIRCRAFT STABILITY AND CONTROL

Includes aircraft handling qualities; piloting; flight controls; and autopilots.

For related information see also *05 Aircraft Design, Testing and Performance.*

N93-29278 Department of the Navy, Washington, DC.
ARTICULATED FIN/WING CONTROL SYSTEM Patent
Charles H. Beauchamp, inventor (to Navy), Manuel Cincotta, Jr., inventor (to Navy), Anthony V. Raffa, inventor (to Navy), and Benoit G. Gauthier, inventor (to Navy) 16 Feb. 1993 9 p Filed 8 Nov. 1991
(AD-D015712; US-Patent-5,186,420; US-Patent-Appl-SN-790607; US-Patent-Class-244-219) Avail: US Patent and Trademark Office

An articulated control surface is provided for hydrodynamic control utilizing a moldable control surface. The central surface is shaped by contracting and elongating wire bundles fabricated with shape-memory alloys located in an adjacent cooling chamber. The shape-memory alloys contract when heated via an applied electric current and elongate when cooled, i.e., the electric current is removed. A pair of wire bundles is anchored inside the cooling chamber. Each bundle is routed over several pulleys in such a manner that a lateral movement is produced at the actuator end of the wire. A pair of bundles act in opposition to maintain dynamic tension at the actuator end. Cooling flow to opposing wire bundles is controlled independently to enhance response time and reduce power requirements. The actuator is a post extending from the cooling chamber to the trailing edge structure of the control surface. DTIC

N93-29985# Michigan Technological Univ., Houghton. Dept. of Mechanical Engineering and Engineering Mechanics.
ROBUST CONTROL OF INTELLIGENT ROTOR
Reza Kashani 22 Feb. 1993 37 p

(Contract DAAL03-92-G-0303)
(AD-A263707; ARO-30299-1-EG-II) Avail: CASI HC A03/MF A01

The performance and robustness of the intelligent rotors under feedback control depend on the fidelity of the models used in designing their controllers. This is also true for other kinds of smart structures. A computer aided robust control design program has been developed that takes the percentage of the variation on the parameters, as well as the desired number of modes to be included in the model and designs a robust controller that guarantees the stability of the system in presence of the formulated uncertainty. Moreover, the use of Terfenol-D magnetostrictive rods for actuation of an intelligent rotor is explored. The challenge in the use of these actuators in intelligent rotor applications is housing them in the structure of the rotor. The packaging of the Terfenol rod actuators, considered in this work, inside the structure of the rotor blade is based on lining the actuators inside the spar along the axis of the blade. This is possible due to the fact that most blades have a hollow D or box spar. The two ends of each actuator is sandwiched between two plates which, for flapwise actuation of the spar, are attached to the top and bottom of the spar, alternatively. This arrangement translate the actuator force to two point moments on the blade at the plate populations. DTIC

N93-30498# Wright Lab., Wright-Patterson AFB, OH.
COMPUTATION OF A DELTA-WING ROLL-AND-HOLD MANEUVER Final Report, 1 Feb. 1992 - 1 Feb. 1993
Raymond E. Gordnier and Miguel Visbal 12 Feb. 1993 46 p
(AD-A264704; WL-TR-93-3016) Avail: CASI HC A03/MF A01

This report presents computations of the flowfield around an 80 degree sweep delta wing undergoing a constant roll-rate maneuver from 0 to 45 degrees. The governing equations for the problem are the unsteady, three-dimensional Navier-Stokes equations. The equations are solved using the implicit, approximately-factored algorithm of Beam-Warming. Fixed roll angle results are also presented and compared with experimental measurements to demonstrate the ability of the numerical technique to accurately capture the flowfield around a rolled delta wing. The dynamic behaviors of the vortex position and strength, as well as their corresponding effect on surface pressure, lift, and roll moment are described. A simple, quasi-static explanation of these vortex behaviors based on effective angle-of-attack and sideslip angle is proposed. DTIC

N93-30550# Johns Hopkins Univ., Baltimore, MD. Dept. of Electrical and Computer Engineering.
ANALYTICAL FOUNDATIONS OF GAIN SCHEDULING Final Report, 1 Mar. 1990 - 28 Feb. 1993
Wilson J. Rugh 15 Mar. 1993 7 p
(Grant AF-AFOSR-0138-90)
(AD-A264682; AFOSR-93-0325TR) Avail: CASI HC A02/MF A01

This final report briefly describes research results on a theory of gain scheduling for flight control applications that were obtained by the Principal Investigator and his students over the three-year period of support. Results reported include development of a basic theory of gain scheduling in nonlinear systems, solution of output regulation problems based on an exogenous system assumption for the exogenous signals (including disturbance and scheduling signals), initial development of methods to alleviate performance degradation in the case of rapidly-varying scheduling signals, and an exploratory application of these results to an autopilot design example. Publications describing the results in detail are listed. DTIC

N93-30604 Aeronautical Research Labs., Melbourne (Australia).
OPTIMAL TRAJECTORIES FOR AIRCRAFT TERRAIN FOLLOWING AND TERRAIN AVOIDANCE: A LITERATURE REVIEW UPDATE
M. E. Halpern Mar. 1993 23 p Limited Reproducibility: More than 20% of this document may be affected by microfiche quality
(AD-A264075; ARL-TR-5; DODA-AR-006-630) Avail: CASI HC A03

This is a literature review relevant to the automated design of flight paths for low-flying military aircraft in terrain following and terrain avoidance roles. Improvements in computer technology continue to widen the range of approaches which may be applied to this important problem. In particular, there is interest in the application of techniques which use elements of artificial intelligence. DTIC

N93-30764*# National Aeronautics and Space Administration. Hugh L. Dryden Flight Research Facility, Edwards, CA.
FLIGHT CONTROL SYSTEM DESIGN FACTORS FOR APPLYING AUTOMATED TESTING TECHNIQUES
Joel R. Sitz and Todd H. Vernon (Planning Research Corp., Edwards, CA.) Washington Oct. 1990 17 p Presented at the 9th Annual Digital Avionics System Conference, Virginia Beach, VA, 15-18 Oct. 1990; sponsored by IEEE Previously announced in IAA as A91-54610
(RTOP 533-02-51)
(NASA-TM-4242; H-1631; NAS 1.15:4242) Avail: CASI HC A03/MF A01

Automated validation of flight-critical embedded systems is being done at ARC Dryden Flight Research Facility. The automated testing techniques are being used to perform closed-loop validation of man-rated flight control systems. The principal design features and operational experiences of the X-29 forward-swept-wing aircraft and F-18 High Alpha Research Vehicle (HARV) automated test systems are discussed. Operationally applying automated testing techniques has accentuated flight control system features that either help or hinder the application of these techniques. The paper also discusses flight control system features which foster the use of automated testing techniques. Derived from text

N93-28851# Defense Advanced Research Projects Agency, Arlington, VA.
X-31 DEMONSTRATION OF INTEGRATED FLIGHT AND PROPULSION CONTROL FOR EFFECTIVE COMBAT AT EXTREME ANGLES OF ATTACK
Michael S. Francis, E. DeVere Henderson (Spectra Research Systems, Inc., Arlington, VA.), Erwin Kunz (Messerschmitt-Boelkow-Blohm G.m.b.H., Munich, Germany.), Sid Powers (Rockwell International Corp., El Segundo, CA.), and Helmut Richter (Ministry of Defence, Germany.) *In* AGARD, Combat Automation for Airborne Weapon Systems: Man/Machine Interface Trends and Technologies Apr. 1993 14 p (For primary document see N93-28850 11-54)
Copyright Avail: CASI HC A03/MF A03

N93-28869*# National Aeronautics and Space Administration. Ames Research Center, Moffett Field, CA.
FLIGHT EVALUATION OF A COMPUTER AIDED LOW-ALTITUDE HELICOPTER FLIGHT GUIDANCE SYSTEM
Harry N. Swenson, Raymond D. Jones (Army Avionics Research and Development Activity, Fort Monmouth, NJ.), and Raymond Clark (Army Avionics Research and Development Activity, Fort Monmouth, NJ.) *In* AGARD, Combat Automation for Airborne Weapon Systems: Man/Machine Interface Trends and Technologies Apr. 1993 11 p (For primary document see N93-28850 11-54)
Copyright Avail: CASI HC A03/MF A03

09 RESEARCH AND SUPPORT FACILITIES (AIR)

Includes airports, hangars and runways; aircraft repair and overhaul facilities; wind tunnels; shock tubes; and aircraft engine test stands.
For related information see also *14 Ground Support Systems and Facilities (Space).*

N93-28467# Air Force Inst. of Tech., Wright-Patterson AFB, OH. School of Engineering.
RENDERING THE OUT-THE-WINDOW VIEW FOR THE AFIT VIRTUAL COCKPIT M.S. Thesis
W. D. McCarty Mar. 1993 50 p
(AD-A262599; AFIT/GCS/ENG/93M-04) Avail: CASI HC A03/MF A01

The Air Force Institute of Technology (AFIT) is developing a distributed interactive flight simulator, the Virtual Cockpit, using commercial graphics workstations and helmet mounted displays. The Virtual Cockpit communicates with other simulators via local and long-haul networks using the SIMNET protocol. The work reported in this thesis focuses on developing the terrain database for the synthetic environment and on rendering the pilot's view of the database. There are many different file formats for describing 3-dimensional geometric polygonal objects. An analysis of three formats, AFIT GEOM, the Naval Postgraduate School (NPS) DRP, and Software Systems' Flight, is presented. Each file format is described, and their attributes are compared in a decision table. A series of C++ classes were developed to render the file format used by the terrain database. These C++ classes, which include classes for stationary and moving entities, and for textures, are discussed. A technique for increasing the rendering speed is also presented. DTIC

N93-28490# Wisconsin Univ., Madison.
UNDULATOR SPECTROMICROSCOPY FACILITY AT THE ADVANCED LIGHT SOURCE Annual Report, 1992
1992 6 p
(Contract DE-FG02-92ER-45468)
(DE93-007964; DOE/ER-45468/1) Avail: CASI HC A02/MF A01

The SpectroMicroscopy Facility is a Participating Research Team (PRT) that was formed to design and build detectors and experimental stations that could take advantage of the specific advantages that the highly coherent undulator source provides. The primary scientific orientation of the team is in materials science and the physics and chemistry of surfaces or interfaces. The SpectroMicroscopy Facility is organized as an ALS 'Type A' project. This report presents progress made on the project for 1992. DOE

N93-29398# Coordinating Research Council, Inc., Atlanta, GA.
AIRCRAFT AND REFUELER BONDING AND GROUNDING STUDY
Feb. 1993 48 p
(AD-A262027; CRC-583) Avail: CASI HC A03/MF A01

The 1990 Edition of NFPA 407, Standard on Aircraft Fuel Servicing, deleted the requirement for grounding during aircraft fueling and tank truck loadings. This change has caused a great deal of concern in the industry since it impacts not only refueling operations, but also airport construction and maintenance. In order to resolve the more controversial aspects of this change, the Coordinating Research Council (CRC) Electrical Discharges Liaison Group conducted a series of tests at Denver Stapleton Airport, 30 October-8 November 1991. This test program culminated in a demonstration of a simulated aircraft refueling operation conducted with and without the use of ground wires. The demonstration was witnessed by representatives from the FAA, the airline, air cargo and aircraft fueling industries, airport design industry and the Denver Fire Department. The program did not address grounding requirements for purposes other than refueling. DTIC

N93-29436# Naval Postgraduate School, Monterey, CA.
MATHEMATICAL MODELING AND CONTROL LAW DEVELOPMENT FOR THE ATMOSPHERIC MONITORING AND CONTROL SYSTEM OF THE CONTROLLED ENVIRONMENT RESEARCH CHAMBER (CERC) AT NASA AMES RESEARCH CENTER M.S. Thesis
Bruce H. Mathers Dec. 1992 127 p
(AD-A261978) Avail: CASI HC A07/MF A02

The objective of this research is to develop a mathematical model and control algorithm for maintenance of the environmental system within the Controlled Environmental Research Chamber (CERC) located at the National Aeronautics and Space Administration (NASA) Ames Research Center, Moffet Field, CA. The hypobaric research chamber is currently undergoing renovation as part of the Human Exploration Development Project (HEDP), an effort on behalf of NASA for advanced life support research. A broad overview of the chamber is provided which includes a physical description, preliminary system hardware and associated performance, and potential experimental uses. A mathematical model of the chamber air mass is developed based on key energy and mass balances. Two methods of adaptive control have been implemented for the coupled control of temperature, composition, pressure and humidity within the closed environment. Simulations testing the control algorithm performance are conducted, including a sup and modified ramp response. The results of the simulations indicate the adaptive methods performed well for the model presented. Further research is required in refining the chamber model for algorithm optimization including integration of hardware dynamics. DTIC

N93-29788# Mitre Corp., McLean, VA.
THE 1991-1992 AVIATION SYSTEM CAPACITY PLAN Report, Jul. 1990 - Jul. 1991
1992 310 p
(AD-A263436; DOT/FAA/ACS-91-1) Avail: CASI HC A14/MF A03

This is a comprehensive review of the Federal Aviation Administration's program to improve the capacity of the National Air Transportation System. The plan identifies the causes and extent of capacity and delay problems currently associated with air travel in the U.S., and outlines various planned and ongoing FAA projects that will reduce the severity of the problems in the future. The major areas of discussion are: (1) Airport Development, (2) Airport and Airspace Capacity, (3) Technology for Capacity Improvement, and (4) Marketplace Solutions. DTIC

N93-29815# Massachusetts Inst. of Tech., Lexington.
TWO SIMULATION STUDIES OF PRECISION RUNWAY MONITORING OF INDEPENDENT APPROACHES TO CLOSELY SPACED PARALLEL RUNWAYS
Ann Marie T. Lind 2 Mar. 1993 129 p
(Contracts DTFA01-89-Z-02033; F19628-90-C-0002)
(AD-A263433; ATC-190; DOT/FAA/NR-92/9) Avail: CASI HC A07/MF A02

This report documents the findings of two simulation studies of air traffic controller reaction to the Precision Runway Monitor (PRM). The PRM is a new system for monitoring independent approaches to closely spaced parallel runways. It consists of a radar which has higher accuracy and a faster update interval than the current system. The PRM radar is accompanied by a high-resolution color display which provides automated visual and vocal warnings to alert controllers of impending and actual penetration of a 'No Transgression Zone' between parallel runways. The studies, were conducted in order to determine the effects of key variables on controller reaction time and to determine controller opinion on system acceptability. Study 1 examined the use of the PRM when the runway separation was both 3,400 ft and 4,300 ft. Study 2 examined the use of the PRM when the runway separation was 3,000 ft. Real-time simulated approach blunders were presented to controllers, and measurements of their reaction times were recorded and analyzed. Independent variables studied included sensor update interval, runway separation, deviation angle, deviation range, flight path condition, approach blunder type, and controller experience level. In addition, controller opinions of the PRM were surveyed. Findings regarding the effects of each of the variables are reported. Survey results of controller opinion are reported. Recommendations for enhancing the realism of the simulation and recommendations of issues for future study are discussed. DTIC

N93-29869# California Univ., Berkeley. Lawrence Berkeley Lab.
X RAY MICROSCOPY RESOURCE CENTER AT THE ADVANCED LIGHT SOURCE
W. Meyer-Ilse, M. Koike, R. Beguiristain, J. Maser, and D. Attwood Jul. 1992 4 p Presented at the SPIE International Symposium on Optical Applied Science and Engineering, San Diego, CA, 19-24 Jul. 1992
(Contract DE-AC03-76SF-00098)
(DE93-010449; LBL-32323; CONF-920792-51) Avail: CASI HC A01/MF A01

An x-ray microscopy resource center for biological x-ray imaging will be built at the Advanced Light Source (ALS) in Berkeley. The unique high brightness of the ALS allows short exposure times and high image quality. Two microscopes, an x-ray microscope (XM) and a scanning x-ray microscope (SXM) are planned. These microscopes serve complementary needs. The XM gives images in parallel at comparable short exposure times, and the SXM is optimized for low radiation doses applied to the sample. The microscopes extend visible light microscopy towards significantly higher resolution and permit images of objects in an aqueous medium. High resolution is accomplished by the use of Fresnel zone plates. Design considerations to serve the needs of biological x-ray microscopy are given. Also, the preliminary design of the microscopes is presented. Multiple wavelength and multiple view images will provide elemental contrast and some degree of 3D information. DOE

N93-29972# Human Resources Research Organization, Alexandria, VA.
DEVELOPMENT OF A CONCEPT FORMULATION PROCESS AID FOR ANALYZING TRAINING REQUIREMENTS AND DEVELOPING TRAINING DEVICES Final Report, Apr. 1991 - Jul. 1992
Paul A. Sticha, Stephens Gibbons, and Michael J. Singer Mar. 1993 39 p
(Contract DAHC35-89-D-0046; DA Proj. 2Q2-63007-A-795)
(AD-A263579; ARI-RR-1637) Avail: CASI HC A03/MF A01

This report describes the development of a concept formulation process decision aid that addresses the tradeoff determination phase. It adapts previously developed models for use during a specific step in the development of a training device. The report identifies the source of information used and explains the rationale for the development of different aspects of the system,. A brief overview of the aiding system is presented. The goals of the aid are introduced and the steps taken to meet those goals are presented. The report describes the data elements, links between elements, and aiding functions and presents and discusses the evaluation of the system by projected users and the results of that evaluation. Difficulties discovered during development and suggestions for future research and development are presented in the conclusion. DTIC

N93-30103# Army Cold Regions Research and Engineering Lab., Hanover, NH.

MATHEMATICAL MODEL OF FROST HEAVE AND THAW SETTLEMENT IN PAVEMENTS

Gary L. Guymon, Richard L. Berg, and Theodore V. Hromadka Apr. 1993 128 p
(Contract DTFA01-84-Z-02038)
(CRREL-REPT-93-2; DOT/FAA/RD-93/15) Avail: CASI HC A07/MF A02

Since 1975, the U.S. Army Corps of Engineers, The Federal Highway Administration, and the Federal Aviation Administration have been working cooperatively to develop a mathematical model to estimate frost heave and thaw weakening under various environmental conditions and for various pavement designs. A model has been developed. It is a 1D representation of vertical heat and moisture flux, is based on a numerical solution technique termed the nodal domain integration method, and estimates frost heave and frost penetration reasonably well for a variety of situations. The model is now ready for additional field evaluation and implementation in appropriate cases. The main objectives are the following: (1) to describe the model, FROST, including modeling uncertainties and errors; (2) to summarize recent comparisons between measured and computed values for frost heave and frost penetration; and (3) to describe parameters necessary for input into the model. Author (revised)

N93-29945# Calspan Advanced Technology Center, Buffalo, NY.

THE USAF ADVANCED TURBINE AEROTHERMAL RESEARCH RIG (ATARR)

C. W. Haldeman, Jr., M. G. Dunn, C. D. MacArthur (Wright Lab., Wright-Patterson AFB, OH.), and C. G. Murawski (Wright Lab., Wright-Patterson AFB, OH.) *In* AGARD, Heat Transfer and Cooling in Gas Turbines Feb. 1993 14 p (For primary document see N93-29926 11-07)
Copyright Avail: CASI HC A03/MF A04

N93-30675*# National Aeronautics and Space Administration. Ames Research Center, Moffett Field, CA.

HELICOPTER SIMULATOR STANDARDS

Edward M. Boothe *In its* NASA/FAA Helicopter Simulator Workshop Apr. 1992 p 31-33 (For primary document see N93-30673 11-01)
Avail: CASI HC A01/MF A02

N93-30678*# National Aeronautics and Space Administration. Ames Research Center, Moffett Field, CA.

SIMULATORS FOR CORPORATE PILOT TRAINING AND EVALUATION

Curt Treichel *In its* NASA/FAA Helicopter Simulator Workshop Apr. 1992 p 45-47 (For primary document see N93-30673 11-01)
Avail: CASI HC A01/MF A02

N93-30681*# National Aeronautics and Space Administration. Ames Research Center, Moffett Field, CA.

HELICOPTER SIMULATOR QUALIFICATION

Brian Hampson *In its* NASA/FAA Helicopter Simulator Workshop Apr. 1992 p 61-64 (For primary document see N93-30673 11-01)
Avail: CASI HC A01/MF A02

N93-30682*# National Aeronautics and Space Administration. Ames Research Center, Moffett Field, CA.

HELICOPTER SIMULATION: MAKING IT WORK

Barry Payne *In its* NASA/FAA Helicopter Simulator Workshop Apr. 1992 p 65-68 (For primary document see N93-30673 11-01)
Avail: CASI HC A01/MF A02

N93-30683*# National Aeronautics and Space Administration. Ames Research Center, Moffett Field, CA.

HELICOPTER TRAINING SIMULATORS: KEY MARKET FACTORS

John McIntosh *In its* NASA/FAA Helicopter Simulator Workshop Apr. 1992 p 69-76 (For primary document see N93-30673 11-01)
Avail: CASI HC A02/MF A02

N93-30685*# National Aeronautics and Space Administration. Ames Research Center, Moffett Field, CA.

DETERMINING THE TRANSFERABILITY OF FLIGHT SIMULATOR DATA

David Green *In its* NASA/FAA Helicopter Simulator Workshop Apr. 1992 p 91-108 (For primary document see N93-30673 11-01)
Avail: CASI HC A03/MF A02

N93-30686*# National Aeronautics and Space Administration. Ames Research Center, Moffett Field, CA.

PROGRESS THROUGH PRECEDENT: GOING WHERE NO HELICOPTER SIMULATOR HAS GONE BEFORE

Richard J. Adams *In its* NASA/FAA Helicopter Simulator Workshop Apr. 1992 p 109-114 (For primary document see N93-30673 11-01)
Avail: CASI HC A02/MF A02

N93-30687*# National Aeronautics and Space Administration. Ames Research Center, Moffett Field, CA.

TRANSFER OF TRAINING AND SIMULATOR QUALIFICATION OR MYTH AND FOLKLORE IN HELICOPTER SIMULATION

Jack Dohme *In its* NASA/FAA Helicopter Simulator Workshop Apr. 1992 p 115-121 (For primary document see N93-30673 11-01)
Avail: CASI HC A02/MF A02

N93-30689*# National Aeronautics and Space Administration. Ames Research Center, Moffett Field, CA.

FREQUENCY-RESPONSE TECHNIQUES FOR DOCUMENTATION AND IMPROVEMENT OF ROTORCRAFT SIMULATORS

Mark B. Tischler *In its* NASA/FAA Helicopter Simulator Workshop Apr. 1992 p 131-146 (For primary document see N93-30673 11-01)
Avail: CASI HC A03/MF A02

N93-30690*# National Aeronautics and Space Administration. Ames Research Center, Moffett Field, CA.

BANDWIDTH AND SIMDUCE AS SIMULATOR FIDELITY CRITERIA

David Key *In its* NASA/FAA Helicopter Simulator Workshop Apr. 1992 p 147-160 (For primary document see N93-30673 11-01)
Avail: CASI HC A03/MF A02

N93-30691*# National Aeronautics and Space Administration. Ames Research Center, Moffett Field, CA.

METHODOLOGY DEVELOPMENT FOR EVALUATION OF SELECTIVE-FIDELITY ROTORCRAFT SIMULATION

William D. Lewis, D. P. Schrage, J. V. R. Prasad, and Daniel Wolfe *In its* NASA/FAA Helicopter Simulator Workshop Apr. 1992 p 161-166 (For primary document see N93-30673 11-01)
Avail: CASI HC A02/MF A02

12 ASTRONAUTICS (GENERAL)

For extraterrestrial exploration see *91 Lunar and Planetary Exploration.*

N93-28699*# National Aeronautics and Space Administration, Washington, DC.

NASA/DOD FLIGHT EXPERIMENTS TECHNICAL INTERCHANGE MEETING PROCEEDINGS

1992 837 p Meeting held in Monterey, CA, 5-9 Oct. 1992
(NASA-TM-108721; NAS 1.15:108721) Avail: CASI HC A99/MF A10

This document contains the proceedings of the Flight Experiments Technical Interchange Meeting held in Monterey California, October 5-9, 1992. Technical sessions 4 through 8 addressing space structures, propulsion, space power systems, space environments and effects, and space operations are covered. Many of the papers are presented in outline and viewgraph form. For individual titles, see N93-28700 through N93-28743.

N93-28700*# National Aeronautics and Space Administration. Marshall Space Flight Center, Huntsville, AL.
LOW-COST ACTIVE STRUCTURAL CONTROL SPACE EXPERIMENT (LASC) **c18**
Rush Robinett (Sandia National Labs., Albuquerque, NM.) and Angelia P. Bukley *In* NASA, Washington, NASA/DOD Flight Experiments Technical Interchange Meeting Proceedings 1992 14 p (For primary document see N93-28699 11-12)
Avail: CASI HC A03/MF A10

The DOE Lab Director's Conference identified the need for the DOE National Laboratories to actively and aggressively pursue ways to apply DOE technology to problems of national need. Space structures are key elements of DOD and NASA space systems and a space technology area in which DOE can have a significant impact. LASC is a joint agency space technology experiment (DOD Phillips, NASA Marshall, and DOE Sandia). The topics are presented in viewgraph form and include the following: phase 4 investigator testbed; control of large flexible structures in orbit; INFLEX; Controls, Astrophysics; and structures experiments in space; SARSAT; and LASC mission objectives. Derived from text

N93-28701*# L'Garde, Inc., Tustin, CA.
IN-STEP INFLATABLE ANTENNA EXPERIMENT **c18**
G. Veal and R. E. Freeland (Jet Propulsion Lab., California Inst. of Tech., Pasadena.) *In* NASA, Washington, NASA/DOD Flight Experiments Technical Interchange Meeting Proceedings 1992 12 p (For primary document see N93-28699 11-12)
Avail: CASI HC A03/MF A10

The topics are presented in viewgraph form and include the following: potential space antenna applications; experiment objectives; experiment technical approach; experiment scenario; spartan services; experiment orbital configuration; experiment canister structure; surface measurement system configuration; and orbital functional sequences. CASI

N93-28702*# McDonnell-Douglas Missile Systems Co., Saint Louis, MO.
NASA INSTEP/MDMSC JITTER SUPPRESSION EXPERIMENT (JITTER) **c37**
Edward V. White *In* NASA, Washington, NASA/DOD Flight Experiments Technical Interchange Meeting Proceedings 1992 9 p (For primary document see N93-28699 11-12)
(Contract NAS1-19245)
Avail: CASI HC A02/MF A10

The objectives are the following: (1) to develop and demonstrate in-space performance of both passive and active damping systems for suppression of micro-amplitude vibration on an actual application structure and operate despite uncertain dynamics and uncertain disturbance characteristics; and (2) to correlate ground and in-space performance - the performance metric is vibration attenuation. The goals are to achieve vibration suppression equivalent to 5 percent passive damping in selected models and 15 percent active damping in selected modes. Various aspects of this experiment are presented in viewgraph form. Derived from text

N93-28703*# Utah State Univ., Logan. Dept. of Mechanical and Aerospace Engineering.
DESCRIPTION OF THE JOINT DAMPING EXPERIMENT (JDX) **c18**
Steven L. Folkman and Frank J. Redd *In* NASA, Washington, NASA/DOD Flight Experiments Technical Interchange Meeting Proceedings 1992 26 p (For primary document see N93-28699 11-12)
Avail: CASI HC A03/MF A10

The overall objective is to develop a small-scale shuttle flight experiment which allows researchers to: (1) characterize the influence of gravity and joint gaps on a small-scale truss model, and (2) evaluate the applicability of low-g aircraft test results for predicting on-orbit behavior. The experiment consists of a three-bay truss and associated hardware for truss excitation and measurement of oscillations. Other aspects of the investigation are presented in viewgraph form. Derived from text

N93-28704*# Phillips Lab., Hanscom AFB, MA. Directorate of Space and Missile Technology.
ADAPTIVE STRUCTURES FLIGHT EXPERIMENTS **c18**
Maurice Martin *In* NASA, Washington, NASA/DOD Flight Experiments Technical Interchange Meeting Proceedings 1992 21 p (For primary document see N93-28699 11-12)
Avail: CASI HC A03/MF A10

The topics are presented in viewgraph form and include the following: adaptive structures flight experiments; enhanced resolution using active vibration suppression; Advanced Controls Technology Experiment (ACTEX); ACTEX program status; ACTEX-2; ACTEX-2 program status; modular control patch; STRV-1b Cryocooler Vibration Suppression Experiment; STRV-1b program status; Precision Optical Bench Experiment (PROBE); Clementine Spacecraft Configuration; TECHSAT all-composite spacecraft; Inexpensive Structures and Materials Flight Experiment (INFLEX); and INFLEX program status. Derived from text

N93-28705*# Massachusetts Inst. of Tech., Cambridge. Space Engineering Research Center.
THE MODE FAMILY OF FACILITY CLASS EXPERIMENTS **c18**
David W. Miller *In* NASA, Washington, NASA/DOD Flight Experiments Technical Interchange Meeting Proceedings 1992 22 p (For primary document see N93-28699 11-12)
Avail: CASI HC A03/MF A10

The objective of the Middeck 0-gravity Dynamics Experiment (MODE) is to characterize fundamental 0-g slosh behavior and obtain quantitative data on slosh force and spacecraft response for correlation of the analytical model. The topics are presented in viewgraph form and include the following: space results; STA objectives, requirements, and approach; comparison of ground to orbital data for the baseline configuration; conclusions of orbital testing; flight experiment resources; Middeck Active Control Experiment (MACE); MACE 1-G and 0-G models; and future efforts. Derived from text

N93-28706*# National Aeronautics and Space Administration. Langley Research Center, Hampton, VA.
CONTROL-STRUCTURES INTERACTION TEST OF THE LACE SATELLITE **c18**
Lawrence W. Taylor, Jr. and Shalom Fisher (Naval Research Lab., Washington, DC.) *In* NASA, Washington, NASA/DOD Flight Experiments Technical Interchange Meeting Proceedings 1992 21 p (For primary document see N93-28699 11-12)
Avail: CASI HC A03/MF A10

It is clear that additional experience and validation of Control Structures Interaction (CSI) techniques are needed in controlling the structural dynamics of flexible spacecraft. It is also clear that the effects of the space environment such as weightlessness dictate that this be done in space. Unfortunately, orbital tests are difficult to achieve because of the high cost of the test article, the launch into orbit, the instrumentation, and communication systems. The Low-power Atmospheric Compensation Experiment (LACE) Satellite has provided an opportunity to achieve a CSI test in space for very little cost. First, the CSI test rode piggy-back and did not interfere with the primary objective of LACE. Second, the novel technique of using ground based measurements of vibration of the orbiting satellite was employed. The LACE has a heavy central body to which is attached booms with lengths as long as 150 feet. The ground measurements were obtained using laser Doppler radar at the MIT Lincoln Laboratory Firepond Facility. The initial tests demonstrated the accuracy of the vibration measurements and obtained structural responses for enhancing the accuracy of the mathematical model of the structural dynamics. Germanium corner-cube retroreflectors attached to the central body and a boom deployed to 18 feet ensured a high strength return signal. Subsequent tests demonstrated the ability of an open-loop damper to attenuate the vibrations of the orbiting satellite. The LACE test results are important in contributing to the validation of a CSI technique, and demonstrating a novel ground measurement technique for orbital tests that is accurate but which has very low cost. Author

N93-28707*# McDonnell-Douglas Space Systems Co., Huntington Beach, CA.
CSI-STAR: A LOW-COST CSI ORBITAL TESTBED **c14**
D. Edberg *In* NASA, Washington, NASA/DOD Flight Experiments Technical Interchange Meeting Proceedings 1992 26 p (For primary document see N93-28699 11-12)
Avail: CASI HC A03/MF A10

The topics are presented in viewgraph form and include the following: rationale for an on-orbit control-structurs interaction (CSI) test facility; CSI flight experiment objectives; feasibility study objectives; CSI free-flyer solution; feasibility study technical status summary; CSI-Star - a low-cost CSI free flyer; conceptual experiment design - option 2 configuration; Delta 2 - Quickstar Interface clambband capability; open and closed loop response of baselined truss with active struts; experiment weight baseline (option 1) configuration; experiment weight option 2 configuration; experiment power baseline (option 1) configuration; experiment power option 2 configuration; CSI Quickstar capabilities/requirements; and remaining work. CASI

N93-28708*# National Aeronautics and Space Administration. Langley Research Center, Hampton, VA.
UPPER ATMOSPHERE RESEARCH SATELLITE JITTER STUDY c18
Stanley Woodard, Mike Garnek (General Electric Co., Philadelphia, PA.), John Molnar (General Electric Co., Philadelphia, PA.), and William Grantham *In* NASA, Washington, NASA/DOD Flight Experiments Technical Interchange Meeting Proceedings 1992 16 p (For primary document see N93-28699 11-12)
Avail: CASI HC A03/MF A10

The study objectives are to analyze in-flight jitter; evaluate different models of the Upper Atmosphere Research Satellite (UARS); and determine jitter prediction accuracy such that adequate (but not excessive) design margins will assume future mission success. The topics are presented in viewgraph form and include the following: UARS chronology; UARS disturbance experiment; microwave limb sounder antenna and mirror time profiles; solar array drive disturbance; roll and yaw jitter correlation with solar array position; solar array rotation; UARS disturbance summary; concept for reduction of jitter effect; jitter reduction using window scheduling; and highlights/lessons learned. Derived from text

N93-28709*# Phillips Lab., Edwards AFB, CA.
ELITE PROGRAM: ELECTRIC INSERTION TRANSFER EXPERIMENT c20
Robert Vondra *In* NASA, Washington, NASA/DOD Flight Experiments Technical Interchange Meeting Proceedings 1992 12 p Prepared in cooperation with Dayton Univ. Research Inst., Edwards AFB, CA (For primary document see N93-28699 11-12)
Avail: CASI HC A03/MF A10

The topics are presented in viewgraph form and include the following: the Cooperative Research & Development Agreement (CRDA); spacecraft; benefits; program milestones; subsystem status; partners; and payloads. CASI

N93-28710*# Southwest Research Inst., San Antonio, TX.
LIQUID MOTION IN A ROTATING TANK EXPERIMENT (LME) c20
F. T. Dodge *In* NASA, Washington, NASA/DOD Flight Experiments Technical Interchange Meeting Proceedings 1992 20 p Sponsored by NASA. Goddard Space Flight Center (For primary document see N93-28699 11-12)
Avail: CASI HC A03/MF A10

The Liquid Motion in Rotating Tank Experiment (LME) will investigate and quantify liquid motions occurring in spin-stabilized spacecraft; acquire representative data to validate ground-test scaling procedures; and obtain scientific understanding to formulate better analytical models. LME eliminates the limitations of ground testing. LME design is nearing the end of phase B: the breadboard hardware model has been completed; the load cells have been fabricated and tested; the experiment computer has been flight qualified; and other electronics have been breadboarded. Various aspects of this experiment are presented in viewgraph form. Derived from text

N93-28711*# Martin Marietta Corp., Denver, CO.
VENTED TANK RESUPPLY EXPERIMENT (VTRE) FOR IN-SPACE TECHNOLOGY EXPERIMENT PROGRAM (IN-STEP) Report, Jun. 1991 - Jul. 1992 c20
In NASA, Washington, NASA/DOD Flight Experiments Technical Interchange Meeting Proceedings 1992 26 p (For primary document see N93-28699 11-12)
(Contract NAS3-25977)
Avail: CASI HC A03/MF A10

An overview of the Vented Tank Resupply Experiment (VTRE) program is presented in outline and graphical form. The goal of the program is to develop, design, build and provide flight and post flight support for a Shuttle Hitchhiker Experiment to investigate and demonstrate vented tank venting in space. Program schedules and experiment subsystem schematics are presented and specific technical objectives, power requirements, payload assemblies, Hitchhiker canister integration, and orbiter mission approach are addressed. CASI

N93-28712*# Boeing Defense and Space Group, Seattle, WA.
TANK PRESSURE CONTROL EXPERIMENT (TPCE) c20
Mike Bentz *In* NASA, Washington, NASA/DOD Flight Experiments Technical Interchange Meeting Proceedings 1992 13 p (For primary document see N93-28699 11-12)
Avail: CASI HC A03/MF A10

The Tank Pressure Control Experiment (TPCE) is a small self-contained STS payload designed to test a jet mixer for cryogenic fluid pressure control. Viewgraphs are presented that describe project organization, experiment objectives and approach, risk management, payload concept and mission plan, and initial test data. CASI

N93-28713*# National Aeronautics and Space Administration. Lewis Research Center, Cleveland, OH.
TANK PRESSURE CONTROL EXPERIMENT/THERMAL PHENOMENA (TPCE/TP) c20
M. M. Hasan and R. H. Knoll *In* NASA, Washington, NASA/DOD Flight Experiments Technical Interchange Meeting Proceedings 1992 18 p (For primary document see N93-28699 11-12)
Avail: CASI HC A03/MF A10

The 'Tank Pressure Control Experiment/Thermal Phenomena (TPCE/TP)' is a reflight of the tank pressure control experiment (TPCE), flown on STS-43 in a standard Get-Away Special (GAS) container in August 1991. The TPCE obtained extensive video and digital data of the jet induced mixing process in a partially filled tank in low gravity environments. It also provided limited data on the thermal processes involved. The primary objective of the reflight of TPCE is to investigate experimentally the phenomena of liquid superheating and pool nucleate boiling at very low heat fluxes in a long duration low gravity environment. The findings of this experiment will be of direct relevance to space based subcritical cryogenic fluid system design and operation. Experiment hardware and results from the first TPCE are described in outline and graphic form. Author (revised)

N93-28714*# L'Garde, Inc., Tustin, CA.
DEVELOPING AN INFLATABLE SOLAR ARRAY c18
Patrick K. Malone, Francis J. Jankowski (Phillips Lab., Edwards AFB, CA.), Geoffery T. Williams, and George J. Vendura, Jr. (SUMM Associates.) *In* NASA, Washington, NASA/DOD Flight Experiments Technical Interchange Meeting Proceedings 1992 15 p (For primary document see N93-28699 11-12)
Avail: CASI HC A03/MF A10

Viewgraphs describing the development of an inflatable solar array as part of the Inflatable Torus Solar Array Technology (ITSAT) program are presented. Program phases, overall and subsystem designs, and array deployment are addressed. CASI

N93-28715*# Space Systems/Loral, Palo Alto, CA.
SODIUM-SULFUR CELL TECHNOLOGY FLIGHT EXPERIMENT (SSCT) c44
Carl R. Halbach *In* NASA, Washington, NASA/DOD Flight Experiments Technical Interchange Meeting Proceedings 1992 8 p (For primary document see N93-28699 11-12)
Avail: CASI HC A02/MF A10

The sodium-sulfur battery is emerging as a prime high-temperature energy storage technology for space flight applications. A Na-S cell demonstration is planned for a 1995-96 NASA Space Shuttle flight which focuses on the microgravity effects on individual cells. The experiment is not optimized for battery performance as such. Rather, it maximizes the variety of operating conditions which the Na-S cell is capable of in a relatively short 5-day flight. The demonstration is designed to reveal the effects of microgravity by comparison with ground test control cells experiencing identical test conditions but with gravity. Specifically, limitations of transport dynamics and associated cell performance characteristics should be revealed. The Na-S Cell Technology Flight Experiment consists of three separate experiments designed to determine cell operating characteristics, detailed electrode kinetics and reactant distributions. Derived from text

N93-28716*# National Aeronautics and Space Administration. Lewis Research Center, Cleveland, OH.
SOLAR ARRAY MODULE PLASMA INTERACTION EXPERIMENT (SAMPIE) **c18**
Dale C. Ferguson *In* NASA, Washington, NASA/DOD Flight Experiments Technical Interchange Meeting Proceedings 1992 23 p (For primary document see N93-28699 11-12)
Avail: CASI HC A03/MF A10

The objective of the Solar Array Module Plasma Interaction Experiment (SAMPIE) is to investigate, by means of a shuttle-based flight experiment and relevant ground-based testing, the arcing and current collection behavior of materials and geometries likely to be exposed to the LEO plasma on high-voltage space power systems, in order to minimize adverse environmental interactions. An overview of the SAMPIE program is presented in outline and graphical form. CASI

N93-28717*# National Aeronautics and Space Administration. Lewis Research Center, Cleveland, OH.
THE PHOTOVOLTAIC ARRAY SPACE POWER PLUS DIAGNOSTICS (PASP PLUS) FLIGHT EXPERIMENT **c44**
Michael F. Piszczor, Henry B. Curtis, Donald A. Guidice (Phillips Lab., Hanscom AFB, MA.), and Paul S. Severance (Phillips Lab., Hanscom AFB, MA.) *In* NASA, Washington, NASA/DOD Flight Experiments Technical Interchange Meeting Proceedings 1992 34 p (For primary document see N93-28699 11-12)
Avail: CASI HC A03/MF A10

An overview of the Photovoltaic Array Space Power Plus Diagnostics (PASP Plus) flight experiment is presented in outline and graphic form. The goal of the experiment is to test a variety of photovoltaic cell and array technologies under various space environmental conditions. Experiment objectives, flight hardware, experiment control and diagnostic instrumentation, and illuminated thermal vacuum testing are addressed. CASI

N93-28718*# Phillips Lab., Hanscom AFB, MA.
SODIUM SULFUR TECHNOLOGY PROGRAM NaSTEC **c33**
Bob Highley and W. Andrew Somerville (Aerospace Corp., El Segundo, CA.) *In* NASA, Washington, NASA/DOD Flight Experiments Technical Interchange Meeting Proceedings 1992 10 p (For primary document see N93-28699 11-12)
Avail: CASI HC A02/MF A10

The NaSTEC program focuses on developing currently available sodium sulfur cells for use in space applications and investigating the operational parameters of the cells. The specific goals of the program are to determine the operational parameters and verify safety limits of Na/S technology battery cells; test long term zero-g operation; and create a life test database. The program approach and ground and flight test objectives are described in textual and graphic form. CASI

N93-28719*# TRW Space and Defense Sector, Redondo Beach, CA.
IN-STEP TWO-PHASE FLOW (TPF) THERMAL CONTROL EXPERIMENT **c34**
In NASA, Washington, NASA/DOD Flight Experiments Technical Interchange Meeting Proceedings 1992 19 p (For primary document see N93-28699 11-12)
Avail: CASI HC A03/MF A10

The Two-Phase Flow Thermal Control Experiment is part of the NASA/OAST In-Space Technology Experiments (In-STEP) Program. The experiment is configured for the Hitchhiker Shuttle payload system and consists of a capillary pumped loop, heatpipe radiator, and two-phase flow heat exchanger. The flight experiment design approach, test plan, payload design, and test components are described in outline and graphic form. CASI

N93-28720*# National Aeronautics and Space Administration. Lewis Research Center, Cleveland, OH.
THERMAL ENERGY STORAGE FLIGHT EXPERIMENT IN MICROGRAVITY **c44**
David Namkoong *In* NASA, Washington, NASA/DOD Flight Experiments Technical Interchange Meeting Proceedings 1992 12 p (For primary document see N93-28699 11-12)
Avail: CASI HC A03/MF A10

The Thermal Energy Storage Flight Experiment was designed to characterize void shape and location in LiF-based phase change materials in different energy storage configurations representative of advanced solar dynamic systems. Experiment goals and payload design are described in outline and graphic form. CASI

N93-28721*# National Aeronautics and Space Administration. Goddard Space Flight Center, Greenbelt, MD.
CRYOGENIC HEAT PIPE EXPERIMENT (CRYOHP) **c44**
Roy McIntosh *In* NASA, Washington, NASA/DOD Flight Experiments Technical Interchange Meeting Proceedings 1992 21 p (For primary document see N93-28699 11-12)
Avail: CASI HC A03/MF A10

The objective of the CRYOHP experiment is to conduct a shuttle experiment that demonstrates the reliable operation of two oxygen heat pipes in microgravity. The experiment will perform the following tasks: (1) demonstrate startup of the pipes from the supercritical state; (2) measure the heat transport capacity of the pipes; (3) measure evaporator and condenser film coefficients; and (4) work shuttle safety issues. The approach for the experiment is as follows: (1) fly two axially grooved oxygen heat pipes attached to mechanical stirling cycle tactical coolers; (2) integrate experiment in hitch-hiker canister; and (3) fly on shuttle and control from ground. Derived from text

N93-28722*# Hughes Aircraft Co., Torrance, CA.
HEAT PIPE PERFORMANCE EXPERIMENT **c44**
George Fleischman *In* NASA, Washington, NASA/DOD Flight Experiments Technical Interchange Meeting Proceedings 1992 40 p (For primary document see N93-28699 11-12)
Avail: CASI HC A03/MF A10

The objective of the heat pipe performance experiment is to answer questions about how heat pipe performance in space differs from heat pipe performance on the ground. This part of the experiment will attempt to account for the following: (1) gravity domination in ground testing; (2) surface tension domination in a microgravity environment; and (3) the effects of underfill and overfill. The secondary objective of the experiment is to obtain quantitative data for axial groove and porous wick heat pipes in a microgravity environment for comparison with the following: (1) analytical models; (2) ground test data; and (3) existing flight data. Derived from text

N93-28723*# Strategic Defense Initiative Organization, Washington, DC.
STRV1-b FLIGHT EXPERIMENT **c18**
In NASA, Washington, NASA/DOD Flight Experiments Technical Interchange Meeting Proceedings 1992 7 p Prepared in cooperation with Defence Research Agency, London, England and Phillips Lab., Hanscom AFB, MA (For primary document see N93-28699 11-12)
Avail: CASI HC A02/MF A10

The Space Technology Research Vehicle (STRV-1b) is discussed. The STRV-1b is a small (100 watt) satellite flown by the British Defense Research Agency (DRA). The mission goal is to fly new and emerging space technologies at a more reasonable cost in a short-term timeframe. The STRV-1b's orbit can be described as a geosynchronous transfer orbit (GTO) with a perigee of 200 km, an apogee of 36,000 km (geosynchronous earth orbit (GEO)), and a period of 10.5 hours. The Phillips Laboratory plans to use the STRV-1b to test up to 20 advanced experimental photovoltaic cells. The discussion is presented in vugraph form. Derived from text

N93-28724*# Phillips Lab., Hanscom AFB, MA.
NEP SPACE TEST PROGRAM OBJECTIVE **c20**
In NASA, Washington, NASA/DOD Flight Experiments Technical Interchange Meeting Proceedings 1992 9 p (For primary document see N93-28699 11-12)
Avail: CASI HC A02/MF A10

The objective of the Nuclear Electric Propulsion (NEP) space test program is to launch an NEP satellite powered by the Russion Topaz 2 reactor by Dec. 1995. The primary goals of the NEP space test program are as follows: (1) demonstrate the feasibility of launching a space nuclear power system; (2) demonstrate and orbit adjust capability using NEP; (3) evaluate

the in-orbit performance of the Topaz 2 reactor and selected electric thrusters; and (4) measure, analyze, and model the NEP self-induced environment. The discussion is presented in vugraph form.
Derived from text

N93-28725*# Alabama Univ., Huntsville.
MEASUREMENT OF THE RELATIVE AND ABSOLUTE MICROGRAVITY ENVIRONMENT OF SPACE PLATFORMS, RECENT FLIGHT RESULTS, AND DETERMINATION OF THE SPATIAL MICROGRAVITY FIELD c29
J. A. Bijvoet, J. Randorf, D. R. Wingo, and J. R. Blakely *In* NASA, Washington, NASA/DOD Flight Experiments Technical Interchange Meeting Proceedings 1992 19 p (For primary document see N93-28699 11-12)
Avail: CASI HC A03/MF A10

Microgravity material processing in space, such as crystal growth, requires specific and accurate knowledge of the very low frequency, very low level microgravity. This means knowledge of absolute microgravity levels. Most acceleration measurement systems for space platforms only measure 'microvibrations,' the measurement of the absolute microgravity level being severely corrupted by bias errors, temperature hysteresis, nonlinearity by-products, and bias changes due to launch vibrations. An advanced system was developed incorporating a fixed 3-axis acceleration measurement system with improved signal conditioning and Invertible Accelerometers for absolute measurements. The higher sensitivity channels have lower frequency low pass filtering to meet crystal growers demands for recording of low level/low frequency disturbances. Also included is a pre-flight bias adjustment feature. Author (revised)

N93-28726*# National Aeronautics and Space Administration. Goddard Space Flight Center, Greenbelt, MD.
ENVIRONMENTAL VERIFICATION EXPERIMENT FOR THE EXPLORER PLATFORM (EVEEP) c18
Bonnie Norris and Chris Lorentson *In* NASA, Washington, NASA/DOD Flight Experiments Technical Interchange Meeting Proceedings 1992 14 p (For primary document see N93-28699 11-12)
Avail: CASI HC A03/MF A10

Satellites and long-life spacecraft require effective contamination control measures to ensure data accuracy and maintain overall system performance margins. Satellite and spacecraft contamination can occur from either molecular or particulate matter. Some of the sources of the molecular species are as follows: mass loss from nonmetallic materials; venting of confined spacecraft or experiment volumes; exhaust effluents from attitude control systems; integration and test activities; and improper cleaning of surfaces. Some of the sources of particulates are as follows: leaks or purges which condense upon vacuum exposure; abrasion of movable surfaces; and micrometeoroid impacts. The Environmental Verification Experiment for the Explorer Platform (EVEEP) was designed to investigate the following aspects of spacecraft contamination control: materials selection; contamination modeling of existing designs; and thermal vacuum testing of a spacecraft with contamination monitors. Derived from text

N93-28727*# National Aeronautics and Space Administration. Goddard Space Flight Center, Greenbelt, MD.
RETURN FLUX EXPERIMENT c18
June L. Tveekrem *In* NASA, Washington, NASA/DOD Flight Experiments Technical Interchange Meeting Proceedings 1992 15 p (For primary document see N93-28699 11-12)
Avail: CASI HC A03/MF A10

All spacecraft emit molecules via outgassing, thruster plumes, vents, etc. The return flux is the portion of those molecules that scatter from the ambient atmosphere and return to the spacecraft. Return flux allows critical spacecraft surfaces to become contaminated even when there is no direct line of sight between the contamination source and the critical surface. Data from the Long Duration Exposure Facility (LDEF) show that contamination of LDEF surfaces could not have come entirely from direct flux. The data suggest significant return flux. Several computer models have been developed to simulate return flux, but the predictions have never been verified in orbit. Large uncertainties in predictions lead to overly conservative spacecraft designs. The purpose of the REturn FLux EXperiment (REFLEX) is to fly a controlled experiment that can be directly compared with predictions from several models. Derived from text

N93-28728*# National Aeronautics and Space Administration. Goddard Space Flight Center, Greenbelt, MD.
SPACECRAFT GLOW AND THE EISG/SKIRT EXPERIMENT c46
Gary R. Swenson (Lockheed Missiles and Space Co., Palo Alto, CA.), Mark Ahmadjian (Phillips Lab., Hanscom AFB, MA.), Don Jennings, and Jim Visentine (National Aeronautics and Space Administration. Lyndon B. Johnson Space Center, Houston, TX.) *In* NASA, Washington, NASA/DOD Flight Experiments Technical Interchange Meeting Proceedings 1992 41 p (For primary document see N93-28699 11-12)
Avail: CASI HC A03/MF A10

The objective of this experiment is to develop an understanding of the physical processes leading to spacecraft glow phenomena. The emphasis is to be on surface temperature and altitude effects. A complete understanding of the phenomena could be used to accomplish the following: (1) characterize optical instrument backgrounds; (2) provide guidelines for thermal insulations; (3) characterize material selection for flight optics and associated spacecraft; and (4) affect flight-operation altitude selection for relevant missions. Author (revised)

N93-28729*# AZ Technology, Huntsville, AL.
THE OPTICAL PROPERTIES MONITOR (OPM): A MULTIPURPOSE OPTICAL LABORATORY IN SPACE c14
Donald R. Wilkes *In* NASA, Washington, NASA/DOD Flight Experiments Technical Interchange Meeting Proceedings 1992 23 p (For primary document see N93-28699 11-12)
Avail: CASI HC A03/MF A10

The Optical Properties Monitor (OPM) is a multifunction in-flight laboratory for in-situ optical studies of materials. Many independent and related studies can be carried out on EURECA with the OPM instruments to address the experiment objectives. Test samples will be selected to address the materials and issues of the greatest interest to NASA, ESA, DoD, and the aerospace community. The objective of the OPM program is to study the effects of the space environment, both natural and induced, on optical, thermal control, solar array, and other materials. Derived from text

N93-28730*# National Aeronautics and Space Administration. Lyndon B. Johnson Space Center, Houston, TX.
RADIATION MONITORING EQUIPMENT DOSIMETER EXPERIMENT c19
Kenneth A. Hardy (Aerospace Medical Research Labs., Brooks AFB, TX.), Michael J. Golightly, and William Quam (EG and G Energy Measurements, Inc., Goleta, CA.) *In* NASA, Washington, NASA/DOD Flight Experiments Technical Interchange Meeting Proceedings 1992 33 p (For primary document see N93-28699 11-12)
Avail: CASI HC A03/MF A10

Spacecraft crews risk exposure to relatively high levels of ionizing radiation. This radiation may come from charged particles trapped in the Earth's magnetic fields, charged particles released by solar flare activity, galactic cosmic radiation, energetic photons and neutrons generated by interaction of these primary radiations with spacecraft and crew, and man-made sources (e.g., nuclear power generators). As missions are directed to higher radiation level orbits, viz., higher altitudes and inclinations, longer durations, and increased flight frequency, radiation exposure could well become a major factor for crew stay time and career lengths. To more accurately define the radiological exposure and risk to the crew, real-time radiation monitoring instrumentation, which is capable of identifying and measuring the various radiation components, must be flown. This presentation describes a radiation dosimeter instrument which was successfully flown on the Space Shuttle, the RME-3. Author

N93-28731*# National Aeronautics and Space Administration. Langley Research Center, Hampton, VA.
THE ORBITER EXPERIMENTS (OEX) PROGRAM
David A. Throckmorton *In* NASA, Washington, NASA/DOD Flight Experiments Technical Interchange Meeting Proceedings 1992 38 p (For primary document see N93-28699 11-12)
Avail: CASI HC A03/MF A10

The objective of the Orbiter Experiments (OEX) program is to obtain research quality flight data for the augmentation and advancement of space transportation technologies. This includes the validation and advancement of analytical theories and of ground-test methods and techniques. The following topics are discussed: aerothermodynamic design tool development

and validation; the freestream environment; trajectory reconstruction; atmospheric reconstruction; the Shuttle Entry Air Data System (SEADS); the Shuttle Upper Atmosphere Mass Spectrometer (SUMS); and aerodynamic forces and moments. The discussion is presented in vugraph form.
Derived from text

N93-28732*# Jet Propulsion Lab., California Inst. of Tech., Pasadena.
LOW EARTH ORBITAL MISSION ABOARD THE SPACE TEST EXPERIMENTS PLATFORM (STEP-3)
David E. Brinza *In* NASA, Washington, NASA/DOD Flight Experiments Technical Interchange Meeting Proceedings 1992 15 p Prepared for Physical Sciences, Inc., Andover, MA (For primary document see N93-28699 11-12)
Avail: CASI HC A03/MF A10

A discussion of the Space Active Modular Materials Experiments (SAMMES) is presented in vugraph form. The discussion is divided into three sections: (1) a description of SAMMES; (2) a SAMMES/STEP-3 mission overview; and (3) SAMMES follow on efforts. The SAMMES/STEP-3 mission objectives are as follows: assess LEO space environmental effects on SDIO materials; quantify orbital and local environments; and demonstrate the modular experiment concept. Derived from text

N93-28733*# Army Strategic Defense Command, Huntsville, AL.
NPB CESIUM SPACE EXPERIMENT c73
George M. Parsons, III *In* NASA, Washington, NASA/DOD Flight Experiments Technical Interchange Meeting Proceedings 1992 11 p (For primary document see N93-28699 11-12)
Avail: CASI HC A03/MF A10

Neutral Particle Beam (NPB) weapons systems are planned to perform the ballistic missile defense functions of nuclear weapon/decoy discrimination and warhead kill at appropriate energy levels and ion currents. Negatively charged ions are produced in a specialized ion source and focused into a high quality particle beam. NPB linear accelerators accelerate and steer the negatively charged ions using electric and magnetic fields. After acceleration and steering the neutralizer system strips away extra electrons from ions to form the electrically neutral particle beam. The neutral beam then travels through space to the target unaffected by the Earth's magnetic fields. Continuing technological advances have greatly reduced the size and weight of NPB accelerator systems. Ion current production has been enhanced by over 100 percent with the intermittent addition of cesium at the NPB ion source device. This increase in current is essential to attain the most light weight, compact NPB platforms and minimize expensive launch costs. Addition of cesium into the ion source has been identified by the NPB community as the highest priority risk reduction space experiment necessary prior to planned NPB accelerator experiments and later weapons systems. The NPB Cesium Space Experiment is planned to successfully demonstrate controlled cesium introduction and vaporization into a simulated ion source chamber. Microgravity effects on the cesium deposition will be studied as will the effects of small amounts of cesium on high voltage accelerator components that might be susceptible to electrical insulator break downs. The experiment design will simulate as closely as possible the environment, physical and operational characteristics of the actual NPB ion source. Author

N93-28734*# National Aeronautics and Space Administration. Lewis Research Center, Cleveland, OH.
TRANSFER ORBIT PLASMA INTERACTION EXPERIMENT (TROPIX)
Mark Hickman *In* NASA, Washington, NASA/DOD Flight Experiments Technical Interchange Meeting Proceedings 1992 12 p (For primary document see N93-28699 11-12)
Avail: CASI HC A03/MF A10

Viewgraphs on the Transfer Orbit Plasma Interaction Experiment (TROPIX) are presented. Objectives of this research are (1) to map the charged particles in Earth's magnetosphere from LEO to GEO at high inclinations; (2) to measure plasma current collection and resulting shifts in vehicle electrical potential from LEO to GEO across range of orbital inclinations; (3) to study spacecraft interaction with plasma environment using solar electric propulsion (SEP) thrusters as plasma contactors; (4) to measure array degradation over mission duration; (5) to evaluate the potential of various microelectronics, spacecraft components, and instruments for future space missions; and (6) to demonstrate SEP technology applied to a flight vehicle. An overview of TROPIX is presented. CASI

N93-28735*# Institute for Space Science and Technology, Inc., Gainesville, FL.
ORBITAL DEBRIS ENVIRONMENT MONITOR (ODEM) c18
John P. Oliver *In* NASA, Washington, NASA/DOD Flight Experiments Technical Interchange Meeting Proceedings 1992 16 p (For primary document see N93-28699 11-12)
Avail: CASI HC A03/MF A10

Viewgraphs on orbital debris environmental monitor (ODEM) are presented. Topics covered include: Long Duration Exposure Facility (LDEF); interplanetary dust experiment; orbital debris clouds; mapping and modeling of orbital debris clouds; and solar maximum mission spacecraft. CASI

N93-28736*# Boeing Defense and Space Group, Kent, WA.
NASA IN-STEP: PERMEABLE MEMBRANE EXPERIMENT c25
In NASA, Washington, NASA/DOD Flight Experiments Technical Interchange Meeting Proceedings 1992 31 p (For primary document see N93-28699 11-12)
Avail: CASI HC A03/MF A10

Viewgraphs on the Permeable Membrane Experiment are presented. An experiment overview is given. The Membrane Phase Separation Experiment, Membrane Diffusion Interference Experiment, and Membrane Wetting Experiment are described. Finally, summary and conclusions are discussed. CASI

N93-28737*# Life Systems, Inc., Cleveland, OH.
ELECTROLYSIS PERFORMANCE IMPROVEMENT AND VALIDATION EXPERIMENT c25
Franz H. Schubert *In* NASA, Washington, NASA/DOD Flight Experiments Technical Interchange Meeting Proceedings 1992 27 p (For primary document see N93-28699 11-12)
Avail: CASI HC A03/MF A10

Viewgraphs on electrolysis performance improvement and validation experiment are presented. Topics covered include: water electrolysis: an ever increasing need/role for space missions; static feed electrolysis (SFE) technology: a concept developed for space applications; experiment objectives: why test in microgravity environment; and experiment description: approach, hardware description, test sequence and schedule. CASI

N93-28738*# California Univ., Los Angeles. Dept. of Mechanical, Aerospace and Nuclear Engineering.
RISK-BASED SPACECRAFT FIRE SAFETY EXPERIMENTS c18
G. Apostolakis, I. Catton, F. Issacci, T. Paulos, S. Jones, K. Paxton, and M. Paul *In* NASA, Washington, NASA/DOD Flight Experiments Technical Interchange Meeting Proceedings 1992 11 p Sponsored by NASA. Lewis Research Center (For primary document see N93-28699 11-12)
Avail: CASI HC A03/MF A10

Viewgraphs on risk-based spacecraft fire safety experiments are presented. Spacecraft fire risk can never be reduced to a zero probability. Probabilistic risk assessment is a tool to reduce risk to an acceptable level. CASI

N93-28739*# Aerospace Medical Research Labs., Wright-Patterson AFB, OH. Visual Display Systems Branch.
ARMSTRONG LABORATORY SPACE VISUAL FUNCTION TESTER PROGRAM c52
Melvin R. ONeal, H. Lee Task, and Gerald A. Gleason *In* NASA, Washington, NASA/DOD Flight Experiments Technical Interchange Meeting Proceedings 1992 6 p (For primary document see N93-28699 11-12)
Avail: CASI HC A02/MF A10

Viewgraphs on space visual function tester program are presented. Many astronauts and cosmonauts have commented on apparent changes in their vision while on-orbit. Comments have included descriptions of earth features and objects that would suggest enhanced distance visual acuity. In contrast, some cosmonaut observations suggest a slight loss in their object discrimination during initial space flight. Astronauts have also mentioned a decreased near vision capability that did not recover to normal until return to earth. Duntley space vision experiment, USSR space vision experiments, and visual function testers are described. Derived from text

N93-28740*# Aerospace Medical Research Labs., Wright-Patterson AFB, OH. Visual Display Systems Branch.

EFFECT OF MICROGRAVITY ON SEVERAL VISUAL FUNCTIONS DURING STS SHUTTLE MISSIONS: VISUAL FUNCTION TESTER-MODEL 1 (VFT-1) **c52**

Melvin R. ONeal, H. Lee Task, and Louis V. Genco *In* NASA, Washington, NASA/DOD Flight Experiments Technical Interchange Meeting Proceedings 1992 14 p (For primary document see N93-28699 11-12)
Avail: CASI HC A03/MF A10

Viewgraphs on the effect of microgravity on several visual functions during STS shuttle missions are presented. The purpose, methods, results, and discussion are discussed. The visual function tester model 1 is used. CASI

N93-28741*# Aerospace Medical Research Labs., Wright-Patterson AFB, OH. Visual Display Systems Branch.

EFFECT OF MICROGRAVITY ON VISUAL CONTRAST THRESHOLD DURING STS SHUTTLE MISSIONS: VISUAL FUNCTION TESTER-MODEL 2 (VFT-2) **c52**

Melvin R. ONeal, H. Lee Task, and Louis V. Genco *In* NASA, Washington, NASA/DOD Flight Experiments Technical Interchange Meeting Proceedings 1992 6 p (For primary document see N93-28699 11-12)
Avail: CASI HC A02/MF A10

Viewgraphs on effect of microgravity on visual contrast threshold during STS shuttle missions are presented. The purpose, methods, and results are discussed. The visual function tester model 2 is used. CASI

N93-28742*# Aerospace Medical Research Labs., Wright-Patterson AFB, OH. Visual Display Systems Branch.

EFFECT OF MICROGRAVITY ON THE VISUAL NEAR POINT: VISUAL FUNCTION TESTER-MODEL 4 (VFT-4) **c52**

Gerald A. Gleason, H. Lee Task, and Melvin R. ONeal *In* NASA, Washington, NASA/DOD Flight Experiments Technical Interchange Meeting Proceedings 1992 8 p (For primary document see N93-28699 11-12)
Avail: CASI HC A02/MF A10

Viewgraphs on effect of microgravity on the visual near point are presented. Background, problem, objectives, approach, benefits, and status are discussed. The visual function tester model 4 is used. CASI

N93-28743*# Alabama Univ., Huntsville. Dept. of Chemistry.

THE EMULSION CHAMBER TECHNOLOGY EXPERIMENT **c35**

John C. Gregory *In* NASA, Washington, NASA/DOD Flight Experiments Technical Interchange Meeting Proceedings 1992 16 p (For primary document see N93-28699 11-12)
Avail: CASI HC A03/MF A10

Photographic emulsion has the unique property of recording tracks of ionizing particles with a spatial precision of 1 micron, while also being capable of deployment over detector areas of square meters or 10's of square meters. Detectors are passive, their cost to fly in Space is a fraction of that of instruments of similar collecting. A major problem in their continued use has been the labor intensiveness of data retrieval by traditional microscope methods. Two factors changing the acceptability of emulsion technology in space are the astronomical costs of flying large electronic instruments such as ionization calorimeters in Space, and the power and low cost of computers, a small revolution in the laboratory microscope data-taking. Our group at UAH made measurements of the high energy composition and spectra of cosmic rays. The Marshall group has also specialized in space radiation dosimetry. Ionization calorimeters, using alternating layers of lead and photographic emulsion, to measure particle energies up to 10(exp 15) eV were developed. Ten balloon flights were performed with them. No such calorimeters have ever flown in orbit. In the ECT program, a small emulsion chamber was developed and will be flown on the Shuttle mission OAST-2 to resolve the principal technological questions concerning space exposures. These include assessments of: (1) pre-flight and orbital exposure to background radiation, including both self-shielding and secondary particle generation; the practical limit to exposure time in space can then be determined; (2) dynamics of stack to optimize design for launch and weightlessness; and (3) thermal and vacuum constraints on emulsion performance. All these effects are cumulative and affect our ability to perform scientific measurements but cannot be adequately predicted by available methods. Author (revised)

N93-29063# Technische Univ., Berlin (Germany). Fachbereich Verkehrswesen.

ANALYSIS OF ORBITAL SYSTEM LOGISTICS IN THE CIS-LUNAR SPACE WITH PARTICULAR CONSIDERATION OF LIFE CYCLE COSTS Ph.D. Thesis [ANALYSE DER LOGISTIK VON ORBITALSYSTEMEN IM CIS-LUNAREN RAUM UNTER BESONDERER BERUECKSICHTIGUNG DER LEBENSZYKLUSKOSTEN]

Stephanos Melissopoulos Feb. 1992 160 p In GERMAN
(ETN-93-93484) Avail: CASI HC A08/MF A02

An attempt to define and analyze the concept of 'logistics of space operation centers' in an infrastructure scenario is presented. A logistics system was designed, which is strongly linked to the transportation system used. A narrow relation between operations in a space operation center and the transport model considered was established. Typical space transportation system designs were adapted and integrated in the logistics/life cycle cost model. A space operation center was conceived from general equations for calculation of module masses of rockets and from the NEPTUN booster project. A simulation model with a mass model, operation model and life cycle cost model was developed for evaluation of life cycle costs of a space operation center. Calculation results give reference costs for exploitation of orbital stations and requirements on space operation center service achievements. These results allow a relation between operations at space operation centers and transportation systems in an orbital infrastructure to be established from a logistic point of view. A sensitivity analysis shows that input parameters must be carefully chosen, because a minimal variation can very strongly modify the results. ESA

N93-30133*# National Aeronautics and Space Administration, Washington, DC.

PAYLOAD FLIGHT ASSIGNMENTS. NASA MIXED FLEET

Norman Starkey Apr. 1993 97 p
(NASA-TM-108255; NAS 1.15:108255) Avail: CASI HC A05/MF A02

This mixed fleet manifest, which serves as the baseline for planning purposes, includes payload flight assignments for the Space Shuttle through FY 1995 and NASA expendable launch vehicle (EVL) missions through FY 1999. The FY 1996-1999 Shuttle manifest planning is omitted pending Space Station redesign. Also included in this document are a list of previous flights, payload requests, and payload/acronyms. CASI

N93-31034*# Boeing Defense and Space Group, Huntsville, AL. Advanced Civil Space Systems.

SPACE TRANSFER CONCEPTS AND ANALYSES FOR EXPLORATION MISSIONS, PHASE 3 Final Report

Gordon R. Woodcock Jun. 1993 347 p
(Contract NAS8-37857)
(NASA-CR-192584; NAS 1.26:192584; D615-10062-2) Avail: CASI HC A15/MF A03

This report covers the third phase of a broad-scoped and systematic study of space transfer concepts for human lunar and Mars missions. The study addressed issues that were raised during Phase 2, developed generic Mars missions profile analysis data, and conducted preliminary analysis of the Mars in-space transportation requirements and implementation from Stafford Committee Synthesis Report. The major effort of the study was the development of the first Lunar Outpost (FLO) baseline which evolved from the Space Station Freedom Hab Module. Modifications for the First Lunar Outpost were made to meet mission requirements and technology advancements. Author (revised)

N93-28770*# Jet Propulsion Lab., California Inst. of Tech., Pasadena.

CLEMENTINE 2: A DOUBLE ASTEROID FLYBY AND IMPACTOR MISSION Abstract Only

R. J. Boain *In* Lunar and Planetary Inst., Workshop on Advanced Technologies for Planetary Instruments, Part 1 1993 p 3 (For primary document see N93-28764 11-91)
Avail: CASI HC A01/MF A01

N93-29725*# California Univ., Los Angeles.

THE 1990/1991 PROJECT SUMMARIES

In Universities Space Research Association, Houston, Proceedings of the Seventh Annual Summer Conference. NASA/USRA: University Advanced Design Program 1991 p 113-116 (For primary document see N93-29712

11-01)
Avail: CASI HC A01/MF A03

N93-29730*# Georgia Inst. for Research, Atlanta.
THE 1990-1991 PROJECT SUMMARIES
In Universities Space Research Association, Houston, Proceedings of the Seventh Annual Summer Conference. NASA/USRA: University Advanced Design Program 1991 p 143-144 (For primary document see N93-29712 11-01)
Avail: CASI HC A01/MF A03

N93-29731*# Georgia Inst. for Research, Atlanta.
THE 1990-1991 PROJECT SUMMARIES
In Universities Space Research Association, Houston, Proceedings of the Seventh Annual Summer Conference. NASA/USRA: University Advanced Design Program 1991 p 145-148 (For primary document see N93-29712 11-01)
Avail: CASI HC A01/MF A03

N93-29742*# Minnesota Univ., Minneapolis.
SINGLE-STAGE MARS MISSION
In Universities Space Research Association, Houston, Proceedings of the Seventh Annual Summer Conference. NASA/USRA: University Advanced Design Program 1991 p 219-226 (For primary document see N93-29712 11-01)
Avail: CASI HC A02/MF A03

N93-29745*# Old Dominion Univ., Norfolk, VA.
FROM ORBITAL DEBRIS CAPTURE SYSTEMS THROUGH INTERNAL COMBUSTION ENGINES ON MARS
In Universities Space Research Association, Houston, Proceedings of the Seventh Annual Summer Conference. NASA/USRA: University Advanced Design Program 1991 p 241-248 (For primary document see N93-29712 11-01)
Avail: CASI HC A02/MF A03

N93-29755*# Texas Univ., Austin.
THE 1990-1991 PROJECT SUMMARIES
In Universities Space Research Association, Houston, Proceedings of the Seventh Annual Summer Conference. NASA/USRA: University Advanced Design Program 1991 p 301-303 (For primary document see N93-29712 11-01)
Avail: CASI HC A01/MF A03

N93-29894# Smith System Engineering Ltd., Guildford (England).
EVOLUTION OR REVOLUTION: THE CATCH 22 OF TACSATS
C. J. Elliott *In* AGARD, TacSats for Surveillance Verification and C3I Feb. 1993 7 p Prepared in cooperation with Smith Associates Ltd., Guildford, England (For primary document see N93-29892 11-32)
Copyright Avail: CASI HC A02/MF A03

N93-29908# Defense Advanced Research Projects Agency, Arlington, VA. Advanced Systems Technology Office.
AN OVERVIEW OF DARPA'S ADVANCED SPACE TECHNOLOGY PROGRAM
E. Nicastri and J. Dodd (Aerospace Corp., Washington, DC.) *In* AGARD, TacSats for Surveillance Verification and C3I Feb. 1993 11 p (For primary document see N93-29892 11-32)
Copyright Avail: CASI HC A03/MF A03

13 ASTRODYNAMICS

Includes powered and free-flight trajectories; and orbital and launching dynamics.

N93-28558*# Dynetics, Inc., Huntsville, AL.
MINIMUM HAMILTONIAN ASCENT TRAJECTORY EVALUATION (MASTRE) PROGRAM (UPDATE TO AUTOMATIC FLIGHT TRAJECTORY DESIGN, PERFORMANCE PREDICTION, AND VEHICLE SIZING FOR SUPPORT OF SHUTTLE AND SHUTTLE DERIVED VEHICLES) USERS MANUAL
J. T. Lyons and William R. Borchers Apr. 1993 238 p
(Contract NAS8-38981)
(NASA-CR-192556; NAS 1.26:192556; TR-93-042) Avail: CASI HC A11/MF A03

Documentation for the User Interface Program for the Minimum Hamiltonian Ascent Trajectory Evaluation (MASTRE) is provided. The User Interface Program is a separate software package designed to ease the user input requirements when using the MASTRE Trajectory Program. This document supplements documentation on the MASTRE Program that consists of the MASTRE Engineering Manual and the MASTRE Programmers Guide. The User Interface Program provides a series of menus and tables using the VAX Screen Management Guideline (SMG) software. These menus and tables allow the user to modify the MASTRE Program input without the need for learning the various program dependent mnemonics. In addition, the User Interface Program allows the user to modify and/or review additional input Namelist and data files, to build and review command files, to formulate and calculate mass properties related data, and to have a plotting capability. Author (revised)

N93-29475# Naval Postgraduate School, Monterey, CA.
AUTOMATED SATELLITE IMAGE NAVIGATION M.S. Thesis
Robert M. Bassett Dec. 1992 89 p
(AD-A262868) Avail: CASI HC A05/MF A01

The automated satellite image navigation method (Auto-Avian) developed and tested by Spaulding (1990) at the Naval Postgraduate School is investigated. The Auto-Avian method replaced the manual procedure of selecting Ground Control Points (GCP's) with an autocorrelation process that utilizes the World Vector Shoreline (WVS) provided by the Defense Mapping Agency (DMA) as a string of GCP's to rectify satellite images. The automatic cross-correlation of binary reference (WVS) and search (image) windows eliminated the subjective error associated with the manual selection of GCP's and produced accuracies comparable to the manual method. The scope of Spaulding's (1990) research was expanded. The worldwide application of the Auto-Avian method was demonstrated in three world regions (eastern North Pacific Ocean, eastern North Atlantic Ocean, and Persian Gulf). Using five case studies, the performance of the Auto-Avian method on 'less than optimum' images (i.e., islands, coastlines affected by lateral distortion and/or cloud cover) was investigated. DTIC

N93-29652*# TRW, Inc., Houston, TX.
REFERENCE EQUATIONS OF MOTION FOR AUTOMATIC RENDEZVOUS AND CAPTURE
David M. Henderson Apr. 1992 40 p
(Contract NAS9-17900)
(NASA-CR-185676; NAS 1.26:185676; TRW-91:J431.1-182) Avail: CASI HC A03/MF A01

The analysis presented in this paper defines the reference coordinate frames, equations of motion, and control parameters necessary to model the relative motion and attitude of spacecraft in close proximity with another space system during the Automatic Rendezvous and Capture phase of an on-orbit operation. The relative docking port target position vector and the attitude control matrix are defined based upon an arbitrary spacecraft design. These translation and rotation control parameters could be used to drive the error signal input to the vehicle flight control system. Measurements for these control parameters would become the bases for an autopilot or feedback control system (FCS) design for a specific spacecraft. Author (revised)

N93-30135*# National Aeronautics and Space Administration. Lyndon B. Johnson Space Center, Houston, TX.
THE +VBAR BREAKOUT DURING APPROACH TO SPACE STATION FREEDOM
Scott D. Dunham Jun. 1993 37 p
(NASA-TM-104772; S-724; NAS 1.15:104772) Avail: CASI HC A03/MF A01

A set of burn profiles was developed to provide bounding jet firing histories for a +vbar breakout during approaches to Space Station Freedom. The delta-v sequences were designed to place the Orbiter on a safe trajectory under worst case conditions and to try to minimize plume impingement on Space Station Freedom structure. Author (revised)

N93-30582# Technische Univ., Berlin (Germany). Fachbereich Verkehrswesen.

DOUBLE SWINGBY AT EARTH-MOON FOR INCREASE OF EXCESS VELOCITY Ph.D. Thesis [DOPPEL-SWING-BY AM ERDMOND ZUR STEIGERUNG DER EXZESSGESCHWINDIGKEIT]

Kok Kiong Ong 1992 111 p In GERMAN
(ETN-93-94177) Avail: CASI HC A06/MF A02

The minimal start velocity for leaving the Earth-Moon system is analytically determined in the framework of the three body problem (spaceprobe, Earth, and Moon). The patched conic method for precise trajectory calculation is presented. Space probe, Earth, and Moon were considered as point objects and motion differential equations were solved with Jacobi integral and Hill curves. Numerical integration was carried out with Runge-Kutta method. Start velocity for the free flight Moon swing by was iteratively ascertained. A sensitivity analysis was conducted for estimating accuracy of space vector of Moon and velocity vector of spaceprobe components. ESA

N93-29589*# Jet Propulsion Lab., California Inst. of Tech., Pasadena.

PRECISE TRACKING OF THE MAGELLAN AND PIONEER VENUS ORBITERS BY SAME-BEAM INTERFEROMETRY. PART 2: ORBIT DETERMINATION ANALYSIS

W. M. Folkner, J. S. Border, S. Nandi, and K. S. Zukor *In its* The Telecommunications and Data Acquisition Report 15 May 1993 p 22-36 (For primary document see N93-29586 11-32)
(RTOP 310-10-63-88-01)
Avail: CASI HC A03/MF A03

14 GROUND SUPPORT SYSTEMS AND FACILITIES (SPACE)

Includes launch complexes, research and production facilities; ground support equipment, e.g., mobile transporters; and simulators.

For related information see also *09 Research and Support Facilities (Air).*

N93-28696*# National Aeronautics and Space Administration. Lewis Research Center, Cleveland, OH.

A NEW FACILITY FOR ADVANCED ROCKET PROPULSION RESEARCH

Joseph G. Zoeckler, James M. Green (Sverdrup Technology, Inc., Brook Park, OH.), and Paul Raitano Jun. 1993 10 p Presented at the 29th Joint Propulsion Conference and Exhibit, Monterey, CA, 28-30 Jun. 1993; cosponsored by AIAA, SAE, ASME, and ASEE
(RTOP 506-42-72)
(NASA-TM-106193; E-7899; NAS 1.15:106193; AIAA Paper 93-1859)
Avail: CASI HC A02/MF A01

A new test facility was constructed at the NASA Lewis Research Center Rocket Laboratory for the purpose of conducting rocket propulsion research at up to 8.9 kN (2000 lbf) thrust, using liquid oxygen and gaseous hydrogen propellants. A laser room adjacent to the test cell provides access to the rocket engine for advanced laser diagnostic systems. The size and location of the test cell provide the ability to conduct large amounts of testing in short time periods, with rapid turnover between programs. These capabilities make the new test facility an important asset for basic and applied rocket propulsion research. Author (revised)

N93-28938# Air Force Inst. of Tech., Wright-Patterson AFB, OH.

ESTIMATING TEST RANGE CAPACITY M.S. Thesis

Paul A. McDaniel 5 Mar. 1993 160 p Limited Reproducibility: More than 20% of this document may be affected by microfiche quality
(AD-A262493; AFIT/GST/ENS/93M-08) Avail: Issuing Activity (Defense Technical Information Center (DTIC)

The main focus of this thesis effort was to develop a means to estimate the capacity of the test range complex at Eglin AFB, Florida. For the purposes of this study, test range capacity was defined as the maximum number of missions, of a given set, that could possibly be supported by range resources on any given day. In trying to determine this number, the complexities of the overall multi-resource constrained scheduling problem dictated a more practical approach be taken in modeling the allocation process of range resources to test missions. Therefore, a series of three single-resource, 0-1 integer programming models depicting the allocation of Test Wing aircraft, radars, and range area resources were developed to produce an upper bound estimate of the range capacity for a given set of missions. In actual testing, the Range Area Allocation Model produced some poor results and therefore, cannot be used in its present form. However, both the Aircraft and Radar Models appear to produce legitimate upper bounds on range capacity in all cases. Nevertheless, to insure the goodness of these two models, further testing is recommended. In addition, a single model depicting the allocation of these two resources and possibly several other, should be developed in order to better estimate range capacity. DTIC

N93-28707*# McDonnell-Douglas Space Systems Co., Huntington Beach, CA.

CSI-STAR: A LOW-COST CSI ORBITAL TESTBED

D. Edberg *In* NASA, Washington, NASA/DOD Flight Experiments Technical Interchange Meeting Proceedings 1992 26 p (For primary document see N93-28699 11-12)
Avail: CASI HC A03/MF A10

N93-28729*# AZ Technology, Huntsville, AL.

THE OPTICAL PROPERTIES MONITOR (OPM): A MULTIPURPOSE OPTICAL LABORATORY IN SPACE

Donald R. Wilkes *In* NASA, Washington, NASA/DOD Flight Experiments Technical Interchange Meeting Proceedings 1992 23 p (For primary document see N93-28699 11-12)
Avail: CASI HC A03/MF A10

N93-29723*# Alabama Univ., Huntsville.

A HIGH-TEMPERATURE FURNACE FOR APPLICATIONS IN MICROGRAVITY

In Universities Space Research Association, Houston, Proceedings of the Seventh Annual Summer Conference. NASA/USRA: University Advanced Design Program 1991 p 97-104 (For primary document see N93-29712 11-01)
Avail: CASI HC A02/MF A03

N93-29729*# Florida Agricultural and Mechanical Univ., Tallahassee.

LUNAR LANDER GROUND SUPPORT SYSTEM

In Universities Space Research Association, Houston, Proceedings of the Seventh Annual Summer Conference. NASA/USRA: University Advanced Design Program 1991 p 139-142 (For primary document see N93-29712 11-01)
Avail: CASI HC A01/MF A03

15 LAUNCH VEHICLES AND SPACE VEHICLES

Includes boosters; operating problems of launch/space vehicle systems; and reusable vehicles.

For related information see also *20 Spacecraft Propulsion and Power.*

N93-28468# Air Force Inst. of Tech., Wright-Patterson AFB, OH. School of Engineering.

AUTOMATING THE SATELLITE RANGE SCHEDULING PROCESS M.S. Thesis

Timothy D. Gooley Mar. 1993 233 p
(AD-A262601; AFIT/GOR/ENS/93M-06) Avail: CASI HC A11/MF A03

Satellite range scheduling is a complex problem that involves scheduling satellite supports in which a satellite and a specific remote tracking station are assigned a time window during which they communicate with each other. As the number and complexity of satellite supports continue to increase, more pressure is placed on the current manual system to efficiently generate a schedule. The objective of this research was to develop a methodology that will automate the generation of the initial 24 hour schedule. The goal of the algorithm developed was to schedule as many conflict free supports as possible. A two phased approach was developed to schedule the supports. The first phase scheduled as many low altitude satellite supports as possible, while the second phase scheduled as many additional high altitude satellite supports as possible. For both phases, schedule generation and schedule improvement algorithms were developed.

The schedule generation algorithms are a mixed integer program linking procedure and an insertion procedure. The schedule improvement algorithms are a two satellite interchange procedure and a three satellite interchange procedure. A schedule was generated for six representative data sets with encouraging results. At least 91% of all satellite support requests were scheduled for each day. These results were comparable to results of the current range schedulers and a previous automation study. Based on the results reported, the methodology presented in this research effort seems to be a valid approach for automating the initial 24 hour schedule. DTIC

N93-29394# Army Research Lab., Aberdeen Proving Ground, MD.
TWO-DIMENSIONAL MODEL FOR CURRENT AND HEAT TRANSPORT IN SOLID-ARMATURE RAILGUNS Final Report, Oct. 1991 - Sep. 1992
John D. Powell, David J. Walbert, and Alexander E. Zielinski Feb. 1993 34 p
(AD-A262014; ARL-TR-74) Avail: CASI HC A03/MF A01

A numerical model is developed for solving the equations which predict current and heat transport in a solid-armature railgun. The model is two dimensional and fully time dependent. Some preliminary calculations are carried out for a 'U-shaped' armature similar to that currently under investigation in the ARDEC small and cannon-caliber railgun programs. The most extensive calculations are for a situation in which the projectile is started at rest and accelerated to about 500 m/s in a time of about 1 ms. Results of the calculations can be used to infer, for example, where melting in the armature is most likely to occur and where the electromagnetic fields are largest. For comparison, calculations are also presented for a situation in which the projectile is held fixed. Some discussion of future efforts is given, with particular emphasis on describing how the model might be used to guide the design of armatures, or provide input for other types of calculations relating to electromagnetic guns. DTIC

N93-29752*# Texas Univ., Austin.
SPACELY'S ROCKETS: PERSONNEL LAUNCH SYSTEM/FAMILY OF HEAVY LIFT LAUNCH VEHICLES
In Universities Space Research Association, Houston, Proceedings of the Seventh Annual Summer Conference. NASA/USRA: University Advanced Design Program 1991 p 291-293 (For primary document see N93-29712 11-01)
Avail: CASI HC A01/MF A03

N93-29759*# Washington Univ., Seattle.
ANTARES: A LOW COST MODULAR LAUNCH VEHICLE FOR THE FUTURE
In Universities Space Research Association, Houston, Proceedings of the Seventh Annual Summer Conference. NASA/USRA: University Advanced Design Program 1991 p 317-328 (For primary document see N93-29712 11-01)
Avail: CASI HC A03/MF A03

N93-29903# Aerospace Corp., Los Angeles, CA.
LAUNCH VEHICLES FOR LIGHTWEIGHT TACSAT DEPLOYMENT
Chester L. Whitehair and Malcolm G. Wolfe *In* AGARD, TacSats for Surveillance Verification and C3I Feb. 1993 17 p (For primary document see N93-29892 11-32)
Copyright Avail: CASI HC A03/MF A03

16 SPACE TRANSPORTATION

Includes passenger and cargo space transportation, e.g., shuttle operations; and space rescue techniques.

For related information see also *03 Air Transportation and Safety* and *18 Spacecraft Design, Testing and Performance.* For space suits see *54 Man/System Technology and Life Support.*

N93-28487# Aerospace Corp., El Segundo, CA. Space Launch Operations.
SPACE TRANSPORTATION ANALYSIS AND DESIGN (REISSUE A)
R. Hartunian, B. Moss, M. G. Wolfe, J. Statsinger, and L. Forrest 17 Feb. 1993 99 p Supersedes TOR-92(2464)-1, AD-A251036
(Contract F04701-88-C-0089)
(AD-A262752; TOR-92(2464)-1-A; XC-SMC) Avail: CASI HC A05/MF A02

The intent of this TOR is to provide a guide to the processes and technical considerations involved in the selection of a launch vehicle for a given satellite mission, the integration of the satellite with the launch vehicle, and the many elements required to derive life-cycle costs of viable launch system candidates. As such, the document is expected to be of interest to satellite mission planners for preliminary assessments of launch vehicle candidate and of general use to experienced specialists and new engineers in both satellites and launch vehicle sectors. Sufficient quantitative data, orbital and vehicle performance formulae, environmental data, and references have been provided to allow preliminary, first-order assessments which should suffice at the very early planning stages. As the planning process matures, the satellite planners are urged to get the much higher fidelity data on both technical and cost information required for programmatic decisions from the appropriate launch vehicle system program offices (SPOs). DTIC

N93-29136*# National Aeronautics and Space Administration. John F. Kennedy Space Center, Cocoa Beach, FL.
DEBRIS/ICE/TPS ASSESSMENT AND INTEGRATED PHOTOGRAPHIC ANALYSIS FOR SHUTTLE MISSION STS-55 Final Report, 22 Mar. - 7 May 1993
Gregory N. Katnik, Barry C. Bowen, and J. Bradley Davis May 1993 136 p Original contains color illustrations
(NASA-TM-107559; NAS 1.15:107559) Avail: CASI HC A07/MF A02; 53 functional color pages

A Debris/Ice/TPS assessment and integrated photographic analysis was conducted for Shuttle mission STS-55. Debris inspections of the flight elements and launch pad were performed before and after launch. Ice/Frost conditions on the External Tank were assessed by the use of computer programs, nomographs, and infrared scanner data during cryogenic loading of the vehicle followed by on-pad visual inspection. High speed photography was analyzed after launch to identify ice/debris sources and evaluate potential vehicle damage and/or in-flight anomalies. This report documents the debris/ice/TPS conditions and integrated photographic analysis of Shuttle mission STS-55, and the resulting effect on the Space Shuttle Program. Author

N93-29215*# Rockwell International Corp., Downey, CA. Space Systems Div.
STRATEGIC AVIONICS TECHNOLOGY DEFINITION STUDIES. SUBTASK 3-1A: ELECTRICAL ACTUATION (ELA) SYSTEMS
Ben T. F. Lum, Charles Pond, and William Dermott 30 Jun. 1993 154 p
(Contract NAS9-18880)
(NASA-CR-193237; NAS 1.26:193237; SSD93D0354) Avail: CASI HC A08/MF A02

This interim report presents the preliminary results of an electrical actuation (ELA) system study (subtask TA3-1A) to support the NASA strategic avionics technology definition studies. The final report of this ELA study is scheduled for September 30, 1993. The topics are presented in viewgraph form and include the following ELA technology demonstration testing; ELA system baseline; power and energy requirements for shuttle effector systems; power efficiency and losses of ELA effector systems; and power and energy requirements for ELA power sources. Derived from text

N93-29387*# White Sands Test Facility, Las Cruces, NM.
APU DIAPHRAGM TESTING. TEST PLAN
Richard Shelley (Lockheed Engineering and Management Services Co., Inc., Las Cruces, NM.) 14 Jan. 1992 14 p Sponsored by NASA. Johnson Space Center
(NASA-TM-108251; TP-WSTF-682; NAS 1.15:108251) Avail: CASI HC A03/MF A01

Auxiliary Power Unit (APU) fuel (hydrazine) tanks have had to be removed from the Columbia Shuttle (OV-102) because they have been in service for 11 years, which is the limit of their useful life. As part of an effort to determine whether the useful life of the fuel tanks can be extended, examination of the ethylene propylene rubber (EPR) diaphragm and the metal from one of the APU tanks is required. The JSC Propulsion and Power Division has requested White Sands Test Facility (WSTF) to examine the EPR diaphragm thoroughly and the metal casing generally from one

tank. The objective is to examine the EPR diaphragm for signs of degradation that may limit the life of its function in the APU propellant tank. The metal casing will also be examined for signs of surface corrosion.
Author (revised)

N93-29501*# National Aeronautics and Space Administration. Lyndon B. Johnson Space Center, Houston, TX.
APU DIAPHRAGM TESTING
Richard Shelley (Lockheed Engineering and Sciences Co., Houston, TX.) and William L. Ross, Sr. (Lockheed Engineering and Sciences Co., Houston, TX.) 1 Mar. 1993 107 p Original contains color illustrations
(NASA-TM-108254; NAS 1.15:108254; TR-682-001) Avail: CASI HC A06/MF A02; 29 functional color pages

The Auxiliary Power Unit (APU) fuel (hydrazine) tanks were removed from the Columbia Shuttle during major modification of the vehicle, because of long-term hydrazine compatibility concerns. The three tanks had been in service for 11 years. As part of an effort to determine whether the useful life of the fuel tanks can be extended, examination of the ethylene propylene rubber (EPR) diaphragm and the metal casing from one of the APU tanks was required. NASA Johnson Space Center Propulsion and Power Division requested the NASA Johnson Space Center White Sands Test Facility to examine the EPR diaphragm for signs of degradation that might limit the life of its function in the APU tank and to examine the metal casing for signs of surface corrosion. No appreciable degradation of the EPR diaphragm was noted. A decrease in the tensile properties was found, but tensile failure is considered unlikely because the metal casing constrains the diaphragm, preventing it from elongating more than a few percent. The titanium casing showed no evidence of surface corrosion.
Author (revised)

N93-30617*# Thiokol Corp., Brigham City, UT. Space Operations.
POSTFLIGHT HARDWARE EVALUATION 360T025 (RSRM-25, STS-46) Final Report
Ferral Morgan Mar. 1993 32 p
(Contract NAS8-38100)
(NASA-CR-192562; NAS 1.26:192562; TWR-60699) Avail: CASI HC A03/MF A01

The final report for the Clearfield disassembly evaluation and a continuation of the KSC postflight assessment for the 360T025 (STS-46) Redesign Solid Rocket Motor (RSRM) flight set is presented. All observed hardware conditions were documented on PFOR's and are included in Appendices A through C. Appendices D and E contain the measurements and safety factor data for the nozzle and insulation components. Along with the KSC Ten-Day Postflight Hardware Evaluation Report (TWR-60687), a summary of the 360T025 hardware evaluation is provided. The as-flown hardware configuration is documented in TWR-60470. Disassembly evaluation photograph numbers are logged in TWA-1986. The 360T025 flight set disassembly evaluations described were performed at the RSRM Refurbishment Facility in Clearfield, Utah. The final factory joint demate occurred on 16 Mar. 1993. Detailed evaluations were performed in accordance with the Clearfield PEEP, TWR-50051, Revision A. All observations were compared against limits that are also defined in the PEEP. These limits outline the criteria for categorizing the observations as acceptable, reportable, or critical. Hardware conditions that were unexpected and/or determined to be reportable or critical were evaluated by the applicable CPT and tracked through the PFAR system. Author (revised)

N93-30618*# Thiokol Corp., Brigham City, UT. Space Operations.
POSTFLIGHT HARDWARE EVALUATION 360T025 (RSRM-25, STS-46). APPENDIX A: INSULATION PFORs Final Report
Mar. 1993 15 p
(Contract NAS8-38100)
(NASA-CR-192563; NAS 1.26:192563; TWR-60699-App-A) Avail: CASI HC A03/MF A01

The final Postflight Hardware Evaluation Report 360T025, Appendix A is presented. Insulation Postflight Observation Records (PFOR's) are provided. Postfire insulation, nozzle insert throat diameter measurements, segment internal insulation condition, and segment liner pattern are addressed.
CASI

N93-30619*# Thiokol Corp., Brigham City, UT. Space Operations.
POSTFLIGHT HARDWARE EVALUATION 360T025 (RSRM-25, STS-46). APPENDIX B: CASE, SEALS, AND JOINTS PFORs Final Report
Mar. 1993 93 p
(Contract NAS8-38100)
(NASA-CR-192564; NAS 1.26:192564; TWR-60699-App-B) Avail: CASI HC A05/MF A01

The final Postflight Hardware Evaluation Report 360T025, Appendix B is presented. The Postflight Observation Record (PFOR) for case, seals, and joints are included.
CASI

N93-30620*# Thiokol Corp., Brigham City, UT. Space Operations.
POSTFLIGHT HARDWARE EVALUATION 360T025 (RSRM-25, STS-46). APPENDIX C: NOZZLE PFORs Final Report
Mar. 1993 75 p
(Contract NAS8-38100)
(NASA-CR-192565; NAS 1.26:192565; TWR-60699-App-C) Avail: CASI HC A04/MF A01

The final Postflight Hardware Evaluation Report 360T025, Appendix C is presented. The Postflight Observation Records (PFOR's) for nozzles is provided.
CASI

N93-30621*# Thiokol Corp., Brigham City, UT. Space Operations.
POSTFLIGHT HARDWARE EVALUATION 360T025 (RSRM-25, STS-46). APPENDIX E: INSULATION POSTFIRE DATA Final Report
Mar. 1993 33 p
(Contract NAS8-38100)
(NASA-CR-192566; NAS 1.26:192566; TWR-60699-App-E) Avail: CASI HC A03/MF A01

The final Postflight Hardware Evaluation Report 360T025, Appendix E is presented. The insulation postfire data is included. Insulation performance is addressed.
CASI

N93-30881# Institute for Defense Analyses, Alexandria, VA.
A REPRESENTATIVE SURVEY OF US SPACE SYSTEMS AND METHODS FOR ESTIMATING THEIR COSTS Final Report, Apr. 1991 - Nov. 1992
J. R. Nelson, James Bui, Mitchell S. Robinson, Jennifer A. Titus, and Stephen K. Welman Nov. 1992 185 p
(AD-A264159; IDA-D-1182; IDA/HQ-92-41994; AD-E501645) Avail: CASI HC A09/MF A02

The purpose of this project was to expand and enhance IDA's capabilities to estimate the future acquisition costs and schedules of space systems. This study accumulated information on launch systems, manned space systems, and interplanetary systems from NASA. Cost and schedule information was collected on representative programs, estimating methods, and supporting databases. The results of the effort include this document, which summarizes costs and schedules of representative space systems along with cost-estimating methods currently being applied, and also a library of over 500 documents that describe technical, schedule, and cost characteristics of U.S. space activities during the past 40 years. Preliminary findings of this study have been applied to estimate the costs of manned access to space.
DTIC

N93-31033*# Ensco, Inc., Melbourne, FL.
SHUTTLE LANDING FACILITY CLOUD COVER STUDY: CLIMATOLOGICAL ANALYSIS AND TWO TENTHS CLOUD COVER RULE EVALUATION
Michael K. Atchison, Robin Schumann, Greg Taylor, John Warburton, Mark Wheeler, and Ann Yersavich May 1993 199 p
(Contract NAS10-11844)
(NASA-CR-193016; NAS 1.26:193016; Rept-93-001) Avail: CASI HC A09/MF A03

The two-tenths cloud cover rule in effect for all End Of Mission (EOM) STS landings at the Kennedy Space Center (KSC) states: 'for scattered cloud layers below 10,000 feet, cloud cover must be observed to be less than or equal to 0.2 at the de-orbit burn go/no-go decision time (approximately 90 minutes before landing time)'. This rule was designed to protect against a ceiling (below 10,000 feet) developing unexpectedly within the next 90 minutes (i.e., after the de-orbit burn decision and before landing). The Applied Meteorological Unit (AMU) developed and analyzed a database of cloud cover amounts and weather conditions at the Shuttle

Landing Facility for a five-year (1986-1990) period. The data indicate the best time to land the shuttle at KSC is during the summer while the worst time is during the winter. The analysis also shows the highest frequency of landing opportunities occurs for the 0100-0600 UTC and 1300-1600 UTC time periods. The worst time of the day to land a shuttle is near sunrise and during the afternoon. An evaluation of the two-tenths cloud cover rule for most data categorizations has shown that there is a significant difference in the proportions of weather violations one and two hours subsequent to initial conditions of 0.2 and 0.3 cloud cover. However, for May, Oct., 700 mb northerly wind category, 1500 UTC category, and 1600 UTC category there is some evidence that the 0.2 cloud cover rule may be overly conservative. This possibility requires further investigation. As a result of these analyses, the AMU developed nomograms to help the Spaceflight Meteorological Group (SMG) and the Cape Canaveral Forecast Facility (CCFF) forecast cloud cover for EOM and Return to Launch Site (RTLS) at KSC. Future work will include updating the two tenths database, further analysis of the data for several categorizations, and developing a proof of concept artificial neural network to provide forecast guidance of weather constraint violations for shuttle landings. Author (revised)

N93-29726*# University of Central Florida, Orlando.
DESIGN, BUILDING, AND TESTING OF THE POSTLANDING SYSTEMS FOR THE ASSURED CREW RETURN VEHICLE
Kenneth C. Hosterman and Loren A. Anderson *In* Universities Space Research Association, Houston, Proceedings of the Seventh Annual Summer Conference. NASA/USRA: University Advanced Design Program 1991 p 117-121 (For primary document see N93-29712 11-01)
Avail: CASI HC A01/MF A03

N93-29749*# Rensselaer Polytechnic Inst., Troy, NY.
THE LIGHTCRAFT PROJECT
Don G. Messitt and Leik N. Myrabo *In* Universities Space Research Association, Houston, Proceedings of the Seventh Annual Summer Conference. NASA/USRA: University Advanced Design Program 1991 p 275-280 (For primary document see N93-29712 11-01)
Avail: CASI HC A02/MF A03

17 SPACE COMM., SPACECRAFT COMM., COMMAND & TRACKING

Includes telemetry; space communications networks; astronavigation and guidance; and radio blackout.

For related information see also *04 Aircraft Communications and Navigation* and *32 Communications and Radar.*

N93-29195*# National Aeronautics and Space Administration. Lewis Research Center, Cleveland, OH.
SYSTEM OVERVIEW ON ELECTROMAGNETIC COMPENSATION FOR REFLECTOR ANTENNA SURFACE DISTORTION
R. J. Acosta, A. J. Zaman, and J. D. Terry Jun. 1993 10 p Presented at the 1993 IEEE AP-S International Symposium, Ann Arbor, MI, 27 Jun. - 2 Jul. 1993
(RTOP 579-50-00)
(NASA-TM-106217; E-7928; NAS 1.15:106217) Avail: CASI HC A02/MF A01

The system requirements and hardware implementation for electromagnetic compensation of antenna performance degradations due to thermal effects was investigated. Future commercial space communication antenna systems will utilize the 20/30 GHz frequency spectrum and support very narrow multiple beams (0.3 deg) over wide angle field of view (15-20 beamwidth). On the ground, portable and inexpensive very small aperture terminals (VSAT) for transmitting and receiving video, facsimile and data will be employed. These types of communication system puts a very stringent requirement on spacecraft antenna beam pointing stability (less than .01 deg), high gain (greater than 50 dB) and very lowside lobes (less than -25 dB). Thermal analysis performed on the advanced communication technology satellite (ACTS) has shown that the reflector surfaces, the mechanical supporting structures and metallic surfaces on the spacecraft body will distort due thermal effects from a varying solar flux. The antenna performance characteristics (e.g., pointing stability, gain, side lobe, etc.) will degrade due to thermal distortion in the reflector surface and supporting structures. Specifically, antenna RF radiation analysis has shown that pointing error is the most sensitive antenna performance parameter to thermal distortions. Other antenna parameters like peak gain, cross polarization level (beam isolation), and side lobe level will also degrade with thermal distortions. In order to restore pointing stability and in general antenna performance several compensation methods were proposed. In general these compensation methods can be classified as being either of mechanical or electromagnetic type. This paper will address only the later one. In this approach an adaptive phased array antenna feed is used to compensate for the antenna performance degradation. Extensive work has been devoted to demonstrate the feasibility of adaptive feed compensation on space communication antenna systems. This paper addresses the system requirements for such a system and identify candidate technologies (analog and digital) for possible hardware implementation. Author (revised)

N93-29306# RADEX, Inc., Bedford, MA.
SPREE INTERACTIVE DATA ANALYSIS TOOL (SIDAT)
C. J. Roth and N. A. Bonito 30 Oct. 1992 34 p
(AD-A262782; RXR-92101; PL-TR-92-2331; SR-6) Avail: CASI HC A03/MF A01

The SPREE Interactive Data Analysis Tool (SIDAT) is a collection of user-friendly display processes for performing real-time and postflight analysis of data from the Shuttle Potential and Return Electron Experiment (SPREE). SPREE was used to study the effects of a potential being induced between a tethered satellite and the Shuttle by the motion of the conductive tether across the Earth's magnetic field lines. Full-color raster graphics and text displays were used for the data presentation, utilizing the X11 and XView X Window System libraries. The SIDAT data display processes allowed the SPREE data and other related data to be viewed in a variety of formats simultaneously. During flight, SIDAT displayed the current or previously captured real-time SPREE telemetry data. SIDAT postflight operations allow the user to perform rapid data survey for analysis. The user specified the times for data survey, displaying either the captured real-time SPREE telemetry data or the SPREE data archived by the Flight Data Recorders. DTIC

N93-29884*# Communications Satellite Corp., Clarksburg, MD.
ON-BOARD B-ISDN FAST PACKET SWITCHING ARCHITECTURES. PHASE 2: DEVELOPMENT. PROOF-OF-CONCEPT ARCHITECTURE DEFINITION REPORT Final Report
Dong-Jye Shyy and Wayne Redman Jun. 1993 126 p
(Contract NASw-4711; RTOP 506-72-21)
(NASA-CR-191151; E-7931; NAS 1.26:191151) Avail: CASI HC A07/MF A02

For the next-generation packet switched communications satellite system with onboard processing and spot-beam operation, a reliable onboard fast packet switch is essential to route packets from different uplink beams to different downlink beams. The rapid emergence of point-to-point services such as video distribution, and the large demand for video conference, distributed data processing, and network management makes the multicast function essential to a fast packet switch (FPS). The satellite's inherent broadcast features gives the satellite network an advantage over the terrestrial network in providing multicast services. This report evaluates alternate multicast FPS architectures for onboard baseband switching applications and selects a candidate for subsequent breadboard development. Architecture evaluation and selection will be based on the study performed in phase 1, 'Onboard B-ISDN Fast Packet Switching Architectures', and other switch architectures which have become commercially available as large scale integration (LSI) devices. Author (revised)

18 SPACECRAFT DESIGN, TESTING AND PERFORMANCE

Includes satellites; space platforms; space stations; spacecraft systems and components such as thermal and environmental controls; and attitude controls.

For life support systems see *54 Man/System Technology and Life Support.* For related information see also *05 Aircraft Design, Testing and Performance, 39 Structural Mechanics,* and *16 Space Transportation.*

N93-28629 California Univ., San Diego.
THE DYNAMICS AND CONTROL OF SPACE TETHERS Ph.D. Thesis
Kurt Voigt Crowder 1992 228 p
Avail: Univ. Microfilms Order No. DA9307210

The dynamics of swinging and spinning space tethered systems are examined, the effects of rapidly spinning tethered systems on their orbit are determined, the phase space positions of unstable and chaotic motion are located, and methods for controlling space tethered systems by manipulating the length and tension of the tether are studied. The dynamics of a system connected by a massless tether are studied. Instabilities are sought for motions corresponding to large librations and rotations in the plane of the orbit. Out of plane instabilities are found for both swinging and spinning motions. The equation for out of plane motion takes the form of Hill's equation, which is well approximated by Mathieu's equation. Instabilities are found from stability charts. The predicted locations of instabilities was checked by integrating the equations of motion numerically and projecting the resulting curves onto one plane to obtain Lissajous plots. Massive tethers are considered. The normal modes of departures from a straight tether were determined. The stability of these modes was analyzed using Mathieu charts. Orbital perturbations are considered. A rapidly spinning tether was assumed. Lagrange's Planetary Equations were solved to find that the size, shape, and inclination of the orbit were unaffected by the tethered system, however, the nodal angle and the argument of periapse were found to precess. A 416km tether could be used to cancel the regression of nodes due to J(sub 2) effects. This method could be used to stabilize orbits with arbitrary inclinations, and could prove useful for many projects, including, for example, a tether mediated low earth orbit to moon transport system. Control laws for spin up, spin down, and reel in are obtained. A method for suppressing out of plane oscillations through parametric damping is also demonstrated. The control methods derived are applied to a numerical model for a massive tether. Most of the control methods stimulate oscillations in the shape of the tether. A method for parametrically damping these oscillations was demonstrated with modest success. The need exists for improved methods to suppress the shape oscillations. Author (revised)

N93-29014# Joint Publications Research Service, Arlington, VA.
JPRS REPORT: SCIENCE AND TECHNOLOGY. CENTRAL EURASIA: ENGINEERING AND EQUIPMENT
29 Jan. 1993 46 p Transl. into ENGLISH from various Russian articles
(JPRS-UEQ-93-001) Avail: CASI HC A03/MF A01

Translated abstracts cover the following areas: space technology, optics, nuclear and non-nuclear energy technology, mechanics, and industrial technology. Some specific topics include efficiency of jet descending module braking methods in planetary atmospheres; examples of evaluating metrological characteristics of solid state sensors for subsatellite systems; on analyzing weak signal detection characteristics in laser ranging tasks; elastic wave precession in rotating body; effect of rotating body on point mass or why planets do not fall on sun; on one solution approximation of kinematic motion equations of rigid body; on spatial collision of rigid bodies; on eigenmode dynamics of rotating axisymmetric elastic body; on theory of elastoplastic superconducting shell reliability; stability of sectional composite cylindrical shell under external pressure; and mathematical modeling of straining dynamics of multifold solar battery during deployment. CASI

N93-29031# DYNACS Engineering Co., Inc., Houston, TX.
SPACE STATION: ORBITER BERTHING
J. Mapar, Y. C. Lin, and M. Kilby 27 Jan. 1992 33 p
Avail: CASI HC A03/MF A01

The berthing/docking maneuver is important for the construction and assembly of the Space Station Freedom (SSF). Berthing has a direct effect on the SSF assembly build up and SSF/Orbiter operations. The dynamics associated with the berthing activities potentially large impacts on the elements ans systems (both the Orbiter and SSF) throughout the assembly sequence. These dynamics will play a major role in the development of operational requirements that need to be identified and validated in order to assure total safety and maneuver execution during the SSF construction. The berthing/docking task will consider those assembly flights where the SSF has the control authority for the combined stack (currently MB-5) and beyond. The purpose of this task is to analyze the effects of berthing dynamics and their impacts on the maneuver and operational requirements. The task objectives are the following: (1) to develop the necessary analytical tool(s) and skills that will enable the verification and certification of berthing/docking for each assembly flight; (2) to perform detailed analyses of the berthing/docking maneuvers during the SSF assembly buildup in order to verify the viability of such maneuvers; and (3) to develop the operational requirements that affect such maneuvers and establish the operational boundaries and envelops for berthing/docking during assembly and mature operations. Various topics are presented in viewgraph form and include the following: analysis tools and capabilities; analysis results; and ongoing work. Derived from text

N93-29108*# Colorado Univ., Boulder. Center for Space Construction.
[SPACE CONSTRUCTION ACTIVITIES] Annual Report
1 Nov. 1991 69 p
(Grant NAGw-1388)
(NASA-CR-192690; NAS 1.26:192690) Avail: CASI HC A04/MF A01

The Center for Space Construction at the University of Colorado at Boulder was established in 1988 as a University Space Engineering Research Center. The mission of the Center is to conduct interdisciplinary engineering research which is critical to the construction of future space structures and systems and to educate students who will have the vision and technical skills to successfully lead future space construction activities. The research activities are currently organized around two central projects: Orbital Construction and Lunar Construction. Summaries of the research projects are included. For individual titles, see N93-29109 through N93-29122.

N93-29109*# Colorado Univ., Boulder.
INTERACTION DYNAMICS OF ON-ORBIT CONSTRUCTION
K. C. Park *In its* Space Construction Activities 1 Nov. 1991 p 3-7
(For primary document see N93-29108 11-18)
Avail: CASI HC A01/MF A01

Deployment and assembly of large structures in orbit is a critical technology to the overall problem of orbital construction. The attendant large configuration changes of structures will cause significant changes in the dynamic characteristics of the entire system, and perturbation to the orbital dynamics of the spacecraft from which the structures are deployed and/or assembled. To better design structures for deployment and assembly, and to better design controlled deployment/assembly processes, accurate modeling techniques are absolutely essential. The problem of modeling the dynamics of deploying and retrieving beam-like structures from a rotating base was addressed. A methodology for discrete modeling, and a computational procedure were developed. These results give us the capability of understanding and predicting the effects on the overall satellite motion of deploying flexible appendages. This is an initial step towards a general capability of treating axially moving three-dimensional beams. The interaction dynamics of the orbiter, its flexible manipulator, and the structures to be assembled/deployed, as a prerequisite in order to simulate incremental in-space structural construction processes are investigated. Preliminary results so obtained indicate that, as the inertia properties of the flexible large space structure under construction change during the space assembly/construction process, the interaction dynamics undergo significant changes in their characteristics, thus revealing the need for a variety of control strategies throughout construction. Author (revised)

N93-29110*# Colorado Univ., Boulder.
HYBRID CMS METHODS WITH MODEL REDUCTION FOR ASSEMBLY OF STRUCTURES
Charbel Farhat *In its* Space Construction Activities 1 Nov. 1991 p 8-9 (For primary document see N93-29108 11-18)
Avail: CASI HC A01/MF A01

Future on-orbit structures will be designed and built in several stages, each with specific control requirements. Therefore there must be a methodology which can predict the dynamic characteristics of the assembled structure, based on the dynamic characteristics of the subassemblies and their interfaces. The methodology developed by CSC to address this issue is Hybrid Component Mode Synthesis (HCMS). HCMS distinguishes itself from standard component mode synthesis algorithms in the following features: (1) it does not require the subcomponents to have displacement compatible models, which makes it ideal for analyzing the deployment of heterogeneous flexible multibody systems, (2) it incorporates a second-level model reduction scheme at the interface, which makes it much faster than other algorithms and therefore suitable for control purposes, and (3) it does answer specific questions such as 'how does the global fundamental frequency vary if I change the physical parameters of substructure k by a specified amount?'. Because it is based on an energy principle rather than displacement compatibility, this methodology can also help the designer to define an assembly process. Current and future efforts are devoted to applying the HCMS method to design and analyze docking and berthing procedures in orbital construction. Author (revised)

N93-29111*# Colorado Univ., Boulder.
CONTROLS OF INTERACTION DYNAMICS OF ORBITAL ASSEMBLY
Renjeng Su *In its* Space Construction Activities 1 Nov. 1991 p 10-15 (For primary document see N93-29108 11-18)
Avail: CASI HC A02/MF A01

Building structures and spacecraft in orbit will require technologies for positioning, docking/berthing, and joining orbital structures. A fundamental problem underlying the operation of docking and berthing is that of controlling the contact dynamics of mechanical structures actuated by active mechanisms such as robotic devices. Control systems must be designed to control these active mechanisms so that both the free space motions and contact motions are stable and satisfy specifications on position accuracy and bounds on contact forces. For the large orbital structures of the future, the problem of interactive dynamics and control is fundamentally different in several ways than it was for spacecraft docking in the past. First, future space structures must be treated as flexible structures - the operations of docking, berthing, and assembly will need to respect the vibrations of the structures. Second, the assembly of these structures will require multiple-point contact, rather than the essentially single-point positioning of conventional spacecraft docking. Third, some assembly operations require the subassemblies to be brought and held in contact so that successful joining can be accomplished. A preliminary study of contact stability and compliance control design has resulted in the development of an analytical method and a design method to analyze stability. The analytical method analyzes the problem of stability when an actively-controlled structure contacts a passive structure. This method makes it possible to accurately estimate the stiffness of the passive structures with which the contact motion will become unstable. The analytic results suggest that passivity is neither achievable in practice, nor necessary as a design concept. A contact control system need only be passive up to a certain frequency; beyond that frequency the system can be stabilized with sufficiently small gains. With this concept the Center developed a design methodology for achieving desired compliant contact motions. This design method is based on H-infinity norm optimization, which makes it possible to consider both driving point mechanical impedance and systems robustness to modeling uncertainty. A laboratory facility was set up to verify experimentally the analytical and design theory. Author (revised)

N93-29112*# Colorado Univ., Boulder.
CONTROLS FOR SPACE STRUCTURES
Mark Balas *In its* Space Construction Activities 1 Nov. 1991 p 16-19 (For primary document see N93-29108 11-18)
Avail: CASI HC A01/MF A01

Assembly and operation of large space structures (LSS) in orbit will require robot-assisted docking and berthing of partially-assembled structures. These operations require new solutions to the problems of controls. This is true because of large transient and persistent disturbances, controller-structure interaction with unmodeled modes, poorly known structure parameters, slow actuator/sensor dynamical behavior, and excitation of nonlinear structure vibrations during control and assembly. For on-orbit assembly, controllers must start with finite element models of LSS and adapt on line to the best operating points, without compromising stability. This is not easy to do, since there are often unmodeled dynamic interactions between the controller and the structure. The indirect adaptive controllers are based on parameter estimation. Due to the large number of modes in LSS, this approach leads to very high-order control schemes with consequent poor stability and performance. In contrast, direct model reference adaptive controllers operate to force the LSS to track the desirable behavior of a chosen model. These schemes produce simple control algorithms which are easy to implement on line. One problem with their use for LSS has been that the model must be the same dimension as the LSS - i.e., quite large. A control theory based on the command generator tracker (CGT) ideas of Sobel, Mabins, Kaufman and Wen, Balas to obtain very low-order models based on adaptive algorithms was developed. Closed-loop stability for both finite element models and distributed parameter models of LSS was proved. In addition, successful numerical simulations on several LSS databases were obtained. An adaptive controller based on our theory was also implemented on a flexible robotic manipulator at Martin Marietta Astronautics. Computation schemes for controller-structure interaction with unmodeled modes, the residual mode filters or RMF, were developed. The RMF theory was modified to compensate slow actuator/sensor dynamics. These new ideas are being applied to LSS simulations to demonstrate the ease with which one can incorporate slow actuator/sensor effects into our design. It was also shown that residual mode filter compensation can be modified for small nonlinearities to produce exponentially stable closed-loop control. A theory for disturbance accommodating controllers based on reduced order models of structures was developed, and stability results for these controllers in closed-loop with large-scale finite element models of structures were obtained. Author (revised)

N93-29113*# Colorado Univ., Boulder.
STRUCTURAL LOAD CONTROL DURING CONSTRUCTION
Martin M. Mikulas, Jr. *In its* Space Construction Activities 1 Nov. 1991 p 20-22 (For primary document see N93-29108 11-18)
Avail: CASI HC A01/MF A01

In the absence of gravitational pull, the major design considerations for large space structures are stiffness for controllability, and transient dynamic loadings (as opposed to the traditional static load associated with earth-based structures). Because of the absence of gravitational loading, space structures can be designed to be significantly lighter than their counterparts on Earth. For example, the Space Shuttle manipulator arm is capable of moving and positioning a 60,000 lb payload, yet weighs less than 1,000 lbs. A recent design for the Space Station which had a total weight of about 500,000 lbs. used a primary loadcarrying keel beam which weighed less than 10,000 lbs. For many large space structures designs it is quite common for the load-carrying structure to have a mass fraction on the order of one or two percent of the total spacecraft mass. This significant weight reduction for large space structures is commonly accompanied by very low natural frequencies. These low frequencies cause an unprecedented level of operational complexity for mission applications which require a high level of positioning and control accuracy. This control problem is currently the subject of considerable research directed towards reducing the flexibility problem. In addition, however, the small mass fraction typically results in structures which are quite unforgiving to inadvertent high loadings. In other words, the structures are 'fragile.' In order to deal with the fragility issue CSC developed a load-limiting concept for space truss structures. This concept is aimed at limiting the levels of load which can occur in a large space structure during the construction process as well as during subsequent operations. Currently, the approach for dealing with large loadings is to make the structure larger. The impact this has on construction is significant. The larger structures are more difficult to package in the launch vehicle, and in fact in some instances the concept must be changed from a deployable truss to an erectable truss to permit packaging. The new load-limiting concept is aimed at permitting the use in large space structures of smaller trusses with a high level of strength robustness, in order to simplify the construction process. To date several analyses conducted on the concept have demonstrated its feasibility, and an experiment is currently being designed to demonstrate its operation. Author

N93-29114*# Colorado Univ., Boulder.
SYSTEMS ENGINEERING STUDIES OF ON-ORBIT ASSEMBLY OPERATION
George W. Morgenthaler *In its* Space Construction Activities 1 Nov.

1991 p 23-26 (For primary document see N93-29108 11-18)
Avail: CASI HC A01/MF A01

While the practice of construction has a long history, the underlying theory of construction is relatively young. Very little has been documented as to techniques of logistic support, construction planning, construction scheduling, construction testing, and inspection. The lack of 'systems approaches' to construction processes is certainly one of the most serious roadblocks to the construction of space structures. System engineering research efforts at CSC are aimed at developing concepts and tools which contribute to a systems theory of space construction. The research is also aimed at providing means for trade-offs of design parameters for other research areas in CSC. Systems engineering activity at CSC has divided space construction into the areas of orbital assembly, lunar base construction, interplanetary transport vehicle construction, and Mars base construction. A brief summary of recent results is given. Several models for 'launch-on-time' were developed. Launch-on-time is a critical concept to the assembly of such Earth-orbiting structures as the Space Station Freedom, and to planetary orbiters such as the Mars transfer vehicle. CSC has developed a launch vehicle selection model which uses linear programming to find optimal combinations of launch vehicles of various sizes (Atlas, Titan, Shuttles, HLLV's) to support SEI missions. Recently, the Center developed a cost trade-off model for studying on orbit assembly logistics. With this model it was determined that the most effective size of the HLLV would be in the range of 120 to 200 metric tons to LEO, which is consistent with the choices of General Stafford's Synthesis Group Report. A second-generation Dynamic Construction Activities Model ('DYCAM') process model has been under development, based on our past results in interruptability and our initial DYCAM model. This second-generation model is built on the paradigm of knowledge-based expert systems. It is aimed at providing answers to two questions: (1) what are some necessary or sufficient conditions for judging conceptual designs of spacecraft?, and (2) can a methodology be formulated such that these conditions may be used to provide computer-aided tools for evaluating conceptual designs and planning for space assembly sequences? Early simulation results indicate that the DYCAM model has a clear ability to emulate and simulate human orbital construction processes. Author (revised)

N93-29115*# Colorado Univ., Boulder.
LUNAR REGOLITH DENSIFICATION **c91**
Hon-Yim Ko and Stein Sture *In its* Space Construction Activities 1 Nov. 1991 p 28-30 (For primary document see N93-29108 11-18)
Avail: CASI HC A01/MF A01

Core tube samples of the lunar regolith obtained during the Apollo missions showed a rapid increase in the density of the regolith with depth. Various hypotheses have been proposed for the possible cause of this phenomenon, including the densification of the loose regolith material by repeated shaking from the seismic tremors which have been found to occur at regular monthly intervals when the moon and earth are closest to one another. A test bed was designed to study regolith densification. This test bed uses Minnesota Lunar Simulant (MLS) to conduct shaking experiments in the geotechnical centrifuge with an inflight shake table system. By reproducing realistic in-situ regolith properties, the experiment also serves to test penetrator concepts. The shake table system was designed and used for simulation experiments to study effects of earthquakes on terrestrial soil structures. It is mounted on a 15 g-ton geotechnical centrifuge in which the self-weight induced stresses are replicated by testing an n-th scale model in a gravity field which is n times larger than Earth's gravity. A similar concept applies when dealing with lunar prototypes, where the gravity ratio required for proper simulation of lunar gravity effects is that between the centrifugal acceleration and the lunar gravity. Records of lunar seismic tremors, or moonquakes, were obtained. While these records are being prepared for use as the input data to drive the shake table system, records from the El Centro earthquake of 1940 are being used to perform preliminary tests, using a soil container which was previously used for earthquake studies. This container has a laminar construction, with the layers free to slide on each other, so that the soil motion during the simulated earthquake will not be constrained by the otherwise rigid boundaries. The soil model is prepared by pluviating the MLS from a hopper into the laminar container to a depth of 6 in. The container is mounted on the shake table and the centrifuge is operated to generate an acceleration of 10 times Earth's gravity or 60 times the lunar gravity, thus simulating a lunar regolith thickness of 30 ft. The shake table is then operated using the scaled 'moonquake' as the input motion. One or more model moonquakes are used in each experiment, after which the soil is analyzed for its density profile with depth. This is accomplished by removing from the soil bed a column of soil contained within a thin rubber sleeve which has been previously embedded vertically in the soil during pluviation. This column of soil is transferred to a gamma ray device, in which the gamma ray transmission transversely through the soil is measured and compared with standard calibration samples. In this manner, the density profile can be determined. Preliminary results to date are encouraging, and the Center plans to study the effects of duration of shaking, intensity of the shaking motion, and the frequency of the motion. Author (revised)

N93-29116*# Colorado Univ., Boulder.
REGOLITH-STRUCTURE MODELING **c91**
Hon-Yim Ko and Stein Sture *In its* Space Construction Activities 1 Nov. 1991 p 31-35 (For primary document see N93-29108 11-18)
Avail: CASI HC A01/MF A01

Early lunar missions have provided a basic understanding of the physical and strength properties of lunar regolith, which have been shown to differ from those of dry terrestrial granular soils. Lunar regolith is predominantly a fine sand of which nearly 40 percent can be characterized as silt with a particle size smaller than 100 micrometers. The top 10 to 20 cm of the regolith can be characterized as being in a loose to medium-loose state. The density of the regolith, however, rapidly increases below a depth of 20 cm. The highly irregular and angular shapes of the regolith particles tend to interlock and create relatively strong mechanical bonds that give the particulate mass substantial cohesive properties and smaller amounts of tensile strength properties. In addition, the friction angle of lunar regolith at medium to high densities is quite high and often exceeds 55 degrees. These known properties of lunar regolith have been matched in a terrestrially-manufactured analog known as Minnesota Lunar Simulant. A variety of experiments were conducted using this simulant to both verify existing information and generate new information on the physical and constitutive properties of lunar regolith. These experiments include maximum and minimum density determinations, specific mass of solids, grain-size distribution, conventional triaxial compression and extension, isotropic compression, one-dimensional compression, direct shear, and direct tension. Direct shear experiments were conducted under atmospheric and vacuum conditions. Results of the physical and strength experiments compare closely to results obtained from lunar missions. Results of simulant strength experiments performed in vacuum indicated no observable difference from results obtained in air. A test bed currently under study is one involving a regolith shield covering a first-generation human habitat module. It is understood that regolith in depths ranging from 3 to 5 meters is required for radiation shielding for habitation and workspace. The habitat module is treated as a rigid cylindrical tube with a smooth exterior. By making the cylinder rigid, a complex interaction problem is reduced to a situation where we can consider the support regolith and the shielding regolith as behaving independently of the structural properties of the cylindrical structure. Medium-dense lunar simulant was placed around a scaled model of the habitat module to provide a radiation shield. This embankment-type shield was constructed in relatively thin but fine layers by compacting, by mechanical vibratory means, layer upon layer of simulant placed adjacent to the horizontally-aligned cylinder. The slope angles were constructed at 55 degrees. The model described above was studied in a geotechnical centrifuge, which allows for the scaling of model dimensions to prototype dimensions by increasing the acceleration of gravity on the model. The deformation response can be scaled up to prototype dimensions to provide an assessment of the deformation patterns of the lunar structure. The actual process of local and/or global growth of instabilities or skip planes can also be observed. Author (revised)

N93-29117*# Colorado Univ., Boulder.
LUNAR REGOLITH PENETRATORS AND CUTTERS **c91**
Frank Barnes and Stein Sture *In its* Space Construction Activities 1 Nov. 1991 p 36-37 (For primary document see N93-29108 11-18)
Avail: CASI HC A01/MF A01

An apparatus was designed and built for conducting simulation experiments on cutting tool penetration in the centrifuge. This equipment is mounted on the laminar container which is used for the regolith densification study, so that the end product of the latter, i.e., a regolith bed with the proper density profile, can be used directly for the penetration tests. In this apparatus, an etching tool is suspended through a pulley system by the action of a double acting air cylinder. By adjusting the air pressure acting on each side of the cylinder, the net downward force acting on the tool can be controlled. The penetration of the tool is measured by an LVDT. This apparatus was proof-tested in the centrifuge and is ready for use in conjunction with the regolith densification experiments.

Author (revised)

N93-29118*# Colorado Univ., Boulder.

LUNAR CRANE SYSTEM c37

Martin M. Mikulas, Jr. *In its* Space Construction Activities 1 Nov. 1991 p 38-41 (For primary document see N93-29108 11-18)

Avail: CASI HC A01/MF A01

In many lunar construction scenarios, mechanical cranes in some form will be indispensible in moving large masses around with various degrees of fine positioning. While thorough experience exists in the use of terrestrial cranes new thinking is required about the design of cranes to be used in extraterrestrial construction. The primary driving force for this new thinking is the need to automate the crane system so that space cranes can be operated as telerobotic machines with a large number of automatic capabilities. This is true because in extraterrestrial construction human resources will need to be critically rationed. The design problems of mechanisms and control systems for a lunar crane must deal with at least two areas of performance. First, the automated crane must be capable of maneuvering a large mass, so that when the mass arrives at the target position there are only small vibrations. Secondly, any residue vibrations must be automatically damped out and a fine positioning must be achieved. For extraterrestrial use there are additional challenges to a crane design - for example, to design a crane system so that it can be transformed for other construction uses. This initial project in crane design does not address such additional issues, although they may be the subject of future CSC research. To date the Center has designed and analyzed many mechanisms. The fundamental problem of trade-offs between passively stabilizing the load and actively controlling the load by actuators was extensively studied. The capability of 3D dynamics modeling now exists for such studies. A scaled model of a lunar crane was set up and it has been most fruitful in providing basic understanding of lunar cranes. Due to an interesting scaling match-up, this scaled model exhibits the load vibration frequencies one would expect in the real lunar case. Using the analytical results achieved to date, a laboratory crane system is now being developed as a test bed for verifying a wide variety of mechanisms and control designs. Future development will be aimed at making the crane system a telerobotic test bed into which external sensors such as computer vision systems, and other small robotic devices such as CSC lunar rovers, will be integrated.

Author (revised)

N93-29119*# Colorado Univ., Boulder.

LUNAR ROVERS AND LOCAL POSITIONING SYSTEM c37

James Avery and Renjeng Su *In its* Space Construction Activities 1 Nov. 1991 p 42-45 (For primary document see N93-29108 11-18)

Avail: CASI HC A01/MF A01

Telerobotic rovers equipped with adequate actuators and sensors are clearly necessary for extraterrestrial construction. They will be employed as substitutes for humans, to perform jobs like surveying, sensing, signaling, manipulating, and the handling of small materials. Important design criteria for these rovers include versatility and robustness. They must be easily programmed and reprogrammed to perform a wide variety of different functions, and they must be robust so that construction work will not be jeopardized by parts failures. The key qualities and functions necessary for these rovers to achieve the required versatility and robustness are modularity, redundancy, and coordination. Three robotic rovers are being built by CSC as a test bed to implement the concepts of modularity and coordination. The specific goal of the design and construction of these robots is to demonstrate the software modularity and multirobot control algorithms required for the physical manipulation of constructible elements. Each rover consists of a transporter platform, bus manager, simple manipulator, and positioning receivers. These robots will be controlled from a central control console via a radio-frequency local area network (LAN). To date, one prototype transporter platform frame was built with batteries, motors, a prototype single-motor controller, and two prototype internal LAN boards. Software modules were developed in C language for monitor functions, i/o, and parallel port usage in each computer board. Also completed are the fabrication of half of the required number of computer boards, the procurement of 19.2 Kbaud RF modems for inter-robot communications, and the simulation of processing requirements for positioning receivers. In addition to the robotic platform, the fabrication of a local positioning system based on infrared signals is nearly completed. This positioning system will make the rovers into a moving reference system capable of performing site surveys. In addition, a four degree mechanical manipulator especially suited for coordinated teleoperation was conceptually designed and is currently being analyzed. This manipulator will be integrated into the rovers as their end effector. Twenty internal LAN cards fabricated by a commercial firm are being used, a prototype manipulator and a range finder for a positioning system were built, a prototype two-motor controller was designed, and one of the robots is performing its first telerobotic motion. In addition, the robots' internal LAN's were coordinated and tested, hardware design upgrades based on fabrication and fit experience were completed, and the positioning system is running. The rover system is able to perform simple tasks such as sensing and signaling; coordination systems which allow construction tasks to begin were established, and soon coordinated teams of robots in the laboratory will be able to manipulate common objects.

Author (revised)

N93-29120*# Colorado Univ., Boulder.

INDIGENOUS LUNAR CONSTRUCTION MATERIALS c31

Wayne P. Rogers and Stein Sture *In its* Space Construction Activities 1 Nov. 1991 p 46-50 (For primary document see N93-29108 11-18)

Avail: CASI HC A01/MF A01

The utilization of local resources for the construction and operation of a lunar base can significantly reduce the cost of transporting materials and supplies from Earth. The feasibility of processing lunar regolith to form construction materials and structural components is investigated. A preliminary review of potential processing methods such as sintering, hot-pressing, liquification, and cast basalt techniques, was completed. The processing method proposed is a variation on the cast basalt technique. It involves liquification of the regolith at 1200-1300 C, casting the liquid into a form, and controlled cooling. While the process temperature is higher than that for sintering or hot-pressing (1000-1100 C), this method is expected to yield a true engineering material with low variability in properties, high strength, and the potential to form large structural components. A scenario for this processing method was integrated with a design for a representative lunar base structure and potential construction techniques. The lunar shelter design is for a modular, segmented, pressurized, hemispherical dome which could serve as habitation and laboratory space. Based on this design, estimates of requirements for power, processing equipment, and construction equipment were made. This proposed combination of material processing method, structural design, and support requirements will help to establish the feasibility of lunar base construction using indigenous materials. Future work will refine the steps of the processing method. Specific areas where more information is needed are: furnace characteristics in vacuum; heat transfer during liquification; viscosity, pouring and forming behavior of molten regolith; design of high temperature forms; heat transfer during cooling; recrystallization of basalt; and refinement of estimates of elastic moduli, compressive and tensile strength, thermal expansion coefficient, thermal conductivity, and heat capacity. The preliminary design of the lunar shelter showed us that joining is a critical technology needed for building a structure from large segments. The problem of joining is important to the design of any structure that is not completely prefabricated. It is especially important when the structure is subjected to tensile loading by an internal pressure. For a lunar shelter constructed from large segments the joints between these large segments must be strong, and they must permit automated construction. With a cast basalt building material which is brittle, there is the additional problem of connecting the joint with the material and avoiding stress concentration that would cause failure. Thus, a well-defined project which we intend to pursue during this coming year is the design of joints for cast basalt structural elements.

Author (revised)

N93-29121*# Colorado Univ., Boulder.

SYSTEMS ENGINEERING STUDIES OF LUNAR BASE CONSTRUCTION c31

George W. Morgenthaler *In its* Space Construction Activities 1 Nov. 1991 p 51 (For primary document see N93-29108 11-18)

Avail: CASI HC A01/MF A01

Many ingenious concepts have been proposed for lunar base construction, but few systematic studies exist which relate time-consistent lunar base construction technologies and the choice of lunar base approach with the long-term SEI objectives - i.e., lunar indigenous base construction and Mars Exploration equipment development. To fill this gap, CSC has taken a two-pronged approach. First, the Center undertook basic geotechnical investigations of lunar soil, fabrication of a scale prototype of a lunar construction crane, a multi-robot construction team laboratory experiment, and a preliminary design of lunar base structures. Second, during Jun. and Jul. 1991 two lunar base construction systems engineering studies were accomplished - a 'near term lunar base' study, and a 'far-term lunar base' study. The goals of these studies were to define the major lunar base construction research problems in consistent technology/construction frameworks, and to define design requirements for construction equipment such as a lunar crane and a regolith mover. The 'near-term lunar base' study examined three different construction concepts for a lunar base comprised of pre-fabricated, pre-tested, Space Station Freedom-type modules, which would be covered with regolith shielding. Concept A used a lunar crane for unloading and transportation; concept B, a winch and cart; and concept C, a walker to move the modules from the landing site to the base site and assemble them. To evaluate the merits of each approach, calculations were made of mass efficiency measure, source mass, reliability, far-term base mass, Mars base mass, and base assembly time. The model thus established was also used to define the requirements for crane speed and regolith mover m(sup 3)/sec rates. A major problem addressed is how to 'mine' the regolith and stack it over the habitats as shielding. To identify when the cost of using indigenous lunar materials to construct the base exceeds the cost of development and delivery of the equipment for processing lunar materials, a study of construction of a candidate sintered regolith 'far term lunar base' was undertaken. A technique was devised for casting slabs of sintered (basaltic) regolith and assembling these into a hemispherical (or geodesic) dome. The major problem occurs with the inner liner. At 14.7 psi and 20 percent oxygen internal atmosphere, the entire structure is in tension, even with the regolith load. Also, another study has indicated that at 14.7 psi major resupply of air will be needed because of leakage, and astronauts may have to engage in extensive pre-breathing and post-breathing for extravehicular activity (EVA) tasks, thus detracting from useful mission work time. An alternative is to operate part of the base at, say, 5 psi and 70 percent oxygen, or to equip the astronauts with hard suits at 8.3 psi or greater. All of these choices directly influence base design and construction techniques. Author (revised)

N93-29122*# Colorado Univ., Boulder.

DESIGN OPTIMIZATION OF SPACE STRUCTURES

Carlos Felippa *In its* Space Construction Activities 1 Nov. 1991 p 52-54 (For primary document see N93-29108 11-18)
Avail: CASI HC A01/MF A01

The topology-shape-size optimization of space structures is investigated through Kikuchi's homogenization method. The method starts from a 'design domain block,' which is a region of space into which the structure is to materialize. This domain is initially filled with a finite element mesh, typically regular. Force and displacement boundary conditions corresponding to applied loads and supports are applied at specific points in the domain. An optimal structure is to be 'carved out' of the design under two conditions: (1) a cost function is to be minimized, and (2) equality or inequality constraints are to be satisfied. The 'carving' process is accomplished by letting microstructure holes develop and grow in elements during the optimization process. These holes have a rectangular shape in two dimensions and a cubical shape in three dimensions, and may also rotate with respect to the reference axes. The properties of the perforated element are obtained through an homogenization procedure. Once a hole reaches the volume of the element, that element effectively disappears. The project has two phases. In the first phase the method was implemented as the combination of two computer programs: a finite element module, and an optimization driver. In the second part, focus is on the application of this technique to planetary structures. The finite element part of the method was programmed for the two-dimensional case using four-node quadrilateral elements to cover the design domain. An element homogenization technique different from that of Kikuchi and coworkers was implemented. The optimization driver is based on an augmented Lagrangian optimizer, with the volume constraint treated as a Courant penalty function. The optimizer has to be especially tuned to this type of optimization because the number of design variables can reach into the thousands. The driver is presently under development. Author (revised)

N93-29134# Air Force Inst. of Tech., Wright-Patterson AFB, OH. Foreign Aerospace Science and Technology Center.

THE INFRARED MEASUREMENT FOR THE REENTRY-BODY-TRANSLATION

Congzhong Zhao 3 Apr. 1993 13 p Transl. into ENGLISH from Hongwai Yaniju (China), v. 7, no. 3, 1988 p 219-223
(AD-A263100; FASTC-ID(RS)T-0311-92) Avail: CASI HC A03/MF A01

The measured results of a reentry-body by a PbS radiometer are described in this paper. The standoff range of the radiometer reaches 100 km. Some features about the target are given. DTIC

N93-29221*# National Aeronautics and Space Administration. Lyndon B. Johnson Space Center, Houston, TX.

THERMAL CERTIFICATION TESTS OF ORBITER THERMAL PROTECTION SYSTEM TILES COATED WITH KSC COATING SLURRIES

James D. Milhoan, Vuong T. Pham, and William D. Sherborne Apr. 1993 90 p
(NASA-TM-104766; JSC-26067; S-716; NAS 1.15:104766) Avail: CASI HC A05/MF A01

Thermal tests of Orbiter thermal protection system (TPS) tiles, which were coated with borosilicate glass slurries fabricated at Kennedy Space Center (KSC), were performed in the Radiant Heat Test Facility and the Atmospheric Reentry Materials & Structures Evaluation Facility at Johnson Space Center to verify tile coating integrity after exposure to multiple entry simulation cycles in both radiant and convective heating environments. Eight high temperature reusable surface insulation (HRSI) tiles and six low temperature reusable surface insulation (LRSI) tiles were subjected to 25 cycles of radiant heat at peaked surface temperatures of 2300 F and 1200 F, respectively. For the LRSI tiles, an additional cycle at peaked surface temperature of 2100 F was performed. There was no coating crack on any of the HRSI specimens. However, there were eight small coating cracks (less than 2 inches long) on two of the six LRSI tiles on the 26th cycle. There was practically no change on the surface reflectivity, physical dimensions, or weight of any of the test specimens. There was no observable thermal-chemical degradation of the coating either. For the convective heat test, eight HRSI tiles were tested for five cycles at a surface temperature of 2300 F. There was no thermal-induced coating crack on any of the test specimens, almost no change on the surface reflectivity, and no observable thermal-chemical degradation with an exception of minor slumping of the coating under painted TPS identification numbers. The tests demonstrated that KSC's TPS slurries and coating processes meet the Orbiter's thermal specification requirements. Author (revised)

N93-29250# Sandia National Labs., Albuquerque, NM.

TESTING IN COMBINED DYNAMIC ENVIRONMENTS

J. D. Rogers 1993 7 p Presented at the 14th Aerospace Testing Seminar, Manhattan Beach, CA, 9-11 Mar. 1993
(Contract DE-AC04-76DP-00789)
(DE93-010679; SAND-93-0090C; CONF-930391-2) Avail: CASI HC A02/MF A01

The combined dynamic environments of vibration and linear acceleration are experienced by a large number of spacecraft components and other devices. Testing such devices has normally been a two step process in which independent vibration and centrifuge tests were performed. There is a concern that combined effects from these two dynamic environments could cause unexpected operational failures which were not predicted from either analysis or the independent tests. This paper describes the design and performance of a testing facility which combines vibration and centrifuge testing in a single operation. The test facility is called the VIBRAFUGE and utilizes Sandia National Laboratory's 29 foot underground centrifuge with an attached electrodynamic shaker. Also addressed are activities underway at SNL on development of a combined vibration and acoustic test facility. DOE

N93-29305# Maxwell Labs., Inc., La Jolla, CA. S-Cubed Div.
SPACECRAFT SURFACE CHARGING HANDBOOK Final Report, Oct. 1989 - Nov. 1992
V. A. Davis and L. W. Gordon Nov. 1992 352 p
(Contract F19628-89-C-0209)
(AD-A262778; AD-E201436; PL-TR-92-2232; SSS-DPR-91-12305) Avail: CASI HC A16/MF A03

Spacecraft surface charging is the buildup of net electric charge - and therefore electrostatic potential - on the external surfaces of a spacecraft due to incident particles with energies in the kilo-electron volt to tens of kilo-electron volts range. Geosynchronous and low-altitude, polar-orbiting spacecraft encounter charging environments. Surface charging causes problems for operational spacecraft. A primary effect is the occurrence of electronic switching anomalies which can be triggered by differential charging related discharges. The discharge induced transients can cause system failures and potentially, material damage. A more common anomaly is a phantom command, requiring intervention from the ground, and possibly resulting in loss of data and/or expendables, thus shortening the operational lifetime of the spacecraft. The work of the early 1980's provided designers with tools to reduce the number and severity of anomalies. Over the past 10 years, concern has arisen regarding charging on low-altitude, polar orbiting spacecraft due to auroral precipitation. Additionally, with the miniaturization of components, modern spacecraft are more vulnerable to EMI. This handbook was developed to address some of these concerns. The scientific issues of concern in spacecraft surface charging are reviewed, the components of a spacecraft surface charging control plan are described, and the techniques used to avoid spacecraft surface charging problems are summarized. Examples are provided of (1) calculational techniques to evaluate the expected effects of a spacecraft design, and (2) experimental techniques to test immunity to spacecraft surface charging effects. Information on the environments found in the geosynchronous and auroral region and the surface material properties that can affect surfaces are also given. DTIC

N93-29648# National Space Development Agency, Tokyo (Japan).
ADVANCED EARTH OBSERVING SATELLITE (ADEOS)
[1993] 27 p In ENGLISH and JAPANESE Original contains color illustrations
Avail: CASI HC A03/MF A01

The objectives of the ADEOS mission are as follows: to acquire data on worldwide environmental changes such as the green house effect, ozone layer depletion, tropical rain forest deforestation, and abnormal climatic conditions; to contribute to international global environmental monitoring; and to further the development of platform bus technology, interorbital data relay technology, etc., which are necessary for the future earth observation systems. To make continuous, thorough observations of the entire earth's surface and its atmosphere, the spacecraft carries two core sensors: the Advanced Visible and Near Infrared Radiometer (AVNIR) and the Ocean Color and Temperature Sensor (OCTS). The two sensors were developed by NASDA. Additionally, the spacecraft carries six (6) Announcement of Opportunity (AO) sensors: the NASA Scatterometer (NSCAT) and Total Ozone Mapping Spectrometer (TOMS); the Polarization and Directionality of the Earth's Surface (POLDER) system; the Interferometric Monitor for Greenhouse Gases (IMG); the Improved Limb Atmospheric Spectrometer (ILAS); and the Retroreflector in Space (RIS). In early 1996, ADEOS will be launched into a sun synchronous sub-recurrent orbit at an altitude of approximately 797 km by an H-2 launcher. Derived from text

N93-29840# Sandia National Labs., Albuquerque, NM.
POWER BEAMING TO COMMUNICATION SATELLITES IN GEO
R. M. Morgan and R. J. Lipinski 1992 8 p Presented at the 1st Annual Wireless Power Transmission Conference, San Antonio, TX, 23-25 Feb. 1993
(Contract DE-AC04-76DP-00789)
(DE93-007608; SAND-92-1974C; CONF-930258-2) Avail: CASI HC A02/MF A01

Batteries normally provide power to geosynchronous satellites during earth eclipse 90 times each year, but the heavy charge-discharge cycle decreases their life expectancy. Battery life, and thus satellite life, could be extended by providing power during eclipses via laser illumination of the photovoltaic array. For a spin-stabilized satellite this would require 35 kill using an 8-m diameter transmission mirror (and 850-nm light) or 180 kW using a 3.5-m mirror. A 3-axis stabilized satellite has a larger span and requires an elongated spot to use a comparable laser. At present, 70 satellites are scheduled to be replaced by the year 2000 at a cost of almost $10 billion. Power beaming could save a substantial portion of this cost. Laser illumination also could augment solar power to increase the power available to new satellites. Increased power could boost the signal strength or allow more channels on the satellite. In addition, high-frequency channels (which require higher power to penetrate the atmosphere) could be used. Removal of waste heat from the satellite limits the amount of power that can be transmitted. Nevertheless, a spin-stabilized satellite with power beaming could generate 0.9 kill per square meter of the collector array, which is six times that of an equivalent conventional satellite using the same size solar panel. A 3-axis stabilized satellite could generate 0.6 kW/sq m (four times conventional). DOE

N93-29988*# Michigan Univ., Ann Arbor. Dept. of Aerospace Engineering.
EFFICIENT REORIENTATION MANEUVERS FOR SPACECRAFT WITH MULTIPLE ARTICULATED PAYLOADS Final Report, 3 Mar. 1992 - 3 Jun. 1993
N. Harris McClamroch 3 Jun. 1993 130 p
(Grant NAG1-1419)
(NASA-CR-193142; NAS 1.26:193142) Avail: CASI HC A07/MF A02

A final report is provided which describes the research program during the period 3 Mar. 1992 to 3 Jun. 1993. A summary of the technical research questions that were studied and of the main results that were obtained is given. The specific outcomes of the research program, including both educational impacts as well as research publications, are listed. The research is concerned with efficient reorientation maneuvers for spacecraft with multiple articulated payloads. For individual titles, see N93-29989 through N93-29995.

N93-29989*# Michigan Univ., Ann Arbor. Dept. of Aerospace Engineering.
CONTROL OF NONLINEAR SYSTEMS WITH APPLICATIONS TO CONSTRAINED ROBOTS AND SPACECRAFT ATTITUDE STABILIZATION Abstract only
Hariharan Krishnan *In its* Efficient Reorientation Maneuvers for Spacecraft with Multiple Articulated Payloads 3 Jun. 1993 2 p (For primary document see N93-29988 11-18)
Avail: CASI HC A01/MF A02

This thesis is organized in two parts. In Part 1, control systems described by a class of nonlinear differential and algebraic equations are introduced. A procedure for local stabilization based on a local state realization is developed. An alternative approach to local stabilization is developed based on a classical linearization of the nonlinear differential-algebraic equations. A theoretical framework is established for solving a tracking problem associated with the differential-algebraic system. First, a simple procedure is developed for the design of a feedback control law which ensures, at least locally, that the tracking error in the closed loop system lies within any given bound if the reference inputs are sufficiently slowly varying. Next, by imposing additional assumptions, a procedure is developed for the design of a feedback control law which ensures that the tracking error in the closed loop system approaches zero exponentially for reference inputs which are not necessarily slowly varying. The control design methodologies are used for simultaneous force and position control in constrained robot systems. The differential-algebraic equations are shown to characterize the slow dynamics of a certain nonlinear control system in nonstandard singularly perturbed form. In Part 2, the attitude stabilization (reorientation) of a rigid spacecraft using only two control torques is considered. First, the case of momentum wheel actuators is considered. The complete spacecraft dynamics are not controllable. However, the spacecraft dynamics are small time locally controllable in a reduced sense. The reduced spacecraft dynamics cannot be asymptotically stabilized using continuous feedback, but a discontinuous feedback control strategy is constructed. Next, the case of gas jet actuators is considered. If the uncontrolled principal axis is not an axis of symmetry, the complete spacecraft dynamics are small time locally controllable. However, the spacecraft attitude cannot be asymptotically stabilized using continuous feedback, but a discontinuous stabilizing feedback control strategy is constructed. If the uncontrolled principal axis is an axis of symmetry, the complete spacecraft dynamics cannot be stabilized. However, the spacecraft dynamics are small time locally controllable in a reduced sense. The reduced spacecraft dynamics cannot be asymptotically stabilized using continuous feedback, but again a discontinuous feedback control strategy is constructed. Author

N93-29990*# Michigan Univ., Ann Arbor. Dept. of Aerospace Engineering.

ATTITUDE STABILIZATION OF A RIGID SPACECRAFT USING TWO MOMENTUM WHEEL ACTUATORS

Hariharan Krishnan, N. Harris McClamroch, and Mahmut Reyhanoglu *In its* Efficient Reorientation Maneuvers for Spacecraft with Multiple Articulated Payloads 3 Jun. 1993 20 p (For primary document see N93-29988 11-18)
(Grant NSF MSS-91-14630)
Avail: CASI HC A03/MF A02

It is well known that three momentum wheel actuators can be used to control the attitude of a rigid spacecraft and that arbitrary reorientation maneuvers of the spacecraft can be accomplished using smooth feedback. If failure of one of the momentum wheel actuators occurs, it is demonstrated that two momentum wheel actuators can be used to control the attitude of a rigid spacecraft and that arbitrary reorientation maneuvers of the spacecraft can be accomplished. Although the complete spacecraft equations are not controllable, the spacecraft equations are small time locally controllable in a reduced nonlinear sense. The reduced spacecraft dynamics cannot be asymptotically stabilized to any equilibrium attitude using a time-variant continuous feedback control law, but discontinuous feedback control strategies are constructed which stabilize any equilibrium attitude of the spacecraft in finite time. Consequently, reorientation of the spacecraft can be accomplished using discontinuous feedback control. Author

N93-29991*# University of Petroleum and Minerals, Dhahran (Saudi Arabia).

NONLINEAR ATTITUDE CONTROL OF PLANAR STRUCTURES IN SPACE USING ONLY INTERNAL CONTROLS

Mahmut Reyhanoglu and N. Harris McClamroch (Michigan Univ., Ann Arbor.) *In* Michigan Univ., Efficient Reorientation Maneuvers for Spacecraft with Multiple Articulated Payloads 3 Jun. 1993 15 p (For primary document see N93-29988 11-18)
(Grant NSF MSS-91-14630)
Avail: CASI HC A03/MF A02

An attitude control strategy for maneuvers of an interconnection of planar bodies in space is developed. It is assumed that there are no exogeneous torques and that torques generated by joint motors are used as means of control so that the total angular momentum of the multibody system is a constant, assumed to be zero. The control strategy utilizes the nonintegrability of the expression for the angular momentum. Large angle maneuvers can be designed to achieve an arbitrary reorientation of the multibody system with respect to an inertial frame. The theoretical background for carrying out the required maneuvers is summarized. Author

N93-29992*# Michigan Univ., Ann Arbor. Dept. of Aerospace Engineering.

ATTITUDE STABILIZATION OF A RIGID SPACECRAFT USING GAS JET ACTUATORS OPERATING IN A FAILURE MODE

Hariharan Krishnan, Mahmut Reyhanoglu, and Harris McClamroch *In its* Efficient Reorientation Maneuvers for Spacecraft with Multiple Articulated Payloads 3 Jun. 1993 6 p Presented at the Conference on Decision and Control, Tucson, AZ, 1992 (For primary document see N93-29988 11-18)
(Grant NSF MSS-91-14630)
Avail: CASI HC A02/MF A02

The attitude stabilization of a rigid spacecraft using control torques supplied by gas jet actuators about only two of its principal axes is considered. First, the case where the uncontrolled principal axis of the spacecraft is not an axis of symmetry is considered. In this case, the complete spacecraft dynamics are small time locally controllable. However, the spacecraft cannot be asymptotically stabilized to an equilibrium attitude using time-invariant continuous feedback. A discontinuous stabilizing feedback control strategy is constructed which stabilizes the spacecraft to an equilibrium attitude. Next, the case where the uncontrolled principal axis of the spacecraft is an axis of symmetry is considered. In this case, the complete spacecraft dynamics are not even accessible. However, the spacecraft dynamics are strongly accessible and small time locally controllable in a reduced sense. The reduced spacecraft dynamics cannot be asymptotically stabilized to an equilibrium attitude using time-invariant continuous feedback, but again a discontinuous stabilizing feedback control strategy is constructed. In both cases, the discontinuous feedback controllers are constructed by switching between one of several feedback functions. Author (revised)

N93-29993*# Michigan Univ., Ann Arbor. Dept. of Aerospace Engineering.

PLANAR REORIENTATION OF A FREE-FREE BEAM IN SPACE USING EMBEDDED ELECTROMECHANICAL ACTUATORS **c39**

Ilya V. Kolmanovsky and N. Harris McClamroch *In its* Efficient Reorientation Maneuvers for Spacecraft with Multiple Articulated Payloads 3 Jun. 1993 12 p Presented at the SPIE Conference on Smart Structures and Materials, 1993 (For primary document see N93-29988 11-18)
(Grant NSF MSS-91-14630)
Avail: CASI HC A03/MF A02

It is demonstrated that the planar reorientation of a free-free beam in zero gravity space can be accomplished by periodically changing the shape of the beam using embedded electromechanical actuators. The dynamics which determine the shape of the free-free beam is assumed to be characterized by the Euler-Bernoulli equation, including material damping, with appropriate boundary conditions. The coupling between the rigid body motion and the flexible motion is explained using the angular momentum expression which includes rotatory inertia and kinematically exact effects. A control scheme is proposed where the embedded actuators excite the flexible motion of the beam so that it rotates in the desired sense with respect to a fixed inertial reference. Relations are derived which relate the average rotation rate to the amplitudes and the frequencies of the periodic actuation signal and the properties of the beam. These reorientation maneuvers can be implemented by using feedback control. Author

N93-29994*# Michigan Univ., Ann Arbor. Dept. of Aerospace Engineering.

EFFICIENT REORIENTATION OF A DEFORMABLE BODY IN SPACE: A FREE-FREE BEAM EXAMPLE

Ilya V. Kolmanovsky and N. Harris McClamroch *In its* Efficient Reorientation Maneuvers for Spacecraft with Multiple Articulated Payloads 3 Jun. 1993 5 p Presented at the American Control Conference, 1993 (For primary document see N93-29988 11-18)
(Grant NSF MSS-91-14630)
Avail: CASI HC A01/MF A02

It is demonstrated that the planar reorientation of a free-free beam in zero gravity space can be accomplished by periodically changing the shape of the beam using internal actuators. A control scheme is proposed in which electromechanical actuators excite the flexible motion of the beam so that it rotates in the desired manner with respect to a fixed inertial reference. The results can be viewed as an extension of previous work to a distributed parameter case. Author

N93-29995*# Michigan Univ., Ann Arbor. Dept. of Aerospace Engineering.

SPACE STATION ATTITUDE DISTURBANCE ARISING FROM INTERNAL MOTIONS

Patrick J. McNally and N. Harris McClamroch *In its* Efficient Reorientation Maneuvers for Spacecraft with Multiple Articulated Payloads 3 Jun. 1993 5 p Presented at the American Control Conference, 1993 (For primary document see N93-29988 11-18)
(Grant NSF MSS-91-14630)
Avail: CASI HC A01/MF A02

A source of space station attitude disturbances is identified. The attitude disturbance is driven by internal space station motions and is a direct result of conservation of angular momentum. Three examples are used to illustrate the effect: a planar three link system, a rigid carrier body with two moveable masses, and a nonplanar five link system. Simulation results are given to show the magnitude of the attitude change in each example. Factors which accentuate or attenuate this disturbance effect are discussed. Author

N93-30038*# Alabama Univ., Huntsville. Center for Microgravity and Materials Research.

RESIDUAL ACCELERATION DATA ON IML-1: DEVELOPMENT OF A DATA REDUCTION AND DISSEMINATION PLAN Final Report, 1 Mar. 1989 - 31 May 1993

Melissa J. B. Rogers and J. Iwan D. Alexander 1993 219 p Original contains color illustrations
(Grant NAG8-759)
(NASA-CR-193224; NAS 1.26:193224) Avail: CASI HC A10/MF A03; 27 functiona l color pages

The research performed consisted of three stages: (1) identification of sensitive IML-1 experiments and sensitivity ranges by order of magnitude estimates, numerical modeling, and investigator input; (2) research and development towards reduction, supplementation, and dissemination of residual acceleration data; and (3) implementation of the plan on existing acceleration databases. Derived from text

N93-30106# European Space Agency, Paris (France).

ASSESSMENT OF COLUMBUS PAYLOAD OPERATIONS CAPABILITIES BY SCHEDULING WITH THE MARS SYSTEM

B. Calvignac (European Space Agency. European Space Research and Technology Center, ESTEC, Noordwijk, Netherlands.) and W. R. Burke, ed. Jul. 1992 50 p
(ESA-STR-235; ISBN-9-29-092168-4; ETN-93-93718) Copyright Avail: CASI HC A03/MF A01; ESA, EPD, ESTEC, Noordwijk, Netherlands, HC

A simulation of Columbus payload operations performed with the aid of the Mission Activities and Resource Scheduler (MaRS) is presented. This exercise was performed to assess the capabilities of the Columbus APM (Attached Pressurized Module) in terms of resources such as crew availability, power supply and video downlink, and to identify any bottlenecks. The data describing the requirements of each of the 58 model experiments (including American and Canadian ones) of the fully outfitted APM was taken from the Columbus Payload Database (CPDB) and from the Columbus Payload Requirements Document. A description of the main features of the MARS system and the set up for this exercise is given. ESA

N93-30142# Howard Univ., Washington, DC. Dept. of Mechanical Engineering.

DYNAMICS AND ROBUST CONTROL OF SAMPLED DATA SYSTEMS FOR LARGE SPACE STRUCTURES Final Report, Sep. 1989 - 1991

Peter M. Bainum, Aprille J. Ericsson, and Xing Quang-Qian Nov. 1992 177 p
(Contract F33615-89-C-3225)
(AD-A264192; WL-TR-92-3088) Avail: CASI HC A09/MF A02

The objective of this research is to develop practical design procedures that can be used in conjunction with optimal digital controllers for future orbiting large space structural systems. In practice, the observational data used to verify the orientation and shape of large flexible systems will, in general, be collected on a sampled basis (discrete-time data system). The system is assumed to be completely observable and deterministic. Systems which will be designed to control both the overall orientation as well as the shape of some of the subsystems (such as antenna mesh form) must function in the discrete-time domain. The aim of this research is to develop methods that can be used to design linear quadratic regulator (LQR) controllers for orbiting large flexible systems. The digital control of an orbiting thin square plate system is analyzed in this volume of the final report. DTIC

N93-30376*# Massachusetts Inst. of Tech., Cambridge. Space Engineering Research Center.

THE MIDDECK 0-GRAVITY DYNAMICS EXPERIMENT Summary Report

Edward F. Crawley, Marthinus C. vanSchoor, and Edward B. Bokhour Washington 1993 107 p
(Contract NAS1-18690; RTOP 589-01-21-01)
(NASA-CR-4500; NAS 1.26:4500; SERC-16-92-R) Avail: CASI HC A06/MF A02

The Middeck 0-Gravity Dynamics Experiment (MODE), flown onboard the Shuttle STS-48 Mission, consists of three major elements: the Experiment Support Module, a dynamics test bed providing computer experiment control, analog signal conditioning, power conditioning, an operator interface consisting of a keypad and display, experiment electrical and thermal control, and archival data storage: the Fluid Test Article assembly, used to investigate the dynamics of fluid-structure interaction in 0-gravity; and the Structural Test Article for investigating the open-loop dynamics of structures in 0-gravity. Deployable, erectable, and rotary modules were assembled to form three one- and two-dimensional structures, in which variations in bracing wire and rotary joint preload could be introduced. Change in linear modal parameters as well as the change in nonlinear nature of the response is examined. Trends in modal parameters are presented as a function of force amplitude, joint preload, and ambient gravity. An experimental study of the lateral slosh behavior of contained fluids is also presented. A comparison of the measured earth and space results identifies and highlights the effects of gravity on the linear and nonlinear slosh behavior of these fluids. Author (revised)

N93-30509# Sandia National Labs., Albuquerque, NM.

BETA/GAMMA MONTE CARLO TRANSPORT IN REPETITIVE STRUCTURES OF SATELLITE SYSTEMS

J. A. Halbleib 1993 5 p Presented at the Nuclear and Space Radiation Effects Conference, Snowbird, UT, 19-23 Jul. 1993
(Contract DE-AC04-76DP-00789)
(DE93-007610; SAND-93-0147C; CONF-930704-1) Avail: CASI HC A01/MF A01

An efficient electron-photon Monte Carlo model, taking advantage of approximate periodicity in repetitive satellite structures, is employed to benchmark a more approximate code and to study the shielding effect of a honeycomb-like structure. DOE

N93-30813# Army Research Lab., Watertown, MA.

DURABILITY OF QUICK REACTION SATELLITE ANTENNA (QRSA) TRUNNION CASTINGS Final Report

Wego Wang and Martin G. Wells Mar. 1993 26 p
(AD-A264095; ARL-TR-89) Avail: CASI HC A03/MF A01

Repeated failures of quick reaction satellite antenna (QRSA) trunnion castings in the field caused alarming concerns about their durability. Arguments over the cause of the failures, ranging from improper installation, unbalanced and/or excess force to poor design and insufficient material strength, have been disputed between the contractor and the government engineers. Incipient melting during solution treatment was also suspected as one of the reasons responsible for cracking in the original aluminum castings. This study compared the microstructures of as-cast and heat-treated samples and concluded that incipient melting did not occur during solution treatment and thus was not the principal cause for cracking in the aluminum castings. Eventually, the light aluminum alloy was replaced by a heavier but stronger ductile iron. As a result, the durability of the QRSA trunnion casting has been significantly improved and the deficiency was remedied. DTIC

N93-30817# Range Commanders Council, White Sands Missile Range, NM.

SATELLITE CALIBRATION REQUIREMENTS

Apr. 1993 8 p
(AD-A264279; RCC-751-93) Avail: CASI HC A02/MF A01

One of the tasks brought before the Joint Range Instrumentation Accuracy Improvement Group was to create a Satellite Calibration Requirements document. This document specifies user requirements for instrumentation onboard any future calibration satellite. The listed satellite user requirements will not necessarily be levied on the satellite; however, these requirements will be considered should funding and equipment or space and weight become available. DTIC

N93-31024# Joint Inst. for Nuclear Research, Dubna (USSR). Lab. of Computing Techniques and Automation.

MATHEMATICAL SIMULATION OF THE INDUCED (GAMMA)-RADIATION IN STRUCTURAL MATERIALS OF SPACESHIPS. TIME DEPENDENCE [MATEMATICHESKOE MODELIROVANIE NAVEDENNOGO GAMMA-IZIUCHENIYA V KONSTRUKTSIONNYKH MATERIALAKH KOSMICHESKIKH APPARATOV. VREMENNAYA ZAVISIMOST]

V. S. Barashenkov, A. N. Sosnin, P. I. Taranenko, and S. N. Fedotov (Moscow Physical-Engineering Inst., Russia.) 1991 10 p In RUSSIAN
(DE93-605312; JINR-R-2-91-242) Avail: CASI HC A02/MF A01 (US Sales Only)

Based on an internuclear model and a computer program for induced gamma-radiation activity calculation, the time-dependence of the gamma-background intensity, induced by cosmic radiation in structural materials Al, Ti, Fe, Cu, W, Pb, and in one of the alloys at different periods is addressed. A table of gamma-emitters, making the main contribution at short and long durations of the flight is presented. DOE

N93-28700*# National Aeronautics and Space Administration. Marshall Space Flight Center, Huntsville, AL.
LOW-COST ACTIVE STRUCTURAL CONTROL SPACE EXPERIMENT (LASC)
Rush Robinett (Sandia National Labs., Albuquerque, NM.) and Angelia P. Bukley *In* NASA, Washington, NASA/DOD Flight Experiments Technical Interchange Meeting Proceedings 1992 14 p (For primary document see N93-28699 11-12)
Avail: CASI HC A03/MF A10

N93-28701*# L'Garde, Inc., Tustin, CA.
IN-STEP INFLATABLE ANTENNA EXPERIMENT
G. Veal and R. E. Freeland (Jet Propulsion Lab., California Inst. of Tech., Pasadena.) *In* NASA, Washington, NASA/DOD Flight Experiments Technical Interchange Meeting Proceedings 1992 12 p (For primary document see N93-28699 11-12)
Avail: CASI HC A03/MF A10

N93-28703*# Utah State Univ., Logan. Dept. of Mechanical and Aerospace Engineering.
DESCRIPTION OF THE JOINT DAMPING EXPERIMENT (JDX)
Steven L. Folkman and Frank J. Redd *In* NASA, Washington, NASA/DOD Flight Experiments Technical Interchange Meeting Proceedings 1992 26 p (For primary document see N93-28699 11-12)
Avail: CASI HC A03/MF A10

N93-28704*# Phillips Lab., Hanscom AFB, MA. Directorate of Space and Missile Technology.
ADAPTIVE STRUCTURES FLIGHT EXPERIMENTS
Maurice Martin *In* NASA, Washington, NASA/DOD Flight Experiments Technical Interchange Meeting Proceedings 1992 21 p (For primary document see N93-28699 11-12)
Avail: CASI HC A03/MF A10

N93-28705*# Massachusetts Inst. of Tech., Cambridge. Space Engineering Research Center.
THE MODE FAMILY OF FACILITY CLASS EXPERIMENTS
David W. Miller *In* NASA, Washington, NASA/DOD Flight Experiments Technical Interchange Meeting Proceedings 1992 22 p (For primary document see N93-28699 11-12)
Avail: CASI HC A03/MF A10

N93-28706*# National Aeronautics and Space Administration. Langley Research Center, Hampton, VA.
CONTROL-STRUCTURES INTERACTION TEST OF THE LACE SATELLITE
Lawrence W. Taylor, Jr. and Shalom Fisher (Naval Research Lab., Washington, DC.) *In* NASA, Washington, NASA/DOD Flight Experiments Technical Interchange Meeting Proceedings 1992 21 p (For primary document see N93-28699 11-12)
Avail: CASI HC A03/MF A10

N93-28708*# National Aeronautics and Space Administration. Langley Research Center, Hampton, VA.
UPPER ATMOSPHERE RESEARCH SATELLITE JITTER STUDY
Stanley Woodard, Mike Garnek (General Electric Co., Philadelphia, PA.), John Molnar (General Electric Co., Philadelphia, PA.), and William Grantham *In* NASA, Washington, NASA/DOD Flight Experiments Technical Interchange Meeting Proceedings 1992 16 p (For primary document see N93-28699 11-12)
Avail: CASI HC A03/MF A10

N93-28714*# L'Garde, Inc., Tustin, CA.
DEVELOPING AN INFLATABLE SOLAR ARRAY
Patrick K. Malone, Francis J. Jankowski (Phillips Lab., Edwards AFB, CA.), Geoffery T. Williams, and George J. Vendura, Jr. (SUMM Associates.) *In* NASA, Washington, NASA/DOD Flight Experiments Technical Interchange Meeting Proceedings 1992 15 p (For primary document see N93-28699 11-12)
Avail: CASI HC A03/MF A10

N93-28716*# National Aeronautics and Space Administration. Lewis Research Center, Cleveland, OH.
SOLAR ARRAY MODULE PLASMA INTERACTION EXPERIMENT (SAMPIE)
Dale C. Ferguson *In* NASA, Washington, NASA/DOD Flight Experiments Technical Interchange Meeting Proceedings 1992 23 p (For primary document see N93-28699 11-12)
Avail: CASI HC A03/MF A10

N93-28723*# Strategic Defense Initiative Organization, Washington, DC.
STRV1-b FLIGHT EXPERIMENT
In NASA, Washington, NASA/DOD Flight Experiments Technical Interchange Meeting Proceedings 1992 7 p Prepared in cooperation with Defence Research Agency, London, England and Phillips Lab., Hanscom AFB, MA (For primary document see N93-28699 11-12)
Avail: CASI HC A02/MF A10

N93-28726*# National Aeronautics and Space Administration. Goddard Space Flight Center, Greenbelt, MD.
ENVIRONMENTAL VERIFICATION EXPERIMENT FOR THE EXPLORER PLATFORM (EVEEP)
Bonnie Norris and Chris Lorentson *In* NASA, Washington, NASA/DOD Flight Experiments Technical Interchange Meeting Proceedings 1992 14 p (For primary document see N93-28699 11-12)
Avail: CASI HC A03/MF A10

N93-28727*# National Aeronautics and Space Administration. Goddard Space Flight Center, Greenbelt, MD.
RETURN FLUX EXPERIMENT
June L. Tveekrem *In* NASA, Washington, NASA/DOD Flight Experiments Technical Interchange Meeting Proceedings 1992 15 p (For primary document see N93-28699 11-12)
Avail: CASI HC A03/MF A10

N93-28735*# Institute for Space Science and Technology, Inc., Gainesville, FL.
ORBITAL DEBRIS ENVIRONMENT MONITOR (ODEM)
John P. Oliver *In* NASA, Washington, NASA/DOD Flight Experiments Technical Interchange Meeting Proceedings 1992 16 p (For primary document see N93-28699 11-12)
Avail: CASI HC A03/MF A10

N93-28738*# California Univ., Los Angeles. Dept. of Mechanical, Aerospace and Nuclear Engineering.
RISK-BASED SPACECRAFT FIRE SAFETY EXPERIMENTS
G. Apostolakis, I. Catton, F. Issacci, T. Paulos, S. Jones, K. Paxton, and M. Paul *In* NASA, Washington, NASA/DOD Flight Experiments Technical Interchange Meeting Proceedings 1992 11 p Sponsored by NASA. Lewis Research Center (For primary document see N93-28699 11-12)
Avail: CASI HC A03/MF A10

N93-29357*# National Aeronautics and Space Administration. Lyndon B. Johnson Space Center, Houston, TX.
CONTINUED INVESTIGATION OF LDEF'S STRUCTURAL FRAME AND THERMAL BLANKETS BY THE METEOROID AND DEBRIS SPECIAL INVESTIGATION GROUP
Thomas H. See (Lockheed Engineering and Sciences Co., Houston, TX.), Kimberly S. Mack (Lockheed Engineering and Sciences Co., Houston, TX.), Jack L. Warren (Lockheed Engineering and Sciences Co., Houston, TX.), Michael E. Zolensky, and Herbert A. Zook *In* NASA. Langley Research Center, LDEF: 69 Months in Space. Second Post-Retrieval Symposium, Part 2 Apr. 1993 p 313-324 (For primary document see N93-29354 11-99)
Avail: CASI HC A03/MF A04

N93-29359*# National Aeronautics and Space Administration. Lyndon B. Johnson Space Center, Houston, TX.

THREE-D CRATER ANALYSIS OF LDEF IMPACT FEATURES FROM STEREO IMAGERY

Clyde A. Sapp (Lockheed Engineering and Sciences Co., Houston, TX.), Thomas H. See (Lockheed Engineering and Sciences Co., Houston, TX.), and Michael E. Zolensky *In* NASA. Langley Research Center, LDEF: 69 Months in Space. Second Post-Retrieval Symposium, Part 2 Apr. 1993 p 339-345 (For primary document see N93-29354 11-99)
Avail: CASI HC A02/MF A04

N93-29362*# Kent Univ., Canterbury (England). Physics Lab.

DERIVATION OF PARTICULATE DIRECTIONAL INFORMATION FROM ANALYSIS OF ELLIPTICAL IMPACT CRATERS ON LDEF

P. J. Newman, N. Mackay, S. P. Deshpande, S. F. Green, and J. A. M. McDonnell *In* NASA. Langley Research Center, LDEF: 69 Months in Space. Second Post-Retrieval Symposium, Part 2 Apr. 1993 p 417-429 Sponsored by the UK Science and Engineering Research Council (For primary document see N93-29354 11-99)
Avail: CASI HC A03/MF A04

N93-29363*# National Aeronautics and Space Administration. Lewis Research Center, Cleveland, OH.

CHARACTERISTICS OF HYPERVELOCITY IMPACT CRATERS ON LDEF EXPERIMENT S1003 AND IMPLICATIONS OF SMALL PARTICLE IMPACTS ON REFLECTIVE SURFACES

Michael J. Mirtich, Sharon K. Rutledge, Bruce A. Banks, Christopher DeVries (Cornell Univ., Ithaca, NY.), and James E. Merrow (Cleveland State Univ., OH.) *In* NASA. Langley Research Center, LDEF: 69 Months in Space. Second Post-Retrieval Symposium, Part 2 Apr. 1993 p 431-451 (For primary document see N93-29354 11-99)
Avail: CASI HC A03/MF A04

N93-29364*# National Aeronautics and Space Administration. Ames Research Center, Moffett Field, CA.

HYPERVELOCITY IMPACT SURVIVABILITY EXPERIMENTS FOR CARBONACEOUS IMPACTORS

T. E. Bunch, Luann Becker (Scripps Institution of Oceanography, La Jolla, CA.), Jeffrey Bada (Scripps Institution of Oceanography, La Jolla, CA.), John Macklin (Washington Univ., Seattle.), Filippo RadicatidiBrozolo (Evans, Charles and Associates, Redwood City, CA.), R. H. Fleming (Evans, Charles and Associates, Redwood City, CA.), and Jozef Erlichman (TMA/Norcal, Richmond, CA.) *In* NASA. Langley Research Center, LDEF: 69 Months in Space. Second Post-Retrieval Symposium, Part 2 Apr. 1993 p 453-477 (For primary document see N93-29354 11-99)
(Contract NAS2-13178; RTOP 199-52-12; RTOP 506-48-00)
Avail: CASI HC A03/MF A04

N93-29365*# Auburn Univ., AL. Space Power Inst.

HYPERVELOCITY IMPACT FACILITY FOR SIMULATING MATERIALS EXPOSURE TO IMPACT BY SPACE DEBRIS

M. F. Rose, S. Best, T. Chaloupka, B. Stephens, and G. Crawford *In* NASA. Langley Research Center, LDEF: 69 Months in Space. Second Post-Retrieval Symposium, Part 2 Apr. 1993 p 479-492 Sponsored by NASA. Marshall Space Flight Center and NASA. Langley Research Center (For primary document see N93-29354 11-99)
Avail: CASI HC A03/MF A04

N93-29369*# National Aeronautics and Space Administration. Lyndon B. Johnson Space Center, Houston, TX.

SCANNING ELECTRON MICROSCOPE/ENERGY DISPERSIVE X RAY ANALYSIS OF IMPACT RESIDUES IN LDEF TRAY CLAMPS

Ronald P. Bernhard (Lockheed Engineering and Sciences Co., Houston, TX.), Christian Durin (Centre National d'Etudes Spatiales, Toulouse, France.), and Michael E. Zolensky *In* NASA. Langley Research Center, LDEF: 69 Months in Space. Second Post-Retrieval Symposium, Part 2 Apr. 1993 p 541-549 (For primary document see N93-29354 11-99)
Avail: CASI HC A02/MF A04

N93-29373*# National Aeronautics and Space Administration. Lyndon B. Johnson Space Center, Houston, TX.

ORIGIN OF ORBITAL DEBRIS IMPACTS ON LDEF'S TRAILING SURFACES

Donald J. Kessler *In* NASA. Langley Research Center, LDEF: 69 Months in Space. Second Post-Retrieval Symposium, Part 2 Apr. 1993 p 585-593 (For primary document see N93-29354 11-99)
Avail: CASI HC A02/MF A04

N93-29374*# POD Associates, Inc., Albuquerque, NM.

DAMAGE AREAS ON SELECTED LDEF ALUMINUM SURFACES

Cassandra R. Coombs, Dale R. Atkinson, Martha K. Allbrooks, Alan J. Watts, Corey J. Hennessy, and John D. Wagner *In* NASA. Langley Research Center, LDEF: 69 Months in Space. Second Post-Retrieval Symposium, Part 2 Apr. 1993 p 595-618 Prepared for Schafer (W. J.) Associates, Inc., Arlington, VA (For primary document see N93-29354 11-99)
(Contracts SDIO-SC-89W-26-11; SDIO-89-C-0034; POD Proj. 019202)
Avail: CASI HC A03/MF A04

N93-29375*# POD Associates, Inc., Albuquerque, NM.

LDEF DATA: COMPARISONS WITH EXISTING MODELS

Cassandra R. Coombs, Alan J. Watts, John D. Wagner, and Dale R. Atkinson *In* NASA. Langley Research Center, LDEF: 69 Months in Space. Second Post-Retrieval Symposium, Part 2 Apr. 1993 p 619-664 Prepared for Lockheed Engineering and Sciences Co., Houston, TX (For primary document see N93-29354 11-99)
(Contract SDIO-SC-02N0165768; POD Proj. 019201)
Avail: CASI HC A03/MF A04

N93-29622*# National Aeronautics and Space Administration. Marshall Space Flight Center, Huntsville, AL.

REFINEMENTS ON THE PINHOLE CAMERA MEASUREMENTS OF THE LDEF ATTITUDE

Palmer N. Peters, Paul N. Whitehouse, and John C. Gregory (Alabama Univ., Huntsville.) *In* NASA. Langley Research Center, LDEF: 69 Months in Space. Part 1: Second Post-Retrieval Symposium Apr. 1993 p 3-12 (For primary document see N93-29621 11-99)
Avail: CASI HC A02/MF A03

N93-29623*# Boeing Defense and Space Group, Seattle, WA.

LDEF MICROENVIRONMENTS, OBSERVED AND PREDICTED

R. J. Bourassa, H. G. Pippin, and J. R. Gillis *In* NASA. Langley Research Center, LDEF: 69 Months in Space. Part 1: Second Post-Retrieval Symposium Apr. 1993 p 13-25 (For primary document see N93-29621 11-99)
(Contract NAS1-19247)
Avail: CASI HC A03/MF A03

N93-29705*# American Space Technology, Inc., Santa Monica, CA.

RETRIEVABLE PAYLOAD CARRIER, NEXT GENERATION LONG DURATION EXPOSURE FACILITY: UPDATE 1992

A. T. Perry, J. A. Cagle, and S. C. Newman *In* NASA. Langley Research Center, LDEF: 69 Months in Space. Part 4: Second Post-Retrieval Symposium Apr. 1993 p 1511-1520 (For primary document see N93-29682 11-99)
Avail: CASI HC A02/MF A03; 2 functional color pages

N93-29724*# Arizona Univ., Tucson.

ADVANCED DESIGN FOR ORBITAL DEBRIS REMOVAL IN SUPPORT OF SOLAR SYSTEM EXPLORATION

In Universities Space Research Association, Houston, Proceedings of the Seventh Annual Summer Conference. NASA/USRA: University Advanced Design Program 1991 p 105-111 (For primary document see N93-29712 11-01)
Avail: CASI HC A02/MF A03

N93-29735*# Maryland Univ., College Park.

DELTA ADVANCED REUSABLE TRANSPORT (DART): AN ALTERNATIVE MANNED SPACECRAFT

T. Lewerenz, M. Kosha, and H. Magazu *In* Universities Space Research Association, Houston, Proceedings of the Seventh Annual Summer

Conference. NASA/USRA: University Advanced Design Program 1991 p 165-175 (For primary document see N93-29712 11-01)
Avail: CASI HC A03/MF A03

N93-29736*# Maryland Univ., College Park.
TAURUS LIGHTWEIGHT MANNED SPACECRAFT EARTH ORBITING VEHICLE
M. Bosset *In* Universities Space Research Association, Houston, Proceedings of the Seventh Annual Summer Conference. NASA/USRA: University Advanced Design Program 1991 p 177-186 (For primary document see N93-29712 11-01)
Avail: CASI HC A02/MF A03

N93-29739*# Michigan Univ., Ann Arbor.
PROJECT MEDSAT
In Universities Space Research Association, Houston, Proceedings of the Seventh Annual Summer Conference. NASA/USRA: University Advanced Design Program 1991 p 197-203 (For primary document see N93-29712 11-01)
Avail: CASI HC A02/MF A03

N93-29740*# Michigan Univ., Ann Arbor.
PROJECT UM-HAUL: A SELF-UNLOADING REUSABLE LUNAR LANDER
In Universities Space Research Association, Houston, Proceedings of the Seventh Annual Summer Conference. NASA/USRA: University Advanced Design Program 1991 p 205-211 (For primary document see N93-29712 11-01)
Avail: CASI HC A02/MF A03

N93-29741*# Minnesota Univ., Minneapolis.
MARS INTEGRATED TRANSPORTATION SYSTEM MULTISTAGE MARS MISSION
In Universities Space Research Association, Houston, Proceedings of the Seventh Annual Summer Conference. NASA/USRA: University Advanced Design Program 1991 p 213-218 (For primary document see N93-29712 11-01)
Avail: CASI HC A02/MF A03

N93-29743*# Naval Postgraduate School, Monterey, CA.
MULTIPURPOSE SATELLITE BUS (MPS)
In Universities Space Research Association, Houston, Proceedings of the Seventh Annual Summer Conference. NASA/USRA: University Advanced Design Program 1991 p 227-236 (For primary document see N93-29712 11-01)
Avail: CASI HC A02/MF A03

N93-29744*# Ohio State Univ., Columbus.
PROJECT WISH: THE EMERALD CITY
In Universities Space Research Association, Houston, Proceedings of the Seventh Annual Summer Conference. NASA/USRA: University Advanced Design Program 1991 p 237-240 (For primary document see N93-29712 11-01)
Avail: CASI HC A01/MF A03

N93-29750*# Texas Univ., Austin.
ASPEC: SOLAR POWER SATELLITE
In Universities Space Research Association, Houston, Proceedings of the Seventh Annual Summer Conference. NASA/USRA: University Advanced Design Program 1991 p 281-285 (For primary document see N93-29712 11-01)
Avail: CASI HC A01/MF A03

N93-29751*# Texas Univ., Austin.
B AND T: LUNAR LANDERS
In Universities Space Research Association, Houston, Proceedings of the Seventh Annual Summer Conference. NASA/USRA: University Advanced Design Program 1991 p 287-289 (For primary document see N93-29712 11-01)
Avail: CASI HC A01/MF A03

N93-29753*# Texas Univ., Austin.
RS LANDERS: LUNAR LANDER
In Universities Space Research Association, Houston, Proceedings of the Seventh Annual Summer Conference. NASA/USRA: University Advanced Design Program 1991 p 295-297 (For primary document see N93-29712 11-01)
Avail: CASI HC A01/MF A03

N93-29754*# Texas Univ., Austin.
SPECS: ORBITAL DEBRIS REMOVAL
In Universities Space Research Association, Houston, Proceedings of the Seventh Annual Summer Conference. NASA/USRA: University Advanced Design Program 1991 p 299-300 (For primary document see N93-29712 11-01)
Avail: CASI HC A01/MF A03

N93-29893# Aerospace Corp., Los Angeles, CA.
TACTICAL SATELLITES
F. H. Newman *In* AGARD, TacSats for Surveillance Verification and C3I Feb. 1993 9 p (For primary document see N93-29892 11-32)
Copyright Avail: CASI HC A02/MF A03

N93-29896# MATRA Marconi Space, Toulouse (France). Espace/Direction des Programmes Militaires.
TACSAT-SPACECRAFT BUS CONCEPT AND DESIGN: APPLICATION OF A MULTIMISSION BUS FOR TACSAT IN LEO
Georges Richard *In* AGARD, TacSats for Surveillance Verification and C3I Feb. 1993 13 p In ENGLISH and FRENCH (For primary document see N93-29892 11-32)
Copyright Avail: CASI HC A03/MF A03

N93-29897# Office National d'Etudes et de Recherches Aerospatiales, Paris (France).
SYSTEM OF NAVIGATION BY SATELLITES WITH EUROPEAN COVERAGE [SYSTEME DE NAVIGATION PAR SATELLITES A COUVERTURE EUROPEENNE]
H. Baranger, J. Bouchard, and T. Michal *In* AGARD, TacSats for Surveillance Verification and C3I Feb. 1993 10 p In FRENCH (For primary document see N93-29892 11-32)
Copyright Avail: CASI HC A02/MF A03

N93-29898# Aerospatiale, Les Mureaux (France). Espace and Defense.
TACTICAL SATELLITES FOR AIR COMMAND AND CONTROL
M. Crochet, J. Cymbalista, and L. Leveque *In* AGARD, TacSats for Surveillance Verification and C3I Feb. 1993 9 p (For primary document see N93-29892 11-32)
Copyright Avail: CASI HC A02/MF A03

N93-29904# Orbital Sciences Corp., Chantilly, VA.
SPACECRAFT AND LAUNCH SYSTEMS FOR TACSAT APPLICATIONS
Chris Schade, Gilbert D. Rye, and Robert H. Meurer *In* AGARD, TacSats for Surveillance Verification and C3I Feb. 1993 11 p (For primary document see N93-29892 11-32)
Copyright Avail: CASI HC A03/MF A03

N93-29905# Ball Corp., Boulder, CO. Space Systems Div.
QuickStar: SYSTEM DESIGN, CAPABILITIES, AND TACTICAL APPLICATIONS OF A SMALL, SMART SPACE SYSTEM
Thomas P. Garrison and Neal T. Anderson *In* AGARD, TacSats for Surveillance Verification and C3I Feb. 1993 12 p (For primary document see N93-29892 11-32)
Copyright Avail: CASI HC A03/MF A03

N93-29906# Messerschmitt-Boelkow-Blohm G.m.b.H., Munich (Germany). Space Communications and Propulsion Systems Div.
ATTITUDE- AND ORBIT CONTROL SUBSYSTEM CONCEPTS FOR TACSATS
H. Bittner, E. Bruederle, M. Surauer, and M. Schwende *In* AGARD, TacSats for Surveillance Verification and C3I Feb. 1993 24 p (For primary document see N93-29892 11-32)
Copyright Avail: CASI HC A03/MF A03

N93-29911# Hughes Aircraft Co., Los Angeles, CA. Remote Sensing Systems.
LOW COST TACSAT FOR NATO SURVEILLANCE
Charles S. Hoff *In* AGARD, TacSats for Surveillance Verification and C3I Feb. 1993 8 p (For primary document see N93-29892 11-32)
Copyright Avail: CASI HC A02/MF A03

N93-29912# Lockheed Missiles and Space Co., Sunnyvale, CA.
COST EFFECTIVE TacSats FOR MILITARY SUPPORT
M. T. Brodsky, M. D. Benz, and J. T. Neer *In* AGARD, TacSats for Surveillance Verification and C3I Feb. 1993 12 p (For primary document see N93-29892 11-32)
Copyright Avail: CASI HC A03/MF A03

N93-30235 Ottawa Univ. (Ontario). Dept. of Electrical Engineering.
VIBRATION CONTROL OF FLEXIBLE SPACE STRUCTURES IN NOISY ENVIRONMENT
S. S. Lim and N. U. Ahmed *In* Engineering Inst. of Canada, Canadian Conference on Electrical and Computer Engineering, Volumes 1 and 2 1990 4 p (For primary document see N93-30215 11-31)
Avail: Engineering Inst. of Canada, 2050 rue Mansfield, Suite 700, Montreal, Quebec H3A 1Z2 Canada

N93-30249 Ottawa Univ. (Ontario). Dept. of Electrical Engineering.
ROBUST BOUNDARY CONTROL OF FLEXIBLE STRUCTURES GOVERNED BY HYBRID DYNAMICS
P. Li, N. U. Ahmed, and S. S. Lim *In* Engineering Inst. of Canada, Canadian Conference on Electrical and Computer Engineering, Volumes 1 and 2 1990 4 p (For primary document see N93-30215 11-31)
Avail: Engineering Inst. of Canada, 2050 rue Mansfield, Suite 700, Montreal, Quebec H3A 1Z2 Canada

19 SPACECRAFT INSTRUMENTATION

For related information see also *06 Aircraft Instrumentation* and *35 Instrumentation and Photography.*

N93-28554*# National Aeronautics and Space Administration. Lewis Research Center, Cleveland, OH.
LOW-FREQUENCY VIBRATION ENVIRONMENT FOR FIVE SHUTTLE MISSIONS
George R. Baugher (National Aeronautics and Space Administration. Marshall Space Flight Center, Huntsville, AL.), Gary L. Martin (National Aeronautics and Space Administration, Washington, DC.), and Richard DeLombard Mar. 1993 13 p Presented at the 31st Aerospace Sciences Meeting, Reno, NV, 11-14 Jan. 1993; sponsored by AIAA
(RTOP 694-03-OH)
(NASA-TM-106059; E-7661; NAS 1.15:106059) Avail: CASI HC A03/MF A01

The Microgravity Science and Applications Division's (MSAD) program to record and analyze the Shuttle's vibration environment is reviewed. This program provides microgravity science investigators with time and frequency analyses of the acceleration environment during their experiments' operation. Information is also provided for future investigators on the expected Shuttle vibration environment. As background, the two major elements of the program are discussed, the Space Acceleration Measurement System (SAMS) and the Acceleration Characterization and Analysis Project (ACAP). A comparison of the acceleration measurements from five Shuttle missions is discussed. Author (revised)

N93-29461# Naval Postgraduate School, Monterey, CA.
DESIGN OF A HIGH RESOLUTION SPATIAL HETERODYNE INTERFEROMETER M.S. Thesis
Kenneth M. Wallace, Jr. Dec. 1992 100 p
(AD-A262867) Avail: CASI HC A05/MF A02

Several new spatial heterodyne interferometers were evaluated using ray tracing analysis. A spherical grating interferometer was examined and found to have nonlinear fringe patterns that are difficult to interpret. A new plane grating interferometer was designed, built, and tested using a visible light laser as the source. The new design uses two mirrors and a single, planar diffraction grating to divide and recombine incident collimated light. The zero and first order ray paths recombine to produce a high contrast, linear, interference fringe pattern suitable for Fourier Transform analysis. The instrument has the potential to perform extremely high resolution spectroscopy in the FUV and EUV portions of the electromagnetic spectrum with resolving powers on the order of 10(exp 6). High resolution analysis of emission line profiles should enable an observer to more accurately determine atmospheric temperature and density profiles. The simple, lightweight, and compact instrument has no moving parts and is suitable for remote sensing from sounding rocket or satellite platforms. DTIC

N93-31032*# Lockheed Engineering and Sciences Co., Houston, TX.
SPACE GENERIC OPEN AVIONICS ARCHITECTURE (SGOAA) REFERENCE MODEL TECHNICAL GUIDE
Richard B. Wray and John R. Stovall Apr. 1993 195 p Supersedes LESC-30347
(Contract NAS9-17900)
(NASA-CR-188246; NAS 1.26:188246; LESC-30347-A) Avail: CASI HC A09/MF A03

This report presents a full description of the Space Generic Open Avionics Architecture (SGOAA). The SGOAA consists of a generic system architecture for the entities in spacecraft avionics, a generic processing architecture, and a six class model of interfaces in a hardware/software system. The purpose of the SGOAA is to provide an umbrella set of requirements for applying the generic architecture interface model to the design of specific avionics hardware/software systems. The SGOAA defines a generic set of system interface points to facilitate identification of critical interfaces and establishes the requirements for applying appropriate low level detailed implementation standards to those interface points. The generic core avionics system and processing architecture models provided herein are robustly tailorable to specific system applications and provide a platform upon which the interface model is to be applied. Author (revised)

N93-28730*# National Aeronautics and Space Administration. Lyndon B. Johnson Space Center, Houston, TX.
RADIATION MONITORING EQUIPMENT DOSIMETER EXPERIMENT
Kenneth A. Hardy (Aerospace Medical Research Labs., Brooks AFB, TX.), Michael J. Golightly, and William Quam (EG and G Energy Measurements, Inc., Goleta, CA.) *In* NASA, Washington, NASA/DOD Flight Experiments Technical Interchange Meeting Proceedings 1992 33 p (For primary document see N93-28699 11-12)
Avail: CASI HC A03/MF A10

N93-28778*# Innovative Concepts Co., McLean, VA.
CLEMENTINE SENSOR PROCESSING SYSTEM Abstract Only
A. A. Feldstein *In* Lunar and Planetary Inst., Workshop on Advanced Technologies for Planetary Instruments, Part 1 1993 p 7-8 (For primary document see N93-28764 11-91)
Avail: CASI HC A01/MF A01

N93-28779*# Arizona Univ., Tucson. Lunar and Planetary Lab.
DESIGN CONCEPT FOR AN IR MAPPING SPECTROMETER FOR THE PLUTO FAST FLYBY MISSION Abstract Only
U. Fink, F. Low, B. Hubbard, M. Rieke, G. Rieke, M. Mumma, S. Nozette, G. Neukum, H. Hamel, and M. DiSanti et al *In* Lunar and Planetary Inst., Workshop on Advanced Technologies for Planetary Instruments, Part 1 1993 p 8 (For primary document see N93-28764 11-91)
Avail: CASI HC A01/MF A01

N93-28781*# National Aeronautics and Space Administration. Goddard Space Flight Center, Greenbelt, MD.
ACOUSTO-OPTIC INFRARED SPECTRAL IMAGER FOR PLUTO FAST FLYBY Abstract Only
D. A. Glenar and J. J. Hillman *In* Lunar and Planetary Inst., Workshop on Advanced Technologies for Planetary Instruments, Part 1 1993 p 8-9 (For primary document see N93-28764 11-91)
Avail: CASI HC A01/MF A01

N93-28784*# Naval Research Lab., Washington, DC. Naval Center for Space Technology.
THE ULTRAVIOLET PLUME INSTRUMENT (UVPI) Abstract Only
D. M. Horan *In* Lunar and Planetary Inst., Workshop on Advanced

Technologies for Planetary Instruments, Part 1 1993 1 p (For *primary document see N93-28764 11-91)*
Avail: CASI HC A01/MF A01

N93-28785*# Spire Corp., Bedford, MA.
MICROTEXTURED METALS FOR STRAY-LIGHT SUPPRESSION IN THE CLEMENTINE STARTRACKER Abstract Only
E. A. Johnson *In* Lunar and Planetary Inst., Workshop on Advanced Technologies for Planetary Instruments, Part 1 1993 p 10-11 (For primary document see N93-28764 11-91)
Avail: CASI HC A01/MF A01

N93-28787*# Physical Sciences, Inc., Andover, MA.
LIGHTWEIGHT MODULAR INSTRUMENTATION FOR PLANETARY APPLICATIONS Abstract Only
P. B. Joshi *In* Lunar and Planetary Inst., Workshop on Advanced Technologies for Planetary Instruments, Part 1 1993 p 11-12 (For primary document see N93-28764 11-91)
Avail: CASI HC A01/MF A01

N93-28790*# KET Canada, Inc., Winnipeg (Manitoba).
A UNIQUE PHOTON BOMBARDMENT SYSTEM FOR SPACE APPLICATIONS Abstract Only
E. J. Klein *In* Lunar and Planetary Inst., Workshop on Advanced Technologies for Planetary Instruments, Part 1 1993 p 13 Prepared in cooperation with Sol-RF Energy Systems, Inc., Winnipeg, Manitoba (For primary document see N93-28764 11-91)
Avail: CASI HC A01/MF A01

N93-28795*# Johns Hopkins Univ., Laurel, MD. Applied Physics Lab.
PROPOSAL FOR A UNIVERSAL PARTICLE DETECTOR EXPERIMENT Abstract Only
J. C. Lesho, R. P Cain, and O. M. Uy *In* Lunar and Planetary Inst., Workshop on Advanced Technologies for Planetary Instruments, Part 1 1993 p 14-15 (For primary document see N93-28764 11-91)
Avail: CASI HC A01/MF A01

N93-28826*# Johns Hopkins Univ., Laurel, MD. Applied Physics Lab.
ENVIRONMENTAL MONITORS IN THE MIDCOURSE SPACE EXPERIMENTS (MSX) Abstract Only
O. M. Uy *In* Lunar and Planetary Inst., Workshop on Advanced Technologies for Planetary Instruments, Part 1 1993 p 27 (For primary document see N93-28764 11-91)
Avail: CASI HC A01/MF A01

N93-28828*# Southwest Research Inst., San Antonio, TX. Instrumentation and Space Research Div.
DEVELOPMENT OF MINIATURIZED OPTIMIZED SMART SENSORS (MOSS) FOR SPACE PLASMAS Abstract Only
D. T. Young *In* Lunar and Planetary Inst., Workshop on Advanced Technologies for Planetary Instruments, Part 1 1993 p 27 (For primary document see N93-28764 11-91)
Avail: CASI HC A01/MF A01

N93-29707*# Chicago Univ., IL. Lab. for Astrophysics and Space Research.
AN LDEF 2 DUST INSTRUMENT FOR DISCRIMINATION BETWEEN ORBITAL DEBRIS AND NATURAL PARTICLES IN NEAR-EARTH SPACE
A. J. Tuzzolino, J. A. Simpson, R. B. McKibben, H. D. Voss (Lockheed Missiles and Space Co., Palo Alto, CA.), and H. Gursky (Naval Research Lab., Washington, DC.) *In* NASA. Langley Research Center, LDEF: 69 Months in Space. Part 4: Second Post-Retrieval Symposium Apr. 1993 p 1535-1549 Sponsored in part by Lockheed Missiles and Space Co. (For primary document see N93-29682 11-99)
(Contract NAGw-3078; N00014-91-J-1716)
Avail: CASI HC A03/MF A03; 2 functional color pages

N93-29909# Alenia Spazio S.p.A., Rome (Italy).
SAR SENSORS ON TACSATS: A FEASIBILITY ASSESSMENT
G. Perrotta *In* AGARD, TacSats for Surveillance Verification and C3I Feb. 1993 9 p (For primary document see N93-29892 11-32)
Copyright Avail: *CASI HC* A02/MF A03

N93-29910# *MATRA Marconi Space (England).*
A TACSAT SAR CONCEPT
C. D. Hall, C. J. Baker (Defence Research Agency, Malvern, England.), G. E. Keyte (Defence Research Agency, Farnborough, England.), and L. M. Murphy (Defence Research Agency, Farnborough, England.) *In* AGARD, TacSats for Surveillance Verification and C3I Feb. 1993 14 p (For primary document see N93-29892 11-32)
Copyright Avail: CASI HC A03/MF A03

20 SPACECRAFT PROPULSION AND POWER

Includes main propulsion systems and components, e.g., rocket engines; and spacecraft auxilliary power sources.

For related information see also *07 Aircraft Propulsion and Power, 28 Propellants and Fuels, 44 Energy Production and Conversion,* and *15 Launch Vehicles and Space Vehicles.*

N93-28474# Air Force Inst. of Tech., Wright-Patterson AFB, OH. School of Engineering.
ANALYSIS OF TOPAZ 2 AND SPACE-R SPACE NUCLEAR POWER PLANTS USING A MODIFIED THERMIONIC MODEL M.S. Thesis
Otto D. Habedank Mar. 1993 107 p
(AD-A262612; AFIT/GNE/ENP/93M-03) Avail: CASI HC A06/MF A02

Models based on the TDS thermionic diode model were developed for TOPAZ 2 and SPACE-R nuclear power systems. Several parameter studies were conducted with the TOPAZ 2 model. These determined system performance and efficiency while varying the following: (1) Coolant flow inlet temperatures. (2) Rate of coolant temperature change. (3) Power profile of the core. (4) Cesium reservoir temperature. Analysis of results indicate the model accurately represented the TOPAZ 2 system, underestimating published data by 10%. Coolant flow studies indicate that raising coolant temperatures up to 100 K higher increases system power by up to 5%. Additional increases in temperature result in gradual performance degradation. Varying the axial power profile of the core from the actual peaked profile to a flat profile results in a negligible 0.3% change in system performance. The peaked profile used in TOPAZ 2 produces the highest system efficiency of all the profiles modeled. The cesium pressure study indicates the system is operating above optimum cesium pressure and system performance is strongly dependent on cesium pressure. Increasing cesium reservoir temperature above design temperature by 30 K decreases system efficiency by 30%. DTIC

N93-28593# Vought Systems Div., Dallas, TX. Missiles Div.
CLUSTERED LANCE BOOSTER (CLB) FEASIBILITY STUDY Report, 29 Sep. 1992 - 28 Jan. 1993
27 Jan. 1993 132 p
(Contract DASG60-92-C-0120)
(AD-A262746) Avail: CASI HC A07/MF A02

Loral Vought (LV) was requested to investigate the feasibility of clustering four Lance propulsion systems as the first stage of a two-stage target vehicle. Two vehicle configurations were considered, both using the Clustered Lance Booster (CLB) as the first stage. On one configuration, the second stage will be the 40-inch diameter Liquid Fueled Target (LFT-40), which was the subject of an LTV Aerospace and Defense Company study in 1991. This configuration is designated as the CLB/LFT-40. The second stage of the other configuration will be a modified Lance having the same external shape as the Lance missile (22-inch diameter). This configuration is designated as the CLB/LFT-22. DTIC

N93-28619*# National Aeronautics and Space Administration. Lewis Research Center, Cleveland, OH.
SMALL HYDROGEN/OXYGEN ROCKET FLOWFIELD BEHAVIOR FROM HEAT FLUX MEASUREMENTS
Brian D. Reed Jun. 1993 30 p Presented at the 29th Joint Propulsion Conference and Exhibit, Monterey, CA, 28-30 Jun. 1993; sponsored by AIAA, SAE, ASME, and ASEE
(RTOP 506-42-31)

(NASA-TM-106233; E-7953; NAS 1.15:106233; AIAA Paper 93-2162)
Avail: CASI HC A03/MF A01

The mixing and heat transfer phenomena in small rocket flow fields with fuel film cooling is not well understood. An instrumented, water-cooled chamber with a gaseous hydrogen/gaseous oxygen injector was used to gather steady-state inner and outer wall temperature profiles. The chamber was tested at 414 kPa (60 psia) chamber pressure, from mixture ratios of 3.41 to 8.36. Sixty percent of the fuel was used for film cooling. These temperature profiles were used as boundary conditions in a finite element analysis program, MSC/NASTRAN, to calculate the local radial and axial heat fluxes in the chamber wall. The normal heat fluxes were then calculated and used as a diagnostic of the rocket's flow field behavior. The normal heat fluxes determined were on the order of 1.0 to 3.0 MW/meters squared (0.6 to 1.8 Btu/sec-inches squared). In the cases where mixture ratio was 5 or above, there was a sharp local heat flux maximum in the barrel section of the chamber. This local maximum seems to indicate a reduction or breakdown of the fuel film cooling layer, possibly due to increased mixing in the shear layer between the film and core flows. However, the flow was thought to be completely laminar, as the throat Reynolds numbers were below 50,000 for all the cases. The increased mixing in the shear layer in the higher mixture ratio cases appeared not to be due to the transition of the flow from laminar to turbulent, but rather due to increased reactions between the hydrogen film and oxidizer-rich core flows.
Author (revised)

N93-28658# Sparta, Inc., Edwards AFB, CA.
MEASUREMENTS OF MAGNETIC FIELDS PRODUCED BY A 30 kWe CLASS ARCJET POWER CONDITIONING UNIT Final Report, period ending Jun. 1992
Daron Bromaghim Jan. 1993 25 p
(DA Proj. 3058)
(AD-A262786; AD-E201429; PL-TR-92-3049) Avail: CASI HC A03/MF A01

The magnetic fields produced by a 30 kWe class Arcjet Power Conditioning Unit were measured using a Gauss meter and an axial magnetic field probe. These tests were conducted at Rocket Research Company in Redmond, WA from 11-12 Jun 1992, using a 30 kWe class Arcjet Power Conditioning Unit (PCU), and associated hardware. The PCU is an engineering model designed by Pacific Electrodynamics for the Electric Propulsion Experiment (ESEX) to be flown on the Advanced Research and Global Observation Satellite (ARGOS). Measurements were recorded at various locations around the PCU at ambient conditions and at power levels of 26, 20, 10, and 6.5 kWe. The results indicate the magnetic field presence is at a level, considering the 'worst case' scenario of test, well below any that would result in damaging effects to the spacecraft or to any other experiment.
DTIC

N93-28680*# Alabama Univ., Huntsville. Dept. of Mechanical Engineering.
ADVANCED EARTH-TO-ORBIT PROPULSION TECHNOLOGY INFORMATION, DISSEMINATION AND RESEARCH Final Report, 13 Jul. 1989 - 31 May 1993
S. T. Wu 31 May 1993 45 p
(Contract NAS8-36955)
(NASA-CR-192561; NAS 1.26:192561; UAH-5-32210FNL) Avail: CASI HC A03/MF A01

A conference was held at MSFC in May 1992 describing the research achievements of the NASA-wide research and technology programs dealing with advanced oxygen/hydrogen and oxygen/hydrocarbon earth-to-orbit propulsion. The purpose of this conference was to provide a forum for the timely dissemination to the propulsion community of the results emerging from this program with particular emphasis on the transfer of information from the scientific/research to the designer.
Author (revised)

N93-28686*# National Aeronautics and Space Administration. Lewis Research Center, Cleveland, OH.
SMALL STIRLING DYNAMIC ISOTOPE POWER SYSTEM FOR ROBOTIC SPACE MISSIONS
D. J. Bents Aug. 1992 18 p Presented at the Nuclear Technologies for Space Exploration, Jackson Hole, WY, 16-19 Aug. 1992; sponsored by American Nuclear Society
(RTOP 596-13-11)
(NASA-TM-105785; E-7215; NAS 1.15:105785) Avail: CASI HC A03/MF A01

The design of a multihundred-watt Dynamic Isotope Power System (DIPS), based on the U.S. Department of Energy (DOE) General Purpose Heat Source (GPHS) and small (multihundred-watt) free-piston Stirling engine (FPSE), is being pursued as a potential lower cost alternative to radioisotope thermoelectric generators (RTG's). The design is targeted at the power needs of future unmanned deep space and planetary surface exploration missions ranging from scientific probes to Space Exploration Initiative precursor missions. Power level for these missions is less than a kilowatt. The incentive for any dynamic system is that it can save fuel and reduce costs and radiological hazard. Unlike DIPS based on turbomachinery conversion (e.g. Brayton), this small Stirling DIPS can be advantageously scaled to multihundred-watt unit size while preserving size and mass competitiveness with RTG's. Stirling conversion extends the competitive range for dynamic systems down to a few hundred watts--a power level not previously considered for dynamic systems. The challenge for Stirling conversion will be to demonstrate reliability and life similar to RTG experience. Since the competitive potential of FPSE as an isotope converter was first identified, work has focused on feasibility of directly integrating GPHS with the Stirling heater head. Thermal modeling of various radiatively coupled heat source/heater head geometries has been performed using data furnished by the developers of FPSE and GPHS. The analysis indicates that, for the 1050 K heater head configurations considered, GPHS fuel clad temperatures remain within acceptable operating limits. Based on these results, preliminary characterizations of multihundred-watt units have been established.
Author (revised)

N93-28694*# National Aeronautics and Space Administration. Lewis Research Center, Cleveland, OH.
PRELIMINARY ENDURANCE TESTS OF WATER VAPORIZERS FOR RESISTOJET APPLICATIONS
W. Earl Morren and Gregory S. MacRae Jun. 1993 27 p Presented at the 29th Joint Propulsion Conference and Exhibit, Monterey, CA, 28-30 Jun. 1993; cosponsored by AIAA, SAE, ASME, and ASEE
(RTOP 506-42-31)
(NASA-TM-106222; E-7871; NAS 1.15:106222; AIAA Paper 93-2403)
Avail: CASI HC A03/MF A01

Three water vaporizers designed for resistojet applications were built and tested for periods up to 500 h and 250 thermal cycles. Two of the vaporizers were not sensitive to orientation with respect to gravity, an indication of likely compatibility with low-gravity environments. Some temperatures and pressures in the third were impacted by orientation, although operation was always stable. The pressure drop across the sand-filled version increased by 147 percent in 38 h and 19 thermal cycles. Bonding of the sand granules in the downstream end of the heat exchanger was the suspected cause of failure of this vaporizer. Pressure drops across the two sintered stainless steel-filled versions were more gradual. One, with a pore size of 60 microns, showed an 80 percent increase in 500 h and 250 thermal cycles and another, with a 10 microns poresize, showed a 29 percent increase in 350 h and 175 thermal cycles. Testing of the latter metal-filled vaporizer was ongoing as of this writing. Oxidation of the porous metal packing materials in these vaporizers, with subsequent deposition of oxide particles within the pores, was believed to have caused the observed increases in pressure drops.
Author (revised)

N93-28946*# Pratt and Whitney Aircraft, West Palm Beach, FL.
ADVANCED ENGINE STUDY PROGRAM Final Report
A. I. Masters, D. E. Galler, T. F. Denman, R. A. Shied, J. R. Black, A. R. Fierstein, G. L. Clark, and B. R. Branstrom Jun. 1993 243 p
(Contract NAS3-23858; RTOP 593-12-11)
(NASA-CR-187217; E-7909; NAS 1.26:187217) Avail: CASI HC A11/MF A03

A design and analysis study was conducted to provide advanced engine descriptions and parametric data for space transfer vehicles. The study was based on an advanced oxygen/hydrogen engine in the 7,500 to 50,000 lbf thrust range. Emphasis was placed on defining requirements for high-performance engines capable of achieving reliable and versatile operation in a space environment. Four variations on the expander cycle were compared, and the advantages and disadvantages of each were assessed. Parametric weight, envelope, and performance data were generated over a range of 7,500 to 50,000 lb thrust and a wide range of chamber pressure and nozzle expansion ratio. Author

N93-28950*# National Aeronautics and Space Administration. Marshall Space Flight Center, Huntsville, AL.

ALTITUDE COMPENSATING ABLATIVE STIFFENING BAND FOR ROCKET MOTOR NOZZLES Patent Application

J. Lynn Brown, inventor (to NASA) (Pratt and Whitney Aircraft, West Palm Beach, FL.), Vaughn W. McIntire, Jr., inventor (to NASA) (Pratt and Whitney Aircraft, West Palm Beach, FL.), Leslie A. Clontz, inventor (to NASA) (Pratt and Whitney Aircraft, West Palm Beach, FL.), Richard J. Peckham, inventor (to NASA) (Pratt and Whitney Aircraft, West Palm Beach, FL.), Alan B. C. Dixon, inventor (to NASA) (Pratt and Whitney Aircraft, West Palm Beach, FL.), and James C. West, inventor (to NASA) (Pratt and Whitney Aircraft, West Palm Beach, FL.) 19 Mar. 1993 8 p
(NASA-Case-MFS-28728-1; NAS 1.71:MFS-28728-1;
US-Patent-Appl-SN-034452) Avail: CASI HC A02/MF A01

A rocket motor nozzle with an ablative internal structural member which provides rigidity to the rocket motor both prior to and during motor operation is described. The rocket motor nozzle of the present invention includes an outer shell which converges to a throat and then diverges to form an entrance. An ablative stiffening band, secured to the inner surface of the nozzle and extending from the aft portion of the nozzle to the throat, is contoured to allow the exhaust gases to flow smoothly through a central longitudinal opening in the band. NASA

N93-29068*# Sverdrup Technology, Inc., Brook Park, OH.

RELIABILITY ASSESSMENT OF THRUST CHAMBER COOLING CONCEPTS USING PROBABILISTIC ANALYSIS TECHNIQUES

Douglas C. Rapp Jun. 1993 20 p Presented at the 29th Joint Propulsion Conference and Exhibit, Monterey, CA, 28-30 Jun. 1993; sponsored by AIAA, SAE, ASME, and ASEE
(Contract NAS3-25266; RTOP 584-04-11)
(NASA-CR-190785; E-7932; NAS 1.26:190785; AIAA Paper 93-2163)
Avail: CASI HC A03/MF A01

The reliability of OFHC (Oxygen Free High Conductivity) copper and NARloy-Z thrust chambers is assessed by applying probabilistic structural analysis techniques to incorporate design parameter variability and uncertainty. Thrust chambers specifically evaluated are the cylindrical test fixtures employed in a plug-nozzle configuration at the NASA Lewis Research Center. Direct sampling Monte Carlo simulations based on a simplified life prediction methodology established probability densities of firing cycles to structural failure. Simulated cyclic lives demonstrated modest agreement to experiment. Similarly, regions of high structural failure probability were determined using a limit state approach employing calculated cumulative distribution functions for effective stress response and an assumed material strength distribution. A probability of failure of 0.012 was calculated at the center of the coolant channel hot-gas-side wall for an OFHC milled channel. Structural response was found to be sensitive to the uncertainties in the thrust chamber thermal environment and the material's thermal expansion coefficient. Author

N93-29091*# Lamar Univ., Beaumont, TX. Coll. of Engineering.

EVALUATION OF ACTUATOR ENERGY STORAGE AND POWER SOURCES FOR SPACECRAFT APPLICATIONS

William E. Simon and Fred M. Young 26 May 1993 74 p
(Grant NAG9-561)
(NASA-CR-193226; NAS 1.26:193226) Avail: CASI HC A04/MF A01

The objective of this evaluation is to determine an optimum energy storage/power source combination for electrical actuation systems for existing (Solid Rocket Booster (SRB), Shuttle) and future (Advanced Launch System (ALS), Shuttle Derivative) vehicles. Characteristic of these applications is the requirement for high power pulses (50-200 kW) for short times (milliseconds to seconds), coupled with longer-term base or 'housekeeping' requirements (5-16 kW). Specific study parameters (e.g., weight, volume, etc.) as stated in the proposal and specified in the Statement of Work (SOW) are included. Author (revised)

N93-29158*# National Aeronautics and Space Administration. Lewis Research Center, Cleveland, OH.

PRELIMINARY INVESTIGATION OF HIGH POWER MICROWAVE PLASMAS FOR ELECTROTHERMAL THRUSTER USE

John L. Power and Daniel J. Sullivan Jun. 1993 18 p Presented at the 29th Joint Propulsion Conference and Exhibit, Monterey, CA, 28-30 Jun. 1993; sponsored by AIAA, SAE, ASME, and ASEE Original contains color illustrations
(RTOP 506-42-31)
(NASA-TM-106207; E-7917; NAS 1.15:106207; AIAA Paper 93-2106)
Avail: CASI HC A03/MF A01; 1 functional color page

Results are reported from preliminary tests to evaluate the high power microwave electrothermal thruster (MET) concept, which employs a free-floating plasma discharge maintained by applied CW microwave power to heat a propellant gas flow. Stable plasmas have been created and maintained in helium (He), nitrogen (N2), and hydrogen (H2) as propellants in both the TM(sub 011) and TM(sub 012) modes at discharge pressures from 10 Pa to 69 kPa. Reproducible starting conditions of pressure and power have been documented for all the plasmas. Vortical inflow of the propellant gas was observed to cause the formation of on-axis 'spike' plasmas. The formation and unformation conditions of these plasmas were studied. Operation in the spike plasma condition enables maximum power absorption with minimum wall heating and offers maximum efficiency in heating the propellant gas. In the spike condition, plasmas of the three propellant gases were investigated in an open channel configuration to a maximum applied power level of 11.2 kW (in N2). Microwave power coupling efficiencies of over 90 percent were routinely obtained at absorbed power levels up to 2 kW. Magnetic nozzle effects were investigated with a superconducting solenoid Al magnet applying a high magnetic field to the plasmas in and exiting from the discharge tube. Author (revised)

N93-29194*# National Aeronautics and Space Administration. Lewis Research Center, Cleveland, OH.

GRAVITY SENSITIVITY OF A RESISTOJET WATER VAPORIZER

W. Earl Morren Jun. 1993 24 p Presented at the 29th Joint Propulsion Conference and Exhibit, Monterey, CA, 28-30 Jun. 1993; cosponsored by AIAA, SAE, ASME, ASEE
(RTOP 506-42-31)
(NASA-TM-106220; E-7870; NAS 1.15:106220; AIAA Paper 93-2402)
Avail: CASI HC A03/MF A01

A laboratory model of a water vaporizer for resistojet applications was designed, fabricated, and steady and transient characteristics were measured. Vaporizer operation was not impacted by rotation about a horizontal axis normal to its own. The vaporizer was operated under low and high accelerations aboard a jet aircraft for periods up to 25 s at flow rates ranging from 159(10)(exp -6) to 230(10)(exp -6) kg/s. Slight changes in inlet and outlet pressures and some heat exchanger temperatures were observed during the low-gravity tests. However, the results of these tests indicated probable compatibility of the vaporizer design tested with a low-gravity environment. Author (revised)

N93-29289# Purdue Univ., West Lafayette, IN. School of Nuclear Engineering.

ENGINEERING CONSIDERATION FOR THE SELF-ENERGIZING MAGNETOPLASMADYNAMIC (MPD): TYPE FUSION PLASMA THRUSTER Annual Report, Jul. 1991 - Jun. 1992

Chan K. Choi and Glen T. Nakafuji Feb. 1993 103 p
(Contract F04611-90-K-0054)
(AD-A262785; AD-E201447; PL-PU/92003; PL-TR-92-3043) Avail: CASI HC A06/MF A02

The major objective of the present study is to perform parametric studies of various DPF electrode configurations using an equivalent circuit model. The operation of the DPF device in the current-rise state is modeled using a transient code simulation of the equivalent circuit. Parametric studies of four DPF electrode configurations which include the tapered, cylindrical anode tip of the Livermore-I experiment, the anode tip with an equilateral triangular shape, the extended triangular anode tip, and the untapered cylindrical anode tip were all performed. Besides the various geometrical shapes, the electrode configurations also depend very sensitively on the dimension of the anode length. The parametric studies indicated that both the equilateral triangular tip and the cylindrical tip configurations generated high sheath currents and F/W values while maintaining relatively similar values of I(sub sp) for all electrode configurations. The extended triangular tip geometry, however, performed less favorably to F/W values and the sheath currents, though the differences compared to the values of other geometries were not very significant. It is thus noted that adequate operating currents can be reached by optimizing the electrode geometry and the charging circuit voltage and that the equivalent circuit modeling provides a realistic basis for analyzing plasma focus pinch dynamics. DTIC

N93-29847*# National Aeronautics and Space Administration. Marshall Space Flight Center, Huntsville, AL.
LIQUID FUEL INJECTION ELEMENTS FOR ROCKET ENGINES Patent Application
George B. Cox, Jr., inventor (to NASA) (Pratt and Whitney Aircraft, West Palm Beach, FL.) 27 Jan. 1993 17 p
(NASA-Case-MFS-28547-1; NAS 1.71:MFS-28547-1; US-Patent-Appl-SN-010037) Avail: CASI HC A03/MF A01

Thrust chambers for liquid propellant rocket engines include three principal components. One of these components is an injector which contains a plurality of injection elements to meter the flow of propellants at a predetermined rate, and fuel to oxidizer mixture ratio, to introduce the mixture into the combustion chamber, and to cause them to be atomized within the combustion chamber so that even combustion takes place. Evolving from these injectors are tube injectors. These tube injectors have injection elements for injecting the oxidizer into the combustion chamber. The oxidizer and fuel must be metered at predetermined rates and mixture ratios in order to mix them within the combustion chamber so that combustion takes place smoothly and completely. Hence tube injectors are subject to improvement. An injection element for a liquid propellant rocket engine of the bipropellant type is provided herein which includes tangential fuel metering orifices, and a plurality of oxidizer tube injection elements whose injection tubes are also provided with tangential oxidizer entry slots and internal reed valves. NASA

N93-30402# Wentworth Inst., Boston, MA.
AEROSPACE PAYLOAD DESIGN AND DEVELOPMENT Final Report, Mar. 1988 - May 1992
Richard B. Gates 4 Nov. 1992 24 p
(Contract F19628-88-C-0031)
(AD-A264502; PL-TR-92-2292) Avail: CASI HC A03/MF A01

Summarized in this report is the work performed under contract F19628-88-C-0031, from March 1988 through May 1992. Efforts consisted of design and fabrication of one-of-a-kind payloads and instruments, field launch services and refurbishment of recovered payloads and instruments. DTIC

N93-30507*# National Aeronautics and Space Administration. Lyndon B. Johnson Space Center, Houston, TX.
HYPERVELOCITY IMPACT TESTING OF THE SPACE STATION UTILITY DISTRIBUTION SYSTEM CARRIER
Scott Lazaroff Jul. 1993 61 p
(NASA-TM-104771; S-723; NAS 1.15:104771) Avail: CASI HC A04/MF A01

A two-phase, joint JSC and McDonnell Douglas Aerospace-Huntington Beach hypervelocity impact (HVI) test program was initiated to develop an improved understanding of how meteoroid and orbital debris (M/OD) impacts affect the Space Station Freedom (SSF) avionic and fluid lines routed in the Utility Distribution System (UDS) carrier. This report documents the first phase of the test program which covers nonpowered avionic line segment and pressurized fluid line segment HVI testing. From these tests, a better estimation of avionic line failures is approximately 15 failures per year and could very well drop to around 1 or 2 avionic line failures per year (depending upon the results of the second phase testing of the powered avionic line at White Sands). For the fluid lines, the initial McDonnell Douglas analysis calculated 1 to 2 line failures over a 30 year period. The data obtained from these tests indicate the number of predicted fluid line failures increased slightly to as many as 3 in the first 10 years and up to 15 for the entire 30 year life of SSF. Author (revised)

N93-30648*# Thiokol Corp., Brigham City, UT. Space Operations.
POSTFLIGHT HARDWARE EVALUATION 360T025 (RSRM-25, STS-46). APPENDIX D: NOZZLE POSTFIRE DATA Final Report
Mar. 1993 15 p
(Contract NAS8-38100)
(NASA-CR-192580; NAS 1.26:192580; TWR-60699-App-D) Avail: CASI HC A03/MF A01

The final Postflight Hardware Evaluation Report 360T025, Appendix D is provided. Nozzle postfire data are included. Char and erosion data are provided. CASI

N93-28709*# Phillips Lab., Edwards AFB, CA.
ELITE PROGRAM: ELECTRIC INSERTION TRANSFER EXPERIMENT
Robert Vondra *In* NASA, Washington, NASA/DOD Flight Experiments Technical Interchange Meeting Proceedings 1992 12 p Prepared in cooperation with Dayton Univ. Research Inst., Edwards AFB, CA (For primary document see N93-28699 11-12)
Avail: CASI HC A03/MF A10

N93-28710*# Southwest Research Inst., San Antonio, TX.
LIQUID MOTION IN A ROTATING TANK EXPERIMENT (LME)
F. T. Dodge *In* NASA, Washington, NASA/DOD Flight Experiments Technical Interchange Meeting Proceedings 1992 20 p Sponsored by NASA. Goddard Space Flight Center (For primary document see N93-28699 11-12)
Avail: CASI HC A03/MF A10

N93-28711*# Martin Marietta Corp., Denver, CO.
VENTED TANK RESUPPLY EXPERIMENT (VTRE) FOR IN-SPACE TECHNOLOGY EXPERIMENT PROGRAM (IN-STEP) Report, Jun. 1991 - Jul. 1992
In NASA, Washington, NASA/DOD Flight Experiments Technical Interchange Meeting Proceedings 1992 26 p (For primary document see N93-28699 11-12)
(Contract NAS3-25977)
Avail: CASI HC A03/MF A10

N93-28712*# Boeing Defense and Space Group, Seattle, WA.
TANK PRESSURE CONTROL EXPERIMENT (TPCE)
Mike Bentz *In* NASA, Washington, NASA/DOD Flight Experiments Technical Interchange Meeting Proceedings 1992 13 p (For primary document see N93-28699 11-12)
Avail: CASI HC A03/MF A10

N93-28713*# National Aeronautics and Space Administration. Lewis Research Center, Cleveland, OH.
TANK PRESSURE CONTROL EXPERIMENT/THERMAL PHENOMENA (TPCE/TP)
M. M. Hasan and R. H. Knoll *In* NASA, Washington, NASA/DOD Flight Experiments Technical Interchange Meeting Proceedings 1992 18 p (For primary document see N93-28699 11-12)
Avail: CASI HC A03/MF A10

N93-28724*# Phillips Lab., Hanscom AFB, MA.
NEP SPACE TEST PROGRAM OBJECTIVE
In NASA, Washington, NASA/DOD Flight Experiments Technical Interchange Meeting Proceedings 1992 9 p (For primary document see N93-28699 11-12)
Avail: CASI HC A02/MF A10

N93-29570*# Cincinnati Univ., OH. Artificial Intelligence and Computer Vision Lab.
A FUZZY CASE BASED REASONING TOOL FOR MODEL BASED APPROACH TO ROCKET ENGINE HEALTH MONITORING
Srinivas Krovvidy, Adam Nolan, Yong-Lin Hu, and William G. Wee *In* NASA. Johnson Space Center, North American Fuzzy Logic Processing Society (NAFIPS 1992), Volume 2 Dec. 1992 p 488-495 (For primary document see N93-29556 11-59)
Avail: CASI HC A02/MF A03

N93-29758*# Virginia Polytechnic Inst. and State Univ., Blacksburg.
SOLAR ELECTRIC PROPULSION CARGO SPACECRAFT FOR MARS MISSIONS
In Universities Space Research Association, Houston, Proceedings of the Seventh Annual Summer Conference. NASA/USRA: University Advanced

Design Program 1991 p 313-316 (For primary document see N93-29712 11-01)
Avail: CASI HC A01/MF A03

N93-29907# Alenia Spazio S.p.A., Rome (Italy).
ELECTRIC PROPULSION FOR LIGHTSATS: A REVIEW OF APPLICATIONS AND ADVANTAGES
G. Perrotta, Gianfranco F. Cirri (Proel Tecnologie, Florence, Italy.), and Giovanni Matticari (Proel Tecnologie, Florence, Italy.) *In* AGARD, TacSats for Surveillance Verification and C3I Feb. 1993 7 p (For primary document see N93-29892 11-32)
Copyright Avail: CASI HC A02/MF A03

23 CHEMISTRY AND MATERIALS (GENERAL)

N93-29067*# National Aeronautics and Space Administration. Langley Research Center, Hampton, VA.
LDEF MATERIALS DATA BASES
Joan G. Funk, John W. Strickland (BAMSI, Inc., Huntsville, AL.), and John M. Davis (National Aeronautics and Space Administration. Marshall Space Flight Center, Huntsville, AL.) Jun. 1993 31 p
(RTOP 506-43-61)
(NASA-TM-107757; NAS 1.15:107757) Avail: CASI HC A03/MF A01

The Long Duration Exposure Facility (LDEF) and the accompanying experiments were composed of and contained a wide variety of materials representing the largest collection of materials flown in low Earth orbit (LEO) and retrieved for ground based analysis to date. The results and implications of the mechanical, thermal, optical, and electrical data from these materials are the foundation on which future LEO space missions will be built. The LDEF Materials Special Investigation Group (MSIG) has been charged with establishing and developing data bases to document these materials and their performance to assure not only that the data are archived for future generations but also that the data are available to the spacecraft user community in an easily accessed, user-friendly form. This paper discusses the format and content of the three data bases developed or being developed to accomplish this task. The hardware and software requirements for each of these three data bases are discussed along with current availability of the data bases. This paper also serves as a user's guide to the MAPTIS LDEF Materials Data Base. Author

N93-29474# Minnesota Univ., Minneapolis. Dept. of Chemistry.
SYNTHESIS OF OLIGOIMIDES AND OLIGOIMIDE ANION RADICALS Final Technical Report
Larry L. Miller 1992 11 p
(Contract N00014-90-J-1569)
(AD-A263129) Avail: CASI HC A03/MF A01

Key to the results described in parts B-D are compounds based on naphthalene dianhydride (A) and dimethoxybenzidine (B). It was demonstrated that AB type oligoimides with lengths up to 80 A (8 nm) (BABABAB) could be synthesized as single molecular weight, pure and usually soluble compounds. Although rotation about the single bonds along the chain is possible, the chains cannot fold. These oligomers constitute the longest, single molecular weight rigid rods that are known. Various end groups could be attached and unsymmetrical rigid rods (different end groups) could be prepared. The compounds were characterized by NMR, IR, MS, and HPLC. In one case, a single crystal was obtained which confirmed the linear structure and that the B units were twisted with respect to the A units. Electrochemical studies showed that the naphthalene diimide group (A) formed anion radical (A-) and dianions (A=), which were stable in DMF in the absence of air. DTIC

N93-30948*# National Aeronautics and Space Administration. Langley Research Center, Hampton, VA.
NATIONAL EDUCATORS' WORKSHOP. UPDATE 92: STANDARD EXPERIMENTS IN ENGINEERING MATERIALS SCIENCE AND TECHNOLOGY
James E. Gardner, comp., James A. Jacobs, comp. (Norfolk State Univ., VA.), and Douglas F. Craig, comp. (Oak Ridge National Lab., TN.) Washington Jun. 1993 443 p Workshop held in Oak Ridge, TN, 11-13 Nov. 1992; sponsored by NASA, DOE, NIST, and Norfolk State University
(RTOP 505-63-50-01)
(NASA-CP-3201; L-17236; NAS 1.55:3201) Avail: CASI HC A19/MF A04

This document contains a collection of experiments presented and demonstrated at the workshop. The experiments related to the nature and properties of engineering materials and provided information to assist in teaching about materials in the education community. For individual titles, see N93-30949 through N93-30979.

N93-30949*# Concurrent Technologies Corp., Johnstown, PA.
NEAR NET SHAPE PROCESSING: A NECESSITY FOR ADVANCED MATERIALS APPLICATIONS
Howard A. Kuhn *In* NASA. Langley Research Center, National Educators' Workshop. Update 92: Standard Experiments in Engineering Materials Science and Technology Jun. 1993 p 1-3 (For primary document see N93-30948 11-23)
Avail: CASI HC A03/MF A04

High quality discrete parts are the backbones for successful operation of equipment used in transportation, communication, construction, manufacturing, and appliances. Traditional shapemaking for discrete parts is carried out predominantly by machining, or removing unwanted material to produce the desired shape. As the cost and complexity of modern materials escalates, coupled with the expense and environmental hazards associated with handling of scrap, it is increasingly important to develop near net shape processes for these materials. Such processes involve casting of liquid materials, consolidation of powder materials, or deformation processing of simple solid shapes into the desired shape. Frequently, several of these operations may be used in sequence to produce a finished part. The processes for near net shape forming may be applied to any type of material, including metals, polymers, ceramics, and their composites. The ability to produce shapes is the key to implementation of laboratory developments in materials science into real world applications. This seminar presents an overview of near net shapemaking processes, some application examples, current developments, and future research opportunities. Derived from text

N93-30950*# Jackson State Univ., MS. Dept. of Technology.
DEVELOPMENT OF AN EXPERIMENTAL METHOD TO DETERMINE THE AXIAL RIGIDITY OF A STRUT-NODE JOINT c39
W. V. Brewer and Hui-Ru Shih *In* NASA. Langley Research Center, National Educators' Workshop. Update 92: Standard Experiments in Engineering Materials Science and Technology Jun. 1993 p 35-42 (For primary document see N93-30948 11-23)
Avail: CASI HC A02/MF A04

The following are presented: the experimental procedure and the results that have been performed to determine the axial rigidity of the strut-node joint; and the method for modifying a simple testing machine to make it capable of performing more accurate tests over a specific load range and able to accept larger test assemblies. Author (revised)

N93-30951*# Texas A&M Univ., College Station. Department of Mechanical Engineering.
MECHANICAL PROPERTIES OF COMPOSITE MATERIALS c24
H. Richard Thornton and L. R. Cornwell *In* NASA. Langley Research Center, National Educators' Workshop. Update 92: Standard Experiments in Engineering Materials Science and Technology Jun. 1993 p 43-48 (For primary document see N93-30948 11-23)
Avail: CASI HC A01/MF A04

A composite material incorporates high strength, high modulus fibers in a matrix (polymer, metal, or ceramic). The fibers may be oriented in a manner to give varying in-plane properties (longitudinal, transverse-stress, strain, and modulus of elasticity). The lay-up of the composite laminates is such that a center line of symmetry and no bending moment exist through the thickness. The laminates are tabbed, with either aluminum or fiberglass, and are ready for tensile testing. The determination of the tensile properties of resin matrix composites, reinforced by continuous fibers, is outlined in ASTM standard D 3039, Tensile Properties of Oriented Fiber Composites. The tabbed flat tensile coupons are placed into the grips of a tensile machine and load-deformation curves plotted. The load-deformation data

are translated into stress-strain curves for determination of mechanical properties (ultimate tensile strength and modulus of elasticity).
Derived from text

N93-30952*# Pennsylvania State Univ., University Park.
NEW MATERIALS: FOUNTAINHEAD FOR NEW TECHNOLOGIES AND NEW SCIENCE
Roy Rustum *In* NASA. Langley Research Center, National Educators' Workshop. Update 92: Standard Experiments in Engineering Materials Science and Technology Jun. 1993 p 49-98 (For primary document see N93-30948 11-23)
Avail: CASI HC A03/MF A04

The role of materials as the benchmark technologies which give epochs of human history their names continues into the present. The discovery of new materials has nearly always been the source of new materials science, and frequently of new technologies. This paper analyzes the actual processes by which new materials are synthesized, i.e. whether driven by serendipitous observations, new knowledge is pulled by the market, or integrated into a technological thrust. This analysis focuses on modern ceramic materials discoveries, since World War 2 and uses 45 years experience in materials synthesis in the author's own laboratory as case studies. A dozen different families of materials or processes are involved: hydrothermal reactions; sol-gel processing; clays and zeolites; electroceramics; zero expansion ceramics; diamond films; and radioactive waste host phases. Nanocomposite concepts introduced by the author a decade ago offer an entire, large, new class of materials which will dominate synthesis for the next period. The future of materials research for the next 25 years cannot be extrapolated from the past 25 years. We are near the asymptote for materials utilization in most metals. Likewise we are approaching saturation in improvement of many useful properties. Justifying much further 'basic' R/D for incremental improvement in civilian-oriented industries will not be easy. In materials synthesis, the near-term future is sure to emphasize not new phases, but tailored micro- and nanocomposites for chemical, electrical, optical, and magnetic uses. Unexpected new discoveries such as the Lanxide process may offer rarer chances for step function advances. The new structure of knowledge management will rely less on local research than on integration of worldwide inputs. Better scientific and technological opportunities will lie in designing knowledge intensive materials to meet the new environmental and conservation goals, and the human needs of the very large numbers at the bottom of the socio-economic structures of the world.
Derived from text

N93-30953*# Duke Univ., Durham, NC. Dept. of Mechanical Engineering and Material Science.
MICROPIPET MANIPULATION OF LIPID MEMBRANES: DIRECT MEASUREMENT OF THE MATERIAL PROPERTIES OF A COHESIVE STRUCTURE THAT IS ONLY TWO MOLECULES THICK **c27**
David Needham *In* NASA. Langley Research Center, National Educators' Workshop. Update 92: Standard Experiments in Engineering Materials Science and Technology Jun. 1993 p 99-120 (For primary document see N93-30948 11-23)
Avail: CASI HC A03/MF A04

The objectives are to demonstrate how we can make direct measurements of the mechanical properties of a special structure in biology, namely the lipid bilayer membrane, using a micromanipulation technique, and how these properties compare and contrast with 'more traditional' technological/engineering materials. Given that the investment in equipment and expertise to carry out these experiments is probably beyond the scope of most teaching labs, the described experiment is not intended as one that can actually be demonstrated in a student laboratory class. The intention behind presenting this work is to begin to raise awareness in the Material Science community about the material properties of biological material that form a new (to us) category of soft engineering materials that have dimensions on the nanoscale. Derived from text

N93-30954*# Purdue Univ., West Lafayette, IN. Mechanical Engineering Technology Dept.
TOOL GRINDING AND SPARK TESTING **c31**
Edward L. Widener *In* NASA. Langley Research Center, National Educators' Workshop. Update 92: Standard Experiments in Engineering Materials Science and Technology Jun. 1993 p 121-126 (For primary document see N93-30948 11-23)
Avail: CASI HC A01/MF A04

The objectives were the following: (1) to revive the neglected art of metal-sparking; (2) to promote quality-assurance in the workplace; (3) to avoid spark-ignited explosions of dusts or volatiles; (4) to facilitate the salvage of scrap metals; and (5) to summarize important references.
Derived from text

N93-30955*# College of Western New England, Springfield, MA. Dept. of Electrical Engineering.
EXPERIMENTS IN CORROSION FOR YOUNGER STUDENTS BY AND FOR OLDER STUDENTS **c26**
James V. Masi *In* NASA. Langley Research Center, National Educators' Workshop. Update 92: Standard Experiments in Engineering Materials Science and Technology Jun. 1993 p 127-136 (For primary document see N93-30948 11-23)
Avail: CASI HC A02/MF A04

The objectives are to illustrate the electrochemical nature of corrosion and to observe the location of anodes and cathodes (arising from differences in composition and cold work) of metals immersed in electrolyte solutions. The magnitudes of voltages and current densities on corroding couples is obtained. Derived from text

N93-30956*# Tulsa Univ., OK. Dept. of Mechanical Engineering.
A MINIATURE FATIGUE TEST MACHINE **c35**
Steven M. Tipton *In* NASA. Langley Research Center, National Educators' Workshop. Update 92: Standard Experiments in Engineering Materials Science and Technology Jun. 1993 p 137-146 (For primary document see N93-30948 11-23)
Avail: CASI HC A02/MF A04

The objective is to enable the student to generate statistically sound fatigue data sets on wire specimens of varying diameter, microstructure, or material. The student can then assess the effect of these parameters of fatigue resistance. The student can also be exposed to ASTM techniques for fatigue data reduction and presentation. Experiments involving variable amplitude block loading are also easily conducted. Derived from text

N93-30957*# National Aeronautics and Space Administration. Langley Research Center, Hampton, VA.
INTRODUCTION TO HIGH PERFORMANCE COMPOSITES **c24**
Norman J. Johnston *In its* National Educators' Workshop. Update 92: Standard Experiments in Engineering Materials Science and Technology Jun. 1993 p 147-192 (For primary document see N93-30948 11-23)
Avail: CASI HC A03/MF A04

The following questions are addressed: What are high performance composites?; How are they used today?; What are their properties?; How do you make them?; and What are the future technology needs for composites? In addition, samples of composite reinforcements such as glass, carbon and Kevlar fibers, matrix materials, and fabricated composite parts will be demonstrated and made available. Author (revised)

N93-30958*# Norfolk State Univ., VA.
MATERIALS EDUCATION ACTIVITIES **c80**
Heidi R. Ries, Jonice Harris (National Inst. of Standards and Technology, Gaithersburg, MD.), Woodrow W. Leake (American Society for Engineering Education, Washington, DC.), L. Roy Bunnell (Battelle Pacific Northwest Labs., Richland, WA.), and Robert Berrettini (Materials Research Society, University Park, PA.) *In* NASA. Langley Research Center, National Educators' Workshop. Update 92: Standard Experiments in Engineering Materials Science and Technology Jun. 1993 p 193-196 (For primary document see N93-30948 11-23)
Avail: CASI HC A01/MF A04

Last year, at NEW: Update '91, a panel discussion was held to address the unique difficulties of attracting and retaining minorities and women in technical studies. Unfortunately, retention in technical majors is a problem of varying proportions for the entire student population, and must be improved in order to maintain the strength of the nation's industrial base. To investigate the cause of student attrition in technical majors, in-depth interviews of both current and former (non-graduating) engineering students at four colleges and universities in Colorado were conducted by Hewitt and Seymour. They found that there was no significant difference in the level of high school preparation and undergraduate academic performance in these two

groups, despite the prevailing faculty perception that most students who switch from technical to nontechnical majors were underprepared. The majority of engineering students who changed majors reported that they were turned off by science, while one-third complained of poor teaching.
Derived from text

N93-30959*# North Carolina Agricultural and Technical State Univ., Greensboro. Dept. of Manufacturing Systems.
IMPROVED MEASUREMENT OF THERMAL EFFECTS ON MICROSTRUCTURE **c76**
Mansur Rastani *In* NASA. Langley Research Center, National Educators' Workshop. Update 92: Standard Experiments in Engineering Materials Science and Technology Jun. 1993 p 197-207 (For primary document see N93-30948 11-23)
Avail: CASI HC A02/MF A04

The objectives were to introduce a simple methodology which could be used to replace the time-consuming and expensive conventional methods of metallographic and quantitative analysis of thermal treatment effect on microstructure. Metallurgical analysis continually calls for the evaluation of thermal treatment effects on microstructure. This commonly demands metallographic sample preparation and microscopic examination, which are time absorbing and costly. These drawbacks are burdensome when large numbers of samples must be levied fast. Mechanical testing can sometimes be substituted, but sample size and shape frequently make these methods impractical. The experiment described here is ideal for the microstructural evaluation of lamp filaments and other wire samples such as copper wire which can be conveniently coiled. Derived from text

N93-30960*# Montana State Univ., Bozeman. Coll. of Engineering.
DIRECT TENSION EXPERIMENTS ON COMPACTED GRANULAR MATERIALS **c39**
Steven W. Perkins *In* NASA. Langley Research Center, National Educators' Workshop. Update 92: Standard Experiments in Engineering Materials Science and Technology Jun. 1993 p 209-220 (For primary document see N93-30948 11-23)
Avail: CASI HC A03/MF A04

The objective of this experiment is to determine the level of tensile strength of uncemented, dry, granular materials. The experimental apparatus does not lend itself to a direct measurement of the material's tensile strength, but must be analyzed as a stress field problem in order to arrive at a tensile strength value. The experiment, and subsequent analysis, serve to instruct the student on the influence of gravitationally induced stresses in frictional granular materials, the importance and difficulty of accurately describing the entire failure envelope for granular materials in the low mean stress range, and the fundamental principles of material modeling.
Derived from text

N93-30961*# Tri-State Univ., Angola, IN.
APPLICATION OF HARDNESS TESTING IN FOUNDRY PROCESSING OPERATIONS: A UNIVERSITY AND INDUSTRY PARTNERSHIP **c26**
Donald H. Martin and Bruce Lash (AL-FE Heat Treating, Inc., Columbia City, IN.) *In* NASA. Langley Research Center, National Educators' Workshop. Update 92: Standard Experiments in Engineering Materials Science and Technology Jun. 1993 p 221-232 (For primary document see N93-30948 11-23)
Avail: CASI HC A03/MF A04

The objectives are the following: (1) to plan a tour of local manufacturing facility to observe hardness testing methods used and how they support the manufacturing process today; (2) to learn the operation of Brinell Hardness Testing and equipment set up with samples of accessory equipment for testing of various materials; (3) to use a Brinell scope (hand magnifier) to measure the diameter of the test indentation (in millimeters); (4) to use the hardness equation to determine the spherical area of the indentation and the calculation of the Brinell Hardness Number; (5) to use standard charts for ASTM standard size indenters to find the hardness number; and (6) to learn a method of conversion of the Brinell number to other hardness scales, their common usage, and also to convert the hardness number to the approximate tensile strength. Derived from text

N93-30962*# Air Force Inst. of Tech., Wright-Patterson AFB, OH. Dept. of Electrical and Computer Engineering.
LABORATORY EXPERIMENTS IN INTEGRATED CIRCUIT FABRICATION **c33**
Thomas J. Jenkins and Edward S. Kolesar *In* NASA. Langley Research Center, National Educators' Workshop. Update 92: Standard Experiments in Engineering Materials Science and Technology Jun. 1993 p 233-272 (For primary document see N93-30948 11-23)
Avail: CASI HC A03/MF A04

The objectives of the experiment are fourfold: to provide practical experience implementing the fundamental processes and technology associated with the science and art of integrated circuit (IC) fabrication; to afford the opportunity for the student to apply the theory associated with IC fabrication and semiconductor device operation; to motivate the student to exercise engineering decisions associated with fabricating integrated circuits; and to complement the theory of n-channel MOS and diffused devices that are presented in the classroom by actually fabricating and testing them. Therefore, a balance between theory and practice can be realized in the education of young engineers, whose education is often criticized as lacking sufficient design and practical content.
Derived from text

N93-30963*# California Polytechnic State Univ., San Luis Obispo. Materials Engineering Dept.
A 69 CENT LOOK AT THERMOPLASTIC SOFTENING **c27**
Linda S. Vanasupa *In* NASA. Langley Research Center, National Educators' Workshop. Update 92: Standard Experiments in Engineering Materials Science and Technology Jun. 1993 p 273-279 (For primary document see N93-30948 11-23)
(Grant NSF USE-91-52078)
Avail: CASI HC A02/MF A04

The objectives are to demonstrate the change in mechanical properties of a thermoplastic polymer when the polymer is heated above the glass transition temperature. The instructor or student can perform this demonstration. In preparation for the demonstration, fill the flask or beaker 3/4 full with water and bring the water to a boil. First observe the initial stiffness of the toothbrush by slightly flexing it. Note that it is fairly stiff and retains its initial shape when the forces are removed. If you were to apply enough force, the toothbrush would break in a somewhat brittle fashion. Now place the toothbrush in the boiling water for 2 minutes. After the 2 minutes are up, remove the toothbrush from the boiling water with the washcloth. At this time, you will be able to bend the toothbrush easily. When it cools it will retain this bent shape. You've just demonstrated heating the polymer above the glass transition temperature, demonstrating thermoplastic softening. Instructor notes are provided. Derived from text

N93-30964*# University of Eastern Illinois, Charleston. School of Technology.
SOLVING A PRODUCT SAFETY PROBLEM USING A RECYCLED HIGH DENSITY POLYETHYLENE CONTAINER **c27**
Ping Liu and T. L. Waskom *In* NASA. Langley Research Center, National Educators' Workshop. Update 92: Standard Experiments in Engineering Materials Science and Technology Jun. 1993 p 281-292 (For primary document see N93-30948 11-23)
Avail: CASI HC A03/MF A04

The objectives are to introduce basic problem-solving techniques for product safety including problem identification, definition, solution criteria, test process and design, and data analysis. The students are given a recycled milk jug made of high density polyethylene (HDPE) by blow molding. The objectives are to design and perform proper material test(s) so they can evaluate the product safety if the milk jug is used in a certain way which is specified in the description of the procedure for this investigation.
Derived from text

N93-30965*# Martin Marietta Energy Systems, Inc., Oak Ridge, TN. Metals and Ceramics Div.
TRIBOLOGY: FRICTION, LUBRICATION, AND WEAR TECHNOLOGY **c37**
Peter J. Blau *In* NASA. Langley Research Center, National Educators' Workshop. Update 92: Standard Experiments in Engineering Materials Science and Technology Jun. 1993 p 293-310 (For primary document

see N93-30948 11-23)
Avail: CASI HC A03/MF A04

The topics are presented in viewgraph form and include the following: introduction and definitions of terms; friction concepts; lubrication technology concepts; wear technology concepts; and tribological transitions. This document is designed for educators who seek to teach these concepts to their students. Derived from text

N93-30966*# Saint John's Univ., Jamaica, NY.
WALKWAY FRICTION: EXPERIMENT AND ANALYSIS **c37**
Mark I. Marpet and Robert J. Brungraber (Bucknell Univ., Lewisburg, PA.) *In* NASA. Langley Research Center, National Educators' Workshop. Update 92: Standard Experiments in Engineering Materials Science and Technology Jun. 1993 p 311-327 (For primary document see N93-30948 11-23)
Avail: CASI HC A03/MF A04

The objectives are to explore the utility and the limitations of the Amontons-Coulomb friction model and to explore design of experiments issues which underlie competent testing. Derived from text

N93-30967*# Ball State Univ., Muncie, IN. Dept. of Industry and Technology.
THERMOFORMING FROM A SYSTEMS VIEWPOINT **c31**
Jerry L. Wickman and Nikhil Kundu (Purdue Univ., Elkhart, IN.) *In* NASA. Langley Research Center, National Educators' Workshop. Update 92: Standard Experiments in Engineering Materials Science and Technology Jun. 1993 p 329-335 (For primary document see N93-30948 11-23)
Avail: CASI HC A02/MF A04

The objectives of this educational exercise are the following: to be able to select and manipulate control charts to adequately reflect processing characteristics and variation; to understand how a manufacturing process can be broken down into its basic components and subsequently analyzed; and to understand how statistics, standards, and metrology are critical to manufacturing. Derived from text

N93-30968*# North Carolina State Univ., Raleigh. Dept. of Materials Science and Engineering.
THE CHARACTERIZATION OF MATERIALS USING X RAY DIFFRACTION **c76**
A. F. Sprecher, Jr., Harvey A. West, and A. A. Fahmy *In* NASA. Langley Research Center, National Educators' Workshop. Update 92: Standard Experiments in Engineering Materials Science and Technology Jun. 1993 p 337-349 (For primary document see N93-30948 11-23)
Avail: CASI HC A03/MF A04

The objectives of this educational exercise are the following: to familiarize the student with x-ray techniques for diffraction pattern generation; to show the student how to utilize x-ray diffraction data for crystal structure determination; and to illustrate systematic and random errors associated with experimental data. Derived from text

N93-30969*# Tulsa Univ., OK. Dept. of Mechanical Engineering.
FRACTURE OF GLASS **c27**
John M. Henshaw *In* NASA. Langley Research Center, National Educators' Workshop. Update 92: Standard Experiments in Engineering Materials Science and Technology Jun. 1993 p 351-358 (For primary document see N93-30948 11-23)
Avail: CASI HC A02/MF A04

The objectives of this educational exercise are the following: to observe and understand the fracture behavior of a brittle material; and to quantify the effects of various treatments on that material designed to modify its strength. A brief introduction to beam bending, fracture mechanics, influence of surface defects, residual stress, and static fatigue is presented. A test procedure for specimen testing is also presented. Derived from text

N93-30970*# State Univ. of Southeast Missouri, Cape Girardeau.
PHASE TRANSITION STUDIES IN BARIUM AND STRONTIUM TITANATES AT MICROWAVE FREQUENCIES **c76**
Jai N. Dahiya *In* NASA. Langley Research Center, National Educators' Workshop. Update 92: Standard Experiments in Engineering Materials Science and Technology Jun. 1993 p 359-370 (For primary document see N93-30948 11-23)
Avail: CASI HC A03/MF A04

The objectives were the following: to understand the phase transformations in barium and strontium titanates as the crystals go from one temperature to the other; and to study the dielectric behavior of barium and strontium titanate crystals at a microwave frequency of 9.12 GHz and as a function of temperature. Phase transition studies in barium and strontium titanate are conducted using a cylindrical microwave resonant cavity as a probe. The cavity technique is quite successful in establishing the phase changes in these crystals. It appears that dipole relaxation plays an important role in the behavior of the dielectric response of the medium loading the cavity as phase change takes place within the sample. The method of a loaded resonant microwave cavity as applied in this work has proven to be sensitive enough to monitor small phase changes of the cavity medium. Derived from text

N93-30971*# Loyola Coll., Baltimore, MD. Dept. of Engineering.
EXPERIMENTS IN MATERIALS SCIENCE FROM HOUSEHOLD ITEMS **c80**
F. Xavier Spiegel *In* NASA. Langley Research Center, National Educators' Workshop. Update 92: Standard Experiments in Engineering Materials Science and Technology Jun. 1993 p 371-375 (For primary document see N93-30948 11-23)
Avail: CASI HC A01/MF A04

Everyday household items are used to demonstrate some unique properties of materials. A coat hanger, rubber band, balloon, and corn starch have typical properties which we often take for granted but can be truly amazing. Author

N93-30972*# Loyola Coll., Baltimore, MD. Dept. of Engineering.
AN AUTOMATED DATA COLLECTION SYSTEM FOR A CHARPY IMPACT TESTER **c39**
Bernard J. Weigman and F. Xavier Spiegel *In* NASA. Langley Research Center, National Educators' Workshop. Update 92: Standard Experiments in Engineering Materials Science and Technology Jun. 1993 p 377-384 (For primary document see N93-30948 11-23)
Avail: CASI HC A02/MF A04

A method for automated data collection has been developed for a Charpy impact tester. A potentiometer is connected to the pivot point of the hammer and measures the angular displacement of the hammer. This data is collected with a computer and, through appropriate software, accurately records the energy absorbed by the specimen. The device can be easily calibrated with minimal effort. Author (revised)

N93-30973*# California Polytechnic State Univ., San Luis Obispo. Materials Engineering Dept.
VISUALIZING WELD METAL SOLIDIFICATION USING ORGANIC ANALOGS **c26**
Daniel W. Walsh and Gary Ray Rogers *In* NASA. Langley Research Center, National Educators' Workshop. Update 92: Standard Experiments in Engineering Materials Science and Technology Jun. 1993 p 385-392 (For primary document see N93-30948 11-23)
Avail: CASI HC A02/MF A04

The objectives of this educational exercise are to allow the student to observe the solidification of a low melting temperature transparent crystalline organic compound that exhibits behavior similar to that of weld metal. A list of equipment and supplies and the procedure for the experiment are presented. Derived from text

N93-30974*# Purdue Univ., Elkhart, IN.
PERFORMANCE OF THERMAL ADHESIVES IN FORCED CONVECTION **c27**
Nikhil K. Kundu *In* NASA. Langley Research Center, National Educators' Workshop. Update 92: Standard Experiments in Engineering Materials Science and Technology Jun. 1993 p 393-401 (For primary document see N93-30948 11-23)
Avail: CASI HC A02/MF A04

Cooling is critical for the life and performance of electronic equipment. In most cases cooling may be achieved by natural convection but forced convection may be necessary for high wattage applications. Use of conventional type heat sinks may not be feasible from the viewpoint of specific applications and the costs involved. In a heat sink, fins can be attached to the well by ultrasonic welding, by soldering, or with a number of industrially available thermal adhesives. In this paper, the author investigates the heat transfer characteristics of several adhesives and compares them with ultrasonic welding and theoretically calculated values. This experiment was conducted in an air flow chamber. Heat was generated by using heaters mounted on the well. Thermstrate foil, Uniset A401, and Aremco 571 adhesives were tested along with an ultrasonically welded sample. Ultrasonic welding performed far better than the adhesives and Thermstrate foil. This type of experiment can be adapted for a laboratory exercise in an upper level heat transfer course. It gives students an exposure to industrial applications that help them appreciate the importance of the course material. Author (revised)

N93-30975*# New Mexico Univ., Albuquerque. Dept. of Mechanical Engineering.
TAGUCHI METHOD OF EXPERIMENTAL DESIGN IN MATERIALS EDUCATION **c80**
Martin W. Weiser *In* NASA. Langley Research Center, National Educators' Workshop. Update 92: Standard Experiments in Engineering Materials Science and Technology Jun. 1993 p 403-414 (For primary document see N93-30948 11-23)
Avail: CASI HC A03/MF A04

Some of the advantages and disadvantages of the Taguchi Method of experimental design as applied to Materials Science will be discussed. This is a fractional factorial method that employs the minimum number of experimental trials for the information obtained. The analysis is also very simple to use and teach, which is quite advantageous in the classroom. In addition, the Taguchi loss function can be easily incorporated to emphasize that improvements in reproducibility are often at least as important as optimization of the response. The disadvantages of the Taguchi Method include the fact that factor interactions are normally not accounted for, there are zero degrees of freedom if all of the possible factors are used, and randomization is normally not used to prevent environmental biasing. In spite of these disadvantages it is felt that the Taguchi Method is extremely useful for both teaching experimental design and as a research tool, as will be shown with a number of brief examples. Author (revised)

N93-30976*# New Mexico Univ., Albuquerque. Dept. of Mechanical Engineering.
POWDER METALLURGY: SOLID AND LIQUID PHASE SINTERING OF COPPER **c26**
Rex Sheldon and Martin W. Weiser *In* NASA. Langley Research Center, National Educators' Workshop. Update 92: Standard Experiments in Engineering Materials Science and Technology Jun. 1993 p 415-430 (For primary document see N93-30948 11-23)
Avail: CASI HC A03/MF A04

Basic powder metallurgy (P/M) principles and techniques are presented in this laboratory experiment. A copper based system is used since it is relatively easy to work with and is commercially important. In addition to standard solid state sintering, small quantities of low melting metals such as tin, zinc, lead, and aluminum can be added to demonstrate liquid phase sintering and alloy formation. The Taguchi Method of experimental design was used to study the effect of particle size, pressing force, sintering temperature, and sintering time. These parameters can be easily changed to incorporate liquid phase sintering effects and some guidelines for such substitutions are presented. The experiment is typically carried out over a period of three weeks. Author (revised)

N93-30977*# Norton Co., Northboro, MA.
HIGH THERMAL CONDUCTIVITY OF DIAMOND **c27**
Patrick M. Stephan *In* NASA. Langley Research Center, National Educators' Workshop. Update 92: Standard Experiments in Engineering Materials Science and Technology Jun. 1993 p 431-439 (For primary document see N93-30948 11-23)
Avail: CASI HC A02/MF A04

The objectives of this educational exercise were to demonstrate the high rate of heat flow from a synthetic diamond coupon and to compare it to a commonly used thermal conductor, such as copper. The principles of heat transfer by conduction and convection may also be demonstrated. A list of equipment and supplies and the procedure for the experiment are presented. Derived from text

N93-30978*# Battelle Pacific Northwest Labs., Richland, WA.
TEMPERATURE-DEPENDENT ELECTRICAL CONDUCTIVITY OF SODA-LIME GLASS **c27**
L. Roy Bunnell and T. H. Vertrees (Kennewick High School, WA.) *In* NASA. Langley Research Center, National Educators' Workshop. Update 92: Standard Experiments in Engineering Materials Science and Technology Jun. 1993 p 441-448 (For primary document see N93-30948 11-23)
Avail: CASI HC A02/MF A04

The objective of this educational exercise was to demonstrate the difference between the electrical conductivity of metals and ceramics. A list of the equipment and supplies and the procedure for the experiment are presented. Derived from text

N93-30979*# Battelle Pacific Northwest Labs., Richland, WA.
CONSTRUCTION AND TESTING OF SIMPLE AIRFOILS TO DEMONSTRATE STRUCTURAL DESIGN, MATERIALS CHOICE, AND COMPOSITE CONCEPTS **c02**
L. Roy Bunnell and Steven W. Piippo (Richland School District, WA.) *In* NASA. Langley Research Center, National Educators' Workshop. Update 92: Standard Experiments in Engineering Materials Science and Technology Jun. 1993 p 449-459 (For primary document see N93-30948 11-23)
Avail: CASI HC A02/MF A04

The objective of this educational exercise is to have students build and evaluate simple wing structures, and in doing so, learn about materials choices and lightweight construction methods. A list of equipment and supplies and the procedure for the experiment are presented. Derived from text

24 COMPOSITE MATERIALS

Includes physical, chemical, and mechanical properties of laminates and other composite materials.

For ceramic materials see *27 Nonmetallic Materials.*

N93-28492# Minnesota Univ., Minneapolis. Dept. of Chemical Engineering and Materials Science.
SYNTHESIS OF CONDUCTING POLYMER COMPOSITE FIBERS IN ELECTROCHEMICAL FLOW CELLS Technical Report, 30 Jun. 1992 - 31 Mar. 1993
Shulong Li and Henry S. White 20 Mar. 1993 20 p
(Contract N00014-91-J-1927)
(AD-A262233; TR-21) Avail: CASI HC A03/MF A01

A one-step electrochemical synthesis of polymer and composite polymer fibers of macroscopic dimensions (greater than 10 cm length and 0.2 mm diameter) is reported. Poly(3-methylthiophene) and polypyrrole fibers are grown from the tip of a Pt microelectrode by oxidation of 3-methylthiophene and pyrrole, respectively, in a capillary flow cell. Hydrodynamic fields within the capillary cell result in unidirectional growth of the polymer along the axis of the flow cell. High strength, conductive, and flexible composite polymer fibers are synthesized by deposition of poly(3-methylthiophene) or polypyrrole on a non conductive Kevlar or polyester string suspended in the solution along the axis of the capillary flow cell. Composite fiber growth rates as large as 30 cm/hr are obtained under optimal conditions. DTIC

N93-28559# Army Research Lab., Aberdeen Proving Ground, MD.
INFLUENCE OF PLY WAVINESS ON STIFFNESS AND STRENGTH REDUCTION OF COMPOSITE LAMINATES Final Report, Jun. 1991 - Aug. 1992
Travis A. Bogetti, Jack W. Gillespie, Jr., and Mark A. Lamontia Apr. 1993 49 p
(DA Proj. 1L1-62618-AH-80)
(AD-A263224; ARL-TR-110) Avail: CASI HC A03/MF A01

An analytic model is developed to investigate the influence of ply waviness on the stiffness and strength of composite laminates. The model predicts the following: elastic properties and thermal expansion coefficients of sublaminates containing wavy layers; ply stress for prescribed mechanical and thermal load cases; and strength reduction associated with ply waviness. Parametric studies are conducted for sublaminates of AS4 Graphite/PEKK and S2 Glass/PEKK which exhibit layer waviness. Results show that stiffness and strength reduction are significant in the direction of ply undulation only. Mechanisms of stiffness reduction are attributed to out-of-plane rotation of wavy layers. This waviness may also create significant interlaminar shear stress that reduces strength. The magnitude of the property reduction increases as the amplitude of the undulation increases and the half-wavelength of the undulation decreases. Ply waviness represents one mechanism that may partially explain why the design and failure analyses of composite structures based on flat, autoclave cured coupon property data (minimal waviness), do not correlate well with test results. DTIC

N93-28592# Battelle Pacific Northwest Labs., Richland, WA.
ULTRAHIGH TEMPERATURE ASSESSMENT STUDY: CERAMIC MATRIX COMPOSITES Final Report, Jul. 1988 - May 1990
E. L. Courtright, H. C. Graham, A. P. Katz, and R. J. Kerans Sep. 1992 143 p
(Contract MIPR-FY1457-88-N-5052; AF Proj. 2420)
(AD-A262740; WL-TR-91-4061) Avail: CASI HC A07/MF A02

As part of the U.S. Air Force initiative to develop high temperature materials for use in future gas turbine engines, a literature survey coupled with an assessment of recently completed experimental programs sponsored by the Air Force was made to evaluate prospective materials capable of operating at 1650 deg C or above in oxidizing environments. The assessment reviews fundamental considerations associated with the use of ceramics and ceramic matrix composites in representative environments and includes discussions on potential performance requirements. Key material categories (e.g., borides, carbides, nitrides, silicides, beryllides, and oxides) are evaluated with respect to their strengths and weaknesses. The reinforcements available for high temperature composite applications are reviewed and several prospective composite systems considered. A principal conclusion relative to possible uses for long-term man-rated gas turbine engines is that oxide/oxide composites-have the best potential for functional use in oxidizing environments above 1650 deg C provided adequate single-crystal reinforcement fibers can be developed. Several nonoxide materials and composites were identified for possible uses in short-duty cycle non-man-rated applications. In addition to materials development, there will be critical need for high-temperature test facilities that can be operated in representative oxidizing environments. DTIC

N93-28624*# National Aeronautics and Space Administration. Lewis Research Center, Cleveland, OH.
SOFT COMPUTING IN DESIGN AND MANUFACTURING OF ADVANCED MATERIALS
George Y Baaklini, Alex Vary, and Krzysztof J. Cios (Toledo Univ., OH.) Apr. 1993 8 p Presented at the ASME Conference, Cincinnati, OH, 24-27 May 1993: sponsored by IGTI and ASME
(RTOP 510-01-50)
(NASA-TM-106032; E-7597; NAS 1.15:106032) Avail: CASI HC A02/MF A01

The potential of fuzzy sets and neural networks, often referred to as soft computing, for aiding in all aspects of manufacturing of advanced materials like ceramics is addressed. In design and manufacturing of advanced materials, it is desirable to find which of the many processing variables contribute most to the desired properties of the material. There is also interest in real time quality control of parameters that govern material properties during processing stages. The concepts of fuzzy sets and neural networks are briefly introduced and it is shown how they can be used in the design and manufacturing processes. These two computational methods are alternatives to other methods such as the Taguchi method. The two methods are demonstrated by using data collected at NASA Lewis Research Center. Future research directions are also discussed. Author (revised)

N93-28657# Army Armament Research, Development and Engineering Center, Watervliet, NY. Benet Lab.
A THERMAL STRESS SOLUTION FOR MULTILAYERED COMPOSITE CYLINDERS Final Report
Mark D. Witherell Feb. 1993 15 p
(AD-A262579; ARCCB-TR-93005) Avail: CASI HC A03/MF A01

An elastic thermal stress solution is presented for a multilayered composite cylinder subjected to a radial temperature field. The solution assumes each layer to be at a uniform temperature, therefore, many layers are required to model regions with large gradients in temperature. Previously developed closed-form solutions for a monolayered cylinder subjected to a uniform temperature change and loadings of internal and external pressures are used to construct the multilayered solution. Results produced by the theoretical solution were compared to those generated from a finite element analysis with excellent agreement. Finally, by combining a previously developed multilayered stress solution for loadings of internal pressure, external pressure, and axial force with the plane-strain thermal stress solution, the multilayered thermal stress solution for generalized plane-strain boundary conditions is shown to be easily obtained. DTIC

N93-28660# Orcon Corp., Union City, CA.
LIGHTWEIGHT FLEXIBLE COMPOSITE TENT MATERIALS Final Report, 4 Jun. 1991 - 31 Dec. 1992
Robert N. King 23 Oct. 1992 30 p
(Contract DAAK60-91-C-0028)
(AD-A263021) Avail: CASI HC A03/MF A01

The program investigated the theory that flexible composite materials can be engineered to provide the physical properties desirable for tent materials, particularly at reduced weights relative to currently available materials. The technology for combining materials into high performance composites is uncommon in the textile industry as a whole, but is commonly practiced by manufacturers specializing in high strength-to-weight ratio materials for applications such as sailcloth and aerospace insulation systems. High strength lightweight composite materials were developed which provide tailored physical properties for use as tent materials. These systems can be produced with commercially-available, reasonably low cost base materials which can be fabricated using existing manufacturing processes. A variety of materials and constructions were shown to meet a majority of the property requirements for the Five-Soldier Crew Tent. Future development of these lightweight constructions should focus on identifying flexible coating systems to improve the hand and durability properties of these continuous film composites. DTIC

N93-28681*# National Aeronautics and Space Administration. Lewis Research Center, Cleveland, OH.
METAL MATRIX LAMINATE TAILORING (MMLT) CODE: USER'S MANUAL
P. L. N. Murthy, M. R. Morel (Sverdrup Technology, Inc., Brook Park, OH.), and D. A. Saravanos (Ohio Aerospace Inst., Brook Park.) May 1993 132 p
(RTOP 510-01-50)
(NASA-TM-106052; E-7644; NAS 1.15:106052) Avail: CASI HC A07/MF A02

The User's Manual for the Metal Matrix Laminate Tailoring (MMLT) program is presented. The code is capable of tailoring the fabrication process, constituent characteristics, and laminate parameters (individually or concurrently) for a wide variety of metal matrix composite (MMC) materials, to improve the performance and identify trends or behavior of MMC's under different thermo-mechanical loading conditions. This document is meant to serve as a guide in the use of the MMLT code. Detailed explanations of the composite mechanics and tailoring analysis are beyond the scope of this document, and may be found in the references. MMLT was developed by the Structural Mechanics Branch at NASA Lewis Research Center (LeRC). Author (revised)

N93-28843*# Pennsylvania State Univ., University Park. Dept. of Engineering Science and Mechanics.
ANALYSIS FOR THERMO-CHEMICAL DECOMPOSITION OF COMPOSITE STRUCTURES Interim Report, Jun. 1992-1993
Ramnath Ganesan, Sunpyo Lee, and N. J. Salamon May 1993 137 p
(Grant NAG8-879)
(NASA-CR-193185; NAS 1.26:193185) Avail: CASI HC A07/MF A02

Research progress for the second year's effort on analysis for thermochemical decomposition of composite structures is presented. The objectives were (1) to develop a fast, yet accurate time integration scheme, and (2) to code the theoretical formulation for a three-dimensional axisymmetric model and verify it against experimental data and results from the one-dimensional axisymmetric model. The objectives were met and surpassed in the case of multidimensional applications. The result is two fully-coupled (through displacement, temperature and pore pressure) and functioning computer codes. Author (revised)

N93-28886# Naval Academy, Annapolis, MD. Div. of Engineering and Weapons.
THE EFFECT OF TEMPERATURE ON THE IMPACT BEHAVIOR OF TiB2 REINFORCED XDTM-TiAl INTERMETALLIC MATRIX COMPOSITES
M. K. Hamm and D. F. Hasson Nov. 1992 21 p
(AD-A262924; USNA-EW-23-92) Avail: CASI HC A03/MF A01

A study was performed to determine the effect of temperature on the impact behavior of two XD(TM) processed TiB2 reinforced TiAl intermetallic composites (IMC's). An existing instrumented tup drop tower apparatus was modified for the program. The IMC compositions were Ti-49 at. % Al + 5 vol. % TiB2 and Ti-48 at. % Al + 10 vol. % TiB2. The specimens were notched to an a/w ratio of 0.2. Details and test procedures for the modified apparatus were presented. Test temperatures ranged from -192 to 1100 C. Impact toughness and maximum bending stress for both IMC's decreased from room temperature to temperatures as high as 1100 C. An important experimental observation which supports these results is the change from transgranular cleavage to intergranular fracture at the 760 C test temperature. Also noted is the possible contribution to decreasing toughness of unfavorable difference in coefficient of thermal expansion between TiB2 and the matrix with increasing temperature. Data repeatability and verification of the ability to observe high temperature brittle-to-ductile transition behavior established confidence in the modification of the existing instrumented tup apparatus. DTIC

N93-28904# Los Alamos National Lab., NM.
ALIGNED, SHORT-FIBER COMPOSITES BY NOVEL FLOW PROCESSING METHODS
D. C. Guell, A. L. Graham, T. Papathanasiou, and J. J. Petrovic 1993 10 p Presented at the Advances in Polymer Processing, Cincinnati, OH, 29-31 Mar. 1993
(Contract W-7405-eng-36)
(DE93-008701; LA-UR-93-569; CONF-9303110-1) Avail: CASI HC A02/MF A01

A hydrodynamic method has been employed to align short, reinforcing fibers in polymer matrix composite materials. Samples of composite materials were prepared and tested two at a time (one with randomly oriented fibers and the other with aligned fibers) to isolate and directly measure the effect on mechanical properties of aligning the fibers. Data were collected for the ultimate tensile strength, modulus of elasticity, and ultimate tensile strain of the composite samples prepared. Results show that the aligned fibers were approximately twice as effective (as randomly oriented fibers) at stiffening and strengthening the composite in the alignment direction. DOE

N93-29001# Texas Univ., Austin. Center for Materials Science and Engineering.
DESIGN OF INTERFACES IN METAL MATRIX COMPOSITES Final Report, 1 Dec. 1989 - 30 Nov. 1992
Harris L. Marcus and Zwy Eliezer 15 Feb. 1993 47 p
(Contract N00014-90-J-1164)
(AD-A262052) Avail: CASI HC A03/MF A01

The main goal of this research was to optimize the interface properties in metal matrix composites by lattice matching the matrix and the dispersoids. Stable, coherent dispersoids can be achieved by mechanically alloying lattice-matched dispersoids into metal matrices and allowing some recrystallization or coarsening to occur, or by internal nitridization or carburization of homogeneous alloys. A model system that has a high probability of forming coherent interfaces is ZrN in Nb. For comparison purposed the relatively poorly matched systems TiN in Nb and TiN in Cu were also studies. The matrix/dispersoid orientation relationship in the Nb/ZrN system has been found to be (011)Nb,Zr (parallel) (001)ZrN. In the Nb/TiN system, the presence of an orientation relationship after extensive nitriding could not be detected. In the Cu/TiN system only external nitridation occurred when bulk Cu-Ti alloys were employed. However uniformly distributed nanosized TiN dispersoids were obtained when alloyed Cu-Ti powders were nitrided and subsequently mechanically alloyed. DTIC

N93-29007# Deutsche Forschungsanstalt fuer Luft- und Raumfahrt, Brunswick (Germany). Abt. Strukturberechnung.
COMPOSITE LAMINATE STIFFNESSES AND THEIR SENSITIVITIES
Bodo Geier Jun. 1992 40 p
(DLR-FB-92-16; ETN-93-93734) Avail: CASI HC A03/MF A01; DLR, VB-PL-DO, Postfach 90 60 58, 5000 Cologne, Germany, HC

An analysis of composite laminate stiffnesses and their sensitivities is presented within the framework of the design of structures made of composite materials. One of the columns upon which optimization of structures is built is the mathematical search method for locating a minimum (or maximum) of a constrained object function. Efficient algorithms will require the evaluation of derivatives of the object function as well as of the constraints. In that context the sensitivities of laminate stiffness matrices may be required. In order to meet such a requirement the derivatives with respect to both ply thicknesses and ply angles, of laminate stiffnesses including transverse shear stiffness, are presented. ESA

N93-29016# Joint Publications Research Service, Arlington, VA.
JPRS REPORT: SCIENCE AND TECHNOLOGY. CENTRAL EURASIA: MATERIALS SCIENCE
12 Aug. 1992 42 p Transl. into ENGLISH from various Russian articles
(JPRS-UMS-92-012) Avail: CASI HC A03/MF A01

Translated abstracts cover the following areas: analysis, testing; coatings; composite materials; corrosion; nonferrous metals, alloys, brazes, solders; nonmetallic materials; preparations; treatments; welding, brazing, soldering; extractive metallury, mining; and miscellaneous. CASI

N93-29017# Joint Publications Research Service, Arlington, VA.
JPRS REPORT: SCIENCE AND TECHNOLOGY. CENTRAL EURASIA: MATERIALS SCIENCE
20 Aug. 1992 33 p Transl. into ENGLISH from various Russian articles
(JPRS-UMS-92-013) Avail: CASI HC A03/MF A01

Translated abstracts cover the following areas: analysis and testing, ferrous metals, nonferrous metals and alloys, welding, preparations and treatments, and extractive metallurgy. Some specific topics include the effect of porosity on breaking stress of powder materials under viscous failure mechanism; characteristic features of the change in the properties of zirconium dioxide-based heat-shield coatings as a function of loading conditions; and the behavior of cylindrical shells made of polymer composite materials with defects under dynamic loading. CASI

N93-29018# Joint Publications Research Service, Arlington, VA.
JPRS REPORT: SCIENCE AND TECHNOLOGY. CENTRAL EURASIA: MATERIALS SCIENCE
13 Nov. 1992 65 p Transl. into ENGLISH from various Russian articles
(JPRS-UMS-92-016) Avail: CASI HC A04/MF A01

Translated abstracts cover the following areas: analysis and testing, coatings, composite materials, corrosion, nonferrous metals and alloys, nonmetallic materials, preparations and treatments, welding, and extractive metallurgy. Some specific topics include a method of design calculation for flywheels made of fibrous composite with binder; strength and fatigue resistance of fabric-based composites under combined effect of static shear stresses and cyclical compressive stresses; structure and atomic dislocation mechanisms of Al-Al9Co2 composite fracture; and long-term strength and creep of molybdenum alloy welds at high temperatures. CASI

N93-29021# Joint Publications Research Service, Arlington, VA.
JPRS REPORT: SCIENCE AND TECHNOLOGY. CENTRAL EURASIA: MATERIALS SCIENCE
12 Jan. 1993 62 p Transl. into ENGLISH from various Russian articles
(JPRS-UMS-93-001) Avail: CASI HC A04/MF A01

Translated abstracts cover the following areas: analysis and testing, coatings, composite materials, ferrous metals, nonferrous metals and alloys, nonmetallic materials, preparations and treatments, welding, and extractive metallurgy. Some specific topics include the inspection of particles in hot gas jet by acoustic emission method; dynamic strength and crack resistance of cryogenic alloys; high-temperature metal-matrix composite; forecasting the lift of hot-pressed ceramic nozzles of closed-drift thrusters by comprehensive nondestructive tests; and predicting ultimate strength of unidirectionally oriented composite material by acoustic emission. CASI

N93-29023* National Aeronautics and Space Administration. Lyndon B. Johnson Space Center, Houston, TX.
METHOD FOR PREPARATION OF A MICROPOROUS STRUCTURE WITH LAYERED INTERSTITIAL SURFACE TREATMENT Patent
Steven L. Koontz, inventor (to NASA) 1 Jun. 1993 10 p Filed 2 Jun.

1992 Continuation-in-part of US-Patent-Appl-SN-429739, filed 31 Oct. 1989
(NASA-Case-MSC-21487-2; US-Patent-5,215,790; US-Patent-Appl-SN-894505; US-Patent-Appl-SN-429739; US-Patent-Class-427-535; US-Patent-Class-427-244; US-Patent-Class-427-269; US-Patent-Class-427-270; US-Patent-Class-427-287; US-Patent-Class-427-377) Avail: US Patent and Trademark Office

A microporous structure with layered interstitial surface treatments, and method and apparatus for preparation thereof are described. The structure is prepared by sequentially subjecting a uniformly surface-treated structure to atomic oxygen treatment to remove an outer layer of surface treatment to a generally uniform depth, and then surface treating the so exposed layer with another surface treating agent. The atomic oxygen/surface treatment steps may optionally be repeated, each successive time to a lesser depth, to produce a microporous structure having multilayered surface treatments. The apparatus employs at least one side arm from a main atomic oxygen-containing chamber. The side arm has characteristic relaxation times such that a uniform atomic oxygen dose rate is delivered to a specimen positioned transversely in the side arm spaced from the main gas chamber. Official Gazette of the U.S. Patent and Trademark Office

N93-29071*# National Aeronautics and Space Administration. Lewis Research Center, Cleveland, OH.
CERAMIC MATRIX COMPOSITES PROPERTIES/MICROSTRESSES WITH COMPLETE AND PARTIAL INTERPHASE BOND
Subodh K. Mital (Toledo Univ., OH.), Pappu L. N. Murthy, and Christos C. Chamis May 1993 13 p Presented at the 38th International SAMPE Symposium/Exhibition, Anaheim, CA, 10-13 May 1993
(RTOP 510-01-50)
(NASA-TM-106136; E-7816; NAS 1.15:106136) Avail: CASI HC A03/MF A01

A multilevel substructuring technique which includes a unique fiber substructuring concept is used for the analysis of continuous fiber reinforced ceramic matrix composites. This technique has four levels of substructuring--from laminate to ply, to supply, and then to fiber. A stand-alone computer code CEMCAN (Ceramic Matrix Composites Analyzer), incorporating this technique and specifically for the simulation of ceramic matrix composites behavior, is currently under development at NASA Lewis Research Center in Cleveland, Ohio. The thermal and mechanical properties, along with the microstresses, for a SiC/RBSN (silicon carbide fiber and reaction bonded silicon nitride matrix) composite at different fiber volume ratios and varying degrees of interfacial bond around the fiber circumference are computed. Values predicted by CEMCAN computer code are shown to bound the experimentally measured values. Results also show that transverse tensile strength test can be a sensitive test method to assess interfacial conditions. Author (revised)

N93-29074*# National Aeronautics and Space Administration. Lewis Research Center, Cleveland, OH.
THERMOVISCOPLASTIC ANALYSIS OF FIBROUS PERIODIC COMPOSITES USING TRIANGULAR SUBVOLUMES
Kevin P. Walker (Engineering Science Software, Inc., Smithfield, RI.), Alan D. Freed, and Eric H. Jordan (Connecticut Univ., Storrs.) Mar. 1993 28 p
(RTOP 505-63-5A)
(NASA-TM-106076; E-7686; NAS 1.15:106076) Avail: CASI HC A03/MF A01

The nonlinear viscoplastic behavior of fibrous periodic composites is analyzed by discretizing the unit cell into triangular subvolumes. A set of these subvolumes can be configured by the analyst to construct a representation for the unit cell of a periodic composite. In each step of the loading history, the total strain increment at any point is governed by an integral equation which applies to the entire composite. A Fourier series approximation allows the incremental stresses and strains to be determined within a unit cell of the periodic lattice. The nonlinearity arising from the viscoplastic behavior of the constituent materials comprising the composite is treated as fictitious body force in the governing integral equation. Specific numerical examples showing the stress distributions in the unit cell of a fibrous tungsten/copper metal matrix composite under viscoplastic loading conditions are given. The stress distribution resulting in the unit cell when the composite material is subjected to an overall transverse stress loading history perpendicular to the fibers is found to be highly heterogeneous, and typical homogenization techniques based on treating the stress and strain distributions within the constituent phases as homogeneous result in large errors under inelastic loading conditions. Author (revised)

N93-29078 Stanford Univ., CA.
AXIAL IMPACT OF COMPOSITES Ph.D. Thesis
Levent Karaoglan 1993 110 p
Avail: Univ. Microfilms Order No. DA9309612

A finite element method was developed to calculate the behavior of an axisymmetric composite body of revolution impacting on an isotropic surface. The composite is made of unidirectional fiber reinforced plies, with no restriction either on the number of plies or on the orientation of the fibers in each ply; hence the laminate may be 'thin' or 'thick', and may be of 'symmetric' or 'unsymmetric' layups. The target may be a semi-infinite body or may be a simple supported or clamped slab. The impact velocity may be zero (static loading) or non-zero with the impactor penetrating the target. A user-friendly computer code AXIMPACT was written which provides the following information: (1) the position of the impactor during impact (including the penetration depth); (2) the stresses and strains in the impactor and the target; (3) the deformations of the impactor and the target; and (4) the failure of the composite impactor and the target. The code was validated by comparing results generated by the code to available analytical and numerical results and to data. In every case the agreement between the present and previous results was excellent. Dissert. Abstr.

N93-29107*# Virginia Polytechnic Inst. and State Univ., Blacksburg. Center for Composite Materials and Structures.
ENVIRONMENTAL EFFECTS ON STITCHED RTM COMPOSITES Interim Report No. 93, Jan. 1991 - May 1993
Keith W. Furrow, Alfred C. Loos, H. Benson Dexter (National Aeronautics and Space Administration. Langley Research Center, Hampton, VA.), and Roberto J. Cano (National Aeronautics and Space Administration. Langley Research Center, Hampton, VA.) Jun. 1993 140 p
(Grant NAG1-343)
(NASA-CR-193221; NAS 1.26:193221; CCMS-93-07; VPI-E-93-06) Avail: CASI HC A07/MF A02

The effects of temperature and humidity cycling on the mechanical properties of AS4/3501-6 quasi-isotropic textile composites were determined. The composites were resin transfer molded from unstitched, Kevlar 29 stitched, and S-2 glass stitched uniweave fabric preforms. Temperature cycling ranged from 60 to -55 C while the relative humidity simultaneously varied between 95 and 0 percent. Data presented include photomicrographs, compression strengths, and compression-compression fatigue results for environmentally cycled and uncycled composites. Photos of microcracks found predominantly around individual stitches were taken at the end of each cycling period. The glass stitched and Kevlar stitched laminates developed significant microcracks before cycling but the microcracks did not grow after cycling. The unstitched uniweave material developed microcracks only after cycling. The glass stitched material had lower baseline compression strength than the unstitched and Kevlar stitched materials. Temperature and humidity cycling reduced the static compression strength of the unstitched and Kevlar stitched uniweave materials nearly 10 percent. Under the same conditions the glass stitched uniweave material lost 3 percent of its baseline strength. Combined temperature and humidity cycling did not affect the fatigue properties of the uniweave materials when the test specimens were dried to their original weights before testing. A second environmental cycle, varying only the temperature at constant 40 percent humidity, resulted in a 5 percent decrease in static compression strength for the unstitched and Kevlar stitched material. Unstitched, glass stitched, and Kevlar stitched materials exposed to constant 60 C and 95 percent relative humidity for 80 days and then saturated in 70 C water, lost 17, 7, and 19 percent of their baseline compression strength, respectively. Moisture absorption at constant temperature and humidity lowered the fatigue strength of the uniweave materials only after saturation. In hot humid conditions moisture diffuses into the composite. The mass diffusivities and maximum moisture uptake for the three uniweave composites were measured. Fick's law was used to predict the moisture absorption. Braided composites, including a stitched 2-D braid, an unstitched 2-D braid, and a 3-D braid, were also exposed to environmental cycling. The moisture absorption in these AS4/E905L systems was lower than the AS4/3501-6 systems and consequently the cycling had little effect on the strengths of braided materials. Author (revised)

N93-29130# Northwestern Univ., Evanston, IL. Dept. of Materials Science and Engineering.
TAILORED INTERFACES FOR METAL-MATRIX COMPOSITES-FUNDAMENTAL CONSIDERATIONS Final Technical Report, 1 Oct. 1988 - 30 Nov. 1992
Morris E. Fine and Julia R. Weertman 28 Jan. 1993 99 p
(Grant AF-AFOSR-0043-89)
(AD-A263048; AFOSR-93-0190TR) Avail: CASI HC A05/MF A02

The objective of this research was to investigate the interface properties needed for successful metal matrix composites. Thermodynamic stability of the interface and the phases in the composite, the nature of the bonding across the interface, and the energy and structure of the interface were studied. With TiC dispersed in Al prepared by the XD process, atomic resolution electron microscopy showed a sharp interface with large areas of partial coherence. The Al-TiC composite is remarkably ductile even at 15 vol.% TiC loading. This attributed to the ability of the Al to recrystallize at the interface forming semicoherent boundaries and to a high level of metallic binding between Al and Ti in TiC. DTIC

N93-29191# California Univ., Berkeley. Lawrence Berkeley Lab.
OXIDATION BEHAVIOR IN REACTION-BONDED ALUMINUM-SILICON ALLOY/ALUMINA POWDER COMPACTS Ph.D. Thesis
S. H. Yokota Dec. 1992 44 p
(Contract DE-AC03-76SF-00098)
(DE93-010407; LBL-33405) Avail: CASI HC A03/MF A01

The goal of this research is to determine the feasibility of producing low-shrinkage mullite/alumina composites by applying the reaction-bonded alumina (RBAO) process to an aluminum-silicon alloy/alumina system. Microstructural and compositional changes during heat treatment were studied by removing samples from the furnace at different steps in the heating schedule and then using optical and scanning electron microscopy, EDS and XRD to characterize the powder compacts. Results suggest that the oxidation behavior of the alloy compact is different from the model proposed for the pure Al/alumina system. DOE

N93-29282# Materials Research Society, Pittsburg, PA.
LOW TEMPERATURE (LT) GaAs AND RELATED MATERIALS Final Report, 15 Sep. 1991 - 14 Sep. 1992
Gerald L. Witt, Robert Calawa, Umesh Mishra, and Eicke Weber 14 Sep. 1992 311 p Symposium held in Boston, MA, 4-6 Dec. 1991
(Grant AF-AFOSR-0399-91)
(AD-A263607; AFOSR-93-0181TR) Avail: CASI HC A14/MF A03

The response to this symposium, less than two years later, accurately reflects the increasing awareness of the rich combination of fundamental materials science and electronic optoelectronic applications that are at play in the subject. The gradual and incomplete understanding of the basic mechanisms responsible for the remarkable properties of these materials have produced a confusion of names. At the time of planning for this symposium the organizers attempted to select a suitable name, one reflecting the understanding to date. However, events would have it otherwise. The then common phrase low temperature of LT GaAs was adopted reluctantly. In doing so, it was realized that this phrase is misleading and inaccurate. More appropriate are two other phrases used in these proceedings. GaAs with arsenic precipitates or GaAsAs and low temperature grown or LTG GaAs. This issue of terminology remains to be resolved. DTIC

N93-29414# Air Force Inst. of Tech., Wright-Patterson AFB, OH. School of Engineering.
AN INVESTIGATION OF GRAPHITE PEEK COMPOSITE UNDER COMPRESSION WITH A CENTRALLY LOCATED CIRCULAR DISCONTINUITY M.S. Thesis
Benjamin Wham, II Mar. 1993 251 p
(AD-A262549; AFIT/GA/93M-01) Avail: CASI HC A12/MF A03

The purpose of this thesis was to determine (both experimentally and analytically) the initiation and progression of failure, stress-strain response, and the failure loads of Graphite/Polyetheretherketone (Gr/PEEK) laminates, incorporating a centrally located circular discontinuity, loading in axial compression at room temperature. The laminates studied were ((0 deg)(sub 16)), ((90 deg)(sub 16)), ((0 deg/90 deg)(SUB 4S)), ((+/- 45 deg)(sub 4S)), and ((0 deg/+/-45 deg/90 deg)(sub 2S)). The specimens were loaded within a Boeing Open Hole Compression Fixture. The micromechanical failure modes were identified using a Scanning Electron Microscope. The analytical progression of failure was predicted using a nonlinear finite element code. The code utilizes a total energy method predicated upon the material properties curves obtained from experimentation to compute the stress-strain response of the material as well as the progression of failure within the model. Results were compared and conclusions were drawn. DTIC

N93-29425# Naval Academy, Annapolis, MD. Div. of Engineering and Weapons.
EFFECTS OF FREEZE/THAW CYCLES ON HYDROSTATICALLY CONDITIONED E-GLASS/J-2 COMPOSITE Final Report, Oct. 1991 - Sep. 1992
D. F. Hasson and M. K. Hamm Sep. 1992 17 p
(AD-A262980) Avail: CASI HC A03/MF A01

A study was performed to determine if freeze/thaw cycles of a polymer matrix composite (PMC) with high moisture content caused increased mechanical property degradation. The PMC was a 36 ply glass fiber with a thermoplast matrix. Moisture was added hydrostatically at high pressure. It was observed that freeze/thaw cycles did not appreciably decrease the maximum load. However, from short beam shear (SBS) specimens taken from the top, middle, and bottom of the hydrostatically conditioned sample, the load characteristics depended on specimen location. The middle SBS specimen had a maximum load very close to that for off the shelf dry samples. From optical microscopy it was observed that the freeze/thaw specimens failed with multiple delaminations while the dry samples failed with single delaminations. Further investigation of this observation is suggested. DTIC

N93-29451*# Allied-Signal Aerospace Co., Torrance, CA. Garrett Ceramic Components.
IMPROVED SILICON NITRIDE FOR ADVANCED HEAT ENGINES Final Report
Harry C. Yeh and Ho T. Fang Apr. 1991 291 p
(Contract NAS3-24385; RTOP 533-05-01)
(NASA-CR-182193; Rept-88-61608; NAS 1.26:182193) Avail: CASI HC A13/MF A03

The results of a four year program to improve the strength and reliability of injection-molded silicon nitride are summarized. Statistically designed processing experiments were performed to identify and optimize critical processing parameters and compositions. Process improvements were monitored by strength testing at room and elevated temperatures, and microstructural characterization by optical, scanning electron microscopes, and scanning transmission electron microscope. Processing modifications resulted in a 20 percent strength and 72 percent Weibull slope improvement of the baseline material. Additional sintering aids screening and optimization experiments succeeded in developing a new composition (GN-10) capable of 581.2 MPa at 1399 C. A SiC whisker toughened composite using this material as a matrix achieved a room temperature toughness of 6.9 MPa m(exp .5) by the Chevron notched bar technique. Exploratory experiments were conducted on injection molding of turbocharger rotors. Author

N93-29609* National Aeronautics and Space Administration. Lewis Research Center, Cleveland, OH.
APPARATUS FOR INTERCALATING LARGE QUANTITIES OF FIBROUS STRUCTURES Patent
James R. Gaier, inventor (to NASA) 6 Jul. 1993 7 p Filed 24 Jul. 1991 Supersedes N91-28289 (29 - 20, p 3304) Division of US-Patent-Appl-SN-608493, filed 2 Nov. 1990
(NASA-Case-LEW-15077-2; US-Patent-5,225,171; US-Patent-Appl-SN-735548; US-Patent-Appl-SN-608493; US-Patent-Class-422-209; US-Patent-Class-422-136; Int-Patent-Class-B01J-19/28) Avail: US Patent and Trademark Office

Apparatus for intercalating large quantities of fibrous structures uses a rotatable reaction chamber containing a liquid phase intercalate. The intercalate liquid phase is controlled by appropriately heating, cooling or pressurizing the reaction. Rotation of the chamber containing the fiber sample ensures total submergence if the fiber during intercalation.

Intercalated graphite fibers having metal-like resistivities are produced and are conceivably useful as electrical conductors.

Official Gazette of the U.S. Patent and Trademark Office

N93-29614* National Aeronautics and Space Administration. Lewis Research Center, Cleveland, OH.

SEMICONDUCTOR COOLING APPARATUS Patent

Bruce A. Banks, inventor (to NASA) and James R. Gaier, inventor (to NASA) 29 Jun. 1993 7 p Filed 11 May 1992 Supersedes N92-34208 (30 - 24, p 4148) Continuation-in-part of abandoned US-Patent-Appl-SN-657238, filed 19 Feb. 1991, which is a continuation-in-part of abandoned US-Patent-Appl-SN-501893, filed 30 Mar. 1990

(NASA-Case-LEW-14162-3; US-Patent-5,224,030; US-Patent-Appl-SN-880851; US-Patent-Appl-SN-657238; US-Patent-Appl-SN-501893; US-Patent-Class-361-386; US-Patent-Class-165-185; US-Patent-Class-174-16.3; US-Patent-Class-428-614; Int-Patent-Class-H05K-7/20) Avail: US Patent and Trademark Office

Gas derived graphite fibers generated by the decomposition of an organic gas are joined with a suitable binder. This produces a high thermal conductivity composite material which passively conducts heat from a source, such as a semiconductor, to a heat sink. The fibers may be intercalated. The intercalate can be halogen or halide salt, alkaline metal, or any other species which contributes to the electrical conductivity improvement of the graphite fiber. The fibers are bundled and joined with a suitable binder to form a high thermal conductivity composite material device. The heat transfer device may also be made of intercalated highly oriented pyrolytic graphite and machined, rather than made of fibers.

Official Gazette of the U.S. Patent and Trademark Office

N93-29802# United Technologies Research Center, East Hartford, CT.

INTERFACIAL STUDIES OF REFRACTORY GLASS-CERAMIC MATRIX/ADVANCED SiC FIBER REINFORCED COMPOSITES Final Report, 1 Feb. 1990 - 1993

J. J. Brennan 1 Apr. 1993 65 p

(Contract N00014-87-C-0699)

(AD-A263264; R93-918246-6) Avail: CASI HC A04/MF A01

The main objective of this program was to characterize the chemistry and structure of new advanced small diameter silicon based fibers and determine how these factors influence the nature of the fiber/matrix interface in refractory glass-ceramic matrix composites. It is the nature of this interface that then determines to a great degree the composite thermal, environmental, and mechanical properties. The fibers under investigation during the course of this program included the lower oxygen Lox M Tyranno SiC fibers from Ube Industries, polymer derived crystalline SiC fibers from Dow Corning Corp., the Si-N-C-O 'Black' fibers from Textron Specialty Materials, low oxygen SiC fibers from the Univ. of Fla., as well as the new low oxygen radiation cured Nicalon SiC type fibers from Nippon Carbon Co. Since the availability of all of these fibers was extremely limited, emphasis was placed on the mechanical, chemical, and microstructural characterization of the fibers through tensile testing, SEM of fiber fracture characteristics, scanning Auger depth profiling of fiber surfaces, and TEM of fiber thin sections, as well as their fracture behavior, bonding characteristics, and interfacial compatibility with various glass-ceramic matrix materials. Results of these analyses are discussed. DTIC

N93-29982# Michigan State Univ., East Lansing. Coll. of Engineering.

RAPIDLY ACTIVATED DYNAMIC PHASE TRANSITIONS IN NONLINEAR SOLIDS Final Report, 1 Aug. 1989 - 15 Dec. 1992

Thomas J. Pence 15 Feb. 1993 22 p

(Contract DAAL03-89-G-0089)

(AD-A263601; ARO-27077.7-MA-SM) Avail: CASI HC A03/MF A01

This research project has addressed critical issues concerned with the mathematical modeling of phase transitions in solids. Detailed microstructural analysis has enabled us to clarify the role of stress waves in the propagation of phase boundaries. The potential for phase boundary movement to damp out stress waves has been demonstrated for certain classes of material response. Nucleation of new phase domains by highly energetic processes has been successfully modeled and new analytical procedures have been developed for the predictive response of phase transforming media during high energy impact. Conversion of mechanical energy to thermal energy has been studied by means of an extended theory which incorporates temperature effects. The role of these dynamical events on the response of devices at the engineering level points to the utility of a mathematical description capable of capturing cumulative microstructural effects. To this end we have also developed mathematical protocols capable of tracking the evolution of thermomechanical austenite/martensite phase variants due to generalized conditions of loading and heating. The associated mathematical model is capable of capturing superelastic response and two-way shape memory in thermoelastic materials. Ohmic heating/convective cooling is a likely activation mechanism for smart devices utilizing these materials, and our numerical simulations have successfully replicated these processes including a smooth transition from isothermal to adiabatic response as the loading rate is increased in a heat convective environment. DTIC

N93-29984# Naval Surface Warfare Center, Bethesda, MD. Survivability Structures and Materials Directorate.

EFFECT OF WATER IMMERSION ON FIBER/MATRIX ADHESION IN THERMOPLASTIC COMPOSITES

Thomas Juska Mar. 1993 27 p

(AD-A263646; CDNSWC/SSM-64-93/02) Avail: CASI HC A03/MF A01

Continuous fiber reinforced thermoplastics were tested for the effect of water immersion on fiber/matrix adhesion. The materials evaluated were E/PPS, AS4/PPS, E/J2, AS4/J2, S2/PEEK, AS4/PEEK, S2/PEKK, AS4/PEKK, and S2/VECTRA. These materials were tested in uniaxial compression, transverse flexure, and short beam shear, both dry and water-conditioned. Scanning electron microscopy was used to assess the quality of the fiber/matrix bond. The carbon reinforced materials retained adhesion after water immersion. However, the glass reinforced thermoplastics were in general degraded by water, which hydrolyzed the fiber/matrix bond and significantly reduced mechanical properties. DTIC

N93-30004 Japan Atomic Energy Research Inst., Tokyo.

EXPERIMENT AND ANALYSIS ON ELASTIC DEFORMATION PROPERTIES OF GRAPHITE AND CARBON MATERIALS FOR HTTR CORE COMPONENTS

Taketoshi Arai, Kazuo Minato, Motokuni Eto, Tatsuo Oku, and Shinichi Yoda Jun. 1992 33 p Limited Reproducibility: More than 20% of this document may be affected by microfiche quality

(DE93-753271; JAERI-M-92-085) Avail: CASI HC A03

Fine-grained isotropic graphite grade IG-110, medium-grained near-isotropic graphite grade PGX and coarse-grained baked carbon grade ASR-ORB are employed as structural materials for the High Temperature Engineering Test Reactor (HTTR). The material properties for design are specified in Structural Design Code for Graphite Components of HTTR. This report describes in detail the experiment on deformation behavior including stress-strain relationship, elastic modulas, and Poisson's ratio of each grade. An analytical method for linear elastic approximation leads to the property values contained in the code. DOE

N93-30137# Army Research Lab., Watertown, MA.

MECHANICAL PROPERTIES OF SEVERAL MAGNESIUM AND ALUMINUM COMPOSITES Final Report

Nikos Tsangarakis and Barmac Taleghani Dec. 1992 16 p

(AD-A262481; ARL-TR-34) Avail: CASI HC A03/MF A01

Several composites of magnesium and aluminum alloys were tested in order to assess and evaluate their mechanical properties. The magnesium alloys were AZ91C, ZE41A, and commercially pure magnesium, reinforced with 40% by volume continuous graphite fiber. The tensile properties of these composites were not superior to those of unreinforced magnesium and estimates of their fracture toughness were low. The matrices of the aluminum composites were 2124-T6, 6061-T4, 2124-T4, and 2219-T4. The reinforcements were either particulate or whiskers of silicon carbide or boron carbide and their volume content was 15% to 30%. The aluminum composites which were reinforced with silicon carbide particulate exhibited improved yield and ultimate tensile stresses, as well as tensile elastic modulus over the unreinforced aluminum alloys. The 2124-T4/B4C/25p composite exhibited the highest ultimate tensile strength which was 511 MPa. The composite which was reinforced with whiskers of silicon carbide exhibited an endurance limit which was 20% higher than that of the matrix alloy. The compressive properties and fracture toughness of some of these aluminum composites were not improved over those of the unreinforced matrix alloy. DTIC

N93-30395# Los Alamos National Lab., NM.
SESAME EQUATION OF STATE NUMBER 8010: BORON LOADED SILICONE POTTING MATERIAL
J. C. Boettger May 1993 10 p
(Contract W-7405-eng-36)
(DE93-012083; LA-12541-MS) Avail: CASI HC A02/MF A01

A new SESAME equation of state (EOS) for boron loaded silicone potting material has been generated using the computer program GRIZZLY. This new EOS has been added to the SESAME EOS library as material number 8010. DOE

N93-30428*# National Aeronautics and Space Administration. Langley Research Center, Hampton, VA.
THE FIRST NASA ADVANCED COMPOSITES TECHNOLOGY CONFERENCE, PART 1
John G. Davis, Jr., comp. and Herman L. Bohon, comp. (Lockheed Engineering and Sciences Co., Hampton, VA.) Jan. 1991 419 p
Conference held in Seattle, WA, 29 Oct. - 1 Nov. 1990
(RTOP 510-02-11)
(NASA-CP-3104-Pt-1; L-16889; NAS 1.55:3104-Pt-1) Avail: CASI HC A18/MF A04

Papers are presented from the conference. The ACT program is a multiyear research initiative to achieve a national goal of technology readiness before the end of the decade. Conference papers recorded results of research in the ACT program on new materials development and processing, innovative design concepts, analysis development and validation, cost effective manufacturing methodology, and cost tracking and prediction procedures. Papers presented on major applications programs approved by the Department of Defense are also included. For individual titles, see N93-30429 through N93-30444.

N93-30429*# Boeing Commercial Airplane Co., Seattle, WA.
COMPOSITES: A VIABLE OPTION
John E. McCarty *In* NASA. Langley Research Center, The First NASA Advanced Composites Technology Conference, Part 1 Jan. 1991 p 3-37 (For primary document see N93-30428 11-24)
Avail: CASI HC A03/MF A04

While it sounded great to be asked to talk about composites, I found it difficult to select subject areas that would be of real interest. My choice is based on saying some things about where the maturity of the composite aircraft structures is today and what that means in terms of future criteria for application. This focus was the basis for my title selection. The other issue that will be addressed was requested by NASA and focuses on composites structures cost. This fits well with the state-of-the-art interpretations I will discuss first, since the cost issue must be viewed from both the current status and future points of view. The difficulty in presenting something in these areas is not in the subjects themselves but in trying to present a real world viewpoint to an audience of composite experts. So, with recognition of the expertise of the audience, I hope you will see something in this presentation about how to view composite aircraft structure. Author

N93-30430*# Lockheed Aeronautical Systems Co., Burbank, CA.
ADVANCED COMPOSITE STRUCTURAL CONCEPTS AND MATERIAL TECHNOLOGIES FOR PRIMARY AIRCRAFT STRUCTURES
Anthony Jackson *In* NASA. Langley Research Center, The First NASA Advanced Composites Technology Conference, Part 1 Jan. 1991 p 39-69 (For primary document see N93-30428 11-24)
Avail: CASI HC A03/MF A04

Structural weight savings using advanced composites have been demonstrated for many years. Most military aircraft today use these materials extensively and Europe has taken the lead in their use in commercial aircraft primary structures. A major inhibiter to the use of advanced composites in the United States is cost. Material costs are high and will remain high relative to aluminum. The key therefore lies in the significant reduction in fabrication and assembly costs. The largest cost in most structures today is assembly. As part of the NASA Advanced Composite Technology Program, Lockheed Aeronautical Systems Company has a contract to explore and develop advanced structural and manufacturing concepts using advanced composites for transport aircraft. Wing and fuselage concepts and related trade studies are discussed. These concepts are intended to lower cost and weight through the use of innovative material forms, processes, structural configurations and minimization of parts. The approach to the trade studies and the downselect to the primary wing and fuselage concepts is detailed. The expectations for the development of these concepts is reviewed. Author

N93-30431*# Douglas Aircraft Co., Inc., Long Beach, CA.
COMPOSITES TECHNOLOGY FOR TRANSPORT PRIMARY STRUCTURE
Victor Chen, Arthur Hawley, Max Klotzsche, Alan Markus, and Ray Palmer *In* NASA. Langley Research Center, The First NASA Advanced Composites Technology Conference, Part 1 Jan. 1991 p 71-126 (For primary document see N93-30428 11-24)
Avail: CASI HC A04/MF A04

The ACT contract activity being performed by the McDonnell Douglas Corporation is divided into two separate activities: one effort by Douglas Aircraft in Long Beach, California with a focus on Transport Primary Wing and Fuselage Structure, and the other effort by McDonnell Aircraft in St. Louis, Missouri with a focus on Advanced Combat Aircraft Center Wing-Fuselage Structure. This presentation is on the Douglas Aircraft Transport Structure portion of the ACT program called ICAPS - Innovative Composite Aircraft Primary Structure. Author

N93-30432*# Boeing Commercial Airplane Co., Seattle, WA.
ADVANCED TECHNOLOGY COMMERCIAL FUSELAGE STRUCTURE
L. B. Ilcewicz, P. J. Smith, T. H. Walker, and R. W. Johnson *In* NASA. Langley Research Center, The First NASA Advanced Composites Technology Conference, Part 1 Jan. 1991 p 127-155 (For primary document see N93-30428 11-24)
(Contract NAS1-18889)
Avail: CASI HC A03/MF A04

Boeing's program for Advanced Technology Composite Aircraft Structure (ATCAS) has focused on the manufacturing and performance issues associated with a wide body commercial transport fuselage. The primary goal of ATCAS is to demonstrate cost and weight savings over a 1995 aluminum benchmark. A 31 foot section of fuselage directly behind the wing to body intersection was selected for study purposes. This paper summarizes ATCAS contract plans and review progress to date. The six year ATCAS program will study technical issues for crown, side, and keel areas of the fuselage. All structural details in these areas will be included in design studies that incorporate a design build team (DBT) approach. Manufacturing technologies will be developed for concepts deemed by the DBT to have the greatest potential for cost and weight savings. Assembly issues for large, stiff, quadrant panels will receive special attention. Supporting technologies and mechanical tests will concentrate on the major issues identified for fuselage. These include damage tolerance, pressure containment, splices, load redistribution, post-buckled structure, and durability/life. Progress to date includes DBT selection of baseline fuselage concepts; cost and weight comparisons for crown panel designs; initial panel fabrication for manufacturing and structural mechanics research; and toughened material studies related to keel panels. Initial ATCAS studies have shown that NASA's Advanced Composite Technology program goals for cost and weight savings are attainable for composite fuselage.
Author (revised)

N93-30433*# Lockheed Aeronautical Systems Co., Burbank, CA.
DESIGN, ANALYSIS, AND FABRICATION OF THE TECHNOLOGY INTEGRATION BOX BEAM
C. F. Griffin and L. E. Meade *In* NASA. Langley Research Center, The First NASA Advanced Composites Technology Conference, Part 1 Jan. 1991 p 157-178 Sponsored in part by Lockheed Aeronautical Systems Company (For primary document see N93-30428 11-24)
(Contracts NAS1-17699; NAS1-18888)
Avail: CASI HC A03/MF A04

Numerous design concepts, materials, and manufacturing methods were investigated analytically and empirically for the covers and spars of a transport wing box. This information was applied to the design, analysis, and fabrication of a full-scale section of a transport wing box. A blade-stiffened design was selected for the upper and lower covers of the box. These covers have been constructed using three styles of AS4/974 prepreg fabrics. The front and rear T-stiffened channel spars were filament wound using AS4/1806 towpreg. Covers, ribs, and spars were assembled using mechanical fasteners. When they are completed later this year, the tests on the technology integration box beam will demonstrate the structural integrity of an advanced composite wing design which is 25 percent lighter than the metal baseline. Author (revised)

N93-30434*# McDonnell Aircraft Co., Saint Louis, MO.
DESIGN AND MANUFACTURING CONCEPTS FOR THERMOPLASTIC STRUCTURES
Michael P. Renieri, Steven J. Burpo, and Lance M. Roundy *In* NASA. Langley Research Center, The First NASA Advanced Composites Technology Conference, Part 1 179-206 (SEE N93-30428 11-24) Jan. 1991 (For primary document see N93-30428 11-24)
Avail: CASI HC A03/MF A04

Results to date on the application of two manufacturing techniques, fiber placement and single diaphragm/coconsolidation, to produce cost-effective, thermoplastic composite (TPC), primary fuselage structure are presented. Applications relative to fuselage upper cover structure indicate potential cost savings relative to conventional approaches. Progress is also presented on efforts concerned with other design details which take advantage of thermoplastic composites such as fastener less stiffener/frame attachments. In addition, results are presented on the development and verification testing of a composite lug analysis program which incorporates through-the-thickness effects. Author (revised)

N93-30435*# National Aeronautics and Space Administration. Langley Research Center, Hampton, VA.
STRUCTURAL EVALUATION OF CURVED STIFFENED COMPOSITE PANELS FABRICATED USING A THERM-Xsm PROCESS
Christos Kassapoglou (Sikorsky Aircraft, Stratford, CT.), Albert J. DiNicola (Sikorsky Aircraft, Stratford, CT.), Jack C. Chou (Sikorsky Aircraft, Stratford, CT.), and Jerry W. Deaton *In its* First NASA Advanced Composites Technology Conference, Part 1 Jan. 1991 p 207-232 (For primary document see N93-30428 11-24)
(Contract NAS1-18799)
Avail: CASI HC A03/MF A04

The use of composites in aircraft structures is often limited by material and manufacturing costs which, for some designs and applications, are prohibitively high. To increase the frequency of application of composites in primary airframe components alternative manufacturing processes are sought that reduce cost and/or enhance structural efficiency. One alternative process involves the use of THERM-Xsm as the pressure transfer medium during autoclave curing. THERM-Xsm, a silicon-based flow able polymer which behaves like a liquid under autoclave presssure, transmits quasi-hydrostatic pressure to all contacting surfaces of the part to be cured. Once the autoclave pressure is relieved, THERM-Xsm reverts back to the powdery solid state and can be reused many times. The THERM-Xsm process to be evaluated is depicted and consists of (1) enclosing the tool and part to be cured by a set of frames that create a box, (2) pouring THERM-Xsm powder onto the part and filling the box, and (3) placing a vacuum bag over the box assembly. In this program, a separating non-porous film (Teflon) was placed between the part to be cured and THERM-Xsm powder to avoid any contamination. The use of THERM-Xsm has two significant advantages over conventional manufacturing procedures. First, it eliminates complicated hard tooling since it guarantees uniform pressure transfer and thus, good compaction at complex structural details (such as frame-stiffener intersections and corners). Second, it greatly simplifies vacuum bagging, since once the part to be cured is covered by THERM-Xsm powder, the vacuum bag need only conform to a relatively flat shape reducing significantly the number of pleats required. A program is on-going at Sikorsky Aircraft to evaluate the structural performance of complex composite fuselage structures made with this THERM-Xsm process and to quantify the impact of THERM-Xsm on manufacturing labor hours and cost. The program involves fuselage panel optimization analysis, a building block test program where structural details representative of the full-scale article are analyzed and tested, and static and fatigue test/analysis of the full-scale test articles. The main results of this program are reported. Author (revised)

N93-30436*# National Aeronautics and Space Administration. Langley Research Center, Hampton, VA.
NOISE TRANSMISSION PROPERTIES AND CONTROL STRATEGIES FOR COMPOSITE STRUCTURES
Richard J. Silcox, Todd B. Beyer, and Harold C. Lester *In its* First NASA Advanced Composites Technology Conference, Part 1 Jan. 1991 p 233-246 (For primary document see N93-30428 11-24)
Avail: CASI HC A03/MF A04

A study of several component technologies required to apply active control techniques to reduce interior noise in composite aircraft structures is described. The mechanisms of noise transmission in an all composite, large-scale, fuselage model are studied in an experimental program and found similar to mechanisms found in conventional aircraft construction. Two primary conditions of structural acoustic response are found to account for the dominant interior acoustic response. A preliminary study of active noise control in cylinders used piezoceramic actuators as force inputs for a simple aluminum fuselage model. These actuators provided effective control for the same two conditions of noise transmission found in the composite fuselage structure. The use of piezoceramic actuators to apply force inputs overcomes the weight and structural requirements of conventional shaker actuators. Finally, in order to accurately simulate these types of actuators in a cylindrical shell, two analytical models are investigated that apply either in-plane forces or bending moments along the boundaries of a finite patch. It is shown that the bending model may not be as effective as the force model for exciting the low order azimuthal modes that typically dominate the structural acoustic response in these systems. This result will affect the arrangement and distribution of actuators required for effective active control systems. Author (revised)

N93-30437*# Delaware Univ., Newark. Dept. of Mechanical Engineering.
LONG DISCONTINUOUS FIBER COMPOSITE STRUCTURE: FORMING AND STRUCTURAL MECHANICS
R. B. Pipes, M. H. Santare, B. J. OToole, A. J. Beaussart, D. C. DeHeer, and R. K. Okine (Du Pont de Nemours, E. I. and Co., Wilmington, DE.) *In* NASA. Langley Research Center, The First NASA Advanced Composites Technology Conference, Part 1 Jan. 1991 p 247-270 (For primary document see N93-30428 11-24)
(Contract NAS1-18758)
Avail: CASI HC A03/MF A04

Cost effective composite structure has motivated the investigation of several new approaches to develop composite structure from innovative material forms. Among the promising new approaches is the conversion of planar sheet to components of complex curvature through sheet forming or stretch forming. In both cases, the potential for material stretch in the fiber direction appears to offer a clear advantage in formability over continuous fiber systems. In the present study, the authors have established a framework which allows the simulation of the anisotropic mechanisms of deformation of long discontinuous fiber laminates wherein the matrix phase is a viscous fluid. The initial study focuses upon the establishment of micromechanics models for prediction of the effective anisotropic viscosities of the oriented fiber assembly in a viscous matrix. Next, the developed constitutive relation is employed through an analogy with incompressible elasticity to exercise the finite element technique for determination of local fiber orientation and laminate thickness after forming. Results are presented for the stretch bending of a curved beam from an arbitrary composite laminate and the bulging of a clamped sheet. Structural analyses are conducted to determine the effect of microstructure on the performance of curved beams manufactured from long discontinuous fiber composites. For the purposes of this study, several curved beams with ideal and non-ideal microstructures are compared for response under pure bending. Material parameters are determined from a separate microstructural analysis.
Author (revised)

N93-30438*# Douglas Aircraft Co., Inc., Long Beach, CA.
RESIN TRANSFER MOLDING FOR ADVANCED COMPOSITE PRIMARY AIRCRAFT STRUCTURES
Alan Markus and Ray Palmer *In* NASA. Langley Research Center, The First NASA Advanced Composites Technology Conference, Part 1 Jan. 1991 p 271-292 (For primary document see N93-30428 11-24)
Avail: CASI HC A03/MF A04

Resin Transfer Molding (RTM) has been identified by Douglas Aircraft Company (DAC) and industry to be one of the promising processes being developed today which can break the cost barrier of implementing composite primary structures into a commercial aircraft production environment. The RTM process developments and scale-up plans Douglas Aircrart will be conducting under the NASA ACT contract are discussed. Author (revised)

N93-30439*# Grumman Aerospace Corp., Bethpage, NY. Aircraft Systems.

CONSOLIDATION OF GRAPHITE THERMOPLASTIC TEXTILE PREFORMS FOR PRIMARY AIRCRAFT STRUCTURE

J. Suarez and J. Mahon *In* NASA. Langley Research Center, The First NASA Advanced Composites Technology Conference, Part 1 Jan. 1991 p 293-338 (For primary document see N93-30428 11-24)
Avail: CASI HC A03/MF A04

The use of innovative cost effective material forms and processes is being considered for fabrication of future primary aircraft structures. Processes that have been identified as meeting these goals are textile preforms that use resin transfer molding (RTM) and consolidation forming. The Novel Composites for Wing and Fuselage Applications (NCWFA) program has as its objective the integration of innovative design concepts with cost effective fabrication processes to develop damage-tolerant structures that can perform at a design ultimate strain level of 6000 micro-inch/inch. In this on-going effort, design trade studies were conducted to arrive at advanced wing designs that integrate new material forms with innovative structural concepts and cost effective fabrication methods. The focus has been on minimizing part count (mechanical fasteners, clips, number of stiffeners, etc.), by using cost effective textile reinforcement concepts that provide improved damage tolerance and out-of-plane load capability, low-cost resin transfer molding processing, and thermoplastic forming concepts. The fabrication of representative Y spars by consolidation methods will be described. The Y spars were fabricated using AS4 (6K)/PEEK 150g commingled angle interlock 0/90-degree woven preforms with +45-degree commingled plies stitched using high strength Toray carbon thread and processed by autoclave consolidation. Author

N93-30440*# Boeing Commercial Airplane Co., Seattle, WA.

COST STUDIES FOR COMMERCIAL FUSELAGE CROWN DESIGNS

T. H. Walker, P. J. Smith, G. Truslove, K. S. Willden, S. L. Metschan, and C. L. Pfahl *In* NASA. Langley Research Center, The First NASA Advanced Composites Technology Conference, Part 1 Jan. 1991 p 339-355 (For primary document see N93-30428 11-24)
(Contract NAS1-18889)
Avail: CASI HC A03/MF A04

Studies were conducted to evaluate the cost and weight potential of advanced composite design concepts in the crown region of a commercial transport. Two designs from each of three design families were developed using an integrated design-build team. A range of design concepts and manufacturing processes were included to allow isolation and comparison of cost centers. Detailed manufacturing/assembly plans were developed as the basis for cost estimates. Each of the six designs was found to have advantages over the 1995 aluminum benchmark in cost and weight trade studies. Large quadrant panels and cobonded frames were found to save significant assembly labor costs. Comparisons of high- and intermediate-performance fiber systems were made for skin and stringer applications. Advanced tow placement was found to be an efficient process for skin lay up. Further analysis revealed attractive processes for stringers and frames. Optimized designs were informally developed for each design family, combining the most attractive concepts and processes within that family. A single optimized design was selected as the most promising, and the potential for further optimization was estimated. Technical issues and barriers were identified. Author

N93-30441*# National Aeronautics and Space Administration. Langley Research Center, Hampton, VA.

A UNIFIED APPROACH FOR COMPOSITE COST REPORTING AND PREDICTION IN THE ACT PROGRAM

W. Tom Freeman, Louis F. Vosteen (Analytical Services and Materials, Inc., Hampton, VA.), and Shahid Siddiqi (Analytical Services and Materials, Inc., Hampton, VA.) *In its* First NASA Advanced Composites Technology Conference, Part 1 Jan. 1991 p 357-369 (For primary document see N93-30428 11-24)
Avail: CASI HC A03/MF A04

The Structures Technology Program Office (STPO) at NASA Langley Research Center has held two workshops with representatives from the commercial airframe companies to establish a plan for development of a standard cost reporting format and a cost prediction tool for conceptual and preliminary designers. This paper reviews the findings of the workshop representatives with a plan for implementation of their recommendations. The recommendations of the cost tracking and reporting committee will be implemented by reinstituting the collection of composite part fabrication data in a format similar to the DoD/NASA Structural Composites Fabrication Guide. The process of data collection will be automated by taking advantage of current technology with user friendly computer interfaces and electronic data transmission. Development of a conceptual and preliminary designers' cost prediction model will be initiated. The model will provide a technically sound method for evaluating the relative cost of different composite structural designs, fabrication processes, and assembly methods that can be compared to equivalent metallic parts or assemblies. The feasibility of developing cost prediction software in a modular form for interfacing with state of the art preliminary design tools and computer aided design (CAD) programs is assessed. Author (revised)

N93-30442*# Northrop Corp., Hawthorne, CA. Aircraft Div.

F-15 COMPOSITE ENGINE ACCESS DOOR

Ramaswamy L. Ramkumar and James C. Watson (McDonnell Aircraft Co., Saint Louis, MO.) *In* NASA. Langley Research Center, The First NASA Advanced Composites Technology Conference, Part 1 Jan. 1991 p 371-384 (For primary document see N93-30428 11-24)
(Contract F33615-87-C-5242)
Avail: CASI HC A03/MF A04

This paper presents a summary of the successfully concluded phase 1 of the two-phase Design and Manufacture of Advanced Thermoplastic Structures (DMATS) program. It addresses the design, manufacture, and validation testing of a thermoplastic F-15E forward engine access door and includes lessons learned during the concurrent product and process design development phases of the program. Author

N93-30443*# Boeing Helicopter Co., Philadelphia, PA.

FABRICATION OF THE V-22 COMPOSITE AFT FUSELAGE USING AUTOMATED FIBER PLACEMENT

Robert L. Pinckney *In* NASA. Langley Research Center, The First NASA Advanced Composites Technology Conference, Part 1 Jan. 1991 p 385-397 (For primary document see N93-30428 11-24)
Avail: CASI HC A03/MF A04

Boeing Helicopters and its subcontractors are working together under an Air Force Wright Research and Development Center (WRDC)-Manufacturing-Technology Large-Composite Primary Structure Fuselage program to develop and demonstrate new manufacturing techniques for producing composite fuselage skin and frame structures. Three sets of aft fuselage skins and frames have been fabricated and assembled, and substantial reductions in fabrication and assembly costs demonstrated. Author

N93-30444*# Northrop Corp., Hawthorne, CA.

LESSONS LEARNED FOR COMPOSITE STRUCTURES

R. S. Whitehead *In* NASA. Langley Research Center, The First NASA Advanced Composites Technology Conference, Part 1 Jan. 1991 p 399-415 (For primary document see N93-30428 11-24)
Avail: CASI HC A03/MF A04

Lessons learned for composite structures are presented in three technology areas: materials, manufacturing, and design. In addition, future challenges for composite structures are presented. Composite materials have long gestation periods from the developmental stage to fully matured production status. Many examples exist of unsuccessful attempts to accelerate this gestation period. Experience has shown that technology transition of a new material system to fully matured production status is time consuming, involves risk, is expensive and should not be undertaken lightly. The future challenges for composite materials require an intensification of the science based approach to material development, extension of the vendor/customer interaction process to include all engineering disciplines of the end user, reduced material costs because they are a significant factor in overall part cost, and improved batch-to-batch pre-preg physical property control. Historical manufacturing lessons learned are presented using current in-service production structure as examples. Most producibility problems for these structures can be traced to their sequential engineering design. This caused an excessive emphasis on design-to-weight and schedule at the expense of design-to-cost. This resulted in expensive performance originated designs, which required costly tooling and led to non-producible parts. Historically these problems have been allowed to persist throughout the production run. The current/future approach for the

production of affordable composite structures mandates concurrent engineering design where equal emphasis is placed on product and process design. Design for simplified assembly is also emphasized, since assembly costs account for a major portion of total airframe costs. The future challenge for composite manufacturing is, therefore, to utilize concurrent engineering in conjunction with automated manufacturing techniques to build affordable composite structures. Composite design experience has shown that significant weight savings have been achieved, outstanding fatigue and corrosion resistance have been demonstrated, and in-service performance has been very successful. Currently no structural design show stoppers exist for composite structures. A major lesson learned is that the full scale static test is the key test for composites, since it is the primary structural 'hot spot' indicator. The major durability issue is supportability of thin skinned structure. Impact damage has been identified as the most significant issue for the damage tolerance control of composite structures. However, delaminations induced during assembly operations have demonstrated a significant nuisance value. The future challenges for composite structures are threefold. Firstly, composite airframe weight fraction should increase to 60 percent. At the same time, the cost of composite structures must be reduced by 50 percent to attain the goal of affordability. To support these challenges it is essential to develop lower cost materials and processes.
Author (revised)

N93-30555# Naval Command, Control and Ocean Surveillance Center, San Diego, CA.

MEASUREMENT OF ELECTROMAGNETIC PROPERTIES OF COMPOSITE MATERIALS Final Report, Oct. 1991 - Sep. 1992

T. Q. Ho, J. C. Logan, J. H. Schukantz, F. W. Shaw, and R. Q. Welch
Feb. 1993 18 p
(AD-A264725; NRAD-TD-2457) Avail: CASI HC A03/MF A01

This report describes four different techniques that may be used for measuring the electromagnetic properties of composite materials. Experimental data obtained from each method are presented. The advantages and disadvantages of each method are also discussed. DTIC

N93-30841*# National Aeronautics and Space Administration. Langley Research Center, Hampton, VA.

FIRST NASA ADVANCED COMPOSITES TECHNOLOGY CONFERENCE, PART 2

John G. Davis, Jr., comp. and Herman L. Bohon, comp. (Lockheed Engineering and Sciences Co., Hampton, VA.) Jan. 1991 622 p
Conference held in Seattle, WA, 29 Oct. - 1 Nov. 1990
(RTOP 510-02-11)
(NASA-CP-3104-Pt-2; L-16889-Pt-2; NAS 1.55:3104-Pt-2) Avail: CASI HC A99/MF A06

Presented here is a compilation of papers presented at the first NASA Advanced Composites Technology (ACT) Conference held in Seattle, Washington, from 29 Oct. to 1 Nov. 1990. The ACT program is a major new multiyear research initiative to achieve a national goal of technology readiness before the end of the decade. Included are papers on materials development and processing, innovative design concepts, analysis development and validation, cost effective manufacturing methodology, and cost tracking and prediction procedures. Papers on major applications programs approved by the Department of Defense are also included. For individual titles, see X91-10208 through X91-10242. For individual titles, see N93-30842 through N93-30876.

N93-30842*# National Aeronautics and Space Administration. Langley Research Center, Hampton, VA.

PRELIMINARY PROPERTIES OF A RESIN FROM ETHYNYL TERMINATED MATERIALS

Paul M. Hergenrother and John W. Connell *In its* First NASA Advanced Composites Technology Conference, Part 2 Jan. 1991 p 419-424
(For primary document see N93-30841 11-24)
Avail: CASI HC A02/MF A06

A blend composed of an ethynyl terminated aspartimide (brittle component) and an ethynyl terminated arylene ether oligomer (tough component) was thermally cured to yield a resin which underwent preliminary evaluation to determine the potential for use in structural applications on aerospace vehicles. The blend exhibited good compression moldability, allowing for fabrication of neat moldings, adhesive specimens and composites at temperatures of 250 C under a pressure of 1.4 MPa (200 psi). Neat resin moldings and adhesive specimens provided relatively high mechanical properties. Composite specimens provided promising results in spite of fiber misalignment, fiber washout, and a small amount of panel warpage.
Author (revised)

N93-30843*# National Aeronautics and Space Administration. Langley Research Center, Hampton, VA.

INFILTRATION/CURE MODELING OF RESIN TRANSFER MOLDED COMPOSITE MATERIALS USING ADVANCED FIBER ARCHITECTURES

Alfred C. Loos (Virginia Polytechnic Inst. and State Univ., Blacksburg.), Mark H. Weideman (Virginia Polytechnic Inst. and State Univ., Blacksburg.), Edward R. Long, Jr., David E. Kranbuehl (College of William and Mary, Williamsburg, VA.), Philip J. Kinsley (College of William and Mary, Williamsburg, VA.), and Sean M. Hart (College of William and Mary, Williamsburg, VA.) *In its* First NASA Advanced Composites Technology Conference, Part 2 Jan. 1991 p 425-441 (For primary document see N93-30841 11-24)
(Grants NAG1-343; NAG1-237)
Avail: CASI HC A03/MF A06

A model was developed which can be used to simulate infiltration and cure of textile composites by resin transfer molding. Fabric preforms were resin infiltrated and cured using model generated optimized one-step infiltration/cure protocols. Frequency dependent electromagnetic sensing (FDEMS) was used to monitor in situ resin infiltration and cure during processing. FDEMS measurements of infiltration time, resin viscosity, and resin degree of cure agreed well with values predicted by the simulation model. Textile composites fabricated using a one-step infiltration/cure procedure were uniformly resin impregnated and void free. Fiber volume fraction measurements by the resin digestion method compared well with values predicted using the model. Author

N93-30844*# National Aeronautics and Space Administration. Langley Research Center, Hampton, VA.

POWDER TOWPREG PROCESS DEVELOPMENT

Robert M. Baucom and Joseph M. Marchello (Old Dominion Univ., Norfolk, VA.) *In its* First NASA Advanced Composites Technology Conference, Part 2 Jan. 1991 p 443-454 (For primary document see N93-30841 11-24)
Avail: CASI HC A03/MF A06

The process for dry powder impregnation of carbon fiber tows being developed at LaRC overcomes many of the difficulties associated with melt, solution, and slurry prepregging. In the process, fluidized powder is deposited on spread tow bundles and fused to the fibers by radiant heating. Impregnated tows have been produced for preform, weaving, and composite materials applications. Design and operating data correlations were developed for scale up of the process to commercial operation. Bench scale single tow experiments at tow speeds up to 50 cm/sec have demonstrated that the process can be controlled to produce weavable towpreg. Samples were woven and molded into preform material of good quality.
Author (revised)

N93-30845*# Boeing Commercial Airplane Co., Seattle, WA.

EFFECTS OF INTRA- AND INTER-LAMINAR RESIN CONTENT ON THE MECHANICAL PROPERTIES OF TOUGHENED COMPOSITE MATERIALS

Dodd H. Grande, Larry B. Ilcewicz, William B. Avery (Boeing Co., Seattle, WA.), and Willard D. Bascom (Utah Univ., Salt Lake City.) *In* NASA. Langley Research Center, First NASA Advanced Composites Technology Conference, Part 2 Jan. 1991 p 455-475 (For primary document see N93-30841 11-24)
(Contract NAS1-18889)
Avail: CASI HC A03/MF A06

Composite materials having multiphase toughened matrix systems and laminate architectures characterized by resin-rich interlaminar layers (RIL) have been the subject of much recent attention. Such materials are likely to find applications in thick compressively loaded structures such as the keel area of commercial aircraft fuselages. The effects of resin content and its interlaminar and intralaminar distribution on mechanical properties were investigated with test and analysis of two carbon-epoxy systems. The RIL was found to reduce the in situ strengthening effect for matrix cracking in laminates. Mode 2 fracture toughness was found to increase with increasing RIL thickness over the range investigated, and Mode 1 interlaminar toughness was negligibly affected. Compressive failure strains were found to increase with increasing resin content for specimens having no damage, holes, and impact damage. Analytical tools for predicting matrix cracking of off-axis plies and damage tolerance in compression after impact (CAI) were successfully applied to materials with RIL. Author (revised)

N93-30846*# Utah Univ., Salt Lake City.
STUDIES OF FIBER-MATRIX ADHESION ON COMPRESSION STRENGTH
Willard D. Bascom, John A. Nairn, and D. J. Boll (Hercules, Inc., Magna, UT.) *In* NASA. Langley Research Center, First NASA Advanced Composites Technology Conference, Part 2 Jan. 1991 p 477-495 (For primary document see N93-30841 11-24)
(Contract NAS1-18883)
Avail: CASI HC A03/MF A06

A study was initiated on the effect of the matrix polymer and the fiber matrix bond strength of carbon fiber polymer matrix composites. The work includes tests with micro-composites, single ply composites, laminates, and multi-axial loaded cylinders. The results obtained thus far indicate that weak fiber-matrix adhesion dramatically reduces 0 degree compression strength. Evidence is also presented that the flaws in the carbon fiber that govern compression strength differ from those that determine fiber tensile strength. Examination of post-failure damage in the single ply tests indicates kink banding at the crack tip. Author (revised)

N93-30847*# Utah Univ., Salt Lake City. Dept. of Material Science and Engineering.
THE INITIATION, PROPAGATION, AND EFFECT OF MATRIX MICROCRACKS IN CROSS-PLY AND RELATED LAMINATES
John A. Nairn, Shoufeng Hu, Siulie Liu, and Jong Bark *In* NASA. Langley Research Center, First NASA Advanced Composites Technology Conference, Part 2 Jan. 1991 p 497-512 (For primary document see N93-30841 11-24)
(Contract NAS1-18833)
Avail: CASI HC A03/MF A06

Recently, a variational mechanics approach was used to determine the thermoelastic stress state in cracked laminates. Described here is a generalization of the variational mechanics techniques to handle other cross-ply laminates, related laminates, and to account for delaminations emanating from microcrack tips. Microcracking experiments on Hercules 3501-6/AS4 carbon fiber/epoxy laminates show a staggered cracking pattern. These results can be explained by the variational mechanics analysis. The analysis of delaminations emanating from microcrack tips has resulted in predictions about the structural and material variables controlling competition between microcracking and delamination failure modes. Author

N93-30848*# National Aeronautics and Space Administration. Langley Research Center, Hampton, VA.
COMPARISON OF IMPACT RESULTS FOR SEVERAL POLYMERIC COMPOSITES OVER A WIDE RANGE OF LOW IMPACT VELOCITIES
C. C. Poe, Jr., M. A. Portanova (Lockheed Engineering and Sciences Co., Hampton, VA.), J. E. Masters (Lockheed Engineering and Sciences Co., Hampton, VA.), B. V. Sankar (Florida Univ., Gainesville.), and Wade C. Jackson (Army Aerostructures Directorate, Hampton, VA.) *In its* First NASA Advanced Composites Technology Conference, Part 2 Jan. 1991 p 513-547 (For primary document see N93-30841 11-24)
Avail: CASI HC A03/MF A06

Static indentation, falling weight, and ballistic impact tests were conducted in clamped plates made of AS4/3501-6 and IM7/8551-7 prepreg tape. The transversely isotropic plates were nominally 7-mm thick. Pendulum and ballistic tests were also conducted on simply supported plates braided with Celion 12000 fibers and 3501-6 epoxy. The 20 degree braided plates were about 5-mm thick. The impactors had spherical or hemispherical shapes with a 12.7 mm diameter. Residual compression strength and damage size were measured. For a given kinetic energy, damage size was least for IM7/8551-7 and greatest for the braided material. Strengths varied inversely with damage size. For a given damage size, strength loss as a fraction of original strength was least for the braided material and greatest for AS4/3501-6 and IM7/8551-7. Strength loss for IM7/8551-7 and AS4/3501-6 was nearly equal. No significant differences were noticed between damage sizes and residual compression strengths for the static indentation, falling weight, and ballistic tests of AS4/3501-6 and IM7/8551-7. For the braided material, sizes of damage were significantly less and compression strengths were significantly more for the falling weight tests than for the ballistic tests. Author (revised)

N93-30849*# Stanford Univ., CA.
DELAMINATIONS IN COMPOSITE PLATES UNDER IMPACT LOADS
Scott R. Finn and George S. Springer *In* NASA. Langley Research Center, First NASA Advanced Composites Technology Conference, Part 2 Jan. 1991 p 549-577 (For primary document see N93-30841 11-24)
(Contract NAS1-18778)
Avail: CASI HC A03/MF A06

A method is presented for calculating the locations, shapes, and sizes of delaminations which occur in a fiber reinforced composite plate subjected to non-penetrating (low velocity) impact of a solid object. The plate may be simply supported, clamped, or free along its edges. A failure model of the delamination formation was developed. This model was then coupled with a finite element analysis. The model and the finite element analysis were then implemented by a computer code (IMPACT-ST) which can be used to estimate the damage initiation load and the locations, shapes, and sizes of the delaminations. Tests were performed measuring the geometries of the delaminations in graphite-epoxy, graphite-toughened epoxy, and graphite-PEEK plates impacted by a projectile with a spherical tip having masses ranging from 0.355 lbm to 0.963 lbm and velocities from 50 in/sec to 225 in/sec. The data were compared to the results of the model, and good agreements were found between the measured and the calculated delamination lengths and widths. Author

N93-30850*# Rockwell International Science Center, Thousand Oaks, CA.
MICROMECHANICS OF FATIGUE IN WOVEN AND STITCHED COMPOSITES
B. N. Cox, M. S. Dadkhah, R. V. Inman, M. R. Mitchell, W. L. Morris, and S. Schroeder *In* NASA. Langley Research Center, First NASA Advanced Composites Technology Conference, Part 2 Jan. 1991 p 579-587 (For primary document see N93-30841 11-24)
(Contract NAS1-18840)
Avail: CASI HC A02/MF A06

The goal is to determine how microstructural factors, especially the architecture of microstructural factors, control fatigue damage in 3D reinforced polymer composites. Test materials were fabricated from various preforms, including stitched quasi-isotropic laminates, and through-the-thickness angle interlock, layer-to-layer angle interlock, and through-the-thickness stitching effect weaves. Preforms were impregnated with a tough resin by a special vacuum infiltration method. Most tests are being performed in uniaxial compression/compression loading. In all cases to date, failure has occurred not by delamination, but by shear failure, which occurs suddenly rather than by gradual macroscopic crack growth. Some theoretical aspects of bridging are also examined. Author (revised)

N93-30851*# National Aeronautics and Space Administration. Langley Research Center, Hampton, VA.
CHARACTERIZATION OF MULTIAXIAL WARP KNIT COMPOSITES
H. Benson Dexter, Gregory H. Hasko (Lockheed Engineering and Sciences Co., Hampton, VA.), and Roberto J. Cano *In its* First NASA Advanced Composites Technology Conference, Part 2 Jan. 1991 p 589-619 (For primary document see N93-30841 11-24)
Avail: CASI HC A03/MF A06

The objectives were to characterize the mechanical behavior and damage tolerance of two multiaxial warp knit fabrics to determine the acceptability of these fabrics for high performance composite applications. The tests performed included compression, tension, open hole compression, compression after impact and compression-compression fatigue. Tests were performed on as-fabricated fabrics and on multi-layer fabrics that were stitched together with either carbon or Kevlar stitching yarn. Results of processing studies for vacuum impregnation with Hercules 3501-6 epoxy resin and pressure impregnation with Dow Tactix 138/H41 epoxy resin and British Petroleum BP E905L epoxy resin are presented. Author

N93-30852*# National Aeronautics and Space Administration. Langley Research Center, Hampton, VA.
DEVELOPMENT OF STITCHING REINFORCEMENT FOR TRANSPORT WING PANELS

Raymond J. Palmer (Douglas Aircraft Co., Inc., Huntington Beach, CA.), Marvin B. Dow, and Donald L. Smith (Lockheed Engineering and Sciences Co., Hampton, VA.) *In its* First NASA Advanced Composites Technology Conference, Part 2 Jan. 1991 p 621-646 (For primary document see N93-30841 11-24)
Avail: CASI HC A03/MF A06

The NASA Advanced Composites Technology (ACT) program has the objective of providing the technology required to obtain the full benefit of weight savings and performance improvements offered by composite primary aircraft structures. Achieving the objective is dependent upon developing composite materials and structures which are damage tolerant and economical to manufacture. Researchers are investigating stitching reinforcement combined with resin transfer molding to produce materials meeting the ACT program objective. Research is aimed at materials, processes, and structural concepts for application in both transport wings and fuselages, but the emphasis to date has been on wing panels. Empirical guidelines are being established for stitching reinforcement in structures designed for heavy loads. Results are presented from evaluation tests investigating stitching types, threads, and density (penetrations per square inch). Tension strength, compression strength, and compression after impact data are reported. Author

N93-30853*# Dow Chemical Co., Midland, MI.

DEVELOPMENT OF RESINS FOR COMPOSITES BY RESIN TRANSFER MOLDING

Edmund P. Woo, Paul M. Puckett, and Shawn J. Maynard *In* NASA. Langley Research Center, First NASA Advanced Composites Technology Conference, Part 2 Jan. 1991 p 647-658 (For primary document see N93-30841 11-24)
(Contract NAS1-18841)
Avail: CASI HC A03/MF A06

Designed to cover a wide range of resin technology and to meet the near-term and long-term needs of the aircraft industry, this research has three objectives: to produce resin transfer molding (RES) resins with improved processability, to produce prepreg systems with high toughness and service temperature, and to produce new resin systems. Progress on reaching the objectives is reported. Author

N93-30854*# BASF Structural Materials, Inc., Charlotte, NC.

ADVANCED FIBER/MATRIX MATERIAL SYSTEMS

J. Timothy Hartness *In* NASA. Langley Research Center, First NASA Advanced Composites Technology Conference, Part 2 Jan. 1991 p 659-676 (For primary document see N93-30841 11-24)
(Contract NAS1-18834)
Avail: CASI HC A03/MF A06

Work completed in Phase 1 of the NASA Advanced Composite Technology program is discussed. Two towpreg forms (commingled yarns and fused powder towpregs) are being characterized under the program. These towpregs will be used to evaluate textile fabrication technologies for advanced aircraft composite structures. The unique characteristic of both of these material forms is that both fiber and matrix resin are handled in a single operation such as weaving, braiding, or fiber placement. The evaluation of both commingled and fused powder towpreg is described. Various polymer materials are considered for both subsonic and supersonic applications. Polymers initially being evaluated include thermoplastic polyimides such as Larc-TPI and New-TPI, thermoplastics such as PEEK and PEKEKK as well as some toughened crosslinked polyimides. Preliminary mechanical properties as well as tow handling are evaluated. Author

N93-30855*# Boeing Defense and Space Group, Philadelphia, PA.

MECHANICAL AND ANALYTICAL SCREENING OF BRAIDED COMPOSITES FOR TRANSPORT FUSELAGE APPLICATIONS

Mark J. Fedro, Christian Gunther, and Frank K. Ko (Drexel Univ., Philadelphia, PA.) *In* NASA. Langley Research Center, First NASA Advanced Composites Technology Conference, Part 2 Jan. 1991 p 677-704 (For primary document see N93-30841 11-24)
(Contract NAS1-18889)
Avail: CASI HC A03/MF A06

The mechanics of materials progress in support of the goal of understanding the application of braided composites in a transport aircraft fuselage are summarized. Composites consisting of both 2-D and 3-D braid patterns are investigated. Both consolidation of commingled graphite/PEEK and resin transfer molding of graphite-epoxy braided composite processes are studied. Mechanical tests were used to examine unnotched tension, open hole tension, compression, compression after impact, in-plane shear, out-of-plane tension, bearing, and crippling. Analytical methods are also developed and applied to predict the stiffness and strengths of test specimens. A preliminary study using the test data and analytical results is performed to assess the applicability of braided composites to a commercial aircraft fuselage. Author

N93-30856*# National Aeronautics and Space Administration. Langley Research Center, Hampton, VA.

ULTRASONIC DETECTION AND IDENTIFICATION OF FABRICATION DEFECTS IN COMPOSITES

Edward R. Long, Jr., Susan M. Kullerd, Patrick H. Johnston, and Eric I. Madaras *In its* First NASA Advanced Composites Technology Conference, Part 2 Jan. 1991 p 705-720 (For primary document see N93-30841 11-24)
Avail: CASI HC A03/MF A06

Methods for deliberate fabrication of porosity into carbon/epoxy composite panels and the influence of three-dimensional stitching on the detection of porosity were investigated. Two methods of introducing porosity were investigated. Porosity was simulated by inclusion of glass microspheres, and a more realistic form of porosity was introduced by using low pressure during consolidation. The panels were ultrasonically scanned and the frequency slope of the ultrasonic attenuation coefficient was used to evaluate the two forms of porosity. The influence of stitching on the detection of porosity was studied using panels which were resin transfer molded from stitched plies of knitted carbon fabric and epoxy resin. Author

N93-30857*# Boeing Co., Seattle, WA.

DEVELOPMENTS IN IMPACT DAMAGE MODELING FOR LAMINATED COMPOSITE STRUCTURES

Ernest F. Dost, William B. Avery, Gary D. Swanson, and Kuen Y. Lin (Washington Univ., Seattle.) *In* NASA. Langley Research Center, First NASA Advanced Composites Technology Conference, Part 2 Jan. 1991 p 721-736 (For primary document see N93-30841 11-24)
(Contract NAS1-18889)
Avail: CASI HC A03/MF A06

Damage tolerance is the most critical technical issue for composite fuselage structures studied in the Advanced Technology Composite Aircraft Structures (ATCAS) program. The objective here is to understand both the impact damage resistance and residual strength of the laminated composite fuselage structure. An understanding of the different damage mechanisms which occur during an impact event will support the selection of materials and structural configurations used in different fuselage quadrants and guide the development of analysis tools for predicting the residual strength of impacted laminates. Prediction of the damage state along with the knowledge of post-impact response to applied loads will allow for engineered stacking sequencies and structural configurations; intelligent decisions on repair requirements will also result. Author

N93-30858*# Washington Univ., Seattle.

MULTI-PARAMETER OPTIMIZATION TOOL FOR LOW-COST COMMERCIAL FUSELAGE CROWN DESIGNS

Zelda Zabinsky, Mark Tuttle, Douglas Graesser, Gun-In Kim, Darrin Hatcher, Gary Swanson (Boeing Commercial Airplane Co., Seattle, WA.), and Larry Ilcewicz (Boeing Commercial Airplane Co., Seattle, WA.) *In* NASA. Langley Research Center, First NASA Advanced Composites Technology Conference, Part 2 Jan. 1991 p 737-748 (For primary document see N93-30841 11-24)
Avail: CASI HC A03/MF A06

The work in progress for developing a methodology and software tool to aid in the optimal design of composite structures is discussed. The methodology is being developed to take advantage of the ability to tailor the composite material in conjunction with the design of the structure. The composites optimization design software UWCODA was found to be very successful in preliminary testing and early experience. UWCODA is a composites design code that uses a number of plies and fiber angles as design variables, employs maximum strain failure criteria for objective function and additional constraints, includes Boeing design tools for stiffened panels, and includes stiffener geometry in the design variables. Author

N93-30859*# National Aeronautics and Space Administration. Langley Research Center, Hampton, VA.
COMPARISON OF HAND LAID-UP TAPE AND FILAMENT WOUND COMPOSITE CYLINDERS AND PANELS WITH AND WITHOUT IMPACT DAMAGE
Dawn C. Jegley and Osvaldo F. Lopez *In its* First NASA Advanced Composites Technology Conference, Part 2 Jan. 1991 p 749-759 (For primary document see N93-30841 11-24)
Avail: CASI HC A03/MF A06

The results of this experimental comparison of filament wound control (unimpacted) cylinders loaded to failure in axial compression indicates that one fiber cross-over location has no effect on the failure mode or strain in thick walled filament wound graphite-epoxy specimens with stacking sequence (plus or minus 45/90) sub 3s. A comparison between filament wound and hand laid-up tape control cylinders indicates that there is little or no difference in the response of cylinders constructed by using two different fabrication methods, however, unimpacted panels with many fiber cross-overs fail at up to 15 percent lower strains than panels with no fiber cross-overs. A comparison of samples subjected to low speed impact damage prior to compressive loading indicates that impact damage reduces the strain at failure by over 60 percent in tape and filament wound graphite-epoxy cylinders and in tape flat panels. The presence of fiber cross-overs was observed to reduce the strength of filament wound impact-damaged panels, but to have no significant effect on the strength of filament wound impact-damaged cylinders. Author (revised)

N93-30860*# Northrop Corp., Hawthorne, CA. Aircraft Div.
EFFECTS OF SCALE IN PREDICTING GLOBAL STRUCTURAL RESPONSE
R. B. Deo and H. P. Kan *In* NASA. Langley Research Center, First NASA Advanced Composites Technology Conference, Part 2 Jan. 1991 p 761-777 (For primary document see N93-30841 11-24)
(Contract NAS1-18842)
Avail: CASI HC A03/MF A06

Analytical techniques for scale-up effects were reviewed. The advantages and limitations of applying the principles of similitude to composite structures is summarized and illustrated by simple examples. An analytical procedure was formulated to design scale models of an axially compressed composite cylinder. A building-block approach was outlined where each structural detail is analyzed independently and the probable failure sequence of a selected component is predicted, taking into account load redistribution subsequent to first element failure. Details of this building-block approach are under development. Author

N93-30861*# National Aeronautics and Space Administration. Langley Research Center, Hampton, VA.
DESIGN AND ANALYSIS OF GRID STIFFENED CONCEPTS FOR AIRCRAFT COMPOSITE PRIMARY STRUCTURAL APPLICATIONS
Damodar R. Ambur *In its* First NASA Advanced Composites Technology Conference, Part 2 Jan. 1991 p 779-789 (For primary document see N93-30841 11-24)
Avail: CASI HC A03/MF A06

An approach to buckling resistant design of general grid stiffened flat plates based on smeared stiffener theory for combined inplane loading is discussed. Some results from parametric studies performed to assess the validity of smeared stiffener for practical stiffener configurations and to illustrate the benefits of different stiffening concepts are given. Details of a design study are discussed where the present analysis method is used to design a grid stiffened panel for a fuselage application and verified using a finite element analysis results. Author

N93-30862*# National Aeronautics and Space Administration. Langley Research Center, Hampton, VA.
OPTIMIZATION OF COMPOSITE SANDWICH COVER PANELS SUBJECTED TO COMPRESSIVE LOADINGS
Juan R. Cruz *In its* First NASA Advanced Composites Technology Conference, Part 2 Jan. 1991 p 791-807 (For primary document see N93-30841 11-24)
Avail: CASI HC A03/MF A06

An analysis and design method is presented for the design of composite sandwich cover panels that includes transverse shear effects and damage tolerance considerations. This method is incorporated into an optimization program called SANDOP (SANDwich OPtimization). SANDOP is used in the present study to design optimized composite sandwich cover panels for transport aircraft wing applications as a demonstration of its capabilities. The results of this design study indicate that optimized composite sandwich cover panels have approximately the same structural efficiency as stiffened composite cover panels designed to identical constraints. Results indicate that inplane stiffness requirements have a large effect on the weight of these composite sandwich cover panels at higher load levels. Increasing the maximum allowable strain and the upper percentage limit of the 0 degree and plus or minus 45 degree plies can yield significant weight savings. The results show that the structural efficiency of these optimized composite sandwich cover panels is relatively insensitive to changes in core density. Author (revised)

N93-30863*# California Univ., Davis.
A COMPARISON OF CLASSICAL MECHANICS MODELS AND FINITE ELEMENT SIMULATION OF ELASTICALLY TAILORED WING BOXES
Lawrence W. Rehfield, Richard D. Pickings, Stephen Chang, and Michael Holl *In* NASA. Langley Research Center, First NASA Advanced Composites Technology Conference, Part 2 Jan. 1991 p 809-815 (For primary document see N93-30841 11-24)
Avail: CASI HC A02/MF A06

Structural tailoring concepts were developed to create wings with elastically produced camber for the purpose of increasing lift during takeoff conditions. Simple models based upon enhancements to the thin walled composite beam theory of Rehfield were developed to investigate prospects for elastic tailoring of the chordwise deformation of wing structures. The purpose here is to provide a comparison of the theoretical results with a finite element model for the bending method of producing camber. Finite element correlation studies were completed for two cases: a bonded unstiffened structural box, and a bolted unstiffened structural box. Results from these studies show an error of less than one percent for the bonded case and less than six percent for the bolted case in predicting camber curvature for the structural box. Examination of the results shows that the theory is very accurate for the cases studied and will provide an excellent basis for conducting further tailoring studies. Author

N93-30864*# Hercules Aerospace Co., Magna, UT. Composite Structures Programs.
ADVANCED FIBER PLACEMENT OF COMPOSITE FUSELAGE STRUCTURES
Robert L. Anderson and Carroll G. Grant *In* NASA. Langley Research Center, First NASA Advanced Composites Technology Conference, Part 2 Jan. 1991 p 817-830 (For primary document see N93-30841 11-24)
Avail: CASI HC A03/MF A06

The Hercules/NASA Advanced Composite Technology (ACT) program will demonstrate the low cost potential of the automated fiber placement process. The Hercules fiber placement machine was developed for cost effective production of composite aircraft structures. The process uses a low cost prepreg tow material form and achieves equivalent laminate properties to structures fabricated with prepreg tape layup. Fiber placement demonstrations planned for the Hercules/NASA program include fabrication of stiffened test panels which represent crown, keel, and window belt segments of a typical transport aircraft fuselage. Author

N93-30865*# Boeing Commercial Airplane Co., Seattle, WA.
PROCESS AND ASSEMBLY PLANS FOR LOW COST COMMERCIAL FUSELAGE STRUCTURE
Kurtis Willden, Stephen Metschan, and Val Starkey *In* NASA. Langley Research Center, First NASA Advanced Composites Technology Conference, Part 2 Jan. 1991 p 831-842 (For primary document see N93-30841 11-24)
Avail: CASI HC A03/MF A06

Cost and weight reduction for a composite structure is a result of selecting design concepts that can be built using efficient low cost manufacturing and assembly processes. Since design and manufacturing are inherently cost dependent, concurrent engineering in the form of a Design-Build Team (DBT) is essential for low cost designs. Detailed cost analysis from DBT designs and hardware verification must be performed to identify the cost drivers and relationships between design and manufacturing processes. Results from the global evaluation are used to quantitatively rank design, identify cost centers for higher ranking design concepts, define and prioritize a list of technical/economic issues and barriers, and identify parameters that control concept response. These results are then used for final design optimization. Author

N93-30866*# National Aeronautics and Space Administration. Langley Research Center, Hampton, VA.

PROGRESSIVE FAILURE METHODOLOGIES FOR PREDICTING RESIDUAL STRENGTH AND LIFE OF LAMINATED COMPOSITES

Charles E. Harris, David H. Allen (Texas A&M Univ., College Station.), and T. Kevin OBrien (Army Aerostructures Directorate, Hampton, VA.) *In its* First NASA Advanced Composites Technology Conference, Part 2 Jan. 1991 p 843-873 (For primary document see N93-30841 11-24)
Avail: CASI HC A03/MF A06

Two progressive failure methodologies currently under development by the Mechanics of Materials Branch at NASA Langley Research Center are discussed. The damage tolerance/fail safety methodology developed by O'Brien is an engineering approach to ensuring adequate durability and damage tolerance by treating only delamination onset and the subsequent delamination accumulation through the laminate thickness. The continuum damage model developed by Allen and Harris employs continuum damage laws to predict laminate strength and life. The philosophy, mechanics framework, and current implementation status of each methodology are presented. Author

N93-30867*# National Aeronautics and Space Administration. Langley Research Center, Hampton, VA.

MULTIPLE METHODS INTEGRATION FOR STRUCTURAL MECHANICS ANALYSIS AND DESIGN

J. M. Housner and M. A. Aminpour (Analytical Services and Materials, Inc., Hampton, VA.) *In its* First NASA Advanced Composites Technology Conference, Part 2 Jan. 1991 p 875-889 (For primary document see N93-30841 11-24)
Avail: CASI HC A03/MF A06

A new research area of multiple methods integration is proposed for joining diverse methods of structural mechanics analysis which interact with one another. Three categories of multiple methods are defined: those in which a physical interface are well defined; those in which a physical interface is not well-defined, but selected; and those in which the interface is a mathematical transformation. Two fundamental integration procedures are presented that can be extended to integrate various methods (e.g., finite elements, Rayleigh Ritz, Galerkin, and integral methods) with one another. Since the finite element method will likely be the major method to be integrated, its enhanced robustness under element distortion is also examined and a new robust shell element is demonstrated. Author

N93-30868*# National Aeronautics and Space Administration. Lewis Research Center, Cleveland, OH.

PROBABILISTIC COMPOSITE ANALYSIS

C. C. Chamis and P. L. N. Murthy *In* NASA. Langley Research Center, First NASA Advanced Composites Technology Conference, Part 2 Jan. 1991 p 891-900 (For primary document see N93-30841 11-24)
Avail: CASI HC A02/MF A06

Formal procedures are described which are used to computationally simulate the probabilistic behavior of composite structures. The computational simulation starts with the uncertainties associated with all aspects of a composite structure (constituents, fabrication, assembling, etc.) and encompasses all aspects of composite behavior (micromechanics, macromechanics, combined stress failure, laminate theory, structural response, and tailoring) optimization. Typical cases are included to illustrate the formal procedure for computational simulation. The collective results of the sample cases demonstrate that uncertainties in composite behavior and structural response can be probabilistically quantified. Author

N93-30869*# Northrop Corp., Hawthorne, CA. Aircraft Div.

A RAYLEIGH-RITZ ANALYSIS METHODOLOGY FOR CUTOUTS IN COMPOSITE STRUCTURES

Steven G. Russell *In* NASA. Langley Research Center, First NASA Advanced Composites Technology Conference, Part 2 Jan. 1991 p 901-920 (For primary document see N93-30841 11-24)
(Contract NAS1-18842)
Avail: CASI HC A03/MF A06

A new Rayleigh-Ritz stress analysis methodology that was developed for composite panels containing cutouts is described. The procedure, which makes use of a general assumed displacement field, accommodates circular and elliptical cutouts in biaxially loaded rectangular composite panels. Symmetric integral padups around the cutout can be included in the analysis. Benchmark results are presented to demonstrate the accuracy of the technique. Strength predictions based on the average stress criterion are generated and compared with experimental data. Finally, the stress analysis methodology is integrated into a design procedure for sizing integral padups around circular cutouts, and a sample problem is solved to illustrate its use. Author

N93-30870*# National Aeronautics and Space Administration. Langley Research Center, Hampton, VA.

EFFECTS OF BOLT-HOLE CONTACT ON BEARING-BYPASS DAMAGE-ONSET STRENGTH

John H. Crews, Jr. and Rajiv A. Naik (Analytical Services and Materials, Inc., Hampton, VA.) *In its* First NASA Advanced Composites Technology Conference, Part 2 Jan. 1991 p 921-937 (For primary document see N93-30841 11-24)
Avail: CASI HC A03/MF A06

A combined experimental and analytical study was conducted to investigate the effects of bolt-hole contact on the bearing bypass strength of a graphite-epoxy laminate. Tests were conducted on specimens consisting of 16-ply quasi-isotropic T300/5208 laminates with a centrally located hole. Bearing loads were applied through a clearance-fit steel bolt. Damage onset strength and damage mode were determined for each test case. A finite element procedure was used to calculate the bolt-hole stresses and bolt contact for each test case. A finite element procedure was used to calculate the bolt-hole stresses and bolt contact for each measured damage-onset strength. For the tension bearing-bypass cases tested, the bolt contact half-angle was approximately 60 degrees at damage onset. For compression, the contact angle was 20 degrees as the bypass load increased. A corresponding decrease in the bearing damage onset strength was attributed to the decrease in contact angle which made the bearing loads more severe. Hole boundary stresses were also computed by superimposing stresses for separate bearing and bypass loading. Stresses at the specimen net section were accurately approximated by the superposition procedure. However, the peak bearing stresses had large errors because the bolt contact angles were not represented correctly. For compression, peak bearing stress errors of nearly 50 percent were calculated. Author

N93-30871*# Northrop Corp., Hawthorne, CA. Aircraft Div.

PREDICTION OF STIFFENER-SKIN SEPARATION IN COMPOSITE PANELS

Han-Pin Kan, Mary A. Mahler, and Ravi B. Deo *In* NASA. Langley Research Center, First NASA Advanced Composites Technology Conference, Part 2 Jan. 1991 p 939-952 (For primary document see N93-30841 11-24)
(Contract NAS1-18842)
Avail: CASI HC A03/MF A06

A methodology was developed to predict the failure of stiffened composite panels by stiffener-skin separation. The methodology is applicable to curved or flat panels under combined uniaxial compression and in-plane shear loads. The analytical crux of the methodology are two different analysis packages: PACL1, which predicts the stress and displacement fields in a stiffened postbuckled panel; and WEBSTER, which predicts the local interfacial (shear and normal) stresses at the skin and stiffener flange junction. PACL1 is a Rayleigh-Ritz analysis of curved composite panels loaded into a post-buckling range. WEBSTER is a two-dimensional elasticity analysis for the skin-stiffener interface. Results of the predictive methodology are given. Author (revised)

N93-30872*# National Aeronautics and Space Administration. Langley Research Center, Hampton, VA.

EXPERIMENTAL BEHAVIOR OF GRAPHITE-EPOXY Y-STIFFENED SPECIMENS LOADED IN COMPRESSION

P. D. Sydow and M. J. Shuart *In its* First NASA Advanced Composites Technology Conference, Part 2 Jan. 1991 p 953-968 (For primary document see N93-30841 11-24)
Avail: CASI HC A03/MF A06

An experimental investigation of the behavior of graphite-epoxy

Y-stiffened specimens loaded in compression is presented. Experimental results are presented for element specimens with a single stiffener and for panel specimens with three stiffeners. Response and failure characteristics of the specimens are described. Effects of impact damage on structural response for both specimen configurations are also presented. Results indicate that impact location may significantly affect the residual strength of the Y-stiffened specimens. The failure results indicate that the critical failure mode is buckling of the stiffener webs for Y-stiffened element specimens and buckling of both stiffener web and stiffener blade for the Y-stiffened panel specimens. Author (revised)

N93-30873*# National Aeronautics and Space Administration. Langley Research Center, Hampton, VA.

STRUCTURAL RESPONSE OF BEAD-STIFFENED THERMOPLASTIC SHEAR WEBS

Marshall Rouse *In its* First NASA Advanced Composites Technology Conference, Part 2 Jan. 1991 p 969-977 (For primary document see N93-30841 11-24)

Avail: CASI HC A02/MF A06

The results of an experimental and analytical study of the structural response and failure characteristics of selected bead-stiffened thermoplastic shear-webs are presented. Results are given for specimens with one stiffeneer, with two stiffeners, and different stiffener geometries. Selected analytical results that were obtained with the Computational Structural Mechanics (CSM) Testbed computer code are presented. Analytical results that describe normal and transverse shear stress are also presented. Author

N93-30874*# Army Aerostructures Directorate, Hampton, VA.

EVALUATION OF SOME SCALE EFFECTS IN THE RESPONSE AND FAILURE OF COMPOSITE BEAMS

Karen E. Jackson and John Morton (Virginia Polytechnic Inst. and State Univ., Blacksburg.) *In* NASA. Langley Research Center, First NASA Advanced Composites Technology Conference, Part 2 Jan. 1991 p 979-1003 (For primary document see N93-30841 11-24)

Avail: CASI HC A03/MF A06

The feasibility of using scale model testing for predicting full-scale behavior of composite beams loaded in tension and flexure was investigated. Classical laws of similitude were applied to fabricate and test replica model beams to identify scaling effects in the load response, strength, and mode of failure. Experiments were conducted using graphite-epoxy composite beams having different laminate stacking sequences and a range of scaled sizes. Results indicated that the elastic response of scaled composite beams was independent of specimen size. However, a significant scale effect in strength was observed. In addition, a transition in failure mode was observed among scaled beams of certain laminate stacking sequences. Weibull statistical and fracture mechanics based models were applied to predict the strength scale effect since standard failure criteria cannot account for the influence of absolute specimen size in failure. Author

N93-30875*# National Aeronautics and Space Administration. Langley Research Center, Hampton, VA.

AN OVERVIEW OF THE CRASH DYNAMICS FAILURE BEHAVIOR OF METAL AND COMPOSITE AIRCRAFT STRUCTURES

Huey D. Carden, Richard L. Boitnott (Army Aerostructures Directorate, Hampton, VA.), Edwin L. Fasanella (Lockheed Engineering and Sciences Co., Hampton, VA.), and Lisa E. Jones (Lockheed Engineering and Sciences Co., Hampton, VA.) *In its* First NASA Advanced Composites Technology Conference, Part 2 Jan. 1991 p 1005-1035 (For primary document see N93-30841 11-24)

Avail: CASI HC A03/MF A06

An overview of failure behavior results is presented from some of the crash dynamics research conducted with concepts of aircraft elements and substructure not necessarily designed or optimized for energy absorption or crash loading considerations. Experimental and analytical data are presented that indicate some general trends in the failure behavior of a class of composite structures that includes fuselage panels, individual fuselage sections, fuselage frames, skeleton subfloors with stringers and floor beams without skin covering, and subfloors with skin added to the frame stringer structure. Although the behavior is complex, a strong similarity in the static/dynamic failure behavior among these structures is illustrated through photographs of the experimental results and through analytical data of generic composite structural models. Author

N93-30876*# California Univ., Davis.

TAILORED COMPOSITE WINGS WITH ELASTICALLY PRODUCED CHORDWISE CAMBER

Lawrence W. Rehfield, Stephen Chang, Peter J. Zischka, Richard D. Pickings, and Michael W. Holl *In* NASA. Langley Research Center, First NASA Advanced Composites Technology Conference, Part 2 Jan. 1991 p 1037-1047 (For primary document see N93-30841 11-24)
(Contract NAS1-18754)

Avail: CASI HC A03/MF A06

Four structural concepts were created which produce chordwise camber deformation that results in enhanced lift. A wing box can be tailored to utilize each of these with composites. In attempting to optimize the aerodynamic benefits, researchers found that there are two optimum designs that are of interest. There is a weight optimum which corresponds to the maximum lift per unit structural weight. There is also a lift optimum that corresponds to maximum absolute lift. Experience indicates that a large weight penalty accompanies the transition from weight to lift optimum designs. New structural models, the basic deformation mechanisms that are utilized, and typical analytical results are presented. It appears that lift enhancements of sufficient magnitude can be produced to render this type of wing tailoring of practical interest. Author

N93-30937 Delaware Univ., Newark.

DAMAGE OF MULTI-DIRECTIONALLY REINFORCED CERAMIC-MATRIX COMPOSITES Ph.D. Thesis

Wen-Shyong Kuo 1992 232 p

Avail: Univ. Microfilms Order No. DA9301765

Ceramic-matrix composites (CMC's) reinforced with continuous fibers exhibit important progressive damage/failure behavior. The performance of CMC's and their damage mechanisms depends on material processing techniques, external loading, and the arrangement of reinforcements. Relationships between constituent properties, fiber arrangements, and the progressive damage behavior of multi-directionally reinforced CMC's, including (1) unidirectional composites, (2) cross-ply composites, and (3) woven fabric composites are studied. The material systems examined include C/borosilicate glass and SiC/CAS unidirectional, SiC/CAS cross-ply, and SiC/SiC woven fabric composites. For unidirectional CMC's, a partial debonding model is introduced. Thermomechanical behavior, with an emphasis on matrix cracking, is examined. The influence of debonding length on the problem is studied through the model. By using an energy balance method two closed form solutions of the critical strains for matrix cracking were obtained. The effects of interface properties, fiber/matrix sliding, matrix surface energy, and fiber volume fraction on the damage of the composite were investigated. For cross-ply CMC's, two kinds of microcracking were observed: transverse cracking in the 90 deg-ply and matrix cracking in the 0 deg-ply with fiber bridging. Through combinations of these two types of microcracking, five damage modes, including one transverse crack and four matrix cracks, are studied. Matrix cracking in the 0 deg-ply is a unique feature of cross-ply CMC's. Using the energy balance method, closed-form equations of critical stresses for the damage modes were obtained. It can be shown that the four matrix cracking equations for cross-ply CMC's reduce to those two for unidirectional CMC's as the thickness of the 90 deg-ply vanishes. The relation between composite performance (stiffness, strength and yielding strain and nonlinear behavior) and constituent properties (thicknesses, thermal properties, surface energies, interfacial shear stress, and fiber volume fraction) was studied. The damage evolution and nonlinear tensile behavior of 2-D woven fabric Nicalon-fiber-reinforced SiC-matrix composites fabricated by chemical vapor infiltration (CVI) were examined. The effect of inter- and intra-yarn pores due to CVI processing and the effect of fiber undulation were stated. The nonlinear portion of the stress strain responses is due to transverse cracks initiated at inter-yarn pores. Strain energy release rates of the cracks in transverse and longitudinal yarns were calculated by a finite element method and a crack closure approach. The results indicate that the composite stiffness reduction due to fiber undulation is insignificant for the SiC/SiC composite. However, the porosity is important to composite stiffness, due to the high-modulus ceramic matrix. The results of strain energy release rates show that using thinner fiber yarns can lead to smaller pores and higher critical stress for transverse cracking. Dissert. Abstr.

N93-29366*# Toronto Univ., North York (Ontario). Inst. for Aerospace Studies.
ANALYSIS OF LDEF MICROMETEOROID/DEBRIS DATA AND DAMAGE TO COMPOSITE MATERIALS
R. C. Tennyson and G. Manuelpillai *In* NASA. Langley Research Center, LDEF: 69 Months in Space. Second Post-Retrieval Symposium, Part 2 Apr. 1993 p 493-511 (For primary document see N93-29354 11-99)
Avail: CASI HC A03/MF A04

N93-30951*# Texas A&M Univ., College Station. Department of Mechanical Engineering.
MECHANICAL PROPERTIES OF COMPOSITE MATERIALS
H. Richard Thornton and L. R. Cornwell *In* NASA. Langley Research Center, National Educators' Workshop. Update 92: Standard Experiments in Engineering Materials Science and Technology Jun. 1993 p 43-48 (For primary document see N93-30948 11-23)
Avail: CASI HC A01/MF A04

N93-30957*# National Aeronautics and Space Administration. Langley Research Center, Hampton, VA.
INTRODUCTION TO HIGH PERFORMANCE COMPOSITES
Norman J. Johnston *In its* National Educators' Workshop. Update 92: Standard Experiments in Engineering Materials Science and Technology Jun. 1993 p 147-192 (For primary document see N93-30948 11-23)
Avail: CASI HC A03/MF A04

25 INORGANIC AND PHYSICAL CHEMISTRY

Includes chemical analysis, e.g., chromatography; combustion theory; electrochemistry; and photochemistry.

For related information see also *77 Thermodynamics and Statistical Physics.*.

N93-28514# Army Research Lab., Aberdeen Proving Ground, MD.
TOMOGRAPHIC ANALYSIS OF LINE-OF-SIGHT INFRARED SPECTRA OF LOW-PRESSURE FLAMES Final Report, May - Oct. 1992
Kevin L. McNesby and Robert A. Fifer Apr. 1993 30 p
(DA Proj. 1L1-61102-AH-43)
(AD-A263185; ARL-TR-108) Avail: CASI HC A03/MF A01

Line-of-sight Fourier transform infrared absorption spectra through a 17-torr methane/nitrous oxide flame have been tomographically analyzed using Abel's equations. Relative absorbances for N2O, CH4, CO2, NO, and CO have been mapped for various 'slices' of the flame at different heights in the flame. Results indicate that the region of maximum NO and CO formation occurs prior to the luminous region of the flame. The technique is shown to be useful in obtaining data from systems for which line of sight data may be unusable. DTIC

N93-28540# IBM Research Lab., San Jose, CA.
ADSORPTION OF SULFATE ON METAL ELECTRODES Technical Report
Leslie A. Barnes, Michael R. Philpott, and Bowen Liu 14 Apr. 1993 22 p
(Contract N00014-92-C-0173)
(AD-A263192; TR-02) Avail: CASI HC A03/MF A01

The adsorption of sulfate SO4(2-) and bisulfate HSO4(-) on copper has been studied using ab initio calculations at the SCF level of theory, to aid in the interpretation of in situ experimental data from the electrochemical interface, in particular, optical and surface x-ray measurements. The calculations are designed to give qualitative insight rather than quantitative accuracy. Optimized structures and harmonic frequencies and intensities are computed for isolated sulfate and bisulfate, and qualitative agreement with experimental data is demonstrated. DTIC

N93-28553# Westinghouse Savannah River Co. Aiken, SC.
TECHNICAL BASES FOR PRECIPITATE HYDROLYSIS PROCESS OPERATING PARAMETERS, REVISION 1
C. J. Bannochie and D. P. Lambert Nov. 1992 28 p
(Contract DE-AC09-89SR-18035)
(DE93-009894; WSRC-TR-92-458-Rev-1) Avail: CASI HC A03/MF A01

The experimental data and rationale in support of the operating parameters for tetraphenylborate precipitate hydrolysis is provided. The report is divided into two sections, the first dealing with lab-scale precipitate hydrolysis experimentation while the second part addresses large-scale runs conducted to demonstrate the revised operating parameters in the Precipitate Hydrolysis Experimental Facility (PHEF). In order to address issues concerning high-boiling organic by-products of precipitate hydrolysis and the concerns about hydroxylamine nitrate (HAN) proposed as a nitrite ion scavenger, an experimental program was intitated in conjuction with the Nitrite Task Team recommendation to reduce the level of nitrite ion in the incoming DWPF feed. DOE

N93-28688# Northwestern Univ., Evanston, IL. Dept. of Chemistry.
SUPPORTED ORGANOMETALLIC COMPLEXES, SURFACE CHEMISTRY, SPECTROSCOPY, AND CATALYSIS
T. J. Marks Apr. 1993 23 p
(Contract DE-FG02-86ER-13511)
(DE93-011930; DOE/ER-13511/7) Avail: CASI HC A03/MF A01

The goal is to elucidate and understand the surface chemistry and catalytic properties of well-defined, highly-reactive organometallic molecules (principally based upon abundant actinide, lanthanide, and early transition elements) adsorbed on metal oxides and halides. Nature of adsorbed species is probed by a battery of chemical and physicochemical techniques, to understand the nature of the molecule-surface coordination chemistry and how this can give rise to extremely high catalytic activity. A complementary objective is to delineate the scope and mechanisms of the heterogeneous catalytic reactions, as well as to relate them both conceptually and functionally to model systems generated in solution. DOE

N93-28750# Delaware Univ., Newark. Center for Catalytic Science and Technology.
DESIGN OF A HIGH ACTIVITY AND SELECTIVITY ALCOHOL CATALYST
H. C. Foley and G. A. Mills 17 Feb. 1993 13 p
(Contract DE-FG22-90PC-90291)
(DE93-012277; DOE/PC-90291/T11) Avail: CASI HC A03/MF A01

Preliminary investigations of these manganese oxide materials show that the different oxides exhibit different selectivity toward methanol and other products. It seems that there is a correlation between the initial O/Mn ratio of the oxide and methanol selectivity. These conclusions are supported by the results. The main product of the manganese oxide-catalyzed CO hydrogenation is methanol except on Mao, which shows the lowest methanol selectivity, but the highest CO2 yield. Preliminarily, the results suggest that the higher the O/Mn ratio of the precursor oxide, the higher will be the methanol selectivity, while the CO2 and methane selectivities will be lower. The higher CO2 and C2, C3, and C4 hydrocarbon selectivities over the Mao catalyst compared to the other manganese oxides tested, indicates that Mao acts more like a water-gas shift and Fischer-Tropsch catalyst. DOE

N93-28880# Brookhaven National Lab., Upton, NY.
AEROSOL PARTICLE ANALYSIS BY RAMAN SCATTERING TECHNIQUE
K. H. Fung and I. N. Tang Oct. 1992 5 p Presented at the Advanced Laser Technology for Chemical Measurements, Santa Fe, NM, 19-21 Oct. 1992
(Contract DE-AC02-76CH-00016)
(DE93-005587; BNL-48146; CONF-9210261-2) Avail: CASI HC A01/MF A01

Laser Raman spectroscopy is a very versatile tool for chemical characterization of micron-sized particles. Such particles are abundant in nature and in numerous energy-related processes. In order to elucidate the formation mechanisms and understand the subsequent chemical transformation under a variety of reaction conditions, it is imperative to develop analytical measurement techniques for in situ monitoring of these suspended particles. In this report, we outline our recent work on spontaneous Raman, resonance Raman, and non-linear Raman scattering as a novel technique for chemical analysis of aerosol particles as well as supersaturated solution droplets. DOE

N93-28911# Oregon Graduate Center for Study and Research, Beaverton.

MEMBRANE-BASED PHOTOCHEMICAL SYSTEMS AS MODELS FOR PHOTOSYNTHETIC CELLS

J. K. Hurst 1992 19 p
(Contract DE-FG06-87ER-13664)
(DE93-009758; DOE/ER-13664/6) Avail: CASI HC A03/MF A01

The objectives of this research are to improve our conceptual view of the ways in which membranes and interfaces can be used to control chemical reactivity. We have focused on understanding three elementary processes that are central to developing membrane-based integrated chemical systems for water photolysis or related photoconversion/photostorage processes. Specifically, we have sought to identify: the influence of interfaces upon charge separation/recombination reactions, pathways for transmembrane charge separation across hydrocarbon bilayer membranes, and mechanisms of water oxidation catalyzed by transition metal coordination complexes. Historically, the chemical dynamics of each of these processes has been poorly understood, with numerous unresolved issues and conflicting viewpoints appearing in the literature. As described in this report our recent research has led to considerable clarification of the underlying reaction mechanisms. DOE

N93-28988# Colorado State Univ., Fort Collins. Dept. of Chemistry.

ELECTROCHEMICAL FABRICATION OF CADMIUM CHALCOGENIDE MICRODIODE ARRAYS Interim Report

Jonathan D. Klein, Charles J. Brumlik, Robert Herrick, Dean Palmer, and Charles R. Martin 9 Apr. 1993 14 p
(Contract N00014-82-K-0612)
(AD-A263169) Avail: CASI HC A03/MF A01

Arrays containing greater than 10(exp 9) 2000A-diameter CdSe or graded CdSe/CdTe cylinders have been electrochemically synthesized within the pores of Anopore(tm) membranes. The alumina template suppresses the 'cauliflower' morphology that is typically observed in electrodeposited CdSe and CdTe films, although X-ray diffraction reveals the materials to be of poor crystallinity. The Anopore membrane template can be removed by treatment with aqueous 1M NaOH, resulting in an array of free-standing CdSe or CdSe/CdTe wires. Current-voltage data show that the Ni/CdSe array is rectifying, with a rectification ratio of 1000 at + or - 2 V. DTIC

N93-29051# City Coll. of the City Univ. of New York, NY.

STUDIES IN PREMIXED COMBUSTION

G. I. Sivashinsky 1993 15 p
(Contract DE-FG02-88ER-13822)
(DE93-007955; DOE/ER-13822/6) Avail: CASI HC A03/MF A01

During the period under review, significant progress was made in studying the intrinsic dynamics of premixed flames and the problems of flame-flow interaction. A weakly nonlinear model for Bunsen burner stabilized flames was proposed and employed for the simulation of three-dimensional polyhedral flames - one of the most graphic manifestations of thermal-diffusive instability in premixed combustion. A high-precision large-scale numerical simulation of Bunsen burner tip structure was conducted. The results obtained supported the earlier conjecture that the tip opening observed in low Lewis number systems is a purely optical effect not involving either flame extinction or leakage of unburned fuel. A one-dimensional model describing a reaction wave moving through a unidirectional periodic flow field is proposed and studied numerically. For long-wavelength fields the system exhibits a peculiar non-uniqueness of possible propagation regimes. The transition from one regime to another occurs in a manner of hysteresis. DOE

N93-29052# Argonne National Lab., IL.

HYDROGEN AND SULFUR PRODUCTION FROM HYDROGEN SULFIDE WASTES

J. B. L. Harkness and R. D. Doctor 1993 8 p Presented at the Industrial Energy Technology Conference and Energy Manager's Workshop, Houston, TX, 24-25 Mar. 1993
(Contract W-31-109-eng-38)
(DE93-008658; ANL/ES/CP-78832; CONF-9303108-1) Avail: CASI HC A02/MF A01

A new hydrogen sulfide waste-treatment process that uses microwave plasma-chemical technology is currently under development in the Soviet Union and in the United States. Whereas the present waste treatment process only recovers sulfur at best, this process recovers both hydrogen and sulfur. The plasma process involves dissociating hydrogen sulfide in a 'nonequilibrium' plasma in a microwave or radio-frequency reactor. After the dissociation process, sulfur is condensed and sold just as is currently done. The remaining gases are purified and separated into streams containing the product hydrogen, the hydrogen sulfide to be recycled to the plasma reactor, and the process purge containing carbon dioxide and water. This process has particular implications for the petroleum refining industry, in which hydrogen is a widely used reagent and must be produced from increasingly scarce hydrocarbon resources. The modular nature of the new process may also offer economic advantages over small-scale waste treatment technologies widely used in the natural-gas industry. Laboratory-scale experiments with pure hydrogen sulfide indicate that conversions exceeding 90% are possible with appropriate reactor design and that the energy required to dissociate hydrogen sulfide is low enough for the plasma process to be economically competitive. In addition, the experiments show that typical refinery acid-gas streams are compatible with the plasma process and that all by-products can be treated with existing technology. DOE

N93-29059# Lawrence Livermore National Lab., CA.

MODIFICATION OF SPECTRAL DISTRIBUTIONS BY MULTILAYER STRUCTURES

P. J. Biltoft May 1992 14 p Presented at the European Conference on Energy Dispersive X Ray Spectrometry, Myconos, Greece, 30 May - 6 Jun. 1992
(Contract W-7405-eng-48)
(DE93-009308; UCRL-JC-109786; CONF-9205319-1) Avail: CASI HC A03/MF A01

Multilayer structures offer the unique ability to control the spectral distribution of x-rays at non-grazing incidence and to provide for the ability to focus x-rays. This combination of attributes offers some exciting possibilities for X-ray spectrometry. Double crystal monochrometers using multilayer structures have shown high energy selectivity with reasonable throughput. X ray optical systems using multilayers deposited onto figured substrates have been used to focus x-rays from a conventional tube to micron size spots. Future x-ray spectrometers will likely take advantage of the energy selection and focussing capabilities of multilayers as they become more readily available. Topics which will be covered in this paper include the following: the modification of spectral emissions from a conventional copper anode x-ray tube by a multilayer, multilayer fabrication, and characterization techniques as they apply to energy-dispersive x-ray spectroscopy (EDXRS). DOE

N93-29125 California Univ., San Diego.

STUDIES OF HYDROGEN-AIR DIFFUSION FLAMES AND OF COMPRESSIBILITY EFFECTS RELATED TO HIGH-SPEED PROPULSION Ph.D. Thesis

Ganeshan Balakrishnan 1992 144 p
Avail. Univ. Microfilms Order No. DA9307178

The structure and the extinction phenomena of hydrogen-air diffusion flames in the counterflow configuration with full and reduced chemical-kinetic mechanisms are investigated. The main reduced mechanism considered is a two-step mechanism. Numerical calculations are performed for strain rates on the air side of 10(exp -4)/s to extinction. The effect of nitrogen chemistry and the uncertainties in elementary rate parameters on flame structure as well as on extinction is investigated. Based on the two-step scheme and on results from numerical integrations, an asymptotic analysis is then performed to derive analytical expressions for predicting extinction strain rates. The flame structure consists of three regions: a thin radical production zone in which H atoms are generated by the global step 3H2 + O2 yields 2H2O + 2H whose rate is largely determined by a high-activation-energy chain-branching elementary reaction, flanked by two thick radical-consumption layers in which the H is consumed by the overall step H + H + M yields H2 + M, the rate of which is controlled by different elementary reactions on the lean and rich sides. The predicted extinction conditions appear to be in reasonable agreement with experiments, although additional work is needed in specific areas that are indicated. Supersonic combustion in turbulent mixing layers locally involve counterflowing streams in which compressibility is important, with the viscous and chemical effects restricted to a narrow layer at the stagnation plane. A theoretical analysis of the inviscid flow is performed for small values of the ratio of the plate separation distance to the lateral extent of the plates, for both planar and axisymmetric geometries. The problem of computing the flow field is reduced to the solution of a single integral equation, which is achieved numerically. The flow exhibits choking at a critical value of the lateral extent of the plate, in the vicinity of which the Mach number approaches unity. The results provide the external boundary-layer conditions needed for studying the flame structure in the viscous region between the two counterflowing streams when compressibility is important. With pressure dependent mass addition along the porous walls, the choking condition is made relevant to the operation of solid-propellant rocket motors. Dissert. Abstr.

N93-29132# University of Northern Illinois, De Kalb. Dept. of Chemistry.

ANALYTICAL APPLICATIONS OF ELECTRIFIED INTERFACES BETWEEN TWO IMMISCIBLE SOLUTIONS

Petr Vanysek 7 Apr. 1993 26 p
(Contract N00014-91-J-1058)
(AD-A263085; TR-051) Avail: CASI HC A03/MF A01

Interfaces between two immiscible electrolyte solutions have some properties that can be investigated and utilized by methods of electrochemistry. This review compares electrochemistry on such interfaces with electrochemistry of metal electrodes immersed in solutions. It builds on knowledge of methods of electroanalysis and shows how it can be applied to the interfaces of immiscible liquids. A simple differential adapter that can convert any potentiostat to the 4-electrode potentiostate needed for the work is described. Experimental techniques involving potentiometry, polarography with dropping electrode, voltammetry and microinterfaces are outlined. DTIC

N93-29133# University of Northern Illinois, De Kalb. Dept. of Chemistry.

EFFECT OF ZINC AND IRON IONS ON THE ELECTROCHEMISTRY OF NICKEL OXIDE ELECTRODE: SLOW CYCLIC VOLTAMMETRY

Ivan Krejci and Petr Vanysek 7 Apr. 1993 25 p
(Contract N00014-91-J-1058)
(AD-A263098; TR-049) Avail: CASI HC A03/MF A01

Porous sintered nickel oxide electrodes were prepared by cathodic electroprecipitation from metal nitrate solutions and characterized by slow (0.1 mV/s) voltammetry in 6 mol/l KOH. The presence of iron or zinc ions resulted in decrease of electrode charging ability and similar changes in voltammograms were observed for both ions. Removal of iron or zinc ions and introduction of lithium ions partially restored the electrode and corresponding voltammogram to original conditions. Presence of cobalt in the electrode material diminished substantially the influence of zinc ions on the electrode properties. DTIC

N93-29182# Massachusetts Univ., Boston.

MAGNETIC RESONANCE STUDIES OF PHOTO-INDUCED ELECTRON TRANSFER REACTIONS

H. vanWilligen Nov. 1992 13 p
(Contract DE-FG02-84ER-13242)
(DE93-012239; DOE/ER-13242/9) Avail: CASI HC A03/MF A01

Fourier Transform Electron Paramagnetic Resonance (FT EPR) is useful in the study of photochemical reactions: a microwave pulse rotates the electron spin magnetization vector from z (magnetic field) into xy plane (pi/2 pulse); the time evolution of magnetization in xy plane, the free induction decay (FID), is sampled. Fourier transform of FID gives the frequency domain EPR spectrum of the free radicals, and the method is ideal for time-resolved studies of free radicals produced by pulsed-laser excitation. Investigations of electron transfer reactions focused on porphyrin (donor) - quinone (acceptor) systems. First, two hydrogen abstraction reactions were studied with FT EPR: photoreduction of acetone with 2-propanol, yielding the acetone ketyl radical, and the reaction of 2-propanol with t-butoxy radicals. Then, the FT EPR study of benzoquinone or duroquinone anion radicals generated by pulsed-laser induced electron transfer from zinc tetraphenylporphyrin (ZnTPP) or tetrasulfonated Zn(TPP), was carried out in homogeneous solution, micellar solutions, and silica gel. Finally, FT EPR was used to study electron transfer quenching of triplet C(sub 60) by electron donors. DOE

N93-29204# Environmental Protection Agency, Research Triangle Park, NC. Atmospheric Research and Exposure Assessment Lab.

ANALYSIS OF PROTOCOL GASES: AN ON-GOING QUALITY ASSURANCE AUDIT

Avis P. Hines Mar. 1993 10 p
(PB93-168839; EPA/600/A-93/055) Avail: CASI HC A02/MF A01

The Environmental Protection Agency (EPA) has initiated a national QA program on the suppliers of protocol gases. In the program, which will operate continuously, protocol gases are obtained and analyzed by EPA. The results of the EPA analysis are then compared to the Certificate of Analysis supplied with the protocol gas. Reported here is a comparison between the assay results obtained by EPA on protocol gases for SO2 and NO and the concentrations provided by the suppliers of the protocol gases. The results are being released on the Technology Transfer Network operated by the Office of Air Quality Planning and Standards of the EPA, Durham, N.C. NTIS

N93-29263# Lawrence Livermore National Lab., CA.

THERMAL PROPERTIES OF ORGANIC AND MODIFIED INORGANIC AEROGELS

R. W. Pekala and L. W. Hrubesh Aug. 1992 10 p Presented at the 1992 International Chlorofluorocarbon (CFC) and Halon Alternatives Conference, Washington, DC, 1 Oct. 1992
(Contract W-7405-eng-48)
(DE93-009230; UCRL-JC-111333; CONF-9210332-1) Avail: CASI HC A02/MF A01

Aerogels are open-cell foams that have already been shown to be among the best thermal insulating solid materials known. Improvements in the thermal insulating properties of aerogels are possible by synthesizing new organic varieties, by using additives within existing aerogel matrix, and by optimizing their nanostructures. We discuss these approaches and give some examples of aerogels which demonstrate the improvements. DOE

N93-29283# Drexel Univ., Philadelphia, PA. Dept. of Mechanical Engineering and Mechanics.

HIGH PRESSURE PREIGNITION CHEMISTRY OF HYDROCARBONS AND HYDROCARBON MIXTURES Final Report, 1 Jan. 1990 - 31 Dec. 1992

Nicholas P. Cernansky, David L. Miller, and David N. Koert 24 Feb. 1993 21 p
(Contract DAAL03-90-G-0024)
(AD-A263611; ARO-27417.6-EG) Avail: CASI HC A03/MF A01

A research program to study the oxidation and ignition characteristics of hydrocarbon fuels and their mixtures has been conducted at Drexel University. The research focused on three major tasks: examination of the chemistry of autoignition during compression ignition processes by performing parametric studies in a variety of experimental facilities listed below; development of chemical models which can simulate the experimental results; and the development of in situ measurement techniques. Several complementary bench scale experiments, which include a static reactor, an atmospheric pressure flow reactor, and a pressurized flow reactor, were used to examine the preignition chemistry and ignition behavior of progressively larger hydrocarbons over a range of temperatures, pressures, and equivalence ratios. Gas chromatography and Gc/Ms were used for chemical analysis of the stable reaction intermediates and products. Fourier Transform Infrared (FTIR) spectroscopy and degenerate four-wave mixing (DFWM) spectroscopy were used in efforts to develop in situ species measurement techniques. The overall program has been successfully completed and has added to our understanding of fuel factors and physical effects on the oxidation and ignition processes of hydrocarbon fuels.... Hydrocarbon Fuels, Preignition Chemistry, Oxidation, Ignition, Chemical Kinetics. DTIC

N93-29291# Minnesota Univ., Minneapolis. Dept. of Aerospace Engineering and Mechanics.

SOME PROBLEMS IN THE MECHANICS OF SOLIDS WITH PHASE MIXTURES Final Report, 1 Jun. 1991 - 30 Nov. 1992

Roger L. Fosdick 19 Feb. 1993 9 p
(Contract DAAL03-91-G-0184)
(AD-A263652; ARO-28986.1-MA) Avail: CASI HC A02/MF A01

This project has concentrated almost entirely on non-convex minimization problems in nonlinear elasticity theory and the existence of deformation-induced microstructure under severe loading conditions. As the microstructure develops and becomes more dense with increasing loads, the material weakens and the body has a softer response. Our minimizing sequences predict this property. To complement our theoretical development, a large scale FEM code was implemented on the CM-200 machine. This code has a high refinement capability which allows us to study those regions of the body where the fine phase mixture occurs and the strain field becomes extremely irregular. DTIC

N93-29389# Calspan-Buffalo Univ. Research Center, NY.
KINETICS OF NITRIC OXIDE FORMATION BEHIND 3 TO 4 KM/S SHOCK WAVES Final Report, 11 Jan. - 14 Dec. 1992
Charles E. Treanor and Marcia J. Williams 15 Feb. 1993 52 p
(Contract DAAL03-92-K-0003)
(AD-A263653; ARO-30404.1-EG-SDI) Avail: CASI HC A04/MF A01

A previously published group of O2/N2 shock-tube experiments, wherein the time history of the NO 5 micrometers radiation was measured, was studied to elicit information about the relevant chemical reactions which produce the radiation. It was found that the calculated radiation was sensitive to the rates used in the Zeldovich mechanism for NO formation, and that the rate measured by Monat et al. for N2 + 0 yields NO + N produced important features of the observed radiation. Vibration-dissociation coupling in this reaction modifies the radiation history in an important way, and is an essential element in obtaining agreement with the experiment. To improve agreement over a range of O2/N2 mixtures, it was necessary to take into account the faster vibrational relaxation of N2 by O2 and O collisions and the subsequent effect on vibration-dissociation coupling. DTIC

N93-29429# State Univ. of New York, Buffalo. Dept. of Chemistry.
MASS SPECTROMETRIC INVESTIGATION OF 2-METHOXYETHANOL AND 2-ETHOXYETHANOL CLUSTERS: MAGIC NUMBERS AND STRUCTURAL IMPLICATIONS
Gopal Vaidyanathan, William J. Herron, and James F. Garvey 3 Apr. 1993 48 p
(Contract N00014-88-K-0483)
(AD-A262822; TR-41) Avail: CASI HC A03/MF A01

We present the results of our mass spectrometric investigations for van der Waals clusters of 2-methoxyethanol and 2-ethoxyethanol. The cluster mass spectra were acquired for a variety of expansion conditions and electron energies. The protonated alkoxyethanol cluster ions (AE)nH(+) form the dominant cluster ion series. A number of fragment ions, that may arise from an unprotonated and/or a protonated alkoxyethanol molecular ion, were solvated by additional alkoxyethanol molecules. The (AE)n(H2O)mH(+) ions were observed with significant intensities only for n greater than or = 5 in neat as well as mixed alkoxyethanol/water expansions. It was also found that (AE)n(H2O)mH(+) cluster ions which satisfy the condition n = 2 (m + 2), for m = 1 and 2, have enhanced ion intensities. The various models that may explain the behavior of (AE)n(H20)mH(+) are discussed. DTIC

N93-29462# Pennsylvania State Univ., University Park. Center for Advanced Materials.
THE 2ND INTERNATIONAL SYMPOSIUM ON ELECTROCHEMICAL IMPEDANCE SPECTROSCOPY (EXTENDED ABSTRACTS) Final Report, 6 Jan. - 31 Dec. 1992
Digby D. MacDonald 1992 286 p Symposium held in Santa Barbara, CA, 12-17 Jul. 1992
(Contract N00014-92-J-1705)
(AD-A262994) Avail: CASI HC A13/MF A03

A workshop on electrochemical impedance spectroscopy was held on 12-17 Jul. 1992. The Symposium provided a forum for recent advances and applications of electrochemical impedance spectroscopy to a variety of problems related to general electrochemical mechanisms and models, passivity, electrochemistry in non-aqueous environments, batteries and fuel cells, mass transport, photoelectrochemistry and semiconductors, and membranes and biological systems. The extended abstracts provided are for talks and posters presented at the workshop. DTIC

N93-29506* National Aeronautics and Space Administration. Langley Research Center, Hampton, VA.
[PROCESS TO PREPARE 1,3-DIAMINO-5-PENTAFLUOROSULFANYLBENZENE] Patent
Terry L. St.Clair, inventor (to NASA), Anne K. St.Clair, inventor (to NASA), and Joseph S. Thrasher, inventor (to NASA) 15 Jun. 1993 6 p Filed 5 Sep. 1991
(NASA-Case-LAR-14773-2-CU; US-Patent-5,220,070;
US-Patent-Appl-SN-755207; US-Patent-Class-564-440;
US-Patent-Class-564-417; US-Patent-Class-562-827;
Int-Patent-Class-C07C-323/09) Avail: US Patent and Trademark Office

A process was developed to prepare 1,3-diamino- 5-pentafluoro sulfanylbenzene. This process involved two steps: preparing the dinitro compound, 1,3-dinitro- 5-pentafluoro sulfanylbenzene, and reducing this compound to form the corresponding diamine. This diamine was reacted with various dianhydrides, diacidchlorides, and epoxy resins to form polyimides, polyamides, and cross linked epoxies. These polymers were used to prepare semi-permeable membranes, wire coatings, and films.
Official Gazette of the U.S. Patent and Trademark Office

N93-29510# Dayton Univ., OH.
AN INVESTIGATION OF RESOLUTION AS ENCOUNTERED IN VARIOUS CHROMATOGRAPHIC OPERATIONAL MODES Final Report, 1 Jan. 1991 - 30 Apr. 1992
Wayne A. Rubey Aug. 1992 75 p
(AF Proj. 3048)
(AD-A262883; UDR-TR-92-53; WL-TR-92-2053) Avail: CASI HC A04/MF A01

An investigation was performed relative to the generation of resolution in isothermal gas chromatography (ITGC), programmed-temperature gas chromatography (PFGC), and a newly evolving technique referred to as thermal gradient programmed gas chromatography (TGPGC). The generation of chromatographic resolution while using open tubular gas chromatographic columns was studied with respect to the influences of dispersion, selectivity, and solute partitioning. Experiments were subsequently conducted to simulate rapid whole column PTGC operation with lengthy open tubular columns. Close agreement between theory and actual generated resolution was obtained during this simulation activity. The major conclusion from this study was that a partition-ratio programming chromatographic operational mode, e.g., TGPGC, possesses considerable promise with respect to rapidly and effectively eluting solutes. Properly implemented TGPGC should be capable of operation whereby selectivity and partitioning are enacted in a near-optimum manner with respect to obtaining maximum useful resolution per unit time. DTIC

N93-29617* National Aeronautics and Space Administration. Lyndon B. Johnson Space Center, Houston, TX.
METHOD FOR PRODUCING OXYGEN FROM LUNAR MATERIALS Patent
Thomas A. Sullivan, inventor (to NASA) 13 Jul. 1993 12 p Filed 24 Sep. 1991 Supersedes N92-12079 (30 - 3, p 367)
(NASA-Case-MSC-21759-1; US-Patent-5,227,032;
US-Patent-Appl-SN-764581; US-Patent-Class-204-129;
US-Patent-Class-204-105R; US-Patent-Class-204-112;
US-Patent-Class-204-104; Int-Patent-Class-C25B-1/02;
Int-Patent-Class-C25B-1/22; Int-Patent-Class-C25C-1/06) Avail: US Patent and Trademark Office

This invention is related to producing oxygen from lunar or Martian materials, particularly from lunar ilmenite in situ. The process includes producing a slurry of the minerals and hot sulfuric acid, the acid and minerals reacting to form sulfates of the metal. Water is added to the slurry to dissolve the minerals into an aqueous solution, the first aqueous solution is separated from unreacted minerals from the slurry, and the aqueous solution is electrolyzed to produce the metal and oxygen.
Official Gazette of the U.S. Patent and Trademark Office

N93-29665 Radian Corp., Austin, TX.
RATES AND MECHANISMS OF REACTION OF HYDROGEN SULFIDE WITH IRON CHELATES Topical Report, Apr. 1993
D. W. DeBerry Apr. 1993 115 p Sponsored by Gas Research Inst. Limited Reproducibility: More than 20% of this document may be affected by microfiche quality
(Contract GRI-5089-260-1875)
(PB93-184299; RCN-296-009-04-01; GRI-93/0019) Avail: CASI HC A06

Chelated iron liquid redox sulfur recovery processes hold promise for providing economical removal of hydrogen sulfide from natural gas with conversion to solid sulfur. They are complex chemical systems. An objective of this project is to identify and characterize the chemical interactions occurring in these liquid redox systems and determine which process parameters impact performance. This report presents the results of this project concerning the mechanism of oxidation of hydrogen sulfide by iron-based compounds in the liquid phase. The rates of reactions of chelated iron sorbing reagents with reduced sulfur species were measured over a wide range of conditions. The effects of relative reactant concentrations, pH, and ionic strength on these rates have been determined using a number of different methods. Effects of temperature and chelate type on the reaction of chelate iron with sulfide are also presented here. A kinetic model was developed to interpret these results and provide an overall framework for the reaction mechanism. This model has proven to be useful for integrating and explaining the results of the kinetics measurements. In addition, the model may become a useful tool for optimizing process chemistry and a key component of a general chemical process model. Details of the model and verification runs are given in this report. NTIS

N93-29766# California Univ., Berkeley. Lawrence Berkeley Lab.
DIFFRACTION AND HOLOGRAPHY WITH PHOTOELECTRONS AND AUGER ELECTRONS: SOME NEW DIRECTIONS
C. S. Fadley (California Univ., Davis.) Jun. 1992 66 p Presented at the 10th International Summer Institute in Surface Science (ISISS) Meeting, Milwaukee, WI, 29 Jun. - 2 Jul. 1992
(Contract DE-AC03-76SF-00098)
(DE93-007664; LBL-33306; CONF-9206332-2) Avail: CASI HC A04/MF A01

The current status of photoelectron and Auger-electron diffraction is reviewed, with emphasis on new directions of activity. The use of forward scattering in the study of adsorbed molecules, epitaxial overlayers, and clean surfaces is one of the most developed applications, and one that will become more powerful as higher energy resolution and perhaps spin analysis are used to resolve emitters on the basis of chemical state, position at a surface, or magnetic state. The use of larger data sets spanning a considerable fraction of the solid angle above a surface will also much enhance the structural information available, for example, in the growth of epitaxial layers or nanostructures on surfaces. Detailed fitting of experimental data to theoretical calculations based upon either single scattering or multiple scattering should also provide more rich structural information, including such parameters as substrate interlayer relaxation. Surface phase transitions in which near-surface layers become highly disordered can also be studied, with results that are complementary to those from such techniques as low energy electron diffraction and medium energy ion scattering. Short-range magnetic order also can be probed by somehow resolving the spin of the outgoing electrons, e.g. by using multiplet-split core levels. DOE

N93-29768# National Inst. of Standards and Technology, Boulder, CO. Thermophysics Div.
TABLES OF EXPERIMENTAL DATA USED FOR THE CORRELATION OF THE THERMOPHYSICAL PROPERTIES OF ETHANE
D. G. Friend, J. F. Ely, and H. Ingham Jan. 1993 306 p
(PB93-173417; NISTIR-3953) Avail: CASI HC A14/MF A03

The authors tabulate experimental data for the thermophysical properties of ethane from an extensive selection of the published literature. A complete tabulation of the data on ethane properties which were used in the development of correlating equations for the fluid state properties is provided. The tables give comparisons between the correlations and the data as well as the weight which was assigned to each point in the development of the correlations. The properties include pressure and densities of the saturated liquid and vapor, the PVT relationship in the single phase, isochoric and isobaric heat capacities, sound speed, viscosity, and thermal conductivity. The general range of the data is from the triple point, near 90.4 K and 1.1 MPa, to about 625 K with pressures to about 100 MPa. Author (revised)

N93-29828# Case Western Reserve Univ., Cleveland, OH. Dept. of Chemistry.
THE ELECTROLYTE FACTOR IN O2 REDUCTION ELECTROCATALYSIS
E. Yeager, M. Razaq, D. Gervasio, A. Razaq, and D. Tryk 23 Apr. 1993 32 p
(Contract N00014-90-J-1212)
(AD-A263565; TR-92-ONR) Avail: CASI HC A03/MF A01

The performance of acid fuel cells operating at moderate temperatures (less than or = 250 C) is limited by the irreversibility of the O2 cathode. Much effort has been directed to identifying more active catalysts than highly dispersed platinum which sets the present bench mark. The optimization of the choice of electrolytes, however, also provides a way to speed up the kinetics. This paper lists, various ways in which the electrolyte can influence the kinetics of the O2 reduction and discusses a few in more detail. The conclusion is reached that the adsorption of electrolyte components has a pronounced effect but that the kinetics do not have a strong dependence on pH or O2 solubility when mass transport control is not involved. Experimental results for a few new acid electrolytes and proton exchange membranes are presented. DTIC

N93-29837# Ames Lab., IA.
THE GLOBAL POTENTIAL ENERGY SURFACES OF THE LOWEST TWO 1A-PRIME STATES OF THE OZONE MOLECULE: THEORETICAL DETERMINATION AND ANALYSIS Ph.D. Thesis
G. J. Atchity Jan. 1993 264 p
(Contract W-7405-eng-82)
(DE93-007537; IS-T-1217) Avail: CASI HC A12/MF A03

The two lowest 1A' potential energy surfaces of the ozone molecule are determined and analyzed using accurate ab-initio MCSCF calculations. The shape-scale perimetric coordinates for triatomic molecules are discussed and further developed. Because the previously determined intersection between these two surfaces of like symmetry is unusual, much of the present work involves this intersection. The relevant theory of intersections is reviewed, and a method for characterizing intersections according to the topology of the surfaces in their vicinity is developed. The reasons for this particular crossing in ozone are investigated. The intersection point in C(sub 2v) symmetry is part of a larger, 1-dimensional intersection seam in C(sub s) symmetry. This seam is shown to consist of four branches. A new method for determining an intersection point in a two-dimensional coordinate space, based on the wavefunction phase-change theorem of Herzberg-Longuet-Higgins, is also developed. Finally, global mappings of the two potential energy surfaces in the scale-shape perimetric coordinates are determined. The minima of the two surfaces, their dissociation and rearrangement paths, and the map of the energy difference between them are all discussed. It is shown that direct formation of the ring structure of ozone from O2 and O is improbable, and that there is no rearrangement pathway on the ground state representing the interchange of two atoms. DOE

N93-30030# Boston Univ., MA.
KINETICS AND DYNAMICS OF REACTING SYSTEMS Final Report, 1 Jan. 1989 - 31 Dec. 1992
Sidney Redner 22 Mar. 1993 12 p
(Contract DAAL03-89-K-0025)
(AD-A264046; ARO-26256.21-CH) Avail: CASI HC A03/MF A01

This project was devoted to a study of the kinetics of diffusion-controlled and surface catalytic reactions. For catalytic reactions, the kinetics of the saturation process were elucidated. The role of interactions between adsorbates on the surface reaction was examined. For the diffusion-controlled reaction, a comprehensive theoretical framework to describe the spatial organization of reactants was developed. Particular attention was devoted to understanding the reaction dynamics at an interface which separates two reactive species. Geometrical features of this interface and the time dependence of the reaction rate were determined. DTIC

N93-30109# Office National d'Etudes et de Recherches Aerospatiales, Paris (France).
IN-SITU TEMPERATURE AND CONCENTRATION MEASUREMENTS OF ORGANOSILICON DECOMPOSITION IN A CHEMICAL VAPOR DEPOSITION REACTOR Ph.D. Thesis - Paris XI Univ., 1989 [MESURES IN-SITU DE TEMPERATURES ET CONCENTRATIONS SUR LE SYSTEME SI-C-H DANS UN REACTEUR DE DEPOT CHIMIQUE EN PHASE VAPEUR]
Nathalie Herlin 1990 124 p In FRENCH Original contains color illustrations
(ONERA-P-1990-3; ETN-93-93720) Avail: CASI HC A06/MF A02

In situ CARS (Coherent Anti-Stokes Raman Scattering) temperature and concentration measurements in a cold wall LPCVD (Low Pressure Chemical Vapor Deposition) vertical reactor are reported. Silicon Carbide (SiC) is deposited from a pure low velocity Tetramethylsilane (TMS) flow. Temperature and concentration maps were measured in the gas phase near a graphite substrate heated by the Joule effect. In situ concentration measurements were made on TMS and hydrogen which is the main product of TMS thermal decomposition. Ex situ partial pressure measurements were made and a temperature discontinuity was observed between the hit surface and the nearby gas in the TMS flow where thermal exchanges and chemical reactions take place simultaneously. This disconinuity is larger in the case of a pure hydrogen flow. These measurements prove incomplete energy transfer between the rotation of molecular species and a hit surface. This is explained using an accommodation coefficient which ranges from 0.05 for hydrogen on SiC to 0.15 for hydrogen on graphite. Thermal exchanges were also studied in the case of hydrogen or nitrogen on tungsten. This last case exhibits a nonBoltzmann rotational distribution when the distance from the hot wall is of the same order of magnitude as the mean free path. An explanation is proposed for this effect. ESA

N93-30139# Office National d'Etudes et de Recherches Aerospatiales, Paris (France).

SCANNING IONIC MICROSCOPY WITH HIGH SPATIAL RESOLUTION: PARALLEL ACQUISITION OF ELEMENTARY IMAGES BY HIGH RESOLUTION MASS SPECTROMETRY Ph.D. Thesis - Paris-Sud Univ., 1989 [MICROSCOPIE IONIQUE A BALAYAGE A HAUTE RESOLUTION SPATIALE: OBTENTION SIMULTANEE D'IMAGES FILTREES PAR UN SPECTROMETRE DE MASSES A FORT POUVOIR SEPARATEUR]

Fabrice Boust Sep. 1990 244 p In FRENCH Original contains color illustrations

(ONERA-NT-1990-7; ETN-93-93726) Avail: CASI HC A11/MF A03

The instrumentation allowing secondary ionic emission processing for the purpose of elementary and isotropic analysis is described. The device enables most of the analytical information contained in the tiny volume of matter sputtered during the impact of a finely focused primary ion beam to be retained. The instrument is built about a central column incorporating an electron microscope and the electrostatic optical system of the ion probe. The lower lens acts both as last demagnifying system and as secondary ion collecting device. Both primary positive ions (cesium) and secondary negative ions run along the same axis. The mass spectrometer, including a spherical electrostatic sector and a magnetic prism, is arranged as in a Mattauch-Herzog configuration, hence allowing simultaneous detection of different ionic species. Very small ion detectors are needed to succeed in parallel detection. Consequently, focus is on developing miniature detectors including conversion dynode followed by a scintillator and a photomultiplier. However, the performance not being satisfactory, small electron multipliers were used. The contribution of parallel acquisition is emphasized through a number of secondary ion images with a 100 nm lateral resolution. ESA

N93-30166# Florida Univ., Gainesville. Dept. of Chemistry.

HIGH MASS RESOLUTION GLOW DISCHARGE MASS SPECTROMETRY USING AN EXTERNAL ION SOURCE FT-ICR MASS SPECTROMETER Technical Report No. 43

C. H. Watson, J. Wronka, F. H. Laukien, C. M. Barshick, and J. R. Eyler 5 Mar. 1993 18 p Prepared in cooperation with Bruker Instruments, Inc., Billerica, MA

(Contract N00014-87-J-1248)

(AD-A264347) Avail: CASI HC A03/MF A01

A glow discharge source has been adapted for use with a commercial external ion source Fourier transform ion cyclotron resonance mass spectrometer. This combination shows promising analytical usefulness. Results on National Institute of Standards and Technology stainless steel standards showed that peaks due to nominally isobaric atomic isotopes can be observed with high mass resolution (m/delta m(sub 1/2) greater than or equal to 290,000). Detection limits in the high parts per billion to low parts per million range were achieved for analysis of trace metals in the standards, and concentrations of the trace elements were determined with good accuracy (better than 15%). DTIC

N93-30188# Pittsburgh Univ., PA. Dept. of Chemical and Petroleum Engineering.

A NOVEL PROCESS FOR METHANOL SYNTHESIS

J. W. Tierney and I. Wender 12 Feb. 1993 14 p

(Contract DE-FG22-89PC-89786)

(DE93-013070; DOE/PC-89786/T15) Avail: CASI HC A03/MF A01

A bench-scale reactor is being used to conduct studies of the conversion of synthesis gas to methanol (MeOH) in the liquid phase by a novel process. In previous reports, we provided evidence for a two step reaction in series, the carbonylation reaction mainly taking place close and the hydrogenolysis reaction taking place on the surface of the copper chromate. The interaction between the two catalyst enhances the rate of MeOH formation. In the last quarter, we showed that under present operating conditions, the methyl formate (MeOH) concentration is not in equilibrium and hence both the carboxylation and the hydrogenolysis reactions influence the rate of MEOH formation. The activities of other alkali and alkaline earth compounds as catalysts, the effect of water and the controlling reaction in the concurrent synthesis is described in this report. DOE

N93-30198# Department of Energy, Washington, DC.

DOE FUNDAMENTALS HANDBOOK: CHEMISTRY

Jan. 1993 130 p

(DE93-012222; DOE-HDBK-1015/2-93) Avail: CASI HC A07/MF A02

This handbook was developed to assist nuclear facility operating contractors in providing operators, maintenance personnel, and the technical staff with the necessary fundamentals training to ensure a basic understanding of chemistry. This volume contains the following modules: reactor water chemistry (effects of radiation on water chemistry, chemistry parameters), principles of water treatment (purpose; treatment processes /ion exchange/; dissolved gases, suspended solids, and pH control; water purity), and hazards of chemicals and gases (corrosives /acids, alkalies/, toxic compounds, compressed gases, flammable/combustible liquids). DOE

N93-30199# Department of Energy, Washington, DC.

DOE FUNDAMENTALS HANDBOOK: MATERIAL SCIENCE

Jan. 1993 94 p

(DE93-012224; DOE-HDBK-1017/1-93) Avail: CASI HC A05/MF A01

This handbook was developed to assist nuclear facility operating contractors in providing operators, maintenance personnel, and the technical staff with the necessary fundamentals training to ensure a basic understanding of the structure and properties of metals. This volume contains the two modules: structure of metals (bonding, common lattice types, grain structure/boundary, polymorphism, alloys, imperfections in metals) and properties of metals (stress, strain, Young modulus, stress-strain relation, physical properties, working of metals, corrosion, hydrogen embrittlement, tritium/material compatibility). DOE

N93-30200# Department of Energy, Washington, DC.

DOE FUNDAMENTALS HANDBOOK: MATERIAL SCIENCE

Jan. 1993 104 p

(DE93-012225; DOE-HDBK-1017/2-93) Avail: CASI HC A06/MF A02

This handbook was developed to assist nuclear facility operating contractors in providing operators, maintenance personnel, and the technical staff with the necessary fundamentals training to ensure a basic understanding of the structure and properties of metals. This volume contains the following modules: thermal shock (thermal stress, pressurized thermal shock), brittle fracture (mechanism, minimum pressurization-temperature curves, heatup/cooldown rate limits), and plant materials (properties considered when selecting materials, fuel materials, cladding and reflectors, control materials, nuclear reactor core problems, plant material problems, atomic displacement due to irradiation, thermal and displacement spikes due to irradiation, neutron capture effect, radiation effects in organic compounds, reactor use of aluminum). DOE

N93-30203# Office National d'Etudes et de Recherches Aerospatiales, Paris (France).

CONTRIBUTION TO THE STUDY OF THE INTERACTION BETWEEN ACOUSTIC WAVES AND COHERENT STRUCTURES INDUCED BY A PRISMATIC CYLINDER IN A RECTANGULAR CAVITY Ph.D. Thesis - Paris VI Univ. [CONTRIBUTION A L'ETUDE DE L'INTERACTION ENTRE DES ONDES ACOUSTIQUES ET DES STRUCTURES TOURBILLONNAIRES EMISES PAR UN OBSTACLE PRIMASTIQUE DANS UNE CAVIT RECTANGULAIRE]

Francois Garnier Sep. 1990 159 p In FRENCH
(ONERA-NT-1990-10; ETN-93-93728) Avail: CASI HC A08/MF A02

Due to the complexity of the problem of the association of large scale vortices to combustion instabilities, the interaction of coherent structures and acoustics are considered in the simplified case of a nonreactive flow. Experimental works were developed on an aerodynamic experiment and in the energetics department. Strouhal number values, associated to coherent structure emission, are similar for the two experiments. A resonance mechanism is observed, and flow visualizations show that vortices are quite symmetric when vortex shedding frequency and that of an acoustic mode are closed. An analytical modeling is developed from the Lighthill theory. Coupling between different modes, observed in experiments, is qualitatively confirmed. The numerical simulation of the interaction between acoustics and coherent structures is made with the help of KIVA code. In the initial version, this code does not describe inflow and outflow. Tests for these boundary conditions have been made with success. This allows a simulation of the aerodynamic experiment. The Strouhal number values, associated to vortex shedding, are in good agreement with the experiments. The transition between a various wake and a vortex street is made easy by an acoustic excitation. The results obtained must give, at term, an efficient action on combustion instabilities. ESA

N93-30209# Los Alamos National Lab., NM.
ISOTHERMAL AND SHOCK COMPRESSION OF HIGH DENSITY AMMONIUM NITRATE AND AMMONIUM PERCHLORATE
F. W. Sandstrom (New Mexico Inst. of Mining and Technology, Socorro.), P. A. Persson (New Mexico Inst. of Mining and Technology, Socorro.), and B. Olinger 1992 9 p Presented at the 10th Detonation Symposium, Boston, MA, 12-16 Jul. 1993
(Contract W-7405-eng-36)
(DE93-000682; LA-UR-92-3008; CONF-930713-5) Avail: CASI HC A02/MF A01

Given the widespread use of ammonium nitrate (AN) and ammonium perchlorate (AP) for energetic materials applications, relatively little data is available regarding their behavior under shock loading. We have evaluated the shock Hugoniots of AN and AP at high initial density (greater than or = 94% TMD) to pressures of approximately 20 GPa. We have used sound speed measurements, isothermal compression x-ray diffraction experiments and shock loading experiments to further explore the behavior of the two materials at elevated pressures. DOE

N93-30365# Chemical Research and Development Center, Aberdeen Proving Ground, MD.
USE OF STATISTICS IN COMPUTATIONAL CHEMISTRY Final Report, Jun. - Aug. 1990
Amnon Birenzvige, Larry M. Sturdivan, George R. Famini, and P. N. Krishnan Sep. 1992 33 p
(AD-A264307; CRDEC-TR-420) Avail: CASI HC A03/MF A01

The physical and chemical properties of various molecules, calculated by three different semi-empirical methods (MNDO, AM1, and PM3) are compared to experimental values using rigorous statistical analysis. The results show that the best method for calculating physical/chemical properties depends on the property and that no one method is adequate to calculate all the physical properties. Furthermore, by employing appropriate statistical tools, the precision and accuracy that each method calculates the different physical/chemical properties was determined. This will make it possible to use computational chemistry as a predictive tool with much better confidence. DTIC

N93-30405# Army Research Lab., Aberdeen Proving Ground, MD.
A NOVEL FLAME THERMOMETER BASED ON THE DOPPLER WIDTH OF RO-VIBRATIONAL TRANSITIONS Final Report, Mar. 1991 - Aug. 1992
David C. Dayton, Rosario C. Sausa, Anthony J. Kotlar, and Andrzej W. Miziolek May 1993 27 p
(DA Proj. IL1-61102-AH-43)
(AD-A264515; ARL-TR-129) Avail: CASI HC A03/MF A01

A complete understanding of the complex network of chemical reactions occurring in flame environment requires the determination of spatially resolved species concentration and temperature profiles which, in turn, can be used as stringent tests for present and developing flame models. Temperature profiles have traditionally been measured using fine wire thermocouples, which can provide a high degree of spatial resolution in a flame given that thermocouple diameters are on the order of ten to hundreds of microns. The thermocouple, however, constitutes a physical interface which may alter the local flame environment. To minimize purtubations to the flame, thermocouples are made as small in diameter as possible and are often coated to reduce or eliminate surface catalytic effects. Another advantage of keeping the diameter of thermocouple as small as possible is that corrections made to the measured temperature for radiation losses and heat conduction are minimal. DTIC

N93-30447# Los Alamos National Lab., NM.
DIRECT MONTE CARLO SIMULATION OF THE CHEMICAL EQUILIBRIUM COMPOSITION OF DETONATION PRODUCTS
M. S. Shaw 1992 5 p Presented at the 10th Detonation Symposium, Boston, MA, 12-16 Jul. 1993
(Contract W-7405-eng-36)
(DE92-040372; LA-UR-92-2793; CONF-930713-3) Avail: CASI HC A01/MF A01

The equation of state of detonation products is a crucial part of any calculation of reacting explosives and their effects. A new Monte Carlo simulation method was developed which allows for chemical equilibration as a natural part of a single simulation; this method is designated N(sub atoms)PT ensemble Monte Carlo since the number of atoms is held constant. The partition function for the collection of atoms is rewritten as a sum over all molecular partition functions. The new method is applied to a variety of test cases relevant to detonation products, such as N(sub 2) + O(sub 2) in equilibrium 2NO at 30 GPa and 3000 K. Work is in progress on combining the N(sub atoms)PT ensemble with the Gibbs ensemble for simulating a fluid-fluid phase segregation. DOE

N93-30526# Pittsburgh Univ., PA. Surface Science Center.
SURFACE CHEMISTRY OF HYDROGEN-PASSIVATED POROUS SILICON-OXIDATION OF SURFACE SI-H GROUPS BY ACETONE
Ling-Fen Rao and John T. Yates, Jr. 12 Apr. 1993 21 p
(Contract N00014-82-0280)
(AD-A264655) Avail: CASI HC A03/MF A01

The oxidation of hydrogen-passivated porous silicon by acetone at room temperature has been observed by using transmission infrared spectroscopy. After reaction with liquid acetone, two infrared absorption modes at 2253 cm(-1) and 2200 cm(-1) develop, and this is accompanied by loss of absorbance of the Si-H stretch modes at 2142, 2110 and 2089 cm(-1). We postulate that oxidation of the surface silicon hydride species by acetone to form (CH3)2HCO-Si-H(x) and ((CH3)2HCO)2Si-H(x) species has occurred. This surface reaction may be utilized for passivation of the silicon surface. DTIC

N93-30534# Florida Univ., Gainesville.
THE 26TH INTERNATIONAL QUANTUM CHEMISTRY SYMPOSIUM ON ATOMIC, MOLECULAR, AND CONDENSED MATTER THEORY AND COMPUTATIONAL METHODS Final Report, 6 Apr. 1992 - 5 Jan. 1993
Rodney J. Bartlett Feb. 1993 921 p Symposium held in St. Augustine, FL, 14-21 March 1992
(Contract DAAL03-92-G-0214)
(AD-A264206; ARO-29669.2-PH-CF) Avail: CASI HC A99/MF A10

The 32nd annual Sanibel Symposium was held March 14 to 21, 1992. The format of the symposium adopted for the past 2 years was followed again this year providing a compact 8-day schedule with an integrated program of quantum biology, quantum chemistry, and condensed matter physics. The topics of the sessions covered by these proceedings include Thirty-five Years of Progress in Electronic Structure Theory, Density Matrices and Other Revelations of 1955, Non-Born-Oppenheimer Methods, Atomic and Molecular Phenomena in Astrophysics, Photoinduced Phenomena, Reactive Molecular Collisions, Quantum Monte Carlo, Density-Functional Theory, Thin Films and Surfaces. A special session on Theoretical Inorganic Chemistry was held in memory of Arnold Karo, one of the real old-timers at Sanibel. All the articles have been subjected to the ordinary refereeing procedures of The International Journal of Quantum Chemistry. The articles presented in the sessions on quantum biology and associated poster sessions are published in a separate volume of The International Journal of Quantum Chemistry. DTIC

N93-30551# State Univ. of New York at Buffalo, Amherst.
STUDIES IN LEWIS ACID AND SUPERACID IONIC LIQUIDS Final Report, 1 Dec. 1989 - 30 Jun. 1992
Robert A. Osteryoung 16 Apr. 1993 33 p
(Grant AF-AFOSR-0099-90)
(AD-A264683; AFOSR-93-0338TR) Avail: CASI HC A03/MF A01

Studies in an ambient temperature chloroaluminate molten salt composed of aluminum chloride and 1-ethyl-3-methylimidazolium chloride were performed. A variety of topics were investigated. The behavior of electroactive polymers, mainly polyaniline, was investigated, and simultaneous EPR and electrochemical experiments were performed. The stoichiometry of several inorganic complexes ions was investigated in a near neutral melt, and a procedure to buffer the neutral melts was examined. A number of electrochemical studies with emphasis on the use of fast pulse voltammetry at very small microelectrodes were performed. Finally, the chemistry and electrochemistry of solutes as influenced by the presence of a proton (Bronsted) acid were investigated by means of electrochemical and NMR techniques. Gutmann donor/acceptor numbers of the melts were obtained, and the behavior of dimethylaniline in the presence and absence of a Bronsted acid was examined. The presence of both Lewis and Bronsted adducts was confirmed. DTIC

N93-30627# Emory Univ., Atlanta, GA. Dept. of Chemistry.
SURFACE CHEMISTRY OF N2H4 ON Si(100)-2X1 Technical Report No. 18
Y. Bu and M. C. Lin 24 May 1993 25 p
(Contract N00014-89-J-1235)
(AD-A264819) Avail: CASI HC A03/MF A01

The adsorption and thermal decomposition of N2H4 on Si(100)-2x1 were investigated using XPS, UPS, HREELS, and LEED. Upon adsorption of 0.2 L N2H4 on the surface at 100 K, partial dissociation of the NH bonds was indicated by the appearance of the Si-H stretching mode at 255 meV in HREELS and the 399.0 eV peak in N(sub 1S) XPS, which is assigned to the N2H(x) (presumably N2H3) species. At lower dosages (D is less than 0.4 L), N2H4 adsorbed on Si(100)-2x1 in a side-on rather than an end-on geometry and hydrogen-bonding is likely to be formed in the overlayer adsorbates. The NN bond breaking process was observed to occur at 600 K; the NH(x) products (x = 0,1,2) could be identified on the surface. At this temperature, the NN stretching mode essentially disappeared and the NH2 deformation and the NH stretching modes shifted from 200 and 413 to 192 and 420 meV, respectively. The same conclusion could also be established from the corresponding XPS and UPS results. Annealing the surface to higher temperatures caused further NH bond breaking, accompanied by the desorption of H2, while N remained on the surface forming Si nitride. DTIC

N93-30646 Stanford Univ., CA.
STUDIES OF CURVATURE, STRAIN, AND UNSTEADY EFFECTS ON PREMIXED FLAMES Ph.D. Thesis
Tarek Echekki 1993 250 p
Avail: Univ. Microfilms Order No. DA9309590

The effects of curvature, strain, and unsteadiness on premixed flames are studied analytically, numerically, and experimentally. The approach includes the development of simplified problem formulations and the study of flames in which the various effects may be isolated. The steady and unsteady (periodic and transient) response to strain are investigated using the one-dimensional strained flame. A simplified reaction rate model is proposed to eliminate the non-linearity associated with Arrhenius models. Solutions using this model agree very well with numerical results based on the Arrhenius model. The analytical treatment, however is much simpler. The effect of flame curvature on stationary cylindrical flames (sink and source configurations) are studied analytically using the simplified reaction rate model. Analytical solutions show that source and sink effects on the flame propagation rates are negligible except when the flame is near the source or sink despite the strong dependence of the preheat zone structure on flame curvature. Consequently, the flame may be considered locally planar. A differential quasi-one dimensional flame model which accounts for flame curvature, lateral flow expansion, and cross-stream diffusion is formulated. It is used to identify the mechanisms that enhance the displacement speed which denotes the velocity of the unburnt gas relative to the flame. Computations of a quasi-one dimensional flame show that the contribution of cross-stream diffusion to displacement speed enhancement may be significant. The results also show that, for a neutrally diffusive mixture, there is a surface in the flame where the mass flux is invariant to lateral flow expansion. The effect of curvature and stretch on the displacement speed are studied experimentally and numerically using the flame tip of a slot burner. The study is limited to a diffusionally neutral mixture to isolate hydrodynamic effects; this is verified by temperature measurements using Rayleigh scattering. The results show that the displacement speed correlates linearly with stretch. The same correlations give a nonlinear dependence on curvature which suggests the existence of a minimum radius of curvature associated with limitations on diffusional transport in highly curved flames. Dissert. Abstr.

N93-30653# Grambling State Univ., LA. Dept. of Physics.
MAGNETIC CHARACTER INVESTIGATION OF HIGHER ALCOHOL SYNTHESIS Cu-Co-Cr CATALYSTS
U. A. Donatto, T. L. Hoard, and A. N. Murty 1992 10 p Presented at the National Science Foundation (NSF) Conference on Diversity in the Scientific and Technological Work Force, Washington, DC, 24-27 Sep. 1992
(Contract DE-FG22-89PC-89762)
(DE93-009732; CONF-9209330-1) Avail: CASI HC A02/MF A01

The selectivity and conversion efficiency of the catalyst are reported to be governed by intermetallic ratios of the three elements. High yields of methanol in a copper-rich field, hydrocarbons in a cobalt-rich field, and mixed alcohols in the intermediate range were observed. The basic mechanism, the extent and effect of intermetallic interactions, or the role and function of chromium still remain unclear. To examine the correspondence between the catalytic and magnetic % behavior of the catalyst, we have investigated the Zero-field Nuclear Magnetic Resonance spectra and Hysteresis character of a series of Cu/Co/Cr trimetallics with Cu/Co ratio varying from 0.2 to 8.0. The magnetic moment of the catalyst system is very low for Cu/Co less than 1.5, dramatically increases when 1.5 less than Cu/Co less than 5.0 and drops for Cu/Co is gre ater than 5.0. The NMR results indicate that chromium serves as a support and inhibits any strong intermetallic interaction between copper and cobalt. DOE

N93-30658 Gas Research Inst., Chicago, IL.
DECOMPOSITION OF HYDROGEN SULFIDE FOR SMALL SCALE GAS PROCESSING. Annual Report, Jan. - Dec. 1992
J. C. S. Wu, C. L. Lin, and P. K. T. Liu 18 Jan. 1993 43 p Sponsored by Gas Research Inst.
(Contract GRI-5089-260-1982)
(PB93-174704; GRI-93/0040) Avail: CASI HC A03/MF A01

Decomposition of H2S with a catalytic membrane reactor was demonstrated in the lab with a ceramic membrane. An existing ceramic membrane with 40 A pore size was modified with silica oxide to have a selectivity of hydrogen over nitrogen of approximately 28. Decomposition was nearly double the thermodynamic equilibrium ratio (12 vs. 6.8%) at 800 C with the modified membrane. Simulation study indicates up to 40% higher than equilibrium conversion could be achieved with the membrane at a higher temperature. Further, an improved membrane with a nearly infinite hydrogen selectivity was developed with a similar modification method. A membrane like this will provide an additional enhancement in the conversion of H2S, which will be experimentally verified in the future. Another process, coupling decomposition with oxidation, was investigated with a straight tube to demonstrate the concept. Generation of SO2 was neligible. An additional 20-30% of enhancement by the concept is expected and will be experimentally verified with the modified membrane. Conceptual design on the membrane reactor utilizing existing engineering and material technology was completed for future field demonstration. NTIS

N93-30661# Brigham Young Univ., Provo, UT.
DIFFUSION COEFFICIENTS AND HEATS OF MIXING IN AQUEOUS ALKANOLAMINES Annual Report, Jan. - Dec. 1992
R. L. Rowley and J. L. Oscarson Jan. 1993 31 p Sponsored by Gas Research Inst.
(Contract GRI-5092-260-2356)
(PB93-176212; GRI-93/0082) Avail: CASI HC A03/MF A01

The objective of the work is to provide accurate data on diffusion coefficients and heats of absorption of acid gases in aqueous amine solutions to assist in the design of economical amine treating systems and to improve the efficiency of existing plants. Specifically covered in the report are measurements of the mutual diffusion coefficient of methyldiethanolamine (MDEA) and diethanolamine in water. Measurements have been made at 25, 50, and 75 C and at 0, 20, 35, and 50 wt.% amine. Heats of absorption of CO2 into aqueous mixtures of MDEA have also been measured calorimetrically. Results are reported at temperatures of 120 and 260 F and pressures of 500 and 1000 psia at total MDEA concentrations of 20, 35, and 50%. NTIS

N93-30664 Case Western Reserve Univ., Cleveland, OH. Dept. of Chemistry.
DIOXYGEN REDUCTION IN VARIOUS ACID ELECTROLYTES
E. B. Yeager, M. Razaq, D. Gervasio, A. Razaq, and D. Tryk 23 Apr. 1993 10 p Limited Reproducibility: More than 20% of this document may be affected by microfiche quality
(Contract N00014-90-J-1212)
(AD-A263564; TR-91-ONR) Avail: Issuing Activity (Defense Technical Information Center (DTIC))

Dioxygen reduction has been examined in several new acid electrolytes and mixtures of these electrolytes with concentrated phosphoric acid (used in present acid H2-O2 fuel cells). The polarization curves have been determined on smooth platinum with the rotating disk and ring-disk electrodes and on high-area platinum with gas-fed electrodes of the semi-hydrophobic-type. The polarization is less than with concentrated H3PO4 in some of these alternative electrolytes. Possible explanations are discussed. DTIC

N93-30667# Pennsylvania State Univ., University Park.
DETAILED STUDIES OF SOOT FORMATION IN LAMINAR DIFFUSION FLAMES FOR APPLICATION TO MODELING STUDIES Annual Report, 1 Feb. 1992 - 31 Jan. 1993
Robert J. Santoro 1 Mar. 1993 52 p
(Grant AF-AFOSR-0285-90)
(AD-A264827; AFOSR-93-0285TR) Avail: CASI HC A04/MF A01

A study of soot particle formation in laminar diffusion flames has been undertaken to investigate soot precursor chemistry, particle inception, and surface growth phenomena. During the first year of this study, emphasis has been given to species concentrations measurements made using mass spectrometric techniques. These measurements have demonstrated that species measurements can be obtained in particle laden regions of diffusion flames using a novel sampling probe approach. In particular, measurements have been obtained of acetylene, diacetylene, benzene, and stable combustion products throughout methane/air and ethene/air laminar diffusion flames. By combining these measurements with previous soot particle and velocity field measurements, it has been possible to follow the soot growth process along individual particle paths. These results establish that soot particle growth ceases due to the depletion of growth species not through the loss of soot particle reactivity as observed in premixed flame studies. Similarly, laser-induced fluorescence measurements of polynuclear aromatic hydrocarbons have been undertaken to follow the evolution of the soot precursor field. These measurements have established that laser-induced fluorescence can be used to reveal the qualitative structure of the molecular growth process leading to soot particle formation. These results need to be extended to provide more quantitative comparisons, particularly regarding fuel structure effect. Additional studies have been carried out to characterize the effects of aggregates on the interpretation of light scattering measurements. The results of these studies have shown that through the incorporation of fractal analysis, a self-consistent treatment of aggregates can be incorporated into the light scattering analysis. DTIC

N93-30760# United Technologies Corp., East Hartford, CT.
NOx CHEMISTRY IN NATURAL GAS FLAMES Final Report, May 1986 - Dec. 1992
M. F. Zabielski, B. A. Woody, and H. H. Hollick Dec. 1992 97 p See also PB92-132927 Sponsored by Gas Research Inst.
(Contract GRI-5086-260-1228)
(PB93-175263; R-95-7376-10; GRI-93/0043) Avail: CASI HC A05/MF A02

The results of a three task NO(x) program are provided. The three tasks covered are as follows: (1) thermal NO production; (2) NO2 formation and removal in flame fronts; and (3) NO removal by natural gas reburning. Detailed descriptions of the species and temperature diagnostics as well as combustion models used in the study are given. Measurements on a low pressure, oxygen-enriched, methane/air flame are described. The rate of the reaction of O + N2 yields NO + N is given for the temperature range from 2185-2413 K. Measurements on low pressure methane flames seeded with NO simulating conditions in natural gas reburning are also described. Results of CH, CN, 1CH2, NH2, NCO, NH, and HNO measurements are compared with modeling results. Moreover, a design study for an atmospheric pressure experiment is described. NTIS

N93-30761# Marathon Oil Co., Littleton, CO.
HYDROGEN SULFIDE DECOMPOSITION INTO HYDROGEN AND SULFUR BY QUINONE CYCLES, PART 1 Final Report, Jun. 1989 - Aug. 1992
M. A. Plummer and S. W. Cowley Feb. 1993 37 p See also PB91-243071 Sponsored by Gas Research Inst.
(Contract GRI-5089-260-1779)
(PB93-175297; GRI-92/0400.1) Avail: CASI HC A03/MF A01

The HYSULF process decomposes hydrogen sulfide using mild conditions. In the process, hydrogen sulfide is first reacted with a quinone in an organic solvent to produce sulfur and hydroquinone. After sulfur removal, hydroquinone is catalytically processed to recover hydrogen and recycle quinone-solvent. The produced sulfur is of excellent quality and easily recoverable from the solvent. The organic solvent should eliminate corrosion problems associated with commercial aqueous redox systems which produce only sulfur. Since no air oxidation is used, the sulfite-sulfate salt problems of aqueous systems will be avoided. The purpose of the GRI contract was to develop a better mechanistic understanding of process chemical reactions and economics. This was to result in the following: (1) Increased quinone conversion and sulfur precipitation rates; (2) Determining the effect of carbon dioxide on first stage chemistry; and (3) Eliminating the anthrone by-product produced in the dehydrogenation step. Essentially, all of the objectives of the project were completed. NTIS

N93-30816# Gordon Research Conferences, Inc., Kingston, RI.
GORDON RESEARCH CONFERENCES, 1991 Final Report, 1 Jun. 1991 - 31 May 1992
Alexander Cruickshank Apr. 1993 61 p
(Grant AF-AFOSR-0268-91)
(AD-A264275; AFOSR-93-0248TR) Avail: CASI HC A04/MF A01

A series of Air Force-supported Gordon Conferences were held during 1991 on the following topics/subtopics: Topic-Inorganic Chemistry/Subtopics-Materials and the Solid-State; Catalysis; New Chemistry of Polymetallic Complexes; Organometallic Chemistry; New Directions in the Chemistry of Coordination Complexes; Bioinorganic Chemistry; Chemistry of Surfaces; Mechanistic Studies and Ligand Transformations; General Inorganic Chemistry. Topic-High Performance Thermosetting Polymeric Materials/Subtopics-None Specified. Topic-Molten Salts and Liquid Metals/Subtopics-Metal-Molten Salt Solutions; Molten Salts; Dynamic Properties; Electrochemistry; Surface Phenomena; Metal-Nonmetal Transitions; Novel States of Matter; Simulations and Theoretical Interpretations. Topic-Elastomers/Subtopics-Flow, Miscibility, and Diffusion; Toughening Plastics; Synthesis; Networks; Thermoplastic Elastomers; History; Fillers and Vulcanization. Topic-Dynamics of Gas-Surface Interactions/Subtopics-Surface Vibrations; Electronic Transitions; Ultrafast Surface Processes; Dynamics of Adsorption; Surface Diffusion; Liquid Interfaces; Dynamics of Film Growth; Surface Chemical Processes; and Special Topics. DTIC

N93-30982# Israel Atomic Energy Commission, Negev. Nuclear Research Center.
METHODS FOR PREPARATION OF MIXTURES OF GASES IN AIR AT THE PARTS-PER-BILLION TO PARTS-PER-MILLION CONCENTRATION RANGE FOR CALIBRATION OF MONITORS
Z. Karpas, S. Melloul, Y. Pollevoy, and A. Matmor May 1992 18 p In HEBREW
(DE92-642433; NRCN(TN)-131) Avail: CASI HC A03/MF A01 (US Sales Only)

Static and dynamic methods for generating mixture of gases and vapors in air at the parts-per-billion (ppb) to parts-per-million (ppm) concentration range were surveyed. The dynamic methods include: a dynamic flow and mixing system; injection of samples into large volumes of air; exponential dilution; permeation and diffusion tubes; and generation of the target gas by chemical reaction or electrolysis. The static methods include preparation of mixtures by weighing the components, by volumetric mixing, and by partial pressure method. The principles governing the utilization of these methods for the appropriate applications were discussed, and examples in which they were used to calibrate an ion mobility spectrometer (IMS) were given. DOE

N93-28736*# Boeing Defense and Space Group, Kent, WA.
NASA IN-STEP: PERMEABLE MEMBRANE EXPERIMENT
In NASA, Washington, NASA/DOD Flight Experiments Technical Interchange Meeting Proceedings 1992 31 p (For primary document see N93-28699 11-12)
Avail: CASI HC A03/MF A10

N93-28737*# Life Systems, Inc., Cleveland, OH.
ELECTROLYSIS PERFORMANCE IMPROVEMENT AND VALIDATION EXPERIMENT
Franz H. Schubert *In* NASA, Washington, NASA/DOD Flight Experiments Technical Interchange Meeting Proceedings 1992 27 p (For primary document see N93-28699 11-12)
Avail: CASI HC A03/MF A10

N93-29367*# Washington Univ., Saint Louis, MO. Center for Space Sciences.
SIMS CHEMICAL ANALYSIS OF EXTENDED IMPACTS ON THE LEADING AND TRAILING EDGES OF LDEF EXPERIMENT AO187-2
S. Amari, J. Foote, P. Swan, R. M. Walker, E. Zinner, and G. Lange (Max-Planck-Inst. fuer Kernphysik, Heidelberg, Germany.) *In* NASA. Langley Research Center, LDEF: 69 Months in Space. Second Post-Retrieval Symposium, Part 2 Apr. 1993 p 513-528 (For primary document see N93-29354 11-99)
Avail: CASI HC A03/MF A04

N93-29627*# Pacific Northwest Lab., Richland, WA.
SENSITIVITY OF LDEF FOIL ANALYSES USING ULTRA-LOW BACKGROUND GERMANIUM VS. LARGE NaI(Tl) MULTIDIMENSIONAL SPECTROMETERS
James H. Reeves, Richard J. Arthur, and Ronald L. Brodzinski *In* NASA. Langley Research Center, LDEF: 69 Months in Space. Part 1: Second Post-Retrieval Symposium Apr. 1993 p 79-86 (For primary document see N93-29621 11-99)
(Contract DE-AC06-76RL-01830)
Avail: CASI HC A02/MF A03

N93-29683*# National Aeronautics and Space Administration. Goddard Space Flight Center, Greenbelt, MD.
OVERVIEW OF THE SYSTEMS SPECIAL INVESTIGATION GROUP INVESTIGATION
James B. Mason, Harry Dursch (Boeing Defense and Space Group, Seattle, WA.), and Joel Edelman (Long Duration Exposure Facility Newsletter, Silver Spring, MD.) *In* NASA. Langley Research Center, LDEF: 69 Months in Space. Part 4: Second Post-Retrieval Symposium Apr. 1993 p 1257-1268 (For primary document see N93-29682 11-99)
Avail: CASI HC A03/MF A03; 2 functional color pages

N93-30064 Emory Univ., Atlanta, GA. Dept. of Chemistry.
THERMAL OXIDATION OF HCN BY NO2 IN SHOCK WAVES
Y. He, M. C. Lin, and Carl F. Melius (Sandia National Labs., Livermore, CA.) *In* JHU, ONR/LANL Workshop on the Fundamental Physics and Chemistry of Combustion, Initiation, and Detonation of Energetic Materials Mar. 1992 p 35-52 (For primary document see N93-30061 11-28)
(Contracts N00014-89-J-1949; N00014-90-F-0078)
Avail: CPIA, 10630 Little Patuxent Pkwy., Suite 202, Columbia, MD 21044-3200 HC

N93-30065 New Mexico Inst. of Mining and Technology, Socorro. Chemistry Dept.
THERMAL DECOMPOSITION OF NITRAMINES
James C. Oxley, R. Szekeres, and A. Kooh *In* JHU, ONR/LANL Workshop on the Fundamental Physics and Chemistry of Combustion, Initiation, and Detonation of Energetic Materials Mar. 1992 p 53-54 (For primary document see N93-30061 11-28)
Avail: CPIA, 10630 Little Patuxent Pkwy., Suite 202, Columbia, MD 21044-3200 HC

N93-30066 Naval Research Lab., Washington, DC.
ION EMISSION DURING HIGH-ENERGY SPUTTERING OF AMMONIUM DINITRAMIDE AND AMMONIUM NITRATE CRYSTALS AND THE DETERMINATION OF ION DECOMPOSITION PATHWAYS USING TANDEM MASS SPECTROMETRY
Robert J. Doyle, Jr. *In* JHL, ONR/LANL Workshop on the Fundamental Physics and Chemistry of Combustion, Initiation, and Detonation of Energetic Materials Mar. 1992 p 55-70 (For primary document see N93-30061 11-28)
Avail: CPIA, 10630 Little Patuxent Pkwy., Suite 202, Columbia, MD 21044-3200 HC

N93-30067 Yale Univ., New Haven, CT. Dept. of Chemistry.
OBSERVATION OF REACTION INTERMEDIATES IN CRYSTALLINE RDX
J. Michael McBride and John P. Toscano *In* JHU, ONR/LANL Workshop on the Fundamental Physics and Chemistry of Combustion, Initiation, and Detonation of Energetic Materials Mar. 1992 p 71-84 (For primary document see N93-30061 11-28)
(Contract N00014-90-J-4015)
Avail: CPIA, 10630 Little Patuxent Pkwy., Suite 202, Columbia, MD 21044-3200 HC

N93-30068 University of Southern California, Los Angeles. Dept. of Chemistry.
NO2 UNIMOLECULAR DECOMPOSITION: STEP-LIKE VARIATION OF k(SUB uni)(E)
G. A. Brucker, S. I. Ionov, Y. Chen, and Curt Wittig *In* JHU, ONR/LANL Workshop on the Fundamental Physics and Chemistry of Combustion, Initiation, and Detonation of Energetic Materials Mar. 1992 p 85-88 (For primary document see N93-30061 11-28)
Avail: CPIA, 10630 Little Patuxent Pkwy., Suite 202, Columbia, MD 21044-3200 HC

N93-30071 Naval Research Lab., Washington, DC. Theoretical Chemistry Section.
CHEMICAL DYNAMICS SIMULATIONS AS A PROBE TO THE INITIATION AND PROPAGATION OF CONDENSED PHASE DETONATIONS
Carter T. White, Daniel H. Robertson, Mark L. Elert (Naval Academy, Annapolis, MD.), and Donald W. Brenner *In* JHU, ONR/LANL Workshop on the Fundamental Physics and Chemistry of Combustion, Initiation, and Detonation of Energetic Materials Mar. 1992 p 127-129 Sponsored by ONR (For primary document see N93-30061 11-28)
Avail: CPIA, 10630 Little Patuxent Pkwy., Suite 202, Columbia, MD 21044-3200 HC

N93-30072 Los Alamos National Lab., NM.
VIBRATIONAL SPECTROSCOPY OF SHOCK-COMPRESSED FLUIDS
Stephen C. Schmidt, James D. Johnson, David S. Moore, Milton S. Shaw, and Richard LeSar *In* JHU, ONR/LANL Workshop on the Fundamental Physics and Chemistry of Combustion, Initiation, and Detonation of Energetic Materials Mar. 1992 p 131-147 (For primary document see N93-30061 11-28)
Avail: CPIA, 10630 Little Patuxent Pkwy., Suite 202, Columbia, MD 21044-3200 HC

N93-30073 Washington State Univ., Pullman. Shock Dynamics Lab.
EXAMINATION OF SHOCK INDUCED CHEMICAL REACTIONS IN LIQUIDS USING TIME-RESOLVED OPTICAL SPECTROSCOPY
Yogendra M. Gupta *In* JHU, ONR/LANL Workshop on the Fundamental Physics and Chemistry of Combustion, Initiation, and Detonation of Energetic Materials Mar. 1992 p 149-162 Sponsored by ONR (For primary document see N93-30061 11-28)
Avail: CPIA, 10630 Little Patuxent Pkwy., Suite 202, Columbia, MD 21044-3200 HC

N93-30075 Massachusetts Inst. of Tech., Cambridge. Dept. of Chemistry.
SINGLE-SHOT FEMTOSECOND SPECTROSCOPY: A METHODOLOGY FOR OBSERVATION OF SOLID-STATE CHEMICAL REACTIONS
Weining Wang and Keith A. Nelson *In* JHU, ONR/LANL Workshop on the Fundamental Physics and Chemistry of Combustion, Initiation, and Detonation of Energetic Materials Mar. 1992 p 167-172 (For primary document see N93-30061 11-28)
Avail: CPIA, 10630 Little Patuxent Pkwy., Suite 202, Columbia, MD 21044-3200 HC

N93-30076 Los Alamos National Lab., NM. Chemical and Laser Sciences Div.
DETONATION MASS SPECTROMETRY
N. Roy Greiner, Herbert A. Fry, and Normand C. Blais *In* JHU, ONR/LANL Workshop on the Fundamental Physics and Chemistry of Combustion, Initiation, and Detonation of Energetic Materials Mar. 1992 p 173-188 (For primary document see N93-30061 11-28)
Avail: CPIA, 10630 Little Patuxent Pkwy., Suite 202, Columbia, MD 21044-3200 HC

N93-30077 Los Alamos National Lab., NM.
STRATEGIES FOR UNDERSTANDING THE DEFLAGRATION-TO-DETONATION TRANSITION
Blaine W. Asay *In* JHU, ONR/LANL Workshop on the Fundamental Physics and Chemistry of Combustion, Initiation, and Detonation of Energetic Materials Mar. 1992 p 227-242 Previously announced as N92-29512 Sponsored by DOE (For primary document see N93-30061 11-28)
Avail: CPIA, 10630 Little Patuxent Pkwy., Suite 202, Columbia, MD 21044-3200 HC

N93-30079 Yale Univ., New Haven, CT. Dept. of Mechanical Engineering.
NUMERICAL MODELING OF MULTIDIMENSIONAL FLAMES WITH APPLICATION TO ENERGETIC MATERIALS Abstract Only
Mitchell D. Smooke *In* JHU, ONR/LANL Workshop on the Fundamental Physics and Chemistry of Combustion, Initiation, and Detonation of Energetic Materials Mar. 1992 p 261 (For primary document see N93-30061 11-28)
Avail: CPIA, 10630 Little Patuxent Pkwy., Suite 202, Columbia, MD 21044-3200 HC

N93-30081 Ballistic Research Labs., Aberdeen Proving Ground, MD.
FLAME STRUCTURE STUDIES OF PROPELLANT LIKE LOW PRESSURE FLAMES USING OPTICAL AND MASS SPECTROMETRIC MEANS
Andrzej W. Miziolek, R. C. Sausa, W. R. Anderson, D. C. Dayton, C. M. Faust, S. L. Howard, and S. A. Barts *In* JHU, ONR/LANL Workshop on the Fundamental Physics and Chemistry of Combustion, Initiation, and Detonation of Energetic Materials Mar. 1992 p 275-297 Sponsored by ONR (For primary document see N93-30061 11-28)
Avail: CPIA, 10630 Little Patuxent Pkwy., Suite 202, Columbia, MD 21044-3200 HC

N93-30082 Lawrence Livermore National Lab., CA.
PRESSURE DEPENDENCE OF THE REACTION PROPAGATION RATE OF TATB TO 40 GPa
M. Frances Foltz and Albert L. Nichols, III *In* JHU, ONR/LANL Workshop on the Fundamental Physics and Chemistry of Combustion, Initiation, and Detonation of Energetic Materials Mar. 1992 p 299-310 (For primary document see N93-30061 11-28)
(Contract W-7405-eng-48)
Avail: CPIA, 10630 Little Patuxent Pkwy., Suite 202, Columbia, MD 21044-3200 HC

N93-30085 Illinois Univ., Urbana-Champaign. Dept. of Mechanical and Industrial Engineering.
UNSTEADY COMBUSTION OF ENERGETIC MATERIALS USING LASER-RECOIL
Quinn Brewster and Steven Son *In* JHU, ONR/LANL Workshop on the Fundamental Physics and Chemistry of Combustion, Initiation, and Detonation of Energetic Materials Mar. 1992 p 359-366 (For primary document see N93-30061 11-28)
Avail: CPIA, 10630 Little Patuxent Pkwy., Suite 202, Columbia, MD 21044-3200 HC

N93-30087 California Univ., Berkeley. Lawrence Berkeley Lab.
METALLIZATION AT DETONATION FRONTS IN SOLIDS
John J. Gilman *In* JHU, ONR/LANL Workshop on the Fundamental Physics and Chemistry of Combustion, Initiation, and Detonation of Energetic Materials Mar. 1992 p 379-394 (For primary document see N93-30061 11-28)
Avail: CPIA, 10630 Little Patuxent Pkwy., Suite 202, Columbia, MD 21044-3200 HC

N93-30090 Princeton Univ., NJ.
HOMOGENEOUS GAS PHASE KINETIC MODEL WITH GRADIENT SENSITIVITY ANALYSIS FOR HIGH TEMPERATURE PARTICULATE BORON COMBUSTION IN FLUORINE ENRICHED ENVIRONMENTS Abstract Only
R. Brown, C. E. Kolb, Richard A. Yetter, Frederick L. Dryer, and H. R. Rabitz *In* JHU, ONR/LANL Workshop on the Fundamental Physics and Chemistry of Combustion, Initiation, and Detonation of Energetic Materials Mar. 1992 p 425 (For primary document see N93-30061 11-28)
Avail: CPIA, 10630 Little Patuxent Pkwy., Suite 202, Columbia, MD 21044-3200 HC

N93-30092 Loyola Coll., Baltimore, MD. Dept. of Electrical Engineering.
MICROSTRUCTURAL BASIS FOR ENHANCED SHOCK-INDUCED CHEMISTRY IN SINGLE CRYSTALS OF AMMONIUM PERCHLORATE
Wayne L. Elban, H. W. Sandusky (Naval Surface Weapons Center, Silver Spring, MD.), B. C. Beard (Naval Surface Weapons Center, Silver Spring, MD.), and B. C. Glancy (Naval Surface Weapons Center, Silver Spring, MD.) *In* JHU, ONR/LANL Workshop on the Fundamental Physics and Chemistry of Combustion, Initiation, and Detonation of Energetic Materials Mar. 1992 p 429-443 Sponsored by ONR and NSWC (For primary document see N93-30061 11-28)
Avail: CPIA, 10630 Little Patuxent Pkwy., Suite 202, Columbia, MD 21044-3200 HC

N93-30093 Naval Surface Weapons Center, Silver Spring, MD.
DEFECT DENSITY MEASUREMENTS IN A SHOCKED SINGLE CRYSTAL OF AMMONIUM PERCHLORATE
B. C. Beard, H. W. Sandusky, B. C. Glancy, and Wayne L. Elban (Loyola Coll., Baltimore, MD.) *In* JHU, ONR/LANL Workshop on the Fundamental Physics and Chemistry of Combustion, Initiation, and Detonation of Energetic Materials Mar. 1992 p 445-461 Sponsored in part by ONR (For primary document see N93-30061 11-28)
Avail: CPIA, 10630 Little Patuxent Pkwy., Suite 202, Columbia, MD 21044-3200 HC

N93-30099 Naval Research Lab., Washington, DC. Lab. for Computational Physics and Fluid Dynamics.
RATE CONSTANT DETERMINATIONS OF REACTIONS H + HNO FROM AB INITIO REACTION PATH CALCULATIONS Abstract Only
Maribel R. Soto and Michael Page *In* JHU, ONR/LANL Workshop on the Fundamental Physics and Chemistry of Combustion, Initiation, and Detonation of Energetic Materials Mar. 1992 p 499 (For primary document see N93-30061 11-28)
Avail: CPIA, 10630 Little Patuxent Pkwy., Suite 202, Columbia, MD 21044-3200 HC

N93-30101 Arkansas Univ., Fayetteville. Dept. of Chemistry.
GAS ELECTRON DIFFRACTION EMPLOYING A PULSED ELECTRON BEAM SYNCHRONOUS WITH PHOTOEXCITATION Abstract Only
John D. Ewbank, Jing Y. Luo, Jeffrey T. English, Walter L. Faust, and Lothar Schafer *In* JHU, ONR/LANL Workshop on the Fundamental Physics and Chemistry of Combustion, Initiation, and Detonation of Energetic Materials Mar. 1992 p 503 (For primary document see N93-30061 11-28)
Avail: CPIA, 10630 Little Patuxent Pkwy., Suite 202, Columbia, MD 21044-3200 HC

N93-30102 Aerodyne Research, Inc., Billerica, MA. Center for Chemical and Environmental Physics.
CONDENSED PHASE DIAGNOSTICS OF NITRAMINE PROPELLANT COMBUSTION Abstract Only
Joda Wormhoudt, P. L. Kebabian, and C. E. Kolb *In* JHU, ONR/LANL Workshop on the Fundamental Physics and Chemistry of Combustion, Initiation, and Detonation of Energetic Materials Mar. 1992 p 505
(For primary document see N93-30061 11-28)
(Contract DAAL03-91-C-0008)
Avail: CPIA, 10630 Little Patuxent Pkwy., Suite 202, Columbia, MD 21044-3200 HC

N93-30277 Barringer Research Ltd., Rexdale (Ontario).
ADVANCED SIGNAL PROCESSING REQUIREMENT IN AN ION MOBILITY EXPLOSIVES DETECTOR
R. Jackson, J. Davies, L. Daubner, L. D. May, and S. Wiles *In* Engineering Inst. of Canada, Canadian Conference on Electrical and Computer Engineering, Volumes 1 and 2 1990 4 p (For primary document see N93-30215 11-31)
Avail: Engineering Inst. of Canada, 2050 rue Mansfield, Suite 700, Montreal, Quebec H3A 1Z2 Canada

26 METALLIC MATERIALS

Includes physical, chemical, and mechanical properties of metals, e.g., corrosion; and metallurgy.

N93-28491# Pennsylvania State Univ., University Park. Dept. of Materials Science and Engineering.
THE TEMPERATURE DEPENDENCE OF THE DEFORMATION AND OXIDATION BEHAVIOR OF AN AGE-HARDENABLE BETA + ALPHA-TWO TITANIUM ALLOY Technical Report
D. M. Goto, L. S. Quattrocchi, and D. A. Koss 5 Mar. 1993 16 p
(Contract N00014-91-J-1414)
(AD-A262232; TR-5) Avail: CASI HC A03/MF A01

The beta Ti alloy Ti-23Nb-11Al (at %) is unique in that it is age hardenable due to the formation of lath-like alpha 2-phase precipitates based on Ti3Al. Furthermore age-hardening occurs at temperatures significantly higher than most conventional beta Ti alloys. This suggests the possibility of the elevated temperature usage of alpha 2-strengthened beta Ti alloys such as Ti-23Nb-11Al. The study examines the compressive deformation behavior of the Ti-23Nb-11Al alloy in the -196 deg. C to 650 deg. C temperature range and demonstrates that very high strengths are possible even at 600 deg. C by precipitation hardening due to the alpha 2 phase. The thermogravimetric oxidation behavior in laboratory air from 600 deg to 700 deg. C indicates parabolic behavior consistent with oxygen diffusion through a scale. DTIC

N93-28499# Purdue Univ., West Lafayette, IN. Metals Information Analysis Center.
REFRACTORY METAL DISILICIDES RESEARCH
K. J. Bowman Dec. 1992 52 p
(Contract DLA900-90-D-0305)
(AD-A262416; MIAC-2) Avail: CASI HC A04/MF A01

Refractory metal disilicides have been a topic of considerable interest to both the metals and ceramics communities in recent years. This report is intended to serve as a status report on fundamental properties and a review of recent research. A major goal of this report has been to incorporate aspects of research for electronic as well as structural applications. Data-reviewed includes physical and mechanical properties as well as phase equilibria, processing and oxidation resistance. Suggested future directions for research are also discussed. DTIC

N93-28529# Japan Atomic Energy Research Inst., Tokyo.
PRELIMINARY TEST OF LIQUID METAL INDUCED EMBRITTLEMENT IN LIQUID LiPb AND STAINLESS-STEEL SYSTEMS
Hiroshi Yoshida, Mikio Enoeda, Yuji Naruse, Takashi Shige, and Misao Hasegawa May 1992 59 p
(DE93-753130; JAERI-M-92-066) Avail: CASI HC A04/MF A01

Corrosion of structural materials with molten metal is one of the major concerns of the feasibility of this concept. Many experimental works have been performed to examine the reactivity of eutectic Li17Pb83 with stainless-steel, and proved that the reactivity of it with structure materials is lower than that of the other molten breeders such as Li and LiF-BeF2. Several investigators have reported that weldments of Cr-Mo ferritic steel degradate with liquid LiPb because of the liquid metal induced embrittlement (LMIE) phenomena. Present study was aimed at the susceptibility of LMIE in the LiPb-steel system under various stress conditions. Tests were done with Li17Pb83 and pure Pb at 500 C. Test specimens of U-bend, tensiled-rod and weldments were prepared from austenitic (SUS316) and ferritic (modified 9Cr-1Mo) steels. At a high stress condition of 70% of the break stress, generation of microcracks was observed. DOE

N93-28545# Pennsylvania State Univ., University Park. Center for Advanced Materials.
FUNDAMENTAL ASPECTS IN THE DESIGN OF PASSIVE ALLOYS
D. D. Macdonald and M. Urquidi-Macdonald 1993 15 p Presented at the European Symposium on Passive Films, Paris, France, 15-19 Feb. 1993
(Contract DE-FG02-91ER-45461)
(DE93-009028; DOE/ER-45461/3; CONF-930271-1) Avail: CASI HC A03/MF A01

Alloying is the most extensively used method for enhancing the passivity of base metals. The art of alloying extends back into antiquity, but it was not until the early part of this century that the highly passive stainless steels were developed. More recently, in response to the need for high strength, corrosion-resistant alloys for gas turbines, various superalloys have been devised that exhibit great resistances to dry oxidation. The role(s) of alloying elements in enhancing passivity in aqueous environments, in terms of the point defect model (PDM) and the solute-vacancy interaction model (SVIM) that was developed a number of years ago is discussed. DOE

N93-28548# Pacific Northwest Lab., Richland, WA.
DEFORMATION MECHANISMS IN Be(SUB 12)X COMPOUNDS
S. M. Bruemmer, J. L. Brimhall, L. A. Charlot, S. Sondhi, R. G. Hoagland, and J. P. Hirth (Washington State Univ., Pullman.) Dec. 1992 8 p Presented at the High-temperature Ordered Intermetallic Alloys V, Boston, MA, 30 Nov. - 3 Dec. 1992
(Contract DE-AC06-76RL-01830)
(DE93-009080; PNL-SA-21288; CONF-9211205-1) Avail: CASI HC A02/MF A01

Dislocation structures were examined, and active slip systems identified, in Be12Nb after compressive deformation at 20, 800, 900, 1000, and 1200 C. A large number of slip systems are active at 1200 C, but these decrease significantly at temperatures below 1000 C. Dislocation structures at low temperatures are limited to 1/2 is less than 101(101) partial dislocations either paired or creating isolated planar faults. Significant ductility is not observed until 1200 C when a second type of partial dislocation, 1/2 is less than 100(011) is present. Dislocations observed in the body-centered tetragonal Be12X compounds (where X can be Nb, Ta, Mo, V, Fe etc.) were modelled atomistically using molecular dynamics. Simulations corroborate the stability of these dislocation systems and indicate that the stacking faults associated with these partial dislocations have very low fault energy. DOE

N93-28564# Oak Ridge National Lab., TN.
PROCESS OPTIMIZATION OF HEXOLOY SX-SiC TOWARDS IMPROVED MECHANICAL PROPERTIES
G. V. Srinivasan (Carborundum Co., Niagara Falls, NY.), S. K. Lau (Carborundum Co., Niagara Falls, NY.), R. S. Storm (Carborundum Co., Niagara Falls, NY.), M. K. Ferber, and M. G. Jenkins 1993 14 p Presented at the 38th ASME International Gas Turbine and Aeroengine Congress and Exhibition, Cincinnati, OH, 24-27 May 1993
(Contract DE-AC05-84OR-21400)
(DE93-007913; CONF-930502-3) Avail: CASI HC A03/MF A01

Results show that SiC materials sintered with additions of Y and Al compounds can achieve the high level of mechanical properties required for use in heat engines. However, the reaction of the second phase with SiC resulting in strength limiting pools, result in increased variability in materials properties. If this variability can be controlled, the relatively low cost of raw materials and processing for Hexoloy SX manufacture would make these materials attractive for low and high temperature engine applications. DOE

N93-28591# Illinois Univ., Urbana.
INTERNATIONAL CONFERENCE ON MARTENSITIC TRANSFORMATIONS (ICOMAT 92) Final Report, 30 Sep. 1991 - 31 Dec. 1992
C. M. Wayman 5 Mar. 1993 104 p
(Grant AF-AFOSR-0380-91)
(AD-A262739; AFOSR-93-0199TR) Avail: CASI HC A06/MF A02

Abstracts of presentations made at the International Conference on Martensitic Transformations are presented. Electronic structure and total energy calculations, matensitic twinning, pre-transitional effects, aging effects, and thermal treatments are addressed. DTIC

N93-28618*# National Aeronautics and Space Administration. Lewis Research Center, Cleveland, OH.
TEXTURING OF InP SURFACES FOR DEVICE APPLICATIONS
Sheila G. Bailey, Navid S. Fatemi (Sverdrup Technology, Inc., Brook Park, OH.), and Geoffrey A. Landis (Sverdrup Technology, Inc., Brook Park, OH.) Apr. 1992 9 p Presented at the Materials Research Society Spring Meeting, San Francisco, CA, 27 Apr. - 1 May 1992;sponsored by the Materials Research Society
(RTOP 506-41-11)
(NASA-TM-106061; E-7664; NAS 1.15:106061) Avail: CASI HC A02/MF A01

A unique process for texturing InP (100) wafers by anisotropic etching was developed. The process produces irregular V-grooves on the surface, which reduce the surface reflectivity. The process does not require photolithography or masking. The etching characteristics depend on doping, with etching tending to proceed more rapidly on the more heavily doped samples. Reduced reflectivity surfaces formed using this process can be applied to solar cells, photodetectors, and other optoelectronic devices. Author

N93-28631# Connecticut Univ., Storrs.
TRANSFORMATION TOUGHENING
M. J. Rafa 19 Apr. 1993 14 p
(Contract DE-FG02-87ER-45318)
(DE93-011805; DOE/ER-45318/6) Avail: CASI HC A03/MF A01

In NiAl, we have succeeded in determining the complete Ginzburg-Landau strain free energy function necessary to model the cubic to tetragonal martensite transformation in a sample of any size. We believe that this is the first time that the parameters of a Ginzburg-Landau functional and the complete strain spinodal for any three-dimensional displacive transformation were used in simulating the transformation near a crack tip under Mode 1 loading; the transformation pattern and toughening are different from standard transformation toughening theories. Furthermore, the strain spinodal has an approximately conical shape which can be specified by two material dependent experimentally accessible parameters, rather than the ellipsoidal shape in standard theories. Stress induced martensitic transformation in a polycrystalline sample of NiAl was simulated. In the ZrO2 system, first principles calculations to determine the semi-empirical potentials for simulating the cubic-tetragonal and tetragonal-monoclinic transformations were started by doing a more elaborate total energy calculation. In the Al2O3 system, we discovered that the first principles calculations and semi-empirical potentials were completed by another group in England. It is these measurements on which we will base our molecular dynamics simulations. DOE

N93-28656# California Inst. of Tech., Pasadena. Div. of Engineering and Applied Science.
A ONE-DIMENSIONAL CONTINUUM MODEL FOR SHAPE-MEMORY ALLOYS
Rohan Abeyaratne, San-Joo Kim, and James K. Knowles Jan. 1993 40 p Prepared in cooperation with Massachusetts Institute of Technology, Cambridge, MA
(Contract N00014-90-J-1871)
(AD-A262505; TR-11) Avail: CASI HC A03/MF A01

An explicit constitutive model that is capable of describing the thermomechanical response of a shape-memory alloy is constructed. The model consists of a Helmholtz free-energy function, a kinetic relation, and a nucleation criterion. The free-energy is associated with a three-well potential energy function; the kinetic relation is based on thermal activation theory; nucleation is assumed to occur at a critical value of the appropriate energy barrier. The predictions of the model in various quasi-static thermomechanical loadings are examined and compared with experimental observations. DTIC

N93-28679# Oak Ridge National Lab., TN.
ENVIRONMENTAL EMBRITTLEMENT OF BINARY AND Zr-DOPED Ni3Al
E. P. George, C. T. Liu, and D. P. Pope 1992 6 p Presented at the 16th Material Research Society International Symposium on the Scientific Basis for Nuclear Waste Management Fall Meeting, Boston, MA, 30 Nov. - 5 Dec. 1992
(Contract DE-AC05-84OR-21400)
(DE93-008575; CONF-921101-98) Avail: CASI HC A02/MF A01

Single crystals of B-free Ni3Al, were cold rolled and recrystallized to produce crack-free polycrystals. Results show that the intrinsic ductility (approximately 16%) of Ni3Al (23.4 at. % Al) is considerably higher than previously thought; however, it is severely embrittled by moisture in air (ductility dropping from a high of approximately 16% when tested in oxygen to a low of approximately 3% in air). Since B-doped Ni3Al does not show such embrittlement, we conclude that a significant part of the beneficial effect of B must be related to suppression of this environmental effect. However, B must also improve grain boundary (GB) cohesion in Ni3Al, since our B-free alloy fractures intergranularly whereas B-doped alloys in general fracture transgranularly. Addition of 0.26 at. % of Zr to Ni3Al significantly improves its ductility: to 11-13% in air, and 48-51% in oxygen. The ductilities observed in oxygen are comparable to the highest ever ductility observed in B-doped Ni3Al, indicating that the GBs in this Zr-doped alloy are not intrinsically brittle (rather, environmental embrittlement is the main reason for its brittleness). Zr dramatically increases the resistance of Ni3Al to GB fracture perhaps by increasing GB cohesion. However, Auger analysis shows little or no Zr segregation on the GB's of Ni3Al, making it unclear how it might actually affect GB cohesion. Zr does not significantly increase the resistance of Ni3Al to environmental embrittlement; nor does it suppress intergranular fracture. In both these respects Zr behaves differently than B. DOE

N93-28902# Northwestern Univ., Evanston, IL.
TRANSFORMATION PLASTICITY IN DUCTILE SOLIDS
G. B. Olson Feb. 1993 5 p
(Contract DE-FG02-88ER-45365)
(DE93-008636; DOE/ER-45365/5) Avail: CASI HC A01/MF A01

Research has addressed the role of martensitic transformation plasticity in the enhancement of toughness in high-strength austenitic steels, and the enhancement of formability in multiphase low-alloy sheet steels. In the austenitic steels, optimal processing conditions have been established to achieve a significant increase in strength level, in order to investigate the interaction of strain-induced transformation with the microvoid nucleation and shear localization mechanisms operating at ultrahigh strength levels. The stress-state dependence of transformation and fracture mechanisms has been investigated in model alloys, comparing behavior in uniaxial tension and blunt-notch tension specimens. A numerical constitutive model for transformation plasticity has been reformulated to allow a more thorough analysis of transformation/fracture interactions. Processing of a new low alloy steel composition has been optimized to stabilize retained austenite by isothermal bainitic transformation after intercritical annealing. Preliminary results show a good correlation of uniform ductility with the austenite amount and stability. DOE

N93-28957# Northwestern Univ., Evanston, IL. Dept. of Materials Science and Engineering.
BAINITIC STABILIZATION OF AUSTENITE IN LOW ALLOY STEELS
M. L. Brandt and G. B. Olson 1992 9 p Presented at the ISS-AIME Symposium on Fundamentals of Aging and Tempering in Bainitic and Martensitic Steel Products, Warrendale, PA, 25-28 Oct. 1992
(Contract DE-FG02-88ER-45365)
(DE93-008275; CONF-9210322-1) Avail: CASI HC A02/MF A01

Stabilization of retained austenite via bainitic transformation was studied in a triple-phase, ferrite/bainite/austenite steel 0.26C1.52Si-1.2Mn. Volume fraction and stability of retained austenite are varied by isothermal transformation time at 752 F following intercritical annealing at 1418 F. Austenite stability is measured using the Bolling-Richman technique. Austenite content is measured by and austenite carbon content is estimated from lattice parameters. Strength and ductility measured in both uniaxial

and plane-strain tension are correlated with austenite amount and stability. While austenite content peaks at 3 minutes transformation time, stability continues to increase out to 5 minutes associated with a saturation of austenite carbon content and continued refinement of austenite particle size. Despite the reduced austenite content of 8 percent, the higher stability provided by the 5 minutes treatment gives superior mechanical properties.
DOE

N93-29002# Martin Marietta Labs., Baltimore, MD.
ELECTROCHEMICAL BEHAVIOR AND SURFACE CHEMISTRY OF ALUMINUM ALLOYS: SOLUTE-RICH INTERPHASE MODEL Annual Report, 1 Dec. 1991 - 30 Nov. 1992
G. D. Davis, B. A. Shaw, B. J. Rees, E. L. Principe, and C. A. Pecile 31 Mar. 1993 41 p
(Contract N00014-85-C-0638)
(AD-A262061; MML-TR-93-04) Avail: CASI HC A03/MF A01

The electrochemical behavior of physical-vapor-deposited nonequilibrium stainless Al-W and Al-Ta alloys and the electrochemical behavior and surface chemistry of sputter-deposited nonequilibrium stainless Al-Ta alloys have been investigated. Results from the vapor-deposited alloys show that these materials possess enhanced passivity despite the presence of nodules and other defects. The stainless aluminum alloys that exhibit better performance are the sputter-deposited thin films that more uniform. Sputter-deposited Al-Ta alloys exhibit enhanced passivity over a pH range of 2 to 12 even though the passive film chemistry varies considerably over this range. This enhanced passivity can be explained by the solute-rich interphace model (SRIM), which claims that formation and passivation of occluded cells are controlled by localized concentrations of solute. The higher concentrations of solute at the metal-oxide interface and around occluded cells stabilize the passive film from continued chloride attack and dissolution.
DTIC

N93-29012# Joint Publications Research Service, Arlington, VA.
JPRS REPORT: SCIENCE AND TECHNOLOGY. CENTRAL EURASIA: MATERIALS SCIENCE
4 Jun. 1992 17 p Transl. into ENGLISH from various Russian articles
(JPRS-UMS-92-008) Avail: CASI HC A03/MF A01

Translated abstracts cover the following areas: ferrous metals, nonferrous metals and alloys, and nonmetallic materials. Some specific topics include method of measuring equivalent stresses in aircraft gas turbine engine blades; structure and properties of titanium alloys with nitrogen; tribological characteristics of steel surfaces with laser carbide hardening under fluid lubrication friction conditions; scandium-doped aluminum alloys; and effect of hydrogen on structure and mechanical properties of VT3-1 titanium alloy.
CASI

N93-29013# Joint Publications Research Service, Arlington, VA.
JPRS REPORT: SCIENCE AND TECHNOLOGY. CENTRAL EURASIA: MATERIALS SCIENCE
15 Apr. 1992 39 p Transl. into ENGLISH from various Russian articles
(JPRS-UMS-92-007) Avail: CASI HC A03/MF A01

Translated abstracts cover the following areas: analysis and testing, corrosion, ferrous metals, nonferrous metals and alloys, welding and brazing, nonmetallic materials, and metal treatments.
CASI

N93-29015# Joint Publications Research Service, Arlington, VA.
JPRS REPORT: SCIENCE AND TECHNOLOGY. CENTRAL EURASIA: MATERIALS SCIENCE
15 Jun. 1992 65 p Transl. into ENGLISH from various Russian articles
(JPRS-UMS-92-009) Avail: CASI HC A04/MF A01

Translated abstracts cover the following areas: analysis and testing, coatings, composite materials, ferrous metals, nonferrous metals and alloys, nonmetallic materials, and material preparations and treatments. Some specific topics include low-temperature shaping of thick-walled composite rings; effect of static and cyclical loads on elasticity moduli of Al-B composite; technique for cyclical bending tests of thin elastic specimens; an investigation of the compatibility of a titanium alloy matrix with ceramic fibers; effect of titanium nitride coat application conditions on its wear under fretting corrosion; tribological characteristics of polymer composite materials and carbon-carbon composites on their basis; and on radiation strength of carbon-carbon composites.
CASI

N93-29019# Joint Publications Research Service, Arlington, VA.
JPRS REPORT: SCIENCE AND TECHNOLOGY. CENTRAL EURASIA: MATERIALS SCIENCE
13 Oct. 1992 61 p Transl. into ENGLISH from various Russian articles
(JPRS-UMS-92-014) Avail: CASI HC A04/MF A01

Translated abstracts cover the following areas: analysis and testing, coatings, composite materials, ferrous metals, nonferrous metals and alloys, nonmetallic materials, preparations and treatments, welding and brazing, and extractive metallurgy. Some specific topics include electronic and crystal structures of Y-Ba-Cu-O superconductor films with anomalous lattice c-parameter; effect of Dy additions on aluminum structure and properties; ceramic composites; electron microscopy of fracture of TiB2-Fe composites; and effect of thermal cycling on structure of hardened Ti-Ta-Nb system alloys.
CASI

N93-29020# Joint Publications Research Service, Arlington, VA.
JPRS REPORT: SCIENCE AND TECHNOLOGY. CENTRAL EURASIA: MATERIALS SCIENCE
16 Oct. 1992 50 p Transl. into ENGLISH from various Russian articles
(JPRS-UMS-92-015) Avail: CASI HC A03/MF A01

Translated abstracts cover the following areas: analysis and testing, coatings, composite materials, ferrous metals, nonferrous metals and alloys, nonmetallic materials, preparations and treatments, welding, and extractive metallurgy and mining. Some specific topics include roller bearings with solid magnetic powder lubricant; and ceramic and composite materials and their properties.
CASI

N93-29043*# National Aeronautics and Space Administration. Marshall Space Flight Center, Huntsville, AL.
THE ROLE OF GRAIN BOUNDARIES IN HYDROGEN DIFFUSION IN METALS AT 25 C
M. D. Danford Jun. 1993 17 p
(NASA-TM-108407; NAS 1.15:108407) Avail: CASI HC A03/MF A01

The effect of grain size on hydrogen diffusion at 25 C was examined for 4340 steel (body-centered cubic) and for Inconel 718 (face-centered cubic). It was found that the effect of grain size is important for body-centered cubic structures, but plays a much less important role in face centered cubic structures. Accurate measurements of hydrogen desorption coefficients during hydrogen desorption show that these are not greatly different for both types of structures.
Author (revised)

N93-29061# Pacific Northwest Lab., Richland, WA.
OPERATIONAL RESULTS OF PILOT CELL TEST WITH CERMET INERT ANODES
T. R. Alcorn (Reynolds Metals Co., Muscle Shoals, AL.), A. T. Tabereaux (Reynolds Metals Co., Muscle Shoals, AL.), N. E. Richards (Reynolds Metals Co., Muscle Shoals, AL.), C. F. Windisch, Jr., D. M. Strachan, J. S. Gregg (Eltech Systems, Inc., Fairport Harbor, OH.), and M. S. Frederick (Eltech Systems, Inc., Fairport Harbor, OH.) Feb. 1993 12 p Presented at the Annual Meeting of The Metallurgical Society, Denver, CO, 21-25 Feb. 1993
(Contract DE-AC06-76RL-01830)
(DE93-009338; PNL-SA-21117; CONF-930202-4) Avail: CASI HC A03/MF A01

The operational performance of a 'six-pack' of cermet anodes and corrosion rates was evaluated in a six kA pilot reduction cell at Reynolds' Manufacturing Technology Laboratory. Two separate test periods were conducted with the cermet anodes; the first period was in conjunction with the Pacific Northwest Laboratory and the second with ELTECH Research Corporation. Both tests used identical NiO-NiFe2O4-Cu anodes manufactured by Ceramic Magnetics, Inc. The ELTECH testing involved the in situ coating of the anodes with cerium oxide. Primary evaluations for both test periods were conducted at target conditions of alumina saturation and 0.5 amp/sq cm anode current density. Individual anodes remained in operation for 25 days during the two and one-half month testing period. Operational difficulties developed throughout the test due to breakage of the anode conductor stems, cracking and breaking of the cermet anodes, unequal anode current distribution, and alumina muck build-up in the cell. These operational problems are discussed as well as an estimate of anode corrosion rates based on metal impurity levels in the aluminum metal pad.
DOE

N93-29092# New Mexico Inst. of Mining and Technology, Socorro.
REPORT ON THE SINTERING AND PROPERTIES OF MgO AND MgO-5 PERCENT TiC
M. Bengisu and O. T. Inal Jul. 1992 21 p Prepared in cooperation with Los Alamos National Lab., NM
(Contract W-7405-eng-36)
(DE93-008676; LA-Sub-93-11/1) Avail: CASI HC A03/MF A01

Sintering of technical grade MgO yields higher fractional densities compared to pure MgO. TiC reacts with MgO under sintering of MgO-TiC composites in air, yielding Mg2TiO4 and CO or CO2. This can be suppressed in vacuum by plasma sintering. Plasma sintering of MgO at 1300 C and short times does not produce satisfactory results. Five vol% TiC increases the sinterability of MgO during conventional air sintering; larger additions (50 vol%) decrease sinterability due to macropores formed by gaseous reaction product. Microwave sintering of MgO is possible. Mechanical properties of MgO are improved by additions of small amounts of TiC to starting powders. DOE

N93-29101# Pacific Northwest Lab., Richland, WA.
MATERIALS CHARACTERIZATION OF CERMET ANODES TESTED IN A PILOT CELL
C. F. Windisch, Jr., D. M. Strachan, C. H. Henager, Jr., T. R. Alcorn (Reynolds Metals Co., Muscle Shoals, AL.), A. T. Tabereaux (Reynolds Metals Co., Muscle Shoals, AL.), and N. E. Richards (Reynolds Metals Co., Muscle Shoals, AL.) Feb. 1993 11 p Presented at the Annual Meeting of The Metallurgical Society, Denver, CO, 21-25 Feb. 1993
(Contract DE-AC06-76RL-01830)
(DE93-008924; PNL-SA-21085; CONF-930202-5) Avail: CASI HC A03/MF A01

Cermet anodes were evaluated as nonconsumable substitutes for carbon anodes using a pilot-scale reduction cell at the Reynolds Manufacturing Technology Laboratory. After pilot cell testing, tile anodes were subjected to extensive materials characterization and physical properties measurements at the Pacific Northwest Laboratory. Significant changes in the composition of the cermet anodes were observed including the growth of a reaction layer and penetration of electrolytes, deep into the cermet matrix. Fracture strength and toughness were measured as a function of temperature and the ductile-brittle transition was reduced by 500 C following pilot cell testing. These results imply difficulties with anode material and control of operating conditions in the pilot cell, and suggest that additional development work be performed before the cermet anodes are used in commercial reduction cells. The results also highlight specific fabrication and operational considerations that should be addressed in future testing. DOE

N93-29102# Argonne National Lab., IL.
INTERIM FATIGUE DESIGN CURVES FOR CARBON, LOW-ALLOY, AND AUSTENITIC STAINLESS STEELS IN LWR ENVIRONMENTS
S. Majumdar, O. K. Chopra, and W. J. Shack Jan. 1993 17 p Presented at the 20th Water Reactor Safety Information Meeting, Bethesda, MD, 21-23 Oct. 1992
(Contract W-31-109-eng-38)
(DE93-009202; ANL/MCT/CP-78588; CONF-921007-23) Avail: CASI HC A03/MF A01

Both temperature and oxygen affect fatigue life; at the very low dissolved-oxygen levels in pressurized water reactors (PWR's) and Boiling Water Reactors (BWR's) with hydrogen water chemistry, environmental effects on fatigue life are modest at all temperatures (T) and strain rates. Between 0.1 and 0.2 ppM, the effect of dissolved-oxygen increases rapidly. In oxygenated environments, fatigue life depends strongly on strain rate and T. A fracture mechanics model is developed for predicting fatigue lives, and interim environmentally assisted cracking (EAC)-adjusted fatigue curves are proposed for carbon steels, low-alloy steels, and austenitic stainless steels. DOE

N93-29144# Wright Lab., Wright-Patterson AFB, OH.
MICROSTRUCTURAL EFFECTS ON THE DEFORMATION AND FRACTURE OF THE ALLOY Ti-25Al-10Nb-3B-1Mo Final Report, 1 Jul. 1988 - 15 Dec. 1992
Charles H. Ward, Jr. Dec. 1992 211 p
(AF Proj. 2306)
(AD-A263095; WL-TR-92-4104) Avail: CASI HC A10/MF A03

The effects of microstructure and temperature on tensile and fracture behavior were explored for the titanium aluminide alloy Ti-25Al-10Nb-3V-1Mo (atomic percent). Three microstructures were selected for this study in an attempt to determine the role of the individual microstructural constituents. The three microstructures studied were an alpha-2 + beta processed microstructure with a fine Widmanstaetten microstructure, a beta processed microstructure with a fine Widmanstaetten microstructure, and a beta processed microstructure with a coarse Widmanstaetten microstructure. Tensile testing of both round and flat specimens was conducted in vacuum at elevated temperature and in air at room and elevated temperatures. Extensive fractography and specimen sectioning were used to study tensile deformation and the effects of environment on this alloy. Room temperature fracture toughness testing using compact tension specimens was conducted. Elevated temperature toughness testing was performed using J-bend bar specimens in an air environment. Again, extensive fractography and specimen sectioning were used to study the elevated temperature toughening mechanisms of this alloy. DTIC

N93-29172*# National Aeronautics and Space Administration. Lewis Research Center, Cleveland, OH.
HIGH TEMPERATURE CREEP AND OXIDATION RESISTANT CHROMIUM SILICIDE MATRIX ALLOY CONTAINING MOLYBDENUM Patent Application
Sai V. Raj, inventor (to NASA) 26 May 1993 14 p
(NASA-Case-LEW-15697-1; NAS 1.71:LEW-15697-1;
US-Patent-Appl-SN-067184) Avail: CASI HC A03/MF A01

Cr3Si is alloyed with molybdenum which produces a two-phase micro structure of (Cr,Mo)3Si and (Cr,Mo)5Si3. The alloy forms two protective oxides over a wide range of temperatures. Chromium and molybdenum oxide volatize under flowing air at high temperatures above 1200 C which facilitates the formation of SiO2 on the surface. Below 1200 C Cr203 is formed. The new alloy has excellent high temperature strength and creep properties. NASA

N93-29256# Brookhaven National Lab., Upton, NY.
POTENTIAL TRANSMISSION AND TRANSIENTS DURING CORROSION: APPLICATIONS TO CORROSION MONITORING
H. S. Isaacs and Jeong-Hwan Cho 1992 11 p Presented at the International Conference on Advances in Corrosion and Protection, Manchester, England, 28 Jun. 1992
(Contract DE-AC02-76CH-00016)
(DE93-010863; BNL-48601; CONF-9206234-2) Avail: CASI HC A03/MF A01

The transmission of potential along a passive metal/electrolyte interface, which is important in corrosion monitoring, has been considered for transitory and sustained corrosion processes. The observed signals are modified and delayed by the passive surface. Using a transmission line as the equivalent circuit of a pipe and incorporating the impedance characteristics of the passive-metal/solution interface, enabled an analysis of the effectiveness of corrosion monitoring methods to be performed. DOE

N93-29259# International Business Machines Corp., San Jose, CA. Almaden Research Center.
IN SITU FOURIER TRANSFORM INFRARED SPECTROSCOPIC STUDY OF BISULFATE AND SULFATE ADSORPTION ON GOLD, WITH AND WITHOUT THE UNDERPOTENTIAL DEPOSITION OF COPPER
Diane B. Parry, Mahesh G. Samant, H. Seki, Michael R. Philpott, and Kevin Ashley 14 Apr. 1993 46 p
(Contract N00014-92-C-0173)
(AD-A263421; TR-05) Avail: CASI HC A03/MF A01

In situ surface infrared (IR) spectroelectrochemistry is used to investigate the adsorption of sulfate (SO4(2-)) and bisulfate (HSO(4-)) ions on polycrystalline gold surfaces in sodium sulfate and sulfuric acid, and also during copper underpotential deposition in sulfuric acid medium. In sodium sulfate solution, IR peaks due to surface sulfate and bisulfate are observed at potentials within the double-layer region on gold, and the ratio of IR peak intensities for sulfate to bisulfate increases as the applied potential is made more negative. In sulfuric acid, surface IR spectra indicate that adsorbed sulfate is favored at more positive potentials, while adsorbed bisulfate is prevalent at more negative voltages; also, a potential-dependent reorientation of water is observed in the spectra. IR spectroelectrochemical data from a sulfuric acid system containing copper sulfate indicate that adsorbed sulfate is present on gold at more positive potentials, and its coverage increases when underpotentially deposited (UPD) copper is present on the gold substrate surface. DTIC

N93-29265# Westinghouse Savannah River Co., Aiken, SC.

EFFECTS OF INTERNAL HELIUM ON MECHANICAL PROPERTIES OF NITRONIC (TM) 40 STAINLESS STEEL

W. C. Mosley 1993 4 p Presented at the 18th Department of Energy (DOE) Compatibility, Aging and Service Life Conference, Aiken, SC, 20-22 Apr. 1993
(Contract DE-AC09-89SR-18035)
(DE93-009902; WSRC-MS-93-134; CONF-9304103-2) Avail: CASI HC A01/MF A01

This report describes results of tests on annealed Nitronic 40 stainless steel containing 0.0, 0.26, and 2.6 appM helium-3 (He-3), over the temperature range 25-842 C. Ultimate tensile strength, 0.2% offset yield strength, total elongation, uniform elongation, nonuniform elongation, and reduction-in-area were measured. The predominant effect of He-3 is decreased ductility caused by inhibition of necking. Annealed Nitronic 40 exhibits greater sensitivity to internal He-3 than solution-annealed Incoloy 903 and high-energy-rate forged 316L stainless steel. DOE

N93-29272# European Space Agency, Paris (France).

ALUMINIUM-HIGH STRENGTH MATERIAL BY MECHANICAL ALLOYING AND REACTION MILLING: BASICS OF PROCESSING AND CHARACTERISATION OF MATERIAL

Hugo Schlich (Bosch, Robert G.m.b.H., Herne, Germany.) and Manfred Thumann (ABB Corporate Research, Baden, Switzerland.) Nov. 1992 90 p Transl. into ENGLISH of Aluminium-Hochleistungswerkstoffe Durch Mechanisches Legieren und Reaktionsmahlen: Grundlagen der Verarbeitung und Werkstoffcharakterisierung (Cologne, Germany, DLR) Jul. 1990 p 1-89 Original language document was announced as N91-18244
(ESA-TT-1249; DLR-FB-90-29; ETN-93-93711) Avail: CASI HC A05/MF A01; Original German version available from DLR, Wissenschaftliches Berichtswesen, VB-PL-DO, Postfach 90 60 58, 5000 Cologne, Germany, HC

Basic investigations in the production and consolidation of atomized, mechanically alloyed and atomized, and additionally milled Al alloy powder are presented and correlated with the mechanical properties of the compacts. By optimization of the processing techniques and parameters, especially of the degassing treatment, an improved strength at elevated temperatures was achieved. However, the ductility is still low and further improvements are necessary. ESA

N93-29391# Defence Research Establishment Suffield, Ralston (Alberta).

EXPERIMENTAL STUDY OF LOCATION AND IDENTIFICATION OF FERROUS SPHEROIDS USING A SMART TOTAL FIELD MAGNETOMETER

John E. McFee, Robert Ellingson, and Yogadhish Das Jan. 1993 109 p
(AD-A263661; DRES-SR-582) Avail: CASI HC A06/MF A02

A microprocessor-controlled magnetometer which accurately locates and identifies compact ferrous objects in real-time is described. The person-portable instrument consists of a cart-mounted cesium magnetometer, optical encoder, microcontroller, interface, and laptop computer. The instrument guides the operator to collect simultaneous magnetic field and position data in a horizontal plane above an object. Custom algorithms estimate location and dipole moment and use the latter to classify the object. Data collection takes 6 - 13 minutes, location and moment estimation 5 seconds, classification 30 seconds. Experiments using two ferrous spheroids and studies using magnetic total field and vertical component magnetic maps generated by a mathematical computer model are described. Limits of error in estimation of location and dipole moment, error in classification, and relative effects of sources of error are quantified. The rms error for location vector components was 0.019 m - 0.045 m compared to the average precision of 0.003 m - 0.005 m. The average magnitude of the difference between estimated and theoretical dipole moment vectors as a percentage of the theoretical dipole moment was 24.5 +/- 11.4% compared to precision of 0.51 - 8.21%. Pattern classification with a computer generated dipole moment design set is described. Deviation between experimental moment estimates and the computer model degraded performance but the misclassification rate for the two objects for which experimental measurements were made was 11.1%. If an experimental design set were used, analysis shows that the limiting misclassification error for the present experimental precision should be between 2 and 5%. DTIC

N93-29786# Oak Ridge National Lab., TN.

LOW TEMPERATURE ENVIRONMENTAL EMBRITTLEMENT IN ORDERED INTERMETALLICS

N. S. Stoloff (Rensselaer Polytechnic Inst., Troy, NY.) and C. T. Liu 1992 43 p Presented at the Workshop on Ordered Intermetallics, Honzhou, China, 28 Sep. - 1 Oct. 1992
(Contract DE-AC05-84OR-21400)
(DE93-009711; CONF-9209328-1) Avail: CASI HC A03/MF A01

There are two types of environmental degradation in intermetallics: hydrogen-induced embrittlement occurring at ambient temperatures, and oxygen-induced embrittlement in air at high temperatures. This review is confined to low-temperature embrittlement and discusses metallurgical means of alleviation. Environmentally induced embrittlement is both pernicious and complex. The low ductility and toughness of many ordered alloys, especially aluminides, at room temperature (RT) is now known to arise from an extrinsic effect. Exclusion of moisture or other sources of H from environment causes Ni3Al, Ni3Si, Fe3Al, and FeAl to display high elongations. However, even when H is excluded, other aluminides (NiAl, CoAl, TiAl, Ti3Al) exhibit little or no RT ductility. Reasons for this difference is complex; the number of independent slip systems, bonding, and differences in environmental susceptibility are the most obvious factors affecting ductility. Grain size/shape, alloy texture, and impurity content are among the factors influencing environmental embrittlement. Each factor needs to be studied for most intermetallics for possible structural applications. DOE

N93-29799# Pennsylvania State Univ., University Park. Dept. of Materials Science and Engineering.

MECHANISMS OF FRACTURE AND CREEP OF STRUCTURAL ALLOYS Annual Report, 1 Jan. 1992 - 28 Feb. 1993

D. A. Koss 29 Mar. 1993 37 p
(Contract N00014-91-J-1414)
(AD-A263108; TR-6) Avail: CASI HC A03/MF A01

Progress is reviewed for research which focuses on two aspects which limit the performance of structural alloys. First, in a study generic to a wide range of materials, we are determining the mechanisms, as well as local failure criteria, by which voids grow, interact and link during ductile fracture due to damage accumulation. Secondly, in a study focused specifically at high strength titanium alloys, we are examining the deformation and fracture behavior of novel beta titanium alloy Ti-23Nb-11Al, which is age-hardenable by the formation of ordered precipates based on Ti3Al. Progress for the period January 1, 1992 to February 28, 1993 is reviewed for the following projects: (1) two-dimensional modeling studies of void linking during ductile, microvoid fracture, (2) a three-dimensional experimental modeling study void growth and linking during ductile fracture, and (3) the influence of temperature on the deformation and oxidation behavior of a new age-hardenable beta titanium alloy. DTIC

N93-29803# Northeastern Univ., Boston, MA. Dept. of Physics.

INTERFACIAL VISCOSITY MEASUREMENTS OF ADSORBED MONOLAYERS ON METAL SURFACES Final Report, 1 May 1990 - 31 Oct. 1992

Jacqueline Krim 31 Oct. 1992 5 p
(Contract N00014-89-J-1853)
(AD-A263288) Avail: CASI HC A01/MF A01

At the outset of this project, we had just developed a technique, employing a quartz crystal microbalance, for measuring the sliding friction coefficient of a molecularly thin film adsorbed on a metal surface. Funding of the project allowed us to carry out a range of measurements documenting the friction coefficient under various circumstances. The measurements were the first of any kind to quantitatively probe how much force is required on average to slide an atom across an interface, and were in the mainstream of the emerging field of nanotribology (a word coined by our group). They hold the world record for the shortest time scale on which friction experiments have been carried out, allowing them to be exactly modelled by molecular dynamics simulations. DTIC

N93-29813# Oak Ridge National Lab., TN.
SOME EFFECTS OF COMPOSITION AND MICROSTRUCTURE ON THE B2 IN EQUILIBRIUM TO DO3 ORDERED PHASE TRANSITION IN Fe3Al ALLOYS
P. J. Maziasz, C. G. McKamey, O. B. Cavin, C. R. Hubbard, and T. Zacharia 1992 9 p Presented at the 16th Material Research Society International Symposium on the Scientific Basis for Nuclear Waste Management Fall Meeting, Boston, MA, 30 Nov. - 5 Dec. 1992
(Contract DE-AC05-84OR-21400)
(DE93-009724; CONF-921101-102) Avail: CASI HC A02/MF A01

Binary Fe-28 at.% Al alloys (Fe3Al-type) transform from B2 yields DO3 ordered phases at 550 C upon cooling. More complex Fe-28Al alloys can have B2 yields DO3 transition temperatures that range from 530 to 670 C. Kinetics of the B2 yields DO3 ordered phase transition also appear to be affected by alloy composition and by matrix dislocation microstructure. The binary and Nb-containing ternary alloys have rapid B2 yields DO3 transition kinetics during cooling. However, the ternary or more complex alloys that contain Cr have relatively slower phase transition kinetics during similar cooling. Deformation of a complex Fe-28Al-5Cr alloy in the B2 phase regime creates a very high matrix dislocation concentration, which coincides with complete suppression of the B2 yields DO3 phase transition during cooling. DOE

N93-29981# Pittsburgh Univ., PA. Dept. of Materials Science and Engineering.
PLATINUM-MODIFIED DIFFUSION ALUMINIDE COATINGS ON NICKEL-BASE SUPERALLOYS Final Report, Jun. 1985 - Jun. 1988
G. M. Kim, G. H. Meier, and F. S. Pettit Mar. 1993 32 p
(Contract DAAG46-85-K-0008)
(AD-A263597; ARL-CR-50) Avail: CASI HC A03/MF A01

Conventional and platinum modified diffusion aluminide coatings on some state-of-the-art single crystal and polycrystalline nickel-base superalloys have been compared in tests designed to establish conditions representative of those existing in gas turbines operating over a range of applications. Resistance of these coatings to oxidation, high temperature hot corrosion, and low temperature hot corrosion have been compared. Platinum has been found to significantly improve the resistance of diffusion aluminides to all of these forms of degradation but the improvement with regard to low temperature hot corrosion is not as great as in the case of the other two forms of attack. Substrate composition has been found to exert a very significant effect on the lives of coatings in the high temperature tests. In the case of high temperature oxidation elements such as Hf are important in that they extend coating lives whereas for high temperature hot corrosion the type and concentration of refractory elements are significant factors affecting coating lives. A limited number of experiments have indicated intermittent hot corrosion exposures degrade the subsequent cyclic oxidation resistance of Pt-aluminide coatings. DTIC

N93-30059# Northwestern Univ., Evanston, IL.
ORGANOMETALLIC AND SURFACE CHEMISTRY OF MIXED-METAL SYSTEMS
D. F. Shriver Apr. 1993 4 p
(Contract DE-FG02-86ER-13640)
(DE93-012686; DOE/ER-13640/6) Avail: CASI HC A01/MF A01

Three new SO2 complexes of metal cluster compounds were prepared: (PPN)(HFe3)(CO9)SO2, and (PPN2)(Ru3)(CO9)SO2, and (PPN2(Ru3)(CO7)(SO2)sub3). The x-ray structures were determined for two of these and the transformation of bound SO2 to duster bound SO and S ligands was investigated. DOE

N93-30060# Maine Univ., Orono.
STRUCTURE, ADHESION, AND STABILITY OF METAL/OXIDE AND OXIDE/OXIDE INTERFACES
R. J. Lad Nov. 1992 9 p
(Contract DE-FG02-90ER-45417)
(DE93-012930; DOE/ER-45417/4) Avail: CASI HC A02/MF A01

Studies of structural, electronic, and chemical properties of metal/oxide and oxide/oxide interfaces were performed on well-defined interfaces that were created by depositing ultra-thin potassium and aluminum films and their oxides onto single crystal TiO2 and NiO surfaces. Work focused on the following: determining the structure, growth mechanisms, and morphologies of metal and oxide films as they are deposited on single crystal oxide surfaces using RHEED and atomic force microscopy; probing electronic structure, bonding, and chemical interactions at the interfaces using x-ray and uv photoelectron spectroscopies (XPS, UPS) and Auger electron spectroscopy (AES); and understanding factors affecting stability and reactivity of the interface regions including the role of defects and impurities. Results indicate that kinetic effects have an important influence on interface structure and composition, and they also show that defects in the oxide substrate induce new electronic states at the interface which play a major role in cation-anion bonding and interface interactions. The results establish a link between electronic and chemical bonding properties and the interface structure and morphology, which is required to successfully manipulate the interfacial properties of advanced ceramic materials. DOE

N93-30105# European Space Agency, Paris (France).
IMPROVEMENT IN DUCTILITY OF THE INTERMETALLIC COMPOUND Ti3Al
Isabelle Ehrhart (Office National d'Etudes et de Recherches Aerospatiales, Paris, France.) Aug. 1992 179 p Transl. into ENGLISH of Contribution a l'Amelioration de la Ductilite du Compose Intermetallique Ti3Al (Paris, France, ONERA) 1991 p 1-143 Original language document was announced as N92-19440
(ESA-TT-1276; ONERA-NT-1991-6; ETN-93-93716) Avail: CASI HC A09/MF A02

Adding a beta-stabilizing element like vanadium to Ti3Al improves ductility by refining the microstructure and retaining the high temperature beta phase. The beta phase has an ordered structure of the B2 type. Its transformation during aging at 400 or 500 C was studied by transmission electron microscopy. The ordered omega phase which precipitates in beta undergoes a complex reordering reaction over prolonged aging times. The equilibrium alpha(sub 2) phase appears within the beta matrix at higher aging temperatures. Investigation of ternary Ti3Al + V alloys with a duplex alpha(sub 2) + beta microstructure revealed that the addition of about 10 at.% V is required to obtain a sufficient degree of ductility at room temperature. Their tensile strength and elongation to rupture depend on the volume fraction and morphology of the two phases, which can be varied by following thermomechanical and heat treatments. An attempt was made to improve the plasticity of the alpha(sub 2) phase by introducing lattice defects in the ordered structure. The effect of deviations from stoichiometry and addition of zirconium or tin was investigated. A decrease in aluminum content enhances ductility quite significantly while zirconium improves the strength and tin has very little effect. A vanadium content of more than 4 at.% has a detrimental effect on the oxidation resistance of Ti3Al. ESA

N93-30115# Messer Griesheim G.m.b.H., Frankfurt am Main (Germany).
LASER GAS ALLOYING OF TITANIUM MATERIALS Final Report [LASERGASLEGIEREN VON TITANWERKSTOFFEN. ABSCHLUSSBERICHT]
D. Mueller (Erlangen-Nuremberg Univ., Germany.), H. W. Bergmann (Erlangen-Nuremberg Univ., Germany.), H. Sibum (Deutsche Titan G.m.b.H., Essen, Germany.), L. Bakowsky, and E. Kappelsberger 1992 36 p In GERMAN
(Contract BMFT-13-N-5439/6)
(ETN-93-93805) Avail: CASI HC A03/MF A01

The production of titanium nitrides and carbides by laser fusion with methane or nitrogen as a reaction gas is considered. The process parameters, such as optical elements, energy, radiation absorption, and their influence in ceramics layer quality, were examined. It is highlighted that nitrogen allows a higher surface hardness and a larger layer thickness than methane. The process gas composition is shown to be important: surface hardness increases with nitrogen/argon mixture ratio and with gas flow angle. A eutectic titanium iron alloy was deposited on cast iron and carbon steel substrates by low pressure plasma spraying and it was melted with a dioxide carbon laser by using varied process gases. TiC is shown to be produced by reaction with carbon of cast iron, and the intermetallic TiFe is produced in the layer. ESA

N93-30138# Office National d'Etudes et de Recherches Aerospatiales, Paris (France).

PLASTIC DEFORMATION BEHAVIOUR OF OXIDE DISPERSION STRENGTHENED TITANIUM ALLOYS Ph.D. Thesis - Paris VI Univ., 1989 [ETUDE DE LA DEFORMATION PLASTIQUE D'ALLIAGES DE TITANE A DISPERSION D'OXYDES DE TERRES RARES]

Christian Perrier Sep. 1990 159 p In FRENCH
(ONERA-NT-1990-6; ETN-93-93725) Avail: CASI HC A08/MF A02

The comparison of plastic deformation behavior of dispersion strengthened titanium (with small Y2O3 particles) with unalloyed titanium is reported. In each temperature domain, the contribution of dispersion strengthening was studied, especially compared with that of interstitial impurities. In high temperature range (500 to 700 C), a detailed study of creep properties showed that dislocation mechanisms control the creep behavior of both binary Ti-Y alloys and unalloyed Ti. The strengthening is the consequence of the increasing of the internal stress (threshold stress). It was shown that dislocation-particle attractive interaction mechanisms control the dislocation motion. It was also apparent that the presence of interstitial impurities (carbon or oxygen) may drastically improve the creep strength of alpha titanium. In the intermediate temperature range (300 to 500 C), the study of Dynamic Strain Aging (DSA) and Static (or relaxation) Aging (SA) was conducted. The experimental results were compared with the most recent developments of DSA and SA models. A model for transients after SA and strain rate change tests is proposed. In the low temperature range (below 300 C and especially below room temperature), the deformation of titanium is controlled by Peierl's mechanisms. The most important strengthening factor is thus the oxygen (or carbon) content. The influence of the oxide dispersion is quite negligible so that the binary Ti-Y alloys are softer than unalloyed Ti (containing oxygen). ESA

N93-30191# Japan Atomic Energy Research Inst., Tokai.

IRRADIATION ASSISTED STRESS CORROSION CRACKING OF STAINLESS STEEL IRRADIATED IN FBR

Takashi Tsukada, Kiyoyuki Shiba, and Hajime Nakajima Nov. 1992 49 p
(DE93-764495; JAERI-M-92-165) Avail: CASI HC A03/MF A01

Japan Atomic Energy Research Institute (JAERI) and Power Reactor and Nuclear Fuel Development Corporation (PNC) initiated a cooperative research on the evaluation of fracture behaviors of neutron irradiated material in 1991. The research program includes a study of stress corrosion cracking (SCC) of the wrapper tube material of fuel assembly irradiated in the experimental fast reactor 'JOYO'. By August 1992 SCC tests by the slow strain rate technique (SSRT) were carried out on the irradiated material. In this cooperative program the wrapper tube material of type 316 stainless steel irradiated in 'JOYO' up to a neutron fluence of 8 x 10(sup 22) n/cm(sup 2) (E greater than 0.1 MeV) at about 425 C was tested by SSRT at 60 C, 200 C and 300 C in the water environment at the hot laboratory of JAERI. The tests showed that the irradiated wrapper tube material fractured by fully ductile mode at 60 C in high purity water with dissolved oxygen of 32 ppm but it was fractured by intergranular cracking at 300 C in the same environment. It is concluded that the stainless steel irradiated in FBR has no susceptibility to SSC at 60 C but susceptibility appears at the higher temperatures in the water. DOE

N93-30389# Lawrence Livermore National Lab., CA.

ORDER-DISORDER TRANSFORMATIONS IN Ni-Al ALLOYS

M. Sluiter and P. E. A. Turchi Aug. 1992 5 p Presented at the 2nd International Conference and Exhibition on Computer Applications to Materials and Molecular Science and Engineering, Yokohama, (Japan), 22-25 Sep. 1992
(Contract W-7405-eng-48)
(DE93-009293; UCRL-JC-109944; CONF-920927-3) Avail: CASI HC A01/MF A01

A brief introduction to the first-principles electronic theory of alloy phase stability is presented and applied to the study of phase equilibria in Ni-rich Ni-Al alloys. The thermodynamics of phases based on the fcc and bcc lattices are treated within various approximate solutions to the Ising Hamiltonian by means of the Cluster Variation Method and phase diagrams are computed. Particular attention is paid to the existence of the ordered phase at Ni5Al3 at low temperatures. It must be noted that only fcc- and bcc-based phases are considered and that the liquid alloy is ignored. DOE

N93-30396 Japan Atomic Energy Research Inst., Tokai.

EXAMINATION OF FORMABILITY TO SEAMLESS TUBES ON Ni-Cr-W SUPERALLOY

Hirokazu Tsuji, Hajime Nakajima, Masao Ohashi, and Masahiro Takemura Oct. 1992 138 p Limited Reproducibility: More than 20% of this document may be affected by microfiche quality
(DE93-764158; JAERI-M-92-148) Avail: CASI HC A07

Research and development have been carried out on the new superalloys as a component material for process heating high-temperature gas-cooled reactors with coolant outlet temperatures of around 1000 C, and the optimum chemical composition has already been proposed. The program had set some targets. One of them is formability to 32-mm-outer dia., 4- to 5-mm-thick, 7-m-long seamless tubes. Hence formability and solution treatment conditions were examined by producing seamless tubes from 2000 kg scale ingot of the proposed optimum Ni-Cr-W superalloy. Based on the obtained results, the following conclusions are drawn: (1) Newly developed Ni-Cr-W superalloy possesses sufficient formability to seamless tubes in both hot- and cold-workability. (2) The grain size of the seamless tubes can be adjusted in a range of ASTM No. 2 to 3 by solution treated at 1230 to 1240 C. DOE

N93-30399 Japan Atomic Energy Research Inst., Tokyo.

DEVELOPMENT OF Ni-Cr-W SUPERALLOYS FOR HIGH TEMPERATURE COMPONENTS IN HIGH TEMPERATURE GAS-COOLED REACTORS, PART 2

Sep. 1992 84 p Limited Reproducibility: More than 20% of this document may be affected by microfiche quality
(DE93-764469; JAERI-M-92-137) Avail: CASI HC A05

Research and development have been carried out on the new superalloys as a component material for process heating high temperature gas-cooled reactors with coolant outlet temperatures of around 1000 C. The program aims at developing new superalloys which are well balanced in high temperature strength, corrosion resistance, producibility, weldability, etc. This report, the second series of development of Ni-Cr-W superalloys, is describing the results of the qualification tests performed by the Subcommittee on Advanced Superalloys from FY 1987 to FY 1990 for the evaluation of the fourth, the fifth and the sixth experimental alloys after the interim report, i.e., the first series. Based on the obtained results, it has been concluded that Ni - 18 to 19 mass % Cr - 20 to 22 mass % W - 0.03 mass % C - 0.08 mass % Ti - 0.02 to 0.05 mass % Zr - 0.002 to 0.007 mass % Y - 0.0035 to 0.006 mass % B is the optimum chemical composition. DOE

N93-30486# Los Alamos National Lab., NM.

CONSTITUTIVE LAWS FOR DEFORMATION AND DYNAMIC RECRYSTALLIZATION IN CUBIC METALS

U. F. Kocks and S. R. Chen 1993 9 p Presented at the 7th International Symposium of the Japan Institute of Metals: Aspects of High Temperature Deformation and Fracture of Crystalline Materials, Nagoya, Japan, 28-31 Jul. 1993
(Contract W-7405-eng-36)
(DE93-010740; LA-UR-93-1065; CONF-930729-1) Avail: CASI HC A02/MF A01

We describe two cases in which constitutive laws for deformation kinetics are available that are both physically well founded and experimentally well obeyed. New experiments on Al-Mg alloys, in the regime of viscous deformation, fit the solute drift equation very well, with n-3 and Q(sub D) unadjustable; they do not fit the solute drag model. The high-stress regime, as well as all data for pure copper, fit the model of hardening and dynamic recovery, at least up to temperatures of 0.6 T(sub m). In both cases, dynamic recrystallization occurs at high temperatures. It seems to follow rather than determine the deformation kinetics. DOE

N93-30490# Lawrence Livermore National Lab., CA.

PHOTO-DESORPTION FROM COPPER ALLOYS

W. A. Barletta, M. Calderon, C. Foerester, H. Halama, and G. Korn Jul. 1992 9 p Presented at the International Conference on High Energy Accelerators, Hamburg, Germany, 20-24 Jul. 1992
(Contract W-7405-eng-48)
(DE93-011872; UCRL-JC-109741; CONF-920706-51) Avail: CASI HC A02/MF A01

In support of PEP-2, a high luminosity B factory, photodesorption of Cu alloys were measured to demonstrate suitability for ultra-high performance under high radiation loads. Results show that eta(sub eff) less than or = 2 x 10(exp -6) mol/photon is a practical design value for Cu vacuum chambers. Commissioning times to attain this value in B factories can be expected to be less than 50 h. Pre-cleaning with Ar glow discharge was shown to be effective. DOE

N93-30538# Army Armament Research, Development and Engineering Center, Watervliet, NY. Benet Lab.
THE ELECTRODEPOSITION OF LOW CONTRACTION CHROMIUM USING HIGH/LOW CURRENT PULSING
Mark D. Miller and Stephen Langston Mar. 1993 17 p
(AD-A264475; ARCCB-TR-93012) Avail: CASI HC A03/MF A01

The effects of high/low current pulse plating on the electrodeposition of low contraction (LC) chromium were evaluated and compared to direct current-electrodeposited LC chromium with respect to microstructure and mechanical properties. A systematic experiment was performed in which three high/low current densities, 200/100, 200/60, and 200/30 A/dm(exp 2), were tested. The high current density time was varied from 0.6 to 60 ms, while the low current density time was kept constant at 30 ms. A high/low condition of 200/100 A/dm(exp 2) for 0.6/30 ms resulted in the overall optimal microstructure and mechanical properties with a resulting hardness value of 900 KHN, a cathode current efficiency of 22.1 percent, and an ultimate tensile strength of 25.8 Ksi. The deposit at this condition was crack-free with a typical columnar microstructure of fine fibrous grains and a (211) preferred orientation. DTIC

N93-30574# Rensselaer Polytechnic Inst., Troy, NY. Dept. of Chemistry.
COORDINATION COMPOUNDS OF ALUMINUM AS PRECURSORS TO ALUMINUM NITRIDE Technical Report No. 8
Leonard V. Interrante May 1993 17 p
(Contract N00014-91-J-1917)
(AD-A264700) Avail: CASI HC A03/MF A01

Two different systems were examined as potential sources of aluminum nitride, an important electronic and structural ceramic material. Cyclic organoaluminium amides obtained as intermediates in the thermolysis of trialkylaluminium: ammonia Lewis acid-base complexes were used to obtain AIN powder and as precursors for the chemical vapor deposition of AIN films. The structures of two of these intermediates were determined by single-crystal x-ray diffraction (XRD) and the kinetics and thermodynamics of their formation and thermal decomposition reactions were also studied. The second system employs ethylenediamine as the Lewis base in combination with the R3Al(R= Me, Et) compounds. A 2:1 ratio of Et3Al with en yields a hydrocarbon-soluble, polymeric amide on thermolysis, which can be used to prepare AIN films by solution coating followed by pyrolysis in NH3. Lower proportions of R3Al to en, on thermolysis, lead to the formation of R(sub m)Al(en-2H)(sub n) cluster species that contain 5- and 6-coordinated Al atoms chelated and bridged by en-2H ligands. On further heating, these cluster species apparently go on to form cross-linked, insoluble, polymeric networks through condensation reactions involving the multiple N-H and R-Al groups on the periphery of the duster molecules. The structures of two of these Al-en duster compounds were determined by single-crystal XRD. DTIC

N93-30623# Joint Publications Research Service, Arlington, VA.
JPRS REPORT: SCIENCE AND TECHNOLOGY. CENTRAL EURASIA: MATERIALS SCIENCE
2 Apr. 1993 26 p Transl. into ENGLISH from various Russian articles
(JPRS-UMS-93-003) Avail: CASI HC A03/MF A01

Papers on Central Eurasia: Materials Science are provided. Topics covered include: analysis and testing, nonmetallic materials, preparation, treatments, and extractive metallurgy and mining. CASI

N93-30652# Oak Ridge National Lab., TN.
REACTIVE SINTERING OF NI3AI INTERMETALLIC ALLOYS UNDER COMPRESSIVE STRESS
K. H. Wu (Florida International Univ., Miami.) and C. T. Liu 1992 6 p
Presented at the 16th Material Research Society International Symposium on the Scientific Basis for Nuclear Waste Management Fall Meeting, Boston, MA, 30 Nov. - 5 Dec. 1992
(Contract DE-AC05-84OR-21400)
(DE93-009729; CONF-921101-109) Avail: CASI HC A02/MF A01

Synthesis of the Ni-25% at. Al intermetallic compound by the thermal explosion mode subject to the application of compressive stress was systematically investigated. The stress was applied prior to the reaction. It was proved that the compressive stress had a profound effect on the reaction, as well as the densification. At a relatively low stress, a full reaction could be completed and the major phase of the final product is Ni3Al. At higher stresses, a partial reaction was resulted, and the final product was primarily the intermediate phases, Ni and NiAl. Three distinct reaction products were obtained in this study. When the stress was below approximately 5 MPa, a fully reacted product was obtained. Between 5 and 15 MPa, a fully and partially reacted zone coexisted. Above 15 MPa, only a partial reaction prevailed. In this experiment, a final product of 99.9% relative density was obtained at the high stress level. DOE

N93-30778# International Centre for Theoretical Physics, Trieste (Italy).
EFFECTIVE INTERACTIONS BETWEEN CONCENTRATION FLUCTUATIONS AND CHARGE TRANSFER IN CHEMICALLY ORDERING LIQUID ALLOYS
Z. Akdeniz and M. P. Tosi Aug. 1992 10 p
(DE93-606724; IC-92/204) Avail: CASI HC A02/MF A01 (US Sales Only)

The correlations between long-wavelength fluctuations of concentration in a liquid binary alloy are determined by a balance between an elastic strain free energy and an Ornstein-Zernike effective interaction. The latter is extracted from thermodynamic data in the case of the Li-Pb system, which is well known to chemically order with stoichiometric composition corresponding to Li4Pb. Strong attractive interactions between concentration fluctuations near the composition of chemical ordering originate from electronic charge transfer, which is estimated from the electron-ion partial structure factors as functions of composition in the liquid alloy. DOE

N93-30812# Army Research Lab., Watertown, MA.
OXIDATION AND HOT CORROSION OF SUPERALLOYS RENE 100 AND X-40 AT TEMPERATURES OF 1475 F TO 2000 F Final Report
M. Levy, J. J. Falco, and F. Pettit Feb. 1993 25 p
(AD-A263747; ARL-TR-87) Avail: CASI HC A03/MF A01

The oxidation resistance and hot corrosion resistance of two superalloys, Rene 100 and X-40, and an aluminide coating for the protection of one of the superalloys are compared. The comparison is made by using tube-furnace oxidation and hot corrosion tests employing a Mettler TGA apparatus at temperatures of 1475 to 2200 F. For hot corrosion tests, the samples were precoated with Na2SO4 prior to heating to the desired temperature and introducing air at a flow rate of 57 cm/min. The oxidation behavior of Rene 100 was poor compared to that of the X-40 alloy, especially at temperatures above 1900 F. The X-40 alloy was found to be more resistant to the initiation of hot corrosion than Rene 100. Both alloys, however, undergo attack at rates consistent with an alloy-induced fluxing mechanism. An aluminide coating on Rene 100 caused the initiation of hot corrosion to be delayed. Attack did occur when cumulative applications of Na2SO4 were used. The coatings were penetrated by the Na2SO4 in localized areas after exposure times of less than 200 hours. The hot corrosion test has validity for mechanisms whereby the degradation process is sustained by reaction products from the alloy. It, therefore, can be used to compare the time to establish such conditions in alloys. Rene 100 is more susceptible to this condition than X-40. DTIC

N93-30815# Brookhaven National Lab., Upton, NY.
MATERIALS STUDIES FOR PREVENTING CORROSION IN CONDENSING ENVIRONMENTS Annual Report, Oct. 1991 - Sep. 1992
L. E. Kukacka and T. Sugama Oct. 1992 102 p See also PB92-172410 Sponsored by Gas Research Inst.
(Contract GRI-5090-260-1948)
(PB93-185478; GRI-92/0511) Avail: CASI HC A06/MF A02

Organic and pre-ceramic coating systems that appear to have high potentials for being cost-effective solutions to corrosion problems encountered in condensing heat exchangers have been identified. The results from the ongoing basic research have been transferred to applied R&D by commercial manufacturers of heat exchangers. Two high performance polyaryl-type polymers, polyphenylene sulfide and polyphenylether-etherketone, have given excellent results when deposited as thin (2-3 mil) coatings on cold-rolled steel substrates. The effectiveness of chemical modification of the steel surface prior to the application of the polymer topcoat as a means for bond enhancement and the formation of chemically resistant reaction products at the interface has been studied, but the results to date are inconclusive. Thin (0.5 to 2.0 micron) coatings of polytitanosiloxane applied to aluminum using sol-gel techniques have also given excellent corrosion resistance. Methods for using the system to chemically bond organic coatings to aluminum and to stabilize interfacial reaction products are currently being evaluated. NTIS

N93-30941# Israel Atomic Energy Commission, Negev. Nuclear Research Center.

EUTECTIC SOLIDIFICATION OF Al-U AT SLOWLY COOLING RATES (10 C PER SECOND)

A. Munitz, V. Y. Zenou, C. Cotler, and E. Nehama May 1992 42 p In HEBREW
(DE92-640082; NRCN-612) Avail: CASI HC A03/MF A01 (US Sales Only)

The solidification of Al-U alloys at slow cooling rates was investigated using optical and scanning microscopy. High purity uranium (99.9%) and high purity aluminum (99.9%) or 'commercially pure' Al-A5 (Al-1050) alloy containing a maximum of 0.5% wt/o of other alloying elements were used to prepare Al-U alloys in a resistance furnace under controlled atmosphere. The observed eutectic composition for U-(Al-A5) was 17 +/- 1 wt/o U, while that for U and pure Al was 19(+-)1 wt/o U. These values are significantly different than the value of 13 wt/o U, reported in the literature. The eutectic morphology and its distribution depends on the type of the aluminum used in preparing the alloy. In both cases eutectic colonies were observed. In alloys prepared with pure Al, the eutectic colonies have a diameter less than 0.2 mm, display a lamellar morphology, and are homogeneously distributed. In alloys prepared with Al-A5, at list 4 different types of eutectic morphologies were observed. Some of the eutectic colonies have diameters as large as 2 to 3 mm. Some interesting nonequilibrium morphological features were observed in the specimen containing hypereutectic compositions. The above results are discussed on the basis of current solidification theories. DOE

N93-31021# Gandhi (Indira) Centre for Atomic Research, Kalpakkam (India).

A REVIEW OF HOT CRACKING IN AUSTENITIC STAINLESS STEEL WELDMENTS

V. Shankar, T. P. S. Gill, S. L. Mannan, and P. Rodriguez 1991 83 p
(DE93-605280; IGC-119) Avail: CASI HC A05/MF A01 (US Sales Only)

The occurrence of hot cracking in austenitic stainless steel weldments is discussed with respect to its origin and metallurgical contributory factors. Of the three types of hot cracking, namely solidification cracking, liquation and ductility dip cracking, solidification cracking occurs in the interdendritic regions in weld metal while liquation and ductility dip cracking occur intergranularly in the heat-affected zone (HAZ). Segregation of impurity and minor elements such as sulphur, phosphorous, silicon, niobium, boron, etc. to form low melting eutectic phases was found to be the major cause of hot cracking. Control of HAZ cracking requires minimization of impurity elements in the base metal. In stabilized stainless steels containing niobium, higher amounts of delta-ferrite were found necessary to prevent cracking than in unstabilized compositions. Titanium compounds were found to cause liquation cracking in maraging steels and titanium containing stainless steels and superalloys. In nitrogen added stainless steels, cracking resistance decreases when the solidification mode changes to primary austenitic due to nitrogen addition. A review of the test methods to evaluate hot cracking behavior showed that several external restraint and semi-self-restraint tests are available. The Finger Test, WRC Fissure Bend Test, the PVR Test, and the Varestraint Test are described along with typical test results. Hot ductility testing to reveal HAZ cracking tendency during welding is described, which is of particular importance to stabilized stainless steels. Based on the literature, recommendations are made for welding stabilized and nitrogen added steels, indicating areas of further work. DOE

N93-31022# Gandhi (Indira) Centre for Atomic Research, Kalpakkam (India).

COMPATIBILITY STUDIES OF AISI TYPE 316 STAINLESS STEEL WITH LEAD-LITHIUM EUTECTIC ALLOY

A. Joseph, K. V. Kasiviswanathan, and Baldev Raj 1991 71 p
(DE93-605281; IGC-122) Avail: CASI HC A04/MF A01 (US Sales Only)

Spent fuel subassemblies from the Fast Breeder Test Reactor (FBTR) are to be stored in leak tight containers until they are required to be sent for reprocessing. Use of advanced fuels like uranium carbides and plutonium carbides, which are known to be highly chemically active with oxygen and moisture demands adequate leak tightness during long term storage to avoid undesirable chemical reactions. Use of low melting alloys which acts as liquid/solid sealants in the storage containers in which fuel subassemblies are to be kept is being considered for this purpose. Lead-lithium (0.7 wt % lithium) eutectic alloy was chosen as one of the candidate alloys for the purpose on the basis of theoretical assessments. The candidate sealing alloy should have good compatibility with the structural materials of fuel subassemblies as well as the fuel and fission products. AISI type 316 stainless steel in solution annealed, ten and twenty percent cold worked condition is the clad and wrapper material used for the fabrication of fuel pins and subassemblies. Compatibility studies between eutectic Pb-Li alloy and AISI type 316 stainless steel material in the above conditions were undertaken at different temperatures and time durations. The studies indicate that the tensile properties of AISI type 316 stainless steel are not subject to any serious jeopardization through contact with this molten Pb-Li eutectic alloy for periods extending even up to 7000 hours at 873 K. Thus use of Pb-Li eutectic alloy would be suitable for the storage of irradiated fuel. DOE

N93-30955*# College of Western New England, Springfield, MA. Dept. of Electrical Engineering.

EXPERIMENTS IN CORROSION FOR YOUNGER STUDENTS BY AND FOR OLDER STUDENTS

James V. Masi *In* NASA. Langley Research Center, National Educators' Workshop. Update 92: Standard Experiments in Engineering Materials Science and Technology Jun. 1993 p 127-136 (For primary document see N93-30948 11-23)
Avail: CASI HC A02/MF A04

N93-30961*# Tri-State Univ., Angola, IN.

APPLICATION OF HARDNESS TESTING IN FOUNDRY PROCESSING OPERATIONS: A UNIVERSITY AND INDUSTRY PARTNERSHIP

Donald H. Martin and Bruce Lash (AL-FE Heat Treating, Inc., Columbia City, IN.) *In* NASA. Langley Research Center, National Educators' Workshop. Update 92: Standard Experiments in Engineering Materials Science and Technology Jun. 1993 p 221-232 (For primary document see N93-30948 11-23)
Avail: CASI HC A03/MF A04

N93-30973*# California Polytechnic State Univ., San Luis Obispo. Materials Engineering Dept.

VISUALIZING WELD METAL SOLIDIFICATION USING ORGANIC ANALOGS

Daniel W. Walsh and Gary Ray Rogers *In* NASA. Langley Research Center, National Educators' Workshop. Update 92: Standard Experiments in Engineering Materials Science and Technology Jun. 1993 p 385-392 (For primary document see N93-30948 11-23)
Avail: CASI HC A02/MF A04

N93-30976*# New Mexico Univ., Albuquerque. Dept. of Mechanical Engineering.

POWDER METALLURGY: SOLID AND LIQUID PHASE SINTERING OF COPPER

Rex Sheldon and Martin W. Weiser *In* NASA. Langley Research Center, National Educators' Workshop. Update 92: Standard Experiments in Engineering Materials Science and Technology Jun. 1993 p 415-430 (For primary document see N93-30948 11-23)
Avail: CASI HC A03/MF A04

27 NONMETALLIC MATERIALS

Includes physical, chemical, and mechanical properties of plastics, elastomers, lubricants, polymers, textiles, adhesives, and ceramic materials.

For composite materials see *24 Composite Materials.*

N93-28489# Nebraska Univ., Lincoln. Dept. of Chemistry.
POLAR ORDER AND RELAXATION OF SECOND ORDER NONLINEAR OPTICAL SUSCEPTIBILITY IN AN ELECTRIC FIELD POLARIZED AMORPHOUS POLYMER
C. H. Wang, S. H. Gu, and H. W. Guan 1993 28 p LIMITED REPRODUCIBILITY: More than 20% of this document may be affected by microfiche quality
(Grant NSF DMR-91-12993)
(AD-A262189; TR-22) Avail: CASI HC A03

The dependence of the second harmonic generation (SHG) signal of an amorphous polymer system containing nonlinear optical (NLO) chromophores on the polarizing electric field is investigated. It is shown that under a weak poling field condition, the SHG intensity is proportional to E sub p squared, provided that the polarizing electric field E sub p is greater than a threshold field, E sub s. Above E sub s the macroscopic polar orientational order is established. The lengthening of the relaxation time for polar orientational order with increasing E sub p is also observed. Theoretical analysis shows that the relaxation time is proportional to the polar order initially induced by the polarizing field. Experiments have been carried out to confirm the theoretical prediction. DTIC

N93-28495# Michigan Univ., Ann Arbor. Dept. of Mechanical Engineering and Applied Mechanics.
MECHANICS OF ELEVATED TEMPERATURE FATIGUE DAMAGE IN FIBER-REINFORCED CERAMICS Final Report, 1 Dec. 1990 - 30 Nov. 1992
John W. Holmes Jan. 1993 73 p
(Grant AF-AFOSR-0106-91)
(AD-A262403; AFOSR-93-0172TR) Avail: CASI HC A04/MF A01

The focus of the research conducted under Grant No. 91-0106 (a two year effort) was to identifying the fundamental mechanisms of fatigue damage that occur in fiber-reinforced ceramics. Several new findings were made during the research effort: (1) the fatigue life of fiber-reinforced ceramics decreased markedly during high frequency fatigue loading, (2) fiber-reinforced ceramics undergo significant internal heating during cyclic loading, (3) because of frictional wear along the fiber-matrix interface, the frictional shear stress in fiber-reinforced ceramics decreases sharply under cyclic loading. Based upon insight gained from the analytical and experimental parts of the investigation, we developed a novel approach to estimate the level of frictional shear stress that exists along the fiber-matrix interface during fatigue. Since this technique allows confirmation of other techniques for estimating frictional shear stress (e.g., fiber pushout technique developed by Marshall at Rockwell Science Center). Moreover, it is the only approach that allows determination of the in-situ change in frictional shear stress during cyclic loading (note that the level of frictional shear stress controls many mechanical properties such as strength, toughness and mechanical damping as well as thermophysical properties such as thermal diffusivity). The analysis that was developed to estimate frictional shear stress can also be used to understand the relationship between composite microstructure and cyclic energy dissipation in fiber-reinforced ceramics. DTIC

N93-28541# Pennsylvania Univ., Philadelphia.
CATALYTIC SYNTHESIS OF SILICON CARBIDE PRECERAMIC POLYMERS: POLYCARBOSILANES
D. H. Berry Oct. 1992 5 p
(Contract DE-FG02-91ER-14173)
(DE93-008634; DOE/ER-14173/T1) Avail: CASI HC A01/MF A01

Polycarbosilanes are the most successful and widely studied class of polymer precursors for silicon carbide, but traditional methods for their synthesis are inefficient and nonselective. This project is focused on developing transition metal catalysts for the synthesis of polycarbosilanes and other preceramic polymers. In recent work, we have developed the first homogeneous transition metal catalysts for the dehydrogenative coupling of simple alkyl silanes to oligomeric and polymeric carbosilanes, H-(SiR2CR')2)n-SiR3. The coupling of alkylgermanes, however, yields the corresponding oligomeric poly(germanes) (Ge-Ge). Future work will help elucidate the mechanisms of these catalytic process, explore the use of hydrogen acceptors as reaction accelerators, and develop new and more active catalysts. DOE

N93-28551# Brookhaven National Lab., Upton, NY.
EVALUATION OF POLYARYL ADHESIVES IN ELASTOMER-STAINLESS STEEL JOINTS
M. Miura, N. Carciello, T. Sugama, and L. E. Kukacka Oct. 1992 26 p
(Contract DE-AC02-76CH-00016)
(DE93-009794; BNL-48089) Avail: CASI HC A03/MF A01

Polyaryl thermoplastic adhesives (polyetheretherketone (PEEK), polyphenylene sulfide (PPS), polyphenylethersulfone (PES)) were evaluated for ability to bond elastomer to metal for use in geothermal environments. Strength of elastomer-to-metal joints adhesives blends (such as in drill pipe or casing protectors) were determined using peel tests. Parameters involved in making the joints were temperature, time, and atmosphere, in addition to type of adhesive. Physical chemical analyses have aided endeavors to determine the cause of adhesion failure in the joint: differential thermal analyses, thermal gravimetric analyses, infrared spectroscopy, and electron spectroscopy for chemical analysis. Tests showed that joints made of adhesive blends which contained greater than 50% PES survived simulated geothermal conditions (200 C, water vapor pressure 200 psi) for weeks without significant decrease in peel strength. Chemical components of the adhesive appear to be highly stable under the conditions required to make the joints and in subsequent exposure to the simulated geothermal environment. DOE

N93-28560# Massachusetts Inst. of Tech., Cambridge. Dept. of Chemical Engineering.
GAS PERMEABILITY OF E/EP SEMICRYSTALLINE DIBLOCK COPOLYMERS Technical Report
P. Kofinas and R. E. Cohen 14 Apr. 1993 30 p
(Contract N00014-91-J-1045)
(AD-A263241; TR-8) Avail: CASI HC A03/MF A01

Gas permeability coefficients P for several gases (He. CO2, CH4, O2, N2) were measured at 25 C in a series of semicrystalline diblock copolymers of poly(ethylene)/ poly(ethylene-propylene) (E/EP). A simple model is presented describing the gas transport in these polymer systems. It predicts the permeability of a randomly oriented spherulitic diblock specimen from the permeabilities of the individual lamellar regions of the copolymer. Model predictions were in excellent agreement with the experimental data. The upper bound (lamellae aligned in parallel with respect to the permeation direction) and lower bound (series lamellar align models were calculated and compared to a limited amount of corresponding experimental data on oriented specimens. DTIC

N93-28561# Aerospace Corp., El Segundo, CA. Mechanics and Materials Technology Center.
THERMAL CONTROL PAINTS ON LDEF: RESULTS OF M0003 SUB-EXPERIMENT 18 Technical Report
Christopher H. Jaggers, Michael J. Meshjishnek, and John M. Coggi 15 Jan. 1993 27 p
(Contract F04701-88-C-0089)
(AD-A263252; TR-93(3935)-3; SMC-TR-93-16) Avail: CASI HC A03/MF A01

Several thermal control paints were flown on LDEF, including the white paints Chemglaze A276, S13GLO, and YB-71, and the black paint D-111. The effects of low earth orbit, which include those induced by UV radiation and atomic oxygen, varied significantly with each paint and its location on LDEF. For example, samples of Chemglaze A276 located on the trailing edge of LDEF darkened significantly due to UV-induced degradation of the paint's binder, while leading-edge samples remained white but exhibited severe atomic oxygen erosion of the binder. Although the response of S13GLO to low earth orbit is much more complicated, it also exhibited greater darkening on trailing edge-samples compared to leading-edge samples. In contrast, YB-71 and D-111 remained relatively stable and showed minimal degradation. This report examines the performance of these paints as determined by changes in their optical and physical properties, including solar absorptance as well as surface chemical changes and changes in surface morphology. It also correlates the optical and physical property changes with the physical phenomena that occurred in these materials during the LDEF mission. DTIC

N93-28600# Los Alamos National Lab., NM.
POLYMERIC MATERIALS FOR USE IN WET HYDROCHLORIC ACID ENVIRONMENTS
J. M. Williams Apr. 1993 28 p
(Contract W-7405-eng-36)
(DE93-010881; LA-12314-MS) Avail: CASI HC A03/MF A01

Of two major operations in plutonium reprocessing, polymeric materials are suitable for use in the wet acid train, but not in the high thermal chloride conversion zone, except in those areas not subjected to excessive heat. This report provides a literature review of available polymeric materials. The discussion is meant to be a guide for corrosion management in hydrochloric acid environments through proper selection from these polymeric materials. DOE

N93-28650# National Inst. of Standards and Technology, Gaithersburg, MD. Ceramics Div.
A STUDY OF THE CHEMICAL MECHANISM IN LUBRICATION
1993 17 p
(Contract DE-AI05-84ER-13230)
(DE93-012230; DOE/ER-13230/T2) Avail: CASI HC A03/MF A01

Boundary lubrication is receiving increased emphasis today, especially with respect to advanced materials. An attempt is made to develop an overall framework to guide developmental efforts. The chemical reaction between the material surface and the lubricant is complex; many reactions occur in parallel between the major elements and their oxides and the minor elements on the surface with lubricant, which usually contain N, O, S, and P compounds. Reaction rates are influenced by surface energy as influenced by rubbing. The reaction products could be inorganic in nature such as hydrides, nitrides; as well as organic in nature, such as organometallic polymers. These products can act as an effective lubricant as well as exhibiting neutral or detrimental effects on friction/wear. Good lubricating film should have strong adhesion to surface, good lateral bonding to form coherent films, and high shear resistance. Detrimental products usually have high corrosivity such as organic acids, weak surface adhesion, and incoherent film structure. DOE

N93-28666# Argonne National Lab., IL. Materials and Components Technology Div.
EFFECT OF METALLIC-COATING PROPERTIES ON THE TRIBOLOGY OF COATED AND OIL-LUBRICATED CERAMICS
O. O. Ajayi, A. Erdemir, G. R. Fenske, R. A. Erck, J. H. Hsieh, and F. A. Nichols Sep. 1992 18 p Presented at the Annual Conference and Exhibition of the Society of Tribologists and Lubrication Engineers, Calgary (Canada), 17-20 May 1993
(Contract W-31-109-eng-38)
(DE93-010663; ANL/MCT/CP-77794; CONF-930513-1) Avail: CASI HC A03/MF A01

Friction and wear behavior was determined for zirconia ceramics lubricated with solid coatings (Ag, Au, and Nb) deposited by ion-beam-assisted-deposition (IBAD) techniques, and a polyol-ester-based synthetic oil. Although the use of soft Ag and Au coatings as solid lubricants in conjunction with the synthetic oil significantly reduced the friction and wear under boundary lubrication at temperatures up to 250 C, these films had poor durability. In contrast, the Nb coating was more durable (in terms of chemical reactivity and adhesion during the tribo-tests) than were the Ag or Au films. However, the friction and wear behavior of the Nb-coated zirconia was poorer than that of the ceramics coated with Ag or Au. DOE

N93-28687# Naval Research Lab., Washington, DC.
ION-BEAM-ASSISTED DEPOSITION OF WEAR-RESISTANT COATINGS
B. D. Sartwell 1993 10 p
(Contract DE-AI02-88CE-90024)
(DE93-011529; DOE/CE-90024/11) Avail: CASI HC A02/MF A01

The adhesion strength and failure modes of ion-beam-assisted deposition (IBAD) TiN coatings were examined using a Revetest acoustic emission scratch tester. It was found that the adhesion strength which is represented as a critical normal load and failure modes of coated system are influenced by coating thickness, coating and substrate material properties, and ratio of incident argon ions to titanium atoms. The critical load increased with increasing substrate hardness. For coatings of thicknesses 0.5, 2.0, and 5.0 micrometers and with R = 0.4, the highest critical load was obtained for the intermediate thickness coating. For coatings of thickness 2 micrometers and with R values of 0.1, 0.4, and 0.7, the highest critical loads were correlated with the spallation of the coating. Further, the change in slope of the coefficient of friction of the diamond stylus sliding on the coated system could be correlated with the removal of the coating from the scratch track. A hot stage for high temperature wear tests on the Revetest apparatus was completed and tests were initiated. DOE

N93-28748# Texas Univ., Austin. Dept. of Chemistry.
SYNTHESIS OF NEW HIGH PERFORMANCE LUBRICANTS AND SOLID LUBRICANTS
R. J. Lagow Apr. 1993 16 p
(Contract DE-FG05-91ER-12119)
(DE93-012237; DOE/ER-12119/2) Avail: CASI HC A03/MF A01

Synthesis and testing was begun on a number of new classes of lubricants: perfluoropolyethers (branching effects), perfluoromethylene oxide ethers, chlorine-substituted fluorocarbon polyethers, fluorine-containing branched ether lubricants, glycerine-based perfluoropolyesters, and perfluoroepoxyether chains. DOE

N93-28761# California Univ., Berkeley. Lawrence Berkeley Lab.
HEALING OF LITHOGRAPHICALLY INTRODUCED FLAWS IN GLASS AND GLASS CONTAINING CERAMICS Ph.D. Thesis
H. D. Ackler Dec. 1992 133 p
(Contract DE-AC03-76SF-00098)
(DE93-010453; LBL-33488) Avail: CASI HC A07/MF A02

The morphological evolution of cylindrical pores or 'channels' and crack-like cavities in glass and glass-containing ceramics at elevated temperatures was studied. The systems studied were: Corning 7056 alkali borosilicate glass, soda-lime glass (microscope slides), a commercially available 96% Al2O3 with approximately 5-10% intergranular glass, 96% Al2O3 bonded to sapphire, and a model sapphire/glass/sapphire system fabricated by diffusion bonding etched and unetched pieces of sapphire onto which 30-50 nm of SiO2 had been sputter deposited. These systems span a broad range of glass contents, and permit observation of healing behavior with varying glass content. The results were compared with analytical models and results of similar studies in completely crystalline systems. DOE

N93-28838# Sandia National Labs., Livermore, CA.
HYDROSTATIC AND UNIAXIAL BEHAVIOR OF A HIGH DENSITY POLYURETHANE FOAM (FR-3720) AT VARIOUS TEMPERATURES
W. Y. Lu, J. S. Korellis, K. L. Lee, and R. Grishaber Mar. 1993 31 p
(Contract DE-AC04-76DR-00789)
(DE93-011486; SAND-93-8227) Avail: CASI HC A03/MF A01

This report describes the foam testing program designed to support a constitutive material response model. Experimental techniques were developed for hydrostatic pressure and uniaxial testing of high density polyurethane foam from ambient to 150 C with deformation greater than 50%. Two chambers were developed to perform the tests. DOE

N93-28839# Westinghouse Savannah River Co., Aiken, SC.
ACID SOLUTION ABSORPTION OF EXTRUDED POLYETHYLENE FOAM
E. A. Kyser Jan. 1993 12 p
(Contract DE-AC09-89SR-18035)
(DE93-011701; WSRC-TR-93-011) Avail: CASI HC A03/MF A01

Water and acid absorption tests of samples of a proposed replacement to current polyethylene foam used as fill material on the FB-Line cation columns have been completed. Water and nitric acid solution absorption of up to 4 volume percent was observed over approximately a 4 month period of time. Because of the nuclear safety implications, liquid absorption of a replacement fill material must be low. Ethafoam (trademark) 220 extruded polyethylene, a product available from Dow Chemical Company appears to be a good candidate material for replacement of the existing fill material. Establishment of 5 volume percent solution absorption specification appears to be both reasonable and achievable for a replacement foam. DOE

N93-29064# Technische Univ., Berlin (Germany). Fachbereich Physikalische Ingenieurwissenschaft.

THERMODYNAMICS OF SWELLING AND COLLAPSE OF POLYELECTROLYTIC GELS Ph.D. Thesis [ZUR THERMODYNAMIK DES SCHWELLENS UND SCHRUMPFENS POLYELEKTROLYTISCHER GELE]

Roland Rydzewski Feb. 1992 141 p In GERMAN
(ETN-93-93485) Avail: CASI HC A07/MF A02

The equilibrium of a polyelectrolytic gel with an electrolyte solution is mathematically described with particular consideration given to unsteadiness occurring in gel state transformation by stationary evolution of electrolyte solution composition. Equilibruim was calculated by minimization of free energy of the gel-bath system. The mixture entropy was considered as that of low molecular, ideal solution. Free energies of interaction between polymer and solvent, of network elasticity, elastrostatic interaction between charge carriers and chemical reactions (pyrolysis), were included in the calculations which were numerically achieved by Newton iterations. Four gel-bath systems were examined, for which the following aspects were discussed: distribution equilibrium of solvent, different ion species and electrical charge between gel and bath, elastic and chemical equilibrium and interaction between them. The systems were: an acrylamid-sodium acrylate-copolymer gel in a sodium chloride solution, with the salt cation similar to the gel counter ion, the same system in which the gel is subjected to uniaxial compression-traction load, the same system, with salt cation different from gel counter ion, and a polyacid gel in sodium hydroxide whose neutralization is studied. ESA

N93-29083* National Aeronautics and Space Administration. Langley Research Center, Hampton, VA.

POLYIMIDES PREPARED FROM 3,5-DIAMINO BENZO TRIFLUORIDE Patent

Margaret K. Gerber, inventor (to NASA) (Proctor and Gamble Co., Cincinnati, OH.), J. Richard Pratt, inventor (to NASA) (PRC Kentron, Inc., Hampton, VA.), Terry L. St.Clair, inventor (to NASA), and Anne K. St.Clair, inventor (to NASA) 8 Jun. 1993 6 p Filed 31 Aug. 1989 Supersedes N91-28425 (30 - 2, p 218)
(NASA-Case-LAR-14206-1; US-Patent-5,218,083;
US-Patent-Appl-SN-429574; US-Patent-Class-528-353;
US-Patent-Class-528-26; US-Patent-Class-528-28; US-Patent-Class-528-125;
US-Patent-Class-528-128; US-Patent-Class-528-170;
US-Patent-Class-528-172) Avail: US Patent and Trademark Office

High performance, thermooxidatively stable polyimides are prepared by reacting aromatic diamines with pendant trifluoromethyl groups and dianhydrides in an amide solvent to form a poly(amic acid), followed by cyclizing the poly(amic acid) to form the corresponding polyimide.
Official Gazette of the U.S. Patent and Trademark Office

N93-29085* National Aeronautics and Space Administration. Langley Research Center, Hampton, VA.

DIPHENYLMETHANE-CONTAINING DIANHYDRIDE AND POLYIMIDES PREPARED THEREFROM Patent

Anne K. St.Clair, inventor (to NASA) (Lockheed Engineering and Sciences Co., Hampton, VA.), Harold G. Boston, inventor (to NASA), and J. Richard Pratt, inventor (to NASA) (Lockheed Engineering and Sciences Co., Hampton, VA.) 8 Jun. 1993 11 p Filed 26 Aug. 1991 Supersedes N92-11200 (30 - 2, p 218)
(NASA-Case-LAR-14487-1; US-Patent-5,218,077;
US-Patent-Appl-SN-750158; US-Patent-Class-528-188;
US-Patent-Class-528-125; US-Patent-Class-528-126;
US-Patent-Class-528-128; US-Patent-Class-528-172;
US-Patent-Class-528-173; US-Patent-Class-528-179) Avail: US Patent and Trademark Office

A high temperature stable, highly optically transparent-to-colorless, low dielectic linear aromatic polyimide is prepared by reacting an aromatic diamine with 3,3'bis (3,4-dicarboxyphenoxy) diphenylmethane dianhydride in an amide solvent to form a linear aromatic polyamic acid. This polyamic acid is then cyclized to form the corresponding polyimide.
Official Gazette of the U.S. Patent and Trademark Office

N93-29088* National Aeronautics and Space Administration. Lyndon B. Johnson Space Center, Houston, TX.

ABLATIVE SHIELDING FOR HYPERVELOCITY PROJECTILES Patent

Michelle A. Rucker, inventor (to NASA) 8 Jun. 1993 7 p Filed 21 May 1992 Supersedes N92-30539 (30 - 21, p 3602)
(NASA-Case-MSC-21884-1; US-Patent-5,217,185;
US-Patent-Appl-SN-887674; US-Patent-Class-244-121;
US-Patent-Class-244-158R; US-Patent-Class-89-36.02;
Int-Patent-Class-B64D-7/00) Avail: US Patent and Trademark Office

A hypervelocity projectile shield which includes a hollow semi-flexible housing fabricated from a plastic like, or otherwise transparent membrane which is filled with a fluid (gas or liquid) is presented. The housing has a inlet valve, similar to that on a tire or basketball, to introduce an ablating fluid into the housing. The housing is attached by a Velcro mount or double-sided adhesive tape to the outside surface of a structure to be protected. The housings are arrayed in a side-by-side relationship for complete coverage of the surface to be protected. In use, when a hypervelocity projectile penetrates the outer wall of a housing it is broken up and then the projectile is ablated as it travels through the fluid, much like a meteorite 'burns up' as it enters the earth's atmosphere, and the housing is deflated. The deflated housing can be easily spotted for replacement, even from a distance. Replacement is then accomplished by simply pulling a deflated housing off the structure and installing a new housing. Official Gazette of the U.S. Patent and Trademark Office

N93-29193*# National Aeronautics and Space Administration. Marshall Space Flight Center, Huntsville, AL.

EFFECTS OF ATOMIC OXYGEN AND ULTRAVIOLET RADIATION ON CANDIDATE ELASTOMERIC MATERIALS FOR LONG DURATION MISSIONS. TEST SERIES NO.1

R. C. Linton, M. M. Finckenor, R. R. Kamenetzky, and P. Gray (Sverdrup Technology, Inc., Huntsville, AL.) Jun. 1993 21 p
(NASA-TM-108408; NAS 1.15:108408) Avail: CASI HC A03/MF A01

Research was conducted at MSFC on the behavior of elastomeric materials after exposure to simulated space environment. Silicone S383 and Viton V747 samples were exposed to thermal vacuum, ultraviolet radiation, and atomic oxygen and then evaluated for changes in material properties. Characterization of the elastomeric materials included weight, hardness, optical inspection under normal and black light, spectrofluorescence, solar absorptance and emittance, Fourier transform infrared spectroscopy, and permeability. These results indicate a degree of sensitivity to exposure and provided some evidence of UV and atomic oxygen synergism. Author (revised)

N93-29201# Bend Research, Inc., OR.

NOVEL POLYMER COMPOSITIONS FOR HIGH-TEMPERATURE MEMBRANE APPLICATIONS, PHASE 1 Final Technical Report

D. J. Brose, M. B. Chidlaw, D. T. Friesen, S. B. McCray, L. D. Nelson, R. J. Ray, and M. E. Schimpf 10 Dec. 1989 66 p
(Grant NSF ISI-88-60947)
(PB93-174126; NSF/ISI-89035-Phase-1) Avail: CASI HC A04/MF A01

The phase 1 program demonstrated the feasibility of using a group of robust polymers to fabricate membranes that are both temperature-resistant and chemically resistant. Whereas control membranes based on conventional polymers degraded at temperatures of 175 C, the robust membranes could withstand exposure to temperatures of 250 C without damage. They also have excellent chemical resistance and unique permselectivity characteristics that make them ideal for a wide variety of separation applications. In addition to fabricating and testing dense-film membranes, researchers were able to fabricate microporous and skinned asymmetric membranes from the robust polymers studied. NTIS

N93-29248# California Univ., Berkeley. Lawrence Berkeley Lab.

A TRANSIENT FGM INTERLAYER BASED APPROACH TO JOINING CERAMICS

A. M. Glaeser, M. L. Shalz, B. J. Dalgleish, and A. P. Tomsia Jan. 1993 17 p Presented at the 2nd International Symposium on Functionally Gradient Materials (FGM), San Francisco, CA, 1-4 Nov. 1992
(Contract DE-AC03-76SF-00098)
(DE93-010415; LBL-33407; CONF-9211218-1) Avail: CASI HC A03/MF A01

In most cases, functionally gradient materials have been designed to produce a desirable property gradient in a material or in a joint region. In this paper, the concept of a transient gradient structure is introduced. The function of the intentional property discontinuities in these multilayer interlayers is to facilitate processing of assemblies and materials combinations that would be difficult to process using conventional bonding approaches. Specifically, the methods make use of a thin or partial layer of a low melting point transient liquid phase to facilitate bonding via brazing, yet produce refractory joints. Several mechanisms for consuming the transient liquid former are outlined, and examples of interlayer designs that exploit these mechanisms are presented. Specific results from experiments joining alumina to alumina via Cu/Pt/Cu, Cu/Ni/Cu, Cu/Nb/Cu, and Sn/Nb/Sn interlayers are presented. DOE

N93-29252# Los Alamos National Lab., NM.
MICROWAVE PROCESSING OF CERAMICS
J. D. Katz 1993 9 p Presented at the Workshop on Microwave-Absorbing Materials for Accelerators, Newport News, VA, 22-24 Feb. 1993
(Contract W-7405-eng-36)
(DE93-010708; LA-UR-93-903; CONF-930296-1) Avail: CASI HC A02/MF A01

Recent work in the areas of microwave processing and joining of ceramics is briefly reviewed. Advantages and disadvantages of microwave processing as well as some of the current issues in the field are discussed. Current state and potential for future commercialization of this technology is also addressed. DOE

N93-29267# Technische Univ., Eindhoven (Netherlands). Electrical Energy Systems Group.
THE DESIGN AND LIFETIME CALCULATION OF MHD GENERATOR WALLS BASED ON SUBCRITICAL CRACK GROWTH IN CERAMICS Ph.D. Thesis
Hubertus Renier Mari vanLierop 1992 157 p
(ISBN-90-9004009-9; ETN-93-93577) Avail: CASI HC A08/MF A02

The design and investigation of the material properties of a wall segment for a closed cycle Magnetohydrodynamic (MHD) generator are described. Because of the maximum size of the available ceramics, the wall of a large generator has to be segmented. Considering the electrical processes in the generator, ceramics should be used as inner materials. Considering the heat flux through the wall a thermal insulating material should be applied. All these considerations are combined in the design. It was found that the bolt in the designed wall segment was loaded with both bending and tensile stresses. Two kinds of diagnostics to measure the load on the bolt are presented. The diagnostics are a laser interferometer in combination with a dynamical model of the construction and a strain gauge measuring system. Models which describe certain aspects of the wall segment are described. These are concerned with: thermal and dynamical modeling of the wall segment; modeling of crack growth; and probabilistic lifetime calculation. An experimental test rig was built to perform the lifetime tests and it proved to be a reliable device to load the wall segment with both thermal and mechanical loads. ESA

N93-29290# Arizona Univ., Tucson.
SYNTHESIS AND POLYMERIZATION OF AZAETHYLENES AND AZA-1,3-DIENES Final Report, 15 Jan. 1990 - 14 Jan. 1993
H. K. Hall, Jr. 8 Apr. 1993 9 p
(Contract DAAL03-91-G-0032)
(AD-A263651; ARO-27440.6-CH) Avail: CASI HC A02/MF A01

The polymerization of compounds containing the C=N bond is investigated. Two families of monomers are synthesized, namely imines (azaethylenes) and aza-1,3-dienes. For the imines, electron-accepting substituents such as cyano and carbomethoxy increase the polymerizability of these monomers. Extremely electrophilic imines are not stable, but do polymerize. Among the azadienes, the ones with the N-CN functionality are the most appropriate for polymerization. Substituents increase the stability of these dienes, but on the other hand hinder their polymerization and an exact balance has to be found. DTIC

N93-29328# Allied-Signal Aerospace Co., Kansas City, MO.
CHARACTERIZATION AND OPTIMIZATION OF A HOT AIR SOLDER-LEVELING SYSTEM
R. R. Penniston, Jr. and D. A. Stockdale Mar. 1993 10 p
(Contract DE-AC04-76DP-00613)
(DE93-010188; KCP-613-5164) Avail: CASI HC A02/MF A01

The characterization and optimization of a new Hot Air Sokkr-Leveling (HASL) System in the Printed Wiring Board Fabrication Area was initiated to reduce the variability and defects in printed wiring board solder coatings. This body of work continues to provide information on the mechanics of solder coating, and allows us to predict the required process adjustments based on board type and geometry. The previous HASL system contained several processes (flux, preheat, solder-coat, cooldown) within one piece of equipment. The new system physically separates these processes using in-line conveyors. Parameters affecting these processes were brainstormed and evaluated using the MaHo Perez-Wilson methodology (MPCpS). The critical parameters were identified and segregated according to individual process. Each process was characterized for materials used, machine settings, and their effect (potential and actual) on product. Due to the wide-ranging affect of the preheat and solder-leveling machine settings, the first decision made was to restrict the characterization to duplication of the coating obtained from the previous system. Adoption of the parameters used on the previous system allowed a reduction in the number of evaluations required to establish initial machine settings (solder pot dwell times, solder temperature, preheat temperature, etc.). Activities in-work include a formal statistical analysis of the solder-leveling capabilities, and completion of optimization activities. DOE

N93-29337# Pennsylvania State Univ., University Park.
PROCEEDINGS OF THE 25TH EUROPEAN CONFERENCE ON THE APPLICATION OF POLAR DIELECTRICS TO CELEBRATE THE 25TH ANNIVERSARY OF THE DIELECTRIC SOCIETY, INCORPORATING THE 1ST INTERNATIONAL WORKSHOP ON INTEGRATED FERROELECTRICS Final Report
J. M. Herbert and R. W. Whatmore 1 Apr. 1993 348 p Meeting held in London, England, 12-15 Apr. 1992
(Contract N00014-92-J-1497)
(AD-A263427) Avail: CASI HC A15/MF A03

The second European Meeting on the Applications of Polar Dielectrics was held in April 1992 to celebrate the 25th Anniversary of the dielectric Society, recognizing the rising importance of thin films of ferroelectrics for a wide range of applications. The meeting also incorporated the 1st International Workshop on Integrated Ferroelectrics. To facilitate international participation, the meeting was held at Imperial College, London. Over 1-50 delegates registered for the meeting from 27 countries. Unfortunately, attendance from Eastern Europe was limited by the present economic and political problems. However, the generous financial support provided by our sponsors enable the organizers to assist the attendance of many from this region and to provide reduced attendance costs for students. Reflecting the current extent of interest in dielectric materials, 175 abstracts were submitted. Topics ranged from stable ceramics for microwave applications to organic crystals and polymers with high nonlinear electro-optical coefficients. About one sixth of the contributions were concerned with the preparation and properties of thin films, particularly those involving ferroelectric materials. DOE

N93-29342# Naval Academy, Annapolis, MD. Dept. of Physics.
HIGH PRESSURE STUDIES OF HYDRATED NAFION MEMBRANES: DIELECTRIC RELAXATION AND DEUTERON NMR Interim Technical Report, Mar. 1992 - Apr. 1993
M. G. McLin, M. C. Wintersgill, J. J. Fontanella, R. S. Chen, and J. P. Jayakody 16 Apr. 1993 16 p
(Contract N00014-93-WR-24016)
(AD-A263511; Rept-TR-1) Avail: CASI HC A03/MF A01

Audio frequency electrical conductivity/dielectric relaxation and nuclear magnetic resonance studies of Nafion-117 have been carried out at pressures up to 0.3 GPa (3 kbar). For some samples, the electrical conductivity exhibits dispersion typical of hopping conductivity in an amorphous material, sigma = sigma(sub o)omega(sub w). The values of m are sample dependent and vary from about 0.55 to 0.75. In addition, the values of m are not strongly pressure sensitive. At a given frequency, the electrical conductivity tends to decrease as pressure increases and yield activation volumes on the order of 5 to 10 cu. cm/mol. The activation volume determined from the NMR spin-lattice relaxation time measurements are also sample dependent. The data shown correspond to an activation volume of about 8.6 cu.cm/mol. DTIC

N93-29344# Wright Lab., Wright-Patterson AFB, OH.
RESULTS OF A ROUND ROBIN TEST PROGRAM: COMPLEX MODULUS PROPERTIES OF A POLYMERIC DAMPING MATERIAL Final Report, Oct. 1986 - May 1992

David I. Jones May 1992 315 p
(AF Proj. 2401)
(AD-A263619; WL-TR-92-3104) Avail: CASI HC A14/MF A03

This report describes the results of a Round Robin test program to evaluate the complex modulus behavior of a typical polymeric damping material, as measured by several different test methods and organizations. The results are analyzed in several different ways, namely wicket plot analysis, temperature by temperature plots of moduli and loss factors versus frequency, and frequency-temperature reduced variables master plots. It is determined that all the test methods used are capable of producing accurate results, but that conditions arise in each case where erroneous results are encountered. These conditions represent extreme values of the specimen stiffness (high or low), system frequencies, (usually high) or situations where small differences between large numbers occur. These conditions define natural limits for each test method and specimen configuration and dimensions. The identification of these limits, and the role of specimen dimension choices in defining the limit boundaries will be invaluable for future testing by each of the test methods and systems examined. DTIC

N93-29404# Naval Command, Control and Ocean Surveillance Center, San Diego, CA.
BORON CARBIDE ALUMINUM CERMETS FOR EXTERNAL PRESSURE HOUSING APPLICATIONS Final Report, FY 1991
J. D. Stachiw, A. Pyzik, D. Carroll, A. Prunier, and T. Allen Sep. 1992 168 p
(AD-A262749; NCCOSC/RDT/E/TR-1574) Avail: CASI HC A08/MF A02

B4C/Al ceramic composites have been found to be excellent candidates for pressure housing applications for use in deep submergence underwater vehicles. These materials have the compressive strengths of a ceramic material but a lower weight/displacement ratio and can be produced in near-net shape. A methodology has been developed in the Dow Chemical Company to form large parts of this material. Nine B4C/Al cylinders with 6-inch diameters and lengths of up to 9 inches were produced in the first phase of the program for development of pressure housing for underwater vehicles. The pressure housing tests showed that the compressive strength of this material in the form of 6-inch diameter by 5-inch-long cylinders was in excess of 300 kpsi. The weight to displacement of cylinders equipped with titanium joint rings for 9000-psi service with safety factor of 2.2 was found to be 0.365, a 27-percent improvement over alumina cylinders with identical dimensions and safety factors. When B4C/Al cylinders are compared to titanium alloy Ti6Al4Va cylinders for 9000-psi service with identical safety factor, the titanium cylinders are found to be 256 percent heavier. DTIC

N93-29441# Nebraska Univ., Lincoln. Dept. of Chemistry.
DIPOLAR ORIENTATIONAL RELAXATION IN GUEST/HOST AMORPHOUS POLYMER PROBED BY SECOND HARMONIC GENERATION
T. Goodson, III and C. H. Wang 1993 21 p
(Grant NSF DMR-91-12993)
(AD-A262006; TR-20) Avail: CASI HC A03/MF A01

The decay of the second harmonic signal of a nonlinear optical chromophore dispersed in an amorphous polymer matrix is investigated. The decay curve can be fit either to the Kohrausch-Williams-Watts (KWW) stretched exponential function or to a bi-exponential function. The bi-exponential fit gives a better description of the decay of the second order nonlinear optical susceptibility of the contact electrode poled amorphous NLO polymer film. The fast decay component of the relaxation curve is attributed to the combined effect of reorientation of NLO dipole and the third order optical nonlinearity. The slow decay is due to the rotational diffusion of the NLO dipole. The temperature dependence of the rotational relaxation time is found to follow the Vogel-Fulcher-Tamman equation. DTIC

N93-29442# Nebraska Univ., Lincoln. Dept. of Chemistry.
ISOTHERMAL ANNEALING AND RELAXATION OF THE SECOND HARMONIC GENERATION SIGNAL FROM A NONLINEAR OPTICAL POLYMER
H. W. Guan, S. H. Gu, and C. H. Wang 1993 11 p
(Grant NSF DMR-91-12993)
(AD-A262007; TR-21) Avail: CASI HC A03/MF A01

Results of the first detailed study of the effect of isothermal annealing on the relaxation behavior of the second harmonic generation signal below T(sub g) of nonlinear optical (NLO) polymers are presented. Lengthening of the NLO chromophore relaxation time by isothermal poling suggests a strategy for preparing a stable NLO material. DTIC

N93-29456 Department of the Navy, Washington, DC.
FLAME OR PLASMA SYNTHESIS OF DIAMOND UNDER TURBULENT AND TRANSITION FLOW CONDITIONS Patent
Keith A. Snail, inventor (to Navy) 29 Dec. 1992 16 p Filed 24 Sep. 1990
(AD-D015689; US-Patent-5,174,983; US-Patent-Appl-SN-587328; US-Patent-Class-423-446) Avail: US Patent and Trademark Office

A method for synthesizing diamond which comprises flowing together a gaseous carbon source and a gaseous hydrogen source to form an at least partially turbulent mixture. The at least partially turbulent mixture is excited to form an at least partially turbulent reactive species which is reacted to form a deposition species. A substrate is disposed in the deposition species while maintaining the substrate at a temperature for the deposition of diamond, thereby, inducing deposition of diamond on the substrate. DTIC

N93-29457 Department of the Navy, Washington, DC.
POLYMERS WITH ELECTRICAL AND NONLINEAR OPTICAL PROPERTIES Patent
John Stenger-Smith, inventor (to Navy) 10 Nov. 1992 5 p Filed 9 Apr. 1991
(AD-D015691; US-Patent-5,162,470; US-Patent-Appl-SN-682169; US-Patent-Class-526-256) Avail: US Patent and Trademark Office

Conjugated stilbenylene polymers are disclosed having nonlinear optical properties, and which can be converted to electrically conductive polymers. Such polymers are produced by reacting a biscycloalkylene sulfonium salt of 2,5-dimethyl stilbene, e.g., 2,5-(4'-methoxy)-stilbene dimethylene bis-(tetramethylene sulfonium bromide), with alkali metal hydroxide to form a cycloalkylene sulfonium salt precursor polymer, and then heating the precursor polymer under conditions to produce the stilbenylene vinylene polymer, e.g., poly(2,5-(4'-methoxy) stilbenylene vinylene). DTIC

N93-29458 Department of the Navy, Washington, DC.
SYNTHETIC LUBRICATING OIL GREASES CONTAINING METAL CHELATES OF SCHIFF BASES Patent
Vinod S. Agarwala, inventor (to Navy), Alfeo A. Conte, Jr., inventor (to Navy), Krishnaswamy S. Rajan, inventor (to Navy), and Prabir K. Sen, inventor (to Navy) 15 Sep. 1992 7 p Filed 9 Apr. 1991
(AD-D015694; US-Patent-5,147,567; US-Patent-Appl-SN-700373; US-Patent-Class-252-42.7) Avail: US Patent and Trademark Office

This invention relates to a method and composition for improving the corrosion resistance and anti-wear properties of synthetic lubricating oil greases comprising the addition to said greases of effective amounts of a chelated Schiff base derived from the condensation of approximately stoichiometic amounts of at least one aldehyde and a polyamine. DTIC

N93-29511# Pennsylvania State Univ., University Park. Materials Research Lab.
CRYSTALLIZATION OF NANOCOMPOSITE GLASSES MADE BY THE SSG PROCESS Final Technical Report, 15 Nov. 1991 - 31 Dec. 1992
Rustum Roy and Sridhar Komarneni 12 Jan. 1993 65 p
(Grant AF-AFOSR-0446-89)
(AD-A262892; AFOSR-93-0177TR) Avail: CASI HC A04/MF A01

The two main objectives of this research were: (1) to crystallize nanocomposite glasses through solid-state epitaxy, and (2) to demonstrate the critical role of epitaxy in crystallization by fabricating sol-gel films on single crystal substrates of a particular orientation. During the last three years we have been able to achieve both these goals using several compositional systems. We have been able to crystallize through seeding albite (NaAlSi3O8) glass which has been considered to be impossible to crystallize. Orthoclase (KAlSi3O8) which is extremely difficult to crystallize has also been crystallized using a compositionally multiphasic gel and crystalline seeds of KA1Si3O8, NaAlSi3O8, CaAl2Si2O8 and SrAl2Si2O8 feldspars. Monoclinic BaAl2Si2O8 has been crystallized at significantly lower temperatures by seeding with monoclinic BaAl2Si2O8 or SrAl2Si2O8 seeds. The effect of seeding has been minor or could not be detected in other glass systems such as Li2O-Al203-SiO2, Rb2O-Al2O3-SiO2 and Cs2O-Al2O3-SiO2. Little or no effect of seeding was found in non-oxide glasses such as silicon oxycarbide glasses. The role of epitaxy in crystallization has been demonstrated convincingly by making dense, epitaxial SrTiO3 and TiO2 thin films on single crystals of SrTiO3 and TiO2 of a particular orientation. The nanocomposite approach which has been discovered and developed through AFOSR support to us is now a well established practice. DTIC

N93-29660# Rutgers - The State Univ., Piscataway, NJ. Dept. of Mechanics and Materials Science.
AN EXTENSION OF A KINETIC THEORY OF POLYMER CRYSTALLIZATION THROUGH THE EXCLUSION OF NEGATIVE BARRIERS Technical Report No. 27, 1 Jun. 1992 - 31 Mar. 1993
Jerry I. Scheinbeim, Louis Petrone, and Brian A. Newman May 1993 54 p
(Contract N00014-91-J-1078)
(AD-A264810) Avail: CASI HC A04/MF A01

The simplest version of the Lauritzen-Hoffman (LH) model of polymer crystallization, which applies to infinitely long model polymer molecules crystallizing on an existing substrate of infinite width, is reexamined. The mathematical expressions for the model free energy barriers are observed to take on negative values at high supercooling. Since such negative barriers appear to be physically unrealizable for the crystallization process, the LH model is extended by imposing a mathematical constraint on the expressions for the barriers, to forbid them from ever being negative. The extended model contains one parameter gamma which varies from 0 to 1 and is analogous to the parameter psi of the LH model. For all values of gamma less than 1, the extended model predicts a finite lamellar thickness at every supercooling; moreover, this thickness at large undercooling, decreases monotonically with increasing undercooling, in agreement with experiment but in marked contrast to the LH model which exhibits the well-known delta l catastrophe. The relative insensitivity of the calculated lamellar thicknesses to the parameter delta supports the use of gamma = 0 as a first approximation for mathematical convenience in practice. DTIC

N93-29767# Oak Ridge National Lab., TN.
MICROWAVE PROCESSING OF SILICON NITRIDE FOR ADVANCED GAS TURBINE APPLICATIONS
T. N. Tiegs and J. O. Kiggans 1993 6 p Presented at the 38th ASME International Gas Turbine and Aeroengine Congress and Exhibition, Cincinnati, OH, 24-27 May 1993
(Contract DE-AC05-84OR-21400)
(DE93-007910; CONF-930502-4) Avail: CASI HC A02/MF A01

Results from previous studies on microwave processing of silicon nitride-based ceramics are reviewed to ascertain the application of this technology to advanced gas turbine (AGT) materials. Areas of microwave processing that have been examined in the past are (1) sintering of powder compacts; (2) heat treatment of dense materials; and (3) nitridation of Si for reaction bonded silicon nitride. The sintering of Si3N4 powder compacts showed improved densification and enhanced grain growth. However, the high additive levels required to produce crack-free parts generally limit these materials to low temperature applications. Improved high-temperature creep resistance was observed for microwave heat-treated materials and therefore has application to materials used in highly demanding service conditions. In contrast to Si3N4, Si couples well in the microwave and sintered reaction-bonded silicon nitride materials were fabricated in a one-step process with cost-effective raw materials. However, these materials are also limited to lower temperature applications, under about 1000 C. DOE

N93-29790# Naval Surface Warfare Center, Bethesda, MD.
PROPERTIES OF SUPERCONDUCTING YBa2Cu3O(6+4) CERAMIC MATERIALS: EFFECT OF PROCESSING PARAMETERS
A. S. Rao Mar. 1993 37 p
(AD-A263441; CARDEROCKDIV-SSM-61-93/04) Avail: CASI HC A03/MF A01

The effect of the sintering temperature, the sintering time and the addition of 5 wt. % silver on the average particle size, bulk density, and the superconducting zero resistance temperature (Tc) YBa2Cu3O(6+x) ceramic materials was investigated in the range 880 - 940 C for 2 hours and at 920 C for different times in the range 0-10 hours. The results suggest that while the density and particle size of the sintered ceramic increases with an increase of the sintering temperature (and 2 hours of sintering), prolonged sintering (at 9200 C) above 4 hours of duration does not improve above properties. However, the superconducting zero resistance temperature (Tc) does not change significantly. In the presence of 5 wt. % silver, it appears that both sintering temperature and duration of sintering significantly improves the bulk density, particle size, and (Tc) of YBa2Cu3O(6+x). DTIC

N93-29795 University Coll., London (England).
CHROMATOGRAPHIC AND SOLVATOCHROMIC MEASUREMENTS ON BUTYL RUBBERS Final Report
Michael H. Abraham and Chau M. Du Jan. 1993 36 p Limited Reproducibility: More than 20% of this document may be affected by microfiche quality
(Contract DAJA45-91-C-0022)
(AD-A263088) Avail: CASI HC A03

The aim of the present work is to characterize polymers in terms of polymer-solute interactions, and hence to understand solubility properties of the polymers concerned. Sorption, desorption and partition are all important processes that could be better understood with such knowledge of solubility-related interactions. The two main methods used in this work to characterize polymers are the solvatochromic method, described in the Third Interim Report, and the method of multiple linear regression analysis (MLRA) based on linear solvation energy relationship (LSER). It is this latter method that will be described here. DTIC

N93-29825# Naval Academy, Annapolis, MD. Dept. of Physics.
SYNTHESIS AND PROPERTIES OF A CATION-CONDUCTING, HIGH TEMPERATURE POLYMER ELECTROLYTE Interim Technical Report, Mar. 1992 - Apr. 1993
Y. Okamoto, Z. S. Xu, M. G. McLin, J. J. Fontanella, and Y. S. Pak 16 Apr. 1993 16 p
(Contract N00014-93-WR-24016)
(AD-A263557; TR-2) Avail: CASI HC A03/MF A01

A new class of polymer electrolyte, high temperature polymer electrolytes, as an electrolyte in high discharge rate batteries is proposed. As an initial effort in the development of these materials, sodium and lithium salts of sulfonated poly(p- phenyleneterephtalamide) have been prepared. DSC and electrical conductivity studies have been performed on these films. The conductivity exhibits Arrhenius behavior over the temperature range in which they are thermally stable (180-240 C) with the material containing sodium being more conductive than those containing lithium. Although the electrical performance of these materials is inadequate from a practical standpoint, it is suggested that with additional development these materials could function as electrolytes for high discharge rate batteries. DTIC

N93-29829# Naval Academy, Annapolis, MD. Div. of Engineering and Weapons.
THE EFFECT OF OXIDATION EMBRITTLEMENT ON THE IMPACT BEHAVIOR OF NICALON REINFORCED CAS 2 CERAMIC MATRIX COMPOSITES
L. A. Gish and D. F. Hasson Apr. 1993 26 p
(Contract N00014-93-WR-24019)
(AD-A263567; USNA-EW-05-93) Avail: CASI HC A03/MF A01

The impact behavior of Nicalon reinforced CAS 2 composites is described. Impact tests of samples loaded to 1.0 microcracking yield and heated to 600 deg C for 10 hours were compared to tests of as received samples to determine the degree of degradation caused by the treatment. In addition, samples which were loaded to 1.0 micro-cracking yield but not heated and samples which were heated to 600 deg C for 10 hours were compared to isolate the effects of pre-cracking and heating. It was demonstrated that oxidation embrittlement has a negative effect on the maximum stress and dynamic fracture toughness of CAS II composites when fractured in impact. It was further demonstrated that specimens reinforced with mica-coated Nicalon fibers are more susceptible to oxidation embrittlement than specimens reinforced with standard Nicalon fibers. DTIC

N93-29856# Case Western Reserve Univ., Cleveland, OH.
MOLECULAR DYNAMICS OF PHYSICAL AGING PROCESSES IN POLYMER GLASSES Final Report, Jan. 1990 - Dec. 1992

J. D. McGervey 23 Feb. 1993 3 p
(Contract DAAL03-90-G-0023)
(AD-A263737; ARO-27037.6-MS) Avail: CASI HC A01/MF A01

We have used the positron as a microscopic probe to clarify the connection between the microscopic properties (e.g., free volume distributions) and macroscopic properties (pressure, volume, and temperature relations) of polymers in the glassy state. Measurements of the positron lifetime distribution in the polymer as a function of temperature, aging, and applied strain have shown that positrons are sensitive to the distribution of free volume elements. However, we have also found that refinements in data analysis are necessary, and that we are far from obtaining an unambiguous free-volume distribution from the current results. Theoretical models are being tested to see if they are consistent with the results. We have also generated simulated positron lifetime distributions to test the validity of our curve-fitting methods, and we have discovered that these methods break down when the instrumental resolution curve exceeds approximately 250 nanoseconds, in width. DTIC

N93-29881# Mar, Inc., Rockville, MD.
DEVELOPMENT OF A TEST PROGRAM TO EVALUATE STRUCTURAL DEFECTS IN GLASS-REINFORCED PLASTIC (GRP), VOLUME 2 Final Report, Dec. 1991 - Nov. 1992
Edward F. McClave and Michael J. Goodwin Nov. 1992 104 p
(Contract DTCG39-91-D-E33A21)
(AD-A263814; R/DC-16B/92-Vol-2; USCG-D-02B-93-Vol-2) Avail: CASI HC A06/MF A02

A mechanical testing program was developed for evaluation of the weakening effects of different types of commonly encountered flaws on the strength of composite boat hulls. A specification was developed for production of test coupons containing realistic and consistently reproducible simulated defects. Tensile and flexural testing procedures were specified, including development of a technique for tensile testing of cored specimens. A statistically-based test plan was developed. A mechanical testing program was conducted in which approximately 400 specimens were subjected to either tensile or flexural testing. This program was conducted to verify specimen production techniques, to validate mechanical testing procedures, and to acquire information about the statistical variability of test results, which is necessary for planning future experiments. The data from the testing also supported a limited number of conclusions about the effects of defects on the strength of composite specimens of solid, balsa-cored, and plastic foam-cored construction. DTIC

N93-29886# Mar, Inc., Rockville, MD.
DEVELOPMENT OF A TEST PROGRAM TO EVALUATE STRUCTURAL DEFECTS IN GLASS-REINFORCED PLASTIC (GRP), VOLUME 1 Final Report, Dec. 1991 - Nov. 1992
Edward F. McClave and Michael J. Goodwin Nov. 1992 260 p
(Contract DTCG39-91-D-E33A21)
(AD-A263813; R/DC-16A/92-Vol-1; USCG-D-02A-93-Vol-1) Avail: CASI HC A12/MF A03

A mechanical testing program was developed for evaluation of the weakening effects of different types of commonly encountered flaws on the strength of composite boat hulls. A specification was developed for production of test coupons containing realistic and consistently reproducible simulated defects. Tensile and flexural testing procedures were specified, including development of a technique for tensile testing of cored specimens. A statistically-based test plan was developed. A mechanical testing program was conducted in which approximately 400 specimens were subjected to either tensile or flexural testing. This program was conducted to verify specimen production techniques, to validate mechanical testing procedures, and to acquire information about the statistical variability of test results, which is necessary for planning future experiments. The data from the testing also supported a limited number of conclusions about the effect's of defects on the strength of composite specimens of solid, balsa-cored, and plastic foam-cored construction. DTIC

N93-30007# Army Research Lab., Watertown, MA.
APPLICATIONS OF LASER LIGHT SCATTERING IN POLYMER DILUTE SOLUTION CHARACTERIZATION Final Report
Marie K. Potts Feb. 1993 31 p
(AD-A263110; ARL-TR-85) Avail: CASI HC A03/MF A01

Dynamic light scattering (or photon correlation spectroscopy, PCS) can be used to determine the frequency distribution of the light scattered from polymer solutions. This distribution contains information about the dynamics of the system. Depending on the wavelength of radiation and the size of the polymer molecule, the translations and rotations of the entire molecule, or the motions of the monomers can be studied. This information, combined with static light scattering (the traditional Zimm Plot analysis), can yield a molecular weight distribution (MWD), z-average radius of gyration (R sub g), hydrodynamic radius (R sub h), translational diffusion coefficient (D sub t), and in some cases a rotational diffusion coefficient (D sub r). Dynamic light scattering (DLS) has been used extensively in the dilute solution regime to determine the type of information listed above, and the theories associated with the various phenomena are well defined. DLS can also be applied to the analyses of semi-dilute solutions and to study the dynamics of entangled systems (e.g., polymer melts or diffusion of polymer chains in a matrix), although the interpretation of this type of DLS is still speculative. This report will focus on the use of DLS to determine translational diffusion coefficients, and the combination of static and dynamic Light scattering to determine molecular weight distributions. DTIC

N93-30024# Office National d'Etudes et de Recherches Aerospatiales, Paris (France).
DETERMINATION OF THE SPACE CHARGE DISTRIBUTION WITHIN AN e-IRRADIATED POLYMER USING THE PRESSURE WAVE PROPAGATION METHOD Ph.D. Thesis - Paris VI Univ. [APPLICATION DE LA METHODE DE L'ONDE DE PRESSION A L'ETUDE DE POLYMERES IRRADIES EN AMBIANCE SPATIALE]
Marie-Pierre Cals 1990 187 p In FRENCH
(ONERA-P-1990-4; ETN-93-92721) Avail: CASI HC A09/MF A02

In the framework of a study of Electro Static Discharges (ESD) on geostationary satellites, a report on the determination of the space charge distribution in e(-) irradiated polymers by the pressure wave propagation method is presented. A pressure pulse generated in the sample by a Nd-YAG pulsed laser is used as a virtual probe of the charge distribution. This method is a powerful tool for measuring space charge distributions in dielectric materials and studying their evolution. An experimental simulation of charging and discharging processes in e(-) irradiated Teflon, Kapton, or PET films is performed. The main results concern the following: charge injection at interface, charge transport in Kapton under high electric field stress, electron range in polymers, and ESD mechanisms. ESA

N93-30028# Massachusetts Inst. of Tech., Cambridge. Dept. of Chemistry.
APPLICATIONS OF TRANSITION METAL COMPOUNDS IN THE PREPARATION OF USEFUL SILICON-CONTAINING CERAMICS
Dietmar Seyferth 20 Apr. 1993 11 p
(Contract N00014-91-J-1590)
(AD-A264028; TR-41) Avail: CASI HC A03/MF A01

There have been many studies of the reactions of organosilicon compounds with diverse transition metal complexes. The original impetus for this research activity was given by the discoveries that heterogeneous platinum and palladium catalysts and chloroplatinic acid were effective hydrosilylation catalysts. In the year that followed, many other transition metal complexes were found to catalyze the addition of silicon hydrides to organic multiple bonds. Also, transition metal complexes were found to catalyze other reactions of organosilicon compounds, such as the insertion of acetylenes and other unsaturated organic compounds into reactive Si-Si bonds and reactions of the Si-C bonds of strained cyclic organosilicon compounds. A different focus on silicon-transition metal chemistry was found in Aylett's preparation of H3Si-transition metal compounds. These were found to be effective precursors for transition metal silicides by chemical vapor deposition. This potentially useful application in materials processing led to further work by others on the synthesis of transition metal complexes containing metal-silicon bonds. DTIC

N93-30047# Oak Ridge National Lab., TN.
THE DRIVE TO COST-EFFECTIVE STRUCTURAL CERAMICS
R. B. Schulz (Department of Energy, Washington, DC.) and D. R. Johnson 1992 7 p Presented at the Annual Automotive Development Technology Contractors' Coordination Meeting, Dearborn, MI, 2-5 Nov. 1992
(Contract DE-AC05-84OR-21400)
(DE93-009722; CONF-9211101-6) Avail: CASI HC A02/MF A01

The Ceramic Technology Program, initiated to develop high-reliability ceramics for applications in advanced automotive heat engines, has broadened its emphasis to cost-effective ceramics for midterm engines as well as long-term advanced engines. The new direction in the program has resulted from the recognition that the high cost of ceramic components is limiting commercial development, even though the reliability of ceramics has been improved significantly. A comprehensive program was undertaken to reduce the cost of ceramic components by reducing the costs associated with powders, forming, densification, and machining processes. Program highlights include a new effort to develop a low-cost source of high-quality silicon nitride powder, recent progress in a program to improve the reliability of silicon nitride ceramics; a forming method called gelcasting; microwave-processed sintered reaction bonded silicon nitride; a low-cost, high-performance silicon carbide; and development of a continuous belt furnace for low-cost densification of silicon nitride. DOE

N93-30051# Sandia National Labs., Albuquerque, NM.
CHROMATE-FREE CORROSION RESISTANT CONVERSION COATINGS FOR ALUMINUM
R. G. Buchheit (Centaur Associates, Inc., Washington, DC.) and G. E. Stoner (Virginia Univ., Charlottesville.) 1993 4 p Presented at the 18th Department of Energy (DOE) Compatibility, Aging and Service Life Conference, Aiken, SC, 20-22 Apr. 1993
(Contract DE-AC04-76DP-00789)
(DE93-009835; SAND-93-0591C; CONF-9304103-1) Avail: CASI HC A01/MF A01

A method for generating chromate-free corrosion resistant coatings on aluminum alloys using a process procedurally similar to standard chromate conversion was developed. These coatings provide good corrosion resistance on 6061-T6 and 1100 A1 under salt spray testing conditions. The resistance of the new coating is comparable to that of chromate conversion coatings in four point probe tests, but higher when a mercury probe technique is used. Initial tests of paint adhesion, and under paint corrosion resistance are promising. Primary advantage of this new process is that no hazardous chemicals are used or produced during the coating operation. DOE

N93-30112# Office National d'Etudes et de Recherches Aerospatiales, Paris (France).
STUDY OF CODEPOSITION OF ALUMINUM-HAFFNIUM AND DEPOSITION OF YTTRIUM BY THE CEMENTATION TECHNIQUE: ELABORATION OF Ni-Cr-Al AND Ni-Cr-Al-Hf FELT MATERIALS Ph.D. Thesis - Orleans Univ., 1989 [ETUDE DU CODEPOT ALUMINIUM-HAFNIUM ET DU DEPOT D'YTTRIUM PAR VOIE THERMOCHIMIQUE: CONTRIBUTION A L'ELABORATION DE FEUTRES METALLIQUES NI-CR-AL ET NI-CR-AL-HF]
Guillaume Leprince Sep. 1990 203 p In FRENCH
(ONERA-NT-1990-9; ETN-93-93727) Avail: CASI HC A10/MF A03

A low pressure gas phase aluminizing technique, where the substrates are treated in the gas phase, over the pack, in a semi-open chamber maintained under reduced pressure, is reported. A stable halide, like aluminum fluoride, is always present in the condensed state in the chamber, and hence, the process is controlled by the metal activities in the pack, the total pressure, and the temperature. The conditions necessary to increase the gaseous transport rate are deduced from a gaseous diffusion model, which takes into account the knudsen diffusion contribution at the lower pressures, inside narrow cavities of complex shaped substrates or porous materials. Using this technique, aluminization of fibers 12 micrometers in diameter of 90 percent porosity, for Ni-20 percent Cr felts and the codeposition of aluminum + hafnium and deposition of ytrrium on the same base material, were performed. Cyclic oxidation tests were performed on these materials at 900, 1000, and 1100 C (lifetime greater than 1000 1 h cycles) whereas hafnium doped specimens resist as high as 1000 C for the same duration. ESA

N93-30129# Los Alamos National Lab., NM.
WHISKER TOUGHENING OF CERAMIC MATERIALS: A REVIEW
M. Bengisu and T. O. Inal 1993 73 p Prepared in cooperation with New Mexico Inst. of Mining and Technology, Socorro, NM
(Contract W-7405-eng-36)
(DE93-011565; LA-SUB-93-11/2) Avail: CASI HC A04/MF A01

Whisker reinforcement of ceramic and glass materials leads to improved toughness along with other mechanical properties. The most significant toughening mechanisms in whisker reinforced ceramics are crack bridging, whisker pullout, and crack deflection, according to a large number of theoretical and experimental studies. Important parameters in whisker toughening are whisker volume fraction, pullout length, whisker strength, and whisker-matrix compatibility. Depending on the whisker-matrix combination selected, limitations may arise at high temperatures due to oxidation, chemical reaction, and creep. Nevertheless, improved mechanical properties and the relative ease in fabrication of whisker reinforced ceramics, compared to fiber reinforced ceramics, opens a wide range of application opportunities for this class of materials. DOE

N93-30169# Massachusetts Inst. of Tech., Cambridge. Dept. of Chemistry.
SYNTHESIS OF CHIRAL MOLYBDENUM ROMP INITIATORS AND ALL-CIS HIGHLY TACTIC POLY-2,3-R2NORBORNADIENE (R = CF3 OR CO2Me) Technical Report
David H. McConville, Jennifer R. Wolf, and Richard R. Schrock 30 Apr. 1993 11 p
(Contract N00014-92-J-1433)
(AD-A264133; TR-19-ONR) Avail: CASI HC A03/MF A01

Well-defined molybdenum ROMP catalysts that contain C2-symmetric diolate ligands (tartrates, binaphtholates, or biphenolates) have been prepared and shown to polymerize 2,3-R2norbornadienes (R = CF3 or CO2Me) to give, in the most favorable case, greater than 99% cis polymers that are much greater than 99% tactic. DTIC

N93-30170# Massachusetts Inst. of Tech., Cambridge. Dept. of Chemistry.
METHYLHYDRIDOPOLYSILAZANE AND ITS PYROLYTIC CONVERSION TO Si3N4/SiC CERAMICS Technical Report No. 39
Neal R. Dando, Anthony J. Perrotta, Carsten Strohmann, and Regina M. Stewart 20 Apr. 1993 34 p
(Contract N00014-91-J-1590)
(AD-A264150) Avail: CASI HC A03/MF A01

The present report explores the use of liquid state nuclear magnetic resonance (NMR) spectroscopy for characterizing the methylhydridopolysilazane (MHPS) prepared by the Seyferth/Wiseman procedure and compares the structure of this polymer with other ceramic precursors derived from similar synthetic routes. X-ray diffraction, cross-polymerization (CP) and single-pulse magic angle spinning (MAS) solid state NMR spectroscopy were employed for characterizing temperature-induced short range bonding and phase evolution in MHPS precursors to SiC/Si3N4 ceramics. The molecular weight and methyl substitution of the preceramic polymers is shown to affect the ceramic yield and phase development of these polysilazanes during pyrolysis. Ceramic yields approaching 90% are observed in these systems. CPMAS-NMR is shown to be uniquely capable of identifying the hydrogen-rich environments and the onset of short range SiC and SiN phase development in these amorphous preceramic materials. DTIC

N93-30182# GTE Labs., Inc., Waltham, MA.
DEVELOPMENT OF ADHERENT CERAMIC COATINGS TO REDUCE CONTACT STRESS DAMAGE OF CERAMICS
S. F. Wayne, J. H. Selverian, and D. ONeil Nov. 1992 220 p Prepared for Oak Ridge National Lab., TN
(Contract DE-AC05-84OR-21400)
(DE93-012518; ORNL/Sub-89-95915/2) Avail: CASI HC A10/MF A03

Strongly adherent coatings were deposited on reaction bonded Si3N4 (RBSN), sintered SiC (SSC), and HIP'ed Si3N4 (HSN) and using a newly developed chemical vapor deposition (CVD) process. Performance of the coating was assessed by oxidation, strength and contact stress testing. A new method was developed to experimentally determine the strength and Weibull modulus of thin brittle films on ceramic substrates. A significant portion of the study was devoted to numerical modeling of the coatings in order to understand the contributions of residual stress as different coating materials and thicknesses were combined. Coating designs were further analyzed by simulating the crack growth behavior in multilayer films while accounting for the interface fracture mechanics. This work has shown that the Al2O3+ZrO2 composite coating developed in this program can provide resistance to oxidation and contact stress. Commercial application of the composite coating has been successfully demonstrated by use of the Al2O3+ZrO2 composite as a protective coating on a Si3N4 cutting tool. DOE

N93-30381# Naval Command, Control and Ocean Surveillance Center, San Diego, CA.
TRIPLET STATES AND OPTICAL ABSORPTIONS IN FINITE POLYENES AND CONJUGATED POLYMERS
David K. Campbell, J. T. Gammel, Hai-Qing Lin, and E. Y. Loh, Jr. Mar. 1993 22 p
(AD-A264552) Avail: CASI HC A03/MF A01

We study the nature of triplet states in correlated, quasi one dimensional bands, with emphasis on the half-filled case relevant to conducting polymers. To incorporate both electron-phonon and electron-electron interaction effects, we use a Peierls-extended Hubbard Hamiltonian, which we solve for finite systems via (numerically) exact diagonalization (Lanczos) techniques. We extend our results to polymers using both standard finite-size extrapolation techniques and a novel boundary condition averaging scheme. First, we examine the nature of the lowest triplet state, focusing on the crossover from the free electron picture of neutral soliton pairs to the strongly correlated limit of spin excitations. We then examine the optical absorption spectra corresponding to (allowed) triplet-triplet transitions; for this purpose it is important that our naval boundary condition averaging method maintains sharp gap-edge features with reducing spurious rapid frequency variations produced by the finite-size approximations to the band-to-band continuum. We compare our results to data on triplet transitions in finite polyenes and discuss possible additional experimental implications, including the interpretation of recent spin-dependent photomodulation (SDPM) experiments in both trans-(CH)x and non-degenerate ground state conjugated polymers. DTIC

N93-30417# Stanford Univ., CA. Dept. of Materials Science and Engineering.
FUNDAMENTAL STUDIES OF THE MECHANICAL BEHAVIOR OF MICROELECTRONICS THIN FILM MATERIALS Final Report, 15 Nov. 1988 - 31 Dec. 1992
William D. Nix Apr. 1993 38 p
(Grant AF-AFOSR-0185-89)
(AD-A264334; AFOSR-93-0272TR) Avail: CASI HC A03/MF A01

This document represents a final technical report for AFOSR Grant No. 89-0185. The research program supported under this grant involved a fundamental study of the mechanical properties of microelectronic thin film materials. The focus of the work was on the microscopic processes that lead to stresses in microelectronic thin films and control the mechanical properties of these materials. Our work ranged from studies of interconnect metals, passivation glasses and heteroepitaxial thin film semiconductors. In previous reports we highlighted work done of the mechanical properties of passivation glasses and interconnect metals and the processes of failure of interconnect metals. In this final report we highlighted our work on misfit dislocation formation in heteroepitaxial thin films. The body of the report contains two reports of our work on misfit dislocations. Our overall understanding of misfit dislocations in Si-Ge layers is described in the first report. That report also describes our work on the effect of capping layers on the formation of misfit dislocations. The second report describes our in situ studies of the kinetics of formation of misfit dislocations in Si-Ge films. By measuring the change of substrates curvature as a function of time during annealing we were able to determine the way in which mobile threading dislocation density changes during the course of annealing. DTIC

N93-30497# Massachusetts Univ., Lowell. Dept. of Chemistry.
CONJUGATED SUBSTITUTED IONIC POLYACETYLENES
Alexandre Blumstein 5 May 1993 76 p
(Contract N00014-91-J-1920)
(AD-A264702) Avail: CASI HC A05/MF A01

A new method for polymerization of the acetylenic bond in 2-ethynyl-pyridine and its trimethylsilyl derivative is described. The acetylenic triple bond is activated by quaternization of the pyridine nitrogen by methyltrifluoro methane-sulfonate (triflate). The resulting N-methylethynyl pyzidinium triflate salts polymerize readily to the corresponding poly(N-methylethynyl pyridinium acetylene)triflates when treated with a nucleophilic initiator such as pyridine, or with a free radical initiator (AIBN). The product polymers are substituted ionic polyacetylenes of low DP with extensive backbone conjugation. Spectral data indicate that the conjugation in these systems is, by far, the highest observed for substituted polyacetylenes. DTIC

N93-30541# Defence Research Establishment Suffield, Ralston (Alberta).
THERMAL CYCLER TEMPERATURE VARIATION AND ITS EFFECT ON THE POLYMERASE CHAIN REACTION
Doug E. Bader Mar. 1993 49 p
(AD-A264660; DRES-SR-583) Avail: CASI HC A03/MF A01

The source of variation in Polymerase Chain Reaction (PCR) amplification assays that were encountered periodically in our studies was investigated. Two approaches, namely, PCR/agarose gel analysis and thermal probe analysis, were used. PCR/agarose gel analysis demonstrated random variation in the quantity and quality of amplified product from well to well, both within and between trials. Several modifications to the procedure did not eliminate variability. Thermal probe analysis indicated significant well to well temperature viability among certain wells or groups of wells within trial ($p = 0.01$) and significant temperature viability among certain well positions from one trial to another ($p = 0.05$). Thermal probe analysis also indicated large differences between the programmed setpoint temperatures and the actual temperatures inside the tubes for all three PCR events at the beginning of the soak period and two of three PCR events at the end of the soak period. The data from this investigation and other studies leads to the conclusion that the source of variability in PCR amplification efficiency experienced is most likely due to the inherent inability of our thermal cycler to maintain consistent temperature homogeneity across the heating block during PCR amplification reactions. It is advisable that replicate samples from amplification be prepared since a particular well cannot be expected to provide consistent results from well to well within a trial or from one trial to the next. DTIC

N93-30552# Clarkson Univ., Potsdam, NY.
COLLOID AND INTERFACE CHEMISTRY ASPECTS OF CERAMICS Final Report, 1989 - 1992
Egon Matijevic 30 Apr. 1993 12 p
(Grant AF-AFOSR-0441-89)
(AD-A264685; AFOSR-93-0329TR) Avail: CASI HC A03/MF A01

The major goal of this project was to address the properties and interactions of fine powders of interest in ceramics. In order to arrive at quantitative conclusions and assure reproducibility of data, the first requirement was to have well defined dispersions consisting of uniform particles of different chemical compositions (simple or mixed) and in different shapes. Thus, one part of the program has dealt with the synthesis of such 'monodispersed' powders. Specifically, we have produced colloidal particles of different metals, metal oxides, and silicon nitride. In addition, internally mixed particles of stoichiometrically defined metal ratios (such as metal niobates) and of variable composition have been obtained. Finally, coated particles of inorganic cores covered with shells of either different inorganic compounds or of polymers were prepared. All these systems were characterized in terms of their bulk and surface properties. In the other part of the program, we studied, theoretically and experimentally, interactions between unlike particles (i.e., the stability of mixed dispersions), in order to evaluate compaction and sintering effects of such powders. The rate of heterocoagulation was followed in aqueous dispersion of different combinations of particles and the obtained data were compared with expected values based on different theoretical models. The significant discrepancies between the experimentally evaluated and calculated stability ratios could be reconciled, if the surface charge segregation was taken into account. DTIC

N93-30557# EIC, Inc., Norwood, MA.
OPTICALLY SWITCHABLE CONDUCTIVE POLYMERS Final Report, 15 Jun. - 14 Dec. 1992
Timothy L. Rose and Allan B. Kon 11 Feb. 1993 158 p
(Contract F49620-92-C-0041)
(AD-A264751; AFOSR-93-0288TR) Avail: CASI HC A08/MF A02

The objectives of the project were to synthesize and characterize a polymer that could be switched to its conductive state by intramolecular electron transfer initiated by absorption of light. By covalently bonding the electron donating moiety to the polymer, the rate of switching should be fast and uniform giving it potential applications in optical processing devices. The initial polymer system selected was a polythiophene substituted at the 3 position with a diphenyliodonium salt. Photodissociation of diphenyliodonium chloride in physical contact with the polymer formed the highly oxidizing phenyliodonium radical cation which in turn oxidized the polythiophene backbone. Several approaches tried to synthesize the covalently bound substituted polythiophene were unsuccessful. Polymerization of 3-ferrocenylpyrrole, which also has potential photodoping properties, was also unsuccessful. DTIC

N93-30565*# National Aeronautics and Space Administration. Marshall Space Flight Center, Huntsville, AL.
METHOD OF FABRICATING A ROCKET ENGINE COMBUSTION CHAMBER Patent Application
Richard R. Holmes, inventor (to NASA) (Rockwell International Corp., Huntsville, AL.), Timothy N. McKechnie, inventor (to NASA) (Rockwell International Corp., Huntsville, AL.), Christopher A. Power, inventor (to NASA) (Rockwell International Corp., Huntsville, AL.), Ronald L. Daniel, inventor (to NASA) (Rockwell International Corp., Huntsville, AL.), and Robert M. Saxelby, inventor (to NASA) (Rockwell International Corp., Huntsville, AL.) 27 Jan. 1993 13 p
(NASA-Case-MFS-28569-1; NAS 1.71:MFS-28569-1; US-Patent-Appl-SN-009908) Avail: CASI HC A03/MF A01

A process for making a combustion chamber for a rocket engine wherein a copper alloy in particle form is injected into a stream of heated carrier gas in plasma form which is then projected onto the inner surface of a hollow metal jacket having the configuration of a rocket engine combustion chamber is described. The particles are in the plasma stream for a sufficient length of time to heat the particles to a temperature such that the particles will flatten and adhere to previously deposited particles but will not spatter or vaporize. After a layer is formed, cooling channels are cut in the layer, than the channels are filled with a temporary filler and another layer of particles is deposited. NASA

N93-30580# Department of the Navy, Washington, DC.
CARBORANE-(SILANE OR SILOXANE)-UNSATURATED HYDROCARBON BASED THERMOSETTING POLYMERS Patent Application
Leslie J. Henderson, inventor (to Navy) and Teddy M. Keller, inventor (to Navy) 17 Dec. 1992 27 p
(AD-D015718; US-Patent-Appl-SN-991940; Navy-Case-74948) Avail: CASI HC A03/MF A01

This invention relates to a new class of inorganic-organic hybrid polymers that are formed from linear inorganic-organic hybrid polymers of varying molecular weight. These new high temperature oxidatively stable thermosetting polymers are formed from linear polymeric materials having repeat units that contain at least one alkynyl group for cross-linking purposes and at least one bis(silyl or siloxanyl)carboranyl group. These organoboron thermoset polymers contain an unsaturated cross-linked hydrocarbon moiety. DTIC

N93-30586# Department of the Navy, Washington, DC.
CARBORANE-(SILOXANE OR SILANE)-UNSATURATED HYDROCARBON BASED POLYMERS Patent Application
Teddy M. Keller, inventor (to Navy) and Leslie J. Henderson, inventor (to Navy) 30 Nov. 1992 21 p
(AD-D015717; US-Patent-Appl-SN-983194; Navy-Case-74945) Avail: CASI HC A03/MF A01

This invention relates to a new class of linear inorganic-organic hybrid polymers of varying molecular weight that are useful for making high temperature, oxidatively stable thermosets, and these novel linear polymers are in themselves oxidatively stable at high temperatures between 600 - 1000 C. These new materials have repeat units that contain at least one alkynyl group and at least one bis(silyl or siloxanyl)carboranyl group within the backbone of these linear polymers. These linear polymers can be further polymerized to form thermosets and ceramics. DTIC

N93-30596# Texas A&M Univ., College Station. Dept. of Chemistry.
CHARACTERIZATION OF SLOW CHROMOPHORE REORIENTATION IN NONLINEAR OPTICAL POLYMERS BY TWO-DIMENSIONAL MAS NMR Technical Report No. 6, 1 Jun. 1992 - 31 May 1993
Sharon Taylor-Myers, James G. Nuzzo, and James F. Haw 14 May 1993 23 p
(AD-A264809) Avail: CASI HC A03/MF A01

Two-dimensional 15N MAS NMR spectrometry was used to characterize slow reorientation of the chromophore at temperatures well below T sub g in the prototypical nonlinear optical (NLO) polymer 10% 4-nitroaniline-15N2/poly(methyl methacrylate). Qualitative analysis of 2D contour plots obtained for various mixing times at 289 K suggests that significant reorientation takes place between 0 ms and 200-300 ms, and little or no further change occurs up to 2000 ms. Straightforward statistical arguments were used to devise a simple model for quantitative analysis of integrated peak intensities in 2D MAS spectra. This analysis demonstrates that the chromophore undergoes random isotropic reorientation at the longest mixing times used and permits a calculation of the fraction of oriented chromophore remaining at any intermediate mixing time. The data at 298 K are well fit by an exponential autocorrelation function with a time constant of 91 ms. Limited data obtained at 323 K demonstrate that the chromophore reorientation is thermally activated and permit a rough estimate of the activation energy. The methods reported here should be readily applied to the characterization of chromophore dynamics at moderately long time scales for a variety of NLO polymer materials. Author (DTIC)

N93-30601# Florida Univ., Gainesville. Dept. of Materials Science and Engineering.
WETTING AND DISPERSION IN CERAMIC/POLYMER MELT INJECTION MOLDING SYSTEMS
M. D. Sacks and J. W. Williams 1993 14 p
(Contract DE-FG05-85ER-45202)
(DE93-013240; DOE/ER-45202/T1) Avail: CASI HC A03/MF A01

This program had two major areas of emphasis: (1) factors influencing state of particulate dispersion and rheological properties of ceramic powder/polymer melt mixtures, and (2) effect of interfacial bonding strength on mechanical and rheological properties of ceramic particle/polymer composites. Alumina and silica in various polyethylenes were used. DOE

N93-30610# Princeton Univ., NJ. Dept. of Chemistry.
ORGANOMETALLIC COMPOUNDS AND POLYMERS WITH SECOND AND THIRD ORDER NONLINEAR OPTICAL PROPERTIES Final Report, 1 Dec. 1989 - 30 Nov. 1992
Mark E. Thompson 6 May 1993 18 p
(Grant AF-AFOSR-0122-90)
(AD-A264774; AFOSR-93-0343TR) Avail: CASI HC A03/MF A01

The chemistry carried out with AFOSR support was aimed at exploring new materials with potentially interesting nonlinear optical properties. All of our work involved transition metal complexes. In these materials we can alter either the metal ion or the ligands independently. In this way it is possible to alter the electronic properties of a given complex without altering its molecular or solid-state structure. Second and third order NLO properties were investigated in these materials. Both molecular and bulk nonlinearities were examined as second order candidates, while only molecular nonlinearities were examined for the third order materials. Second order properties in coordination compounds were found to scale Sc approximately equal to Cr greater than or approximately equal to Fe greater than Co. Polar coordination polymers were prepared in which excellent polar order was found in the polyermic chains, however, the adjacent chains pack antiparallel in the crystal leading to no bulk second order activity. Group 4 organometallic complexes were examined for their third order properties. Here the order based on metal was found to be Ti greater than Zr greater than Hf. The nonlinearity is thought to arise from extended molecular orbitals. DTIC

N93-30628# California Univ., Los Angeles. Dept. of Chemistry and Biochemistry.
THE ADHESION OF AgI MOLECULES TO GASEOUS METALLIC SILVER CLUSTER CATIONS Technical Report No. 1974
Clifton K. Fagerquist, Dilip K. Sensharma, Temer S. Ahmadi, and M. A. El-Sayed 6 May 1993 23 p
(Contract N00014-89-J-1350)
(AD-A264820) Avail: CASI HC A03/MF A01

The evaporative channels for the unimolecular dissociation of metastable Ag(X)I(Y)(+) (X = 5-25; Y = 0-4) clusters made by fast atom bombardment of silver foil in the presence of CH3I vapor are observed in the first field free region of a double focussing mass spectrometer. Three dominant neutral evaporative channels were found: Ag loss, Ag2 loss, and AgI loss. Only Ag12I3(+) is found to have an additional channel involving an (AgI)3 loss. Consistent with our previous studies of stable Ag(X)I(Y)(+) clusters, a structural formula of (Ag(X-Y)) + (AgI)(Y) was assumed where the metallic part of the cluster conforms to Jellium model predictions. In comparing the relative evaporative loss of AgI from these metastable clusters, the following were observed: (1) evidence for significant AgI-AgI interaction for clusters whose metallic part has a 1s(sup 2), 1P(sup 2), or 1s(sup 2),1p(sup 4) Jellium configuration; (2) a near constant fractional loss of AgI as the number of AgI units in the parent cluster increases for clusters whose metallic part has a closed main Jellium shell; (3) a relative increase in the fraction loss of AgI as the number of AgI molecules in the parent cluster increases for clusters with an open shell configuration for the metallic part. These observations are discussed in terms of evaporative loss of AgI from structures in which the AgI molecules solvate the metallic part of the cluster. It is proposed that the heat of AgI evaporation is greatly determined by dipole/induced-dipole interactions between the permanent dipole of AgI and the polarizable delocalized electron density of the metallic part of the cluster. DTIC

N93-30656# Sandia National Labs., Albuquerque, NM.
ADHESION OF THICK FILM Au TO ALUMINA CERAMICS
G. C. Nelson, J. J. Stephens, and P. F. Hlava 1993 3 p Presented at the 18th Department of Energy (DOE) Compatibility, Aging and Service Life Conference, Aiken, SC, 20-22 Apr. 1993
(Contract DE-AC04-76DP-00789)
(DE93-009802; SAND-93-0335C; CONF-9304103-3) Avail: CASI HC A01/MF A01

Thick film Au metallizations are commonly used as conductors in hybrid microelectronics that operate at high frequencies. Discrete components are attached to these conductors with Pb/In solder. Intermetallic compounds form and grow in the solid state with time; AuIn2 is the primary compound formed in the Au-Pb/In system. A hybrid unit using this technology failed to consume all of the Au after being artificially aged and then subjected to normal thermal cycle and vibration testing. Postmortem analysis revealed that three capacitors had debonded. The failed parts were studied to determine the failure mechanism(s) and to define a parametric study to characterize the mechanisms that bond the Au thick film to the ceramic substrate. DOE

N93-30773# Instituto de Pesquisas Energeticas e Nucleares, Sao Paulo (Brazil).
EFFECT OF LEAD ADDITION ON THE FORMATION OF SUPERCONDUCTING PHASES IN Bi-Sr-Ca-Cu-O CERAMICS M.S. Thesis [EFEITO DA ADICAO DE CHUMBO NA FORMACAO DE FASES SUPERCONDUTORAS EM CERAMICAS DE BI-SR-CA-CU-O]
A. E. Martinelli 1991 82 p In PORTUGESE
(DE93-606893; INIS-BR-2988) Avail: CASI HC A05/MF A01 (US Sales Only)

Superconducting ceramics with starting composition Bi(2-x)Pb-(x)Sr2Ca2Cu3O(y) (0.0 is less than or equal to x is less than or equal to 0.6) were prepared in order to investigate the effects of partial substitution of Pb for Bi and sintering time and atmosphere in the formation of superconducting phases. For all samples x-ray diffraction analyses were performed to estimate the amount of superconducting phases; superconductivity was analyzed by dc electrical resistance and ac magnetic susceptibility measurements. The main results show that: (1) the longer the sintering time (up to 168 h), the larger the volume fraction of superconducting phases with critical temperature (T(sub c)) greater than the temperature of nitrogen liquefaction; (2) by partially substituting Pb for Bi it is possible to restrain the formation of 2212 phase (T(sub c) = 80 K) and to enhance the amount of 2223 phase (T(sub c) = 105 K); and (3) a heat treatment under oxygen atmosphere before sintering enhances the formation of 2223 phase. DOE

N93-30774# Instituto de Pesquisas Energeticas e Nucleares, Sao Paulo (Brazil).
THE EFFECT OF Bi2 O3 ON THE ELECTRICAL PROPERTIES OF Zr O2: 3 PERCENT Mg O CERAMIC SOLID ELECTROLYTES M.S. Thesis [EFEITO DA ADICAO DE OXIDO DE BISMUTO NAS PROPRIEDES ELETRICAS DE ELETROLITOS SOLIDOS DE ZIRCONIA: 3 PERCENT MAGNESIA]
I. C. Cosentino 1991 64 p In PORTUGESE
(DE93-607029; INIS-BR-2989) Avail: CASI HC A04/MF A01 (US Sales Only)

Three wt% MgO ceramic solid electrolytes were prepared to study the effect of Bi2O3 addition on densification and electrical conductivity. Microstructural characterization was done by x-ray diffractometry, scanning electron microscopy, and electron microprobe analyses. Electrical conductivity measurements were done by two probe dc techniques in the 400 C - 700 C temperature range. The results show that 5 wt% Bi2O3 addition improves densification: 93% TD and 98% TD specimens are obtained from zirconia stabilized by powder mixture and by coprecipitation of oxides, respectively. Moreover, electrical conductivity values are found to be two orders of magnitude higher for ZrO2: 3 wt% MgO with 5% Bi2O3. DOE

N93-30883# Lehigh Univ., Bethlehem, PA. Materials Research Center.
PROCESSING OF NOVEL NANOPARTICLE DISPERSION STRENGTHENED CERAMICS FOR IMPROVED MECHANICAL PERFORMANCE Annual Report No. 1
Helen M. Chan, Martin P. Harmer, and Gary A. Miller 14 Dec. 1992 106 p
(Contract N00014-92-J-1635)
(AD-A264191) Avail: CASI HC A06/MF A02

Nanocomposites have continued to show promise both as structural ceramic materials and as ideal systems in which to design multiphase microstructures. This report focuses on successful techniques for fabricating Al2O3/SiC nanocomposites, the strengthening obtained by the addition of sub-micron SiC particles to Al2O3, and the technological advantages of the nanocomposite. Some of the most significant conclusions of this work are as follows: (1) A technique has been developed to reproducibly fabricate fine-grained nanocomposites of Al2O3 containing 0.15 micrometer SiC particles. (2) It has been confirmed that nanocomposites of Al2O3 containing 5 vol% 0.15 micrometer SiC have exceptionally high unindented strengths. A subsequent annealing step improves these unindented strengths to greater than 1 GPa. (3) The strengthening effect appears to be grain size independent; the strengthening does not diminish even after the matrix grain size is coarsened to the level of 60 microns. This is in marked contrast to undoped Al2O3 in which the unindented strengths decrease significantly as the grain size coarsens. (3) The strengthening mechanism in the nanocomposite is believed to arise from machining-induced residual surface stresses. The function of the annealing step is to relax these stresses slightly (as indicated in preliminary x-ray stress measurements) while significantly decreasing the size of the machining flaws. DTIC

N93-30885# Massachusetts Inst. of Tech., Cambridge. Ceramics Processing Research Lab.
DESIGN, SYNTHESIS, AND CHEMICAL PROCESSING OF HIERARCHICAL CERAMIC STRUCTURES FOR AEROSPACE APPLICATIONS Final Report, 1 Aug. 1989 - 28 Feb. 1993
Wendell E. Rhine, Michael J. Cima, and H. K. Bowen 30 Mar. 1993 218 p
(Contract F49620-89-C-0102)
(AD-A264227; AFOSR-93-0294TR) Avail: CASI HC A10/MF A03

Ceramic materials are beginning to replace conventional materials in high temperature structural applications, but further advances are needed to improve their reliability. To analyze the complex behavior of ceramics, it is useful to consider the structure on four hierarchical levels--namely the molecular-, nano-, micro-, and macroscales. Interactions at and between these various levels of structure exert important and often quite specific influences. The research conducted for this effort involved using chemical approaches to synthesize and process ceramic powders to create and control these hierarchical structures in ceramic materials. With the development of chemical approaches for synthesizing and processing ceramics, it is possible to develop synthetic and processing methods to control the molecular and nanostructure of ceramic powders. This report describes our efforts to synthesize submicron SiC, TiB2, TiC, and TiN powders and nanocomposites from preceramic polymers. Efforts to synthesize epitaxial LiNbO3 films from alkoxide precursors are also described. DTIC

N93-30898# Carnegie-Mellon Univ., Pittsburgh, PA.
PHYSICAL CHEMICAL STUDIES ON MOLECULAR COMPOSITE COMPOSITIONS Final Report, 1 Jan. 1988 - 31 Jul. 1992
Guy C. Berry 20 Feb. 1993 99 p
(Grant AF-AFOSR-0206-89)
(AD-A264834; AFOSR-93-0206TR) Avail: CASI HC A05/MF A02

Research in three areas is described: nonlinear optical (NLO) properties of nematic solutions of PBT; the refractive indices of nematic solutions of

PBT; and the rheological properties of blends of PBT and nylon-66, or PBO and PabBO, where PBT is trans-poly(1,4-phenylene 2,6-benzobisthia-zole), PBO is cis-poly(1,4-phenylene 2,6-benzobisoxazole), PabBO is poly(2,5-benzoxazole), and nylon-66 is poly(hexamethylene adipamide). Fully aligned monodomains of nematic solutions of PBT were used in the first two parts. An unexpected NLO behavior was observed in which the maximum NLO third-harmonic generation did not occur with light polarized along the molecular axis of the rodlike PBT, even though the refractive index is maximum for that case-possible reasons for this behavior are discussed. The rheology of miscible blends of the rodlike chains with flexible or semiflexible chains is discussed using a model accounting for constraints on the rodlike dynamics imposed by the flexible or semiflexible components. It is shown that information from phase equilibria is essential to such an analysis, as the dynamic constraints are correlated with the factors that cause the formation of the nematic phase in such blends. DTIC

N93-30900# California Inst. of Tech., Pasadena.
CONJUGATED POLYMERS FROM CYCLOHEXADIENEDIOL MONOMERS Final Technical Report, 1 Oct. 1991 - 30 Sep. 1992
Robert H. Grubbs 17 Mar. 1993 7 p
(Grant AF-AFOSR-0094-88)
(AD-A264837; AFOSR-93-0216TR) Avail: CASI HC A02/MF A01

A high yield synthetic scheme for poly(paraphenylene) starting from biologically produced cis-5,6-dihydroxy 1,3-cyclohexadiene was developed in which trimethylsiloxy groups on the diol precursor polymer are quantitatively transformed to ester functionalities for facile cis-pyrolytic elimination. The final pyrolysis step appears to be very sensitive to reaction conditions and additives, and can result in some degradation of the polymer backbone. The use of Lewis acid salts such as anhydrous zinc halides or Bronsted acids such as 3,4-dichlorobenzenesulfonic acid as aromatization catalysts was found to lower the aromatization temperature and prevent degradation. The Lewis acid salt catalysts afford dark colored, tough films while the Bronsted acid catalysts afford light colored, malleable foams. Polyphenylenevinylene was also prepared from cis-5,6-dihydroxy 1,3-cyclohexadiene through a precursor polymer route. DTIC

N93-30909# Pennsylvania State Univ., University Park. Dept. of Chemistry.
WATER-SOLUBLE POLYPHOSPHAZENES AND THEIR HYDROGELS
Harry R. Allcock 18 May 1993 11 p
(Contract N00014-91-J-1194)
(AD-A264883; TR-11) Avail: CASI HC A03/MF A01

Descriptions of polyphosphazenes and their relationship to: bioerodible systems; radiation-crosslinking to give hydrogels; surface hydrogel grafting; membranes, blends, and IPN's; gel-immobilized enzymes; and ion-cross-linked hydrogels are summarized. DTIC

N93-30938*# National Aeronautics and Space Administration. Lewis Research Center, Cleveland, OH.
TENSILE CREEP BEHAVIOR OF POLYCRYSTALLINE ALUMINA FIBERS
H. M. Yun and J. C. Goldsby Jul. 1993 11 p
(RTOP 537-04-21)
(NASA-TM-106269; E-7995; NAS 1.15:106269) Avail: CASI HC A03/MF A01

Tensile creep studies were conducted on polycrystalline Nextel 610 and Fiber FP alumina fibers with grain sizes of 100 and 300 nm, respectively. Test conditions were temperatures from 800 to 1050 C and stresses from 60 to 1000 MPa. For both fibers, only a small primary creep portion occurred followed by steady-state creep. The stress exponents for steady-state creep of Nextel 610 and Fiber FP were found to be about 3 and 1, respectively. At lower temperatures, below 1000 C, the finer grained Nextel 610 had a much higher 0.2 percent creep strength for 100 hr than the Fiber FP; while at higher temperatures, Nextel 610 had a comparable creep strength to the Fiber FP. The stress and grain size dependencies suggest Nextel 610 and Fiber FP creep rates are due to grain boundary sliding controlled by interface reaction and Nabarro-Herring mechanisms, respectively. Author (revised)

N93-28829*# Alabama Univ., Huntsville. Dept. of Physics.
X RAY, FAR, AND EXTREME ULTRAVIOLET COATINGS FOR SPACE APPLICATIONS Abstract Only
M. Zukic and D. G. Torr *In* Lunar and Planetary Inst., Workshop on Advanced Technologies for Planetary Instruments, Part 1 1993 p 27-28 (For primary document see N93-28764 11-91)
Avail: CASI HC A01/MF A01

N93-29368*# Vanderbilt Univ., Nashville, TN. Dept. of Materials Science and Engineering.
CRATERING IN GLASSES IMPACTED BY DEBRIS OR MICROMETEORITES
David E. Wiedlocher and Donald L. Kinser *In* NASA. Langley Research Center, LDEF: 69 Months in Space. Second Post-Retrieval Symposium, Part 2 Apr. 1993 p 529-539 (For primary document see N93-29354 11-99)
(Contracts NAS8-156; NAS8-32695; NASA Order L-17761-D)
Avail: CASI HC A03/MF A04

N93-30953*# Duke Univ., Durham, NC. Dept. of Mechanical Engineering and Material Science.
MICROPIPET MANIPULATION OF LIPID MEMBRANES: DIRECT MEASUREMENT OF THE MATERIAL PROPERTIES OF A COHESIVE STRUCTURE THAT IS ONLY TWO MOLECULES THICK
David Needham *In* NASA. Langley Research Center, National Educators' Workshop. Update 92: Standard Experiments in Engineering Materials Science and Technology Jun. 1993 p 99-120 (For primary document see N93-30948 11-23)
Avail: CASI HC A03/MF A04

N93-30963*# California Polytechnic State Univ., San Luis Obispo. Materials Engineering Dept.
A 69 CENT LOOK AT THERMOPLASTIC SOFTENING
Linda S. Vanasupa *In* NASA. Langley Research Center, National Educators' Workshop. Update 92: Standard Experiments in Engineering Materials Science and Technology Jun. 1993 p 273-279 (For primary document see N93-30948 11-23)
(Grant NSF USE-91-52078)
Avail: CASI HC A02/MF A04

N93-30964*# University of Eastern Illinois, Charleston. School of Technology.
SOLVING A PRODUCT SAFETY PROBLEM USING A RECYCLED HIGH DENSITY POLYETHYLENE CONTAINER
Ping Liu and T. L. Waskom *In* NASA. Langley Research Center, National Educators' Workshop. Update 92: Standard Experiments in Engineering Materials Science and Technology Jun. 1993 p 281-292 (For primary document see N93-30948 11-23)
Avail: CASI HC A03/MF A04

N93-30969*# Tulsa Univ., OK. Dept. of Mechanical Engineering.
FRACTURE OF GLASS
John M. Henshaw *In* NASA. Langley Research Center, National Educators' Workshop. Update 92: Standard Experiments in Engineering Materials Science and Technology Jun. 1993 p 351-358 (For primary document see N93-30948 11-23)
Avail: CASI HC A02/MF A04

N93-30974*# Purdue Univ., Elkhart, IN.
PERFORMANCE OF THERMAL ADHESIVES IN FORCED CONVECTION
Nikhil K. Kundu *In* NASA. Langley Research Center, National Educators' Workshop. Update 92: Standard Experiments in Engineering Materials Science and Technology Jun. 1993 p 393-401 (For primary document see N93-30948 11-23)
Avail: CASI HC A02/MF A04

N93-30977*# Norton Co., Northboro, MA.
HIGH THERMAL CONDUCTIVITY OF DIAMOND
Patrick M. Stephan *In* NASA. Langley Research Center, National Educators' Workshop. Update 92: Standard Experiments in Engineering Materials Science and Technology Jun. 1993 p 431-439 (For primary document see N93-30948 11-23)
Avail: CASI HC A02/MF A04

N93-30978*# Battelle Pacific Northwest Labs., Richland, WA.

TEMPERATURE-DEPENDENT ELECTRICAL CONDUCTIVITY OF SODA-LIME GLASS

L. Roy Bunnell and T. H. Vertrees (Kennewick High School, WA.) *In* NASA. Langley Research Center, National Educators' Workshop. Update 92: Standard Experiments in Engineering Materials Science and Technology Jun. 1993 p 441-448 (For primary document see N93-30948 11-23)

Avail: CASI HC A02/MF A04

28 PROPELLANTS AND FUELS

Includes rocket propellants, igniters, and oxidizers; their storage and handling procedures; and aircraft fuels.

For related information see also *07 Aircraft Propulsion and Power, 20 Spacecraft Propulsion and Power,* and *44 Energy Production and Conversion.*

N93-28515# Army Research Lab., Aberdeen Proving Ground, MD.

EXPLOSIVE CONSOLIDATION OF COMBUSTION SYNTHESIZED TiC AND TiB2: PRECURSOR MORPHOLOGY EFFECTS Final Report, 1 Oct. 1987 - 1 Oct. 1989

Laszlo J. Kecskes, Andrus Niiler, Thomas Kottke, Sharon H. Robinson, and Frederick B. Pierce Apr. 1993 41 p

(DA Proj. 1L1-61102-AH-43)

(AD-A263186; ARL-TR-107) Avail: CASI HC A03/MF A01

The combustion synthesis/dynamic consolidation (CS/DC) technique has been applied to titanium-carbon and titanium-boron mixture with different initial precursor carbon and boron powder morphologies. The evolution of the CS/DC product structure was investigated by analyzing and comparing the combustion synthesis products following three fabrication process steps: reacted loose powders, reacted green compacts, and reacted green compacts which were dynamically consolidated shortly after the synthesis. In all cases, the purity of the precursor carbon and boron powders was found to affect the products' residual porosity. However, the dependence of the resultant product grain morphology on the precursors' morphology was not as straightforward. Correlations between the respective product structures and possible reaction mechanisms are discussed. DTIC

N93-28517# Phillips Lab., Edwards AFB, CA.

SPECIFIC IMPULSE CALCULATIONS OF HIGH ENERGY DENSITY SOLID CRYOGENIC ROCKET PROPELLANTS. 1. ATOMS IN SOLID H2 Final Report, period ending Feb. 1993

Patrick G. Carrick Apr. 1993 63 p

(AD-A263208; PL-TR-93-3014) Avail: CASI HC A04/MF A01

Specific impulse calculations for a wide range of input concentrations are reported for atomic additives to solid hydrogen, combusted with liquid oxygen. These specific impulse values are presented in the form of 3D contour plots that reveal information about an entire region of interest. The output product species are also presented in this manner. These plots can be used to determine the optimum performance of any particular additive concentration and provide insight into how the performance level changes with concentration of the additive, temperature in the chamber, and exhaust product species. DTIC

N93-28668# Air Products and Chemicals, Inc., Allentown, PA.

DEVELOPMENT OF ALTERNATIVE FUELS FROM COAL-DERIVED SYNGAS

D. M. Brown 19 May 1992 153 p

(Contract DE-AC22-91PC-90018)

(DE93-011629; DOE/PC-90018/T6) Avail: CASI HC A08/MF A02

The overall objectives of this program are to investigate potential technologies for the conversion of coal-derived synthesis gas to oxygenated fuels, hydrocarbon fuels, fuel intermediates, and octane enhancers; and to demonstrate the most promising technologies at DOE's LaPorte, Texas, Slurry Phase Alternative Fuels Development Unit (AFDU). BASF continues to have difficulties in scaling-up the new isobutanol synthesis catalyst developed in Air Products' laboratories. Investigations are proceeding, but the proposed operation at LaPorte in April is now postponed. DOE has accepted a proposal to demonstrate Liquid Phase Shift (LPS) chemistry at LaPorte as an alternative to isobutanol. There are two principal reasons for carrying out this run. First, following the extensive modifications at the site, operation on a relatively 'benign' system is needed before we start on Fischer-Tropsch technology in July. Second, use of shift catalyst in a slurry reactor will enable DOE's program on coal-based Fischer-Tropsch to encompass commercially available cobalt catalysts - up to now they have been limited to iron-based catalysts which have varying degrees of shift activity. In addition, DOE is supportive of continued fuel testing of LaPorte methanol - tests of MIOO at Detroit Diesel have been going particularly well. LPS offers the opportunity to produce methanol as the catalyst, in the absence of steam, is active for methanol synthesis. DOE

N93-28695*# National Aeronautics and Space Administration. Lewis Research Center, Cleveland, OH.

BENEFITS OF IN SITU PROPELLANT UTILIZATION FOR A MARS SAMPLE RETURN MISSION

Mary F. Wadel Jun. 1993 13 p Presented at the 29th Joint Propulsion Conference and Exhibit, Monterey, CA, 28-30 Jun. 1993; cosponsored by AIAA, SAE, ASME, ASEE

(RTOP 506-42-72)

(NASA-TM-106243; E-7926; NAS 1.15:106243; AIAA Paper 93-2244)

Avail: CASI HC A03/MF A01

Previous Mars rover sample return mission studies have shown a requirement for Titan 4 or STS Space Shuttle launch vehicles to complete a sample return from a single Mars site. These studies have either used terrestrial propellants or considered in situ production of methane and oxygen for the return portion of the mission. Using in situ propellants for the return vehicles reduces the Earth launch mass and allows for a smaller Earth launch vehicle, since the return propellant is not carried from Earth. Carbon monoxide and oxygen (CO/O2) and methane and oxygen (CH4/O2) were investigated as in situ propellants for a Mars sample return mission and the results were compared to a baseline study performed by the Jet Propulsion Laboratory using terrestrial propellants. Capability for increased sample return mass, use of an alternate launch vehicle, and an additional mini-rover as payload were included. CO/O2 and CH4/O2 were found to decrease the baseline Earth launch mass by 13.6 and 9.2 percent, respectively. This resulted in higher payload mass margins for the baseline Atlas 2AS launch vehicle. CO/O2 had the highest mass margin. And because of this, it was not only possible to increase the sample return mass and carry an additional mini-rover, but was also possible to use the smaller Atlas 2A launch vehicle. Author (revised)

N93-28752# Lehigh Univ., Bethlehem, PA.

HIGH OCTANE ETHERS FROM SYNTHESIS GAS-DERIVED ALCOHOLS

K. Klier, R. G. Herman, M. A. Johansson, and O. C. Feeley Feb. 1993 20 p

(Contract DE-AC22-90PC-90044)

(DE93-012470; DOE/PC-90044/9) Avail: CASI HC A03/MF A01

The testing of strongly acidic catalysts for the conversion of a mixture of methanol and isobutanol to ethers and hydrocarbons was continued. Under standardized test conditions the catalysts tested this quarter were: phosphotungstic acid supported on zirconia (PW12/ZrO2), 'niobic acid' (Nb2O5 x H20), and an iron and manganese doped sulfate-modified zirconia (Fe/Mn/ZrO2/SO4(2-)). The overall activity of these catalysts followed the order of Fe/Mn/ZrO2/SO4(2-) is greater than PW12/ZrO2 is greater than Nb2O5 x H2O with the Fe/Mn/ZrO2/SO4(2-) catalyst approaching ZrO2/SO4 (2-) in both activity and selectivity for isobutene production. The effect of the presence of water on the reaction of methanol and isobutanol over ZrO2/SO4(2-) was determined to be insignificant. At 157 C and a feed of 2/1 molar ratio methanol/isobutanol, the production of isobutene was unaffected by the addition of 0.05 and 0.10 parts of water to the 2/1 alcohol feed. Surface areas have been determined for Fe/Mn/ZrO2/SO4(2-) niobic acid, and phosphotungstic acid on silica. After calcination, the surface area for Fe/Mn/ZrO2/SO4(2-) was found to be 83 M2/g. Niobic acid and phosphotungstic acid on silica (PW12/SiO2) were found to have surface areas of 118 and 218 sq m/g, respectively. H-1 NMR was used to determine if and how much 1-butene was present as a product when isobutanol is dehydrated over sulfate-modified zirconia. It was found to be present in small amounts, less than 3% of the product stream. DOE

N93-29251# Los Alamos National Lab., NM.

A SIMPLE MODEL FOR EXPLOSIVES FORMULATION

T. Rivera 1993 5 p Presented at the 1993 MAES National Symposium

on Super Critical Water Oxidation on Energetic Materials, Long Beach, CA, Apr. 1993
(Contract W-7405-eng-36)
(DE93-010703; LA-UR-93-922; CONF-9304110-1) Avail: CASI HC A01/MF A01

A simple model based on surface chemistry is developed, based on simple concepts of contact angle, wetting, and spreading. Results of the modeling can be stated by two simplified rules of thumb: (1) A liquid will spread on the surface of a solid if the surface tension of the liquid is less than the surface free energy of the solid, and (2) The liquid having the surface tension nearest that of the solid will preferentially wet the surface of the solid. These two rules can then be used to define the parameters that constitute a process for formulating a plastic bonded explosive (PBX), which is a crystalline high-explosive material coated with a small amount of plastic polymeric material (the binder). The PBX then can be pressed to a high density, and machined to a specific shape. The pressed and machined explosive material can then be used in a physics experiment to study fundamental properties of either the explosive or some other material. DOE

N93-29296# Illinois Univ., Urbana.
RESPONSE OF ENERGETIC SOLIDS TO LIGHT, HEAT AND SHOCK PULSES Final Report, 1 Jan. 1990 - 31 Dec. 1992
Dana D. Dlott 12 Mar. 1993 6 p
(Contract DAAL03-90-G-0030)
(AD-A263702; ARO-27025.16-CH) Avail: CASI HC A02/MF A01

Despite wide ranging efforts, little is known about the molecular basis of initiation to detonation by shock waves of energetic solid materials. Ultrafast optical spectroscopy was used to study molecular energy transfer and shock wave induced chemistry in energetic materials and related systems. Theoretical models were developed to gain further understanding of these important processes. DTIC

N93-29312# Los Alamos National Lab., NM.
SUPER CRITICAL WATER OXIDATION ON ENERGETIC MATERIALS
J. A. Sanchez 1993 13 p Presented at the 1993 MAES National Symposium on Super Critical Water Oxidation on Energetic Materials, Long Beach, CA, Apr. 1993
(Contract W-7405-eng-36)
(DE93-010704; LA-UR-93-921; CONF-9304110-2) Avail: CASI HC A03/MF A01

Supercritical water oxidation (SCWO) is an innovative process for the destruction of hazardous wastes that occurs above the critical temperature and pressure of water. In this paper we present results for the oxidation of simple organic wastes and the destruction of explosives. We have tested a 50 gal./day mobile tubular reactor using both acetone and hexane as surrogate aqueous wastes in reaction with excess oxygen. For acetone, our results indicate that the fuel and oxidant can be conveniently premixed before heating and the acetone effectively destroyed (greater than 99.999%). By contrast, hexane, and likely other insoluble flammable organics must be separately preheated to above the critical temperature of water to avoid detonation. With regards to the treatment of explosives, we have demonstrated detection-sensitivity-limited destruction (typically greater than 99.9%) of five explosives, HMX, RDX, TNT, NQ, and PETN, in a smaller scale SCWO reactor. Two alternative methods of increasing processing throughput for explosives, which have very low solubility in water at room temperature, were also investigated. They are the use of slurries and the SCWO postprocessing of the products of explosives hydrolyzed in low-temperature, basic solutions. DOE

N93-29402# Wright Lab., Wright-Patterson AFB, OH.
ADVANCED THERMALLY-STABLE, COAL-DERIVED, JET FUELS PROGRAM: EXPERIMENT SYSTEM AND MODEL DEVELOPMENT Annual Report, Jul. 1991 - Sep. 1992
Elmer Klavetter, Steve Martin, Wayne Trott, Tim OHern, and Gerald Nelson Feb. 1993 93 p
(Contract MIPR-FY1455-91N-0638; AF Proj. 3048)
(AD-A262747; WL-TR-92-2105) Avail: CASI HC A05/MF A01

A program entitled 'Thermally-Stable Jet Fuels Development' was initiated in FY89 by the U.S. Air Force, Aero Propulsion and Power Directorate, working jointly with the Department of Energy, Pittsburgh Energy Technology Center. Thermal stability of aviation fuels is of concern because of the potential operation problems arising from fuel degradation under thermal stress conditions. Sandia National Laboratories has been conducting efforts to develop instrumentation for monitoring characteristics of jet fuel degradation and solids deposition and develop models of those mechanisms from the data acquired using that instrumentation. This report describes the instrumentation development, data acquisition, and model parameter determination. Analysis of solid deposits is also described. DTIC

N93-29494# Army Missile Command, Redstone Arsenal, AL. Systems Simulation and Development Directorate.
THE EQUIVALENT FLAT NOSE DIAMETER OF HEMISPHERICAL NOSE CYLINDRICAL PROJECTILES FOR IMPACT INDUCED DETONATION OF ENERGETIC MATERIALS Final Technical Report, Sep. 1991 - 1992
James P. Billingsley and James M. Oliver Dec. 1992 39 p
(AD-A263244; AD-E951998; AMSMI/TR-RD-SS-92-11) Avail: CASI HC A03/MF A01

The analysis of explosive detonation via projectile impact is inherently complex because of the many variables which must be considered. One very important variable is the nose or tip shape of the projectile which contacts the bare unprotected planar surface of the energetic material. This report demonstrates that Hemispherical Nose (HN) projectiles (cylindrical, rods, or spheres) are equivalent to a much smaller Flat Nose (FN) surface. This equivalence is suggested by comparison with appropriate theory and a very limited amount of experimental data for two explosives (PBX-9404 and COMP-B). Author (DTIC)

N93-29762# Army Research Lab., Aberdeen Proving Ground, MD.
THE XNOVAKTC RHEOLOGICAL MODEL Final Report, Nov. 1990 - Apr. 1991
Paul J. Conroy Mar. 1993 36 p
(DA Proj. 1L1-61102-AH-43)
(AD-A263298; ARL-MR-47) Avail: CASI HC A03/MF A01

The rheological model, which is incorporated in the NOVA family of interior ballistic codes (Gough 1974), of which XNOVAKTC is the latest version, is examined in detail. The assumptions which are made in this model are also examined in detail. These assumptions are linked to the availability of experimental data, which may be used to guide constitutive modeling. Both empirical as well as analytical/experimental models are presented to provide the required mathematical closure of the solid-phase model. Previous work in this constitutive modeling area is discussed. Interior ballistic simulations of realistic systems by XNOVAKTC are shown to predict values of intrinsic intergranular bed stress in excess of 100 MPa. However, available mixture stress vs. mixture density measurements have shown pronounced nonlinear behavior at values well below 100 MPa, which suggests that measurements are needed over a wider range of intrinsic stresses. DTIC

N93-29835# Electro Magnetic Applications, Inc., Denver, CO.
MICROSTRUCTURAL MODELING OF ELECTRICAL BREAKDOWN IN SOLID FUEL PROPELLANTS Final Report, 14 Aug. 1987 - 14 Oct. 1990
Ronal W. Larson, Paul D. Beale, John D. Curry, Fred Eriksen, and Michael Frisoni 23 Mar. 1993 33 p
(Contract DAAL03-87-C-0021)
(AD-A263466; EMA-90-R-51; ARO-24927.4-EGS) Avail: CASI HC A03/MF A01

The subject matter in this report is an analytical treatment of the microstructural aspects of Electrostatic Discharge (ESD) ignition of solid rocket motors. ESD hazards of the type described herein are now well known to the solid propellant industry. Since 1985, two accidents involving solid rocket motors have caused the loss of eight lives. These are now accepted to have been initiated by ESD, causing ESD to have become the leading safety hazard within the solid propellant industry. The report describes features of solid propellants that make them particularly susceptible to ESD. Primary emphasis was placed on microstructural modeling to better understand how to mitigate these hazards by understanding the details of the hazard. Attempts were made in this and a companion doctoral thesis to explain (among other things) effects of time (or frequency), propellant formulation, temperature, pressure, and relative humidity. This report explains, but is not intended as a final definitive explanation of, much of the experimental phenomena that is summarized herein. DTIC

N93-30042# Neste Oy, Helsinki (Finland).
NEW HYDROGEN TECHNOLOGIES
1992 29 p
(DE93-778353; NEI-FI-184) Avail: CASI HC A03/MF A01

An overview of the overall hydrogen system is presented. There are separate sections for production, distribution, transport, storage, and applications of hydrogen. The most important methods for hydrogen production are steam reformation of natural gas and electrolysis of water. Of the renewable energy options, production of hydrogen by electrolysis using electricity from wind turbines or by gasification of biomass were found to be the most economic for Finland. Direct use of this electricity or the production of liquid fuels from biomass will be competing alternatives. When hydrogen is produced in the solar belt or where there is cheap hydropower, it must be transported over long distances. The overall energy consumed for the transport is from 25 to 40 % of the initial available energy. Hydrogen storage can be divided into stationary and mobile types. The most economic, stationary, large scale hydrogen storage for both long and short periods is underground storage. When suitable sites are not available, then pressure vessels are the best for short period and liquid H2 for long period. Vehicle storage of hydrogen is by either metal hydrides or liquid H2. Hydrogen is a very versatile energy carrier. It can be used to produce heat directly in catalytic burners without flame, to produce electricity in fuel cells with high efficiency for use in vehicles or for peak power shaving, as a fuel component with conventional fuels to reduce emissions, as a way to store energy, and as a chemical reagent in reactions. DOE

N93-30061 Johns Hopkins Univ., Columbia, MD. Chemical Propulsion Information Agency.
ONR/LANL WORKSHOP ON THE FUNDAMENTAL PHYSICS AND CHEMISTRY OF COMBUSTION, INITIATION, AND DETONATION OF ENERGETIC MATERIALS
Camille T. Hudson, ed. Mar. 1992 508 p Workshop held in Los Alamos, NM, 3-6 Mar. 1992
(Contract N00014-91-C-0001)
(CPIA-Publ-589) Avail: CPIA, 10630 Little Patuxent Pkwy., Suite 202, Columbia, MD 21044-3200 HC

This document contains the abstracts, papers, and selected posters presented at the Office of Naval Research/Los Alamos National Laboratory (ONR/LANL) workshop that was held at the Los Alamos National Laboratory, Los Alamos, New Mexico, 3-6 Mar. 1992. The workshop focused on the fundamental physics and chemistry of the combustion, initiation, and detonation of energetic materials. For individual titles, see N93-30062 through N93-30102.

N93-30062 Delaware Univ., Newark. Dept. of Chemistry.
COMBUSTION/EXPLOSION CHEMISTRY OF BULK MATERIALS
Thomas B. Brill *In* JHU, ONR/LANL Workshop on the Fundamental Physics and Chemistry of Combustion, Initiation, and Detonation of Energetic Materials Mar. 1992 p 1-19 Sponsored by AFOSR and Air Force Avionics Lab. (For primary document see N93-30061 11-28)
Avail: CPIA, 10630 Little Patuxent Pkwy., Suite 202, Columbia, MD 21044-3200 HC

Introduction of new explosive and propellant compounds presents an enormous challenge for persons responsible for performance and safety. Predictive modeling of the ignition, combustion, and explosion process will become an increasingly important contribution of the research arm of the combustion and explosives community. This is because good models can help guide the introduction of new materials into practice in the face of cost, safety, and environmental constraints. Trustworthy models require sound experimental parameters as input. Many of the required variables cannot be obtained during the combustion or explosion process and can only be obtained by simulations. Hence, new experimental methods that can establish chemical and physical details about ignition, combustion, and explosion in a relevant manner are in great demand. Microscale fast thermolysis techniques combined with time-resolved spectroscopy have finally advanced to the point where a direct connection can be made to the macroscale combustion/explosion domain of bulk materials. This connection was made by recognizing that the heterogeneous reaction zone that defines a burning surface is instantly simulated by a rapidly heated thin film of material. This simulation is made with SMATCH/FTIR spectroscopy where the dynamic mass and temperature change are simultaneously measured on a thin film heated at 100 - 350 C/sec. The Arrhenius constants calculated from these data predict the linear regression rate of the bulk material burning at the same temperature and pressure. In this way, fast thermolysis can simulate a burning surface. Chemical details about the burning surface that are obtained by these microscale fast thermolysis techniques are found to be correlated well with findings by others who have investigated the macroscale behavior of the bulk material. The chemical details are explained in viewgraph form. Author (revised)

N93-30063 Sandia National Labs., Livermore, CA. Combustion Research Facility.
THE THERMOCHEMISTRY AND REACTION PATHWAYS OF THE DECOMPOSITION AND COMBUSTION OF ENERGETIC MATERIALS
Carl F. Melius *In* JHU, ONR/LANL Workshop on the Fundamental Physics and Chemistry of Combustion, Initiation, and Detonation of Energetic Materials Mar. 1992 p 21-34 Sponsored in part by DOE (For primary document see N93-30061 11-28)
(Contract N00014-90-F-0078)
Avail: CPIA, 10630 Little Patuxent Pkwy., Suite 202, Columbia, MD 21044-3200 HC

The application of theoretical chemistry and detailed chemical kinetics modeling provides a powerful approach to the understanding of the processes occurring in the decomposition and combustion of energetic materials. Combined with experimental chemical kinetic and flame measurements, it is unraveling the complex chemistry that occurs during the various stages of propellant combustion. In particular, the gas phase thermochemistry and reaction pathways have been investigated theoretically using quantum chemical methods such as Bond-Additivity-Corrected Moeller-Plesset 4th order perturbation theory (BAC-MP4). This approach was used to determine accurate heats of formation and free energies for reaction intermediates of decomposition and combustion of nitramines. The BAC-MP4 method is also used to calculate reaction pathways involving these intermediates. Using a fluid dynamics model for heat and mass transport combined with detailed chemical kinetics modeling, this information can be used to develop a chemical model for nitramine combustion. Important issues regarding the chemical processes of nitramine decomposition, ignition, and combustion are discussed. Differences in decomposition mechanisms for the condensed phase and gas phase are identified. New theoretical chemistry approaches for investigating condensed phase reaction mechanisms are presented. These new methods are applied to nitromethane decomposition. Author (revised)

N93-30064 Emory Univ., Atlanta, GA. Dept. of Chemistry.
THERMAL OXIDATION OF HCN BY NO2 IN SHOCK WAVES **c25**
Y. He, M. C. Lin, and Carl F. Melius (Sandia National Labs., Livermore, CA.) *In* JHU, ONR/LANL Workshop on the Fundamental Physics and Chemistry of Combustion, Initiation, and Detonation of Energetic Materials Mar. 1992 p 35-52 (For primary document see N93-30061 11-28)
(Contracts N00014-89-J-1949; N00014-90-F-0078)
Avail: CPIA, 10630 Little Patuxent Pkwy., Suite 202, Columbia, MD 21044-3200 HC

Both NO2 and HCN are early products of cyclic/polycyclic nitramine decomposition reactions. The kinetics and mechanism of the thermal reaction between these two important species are not yet understood. In this work, we have studied the thermal oxidation of HCN by NO2 at temperatures between 1500 and 2400 k, using a shock tube equipped with two stabilized cw CO lasers. One pair of reaction products, either CO and NO or CO and H2O, could be simultaneously monitored. Kinetic modeling was carried out for these products employing an improved mechanism, which incorporates several new processes involving HNC, the structural isomer of HCN, as well as many newly established reactions involving HNCO. The implications of HNC to the HCN-NO2 chemistry under the present shock tube conditions will be discussed in terms of the BAC-MP4 results. Author (revised)

N93-30065 New Mexico Inst. of Mining and Technology, Socorro. Chemistry Dept.
THERMAL DECOMPOSITION OF NITRAMINES **c25**
James C. Oxley, R. Szekeres, and A. Kooh *In* JHU, ONR/LANL Workshop on the Fundamental Physics and Chemistry of Combustion, Initiation, and Detonation of Energetic Materials Mar. 1992 p 53-54 (For primary document see N93-30061 11-28)

Avail: CPIA, 10630 Little Patuxent Pkwy., Suite 202, Columbia, MD 21044-3200 HC

The thermal decomposition of a number of nitramines was examined in dilute solution. The nitramines examined included aliphatic mononitramines (dimethylnitramine (DMN), diethylnitramine (DEN), dipropylnitramine (DPN), and diisopropylnitramine (DIPN)), cyclic mononitramines (N-nitropiperidine (NPIP) and N-nitropyrrolidine (DP)), cyclic dinitramines (N-dinitropiperazine (pDNP), 1,3-dinitro- 1,3-diazacyclopentane (DNI), and 1,3-dinitro-1,3-diazacyclohexane (mDNP)), and nitramines of military interest RDX, HMX, CL20, and TNAZ. For the aliphatic and cyclic mono- and di-nitramines, the corresponding nitrosamines were the only or major condensed-phase product. For D-MN the products were completely characterized.
Author (revised)

N93-30066 Naval Research Lab., Washington, DC.
ION EMISSION DURING HIGH-ENERGY SPUTTERING OF AMMONIUM DINITRAMIDE AND AMMONIUM NITRATE CRYSTALS AND THE DETERMINATION OF ION DECOMPOSITION PATHWAYS USING TANDEM MASS SPECTROMETRY **c25**
Robert J. Doyle, Jr. *In* JHL, ONR/LANL Workshop on the Fundamental Physics and Chemistry of Combustion, Initiation, and Detonation of Energetic Materials Mar. 1992 p 55-70 (For primary document see N93-30061 11-28)
Avail: CPIA, 10630 Little Patuxent Pkwy., Suite 202, Columbia, MD 21044-3200 HC

The instrument used in this study is a ZAB-2FQ three-stage, high-resolution mass spectrometer that is uniquely configured to study dissociation processes. The geometry of the major components of the instrument is shown. Selected ions may undergo dissociating collisions with gases or unimolecular reactions in the regions between the ion source and the magnet and/or between the magnet and the electric sector and/or in the first quadrupole of the dual quadrupole stage. The stage following each collision region analyzes the collision product ions or is used to isolate a selected ion for further collisions. The preferred method of ion formation is fast-atom bombardment (FAB). Using this method, ions are sputtered directly from the surface of crystalline ammonium dinitramide (ADN) by the application of a high-energy (6-7 keV) beam of xenon atoms. ADN crystals are pressed into soft indium metal for support and are inserted by a probe into the FAB ion source. The ions formed by sputtering are extracted from the ion source and accelerated at high voltage into the mass spectrometer. The four main areas of this work-in-progress are summarized.
Author (revised)

N93-30067 Yale Univ., New Haven, CT. Dept. of Chemistry.
OBSERVATION OF REACTION INTERMEDIATES IN CRYSTALLINE RDX **c25**
J. Michael McBride and John P. Toscano *In* JHU, ONR/LANL Workshop on the Fundamental Physics and Chemistry of Combustion, Initiation, and Detonation of Energetic Materials Mar. 1992 p 71-84 (For primary document see N93-30061 11-28)
(Contract N00014-90-J-4015)
Avail: CPIA, 10630 Little Patuxent Pkwy., Suite 202, Columbia, MD 21044-3200 HC

We have studied low-temperature electron paramagnetic resonance (EPR) and Fourier-transform infrared (FTIR) spectra in single-crystal samples of RDX after photolysis at very low temperatures and with subsequent warming. Only a small fraction of the material was decomposed, probably less than 0.1 percent. The primary goal of this work was to establish reaction schemes for this energetic solid under conditions suitable for the kind of detailed spectroscopic investigation that can identify chemical intermediates and reveal the structure and mechanical properties of their surroundings. Knowledge of these intermediates, their spectral characteristics, and their reaction schemes should prove useful to those who use other techniques to study thermal or shock-induced decomposition of solid RDX.
Author (revised)

N93-30068 University of Southern California, Los Angeles. Dept. of Chemistry.
NO2 UNIMOLECULAR DECOMPOSITION: STEP-LIKE VARIATION OF k(SUB uni)(E) **c25**
G. A. Brucker, S. I. Ionov, Y. Chen, and Curt Wittig *In* JHU, ONR/LANL Workshop on the Fundamental Physics and Chemistry of Combustion, Initiation, and Detonation of Energetic Materials Mar. 1992 p 85-88 (For primary document see N93-30061 11-28)
Avail: CPIA, 10630 Little Patuxent Pkwy., Suite 202, Columbia, MD 21044-3200 HC

The photoinitiated unimolecular reaction of NO2 is the only case in which a stable triatomic can be excited optically via an allowed one-photon transition to levels above the reaction threshold that have predominantly ground electronic state character. It is known that near-infrared, visible, and ultraviolet photons excite NO2 into a region of strong mixing between the (2)A1 ground state and the (2)B2 electronically excited state. Moreover, excitation between 250 and 398 nm results in NO2 decomposition to NO and O in their electronic ground states. Energies above reaction threshold, 25130.6/cm, are spectroscopically accessible over a broad, continuously tunable range, and NO is particularly amenable to sensitive, state-selective detection. Recent studies have successfully assigned NO2 vibrational levels of the ground electronic state up to 10,000/cm and the density of vibronic levels on the strongly coupled (2)A1 and (2)B2 electronic surfaces has been experimentally estimated in the region 16,500-18,500/cm. Moreover, spectra of extremely cold expansion-cooled samples have been taken in the region just below D(sub 0). Such data provide experimental assessments of level densities near D(sub 0) facilitating comparisons between theoretical predictions and measured reaction rates.
Author (revised)

N93-30069 Sandia National Labs., Albuquerque, NM.
THERMAL DECOMPOSITION CHEMISTRY AND SHOCK SENSITIVITY OF THERMALLY AGED EXPLOSIVES
Anita M. Renlund, Kenneth L. Erickson, and Wayne M. Trott *In* JHU, ONR/LANL Workshop on the Fundamental Physics and Chemistry of Combustion, Initiation, and Detonation of Energetic Materials Mar. 1992 p 89-121 Sponsored in part by ONR (For primary document see N93-30061 11-28)
(Contract DE-AC04-76DP-00789)
Avail: CPIA, 10630 Little Patuxent Pkwy., Suite 202, Columbia, MD 21044-3200 HC

Thin-film samples of energetic material were used in the investigation of thermal decomposition chemistry under a variety of conditions. Decomposition was examined by utilizing the following: (1) confined samples of RDX or TATB maintained at an elevated temperature for up to 20 hours; (2) confined samples of RDX, HMX, TATB, HNS, or PCN heated at rates of 5-10 C/sec; and (3) pulsed laser heated (greater than 10 C/sec) RDX samples with no confinement. In the first two experiments, condensed-phase processes were examined using IR absorption spectroscopy (conventional IR and time-resolved infrared spectral photography). Observed products include H2O (consistently seen in heated nitramines), CH2O, and HCN. Gas-phase products of the rapidly heated RDX films were detected by time-of-flight mass spectrometry. Observed signals include clear signatures of decomposition products (m/z = 15 and m/z = 97) as well as ion masses arising from fragmentation of the parent molecule. In related experiments, the Velocity Interferometer System for Any Reflector (VISAR) was used to monitor reactive wave growth in energetic materials subjected to combined thermal and impact events. Sustained shocks were introduced into heated and confined samples of PBX 9502 and PBX 9404 using projectiles driven by a 63-mm-diameter light gas gun. Enhanced sensitivity to shock initiation was observed at sample temperatures as low as 140 C. The roles of elevated temperature, temperature-dependent sample density, and decomposition chemistry are discussed.
Author (revised)

N93-30070 Societe Nationale des Poudres et Explosifs, Paris (France).
PROPULSION AND DETONICS RESEARCH IN FRANCE
Jacques Boileau *In* JHU, ONR/LANL Workshop on the Fundamental Physics and Chemistry of Combustion, Initiation, and Detonation of Energetic Materials Mar. 1992 p 123-125 (For primary document see N93-30061 11-28)
Avail: CPIA, 10630 Little Patuxent Pkwy., Suite 202, Columbia, MD 21044-3200 HC

We present an overview of the present situation in France in the areas of Propulsion and Detonics. In each part, we begin with a short explanation of the French organization and of the research programs' targets. This is followed by the description of some recent results. Additionally, we provide information on future projects. The following topics are discussed: research into improved performance; economic considerations; and increased knowledge of the combustion or detonation mechanisms at the macroscopic and molecular levels. Author (revised)

N93-30071 Naval Research Lab., Washington, DC. Theoretical Chemistry Section.

CHEMICAL DYNAMICS SIMULATIONS AS A PROBE TO THE INITIATION AND PROPAGATION OF CONDENSED PHASE DETONATIONS **c25**

Carter T. White, Daniel H. Robertson, Mark L. Elert (Naval Academy, Annapolis, MD.), and Donald W. Brenner *In* JHU, ONR/LANL Workshop on the Fundamental Physics and Chemistry of Combustion, Initiation, and Detonation of Energetic Materials Mar. 1992 p 127-129 Sponsored by ONR (For primary document see N93-30061 11-28)

Avail: CPIA, 10630 Little Patuxent Pkwy., Suite 202, Columbia, MD 21044-3200 HC

A detonation propagates through a solid explosive as a shock wave accompanied by a rapid rise in temperature, pressure, and density, which induce the exothermic chemical reactions that are necessary to sustain it. Because of the extremely short time and length scales involved, molecular dynamics simulations provide a potentially powerful probe of the interplay between shock waves and chemistry at the detonation front. This approach may also yield insight into the processes that lead to the onset of detonation as well as clarify the relationship between the discrete shock induced chemistry and those properties of solid explosives that can be understood based on continuum (hydrodynamic) theories. For these simulations to be at all convincing, however, a model must be devised that is sufficiently simple to treat condensed phase systems while incorporating traditional chemical concepts such as concerted reactions and energy release via the formation of strong chemical bonds. We have developed a model for a two-dimensional diatomic energetic molecular solid using Tersoff-type potentials that does have these essential ingredients. Simulations using this model display characteristics expected of a macroscopic detonation while exhibiting rich properties such as shock wave splitting which can be understood based on classical continuum concepts. Our results suggest the potential importance of dissociative transitions and rarefaction shock waves in understanding detonations. Author

N93-30072 Los Alamos National Lab., NM.

VIBRATIONAL SPECTROSCOPY OF SHOCK-COMPRESSED FLUIDS **c25**

Stephen C. Schmidt, James D. Johnson, David S. Moore, Milton S. Shaw, and Richard LeSar *In* JHU, ONR/LANL Workshop on the Fundamental Physics and Chemistry of Combustion, Initiation, and Detonation of Energetic Materials Mar. 1992 p 131-147 (For primary document see N93-30061 11-28)

Avail: CPIA, 10630 Little Patuxent Pkwy., Suite 202, Columbia, MD 21044-3200 HC

Coherent anti-Stokes Raman spectroscopy is being used to study the structure and energy transfer in simple molecular liquids at high pressures and temperatures. Dense fluids to several thousand degrees temperature and several hundred kilobars pressure are obtained using the shock compression technique. These pressures and temperatures are comparable to those experienced during explosive detonation and product expansion. Vibrational frequencies, third-order susceptibility ratios and line widths have been determined for N2, O2, CO, mixtures of N2, O2, and CO, and N2O by comparing experimental data to spectra calculated using a semiclassical model. Frequencies are found to increase with pressure. Transition intensity and line width data suggest that thermal equilibrium of the vibrational levels is attained in less than a few nanoseconds at the high pressures and temperatures. Vibrational temperatures obtained are compared to those derived from equation of state calculations. Author (revised)

N93-30073 Washington State Univ., Pullman. Shock Dynamics Lab.

EXAMINATION OF SHOCK INDUCED CHEMICAL REACTIONS IN LIQUIDS USING TIME-RESOLVED OPTICAL SPECTROSCOPY **c25**

Yogendra M. Gupta *In* JHU, ONR/LANL Workshop on the Fundamental Physics and Chemistry of Combustion, Initiation, and Detonation of Energetic Materials Mar. 1992 p 149-162 Sponsored by ONR (For primary document see N93-30061 11-28)

Avail: CPIA, 10630 Little Patuxent Pkwy., Suite 202, Columbia, MD 21044-3200 HC

The overall objective of our work is to develop a detailed understanding of shock induced chemical changes in condensed energetic materials. An extensive experimental effort was undertaken at Washington State University during the 1980's to permit time-resolved, spectroscopic measurements in shocked materials. Because of practical constraints at an academic institution, our work to date has focused on liquid CS2 which was known to undergo a shock-induced chemical change from the continuum measurements and analyses reported by Sheffield. Time-resolved absorption, reflection and Raman (preliminary) experiments have been carried out on liquid CS2 shocked to 115 kbar. Most of the experiments involved reverberation shocks or step-wise-loading (SWL); some of the reflection spectroscopy experiments involved double shock loading to relate the absorption results (SWL) to continuum results (single and double shock loading). Absorption results from very thin sample (1 micrometer) measurements were noteworthy in that the full absorption band (centered at 320 nanometers) could be examined. Our results show that both pressure and temperature alter the electronic properties of CS2. Threshold pressure for chemical reactions ranged from 88-115 kbar in step-wise-loading experiments depending on the temperature. The primary roles of pressure and temperature are the delocalization of pi-electrons and formation of hot bands. The electron delocalization is likely a precursor to the chemical reaction. An important finding of the present work was the result that kinetics and molecular reorientation may be important factors in understanding shock-induced chemical reactions and in relating these data to static pressure results. The reflection experiments validate most of the conclusions from the absorption work. These results link the continuum and spectroscopic results for different thermodynamic states. Despite the many advances in the present work, the exact nature of shocked CS2 over the nanosecond to microsecond time scale has not been established. Vibrational spectroscopy is needed to address this issue. We have started work on nitromethane and preliminary results to date suggest that time-resolved Raman, absorption and reflection data can be obtained for this material. Author (revised)

N93-30074 Los Alamos National Lab., NM.

A STERIC HINDRANCE MODEL FOR THE CRYSTAL ORIENTATION DEPENDENCE OF THE SHOCK INITIATION SENSITIVITY OF PETN EXPLOSIVE

Jerry J. Dick *In* JHU, ONR/LANL Workshop on the Fundamental Physics and Chemistry of Combustion, Initiation, and Detonation of Energetic Materials Mar. 1992 p 163-165 (For primary document see N93-30061 11-28)

(Contract W-7405-eng-36)

(LA-UR-92-1427) Avail: CPIA, 10630 Little Patuxent Pkwy., Suite 202, Columbia, MD 21044-3200 HC

Shock initiation sensitivity of PETN is strongly dependent on crystal orientation. This is explained by a model of steric hindrance at the molecular level due to shear flow associated with shock-induced uniaxial strain. The hindered shear is an endothermic, nonequilibrium process leading to bond breaking and subsequent exothermic decomposition reactions. In an earlier paper it was claimed that the (100) and (010) shock directions were not equivalent in terms of steric hindrance. If one considers the steric hindrance to shear motion of both the body-centered and corner molecules, then it appears that the directions are equivalent. The previous analysis had focussed on steric hindrance to motion of the body-centered molecule. In sensitive, hindered orientations the shear flow may be supercritical, that is, simultaneous shear may be occurring as the strength of the perfect lattice is exceeded. Examination of previously published elastic precursor strengths in inert materials makes it seem likely that simultaneous shear may occur in other materials where the primary slip system is not available, especially in quartz. Derived from text

N93-30075 Massachusetts Inst. of Tech., Cambridge. Dept. of Chemistry.

SINGLE-SHOT FEMTOSECOND SPECTROSCOPY: A METHODOLOGY FOR OBSERVATION OF SOLID-STATE CHEMICAL REACTIONS **c25**

Weining Wang and Keith A. Nelson *In* JHU, ONR/LANL Workshop on the Fundamental Physics and Chemistry of Combustion, Initiation, and Detonation of Energetic Materials Mar. 1992 p 167-172 (For primary document see N93-30061 11-28)

Avail: CPIA, 10630 Little Patuxent Pkwy., Suite 202, Columbia, MD 21044-3200 HC

We have constructed and begun testing an apparatus for single-shot femtosecond spectroscopy. A single probe pulse is split with n beam splitters to produce 2(n) separate probe pulses, each of which is delayed by a different amount and directed into the sample. In this manner 2(n) points on the time axis are monitored in a single laser shot. We have now recorded the first test data, using the apparatus with 16 probe pulses. This methodology will permit time-resolved solid-state photochemistry experiments in which absorption of the excitation pulse initiates chemistry in an electronic excited state. Another class of experiment involves not absorption but 'impulsive' stimulated Raman scattering (ISRS) of the femtosecond excitation pulse. Through ISRS, coherent lattice vibrations can be driven. It should be possible to reach large lattice vibrational amplitudes, comparable to those characteristic of shock waves (but with just a few, selected lattice modes excited). However this involves high light intensities which cause sample damage due to various nonlinear optical mechanisms. Recording the full time-resolved material response to ISRS 'microshock' excitation with just one laser shot will permit high intensities to be used. Sample damage will be greatly reduced, and will not prevent data collection even when it does occur. Derived from text

N93-30076 Los Alamos National Lab., NM. Chemical and Laser Sciences Div.

DETONATION MASS SPECTROMETRY c25

N. Roy Greiner, Herbert A. Fry, and Normand C. Blais *In* JHU, ONR/LANL Workshop on the Fundamental Physics and Chemistry of Combustion, Initiation, and Detonation of Energetic Materials Mar. 1992 p 173-188 (For primary document see N93-30061 11-28)

Avail: CPIA, 10630 Little Patuxent Pkwy., Suite 202, Columbia, MD 21044-3200 HC

Detonation reactions in laboratory-scale (30-250 mg) pellets of solid high explosives are quenched in a series of stages by unconfined free expansion into a high vacuum, and molecular species in the quenched reaction mixtures from 95 contiguous stages (volume elements) are characterized by dynamic time-of-flight mass spectrometry while the material is still expanding freely. The stage at which the detonation reaction begins to quench and the rate of quenching depend on the depth of the volume element in the pellet and the velocity of the rarefaction wave coming from the vacuum interface. Time-sequenced laser-schlieren images of the detonation and quench processes validate a computer model that links the observed chemical composition at each stage to the hydrodynamic history of the corresponding volume element based on the equation of state of the products from the explosive under study. From this analysis we deduce that each volume element to about 20 micrometers deeper in the pellet than the previous one. Sound speed estimates indicate that quenching begins about 3 nanoseconds later for additional layer, and the time-constant for the quench processes is also 3 nanoseconds per layer. These time and length scales should allow resolution of the reaction zone and reactions behind the reaction zone. Molecular models of detonation are challenged and refined by comparing observed mass spectra with spectra predicted by the models. Improved understanding of how molecular structure and reaction dynamics determine the sensitivity and performance of energetic materials is expected to guide both the development of better detonation models and the synthesis of new less sensitive and more powerful high explosives. Derived from text

N93-30077 Los Alamos National Lab., NM.

STRATEGIES FOR UNDERSTANDING THE DEFLAGRATION-TO-DETONATION TRANSITION c25

Blaine W. Asay *In* JHU, ONR/LANL Workshop on the Fundamental Physics and Chemistry of Combustion, Initiation, and Detonation of Energetic Materials Mar. 1992 p 227-242 Previously announced as N92-29512 Sponsored by DOE (For primary document see N93-30061 11-28)

Avail: CPIA, 10630 Little Patuxent Pkwy., Suite 202, Columbia, MD 21044-3200 HC

The deflagration-to-detonation (DDT) phenomenon has been studied for many years. However, no comprehensive model of the DDT process is available. It is important to understand the mechanism by which an explosive will detonate when the source of ignition is a weak shock or flame, and to be able to predict this response. We have identified several key areas of the DDT problem which need to be understood before any such prediction can be made, and have established a modest program to obtain a more fundamental understanding of the behavior of explosive under the conditions that can lead to DDT. Author

N93-30078 Georgia Inst. of Tech., Atlanta. School of Aerospace Engineering.

THE OUTLOOK FOR UNDERSTANDING THE COMBUSTION OF SOLID PROPELLANTS AND WHAT IT WILL TAKE

Edward W. Price *In* JHU, ONR/LANL Workshop on the Fundamental Physics and Chemistry of Combustion, Initiation, and Detonation of Energetic Materials Mar. 1992 p 243-260 Sponsored by ONR (For primary document see N93-30061 11-28)

Avail: CPIA, 10630 Little Patuxent Pkwy., Suite 202, Columbia, MD 21044-3200 HC

An outlook for the development of an understanding of solid propellant combustion is presented. 'Understanding propellant combustion' is characterized as the description of the process in every nontrivial detail, in quantitative form suitable for prediction of the answers to any questions that might be posed by the propellant and rocket propulsion community, and prediction of new technological opportunities. The current understanding of steady state burning of heterogeneous propellants is reviewed and a research strategy for the investigation of propellants with new ingredients is outlined. CASI

N93-30079 Yale Univ., New Haven, CT. Dept. of Mechanical Engineering.

NUMERICAL MODELING OF MULTIDIMENSIONAL FLAMES WITH APPLICATION TO ENERGETIC MATERIALS Abstract Only c25

Mitchell D. Smooke *In* JHU, ONR/LANL Workshop on the Fundamental Physics and Chemistry of Combustion, Initiation, and Detonation of Energetic Materials Mar. 1992 p 261 (For primary document see N93-30061 11-28)

Avail: CPIA, 10630 Little Patuxent Pkwy., Suite 202, Columbia, MD 21044-3200 HC

The coupling of adaptive numerical methods with large memory parallel/vector computers has produced an extremely powerful tool with which to probe flame structure. One such reacting system - the axisymmetric laminar diffusion flame is investigated numerically. The ability to predict the coupled effects of complex transport phenomena with detailed chemical kinetics in these flames is critical in the modeling of energetic materials such as heterogeneous propellants. An unconfined configuration in which a cylindrical fuel stream is surrounded by a coflowing oxidizer jet is considered. Computationally, the governing conservation equations of mass, momentum, species balance, and energy are solved with detailed transport and finite rate chemistry submodels. Up to six processors of an IBM ES/3090 600J in parallel are used to obtain a discrete solution on a two-dimensional grid with Newton's method and adaptive mesh refinement. Unlike some models in which diffusion in the axial direction is neglected, the fully elliptic problem is considered. Author (revised)

N93-30080 Pennsylvania State Univ., University Park. Dept. of Mechanical Engineering.

DETERMINATION OF GAS PHASE SPECIES AND TEMPERATURE PROFILES ABOVE SOLID PROPELLANTS

B. L. Fetherolf and Thomas A. Litzinger *In* JHU, ONR/LANL Workshop on the Fundamental Physics and Chemistry of Combustion, Initiation, and Detonation of Energetic Materials Mar. 1992 p 263-274 (For primary document see N93-30061 11-28)

Avail: CPIA, 10630 Little Patuxent Pkwy., Suite 202, Columbia, MD 21044-3200 HC

Through the support of the Office of Naval Research a microprobe mass spectrometer (MPMS) system has been developed to study the species profiles above the surface of oxidizers, binders and solid propellants during laser heating and laser supported combustion. The objective of the research is to measure the species profiles above the surface of the reacting materials so that the reaction paths responsible for the observed profiles can be determined. The MPMS system has been used to study HTPB, BAMO/NMMO, RDX, BLX-9, XM-39 and most recently ADN. During testing samples are withdrawn from the reacting gases using a quartz microprobe with an orifice diameter of approximately 20 microns which results in a spatial resolution of approximately 100 microns. The gases then enter the MS that can monitor twelve individual molecular weights or execute continuous scans of molecular weight over the range of 2 to 500 amu at rates up to 2000 amu/s. To obtain the spatial variation of the species above the sample surface, the sample position is controlled by a linear actuator which is linked to the microcomputer that controls the MPMS. In addition to the species profiles, temperature profiles in the gas phase are determined using micro thermocouples. In the ADN results reported here, the initial atmosphere was Argon at pressures up to three atmospheres, and the heat flux was 100 W/sq cm for all tests. Testing included molecular weight scans and selected ion monitoring as well as testing with and without movement of the sample. In the molecular weight scans no species with molecular weight above 50 were detected. The major products leaving the sample surface were, in decreasing order of concentration, N2O, H2O, N2, NO2 and NH3. Several tests also indicated reaction of these species which resulted in increases in the concentration of H2O and N2 as well as the production of NO and O2. Based upon the observed species profiles possible reaction routes are suggested and preliminary modeling is performed. The initial modeling is done with an experimentally derived temperature profile imposed on the reaction. The results of the modeling study show the correct trends in major species. Derived from text

N93-30081 Ballistic Research Labs., Aberdeen Proving Ground, MD.

FLAME STRUCTURE STUDIES OF PROPELLANT LIKE LOW PRESSURE FLAMES USING OPTICAL AND MASS SPECTROMETRIC MEANS c25

Andrzej W. Miziolek, R. C. Sausa, W. R. Anderson, D. C. Dayton, C. M. Faust, S. L. Howard, and S. A. Barts *In* JHU, ONR/LANL Workshop on the Fundamental Physics and Chemistry of Combustion, Initiation, and Detonation of Energetic Materials Mar. 1992 p 275-297 Sponsored by ONR (For primary document see N93-30061 11-28)
Avail: CPIA, 10630 Little Patuxent Pkwy., Suite 202, Columbia, MD 21044-3200 HC

The chemistry of propellant like flames is being studied using a well-instrumented flame structure research apparatus which incorporates a number of flame diagnostic techniques for determining flame structure parameters such as temperature, major stable and reactive species profiles. Optical techniques include laser induced fluorescence (LIF), resonance enhanced multiphoton ionization (REM PI), Fourier Transform Infrared (FTIR) spectrometry, and a tunable diode laser (TDL). Also included is a molecular beam mass spectrometer (MB/MS) system consisting of a quartz sampler and a triple quadrupole mass spectrometer. The MB/MS system is a very powerful flame diagnostic tool since it can detect virtually all major and minor flame species. However, the quartz sampler is a potential source of considerable flame perturbation since it can be a substantial heat sink as well as a possible disturbance to the flow field. One of our first studies was aimed at the determination of the flame perturbation by the quartz sampler. In this work we compared the flame profiles for H, O, OH, and CO in a C2H4/O2/Ar flame using optical diagnostics (REM PI for H, LIF for O and OH, and TDL for CO) and the MB/MS technique. In all cases the agreement was found to be good, thus giving us confidence concerning the validity of using the MB/MS flame profile data for flame model comparisons. In a related study using a C2H4/N2O/Ar flame we demonstrated the usefulness of the triple quadruple by distinguishing between CO, N2, and C2H4 which all have a nominal m/z = 28. Similarly, we were able to discriminate between CO2 and N2O at m/z = 44. We have completed a comprehensive experimental and modeling study of a stoichiometric H2/N2O/Ar flame which is one of the simplest nitrogen oxide flames. In this study we have been able to investigate the importance of certain key elementary reactions and to determine the reaction mechanisms for the flame nitrogen species. Upcoming flame structure studies will involve nitrogen dioxide as the primary oxidizer. Author (revised)

N93-30082 Lawrence Livermore National Lab., CA.

PRESSURE DEPENDENCE OF THE REACTION PROPAGATION RATE OF TATB TO 40 GPa c25

M. Frances Foltz and Albert L. Nichols, III *In* JHU, ONR/LANL Workshop on the Fundamental Physics and Chemistry of Combustion, Initiation, and Detonation of Energetic Materials Mar. 1992 p 299-310 (For primary document see N93-30061 11-28)
(Contract W-7405-eng-48)
Avail: CPIA, 10630 Little Patuxent Pkwy., Suite 202, Columbia, MD 21044-3200 HC

The insensitive high explosive 1,3,5-triamino 2,4,6-trinitro-benzene (TATB), laser ignited under high pressure in a diamond anvil cell, exhibits strongly pressure-dependent reaction propagation rates (RPR). Discontinuities in the RPR as a function of pressure (3-40 GPa) were observed at 19, 30, and 40 +/- 1 GPa. Increasing pressure caused a progressive shift in color of the TATB, from yellow at ambient pressure to red, then to black above 30 GPa. In addition, the appearance of high pressure inclusions (sharply delineated polycrystalline zones) was noted. A phase transition analogous to that between graphite and diamond to produce a dense 3-D network wurtzitane structure is postulated. Preliminary work on the high pressure behavior of TATB analogs and aromatic complexes is discussed. A comparison of present data is made with the previously published pressure-dependent RPR curve for nitromethane. Viewgraphs are provided. Author (revised)

N93-30083 Sandia National Labs., Livermore, CA. Combustion Research Facility.

THERMAL DECOMPOSITION PATHWAYS OF RDX IN THE CONDENSED PHASE

Richard Behrens, Jr. and Suryanarayana Bulusu (Army Armament Research, Development and Engineering Center, Picatinny Arsenal, NJ.) *In* JHU, ONR/LANL Workshop on the Fundamental Physics and Chemistry of Combustion, Initiation, and Detonation of Energetic Materials Mar. 1992 p 311-340 Submitted for publication Sponsored by ARO and Army Armament Research, Development and Engineering Center (For primary document see N93-30061 11-28)
Avail: CPIA, 10630 Little Patuxent Pkwy., Suite 202, Columbia, MD 21044-3200 HC

Through the use of simultaneous thermogravimetry modulated beam mass spectrometry (STMBMS) measurements, time-of-flight (TOF) velocity spectra analysis, and H-2, C-13, N-15, and O-18 labeled analogues of RDX, the thermal decomposition products of RDX were identified as H2O, HCN, CO, CH2O, NO, N2O, NH2CHO, NO2, HONO, (CH3)NHCHO, oxy-s-triazine (OST) and 1-nitroso-3, 5-dinitro-hexahydro-s-triazine (ONDNTA). By measuring the temporal behaviors of the gas formation rates of each of these products during a decomposition experiment, the primary reaction pathways that control the decomposition of RDX in both the solid and liquid phases were discovered. Viewgraphs and a description are presented. Author (revised)

N93-30084 Princeton Univ., NJ. Dept. of Mechanical and Aerospace Engineering.

KINETIC STUDIES ON GAS-PHASE REACTION MECHANISMS IMPORTANT TO THE COMBUSTION OF ENERGETIC MATERIALS: THE CO/N2O REACTION

Richard A. Yetter, Frederick L. Dryer, M. Allen, and N. Ilincic *In* JHU, ONR/LANL Workshop on the Fundamental Physics and Chemistry of Combustion, Initiation, and Detonation of Energetic Materials Mar. 1992 p 341-357 (For primary document see N93-30061 11-28)
Avail: CPIA, 10630 Little Patuxent Pkwy., Suite 202, Columbia, MD 21044-3200 HC

Kinetic experiments and modeling calculations on the high temperature reaction of gas phase intermediates associated with the combustion process of energetic polycyclic nitramines and energetic polymers are reported. The chemical systems of interest include the fuels H2, CO, CH2O, CH4, C2H4, HCN, and NH3 and the oxidizers NO2 and N2O. Many of these species have been observed experimentally and/or predicted numerically in the gas-phase above burning propellants. The combinations of these fuels and oxidizers form basic sets of gas-phase kinetic systems necessary to understand in order to build hierarchical reaction mechanisms for the combustion of energetic materials. Results are presented for CO reacting with N2O. The experiments are conducted in a variable temperature (600 K less than T less than 1200 K), variable pressure (1 atm. less than P less than 15 atm.) flow reactor with residence times ranging from 10 ms to 10 s. Reactant, intermediate, and product species concentrations as a function of reaction time are obtained via continuous sampling/thermal quenching of a small fraction of the total gas flow with a stainless steel, water-cooled probe which traverses the length of the 10 cm. diameter reactor tube along its center-line. Analytical detection and quantification of stable species is performed in the sample line by on-line Fourier transform infrared analysis. Additional continuous monitoring of several species is obtained by non-dispersive infrared analysis for CO and CO2 concentrations, by chemiluminescence analysis for NO and NO2 concentrations, by electrochemical analysis for O2 concentration, and by selective thermal conductivity analysis for H2 concentration. Off-line analysis of stable species includes gas chromatography and gas chromatography/mass spectrometry. Temperature measurements are obtained by fine wire silica-coated Pt/Pt-13%Rh thermocouples. The modeling aspects emphasize the use of hierarchical reaction mechanism construction and validation along with reaction flux and gradient sensitivity analysis. Validations of the reaction mechanisms are obtained by comparison of the predicted concentration profiles with the experimentally measured profiles and by sensitivity analysis calculations. Sensitivity analysis is used for coordinating experiment and model development and to identify key species and reactions, and hence, suggest thermochemical and kinetic parameters for future theoretical and experimental study. The results show that in near dry CO/N2O systems, the reaction of CO + N2O yields CO2 + N2 is important and found to have a rate the order of 10(exp 6) cu cm/mol(s). Hydrogen impurities are shown to lower the overall activation energy of the reaction. In the wet CO/O2 system, the rate of CO + HO2 yields CO2 + OH is likely four times larger than recommended literature values. Author (revised)

N93-30085 Illinois Univ., Urbana-Champaign. Dept. of Mechanical and Industrial Engineering.

UNSTEADY COMBUSTION OF ENERGETIC MATERIALS USING LASER-RECOIL **c25**

Quinn Brewster and Steven Son *In* JHU, ONR/LANL Workshop on the Fundamental Physics and Chemistry of Combustion, Initiation, and Detonation of Energetic Materials Mar. 1992 p 359-366 (For primary document see N93-30061 11-28)

Avail: CPIA, 10630 Little Patuxent Pkwy., Suite 202, Columbia, MD 21044-3200 HC

A theoretical and experimental investigation is being conducted on the unsteady combustion of various energetic materials and solid propellants under dynamic radiant heating conditions. The basis of the experimental study is a laser-recoil technique. This technique uses a spatially uniform laser beam to augment and perturb the combustion of the propellant. The recoil thrust is measured using a microforce transducer. Fiber optic transmission measurements are conducted to quantify the laser transmission loss upon passing through the combustion product plume. The analysis is currently being carried out under the assumptions of quasi-steady gas and surface reaction, homogeneous propellant, and one-dimensional flame (or QSHOD theory). The classical linear QSHOD theory was generalized to include the effect of external radiant flux with in-depth absorption. This was done in both the framework of the Zeldovich-Novozkilov (ZN) phenomenological theory and that of the flame description (FD) approach. The relationship of these two approaches was demonstrated for the generalized radiant flux case. The general (non-linear) QSHOD theory was also extended to include external radiation with in-depth absorption and some numerical studies of non-linear effects were conducted. These studies illustrate an effect of the mean radiant flux on the combustion response (both linear and non-linear) which has previously been neglected by most researchers in this area. The theoretical results also indicate the importance of in-depth absorption for most wavelength-material combinations. Also, a method for obtaining the linear response function over a range of frequencies from a single test using a series of radiant pulses is demonstrated. Experimental results were obtained for conventional propellants and energetic materials such as double base propellants and AP/HTPB. These results demonstrate that the laser-recoil technique, when combined with combustion modeling comparisons, offers significant promise as a laboratory technique for characterizing the unsteady combustion of propellants and energetic materials. In this regard, laser-recoil tests offer a significant savings in time and cost relative to T-burner testing. It also appears to be a very sensitive technique for obtaining kinetic parameters under combustion-like conditions. The need for such techniques has been receiving increasing recognition lately. And finally, laser-recoil tests offer a new experimental technique for studying the fundamental mechanism of propellant and energetic material combustion, allowing investigation of the classical QSHOD assumptions as well as the basic behavior of the leading edge flame in multi-dimensional composite propellants. Author (revised)

N93-30086 Maryland Univ., College Park. Dept. of Mechanical Engineering.

DISLOCATION ROLES IN ENERGETIC CRYSTAL RESPONSES

Ronald W. Armstrong and Wayne L. Elban (Loyola Coll., Baltimore, MD.) *In* JHU, ONR/LANL Workshop on the Fundamental Physics and Chemistry of Combustion, Initiation, and Detonation of Energetic Materials Mar. 1992 p 367-378 (For primary document see N93-30061 11-28)

Avail: CPIA, 10630 Little Patuxent Pkwy., Suite 202, Columbia, MD 21044-3200 HC

Energetic crystals show an unusual combination of mechanical properties in being elastically-compliant, but also being relatively hard and brittle. Evidence is presented for the important role that dislocations play in providing an understanding of these strength properties and how they relate to the responses of energetic crystals to mechanical forces or imposed deformations, as occur in impact tests, shocks, and combustion processes. Author (revised)

N93-30087 California Univ., Berkeley. Lawrence Berkeley Lab.

METALLIZATION AT DETONATION FRONTS IN SOLIDS **c25**

John J. Gilman *In* JHU, ONR/LANL Workshop on the Fundamental Physics and Chemistry of Combustion, Initiation, and Detonation of Energetic Materials Mar. 1992 p 379-394 (For primary document see N93-30061 11-28)

Avail: CPIA, 10630 Little Patuxent Pkwy., Suite 202, Columbia, MD 21044-3200 HC

Detonation fronts propagate too fast for thermal activation of the chemical reactions that drive them. Direct electronic excitation is needed. It is proposed that the compression in the front causes metallization of the energetic solid; making it an insulator-metal interface. The compressed conduction electrons provide the high pressure gradient needed to accelerate the ions at the front up to the detonation velocity. A simple method (based on the Keyes antibonding potential) for estimating the pressure peak is given. The calculated peak pressure is about 3B/2 where B is the bulk modulus of the initial solid (compressed state of the material). Thus it is in the megabar range. Herzfeld's theory of the insulator-metal transition which is used to estimate the critical compression for lead azide, and other ionic materials, is presented. It is consistent with the relative sensitivities of the azides. Another model for electronic excitation, Zener band-to-band tunneling, is discussed briefly. In addition to being induced by volumetric compression, metallization can be induced by large shear strains; that is, by large changes in covalent bond angles. This is known to cause metallization in semiconductors (C, Si, Ge, and Sn) when the tetrahedral angle is increased from 109.5 deg to 149.5 deg. It is shown that this critical angular change is consistent with the simple Pauling theory of the covalent bond. The implications for energetic materials such as PETN is discussed. Metallization can be phonon assisted so it is temperature, as well as deformation, dependent. In organic-type materials, it is also facilitated by electron delocalization. This is why the sensitivities of organic explosives tend to depend on the amount of resonance in their bonding. Viewgraphs are provided. Author

N93-30088 Texas Univ., Austin. Dept. of Aerospace Engineering and Engineering Mechanics.

DAMAGE GROWTH IN COMPOSITE PROPELLANTS

Richard A. Schapery *In* JHU, ONR/LANL Workshop on the Fundamental Physics and Chemistry of Combustion, Initiation, and Detonation of Energetic Materials Mar. 1992 p 395-407 (For primary document see N93-30061 11-28)

(Contract N00014-91-J-1738)

Avail: CPIA, 10630 Little Patuxent Pkwy., Suite 202, Columbia, MD 21044-3200 HC

Macrocracking and distributed microcracking in particle-filled rubber are addressed, assuming quasi-static growth (crack speed approx. less than 30 m/s). As an increase in fracture surface area may lead to an increase in sensitivity, interest is in those factors that influence crack growth as well as ways in which this growth can be minimized. Crack growth depends on the driving force as well as the material parameters which determine the resistance to growth. First the driving force and these parameters are discussed, and then behavior for macrocracking at various strain rates, pressures, and temperatures is illustrated. Next, a micromechanical model for predicting microcrack growth in particle-filled rubber is described. The same principles that are used for predicting macrocracking are applied to microcracking. For a propellant which is elastic (except for damage growth), this model leads to an equation that relates the amount of microcracking at a given time to the applied strain Epsilon, undamaged Young's modulus E, characteristic particle size R, and fracture energy G(sub c) (for adhesive or cohesive cracks). Thus, there is a basic dimensionless ratio involving only material parameters and which directly controls the extent of microcracking, Pi(sub 1) = RE/G(sub c). The smaller Pi(sub 1) is the smaller will be the degree of microcracking at a given strain and time. For viscoelastic propellant behavior, a similar result is obtained, but E must be replaced by a suitably defined, effective modulus. The modulus E depends on the shape of the distribution function for particle sizes but not on the size itself. Increased resistance to microcrack growth, for a given strain and particle volume fraction, may be achieved by increasing G(sub c) or by minimizing the product RE through the selection of the distribution of particle sizes. As the last topic, how this latter change can be accomplished is illustrated. The approach consists of first recognizing that the particle size distribution which minimizes the viscosity eta of the uncured propellant mix also minimizes E because E is proportional to eta. Principles for minimizing RE, for any given particle volume fraction and minimum particle size, are described. Author (revised)

N93-30089 Los Alamos National Lab., NM. Theoretical Div.

INTERFACIAL MELTING IN CRACKED EXPLOSIVES

John K. Dienes *In* JHU, ONR/LANL Workshop on the Fundamental Physics and Chemistry of Combustion, Initiation, and Detonation of Energetic Materials Mar. 1992 p 409-421 (For primary document see N93-30061 11-28)

Avail: CPIA, 10630 Little Patuxent Pkwy., Suite 202, Columbia, MD 21044-3200 HC

Research on the role of hot spots in the sensitivity of explosives goes back over a century, but has accelerated significantly in recent years. The difficulty of observing very small regions that are hot for only a very short time makes theoretical results, which can provide important insights, particularly relevant. Hot spots are often associated with void collapse, but there is increasing evidence that the heating localized in shear cracks and shear bands can lead to ignition, and I proposed some years ago that this is the mechanism underlying XDT. Experimental results of Howe and others show that melting occurs in these defects. I will describe how melting was incorporated into the SCRAM code and illustrate its importance with sample calculations for TNT, the explosive used in Howe's BRL experiments. It is emphasized that the thickness of the melted zone is on the order of microns, whereas the HE dimensions are on the order of 10 cm. Thus, special sub-grid methods are required to carry out such calculations. The unified theory of flow, fracture, and fragmentation underlying SCRAM has been developed over a twenty-year period in connection with a variety of applied programs. Author (revised)

N93-30090 Princeton Univ., NJ.

HOMOGENEOUS GAS PHASE KINETIC MODEL WITH GRADIENT SENSITIVITY ANALYSIS FOR HIGH TEMPERATURE PARTICULATE BORON COMBUSTION IN FLUORINE ENRICHED ENVIRONMENTS Abstract Only **c25**

R. Brown, C. E. Kolb, Richard A. Yetter, Frederick L. Dryer, and H. R. Rabitz *In* JHU, ONR/LANL Workshop on the Fundamental Physics and Chemistry of Combustion, Initiation, and Detonation of Energetic Materials Mar. 1992 p 425 (For primary document see N93-30061 11-28)

Avail: CPIA, 10630 Little Patuxent Pkwy., Suite 202, Columbia, MD 21044-3200 HC

Advanced underwater explosive all-gas-product concepts have evolved that may employ mixed nitramine difluoroamino explosives, dinitramino salts, energetic polymers, and aluminum or boron particles. Achieving maximum effectiveness in the application of these new concepts requires the ability to control the post-detonation bubble energy release rates. These rates are intimately coupled to the boron and/or aluminum particle combustion processes that would occur in high pressure, fluorine rich detonation product gases. A homogeneous gas phase kinetic model for high temperature B/O/H/C/F combustion systems is presented. Model results are presented which illustrate the effects of mixture temperature, pressure, and composition on the reaction dynamics of boron oxides, oxyhydrides, fluorides, and oxyfluorides. Reaction flux/pathway techniques and sensitivity analysis theory of isothermal systems are used to identify important reactions. Model results indicate that OBF(g) is a key high temperature intermediate that plays a role similar to HOBO(g) in B/O/C/H combustion systems. Author (revised)

N93-30091 Texas Univ., Austin. Dept. of Physics.

ATOMIC FORCE MICROSCOPY OF AMMMONIUM PERCHLORATE Abstract Only

Alex deLozanne and Minsun Yoo *In* JHU, ONR/LANL Workshop on the Fundamental Physics and Chemistry of Combustion, Initiation, and Detonation of Energetic Materials Mar. 1992 p 427-428 (For primary document see N93-30061 11-28)

(Contract N00014-90-J-1858)

Avail: CPIA, 10630 Little Patuxent Pkwy., Suite 202, Columbia, MD 21044-3200 HC

The (210) surface of ammonium perchlorate (NH4ClO4) with an atomic force microscope in air is studied. Large scale images show monomolecular steps that are often aligned with major crystalline directions. Surface modification is clearly observed with forces as low as 3O nN, but is usually limited to the bottom and the sides of the field of view, where the tip scans for a long time and where it turns around, respectively. At the molecular scale, structures with substantial order, with minimum lateral sizes of 3A were observed. The identification of these features is difficult due to the large unit cell of this compound (40 atoms per unit cell), and the lack of perfect order in the images. The SARCH/LATUSE program developed by Van Hove and Hermann was used to analyze this structure. Ammonium perchlorate is hygroscopic; it is therefore possible that surface modification is enhanced by the moisture present in air. Experiments in a dry atmosphere have recently confirmed this explanation. Author (revised)

N93-30092 Loyola Coll., Baltimore, MD. Dept. of Electrical Engineering.

MICROSTRUCTURAL BASIS FOR ENHANCED SHOCK-INDUCED CHEMISTRY IN SINGLE CRYSTALS OF AMMONIUM PERCHLORATE **c25**

Wayne L. Elban, H. W. Sandusky (Naval Surface Weapons Center, Silver Spring, MD.), B. C. Beard (Naval Surface Weapons Center, Silver Spring, MD.), and B. C. Glancy (Naval Surface Weapons Center, Silver Spring, MD.) *In* JHU, ONR/LANL Workshop on the Fundamental Physics and Chemistry of Combustion, Initiation, and Detonation of Energetic Materials Mar. 1992 p 429-443 Sponsored by ONR and NSWC (For primary document see N93-30061 11-28)

Avail: CPIA, 10630 Little Patuxent Pkwy., Suite 202, Columbia, MD 21044-3200 HC

A number of single crystals of ammonium perchlorate (AP) were shock loaded near the reaction threshold to investigate the effects of concentrated lattice defects (dislocations) and differing crystal orientations on chemical reactivity. Large, optical quality crystals of pure AP were immersed in mineral oil and shocked through either the (001) or (210) surfaces by a detonator. Prior to shock loading, some crystals had localized regions of increased lattice defects and strain created by placing diamond pyramid (Vickers) hardness impressions into their exterior cleavage surfaces. High-speed photographs showed the occurrence of the same slip deformation that was previously determined from hardness testing, and preferential cracking and luminosity near some of the hardness impressions. The shocked crystals were recovered, sometimes intact, for microstructural characterization and chemical analyses. Crystal orientation relative to the shock propagation direction changed the dynamic response and threshold for decomposition of the crystal, much as accommodating the hardness indenter required different slip and crack systems for the various surfaces of unshocked crystals. One recovered crystal was cleaved twice through hardness impressions on the (001) and shock-entry (210) surfaces, allowing spatial analysis of the interior regions of the crystal using x-ray photoelectron spectroscopy (XPS). Along these freshly cleaved surfaces, the XPS results showed enhanced lattice disruption and perchlorate decomposition as a result of the hardness impressions. The greatest decomposition was not immediately adjacent to the impressions, but near the tips of cracks and along slip planes emanating from the impressions a long way into the crystal. Author

N93-30093 Naval Surface Weapons Center, Silver Spring, MD.

DEFECT DENSITY MEASUREMENTS IN A SHOCKED SINGLE CRYSTAL OF AMMONIUM PERCHLORATE **c25**

B. C. Beard, H. W. Sandusky, B. C. Glancy, and Wayne L. Elban (Loyola Coll., Baltimore, MD.) *In* JHU, ONR/LANL Workshop on the Fundamental Physics and Chemistry of Combustion, Initiation, and Detonation of Energetic Materials Mar. 1992 p 445-461 Sponsored in part by ONR (For

primary document see N93-30061 11-28)
Avail: CPIA, 10630 Little Patuxent Pkwy., Suite 202, Columbia, MD 21044-3200 HC

The line widths of x-ray photoelectron spectra have been correlated with dislocation densities in a shock-damaged crystal of ammonium perchlorate (AP). A centimeter-size AP crystal was initially transparent except for several diamond pyramid (Vickers) hardness impression, which provided localized strain centers. The crystal was non-uniformly damaged by a rapidly decaying shock (peak pressure of 24.4 kbar at the entry surface), recovered intact, and cleaved through the impressions. Those cleaved planes permitted interior analysis of the crystal by x-ray photoelectron spectroscopy (XPS) over 1 mm by 1 mm areas. The Cl(2p3,2) line width of the spectra ranged from 1.70 eV for the region of greatest visible damage to 1.22 eV for the region of no visible damage, the same line width as that for unshocked AP (control). The observed damage was compared to photographs in the literature of irradiated AP crystals, for which dislocations densities were reported. This provided an approximate correlation of dislocation density versus XPS line width that was refined by chemically etching and counting dislocations on another cleaved plane in the recovered crystal. By this technique, an approximate 100 times increase in dislocation density was determined for the region of greatest shock damage. While XPS line widths were relatively unaffected by the hardness impressions, their associated strain fields enhanced perchlorate decomposition. Assuming that those perchlorate anions in the vicinity adjacent to dislocations were distorted, ab initio calculations predicted variations in the 2p orbital energy of 0.01 to 0.46 eV, thereby producing the observed line width broadening.
Author (revised)

N93-30094 Naval Surface Weapons Center, Silver Spring, MD.
COMPARISON OF DEFORMATION AND SHOCK REACTIVITY FOR SINGLE CRYSTALS OF RDX AND AMMONIUM PERCHLORATE
H. W. Sandusky, B. C. Glancy, B. C. Beard, Wayne L. Elban (Loyola Coll., Baltimore, MD.), and Ronald W. Armstrong (Maryland Univ., College Park.) *In* JHU, ONR/LANL Workshop on the Fundamental Physics and Chemistry of Combustion, Initiation, and Detonation of Energetic Materials Mar. 1992 p 463-481 Sponsored in part by ONR (For primary document see N93-30061 11-28)
Avail: CPIA, 10630 Little Patuxent Pkwy., Suite 202, Columbia, MD 21044-3200 HC

The role of microstructure on the shock reactivity of large single crystals of cyclotrimethylenetrinitramine (RDX) and ammonium perchlorate (AP) is being studied. Variation in material microstructure was controlled by putting strain centers in external surfaces with indentation hardness testing prior to shock loading and by changing crystal orientation relative to shock propagation direction. Preparatory to the shock experiments, diamond pyramid (Vickers and Knoop) microindentation hardness testing was performed at low strain rates. The resultant plastic impressions were analyzed in detail to yield information about slip and cracking systems, the size and character of the cumulative dislocation strain fields surrounding the impressions, and the effect of cracking on hardness with increasing applied load. The crystals were shock loaded by a detonator at a known standoff distance in an aquarium apparatus containing mineral oil. An image converter camera operating at 1 to 5 million frames per second recorded the spherically expanding shock in the mineral oil, the passage of the shock through the crystal, and the crystal response after shock loading. A number of the shocked crystals were recovered for subsequent microstructural characterization and chemical analysis. Author (revised)

N93-30095 Sandia National Labs., Albuquerque, NM.
ENERGETIC MATERIAL RESPONSE TO ABNORMAL ENVIRONMENTS
Susan H. Fischer, Steven M. Harris, and Anita M. Renlund *In* JHU, ONR/LANL Workshop on the Fundamental Physics and Chemistry of Combustion, Initiation, and Detonation of Energetic Materials Mar. 1992 p 483-484 (For primary document see N93-30061 11-28)
Avail: CPIA, 10630 Little Patuxent Pkwy., Suite 202, Columbia, MD 21044-3200 HC

Although our knowledge of energetic-material phenomena such as detonation, combustion, decomposition, deflagration-to-detonation transition (DDT), and shock initiation has increased greatly, there are still many mechanisms that we do not understand well and cannot predict accurately. The response of energetic materials plays an integral role in intrinsic-surety issues such as safeguarding, refitting, or retiring weapons in stockpile as well as in commercial enterprises. The Nuclear Safety Department at Sandia National Laboratories (SNL) is responsible for characterizing energetic-material response relating to such issues. A number of test series are planned and in progress to investigate the violence of reaction in cookoff, the shock initiation as a function of thermal degradation and mechanical damage, and early phases of combustion and DDT. Some of these activities are described. Author (revised)

N93-30096 New Mexico Inst. of Mining and Technology, Socorro. Center for Explosives Technology Research.
DETONATION SHOCK DYNAMICS OF COMPOSITE ENERGETIC MATERIALS
Jaimin Lee, Per-Anders Persson, and John B. Bdzil (Los Alamos National Lab., NM.) *In* JHU, ONR/LANL Workshop on the Fundamental Physics and Chemistry of Combustion, Initiation, and Detonation of Energetic Materials Mar. 1992 p 485-494 (For primary document see N93-30061 11-28)
Avail: CPIA, 10630 Little Patuxent Pkwy., Suite 202, Columbia, MD 21044-3200 HC

The relationship between the detonation velocity normal to the shock-front and the shock-front curvature was obtained from experimental detonation velocities and shock front shapes for an ammonium nitrate-based emulsion explosive with a density of 1.248 g/cc. By using this relationship in the quasi one-dimensional Euler equations obtained from the detonation shock dynamics theory (DSD), the reaction rate for this material was determined as a function of pressure and density. The one-dimensional initiation experiment (wedge test) was numerically modeled using this rate law. The calculated shock trajectories agreed with the experimental wedge test data over a wide range of initial pressures. This agreement suggests that the small shock-curvature asymptotics that underlies DSD may be valid even for relatively large shock curvatures. The reaction-rate equation obtained for this emulsion explosive shows that the rate is very slow and weakly state dependent. These characteristics of the rate indicated that the nonideal behavior of most emulsion-type explosives can be attributed to their slow and state-insensitive rates. The calibration method developed in this study is independent of the form of the rate. Realistic rate equations for explosives can be obtained in a very systematic way from two-dimensional steady-state experiments interpreted with DSD. Author (revised)

N93-30097 Naval Research Lab., Washington, DC.
MOLECULAR DYNAMICS OF DETONATION IN CRYSTALS WITH DEFECTS **c72**
Lee Phillips and Robert S. Sinkovits *In* JHU, ONR/LANL Workshop on the Fundamental Physics and Chemistry of Combustion, Initiation, and Detonation of Energetic Materials Mar. 1992 p 495-496 Sponsored in part by ONR (For primary document see N93-30061 11-28)
Avail: CPIA, 10630 Little Patuxent Pkwy., Suite 202, Columbia, MD 21044-3200 HC

We examined, using computational molecular dynamics, shocks produced in two- and three dimensional atomic and molecular crystals through impact and end loading. The effect of various lattice defects on the shock propagation and the transition to detonation is investigated. It is observed that small defects in the lattice structure have a large effect on the shock and detonation dynamics. Intermolecular potentials are of the Lennard-Jones type, with chemical bonds represented by predissociative classical potentials and elaborations thereof. In a three-dimensional simulation of a shock in a crystal containing a vacancy cluster defect (a small void), we find that the earliest release of chemical energy occurs at the site of the defect, aside from the crystal surface. This is also the site of a small hot spot. Further conclusions about the effect of defects on the subsequent propagation of the detonation front, and, especially, on shock sensitivity, must await simulations on larger three-dimensional systems. Our earlier computational experiments on shocks in nonreacting crystals indicate that the detailed dynamics of the shock-defect interaction, and the resulting thermalization of the fluid-phase inclusion that results, is rather different in two- and three-dimensions, and therefore realistic conclusions concerning the role of crystallographic defects on shock sensitivity should be based on three-dimensional computations. As a well-resolved molecular dynamics simulation in a 3-d condensed phase requires the forces due to approximately a thousand nearest neighbors to be calculated for each atom, the computing requirements for even moderately large systems (greater than 104 particles) are substantial. We have found massively parallel computer architectures to be helpful in dealing with this problem; the computations shown here were carried out on a 16 kiloprocessor Connection Machine, for which we have developed a parallelized version of the MLG particle tracking algorithm. Author (revised)

N93-30098 New Orleans Univ., LA. Dept. of Chemistry.
APPLICATIONS OF DENSITY FUNCTIONAL THEORY TO CALCULATION OF REACTION ENERGETICS Abstract Only
Peter Politzer *In* JHU, ONR/LANL Workshop on the Fundamental Physics and Chemistry of Combustion, Initiation, and Detonation of Energetic Materials Mar. 1992 p 497 (For primary document see N93-30061 11-28)
Avail: CPIA, 10630 Little Patuxent Pkwy., Suite 202, Columbia, MD 21044-3200 HC

We are increasingly using the methodology of density functional theory for computational studies of energetic molecules. This approach focuses upon the electron density rather than upon a wave function, with a consequent considerable saving of computer time and resources. Density functional procedures do take account of electronic correlation; accordingly it is possible to obtain results of accuracy comparable to post-Hartree-Fock ab initio methods (e.g. Moeller-Plesset and configuration interaction). Most of our density functional work in the past has invoked the local density approximation (LDA), whereby exchange and correlation effects are treated by means of the uniform electron gas model. However, we are increasingly going above the LDA level, and using nonlocal formulations. In this presentation, we report five sets of results: (1) activation energies for the concerted ring-opening dissociations of four cyclic molecules -- 1,3-diaza cyclobutane, 1,3-dinitro diazacyclobutane, 1,3,5-triaza cyclohexane, and 1,3,5-trinitro triazacyclohexane (RDX); (2) activation and total energies of isomerization of unsaturated molecules to highly-strained cage-like systems; (3) heterolytic C-N dissociation energies for cubane dinitramine and methyl dinitramine; (4) C-NO2 and N-NO2 rotational barriers; and (5) general comparison of dissociation energies computed at local and nonlocal levels. Author (revised)

N93-30099 Naval Research Lab., Washington, DC. Lab. for Computational Physics and Fluid Dynamics.
RATE CONSTANT DETERMINATIONS OF REACTIONS H + HNO FROM AB INITIO REACTION PATH CALCULATIONS Abstract Only **c25**
Maribel R. Soto and Michael Page *In* JHU, ONR/LANL Workshop on the Fundamental Physics and Chemistry of Combustion, Initiation, and Detonation of Energetic Materials Mar. 1992 p 499 (For primary document see N93-30061 11-28)
Avail: CPIA, 10630 Little Patuxent Pkwy., Suite 202, Columbia, MD 21044-3200 HC

The reaction of H + HNO has been proposed as an intermediate step in the rate mechanism of processes such as the inhibition of hydrocarbon combustion by nitric oxide, the reaction of radicals with NO in the atmosphere, and the combustion of nitrogen-containing species. A facile and substantially exothermic channel for this reaction is hydrogen-atom abstraction, H + HNO yields H2 + NO (reaction (1)). This reaction is more than 50 kcal/mol exothermic; therefore, it is expected to have a negligible barrier or none at all. Kinetic data for reaction (1) exists for flame temperatures except they disagree by as much as an order of magnitude. The most widely accepted value is 0.8 x 10 exp -11 cc/(molecule x sec.) determined at 2000 K by Halstead and Jenkins. At low temperatures, there have been several indirect determinations which also disagree markedly. Furthermore, the temperature-dependence of this reaction is poorly understood. Another possible pathway for H + HNO is H-atom addition to the nitrogen atom of HNO: H + HNO yields H2NO ((sup 2) A') (reaction (2)) and H + HNO yields H2NO ((sup 2) A') (reaction (3)). Like the abstraction, these reactions are also expected to be substantially exothermic; therefore, they may also have a low barrier. At high pressures, an addition complex can be collisionally stabilized, and one of these addition reactions might compete effectively with the abstraction reaction. In our work, we investigate the reaction pathways of reactions (1) and (2) using ab initio multi-configuration self-consistent field (MCSCF) and configuration interaction (CI) methods. Also, we use transition state theory to calculate the temperature-dependent rate constants of these reactions. Our objective is to address the controversy about the rate of reaction (1) and to understand the possible competition between these two reactive channels. Author (revised)

N93-30100 Naval Research Lab., Washington, DC. Theoretical Chemistry Section.
SHOCK WAVES AND POLYMORPHIC PHASE TRANSITIONS IN ENERGETIC MATERIALS Abstract Only
Daniel H. Robertson, D. W. Brenner, and Carter T. White *In* JHU, ONR/LANL Workshop on the Fundamental Physics and Chemistry of Combustion, Initiation, and Detonation of Energetic Materials Mar. 1992 p 501 Sponsored by ONR (For primary document see N93-30061 11-28)
Avail: CPIA, 10630 Little Patuxent Pkwy., Suite 202, Columbia, MD 21044-3200 HC

Molecular dynamics has been shown to be ideally suited for studying shock wave phenomena giving results consistent with continuum theory. In this paper, we use reactive potentials together with molecular dynamics techniques to simulate at the atomic scale the onset and propagation of chemically-sustained shock waves in a model energetic molecular solid. Once this material initiates, physical properties such as temperature, particle flow and detonation velocities, pressure and power generation are all consistent with a detonation. The shock wave is chemically-sustained by the consumption of the initial energetic AB material to form A2 and B2 products with an associated release of energy that sustains the propagation of the shock wave at a constant velocity. These identifiable products form at the rear of a high-density dissociative phase with an associated release of potential energy. A lower density compressional wave preceeds this dissociative phase allowing these simulations to exhibit a stable growing split shock wave. This split shock wave can be modeled in a nonenergetic material and results from the polymorphic phase transition of the molecular solid to the close-packed solid of the dissociative phase. The presence of this dissociative phase and its associated polymorphic phase transition appear to be key factors for the formation of a chemically-sustained shock wave in these simulations. Our results suggest the potential importance of dissociative phases, polymorphic phase transitions, and rarefaction shocks in understanding the formation and evolution of detonations in condensed energetic materials. Author (revised)

N93-30101 Arkansas Univ., Fayetteville. Dept. of Chemistry.
GAS ELECTRON DIFFRACTION EMPLOYING A PULSED ELECTRON BEAM SYNCHRONOUS WITH PHOTOEXCITATION Abstract Only **c25**
John D. Ewbank, Jing Y. Luo, Jeffrey T. English, Walter L. Faust, and Lothar Schafer *In* JHU, ONR/LANL Workshop on the Fundamental Physics and Chemistry of Combustion, Initiation, and Detonation of Energetic Materials Mar. 1992 p 503 (For primary document see N93-30061 11-28)
Avail: CPIA, 10630 Little Patuxent Pkwy., Suite 202, Columbia, MD 21044-3200 HC

Work was continued to put a GED instrument into operation that uses a pulsed electron beam synchronous with photoexcitation. Excimer laser pulses (ArF, 193 nm, 15 ns FWHM, 30 mJ) are directed onto a tantalum photocathode within a Pierce-type electron gun. Electron pulses, generated by photoemission, are accelerated through a potential of 40 keV, and focused onto target molecules entering the diffraction chamber through a nozzle orifice. Pulses from a second excimer laser, synchronized with the first, excite the target gases in the scattering center. Within a well defined and variable time interval r (including r less than or = O) the diagnostic electron pulses are scattered by the excited species. The diffraction intensities are recorded by the real-time technique developed at the University of Arkansas. Author (revised)

N93-30102 Aerodyne Research, Inc., Billerica, MA. Center for Chemical and Environmental Physics.
CONDENSED PHASE DIAGNOSTICS OF NITRAMINE PROPELLANT COMBUSTION Abstract Only **c25**
Joda Wormhoudt, P. L. Kebabian, and C. E. Kolb *In* JHU, ONR/LANL Workshop on the Fundamental Physics and Chemistry of Combustion, Initiation, and Detonation of Energetic Materials Mar. 1992 p 505 (For primary document see N93-30061 11-28)
(Contract DAAL03-91-C-0008)
Avail: CPIA, 10630 Little Patuxent Pkwy., Suite 202, Columbia, MD 21044-3200 HC

Our poster presents a first report on a program whose goal is to develop the technique of fast-response spectral infrared fiber optic probing of burning propellant strands, and demonstrate it in mechanism studies of condensed phase processes in nitramine propellant combustion. We are beginning the second year of a three-year program and, having assembled most of our experimental apparatus, are turning to a series of preliminary observations which will allow better understanding of the full experiments. The basic experiment involves a modulated infrared source, a pair of fibers meeting in the propellant strand with a small absorption gap between them, and (initially) infrared detectors with interference filters which select spectral regions including absorption bands of decomposition product molecules (an infrared detector array and monochromator is clearly the ideal detection system). Also included in the experimental apparatus are a high pressure strand burner and a video camera and recorder system which will allow both observation of the burning strand and high magnification viewing of the fibers during setup and testing. We have begun burning propellant strands, and have found conditions which seem adequate for first experiments. Transmission measurements on thin slices of propellant indicate a useful spectral window within which a number of decomposition product molecules might be observed. We have also started transient heating studies using a hot filament rather than burning propellant to heat the fiber. These seem to indicate that the fibers may be useful well above their melting point. Next, we will be developing techniques to insert fibers into propellant strands, and to monitor whether they are properly aligned as insertion is performed. Author (revised)

N93-30424# Naval Surface Warfare Center, Dahlgren, VA.
THE MEASUREMENT OF ELECTRICAL CONDUCTIVITY IN DETONATING CONDENSED EXPLOSIVES
Douglas G. Tasker, Richard J. Lee, and Paul K. Gustavson Mar. 1993 59 p
(AD-A264482; NSWCDD/TR-92/218) Avail: CASI HC A04/MF A01

The time-resolved measurement of electrical conductivity provides a unique means of studying detonating explosives. The results of a large number of experiments are reported. Two types of experiments were performed; they measured bulk resistance and time-resolved conductivity. Some interesting effects, due to detonation wave instabilities, were observed when the explosives dimensions were close to criticality, i.e., close to failure diameter or thickness. The conductivity profile observed in the aluminized explosive PBXN-111 (formerly PBXW-1 15) is interesting and unusual. The results are probably due to a combination of wave instabilities and late reaction effects. This demonstrates one of the advantages of using conductivity measurements as a diagnostic tool. Wave instabilities are apparent that could not be determined by other means. DTIC

N93-30446# Los Alamos National Lab., NM.
THE USE OF QUANTUM CHEMISTRY TO ESTIMATE THE PERFORMANCE AND PROPERTIES OF EXPLOSIVES
J. P. Ritchie 1992 17 p Presented at the 10th Detonation Symposium, Boston, MA, 12-16 Jul. 1993
(Contract W-7405-eng-36)
(DE92-040369; LA-UR-92-2824; CONF-930713-2) Avail: CASI HC A03/MF A01

The ready availability of high speed computers has led to the development of quantum chemistry techniques that can provide a variety of information about molecules. Heats of formation, geometries, vibrational frequencies, and charge distributions can be obtained with reasonable reliability. Depending upon the quantity of interest and the chemical composition of the molecule, the associated computer costs may range from moderate, requiring only scientific workstations, to immense, requiring current generation supercomputers and beyond. In addition, a wide assortment of techniques and programs from which to choose exist, each with its own strengths and weaknesses. This variety may seem baffling to the applications oriented non-specialist. Moreover, it is prudent to acknowledge that many quantities commonly used in estimating the performance of explosives can be obtained more cheaply and more accurately using methods that are not quantum chemical in nature. Such methods can be used quite effectively, provided that they have been properly parametrized in the regime of interest and that they are capable of producing information that is physically realistic. Nevertheless, quantum chemical techniques offer the opportunity of going beyond the familiar territory of C,H,N,O compounds. In addition, they also are capable of providing information about hypothetical molecules and states of matter. Two applications of quantum chemistry are described. The approach in each of these cases illustrates an informed choice of state-of-the-art techniques to obtain the desired results in a timely fashion. DOE

N93-30663# Gas Research Inst., Chicago, IL.
POWER GENERATION AND TRANSPORTATION SYSTEMS RESEARCH DEPARTMENT
A. Benedict Sep. 1992 178 p See also PB92-108869
(PB93-178309; GRI-92/0317) Avail: CASI HC A09/MF A02

Activities of the Gas Research Institute's Power Generation and Transportation Systems subprogram for the period between 1 Oct. 1991 and 30 Sep. 1992 are summarized. The particular project areas covered in the report are Cogeneration and Power Systems, Engine Technology and Component Development, Natural Gas Vehicles Research, and Electric Power Generation. For each project area a separate chapter is provided. Each chapter includes a rationale for funding the research effort, the goals and objectives to be achieved, a general statement on research accomplishments, and the strategy employed in the project area. Each chapter also contains a series of summary reports on the status of each contract. NTIS

29 MATERIALS PROCESSING

Includes space-based development of products and processes for commercial applications.

For biological materials see *55 Space Biology.*

N93-30939*# National Aeronautics and Space Administration. Lewis Research Center, Cleveland, OH.
PREDICTION OF GAS-LIQUID TWO-PHASE FLOW REGIME IN MICROGRAVITY
Jinho Lee (National Academy of Sciences - National Research Council, Washington, DC.) and Jonathan A. Platt Jul. 1993 41 p
(RTOP 694-03-0A)
(NASA-TM-106274; E-7079; NAS 1.15:106274) Avail: CASI HC A03/MF A01

An attempt is made to predict gas-liquid two-phase flow regime in a pipe in a microgravity environment through scaling analysis based on dominant physical mechanisms. Simple inlet geometry is adopted in the analysis to see the effect of inlet configuration on flow regime transitions. Comparison of the prediction with the existing experimental data shows good agreement, though more work is required to better define some physical parameters. The analysis clarifies much of the physics involved in this problem and can be applied to other configurations. Author

N93-31031*# Science Applications International Corp., Torrance, CA. Thermal Sciences Div.
EFFECTS OF BUOYANCY ON GAS JET DIFFUSION FLAMES Final Report
M. Yousef Bahadori and Raymond B. Edelman Apr. 1993 364 p
(Contract NAS3-22822; RTOP 694-03-0A)
(NASA-CR-191109; E-7720; NAS 1.26:191109) Avail: CASI HC A16/MF A03

The objective of this effort was to gain a better understanding of the fundamental phenomena involved in laminar gas jet diffusion flames in the absence of buoyancy by studying the transient phenomena of ignition and flame development, (quasi-) steady-state flame characteristics, soot effects, radiation, and, if any, extinction phenomena. This involved measurements of flame size and development, as well as temperature and radiation. Additionally, flame behavior, color, and luminosity were observed and recorded. The tests quantified the effects of Reynolds number, nozzle size, fuel reactivity and type, oxygen concentration, and pressure on flame characteristics. Analytical and numerical modeling efforts were also performed. Methane and propane flames were studied in the 2.2 Second Drop Tower and the 5.18-Second Zero-Gravity Facility of NASA LeRC. In addition, a preliminary series of tests were conducted in the KC-135 research aircraft. Both micro-gravity and normal-gravity flames were studied in this program. The results have provided unique and new information on the behavior and characteristics of gas jet diffusion flames in micro-gravity environments. Author (revised)

N93-28725*# Alabama Univ., Huntsville.
MEASUREMENT OF THE RELATIVE AND ABSOLUTE MICROGRAVITY ENVIRONMENT OF SPACE PLATFORMS, RECENT FLIGHT RESULTS, AND DETERMINATION OF THE SPATIAL MICROGRAVITY FIELD
J. A. Bijvoet, J. Randorf, D. R. Wingo, and J. R. Blakely *In* NASA, Washington, NASA/DOD Flight Experiments Technical Interchange Meeting Proceedings 1992 19 p (For primary document see N93-28699 11-12)
Avail: CASI HC A03/MF A10

31 ENGINEERING (GENERAL)

Includes vacuum technology; control engineering; display engineering; cryogenics; and fire prevention.

N93-28570# California Univ., Berkeley. Lawrence Berkeley Lab.
ADVANCED INSULATIONS FOR REFRIGERATOR/FREEZERS: THE POTENTIAL FOR NEW SHELL DESIGNS INCORPORATING POLYMER BARRIER CONSTRUCTION
B. T. Griffith and D. Arasteh Nov. 1992 23 p
(Contract DE-AC03-76SF-00098)
(DE93-010600; LBL-33376) Avail: CASI HC A03/MF A01

The impending phase-out of chlorofluorocarbons (CFC's) used to expand foam insulation, combined with requirements for increased energy efficiency, make the use of non-CFC-based high performance insulation technologies increasingly attractive. The majority of current efforts are directed at using advanced insulations in the form of thin, flat low-conductivity gas-filled or evacuated orthogonal panels, which are referred to as Advanced Insulation Panels (AIP's). AIP's can be used in composite with blown polymer foams to improve insulation performance in refrigerator/freezers (R/F's) of conventional design and manufacture. This AIP/foam composite approach is appealing because it appears to be a feasible, near-term method for incorporating advanced insulations into R/F's without substantial redesign or retooling. However, the requirements for adequate flow of foam during the foam-in-place operation impose limitations on the allowable thickness and coverage area of AIP's. Design alternatives which may offer a greater increase in overall thermal resistance than is possible with the use of AIP/foam composites in current R/F design are examined. These design alternatives generally involve a basic redesign of the R/F taking into account the unique requirements of advanced insulations and the importance of minimizing thermal bridging with high thermal resistance insulations. The focus is on R/F doors because they are relatively simple and independent R/F components and are therefore good candidates for development of alternative designs. R/F doors have significant thermal bridging problems due to the steel outer shell construction. A three dimensional finite difference computer modeling exercise of a R/F door geometry was used to compare the overall levels of thermal resistance (R-value) for various design configurations. DOE

N93-28632# Technical Research Centre of Finland, Espoo. Structural Engineering Lab.
DYNAMIC ICE STRUCTURE INTERACTION: THEORY AND APPLICATIONS Ph.D. Thesis - Helsinki Univ. of Technology
Esa Eranti (Pitkala, Lauri Ltd. Consulting Engineers, Helsinki, Finland.) 1992 84 p Sponsored by Technology Development Center of Finland; Academy of Finland; and Foundation of Civil Engineering
(VTT-Pubs-90; ISBN-9-51-384068-9; ETN-93-93777) Copyright Avail: CASI HC A05/MF A01

A theory of dynamic ice-structure interaction is described with transverse and torsional vibrations included. The theory is applicable to cases of pure crushing of ice against vertical structures as well as combined crushing and shearing of ice against inclined structures. The zonal ice failure approach is adapted, the structure being locally in contact with solid and broken ice alternatively. Simple rules are given for the development of the zonal ice force in the interaction process. The structural response, the zonal ice force components and the global ice force are found in an iterative step by step procedure based on the development of the theoretical distance between the zonal contact point and the ice edge. Medium scale ice-structure interaction tests performed on the ice tank using freshwater columnar grained ice are described. The practice of using aspect ratio curves or pressure area curves to predict effective ice pressures caused by columnar grained level ice is concluded to be generally invalid and may in some cases be even dangerous. Each situation is a special case of dynamic ice structure interaction and the effective ice pressure and the structural response records depend strongly on the geometric and dynamic properties of the structure. The proposed approach provides an upper bound solution for global ice force and structural response, in the sense that it assumes pure crushing or combined crushing and shearing failure of ice, and ignores reductions that may result from the failure modes. ESA

N93-28635# Joint Publications Research Service, Arlington, VA.
JPRS REPORT: SCIENCE AND TECHNOLOGY. CENTRAL EURASIA: ENGINEERING AND EQUIPMENT
8 Jun. 1992 52 p Transl. into ENGLISH from various Russian articles
(JPRS-UEQ-92-007) Avail: CASI HC A04/MF A01

Translated articles cover the following topics: aviation and space technology; optics, high energy devices; nuclear energy; non-nuclear energy; and mechanics of gases, liquids, and solids. CASI

N93-28636# Joint Publications Research Service, Arlington, VA.
JPRS REPORT: SCIENCE AND TECHNOLOGY. CENTRAL EURASIA: ENGINEERING AND EQUIPMENT
30 Apr. 1992 46 p Transl. into ENGLISH from various Russian articles
(JPRS-UEQ-92-006) Avail: CASI HC A03/MF A01

Translated articles cover the following topics: aviation and space technology; optics, high energy devices; nuclear energy; non-nuclear energy; mechanics of gases, liquids, and solids; and industrial technology, planning, and productivity. CASI

N93-28674# Joint Publications Research Service, Arlington, VA.
JPRS REPORT: SCIENCE AND TECHNOLOGY. CENTRAL EURASIA: ENGINEERING AND EQUIPMENT
21 Sep. 1992 55 p Transl. into ENGLISH from various Russian articles
(JPRS-UEQ-92-010) Avail: CASI HC A04/MF A01

Translated articles cover the following topics: aviation and space technology; optics, high energy devices; nuclear energy; non-nuclear energy; mechanics of gases, liquids, and solids; and industrial technology, planning, and productivity. CASI

N93-28675# Joint Publications Research Service, Arlington, VA.
JPRS REPORT: SCIENCE AND TECHNOLOGY. CENTRAL EURASIA: ENGINEERING AND EQUIPMENT
8 Jul. 1992 44 p Transl. into ENGLISH from various Russian articles
(JPRS-UEQ-92-008) Avail: CASI HC A03/MF A01

Translated articles cover the following topics: aviation and space technology; optics, high energy devices; nuclear energy; mechanics of gases, liquids, and solids; and industrial technology, planning, and productivity. CASI

N93-28691# Joint Publications Research Service, Arlington, VA.
JPRS REPORT: SCIENCE AND TECHNOLOGY. CENTRAL EURASIA: ENGINEERING AND EQUIPMENT
22 Feb. 1993 38 p Transl. into ENGLISH from various Russian articles
(JPRS-UEQ-93-003) Avail: CASI HC A03/MF A01

Translated articles cover the following topics: aviation and space technology; nuclear energy; non-nuclear energy; mechanics of gases, liquids, and solids; and industrial technology, planning, and productivity. Author

N93-28698*# Krug Life Sciences, Inc., Houston, TX.
ADVANCED COLLAPSIBLE TANK FOR LIQUID CONTAINMENT
David T. Flanagan and Robert C. Hopkins (Houston Univ., Clear Lake, TX.) Jun. 1993 47 p
(Contract NAS9-18492)
(NASA-CR-188247; NAS 1.26:188247) Avail: CASI HC A03/MF A01

Tanks for bulk liquid containment will be required to support advanced planetary exploration programs. Potential applications include storage of potable, process, and waste water, and fuels and process chemicals. The launch mass and volume penalties inherent in rigid tanks suggest that collapsible tanks may be more efficient. Collapsible tanks are made of lightweight flexible material and can be folded compactly for storage and transport. Although collapsible tanks for terrestrial use are widely available, a new design was developed that has significantly less mass and bulk than existing models. Modelled after the shape of a sessible drop, this design features a dual membrane with a nearly uniform stress distribution and a low surface-to-volume ratio. It can be adapted to store a variety of liquids in nearly any environment with constant acceleration field. Three models of 10L, 50L, and 378L capacity have been constructed and tested. The 378L (100 gallon) model weighed less than 10 percent of a commercially available collapsible tank of equivalent capacity, and required less than 20 percent of the storage space when folded for transport. Author (revised)

N93-28893# Pacific Northwest Lab., Richland, WA.
OVERVIEW OF PIPING ISSUES AND TRENDS
S. H. Bush Dec. 1992 25 p Presented at the 4th Symposium on Current Issues Related to Nuclear Power Plant Structure, Equipment and Piping, Orlando, FL, 9-11 Dec. 1992
(Contract DE-AC06-76RL-01830)
(DE93-006628; PNL-SA-21260; CONF-921262-1) Avail: CASI HC A03/MF A01

A variety of failure mechanisms that have contributed to failures in nuclear reactor piping systems are discussed. These include general corrosion, intergranular stress corrosion, erosion-corrosion, mechanical fatigue, and thermal fatigue covering the spectrum from mixing-tee to stratification. Actions to minimize or eliminate these failure mechanisms are discussed where these actions are based on the experience amassed over the past three decades. DOE

N93-29090# Joint Publications Research Service, Arlington, VA.
JPRS REPORT: SCIENCE AND TECHNOLOGY. CENTRAL EURASIA: ENGINEERING AND EQUIPMENT
26 May 1993 19 p Transl. into ENGLISH from various Russian articles
(JPRS-UEQ-93-004) Avail: CASI HC A03/MF A01

Translated abstracts cover the following areas: optics, nuclear energy, fluid dynamics, and industrial technology. Some specific topics include internal source optimization in problem of sphere in MHD flow; on development of oblique waves in planar subsonic boundary layer; variational method of plotting subsonic airfoil profiles; and gas dynamics of pulsed jets and pressure oscillations on laser-irradiated target. CASI

N93-29611* National Aeronautics and Space Administration. Langley Research Center, Hampton, VA.
METHOD AND APPARATUS FOR WEAVING A WOVEN ANGLE PLY FABRIC Patent
Gary L. Farley, inventor (to NASA) 6 Jul. 1993 14 p Filed 26 Sep. 1991 Supersedes N92-11220 (30 - 2, p 222)
(NASA-Case-LAR-14048-1; US-Patent-5,224,519;
US-Patent-Appl-SN-766609; US-Patent-Class-139-11;
US-Patent-Class-139-DIG.1; US-Patent-Class-428-225;
Int-Patent-Class-D03D-41/00; Int-Patent-Class-D03D-13/00;
Int-Patent-Class-D03C-13/00) Avail: US Patent and Trademark Office

Planar or multilayer structural preforms are made having yarns extending in a bias direction of the preform. Angularly directed yarns can be inserted in planar and multilayer fabrics to increase shear strength of structural preforms made from the fabrics. In multilayer fabrics, the angle yarns can extend between layers to provide through-the-thickness reinforcement. Fabrics are formed by carrying yarns transversely across the fabric as the fabric advances. Fill yarns may be inserted by an insertion technique employing a pneumatic beating element. Angle yarn feeding arrangements are made readily removable to provide for the use of other weaving assemblies. Official Gazette of the U.S. Patent and Trademark Office

N93-29663 National Inst. of Standards and Technology, Gaithersburg, MD.
PROGRAMMER'S REFERENCE GUIDE TO FDMS FILE FORMATS
R. W. Portier Apr. 1993 45 p Limited Reproducibility: More than 20% of this document may be affected by microfiche quality
(PB93-182038; NISTIR-5162) Avail: CASI HC A03

Fire Data Management System, FDMS, is a computer database specifically designed to store and retrieve fire test results. The guide provides detailed descriptions of the current, beta version, file formats as well as revisions planned for the immediate future. NTIS

N93-29666# National Inst. of Standards and Technology, Gaithersburg, MD. Precision Engineering Div.
ISSUES, CONCEPTS, AND STANDARD TECHNIQUES IN ASSESSING ACCURACY OF COORDINATE MEASURING MACHINES
D. A. Swyt Feb. 1993 91 p
(PB93-184331; NIST/TN-1400) Avail: CASI HC A05/MF A01

The report deals with a variety of issues, concepts and standard techniques in assessing the accuracy of measurements of modern laser-based computer-controlled coordinate measuring machines. It outlines technical issues in assessing conformity of dimensions of manufactured parts to design tolerances with such CMM's, uses a new system of length-dimensional types (displacement, position, distance and extension) as the basis for an error-budget analysis of CMM measurement capabilities and, based on that system, intercompares U.S., German, British and Japanese CMM performance standards, showing that the U.S. standard provides separate test of a CMM's capability to measure of each length-dimensional type and the part features associated with them. NTIS

N93-29969# Naval Postgraduate School, Monterey, CA.
PRELIMINARY DEVELOPMENT OF A VTOL UNMANNED AIR VEHICLE FOR THE CLOSE-RANGE MISSION M.S. Thesis
Gregory A. Kress 29 Sep. 1992 88 p
(AD-A263514) Avail: CASI HC A05/MF A01

The preliminary development of a full-scale Vertical Takeoff and Landing (VTOL) Unmanned Air Vehicle (UAV) for the Close-Range mission was completed at the Naval Postgraduate School (NPS). The vehicle was based on half-scale ducted-fan investigations performed at the UAV Flight Research Lab. The resulting design is a fixed-duct, tail-sitter UAV with a canard-configured horizontal stabilizer. Major airframe components are used from previous UAV's and include the wings from a U.S. Army Aquila and the ducted fan from the U.S. Marine Corps AROD. Accomplishments include: (1) the design and fabrication of a carry-through spar, and (2) the design and construction of an engine test stand. The through spar was designed using finite element analysis and constructed from composite materials. The purpose of the test stand is to measure torque, horsepower, and thrust of an entire ducted fan or an individual engine. Completion of this thesis will pave the way for future NPS research into the growing interest in VTOL UAV technology. DTIC

N93-30215 Engineering Inst. of Canada, Montreal (Quebec). Canadian Society for Electrical and Computer Engineering.
CANADIAN CONFERENCE ON ELECTRICAL AND COMPUTER ENGINEERING, VOLUMES 1 AND 2 [CONGRES CANADIEN EN GENIE ELECTRIQUE ET INFORMATIQUE, TOMES 1 ET 2]
1990 1453 p In ENGLISH and FRENCH Conference held in Ottawa, Ontario, 4-6 Sep. 1990; sponsored by IEEE
(ISBN-0-9694170-1-2; CTN-93-60717) Avail: Engineering Inst. of Canada, 2050 rue Mansfield, Suite 700, Montreal, Quebec H3A 1Z2 Canada

At a conference on electrical and computer engineering, papers were presented in the fields of power systems, wireless communication, information systems, speech and image processing, neural networks, control systems, robotics, electronic devices, software engineering, coding, signal processing, artificial intelligence, computer architectures and networks, fiber optics, fuzzy logic, computer vision, aviation meteorology, electromagnetics, motors, digital filters, computer hardware, synchronous machines, integrated systems in aviation, instrumentation, numerical simulation, and radar. For individual titles, see N93-30216 through N93-30358.

N93-30216 Queens Univ., Kingston (Ontario). Dept. of Electrical Engineering.
ROBUST CONTROL VIA H-INFINITY OPTIMIZATION **c63**
J. R. Sveinsson and F. W. Fairman *In* Engineering Inst. of Canada, Canadian Conference on Electrical and Computer Engineering, Volumes 1 and 2 1990 3 p (For primary document see N93-30215 11-31)
Avail: Engineering Inst. of Canada, 2050 rue Mansfield, Suite 700, Montreal, Quebec H3A 1Z2 Canada

Two motivations for using a feedback controller are both concerned with reducing the system's sensitivity. One is the robust stability problem wherein a single controller is to be determined so as to stabilize any one of a number of possible plants drawn from a plant uncertainty set. Another example is the H-infinity optimization problem, in which the plant is assumed to have two sets of inputs (w and u) and two sets of outputs (z and y).

The controller which has input y and output u is then designed so as to stabilize the complete feedback system and to minimize the infinity norm of the resulting transfer function from w to z. Although the H-infinity problem was originally formulated and solved in the frequency domain, the recent emergence of a state space approach involving the solution of two indefinite Riccati equations is proving to be more practical. The robust stabilization problem is converted to an H-infinity optimal control problem, and the two Riccati equation approach is used to determine both the maximum allowable bound on the perturbations and the controller which stabilizes all members of the uncertainty set. Author (CISTI)

N93-30217 Quality Management Control, Inc., Ottawa (Ontario).
CONTROL SYSTEM DESIGN AND MULTIPARAMETER VARIATIONS **c63**
James Morris Overton *In* Engineering Inst. of Canada, Canadian Conference on Electrical and Computer Engineering, Volumes 1 and 2 1990 4 p (For primary document see N93-30215 11-31)
Avail: Engineering Inst. of Canada, 2050 rue Mansfield, Suite 700, Montreal, Quebec H3A 1Z2 Canada

A new technique for designing control systems is presented and illustrated for the case of a position control servo with velocity feedback. According to this technique, an isomorphic comparison is made between a standard transfer function and the transfer function of the system to be designed. This comparison leads to a set of sensitivity functions for a corresponding set of control system network components. The derivatives of the ratios of the pole or zero position of the network transfer functions are calculated and a set of independent simultaneous equations are produced, one for each component. The equations are solved to obtain the specific values of the component parameters. This technique differs from the classical frequency domain design techniques in that the values of components are calculated rather than selected; in addition, it requires no high-level mathematics, is independent of both time and frequency, and does not require compensation. Author (CISTI)

N93-30218 Victoria Univ. (British Columbia). Dept. of Electrical and Computer Engineering.
A CLOSED-FORM FORMULA FOR THE MANIPULATOR REGRESSOR **c63**
W.-S. Lu and Q.-H. Meng *In* Engineering Inst. of Canada, Canadian Conference on Electrical and Computer Engineering, Volumes 1 and 2 1990 4 p (For primary document see N93-30215 11-31)
Avail: Engineering Inst. of Canada, 2050 rue Mansfield, Suite 700, Montreal, Quebec H3A 1Z2 Canada

An attempt is made to provide a closed-form formula for the regressor of a general n-degree of freedom robotic system in which the mass, center of mass, and inertia tensor of the payload are unknown. In practice, this is the most common case where parameter uncertainties are encountered. The approach to this problem is based on the observation that the unknown part of the Lagrangian for a working robot can be separated from the Lagrangian of the same robot with no payload. Owing to the additive nature of the Lagrangian, the approach adopted can readily be extended to treat robots with other unknown dynamic parameters such as the mass and inertia tensor of a certain link. Moreover, the formula obtained is found suitable as a starting point to further derive a closed-form formula for the so-called filtered regressor which was used in several globally stable adaptation laws. Author (CISTI)

N93-30219 Ottawa Univ. (Ontario). Dept. of Electrical Engineering.
NONLINEAR PROCESSING OF PHASE VOCODED SPEECH **c32**
Luc Gagnon and W. F. McGee *In* Engineering Inst. of Canada, Canadian Conference on Electrical and Computer Engineering, Volumes 1 and 2 1990 4 p (For primary document see N93-30215 11-31)
Avail: Engineering Inst. of Canada, 2050 rue Mansfield, Suite 700, Montreal, Quebec H3A 1Z2 Canada

Although adaptive coding is in widespread use, the availability of very large scale integrated digital signal processing chips makes filterbank analysis and synthesis of speech signals very economical. This ear modeling simplifies the application of masking properties of the ear. Experiments were conducted to determine the number of filterbank outputs needed to reconstruct speech signals using a logarithmic bandpass filterbank consisting of an analysis and a synthesis filterbank. With eight outputs, the original speech sentence is found to be very clear; addition of 32 more outputs restores the breathiness to the sentence. A surprising degree of intelligibility is retained even with one output. The bandwidth of the speech signals is limited. The use of these filterbanks for speech enhancement and modest bitrate transmission appears favorable. Author (CISTI)

N93-30220 Waterloo Univ. (Ontario). Dept. of Electrical and Computer Engineering.
ON SUBBAND CODING/EMBEDDED VECTOR QUANTIZATION FOR SPEECH CODING **c32**
Lise Vanterpool and Jon W. Mark *In* Engineering Inst. of Canada, Canadian Conference on Electrical and Computer Engineering, Volumes 1 and 2 1990 4 p (For primary document see N93-30215 11-31)
Avail: Engineering Inst. of Canada, 2050 rue Mansfield, Suite 700, Montreal, Quebec H3A 1Z2 Canada

A procedure for constructing a subband/embedded vector quantization coder for speech coding is presented. The proposed coder has three major components: a bank of filters for partitioning the full-band signal into subbands; a quantizing scheme for the subband signals; and a suitable bit allocation algorithm. To reduce the complexity of the coding process, a form of hierarchical vector quantization is adopted in which each of the subband signals is decomposed into two roughly independent signals (gain and shape) that are coded individually. Experiments indicate that at a rate of 32 kbps, the coded speech is quite pleasant. However, at the design rate of 16 kbps, the system performance is poor. Nevertheless, the embedded coder developed is a fairly good design. Four subbands were used in the design; increasing the number of subbands should improve the system performance. Author (CISTI)

N93-30221 National Research Council of Canada, Ottawa (Ontario). Speech Research Centre.
IMPROVEMENT OF THE NRC AUTOMATIC SPEECH RECOGNITION SYSTEM **c32**
Dariusz A. Zwierzynski and C. Lefebvre *In* Engineering Inst. of Canada, Canadian Conference on Electrical and Computer Engineering, Volumes 1 and 2 1990 4 p (For primary document see N93-30215 11-31)
Avail: Engineering Inst. of Canada, 2050 rue Mansfield, Suite 700, Montreal, Quebec H3A 1Z2 Canada

The ongoing research being conducted at Canada's National Research Council on the improvement of an automatic speech recognition (ASR) system is reviewed. The current speech recognizer is first described, and some examples of its performance are provided. Tests have demonstrated that the system performs well, particularly in adverse acoustic conditions, in comparison with other ASR algorithms. The rationale for work on the extraction and integration of segmental and prosodic features for enhancing recognition of plosive consonants is given. It is argued that the substitution error for word-initial plosives can be lowered if pitch information at voicing onset is used in recognition, along with segmental cues such as burst characteristics, voice onset time, and first formant transition. A robust pitch detection algorithm is outlined, and the strategy employing neurocomputing in a three-layer neural network for the processing of segmental and prosodic cues is explained. Author (CISTI)

N93-30222 Windsor Univ. (Ontario). Dept. of Electrical Engineering.
REALIZATION OF HIGH SPEED ADAPTIVE FIR DIGITAL FILTERS **c33**
H. K. Kwan and Q. P. Li *In* Engineering Inst. of Canada, Canadian Conference on Electrical and Computer Engineering, Volumes 1 and 2 1990 4 p (For primary document see N93-30215 11-31)
Avail: Engineering Inst. of Canada, 2050 rue Mansfield, Suite 700, Montreal, Quebec H3A 1Z2 Canada

A structure of high-speed adaptive finite impulse response (FIR) digital filters is presented. The filters are based on delayed multipath implementation. The corresponding adaptive algorithm is developed for this structure which is applicable to arbitrary N-path realization, where N is greater than or equal to 2. The throughput rate of the present system can be N squared times that of a conventional adaptive FIR digital filter. Simulation results are included pertaining to the use of this structure and algorithm in an adaptive modeling system which is suitable for seismic exploration and other applications. Author (CISTI)

N93-30223 Manitoba Univ., Winnipeg. Dept. of Electrical and Computer Engineering.
ANALOG CMOS CIRCUITS FOR NEURAL NETWORKS **c33**

Christian Schneider, Roland Schneider, Gordon McGonigal, and Howard Card *In* Engineering Inst. of Canada, Canadian Conference on Electrical and Computer Engineering, Volumes 1 and 2 1990 4 p (For primary document see N93-30215 11-31)
Avail: Engineering Inst. of Canada, 2050 rue Mansfield, Suite 700, Montreal, Quebec H3A 1Z2 Canada

A compact analog complementary metal oxide semiconductor (CMOS) synaptic circuit with in-situ Hebbian learning was developed and used to construct a deterministic Boltzmann neural network. Investigations have shown that, because of the error compensating properties of the learning algorithm, neural network architectures such as the deterministic Boltzmann machine are robust even when constructed from compact, highly non-ideal analog CMOS components. The use of floating-gate field effect transistors for nonvolatile storage is also discussed. Author (CISTI)

N93-30224 Ottawa Univ. (Ontario). Dept. of Electrical Engineering.
A MOTION DETECTOR BASED ON A NEURAL NETWORK **c33**
T. H. Yeap, J. K. Tsotsos (Toronto Univ., Ontario.), S. G. Zaky (Toronto Univ., Ontario.), and H. C. Kwan (Toronto Univ., Ontario.) *In* Engineering Inst. of Canada, Canadian Conference on Electrical and Computer Engineering, Volumes 1 and 2 1990 4 p (For primary document see N93-30215 11-31)
Avail: Engineering Inst. of Canada, 2050 rue Mansfield, Suite 700, Montreal, Quebec H3A 1Z2 Canada

The architecture of a motion detector using a modular neural network is presented. Each network module contains a number of sequence nodes connected in a chain, where each node is responsible for recognizing only one image in a sequence. When a correct sequence is presented, the nodes are activated one at a time, with each node providing an excitatory signal to its successor on the chain. The time element is modeled by providing the nodes with a fading memory. Temporal integration of the sequence nodes' activities by a result node is used to generate an output response representing the input sequence. Given a sequence of images of an object moving in a plane parallel to the image plane, the motion detector can be trained to estimate quantities such as the speed and direction of movement of the object. The network has been tested and simulated. Results show that the detector is insensitive to small differences between the training and test trajectories, can recognize partial sequences, and is tolerant to noise in the input. Author (CISTI)

N93-30225 Saskatchewan Univ., Saskatoon. Biomedical Engineering Div.
AN ARTIFICIAL NEURAL NETWORK MODEL FOR PERIODIC TRAJECTORY GENERATION **c33**
S. Shankar, R. E. Gander, and H. C. Wood *In* Engineering Inst. of Canada, Canadian Conference on Electrical and Computer Engineering, Volumes 1 and 2 1990 4 p (For primary document see N93-30215 11-31)
Avail: Engineering Inst. of Canada, 2050 rue Mansfield, Suite 700, Montreal, Quebec H3A 1Z2 Canada

A neural network model based on biological systems was developed for potential robotic application. The model consists of three interconnected layers of artificial neurons or units: an input layer subdivided into state and plan units, an output layer, and a hidden layer between the two outer layers which serves to implement nonlinear mappings between the input and output activation vectors. Weighted connections are created between the three layers, and learning is effected by modifying these weights. Feedback connections between the output and the input state serve to make the network operate as a finite state machine. The activation vector of the plan units of the input layer emulates the supraspinal commands in biological central pattern generators in that different plan activation vectors correspond to different sequences or trajectories being recalled, even with different frequencies. Three trajectories were chosen for implementation, and learning was accomplished in 10,000 trials. The fault tolerant behavior, adaptiveness, and phase maintenance of the implemented network are discussed. Author (CISTI)

N93-30226 Concordia Univ., Montreal (Quebec). Center for Signal Processing and Communications.
PARAMETER IDENTIFICATION OF TIME-VARYING SYSTEMS USING NEURAL NETWORKS **c33**
Keqin Gao, M. Omair Ahmad, and M. N. S. Swamy *In* Engineering Inst. of Canada, Canadian Conference on Electrical and Computer Engineering, Volumes 1 and 2 1990 4 p (For primary document see N93-30215 11-31)
Avail: Engineering Inst. of Canada, 2050 rue Mansfield, Suite 700, Montreal, Quebec H3A 1Z2 Canada

A neural network solution is introduced for the problem of parameter identification of time-varying systems. An autoregressive (AR) model is used to identify the unknown system. The problem is formulated to minimize the least squares (LS) error between the output of the unknown system and the output of the AR model when they are driven by a white Gaussian noise. Because of the time-varying nature of the unknown system, an exponentially weighted LS scheme is employed to attach more weight to the current data. A neural network is designated to estimate the solution of the weighted LS problem that gives the parameter of the AR model. Since this is an unconstrained quadratic optimization problem and the AR parameters can assume either + or - values, a hyperbolic tangent function is used as the nonlinear activation function for the neurons. A space iterative search technique is incorporated into the computational procedure of the neural network such that it can find solution in an open space rather than within a hypercube. In order to identify the time-varying parameters efficiently, recursive formulations are derived so that the coefficient of the neural network can be updated whenever a new observation is available. Finally, computer simulation results are presented to demonstrate the performance of the scheme. Author (CISTI)

N93-30227 Ottawa Univ. (Ontario). Dept. of Computer Science.
PERFORMANCE ANALYSIS OF COMMUNICATION PROTOCOLS USING D-TIMED PETRI NET **c32**
G. H. Masapati and George M. White *In* Engineering Inst. of Canada, Canadian Conference on Electrical and Computer Engineering, Volumes 1 and 2 1990 4 p (For primary document see N93-30215 11-31)
Avail: Engineering Inst. of Canada, 2050 rue Mansfield, Suite 700, Montreal, Quebec H3A 1Z2 Canada

The application of D-timed Petri nets to performance analysis of the stop-and-wait communications protocol is examined. The model of this protocol includes the explicit modeling of losing messages, messages being damaged, and losing acknowledgements. The advantage of such a model is that it helps in understanding the effect of these errors on the performance of the stop-and-wait protocol. A calculation is presented of the optimum message block size for which the performance is maximum. For a transmission speed of 4800 bits/s, 32 non-data bits per block, an average of 0.00001 errors per bit, and a timeout interval of 4 seconds, the optimum message block size is found to be 20305 bits, with a maximum value of performance of 0.3716. Author (CISTI)

N93-30228 Ottawa Univ. (Ontario). Dept. of Computer Science.
AUTOMATIC SYNTHESIS OF PROTOCOL SPECIFICATIONS **c32**
Kassem Saleh *In* Engineering Inst. of Canada, Canadian Conference on Electrical and Computer Engineering, Volumes 1 and 2 1990 4 p (For primary document see N93-30215 11-31)
Avail: Engineering Inst. of Canada, 2050 rue Mansfield, Suite 700, Montreal, Quebec H3A 1Z2 Canada

A new method is proposed for the automatic synthesis of a computer communications protocol specification from a service specification. Both the service and the protocol specifications are modeled by finite state machines. The resulting synthesized protocol is guaranteed to be free from logical design (syntactic) errors and to conform to the service specification. In addition, the synthesized protocol is augmented by error-recovery patterns to enable recovery from transmission errors caused by an unreliable communication medium. An application of the new method to a service specification example is presented. Author (CISTI)

N93-30229 Victoria Univ. (British Columbia). Dept. of Electrical and Computer Engineering.
MODELLING OF CHANNEL THICKNESS MODULATION EFFECT IN SI GaAs MESFET'S **c76**
H. L. Kwok *In* Engineering Inst. of Canada, Canadian Conference on Electrical and Computer Engineering, Volumes 1 and 2 1990 4 p (For primary document see N93-30215 11-31)
Avail: Engineering Inst. of Canada, 2050 rue Mansfield, Suite 700, Montreal, Quebec H3A 1Z2 Canada

The current-voltage characteristics of metal semiconductor field effect transistors built on semi-insulating GaAs substrates is examined by taking into account the effect of channel thickness modulation due to carrier trapping. It is shown that, to a first-order approximation, the effect can be modeled by an additional term proportional to the drain current. A single equation with five parameters was used for the current-voltage characteristics in both the linear and the saturation regions. The equation agreed reasonably well with experimental results for small and large threshold voltages. Some detailed discussion is provided on the variations of the equation parameters under different biasing conditions. Author (CISTI)

N93-30230 Defence Research Establishment, Ottawa (Ontario).
SIMULATION OF TRANSIENT RADIATION EFFECTS ON SEMICONDUCTOR DEVICES USING A PULSED Q-SWITCHED Nd:YAG LASER c76
G. T. Pepper and S. M. Khanna *In* Engineering Inst. of Canada, Canadian Conference on Electrical and Computer Engineering, Volumes 1 and 2 1990 4 p (For primary document see N93-30215 11-31)
Avail: Engineering Inst. of Canada, 2050 rue Mansfield, Suite 700, Montreal, Quebec H3A 1Z2 Canada

Nuclear and space radiation can produce transient and permanent changes in the properties of semiconductor materials and devices, generally leading to performance degradation. A good understanding of the basic physical processes that affect semiconducting materials/devices is an essential first step in the process of achieving radiation hard devices. Electron linear accelerators and flash x-ray machines have been traditionally used for studying transient radiation effects in semiconducting devices and circuits. Preliminary results are presented which demonstrate that a Nd-YAG laser can be used as a low-cost alternative for such investigations. Short pulses of 1064 nm radiation from a pulsed Q-switched Nd-YAG laser were used to study transient photocurrent in a variety of Si and GaAs devices. Results show that militarily significant dose rates, in excess of 10(exp 11) rad(Si)/s, can be easily obtained with a relatively low-power Nd-YAG laser. This system may also be used for the simulation of single-event upsets that occur in spaceborne electronics. Author (CISTI)

N93-30231 Carleton Univ., Ottawa (Ontario).
RIB ARROW INTEGRATED OPTIC POLARIZER c74
S. Yuen, B. Syrett, W. Jiang (Canadian Marconi Co. Ltd., Montreal, Quebec.), J. Chrostowski (National Research Council of Canada, Ottawa, Ontario.), and J. Wartak (National Research Council of Canada, Ottawa, Ontario.) *In* Engineering Inst. of Canada, Canadian Conference on Electrical and Computer Engineering, Volumes 1 and 2 1990 4 p (For primary document see N93-30215 11-31)
Avail: Engineering Inst. of Canada, 2050 rue Mansfield, Suite 700, Montreal, Quebec H3A 1Z2 Canada

A new type of integrated optical polarizer employs the antiresonant reflecting optical waveguide (ARROW) structure. The criteria for achieving optimal polarization extinction with these waveguide devices are discussed. Experimental results from testing of the prototype devices are then presented. Field distributions perpendicular to the core and cladding interfaces were analyzed using the transverse resonance method to arrive at the optimal ARROW structure. In addition, field confinement by the rib waveguide in the horizontal direction was examined using the effective index method. Excellent correlations between the theoretical and experimental beam profiles were obtained. Author (CISTI)

N93-30232 Ottawa Univ. (Ontario).
TACTILE SENSING FOR 3-DIMENSIONAL SHAPE ESTIMATION c35
E. Petriu, M. Greenspan, F. Gelinas, W. S. McMath (Canadian Space Agency, Ottawa, Ontario.), and S. K. Yeung (Canadian Space Agency, Ottawa, Ontario.) *In* Engineering Inst. of Canada, Canadian Conference on Electrical and Computer Engineering, Volumes 1 and 2 1990 4 p (For primary document see N93-30215 11-31)
Avail: Engineering Inst. of Canada, 2050 rue Mansfield, Suite 700, Montreal, Quebec H3A 1Z2 Canada

The conceptual and implementation aspects are presented for a cutaneous tactile sensor developed for the contact measurement of a local three dimensional object shape. Most of the available tactile sensing technologies measure the contact force transmitted through an elastic pad which contacts the object of interest. A force-sensitive array of strain gauges is used in an experimental 8-by-8 sensor array to provide a de facto two dimensional sampling of the continuous spatial field of the strain in the elastic pad. Each gauge also provides a quantization of strain intensity in the third direction of three dimensional space. The different functional steps in the sensing process were studied using the experimental tactile sensor array. The results show that the tested approach is robust and has a number of functional characteristics which favor further investigation for potential space applications. Author (CISTI)

N93-30233 McMaster Univ., Hamilton (Ontario). Dept. of Electrical and Computer Engineering.
DIVISION BY POLYNOMIAL MATRIX AND ITS APPLICATION TO MULTIVARIABLE LINEAR SYSTEMS c63
Jianguo Fu and N. K. Sinha *In* Engineering Inst. of Canada, Canadian Conference on Electrical and Computer Engineering, Volumes 1 and 2 1990 3 p (For primary document see N93-30215 11-31)
Avail: Engineering Inst. of Canada, 2050 rue Mansfield, Suite 700, Montreal, Quebec H3A 1Z2 Canada

The concept of division by a polynomial matrix is introduced and applied for solving a polynomial matrix equation that arises in applications such as the design of compensators for multivariable systems. It is shown that the proposed division by a polynomial matrix can be easily implemented on a computer, since this approach converts the operation on a polynomial matrix into an operation on a numerical coefficient matrix. This approach can also be utilized in the design of adaptive controllers for multivariable linear systems in the presence of uncertainty. Author (CISTI)

N93-30234 Ottawa Univ. (Ontario). Dept. of Electrical Engineering.
OPTIMAL FILTERING AND LQR THEORY WITH CONSTRAINTS ON SYSTEM AND CONTROL MATRICES c33
N. U. Ahmed and Peng Li *In* Engineering Inst. of Canada, Canadian Conference on Electrical and Computer Engineering, Volumes 1 and 2 1990 4 p (For primary document see N93-30215 11-31)
Avail: Engineering Inst. of Canada, 2050 rue Mansfield, Suite 700, Montreal, Quebec H3A 1Z2 Canada

Some recent results are presented from the formulation of the classical linear quadratic regulator problem. The approach is based on direct optimization in the space of operators, thereby allowing constraints on the operator types and norms. It is shown that the constrained optimal regulators and optimum filters converge to the classical ones as the constraints are removed. In addition, some generalities and possible generalizations for filtering problem solutions are presented. As a bonus, the developed approach provides a simple and direct derivation of the Kalman-Bucy filter equations. For illustration, some numerical results are shown comparing constrained and unconstrained linear filters. Author (CISTI)

N93-30235 Ottawa Univ. (Ontario). Dept. of Electrical Engineering.
VIBRATION CONTROL OF FLEXIBLE SPACE STRUCTURES IN NOISY ENVIRONMENT c18
S. S. Lim and N. U. Ahmed *In* Engineering Inst. of Canada, Canadian Conference on Electrical and Computer Engineering, Volumes 1 and 2 1990 4 p (For primary document see N93-30215 11-31)
Avail: Engineering Inst. of Canada, 2050 rue Mansfield, Suite 700, Montreal, Quebec H3A 1Z2 Canada

Based on a dynamic model developed for large flexible spacecraft, a stabilizing control is designed which can suppress the vibrations induced by random perturbation. The problem considered is that of asymptotic stabilization in the presence of random disturbances by application of simple feedback controls. A flexible spacecraft consisting of a rigid body with a long flexible beam attached to it and undergoing three types of motion (rigid body translation and rotation, and beam vibration) is modeled. The results indicate that the feedback controls are robust with respect to the disturbances. Some numerical simulation results are also presented for illustration of the impact of random perturbation on the dynamic behavior of the system and the effectiveness of the suggested controls.
Author (CISTI)

N93-30236 Concordia Univ., Montreal (Quebec). Dept. of Electrical and Computer Engineering.
A SYSTOLIC-ARRAY STRUCTURE FOR MTCM RECEIVERS c33
S. H. Jamali and Tho Le-Ngoc *In* Engineering Inst. of Canada, Canadian Conference on Electrical and Computer Engineering, Volumes 1 and 2 1990 4 p (For primary document see N93-30215 11-31)

Avail: Engineering Inst. of Canada, 2050 rue Mansfield, Suite 700, Montreal, Quebec H3A 1Z2 Canada

Multiple trellis-coded modulation (MTCM) schemes, which represent a performance on the fading channels superior to the conventional trellis-coded modulated schemes, have a highly connected trellis diagram with parallel paths between states. Optimum detection of these schemes is achieved by the Viterbi algorithm (VA). For the schemes with a large number of states or parallel paths, this algorithm requires many computations during each symbol interval. Applications where the data rate is high necessitate a parallel processing implementation of the VA rather than the sequential solution. A highly concurrent implementation of the VA is proposed, based on systolic array processors for MTCM receivers. It is shown that the throughput rate gain of this systolic array decoder increases exponentially with the multiplicity of the MTCM schemes. This allows designing the MTCM schemes with higher multiplicities, with such schemes having more coding gain than the MTCM codes with smaller multiplicities.
Author (CISTI)

N93-30237 Simon Fraser Univ., Burnaby (British Columbia). Communications Science Lab.

AN ERROR CONTROL PROTOCOL BASED ON TRELLIS CODED MODULATIONS **c32**

Paul Ho and Yan Wu *In* Engineering Inst. of Canada, Canadian Conference on Electrical and Computer Engineering, Volumes 1 and 2 1990 6 p (For primary document see N93-30215 11-31)
Avail: Engineering Inst. of Canada, 2050 rue Mansfield, Suite 700, Montreal, Quebec H3A 1Z2 Canada

Instead of using binary forward error correcting codes for hybrid automatic repeat request systems, it is proposed to use joint power and bandwidth efficient trellis-coded modulations (TCM). Due to their bandwidth efficiency, error control systems using TCM can achieve much higher throughput, in the range of signal-to-noise ratios of interest, than systems using more conventional coding and modulation methods. By making use of the fact that rate-compatible TCM schemes can be obtained by periodically puncturing and/or repeating modulation symbols from a mother TCM scheme, the effective code rate, and hence the error correction capability, of the TCM subsystem can be varied by adopting a retransmission strategy that sends only incremental redundant symbols, and by adopting a decoding strategy that performs code combining. Such rate-adaptive hybrid error control systems are quite suitable for mobile radio application. Using analysis and computer simulation, the performance of three such systems was studied in a Rayleigh fading environment. The tradeoff of these systems, in terms of throughput, decoding complexity, and frame-error rate, is discussed. The system giving the best compromise among these three performance measures uses rate-compatible TCM schemes obtained from the Ungerboeck 8-state 8PSK code. Author (CISTI)

N93-30238 Gandalf Technologies, Inc., Nepean (Ontario).

A SINGLE CHIP HIGH-SPEED CMOS VITERBI DECODER **c33**

David Peter Noel and Tad Kwasniewski (Carleton Univ., Ottawa, Ontario.) *In* Engineering Inst. of Canada, Canadian Conference on Electrical and Computer Engineering, Volumes 1 and 2 1990 4 p (For primary document see N93-30215 11-31)
Avail: Engineering Inst. of Canada, 2050 rue Mansfield, Suite 700, Montreal, Quebec H3A 1Z2 Canada

To provide an improved coding gain at high transmission rates, a single-chip complementary metal oxide semiconductor (CMOS) Viterbi decoder was developed. A close examination of an implementation of error control coding utilizing the Viterbi algorithm as a method of improving forward error correction schemes has uncovered sub-circuits within most designs which could be modified for use at higher rates of operation. By capitalizing upon the strength of those portions of the various designs capable of high speed operation, an optimal high speed Viterbi decoder was then designed. The major sub-circuits modified for use in the optimal design are primarly the add-compare-select circuitry and the path memory as it exists in several of the reviewed designs. With the use of the 1.2 micron CMOS process, high-speed operations exceeding 100 megasymbols per second is achieved. The reduced-area technology permits the implementation to be placed on an individual silicon die. Author (CISTI)

N93-30239 McMaster Univ., Hamilton (Ontario). Communications Research Lab.

QR DECOMPOSITION BASED LEAST SQUARES LATTICE ALGORITHM **c61**

Simon Haykin *In* Engineering Inst. of Canada, Canadian Conference on Electrical and Computer Engineering, Volumes 1 and 2 1990 3 p (For primary document see N93-30215 11-31)
Avail: Engineering Inst. of Canada, 2050 rue Mansfield, Suite 700, Montreal, Quebec H3A 1Z2 Canada

The QR decomposition provides a mathematical tool for the factorization of a rectangular complex-valued data matrix. Highlights are presented of a new algorithm, based on the numerically robust QR decomposition, for a fast recursive solution of the linear least squares problem. The algorithm has a lattice-like structure and its development is based on a hybridization of ideas. Three distinct elements may be identified in the new algorithm: initial values specified by the input data and desired response; order updates (recursions) for computing angle normalized estimation errors, including the adaptive filter output; and time update (recursions) for the direct computation of a corresponding set of auxiliary parameters. The new algorithm has operational and implementational advantages including fast rate of convergence, numerical stability, high level of computational efficiency, a modular structure, and an integral set of desired variables and parameters.
Author (CISTI)

N93-30240 Alberta Telecommunications Research Centre, Edmonton.

ENHANCED RESOLUTION AND DE-ALIASING TECHNIQUES FOR FAST FOURIER TRANSFORMS **c61**

G. D. Cormack and J. N. McMullin *In* Engineering Inst. of Canada, Canadian Conference on Electrical and Computer Engineering, Volumes 1 and 2 1990 5 p (For primary document see N93-30215 11-31)
Avail: Engineering Inst. of Canada, 2050 rue Mansfield, Suite 700, Montreal, Quebec H3A 1Z2 Canada

Improvements in fast Fourier transform (FFT) procedures for rapid spectral analysis of large sets of signal data are described. Final-value padding prior to FFT transformation of a steplike function, such as zero padding for a limited duration function, is found to increase the spectral resolution. In an example considered, a sixteen-fold enhancement is obtained. Frequency domain de-aliasing algorithms based on interpolative modeling between data points are presented and are used to remove aliasing error from FFT results. These algorithms are uniquely attractive because of their accuracy and their computational efficiency. The algorithms can be up to eight orders of magnitude more accurate than the ordinary FFT, even above the Nyquist frequency. The frequency domain de-aliasing method presented is also shown to be valid for increasing the accuracy of an FFT of a steplike data set. Author (CISTI)

N93-30241 Atlantis Scientific Systems Group, Inc., Ottawa (Ontario).

THE USE OF DATA TURNING IN AIRBORNE RADARS **c32**

L. Lightstone and D. Faubert *In* Engineering Inst. of Canada, Canadian Conference on Electrical and Computer Engineering, Volumes 1 and 2 1990 4 p (For primary document see N93-30215 11-31)
Avail: Engineering Inst. of Canada, 2050 rue Mansfield, Suite 700, Montreal, Quebec H3A 1Z2 Canada

Data turning is a digital signal processing method that achieves good signal-to-noise ratio and target/interference resolution while reducing the number of pulses processed in the discrete Fourier transform/fast Fourier transform operation. A mathematical description is provided of data turning, along with a mathematical example of the impact of data turning on a bank of discrete Fourier transform filters. Data turning is discussed from the frequency domain and time domain perspectives, and a simulated performance example is taken from an airborne pulse doppler radar system. It is shown that data turning can, with a proper choice of signal processing parameters, approximate the integration improvement of non-coherent integration. Data turning can be significantly faster than either full coherent processing or non-coherent processing. Author (CISTI)

N93-30242 Queens Univ., Kingston (Ontario). Dept. of Electrical Engineering.

SYNCHRONIZATION OF THE LAPTV ADATIVE FILTER WITH INPUT STATISTICS **c33**

Heping Ding and Moustafa M. Fahmy *In* Engineering Inst. of Canada, Canadian Conference on Electrical and Computer Engineering, Volumes 1

and 2 1990 4 p (For primary document see N93-30215 11-31)
Avail: Engineering Inst. of Canada, 2050 rue Mansfield, Suite 700, Montreal, Quebec H3A 1Z2 Canada

A discrete-time linear, almost periodically time-varying (LAPTV) adaptive filter (AF) that admits the output modulator structure (OMS) was proposed for processing almost cyclostationary (ACS) signals. The problem of synchronization of this LAPTV AF with the input ACS signals is encountered in practical applications. An intrinsic frequency tracking scheme is proposed for synchronizing the LAPTV AF with varying input statistics. The tracking algorithm is presented and analyzed and it is shown that the algorithm converges if the step size (a positive constant controlling the rate of adjustment) meets specified criteria. Two simulations were performed to evaluate the transient and steady-state behaviors of the tracking scheme. It is concluded that the proposed scheme succeeds in keeping the LAPTV AF synchronous with the input statistics, with a controllable performance degradation. Author (CISTI)

N93-30243 Ottawa Univ. (Ontario). Dept. of Electrical Engineering.
FEATURE SEGMENTATION USING A MULTIPLE-STACK BASED CHAIN CODING ALGORITHM **c61**
Dan Ionescu and Michael A. Sasarman *In* Engineering Inst. of Canada, Canadian Conference on Electrical and Computer Engineering, Volumes 1 and 2 1990 4 p (For primary document see N93-30215 11-31)
Avail: Engineering Inst. of Canada, 2050 rue Mansfield, Suite 700, Montreal, Quebec H3A 1Z2 Canada

A new pixel labeling method is introduced for use in contour tracing in images with linear features, as a way to improve the performance of existing generalized chain codes. The proposed algorithm employs a multiple stack (MS) to track intersection points, referred to as T-joints, between blobs and lines in edge images. The stack mechanism is activated only in the presence of one-pixel-wide features. The MS algorithm is suitable for interpretation of aerial images where small features are quite frequent. The algorithm was implemented on a massively parallel architecture using LANDSAT multispectral images, and an example of analysis of an aerial test image is included. Author (CISTI)

N93-30244 McGill Univ., Montreal (Quebec). Computer Vision and Robotics Lab.
AN ARCHITECTURE FOR AN ANALOG VLSI NEURAL NETWORK FOR EARLY COMPUTER VISION PROCESSING **c33**
D. D. Haule, M. E. Malowany, D. Lambidonis, S. Nemawarkar, S. Sayegh, and A. S. Malowany *In* Engineering Inst. of Canada, Canadian Conference on Electrical and Computer Engineering, Volumes 1 and 2 1990 4 p (For primary document see N93-30215 11-31)
Avail: Engineering Inst. of Canada, 2050 rue Mansfield, Suite 700, Montreal, Quebec H3A 1Z2 Canada

A two-stage early vision algorithm for curve description in images has been targeted for an analog very large scale integration (VLSI) implementation. Similarity between the processing in the two algorithm stages is exploited, resulting in a single modular chip capable of performing either processing stage. The core of the circuitry is a parallel convolution array modeled after connectionist artificial neural network structures. Pipelining of the image data is applied, using on-chip temporary analog storage to implement neighborhood operations. On-chip long-term analog storage for algorithm parameters is proposed using floating-gate electronically erasable programmable read-only memory technology. The chip, whose approximate transistor count is 15,000, is designed for a complementary metal oxide semiconductor (CMOS) 1.2 micron double-metal process. An effort is made to maintain the transistors in the subthreshold region of operation to decrease power requirements, particularly in the analog convolution array which forms the bulk of the chip and is of concern for scaling up the array size in the future. Author (CISTI)

N93-30245 Carleton Univ., Ottawa (Ontario). Dept. of Electronics.
HIGH-SPEED, CMOS DUAL MODULUS FREQUENCY DIVIDER FOR RF FREQUENCY SYNTHESIS **c33**
Navid Foroudi and Tad A. Kwasniewski *In* Engineering Inst. of Canada, Canadian Conference on Electrical and Computer Engineering, Volumes 1 and 2 1990 3 p (For primary document see N93-30215 11-31)
Avail: Engineering Inst. of Canada, 2050 rue Mansfield, Suite 700, Montreal, Quebec H3A 1Z2 Canada

With a trend towards integrating the radio frequency (RF) component of a mobile/satellite/indoor wireless transceiver into a single integrated circuit, the issue of high-speed, high resolution frequency synthesis becomes highly important. To achieve high resolution, a fractional division frequency divider can be used. A dual modulus frequency divider has been designed for a 3-micrometer CMOS process. The speed is enhanced by using a novel fast digital counter in a circuit in which only the first stage works with high frequency. Decoding hardware passes the division-ratio control signal to the first stage only during one of the states of the second stage, which is clocked by the output of the first stage. The proposed circuit configuration works with a single phase clock, which eliminates skew problems. After optimization, a simulation indicates that the circuit can operate with a frequency as high as 165 MHz. Author (CISTI)

N93-30246 Laval Univ. (Quebec). Dept. of Electrical Engineering.
LOGARITHMIC TIME SCALE IN THERMOGRAPHIC NON DESTRUCTIVE EVALUATION (NDE) OF MATERIALS **c38**
X. Maldague, J. C. Krapez (National Research Council of Canada, Boucherville, Quebec.), and P. Cielo (National Research Council of Canada, Boucherville, Quebec.) *In* Engineering Inst. of Canada, Canadian Conference on Electrical and Computer Engineering, Volumes 1 and 2 1990 4 p (For primary document see N93-30215 11-31)
Avail: Engineering Inst. of Canada, 2050 rue Mansfield, Suite 700, Montreal, Quebec H3A 1Z2 Canada

Active thermography is an attractive new technique for the nondestructive inspection of materials and structures. This technique uses a thermal perturbation to stimulate the response of the part being evaluated. Dedicated image processing is necessary to recover quantitative information about possible buried low thermal conductance defects. A technique is presented which allows recovery of the complete temporal history curve of the sample following the thermal stimulation, taking into account the typical limitations of digital systems both in terms of speed to capture images and available memory to hold them. The technique is based on the use of a logarithmic time scale to record the observational data. Such a time scale is shown to allow acquisition of infrared images over long periods of time without exceeding the computer memory capacity while retaining all the important features of the temperature history curve following the thermal perturbation necessary to detect low thermal conducting defects. Author (CISTI)

N93-30247 Quebec Univ., Montreal. Dept. of Mathematics and Computer Science.
AN INFORMATION THEORETIC APPROACH TO STOCHASTIC ADAPTIVE CONTROL APPLICATION TO MANIPULATORS WITH ACTIVE INERTIA **c63**
Guy Jumarie *In* Engineering Inst. of Canada, Canadian Conference on Electrical and Computer Engineering, Volumes 1 and 2 1990 4 p (For primary document see N93-30215 11-31)
Avail: Engineering Inst. of Canada, 2050 rue Mansfield, Suite 700, Montreal, Quebec H3A 1Z2 Canada

An alternative approach is presented to tackling the problem of the control of stochastic systems, in which the control of the continuous plant itself is designed and then the effects of discretization in the computerized implementation are analyzed. To this end, the Fokker-Planck equation which defines the state probability density of the process is combined with some basic concepts of Shannon's information theory. A model reference adaptive control is suggested in which the cross-entropy between the actual system and the system to be tracked is minimized. The application of the adaptive control scheme to robotic manipulators is outlined. Author (CISTI)

N93-30248 Nova Scotia Technical Coll., Halifax.
AN ADAPTIVE CONTROLLER FOR A CLASS OF MIMO NON-MINIMUM PHASE SYSTEMS WITH DISTURBANCE REJECTION DESIGN **c63**
X. Li and C. R. Baird *In* Engineering Inst. of Canada, Canadian Conference on Electrical and Computer Engineering, Volumes 1 and 2 1990 4 p (For primary document see N93-30215 11-31)
Avail: Engineering Inst. of Canada, 2050 rue Mansfield, Suite 700, Montreal, Quebec H3A 1Z2 Canada

The problem of disturbances rejection in an adaptive controller design is addressed. A new adaptive control algorithm is derived to obtain the complete measurable disturbances rejection in both static and dynamic states for a class of non-minimum phase multiple-input multiple-output systems by reassigning the system zeros to the stable region. The controller design scheme incorporates three steps. First, the system model is modified

by using a control signal which takes two values during a sampling period. Then two precompensators are established to the decoupling end. Finally, the generalized minimum variance approach is applied to each decoupled loop, and the complete measurable disturbance rejection is achieved through the feedforward compensating. A simulated example is presented to demonstrate the performance of the proposed controller. Perfect reference following and complete measurable disturbance rejection are achieved at sampling instants after the estimated parameters converged.
Author (CISTI)

N93-30249 Ottawa Univ. (Ontario). Dept. of Electrical Engineering.
ROBUST BOUNDARY CONTROL OF FLEXIBLE STRUCTURES GOVERNED BY HYBRID DYNAMICS **c18**
P. Li, N. U. Ahmed, and S. S. Lim *In* Engineering Inst. of Canada, Canadian Conference on Electrical and Computer Engineering, Volumes 1 and 2 1990 4 p (For primary document see N93-30215 11-31)
Avail: Engineering Inst. of Canada, 2050 rue Mansfield, Suite 700, Montreal, Quebec H3A 1Z2 Canada

The robust control and stabilization of a simplified spacecraft control laboratory experiment (SCOLE) model are analyzed. In this model, a long flexible mast or elastic beam joins two rigid bodies. Boundary conditions are imposed at one end by the control forces and torques acting on one body, with the other end at rest. A mathematical model is rigorously derived and it is shown that the vibrations in the flexible mast can be completely eliminated by applying appropriate feedback control forces and torques. Moreover, it is proved that the boundary feedback control is robust in the sense that the stability properties remain invariant under a broad class of perturbations by the same feedback law. Simulation results for the SCOLE model are also included. Author (CISTI)

N93-30250 Gandalf Technologies, Inc., Nepean (Ontario).
A SLOTTED ALOHA SATELLITE CHANNEL SIMULATOR **c32**
D. Peter Noel and Arthur F. Guibord (Telesat Canada, Ottawa, Ontario.) *In* Engineering Inst. of Canada, Canadian Conference on Electrical and Computer Engineering, Volumes 1 and 2 1990 4 p (For primary document see N93-30215 11-31)
Avail: Engineering Inst. of Canada, 2050 rue Mansfield, Suite 700, Montreal, Quebec H3A 1Z2 Canada

The task of developing a data communication system for mobile applications may be aided through the use of a customized simulator. By modeling the communications channel, the user population and traffic density may be optimized for peak performance under most conditions. A flexible slotted Aloha channel simulator, capable of customization to various channel configurations and user profiles, was developed as a flexible tool for analyzing the transient and steady-state performance of a multiple access network. The design of the simulator was based on the specifications associated with the satellite messaging protocol within the Telesat Mobile satellite data service. Sample simulation results are presented and analyzed, showing such phenomena as the effects of channel loading on queueing delay.
Author (CISTI)

N93-30251 Raytheon Canada Ltd., Waterloo (Ontario).
IMPROVED BOUNDS FOR SYNCHRONIZATION JITTER **c32**
Stuart C. White and Norman C. Beaulieu (Queens Univ., Kingston, Ontario.) *In* Engineering Inst. of Canada, Canadian Conference on Electrical and Computer Engineering, Volumes 1 and 2 1990 7 p (For primary document see N93-30215 11-31)
Avail: Engineering Inst. of Canada, 2050 rue Mansfield, Suite 700, Montreal, Quebec H3A 1Z2 Canada

The application of the detection theory (DT) bound is developed for the symbol timing recovery problem. It is shown that this bound is particularly well suited to the symbol synchronization problem, and provides useful information in a wide variety of situations. The Cramer-Rao (CR) and DT bounds are compared for this application. In order to assess the comparative usefulness of the two bounds, a different form of the CR bound is first derived which is more applicable to the symbol timing problem than the usual statement of the CR bound. It is shown that the DT bound yields useful results for signaling pulses with jump discontinuities and for small signal-to-noise ratios. In addition, the DT bound provides information about the variation in performance achievable for different symbol sequences. In contrast, the CR bound gives no useful information about any of these three cases. Author (CISTI)

N93-30252 McMaster Univ., Hamilton (Ontario). Communications Research Lab.
PROPAGATION CHANNEL MODELING FOR ANGLE-DIVERSITY COMBINING SIMULATION **c32**
Milan Despinic and Desmond P. Taylor *In* Engineering Inst. of Canada, Canadian Conference on Electrical and Computer Engineering, Volumes 1 and 2 1990 4 p (For primary document see N93-30215 11-31)
Avail: Engineering Inst. of Canada, 2050 rue Mansfield, Suite 700, Montreal, Quebec H3A 1Z2 Canada

The design and analysis of digital microwave radio systems employing antenna pattern/angle or space diversity to combat multipath fading requires knowledge of the channel characteristics for each diversity branch. A method is described for deriving the statistical channel models for each diversity branch in any line-of-sight microwave link. The method is based on statistically modeling the link's atmospheric refractivity profile so that, by using ray tracing techniques to estimate the received raypath parameters for each profile, and including the effects of the diversity antenna patterns, an ensemble of channel responses can be formed for each diversity branch. Performance factor distributions could then be computed and used to find the optimum diversity antenna patterns, as well as to estimate outage, for a particular link. Author (CISTI)

N93-30253 Defence Research Establishment, Ottawa (Ontario).
ACOUSTO-OPTIC TIME-INTEGRATING CORRELATORS FOR PROCESSING WIDEBAND DIGITAL DATA **c74**
N. Brousseau and J. W. A. Salt *In* Engineering Inst. of Canada, Canadian Conference on Electrical and Computer Engineering, Volumes 1 and 2 1990 3 p (For primary document see N93-30215 11-31)
Avail: Engineering Inst. of Canada, 2050 rue Mansfield, Suite 700, Montreal, Quebec H3A 1Z2 Canada

The development of high quality optical components has made possible the implementation of high performance optical data processors of many kinds. The research on time integrating correlators (TIC) performed at the Defence Research Establishment Ottawa is described. TIC's are acousto-optic data processors designed to produce at high speed the cross correlation between any two input signals. The principle of operation of TIC's is briefly reviewed and the characteristics of the signal that they produce are discussed. Three implementations being currently developed are presented together with an analysis of the factors affecting the performance of TIC's. TIC's are characterized by a sensitivity comparable to that of a radiometer and by processing speeds on the order of 10 to the 12th operations per second. Their dynamic range is usually limited by the dynamic range of the detector array. TIC's correlating two signals of different intensity have demonstrated a dynamic range of 43 dB in a system having a time-bandwidth product of 180,000. Author (CISTI)

N93-30254 Naval Surface Warfare Center, Silver Spring, MD. Information and Mathematical Sciences Branch.
ZERO-CROSSING RATE OF SOME NON-GAUSSIAN PROCESSES **c64**
John Barnett and Benjamin Kedem (Maryland Univ., College Park.) *In* Engineering Inst. of Canada, Canadian Conference on Electrical and Computer Engineering, Volumes 1 and 2 1990 4 p (For primary document see N93-30215 11-31)
Avail: Engineering Inst. of Canada, 2050 rue Mansfield, Suite 700, Montreal, Quebec H3A 1Z2 Canada

It is a curious fact that the formulae for the expected zero-crossing rate of some non-Gaussian processes may be obtained using monotone transformations of Gaussian processes. This is shown using two different techniques. The first technique involves the derivation of the expected zero-crossing rate for discrete time and then extending the result to the continuous time case. The second is a direct method that makes use, successively, of Price's theorem, the chain rule, and Rice's formula. The two methods should prove useful for the general level-crossing problem of a variety of random processes. Author (CISTI)

N93-30255 McMaster Univ., Hamilton (Ontario). Communications Research Lab.
AN ADAPTIVE ALGORITHM FOR LINEAR ASSOCIATIVE MEMORY PROBLEM **c61**
Sanzheng Qiao *In* Engineering Inst. of Canada, Canadian Conference on Electrical and Computer Engineering, Volumes 1 and 2 1990 4 p

(For primary document see N93-30215 11-31)
Avail: Engineering Inst. of Canada, 2050 rue Mansfield, Suite 700, Montreal, Quebec H3A 1Z2 Canada

Associative memory is one of a number of neural computing techniques. The linear adaptive combiner model for associative memory is outlined and an adaptive algorithm is presented for the linear associative memory problem. The algorithm is based on Kishi's (1964) theorem and uses different schemes for initialization and recursion, showing good numerical properties. A parallel implementation of the algorithm is also proposed.
Author (CISTI)

N93-30256 Ottawa Univ. (Ontario). Dept. of Electrical Engineering.
ANALYTICAL PREDICTIONS OF THE INTERMODULATION NOISE OF SEMICONDUCTOR LASER DIODE **c36**
Tapan Biswas and W. F. McGee *In* Engineering Inst. of Canada, Canadian Conference on Electrical and Computer Engineering, Volumes 1 and 2 1990 4 p (For primary document see N93-30215 11-31)
Avail: Engineering Inst. of Canada, 2050 rue Mansfield, Suite 700, Montreal, Quebec H3A 1Z2 Canada

Theoretical models for semiconductor laser diode nonlinearities are investigated. Volterra transfer functions are calculated from the laser rate equations using an output-to-input approach. Nonlinear models for second harmonic, third harmonic, and two-tone third-order intermodulation distortions are calculated from the Volterra transfer functions. Variations of distortion level with frequency and bias are shown along with previously published theoretical, simulation, and experimental results. The advantage of the approach presented is that it offers a more general analysis framework and an accurate rapid evaluation of the device performance.
Author (CISTI)

N93-30257 Ecole Polytechnique, Montreal (Quebec).
PERFORMANCE ENHANCEMENT OF DYNAMIC CMOS LOGIC CIRCUITS **c33**
Azzedine Boulguira and Yvon Savaria *In* Engineering Inst. of Canada, Canadian Conference on Electrical and Computer Engineering, Volumes 1 and 2 1990 4 p (For primary document see N93-30215 11-31)
Avail: Engineering Inst. of Canada, 2050 rue Mansfield, Suite 700, Montreal, Quebec H3A 1Z2 Canada

Dynamic complementary metal oxide semiconductor (CMOS) circuits have been a privileged target for the optimization of characteristics such as speed, area, and power dissipation. Research was conducted to reduce the delay of classes of CMOS logic circuits by inserting a parallel regenerator at specific nodes. The new design method presented is shown to reduce the delay by as much as 80% and the delay-area product by up to 35%. Results of different circuit simulations using the HSPICE simulator, assuming Northern Telecom CMOS3DLM technology parameters are summarized.
Author (CISTI)

N93-30258 Transport Canada, Winnipeg (Manitoba).
FAULT TOLERANCE AND TESTING FOR WSI SYSTEMS **c33**
Alan W. Ptak and R. D. McLeod (Manitoba Univ., Winnipeg.) *In* Engineering Inst. of Canada, Canadian Conference on Electrical and Computer Engineering, Volumes 1 and 2 1990 3 p (For primary document see N93-30215 11-31)
Avail: Engineering Inst. of Canada, 2050 rue Mansfield, Suite 700, Montreal, Quebec H3A 1Z2 Canada

Fault tolerance and testing for wafer scale integration (WSI) processor arrays using boundary scan and built-in self-test (BIST) technology are discussed. A test strategy for verification of all components within an integrated circuit wafer is presented, and a fault tolerance technique using semi-concurrent fault detection is described. The test strategy consists of four steps taken to verify test bus continuity, boundary scan register continuity, interconnection network connectivity, and processor element integrity. The component-level area overhead for boundary scan and BIST is modest for present-day fabrication processes, and will diminish to an insignificant level as integrated circuit fabrication technology continues to improve.
Author (CISTI)

N93-30259 Manitoba Univ., Winnipeg.
GENERATION OF CONFIGURABLE SELF-SYNCHRONIZING SYNCHRONOUS CMOS STATIC RAMs **c60**
W. Kinsner *In* Engineering Inst. of Canada, Canadian Conference on Electrical and Computer Engineering, Volumes 1 and 2 1990 4 p
(For primary document see N93-30215 11-31)
Avail: Engineering Inst. of Canada, 2050 rue Mansfield, Suite 700, Montreal, Quebec H3A 1Z2 Canada

A new configurable self synchronizing synchronous complementary metal oxide semiconductor static random access memory is described. A new memory generation approach has been developed that results in memories of any bit size. The memory is limited in size only by physical considerations. The memory generator not only produces a layout that can be used directly in any physical location in the design of application specific integrated circuits, but also generates data bases for the desired memory simulation in order to verify its actual timing to be used in the rest of the design. A self synchronizing memory architecture has been selected to assure the worst-case timing with temperature variations, process variations, and aging of each memory generated. The memories can be implemented in either a two dimensional or a two and one-half dimensional architecture.
Author (CISTI)

N93-30260 Bell-Northern Research Ltd., Ottawa (Ontario).
A NUMERICAL SIMULATOR FOR TESTING SLIDING MODE CONTROLS IN STOCHASTIC SYSTEMS **c64**
P. Gauthier and R. P. Malhame (Ecole Polytechnique, Montreal, Quebec.) *In* Engineering Inst. of Canada, Canadian Conference on Electrical and Computer Engineering, Volumes 1 and 2 1990 4 p (For primary document see N93-30215 11-31)
Avail: Engineering Inst. of Canada, 2050 rue Mansfield, Suite 700, Montreal, Quebec H3A 1Z2 Canada

Hybrid stochastic models can be used to characterize the stochastic behavior of a great variety of systems which have a discontinuous character or follow a jump process. One of these systems is the stochastic variable structure controller. A mathematical model of such a controller is outlined, in which the system dynamics is completely specified by a vector of the usual continuous state and the discrete state. The discrete variable characterizes the structures between which the process oscillates to create a nonideal sliding mode. It is shown that the evolution of the probability density functions in each of these structures can be described by a system of coupled Fokker-Planck equations. Using a finite difference approximation, a numerical simulation of the resulting system of partial differential equations has been constructed. The invariance properties in a sliding mode in the presence of noise are evaluated. The simulations suggest the possible existence of a Riccati type equation for the propagation of covariances which would extend in a certain way the well-known invariance properties of deterministic systems in sliding modes to the second moments of the state dynamic probability distribution.
Author (CISTI)

N93-30261 Royal Military Coll. of Canada, Kingston (Ontario). Dept. of Mechanical Engineering.
ANALYSIS AND SIMULATION OF A TWO DEGREES-OF-FREEDOM ONE-LINK FLEXIBLE FOREARM **c37**
J. C. Piedboeuf and R. Hurteau (Ecole Polytechnique, Montreal, Quebec.) *In* Engineering Inst. of Canada, Canadian Conference on Electrical and Computer Engineering, Volumes 1 and 2 1990 6 p (For primary document see N93-30215 11-31)
Avail: Engineering Inst. of Canada, 2050 rue Mansfield, Suite 700, Montreal, Quebec H3A 1Z2 Canada

Reliable models are necessary to study flexible robots. A nonlinear model for a two degrees of freedom robot with a flexible forearm is presented. Both a continuous form and a discrete form of the model are given. The flexibility of the link is represented along three planes: horizontal, vertical, and longitudinal. Nonlinear phenomena such as Coriolis and centrifugal forces, and the coupling between horizontal and vertical deflections are clearly illustrated. A simulation program termed E.S.A., developed to analyze the model, has allowed the nonlinear model to be studied, analyzed, and compared to the linear one. Two terrestrial robots and a robot configured to operate in space were analyzed. A criterion has been defined and a rule is proposed to determine whether the nonlinearities have to be taken into account or not. This rule indicates the angular speed at which a divergence of more than 5 percent will be observed between the nonlinear and the linear models. Small amplitude phenomena were also investigated, such as the coupling between the rigid and flexible modes and the coupling between the deformation due to the payload.
Author (CISTI)

N93-30262 McGill Univ., Montreal (Quebec). Dept. of Biomedical Engineering.
A PARALLEL PROCESSING SYSTEM FOR INTENSIVE I/O **c62**
Sylvain Martel, Serge Lafontaine, and Ian Hunter *In* Engineering Inst. of Canada, Canadian Conference on Electrical and Computer Engineering, Volumes 1 and 2 1990 5 p (For primary document see N93-30215 11-31)
Avail: Engineering Inst. of Canada, 2050 rue Mansfield, Suite 700, Montreal, Quebec H3A 1Z2 Canada

A computer for controlling a high performance micro-robot has been developed. The interprocessor communication scheme as well as the programmable input/output (I/O) subsystem constitute the main characteristics of this loosely coupled system with minimum interprocessor communication overhead. To achieve a high throughput, the major bottlenecks encountered in other systems have been reduced significantly. The general architecture allows large bus bandwidths and guarantees fast response time to asynchronous external events that must be dealt with in real time. The main features include memory, cache, I/O channels, and the interfacing procedure to various types of analog to digital and digital to analog converters, serial ports, timers, expansion ports with programmable lines, and network interface. The system allows simple implementation of free-running or computer controlled modes for analog to digital converters. The multiprocessor facilities provide interprocessor signalling, arbitration, synchronization, multicast transfers, burst accesses, and avoidance of communication deadlocks. Bus sharing is also possible. Pipelined and master/slave configuration strategies are available for obtaining maximum throughput for distributed real-time processes in this computer. Tools including macros and system calls are provided to help the programmer extract maximum performance from the system. Author (CISTI)

N93-30263 McMaster Univ., Hamilton (Ontario). Dept. of Electrical and Computer Engineering.
A TRANSPUTER BASED PARALLEL PROCESSING ARCHITECTURE FOR ROBOTICS APPLICATIONS **c62**
Akilesh Parameswar and Naresh K. Sinha *In* Engineering Inst. of Canada, Canadian Conference on Electrical and Computer Engineering, Volumes 1 and 2 1990 4 p (For primary document see N93-30215 11-31)
Avail: Engineering Inst. of Canada, 2050 rue Mansfield, Suite 700, Montreal, Quebec H3A 1Z2 Canada

Calculation of inverse dynamics renders robot control schemes computationally intensive. Practical implementation of these schemes requires stringent real-time constraints to be satisfied by the processing hardware. A new computer architecture is presented which makes possible high sample rate controllers. A parallel processing system, based on the INMOS transputer, is proposed. The transputer is a 32-bit processor desiged to be a building block of parallel processing systems, and is ideally suited to robotics applications. The architecture is based upon a data flow decomposition of the inverse dynamics algorithm with calculations being performed in a pipelined fashion. The proposed design yields high performance at low cost. Author (CISTI)

N93-30264 Defence Research Establishment, Ottawa (Ontario).
CANADIAN EHF MILSATCOM RESEARCH AND DEVELOPMENT PROJECT **c32**
Robert J. Keightley *In* Engineering Inst. of Canada, Canadian Conference on Electrical and Computer Engineering, Volumes 1 and 2 1990 4 p (For primary document see N93-30215 11-31)
Avail: Engineering Inst. of Canada, 2050 rue Mansfield, Suite 700, Montreal, Quebec H3A 1Z2 Canada

A portion of any future Canadian Military Satellite Communication (MILSATCOM) system may be implemented in the extremely high frequency (EHF) band. The wide bandwidths available at EHF may be exploited to provide reliable, secure, and very robust communications. The EHF Satellite Communications Research and Development Project has been implemented to develop a Canadian industrial technology base capable of supporting an operational EHF MILSATCOM system. The principal project activity is the contracted development of functional advanced development models of an EHF satellite payload and ground terminals. Other significant activities include a technology exploration program as well as an in-house system and technology evaluation program. The goals of this project are outlined and the characteristics anticipated to be required in a Canadian MILSATCOM system are identified. Author (CISTI)

N93-30265 COM DEV Ltd., Cambridge (Ontario).
SAW TECHNOLOGY FOR ON-BOARD PROCESSING IN MILITARY SATELLITE COMMUNICATIONS **c32**
Alastair Malarky and Michael Shaw *In* Engineering Inst. of Canada, Canadian Conference on Electrical and Computer Engineering, Volumes 1 and 2 1990 4 p (For primary document see N93-30215 11-31)
Avail: Engineering Inst. of Canada, 2050 rue Mansfield, Suite 700, Montreal, Quebec H3A 1Z2 Canada

Military satellite communications require onboard signal processing and highly directive antennas to reduce the risk of jamming. Elements of signal processing include frequency hopping over wide bandwidths, sophisticated coding, and robust modulation techniques. Surface acoustic wave (SAW) devices are ideally suited to carry out some of these onboard processing functions. The work being carried out on low and medium data rate processing for application in the Canadian extremely high frequency SATCOM program is reviewed. It is shown how SAW technology is capable of meeting many requirements for onboard processing in military communications. SAW devices are designed in the time domain and are best described as finite impulse response filters. They have applications as time delay devices, matched filters, and dispersers for frequency discrimination and block demodulation. The block demodulation capability is based on the use of a SAW chirp-Z Fourier transform (CFT), and the CFT response characteristics of SAW devices are noted. Advantages of SAW devices for onboard applications include small size, ruggedness, insensitivity to radiation, stable characteristics over a range of temperatures, and inherent reliability. Author (CISTI)

N93-30266 Raytheon Canada Ltd., Waterloo (Ontario).
COMPARISON OF DIVERSITY COMBINING, INTERLEAVING, AND DECODING TECHNIQUES OF A SCINTILLATED CHANNEL **c32**
R. Yang and P. VanMinnen (COM DEV Ltd., Cambridge, Ontario.) *In* Engineering Inst. of Canada, Canadian Conference on Electrical and Computer Engineering, Volumes 1 and 2 1990 4 p (For primary document see N93-30215 11-31)
Avail: Engineering Inst. of Canada, 2050 rue Mansfield, Suite 700, Montreal, Quebec H3A 1Z2 Canada

The effectiveness of convolutional coding, various diversity combining schemes, interleaving, and non-coherent frequency shift keying (NCFSK) / differential binary phase shift keying (DBPSK) schemes in a scintillated channel is evaluated. The scintillation process is assumed to be Rayleigh distributed, and the process under consideration is that caused by a high altitude nuclear detonation in the ionosphere which may especially affect the signal propagation in a satellite communication system. Bit error probability calculations are presented for the various schemes. It is concluded that the performances of frequency hopping (FH)/DPSK and FH/NCFSK systems are similar. With the interleaver placed after the diversifier, linear combining and soft-decision Viterbi decoding are the best options for combatting scintillation. In FH/NCFSK, a suboptimal configuration is the substitution of the linear combiner by a nonlinear combiner, where the nonlinear combiner performs envelope detection normalized by the sum of the voltages at the outputs of the tone detectors. Author (CISTI)

N93-30267 Communications Research Centre, Ottawa (Ontario).
A SATELLITE DOWNLINK SPREAD SPECTRUM TIMING BEACON **c32**
W. R. Seed, J. L. Pearce (Defence Research Establishment, Ottawa, Ontario.), and J. S. Wight (Carleton Univ., Ottawa, Ontario.) *In* Engineering Inst. of Canada, Canadian Conference on Electrical and Computer Engineering, Volumes 1 and 2 1990 4 p (For primary document see N93-30215 11-31)
Avail: Engineering Inst. of Canada, 2050 rue Mansfield, Suite 700, Montreal, Quebec H3A 1Z2 Canada

The design and laboratory performance of a satellite downlink spread-spectrum timing beacon is discussed. The timing beacon is required to provide the users of a multiple-access system with a highly accurate timing reference. A 300 bit per second data signal, comprised of satellite timing and orbital ephemeris information, is spread using a 1 MHz clocked direct-sequence pseudonoise code. By synchronizing the receiver to this sequence, the user has access to a 1 microsecond duration timing mark. Code acquisition is achieved using serial search synchronization techniques. A one-chip delay-locked loop, having a loop filter bandwidth reduction circuit for transition from acquisition to track mode, is used to track and despread the received signal. A squaring loop with frequency searching and lock detection is used to provide coherent data demodulation. The ability to achieve better than a 1-microsecond timing accuracy and an uncoded error rate below 0.00001 for input signal-to-noise ratios below minus 20 dB is demonstrated. Author (CISTI)

N93-30268 MPR Teltech Ltd., Ottawa (Ontario).
FASSET: A DEVELOPMENT MODEL FOR A CANADIAN EHF MILSATCOM SYSTEM **c32**
Gary Boudreau and R. J. Keightley (Defence Research Establishment, Ottawa, Ontario.) *In* Engineering Inst. of Canada, Canadian Conference on Electrical and Computer Engineering, Volumes 1 and 2 1990 4 p (For primary document see N93-30215 11-31)
Avail: Engineering Inst. of Canada, 2050 rue Mansfield, Suite 700, Montreal, Quebec H3A 1Z2 Canada

FASSET (Functional Advanced Development EHF SATCOM System for Evaluation and Test) is an advanced development model of an extremely high frequency (EHF) military satellite communication system or SATCOM. The model will be employed by the Canadian Department of National Defence to demonstrate and evaluate the capabilities of the EHF SATCOM for Canada. As part of the Canadian EHF SATCOM Research and Development Project, FASSET will develop the concepts and technology that would be required in any future operational EHF military SATCOM system. The present effort was preceded by several phases of extensive analysis and study to define and specify the system. FASSET is a ground-based facility that consists of two functional Advanced Development Model (ADM) ground terminals and a functional ADM communications payload along with associated equipment necessary to emulate various satellite system configurations under a variety of channel conditions and jamming threats. The capabilities of the FASSET facility are described, including communication at low data rates (75-19,200 bits/second) and medium data rates (32,000 to 1.544 million bits/second) and synchronization of the system in both acquisition and tracking processes. Author (CISTI)

N93-30269 Simon Fraser Univ., Burnaby (British Columbia).
MODELLING AND SIMULATION OF HUMAN RETINAL VISION PROCESSING **c52**
Philip J. Scheltens, Andrew H. Rawicz, and Marek J. Syrzycki *In* Engineering Inst. of Canada, Canadian Conference on Electrical and Computer Engineering, Volumes 1 and 2 1990 4 p (For primary document see N93-30215 11-31)
Avail: Engineering Inst. of Canada, 2050 rue Mansfield, Suite 700, Montreal, Quebec H3A 1Z2 Canada

Examination of biological vision processing systems has been used to develop a model of retinal vision processing. The model features differently sized photoreceptors with programmable light adaptation and lateral interaction mechanisms. Each specific effect can be invoked by a proper choice of model parameters responsible for static and temporal rod response, lateral inhibition, scaling of bipolar summation, and filter kernel size. This model has been simulated in various illumination conditions, producing outputs that resemble psychophysical results with human vision such as Mach bands. The model and its algorithms were found useful for performing such image processing tasks as image deblurring, edge enhancement, and edge extraction. Author (CISTI)

N93-30270 Simon Fraser Univ., Burnaby (British Columbia). School of Engineering Science.
QUANTIZATION EFFECTS IN SEGMENTATION OF RANGE IMAGES **c61**
Troy L. Yee and Kamal Kant Gupta *In* Engineering Inst. of Canada, Canadian Conference on Electrical and Computer Engineering, Volumes 1 and 2 1990 4 p (For primary document see N93-30215 11-31)
Avail: Engineering Inst. of Canada, 2050 rue Mansfield, Suite 700, Montreal, Quebec H3A 1Z2 Canada

With recent developments in range imaging systems, considerable research effort has been devoted to acquiring three dimensional models from range images. A project has been undertaken with the objective of developing theory and implementing algorithms for decomposing complex surfaces into meaningful parts. Some preliminary results are presented on segmenting range images into meaningful entities, or surface patches representing certain invariant characteristics (derived from differential geometric properties) of the surfaces in the image. A segmentation algorithm proposed by Besl (1988) has been implemented in the C language for running on Sparc stations under the UNIX operating system. A brief overview of Besl's method is given, assessing its sensitivity to quantization error. Testing of the algorithm on a simple synthetic image has shown that reasonable surface segmentation can be obtained at a substantial cost in computing time. A higher resolution in range values in the devices which generate the range images is required; this would reduce the quantization errors and thereby, improve surface segmentation and reduce computing time. Author (CISTI)

N93-30271 Ecole Polytechnique, Montreal (Quebec).
RECURSIVE-BATCH ESTIMATION OF STRUCTURE AND MOTION FROM STEREO IMAGE SEQUENCES **c74**
Juyang Weng and Paul Cohen *In* Engineering Inst. of Canada, Canadian Conference on Electrical and Computer Engineering, Volumes 1 and 2 1990 4 p (For primary document see N93-30215 11-31)
Avail: Engineering Inst. of Canada, 2050 rue Mansfield, Suite 700, Montreal, Quebec H3A 1Z2 Canada

Using long stereo image sequences, a recursive-batch approach is used to fuse multiple stereo views. The objective of this recursive-batch approach is to achieve higher performance without suffering from excessive computational cost. The information about the object structure is preserved from one image frame to the next, and it is refined recursively. The structure is represented in a camera-centered and a world-centered coordinate system. The former is useful for continuous navigation and the latter for visual map generation. In the presence of noise, the expected accuracy is provided together with the estimated solutions. With this recursive-batch method, the estimated motion trajectory closely tracks actual motions and it has eliminated the long divergence time period, which typically covers about 20 to 30 image frames, with a conventional Kalman filtering method. Author (CISTI)

N93-30272 Laval Univ. (Quebec).
A SINGLE BAND PROCESSOR FOR THE COMPUTATION OF RANGE FROM OPTICAL ABSORBANCE **c74**
Paul Fortier, Denis Laurendeau, Stephane Morin, and Louis Begin *In* Engineering Inst. of Canada, Canadian Conference on Electrical and Computer Engineering, Volumes 1 and 2 1990 4 p (For primary document see N93-30215 11-31)
Avail: Engineering Inst. of Canada, 2050 rue Mansfield, Suite 700, Montreal, Quebec H3A 1Z2 Canada

A single-board processor for the computation of range data from optical absorbance is presented. The concept of range from optical absorbance is reviewed and the architecture adopted for efficient computation of range is detailed. The processor is based on a Texas Instruments TMS32020 programmable digital signal processor chip and is interfaced with a host microcomputer. The processor serves to calibrate the system and to compute the illuminance ratio required to calculate the range. The host computer is responsible for the overall control of the system, graphic display of the range maps, and interface with the user. A 256-by-256 pixel range image is obtained in less than one second using the processor. Author (CISTI)

N93-30273 Kansas State Univ., Manhattan. Dept. of Electrical and Computer Engineering.
A NEW WAY TO USE FUZZY SETS IN IMAGE SHARPENING **c61**
Yiming Yu and Eddie R. Fowler *In* Engineering Inst. of Canada, Canadian Conference on Electrical and Computer Engineering, Volumes 1 and 2 1990 4 p (For primary document see N93-30215 11-31)
Avail: Engineering Inst. of Canada, 2050 rue Mansfield, Suite 700, Montreal, Quebec H3A 1Z2 Canada

The concept of fuzzy sets has been applied to digital image processing, especially image enhancement. It has been shown that fuzzy set theory can be advantageously applied in image enhancement techniques because the theory is capable of describing and analyzing vagueness of objects in an image. However, in most of these applications, the images are always interpreted the same way into their fuzzy property domains. This type of interpretation is much like normalizing gray levels in image which is an inadequate procedure for image sharpening. A new way to define images using fuzzy sets is provided, in which the image definitions do not have to be the same everywhere. For different image processing purposes, different definitions of images using fuzzy sets can be selected for better results. The new definition procedure is more appropriate for image sharpening and an algorithm for implementing this approach is listed. The performance of this algorithm in image sharpening of three standard images is compared to that of the De and Chatterji (1988) fuzzy set approach and shown to yield more image contrast with less computational time. Author (CISTI)

N93-30274 Senstar Corp., Kanata (Ontario).
FUTURE DIRECTIONS IN AVIATION SECURITY **c03**
M. C. Maki *In* Engineering Inst. of Canada, Canadian Conference on Electrical and Computer Engineering, Volumes 1 and 2 1990 4 p (For primary document see N93-30215 11-31)
Avail: Engineering Inst. of Canada, 2050 rue Mansfield, Suite 700, Montreal, Quebec H3A 1Z2 Canada

Advances in airport security technology based on the guided radar principle are reviewed. Such technology utilizes very high frequency radio waves, optimal for detection of human intruders in terms of radar cross-section. The Rapidly Extendible Perimeter Line Sensor uses a discrete wave coupling device as the sensing element. The system incorporates a pair of externally attached transmit/receive inductive couplers at opposite ends of a single conductor. For installation, the cable is unwound and clipped to support poles, with transmit and receive couplers at either end of the desired detection zone. A dual magnetically coupled slow propagation attenuating cable has been designed to provide its own attenuation of external modes of propagation, and both the transmit and receive coaxial components are contained within the same jacket. The cable can be used either in buried or surface (relocatable) modes. The Area Illuminated Leaky Cable Sensor is a variant of the leaky cable technology intended to secure a number of individual resources located in a cluster arrangement. The Tactical VHF/Volumetric Surveillance Radar provides volumetric (surface and overhead) coverage using send and receive antennas which can be configured according to the zone needing protection. The antennas can be mounted on buildings or aircraft, or can be portable types for fast temporary setup of a security perimeter. Author (CISTI)

N93-30275 American Science and Engineering, Inc., Cambridge, MA.
AUTOMATIC DETECTION OF EXPLOSIVES USING X RAY IMAGING **c03**
David Schafer and Martin Annis *In* Engineering Inst. of Canada, Canadian Conference on Electrical and Computer Engineering, Volumes 1 and 2 1990 4 p (For primary document see N93-30215 11-31)
Avail: Engineering Inst. of Canada, 2050 rue Mansfield, Suite 700, Montreal, Quebec H3A 1Z2 Canada

Backscatter imaging has been developed as a new technique for the x-ray imaging of checked baggage. In the scatter image, the contrast for explosives in an image is dramatically increased and the image confusion is decreased. An explosive detection system is being developed based on measuring the bulk x-ray characteristics of scatter images of checked baggage. In the simplified version of this system, it is proposed that normal checked baggage as a group has rather similar scatter characteristics. To test this hypothesis, bags from a lost-baggage agency were obtained and measurements were made of their scattering characteristics. Several simulated bombs were added to some of the bags and the changes in the characteristics were used to develop an automatic detection algorithm. Preliminary results show that the system was able to detect 2.3-pound bombs 100% of the time with only a 2% false alarm rate, and to detect 80% of 0.7-pound bombs at a similar false alarm rate. Author (CISTI)

N93-30276 Scintrex Ltd., Concord (Ontario).
EXPLOSIVES DETECTION SYSTEMS FOR AIRPORT SECURITY GAS CHROMATOGRAPHIC BASED DEVICES **c03**
S. Nacson, C. Castledine, T. Siu, T. Lu, and O. Legrady *In* Engineering Inst. of Canada, Canadian Conference on Electrical and Computer Engineering, Volumes 1 and 2 1990 3 p (For primary document see N93-30215 11-31)
Avail: Engineering Inst. of Canada, 2050 rue Mansfield, Suite 700, Montreal, Quebec H3A 1Z2 Canada

A high-speed explosive vapors monitoring system has been developed which is suitable for use at an airport security gate for detecting the presence of explosives on passengers and in baggage. The system consists of a rapid vapor concentration manifold, an explosive vapor preconcentrator, and a fast gas chromatograph/electron capture detection system. Different configurations of vapor concentration manifolds are used for examination of passengers and of baggage. The system was tested in two months of full-scale trials at a throughput of 7 passengers or bags per minute. An alarm rate of about one in a thousand for the walk-through unit and two in a thousand for the baggage unit were recorded. The system has shown exceptional sensitivity to explosive vapors, being capable of detecting less than 5 parts per trillion of ethylene glycol dinitrate at a low rate of false alarms. Author (CISTI)

N93-30277 Barringer Research Ltd., Rexdale (Ontario).
ADVANCED SIGNAL PROCESSING REQUIREMENT IN AN ION MOBILITY EXPLOSIVES DETECTOR **c25**
R. Jackson, J. Davies, L. Daubner, L. D. May, and S. Wiles *In* Engineering Inst. of Canada, Canadian Conference on Electrical and Computer Engineering, Volumes 1 and 2 1990 4 p (For primary document see N93-30215 11-31)
Avail: Engineering Inst. of Canada, 2050 rue Mansfield, Suite 700, Montreal, Quebec H3A 1Z2 Canada

Ion mobility spectroscopy (IMS), also called plasma chromatography, can be used to detect trace quantities of explosives in the presence of many other materials and natural interferents. IMS offers significant practical advantages over many other techniques used in airport security systems, including near real-time detection, good specificity and excellent sensitivity, no health hazard, simplicity of operation, comparatively light weight, and low cost. The principles of IMS are discussed along with the methods of processing IMS signals. The identification of the respective analytes by calculating analyte drift time, and the assessment of half-widths of pulses for both the target and background ions, present a challenge to signal deconvolution and processing. Algorithms have been developed to maximize signal abstraction from varying backgrounds. The use of algorithm-based processing greatly reduces false alarm rates which otherwise would seriously degrade the usefulness of the detection system. Author (CISTI)

N93-30278 Queens Univ., Kingston (Ontario). Dept. of Electrical Engineering.
TASK ALLOCATION AND REAL-TIME CONSIDERATIONS FOR THE ROBOT CONTROLLER TEST STATION (RCTS) **c63**
R. Allard, M. A. Ramsay, and M. M. Bayoumi *In* Engineering Inst. of Canada, Canadian Conference on Electrical and Computer Engineering, Volumes 1 and 2 1990 4 p (For primary document see N93-30215 11-31)
Avail: Engineering Inst. of Canada, 2050 rue Mansfield, Suite 700, Montreal, Quebec H3A 1Z2 Canada

The Robot Controller Test Station (RCTS) developed at Queen's University has emerged as a valuable tool for testing and integrating control and sensing schemes within a complete robot environment. RCTS is based on a modular approach that is both flexible and easy to use and modify. The system also features a menu interface and analysis functions for monitoring purposes. Version 2 of RCTS features an expanded communication system giving the ability to share the computing workload among several processors. The efficient allocation of software partitions to the different processors then becomes important. The goal is to choose a configuration permitting an optimal utilization of the computing resources. Once the user proceeds with the implementation, the fine tuning of real-time parameters may take place using the menu interface. The allocation model also gives a crude indication of the amount of excess computing resources available. The real-time constraints within RCTS are exposed and an allocation algorithm is developed. The algorithm produces an optimum solution, providing the number of processors is kept small. It takes into account transient loads as well as precedence relations between the modules. The method may be generalized to other periodic systems, particularly in robotics. Author (CISTI)

N93-30279 Carleton Univ., Ottawa (Ontario).
ON ANALYTICAL PERFORMANCE MODELLING OF SOFTWARE FOR DISTRIBUTED SYSTEMS **c61**
D. C. Petriu, C. M. Woodside, J. E. Neilson, and S. Majumdar *In* Engineering Inst. of Canada, Canadian Conference on Electrical and Computer Engineering, Volumes 1 and 2 1990 4 p (For primary document see N93-30215 11-31)
Avail: Engineering Inst. of Canada, 2050 rue Mansfield, Suite 700, Montreal, Quebec H3A 1Z2 Canada

Specific issues of software modeling for performance evaluation are addressed, such as the abstraction process necessary to build manageable performance models, the difference between the abstract representation of

software for development purposes and for performance analysis, the ability of various modeling techniques to capture relevant features of concurrent software, and the use of analytical performance models in the software development process. Three analytical modeling methods are compared from the point of view of their capability to model software for distributed systems, emphasizing their strengths and shortcomings. The methods are queueing networks, Petri nets, and stochastic rendezvous networks.
Author (CISTI)

N93-30280 Concordia Univ., Montreal (Quebec). Faculty of Engineering and Computer Science.
OPTIMIZED PARTITIONING AND BALANCING FOR PARALLEL PROCESSING **c62**
Y. C. Zhao, L. Tao, K. Thulasiraman, and M. N. S. Swamy *In* Engineering Inst. of Canada, Canadian Conference on Electrical and Computer Engineering, Volumes 1 and 2 1990 4 p (For primary document see N93-30215 11-31)
Avail: Engineering Inst. of Canada, 2050 rue Mansfield, Suite 700, Montreal, Quebec H3A 1Z2 Canada

For loosely-coupled and synchronized parallel systems, a new mathematical formulation is proposed to minimize the maximal processor computation time and the maximal interprocessor communication time. For this partitioning problem, an equivalent multiobjective zero-one quadratic programming formulation is developed. A two-phase heuristic algorithm bounded in polynomial time is presented for solving the problem. Some comparisons of this algorithm with those in the literature for different graph partitioning problems are given. The computational results for a set of random problem instances are provided for evaluation. Author (CISTI)

N93-30281 Queens Univ., Kingston (Ontario). Dept. of Electrical Engineering.
COARSE SYNCHRONIZATION IN AN EHF FREQUENCY-HOPPED SATELLITE COMMUNICATIONS SYSTEM **c32**
S. J. Simmons and P. Lamers *In* Engineering Inst. of Canada, Canadian Conference on Electrical and Computer Engineering, Volumes 1 and 2 1990 4 p (For primary document see N93-30215 11-31)
Avail: Engineering Inst. of Canada, 2050 rue Mansfield, Suite 700, Montreal, Quebec H3A 1Z2 Canada

A study is presented of the problem of users first attempting to synchronize their M-ary frequency shift keying (FSK) transmissions to the dehopper of a signal processing satellite in a multi-user frequency division multiple access frequency hopped extremely high frequency satellite system. A simple and robust scheme is examined, based on using one of the FSK tones as a sync probe, comparing its energy to that seen in M-minus-one other tone bins during each hop. Multi-tone jamming is considered, at signal/jamming ratios of 0 dB and higher with background noise. It is shown that coarse sync alignment to within a fraction of a hop period can be reliably established for all but the very highest jammer powers (larger by the full processing gain). The resulting average time to acquisition is on the order of 0.5 to 2 seconds. Author (CISTI)

N93-30282 National Defence Headquarters, Ottawa (Ontario).
SECURITY OF THE REMOTE CONTROL LINK OF ANIK E SATELLITES [SECURITE DU LIEN DE TELECOMMANDE DES SATELLITES ANIK E] **c32**
Michael J. J. Drapeau *In* Engineering Inst. of Canada, Canadian Conference on Electrical and Computer Engineering, Volumes 1 and 2 1990 4 p In FRENCH (For primary document see N93-30215 11-31)
Avail: Engineering Inst. of Canada, 2050 rue Mansfield, Suite 700, Montreal, Quebec H3A 1Z2 Canada

The consequences of the loss of communication capability of a communications satellite in Canada would probably be catastrophic. It, thus, becomes important to protect the satellite system against any organization which is or could be hostile. A preliminary study has been initiated with the objective of determining the main threats to the Anik C and D satellites and to define the possible measures which could minimize their effects. It is concluded that the remote control links of the new generations of satellites must be protected against intrusion and jamming. Consequently, an agreement has been reached with Telesat Canada to encode the remote control links with the Anik E satellites and to transmit using a narrow beam directed only towards a restricted number of terrestrial control stations. Telesat will also engage in improving the security of its infrastructure and to ensure that the entire ground-based control and location system for the satellite will incorporate a sufficient degree of redundancy.
Author (CISTI)

N93-30283 Victoria Univ. (British Columbia). Dept. of Electrical and Computer Engineering.
CODING FOR FREQUENCY HOPPED SPREAD SPECTRUM SATELLITE COMMUNICATIONS **c32**
Qiang Wang, Vijay K. Bhargava, T. Aaron Gulliver (Defence Research Establishment, Ottawa, Ontario.), and Ian F. Blake (Waterloo Univ., Ontario.) *In* Engineering Inst. of Canada, Canadian Conference on Electrical and Computer Engineering, Volumes 1 and 2 1990 4 p (For primary document see N93-30215 11-31)
Avail: Engineering Inst. of Canada, 2050 rue Mansfield, Suite 700, Montreal, Quebec H3A 1Z2 Canada

Fast frequency hopped M-ary frequency shift keying (FSK) has drawn great attention recently due to its practicality. In such systems, the use of error correction coding and diversity has been shown to be very effective against jamming. A comparative view is presented of the system performances based on two different assumptions: a fixed data rate and a fixed hop rate. It is shown that while under partial-band noise jamming there is little difference in the system performances under those two assumptions, there is a significant difference when the jamming is multi-tone. Specifically, due to multi-tone jamming, a fixed hop rate system has an optimum M for M-ary FSK which is monotonically increasing with the ratio of energy-per-hop to jamming spectral density (Eh/Jo). Furthermore, if a coding system has a parameter related to M such as a dual-K code, optimum choice of the parameter value is also related to the optimum M and thus, Eh/Jo. For a fixed data rate system, the optimum K is either 2 or 3, depending on the coding scheme but not depending on the signal to jamming ratio. Author (CISTI)

N93-30284 COM DEV Ltd., Cambridge (Ontario).
ADAPTIVE JAMMER NULLING IN EHF COMMUNICATIONS SATELLITES **c32**
Jai Bhagwan, Stephen Kavanagh, and J. L. Yen (Toronto Univ., Ontario.) *In* Engineering Inst. of Canada, Canadian Conference on Electrical and Computer Engineering, Volumes 1 and 2 1990 4 p (For primary document see N93-30215 11-31)
Avail: Engineering Inst. of Canada, 2050 rue Mansfield, Suite 700, Montreal, Quebec H3A 1Z2 Canada

A preliminary investigation is reviewed concerning adaptive null steering multibeam uplink receiving system concepts for future extremely high frequency communications satellites. Primary alternatives in the design of the uplink antenna, the multibeam adaptive nulling receiver, and the processing algorithm and optimization criterion are discussed. The alternatives are phased array, lens or reflector antennas, nulling at radio frequency or an intermediate frequency, wideband versus narrowband nulling, and various adaptive nulling algorithms. A primary determinant of the hardware complexity is the receiving system architecture, which is described for the alternative antenna and nulling concepts. The final concept chosen will be influenced by the nulling performance requirements, cost, and technological readiness. Author (CISTI)

N93-30285 Communications Research Centre, Ottawa (Ontario).
TEMPORAL SYNCHRONIZATION OF FREQUENCY HOPPED DPSK **c32**
W. R. Seed *In* Engineering Inst. of Canada, Canadian Conference on Electrical and Computer Engineering, Volumes 1 and 2 1990 4 p (For primary document see N93-30215 11-31)
Avail: Engineering Inst. of Canada, 2050 rue Mansfield, Suite 700, Montreal, Quebec H3A 1Z2 Canada

The downlink temporal synchronization strategies for a frequency hopped differentially encoded phase shift keying (FH/DPSK) signal are examined. Arguments are presented to support the concept of a burst distribution of sync hops, or 13-bit encoded hops used only for synchronization. The burst distribution is shown to provide a favorable tradeoff between input signal-to-noise ratio and probability of a false alarm. The synchronization process, which includes acquisition, verification, and track modes is reviewed. Envelope detection of the dehopped signal is used to provide an indication of initial acquisition as well as a coarse timing estimate of the sync hop time-of-arrival. The sync hop is also quadrature detected to verify the presence of the sync hop and to provide a fine timing estimate accurate to within a small fraction of a data bit. Simulations of the coarse and fine root mean square timing estimate error are shown to approach the theoretical lower bounds. Author (CISTI)

N93-30286 National Research Council of Canada, Ottawa (Ontario). Inst. for Information Technology.

ON THE IMPLEMENTATION OF THE BIRIS RANGE SENSOR FOR APPLICATIONS IN ROBOTIC CONTROL AND AUTONOMOUS NAVIGATION **c74**

F. Blais, M. Rioux, J. Domey, and J. A. Beraldin *In* Engineering Inst. of Canada, Canadian Conference on Electrical and Computer Engineering, Volumes 1 and 2 1990 4 p (For primary document see N93-30215 11-31)

Avail: Engineering Inst. of Canada, 2050 rue Mansfield, Suite 700, Montreal, Quebec H3A 1Z2 Canada

A real-time implementation of the range sensor called BIRIS (for bi-iris) on a commercially available image processing system is described. The optical principle of the range sensor and its performance is reviewed. The high immunity of the sensor to ambient illumination and external perturbations is also demonstrated. The different options available to integrate BIRIS with existing computers/controllers are shown. Cost and safety questions are addressed. Experimental results are also presented to demonstrate the possibilities of range sensing for applications in robotics and semi-autonomous navigation. Author (CISTI)

N93-30287 National Research Council of Canada, Ottawa (Ontario).

APPLICATIONS OF DIGITAL 3-D IMAGING **c61**

M. Rioux *In* Engineering Inst. of Canada, Canadian Conference on Electrical and Computer Engineering, Volumes 1 and 2 1990 10 p (For primary document see N93-30215 11-31)

Avail: Engineering Inst. of Canada, 2050 rue Mansfield, Suite 700, Montreal, Quebec H3A 1Z2 Canada

The technology and applications of digital three dimensional (3-D) imaging are reviewed. Its advantages over two dimensional imaging are discussed. Current applications under development are presented, mainly in the fields of robotics and dimensional inspections. Digital 3-D imaging possesses some unique features. Among all the imaging systems, only digital 3-D provides the data useful to make a direct copy of an object using numerically controlled milling or stereo lithography. In addition, 3-D views of a scene or object can be reconstructed from a single image transmitted over a communications link. Another feature is the absence of scaling effect (or apparent size) with distance from a 3-D camera; this is a highly desirable feature for machine vision. Future applications are suggested, including automated vision for the Freedom space station, protection of high security areas, and traffic volume monitoring. Author (CISTI)

N93-30288 Laval Univ. (Quebec). Lab. de Vision et Systemes Numeriques.

A ROBUST MULTI-OPERATOR 3-D EDGE DETECTION APPROACH FOR RANGE IMAGE SEGMENTATION **c61**

Marc Soucy and Denis Laurendeau *In* Engineering Inst. of Canada, Canadian Conference on Electrical and Computer Engineering, Volumes 1 and 2 1990 4 p (For primary document see N93-30215 11-31)

Avail: Engineering Inst. of Canada, 2050 rue Mansfield, Suite 700, Montreal, Quebec H3A 1Z2 Canada

An approach is presented for detecting and locating occluding contours and surface orientation discontinuities. Several directional operators with complementary characteristics are computed on the whole image. Local maxima of these operators are extracted and thresholded automatically. Then four directional edge maps are obtained through structured matching. These maps are finally merged by a local weighted averaging technique based on a metric that measures the quality of directional edge information. Experimental results obtained from a synchronized geometry range finder demonstrate that the proposed edge-detection approach is very efficient. All major edges of the objects are detected while spurious edges were eliminated. Author (CISTI)

N93-30289 Ottawa Univ. (Ontario).

RECOGNIZING PARTIALLY OVERLAPPING OBJECTS **c61**

Tayeb Damerji, Badreddine Karoui, and Dan Ionescu *In* Engineering Inst. of Canada, Canadian Conference on Electrical and Computer Engineering, Volumes 1 and 2 1990 4 p (For primary document see N93-30215 11-31)

Avail: Engineering Inst. of Canada, 2050 rue Mansfield, Suite 700, Montreal, Quebec H3A 1Z2 Canada

A model-based vision system that uses the parameters of an autoregressive model as features to model local sub-parts of the boundary is presented. A decomposition algorithm detects sub-parts of one object, when the object is not occluded, and sub-parts of the boundaries of different objects in the case of occlusion. The autoregressive model parameters representing the detected sub-parts are matched to features of known sub-parts according to the hypothesize verify paradigm. In order to reduce the recognition time, a pruning phase is added to eliminate obvious mismatches. The recognition process ends when all of the sub-parts in the scene are identified. Author (CISTI)

N93-30290 Laval Univ. (Quebec). Dept. of Electrical Engineering.

RADIATED FIELDS FROM AN ELECTROMAGNETIC PULSE SIMULATOR [CHAMPS RAYONNES PAR UN SIMULATEUR D'IMPULSIONS ELECTROMAGNETIQUES] **c32**

M. Pelletier, G. Y. Delisle, and S. Kashyap (Defence Research Establishment, Ottawa, Ontario.) *In* Engineering Inst. of Canada, Canadian Conference on Electrical and Computer Engineering, Volumes 1 and 2 1990 4 p In FRENCH (For primary document see N93-30215 11-31)

Avail: Engineering Inst. of Canada, 2050 rue Mansfield, Suite 700, Montreal, Quebec H3A 1Z2 Canada

Simulators of electromagnetic pulses allow generation within a limited time of very high-intensity fields such as those produced in a nuclear explosion. These fields can be radiated out of the test zone at a lower but nevertheless significant level; if the intensity of these fields is sufficiently high, damage to humans and electronic equipment can result. An evaluation of the potential danger of these simulator emissions requires knowledge of the amplitude, duration, and the energy of the radiated impulses. A technique is presented for calculating the fields radiated by a parallel-plane electromagnetic pulse simulator. The same method can also be applied to a rhombic type simulator. Sample numerical results are presented along with the calculations of the energy and power density and a discussion of the formation of the field in the frequency domain. Author (CISTI)

N93-30291 Concordia Univ., Montreal (Quebec).

MODELS FOR PERFORMANCE ASSESSMENT OF HF ANTENNAS ON THE CH-135/TWIN HUEY HELICOPTER **c32**

Stanley J. Kubina and Shahram Esfandiari *In* Engineering Inst. of Canada, Canadian Conference on Electrical and Computer Engineering, Volumes 1 and 2 1990 3 p (For primary document see N93-30215 11-31)

Avail: Engineering Inst. of Canada, 2050 rue Mansfield, Suite 700, Montreal, Quebec H3A 1Z2 Canada

The performance of two practical radio-antenna designs for the Bell CH-135 helicopter was evaluated by developing wire-grid models for moment-method modeling of the corresponding radiating system. The first model evaluated a tranline antenna, with the rotor lined up along the helicopter's length. The second model involved a zig-zag antenna with the rotor in the same position. Other models were developed for the same two antenna types with the rotor blade at different positions. The validity of each model was assessed by comparing the computed radiation patterns with scale-model measured patterns, and by comparing the high-frequency assessment parameters. The effect of rotor modulation on these parameters is discussed. Computer model validation for shorted loop antennas was achieved throughout the 2-30 MHz range. Author (CISTI)

N93-30292 Manitoba Univ., Winnipeg. Dept. of Electrical and Computer Engineering.

TRANSIENT FIELD COMPUTATIONS WITHIN OR PROXIMITY OF COMPLEX STRUCTURES: FD-TD APPROACH **c32**

W. A. Chamma and L. Shafai *In* Engineering Inst. of Canada, Canadian Conference on Electrical and Computer Engineering, Volumes 1 and 2 1990 4 p (For primary document see N93-30215 11-31)

Avail: Engineering Inst. of Canada, 2050 rue Mansfield, Suite 700, Montreal, Quebec H3A 1Z2 Canada

The effects of impulsively excited electromagnetic bursts, resulting from lightning or nuclear explosions on electronic equipment have raised interest in electromagnetic transient field penetration and coupling into complex structures. A numerical technique in which the Maxwell equations are solved using the finite difference time domain technique is presented for computing the transient response of a sphere illuminated by a Gaussian plane wave. Results are compared with the corresponding Rayleigh-Mie analytic solution and showed good agreement. The field penetration and frequency response of open-top conducting boxes was also explored. The addition of a lossy material on the top of one of the boxes was shown to reduce the field magnitudes inside the box. Author (CISTI)

N93-30293 Manitoba Univ., Winnipeg. Dept. of Electrical and Computer Engineering.

COMPUTER-AIDED MODELING FOR ANALYSIS OF ARBITRARY SCATTERERS AND FEEDS **c32**

H. Moheb and L. Shafai *In* Engineering Inst. of Canada, Canadian Conference on Electrical and Computer Engineering, Volumes 1 and 2 1990 4 p (For primary document see N93-30215 11-31)

Avail: Engineering Inst. of Canada, 2050 rue Mansfield, Suite 700, Montreal, Quebec H3A 1Z2 Canada

Surface integral equations are formulated to relate the radiation and scattering fields of primary feeds and scatterers to the current distributions on their surface. These currents are determined by reducing surface integral equations to a matrix equation via a moment method. The computed currents are utilized to determine the co-polar and cross-polar fields of feeds and the far field of the scatterers. The technique is subsequently applied to study the radar cross-section of complex geometries such as conducting and dielectric spheres, finite cylinders, cubes and prisms, as well as to the rectangular waveguides representing an antenna problem. The developed method is general enough to handle various antenna and scattering problems and to generate solutions with a high degree of accuracy. Author (CISTI)

N93-30294 Defence Research Establishment, Ottawa (Ontario). Electronics Div.

AN IMPROVED MODEL-CREATION PROGRAM FOR EM INTERACTION ANALYSIS **c32**

S. Kashyap, M. Dion, and A. Louie *In* Engineering Inst. of Canada, Canadian Conference on Electrical and Computer Engineering, Volumes 1 and 2 1990 3 p (For primary document see N93-30215 11-31)

Avail: Engineering Inst. of Canada, 2050 rue Mansfield, Suite 700, Montreal, Quebec H3A 1Z2 Canada

Several codes are available for computation of the interaction of electromagnetic waves with simple and complicated structures. All existing codes require as an input the geometry of the object under study. This geometry is supplied as a wire-grid, surface-patch, or cell model, depending on the simulation code. The difficulty of creating such geometric data increases with the complexity of the structure, as is the case with aircraft. To aid in this process, the DIDEC program was created, starting as a program that created wire models using a digitizing tablet. Initially, it created Numerical Electromagnetic Code input files for wire-grid structures. Since then, it has developed into an interactive program, DIDEC/DREO, for designing wire-grid, patch, and cell models of complex structures for solving electromagnetic interaction problems. The various features of the current version of DIDEC/DREO are described, with examples provided of graphic displays. Author (CISTI)

N93-30295 Canadian Forces Base Trenton, Astra (Ontario). Forecast Centre.

STAND ALONE LIGHTNING DETECTION EQUIPMENT USED AT CANADIAN FORCES AIR BASES **c47**

Pierre Pommainville and Robert Cross (National Defence Headquarters, Ottawa, Ontario.) *In* Engineering Inst. of Canada, Canadian Conference on Electrical and Computer Engineering, Volumes 1 and 2 1990 3 p (For primary document see N93-30215 11-31)

Avail: Engineering Inst. of Canada, 2050 rue Mansfield, Suite 700, Montreal, Quebec H3A 1Z2 Canada

Stand alone lightning detection systems were installed at 15 Canadian Forces air bases across Canada and in Germany. The basic operation of this system is explained. The detection process begins when the large electric currents associated with the lightning return stroke radiate radio frequency energy. Incoming signals are analyzed by discrimination logic circuits, and the direction and range of any lightning signals are computed. A display screen shows the number of lightning flashes within the last 15 minutes in each of a number of radially partitioned segments in the surrounding area of the detection station. A case study of the operational use of the system is presented, revealing its advantage as an observational tool that fills the gap between the relatively large-scale resolution of meteorological satellite imagery and that of small-scale local weather reports. As a result of experience with the system, changes to the display output are currently under investigation to enhance the usefulness of the system as a local thunderstorm warning device. Author (CISTI)

N93-30296 Quebec Univ., Montreal. Centre de Recherche Informatique de Montreal.

STRATUS: A PROTOTYPE EXPERT ADVISORY SYSTEM FOR TERMINAL WEATHER FORECASTING **c47**

Michel C. Desmarais, Fances deVerteuil, Denis Jacob (Atmospheric Environment Service, Saint-Laurent, Quebec.), and Peter Zwack *In* Engineering Inst. of Canada, Canadian Conference on Electrical and Computer Engineering, Volumes 1 and 2 1990 4 p (For primary document see N93-30215 11-31)

Avail: Engineering Inst. of Canada, 2050 rue Mansfield, Suite 700, Montreal, Quebec H3A 1Z2 Canada

The methodology used to develop an expert system to predict low clouds at airport terminals is described. The expert system is based on the fundamental physical rules that govern the existence of low clouds. Emphasis is placed on the validation and testing of a qualitative model which is used to determine the low cloud cover. A sensitivity analysis of the system has provided invaluable feedback which will improve the ability to model the physical phenomena involved in forecasting low clouds. The results of this analysis indicated that the turbulence and stability parameters used in the model had little contribution to the diagnostic process. The contribution of vertical motion is significant, but small. The contribution of the dew point depression is overwhelming compared to the other parameters, showing that the bulk of the forecasting effort should be spent arriving at good estimates for the temperature and the dew point temperature. Author (CISTI)

N93-30297 CompEngServ Ltd., Ottawa (Ontario).

CLOUD CLASSIFICATION FROM SATELLITE IMAGERY USING NEURAL COMPUTING **c47**

B. Archie Bowen and J. David Steenbergen (Atmospheric Environment Service, Downsview, Ontario.) *In* Engineering Inst. of Canada, Canadian Conference on Electrical and Computer Engineering, Volumes 1 and 2 1990 3 p (For primary document see N93-30215 11-31)

Avail: Engineering Inst. of Canada, 2050 rue Mansfield, Suite 700, Montreal, Quebec H3A 1Z2 Canada

A study was conducted to determine the feasibility of using neural computing for automatically classifying cloud types as seen in meteorological satellite imagery. A parallel approach to the problem is appealing due to the very large quantities of data involved and the short lifetime of the information. In a feasibility study, neural networks were trained and tested on simulated cloud patterns representing 11 cloud types. The input to the network was preprocessed using pre-attentive filters to create a representation of lower dimensionality. Three types of filters were tested: Fourier-Mellin filters, Gabor filters, and a new type of filter called a prototype image filter. The networks typically consisted of less than 60 neurons with 10 to 24 filters. It was not possible to obtain results for each filter using exactly the same training and test sets. However, classification accuracies for each type of filter were above 90%. Author (CISTI)

N93-30298 MacDonald, Dettwiler and Associates Ltd., Richmond (British Columbia).

METEOROLOGICAL INFORMATION FOR AVIATION: A SYSTEMS APPROACH **c47**

R. G. Humphries, J. N. Geddes, W. C. Cree, and L. W. Diehl *In* Engineering Inst. of Canada, Canadian Conference on Electrical and Computer Engineering, Volumes 1 and 2 1990 4 p (For primary document see N93-30215 11-31)

Avail: Engineering Inst. of Canada, 2050 rue Mansfield, Suite 700, Montreal, Quebec H3A 1Z2 Canada

The use of meteorological information by the aviation community, particularly by air traffic control, is reviewed. Meteorological data are available in three basic forms: alphanumeric, binary, and graphics. Current informational systems do not allow for manipulation or analysis of the data to provide specially derived products and weather alerts, or to select significant information of interest to a particular user. A modernization program is under way at Canada's Atmospheric Environment Service (AES) to improve support for weather office operations and data transfer. The program is providing the potential for accessing new types of information and for accessing information in digital form. In aviation applications, a modernized weather information system would have three principal components: ingestion of data from weather radar, weather satellite, and AES products; data processing to allow extraction and organizing of relevant information from the data stream; and information delivery at fully interactive workstations. An example of such an information system is outlined, based on the MacDonald Dettwiler VORTEX system. Author (CISTI)

N93-30299 McMaster Univ., Hamilton (Ontario). Communications Research Lab.

CLASSIFICATION OF RADAR CLUTTER IN AN AIR TRAFFIC CONTROL ENVIRONMENT **c04**

Simon Haykin, Wolfgang Stehwien (Litton Systems, Canada Ltd., Etobicoke, Ontario.), Cong Deng, Peter Weber, and Richard Mann *In* Engineering Inst. of Canada, Canadian Conference on Electrical and Computer Engineering, Volumes 1 and 2 1990 3 p (For primary document see N93-30215 11-31)

Avail: Engineering Inst. of Canada, 2050 rue Mansfield, Suite 700, Montreal, Quebec H3A 1Z2 Canada

Highlights are presented from an experimental study aimed at the classification of radar clutter as experienced in an air traffic control environment. The results are based on recorded radar data obtained from two operational radar sites. The Burg algorithm for computing reflection coefficients is the basic mathematical tool used for extraction of radar features based on second-order statistics. Two methods for the classification are described: a parametric Bayes procedure and a neural network approach based on the backpropagation algorithm. The classification accuracies of the two methods were found to be about 82% and 90% respectively. The reasons for the superiority of the latter are discussed. Author (CISTI)

N93-30300 Saskatchewan Univ., Saskatoon. Dept. of Electrical Engineering.

AN EXPERT SYSTEM FOR IDENTIFICATION OF THE TASK STATUS FROM TACTILE SENSOR DATA **c37**

C. S. Vaidyanathan and H. C. Wood *In* Engineering Inst. of Canada, Canadian Conference on Electrical and Computer Engineering, Volumes 1 and 2 1990 4 p (For primary document see N93-30215 11-31)

Avail: Engineering Inst. of Canada, 2050 rue Mansfield, Suite 700, Montreal, Quebec H3A 1Z2 Canada

Tactile data from tactile sensors for robotic applications can be characterized in the form of dynamic force images and processed to obtain decision parameters suitable for task status identification. Decision parameters were obtained by processing raw tactile data from a prototype intelligent manipulator system. The interpretation of these decision parameters was carried out in an experiment using an embedded expert system which was designed using the KES expert system development tool and implemented to interpret the task status of the prototype system. The status displayed by the expert system provides a complete set of information about the task including the direction of any object displacement relative to the gripper. The system performance was validated using test data obtained while grasping a sample object weighing 21 g and was found to be satisfactory. The design of control strategies using the task status information is currently in progress. Author (CISTI)

N93-30301 Carleton Univ., Ottawa (Ontario). Dept. of Systems and Computer Engineering.

MLOG: A LANGUAGE FOR PROTOTYPING CONCURRENT SYSTEMS **c61**

Gerald M. Karam and Jeff T. Wilson *In* Engineering Inst. of Canada, Canadian Conference on Electrical and Computer Engineering, Volumes 1 and 2 1990 6 p (For primary document see N93-30215 11-31)

Avail: Engineering Inst. of Canada, 2050 rue Mansfield, Suite 700, Montreal, Quebec H3A 1Z2 Canada

The design of embedded concurrent systems is a challenging activity because of the complex communications relationships that are usually present. Examples of such applications include telecommunications, process control, avionics, and weapons systems. The MLog language is a multitasking, object oriented Prolog for which the primary application is prototyping embedded concurrent systems. MLog supports the object oriented programming concepts of active and passive objects, classes, meta-classes, inheritance, methods, message passing, and instance variables. Active objects are large-grain communicating sequential processes that communicate with each other using rendezvous and asynchronous message-passing. Passive objects, invoked like procedure calls, have no protection for mutual exclusion. Execution in MLog is based on the top-down resolution mechanism of conventional Prolog, where the object oriented programming systems methods are actually Prolog procedures, and message-passing equates to solving goals. The MLog environment, in particular ProtoTool (a prototyping support facility) and DMLog (a sophisicated debugger) provides the infrastructure for building and studying prototypes of concurrent systems. Author (CISTI)

N93-30302 Ottawa Univ. (Ontario). Dept. of Computer Science.

COMMUNICATIONS SYSTEMS DESIGN FOR TESTABILITY: GREY-BOX TESTING **c32**

Robert L. Probert and Cecilia Geldrez *In* Engineering Inst. of Canada, Canadian Conference on Electrical and Computer Engineering, Volumes 1 and 2 1990 5 p (For primary document see N93-30215 11-31)

Avail: Engineering Inst. of Canada, 2050 rue Mansfield, Suite 700, Montreal, Quebec H3A 1Z2 Canada

Large systems such as telecommunications systems may involve several million lines of executable code and tend to evolve incrementally, thus rendering testing and maintainability a very complex task. For this reason, testing and verification requirements must be defined and incorporated into the development process early in the software development cycle. Thus, design becomes a key component of these systems. An approach to assist in enhancing the testability of software designs is proposed, termed grey-box testing. One particular grey-box testing paradigm named semantic instrumentation is illustrated. Designs are represented as design machines, an extension of finite-state machines. A design-level plan for verification/test is then derived to guarantee branch coverage of the design machine for both normal behaviors and for processing of exceptions. Finally, semantic probes are defined to provide a mapping from the design machine to implemented code. These probes are used to document design decisions, implementation decisions, and execution traces during code verification and test. The process of semantic instrumentation is illustrated on communications services, more precisely, on the service of the alternating bit protocol. Author (CISTI)

N93-30303 National Defence Headquarters, Ottawa (Ontario).

PERFORMANCE OF FREQUENCY HOPPED M-ARY FSK IN RAYLEIGH FADING AND PARTIAL-BAND JAMMING **c32**

D. C. Leal *In* Engineering Inst. of Canada, Canadian Conference on Electrical and Computer Engineering, Volumes 1 and 2 1990 4 p (For primary document see N93-30215 11-31)

Avail: Engineering Inst. of Canada, 2050 rue Mansfield, Suite 700, Montreal, Quebec H3A 1Z2 Canada

Military satellite communications systems must have waveforms that ensure reliable performance during jamming and fading situations. An analysis is provided for the performance of M-ary frequency shift keying (FSK) in the presence of system noise, using the Rician fading model. Frequency hopping and worst-case partial-band noise (PBN) jamming are then added to the model and analyzed. Results are displayed showing the worst-case values of the bit error rate (BER) as a function of the signal to jamming ratio (SJR). A straight-line relationship is observed, as was also seen for Rayleigh fading without jamming. The jammer fill fraction and the BER are shown as a function of the fixed to scatter ratio F for a fixed value of the signal to noise ratio and SJR. For high values of F, the Gaussian model may be assumed and a low value of jammer fill fraction is needed to achieve the worst-case result. For low F, the Rayleigh model may be assumed and broad-band jamming is the optimum strategy. For intermediate F values, the Rician model can be assumed. A rapid transition is shown through the few decibels separating the worst-case PBN jamming Gaussian result and the Rayleigh fading result. The ratio F can be considered as a single-parameter bridge beween the worst-case PBN jamming straight line in the Gaussian model and the Rayleigh fading straight line.
Author (CISTI)

N93-30304 Bell-Northern Research Ltd., Ottawa (Ontario).
GENERALIZED OCTREES FOR CONSTRAINED OBJECT MODELING **c61**
David J. Brewer and Andrew K. C. Wong (Waterloo Univ., Ontario.) *In* Engineering Inst. of Canada, Canadian Conference on Electrical and Computer Engineering, Volumes 1 and 2 1990 4 p (For primary document see N93-30215 11-31)
Avail: Engineering Inst. of Canada, 2050 rue Mansfield, Suite 700, Montreal, Quebec H3A 1Z2 Canada

A computer vision methodology for three dimensional object modeling is discussed. The model consists of a modified form of the classic octree for object representation and selected attributes for object recognition. The generalized octree allows both volume-based and surface-based attributes to be stored and retrieved for object recognition. The object model is constrained to applications in which object orientation measured along primary, secondary, and tertiary axes can be derived during sensor data preprocessing. The model is not based upon or optimized for a specific sensor, but does require a specific form of information to be extracted from the sensor(s) that are selected. The model allows information from multiple sensors to be combined and stored in a single structure, and the model is therefore relevant to sensor/data fusion applications. Results achieved with the model are presented for vehicle recognition applications using an active laser radar and passive infrared airborne sensor system. Simulated dual-mode sensor data was used to generate object prototypes. The object prototypes were then employed to evaluate recognition performance for simulated unlabelled samples. The object model was not tested using live sensor data. The model is well suited for vehicle recognition (e.g., tank versus truck) but is less suited for vehicle identification.
Author (CISTI)

N93-30305 Toronto Univ. (Ontario). Computer Integrated Manufacturing Lab.
DESIGN AND IMPLEMENTATION OF AN INTERACTIVE ISOCHROMATIC FRINGE-ANALYSIS SYSTEM USING MACHINE-VISION TECHNIQUES **c39**
A. Mitu, B. Benhabib, K. C. Smith, and S. A. Meguid *In* Engineering Inst. of Canada, Canadian Conference on Electrical and Computer Engineering, Volumes 1 and 2 1990 4 p (For primary document see N93-30215 11-31)
Avail: Engineering Inst. of Canada, 2050 rue Mansfield, Suite 700, Montreal, Quebec H3A 1Z2 Canada

Photoelastic stress analysis is a powerful technique which enables a complete stress analysis to be carried out on engineering components or structures at the design stage. However, the analysis can be a long and tedious process and is normally carried out by an expert. A study was undertaken to create an automated stress and strain analysis system making use of a dynamically controlled stress field to facilitate the acquisition and interpretation of photoelastic data. The first step towards this goal was taken by implementing an interactive isochromatic fringe analysis system (IIFAS) to serve as a basis for further research and development. The algorithms developed for this system are presented together with an analysis of their performance based on actual tests. The IIFAS performs an analysis of isochromatic fringes in several steps. First, the image containing the fringes is cleaned of noise using a median filter. Next, the image is segmented by grey-level thresholding into background and fringes. The thresholding point is determined by an automatic threshold selection algorithm. Finally, the orders of the fringes are assigned by a fringe counting algorithm. The IIFAS performed well during tests using photoelastic images of a disk under diametrical compression. Author (CISTI)

N93-30306 Ottawa Univ. (Ontario). Dept. of Electrical Engineering.
PROGRESS IN THE DEVELOPMENT OF BROADBAND ELECTRIC-FIELD SENSORS FOR TRANSIENT FIELDS **c32**
Art Thansandote, Stan S. Stuchly, Mariusz Barski, and Maria A. Stuchly (Health and Welfare Canada, Ottawa, Ontario.) *In* Engineering Inst. of Canada, Canadian Conference on Electrical and Computer Engineering, Volumes 1 and 2 1990 4 p (For primary document see N93-30215 11-31)
Avail: Engineering Inst. of Canada, 2050 rue Mansfield, Suite 700, Montreal, Quebec H3A 1Z2 Canada

Several broadband active E-field sensors in the frequency range from 30 Hertz to 350 megaHertz based on electrically small spherical antennas for measurement of continuous wave and transient fields were developed. Such sensors are suitable for electromagnetic pulse and electrostatic discharge research, lightning measurement, and investigation of biological effects of pulsed electromagnetic fields. Wideband performance of the sensor was achieved by using buffer amplifiers with a very high output impedance. Two monopole configuration sensors and one free-field sensor were built, tested, and calibrated in a transient electromagnetic (TEM) cell in both the frequency domain and the time domain. Each sensor provides a flat frequency independent response up to almost 6 decades. For example, the 5.6 cm diameter hemispherical sensor has the flat response region extending from 30 Hertz to 42 megaHertz with a sensitivity of 1.9 millivolts/(volt/meter). The dynamic range of all sensors was estimated to be over 75 decibels. The rise time of the output pulse for a Gaussian pulse incident field of 450 picosecond width is less than one nanosecond.
Author (CISTI)

N93-30307 Manitoba Univ., Winnipeg. Dept. of Electrical and Computer Engineering.
TOLERANCE THEORY OF PHASED ARRAY ANTENNAS: A STATISTICAL APPROACH **c32**
A. Sebak, L. Shafai, and G. Bridges *In* Engineering Inst. of Canada, Canadian Conference on Electrical and Computer Engineering, Volumes 1 and 2 1990 4 p (For primary document see N93-30215 11-31)
Avail: Engineering Inst. of Canada, 2050 rue Mansfield, Suite 700, Montreal, Quebec H3A 1Z2 Canada

Random errors, due to perturbations in the excitation coefficients, errors in the placement of antenna elements, mutual coupling, frequency variations in the signal, environmental and manufactring tolerances, etc., have a significant effect on the directivity, beamwidth, pointing angle, and sidelobe levels of the radiation pattern of phased-array antennas. The effect of amplitude and phase errors, and amplifier and phase shifter failures on the antenna performance was studied. The antenna considered is a linear array with amplitude distribution symmetric about the center of the antenna, but is otherwise arbitrary. The phase gradient across the array is assumed to be generated using digital phase shifters of arbitrary number of bits. The mathematical formulations and their numerical implementation are valid for a linear array of arbitrary aperture distribution and number of radiating elements at an arbitrary scan angle. Author (CISTI)

N93-30308 Canadian Space Agency, Ottawa (Ontario). David Florida Lab.
DEVELOPMENT OF AN ANTENNA MEASUREMENT FACILITY OPERATING IN THE 2 GHz - 100 GHz FREQUENCY RANGE **c32**
S. R. Mishra and G. A. Morin (Defence Research Establishment, Ottawa, Ontario.) *In* Engineering Inst. of Canada, Canadian Conference on Electrical and Computer Engineering, Volumes 1 and 2 1990 4 p (For primary document see N93-30215 11-31)
Avail: Engineering Inst. of Canada, 2050 rue Mansfield, Suite 700, Montreal, Quebec H3A 1Z2 Canada

A multipurpose research and development facility for antenna pattern measurement in the 2-100 GHz range is being commissioned at the David Florida Laboratory of the Canadian Space Agency. The facility incorporates an anechoic chamber 20 by 14 by 9.5 feet, an antenna positioner with precision encoders, automated control equipment, and a wide frequency coverage network analyzer. The design considerations, equipment details, performance, and salient features of the facility's hardware and software are described. The facility will be used to develop antenna measurement technology for next generation spacecraft, communications, and radar systems, and to provide support for various antenna development projects.
Author (CISTI)

N93-30309 Concordia Univ., Montreal (Quebec). Dept. of Electrical and Computer Engineering.
COUPLING GAIN COMPUTATION BETWEEN ANTENNAS ON CIRCULAR CYLINDERS AT SHF/EHF FREQUENCIES **c32**
D. Chatterjee, S. J. Kubina, and R. Paknys *In* Engineering Inst. of Canada, Canadian Conference on Electrical and Computer Engineering, Volumes 1 and 2 1990 3 p (For primary document see N93-30215 11-31)
Avail: Engineering Inst. of Canada, 2050 rue Mansfield, Suite 700, Montreal, Quebec H3A 1Z2 Canada

In analysis of electromagnetic compatibility of collocated avionics systems, aircraft fuselages are modeled by circular cylinders and antennas by a set of keyhole gains at their individual locations. When the antennas are completely hidden from each other by the fuselage, the unwanted signal reaching the receiver antenna travels round the fuselage in a creeping wave. The creeping wave shading loss between a pair of isotropic sources is simulated using half-wave, magnetic type, axial dipoles on a circular cylinder via the basic scattering code (NECBSC2). The results presented were obtained without modifying the NECBSC2 code and compare fairly well with previously published data. This simulation technique and a probable cause for the discrepancies between the NECBSC2 and AAPG codes are discussed. Author (CISTI)

N93-30310 Ottawa Univ. (Ontario). Dept. of Mechanical Engineering.
TRAJECTORY GENERATION FOR DUAL-ARM ROBOTS USING ARTIFICIAL IMPEDANCE APPROACH **c37**
D. S. Necsulescu, R. Jassemi-Zargani, and W. B. Graham (Canadian Space Agency, Ottawa, Ontario.) *In* Engineering Inst. of Canada, Canadian Conference on Electrical and Computer Engineering, Volumes 1 and 2 1990 4 p (For primary document see N93-30215 11-31)
Avail: Engineering Inst. of Canada, 2050 rue Mansfield, Suite 700, Montreal, Quebec H3A 1Z2 Canada

Recent research has shown that the trajectory of a robot arm can be generated in real time by assuming artificial mechanical impedances in the robot workvolume. The artificial impedance approach is applied to dual arm robots via an analytical model of the impedance control of a dual-arm planar robot. Simulations are presented to illustrate the manipulation of non-rigid bodies such as a flexible rod and a string, and to illustrate the operation of an impedance controller in the approaching and the coordination phases of the motion of the two arms. The results show that this approach is a candidate for solving some of the difficulties of coordinated dual-arm robot operation, both in the approaching phase and in the object handling phase. In particular, simulation results are obtained for the case of handling a string with sag constraints. Author (CISTI)

N93-30311 Thomson-CSF Systems Canada, Inc., Nepean (Ontario).
A FUNCTIONAL SYSTEM ARCHITECTURE FOR FULLY AUTONOMOUS ROBOT **c37**
S. Kalaycioglu *In* Engineering Inst. of Canada, Canadian Conference on Electrical and Computer Engineering, Volumes 1 and 2 1990 4 p (For primary document see N93-30215 11-31)
Avail: Engineering Inst. of Canada, 2050 rue Mansfield, Suite 700, Montreal, Quebec H3A 1Z2 Canada

The Mobile Servicing System (MSS) Autonomous Robotics Program intends to define and plan the development of technologies required to provide a supervised autonomous operation capability for the Special Purpose Dexterous Manipulator (SPDM) on the MSS. The operational functions for the SPDM to perform the required tasks, both in fully autonomous or supervised modes, are identified. Functional decomposition is performed using a graphics oriented methodology called Structural Analysis Design Technique. This process defines the functional architecture of the system, the types of data required to support its functionality, and the control processes that need to be emplaced. On the basis of the functional decomposition, a technology breakdown structure is also developed. A preliminary estimate of the status and maturity of each relevant technology is made, based on this technology breakdown. The developed functional hierarchy is found to be very effective for a robotic system with any level of autonomy. Moreover, this hierarchy can easily be applied to an existing very low level autonomous system and can provide a smooth transition towards a higher degree of autonomy. The effectiveness of the developed functional hierarchy will also play a very significant role both in the system design as well as in the development of the control hierarchy. Author (CISTI)

N93-30312 Canadian Space Agency, Ottawa (Ontario).
ROBOT ARM WITH POSITIONAL ABSOLUTE ENCODED JOINTS **c37**
S. K. Yeung, C. Baribeau (Ottawa Univ., Ontario.), A. Pharand (Ottawa Univ., Ontario.), and E. Petriu (Ottawa Univ., Ontario.) *In* Engineering Inst. of Canada, Canadian Conference on Electrical and Computer Engineering, Volumes 1 and 2 1990 4 p (For primary document see N93-30215 11-31)
Avail: Engineering Inst. of Canada, 2050 rue Mansfield, Suite 700, Montreal, Quebec H3A 1Z2 Canada

An absolute position measurement method used for control of an experimental three-joint robot arm is based on pseudo random binary sequence properties. A scanning technique is used to solve the code reading ambiguity problems. An 8-bit absolute position encoder was implemented in each robot joint and tested. The absolute encoder is used in conjunction with a conventional incremental encoder mounted on the input motor shaft. This solution provides the advantages of both position measuring techniques, the absolute encoder's noise immunity, and the incremental encoder's very high resolution. The control algorithm and hardware implementation are discussed. Author (CISTI)

N93-30313 Spar Aerospace Ltd., Weston (Ontario).
JOINT DRIVE DEVELOPMENT FOR THE SPACE STATION REMOTE MANIPULATOR SYSTEM **c37**
W. J. Ballantyne *In* Engineering Inst. of Canada, Canadian Conference on Electrical and Computer Engineering, Volumes 1 and 2 1990 5 p (For primary document see N93-30215 11-31)
Avail: Engineering Inst. of Canada, 2050 rue Mansfield, Suite 700, Montreal, Quebec H3A 1Z2 Canada

Parts of the design of the Space Station Remote Manipulator System's joint drive (the motor and drive electronics) have reached the proof of concept phase, while other parts (the joint drive module, joint housing, and joint electronic unit packaging) exist at present only as mockups of design concepts. The system requirements for the joint drive are outlined and the drive system architectures are described. Drive electromechanics are located within each joint and drive electronics are physically distributed over the length of the manipulator arm. The drives system has a modular design for ready maintainability in orbit. Equipment features are also described along with the considerations that led to their incorporation. These include the brushless motors, friction disc brakes, compound differential planetary gear train, and resolver based position and velocity sensing devices. Author (CISTI)

N93-30314 Ottawa Univ. (Ontario). Dept. of Electrical Engineering.
COMPARISON OF MULTIPLE ACCESS TECHNIQUES FOR BANDWIDTH LIMITED LAND-MOBILE SATELLITE COMMUNICATIONS **c32**
A. Yongacoglu, R. G. Lyons (SkyWave Electronics Ltd., Kanata, Ontario.), and B. A. Mazur (Calian Communications, Kanata, Ontario.) *In* Engineering Inst. of Canada, Canadian Conference on Electrical and Computer Engineering, Volumes 1 and 2 1990 4 p (For primary document see N93-30215 11-31)
Avail: Engineering Inst. of Canada, 2050 rue Mansfield, Suite 700, Montreal, Quebec H3A 1Z2 Canada

A capacity analysis and comparison of code division multiple access (CDMA) and frequency division multiple access (FDMA) approaches is presented as applicable to the voice service of a land/mobile satellite system. Both digital and amplitude companded single sideband analog modulations are considered with FDMA. Systems capacities are compared on the basis of identical link availabilities and physical propagation models. Parameters are optimized for a bandwidth limited, multi-beam environment. For CDMA, the benefits of voice activated carriers, antenna discrimination, polarization reuse, return link power control, and multipath suppression are included in the analysis. For FDMA, the advantages of bandwidth efficient modulation or coding combinations, voice activated carriers, polarization reuse, beam placement, and frequency staggering were taken into account. It can be concluded that all systems considered possess various possibilities for capacity enhancement with greater complexity, but the capacity improvements available to the CDMA forward link are probably larger and more easily attainable. Author (CISTI)

N93-30315 Communications Research Centre, Ottawa (Ontario). Dept. of Communications.
COMPARISON OF TWO RANDOM ACCESS TECHNIQUES FOR THE NORTH AMERICAN MSAT SYSTEM **c32**
Stewart Crozier and Brian Skerry (Telesat Mobile, Inc., Ottawa, Ontario.) *In* Engineering Inst. of Canada, Canadian Conference on Electrical and Computer Engineering, Volumes 1 and 2 1990 4 p (For primary document see N93-30215 11-31)
Avail: Engineering Inst. of Canada, 2050 rue Mansfield, Suite 700, Montreal, Quebec H3A 1Z2 Canada

Two random access techniques for the North American mobile satellite system are investigated and compared. The first approach uses only random access inbound signaling channels. The second approach is a type of reservation scheme, and uses a combination of time division multiple access and random access request inbound signaling channels. The performance for both approaches is heavily dependent on the probability of collision in the random access channels. The random access channels are assumed to operate under sloppy slotted ALOHA conditions, to maximize channel capacity. Equating the average number of transmissions per successful inbound information unit for the two approaches, it is shown that the reservation approach is much more bandwidth efficient. Author (CISTI)

N93-30316 McMaster Univ., Hamilton (Ontario). Communications Research Lab.

AN ADAPTIVE MAXIMUM LIKELIHOOD RECEIVER FOR CORRELATED RAYLEIGH FADING CHANNELS **c32**

Wayne C. Dam and Desmond P. Taylor *In* Engineering Inst. of Canada, Canadian Conference on Electrical and Computer Engineering, Volumes 1 and 2 1990 4 p (For primary document see N93-30215 11-31)

Avail: Engineering Inst. of Canada, 2050 rue Mansfield, Suite 700, Montreal, Quebec H3A 1Z2 Canada

Previous work on receivers suitable for correlated Rayleigh fading channels is examined. The analysis is generalized to complex signaling. It is demonstrated that the error performance of a standard receiver is weakly dependent on the structure of the fading process, and that an appropriate receiver may exploit this structure to give greatly improved performance. Two receiver structures, based on the classic estimator correlator derivation of Kailath, are considered. These structures are able to lower the error floor of a receiver in a correlated, Rayleigh fading channel. The performance limitation is found to be due to the form of the receiver used, rather than a fundamental channel capacity type of limit, and the appropriate receiver structure is able to virtually eliminate the asymptotic error. The performance of both standard and optimal receivers is examined analytically and verified through simulation. Author (CISTI)

N93-30317 Teleglobe Canada, Montreal (Quebec).

TELEGLOBE'S INTERNATIONAL MOBILE EARTH TERMINAL SERVICE **c32**

Joel Duchoeny *In* Engineering Inst. of Canada, Canadian Conference on Electrical and Computer Engineering, Volumes 1 and 2 1990 4 p (For primary document see N93-30215 11-31)

Avail: Engineering Inst. of Canada, 2050 rue Mansfield, Suite 700, Montreal, Quebec H3A 1Z2 Canada

In 1990, Teleglobe Canada initiated a developmental Mobile Earth Terminal (MET) service. By the use of the INMARSAT satellite, the service can provide voice and data communication capabilities between lightweight, self-contained terminals and the international public telephone network. Initially, the developmental program provides service to a test group of up to 18 terminals. Plans are under way to introduce a global digital service to the public by 1991-92. Such a service will have the potential to solve communication problems for such users as news media, diplomatic corps, disaster relief teams, construction teams in remote areas, and expeditions. The terminals are briefcase size and include L-band transmitter, receiver, and antenna, a power supply, and batteries. Equipment setup can be easily done in 1-2 minutes. Calls are made by aiming the antenna at the MARECS B2 satellite (covering the Atlantic Ocean region) and dialing the appropriate number. Author (CISTI)

N93-30318 Chan Technologies, Inc., Kirkland (Quebec).

ARRAY-FED REFLECTOR SYSTEMS WITH LIMITED SCAN **c32**

K. K. Chan and R. Martin (Defence Research Establishment, Ottawa, Ontario.) *In* Engineering Inst. of Canada, Canadian Conference on Electrical and Computer Engineering, Volumes 1 and 2 1990 4 p (For primary document see N93-30215 11-31)

Avail: Engineering Inst. of Canada, 2050 rue Mansfield, Suite 700, Montreal, Quebec H3A 1Z2 Canada

Results of an investigation of single parabolic reflector systems with small focal length/diameter ratio and limited electronic scan capability are presented. Such systems have been proposed for space-based radar surveillance application in the form of a rotating reflector antenna sweeping the earth's surface. Center-fed and offset-fed reflectors with focused, defocused, and transform feed arrays are the configurations studied. The performance goal is to achieve a minimum of three or four beamwidths of electronic scan in both elevation and azimuth with sidelobes of less than -40 dB in the receive mode. On transmit, maximum directivity is sought. High power distribution and switching among feed elements is to be avoided. The offset reflector fed by a defocused array with a corporate beamforming network or a transform feed is found to meet these requirements. Author (CISTI)

N93-30319 Chan Technologies, Inc., Kirkland (Quebec).

A DUAL POLARIZED BROADBAND MULTIFREQUENCY EARTH STATION FEED **c32**

K. K. Chan, S. R. Gauthier (Department of National Defence, Ottawa, Ontario.), and G. Dinham (Department of National Defence, Ottawa, Ontario.) *In* Engineering Inst. of Canada, Canadian Conference on Electrical and Computer Engineering, Volumes 1 and 2 1990 4 p (For primary document see N93-30215 11-31)

Avail: Engineering Inst. of Canada, 2050 rue Mansfield, Suite 700, Montreal, Quebec H3A 1Z2 Canada

Communications satellites are increasingly designed to operate in more than two frequency bands. To communicate with these satellites, it is more cost-effective to use a single multiband feed with a suitably designed Cassegrain reflector system than having several separate ground stations. Procedures for designing such a feed, which can operate simultaneously in three bands are presented. The feed has well-matched orthogonally polarized ports, with dual circular polarization in the C and X bands and dual circular or dual linear polarization in the Ku band. Measured results are given from the integrated feed system alone and when installed on a reflector antenna. These results fully validate the design concept adopted. Author (CISTI)

N93-30320 Concordia Univ., Montreal (Quebec).

RCS OF FUNDAMENTAL SCATTERERS IN THE HF BAND BY WIRE-GRID MODELLING **c32**

C. W. Trueman and S. J. Kubina *In* Engineering Inst. of Canada, Canadian Conference on Electrical and Computer Engineering, Volumes 1 and 2 1990 4 p (For primary document see N93-30215 11-31)

Avail: Engineering Inst. of Canada, 2050 rue Mansfield, Suite 700, Montreal, Quebec H3A 1Z2 Canada

To extract the maximum information from the return of a radar target such as an aircraft, the target's scattering properties must be well known. Wire grid modeling allows a detailed representation of the surface of a complex scatterer such as an aircraft, in the frequency range where the aircraft size is comparable to a wavelength. A moment method analysis determines the currents on the wires of the grid including the interactions between all parts of the structure. Wire grid models of fundamental scatterers (plates, strips, cubes, and spheres) of sizes comparable to the wavelength in the 2-30 MHz range are analyzed. The study of the radar cross section (RCS) of wire grids in comparison with measured RCS data helps to establish guidelines for building wire grid models, specifying such parameters as where to locate wires, how short the segments must be, and what radius to use. The guidelines so developed can then be applied to build wire grid models of much more complex bodies such as aircraft with much greater confidence. Author (CISTI)

N93-30321 Canadian Space Agency, Ottawa (Ontario). David Florida Lab.

WIDE FREQUENCY POLARIMETRIC RADAR CROSS SECTION MEASUREMENTS **c32**

S. R. Mishra, P. Charron, J. Smithson, and J. Mantz *In* Engineering Inst. of Canada, Canadian Conference on Electrical and Computer Engineering, Volumes 1 and 2 1990 4 p (For primary document see N93-30215 11-31)

Avail: Engineering Inst. of Canada, 2050 rue Mansfield, Suite 700, Montreal, Quebec H3A 1Z2 Canada

Modern radar cross section (RCS) measurements require determination of the full polarimetric scattering matrix on complex targets. Some of the special considerations necessary for these measurements include appropriate choice of calibration targets, proper equipment setting for full target response, and effect of target support system. A polarimetric RCS measurement facility having a target support column and positioner, transmit and receive antennas, a network analyzer, and automated data measurement and analysis capability is described. The target and antennas are mounted within an anechoic chamber. The facility is presently configured for X band

monostatic measurements and results are presented in the form of maps of amplitude and phase contours for a 7 cm metallic cube.
Author (CISTI)

N93-30322 Hickling (James F.) Management Consultants Ltd., Ottawa (Ontario).
THE AIR TRAFFIC CONTROLLER'S MENTAL MODEL AND IT'S IMPLICATIONS FOR EQUIPMENT DESIGN AND TRAINEE SELECTION **c53**
Richard H. Mogford *In* Engineering Inst. of Canada, Canadian Conference on Electrical and Computer Engineering, Volumes 1 and 2 1990 4 p (For primary document see N93-30215 11-31)
Avail: Engineering Inst. of Canada, 2050 rue Mansfield, Suite 700, Montreal, Quebec H3A 1Z2 Canada

In the context of air traffic control, a controller's mental model is a hypothetical construct which refers to the operator's learning and concepts about a system and what it is supposed to do. It is suggested that the controller's picture of the various elements of the air traffic control system is an aspect of the mental model which is worthwhile investigating in order to assist in system design and the selection of controllers. Previous research on air traffic control mental models is reviewed and applied to air traffic control systems. It is seen that objective tools exist for exploring some facets of the operator's mental model of a complex system. There are promising indications that these tools can help measure some aspects of the controller's mental model or picture. There is also evidence that the quality of a controller's picture is related to operational skill level.
Author (CISTI)

N93-30323 Hughes Aircraft Co., Goleta, CA. Systems Div.
THE CANADIAN AUTOMATED AIR TRAFFIC SYSTEM **c04**
Don E. Ludwig *In* Engineering Inst. of Canada, Canadian Conference on Electrical and Computer Engineering, Volumes 1 and 2 1990 4 p (For primary document see N93-30215 11-31)
Avail: Engineering Inst. of Canada, 2050 rue Mansfield, Suite 700, Montreal, Quebec H3A 1Z2 Canada

The Canadian Automated Air Traffic System (CAATS) provides a model for future air traffic systems operating in the year 2000 and beyond. The design has configuration flexibility and extensibility provisions which will enable the system currently being implemented to adapt to the requirements of the 2000s. Key elements of this design are described. These are: an architecture which uses an open system interconnect for inter- and intra-system interfacing of distributed data processing and display elements; use of commercial off-the-shelf components and software with provision for substitution of evolving technology; use of Ada software and a partitioning which will facilitate maintenance and adaptation to future operational needs; introduction of a computer human interface design and state of the art workstations which facilitate efficient controller interaction and have flexibility for adaptation to a changing environment; and incorporation of automated on-line maintenance reporting and system configuration control from a centralized position. Author (CISTI)

N93-30324 Sony Corp. of America, San Diego, CA.
COMPUTER-CONTROLLED ALIGNMENT FOR A 2000-LINE COLOR MONITOR **c04**
David A. Eccles, Manabu Suzuki (Sony Corp., Tokyo, Japan.), Hiroshi Nakano (Sony Corp., Tokyo, Japan.), Yuki Okamoto (Sony Corp., Tokyo, Japan.), and Kazuo Kii (Sony Corp., Tokyo, Japan.) *In* Engineering Inst. of Canada, Canadian Conference on Electrical and Computer Engineering, Volumes 1 and 2 1990 4 p (For primary document see N93-30215 11-31)
Avail: Engineering Inst. of Canada, 2050 rue Mansfield, Suite 700, Montreal, Quebec H3A 1Z2 Canada

Field alignment of a new 2048 line, 20-by-20 inch color monitor used for air traffic control is made easier by means of a new remote digital alignment system. The system includes a video processor, a digital processor for alignment data, and deflection and correction circuits. A personal computer running the alignment software is used to perform adjustments on the production line. A remote controller similar to that used with a television is provided to support field maintenance. The alignment system allows menu-driven convergence, color purity, focus, and distortion adjustment via a digital interface. Automatic setup functions for white balance and color purity have also been developed. Touchup alignment by unskilled customers can be done in about 15 minutes. Author (CISTI)

N93-30325 Centre d'Etudes de la Navigation Aerienne, Toulouse (France).
EVOLUTION OF RADAR DATA PROCESSING IN THE FRENCH AIR TRAFFIC CONTROL SYSTEM **c04**
D. Figarol and B. Kriner *In* Engineering Inst. of Canada, Canadian Conference on Electrical and Computer Engineering, Volumes 1 and 2 1990 4 p (For primary document see N93-30215 11-31)
Avail: Engineering Inst. of Canada, 2050 rue Mansfield, Suite 700, Montreal, Quebec H3A 1Z2 Canada

A research study called HADAMARD is described which is aimed at providing a new multiradar multiplot tracking system for air traffic control in France. The system is based on state of the art and advanced tracking technology to take full advantage of monopulse radar coverage that will be implemented at the present time. This system will help to reduce minimal radar separations between aircraft without a loss in safety. After an overview of the more general context of radar data processing evolution in France, functional characteristics of HADAMARD are described in the areas of system design, input management, track initiation, data association, track update and maneuver detection, and estimation of radar bias. The HADAMARD prototype has been developed in Ada software, and its evaluation phase was completed in the summer of 1990. HADAMARD is on its way to integration into the CAUTRA 4.1 software which will be rehosted on new Data General MV computers. Author (CISTI)

N93-30326 National Research Council of Canada, Ottawa (Ontario). Inst. for Information Technology.
SUPERVISED AUTONOMY IN TELEROBOTICS **c63**
N. Burtnyk and J. Basran (Ottawa Univ., Ontario.) *In* Engineering Inst. of Canada, Canadian Conference on Electrical and Computer Engineering, Volumes 1 and 2 1990 7 p (For primary document see N93-30215 11-31)
Avail: Engineering Inst. of Canada, 2050 rue Mansfield, Suite 700, Montreal, Quebec H3A 1Z2 Canada

Advanced autonomous robots are envisaged for applications in harsh, demanding or dangerous environments such as nuclear, underwater operations, space, mining and tunneling, civil engineering and construction, etc. A major challenge in telerobotics development is to incorporate the robot's capability for autonomous operation wherever possible. A supervisory control concept for exploiting autonomous functionality in an unstructured environment is presented. Through an effective man-machine dialogue, the operator uses human perceptual and planning abilities to assist the robot in acquiring a model of its environment. Once this structure is acquired, the operator instructs the robot on how to perform a task as a sequence of actions based on generic skills. A discussion of the technical solutions that are essential to implement this concept and the results of a study to develop a robot operating under supervised autonomy are presented.
Author (CISTI)

N93-30327 National Research Council of Canada, Ottawa (Ontario). Inst. for Information Technology.
A MULTIPROCESSOR ARCHITECTURE FOR REALTIME ROBOT CONTROL **c60**
Shadia Elgazzar *In* Engineering Inst. of Canada, Canadian Conference on Electrical and Computer Engineering, Volumes 1 and 2 1990 5 p (For primary document see N93-30215 11-31)
Avail: Engineering Inst. of Canada, 2050 rue Mansfield, Suite 700, Montreal, Quebec H3A 1Z2 Canada

The control of autonomous robots and their operation in unstructured environments offer a challenging problem to the researchers in the field of robotics. Hardware and software architectures must be reconsidered, as the real-time requirements cannot be met using conventional machines. A configurable and adaptable architecture for real-time robot control has been developed based on a multi-processor based architecture and Harmony, an object-based, real-time, multiprocessing, multitasking operating system. This architecture is capable of supporting, in a consistent manner, every aspect of an intelligent robot system. The modular construction of the hardware and software components of this controller has minimized robot dependencies, which makes it capable of controlling many types of robots. The necessary requirements for a versatile robot system controller and the implementation of an open architecture for controlling single/dual robot manipulators are described. The porting of Kali, a powerful low-level programming system for multiple robot control, to Harmony is also described. Author (CISTI)

N93-30328 CAE Electronics Ltd., Saint Laurent (Quebec).
RADAR BEAM EFFECTS FOR A FLIGHT SIMULATOR USING SIGNAL PROCESSOR BASED HARDWARE **c32**
E. J. Nemer, R. C. Bridegeman, and A. S. Malowany (McGill Univ., Montreal, Quebec.) *In* Engineering Inst. of Canada, Canadian Conference on Electrical and Computer Engineering, Volumes 1 and 2 1990 5 p (For primary document see N93-30215 11-31)
Avail: Engineering Inst. of Canada, 2050 rue Mansfield, Suite 700, Montreal, Quebec H3A 1Z2 Canada

The design of a signal processor based system to simulate the beam-forming effects of airborne radars is presented. The problem is first formulated as a digital filtering operation with the filter response derived from the power distribution function of the radiating antenna. To lighten the computational load required for real-time simulation, an efficient finite impulse response (FIR) filter implementation proposed by Chu and Burrus (1984) is used. The algorithm, a unique implementation of FIR filters, is based on a polynomial approximation of the filter's response and results in significant reduction in the number of operations. In spite of this optimization, very high arithmetic throughput is still needed for real-time simulation. To design a system with the required capability, a high performance signal processor, the TMS320C30, was selected. The system also includes a data channel controller, an arbitration logic, fast memory elements, and a parallel interface to the host computer. The architecture is made modular, allowing many similar units to be teamed up and provide virtually unlimited computing power. The system is programmable and can simulate a variety of radar systems of different characteristics. Author (CISTI)

N93-30329 National Research Council of Canada, Ottawa (Ontario). Flight Research Lab.
AIRBORNE DATA ACQUISITION USING A FRONT-END PROCESSOR ARCHITECTURE **c60**
J. E. Jordan and K. K. Lum *In* Engineering Inst. of Canada, Canadian Conference on Electrical and Computer Engineering, Volumes 1 and 2 1990 4 p (For primary document see N93-30215 11-31)
Avail: Engineering Inst. of Canada, 2050 rue Mansfield, Suite 700, Montreal, Quebec H3A 1Z2 Canada

An airborne data gathering and processing system is described, employing front-end data acquisition processors in a multiprocessor architecture. The system is used to make measurements of the earth's magnetic field using three sensors mounted in the wing tips and tail of an aircraft. In addition, data are acquired from a series of navigation and avionics systems so that measurements recorded by the system can be referenced spatially. The system uses a central host processor as well as a coprocessor to process data acquired from the front-end data acquisition processors. Real-time processing includes magnetic compensation of the aircraft, optimal estimation of the position of the aircraft, and informational displays for the pilots, navigator, and equipment operator. Author (CISTI)

N93-30330 Canadian Marconi Co. Ltd., Kanata (Ontario).
EMBEDDED GPS: THE CANADIAN MARCONI APPROACH **c04**
James M. Brown and R. K. Tiedemann *In* Engineering Inst. of Canada, Canadian Conference on Electrical and Computer Engineering, Volumes 1 and 2 1990 4 p (For primary document see N93-30215 11-31)
Avail: Engineering Inst. of Canada, 2050 rue Mansfield, Suite 700, Montreal, Quebec H3A 1Z2 Canada

A new, embeddable global positioning system (GPS) card set uses the same software algorithms and very similar hardware architecture as the Canadian Marconi CMA-786 GPS navigation receiver. Three circuit cards totalling 50 square inches and typically consuming only 7.5 watts implement a complete 2-channel GPS sensor suitable for embedding in other avionics navigation equipment, land vehicle navigation equipment, or time transfer devices. A high speed 8-bit parallel interface and an RS-232 interface are provided to facilitate this integration. A separate power supply, mechanical housing and integrated microstrip antenna / preamplifier are required. Satellite acquisition and tracking algorithms, Kalman filter and navigation software, and hardware implementation are described. Author (CISTI)

N93-30331 Communications Research Centre, Ottawa (Ontario).
CONSTANT AVERAGE POWER SINGLE SIDEBAND (CAPSSB) MODULATION **c32**
E. E. Matt and J. H. Lodge *In* Engineering Inst. of Canada, Canadian Conference on Electrical and Computer Engineering, Volumes 1 and 2 1990 4 p (For primary document see N93-30215 11-31)
Avail: Engineering Inst. of Canada, 2050 rue Mansfield, Suite 700, Montreal, Quebec H3A 1Z2 Canada

In a mobile satellite environment, amplitude companded single sideband (ACSSB) schemes for speech transmission can offer a degree of robustness to fading and shadowing that is difficult for alternate approaches to match. One drawback to ACSSB signals is that neither their average nor instantaneous transmit powers are constant. A new single sideband scheme is described which exhibits a nearly constant average transmit power and limits the peak instantaneous transmit power to only a few dB above the average level. In this scheme, a single digital signal processing microprocessor performs all the modulator functions. The architectures of the modulator and demodulator sections are described, and the technique for peak-to-average ratio reduction is discussed. The soft voice activation algorithm is also presented. The system has successfully transmitted speech over the MARECS-B satellite using constant average power single sideband radio in the vehicle and matching equipment in the hub station. These tests showed that the system can transmit voice over a 5 kHz channel with good communications quality when the received carrier to noise power spectral density ratio is 50 dB-Hz or greater. Author (CISTI)

N93-30332 Queens Univ., Kingston (Ontario). Dept. of Electrical Engineering.
SIGNAL PROCESSOR BASED MSAT TRELLIS CODED M-DPSK WITH ADAPTIVE DOPPLER PHASOR CORRECTION **c32**
P. Bengough, L. Berg, B. Koblents, and P. J. McLane *In* Engineering Inst. of Canada, Canadian Conference on Electrical and Computer Engineering, Volumes 1 and 2 1990 4 p (For primary document see N93-30215 11-31)
Avail: Engineering Inst. of Canada, 2050 rue Mansfield, Suite 700, Montreal, Quebec H3A 1Z2 Canada

A trellis coded M-differential phase shift keying (DPSK) modem with convolutional interleaving and deinterleaving has been developed and tested on a system consisting of three signal processing chips. The coded modem is either 2400 or 4800 bps in a 5 kHz bandwidth, whereas 1200 to 7200 bps can be supported without coding. All digital transmitters and receivers are designed using a 4 kHz carrier. Integrate and dump driven Viterbi decoding is used. Timing recovery is based on early/late gate principles which are extended to 8-DPSK modulation. This involves a novel threshold scheme. Open-loop Doppler correction is used in the setup mode and the tracking technique of Ungerboeck, Edbauer, and Natali (1982, 1989, 1986) for the data mode. The Doppler phasor is corrected rather than the Doppler frequency as it is easier to implement in digital signal processing realizations. The modem has been tested in the laboratory for a noise channel and no Doppler frequency correction. Author (CISTI)

N93-30333 Queens Univ., Kingston (Ontario). Dept. of Electrical Engineering.
TWO-STAGE DOPPLER PHASOR CORRECTED TCM/DMPSK FOR SHADOWED MOBILE SATELLITE CHANNELS **c32**
P. J. McLane *In* Engineering Inst. of Canada, Canadian Conference on Electrical and Computer Engineering, Volumes 1 and 2 1990 5 p (For primary document see N93-30215 11-31)
Avail: Engineering Inst. of Canada, 2050 rue Mansfield, Suite 700, Montreal, Quebec H3A 1Z2 Canada

A two-stage Doppler correction algorithm is presented for mobile satellite, digital signal processing based modems. The modulation considered is trellis coded differential phase shift keying (DPSK) involving eight signal points. The Doppler phasor rather than the Doppler angle is corrected as it leads to easy realization in digital signal processing software. The Doppler phasor correction algorithm presented has a set-up mode where the data are known and a data mode where the data are unknown. Both digital simulation and analytical techniques are used in the performance analysis. Author (CISTI)

N93-30334 Defence Research Establishment, Ottawa (Ontario).
STATUS OF THE CANADIAN MILITARY MULTIBEAM ANTENNA (MBA) DEVELOPMENT FOR EHF SATCOM **c32**
G. A. Morin, E. B. Felstead (Communications Research Centre, Ottawa, Ontario.), K. S. Rao (Spar Aerospace Ltd., Sainte-Anne-de-Bellevue, Quebec.), and K. K. Chan (Chan Technologies, Inc., Kirkland, Quebec.) *In* Engineering Inst. of Canada, Canadian Conference on Electrical and Computer Engineering, Volumes 1 and 2 1990 3 p (For primary document see N93-30215 11-31)
Avail: Engineering Inst. of Canada, 2050 rue Mansfield, Suite 700, Montreal, Quebec H3A 1Z2 Canada

In support of ongoing research on extremely high frequency military satellite communications, exploratory development work is being conducted on multibeam antennas for use on board satellites having Canada-wide coverage. The emphasis is on receive antennas that possess narrow beams, fast beam hopping, and low sidelobes for rejection of interference outside the beam area. To attain the stringent specifications required, a number of approaches were considered. A method of combining seven adjacent beams into one composite beam was found to be the best way to meet the specifications. This method uses a single aperture (lens or reflector) and standard focusing but combines a septet of adjacent beams (or horns). Among the focusing configurations studied, it was found that the single offset reflector gave the best results. Author (CISTI)

N93-30335 Chan Technologies, Inc., Kirkland (Quebec).
COMPARISON AND DESIGN OF MULTIPLE BEAM ANTENNA FEED NETWORKS **c32**
K. K. Chan, D. Faubert (Defence Research Establishment, Ottawa, Ontario.), and R. Martin (Defence Research Establishment, Ottawa, Ontario.) *In* Engineering Inst. of Canada, Canadian Conference on Electrical and Computer Engineering, Volumes 1 and 2 1990 4 p (For primary document see N93-30215 11-31)
Avail: Engineering Inst. of Canada, 2050 rue Mansfield, Suite 700, Montreal, Quebec H3A 1Z2 Canada

The architectures of three types of multiple beam networks are discussed along with their performance and capability. The networks considered are the Blass matrix, the Butler matrix, and the Rotman lens. To illustrate their properties, representative networks are characterized by their scattering parameters. Realistic models, verified by measured results, are used in the performance analysis. The relative merits of these networks are evaluated. Areas of applicability best suited to each type of network are indicated. The Blass matrix is preferred when the number of beams required is about two to four. The Butler matrix can produce a larger number of high quality beams with fewer components than the Blass matrix. Because the lens is a true time delay device, the scanned beam pointing remains invariant with frequency; this is desirable for electronic countermeasures systems. Author (CISTI)

N93-30336 Chan Technologies, Inc., Kirkland (Quebec).
RECENT ADVANCES IN BOOTLACE LENS DESIGN **c32**
K. K. Chan, W. B. Wallace (AeroSmith Systems Corp., Los Altos, CA.), and R. R. Blasing (AeroSmith Systems Corp., Los Altos, CA.) *In* Engineering Inst. of Canada, Canadian Conference on Electrical and Computer Engineering, Volumes 1 and 2 1990 4 p (For primary document see N93-30215 11-31)
Avail: Engineering Inst. of Canada, 2050 rue Mansfield, Suite 700, Montreal, Quebec H3A 1Z2 Canada

A bootlace lens is a beamformer which produces simultaneous multiple beams that span a given coverage area. It comprises a cavity region fed by input ports, output ports and dummy loaded ports. Bootlace lenses are used in applications which demand frequency invariant beams such as feed networks in electronic countermeasures or surveillance systems; they are also well suited as transform feeds for reflector and space-fed lens antennas. Until recently, design of these lenses has been based on experimentation, adjustments, and proprietary knowledge. An analytical alternative to the experimental approach is presented. The lens is analyzed, when implemented in stripline or microstrip, as a planar multiport network with an arbitrary contour. Entire domain basis functions are used for the port apertures to achieve fast convergence to the final solution. Experimental results from a microstrip lens and a stripline lens are presented to verify this method of analysis. With the ability to predict lens behavior accurately, a design approach is established that will yield lenses possessing prescribed properties such as matched ports and low ripple level in the transmission responses at the array ports. Author (CISTI)

N93-30337 Thompson-Hickling Aviation, Inc., Ottawa (Ontario).
ENGINEERING MANAGEMENT CONSIDERATION FOR AN INTEGRATED AERONAUTICAL MOBILE SATELLITE SERVICE **c32**
John M. Belcher *In* Engineering Inst. of Canada, Canadian Conference on Electrical and Computer Engineering, Volumes 1 and 2 1990 4 p (For primary document see N93-30215 11-31)
Avail: Engineering Inst. of Canada, 2050 rue Mansfield, Suite 700, Montreal, Quebec H3A 1Z2 Canada

In order to meet local air traffic control terminal requirements as well as national and transborder requirements, countries have developed communications, navigation, and surveillance (CNS) systems having little systems integration and a solely ground-based solution to air traffic control problems. It is believed that the application of satellite technology is the only currently viable solution that will enable international civil aviation to overcome the shortcomings of the presently available CNS systems. If properly implemented, available satellite system technology integrated with avionics and ground based capabilities, can be used to meet new global aviation demands. A clear transition plan has to be implemented so as to ensure continuity of service, recognize user-borne costs, and satisfy institutional and national objectives in the progress toward a universal air traffic management (ATM) system. ATM systems design should rely on a modular approach for flexibility and upgrading. An aeronautical mobile satellite service is intended to provide a worldwide satellite data link and direct air/ground voice communication. Institutional and financial roadblocks for implemetation of a global based approach will likely be far greater than technical constraints. Author (CISTI)

N93-30338 Transport Canada, Ottawa (Ontario).
ADAPTING SYSTEM ENGINEERING PRINCIPLES TO THE CANADIAN AIRSPACE SYSTEM **c04**
T. E. Thompson and R. G. Lewis (Martin Marietta Canada Ltd., Ottawa, Ontario.) *In* Engineering Inst. of Canada, Canadian Conference on Electrical and Computer Engineering, Volumes 1 and 2 1990 4 p (For primary document see N93-30215 11-31)
Avail: Engineering Inst. of Canada, 2050 rue Mansfield, Suite 700, Montreal, Quebec H3A 1Z2 Canada

Adaptations have been made to published textbook methodologies for system engineering to allow practical application to the Canadian Airspace System (CAS) redesign. The CAS is the collection of equipment and facilities which, together with skilled personel, processes, and procedures, makes up the Canadian air navigation and traffic control system. The CAS design process must put into place a complete design for the year 2000 CAS as well as a process for making controlled design changes in the future. The application of systems engineering principles in this design process is absolutely necessary to avoid expensive duplication or incompatibilities. The following six steps that are being used in the CAS redesign are described: preparing operational requirements for the systems; developing the operational and support concepts for the system; specifying system requirements; specifying system design at four different levels; developing a transition plan; and developing an integration strategy to control and manage system implementation. Support tools used in the redesign are briefly discussed, including computer aided design tools and an engineering data base. Author (CISTI)

N93-30339 MacDonald, Dettwiler and Associates Ltd., Ottawa (Ontario).
APPLICATION AND INTEGRATION OF DIVERSE TECHNOLOGY IN AN AVIATION SYSTEM: THE NATIONAL AERONAUTICAL INFORMATION PROCESSING SYSTEM **c04**
Karl Snider and Tim Daniel *In* Engineering Inst. of Canada, Canadian Conference on Electrical and Computer Engineering, Volumes 1 and 2 1990 4 p Prepared in cooperation with MacDonald, Dettwiler Proprietary Ltd., New South Wales, Australia (For primary document see N93-30215 11-31)
Avail: Engineering Inst. of Canada, 2050 rue Mansfield, Suite 700, Montreal, Quebec H3A 1Z2 Canada

The National Aeronautical Information Processing System is under development for the Australian civil aviation authorities. It will be an advanced automated aeronautical information service for providing flight briefing and flight plan filing in a flexible manner. The system development involves the combination and integration of diverse technologies including voice synthesis, aircraft flight calculations, image processing, facsimile data transmission, optical scanner inputs, geographical information systems, airspace and aircraft databases, fault tolerant computer hardware and software, telephone call distribution, geographic projections developed for satellite image correction systems, and special algorithms which permit pilots to plan flights along geographic features. The system architecture is described along with typical usage scenarios and human-machine interface design. Author (CISTI)

N93-30340 Calgary Univ. (Alberta). Dept. of Electrical Engineering.
AN AUTO-GUIDING SYSTEM FOR MID-SIZED TELESCOPES **c89**
J. W. Haslett, W. Gonnason, S. Balasubramanian, R. J. Condon, F. N. Trofimenkoff, and S. E. Nordquist *In* Engineering Inst. of Canada, Canadian Conference on Electrical and Computer Engineering, Volumes 1 and 2 1990 6 p (For primary document see N93-30215 11-31)
Avail: Engineering Inst. of Canada, 2050 rue Mansfield, Suite 700, Montreal, Quebec H3A 1Z2 Canada

Some aspects of mid-sized telescope auto-guiding are introduced along with the special guidance problems associated with the Univerisity of Calgary's infrared telescope, a 1.5 meter aperture instrument with an alt-alt mount and two-channel photometry system. Two new types of position detecting sensors are discussed as candidates for inclusion in auto-guiding schemes that solve the telescope's tracking problems. One is a monolithic complementary metal oxide semiconductor implementation and the other is a short integration time sensor. Both of these devices calculate the centroid of a diffuse optical source that is focused on them. A description of the centroiding system is provided and the main sensitivities associated with the guiding method are identified. Performance guidelines are given for these sensors along with some results of low flux level testing of these devices. It is found that both sensors are suitable, with some prior intensification, for use in an auto-guider for the infrared telescope and any other mid-sized telescope tracking system. Author (CISTI)

N93-30341 Quebec Univ., Hull.
FIBER-OPTIC POLARIMETRIC STRAIN GAUGE **c35**
Wojtek J. Bock and Tomasz R. Wolinski (Warsaw Univ., Poland.) *In* Engineering Inst. of Canada, Canadian Conference on Electrical and Computer Engineering, Volumes 1 and 2 1990 4 p (For primary document see N93-30215 11-31)
Avail: Engineering Inst. of Canada, 2050 rue Mansfield, Suite 700, Montreal, Quebec H3A 1Z2 Canada

A prototype fiber-optic polarimetric strain gauge based on the polarization mode coupling that occurs in highly birefringent optical fibers under the influence of axial strain is presented. Measurement set-up for a bonded strain gauge and its metrological characteristics are discussed together with the interpretation of observed physical effects in terms of changes in beat-length parameter under axial strain. The device is far more sensitive than conventional strain gauges, and can also be readily adjusted to a specified range of strain through an appropriate choice of fiber length and optical signal wavelength. The temperature drift of the device can be compensated in a straightforward procedure. The device is immune to electromagnetic interference, and is intrinsically safe in electrically dangerous, hazardous or explosive environments. Another attraction of this technology is its direct compatibility with fiber-optic telemetry, optical data transmission systems and multiplexing / demultiplexing technology. Author (CISTI)

N93-30342 Communications Research Centre, Ottawa (Ontario).
DESIGN ISSUES AND INITIAL PERFORMANCE OF AN ADAPTIVE AIR/GROUND/AIR HF COMMUNICATION SYSTEM **c32**
G. R. Nourry and D. G. McLachlan *In* Engineering Inst. of Canada, Canadian Conference on Electrical and Computer Engineering, Volumes 1 and 2 1990 7 p (For primary document see N93-30215 11-31)
Avail: Engineering Inst. of Canada, 2050 rue Mansfield, Suite 700, Montreal, Quebec H3A 1Z2 Canada

Airplanes flying in the Canadian Arctic are often without communication to an appropriate air traffic control center for substantial periods of time. Attempts to provide continuous communication coverage for such aircraft must take the special geography of the region into account. High frequency communications appears to be the only practical single medium that can potentially provide this service. The constraints and the issues involved in the design of an air-ground-air high frequency communication system for arctic operation are discussed. The system design incorporates both the Link-11 standard and an automatic link establishment (ALE) unit. It is demonstrated that Link-11 and ALE techniques are, in some cases, complementary and that for the specific case of high frequency skywave propagation, ALE techniques are necessary for efficient operation of a Link-11 system. The system has been implemented in an experimental configuration at four stations in the Canadian Arctic, which will be operated for a year at a period of sunspot maximum in order to evaluate system performance and to study high frequency transmission in polar regions. Author (CISTI)

N93-30343 Harris Corp., Rochester, NY.
ADVANCED HF DIGITAL NETWORKS **c32**
Marvin Baker and N. P. Robinson (Rome Air Development Center, Griffiss AFB, NY.) *In* Engineering Inst. of Canada, Canadian Conference on Electrical and Computer Engineering, Volumes 1 and 2 1990 4 p (For primary document see N93-30215 11-31)
Avail: Engineering Inst. of Canada, 2050 rue Mansfield, Suite 700, Montreal, Quebec H3A 1Z2 Canada

Technology developments in high frequency digital communications, being applied to mobile users spread over a large continental size area, are reviewed. The objective of these developments is to integrate efficient multiple access methods, prudent frequency management, and improved link quality analysis (LQA) into a user friendly communications network for military and civilian users of land vehicles, ships, and aircraft. The network scenario envisaged comprises a variable number (up to 100) of users distributed randomly over a circular area of 6400 km radius, with 3-10 members active at any given time. Members shall be frequency hopping while sharing a common hop set in a subset of the high frequency band using skywave, near vertical incidence skywave, multi-hop, and groundwave propagation. Network specifications include digital voice or data at 75 to 2400 bps in a 3 kHz bandwidth, Doppler shift of up to 50 Hz, multipath delay of up to 5 milliseconds, and long (1/4 Hz) and short (2 Hz) duration receive signal fades. A three stage approach is used for development of this network. Results to date are presented in the areas of bit error rate measurements, channel evaluation, access methods evaluation, and network simulator development. Author (CISTI)

N93-30344 Bell-Northern Research Ltd., Ottawa (Ontario).
SEMI-BLIND RESTORATION OF IMAGES DISTORTED BY RANDOM TIME VARYING POINT SPREAD FUNCTIONS **c65**
Edward Lam and Rabab K. Ward (British Columbia Univ., Vancouver.) *In* Engineering Inst. of Canada, Canadian Conference on Electrical and Computer Engineering, Volumes 1 and 2 1990 4 p (For primary document see N93-30215 11-31)
Avail: Engineering Inst. of Canada, 2050 rue Mansfield, Suite 700, Montreal, Quebec H3A 1Z2 Canada

The problem of restoring images from multiple observations in the presence of noise is considered. The distortion is due to a random, time varying inhomogeneous medium such as atmospheric turbulence. The point spread function at the time of observing each image is also recorded. The observation of the point spread function is also contaminated by noise. Since the correlation from one frame to the other is unknown, conventional restoration methods have mainly been based on averaging. A maximum likelihood solution is developed for this problem and it is shown that its results are better than those based on averaging. It has also been found that compared to the linear regression method, the maximum likelihood method is less stable when the number of observations is not large, or when the distortion is not small. Author (CISTI)

N93-30345 Toronto Univ. (Ontario). Dept. of Electrical Engineering.
MORPHOLOGICAL AND ORDER STATISTIC FILTERS: A COMPARATIVE STUDY **c33**
Renee L. J. Martens, Ziheng Zhou, and Anastasios N. Venetsanopoulos *In* Engineering Inst. of Canada, Canadian Conference on Electrical and Computer Engineering, Volumes 1 and 2 1990 4 p (For primary document see N93-30215 11-31)
Avail: Engineering Inst. of Canada, 2050 rue Mansfield, Suite 700, Montreal, Quebec H3A 1Z2 Canada

The performance of five order statistic filter and four morphological filters is compared based on criteria which were chosen to be close to the characteristics of the human visual system. Four different noise distributions were used in the experiments conducted for the comparison: Gaussian noise, impulsive noise, the mixture of those two, and double exponential noise. The fact that the performance of a filter is image-dependent, even with identical noise distribution, was also considered. Three different types of test images were used in the evaluations: a synthetic image created for examining edge- and line-preserving properties of a filter; a real image containing many edges and small details to test detail preserving capability; and a background of clouds, which is a simulation of real infrared radar images. The results suggest that some order statistic filters are better suited for edge preservation and noise removal than the morphological filters. It is noted that for cloud removal, the open-closing, adaptive window edge detecting, median, signal adaptive median, and moving average filters all detected the targets with very low false alarm rates, although they were not originally designed for such a task. Author (CISTI)

N93-30346 Wilfrid Laurier Univ., Waterloo (Ontario).
IMAGE ENHANCEMENT USING AN ANALOG DEVICE NEURAL NETWORK **c33**
Nora M. Znotinas and Franklin M. McGovern *In* Engineering Inst. of Canada, Canadian Conference on Electrical and Computer Engineering, Volumes 1 and 2 1990 4 p (For primary document see N93-30215 11-31)
Avail: Engineering Inst. of Canada, 2050 rue Mansfield, Suite 700, Montreal, Quebec H3A 1Z2 Canada

A fully parallel analog device neural network which simulates the outer plexiform layer of the retina is presented. The prototype network is a 36 cell linear array with the option of first and/or second neighbor interaction. Results focus on lateral inhibition due to: (1) the first nearest neighbors where a cell's output is mediated by the value of the neighboring cells to the immediate left and right; and (2) the second nearest neighbors where a cell's output is mediated by the value of two neighboring cells to the left and also to the right. Results focus only on the static and spatial aspects of images. It is apparent from the results that it is contrast, not absolute changes in background illumination, that primarily determine the response amplitude. The network shows pulse responses that are consistent with the response of the outer plexiform layer of the retina. The impulse response of the network demonstrates contrast invariance under variable illumination, dynamic range compression, and pulse and edge enhancement. Author (CISTI)

N93-30347 Atlantis Scientific Systems Group, Inc., Ottawa (Ontario).
SIMILARITIES BETWEEN SYNTHETIC APERATURE RADAR AND GROUND PROBING RADAR IMAGING **c32**
Bernard Armour, Alan Judge (Geological Survey of Canada, Ottawa, Ontario.), and Ron Saper *In* Engineering Inst. of Canada, Canadian Conference on Electrical and Computer Engineering, Volumes 1 and 2 1990 5 p (For primary document see N93-30215 11-31)
Avail: Engineering Inst. of Canada, 2050 rue Mansfield, Suite 700, Montreal, Quebec H3A 1Z2 Canada

Two radar imaging techniques of synthetic aperture radar (SAR) and pulsed ground probing radar (GPR) are reviewed, drawing attention to the fundamental similarities in the image formation processing. An airborne SAR image of the ground terrain is formed by flying along a track and collecting radar echo measurements with the side-looking antenna sweeping out a strip along the ground surface. A pulsed GPR image profiling a cross-section of the subsurface is formed by repeated radar measurements at discrete intervals along a straight line on the ground surface. In both cases, the image is formed by combining the set of discrete measurements along the track to achieve a high resolution image in two dimensions. The processing consists of two steps: pulse compression and azimuth compression. Range processing and azimuth processing are described with reference to the filtering used and the reflectivity functions involved. Examples of SAR and GPR images are included. Author (CISTI)

N93-30348 Laval Univ. (Quebec).
SEGMENTATION OF SAR IMAGES **c32**
N. Kaliaguine and J.-N. Beaulieu *In* Engineering Inst. of Canada, Canadian Conference on Electrical and Computer Engineering, Volumes 1 and 2 1990 4 p (For primary document see N93-30215 11-31)
Avail: Engineering Inst. of Canada, 2050 rue Mansfield, Suite 700, Montreal, Quebec H3A 1Z2 Canada

A new and simple filter is presented which is useful for the segmentation of a synthetic aperture radar picture. The filter used corresponds to an adiabatic transformation, is reversible, and does not introduce information loss. The purpose of the filter is to transform the noise model of the image from multiplicative Gaussian to additive Gaussian, the latter being easier to process. Two assumptions are used in processing an image: that the image had a multiplicative noise (always a good approximation for a synthetic aperature radar image) and that the regions in the image can be discriminated by the average of their pixels. A hierarchical stepwise optimization algorithm is used in conjunction with the filter to segment images. Experimental results are presented to illustrate the segmentation of an aerial agricultural image under various filtering methods. Author (CISTI)

N93-30349 MPR Teltech Ltd., Burnaby (British Columbia).
THE EVOLUTION OF GLOBAL MOBILE COMMUNICATIONS **c32**
A. I. Spolsky and J. R. Brasic *In* Engineering Inst. of Canada, Canadian Conference on Electrical and Computer Engineering, Volumes 1 and 2 1990 6 p (For primary document see N93-30215 11-31)
Avail: Engineering Inst. of Canada, 2050 rue Mansfield, Suite 700, Montreal, Quebec H3A 1Z2 Canada

A long term, global viewpoint is presented on the subject of communications access which may be the key to resolving many of the world's current requirements for developing a truly global, ubiquitous mobile/personal voice and data communications capability. The solutions are multi disciplinary, some using terrestrial techniques, some by satellite, but both using a variety of technologies and techniques. In the area of satellite communications, the focus is on inexpensive, efficient antennas, high gain spacecraft amplifiers and efficient power and bandwidth modulation techniques including high performance, low bit rate voice codecs. Terrestrially, many of the same technologies apply to cellular telephone systems. A key issue is the electromagnetic spectrum and its utilization efficiency, especially if the popularity of cellular telephones is repeated in the development of mobile satellite systems. Integration of diverse systems depends on formulating a framework that will allow systems to be interoperable by specifying logical interfaces among most or all evolving niche systems. Author (CISTI)

N93-30350 CompEngServ Ltd., Ottawa (Ontario).
ISSUES OF ATC CONFLICT RESOLUTION UNDER REAL-TIME CONSTRAINTS **c04**
I. G. Smith and C. A. Crabb *In* Engineering Inst. of Canada, Canadian Conference on Electrical and Computer Engineering, Volumes 1 and 2 1990 4 p (For primary document see N93-30215 11-31)
Avail: Engineering Inst. of Canada, 2050 rue Mansfield, Suite 700, Montreal, Quebec H3A 1Z2 Canada

The CORES 2 (COnflict REsolution System) project has the goal to produce a developmental system that provides conflict detection, prediction, and resolution advice to air traffic controllers in an enroute radar controlled airspace. Unlike several other developmental efforts, the project attempts to address many of the real-time and other temporal issues involved in this area. Some of the issues which are currently under investigation as part of the implementation of the system are described. These issues include prediction mechanisms, priorities for resolving concurrent conflicts, time allowed for presentation of solutions, validity intervals of solutions, interactions between conflicts and solutions, and presentation of conflicts and solutions. An object oriented rule-based system was chosen as a suitable development environment for the CORES system, which also includes an air traffic simulator. Author (CISTI)

N93-30351 Mitre Corp., McLean, VA.
NATIONAL AIRSPACE SYSTEM PERFORMANCE ANALYSIS CAPABILITY (NASPAC) SIMULATION MODEL **c04**
Lynne Fellman *In* Engineering Inst. of Canada, Canadian Conference on Electrical and Computer Engineering, Volumes 1 and 2 1990 4 p (For primary document see N93-30215 11-31)
Avail: Engineering Inst. of Canada, 2050 rue Mansfield, Suite 700, Montreal, Quebec H3A 1Z2 Canada

The National Airspace System Performance Analysis Capability (NASPAC) simulation model was developed to assist in analyzing the performance of the US National Airspace System and to estimate the effects of proposed changes in the system. An early version of the model was used to identify entities such as airports and airspace that limit system performance and to evaluate the impacts of changes to some of these entities. Subsequently, the NASPAC simulation model was enhanced and has been used to analyze the impact of planned and proposed improvements to major airports, potential changes to airspace structures, anticipated future growth in air traffic demand, and changes in airline scheduling practices. Principal inputs to the model include air traffic demand, airport and airspace network structures and capacities, and flight or aircraft characteristics. Principal outputs include operations per hour, instantaneous aircraft counts, and aircraft delays. Three recent applications of the NASPAC model are described: analysis of national impacts of the Dallas-Fort Worth Metroplex plan; analysis of impacts of a new air carrier hub at Philadelphia; and a national airspace saturation analysis. Author (CISTI)

N93-30352 Mitre Corp., McLean, VA.

PROCEDURAL DEVELOPMENT PROTOTYPE IN AUTOMATED EN ROUTE AIR TRAFFIC CONTROL **c04**

C. Vanessa Fong *In* Engineering Inst. of Canada, Canadian Conference on Electrical and Computer Engineering, Volumes 1 and 2 1990 3 p (For primary document see N93-30215 11-31)

Avail: Engineering Inst. of Canada, 2050 rue Mansfield, Suite 700, Montreal, Quebec H3A 1Z2 Canada

A key element in the US Federal Aviation Administration's plan to modernize the air traffic control system is the Advanced Automation System which incorporates the collection of automation capabilities known as Automated En Route Air Traffic Control (AERA). AERA has three components: AERA 1, with the capabilities of aircraft trajectory estimation, automated problem detection, and trial planning; AERA 2, summarized below; and AERA 3, currently in the concept development phase. In order to support the evaluation of AERA 2 capabilities, a procedural development prototype is being developed for use in defining, evaluating, and revising air traffic control operational and training materials for AERA 2. The prototype is implemented on a VAX 8700/VMS system in PL/1. The AERA 2 traffic simulation and other capabilities are displayed on color monitors with graphics controllers. Capabilities of the prototype include automated problem resolution, computer human interfacing, automated controller aids, air traffic control scenario generation, data collection, and other graphics image capture and replay tools. The overall characteristics of this prototype are discussed. Author (CISTI)

N93-30353 Mitre Corp., McLean, VA.

ENHANCING AVAILABILITY, PERFORMANCE, AND FLEXIBILITY OF AIR TRAFFIC CONTROL AIR-GROUND SERVICES **c04**

Gian P. Jain, Douglas L. Bamford, and Leone C. Monticone *In* Engineering Inst. of Canada, Canadian Conference on Electrical and Computer Engineering, Volumes 1 and 2 1990 5 p (For primary document see N93-30215 11-31)

Avail: Engineering Inst. of Canada, 2050 rue Mansfield, Suite 700, Montreal, Quebec H3A 1Z2 Canada

The air-ground (A/G) communications service for the air traffic control (ATC) community must be designed to provide end-to-end communications that meets high availability and performance requirements. These service requirements, such as voice quality, can be satisfied by the proper selection of network elements and design of the A/G network. The terrestrial portion of the A/G voice service is discussed along with the radio frequency link portion of this service. The evolution of the A/G network operations from a manual to an automated process for restoration and management is demonstrated, such evolution leading to new configurations with the potential for better availability, performance, and flexibility in an ATC environment. In addition, preliminary work is presented on a procedure that can be used to take into account the dependencies that may occur between failures (such as dependencies between circuit failures in the terrestrial environment) in any availability analysis. Author (CISTI)

N93-30354 Mitre Corp., McLean, VA.

CHANGING ROLE OF TELECOMMUNICATIONS MANAGEMENT IN AIR TRAFFIC CONTROL IN THE FAA **c04**

Kikram Prabhu *In* Engineering Inst. of Canada, Canadian Conference on Electrical and Computer Engineering, Volumes 1 and 2 1990 4 p (For primary document see N93-30215 11-31)

Avail: Engineering Inst. of Canada, 2050 rue Mansfield, Suite 700, Montreal, Quebec H3A 1Z2 Canada

The mission of the US Federal Aviation Administration (FAA) is air traffic control (ATC). As the ATC function has evolved over the years from being primarily manual to one supported by many interconnected automated systems, the associated telecommunications requirements have become more specialized. Consequently, the FAA telecommunications network has changed over time and consists of a number of subnetworks and subsystems, some of which are interconnected in a complex manner. More subsystems are planned and will be added over the next few years. Since there is a combination of FAA-owned and leased subsystems, management of the overall network and its evolution is becoming very important. The rapidly changing telecommunications market environment in the USA has increased available equipment and service offerings; it has also made it necessary to deal with multiple carriers and vendors. The telecommunications management infrastructure for Operations, Administration, and Maintenance (OA&M) in the FAA is described along with the undergoing changes in its role. As the overall network is becoming very complex, the telecommunications management structure has to emphasize the end-to-end service perspective rather than that of individual subsystems to ensure responsiveness to ATC users. Author (CISTI)

N93-30355 Memorial Univ. of Newfoundland, Saint Johns. Centre for Cold Ocean Resources Engineering.

ADAPTIVE FILTERING FOR CLUTTER SUPPRESSION IN HIGH FREQUENCY RADAR **c32**

Rafaat H. Khan *In* Engineering Inst. of Canada, Canadian Conference on Electrical and Computer Engineering, Volumes 1 and 2 1990 4 p (For primary document see N93-30215 11-31)

Avail: Engineering Inst. of Canada, 2050 rue Mansfield, Suite 700, Montreal, Quebec H3A 1Z2 Canada

High frequency (HF) radar has the unique potential for over the horizon detection of ocean surface targets. However, ocean waves are also strong reflectors for HF radar and this high clutter level has limited its application for target detection. New results from the time domain analysis of ocean clutter show that it can be modelled as two angle modulated signals. This may be used to selectively suppress the clutter component and enhance the target detection performance. The practical implementation of clutter suppression, based upon this model, involves tracking of multiple time-varying sinusoids. An adaptive filtering technique to track time-varying sinusoids is discussed and initial results are presented. Author (CISTI)

N93-30356 Mitre Corp., McLean, VA.

DEVELOPING AUTOMATION FOR TERMINAL AIR TRAFFIC CONTROL: CASE STUDY OF THE IMAGING AID **c04**

Anand D. Mundra and Kerry M. Levin *In* Engineering Inst. of Canada, Canadian Conference on Electrical and Computer Engineering, Volumes 1 and 2 1990 4 p (For primary document see N93-30215 11-31)

Avail: Engineering Inst. of Canada, 2050 rue Mansfield, Suite 700, Montreal, Quebec H3A 1Z2 Canada

A passive automation aid called the imaging aid or ghosting aid has recently been developed for the US Federal Aviation Administration to help air traffic controllers stagger aircraft to converging runways in instrument flight rule conditions. This aid has been prototyped in a real-time simulation facility with the help of full performance level controllers, has been approved for operational evaluation at Lambert St. Louis International Airport during 1990, and is expected to be deployed nationally in the USA starting in 1992. The prototyping process used in the development of the imaging aid is described as a case study in developing air traffic control (ATC) automation. In this process, the imaging aid was designed to solve the difficulty of precise staggering on a sustained basis by converting the converging approaches geometry to simulate a single runway approach geometry. A methodology is proposed for the development of automation for terminal ATC based on the lessons learned from this prototype. Author (CISTI)

N93-30357 Transport Canada, Ottawa (Ontario).

AIRSPACE DESIGN EXPERT SYSTEM (ADES), A 2D/3D MAPPING AND MODELLING TOOL INCORPORATING AN EXPERT SYSTEM FOR USE IN INSTRUMENT APPROACH DESIGN **c04**

J. C. Ainsworth, L. Lam (Virtual Prototypes, Inc., Montreal, Quebec.), B. Schoor (Virtual Prototypes, Inc., Montreal, Quebec.), and M. McQueen (Virtual Prototypes, Inc., Montreal, Quebec.) *In* Engineering Inst. of Canada, Canadian Conference on Electrical and Computer Engineering, Volumes 1

and 2 1990 4 p (For primary document see N93-30215 11-31)
Avail: Engineering Inst. of Canada, 2050 rue Mansfield, Suite 700, Montreal, Quebec H3A 1Z2 Canada

ADES (Airspace Design Expert System) provides Transport Canada with a two and three dimensional graphic environment for the design of flight procedures. ADES brings together data for the air navigation facilities and obstacles, criteria for the flight procedure design, and information of the physical world to provide an integrated computer environment that replaces the existing manual environment. A carefully designed graphical user interface provides a uniform and simple medium with which the design specialist can communicate. The expert knowledge used in ADES can be modified to adapt the system to different requirements in the present or future. A flexible data management strategy is also used to provide a centralized information data base that can be easily maintained and expanded. There are three distinct parts to the ADES system: the Interactive Design Environment, with software modules for flight procedure design, utilities, data, and graphics; the Design Support Environment, consisting of the Nexpert Object Expert system tools, the INFORMIX Relational Database Management System, and a graphics environment provided by the workstation and proprietary graphics tools; and the external knowledge bases and data bases. A computer aided learning component is also provided to train users and to serve as a refresher for infrequent users. Author (CISTI)

N93-30358 MiTech, Inc., Washington, DC.
EVALUATION OF CATEGORY 3 MLS DESIGNS **c04**
Rick Cassell, Kelly R. Markin (Mitre Corp., McLean, VA.), and Alex E. Smith *In* Engineering Inst. of Canada, Canadian Conference on Electrical and Computer Engineering, Volumes 1 and 2 1990 4 p (For primary document see N93-30215 11-31)
Avail: Engineering Inst. of Canada, 2050 rue Mansfield, Suite 700, Montreal, Quebec H3A 1Z2 Canada

A key aspect of the implementation of microwave landing systems (MLS) is their compliance with US Federal Aviation Administration and International Civil Aviation Organization requirements for Category 3 landing operations, the lowest visibility operation. Since the landing system is used in such operations as the sole means of guidance, safety is the primary consideration. The safety of the landing system is related to two different items, continuity of service (COS) and integrity. The COS quantifies the probability of maintaining guidance throughout the critical phase of the landing operation. Integrity quantifies the probability of not transmitting potentially hazardous guidance to the aircraft. Three MLS ground equipment design architectures are evaluated for compliance with Category 3 COS and integrity requirements. These designs include a basic design consisting of redundant transmitters and monitors; a second design, the same as the first but with periodic switchover between two transmitters and executive monitors; and a third design, the same as the first except for the addition of a redundant shutdown capability. In addition, tradeoffs between the designs and several alternatives are analyzed. It is shown that relatively small changes in design architecture and implementation can result in large differences in the calculated integrity and COS. Author (CISTI)

N93-30508# Sandia National Labs., Albuquerque, NM.
STEPS REQUIRED IN THE PURSUIT OF QUANTITATIVE RISK MANAGEMENT PROCESSES FOR HIGH PRESSURE SYSTEMS
T. G. Priddy Jul. 1993 12 p Presented at the Pressure Vessel and Piping Conference, Denver, CO, 25-29 Jul. 1993
(Contract DE-AC04-76DP-00789)
(DE93-007586; SAND-93-0170C; CONF-930702-11) Avail: CASI HC A03/MF A01

Codes and standards have served remarkably well in reducing both the frequency and the consequences of pressure vessel and piping system failures. Past successful uses of safety standards show that safety can indeed be designed into potentially hazardous systems. Operational maintenance and inspection programs can also ensure and perpetuate design and manufactured reliability. However, as more advanced and challenging applications with high pressure systems and potentially hazardous operations are encountered, it is necessary to sharpen our technology, estimate reliability, quantify consequences, and manage risks with cost-effective processes. Practical systems are constructed of several components, and design standards are not always available for every component. A variable level of safety is, therefore, admitted within a system and some assessment of the overall safety is desired. Additionally, when potential personnel safety consequences are large but isolated, secondary protective steps should be considered such as barricading, protective enclosures, or remote operation. Rationale and activities that are based on probabilistic risk assessment (PRA) methods are discussed. While general application of PRA is not advocated at this time, certain derivative parts are suggested for use in closed-loop, risk management activities. DOE

N93-30581# Technical Research Centre of Finland, Espoo. Electrical and Automation Engineering Lab.
USES OF RISK IMPORTANCE MEASURES [RISKITARKEYSMITAT]
Tuomas Mankamo (Avaplan Oy, Finland.), Kurt Porn (Studsvik Nuclear, Nykoping, Sweden.), and Jan Holmberg May 1991 49 p Sponsored by Ministry of Trade and Industry
(VTT-TIED-1245; ISBN-951-38-3877-3; ETN-93-93772) Copyright Avail: CASI HC A03/MF A01

The definitions, relationships, and interpretations of the three most basic measures of risk importance measures are outlined: risk increase factor, risk decrease factor, and fractional contribution. Risk importance measures provide an understandable and practical way of presenting probabilistic safety analysis results which too often tend to remain abstract numbers without real insight into the content. The fundamental aspect of importance measures is that they express some specific influence of a basic event in the total risk. The basic failure or error events are the elements from which the reliability and risk models are constituted. The importance measures are relative, which is an advantage compared to absolute risk numbers, due to insensitivity with respect to quantification uncertainties. Therefore, they are particularly adapted to give first hand guidance on where to focus the main interest from the system's risk and reliability point of view, and from where to continue the analysis with more sophisticated methods requiring more effort. ESA

N93-28802*# Little (Arthur D.), Inc., Cambridge, MA.
SPACEBORNE PASSIVE RADIATIVE COOLER Abstract Only
S. Mathias *In* Lunar and Planetary Inst., Workshop on Advanced Technologies for Planetary Instruments, Part 1 1993 p 17 (For primary document see N93-28764 11-91)
Avail: CASI HC A01/MF A01

N93-28825*# TRW, Inc., Redondo Beach, CA.
MINIATURE LONG-LIFE SPACE CRYOCOOLERS Abstract Only
E. Tward *In* Lunar and Planetary Inst., Workshop on Advanced Technologies for Planetary Instruments, Part 1 1993 p 26-27 (For primary document see N93-28764 11-91)
Avail: CASI HC A01/MF A01

N93-29120*# Colorado Univ., Boulder.
INDIGENOUS LUNAR CONSTRUCTION MATERIALS
Wayne P. Rogers and Stein Sture *In its* Space Construction Activities 1 Nov. 1991 p 46-50 (For primary document see N93-29108 11-18)
Avail: CASI HC A01/MF A01

N93-29121*# Colorado Univ., Boulder.
SYSTEMS ENGINEERING STUDIES OF LUNAR BASE CONSTRUCTION
George W. Morgenthaler *In its* Space Construction Activities 1 Nov. 1991 p 51 (For primary document see N93-29108 11-18)
Avail: CASI HC A01/MF A01

N93-30954*# Purdue Univ., West Lafayette, IN. Mechanical Engineering Technology Dept.
TOOL GRINDING AND SPARK TESTING
Edward L. Widener *In* NASA. Langley Research Center, National Educators' Workshop. Update 92: Standard Experiments in Engineering Materials Science and Technology Jun. 1993 p 121-126 (For primary document see N93-30948 11-23)
Avail: CASI HC A01/MF A04

N93-30967*# Ball State Univ., Muncie, IN. Dept. of Industry and Technology.
THERMOFORMING FROM A SYSTEMS VIEWPOINT
Jerry L. Wickman and Nikhil Kundu (Purdue Univ., Elkhart, IN.) *In* NASA. Langley Research Center, National Educators' Workshop. Update 92:

Standard Experiments in Engineering Materials Science and Technology Jun. 1993 p 329-335 (For primary document see N93-30948 11-23) Avail: CASI HC A02/MF A04

32 COMMUNICATIONS AND RADAR

Includes radar; land and global communications; communications theory; and optical communications.

For related information see also *04 Aircraft Communications and Navigation* and *17 Space Communications, Spacecraft Communications, Command and Tracking.* For search and rescue see *03 Air Transportation and Safety,* and *16 Space Transportation.*

N93-28476# Air Force Inst. of Tech., Wright-Patterson AFB, OH. School of Engineering.
FREQUENCY DOMAIN SPEECH COMPRESSION USING THE KARHUNEN-LOEVE TRANSFORM M.S. Thesis
Donald W. Dryley Mar. 1993 170 p
(AD-A262613; AFIT/GEO/ENG/93M-02) Avail: CASI HC A08/MF A02

The purpose of this study was to test the influence of phase on the quality of speech reproduced by a speaker dependent compression system. The tests consisted of compressing frequency domain speech vectors using the Karhunen-Loeve Transform, with and without phase, then making subjective judgements as to the reproduced quality. Error Metrics were then tested for their suitability as predictors of reproduced quality. The compression software transformed each speech vector into a vector of complex Fourier coefficients (only half of the coefficients are needed as transform is hermitian). Phase was preserved by using the real frequency components to form one vector and the corresponding imaginary components to form a second vector of real numbers which were then separately compressed. The expanded vectors were recombined and speech reconstructed by Inverse Fourier Transformation. Compression ratios of 8:1 could be achieved without any perceivable difference between the original speech and reconstructed speech by minimizing the MSE of each vector of the pair. The 8:1 Compression Ratio corresponded to a covariance matrix Condition Number of 200. Recommendations for further study into voice characterization and an optimal transform for speech are made. DTIC

N93-28502# Universiteit Twente, Enschede (Netherlands). Tele-Informatics and Open Systems Group.
A SURVEY OF NETWORK INTERFACE DESIGNS
Andras Olah 31 Aug. 1992 33 p LIMITED REPRODUCIBILITY: More than 20% of this document may be affected by microfiche quality
(MEMO-INF-92-59; TIOS-92-26; ETN-93-93837) Copyright Avail: CASI HC A03

Due to the protocol processing bottleneck in communication nodes being the most significant limiting factor of high speed networks, solutions for efficient implementations have to be developed. Dedicated hardware implementations can exploit the parallelism inherent in protocol processing. A discussion on network interfaces designed to offload protocol processing from the host computer is presented. The designs are analyzed in order to answer some questions about the necessity of the automatic synthesis of protocol processing hardware. ESA

N93-28534# Nagoya Univ. (Japan). Plasma Science Center.
LARGE AMPLITUDE STRIATIONS IN AN RF DISCHARGE
Teruyuki Sato, Tatsuo Shoji, Youichi Sakawa, and Mitsuyoshi Hori May 1992 14 p
(DE93-753244; PSC-19) Avail: CASI HC A03/MF A01

Paired luminous rings separated by a narrow dark-gap are observed in a radio-frequency discharge. In the discharge, a 0.8 - 5 MHz radio-frequency field with an amplitude of (+-)0.5 - (+-)1.7 kV is applied to two 100 mm wide electrodes, separated by 20 - 100 mm, surrounding a 100 mm diameter pyrex glass tube containing hydrogen gas of 1 - 50 Torr. The number of paired rings, which are axially symmetric with respect to the midplane of two electrodes, increases with the hydrogen gas pressure. The time resolved light intensity measurements show that the outer rings near the electrodes start to appear early in time then the inner rings are produced later. DOE

N93-28555# Federal Aviation Administration, Atlantic City, NJ.
TIME DELAY MEASUREMENTS OF CURRENT PRIMARY FAA AIR/GROUND TRANSMITTERS AND RECEIVERS
John Petro and Philip Randazzo Jun. 1993 25 p
(DOT/FAA/CT-TN93/14) Avail: CASI HC A03/MF A01

The results of tests performed by ACW-300B, Spectrum Engineering Group, in determining the amount of time delay present in various air/ground communications equipment are detailed. This test was comprised of an Federal Aviation Administration (FAA) Air Navigation Ground Radio Transmitter (AN-GRT-21) and an FAA Air Navigation Ground Radio Receiver (AN-GRR-23): two aircraft transceivers, a King KTR-905 very high frequency (VHF) transceiver, and a Collins VHF-251 Technical Standard Order (TSO) transceiver Author (revised)

N93-28588# Dartmouth Coll., Hanover, NH.
DEVELOPMENT OF AN AIRBORNE MMW FM-CW RADAR FOR MAPPING RIVER ICE
Norbert E. Yankielum, Michael G. Ferrick, and Patricia B. Weyrick Jan. 1993 15 p
(Contract DACA89-90-K-0003; DA Proj. 4A7-62784-AT-42)
(AD-A262655; CRREL-93-1) Avail: CASI HC A03/MF A01

Analyses of a river's freezeup ice cover stability and its breakup rely on detailed knowledge of the cover's thickness and the variability of that thickness. A high-resolution, millimeter wave (26.5- to 40-GHz) Frequency Modulated-Continuous Wave radar with real-time data acquisition and digital signal processing and display capability was deployed from a low-flying (3-10 m) helicopter to continuously acquire, process and display data during an ice thickness profiling survey of a 24-km study reach. A nominal sheet ice thickness of 50 cm, occasional areas of new ice sheet as thin as 5 cm, open leads, and massive ice accumulations on the order of 5 m thick were encountered. Radar profiling data agreed with ground truth from borehole measurements of the sheet ice, and provided a more detailed view of the ice conditions than that obtained from a low altitude video survey. The radar system provided rapid, safe and accurate data acquisition, allowing detailed mapping of the ice conditions throughout the reach. DTIC

N93-28654# Naval Postgraduate School, Monterey, CA.
PREDICTING RADIATION CHARACTERISTICS FROM ANTENNA PHYSICAL DIMENSIONS M.S. Thesis
Daniel S. Dietrich Dec. 1992 286 p
(AD-A262462) Avail: CASI HC A13/MF A03

The fundamental theory and equations used in writing a set of software applications which predict antenna radiation parameters are explained. Each application predicts the radiation characteristics of a particular type of antenna over a planar surface which serves as a model of either earth or seawater. The radiation parameter predictions are based solely on an antenna's physical dimensions, the properties of the underlying surface, and electromagnetic theory. Existing electric field equations provide the basis for radiation parameter predictions, and the accuracy of the predicted radiation parameters is totally dependent upon the extent to which the electric field equations used realistically model the actual radiated electromagnetic fields of the antennas. In addition to a review of applicable electromagnetic field theory, this report is also intended to be a user's guide for the corresponding computer applications. The appendices contain computer hardcopies of sample calculations for several antenna types and remarks regarding the conformity of predicted radiation parameters to expectations. Radiation parameters computed thus far are consistent with expectations based on other computational programs and empirical measurements. DTIC

N93-28655# Massachusetts Inst. of Tech., Cambridge.
GROUND CLUTTER MEASUREMENTS FOR SURFACE-SITED RADAR
J. B. Billingsley 1 Feb. 1993 96 p
(Contract F19628-90-C-0002)
(AD-A262472; MIT-TR-786-Rev-1; ESC-TR-92-135) Avail: CASI HC A05/MF A01

A large volume of radar ground clutter measurement data was collected from many sites that are widely dispersed over the North American continent. At each site backscatter was recorded from all the terrain within the field of view, typically to ranges extending to 25 or 50 km. As a result, in most of these measurements the angle of illumination of the earth's surface was usually very low, typically within a degree or so of grazing incidence, with much intermittent shadowing of low regions. The nature of low-angle radar ground clutter as it has come to be understood through analysis of this extensive new base of measurements is examined. Depression angle, that is, the angle below the horizontal at which the backscattering terrain point is observed at the radar antenna, is shown to be the principal parametric influence on clutter amplitude statistics, even for the very low angles and small (i.e., typically fractional) variations in angle that occur in surface-sited radar. This principal role of depression angle is the result of its effect on shadowing in a sea of patchy visibility and discrete or localized scattering sources. Following this understanding, a general predictive model for ground clutter spatial amplitude statistics is developed based on very precise computation of depression angle but on only relatively gross specification of terrain type. The important radar parameters entering the model are radar frequency as it affects mean strength of clutter amplitude distributions and spatial resolution as it affects spread in these distributions. DTIC

N93-28689 North Carolina Univ., Chapel Hill.
MULTIFRACTAL ANALYSIS OF RADIO LOBES Ph.D. Thesis
David Reed DeGraff 1992 241 p
Avail: Univ. Microfilms Order No. DA9309863

The synchrotron surface brightness of several large angular size radio sources (the radio galaxies Cygnus A (at both 6 and 20 centimeters) 3C436, 3C353 (both at 20 cm) as well as the quasar 3C 175 (at 6 cm)) were analyzed in terms of their fractal properties. All the galaxies show remarkably similar fractal spectra, different from those seen in terrestrial examples of hydrodynamic turbulence. The quasar has a slightly different spectrum, more closely resembling terrestrial examples. To reach a physical interpretation of these results, multifractal models were used to simulate synchrotron radio emission in four different cases: (1) a multifractal distribution of electron energies with uniform magnetic field, (2) a multifractal distribution of magnetic field strengths containing a monoenergetic electron distribution, (3) multifractal distribution of electron number densities with uniform magnetic field, and (4) a power law electron energy distribution in a multifractal distribution of magnetic field strengths. With the additional constraint that the simulations produce the observed synchrotron emission spectrum, the fractal spectra of the simulations were compared to the observed fractal spectra of the radio lobes. Only the quasar was well represented by the fractal spectrum both in terms of the width of the spectrum, and the fractal dimension of the minimum and maximum alpha values. The simulations were too wide, and did not have elevated values for f(alpha(sub min)) even when the magnetic fields fractal spectrum f(alpha(sub min)) values were elevated. Multifractal analysis is shown to be a powerful tool for interpreting the turbulence inside the lobes of radio galaxies and quasars. By comparing the fractal spectra of observed radio lobes at different frequencies, to various simulated multifractal spectra, one can infer details of the lobe physics. This will have implications for numerical magnetohydrodynamic (MHD) simulations of these objects. Author (revised)

N93-28896# Oxford Univ. (England). Robotics Research Group.
A CORNER MATCHING AND TRACKING STRATEGY APPLIED TO VIDEOPHONY
Larry S. Shapiro, Han Wang, and J. Michael Brady May 1992 64 p
Sponsored in part by ORS, United Kingdom, and Foundation for Research Development, Republic of South Africa
(OUEL-1933/92; ETN-93-93876) Avail: CASI HC A04/MF A01

The problem of tracking independently moving (and possibly non rigid) objects over long periods of time, where object motion occurs relative to a single camera, is addressed. This research was motivated by the videoconferencing application, which requires a reliable matching algorithm to operate at high speed on lengthy image sequences. Focus is primarily on the low level 'front end' of such a system; the data that emerge are intended to feed into trajectory analysis modules which will group features into coherently moving objects and estimate their three dimensional motion. One such module, to segment moving features from stationary ones, is also described. The study builds upon a previously developed 'corner' finder that runs at 14 Hz on T800 transputers. These 'corners' are curvature extrema in the image intensity surface, and have already served successfully as features in a stereomatching algorithm. This work is extended to the general motion case (single camera), which introduces both benefits and complications: the former because temporal integration facilitates noise resistance and allows ambiguities to be resolved in time, and the latter because objects can change over time in ways they can not change over space alone. The framework presented has two parts: a matcher, which performs short range correspondence on the basis of just two frames, and a tracker, which interprets this information and maintains a spatio-temporal trajectory for each feature. The utility of corners as correspondence tokens is demonstrated and their extraction mechanism is described. The matcher and tracker subsystems are discussed, with a review of relevant literature and experimental results. A simple module to distinguish between moving and stationary points is presented and directions for future research are given. ESA

N93-28900# Los Alamos National Lab., NM.
A PROPOSED APPROACH FOR DEVELOPING NEXT-GENERATION COMPUTATIONAL ELECTROMAGNETICS SOFTWARE
E. K. Miller, R. P. Kruger, and S. Moraites (Simulated Life Systems, Inc., Chambersburg, PA.) 1993 29 p Presented at the 7th Annual Review of Progress in Applied Computational Electromagnetics, Monterey, CA, 19-21 Mar. 1991
(Contract W-7405-eng-36)
(DE93-007326; LA-UR-93-428; CONF-9103123-4) Avail: CASI HC A03/MF A01

Computations have become a tool coequal with mathematics and measurements as a means of performing electromagnetic analysis and design. This is demonstrated by the volume of articles and meeting presentations in which computational electromagnetics (CEM) is routinely employed to address an increasing variety of problems. Yet, in spite of the substantial resources invested in CEM software over the past three decades, little real progress seems to have been made towards providing the EM engineer software tools having a functionality equivalent to that expected of hardware instrumentation. Furthermore, the bulk of CEM software now available is generally of limited applicability to large, complex problems because most modeling codes employ a single field propagator, or analytical form, of Maxwell's Equations. The acknowledged advantages of hybrid models, i.e., those which employ different propagators in differing regions of a problem, are relatively unexploited. The thrust of this discussion is to propose a new approach designed to address both problems outlined above, integrating advances being made in both software and hardware development. After briefly reviewing the evolution of modeling CEM software to date and pointing out the deficiencies thereof, we describe an approach for making CEM tools more truly 'user friendly' called EMSES (Electromagnetic Modeling and Simulation Environment for Systems). This will be achieved through two main avenues. One is developing a common problem-description language implemented in a visual programming environment working together with a translator that produces the specific model description needed by various numerical treatments, in order to optimize user efficiency. The other is to employ a new modeling paradigm based on the idea of field propagators to expedite the development of the hybrid models that are needed to optimize computation efficiency. DOE

N93-28909# Los Alamos National Lab., NM.
HIGH-RESOLUTION SIGNAL SYNTHESIS FOR TIME-FREQUENCY DISTRIBUTIONS
G. S. Cunningham and W. J. Williams 1993 5 p Presented at the IEEE International Conference on Acoustics, Speech, and Signal Processing, Minneapolis, MN, 27-30 Apr. 1993
(Contract W-7405-eng-36)
(DE93-008735; LA-UR-93-638; CONF-930489-2) Avail: CASI HC A01/MF A01

Bilinear time-frequency distributions (TFD's) offer improved resolution over linear nine-frequency representations (TFR's), but many TFD's are costly to evaluate and are not associated with signal synthesis algorithms. Recently, the spectrogram (SP) decomposition and weighted reversal correlator decomposition have been used to define low-cost, high-resolution TFD's. In this paper, we show that the vector-valued 'square-root' of a TFD (VVTFR) provides a representational underpinning for the TFD. By synthesizing signals from modified VVTFR's, we define high-resolution signal synthesis algorithms associated with TFD's. The signal analysis and synthesis packages can be implemented as weighted sums of SP/short-time Fourier Transform signal analysis and synthesis packages, which are widely available, allowing the interested non-specialist easy access to high-resolution methods. DOE

N93-28955*# National Aeronautics and Space Administration. Pasadena Office, CA.
A SATELLITE-TRACKING MILLIMETER-WAVE REFLECTOR ANTENNA SYSTEM FOR MOBILE SATELLITE-TRACKING Patent Application
Arthur C. Densmore, inventor (to NASA) (Jet Propulsion Lab., California Inst. of Tech., Pasadena.), Vahraz Jamnejad, inventor (to NASA) (Jet Propulsion Lab., California Inst. of Tech., Pasadena.), and Kenneth E. Woo, inventor (to NASA) (Jet Propulsion Lab., California Inst. of Tech., Pasadena.) 30 Nov. 1992 37 p
(Contract NAS7-918)
(NASA-Case-NPO-18772-1-CU; NAS 1.71:NPO-18772-1-CU; US-Patent-Appl-SN-999794) Avail: CASI HC A03/MF A01

A miniature dual-band two-way mobile satellite tracking antenna system mounted on a movable ground vehicle includes a miniature parabolic reflector dish having an elliptical aperture with major and minor elliptical axes aligned horizontally and vertically, respectively, to maximize azimuthal directionality and minimize elevational directionality to an extent corresponding to expected pitch excursions of the movable ground vehicle. A feed-horn has a back end and an open front end facing the reflector dish and has vertical side walls opening out from the back end to the front end at a lesser horn angle and horizontal top and bottom walls opening out from the back end to the front end at a greater horn angle. An RF circuit couples two different signal bands between the feed-horn and the user. An antenna attitude controller maintains an antenna azimuth direction relative to the satellite by rotating it in azimuth in response to sensed yaw motions of the movable ground vehicle so as to compensate for the yaw motions to within a pointing error angle. The controller sinusoidally dithers the antenna through a small azimuth dither angle greater than the pointing error angle while sensing a signal from the satellite received at the reflector dish, and deduces the pointing angle error from dither-induced fluctuations in the received signal. NASA

N93-28997# Rome Lab., Griffiss AFB, NY.
MODIFIED ACOUSTO-OPTIC ADAPTIVE PROCESSOR (MOD-AOAP) Inhouse Report, Feb. 1989 - Jun. 1992
Christopher W. Keefer, John E. Malowicki, and Paul M. Payson Dec. 1992 35 p
(AD-A261983; RL-TR-92-310) Avail: CASI HC A03/MF A01

Multipath jamming noise introduced into a radar antenna's sidelobes effectively reduces the radar's target detection capability. The acousto-optic adaptive processor (AOAP) was developed to demonstrate an optical implementation of the least mean square (LMS) algorithm for adaptively cancelling noise jamming. The AOAP system demonstrated 30 dB cancellation of monotone CW signals, with degraded performance as the bandwidth increased. The liquid crystal light valve (LCLV), used as the integrator/ spatial light modulator in the AOAP, has been identified as limiting system performance. In this report we report on modifications to the AOAP. Specifically, the LCLV has been replaced with a photorefractive crystal. Cancellation performance and cancellation speed of the mod-AOAP are presented and compared to the original results. DTIC

N93-28998# Rome Lab., Griffiss AFB, NY.
MULTICHANNEL DETECTION OF PARTIALLY CORRELATED SIGNALS IN CLUTTER Inhouse Report, Nov. 1991 - Oct. 1992
James H. Michels Dec. 1992 53 p
(AD-A261984; RL-TR-92-332) Avail: CASI HC A04/MF A01

This report considers the Gaussian multichannel binary detection problem in which the signal and non-white clutter noise are Gaussian vector processes with unknown statistics. A generalized likelihood ratio using multichannel innovations processes is implemented via a model-based approach where the signal and clutter are assumed to be characterized by autoregressive vector processes with arbitrary temporal and cross-channel correlation. The innovations processes are obtained through linear estimation using multichannel parameter estimates. Detection performance is considered as the estimates approach steadystate with increasing data block sample sizes. Results for two-channel signal and clutter noise vectors with various temporal and cross-channel correlation are obtained using a Monte-Carlo procedure. In the transient-state (estimation with limited data), the detection results are considered as a function of the data batch sizes used in parameter estimation. Furthermore, it is noted that the detection performance in the transient-state is related to that of the estimator which, in turn, has its own dependence upon process correlation. The results provide insight regarding the factors which control the processing time requirements to achieve a specified level of detection performance. DTIC

N93-29011# Mission Research Corp., Santa Barbara, CA.
ELECTROMAGNETIC DIFFUSION AND WIRE COUPLING Final Report, Sep. 1987 - Apr. 1988
Bart Goldstein and Rudolf Goldflam Apr. 1993 107 p
(Contract DAAL02-87-C-0113)
(AD-A263183; MRC-R-1156; ARL-CR-54) Avail: CASI HC A06/MF A02

This report documents the research performed to develop physical insight into the coupling of radiated, pulsed, electromagnetic energy to a thin wire located inside a rectangular metallic enclosure. The electromagnetic fields diffuse into the rectangular cavity. The cavity size is not small compared to the wavelengths in the exciting field. A prime objective was to determine how the wire transients will change due to the parameters of cavity size, wire locations and orientation, and incident pulse parameters such as polarization, risetime, and decay time. The approach involved frequency domain analysis based on three distinct frequency regimes: low, intermediate, and high. In the low frequency region the skin depth is larger than the wall thickness of the enclosure. The intermediate region extends to the lowest internal mode of the enclosure. The high frequency region extends upward from the lowest mode. validation of the analytical results, planned under Phase 2 of the SBIR, were not performed. DTIC

N93-29087* National Aeronautics and Space Administration. Pasadena Office, CA.
MINIATURE MODULAR MICROWAVE END-TO-END RECEIVER Patent
Lin M. Sukamto, inventor (to NASA) (Jet Propulsion Lab., California Inst. of Tech., Pasadena.), Thomas W. Cooley, inventor (to NASA) (Jet Propulsion Lab., California Inst. of Tech., Pasadena.), Michael A. Janssen, inventor (to NASA) (Jet Propulsion Lab., California Inst. of Tech., Pasadena.), and Gary S. Parks, inventor (to NASA) (Jet Propulsion Lab., California Inst. of Tech., Pasadena.) 8 Jun. 1993 17 p Filed 3 Dec. 1991 Supersedes N92-30103 (30 - 20, p 3437)
(Contract NAS7-918)
(NASA-Case-NPO-18713-1-CU; US-Patent-5,218,357; US-Patent-Appl-SN-802078; US-Patent-Class-342-351; US-Patent-Class-343-700; US-Patent-Class-361-394; US-Patent-Class-257-712; Int-Patent-Class-G01S-3/02; Int-Patent-Class-H05K-5/00; Int-Patent-Class-H01L-23/02) Avail: US Patent and Trademark Office

An end-to-end microwave receiver system contained in a single miniature hybrid package mounted on a single heatsink is presented. It includes an input end connected to a microwave receiver antenna and an output end which produces a digital count proportional to the amplitude of a signal of a selected microwave frequency band received at the antenna and corresponding to one of the water vapor absorption lines near frequencies of 20 GHz or 30 GHz. The hybrid package is on the order of several centimeters in length and a few centimeters in height and width. The package includes an L-shaped carrier having a base surface, a vertical wall extending up from the base surface and forming a corner therewith, and connection pins extending through the vertical wall. Modular blocks rest on the base surface against the vertical wall and support microwave monolithic integrated circuits on top surfaces thereof connected to the external connection pins. The modular blocks lie end-to-end on the base surface so as to be modularly removable by sliding along the base surface beneath the external connection pins away from the vertical wall.
Official Gazette of the U.S. Patent and Trademark Office

N93-29105*# Arizona Univ., Tucson. Inst. of Atmospheric Physics.
DEVELOPMENT OF A 9.3 MICROMETER CW LIDAR FOR THE STUDY OF ATMOSPHERIC AEROSOL Final Technical Report, 14 Feb. 1989 - 12 Jan. 1993
B. N. Whiteside and R. M. Schotland 29 Jun. 1993 100 p
(Grant NAG8-766)
(NASA-CR-193227; NAS 1.26:193227) Avail: CASI HC A05/MF A02

This report provides a brief summary of the basic requirements to obtain coherent or heterodyne mixing of the optical radiation backscattered by atmospheric aerosols with that from a fixed frequency source. The

continuous wave (CW) mode of operation for a coherent lidar is reviewed along with the associated lidar transfer equation. A complete optical design of the three major subsystems of a CW, coherent lidar is given. Lens design software is implemented to model and optimize receiver performance. Techniques for the opto-mechanical assembly and some of the critical tolerances of the coherent lidar are provided along with preliminary tests of the subsystems. Included in these tests is a comparison of the experimental and the theoretical average power signal-to-noise ratio. The analog to digital software used to evaluate the power spectrum of the backscattered signal is presented in the Appendix of this report.
Author (revised)

N93-29131# Cornell Univ., Ithaca, NY.
FEMTOSECOND CARRIER PROCESSES IN COMPOUND SEMICONDUCTORS AND REAL TIME SIGNAL PROCESSING Annual Report
J. P. Krusius 10 Mar. 1993 279 p
(Contract F49620-90-C-0039)
(AD-A263076) Avail: CASI HC A13/MF A03

This report is the annual report on research conducted under the auspices of the Joint Services Electronics Program at Cornell University. The research is grouped under two themes: (1) femtosecond carrier processes in compound semiconductors; and (2) real time signal processing. Results on OMVPE materials growth, femtosecond laser probing of hot carriers, and ensemble Monte Carlo simulations are reported on under the first theme. Accomplishments on VLSI algorithms, fault tolerant architectures, and architectures with multiple functional units for signal processing are given under the second theme. DTIC

N93-29202# National Telecommunications and Information Administration, Boulder, CO. Inst. for Telecommunication Sciences.
WIDEBAND PROPAGATION MEASUREMENTS FOR WIRELESS INDOOR COMMUNICATION
Peter B. Papazian, Yeh Lo, Elizabeth E. Pol, Michael P. Roadifer, Thomas G. Hoople, and Robert J. Achatz Jan. 1993 39 p
(PB93-175123; NTIA-93-292) Avail: CASI HC A03/MF A01

Wideband impulse response measurements were made to characterize proposed radio data channels in three indoor environments. The measurement system employed a 1.5 GHz carrier which was biphase shift key (BPSK) modulated using a 100 Mb/s pseudo-random code. By using a correlation receiver, the channel cophase and quadphase responses were measured and stored for later processing. Data processing included calculation of delay spread, correlation bandwidth (BW), and signal attenuation. The raw data are stored in binary form on tape and disk for further indoor propagation channel studies. NTIS

N93-29217*# Interferometrics, Inc., Vienna, VA.
INTERFEROMETRIC TRACKING SYSTEM FOR THE TRACKING AND DATA RELAY SATELLITE
John E. Effland, Curtis A. Knight, and John C. Webber 26 May 1993 22 p
(Contract NAS5-30313)
(NASA-CR-193274; NAS 1.26:193274; SBIR-07.03-8500) Avail: CASI HC A03/MF A01

This report documents construction and testing of the Interferometric Tracking System project developed under the NASA SBIR contract NAS5-30313. Manuals describing the software and hardware, respectively entitled: 'Field Station Guide to Operations' and 'Field Station Hardware Manual' are included as part of this final report. The objective of this contract was to design, build, and operate a system of three ground stations using Very Long Baseline Interferometry techniques to measure the TDRS orbit. The ground stations receive signals from normal satellite traffic, store these signals in co-located computers, and transmit the information via phone lines to a central processing site which correlates the signals to determine relative time delays. Measurements from another satellite besides TDRS are used to determine clock offsets. A series of such measurements will ultimately be employed to derive the orbital parameters, yielding positions accurate to within 50 meters or possibly better. Author

N93-29244# Oak Ridge National Lab., TN.
WAVELET TRANSFORM TECHNIQUES AND SIGNAL ANALYSIS
R. B. Perez (Tennessee Univ., Knoxville.), J. K. Mattingly (Tennessee Univ., Knoxville.), and J. S. Perez (Universidad Politecnica de Madrid, Spain.) 1993 8 p Presented at the American Nuclear Society (ANS) Annual Meeting, San Diego, CA, 20-24 Jun. 1993
(Contract DE-AC05-84OR-21400)
(DE93-007919; CONF-930601-4) Avail: CASI HC A02/MF A01

Traditionally, the most widely used signal analysis tool is the Fourier transform which, by producing power spectral densities (PSD's), allows time dependent signals to be studied in the frequency domain. However, the Fourier transform is global - it extends over the entire time domain - which makes it ill-suited to study nonstationary signals which exhibit local temporal changes in the signal's frequency content. To analyze nonstationary signals, the family of transforms commonly designated as short-time Fourier transforms (STFT's), capable of identifying temporally localized changes in the signal's frequency content, were developed by employing window functions to isolate temporal regions of the signal. For example, the Gabor STFT uses a Gaussian window. However, the applicability of STFT's is limited by various inadequacies. The Wavelet transform (WT), recently developed by Grossman and Morlet and explored in depth by Daubechies and Mallat, remedies the inadequacies of STFT's. Like the Fourier transform, the WT can be implemented as a discrete transform (DWT) or as a continuous (integral) transform (CWT). Some of the potential applications of the wavelet transform algorithms to signal analysis is briefly illustrated.
DOE

N93-29245# Fermi National Accelerator Lab., Batavia, IL.
A COMPARISON OF HIGH-SPEED LINKS, THEIR COMMERCIAL SUPPORT AND ONGOING R/D ACTIVITIES
H. L. Gonzalez, E. Barsotti, S. Zimmermann, M. Nomachi, and O Sasaki Oct. 1992 5 p Presented at the Institute of Electrical and Electronic Engineers (IEEE) Nuclear Science Symposium and Medical Imaging Conference, Orlando, FL, 26-31 Oct. 1992
(Contract DE-AC02-76CH-03000)
(DE93-008134; FNAL/C-92/288; CONF-921005-28) Avail: CASI HC A01/MF A01

Technological advances and a demanding market have forced the development of higher bandwidth communication standards for networks, data links, and busses. Most of these emerging standards are gathering enough momentum that their widespread availability and lower prices are anticipated. The hardware and software that support the physical media for most of these links is currently available, allowing the user community to implement fairly high-bandwidth data links and networks with commercial components. Also, switches needed to support these networks are available or being developed. The commercial support of high-bandwidth data links, networks, and switching fabrics provides a powerful base for the implementation of high-bandwidth data acquisition systems. A large data acquisition system like the one for the Solenoidal Detector Collaboration (SDC) at the SSC can benefit from links and networks that support an integrated systems engineering approach, for initialization, downloading, diagnostics, monitoring, hardware integration, and event data readout. The issue that our current work addresses is the possibility of having a channel/network that satisfies the requirements of an integrated data acquisition system. A brief description of high-speed communication links and protocols that we consider of interest for high energy physics data acquisition systems are presented. The protocols to be covered are High Performance Parallel Interface (HIPPI), Serial HIPPI, Fibre Channel (FC), and Scalable Coherent Interface (SCI). In addition, the initial work required to implement an SDC-like data acquisition system is described. DOE

N93-29266# Technische Univ., Eindhoven (Netherlands).
SPEECH RECOGNITION BY RECURSIVE STOCHASTIC MODELLING Ph.D. Thesis
Joannes Josephus Nijtmans 1992 174 p
(ISBN-90-9005038-8; ETN-93-93576) Copyright Avail: CASI HC A08/MF A02

The application of algorithms for automatic speech recognition is described. Parameters to describe a speech signal were searched for from which log area ratio parameters were chosen. Based on these parameters, a segmentation algorithm was developed. The recognition process was then discussed. A new method was developed based on a new model: the Recursive Markov Model (RMM) which is an extension of the existing Hiddem Markov Model (HMM) and has the advantage of shorter computations, hierarchical modeling, and state sharing. Results of tests of the implemented algorithms are given and the relative merits of the methods of speech recognition are considered. ESA

N93-29275 Department of the Navy, Washington, DC.
TIME-INTERPOLATION METHOD FOR DIGITAL BEAMFORMERS Patent
John Green, inventor (to Navy) 2 Mar. 1993 6 p Filed 22 Jan. 1991
(AD-D015709; US-Patent-5,191,546; US-Patent-Appl-SN-643257; US-Patent-Class-364-723) Avail: US Patent and Trademark Office

An improved time-interpolation method for digital time-domain beamformers is provided. The method determines an input channel value at a known fractional delay as a two-stage process. In a first stage, input channel parameters common to all beams and independent of the known fractional delay are determined. In a second stage, the input channel parameters are weighted and summed for each beam to determine the input channel value at the known fractional delay. Weighting of the parameters is based upon the known fractional delay and the frequency band of interest. DTIC

N93-29280 Department of the Navy, Washington, DC.
HYBRID DATA LINK Patent
Jack E. Holzschuh, inventor (to Navy) and John D. Hightower, inventor (to Navy) 16 Feb. 1993 6 p Filed 20 Apr. 1992
(AD-D015714; US-Patent-5,186,414; US-Patent-Appl-SN-871255; US-Patent-Class-244-3.12) Avail: US Patent and Trademark Office

A high data rate over-the-horizon communications capability is provided between two or more platforms at rest or in motion, in the air or on the surface. An RF transmitter/receiver-optical fiber interface unit is launched from a launch platform and is supported via a deployed parachute or balloon to provide a bidirectional RF data link with the launch platform and a bidirectional optical data link over an optical fiber extending to an autonomous vehicle platform, such as a missile. DTIC

N93-29308# Pacific Northwest Lab., Richland, WA.
STABILIZED PLATFORM FOR TETHERED BALLOON SOUNDINGS OF BROADBAND LONG- AND SHORT-WAVE RADIATION
J. M. Alzheimer, G. A. Anderson, and C. D. Whiteman Jan. 1993 7 p Presented at the 73rd American Meteorological Society (AMS) Annual Meeting, Anaheim, CA, 17-22 Jan. 1993
(Contract DE-AC06-76RL-01830)
(DE93-007876; PNL-SA-21089; CONF-930133-8) Avail: CASI HC A02/MF A01

Changes in the composition of trace gases in the earth's atmosphere have been reported by many observers, and a general concern has been expressed regarding possible changes to the earth's climate that may be caused by radiatively active gases introduced into the earth's atmosphere by man's activities. Radiatively active trace gases produce temperature changes in the earth's atmosphere through changes in radiative flux divergence. Our knowledge of and means of measuring radiative flux divergence is very limited. A few observations of vertical radiative flux divergences have been reported from aircraft from radiometersondes from towers and from large tethered balloons. These measurement techniques suffer from one or more drawbacks, including shallow sounding depths (towers), high cost (aircraft), complicated logistics (large tethered balloons), and limitation to nighttime hours (radiometersondes). Changes in radiative flux divergence caused by anthropogenic trace gases are expected to be quite small, and will be difficult to measure with existing broadband radiative flux instruments. The emphasis of present research in global climate change is thus being focused on improving radiative transfer algorithms in global climate models. The radiative parameterizations in these models are at an early stage of development and information is needed regarding their performance, especially in cloudy conditions. The impetus for the research reported is the need for a device that can supplement existing means of measuring vertical profiles of long- and short-wave irradiance and radiative flux divergence. A small tethered-balloon-based system that can make radiometric soundings through the atmospheric boundary layer was designed. The concept, the design considerations, and the design and construction of this sounding system are discussed. The performance of the system will be tested in a series of balloon flights scheduled for the fall and winter of 1992. DOE

N93-29348# Oak Ridge National Lab., TN.
LEAKY COAXIAL CABLE SIGNAL TRANSMISSION FOR REMOTE FACILITIES
S. F. Smith and R. I. Crutcher 1993 8 p Presented at the 5th Topical Meeting on Robotics and Remote Systems, Knoxville, TN, 26-29 Apr. 1993
(Contract DE-AC05-84OR-21400)
(DE93-007916; CONF-930403-20) Avail: CASI HC A02/MF A01

To develop reliable communications methods to meet the rigorous requirements for nuclear hot cells and similar environments, including control of cranes, transporters, and advanced servomanipulators, the Consolidated Fuel Reprocessing Program (CFRP) at Oak Ridge National Laboratory (ORNL) has conducted extensive tests of numerous technologies to determine their applicability to remote operations. To alleviate the need for large bundles of cables that must accommodate crane/transporter motion relative to the boundaries of the cell, several transmission techniques are available, including slotted-line radio-frequency couplers, infrared beams, fiber-optic cables, free-space microwave, and inductively coupled leaky coaxial cable. This paper discusses the general characteristics, mode of operation, and proposed implementation of leaky coaxial cable technology in a waste-handling facility scheduled to be built in the near future at ORNL. In addition, specific system hardware based around the use of leaky coaxial cable is described in detail. Finally, data from a series of radiation exposure tests conducted by the CFRP on several samples of the basic leaky coaxial cable and associated connectors are presented. DOE

N93-29407# Defence Research Establishment, Ottawa (Ontario).
THEORETICAL BIT ERROR RATE PERFORMANCE OF THE KALMAN FILTER EXCISOR FOR FM INTERFERENCE
Brian Kozminchuk Dec. 1992 46 p
(AD-A263018; DREO-1163) Avail: CASI HC A03/MF A01

This technical report develops a theoretical bit error rate expression for a Kalman filtering technique that is used for filtering narrowband interferers out of direct sequence spread spectrum signals. The approach is based on the digital phase-locked loop Kalman filter and is close to optimum in so far as demodulating an FM-type of interferer. Because the interference is assumed to be much stronger than either the signal or noise, the Kalman filter locks onto the interference and produces estimates of its phase and envelope. Several assumptions are made in the development of the theoretical bit error rate expression and these are expanded upon. It is shown and illustrated that theory agrees well with simulation as long as the bandwidth of the low pass filter used to determine the envelope of the interference is much less than the sampling rate, otherwise the interference estimate at the input to the interference canceller will have significant cross-correlation with the signal, leading to some cancellation of the spread spectrum signal. DTIC

N93-29438# Defence Research Establishment, Ottawa (Ontario).
SOFTWARE DEVELOPMENT AND ANALYSIS FOR EXPERIMENTAL HIGH FREQUENCY SURFACE WAVE RADAR DATA
H. C. Chan Dec. 1992 59 p
(AD-A261982; DREO-1153) Avail: CASI HC A04/MF A01

Processing software for data collected in an experimental High Frequency Surface Wave Radar (HFSWR) project is implemented in the VAX-3800 computer and the FPS-5000 floating point array process. The software is used to process the data in-house so as to obtain insights in HFSWR sea clutter, noise, and target characteristics. The data are examined to assess quality. Several deficiencies are observed in the data, including 60 Hz power source harmonic interferences and discontinuities in data sequences. Preliminary analysis of some of the data shows that conventional Doppler processing of the data permits the detection of ship and large aircraft targets at fairly long ranges. Plans for further analysis of these data are discussed. DTIC

N93-29455 Department of the Navy, Washington, DC.
OPTICAL ANTENNA BEAM STEERING USING DIGITAL PHASE SHIFTER CONTROL Patent
William D. Jemison, inventor (to Navy), R. Herczfeld, inventor (to Navy), and Arthur Paolella, inventor (to Navy) 17 Nov. 1992 11 p Filed 11 Mar. 1992

(AD-D015688; US-Patent-5,164,736; US-Patent-Appl-SN-853229; US-Patent-Class-342-368) Avail: US Patent and Trademark Office

A method and system for steering an antenna beam are provided. A light source emits light wherein at least one parameter of the emitted light is modulated. Modulated light is received by an optical detector and an analog control signal is provided by the optical detector in response to the modulated parameter. The control signal is applied to an analog-to-digital converter to convert the signal from analog to digital. The digital converter output signal is applied to a digital phase shifter for controlling the phase shift of the phase shifter and thereby steering an antenna beam according to the modulated parameter. The modulated parameter may be, for example, the intensity of the emitted light or the frequency of the emitted light. A plurality of converters and phase shifters may be provided for steering of phased array antennas. DTIC

N93-29507* National Aeronautics and Space Administration. Pasadena Office, CA.

PLANAR MICROSTRIP YAGI ANTENNA ARRAY Patent

John Huang, inventor (to NASA) 15 Jun. 1993 10 p Filed 28 Feb. 1991 Continuation-in-part of abandoned US-Patent-Appl-SN-501892, filed 30 Mar. 1990
(NASA-Case-NPO-17873-2-CU; US-Patent-5,220,335; US-Patent-Appl-SN-664445; US-Patent-Appl-SN-501892; US-Patent-Class-343-700MS; US-Patent-Class-343-819; US-Patent-Class-343-833; US-Patent-Class-343-834; Int-Patent-Class-H01Q-1/380; Int-Patent-Class-H01Q-19/300) Avail: US Patent and Trademark Office

A directional microstrip antenna includes a driven patch surrounded by an isolated reflector and one or more coplanar directors, all separated from a ground plane on the order of 0.1 wavelength or less to provide end fire beam directivity without requiring power dividers or phase shifters. The antenna may be driven at a feed point a distance from the center of the driven patch in accordance with conventional microstrip antenna design practices for H-plane coupled or horizontally polarized signals. The feed point for E-plane coupled or vertically polarized signals is at a greater distance from the center than the first distance. This feed point is also used for one of the feed signals for circularly polarized signals. The phase shift between signals applied to feed points for circularly polarized signals must be greater than the conventionally required 90 degrees and depends upon the antenna configuration.
Official Gazette of the U.S. Patent and Trademark Office

N93-29514# Cornell Univ., Ithaca, NY.

FEMTOSECOND CARRIER PROCESSES IN COMPOUND SEMICONDUCTORS AND REAL TIME SIGNAL PROCESSING Annual Report, 1 May 1992 - 30 Apr. 1993

J. P. Krusius 10 Mar. 1993 59 p
(Contract F49620-90-C-0039)
(AD-A262966) Avail: CASI HC A04/MF A01

This report is the annual report on research conducted under the auspices of the Joint Services Electronics Program at Cornell University. The research is grouped under two themes: (1) femtosecond carrier processes in compound semiconductors, and (2) real time signal processing. Results on OMVPE materials growth, femtosecond laser probing of hot carriers, and ensemble Monte Carlo simulations are reported on under the first theme. Accomplishments on VLSI algorithms, fault tolerance architectures, and architectures with multiple functional units for signal processing are given under the second theme. DTIC

N93-29586*# Jet Propulsion Lab., California Inst. of Tech., Pasadena.

THE TELECOMMUNICATIONS AND DATA ACQUISITION REPORT Progress Report, Jan. - Mar. 1993

Edward C. Posner, ed. 15 May 1993 209 p
(NASA-CR-193144; TDA-PR-42-113; NAS 1.26:193144) Avail: CASI HC A10/MF A03

This quarterly publication provides archival reports on developments in programs managed by JPL's Office of Telecommunications and Data Acquisition (TDA) in the following areas: space communications, radio navigation, radio science, and ground-based radio and radar astronomy. This document also reports on the activities of the Deep Space Network (DSN) in planning, supporting research and technology, implementation, and operations. Also included are standards activity at JPL for space data and information systems and reimbursable DSN work performed for other space agencies through NASA. The preceding work is all performed for NASA's Office of Space Communications (OSC). The TDA Office also performs work funded by another NASA program office through and with the cooperation of OSC. This is the Orbital Debris Radar Program with the Office of Space Systems Development. For individual titles, see N93-29587 through N93-29603.

N93-29587*# Jet Propulsion Lab., California Inst. of Tech., Pasadena.

AN IMPROVED LINEAR ION TRAP PHYSICS PACKAGE

J. D. Prestage *In its* The Telecommunications and Data Acquisition Report 15 May 1993 p 1-6 (For primary document see N93-29586 11-32)
(RTOP 310-10-62-15)
Avail: CASI HC A02/MF A03

This article describes an improvement in the architecture of the physics package used in the Linear Ion Trap (LIT)-based frequency standard recently developed at JPL. This new design is based on the observation that ions can be moved along the axis of an LIT by applied dc voltages. The state selection and interrogation region can be separated from the more critical microwave resonance region where the multiplied local oscillator signal is compared with the stable atomic transition. This separation relaxes many of the design constraints of the present units. Improvements include increased frequency stability and a substantial reduction in size, mass, and cost of the final frequency standard. Author (revised)

N93-29588*# Jet Propulsion Lab., California Inst. of Tech., Pasadena.

THE EFFECT OF CLOCK, MEDIA, AND STATION LOCATION ERRORS ON DOPPLER MEASUREMENT ACCURACY c04

J. K. Miller *In its* The Telecommunications and Data Acquisition Report 15 May 1993 p 7-21 (For primary document see N93-29586 11-32)
(RTOP 310-10-63-84-02)
Avail: CASI HC A03/MF A03

Doppler tracking by the Deep Space Network (DSN) is the primary radio metric data type used by navigation to determine the orbit of a spacecraft. The accuracy normally attributed to orbits determined exclusively with Doppler data is about 0.5 microradians in geocentric angle. Recently, the Doppler measurement system has evolved to a high degree of precision primarily because of tracking at X-band frequencies (7.2 to 8.5 GHz). However, the orbit determination system has not been able to fully utilize this improved measurement accuracy because of calibration errors associated with transmission media, the location of tracking stations on the Earth's surface, the orientation of the Earth as an observing platform, and timekeeping. With the introduction of Global Positioning System (GPS) data, it may be possible to remove a significant error associated with the troposphere. In this article, the effect of various calibration errors associated with transmission media, Earth platform parameters, and clocks are examined. With the introduction of GPS calibrations, it is predicted that a Doppler tracking accuracy of 0.05 microradians is achievable.
Author (revised)

N93-29589*# Jet Propulsion Lab., California Inst. of Tech., Pasadena.

PRECISE TRACKING OF THE MAGELLAN AND PIONEER VENUS ORBITERS BY SAME-BEAM INTERFEROMETRY. PART 2: ORBIT DETERMINATION ANALYSIS c13

W. M. Folkner, J. S. Border, S. Nandi, and K. S. Zukor *In its* The Telecommunications and Data Acquisition Report 15 May 1993 p 22-36 (For primary document see N93-29586 11-32)
(RTOP 310-10-63-88-01)
Avail: CASI HC A03/MF A03

A new radio metric positioning technique has demonstrated improved orbit determination accuracy for the Magellan and Pioneer Venus Orbiter orbiters. The new technique, known as Same-Beam Interferometry (SBI), is applicable to the positioning of multiple planetary rovers, landers, and orbiters which may simultaneously be observed in the same beamwidth of Earth-based radio antennas. Measurements of carrier phase are differenced between spacecraft and between receiving stations to determine the plane-of-sky components of the separation vector(s) between the spacecraft. The SBI measurements complement the information contained in line-of-sight Doppler measurements, leading to improved orbit determination accuracy. Orbit determination solutions have been obtained for a number of 48-hour data arcs using combinations of Doppler, differenced-Doppler, and SBI data acquired in the spring of 1991. Orbit determination accuracy is assessed by comparing orbit solutions from adjacent data arcs. The orbit solution differences are shown to agree with expected orbit determination uncertainties. The results from this demonstration show that the orbit determination accuracy for Magellan obtained by using Doppler plus SBI data is better than the accuracy achieved using Doppler plus differenced-Doppler by a factor of four and better than the accuracy achieved using only Doppler by a factor of eighteen. The orbit determination accuracy for Pioneer Venus Orbiter using Doppler plus SBI data is better than the accuracy using only Doppler data by 30 percent. Author

N93-29590*# Jet Propulsion Lab., California Inst. of Tech., Pasadena.
HIGH-POWER Ka-BAND AMPLIFIER c33
R. Cormier *In its* The Telecommunications and Data Acquisition Report 15 May 1993 p 37-45 (For primary document see N93-29586 11-32)
(RTOP 310-20-64-22)
Avail: CASI HC A02/MF A03

Development of a high-power tube suitable to power a Ka-band (34.5-GHz) antenna transmitter located at the Goldstone, California, tracking station is continuing. The University of Maryland Laboratory for Plasma Research and JPL are conducting a joint effort to test the feasibility of phase locking a second-harmonic gyrotron both by direct injection at the output cavity and by using a priming cavity to bunch the electrons in the beam. This article describes several design options and the results of computer simulation testing. Author

N93-29591*# Jet Propulsion Lab., California Inst. of Tech., Pasadena.
EXPERIMENTAL AND MODAL VERIFICATION OF AN INTEGRAL EQUATION SOLUTION FOR A THIN-WALLED DICHROIC PLATE WITH CROSS-SHAPED HOLES c33
L. W. Epp and P. H. Stanton *In its* The Telecommunications and Data Acquisition Report 15 May 1993 p 46-62 (For primary document see N93-29586 11-32)
(RTOP 310-20-64-86-02)
Avail: CASI HC A03/MF A03

In order to add the capability of an X-band uplink onto the 70-m antenna, a new dichroic plate is needed to replace the Pyle-guide-shaped dichroic plate currently in use. The replacement dichroic plate must exhibit an additional passband at the new uplink frequency of 7.165 GHz, while still maintaining a passband at the existing downlink frequency of 8.425 GHz. Because of the wide frequency separation of these two passbands, conventional methods of designing air-filled dichroic plates exhibit grating lobe problems. A new method of solving this problem by using a dichroic plate with cross-shaped holes is presented and verified experimentally. Two checks of the integral equation solution are described. One is the comparison to a modal analysis for the limiting cross shape of a square hole. As a final check, a prototype dichroic plate with cross-shaped holes was built and measured. Author (revised)

N93-29592*# Jet Propulsion Lab., California Inst. of Tech., Pasadena.
GRAVITY REFERENCED ELEVATION ENCODER DEVELOPMENT c35
R. E. Goddard *In its* The Telecommunications and Data Acquisition Report 15 May 1993 p 63-73 (For primary document see N93-29586 11-32)
(RTOP 310-20-65-67)
Avail: CASI HC A03/MF A03

Recent progress in the development of a gravity-sensor-based instrument for determining the elevation angle of DSN antennas is described. The benefits of such a system include the capability to locate the Gravity Referenced Elevation Encoder (GREE) directly on the primary reflector (thus bypassing structural flexure and deformation error sources), anticipated lower maintenance costs compared to the present gimbal encoders, direct replaceability, or supplementation of the present gimbal encoders and the utilization of off-the-shelf components to construct the GREE. This article includes a description of the nominal GREE design. Test results on a laboratory breadboard model are given. Rigid-body dynamics of the GREE are derived and the simulated performance in response to measured antenna vibrations is given. Author (revised)

N93-29593*# Jet Propulsion Lab., California Inst. of Tech., Pasadena.
A NOTE ON THE COMPUTATION OF ANTENNA-BLOCKING SHADOWS
R. Levy *In its* The Telecommunications and Data Acquisition Report 15 May 1993 p 74-79 (For primary document see N93-29586 11-32)
(RTOP 310-20-65-86-04)
Avail: CASI HC A02/MF A03

A simple and readily applied method is provided to compute the shadow on the main reflector of a Cassegrain antenna, when cast by the subreflector and the subreflector supports. The method entails some convenient minor approximations that will produce results similar to results obtained with a lengthier, mainframe computer program. Author

N93-29594*# Jet Propulsion Lab., California Inst. of Tech., Pasadena.
MAXIMUM AND MINIMUM RETURN LOSSES FROM A PASSIVE TWO-PORT NETWORK TERMINATED WITH A MISMATCHED LOAD
T. Y. Otoshi *In its* The Telecommunications and Data Acquisition Report 15 May 1993 p 80-88 (For primary document see N93-29586 11-32)
(RTOP 310-20-65-86-08)
Avail: CASI HC A02/MF A03

This article presents an analytical method for determining the exact distance a load is required to be offset from a passive two-port network to obtain maximum or minimum return losses from the terminated two-port network. Equations are derived in terms of two-port network S-parameters and load reflection coefficient. The equations are useful for predicting worst-case performances of some types of networks that are terminated with offset short-circuit loads. Author

N93-29595*# Jet Propulsion Lab., California Inst. of Tech., Pasadena.
THE GENERAL THEORY OF CONVOLUTIONAL CODES c61
R. J. McEliece (California Inst. of Tech., Pasadena.) and R. P. Stanley (California Inst. of Tech., Pasadena.) *In its* The Telecommunications and Data Acquisition Report 15 May 1993 p 89-98 (For primary document see N93-29586 11-32)
(RTOP 310-30-71-83-04)
Avail: CASI HC A02/MF A03

This article presents a self-contained introduction to the algebraic theory of convolutional codes. This introduction is partly a tutorial, but at the same time contains a number of new results which will prove useful for designers of advanced telecommunication systems. Among the new concepts introduced here are the Hilbert series for a convolutional code and the class of compact codes. Author (revised)

N93-29596*# Jet Propulsion Lab., California Inst. of Tech., Pasadena.
UNCORRECTABLE SEQUENCES AND TELECOMMAND
Laura Ekroot, R. McEliece (California Inst. of Tech., Pasadena.), S. Dolinar, and L. Swanson *In its* The Telecommunications and Data Acquisition Report 15 May 1993 p 99-105 (For primary document see N93-29586 11-32)
(RTOP 310-30-71-83-04)
Avail: CASI HC A02/MF A03

The purpose of a tail sequence for command link transmission units is to fail to decode, so that the command decoder will begin searching for the start of the next unit. A tail sequence used by several missions and recommended for this purpose by the Consultative Committee on Space Data Standards is analyzed. A single channel error can cause the sequence to decode. An alternative sequence requiring at least two channel errors before it can possibly decode is presented. (No sequence requiring more than two channel errors before it can possibly decode exists for this code.) Author

N93-29597*# Jet Propulsion Lab., California Inst. of Tech., Pasadena.
GALILEO POST-GASPRA CRUISE AND EARTH-2 ENCOUNTER c91
P. E. Beyer and M. M. Andrews *In its* The Telecommunications and Data Acquisition Report 15 May 1993 p 106-117 (For primary document see N93-29586 11-32)
(RTOP 314-40-22-37-01)
Avail: CASI HC A03/MF A03

This article documents DSN support for the Galileo cruise after the Oct. 1991 encounter with the asteroid Gaspra. This article also details the Earth-2 encounter and the special non-DSN support provided during the Earth-2 closest approach. Author (revised)

N93-29598*# Jet Propulsion Lab., California Inst. of Tech., Pasadena.
DSN SUPPORT OF MARS OBSERVER c81
M. R. Traxler *In its* The Telecommunications and Data Acquisition

Report 15 May 1993 p 118-122 (For primary document see N93-29586 11-32)
(RTOP 314-40-22-30-01)
Avail: CASI HC A01/MF A03

This article provides a summary of the DSN prelaunch, launch, and cruise support of the Mars Observer through Trajectory Correction Maneuver 2 (TCM-2) on 8 Feb. 1993. This summary includes planning, implementation, testing, DSN special configurations and DSN operational problems, and successes and challenges to date. Author (revised)

N93-29599*# Jet Propulsion Lab., California Inst. of Tech., Pasadena.
SIGNAL-TO-NOISE RATIO LOSSES IN FULL SPECTRUM COMBINING OF SIGNALS WITH A DOWNCONVERTED SUBCARRIER
Y. Feria and J. Statman *In its* The Telecommunications and Data Acquisition Report 15 May 1993 p 123-129 (For primary document see N93-29586 11-32)
(RTOP 314-30-61-02-10)
Avail: CASI HC A02/MF A03

This article presents the results of the signal-to-noise ratio loss in the process of full spectrum combining of signals with a downconverted subcarrier under imperfect conditions. These imperfect conditions not only include the misalignment of the carrier, the subcarrier, and the symbols, but they also include the nonideal filtering in the subcarrier downconversion process, the cutoff of the data bandwidth, and the distortion in signal waveform. Author

N93-29600*# Jet Propulsion Lab., California Inst. of Tech., Pasadena.
DSS-14 SUBREFLECTOR ACTUATOR DYNAMICS DURING THE LANDERS EARTHQUAKE **c46**
R. Levy and D. Strain *In its* The Telecommunications and Data Acquisition Report 15 May 1993 p 130-146 (For primary document see N93-29586 11-32)
(RTOP 314-30-45-10-21)
Avail: CASI HC A03/MF A03

The 28 Jun. 1992 Landers earthquake ground motion records at the Echo site (DSS-12 antenna) were adjusted to provide a better match with spectra from the measured Mars site (DSS-14 antenna) instrument tower response. A finite-element model of the antenna structural system was analyzed for response to this ground motion. Dynamic forces and displacements were computed in the locality of components that had failed during the earthquake. Calculated forces in the range of 30,000 to 35,000 lb on failed Y-axis actuator U-joints were consistent with laboratory load tests. The load capacity of these joints was found to be below the range of 34,000 to 42,000 lb. Dynamic amplification factors of from 6 to 16 were computed for the quadripod apex accelerations with respect to the ground accelerations. The largest factor--25--was found at the outboard end of the X-actuator. Author (revised)

N93-29601*# Jet Propulsion Lab., California Inst. of Tech., Pasadena.
AN ANALYSIS OF THE 70-METER ANTENNA HYDROSTATIC BEARING BY MEANS OF COMPUTER SIMULATION **c37**
R. D. Bartos *In its* The Telecommunications and Data Acquisition Report 15 May 1993 p 147-173 (For primary document see N93-29586 11-32)
(RTOP 314-30-42-10-87)
Avail: CASI HC A03/MF A03

Recently, the computer program 'A Computer Solution for Hydrostatic Bearings with Variable Film Thickness,' used to design the hydrostatic bearing of the 70-meter antennas, was modified to improve the accuracy with which the program predicts the film height profile and oil pressure distribution between the hydrostatic bearing pad and the runner. This article presents a description of the modified computer program, the theory upon which the computer program computations are based, computer simulation results, and a discussion of the computer simulation results. Author (revised)

N93-29602*# Jet Propulsion Lab., California Inst. of Tech., Pasadena.
ACOUSTIC CHARGE TRANSPORT TECHNOLOGY INVESTIGATION FOR ADVANCED DEVELOPMENT TRANSPONDER
S. Kayalar *In its* The Telecommunications and Data Acquisition Report 15 May 1993 p 174-183 (For primary document see N93-29586 11-32)
(RTOP 315-91-10-13-12)
Avail: CASI HC A02/MF A03

Acoustic charge transport (ACT) technology has provided a basis for a new family of analog signal processors, including a programmable transversal filter (PTF). Through monolithic integration of ACT delay lines with GaAs metal semiconductor field effect transistor (MESFET) digital memory and controllers, these devices significantly extend the performance of PTF's. This article introduces the basic operation of these devices and summarizes their present and future specifications. The production and testing of these devices indicate that this new technology is a promising one for future space applications. Author (revised)

N93-29603*# Jet Propulsion Lab., California Inst. of Tech., Pasadena.
THE FLIGHT PERFORMANCE OF THE GALILEO ORBITER USO
D. D. Morabito, T. P. Krisher, and S. W. Asmar *In its* The Telecommunications and Data Acquisition Report 15 May 1993 p 184-202 (For primary document see N93-29586 11-32)
(RTOP 314-40-31-30-26; RTOP 889-54-62-01)
Avail: CASI HC A03/MF A03

Results are presented in this article from an analysis of radio metric data received by the DSN stations from the Galileo spacecraft using an Ultrastable Oscillator (USO) as a signal source. These results allow the health and performance of the Galileo USO to be evaluated, and are used to calibrate this Radio Science instrument and the data acquired for Radio Science experiments such as the Redshift Observation, Solar Conjunction, and Jovian occultations. Estimates for the USO-referenced, spacecraft-transmitted frequency and frequency stability were made for 82 data acquisition passes conducted between launch (Oct. 1989) and Nov. 1991. Analyses of the spacecraft-transmitted frequencies show that the USO is behaving as expected. The USO was powered off and then back on in Aug. 1991 with no adverse effect on its performance. The frequency stabilities measured by Allan deviation are consistent with expected values due to thermal wideband noise and the USO itself at the appropriate time intervals. The Galileo USO appears to be healthy and functioning normally in a reasonable manner. Author (revised)

N93-29680 National Oceanic and Atmospheric Administration, Boulder, CO. Wave Propagation Lab.
RTE: A UNIX LIBRARY WITH ON-LINE DOCUMENTATION AND SAMPLE PROGRAMS FOR MICROWAVE RADIATIVE TRANSFER CALCULATIONS
J. C. Reynolds and J. A. Schroeder Mar. 1993 92 p See also PB92-129931 and PB92-227198 Limited Reproducibility: More than 20% of this document may be affected by microfiche quality
(PB93-180248; NOAA-TM-ERL-WPL-229) Avail: CASI HC A05

The FORTRAN library that the NOAA Wave Propagation Laboratory (WPL) developed to perform radiative transfer calculations for an upward-looking microwave radiometer is described. Although the theory and algorithms have been used for many years in WPL radiometer research, the Radiative Transfer Equation (RTE) software has combined them into a toolbox that is portable, readable, application independent, and easy to update. RTE has been optimized for the UNIX environment. However, the FORTRAN source code can be compiled on any platform that provides a Standard FORTRAN 77 compiler. RTE allows a user to do cloud modeling, calibrate radiometers, simulate hypothetical radiometer systems, develop retrieval techniques, and compute weighting functions. The radiative transfer model used is valid for channel frequencies below 1000 GHz in clear conditions and for frequencies below 100 GHz when clouds are present. NTIS

N93-29765# Los Alamos National Lab., NM.
OPTIMIZATION OF HPM DEVICE PARAMETERS FOR MAXIMUM AIR TRANSMISSION
R. Roussel-Dupre and T. Tunnell (EG and G Energy Measurements, Inc., Los Alamos, NM.) 1993 23 p Presented at the International Society for Optical Engineering (SPIE) Conference, Los Angeles, CA, 16-23 Jan. 1993
(Contract W-7405-eng-36)
(DE93-007332; LA-UR-93-361; CONF-930159-17) Avail: CASI HC A03/MF A01

The propagation of high-power microwave (HPM) pulses through the atmosphere is a subject that has received renewed attention in the last decade. For sufficiently high-power pulses, it is possible for air breakdown to be initiated by the front end of the pulse and for ohmic dissipation of the tail end to proceed as the tail propagates through the newly created plasma. Generally, this nonlinear process termed tail erosion is modeled with time-dependent fluid or kinetic codes that require a fine mesh of range and time points. The computational time to run these codes, however, precludes their use in determining the optimum pulse characteristics and propagation paths for transmission of a desired fluence. In this paper, a new frequency scaling law that greatly reduces computational requirements and at the same time incorporates the nonlinear effects inherent to HPM propagation is discussed. Results of a comparison between predictions of air breakdown thresholds made using the frequency scaling law and experimental data taken at various frequencies are presented. The scaling law is implemented in an existing HPM propagation code and has been used recently to develop a new predictive capability that calculates the optimum energy, power, and antenna requirements necessary to transmit a desired fluence. These capabilities provide both the accuracy and rapid computational turnaround necessary for system studies that assess the effects of HPM propagation for particular HPM devices and that attempt to open device parameters for maximum air transmission. Samples of both forward propagation, predictive calculations, and inverse, optimization calculations are presented. DOE

N93-29875# California Univ., Los Angeles. School of Engineering and Applied Science.
PLANAR ACTIVE ANTENNAS AND QUASI-OPTICAL POWER COMBINING ARRAYS USING FET'S AND SLOTS
Shigeo Kawasaki and Tatsuo Itoh 20 Mar. 1993 161 p
(Contract DAAH04-93-G-0068)
(AD-A263759; UCLA-ENG-93-22; ARO-30921.1-EL) Avail: CASI HC A08/MF A02

This report presents design concepts and experimental data for planar active antenna and quasi-optical power combining arrays with strong coupling to realize a compact and low-cost radar and communication system. The prototype circuits for this purpose were made in a layered configuration using microstrip lines and in a uniplanar structure using CPW's. As an active source, an FET was selected. As a unit cell of the power combining array, a single layered active antenna using microstrip lines and slots was fabricated. In the design, small signal S-parameters were used to determine the circuit configuration while a large signal analysis to the entire circuit involving the slot antenna input impedance was carried out. The circuit designed for 10 GHz was found to operate at 9.3 GHz and the other designed for 25 GHz at 24 GHz. In addition, the circuit with CPW's and slots designed for 10 GHz was found to operate at 8.6 GHz. Based on these successful results, linear power combining arrays were made. For the strong coupling, each oscillator output is connected by a single transmission line. Several 6-element microstrip arrays and a 4-element CPW array were fabricated. In the former, sharp main beams were obtained. To obtain a millimeter-wave operating frequency, the second harmonic spatial power combining array made with FET's were demonstrated around 40 GHz. To show a topology of a 2-dimensional array, a 16-element dual polarized array at 7.8 GEL was made. To obtain the maximum in-phase radiation signal, impedance matching, a phase of the radiation signal and a signal phase of each oscillator were taken into account. DTIC

N93-29877 Ludwig-Maximilians-Univ., Munich (Germany).
INTERNATIONAL JOURNAL OF NUMERICAL MODELING: ELECTRONIC NETWORKS, DEVICES, AND FIELDS, VOLUME 5, NUMBER 3, AUGUST 1992
Wolfgang Hoefer and Brian Tuck Aug. 1992 79 p Limited Reproducibility: More than 20% of this document may be affected by microfiche quality
(Contract DAJA-91-M-0311)
(AD-A263765) Avail: CASI HC A05

The contents of this report are as follows: Modeling in the Time Domain; Panel Discussion and Open Forum--Summary Report; Radiation and Scattering of Transient Electromagnetic Fields; Finite Difference Time-domain Simulation of Electromagnetic Fields and Microwave Circuits; Multidimensional Wave Digital Filters for Discrete-Time Modelling of Maxwell's Equations; and Parallel Implementation of Cellular Systems for Numerical Modelling. DTIC

N93-29882# Naval Postgraduate School, Monterey, CA. Dept. of Electrical and Computer Engineering.
WIDEBANDING TECHNIQUES FOR VHF ANTENNAS 2 Technical Report, 10 Jan. 1992 - 30 Mar. 1993
Keem B. Thiem and Ramakrishna Janaswamy Mar. 1993 140 p
(AD-A263998; NPSEC-93-007) Avail: CASI HC A07/MF A02

For a variety of mechanical and electrical reasons, the U.S. Army prefers to use a wire antenna for its mobile applications in the HF and VHF bands. However, due to the rapid fluctuation of impedance with frequency, a simple wire antenna is not suitable. This research will look into the aspects of electronic switching of the antenna length and electronic switching of the accompanying tuning network for frequency hopping applications. Two separate schemes will be studied. The first one involves a chosen wire antenna loaded with PIN diodes. The diodes will be selectively switched ON or OFF at different frequencies to control the input impedance of the antenna. In the second scheme, a monopole antenna of fixed length will be considered and data on its input impedance over many sub-bands within 30 to 90 MHz will be generated. Tuning networks composed of resistors, inductors, and capacitors will be designed over each sub-band. The various networks will then be connected via PIN diodes and selectively switched to provide matching over a much wider band. DTIC

N93-29890# Mitre Corp., Bedford, MA.
ETHERNET PERFORMANCE OF THE MOTOROLA ALTAIR WIN SYSTEM Final Report
Marie B. Normoyle Mar. 1993 42 p
(Contract F19628-89-C-0001)
(AD-A263877; MTR-92B0000122; ESC-TR-92-276) Avail: CASI HC A03/MF A01

Wireless networks offer an attractive alternative to physical cabling for rapid deployment systems. These networks emphasize ease of installation and configuration maintenance. The Motorola Altair wireless in-building network (WIN) offers the additional benefit of compatibility with existing Ethernet devices and wired segments, allowing it to grow as required. Tests were performed to determine the performance capabilities of the WIN system versus wired-Ethernet-configurations. For these tests, the WIN components were integrated into several typical Ethernet topologies that were compared against equivalent wired topologies. Performance was measured using the elapsed time required for a single file transfer as simulated background traffic was increased. Results show that for average Ethernet utilization under 2 Mbits per second, the WIN system performs as well as a wired topology, although individual instances of poor performance may be experienced. In topologies where traffic is routed across a path operating at less than 2 Mbits per second, such as T1 data link, the WIN system is essentially transparent to the network. Performance within the WIN microcell is optimum for handshaking protocols implemented with small to medium-sized Ethernet packets. DTIC

N93-29892# Advisory Group for Aerospace Research and Development, Neuilly-Sur-Seine (France). Avionics Panel.
T(LC2)ACS(LC3)ATS FOR SURVEILLANCE VERIFICATION AND C3I [LES SATELLITES TACTIQUES (TACSATS) POUR LA SURVEILLANCE, LA VERIFICATION ET LA C3I]
Feb. 1993 252 p Symposium held in Brussels, Belgium, 19-22 Oct. 1992
(AGARD-CP-522; ISBN-92-835-0700-2; AD-A264371) Copyright Avail: CASI HC A12/MF A03

The symposium dealt with small satellites used for tactical applications that might be of value to NATO. The 11 sessions covered TacSat concepts and needs, aspects of TacSat applications, TacSat system applications, communication concepts, launch systems, spacecraft bus, advanced technology, radar concepts, electro-optics concepts, and two panel discussions. The information generated by the symposium will be used by Working Group 16 to report on the utility of such satellites and applications to meet future NATO needs. For individual titles, see N93-29893 through N93-29913.

N93-29893# Aerospace Corp., Los Angeles, CA.
TACTICAL SATELLITES **c18**
F. H. Newman *In* AGARD, TacSats for Surveillance Verification and C3I Feb. 1993 9 p (For primary document see N93-29892 11-32)
Copyright Avail: CASI HC A02/MF A03

The concept of a Tactical Space System (TACSAT) is a means to provide a rapid, on demand, augmentation of the backbone U.S. military space systems. Such augmentation would be valuable to temporarily replace lost capability or in times of crisis, to accommodate surge demands. Because augmentation needs are not always known a-priori, it would be desirable to be able to rapidly constitute the appropriate payload-satellite bus combination to accommodate the need for a specific space capability. To do this, one can envision a standard bus capable of accepting a variety of payloads, or better yet, a single spacecraft designed to perform several different missions. Both options are considered. A number of potential missions exist in the areas of surveillance, navigation, environmental sensing, and communications. Of these, two are presented as strawman concepts: surveillance and communication. For surveillance, an electro-optical payload is described that could be used for missile surveillance, theater targeting, or weather data using the same optics, focal plane, and processor. The satellite orbit selected dictates which mission is performed. For communication, both SHF and EHF payloads are defined to provide theater coverage for the tactical user. The advantages and penalties that accrue to the use of a common bus are also explored. In addition, launch options are identified and a comparison made between 'launch-on-demand' and 'launch-on-schedule' strategies. Potential timelines for rapid launch are shown based on parallel processing and checkout of spacecraft and launcher. This technique is compared with launching satellites on a routine basis and storing them in orbit. Energy requirements for repositioning these stored satellites after they are activated in time of need are defined.
Author (revised)

N93-29894# Smith System Engineering Ltd., Guildford (England).
EVOLUTION OR REVOLUTION: THE CATCH 22 OF TACSATS c12
C. J. Elliott *In* AGARD, TacSats for Surveillance Verification and C3I Feb. 1993 7 p Prepared in cooperation with Smith Associates Ltd., Guildford, England (For primary document see N93-29892 11-32)
Copyright Avail: CASI HC A02/MF A03

The potential exploitation of TACSATs is limited by a vicious circle in which users do not specify requirements which they believe to be infeasible and the space industry does not offer radically new solutions because it perceives no demand. This is the Catch 22 of the title. This paper aims to show some of the possibilities if we break out of that vicious circle. A private civilian Earth observation mission (SeaStar) is adopted as a baseline. In order to illustrate what might be possible, military payloads for surveillance, verification, and C3I are suggested, derived from land or air bases systems that either already exist or are known to be under development. It must be appreciated that these are not presented as proposed designs, merely as a kind of 'existence proof' for high performance and low cost satellites. It is possible, on the basis of this 'existence proof', to explore some of the operational consequences of the more general use of TACSATs.
Author (revised)

N93-29895# MATRA Marconi Space (England).
TACSAT GROUND CONTROL AND DATA COLLECTION
C. G. Cochrane *In* AGARD, TacSats for Surveillance Verification and C3I Feb. 1993 6 p (For primary document see N93-29892 11-32)
Copyright Avail: CASI HC A02/MF A03

This paper addresses the concept of a satellite based system serving the needs of tactical users for direct access to communications and various forms of surveillance. Such a system must take account of the most effective methods for deployment and maintenance during its intended period of operation. In terms of the mission needs, the Tactical Satellite System (TACSAT) is required to provide the services for tactical users over a relatively small region of maybe some 1000-2000 km diameter. Also, the concept is likely to involve relatively short periods of operation of about 3 to 6 months for a typical operation scenario. The paper, therefore, addresses a system concept in which the emphasis is placed on reducing the scale of the logistics involved in the deployment of TACSAT elements and simplifying the ground operations and facilities necessary for the users to gain access to the services provided. This paper addresses the following: (1) the need for 'launch on demand'; (2) the possibility of launches being directly under the control of the area commander; (3) operating concepts for TACSATs, comparing the approach of launch-via-residual-mass as part of a larger mission, not dedicated to the TACSAT mission with the approach of dedicated, launch-on-demand; (4) identification of information flow requirements for TACSAT integrity and status evaluation and for surveillance data recovery; (5) determination of technical and cost drivers influencing the form and cost of ground installation and logistic issues; (6) integration of TACSAT facilities and services with other communications and surveillance systems available to the Tactical Commander; and (7) investigation of techniques minimize the ground control and data collection overhead.
Author (revised)

N93-29896# MATRA Marconi Space, Toulouse (France). Espace/Direction des Programmes Militaires.
TACSAT-SPACECRAFT BUS CONCEPT AND DESIGN: APPLICATION OF A MULTIMISSION BUS FOR TACSAT IN LEO c18
Georges Richard *In* AGARD, TacSats for Surveillance Verification and C3I Feb. 1993 13 p In ENGLISH and FRENCH (For primary document see N93-29892 11-32)
Copyright Avail: CASI HC A03/MF A03

Some details as to what is a tactical satellite, as far as such satellites are very often associated with the notion of cheap small satellites, are analyzed. The design process of a low earth orbit multimission bus for tactical application is described. Derived from text

N93-29897# Office National d'Etudes et de Recherches Aerospatiales, Paris (France).
SYSTEM OF NAVIGATION BY SATELLITES WITH EUROPEAN COVERAGE [SYSTEME DE NAVIGATION PAR SATELLITES A COUVERTURE EUROPEENNE] c18
H. Baranger, J. Bouchard, and T. Michal *In* AGARD, TacSats for Surveillance Verification and C3I Feb. 1993 10 p In FRENCH (For primary document see N93-29892 11-32)
Copyright Avail: CASI HC A02/MF A03

The object of this presentation is to propose a navigation system functioning according to the same principle as the GPS system but which would offer a permanent service in Europe using a limited number of satellites. The constellation presented here requires only 4 satellites including one geostationary and three satellites on geosynchronous orbits of weak inclination and eccentricity. This constellation makes it possible to completely cover Europe, the Middle-East and Africa. Moreover, the use of relatively simple satellites is possible. Indeed, all the satellites being permanently visible from the same point of the globe, it is possible to leave on the ground the ultrastable clock which provides the time reference for measurements of user-satellite distance. This constellation appears promising and a more thorough analysis is in hand in order to judge the feasibility of such a system. In particular, the problems arising from the setting and the maintenance in position of such a constellation are being analyzed right now. Several possible solutions for the installation, with single or multiple launches, from standard transfer orbits or not, are presented here. In order to provide a first evaluation of the cost of maintaining it in position, the influence of the main disturbances of orbit on the service provided was analyzed. Some examples of the maintenance in position are also provided. Transl. by FLS

N93-29898# Aerospatiale, Les Mureaux (France). Espace and Defense.
TACTICAL SATELLITES FOR AIR COMMAND AND CONTROL c18
M. Crochet, J. Cymbalista, and L. Leveque *In* AGARD, TacSats for Surveillance Verification and C3I Feb. 1993 9 p (For primary document see N93-29892 11-32)
Copyright Avail: CASI HC A02/MF A03

This paper is divided in three parts corresponding to the following items: (1) air command and control functions and deficiencies; (2) contribution of TACSATS to air command and control; and (3) operational improvements due to TACSATS.
Author (revised)

N93-29899# Marmara Research Inst., Gebze (Turkey).
CONSIDERATIONS FOR NATO SATELLITE COMMUNICATIONS IN THE POST-2000 ERA
A. Nejat Ince *In* AGARD, TacSats for Surveillance Verification and C3I Feb. 1993 8 p (For primary document see N93-29892 11-32)
Copyright Avail: CASI HC A02/MF A03

The National Delegates Board of AGARD, upon recommendation by the Avionics Panel of AGARD, approved in March 1986 the establishment of WG-13 to study satellite communications for NATO under the direction of Prof. Dr. Nejat Ince of Turkey. Some 14 scientists/engineers, from research and industrial establishments of Canada, France, the Federal

Republic of Germany, Norway, Turkey, the United Kingdom, the United States of America as well as from International Military Staff of NATO and SHAPE Technical Centre, participated in the work of WG-13. This paper is a brief summary of the studies carried out by the group in the period 1988-1990 on the type of satellite communication systems which NATO can have in the post-2000 era including the critical techniques and technologies that need to be developed for this purpose.

Derived from text

N93-29900# Massachusetts Inst. of Tech., Lexington. Lincoln Lab.

ADVANCED TECHNOLOGIES FOR LIGHTWEIGHT EHF TACTICAL COMMUNICATIONS SATELLITES

David R. McElroy, Dean P. Kolba, William L. Greenberg, and Marilyn Semprucci *In* AGARD, TacSats for Surveillance Verification and C3I Feb. 1993 9 p (For primary document see N93-29892 11-32)
(Contract F19628-90-C-0002)
Copyright Avail: CASI HC A02/MF A03

The communications capabilities provided by EHF satellites can range from low data rate services (75 to 2400 bps per channel) to medium data rate links (4.8 kbps to 1.544 Mbps per link) depending on the payload configuration. Through the use of EHF waveform standards, the EHF payloads will be compatible with existing and planned EHF terminals. Advanced technologies permit the development of highly capable, lightweight payloads which can be utilized in a variety of roles. The key payload technologies include adaptive uplink antennas; high speed, low power digital signal processing subsystems; lightweight frequency hopping synthesizers; and efficient solid-state transmitters. The focus in this paper is on the signal processing and frequency generation technologies and their application in a lightweight EHF payload for tactical applications. Author

N93-29901# MPR Teltech Ltd., Ottawa (Ontario).

SYNCHRONIZATION TECHNIQUES FOR MEDIUM DATA RATE EHF MILSATCOM SYSTEMS

G. Boudreau and M. Schefter *In* AGARD, TacSats for Surveillance Verification and C3I Feb. 1993 9 p (For primary document see N93-29892 11-32)
Copyright Avail: CASI HC A02/MF A03

In the area of MILSATCOM, considerable effort is currently being expended on the development of systems operating in the EHF frequency bands and employing onboard processing. Two of the principal advantages of employing these features are that the MILSATCOM system will be capable of increased throughput and will possess increased immunity to jamming and other channel impairments. Most of the previous research and development in EHF MILSATCOM has concentrated on Low Data Rate (LDR) waveforms, for data rates up to 2.4 kbps. In order to meet the requirements for increased throughput, Medium Data Rate (MDR) waveforms are being developed. These systems include data rates up to and including T1. This paper examines the constraints that communicating at MDR data rates places on synchronization and provides an overview of some of the various techniques and algorithms that can be employed for both spatial and time acquisition as well as tracking. Both channel and equipment impairments affecting synchronization are examined. Robust open and closed loop acquisition and tracking algorithms are examined in conjunction with onboard processing techniques. Performance is discussed in terms of SNR, acquisition time, probability of correct acquisition and probability of false acquisition. Tradeoffs in a MILSATCOM system design based on various user requirements are also presented. Author

N93-29902# Microtel Pacific Research Ltd., Burnaby (British Columbia).

TERRAIN AND COVERAGE PREDICTION ANALYSES FOR NON-GEOSTATIONARY ORBIT EHF SATELLITE COMMUNICATIONS

M. Jamil Ahmed *In* AGARD, TacSats for Surveillance Verification and C3I Feb. 1993 11 p (For primary document see N93-29892 11-32)
Copyright Avail: CASI HC A03/MF A03

This paper examines communications coverage from five non-geostationary satellite orbits. These orbits are as follows: circular inclined synchronous; GPS; Molniya 12 and 24 hour; and Tundra orbits. It also shows the increase in propagation loss due to irregular terrain and the foliage loss at mm waves, as well as the combined effect of terrain and foliage on satellite view duration. It is concluded that coverage calculations for EHF satcom earth terminals need to take into account terrain and foliage losses. Author (revised)

N93-29903# Aerospace Corp., Los Angeles, CA.

LAUNCH VEHICLES FOR LIGHTWEIGHT TACSAT DEPLOYMENT c15

Chester L. Whitehair and Malcolm G. Wolfe *In* AGARD, TacSats for Surveillance Verification and C3I Feb. 1993 17 p (For primary document see N93-29892 11-32)
Copyright Avail: CASI HC A03/MF A03

The need for tacsats is discussed, and typical tacsat mission requirements are identified. A spectrum of potential tacsat launch systems is identified and characterized, including both U.S. and non-U.S. systems, and ranging from existing operational vehicles to very advanced vehicles that will not become available until well into the next century. The six basic launch system design drivers are presented: performance, cost, operability, launch responsiveness, launch flexibility, and survivability. These design drivers are discussed as they relate to tacsat launch requirements. The launch systems that are described are placed in the following categories: (1) mainline launch systems; (2) small fixed/relocatable/mobile launch systems; (3) ballistic missile-derived launch systems; and (4) far-term launch systems. The impact of the U.S./CIS Strategic Arms Reduction Talks (START) agreements on the availability of surplus ballistic missiles is discussed. The availability and utility of a wide selection of global launch sites are also examined. It is concluded that the general tacsat mission is a viable concept, and possibly satisfies a very critical future need. It is demonstrated that the tacsat launch services needs into the foreseeable future can be supported by current and planned launch systems launched from existing launch sites. However, numerous other options are available and should be investigated by the tacsat system designer/planner for viability and cost effectiveness. Author (revised)

N93-29904# Orbital Sciences Corp., Chantilly, VA.

SPACECRAFT AND LAUNCH SYSTEMS FOR TACSAT APPLICATIONS c18

Chris Schade, Gilbert D. Rye, and Robert H. Meurer *In* AGARD, TacSats for Surveillance Verification and C3I Feb. 1993 11 p (For primary document see N93-29892 11-32)
Copyright Avail: CASI HC A03/MF A03

The ability of a tactical communication satellite (TACSAT) space system to fulfill its mission application with the desired capability, responsiveness, reliability, and survivability, while at the same time achieving low cost objectives, is a tremendous challenge that can only be met if all of the system segments - launch, space, and ground - contribute to meeting mission unique requirements. The emerging concepts for the development, deployment, and operation of cost-effective TACSAT space systems are especially dependent on the flexibility and operability of their launch vehicle and spacecraft bus systems. Orbital Sciences Corporation (OSC) has privately developed two flexible yet cost-effective space launch vehicles--Pegasus (TM) and Taurus (TM)--with significant and unique operational capabilities that enable TACSAT space systems to meet these challenges. The Defense Advanced Research Projects Agency (DARPA) has sponsored the first launch of both systems, with follow-on launches scheduled in support of U.S. Air Force, NASA, SDIO, and commercial programs. In addition, OSC has developed a flexible, cost-effective, spacecraft bus--PegaStar (TM)--that makes common use of the Pegasus or Taurus final stage avionics and structure in an integrated systems approach, thereby optimizing the mass and volume available for payload sensors. PegaStar spacecraft for the Air Force and NASA are now in engineering and production. Author (revised)

N93-29905# Ball Corp., Boulder, CO. Space Systems Div.

QuickStar: SYSTEM DESIGN, CAPABILITIES, AND TACTICAL APPLICATIONS OF A SMALL, SMART SPACE SYSTEM c18

Thomas P. Garrison and Neal T. Anderson *In* AGARD, TacSats for Surveillance Verification and C3I Feb. 1993 12 p (For primary document see N93-29892 11-32)
Copyright Avail: CASI HC A03/MF A03

The QuickStar System is not a concept--it is a flight-proven design. QuickStar is a small, highly capable, low-cost, lightweight spacecraft using modern design techniques that can carry tactical assets into space at a tenth of the cost of current systems. System design, relevant technologies, payload capabilities (mass, power, data rate, pointing, volume), and tactical mission applications of this lightweight satellite are described. As part of the overall small satellite system architecture, a portable, low-cost multipurpose ground station to support production, test, launch, and orbit operations of the space segment is also available. The versatility and transportability built into the ground station allows placement at any government installation or field site. The prototype QuickStar space segment was developed to ride as a secondary payload on a McDonnell Douglas Delta 2 series expendable launch vehicle (ELV). With the extra performance provided by the Delta 2 or other ELV of similar configuration, as many as four satellites could be orbited at one time. In addition, the paper describes a QuickStar satellite configuration, incorporating the same subsystems and capabilities as the prototype QuickStar, designed for stand-alone ELV (Scout or Pegasus) launchings. The program schedule for the design, fabrication, and test of a QuickStar satellite system reflects the fast-paced environment of a low-cost program. Minimal paper and much concurrent engineering goes into a schedule that provides a flight-ready spacecraft and supporting ground station in only 15 months. Author (revised)

N93-29906# Messerschmitt-Boelkow-Blohm G.m.b.H., Munich (Germany). Space Communications and Propulsion Systems Div.
ATTITUDE- AND ORBIT CONTROL SUBSYSTEM CONCEPTS FOR TACSATS **c18**
H. Bittner, E. Bruederle, M. Surauer, and M. Schwende *In* AGARD, TacSats for Surveillance Verification and C3I Feb. 1993 24 p (For primary document see N93-29892 11-32)
Copyright Avail: CASI HC A03/MF A03

An attempt has been made to identify the configuration, the equipment, and the necessary technology of an Attitude- and Orbit Control Subsystem (AOCS), which can provide the necessary flexibility for serving the large variety of TACSAT mission objectives and the associated performance requirements. This discussion is based on more than 20 years of experience in AOCS design and development for communication and application spacecraft (S/C). Author (revised)

N93-29907# Alenia Spazio S.p.A., Rome (Italy).
ELECTRIC PROPULSION FOR LIGHTSATS: A REVIEW OF APPLICATIONS AND ADVANTAGES **c20**
G. Perrotta, Gianfranco F. Cirri (Proel Tecnologie, Florence, Italy.), and Giovanni Matticari (Proel Tecnologie, Florence, Italy.) *In* AGARD, TacSats for Surveillance Verification and C3I Feb. 1993 7 p (For primary document see N93-29892 11-32)
Copyright Avail: CASI HC A02/MF A03

The paper reviews the advantages and limitations of electric propulsion for lightsats characterized by a launch mass in the 300 to 800 kg range. The considered systems include ion propulsion, arc jets, and stationary plasma thrusters for different applications such as drag compensation, orbit raising, fine trimming of orbital parameters, and various orbit transfers. Electric propulsion provides substantial mass savings and turns out to be an enabling technology for certain lightsat missions. The constraints resulting from DC power limitations on board small satellites are discussed, along with the implications on candidate technologies and system solutions. A review of near term prospectives of low power ion thrusters, for lightsats applications, concludes the paper. Author (revised)

N93-29908# Defense Advanced Research Projects Agency, Arlington, VA. Advanced Systems Technology Office.
AN OVERVIEW OF DARPA'S ADVANCED SPACE TECHNOLOGY PROGRAM **c12**
E. Nicastri and J. Dodd (Aerospace Corp., Washington, DC.) *In* AGARD, TacSats for Surveillance Verification and C3I Feb. 1993 11 p (For primary document see N93-29892 11-32)
Copyright Avail: CASI HC A03/MF A03

The Defense Advanced Research Projects Agency (DARPA) is the central research and development organization of the DoD and, as such, has the primary responsibility for the maintenance of U.S. technological superiority over potential adversaries. DARPA's programs focus on technology development and proof-of-concept demonstrations of both evolutionary and revolutionary approaches for improved strategic, conventional, rapid deployment and sea power forces, and on the scientific investigation into advanced basic technologies of the future. DARPA can move quickly to exploit new ideas and concepts by working directly with industry and universities. For four years, DARPA's Advanced Space Technology Program (ASTP) has addressed various ways to improve the performance of small satellites and launch vehicles. The advanced technologies that are being and will be developed by DARPA for small satellites can be used just as easily on large satellites. The primary objective of the ASTP is to enhance support to operational commanders by developing and applying advanced technologies that will provide cost-effective, timely, flexible, and responsive space systems. Fundamental to the ASTP effort is finding new ways to do business with the goal of quickly inserting new technologies into DoD space systems while reducing cost. In our view, these methods are prime examples of what may be termed 'technology leveraging.' The ASTP has initiated over 50 technology projects, many of which were completed and transitioned to users. The objectives are to quickly qualify these higher risk technologies for use on future programs and reduce the risk of inserting these technologies into major systems, and to provide the miniaturized systems that would enable smaller satellites to have significant - rather than limited - capability. Only a few of the advanced technologies are described, the majority of which are applicable to both large and small satellites. Derived from text

N93-29909# Alenia Spazio S.p.A., Rome (Italy).
SAR SENSORS ON TACSATS: A FEASIBILITY ASSESSMENT **c19**
G. Perrotta *In* AGARD, TacSats for Surveillance Verification and C3I Feb. 1993 9 p (For primary document see N93-29892 11-32)
Copyright Avail: CASI HC A02/MF A03

The feasibility of installing SAR's on board lightsats for tactical and strategic observation missions is discussed, emphasizing high resolution and short revisit intervals as main system drivers. Lightsat constellations design criteria are presented for both global and limited latitude belt coverage. Pros and cons of sunsynchronous versus medium inclination non-sunsynchronous orbits are discussed. Gross system trade offs for the SAR sensor are then addressed, in the specific context of a resource-limited lightsat, stressing the achievement of resolutions better than 5 m, swaths greater than 20 Km, access angles of at least 30 deg, small antenna dimensions, and a reasonable power consumption. Both X and C band SAR solutions are outlined. Data transmission alternatives are also discussed, in the context of tactical and strategic scenarios, outlining their projected performance. Constellation orbits control and platform attitude are also addressed for their impact on mission, SAR image quality and satellite design requirements. Key aspects of critical platform subsystems are also identified. Author (revised)

N93-29910# MATRA Marconi Space (England).
A TACSAT SAR CONCEPT **c19**
C. D. Hall, C. J. Baker (Defence Research Agency, Malvern, England.), G. E. Keyte (Defence Research Agency, Farnborough, England.), and L. M. Murphy (Defence Research Agency, Farnborough, England.) *In* AGARD, TacSats for Surveillance Verification and C3I Feb. 1993 14 p (For primary document see N93-29892 11-32)
Copyright Avail: CASI HC A03/MF A03

The payload concept covered is that of a low cost, high performance radar sensor capable of detecting and recognizing static objects within an imaged scene of the Earth's surface using the Synthetic Aperture Radar (SAR) technique. The overall system is integrated with a TACSAT platform in Low Earth Orbit (LEO) and, although only passing reference is made to this feature, the radar could also have a capability for the detection of Ground Moving Targets (GMTI). A parametric review of such a sensor in the light of the target and background features to be observed is provided. A design concept is included showing the possible hardware realization of a candidate system, as well as budgets for the mass, size, power, and pointing requirements of the instrument. Additional design features considered are the influence that short duration missions may have on hardware redundancy and the effect of short, low duty-cycle observation periods on solar array and battery sizing. The way towards a low cost R and D demonstrator system allowing a practical investigation of the key techniques and technologies is addressed. Author (revised)

N93-29911# Hughes Aircraft Co., Los Angeles, CA. Remote Sensing Systems.
LOW COST TACSAT FOR NATO SURVEILLANCE **c18**
Charles S. Hoff *In* AGARD, TacSats for Surveillance Verification and C3I Feb. 1993 8 p (For primary document see N93-29892 11-32)
Copyright Avail: CASI HC A02/MF A03

Cost and performance technology breakthroughs in recent years have made possible the near term development and deployment of a low cost TACSAT surveillance system. The potential for both the spacecraft and sensor to be launched on lower cost launch systems is the fundamental basis for reduced system cost. Additionally, the spacecraft and sensor must be amenable to low cost mass production. For all weather, day/night surveillance, an active synthetic aperture radar (SAR) is the ideal instrument, and the ability to mass manufacture thousands of very low cost transmit/receive (T/R) modules was developed at Hughes. Since the size of a SAR increases as the orbital altitude is increased, a final element of the economical basis for a low cost TACSAT is the definition of low earth orbit (LEO) space constellations with high mission utility. Tradeoffs are also provided to compare sparse or zero based peacetime constellations with surge launch capabilities to small peacetime early warning space constellations that can also instantly provide regional combat support on demand. Author

N93-29912# Lockheed Missiles and Space Co., Sunnyvale, CA.
COST EFFECTIVE TacSats FOR MILITARY SUPPORT c18
M. T. Brodsky, M. D. Benz, and J. T. Neer *In* AGARD, TacSats for Surveillance Verification and C3I Feb. 1993 12 p (For primary document see N93-29892 11-32)
Copyright Avail: CASI HC A03/MF A03

The key space system features required to provide effective support to military field units are discussed and Lockheed's concept to fill critical niches in military surveillance and remote sensing is discussed. The military is aware of benefits available from more effective use of space. To provide those benefits, space systems must be dependable, easy to use, flexible, responsive, and affordable. How a programmable, multi-spectral E-O sensor combined with a new small satellite bus and supporting command and control and data processing tools can provide environmental and surveillance support to users in peacetime, crisis, and combat is discussed. Also discussed are how such a system meets essential military utility criteria and an approach for rapid TacSat system development, evaluation, and deployment. Author (revised)

N93-29913# MATRA Marconi Space (England).
TACSAT METEOROLOGICAL PAYLOADS c47
D. Hickman *In* AGARD, TacSats for Surveillance Verification and C3I Feb. 1993 8 p (For primary document see N93-29892 11-32)
Copyright Avail: CASI HC A02/MF A03

Information derivable from meteorological satellites are reviewed in terms of their applicability to military use. Potential TACSAT meteorological systems are discussed in terms of GEO and LEO payloads currently in operation. Author

N93-29975# Naval Research Lab., Bay Saint Louis, MS.
ARSRP SIGNAL PROCESSING SOFTWARE
Lisa Pflug, Jerald W. Caruthers, and Richard R. Slater Feb. 1993 61 p
(AD-A263543; NRL/MR/7173-92-7004) Avail: CASI HC A04/MF A01

Software written in PV-WAVE to process data collected aboard the RV Cory Chouest during the Acoustic Reverberation Special Research Program Reconnaissance (ARSRP) Experiment conducted in the summer of 1991 is documented in this memorandum report. Although developed specifically for ARSRP-collected data, the software will work on any data collected aboard the RV Cory Chouest and written to 9-track tape for processing with the Off Line Processor (OLP) software in the 'beam tape' (BTS) format - this includes beamformed and hydrophone pass-through data. Software written by the Scripps Institution of Oceanography to read OLP tapes and output files in Society of Exploration Geophysicists 'Y' (SEGY) format is discussed. ARSRP Signal Processing Software (ASPS) discussed in the report includes reading SEGY format archive tapes into ASCII format, conversion of ASCII data files to unformatted form for compact storage and fast access by PV-WAVE, and beamforming and matched filtering with PV-WAVE programs. A program to create waterfall display plots of hydrophone data, beamformed data, or matched filtered data is included. DTIC

N93-29987# Naval Postgraduate School, Monterey, CA.
A COMPARISON OF TRANS-EQUATORIAL IONOSPHERE PROPAGATION PREDICTIONS FROM AMBCOM WITH MEASURED DATA M.S. Thesis
John W. McKinstry Mar. 1993 92 p
(AD-A264006) Avail: CASI HC A05/MF A01

This thesis examines radio propagation conditions over trans-equatorial (TE) paths. The study precedes Project PENEX, a field experiment to measure and collect calibrated HF skywave signal strength data for polar, equatorial, and near-vertical incidence propagation paths. PENEX will benchmark the absolute accuracy of the signal-to-noise models in the MEDUSA propagation model now being developed by the Naval Command, Control and Ocean Surveillance Center. Since only minimal information is available about TE paths, a comprehensive review of the published literature on TE experiments was completed, with emphasis on TE paths between magnetic conjugate points. Data from such paths have revealed the presence of unusual propagation i-nodes which are not predicted bv standard propagation programs such as PROPHET, IONCAP, and AMBCOM. The review of the literature revealed that Stanford Research Institute (SRI) published measured data on a TE path between the Pacific islands of Kauai and Rarotonga. A comparison was made between the SRI data and predictions for the same path to assess the usefulness of current prediction programs for TE paths. The SRI AMBCOM program was used for this comparison. As expected, sizeable differences were found between the predicted and measured results, especially during times when unusual propagation modes were present. This suggests that prediction programs should be modified to include the observed TE modes. DTIC

N93-30010 Utah Univ., Salt Lake City.
APPLICATIONS OF THREE-DIMENSIONAL MODELING IN ELECTROMAGNETIC EXPLORATION Ph.D. Thesis
Louise Donna Pellerin 1992 183 p
Avail: Univ. Microfilms Order No. DA9308492

Numerical modeling is used in geophysical exploration to understand physical mechanisms of a geophysical method, compare different exploration techniques, and interpret field data. Exploring the physics of a geophysical response enhances the geophysicist's insight, resulting in better survey design and interpretation. Comparing exploration methods numerically can eliminate the use of a technique that cannot resolve the exploration target. Interpreting field data to determine the structure of the earth is the ultimate goal of the exploration geophysicist. Applications of three-dimensional (3-D) electromagnetic (EM) modeling in mining, geothermal and environmental exploration demonstrate the importance of numerical modeling as a geophysical tool. Detection of a confined, conductive target with a vertical electric source (VES) can be an effective technique if properly used. The vertical magnetic field response is due solely to multi-dimensional structures, and current channeling is the dominant mechanism. A VES is deployed in a bore hole, hence the orientation of the hole is critical to the response. A deviation of more than a degree from the vertical can result in a host response that overwhelms the target response. Only the in-phase response at low frequencies can be corrected to a purely vertical response. The geothermal system studied consists of a near-surface clay cap and a deep reservoir. The magnetotelluric (MT), controlled-source audio magnetotelluric (CSAMT), long-offset time-domain electromagnetic (LOTEM) and central-loop transient electromagnetic (TEM) methods are appraised for their ability to detect the reservoir and delineate the cap. The reservoir anomaly is supported by boundary charges and therefore is detectable only with deep sounding electric field measurement MT and LOTEM. The cap is easily delineated with all techniques. For interpretation I developed an approximate 3-D inversion that refines a 1-D interpretation by removing lateral distortions. An iterative inverse procedure invokes EM reciprocity while operating on a localized portion of the survey area thereby greatly reducing the computational requirements. The scheme is illustrated with three synthetic data sets representative of problems in environmental geophysics. Dissert. Abstr.

N93-30016# Colorado Univ., Colorado Springs.
QUANTIFICATION OF THERMOGRAPHIC MAPPING TECHNIQUES Final Report
John Norgard and Don Metzger Dec. 1992 90 p
(Contract F30602-91-C-0113)
(AD-A264020; RL-TR-92-320) Avail: CASI HC A05/MF A01

Thermographic mapping of microwave fields is a method of imaging the electromagnetic field in a region of space by viewing the heating it produces when interacting with a material. As the microwave field interacts with a material, some of the electromagnetic energy may be converted into heat. This heat can be viewed in several ways; the most useful technique developed to date involves an infrared camera. The objective is to develop appropriate theoretical and experimental practices to allow for the design and manufacture of an electromagnetic absorbing screen. The absorbing screen must exhibit a significant heat rise for a small amount of incident electromagnetic energy while not disturbing the electromagnetic field it is measuring. Thus, the design of the absorber involves a trade-off between these two desirable properties. DTIC

N93-30018# Office National d'Etudes et de Recherches Aerospatiales, Paris (France).
SCATTERING THROUGH APERTURES AND BY THREE-DIMENSIONAL STRUCTURES. APPLICATION TO THE MEASUREMENT OF THE SURFACE IMPEDANCE OF CONDUCTIVE MATERIALS Ph.D. Thesis - Univ. des Sciences et Techniques, 1989 [DIFFRACTION PAR DES OUVERTURES ET PAR DES OBJETS TRIDIMENSIONNELS. APPLICATION A LA MESURE DES IMPEDANCES DE SURFACE DES MATERIAUX BONS CONDUCTEURS]
Vincent Gobin 1990 184 p In FRENCH
(ONERA-P-1990-2; ETN-93-93719) Avail: CASI HC A09/MF A02

The influence of conductive materials (such as carbon composite materials) in the propagation of electromagnetic perturbations into aircraft is studied. The method of moments (in frequency domain) is used to calculate the current distribution on a three dimensional structure of any shape. Two integral equations are constructed to calculate the scattering of a known wave through apertures and the current distribution in an object (characterized by its surface impedance) divided into surfaces and wires. The basis functions for wires and surfaces are generalized to modelize the wire/surface junctions. Various numerical applications are presented. The scattering through a loaded aperture is studied, both experimentally and theoretically and the influence of junctions between materials is emphasized. A method of measurement of surface impedance (from a few micro-Ohms to a few Ohms) is presented. ESA

N93-30025# PTT Research, Leidschendam (Netherlands).
ACTIVITIES REPORT OF PTT RESEARCH Annual Report, 1991 [JAARBOEK PTT RESEARCH 1991]
1992 162 p In DUTCH
(ISBN-9-07-212514-2; ETN-93-93341) Copyright Avail: CASI HC A08/MF A02

In the field of postal infrastructure research, activities were performed on postcode readers, radiolabels, and techniques of operations research and artificial intelligence. In the field of telecommunication, transportation, and information, research was made on multipurpose coding schemes, speech recognition, hypertext, a multimedia information server, security of electronic data interchange, document retrieval, improvement of the quality of user interfaces, domotics living support (techniques), and standardization of telecommunication prototcols. In the field of telecommunication infrastructure and provisions research, activities were performed on universal personal telecommunications, advanced broadband network technologies, coherent techniques, measurement of audio quality, near field facilities, local beam communication, local area networks, network security, coupling of broadband and narrowband integrated services digital networks, digital mapping, and standardization of protocols. ESA

N93-30126# Norfolk State Univ., VA.
POLARIZATION EXPERIMENTS WITH HADRONIC AND ELECTROMAGNETIC PROBES
V. Punjabi 30 Mar. 1993 30 p
(Contract DE-FG05-89ER-40525)
(DE93-011375; DOE/ER-40525/6) Avail: CASI HC A03/MF A01

The following research activities were carried out during the past year: (1) calibration of focal plane polarimeter POMME up to 2.4 GeV at Saturne National Laboratory (LNS) in Saclay; (2) measurement of tensor analyzing power T(sub 20) and polarization transfer kappa(sub 0) at Saturne up to 2.1 GeV in elastic backward dp scattering (d-bar)p yields (p-bar)d; (3) measurement of tensor analyzing power T(sub 20) at synchrophasotron in Dubha up to 4.4 Gev in elastic backward dp scattering (d-bar)p yields pd; (4) resubmission of conditionally approved G(sub EP) proposal 89-14 at CEBAF; and (5) start construction of focal plane polarimeter (FPP) for CEBAF hall A hadron spectrometer. The planned work for the next year includes: (1) construction of FPP for CEBAF hall A hadron spectrometer; (2) measurement of polarization transfer kappa(sub 0) and tensor analyzing power T(sub 20) in elastic backward dp scattering at Saturne; (3) measurements of tensor analyzing power in (H-1)((Li-6),d)X, (H-1)((Li-6),alpha)X, (H-1)((Li-6),t)X and (H-1)((Li-6),(He-3))X reactions at Saturne; and study of polarization transfer in (H-2)((e-bar),e'(p-bar))n reaction at Bates. DOE

N93-30145# Electronics Research Lab., Adelaide (Australia).
ELECTRO-OPTIC CHARACTERISATION OF EXTREMELY WIDE BANDWIDTH ELECTRICAL SIGNALS
A. C. Lindsay, G. A. Knight, S. C. Troedson, and I. G. Fuss Feb. 1993 43 p
(AD-A264202; ERL-0673-RR; DODA-AR-008-114) Avail: CASI HC A03/MF A01

In this report an ultrafast electro-optic sampling system suitable for applications such as device characterization is described. The aperture time of the sampler is calculated to be about 290 fs, implying an attainable device bandwidth in excess of 300 GHz. The sampler was characterized using a test pulse with approximately 12 GHz of frequency content, and the results compared to those obtained from an 18 GHz digital sampling oscilloscope. DTIC

N93-30150# Office of Technology Assessment, Washington, DC.
THE 1992 WORLD ADMINISTRATIVE RADIO CONFERENCE: TECHNOLOGY AND POLICY IMPLICATIONS
May 1993 199 p Conference held in Malaga-Torremolinos, Spain, Feb. 1992
(OTA-TCT-549; ISBN-0-16-041766-X) Avail: CASI HC A09/MF A03; SOD HC

As the 20th century draws to a close, new radio technologies and services are poised to change the ways we communicate. Radio waves already make possible a wide range of services considered commonplace--AM and FM radio broadcasting, television, cellular telephones, remote garage-door openers, and baby monitors. Advances in radio technology are giving birth to even more new products and services, including pocket-sized telephones that may allow people to make and receive calls anywhere in the world, high-definition televisions (HDTV) with superior quality pictures and sound, and static-free digital radios. The 1992 World Administrative Radio Conference (WARC-92) authorized frequencies for many of these new radio communication services, and granted additional frequencies for many existing services, including international broadcasting, satellite-based mobile communications, and communications in space. The effects of these changes will be felt well into the 21st century as countries around the world develop and deploy new communications systems to serve the needs of consumers, businesses, and governments. For the United States, the decisions made at the conference will critically affect how we develop new radio technologies and applications, how competitive this country will be in radio communications equipment and services, and how effectively the United States can exercise its role as a leader in world radio communication policymaking. This study of the outcomes and implications of WARC-92 was requested by the House Committee on Energy and Commerce and the Senate Committee on Commerce, Science, and Transportation. OTA was asked to evaluate the success of U.S. proposals at the conference, discuss the implications of the decisions made for U.S. technology and policy development, and identify options for improving U.S. participation in future world radio communication conferences. Author (revised)

N93-30362# Navy Personnel Research and Development Center, San Diego, CA.
REVIEW OF THE EFFECTIVENESS OF VIDEO MEDIA IN INSTRUCTION Final Report, Jan. 1991 - Sep. 1992
C. D. Wetzel, Paul H. Radtke, Hervey W. Stern, Jan Dickieson, and J. C. McLachlan Apr. 1993 218 p
(AD-A264228; NPRDC-TR-93-4) Avail: CASI HC A10/MF A03

Visual forms of instruction are increasingly used as a result of the widespread use of video technologies such as broadcasts, teleconferencing, tapes, videodiscs, and emerging multimedia combinations of computer and digital video technologies. The considerable amount of research that stretches back to early work with film, television, and static visual materials can be of benefit in developing these new forms of instruction. The objective is to present a review of the current research literature regarding the use of dynamic video media in instruction. Research on the following topics was reviewed: general reviews of the effectiveness, acceptance, and costs of several forms of educational television; teaching techniques used effectively with video media; combining visual and verbal information; the effects of motion, animation, and interactivity, the relationship between media perceptions and learning; the effect of various video production techniques on learning; and critical perspectives on learning from media. This review can be used as background material for future research or instructional development efforts concerned with learning from video-based media. DTIC

N93-30371*# National Aeronautics and Space Administration, Washington, DC.
CONSULTATIVE COMMITTEE FOR SPACE DATA SYSTEMS RECOMMENDATION FOR SPACE DATA SYSTEM STANDARDS: TELECOMMAND. PART 2.1: COMMAND OPERATION PROCEDURES
Jan. 1991 71 p Prepared in cooperation with CNES, Paris, France, DFVLR, Berlin, Germany, ESA, Paris, France, ISRO, Bangalore, India, INPE, Sao Jose dos Campos, Brazil, and NASDA, Tokyo, Japan
(NASA-TM-108158; Red-Book-Issue-4; CCSDS-202.1-R-4; NAS 1.15:108158) Avail: CASI HC A04/MF A01

This recommendation contains the detailed specification of the logic required to carry out the Command Operations Procedures of the Transfer Layer. The Recommendation for Telecommand--Part 2, Data Routing Service contains the standard data structures and data communication procedures used by the intermediate telecommand system layers (the Transfer and Segmentation Layers). In particular, it contains a brief description of the Command Operations Procedures (COP) within the Transfer Layer. This recommendation contains the detailed definition of the COP's in the form of state tables, along with definitions of the terms used. It is assumed that the reader of this document is familiar with the data structures and terminology of part 2. In case of conflict between the description of the COP's in part 2 and in this recommendation, the definition in this recommendation will take precedence. In particular, this document supersedes section 4.3.3.1 through 4.3.3.4 of part 2. Author

N93-30386# Minnesota Univ., Minneapolis. Dept. of Electrical Engineering.
MULTISCALE AND MULTIGRID INFORMATION REPRESENTATION, EXTRACTION AND FUSION Final Report, 1 Feb. 1992 - 31 Jan. 1993
Ahmed Tewfik Apr. 1993 71 p
(Contract F49620-92-J-0134)
(AD-A264623; AFOSR-93-0322TR) Avail: CASI HC A04/MF A01

The basic goal of this research was to study the role that wavelet theory can play in information representation and extraction. The researchers focused their attention primarily on surveillance applications. As part of their research, they studied two problems that arise in surveillance. The first problem was that of determining the directions of arrivals of a set of plane waves in the presence of a background noise of unknown correlation structure. The second problem involved selecting an optimal set of N waveforms, with N fixed, to obtain the best reconstruction of a distributed range-doppler target reflectivity function. DTIC

N93-30423# Naval Research Lab., Washington, DC.
CHARACTERISTICS OF HIGH-FREQUENCY SIGNALS, NOISE, AVAILABILITY, AND DURATION OF BANDWIDTHS BASED ON ROTHR AMCHITKA SPECTRUM MEASUREMENTS
G. D. McNeal 16 Apr. 1993 43 p
(AD-A264480; NRL/FR/5324-93-9536) Avail: CASI HC A03/MF A01

The successful performance of a High-Frequency (HF) Over-The-Horizon Radar (OTHR) is dependent upon the environment in which the radar must operate. This study investigates measured power levels of noise and signal characteristics in the HF environment of an operational OTHR system located in Amchitka, Alaska. These measurements were acquired by the Navy's AN/TPS-71 Relocatable OTHR (ROTHR) spectrum monitor, and represent a new source of HF environmental measurements for noise characteristics, channel availability, and expected duration of various channel widths as a function of frequency, time-of-day, and season-of-year. The analysis and results presented are based on HF environmental measurements obtained over the 5 to 28 MHz frequency band by a receiver with a very low noise figure, an efficient antenna, a high dynamic range, and which was seldom internally noise limited. The analysis of this data has provided information on power levels associated with noise and HF users in the geographic region of the radar. Clear channel availability results are based on a threshold level defined by empirical distribution functions (EDF) of the measured power levels from the ROTHR site in Amchitka. Discussions are also provided on how the noise power levels measured by the spectrum monitor compare with CCIR predictions for this geographical location. Directional characteristics are inferred by comparing spectrum monitor noise levels with those seen on the radar. DTIC

N93-30514# Mitre Corp., Bedford, MA.
ADAPTIVE AIRBORNE RADAR SIMULATION WITH EQUALIZATION FILTER TAPS
B. N. Babu and J. A. Torres Apr. 1993 11 p
(AD-A264722; M-93B0000041) Avail: CASI HC A03/MF A01

Space-time processing (STP) provides an adaptive filter for an airborne phased-array radar to detect targets in clutter and jamming that have spatial and Doppler spread. We developed a flexible airborne radar simulation to identify limitations in the techniques and to evaluate the capabilities of different STP designs. One of the space-time architectures, jointly adaptive STP in the element space, employs joint processing of array elements and pulse train data. The array elements provide the azimuth (spatial) information, and the pulse repetition interval (PRI) taps or pulses provide the Doppler information required to form the two-dimensional azimuth-Doppler filter. In the adaptive mode, additional temporal information from taps separated by a sampling rate interval (greater than Nyquist) provide additional degrees of freedom to mitigate interference due to wideband, narrowband, and multipath jamming. This paper discusses the theory and implementation of STD using temporal equalization filter taps, and presents three different examples illustrating the features of the simulation. DTIC

N93-30537# Defence Research Establishment, Ottawa (Ontario).
EFFECTS OF IMBALANCES AND DC OFFSETS ON I/Q DEMODULATION
Jim P. Lee Dec. 1992 55 p
(AD-A264466; DREO-1148) Avail: CASI HC A04/MF A01

The effects of imbalances and DC offsets, in an I/Q demodulator, on the demodulation of radar signals are addressed in this report. Three normalized parameters, namely the peak-to-peak-ripple to mean, phase error and normalized instantaneous frequency deviation are used to characterize distortions introduced on the envelope, phase and instantaneous frequency respectively. The effect on the distortions, due to aliasing and approximation use in deriving the instantaneous frequency in a discrete-time processor, is also analyzed. When there are imbalances and DC offsets, a bias is produced on both the demodulated envelope and phase. AC ripples with frequency components which are multiples of the baseband frequency are also generated on all of the three demodulated signal waveforms. In EW applications, the instantaneous bandwidth of the I/Q demodulator is usually much wider than the demodulated signal bandwidth. As a result, when the baseband frequency of the signal is high and comparable to its modulation bandwidth, the higher frequency components of the distortion can be effectively reduced by low-pass filtering. DTIC

N93-30576# New York Univ., New York. Courant Inst. of Mathematical Sciences.
MULTIRESOLUTION ANALYSIS OF SAR DATA Final Report, Sep. 1989 - 1992
Robert Hummel Jan. 1993 19 p
(Contract F33615-89-C-1087)
(AD-A264727; WL-TR-93-1011) Avail: CASI HC A03/MF A01

The 'Multiresolution Analysis of SAR Data' program supported research work in five areas. Geometric hashing theory can now be viewed as a Bayesian approach to object recognition. False alarm rates can be greatly reduced by using certain enhancements and modifications developed under this project. Geometric hashing algorithms now exist for the Connection Machine. Recognition of synthetically-produced dot arrays was demonstrated using a model base of 1024 objects. The work represents a substantial advance over existing model-based vision capabilities. Algorithms were developed for determining the translation and rotation of a sensor given only the image flow field data. These are new algorithms, and are much more stable than existing computer vision algorithms for this task. The algorithms might provide independent verification of gyroscopic data, or might be used to compute relative motion with respect to a moving scene object, or may be useful for motion-based segmentation. Our theories explaining the Dempster/Shafer calculus and developing new uncertainty reasoning calculi were extended, and presented at a conference and were incorporated into the Bayesian interpretation of geometric hashing. 'Wavelet Slice Theorem' was developed in several different versions, any of which yields an alternate approach to image formation. The result may well provide a more stable approach to image formation than the standard Fourier-based projection slide theorem, since interpolation of unknown spectra values is better-founded. DTIC

N93-30595# Naval Command, Control and Ocean Surveillance Center, San Diego, CA.
VARIABILITY OF THE ELECTRIC FIELD STRENGTH IN THE EARTH-IONOSPHERE WAVEGUIDE DUE TO VARIATIONS IN THE ELECTRON DENSITY PROFILE Final Report, Jul. 1990 - Dec. 1991
C. H. Shellman Dec. 1992 25 p
(AD-A264808; NRAD-TD-2410) Avail: CASI HC A03/MF A01

A method is developed for finding the standard deviation of the field strength in the earth-ionosphere at very low frequencies. This method uses derivatives of the waveguide eigenangles for height and slope variations in the electron density profile. The calculated results are in reasonable agreement with available data. DTIC

N93-30597# South Carolina Univ., Columbia.
APPLICATION OF INTEGRAL AND DIFFERENTIAL EQUATION METHODS FOR VARIOUS EM INTERACTION PROBLEMS
Mar. 1993 43 p
(AD-A264821; NRAD-TD-2453) Avail: CASI HC A03/MF A01

This document reviews the application of integral equation methods that are commonly used to study the interaction of EM fields with two-dimensional lossy anisotropic objects. The study focuses on plane wave scattering done by arbitrarily shaped cylindrical geometries that have circular and rectangular cross sections. In addition to discussing solid material objects, the document investigates the bistatic radar cross section of several metallic circular cylinders that are coated with a single layer of anisotropic material. The document concludes by investigating the radiation effects from a uniform line source that runs through a lossy anisotropic shell of finite thickness. The document discusses combined-field surface integral equations (CFSIE's). It presents highlights of the method of moments (MOM) numerical solution to CFSIE's and gives numerical results for solid, hollow, and coated cylindrical scatterers. The effects of material anisotrophy in the EM response of the scatterer are emphasized. DTIC

N93-30611# Federal Aviation Administration, Cambridge, MA.
AN ANALYSIS OF EN ROUTE CONTROLLER-PILOT VOICE COMMUNICATIONS
Kim M. Cardosi Mar. 1993 25 p
(AD-A264784; DOT-VNTSC-FAA-93-2; DOT/FAA/RD-93/11) Avail: CASI HC A03/MF A01

The purpose of this analysis was to examine current pilot-controller communication practices in the en route environment. Forty-eight hours of voice tapes from eight different Air Route Traffic Control Centers (ARTCC's) were examined. There were 5,032 controller-to-pilot transmissions and 3,576 clearances (e.g., instructions to maneuver or change radio frequencies, routing changes, etc.) in this sample. The complexity of the clearance (i.e., the number of pieces of information) was examined and the number of erroneous readbacks and pilot requests for repeats were analyzed as a function of clearance complexity. Pilot acknowledgements were also analyzed; the numbers of full and partial readbacks, and acknowledgements only (i.e., 'roger') were tallied. Fewer than one percent of the clearances resulted in communications errors. Among the error factors examined were the following: complexity of the clearance, type of acknowledgement, use of call sign in the acknowledgement, type of information in error, and whether or not the controller responded to the readback error. Instances in which the controller contacted the aircraft with one call sign and the pilot acknowledged the transmission with another call sign were also examined. The report concludes with recommendations to further reduce the probability of communication problems. DTIC

N93-30631# Oak Ridge National Lab., TN.
RADIATION-HARDENED MICROWAVE COMMUNICATIONS SYSTEM
S. F. Smith, D. W. Bible, R. I. Crutcher, J. H. Hannah, J. A. Moore, C. H. Nowlin, R. I. Vandermolen, D. Chagnot (Commissariat a l'Energie Atomique, Grenoble, France.), and A. LeRoy (Commissariat a l'Energie Atomique, Grenoble, France.) 1993 9 p Presented at the 5th Topical Meeting on Robotics and Remote Systems, Knoxville, TN, 26-29 Apr. 1993
(Contract DE-AC05-84OR-21400)
(DE93-007915; CONF-930403-21) Avail: CASI HC A02/MF A01

To develop a wireless communication system to meet the stringent requirements for a nuclear hot cell and similar environments, including control of advanced servomanipulators, a microwave signal transmission system development program was established to produce a demonstration prototype for the Consolidated Fuel Reprocessing Program at Oak Ridge National Laboratory (ORNL). Proof-of-principle tests in a partially metal lined enclosure at ORNL successfully demonstrated the feasibility of directed microwave signal transmission techniques for remote systems applications. The potential for much more severe radio-frequency (RF) multipath propagation conditions in fully metal lined cells led to a programmatic decision to conduct additional testing in more typical hot-cell environments at other sites. Again, the test results were excellent. Based on the designs of the earlier systems, an advanced microwave signal transmission system configuration was subsequently developed that, in highly reflective environments, will support both high-performance video channels and high baud-rate digital data links at total gamma dose tolerance levels exceeding 10(exp 7) rads and at elevated ambient temperatures. DOE

N93-30662# National Oceanic and Atmospheric Administration, Miami, FL.
RECEPTION AT ASCENSION ISLAND, SOUTH ATLANTIC, OF THE TRANSMISSIONS FROM THE HEARD ISLAND FEASIBILITY TEST
D. R. Palmer, T. M. Georges, J. J. Wilson, L. D. Weiner, and J. A. Paisley Feb. 1993 35 p Prepared in cooperation with Computer Sciences Raytheon Co., Patrick AFB, FL
(PB93-176261; NOAA-TM-ERL-AOML-73) Avail: CASI HC A03/MF A01

The objective of the Heard Island Feasibility Test (HIFT) is to ensonify the global ocean with a single source to determine the feasibility of measuring the extent of ocean warming due to the greenhouse effect. The signal-to-noise ratios and the precision of arrival times measured at the listening stations will help determine the feasibility of a long-term effort to monitor average oceanic temperature change. The report describes the observational effort undertaken at ascension and discusses general features of the data set collected there. Emphasis is on the spectral characteristics of the received signals and their temporal characteristics before demodulation. NTIS

N93-30672# Technische Univ., Berlin (Germany). Fachbereich Elektrotechnik.
EXAMINATIONS OF PERTURBATION REDUCTION BY AUTOMATIC SPEECH DEPENDENT RECOGNITION OF SEPARATELY SPOKEN SINGLE WORDS Ph.D. Thesis [UNTERSUCHUNGEN ZUR STOERREDUKTION BEI DER AUTOMATISCHEN SPRECHERABHAENGIGEN ERKENNUNG VON ISOLIERT GESPROCHENEN EINZELWOERTERN]
Dieter Becker 1992 118 p In GERMAN
(ETN-93-94180) Avail: CASI HC A06/MF A02

Algorithms for combination of speech recognition with integrated disturbance cancellation are developed. Some processes of disturbance insensitive speech recognition systems are described, such as extraction of disturbance insensitive speech parameters, training of the reference data base in perturbed environment and a combination of both systems, which uses the Mel frequency cepstral coefficients and the dynamic programming. Several methods of disturbance reduction are presented, which are characterized as one, two and four channel processes, and are based on spectral substraction, adaptive filtration and adaptive Wiener filtration algorithms. Results of speech recognition system simulation without perturbation reduction algorithm and under noise influence are presented, and strategies for speech recognition systems with integrated one, two, and four channel noise reduction are depicted. ESA

N93-30727# Advisory Group for Aerospace Research and Development, Neuilly-Sur-Seine (France). Electromagnetic Wave Propagation Panel.
ELF/VLF/LF RADIO PROPAGATION AND SYSTEMS ASPECTS [LA PROPAGATION DES ONDES RADIO ELF/VLF/LF ET LES ASPECTS SYSTEMES]
May 1993 343 p Symposium held in Brussels, Belgium, 28 Sep. - 2 Oct. 1992

(AGARD-CP-529; ISBN-92-835-0712-6) Copyright Avail: CASI HC A15/MF A03

This publication reports the papers presented to a specialists' meeting held by the Electromagnetic Wave Propagation Panel at its Fall 1992 meeting. The topics covered on the occasion of that symposium include the following: (1) propagation aspects--numerical modelling, propagation measurements, and propagation in sea water; (2) radio noise and interference--long wave TE/TM noise prediction model, measurements, and ELF generated by auroral electrojet modulation; (3) antenna considerations--antenna fundamentals, scale modelling, measurements of pattern and bandwidth, and tethered aerostat VLF/LF transmitting antennas; (4) System aspects--viability assessment for reliable LW communication links; and (5) future satellite systems--orbiting system for ELF/VLF strategic communications, and tethered satellite systems. For individual titles, see N93-30728 through N93-30755.

N93-30728# Communications Research Centre, Ottawa (Ontario).
INTRODUCTION
John S. Belrose *In* AGARD, ELF/VLF/LF Radio Propagation and Systems Aspects May 1993 12 p (For primary document see N93-30727 11-32)
Copyright Avail: CASI HC A03/MF A03

An introduction and welcome to the Specialists' Meeting on 'ELF/VLF/LF Radio Propagation and System Aspects' given at the Electromagnetic Wave Propagation Panel Symposium, held at the Quartier Reine Elisabeth, Brussels, Belgium, 28 Sep. - 2 Oct. 1992, is presented. The following topics are discussed: the early history of radio communications, NATO interest in ELF/VLF/LF, propagation mode, effect of the finite conductivity of the ground, and VLF antennas. CASI

N93-30729# Naval Command, Control and Ocean Surveillance Center, San Diego, CA. Ocean and Atmospheric Sciences Div.
NUMERICAL MODELING OF THE PROPAGATION MEDIUM AT VLF/LF
J. A. Ferguson *In* AGARD, ELF/VLF/LF Radio Propagation and Systems Aspects May 1993 9 p (For primary document see N93-30727 11-32)
Copyright Avail: CASI HC A02/MF A03

A reliable knowledge of radio signal amplitude and phase characteristics is required to design and maintain communications and navigational circuits at VLF and LF. The ability to accurately calculate signal levels as a function of frequency, position, and time is of considerable importance in achieving reliable assessment of communication and navigation coverage. Detailed computer models based on multiple mode waveguide theory were developed. These models were found to produce good comparisons between measurements and calculations of signal variations as a function of propagation distance. However, results can be very sensitive to the ionospheric inputs to these computer models. This paper presents an overview of the computer model and results of empirical modeling of the propagation medium. Author (revised)

N93-30730# Naval Undersea Warfare Center, New London, CT.
ELF PROPAGATION HIGHLIGHTS
Peter R. Bannister *In* AGARD, ELF/VLF/LF Radio Propagation and Systems Aspects May 1993 15 p (For primary document see N93-30727 11-32)
Copyright Avail: CASI HC A03/MF A03

In this paper, we have presented a tutorial overview of ELF propagation. We have also compared the Greifingers simple form approximate expressions (which relate ELF propagation constants to realistic ionospheric conductivity profiles) with experimentally derived results for both daytime and nighttime ambient propagation conditions. The inverse problem has also been considered. We have used the experimentally determined values of effective attenuation rate and excitation factor, along with the modified Greifinger equations, to establish representative ionospheric parameters for each propagation path considered. These parameters include the reflection height h(sub o), the inverse scale height Beta (which is equal to 1/Zeta(sub 0)), and the reference height H of the equivalent exponential ionospheric conductivity profile. We have recently analyzed some of the field strength data taken at the U.S. Navy's four land based ELF monitoring sites (New London, CT; Norfolk, VA; Kings Bay, GA; and Pearl City, HI). Both the daytime and nighttime inferred values of excitation factors and daytime attenuation rates are in good agreement with previous 75 Hz band measurements taken over various propagation paths. However, the summertime nighttime attenuation rates are substantially lower (approximately 0.6 dB/Mm compared to approximately 1.0 dB/Mm). Also, the summertime daytime attenuation rates (approximately 1.25 dB/Mm) are lower than measured during other times of the year (approximately 1.50 dB/Mm). Author (revised)

N93-30731*# National Aeronautics and Space Administration. Goddard Space Flight Center, Greenbelt, MD.
THE CONE STRUCTURE AND FOCUSING OF THE ELECTRIC FIELD OF VLF AND LF WAVES AT HIGH ALTITUDES OF THE IONOSPHERE
Y. L. Alpert (Harvard-Smithsonian Center for Astrophysics, Cambridge, MA.) and J. L. Green *In* AGARD, ELF/VLF/LF Radio Propagation and Systems Aspects May 1993 11 p (For primary document see N93-30727 11-32)
Copyright Avail: CASI HC A03/MF A03

This paper presents a short review of the frequency and angle dependencies of the electric field radiated by an electric dipole E = E(sub 0)cos(omega)t in a magnetoplasma and detailed results of numerical calculations of (E) in the VLF and LF frequency bands 0.02f(sub b) is less than or equal to F is less than or equal to 0.5f(sub b) in the ionosphere and magnetosphere in the altitude region Z = (800 - 6000) km (F is approximately (4 - 500) kHz and f(sub b) is approximately equal to (1.1 to 0.2) MHz is the electron gyro-frequency). The amplitudes of the electric field have large maxima in four regions: close to the direction of the Earth magnetic field line B(sub 0) (it is the so called Axis field E(sub 0); in the Storey E(sub St); Reversed Storey E(sub RevSt); and Resonance E(sub Res) Cones. The maximal values of E(sub 0), E(sub Res), and E(sub Rev ST) are the most pronounced close to the low hybrid frequency, F is approximately F(sub L). The flux of the electric field is concentrated in very narrow regions, with the apexes angles of the cones delta(beta) is approximately (0.1 - 1) degree. The enhancement and focusing of the electric field increases with altitude starting at Z is greater than 800 km. At Z is greater than or equal to 1000 up to 6000 km, the relative value of E, in comparison with its value at Z equals 800 km is about (10(exp 2) to 10(exp 10)) times larger. Thus, the flux of VLF and LF electromagnetic waves in the Earth magnetoplasma produces and is guided by very narrow pencil beams, similar, let us say, to laser beams. Author (revised)

N93-30732# Naval Command, Control and Ocean Surveillance Center, San Diego, CA. Ocean and Atmospheric Sciences Div.
VLF/LF PROPAGATION MEASUREMENTS
John E. Bickel *In* AGARD, ELF/VLF/LF Radio Propagation and Systems Aspects May 1993 14 p (For primary document see N93-30727 11-32)
Copyright Avail: CASI HC A03/MF A03

The Research, Development, Test, and Evaluation (RDT&E) division of the Naval Command, Control and Ocean Surveillance Center (NCCOSC), and its predecessors, Navy Electronics Laboratory (NEL), Naval Electronics Laboratory Center (NELC), and Naval Ocean Systems Center (NOSC), have had a continuing program to develop a reliable VLF/LF communications coverage prediction capability for the U.S. Navy. This involves the measurement of field intensity of many communication stations, the development of propagation models to fit the data measured, and the validation of these models to verify predictions for all seasons world-wide, including possible solar cycle effects. During the current campaigns, data were recorded using various platforms including numerous aircraft, six ships, three submarines, and up to 28 fixed sites since 1981. Currently, data are being recorded aboard two ships and at seven fixed sites. An attempt is made to maintain an overall root-mean-square (rms) accuracy of 0.5 dB, with system calibration and stability measured to the order of 0.1 dB ring. The goal for the model under development is to fit these data and extrapolate predictions to other propagation conditions to within 1 dB. This was a challenging task where local environmental effects can cause significantly larger perturbations. A review of the literature is presented summarizing and comparing methods and techniques used by other researchers in the field. This is followed by discussion of the commercial equipment used, the calibration and recording procedures followed, a comparison of results obtained simultaneously using various platforms and sites, and an estimate of the overall accuracy/reliability of the data obtained. Author (revised)

N93-30733# Communications Research Centre, Ottawa (Ontario).

VLF PROPAGATION MEASUREMENTS IN THE CANADIAN ARCTIC

Wilfred R. Lauber and Jean M. Bertrand *In* AGARD, ELF/VLF/LF Radio Propagation and Systems Aspects May 1993 12 p (For primary document see N93-30727 11-32)

Copyright Avail: CASI HC A03/MF A03

For the past three years, during a period of high sun spot numbers, propagation measurements were made on the reception of VLF signals in the Canadian Arctic. Between Aug. and Dec. 1989, the received signal strengths were measured on the Canadian Coast Guard icebreaker, John A. MacDonald in the Eastern Canadian Arctic. Between Jul. 1991 and Jun. 1992, the received signal strengths were measured at Nanisivik, Baffin Island. The purposes of this work were to check the accuracy and estimate variances of the Naval Ocean Systems Center's (NOSC) Long Wave Propagation Capability (LWPC) predictions in the Canadian Arctic and to gather ionospheric storm data. In addition, the NOSC data taken at Fort Smith and our data at Nanisivik were used to test the newly developed Longwave Noise Prediction (LNP) program and the CCIR noise predictions, at 21.4 and 24.0 kHz. The results of the work presented and discussed in this paper show that in general the LWPC predicts accurate values of received signal strength in the Canadian Arctic with standard deviations of 1 to 2 dB over several months. Ionospheric storms can gauge the received signal strengths to decrease some 10 dB for a period of several hours or days. However, the effects of these storms are highly dependent on the propagation path. Finally the new LNP atmospheric noise model predicts lower values of noise in the Arctic than the CCIR model and our limited measurements tend to support these lower values. Author (revised)

N93-30734# Telefunken System Technik G.m.b.H., Ulm (Germany). Radio Communications Subdivision.

THEORETICAL AND EXPERIMENTAL COVERAGE ANALYSIS OF A VLF TRANSMITTER

Detlev Borgmann *In* AGARD, ELF/VLF/LF Radio Propagation and Systems Aspects May 1993 5 p (For primary document see N93-30727 11-32)

Copyright Avail: CASI HC A01/MF A03

The coverage area of a VLF transmitting station, located in the northern part of Germany, is analyzed. In order to predict the receiving skin depth for the complete operation area of the VLF station, some investigations were made in theoretical propagation models. Then a computer program based on the wave guide mode theory was implemented. To verify the validation of the theoretical model, measurements of field strength in some specific areas were carried out. The first part of the paper is concerned with a description of the theoretical approach of the coverage analysis. The second part describes some properties of the operation area and gives in detail results from measurements. Finally, a comparison of theoretical and measured data then shows the quality of agreement between theory and praxis. Author (revised)

N93-30735# IWG Corp., San Diego, CA.

INVESTIGATIONS OF EQUATORIAL IONOSPHERE NIGHTTIME MODE CONVERSION AT VLF

Verne Hildebrand *In* AGARD, ELF/VLF/LF Radio Propagation and Systems Aspects May 1993 11 p Sponsored in part by ONR (For primary document see N93-30727 11-32)

Copyright Avail: CASI HC A03/MF A03

VLF Radiowave propagation provides one of the few viable tools for exploring the properties of the lower D-region ionosphere. Conversely, VLF communications coverage analysis and prediction is directly dependent on the quality of models for the D-region ionosphere. The VLF Omega navigation signals are an excellent and under-utilized resource for conducting D-region research in direct support of VLF communications. Stations are well placed for investigating polar, mid latitude, and equatorial phenomena. Much can be learned by fully utilizing the very stable signals radiated at five frequencies, available from each of the eight transmitters, and taking full advantage of modal structure. While the Omega signals, 10.2 to 13.6 kHz, are well below the VLF communications band, we contend that much of the knowledge gained on D-region characteristics can be directly applied at the higher frequencies. The opportunity offered by Omega needs to be exploited. With the Global Positioning System (GPS) coming onboard as the prime means for global navigation, pressure is mounting to phase out Omega. In this paper we describe how we are using Omega along with computer codes of full wave VLF propagation, provided to us by the U.S. Naval Ocean Systems Center (NOSC), for ionosphere research and by example illustrate the potential for other investigations. Author (revised)

N93-30736# British Antarctic Survey, Cambridge (England).

TRANSIENT (APPROXIMATELY EQUALS 10 s) VLF AMPLITUDE AND PHASE PERTURBATIONS DUE TO LIGHTNING-INDUCED ELECTRON PRECIPITATION INTO THE IONOSPHERE (THE TRIMPI EFFECT)

A. J. Smith, P. D. Cotton, and J. S. Robertson *In* AGARD, ELF/VLF/LF Radio Propagation and Systems Aspects May 1993 7 p (For primary document see N93-30727 11-32)

Copyright Avail: CASI HC A02/MF A03

This paper describes certain characteristics and statistics of the Trimpi effect, as observed near to and equatorward of the Antarctic Peninsula region, inferred using data from specially designed narrowband OPAL (Omega Phase and Amplitude Logger) receivers deployed in 1989 at Faraday and Halley stations, Antarctica. The amplitude and phase of signals from four Omega VLF transmitters were recorded in each Omega segment (8 segments per 10 s). A 12 month data set was scanned for Trimpi events which, however, were observed on only three of the eight paths, namely Hawaii-Faraday, Argentina-Faraday, and Argentina-Halley, due to inadequate signal-noise ratio on the other paths. The great majority of the approximately 3500 observed events occurred at night. For the all-sea, Hawaii-Faraday path at night, with a single mode dominant at the receiver, lightning-induced electron precipitation (LEP) was inferred to be occurring up to approximately 1.8 Mm from Faraday. A scatter plot of Trimpi amplitude versus phase for this path is interpreted to infer that LEP regions responsible for the events occurred mostly in the L-range 2-3, with the horizontal size of an affected region in the ionosphere being typically 50 km latitudinally and 200 km longitudinally. Author (revised)

N93-30737*# Stanford Univ., CA. Space, Telecommunications and Radioscience Lab.

LIGHTNING-INDUCED EFFECTS ON VLF/LF RADIO PROPAGATION

U. S. Inan and J. V. Rodriguez *In* AGARD, ELF/VLF/LF Radio Propagation and Systems Aspects May 1993 10 p Sponsored by NASA, Washington (For primary document see N93-30727 11-32)
(Contracts N00014-82-K-0489; N00014-92-J-1579; NSF DPP-90-20687; NSF ATM-91-13012)

Copyright Avail: CASI HC A02/MF A03

In recent years, at least two different ways in which energy from lightning discharges couples into the lower ionosphere and the radiation belts have come to the fore. In this paper, we briefly review these recent results especially from the point of view of their effects on VLF/LF radio propagation in the earth-ionosphere wave guide. We separately discuss two different mechanisms of coupling, namely lightning-induced electron precipitation, and lightning-induced heating and ionization of the lower ionosphere. We also discuss a planned active VLF wave-injection experiment designed to investigate ionospheric heating by VLF waves under controlled conditions and to generate ELF waves by modulated VLF heating. Author (revised)

N93-30738# Leicester Univ. (England). Dept. of Engineering.

STUDIES OF THE PROPAGATION OF LOW FREQUENCY (LF) RADIO WAVES

E. M. Warrington and T. B. Jones *In* AGARD, ELF/VLF/LF Radio Propagation and Systems Aspects May 1993 20 p Sponsored in part by Defence Research Agency (For primary document see N93-30727 11-32)

Copyright Avail: CASI HC A03/MF A03

Low frequency (30-300 kHz) radio waves can propagate to great distances with little attenuation in the cavity formed by the earth and the ionosphere. Because of the relatively high frequency at LF, many active propagation modes can occur between the transmitter and receiver. Changes in the ionospheric conductivity or reflection height can influence the phase and amplitude of these modes and, hence, produce mutual interference. Because of these interference effects, the propagation is less stable than at VLF and the received field strength becomes more difficult to predict. In the present investigation, the WAVEHOP program was employed in conjunction with a range of ionospheric models to estimate the receiver field strength over a number of experimental paths. The predicted values were compared with those measured in an attempt to validate the ionospheric models and the method of calculation. Author (revised)

N93-30739# Kings Coll., London (England). Dept. of Physics.
ELF PROPAGATION IN DEEP AND SHALLOW SEA WATER
C. P. Burke and D. LlanwynJones *In* AGARD, ELF/VLF/LF Radio Propagation and Systems Aspects May 1993 8 p Sponsored in part by Defence Research Agency (For primary document see N93-30727 11-32)
Copyright Avail: CASI HC A02/MF A03

In this paper, electromagnetic wave propagation at Extremely Low Frequencies (ELF) in deep and shallow sea water is considered. The term 'ELF' is used here somewhat loosely to refer to the frequency band 0-3 kHz. The radiation source is considered to be located in the sea water and is taken to be a horizontal electric dipole (HED) or a vertical electric dipole (VED). For the deep water ease, a comparison is made between results computed using complex image theory and results calculated using the full Sommerfeld integral formulation. Both of these formulations include the lateral waves which propagate along the air-sea interface. Moving on to the case of shallow water, there are two lateral wave modes of propagation-lateral waves which propagate on the sea surface and along the seabed. These modes are included by numerical evaluation of the Sommerfeld integrals which appear in the complete solution. We also compare the relative efficacy of subsurface horizontal electric dipoles and vertical electric dipoles as radiators. For the case of zero frequency (dc), the Sommerfeld integrals simplify considerably enabling the fields to be evaluated as the sums of infinite series. This dc formulation leads to much reduced computation time. Finally, the effects on propagation of long-wavelength water gravity waves or tides on the surface of the sea are examined by considering these waves as a perturbation to the sea-air interface. Author (revised)

N93-30740# Vrije Univ., Brussels (Belgium).
COMPARATIVE STUDY OF UNDERSEA FIELDS PRODUCED BY VARIOUS DIPOLES
G. Annaert and A. Barel *In* AGARD, ELF/VLF/LF Radio Propagation and Systems Aspects May 1993 9 p (For primary document see N93-30727 11-32)
Copyright Avail: CASI HC A02/MF A03

ELF/VLF/LF-radiation by electric or magnetic dipoles located above or on the surface of the earth or sea is investigated from the exact Sommerfeld potentials. Due to the nonzero conductivity of the ground or sea water, the waves are strongly attenuated and only a small near field can be effectively used for communication in a low frequency range. The Fresnel coefficient approximation technique, which presumes a planar plane wave propagation, is correct in the far-field but loses great accuracy in a region close to the radiator. It is the purpose of this paper to review the electromagnetic propagation in layered media based on the rigorous spectral domain method. This theory expresses the Hertz potentials, either of the magnetic type A or the electric type F, in terms of Sommerfeld integrals. A communication range, as the maximum depth at which satisfactory signal reception is still possible, is derived in function of ground parameters, frequency, and dipole orientation. Author (revised)

N93-30741# Defence Research Agency, London (England).
A METHODOLOGY AND TOOL FOR THE PREDICTION OF DEPTH OF RECEPTION IN THE SEA FOR A VLF/LF COMMUNICATIONS SYSTEM
D. M. Nicholls *In* AGARD, ELF/VLF/LF Radio Propagation and Systems Aspects May 1993 12 p Sponsored in part by Ministry of Defence (For primary document see N93-30727 11-32)
Copyright Avail: CASI HC A03/MF A03

This paper describes a method of predicting the depth performance of a VLF/LF (Very Low Frequency/Low Frequency) communications system for submarine reception. The method uses a Long Wave Propagation Capability program which includes parameters of the system to be considered, such as transmitter power, aerial, and receiver sensitivities. Results from an analysis for a particular communications system are presented including an audio visual format to show the expected variations in depth performance with reference to operational frequency, transmitter power, time of day and year, and the signal to noise requirements for the system. The analysis method is flexible and could be adapted for similar communications systems. Author (revised)

N93-30742# Pacific-Sierra Research Corp., Santa Monica, CA.
A LONG WAVE TE/TM NOISE PREDICTION MODEL
C. R. Warber and E. C. Field, Jr. *In* AGARD, ELF/VLF/LF Radio Propagation and Systems Aspects May 1993 12 p (For primary document see N93-30727 11-32)
Copyright Avail: CASI HC A03/MF A03

A computer model that predicts both horizontally and vertically polarized noise in the ELF to LF band (10 Hz-60 kHz) is described. Since naturally occurring radio noise in this band is produced by lightning, and propagates to the receiver via the earth-ionosphere waveguide, the model starts with average lightning flash density data which it turns into radiated power for horizontal and vertical noise. Adjustments are made to the radiated power to account for seasonal and latitudinal differences in the lightning processes. The noise power is then integrated over fairly large geographic areas into horizontal and vertical equivalent noise transmitters. The power radiated from each of these transmitters is propagated to the receiver location using standard anisotropic long wave propagation algorithms and well-known models of the earth-ionosphere waveguide. From the received power, the model predicts RMS noise, standard deviation, voltage deviation VD, and the amplitude probability distribution of the noise for both polarizations. Since the model is based on theory, it can also predict these parameters under disturbed ionospheric conditions. The model's agreement with data is demonstrated. Author (revised)

N93-30743# Genoa Univ. (Italy). Dept. of Biophysical and Electronic Engineering.
APPLICATION OF NON-STANDARD SIGNAL PROCESSING TO ELF NOISE CHARACTERIZATION FOR THE TSS1-OESEE PROGRAMME
G. Tacconi, A. Tiano (Pavia Univ., Italy.), and S. Pagnan (Consiglio Nazionale delle Ricerche, Genoa, Italy.) *In* AGARD, ELF/VLF/LF Radio Propagation and Systems Aspects May 1993 8 p Sponsored in part by Italian Space Agency (For primary document see N93-30727 11-32)
Copyright Avail: CASI HC A02/MF A03

Within the framework of the TSS1 (Tethered Satellite System)-Project, a measurement program on the electromagnetic background noise was performed. This program, called OESEE (Observation on the Earth Surface of Electromagnetic Emissions), intends to carry out a number of passive detections of possible emissions by the orbiting tethered system. From theoretical considerations on the cold plasma theory in the ionosphere, the expected frequency band of these emissions should be in the order of about 1 Hz up to 60 Hz. In order to design an optimal receiver of such a signal, the noise statistical characteristics have to be taken into account. From the literature, it was shown that this noise is characterized, from the statistical viewpoint, by a non-gaussian and non-stationary behavior. This paper outlines some recently proposed applications of non-gaussian and non-stationary signal processing techniques which can be usefully applied to ELF (Extremely Low Frequency) electromagnetic noise characterization for detection and parameter estimation purposes. Some simulation examples are presented together with some results obtained from experimental data of natural background noise in the ELF range recorded at Canary Islands as a preliminary test of the TSS1 mission. The TSS1 (Tethered Satellite System) is a NASA/ASI (Agenzia Spaziale Italiana) research project. Author (revised)

N93-30744# Stanford Univ., CA. Space, Telecommunications and Radioscience Lab.
ELF/VLF RADIO NOISE MEASUREMENTS AT HIGH LATITUDES DURING SOLAR PARTICLE EVENTS
A. C. Fraser-Smith and J. P. Turtle (Rome Lab., Hanscom AFB, MA.) *In* AGARD, ELF/VLF/LF Radio Propagation and Systems Aspects May 1993 8 p (For primary document see N93-30727 11-32)
(Contracts F19628-89-K-0015; N00014-81-K-0382; N00014-90-J-1080; N00014-92-J-1576; NSF ATM-88-22560; NSF DPP-87-20167; NSF DPP-91-19552)
Copyright Avail: CASI HC A02/MF A03

We report simultaneous measurements of ELF/VLF radio noise (10 Hz-32 kHz) at three high latitude locations (Thule and Sondrestromfjord, Greenland; and Arrival Heights, Antarctica) during a number of moderately large and large solar particle events (SPE's) including some of the largest that have been observed during the last three decades. Thule is close to the center of the northern polar cap and thus the ELF/VLF noise signals reaching it are particularly exposed to the ionospheric effects of the SPE's, whereas the ELF/VLF noise signals at Sondrestromfjord and Arrival Heights, which are located closer to their corresponding auroral zones, should be less affected. These general expectations are supported by the results of our measurements, which show major changes occurring in the Thule noise statistics following the start of the polar cap absorption (PCA) caused by the SPE's and smaller changes at Sondrestromfjord and Arrival Heights. The changes depend markedly on the frequency of the noise signals. At Thule, for frequencies in the approximate range 250 Hz to 1.5 kHz, the diurnal variation in the ring noise amplitudes is typically suppressed during the 2-3 days following the start of the PCA, and in most of the examples we have examined there tends to be a decrease in the average amplitude. Nevertheless, increases can occur. Following the event of 12 Aug. 1989, the noise amplitudes increased by as much as 10-15 dB. For most other frequencies in the range 10 Hz-32 kHz there is little change in the noise statistics. However, in the range 3-10 kHz there tends to be a marked decline in the ring noise amplitudes at Thule in the 24 hours following the start of the PCA, after which there is a rapid recovery to the undisturbed levels. At Sondrestromfjord and, to a lesser extent, at Arrival Heights, the most marked change appears to be the suppression of the diurnal variation noise peaks and thus lower average noise amplitudes in the 2-3 days following the start of the PCA. Author (revised)

N93-30745# Institute for Telecommunication Sciences, Boulder, CO.
ELF/VLF SPECTRUM MEASUREMENTS
M. G. Laflin *In* AGARD, ELF/VLF/LF Radio Propagation and Systems Aspects May 1993 12 p (For primary document see N93-30727 11-32)
Copyright Avail: CASI HC A03/MF A03

A 16-bit digital spectrum analysis system was designed and built to provide measurement capabilities not currently available in commercial systems. The system provides the wide dynamic range necessary to observe very weak signals in the presence of strong signals. Large sample size allows for high frequency resolution. System outputs include spectral densities, amplitude probability distributions, diurnal amplitude variations, and time domain plots. Measurements were made to characterize the ELF/VLF H-field noise environment in a sampling of office buildings. These include two buildings in New York City and two Denver office buildings. Measurements were made for all hours of the day and include business day and weekend coverage. Results reveal a complicated signal environment. Associated with the power distribution frequencies were strong odd harmonics with higher harmonics evident into the kilo Hertz range; other man-made noise components were also evident. Author

N93-30746# Naval Underwater Systems Center, New London, CT.
RESULTS OF THE JOINT HIPAS/NUWC CAMPAIGNS TO INVESTIGATE ELF GENERATED BY AURORAL ELECTROJET MODULATION
Peter R. Bannister, Raymond F. Ingram, Michael J. McCarrick (California Univ., Los Angeles.), and Alfred Y. Wong (California Univ., Los Angeles.) *In* AGARD, ELF/VLF/LF Radio Propagation and Systems Aspects May 1993 12 p (For primary document see N93-30727 11-32)
Copyright Avail: CASI HC A03/MF A03

This paper reports the results of the first concerted effort (both experimentally and theoretically) to characterize the various parameters of the Extremely Low Frequency (ELF) and HIgh Power Auroral Stimulation (HIPAS) polar electrojet antenna excited by the HIPAS radiating facility. These parameters include the magnetic dipole moment, excitation height, and range and bearing dependence. The experimentally determined values of these various parameters, using a mobile ELF receiver, as well as a long distance station, are in agreement with predictions. Author (revised)

N93-30747# Communications Research Centre, Ottawa (Ontario).
VLF/LF TRANSMITTING ANTENNAS
John S. Belrose *In* AGARD, ELF/VLF/LF Radio Propagation and Systems Aspects May 1993 22 p Sponsored in part by Dept. of National Defence (For primary document see N93-30727 11-32)
Copyright Avail: CASI HC A03/MF A03

Very Low Frequency (VLF) transmitting antenna design is a specialized field of engineering that requires the combined skill of radio, civil, and mechanical engineers. The antenna systems used for this band (15-30 kHz) are enormous structures. Vertical radiators with very extensive top-loading (non-radiating top-hats) are necessary because the electrical height of practical towers is small. For tower heights of 300-450 meters (1000-1500 feet) the electrical heights are only fifteen to forty-five one thousandths of a wavelength. This presentation discusses the following topics: antenna design concepts, antenna fundamentals, tools for antenna modeling, a mini-study of conventional antennas, multiple tuned antenna systems, and a comparison between performance (measured and predicted) for multiple tuned antennas vs. single tuned antennas. Author (revised)

N93-30748# Defence Research Agency, London (England).
A DYNAMIC BANDWIDTH AND PHASE LINEARITY MEASUREMENT TECHNIQUE FOR 4-CHANNEL MSK VLF ANTENNA SYSTEMS
M. D. Harrington *In* AGARD, ELF/VLF/LF Radio Propagation and Systems Aspects May 1993 8 p Sponsored in part by Ministry of Defence (For primary document see N93-30727 11-32)
Copyright Avail: CASI HC A02/MF A03

This paper presents a method for performing dynamic measurements of antenna bandwidth and phase linearity parameters for VLF transmitter systems. These measurements were undertaken in support of both National and NATO VLF MSK upgrade programs and relate to VLF transmitting antenna characteristics required in order to comply with STANAG 5030. Author (revised)

N93-30749# Defence Research Agency, London (England).
STUDY OF A VLF DISTRIBUTED ANTENNA ARRAY
G. A. Ashdown *In* AGARD, ELF/VLF/LF Radio Propagation and Systems Aspects May 1993 13 p Sponsored in part by Ministry of Defence (For primary document see N93-30727 11-32)
Copyright Avail: CASI HC A03/MF A03

This study considers the use of an array of VLF antennas distributed throughout the UK, instead of a single, high powered antenna, for submarine command broadcasts. Such an array offers survivability and environmental advantages. The coverage of the array would, however, not be omni-azimuthal, but would have nulls every few degrees as a result of the interference between the signals from the individual antennas. The study investigates the effect on the array coverage of a number of impairments (operating frequency, phase and frequency errors, and antenna loss) and discusses the advantages and disadvantages of steering the main beam to the receiving platform. Consideration is also given to how the received signal will be distorted depending on the location of the receiving platform. It was concluded that a VLF array would not be suitable for providing wide area continuous and assured communications. Author (revised)

N93-30750# Porto Univ. (Portugal). Dept. de Engenharia Electrotecnica e de Computadores.
APPLICATION OF THE FOURIER TRANSFORM TO SHORT ANTENNAS
Francisco C. V. Grilo *In* AGARD, ELF/VLF/LF Radio Propagation and Systems Aspects May 1993 7 p (For primary document see N93-30727 11-32)
Copyright Avail: CASI HC A02/MF A03

As is well known, the far field pattern of an aperture is related to a distribution of radiating sources by the Fourier Transform. In this paper, we show that it is also possible to use a Fourier Transform to perform the analysis and synthesis of short antennas. In this way, we can easily have both the analytical and graphical representation of the antenna pattern and the errors that we make with the usual approximating models. It is also possible to make use of know how from the field of signal processing to perform the analysis and synthesis of the radiation pattern. All the theory is based on the Theorem of the Small Complex Translation meaning that we can represent all the current distribution on the antenna by complex translations of an infinitesimal element of current. The correspondent pattern can be found using an adequate spatial variable representation. Author (revised)

N93-30751# IDS Ingegneria dei Sistemi S.p.A., Pisa (Italy).
ANTENNA MODELING AND ANALYSIS FOR ELF/VLF/LF APPLICATIONS
M. Bandinelli, S. Chiti, and R. Cioni *In* AGARD, ELF/VLF/LF Radio Propagation and Systems Aspects May 1993 9 p (For primary document see N93-30727 11-32)
Copyright Avail: CASI HC A02/MF A03

This paper presents a numerical procedure which can be effectively used for the analysis/design of a very-low frequency capacitive antenna system on complex platforms and for charge distribution computation. The 'quasi static' radiation problem was solved by means of the corresponding electrostatic solution, by using a Method Of Moments (MOM) procedure.

Pulse basis functions, defined on surface patch domains, and the point-matching test procedure are used in conjunction with a powerful postprocessing numerical tool. Given the platform model, the postprocessing tool allows us to analyze all possible antenna configurations by running the MOM computer code only once. The following parameters can be evaluated: (1) antenna radiation pattern; (2) antenna Norton equivalent circuit, from which the effective voltage at the input of the receiver can be evaluated; (3) induced charge distribution; and (4) scattered electric field distribution near the platform. The proposed solution is particularly useful for applications where the criticality of the structure requires a peculiar attention in defining structural elements that constitute the 'electrical doublet' (conformal antenna). Author (revised)

N93-30752# Naval Undersea Warfare Center, New London, CT. Submarine Electromagnetic Systems Dept.

PATTERN MEASUREMENTS OF US NAVY ELF ANTENNAS

E. A. Wolkoff and W. A. Kraimer *In* AGARD, ELF/VLF/LF Radio Propagation and Systems Aspects May 1993 10 p (For primary document see N93-30727 11-32)

Copyright Avail: CASI HC A02/MF A03

The radiation pattern of an Extremely Low Frequency (ELF) transmitting antenna can be determined from field components measured at a single point. Horizontal magnetic fields from the four US Navy ELF antennas in the north central United States were measured at three receiving locations. The three resulting pattern factors for each antenna are compared and shown to be in good agreement. Author (revised)

N93-30753# SRI International Corp., Arlington, VA.

TETHERED AEROSTAT VLF/LF TRANSMITTER SYSTEM DESIGN CONSIDERATIONS

Richard L. Crawford, Thomas C. LaManna, and Kenneth L. Jordon (Science Applications International Corp., Vienna, VA.) *In* AGARD, ELF/VLF/LF Radio Propagation and Systems Aspects May 1993 6 p (For primary document see N93-30727 11-32)

Copyright Avail: CASI HC A02/MF A03

A tethered aerostat VLF/LF transmitter (TAVT) system is a cost-effective, survivable alternative for reconstituting VLF/LF communications connectivity to strategic forces in a post-attack environment. This paper describes the tradeoff design considerations that led to recommending a TAVT system with a 50,000-cubic-foot aerostat and a 5,000-foot tether used as the transmitting radio antenna. The major tradeoff factors considered in choosing this design were: survivability, transportability, coverage area, operating frequency range, maximum effective radiated power, cost, and corona avoidance. Author

N93-30754# E-Systems, Inc., Greenville, TX.

VIABILITY ASSESSMENT FOR RELIABLE LONG-WAVE COMMUNICATION LINKS

T. S. Cory and T. R. Holzheimer *In* AGARD, ELF/VLF/LF Radio Propagation and Systems Aspects May 1993 17 p (For primary document see N93-30727 11-32)

Copyright Avail: CASI HC A03/MF A03

This paper illustrates the viability of reliable global communications at VLF as a consequence of the insight gained by performing link analyses vs. frequency. The physical and economic reality of implementing these possibilities depends on the availability of transmit resources, possibly on a shared basis. Author (revised)

N93-30755*# National Aeronautics and Space Administration. Marshall Space Flight Center, Huntsville, AL.

ORBITING TRANSMITTER AND ANTENNA FOR SPACEBORNE COMMUNICATIONS AT ELF/VLF TO SUBMERGED SUBMARINES

P. R. Bannister (Naval Undersea Warfare Center, New London, CT.), J. K. Harrison, C. C. Rupp, R. W. P. King (Harvard Univ., Cambridge, MA.), M. L. Cosmo (Harvard-Smithsonian Center for Astrophysics, Cambridge, MA.), E. C. Lorenzini (Harvard-Smithsonian Center for Astrophysics, Cambridge, MA.), C. J. Dyer (Raytheon Co., Portsmouth, RI.), and M. D. Grossi (Raytheon Co., Portsmouth, RI.) *In* AGARD, ELF/VLF/LF Radio Propagation and Systems Aspects May 1993 14 p (For primary document see N93-30727 11-32)

Copyright Avail: CASI HC A03/MF A03

An orbital emplacement for the transmitter and the antenna of a communications link at ELF (30 to 300 Hz) and VLF (3 kHz to 30 kHz) to submerged submarines has been considered since the very inception of the space age. However, only recently has space technology reached a sufficient level of maturity for system designers to undertake serious studies of this link configuration. The optimistic outlook stems from recent space technology developments, such as the design and construction by NASA of long orbiting tethers, and the testing, onboard Shuttle Orbiter ATLANTIS, of the first spaceborne 20 km metal wire. This is known as the Tethered Satellite System-1 (TSS-1), a space mission that might be possibly followed by other flights, with tether lengths that could reach 100 km. Once deployed at a height of, say, 300 km, from a Shuttle Orbiter, or from another suitable platform, a long, thin tether aligns itself along the local vertical by virtue of the gradient of the Earth gravity field. If made of metal, the tether can function as a VED (Vertical Electric Dipole) transmitting antenna at ELF and VLF. Author (revised)

N93-30757# Phillips Lab., Hanscom AFB, MA.

PERFORMANCE STATISTICS BULLETIN. HIGH LATITUDE METEOR SCATTER PROPAGATION, MAY, JUNE, JULY 1989 Interim Report

Alan D. Bailey, Jens C. Ostergaard, Regina M. Burton, Carlton H. Curtis, and Wayne I. Klemetti 25 Aug. 1992 211 p

(AF Proj. 4643)

(AD-A264003; PL-TR-92-2222; ERP-1107) Avail: CASI HC A10/MF A03

A representative sampling of meteor scatter propagation performance statistics is presented from the PL/GP High Latitude Meteor Scatter Test Bed (HLMSTB). The data address questions of meteor scatter propagation under disturbed ionospheric conditions, as well as normal meteor scatter propagation in the polar region. The time and frequency variations of the propagation transfer function are characterized over the 35 to 147 MHz range, including the availability of useful meteor trails, the potential communication capacity associated with those trails, the occurrence and persistence of ionospheric scatter and sporadic E-layers, variations in the signal-to-noise ratios of each scatter return, and the effects of auroral and polar cap absorption (PCA) events on meteor scatter propagation and communications. Statistics presented include: Arrival Rate, Duration Duty Cycle and Noise Temperature as functions of Day, Time of Day, Signal Threshold, and SNR Threshold. This bulletin is one of a periodic series of polar meteor scatter data bulletins. DTIC

N93-30836# Nationaal Inst. voor Kernfysica en Hoge Energiefysica, Amsterdam (Netherlands).

MODIFICATION OF THE S-BAND PHASE SHIFTER MODEL 331A-3 OF ELECTROMAGNETIC SCIENCES INC. [MODIFICATIE VAN DE S-BAND FASEDRAAIER MODEL 331A-3 VAN ELECTROMAGNETIC SCIENCES INC.]

J. D. Schipper 1992 16 p In DUTCH

(DIGEL-1992-5; ETN-93-93308) Avail: CASI HC A03/MF A01

A phase shifter consisting of a variable delay line was modified. The range of this delay line is about 500 ps, which is more than sufficient to shift the phase 360 deg at a frequency of 2.861 GHz. The phase shifter is a piece of waveguide with an N-connector adaptor at each end. A ferrite core in the waveguide was subject to a magnetic field for a short time, causing remanescent magnetism in the core. This magnetism determines the electrical length of the waveguide. ESA

N93-30879# Cornell Univ., Ithaca, NY. Dept. of Electrical Engineering.

ENHANCED CONVERGENCE ADAPTIVE DETECTION Final Report, 1 Feb. - 30 Nov. 1991

Allan O. Steinhardt 28 Feb. 1993 8 p

(Grant AF-AFOSR-0149-91)

(AD-A264100; AFOSR-93-0313TR) Avail: CASI HC A02/MF A01

We addressed the problem of detecting targets using an array of active sensors. We have been concerned with devising means of obtaining reliable detection with a small number of samples (small relative to the number of unknown parameters). This problem arises with large arrays, and/or low cross section targets. Past techniques for addressing this problem incorporated prior structure into likelihood procedures. Such approaches are as follows: (1) intractable, requiring iterative solution, (2) not CFAR, and (3) not optimal. We have approached this problem using group symmetries. Specifically, we introduce a framework for exploring array detection problems in a reduced dimensional space by exploiting the theory of invariance in hypothesis testing. This involves calculating a low dimensional basis set of functions called the maximal invariant, the statistics of which are often tractable to obtain, thereby making analysis feasible and facilitating the search for tests with some optimality property. Using this approach, we obtain a locally most powerful test for the unstructured covariance case and show that the Kelly and AMF detectors form an algebraic span for any invariant detector. Applying the same framework to structured covariance matrices, we gain some insights and propose several new detectors which are shown to outperform existing detectors. DTIC

N93-30880# Massachusetts Inst. of Tech., Cambridge. Research Lab. of Electronics.
MICROWAVE EMISSION FROM RELATIVISTIC ELECTRON BEAMS Final Report, 1 Nov. 1988 - 31 Oct. 1989
George Bekefi 16 Apr. 1993 188 p
(Grant AF-AFOSR-0082-89)
(AD-A264102; AFOSR-93-0309TR) Avail: CASI HC A09/MF A02

This is a continuation proposal on Microwave Emission from Relativistic electron Beams. Below we summarize the various research activities. All of the experimental studies described below will be performed using our Physics International 615MR Pulserad Accelerator with a maximum voltage of 500 kV and peak currents of 4 kA and the 1.5MV, 30kA Pulserad 110A. The electron beam is presently generated by a thermionically emitting, electrostatically focused, Pierce-type electron gun (250 kV, 250 A) removed from a SLAC klystron. An assembly of six focusing coils is designed so that their magnetic field lines lie along the zero-magnetic field electron trajectories. This field configuration gives the least scalloping of the electron beam (low transverse temperature) and allows the magnetic field amplitude to be varied over a wide range without greatly affecting the electron beam temperature. Only the inner portion of the beam is used; an aperture limits the beam radius to r(sub b) = 0.254 cm. Consequently, the net current available for the different experiments is in the range of 1-8 A. In addition to the above gun, we have recently procured from SLAC a brand-new, state of the art, electron gun that can operate at 450 kV and a peak current of approximately 500 A. The advantage of this system over the previous one is our ability to operate at higher voltages and thus study the various coherent radiation mechanisms at considerably shorter wavelengths. DTIC

N93-30923# Joint Inst. for Nuclear Research, Dubna (USSR). Lab. of High Energy.
SOME PROBLEMS OF RELATIVISTIC ELECTRODYNAMICS
V. N. Streltsov 1991 14 p
(DE92-644738; JINR-E-2-91-184) Avail: CASI HC A03/MF A01 (US Sales Only)

Some problems of electrodynamics are considered from the point of view of the radar formulation of relativity theory. This formulation is based on light or retarded distances, the increasing of longitudinal sizes of moving objects is its consequence. Based of Lienard-Wiechert potentials, it is shown that in terms of retarded distances equipotential surfaces take the form of rotation ellipsoids, stretched in the direction of electric charge motion. The difficulty connected with the appearance of charge in a moving (neutral) current-carrying conductor is overcome. DOE

N93-30993# Academy of Sciences (USSR), Novosibirsk. Inst. Yadernoj Fiziki.
MICROSECOND RIBBON RELATIVISTIC ELECTRON BEAM IN A PLANE UNDULATOR AND GENERATION OF MICROWAVE RADIATION [MIKROSEKUNDNYJ LENTOCHNYJ REHP V PLOSKOM ONDULYATORE I GENERATSIYA V EHTOJSISTEME MILLIMETROVOGO IZLUCHENLYA]
A. V. Arzhannikov, S. L. Sinitskij, and M. V. Yushkov 1991 17 p In RUSSIAN
(DE93-605693; IYaF-91-85) Avail: CASI HC A03/MF A01 (US Sales Only)

Results of experiments on the transport of a microsecond ribbon REB with some kiloampers current in the plane magnetic undulator at the longitudinal guiding magnetic field were described. Influence of the guiding magnetic field strength on the passing of the beam in the 1 meter undulator and generation of microwave radiation was studied in the experiments. DOE

N93-30995# Naval Command, Control and Ocean Surveillance Center, San Diego, CA. Research, Development, Test and Evaluation.
OPTIMUM DESIGN OF MULTIWIRE CAGES FOR HIGH-VOLTAGE APPLICATIONS
P. M. Hansen Aug. 1992 73 p
(AD-A264310; NRAD-TR-1495) Avail: CASI HC A04/MF A01

This report examines the parameters for systems of multiwire cages carrying high voltages above ground in order to minimize the maximum electric field on the surface of the wires. For the two-wire case, the following methods of calculation were compared (1) a simple geometric theory (SGT); (2) a complete geometric theory (CGT); (3) an infinite series of images (exact solution for given constraints); and (4) a computer-based method of moments (MOM) solution. The MOM results were calculated for cages with 2 through 6 wires, and for 12 wires. This work resulted in two design procedures: one based on minimum wire spacing for a given wire diameter, and the other based on minimizing the total wire cross section of the cage. These procedures are presented along with three examples that include antenna and transmission line applications. DTIC

N93-31036*# Arizona State Univ., Tempe. Telecommunications Research Center.
ADVANCED ELECTROMAGNETIC METHODS FOR AEROSPACE VEHICLES Semiannual Progress Report, 1 Jan. - 30 Jun. 1993
Constantine A. Balanis, Weimin Sun, El-Budawy El-Sharawy, James T. Aberle, Craig R. Birtcher, Jian Peng, Panayiotis A. Tirkas, David Kokotoff, and Frank Zavosh 1993 91 p Conference held at Tempe, AZ, 28-29 Oct. 1992, and meeting held on 19-20 May 1993
(Grant NAG1-1082)
(NASA-CR-193468; NAS 1.26:193468; TRC-EM-CAB-9306) Avail: CASI HC A05/MF A01

The Advanced Helicopter Electromagnetics (AHE) Industrial Associates Program has continuously progressed with its research effort focused on subjects identified and recommended by the Advisory Task Force of the program. The research activities in this reporting period have been steered toward practical helicopter electromagnetic problems, such as HF antenna problems and antenna efficiencies, recommended by the AHE members at the annual conference held at Arizona State University on 28-29 Oct. 1992 and the last biannual meeting held at the Boeing Helicopter on 19-20 May 1993. The main topics addressed include the following: Composite Materials and Antenna Technology. The research work on each topic is closely tied with the AHE Consortium members' interests. Significant progress in each subject is reported. Special attention in the area of Composite Materials has been given to the following: modeling of material discontinuity and their effects on towel-bar antenna patterns; guidelines for composite material modeling by using the Green's function approach in the NEC code; measurements of towel-bar antennas grounded with a partially material-coated plate; development of 3-D volume mesh generator for modeling thick and volumetric dielectrics by using FD-TD method; FDTD modeling of horn antennas with composite E-plane walls; and antenna efficiency analysis for a horn antenna loaded with composite dielectric materials. Author (revised)

N93-28820*# Utah State Univ., Logan. Space Dynamics Lab.
PLASMA DIAGNOSTICS BY ANTENNA IMPEDANCE MEASUREMENTS Abstract Only
C. M. Swenson, K. D. Baker, E. Pound, and M. D. Jensen *In* Lunar and Planetary Inst., Workshop on Advanced Technologies for Planetary Instruments, Part 1 1993 p 24 (For primary document see N93-28764 11-91)
Avail: CASI HC A01/MF A01

N93-30219 Ottawa Univ. (Ontario). Dept. of Electrical Engineering.
NONLINEAR PROCESSING OF PHASE VOCODED SPEECH
Luc Gagnon and W. F. McGee *In* Engineering Inst. of Canada, Canadian Conference on Electrical and Computer Engineering, Volumes 1 and 2 1990 4 p (For primary document see N93-30215 11-31)
Avail: Engineering Inst. of Canada, 2050 rue Mansfield, Suite 700, Montreal, Quebec H3A 1Z2 Canada

N93-30220 Waterloo Univ. (Ontario). Dept. of Electrical and Computer Engineering.
ON SUBBAND CODING/EMBEDDED VECTOR QUANTIZATION FOR SPEECH CODING
Lise Vanterpool and Jon W. Mark *In* Engineering Inst. of Canada, Canadian Conference on Electrical and Computer Engineering, Volumes 1 and 2 1990 4 p (For primary document see N93-30215 11-31)
Avail: Engineering Inst. of Canada, 2050 rue Mansfield, Suite 700, Montreal, Quebec H3A 1Z2 Canada

N93-30221 National Research Council of Canada, Ottawa (Ontario). Speech Research Centre.
IMPROVEMENT OF THE NRC AUTOMATIC SPEECH RECOGNITION SYSTEM
Dariusz A. Zwierzynski and C. Lefebvre *In* Engineering Inst. of Canada, Canadian Conference on Electrical and Computer Engineering, Volumes 1 and 2 1990 4 p (For primary document see N93-30215 11-31)
Avail: Engineering Inst. of Canada, 2050 rue Mansfield, Suite 700, Montreal, Quebec H3A 1Z2 Canada

N93-30227 Ottawa Univ. (Ontario). Dept. of Computer Science.
PERFORMANCE ANALYSIS OF COMMUNICATION PROTOCOLS USING D-TIMED PETRI NET
G. H. Masapati and George M. White *In* Engineering Inst. of Canada, Canadian Conference on Electrical and Computer Engineering, Volumes 1 and 2 1990 4 p (For primary document see N93-30215 11-31)
Avail: Engineering Inst. of Canada, 2050 rue Mansfield, Suite 700, Montreal, Quebec H3A 1Z2 Canada

N93-30228 Ottawa Univ. (Ontario). Dept. of Computer Science.
AUTOMATIC SYNTHESIS OF PROTOCOL SPECIFICATIONS
Kassem Saleh *In* Engineering Inst. of Canada, Canadian Conference on Electrical and Computer Engineering, Volumes 1 and 2 1990 4 p (For primary document see N93-30215 11-31)
Avail: Engineering Inst. of Canada, 2050 rue Mansfield, Suite 700, Montreal, Quebec H3A 1Z2 Canada

N93-30237 Simon Fraser Univ., Burnaby (British Columbia). Communications Science Lab.
AN ERROR CONTROL PROTOCOL BASED ON TRELLIS CODED MODULATIONS
Paul Ho and Yan Wu *In* Engineering Inst. of Canada, Canadian Conference on Electrical and Computer Engineering, Volumes 1 and 2 1990 6 p (For primary document see N93-30215 11-31)
Avail: Engineering Inst. of Canada, 2050 rue Mansfield, Suite 700, Montreal, Quebec H3A 1Z2 Canada

N93-30241 Atlantis Scientific Systems Group, Inc., Ottawa (Ontario).
THE USE OF DATA TURNING IN AIRBORNE RADARS
L. Lightstone and D. Faubert *In* Engineering Inst. of Canada, Canadian Conference on Electrical and Computer Engineering, Volumes 1 and 2 1990 4 p (For primary document see N93-30215 11-31)
Avail: Engineering Inst. of Canada, 2050 rue Mansfield, Suite 700, Montreal, Quebec H3A 1Z2 Canada

N93-30250 Gandalf Technologies, Inc., Nepean (Ontario).
A SLOTTED ALOHA SATELLITE CHANNEL SIMULATOR
D. Peter Noel and Arthur F. Guibord (Telesat Canada, Ottawa, Ontario.) *In* Engineering Inst. of Canada, Canadian Conference on Electrical and Computer Engineering, Volumes 1 and 2 1990 4 p (For primary document see N93-30215 11-31)
Avail: Engineering Inst. of Canada, 2050 rue Mansfield, Suite 700, Montreal, Quebec H3A 1Z2 Canada

N93-30251 Raytheon Canada Ltd., Waterloo (Ontario).
IMPROVED BOUNDS FOR SYNCHRONIZATION JITTER
Stuart C. White and Norman C. Beaulieu (Queens Univ., Kingston, Ontario.) *In* Engineering Inst. of Canada, Canadian Conference on Electrical and Computer Engineering, Volumes 1 and 2 1990 7 p (For primary document see N93-30215 11-31)
Avail: Engineering Inst. of Canada, 2050 rue Mansfield, Suite 700, Montreal, Quebec H3A 1Z2 Canada

N93-30252 McMaster Univ., Hamilton (Ontario). Communications Research Lab.
PROPAGATION CHANNEL MODELING FOR ANGLE-DIVERSITY COMBINING SIMULATION
Milan Despinic and Desmond P. Taylor *In* Engineering Inst. of Canada, Canadian Conference on Electrical and Computer Engineering, Volumes 1 and 2 1990 4 p (For primary document see N93-30215 11-31)
Avail: Engineering Inst. of Canada, 2050 rue Mansfield, Suite 700, Montreal, Quebec H3A 1Z2 Canada

N93-30264 Defence Research Establishment, Ottawa (Ontario).
CANADIAN EHF MILSATCOM RESEARCH AND DEVELOPMENT PROJECT
Robert J. Keightley *In* Engineering Inst. of Canada, Canadian Conference on Electrical and Computer Engineering, Volumes 1 and 2 1990 4 p (For primary document see N93-30215 11-31)
Avail: Engineering Inst. of Canada, 2050 rue Mansfield, Suite 700, Montreal, Quebec H3A 1Z2 Canada

N93-30265 COM DEV Ltd., Cambridge (Ontario).
SAW TECHNOLOGY FOR ON-BOARD PROCESSING IN MILITARY SATELLITE COMMUNICATIONS
Alastair Malarky and Michael Shaw *In* Engineering Inst. of Canada, Canadian Conference on Electrical and Computer Engineering, Volumes 1 and 2 1990 4 p (For primary document see N93-30215 11-31)
Avail: Engineering Inst. of Canada, 2050 rue Mansfield, Suite 700, Montreal, Quebec H3A 1Z2 Canada

N93-30266 Raytheon Canada Ltd., Waterloo (Ontario).
COMPARISON OF DIVERSITY COMBINING, INTERLEAVING, AND DECODING TECHNIQUES OF A SCINTILLATED CHANNEL
R. Yang and P. VanMinnen (COM DEV Ltd., Cambridge, Ontario.) *In* Engineering Inst. of Canada, Canadian Conference on Electrical and Computer Engineering, Volumes 1 and 2 1990 4 p (For primary document see N93-30215 11-31)
Avail: Engineering Inst. of Canada, 2050 rue Mansfield, Suite 700, Montreal, Quebec H3A 1Z2 Canada

N93-30267 Communications Research Centre, Ottawa (Ontario).
A SATELLITE DOWNLINK SPREAD SPECTRUM TIMING BEACON
W. R. Seed, J. L. Pearce (Defence Research Establishment, Ottawa, Ontario.), and J. S. Wight (Carleton Univ., Ottawa, Ontario.) *In* Engineering Inst. of Canada, Canadian Conference on Electrical and Computer Engineering, Volumes 1 and 2 1990 4 p (For primary document see N93-30215 11-31)
Avail: Engineering Inst. of Canada, 2050 rue Mansfield, Suite 700, Montreal, Quebec H3A 1Z2 Canada

N93-30268 MPR Teltech Ltd., Ottawa (Ontario).
FASSET: A DEVELOPMENT MODEL FOR A CANADIAN EHF MILSATCOM SYSTEM
Gary Boudreau and R. J. Keightley (Defence Research Establishment, Ottawa, Ontario.) *In* Engineering Inst. of Canada, Canadian Conference on Electrical and Computer Engineering, Volumes 1 and 2 1990 4 p (For primary document see N93-30215 11-31)
Avail: Engineering Inst. of Canada, 2050 rue Mansfield, Suite 700, Montreal, Quebec H3A 1Z2 Canada

N93-30281 Queens Univ., Kingston (Ontario). Dept. of Electrical Engineering.
COARSE SYNCHRONIZATION IN AN EHF FREQUENCY-HOPPED SATELLITE COMMUNICATIONS SYSTEM
S. J. Simmons and P. Lamers *In* Engineering Inst. of Canada, Canadian Conference on Electrical and Computer Engineering, Volumes 1 and 2 1990 4 p (For primary document see N93-30215 11-31)
Avail: Engineering Inst. of Canada, 2050 rue Mansfield, Suite 700, Montreal, Quebec H3A 1Z2 Canada

N93-30282 National Defence Headquarters, Ottawa (Ontario).
SECURITY OF THE REMOTE CONTROL LINK OF ANIK E SATELLITES [SECURITE DU LIEN DE TELECOMMANDE DES SATELLITES ANIK E]
Michael J. J. Drapeau *In* Engineering Inst. of Canada, Canadian Conference

on Electrical and Computer Engineering, Volumes 1 and 2 1990 4 p In FRENCH (For primary document see N93-30215 11-31)
Avail: Engineering Inst. of Canada, 2050 rue Mansfield, Suite 700, Montreal, Quebec H3A 1Z2 Canada

N93-30283 Victoria Univ. (British Columbia). Dept. of Electrical and Computer Engineering.
CODING FOR FREQUENCY HOPPED SPREAD SPECTRUM SATELLITE COMMUNICATIONS
Qiang Wang, Vijay K. Bhargava, T. Aaron Gulliver (Defence Research Establishment, Ottawa, Ontario.), and Ian F. Blake (Waterloo Univ., Ontario.) *In* Engineering Inst. of Canada, Canadian Conference on Electrical and Computer Engineering, Volumes 1 and 2 1990 4 p (For primary document see N93-30215 11-31)
Avail: Engineering Inst. of Canada, 2050 rue Mansfield, Suite 700, Montreal, Quebec H3A 1Z2 Canada

N93-30284 COM DEV Ltd., Cambridge (Ontario).
ADAPTIVE JAMMER NULLING IN EHF COMMUNICATIONS SATELLITES
Jai Bhagwan, Stephen Kavanagh, and J. L. Yen (Toronto Univ., Ontario.) *In* Engineering Inst. of Canada, Canadian Conference on Electrical and Computer Engineering, Volumes 1 and 2 1990 4 p (For primary document see N93-30215 11-31)
Avail: Engineering Inst. of Canada, 2050 rue Mansfield, Suite 700, Montreal, Quebec H3A 1Z2 Canada

N93-30285 Communications Research Centre, Ottawa (Ontario).
TEMPORAL SYNCHRONIZATION OF FREQUENCY HOPPED DPSK
W. R. Seed *In* Engineering Inst. of Canada, Canadian Conference on Electrical and Computer Engineering, Volumes 1 and 2 1990 4 p (For primary document see N93-30215 11-31)
Avail: Engineering Inst. of Canada, 2050 rue Mansfield, Suite 700, Montreal, Quebec H3A 1Z2 Canada

N93-30290 Laval Univ. (Quebec). Dept. of Electrical Engineering.
RADIATED FIELDS FROM AN ELECTROMAGNETIC PULSE SIMULATOR [CHAMPS RAYONNES PAR UN SIMULATEUR D'IMPULSIONS ELECTROMAGNETIQUES]
M. Pelletier, G. Y. Delisle, and S. Kashyap (Defence Research Establishment, Ottawa, Ontario.) *In* Engineering Inst. of Canada, Canadian Conference on Electrical and Computer Engineering, Volumes 1 and 2 1990 4 p In FRENCH (For primary document see N93-30215 11-31)
Avail: Engineering Inst. of Canada, 2050 rue Mansfield, Suite 700, Montreal, Quebec H3A 1Z2 Canada

N93-30291 Concordia Univ., Montreal (Quebec).
MODELS FOR PERFORMANCE ASSESSMENT OF HF ANTENNAS ON THE CH-135/TWIN HUEY HELICOPTER
Stanley J. Kubina and Shahram Esfandiari *In* Engineering Inst. of Canada, Canadian Conference on Electrical and Computer Engineering, Volumes 1 and 2 1990 3 p (For primary document see N93-30215 11-31)
Avail: Engineering Inst. of Canada, 2050 rue Mansfield, Suite 700, Montreal, Quebec H3A 1Z2 Canada

N93-30292 Manitoba Univ., Winnipeg. Dept. of Electrical and Computer Engineering.
TRANSIENT FIELD COMPUTATIONS WITHIN OR PROXIMITY OF COMPLEX STRUCTURES: FD-TD APPROACH
W. A. Chamma and L. Shafai *In* Engineering Inst. of Canada, Canadian Conference on Electrical and Computer Engineering, Volumes 1 and 2 1990 4 p (For primary document see N93-30215 11-31)
Avail: Engineering Inst. of Canada, 2050 rue Mansfield, Suite 700, Montreal, Quebec H3A 1Z2 Canada

N93-30293 Manitoba Univ., Winnipeg. Dept. of Electrical and Computer Engineering.
COMPUTER-AIDED MODELING FOR ANALYSIS OF ARBITRARY SCATTERERS AND FEEDS
H. Moheb and L. Shafai *In* Engineering Inst. of Canada, Canadian Conference on Electrical and Computer Engineering, Volumes 1 and 2 1990 4 p (For primary document see N93-30215 11-31)
Avail: Engineering Inst. of Canada, 2050 rue Mansfield, Suite 700, Montreal, Quebec H3A 1Z2 Canada

N93-30294 Defence Research Establishment, Ottawa (Ontario). Electronics Div.
AN IMPROVED MODEL-CREATION PROGRAM FOR EM INTERACTION ANALYSIS
S. Kashyap, M. Dion, and A. Louie *In* Engineering Inst. of Canada, Canadian Conference on Electrical and Computer Engineering, Volumes 1 and 2 1990 3 p (For primary document see N93-30215 11-31)
Avail: Engineering Inst. of Canada, 2050 rue Mansfield, Suite 700, Montreal, Quebec H3A 1Z2 Canada

N93-30302 Ottawa Univ. (Ontario). Dept. of Computer Science.
COMMUNICATIONS SYSTEMS DESIGN FOR TESTABILITY: GREY-BOX TESTING
Robert L. Probert and Cecilia Geldrez *In* Engineering Inst. of Canada, Canadian Conference on Electrical and Computer Engineering, Volumes 1 and 2 1990 5 p (For primary document see N93-30215 11-31)
Avail: Engineering Inst. of Canada, 2050 rue Mansfield, Suite 700, Montreal, Quebec H3A 1Z2 Canada

N93-30303 National Defence Headquarters, Ottawa (Ontario).
PERFORMANCE OF FREQUENCY HOPPED M-ARY FSK IN RAYLEIGH FADING AND PARTIAL-BAND JAMMING
D. C. Leal *In* Engineering Inst. of Canada, Canadian Conference on Electrical and Computer Engineering, Volumes 1 and 2 1990 4 p (For primary document see N93-30215 11-31)
Avail: Engineering Inst. of Canada, 2050 rue Mansfield, Suite 700, Montreal, Quebec H3A 1Z2 Canada

N93-30306 Ottawa Univ. (Ontario). Dept. of Electrical Engineering.
PROGRESS IN THE DEVELOPMENT OF BROADBAND ELECTRIC-FIELD SENSORS FOR TRANSIENT FIELDS
Art Thansandote, Stan S. Stuchly, Mariusz Barski, and Maria A. Stuchly (Health and Welfare Canada, Ottawa, Ontario.) *In* Engineering Inst. of Canada, Canadian Conference on Electrical and Computer Engineering, Volumes 1 and 2 1990 4 p (For primary document see N93-30215 11-31)
Avail: Engineering Inst. of Canada, 2050 rue Mansfield, Suite 700, Montreal, Quebec H3A 1Z2 Canada

N93-30307 Manitoba Univ., Winnipeg. Dept. of Electrical and Computer Engineering.
TOLERANCE THEORY OF PHASED ARRAY ANTENNAS: A STATISTICAL APPROACH
A. Sebak, L. Shafai, and G. Bridges *In* Engineering Inst. of Canada, Canadian Conference on Electrical and Computer Engineering, Volumes 1 and 2 1990 4 p (For primary document see N93-30215 11-31)
Avail: Engineering Inst. of Canada, 2050 rue Mansfield, Suite 700, Montreal, Quebec H3A 1Z2 Canada

N93-30308 Canadian Space Agency, Ottawa (Ontario). David Florida Lab.
DEVELOPMENT OF AN ANTENNA MEASUREMENT FACILITY OPERATING IN THE 2 GHz - 100 GHz FREQUENCY RANGE
S. R. Mishra and G. A. Morin (Defence Research Establishment, Ottawa, Ontario.) *In* Engineering Inst. of Canada, Canadian Conference on Electrical and Computer Engineering, Volumes 1 and 2 1990 4 p (For primary document see N93-30215 11-31)
Avail: Engineering Inst. of Canada, 2050 rue Mansfield, Suite 700, Montreal, Quebec H3A 1Z2 Canada

N93-30309 Concordia Univ., Montreal (Quebec). Dept. of Electrical and Computer Engineering.
COUPLING GAIN COMPUTATION BETWEEN ANTENNAS ON CIRCULAR CYLINDERS AT SHF/EHF FREQUENCIES
D. Chatterjee, S. J. Kubina, and R. Paknys *In* Engineering Inst. of Canada, Canadian Conference on Electrical and Computer Engineering, Volumes 1 and 2 1990 3 p (For primary document see N93-30215

11-31)
Avail: Engineering Inst. of Canada, 2050 rue Mansfield, Suite 700, Montreal, Quebec H3A 1Z2 Canada

N93-30314 Ottawa Univ. (Ontario). Dept. of Electrical Engineering.
COMPARISON OF MULTIPLE ACCESS TECHNIQUES FOR BANDWIDTH LIMITED LAND-MOBILE SATELLITE COMMUNICATIONS
A. Yongacoglu, R. G. Lyons (SkyWave Electronics Ltd., Kanata, Ontario.), and B. A. Mazur (Calian Communications, Kanata, Ontario.) *In* Engineering Inst. of Canada, Canadian Conference on Electrical and Computer Engineering, Volumes 1 and 2 1990 4 p (For primary document see N93-30215 11-31)
Avail: Engineering Inst. of Canada, 2050 rue Mansfield, Suite 700, Montreal, Quebec H3A 1Z2 Canada

N93-30315 Communications Research Centre, Ottawa (Ontario). Dept. of Communications.
COMPARISON OF TWO RANDOM ACCESS TECHNIQUES FOR THE NORTH AMERICAN MSAT SYSTEM
Stewart Crozier and Brian Skerry (Telesat Mobile, Inc., Ottawa, Ontario.) *In* Engineering Inst. of Canada, Canadian Conference on Electrical and Computer Engineering, Volumes 1 and 2 1990 4 p (For primary document see N93-30215 11-31)
Avail: Engineering Inst. of Canada, 2050 rue Mansfield, Suite 700, Montreal, Quebec H3A 1Z2 Canada

N93-30316 McMaster Univ., Hamilton (Ontario). Communications Research Lab.
AN ADAPTIVE MAXIMUM LIKELIHOOD RECEIVER FOR CORRELATED RAYLEIGH FADING CHANNELS
Wayne C. Dam and Desmond P. Taylor *In* Engineering Inst. of Canada, Canadian Conference on Electrical and Computer Engineering, Volumes 1 and 2 1990 4 p (For primary document see N93-30215 11-31)
Avail: Engineering Inst. of Canada, 2050 rue Mansfield, Suite 700, Montreal, Quebec H3A 1Z2 Canada

N93-30317 Teleglobe Canada, Montreal (Quebec).
TELEGLOBE'S INTERNATIONAL MOBILE EARTH TERMINAL SERVICE
Joel Duchoeny *In* Engineering Inst. of Canada, Canadian Conference on Electrical and Computer Engineering, Volumes 1 and 2 1990 4 p (For primary document see N93-30215 11-31)
Avail: Engineering Inst. of Canada, 2050 rue Mansfield, Suite 700, Montreal, Quebec H3A 1Z2 Canada

N93-30318 Chan Technologies, Inc., Kirkland (Quebec).
ARRAY-FED REFLECTOR SYSTEMS WITH LIMITED SCAN
K. K. Chan and R. Martin (Defence Research Establishment, Ottawa, Ontario.) *In* Engineering Inst. of Canada, Canadian Conference on Electrical and Computer Engineering, Volumes 1 and 2 1990 4 p (For primary document see N93-30215 11-31)
Avail: Engineering Inst. of Canada, 2050 rue Mansfield, Suite 700, Montreal, Quebec H3A 1Z2 Canada

N93-30319 Chan Technologies, Inc., Kirkland (Quebec).
A DUAL POLARIZED BROADBAND MULTIFREQUENCY EARTH STATION FEED
K. K. Chan, S. R. Gauthier (Department of National Defence, Ottawa, Ontario.), and G. Dinham (Department of National Defence, Ottawa, Ontario.) *In* Engineering Inst. of Canada, Canadian Conference on Electrical and Computer Engineering, Volumes 1 and 2 1990 4 p (For primary document see N93-30215 11-31)
Avail: Engineering Inst. of Canada, 2050 rue Mansfield, Suite 700, Montreal, Quebec H3A 1Z2 Canada

N93-30320 Concordia Univ., Montreal (Quebec).
RCS OF FUNDAMENTAL SCATTERERS IN THE HF BAND BY WIRE-GRID MODELLING
C. W. Trueman and S. J. Kubina *In* Engineering Inst. of Canada, Canadian Conference on Electrical and Computer Engineering, Volumes 1 and 2 1990 4 p (For primary document see N93-30215 11-31)
Avail: Engineering Inst. of Canada, 2050 rue Mansfield, Suite 700, Montreal, Quebec H3A 1Z2 Canada

N93-30321 Canadian Space Agency, Ottawa (Ontario). David Florida Lab.
WIDE FREQUENCY POLARIMETRIC RADAR CROSS SECTION MEASUREMENTS
S. R. Mishra, P. Charron, J. Smithson, and J. Mantz *In* Engineering Inst. of Canada, Canadian Conference on Electrical and Computer Engineering, Volumes 1 and 2 1990 4 p (For primary document see N93-30215 11-31)
Avail: Engineering Inst. of Canada, 2050 rue Mansfield, Suite 700, Montreal, Quebec H3A 1Z2 Canada

N93-30328 CAE Electronics Ltd., Saint Laurent (Quebec).
RADAR BEAM EFFECTS FOR A FLIGHT SIMULATOR USING SIGNAL PROCESSOR BASED HARDWARE
E. J. Nemer, R. C. Bridegeman, and A. S. Malowany (McGill Univ., Montreal, Quebec.) *In* Engineering Inst. of Canada, Canadian Conference on Electrical and Computer Engineering, Volumes 1 and 2 1990 5 p (For primary document see N93-30215 11-31)
Avail: Engineering Inst. of Canada, 2050 rue Mansfield, Suite 700, Montreal, Quebec H3A 1Z2 Canada

N93-30331 Communications Research Centre, Ottawa (Ontario).
CONSTANT AVERAGE POWER SINGLE SIDEBAND (CAPSSB) MODULATION
E. E. Matt and J. H. Lodge *In* Engineering Inst. of Canada, Canadian Conference on Electrical and Computer Engineering, Volumes 1 and 2 1990 4 p (For primary document see N93-30215 11-31)
Avail: Engineering Inst. of Canada, 2050 rue Mansfield, Suite 700, Montreal, Quebec H3A 1Z2 Canada

N93-30332 Queens Univ., Kingston (Ontario). Dept. of Electrical Engineering.
SIGNAL PROCESSOR BASED MSAT TRELLIS CODED M-DPSK WITH ADAPTIVE DOPPLER PHASOR CORRECTION
P. Bengough, L. Berg, B. Koblents, and P. J. McLane *In* Engineering Inst. of Canada, Canadian Conference on Electrical and Computer Engineering, Volumes 1 and 2 1990 4 p (For primary document see N93-30215 11-31)
Avail: Engineering Inst. of Canada, 2050 rue Mansfield, Suite 700, Montreal, Quebec H3A 1Z2 Canada

N93-30333 Queens Univ., Kingston (Ontario). Dept. of Electrical Engineering.
TWO-STAGE DOPPLER PHASOR CORRECTED TCM/DMPSK FOR SHADOWED MOBILE SATELLITE CHANNELS
P. J. McLane *In* Engineering Inst. of Canada, Canadian Conference on Electrical and Computer Engineering, Volumes 1 and 2 1990 5 p (For primary document see N93-30215 11-31)
Avail: Engineering Inst. of Canada, 2050 rue Mansfield, Suite 700, Montreal, Quebec H3A 1Z2 Canada

N93-30334 Defence Research Establishment, Ottawa (Ontario).
STATUS OF THE CANADIAN MILITARY MULTIBEAM ANTENNA (MBA) DEVELOPMENT FOR EHF SATCOM
G. A. Morin, E. B. Felstead (Communications Research Centre, Ottawa, Ontario.), K. S. Rao (Spar Aerospace Ltd., Sainte-Anne-de-Bellevue, Quebec.), and K. K. Chan (Chan Technologies, Inc., Kirkland, Quebec.) *In* Engineering Inst. of Canada, Canadian Conference on Electrical and Computer Engineering, Volumes 1 and 2 1990 3 p (For primary document see N93-30215 11-31)
Avail: Engineering Inst. of Canada, 2050 rue Mansfield, Suite 700, Montreal, Quebec H3A 1Z2 Canada

N93-30335 Chan Technologies, Inc., Kirkland (Quebec).
COMPARISON AND DESIGN OF MULTIPLE BEAM ANTENNA FEED NETWORKS
K. K. Chan, D. Faubert (Defence Research Establishment, Ottawa, Ontario.), and R. Martin (Defence Research Establishment, Ottawa, Ontario.) *In* Engineering Inst. of Canada, Canadian Conference on Electrical and Computer Engineering, Volumes 1 and 2 1990 4 p (For primary document see N93-30215 11-31)

Avail: Engineering Inst. of Canada, 2050 rue Mansfield, Suite 700, Montreal, Quebec H3A 1Z2 Canada

N93-30336 Chan Technologies, Inc., Kirkland (Quebec).
RECENT ADVANCES IN BOOTLACE LENS DESIGN
K. K. Chan, W. B. Wallace (AeroSmith Systems Corp., Los Altos, CA.), and R. R. Blasing (AeroSmith Systems Corp., Los Altos, CA.) *In* Engineering Inst. of Canada, Canadian Conference on Electrical and Computer Engineering, Volumes 1 and 2 1990 4 p (For primary document see N93-30215 11-31)
Avail: Engineering Inst. of Canada, 2050 rue Mansfield, Suite 700, Montreal, Quebec H3A 1Z2 Canada

N93-30337 Thompson-Hickling Aviation, Inc., Ottawa (Ontario).
ENGINEERING MANAGEMENT CONSIDERATION FOR AN INTEGRATED AERONAUTICAL MOBILE SATELLITE SERVICE
John M. Belcher *In* Engineering Inst. of Canada, Canadian Conference on Electrical and Computer Engineering, Volumes 1 and 2 1990 4 p (For primary document see N93-30215 11-31)
Avail: Engineering Inst. of Canada, 2050 rue Mansfield, Suite 700, Montreal, Quebec H3A 1Z2 Canada

N93-30342 Communications Research Centre, Ottawa (Ontario).
DESIGN ISSUES AND INITIAL PERFORMANCE OF AN ADAPTIVE AIR/GROUND/AIR HF COMMUNICATION SYSTEM
G. R. Nourry and D. G. McLachlan *In* Engineering Inst. of Canada, Canadian Conference on Electrical and Computer Engineering, Volumes 1 and 2 1990 7 p (For primary document see N93-30215 11-31)
Avail: Engineering Inst. of Canada, 2050 rue Mansfield, Suite 700, Montreal, Quebec H3A 1Z2 Canada

N93-30343 Harris Corp., Rochester, NY.
ADVANCED HF DIGITAL NETWORKS
Marvin Baker and N. P. Robinson (Rome Air Development Center, Griffiss AFB, NY.) *In* Engineering Inst. of Canada, Canadian Conference on Electrical and Computer Engineering, Volumes 1 and 2 1990 4 p (For primary document see N93-30215 11-31)
Avail: Engineering Inst. of Canada, 2050 rue Mansfield, Suite 700, Montreal, Quebec H3A 1Z2 Canada

N93-30347 Atlantis Scientific Systems Group, Inc., Ottawa (Ontario).
SIMILARITIES BETWEEN SYNTHETIC APERATURE RADAR AND GROUND PROBING RADAR IMAGING
Bernard Armour, Alan Judge (Geological Survey of Canada, Ottawa, Ontario.), and Ron Saper *In* Engineering Inst. of Canada, Canadian Conference on Electrical and Computer Engineering, Volumes 1 and 2 1990 5 p (For primary document see N93-30215 11-31)
Avail: Engineering Inst. of Canada, 2050 rue Mansfield, Suite 700, Montreal, Quebec H3A 1Z2 Canada

N93-30348 Laval Univ. (Quebec).
SEGMENTATION OF SAR IMAGES
N. Kaliaguine and J.-N. Beaulieu *In* Engineering Inst. of Canada, Canadian Conference on Electrical and Computer Engineering, Volumes 1 and 2 1990 4 p (For primary document see N93-30215 11-31)
Avail: Engineering Inst. of Canada, 2050 rue Mansfield, Suite 700, Montreal, Quebec H3A 1Z2 Canada

N93-30349 MPR Teltech Ltd., Burnaby (British Columbia).
THE EVOLUTION OF GLOBAL MOBILE COMMUNICATIONS
A. I. Spolsky and J. R. Brasic *In* Engineering Inst. of Canada, Canadian Conference on Electrical and Computer Engineering, Volumes 1 and 2 1990 6 p (For primary document see N93-30215 11-31)
Avail: Engineering Inst. of Canada, 2050 rue Mansfield, Suite 700, Montreal, Quebec H3A 1Z2 Canada

N93-30355 Memorial Univ. of Newfoundland, Saint Johns. Centre for Cold Ocean Resources Engineering.
ADAPTIVE FILTERING FOR CLUTTER SUPPRESSION IN HIGH FREQUENCY RADAR
Rafaat H. Khan *In* Engineering Inst. of Canada, Canadian Conference on Electrical and Computer Engineering, Volumes 1 and 2 1990 4 p (For primary document see N93-30215 11-31)
Avail: Engineering Inst. of Canada, 2050 rue Mansfield, Suite 700, Montreal, Quebec H3A 1Z2 Canada

33 ELECTRONICS AND ELECTRICAL ENGINEERING

Includes test equipment and maintainability; components, e.g., tunnel diodes and transistors; microminiaturization; and integrated circuitry.

For related information see also *60 Computer Operations and Hardware* and *76 Solid-State Physics.*

N93-28483# SRI International Corp., Menlo Park, CA.
FIELD-EMITTER ARRAYS FOR RF VACUUM MICROELECTRONICS Quarterly Report No. 5, 1 Oct. - 31 Dec. 1992
C. A. Spindt, A. Rosengreen, and P. R. Schwoebel Mar. 1993 36 p
(Contract MDA972-91-C-0029; ARPA Order 8162)
(AD-A262677; SRI-2743) Avail: CASI HC A03/MF A01

SRI International has completed the fifth quarter of a program to develop field-emitter arrays for vacuum microelectronics. The goals of the effort are 5 mA at 5 A/sq cm for at least 2 hours, and demonstrated modulation of the emission at 1 GHz. Low-capacitance cathodes were fabricated that produced 10 mA emission with an applied voltage of 130V, using a chemical vapor deposition process to produce SiO2 layers. One year of continuous 1000-tip cathode operation was achieved for a low-frequency emission test, significantly exceeding the program current density goal. Fabrication and assembly were completed for an apparatus required for microwave testing. In the program to optimize performance of field-emitter arrays, a series of plasma-cleaning experiments, involving hydrogen glow discharge, was performed. DTIC

N93-28523# Oak Ridge National Lab., TN.
ORNL SUPERCONDUCTING TECHNOLOGY PROGRAM FOR ELECTRIC ENERGY SYSTEMS
R. A. Hawsey, comp. Feb. 1993 77 p
(Contract DE-AC05-84OR-21400)
(DE93-009588; ORNL/HTSPC-4) Avail: CASI HC A05/MF A01

The Oak Ridge National Laboratory (ORNL) Superconducting Technology Program is conducted as part of a national effort by the US Department of Energy's (DOE's) Office of Conservation and Renewable Energy to develop the technology base needed by US industry for commercial development of electric power applications of high-temperature superconductivity. The two major elements of this program are wire development and systems development. This document describes the major research and development activities for this program together with related accomplishments. The technical progress reported was summarized from information prepared for the FY-92 Peer Review of Projects, which was conducted by DOE's Office of Program Analysis, Office of Energy Research. This ORNL program is highly leveraged by the staff and other resources of US industry and universities. Interlaboratory teams are also in place on a number of industry-driven projects. Patent disclosures, working group meetings, staff exchanges, and joint publications and presentations ensure that there is technology transfer to US industry. Working together, the collaborative teams are making tremendous progress in solving the scientific and technical issues necessary for the commercialization of long lengths of practical high-temperature superconductor wire and wire products. DOE

N93-28539*# Virginia Polytechnic Inst. and State Univ., Blacksburg. Dept. of Electrical Engineering.
DESIGN AND CONSTRUCTION OF A PROTOTYPE ACTS PROPAGATION TERMINAL Final Report, period ending 26 Apr. 1993
Warren Stutzman, Tim Pratt, Charles Nunnally, Randall Nealy, Will Remaklus, Bill Sylvester, Andrew Predoehl, and Doug Gaff 26 Apr. 1993 21 p
(Grant NAGw-2335)
(NASA-CR-193071; NAS 1.26:193071; SATCOM-93-5) Avail: CASI HC A03/MF A01

The launch schedule for the Advanced Communication Technology Satellite (ACTS) spacecraft did not leave sufficient time for completion of the prototype ACTS Propagation Terminals (APT) prior to initiation of the APT production phase. In fact, the approach used was to construct and test all subassemblies of the terminal with special emphasis on the technically challenging portions. These include the RF front end that uses a state-of-the-art down converter which integrates a low noise amplifier, mixer, post amplifier, filter, and local oscillator port frequency doubler into a single small package. In addition, a new digital receiver that uses the latest DSP technology was developed. Both of these subassemblies were thoroughly tested. The highest risk technology in the APT program was the digital receiver. Several candidate algorithms and DSP chips were investigated early on, primarily under JPL sponsorship. A receiver was constructed based on Texas Instruments chip. The final prototype digital receiver was one based on an Analog Devices chip. The design and test results are documented in a report prepared for this grant. A Primary Design Review (PDR) was conducted 30 May 1991, and a Critical Design Review was held 7 Jul. 1992. Final complete documentation of the APT's will appear in the form of three reports: a hardware description report, a report on the data collection code (ACTS VIEW), and a report on the preprocessing code. Author (revised)

N93-28563# Defence Research Establishment, Ottawa (Ontario).
NEUTRON RADIATION INDUCED DEGRADATION OF DIODE CHARACTERISTICS
S. M. Khanna, G. T. Pepper, and R. E. Stone Dec. 1992 40 p
(AD-A263277; DREO-1155) Avail: CASI HC A03/MF A01

Neutron radiation effects on diode current-voltage characteristics have been studied for a variety of diode over 1(10)(exp 13) - 3(10)(exp 15) n/sq cm 1 MeV equivalent neutron fluence range. A classification scheme consisting of three types of neutron effects on diode forward characteristics is proposed here for the first time. For constant forward current I(sub F) higher than that in the generation-recombination regime, the diode voltage V(sub F) either increases with fluence phi (Type 1 diode), on V(sub F) first decreases with phi at lower fluence levels and then increases with phi at higher fluence levels (Type 2 diode), or V(sub F) decreases with phi at all fluence levels used in this work (Type 3 diode). Most of the previous results on p-n junction diodes correspond to Type 1 diode results. Type 2 diode results are rather rare in the literature. Several examples of Type 2 diode results are presented here. Type 3 diode results are reported here for other types of diodes not reported earlier. These results are explained qualitatively in terms of the theories for a p-n junction and for radiation effects on semiconductors. It is shown here that a type 3 diode could be developed as a high neutron fluence monitor with three orders of magnitude higher upper limit than the Harshaw p-i-n diode neutron fluence monitor under evaluation at the US Army Aberdeen Proving Grounds, Aberdeen, Md. The results also suggest a methodology for radiation hard diode development. DTIC

N93-28581# California Univ., Berkeley. Lawrence Berkeley Lab.
IN SITU CHARACTERIZATION OF INTERFACIAL AND BULK PROPERTIES OF LITHIUM POLYMER BATTERIES USING 4-PROBE DC TECHNIQUES
Meilin Liu (Georgia Inst. of Tech., Atlanta.), S. J. Visco, and L. C. DeJonghe Nov. 1992 11 p Presented at the 16th Material Research Society International Symposium on the Scientific Basis for Nuclear Waste Management Fall Meeting, Boston, MA, 30 Nov. - 5 Dec. 1992
(Contract DE-AC03-76SF-00098)
(DE93-007699; LBL-33367; CONF-921101-90) Avail: CASI HC A03/MF A01

The use of transient and steady-state 4-probe techniques for the evaluation of the limitations to performance in solid-state electrochemical devices is described. The application of sequential, bipolar square-wave current pulses to a solid polymer cell with two internal reference electrodes allows separation of the polarization behavior of the various components of the cell, and indicates the rate limiting processes in the cell. Careful design of the experimental cell and appropriate selection of current pulse width allows evaluation of fundamental kinetic and transport properties, as well as activation parameters. Steady state constant-current measurements using 4-probe cells allows in situ observation of interface stability and/or polarization as a function of time as the cell is cycling. DOE

N93-28589# Texas Univ., Austin. Electronics Research Center.
ELECTRONICS RESEARCH REPORT Annual Report, 15 May 1992 - 14 Feb. 1993
Edward J. Powers 14 Feb. 1993 95 p
(Contract F49620-92-C-0027)
(AD-A262733; Rept-46) Avail: CASI HC A05/MF A01

This report summarizes scientific progress on 'Basic Research in Electronics' which has been conducted under the auspices of the DoD Joint Services Electronics Program during the period 15 May 1992 - 14 February 1993. Progress on five solid-state, two information electronics, and two electromagnetic projects is described. DTIC

N93-28597# Lawrence Livermore National Lab., CA.
IMPROVING THE JITTER OF THE 150 kJ EXPERIMENTS SOLID DIELECTRIC SWITCHES
E. E. Domning Jan. 1993 189 p
(Contract W-7405-eng-48)
(DE93-009459; UCRL-ID-112497) Avail: CASI HC A09/MF A02

The 150 kJ experiment has four capacitor modules that are individually switched into a central transmission line. Each switch must carry a peak current of 2 MA, have an inductance of under 5 nH, a resistance of under 1 mil, a jitter of 25 nS and be able to hold off 60 kV. We determined that a metal to metal contact solid dielectric switch (SDS) that uses the force from an exploding bridge foil (EBF) to rupture the dielectric would meet these specifications given that we were able to improve its jitter performance. The jitter reported by other experimenters on EBF triggers is in the 100 nS range. To develop a low jitter trigger we designed and tested triggers on an experimental test stand built to simulate a 150 kJ capacitor module. On this test stand we developed an EBF trigger with jitter under 25 nS and a new type of trigger we called the magnetic push trigger also with jitter under 25 nS. The magnetic push trigger uses the magnetic expansion of a stripline due to the Lorentz force to rupture the dielectric. We found that our magnetic push trigger did less damage to switch components and was easier to apply than EBF trigger. DOE

N93-28610*# National Aeronautics and Space Administration. Lewis Research Center, Cleveland, OH.
DEVELOPMENT OF Si(1-x)Ge(x) TECHNOLOGY FOR MICROWAVE SENSING APPLICATIONS
Rafael A. Mena, Susan R. Taub, Samuel A. Alterovitz, Paul E. Young (Toledo Univ., OH.), Rainee N. Simons (Sverdrup Technology, Inc., Brook Park, OH.), and David Rosenfeld May 1993 13 p
(RTOP 505-44-2C)
(NASA-TM-106157; E-7843; NAS 1.15:106157) Avail: CASI HC A03/MF A01

The progress for the first year of the work done under the Director's Discretionary Fund (DDF) research project entitled, 'Development of Si(1-x)Ge(x) Technology for Microwave Sensing Applications.' This project includes basic material characterization studies of silicon-germanium (SiGe), device processing on both silicon (Si) and SiGe substrates, and microwave characterization of transmission lines on silicon substrates. The material characterization studies consisted of ellipsometric and magneto-transport measurements and theoretical calculations of the SiGe band-structure. The device fabrication efforts consisted of establishing SiGe device processing capabilities in the Lewis cleanroom. The characterization of microwave transmission lines included studying the losses of various coplanar transmission lines and the development of transitions on silicon. Each part of the project is discussed individually and the findings for each part are presented. Future directions are also discussed. Author (revised)

N93-28641# Sandia National Labs., Albuquerque, NM.
THERMAL AND MECHANICAL ANALYSIS OF FLIP-CHIPS ON A LIQUID COOLED MULTICHIP MODULE
R. Narayanan (North Carolina Univ., Charlotte.), P. M. Hall (Johnson C. Smith Univ., Charlotte, NC.), and R. Chanchani 1992 34 p Presented at the 43th Electronic Component and Technology Conference, Orlando, FL, 1-3 Jun. 1993
(Contract DE-AC04-76DP-00789)
(DE93-007609; SAND-92-2554C; CONF-9306104-3) Avail: CASI HC A03/MF A01

In this paper, thermal analysis of a three dimensional quarter model of a 156 pad flip-chip on a liquid cooled multichip module with 75 other chips is simulated using COSMOS -- finite element software. Both flip-chip (pad grid array type) and TAB type of interconnections are used for the module. The total power on the board is 67 watts, the flip-chips generating up to 1.5 watts each, and the one TAB type generating 12 watts. Each chip can be modeled independently due to the absence of cross-heating by its neighbors. Forced convection liquid cooling using an organic coolant with various flow rates and thus various convection coefficients are used for the study. The temperature rise in the boundary layer of the coolant was 8 F at the coolant flow rate of 0.08 gallons per minute for the flip-chip with 1.5 watts. The maximum thermal strains calculated were found to be 0.35% (if the temperature of zero strain is assumed to be 0 F, and Young's modulus of solder is 2 Mpsi). The maximum shears were found in the corner bump, and they differed from the next bump by 20%. Polyimide layers above and below the solder bumps were found to contribute about 80% of the thermal resistance! These results are used in a Coffin-Manson analysis to predict adequate life (cycles) for the high lead solder bumps (95%Pb-5%Sn). DOE

N93-28669# Central Research Inst. of Electric Power Industry, Tokyo (Japan). Energy and Environment Lab.
DEVELOPMENT OF NICKEL/METAL HYDRIDE SECONDARY BATTERY
T. Ikeya, K. Kumai, and T. Iwahori Jun. 1992 31 p
(DE93-781330; CRIE-T-91084) Avail: CASI HC A03/MF A01

The paper studies reformation of hydrogen storage alloys for improvement of the performance of nickel/metal hydride batteries using hydrogen storage alloys. A method in which cobalt-added alloys are mixed and ground is considered as a substitute for plating based methods. The nickel/metal hydride battery is assembled by controlling the nickel electrode using the reformed alloys produced by this method. The battery shows a life of about 1000 cycles. After reforming the hydrogen storage alloys by nickel-plating, the cycle life is prolonged to over 2000 cycles. It is clear that the hydrogen storage alloys can be reformed by appropriate mechanical treatment by such an easy method as grinding. Additionally, long-time grinding decreases discharge capacity. DOE

N93-28746# Central Research Inst. of Electric Power Industry, Tokyo (Japan). Energy and Environment Lab.
RESEARCH AND DEVELOPMENT OF CARBON BLACK ANODES FOR LITHIUM SECONDARY CELLS
K. Takei, K. Kumai, T. Iwahori, T. Uwai, and M. Furusho May 1992 34 p
(DE93-781331; CRIE-T-91054) Avail: CASI HC A03/MF A01

Experimental studies are made on basic anode characteristics of carbon black as a substituting material for metal lithium for lithium secondary batteries. Carbon black is employed because of its controllable crystallinity as carbon material to study changes of states under treatment conditions after synthesis, reversibility of charge/discharge, and the amount of side reaction. As a result, carbon black is found out to be applicable to the lithium secondary battery, with further improvement required, though. As for heat treatment after synthesis of carbon black, it is clarified that low temperature treatment (1200 C) is more effective for increase in reversible anode capacity. This is considered to be caused by changes in microstructure of the carbon black associated with the heat treatment. Charge/discharge electric potential is closed to that of metal lithium, and electromotive force reduces only by about 0.2V when assembled as battery. The side reaction occurs only at the initial reaction (charge) time, but the gas generation reaction which increases internal pressure of the battery is approximately 1% of all the reaction. Moreover, in charge/discharge in and after the second cycle, no gas generation reaction is observed, which shows that carbon black is applicable to the lithium battery which is a closed system. DOE

N93-28830# Los Alamos National Lab., NM.
UPGRADING THE LAMPF 201 MHz RF GENERATORS
W. M. Parsons, J. T. M. Lyles, and H. W. Harris 1993 8 p Presented at the Workshop on Accelerators for Future Spallation Neutron Sources, Santa Fe, NM, 15-21 Feb. 1993
(Contract W-7405-eng-36)
(DE93-010715; LA-UR-93-823; CONF-930292-1) Avail: CASI HC A02/MF A01

Radio-frequency generators, operating at 201 MHz, power the first four stages of the Los Alamos Meson Physics Facility (LAMPF) accelerator. Each generator consists of four stages of series-connected, vacuum-tube amplifiers. The first amplifier is a grid-modulated tetrode that produces 500 W peak-power. The second amplifier is a drive-modulated tetrode that produces 5 kW peak-power. The third stage is a grid- and plate-modulated tetrode that produces 130 kW peak-power. The last stage is a plate-modulated triode that produces 2.5 MW peak power. A modernization program has been initiated to improve the reliability of each of these stages. The first two stages of each generator are being replaced with a single, drive-modulated, solid-state amplifier. Specifications for the amplifier design, and requirements for integration into the system are presented. The third stage will be converted to a drive-modulated system using the current tetrode. This modification involves the development of a 17-kV, 15-A switching supply to replace the present plate-modulator. Design requirements for this switching supply are presented. The final stage will remain plate-modulated but will contain a new driver unit for the modulator tube. DOE

N93-28940# Westinghouse Electric Corp., Pittsburgh, PA.
PROCESSING, FABRICATION, AND DEMONSTRATION OF HTS INTEGRATED MICROWAVE CIRCUITS Status Report No. 6, 26 Oct. 1992 - 24 Jan. 1993
G. R. Wagner 24 Jan. 1993 15 p
(Contract N00014-91-C-0112; ARPA Order 7932)
(AD-A263161) Avail: CASI HC A03/MF A01

Work is in progress to determine the dynamic range of superconducting filters by studying their noise and power handling characteristics. The goal is to establish their usefulness in receiver front-end applications. The thermal noise figure of HTS filters and its effect on a filter-low-noise-amplifier chain are being examined. Calculations of the noise figures for the filter alone and for the filter-amplifier chain are shown as a function of filter loss. Notice that, for cooled passive devices, the noise figure is lower than the insertion loss. DTIC

N93-28944# Sandia National Labs., Albuquerque, NM.
SUBNANOSECOND HIGH POWER PERFORMANCE OF A BISTABLE OPTICALLY-CONTROLLED GaAs SWITCH
D. C. Stoudt (Naval Surface Warfare Center, Dahlgren, VA.), R. A. Roush (Naval Surface Warfare Center, Dahlgren, VA.), M. S. Mazzola (Naval Surface Warfare Center, Dahlgren, VA.), F. J. Zutavern, and G. M. Loubriel 1992 2 p Presented at the 9th IEEE Pulsed Power Conference, Albuquerque, NM, 21-23 Jun. 1993
(Contract DE-AC04-76DP-00789)
(DE93-006285; SAND-92-2874C; CONF-930616-1) Avail: CASI HC A01/MF A01

Results are presented which demonstrate the ability of the Bistable (or bulk) Optically controlled Semiconductor Switch (BOSS) to open against a rising electric field on the time scale of less than one nanosecond. The BOSS device is fabricated from semi-insulating, copper-compensate, silicon-doped GaAs. DOE

N93-28983# Central Research Inst. of Electric Power Industry, Tokyo (Japan). Energy and Environment Lab.
APPROACH TO EXTENDING THE CYCLE LIFE OF LITHIUM SECONDARY BATTERY
K. Kumai, T. Ikeya, K. Ishihara, and T. Iwahori May 1992 24 p
(DE93-776266; CRIE-T-91052) Avail: CASI HC A03/MF A01

With an objective to elucidate life extending requirement in lithium secondary battery, discussions were given on effects of operating conditions on cycle life and integrated capacity using commercially available Li/MoS2 cells. The following matters were made clear. A trend was observed that the battery life extends when discharge depths are held shallow, but the integrated capacity remains constant in low discharge conditions (0.1 C to 0.125 C) regardless of discharge depths, and the total charge amount required for batteries discharged to various depths remained the same: the integrated discharge capacity at high-rate discharge (0.3 C) increased largely (about seven times) over the case of low-rate discharge to the same depth; and the cycle life of a lithium battery is affected not only by discharge depths, but also by charge/discharge currents and charge/discharge voltages, wherein the targeted cycle life for this cell (2,500 cycles or more) was achieved when the cell was charged and discharged at 1.5 V to 2.0 V with the discharge depth held low (30%

D.O.D.) at a low-rate discharge (0.1 C) and high-rate discharge (0.3 C). DOE

N93-28999# Naval Surface Warfare Center, Dahlgren, VA.
HIGH-VOLTAGE PULSE GENERATOR CAPABLE OF 2000 J AT 10 kV
Harry E. Cleaver 31 Jul. 1992 88 p
(AD-A262034; NSWCDD/MP-92/222) Avail: CASI HC A05/MF A01

The 10-kV High-Voltage Pulse Generator is used to deliver high-energy pulses to exploding wire or flash-lamp illuminators used in high-speed photography of explosive tests. With properly rated components, the pulser is capable of an energy content of 2000 J at 10 kV. Components presently installed limit the output to 900 J at 6 kV. At this limit, the pulser delivers a peak current of 3500 A into a 1.25-ohms resistive load. DTIC

N93-29010# Army Armament Research, Development and Engineering Center, Watervliet, NY. Benet Lab.
STUDY ON DECREASING TORQUE NOISE RESULTING FROM FEEDBACK NOISE FOR THE MODIFIED BANG-BANG CONTROLLER Final Report
Ronald L. Racicot Mar. 1993 18 p
(AD-A263178; ARCCB-TR-93008) Avail: CASI HC A03/MF A01

The main problem with using the modified bang-bang controller is the moderate amounts of feedback noise can lead to high levels of torque noise. This stems from a velocity squared term in the controller. This report presents computer simulation results from a study aimed at decreasing torque noise. Two approaches are (1) decrease feedback noise directly, and (2) modify the controller so that it is less sensitive to feedback noise. We recommend that the control designer decrease feedback noise as much as practical and then decrease controller gains as a function of velocity until acceptable levels of torque noise are achieved. DTIC

N93-29036# Argonne National Lab., IL.
BATTERY TESTING AT ARGONNE NATIONAL LABORATORY
W. H. DeLuca, K. R. Gillie, J. E. Kulaga, J. A. Smaga, A. F. Tummillo, and C. E. Webster 1992 7 p Presented at the Annual Automotive Development Technology Contractors' Coordination Meeting, Dearborn, MI, 2-5 Nov. 1992
(Contract W-31-109-eng-38)
(DE93-009204; ANL/CMT/CP-77168; CONF-9211101-5) Avail: CASI HC A02/MF A01

Advanced battery technology evaluations are performed under simulated electric-vehicle operating conditions at the Analysis & Diagnostic Laboratory (ADL) of Argonne National Laboratory. The ADL results provide insight into those factors that limit battery performance and life. The ADL facilities include a test laboratory to conduct battery experimental evaluations under simulated application conditions and a post-test analysis laboratory to determine, in a protected atmosphere if needed, component compositional changes and failure mechanisms. This paper summarizes the performance characterizations and life evaluations conducted during FY-92 on both single cells and multi-cell modules that encompass six battery technologies (Na/S, Li/FeS, Ni/Metal-Hydride, Ni/Zn, Ni/Cd, Ni/Fe). These evaluations were performed for the Department of Energy, Office of Transportation Technologies, Electric and Hybrid Propulsion Division, and the Electric Power Research Institute. The ADL provides a common basis for battery performance characterization and life evaluations with unbiased application of tests and analyses. The results help identify the most promising R&D approaches for overcoming battery limitations, and provide battery users, developers, and program managers with a measure of the progress being made in battery R&D programs, a comparison of battery technologies, and basic data for modeling. DOE

N93-29037 Polish Academy of Sciences, Warsaw. Inst. Podstawowych Problemow Techniki.
BIFURCATIONS PHENOMENA IN A NONLINEAR OSCILLATOR: APPROXIMATE ANALYTICAL STUDIES VERSUS COMPUTER SIMULATION RESULTS
Wanda Szemplinska-Stupnicka and Jerzy Rudowski 1992 41 p
Avail: Issuing Activity

The behavior of a driven single-well oscillator with quadratic nonlinearity is studied and an attention is focused on exploring a relationship between classic concepts of the approximate theory of nonlinear oscillations and the complex bifurcations and escape phenomena obtained by computer simulations. An analytical analysis of the Hill's type variational equation leads to approximate estimates for the blue-sky catastrophe and period doubling instability and eventually results in the approximate predictive criteria for the main escape region. The theoretical study and computer simulations are extended to the 1/2 subharmonic resonance and the analysis brings a new insight into the nonlinear phenomena, which occur in the higher frequency region. Author

N93-29048# Fermi National Accelerator Lab., Batavia, IL.
TESLA TEST CELL CRYOSTAT SUPPORT POST THERMAL AND STRUCTURAL ANALYSIS
T. H. Nicol 15 Aug. 1992 36 p
(Contract DE-AC02-76CH-03000)
(DE93-008365; FNAL-TM-1794) Avail: CASI HC A03/MF A01

TeV Superconducting Linear Accelerator (TESLA) cryostats consist of eight, 1-meter-long radio frequency (RF) cavity modules cryogenically connected in series with one focusing quadrupole. Each module contains one, 9-cell superconducting RF cavity operating at 1.3 GHz in a 1.8K helium bath. Individual modules are self-contained in the that they have their own input couplers, high order mode couplers, and tuning mechanisms. Services common to the entire cryostat consist of 70K and 4.5K thermal radiation shields, shield supply and return lines, a 1.8K helium supply line, and a gas helium return pipe. All cavity modules, the quadrupole, and cryogenic seances are contained in a single 12-meter-long vacuum vessel. The goal on TESLA is the successful fabrication and test of four complete cryostat assemblies. These cryostats will be installed in a string cooled to operating temperature, and powered. This test will address problems which may arise when modules are installed in a tunnel environment. It will also permit testing of the basic cooling concepts, measurement of static heat losses, and measurement of the RF performance of all cavities. DOE

N93-29173*# National Aeronautics and Space Administration. Langley Research Center, Hampton, VA.
HEATING HEAD FOR INDUCTION HEATING APPARATUS Patent Application
Robert H. Coultrip, inventor (to NASA) (Inductron Corp., Yorktown, VA.), Samuel D. Johnson, inventor (to NASA) (Inductron Corp., Yorktown, VA.), Carl E. Copeland, inventor (to NASA) (Inductron Corp., Yorktown, VA.), Robert J. Swaim, inventor (to NASA), Robert L. Fox, inventor (to NASA), and William M. Phillips, Jr., inventor (to NASA) (Inductron Corp., Yorktown, VA.) 15 Mar. 1993 11 p
(NASA-Case-LAR-14429-1; NAS 1.71:LAR-14429-1; US-Patent-Appl-SN-030894) Avail: CASI HC A03/MF A01

A heating head is presented for an induction heating apparatus that includes an elongated pole piece being substantially E-shaped in cross section and has a base, two outer legs, and a middle leg spaced from the two outer legs by two parallel gaps. A capacitor is connectable to a power source, and a coil wrapped around the middle leg of the pole piece. The coil has first and second ends connected to the capacitor. When a susceptor is placed in juxtaposition to distal ends of the two outer legs and the middle leg, the susceptor is heated by eddy currents induced in the susceptor due to the magnetic flux passing between the two outer legs and the middle leg along two parallel heating zones substantially centered over the two parallel gaps. NASA

N93-29203# National Inst. of Standards and Technology, Gaithersburg, MD. Automated Electronics Manufacturing Programs.
INITIAL GRAPHICS EXCHANGE SPECIFICATION HYBRID MICROCIRCUIT APPLICATION PROTOCOL Final Report
Curtis Parks, Roger McCollough (Naval Command, Control and Ocean Surveillance Center, San Diego, CA.), Charles Azu (Naval Command, Control and Ocean Surveillance Center, San Diego, CA.), Larry Savage (Raytheon Co., Lexington, MA.), Patrick Toomey (Raytheon Co., Lexington, MA.), and Thomas Makoski (International TechneGroup, Inc., Milford, OH.) Jan. 1993 199 p Sponsored by Naval Command, Control and Ocean Surveillance Center
(PB93-175404; NIST/TN-1295) Avail: CASI HC A09/MF A03; SOD HC

An application protocol is an information systems view of a specific product. The view represents an agreement on the generic activities needed to design and fabricate the product, the agreement on the information needed to support those activities, and the specific constructs of a product data standard for use in transferring some or all of the information required.

This applications protocol describes the data for hybrid microcircuits products in terms of a product description standard called the Initial Graphics Exchange Specifications (IGES). More specifically, the Hybrid Microcircuit Assembly (HMA or hybrid) IGES Application Protocol (AP) specifies the mechanisms for defining and exchanging computer-models and their associated data for hybrid microcircuits in IGES format. The AP defines the appropriateness of the data items for describing the geometry of the various parts of a hybrid microcircuit (shape and location), the connectivity, and the processing and material characteristics. NTIS

N93-29269# Technische Univ., Eindhoven (Netherlands).
HANDSHAKE CIRCUITS: AN INTERMEDIARY BETWEEN COMMUNICATING PROCESSES AND VLSI Ph.D. Thesis - Philips Gloeilampenfabrieken N.V.
Cornelis Hermanus vanBerkel 1992 250 p
(ETN-93-93579) Avail: CASI HC A11/MF A03

Tangram and handshake circuits are introduced. The cost and performance of the circuits is the primary concern, as they make Very Large Scale Integration (VLSI) programming different from (and also more difficult than) traditional computer programming. The theory for handshake circuits makes up the body of the thesis. The key motion is that of the handshake process. A handshake process is a mathematical object that describes a handshake communication behavior. This handshake behavior may be that of the components of a handshake circuit. A handshake circuit is a set of handshake processes that satisfy a simple compositional rule. The behavior of the handshake circuit is defined through parallel composition of its constituents components and is, again, a handshake process. In appendix A, the delay insensitivity of handshake circuits is related to the theory reported in the literature. A calculus for handshake processes is developed. This calculus allows concise descriptions of behaviors of handshake components. A precise definition of Tangram is given. For a subset of Tangram, which we call Core Tangram, a formal denotation 'H' is given in terms of handshake processes. In appendix B, a link to the well known failure semantics of CSP (Communication Sequential Processes) is established. The translation of Tangram programs into handshake circuits by means of the mathematical function 'C' is described. For Core Tangram it is proven that the behavior of the compiled handshake circuit is equivalent to that of the original program in a well defined sense. The realization of handshake circuits in VLSI is considered. Issues such as peephole optimization, handshake refinement, data encoding, decompositions into VLSI operator networks, initialization, and testing are discussed. Some practical experiences with VLSI programming and silicon compilation are discussed. ESA

N93-29271# Technische Univ., Eindhoven (Netherlands).
INSTRUMENTAL NEUTRON ACTIVATION ANALYSIS DEVELOPED FOR SILICON INTEGRATED CIRCUIT TECHNOLOGY Ph.D. Thesis - Philips Gloeilampenfabrieken N.V.
Marinus Leendert Verheijke 1992 225 p
(ETN-93-93581) Avail: CASI HC A10/MF A03

The merits of neutron activation analysis as a trace and ultratrace element analysis technique, as well as its relevance to silicon integrated circuit technology, were studied. The work was divided into four parts: the theory of the neutron activation process, the calibration method, and the influence of interfering reactions; the irradiation facilities and the determination of their characteristic parameters; the spectrometer system for the measurement of the gamma radiation and the evaluation of the spectra; and the accuracy of the method, the limits of detection, the practical performance of the analyses, and typical results in the field of silicon integrated circuit technology. The method is briefly compared with other modern trace analysis techniques which are also used for silicon integrated circuit technology, and the future possibilities of neutron activation analysis in this area are considered. ESA

N93-29281 Department of the Navy, Washington, DC.
OPTICALLY CONTROLLED ACTIVE IMPEDANCE ELEMENT PARTICULARLY SUITED FOR A MICROWAVE OSCILLATOR Patent
William D. Jemison, inventor (to Navy) and Peter R. Herezfeld, inventor (to Navy) 30 Mar. 1993 11 p Filed 28 Feb. 1992
(AD-D015723; US-Patent-5,198,783; US-Patent-Appl-SN-843677; US-Patent-Class-331-66) Avail: US Patent and Trademark Office

An optically controlled active impedance element particularly suited to serve as a tuneable inductive element for a microwave oscillator is disclosed. The optically controlled active inductive element is comprised of a circuit arrangement, preferably consisting of MESFET devices which exhibit a composite inductive characteristic, and whose inductance may be determined and controlled by direct illumination impinging on the MESFET's. The optically controlled active inductive element lends itself to being adapted to monolithic microwave integrated circuit (MMIC) applications and may find use in a wide variety of microwave circuits. Also disclosed, is an embodiment which used the optical controlled active impedance element, in a prescribed manner, to serve as a tunable capacitor for use in various microwave circuits. DTIC

N93-29311# Argonne National Lab., IL.
THE ANL ELECTRIC VEHICLE BATTERY R/D PROGRAM FOR DOE-EHP
1 Mar. 1993 10 p
(Contract W-31-109-eng-38)
(DE93-010658; ANL/CMT/RP-79188) Avail: CASI HC A02/MF A01

The Electrochemical Technology Program at Argonne National Laboratory (ANL) provides technical and programmatic support to DOE's Electric and Hybrid PropuLsion Division (DOE-EHP). The goal of DOE-EHP is to advance promising electric-vehicle (EV) propulsion technologies to levels where industry will continue their commercial development and thereby significantly reduce air pollution and petroleum consumption. In support of this goal, ANL provides research, development, testing/evaluation, post-test analysis, modeling, and technical management of industrial R&D contracts on advanced battery technologies for DOE-EHP. This report summarizes the battery-related activities undertaken during the period of 1 Oct. 1992 - 31 Dec. 1992. In this report, the objective, background, technical progress, and status are described for each task. The work is organized into the following task areas: 1.0 Project Management and Coordination; 2.0 Sodium/Metal Chloride R&D; 3.0 Microreference Electrodes for Lithium/Polymer Batteries; and 4.0 USABC Support. The Project Management and Coordination Task Area encompasses planning, organization, coordination, integration, and overall management of battery R&D projects for DOE-EHP, as well as work performed in behalf of DOE-directed inter-laboratory tasks. Section 3 of this report recounts the work performed during this reporting period on each task within these task areas. DOE

N93-29408# Office of the Under Secretary of Defense (Acquisitions), Washington, DC.
DEPARTMENT OF DEFENSE ADVISORY GROUP ON ELECTRON DEVICES: APPENDIX TO SPECIAL TECHNOLOGY AREA REVIEW ON MICROWAVE PACKAGING TECHNOLOGY
Feb. 1993 143 p
(AD-A262136) Avail: CASI HC A07/MF A02

Electronic packaging is identified as an area providing opportunity for system performance enhancement for both defense and commercial applications. The move to microwave/millimeter wave multi-chip assemblies with high density interconnects is causing a significant shift in the current practices of how packages are being designed and manufactured. The longer term trend is to move to subsystem or multi-level packaging schemes to achieve higher levels of system integration. Packaging costs are being emphasized early in system developments. Workshop goals include the following: (1) define packaging and interconnect technology and manufacturing problems/issues; (2) recommend solutions to these problems by developing an investment strategy that can be used by government and industry; and (3) build upon and couple to the 2-4 Mar. 92 aged electronics packaging technology star. DTIC

N93-29427# Columbia Univ., New York, NY. Dept. of Electrical Engineering.
MULTICHIP MODULE HIGH SPEED TESTING Quarterly Progress Report, 1 Jan. - 31 Mar. 1993
Robert J. Davis and David H. Auston 31 Mar. 1993 4 p
(Contract N00014-91-J-4045)
(AD-A262989) Avail: CASI HC A01/MF A01

Progress in the testing of multichip module electronic circuit packages for the period 1 Jan. 1993 - 31 Mar. 1993 is described, in the areas of the testing of multichip modules using electrooptic polymers and organic crystals. DTIC

N93-29435 Naval Air Warfare Center, China Lake, CA. Weapons Div.
THE 17TH ANNUAL ELECTRONICS MANUFACTURING SEMINAR PROCEEDINGS
Dec. 1992 319 p Seminar held in Ridgecrest, CA, 2-4 Feb. 1993
Limited Reproducibility: More than 20% of this document may be affected by microfiche quality
(AD-A261963; NAWCWPNS-TP-8096) Avail: Issuing Activity (Defense Technical Information Center (DTIC))

Presented are the proceedings of the 17th Annual Electronics Manufacturing Seminar, held on 2-4 Feb. 1993, in Ridgecrest, Calif. The proceedings include the papers presented at the Seminar and cover all aspects of soldering technology and electronics manufacturing. The proceedings are a compilation of information provided by both nongovernment and government sources. The proceedings are published in the interest of furthering communication and broadening awareness of current activities among soldering technology and electronics manufacturing specialists. DTIC

N93-29478# Naval Research Lab., Washington, DC.
STUDY OF GAIN IN C-BAND DEFLECTION CAVITIES FOR A FREQUENCY-DOUBLING MAGNICON AMPLIFIER
S. H. Gold, C. A. Sullivan, B. Hafizi, and W. M. Manheimer 26 Mar. 1993 20 p
(AD-A263132; NRL/MR/6793-93-7197) Avail: CASI HC A03/MF A01

We report an experimental study of the gain between two half-wavelength, 5.7 GHz TM 110 pillbox cavities, separated by a quarter-wavelength drift space, and powered by a 170A, 500 keV electron beam immersed in an 8.1 kG magnetic field. These cavities constitute the first section of a planned multicavity detection system, whose purpose is to spin up an electron beam to high transverse momentum for injection into the output cavity of a frequency-doubling magnicon amplifier. We have observed a gain of approximately 15 dB in the preferred circular polarization, at a frequency shift of approximately -0.18%, and a gain of approximately 3 dB in the opposite circular polarization, at a frequency shift of approximately +0.06%. These results are in good agreement with theory. DTIC

N93-29485# Texas Univ., Austin. Electronics Research Center.
ELECTRONICS RESEARCH AT THE UNIVERSITY OF TEXAS AT AUSTIN. APPENDIX: JSEP SPONSORED PUBLICATIONS Annual Report, 15 May 1992 - 14 Feb. 1993
Edward J. Powers 14 Feb. 1993 265 p
(Contract F49620-92-C-0027)
(AD-A262993; Rept-47) Avail: CASI HC A12/MF A03

This Appendix to the Annual Report contains reprints of publications relating to basic research in information electronics, electromagnetics, and solid-state electronics. The research is described in Annual Report No. 46 and was carried out at the University of Texas at Austin under the auspices of the DoD Joint Services Electronics Program. DTIC

N93-29495# Columbia Univ., New York, NY. School of Mines.
SYMPOSIUM ON HIGH TEMPERATURE SUPERCONDUCTORS: MATERIALS RESEARCH FOR EMERGING TECHNOLOGIES
Siu-Wai Chan 25 Feb. 1993 10 p Symposium held in Boston, MA, 2-6 Dec. 1991
(Contract N00014-91-J-1997)
(AD-A263120) Avail: CASI HC A02/MF A01

The emergence of thin film and bulk technologies has resulted in an increasing emphasis in applications. The purpose of this symposium is to bring together a group of interdisciplinary scientists and engineers to help identify and solve the material related issues that still hamper the application of HTS materials. Specific topics to be emphasized include: Transport in bulk superconductors; Weak links and Josephson junctions: formation and control of properties; Effect of processing on properties of thin films; Correlation between the microstructure and transport (DC and microwave) in thin films; Noise in HTS materials; Multilayered structures; Grain Boundaries and Interfaces; and New HTS materials--bulk materials and thin films. DTIC

N93-29513# Microelectronics and Computer Technology Corp., Austin, TX.
AN MCM/CHIP CONCURRENT ENGINEERING VALIDATION Final Quarterly Report, Jul. - Sep. 1992
Hector Moreno and Shuane Stark 31 Dec. 1992 32 p
(Contract MDA972-92-C-0022; ARPA Order 8363)
(AD-A262959; HVE-042-93) Avail: CASI HC A03/MF A01

We report on the MOST software system, which implements a concurrent physical design environment for Multi-Chip Modules. The system integrates the work of design teams distributed across a network and using different CAD systems. At present the following systems have been integrated: Cadence's Edge 2.1, Cadence's Allegro 6.1, AutoDesk's AutoCad 12.0, and Harris' Finesse. Software links were established allowing data from those systems to be shared through a ROSE (Rensselaer Object Storage Environment) database management developed under the sponsorship of the DICE program. The code was written in C++ and uses various methods to feed the information in and obtain it out of the design systems: IGES for Allegro, SKILL for Edge and dfile for Finesse, while the AutoCad link is a direct one. The DDR2 (Digital Drop Receiver, version 2) multi-chip module from Harris was entered into the system and routed utilizing a redundant route scheme. The exercise used a concurrent approach, the data defining parts and placement entered through Finesse, the parts modified in Edge, the route done in Allegro and the final merge and verification performed with the Edge tool. DTIC

N93-29605 Department of the Navy, Washington, DC.
TEMPERATURE COMPENSATED LITHIUM BATTERY ENERGY MONITOR Patent
Albert M. Bates, inventor (to Navy) 10 Nov. 1992 10 p Filed 3 Apr. 1991
(AD-D015680; US-Patent-5,162,741; US-Patent-Appl-SN-682159; US-Patent-Class-324-431) Avail: US Patent and Trademark Office

A system is provided for temperature compensating and monitoring the energy of a lithium battery. In this method, a temperature compensation factor is determined according to a value of temperature. A determination is made of the energy usage while the battery operates at that temperature. The temperature usage is then compensated in accordance with the temperature compensation factor. A second temperature, along with a second temperature compensation factor, is determined. A second energy level is determined and compensated as described for the first. A cumulative energy usage is determined according to the first and second compensated energy usage values. DTIC

N93-29654# Texas A&M Univ., College Station.
SYNTHESIS TECHNIQUES AND ANALYSIS TOOLS FOR ON-CHIP FAULT-TOLERANCE Final Report
Dhiraj K. Pradhan 1992 17 p
(Contract N00014-91-J-1404)
(AD-A263167) Avail: CASI HC A03/MF A01

Significant research performed on a broad range of issues related to fault-tolerant design both at the chip and system level are summarized. First discussed is an integrated approach, currently under development for integrating concurrent checking with BIST. The goal is to generate synthesis tools to develop low-cost fault-tolerant VLSI chip design tools that are both easy to test as well as being robust against operational errors. REACT, a tool currently under development for fault-tolerant architecture characterization is reviewed. An on-going research on the development of fault-tolerant architectures is presented. DTIC

N93-29655# Army Missile Command, Redstone Arsenal, AL. Weapons Science Directorate.
PROTOTYPE AND SHORT-RUN PRINTED CIRCUIT BOARD CREATION Final Technical Report, Sep. 1990 - 1992
Darryl Hoelder Mar. 1993 23 p
(AD-A263245; AD-E952002; AMSMI/TR-RD-WS-92-13) Avail: CASI HC A03/MF A01

The knowledge and experience developed within this directorate over the past several months in the fabrication of Printed Circuit Board (PCB) techniques is described. Due to the limited quantity of identical, custom-made PCB's needed for use in the laboratory, it is both cost-effective and less time-consuming to fabricate PCB's in-house, than to employ an outside supplier. The combination of equipment and techniques permits the fabrication of single and short-run PCB's of up to 8 by 10 inches, with little problem. The system described has been in place for about two years after being developed over a longer period. As with any technique-dependent process, experience and learning will contribute to better quality in the product. However, this set of equipment and the techniques described should yield reasonable results very quickly after the start of operation. Continuing improvement of these techniques is taking place, but there now exists a capability for the creation of small quantities of PCB's sufficient for laboratory uses. The design techniques used are directly useful for the creation of materials required by an outside jobber for producing a large quantity of PCB's, should that be required. DTIC

N93-29671# National Science Foundation of US, Tokyo (Japan).
NSF TOKYO REPORTS: JAPANESE R AND D PROJECTS ON MICRO- AND NANOFABRICATION AND RELATED BASIC RESEARCH PROJECTS
Jan. 1993 31 p
(PB93-181261) Avail: CASI HC A03/MF A01

The report examines Japanese projects believed to fall in the general area of micro- and nanofabrication technologies or nanoscopic materials and structures, including basic research projects with the potential of leading to future development of relevant technologies. Listed projects were selected as a result of discussions with officials of the respective agencies, in the absence of any ready-made or official list of such projects. Projects are grouped together under the government programs supporting them, with information on title, duration, and total budget in Japanese yen. NTIS

N93-29673# Central Research Inst. of Electric Power Industry, Tokyo (Japan). Energy and Environment Lab.
RESEARCH AND DEVELOPMENT OF LITHIUM SECONDARY BATTERIES FOR LOAD CONDITIONER USE, VOLUME 2
N. Terada, K. Takei, K. Ishihara, T. Iwahori, T. Tanaka, H. Mishima, and K. Takeuchi Jun. 1992 28 p
(DE93-781329; CRIE-T-91078) Avail: CASI HC A03/MF A01

Results of evaluation are reported on cycle life/power performance of square lithium/vanadium oxide secondary batteries (25Wh class) trially manufactured as a basic unit for the battery energy storage system which can be installed at home. Experimental results of charge/discharge cycle and power characteristics verify that the battery is highest in performance of all the large capacity lithium secondary batteries which have been made public. The lithium secondary battery with a large capacity more than 10Wh by operation of 50% DOD (depth of discharge) achieves 420 cycles, the highest level. The amount of energy taken out by about one-hour rate discharge is reduced only to about 85% of that by 8-hour rate discharge, which is a favorable result as the lithium secondary battery which operates at normal temperature. However, at the end of one-hour rate discharge, some of the battery surface temperatures rise about 10 C, and this may cause inhibition in the structure as a pair battery. The following method is suggested for improvement: thickness of the cathode of the main heating part is reduced to promote thermal radiation, and the cathode area is enlarged to decrease the current density. DOE

N93-29793# Lawrence Livermore National Lab., CA.
FREQUENCY DEPENDENT ELECTRICAL PROPERTIES OF MINERALS AND PARTIAL-MELTS
J. J. Roberts and J. A. Tyburczy (Arizona State Univ., Tempe.) 26 Aug. 1992 35 p Presented at the 11th Workshop on Electromagnetic Induction in the Earth, Wellington, New Zealand, 26 Aug. - 2 Sep. 1992
(Contract W-7405-eng-48)
(DE93-009254; UCRL-JC-111340; CONF-9208215-1) Avail: CASI HC A03/MF A01

Frequency-dependent impedance of olivine, dunites, metapelites, and partial-melts between 10(sup -4) and 10(sup 5) Hz, when plotted in complex impedance plane, reveal arcs corresponding to different conduction mechanisms. In polycrystalline materials, two impedance arcs related to material properties (as opposed to electrode properties) are observed. The mechanisms occur in series; they are interpreted as grain interior or bulk conduction, grain boundary conduction, and sample-electrode interface effects, from highest to lowest frequency, respectively. Natural dunitic rocks show similar behavior. The grain boundaries do not enhance the conductivity of any of the materials (series electrical behavior) and sometimes limit the total conductivity of the grain interior-grain boundary system. Olivine-basalt partial-melts also show at least two conduction mechanisms occurring in series over 10(sup -4)-10(sup 5) Hz. Isolated melt pockets show series conduction, while interconnected melt phase show parallel conduction. Because laboratory electrical measurements are used in inversion of field EM data to derive conductivity vs depth profiles, it is important to understand the frequency dependent behavior of Earth materials. Activation energies determined from studies that measure conductivity at a single frequency may be erroneous because of the shift in frequency of different conduction mechanisms as temperature is varied. DOE

N93-29798# Air Force Systems Command, Wright-Patterson AFB, OH. Foreign Aerospace Science and Technology Center.
NEW DEVELOPMENTS IN VACUUM MICROELECTRONICS
Fujian Liao 2 Apr. 1993 25 p Transl. into ENGLISH from Dianzi Xuebao (China), v. 19, no. 3, May 1991 p 89-95
(AD-A263103; FASTC-ID(RS)T-0314-92) Avail: CASI HC A03/MF A01

This paper describes a new field-vacuum microelectronics or vacuum integrated circuits (VIC). Its principle, the structure of the field emission microtriodes and microfabrication techniques and processing are given in detail. The processing for the thin field emission cathodes is also reviewed. The application of VIC and the related problems for its future development are discussed. DTIC

N93-29812# Los Alamos National Lab., NM.
ANALYSIS OF AN MCG/FUSE/PFS EXPERIMENT
I. R. Lindemuth, D. G. Rickel, and R. E. Reinovsky 1993 9 p Presented at the 6th International Conference on Megagauss Magnetic Field Generation and Related Topics, Albuquerque, NM, 9-12 Nov. 1992
(Contract W-7405-eng-36)
(DE93-007355; LA-UR-93-0044; CONF-921133-17) Avail: CASI HC A02/MF A01

The Los Alamos PROCYON high-explosive pulsed power (HEPP) implosion system is intended to produce 1 MJ of soft x-radiation for fusion and material studies. The system uses the MK-IX magnetic flux compression generator to drive a 'slow' opening switch which, upon operation, connects the output of the MK-IX generator to a plasma flow switch, which, in turn, delivers current to a rapidly imploding load. The closing switch isolates the plasma flow switch (PFS) and load from any precursor current which might arise due to the finite impedance of the opening switch during its closed phase. In that experiment, our first test, the MK-IX generated approximately 16 MA and 8.2 MJ, and approximately 9.8 MA and 1.15 MJ were delivered to a fixed inductive load in 8-10 microseconds. Computations performed after the experiment, taking into account experimental variables which could not be accurately predicted prior to the experiment, were in satisfactory agreement with all experimental observations, including a double-peaked dI/dt signal which indicated a particular trajectory of the copper fuse material through density-temperature space. Prompted by our success with a fixed load, a second experiment was performed using the MK-IX/fuse/STS combination to drive a plasma flow switch. The objectives of the experiment were to observe the ability of the fuse/STS combination to drive a plasma flow switch and to evaluate our ability to predict system performance. The details of the experiment, the measurements taken, and the data reduction process have previously been reported. The MK-IX produced approximately 22 MA, and approximately 10 MA was delivered to the PFS, which moved down the coaxial barrel of the assembly in an intact manner in about 8 microseconds. The results of our computational analysis of the experiment are presented. DOE

N93-29814# Wyoming Univ., Laramie. Dept. of Electrical Engineering.
ENERGY EFFICIENT DRIVEPOWER, VOLUME 2
S. Ula, D. L. Jordan, and L. E. Birnbaum 1993 46 p
(Contract DE-AI79-90BP-08212)
(DE93-012437; DOE/BP-08212/T3-Vol-2) Avail: CASI HC A03/MF A01

A large number of information sources in the area of the efficient use of drivepower are listed. The main list is for the general user of drivepower systems. The other list is a supplemental reference list for the design engineer. DOE

N93-29826# Naval Academy, Annapolis, MD. Dept. of Physics.
ELECTRICAL RELAXATION IN ACID-FORM NAFION Interim Technical Report, Mar. 1992 - Apr. 1993
J. J. Fontanella, M. G. McLin, and M. C. Wintersgill 16 Apr. 1993 29 p
(Contract N00014-93-WR-24016)
(AD-A263558; Rept-TR-3) Avail: CASI HC A03/MF A01

Electrical relaxation studies of acid-form NAFION-117 membranes dried in situ at 380 K in vacuum have been performed. Significant electrical conductivity is found and the data are found to be non-Arrhenius. The results are converted to the electrical modulus representation and a conductivity relaxation is observed. A stretched exponential is best-fit to the conductivity relaxation and again, non-Arrhenius behavior is observed for the peak position. Finally, at low temperatures, a new dielectric relaxation peak is found which has an activation enthalpy of about 0.57 eV (13 kcal/mol). This relaxation is analogous to the Gamma-relaxation observed in mechanical relaxation studies. DTIC

N93-29833# Varian Associates, Palo Alto, CA.
IMPROVED FIELD EMITTER CURRENT DENSITIES AND STABILITY THROUGH THE APPLICATION OF A PROPRIETARY PROCESS Quarterly Report No. 4, Dec. 1992 - Feb. 1993
Feb. 1993 14 p
(Contract MDA972-92-C-0033)
(AD-A263464) Avail: CASI HC A03/MF A01

As detailed in the previous reports, the necessary current densities (60 A/sq cm), linear current densities (3 mA/mm), and stability (greater than 2 days) to meet the contract goals (at least theoretically) have been achieved. The next step is to fabricate three terminal devices to demonstrate the remaining contract goal--a one GHz current gain cutoff frequency (f(sub t)). During this period the design of the three terminal devices was completed, and the mask set was received at the end of the period. RF modulation at one GHz was also demonstrated as high as 2 GHz with an incremental gain in s(sub 21) of 0.5 dB. DTIC

N93-29922# Maryland Univ., College Park. Dept. of Electrical Engineering.
IMPROVED DESIGN CONCEPTS FOR MILLIMETER WAVE POWER SOURCES Final Report, 15 Mar. 1992 - 14 Mar. 1993
V. L. Granatstein, H. Guo, and Y. Carmel 14 Mar. 1993 23 p
(Grant AF-AFOSR-0142-90)
(AD-A264060; AFOSR-93-0311TR) Avail: CASI HC A03/MF A01

This progress report summarizes the work done during the period from 15 Mar. 1992 to 14 Mar. 1993. In the past year, we have designed a phase-locked, harmonic, inverted gyro-twistron, known as the phigtron. The phigtron combines a subharmonic gyro-TWT amplifier input section with a gyroklystron type output cavity. The phigtron is expected to reach much higher phase-locking gain and wider bandwidth than the two cavity phase-locked gyroklystron oscillator. The efficient and stable operation of this phase-locked harmonic gyrotron will be obtained through the implementation of mode selective interaction circuits. The proof-of-principle cold test results of such circuitry have recently been obtained indicating that the technical realization of this research concept is feasible. The construction of the phigtron hot test laboratory facility is now actively proceeding. DTIC

N93-29986# Jackson State Univ., MS. Dept. of Chemistry.
CHARACTERIZATION OF LITHIUM ELECTRODE SURFACE IN LITHIUM SECONDARY BATTERIES BY IN SITU RAMAN SPECTROSCOPIC METHODS Final Report, 1 Sep. 1989 - 31 Dec. 1992
Hiroyasu Tachikawa 24 Mar. 1993 23 p
(Contract DAAL03-89-G-0105)
(AD-A263728; ARO-27241.1-CH-SAH) Avail: CASI HC A03/MF A01

Surface layers on lithium electrodes formed in several solvents including dimethyl carbonate (DMC), diethyl carbonate (DEC), polyethylene glycol 400 dimethyl ether (PEG400DME), and propylene carbonate (PC) have been studied by Raman spectroscopy. Both DMC and DEC were used singly, and also mixed with either methyl acetate or methyl formate. The Raman spectra showed that passive films formed on the Li surface in different solvents may have different chemical structures, which changed during the charging and discharging processes. A solid film of fullerene C60, which could be used as a cathode in Li rechargeable batteries, was examined in the PEG400DME solution by both electrochemical and Raman spectroscopy. Cyclic voltammograms (CV's) showed five redox peaks which suggested the formation of C60(-), C60(2-), C60(3-), C60(4-), and C60(5-). Raman spectra obtained from thin C60 film indicated that the thin fulleride film dissolved in the PEG400DME/LiClO4 solution at negative potentials. DTIC

N93-30021# Naval Surface Warfare Center, Dahlgren, VA.
AN EXPLOSIVELY ACTUATED ELECTRICAL SWITCH USING KAPTON INSULATION
Douglas G. Tasker, Richard J. Lee, and Paul K. Gustavson Mar. 1993 52 p
(AD-A263835; NSWCDD/TR-92/124; ARO-29354.3-MA) Avail: CASI HC A04/MF A01

The designs and manufacture of several explosively-actuated, electrical closing switches are described. The switches are fast operating; can handle very high electrical power; are highly energy efficient, with low inductance and low resistance, when closed; but are able to withstand very high voltages when open. The switches exploit shock-induced conductivity effects in polypyromellitimide insulators (PPMI), e.g., Kapton. The key to the successful operation of the switches is to use them in the transverse mode of operation, i.e., where the detonation wave travels transverse to the applied electric field. Through the research described in this report, the many factors that are crucial to the design of an effective switch have been identified. Various switch designs and the results of using them in numerous applications are provided. DTIC

N93-30031# Varian Associates, Palo Alto, CA.
IMPROVED FIELD EMITTER CURRENT DENSITIES AND STABILITY THROUGH THE APPLICATION OF A PROPRIETARY PROCESS Quarterly Report No. 2, Jun. - Aug. 1992
Aug. 1992 5 p
(Contract MDA972-92-C-0033)
(AD-A264048) Avail: CASI HC A01/MF A01

This brief report highlights the technical progress made during the three-month period covered on the contract. The contract goals are to demonstrate a three-terminal vacuum microelectronic device having a current gain cutoff frequency f(sub t) of at least one GHz at a current density of at least 5 A/sq cm, stable over a period of 2 hours or more. The previous report described the advantages of the single-crystal approach being employed for the contract. Linear current densities of 0.8 mA/mm were reported, within a factor of 3 needed to theoretically satisfy the performance goals of the contract (Task 1 of the SOW). Furthermore, these current densities were realized in conventional 10(exp 9) Torr vacuum levels without a UHV bake-out as is necessary for non-crystalline structures. The current emission would remain stable over a period in excess of several days. During this period the focus was on improving the linear current density to the value needed to achieve f(sub t) greater than or equal to 1 GHz. To better communicate the impact of the work done during the period, the results are presented first, followed by the experimental work behind these results. DTIC

N93-30057# Wyoming Univ., Laramie. Dept. of Electrical Engineering.
ENERGY EFFICIENT DRIVEPOWER: AN OVERVIEW
S. Ula, L. E. Birnbaum, and D. Jordan 1993 48 p
(Contract DE-AI79-90BP-08212)
(DE93-012435; DOE/BP-08212/T2) Avail: CASI HC A03/MF A01

This report examines energy efficiency in drivepower systems. Only systems where the prime movers are electrical motors are discussed. A systems approach is used to examine all major aspects of drivepower including motors, controls, electrical tune-ups, mechanical efficiency, maintenance, and management. Potential annual savings to the US society of $25 to $50 billion are indicated. The report was written for readers with a semi-technical background. DOE

N93-30058# Wyoming Univ., Laramie. Dept. of Electrical Engineering.
ENERGY EFFICIENT DRIVEPOWER
S. Ula, D. L. Jordan, and L. E. Birnbaum 1993 82 p
(Contract DE-AI79-90BP-08212)
(DE93-012436; DOE/BP-08212/T3-Vol-1) Avail: CASI HC A05/MF A01

This document lists a large number of information sources in the area of the efficient use of drivepower. This is a broad area, covering not just electric motors, but all of the parts of a system which transfers the power from when it enters a facility to when the load is driven and controlled. DOE

N93-30108# Technical Research Centre of Finland, Espoo. Computer Technology Lab.
TOTAL DOSE TESTS FOR THE PROMICS-3 INSTRUMENT

Raimo Verkasalo Jan. 1991 43 p
(VTT-TIED-1203; ISBN-9-51-383929-X; ETN-93-93770) Copyright Avail: CASI HC A03/MF A01

The sensitivity of some analog and digital Integrated Circuits (IC's) to ionizing radiation was tested in order to evaluate their potential usefulness especially in the PROMICS-3 instrument. The PROMICS-3 is a plasma instrument to be flown on the Russian Interball satellites. The radiation tolerance requirement of the auroral Interball satellite is about 45 krad/year inside a shielding of 4 mm aluminum. The IC's tested were: AD571 A/D-converter, ADDAC80 D/A-converter, LF442A and PM108A operational amplifiers, MPREF01 voltage reference, STC SPXO 6 MHZ oscillator, 4N55 optocoupler, MC51C98 and CY7C164 16k*4 static CMOS RAM. Co-60 was used as the irradiation source. The test methods and results are described. The RAM circuits failed between 10 and 20 krad. D/A- and A/D-converters degraded only slightly after 100 krad, but one of the A/D converters failed functionally at 190 krad. The LF442A began to degrade in the test connection at 100 krad, and PM108A at 30 krad. The output voltage of the voltage reference MPREF101 increased about 20 mV after 100 krad. No change was observed in the output frequency of the STC SPXO oscillator even after 300 krad. The current transfer ratio of the 4N55 decreased continuously to about 75% of the initial value after 100 krad. ESA

N93-30118# Sandia National Labs., Albuquerque, NM.
CHARACTERISTIC AND DEVELOPMENT REPORT SA3581/MC4196 LIGHTNING ARRESTOR CONNECTOR (LAC)
P. J. Konnick, G. Gabert (Martin Marietta Specialty Components, Inc., Largo, FL.), K. Bradley (Martin Marietta Specialty Components, Inc., Largo, FL.), and W. Washington (Martin Marietta Specialty Components, Inc., Largo, FL.) Mar. 1993 121 p
(Contract DE-AC04-76DP-00789)
(DE93-010610; SAND-92-0406) Avail: CASI HC A06/MF A02

This report describes the design, development, manufacturing processes, acceptance equipment, test results, and conclusions for the SA3581/MC4196 LAC program. Four development groups (Identified as Groups 1 through 3 and a Proof of Development Build) provided the evaluation criteria for the PPI/TMS production units. DOE

N93-30127# Sandia National Labs., Albuquerque, NM.
FOREIGN TECHNOLOGY ASSESSMENT: ENVIRONMENTAL EVALUATION OF A RADIATION-HARD OSCILLATOR/DIVIDER
M. A. Dvorack Mar. 1993 41 p
(Contract DE-AC04-76DP-00789)
(DE93-011481; SAND-92-2473) Avail: CASI HC A03/MF A01

Salford Electrical Instruments, Ltd., and the General Electric Company's Hirst Research Center, under contract to the United Kingdom's (UK) Ministry of Defence, developed a radiation-hard, leadless chip-carrier-packaged oscillator/divider. Two preproduction clocks brought to Sandia National Laboratories (SNL) by a potential SNL customer underwent mechanical and thermal environmental evaluation. Because of the subsequent failure of one device and the deteriorating condition of another device, the devices were not subjected to radiation tests. The specifics of the environmental evaluation performed on these two clocks and the postmortem analysis of one unit, which ultimately failed, are described. Clock startup time versus temperature studies were also performed and compared to an SNL-designed clock having the same fundamental frequency. DOE

N93-30152# Mission Research Corp., Albuquerque, NM.
TEST STRUCTURE TO MICROCIRCUIT CORRELATION Final Report, Mar. 1990 - Jun. 1992
Edward W. Enlow Apr. 1993 38 p
(Contract F29601-89-C-0014)
(AD-A264157; MRC/ABQ-R-1467; PL-TR-92-1013) Avail: CASI HC A03/MF A01

This Parametric Analysis of Radiation effects software development is given the general title PARA. This report describes the development of algorithms and source codes for the simulation of radiation effects on CMOS IC's. The project concentrated on the simulation of total dose effects and the ways to establish/predict the operational lifetime and radiation tolerance of IC's. The PARA switch level simulator incorporates the capability to assign bias dependent postirradiation drive parameters to transistors within a microcircuit and to calculate propagation delays based on those parameters. This permits test vectors to be assigned based on worst case postirradiation propagation delays. DTIC

N93-30201 Department of the Navy, Washington, DC.
ORDNANCE THERMAL BATTERY Patent
Louis Pracchia, inventor (to Navy), Ronald F. Vetter, inventor (to Navy), and Darwin Rosenlof, inventor (to Navy) 27 Apr. 1993 7 p Filed 5 Nov. 1990
(AD-D015722; US-Patent-Class-102-207) Avail: US Patent and Trademark Office

This invention pertains to thermal battery activated by external heat comprising an anode, e.g., composed of a lithium-aluminum alloy, a cathode, e.g., composed of iron disulfide, and an electrolyte, e.g., a lithium chloride-potassium chloride eutectic, the electrolyte being inactive at ambient temperature but being activated by melting at a predetermined temperature when exposed to external heating. The battery can be used as a sensor or to ignite pyrotechnic and power electronic devices, in system for reducing the hazard of ordnance exposed to detrimental heating. A particular application is the use of the battery to activate a squib to function in conjunction with one or more other components, to vent an ordnance case, preventing its explosion in a fire. DTIC

N93-30370# Sandia National Labs., Albuquerque, NM.
DETECTING RESIDUE ON A PRINTED CIRCUIT BOARD: AN APPLICATION OF THE BOUNDARY CONTOUR/FEATURE CONTOUR SYSTEM
M. W. Koch and M. M. Moya 1992 4 p Presented at the World Congress on Neural Networks, Portland, OR, 11-15 Jul. 1993
(Contract DE-AC04-76DP-00789)
(DE93-006283; SAND-92-2901C; CONF-930741-2) Avail: CASI HC A01/MF A01

We have developed a video detection algorithm for measuring the residue left on a printed circuit board after a soldering process. Oblique lighting improves the contrast between the residue and the board substrate, but also introduces an illumination gradient. The algorithm uses the Boundary Contour System/Feature Contour System to produce an idealized clean board image by discounting the illuminant, detecting trace boundaries, and filling the trace and substrate regions. The algorithm then combines the original input image and ideal image using mathematical models of the normal and inverse Weber Law to enhance the residue on the traces and substrate. The paper includes results for a clean board and one with residue. DOE

N93-30406# Battelle Columbus Labs., OH.
HIGH RELIABILITY, MAINTENANCE-FREE INS BATTERY DEVELOPMENT Interim Report, 27 Sep. 1991 - 31 Jul. 1992
David G. Vutetakis and David J. Surd 31 Jul. 1992 136 p
(Contract F33657-90-D-2190)
(AD-A264521; WL-TR-92-2082) Avail: CASI HC A07/MF A02

This report documents the findings of a study undertaken to develop a high reliability, maintenance-free battery (HRMFB) for application in the Litton LTN-72 and Delco Carousel 4 Inertial Navigation Systems (INS). The results indicated that the sealed lead-acid battery technology is the best candidate from a cost and risk standpoint. A specification sheet was developed detailing the performance and test requirements for the proposed INS HRMFB. DTIC

N93-30409# Honeywell, Inc., Bloomington, MN. Sensor and System Development Center.
RF VACUUM MICROELECTRONICS Quarterly Technical Report, 1 Jan. - 31 Mar. 1993
A. I. Akinwande and D. K. Arch 7 May 1993 11 p
(Contract MDA972-91-C-0030; ARPA Order 8162)
(AD-A264528) Avail: CASI HC A03/MF A01

We summarize our technical progress towards developing a thin-film edge emitter vacuum transistor capable of 1 GHz modulation. Extensive DC characterization of vacuum triode devices was carried out. Low frequency (10 KHz) modulation was demonstrated. Impedance mismatch between the fabricated devices and the test system prevented high frequency measurements. Redesign of the vacuum triodes is planned to achieve the 1 GHz program goal. DTIC

N93-30516# Sandia National Labs., Albuquerque, NM.
EFFECTS OF DEVICE SCALING AND GEOMETRY ON MOS RADIATION HARDNESS ASSURANCE
M. R. Shaneyfelt, D. M. Fleetwood, and P. S. Winokur 1993 5 p
Presented at the Nuclear and Space Radiation Effects Conference, Snowbird, UT 19-23 Jul. 1993
(Contract DE-AC04-76DP-00789)
(DE93-009832; SAND-93-0531C; CONF-930704-6) Avail: CASI HC A01/MF A01

MOS total-dose response is shown to depend strongly on transistor gate length. Simple scaling models cannot predict short-channel device response from long-channel results. Hardness assurance implications are discussed for weapon and space environments. DOE

N93-30539# Army Research Lab., Aberdeen Proving Ground, MD.
ON THE IDEALITY OF USING A STEP-FUNCTION CURRENT IN A METALLIC FOIL TO SIMULATE A STEP-FUNCTION HEAT-FLUX SOURCE Final Report, Jan. - Feb. 1992
Martin S. Miller May 1993 23 p
(DA Proj. 1L1-61102-AH-43)
(AD-A264627; ARL-MR-65) Avail: CASI HC A03/MF A01

An exact solution is derived to the one-dimensional, time-dependent, heat-conduction equation for a two-layer, semi-infinite, composite solid with sudden uniform heat generation in the surface layer, no heat transfer through the surface plane, and uniform initial temperature. The interface between the two layers is assumed to have no thermal contact resistance. This solution enables a discussion of the ideality with which a step-function electric current in a metallic foil can generate a step-function heat flux into a contacting semi-infinite solid. Previous measurements of thermal diffusivity (based on the above conditions) have relied on the idealized constant-flux solution for data reduction. It is shown here that the temperature errors in the substrate arising from non-ideality of the constant-flux boundary condition increase with depth into the substrate, foil thickness, and decreasing thermal conductivity/diffusivity of the substrate. DTIC

N93-30616# Technische Univ., Berlin (Germany). Fachbereich Mathematik.
PLACEMENT OF CELLS: THEORY AND SOLUTION OF A QUADRATIC 0/1 OPTIMIZATION PROBLEM Ph.D. Thesis [PLAZIEREN VON ZELLEN: THEORIE UND LOESUNG EINES QUADRATISCHEN 0/1-OPTIMIERUNGSPROBLEMS]
Robert Weismantel 1992 234 p In GERMAN
(ETN-93-94182) Avail: CASI HC A11/MF A03

The placement problem by design of electronic chips is studied in the framework of very large scale integration. Methods for modeling placement are presented, such as min-cut heuristics, simulated annealing, and a continuous quadratic optimization method based on relaxation. The 'sea of cells' concept was chosen and a quadratic 0/1 optimization problem was described with a graph theory formulation. Variations of the problem and existence of polynomial, epsilon approximative algorithms were discussed. The problem was solved with heuristic decomposition method, with 16 locations for each cell and with 9 locations for each cell. A dynamic decomposition process was also described and a linear Lagrange relaxation solution was proposed. The clustering problem was introduced to reduce magnitude order of placement problem. The r-clustering polytope was presented from a polyhedral point of view. Several classes of facets were described by inequalities, which combine nodes and branches in the following cases: roof dual and disjuncted stars, roof dual and a tree, roof dual and a star, and roof dual and a branch. ESA

N93-30622# National Inst. for Research in Inorganic Materials, Ibaraki (Japan).
STUDY ON DIAMOND SEMICONDUCTOR
27 Nov. 1991 31 p
(DE92-531076; ETDE/JP-MF-92531076) Avail: CASI HC A03/MF A01 (US Sales Only)

The objectives of this study were to synthesize a diamond semiconductor using the CVD process, clarify the basic characteristics of the particular semiconductor, and establish a method to synthesize semiconductors having high crystallinity. The synthesizing method used was a microwave plasma CVD process. This method has a slow growth rate, but has good plasma stability and good reproducibility of the synthesizing condition with less contamination from electrodes. The dopants used were boron and phosphorus. The study included an experiment on deposition onto a diamond substrate in addition to polycrystalline films, which enabled a deposition onto a substrate with a diameter of 10 cm. A secondary ionic mass analyzer was used to discuss the relative change in impurity concentrations according to the synthesizing conditions and the crystal face dependence under identical conditions. The crystallinity received appreciable effects from the carbon concentration and the substrate temperature among the synthesizing conditions. Temperature dependence of the electric conductivity and activation energies were derived. The hole mobility was measured on mono-crystal film specimens grown on the face of a high-pressure synthesized diamond (100). DOE

N93-30650# Sandia National Labs., Albuquerque, NM.
CHARGE SEPARATION IN BIPOLAR TRANSISTORS
R. N. Nowlin (Arizona Univ., Tucson.), S. L. Kosier (Arizona Univ., Tucson.), R. D. Schrimpf (Arizona Univ., Tucson.), W. E. Combs (Naval Surface Warfare Center, Crane, IN.), and D. M. Fleetwood 1993 5 p Presented at the Nuclear and Space Radiation Effects Conference, Snowbird, UT, 19-23 Jul. 1993
(Contract DE-AC04-76DP-00789)
(DE93-009624; SAND-93-0381C; CONF-930704-4) Avail: CASI HC A01/MF A01

The effects of the midgap-level interface trap density and net oxide charge on the total-dose gain degradation of a bipolar transistor are separately identified. The superlinear dose dependence of the excess base current is explained. DOE

N93-30763# Nationaal Inst. voor Kernfysica en Hoge Energiefysica, Amsterdam (Netherlands).
INVESTIGATION OF METHODS FOR THE MEASUREMENT OF SMALL ELECTRON BUNDLE CURRENTS Thesis - Amsterdam Univ. [EEN ONDERZOEK NAAR METHODEN VOOR HET METEN VAN LAGE ELEKTRONENBUNDELSTROMEN]
H. J. Hollander May 1992 56 p In DUTCH
(DIGEL-1992-4; ETN-93-93307) Avail: CASI HC A04/MF A01

Methods for the measurement of the current of an electron bundle in a linear electron accelerator were investigated. The bundle is in vacuum and should not be affected by the measurement. The maximum current is 250 microA. The Faraday effect is too weak for the current detection. A measurement based on a glass fiber with a magnetostrictive coating is possible but only with a bandwidth of 8 Kkz. The signal to noise ratio of an inductive detection method depends strongly on the core material, the properties of which have to be further investigated. A capacitive transducer consisting of two conducting cylinders axially suspended around the bundle has to be preferred. A method to determine the signal to noise ratio of capacitive and inductive detectors is outlined. ESA

N93-30835# Nationaal Inst. voor Kernfysica en Hoge Energiefysica, Amsterdam (Netherlands).
A 250 mA TOROID MONITOR FOR THE MEASUREMENT OF THE BUNDLE CURRENT IN THE STRETCHER MODE OF AmPS [250 MA TOROIDE MONITOR VOOR HET METEN VAN DE BUNDELSTROOM IN DE STRETCHERMODE VAN AMPS]
J. T. vanEs and J. C. Boes 1992 13 p In DUTCH
(DIGEL-1992-1; ETN-93-93305) Avail: CASI HC A03/MF A01

Toroid monitors were developed to measure the bundle current of the storage ring AmPS (Amsterdam Pulse Stretcher). A toroid monitor consists of a current transformer around the bundle pipe and a current to voltage converter. The transformer is located in a radiation free environment. Therefore, since the required bandwidth is between 100 and 3 MHz, a transmission line to the converter electronics is necessary. This leads to special requirements for the converter, which also contains a zero line restorer and an output circuit that can drive 50 ohm lines. ESA

N93-30838# Nationaal Inst. voor Kernfysica en Hoge Energiefysica, Amsterdam (Netherlands).
ELECTRONICS FOR A NEUTRON DETECTOR AND A GEIGER-MUELLER DETECTOR FOR THE RADIATION PROTECTION AROUND MEA AND AmPS [NEUTRONE- EN G.M.-DETECTOR ELEKTRONICA VOOR DE STRALINGSBEVEILIGING ROND MEA EN

AMPS]
J. D. Schipper 1992 25 p In DUTCH
(DIGEL-1992-6; ETN-93-93310) Avail: CASI HC A03/MF A01

Electronic circuits were developed for the radiation protection set up around the accelerators AmPS (Amsterdam Pulse Stretcher) and MEA. This set up consists of a neutron detector and a Geiger-Mueller detector. The electronics fulfill the requirements of the security service. The amplifier of the neutron detector, the high voltage power supply for the detector, the discriminators, and the power supplies for the electronic circuits are described. ESA

N93-30896# Advanced Fuel Research, Inc., East Hartford, CT.
SUPERCONDUCTING FLUX COUPLED FAST SWITCHING DEVICE FROM YBCO FILMS Final Report, 1 Sep. 1991 - 29 Feb. 1992
David B. Fenner 30 Apr. 1992 24 p
(Contract F49620-91-C-0067)
(AD-A264301; AFOSR-93-0292TR) Avail: CASI HC A03/MF A01

Applications of high-temperature superconducting (HTSC) materials, especially thin-film YBaCuO, to microelectronic devices have been limited by materials-related fabrication problems. Magnetic-flux-coupled devices are less limited by these problems but have not been widely explored. The innovation for this program was demonstration of a flux-coupled device that was: (1) simple to fabricate, (2) based on silicon substrates, (3) shows excellent flux-flow dynamics, and (4) can be implemented in switching or amplifying circuits. In Phase 1 we have demonstrated our potential for developing this device utilizing high critical-current YBCO thin films on yttria-stabilized zirconia (YSZ)-buffered Si substrates. Our devices are designed to take advantage of these new materials opportunities, are within realistic materials and fabrication constraints, and are projected to operate from dc to at least 10 GHz. The flux-flow devices (FFD) we have fabricated, include: externally-activated magnetic switch, superconducting transformer, and flux-flow (transistor-like) switch. The use of Si wafers not only allows high-quality quality films on large (or very thin) and inexpensive substrates, but also many design configurations with great potential for wafer-scale, hybrid integration with semiconductor electronics. DTIC

N93-31030# Laboratoire d'Automatique et d'Analyse des Systemes, Toulouse (France). Groupe Circuits et Composants Micro-Ondes.
DESIGN AND INTEGRATION OF HIGH BIT RATE FOUR PHASE MONOLITHIC DEMODULATORS AND MODULATORS AT X BAND Ph.D. Thesis - Toulouse Univ. [CONCEPTION ET INTEGRATION MONOLITHIQUE DE MODULATEURS ET DEMODULATEURS QUADRIPHASE HAUT DEBIT EN BANDE X]
Antoine Primerose 1992 243 p In FRENCH Prepared in cooperation with CNES, Toulouse, France Original contains color illustrations
(LAAS-92354; ETN-93-94235) Avail: CASI HC A11/MF A03

The design and the fabrication of electronic functions in Microwave Monolithic Integrated Circuits (MMIC) are presented. These functions have applications in telecommunication satellites with onboard regeneration and high bit rate telemetry for new generations of Earth observation satellites. The four phase modulator was processed in two foundry runs with the goal to improve its performances. Particularities of the developed modulator are no bias power requirement and the absence of any tuning. The first versions of a four phase demodulator and of a phase comparator were implemented and tested. The design of these circuits needed a full simulation and modeling work in the nonlinear domain. Other functions required for applications were processed. The good results obtained in all the circuits validate demodulator and modulator concepts. Developed functions could be used in high bit rate telemetry and in onboard regeneration microwave subsystems. ESA

N93-28718*# Phillips Lab., Hanscom AFB, MA.
SODIUM SULFUR TECHNOLOGY PROGRAM NaSTEC
Bob Highley and W. Andrew Somerville (Aerospace Corp., El Segundo, CA.) *In* NASA, Washington, NASA/DOD Flight Experiments Technical Interchange Meeting Proceedings 1992 10 p (For primary document see N93-28699 11-12)
Avail: CASI HC A02/MF A10

N93-29590*# Jet Propulsion Lab., California Inst. of Tech., Pasadena.
HIGH-POWER Ka-BAND AMPLIFIER
R. Cormier *In its* The Telecommunications and Data Acquisition Report 15 May 1993 p 37-45 (For primary document see N93-29586 11-32)
(RTOP 310-20-64-22)
Avail: CASI HC A02/MF A03

N93-29591*# Jet Propulsion Lab., California Inst. of Tech., Pasadena.
EXPERIMENTAL AND MODAL VERIFICATION OF AN INTEGRAL EQUATION SOLUTION FOR A THIN-WALLED DICHROIC PLATE WITH CROSS-SHAPED HOLES
L. W. Epp and P. H. Stanton *In its* The Telecommunications and Data Acquisition Report 15 May 1993 p 46-62 (For primary document see N93-29586 11-32)
(RTOP 310-20-64-86-02)
Avail: CASI HC A03/MF A03

N93-29685*# Martin Marietta Labs., Baltimore, MD.
RADIATION SENSITIVITY OF QUARTZ CRYSTAL OSCILLATORS EXPERIMENT FOR THE LONG DURATION EXPOSURE FACILITY (LDEF), PART 2
J. S. Ahearn and J. D. Venables *In* NASA. Langley Research Center, LDEF: 69 Months in Space. Part 4: Second Post-Retrieval Symposium Apr. 1993 p 1285-1289 (For primary document see N93-29682 11-99)
Avail: CASI HC A01/MF A03; 2 functional color pages

N93-29690*# TRW Space Technology Labs., Redondo Beach, CA.
LDEF SPACE PLASMA-HIGH VOLTAGE DRAINAGE EXPERIMENT POST-FLIGHT RESULTS
J. Y. Yaung, B. K. Blakkolb, W. C. Wong, L. E. Ryan, H. J. Schurig, and W. W. L. Taylor *In* NASA. Langley Research Center, LDEF: 69 Months in Space. Part 4: Second Post-Retrieval Symposium Apr. 1993 p 1343-1354 (For primary document see N93-29682 11-99)
Avail: CASI HC A03/MF A03; 2 functional color pages

N93-30222 Windsor Univ. (Ontario). Dept. of Electrical Engineering.
REALIZATION OF HIGH SPEED ADAPTIVE FIR DIGITAL FILTERS
H. K. Kwan and Q. P. Li *In* Engineering Inst. of Canada, Canadian Conference on Electrical and Computer Engineering, Volumes 1 and 2 1990 4 p (For primary document see N93-30215 11-31)
Avail: Engineering Inst. of Canada, 2050 rue Mansfield, Suite 700, Montreal, Quebec H3A 1Z2 Canada

N93-30223 Manitoba Univ., Winnipeg. Dept. of Electrical and Computer Engineering.
ANALOG CMOS CIRCUITS FOR NEURAL NETWORKS
Christian Schneider, Roland Schneider, Gordon McGonigal, and Howard Card *In* Engineering Inst. of Canada, Canadian Conference on Electrical and Computer Engineering, Volumes 1 and 2 1990 4 p (For primary document see N93-30215 11-31)
Avail: Engineering Inst. of Canada, 2050 rue Mansfield, Suite 700, Montreal, Quebec H3A 1Z2 Canada

N93-30224 Ottawa Univ. (Ontario). Dept. of Electrical Engineering.
A MOTION DETECTOR BASED ON A NEURAL NETWORK
T. H. Yeap, J. K. Tsotsos (Toronto Univ., Ontario.), S. G. Zaky (Toronto Univ., Ontario.), and H. C. Kwan (Toronto Univ., Ontario.) *In* Engineering Inst. of Canada, Canadian Conference on Electrical and Computer Engineering, Volumes 1 and 2 1990 4 p (For primary document see N93-30215 11-31)
Avail: Engineering Inst. of Canada, 2050 rue Mansfield, Suite 700, Montreal, Quebec H3A 1Z2 Canada

N93-30225 Saskatchewan Univ., Saskatoon. Biomedical Engineering Div.
AN ARTIFICIAL NEURAL NETWORK MODEL FOR PERIODIC TRAJECTORY GENERATION
S. Shankar, R. E. Gander, and H. C. Wood *In* Engineering Inst. of Canada, Canadian Conference on Electrical and Computer Engineering, Volumes 1 and 2 1990 4 p (For primary document see N93-30215 11-31)
Avail: Engineering Inst. of Canada, 2050 rue Mansfield, Suite 700, Montreal, Quebec H3A 1Z2 Canada

N93-30226 Concordia Univ., Montreal (Quebec). Center for Signal Processing and Communications.
PARAMETER IDENTIFICATION OF TIME-VARYING SYSTEMS USING NEURAL NETWORKS
Keqin Gao, M. Omair Ahmad, and M. N. S. Swamy *In* Engineering Inst. of Canada, Canadian Conference on Electrical and Computer Engineering, Volumes 1 and 2 1990 4 p (For primary document see N93-30215 11-31)
Avail: Engineering Inst. of Canada, 2050 rue Mansfield, Suite 700, Montreal, Quebec H3A 1Z2 Canada

N93-30234 Ottawa Univ. (Ontario). Dept. of Electrical Engineering.
OPTIMAL FILTERING AND LQR THEORY WITH CONSTRAINTS ON SYSTEM AND CONTROL MATRICES
N. U. Ahmed and Peng Li *In* Engineering Inst. of Canada, Canadian Conference on Electrical and Computer Engineering, Volumes 1 and 2 1990 4 p (For primary document see N93-30215 11-31)
Avail: Engineering Inst. of Canada, 2050 rue Mansfield, Suite 700, Montreal, Quebec H3A 1Z2 Canada

N93-30236 Concordia Univ., Montreal (Quebec). Dept. of Electrical and Computer Engineering.
A SYSTOLIC-ARRAY STRUCTURE FOR MTCM RECEIVERS
S. H. Jamali and Tho Le-Ngoc *In* Engineering Inst. of Canada, Canadian Conference on Electrical and Computer Engineering, Volumes 1 and 2 1990 4 p (For primary document see N93-30215 11-31)
Avail: Engineering Inst. of Canada, 2050 rue Mansfield, Suite 700, Montreal, Quebec H3A 1Z2 Canada

N93-30238 Gandalf Technologies, Inc., Nepean (Ontario).
A SINGLE CHIP HIGH-SPEED CMOS VITERBI DECODER
David Peter Noel and Tad Kwasniewski (Carleton Univ., Ottawa, Ontario.) *In* Engineering Inst. of Canada, Canadian Conference on Electrical and Computer Engineering, Volumes 1 and 2 1990 4 p (For primary document see N93-30215 11-31)
Avail: Engineering Inst. of Canada, 2050 rue Mansfield, Suite 700, Montreal, Quebec H3A 1Z2 Canada

N93-30242 Queens Univ., Kingston (Ontario). Dept. of Electrical Engineering.
SYNCHRONIZATION OF THE LAPTV ADATIVE FILTER WITH INPUT STATISTICS
Heping Ding and Moustafa M. Fahmy *In* Engineering Inst. of Canada, Canadian Conference on Electrical and Computer Engineering, Volumes 1 and 2 1990 4 p (For primary document see N93-30215 11-31)
Avail: Engineering Inst. of Canada, 2050 rue Mansfield, Suite 700, Montreal, Quebec H3A 1Z2 Canada

N93-30244 McGill Univ., Montreal (Quebec). Computer Vision and Robotics Lab.
AN ARCHITECTURE FOR AN ANALOG VLSI NEURAL NETWORK FOR EARLY COMPUTER VISION PROCESSING
D. D. Haule, M. E. Malowany, D. Lambidonis, S. Nemawarkar, S. Sayegh, and A. S. Malowany *In* Engineering Inst. of Canada, Canadian Conference on Electrical and Computer Engineering, Volumes 1 and 2 1990 4 p (For primary document see N93-30215 11-31)
Avail: Engineering Inst. of Canada, 2050 rue Mansfield, Suite 700, Montreal, Quebec H3A 1Z2 Canada

N93-30245 Carleton Univ., Ottawa (Ontario). Dept. of Electronics.
HIGH-SPEED, CMOS DUAL MODULUS FREQUENCY DIVIDER FOR RF FREQUENCY SYNTHESIS
Navid Foroudi and Tad A. Kwasniewski *In* Engineering Inst. of Canada, Canadian Conference on Electrical and Computer Engineering, Volumes 1 and 2 1990 3 p (For primary document see N93-30215 11-31)
Avail: Engineering Inst. of Canada, 2050 rue Mansfield, Suite 700, Montreal, Quebec H3A 1Z2 Canada

N93-30257 Ecole Polytechnique, Montreal (Quebec).
PERFORMANCE ENHANCEMENT OF DYNAMIC CMOS LOGIC CIRCUITS
Azzedine Boulguira and Yvon Savaria *In* Engineering Inst. of Canada, Canadian Conference on Electrical and Computer Engineering, Volumes 1 and 2 1990 4 p (For primary document see N93-30215 11-31)
Avail: Engineering Inst. of Canada, 2050 rue Mansfield, Suite 700, Montreal, Quebec H3A 1Z2 Canada

N93-30258 Transport Canada, Winnipeg (Manitoba).
FAULT TOLERANCE AND TESTING FOR WSI SYSTEMS
Alan W. Ptak and R. D. McLeod (Manitoba Univ., Winnipeg.) *In* Engineering Inst. of Canada, Canadian Conference on Electrical and Computer Engineering, Volumes 1 and 2 1990 3 p (For primary document see N93-30215 11-31)
Avail: Engineering Inst. of Canada, 2050 rue Mansfield, Suite 700, Montreal, Quebec H3A 1Z2 Canada

N93-30345 Toronto Univ. (Ontario). Dept. of Electrical Engineering.
MORPHOLOGICAL AND ORDER STATISTIC FILTERS: A COMPARATIVE STUDY
Renee L. J. Martens, Ziheng Zhou, and Anastasios N. Venetsanopoulos *In* Engineering Inst. of Canada, Canadian Conference on Electrical and Computer Engineering, Volumes 1 and 2 1990 4 p (For primary document see N93-30215 11-31)
Avail: Engineering Inst. of Canada, 2050 rue Mansfield, Suite 700, Montreal, Quebec H3A 1Z2 Canada

N93-30346 Wilfrid Laurier Univ., Waterloo (Ontario).
IMAGE ENHANCEMENT USING AN ANALOG DEVICE NEURAL NETWORK
Nora M. Znotinas and Franklin M. McGovern *In* Engineering Inst. of Canada, Canadian Conference on Electrical and Computer Engineering, Volumes 1 and 2 1990 4 p (For primary document see N93-30215 11-31)
Avail: Engineering Inst. of Canada, 2050 rue Mansfield, Suite 700, Montreal, Quebec H3A 1Z2 Canada

N93-30962*# Air Force Inst. of Tech., Wright-Patterson AFB, OH. Dept. of Electrical and Computer Engineering.
LABORATORY EXPERIMENTS IN INTEGRATED CIRCUIT FABRICATION
Thomas J. Jenkins and Edward S. Kolesar *In* NASA. Langley Research Center, National Educators' Workshop. Update 92: Standard Experiments in Engineering Materials Science and Technology Jun. 1993 p 233-272 (For primary document see N93-30948 11-23)
Avail: CASI HC A03/MF A04

34 FLUID MECHANICS AND HEAT TRANSFER

Includes boundary layers; hydrodynamics; fluidics; mass transfer; and ablation cooling.

For related information see also *02 Aerodynamics* and *77 Thermodynamics and Statistical Physics.*

N93-28557*# Wooster Coll., OH. Dept. of Physics.
LOADING AND TESTING A LIGHT SCATTERING CELL WITH A BINARY FLUID MIXTURE NEAR ITS CRITICAL COMPOSITION Final Report, 1 Jun. - 30 Aug. 1992
Donald T. Jacobs and James S. Becker Jun. 1993 27 p
(Grant NAG3-1354)
(NASA-CR-193147; NAS 1.26:193147) Avail: CASI HC A03/MF A01

Critical phenomena has been the subject of physics research for many years. However, only in recent years has the research effort become intense. The current intensity has caused the study of critical phenomena to be grouped into a previous older era and a present contemporary era. Turbidity cell filling with methanol cyclohexane is one of the first steps toward a further understanding of critical phenomena. Work performed during the research period is outlined. During this period, research was spent developing apparatus and techniques that will make it possible to study critical phenomena through turbidity measurements on methanol cyclohexane. Topics covered range from the orientation of turbidity cell parts for assembly to the filling apparatus and procedure used when th cell is built. The last section will briefly cover some of the observations made when viewing the cell in a controlled water bath. However, before mention is made of the specifics of the summer research, a short introduction to critical phenomena and turbidity and how they relate to this experiment is provided. CASI

N93-28566# National Inst. of Standards and Technology, Gaithersburg, MD. Chemical Science and Technology Lab.
ESTIMATION OF DROPLET COLLISION FREQUENCY IN A SPRAY
J. R. Zurlo (Wisconsin Univ., Madison.), C. Presser, and H. G. Semerjian 1992 6 p Presented at the ILASS-AMERICAS 1992, San Ramon, CA, 18-20 May 1992
(Contract DE-AI01-86CE-90213)
(DE93-007991; CONF-9205307-1) Avail: CASI HC A02/MF A01

An estimate of droplet collision frequency was obtained in a pressure-atomized fuel spray. Measurement of the vertical linear depolarization ratio was used to provide information on droplet sphericity which in turn was used to determine droplet collision frequency. The results indicate that droplet collision frequency increases near the spray boundary where the droplet number density is a maximum. DOE

N93-28595# Sandia National Labs., Livermore, CA.
LIMITATIONS OF THE IDEAL PHASE-DOPPLER SYSTEM: EXTENSION TO SPATIALLY AND TEMPORALLY INHOMOGENEOUS PARTICLE FLOWS WITH AN APPLICATION TO DIESEL SPRAYS
K. D. Marx and C. F. Edwards Dec. 1992 58 p Presented at the 6th International Symposium on the Application of Laser Techniques to Fluid Mechanics, Lisbon, Portugal, 20 Jul. 1992
(Contract DE-AC04-76DR-00789)
(DE93-009447; SAND-92-8540; CONF-9207151-1) Avail: CASI HC A04/MF A01

The effect of the single-particle constraint on the response of phase-Doppler instruments is determined for particle flows which are spatially nonuniform and time-dependent. Poisson statistics are applied to particle positions and arrival times within the phase-Doppler probe volume to determine the probability that a particle is measured successfully. It is shown that the single-particle constraint can be viewed as applying spatial and temporal filters to the particle flow. These filters have the same meaning as those that were defined previously for uniform, steady-state sprays, but in space- and time-dependent form. Criteria are developed for determining when a fully inhomogeneous analysis of a flow is required and when a quasi-steady analysis will suffice. A new bias due to particle arrival time displacement is identified and the conditions under which it must be considered are established. The present work provides the means to rigorously investigate the response of phase-Doppler measurement systems to transient sprays such as those which occur in diesel engines. To this end, the results are applied to a numerical simulation of a diesel spray. The calculated hypothetical response of the ideal instrument provides a quantitative demonstration of the regimes within which measurements can accurately be made in such sprays. DOE

N93-28612 Brown Univ., Providence, RI.
ACCELERATED MOTION OF RIGID SPHERES IN UNSTEADY FLOWS AT LOW TO MODERATE REYNOLDS NUMBERS Ph.D. Thesis
Eugene Jen-Ming Chang 1992 228 p
Avail: Univ. Microfilms Order No. DA9308787

A direct numerical simulation, based on spectral methods, has been used to compute the time dependent, axisymmetric viscous flow past a rigid sphere. Both oscillatory flow about a zero mean and flows with a constant acceleration or deceleration have been investigated. The simulation has been verified for steady flow conditions, and for unsteady flow there is excellent agreement with Stokes flow theory at very low Reynolds numbers. At moderate Reynolds numbers, around 20, there is good general agreement with available experimental data for oscillatory motion. Under steady flow conditions no separation occurs at Reynolds numbers below 20, however in an oscillatory flow a separation bubble forms on the decelerating portion of each cycle at Reynolds numbers well below this. As the flow accelerated again, the bubble detaches and decays, while the formation of a new bubble is inhibited till the flow again decelerates. Similar features are observed for constant deceleration or acceleration of the flow. The contribution of the pressure to the resultant force on the sphere includes a component that is well described by the usual added mass term even when there is separation. However the reversed flow within the separation bubble, under decelerating flow conditions, strongly modifies the frictional component of the force and may produce an effective negative drag. Dissert. Abstr.

N93-28613 Michigan Univ., Ann Arbor.
APPLICATIONS OF UNITARITY IN THE STANDARD MODEL Ph.D. Thesis
Leo P. H. M. deWit 1992 72 p
Avail: Univ. Microfilms Order No. DA9308301

Unitarity is a crucial ingredient of any quantum field theory. The requirement that the sum of probabilities of all possible consequences resulting out of a given initial situation equals 100 percent is inescapable. We study the practical consequences that can be derived from the unitarity requirement. We show how unitarity can be proved in a quantum field theory. First the old proof by Veltman is reviewed. Next a new derivation of the Cutkosky-Veltman cutting rules is given. As an application, we discuss the constraints on the photon self energy and the resulting effect on the photon propagator. Next the decomposition of transition amplitudes into partial wave amplitudes is discussed. Bounds on these partial waves are derived. The concept of 'partial wave unitarity' is explained. Assuming that for weak interactions the lowest order Feynman diagrams will always dominate the higher order diagrams, bounds can be put on certain parameters in the standard model Lagrangian. An upper limit for the Higgs mass is derived, and the four vector boson vertex is constrained. Finally we study the partial wave decomposition for off-shell scattering processes. We find that such off-shell partial waves cannot be constrained, as opposed to the on-shell partial waves. Dissert. Abstr.

N93-28626*# National Aeronautics and Space Administration. Lewis Research Center, Cleveland, OH.
A NEW FLUX CONSERVING NEWTON'S METHOD SCHEME FOR THE TWO-DIMENSIONAL, STEADY NAVIER-STOKES EQUATIONS
James R. Scott and Sin-Chung Chang Jun. 1993 47 p Sponsored by NASA, Washington
(RTOP 505-62-52)
(NASA-TM-106160; E-7895; NAS 1.15:106160) Avail: CASI HC A03/MF A01

A new numerical method is developed for the solution of the two-dimensional, steady Navier-Stokes equations. The method that is presented differs in significant ways from the established numerical methods for solving the Navier-Stokes equations. The major differences are described. First, the focus of the present method is on satisfying flux conservation in an integral formulation, rather than on simulating conservation laws in their differential form. Second, the present approach provides a unified treatment of the dependent variables and their unknown derivatives. All are treated as unknowns together to be solved for through simulating local and global flux conservation. Third, fluxes are balanced at cell interfaces without the use of interpolation or flux limiters. Fourth, flux conservation is achieved through the use of discrete regions known as conservation elements and solution elements. These elements are not the same as the standard control volumes used in the finite volume method. Fifth, the discrete approximation obtained on each solution element is a functional solution of both the integral and differential form of the Navier-Stokes equations. Finally, the method that is presented is a highly localized approach in which the coupling to nearby cells is only in one direction for each spatial coordinate, and involves only the immediately adjacent cells. A general third-order formulation for the steady, compressible Navier-Stokes equations is presented, and then a Newton's method scheme is developed for the solution of incompressible, low Reynolds number channel flow. It is shown that the Jacobian matrix is nearly block diagonal if the nonlinear system of discrete equations is arranged approximately and a proper pivoting strategy is used. Numerical results are presented for Reynolds numbers of 100, 1000, and 2000. Finally, it is shown that the present scheme can resolve the developing channel flow boundary layer using as few as six to ten cells per channel width, depending on the Reynolds number. Author (revised)

N93-28627*# National Aeronautics and Space Administration. Lewis Research Center, Cleveland, OH.
PRELIMINARY EXPERIMENTAL RESULTS FOR A CRYOGENIC BRUSH SEAL CONFIGURATION
J. A. Carlile, R. C. Hendricks, R. I. Hibbs (Rockwell International Corp.,

Canoga Park, CA.), S. E. McVey (Rockwell International Corp., Canoga Park, CA.), and J. K. Scharrer (Rockwell International Corp., Canoga Park, CA.) Jun. 1993 13 p Presented at the 29th AIAA Joint Propulsion Conference and Exhibit, Monterey, CA, 28-30 Jun. 1993; cosponsored by AIAA, SAE, ASME, and ASEE
(RTOP 584-03-11)
(NASA-TM-106236; E-7952; NAS 1.15:106236; AIAA Paper 93-2535)
Avail: CASI HC A03/MF A01

Preliminary fluid nitrogen flow data are reported for a five-brush, ceramic-coated-rub-runner brush seal system, where the brushes and the rub runner were placed at each end of a centrally pressurized multifunction tester ('back-to-back' set of brushes) and tested at rotor speeds of 0, 10, 18, and 22.5 krpm. After testing, both the brushes and the ceramic-coated rub runner appeared pristine. The coating withstood both the thermomechanical and dynamic loadings with minor wear track scarring. The bristle tips showed some indication of material shearing (smearing) wear. The Ergun porous flow equation was applied to the brush seal data. The Ergun relation, which required heuristic information to characterize the coefficients, fit the gaseous data but was in poor agreement with the fluid results. The brush seal exit conditions were two phase. Two-phase, choked-flow design charts were applied but required one data point at each rotor speed to define the (C(sub f)A x Constant) flow and area coefficients. Reasonable agreement between prediction and data was found, as expected, but such methods are not to be construed as two-phase-flow brush seal analyses. Author (revised)

N93-28630# Cornell Univ., Ithaca, NY.
DENSE INCLINED FLOWS: THEORY AND EXPERIMENTS
1992 7 p
(Contract DE-AC22-91PC-90183)
(DE93-011452; DOE/PC-90183/T6) Avail: CASI HC A02/MF A01

Rapid, gravity-driven flows of granular materials down inclines pose a challenge to our understanding. Even in situations in which the flow is steady and two-dimensional, the details of how momentum and energy are balanced within the flow and at the bottom boundary are not well understood. Thus we have undertaken a research program integrating theory, computer simulation, and experiment that will focus on dense entry flows down inclines. Its goal is to understand the regime of inclined flow that involves a large, relatively passive mass of granular material moving above a narrow region of intensely sheared, colliding grains. The effort involves the development of theory informed by the results of simultaneous computer simulations and the construction, instrumentation, and use of an experimental facility in which the variables necessary to assess the success or failure of the theory can be measured. In the present reporting period, we have completed a series of experiments to measure the collision properties of various small particles. Results for 3mm glass beads are presented here. In addition, we have made progress in the design of a new sensor to measure simultaneously the particle volume fraction near the wall and the normal force of impact from individual collisions. Finally, we have conducted additional simulations of the rapid granular flows of spheres interacting with a flat, frictional wall. The objective was to generate semi-empirical expressions for the boundary conditions imposed by the wall on the flow. DOE

N93-28639# Sandia National Labs., Albuquerque, NM.
A GRID REFINEMENT STUDY OF TWO-DIMENSIONAL TRANSIENT FLOW OVER A BACKWARD-FACING STEP USING A SPECTRAL-ELEMENT METHOD
J. R. Torczynski 1992 18 p Presented at the American Society of Mechanical Engineers (ASME) Fluids Engineering Conference, Washington, DC, 20-24 Jun. 1993
(Contract DE-AC04-76DP-00789)
(DE92-018262; SAND-92-1561C; CONF-930621-1) Avail: CASI HC A03/MF A01

The two-dimensional transient flow over a backward-facing step is numerically simulated using the spectral-element computational fluid dynamics code NEKTON. The simulated geometry corresponds to that of Kaiktsis et al. (1991) and Armaly et al. (1983), and flow is examined at Reynolds numbers of 500 and 800. A systematic grid refinement study is performed by varying both the element size and the order of the polynomial representation within the elements. For both values of the Reynolds number, it is observed that low-resolution cases exhibit sustained chaotic temporal behavior but that high-resolution cases evolve toward asymptotically steady flow by a monotonic decay of the transient. The resolution required to obtain asymptotically steady behavior is seen to increase with Reynolds number. These results suggest that the recently reported transition to chaotic flow at Reynolds numbers around 700 is an artifact of inadequate spatial resolution. The cause of resolution-dependent temporal behavior of spectral-element methods is explored. DOE

N93-28663# California Univ., Berkeley. Lawrence Berkeley Lab.
THE ONSET OF VORTEX TURBULENCE Ph.D. Thesis
G. Huber Dec. 1992 98 p
(Contract DE-AC03-76SF-00098)
(DE93-010424; LBL-33517) Avail: CASI HC A05/MF A02

The goal is to investigate some of the unusual and spectacular properties near the transition to turbulence in a two-dimensional field of limit-cycle oscillators. Of particular interest are the dynamics of topological defects (vortices) associated with the onset of turbulence. The complex Ginzburg-Landau equation describes an extended reaction-diffusion system close to the bifurcation of a steady state into a stable, periodic orbit. In the jargon of nonlinear dynamics, it is the amplitude equation corresponding to a Hopf bifurcation. Because of the generality of the assumptions under which it is derived, the complex Ginzburg-Landau equation describes systems in contexts other than chemical reactions with diffusion. Examples include Rayleigh-Benard convection and the phase fields of multimode lasers. The reaction-diffusion model is however, a sufficiently general model to frame our discussion. DOE

N93-28744# Office National d'Etudes et de Recherches Aerospatiales, Paris (France). Direction de l'Aerodynamique.
DEVELOPMENT OF A 3-D IMPLICIT EULER CODE FOR HYPERSONIC AND HIGH SUPERSONIC FLOWS Final Summary Report [DEVELOPPEMENT D'UN CODE EULER 3D IMPLICITE POUR DES ECOULEMENTS EN REGIME HYPERSONIQUE OU SUPERSONIQUE ELEVE]
P. Guillen, Olivier Pierre Jacquotte, and M. Borrel Oct. 1990 50 p In ENGLISH and FRENCH
(Contract DRET-88-34-001)
(ONERA-RSF-23/1123-AY-230A; ONERA-RSF-23/1123-AY-232A; ETN-91-90083) Avail: CASI HC A03/MF A01

The progress made in developing a three dimensional Euler code for complex configurations of hypersonic and high supersonic flows is described. A multidomain method is studied on one hand in order to better obtain a grid, as well as develop implicit schemes. The industrial applications of the three dimensional code are discussed. For individual titles, see N93-28745 through N93-28745.

N93-28745# Office National d'Etudes et de Recherches Aerospatiales, Paris (France). Aerodynamics Dept.
NUMERICAL SIMULATION OF PERFECT FLUID FLOWS AROUND COMPLEX 3D CONFIGURATIONS BY A MULTIDOMAIN SOLVER USING THE MUSCL APPROACH
Ph. Guillen, M. Borrel, and M. Dormieux (Aerospatiale, Chatillon, France.) *In its* Development of a 3-D Implicit Euler Code for Hypersonic and High Supersonic Flows Oct. 1990 p 33-44 (For primary document see N93-28744 11-34)
Avail: CASI HC A03/MF A01

A numerical scheme of the MUSCL type used for the numerical simulation of gas flow of different types around complex configurations is described. Approximate Riemann solvers of the Van Leer, Roc, and Osher types, developed for perfect gas flows are used. These solvers have been extended to non-reactive mixtures of two species and real gas flows by Abgrall, Montagne and Vinokur. The architecture of the code, dictated by constraints in geometrical considerations, computational aspects, the specific nature of the flow, and ergonomy, is described. ESA

N93-28751# Massachusetts Inst. of Tech., Cambridge. Dept. of Chemical Engineering.
MACROSTATISTICAL HYDRODYNAMICS
H. Brenner 1993 15 p
(Contract DE-FG02-88ER-13896)
(DE93-012289; DOE/ER-13896/5) Avail: CASI HC A03/MF A01

This research aims to correlate the macroscopic rheological behavior of suspensions with their statistical microstructure. This fundamental knowledge will benefit a host of technologies, including geothermal energy production, petroleum production and refining, and synfuels processing. The approach involves a novel combination of experiments, numerics, and theory. Experiments primarily involve tracking small balls as they fall slowly through otherwise quiescent suspensions of neutrally buoyant particles. Detailed trajectories of the balls, obtained either with new experimental techniques or by numerical simulation, are statistically interpreted in terms of the mean settling velocity and the dispersion about the mean. Determining the mean settling velocity of balls that are small relative to the suspended particles is a means of measuring the macroscopic zero-shear-rate viscosity without significantly disturbing the original microstructure; therefore, falling-ball rheometry is a powerful tool for use in studying the effects of microstructure on the macroscopic properties of suspensions. The dispersion about the mean yields information about the particle interactions. To date, the mean and dispersivity of a falling sphere's velocity has been determined as a function of the tracer sphere size and the suspended particle size, shape, and concentration. Currently, the pressure drop caused by the falling ball is also being measured. This will provide a much needed benchmark problem for numerical studies, as well as provide another measure of the macroscopic response of a suspension as a function of its microstructure. Also begun recently are two studies of boundary effects in two-phase fluids: the determination of the torque on a small ball spinning in a suspension, and the determination of the velocity of a small ball rolling down the wall of a container holding a suspension. DOE

N93-28878# Chicago Univ., IL.
STUDIES OF COMPLEXITY IN FLUID SYSTEMS
L. P. Kadanoff, P. Constantin, T. F. Dupont, and S. Nagel Feb. 1993 12 p
(Contract DE-FG02-92ER-25119)
(DE93-010776; DOE/ER-25119/1) Avail: CASI HC A03/MF A01

The objective is to bring together researchers from several disciplines (mathematics, numerical computation, and theoretical and experimental physics) who share an interest in the development of complexity in fluid systems. Work is in progress on development of singular interfluid interfaces on several fronts. Striking variations in droplet formation can be observed in physical experiments and simulations based on simple models. High-speed photographs are being taken of small liquid drop breaking into droplets. Experimental studies of granular materials are being continued. DOE

N93-28947*# National Aeronautics and Space Administration. Lewis Research Center, Cleveland, OH.
THE DEVELOPMENT OF A MIXING LAYER UNDER THE ACTION OF WEAK STREAMWISE VORTICES
Marvin E. Goldstein and Joseph Mathew Mar. 1993 36 p
(Contract NCC3-233; RTOP 505-62-21)
(NASA-TM-106089; E-7724; NAS 1.15:106089; ICOMP-93-9) Avail: CASI HC A03/MF A01

The action of weak, streamwise vortices on a plane, incompressible, steady mixing layer is examined in the large Reynolds-number limit. The outer, inviscid region is bounded by a vortex sheet to which the viscous region is confined. It is shown that the local linear analysis becomes invalid at streamwise distances O(epsilon(sup -1)), where epsilon is much less than 1 is the cross flow amplitude, and a new nonlinear analysis is constructed for this region. Numerical solutions of the nonlinear problem show that the vortex sheet undergoes an O(1) change in position and that the solution is ultimately terminated by the appearance of a singularity. The corresponding viscous layer shows downstream thickening, but appears to remain well behaved up to the singular location. Author (revised)

N93-28975*# Institute for Computer Applications in Science and Engineering, Hampton, VA.
SOME ASPECTS OF THE AEROACOUSTICS OF HIGH-SPEED JETS Final Report
James Lighthill (University Coll., London, England.) Washington May 1993 47 p Submitted for publication
(Contract NAS1-19480; RTOP 50-90-52-01)
(NASA-CR-191458; NAS 1.26:191458; ICASE-93-20) Avail: CASI HC A03/MF A01

Some of the background to contemporary jet aeroacoustics is addressed. Then scaling laws for noise generation by low-Mach-number airflows and by turbulence convected at 'not so low' Mach number is reviewed. These laws take into account the influence of Doppler effects associated with the convection of aeroacoustic sources. Next, a uniformly valid Doppler-effect approximation exhibits the transition, with increasing Mach number of convection, from compact-source radiation at low Mach numbers to a statistical assemblage of conical shock waves radiated by eddies convected at supersonic speed. In jets, for example, supersonic eddy convection is typically found for jet exit speeds exceeding twice the atmospheric speed of sound. The Lecture continues by describing a new dynamical theory of the nonlinear propagation of such statistically random assemblages of conical shock waves. It is shown, both by a general theoretical analysis and by an illustrative computational study, how their propagation is dominated by a characteristic 'bunching' process. That process associated with a tendency for shock waves that have already formed unions with other shock waves to acquire an increased proneness to form further unions - acts so as to enhance the high-frequency part of the spectrum of noise emission from jets at these high exit speeds. Author (revised)

N93-28993# Aeronautical Research Inst. of Sweden, Bromma.
INVISCID QUASI ONE-DIMENSIONAL NONEQUILIBRIUM FLOW
Tor Arne Gronland 23 Nov. 1992 44 p
(Proj. AE-4051)
(FFA-TN-1992-35) Avail: CASI HC A03/MF A01

This work deals with numerical methods for nozzle flow in the quasi one-dimensional approximation. A point implicit scheme is used as a remedy to the numerical difficulties arising from the stiff equation system of nonequilibrium flow. The gas considered is air in thermal and chemical nonequilibrium. Two different chemistry models are used. One follows the Park formulation and another the Dunn & Kang formulation. Both using a 5 species, 17 reactions, air model. Boundary conditions are critical for internal flows. An accurate formulation by the method of characteristics is given. By setting a subsonic outflow condition for a choked flow, a stationary shock is captured inside the nozzle. The work performed is tested and implemented in a quasi one-dimensional Euler code, NOZWS. Author

N93-28994# Aeronautical Research Inst. of Sweden, Bromma. Dept. of Aerodynamics.
IMPLEMENTATION OF A MULTIDOMAIN NAVIER-STOKES CODE ON THE INTEL iPSC2 HYPERCUBE
Peter Eliasson, Ingemar Lindblad, and Per Wahlund 18 Nov. 1992 19 p
(Contract NUTEK-90-02278P; Proj. AU-4093)
(FFA-TN-1992-37) Avail: CASI HC A03/MF A01

This report describes the implementation of a multidomain/multigrid 3D Navier-Stokes code on a parallel computer, namely the Intel iPSC2 hypercube. The sequential flow code was the EURANUS code, developed at VUB, Brussels and FFA, Stockholm. In addition to the Navier-Stokes and multigrid algorithms, this code is characterized by a software-engineering-based coding approach to produce a structured and flexible program. It has a dynamic memory handling to facilitate the storage and maintenance of multiple domains of different sizes. The data structure supports more than one (super)computer architecture and facilitates parallel processing. Multidomain calculations are handled in the code in a flexible manner which can be used on MIMD type computers as well as supercomputers. The host-node program structure and explicit send-receive routines for data exchange between domains on the hypercube meant that the start-up of the code and the handling of external files had to undergo the largest changes. The code was tested on a realistic hypersonic problem, a delta wing at Mach 10. This is a one domain problem, to run it parallel the domain was split up into several smaller equally sized domains. The domains were then distributed to the nodes, one domain per node. Due to the small memory of the machine (4 Mbytes/nodes) rather small problems fit into the memory. Two different cases were run using 1 to 16 nodes (domains). The results revealed that the overhead from the data structure and boundary conditions is rather high. This indicates that the subdivided domains are too small for good efficiency. High speedups require larger cases and machines with much larger memory. Author (revised)

N93-29009# Aeronautical Research Inst. of Sweden, Bromma. Dept. of Aerodynamics.
AN EFFICIENT SPECTRAL INTEGRATION METHOD FOR THE SOLUTION OF THE NAVIER-STOKES EQUATIONS

Anders Lundbladh, Dan S. Henningson, and Arne V. Johansson (Royal Inst. of Tech., Stockholm, Sweden.) 30 Nov. 1992 53 p
(Contract NUTEK-5622-92-04537; Proj. AU-4109)
(FFA-TN-1992-28) Avail: CASI HC A04/MF A01

An efficient spectral integration technique for the solution of the incompressible Navier-Stokes equations in the channel flow geometry is described and implemented in a computer code using the FORTRAN language. The horizontal directions are discretized using Chebyshev series. Time integration is done using second order Adams-Bashforth or third order Runge-Kutta methods for the non-linear terms and Crank-Nicholson for the viscous terms. The computer code is available using electronic mail. Author

N93-29025# Royal Inst. of Tech., Stockholm (Sweden). Dept. of Numerical Analysis and Computing Science.

NONLINEAR STABILITY OF VISCOUS SHOCK WAVES

Anders Szepessy and Zhouping Xin 1990 63 p
(Contract DE-FG02-88ER-25053; NSF DMS-90-02286)
(TRITA-NA-9205) Avail: CASI HC A04/MF A01

The large time asymptotic stability of solutions for systems of nonlinear viscous conservation laws are studied. Systems which are strictly hyperbolic and either genuinely nonlinear or linear degenerate in each characteristic field are addressed. Such systems possess a smooth travelling wave solution, which is called a viscous p-shock wave solution, provided that the shock strength epsilon is equivalent to the absolute value of the sum of u(sub +) - u(sub -) is small, the constant states u(sub +/-) and the wave speed sigma are related by the Rankine-Hugoniot condition and the Lax entropy condition. Derived from text

N93-29039 Stanford Univ., CA.

STATE VECTOR SPLITTING: A NUMERICAL SCHEME FOR THE EULER EQUATIONS Ph.D. Thesis

Hakan Oksuzoglu 1993 70 p
Avail: Univ. Microfilms Order No. DA9309644

A new numerical scheme was developed for the solution of the Euler equations in multi-dimensions. The scheme removes the critical dependency on the choice of a 'good' grid by making use of the multidimensional character of the Euler Equations. In addition, a new procedure for implementing solid wall boundary conditions was introduced which does not require body-fitted grids. This grid independent nature of the scheme allows one to solve complicated geometry problems on simple regular grids. The scheme uses an upwind direction which is independent of the underlying coordinate system. This direction is determined only by the local state of the fluid. The scheme is explicit and easy to implement for both serial and parallel computation. The current implementation of the algorithm for two space dimensions can handle unsteady flows around almost arbitrary geometries using a simple cartesian mesh. Several numerical experiments were done to show the flexibility and the robustness of the algorithm. Dissert. Abstr.

N93-29040 Minnesota Univ., Minneapolis.

STABILIZED SPACE-TIME FINITE ELEMENT FORMULATIONS FOR UNSTEADY INCOMPRESSIBLE FLOWS INVOLVING FLUID-BODY INTERACTIONS Ph.D. Thesis

Sanjay Mittal 1992 177 p
Avail: Univ. Microfilms Order No. DA9308739

Stabilized space-time finite element formulations are presented for unsteady incompressible flows involving fluid-body interactions. A detailed numerical investigation is carried out for flows past an elastically mounted cylinder. The non-linear coupling between the flow field and the motion of the cylinder leads to interesting phenomena like 'hysteresis' and 'lock-in'. Flows past a horizontally oscillating cylinder and a pitching airfoil are also studied. The method is also applied to compute the dynamics of a freely falling airfoil and a projectile that has certain initial velocity. In all these computations, smart mesh moving schemes are used that minimize the projection errors and increase the parallelization potential. The formulations are used to study laminar flow past a fixed airfoil at high Reynolds numbers. Preliminary results are presented for a three-dimensional simulation that involves time-dependent Taylor instabilities in Couette flow. Efficient iteration techniques are employed to solve the equation systems resulting from the finite element discretizations of these large-scale problems. A large fraction of these computations are carried out on massively parallel supercomputers. Dissert. Abstr.

N93-29050# Lawrence Livermore National Lab., CA.

LARGE EDDY SIMULATIONS OF SHOCKWAVE PASSAGE THROUGH TURBULENCE

A. C. Buckingham Jul. 1992 16 p Presented at the American Society of Mechanical Engineers (ASME) Fluids Engineering Conference, Washington, DC, 20-24 Jun. 1993
(Contract W-7405-eng-48)
(DE92-019503; UCRL-JC-111080; CONF-930621) Avail: CASI HC A03/MF A01

This is a discussion of progress in continuing efforts to understand and predict the influence of shock waves on turbulent fields during shock-turbulence interactions. Observations show that the Reynolds stress tensor magnitude increases. Strong support for tensor amplification is supplied by the sharply distorted strain field localized to the immediate neighborhood of the shock surface. Beyond this there develops a gradual decay to a new more modestly amplified state relative to the pre-shocked level. Practical interest centers on the significantly altered, albeit shock localized, values of post-shock turbulent kinetic energy, transport, component mixing, wall shear, and heat transfer. The first phase makes use of a direct two dimensional Monte Carlo simulation procedure to examine the influence of upstream turbulence on shock structure and front topography. Linear viscoelastic turbulence response parameters are developed to model the interaction. In the post-shock region, compressible two dimensional large eddy simulations (LES) are applied. Initially a compressibility modified Smagorinsky model with random subgrid scale backscatter is adopted for the non-resolved scales. Favre averaged conservation equations apply to the explicitly resolved scales. Predicted amplification levels, modal energy partition, shock translational to turbulence kinetic energy transfer, and viscoelastic response of turbulence to shock interaction are examined in comparison with available experimental evidence. Recent developments in two-band dynamic eddy viscosity modeling for the subgrid scales are then examined for improvement of the results of the LES in the near wall region, under the influence of stochastic subgrid scale backscatter, and in the neighborhood of the shock. DOE

N93-29075*# National Aeronautics and Space Administration. Lewis Research Center, Cleveland, OH.

APPLICATION OF RAY TRACING IN RADIATION HEAT TRANSFER

Joseph F. Baumeister Aug. 1993 52 p Presented at the Computer Applications Symposium, Los Angeles, CA, 12 Mar. 1993, and the Thermal and Fluids Analysis Workshop, Cleveland, OH, 16-20 Aug. 1993; cosponsored by ASME and LMU
(NASA-TM-106206; E-7915; NAS 1.15:106206) Avail: CASI HC A04/MF A01

This collection of presentation figures displays the capabilities of ray tracing for radiation propagation calculations as compared to an analytical approach. The goal is to introduce the terminology and solution process used in ray tracing, and provide insight into radiation heat transfer principles and analysis tools. A thermal analysis working environment is introduced that solves demanding radiation heat transfer problems based on ray tracing. This information may serve as a reference for designing and building ones own analysis environment. Author

N93-29077 California Inst. of Tech., Pasadena.

DIRECT NUMERICAL SIMULATIONS OF UNSTEADY SEPARATED FLOWS USING VORTEX METHODS Ph.D. Thesis

Petros D. Koumoutsakos 1993 184 p
Avail: Univ. Microfilms Order No. DA9307040

Numerical simulations are presented for viscous incompressible flows with and without solid wall boundaries. Our numerical method is based on vortex methods. The classical inviscid scheme is enhanced to account for viscous effects via the method of particle strength exchange. The method is extended to account for the enforcement of the no-slip boundary condition as well by appropriately modifying the strength of the particles. Computations are possible for extended times by periodically remeshing the vorticity field. The particles are advanced using the Biot-Savart law for the evaluation of the velocity. Computations are made using up to O(10(exp 6)) vortex particles by efficiently implementing the method of multipole expansions for vector computer architectures to obtain an O(N) algorithm. The method is used to simulate the inviscid evolution of an elliptical vortex in an unbounded fluid as well as unsteady separated flows around circular cylinders for a wide range of Reynolds numbers (40-9500). Direct comparisons are made of the results of the present method with those from a variety of theoretical, computational, and experimental studies. The results exhibit the robustness and validity of the present method and allow to gain physical insight as to vorticity formation and its relation to the forces experienced by the body. Dissert. Abstr.

N93-29126# Pacific Northwest Lab., Richland, WA.

A FOUR-FIELD APPROACH TOWARDS DEVELOPING A MECHANISTIC MODEL FOR MULTIPHASE FLOW

J. M. Kelly 1993 35 p Sponsored by DOE

(DE93-006572; PNL-SA-18878) Avail: CASI HC A03/MF A01

A four-field model has been developed to provide a more mechanistic treatment of multiphase flow. In a gas/liquid system, the four-field approach considers two continuous (liquid and vapor) and two discrete (bubbles and drops) fields. Modeling each phase as a combination of two forms, each with a distinct interface geometry and velocity field, provides a more physically realistic framework for two-phase flow analysis than the commonly used two-fluid model. The four-field model and first-generation constitutive models are described. Simulations of air/water bubble coalescence tests are presented and correlation deficiencies noted. Further efforts to develop mechanistic models for the processes that create or destroy interfacial area are planned as part of this program. DOE

N93-29141# Massachusetts Inst. of Tech., Cambridge. Dept. of Aeronautics and Astronautics.

FLOW PHENOMENA IN TURBOMACHINES Final Technical Report, 20 Oct. 1989 - 19 Oct. 1992

E. M. Creitzer, A. H. Epstein, M. B. Giles, J. E. McCune, and C. S. Tan 20 Jan. 1993 181 p

(Grant AF-AFOSR-0035-90)

(AD-A263049; AFOSR-93-0194TR) Avail: CASI HC A09/MF A02

This report describes work carried out at the Gas Turbine Laboratory at MIT during the period 10/20/89 - 10/19/92, as part of our multi-investigator effort on basic unsteady flow phenomena in turbomachines. Within the overall project four separate tasks are specified. These are, in brief: (1) The Influence of Inlet Temperature Nonuniformities on Turbine Heat Transfer and Dynamics; (2) Assessment of Unsteady Losses in Stator/ Rotor Interactions; (3) Unsteady Phenomena and Flowfield instabilities in Multistage Axial Compressors; (4) Vortex Wake-Compressor Blade Interaction in Cascades - A New Rapid Method for Unsteady Separation and Vorticity Flux Calculations. DTIC

N93-29155*# National Aeronautics and Space Administration. Langley Research Center, Hampton, VA.

THE THREE-DIMENSIONAL MULTI-BLOCK ADVANCED GRID GENERATION SYSTEM (3DMAGGS)

Stephen J. Alter (Lockheed Engineering and Sciences Co., Hampton, VA.) and Kenneth J. Weilmuenster May 1993 73 p

(RTOP 506-40-91-02)

(NASA-TM-108985; NAS 1.15:108985) Avail: CASI HC A04/MF A01

As the size and complexity of three dimensional volume grids increases, there is a growing need for fast and efficient 3D volumetric elliptic grid solvers. Present day solvers are limited by computational speed and do not have all the capabilities such as interior volume grid clustering control, viscous grid clustering at the wall of a configuration, truncation error limiters, and convergence optimization residing in one code. A new volume grid generator, 3DMAGGS (Three-Dimensional Multi-Block Advanced Grid Generation System), which is based on the 3DGRAPE code, has evolved to meet these needs. This is a manual for the usage of 3DMAGGS and contains five sections, including the motivations and usage, a GRIDGEN interface, a grid quality analysis tool, a sample case for verifying correct operation of the code, and a comparison to both 3DGRAPE and GRIDGEN3D. Since it was derived from 3DGRAPE, this technical memorandum should be used in conjunction with the 3DGRAPE manual (NASA TM-102224). Author (revised)

N93-29157*# National Aeronautics and Space Administration. Lewis Research Center, Cleveland, OH.

HIGH REYNOLDS NUMBER AND TURBULENCE EFFECTS ON AERODYNAMICS AND HEAT TRANSFER IN A TURBINE CASCADE

Frederick C. Yeh, Steven A. Hippensteele, G. James VanFossen, Philip E. Poinsatte, and Ali Ameri (Kansas Univ. Center for Research, Inc., Lawrence.) Jun. 1993 17 p Presented at the 29th Joint Propulsion Conference and Exhibit, Monterey, CA, 28-30 Jun. 1993; cosponsored by AIAA, SAE, ASME, and ASEE

(RTOP 505-62-52)

(NASA-TM-106187; E-7791; NAS 1.15:106187; AIAA Paper 93-2252)

Avail: CASI HC A03/MF A01

Experimental data on pressure distribution and heat transfer on a turbine airfoil were obtained over a range of Reynolds numbers from 0.75 to 7.5 x 10 exp 6 and a range of turbulence intensities from 1.8 to about 15 percent. The purpose of this study was to obtain fundamental heat transfer and pressure distribution data over a wide range of high Reynolds numbers and to extend the heat transfer data base to include the range of Reynolds numbers encountered in the Space Shuttle main engine (SSME) turbopump turbines. Specifically, the study aimed to determine (1) the effect of Reynolds number on heat transfer, (2) the effect of upstream turbulence on heat transfer and pressure distribution, and (3) the relationship between heat transfer at high Reynolds numbers and the current data base. The results of this study indicated that Reynolds number and turbulence intensity have a large effect on both the transition from laminar to turbulent flow and the resulting heat transfer. For a given turbulence intensity, heat transfer for all Reynolds numbers at the leading edge can be correlated with the Frossling number developed for lower Reynolds numbers. For a given turbulence intensity, heat transfer for the airfoil surfaces downstream of the leading edge can be approximately correlated with a dimensionless parameter. Comparison of the experimental results were also made with a numerical solution from a two-dimensional Navier-Stokes code. Author (revised)

N93-29159*# Arizona State Univ., Tempe. Coll. of Engineering and Applied Sciences.

SUPERSONIC FLOW CALCULATION USING A REYNOLDS-STRESS AND AN EDDY THERMAL DIFFUSIVITY TURBULENCE MODEL

T. P. Sommer, R. M. C. So, and H. S. Zhang Washington Jun. 1993 38 p

(Grant NAG1-1080; RTOP 505-70-59-08)

(NASA-CR-4515; NAS 1.26:4515) Avail: CASI HC A03/MF A01

A second-order model for the velocity field and a two-equation model for the temperature field are used to calculate supersonic boundary layers assuming negligible real gas effects. The modeled equations are formulated on the basis of an incompressible assumption and then extended to supersonic flows by invoking Morkovin's hypothesis, which proposes that compressibility effects are completely accounted for by mean density variations alone. In order to calculate the near-wall flow accurately, correction functions are proposed to render the modeled equations asymptotically consistent with the behavior of the exact equations near a wall and, at the same time, display the proper dependence on the molecular Prandtl number. Thus formulated, the near-wall second order turbulence model for heat transfer is applicable to supersonic flows with different Prandtl numbers. The model is validated against flows with different Prandtl numbers and supersonic flows with free-stream Mach numbers as high as 10 and wall temperature ratios as low as 0.3. Among the flow cases considered, the momentum thickness Reynolds number varies from approximately 4,000 to approximately 21,000. Good correlation with measurements of mean velocity, temperature, and its variance is obtained. Discernible improvements in the law-of-the-wall are observed, especially in the range where the big-law applies. Author (revised)

N93-29161*# National Aeronautics and Space Administration. Lewis Research Center, Cleveland, OH.

A NUMERICAL STUDY OF CONFINED TURBULENT JETS

J. Zhu and T.-H. Shih Jun. 1993 27 p Prepared for the Winter Annual Meeting, New Orleans, LA, 28 Nov. - 3 Dec. 1993; sponsored by ASME

(RTOP 505-90-5K)

(NASA-TM-106197; E-7906; NAS 1.26:106197; ICOMP-93-18; CMOTT-93-07) Avail: CASI HC A03/MF A01

A numerical investigation is reported of turbulent incompressible jets confined in two ducts, one cylindrical and the other conical with a 5 degree divergence. In each case, three Craya-Curtet numbers are considered which correspond, respectively, to flow situations with no moderate and strong recirculation. Turbulence closure is achieved by using the k-epsilon model and a recently proposed realizable Reynolds stress algebraic equation model that relates the Reynolds stresses explicitly to the quadratic terms of the mean velocity gradients and ensures the positiveness of each component of the turbulent kinetic energy. Calculations are carried out with a finite-volume procedure using boundary-fitted curvilinear coordinates. A second-order accurate, bounded convection scheme and sufficiently fine grids are used to prevent the solutions from being contaminated by numerical diffusion. The calculated results are compared extensively with the available experimental data. It is shown that the numerical methods presented are capable of capturing the essential flow features observed in the experiments and that the realizable Reynolds stress algebraic equation model performs much better than the k-epsilon model for this class of flows of great practical importance. Author (revised)

N93-29177 North Carolina State Univ., Raleigh.
NONLINEAR RELAXATION ALGORITHMS FOR THE COMPRESSIBLE NAVIER-STOKES EQUATIONS IN TWO AND THREE DIMENSIONS Ph.D. Thesis
Jack Ray Edwards 1993 158 p
Avail: Univ. Microfilms Order No. DA9309786

An efficient new class of implicit algorithms for the computation of steady, two- and three-dimensional, compressible Navier-Stokes flow fields is presented. A nonlinear relaxation strategy based on a fully coupled sequence of line or planar Gauss-Seidel sweeps is used to drive the solution toward a steady state. Quasi-Newton techniques are used to accelerate the convergence of the 2-D algorithm and to reduce approximate factorization errors in the 3-D version. Convergence characteristics are further improved through the addition of a coarse-grid correction procedure. The discretization of the Navier-Stokes set is hybrid in nature, with flux-vector splitting utilized for the streamwise inviscid fluxes and central differences with flux-limited artificial dissipation used for the transverse inviscid fluxes. Viscous fluxes are central-differenced. Both laminar and turbulent cases are considered, with turbulent closure provided by a modification of the Baldwin-Barth one-equation model. Convergence histories and comparisons with experimental data are presented for several 2-D and 3-D shock wave-boundary layer interactions. Several numerical simulations of the Mach 10 flow through a generic 3-D sidewall compression scramJet inlet configuration are also presented. For the medium-sized (175,000-325,000 mesh points) 3-D validation cases, the algorithm provides steady-state convergence in 15 to 17 Cray Y-MP CPU minutes. Converged solutions for some of the inlet flow fields (375,000-395,000 mesh points) are obtained in about one CPU hour. Dissert. Abstr.

N93-29208*# National Aeronautics and Space Administration. Lewis Research Center, Cleveland, OH. Inst. for Computational Mechanics in Propulsion.
ACCURACY OF LEAST-SQUARES METHODS FOR THE NAVIER-STOKES EQUATIONS
Pavel B. Bochev (Virginia Polytechnic Inst. and State Univ., Blacksburg.) and Max D. Gunzburger Jun. 1993 22 p
(Contract NCC3-233; RTOP 505-90-5K)
(NASA-TM-106209; E-7919; ICOMP-93-19; NAS 1.15:106209) Avail: CASI HC A03/MF A01

Recently there has been substantial interest in least-squares finite element methods for velocity-vorticity-pressure formulations of the incompressible Navier-Stokes equations. The main cause for this interest is the fact that algorithms for the resulting discrete equations can be devised which require the solution of only symmetric, positive definite systems of algebraic equations. On the other hand, it is well-documented that methods using the vorticity as a primary variable often yield very poor approximations. Thus, here we study the accuracy of these methods through a series of computational experiments, and also comment on theoretical error estimates. It is found, despite the failure of standard methods for deriving error estimates, that computational evidence suggests that these methods are, at the least, nearly optimally accurate. Thus, in addition to the desirable matrix properties yielded by least-squares methods, one also obtains accurate approximations. Author (revised)

N93-29213*# Purdue Univ., West Lafayette, IN. School of Aeronautics and Astronautics.
DEVELOPMENT OF AN UNSTRUCTURED SOLUTION ADAPTIVE METHOD FOR THE QUASI-THREE-DIMENSIONAL EULER AND NAVIER-STOKES EQUATIONS Final Report, 2 Jan. 1990 - 31 Aug. 1993
Yi-Tsann Jiang and William J. Usab, Jr. 31 Aug. 1993 269 p
(Grant NAG3-1127)
(NASA-CR-193241; NAS 1.26:193241) Avail: CASI HC A12/MF A03

A general solution adaptive scheme based on a remeshing technique is developed for solving the two-dimensional and quasi-three-dimensional Euler and Favre-averaged Navier-Stokes equations. The numerical scheme is formulated on an unstructured triangular mesh utilizing an edge-based pointer system which defines the edge connectivity of the mesh structure. Jameson's four-stage hybrid Runge-Kutta scheme is used to march the solution in time. The convergence rate is enhanced through the use of local time stepping and implicit residual averaging. As the solution evolves, the mesh is regenerated adaptively using flow field information. Mesh adaptation parameters are evaluated such that an estimated local numerical error is equally distributed over the whole domain. For inviscid flows, the present approach generates a complete unstructured triangular mesh using the advancing front method. For turbulent flows, the approach combines a local highly stretched structured triangular mesh in the boundary layer region with an unstructured mesh in the remaining regions to efficiently resolve the important flow features. One-equation and two-equation turbulence models are incorporated into the present unstructured approach. Results are presented for a wide range of flow problems including two-dimensional multi-element airfoils, two-dimensional cascades, and quasi-three-dimensional cascades. This approach is shown to gain flow resolution in the refined regions while achieving a great reduction in the computational effort and storage requirements since solution points are not wasted in regions where they are not required. Author

N93-29253# Los Alamos National Lab., NM.
EXPERIMENTAL STUDY OF INSTABILITY GROWTH PATTERNS OF A SHOCK-ACCELERATED, THIN FLUID LAYER
J. W. Jacobs (Arizona Univ., Tucson.), D. G. Jenkins, D. L. Klein, and R. F. Benjamin 1993 7 p Presented at the 4th International Workshop on the Physics of Compressible Turbulent Mixing, Cambridge, England, 29 Mar. - 1 Apr. 1993
(Contract W-7405-eng-36)
(DE93-010741; LA-UR-93-1059; CONF-9303126-2) Avail: CASI HC A02/MF A01

We have discovered a remarkable set of flow patterns induced by shock acceleration of two nearby, perturbed interfaces. Using planar laser-induced fluorescence (PLIF), we observe three distinct patterns in the nonlinear evolution of Richtmyer-Meshkov (RM) instabilities associated with this flow. We observe two patterns dominated by vortex pairs and one pattern showing no vortex pairing (until late time) for initial conditions that are indistinguishable by measurement techniques available for our work. The flow is initiated by spatially periodic perturbations imposed on a 'gas curtain' interacting with a planar shock wave. These flow patterns are not predictable nor controllable in our experiments. Our measurements appear to be the first observations of a shock-driven flow exhibiting characteristics of bifurcation. Results were recently published, and more detailed results are forthcoming. We present here a brief description of the experiment, summary of results, and a vortex-based explanation of the phenomena. DOE

N93-29260# Air Force Inst. of Tech., Wright-Patterson AFB, OH. Foreign Aerospace Science and Technology Center.
NUMERICAL COMPUTATION OF INVISCID FLOW AROUND NOSE TIP OF SPACE SHUTTLE WITH NND SCHEME
Ye Youda and Guo Zhiquan 27 Apr. 1993 18 p Transl. into ENGLISH from unidentified document (China) p 282-290
(AD-A264012; FASTC-ID(RS)T-0867-92) Avail: CASI HC A03/MF A01

The NND scheme presented by Professor Zhang Hanxin of the CARDC has been used in this paper to complete the following computations: the two-dimensional inviscid flow around the symmetric plane of the nose tip of the space shuttle; the three-dimensional inviscid flow around the nose tip of the space shuttle; and the three dimensional inviscid flow around the axisymmetric indented body. Under the general coordinate system, the computation grids have been generated by algebra equations. The characteristic compatibility equations have been used to treat the shock and body surface boundaries, and there is a special treatment in translation of the coordinate system. Finally, the comparative computations have been completed using second order SCM schemes. The results of computation illustrate that the NND scheme used in this paper can avoid numerical oscillations and high resolution to shock-capturing. DTIC

N93-29273# European Space Agency, Paris (France).
FLOW VISUALIZATION ON HELICOPTER BLADES USING ACENAPHTHEN
Claas-Hinrik Rohardt (Deutsche Forschungsanstalt fuer Luft- und Raumfahrt, Brunswick, Germany.) Nov. 1992 41 p Transl. into ENGLISH of Stroemungssichtbarmachung an Hubschrauberrotorblaettern Mittels Acenaphthen (Brunswick, Germany, DLR) Jul. 1990 p 1-42 Original language document was announced as N91-21466
(ESA-TT-1255; DLR-FB-90-37; ETN-93-93712) Avail: CASI HC A03/MF A01; Original German version available from DLR, Wissenschaftliches Berichtswesen, VB-PL-DO, Postfach 90 60 58, 5000 Cologne, Germany, HC

Results of visualization of boundary layer characteristics on a helicopter blade under practical conditions are described. The acenaphthene visualization method was used. It was found to be effective in ascertaining the laminar turbulent transition point. The results confirm the design philosophy of generating the longest possible laminar paths in order to minimize skin friction drag. Despite some inadequacy of surface quality (especially in the front area of the blade), there are prolonged laminar boundary layer paths in the hover. It is nonetheless found that aerofoil disturbances, such as those arising due to the anti-erosion strip, should be avoided. Likewise, regular cleaning of the rotor blades to remove insect residues is important in order to maintain high aerofoil performance levels. Calculations with a two dimensional method tended to indicate satisfactory consistency with transition points obtained by experimental means. ESA

N93-29300# Lawrence Livermore National Lab., CA.
THE MICROCHANNEL HEATSINK WITH LIQUID NITROGEN COOLING
R. A. Riddle and A. F. Bernhardt Jun. 1992 11 p Presented at the Society of Photo-Optical Instrumentation Engineers (SPIE) International Symposium on Optical Applied Science and Engineering, San Diego, CA, 19-24 Jul. 1992
(Contract W-7405-eng-48)
(DE93-009258; UCRL-JC-109267; CONF-920792-49) Avail: CASI HC A03/MF A01

Excellent thermal performance of a silicon microchannel heatsink is demonstrated using liquid nitrogen as the coolant over a wide range of heat loads up to 1 kW/sq cm. This performance is partly due to the order of magnitude increase in the thermal conductivity of silicon near 77 K compared to room temperature. Subcooled boiling of the liquid nitrogen in the microchannel heatsink further enhances the thermal performance but makes the thermal resistance a nonlinear function of heat load. For a 500 W/sq cm heat load, a thermal resistances of 0.052 sq cm C/W for a 9:1 aspect ratio heatsink was measured. DOE

N93-29319# Technische Univ., Eindhoven (Netherlands). Faculty of Physics.
NON-LINEAR WAVE PHENOMENA IN A GAS-VAPOUR MIXTURE WITH PHASE TRANSITION Ph.D. Thesis
Hubertus Josephus Smolders 1992 191 p
(ETN-93-93582) Avail: CASI HC A09/MF A02

An experimental and theoretical investigation of two types of gasdynamic flow with phase transition is reported. The flow phenomena studied are: the unsteady nonlinear rarefaction wave in a gas-vapor mixture with stimulated condensation on foreign particles added to the mixture; and the shock wave in a fog, which causes the evaporation of droplets that are presented. The structure of these types of waves, influenced by the phase transitions processs, was investigated and the validity of models to describe droplet formation and growth was established. ESA

N93-29326# Notre Dame Univ., IN. Dept. of Chemical Engineering.
EVOLUTION OF FLOW DISTURBANCES IN COCURRENT GAS-LIQUID FLOWS
M. J. McCready Oct. 1992 19 p
(Contract DE-FG02-88ER-13913)
(DE93-010083; DOE/ER-13913/5) Avail: CASI HC A03/MF A01

Studies of interfacial waves in horizontal gas-liquid flows, close to neutral stability, suggest that the rate of evolution of the interface may be linked to nonlinear interactions between the fundamental mode and the subharmonic -- even if the subharmonic is linearly stable. The rate of evolution increases as the subharmonic becomes more unstable. A comparison of linear stability techniques used to predict the initial behavior of waves reveals similar predictions of growth rates and almost identical speeds between a two layer laminar Orr-Sommerfeld theory and an Orr-Sommerfeld theory when the effect of the (turbulent) gas flow enters as boundary conditions on the liquid layer. However, there is disagreement at small wavenumbers as to the point at which the growth curve crosses 0. This is a significant problem because longwave disturbances, in our case roll waves, form by growth of (initially) small amplitude waves that have frequencies which are 0.5 to 1 Hz, which is in the range where the two theories disagree about the sign of the growth rate. While nonlinear effects are probably involved in the formation of the peak (at least while its amplitude is small), the linear growth rate must play an important role when the amplitude is small. DOE

N93-29335# Vermont Univ., Burlington.
VELOCITY MEASUREMENTS OF LOW REYNOLDS NUMBER TUBE FLOW USING FIBER-OPTIC TECHNOLOGY Ph.D. Thesis
J. C. Bianchi Mar. 1993 78 p
(Contract DE-FG02-91ER-61173)
(DE93-009865; DOE/ER-61173/T1) Avail: CASI HC A05/MF A01

In 1988, Nielsen started work to measure the spatial variability of the mass flux vector being transported in a porous medium. To measure the spatial variability of the mass flux vector, the spatial variability of its components (velocity, concentration) must be measured. Nielsen was successful in measuring the pore level concentration at many different pores and in verifying the assumption that a nonuniform concentration field exists within the mixing zone between two miscible fluids. However, Nielsen was unable to conduct the necessary pore level velocity measurements needed. Nielsen's work is being continued and a probe is being developed that will measure both velocity and concentration components at pore level. The probe is essentially the same probe used to make the pore level concentration measurements with added capabilities needed to make the velocity measurements. This probe has several design variables, dealing primarily with the velocity component, that need further investigation. The research presented in this thesis investigates these parameters by performing experiments in a capillary tube. The tube is a controlled system where the velocity of the fluid can be determined from the volumetric flow rate using Poiseuille's solution for viscous flow. Also, a statistically based relationship between the velocity measured with the probe and the velocity determined from the volumetric flow rate has been developed. DOE

N93-29338# Kentucky Univ., Lexington. Dept. of Mechanical Engineering.
PULSE MITIGATION AND HEAT TRANSFER ENHANCEMENT TECHNIQUES. VOLUME 3: LIQUID SODIUM HEAT TRANSFER FACILITY AND TRANSIENT RESPONSE OF SODIUM HEAT PIPE TO PULSE FORWARD AND REVERSE HEAT LOAD Final Report, 1 Jul. 1987 - 31 Jul. 1992
L. C. Chow, O. J. Hahn, and H. X. Nguyen Aug. 1992 97 p
(Contract F33615-87-C-2777)
(AD-A263496; UK-ME-92-03; WL-TR-92-2097) Avail: CASI HC A05/MF A02

This report presents the description of a liquid sodium heat transfer facility (sodium loop) constructed to support the study of transient response of heat pipes. The facility, consisting of the loop itself, a safety system, and a data acquisition system, can be safely operated over a wide range of temperature and sodium flow rate. The transient response of a heat pipe to pulse heat load at the condenser section was experimentally investigated. A 0.457 m screen wick, sodium heat pipe with an outer diameter of 0.127 m was tested under different heat loading conditions. A major finding was that the heat pipe reversed under a pulse heat load applied at the condenser. The time of reversal was approximately 15 to 25 seconds. The startup of the heat pipe from frozen state was also studied. It was found that during the startup process, at least part of the heat pipe was active. The active region extended gradually down to the end of the condenser until all of the working fluid in the heat pipe was molten. DTIC

N93-29339# Kentucky Univ., Lexington. Dept. of Mechanical Engineering.
PULSE MITIGATION AND HEAT TRANSFER ENHANCEMENT TECHNIQUES. VOLUME 4: TRANSIENT BEHAVIOR OF HEAT PIPE WITH THERMAL ENERGY STORAGE UNDER PULSE HEAT LOADS Final Report, 1 Jul. 1987 - 31 Jul. 1992
L. C. Chow and M. J. Chang Aug. 1992 201 p
(Contract F33615-87-C-2777)
(AD-A263497; UK-ME-92-04; WL-TR-92-2098) Avail: CASI HC A10/MF A03

A novel design of a high-temperature axially grooved heat pipe (HP), which utilizes thermal energy storage (TES) to mitigate pulse heat loads, was presented. Phase-change material (PCM) encapsulated in cylindrical containers was used for thermal energy storage. The transient responses of the HP/TES system under two types of pulse heat loads were studied numerically. The first type is pulse heat loads applied at the heat pipe evaporator; the second type is reversed-pulse heat loads applied at the condenser. The transient response of three different HP/TES configurations were compared: (1) a heat pipe with a large empty cylinder installed in the vapor core, (2) a heat pipe with a large PCM cylinder, and (3) a heat pipe with six small PCM cylinders. It was found that the PCM is very effective in mitigating the adverse effect of pulse heat loads. The six small PCM cylinders are more efficient than the large PCM cylinder in relaxing the heat pipe temperature increase under pulse heat loads. DTIC

N93-29352# Kentucky Univ., Lexington. Dept. of Mechanical Engineering.
PULSE MITIGATION AND HEAT TRANSFER ENHANCEMENT TECHNIQUES. VOLUME 1: SPRAY COOLING Final Report, 1 Jul. 1987 - 31 Jul. 1992
L. C. Chow, D. E. Tilton, and M. R. Pais Aug. 1992 94 p
(Contract F33615-87-C-2777)
(AD-A263495; UK-ME-92-02; WL-TR-92-2086) Avail: CASI HC A05/MF A01

This report presents an experimental and theoretical investigation of spray cooling. A complete study is presented for surfaces maintained between the fluid saturation temperature and the Leidenfrost temperature. Experiments were conducted to analyze the effects of spray and surface conditions on the heat transfer. Different mechanisms causing the critical heat flux (CHF) are identified. For dropwise evaporation, CHF results when the surface heat flux exceeds the latent heat content of the spray. As the flow rate is increased, droplet conglomeration and surface flooding result. For low flow rate cases with a flooded surface, CHF is caused by a liquid deficiency resulting from droplet expulsion caused by the nucleating bubbles within the liquid film. For higher flow rate cases, CHF occurs when the vapor generation rate on the surface is so high that a vapor barrier is formed. DTIC

N93-29353# Nielsen Engineering and Research, Inc., Mountain View, CA.
METHODS FOR REDUCING TURBULENT FLOW AERO-OPTICAL DISTORTION Final Report, 1 Jun. 1992 - 30 Jun. 1993
Robert E. Childs 31 Mar. 1993 47 p
(Contract DAAL03-92-C-0015)
(AD-A263698; NEAR-TR-460; ARO-30431.1-EG-SBI) Avail: CASI HC A03/MF A01

Methods for reducing the aero-optical distortion which affects jet-cooled seeker windows on high-speed, endo-atmospheric interceptors were studied. Reductions in turbulence were achieved by curving the shear layer in the streamwise direction. This type of curvature corresponds to a window whose outer surface is convex in the axial direction. For a case with moderate curvature, the peak shear stress and density fluctuations were reduced by 85% compared to an otherwise similar flat shear layer. The optical properties of the shear layers were evaluated using a simple ray-tracing method, and the aero-optical distortion was significantly reduced by the stabilizing curvature. Another control concept that was tested involved lateral convergence imposed upon the shear layer. This concept was unsuccessful from an aero-optics view point because the turbulent shear stress roughly doubled relative to the unmodified shear layer. DTIC

N93-29419# Air Force Inst. of Tech., Wright-Patterson AFB, OH.
MITIGATION OF SHOCK WAVES IN A CYLINDRICAL TUNNEL BY FOAM M.S. Thesis
Grant W. Fondaw Mar. 1993 115 p
(AD-A262491; AFIT/GNE/ENP/93M-2) Avail: CASI HC A06/MF A02

The effectiveness of foam linings in mitigating shock waves in tunnels is investigated. A polyurethane foam liner of varying density, crush strength, and thickness was modeled inside a 1 meter radius tunnel and an explosion of 1.25 kg of plastic explosive was simulated. Using CTH, an Eulerian-Lagrangian hydrodynamics code from Sandia National Laboratories, the overpressures were computed and compared graphically to determine the effect of varying each foam parameter. The walls of the tunnel consisted of a perfectly reflecting boundary, and in some cases, a foam liner. Low density foam provided the most shock attenuation, with a 20 cm thick layer of 90% void 0.1265 g/cm(sup 3) foam reducing the shock overpressure by 70% at 50 meters. The effects of foam thickness on the shock pressure varied with the distance from the explosion. The thicker foams raised the initial pressure near the explosion due to constriction of the tunnel area. However, the thicker layers reduced the shock faster. Varying the crush strength of the foam from 1 atm to 3 atm overpressure did not affect its ability to mitigate shock propagation in the tunnel. The results strongly suggest that foam can mitigate shock waves significantly. DTIC

N93-29426# Wright Lab., Wright-Patterson AFB, OH.
THE EFFECT OF HIGH TEMPERATURE ON WALL SHEAR IN A TWO DIMENSIONAL WALL JET Final Report, 1 Oct 1991 - 21 Oct. 1992
M. A. Narayanan and Richard B. Rivir Oct. 1992 61 p
(AD-A262982; WL-TR-92-2091) Avail: CASI HC A04/MF A01

The effect of turbulence on skin friction was examined in the developing stage of a high Reynolds number wall jet. Skin friction was computed from the law of the wall measurements of mean velocity profiles in the sublayer. It was observed that constant 'A' in the law of the wall relation U/U* = A log YU*/upsilon + B was a universal one equal to 5.6 while 'B' was linearly dependent on the turbulence intensity near the wall. The wall shear was not significantly altered from that of an ordinary flat plate turbulent boundary layer even at high turbulence levels. The decay of the mean velocity in the longitudinal direction was found to be independent of the momentum flux of the jet at the nozzle exit. DTIC

N93-29472# Wright Lab., Wright-Patterson AFB, OH.
AN UPWIND METHOD FOR THE SOLUTION OF THE 3D EULER AND NAVIER-STOKES EQUATIONS ON ADAPTIVELY REFINED MESHES Final Report, Mar. 1991 - Jun. 1992
Michael J. Aftosmis 17 Oct. 1992 49 p
(AD-A262863; WL-TR-92-3107) Avail: CASI HC A03/MF A01

A new node based upwind scheme for the solution of the 3D Navier-Stokes equations on adaptively refined meshes is presented. The method uses a second-order upwind TVD scheme to integrate the convective terms, and discretizes the viscous terms with a new compact central difference technique. Grid adaptation is achieved through directional division of hexahedral cells in response to evolving features as the solution converges. The method is advanced in time with a multistage Runge-Kutta time stepping scheme. Two- and three-dimensional examples establish the accuracy of the inviscid and viscous discretization. These investigations highlight the ability of the method to produce crisp shocks, while accurately and economically resolving viscous layers. The representation of these and other structures is shown to be comparable to that obtained by structured methods. Further 3D examples demonstrate the ability of the adaptive algorithm to effectively locate and resolve multiple scale features in complex 3D flows with many interacting, viscous, and inviscid structures. DTIC

N93-29804# Texas Univ., Austin. Inst. for Fusion Studies.
VERTICAL SLOT CONVECTION: A LINEAR STUDY
A. McAllister (Tokyo Univ., Japan.), R. Steinolfson (Southwest Research Inst., San Antonio, TX.), and T. Tajima Nov. 1992 65 p
(Contract DE-FG05-80ET-53088)
(DE93-007643; DOE/ET-53088/584; IFSR-584) Avail: CASI HC A04/MF A01

The linear stability properties of fluid convection in a vertical slot were studied. We use a Fourier-Chebychev decomposition to set up the linear eigenvalue problems for the Vertical Slot Convection and Benard problems. The eigenvalues, neutral stability curves, and critical point values of the Grashof number, G, and the wavenumber were determined. Plots of the real and imaginary parts of the eigenvalues as functions of G and (alpha) are given for a wide range of the Prandtl number, Pr, and special note is made of the complex mode that becomes linearly unstable above Pr approximately 12.5. A discussion comparing different special cases facilitates the physical understanding of the VSC equations, especially the interaction of the shear-flow and buoyancy induced physics. Making use of the real and imaginary eigenvalues and the phase properties of the eigenmodes, the eigenmodes were characterized. One finds that the mode structure becomes progressively simpler with increasing Pr, with the greatest complexity in the mid ranges where the terms in the heat equation are of roughly the same size. DOE

N93-29836# Los Alamos National Lab., NM.
WEAKLY NONLINEAR DYNAMICS OF NEAR-CJ DETONATION WAVES
J. B. Bdzil and R. Klein (Technische Hochschule, Aachen, Germany.) 1993 28 p Presented at the ICASE Symposium on Hypersonic Propulsion, Langely, VA, Oct. 1992
(Contract W-7405-eng-36)
(DE93-007344; LA-UR-93-165; CONF-9210298-1) Avail: CASI HC A03/MF A01

The renewed interest in safety issues for large scale industrial devices and in high speed combustion has driven recent intense efforts to gain a deeper theoretical understanding of detonation wave dynamics. Linear stability analyses, weakly nonlinear bifurcation calculations, as well as full scale multi-dimensional direct numerical simulations have been pursued for a standard model problem based on the reactive Euler equations for an ideal gas with constant specific heat capacities and simplified chemical reaction models. Most of these studies are concerned with overdriven detonations. This is true despite the fact that the majority of all detonations observed in nature are running at speeds close to the Chapman-Jouguet (CJ) limit value. By focusing on overdriven waves, one removes an array of difficulties from the analysis that is associated with the sonic flow conditions in the wake of a CJ-detonation. In particular, the proper formulation of downstream boundary conditions in the CJ-case is a yet unsolved analytical problem. A proper treatment of perturbations in the back of a Chapman-Jouguet detonation has to account for two distinct weakly nonlinear effects in the forward acoustic wave component. The first is a nonlinear interaction of highly temperature sensitive chemistry with the forward acoustic wave component in a transonic boundary layer near the end of the reaction zone. The second is a cumulative three-wave-resonance in the sense of Majda et al., which is active in the near-sonic burnt gas flow and which is essentially independent of the details of the chemical model. In this work, we consider detonations in mixtures with moderate state sensitivity of the chemical reactions. Then, the acoustic perturbations do not influence the chemistry at the order considered and we may concentrate on the second effect: the three-wave resonance. DOE

N93-29838# California Univ., San Diego, La Jolla. Dept. of Physics.
HAMILTONIAN DYNAMICS OF COUPLED POTENTIAL VORTICITY AND INTERNAL WAVE MOTION: 1. LINEAR MODES Final Technical Report, 1 Jun. 1989 - 30 Nov. 1992
Henry D. Abarbanel and Ali Rouhi 17 Feb. 1993 29 p
(Contract N00014-89-J-1912)
(AD-A263469) Avail: CASI HC A03/MF A01

This proposal describes work to be carried out extending the study of phase-space density representations of the fluids dynamics to the case where the fluid density is not constant, but the fluid is incompressible, so the fluid velocity satisfies Delta(u) = 0. This will allow the phase-space density representation to describe inhomogeneous fluids. Since the phase space density representation is ideally suited to making time scale separations of the form needed for isolating geostrophic and quasi-geostrophic motions of the full fluid equations and doing so in a fully Hamiltonian fashion, this improvement on past work will enable the inclusion of density variations into the Hamiltonian formulation of these mesoscale geophysical motions. The extension of phase space density formulation of fluids to this case will allow the study of the interplay between internal wave motions--fast density variations--and mesoscale motions--far slower geostrophic and quasi-geostrophic motions. The proposal describes, in outline, the work which will be carried out by the principal investigator and a graduate student over a period of three years which will formulate the Hamiltonian version of inhomogeneous, incompressible flows in phase space density form and separate out the slow and fast motions relevant to geophysical flows. DTIC

N93-29851# Naval Research Lab., Washington, DC.
A PARALLEL IMPLICIT INCOMPRESSIBLE FLOW SOLVER USING UNSTRUCTURED MESHES Interim Report
Ravi Raniamurti and Rainald Lohner 17 Jan. 1993 33 p
(AD-A263395; NRL/MR/6410-93-7178) Avail: CASI HC A03/MF A01

An incompressible flow solver based on unstructured grids is implemented on a parallel distributed memory computer architecture. An important phase in the flow solver is the solution of the elliptic equations for the velocities and pressure. This elliptic solver is parallelized and incorporated into both the explicit and implicit versions of the incompressible flow solver. Performance and scalability studies are carried out on both Intel iPSC 860 and the Intel Delta prototype, and show that the code is scalable. A parallelizable load balancing algorithm is developed to be used in conjunction with the incompressible flow solver. Steady and unsteady flows over a tri-element airfoil and NACA0012 airfoil are computed using the parallel incompressible flow solver. DTIC

N93-29966# Spire Corp., Bedford, MA.
IMPROVED HEAT REMOVAL BY MICROSCOPIC SURFACE TEXTURING OF CAPILLARIES Final Report, 1 Apr. - 30 Oct. 1992
Charles C. Blatchley Oct. 1992 39 p
(Contract F33615-92-C-2252)
(AD-A263483; WL-TR-93-1060) Avail: CASI HC A03/MF A01

Phase 1 demonstrated that ion beam microtexturing of metal surfaces enhances heat transfer under three conditions: (1) thermal radiation emission at relatively high temperatures, (2) forced convection, and (3) nucleate boiling. Features were too small to significantly affect heat transfer under non-flowing constant phase conditions. For nucleate boiling, combining microtexture with large scale structures, and after optimizing the texturing process, it should be possible to achieve a composite enhancement better than 20 times the nucleate-boiling heat transfer from a smooth surface. Ion texturing processes produce rugged broadband light absorbers, completely black from the visible to long wavelength IR. At higher temperature ranges, enhanced radiation adds significantly to total heat transferred. Thus, heat pipes, capillaries, and higher temperature radiators would all perform better with microtextured surfaces. DTIC

N93-29968# Naval Postgraduate School, Monterey, CA.
THREE-DIMENSIONAL FIBER-OPTIC LDV MEASUREMENTS IN THE ENDWALL REGION OF A LINEAR CASCADE OF CONTROLLED-DIFFUSION STATOR BLADES M.S. Thesis
David M. Dober 25 Mar. 1993 127 p
(AD-A263513) Avail: CASI HC A07/MF A02

Measurements were taken of the vortex system that results from the interaction between a stator blade tip and the approaching endwall boundary layer in a linear cascade of controlled-diffusion compressor stator blades. Measurements were taken at Reynolds numbers based on stator blade chord of 240000 and 711000. Total pressure measurements were first conducted upstream and downstream of the controlled-diffusion stator blades. The approaching boundary layer was characterized and the location of the downstream vortices were approximated. Upstream and downstream three-dimensional fiber-optic LDV surveys were then conducted to observe the velocity profiles of the approaching boundary layer and to map the location and velocity characteristics of the downstream vortex system. Results clearly show the effect that the over-all secondary flow in the blade passage has on the location of the two oppositely rotating vortices. The downstream flow characteristics were also shown to be periodic.
DTIC

N93-30035# Michigan Univ., Ann Arbor. Dept. of Mechanical Engineering and Applied Mechanics.
HYDRODYNAMIC INTERACTIONS AMONG FIBERS IN HIGH EFFICIENCY FILTERS
M. Sahraoui, H. Marshall, and M. Kaviany 29 Oct. 1992 37 p Prepared for Lawrence Livermore National Lab., CA

(Contract W-7405-eng-48)
(DE93-007117; UCRL-CR-111783) Avail: CASI HC A03/MF A01

In this report we present a review of the various analytical solutions for the two-dimensional flow in a model fibrous filter made of periodic arrangements of cylinders. These two-dimensional analytical solutions include the various treatments, namely the creeping flow, the inviscid flow, the swarm theory, and the Oseen approximation. We examine in detail the commonly used solutions of Happel, Kuwabara, and the swarm theory of Neale and Nader. We also examine the three-dimensional solutions of Banks obtained by the superposition of the two-dimensional analytical solutions. A review of the different numerical solutions for the flow over cylinders is also given. In addition, we also present an analytical solution which is an extension to the Kuwabara solution and uses the actual boundaries of the square unit cell. The first term of this extended analytical solution is the Kuwabara solution. A two-dimensional numerical solution is also presented for the rectangular and square unit cells. This numerical solution is used to determine the effect of the unit cell anisotropy on the pressure drop across the unit cell. The numerical solution is used for comparison with the analytical solutions of Kuwabara, Happel, and our extended solution. The analytical solution of Kuwabara and Happel show significant error, especially near the boundaries of the unit cell. The extended analytical solution shows good agreement with the numerical results. The ongoing three-dimensional numerical solution of flow over cylinders is also discussed. DOE

N93-30132# Idaho State Univ., Pocatello.
SIPHON BREAKER DESIGN REQUIREMENTS
D. T. Neill and A. G. Stephens Mar. 1993 222 p
(Contract DE-FG07-88ER-12820)
(DE93-011799; DOE/ER-12820/T1) Avail: CASI HC A10/MF A03

The Siphon Breaker Design Requirements Project was intended to provide experimental data on siphon flow effects. In addition, the experimental system was to be modeled with the RELAP code and the predicted and measured performances compared. The design and operation of the siphon breaker experimental equipment from 1989 to 1991 are described. In addition the test results for all the experimental runs made in 1990 and 1991 are presented and described. Unfortunately, useful results were not obtained from a RELAP 5 model of the siphon system; consequently, we are unable to present any predictive calculations for comparison with the data presented. We have had lots of expert advice from several sources on using the RELAP code but to date our efforts have remained unsuccessful. After an extra year of effort, admittedly part-time but a lot of that, the modeling efforts was abandoned and the experimental equipment and test results are described. DOE

N93-30155# Kentucky Univ., Lexington. Dept. of Mechanical Engineering.
PULSE MITIGATION AND HEAT TRANSFER ENHANCEMENT TECHNIQUES. VOLUME 2: EFFECT OF SURFACE WETTABILITY AND ROUGHNESS IN EVAPORATIVE SPRAY COOLING Final Report, 1 Jul. 1987 - 31 Jul. 1992
L. C. Chow, M. S. Sehmbey, and M. R. Pais 31 Jul. 1992 141 p
(Contract F33615-87-C-2777)
(AD-A264174; UK-ME-92-05; WL-TR-92-2096) Avail: CASI HC A07/MF A02

In the spray cooling of a heat surface, variations in the surface contact angle cause a change in nucleation characteristics and thereby influence the heat transfer process. The surface roughness variations affect the thickness of the liquid film formed by the spray; this has a profound effect on the heat transfer from the surface. The effect of these two parameters is studied experimentally under different spray conditions involving an air atomizing nozzle. DTIC

N93-30156# Materials Research Labs., Ascot Vale (Australia).
THE WAKE SOFTWARE SUITE: USER'S GUIDE
M. A. Carroll Jan. 1993 45 p
(AD-A264181; MRL-GD-0050; DODA-AR-008-249) Avail: CASI HC A03/MF A01

This report provides details of the requirements needed to run the computer program WAKE. WAKE was developed during Feb. - Mar. 1992 as a result of a research project which was undertaken within DSTO Salisbury. WAKE calculates the internal wave velocity field generated by a moving subsurface body in a density stratified ocean. DTIC

N93-30162# Yale Univ., New Haven, CT. Dept. of Applied Physics.
NONLINEAR SPECTROSCOPY OF MULTICOMPONENT DROPLETS AND TWO- AND THREE-DIMENSIONAL MEASUREMENTS IN FLAMES Annual Report, 1 Feb. 1992 - 31 Jan. 1993
Richard K. Chang and Marshall B. Long 5 Mar. 1993 24 p
(Grant AF-AFOSR-0150-91)
(AD-A264341; AFOSR-93-0240TR) Avail: CASI HC A03/MF A01

Significant progress has been made in the following areas: (1) nonlinear spectroscopy of micrometer sized droplets, and (2) development and application of two- and three-dimensional scalar and velocity measurement techniques in flames. In the nonlinear spectroscopy area, the following achievements are reported: (1) fluorescence seeding of the stimulated Raman scattering (SRS) in order to increase the detectivity (by as much as 10X) of minor species in a multicomponent liquid droplet that contains a fluorescent dye; (2) temporal precession of the SRS as a means of determining the shape distortion (7 parts out of 10(exp 3)) of a flowing droplet because of inertial force; (3) preliminary measurements of the relative evaporation rates of 15 droplets in a segmented stream where the few lead droplets evaporate faster than the remaining droplets; and (4) suppression of lasing by the SRS and amplification of the SRS in microdroplets, leading to an increased SRS signal. DTIC

N93-30184# Sandia National Labs., Albuquerque, NM.
USE OF A GENETIC ALGORITHM TO SOLVE TWO-FLUID FLOW PROBLEMS ON AN NCUBE MULTIPROCESSOR COMPUTER
R. J. Pryor and D. D. Cline 1992 13 p Presented at the International Topical Meeting on Mathematical Methods and Supercomputing in Nuclear Applications (M/C+SNA 1993), Karlsruhe, Germany, 19-23 Apr. 1993
(Contract DE-AC04-76DP-00789)
(DE93-009630; SAND-92-2847C; CONF-930404-9) Avail: CASI HC A03/MF A01

A method of solving the two-phase fluid flow equations using a genetic algorithm on a NCUBE multiprocessor computer is presented. The topics discussed are the two-phase flow equations, the genetic representation of the unknowns, the fitness function, the genetic operators, and the implementation of the algorithm on the NCUBE computer. The efficiency of the implementation is investigated using a pipe blowdown problem. Effects of varying the genetic parameters and the number of processors are presented. DOE

N93-30369# Cincinnati Univ., OH.
SIMULATION, CHARACTERIZATION AND CONTROL OF FORCED UNSTEADY VISCOUS FLOWS USING NAVIER-STOKES EQUATIONS Final Report, Feb. 1990 - May 1992
K. N. Ghia and U. Ghia Nov. 1992 133 p
(Grant AF-AFOSR-0249-90)
(AD-A264333; AFL-RN-92-11-78; AFOSR-93-0207TR) Avail: CASI HC A07/MF A02

A two-and-a-quarter-year multi-tasked research project was pursued by the present investigators to study dynamic stall phenomenon under AFOSR sponsorship between Feb. 1990 - May 1992. The major objective was to predict and control the dynamic stall phenomenon in 2-D and 3-D flows. In the process of achieving these objectives, significant effort was directed towards developing mathematical models and the corresponding computational methods which were made available to interested researchers and organizations involved in computational fluid dynamics (CFD) research. The analyses developed included a two-dimensional Navier-Stokes (NS) analysis for a general body undergoing arbitrary three-degree-of-freedom maneuvers; detailed results are provided for this class of flows. For enhancement of accuracy and efficiency, an adaptive-grid time-accurate flow solution technique was developed to enable improved resolution of the various length scales in a vortex-dominated unsteady flow. A multi-block grid generation analysis is developed for a 3-D rectangular planform wing. For the corresponding flow analysis using velocity-vorticity variables and direct-solution philosophy, the difficulties experienced were clearly discussed in the annual report submitted a year ago in November 1991. This 3-D flow analysis was therefore temporarily set aside. It will be pursued further in a subsequent grant, and the progress made on it will be reported in a forthcoming annual report for that grant. In the current grant, the study of

3-D flows was continued, using an iterative solution methodology. Hence, a 3-D unsteady Navier-Stokes analysis, again using velocity-vorticity variables, and an iterative solution technique with multi-grid acceleration were developed. DTIC

N93-30375*# Old Dominion Univ., Norfolk, VA. Dept. of Mechanical Engineering and Mechanics.
TOPOLOGY AND GRID ADAPTION FOR HIGH-SPEED FLOW COMPUTATIONS Final Report, 1 Jan. - 31 Dec. 1987
Jamshid S. Abolhassani and Surendra N. Tiwari Washington Mar. 1989 139 p
(Contract NCC1-68; RTOP 505-90-21-02)
(NASA-CR-4216; NAS 1.26:4216) Avail: CASI HC A07/MF A02

This study investigates the effects of grid topology and grid adaptation on numerical solutions of the Navier-Stokes equations. In the first part of this study, a general procedure is presented for computation of high-speed flow over complex three-dimensional configurations. The flow field is simulated on the surface of a Butler wing in a uniform stream. Results are presented for Mach number 3.5 and a Reynolds number of 2,000,000. The O-type and H-type grids have been used for this study, and the results are compared together and with other theoretical and experimental results. The results demonstrate that while the H-type grid is suitable for the leading and trailing edges, a more accurate solution can be obtained for the middle part of the wing with an O-type grid. In the second part of this study, methods of grid adaption are reviewed and a method is developed with the capability of adapting to several variables. This method is based on a variational approach and is an algebraic method. Also, the method has been formulated in such a way that there is no need for any matrix inversion. This method is used in conjunction with the calculation of hypersonic flow over a blunt-nose body. A movie has been produced which shows simultaneously the transient behavior of the solution and the grid adaption. Author (revised)

N93-30379 Waterloo Univ. (Ontario).
ANALYTICAL AND EXPERIMENTAL STUDY OF LAMINAR FREE CONVECTIVE HEAT TRANSFER FROM ISOTHERMAL CONVEX BODIES OF ARBITRARY SHAPE Ph.D. Thesis
Khosrow Jafarpur 1992 375 p
(ISBN-0-315-72512-5) Avail: Univ. Microfilms Order No. DANN72512

An analytical and experimental study of laminar free convection from bodies of arbitrary convex shape is performed to determine the effect of shape, aspect ratio, and orientation of isothermal bodies on the area-averaged Nusselt number over a wide range of Rayleigh and Prandtl numbers. Also, a simple procedure is provided for predicting laminar free convection heat transfer from bodies of arbitrary convex shape, based upon a characteristic length using the square root of the total body surface area, square root of A. To examine the theoretical basis for the Nu-Ra expressions, a new simple, but accurate, approximate analytical method is developed. The proposed method is novel in: linearizing the convective terms, reducing a convective problem to a simpler transient conduction problem for which a solution may exist, and also obtaining an explicit expression for an 'effective velocity' in free convection boundary layer flow, as a function of the Prandtl number. The end result of this method is an explicit expression in terms of a simple superposition of two limits: diffusive limit and laminar boundary layer solution. To predict the laminar boundary layer limit, information regarding the dependency on Prandtl number and the body gravity function is required. By providing different exact and approximate methods, such as the same characteristic lengths and aspect ratios method or the inscribing and circumscribing method (the bounds method), the two asymptotes can be determined for any given shape. This includes body shapes such as the so-called two-dimensional bodies, disks, bodies of small aspect ratios and vertical cylinders of different aspect ratios. In the experimental program, through a transient cooling process and pressure variation technique, the measurement of heat transfer by free convection from isothermal bodies to air is conducted. Due to the nature of the experimental technique adopted and the need for the heat capacity, in a separate and single test at pressures below 10(exp -6) torr, the effective surface emissivity and heat capacity of each body are estimated. The predictions are compared with the experimental data and other sources; very good agreement in almost all of the cases is observed. The simplicity, generality, and accuracy used in the analytical models make the proposed method superior for predicting free convection heat transfer from isothermal convex bodies for the laminar range of Ra and all Prandtl numbers. Dissert. Abstr.

N93-30403# Kentucky Univ., Lexington. Dept. of Mechanical Engineering.
PULSE MITIGATION AND HEAT TRANSFER ENHANCEMENT TECHNIQUES. VOLUME 5: TRANSIENT LIQUID MOVEMENT IN HEAT PIPE WICKS Final Report, 1 Jul. 1987 - 31 Jul. 1992
L. C. Chow and J. H. Abrose Aug. 1992 165 p
(Contract F33615-87-C-2777)
(AD-A264513; UK-ME-92-01; WL-TR-92-2099) Avail: CASI HC A08/MF A02

A new transient model for the liquid flow is presented. The continuous distribution of the saturation in the wick is modeled, where previous models had assumed a uniformly saturated structure. Solution of the liquid flow model requires that the saturation dependence of the capillary flow properties be known. These properties must be determined experimentally because of the complex geometry of the porous wick structures. An experimental study of the flow properties was performed for the case of multilayer mesh wicks. X-ray radiography was used to determine saturation distributions in the wicks for a variety of conditions. Capillary pressure and relative permeability were determined from independent experiments. Results of the transient liquid flow model compare favorably with the results from the heat pipe experiments. DTIC

N93-30484# Los Alamos National Lab., NM.
ERRORS WHEN SHOCK WAVES INTERACT DUE TO NUMERICAL SHOCK WIDTH
R. Menikoff Mar. 1993 16 p Presented at the MSI/Stony Brook Conference on Nonlinear Analysis and Computation, Stony Brook, NY, 8-9 Apr. 1993
(Contract W-7405-eng-36)
(DE93-010699; LA-UR-93-958; CONF-9304105-1) Avail: CASI HC A03/MF A01

A simple test problem proposed by Noh, a strong shock reflecting from a rigid wall, demonstrates a generic problem with numerical shock capturing algorithms at boundaries that Noh called 'excess wall heating'. We show that the same type of numerical error occurs in general when shock waves interact. The underlying cause is the non-uniform convergence to the hyperbolic solution of the inviscid limit of the solution to the PDE's with viscosity. The error can be understood from an analysis of the asymptotic solution. For a propagating shock, there is a difference in the total energy of the parabolic wave relative to the hyperbolic shock. Moreover, the relative energy depends on the strength of the shock. The error when shock waves interact is due to the difference in the relative energies between the incoming and outgoing shock waves. It is analogous to a phase shift in a scattering matrix. A conservative differencing scheme correctly describes the Hugoniot jump conditions for a steady propagating shock. Therefore, the error from the asymptotics occurs in the transient when the waves interact. The entropy error that occurs in the interaction region remains localized but does not dissipate. A scaling argument shows that as the viscosity coefficient goes to zero, the error shrinks in spatial extention but is constant in magnitude. Noh's problem of the reflection of a shock from a rigid wall is equivalent to the symmetric impact of two shock waves of the opposite family. The asymptotic argument shows that the same type of numerical error would occur when the shocks are of unequal strength. Thus, Noh's problem is indicative of a numerical error that occurs when shocks interact due to the numerical shock width. DOE

N93-30485# Los Alamos National Lab., NM.
TOWARDS A BETTER HYDRO FOR DYNAMIC MIX CALCULATIONS
J. Binstock 1993 14 p Presented at the 4th International Workshop on the Physics of Compressible Turbulent Mixing, Cambridge, England, 29 Mar. - 1 Apr. 1993
(Contract W-7405-eng-36)
(DE93-010702; LA-UR-93-923; CONF-9303126-1) Avail: CASI HC A03/MF A01

A difference equation technique suitable for clean, dynamic mix, and turbulence Lagrangian calculations is shown. This new technique is compared to the standard one for clean one-dimensional calculations of the Noh, Sedov Blast Wave, and Strong Shock Tube test problems, and for a one-dimensional two-phase flow dynamic mix calculation of a modified Noh problem: all test problems involving shocks. The new technique is shown to dramatically reduce the noise in the calculated hydrodynamic quantities of pressure, density, specific internal energy, and Lagrangian interface velocity. DOE

N93-30489# Texas A&M Univ., College Station. Dept. of Nuclear Engineering.
MULTIPARTICLE IMAGING TECHNIQUE FOR TWO-PHASE FLUID FLOWS USING PULSED LASER SPECKLE VELOCIMETRY
T. A. Hassan Dec. 1992 114 p
(Contract DE-FG02-88ER-12813)
(DE93-011734; DOE/ER-12813/1) Avail: CASI HC A06/MF A02

The practical use of Pulsed Laser Velocimetry (PLV) requires the use of fast, reliable computer-based methods for tracking numerous particles suspended in a fluid flow. Two methods for performing tracking are presented. One method tracks a particle through multiple sequential images (minimum of four required) by prediction and verification of particle displacement and direction. The other method, requiring only two sequential images uses a dynamic, binary, spatial, cross-correlation technique. The algorithms are tested on computer-generated synthetic data and experimental data which was obtained with traditional PLV methods. This allowed error analysis and testing of the algorithms on real engineering flows. A novel method is proposed which eliminates tedious, undesirable, manual, operator assistance in removing erroneous vectors. This method uses an iterative process involving an interpolated field produced from the most reliable vectors. Methods are developed to allow fast analysis and presentation of sets of PLV image data. Experimental investigation of a two-phase, horizontal, stratified, flow regime was performed to determine the interface drag force, and correspondingly, the drag coefficient. A horizontal, stratified flow test facility using water and air was constructed to allow interface shear measurements with PLV techniques. The experimentally obtained local drag measurements were compared with theoretical results given by conventional interfacial drag theory. Close agreement was shown when local conditions near the interface were similar to space-averaged conditions. However, theory based on macroscopic, space-averaged flow behavior was shown to give incorrect results if the local gas velocity near the interface was unstable, transient, and dissimilar from the average gas velocity through the test facility. DOE

N93-30492*# Engineering Research and Consulting, Inc., Huntsville, AL.
DEVELOPMENT OF A CFD CODE FOR CASTING SIMULATION Final Report
Jesse E. Murph 15 Jan. 1993 71 p Original contains color illustrations
(Contract NAS8-39241)
(NASA-CR-192577; NAS 1.26:192577; ERC/HSV-TR93-01) Avail: CASI HC A04/MF A01; 9 functional color pages

Because of high rejection rates for large structural castings (e.g., the Space Shuttle Main Engine Alternate Turbopump Design Program), a reliable casting simulation computer code is very desirable. This code would reduce both the development time and life cycle costs by allowing accurate modeling of the entire casting process. While this code could be used for other types of castings, the most significant reductions of time and cost would probably be realized in complex investment castings, where any reduction in the number of development castings would be of significant benefit. The casting process is conveniently divided into three distinct phases: (1) mold filling, where the melt is poured or forced into the mold cavity; (2) solidification, where the melt undergoes a phase change to the solid state; and (3) cool down, where the solidified part continues to cool to ambient conditions. While these phases may appear to be separate and distinct, temporal overlaps do exist between phases (e.g., local solidification occurring during mold filling), and some phenomenological events are affected by others (e.g., residual stresses depend on solidification and cooling rates). Therefore, a reliable code must accurately model all three phases and the interactions between each. While many codes have been developed (to various stages of complexity) to model the solidification and cool down phases, only a few codes have been developed to model mold filling. Author (revised)

N93-30499# Yale Univ., New Haven, CT. Dept. of Mathematics.
ANALYSIS AND COMPUTATION FOR VORTEX DYNAMICS AND RAREFIED GASES Final Report, 1 Nov. 1989 - 31 Oct. 1992
Russel Caflisch Dec. 1992 3 p
(Grant AF-AFOSR-0013-90)
(AD-A264705; AFOSR-93-0324TR) Avail: CASI HC A01/MF A01

The researchers have developed a variety of adapted orthogonal transforms for signal compression and analysis. These methods have been used successfully in sound and high resolution image compression and are currently being tested for their technological value. In parallel, the best basis algorithm has been used by K. Sreenivasan for analysis of experimental turbulence data, and by M. Farge and V. Wickerhauser for the analysis of simulated two dimensional vorticity fields. This analysis permits a more careful comparison between simulation and experiment by detecting subtle differences in structures. By extracting coherent structures in the flows, it promises to permit efficient tracking of these structures. In particular, as a result of testing by the FBI and Scotland Yard, a variant of these algorithms has been chosen as a standard for fingerprint image compression with an estimated initial saving to the FBI in storage hardware alone of $25,000,000. These methods are also being tested, in collaboration with Martin Marietta, for automatic target recognition. DTIC

N93-30571# Naval Surface Warfare Center, Bethesda, MD. Machinery Research and Development Directorate.
SOME IMPLICATIONS OF A DIFFERENTIAL TURBOMACHINERY EQUATION WITH VISCOUS CORRECTION
Herman B. Urbach Mar. 1993 27 p
(AD-A264693; CDNSWC-MRD-80-93-10) Avail: CASI HC A03/MF A01

A differential equation describing the energy transfer between a fluid and a body moving in that fluid was derived. The derivation, based upon the Coriolis form of the Navier-Stokes equation, contains a rigorous viscous correction. For inviscid ideal cases, the equation demonstrates that the rate of total enthalpy transfer from (or to) the system is a function of the transverse component of the pressure gradient. Therefore, for practical turbomachinery rotors, the derivative, del(p)/del(theta) can never vanish. On integration of the differential equations, a form of the Euler Turbomachinery Equation with viscous correction is derived. The resultant form contains two distinct work rate terms for the axial and radial components of the flow. The fact that integration yields a result which approximates the classic Euler Turbomachinery Equation constitutes confirmation of the derivation. An application of the equation to an ideal infinite linear cylinder with bound vorticity was developed, yielding the expected known result. DTIC

N93-30625 Brown Univ., Providence, RI.
THE STRUCTURE AND DYNAMICS OF THE VORTICITY AND PASSIVE SCALAR FIELDS AT SMALL SCALES IN HOMOGENEOUS ISOTROPIC TURBULENCE Ph.D. Thesis
Gregory R. Ruetsch 1992 127 p
Avail. Univ. Microfilms Order No. DA9308880

Using direct numerical simulations of homogeneous isotropic turbulence, the small-scale structures of the vorticity and passive scalar fields were investigated. Both statistical and visual techniques were used to examine quantities that appear in the evolutions equations for the enstrophy and scalar gradient. Tube like regions of intense enstrophy contain large positive, and sometimes negative, enstrophy production, and regions of mostly moderate-valued kinetic energy dissipation surround these tubes. The statistical techniques show that although activity in these vortex tubes is large, on a volume normalized basis, by far the largest contributions to the terms in the evolution equations, along with the energy dissipation, are from low-level 'background' activity. Although sheets of intense scalar gradient are found to wrap around the vortex tubes, the most intense scalar gradient sheets are dissociated from the vortex tubes. Both the enstrophy and strain-rate are small in the vicinity of these sheets. It was determined that the persistence and not the strength of the strain field is responsible for the production of these intense scalar gradient sheets. Persistent strain fields are set up by pairs of vortices with approximately equal circulation, which most frequently occur when the vortices are weak. Both antiparallel and parallel configurations of such vortices are observed. The temporal evolution of these structures was also investigated. Sheets of vorticity are found to undergo a transition which can be qualitatively described by the Kelvin-Helmholtz instability. This process is responsible for the formation of the vortex tubes. In addition, antiparallel regions of vorticity were found to collapse and produce vortex sheets. These pairs of vortex sheets are effective in producing persistent strain, and therefore intense scalar gradient sheets. Dissert. Abstr.

N93-30630# Iowa State Univ. of Science and Technology, Ames.
COMPUTATIONAL FLUID DYNAMICS RESEARCH ON DYNAMICALLY ADAPTIVE MESH METHODS FOR TRANSONIC FLOWS Final Report, 1 Nov. 1990 - 31 Dec. 1992
Richard G. Hindman 24 Nov. 1992 48 p
(Grant AF-AFOSR-0034-90)
(AD-A264833; AFOSR-93-0205TR) Avail: CASI HC A03/MF A01

Dynamic mesh adaptation strategies are investigated. These include software development, dynamically adaptive mesh schemes, errors arising from generalized mappings, and orthogonality. The strategies developed are tested against the Euler and viscous Burgers Equations. DTIC

N93-30759# Pennsylvania Univ., Philadelphia. Dept. of Chemical Engineering.
FLUIDS IN POROUS MEDIA. Final Report
E. D. Glandt and A. L. Myers Feb. 1993 37 p Sponsored by Gas Research Inst.
(Contract GRI-5086-260-1252)
(PB93-175198; GRI-93/0088) Avail: CASI HC A03/MF A01

First, second, and third generation models of microporous activated carbon adsorbents were tested and compared with experiment. Isotherms, isosteric heats, selectivities, and configurational properties (energy and density distributions) were calculated by grand canonical ensemble Monte Carlo (GCMC) simulation. The simulations yielded a result of 220 V/V for the theoretical capacity of monolithic porous carbon. The figure is a theoretical but unattainable limit, as it refers to an adsorbent with a uniform, optimum pore size, containing no mesopores, no macropores, and no void space. NTIS

N93-30902 California Inst. of Tech., Pasadena.
AN ADAPTIVE LAGRANGIAN METHOD FOR COMPUTING 1-D REACTING FLOWS AND THE THEORY OF RIEMANN INVARIANT MANIFOLDS FOR THE COMPRESSIBLE EULER EQUATIONS Ph.D. Thesis
Tasso Lappas 1993 126 p
Avail: Univ. Microfilms Order No. DA9307041

A method for computing one dimensional unsteady compressible flows, with and without chemical reactions is presented. Focus was on the accurate computation of the discontinuous waves that arise in such flows. The main feature of the method is the use of an adaptive Lagrangian grid. This allows the computation of discontinuous waves and their interactions with the accuracy of front-tracking algorithms. This is done without the use of additional grid points representing shocks, in contrast to conventional front-tracking schemes. The Lagrangian character of the present scheme also allows contact discontinuities to be captured easily. The algorithm avoids interpolation across discontinuities in a natural and efficient way. The method was used on a variety of reacting and non-reacting flows in order to test its ability to compute accurately and in a robust way complicated wave interactions. A new approach for computing multidimensional flows of an inviscid gas is presented. The goal is to use the knowledge of the one-dimensional characteristic problem for gasdynamics to compute genuinely multidimensional flows in a mathematically consistent way. A family of spacetime manifolds is found on which an equivalent 1-D problem holds. These manifolds are referred to as Riemann Invariant Manifolds. Their geometry depends on the local spatial gradients of the flow and they provide locally a convenient system of coordinate surfaces for space time. In the case of zero entropy gradients, functions analogous to the Riemann invariants of 1-D gasdynamics can be introduced. These generalized Riemann Invariants are constant on the Riemann Invariant Manifolds. The equations of motion are integrable on these manifolds and the problem of computing the solution becomes that of determining the geometry of these manifolds locally in space time. Their geometry is examined and, in particular, their relation to the characteristic surfaces. It turns out that they can be space-like or time-like, depending on the flow gradients. An important parameter is introduced which plays the role of a Mach number for the wave fronts that these manifolds represent. This theory can be viewed as the extension of the method of characteristics to multidimensional unsteady flows. There are many ways of using the theory to develop practical numerical schemes. It is shown how it is possible to correct a conventional second-order Godunov scheme for multidimensional effects, using this theory. A family of second-order conservative Godunov schemes is derived using the theory of Riemann Invariant Manifolds, for the case of two-dimensional flow. The extension to three dimensions is straightforward. One of these schemes is used to compute two standard test cases and a two dimensional inviscid shear layer. Dissert. Abstr.

N93-30999 Michigan Univ., Ann Arbor.
NUMERICAL WAVE PROPAGATION AND STEADY-STATE SOLUTIONS Ph.D. Thesis
Karim MazaheriBody 1992 232 p
Avail: Univ. Microfilms Order No. DA9308394

In solving steady-state problems (governed by the Euler equations) with unsteady solution process, error waves can be damped or eliminated at three different places: the inner boundary; the computational field; and the outer boundary. Presented are techniques for doing this leading to faster convergence to a steady state. Visualization techniques which help to understand, design, and develop new ideas regarding this view point of convergence acceleration, are also presented. Error waves are damped at the inner boundary by using a soft wall condition, instead of the common rigid wall boundary condition. This boundary condition is analyzed, and the optimum way to implement it is derived. Its application in two space dimensions for both upwind and central differencing codes is developed, and in subsonic flows with no shocks, gains of more than 50 percent in running time are reported. Error waves in the computational field are damped by adding a bulk viscosity term to the momentum equations. After analysis of its effects in linearized equations, its explicit and implicit implementation in one and two space dimensions are studied. Its successful performance in combination with the soft-wall boundary condition and residual smoothing is also reviewed. It is shown how this new term can stabilize and accelerate the computation of low-Mach-number flows. Finally to improve the convergence acceleration via the outer boundary, the well-known topic of absorbing boundary conditions is partially reviewed. It is shown that in many cases the outgoing waves are not, as commonly assumed, normal to the outer boundary. It is shown how slowing down the waves near the outer boundary can accelerate the convergence, and some new boundary models are introduced which take into account the angle of incidence to minimize the reflections. Dissert. Abstr.

N93-31020# Kernforschungszentrum G.m.b.H., Karlsruhe (Germany). Inst. fuer Neutronenphysik und Reaktortechnik.
GODUNOV-TYPE METHODS FOR THE EQUATIONS OF COMPRESSIBLE FLUID MECHANICS Thesis - Karlsruhe Univ. [GODUNOV-TYP VERFAHREN FUER DIE GLEICHUNGEN DER KOMPRESSIBLEN STROEMUNGSMECHANIK]
C.-D. Munz Aug. 1992 165 p In GERMAN
(KfK-5058; ETN-93-94190) Copyright Avail: CASI HC A08/MF A02

The construction of a family of shock capturing schemes is considered: the Godunov type schemes. A review of these schemes is given in the case of the time dependent one dimensional equations of compressible fluid mechanics, as developed in recent years. The construction of the Godunov type schemes are examined for two dimensional problems in space and applied to the compressible Navier-Stokes equations. Numerical results of the study of the instability of transonic and supersonic shear flows are shown. Godunov type schemes for the one dimensional equations of compressible fluid mechanics in Lagrange coordinates were constructed. A simple Godunov type scheme for the equations of relativistic hydrodynamics was proposed. Numerical results for several test problems are presented. ESA

N93-28719*# TRW Space and Defense Sector, Redondo Beach, CA.
IN-STEP TWO-PHASE FLOW (TPF) THERMAL CONTROL EXPERIMENT
In NASA, Washington, NASA/DOD Flight Experiments Technical Interchange Meeting Proceedings 1992 19 p (For primary document see N93-28699 11-12)
Avail: CASI HC A03/MF A10

N93-29624*# Lockheed Engineering and Sciences Co., Hampton, VA.
A GENERALIZED APPROACH TO THE THERMAL ANALYSIS OF THE LONG DURATION EXPOSURE FACILITY'S FLIGHT EXPERIMENTS

Thomas R. Sampair *In* NASA. Langley Research Center, LDEF: 69 Months in Space. Part 1: Second Post-Retrieval Symposium Apr. 1993 p 27-50 (For primary document see N93-29621 11-99)
Avail: CASI HC A03/MF A03

N93-29701*# National Aeronautics and Space Administration. Goddard Space Flight Center, Greenbelt, MD.
LONG DURATION EXPOSURE FACILITY (LDEF) LOW TEMPERATURE HEAT PIPE EXPERIMENT PACKAGE (HEPP) FLIGHT RESULTS
Roy McIntosh, Craig McCreight (National Aeronautics and Space Administration. Ames Research Center, Moffett Field, CA.), and Patrick J. Brennan (OAO Corp., Greenbelt, MD.) *In* NASA. Langley Research Center, LDEF: 69 Months in Space. Part 4: Second Post-Retrieval Symposium Apr. 1993 p 1455-1475 (For primary document see N93-29682 11-99)
Avail: CASI HC A03/MF A03; 2 functional color pages

N93-29757*# Utah State Univ., Logan.
THERMION: VERIFICATION OF A THERMIONIC HEAT PIPE IN MICROGRAVITY
In Universities Space Research Association, Houston, Proceedings of the Seventh Annual Summer Conference. NASA/USRA: University Advanced Design Program 1991 p 309-312 (For primary document see N93-29712 11-01)
Avail: CASI HC A01/MF A03

N93-29761*# Worcester Polytechnic Inst., MA.
ROTATIONAL FLUID FLOW EXPERIMENT
In Universities Space Research Association, Houston, Proceedings of the Seventh Annual Summer Conference. NASA/USRA: University Advanced Design Program 1991 p 335-338 (For primary document see N93-29712 11-01)
Avail: CASI HC A01/MF A03

N93-29935# Wright Lab., Wright-Patterson AFB, OH. Aero Propulsion and Power Directorate.
HEAT TRANSFER IN HIGH TURBULENCE FLOWS: A 2-D PLANAR WALL JET
R. B. Rivir, W. T. Troha, W. A. Eckerle (Cummins Engine Co., Inc., Columbus, IN.), and W. J. Schmoll (Dayton Univ. Research Inst., OH.) *In* AGARD, Heat Transfer and Cooling in Gas Turbines Feb. 1993 12 p (For primary document see N93-29926 11-07)
Copyright Avail: CASI HC A03/MF A04

N93-29936# Purdue Univ., West Lafayette, IN. School of Mechanical Engineering.
HEAT TRANSFER WITH MODERATE FREE STREAM TURBULENCE
S. N. B. Murthy *In* AGARD, Heat Transfer and Cooling in Gas Turbines Feb. 1993 33 p (For primary document see N93-29926 11-07)
(Contract F49620-87-K-0008)
Copyright Avail: CASI HC A03/MF A04

N93-29937# University Coll. of Swansea (Wales). Dept. of Mechanical Engineering.
THE EFFECT OF ORTHOGONAL-MODE ROTATION ON FORCED CONVECTION IN A CIRCULAR-SECTIONED TUBE FITTED WITH FULL CIRCUMFERENTIAL TRANSVERSE RIBS
W. D. Morris and R. Salemi *In* AGARD, Heat Transfer and Cooling in Gas Turbines Feb. 1993 11 p Sponsored in part by Science Research Council and Rolls-Royce Ltd. (For primary document see N93-29926 11-07)
Copyright Avail: CASI HC A03/MF A04

N93-29940# Oxford Univ. (England). Dept. of Engineering Science.
FUNDAMENTAL STUDIES OF IMPINGEMENT COOLING THERMAL BOUNDARY CONDITIONS
M. G. Lucas, P. T. Ireland, Z. Wang, T. V. Jones, and W. J. Pearce (Rolls-Royce Ltd., Bristol, England.) *In* AGARD, Heat Transfer and Cooling in Gas Turbines Feb. 1993 10 p Sponsored in part by Ministry of Defence; Science Research Council; and Rolls-Royce Ltd. (For primary document see N93-29926 11-07)
Copyright Avail: CASI HC A02/MF A04

N93-29941# Pratt and Whitney Aircraft of Canada Ltd., Longueuil (Quebec).
PREDICTION OF JET IMPINGEMENT COOLING SCHEME CHARACTERISTICS (AIRFOIL LEADING EDGE APPLICATION)
A. Riahi, H. J. Saabas, and W. Abdel Messeh *In* AGARD, Heat Transfer and Cooling in Gas Turbines Feb. 1993 14 p (For primary document see N93-29926 11-07)
Copyright Avail: CASI HC A03/MF A04

N93-29944# Nottingham Univ. (England). Dept. of Mechanical Engineering.
THE SWOLLEN POLYMER TECHNIQUE AND ITS USE FOR HEAT TRANSFER INVESTIGATIONS ON FILM COOLED SURFACES
N. Hay, D. Lampard, and N. MacLeod (Edinburgh Univ., Scotland.) *In* AGARD, Heat Transfer and Cooling in Gas Turbines Feb. 1993 21 p (For primary document see N93-29926 11-07)
Copyright Avail: CASI HC A03/MF A04

N93-29948# Institut de Mecanique des Fluides de Marseille (France).
STUDY OF FLOW STRUCTURE IN ROTATING CAVITIES: NUMERICAL PREDICTIONS OF LAMINAR AND TURBULENT, STEADY, AND UNSTEADY FLOWS
P. Maubert, R. Schiestel, L. Elena, A. Randriamampianina, A. M. Chaouche, E. CrespodelArco, and P. Bontoux *In* AGARD, Heat Transfer and Cooling in Gas Turbines Feb. 1993 23 p Sponsored in part by CCVR; CNRS; IMT; Conseil Regional PACA; Defence Research Establishment Toronto; International Exchange Program; and Ministere des Affaires Etrangeres (For primary document see N93-29926 11-07)
Copyright Avail: CASI HC A03/MF A04

N93-29952# Technische Univ., Darmstadt (Germany). Inst. fuer Technische Thermodynamik.
FLUID FLOW AND HEAT TRANSFER IN THE ENTRANCE REGION OF AN ANNULUS BETWEEN INDEPENDENTLY ROTATING TUBES WITH A TURBULENT AXIAL FLOW
H. Pfitzer, T. Rothe, and H. Beer *In* AGARD, Heat Transfer and Cooling in Gas Turbines Feb. 1993 11 p (For primary document see N93-29926 11-07)
Copyright Avail: CASI HC A03/MF A04

N93-29953# Technische Univ., Darmstadt (Germany).
THE EFFECT OF MAIN STREAM FLOW ANGLE ON FLAME TUBE FILM COOLING
H. Klinger and D. K. Hennecke *In* AGARD, Heat Transfer and Cooling in Gas Turbines Feb. 1993 12 p Sponsored in part by BMFT (For primary document see N93-29926 11-07)
Copyright Avail: CASI HC A03/MF A04

N93-29954# Leeds Univ. (England). Dept. of Fuel and Energy.
IMPINGEMENT/EFFUSION COOLING
G. E. Andrews, A. M. AlDabagh, A. A. Asere, F. Bazdidi-Tehrani, M. C. Mkpadi, and A. Nazari *In* AGARD, Heat Transfer and Cooling in Gas Turbines Feb. 1993 10 p (For primary document see N93-29926 11-07)
(Contract SRC-GR/D/53029)
Copyright Avail: CASI HC A02/MF A04

N93-29955# Middle East Technical Univ., Ankara (Turkey). Dept. of Chemical Engineering.
EVALUATION OF MULTI-DIMENSIONAL FLUX MODELS FOR RADIATIVE TRANSFER IN CYLINDRICAL COMBUSTION CHAMBERS
Nevin Selcuk *In* AGARD, Heat Transfer and Cooling in Gas Turbines Feb. 1993 6 p (For primary document see N93-29926 11-07)
Copyright Avail: CASI HC A02/MF A04

N93-29956# Office National d'Etudes et de Recherches Aerospatiales, Paris (France).
CALCULATIONS OF REACTIVE TURBULENT FLOWS IN AERONAUTICAL CHAMBERS [CALCULS D'ECOULEMENTS TURBULENTS REACTIFS DANS LES FOYERS AERONAUTIQUES]
P. Caillau and F. Dupoirieux *In* AGARD, Heat Transfer and Cooling in

Gas Turbines Feb. 1993 13 p In FRENCH (For primary document see N93-29926 11-07)
Copyright Avail: CASI HC A03/MF A04

N93-29959# Von Karman Inst. for Fluid Dynamics, Rhode-Saint-Genese (Belgium).
ON THE DEVELOPMENT OF A FILM COOLING LAYER
F. Lopez Pena and T. Arts *In* AGARD, Heat Transfer and Cooling in Gas Turbines Feb. 1993 12 p Sponsored by Commission of the European Communities (For primary document see N93-29926 11-07)
Copyright Avail: CASI HC A03/MF A04

35 INSTRUMENTATION AND PHOTOGRAPHY

Includes remote sensors; measuring instruments and gages; detectors; cameras and photographic supplies; and holography.

For aerial photography see *43 Earth Resources and Remote Sensing.* For related information see also *06 Aircraft Instrumentation,* and *19 Spacecraft Instrumentation.*

N93-28488# Aerospace Corp., El Segundo, CA. Lab. Operations.
THE DESIGN AND TESTING OF A HIGH-TEMPERATURE GRAPHITE DILATOMETER Technical Report
Patrick M. Sheaffer and George W. Henderson 24 Jun. 1992 46 p
(Contract F04701-85-C-0086)
(AD-A262185; TR-0088(3935-06)-2; SSD-TR-92-25) Avail: CASI HC A03/MF A01

A dilatometer for investigating the high-temperature behavior of carbonaceous materials has been constructed within a graphite tube furnace in the Composites Section of the Mechanics and Materials Technology Center of The Aerospace Corporation. The dilatometer is a single-pushrod type with a linear variable differential transformer (LVDT) dilation measurement system and employs computer data acquisition and analysis. It can measure thermally induced strain of a sample from room temperature to over 3000 deg C, a temperature that has been difficult to reach with currently available laboratory apparatus. The estimated uncertainty of the dilation measurement system is about +/- 5 microns over the entire temperature range. All components in the hot zone, including the sample holder and pushrod, are made of polycrystalline graphite. A three-point-bend fixture can be placed in the apparatus to measure the rheological properties of a pyrolyzing carbon precursor or the high-temperature creep properties of a carbon under conditions of constant flexural stress. DTIC

N93-28520# Lawrence Livermore National Lab., CA.
RADIOMETRIC CALIBRATION SYSTEM FOR IR CAMERAS
H. S. Park, D. W. Dobie, T. E. Ferretta, D. B. Hakala, M. P. Nolan, and E. L. Parker 15 May 1992 8 p Presented at the International Society for Photo Optical Engineering Conference, Orlando, FL, 20-24 Apr. 1992
(Contract W-7405-eng-48)
(DE93-009237; UCRL-JC-108444; CONF-920471-6) Avail: CASI HC A02/MF A01

An automated calibration system that was developed to calibrate IR flight cameras for a series of sub-orbital experiments is described. Short schedules as well as concern over cryo-cooler lifetimes dictated a totally automated calibration system that obtained as much data as possible over a short period of time. The data must be as complete as possible since the cameras are not recovered. For this reason the system calibrates each pixel individually. The output of the calibration is a set of calibration coefficients which convert the gray level output of the camera into physical units of radiance (Watts/cm(sub 2)-str-microns). The Hughes 256 x 256 pixels PtSi cameras and 128 x 128 pixels HgCd cameras and Amber 128 x 128 pixels InSb cameras were calibrated. These cameras put out 8 bit digital data and sync signal at a given camera setting. The calibration acquisition system is described and the results for the Hughes 256 x 256 PtSi camera are shown. DOE

N93-28645# Sandia National Labs., Albuquerque, NM.
FLASH X RAY SYSTEM: TECHNIQUES AND APPLICATIONS
J. C. Lanoue and R. B. Berry Mar. 1993 19 p
(Contract DE-AC04-76DP-00789)
(DE93-011477; SAND-92-2442) Avail: CASI HC A03/MF A01

High speed flash radiography has been used to record phenomena that occur during rapid dynamic events. The events are difficult, if not impossible, to record by other means due to the speed of the event or the obscuration associated with it. To eliminate the motion blur of objects moving at high speeds, it is necessary to have extremely short exposure times. This short exposure time requires the use of high speed intensifying screens and high speed x-ray film to record the radiographic image. Technicians who use flash x-rays have to depend on recommendations from present and former flash x-ray users for film and screen selection. The film and screen industry has made many changes in the last few years. It is not uncommon to find that the particular film or screen used in the past is no longer manufactured. This paper will describe some of the films and screens that are currently used for testing. It will also describe the optimum experimental setup used to obtain the best images. DOE

N93-28659# Chemical Research and Development Center, Aberdeen Proving Ground, MD.
MEASUREMENT OF A MICHELSON INTERFEROMETER MIRROR VELOCITY WITH A TIME INTERVAL ANALYZER Final Report, Feb. - Jun. 1992
R. J. Combs, R. B. Knapp, and C. T. Cathey (Tri-Square Corp., Ormand Beach, FL.) Jul. 1992 46 p
(AD-A263009; CRDEC-TR-356) Avail: CASI HC A03/MF A01

This report documents the design, construction, and implementation of a time interval analyzer (TIA). The TIA is a precision counter that measures the dynamic variation in the time intervals (i.e., frequency) of a signal. The helium-neon (HeNe) laser signal from the servo-mirror control circuitry of the interferometer provides a nearly constant frequency source. The HeNe signal frequency is directly proportional to the interferometer mirror velocity. A constant velocity is crucial for the proper operation of a Michelson interferometer, which is used in a Fourier transform spectrometer. The TIA provides a critical evaluation of velocity variations in a single interferometer mirror scan via analysis of the HeNe laser signal. DTIC

N93-28664# California Univ., Berkeley. Lawrence Berkeley Lab.
NOVEL LOW TEMPERATURE SUPERCONDUCTING BOLOMETERS
M. Nahum, P. L. Richards, M. Gaidis (Yale Univ., New Haven, CT.), and D. E. Prober (Yale Univ., New Haven, CT.) Nov. 1992 3 p Presented at the 17th Annual SPIE International Conference on Infrared and Millimeter Wave Sources, Pasadena, CA, 14-18 Dec. 1992
(Contract DE-AC03-76SF-00098)
(DE93-010433; LBL-33349; CONF-921217-5) Avail: CASI HC A01/MF A01

Antenna-coupled superconducting bolometers for submillimeter and millimeter waves, which make use of the thermal boundary resistance between metals and insulators and the trapping of quasiparticles at metal-superconductor interfaces, were designed and fabricated. These devices were used to make measurements of the frequency response and optical efficiency of the log-periodic antennas between 90 GHz to 1.8 THz. DOE

N93-28989# OPTRA, Inc., Beverly, MA.
ENHANCED NONCONTACTING LASER EXTENSOMETER FOR BIAXIAL STRAIN MEASUREMENTS Final Report, Jan. - Aug. 1992
James J. Connolly, James R. Engel, and Andrew T. Lintz Sep. 1992 42 p
(Contract DAAL04-92-C-0005)
(AD-A263170; MTL-TR-92-60) Avail: CASI HC A03/MF A01

In the proposed program, OPTRA will develop and commercialize a non-contact biaxial extensometer for the material testing market. The optical technology, based on an existing OPTRA single axis product, allows the accurate measurement of surface strains on any test specimen without contact and without material preparation. The non-contact measurement in ideal for high temperature testing, single fiber testing, high humidity/liquid immersed testing, high strain elastomer testing and many other applications that are unsuitable for bonded gages. The incorporation of two axes of strain measurement in a single instrument allows users to measure shear strain, Poisson's ratio, and other biaxial strain conditions. The ability to reorient the measurement axes relative to the test specimen in real time with small cyclic loading allows the user to rapidly identify the maximum and minimum normal strain axes and thereby fully define an unknown state of plane strain. The product development will be focussed on meeting a wide range of material test requirements and on keeping production costs low to insure that a commercially viable product is produced. DTIC

N93-29046# Department of the Navy, Washington, DC.
GYROSCOPE WITH EXCESS NOISE SUBTRACTION Patent Application
Robert P. Moeller, inventor (to Navy) and William K. Burns, inventor (to Navy) 30 Nov. 1992 22 p
(AD-D015698; US-Patent-Appl-SN-983335; Navy-Case-73910) Avail: CASI HC A03/MF A01

A system and method for subtracting excess noise from a high sensitivity gyroscope system in which a laser diode array is focused into an Nd-doped active fiber is described. A resultant gyro signal is polarized, detected, and amplified. A noise signal is polarized, delayed, detected, and amplified such that the noise signal is polarized parallel to the gyro signal and delayed by a fiber delay of a length equal to a length of gyroscope fiber coil. The excess noise component in the amplified gyro signal is reduced by modulating the amplified noise signal with a portion of the amplified gyro signal and subtracting the amplitude-modulated noise signal from the amplified gyro signal to produce a reduced noise gyro signal. DTIC

N93-29066*# Cuyuna Corp., Austin, TX.
PROGRAM FOR AN IMPROVED HYPERSONIC TEMPERATURE-SENSING PROBE
Richard J. Reilly Jun. 1993 63 p
(Contract NAS2-13457; RTOP 505-68-50)
(NASA-CR-186025; H-1893; NAS 1.26:186025) Avail: CASI HC A04/MF A01

Under a NASA Dryden-sponsored contract in the mid 1960s, temperatures of up to 2200 C were successfully measured using a fluid oscillator. The current program, although limited in scope, explores the problem areas which must be solved if this technique is to be extended to 10,000 R. The potential for measuring extremely high temperatures, using fluid oscillator techniques, stems from the fact that the measuring element is the fluid itself. The containing structure of the oscillator need not be brought to equilibrium temperature with with the fluid for temperature measurement, provided that a suitable calibration can be arranged. This program concentrated on review of high-temperature material developments since the original program was completed. Other areas of limited study included related pressure instrumentation requirements, dissociation, rarefied gas effects, and analysis of sensor time response. Author

N93-29084* National Aeronautics and Space Administration. Langley Research Center, Hampton, VA.
CONSTANT FREQUENCY PULSED PHASE-LOCKED LOOP MEASURING DEVICE Patent
William T. Yost, inventor (to NASA) (PRC Kentron, Inc., Hampton, VA.), Peter W. Kushnick, inventor (to NASA) (PRC Kentron, Inc., Hampton, VA.), and John H. Cantrell, inventor (to NASA) 1 Jun. 1993 12 p Filed 26 Aug. 1991 Supersedes N92-10182 (30 - 1, p 34)
(NASA-Case-LAR-13823-1; US-Patent-5,214,955; US-Patent-Appl-SN-749737; US-Patent-Class-73-24.05; US-Patent-Class-374-119; US-Patent-Class-73-5.97; US-Patent-Class-73-32A; US-Patent-Class-73-61.75; US-Patent-Class-73-61.79; US-Patent-Class-73-64.53) Avail: US Patent and Trademark Office

A measuring apparatus is presented that uses a fixed frequency oscillator to measure small changes in the phase velocity ultrasonic sound when a sample is exposed to environmental changes such as changes in pressure, temperature, etc. The invention automatically balances electrical phase shifts against the acoustical phase shifts in order to obtain an accurate measurement of electrical phase shifts.
Official Gazette of the U.S. Patent and Trademark Office

N93-29149# California Univ., Berkeley. Lawrence Berkeley Lab.
SUPERCONDUCTING SUBMILLIMETER AND MILLIMETER WAVE DETECTORS Ph.D. Thesis
M. Nahum 20 Oct. 1992 133 p
(Contract DE-AC03-76SF-00098)
(DE93-007656; LBL-33039) Avail: CASI HC A07/MF A02

The series of projects described in this dissertation was stimulated by the discovery of high temperature superconductivity. Our goal was to develop useful applications which would be competitive with the current state of technology. The high-T(c) microbolometer was developed into the most sensitive direct detector of millimeter waves, when operated at liquid nitrogen temperatures. The thermal boundary resistance of thin YBa(2)Cu(3)O(7-delta) films was subsequently measured and provided direct evidence for the bolometric response of high-T(c) films to fast (ns) laser pulses. The low-T(c) microbolometer was developed and used to make the first direct measurements of the frequency dependent optical efficiency of planar lithographed antennas. The hot-electron microbolometer was invented less than a year prior to the writing of this dissertation. Our analysis, presented here, indicates that it should be possible to attain up to two orders of magnitude higher sensitivity than that of the best available direct detectors when operated at the same temperature. The temperature readout scheme for this device could also be used to measure the intrinsic interaction between electrons and phonons in a metal with a sensitivity that is five orders of magnitude better than in previous measurements. Preliminary measurements of quasiparticle trapping effects at the interface between a metal and a superconductor are also presented. DOE

N93-29209*# National Aeronautics and Space Administration. Langley Research Center, Hampton, VA.
ENHANCED REDUCTION OF VELOCITY DATA OBTAINED DURING CETA FLIGHT EXPERIMENT
Tom D. Finley, Douglas T. Wong, and John S. Tripp Washington May 1993 13 p
(RTOP 472-47-12-50)
(NASA-TM-4460; L-17168; NAS 1.15:4460) Avail: CASI HC A03/MF A01

A newly developed technique for enhanced data reduction provides an improved procedure that allows least squares minimization to become possible between data sets with an unequal number of data points. This technique was applied in the Crew and Equipment Translation Aid (CETA) experiment on the STS-37 Shuttle flight in April 1991 to obtain the velocity profile from the acceleration data. The new technique uses a least-squares method to estimate the initial conditions and calibration constants. These initial conditions are estimated by least-squares fitting the displacements indicated by the Hall-effect sensor data to the corresponding displacements obtained from integrating the acceleration data. The velocity and displacement profiles can then be recalculated from the corresponding acceleration data using the estimated parameters. This technique, which enables instantaneous velocities to be obtained from the test data instead of only average velocities at varying discrete times, offers more detailed velocity information, particularly during periods of large acceleration or deceleration. Author

N93-29297# North Carolina Univ., Charlotte. Dept. of Electrical Engineering.
ITERATIVE ENCODING METHODS FOR COMPUTER GENERATED HOLOGRAMS Final Report, 1 Oct. 1991 - 30 Sep. 1992
Michael R. Feldman 8 Feb. 1993 4 p
(Contract DAAL03-91-G-0091)
(AD-A263705; ARO-28416.2-PH) Avail: CASI HC A01/MF A01

Iterative encoding methods capable of greatly increasing the performance of CGH's were investigated. An F/l holographic lens, designed with an iterative encoding method was measured to have a diffraction efficiency of 87%. This is the highest reported efficiency for an F/l element. A recursive Mean Squared Error Algorithm was developed to reduce the computation time. A hologram was fabricated to generate a 32x32 spot array. The experimental measurements indicated a diffraction efficiency of 72% and uniformity of + or -1%. This is the highest reported diffraction efficiency for such large-sized spot arrays. DTIC

N93-29325# Westinghouse Savannah River Co., Aiken, SC.
TRANSIENT RESPONSE OF EMBEDDED THERMOCOUPLES
D. A. Coutts Nov. 1992 36 p Revised
(Contract DE-AC09-89SR-18035)
(DE93-009889; WSRC-TR-92-73-Rev-1) Avail: CASI HC A03/MF A01

There is an increasing interest in the ability to measure transient behavior in heated systems in the Heat Transfer Laboratory. To accomplish this, an understanding of transient instrument behavior is necessary. This report discusses the transient behavior of small diameter thermocouples which are imbedded in an aluminum plate and provides an estimate of the composite time constant for different imbedded arrangements. It also describes a technique which can be used to estimate the time constant. The primary purpose of the data presented in this report was to evaluate manufacturing, installation, and calibration techniques. Use of the data in this report for critical applications should be limited to generalizations of behavior and uncertainty analysis. DOE

N93-29390# Illinois Univ. at Urbana-Champaign, Savoy. Advanced Construction Technology Center.
ADVANCED CONSTRUCTION TECHNOLOGY CENTER RESEARCH Final Report, 20 Jan. 1987 - 19 Jan. 1993
J. P. Murtha 19 Mar. 1993 112 p
(Contract DAAL03-87-K-0006)
(AD-A263654; ARO-24605.164-EG-UIR) Avail: CASI HC A06/MF A02

The research reported was part of the Department of Defense Universities Research Initiative (URI) Program. Because of the heavy investment in planning, design, construction, maintenance, and operation of its huge physical plant, the U.S. Army included Advanced Construction Technology as one of the areas of concentration in the URI program. The research program consisted of 28 research projects conducted in the following five areas: nondestructive evaluation technologies for constructed works, construction site metrology, new materials and material technologies for construction, computer-aided construction, and special technologies. Accordingly, the research program was a multi-disciplinary program conducted by faculty and graduate students at the University of Illinois. DTIC

N93-29476# New Mexico Univ., Albuquerque. Dept. of Chemistry.
SCANNING PROBE LITHOGRAPHY. PART 1: SCANNING TUNNELING MICROSCOPE-INDUCED LITHOGRAPHY OF SELF-ASSEMBLED n-ALKANETHIOL MONOLAYER RESISTS Technical Report
Claudia B. Ross, Li Sun, and Richard M. Crooks 19 Mar. 1993 27 p
(Contract N00014-91-J-1991)
(AD-A263130; TR-5) Avail: CASI HC A03/MF A01

The tip of a scanning tunneling microscope was used to fabricate geometrically well structures within organized, self-assembled monolayer resist that have critical dimensions ranging from 60 nm to 5 micrometers. To achieve nanometer-scale lithography, a Au(111) substrate was coated with a self-assembled monolayer of HS(CH2)17CH3, which functions as an ultrathin (approx. 2.5 nm) resist, and then the resist was etched by an STM tip. This treatment results in window-like features that penetrate the organic monolayer. Nanolithographically defined features have been characterized by scanning tunneling microscopy, scanning electron microscopy, and electrochemical methods. For example, since mass and electron transfer to the conductive Au substrate are blocked by the monolayer everywhere except in the STM-etched regions, the windows serve as ultramicroelectrodes. The limiting current that results from radial diffusion of a bulk-phase redox species to the etched window is in close agreement with that predicted by theory. DTIC

N93-29503* National Aeronautics and Space Administration. Marshall Space Flight Center, Huntsville, AL.
VALVE MALFUNCTION DETECTION APPARATUS Patent
Richard K. Burley, inventor (to NASA) 13 Jul. 1993 6 p Filed 7 Oct. 1992
(NASA-Case-MFS-29904-1; US-Patent-5,226,447;
US-Patent-Appl-SN-957127; US-Patent-Class-137-554;
US-Patent-Class-137-557; US-Patent-Class-116-70;
US-Patent-Class-340-611; Int-Patent-Class-F16K-37/00) Avail: US Patent and Trademark Office

A detection system is provided for sensing a malfunction of a valve having an outlet connected to an end of a first pipe through which pressurized fluid may be flowed in a downstream direction away from the valve. The system includes a bypass pipe connected at its opposite ends to the first pipe and operative to bypass a portion of the fluid flow therethrough around a predetermined section thereof. A housing is interiorly divided by a flexible diaphragm into first and second opposite chambers which are respectively communicated with the first pipe section and the bypass pipe, the diaphragm being spring-biased toward the second chamber. The diaphragm housing cooperates with check valves and orifices connected in the two pipes to create and maintain a negative pressure in the first pipe section in response to closure of the valve during pressurized flow through the first pipe. A pressure switch senses the negative pressure and transmits a signal indicative thereof to a computer. Upon cessation of the signal while the valve is still closed, the computer responsively generates a signal indicating that the valve, or another portion of the detection system, is leaking. Official Gazette of the U.S. Patent and Trademark Office

N93-29773# Lawrence Livermore National Lab., CA.
A NEW MULTICHANNEL SOFT X RAY FRAMING CAMERA FOR FUSION EXPERIMENTS
F. Ze, R. L. Kauffman, J. D. Kilkenny, J. Wielwald, P. M. Bell, R. Hanks, J. Stewart, D. Dean, J. Bower, and R. Wallace 20 Mar. 1992 14 p
Presented at the 9th Topical Conference on High-Temperature Plasma Diagnostics, Santa Fe, NM, 15-19 Mar. 1992
(Contract W-7405-eng-48)
(DE93-009302; UCRL-JC-110094; CONF-920362-43) Avail: CASI HC A03/MF A01

Two dimensional, time resolved x-ray imaging is a principal technique used to study hot plasmas produced in laser heated targets. It can be used to study laser energy deposition within the irradiation spot, the spatial and temporal dependence of laser to x-ray conversion efficiency, electron transport and density profiles, mass ablation rates as well as x-ray driven implosions in inertial confinement fusion experiments. A new soft x-ray framing camera which will allow us to record two-dimensional images at different times almost simultaneously was successfully developed. It is a broad band diagnostic (100 eV less than or equal to delta(h(radical)) less than or equal to 400 eV) having three channels which can obtain x-ray images at four different times from laser driven targets. Its current configuration includes one 500 eV, one 1.0 keV, and one approximately 2.5 keV channels. The two low energy channels resulted from pairing transmission filters to grazing x-ray mirrors. Other channel options can be implemented easily to measure other x-ray energies. Four different striplines coated on a microchannel plate are gated at different times. Each strip records three different images taken nearly simultaneously, one image per channel. The result is twelve x-ray images on film, four images per channel taken at four different times, with a nominal resolution of approximately 100 ps per image. The diagnostics' spatial resolution is approximately 10 microns. This new instrument was already fielded during x-ray conversion experiments, using both low and high Z targets driven by 1ns-2ns, 'flat top' laser pulses. The details of the instrument design and sample results from conversion experiments are shown. DOE

N93-29842# Sandia National Labs., Livermore, CA.
ADVANCED COORDINATE MEASURING MACHINE AT SANDIA NATIONAL LABORATORIES
R. D. Pilkey and P. A. Klevgard Mar. 1993 32 p
(Contract DE-AC04-76DR-00789)
(DE93-010618; SAND-93-8208) Avail: CASI HC A03/MF A01

Sandia National Laboratories/California has acquired a new Moore M-48V CNC five-axis universal coordinate measuring machine (CMM). Site preparation, acceptance testing, and initial performance results are discussed. Unique features of the machine include a ceramic ram and vacuum evacuated laser pathways (VELPS). The implementation of a VELPS system on the machine imposed certain design requirements and entailed certain start-up problems. The machine's projected capabilities, workload, and research possibilities are outlined. DOE

N93-30032# Army Research Lab., Aberdeen Proving Ground, MD.
MEASUREMENT OF PROJECTILE SURFACE TEMPERATURE BY MEANS OF ITS INFRARED RADIATION: A PRELIMINARY STUDY Final Report, Jan. - Apr. 1992
Keith P. Soencksen Apr. 1993 32 p
(DA Proj. 1L1-61102-AH-43)
(AD-A264053; ARL-MR-62) Avail: CASI HC A03/MF A01

The current work is a preliminary study to the planned direct measurement of the infrared emissions of a projectile in flight, from which surface temperature will be estimated. If the planned experiment is to be meaningful, the projectile surface temperature must be high enough such that the incident infrared radiation is significant enough to be measured by the detectors. In this report, detector threshold is calculated and compared to the computed infrared radiation reaching the detector from an M735 projectile nosecone at a distance from the muzzle of 225 meters. In the wavelength band 2.0-2.5 microns, the results predict that the detector will not be able to see the projectile emissions, and in the wavelength band 3.5-4.0 microns, the results show probable detection of most of the projectile only if the flow is turbulent. DTIC

N93-30491# Lawrence Livermore National Lab., CA.
A NEW TUBELESS NANOSECOND STREAK CAMERA BASED ON OPTICAL DEFLECTION AND DIRECT CCD IMAGING
C. C. Lai Dec. 1992 15 p Presented at the 20th International Congress on High Speed Photography and Photonics, Victoria, Ontario, 25-26 Sep. 1992
(Contract W-7405-eng-48)
(DE93-011893; UCRL-JC-109615; CONF-9209188-10) Avail: CASI HC A03/MF A01

A new optically deflected streaking camera with performance of nanosecond-range resolution, superior imaging quality, high signal detectability, and large format recording has been conceived and developed. Its construction is composed of an optomechanical deflector that deflects the line-shape image of spatial-distributed time-varying signals across the sensing surface of a cooled scientific two-dimensional CCD array with slow readout driving electronics, a lens assembly, and a desk-top computer for prompt digital data acquisition and processing. Its development utilizes the synergism of modern technologies in sensor, optical deflector, optics, and microcomputer. With laser light as signal carrier, the deflecting optics produces near diffraction-limited streak images resolving to a single pixel size of less than or = 25 microns. A 1kx1k-pixel array can thus provide a vast record of 1,000 digital data points along each spatial or temporal axis. Since only one photon-to-electron conversion exists in the entire signal recording path, the camera responses linearly to the incident light over a wide dynamic range in excess of 10(exp 4):1. Various image deflection techniques are assessed for imaging fidelity, deflection speed, and capacity for external triggering. Innovative multiple-pass deflection methods for utilizing optomechanical deflector have been conceived and developed to attain multi-fold amplification for the optical scanning speed across the CCD surface at a given angular deflector speed. Without significantly compromising imaging. quality, or flux throughput efficiency, these optical methods enable a sub-10 ns/pixel streak speed with the deflector moving benignly at less than 500 radians/second, or equivalently 80 revolutions/second. Test results of the prototype performance are summarized including a spatial resolution of 10 lp/mm at 65% CTF and a temporal resolution of 11.4 ns at 3.8 ns/pixel. DOE

N93-30510# Sandia National Labs., Albuquerque, NM.
PORTABLE FIBER OPTIC COUPLED DOPPLER INTERFEROMETER SYSTEM FOR DETONATION AND SHOCK WAVE DIAGNOSTICS
K. J. Fleming 1993 7 p Presented at the 6th Test Technology Symposium, Baltimore, MD, 30 Mar. 1993
(Contract DE-AC04-76DP-00789)
(DE93-009827; SAND-93-0712C; CONF-9303128-1) Avail: CASI HC A02/MF A01

Testing and analysis of shock wave characteristics such as produced by detonators and ground shock propagation frequently require a method of measuring velocity and displacement of the surface of interest. One method of measurement is doppler interferometry. The VISAR (Velocity Interferometer System for Any Reflector) uses doppler interferometry and has pined wide acceptance as the preferred tool for shock measurement. An important asset of VISAR is that it measures velocity and displacement non-intrusively. The conventional VISAR is not well suited for portability because of its sensitive components, large power and cooling requirements, and hazardous laser beam. A new VISAR using the latest technology in solid state lasers and detectors was developed and tested. To further enhance this system's versatility, the unit is fiber optic coupled which allows remote testing, permitting the VISAR to be placed over a kilometer away from the target being measured. Because the laser light is contained in the fiber optic, operation of the system around personnel is far less hazardous. A software package for data reduction was also developed for use with a personal computer. These new advances have produced a very versatile system with full portability which can be totally powered by batteries or a small generator. The solid state VISAR and its peripheral components, fiber optic coupling methods, and the fiber optic coupled sensors used for sending and receiving laser radiation is described. DOE

N93-30531# California Univ., Berkeley. Lawrence Berkeley Lab.
THE X RAY MICROSCOPY RESOURCE CENTER AT THE ADVANCED LIGHT SOURCE
W. Meyer-Ilse, D. Attwood, and M. Koike Aug. 1992 12 p Presented at the 4th International Conference on Biophysics and Synchrotron Radiation, Tsukuba, Japan, 30 Aug. - 5 Sep. 1992
(Contract DE-AC03-76SF-00098)
(DE93-010443; LBL-32367; CONF-920821-3) Avail: CASI HC A03/MF A01

The high spectral brightness of undulator radiation from the Advanced Light Source (ALS) offers a great scientific opportunity for biological x-ray microscopy. X-ray microscopy extends visible light microscopy to higher resolution and makes use of unique contrast mechanisms. It does not compete with techniques such as electron microscopy in terms of resolution, but rather offers unique advantages, including the opportunity to take images of samples in an aqueous environment. For a considerable range of resolution and sample thickness the radiation dose in x-ray microscopy is lower than in electron microscopy under the same imaging conditions. To exploit this opportunity a Biological X-ray Microscopy Resource Center will be built at the ALS. An x-ray microscope (XM) and a scanning x-ray microscope (SXM) are to be built. These two microscopes serve complementary needs. The XM gives high quality images at comparably short exposure times, while the SXM is optimized for low radiation dose. High resolution is accomplished in both microscopes with Fresnel zone plate lenses. The SXM produces a diffraction-limited focus point, which is scanned across the sample; therefore the SXM can use only the spatially coherent portion of the radiation. The SXM is best operated on an undulator source with its small phase space. An XM can use the full brightness, including the incoherent fraction of the source. It can be operated with either a bending magnet or an undulator source. The XM can be installed initially at a bending magnet, which can be available at an earlier time, and thus permits the development of diverse biological community at an earlier time. Later this XM can be moved to the undulator, or left at the bending magnet for developmental and less demanding experiments. DOE

N93-30584 Wright Lab., Wright-Patterson AFB, OH.
LOW COST INSTRUMENTATION: PARALLEL PORT ANALOG TO DIGITAL CONVERTER Interim Technical Report, Jul. - Dec. 1992
Matthew P. Dierking Feb. 1993 12 p Limited Reproducibility: More than 20% of this document may be affected by microfiche quality
(AD-A263468; WL-TM-93-102) Avail: CASI HC A03

The personal computer (PC) has become a powerful and cost effective computing platform for use in the laboratory and industry. This Technical Memorandum presents the use of the PC parallel port adapter to implement a low cost analog to digital converter for general purpose instrumentation and automated data acquisition. DTIC

N93-30655# Sandia National Labs., Albuquerque, NM.
THE USE OF DFT WINDOWS IN SIGNAL-TO-NOISE RATIO AND HARMONIC DISTORTION COMPUTATIONS
O. M. Solomon, Jr. 1993 10 p Presented at the Instrumentation and Measurement Technology Conference, Irvine, CA, 18-20 May 1993
(Contract DE-AC04-76DP-00789)
(DE93-009800; SAND-93-0518C; CONF-930577-1) Avail: CASI HC A02/MF A01

The discrete Fourier transform (DFT) is frequently used in the computation of the signal-to-noise ratio (SNR) and harmonic distortion. To estimate the SNR or harmonic distortion, a sine wave is applied to the digitizing system under test. When the data record contains an integer number of cycles of the sine wave, energy from the sine wave and its harmonics does not leak into adjacent DFT frequency bins. Each harmonic occupies one and only one DFT frequency bin. To find the root-mean-square (RMS) value of a harmonic from its DFT, one computes the magnitude of the DFT value at the single frequency of the harmonic. When the DFT's of the fundamental and its harmonics are single lines, the SNR and harmonic distortion are easy to compute. When the data record contains a non-integer number of cycles of the sine wave, energy leaks from the sine wave and its harmonics to adjacent frequencies. The literature contains several approaches to the problem of determining which DFT components correspond to a sine wave harmonic. This paper describes how to estimate the RMS value of a sine wave from its DFT with special attention to the selection of the DFT window. The set of DFT frequencies which comprise a harmonic depends on the DFT window, the length of the DFT, and the number of bits of the digitizer. Criteria are developed for choosing the DFT frequencies that correspond to a sine wave. These criteria lead to better choices of DFT windows for SNR and harmonic distortion calculations. DOE

N93-28743*# Alabama Univ., Huntsville. Dept. of Chemistry.
THE EMULSION CHAMBER TECHNOLOGY EXPERIMENT
John C. Gregory *In* NASA, Washington, NASA/DOD Flight Experiments Technical Interchange Meeting Proceedings 1992 16 p (For primary document see N93-28699 11-12)
Avail: CASI HC A03/MF A10

N93-28765*# Jet Propulsion Lab., California Inst. of Tech., Pasadena.
A MICROSEISMOMETER FOR TERRESTRIAL AND EXTRATERRESTRIAL APPLICATIONS Abstract Only
W. Banerdt, W. Kaiser, and T. VanZandt *In* Lunar and Planetary Inst., Workshop on Advanced Technologies for Planetary Instruments, Part 1 1993 p 1 (For primary document see N93-28764 11-91)
Avail: CASI HC A01/MF A01

N93-28766*# Hughes Danbury Optical Systems, Inc., CT.
THE HYDICE INSTRUMENT DESIGN AND ITS APPLICATION TO PLANETARY INSTRUMENTS Abstract Only
R. Basedow, P. Silverglate, W. Rappoport, R. Rockwell, D. Rosenberg, K. Shu, R. Whittlesey, and E. Zalewski *In* Lunar and Planetary Inst., Workshop on Advanced Technologies for Planetary Instruments, Part 1 1993 p 1 (For primary document see N93-28764 11-91)
Avail: CASI HC A01/MF A01

N93-28767*# National Oceanic and Atmospheric Administration, Boulder, CO. Wave Propagation Lab.
RUGGED, NO-MOVING-PARTS WINDSPEED AND STATIC PRESSURE PROBE DESIGNS FOR MEASUREMENTS IN PLANETARY ATMOSPHERES Abstract Only
A. J. Bedard, Jr. and R. T. Nishiyama (Colorado Univ., Boulder.) *In* Lunar and Planetary Inst., Workshop on Advanced Technologies for Planetary Instruments, Part 1 1993 p 1-2 (For primary document see N93-28764 11-91)
Avail: CASI HC A01/MF A01

N93-28768*# Grumman Aerospace Corp., Bethpage, NY.
DESIGN OF A PARTICLE BEAM SATELLITE SYSTEM FOR LUNAR PROSPECTING Abstract Only
D. H. Berwald and P. Nordin *In* Lunar and Planetary Inst., Workshop on Advanced Technologies for Planetary Instruments, Part 1 1993 p 2 (For primary document see N93-28764 11-91)
(Contract DASG60-90-C-0103)
Avail: CASI HC A01/MF A01

N93-28769*# Los Alamos National Lab., NM. Geology and Geochemistry Group.
LAER-INDUCED BREAKDOWN SPECTROSCOPY INSTRUMENT FOR ELEMENT ANALYSIS OF PLANETARY SURFACES Abstract Only
J. Blacic, D. Pettit, D. Cremers, and N. Roessler (McDonnell-Douglas Electronics Co., Saint Louis, MO.) *In* Lunar and Planetary Inst., Workshop on Advanced Technologies for Planetary Instruments, Part 1 1993 p 2-3 (For primary document see N93-28764 11-91)
Avail: CASI HC A01/MF A01

N93-28771*# Massachusetts Inst. of Tech., Lexington. Lincoln Lab.
HIGH-PERFORMANCE VISIBLE/UV CCD FOCAL PLANE TECHNOLOGY FOR SPACEBASED APPLICATIONS Abstract Only
B. E. Burke, R. W. Mountain, J. A. Gregory, J. C. M. Huang, M. J. Cooper, E. D. Savoye, and B. B. Kosicki *In* Lunar and Planetary Inst., Workshop on Advanced Technologies for Planetary Instruments, Part 1 1993 p 3-4 Sponsored in part by AF (For primary document see N93-28764 11-91)
Avail: CASI HC A01/MF A01

N93-28774*# Jet Propulsion Lab., California Inst. of Tech., Pasadena.
POLARIMETRIC MULTISPECTRAL IMAGING TECHNOLOGY Abstract Only
L.-J. Cheng, T.-H. Chao, M. Dowdy, C. Mahoney, and G. Reyes *In* Lunar and Planetary Inst., Workshop on Advanced Technologies for Planetary Instruments, Part 1 1993 p 4-5 (For primary document see N93-28764 11-91)
Avail: CASI HC A01/MF A01

N93-28775*# National Aeronautics and Space Administration. Langley Research Center, Hampton, VA.
A REMOTE LASER-MASS SPECTROMETER FOR DETERMINATION OF ELEMENTAL COMPOSITION Abstract Only
R. J. DeYoung and W. Situ (Hampton Univ., VA.) *In* Lunar and Planetary Inst., Workshop on Advanced Technologies for Planetary Instruments, Part 1 1993 p 5-6 (For primary document see N93-28764 11-91)
Avail: CASI HC A01/MF A01

N93-28776*# Laboratory for Astrophysics and Space Research, Chicago, IL.
THE APX SPECTROMETER FOR MARTIAN MISSIONS Abstract Only
T. Economou *In* Lunar and Planetary Inst., Workshop on Advanced Technologies for Planetary Instruments, Part 1 1993 p 6-7 (For primary document see N93-28764 11-91)
Avail: CASI HC A01/MF A01

N93-28783*# Terra Systems, Inc., Kailua, HI.
IMAGING SPECTROMETERS USING CONCAVE HOLOGRAPHIC GRATINGS Abstract Only
J. Gradie and S. Wang (SETS Technology, Inc., Mililani, HI.) *In* Lunar and Planetary Inst., Workshop on Advanced Technologies for Planetary Instruments, Part 1 1993 p 9-10 (For primary document see N93-28764 11-91)
Avail: CASI HC A01/MF A01

N93-28794*# Lockheed Missiles and Space Co., Palo Alto, CA. Research Lab.
RESOLUTION-ENHANCED MAPPING SPECTROMETER Abstract Only
J. B. Kumer, J. N. Aubrun, W. J. Rosenberg, and A. E. Roche *In* Lunar and Planetary Inst., Workshop on Advanced Technologies for Planetary Instruments, Part 1 1993 p 14 (For primary document see N93-28764 11-91)
Avail: CASI HC A01/MF A01

N93-28804*# National Aeronautics and Space Administration. Lyndon B. Johnson Space Center, Houston, TX.
SOURCES SOUGHT FOR INNOVATIVE SCIENTIFIC INSTRUMENTATION FOR SCIENTIFIC LUNAR ROVERS Abstract Only
C. Meyer *In* Lunar and Planetary Inst., Workshop on Advanced Technologies for Planetary Instruments, Part 1 1993 p 18 (For primary document see N93-28764 11-91)
Avail: CASI HC A01/MF A01

N93-28817*# Jet Propulsion Lab., California Inst. of Tech., Pasadena.
A LOW-COST, LIGHTWEIGHT, AND MINIATURIZED TIME-OF-FLIGHT MASS SPECTROMETER (TOFMS) Abstract Only
S. K. Srivastava *In* Lunar and Planetary Inst., Workshop on Advanced Technologies for Planetary Instruments, Part 1 1993 p 23 (For primary document see N93-28764 11-91)
Avail: CASI HC A01/MF A01

N93-29592*# Jet Propulsion Lab., California Inst. of Tech., Pasadena.
GRAVITY REFERENCED ELEVATION ENCODER DEVELOPMENT
R. E. Goddard *In its* The Telecommunications and Data Acquisition Report 15 May 1993 p 63-73 (For primary document see N93-29586 11-32)
(RTOP 310-20-65-67)
Avail: CASI HC A03/MF A03

N93-29696*# Jobin et Yvon S.A., Longjumeau (France).
RULED AND HOLOGRAPHIC EXPERIMENT (AO 138-5) Abstract Only
Francis Bonnemason *In* NASA. Langley Research Center, LDEF: 69

Months in Space. Part 4: Second Post-Retrieval Symposium Apr. 1993 p 1401 (For primary document see N93-29682 11-99)
Avail: CASI HC A01/MF A03; 2 functional color pages

N93-29697*# Georgia Inst. of Tech., Atlanta. School of Electrical Engineering.
HOLOGRAPHIC DATA STORAGE CRYSTALS FOR THE LDEF
W. Russell Callen and Thomas K. Gaylord *In* NASA. Langley Research Center, LDEF: 69 Months in Space. Part 4: Second Post-Retrieval Symposium Apr. 1993 p 1403-1411 (For primary document see N93-29682 11-99)
(Contract NAS1-15370)
Avail: CASI HC A02/MF A03; 2 functional color pages

N93-29779*# Kansas Univ. Center for Research, Inc., Lawrence. Dept. of Aerospace Engineering.
SELECTION AND STATIC CALIBRATION OF THE MARSH J1678 PRESSURE GAUGE
Charles R. Oxendine and Howard W. Smith *In its* The Ultra Light Aircraft Testing 1993 32 p (For primary document see N93-29774 11-05)
(Grant NAG1-345)
Avail: CASI HC A03/MF A02

N93-29942# Deutsche Forschungsanstalt fuer Luft- und Raumfahrt, Cologne (Germany). Inst. for Propulsion Technology.
AN L2F-MEASUREMENT DEVICE WITH IMAGE ROTATOR PRISM FOR FLOW VELOCITY ANALYSIS IN ROTATING COOLANT CHANNELS
M. Beversdorff, O. Hein, and R. Schodl *In* AGARD, Heat Transfer and Cooling in Gas Turbines Feb. 1993 7 p (For primary document see N93-29926 11-07)
Copyright Avail: CASI HC A02/MF A04

N93-30232 Ottawa Univ. (Ontario).
TACTILE SENSING FOR 3-DIMENSIONAL SHAPE ESTIMATION
E. Petriu, M. Greenspan, F. Gelinas, W. S. McMath (Canadian Space Agency, Ottawa, Ontario.), and S. K. Yeung (Canadian Space Agency, Ottawa, Ontario.) *In* Engineering Inst. of Canada, Canadian Conference on Electrical and Computer Engineering, Volumes 1 and 2 1990 4 p (For primary document see N93-30215 11-31)
Avail: Engineering Inst. of Canada, 2050 rue Mansfield, Suite 700, Montreal, Quebec H3A 1Z2 Canada

N93-30341 Quebec Univ., Hull.
FIBER-OPTIC POLARIMETRIC STRAIN GAUGE
Wojtek J. Bock and Tomasz R. Wolinski (Warsaw Univ., Poland.) *In* Engineering Inst. of Canada, Canadian Conference on Electrical and Computer Engineering, Volumes 1 and 2 1990 4 p (For primary document see N93-30215 11-31)
Avail: Engineering Inst. of Canada, 2050 rue Mansfield, Suite 700, Montreal, Quebec H3A 1Z2 Canada

N93-30461*# Sony Magnetic Products, Inc., Cypress, CA.
THE NT DIGITAL MICRO TAPE RECORDER
Toshikazu Sasaki, John Alstad, and Mike Younker *In* NASA. Goddard Space Flight Center, Goddard Conference on Mass Storage Systems and Technologies, Volume 1, 1993 p 143-157 (For primary document see N93-30449 11-82)
Avail: CASI HC A03/MF A03

N93-30466*# National Media Lab., Saint Paul, MN.
EVALUATION OF D-1 TAPE AND CASSETTE CHARACTERISTICS: MOISTURE CONTENT OF SONY AND AMPEX D-1 TAPES WHEN DELIVERED
Gary Ashton *In* NASA. Goddard Space Flight Center, Goddard Conference on Mass Storage Systems and Technologies, Volume 1, 1993 p 217-238 (For primary document see N93-30449 11-82)
Avail: CASI HC A03/MF A03

N93-30468*# Penny and Giles Data Recorders Ltd. (England).
THE MODERN HIGH RATE DIGITAL CASSETTE RECORDER
Martin Clemow *In* NASA. Goddard Space Flight Center, Goddard Conference on Mass Storage Systems and Technologies, Volume 1, 1993 p 245-249 (For primary document see N93-30449 11-82)
Avail: CASI HC A03/MF A03

N93-30469*# Laboratoire Central de Recherches Thomson-CSF, Orsay (France).
TOWARDS A 1000 TRACKS DIGITAL TAPE RECORDER
J. M. Coutellier, J. P. Castera, J. Colineau, J. C. Lehureau, F. Maurice (Thomson Consumer Electronics, Illkirch, France.), and C. Hanna (Thomson Consumer Electronics, Illkirch, France.) *In* NASA. Goddard Space Flight Center, Goddard Conference on Mass Storage Systems and Technologies, Volume 1, 1993 p 251-252 (For primary document see N93-30449 11-82)
Avail: CASI HC A01/MF A03

N93-30470*# Datatape, Inc., Pasadena, CA.
EVOLUTION OF A HIGH-PERFORMANCE STORAGE SYSTEM BASED ON MAGNETIC TAPE INSTRUMENTATION RECORDERS
Bruce Peters *In* NASA. Goddard Space Flight Center, Goddard Conference on Mass Storage Systems and Technologies, Volume 1, 1993 p 253-256 (For primary document see N93-30449 11-82)
Avail: CASI HC A01/MF A03

N93-30477*# Digital Equipment Corp., Maynard, MA.
ANALYSIS OF CACHE FOR STREAMING TAPE DRIVE
V. Chinnaswamy *In* NASA. Goddard Space Flight Center, Goddard Conference on Mass Storage Systems and Technologies, Volume 1, 1993 p 299-310 (For primary document see N93-30449 11-82)
Avail: CASI HC A03/MF A03

N93-30479*# Exabyte Corp., Boulder, CO.
OPTIMIZING DIGITAL 8MM DRIVE PERFORMANCE
Gerry Schadegg *In* NASA. Goddard Space Flight Center, Goddard Conference on Mass Storage Systems and Technologies, Volume 1, 1993 p 317-328 (For primary document see N93-30449 11-82)
Avail: CASI HC A03/MF A03

N93-30956*# Tulsa Univ., OK. Dept. of Mechanical Engineering.
A MINIATURE FATIGUE TEST MACHINE
Steven M. Tipton *In* NASA. Langley Research Center, National Educators' Workshop. Update 92: Standard Experiments in Engineering Materials Science and Technology Jun. 1993 p 137-146 (For primary document see N93-30948 11-23)
Avail: CASI HC A02/MF A04

36 LASERS AND MASERS

Includes parametric amplifiers.
For related information see also *76 Solid-State Physics.*

N93-28594# Brookhaven National Lab., Upton, NY.
ULTRAVIOLET FREE ELECTRON LASER FACILITY PRELIMINARY DESIGN REPORT
I. Ben-Zvi, ed. Feb. 1993 458 p
(Contract DE-AC02-76CH-00016)
(DE93-009360; BNL-48565) Avail: CASI HC A20/MF A04

This document, the Preliminary Design Report (PDR) for the Brookhaven Ultraviolet Free Electron Laser (UV FEL) facility, describes all the elements of a facility proposed to meet the needs of a research community which requires ultraviolet sources not currently available as laboratory based lasers. Further, for these experiments, the requisite properties are not extant in either the existing second or upcoming third generation synchrotron light sources. This document is the result of our effort at BNL to identify potential users, determine the requirements of their experiments, and to design a facility which can not only satisfy the existing need, but have adequate flexibility for possible future extensions as need dictates and as evolving technology allows. The PDR is comprised of three volumes. In this, the first volume, background for the development of the proposal is given, including descriptions of the UV FEL facility, and representative examples of the science it was designed to perform. Discussion of the limitations and potential directions for growth are also included. A detailed description of the facility design is then provided, which addresses the accelerator, optical, and experimental systems. Information regarding the conventional construction for the facility is contained in an addendum to volume one (IA). DOE

N93-28614# Technische Univ., Berlin (Germany). Fachbereich Elektrotechnik.
INFLUENCE OF OPTICAL FEEDBACK ON THE PULSE BEHAVIOR OF SEMICONDUCTOR LASERS Ph.D. Thesis [EINFLUSS OPTISCHER RUECKWIRKUNG AUF DAS PULSVERHALTEN VON HALBLEITERLASERN]
Jianmin Wang 1992 132 p In GERMAN
(ETN-93-93798) Avail: CASI HC A07/MF A02

The influence of optical feedback and dispersion on the intensity noise of modulated laser diodes and their effect on optical transmission systems is studied in order to establish if laser diodes can be used in the coherence collapse area to be implemented in pulse code modulation transmission systems. A numerical process was developed to simulate the relative intensity noise of the single mode laser diode, which was shown to be worsened by jitter and overoscillations due to laser diode modulation, which can be reduced with a high relaxation frequency. A similar behavior was observed in the transition to coherence collapse area and it was noticed that at high reflection level the relative intensity noise is so important that jitter and overrelation can be neglected. A model was developed for calculation of laser diode noise on coherence collapse area, so that intensity and frequency noise and line width of laser diodes could be analytically obtained. It was established that relaxation oscillation damping is increased by optical feedback and reflection sensitivity is reduced by growing line width. ESA

N93-28623*# Lightwave Electronics Corp., Mountain View, CA.
ALL SOLID-STATE HIGH POWER VISIBLE LASER Final Report, 22 May 1991 - 22 May 1993
William M. Grossman 16 Jun. 1993 92 p Original contains color illustrations
(Contract NAS7-1145)
(NASA-CR-193163; NAS 1.26:193163) Avail: CASI HC A05/MF A01; 6 functional color pages

The overall objective of this Phase 2 effort was to develop and deliver to NASA a high repetition rate laser-diode-pumped solid-state pulsed laser system with output in the green portion of the spectrum. The laser is for use in data communications, and high efficiency, short pulses, and low timing jitter are important features. A short-pulse 1 micron laser oscillator, a new multi-pass amplifier to boost the infrared power, and a frequency doubler to take the amplified infrared pulsed laser light into the green. This produced 1.5 W of light in the visible at a pulse repetition rate of 20 kHz in the laboratory. The pulses have a full-width at half maximum of near 1 ns. The results of this program are being commercialized. Author (revised)

N93-28653# Harvard Univ., Boston, MA.
LASER SPECTROSCOPY OF HYDROCARBON RADICALS
1993 8 p
(Contract DE-FG02-90ER-14132)
(DE93-012555; DOE/ER-14132/3) Avail: CASI HC A02/MF A01

Several hydrocarbon reactive intermediates (carbenes, biradicals, etc.) were prepared in a supersonic jet expansion. Heats of formation were determined for the isomeric C_3H_2 carbenes. Fits were made to the photoelectron spectra of c-C_3H_2 and c-C_4H_4. Resonant MPI spectra were obtained for allyl radical and its deuterated isotopomers. DOE

N93-28847# California Univ., Berkeley. Lawrence Berkeley Lab.
A TECHNIQUE FOR SINGLE-PULSE SPECTRUM AND PULSE WIDTH MEASUREMENTS FOR AN IR-FEL
W. P. Leemans, J. A. Edighoffer, K. J. Kim, S. Chattopadhyay, and H. A. Schwettman (Stanford Univ., CA.) Aug. 1992 14 p Presented at the 14th International Free Electron Laser Conference, Kobe, Japan, 23-28 Aug. 1992
(Contract DE-AC03-76SF-00098)
(DE93-007732; LBL-32284; ESG-188; CONF-9208142-20) Avail: CASI HC A03/MF A01

A diagnostic system has been designed to measure the spectrum and pulse width of infrared FEL pulses. Use of an image dissector and a single element high speed detector with integrating sphere, allows one to obtain spectral or temporal information for each individual micro-pulse inside the pulse train. The spectral diagnostic consists of a mode matching telescope, a high resolution spectrometer, an imaging telescope, and an image dissector system. The imaging telescope between the spectrograph and the image dissector provides for variable magnification (and hence resolution) of the spectrum onto the image dissector. The pulse width measurement uses single pulse autocorrelation through non-collinear optical mixing in a frequency doubling crystal, an imaging telescope, and again an image dissector system. Here, the imaging telescope relays the image of the region in the nonlinear crystal in which second harmonic light was generated onto the image dissector. The design and implementation of these diagnostics for the 1-11 microns on the IR-FEL at Stanford University are discussed. DOE

N93-28887# Los Alamos National Lab., NM.
SMART SKIN STRUCTURES FOR IDENTIFYING AND LOCATING LASER IRRADIATION
P. C. LaDelfe, R. M. Goeller, and H. S. Murray 1992 11 p Presented at the SPIE 1993 North American Conference on Smart Structures and Materials, Albuquerque, NM, 1-4 Feb. 1992
(Contract W-7405-eng-36)
(DE93-005464; LA-UR-92-4353; CONF-9202154-1) Avail: CASI HC A03/MF A01

A pyramidal arrangement of wavelength-selective optical detectors can be used to determine the identity (wavelength), intensity, and direction-of-arrival of laser irradiation. The advantages of this technique are that only unobtrusive, skin-like structures are required and that large collection areas provide high sensitivity. The disadvantage is that the angular resolution (approximately 5 degrees in a 60 degree field-of-view) is less than that which can be achieved using methods requiring thicker structures. The detector elements are large-area, polyvinylidine fluoride, pyroelectric devices with wavelength selective coatings. Four identical arrays of these elements are situated on the top and sides of a frustrated, three-sided prism. Since only the relative orientations are significant, these faces can be selected regions on the surface of an existing structure. We first describe the construction of the detectors and the system, then develop the mathematical description of the system. Using coated detectors whose performance has been experimentally verified, we will model the response to in-channel, monochromatic irradiation and then describe the data analysis algorithm. Although we will limit our model to a simple, two-channel system, the concept and algorithm can easily be extended to a system of any reasonable number of nonoverlapping channels. DOE

N93-28980# National Inst. for Fusion Science, Nagoya (Japan).
DEVELOPMENT OF HIGH POWER MICROWAVE SOURCE
Shoichi Ono (Tohoku Univ., Sendai, Japan.) Apr. 1992 42 p
(DE93-753316; NIFS-MEMO-6) Avail: CASI HC A03/MF A01

To achieve thermonuclear fusion it is inevitable to develop high power microwave and millimeter wave sources for plasma heating. In 1990, working group was organized as a collaboration study in National Institute for Fusion Science to review the present status of development on high microwave source. The review of development on high power klystron and gyrotron, FEL and microwave power source by REB is reported. Development of high power klystron is almost finished except for cooling of the window, cavity, and collector. As for the gyrotron oscillating with the whispering gallery mode, one must overcome the same problem for CW operation. In the quasi-optical gyrotron, there is no special progress for increasing the frequency and efficiency. Though the experimental evidence on autoresonance in the development of peniotron is performed, output power and frequency is much smaller than that of the gyrotron. It is difficult to increase in the pulse width of FEL having giant power of GW level with several ten ns and the utilization for plasma heating is limited. In addition, microwave and millimeter wave oscillators with high power which are running in the laboratories and the institutes are summarized. DOE

N93-29097# Lawrence Livermore National Lab., CA.
DESIGN OF THE NOVA UPGRADE LASER SYSTEM FOR IGNITION FUSION EXPERIMENTS
E. M. Campbell Oct. 1992 5 p Presented at the 14th International Conference on Plasma Physics and Controlled Nuclear Fusion Research,

Wurzburg, Germany, Oct. 1992
(Contract W-7405-eng-48)
(DE93-009077; UCRL-JC-109893; CONF-9210315-2) Avail: CASI HC
A01/MF A01

A 1-2 Mj, 500 TW 0.35 micron solid state laser has been proposed to demonstrate the scientific feasibility of ICF at laboratory scale for national security applications and to develop ICF technology and science for long term commercial electric power generation and for basic scientific applications. In this paper, we describe the design of this facility, designated by LLNL as the Nova Upgrade. This facility consists of a frequency converted neodymium-doped glass laser utilizing advanced optical components and a cost effective multipass architecture and a target area capable of safely containing TN fusion yields up to 45 MJ. DOE

N93-29098# Lawrence Livermore National Lab., CA.
HIGH-EFFICIENCY HIGH-RELIABILITY OPTICAL COMPONENTS FOR A LARGE, HIGH-AVERAGE-POWER VISIBLE LASER SYSTEM
J. R. Taylor and C. J. Stolz 29 Dec. 1992 13 p Presented at the International Symposium on Advanced Electronic and Optoelectronic Materials, Los Angeles, CA, 20-23 Jan. 1993
(Contract W-7405-eng-48)
(DE93-009225; UCRL-JC-112499; CONF-930135-2) Avail: CASI HC
A03/MF A01

Laser system performance and reliability depends on the related performance and reliability of the optical components which define the cavity and transport subsystems. High-average-power and long transport lengths impose specific requirements on component performance. The complexity of the manufacturing process for optical components requires a high degree of process control and verification. Qualification has proven effective in ensuring confidence in the procurement process for these optical components. Issues related to component reliability have been studied and provide useful information to better understand the long term performance and reliability of the laser system. DOE

N93-29104# Lawrence Livermore National Lab., CA.
DEVELOPMENT OF COHERENT X RAY LASERS
R. A. London Dec. 1992 24 p Presented at the Meeting of the Division of Plasma Physics of the American Physical Society, Seattle, WA, 16-20 Nov. 1992
(Contract W-7405-eng-48)
(DE93-009288; UCRL-JC-105899; CONF-921103-8) Avail: CASI HC
A03/MF A01

Proposed x-ray laser applications such as interferometry and holography require coherent radiation. The fact that x-ray laser media are short-lived, high-temperature plasmas leads to very different coherence properties from those of ordinary lasers. Research aimed at developing theoretical models and experimentally characterizing and improving x-ray laser coherence is discussed. Longitudinal coherence is already sufficient for several applications due to the narrow linewidths. However, transverse coherence is estimated to be poor for most current x-ray lasers. To quantify these estimates and to design better lasers, both wave and geometric optics propagation and coherence theories have been developed. These theories and resulting predictions of the coherence length are presented and compared. Measurements of x-ray laser beampatterns and coherence lengths are presented and compared to detailed theoretical simulations. Designs for more coherent lasers are given. DOE

N93-29180# Sandia National Labs., Albuquerque, NM.
LOW-PUMP-RATE MULTI-MILLISECOND ATOMIC XENON LASER
E. L. Patterson and G. E. Samlin Feb. 1993 26 p
(Contract DE-AC04-76DP-00789)
(DE93-011484; SAND-93-0057) Avail: CASI HC A03/MF A01

Characteristics of a long pulse, low-pump rate, atomic xenon (Xe I) laser are described. Energy loading up to 170 mJ/cc at pulse widths between 5 and 55 ms is achieved with an electron beam in transverse geometry. The small-signal gain coefficient, loss coefficient, and saturation intensity are inferred from a modified Rigrod analysis. For pump rates between 12 and 42 W/cc the small-signal gain coefficient varies between 0.64 and 0.91%/cm, the loss coefficient varies between 0.027 and 0.088%/cm, and the saturation intensity varies between 61 and 381 W/cm(sup 2). Laser energy as a function of pulse width and the effects of air and CO2 impurities are described. The intrinsic laser energy efficiency has a maximum at a pulse width of 10 ms corresponding to a pump rate of 1.6 W/cc. No maximum is observed in the intrinsic power efficiency. A drastic reduction of laser output power is observed for impurity concentrations of greater than (approx)0.01%. An investigation of the dominant laser wavelength in a high Q cavity indicates that the 2.6-(mu)m radiation dominates. A comparison of dominant wavelength with reactor pumped results indicates good agreement when the same cavity optics are used. DOE

N93-29207# Lawrence Livermore National Lab., CA.
EFFECTS OF VACUUM EXPOSURE ON STRESS AND SPECTRAL SHIFT OF HIGH REFLECTIVE COATINGS
C. J. Stolz, J. R. Taylor, W. K. Eickelberg, and J. D. Lindh Jun. 1992 23 p Presented at the 5th Topical Meeting on Optical Interference Coating, Tucson, AZ, 1-5 Jun. 1992
(Contract W-7405-eng-48)
(DE93-009318; UCRL-JC-109480; CONF-9206138-2) Avail: CASI HC
A03/MF A01

The Atomic Vapor Laser Isotope Laser Separation (AVLIS) program operates the world's largest average power dye laser; the dye laser beams are combined, formatted, and transported in vacuum. The optical system is aligned at atmosphere, while the system must meet requirements in vacuum. Therefore, coating performance must be characterized in both atmosphere and vacuum. Changes in stress and spectral shift in ambient and vacuum environments are reported for conventional and dense multilayer dielectric coatings. DOE

N93-29264# Sandia National Labs., Albuquerque, NM.
COMPUTATIONAL SIMULATIONS OF A SOFT X RAY PROJECTION LITHOGRAPHY LASER PLASMA SOURCE
R. E. Olson, W. C. Sweatt, and P. D. Rockett 1993 4 p Presented at the Optical Society of America (OSA) Topical Meeting on Soft X Ray Projection Lithography, Monterey, CA, 10-12 May 1993
(Contract DE-AC04-76DP-00789)
(DE93-009625; SAND-93-0211C; CONF-9305159-1) Avail: CASI HC
A01/MF A01

A Sandia National Laboratories/AT&T Bell Laboratories Team is developing a soft x-ray projection lithography tool that uses a compact laser plasma as a source of 14 nm x-rays. Optimization of the 14 nm x-rays source brightness is a key issue in this research. This paper describes our understanding of the source as it has been obtained through the use of computer simulations utilizing the LASNEX radiation-hydrodynamics code. DOE

N93-29276 Department of the Navy, Washington, DC.
METHOD OF EMITTING ON A SPECIFIC WAVELENGTH FRAUNHOFER LINE USING A NEODYMIUM DOPED LASER TRANSMITTER Patent
Victor L. Moberg, inventor (to Navy) 19 Jan. 1993 14 p Filed 31 Dec. 1991
(AD-D015710; US-Patent-5,181,212; US-Patent-Appl-SN-816514;
US-Patent-Class-372-22) Avail: US Patent and Trademark Office

A method of emitting on a specific wavelength Fraunhofer line of peak seawater transmission and minimum solar radiation is disclosed. This method includes the steps of emitting at least on a specific wavelength of an infrared transition line from a neodymium gain element in an optical resonator; frequency tripling the infrared line from the resonator to a specific ultraviolet wavelength in a frequency multiplier; and Raman down shifting the specific ultraviolet wavelength a predetermined degree by a predetermined number of Stokes shifts in a predetermined medium in a Raman shifter to produce a high peak-power output at the specific wavelength Fraunhofer line. DTIC

N93-29277 Department of the Navy, Washington, DC.
ND LASER WITH CO-DOPED ION(S) PUMPED BY VISIBLE LASER DIODES Patent
Richard Scheps, inventor (to Navy) 6 Apr. 1993 11 p Filed 17 Jun. 1991
(AD-D015711; US-Patent-5,200,972; US-Patent-Appl-SN-718316;
US-Patent-Class-372-69) Avail: US Patent and Trademark Office

The 1.06 microns Nd transition in a co-doped Cr,Nd:Gd3Sc2Ga3O12 (Cr,Nd:GSGG) gain element is obtained by diode pumping Cr(3+) at 670 run and produces efficient, low threshold laser operation. Although co-doped

Cr,Nd:GSGG was developed for more efficient flashlamp pumping, it has the desirable property of having an extraordinarily broad absorption to allow for efficient diode pumping relative to the ND:YAG laser. The consequent broad bandwidth tolerance of the Cr,Nd:GSGG for the diode pumping radiation allows diode pumping of the 1.06 microns transition without regard to the wavelength of the visible diodes which has the potential for reducing the cost of the semiconductor pump and also demonstrates the extended versatility of these diodes which previously had been restricted to pump the Cr(3+) tunable vibronic lasers. CW and long pulse diode pumping provided pump power levels as high as 300 mW CW and 1 W pulsed. The lowest threshold power was measured at 938 micron W and the highest output power was obtained at 43 mW CW and 173 mW pulsed. The best slope efficiency obtained was 42.1%, 78% of the theoretical maximum. Loss measurements indicate a value of 0.4%/cm. DTIC

N93-29287 Department of the Navy, Washington, DC.
LASER RADIATION DETECTION SYSTEM Patent
Keith L. Gardner, inventor (to Navy) 27 Apr. 1993 5 p Filed 21 Oct. 1976
(AD-D015724; US-Patent-5,206,502; US-Patent-Appl-SN-735471; US-Patent-Class-250-226) Avail: US Patent and Trademark Office

This invention pertains to a laser radiation detection system using a spatial/wavelength filter to modulate the response of a detector as a function of wavelength, allowing discrimination of laser sources against broad spectral sources, as well as wavelength determination. DTIC

N93-29309# Lawrence Livermore National Lab., CA.
INNER-SHELL PHOTO-IONIZED X RAY LASER SCHEMES
G. L. Strobel, D. C. Eder, R. A. London, M. D. Rosen, R. W. Falcone (California Univ., Berkeley.), and S. P. Gordon (California Univ., Berkeley.) Jan. 1993 14 p Presented at the OE/LASE 1993: International Society for Optical Engineering (SPIE) Conference, Los Angeles, CA, 16-23 Jan. 1993
(Contract W-7405-eng-48)
(DE93-009285; UCRL-JC-110956; CONF-930159-19) Avail: CASI HC A03/MF A01

Current x-ray lasers operate in the 35 to 500 A wavelength regimes with 21.5 A being the limit for the successful collisional excitation approach using Nickel-like ions. In this paper, we discuss an x-ray laser scheme in the 5 to 15 A regime. The scheme uses an ultra-short (100 fsec FWHM) intense (10(exp 17) Watts/sq cm) laser pulse to produce a hot plasma at a laser line focus. This plasma serves as an x-ray source that photo-ionizes the K shell of a nearby concentration of lasant atoms. This produces a population inversion, and resulting positive gain for an allowed 2p-1s radiative transition in the singly charged ion. This x-ray laser scheme has been studied for a number of years with some recent work by Kapteyn. There are three major differences between this work and that of Kapteyn. First, a two temperature black body is used in the kinetic calculation to model the ionizing spectrum as compared to a single temperature model Second, the modeled spectrum is obtained directly from simulations of the x-ray source using a target material with x-ray spectra matched to the particular lasant material. Third, the effect of excitation in hydrogen, which is added to the lasant material to slow down energetic electrons, is included in addition to the effect of ionization of hydrogen discussed by Kapteyn. DOE

N93-29395# Krug Life Sciences, Inc., San Antonio, TX.
OPERATING MANUAL FOR SINGLE-SHOT AUTOCORRELATOR Final Technical Report, Jan. - Jun. 1992
Clarence P. Cain and Gary D. Noojin Jan. 1993 30 p
(Contract F33615-88-C-0631)
(AD-A262016; AL-TR-1992-0113) Avail: CASI HC A03/MF A01

Special instrumentation is required to measure and analyze laser pulses below one nanosecond because of the limitations of standard instrumentation used to measure real-time signals. We have designed and developed an instrument with unique features to measure the pulsewidth of single laser pulses below one nanosecond using the standard autocorrelation technique. A single laser pulse is divided into two equal pulses by a 50/50 beamsplitter and recombined in space and in time inside a wafer of KDP crystal which generates a second harmonic of the combined pulses. These three pulses are then focused on a charge-coupled device (CCD) camera and analyzed by a laser beam analyzer to yield information on the FWHM (full-width-half-maximum) time of the original pulse. By using a CCD camera, the full two-dimensional image can be recorded to insure that the correct horizontal profile is analyzed within the vertical profile. The delay for overlapping the beams in time is obtained by translating the beamsplitter while the positioning is obtained by rotating the beamsplitter. The design and results are discussed. DTIC

N93-29781# Lawrence Livermore National Lab., CA.
PROBLEMS IN THE IMPLEMENTATION OF X RAY OPTICS WITH X RAY LASERS
B. J. MacGowan, S. Mrowka, T. W. Barbee, Jr., L. B. DaSilva, D. C. Eder, J. A. Koch, and J. H. Underwood (California Univ., Berkeley. Lawrence Berkeley Lab.) 22 Jul. 1992 8 p Presented at the 3rd International Colloquium on X Ray Lasers, Schliersee, Germany, 18-22 May 1992
(Contract W-7405-eng-48)
(DE93-009297; UCRL-JC-111376; CONF-920523-8) Avail: CASI HC A02/MF A01

When using multilayer mirrors in x-ray laser cavities, damage from intense optical and x-ray pulses, is a major problem. X-ray damage to WC-/C and Cr3C2/C multilayer mirrors has been studied using short pulses (500 psec) of soft x-rays from a laser produced plasma. The effect of damage on the mirror reflectivity and position and shape of the bandpass were resolved temporally and spectrally. Simulations of the behavior of the mirrors are found to be broadly consistent with the observed damage thresholds. DOE

N93-29789# Naval Postgraduate School, Monterey, CA.
INVESTIGATIONS OF SELF-PUMPED PHASE CONJUGATE LASER BEAMS AND COHERENCE LENGTH M.S. Thesis
George M. Sutton Mar. 1993 54 p
(AD-A263438) Avail: CASI HC A04/MF A01

The phase conjugation process by a nonlinear, photorefractive crystal is not completely ideal and losses should be expected to occur after a beam is conjugated. This thesis research investigates possible changes in coherence length as a result of internal losses in barium titanate (BaTiO3). Additionally, laser reflections from a corner cube reflector is also examined for changes in coherence length. Experimental findings are inconclusive because the conventional spectrometer used to measure coherence length did not possess the required resolution. It is recommended that an interferometer which can resolve the laser line width be utilized for future coherence length measurements, together with a means of blocking the conjugated beam from entering the laser cavity and destabilizing the oscillations within. DTIC

N93-29797# Air Force Systems Command, Wright-Patterson AFB, OH. Foreign Aerospace Science and Technology Center.
CONSTRUCTION AND OPERATION OF A GAS TRANSPORT CO2 LASER
I. Gutu, M. V. Udrea, D. Dumitras, and V. Draganescu 2 Apr. 1993 10 p Transl. into ENGLISH from Zhongguo Jiguang (China), v. 12, no. 9, 1985 p 518-520
(AD-A263102; FASTC-ID(RS)T-0307-92) Avail: CASI HC A02/MF A01

The construction and operation of a CO2 gas transport laser with cylindrical geometry is presented. This work aims at small size and light weight gas transport laser at high output level. This has been accomplished by a single metallic cylinder for electric discharge, recirculation and the cooling of the gas mixture. More than 1kW laser power was obtained from a laser of the length of 1.45m, diameter 0.54m and cca weight 180 kg. Typical parameters were: pressure 40 Torr, CO2:N2:He = 1:8:11, discharge current 8 A, efficiency 12%, and laser spot 28 x 22mm sq. DTIC

N93-29800# Army Missile Command, Redstone Arsenal, AL. Weapons Science Directorate.
SELECTIVE NITRATIONS. VOLUME 2: THE LASER-INDUCED NITRATION OF THREE CYCLOALKANES Final Technical Report, Jul. 1991 - Sep. 1992
Ann E. Stanley, Judith M. Bonicamp, Susan E. Godbey, and Larry M. Ludwick Mar. 1993 99 p
(AD-A263250; AD-E952001; AMSMI/TR-RD-WS-93-1) Avail: CASI HC A05/MF A02

The army uses nitrated compounds as explosives and propellants.

There is a special need for propellants with the chemical composition necessary to burn exactly with high energy production, but with a minimum of side products which create smoke. Laser-induced chemistry possesses the potential to drive some reactions in an efficient and selective manner, and may be useful in driving nitration reactions toward specific products. Reported here are the results of several successful attempts to laser-induce the reactions of nitrogen oxides with three cycloalkanes. Specifically, the tunable, continuous wave, carbon dioxide infrared laser was used to drive the reaction between the nitrogen dioxide and cyclopropane, cyclobutane, and cyclopentane under a variety of reaction conditions. The spectrochemical analyses of the product mixtures are presented here. In addition to nitrocycloalkanes, other products resulting were either from ring cleavage, or from nitration or oxidation of ring fragments. By examining the effects of various reaction conditions on the product arrays, it was possible to find optimum conditions for producing the nitrocycloalkanes while minimizing side products. Author (DTIC)

N93-29827# Wright Lab., Wright-Patterson AFB, OH.
ATMOSPHERIC TRANSVERSE COHERENCE LENGTH MEASUREMENT SYSTEM FOR LASER COMMUNICATIONS Final Report, 1 Sep. 1989 - 31 Jul. 1992
Gary D. Wilkins Feb. 1993 54 p
(AF Proj. ILI-R)
(AD-A263563; WL-TR-93-1023) Avail: CASI HC A04/MF A01

This paper summarizes the Wright Laboratory In-House Laboratory Independent Research (ILIR) conducted to determine the feasibility of using inherent information, such as angle-of-arrival fluctuations of incident radiation and spreading of the focused spot size, obtained through the measurement of the diffraction limited aperture of the atmosphere, to adaptively optimize laser communications system parameters. DTIC

N93-29853# Duke Univ., Durham, NC.
HIGH RESOLUTION FREE-ELECTRON LASER SPECTROSCOPY Ph.D. Thesis Final Technical Report, 1 Jun. 1988 - 30 Sep. 1991
John M. Madey and Eric B. Szarmes 23 Mar. 1993 155 p
(Contract DAAL03-88-K-0109)
(AD-A263734; ARO-25349.1-PH) Avail: CASI HC A08/MF A02

High peak power infrared pulses as short as 350 femtoseconds were generated using the MK 3 FEL. Small signal analyses were developed for operating the FEL with electron pulses whose energy varies linearly with time. Chirped-pulse simulations using modest energy chirps have demonstrated a x15 compression ratio at saturated power levels for 3.4 ps optical pulses at 3.35 microns, and coupled pulse simulations have indicated substantial longitudinal mode reduction on microsecond time scales. A Michelson mirror resonator was operated for the first time on the MK 3 FEL, along with phase-locked operation using a beamsplitter reflectance of only 1.4%. DTIC

N93-29867# Naval Postgraduate School, Monterey, CA.
MAGNETIC FIELD MEASUREMENTS OF THE CEBAF (NIST) WIGGLER USING THE PULSED WIRE METHOD M.S. Thesis
Stephen M. Wallace Sep. 1992 51 p
(AD-A263997) Avail: CASI HC A04/MF A01

The Free Electron Laser (FEL) has proven to be a versatile photon source for many applications in science, industry, and defense. It is capable of providing wide tunability and high efficiency, but has yet to yield high average power required as a weapon system. The proposed infrared and ultraviolet FELs at the Continuous Electron Beam Accelerator Facility (CEBAF) have been projected to provide high average power. The first section of this thesis will study the necessity of a FEL for shipboard defense, and state the advantages over other defense systems. The remainder will focus on use of the pulsed wire method for measuring the magnetic field errors of the CEBAF/National Institute of Science and Technology (NIST) wiggler. Data analysis indicates the wiggler will have a net electron beam deflection of x = 5.2 mm, which is much greater than the electron beam radius of re = 0.4 mm and the optical mode waist of wo = 1 mm. DTIC

N93-29883# Naval Postgraduate School, Monterey, CA. Dept. of Mathematics.
NONLINEAR MODE COUPLING IN FREE ELECTRON LASERS Technical Report, Jan. - Mar. 1993
C. L. Frenzen 11 Mar. 1993 18 p
(AD-A263999; NPS-MA-93-012) Avail: CASI HC A03/MF A01

The optical field in free electron lasers can sometimes develop sidebands and exhibit very complex behavior. The purpose of this report is to develop a two mode model of the optical field in a free electron laser in which the optical modes are coupled by the free electrons in the laser. This model may be used to study the long term stability of the optical wave and the development of sidebands in the optical field. In this report, the equations of motion governing the interaction of an electron with the optical modes will be derived. DTIC

N93-29918# IBM Federal Systems Div., Yorktown Heights, NY.
FEMTOSECOND LASER STUDIES OF EXCITED STATE DYNAMICS Final Report, 1 Jun. 1990 - 31 Mar. 1993
Peter P. Sorokin and J. H. Glownia Mar. 1993 15 p
(Contract DAAL03-90-C-0006)
(AD-A263708; ARO-27508.9-PH) Avail: CASI HC A03/MF A01

Considerable progress has been made in the two main (and interrelated) areas in which the recent research has been focussed. These are (1) the development of novel, intense, femtosecond time-scale, VUV laser sources, and (2) the development of femtosecond time-scale, transition-state absorption spectroscopy of photodissociating gas-phase molecules. In both of these areas, some trails have been blazed that will undoubtedly soon be followed by others. A third area of investigation was to examine the possibility of two-photon amplification in the molecular system diphenyl hexatriene (DPH). Here the critical experiment still remains to be done. However, researchers were able to show that DPH does satisfy one stringent requirement for a potential two-photon amplifying system, namely, that it be completely stable against one-photon lasing under conditions of very heavy optical pumping. DTIC

N93-29983# Arizona Univ., Tucson. Optical Sciences Center.
NONEQUILIBRIUM SCREENING AND EXCITON DYNAMICS PROBED BY FEMTOSECOND LASER PULSES Final Report, 15 May 1989 - 14 Nov. 1992
N. Peyghambarian and S. W. Koch 15 Feb. 1993 74 p
(Contract DAAL03-89-K-0100)
(AD-A263603; ARO-26974.15-PH) Avail: CASI HC A04/MF A01

Our efforts were aimed at the study of nonequilibrium properties of a high-density electron-hole-pair system, which was generated resonantly by femtosecond laser excitation. The investigation consisted of joint theoretical and experimental approaches. Using state of the art femtosecond experimental techniques, we studied extremely rapid physical phenomena. We have succeeded not only in completing the proposed tasks, but have also initiated some new projects and obtained very interesting results. During the last three years in this program, we have published three physical Review Letters, nine Physical Reviews, several other papers in good journals such as Appl. Phys. Lett., J. Opt. Soc. Am., etc., nineteen invited presentations at important conferences, and several contributed papers at international conferences. The list of publications is given in the next section. Here, we summarize the highlights of our achievements during the last three years of this contract. DTIC

N93-30186# Wisconsin Univ., Madison. Fusion Technology Inst.
SIRIUS-P: AN INERTIALLY CONFINED DIRECT DRIVE LASER FUSION POWER REACTOR
I. N. Sviatoslavsky, G. L. Kulcinski, G. A. Moses, D. Bruggink, R. L. Engelstad, H. Y. Khater, E. M. Larsen, E. G. Lovell, J. J. MacFarlane, and E. A. Mogahed et al Mar. 1993 297 p
(Contract DE-AS03-88DP-10754)
(DE93-012433; DOE/DP-10754/1) Avail: CASI HC A13/MF A03

The SIRIUS-P conceptual design study is of a 1000 MWe laser driven inertial confinement fusion power reactor utilizing near symmetric illumination of direct drive targets. The reference driver is a KrF laser; however, any other laser capable of delivering short wavelength energy can be substituted. Sixty beams providing a total of 3.4 MJ of energy are used at a repetition rate of 6.7 Hz and a target gain of 118. The spherical chamber has an internal diameter of 6.5 m and consists of two independent components, a first wall assembly fabricated from a c/c composite and a blanket assembly made of SiC. First wall protection is provided by a xenon buffer gas at a pressure of 0.5 torr. The chamber is cooled by a flowing granular bed of solid ceramic material, TiO2 for the first wall assembly and Li2O for the blanket assembly. The chamber is housed within a 42 m radius cylindrical reactor building which is 86 m high and which shares the same vacuum space as the chamber. All the laser beams are brought in at the bottom of the building, first onto a dielectrically coated final focusing mirror and finally onto a metallic grazing incidence mirror which reflects them into the chamber through beam ports open to the building. Neutron traps behind the grazing incidence mirrors are used to prolong the lifetimes of the final focusing optics. The nominal cost of electricity from this system is 65 mills/kwh assuming an 8% interest rate on capital. DOE

N93-30394# Lawrence Livermore National Lab., CA.

HIGH-REPETITION RATE X RAY LASERS AND APPLICATIONS

D. C. Eder, P. Amendt, C. B. Dane, L. B. DaSilva, L. A. Hackel, M. R. Hermann, R. A. London, B. J. MacGowan, D. L. Matthews, and M. D. Rosen et al Feb. 1993 6 p Presented at the 1992 International Conference on Lasers, Houston, TX, 7-11 Dec. 1992
(Contract W-7405-eng-48)
(DE93-011882; UCRL-JC-110878; CONF-921256-3) Avail: CASI HC A02/MF A01

The unique attributes of high repetition rate x-ray lasers can aid in the understanding of the structure and chemistry of free clusters, dynamical processes such as chemical reactions in surface layers, and general material properties studied with pump/probe techniques. Standard x-ray sources such as synchrotrons and laser plasmas are inadequate in many situations because of the quasi-continuous temporal output property of synchrotrons and the large bandwidth associated with plasma sources. Two approaches to achieving high repetition rate x-ray lasers are presented. The first utilizes conventional x-ray lasers combined with new high repetition rate optical drivers. The second is based on rapid recombination following field ionization of a plasma by a high-intensity short-pulse driving laser. Applications appropriate for each of these approaches are discussed. DOE

N93-30401# Stanford Univ., CA. Edward L Ginzton Lab. of Physics.

RESEARCH STUDIES ON SHORT WAVELENGTH BY SELECTIVE AUGER PROCESSES Final Technical Report

S. E. Harris Jan. 1993 10 p
(Contract N00014-87-K-2016)
(AD-A264493) Avail: CASI HC A02/MF A01

Efforts are divided into two areas: (1) development of short wavelength coherent sources, and (2) studies of lasers without inversion. In the first area, gain in the vacuum ultraviolet (VUV) and extreme ultraviolet (XUV) was observed in Xe, Zn, Kr, Cs, and H2 gases. Methods for saturating the laser transitions in Xe and Cs were developed and produced microjoule level fully saturated outputs at 109 nm and 96.9 nm, respectively. Efforts to construct the next generation laser driver for such studies were also completed during this time period. In the second area, theoretical studies of different methods for creating transparency in atomic vapors were explored. Various applications of these transparencies were investigated, including the possibility of systems which would exhibit laser gain without the necessity for population inversion and the enhancement of nonlinear optical processes in the presence of such a transparency. Experiments demonstrated enhanced sum-frequency generation of 104.8-nm radiation with a naturally occurring transparency in Zn vapor. DTIC

N93-30415*# National Aeronautics and Space Administration. Pasadena Office, CA.

TUNABLE CW DIODE-PUMPED Tm,Ho:YLiF4 LASER OPERATING AT OR NEAR ROOM TEMPERATURE Patent Application

Brendan T. McGuckin, inventor (to NASA) (Jet Propulsion Lab., California Inst. of Tech., Pasadena.) and Robert T. Menzies, inventor (to NASA) (Jet Propulsion Lab., California Inst. of Tech., Pasadena.) 30 Mar. 1993 29 p
(Contract NAS7-918)
(NASA-Case-NPO-18611-1-CU; NAS 1.71:NPO-18611-1-CU; US-Patent-Appl-SN-044668) Avail: CASI HC A03/MF A01

A conversion efficiency of 42 percent and slope efficiency of 60 percent relative to absorbed pump power are obtained from a continuous wave diode-pumped Tm,Ho:YLiF4 laser at 2 microns with output power of 84mW at a crystal temperature of 275K. The emission spectrum is etalon tunable over a range of 7nm (16.3 cm(sup -1) centered on 2.067 microns with fine tuning capability of the transition frequency with crystal temperature at a measured rate of -0.03/(cm)K. The effective emission cross-section is measured to be 5 x 10(sup -21) cm squared. These and other aspects of the laser performance are disclosed in the context of calculated atmospheric absorption characteristics in this spectral region and potential use in remote sensing applications. Single frequency output and frequency stabilization are achieved using an intracavity etalon in conjunction with an external reference etalon. NASA

N93-30427# Department of the Navy, Washington, DC.

HOLMIUM QUASI-TWO LEVEL LASER Patent Application

Steven R. Bowman, inventor (to Navy) and Barry J. Feldman, inventor (to Navy) 30 Dec. 1992 33 p
(AD-D015706; US-Patent-Appl-SN-998347; Navy-Case-74205) Avail: CASI HC A03/MF A01

According to the invention, a directly pumped holmium quasi-two level laser is provided which affords a number of important advantage over sensitized holmium lasers. These advantages include reducing the thermal loading of the laser medium, reducing the upconversion losses, increasing the short pulse extraction efficiency, reducing the sensitivity of the gain provided to temperature effects, and increasing the flexibility in the selection of holmium ion concentrations and holmium host materials. In accordance with the invention, a laser system or device is provided which comprises a holmium laser having an output wavelength of 2.1 micrometers and a further, pumping laser having an output wavelength of 2.0 micrometers for directly pumping the holmium laser. DTIC

N93-30530# California Univ., Berkeley. Lawrence Berkeley Lab.

EXPERIMENTAL TEST OF HOLE-COUPLED FEL RESONATOR DESIGNS USING A CW-HeNe LASER

W. P. Leemans, E. W. Wallace, M. Xie, and K. J. Kim Jan. 1993 8 p Presented at the OE/LASE 1993 International Society for Optical Engineering Conference, Los Angeles, CA, 16-23 Jan. 1993
(Contract DE-AC03-76SF-00098)
(DE93-010439; LBL-33603; ESG-246; CONF-930159-20) Avail: CASI HC A02/MF A01

We report on ongoing experiments and simulations which model the performance of hole-coupled resonators. We have previously studied a hole-coupled resonator which was well inside the stable region (stability parameter g = -0.8). In the far field, good agreement between experiment and simulation was obtained for both the intracavity and outcoupled mode-profile. The present study involves a resonator with a stability parameter of -0.987, identical to the stability parameter of the proposed Infrared Free Electron Laser (IRFEL) at Lawrence Berkeley Laboratory. The experiments were carried out with a frequency stabilized CW-HeNe laser beam at a wavelength of 632.8 nm. Both intracavity and outcoupled mode profiles and power levels were measured. The simulations were done using the code HOLD, which is based on the Fresnel approximation for the Huygens kernel. Within the experimental uncertainties, magnified due to the 1/(1+g) dependence of the mode characteristics on errors in measured resonator parameters, we have obtained fair agreement between experiment and simulation. DOE

N93-30553# Naval Command, Control and Ocean Surveillance Center, San Diego, CA.

UPLINK LASER PROPAGATION MEASUREMENTS THROUGH THE SEA SURFACE, HAZE AND CLOUDS

G. T. Kaye, Roger Nies, and Michael Lovern Mar. 1993 14 p
(AD-A264687) Avail: CASI HC A03/MF A01

An Airborne Optical Receiver (AOR) was developed and tested to investigate the propagation and reception of optical communications uplinks from a submerged laser source to an overflying fleet aircraft. The AOR was flown in a P-3C Orion aircraft for an at-sea test off the southern California coast in August, 1990. A green laser transmitter was suspended from the Research Platform FLIP at depths of 15 to 45 m. During six nights of operations, the AOR received the laser light at various test geometries and through clear and cloudy conditions. This represents the first optical uplink cloud experiment at visible wavelengths. Results show that optical pulses in clouds are significantly more forward-scattered than modeled. The results can be explained by Mie scattering theory. Measured cloud attenuation and pulse stretching agreed with an existing optical propagation model. Significant attenuation and signal spreading due to haze and fog was measured and compared with theory. DTIC

N93-30587# Department of the Navy, Washington, DC.
INTRACAVITY-PUMPED 2.1 MICROMETER Ho(3+): YAG LASER Patent Application
Leon Esterowitz, inventor (to Navy) and Robert S. Stoneman, inventor (to Navy) 30 Dec. 1992 23 p
(AD-D015728; US-Patent-Appl-SN-998348; Navy-Case-74075) Avail: CASI HC A03/MF A01

In a preferred embodiment, a Tm(3+):YAG laser crystal and a Ho(3+):YAG laser crystal are placed within a reflective path of a laser cavity for intracavity pumping the Ho(3+):YAG laser crystal. The Tm(3+):YAG laser crystal emits a substantially 2.0 micrometers laser emission after being resonantly end-pumped by a pump beam at a wavelength of about 785 nm and the substantially 2.0 micrometers laser emission is used to pump the Ho(3+): YAG laser crystal. The intracavity-pumped Ho(3+):YAG laser crystal emits an output laser emission at substantially 2.1 micrometers. The slope efficiency of the Ho(3+):YAG laser crystal output power is about 40% of the pump power absorbed by the Tm(3+):YAG laser crystal. DTIC

N93-30599# Naval Command, Control and Ocean Surveillance Center, San Diego, CA.
LASER BASED 3D VOLUMETRIC DISPLAY SYSTEM
Parviz Soltan, John Trias, Waldo Robinson, and Weldon Dahlke Mar. 1993 18 p
(AD-A264825) Avail: CASI HC A03/MF A01

In the past several years, the Display Systems Branch, Naval Ocean Systems Center (NOSC), has been involved in the development of laser based display systems with the goal of upgrading the image quality of shipboard displays. In the paper we report work on: (1) developing laser generated 3D volumetric images on a rotating double helix (where the 3D displays are computer controlled for group viewing with the naked eye), and (2) system feasibility results along with the first and second generation component parameters. DTIC

N93-30640 Max-Planck-Inst. fuer Extraterrestrische Physik, Garching (Germany).
A VARIABLE REFLECTIVITY OUTPUT COUPLER FOR OPTICALLY PUMPED FAR INFRARED LASERS
U. U. Graf (Texas Univ., Austin.), A. I. Harris, J. Stutzki (Cologne Univ., Germany.), and R. Genzel Jun. 1992 9 p Submitted for publication
(MPE-Preprint-225; ETN-93-93937) Copyright Avail: Fachinformationszentrum Karlsruhe, 7514 Leopoldshafen-Eggenstein 2, Germany

The design and performance of a variable reflectivity output coupler for optically pumped far infrared lasers are investigated. The output coupler is a compact, tunable Michelson interferometer. The output coupling ratio is adjustable between 0 and equal to or greater than 60% for laser line wavelengths between 110 and 500 micrometers. This output coupler provides increased output power and flexibility. Beam profile measurements show that the Michelson output coupler produces a well collimated Gaussian laser beam. Design features are: the use of a 10 micrometers reflection coated quartz vacuum window which acts as a dichroic mirror for the pump radiation; the high mechanical stability obtained by leaf sping flexure mount of the movable Michelson mirror and by restricted alignment devices. ESA

N93-30767# Academy of Sciences (USSR), Novosibirsk. Inst. Yadernoj Fiziki.
ANALYSIS OF POSSIBILITIES FOR USING LASER SCATTERING FOR MeV ELECTRON BEAM DIAGNOSTICS [ANALIZ VOZMOZHNOSTEJ PRIMENENIYA IAZERNOGO RASSEYANIYA DIYA DIAGNOSTIKI PUCHKOV MEHVNYKH EHLEKTRONOV]
A. V. Arzhannikov 1991 24 p In RUSSIAN
(DE93-606223; IYaF-91-102) Avail: CASI HC A03/MF A01 (US Sales Only)

Analysis of a possibility of measuring the longitudinal speed spread of MeV electrons by laser scattering is performed. The choice of the wavelength and the power of an initial laser beam as well as its incidence angle to the beam and scattered radiation detection angle is discussed therewith. Shapes of spectra of radiation scattered on the beams with different distribution functions are presented and effects of movement of electrons in intrinsic beam fields on them is discussed. DOE

N93-30775# Instituto de Pesquisas Energeticas e Nucleares, Sao Paulo (Brazil).
THEORETICAL-EXPERIMENTAL STUDY OF THE NON-THERMAL EFFECTS OF THE POLARIZED LASER RADIATION IN LIVING TISSUES M.S. Thesis [ESTUDO TEORICO-EXPERIMENTAL DOS EFEITOS NAO TERMICOS DA RADIACAO LASER POLARIZADA EM TECIDOS VIVOS]
M. S. Ribeiro 1991 116 p In PORTUGESE
(DE93-607212; INIS-BR-2958) Avail: CASI HC A06/MF A02 (US Sales Only)

A fundamental objective was to analyze the non-thermal effects of the laser polarized light in biological tissues. These effects were performed with low power laser output. The theoretical procedure consisted of looking for a simple model which connects the effect of light polarized with microscopically rough tissues using well established physical concepts. Experimentally, artificial wounds were created on the back of animals using liquid nitrogen (this method was chosen because it does not interfere in the biochemistry of the animal tissue). For the wound irradiation a He-Ne attached to an optical system was used. DOE

N93-30801# Bhabha Atomic Research Centre, Bombay (India).
COMPUTER CONTROL OF PULSED TUNABLE DYE LASERS
S. S. Thattey, A. S. Dongare, B. M. Suri, and L. G. Nair 1992 25 p
(DE93-605896; BARC-1992/E/005) Avail: CASI HC A03/MF A01 (US Sales Only)

Pulsed tunable dye lasers are being used extensively for spectroscopic and photo-chemical experiments, and a system for acquisition and spectral analysis of a volume of data generated will be quite useful. The development of a system for wavelength tuning and control of tunable dye lasers and an acquisition system for spectral data generated in experiments with these lasers are described. With this system, it is possible to control the tuning of three lasers, and acquire data in four channels, simultaneously. It is possible to arrive at the desired dye laser wavelength with a reproducibility of (+-) 0.012 cm(exp -1), which is within the absorption width (atomic interaction) caused by pulsed dye lasers of linewidth 0.08 cm(exp -1). The spectroscopic data generated can be analyzed for spectral identification within absolute accuracy (+-) 0.012 cm(exp -1). DOE

N93-30910# Naval Command, Control and Ocean Surveillance Center, San Diego, CA.
EFFICIENT LASER ACTION FROM TWO CW LASER PUMPED PYRROMETHENE-BF2 COMPLEXES
S. C. Guggenheimer, J. H. Boyer, K. Thangaraj, M. Shah, and M. L. Soong 17 May 1993 12 p
(AD-A264887; NCCOSC/RDT/E-TR-26) Avail: CASI HC A03/MF A01

Two new pyrromethene-BF2 dyes P-556 and P-567 were tested for CW laser operation. P-556 demonstrated a significant advance in the 530-620 nm region over commercial dyes currently available, where the best CW dyes in any range have peak efficiencies on the order of 35% and dyes in this range typically less than 25%. The P-556 has a CW efficiency of 45% at the peak. DTIC

N93-31023# Bhabha Atomic Research Centre, Bombay (India).
PULSED LASER PHOTOACOUSTIC SPECTROMETER FOR STUDY OF SOLID MATERIALS
N. D. Patel and V. B. Kartha (Bhabha Atomic Research Centre, Bombay, India.) 1991 17 p
(DE93-605290; BARC-1991/E/017) Avail: CASI HC A03/MF A01 (US Sales Only)

The technique of photoacoustic spectroscopy has wide applications because it is extremely sensitive, and can be used to obtain spectra in wide spectral range for solids, liquids, gases, solutions, crystals etc. which may be usually difficult by conventional methods. For studying a variety of materials, a pulsed laser photoacoustic spectrometer was set up in the laboratory. The design and performance of the instrument is discussed. Some of the spectra of materials like Nd2O9 powder, Nd-YAG crystal, CoCl2 6H2O etc. are shown. A detailed discussion on assignment of the spectra of Nd-YAG is also presented. DOE

N93-28772*# Hunter Coll., New York, NY. Dept. of Physics.
EVERY GOOD VIRTUE YOU EVER WANTED IN A Q-SWITCHED SOLID-STATE LASER AND MORE: MONOLITHIC, DIODE-PUMPED, SELF-Q-SWITCHED, HIGHLY REPRODUCIBLE, DIFFRACTION-LIMITED Nd:YAG LASER Abstract Only
Y. C. Chen and K. K. Lee (Colorado Univ., Colorado Springs.) *In* Lunar and Planetary Inst., Workshop on Advanced Technologies for Planetary Instruments, Part 1 1993 p 4 (For primary document see N93-28764 11-91)
Avail: CASI HC A01/MF A01

N93-28780*# National Aeronautics and Space Administration. Goddard Space Flight Center, Greenbelt, MD.
MULTIBEAM LASER ALTIMETER FOR PLANETARY TOPOGRAPHIC MAPPING Abastract Only
J. B. Garvin, J. L. Bufton, and D. J. Harding *In* Lunar and Planetary Inst., Workshop on Advanced Technologies for Planetary Instruments, Part 1 1993 p 8 (For primary document see N93-28764 11-91)
Avail: CASI HC A01/MF A01

N93-28823*# Jet Propulsion Lab., California Inst. of Tech., Pasadena.
SUBNANORADIAN, GROUNDBASED TRACKING OF SPACEBORNE LASERS Abstract Only
R. N. Treuhaft *In* Lunar and Planetary Inst., Workshop on Advanced Technologies for Planetary Instruments, Part 1 1993 p 25-26 (For primary document see N93-28764 11-91)
Avail: CASI HC A01/MF A01

N93-30256 Ottawa Univ. (Ontario). Dept. of Electrical Engineering.
ANALYTICAL PREDICTIONS OF THE INTERMODULATION NOISE OF SEMICONDUCTOR LASER DIODE
Tapan Biswas and W. F. McGee *In* Engineering Inst. of Canada, Canadian Conference on Electrical and Computer Engineering, Volumes 1 and 2 1990 4 p (For primary document see N93-30215 11-31)
Avail: Engineering Inst. of Canada, 2050 rue Mansfield, Suite 700, Montreal, Quebec H3A 1Z2 Canada

37 MECHANICAL ENGINEERING

Includes auxiliary systems (nonpower); machine elements and processes; and mechanical equipment.

N93-28501*# National Aeronautics and Space Administration. Lyndon B. Johnson Space Center, Houston, TX.
MAGNETICALLY OPERATED CHECK VALVE Patent Application
Brian G. Morris, inventor (to NASA) and Richard J. Bozeman, Jr., inventor (to NASA) 19 Mar. 1993 26 p
(NASA-Case-MSC-22046-1; NAS 1.71:MSC-22046-1; US-Patent-Appl-SN-038748) Avail: CASI HC A03/MF A01

A magnetically operated check valve is disclosed having, in one aspect, a valve body and a movable poppet disposed therein. A magnet attracts the poppet to hold the valve shut until the force of fluid flow through the valve overcomes the magnetic attraction and moves the poppet to an unseated, open position. The poppet and magnet are configured and disposed to trap a magnetically attracted particulate and prevent it from flowing to a valve seating region. NASA

N93-28552# Allied-Signal Aerospace Co., Kansas City, MO.
DEVELOPMENT OF AN UPDATED PINCH-WELDING CAPABILITY Final Report
J. A. Samayoa Feb. 1993 168 p
(Contract DE-AC04-76DP-00613)
(DE93-009823; KCP-613-4863) Avail: CASI HC A08/MF A02

An updated pinch-welding capability was developed. The work included development and implementation of unique tooling to allow reproduction of the Savannah River Plant (SRP) confined pinch-welding process using a 3-phase, 100 KVA resistance welder. The new process replaced an existing process in use at Kansas City Division (KCD) since about 1978. A statistical experiment was designed and utilized to define the operational envelope of the new process and to define acceptable machine parameters to produce the pinch-weld. An acceptance criteria for production welds was developed and implemented. DOE

N93-28578# Naval Undersea Warfare Center, New London, CT. New London Detachment.
A COMPLETE SET OF FIELD EQUATIONS FOR THE DYNAMIC SIMULATION OF A TOWED CABLE SYSTEM Final Report
A. A. Ruffa and N. Toplosky 11 Jan. 1993 38 p
(AD-A262570; NUWC-NL-TR-10231) Avail: CASI HC A03/MF A01

The development of a complete set of field equations describing the dynamic behavior of a towed cable is presented. The model includes inertial effects, as well as bending, torsional, and extensional rigidity. The resulting field equations are a generic set of 13 coupled, nonlinear, partial differential equations in time and unstretched cable scope. Hydrodynamic loading and added mass are left as user-defined functions. DTIC

N93-28837# Sandia National Labs., Albuquerque, NM.
DIFFUSION BONDING
L. E. Brown Mar. 1993 52 p
(Contract DE-AC04-76DP-00789)
(DE93-011480; SAND-92-1941) Avail: CASI HC A04/MF A01

A temperature between 400 and 500 and a pressure between 40 MPa and 160 MPa were indicated by a two-factor, three-level factorial experiment for diffusion bonding of molybdenum sheet substrates. These substrates were sputter ion plated with palladium (0.5 microns) and silver (10 microns) films on the mating surfaces, with the silver used as a bonding interlayer. The palladium acted as an adhesive layer between the silver film and molybdenum substrate. The silver diffusion bonds that resulted were qualitatively characterized at the interfacial regions, and bonds with no visible interface were obtained at 7500X magnification. Correlations were obtained for voids found optically at the silver/silver bonding interface and colored image maps, illustrating bond quality, produced by nondestructive ultrasonic imaging. Above 160 MPa, the bonding process produces samples with a nonuniform load distribution. These samples contained regions with gaps and well-bonded regions at the silver/silver interface, and all had macroscopic deformation of the silver films. DOE

N93-28903# Argonne National Lab., IL. Materials and Components Technology Div.
SURFACE MODIFICATION OF TRIBOLOGICAL COMPONENTS IN TRANSPORTATION
G. R. Fenske Nov. 1992 36 p Presented at the Annual Automotive Development Technology Contractors' Coordination Meeting, Dearborn, MI, 2-5 Nov. 1992
(Contract W-31-109-eng-38)
(DE93-008647; ANL/MCT/CP-77166; ANL/VU-77166; CONF-9211101-4)
Avail: CASI HC A03/MF A01

This paper reviews a number of programs funded through the Engineered Tribological Interfaces (ETI) Task area of the Tribology Program that utilize energetic beams of atoms to enhance the mechanical and microstructural properties of near-surface regions to improve the tribological performance of critical components. The processes used in these programs include techniques based on chemical vapor deposition, physical vapor deposition, and ion implantation. A common feature of these techniques is their ability to produce dense and adherent modified surfaces without need for subsequent grinding/polishing treatments. Another feature of these techniques is their ability to introduce a wide range of elements into near-surface regions. DOE

N93-28951*# National Aeronautics and Space Administration. Marshall Space Flight Center, Huntsville, AL.
WELDING WIRE PRESSURE SENSOR ASSEMBLY Patent Application
Timothy B. Morris, inventor (to NASA) (Nichols Research Corp., Huntsville, AL.), Peter F. Milly, inventor (to NASA) (Nichols Research Corp., Huntsville, AL.), and J. Kevin White, inventor (to NASA) (Nichols Research Corp., Huntsville, AL.) 27 May 1993 9 p
(NASA-Case-MFS-26216-1; NAS 1.71:MFS-26216-1; US-Patent-Appl-SN-070132) Avail: CASI HC A02/MF A01

The present invention relates to a device which is used to monitor the position of a filler wire relative to a base material being welded as the filler wire is added to a welding pool. The device is applicable to automated welding systems wherein nonconsumable electrode arc welding processes are utilized in conjunction with a filler wire which is added to a weld pool created by the electrode arc. The invention senses pressure deviations from a predetermined pressure between the filler wire and the base material, and provides electrical signals responsive to the deviations for actuating control mechanisms in an automatic welding apparatus so as to minimize the pressure deviation and to prevent disengagement of the contact between the filler wire and the base material. NASA

N93-28954*# National Aeronautics and Space Administration. Pasadena Office, CA.
DUAL ARM GENERALIZED COMPLIANT MOTION WITH SHARED CONTROL Patent Application
Paul G. Backes, inventor (to NASA) (Jet Propulsion Lab., California Inst. of Tech., Pasadena.) 24 Mar. 1993 60 p
(Contract NAS7-918)
(NASA-Case-NPO-18738-1-CU; NAS 1.71:NPO-18738-1-CU; US-Patent-Appl-SN-034608) Avail: CASI HC A04/MF A01

A multiple arm generalized compliant motion robot control system governs dual multi-joint robot arms handling an object with both of the arms in accordance with input parameters governing plural respective behaviors to be exhibited by the robot in respective behavior spaces simultaneously. A move-squeeze decomposition processor computes actual move and squeeze decomposition forces based upon current robot force sensor outputs. A compliant motion processor transforms plural object position perturbations of the plural behaviors from the respective behavior spaces to a common space and computes a relative transformation to a behavior-commanded object position in accordance with the object position perturbations of the plural behaviors. A kinematics processor updates a transformation to a current commanded object position based upon the relative transformation to the behavior-commanded object position. A multiple arm squeeze control processor computes from appropriate squeeze force input parameters and from actual squeeze forces for each of the arms, a squeeze control position perturbation for each of the arms, to provide squeeze control. An inverse kinematics processor computes from the commanded object position transformation and from the squeeze control position perturbation, new robot joint angles, and controls respective joints of the robot arms in accordance with the new robot joint angles. NASA

N93-28968# Oak Ridge National Lab., TN.
INSERVICE DIAGNOSTIC METHODS FOR SOLENOID-OPERATED VALVES
R. C. Kryter 1993 8 p Presented at the Meeting on Nuclear Plant Instrumentation, Control and Man-Machine Interface Technologies, Oak Ridge, TN, 18-21 Apr. 1993
(Contract DE-AC05-84OR-21400)
(DE93-007823; CONF-930401-1) Avail: CASI HC A02/MF A01

Solenoid-operated valves (SOV's) were studied at Oak Ridge National Laboratory as part of the USNRC Nuclear Plant Aging Research (NPAR) Program. The primary objective of the study was to identify, evaluate, and recommend methods for inspection, surveillance, monitoring, and maintenance of SOV's that can help ensure their operational readiness-that is, their ability to perform required safety functions under all anticipated operating conditions, since failure of one of these small and relatively inexpensive devices could have serious consequences under certain circumstances. An earlier (Phase 1) NPAR program study described SOV failure modes and causes and had identified measurable parameters thought to be linked to the progression of everpresent degradation mechanisms that may ultimately result in functional failure of the valve. Using this earlier work as a guide, the present (Phase 11) study focused on devising and then demonstrating the effectiveness of techniques and equipment with which to measure performance parameters that show promise for detecting the presence and trending the progress of such degradations before they reach a critical stage. Intrusive techniques requiring the addition of magnetic or acoustic sensors or the application of special test signals were investigated briefly, but major emphasis was placed on the examination of condition-indicating techniques that can be applied with minimal cost and impact on plant operation. Experimental results are presented that demonstrate the technical feasibility and practicality of the monitoring techniques assessed in the study, and recommendations for further work are provided. DOE

N93-29080*# Draper (Charles Stark) Lab., Inc., Cambridge, MA.
MULTIVARIABLE CONTROL OF THE SPACE SHUTTLE REMOTE MANIPULATOR SYSTEM USING LINEARIZATION BY STATE FEEDBACK M.S. Thesis
Chang-Ching Lo Gettman May 1993 129 p
(Contract NAS9-18426)
(NASA-CR-188248; NAS 1.26:188248; CSDL-T-1176) Copyright Avail: CASI HC A07/MF A02

This thesis develops and demonstrates an approach to nonlinear control system design using linearization by state feedback. The design provides improved transient response behavior allowing faster maneuvering of payloads by the SRMS. Modeling uncertainty is accounted for by using a second feedback loop designed around the feedback linearized dynamics. A classical feedback loop is developed to provide the easy implementation required for the relatively small on board computers. Feedback linearization also allows the use of higher bandwidth model based compensation in the outer loop, since it helps maintain stability in the presence of the nonlinearities typically neglected in model based designs. Author (revised)

N93-29082 Notre Dame Univ., IN.
AN AUTONOMOUS VISION-BASED MOBILE ROBOT Ph.D. Thesis
Eric Thomas Baumgartner 1993 146 p
Avail: Univ. Microfilms Order No. DA9308220

This dissertation describes estimation and control methods for use in the development of an autonomous mobile robot for structured environments. The navigation of the mobile robot is based on precise estimates of the position and orientation of the robot within its environment. The extended Kalman filter algorithm is used to combine information from the robot's drive wheels with periodic observations of small, wall-mounted, visual cues to produce the precise position and orientation estimates. The visual cues are reliably detected by at least one video camera mounted on the mobile robot. Typical position estimates are accurate to within one inch. A path tracking algorithm is also developed to follow desired reference paths which are taught by a human operator. Because of the time-independence of the tracking algorithm, the speed that the vehicle travels along the reference path is specified independent from the tracking algorithm. The estimation and control methods have been applied successfully to two experimental vehicle systems. Finally, an analysis of the linearized closed-loop control system is performed to study the behavior and the stability of the system as a function of various control parameters. Dissert. Abstr.

N93-29175*# National Aeronautics and Space Administration. Langley Research Center, Hampton, VA.
SINGLE ACTING TRANSLATION/ROTATIONAL BRAKE Patent Application
Johnny W. Allred, inventor (to NASA) and Vincent J. Fleck, inventor (to NASA) 12 May 1993 15 p
(NASA-Case-LAR-14738-1; NAS 1.71:LAR-14738-1; US-Patent-Appl-SN-064324) Avail: CASI HC A03/MF A01

A brake system is provided that applies braking forces on surfaces in both the translational and rotational directions using a single acting self-contained actuator that travels with the translational mechanism. The brake engages a mechanical lock and creates a frictional force on the translational structure preventing translation while simultaneously creating a frictional torque that prevents rotation of the vertical support. The system may include serrations on the braking surfaces to provide increased breaking forces. NASA

N93-29185# Sandia National Labs., Albuquerque, NM.
THE DESIGN AND MODELLING OF A COMB-DRIVE-BASED MICROENGINE FOR MECHANISM DRIVE APPLICATIONS
E. J. Garcia and J. J. Sniegowski 1992 5 p Presented at the 7th International Conference on Solid-state Sensors and Actuators, Yokohama, Japan , 7-10 Jun. 1993
(Contract DE-AC04-76DP-00789)
(DE93-009826; SAND-92-2497C; CONF-9306118-1) Avail: CASI HC A01/MF A01

The design and modelling of a comb-drive-based microengine is presented. The motivation for developing such a device came from our own need to drive specific micromechanisms. Difficulty in connecting an external load to an existing micromotor and insufficient torque led us to a design which uses the comb drive concept of Tang, Nguyen, and Howe, to convert linear oscillatory motion into rotational motion. The microengine provides output in the form of a continuously rotating output gear that is capable of delivering torque to a micromechanism. The microengine can be operated at varying speeds and its motion can be reversed. Modelling of the system indicates that dynamic effects are important and that the device behaves in ways similar to that of 'high speed' machinery. Processing considerations address the elimination of natural interferences that arise when conformally deposited polysilicon films form the links, joints, and gears. The resultant device is completely batch fabricated without the need for manual assembly steps. DOE

N93-29205# Babcock and Wilcox Co., Lynchburg, VA. Research and Development Div.

SENSOR SYSTEMS FOR MONITORING MAGLEV GUIDEWAY STRUCTURES Final Report

J. W. Berthold, J. R. Bower, J. D. Buttram, L. R. Okes, and M. O. Robertson Jul. 1992 85 p
(Contract DTFR53-91-C-00064)
(PB93-154821; DOT/FRA/NMI-92/12) Avail: CASI HC A05/MF A01

The report is an assessment of the technologies available for continuous monitoring of the physical condition and structural integrity of maglev guideways. The detection of obstructions on the guideway is not included. No particular guideway design is assumed, other than that the largest part of the system will consist of repetitive reinforced concrete structures, probably elevated, that are aligned with close tolerances. It is assumed that the guideway is to be monitored for the correct alignment of the sections, any unusual vibrations or motions, detection of catastrophic failure, and possibly accumulation of ice and snow. The technologies covered are acoustic emission monitoring (a passive acoustic method of listening for crack growth or other unusual structure borne sound), infrared and visible light monitoring (ranging from cameras to displacement sensors), ultrasonics (for vibration, displacement, snow and ice), microwave monitors (for vibration and displacement sensors), and fiber optics (for networks of strain gauges). It is the conclusion of the report that the technologies described are sufficiently mature to meet the requirements. Any particular application will certainly need development, and some may need extensive development, but the basic capabilities are there. NTIS

N93-29247# Oak Ridge National Lab., TN.

A MANIPULATOR KINEMATIC DESIGN FOR HIGH-VACUUM OPERATION

S. M. Killough 1993 8 p Presented at the 5th Topical Meeting on Robotics and Remote Systems, Knoxville, TN, 26-29 Apr. 1993
(Contract DE-AC05-84OR-21400)
(DE93-010264; CONF-930403-36) Avail: CASI HC A02/MF A01

To meet the special requirements for remote maintenance in vacuum environments, a unique manipulator was designed that could be adapted easily to vacuum use. Rather than being concerned with the components that traditionally have made vacuum use difficult, such as flexible wiring, we have developed a new kinematic design that will eliminate the use of these troublesome components. This new manipulator uses a parallel-link configuration to eliminate the need for mounting the motors on moving links, thus also removing the need for flexible cables. The configuration also provides several other unique and beneficial characteristics for nonvacuum USC. DOE

N93-29254# Oak Ridge National Lab., TN.

A PORTABLE MODULAR ARCHITECTURE FOR ROBOTIC MANIPULATOR CONTROL

P. L. Butler 1993 7 p Presented at the 5th Topical Meeting on Robotics and Remote Systems, Knoxville, TN, 26-29 Apr. 1993
(Contract DE-AC05-84OR-21400)
(DE93-010819; CONF-930403-35) Avail: CASI HC A02/MF A01

A control architecture has been developed to provide a framework for robotic manipulator control. This architecture, called the Modular Integrated Control Architecture (MICA), has been successfully applied to two different manipulator systems. MICA is a portable system in two respects. First, it can be used for the control of different types of manipulator systems. Second, the MICA code is portable across several operating environments. This portability allows the sharing of common control code among various systems. A major portion of MICA is the precise control of multiple processors that have to be coordinated to control a manipulator system. By having MICA control the processor synchronization, the system developer can concentrate on the specific aspects of a new manipulator system. MICA also provides standard functions for trajectory generation that can be used for most manipulators. Custom trajectory generators can be easily added to suit the needs of a particular robotic control system. Another facility that MICA provides is a simulation of the manipulator, allowing the control code to be simulated before trying it on a manipulator system. Using this technique, one can develop code for a manipulator system without risking damage to the arm during development. DOE

N93-29288 Department of the Navy, Washington, DC.

COMBINED CENTRIFUGAL FORCE/GRAVITY GAS/LIQUID SEPARATOR SYSTEM Patent

Luis E. Lema, inventor (to Navy) 13 Apr. 1993 6 p Filed 3 Apr. 1992
(AD-D015726; US-Patent-5,202,026; US-Patent-Appl-SN-862689; US-Patent-Class-210-512.1) Avail: US Patent and Trademark Office

A gas/liquid separator system has an outer enclosing tank filled with a demisting packing material. The tank has a gas outlet port and a liquid outlet port located at its top and bottom, respectively. At least one cylindrical, centrifugal force gas/liquid separator is vertically aligned and centrally located within the tank and is surrounded by the packing material. The cylindrical separator receives a gas/liquid mixture, separates the mixture into respective substantially gas and substantially liquid components, and allows the substantially gas components to exit its gas escape port. It also allows the substantially liquid components to exit its liquid escape port. The packing material in the tank further separates the substantially gas and liquid components as they rise and fall, respectively, through the packing material. An inflow line introduces the mixture into the cylindrical separator. The inflow line is upwardly inclined in a direction of flow of the mixture at a point where the inflow line communicates with the cylindrical separator. DTIC

N93-29316# Oak Ridge National Lab., TN.

AN ARCHITECTURE FOR ROBOTIC SYSTEM INTEGRATION

P. L. Butler, D. B. Reister, C. S. Gourley (Tennessee Univ., Knoxville.), and S. M. Thayer (Tennessee Univ., Knoxville.) 1993 8 p Presented at the 5th Topical Meeting on Robotics and Remote Systems, Knoxville, TN, 26-29 Apr. 1993
(Contract DE-AC05-84OR-21400)
(DE93-010829; CONF-930403-34) Avail: CASI HC A02/MF A01

An architecture was developed to provide an object-oriented framework for the integration of multiple robotic subsystems into a single integrated system. By using an object-oriented approach, all subsystems can interface with each other, and still be able to be customized for specific subsystem interface needs. The object-oriented framework allows the communications between subsystems to be hidden from the interface specification itself. Thus, system designers can concentrate on what the subsystems are to do, not how to communicate. This system was developed for the Environmental Restoration and Waste Management Decontamination and Decommissioning Project at Oak Ridge National Laboratory. In this system, multiple subsystems are defined to separate the functional units of the integrated system. For example, a Human-Machine Interface (HMI) subsystem handles the high-level machine coordination and subsystem status display. The HMI also provides status-logging facilities and safety facilities for use by the remaining subsystems. Other subsystems have been developed to provide specific functionality, and many of these can be reused by other projects. DOE

N93-29330# Carnegie-Mellon Univ., Pittsburgh, PA.

RESEARCH ON RECONFIGURABLE AND RELIABLE MANIPULATORS

P. K. Khosla and T. Kanade 1993 5 p
(Contract DE-FG02-89ER-14042)
(DE93-010244; DOE/ER-14042/4) Avail: CASI HC A01/MF A01

We have proposed the concept of reconfigurable manipulators as a solution to tasks that require varied configurations of manipulators. Using modules of varying sizes and performance specifications, it is possible to build manipulators to suit the task at hand. Our research is not only addressing the issue of creating such manipulators but also the interesting theoretical challenges posed in mapping tasks to manipulators. We have developed strategies that allow us to determine the kinematic and dynamic configuration of a non-redundant manipulator from task specifications such as reachability, obstacle avoidance, manipulability, joint, limits, and joint velocities and accelerations. We are presently extending this design methodology for design of redundant and fault tolerant manipulator systems. Further, we are also addressing issues in automatic generation of software for kinematics, dynamics, and controllers for the configured manipulators. During the next year, we will be demonstrating automatic generation of software on the prototype system that we are building. We expect to have 4 joint and link modules available for this demonstration. The joint and link modules will also incorporate concepts for making power and data connections when the mechanical connection is made. Further, they will also include electronics, housed within the module, for communication and real-time control. DOE

N93-29388# Wisconsin Univ. Hospital, Madison. Engine Research Center.

MODELING THE EFFECTS OF DROP DRAG AND BREAKUP ON FUEL SPRAYS

Alex B. Liu, Daniel Mather, and Rolf D. Reitz Mar. 1993 17 p
(Contract DAAL03-86-K-0174)
(AD-A263650; TP-930072; ARO-24623.126-EG-UIR) Avail: CASI HC A03/MF A01

Spray models were evaluated using experimentally measured trajectories and drop sizes of single drops injected into a high relative velocity gas flow. The computations were made using a modified version of the KIVA-2 code. It was found that the drop drag coefficient and the drop breakup time model constant had to be adjusted in order to match the measurements. Based on these findings, a new drop drag submodel is proposed in which the drop drag coefficient changes dynamically with the flow conditions. The model accounts for the effects of drop distortion and oscillation due to the relative motion between the drop and the gas. The value of the drag coefficient varies between the two limits of that of a rigid sphere (no distortion) and that of a disk (maximum distortion). The modified model was also applied to diesel sprays. The results show that the spray tip penetration is relatively insensitive to the value used for the drop drag coefficient. However, the distribution of drop sizes within sprays is influenced by drop drag. This is due to the fact that changes in drop drag produce changes in the drop-gas relative velocity. This, in turn, causes changes in the spray drop size through the drop breakup and coalescence processes. The changes occur in such a way that the net effect on the spray penetration is small over the tested ranges of conditions. These results emphasize that measurements of spray penetration are not sufficient to test and produce improved spray models. Instead, local measurements of drop size and velocity are needed to develop accurate spray models. DTIC

N93-29505* National Aeronautics and Space Administration. Goddard Space Flight Center, Greenbelt, MD.

SPLINE SCREW AUTOCHANGER Patent

John M. Vranish, inventor (to NASA) 15 Jun. 1993 7 p Filed 27 Jul. 1992
(NASA-Case-GSC-13435-1; US-Patent-5,219,318;
US-Patent-Appl-SN-918746; US-Patent-Class-483-16;
US-Patent-Class-414-729; US-Patent-Class-483-901;
US-Patent-Class-901-30; US-Patent-Class-901-41;
Int-Patent-Class-B23Q-3/155; Int-Patent-Class-B25J-15/04) Avail: US Patent and Trademark Office

A captured nut member is located within a tool interface assembly and being actuated by a spline screw member driven by a robot end effector. The nut member lowers and rises depending upon the directional rotation of the coupling assembly. The captured nut member further includes two winged segments which project outwardly in diametrically opposite directions so as to engage and disengage a clamping surface in the form of a chamfered notch respectively provided on the upper surface of a pair of parallel forwardly extending arm members of a bifurcated tool stowage holster which is adapted to hold and store a robotic tool including its end effector interface when not in use. A forward and backward motion of the robot end effector operates to insert and remove the tool from the holster.
Official Gazette of the U.S. Patent and Trademark Office

N93-29618* National Aeronautics and Space Administration. Marshall Space Flight Center, Huntsville, AL.

SYSTEM FOR TESTING BEARINGS Patent

John C. Gibson, inventor (to NASA) 13 Jul. 1993 5 p Filed 26 Dec. 1991 Supersedes N92-17584 (30 - 8, p 1306)
(NASA-Case-MFS-28589-1; US-Patent-5,226,308;
US-Patent-Appl-SN-813628; US-Patent-Class-73-9;
Int-Patent-Class-G01N-19/02) Avail: US Patent and Trademark Office

Disclosed here is a system for testing bearings wherein a pair of spaced bearings provides support for a shaft on which is mounted a bearing to be tested, this bearing being mounted in a bearing holder spaced from and in alignment with the pair of bearings. The bearing holder is provided with an annular collar positioned in an opening in the bearing holder for holding the bearing to be tested. A screw threaded through the bearing holder into engagement with the annular collar can be turned to force the collar radially out of alignment with the pair of bearings to apply a radial load to the bearing.
Official Gazette of the U.S. Patent and Trademark Office

N93-29846*# National Aeronautics and Space Administration. Marshall Space Flight Center, Huntsville, AL.

QUICK CONNECT FASTENER Patent Application

Bruce Weddendorf, inventor (to NASA) 1 Jun. 1993 16 p
(NASA-Case-MFS-28833-1; NAS 1.71:MFS-28833-1;
US-Patent-Appl-SN-069481) Avail: CASI HC A03/MF A01

This invention relates to a quick connect fastener for attachment to an axially elongated externally threaded member by axially thrusting the fastener onto the member, the fastener having an outer casing including a passageway having a frustoconical surface. A segmented core having four internally threaded shells is positioned within the casing, the shells having a frustoconical outer surface and a cylindrical annulus including a standard thread profile. The shells include a groove at each end for receiving a C-shaped clip which urge the shells radially outwardly and toward the larger end of the passageway. A coil spring positioned within the nut casing at the larger end acts to urge the shells toward a surface acting as a stop at the smaller end which limits movement of the shells and counteracts a substantial amount of the tension of the externally threaded member. Raised keys on the surfaces of the shells are received within grooves in the casing so that the shells rotate upon rotation of the shell. NASA

N93-30149 Stanford Univ., CA.

OPTIMAL GEOMETRIC DESIGN OF ROBOTS FOR ENVIRONMENTS WITH OBSTACLES Ph.D. Thesis

Krasimir Dobromirov Kolarov 1993 214 p
Avail: Univ. Microfilms Order No. DA9309623

The problem discussed is: given an environment with obstacles, what is the optimal design of a robot that can reach everywhere in this environment without collision with the obstacles. The main questions of concern are: what is the most appropriate type for the links of the robot; what is the minimum number of links that are needed to cover every point in the free space; and what is the best placement for the robot in the environment. The primary joint type employed is a one degree of freedom prismatic joint which folds into itself like a telescope to some minimal length. Our robot is formed by connecting each telescopically jointed link to a revolute joint at its other end. The revolute axes are perpendicular to the prismatic axes. The links thus formed are called 'telescoping links.' All links of the robots that are considered have telescoping structure. In the first part, some algorithms for finding the set of points in the environment (the link center) that can reach all other points with minimum number of telescoping links is discussed. The description and implementation of an algorithm that finds all visibility polygons from a given point when the obstacles are modeled as convex polygons are discussed. This algorithm is used in the implementation of algorithms for finding the link center and an approximate link center. The modifications and the additions that these algorithms require to cover curvilinear, non-convex and three-dimensional obstacles are discussed. In the second part, several theorems that establish upper and lower bounds on the number of links needed to cover the free space in both planar and spatial cases are derived. Some algorithms for minimizing the upper bounds to, hopefully, the optimal number of links for the environment are described. Finally, several generalizations to the basic problem for the cases when we design both the robot and the environment simultaneously, when we deal with moving robots and obstacles, multiple robots or robots with variable structure are considered. Dissert. Abstr.

N93-30210# Oak Ridge National Lab., TN.
INPUT RELEGATION CONTROL FOR GROSS MOTION OF A KINEMATICALLY REDUNDANT MANIPULATOR
M. A. Unseren 1993 26 p Presented at the 1993 Institute of Electrical and Electronics Engineers/Robotics Society of Japan (IEEE/RSJ) International Conference on Intelligent Robots and Systems (IROS), Yokohama, Japan, 26-30 Jul. 1993
(Contract DE-AC05-84OR-21400)
(DE93-005301; CONF-930736-1) Avail: CASI HC A03/MF A01

This paper proposes a method for resolving the kinematic redundancy of a serial link manipulator moving in a three-dimensional workspace. The underspecified problem of solving for the joint velocities based on the classical kinematic velocity model is transformed into a well-specified problem. This is accomplished by augmenting the original model with additional equations which relate a new vector variable quantifying the redundant degrees of freedom (DOF) to the joint velocities. The resulting augmented system yields a well specified solution for the joint velocities. Methods for selecting the redundant DOF quantifying variable and the transformation matrix relating it to the joint velocities are presented so as to obtain a minimum Euclidean norm solution for the joint velocities. The results obtained from experimentally implementing the proposed scheme on the CESARM research manipulator are presented. DOE

N93-30211# Los Alamos National Lab., NM.
CONTAINMENT OF EXPLOSIONS IN SPHERICAL VESSELS
T. A. Duffey, J. M. Greene, W. E. Baker (New Mexico Univ., Albuquerque.), and B. B. Lewis (APTEK, Inc., Colorado Springs, CO.) 1992 22 p Presented at the Pressure Vessel and Piping Conference, Denver, CO, 25-29 Jul. 1993
(Contract W-7405-eng-36)
(DE93-005445; LA-UR-92-4061; CONF-930702-2) Avail: CASI HC A03/MF A01

A correlation of the experimentally recorded dynamic response of a spherical containment vessel with theoretical finite element calculations is presented. Three experiments were performed on the 6-ft-diameter steel vessel using centrally located 12-lb. and 40-lb. high explosive charges. Pressure-time loading on the inner wall of the vessel was recorded for each test using pressure transducers. Resulting dynamic response of the vessel was recorded for each test using strain gages mounted at selected locations on the outer surface of the vessel. Response of the vessel was primarily elastic. A finite element model of the vessel was run using DYNA3D, a dynamic structural analysis code. Pressure loading for the finite element model was based on results from a one-dimensional reactive hydrodynamics code. Correlations between experiments and analysis were generally good for the tests for frequency and strain magnitude at most locations. Comparisons of experimental and calculated pressure-time histories were less satisfactory. DOE

N93-30378 California Univ., Berkeley.
EXPERIMENTAL AND ANALYTICAL INVESTIGATION OF FINGER-FOLLOWER CAM SYSTEMS Ph.D. Thesis
Wensyang Hsu 1992 164 p
Avail: Univ. Microfilms Order No. DA9304948

A predictive dynamic model to compute the motions of components in cam systems, along with the experimental work to verify the model are described. The major components in finger-follower cam systems include the cam, the follower, the hydraulic lash adjuster, and the valve spring, equipped sometimes with a helical valve spring cup damper. In order to fully describe the dynamics of such a system, a lumped/distributed parameter model for the finger-follower cam system with a moving follower pivot is proposed. The valve spring is modeled as a distributed parameter element, and the adjuster is modeled as a stiff spring with viscous damping. The coulomb friction combined with viscous damping between sliding surfaces are also considered. The model predicts toss between the adjuster and the follower at 2535 rpm, and experiment indicates toss starting at 2520 rpm. It is found by simulation that designing hydraulic lash adjuster to be as rigid as possible is essential to successful high speed operation of finger-follower valve trains because a 50 percent decrease in the compliance of the adjuster could increase the maximum camshaft operating speed 150 rpm. Total elimination of the hydraulic lash adjuster is not always feasible because hydraulic lash adjusters can eliminate the clearance between components and do not need to be mechanically, manually adjusted. In order to provide a more stable and precise description on the dynamic response of the adjuster, a two-mode dynamic model for the adjuster is proposed by considering the oil compressibility in the oil chamber, as well as the oil leakage through the annular gap. Furthermore, the effect due to the oil flow from the central orifice to the oil chamber is also studied analytically and experimentally. The inertia effects of the helical valve spring can be suppressed by a cup damper. Damping between the damper and spring wire is found to depend only weakly on relative sliding velocity. The current formula in computing spring force including the effects of coulomb friction, spring coil dilation, bending moments on both the spring wire and the damper, is verified by comparison between different models and experimental data. Dissert. Abstr.

N93-30384# Naval Command, Control and Ocean Surveillance Center, San Diego, CA.
A TESTBED FOR AUTONOMOUS REFLEXIVE GRASPING
David A. Kemme and John R. McDonnell Mar. 1993 8 p
(AD-A264557) Avail: CASI HC A02/MF A01

This work describes the development of a testbed which combines a subsumption architecture approach with neural network processing of tactile information in a reflexive behavior feasibility study. An overview of the tactile sensor, the neural network processor, and subsumption architecture is provided along with a plan for integrating these components into a single system. By incorporating local (reflexive) processing capabilities within a robot gripper, an additional layer of control is attained without an increased computing burden being placed on the system controller. DTIC

N93-30404# Martin Marietta Corp., Baltimore, MD.
DRIVE-REINFORCEMENT LEARNING SYSTEM APPLICATIONS Final Report, 1 Jan. 1989 - 1 Jul. 1992
Daniel W. Johnson 31 Jul. 1992 76 p
(Contract F33615-89-C-1023)
(AD-A264514; WL-TR-92-1122) Avail: CASI HC A05/MF A01

The application of Drive-Reinforcement (D-R) to the unsupervised learning of manipulator control functions was investigated. In particular, the ability of a D-R neuronal system to learn servo-level and trajectory-level controls for a robotic mechanism was assessed. Results indicate that D-R based systems can be successful at learning these functions in real-time with actual hardware. Moreover, since the control architectures are generic, the evidence suggests that D-R would be effective in control system applications outside the robotics arena. DTIC

N93-30512# Honeywell, Inc., Glendale, AZ. Satellite Systems Operations.
CRYOGENIC MAGNETIC BEARING Final Report, 1 Nov. 1985 - 1 May 1991
James Andrus, John Kendig, and John Kroeger Dec. 1992 98 p
(Contract F33615-86-C-5015)
(AD-A264716; S71-1180-1.0-1; WL-TR-91-4150) Avail: CASI HC A05/MF A02

Magnetic suspension provides an alternative to rolling-element bearings for some precision gimbal applications. The Cryogenic Magnetic Bearing program includes studies of magnetic suspension for a gimbal bearing requiring long life (greater than 7 years); low runout (less than 5 microrads bore-sight error due to runout); and low, uniform drag torque. Additionally, the bearing is to operate in an oscillating mode, from room-ambient (300 K) to liquid nitrogen (77 K) temperatures at ambient pressure and in a hard vacuum (10 (exp-6) torr). Two magnetic suspension alternatives were studied: an all-active approach using electromagnets to control all five bearing degrees-of-freedom and a Passive-Radial Active-Axial (PRAA) approach using passive magnetics to stabilize four of the five bearing degrees-of-freedom and an electromagnet to control the fifth. The all-active approach provides a lower weight, better-accuracy bearing system than the PRAA system, but requires more quiescent operating power and is electrically more complex. The PRAA was selected for hardware study to produce a simple, low-power magnetic system. DTIC

N93-30524# IBM Research Lab., San Jose, CA.
FUNDAMENTAL STUDIES OF FRICTION, LUBRICATION, AND WEAR BY ATOMIC FORCE MICROSCOPY
Gary M. McCleeland 14 Apr. 1993 40 p

(Contract F49620-89-C-0068)
(AD-A264647; AFOSR-93-0333TR) Avail: CASI HC A03/MF A01

To probe friction, lubrication, and wear on an atomic scale, a capacitance-based ultrahigh vacuum force microscope was developed. It measures both parallel and perpendicular forces between a tip and a surface. Friction between a diamond tip and chemical-vapor-deposited (CVD) diamond films at loads below one micronewton showed a sublinear dependence of friction on load, with the effective friction coefficient varying between 0.2 and 0.8 depending on load and location. Stick-slip behavior resulting from both surface heterogeneity and static/dynamic friction was observed. A CVD process was developed for growing single crystal diamond tips with radii as small as 30 nm. The normal force between these tips and diamond (100) and (111) surfaces agrees with calculated dispersion forces. The frictional force variation on the (100) surface are tentatively associated with a reconstructed geometry convoluted over an asymmetric tip shape, while the (111) surface exhibits features which cannot be simply associated with the surface structure. Friction is approximately 3 nanonewtons independent of loads up to 100 nanonewtons. A field emission technique was developed for continuously observing the motion of individual adsorbed atoms and molecules. The hopping of individual Cs atoms between sites on a tungsten tip was observed with 2 ps and 5 Angstrom resolution. DTIC

N93-30567*# National Aeronautics and Space Administration. Marshall Space Flight Center, Huntsville, AL.
MOLD BOLT AND MEANS FOR ACHIEVING CLOSE TOLERANCES BETWEEN BOLTS AND BOLT HOLES Patent Application
David Johnston, inventor (to NASA) and Phillip G. Bryant, inventor (to NASA) (Teledyne Brown Engineering, Huntsville, AL.) 27 Jan. 1993 12 p
(NASA-Case-MFS-28720-1; NAS 1.71:MFS-28720-1; US-Patent-Appl-SN-009909) Avail: CASI HC A03/MF A01

In the space shuttle, a cargo bay storage rack was required which was to be manufactured from a metal-plastic composite and bolted to a cargo structure. Following completion, utilization of the rack was disallowed due to tolerances, that is, the size differences between the outside bolt diameter and the inside hole diameter. In addition to the space shuttle problem there are other close tolerance requirements for bolts. Such environments often benefit from close tolerance bolting. Frequently such fabrication is not cost effective. Consequently there is a need for means of achieving close tolerances between bolts and bolt holes. Such means are provided. After compressing the elements together a strong rigid plastic, ceramic, or ceramic plastic fluid is forced into a channel extending through the bolt. NASA

N93-30632# Westinghouse Hanford Co., Richland, WA.
STRUCTURAL DESIGN, ANALYSIS, AND CODE EVALUATION OF AN ODD-SHAPED PRESSURE VESSEL
M. A. Rezvani and H. H. Ziada Dec. 1992 8 p Presented at the Pressure Vessel and Piping Conference, Denver, CO, 25-29 Jul. 1993
(Contract DE-AC06-87RL-10930)
(DE93-008182; WHC-SA-1684; CONF-930702-8) Avail: CASI HC A02/MF A01

An effort to design, analyze, and evaluate a rectangular pressure vessel is described. Normally pressure vessels are designed in circular or spherical shapes to prevent stress concentrations. In this case, because of operational limitations, the choice of vessels was limited to a rectangular pressure box with a removable cover plate. The American Society of Mechanical Engineers (ASME) Boiler and Pressure Vessel Code is used as a guideline for pressure containments whose width or depth exceeds 15.24 cm (6.0 in.) and where pressures will exceed 103.4 KPa (15.0 lbf/in(sup 2)). This evaluation used Section 8 of this Code, hereafter referred to as the Code. The dimensions and working pressure of the subject vessel fall within the pressure vessel category of the Code. The Code design guidelines and rules do not directly apply to this vessel. Therefore, finite-element methodology was used to analyze the pressure vessel, and the Code then was used in qualifying the vessel to be stamped to the Code. Section 8, Division 1 of the Code was used for evaluation. This action was justified by selecting a material for which fatigue damage would not be a concern. The stress analysis results were then checked against the Code, and the thicknesses adjusted to satisfy Code requirements. Although not directly applicable, the Code design formulas for rectangular vessels were also considered and presented. DOE

N93-30654# Sandia National Labs., Albuquerque, NM.
GRAPHICAL PROGRAMMING: ON-LINE ROBOT SIMULATION FOR TELEROBOTIC CONTROL
M. J. McDonald and R. D. Palmquist 1993 15 p Presented at the International Robots and Vision Conference, Detroit, MI, 6-8 Apr. 1993
(Contract DE-AC04-76DP-00789)
(DE93-009796; SAND-93-0003C; CONF-930491-2) Avail: CASI HC A03/MF A01

Sandia has developed an advanced operational control system approach, caged Graphical Programming, to design and operate robotic waste cleanup and other hazardous duty robotic systems. The Graphical Programming approach produces robot systems that are faster to develop and use, safor in operation, and cheaper overall than alternative teleoperation or autonomous robot control systems. The Graphical Programming approach uses 3-D visualization and simulation software with intuitive operator interfaces for the programming and control of complex robotic systems. Graphical Programming Supervisor software modules allow an operator to command and simulate complex tasks in a graphic preview mode and, when acceptable, command the actual robots and monitor their motions with the graphic system. Graphical Programming Supervisors maintain registration with the real world and allow the robot to perform tasks that cannot be accurately represented with models alone by using a combination of model and sensor-based control. This paper describes the Graphical Programming approach, several example control systems that use Graphical Programming, and key features necessary for implementing successful Graphical Programming systems. DOE

N93-30820# Babcock and Wilcox Co., Lynchburg, VA. Contract Research Div.
GUIDEWAY STRUCTURAL DESIGN AND POWER/PROPULSION/BRAKING IN RELATION TO GUIDEWAYS, VOLUME 1 Final Report, Aug. 1991 - Jan. 1992
K. M. Falkowski, F. S. Key, and S. B. Kuznetsov Jan. 1993 269 p See also PB93-169910 Sponsored by National Maglev Initiative (FRA), Washington, DC
(Contract DTFR53-91-C-00065)
(PB93-169902; DOT/FRA/NMI-92/25-Vol-1) Avail: CASI HC A12/MF A03

The report summarizes work completed in the investigation of the power, propulsion, and braking systems for five different electrodynamic (EDS) Maglev configurations. System requirements and recommendations, including a cost analysis, are determined for each configuration. The analysis considers variations in vehicle length, acceleration/deceleration criteria, airgap clearance, and maximum propulsion thrust. Five different guideway configurations have been considered, each of which is based on air-core magnets made from low-temperature superconductors (LTSC) or the new high-T(sub c) ceramic superconductors (HTSC's). The material requirements and cost of the guideway electrical components were studied as a function of the energy conversion efficiency, the stator block length, armature current density, stator temperature rise, and other parameters. The propulsion design focused on a dual-parallel, linear synchronous motor (LSM) with thrust modulation achieved by applying a variable frequency and voltage along the guideway. Critical design parameters were estimated using a three-dimensional computer model for the inductances, magnetic fields, and electromagnetic forces. NTIS

N93-30828# Systems Technology, Inc., Hawthorne, CA.
VEHICLE DYNAMIC STABILITY AND ROLLOVER Final Report
R. W. Allen, H. T. Szostak, D. H. Klyde, T. J. Rosenthal, and K. J. Owens Jun. 1992 300 p See also PB90-115445 Sponsored by National Highway Traffic Safety Administration, Washington, DC
(Contract DTNH22-88-C-07384)
(PB93-185437; STI-TR-1268-1; DOT-HS-807 956) Avail: CASI HC A13/MF A03

The report considers ground vehicle lateral/directional stability which is of primary concern in traffic safety. Lateral/directional dynamics involve yawing, rolling, and lateral acceleration motions, and stability concerns include spinout and rollover. The report describes accident analysis, vehicle testing, and computer simulation analysis designed to give insight into basic vehicle design variables that contribute to stability problems. The results of vehicle testing and simulation analysis indicate that a vehicle that has both a relatively low ratio of track width to center of gravity height and is equipped with tires which have a relatively high peak coefficient of friction will have a propensity to rollover during steering maneuvers on a flat surface. Vehicle testing and computer simulation analysis also indicate that directional stability is significantly influenced by the relationship between vehicle weight distribution and lateral load transfer distribution that is greater than or equal to the percent weight on the front axle. NTIS

N93-31039*# Aerojet-General Corp., Sacramento, CA. Propulsion Div.
ORBITAL TRANSFER VEHICLE OXYGEN TURBOPUMP TECHNOLOGY. VOLUME 3: HOT OXYGEN TESTING Final Report, 17 Jul. - 31 Dec. 1989
Robert L. Urke Oct. 1992 94 p
(Contract NAS3-23772)
(NASA-CR-191036; NAS 1.26:191036) Avail: CASI HC A05/MF A01

This report covers the work done in preparation for a liquid oxygen rocket engine turbopump test utilizing high pressure hot oxygen gas for the turbine drive. The turbopump (TPA) is designed to operate with 400 F oxygen turbine drive gas. The goal of this test program was to demonstrate the successful operation of the TPA under simulated engine conditions including the hot oxygen turbine drive. This testing follows a highly successful series of tests pumping liquid oxygen with gaseous nitrogen as the turbine drive gas. That testing included starting of the TPA with no assist to the hydrostatic bearing. The bearing start entailed a rubbing start until the pump generated enough pressure to support the bearing. The articulating, self-centering hydrostatic bearing exhibited no bearing load or stability problems. The TPA was refurbished for the hot gas drive tests and facility work was begun, but unfortunately funding cuts prohibited the actual testing. Author (revised)

N93-28702*# McDonnell-Douglas Missile Systems Co., Saint Louis, MO.
NASA INSTEP/MDMSC JITTER SUPPRESSION EXPERIMENT (JITTER)
Edward V. White *In* NASA, Washington, NASA/DOD Flight Experiments Technical Interchange Meeting Proceedings 1992 9 p (For primary document see N93-28699 11-12)
(Contract NAS1-19245)
Avail: CASI HC A02/MF A10

N93-29118*# Colorado Univ., Boulder.
LUNAR CRANE SYSTEM
Martin M. Mikulas, Jr. *In its* Space Construction Activities 1 Nov. 1991 p 38-41 (For primary document see N93-29108 11-18)
Avail: CASI HC A01/MF A01

N93-29119*# Colorado Univ., Boulder.
LUNAR ROVERS AND LOCAL POSITIONING SYSTEM
James Avery and Renjeng Su *In its* Space Construction Activities 1 Nov. 1991 p 42-45 (For primary document see N93-29108 11-18)
Avail: CASI HC A01/MF A01

N93-29601*# Jet Propulsion Lab., California Inst. of Tech., Pasadena.
AN ANALYSIS OF THE 70-METER ANTENNA HYDROSTATIC BEARING BY MEANS OF COMPUTER SIMULATION
R. D. Bartos *In its* The Telecommunications and Data Acquisition Report 15 May 1993 p 147-173 (For primary document see N93-29586 11-32)
(RTOP 314-30-42-10-87)
Avail: CASI HC A03/MF A03

N93-29688*# Centre National d'Etudes Spatiales, Toulouse (France).
NEW RESULTS FROM FRECOPA ANALYSIS
Christian Durin *In* NASA. Langley Research Center, LDEF: 69 Months in Space. Part 4: Second Post-Retrieval Symposium Apr. 1993 p 1315-1331 (For primary document see N93-29682 11-99)
Avail: CASI HC A03/MF A03; 2 functional color pages

N93-29737*# Maryland Univ., College Park. Mechanical Engineering.
WALKING ROBOT: A DESIGN PROJECT FOR UNDERGRADUATE STUDENTS
In Universities Space Research Association, Houston, Proceedings of the Seventh Annual Summer Conference. NASA/USRA: University Advanced Design Program 1991 p 187-190 (For primary document see N93-29712 11-01)
Avail: CASI HC A01/MF A03

N93-30261 Royal Military Coll. of Canada, Kingston (Ontario). Dept. of Mechanical Engineering.
ANALYSIS AND SIMULATION OF A TWO DEGREES-OF-FREEDOM ONE-LINK FLEXIBLE FOREARM
J. C. Piedboeuf and R. Hurteau (Ecole Polytechnique, Montreal, Quebec.) *In* Engineering Inst. of Canada, Canadian Conference on Electrical and Computer Engineering, Volumes 1 and 2 1990 6 p (For primary document see N93-30215 11-31)
Avail: Engineering Inst. of Canada, 2050 rue Mansfield, Suite 700, Montreal, Quebec H3A 1Z2 Canada

N93-30300 Saskatchewan Univ., Saskatoon. Dept. of Electrical Engineering.
AN EXPERT SYSTEM FOR IDENTIFICATION OF THE TASK STATUS FROM TACTILE SENSOR DATA
C. S. Vaidyanathan and H. C. Wood *In* Engineering Inst. of Canada, Canadian Conference on Electrical and Computer Engineering, Volumes 1 and 2 1990 4 p (For primary document see N93-30215 11-31)
Avail: Engineering Inst. of Canada, 2050 rue Mansfield, Suite 700, Montreal, Quebec H3A 1Z2 Canada

N93-30310 Ottawa Univ. (Ontario). Dept. of Mechanical Engineering.
TRAJECTORY GENERATION FOR DUAL-ARM ROBOTS USING ARTIFICIAL IMPEDANCE APPROACH
D. S. Necsulescu, R. Jassemi-Zargani, and W. B. Graham (Canadian Space Agency, Ottawa, Ontario.) *In* Engineering Inst. of Canada, Canadian Conference on Electrical and Computer Engineering, Volumes 1 and 2 1990 4 p (For primary document see N93-30215 11-31)
Avail: Engineering Inst. of Canada, 2050 rue Mansfield, Suite 700, Montreal, Quebec H3A 1Z2 Canada

N93-30311 Thomson-CSF Systems Canada, Inc., Nepean (Ontario).
A FUNCTIONAL SYSTEM ARCHITECTURE FOR FULLY AUTONOMOUS ROBOT
S. Kalaycioglu *In* Engineering Inst. of Canada, Canadian Conference on Electrical and Computer Engineering, Volumes 1 and 2 1990 4 p (For primary document see N93-30215 11-31)
Avail: Engineering Inst. of Canada, 2050 rue Mansfield, Suite 700, Montreal, Quebec H3A 1Z2 Canada

N93-30312 Canadian Space Agency, Ottawa (Ontario).
ROBOT ARM WITH POSITIONAL ABSOLUTE ENCODED JOINTS
S. K. Yeung, C. Baribeau (Ottawa Univ., Ontario.), A. Pharand (Ottawa Univ., Ontario.), and E. Petriu (Ottawa Univ., Ontario.) *In* Engineering Inst. of Canada, Canadian Conference on Electrical and Computer Engineering, Volumes 1 and 2 1990 4 p (For primary document see N93-30215 11-31)
Avail: Engineering Inst. of Canada, 2050 rue Mansfield, Suite 700, Montreal, Quebec H3A 1Z2 Canada

N93-30313 Spar Aerospace Ltd., Weston (Ontario).
JOINT DRIVE DEVELOPMENT FOR THE SPACE STATION REMOTE MANIPULATOR SYSTEM
W. J. Ballantyne *In* Engineering Inst. of Canada, Canadian Conference on Electrical and Computer Engineering, Volumes 1 and 2 1990 5 p (For primary document see N93-30215 11-31)
Avail: Engineering Inst. of Canada, 2050 rue Mansfield, Suite 700, Montreal, Quebec H3A 1Z2 Canada

N93-30965*# Martin Marietta Energy Systems, Inc., Oak Ridge, TN. Metals and Ceramics Div.
TRIBOLOGY: FRICTION, LUBRICATION, AND WEAR TECHNOLOGY
Peter J. Blau *In* NASA. Langley Research Center, National Educators' Workshop. Update 92: Standard Experiments in Engineering Materials Science and Technology Jun. 1993 p 293-310 (For primary document see N93-30948 11-23)
Avail: CASI HC A03/MF A04

N93-30966*# Saint John's Univ., Jamaica, NY.
WALKWAY FRICTION: EXPERIMENT AND ANALYSIS
Mark I. Marpet and Robert J. Brungraber (Bucknell Univ., Lewisburg, PA.) *In* NASA. Langley Research Center, National Educators' Workshop. Update 92: Standard Experiments in Engineering Materials Science and Technology Jun. 1993 p 311-327 (For primary document see N93-30948 11-23)
Avail: CASI HC A03/MF A04

38 QUALITY ASSURANCE AND RELIABILITY

Includes product sampling procedures and techniques; and quality control.

N93-28685# Sandia National Labs., Albuquerque, NM.
RELIABILITY ASSESSMENT AT AIRLINE INSPECTION FACILITIES. VOLUME 2: PROTOCOL FOR AN EDDY CURRENT INSPECTION RELIABILITY EXPERIMENT Final Report
Floyd Spencer, Giancarlo Borgonovi (Science Applications, Inc., Albuquerque, NM.), Dennis Roach, Don Schurman (Science Applications, Inc., Albuquerque, NM.), and Ron Smith (AEA Technology, London, England.) May 1993 62 p
(DOT/FAA/CT-92/12-Vol-2) Avail: CASI HC A04/MF A01

The Aging Aircraft NDI Development and Demonstration Center (AANC) at Sandia National Laboratories is charged by the FAA to support technology transfer, technology assessment, and technology validation. A key task facing the center is the establishment of a consistent and systematic methodology to assess the reliability of inspections through field experiments. This task is divided into three major areas: reliability of eddy current lap splice inspections at transport aircraft maintenance facilities; reliability of inspection at commuter aircraft maintenance facilities; and reliability of inspection associated with visual inspection of aircraft structural parts. Volume 2 is the second document in a series of three describing the planning, execution, and results of an eddy current inspection field experiment. This document provides a detailed description of the experimental hardware and protocols. It also describes the methodology to be used in the analysis of the data. Author (revised)

N93-28943# Argonne National Lab., IL. Materials and Components Technology Div.
USE OF LOCAL X RAY COMPUTERIZED TOMOGRAPHY FOR HIGH-RESOLUTION, REGION-OF-INTEREST INSPECTION OF LARGE CERAMIC COMPONENTS FOR ENGINES
E. A. Sivers, D. A. Holloway, and W. A. Ellingson 1993 21 p Presented at the 38th ASME International Gas Turbine and Aeroengine Congress and Exhibition, Cincinnati, OH, 24-27 May 1993
(Contract W-31-109-eng-38)
(DE93-005564; ANL/MCT/CP-77501; CONF-930502-2) Avail: CASI HC A03/MF A01

Reliability continues to be an issue in ceramic components for high-temperature, high-wear applications in advanced engine designs. Recently, high-resolution, three-dimensional, X-ray computerized tomography (XRCT) has been shown to be invaluable for inspecting relatively small components. However, the time and system capacity required to collect complete high-resolution data for large ceramic objects is often prohibitive. When only the critical regions of a large component need be inspected with high resolution, region-of-interest XRCT is a viable alternative. With local XRCT methods used on data taken through only the critical area, it is possible to reconstruct flat, 'edge-enhanced' images in which density differences are clearly delineated. We present XRCT results from local scans of critical regions in a large, pressure-slip-cast, Si3N4 turbine rotor and two Si3N4 test phantoms. We also illustrate how the method can be extended to larger assemblies of ceramic components. DOE

N93-29073*# National Aeronautics and Space Administration. Lewis Research Center, Cleveland, OH.
ACOUSTO-ULTRASONIC ANALYSIS OF FAILURE IN CERAMIC MATRIX COMPOSITE TENSILE SPECIMENS
Harold E. Kautz and Abhisak Chulya (Cleveland State Univ., OH.) Jun. 1993 10 p Presented at the Second International Conference on Acousto-Ultrasonics, Atlanta, GA, 24-25 Jun. 1993; sponsored by American Society for Nondestructive Testing, Inc.
(RTOP 510-01-50)
(NASA-TM-106219; E-7930; NAS 1.15:106219) Avail: CASI HC A02/MF A01

Three types of acousto-ultrasonic (AU) measurements, stress-wave factor (SWF), lowest antisymmetric plate mode group velocity (VS), and lowest symmetric plate mode group velocity (VL), were performed on specimens before and after tensile failure. Three different Nicalon fiber architectures with ceramic matrices were tested. These composites were categorized as 1D (unidirectional fiber orientation) SiC/CAS glass ceramic, and 2D and 3D woven SiC/SiC ceramic matrix materials. SWF was found to be degraded after tensile failure in all three material categories. VS was found to be degraded only in the 1D SiC/CAS. VL was difficult to determine on the irregular specimen surfaces but appeared unchanged on all failed specimens. 3D woven specimens with heat-treatment at high temperature exhibited degradation only in SWF. Author

N93-29220*# National Aeronautics and Space Administration. John F. Kennedy Space Center, Cocoa Beach, FL.
GUIDE FOR CERTIFYING PRESSURE VESSELS AND SYSTEMS
Floyd Lundy and Paul W. Krusa Jul. 1992 94 p
(NASA-TM-107549; NAS 1.15:107549) Avail: CASI HC A05/MF A01

This guide is intended to provide methodology and describe the intent of the Pressure Vessel and System (PV/S) Certification program. It is not meant to be a mandated document, but is intended to transmit a basic understanding of the PV/S program, and include examples. After the reader has familiarized himself with this publication, he should have a basic understanding of how to go about developing a PV/S certification program. Author

N93-29443# Ames Lab., IA.
ADVANCED NDE TECHNOLOGY PROGRAM Final Report, 11 Oct. 1990 - 30 Sep. 1991
D. O. Thompson Aug. 1992 159 p
(Contract FY1457-91-N-5014)
(AD-A262008; WL-TR-92-4068) Avail: CASI HC A08/MF A02

The final reports of the various projects included in the Advanced Nondestructive Evaluation (NDE) Technology Program at the Ames Laboratory (DOE), Iowa State University are included. The technologies covered include thermal wave methods, image enhancement, laser based ultrasonics, detection of brittle phase in Ti alloys, adhesive bond characterization, and eddy current methods. DTIC

N93-30413*# National Aeronautics and Space Administration. Pasadena Office, CA.
HIDDEN MARKOV MODELS FOR FAULT DETECTION IN DYNAMIC SYSTEMS Patent Applications
Padhraic J. Smyth, inventor (to NASA) (Jet Propulsion Lab., California Inst. of Tech., Pasadena.) 7 Apr. 1993 60 p
(Contract NAS7-918)
(NASA-Case-NPO-18982-1-CU; NAS 1.71:NPO-18982-1-CU; US-Patent-Appl-SN-047135) Avail: CASI HC A04/MF A01

The invention is a system failure monitoring method and apparatus which learns the symptom-fault mapping directly from training data. The invention first estimates the state of the system at discrete intervals in time. A feature vector x of dimension k is estimated from sets of successive windows of sensor data. A pattern recognition component then models the instantaneous estimate of the posterior class probability given the features, p(w(sub i) perpendicular to x), 1 less than or equal to i is less than or equal to m. Finally, a hidden Markov model is used to take advantage of temporal context and estimate class probabilities conditioned on recent past history. In this hierarchical pattern of information flow, the time series data is transformed and mapped into a categorical representation (the fault classes) and integrated over time to enable robust decision-making. Author (revised)

N93-30414*# National Aeronautics and Space Administration. Langley Research Center, Hampton, VA.
A QUALITY MONITOR AND MONITORING TECHNIQUE EMPLOYING OPTICALLY STIMULATED ELECTRON EMISSION Patent Application
William T. Yost, inventor (to NASA), Christopher S. Welch, inventor (to NASA) (College of William and Mary, Gloucester Point, VA.), Edmond J.

Joe, inventor (to NASA) (AS&M, Inc., Hampton, VA.), and Bill Bryan Hefner, Jr., inventor (to NASA) (AS&M, Inc., Hampton, VA.) 11 May 1993 43 p
(NASA-Case-LAR-15063-1; NAS 1.71:LAR-15063-1;
US-Patent-Appl-SN-060617) Avail: CASI HC A03/MF A01

A light source directs ultraviolet light onto a test surface and a detector detects a current of photoelectrons generated by the light. The detector includes a collector which is positively biased with respect to the test surface. Quality is indicated based on the photoelectron current. The collector is then negatively biased to replace charges removed by the measurement of a nonconducting substrate to permit subsequent measurements. Also, the intensity of the ultraviolet light at a particular wavelength is monitored and the voltage of the light source varied to maintain the light a constant desired intensity. The light source is also cooled via a gas circulation system. If the test surface is an insulator, the surface is bombarded with ultraviolet light in the presence of an electron field to remove the majority of negative charges from the surface. The test surface is then exposed to an ion field until it possesses no net charge. The technique described above is then performed to assess quality. NASA

N93-30636# Los Alamos National Lab., NM.

THE QUALITY ASSURANCE LIAISON: COMBINED TECHNICAL AND QUALITY ASSURANCE SUPPORT

S. L. Bolivar and J. L. Day (Los Alamos Technical Associates, Inc., NM.) 1993 8 p Presented at the 17th Annual Rocky Mountain Quality Conference, Denver, CO, 6-8 Jun. 1993
(Contract W-7405-eng-36)
(DE93-008725; LA-UR-93-690; CONF-9306114-1) Avail: CASI HC A02/MF A01

The role of the quality assurance liaison, the responsibilities of this position, and the evolutionary changes in duties over the last six years are described. The role of the quality assurance liaison has had a very positive impact on the Los Alamos Yucca Mountain Site Characterization (YW) quality assurance program. Having both technical and quality assurance expertise, the quality assurance liaisons are able to facilitate communications with scientists on quality assurance issues and requirements, thereby generating greater productivity in scientific investigations. The quality assurance liaisons help ensure that the scientific community knows and implements existing requirements, is aware of new or changing regulations, and is able to conduct scientific work within Project requirements. The influence of the role of the quality assurance liaison can be measured by an overall improvement in attitude of the staff regarding quality assurance requirements and improved job performance, as well as a decrease in deficiencies identified during both internal and external audits and surveillances. This has resulted in a more effective implementation of quality assurance requirements. DOE

N93-30246 Laval Univ. (Quebec). Dept. of Electrical Engineering.

LOGARITHMIC TIME SCALE IN THERMOGRAPHIC NON DESTRUCTIVE EVALUATION (NDE) OF MATERIALS

X. Maldague, J. C. Krapez (National Research Council of Canada, Boucherville, Quebec.), and P. Cielo (National Research Council of Canada, Boucherville, Quebec.) *In* Engineering Inst. of Canada, Canadian Conference on Electrical and Computer Engineering, Volumes 1 and 2 1990 4 p (For primary document see N93-30215 11-31)
Avail: Engineering Inst. of Canada, 2050 rue Mansfield, Suite 700, Montreal, Quebec H3A 1Z2 Canada

39 STRUCTURAL MECHANICS

Includes structural element design and weight analysis; fatigue; and thermal stress.

For applications see *05 Aircraft Design, Testing and Performance* and *18 Spacecraft Design, Testing and Performance.*

N93-28516# Naval Postgraduate School, Monterey, CA. Dept. of Mathematics.

THE CURVATURE OF PLANE ELASTIC CURVES Tech Report, Jan. 1993 - Mar. 1993

Guido Brunnett 17 Mar. 1993 19 p
(AD-A263198; NPS-MA-93-013) Avail: CASI HC A03/MF A01

In this paper, plane elastic curves are revisited from a viewpoint that emphasizes curvature properties of these curves. The family of elastic curves is considered in dependence of a tension parameter Sigma and the squared global curvature maximum K2/m. It is shown that for any elastic curve K2/m is bigger than the tension parameter Sigma. A curvature analysis of the fundamental forms of the elastic curves is presented. A formula is established that gives the maximum turning angle of an elastica as a function depending on K2/m and Sigma. Finally, it is shown that an elastic curve can be represented as a linear combination of its curvature, arc length, and energy function and that any curve with this property is an elastic. DTIC

N93-28556*# Colorado Univ., Boulder. Dept. of Aerospace Engineering Sciences and Center for Space Structures and Controls.

FINITE ELEMENT ANALYSIS OF TIME-INDEPENDENT SUPERCONDUCTIVITY Ph.D. Thesis Final Report

James J. Schuler May 1993 257 p
(Grant NAG3-934; RTOP 509-10-11)
(NASA-CR-191140; E-7852; NAS 1.26:191140) Avail: CASI HC A12/MF A03

The development of electromagnetic (EM) finite elements based upon a generalized four-potential variational principle is presented. The use of the four-potential variational principle allows for downstream coupling of EM fields with the thermal, mechanical, and quantum effects exhibited by superconducting materials. The use of variational methods to model an EM system allows for a greater range of applications than just the superconducting problem. The four-potential variational principle can be used to solve a broader range of EM problems than any of the currently available formulations. It also reduces the number of independent variables from six to four while easily dealing with conductor/insulator interfaces. This methodology was applied to a range of EM field problems. Results from all these problems predict EM quantities exceptionally well and are consistent with the expected physical behavior. Author

N93-28567# Ames Lab., IA.

CRACK LENGTH DETERMINATION BY ULTRASONIC METHODS

D. K. Rehbein, R. B. Thompson, and O. Buck 1992 7 p Presented at the Review of Progress in Quantitative Non Destructive Evaluation (NDE), La Jolla, CA, 19-24 Jul. 1992
(Contract W-7405-eng-82)
(DE93-008075; IS-M-739; CONF-920799-6) Avail: CASI HC A02/MF A01

Under the restriction of being able to operate in through transmission with focussed transducers, it has been shown that the location of the tip of a fatigue crack can be determined to within 0.5 mm in those cases where curvature of the crack front is significant with correspondingly better accuracy as the curvature decreases. Location of the crack tip is accomplished through use of the distributed spring model and also yields information on the residual stresses due to closure. The technique used is able to determine the crack length to within (plus minus) 0.5 mm in the unloaded condition in contrast to most of the work done previously, removing the necessity for application of a load sufficient to fully open the crack. DOE

N93-28596# Lawrence Livermore National Lab., CA.

THE WAVE, THE CYLINDER, AND THE PLATE

S. Govindjee Aug. 1992 18 p
(Contract W-7405-eng-48)
(DE93-009458; UCRL-ID-111489) Avail: CASI HC A03/MF A01

In this report, a simple fluid-structure interaction problem is proposed as a benchmark test for fluid-structure codes. The report details the solution to the problem of a plane wave scattering off an elastic cylinder with internal structure in an acoustic medium. The particular system analyzed is an infinitely long cylinder with an internal hinged plate. and as such, the problem is two dimensional in nature. The analysis sets up the basics of acoustic scattering from elastic structures and then proceeds to develop the particular solution for the chosen structure. The complete solution to the steady state problem is developed in terms of harmonic series in the polar angle. The final expressions are in terms of infinite series over the cylindrical shell harmonics and permit comparisons and validation of results from numerical techniques such as finite difference and finite element methods. It is noted that the geometry, although simple, embodies some of the main features of more complicated problems and thus makes the given problem suitable for use in benchmarking and verification. DOE

N93-28633*# National Aeronautics and Space Administration. Lewis Research Center, Cleveland, OH.

PROBABILISTIC SIMULATION OF MULTI-SCALE COMPOSITE BEHAVIOR

D. G. Liaw (Sverdrup Technology, Inc., Brook Park, OH.), M. C. Shiao (Sverdrup Technology, Inc., Brook Park, OH.), S. N. Singhal (Sverdrup Technology, Inc., Brook Park, OH.), and Christos C. Chamis Jun. 1993 14 p Presented at the 6th Japan-US Conference on Composite Materials, Orlando, FL, 22-25 Jun. 1992
(RTOP 510-02-12)
(NASA-TM-106196; E-7904; NAS 1.15:106196) Avail: CASI HC A03/MF A01

A methodology is developed to computationally assess the probabilistic composite material properties at all composite scale levels due to the uncertainties in the constituent (fiber and matrix) properties and in the fabrication process variables. The methodology is computationally efficient for simulating the probability distributions of material properties. The sensitivity of the probabilistic composite material property to each random variable is determined. This information can be used to reduce undesirable uncertainties in material properties at the macro scale of the composite by reducing the uncertainties in the most influential random variables at the micro scale. This methodology was implemented into the computer code PICAN (Probabilistic Integrated Composite ANalyzer). The accuracy and efficiency of this methodology are demonstrated by simulating the uncertainties in the material properties of a typical laminate and comparing the results with the Monte Carlo simulation method. The experimental data of composite material properties at all scales fall within the scatters predicted by PICAN. Author

N93-28832# Oak Ridge Y-12 Plant, TN.

DESIGN AND EVALUATION OF A UNIAXIAL PULL TEST FOR LITHIUM HYDRIDE/DEUTERIDE

D. A. Waldrop, M. J. Marsicek, and K. C. Liu (Oak Ridge National Lab., TN.) Dec. 1992 20 p
(Contract DE-AC05-84OS-21400)
(DE93-010760; Y-2447) Avail: CASI HC A03/MF A01

A uniaxial pull test was developed for determining tensile strength of lithium hydride (LiH). Objectives were to establish the capability of acquiring highly credible uniaxial strength data using a conventional pull specimen and to assess compatibility of existing data bases from disk flexure, four-point bend, and ring tensile tests. A specimen was designed using elliptic contours between gage section and button-head ends to minimize stress concentrations. A finite-element stress analysis was performed. Bending strains resulting from load train misalignment were also minimized by close tolerancing of the gripping fixture and the use of hydraulic-universal joints. Twenty specimens were fabricated and tested for a preliminary date base. Bending studies were conducted on two specimens. Within the load range of interest, bending stresses accounted for about 1% of the nominal stress. The test provided reliable, true-uniaxial strength data. Comparison with existing data bases suggests that high-stress gradients within a specimen may alter strength distribution. DOE

N93-29069*# National Aeronautics and Space Administration. Langley Research Center, Hampton, VA.

THE GROWTH OF SMALL CORROSION FATIGUE CRACKS IN ALLOY 2024

Robert S. Piascik and Scott A. Willard (Lockheed Engineering and Sciences Co., Hampton, VA.) Apr. 1993 31 p
(RTOP 538-02-10-01)
(NASA-TM-107755; NAS 1.15:107755) Avail: CASI HC A03/MF A01

The corrosion fatigue crack growth characteristics of small surface and corner cracks in aluminum alloy 2024 is established. The damaging effect of salt water on the early stages of small crack growth is characterized by crack initiation at constituent particle pits, intergranular microcracking for a less than 100 micrometers, and transgranular small crack growth for a micrometer. In aqueous 1 percent NaCl and at a constant anodic potential of -700 mV(sub SCE), small cracks exhibit a factor of three increase in fatigue crack growth rates compared to laboratory air. Small cracks exhibit accelerated corrosion fatigue crack growth rates at low levels of delta-K (less than 1 MPa square root of m) below long crack delta-K (sub th). When exposed to Paris regime levels of crack tip stress intensity, small corrosion fatigue cracks exhibit growth rates similar to that observed for long cracks. Results suggest that crack closure effects influence the corrosion fatigue crack growth rates of small cracks (a less than or equal to 100 micrometers). This is evidenced by similar small and long crack growth behavior at various levels of R. Contrary to the corrosion fatigue characteristics of small cracks in high strength steels, no pronounced chemical crack length effect is observed for Al by 2024 exposed to salt water. Author

N93-29076# Aeronautical Research Inst. of Sweden, Bromma.

FACTORS INFLUENCING THE INTERLAMINAR FRACTURE TOUGHNESS AND ITS EVALUATION IN COMPOSITES

Robin Olsson Dec. 1992 54 p Sponsored by Swedish Defence Materials Administration
(FFA-TN-1991-34) Avail: CASI HC A04/MF A01

This review discusses in qualitative terms different physical factors that have to be considered when characterizing delamination toughness of polymetric continuous fiber composites. The mere determination of delamination toughness is not trivial and is discussed first. The resistance to delamination of composites is highly dependent on the mode of fracture and the fiber angles of the plies adjacent to the crack. Loading rate and hygrothermal effects can have a large influence on the material toughness and are discussed. The toughness of the composite is highly dependent on the properties of the constituents and their interaction in the composite. This question is discussed and the physical causes for poor transfer of neat resin toughness to the composite are clarified. Author

N93-29106# Queensland Univ., Brisbane (Australia). Dept. of Civil Engineering.

WIND LOADS ON CANOPY ROOFS

J. D. Ginger and C. W. Letchford Jun. 1991 80 p Sponsored by Australian Research Council
(RR-CE132; ISBN-0-86776-462-7) Avail: CASI HC A05/MF A01

Wind pressure distributions on 30 m x 30 m canopy roofs over a range of roof pitch angles were determined in the wind tunnel, in a simulated, terrain category 3 (AS-1170) atmospheric boundary layer flow at a length scale of 1/100. Contour plots of local point pressures indicate that the largest pressures were experienced close to the leading edges and the ridge line at a wind orientation of 30 degrees. These contour plots also provide information on the flow mechanisms over the roof. The largest area averaged pressure coefficients were obtained on the leading sections of the roof at a wind orientation of between 20 and 30 degrees. Area averaged pressures on rectangular strips in regions close to the leading edges and ridge line experience pressures substantially larger than those on the rest of the roof. Author

N93-29154*# Old Dominion Univ., Norfolk, VA. Coll. of Engineering and Technology.

NONLINEAR ANALYSES OF COMPOSITE AEROSPACE STRUCTURES IN SONIC FATIGUE Progress Report, 16 Dec. 1992 - 15 Jun. 1993

Chuh Mei Jun. 1993 21 p
(Grant NAG1-1358)
(NASA-CR-193124; NAS 1.26:193124) Avail: CASI HC A03/MF A01

This report summarizes the semiannual research progress, accomplishments, and future plans performed under the NASA Langley Research Center Grant No. NAG-1-1358. The primary research effort of this project is the development of analytical methods for the prediction of nonlinear random response of composite aerospace structures subjected to combined acoustic and thermal loads. The progress, accomplishments, and future plates on four sonic fatigue research topics are described. The sonic fatigue design and passive control of random response of shape memory alloy hybrid composites presented in section 4, which is suited especially for HSCT, is a new initiative. Derived from text

N93-29196*# National Aeronautics and Space Administration. Lewis Research Center, Cleveland, OH.

BOUNDS ON INTERNAL STATE VARIABLES IN VISCOPLASTICITY

Alan D. Freed Jun. 1993 6 p Prepared for Plasticity 1993, Baltimore, MD, 19-23 Jul. 1993; sponsored by Univ. of Maryland

(RTOP 505-63-5A)
(NASA-TM-106215; E-7924; NAS 1.15:106215) Avail: CASI HC A02/MF A01

A typical viscoplastic model will introduce up to three types of internal state variables in order to properly describe transient material behavior; they are as follows: the back stress, the yield stress, and the drag strength. Different models employ different combinations of these internal variables--their selection and description of evolution being largely dependent on application and material selection. Under steady-state conditions, the internal variables cease to evolve and therefore become related to the external variables (stress and temperature) through simple functional relationships. A physically motivated hypothesis is presented that links the kinetic equation of viscoplasticity with that of creep under steady-state conditions. From this hypothesis one determines how the internal variables relate to one another at steady state, but most importantly, one obtains bounds on the magnitudes of stress and back stress, and on the yield stress and drag strength. Author (NASDA)

N93-29349 Rice Univ., Houston, TX. Dept. of Mathematical Sciences.
INTEGRATED APPROACHES TO PARALLELISM IN OPTIMIZATION AND SOLUTION OF INVERSE PROBLEMS Final Report, 15 May 1989 - 31 Mar. 1992
William Symes 1 Jan. 1993 3 p Limited Reproducibility: Document partially illegible
(Grant AF-AFOSR-0363-89)
(AD-A262259; AFOSR-93-0196TR) Avail: Issuing Activity (Defense Technical Information Center (DTIC))

Mathematical models for mechanical design problems and development of analytical and numerical tools for their solution was studied under this grant. The mathematical problems separate into ones of rods and membranes. Regarding the former, with M. Overton, the PI provided the first rigorous study of the shape of the strongest rod. In particular, within the context of the Euler-Bernoulli model, we established existence, necessary conditions, regularity, and a general, though efficient, means of computing an optimal shape. Previous studies had not fully dealt with the fact that the strength of a rod (the axial load under which it commences to bucle) need not be a differentiable function of its shape. The Mathematical Intelligence solicited an expository account of this work. This article was picked up by Discover magazine, where the review appears. Engineers in off-shore oil rig design at Exxon Production Research in Houston have approached the PI regarding the research. Via the rolling of thin plates they have the means to create rods with piecewise conical cross-sections. With J. Maddocks, the PI has extended all of the above analytical findings to a much richer class of rods. In particular, they are able to accommodate hyperelastic rods with nonlinear bending laws and vanishing cross-sections in both the interior and at the boundary. In this new framework, they are also finally able to carefully pose and settle bifurcation questions as to whether the branches of equilibria stemming from the buckling load of the optimal column are indeed supercritical, i.e., rightward. DTIC

N93-29432# Massachusetts Inst. of Tech., Cambridge. Dept. of Mechanical Engineering.
A RIEMANN PROBLEM FOR AN ELASTIC BAR THAT CHANGES PHASE Technical Report No. 10
Yier Lin Nov. 1992 45 p
(Contract N00014-90-J-1871)
(AD-A262827) Avail: CASI HC A03/MF A01

This paper is concerned with the dynamics of an elastic bar that can undergo reversible stress-induced phase transformations. We consider a Riemann problem in which the initial strains belong to a single metastable phase and prove uniqueness of solution that satisfy a nucleation criterion and a kinetic law at all subsonic and sonic phase boundaries. This paper generalizes the results of a previous paper, which considered a piecewise linear material for which the following are true: no wave fans exist, shock waves always travel at the acoustic speed, and shock waves are dissipation-free. The material model of the present paper does not suffer from these degeneracies. DTIC

N93-29515# New Mexico Univ., Albuquerque. Dept. of Chemistry.
THE MECHANICAL RESPONSE OF GOLD SUBSTRATES MODIFIED WITH SELF-ASSEMBLING MONOLAYER FILMS
Ross C. Thomas, Richard M. Crooks, J. E. Houston (Sandia National Labs., Albuquerque, NM.), and Terry A. Michalske (Sandia National Labs., Albuquerque, NM.) 19 Mar. 1993 22 p
(Contract N00014-91-J-1991)
(AD-A262997; TR-4) Avail: CASI HC A03/MF A01

We have used the newly developed interfacial force microscope (IFM) to study the adhesive and mechanical properties of a Au substrate. We show that a W probe interacting with a Au surface results in plastic deformation under very small repulsive loads and transfers Au to the probe surface in a galling interaction upon removal. However, when the Au surface is passivated by a self-assembling monolayer of n-docosanethiol molecules ($CH3(CH2)21SH$), the substrate is able to elastically support large repulsive loads with no attractive interactions. Within this elastic region, the load/deformation relationship closely follows the classic Hertzian model for a rigid punch deforming an elastic half space. As a result, we are able to determine the maximum values for the shear-stress threshold for plastic deformation to be approximately 1 GPa in agreement with theoretical determinations. Above this value, the substrate permanently deforms. Remarkably, however, the strong binding of the molecular film to the Au surface permits it to maintain its passivating properties even after gross plastic damage. DTIC

N93-29612* National Aeronautics and Space Administration. Langley Research Center, Hampton, VA.
METHOD OF CONTINUOUSLY DETERMINING CRACK LENGTH Patent
Ramamurthy Prabhakaran, inventor (to NASA) and Osvaldo F. Lopez, inventor (to NASA) 13 Jul. 1993 14 p Filed 24 May 1991 Supersedes N92-11374 (30 - 2, p 247)
(NASA-Case-LAR-14480-1-CU; US-Patent-5,227,731; US-Patent-Appl-SN-705474; US-Patent-Class-324-718; US-Patent-Class-324-699; US-Patent-Class-73-799; Int-Patent-Class-G01R-27/02; Int-Patent-Class-G01N-19/08) Avail: US Patent and Trademark Office

The determination of crack lengths in an accurate and straight forward manner is very useful in studying and preventing load created flaws and cracks. A crack length sensor according to the present invention is fabricated in a rectangular or other geometrical form from a conductive powder impregnated polymer material. The long edges of the sensor are silver painted on both sides and the sensor is then bonded to a test specimen via an adhesive having sufficient thickness to also serve as an insulator. A lead wire is connected to each of the two outwardly facing silver painted edges. The resistance across the sensor changes as a function of the crack length in the specimen and sensor. The novel aspect of the present invention includes the use of relatively uncomplicated sensors and instrumentation to effectively measure the length of generated cracks. Official Gazette of the U.S. Patent and Trademark Office

N93-29613* National Aeronautics and Space Administration. Langley Research Center, Hampton, VA.
SHEAR SENSITIVE MONOMER-POLYMER LAMINATE STRUCTURE AND METHOD OF USING SAME Patent
Jag J. Singh, inventor (to NASA), Abe Eftekhari, inventor (to NASA), and Devendra S. Parmar, inventor (to NASA) 29 Jun. 1993 13 p Filed 2 Mar. 1992 Supersedes N92-30317 (30 - 21, p 3662)
(NASA-Case-LAR-14654-1-CU; US-Patent-5,223,310; US-Patent-Appl-SN-849612; US-Patent-Class-428-1; US-Patent-Class-428-409; US-Patent-Class-428-480; US-Patent-Class-428-913; US-Patent-Class-359-67; US-Patent-Class-359-74; US-Patent-Class-359-82) Avail: US Patent and Trademark Office

Monomer cholesteric liquid crystals have helical structures which result in a phenomenon known as selective reflection, wherein incident white light is reflected in such a way that its wavelength is governed by the instantaneous pitch of the helix structure. The pitch is dependent on temperature and external stress fields. It is possible to use such monomers in flow visualization and temperature measurement. However, the required thin layers of these monomers are quickly washed away by a flow, making their application time dependent for a given flow rate. The laminate structure according to the present invention comprises a liquid crystal polymer substrate attached to a test surface of an article. A light absorbing coating is applied to the substrate and is thin enough to permit bonding steric interaction between the liquid crystal polymer substrate and an overlying liquid crystal monomer thin film. Light is directed through and reflected by the liquid crystal monomer thin film and unreflected light is absorbed by

the underlying coating. The wavelength of the reflected light is indicative of the shear stress experienced by the test surface. Novel aspects of the invention include its firm bonding of a liquid crystal monomer to a model and its use of a coating to reduce interference from light unreflected by the monomer helical structure.
Official Gazette of the U.S. Patent and Trademark Office

N93-29801# Army Research Lab., Aberdeen Proving Ground, MD.
THE EFFECT OF MATERIAL STRENGTH ON SEGMENT PENETRATION BEHAVIOR Final Report, Jan. 1992 - Feb. 1993
Todd W. Bjerke Apr. 1993 23 p
(DA Proj. 1L1-62618-AH-80)
(AD-A263262; ARL-MR-51) Avail: CASI HC A03/MF A01

The effects of penetrator material strength on the terminal ballistic behavior of tungsten alloy segments fired into armor plate was determined by a series of impact experiments. Three different strength tungsten alloys were machined into cylinders with an aspect ratio of 4 and were subsequently impacted into rolled homogeneous armor at 1.5 km/s. The depth of penetration and the shape of the penetrator material remaining in the penetration cavity were recorded and compared. Decreasing the penetrator material strength was observed to slightly decrease the length of residual material and the depth of penetration. The diameter of the plastically deformed residual material was observed to increase with decreasing penetrator material strength. DTIC

N93-29843# Sandia National Labs., Livermore, CA.
AN EXPERIMENTAL/ANALYTICAL EVALUATION OF BIAXIAL SHEET FAILURE
K. L. Lee, S. L. Brandon, M. F. Horstemeyer, and J. S. Korellis Mar. 1993 26 p
(Contract DE-AC04-76DR-00789)
(DE93-010620; SAND-93-8226) Avail: CASI HC A03/MF A01

An experimental test system has been developed to support numerical modeling analysis of sheet metal failure. The system consists of a planar biaxial test frame, cruciform specimens and grips, and custom software to control the frame's actuators. Thin aluminum 6061-0 specimens are loaded to the point of incipient failure under different biaxial stress ratios. The data from these tests are used in validating a constitutive plasticity/failure model for aluminum 6061-0 by comparison with finite element predictions. DOE

N93-29855# Tufts Univ., Medford, MA. Dept. of Mechanical Engineering.
THREE-DIMENSIONAL ELASTIC STRESS ANALYSIS IN MATERIALS WITH MANY INHOMOGENEITIES Final Report, 1 Apr. 1988 - 31 Dec. 1992
Mark Kachanov Feb. 1993 8 p
(Contract DAAL03-88-K-0027)
(AD-A263736; ARO-25345.13-EG) Avail: CASI HC A02/MF A01

The research effort was concentrated on micromechanics of brittle materials with multiple interacting defects and on the impact of the defects on the overall (effective) properties. The work addressed the following problems: (1) three-dimensional mechanics of crack interactions; (2) three-dimensional mechanics of crack-microcrack interactions; (3) relationship between fracturing of a brittle microcracking material and reduction of its effective stiffness; (4) effective elastic properties of cracked solids and continuum characterization of crack arrays; (5) mechanics of solids filled with compressible fluid; and (6) anisotropic materials with interacting cracks. DTIC

N93-29863# California Univ., San Diego, La Jolla. Dept. of Applied Mechanics and Engineering Sciences.
BALANCED TECHNOLOGY INITIATIVE ON COMPUTATIONAL MECHANICS OF MATERIALS Final Technical Report, 15 Aug. 1989 - 30 Sep. 1991
Robert J. Asaro 7 Apr. 1993 4 p
(Contract N00014-89-J-3235)
(AD-A263906) Avail: CASI HC A01/MF A01

The goal of this project, which was part of the DARPA Balanced Technology Initiative on Computational Mechanics, was to develop a comprehensive approach to the numerical modeling of the mechanical behavior of materials. Particular areas for focus in the project were the inelastic deformation of highly anisotropic materials such as single crystals and textured polycrystals, as well as evolving microstructural damage in ceramics and ductile metals in both slow and high rate deformation processes. While the contract was awarded for a period of three years, it was actually funded only for the first year. Nonetheless, significant progress can be reported as a direct result of this project. DTIC

N93-30147# Washington Univ., Seattle. Dept. of Mechanical Engineering.
TWO-PARAMETER CRACK TIP FIELD ASSOCIATED WITH STABLE CRACK GROWTH IN A THIN PLATE: A HYBRID ANALYSIS Technical Report, Jun. 1992 - Apr. 1993
G. B. May, F. X. Wang, and A. S. Kobayashi Apr. 1993 20 p
(Contract N00014-89-J-1276)
(AD-A264221; UWA/DME/TR-93-71) Avail: CASI HC A03/MF A01

Moire interferometry was used to determine the two orthogonal displacement fields surrounding a stably growing crack in a thin 2024-T3 aluminum alloy, single-edge notched (SEN) specimen. The measured displacements were used to compute the J-integral and the associated HRR and the second order Q displacement fields. Also, a 2-D elastic-plastic finite element model of the fracturing specimen was executed in its generation mode to compute the crack tip displacement field and the J-integral for small crack extension. The numerically computed and experimentally derived J-values agreed prior to crack extension but differed increasingly with stable crack growth. The HRR and measured v-displacements agreed well but significant difference between the HRR and measured u displacements was noted. Thus, the Q component of the v-displacement was negligible but the corresponding u-component varied nonlinearly with radial distance from the crack tip. DTIC

N93-30159# Purdue Univ., West Lafayette, IN. Dept. of Materials Engineering.
DAMAGE MECHANICS IN 2-D AND 3-D MICROSTRUCTURES Final Report, Jul. 1989 - Jun. 1992
Keith J. Bowman and Martin Ostoja-Starzewski 26 Feb. 1993 50 p
Prepared in cooperation with Michigan State University
(Grant AF-AFOSR-0423-89)
(AD-A264337; AFOSR-93-0213TR) Avail: CASI HC A03/MF A01

The evolution of damage and strategies for assessing damage when it has occurred in structural materials is the primary focus of this research program. The research effort is a collaborative one on mesomechanics called 'Damage in 2D and 3D Microstructures.' What distinguishes this effort from others is the attempt to perform incisive model experiments to assist in evaluating stochastic models for constitutive laws (elasticity and conductivity), mechanical response plasticity, and hardness and associated damage processes. The theoretical models are designed to be elegant and efficient in the use of computing resources as opposed to brute force procedures which handle systems with different scales by scaling up the size of the computer. The essence of this work is to explore sample size microstructure relationships via stochastic models which reflect the same types of variability present in the response of real materials. This leads directly to concerns with effective properties of materials. Thus, research integrates the effects of microstructure and preferred orientation on the effective tensorial properties of polycrystalline materials. DTIC

N93-30185# Sandia National Labs., Albuquerque, NM.
CHARACTERIZING TRANSIENT VIBRATIONS USING BAND LIMITED TEMPORAL MOMENTS
D. O. Smallwood 1993 12 p Presented at the 39th Annual Technical Meeting of the Institute of Environmental Sciences, Las Vegas, NV, 2-7 May 1993
(Contract DE-AC04-76DP-00789)
(DE93-009639; SAND-93-0416C; CONF-930529-2) Avail: CASI HC A03/MF A01

A method is described to characterize shocks (transient time histories) in terms of the Fourier energy spectrum and the temporal moments of the shock passed through a contiguous set of bandpass filters. This method is compared for two transient time histories with the more conventional methods of shock response spectra (SRS) and a nonstationary random characteristic. DOE

N93-30213# Oak Ridge National Lab., TN.
STRESS-INTENSITY-FACTOR INFLUENCE COEFFICIENTS FOR AXIAL AND CIRCUMFERENTIAL FLAWS IN REACTOR PRESSURE VESSELS
J. W. Bryson and T. L. Dickson 1993 20 p Presented at the Pressure Vessel and Piping Conference, Denver, CO, 25-29 Jul. 1993
(Contract DE-AC05-84OR-21400)
(DE93-006206; CONF-930702-4) Avail: CASI HC A03/MF A01

Weight-function techniques in linear elastic fracture mechanics utilize stress-intensity-factor influence coefficients K* and superposition principles to compute stress intensity factors. This paper presents influence coefficients for two flaw geometries often employed in fracture analyses of reactor pressure vessels: (1) infinitely long, axial, inside-surface flaws and (2) 360 degree, circumferential, inside-surface flaws. Calculations were performed using ABAQUS, a nuclear quality assurance (NQA-1) certified finite-element program which employs a highly accurate crack extension technique for the computation of the J-integral. Influence coefficients are computed for flaw depths in the range 0.01 less than or = a/T less than or = 0.9 with particular emphasis on shallow flaws (a/T less than or = 0.1). This study addresses vessels having R/T = 10 which is appropriate for most PWR's in USA. The influence coefficients have been implemented in the FAVOR fracture-mechanics code currently being developed under the NRC-funded HSST Program at ORNL. DOE

N93-30374*# Virginia Polytechnic Inst. and State Univ., Blacksburg. Dept. of Engineering Science and Mechanics.
STATIC AND DYNAMIC LARGE DEFLECTION FLEXURAL RESPONSE OF GRAPHITE-EPOXY BEAMS
Mark D. Sensmeier, O. Hayden Griffin, Jr., and Eric R. Johnson Washington Mar. 1988 251 p
(Grant NAG1-343; RTOP 505-63-01-11)
(NASA-CR-4118; NAS 1.26:4118; VPI-E-87-7) Avail: CASI HC A12/MF A03

An experimental and analytical study of large deflection flexural response of graphite-epoxy beams subjected to eccentric axial compression was conducted. The beam specimens were subjected to axial impact and to static axial loads, in order to assess the damage caused by impact. A one-dimensional geometrically and materially nonlinear finite element model was developed to predict static beam response. The model incorporated width-wise effects by assuming specific forms of the displacements across the width, with lengthwise variation introduced as a degree of freedom. The resulting 22 degree of freedom element accurately predicted the load deflection and strain-deflection responses of the static test specimens. Author (revised)

N93-30545# Wright Lab., Eglin AFB, FL. Armament Directorate.
A CERAMIC FRACTURE MODEL FOR HIGH VELOCITY IMPACT Final Report, Oct. 1985 - Feb. 1993
William H. Cook May 1993 184 p
(AF Proj. 2302)
(AD-A264728; WL-TR-93-7023) Avail: CASI HC A09/MF A02

The objectives of this research program were to develop, implement, and demonstrate a failure model for aluminum oxide ceramic under impact loading. A comprehensive test program for Coors AD-85 was conducted. Four types of experiments provided a basis for the development of the ceramic failure model. A phenomenological damage-based failure model for compressive fracture of impacted aluminum oxide was developed with emphasis placed on predicting fragment sizes of failed ceramic. Test data suggested a fragment size correlation with loading rate. A model was developed incorporating the data and implemented in the EPIC hydrocode. Comparisons of the results of this model to penetration test were positive. DTIC

N93-30598# Naval Command, Control and Ocean Surveillance Center, San Diego, CA.
ELASTIC STABILITY CONSIDERATIONS FOR DEEP SUBMERGENCE CERAMIC PRESSURE HOUSING
Ramon R. Kurkchubasche Mar. 1993 10 p
(AD-A264824) Avail: CASI HC A02/MF A01

This paper discusses considerations in the design of ceramic pressure housings to prevent catastrophic failure of the housing under hydrostatic load. Emphasis is on trends discovered in the stability analysis, using the program BOSOR4, of cylindrical housings closed on both ends with hemispherical caps. Design of metallic rings for the joining of two or more cylindrical sections is also discussed. DTIC

N93-30626 Michigan Univ., Ann Arbor.
VIBRATION LOCALIZATION IN ROTATING SHAFTS Ph.D. Thesis
Suhyun Choi 1992 155 p
Avail: Univ. Microfilms Order No. DA9308289

The mode localization phenomenon between two orthogonal principal directions in flexible rotating shafts with slightly dissimilar lateral moments of inertia is investigated theoretically and experimentally. A consistent model is derived which describes the flexural vibration in two orthogonal planes, and the torsional vibrations of a straight rotating Timoshenko shaft with dissimilar lateral principal moments of inertia subject to a constant compressive axial load. In particular, a new approach for calculating correctly the effect of an axial load for a Timoshenko beam is developed based on the change in length of the centroidal line. The analysis of mode localization in a rotating shaft is carried out in an exact closed-form for a Rayleigh beam model using a separation of variables approach, and using a Galerkin approximation and perturbation methods which yield insights into the occurrence of localization. The analysis of eigenvalue loci veering is also performed using the perturbation techniques. Analytical and numerical results for a rotating shaft with simply supported, and with fixed-free, boundary conditions are presented: (1) the parameters which determine the degree of vibration localization are the difference between the two lateral moments of inertia, the rotational speed of the shaft, and the mode number; (2) for the strongly coupled case, the classical perturbation solutions are good approximations to the exact solutions; (3) for the weakly coupled case, the first-order modified perturbation solutions provide good approximations, and the second-order results yield excellent agreement with the exact solutions except for very small values of disorder; and (4) for the weakly coupled system, both strong localization and eigenvalue loci veering occur. To verify the theoretical results, a series of experiments are performed. Measurements of the natural frequencies are presented for non-rotating/rotating and tuned/mistuned shafts with simply supported boundary conditions. The localization phenomenon was demonstrated through measurements of the forced response due to unbalanced mass. The results of the theoretical and experimental studies indicate that indeed localization may occur in rotating shafts. Dissert. Abstr.

N93-31013# Los Alamos National Lab., NM.
A CONTINUUM CODE INVESTIGATION OF STRESS INTEGRATION USING EXACT AND APPROXIMATE MATERIAL ROTATION
R. F. Davidson and P. J. Maudlin Nov. 1992 28 p
(Contract W-7405-eng-36)
(DE93-001892; LA-12389-MS) Avail: CASI HC A03/MF A01 (US Sales Only)

The accuracy of the Zaremba-Jaumann-Noll stress rate (referred to as the Jaumann Stress Rate) used in various continuum mechanics codes is investigated using two realistic warhead formation problems that involve isotropic plasticity, large deformations, and large rigid body rotation. It was demonstrated in the literature for simple problems that, although the Jaumann Stress Rate is objective (i.e., under superimposed rigid body rotation, it transforms in like manner as the stress or strain rate), it is not kinematically consistent because it uses the anti-symmetric part of the velocity gradient tensor to approximate rigid body rotation. A theoretically correct approach would use an objective stress rate that is kinematically consistent via the use of the exact rigid body rotation rate. It is shown that, although the Jaumann Stress Rate is sufficiently accurate for gross deformation, inspection of the stress-strain details show kinetical errors. The computational expense of using an exact rotation rate is shown to be insignificant. DOE

N93-31015# Technische Univ., Berlin (Germany). Inst. fuer Luft- und Raumfahrt.
THE CONTACT MECHANICAL NONLINEARITIES OF A MATHEMATICAL MODEL OF A RAILWAY WHEEL ROLLING OVER CORRUGATED RAIL
Jerzy Piotrowski Sep. 1991 43 p
(ILR-Mitt-266(1991); ETN-93-94171) Avail: CASI HC A03/MF A01

The results of the investigations carried out on possible nonlinear contact mechanical effects of a wheel rolling over corrugated rail are discussed. The applied method of investigation takes as a starting point normal force and creep variations calculated by using a linear model of corrugations. Predicted normal loads between wheel and rail were taken as an input for the solution of the normal contact problem using an approximate, numerical method for non-Hertzian contact. The results of normal contact calculations were analyzed from the point of view of the geometry of contact and basic contact mechanical quantities which influence vertical dynamics of the system, generating the creep forces and wear. Similar analysis was carried out for Hertzian assumptions with the use of the same method for non-Hertzian normal contact problem. The main conclusion arrived at is that the discrepancies due to Hertzian description of the contact mechanical part of the linear model against the non-Hertzian description are most strongly pronounced when the wheel traverses the trough of the corrugation and, that might lead to the significant overall discrepancies in predictions obtained with the two different contact mechanical parts of the model. ESA

N93-31016# Technische Univ., Berlin (Germany). Inst. fuer Luft- und Raumfahrt.

THE STEADY-STATE TANGENTIAL CONTACT PROBLEM FOR A FALLING DROP TYPE OF CONTACT AREA ON CORRUGATED RAIL BY SIMPLIFIED THEORY OF ROLLING CONTACT

Jerzy Piotrowski Oct. 1991 30 p
(ILR-Mitt-267(1991); ETN-93-94172) Avail: CASI HC A03/MF A01

Investigation of contact mechanical nonlinearities of a mathematical model of corrugation revealed that the typical shape of contact patch resembles a falling drop of water. A contact patch of that shape was approximated with a figure composed of two parts of ellipses with different eccentricities. The contact pressure distribution was assumed as a smoothing ensemble of two paraboloidal distributions. The description of a general case of double half elliptical contact area was given but a special case of double half elliptical contact is more interesting as it possesses some Hertzian properties. It was shown how three geometrical parameters of double half elliptical contact can be chosen when actual, non-Hertzian contact is known. A linear theory was written which indicates that the lateral vibrations of the rail may be excited only due to shape variation on corrugation even if any other cause for these vibrations does not exist. For nonlinear theory a computer program, based on FASTSIM algorithm by Kalker, was written. The aim is to calculate the creep forces and frictional power density distribution over the contact area. Also, a graphic program visualizing the solution was written. Numerical results are not provided; unattended and unsolved problems relevant for this type of contact are listed. ESA

N93-31017# Technische Univ., Berlin (Germany). Inst. fuer Luft- und Raumfahrt.

DETERMINATION OF LOW FREQUENCY REFERENCE SLIPPING FOR HIGH FREQUENCY UNSTATIONARY MOTION PROCESSES [ERMITTLUNG NIEDERFREQUENTER REFERENZSCHLUEPFE FUER HOCHFREQUENTE, INSTATIONAERE BEWEGUNGSVORGAENGE]

Sebastian Stichel 1992 49 p In GERMAN
(ILR-Mitt-273(1992); ETN-93-94173) Avail: CASI HC A03/MF A01

Slips and slipping forces, which occur by unrolling of the set of wheels in a defective rail, are obtained in reference states, with focus on locomotive propulsion parameters influence in hackle formation. It is assumed that rail defects are described by a stochastic distribution and that slipping properties can be determined by the quadratic mean value of low frequency reference states. Calculations were performed by linear vehicle models with the covariance method. Geometric quantities for the wheel/trail contact are identical for all parameter variations. The results show a real dependence of slipings on vehicle excitation intensity. Calculations were carried out with the spectral density method and were shown to be in agreement, but the covariance method is proved to be a more rapid numerical process. ESA

N93-31028 Michigan Univ., Ann Arbor.

THEORETICAL AND EXPERIMENTAL INVESTIGATION OF SLACK CABLE/MASS SYSTEM DYNAMICS Ph.D. Thesis

Hai-Ping Lin 1992 177 p
Avail: Univ. Microfilms Order No. DA9308381

A theoretical model is presented that describes the three-dimensional nonlinear motion of a sagged cable that supports an array of discrete masses. A closed-form solution procedure is used to determine the equilibrium state of an arbitrarily suspended cable with an arbitrarily complex mass array. The equations of motion are linearized about equilibrium and the natural frequencies and mode shapes are determined from the associated eigenvalue problem governing free response. A global discretization based on Galerkin's method is used to solve this eigenvalue problem. With a judicious choice of the admissible functions, the convergence of the eigensolutions can be substantially accelerated over that found using 'traditional' admissible functions. A convergence study is pursued to determine the source of accelerated convergence. It is also noted that the convergence problem associated with the cable/mass system is generic. Similar convergence problems arise in other structural dynamics applications where the eigenfunctions have limited continuity; e.g., structures containing discrete elements, voids, or concentrated loads. The numerical results reveal that, for a general cable/mass system, there are three principal transitions in the frequency spectrum as the suspension parameter lambda(sup 2) is varied. These include: (1) rod-string transition, (2) the string/inextensible cable transition, and (3) slack cable transition. While the first two transitions have been noted in the previous studies, the third one has not. During this third transition, the cable is nearly decoupled into a number of segments and the vibration modes become localized. An asymptotic/numerical solution is also derived based on the assumptions of piecewise constant equilibrium cable tension and equilibrium inclination angle distributions. The advantage of this asymptotic/numerical solution is its ability to provide results for higher-order eigensolutions of complex mass arrays. Experimental results based on the measurements of frequency response functions are provided and serve to validate the theoretical model. Dissert. Abstr.

N93-31038*# National Aeronautics and Space Administration. Langley Research Center, Hampton, VA.

ON NEURAL NETWORKS IN IDENTIFICATION AND CONTROL OF DYNAMIC SYSTEMS

Minh Phan (Lockheed Engineering and Sciences Co., Hampton, VA.), Jer-Nan Juang, and David C. Hyland (Harris Corp., Melbourne, FL.) Jun. 1993 34 p
(RTOP 585-03-11-09)
(NASA-TM-107702; NAS 1.15:107702) Avail: CASI HC A03/MF A01

This paper presents a discussion of the applicability of neural networks in the identification and control of dynamic systems. Emphasis is placed on the understanding of how the neural networks handle linear systems and how the new approach is related to conventional system identification and control methods. Extensions of the approach to nonlinear systems are then made. The paper explains the fundamental concepts of neural networks in their simplest terms. Among the topics discussed are feed forward and recurrent networks in relation to the standard state-space and observer models, linear and nonlinear auto-regressive models, linear, predictors, one-step ahead control, and model reference adaptive control for linear and nonlinear systems. Numerical examples are presented to illustrate the application of these important concepts. Author (revised)

N93-29777*# Kansas Univ. Center for Research, Inc., Lawrence. Dept. of Aerospace Engineering.

NASTRAN ANALYSIS FOR THE AIRMASS SUNBURST MODEL 'C' ULTRALIGHT AIRCRAFT

John Verbestel and Howard W. Smith *In its* The Ultra Light Aircraft Testing 1993 32 p (For primary document see N93-29774 11-05)
(Grant NAG1-345)
Avail: CASI HC A03/MF A02

N93-29993*# Michigan Univ., Ann Arbor. Dept. of Aerospace Engineering.

PLANAR REORIENTATION OF A FREE-FREE BEAM IN SPACE USING EMBEDDED ELECTROMECHANICAL ACTUATORS

Ilya V. Kolmanovsky and N. Harris McClamroch *In its* Efficient Reorientation Maneuvers for Spacecraft with Multiple Articulated Payloads 3 Jun. 1993 12 p Presented at the SPIE Conference on Smart Structures and Materials, 1993 (For primary document see N93-29988 11-18)
(Grant NSF MSS-91-14630)
Avail: CASI HC A03/MF A02

N93-30305 Toronto Univ. (Ontario). Computer Integrated Manufacturing Lab.
DESIGN AND IMPLEMENTATION OF AN INTERACTIVE ISOCHROMATIC FRINGE-ANALYSIS SYSTEM USING MACHINE-VISION TECHNIQUES
A. Mitu, B. Benhabib, K. C. Smith, and S. A. Meguid *In* Engineering Inst. of Canada, Canadian Conference on Electrical and Computer Engineering, Volumes 1 and 2 1990 4 p (For primary document see N93-30215 11-31)
Avail: Engineering Inst. of Canada, 2050 rue Mansfield, Suite 700, Montreal, Quebec H3A 1Z2 Canada

N93-30950*# Jackson State Univ., MS. Dept. of Technology.
DEVELOPMENT OF AN EXPERIMENTAL METHOD TO DETERMINE THE AXIAL RIGIDITY OF A STRUT-NODE JOINT
W. V. Brewer and Hui-Ru Shih *In* NASA. Langley Research Center, National Educators' Workshop. Update 92: Standard Experiments in Engineering Materials Science and Technology Jun. 1993 p 35-42 (For primary document see N93-30948 11-23)
Avail: CASI HC A02/MF A04

N93-30960*# Montana State Univ., Bozeman. Coll. of Engineering.
DIRECT TENSION EXPERIMENTS ON COMPACTED GRANULAR MATERIALS
Steven W. Perkins *In* NASA. Langley Research Center, National Educators' Workshop. Update 92: Standard Experiments in Engineering Materials Science and Technology Jun. 1993 p 209-220 (For primary document see N93-30948 11-23)
Avail: CASI HC A03/MF A04

N93-30972*# Loyola Coll., Baltimore, MD. Dept. of Engineering.
AN AUTOMATED DATA COLLECTION SYSTEM FOR A CHARPY IMPACT TESTER
Bernard J. Weigman and F. Xavier Spiegel *In* NASA. Langley Research Center, National Educators' Workshop. Update 92: Standard Experiments in Engineering Materials Science and Technology Jun. 1993 p 377-384 (For primary document see N93-30948 11-23)
Avail: CASI HC A02/MF A04

42 GEOSCIENCES (GENERAL)

N93-29089# Joint Publications Research Service, Arlington, VA.
JPRS REPORT: SCIENCE AND TECHNOLOGY. CENTRAL EURASIA: EARTH SCIENCE
23 Jun. 1993 16 p Transl. into ENGLISH from various Russian articles
(JPRS-UES-93-003) Avail: CASI HC A03/MF A01

Translated abstracts cover the following areas: geology, meteorology, oceanography, atmospheric physics, and ecology. Some specific topics include the possibility of obtaining information on climate parameters from American operational satellite data; dispersion relation and phase velocity of surface waves in a sea of finite depth; efficiency of adaptive correction for random tilts of wave front of laser beams propagating through turbulent atmosphere; probability density of saturated fluctuations in intensity of optical wave in turbulent atmosphere; and possibility of determining microphysical parameters of noctilucent and mesospheric clouds using data from remote twilight sounding from space. CASI

N93-30624# Joint Publications Research Service, Arlington, VA.
JPRS REPORT: SCIENCE AND TECHNOLOGY. CENTRAL EURASIA: EARTH SCIENCES
11 May 1993 19 p Transl. into ENGLISH from various Russian articles
(JPRS-UES-93-002) Avail: CASI HC A03/MF A01

Papers on Central Eurasia: Earth Sciences are included. Topics covered include: arctic and antarctic research, oceanography, physics of atmospheres, and ecology. CASI

N93-30634# National Academy of Sciences - National Research Council, Washington, DC. Mapping Science Committee.
TOWARD A COORDINATED SPATIAL DATA INFRASTRUCTURE FOR THE NATION
1993 183 p Original contains color illustrations
(B-149; ISBN-0-309-04899-0; LC-93-84335) Avail: CASI HC A09/MF A02

The Mapping Science Committee (MSC) was established in 1987 at the request of the U.S. Geological Survey (USGS) to provide advice on their cartographic and geographic activities. During the course of its studies, the MSC was exposed to activities in several other federal agencies and recognized several generic problems involving the conduct of mapping and spatial analysis. In response to the initial charges developed for the earlier USGS activity, the MSC issued two reports, Spatial Data Needs: The Future of the National Mapping Program (1990) and Research and Development in the National Mapping Division, USGS: Trends and Prospects (1991). In both reports, the MSC recognized the utility of its advice to the broader governmental agencies that utilize mapping or the analyses of spatially referenced digital data. Because of this recognition, the MSC initiated this study. The question that this study addresses is the following: What could be done better or more efficiently if the content, accuracy, organization, and control of spatial data were different? The study examines the current national spatial data infrastructure, encompassing the roles of private institutions as well as local, state, and federal governments in using and sharing geographic information. In addition it identifies barriers that prevent these groups from acquiring knowledge, making decisions, or performing the duties that rely on the timely availability and easy access to an organized body of geographically referenced information. The scope of spatial data can be enormous, and spatial data can be important components of a wide variety of scientific, technical, and social disciplines and applications. The MSC focused its efforts on the generic issues of spatial data management, collection, and use, particularly regarding the data bases that drive geographic information systems and other similar methods of analyses. Author (revised)

43 EARTH RESOURCES AND REMOTE SENSING

Includes remote sensing of earth resources by aircraft and spacecraft; photogrammetry; and aerial photography.
For instrumentation see *35 Instrumentation and Photography.*

N93-28620*# Daedalus Enterprises, Inc., Ann Arbor, MI.
RESEARCH AND DEVELOPMENT OF AN AIRBORNE MULTISPECTRAL SCANNER TO MEASURE FIRE, TERRESTRIAL AND ATMOSPHERIC CHARACTERISTICS (50 CHANNEL) Final Report, 10 May 1989 - 28 Feb. 1991
Steven D. Cech 13 Mar. 1991 24 p
(Contract NAS2-13036; SBIR-08.29-5649)
(NASA-CR-193121; NAS 1.26:193121) Avail: CASI HC A03/MF A01

The AB184 Spectrometer and the AC12206 High Temperature Blackbody Reference Source Assembly were both successfully developed during this contract effort. The newly developed hardware provide a means of quantifying the spectral characteristics of high temperature fire scenes. Author

N93-28915# Deutsche Forschungsanstalt fuer Luft- und Raumfahrt, Oberpfaffenhofen (Germany). Abt. Fernerkundungsanwendungen.
PROCEEDINGS OF THE 8TH USER SEMINAR OF THE GERMAN REMOTE SENSING DATA CENTER OF THE GERMAN AEROSPACE ESTABLISHMENT (DLR) [TAGUNGSBAND: 8. NUTZERSEMINAR DES DEUTSCHEN FERNERKUNDUNGSDATENZENTRUMS DER DLR]
Rudolf Winter and Winfried Markwitz May 1992 88 p In GERMAN Proceedings held in Oberpfaffenhofen, Germany, 16-17 Sep. 1991 Original contains color illustrations
(DLR-Mitt-92-09; ETN-93-93575) Avail: CASI HC A05/MF A01; DLR, Zentrale Allgemeine Dienste, Versand, Postfach 90 60 58, 5000 Cologne 90, Germany, HC

The application potential of data from NOAA, LANDSAT, and ERS-1 satellites was presented in 18 scientific papers. The main emphasis was on the processing and application of radar data as well as preparations for the ERS-1. Another important subject was the results of applications in forestry in the old and new German Federal States, in Alpine regions and the Soviet Union, investigations in urban areas and for monitoring in Kenya. Status reports were given on the funding concept of ecological research of the Federal Ministry of Research and Technology (BMFT), on the International Space Year (ISY 92), and on the processing and archiving of data of the ERS-1. For individual titles, see N93-28916 through N93-28932.

N93-28916# Deutsche Forschungsanstalt fuer Luft- und Raumfahrt, Oberpfaffenhofen (Germany). Deutsches Fernerkundungsdatenzentrum.

THE GERMAN PAF (PROCESSING AND ARCHIVING FACILITIES) FOR ERS-1 [DAS DEUTSCHE PAF FUER ERS-1]

Joerg Gredel *In its* Proceedings of the 8th User Seminar of the German Remote Sensing Data Center of the German Aerospace Establishment (DLR) May 1992 p 11-15 In GERMAN (For primary document see N93-28915 11-43)

Avail: CASI HC A01/MF A01; DLR, Zentrale Allgemeine Dienste, Versand, Postfach 90 60 58, 5000 Cologne 90, Germany, HC

The first European remote sensing ERS-1 satellite was launched in 1991 on a polar orbit for environmental observations. Data processing and product distribution are carried out in four centers, namely Processing and Archiving Facilities (PAF). The German PAF is involved in high precision data processing. The most important Synthetic Aperture Radar (SAR) products are: precision image, geocoded ellipsoid corrected image, and geocoded terrain corrected image. A sensor calibration by the European Space Agency and a careful validation of products by the PAF must be carried out before product delivery to users. ESA

N93-28917# Deutsches Geodaetisches Forschungsinst., Munich (Germany).

PROCESSING OF ALTIMETER DATA BY THE GERMAN ERS-1 PROCESSING AND ARCHIVING FACILITY (D-PAF) [VERARBEITUNG VON ALTIMETERDATEN BEIM DEUTSCHEN ERS-1 AUSWERTEZENTRUM (D-PAF)]

Wolfgang Bosch *In* DLR, Proceedings of the 8th User Seminar of the German Remote Sensing Data Center of the German Aerospace Establishment (DLR) May 1992 p 16-17 In GERMAN Original contains color illustrations (For primary document see N93-28915 11-43)

Avail: CASI HC A01/MF A01; DLR, Zentrale Allgemeine Dienste, Versand, Postfach 90 60 58, 5000 Cologne 90, Germany, HC

The possibilities of satellite altimetry for sea surface measurements and time variations are described. Double measurements analysis allow an increase of satellite flight precision by interpolation in the cross points of up and down flight curves. Models for height errors are then determined by compensation to reduce flight errors. With knowledge of the improved satellite attitude and careful corrected shift measurements of the altimeters, sea level curves can be calculated along the subsatellite tracking. By interpolation these levels are finally transferred onto a regular grid. Altimeter data are systematically archived and processed to obtain a relief representation of the sea level surface. ESA

N93-28918# Deutsches Geodaetisches Forschungsinst., Munich (Germany).

EXACT TRAJECTORY DETERMINATOR FOR ERS-1 [GENAUE BAHNBESTIMMUNG FUER ERS-1]

Franz-Heinrich Massmann *In* DLR, Proceedings of the 8th User Seminar of the German Remote Sensing Data Center of the German Aerospace Establishment (DLR) May 1992 p 18-20 In GERMAN (For primary document see N93-28915 11-43)

Avail: CASI HC A01/MF A01; DLR, Zentrale Allgemeine Dienste, Versand, Postfach 90 60 58, 5000 Cologne 90, Germany, HC

The calculation of temporary and precise flight ephemerides was performed in German processing and archiving facilities. These exact trajectories can be used for correction of ERS-1 Earth observation measurements. Initially, only laser and radar altimeter observations were available for trajectory calculations. These were more precise after classification of data materials and files and geographic distribution and when the measure concept was demonstrated. The worldwide distributed laser stations transfer the data to German processing and archiving facilities. Trajectory determination is carried out by means of a geodetic parameter estimation system. Motion equations are numerically integrated in a trajectory determination module by taking into account perturbation factors, and the trajectory is then iteratively improved. ESA

N93-28919# Stuttgart Univ. (Germany). Inst. fuer Navigation.

THE INTERFEROMETRIC SAR TECHNOLOGY AND ITS USABILITY IN THE FRAMEWORK OF ERS-1 [DIE INTERFEROMETRISCHE SAR-TECHNIK UND IHRE NUTZUNGSMOEGLICHKEITEN IM RAHMEN VON ERS-1]

Philipp Hartl *In* DLR, Proceedings of the 8th User Seminar of the German Remote Sensing Data Center of the German Aerospace Establishment (DLR) May 1992 p 21-23 In GERMAN (For primary document see N93-28915 11-43)

Avail: CASI HC A01/MF A01; DLR, Zentrale Allgemeine Dienste, Versand, Postfach 90 60 58, 5000 Cologne 90, Germany, HC

Phase measurement of radar echo by interferometric SAR (Synthetic Aperture Radar) technology is explained. Data of at least two recordings of the sample scene must be simultaneously processed provided that they are issued from narrowly neighboring satellite positions and no differences in direction slant range occur. These differences are measured point by point while the phase differences of corresponding echo signals are evaluated. Since two points with equal geographic coordinates and different topographic height have a different direction angle, this can be measured by interferometry and a digital height model can be obtained. The method is shown to be hardly usable for surfaces with strong reliefs and for forests, because radar scattering properties of observed surfaces must be time-independent. ESA

N93-28920# Zurich Univ. (Switzerland). Inst. fuer Geographie.

RECORDING OF FOREST SURFACE IN SAR-IMAGES WITH STATISTICAL METHODS IN AREAS OF PRONOUNCED RELIEF [ERFASSUNG DER WALDFLAECHE IN SAR-BILDERN MIT HILFE STATISTISCHER METHODEN IN GEBIETEN MIT AUSGEPRAEGTEM RELIEF]

F. Holecz and D. Nueesch *In* DLR, Proceedings of the 8th User Seminar of the German Remote Sensing Data Center of the German Aerospace Establishment (DLR) May 1992 p 24-27 In GERMAN (For primary document see N93-28915 11-43)

Avail: CASI HC A01/MF A01; DLR, Zentrale Allgemeine Dienste, Versand, Postfach 90 60 58, 5000 Cologne 90, Germany, HC

The correction of the SAR (Synthetic Aperture Radar) images for an optimal interpretation, is studied. Measure noises were considered, such as speckle effect and geometric or radiometric distortions. Appropriate adaptative filters must be chosen, and a correction process based on a distance Doppler algorithm must be used, to build a topographic map. Errors can be minimized through optimal image raster width and interpolation process. Interaction between incident microwaves and natural surfaces, topographical influence on obtained signatures, statistic or semi-empirical backscattering model, as well as a parameter for precise relief detailing, play an important role in the quality of information recovery. To statistically describe the anisotropic texture of a forest, Gray level run length matrix, Gray level difference matrix, spatial Gray level dependence matrix, and the power spectrum method were used. Another method, related to the extraction of basis vectors with an adaptive system, was used to calculate eigenvectors and eigenvalues from the covariance matrix, which gives an approximation of second order or statistical dependences. ESA

N93-28921# Ludwig-Maximilians-Univ., Munich (Germany). Lehrstuhl fuer Landschaftstechnik.

FOREST EXAMINATION WITH POLARIMETRIC RADAR IMAGE DATA [WALDUNTERSUCHUNGEN MIT POLARIMETRISCHEN RADARBILDDATEN]

Barbara Koch and Bernhard Foerster *In* DLR, Proceedings of the 8th User Seminar of the German Remote Sensing Data Center of the German Aerospace Establishment (DLR) May 1992 p 28-31 In GERMAN Original contains color illustrations (For primary document see N93-28915 11-43)

Avail: CASI HC A01/MF A01; DLR, Zentrale Allgemeine Dienste, Versand, Postfach 90 60 58, 5000 Cologne 90, Germany, HC

Data in C band, L band, and P band in four polarizations were obtained from a DC-8 radar flight experimentation to evaluate the information content of polarimetric radar data in view of vegetal cover age and three variety estimation. DC-8 data transformation in equivalent gray scale values and polarization angles psi and khi calculation were carried out. The study shows differences in information content between C band, L band, and P band. The last two allow forests to be distinguished from agricultural surfaces and deciduous from conifer trees. In P band three age distributions are also available. Polarization angle effect on radar signal is characterized to show that forestry class separability with wave length is influenced by polarization state. ESA

N93-28922# Bonn Univ. (Germany). Lehrstuhl fuer Allgemeinen Pflanzenbau.

REMOTE SENSING OF AGRICULTURAL VEGETATION: STATUS AND PERSPECTIVES [FERNERKUNDUNG DER LANDWIRTSCHAFTLICH GENUTZTEN VEGETATION: STAND DER ANWENDUNG UND PERSPEKTIVEN]

W. Kuehbauch *In* DLR, Proceedings of the 8th User Seminar of the German Remote Sensing Data Center of the German Aerospace Establishment (DLR) May 1992 p 32-34 In GERMAN (For primary document see N93-28915 11-43)

Avail: CASI HC A01/MF A01; DLR, Zentrale Allgemeine Dienste, Versand, Postfach 90 60 58, 5000 Cologne 90, Germany, HC

The possibilities of optical and microwave sensors for variety identification and situation descriptions of cultivated plants are reviewed. It is important to develop model formulations in which the plant cover can be defined in simple geometric coordinates. It is proved that for vegetation cover description by optical sensors the interpretation is better in red/infrared area and a good estimation of plant biomass and its chlorophyll content can be obtained. High resolution spectroscopy allowed measurement of nitrogen fertilizing effect in meadowland. It is concluded that remote sensing can be used for agriculture only by combining data with other information sources such as statistics and geologic or meteorologic charts. ESA

N93-28923# Zeiss (Carl), Jena (Germany).

SAR SHAPE-FROM-SHADING FOR A POPULATED ALPINE AREA [SAR SHAPE-FROM-SHADING FUER EIN BESIEDELTES ALPINES GEBIET]

Rolf Hartmann *In* DLR, Proceedings of the 8th User Seminar of the German Remote Sensing Data Center of the German Aerospace Establishment (DLR) May 1992 p 35-39 In GERMAN Original contains color illustrations (For primary document see N93-28915 11-43)

Avail: CASI HC A01/MF A01; DLR, Zentrale Allgemeine Dienste, Versand, Postfach 90 60 58, 5000 Cologne 90, Germany, HC

The use of satellite-borne radar recordings for developing digital ground models is explained. Shape-from-shading methods allow a ground height value to be assigned to each image pixel with high spatial resolution. These processes are full of serious reconstruction faults at lower spatial frequencies, due to nonhomogeneity of radar backscattering coefficients, integration methods, radiometric calibration and speckle noise of radar signal. It is established that angle dependence of radar backscattering coefficients can be neglected and geometry factor of radar cross section linearly depends on height difference in the image pixel in range direction, so that linear filter can be used to estimate errors in reconstructed height values. ESA

N93-28924# Deutsche Forschungsanstalt fuer Luft- und Raumfahrt, Oberpfaffenhofen (Germany). Deutsches Fernerkundungsdatenzentrum.

THE GERMAN SATELLITE GROUND STATION IN ANTARCTICA: REALIZATION AND FIRST RESULTS [DIE DEUTSCHE SATELLITENBODENSTATION IN DER ANTARKTIS: REALISIERUNG UND ERSTE ERGEBNISSE]

Klaus-Dieter Reiniger, Alfons Max Zimmer, and Stefan Werner Dech *In its* Proceedings of the 8th User Seminar of the German Remote Sensing Data Center of the German Aerospace Establishment (DLR) May 1992 p 40-45 In GERMAN Original contains color illustrations (For primary document see N93-28915 11-43)

Avail: CASI HC A02/MF A01; DLR, Zentrale Allgemeine Dienste, Versand, Postfach 90 60 58, 5000 Cologne 90, Germany, HC

A satellite ground station was built on the Antarctic peninsula for receiving SAR (Synthetic Aperture Radar) data of ERS satellite, supplementing systems such as NOAA satellite and for measuring the Antarctic continental drift by very long base interferometry. First image data from ERS-1 satellite give information about Stancomb-Wills ice river, channel glaciers, ice flows, and sea ice motions. NOAA-AVHRR (Advanced Very High Resolution Radiometer) photography recordings are presented, which allow observations of clouds, ice surface, meteorological phenomena, and coast in South America and Antarctica. ESA

N93-28925# Bonn Univ. (Germany). Geographisches Inst.

FOG STUDIES IN THE ALPINE REGION WITH DIGITAL NOAA/AVHRR DATA [NEBELSTUDIEN IM ALPENRAUM MIT DIGITALEN NOAA/AVHRR-DATEN]

Matthias Bachmann, Joerg Bendix, and Matthias Winiger *In* DLR, Proceedings of the 8th User Seminar of the German Remote Sensing Data Center of the German Aerospace Establishment (DLR) May 1992 p 46-49 In GERMAN Original contains color illustrations (For primary document see N93-28915 11-43)

Avail: CASI HC A01/MF A01; DLR, Zentrale Allgemeine Dienste, Versand, Postfach 90 60 58, 5000 Cologne 90, Germany, HC

Multispectral data of Earth orbit NOAA satellite are particularly useful for extensive observation of fog distribution. Data processing methods developed for fog identification image correction and fog thickness estimation are explained. Fog identification is based on radiation temperature difference in AVHRR (Advanced Very High Resolution Radiometer) channels 3 and 4. Fog frequency charts could be calculated from NOAA/AVHRR data in Swiss foothills of the Alps and in the Milan region. Regional boundary layer airflow patterns can be derived by regression analysis from digital NOAA/AVHRR data and correlated with harmful substance emissions. ESA

N93-28926# Freiburg Univ. (Germany). Inst. fuer Physische Geographie.

UTILIZATION OF NOAA/AVHRR DATA FOR ENERGY BALANCE OF LAKE CONSTANCE (SWITZERLAND) [DIE ANWENDUNG VON NOAA-AVHRR DATEN ZUR ENERGIEBILANZIERUNG DES BODENSEES]

Karl Schneider and Wolfram Mauser (Technische Univ., Munich, Germany.) *In* DLR, Proceedings of the 8th User Seminar of the German Remote Sensing Data Center of the German Aerospace Establishment (DLR) May 1992 p 50-53 In GERMAN Original contains color illustrations (For primary document see N93-28915 11-43)

Avail: CASI HC A01/MF A01; DLR, Zentrale Allgemeine Dienste, Versand, Postfach 90 60 58, 5000 Cologne 90, Germany, HC

The use of satellite data to allow direct and extensive measurements of some parameters involved in energy fluxes at water surface in a lake is shown. By means of continuous radiometric measurements of surface temperature, upper water column temperature curves and meteorological parameters, the effect of energy fluxes in boundary surface temperatures can be examined. A modified split-window process and the radiation transfer model LOWTRAN-7 were used for atmosphere corrections of temperature images from NOAA/AVHRR (Advanced Very High Resolution Radiometer). The energy balance was calculated from energy fluxes between atmosphere and water, as the sum of latent and conduction heat from short and long wave radiation and long wave transmission. ESA

N93-28927# Deutsche Forschungsanstalt fuer Luft- und Raumfahrt, Oberpfaffenhofen (Germany). Inst. fuer Physik der Atmosphaere.

DERIVATION OF CONDUCTIVE HEAT TRANSFER IN MOUNTAINS FROM AVHRR DATA [DIE ABLEITUNG DES FUEHLBAREN WAERMESTROMES IM GEBIRGE AUS AVHRR-DATEN]

Hermann Mannstein *In its* Proceedings of the 8th User Seminar of the German Remote Sensing Data Center of the German Aerospace Establishment (DLR) May 1992 p 54-57 In GERMAN Original contains color illustrations (For primary document see N93-28915 11-43)

Avail: CASI HC A01/MF A01; DLR, Zentrale Allgemeine Dienste, Versand, Postfach 90 60 58, 5000 Cologne 90, Germany, HC

The conductive heat transfer can be calculated from AVHRR (Advanced Very High Resolution Radiometer) data and measurements of air temperature profiles by taking into consideration height information of a digital ground model. It is described as a function of surface roughness atmosphere state and slope and was estimated apart from simulations of up-slope boundary layers, which establish a relation between conduction heat and temperature difference between ground and free atmosphere. This method allows an extensive recording of data and a pixel integration in a surface defined by the sensor geometric resolution. ESA

N93-28928# Wuerzburg Univ. (Germany). Geographisches Inst.
DIGITAL IMAGE PROCESSING OF DESCANNED TERRESTRIAL GROUND PHOTOGRAPHS [DIGITALE BILDVERARBEITUNG AN ABGESCANNTEN TERRESTRISCHEN GELAENDEFOTOS]
Ingrid Stengel *In* DLR, Proceedings of the 8th User Seminar of the German Remote Sensing Data Center of the German Aerospace Establishment (DLR) May 1992 p 58-63 In GERMAN Original contains color illustrations (For primary document see N93-28915 11-43)
Avail: CASI HC A02/MF A01; DLR, Zentrale Allgemeine Dienste, Versand, Postfach 90 60 58, 5000 Cologne 90, Germany, HC

The problem of the bad quality of photographs of sandy terrains such as deserts and dunes is studied. The possibilities of improvement by digital image processing are examined: normed or interactive histogram spreading for a stronger contrast, equidensity lining for distinguishing areas of same color, luminosity, exposition, slope and grain size, and reduction of indistinctness by high-pass filtration. Image processing for separation of surface textures from various directions is given as an example: the original picture was recorded at a plane aeolicen sand layer in the North Sea, which resulted from accumulations due to several wind directions and intensities. Sand layer surface was weakly and diffusively wrinkled with very regular crest shifts, so that shadow gives little information. Image contrast was optimized and specially defined direction filtration (5 by 5 pixel matrix) was applied to examine crest distribution of sand layer. ESA

N93-28929# Freiburg Univ. (Germany). Abt. Luftbildmessung und Fernerkundung.
ATMOSPHERIC CORRECTION OF LANDSAT-TM-DATA FOR FOREST INVENTORY [ATMOSPHAERENKORREKTUR VON LANDSAT-TM-DATEN FUER ZWECKE DER FORSTINVENTUR]
Gilbert Kattenborn *In* DLR, Proceedings of the 8th User Seminar of the German Remote Sensing Data Center of the German Aerospace Establishment (DLR) May 1992 p 64-67 In GERMAN Original contains color illustrations (For primary document see N93-28915 11-43)
Avail: CASI HC A01/MF A01; DLR, Zentrale Allgemeine Dienste, Versand, Postfach 90 60 58, 5000 Cologne 90, Germany, HC

An algorithm is presented for atmospheric correction of multispectral satellite data in solar spectral area. This process was achieved and tested for forest evaluations of LANDSAT-TM (Thematic Mapper) recordings above distorted relief but can be adapted to other sensors and similar problems. A routine identifies surfaces with thick, dark vegetation as objects of well known reflection, according to a vegetation index and a low reflection in near infrared area. A net of reference points can then be stretched. These points are chosen to represent horizontal, terrain dependent or vertical variations of atmospheric conditions and allow calculation of transmission, air light and irradiation values with LOWTRAN-7 software. A three dimensional model of current and local atmosphere conditions in the considered region is, therefore, obtained. After estimation of mean region albedo, atmosphere corrected albedos are calculated by considering the isotropic reflection of the surface with iterative utilization of a correction model. ESA

N93-28930# Geosystems G.m.b.H., Germering (Germany).
MODEL-ORIENTED CORRECTION OF THEMATIC MAPPER RAW DATA [MODELLORIENTIERTE ENTZERRUNG VON THEMATIC MAPPER ROHDATEN]
Hardy M. Ehrhardt *In* DLR, Proceedings of the 8th User Seminar of the German Remote Sensing Data Center of the German Aerospace Establishment (DLR) May 1992 p 68-71 In GERMAN (For primary document see N93-28915 11-43)
Avail: CASI HC A01/MF A01; DLR, Zentrale Allgemeine Dienste, Versand, Postfach 90 60 58, 5000 Cologne 90, Germany, HC

Perturbations of the geometry of the original recorded image from thematic mappers are examined; their magnitude is estimated, and a model for compensation is presented. The following parameters were considered: irregularity of mirror rotation, attitude, Earth rotation, Earth curvature, and perspective distortion. Several versions of the same photograph are presented to allow a comparison of some existing correction systems. ESA

N93-28931# Deutsche Forschungsanstalt fuer Luft- und Raumfahrt, Oberpfaffenhofen (Germany). Deutches Fernerkundungsdatenzentrum.
EVIDENCE-BASED CLASSIFICATION OF SATELLITE IMAGE DATA [EVIDENZBASIERTE KLASSIFIZIERUNG VON SATELLITENBILDDATEN]
Gabriele Lohmann *In its* Proceedings of the 8th User Seminar of the German Remote Sensing Data Center of the German Aerospace Establishment (DLR) May 1992 p 72-73 In GERMAN (For primary document see N93-28915 11-43)
Avail: CASI HC A01/MF A01; DLR, Zentrale Allgemeine Dienste, Versand, Postfach 90 60 58, 5000 Cologne 90, Germany, HC

A new method for classification of satellite image data is presented which is particularly adapted to cartography of forest regions in Germany but can be applied to other areas such as tropical rain forests. The process is based on varied distribution functions and several independent feature spaces, which are considered as 'sources of evidence' according to the Dempster-Shafer Theory. The method allows the identification of information from different sources, for example several sensors. ESA

N93-28932# Klein und Stekl G.m.b.H., Stuttgart (Germany).
NEW CLASSIFICATION METHODS [NEUE KLASSIFIZIERUNGSMETHODEN]
Helmut Schumacher *In* DLR, Proceedings of the 8th User Seminar of the German Remote Sensing Data Center of the German Aerospace Establishment (DLR) May 1992 p 74-75 In GERMAN (For primary document see N93-28915 11-43)
Avail: CASI HC A01/MF A01; DLR, Zentrale Allgemeine Dienste, Versand, Postfach 90 60 58, 5000 Cologne 90, Germany, HC

The implementation of the maximum likelihood method is proposed by carrying out a component transformation by class. The robustness of this implementation towards badly conditioned covariance matrices is demonstrated. Fuzzy sets were used and distances to cluster centers were reproduced in the classes according to their membership degree to obtain fuzzy classifications. Beside the use of by class-different features and of various classifications inside a classification operation, a new formulation arises for the multitemporal classifying, and consequently a new method is proposed for realization of a geocoded thematic database. Performances of the method are demonstrated by means of synthetic and real thematic mapper data and by comparison with probabilistic relaxation process. ESA

N93-29000# Industrial Coll. of the Armed Forces, Washington, DC.
EARTH OBSERVATION FROM SPACE: COMPETITION OR COOPERATION? Research Report, Aug. 1991 - Apr. 1992
David P. Oberthaler Apr. 1992 36 p
(AD-A262044; NDU-ICAF-92-A208) Avail: CASI HC A03/MF A01

The purpose of this paper is to examine how the United States should balance its international cooperation and competition as it pertains to earth observations or remote sensing from space. Earth observations or remote sensing includes all forms of observation by sensors borne by a space object including visual, optical or any form of radiometrically produced images and any measurements taken of the earth's surface, its atmosphere or its weather systems. The capabilities of remote sensing are as varied as the sensors that are built and put in orbit, but capabilities fall into two general categories; imagery and measurement. Imagery includes visible light photography, infrared photography, and radar images of the earth's surface. Imagery also has the broadest application cutting across scientific, economic and national security lines. Accurate and detailed images of the earth's surface can be produced through cameras, radar, and specialized scanners to improve the accuracy of maps, observe and assist in weather reporting and prediction, assess the impact of man on his environment, and assess the status of crops and natural resources. Measurement accomplished using remote sensing has largely scientific applications including the production of data on the chemical composition of the earth's atmosphere, measurement of radiation, and precise measurement of landmass position and movement. DTIC

N93-29146# Goodwin (R. Christopher) and Associates, Inc., New Orleans, LA.
REMOTE SENSING SURVEY OF MISSISSIPPI RIVER-GULF OUTLET, BRETON SOUND DISPOSAL AREA, PLAQUEMINES PARISH, LOUISIANA Final Report
Jack D. Irion, Peter Morrison, Paul V. Heinrich, and Danton Kostandarithes

Feb. 1993 80 p
(Contract DACW29-90-D-0018)
(AD-A263097; COELMN/PD-93/05) Avail: CASI HC A05/MF A01

A magnetic and acoustic remote sensing survey for submerged cultural resources was conducted over a 1,600-acre project area off shore of Breton Island, Plaquemines Parish, Louisiana. The project area, which measures a mile wide and 2.5 miles long, encompasses the proposed site of the Mississippi River-Gulf Outlet Breton Sound Disposal Area. The survey was conducted for the U.S. Army Corps of Engineers, New Orleans District, pursuant to Delivery Order 0010, of Contract DACW29-90-D-0018. The proposed disposal of dredge spoil may impact several of the anomalies recorded during the survey. A controlled hydrographic survey was performed over the project area utilizing a proton precession magnetometer to collect magnet data, a side scan sonar to record acoustic anomalies, and a precision echosounder to acquire bathymetry. Real time positioning was maintained by a Differential Global Positioning System (DGPS) linked to a computer navigation program. Seventy-eight magnetic anomalies and one acoustic anomaly were recorded during the survey. The acoustic anomaly, which is associated with a cluster of magnetic targets, appears to be related to modern steel wreckage. In addition to this target, six other clusters of anomalies were distinguished. Of the seven anomaly clusters, additional archeological investigations are recommended for five. DTIC

N93-29179*# Stanford Univ., CA. Physics Lab.
INVESTIGATION OF A GEODESY COEXPERIMENT TO THE GRAVITY PROBE B RELATIVITY GYROSCOPE PROGRAM Final Report, Jun. 1993
C. W. F. Everitt, Bradford W. Parkinson, and Mark Tapley 25 Jun. 1993 14 p
(Grant NAG5-1155)
(NASA-CR-193263; NAS 1.26:193263) Avail: CASI HC A03/MF A01

Geodesy is the science of measuring the gravitational field of and positions on the Earth. Estimation of the gravitational field via gravitation gradiometry, the measurement of variations in the direction and magnitude of gravitation with respect to position, is this dissertation's focus. Gravity Probe B (GP-B) is a Stanford satellite experiment in gravitational physics. GP-B will measure the precession the rotating Earth causes on the space time around it by observing the precessions of four gyroscopes in a circular, polar, drag-free orbit at 650 km altitude. The gyroscopes are nearly perfect niobium-coated spheres of quartz, operating at 1.8 K to permit observations with extremely low thermal noise. The permissible gyroscope drift rate is miniscule, so the torques on the gyros must be tiny. A drag-free control system, by canceling accelerations caused by nongravitational forces, minimizes the support forces and hence torques. The GP-B system offers two main possibilities for geodesy. One is as a drag-free satellite to be used in trajectory-based estimates of the Earth's gravity field. We described calculations involving that approach in our previous reports, including comparison of laser only, GPS only, and combined tracking and a preliminary estimate of the possibility of estimating relativistic effects on the orbit. The second possibility is gradiometry. This technique has received a more cursory examination in previous reports, so we concentrate on it here. We explore the feasibility of using the residual suspension forces centering the GP-B gyros as gradiometer signals for geodesy. The objective of this work is a statistical prediction of the formal uncertainty in an estimate of the Earth's gravitation field using data from GP-B. We perform an instrument analysis and apply two mathematical techniques to predict uncertainty. One is an analytical approach using a flat-Earth approximation to predict geopotential information quality as a function of spatial wavelength. The second estimates the covariance matrix arising in a least-squares estimate of a spherical harmonic representation of the geopotential using GP-B gradiometer data. The results show that the GP-B data set can be used to create a consistent estimate of the geopotential up to spherical harmonic degree and order 60. The formal uncertainty of all coefficients between degrees 5 and 50 is reduced by factors of up to 30 over current satellite-only estimates and up to 7 over estimates which include surface data. The primary conclusion resulting from this study is that the gravitation gradiometer geodesy coexperiment to GP-B is both feasible and attractive. Author (revised)

N93-29255# Oak Ridge National Lab., TN.
REMOTE VEHICLE SURVEY TOOL
G. A. Armstrong, B. L. Burks, R. L. Kress, D. G. Wagner (Westinghouse Savannah River Co., Aiken, SC.), and C. R. Ward (Westinghouse Savannah River Co., Aiken, SC.) 1993 9 p Presented at the 5th Topical Meeting on Robotics and Remote Systems, Knoxville, TN, 26-29 Apr. 1993
(Contract DE-AC05-84OR-21400)
(DE93-010822; CONF-930403-41) Avail: CASI HC A02/MF A01

The Remote Vehicle Survey Tool (RVS7) is a color graphical display tool for viewing remotely acquired scientific data. The RVST displays the data in the form of a color two-dimensional world model map. The world model map allows movement of the remote vehicle to be tracked by the operator and the data from sensors to be graphically depicted in the interface. Linear and logarithmic meters, dual channel oscilloscopes, and directional compasses are used to display sensor information. The RVST is user-configurable by the use of ASCII text files. The operator can configure the RVST to work with any remote data acquisition system and teleoperated or autonomous vehicle. The modular design of the RVST and its ability to be quickly configured for varying system requirements make the RVST ideal for remote scientific data display in all environmental restoration and waste management programs. DOE

N93-29307# Beleidscommissie Remote Sensing, Delft (Netherlands).
INFORMATION SYSTEM FOR CO-REGISTRATION OF CAESAR SEA-IMAGES BASED ON TWO DIMENSIONAL IMAGE MATCHING TECHNIQUES (SCORE). PART 1: INTRODUCTION, USER REQUIREMENTS, AND FEASIBILITY TESTS
G. M. H. J. Habets (National Aerospace Lab., Amsterdam, Netherlands.), W. J. Looijen (National Aerospace Lab., Amsterdam, Netherlands.), A. J. Rietveld (National Aerospace Lab., Amsterdam, Netherlands.), M. J. P. M. Lemmens (Technische Univ., Delft, Netherlands.), and B. Spiering (Technische Univ., Delft, Netherlands.) Aug. 1992 19 p
(BCRS Proj. TE-2.11)
(BCRS-90-40a-Pt-1; NLR-CR-92045-L-Pt-1; TD-92-2791-Pt-1; ISBN-90-5411-044-9; ETN-93-93750) Avail: CASI HC A03/MF A01

Part one of the three part feasibility study to see if accurate high precision coregistration of the Charge Coupled Device (CCD) Airborne Experimental Scanner for Applications in Remote sensing (CAESAR) channels, which is required for sea images, can be obtained using image control points is reported. This strategy is performed by using image matching techniques. An introduction to the coregistration of CAESAR sea images is given and the user requirements for coregistration of sea observations with CAESAR is described. In part two an image matching strategy for CAESAR sea images is developed, and the functional and detailed design of SCORE are given in part three. ESA

N93-29320# Beleidscommissie Remote Sensing, Delft (Netherlands).
THE MAESTRO-1 CAMPAIGN: ANALYSES OF POLARIMETRIC SAR DATA OF AGRICULTURAL FIELDS AND FORESTS
D. H. Hoekman (Wageningen Agricultural Univ., Netherlands.), G. G. Lemoine (Joint Research Centre of the European Communities, Ispra, Italy.), and J. J. vanderSanden (Wageningen Agricultural Univ., Netherlands.) Aug. 1992 107 p Original contains color illustrations
(BCRS Proj. AO-2.24)
(BCRS-92-06; TD-92-2904; ISBN-90-5411-037-6; ETN-93-93751) Avail: CASI HC A06/MF A02

The Maestro-1 radar campaign which focused on the deployment of AIRSAR, a model, polarimetric multiband imaging radar system, to study the capabilities of multiband polarimetric radar data is addressed. The introduction of P band data, acquired simultaneously with the C and L band data, was recognized as interesting for the development of certain applications, notably on forestry and soil studies. On 16 Aug. 1989 three sites in The Netherlands, an agricultural area, the Hosterwold forest in Southern Flevoland, and the Speulderbos forest at The Veluwe are flown over and an extensive ground dataset was collected. The following are discussed: the polarimetric calibration; the database; the polarimetric features of agricultural fields and forests; the polarimetric contrast classification of agricultural fields and forests; the analysis of Maestro data in bare soil; and the results for forests. ESA

N93-29321# Beleidscommissie Remote Sensing, Delft (Netherlands).
PREPROCESSING AIRBORNE REMOTE SENSING PARES CALIBRATION MAINTENANCE FUNCTIONAL DESIGN DOCUMENT
G. M. H. J. Habets (National Aerospace Lab., Amsterdam, Netherlands.), A. J. Rietveld (National Aerospace Lab., Amsterdam, Netherlands.), and W.

J. Looijen Aug. 1992 . 54 p
(BCRS Proj. TE-2.10)
(BCRS-92-07; NLR-CR-92043-L; TD-92-2906; ISBN-90-5411-040-6; ETN-93-93752) Avail: CASI HC A04/MF A01

The functional design of the calibration maintenance part of the Preprocessing Airborne Remote Sensing (PARES) information system, a general software package for radiometric and geometric correction of image data recorded by airborne remote sensing scanning systems, is described. Images of two scanning systems can be corrected by PARES: Side Looking Airborne Radar (SLAR) images, and Charge Coupled Device (CCD) Airborne Experimental Scanner for Applications in Remote sensing (CAESAR) images. The calibration of SLAR images is contained inside the image data itself. The results of the calibration of the antenna gain of SLAR are included in the PARES software. The CAESAR scanner needs calibration of the A/D converter and of the charge coupled device arrays it uses to be able to correct the image data radiometrically. The calibration maintenance is mainly dedicated to the CAESAR scanner. Since the operating modes of CAESAR are gradually incremented and since existing modes are repeatedly calibrated during the lifecycle of the sensor, new calibrations are unavoidable. As a result, the calibration maintenance comprises functions to add, test, validate, analyze, and visualize calibrations in order to assure that the radiometric specifications of the scanner are being fulfilled. ESA

N93-29465# Beleidscommissie Remote Sensing, Delft (Netherlands).
NATIONAL REMOTE SENSING PROGRAMME 2 ACMS PROJECT. PHASE 1: VALIDATION. PART 1: DEFINITION OF VALIDATION EXPERIMENT
Jul. 1992 17 p Prepared in cooperation with Environmental Analysis and Remote Sensing, Delft, Netherlands
(BCRS Proj. 3.2/CO-01)
(BCRS-92-10-Phase-1-Pt-1; TD-92-9548-Phase-1-Pt-1; ISBN-90-5411-048-1; ETN-93-93753) Avail: CASI HC A03/MF A01

On the basis of the study entitled 'Product development plan in agrometeorology and crop forecasting' an Agromet Crop Monitoring System (ACMS) was proposed. This consists of a PC based Meteosat PDFUS, a PC based processing system (to produce rainfall, actual evapotranspiration, relative growth and thermal inertial maps from Meteosat imagery); and a PC based GIS which will allow the user to integrate the Meteosat products, as well as externally aquired satellite products, particularly NOAA, in a GIS environment, dedicated to his own needs. For this purpose a modified ILWIS system was suggested, which could be adapted to two kinds of applications: agrometeorology and crop monitoring, and hydrology. The set up of an experiment to validate the monitoring techniques in question particularly those concerning the mapping of actuall evapotranspiration and crop growth, is discussed. The possibility of comparison with the NOAA-NDVI (Normalized Difference Vegetation Index) approach is also considered. A validation experiment is finally proposed. ESA

N93-29466# Beleidscommissie Remote Sensing, Delft (Netherlands).
REMOTE SENSING IN CZECHOSLOVAKIA AND HUNGARY: AN ANALYSIS OF THE POSSIBLE CO-OPERATION OF THE NETHERLANDS WITH CZECHOSLOVAKIA AND HUNGARY IN THE FIELD OF REMOTE SENSING
A. vanDijk (DHV Raadgevend Ingenieursbureau B.V., Amersfoort, Netherlands.), P. Hesen (Bongaerts, Kuyper and Huiswaard, Consulting Engineers, The Hague, Netherlands.), and A. Rosema (Environmental Analysis and Remote Sensing, Delft, Netherlands.) Aug. 1992 206 p Original contains color illustrations
(BCRS Proj. 6.5/IS-08)
(BCRS-92-12; ISBN-90-5411-050-3; TD-92-2907; ETN-93-93754) Avail: CASI HC A10/MF A03

Possibilities of cooperation, with regard to remote sensing (RS), of the Netherlands with Czechoslovakia and Hungary are addressed. In both countries information was collected through interviews with people involved in this field. The report can be regarded as a cookbook for cooperation of the Netherlands with Hungary and Czechoslovakia, to be used by Dutch agencies (consultancy firms, institutes etc.) working in this field and seeking cooperation with RS agencies in the two East European countries. Its recipes state: who is who in Czechoslovakia and in Hungary in remote sensing; what are their specific interests and specialities; who is active in RS research, application or training; what kind of equipment is available; which goods and services are either offered or needed; how is the RS organization and cooperation in the two countries; and who are the main finding agencies. ESA

N93-29615 Ohio State Univ., Columbus.
MULTIPLE IMAGE MULTIPOINT MATCHING FOR AUTOMATIC AEROTRIANGULATION Ph.D. Thesis
Panayota Agouris 1992 133 p
Avail: Univ. Microfilms Order No. DA9307712

Performing an automatic aerotriangulation using digital image processing methods and images available exclusively in digital format is addressed. A conceptual system was developed and implemented which allows the determination of exterior orientation parameters and positions of selected points in object space using a minimal number of assumptions. In direct analogy to the preparation phase of the conventional approach, a photomosaic was automatically generated to describe the interrelationship of all photos within the available block. It was created using matched pairs of conjugate points in all stereo pairs formed within the block and it provides the necessary transition from stereo to n-stage operations. This photomosaic was subsequently used for the automatic extraction of approximate conjugate image coordinates. By examining its accuracy at various levels of resolution, the finer resolution for which the photomosaic produces sufficiently accurate conjugate points is selected as the first level at which precise least squares matching is executed. Thus, the system becomes more economical by having multiphoto matching performed at the minimum necessary number of levels of resolution. A multiple image multipoint matching strategy was developed to identify and precisely match conjugate points in the triple, quadruple or multiple overlapping areas of the block. By taking into account the geometric relationship between conjugate points as it is expressed by their corresponding image forming rays, and using image coordinates rather than the widely used local template coordinates, matching and block adjustment can be combined in a unique way. Thus, the mensuration and adjustment phases of classical aerotriangulation are substituted by a single digital process. Even though, strictly speaking, matching is not carried out in the object space, it is actually performed through the object space. The obtained solution is forced not only to be radiometrically coherent like all typical least squares matching techniques, but to be geometrically coherent as well. The accuracy of the results is improved by repeating the process through finer levels of image pyramids and thus reducing the pixel size. Experimental results confirmed the derived theoretical strategy and support its quality and feasibility. The introduction of digital techniques offers a solution to the problem of subjective point identification errors associated with a human operator who is unable to observe more than two photos at a time. Instead, multiphoto matching is essentially a digitally implemented n-stage comparator. Having this as its core module, the presented digital aerotriangulation scheme, apart from flexible and efficient, is also really close to becoming fully automatic. Dissert. Abstr.

N93-29817# Scripps Institution of Oceanography, La Jolla, CA. Geological Research Div.
CHARTING THE REMOTE SOUTHERN OCEANS WITH GEOSAT ALTIMETRY Final Technical Report
David T. Sandwell, Walter Smith, Jacqueline Mammerickx, and Robert Parker 13 Apr. 1993 11 p
(Contract N00014-91-J-1642)
(AD-A263452) Avail: CASI HC A03/MF A01

The Geosat satellite altimeter has mapped the marine gravity field over nearly all of the world's oceans to a high accuracy and high spatial resolution. In the wavelength band 15 to 200 km, variations in gravity anomaly are highly correlated with seafloor topography. Since many southern ocean areas are sparsely surveyed, these new Geosat data reveal many previously unsurveyed features such as seamounts and fracture zones. The objectives of our proposed research were as follows: (1) Develop a method of combining geoid heights (or gravity anomalies) with shipboard profiles in order to improve bathymetric charts. (2) Evaluate the method by comparing bathymetric predictions with measured seafloor depths in two areas south of 60 deg S. (3) Produce an improved unclassified version of the Navy's standard bathymetric data base of the southern ocean (i.e. between 60 deg S and 72 deg S). (4) Produce an improved classified version of the Navy's standard bathymetric data base of the Southern Hemisphere (i.e. south of the equator). The original cost of the proposed research to be conducted over a 3 year period was $485,237. Due to a budget cut at DMA our budget was reduced to $40,000. Thus we completed only a small fraction of the proposed research as outlined in the attached progress reports. DTIC

N93-29830# Phillips Lab., Hanscom AFB, MA.

MODELING THE BIDIRECTIONAL REFLECTANCE AND SPECTRA

Crystal B. Schaaf and Alan H. Strahler 20 Apr. 1993 9 p
(AD-A263570; PL-TR-93-2096) Avail: CASI HC A02/MF A01

Analysis of aircraft imagery and ground measurements acquired for a spruce forest stand in Howland, Maine as part of the 1990 Forest Ecosystem Dynamics Multisensor Aircraft Campaign (FEDMAC), show that the Li-Strahler geometric-optical forest canopy reflectance model can estimate spectral bidirectional reflectance factors and spectral albedo with some success. In this model, the vegetated surface is treated as an assemblage of partially illuminated tree crowns of ellipsoidal shape, and through geometric-optics and Boolean set theory, the proportion of sunlit and shadowed canopy and background is modeled as a function of view angle. Tne model is driven by ground measurements of spectral reflectance and tree crown shape, size, and spacing. Atmospherically corrected multiangular radiance measurements from the Advanced Solid State Array Spectroradiometer (ASAS) fit the shape of the modeled reflectance function quite well. Integration of the reflectance function yields a spectral albedo, which, when extended to the full solar spectrum, agrees with pyranometer measurements obtained at the site. DTIC

N93-29834# Cooperative Inst. for Research in the Atmosphere, Fort Collins, CO.

GEOSCIENCE CENTER RESEARCH Final Report, 1 Sep. 1986 - 15 Jun. 1992

Thomas H. VonderHaar and Jan L. Behunek Nov. 1992 199 p
(Contract DAAL03-86-K-0175)
(AD-A263465; ARO-24608.15-GS-UIR) Avail: CASI HC A09/MF A03

The research grant was supported by the Army Research Office (ARO) Center for Geosciences located at the Foothills Campus at Colorado State University under the auspices of the Cooperative Institute for Research in the Atmosphere (CIRA). The Center for Geoscience at Colorado State University was established in collaboration with the ARO on 1 Oct. 1986. The Center brought together a wide range of expertise into one focused multi-disciplinary research framework. Under the administrative structure of CIRA, the Center involved investigators from the University's Departments of Atmospheric Science, Civil Engineering, Electrical Engineering, Earth Resources, Forest and Wood Science, Physics, and Psychology. The technical components of the Center are in Atmospheric and Surface Remote and In-Situ Sensing; Atmospheric Modeling; Hydrologic Modeling; and Geoscience Information Extraction. DTIC

N93-30045 Arizona Univ., Tucson.

THE ESTIMATION AND SCALING OF LAND-SURFACE FLUXES OF LATENT AND SENSIBLE HEAT WITH REMOTELY SENSED DATA OVER A GRASSLAND SITE Ph.D. Thesis

Karen Sue Humes 1992 259 p
Avail: Univ. Microfilms Order No. DA9309021

The overall topic of the research described was the partitioning of available energy at the Earth's surface into sensible and latent heat flux, with an emphasis on the development of techniques which utilize remotely sensed data. One of the major objectives was to investigate the modification of existing techniques, developed over agricultural surfaces, to 'natural' ecosystems (i.e., non-agricultural vegetation types with variable and incomplete canopy cover). Ground-based measurements of surface fluxes, vegetation cover, and surface and root-zone soil moisture from the First ISLSCP (International Land Surface Climatology Program) Field Experiment (FIFE) were used to examine the factors controlling the partitioning of energy at ground stations with contrasting surface characteristics. Utilizing helicopter-based and satellite-based data acquired directly over ground-based flux stations at the FIFE experimental area, relatively simple algorithms were developed for estimating the soil heat flux and sensible heat flux from remotely sensed data. The root mean square error (RMSE) between the sensible heat flux computed with the remotely sensed data and the sensible heat flux measured at the ground stations was 33 Wm(sup 2). These algorithms were then applied on a pixel-by-pixel basis to data from a Landsat-TM (Thematic Mapper) scene acquired over the FIFE site on 15 Aug. 1987 to produce spatially distributed surface energy-balance components for the FIFE site. A methodology for quantifying the effect of spatial scaling on parameters derived from remotely sensed data was presented. As an example of the utility of this approach, NDVI values for the FIFE experimental area were computed with input data of variable spatial resolution. The differences in the values of NDVI computed at different spatial resolutions were accurately predicted by an equation which quantified those differences in terms of variability in input observations. Dissert. Abstr.

N93-30049# Department of Energy, Washington, DC. Environmental Sciences Div.

THE POSSIBLE DIRECT USE OF SATELLITE RADIANCE MEASUREMENTS BY THE ATMOSPHERIC RADIATION MEASUREMENT PROGRAM

Mar. 1993 76 p
(DE93-009819; DOE/ER-0585T) Avail: CASI HC A05/MF A01

The Atmospheric Radiation Measurement (ARM) Program is a major research program initiated by the Department of Energy to improve our understanding of radiative and cloud processes critical to predicting the Earth's climate and its changes. Central to this concept is the use of four to six intensively instrumented sites for long-term study and characterization of the processes of interest. The instrumentation suites will include ground-based, high-accuracy radiometers for measuring the short and longwave surface flux, as well as an extensive set of ground-and air-based instrumentation for characterizing the intervening atmospheric column. Satellite-based measurements are expected to play a very important role in providing top-of-the-atmosphere measurements. The possibility of comparing ARM outputs directly with satellite measurements, thereby ensuring the independence of these two important data sets, is examined. Thus focus was on what do satellites really measure and how well do they measure it; on what can we do about the general lack of adequate visible channel calibration; on what is the best way for ARM to obtain near-real-time access to this unprocessed data; and on what is the optimum way for ARM to make use of satellite data. DOE

N93-30107# Loughborough Univ. of Technology (England). Dept. of Mathematical Sciences.

ANALYSIS OF THERMAL BAR USING BOUNDARY-LAYER INTEGRAL EQUATIONS GRADIENTS

Anthony Kay Sep. 1992 13 p
(MATHS-Rept-A-177; ETN-93-93741) Avail: CASI HC A03/MF A01

The possibility of modeling lakes by examination of the thermal bar in isolation is discussed. Taking advantage of an analogy with a heated vertical plate immersed in fluid, an analysis of the thermal bar (which occurs at the isotherm of the temperature of maximum density in water) by means of boundary layer integral equations, is presented. Similar scalings to those for the heated plate are found, but the effects of viscosity appear to be only of secondary importance. ESA

N93-30637# Tennessee Valley Authority, Chattanooga. Div. of Water Resources.

REMOTE SENSING FOR WATER QUALITY MONITORING IN THE TENNESSEE VALLEY: FIELD TESTS OF TWO SYSTEMS

F. Dierberg 25 Aug. 1992 123 p
(DE93-008997; TVA/WR-92/17) Avail: CASI HC A06/MF A02

Two airborne remote sensing systems, the Compact Airborne Spectrographic Imager (CASI), and the Airborne Multispectral Measurement System (AMMS) were field tested over reservoirs in the Tennessee River valley during the summer of 1991 and winter (AMMS only) of 1992. Univariate, linear regression analyses using single or ratioed wavelength bands and line height algorithms for spectral energy in the 625-725 nm wavelength range provided the best correlations to ground-truthed uncorrected chlorophyll A, turbidity, suspended solids, and Secchi disk transparency. Details of these monitoring studies are included. DOE

N93-30833# Environmental Protection Agency, Washington, DC. Office of Assistant Administrator for Water.

OFFICE OF WATER ENVIRONMENTAL AND PROGRAM INFORMATION SYSTEMS COMPENDIUM, FY 1992

Apr. 1992 158 p
(PB93-186203; EPA/800/B-92/001) Avail: CASI HC A08/MF A02

The compendium combines text and graphics in profiling 20 key Office of Water Information Systems. These profiles highlight the type of information contained in the 20 systems and the management tools (statistical, graphical, and linkage packages) associated with each. The compendium also includes descriptions of nearly 100 additional Office of Water Environmental and Program Information Systems and 35 water-related systems from other areas of the government. NTIS

N93-30839# Beleidscommissie Remote Sensing, Delft (Netherlands).
LAND USE DATABASE FOR THE NETHERLANDS USING LANDSAT THEMATIC MAPPER PICTURES [GRONDGEBRUIKSDATABANK VAN NEDERLAND VERVAARDIGD MET BEHULP VAN LANDSAT THEMATIC MAPPER OPNAMEN]
H. Thunnissen (Winand Staring Centre, Wageningen, Netherlands.), R. Olthof (Winand Staring Centre, Wageningen, Netherlands.), P. Getz (DHV Raadgevend Ingenieursbureau B.V., Amersfoort, Netherlands.), and L. Vels (DHV Raadgevend Ingenieursbureau B.V., Amersfoort, Netherlands.) Aug. 1992 211 p In DUTCH
(BCRS-91-32; DLO-168; ISBN-9-05-411053-8; ETN-93-93315) Copyright Avail: CASI HC A10/MF A03

A land use data base for the Netherlands was drawn up using satellite images. This data base can be used on national scale with a view to water management, protection of soil and ground water, and country planning. The data base consists of a raster with pixels of 25 by 25 m covering the whole country. Fifteen land use classes can be distinguished with emphasis on agricultural land use. The applicability on a regional scale depends on land use, vegetation growth, and satellite image recording. ESA

N93-31009# Beleidscommissie Remote Sensing, Delft (Netherlands).
CAESAR DEVELOPMENT PLAN 1992-1995 Final Report
J. Boerger (National Aerospace Lab., Amsterdam, Netherlands.), M. vanPersie (National Aerospace Lab., Amsterdam, Netherlands.), G. Habets (National Aerospace Lab., Amsterdam, Netherlands.), G. Lamers (National Aerospace Lab., Amsterdam, Netherlands.), H. Pouwels (National Aerospace Lab., Amsterdam, Netherlands.), and C. Smorenburg (Netherlands Organization for Applied Scientific Research TNO, Delft.) Aug. 1992 103 p
(BCRS-92-17; ISBN-9-05-411059-7; ETN-93-94089) Avail: CASI HC A06/MF A02

The CAESAR (CCD (Charge Coupled Device) Airborne Experimental Scanner for Applications in Remote sensing) development plan is presented. CAESAR is a multispectral pushroom scanner using linear charge coupled device detector arrays. An overview of the existing CAESAR system is presented in order to understand the proposed modifications. A list of the proposed modifications is given. These modifications concern the sensors, filters, mounting, data handling, electronics, calibration and operational aspects. The feasibility of the proposed modifications is elaborated on and conclusions are given. A product description of a stabilization platform is included in the appendix. ESA

N93-31010# Beleidscommissie Remote Sensing, Delft (Netherlands).
ERS-1 DIRECTIONAL WAVE SPECTRA VALIDATION WITH THE AIRBORNE SAR PHARS
J. C. M. Kleijweg (Physics and Electronics Lab. TNO, The Hague, Netherlands.) and H. Greidanus (Physics and Electronics Lab. TNO, The Hague, Netherlands.) Oct. 1992 57 p
(BCRS-92-18; FEL-92-C282; ISBN-9-05-411061-9; ETN-93-94090) Avail: CASI HC A04/MF A01

The ERS-1 calibration/validation campaign 'RENE91' is reported. The purpose was to validate ERS-1 geophysical products using other remotely sensed data and in situ measurements. For three days during this campaign, the airborne 'PHARS' (Phased Array SAR (Synthetic Aperture Radar)) measured ocean wave spectra concurrent with the ERS-1 and with a surface radar system and a wave buoy. The results of these instruments are compared, and subsequently interpreted on the basis of SAR ocean wave imaging theory. A total of seven ERS-1 and 14 PHARS wave spectra are analyzed, together with numerous surface radar and buoy spectra. All these spectra contained a total of 13 different wave systems. From the intercomparison, it was found that: very short waves (less than 70 m wavelength) are not seen by ERS-1, nor by PHARS; roughly half the wave occurrences are detected by both ERS-1 and PHARS, the remaining are missed by either or both; peak wavelength and direction of the same wave component can differ considerably as imaged by the various sensors; ERS-1 misses more wave systems than PHARS, especially azimuth traveling ones. All these effects can be understood in terms of the elements of the SAR ocean wave imaging process: scanning distortion, velocity bunching, and defocusing. ESA

N93-31011# Beleidscommissie Remote Sensing, Delft (Netherlands).
BAYESIAN LINEAR ANALYSIS WITH APPLICATION TO REMOVAL OF ATMOSPHERIC INFLUENCES ON OPTICAL REMOTE SENSING IMAGES
V. L. Dolman (Vrije Univ., Amsterdam, Netherlands.), J. F. deHaan (Vrije Univ., Amsterdam, Netherlands.), and J. W. Hovenier (Vrije Univ., Amsterdam, Netherlands.) Oct. 1992 137 p
(BCRS-92-19; ISBN-9-05-411060-0; ETN-93-94091) Avail: CASI HC A07/MF A02

Research aimed at the development of methods for removal of atmospheric influences on visual and near infrared remote sensing imagery is presented. Remote sensing of the Earth involves an exceedingly complex system. Structural progress in quantitative analysis of the system requires combination of data from different sources. A major problem is reliable estimation of errors due to measurement errors and to uncertainty about the system's properties that are not measured. It is shown that Bayesian analysis provides a general strategy to incorporate data from different sources in the estimation of any quantity of interest and its error. In the analysis, the role of physical models is crucial. The maximum entropy principle is applied to ensure that the analysis is based only upon information that is actually available. A dramatic simplification results if several relations between quantities are linearized. This leads to a very simple algorithm to analyze remote sensing and related data which requires only a tiny computational effort. This algorithm and the underlying formalism is presented. It is also shown that Bayesian linear analysis allows various types of analytical insight. The analysis is applied to the problem of removal of atmospheric influences on optical satellite imagery. Here, linearization errors turn out to be rather small. Various aspects of the atmospheric correction problem are investigated, analytically as well as numerically. It is concluded that Bayesian linear analysis is a useful approach for the analysis of remote sensing and related data. ESA

N93-28797*# Naval Research Lab., Washington, DC.
FILTERING INTERPOLATORS FOR IMAGE COMPARISON ALGORITHMS Abstract Only
R. L. Lucke and A. D. Stocker (Space Computer Corp., Santa Monica, CA.) *In* Lunar and Planetary Inst., Workshop on Advanced Technologies for Planetary Instruments, Part 1 1993 p 15 (For primary document see N93-28764 11-91)
Avail: CASI HC A01/MF A01

N93-29738*# Massachusetts Inst. of Tech., Cambridge.
PROJECT COPERNICUS: AN EARTH OBSERVING SYSTEM
In Universities Space Research Association, Houston, Proceedings of the Seventh Annual Summer Conference. NASA/USRA: University Advanced Design Program 1991 p 191-196 (For primary document see N93-29712 11-01)
Avail: CASI HC A02/MF A03

44 ENERGY PRODUCTION AND CONVERSION

Includes specific energy conversion systems, e.g., fuel cells; global sources of energy; geophysical conversion; and windpower.

For related information see also *07 Aircraft Propulsion and Power, 20 Spacecraft Propulsion and Power,* and *28 Propellants and Fuels.*

N93-28603# Sandia National Labs., Albuquerque, NM. Experimental Mechanics Dept.
THE NATURAL EXCITATION TECHNIQUE (NExT) FOR MODAL PARAMETER EXTRACTION FROM OPERATING WIND TURBINES
George H. James, III, Thomas G. Carne, and James P. Lauffer Feb. 1993 46 p
(Contract DE-AC04-76DP-00789)
(DE93-010611; SAND-92-1666) Avail: CASI HC A03/MF A01

The Natural Excitation Technique (NExT) is a method of modal testing that allows structures to be tested in their ambient environments. This report is a compilation of developments and results since 1990, and contains a new theoretical derivation of NExT, as well as a verification using analytically generated data. In addition, we compare results from NExT with conventional modal testing for a parked, vertical-axis wind turbine, and, for a rotating turbine, NExT is used to calculate the model parameters as functions of the rotation speed, since substantial damping is derived from the aeroelastic interactions during operation. Finally, we compare experimental results calculated using NExT with analytical predictions of damping using aeroelastic theory. DOE

N93-28971# Purdue Univ., West Lafayette, IN.

NEW III-V CELL DESIGN APPROACHES FOR VERY HIGH EFFICIENCY

M. S. Lundstrom, M. R. Melloch, G. B. Lush, M. P. Patkar, and M. P. Young Apr. 1993 110 p Prepared for Midwest Research Inst., Golden, CO
(Contract DE-AC02-83CH-10093)
(DE93-000097; NREL/TP-451-5355) Avail: CASI HC A06/MF A02

This report describes to examine new solar cell design approaches for achieving very high conversion efficiencies. The program consists of two elements. The first centers on exploring new thin-film approaches specifically designed for M-3 semiconductors. Substantial efficiency gains may be possible by employing light trapping techniques to confine the incident photons, as well as the photons emitted by radiative recombination. The thin-film approach is a promising route for achieving substantial performance improvements in the already high-efficiency, single-junction, 3-5 cell. The second element of the research involves exploring design approaches for achieving high conversion efficiencies without requiring extremely high-quality material. This work has applications to multiple-junction cells, for which the selection of a component cell often involves a compromise between optimum band pp and optimum material quality. It could also be a benefitial manufacturing environment by making the cell's efficiency less dependent on material quality. DOE

N93-28974* National Aeronautics and Space Administration. Lewis Research Center, Cleveland, OH.

ALKALI METAL CARBON DIOXIDE ELECTROCHEMICAL SYSTEM FOR ENERGY STORAGE AND/OR CONVERSION OF CARBON DIOXIDE TO OXYGEN Patent

Norman H. Hagedorn, inventor (to NASA) 25 May 1993 7 p Filed 26 Sep. 1991 Supersedes N92-10222 (30 - 1, p 42)
(NASA-Case-LEW-14973-1; US-Patent-5,213,908;
US-Patent-Appl-SN-766593; US-Patent-Class-429-16;
US-Patent-Class-429-27; US-Patent-Class-429-29; US-Patent-Class-429-30;
US-Patent-Class-429-46; US-Patent-Class-429-103;
Int-Patent-Class-H01M-8/14) Avail: US Patent and Trademark Office

An alkali metal, such as lithium, is the anodic reactant; carbon dioxide or a mixture of carbon dioxide and carbon monoxide is the cathodic reactant; and carbonate of the alkali metal is the electrolyte in an electrochemical cell for the storage and delivery of electrical energy. Additionally, alkali metal-carbon dioxide battery systems include a plurality of such electrochemical cells. Gold is a preferred catalyst for reducing the carbon dioxide at the cathode. The fuel cell of the invention produces electrochemical energy through the use of an anodic reactant which is extremely energetic and light, and a cathodic reactant which can be extracted from its environment and therefore exacts no transportation penalty. The invention is, therefore, especially useful in extraterrestrial environments.
Official Gazette of the U.S. Patent and Trademark Office

N93-29147# Los Alamos National Lab., NM.

POLYMER ELECTROLYTE FUEL CELLS FOR TRANSPORTATION APPLICATIONS

T. E. Springer, M. S. Wilson, F. H. Garzon, T. A. Zawodzinski, and S. Gottesfeld 1993 13 p Presented at the Electric Vehicle Symposium, Honolulu, HI, 16-23 May 1993
(Contract W-7405-eng-36)
(DE93-008721; LA-UR-93-728; CONF-9305150-1) Avail: CASI HC A03/MF A01

The application of the polymer electrolyte fuel cell (PEFC) as a primary power source in electric vehicles has received increasing attention during the last few years. This increased attention has been fueled by a combination of significant technical advances in this field and by the initiation of some projects for the demonstration of a complete, PEFC-based power system in a bus or in a passenger car. Such demonstration projects reflect an increased faith of industry in the potential of this technology for transportation applications, or, at least, in the need for a detailed evaluation of this potential. Nevertheless, large scale transportation applications of PEFC's require a continued concerted effort of research on catalysis, materials and components, combined with the engineering efforts addressing the complete power system. This is required to achieve cost effective, highly performing PEFC stack and power system. We describe in this contribution some recent results of work performed within the Core Research PEFC Program at Los Alamos National Laboratory, which has addressed transportation applications of PEFC's. DOE

N93-29844# Argonne National Lab., IL.

SOLID OXIDE FUEL CELLS FOR TRANSPORTATION: A CLEAN, EFFICIENT ALTERNATIVE FOR PROPULSION

R. Kumar, M. Krumpelt, and K. M. Myles 1993 9 p Presented at the 183rd Electrochemical Society Meeting, Honolulu, HI, 16-21 May 1993
(Contract W-31-109-eng-38)
(DE93-010662; ANL/CMT/CP-77865; CONF-930571-8) Avail: CASI HC A02/MF A01

Fuel cells show great promise for providing clean and efficient transportation power. Of the fuel cell propulsion systems under investigation, the solid oxide fuel cell (SOFC) is particularly attractive for heavy duty transportation applications that have a relatively long duty cycle, such as locomotives, trucks, and barges. Advantages of the SOFC include a simple, compact system configuration; inherent fuel flexibility for hydrocarbon and alternative fuels; and minimal water management. The specific advantages of the SOFC for powering a railroad locomotive are examined. Feasibility, practicality, and safety concerns regarding SOFCs in transportation applications are discussed. DOE

N93-29925# Midwest Research Inst., Golden, CO.

MODIFICATION OF FLUX PROFILES USING A FACETED CONCENTRATOR

A. Lewandowski, K. Scholl, and C. Bingham Jan. 1993 7 p Presented at the SOLAR 1993: American Society of Mechanical Engineers (ASME)/American Solar Energy Society (ASES) Joint Solar Energy Conference, Washington, DC, 22-28 Apr. 1993
(Contract DE-AC02-83CH-10093)
(DE93-000087; NREL/TP-471-5352; CONF-930435-7) Avail: CASI HC A02/MF A01

The use of a faceted solar concentrator allows for some flexibility in aiming strategy and in the intensity of the resulting flux profile at the target. This can be an advantage when considering applications that do not necessarily require maximum concentration, particularly emerging, new applications in solar processed advanced materials. This paper will describe both an analysis of predicted flux profiles for several different aiming strategies using the SOLFUR computer code and experiments to characterize the actual flux profiles realized with a selected aiming strategy. The SOLFUR code models each of the furnace components explicitly. Aim points for each facet can be specified. Thus, many strategies for adjusting aim points can be easily explored. One strategy calls for creating as uniform a flux over as large an area as possible. We explored this strategy analytically and experimentally. The experimental data consist of flux maps generated by a video imaging system calibrated against absolute flux measurements taken with circular foil calorimeters. Results from the analytical study and a comparison with the experimental data indicate that uniform profiles can be produced over fairly large areas. DOE

N93-29965# Spire Corp., Bedford, MA.

LOW-COST, HIGH-EFFICIENCY SOLAR CELLS UTILIZING GaAs-ON-Si TECHNOLOGY

S. M. Vernon Apr. 1993 25 p Prepared for Midwest Research Inst., Golden, CO
(Contract DE-AC02-83CH-10093)
(DE93-000096; NREL/TP-451-5353) Avail: CASI HC A03/MF A01

This report describes work to develop technology to deposit GaAs on Si using a nucleation layer of atomic-layer-epitaxy-grown GaAs or AlAs on Si. This ensures two-dimensional nucleation and should lead to fewer defects in the final GaAs layer. As an alternative, we also developed technology for depositing GaAs on sawtooth-patterned Si. Preliminary studies showed that this material can have a very low defect density, approximately 1 x 10(exp 5) cm(exp -5), as opposed to our conventionally grown GaAs on SL which has a typical defect density of over 1 x 10(exp 7) cm(exp -2). Using these two new methods of GaAs-on-Si material growth, we made solar cells that are expected to show higher efficiencies than those of previous cells. DOE

N93-30001 American Solar Energy Society, Boulder, CO.
SOLAR WORLD CONGRESS: PROCEEDINGS OF THE BIENNIAL CONGRESS OF THE INTERNATIONAL SOLAR ENERGY SOCIETY, VOLUME 1, PART 2
M. E. Arden, S. M. A. Burley, and M. Coleman 1992 583 p Conference held in Denver, CO, 19-23 Aug. 1991 See also Volume 1, Part 1, PB93-174761 and Volume 2, Part 1, PB93-174787 Sponsored by Environmental Protection Agency, Research Triangle Park, NC, Air and Energy Engineering Research Lab.
(PB93-174779; EPA/600/R-93/058B) Copyright Avail: Issuing Activity

Contents: Wind Energy Experiences; Wind Energy Systems Performance; Wind Systems Applications and Hydropower; Utility and Regulatory Issues; Solar Hydrogen Technologies; Biotechnology; Bio-Chemical Conversion; Biofuels; Radiation Instruments, Measurements; Radiation Models; Simulation; Radiation Resources; Use of Radiation Data; and Renewable Resource Posters. NTIS

N93-30011# Oregon Inst. of Tech., Klamath Falls. Geo-Heat Center.
DIRECT USE GEOTHERMAL APPLICATIONS FOR BRAZED PLATE HEAT EXCHANGERS
K. Rafferty Feb. 1993 66 p
(Contract DE-FG07-90ID-13040)
(DE93-008559; DOE/ID-13040/18) Avail: CASI HC A04/MF A01

Brazed plate heat exchanger were placed in three geothermal fluids (Klamath Falls, OR; Boise, ID; and Pagosa Springs, CO) in order to determine the effect of H2S on braze material. Based on subsequent analysis, it appears that the rate of corrosion of the braze material is much slower than corrosion of copper tube materials in the same fluids. Minimum expected life of the heat exchangers based on these corrosion rates is reported to be 12 years in fluids of less than 1 ppm H2S and 10 years in fluids of less than 5 ppm. Based on these expected lives, and using a 3% inflation rate and 8% discount rate, brazed plate heat exchangers are a clear economic choice in which the capital cost is 50% or less of the cost of a plate and frame heat exchanger for the same duty. Due to their single pass design, brazed plate heat exchangers are generally limited to approach temperatures of 10 deg or greater. Size limitations restrict applications to 100 gpm and/or 200 sq ft heat transfer surface area. DOE

N93-30111# Technical Research Centre of Finland, Espoo. Electrical and Automation Engineering Lab.
PREFEASIBILITY STUDY ON COMPRESSED AIR ENERGY STORAGE SYSTEMS [PAINEILMAVARASTON KAYTTO SAHKON TUOTANNOSSA]
Yehia ElMahgary, Esa Peltola, Kari Sipila, and Anne Vaatainen Aug. 1991 66 p
(VTT-TIED-1267; ISBN-9-51-383899-4; ETN-93-93774) Copyright Avail: CASI HC A04/MF A01

A prefeasibility study on Compressed Air Energy Storage (CAES) systems is presented. The costs of excavating rock caverns for compressed air storage and those for forming suitable storage caverns in existing mines were estimated, and this information was used to calculate the economics of CAES. An analysis of the different possible systems is given following a review of literature on CAES. This was followed by an economic analysis which comprised two separate systems. The first consisted of conventional oil fueled gas turbine plants provided with CAES system. In the second system wind turbines were used to run the compressors which are used in charging the compressed air storage cavern. The results of the current prefeasibility study confirmed the economic attractiveness of the CAES in the first system. Wind turbines still seem, however, to be too expensive to compete with coal power plants. More accurate and straightforward results could be obtained only in a more comprehensive study. ESA

N93-30206# Midwest Research Inst., Golden, CO.
STUDY OF PARAMETERS AFFECTING THE PERFORMANCE OF SOLAR DESICCANT COOLING SYSTEMS
A. A. Pesaran and E. A. Hoo Jan. 1993 7 p Presented at the SOLAR 1993: American Society of Mechanical Engineers (ASME)/American Solar Energy Society (ASES) Joint Solar Energy Conference, Washington, DC, 22-28 Apr. 1993
(Contract DE-AC02-83CH-10093)
(DE93-000088; NREL/TP-471-5375; CONF-930435-6) Avail: CASI HC A02/MF A01

The performance of a solar desiccant cooling system depends on the performance of its components, particularly the desiccant dehumidifier and solar collectors. The desiccant dehumidifier performance is affected by the properties of the desiccant, particularly the shape of the isotherm and the regeneration temperature. The performance of a solar collector, as one would expect, depends on its operating temperature, which is very close to the desiccant regeneration temperature. The purpose of this study was to identify the desiccant isotherm shape (characterized by separation factor) that would result in the optimum performance - based on thermal coefficient of performance and cooling capacity - of a desiccant cooling cycle operating in ventilation mode. Different regeneration temperatures ranging from 65 to 160 C were investigated to identify the corresponding optimum isotherm shape at each. Thermal COP dictates the required area of the solar collectors, and the cooling capacity is an indication of the size and cost of the cooling equipment. Staged and no-staged regeneration methods were studied. DOE

N93-30207# Midwest Research Inst., Golden, CO.
MEASUREMENTS AND CHARACTERIZATION BRANCH Annual Report, FY 1992
P. Dippo, ed. Mar. 1993 27 p
(Contract DE-AC02-83CH-10093)
(DE93-000094; NREL/TP-412-5422) Avail: CASI HC A03/MF A01

The Measurements and Characterization Branch actively supports the advancement of DOE/NREL goals for the development and implementation of the solar photovoltaic (PV) technology. The primary focus of the laboratories is to provide state-of-the-art analytical capabilities for materials and device characterization and fabrication. The branch houses a comprehensive facility that is capable of providing information on the full range of PV components. A major objective of the branch is to aggressively pursue collaborative research with other government laboratories, universities, and industrial firms for the advancement of Pv technologies. Members of the branch disseminate research findings to the technical community in publications and presentations. The Measurements and Characterization Branch encompasses seven coordinated research groups, providing integrated research and development that covers all aspects of photovoltaic materials/devices characterization. DOE

N93-30208# Research Triangle Inst., Research Triangle Park, NC.
GROWTH AND DEVELOPMENT OF GaInAsP FOR USE IN HIGH-EFFICIENCY SOLAR CELLS
P. R. Sharps Apr. 1993 18 p Prepared for Midwest Research Inst., Golden, CO
(Contract DE-AC02-83CH-10093)
(DE93-000098; NREL/TP-451-5414) Avail: CASI HC A03/MF A01

This report describes work done during Phase 2 of the subcontract. Goals for Phase 2 include the following: (1) Optimize the GaInAsP cell on GaAs and demonstrate a 500-sun at air mass (AM) 1.5 efficiency of greater than 23%; (2) Develop a window layer, including the evaluation of AlGaAs, GaInP, AlGaAsP, AlGaInP, and GaP; (3) Develop a front-surface contact, with a grid designed for 500-sun concentration, and a goal of a contact resistivity of approximately 10(exp 5) ohm-cm(exp 2); (4) Grow GaInAsP cells on Ge, with a goal of a 1-sun (AM 1.5) efficiency of greater than 15%. Accomplishments reported herein include (1) the fabrication of p-on-n and n-on-p GaInAsP cells on GaAs, with the n-on-p cell demonstrating a 10-sun (AM 1.5) active-area efficiency of 23.4% as measured at NREL, (2) the evaluation of Al(x)Ga(1-x)As, GaInP2, and AlInP2 window layers; and (3) the fabrication of GaInAsP cells on Ge, with the demonstration of a p-on-n GaInAsP cell grown on Ge with a 1-sun (AM 1.5) active-area efficiency of 14.4%. DOE

N93-30391# Sandia National Labs., Albuquerque, NM.
THERMAL EFFECTS TESTING AT THE NATIONAL SOLAR THERMAL TEST FACILITY
M. E. Ralph, C. P. Cameron, and C. M. Ghanbari 1992 13 p Presented

at the 39th International Instrumentation Symposium, Albuquerque, NM, 2-6 May 1993
(Contract DE-AC04-76DP-00789)
(DE93-009825; SAND-92-2167C; CONF-930561-3) Avail: CASI HC A03/MF A01

The National Solar Thermal Test Facility is operated by Sandia National Laboratories and located on Kirkland Air Force Base in Albuquerque, New Mexico. The permanent features of the facility include a heliostat field and associated receiver tower, two solar furnaces, two point-focus parabolic concentrators, and Engine Test Facility. The heliostat field contains 220 computer-controlled mirrors, which reflect concentrated solar energy to test stations on a 61-m tower. The field produces a peak flux density of 250 W/cm(sup 2) that is uniform over a 15-cm diameter with a total beam power of over 5 MW(sub t). The solar beam has been used to simulate aerodynamic heating for several customers. Thermal nuclear blasts have also been simulated using a high-speed shutter in combination with heliostat control. The shutter can accommodate samples up to 1 m (times) 1 m and it has been used by several US and Canadian agencies. A glass-windowed wind tunnel is also available in the Solar Tower. It provides simultaneous exposure to the thermal flux and air flow. Each solar furnace at the facility includes a heliostat, an attenuator, and a parabolic concentrator. One solar furnace produces flux levels of 270 W/cm(sup 2) over and delivers a 6-mm diameter and total power of 16 kW(sub t). A second furnace produces flux levels up to 1000 W/cm(sup 2) over a 4 cm diameter and total power of 60 kW(sub t). Both furnaces include shutters and attenuators that can provide square or shaped pulses. The two 11 m diameter tracking parabolic point-focusing concentrators at the facility can each produce peak flux levels of 1500 W/cm(sup 2) over a 2.5 cm diameter and total power of 75 kW(sub t). High-speed shutters have been used to produce square pulses. DOE

N93-30573# Technische Univ., Berlin (Germany). Fachbereich Elektrotechnik.
TECHNICAL EXAMINATION AND SIMULATION OF A PHOTOVOLTAIC SYSTEM: SOLAR GENERATOR, BATTERY, DOWNLOAD Ph.D. Thesis [MESSTECHNISCHE UNTERSUCHUNG UND SIMULATION EINES PHOTOVOLTAIKSYSTEMS: SOLARGENERATOR, BATTERIE, TIEFSETZSTELLER, LAST]
Armin Thoma 1992 145 p In GERMAN
(ETN-93-94179) Avail: CASI HC A07/MF A02

Examinations of each component behavior of a solar generator system are carried out. A solar tank station was supplied to an electric car on a low loss regulator. By using a large system battery, the vehicle battery could be fully loaded. Several loading processes were used for the electric car by using the system battery with an intelligent regulator. Examinations for range optimization were achieved with integration of a measure data acquisition system in the electric car. A measuring process was developed for recording the current-voltage curve of high power solar generators with low-loss load simulators. A state analysis of solar generator was obtained by comparison of data sets. A software tool was realized for analysis of operation state. By converting equivalent schemes into simulation programs, device optimization was carried out with parameter variation. ESA

N93-30777# Academy of Sciences of the Ukraine, Kiev. Inst. Yadernykh Issledovanij.
CHANGE OF SOLAR CELL ELEMENT PROPERTIES INFLUENCED BY ADSORBED ATOMS [IZMENENIE EHIEKTROFIZICHESKIKH SVOJSTV SOINECHNYKH EHLEMENTOV PRI VOZDEJSTVII ADSORBIROVANNYKH ATOMOV]
A. I. Livshits, Y. A. Romanovskij, A. N. Zavilopulo, A. I. Zhukov, and A. V. Snegurskij 1991 26 p In RUSSIAN
(DE93-606694; KIYal-91-8) Avail: CASI HC A03/MF A01 (US Sales Only)

A series of experimental studies on the influence of alkali and alkaline-earth metal films on electro-physical properties of solar elements used for spacecraft energy supply was carried out. Metal films of different thicknesses were deposited using an effusion source, the mass of the film was calculated using measured atomic beam density. The Mg film thickness was determined by means of microscopic technique. The dynamics of current-to-voltage characteristic variation was studied for different film thickness and chemical composition in vacuum and in oxygen atmosphere. DOE

N93-30814# Rocky Research Corp., Boulder City, NV.
COMPLEX-COMPOUND HEAT PUMP: TOPICAL REPORT ON PHASE 1 RESULTS Final Report, Jan. 1990 - Jul. 1992
U. Rockenfeller, L. D. Kirol, W. T. Dooley, J. Langeliers, and P. Sarkisian Aug. 1992 98 p See also PB90-163007 Sponsored by Gas Research Inst.
(Contract GRI-5089-243-1903)
(PB93-185460; GRI-93/0113) Avail: CASI HC A05/MF A02

A gas-fired heat pump using complex compound chemisorption media and ammonia refrigerant is being developed. Complex compounds are advantageous because they adsorb large amounts of refrigerant (up to 80 percent of the adsorbent dry weight), exhibit vapor pressure independent of refrigerant concentration, can be made to adsorb very rapidly, and can be formulated to have different vapor pressures. The heat pump being developed has three stages, each using a different formulation. Multiple stages are used to increase efficiency, giving cooling COPs near one. Heating-mode operation at ambient temperatures of -20 F and below can also be achieved. The report presents results from Phase 1 of the development project. Phase 1 efforts focused on generation of engineering data to ensure that no major obstacles would be met in future development, and to provide data necessary for design of a breadboard system. Work included the following: (1) optimization of the sorbers internal heat and mass transfer hardware to maximize sorption rates and minimize cost, (2) qualification of sorbent media with respect to stability and corrosion, (3) estimation of manufacturing and operating costs, and (4) development of preliminary designs for heat pump and AC systems. NTIS

N93-30891# Midwest Research Inst., Golden, CO.
SILICON FILM(TRADEMARK) PHOTOVOLTAIC MANUFACTURING TECHNOLOGY
W. R. Bottenberg, R. B. Hall, E. L. Jackson, S. Lampo, W. E. Mulligan (Astropower, Inc., Newark, DE.), and A. M. Barnett (Astropower, Inc., Newark, DE.) Apr. 1993 25 p Prepared in cooperation with AstroPower, Inc., Newark, DE
(Contract DE-AC02-83CH-10093)
(DE93-010008; NREL/TP-411-5455) Avail: CASI HC A03/MF A01

This report describes work on a project to develop an advanced low-cost manufacturing process for a new utility-scale flatplate module based on thin active layers of polycrystalline silicon on a low-cost substrate. This is called the Silicon-Film(trademark) process. This new power module is based on a new large solar cell that is 675 sq cm in area. Eighteen of these solar cells form a 170-W module. Twelve of these modules form a 2-kW array. The program has three components: (1) development of a Silicon-Film(trademark) wafer machine that can manufacture wafer 675 sq cm in size with a total product cost reduction of 70%; (2) development of an advanced solar cell manufacturing process that will turn the Silicon-Film(trademark) wafer into a 14%-efficient solar cell; and (3) development of an advanced module design based on these large-area, efficient silicon solar cells with an average power of 170 watts. The completion of these three tasks will lead to a new power module designed for utility and other power applications with a substantially lower cost. DOE

N93-30935 American Solar Energy Society, Boulder, CO.
SOLAR WORLD CONGRESS: PROCEEDINGS OF THE BIENNIAL CONGRESS OF THE INTERNATIONAL SOLAR ENERGY SOCIETY, VOLUME 2, PART 2
M. E. Arden, S. M. A. Burley, and M. Coleman 1992 691 p Meeting held in Denver, CO, 19-23 Aug. 1991 See also volume 2, part 1, PB93-174787 and volume 3, part 1, PB93-174803 Sponsored by EPA, Research Triangle Park, NC Limited Reproducibility: More than 20% of this document may be affected by microfiche quality
(PB93-174795; EPA/600/R-93/058D) Copyright Avail: Issuing Activity (National Technical Information Service (NTIS))

Topics covered in Volume 2, Part 2, include concentrating collectors; solar heat storage; central receivers; dish collectors; line-focus collectors; detoxification and materials; solar heat; desalination; solar ponds; and solar drying. NTIS

N93-28715*# Space Systems/Loral, Palo Alto, CA.
SODIUM-SULFUR CELL TECHNOLOGY FLIGHT EXPERIMENT (SSCT)
Carl R. Halbach *In* NASA, Washington, NASA/DOD Flight Experiments

Technical Interchange Meeting Proceedings 1992 8 p (For primary document see N93-28699 11-12)
Avail: CASI HC A02/MF A10

N93-28717*# National Aeronautics and Space Administration. Lewis Research Center, Cleveland, OH.
THE PHOTOVOLTAIC ARRAY SPACE POWER PLUS DIAGNOSTICS (PASP PLUS) FLIGHT EXPERIMENT
Michael F. Piszczor, Henry B. Curtis, Donald A. Guidice (Phillips Lab., Hanscom AFB, MA.), and Paul S. Severance (Phillips Lab., Hanscom AFB, MA.) *In* NASA, Washington, NASA/DOD Flight Experiments Technical Interchange Meeting Proceedings 1992 34 p (For primary document see N93-28699 11-12)
Avail: CASI HC A03/MF A10

N93-28720*# National Aeronautics and Space Administration. Lewis Research Center, Cleveland, OH.
THERMAL ENERGY STORAGE FLIGHT EXPERIMENT IN MICROGRAVITY
David Namkoong *In* NASA, Washington, NASA/DOD Flight Experiments Technical Interchange Meeting Proceedings 1992 12 p (For primary document see N93-28699 11-12)
Avail: CASI HC A03/MF A10

N93-28721*# National Aeronautics and Space Administration. Goddard Space Flight Center, Greenbelt, MD.
CRYOGENIC HEAT PIPE EXPERIMENT (CRYOHP)
Roy McIntosh *In* NASA, Washington, NASA/DOD Flight Experiments Technical Interchange Meeting Proceedings 1992 21 p (For primary document see N93-28699 11-12)
Avail: CASI HC A03/MF A10

N93-28722*# Hughes Aircraft Co., Torrance, CA.
HEAT PIPE PERFORMANCE EXPERIMENT
George Fleischman *In* NASA, Washington, NASA/DOD Flight Experiments Technical Interchange Meeting Proceedings 1992 40 p (For primary document see N93-28699 11-12)
Avail: CASI HC A03/MF A10

N93-29686*# National Aeronautics and Space Administration. Lewis Research Center, Cleveland, OH.
THE EFFECT OF THE LOW EARTH ORBIT ENVIRONMENT ON SPACE SOLAR CELLS: RESULTS OF THE ADVANCED PHOTOVOLTAIC EXPERIMENT (S0014)
David J. Brinker, John R. Hickey (Eppley Lab., Inc., Newport, RI.), and David A. Scheiman (Sverdrup Technology, Inc., Brook Park, OH.) *In* NASA. Langley Research Center, LDEF: 69 Months in Space. Part 4: Second Post-Retrieval Symposium Apr. 1993 p 1291-1302 (For primary document see N93-29682 11-99)
Avail: CASI HC A03/MF A03; 2 functional color pages

N93-29687*# Jet Propulsion Lab., California Inst. of Tech., Pasadena.
LEO EFFECTS ON CANDIDATE SOLAR CELL COVER MATERIALS
Paul M. Stella *In* NASA. Langley Research Center, LDEF: 69 Months in Space. Part 4: Second Post-Retrieval Symposium Apr. 1993 p 1303-1313 (For primary document see N93-29682 11-99)
Avail: CASI HC A03/MF A03; 2 functional color pages

N93-29732*# Houston Univ., TX.
SOLAR ENERGY EMPLACEMENT DEVELOPER
Michael Mortensen and Bob Sauls *In* Universities Space Research Association, Houston, Proceedings of the Seventh Annual Summer Conference. NASA/USRA: University Advanced Design Program 1991 p 149-154 (For primary document see N93-29712 11-01)
Avail: CASI HC A02/MF A03

45 ENVIRONMENT POLLUTION

Includes atmospheric, noise, thermal, and water pollution.

N93-28536# Japan Atomic Energy Research Inst., Tokyo.
HIGH PERFORMANCE DISPERSION MODEL PHYSIC
Hiromi Yamazawa (Japan Atomic Energy Research Inst., Ibaraki.) Jul. 1992 59 p
(DE93-753303; JAERI-M-92-102) Avail: CASI HC A04/MF A01

The description and usage of the dispersion calculation model PHYSIC were summarized. The model was developed in the study of developing high performance SPEEDI with the purpose of introducing meteorological forecast function into the environmental emergency response system. PHYSIC consists of two parts, the three-dimensional meteorological model and the dispersion model. The former comprises primitive equations with Boussinesq approximation, which are solved by a finite difference method. The latter employs a particle dispersion method. PHYSIC can be used to evaluate the meteorological condition as well as the dispersion from a point source located in a complex terrain. The spatial and temporal scales of the model are 10 to 1000 km horizontally, 1 to 10 km vertically and 1 hour to 1 day, respectively. DOE

N93-28543# Harvard Univ., Cambridge, MA. Dept. of Organismic and Evolutionary Biology.
PREDICTING THE RESPONSE OF A TEMPERATE FOREST ECOSYSTEM TO ATMOSPHERIC CO2 INCREASE
F. A. Bazzaz 1993 11 p
(Contract DE-FG02-84ER-60257)
(DE93-010081; DOE/ER-60257/7) Avail: CASI HC A03/MF A01

This report summarizes the second year of research progress. Included are progress reports for the following studies: the responses of temperate forest tree to 3 years of exposure to elevated carbon dioxide, and high and low nutrient and light levels; pot-size limitations in carbon dioxide studies, interactive effects of carbon dioxide and soil moisture availability on tree seedling's tissue water relations, growth, and niche characteristics; individual versus population responses to elevated carbon dioxide levels in two species of annual weeds; and the development of gypsy moth larvae raised on gray and yellow birth foliage grown in ambient and elevated carbon dioxide environments. DOE

N93-28682*# National Aeronautics and Space Administration. Goddard Space Flight Center, Greenbelt, MD.
RESULTS FROM THE US/RUSSIAN METEOR-3/TOTAL OZONE MAPPING SPECTROMETER Interim Report, 15 Aug. 1991 - 1 Jun. 1992
Jay R. Herman, ed. Jan. 1993 114 p Original contains color illustrations
(NASA-TM-104576; Rept-93B00029; NAS 1.15:104576) Avail: CASI HC A06/MF A02; 9 functional color pages

The development of Meteor-3/TOMS (Total Ozone Mapping Spectrometer) was a joint project of the United States and Russia to fly a U.S. ozone measuring instrument (TOMS) onboard a Russian spacecraft (Meteor-3) and rocket (Cyclone), launched from Plesetsk, Russia. The Meteor-3/TOMS (M3TOMS) was launched into a 1202-km-high, near-polar orbit on 15 Aug. 1991, where it can obtain complete global coverage for most of each year. Both the U.S. and Russian sides have successfully received and processed data into ozone amounts from 25 Aug. 1991 to 1 Jun. 1992, and expect to continue for the life of the instrument and spacecraft. The successful development of the instrument hardware, spacecraft interface, data memory, telemetry systems, and software are described. Descriptions are given of the U.S. and Russian ground stations for receiving M3TOMS data. In addition, the data reduction software was independently developed by the U.S. and by the Russians, and is shown to agree to better than the precision of the measurements. Author (revised)

N93-28873# Capone (Ronald L.) and Associates, Arlington, VA.
USING A NEURAL NETWORK TO ESTIMATE SOLVENT CONSUMPTION Report, Apr. - Jun. 1992
Ronald L. Capone and P. Jeff Chappell 1993 6 p Presented at the 9th Conference on Artificial Intelligence for Applications, Orlando, FL, 1-5

Mar. 1993 Sponsored by EPA and Air and Energy Engineering Research Lab.
(PB93-173110; EPA/600/A-93/063) Avail: CASI HC A02/MF A01

A neural network, using the backpropagation paradigm, that is taught the relationship between employment in the graphic arts industry - (Standard Industrial Classification Code (SIC) 27) - and economic variables and solvent consumption by SIC 27 is discussed. The project is a proof of concept whose objective is to a relationship using national-level data, which are known, and apply it to estimating solvent consumption on the county level, where data are thus far not available. The network accurately learns a relationship from national data. Although definitive testing is not yet possible due to data limitations, there are indications that the national relationship can be used to estimate county-level solvent consumption. Network inputs are SIC 27 employment, productivity for the current and 1 prior year, and an eight-element 'signature' of quarterly economic changes in output from non-durable industries. One hidden layer of two processing elements connects the 11-element input layer to a 1-element output layer. NeuralWare Professional II Plus Version 4.0 was used as the platform. Training requires 30,000 iterations and results in a Pearson's r value of 0.99. The best result achieved by ordinary least squares regression was 0.93. NTIS

N93-28881# Institute of Energy Economics of Japan.
GLOBAL WARMING ISSUE AND GLOBAL ECONOMIC MODEL
10 Nov. 1992 215 p
(DE93-781334; IEE-SR-237) Avail: CASI HC A10/MF A03

Global economic models for CO2 emission control are studied to cope with the global warming problem. Various models simulate macro-economically economic effects associated with CO2 emission control, that is, carbon tax, gross domestic product (GDP) losses, the market of CO2 emission rights, effects on the international trade, changes in structure of energy sources, effects on each region, etc. and provide the data to judge what control measures should be taken. Each model brings different results. Therefore, in the model comparison project of OECD, by using six models and standardizing among the models, preconditions, region, framework of time, and CO2 reduction scenario of the business-as-usual case which is the standard are addressed and the differences between the models on the carbon tax and economic costs in case of achieving reduction of emission of a certain amount of CO2 are clarified. Moreover, the same model comparison project by Stanford University is introduced which places emphasis on production in the energy sector. The details of various models made for simulation are reported in the itemized discussions. DOE

N93-28882# New Energy and Industrial Technology Development Organization, Tokyo (Japan).
ASSESSMENT OF ENERGY TECHNOLOGIES CONTRIBUTING TO ENVIRONMENTAL CONSERVATION
Mar. 1992 158 p
(DE93-781439; NEDO-ITE-9105) Avail: CASI HC A08/MF A02

Paying attention to energy technologies which have great effects on control of greenhouse effect gas emissions, analysis, and assessment are made on effectiveness of each technology (effect, cost, usability, and quality of technology) to study an outlook for future development. Assessment of technological options is explained. Energy conservation and improvement of efficiency in production, conversion, distribution, and end use of energy are one of the most effective measures. The technology to recover and isolate CO2 emitted in burning fossil fuels is worth studying. The photovoltaic power generation has a possibility of being applied to deserts and the surface of the ocean on a large scale, if energy transportation technology is substantially advanced. Assessment of factors affecting regional and sectoral differences in CO2 emission indicates that clearly such factors as economic development, population growth, energy conservation, changes in industrial structure, fuel switching, and technological advance influence the regional and sectoral patterns of historical energy consumption and CO2 emissions. DOE

N93-28883# New Energy and Industrial Technology Development Organization, Tokyo (Japan).
STUDY ON TECHNOLOGY FOR EFFECTIVE UTILIZATION OF CARBON DIOXIDE IN VIEW OF GLOBAL ENVIRONMENT
Mar. 1992 201 p
(DE93-781440; NEDO-ITE-9106) Avail: CASI HC A10/MF A03

Research and study are made on the total system used for EOR (Enhanced Oil Recovery) as a means to recover CO2 from fixed emission sources and fix it. An EOR feasibility study is carried out in East Kalimantan, Indonesia. Further, researches at home and overseas are made on iron making, oil refining, cement and natural gas refining as well as electric power as CO2 fixed emission sources, and it is found that the system which uses the local fixed emission source is also possible. For optimization of the total system, EOR, CO2 recovery/liquefaction, transport vessels carrying both LPG and LCO2, and recycle plants are studied. In the estimation, the cost of CO2 is higher than that of CO2 used in the injection of CO2 presently conducted on a commercial base, but the cost is expected to be reduced by future technical development. The method in which CO2 is fixed while performing EOR is an extension of the technology already carried out and seems to have the earliest materialization as a system. DOE

N93-28899# ABB Environmental Services, Inc., Portland, ME.
FUGITIVE HYDROCARBON EMISSIONS FROM PACIFIC OCS FACILITIES, VOLUME 1 Final Report
30 Nov. 1992 575 p See also PB82-217126 and PB93-173805
(Contract DI-14-35-0001-30428)
(PB93-173797; OCS/MMS-92/0043-Vol-1) Avail: CASI HC A24/MF A04

In January 1989, the Minerals Management Service (MMS) conducted a study using the latest approved methods for emission screening and sampling solely on Outer Continental Shelf (OCS) oil and gas platforms in the Santa Barbara Channel in order to determine platform emission rates more representative of that region. The study was designed and reviewed throughout its conduct by a Quality Review Board (QRB) composed of air resource agencies and industry. Representatives from the Tri-county Air Pollution Control Districts and the MMS actively participated at these meetings. Some participants expressed concerns about some of the methods used and the study results. ABB's thorough responses to these questions and comments were submitted to all reviewers before the printing of the final report, and are contained in appendices of the study final report now available to the public. The results of the MMS study show that the average emission factors for the Pacific OCS oil and gas facilities measured in 1989 are 3.5 times lower than those Pacific OCS facilities sampled in the 1979 API/Rockwell study, and 7.8 times lower than the Gulf of Mexico OCS facilities sampled in the same 1979 study. Efforts to determine the quantitative effect of inspection and maintenance programs on controlling emissions were inconclusive. NTIS

N93-28949 Houston Univ., TX.
DEVELOPMENT OF ULTRAVIOLET ABSORPTION PHOTOMETER FOR ATMOSPHERIC OZONE MEASUREMENTS AND RESULTS FROM MID-LATITUDE INVESTIGATIONS Ph.D. Thesis
Bhaswar Sen 1992 254 p
Avail: Univ. Microfilms Order No. DA9309710

The design and construction of a dual-beam ultraviolet-absorption photometer, as a balloon payload, for ozone measurements is described. Then, the construction of a rocket-borne version of the instrument and results of tests performed in the laboratory are described. Results of balloon sights using this instrument and a NASA-JSC/UH ultraviolet photometer are finally presented. Measurement of ozone in the atmosphere can be made using the strong photometric absorption feature of the gas at 253.7 nanometers. An ultraviolet lamp produces identical optical paths through two absorption columns. Two photodetectors measure the intensity of light through the two columns and a third detector just adjacent to the lamp provides a monitor of integrated light intensity, thus allowing detection of (and on board corrections to) changes in lamp output. A four-port valve in series with an ozone scrubber periodically reverses the two columns between ozone measurement and reference cycles. In this way, instrumental drifts and differences in the two optical paths can be monitored, and corrections, both scientific and engineering, can be deduced. Fast ozone measurements can be made along with other meteorological parameters, allowing good determination of the vertical profile of ozone. Ozone profiles computed from standard photochemical models are usually lower than those determined from satellite measurements; the discrepancies are typically forty percent of measured values at 50 km, and fifty percent at 80 km. Ozone column density measurements with ground based instruments and rocket-borne detectors agree with satellite data, but with a wide variation in accuracy and precision. In situ measurement of ozone with high accuracy, precision, and good spatial resolution would allow testing of (1) current and future photochemical models, and (2) predicted diurnal and seasonal variation in the mesosphere. Details are presented of our ultraviolet photometer adapted for rocket operation and laboratory test results are discussed. Mid-latitude stratospheric ozone measurements using the NASA-JSC/UH and the dual-beam ultraviolet-absorption photometer are presented. Enhancement in tropospheric ozone is evident in data from the summer (1988, 1989, and 1990) flights. Fine structures in the vertical ozone profile correlate closely with structures in the ambient air temperature. Intercomparison of the two photometers and the 1986 Ozone Reference Model for the Middle Atmosphere verifies the high precision and accuracy of the ultraviolet photometers. The overall agreement between the ultraviolet photometer data, the ozone model, and the TOMS total column ozone measurements are very good. Dissert. Abstr.

N93-28965# Lawrence Livermore National Lab., CA.
EMISSION INVENTORIES: A GLOBAL MODELING PERSPECTIVE
J. Dignon and T. E. Graedel (Bell Telephone Labs., Inc., Murray Hill, NJ.) 18 Nov. 1992 8 p Presented at the Air and Waste Management Association (AWMA) Conference, Durham, NC, 19-22 Oct. 1992
(Contract W-7405-eng-48)
(DE93-005817; UCRL-JC-110372; CONF-9210280-1) Avail: CASI HC A02/MF A01

Concern regarding human induced changes in the chemical and radiative properties of our atmosphere through increased emission of trace gas species has received considerable attention. Effective models are needed to understand the future of ozone, global warming, and other important anthropogenic perturbations before policy decisions can be considered. In order to model accurately, knowledge of the temporal and spatial trends in the emissions of the radiatively and chemically important trace species is required. Since many models are currently being used to understand these issues, model validation with experimental measurement becomes extremely important. Emissions inventories commonly pay a bridging role between atmospheric measurement and model studies. DOE

N93-28967# Lawrence Livermore National Lab., CA.
ATMOSPHERIC AND GEOPHYSICAL SCIENCES DIVISION: G-DIVISION DID YOU KNOW?
M. C. MacCracken Sep. 1992 7 p
(Contract W-7405-eng-48)
(DE93-007412; UCRL-ID-112018) Avail: CASI HC A02/MF A01

This report briefly describes environmental consequences of the Kuwaiti oil fires, global warming, and the Southern Oscillation (El Nino events). DOE

N93-28972# Lawrence Livermore National Lab., CA.
GLOBAL WARMING POTENTIAL FOR SF6
A. S. Grossman and D. J. Wuebbles Dec. 1992 3 p
(Contract W-7405-eng-48)
(DE93-007394; UCRL-ID-112944) Avail: CASI HC A01/MF A01

Sulfur hexaflouride (SF(sub 6)) is a trace gas in the atmosphere which, due to its long lifetime of approximately 3200 years (Ravishankara, 1992), could contribute significantly, if concentrations grew large enough, to concerns about global warming via the greenhouse effect. According to Rinsland et al. (1990), SF6 is widely used as an insulating gas in the high voltage electrical equipment industry. While the present day concentration of SF6 is small, Watson and Siddicoat (1985) show a linear increase rate of 0.084 pptv/yr. between 1970 and 1984. This increase coupled with the long lifetime of SF6 could, over an extended period of time, cause measurable contributions to global warming concerns. In a recent publication, an approximate model for the calculation of the Global Warming Potentials (GWP's) of trace gases in the atmosphere was described. The main purpose of this paper is to use the GWP model to calculate the GWP of SF6. DOE

N93-28992# Oak Ridge National Lab., TN.
STATE OF THE ART: ECOLOGICAL BIOMARKERS
L. R. Shugart 1992 9 p Presented at the NATO ARW on Use of Biomarkers in Assessing Health and Environmental Impacts of Chemical Pollutants, Luso, Portugal, 1-5 Jun. 1992
(Contract DE-AC05-84OR-21400)
(DE93-006621; ESD-Publ-4018; CONF-9206339-1) Avail: CASI HC A02/MF A01

It is especially difficult to demonstrate the effect of environmental pollution at the Ecosystem level, where populations and communities are studied. Although pollution can produce stress at the Ecosystem level, the response observed is latent and so far removed from the initial event of exposure that causality is almost impossible to establish. Risk assessment to date has relied on models that use toxicity data and physical properties of chemicals. This approach has been ineffective at the Ecosystem level because of the complexity of pollutants in the environment and the variability in susceptibility of the numerous species present. The use of biological responses (biomarkers) in organisms present in a polluted environment is an approach that may resolve some of the problems outlined. Chemicals are known to elicit measurable and characteristic biological responses in exposed organisms. Such evidence can provide a link between exposure and effect. Unfortunately, this area of endeavor has received little attention until recently. It has only been within the past several years that authoritative texts have become available to document the application of this promising approach. DOE

N93-29029*# Universities Space Research Association, Huntsville, AL.
NATURAL ENVIRONMENTAL SERVICE SUPPORT TO NASA VEHICLE, TECHNOLOGY, AND SENSOR DEVELOPMENT PROGRAMS Final Report, 7 Jul. 1987 - 31 Mar. 1993
30 Apr. 1993 11 p
(Contract NAS8-36639)
(NASA-CR-192554; NAS 1.26:192554) Avail: CASI HC A03/MF A01

The research performed under this contract involved definition of the natural environmental parameters affecting the design, development, and operation of space and launch vehicles. The Universities Space Research Association (USRA) provided the manpower and resources to accomplish the following tasks: defining environmental parameters critical for design, development, and operation of launch vehicles; defining environmental forecasts required to assure optimal utilization of launch vehicles; and defining orbital environments of operation and developing models on environmental parameters affecting launch vehicle operations. Derived from text

N93-29033# Nevada Univ., Las Vegas. Environmental Research Center.
TANK ISSUES: DESIGN AND PLACEMENT OF FLOATING LIQUID MONITORING WELLS Final Report
M. S. Bedinger Feb. 1993 6 p See also PB93-161156 and PB93-161131
(Grant EPA-R-814701)
(PB93-161149; EPA/600/9-90/045) Avail: CASI HC A02/MF A01

Liquid product monitoring is the predominant method of external leak detection where the water table is within the zone of excavation. The paper discusses the use of liquid product monitors at new and old tank installations for detecting leaks from underground hydrocarbon storage tanks. The paper discusses the site conditions under which liquid product monitors can be effectively used, conditions which may mitigate or prevent the effective use of liquid product monitors and the construction and placement of liquid product monitoring wells. Liquid product monitors are not used to determine the rate of tank leak. The rate of tank lead can be determined by other methods such as inventory or internal monitoring methods. Effective use of liquid product monitors or any other method of leak detection requires training and experience on the part of the user. NTIS

N93-29034# Nevada Univ., Las Vegas. Environmental Research Center.
TANK ISSUES: SITE CHARACTERIZATION FOR EXTERNAL LEAK MONITORING Final Report
M. S. Bedinger Feb. 1993 10 p See also PB93-161149 and PB93-161131
(Grant EPA-R-814701)
(PB93-161156; EPA/600/9-90/046) Avail: CASI HC A02/MF A01

Before designing an external monitoring system, information is needed about the natural and man-made characteristics of the site. Site characteristics are important in selecting the appropriate monitoring method. The paper discusses site characteristics with respect to external monitoring by liquid product monitoring and vapor monitoring. NTIS

N93-29055# Lawrence Livermore National Lab., CA.
ATMOSPHERIC AND GEOPHYSICAL SCIENCES PROGRAM REPORT, 1990-1991
M. C. MacCracken, ed., J. R. Albritton, ed., and P. M. MacGregor, ed. Jun. 1992 163 p
(Contract W-7405-eng-48)
(DE93-007390; UCRL-51444-90/91) Avail: CASI HC A08/MF A02

Research programs from Lawrence Livermore Laboratory from 1990-1991 in atmospheric chemistry and geophysics are described. Programs such as mathematical modeling of atmospheric dispersions of pollutants and radionuclides, tropospheric chemistry, clouds, climate models, and the effects of atmospheric trace constituents on ozone are described. DOE

N93-29135# Westinghouse Hanford Co., Richland, WA.
HANFORD ENVIRONMENTAL INFORMATION SYSTEM (HEIS) USER'S MANUAL, VOLUME 1
P. A. Edwards, ed. 1992 911 p Revised
(Contract DE-AC06-87RL-10930)
(DE93-007465; WHC-EP-0372-Vol-1-Rev-1) Avail: CASI HC A99/MF A10

The Hanford Environmental Information System (HEIS) is a consolidated set of automated resources that effectively manage the data gathered during environmental monitoring and restoration of the Hanford Site. The HEIS includes an integrated database that provides consistent and current data to all users and promotes sharing of data by the entire user community. This manual, the HEIS User's Manual, describes the facilities available to the scientist, engineer, or manager who uses the system for environmental monitoring, assessment, and restoration planning; the manual is also intended for the regulator who is responsible for reviewing Hanford Site operations against regulatory requirements and guidelines. DOE

N93-29200# Environmental Protection Agency, Research Triangle Park, NC. Atmospheric Research and Exposure Assessment Lab.
SUMMER 1990 ATLANTA OZONE PRECURSOR STUDY (JANUARY 1993)
Larry J. Purdue 1993 15 p Presented at the VOC Workshop Assessment and Evaluation, Amersfoot, The Netherlands, 26-28 Jan. 1993
(PB93-167203; EPA/600/A-93/044) Avail: CASI HC A03/MF A01

During the summer of 1990, the U.S. Environmental Protection Agency (EPA) conducted a major monitoring study in Atlanta, Georgia, addressing the measurement of ozone and its precursors. The study was undertaken to obtain an information base to support the development and implementation of improved strategies for reducing ozone in U.S. cities that are out of compliance with EPA's National Ambient Air Quality Standard (NAAQS) for ozone. The primary objective of the study was to collect a comprehensive data base of ambient concentrations of ozone and ozone precursors during the summer ozone season at six sites distributed across the Atlanta metropolitan area. A report describing the details of the experiment and summarizing the resulting data base is available. The data base containing more than 300,000 hourly measurements of the 60 parameters addressed is also available on a 3.5 inch disk. The lecture provides an overview of the study, focusing on its objectives and its experimental design with a limited discussion on results and interpretation. NTIS

N93-29262# Department of Energy, Washington, DC. Environmental Sciences Div.
OCEAN MARGINS PROGRAM
Mar. 1993 23 p
(DE93-008937; DOE/ER-0579T) Avail: CASI HC A03/MF A01

The Ocean Margins Program addresses a quantitative understanding of the dispersal and fate of energy-related materials at the land/ocean interface. The principal focus of this program is on the fluxes of carbon in the coastal ocean and their implications for global carbon cycle and global climate change. Over 30 research abstracts are included. DOE

N93-29318# Maryland Univ., Baltimore.
EXPLOITATION OF PARALLELISM IN CLIMATE MODELS
F. Baer, J. J. Tribbia, and D. L. Williamson 1993 9 p
(Contract DE-FG05-91ER-61219)
(DE93-011259; DOE/ER-61219/2) Avail: CASI HC A02/MF A01

The US Department of Energy (DOE), through its CHAMMP initiative, hopes to develop the capability to make meaningful regional climate forecasts on time scales exceeding a decade. This capability is to be based on numerical prediction type models. We propose research to consider theoretical limits for prediction of climate and climate change on appropriate time scales, to develop new mathematical techniques to utilize massively parallel processors (MPP), to actually utilize MPP's as a research tool, and to develop improved representations of some processes essential to climate prediction. In particular, our goals are as follows: reconfigure the prediction equations such that the time iteration process can be compressed by use of MMP architecture, and to develop appropriate algorithms; develop local subgrid scale models which can provide time and space dependent parameterization for a state-of-the-art climate model to minimize the scale resolution necessary for a climate model, and to utilize MPP capability to simultaneously integrate those subgrid models and their statistics; and capitalize on the MPP architecture to study the inherent ensemble nature of the climate problem. DOE

N93-29669 Sonoma Technology, Inc., Santa Rosa, CA.
STUDY TO DETERMINE THE NATURE AND EXTENT OF OZONE AND OZONE PRECURSOR TRANSPORT IN SELECTED AREAS OF CALIFORNIA Final Report
P. T. Roberts, S. Musarra, T. B. Smith, and F. W. Lurmann Apr. 1992 359 p Sponsored by California State Air Resources Board, Sacramento, Research Div. Limited Reproducibility: More than 20% of this document may be affected by microfiche quality
(Contract ARB-A932-129)
(PB93-184828) Avail: CASI HC A16

The project was designed to assess the contribution of transported pollutants to violations of the state ozone standard within the air basins covered by the report using existing data and advanced data analysis techniques. The objectives of the project were to determine the characteristics of ozone and ozone precursor transport within the California air basins covered by the report and to identify whether the contribution of transported pollutants to ozone violations in each downwind area was inconsequential, significant, or overwhelming, relative to locally-emitted pollutants. The precursor pollutants of interest were nitrogen oxides and reactive organic gases. The project evaluated transport to the following areas: The Broader Sacramento Area and the Upper Sacramento Valley; The North Central Coast Air Basin; The Southeast Desert Air Basin (SEDAB); and the Imperial County portion of the SEDAB. NTIS

N93-29672# New Energy and Industrial Technology Development Organization, Tokyo (Japan).
TREND SURVEY ON THE ELUCIDATION OF THE GLOBAL WARMING MECHANISM BY THE GOVERNMENTS OF MAJOR INDUSTRIALIZED NATIONS
Mar. 1992 18 p
(DE93-776427; NEDO-ITE-9108) Avail: CASI HC A03/MF A01

This report reviewed 'Trend survey on the elucidation of the global warming mechanism in the governments of major industrialized nations', which has been conducted by EPDC (Electric Power Development Co.) in FY 1991 and is administered by NEDO. Presented are positive stances of the governments of major industrialized nations on their science and technology policies to carry out international tasks, such as global environmental issues, resources and energy problems, etc., or to strengthen their industrial competitive abilities. Also described are the energy policies of world nations, which reflect their global environmental policies and strategies. In taking approaches to global environmental issues of major nations, the U.S. administration spends by far the largest funds for survey and studies to elicidate the scientific mechanism of these problems, which is reflected in the U.S. policy of giving priority to the accumulation of scientific knowledge in dealing with problems of climate changes. Furthermore, a feasibility study on CO2 recovery, transportation and disposal technologies is introduced, which is currently planned by the IEA. DOE

N93-29674 Council on Environmental Quality, Washington, DC.
BUILDING ALLIANCES TO RESTORE COASTAL ENVIRONMENTS: A COASTAL AMERICA PROGRESS REPORT
Jan. 1993 31 p Limited Reproducibility: More than 20% of this document may be affected by microfiche quality
(PB93-169464) Avail: CASI HC A03

Coastal America is a unique partnership created for one purpose: to join the forces of federal agencies with state, local, and private alliances to collaboratively address environmental problems along U.S. shorelines. In particular, Coastal America focuses on three wide-spread problems that are the result of rising populations in coastal areas and associated increases in demands on coastal resources: loss and degradation of habitat; pollution from nonpoint sources; and contaminated sediments. The challenge is to integrate capabilities and existing resources with state, local, and nongovernmental efforts to address specific local problems by sharing information, pooling field expertise, and combining management skills and resources. Coastal America partners come to the table not just as representatives of their offices, but with a broader, problem-solving orientation, to produce demonstrable environmental results. NTIS

N93-29676 California Univ., Santa Barbara.
ACID GAS TREATING BY AQUEOUS ALKANOLAMINES Annual Report, Jul. - Dec. 1992
O. C. Sandall, E. B. Rinker, A. Tamimi, R. A. Davis, and D. W. Oelschlager Dec. 1992 148 p Sponsored by Gas Research Inst. Limited Reproducibility: More than 20% of this document may be affected by microfiche quality
(Contract GRI-5092-260-2345)
(PB93-176188; GRI-92/0528) Avail: CASI HC A07

The objective of the work is to investigate the simultaneous absorption or desorption of CO2 and H2S into and from a mixed aqueous amine solvent consisting of methyldiethanolamine (MDEA) and diethanolamine (DEA). In work completed thus far models have been developed for single gas (either H2S or CO2) absorption into a single amine solution (MDEA or DEA). Density and viscosity measurements have been made for aqueous MDEA, DEA and MDEA/DEA mixtures over the temperature range 20 to 100 C and for concentrations up to 50 weight %. NTIS

N93-29681# Agency for International Development, Washington, DC.
TROPICAL FORESTS AND BIOLOGICAL DIVERSITY: USAID REPORT TO CONGRESS 1990-1991
May 1992 58 p
(PB93-180453; AID-PN-ABL-711) Avail: CASI HC A04/MF A01

Over the last few years environmental concerns have moved to the forefront of USAID's agenda. The report to Congress reviews USAID's efforts to conserve and protect tropical forests and biological diversity during FY's 1990-91. Following an introduction that summarizes the mounting worldwide problems of biodiversity loss and deforestation, Section 1 reviews funding trends for and initiatives in these two areas. Section 2 provides an overview of centrally funded activities, including the Forest Resources Management Project, the Biodiversity Support Program, the Development Strategies for Fragile Lands Project, and the Coastal Resources Management Project. Individual sections then cover USAID activities in Africa, Asia, and Latin America and the Caribbean. Interspersed throughout the report are brief topical summaries which discuss subjects such as U.S. legislative mandates, the Global Environmental Facility, USAID agroforestry activities, African elephant conservation, and the protection of threatened national parks. NTIS

N93-29770# Department of Energy, Washington, DC. Environmental Sciences Div.
OVERVIEW OF THE DOE ATMOSPHERIC CHEMISTRY PROGRAM'S OZONE PROJECT
Jan. 1993 51 p
(DE93-007416; DOE/ER-0575T) Avail: CASI HC A04/MF A01

The global atmospheric ozone issue presents a demanding challenge to Department of Energy (DOE) policy analysts, planners, and decision makers, who are responsible for developing and implementing a National Energy Strategy (NES) that maximizes efficient and economical use of US energy resources and, at the same time, minimizes associated impacts on the natural and human environment. On the one hand, recent evaluations of stratospheric and global tropospheric ozone trends indicate substantial anthropogenic impacts that, if allowed to continue, could result in widespread and unacceptable environmental damage. On the other hand, current and proposed remediation efforts have resulted and will result in severe, and potentially unacceptable, socioeconomic impacts. Numerous scientific uncertainties exist concerning changes to the ozone distribution, which complicate the DOE's strategic planning process. Moreover, many ozone-related energy-policy decisions are currently being formulated with minimum participation by DOE. In view of these features, a strong need exists for active DOE participation in global ozone research. This document, which describes the background and initial design for the DOE Ozone Project, defines initial DOE plans for this participation. DOE

N93-29792# Lawrence Livermore National Lab., CA.
POTENTIAL EFFECTS OF HFC-152a ON GLOBAL OZONE AND CLIMATE
D. J. Wuebbles Jan. 1993 5 p Presented at the Bay Area Air Quality Management District Workshop, San Francisco, CA, 26 Jan. 1993
(Contract W-7405-eng-48)
(DE93-008018; UCRL-JC-112945; CONF-930178-1) Avail: CASI HC A01/MF A01

The hydrofluorocarbon, CH3CHF2, also referred to as HFC-152a, is being considered by the chemical industry for a variety of potential uses, including as a refrigerant, aerosol propellant, and foam blowing agent. Many of these uses of HFC-152a will be as replacements for chlorofluorocarbons (CFCs) such as CFC-11 and CFC-12 that are of concern because of their effects on stratospheric ozone and on climate. The purpose of this paper is to review the current scientific understanding of the potential for HFC-152a to have an impact on the atmospheric environment, with emphasis on the potential effects on global ozone and climate. DOE

N93-29858# Office of the Secretary of Defense, Washington, DC.
STRATEGIC ENVIRONMENTAL RESEARCH AND DEVELOPMENT PROGRAM (SERDP) Annual Report, FY 1992
1992 32 p
(AD-A263745) Avail: CASI HC A03/MF A01

The Strategic Environmental Research and Development Program (SERDP) is intended to identify and develop technology that will enhance the capability of the Department of Defense and the Department of Energy to meet their environmental obligations. Also the program is intended to provide technology and information that may be useful to other government and private organizations in addressing environment concerns. SERDP provides a vehicle to facilitate the transfer of appropriate technology from the private sector to address DoD and DOE environmental and energy issues. Specifically, the purposes of the program are as follows: (1) address environmental matters of concern to DoD and DOE through support for basic and applied research and the development technologies that can enhance the capabilities of the departments to meet their environmental obligations; (2) identify and share research, technologies, and other information developed by DoD and DOE for national defense purposes, involved in the development of energy technologies and of technologies to address environmental restoration, waste minimization, hazardous waste substitution, and other environmental concerns; (3) furnish other governmental and private organizations with data, and enhance collection and analytical capabilities for use by such organizations in the conduct of environmental research; and (4) identify technologies developed by the private sector that are useful to DoD and DOE defense activities concerning environmental restoration, hazardous and solid waste minimization and prevention, and hazardous material substitution, and provide for the use of such technologies. DTIC

N93-29861 ABB Environmental Services, Inc., Portland, ME.
FUGITIVE HYDROCARBON EMISSIONS FROM PACIFIC OCS FACILITIES. VOLUME 2: EXECUTIVE SUMMARY AND USER'S GUIDE
30 Nov. 1992 49 p See also Volume 1, PB93-173797 Sponsored by Minerals Management Service, Camarillo, CA, Pacific OCS Region Limited Reproducibility: More than 20% of this document may be affected by microfiche quality
(Contract DI-14-35-0001-30428)
(PB93-173805-Vol-2; OCS/MMS-92/0044-Vol-2) Avail: Issuing Activity (National Technical Information Service (NTIS))

Offshore oil and gas production and processing activities may exacerbate existing air quality problems as a result of the release of fugitive hydrocarbon emissions into the atmosphere. In order to address the issue of fugitive emissions from platforms located in Pacific Outer Continental Shelf (OCS) waters, the Minerals Management Service (MMS) of the U.S. Department of the Interior contracted with ABB Environmental Services, Inc. (ABB-ES) in early 1989 to perform emission rate measurements and data analysis on seven platforms off the Southern California coast in outer continental shelf (OCS) waters. The program objectives were to (1) determine fugitive hydrocarbon emission rates from the seven Pacific OCS facilities, (2) develop and evaluate methods for estimating fugitive hydrocarbon emission rates from existing and future Pacific OCS facilities, and (3) evaluate the effectiveness of inspection and maintenance (I & M) programs in the reduction of fugitive hydrocarbon emissions on the seven Pacific OCS facilities. The executive summary briefly describes the methodology used in the current study, as well as the results and conclusions of the study. A Users' Guide for predicting total platform fugitive hydrocarbon emission rates for Pacific OCS oil and gas production facilities based on the data collected in the current study is included as an appendix. NTIS

N93-30008# Los Alamos National Lab., NM.
MULTI-ATTRIBUTE DECISION THEORY METHODOLOGY FOR POLLUTION CONTROL MEASURE ANALYSIS
A. S. BarreraRoldan (Instituto Mexicano de Petroleo, Mexico City.), A. CoronaJuarez (Instituto Mexicano de Petroleo, Mexico City.), R. W. Hardie, and G. R. Thayer 1992 12 p Presented at the International Symposium on Air Pollution, Monterrey, Mexico, 16-25 Feb. 1993
(Contract W-7405-eng-36)
(DE93-005444; LA-UR-92-4063; CONF-930208-2) Avail: CASI HC A03/MF A01

A methodology based in Multi-Attribute Decision Theory was developed to prioritize air pollution control measures and strategies (a set of measures) for Mexico City Metropolitan Area (MCMA). We have developed a framework that takes into account economic, technical feasibility, environmental, social, political, and institutional factors to evaluate pollution mitigation measures and strategies utilizing a decision analysis process. In a series of meetings with a panel of experts in air pollution from different offices of the Mexican government, we have developed general and specific criteria for a decision analysis tree. With these tools the measures or strategies can be graded and a figure of merit can be assigned to each of them, so they can be ranked. Two pollution mitigation measures were analyzed to test the methodology, the results are presented. This methodology was developed specifically for Mexico City, though the experience gained in this work can be used to develop similar methodologies for other metropolitan areas throughout the world. DOE

N93-30009# Oak Ridge National Lab., TN.
WHAT'S PAST IS PROLOGUE: SUPPORTING GLOBAL CHANGE RESEARCH WITH HISTORICAL DATA
R. B. Honea, C. L. Floyd (Communication and Information Technology, Inc., TN.), and R. W. Peplies (East Tennessee State Univ., Johnson City.) 1993 9 p Presented at the Annual Meeting of the American Society of Photogrammetry and Remote Sensing, New Orleans, LA, 16-18 Feb. 1993
(Contract DE-AC05-84OR-21400)
(DE93-005777; CONF-930244-2) Avail: CASI HC A02/MF A01

This paper discusses an ongoing effort to analyze historical remote sensing data and to develop a technology to integrate this analysis into a common framework with the satellite imagery. Historical data and metadata from aircraft remote sensor missions, satellite overflights, and other sources from around the world will be used to develop detailed information on the historical changes in the earth's land, water, and atmospheric resources. DOE

N93-30015# Mitre Corp., McLean, VA. JASON Program Office.
A PRELIMINARY REVIEW OF GLOBAL CO2 EXCHANGE BETWEEN OCEAN AND ATMOSPHERE
R. Davis and M. Gregg 16 Mar. 1993 50 p Sponsored by DOD
(AD-A264019; JSR-90-302) Avail: CASI HC A03/MF A01

Although the present rate of increase of CO2 in the atmosphere is well documented, changes in the next century cannot be accurately predicted because the CO2 budget is so poorly understood. The atmospheric concentration is increasing 1.4 ppm/year, corresponding to an increase in the atmospheric inventory of 3 Gt/year (1 Gt is 10(exp 9) metric tons or 10(exp 12) kg). This observed increase is less than half of the estimated 8.7 Gt/year released by all sources to the atmosphere. Most of the residual has been assumed to enter the ocean. This cannot be verified directly, however, since the total dissolved inorganic CO2 in the ocean is so much larger than the cumulative release of fossil fuel since 1850 that the change due to fossil fuel is small compared to natural variability. As a result, global CO2 budgets are attempted by calculating the fluxes between ocean and atmosphere and between land and atmosphere. DTIC

N93-30043*# National Aeronautics and Space Administration. Goddard Space Flight Center, Greenbelt, MD.
QUANTIFYING AND MINIMIZING UNCERTAINTY OF CLIMATE FORCING BY ANTHROPOGENIC AEROSOLS
J. E. Penner (Lawrence Livermore National Lab., CA.), R. J. Charlson (Washington Univ. Hospital, Seattle.), J. M. Hales (Envair, Richland, WA.), N. Laulainen (Pacific Northwest Lab., Richland, WA.), R. Leifer (Department of Energy, New York, NY.), T. Novakov (California Univ., Berkeley. Lawrence Berkeley Lab.), J. Ogren (National Oceanic and Atmospheric Administration, Boulder, CO.), L. F. Radke (National Center for Atmospheric Research, Boulder, CO.), S. E. Schwartz (Brookhaven National Lab., Upton, NY.), and L. Travis Mar. 1993 63 p
(Contract W-7405-eng-48)
(NASA-TM-108259; NAS 1.15:108259; DE93-009820; DOE/NBB-0092T)
Avail: CASI HC A04/MF A01

The clear-sky climate forcing by anthropogenic aerosols was shown to be of sufficient magnitude to mask the effects of anthropogenic greenhouse gases over large regions. Anthropogenic aerosols are composed of a variety of aerosol types including water-soluble inorganic species (e.g., sulfate, nitrate, ammonium), organic condensed species, elemental or black carbon, and mineral dust. Estimates of the clear-sky forcing by anthropogenic sulfate aerosols and by organic biomass-burning aerosols were published previously. The uncertainty in the forcing by these aerosol types is estimated. Estimates of the clear-sky forcing by other anthropogenic aerosol types do not even exist though the forcing by these aerosol types is thought to be smaller than that by sulfate and biomass burning aerosols. DOE

N93-30131# Kansas Univ., Lawrence. Dept. of Geography.
SIMULATION OF LANDSCAPE DISTURBANCES AND THE EFFECT OF CLIMATIC CHANGE
W. L. Baker 29 Jan. 1993 87 p
(Contract DE-FG02-89ER-60883)
(DE93-011615; DOE/ER-60883/3) Avail: CASI HC A05/MF A01

The purpose of this research is to understand how changes in climate may affect the structure of landscapes that are subject to periodic disturbances. A general model useful for examining the linkage between climatic change and landscape change was developed. The model makes use of synoptic climatic data, a geographical information system (GRASS), field data on the location of disturbance patches, simulation code written in the SIMSCRIPT language, and a set of landscape structure analysis programs written specifically for this research project. A simplified version of the model, lacking the climatic driver, was used to analyze how changes in disturbance regimes (in this case settlement and fire suppression) affect landscape change. Landscape change lagged in its response to changes in the disturbance regime, but the lags differed depending upon the character of the change and the particular measure considered. The model will now be modified for use in a specific setting to analyze the effects of changes in climate on the structure of flood-disturbed patches along the Animas River, Colorado. DOE

N93-30154# Naval War Coll., Newport, RI.
THE ENVIRONMENT AS AN OPERATIONAL CENTER OF GRAVITY Final Report
Gordan E. VanHook 22 Feb. 1993 57 p
(AD-A264170) Avail: CASI HC A04/MF A01

The increasing influence of environmentalism on the military is analyzed with an emphasis on ecological trends and factors that effect the operational commander. An analysis is conducted to determine the ecological factors within society, government, and international law that impact armed conflict. The potential of means and methods of warfare to damage the environment is described from an historical and ecological domain (air, land, water, and living organisms) perspective. The importance of operational commanders making environmentally sound decisions is determined to be a key component of public support. The growing knowledge of the impact of environmental degradation and the decreasing global threat mean the operational commanders will need to consider the environmental ramifications during target and weapons selection. A list of ecological considerations is provided for the operational commander. DTIC

N93-30180# Oak Ridge National Lab., TN.
POLLUTION PREVENTION: A REGULATORY UPDATE
Ann E. Walzer (Martin Marietta Energy Systems, Inc., Oak Ridge, TN.) and

Jay W. Maynard (Maynard, Jay W., Columbus, OH.) 1993 9 p Presented at the Waste Management 1993, Tucson, AZ, 28 Feb. - 4 Mar. 1993
(Contracts DE-AC05-84OR-21400; DE-AC05-76OR-00001)
(DE93-009727; CONF-930205-54) Avail: CASI HC A02/MF A01

Pollution prevention is the emphasis of the 1990s environmental philosophy. This new environmental era was ushered in when President Bush signed the Pollution Prevention Act in October 1990. This law, with its accompanying philosophy, was in response to the realization that end-of-the-pipe treatment, which frequently changed the media in which a pollutant or waste was discharged, was inadequate to protect the environment and human health. Pollution prevention advocates source reduction, where material substitutions and engineering solutions are sought to reduce the volume and toxicity of waste and pollutants. This proactive approach reduces environmental impacts such as those of former waste sites which have produced environmental legacies that will cost billions of dollars and take decades to remediate. This paper describes pollution prevention philosophy and summarizes regulatory pollution prevention requirements. It describes current regulatory trends in the area of pollution prevention, including voluntary programs and enforcement actions. The Pollution Prevention Act of 1990 is described, and pollution prevention initiatives embodied in other laws, including the Clean Air Act, the Clean Water Act, the Emergency Planning and Community Right-To-Know Act, the Resource Conservation and Recovery Act, and the Toxic Substances Control Act, are discussed. A historical overview of waste minimization initiatives within the Department of Energy is given, and other pollution prevention initiatives that affect federal facilities, such as Executive Order 12780, which mandates recycling and the procurement of recycled materials, are also outlined. DOE

N93-30183# Pacific Northwest Lab., Richland, WA.

CASE STUDY OF FRONTAL BOUNDARY STUDY MISSION 03

W. R. Barchet, M. T. Dana, and J. M. Thorp Sep. 1992 70 p
(Contract DE-AC06-76RL-01830)
(DE93-007176; PNL-8384) Avail: CASI HC A04/MF A01

The Frontal Boundary Study was conducted by the Pacific Northwest Laboratory (PNL) for the US Department of Energy in October and November 1989 in central Ohio. This report, which was prepared for the US Environmental Protection Agency, presents the results of the aircraft and surface observations made for one precipitation event during the study, on October 10, 1989. This particular event was selected because of its relatively simple meteorological setting. PNL's Gulfstream (G-1) aircraft was used to sample trace gas concentrations aloft in the inflow region of the precipitation system. Precipitation chemistry and rainfall rate data are presented for the October 10, 1989 event from the network of surface precipitation samplers. Trace gas concentrations and other meteorological variables measured with the G-1 during flight 03 on this date are included. Meteorological observations obtained with radiosondes and radar are also presented. These data sets can be used to evaluate air quality and wet deposition models. DOE

N93-30187# Idaho Univ., Moscow. Idaho Water and Energy Resources Research Inst.

ANNUAL REPORT ON MONITORING OF THE UNSATURATED ZONE AND RECHARGE AREAS AT INEL TO THE STATE OF IDAHO INLEL OVERSIGHT COMMITTEE

D. Horn, J. Liou, and J. Finnie Mar. 1993 121 p
(Contract DE-FG07-91ID-13042)
(DE93-012947; DOE/ID-13042/22) Avail: CASI HC A06/MF A02

This project, begun in March 1991, was originally structured as two separate research efforts: An investigation of the recharge phenomenon and surface water-ground water interactions at the INEL; and a study of water and contaminant movement through the unsaturated zone, including a review of computer models used to described this process. During the initial months of work, it became obvious to those involved in these studies that the two topic areas were intimately related, and work since that time has proceeded with no firm boundaries between the two efforts. Much of the Phase 1 work (March 1991--March 1992) consisted of a detailed review of available literature pertinent to the two research topics and to the INEL site. This Annual Report summarizes the other project activities during Phase 3, and is organized into three sections: Section I -- an overview of the ongoing efforts related to computer model algorithms and data requirements for modeling the transport process in the unsaturated zone (Dr. Jim Liou). Section H -- a review of ongoing work to predict the growth and decay of the ground water mound beneath the INEL spreading basins, using the computer model UNSAT-2 (Dr. John Finnie). Section M -- a final report of the completed study effort examining the recharge rates associated with stream flow in the Big Lost River, and the effects of this recharge on ground water levels at the INEL site (Dr. Dennis Horn). Phase M of the project has now begun, and will conclude in December 1993 with two final reports documenting the work that has been briefly described in Sections I and H of this report. DOE

N93-30197# Army Engineer Waterways Experiment Station, Vicksburg, MS. Environmental Lab.

AN EVALUATION OF FACTORS AFFECTING THE SOLIDIFICATION/STABILIZATION OF HEAVY METAL SLUDGE Final Report

R. M. Bricka and Larry W. Jones Mar. 1993 166 p
(AD-A264128; WES/TR/EL-93-4) Avail: CASI HC A08/MF A02

Solidification/stabilization of hazardous waste involves mixing the waste with a binder material to enhance the physical properties of the waste and to immobilize contaminants that may be detrimental to the environment. Many hazardous wastes contain materials that are known to inhibit the setting and strength development properties of cement and pozzolan binding agents commonly used in solidification/stabilization processes. This study presents the results of an evaluation into the effects of ten interfering substances (oil, grease, lead, copper, zinc, sodium hydroxide, sodium sulfate, phenol, trichloroethylene, and hexachlorobenzene) on the physical and contaminant mobility properties of a solidified/stabilized heavy metal sludge. Three binder materials (Portland cement, lime/fly ash, and cement/fly ash) were used to solidify/stabilize a synthetic metal plating waste sludge containing substantial concentrations of four metals (cadmium, chromium, nickel, and mercury). The effects of these interfering materials were evaluated using five physical tests: unconfined compressive strength (UCS), cone index, bulk density, wet/dry cycling, and permeability. Contaminant leaching properties were evaluated using the U.S. Environmental Protection Agency's Extraction Procedure test. Microchemical/micromorphological analyses were also performed on the treated sludges. DTIC

N93-30360# Minnesota Univ., Minneapolis. Inst. for Mathematics and its Applications.

ENVIRONMENTAL STUDIES: MATHEMATICAL, COMPUTATIONAL AND STATISTICAL ANALYSES Final Report, 1 Jul. - 31 Dec. 1992

Avner Friedman and Willard Miller, Jr. 3 Mar. 1993 34 p
(Contract F49620-92-J-0410)
(AD-A264223; AFOSR-93-0317TR) Avail: CASI HC A03/MF A01

As we enter the final decade of the twentieth century, environmental protection has become a universal issue with world-wide support. Destruction of the stratospheric ozone-layer, global increase in carbon dioxide and other radiatively important trace gases, acid rain, urban smog, water pollution of various types, and improper disposal of toxic wastes have all been shown as pressing problems for the 1990's. Environmental studies have now bridged the realms of academic research and societal applications. Mathematical modeling and large-scale data collection and analysis lie at the core of all environmental studies. Examples of such issues are the protection of the ozone-layer, climate change, regional and urban pollution, toxic waste disposal, and water pollution. While each of these environmental problems involves extremely complex interplay of many physical, chemical, and even human interactions, mathematical analysis serves as the single unifying foundation. Because of the well-recognized highly intensive and perturbing impact of direct environmental experiments, computational models become the prevalent tool in identifying, assessing, and resolving these problems. Unfortunately, scientists, mathematicians, and engineers immersed in developing and applying environmental models, computational methods, statistical, techniques and computational hardware advance with separate and often discordant paces. The Summer Program on Mathematical, Computational, and Statistical Analyses in Environmental Studies was designed to provide a much needed interdisciplinary forum for joint exploration of recent advances in the formulation and application of (1) environmental models, (2) environmental data and data assimilation, (3) stochastic modeling and optimization, and (4) Global climate modeling. DTIC

N93-30504# Lawrence Livermore National Lab., CA.
A CORRELATED k-DISTRIBUTION MODEL OF THE ATMOSPHERIC HEATING RATES FOR OVERLAPPING SPECTRA OF CO2 AND H2O
K. E. Grant and A. S. Grossman Dec. 1992 5 p
(Contract W-7405-eng-48)
(DE93-007391; UCRL-ID-112628) Avail: CASI HC A01/MF A01

The problem of overlapping the spectra of CO2 and H2O in the 0-2500 cm(sup -1) wavenumber region was considered using a correlated k-distribution model for the transmission in the atmosphere between 0 and 60 km. Individual k-distributions for the two gases were combined using an overlapping algorithm to produce k-distributions for the mixture of CO2 plus H2O. A prototype radiative transfer model was used to calculate atmospheric fluxes and heating rates. The hearing rates for the overlapped mixture agree to better than eight percent with those calculated for a single precombined mixture of CO2 and H2O. DOE

N93-30506# Syracuse Univ., NY. Dept. of Chemical Engineering and Materials Science.
SIMULATION AND CALCULATION OF DIFFUSIVE AEROSOL DEPOSITION
C. Tien and B. V. Ramarao Oct. 1992 67 p Prepared for Lawrence Livermore National Lab., CA
(Contract W-7405-eng-48)
(DE93-007518; UCRL-CR-111779; B-160439) Avail: CASI HC A04/MF A01

A simulation method for predicting the deposition of diffusive aerosols in two dimensional flows was developed and applied to the calculation of the unit fiber efficiency in Kuwabara flow. Contrary to conventional thinking, the inertial effect may become important even for submicron aerosols under certain conditions. The commonly applied format of considering the collection efficiency as the sum of the collection efficiencies due to interception and Brownian diffusion was found inadequate in most cases although the additive principle is applicable in most cases if the inertial effect is included. It was also found that by ignoring the inertial effect, the most penetrating particle size may differ significantly from the correct value when the inertial effect is included. DOE

N93-30660# Abt Associates, Inc., Cambridge, MA.
EVALUATION OF ENVIRONMENTAL MARKETING TERMS IN THE UNITED STATES
5 Feb. 1993 203 p Sponsored by Environmental Protection Agency, Washington, DC. Office of Pollution, Prevention, and Toxics
(Contract EPA-68-D9-0169)
(PB93-175784; EPA/741/R-92/003) Avail: CASI HC A10/MF A03

The study is a comprehensive examination of the use of environmental marketing terms in the United States as of mid-1992. Topics discussed in the report include the following: (1) issues involved in the use of environmental marketing terms; (2) consumer understanding of these terms; (3) trends in the use of environmental terms in consumer product labeling and advertising; (4) cases where environmental marketing claims have been avoided or discontinued; and (5) proposed and existing definitions of environmental marketing terms. The report was prepared in response to a call for federal action by many groups involved in environmental marketing and is designed to serve two main purposes. For state and federal policy makers seeking to promulgate guidelines or regulations governing environmental marketing terms, it provides an analytical foundation on which to base policy decisions. For those generally interested in environmental marketing, it serves as a comprehensive source of information about the major issues involved. It does not advocate a particular position or course of action. NTIS

N93-30762# Kerr (Robert S.) Water Research Center, Ada, OK.
PERFORMANCE AND COST EVALUATION OF BIOREMEDIATION TECHNIQUES FOR FUEL SPILLS
C. H. Ward (Rice Univ., Houston, TX.), J. T. Wilson, D. H. Kampbell, and S. Hutchins 1993 10 p See also PB89-219976 Prepared in cooperation with Rice Univ.
(PB93-175545; EPA/600/A-93/073) Avail: CASI HC A02/MF A01

Soils and ground water beneath the U.S. Coast Guard Air Station at Traverse City, MI, have been contaminated with separate spills of aviation gasoline and JP-4 jet fuel. Contamination from both plumes has affected a shallow water table aquifer consisting of a medium grained sand. This site has been the location of a cooperative effort between the U.S. Coast Guard and U.S. EPA to extensively characterize the site to determine the three dimensional extent of contamination, local hydrogeology, geochemistry of the solids and water, and nature of microbial activity. Evaluation concerning feasibility and cost of three innovative bioremediation techniques has also been completed at the Air Station. One evaluation demonstrated the use of hydrogen peroxide as the electron acceptor to enhance aerobic biodegradation in a portion of the aviation gasoline area. Nitrate was used as the electron acceptor for a portion of the JP-4 jet fuel contamination. Bioventing of a second portion of the aviation gasoline contamination was the third innovative technique evaluated. Each treatment reduced benzene levels to less than 5 micrograms/l, with 25% to 60% reduction in total fuel levels. For these evaluations, bioventing had the lowest capital and operating costs, followed by nitrate addition, and finally hydrogen peroxide. NTIS

N93-30823# Desert Research Inst., Reno, NV.
ENVIRONMENTAL MONITORING AND ASSESSMENT PROGRAM. EMAP: ARID COLORADO PLATEAU PILOT STUDY
S. E. Franson, ed. Jan. 1993 175 p See also PB91-141796 and PB93-100139 Prepared in cooperation with Nevada Univ.
(PB93-181618; EPA/620/R-93/001) Avail: CASI HC A08/MF A02

The 1992 Colorado Plateau Indicator Pilot Study, the first field activity for the EMAP-Arid group, is designed to evaluate several indicators of arid ecosystem condition for continued development and implementation for monitoring. This Implementation Plan describes the conceptual approach for the pilot study; questions that will be addressed in the study; the rationale and process that led to the choice of a portion of the Colorado Plateau for the study site; and the rationale and process for selection of the indicators to be tested. The overall EMAP-Arid design is presented along with the specifics for the pilot study and the sampling plot designs. Logistics, quality assurance, information management and GIS, and analysis and reporting of the pilot study results also are addressed. The bulk of the implementation plan describes the indicators that are to be evaluated in the pilot study: vegetation composition, structure, and abundance; soil properties including erosion potential; and spectral properties of vegetation and soils from both on-ground and remote sensors. An appendix describes retrospective and landscape indicators that will be further developed by EMAP-Arid in the future. NTIS

N93-30825# Geological Survey, Louisville, KY. Water Resources Div.
CONTAMINATION OF SOIL, SOIL GAS, AND GROUND WATER BY HYDROCARBON COMPOUNDS NEAR GREEAR, MORGAN COUNTY, KENTUCKY Water Resources Investigation
A. G. Alexander, D. D. Zettwoch, M. D. Unthank, and R. B. Burns (Kentucky Dept. of Natural Resources and Environmental Protection, Frankfort.) 1993 46 p Prepared in cooperation with Kentucky Natural Resources and Environmental Protection Cabinet, Frankfort
(PB93-182244; USGS/WRI-92-4138) Avail: CASI HC A03/MF A01

The purpose of the report is to present the results of an investigation of hydrocarbon contamination near Greear, KY. Specifically, the report describes the areal extent and migration of the hydrocarbon contamination in the soil, soil gas, and ground water in the study area. The report also includes a description of the hydrogeologic framework of the Greear area. The application and use of soil-gas surveys and the on-site analysis of soil gases also are described. NTIS

N93-30826# Geological Survey, Lawrence, KS. Water Resources Div.
HYDROGEOLOGY AND GROUND-WATER-QUALITY CONDITIONS AT THE RENO COUNTY LANDFILL, SOUTH-CENTRAL KANSAS, 1990-1991 Water Resources Investigation
B. A. Heck, N. C. Myers, and D. A. Hargadine 1992 67 p Prepared in cooperation with Reno County, KS
(PB93-183085; USGS/WRI-92-4169) Avail: CASI HC A04/MF A01

The report describes the physical setting of the Reno County Landfill, the fate of waste materials in landfills, and the investigative methods used. Data collected during installation of temporary and monitoring wells and subsequent water-level measurements are used to describe the geology and hydrology in the vicinity of the landfill. Analysis of samples from private-supply and monitoring wells, and from a nearby creek define water-quality conditions near the landfill and the effects of the landfill on ground-water quality. NTIS

N93-30829# Environmental Protection Agency, Washington, DC. Office of Radiation and Indoor Air.

ENVIRONMENTAL CHARACTERISTICS OF EPA, NRC, AND DOE SITES CONTAMINATED WITH RADIOACTIVE SUBSTANCES

Mar. 1993 93 p See also DE90013615 Prepared in cooperation with Department of Energy, Washington, DC. Office of Environmental Restoration, and Nuclear Regulatory Commission, Washington, DC. Office of Nuclear Material Safety and Safeguards

(PB93-185551; EPA/402/R-93/011) Avail: CASI HC A05/MF A01

The U.S. EPA offices of Radiation and Indoor Air and Solid Waste and Emergency Response, the U.S. Department of Energy Office of Environmental Restoration and Waste Management, and the Nuclear Regulatory Commission Office of Nuclear Material Safety and Safeguards initiated preliminary efforts to promote the more appropriate and consistent use of computer models in remediating sites contaminated by radioactive substances and managed by the participating federal agencies. As a baseline for these efforts, the nature and types of problems present at these sites must be understood. The report responds to this need. It presents in textual, tabular, and graphical formats the following: a list of the 45 EPA National Priorities List Superfund sites and the 38 NRC Site Decommissioning Management Plan sites containing radioactive waste materials, the types of waste found at each site, a description of the physical form of the waste, physical characteristics of the site, and demographic characteristics of the region surrounding the site. NTIS

N93-30831# Environmental Protection Agency, Cincinnati, OH. Risk Reduction Engineering.

PLANNING AND PROGRESS OF EPA'S POLLUTION PREVENTION RESEARCH PROGRAM

J. S. Bridges 1993 9 p

(PB93-185767; EPA/600/A-93/093) Avail: CASI HC A02/MF A01

The purpose of the paper is as follows: (1) present an awareness for environmental stewardship using pollution prevention (P2) as an approach by the public administrator for decision-making, and (2) present the EPA's pollution prevention research strategy. The paper was presented at the American Society for Public Administration, Region 6 Conference on 3 Oct. 1991. NTIS

N93-30834# Environmental Protection Agency, Washington, DC. Office of Policy, Planning and Evaluation.

GUIDE TO FEDERAL WATER QUALITY PROGRAMS AND INFORMATION: A GUIDE WITH COMPUTER SOFTWARE DEVELOPED BY THE INTERAGENCY WORKING GROUP ON WATER QUALITY

Feb. 1993 187 p See also PB92-201144

(PB93-186245; EPA/230/B-93/001) Avail: CASI HC A09/MF A02

The publication makes key Federal information on water quality available to environmental analysts. The Guide includes information on the following: (1) underlying demographic pressures; (2) the use of land, water, and resources; (3) pollutant loadings; (4) ambient water quality; (5) other effects of water pollution; and (6) a listing of programs established to preserve, protect, and restore water quality. NTIS

N93-30887 National Inst. of Standards and Technology, Gaithersburg, MD.

HORIZONTAL NUCLEATE FLOW BOILING HEAT TRANSFER COEFFICIENT MEASUREMENTS AND VISUAL OBSERVATIONS FOR R12, R134a, AND R134a/ESTER LUBRICANT MIXTURES

M. A. Kedzierski and M. P. Kaul Mar. 1993 34 p See also PB93-120756 Sponsored by Department of Energy, Washington, DC Limited Reproducibility: More than 20% of this document may be affected by microfiche quality

(PB93-178598; NISTIR-5144) Avail: CASI HC A03

The paper presents a calorimetric and visual investigation of horizontal nucleate flow boiling of five different fluids: (1) dichlorodifluoromethane (R12), (2) 1,1,1,2-tetrafluoroethane (R134a), (3) R134a/1.7% proprietary polyol ester lubricant, (4) R134a/0.9% neopentyle polyol ester lubricant, and (5) R134a/2.3% neopentyle polyol ester lubricant. The calorimetric aspect of the study concentrates on the measurement of the local two-phase heat transfer coefficient (h(sub 2(phi))). The visual measurements obtained from high-speed 16 mm film of the boiling were taken simultaneously with the calorimetric measurements. The bubble diameters (D(sub b)) and the bubble density were derived from over 50 high-speed films. The purpose of the study is to provide a source of heat transfer information for the boiling of R12 and R134a/ester lubricant mixtures. Automotive and supermarket companies have begun to manufacture original air conditioning/refrigeration equipment with R134a as the operating fluid. The evaporator predominantly utilized by these industries is the in-tube heat exchanger. Naturally, designers of such evaporators require heat transfer coefficients for the horizontal flow boiling of R134a/ester mixtures. Only the nucleate flow boiling regime was investigated in the study with the aim of furthering the understanding of the fundamental heat transfer mechanisms responsible for the phenomenon. NTIS

N93-30996# International Atomic Energy Agency, Vienna (Austria).

STATEMENT ON THE UNITED NATIONS CONFERENCE ON ENVIRONMENT AND DEVELOPMENT

H. Blix Jun. 1992 5 p Conference held in Rio de Janeiro, Brazil, 1-12 Jun. 1992

(DE93-601878; INIS-MF-13356; CONF-9206148) Avail: CASI HC A01/MF A01 (US Sales Only)

Energy generation contributes greatly to environmental damage, and its impacts now pose a threat to the entire planet. The demand for energy is certain to increase in the coming decades, and the world will have to assess carefully what mix of energy sources is compatible with sustainable development and how best to use energy. The present heavy use of fossil fuels is at the root of some of the most serious environmental problems we face. Nuclear power can play an important part in combusting climate change and other energy-related problems such as urban air pollution and acid deposition. It too poses problems, such as the risk of serious accidents and the difficulties in managing radioactive wastes. The IAEA has an important role in laying down international guidelines for nuclear power plant safety and radioactive waste management. DOE

46 GEOPHYSICS

Includes aeronomy; upper and lower atmosphere studies; ionospheric and magnetospheric physics; and geomagnetism.

For space radiation see *93 Space Radiation.*

N93-28475# Forschungszentrum Juelich G.m.b.H. (Germany). Inst. fuer Chemie und Dynamik, der Geosphaere 3: Atmosphaerische Chemie.

DISTRIBUTION OF C1-C2 ALDEHYDES IN THE FREE TROPOSPHERE Thesis - Cologne Univ.

D. W. Arlander, U. Schmidt, and D. H. Ehhalt Jul. 1992 135 p

(JUEL-2650; ETN-93-93806) Avail: CASI HC A07/MF A02

A sensitive and selective measurement technique for the determination of tropospheric formaldehyde and acetaldehyde in background air is described. The method is based on the derivatization of aldehydes with 2,4-dinitrol phenyl hydrazine. The derivative aldehyde hydrazones are then separated using High Performance Liquid Chromatography (HPLC) and detected at 355 nm using a conventional HPLC-UV/VIS absorbance detector. Ground level measurements for formaldehyde and acetaldehyde were shown to vary from 0.5 to 7 ppb and 0.1 to 2.0 ppb, respectively. Diurnal mean mixing ratios of formaldehyde and acetaldehyde were 2.8 +/- 1.5 ppb and 0.7 +/- 0.4 ppb, respectively. Significant diurnal patterns were observed with maximum mixing ratios in the early afternoons, and minimum mixing ratios shortly before sunrise. A potential interference from organic hydroperoxides is also discussed. Aircraft measurements showed the potential of cartridge based methods for aldehyde measurements in the free troposphere. These test flights indicated that formaldehyde vertical profiles can be dependent on inversion height and cloud frequency. In-cloud formaldehyde measurements tended to be lower than gas phase measurements. This effect is most likely due to efficient absorption of formaldehyde into the droplets followed by rapid aqueous phase oxidation. Mixing ratios of tropospheric formaldehyde and acetaldehyde were determined. Vertical profiles were obtained which yielded a characterization of formaldehyde and acetaldehyde distributions throughout the free troposphere. Above the mixing layer, aldehyde mixing ratios typically decreased with increasing altitude. Lowest values of formaldehyde were detected in the upper troposphere. At this altitude, the practical detection limit of the method is reached. Comparison of formaldehyde measurements with model results indicate that although methane is a very significant formaldehyde precursor, the inclusion of naturally emitted nonmethane hydrocarbons and possibly industrial sources are necessary in order to predict troposphere formaldehyde mixing ratios more accurately. ESA

N93-28538*# California Univ., Irvine. Dept. of Physics.
LABORATORY SIMULATION OF FIELD-ALIGNED CURRENTS Annual Progress Report, Mar. 1992-1993
Frank J. Wessel and Norman Rostoker Mar. 1993 51 p
(Grant NAGw-2655)
(NASA-CR-193091; NAS 1.26:193091) Avail: CASI HC A04/MF A01

A summary of progress during the period Apr. 1992 to Mar. 1993 is provided. Objectives of the research are (1) to simulate, via laboratory experiments, the three terms of the field-aligned current equation; (2) to simulate auroral-arc formation processes by configuring the boundary conditions of the experimental chamber and plasma parameters to produce highly localized return currents at the end of a field-aligned current system; and (3) to extrapolate these results, using theoretical and computational techniques, to the problem of magnetospheric-ionospheric coupling and to compare them with published literature signatures of auroral-arc phenomena. Derived from text

N93-28677# Iowa State Univ. of Science and Technology, Ames.
MODELING LAND-SURFACE/ATMOSPHERE DYNAMICS FOR CHAMMP
W. J. Gutowski, Jr. Jan. 1993 6 p
(Contract DE-FG02-92ER-61473)
(DE93-008520; DOE/ER-61473/1) Avail: CASI HC A02/MF A01

Project progress is described on a DOE CHAMMP project to model the land-surface/atmosphere coupling in a heterogeneous environment. This work is a collaboration between scientists at Iowa State University and the University of New Hampshire. Work has proceeded in two areas: baseline model coupling and data base development for model validation. The core model elements (land model, atmosphere model) were ported to the Principal Investigator's computing system, and baseline coupling has commenced. The initial target data base is the set of observations from the FIFE field campaign, which is in the process of being acquired. For the remainder of the project period, additional data from the region surrounding the FIFE site and from other field campaigns will be acquired to determine how to best extrapolate results from the initial target region to the rest of the globe. In addition, variants of the coupled model will be used to perform experiments examining resolution requirements and coupling strategies for land-atmosphere coupling in a heterogeneous environment. DOE

N93-28842*# SRI International Corp., Menlo Park, CA.
THE DYNAMIC CUSP AT LOW ALTITUDES: A CASE STUDY COMBINING VIKING, DMSP, AND SONDRESTROM INCOHERENT SCATTER RADAR OBSERVATIONS
Jurgen Watermann, Odile delaBeaujardiere, Dirk Lummerzheim (Alaska Univ., Fairbanks.), Joachim Woch (Swedish Inst. of Space Physics, Kiruna.), Patrick T. Newell (Johns Hopkins Univ., Laurel, MD.), Thomas A. Potemra (Johns Hopkins Univ., Laurel, MD.), Frederick J. Rich (Phillips Lab., Hanscom AFB, MA.), and Mans Shapshak (Royal Inst. of Tech., Stockholm, Sweden.) 1992 40 p
(Contract NASw-4603; NAGw-3037; NSF ATM-90-22197; NSF ATM-91-08193; NSF ATM-91-12680; NSF ATM-92-02795; NSF ATM-88-22560)
(NASA-CR-193152; NAS 1.26:193152) Avail: CASI HC A03/MF A01

A case study involving data from three satellites and a ground-based radar are presented. Focus is on a detailed discussion of observations of the dynamic cusp made on 24 Sep. 1986 in the dayside high-latitude ionosphere and interior magnetosphere. The relevant data from space-borne and ground-based sensors is presented. They include in-situ particle and field measurements from the DMSP-F7 and Viking spacecraft and Sondrestrom radar observations of the ionosphere. These data are augmented by observations of the IMF and the solar wind plasma. The observations are compared with predictions about the ionospheric response to the observed particle precipitation, obtained from an auroral model. It is shown that observations and model calculations fit well and provide a picture of the ionospheric footprint of the cusp in an invariant latitude versus local time frame. The combination of Viking, Sondrestrom radar, and IMP-8 data suggests that we observed an ionospheric signature of the dynamic cusp. Its spatial variation over time which appeared closely related to the southward component of the IMF was monitored. Author (revised)

N93-28889# Department of Energy, Washington, DC. Environmental Sciences Div.
PROCEEDINGS OF THE SECOND ATMOSPHERIC RADIATION MEASUREMENT (ARM) SCIENCE TEAM MEETING
Dec. 1992 169 p Meeting held in Denver, CO, 26-30 Oct. 1991
(DE93-005886; CONF-911033-6) Avail: CASI HC A08/MF A02

The second Atmospheric Radiation Measurement (ARM) Science Team Meeting was held in Denver, CO, in Oct. 1991. The five-day meeting provided a forum for a technical exchange among the members of the ARM Science Team and a discussion of the technical aspects of the project infrastructure. The meeting included several activities: Science Team presentations, discussions of the first site occupation plan, experiment design sessions, and poster sessions. This Proceedings document includes papers presented at the meeting. The papers included are those from the technical sessions, the experiment design sessions, the first site occupation, and descriptions of locales for future sites. Individual projects are processed separately for the database. DOE

N93-29032*# Alabama Univ., Huntsville. Dept. of Chemistry.
FNAS CRRES PROGRAM COMPLETION Final Report, 21 Oct. - 21 Dec. 1992
George P. Miller 21 Dec. 1992 18 p
(Contract NAS8-38609)
(NASA-CR-192468; NAS 1.26:192468) Avail: CASI HC A03/MF A01

An agenda and the list of attendees at the Combined Release and Radiation Effects Satellite (CRRES) IWG meeting, held on 14-15 Dec. 1992, are presented. Short summaries of the work that has been completed to date, in support of the contract, are presented. CASI

N93-29197# National Center for Atmospheric Research, Boulder, CO. Atmospheric Chemistry Div.
ANALYSIS OF MASS TRANSPORT AND POTENTIAL VORTICITY BUDGET IN A SIMULATED TROPOPAUSE FOLDING Ph.D. Thesis-Univ. Catholoique de Louvain
Jean-Francois Lamarque 1993 214 p Sponsored by NSF
(PB93-156792; NCAR/CT-142) Avail: CASI HC A10/MF A03

In chapter 1, after a review of the different definitions of the tropopause, an historic review of cross-tropopause mass exchange is given and the tropopause folding dynamics is explained qualitatively. In chapter 2, the authors present the regional (or meso) scale model the NCAR mesoscale model or MM4) used to simulate the tropopause fold. In chapter 3, the event they have chosen to simulate is depicted in terms of potential vorticity evolution on isentropic surface, total ozone column evolution, and three-dimensional isosurface of potential vorticity evolution. The mathematical formulation of the cross-tropopause mass exchange is presented in chapter 4. It is also applied to the particular case described in chapter 3. In chapters 5 and 6, the effect of the cross-tropopause exchange on chemical species is discussed. For these chapters, a new offline tracer transport model is developed. In chapter 5, the cross-tropopause transport of ozone is estimated. Chapter 6 applies the formalism developed in the previous chapters to proposed high flying stratospheric aircrafts as the effect of the effluents released by these planes on the stratosphere depends, to an important extent, on their residence time in the stratosphere. Finally, the conclusions and prospectives are drawn. NTIS

N93-29343# Boston Coll., Chestnut Hill, MA. Inst. for Space Research.
IONOSPHERIC STRUCTURE SPECIFICATIONS AND SYSTEMS EFFECTS
Sunanda Basu 31 Dec. 1992 35 p
(Contract F19628-90-K-0007)
(AD-A263573; PL-TR-93-2018; SR-2) Avail: CASI HC A03/MF A01

Ionospheric scintillation measurements are examined in relation to the satellite in-situ measurements of electron density structures in the ionosphere and the plasma processes responsible for the generation of these structures. Radio waves from satellites are scattered and ionospheric scintillation is recorded on the ground in the presence of a relative motion between the satellite, the ionosphere, and the observer. The electron density irregularity spectrum of extended equatorial spread F structures, generated by a Rayleigh-Taylor instability process, is found to be compatible with multi-frequency satellite scintillation measurements. In the case of equatorial bottomside sinusoidal irregularities, however, the power-law spectral index of scintillations is found to be considerably shallower than that expected.

At high latitudes, two distinct classes of plasma instabilities, namely, the gradient-drift and shear-driven instability processes are identified. The observed difference of 0.5 between the spectral indices of high latitude scintillation and in-situ irregularity spectra has been explained in the context of an anistropic irregularity spectrum. DTIC

N93-29346# Los Alamos National Lab., NM.
SENSITIVITY STUDY OF CLOUD/RADIATION INTERACTION USING A SECOND ORDER TURBULENCE RADIATIVE-CONVECTIVE MODEL
C. Y. J. Kao and W. S. Smith 1993 17 p Presented at the International Specialty Conference: The Role of Meteorology in Managing the Environment in the 1990s, Scottsdale, AZ, 26-28 Jan. 1993
(Contract W-7405-eng-36)
(DE93-007365; LA-UR-93-315; CONF-930140-2) Avail: CASI HC A03/MF A01

A high resolution one-dimensional version of a second order turbulence convective/radiative model, developed at the Los Alamos National Laboratory, was used to conduct a sensitivity study of a stratocumulus cloud deck, based on data taken at San Nicolas Island during the intensive field observation marine stratocumulus phase of the First International Satellite Cloud Climatology Program (ISCCP) Regional Experiment (FIRE IFO), conducted in Jul. 1987. Initial profiles for liquid water potential temperature, and total water mixing ratio were abstracted from the FIRE data. The dependence of the diurnal behavior on liquid water content, cloud top height, and cloud base height were examined for variations in subsidence rate, sea surface temperature, and initial inversion strength. The modelled diurnal variation in the column integrated liquid water agrees quite well with the observed data, for the case of low subsidence. The modelled diurnal behavior for the height of the cloud top and base show qualitative agreement with the FIRE data, although the overall height of the cloud layer is about 200 meters too high. DOE

N93-29401# Naval Air Systems Command, Point Mugu, CA. Weapons Div.
TIDAL AND LUNAR DATA FOR POINT MUGU, SAN NICOLAS ISLAND, AND THE BARKING SANDA AREA DURING 1993 Annual Report
Charles J. Fisk and Bernard C. Cohenour Dec. 1992 39 p
(AD-A262725; NAWCWPNS-TM-7469) Avail: CASI HC A03/MF A01

Basic lunar and tidal data for Point Mugu, San Nicolas Island and the Barking Sands area during 1993 are provided. The data presented are: (1) tidal data; (2) times of moonrise and moonset; (3) times of lunar phases; and (4) times of sunrise and sunset. DTIC

N93-29405# Woods Hole Oceanographic Inst., MA.
GEOCHEMICAL AND FLUID DYNAMIC INVESTIGATIONS INTO THE NATURE OF CHEMICAL HETEROGENEITY IN THE EARTH'S MANTLE Ph.D. Thesis
Erik H. Hauri Sep. 1992 238 p
(Grant NSF EAR-87-08372)
(AD-A262753; WHOI-92-32) Avail: CASI HC A11/MF A03

Variations in the abundances of elements and radiogenic isotopes in mantle derived periodotites and volcanic rocks are chemical integrals over time, space, and process, which ultimately contain information about the role of convection in the earth's mantle in creating, maintaining, and destroying geochemical heterogeneities. Successful inversion of these integrals extensive of these integrals requires extensive knowledge of the geochemical behavior of elements, the length scales of chemical variability, the evolution with time of geologic systems, the physical properties of mantle rocks, and the driving forces of phenomena which govern heat and mass transport in a dynamic earth. This dissertation attempts to add to this knowledge by examining the trace element and isotope geochemistry of mantle periodotites and oceanic island basalts, and by studying aspects of the flow of viscous fluids driven by thermal buoyancy. DTIC

N93-29412# Scripps Institution of Oceanography, La Jolla, CA.
MODERN SEISMIC TRAVEL TIME TABLES AND STATION CORRECTIONS FOR P AND S WAVES Final Report, 13 Sep. 1990 - 13 Dec. 1992
John A. Orcutt 13 Dec. 1992 36 p
(Contract F19628-90-K-0053)
(AD-A262536; PL-TR-93-2001) Avail: CASI HC A03/MF A01

We refine estimates of inner core structure by examining PKP travel times and find that anisotropy is a simpler explanation than heterogeneity for the observed residual patterns. Our preferred model of inner core anisotropy contains velocities that are 0.5% faster in a N-S direction than an E-W direction. We also studied various mantle differential travel times including SS-S, ScS-S, PP-P, and PcP-P and compare these results to those obtained from handpicked waveform data. Large-scale coherent patterns of residuals are seen which indicate mantle heterogeneity. Further, we examined PKP travel times to study the possibility of outer core heterogeneity models which are suggested by observations of anomalous splitting in normal modes. We find that the travel times limit the scale of possible outer core heterogeneity to models much smaller than those required to explain the mode splitting data. Finally, we developed computer codes which return travel time and ray geometries for a given seismic phase, source-receiver pair, and arbitrary 3-d earth models specified by their spherical harmonic expansions. DTIC

N93-29467 Michigan Univ., Ann Arbor.
SPECTRAL ENERGETICS OF THE LOWER THERMOSPHERE Ph.D. Thesis
Robert Gary Raskin 1992 198 p
Avail: Univ. Microfilms Order No. DA9308429

A spectral energetics analysis of the lower thermosphere is carried out using simulated data from the NCAR Thermosphere-Ionosphere General Circulation Model (TIGCM). The results clarify the physical processes through which upwardly propagating semidiurnal tides dissipate and release their energy into the lower thermosphere. Energy residing within the study region is partitioned into reservoirs of available potential energy, irrotational kinetic energy, and nondivergent kinetic energy at four vertical levels. A definition of available potential energy is used that is appropriate for regions of variable mean molecular weight. The reservoirs are further subdivided by vector spherical harmonic wave numbers, and an energy budget is computed for each mode. The source, sink, and transformation terms are obtained using a post-processor that reproduces the contribution of each term in the momentum and thermodynamic equations. The loss terms for the tonal wave number two modes represent the dissipating forces for the semidiurnal tides. Viscosity, heat conduction, and ion drag represent the primary dissipative forces. Numerical smoothing within the TIGCM, representing subgrid-scale diffusion, is found to have a non-negligible contribution to the tidal dissipation. A small terdiurnal tide that is excited by ion drag is also observed in the model. A sensitivity analysis is carried out to ascertain the effects of the seasonal cycles solar cycle, UT, and geomagnetic activity. At solar maximum, solar heating at the trough of the tide is an important dissipative force; the altitude of tidal dissipation is correspondingly lower. At high values of geomagnetic forcing, the propagating semidiurnal tide is completely dissipated within the study region. Dissert. Abstr.

N93-29831# Oslo Univ. (Norway). Inst. of Physics.
ELECTRODYNAMICS OF THE DAYSIDE CLEFT REGION BASED ON GROUND OBSERVATIONS AT SVALBARD Final Report, Dec. 1991 - Jan. 1992
A. Egeland, J. A. Holtet, and P. E. Sandholt 20 Jan. 1993 15 p
(Grant AF-AFOSR-0082-90)
(AD-A263571; PL-TR-93-2022) Avail: CASI HC A03/MF A01

Based on extensive, diagnostic ground observations in the Svalbard region (mainly at Ny Alesund at 76 deg lambda) together with simultaneous, coordinated measurements from Greenland and Heiss Island spanning - 4 hours in magnetic local time - together with the EISCAT radars as well as DMSP satellite-recordings, essential information on the dynamics of the dayside cleft and polar cap region (auroral, ionospheric, and electric field) have been obtained. This is an important prerequisite to the understanding of the physics of the dayside boundary layers. Several papers have been presented and many lectures given related to this program. Possible generation mechanisms of dayside cusp/cleft auroras including magnetic merging, external pressure pulses, Kelvin-Helmholtz-instabilities, and dynamo processes by intruding plasma elements are discussed. To determine the characteristic auroral signatures of these boundary layer processes is a major objective of these studies. DTIC

N93-29879# Hawaii Univ., Honolulu.
ARI: INTERNAL GRAVITY WAVES AT ABRUPT TOPOGRAPHY Final Report

Peter Muller 1993 1 p
(Contract N00014-89-J-1315)
(AD-A263795) Avail: CASI HC A01/MF A01

The objective of the grant was to describe and model the interaction between internal gravity waves and irregular bottom topography, to determine the significance of the interaction, and to identify the appropriate theoretical tools to describe the interaction in oceanographically relevant parameter ranges. DTIC

N93-30005 California Inst. of Tech., Pasadena.
MODELING EARTHQUAKES WITH LOCAL AND REGIONAL BROADBAND DATA Ph.D. Thesis
Douglas Scott Dreger 1993 215 p
Avail: Univ. Microfilms Order No. DA9307034

Waveform modeling techniques were applied to several recent, moderate sized earthquakes recorded by the broadband, high dynamic range TERRAscope array in southern California. A method for the determination of source parameters at regional distances with three-component, sparse network data is developed, and applied to several events that occurred both within and outside the array. In some cases only the data from a single, three-component station was required to recover the source parameters. The source characteristics of the 1990 Upland mainshock (M(sub l) = 5.2) were investigated utilizing the broadband data recorded by the Pasadena station of the TERRAscope array. Green's functions developed by forward-modeling the waveforms of two smaller earthquakes that occurred in the Upland source region in 1988 were used in the analysis. Comparisons of the 1990 mainshock with the 1988 events revealed that the mainshock source was relatively complicated. Multi-point source and distributed finite slip models show that the mainshock ruptured down dip (6 km to 9 km) with a non-uniform slip distribution in which 30 percent of the total seismic moment was released from a relatively small area at 9 km depth. The overall area of the mainshock was found to be significantly smaller than the aftershock zone. The source process of the 28 Jun. 1991 Sierra Madre earthquake (M(sub L) = 5.8) is investigated using the broadband data recorded at 6 TERRAscope stations. Ratios of the peak amplitudes of simulated short-period and long-period Wood-Anderson seismograms show that stations southwest of the epicenter have elevated levels of short-period energy relative to stations to the east suggesting the presence of source directivity. The displacement waveforms were forward modeled using distributed finite slip models. The best fitting model consists of an up dip rupture toward the west. This model fails however to explain the amplitudes of the short-period waves. A non-uniform slip model was developed that better explains the short-period amplitudes. The results of this analysis indicate that the shorter-period energy is controlled more by the patches on the fault that experience the greatest slip, rather than the accumulative motions due to slip on the whole fault surface. Dissert. Abstr.

N93-30113 Royal Netherlands Meteorological Inst., De Bilt. Centrale Weerdienst.
DAILY SUM OF THE GLOBAL RADIATION: CALCULATION METHOD AND VERIFICATION OF FORECAST [DAGSOM VAN DE GLOBALE STRALING: EEN REKENMETHODE EN VERWACHTINGSVERIFICATIE]
M. C. Nolet 1991 17 p In DUTCH
(KNMI-TR-138; ISBN-9-03-692007-8; ETN-93-93588) Copyright Avail: Royal Netherlands Meteorological Inst., PO Box 201, 3730 AE De Bilt, Wilhelminalaan 10, Netherlands

The daily global radiation was calculated and compared with observations. It was calculated from the hourly averages deduced from the elevation of the Sun and the cloud cover. The calculated daily sums are on the average somewhat higher than the observed ones, and have to be slightly corrected. The correlation coefficient between calculated and observed daily sums is very high (0.98). The forecast of the daily sum of the global radiation (i.e. of the cloud cover degree) is difficult. The correlation coefficient between expected and real daily sum varies from 0.62 to 0.88, and the average absolute error is about 13% of the maximum possible daily sum. ESA

N93-30174# Northwest Research Associates, Inc., Bellevue, WA.
LABORATORY STUDIES OF GRAVITY WAVE/MEAN FLOW INTERACTIONS Annual Report, 15 Nov. 1991 - 14 Nov. 1992
Donald P. Delisi 4 Mar. 1993 32 p
(Contract F49620-92-C-0005)
(AD-A264226; NWRA-CR-92-R095; AFOSR-93-0265TR) Avail: CASI HC A03/MF A01

Progress is reported on laboratory measurements of gravity wave/critical layer interactions. Previous results have been reported for the interactions of single monochromatic waves propagating in a stratified fluid with a vertical velocity shear. The new results presented here are for two monochromatic forcing waves, each propagating with a different phase speed. Thus, the critical layer for each wave is distinct in the vertical. The results for the two-wave case are compared to similar results for the one-wave case. In the one-wave case, only weak overturning appeared in the upper part of the tank for interaction times longer than about 13 minutes, and regular, periodic turbulence was observed in the lower part of the tank. In contrast, in the two-wave case, sustained overturning was observed in the upper part of the tank and packets of turbulence were seen in the lower part of the tank. Velocity profiles are currently being examined to attempt to understand these observed differences. Other improvements in the hardware and software of the facility are also reported, and plans for the coming year are discussed. DTIC

N93-30367# Colorado Univ., Boulder. Lab. for Atmospheric and Space Physics.
NUMERICAL MODELING AND PARAMETERIZATION OF GRAVITY WAVE PROCESSES AND EFFECTS IN THE ATMOSPHERE Annual Report, 1 Jan. - 31 Dec. 1992
David C. Fritts 31 Dec. 1992 5 p
(Contract F49620-92-J-0138)
(AD-A264331; AFOSR-93-0262TR) Avail: CASI HC A01/MF A01

A nonlinear, compressible, spectral collocation code was developed to examine gravity wave breaking and instability processes in two and three spatial dimensions. Initial studies demonstrated that the preferred mode of instability within a high-frequency gravity wave is a convective instability comprised of counter-rotating vortices aligned transverse to the direction of wave propagation (a horizontal wavenumber normal to that of the gravity wave). Thus, wave instability is inherently three-dimensional, and two-dimensional models are unlikely to adequately describe either the physics of wave breaking or the implications for wave transports and eddy mixing. A parallel effort emphasized the statistical effects of wave interactions and dissipation processes and developed a new spectral parameterization of gravity wave transports of energy and momentum and their atmospheric effects. This scheme relies on the approximately universal spectral shape of the gravity wave motion field throughout the atmosphere to assess the potential for wave transports and variations with background wind and stability profiles. DTIC

N93-30487# Los Alamos National Lab., NM.
A COMPUTER SIMULATION OF THE PRODUCTION OF AN ARTIFICIALLY IONIZED LAYER USING THE ARECIBO FACILITY
G. M. Milikh, J. M. Hinds, and L. M. Duncan (Clemson Univ., SC.) 1993 46 p
(Contract W-7405-eng-36)
(DE93-010817; LA-Sub-93-152) Avail: CASI HC A03/MF A01

A computer model simulating the formation of an artificially ionized layer in the atmosphere by a series of microwave pulses was developed and is presented. The approach utilizes possible opportunities offered by the existing Arecibo transmitter and antenna. A modified version of the kinetic theory of the breakdown of air by a powerful microwave emission was incorporated into a model of electromagnetic propagation through the atmosphere by a converging ionizing microwave pulse. This model takes into consideration radio wave self-action as well as absorption, and produces profiles of electron concentration formed in the atmosphere by both an isolated pulse and a series of pulses. Effects of varying the shape of the ionizing pulse are considered as well as the influence of the ambient electron concentration. Also, the dependence of the electron concentration on the energy and duration of the pulse is investigated. The possible increase in the rate of electron production is considered when using an intense pulse to initiate the breakdown followed by a series of pulses of lesser energy. The influence of the refraction of the microwave beam is estimated. The computer model presented shows that an AIL (Artificial Ionized Layer) of electrons reaching concentrations on the order of 10(sup 8) cm(sup -3) could be formed over a height range of 40-70 km, if the Arecibo antenna and radio facility were reconfigured so that it would be able to generate microwaves with f = 2.38 GHz and a power of approximately 1-4 MW. In addition, a pulse compressor would be used to form pulses with durations of approximately 0.1-0.15 (mu)s with a repetition frequency of 103 Hz. DOE

N93-30562# SRI International Corp., Menlo Park, CA.
MITHRAS STUDIES OF THE BOUNDARY BETWEEN OPEN AND CLOSED FIELD LINES Annual Report, 1 Dec. 1991 - 30 Nov. 1992
Odile DelaBeaujardiere Mar. 1993 9 p
(Contract F49620-92-C-0011)
(AD-A264758; AFOSR-93-0243TR) Avail: CASI HC A02/MF A01

The coupling between the solar wind, the magnetosphere, and the ionosphere was studied using data from multi-instrument campaigns. One study showed that, even under quiescent conditions, the polar cap boundary was quite active. Repeated disturbances in particle precipitation and the electric field were observed at intervals of 10 to 20 minutes. Some of these perturbations propagated westward at a velocity of around 1000 m/s. It was argued that these perturbations are the ionospheric signature of rapid increases in the midnight-sector magnetic reconnection. In a separate study, the transition from active to quiet conditions was examined. The interplanetary magnetic field northward component switched suddenly from a northward to a southward orientation. The ionosphere responded within about two minutes: the electric field intensity diminished, and the F-region large and small scale irregularities changed dramatically. This response time is much shorter than had previously been assumed. DTIC

N93-30564 Michigan Univ., Ann Arbor.
OBSERVING AND MODELLING F-REGION IONOSPHERIC DYNAMICS USING THE OII 7320A EMISSION Ph.D. Thesis
Stephen Scott Carr 1992 328 p
Avail: Univ. Microfilms Order No. DA9308284

Limb-scan observations of Doppler line profiles from the (OII) lambda 7320A emission at F-Region altitudes, made with the Fabry-Perot interferometer (FPI) on the Dynamics Explorer-2 (DE-2) spacecraft, were analyzed to provide measurements of the meridional component of the ion convection velocity along the instrument line-of-sight. The DE-2 results presented demonstrate the first spaceborne use of the remote-sensing Doppler technique for measurements of ionospheric convection. The FPI meridional ion drift measurements were compared with nearly simultaneous in situ ion drift measurements from the Retarding Potential Analyzer (RPA) on DE-2. Once allowance is made for the temporal lag between the in situ and remove measurements, the results from the two techniques are found to be in good agreement, within specified experimental errors, giving confidence in the FPI measurements. The spaceborne interferometric technique has future utility for 2-dimensional imaging of polar ionospheric convection. Results from a simulated space-based observing platform, based on the DE-2 technique and an extension of a 7320A aeronomical model, are presented to demonstrate that a large fraction of the entire polar ionospheric convection pattern can be monitored from space during approximately 16-minute polar passes of a suitably-instrumented satellite. In the simulation, the polar-orbiting satellite's FPI system views the 7320A emission at various tangent point altitudes at +/- 45 deg and +/- 135 deg to the satellite velocity vector. By adjusting the horizon scan angle, several swaths of vectors at different horizontal spacing from the satellite can be recovered. Doppler line profiles from the (OII) 7320A emission at F-Region altitudes, made with the FPI at Sondre Stromfjord, Greenland, were analyzed to provide ion drift vectors and temperatures. These measurements demonstrate a unique ground-based use of the remote sensing technique from within the auroral zone since they are compared to simultaneous incoherent scatter radar (ISR) measurements. Results from the two techniques are in reasonable agreement, within specified instrumental errors, giving confidence in ground-based FPI measurements of the high-latitude ionospheric convection pattern and temperature field. Dissert. Abstr.

N93-30593# Mission Research Corp., Newington, VA.
ACOUSTIC-GRAVITY WAVES FROM LOW-ALTITUDE LOCALIZED DISTURBANCES Technical Report, 23 Sep. 1988 - 7 Oct. 1992
Steven Bottone 1 May 1993 62 p
(Contract DNA001-88-C-0223)
(AD-A264804; MRC/WDC-R-296; DNA-TR-92-140) Avail: CASI HC A04/MF A01

A physics-based analytic model of the ionospheric effects of low-altitude nuclear explosions due to acoustic-gravity waves (AGW) is produced. The model contains the essence of AGW theory predictions while including basic atmospheric chemistry effects to allow descriptions of AGW induced changes for both nighttime and daytime ionospheres. The model allows multiple explosions at arbitrary times and locations although its experimental basis is, of course, from single explosion data. DTIC

N93-30756# California Inst. of Tech., Pasadena. Seismological Lab.
MODELING REGIONAL SEISMIC WAVES
Donald V. Helmberger and David G. Harkrider 29 Jun. 1992 115 p
(Contract F19628-90-K-0049)
(AD-A264002; PL-TR-92-2186; SR-1) Avail: CASI HC A06/MF A02

This research performed under the contract, during the period 26 Sep. 1990 through 25 Sep. 1991, can be divided into two main topics; determining compressional velocity by modeling waveforms and travel time data from long-period and short-period recordings and determining surface wave magnitudes for NTS events using regional data. In section 1, a compressional velocity model for the northwest Atlantic Ocean was derived by modeling wave form and travel time data from long-period and short-period WWSSN and Canadian network station recordings. A ninety kilometer thick lid with the velocity of 8.1 km/sec at the top gradually changing to 8.3 km/sec at the bottom is obtained by fitting the travel time data of first arrivals and waveform data of pure oceanic paths at distance of 8 - 20 degrees. Triplication P waveform data constrains the structure below the lid. A distinct low velocity zone is located at depth of about 170 km. Combining with the shear wave structure derived by Grand and Helmberger for the same region, we can infer a very oliving-rich mineralogy in the upper 100 km and a very garnet-rich mineralogy at the depth of 200 - 400 km, at which partial melting should be also responsible for the very high VP/VS ratio. In section 2, the use of surface wave magnitudes as a determination of yield of under-ground explosions and the associated magnitude-yield scaling relationship was re-examined. Surface wave magnitudes for 190 Nevada Test Site (NTS) underground nuclear explosions were calculated from a data set of regional long-period seismograms from a combined super-network of 55 North American stations. Great effort went towards making the data set comprehensive and diverse in terms of yield, source location, and shot medium in order to determine the portability of surface wave magnitude scales. DTIC

N93-30785# Academy of Sciences (USSR), Novosibirsk. Inst. Yadernoj Fiziki.
ON THE PHOTONIC CHIRAL ANOMALY IN AN EXTERNAL GRAVITATIONAL FIELD
A. D. Dolgov, S. V. Kostyuk, and I. B. Khriplovich 1991 12 p
(DE93-606082; IYaF-91-31) Avail: CASI HC A03/MF A01 (US Sales Only)

The anomalous photonic chiral current in an external gravitational field is discussed. The current is parallel to the gravitational field. The parallel configuration is achieved by means of the ultraviolet and infrared regularization for spins 1/2 and 1. DOE

N93-30940# International Centre for Theoretical Physics, Trieste (Italy).
GENERAL SCALAR-TENSOR THEORIES FOR INDUCED GRAVITY INFLATION
H. BoutalebJ (Mohammed V Univ., Rabat, Morocco.) and A. L. Marrakchi Jul. 1992 17 p
(DE93-602505; IC-92/132) Avail: CASI HC A03/MF A01 (US Sales Only)

Some cosmological implications of a general scalar-tensor theory for induced gravity are discussed. The model exhibits a slow-rolling phase provided that the coupling function epsilon(phi) varies slowly enough such that (phi) dl(n)(epsilon)(phi)/d(phi) much less than 2 during almost the inflationary epoch. It is then shown that, as in the ordinary induced gravity inflation, the chaotic scenario is more natural than the new scenario which proves to be even not self-consistent. The results are applied, for illustration, to a scalar-tensor theory of the Barker type. DOE

N93-30991# Academy of Sciences (USSR), Novosibirsk. Inst. Yadernoj Fiziki.

COMPLEX APPARATUS AND RESULTS OF ACTIVE EXPERIMENT ELECTRON-1 WITH INJECTION OF ELECTRONIC BEAM IN THE IONOSPHERE [KOMPLEKS APPARATURY I REZULTATY AKTIVNOGO EHKSPERIMENTA EHIEKTRON-1 S INZHEKTSIEJ EHLEKTRONNOGO PUCHKA V IONOSFERU]

V. F. Bykovskij, S. B. Goryachev, and A. A. Doroshkin 1991 45 p In RUSSIAN

(DE93-605452; IYaF-91-62) Avail: CASI HC A03/MF A01 (US Sales Only)

The 'Electron' scientific apparatus complex, which was designed for experimentation with electron beam injection from space vehicles, is described. The complex is comprised of an electron injector with a high-frequency modulator, a set of board diagnostic equipment, and three ejection diagnostic containers. Results of an experiment on the modulated electron beam interaction (0.5A current and 6.5-8 keV energy) with ionospheric plasma at 90-150 km altitudes are presented. Energy spectra of recurrent electrons and ions arriving at a meteorocket are presented. DOE

N93-30992# Gandhi (Indira) Centre for Atomic Research, Kalpakkam (India).

ATMOSPHERIC STUDIES WITH SODAR AT KALPAKKAM

K. M. Somayaji 1991 70 p

(DE93-605544; IGC-125) Avail: CASI HC A04/MF A01 (US Sales Only)

A Doppler SODAR for measurement of wind characteristics at different heights has been installed at HASL, IGCAR, Kalpakkam and has been in operation since Jan. 1990. The technical specifications and the basic aspects of SODAR, siting considerations, and installation details are given. The report also discusses some observations regarding the site selection, installation, and operation of SODAR's. The basic theory of SODAR's, some aspects of turbulence and dispersion in atmosphere, and the various stability classification schemes are outlined. Some details regarding land/sea-breeze circulations and inversions are also given. DOE

N93-31002# International Centre for Theoretical Physics, Trieste (Italy).

A NON DEGENERATE SEMI-CLASSICAL LAGRANGIAN FOR DILATON-GRAVITY IN TWO DIMENSIONS

N. Mohammedi May 1992 13 p

(DE92-641339; IC-92/73) Avail: CASI HC A03/MF A01 (US Sales Only)

An action for two dimensional gravity conformally coupled to two dilaton-type fields is analyzed. Classically, the theory has some exact solutions. These include configurations representing black holes. A semi-classical theory is obtained by assuming that these singular solutions are caused by the collapse of some matter fields. The semi-classical equations of motion reveal then that any generic solution must have a flat geometry. DOE

N93-28728*# National Aeronautics and Space Administration. Goddard Space Flight Center, Greenbelt, MD.

SPACECRAFT GLOW AND THE EISG/SKIRT EXPERIMENT

Gary R. Swenson (Lockheed Missiles and Space Co., Palo Alto, CA.), Mark Ahmadjian (Phillips Lab., Hanscom AFB, MA.), Don Jennings, and Jim Visentine (National Aeronautics and Space Administration. Lyndon B. Johnson Space Center, Houston, TX.) *In* NASA, Washington, NASA/DOD Flight Experiments Technical Interchange Meeting Proceedings 1992 41 p (For primary document see N93-28699 11-12)

Avail: CASI HC A03/MF A10

N93-29600*# Jet Propulsion Lab., California Inst. of Tech., Pasadena.

DSS-14 SUBREFLECTOR ACTUATOR DYNAMICS DURING THE LANDERS EARTHQUAKE

R. Levy and D. Strain *In its* The Telecommunications and Data Acquisition Report 15 May 1993 p 130-146 (For primary document see N93-29586 11-32)

(RTOP 314-30-45-10-21)

Avail: CASI HC A03/MF A03

47 METEOROLOGY AND CLIMATOLOGY

Includes weather forecasting and modification.

N93-28465# Air Force Inst. of Tech., Wright-Patterson AFB, OH. School of Engineering.

CHARACTERIZATION OF LABORATORY GENERATED TURBULENCE BY OPTICAL PHASE MEASUREMENTS M.S. Thesis

Eric P. Magee 23 Mar. 1993 174 p

(AD-A262596; AFIT/GEO/ENG/93M-03) Avail: CASI HC A08/MF A02

The resolution achieved by an optical imaging system in the presence of the random effects of the atmosphere is severely degraded from the theoretical diffraction limit. Techniques exist for recovering near diffraction limited performance of an imaging system in the presence of atmospheric turbulence. As opposed to laboratory testing, testing image enhancement techniques in the Earth's atmosphere imposes many limitations. Unfavorable weather conditions could result in the loss of time and money invested in conducting the experiments. With a properly characterized turbulence generator, with statistics that match those of the atmosphere, experimental testing of image enhancement techniques can be conducted in a controlled laboratory environment. A turbulence chamber has been designed and built for laboratory testing of current and future adaptive optics and image enhancement techniques. The turbulence is produced within a chamber consisting of two small fans and a heating element. A unique method of characterizing the statistics of the turbulence has been developed. The wavefront phase perturbations are measured using a shearing interferometer. The statistical properties of the turbulence are then characterized by estimating the phase structure function from the wavefront phase measurements. The phase structure function is a measure of the correlation of the phase between two points in a plane perpendicular to the direction of propagation. It has been found that the estimate of the phase structure function depends only on the magnitude of the separation between the spatially separated points, and follows the Kolmogorov r(5/3) power law. DTIC

N93-28518# New Mexico Univ., Albuquerque. Dept. of Physics and Astronomy.

DISCHARGE OF ELECTRICALLY CHARGED CLOUDS Final Report, Sep. 1990 - Sep. 1992

Jean-Claude Diels, Xin M. Zhao, Chao-Yuen Yeh, and Cai Y. Wang 26 Oct. 1992 29 p

(Contract F19628-90-K-0056)

(AD-A263212; PL-TR-92-2266) Avail: CASI HC A03/MF A01

In a one year program, we have established a new mechanism for triggering lightning using low energy (less than 1 mJ) ultrashort (subpicosecond) pulses. A pre-ionized 'needle-shaped' path is created by three to four photon ionization of oxygen or applied field results in a local enhancement of the field, sufficient to reach avalanche breakdown. Measurement of multiphoton ionization cross section have established that a few mJ/sq cm in 200 fs at 248nm are sufficient to create 1013 electrons/cc. Laser induced discharge of 90 KV over 25 cm have been demonstrated with ns pulses at 248 nm, at pressure of 1/7 atm. This result and the theory indicate that less than 1 mJ in less than 1 ps duration pulses at 248 nm should induce the discharge at atmospheric pressure. A fs laser oscillator-amplifier has been assembled to perform such tests. DTIC

N93-28519# International Meteorological Inst., Stockholm (Sweden).

ACTIVITIES REPORT OF THE INTERNATIONAL METEOROLOGICAL INSTITUTE, STOCKHOLM (SWEDEN) Annual Report, Jul. 1991 - Jun. 1992

Aug. 1992 76 p

(ETN-93-93768) Avail: CASI HC A05/MF A01

The annual report of the International Meteorological Institute (IMI), which conducts research in meteorology and associated fields and promotes international scientific cooperation within meteorology, is presented. The international activities are summarized. Research activities are described which covered dynamic meteorology (mesoscale circulation, synoptic large scale dynamics); chemical meteorology (precipitation chemistry, trace exchange between the atmosphere and the underlying surfaces, atmospheric oxidants, modeling of tropospheric chemistry, the global carbon cycle); atmospheric physics (minor constituents, airglow studies, studies of the mesopause region, and stratospheric composition studies); atmospheric aerosol science (airborne particles and CO2, cloud chemistry and physics, and ice core research). ESA

N93-28875# Scripps Institution of Oceanography, La Jolla, CA. Marine Physical Lab.

AN AUTOMATED OBSERVING SYSTEM FOR PASSIVE EVALUATION OF CLOUD COVER AND VISIBILITY Final Report, Sep. 1988 - Jan. 1992

J. E. Shields, R. W. Johnson, and M. E. Karr Jul. 1992 40 p
(Contract F19628-88-C-0154)
(AD-A263207; SIO-REF-92-22; MPL-U-65/92; PL-TR-92-2202; XC-PL/HANSCOM) Avail: CASI HC A03/MF A01

The Automated Observing System is a passive system for determination of cloud cover and sector visibility. This system was developed from related systems, the Whole Sky Imager for cloud field assessment, and the Horizon Scanning Imager for determination of the sector visibility. During the past funding interval, much of the effort on this system was directed toward development of night visibility capability. This report discusses the theoretical development of the equations and analytic approaches to night visibility. A variety of hardware and software adaptations are discussed, which allow the sensor to utilize multiple integration periods for increased system sensitivity. Sample results are included. Secondary developments discussed in this report include an in-depth sensitivity analysis of the daytime visibility system, as well as achievement of more accurate cloud algorithms and night cloud capability funded separately. This is followed by recommendations for improvements to tile current system, and for development of tactical systems based on the existing capability. DTIC

N93-28876# Naval Research Lab., Monterey, CA.

LEADEX DATA REPORT. PART 1: WEATHER ANALYSIS AND SATELLITE IMAGES Final Report, 25 Mar. - 24 Apr. 1992

Robert W. Fett, Thomas F. Lee, Warren W. Rodie, Stephen D. Burk, and William T. Thompson Dec. 1992 309 p
(DA Proj. 3103)
(AD-A263217; NRL/PU/7531-92-0003) Avail: CASI HC A14/MF A03

This document contains weather analyses, forecast products, and selected satellite images obtained during the Leads Experiment (Leadex) from 25 Mar. - 24 Apr. 1992. This NRL Publication is Part 1 of a two-part data compilation report. Part 2 contains daily rawinsonde data obtained at Deadhorse and at the ice camp, and buoy data from four buoys surrounding the ice camp. A special section of Part 1 introduces the European spacecraft ERS-1 Synthetic Aperture Radar (SAR) data and shows some of the unique images from this sensor--courtesy of the European Space Agency (ESA). The report affords an opportunity to compare SAR data over selected locations with visible and infrared data from the DMSP satellite, with microwave imager (SSM/I) data from the same satellite, and with multispectral images from the NOAA satellite system. Special mesoscale weather depictions over the Leadex area, derived from the Navy's Second Order Closure Mesoscale Model (SOCMM), are shown for each day of the experiment. DTIC

N93-28991# Air Force Environmental Technical Applications Center, Scott AFB, IL.

SEASONAL SNOWFALL STATISTICS FOR SELECTED STATIONS

Jan. 1993 39 p Superseded Oct. 1988, AD-A203965
(AD-A263173; USAFETAC/TN-88/005-REV) Avail: CASI HC A03/MF A01

A convenient reference to seasonal snowfall statistics at 63 selected locations worldwide is discussed. Revised data is for the 10-year period from 1980 to 1990. Total snowfall amounts for each season (defined as July of one year to June of the next) is provided, along with 24-hour snowfall extremes, and dates. Seasonal means and standard deviations are also given. All values are in inches. DTIC

N93-29054# Battelle Pacific Northwest Labs., Richland, WA.

THE METEOROLOGICAL DATABASE Interim Report

S. A. Stage, J. V. Ramsdell, C. A. Simonen, and K. W. Burk Jan. 1993 70 p
(Contract DE-AC06-76RL-01830)
(DE93-007289; PNWD-2090-HEDR) Avail: CASI HC A04/MF A01

The Hanford Environmental Dose Reconstruction (HEDR) Project is estimating radiation doses that individuals may have received from operations at Hanford from 1944 to the present. An independent Technical Steering Panel (TSP) directs the project, which is being conducted by the Battelle, Pacific Northwest Laboratories in Richland, Washington. The goals of HEDR, as approved by the TSP, include dose estimates and determination of confidence ranges for these estimates. The current status of the meteorological database is described. The meteorological data available for use in climate model calculations, the data collection procedures, and the preparation and control of the meteorological database are described. An initial assessment of the data quality is provided. The available meteorological data are adequate for atmospheric calculations. Initial checks of the data indicate the data entry accuracy meets the data quality objectives. DOE

N93-29095# Los Alamos National Lab., NM.

DOPPLER-RADAR WIND-SPEED MEASUREMENTS IN TORNADOES: A COMPARISON OF REAL AND SIMULATED SPECTRA

H. B. Bluestein (Oklahoma Univ., Norman.), J. G. LaDue (Oklahoma Univ., Norman.), H. Stein (Oklahoma Univ., Norman.), D. Speheger (Oklahoma Univ., Norman.), and W. P. Unruh 1993 4 p Presented at the Radar Meteorology Meeting, Norman, OK, 24-28 May 1993
(Contract W-7405-eng-36)
(DE93-008734; LA-UR-93-639; CONF-9305139-1) Avail: CASI HC A01/MF A01

Bluestein and Unruh have discussed the advantages of using a portable Doppler radar to map the wind field in tornadoes. During the spring of 1991, a storm-intercept team from the University of Oklahoma (OU) collected data near five supercell tornadoes in Oklahoma and Kansas. Details about the 1-W, 3-cm, 5-deg half-power beamwidth, CW/FM-CW Doppler radar we used and the methods of data collection and analysis are found in Bluestein and Unruh and Bluestein et al. Using the portable radar, we approximately doubled in only one year the number of tornado spectra that had been collected over a period of almost 20 years by NSSL's fixed-site Doppler radar. In this paper, we will compare observed tornado wind spectra with simulated wind spectra (Zmic and Doviak 1975) in order to learn more about tornado structure. DOE

N93-29198# National Weather Service, Bohemia, NY. Scientific Services Div.

RHODE ISLAND HURRICANES AND TROPICAL STORMS: A FIFTY-SIX YEAR SUMMARY, 1936-1991

David R. Vallee (National Weather Service, Providence, RI.) Mar. 1993 70 p
(PB93-162006; NOAA-TM-NWS-ER-86) Avail: CASI HC A04/MF A01

The paper was compiled to provide a general overview of all tropical cyclone activity near Rhode Island since 1936. The year of 1936 is arbitrary, chosen mainly to include a not so well known system prior to the well documented Great New England Hurricane of 1938. Thirty-one such storms have affected the state in the past 56 years, either making landfall along the coast of southern New England, or passing close enough over the offshore waters to spread tropical storm or hurricane force conditions into the area. The intensities of these systems have ranged from weak, disorganized tropical storms to full fledged major hurricanes. The one feature common to almost all of the storms was a rapid acceleration toward Rhode Island, which greatly reduced the time to prepare and evacuate. NTIS

N93-29257# Massachusetts Inst. of Tech., Lexington. Lincoln Lab.

CONTRIBUTIONS TO THE AMERICAN METEOROLOGICAL SOCIETY'S 26TH INTERNATIONAL CONFERENCE ON RADAR METEOROLOGY

Marilyn W. Wolfson 1 Apr. 1993 36 p Conference held in Norman, OK, 24-28 May 1993
(Contracts DTFA-01-91-Z-02036; F19628-90-C-0002)
(AD-A263385; ATC-199; DOT/FAA/RD-93/14) Avail: CASI HC A03/MF A01

The work reported included Terminal Doppler Weather Radar (TDWR), Air Surveillance Radar-9, and Integrated Terminal Doppler Weather Radar Surveillance Systems (TASS). The staff members of the Weather Sensing Group have documented their studies in four major areas: Operational Systems (TDWR Operational Test and Evaluation results); Radar Operations (future airport weather surveillance requirements, a 'machine intelligent' gust front detection algorithm, microburst asymmetry study results, a shear-based microburst detection algorithm, and a hazard index for TWDR-detected microbursts); Signal Processing (coherent processing across multi-PRI waveforms, clutter filter design for multiple-PRT signals, and identification of anomalous propagation associated with thunderstorm outflows); and Analysis Methods (multiple-single Doppler wind analysis using NEXRAD data, and an adjoint method wind retrieval scheme). DTIC

N93-29304# Range Commanders Council, White Sands Missile Range, NM. Meteorology Group.

PROCEEDINGS OF THE THUNDER AND LIGHTING SEMINAR AND THE 3D LIGHTNING WARNING WORKSHOP

Feb. 1993 263 p Workshop held in Las Cruces, NM, 27 Feb. 1990
(AD-A262766) Avail: CASI HC A12/MF A03

The primary objective of the seminar was to provide information and exchange theories on sensors, techniques, and applications relating to lightning and thunderstorms. Information on the operational aspects of lightning detection sensors and how they may be used as well as advantages and limitations of the various systems and sensors discussed are provided. The lighting workshop was conducted as an objective of the Lightning Prediction and Detection Committee of the RCC Meteorology Group. The committee initiated a survey of lightning instruments and procedures used at the various ranges and organizations. The results of this survey are included. DTIC

N93-29347# Los Alamos National Lab., NM.

PROGNOSTIC CLOUD WATER IN THE LOS ALAMOS GENERAL CIRCULATION MODEL

J. E. Kristjansson and C. Y. J. Kao 1993 8 p Presented at the International Specialty Conference: The Role of Meteorology in Managing the Environment in the 1990s, Scottsdale, AZ, 26-28 Jan. 1993
(Contract W-7405-eng-36)
(DE93-007381; LA-UR-93-201; CONF-930140-3) Avail: CASI HC A02/MF A01

Most of today's general circulation models (GCM's) have a greatly simplified treatment of condensation and clouds. Recent observational studies of the earth's radiation budget have suggested cloud-related feedback mechanisms to be of tremendous importance for the issue of global change. Thus, there has arisen an urgent need for improvements in the treatment of clouds in GCM's, especially as the clouds relate to radiation. In the present paper, we investigate the effects of introducing pregnostic cloud water into the Los Alamos GCM. The cloud water field, produced by both stratiform and convective condensation, is subject to 3-dimensional advection and vertical diffusion. The cloud water enters the radiation calculations through the long wave emissivity calculations. Results from several sensitivity simulations show that realistic cloud water and precipitation fields can be obtained with the applied method. Comparisons with observations show that the most realistic results are obtained when more sophisticated schemes for moist convection are introduced at the same time. The model's cold bias is reduced and the zonal winds become stronger, due to more realistic tropical convection. DOE

N93-29393# Naval Postgraduate School, Monterey, CA.

THE SENSITIVITY OF AGEOSTROPHIC CIRCULATIONS TO MODEL RESOLUTION: A CASE STUDY USING NGM FORECASTS OF ERICA IOP-4 M.S. Thesis

James Berdeguez Dec. 1992 144 p
(AD-A262011) Avail: CASI HC A07/MF A02

The effect of model resolution on the ageostrophic circulations and dynamics of a rapidly deepening extratropical cyclone that occurred during the Intensive Observing Period (IOP) 4 (4-5 January 1989) of the Experiment on Rapidly Intensifying Cyclones over the Atlantic (ERICA) is examined using the psi-vector technique proposed by Keyser et al. (1989). A comparison of forecasts made by the National Meteorological Center's Nested Grid Model (NGM) using operational (C-grid) and double-resolution (D-grid) versions indicated central pressure and frontal evolution differences between the two forecasts IW IOP-4 cyclone was observed to deepen by 60 mb in 24 h to a central pressure of 936 mb. The NGM C-grid forecast attained a central pressure at 0000 UTC 5 Jan. of 959 mb, while the D-grid forecast attained a central pressure of 949 mb. Differences in the laterally coupled jet streaks between the C- and D-grid forecasts enabled the D-grid forecast to depict stronger transverse ageostrophic circulations that produced stronger ascent and greater spin-up of the low-level cyclone. DTIC

N93-29399# Argonne National Lab., IL. Environmental Assessment and Information Sciences Div.

EVALUATION OF ATMOSPHERIC WIND FIELD AND DISPERSION MODELS FOR FOG-OIL SMOKE DISPERSION IN COMPLEX TERRAIN: FIELD MEASUREMENT AND MODEL EVALUATION PROGRAM FOR ASSESSMENT OF THE ENVIRONMENTAL EFFECTS OF MILITARY SMOKES Final Report

D. M. Maloney, A. J. Policastro, W. E. Dunn (Illinois Univ., Urbana-Champaign.), and D. F. Brown (Illinois Univ., Urbana-Champaign.) Jul. 1992 107 p
(DA Proj. 3E1-62720-A-835)
(AD-A262051) Avail: CASI HC A06/MF A02

Three models used to predict the wind field and pollutant dispersion in complex terrain are compared with smoke dispersion data acquired as part of the AMADEUS field experiments in 1987 near Red Bluff, California. The models evaluated were WADOCT, HOTMAC/RAPTAD, and RAMS. The data base for model testing encompassed 7 fog-oil smoke releases from ground level under stable meteorological conditions. Smoke concentrations were measured out to 4 km downwind. Time-dependent meteorological and source data were available from these tests to be used as model input. The results showed that the WADOCT model predicted quite well for the first 300 m downwind but then underpredicted the plume concentration by an order of magnitude at distances of 4 km downwind. The HOTMAC/RAPTAD model revealed a similar behavior. The inability of those two models to predict the trajectory of the plume and the observed limited vertical growth of the plume, in the downwind valley, are the likely causes of the underprediction. The RAMS model revealed very poor wind field and dispersion predictions based on the large grid spacing that was required (for this application) in order to make the computer run times manageable. DTIC

N93-29448*# National Aeronautics and Space Administration. Goddard Space Flight Center, Greenbelt, MD.

CONVECTIVE AND STRATIFORM RAIN: MULTICHANNEL MICROWAVE SENSING OVER OCEANS

C. Prabhakara, J. J. Nucciarone (Hughes STX, Inc., Lanham, MD.), and G. Dalu (Consiglio Nazionale delle Ricerche, Cagliari, Italy.) Washington Jun. 1993 44 p
(NASA-TM-104586; Rept-93B00084; NAS 1.15:104586) Avail: CASI HC A03/MF A01

Measurements made by the Special Sensor Microwave/Imager (SSM/I) radiometer over the oceans, at 19, 37, and 85 GHz in dual polarization, are used to develop a model to classify rain into light-stratiform, moderately convective, and heavy convective types in the mesoscale convective systems (MCS). It is observed that the bulk of the 19- and 37-GHz data are linearly correlated with respect to one another, and generally increase together in brightness as the mean rain rate in the field of view (FOV) of the radiometer increases. However, a significant fraction of the data from these channels departs from this linear relationship, reflecting the nonuniform rain that is convective vs. the relatively light stratiform rain. It is inferred from the SSM/I data, in a MCS, when the slope dT sub 3/dT sub 19 is greater than unity there are optically thin clouds which produce light uniform rain. On the other hand, when dT sub 3/dT sub 19 is close to unity, the rain cells have an open structure and correspond to the convective type of rain. The openings between the cells are apparently a result of the downdrafts and/or entrainment. Relatively low values of 85-GHz brightness temperatures that are present when dT sub 37/dT sub 19 is close to unity support these views and, in addition, leads us to conclude that when the convection is heavy this brightness temperature decreases due to scattering by hydrometeors. On the basis of this explanation of the SSM/I data, an empirical rain retrieval algorithm is developed. Radar backscatter observations over the Atlantic Ocean next to Florida are used to demonstrate the applicability of this method. Three monthly mean maps of rainfall over the oceans from 50 degrees N to 50 degrees S, are presented to illustrate the ability of this method to sense seasonal and interannual variations of rain. Author

N93-29479# Mitre Corp., McLean, VA. Jason Program Office.

CLOUDS AND RADIATION: A PRIMIER

F. Zachariasen 25 Feb. 1993 29 p
(AD-A263136; JSR-90-307) Avail: CASI HC A03/MF A01

This paper addresses a previously unknown complex interdisciplinary process providing a feedback loop which may have a major impact on the effect on global climate of the steadily increasing growth of greenhouse gases in the atmosphere. DTIC

N93-29491# Naval Research Lab., Monterey, CA.
LEADEX DATA REPORT. PART 2: RAWINSONDE AND ICE STATION DATA Final Report, 25 Mar. - 24 Apr. 1992
Kenneth L. Davidson, James E. Overland, and Daniel E. Wolfe Dec. 1992 560 p
(NR Proj. 3103)
(AD-A263218; NRL/PU/7541-92-0004) Avail: CASI HC A24/MF A04

This document contains surface and upper air observations and aircraft flight information obtained during the Leads Experiment (Leadex) period of 25 March to 24 April 1992. The data consist of rawinsonde observations taken at Deadhorse, Alaska, and the ice camp; surface observations from five ice stations; and a list of aircraft flight dates, purposes, and related operational aspects. This report is Part 2 of a series of data compilation reports; part 1 contains weather analyses, forecast products, and selected satellite images. DTIC

N93-29664 National Weather Service, Washington, DC. Climate Analysis Center.
THE 17TH ANNUAL CLIMATE DIAGNOSTICS WORKSHOP
Mar. 1993 460 p Workshop held in Norman, OK, 18-23 Oct. 1992 See also PB92-167378 Limited Reproducibility: More than 20% of this document may be affected by microfiche quality
(PB93-183895) Avail: CASI HC A20

The Seventeenth Annual Climate Diagnostics Workshop was hosted by the University of Oklahoma in Norman, OK, October 19-23, 1992. These Proceedings provide a published record of the presentations made at the Workshop. Sessions were conducted on the following topics: Recent Climate Anomalies; ENSO; Air-Sea Interaction, Regional Climate Studies, Hydrology/Precipitation, etc. NTIS

N93-29810# Air Force Environmental Technical Applications Center, Scott AFB, IL.
THUNDERSTORM FORECAST STUDY FOR EGLIN AFB, FLORIDA
Daniel Comell Mar. 1993 48 p
(AD-A263423; USAFETAC/PR-93/001) Avail: CASI HC A03/MF A01

This report describes the evaluation of an empirical technique (WINNDEX) for predicting air-mass thunderstorms at Eglin AFB, FL. Results showed that the WINNDEX objective forecast technique had a Heidke skill score of .18 in predicting thunderstorm activity on the Eglin Range complex. A discriminant analysis model was developed that improved this skill to .32 in predicting the occurrence of thunderstorms during four 3-hour periods beginning at 1200Z. The study demonstrates the utility of USAFETAC's lightning database in developing and verifying a thunderstorm forecast model for remote locations. DTIC

N93-29832# Phillips Lab., Hanscom AFB, MA.
WIND MEASUREMENT ACCURACY OF A LORAN RADIOSONDE
James F. Morrissey 26 Oct. 1992 26 p
(AD-A263572; PL-TR-92-2262; ERP-1110) Avail: CASI HC A03/MF A01

A comparison of winds obtained using a Loran radiosonde system developed at Phillips Laboratory and winds derived using radar tracking of targets attached to the radiosonde balloon train are presented. The tests involve 10 ascents with dual Loran ground stations on most flights and dual radar tracking on two flights. The tests were performed at the Goddard Space Flight Center/Wallops Flight Facility in June 1990. The radiosonde is sufficiently accurate (0.32 m/s) to evaluate a wind profiler that has an error budget of 1.0 m/s. The wind profiler has been proposed to satisfy day of launch missile range wind measurement requirements. DTIC

N93-29850# Air Weather Service, Scott AFB, IL.
THE BASICS OF WEATHER MODELS
W. D. Meyer Mar. 1993 15 p
(AD-A263386; AWS/FM-93/001) Avail: CASI HC A03/MF A01

Without using mathematics, the important information weather forecasters need to know to apply numerical weather prediction (NWP) forecasts are summarized. Some tough choices regarding what material to include were made. The more technically rigorous information was put in an appendix. The material is organized under three main topics: history of NWP, components of an NWP model, and strengths and weaknesses of NWP models. Author (revised)

N93-29967# Air Weather Service, Scott AFB, IL.
CLOUDIEST YEAR STUDY: AN ANALYSIS OF THE 3DNEPH AND RTNEPH DATABASES
Billy D. Bainter Apr. 1993 25 p
(AD-A263409; AWS/PR-93/004) Avail: CASI HC A03/MF A01

Nephanalysis data from the Air Force Global Weather Central's (AFGWC's) two nephanalysis models (3-Dimensional Nephanalysis, or 3DNEPH, and Real-Time Nephanalysis, or RTNEPH) has been archived by USAFETAC's Operating Location A at Asheville, NC, since 1973. It has been used and applied by USAFETAC analysts since the data became part of the Air Weather Service's overall operational database. USAFETAC is frequently asked how one year's nephanalysis data compares with another in terms of global cloudiness. Up to now, that question has not been answered because of the immensity of the 3DNEPH and RTNEPH databases. But by combining new technologies with a scheme to reduce data volume, USAFETAC/DOS was recently able to rank data by years and months to determine the existence or non-existence of so-called 'cloudiest' periods. The study, the results of which are documented, used 3DNEPH and RTNEPH data from 1977 to 1991 to determine the years and months with maximum mean total cloudiness. DTIC

N93-30013 Royal Netherlands Meteorological Inst., De Bilt.
SYSTEMS DESCRIPTION OF MIVOS (MIST FORECAST SYSTEM), PART 1 [SYSTEEMBESCHRIJVING MIST VOORSPEL SYSTEEM MIVOS, DEEL 1]
D. Blaauboer, H. R. A. Wessels, S. Kruizinga, and J. vanLierop Jan. 1992 39 p In DUTCH
(KNMI-TR-141-Pt-1; ISBN-9-03-692012-4; ETN-93-93591) Copyright
Avail: Royal Netherlands Meteorological Inst., PO Box 201, 3730 AE De Bilt, Wilhelminalaan 10, Netherlands

A mainly technical description of MIVOS (Dutch acronym for mist forecast system) is given for the users. The systems concept (basic ideas behind the knowledge system MIVOS, numerical models used, and integration in the environment) is outlined. Hardware and software are described. MIVOS was evaluated with respect to future developments. The knowledge acquisition system is explained. ESA

N93-30044 Cornell Univ., Ithaca, NY.
SURFACE SHEAR STRESS ESTIMATES FROM GEOSTROPHIC WINDS FOR USE IN SENSIBLE AND LATENT HEAT FLUX FORMULATIONS Ph.D. Thesis
Richard D. Crago 1993 251 p
Avail: Univ. Microfilms Order No. DA9309552

The surface shear stress (or friction velocity, u(sub *)) is found in many formulations for evapotranspiration (LE) and sensible heat flux (H) from land surfaces, but is difficult to estimate without actually measuring wind speeds. ABL (Atmospheric Boundary Layer) similarity theory is used to estimate u(sub *) from the geostrophic wind (i.e., from the atmospheric pressure field). Atmospheric pressure is routinely measured at most weather stations across many continents on an hourly basis. Data from the First ISLSCP (International Satellite Land Surface Climatology Project) Field Experiment (FIFE) were analyzed. The values of the similarity variables B and B(sub W) were determined, and several formulations for the variables were compared. The optimal formulation (i.e., the one which produced the best match with the reference u(sub *) values obtained from surface layer similarity) used the magnitude (G) of the geostrophic wind and a stability-dependent B(sub W) function. The effects of random errors, baroclinicity, and inertial effects on the results were analyzed. Random measurement errors and the omission of inertial effects in the optimal formulation may cause considerable scatter. No dependence of the similarity variables on baroclinicity or scale-height ratio was discernable amidst the scatter, but they may still at times be important. Contrary to the findings of Hasse and Wagner, no tendency was found in the low wind speed range for near surface wind speeds to be greater than geostrophic wind

speeds. The geostrophic drag coefficient (i.e., u(sub *)/G) did not vary with stability or baroclinicity; a constant value of 0.1006 (for z(sub 0) = 1.05 m) gave unbiased estimates of u(sub *) and a higher correlation with the reference values than the optimal ABL similarity formulation. Estimates of H and LE using ABL similarity for temperature, the surface energy budget for LE, and the optimal B(sub W) formulation for u(sub *) gave correlations with values measured at the surface wing the Bowen-ratio with energy-budget method of 0.73 and 0.92, respectively. ABL similarity with measured winds provided better estimates, but is less applicable for widespread use in hydrology. Reduction of measurement error and incorporation of accurate acceleration estimates could improve results.
Dissert. Abstr.

N93-30055# Colorado State Univ., Fort Collins. Dept. of Atmospheric Science.

A STOCHASTIC FORMATION OF RADIATIVE TRANSFER IN CLOUDS

G. L. Stephens and P. M. Gabriel Mar. 1993 23 p
(Contract DE-FG02-90ER-61067)
(DE93-011372; DOE/ER-61067/2) Avail: CASI HC A03/MF A01

The research carried out under this award dealt with issues involving deterministic radiative transfer, remote sensing, Stochastic radiative transfer, and parameterization of cloud optical properties. A number of different forms of radiative transfer models in one, two, and three dimensions were developed in an attempt to build an understanding of the radiative transfer in clouds with realistic spatial structure and to determine the key geometrical parameter that influence this transfer. The research conducted also seeks to assess the relative importance of these geometrical effects in contrast to microphysical effects of clouds. The main conclusion of the work is that geometry has a profound influence on all aspects of radiative transfer and the interpretation of this transfer. We demonstrate how this geometry can influence an estimate of the particle effective radius to the 30-50% level and also how geometry can significantly bias the remote sensing of cloud optical depth.
DOE

N93-30114 Royal Netherlands Meteorological Inst., De Bilt. Afd. Fysische Meteorologie.

SYLLABUS PHYSICAL METEOROLOGY, PART 1 [SYLLABUS FYSISCHE METEOROLOGIE 1]

H. R. A. Wessels 1991 60 p In DUTCH
(KNMI-TR-140-Pt-1; ISBN-9-03-692010-8; ETN-93-93590) Copyright
Avail: Royal Netherlands Meteorological Inst., PO Box 201, 3730 AE De Bilt, Wilhelminalaan 10, Netherlands

The syllabus physical meteorology was made for the extensive education of senior meteorologists. Part 1 treats atmospheric radiation, thermodynamics of humid air, vertical transport processes, and microphysics of clouds.
ESA

N93-30176 Mitre Corp., Bedford, MA.

NEURAL NETWORK CLOUD CLASSIFICATION RESEARCH

Ira G. Smotroff Mar. 1993 71 p Limited Reproducibility: More than 20% of this document may be affected by microfiche quality
(AD-A264628; MTR-93B0000039) Avail: CASI HC A04

Neural networks are appropriate for meteorological classification tasks for a number of reasons. First, their associative properties allow graceful degradation of performance under conditions of ambiguity and noise, thus avoiding the brittle behavior of many standard approaches. Second, they learn to perform tasks which cannot easily be specified analytically, such as non-linear discriminate functions. Finally, they can be executed in realtime on appropriate hardware. To exploit these properties, this research developed a general approach to meteorological classification based on neural network data fusion. The system was applied to cloud type identification from satellite imagery. The current experiment is one of the first to provide a large cloud database on which to train, and as such is one of the first true cross-validation experiments in this area. While the 27 days of data provides many pixel samples of the cloud types present at a particular hour, the question to be answered here was whether the samples collected on particular types of clouds sufficiently represent the variations of that cloud that can appear on a different day. The promising results point to the applicability of neural networks for automated generation of meteorological products in real time.
DTIC

N93-30521# Air Force Systems Command, Wright-Patterson AFB, OH. Aeronautical Systems Center.

GRAPHICAL COMPARISON OF U.S. STANDARD ATMOSPHERES AND MILITARY STANDARD CLIMATIC EXTREMES Final Report, Jan. 1990 - Jul. 1991

Joseph C. Zuppardo Feb. 1993 272 p
(AD-A264639; ASC-TR-93-5002) Avail: CASI HC A12/MF A03

This report provides a compilation of the most commonly used atmosphere and climatic extremes. This compilation has been formed to aid the user in understanding the differences between the atmospheres. This may, therefore, be used as a tool to aid the user in choosing the best atmospheric model for their application.
DTIC

N93-30535# Phillips Lab., Hanscom AFB, MA.

CLOUD IMPACTS ON DOD OPERATIONS AND SYSTEMS CONFERENCE (CIDOS-91)

D. D. Grantham and J. W. Snow 18 Dec. 1992 47 p Conference held in El Segundo, CA, 9-12 Jul. 1991
(AF Proj. 6670)
(AD-A264463; PL-TR-92-2336; ERP-1116) Avail: CASI HC A03/MF A01

The Tri-Service Cloud Modeling Program was established by OUSDR&E and is chaired by the Phillips Lab, Geophysics Directorate/GPA. As a part of this program, the CIDOS conference is held at 18-month intervals. This forum was attended by about 140 researchers and DoD systems designers/users to exchange information on requirements and ongoing research for cloud effects on weapon, communications and surveillance systems. The theme of CIDOS-91 was 'Clouds - The First Order Impact for Defense and Climate Change'. Two Keynote addresses were presented: 'Cloud Forecasting: The Challenge During Operation Desert Storm, by Lt. Col. Gerald Riley, Staff Weather Officer to DS Field HQ; and, a review of the International Satellite Cloud Climatology Project by Dr. W. B. Rossow, NASA, Director ISCCP. The latter keynote emphasized the need for greater exchange of cloud data between the civilian and military communities, especially in light of the Congressional Strategic Environmental Research & Development Program (SERDP). Three working groups deliberated on the topics: Better Customer Interface; New Model/Database Requirements; and the development of a new DoD Clouds Handbook. The recommendations from the working groups and the CIDOS Executive Committee will be submitted to OUSDR and E and will form new statements of need to the tri-service agencies.
DTIC

N93-30608# Air Force Environmental Technical Applications Center, Asheville, NC.

AIR WEATHER SERVICE MASTER STATION CATALOG USAFETAC CLIMATIC DATABASE USERS HANDBOOK NO. 6

Tom Kotz and Phil Clouse Mar. 1993 51 p
(AD-A264761; USAFETAC/UH-93/001) Avail: CASI HC A04/MF A01

This document provides users of the Air Weather Service Master Station Catalog with information on database history, production, and content. This document also discusses processing and quality control, and it informs users on how to obtain the data.
DTIC

N93-30651# Sandia National Labs., Albuquerque, NM.

ROCKET-TRIGGERED LIGHTNING STUDIES FOR THE PROTECTION OF CRITICAL ASSETS

M. E. Morris, R. J. Fisher, G. H. Schnetzer, K. O. Merewether, and R. E. Jorgenson 1993 15 p Presented at the Industrial and Commercial Power System Conference, Tampa, FL, 3-6 May 1993
(Contract DE-AC04-76DP-00789)
(DE93-009633; SAND-93-0530C; CONF-930514-1) Avail: CASI HC A03/MF A01

Lighting protection systems (LPS's) for explosives handling and storage facilities have long been designed similarly to those used for more conventional facilities, but their overall effectiveness in controlling interior electromagnetic (EM) environments has still not been rigorously assessed. Frequent lightning-caused failures of a security system installed in earth-covered explosives storage structures prompted the U.S. Army and Sandia National Laboratories to conduct a program to determine quantitatively the EM environments inside an explosives storage structure that is struck by lightning. These environments were measured directly during rocket-triggered lightning (RTL) tests in the summer of 1991 and were computed using linear finite-difference, time-domain (FDTD) EM solvers. The experimental and computational results were first compared in order to validate the code and were also used to construct bounds for interior environments corresponding to seven incident lightning flashes. The code insults were also used to develop simple circuit models for the EM field behavior--a process that resulted in a very simple and somewhat surprising physical interpretation of the structure's response that has significant practical and economic implications for design, construction, and maintenance of such facilities. DOE

N93-30758# National Hurricane Center, Coral Gables, FL.
DEADLIEST, COSTLIEST, AND MOST INTENSE US HURRICANES OF THIS CENTURY (AND OTHER FREQUENTLY REQUESTED HURRICANE FACTS)
P. J. Herbert, J. D. Jarrell, and M. Mayfield Feb. 1993 46 p Supersedes PB91-178004
(PB93-174993; NOAA-TM-NWS-NHC-31) Avail: CASI HC A03/MF A01

Lists of United States hurricanes which have caused 25 or more deaths and more than one hundred million dollars in damages have been compiled from all data sources available at the National Hurricane Center. The document is an update through the 1992 hurricane season. Hurricane Andrew, an intense hurricane causing about $25 billion damage to the coasts of Florida and Louisiana, requires nearly all of the damage and intensity tables to be revised. Because of Hurricane Iniki in the Hawaiian islands in 1992, Table 14 has been added covering Hawaiian hurricanes of this century, and certain tables have been modified to include Hawaiian and eastern Pacific hurricanes. The Hawaiian information, given in Table 14 was provided by the Honolulu Weather Service Forecast Office. NTIS

N93-30889# San Francisco State Univ., CA. Dept. of Geosciences.
CASE STUDY OF THE OPERATIONAL USEFULNESS OF THE SHARP WORKSTATION IN FORECASTING A MESOCYCLONE-INDUCED COLD SECTOR TORNADO EVENT IN CALIFORNIA
J. P. Monteverdi Mar. 1993 32 p See also PB89-121297 Sponsored by National Weather Service, Salt Lake City, UT
(PB93-178697; NOAA-TM-NWS-WR-219) Avail: CASI HC A03/MF A01

An illustration of the operational usefulness of the SHARP Workstation in providing supplementary guidance to forecasters in a situation in which two tornadoes occurred in California's Sacramento Valley is presented. Use of the SHARP Workstation in analyzing the initial hodograph and in producing a bogus afternoon sounding and hodograph for the Sacramento Valley indicated that buoyancy and shear were in the correct range for moderate to strong mesocyclone-induced tornadoes. Conventional wisdom would have suggested that weak funnel clouds and small hail were the chief threats in the weather pattern. However, forecasters, aware of the role of shear in inducing storm rotation and of the potential for the weather pattern to be associated with favorable buoyancy and shear parameters in certain regions of California, would have been alert to the possibility of damaging and potentially life-threatening tornadoes. NTIS

N93-31006# International Centre for Theoretical Physics, Trieste (Italy).
THE DISTRIBUTION OF THE ANNUAL AND SEMIANNUAL CYCLES IN THE TROPICS
W. L. Sumathipala Jun. 1992 24 p
(DE92-642213; IC-92/111) Avail: CASI HC A03/MF A01 (US Sales Only)

The distributions of annual and semiannual cycles in the tropics are studied using outgoing long-wave radiation (OLR), and FGGE level 3 b wind data. Amplitudes and variances of first and second harmonics (in the time domain) of low level zonal wind (U) are largest over monsoon regions of the eastern hemisphere and account for more than 80% of the variance. The first harmonic of OLR shows largest amplitudes over the continental regions between 10-15 degrees from the equator. The first harmonics of both low-level wind and OLR show standing character. The second and third harmonics of U are characterized by cross equatorial and clockwise phase propagation. All three harmonics are 'phase locked' in the monsoon region of the eastern hemisphere during summer. Amplitude of the first harmonic of low level meridional wind (V) is prominent at the Somalia coast and Malaysia. Amplitude variations of first and second harmonics of upper level zonal wind exhibit the response of subtropical jet streams to monsoon and inter-monsoon convective activity. Fairly strong amplitudes of OLR are found over the equatorial land areas where rainfall is maximum during the transition periods. DOE

N93-31018# GKSS-Forschungszentrum Geesthacht (Germany). Inst. fuer Physik.
MEASUREMENT OF THE ROTATION RAMAN SPECTRA OF NITROGEN, OXYGEN, AND WATER VAPOR UNDER CONDITIONS OF A TEMPERATURE HUMIDITY LIDAR Thesis - Hamburg Univ. [MESSUNG DER ROTATIONS-RAMAN-SPEKTREN VON STICKSTOFF, SAUERSTOFF UND WASSERDAMPF UNTER DEN BEDINGUNGEN EINES TEMPERATUR-FEUCHTE-LIDARS]
J. Zeyn 20 Mar. 1992 91 p In GERMAN
(GKSS-92/E/32; ETN-93-94188) Copyright Avail: CASI HC A05/MF A01

Spectroscopic investigations of nitrogen, oxygen, and water vapor are described. For the measurements of the pure rotational Raman spectra of these gases, a monochromator was designed. The source of radiation was a KrF excimer laser frequency shifted by stimulated Raman scattering in hydrogen. A thallium atom vapor filter was used for Mie and Rayleigh scattering suppression. An interference filter was implemented for weakening vibration rotation Raman lines. The design of the monochromator and the selection of the radiation source meet the requirements of a lidar system. It was possible to separate individual lines of the pure rotational Raman spectra and to verify the ratio of cross sections of nitrogen and oxygen. For the rotational Raman cross sections of water vapor an upper limit is given. ESA

N93-29913# MATRA Marconi Space (England).
TACSAT METEOROLOGICAL PAYLOADS
D. Hickman *In* AGARD, TacSats for Surveillance Verification and C3I Feb. 1993 8 p (For primary document see N93-29892 11-32)
Copyright Avail: CASI HC A02/MF A03

N93-30295 Canadian Forces Base Trenton, Astra (Ontario). Forecast Centre.
STAND ALONE LIGHTNING DETECTION EQUIPMENT USED AT CANADIAN FORCES AIR BASES
Pierre Pommainville and Robert Cross (National Defence Headquarters, Ottawa, Ontario.) *In* Engineering Inst. of Canada, Canadian Conference on Electrical and Computer Engineering, Volumes 1 and 2 1990 3 p (For primary document see N93-30215 11-31)
Avail: Engineering Inst. of Canada, 2050 rue Mansfield, Suite 700, Montreal, Quebec H3A 1Z2 Canada

N93-30296 Quebec Univ., Montreal. Centre de Recherche Informatique de Montreal.
STRATUS: A PROTOTYPE EXPERT ADVISORY SYSTEM FOR TERMINAL WEATHER FORECASTING
Michel C. Desmarais, Fances deVerteuil, Denis Jacob (Atmospheric Environment Service, Saint-Laurent, Quebec.), and Peter Zwack *In* Engineering Inst. of Canada, Canadian Conference on Electrical and Computer Engineering, Volumes 1 and 2 1990 4 p (For primary document see N93-30215 11-31)
Avail: Engineering Inst. of Canada, 2050 rue Mansfield, Suite 700, Montreal, Quebec H3A 1Z2 Canada

N93-30297 CompEngServ Ltd., Ottawa (Ontario).
CLOUD CLASSIFICATION FROM SATELLITE IMAGERY USING NEURAL COMPUTING
B. Archie Bowen and J. David Steenbergen (Atmospheric Environment Service, Downsview, Ontario.) *In* Engineering Inst. of Canada, Canadian Conference on Electrical and Computer Engineering, Volumes 1 and 2 1990 3 p (For primary document see N93-30215 11-31)
Avail: Engineering Inst. of Canada, 2050 rue Mansfield, Suite 700, Montreal, Quebec H3A 1Z2 Canada

N93-30298 MacDonald, Dettwiler and Associates Ltd., Richmond (British Columbia).
METEOROLOGICAL INFORMATION FOR AVIATION: A SYSTEMS APPROACH
R. G. Humphries, J. N. Geddes, W. C. Cree, and L. W. Diehl *In* Engineering Inst. of Canada, Canadian Conference on Electrical and Computer

Engineering, Volumes 1 and 2 1990 4 p (For primary document see N93-30215 11-31)
Avail: Engineering Inst. of Canada, 2050 rue Mansfield, Suite 700, Montreal, Quebec H3A 1Z2 Canada

48 OCEANOGRAPHY

Includes biological, dynamic, and physical oceanography; and marine resources.

For related information see also *43 Earth Resources and Remote Sensing.*

N93-28497*# National Aeronautics and Space Administration. Goddard Space Flight Center, Greenbelt, MD.

SeaWIFS TECHNICAL REPORT SERIES. VOLUME 2: ANALYSIS OF ORBIT SELECTION FOR SeaWiFS: ASCENDING VERSUS DESCENDING NODE

Stanford B. Hooker, ed., Elaine R. Firestone, ed. (General Sciences Corp., Laurel, MD.), and Watson W. Gregg Washington Sep. 1992 20 p
(NASA-TM-104566-Vol-2; NAS 1.15:104566-Vol-2; Rept-92B00122) Avail: CASI HC A03/MF A01

Due to range safety considerations, the Sea-viewing Wide Field-of-view Sensor (SeaWiFS) ocean color instrument may be required to be launched into a near-noon descending node, as opposed to the ascending node used by the predecessor sensor, the Coastal Zone Color Scanner (CZCS). The relative importance of ascending versus descending near-noon orbits was assessed here to determine if descending node will meet the scientific requirements of SeaWiFS. Analyses focused on ground coverage, local times of coverage, solar and viewing geometries (zenith and azimuth angles), and sun glint. Differences were found in the areas covered by individual orbits, but were not important when taken over a 16 day repeat time. Local time of coverage was also different: for ascending node orbits the Northern Hemisphere was observed in the morning and the Southern Hemisphere in the afternoon, while for descending node orbits the Northern Hemisphere was observed in the afternoon and the Southern in the morning. There were substantial differences in solar azimuth and spacecraft azimuth angles both at equinox and at the Northern Hemisphere summer solstice. Negligible differences in solar and spacecraft zenith angles, relative azimuth angles, and sun glint were obtained at the equinox. However, large differences were found in solar zenith angles, relative azimuths, and sun glint for the solstice. These differences appeared to compensate across the scan, however, an increase in sun glint in descending node over that in ascending node on the western part of the scan was compensated by a decrease on the eastern part of the scan. Thus, no advantage or disadvantage could be conferred upon either ascending node or descending node for noon orbits. Analyses were also performed for ascending and descending node orbits that deviated from a noon equator crossing time. For ascending node, afternoon orbits produced the lowest mean solar zenith angles in the Northern Hemisphere, and morning orbits produced the lowest angles for the Southern Hemisphere. For descending node, morning orbits produced the lowest mean solar zenith angles for the Northern Hemisphere; afternoon orbits produced the lowest angles for the Southern Hemisphere. Author (revised)

N93-28500*# National Aeronautics and Space Administration. Goddard Space Flight Center, Greenbelt, MD.

SeaWIFS TECHNICAL REPORT SERIES. VOLUME 6: SeaWiFS TECHNICAL REPORT SERIES CUMULATIVE INDEX: VOLUMES 1-5

Stanford B. Hooker, ed. and Elaine R. Firestone, ed. (General Sciences Corp., Laurel, MD.) Washington Nov. 1992 12 p
(NASA-TM-104566-Vol-6; NAS 1.15:104566-Vol-6; Rept-93B00016) Avail: CASI HC A03/MF A01

The Sea-viewing Wide Field-of-view Sensor (SeaWiFS) is the follow-on ocean color instrument to the Coastal Zone Color Scanner (CZCS), which ceased operations in 1986, after an eight year mission. SeaWiFS is expected to be launched in August 1993, on the Sea Star satellite, being built by Orbital Sciences Corporation (OSC). The SeaWiFS Project at the NASA/Goddard Space Flight Center (GSFC) has undertaken the responsibility of documenting all aspects of this mission, which is critical to the ocean color and marine science communities. This documentation, entitled the SeaWiFS Technical Report Series, is in the form of NASA Technical Memoranda Number 104566. All reports published are volumes within the series. This volume serves as a reference, or guidebook, to the previous five volumes and consists of four main sections including an index to key words and phrases, a list of all references cited, and lists of acronyms and symbols used. It is our intention to publish a summary index of this type after every five volumes in the series. This will cover the topics published in all previous editions of the indices, that is, each new index will include all of the information contained in the preceding indices. Author

N93-28670# Columbia Univ., Palisades, NY.

STEADY-STATE AND TRANSIENT MODELING OF TRACER AND NUTRIENT DISTRIBUTIONS IN THE GLOBAL OCEAN

T. F. Stocker and W. S. Broecker Mar. 1993 10 p
(Contract DE-FG02-91ER-61202)
(DE93-011043; DOE/ER-61202/2) Avail: CASI HC A02/MF A01

The balance of stable and decaying tracers was incorporated into a latitude-depth ocean circulation model which resolves the major ocean basin and is coupled to an atmospheric energy balance model. The modern distribution of radiocarbon and the analysis of artificial color tracers enabled the census of the deep water masses. We show that good agreement with the observation can be achieved if the surface forcing is modified. The same process could also account for long-term, large-scale changes of the global thermohaline circulation. Uptake rates of carbon are investigated using an inorganic carbon cycle model and performing 2 x CO2 experiments. We prescribe the industrial evolution of pCO2 in the atmosphere from 1792 to 1988 and calculate the total flux of carbon into the world ocean. Results are in good agreement with two recent 3-dimensional model simulations. First results using an organic carbon cycle in this model are presented. Changes in the hydrological cycle can stabilize the thermohaline circulation in the Atlantic and enable simulation of climate events resembling the Younger Dryas. By adding the balance of radiocarbon the evolution of its atmospheric concentration is studied during rapid changes of deep ocean ventilation. A resumption of ventilation creates a rapid decrease of atmospheric radiocarbon which is able to mask the natural decay. DOE

N93-28885# Scripps Institution of Oceanography, La Jolla, CA. Center for Coastal Studies.

ANALYSES OF DATA FROM FINE STRUCTURE AND CIRCULATION STUDIES IN THE GULF OF CALIFORNIA Final Report, 1 Mar. 1991 - 30 Sep. 1992

Myrl C. Hendershott Apr. 1993 3 p
(Contract N00014-91-J-1791)
(AD-A262910) Avail: CASI HC A01/MF A01

The objective of this proposal was to complete the analysis and manuscripts of the CTD data collected in the Gulf of California. The most important accomplishment of the present reporting period has been completion, submission for publication to Deep Sea Research, and acceptance, subject to minor modifications requested by a referee, of a paper by Ph.D. student Juan Rodrigues-Sero and M.C. Hendershott describing fine structure in the Gulf of California. The title is 'Vertical Temperature Gradient Fine Structure Spectra in the Gulf of California.' We have also made significant progress on a manuscript with A. de Leon and A. Badan Dangon, of CICESE (Ensenada, Mexico) in which ADCP data collected in the northern Gulf of California in Jan. 1990 are processed to extract the tidal velocity field there. The initial reduction of observations is complete, but we wish to include in the publication a comparison with tidal model results to be provided by researchers at CICESE and then to re-analyze the data using the model fields as a basis set rather than simple polynomials in the space coordinates. DTIC

N93-28996# Woods Hole Oceanographic Inst., MA.

OPTICAL MEASUREMENTS OF RIPPLES USING A SCANNING LASER SLOPE GAUGE. PART 1: INSTRUMENTATION AND PRELIMINARY RESULTS

Robert J. Martinsen and Erik J. Bock Mar. 1993 15 p
(Contract N00014-90-J-1717)
(AD-A261939; WHOI-Contrib-8701) Avail: CASI HC A03/MF A01

We describe the design, implementation, and deployment of a laser slope gauge developed at the Woods Hole Oceanographic Institution for the purpose of studying the propagation characteristics of capillary ripples, and how currents and natural slicks on the ocean surface modify ripple spectra. The laser slope gauge constitutes a nondisruptive optical technique for determining the slope spectrum for a range of waves with wavelengths between 2 mm and 20 cm using both spatial and temporal information. Operation of the sensor and data acquisition system is discussed and a sample data record collected in the Gulf Stream off Cape Hatteras, NC is interpreted and analyzed. DTIC

N93-29003# Woods Hole Oceanographic Inst., MA.
NEAR REAL-TIME GIS IN DEEP-OCEAN EXPLORATION
Jonathan C. Howland, Martin Marra, Daniel F. Potter, and W. K. Stewart Mar. 1993 9 p
(Contracts N00014-90-J-1848; N00014-90-J-1912)
(AD-A262073; WHOI-Contrib-8046) Avail: CASI HC A02/MF A01

During a 1991 oceanographic research expedition to the Juan de Fuca Ridge, the Deep Submergence Laboratory (DSL) of the Woods Hole Oceanographic Institution (WHOI) applied interactive mapping with a geographic information system (GIS) in conjunction with real-time navigation. As DSL's remotely operated vehicle (ROV), Jason, surveyed a hydrothermal vent field, acoustic navigation updates were combined with maps generated to the specifications of participating scientists. The maps, which were generated in near-real time, were used to plan vehicle operations in a hazardous environment and to monitor survey progress and data quality. Geologic observations made in real-time by scientists monitoring ROV sensors were logged into data files, combined with processed navigation, and used to produce preliminary updates to maps of the vent field. This experimental combination of GIS technology with navigation and visualization software was highly successful. Future scientific efforts will include further processing of sensor data, integration of image products into the GIS database, and the production of high-quality mapping products. DTIC

N93-29295# Office of Naval Research, Arlington, VA.
OCEAN WAVES IN SAMSON/SWADE Final Technical Report
1993 4 p
(Contract N00014-90-J-1255)
(AD-A263681) Avail: CASI HC A01/MF A01

The scientific objective of this project was to determine the origin and governing dynamics of the low frequency (nominally 0.01 Hz) infragravity waves which are sometimes very energetic in shallow water. Possible generation mechanisms include local nonlinear forcing of bound infragravity waves by groups of sea and swell, excitation of freely propagating edge waves in nearby surf zones, and ocean-basin-wide propagation of infragravity waves excited by large, distant storms. Important dynamical questions include what are the amounts of infragravity energy reflected by the beach face, refractively trapped during propagation across the shelf, and lost by bottom friction. DTIC

N93-29298# Alaska Univ., Fairbanks.
A FIELD INVESTIGATION OF WATER AND SALT MOVEMENT IN PERMAFROST AND THE ACTIVE LAYER Final Report, 1 Jul. 1989 - 31 Dec. 1992
T. E. Osterkamp Feb. 1993 46 p
(Contract DAAL03-89-K-0106)
(AD-A263706; ARO-26281.5-GS) Avail: CASI HC A03/MF A01

Evidence from subsea permafrost, permafrost in coastal regions of the Arctic and Antarctic, and in the cold and sometimes arid regions of China, the Soviet Union, Antarctica, and North America, indicates that saline permafrost is very widespread - perhaps more common than non-saline permafrost. This salty permafrost is found near the surface at depths of geotechnical interest, within, and under continuous and discontinuous permafrost. These salts can produce significant changes in permafrost properties and processes and it is possible for these salts to become mobile under potential energy gradients. It is concluded that saline permafrost will become increasingly important in the rational assessment of scientific, engineering, environmental, and agricultural problems of the future. DTIC

N93-29327# Washington Univ., Seattle.
UPPER OCEAN MODEL OF DISSOLVED ATMOSPHERIC GASES
R. Schudlich and S. Emerson 1992 13 p
(Contract DE-FG06-90ER-61037)
(DE93-010151; DOE/ER-61037/1) Avail: CASI HC A03/MF A01

The goal of this project is to estimate the rate of biological oxygen production at Hawaiian Ocean Time-series station ALOHA in the central North Pacific ocean. Our approach is to use an upper ocean model together with measurements to interpret an annual cycle of temperature, salinity, dissolved oxygen, argon, nitrogen, and the stable isotope ratio of oxygen at station ALOHA. This project represents the first upper ocean geochemical study in which model predictions are verifiable by independent measurements. Using the model, we will be able to assess the relative roles played by physical processes (air-sea gas exchange, air injection by bubbles, temperature-induced changes in gas solubility, trapping below the mixed layer, and diffusion) and biological processes (photosynthesis, respiration, and nutrient recycling) in producing the observed distribution of dissolved atmospheric gases. The long term goal of this project is to understand the utility of chemical tracers for quantifying biological processes in the ocean. DOE

N93-29422# Scripps Institution of Oceanography, La Jolla, CA.
OPTICAL SLOPE/HEIGHT MEASUREMENTS OF SMALL SCALE WAVES WITHIN THE SAXON-FPN EXPERIMENT Final Report, 30 Sep. 1989 - 29 Sep. 1992
B. Jahne, S. Waas, and J. Klinke 16 Feb. 1993 10 p
(Contract N00014-89-J-3222)
(AD-A262572) Avail: CASI HC A02/MF A01

This research focused on measurements of short wind waves in the open ocean with optical techniques using a triple strategy. First, optical imaging of short wind waves was reviewed using an unified approach based on the shape from shading and shape from stereo paradigms from computer vision. This analysis revealed the weaknesses of conventional stereo and Stilwell photography. Refraction-based techniques perform much better, but reflection-based can also be used to obtain statistical wave slope data. Second, laboratory measurements of short wind waves in three different wind wave facilities revealed some surprising new features of the wave number spectra that seem also to be valid for oceanic conditions but in contrast to existing theory. Third, a new optical system, the Reflective Stereo Slope Gauge (RSSG), was developed that measures the slope and height of large waves and statistical parameters of short waves. The feasibility of the new concept was demonstrated with measurements at Scripps Pier and the Noordwijk Research Platform. A second-generation instrument will be built for routine measurements in a follow-up project. DTIC

N93-29437# Naval Postgraduate School, Monterey, CA.
USING C-VECTOR METHOD TO DERIVE THE THREE-DIMENSIONAL CIRCULATION PATTERN NEAR THE EAST GREENLAND POLAR FRONT M.S. Thesis
Wei-Szu Li Dec. 1992 111 p
(AD-A261979) Avail: CASI HC A06/MF A02

The C-vector method is used to determine the three-dimensional pseudo-vorticity field of the East Greenland Current by using a CTD data set acquired during the 1984 Northwind cruise. The value of the ageostrophic pseudo-vorticity, the total (geostrophic and ageostrophic) pseudo vorticity, and the vertical component of the C-vector curl, Psi, can be calculated by the C-vector method. From these values the pseudo-vorticity can be investigated for the East Greenland Current. Additionally, the positive and the negative vertical motion at each level can be investigated from the Psi value. A two-cell structure with downward motion around the East Greenland Polar Front was found. The C-vector method also demonstrates that the vertical circulation induced by an anticyclonic gyre and the cross-coastal circulation generated by the surface wind can be depicted. DTIC

N93-29659# Naval Command, Control and Ocean Surveillance Center, San Diego, CA.
OCEAN AEROSOL MEASUREMENTS AND MODELS IN THE STRAITS OF FLORIDA (THE KEY-90 EXPERIMENT)
Stuart G. Gathman 1992 15 p Previously announced in IAA as A93-37103
(AD-A264777) Avail: CASI HC A03/MF A01

The Navy Oceanic Vertical Aerosol Model (NOVAM) has been under development for some time. The model showed considerable promise in its first verification test during the First International Satellite Cloud Climatology Project (ISCCP) Regional Experiment (FIRE) in the eastern Pacific. Because much of the development work on NOVAM was done in this oceanic region, the model needed to be tested in very different environments to see just how universally it could be applied to other regions. KEY-90 was an experiment carried out in the tropical waters between the Florida Keys and Cuba in July 1990 to test the model. It included investigators from the U.S., U.K., and the Netherlands. The experiment included two lidars, two aircraft, a small boat, buoys, and several shore installations. The experiment provided an excellent data base not only to test the model for the tropical water scenario, but also to further investigate the convective marine boundary layer and to enhance further modeling schemes in this region. This paper describes the optical, IR, and meteorological measurements made during KEY-90 and shows the comparison between the NOVAM model predictions and measurement. DTIC

N93-29670 American Chemical Society, Washington, DC.

CHEMISTRY OF THE ATMOSPHERE: ITS IMPACT ON GLOBAL CHANGE. CHEMRAWN 7: PERSPECTIVES AND RECOMMENDATIONS

John W. Birks, ed., Jack G. Calvert, ed., and Robert E. Sievers, ed. 1992 168 p The International Conference on the Chemistry of the Atmosphere, Baltimore, MD, 2-6 Dec. 1991 Prepared in cooperation with American Chemical Society, Washington, DC Sponsored by Agency for International Development, Washington, DC, Office of Energy and Infrastructure

(PB93-180644; AID-PN-ABM-278) Copyright Avail: Issuing Activity

Contents: An Approach to Global Climatic Change: A U.S. Perspective; Atmospheric Chemistry and Global Change: The Scientist's Viewpoint; Global Environmental Change Overview: Developing Countries; Control of Global Change: Industrial View; Control of Global Climate Alteration: Power Industry Perspective; Future Energy Sources and the Atmospheric Challenges for Research and Development; International Cooperation and Some Research Needs to Improve Our Understanding of the Chemistry of the Atmosphere; Global Change and the Role of Governments. NTIS

N93-29819# Naval Postgraduate School, Monterey, CA.

A WATER MASS ANALYSIS OF THE 1991-1992 EL NINO SIGNAL IN THE FARALLON ISLANDS REGION M.S. Thesis

Kevin A. Hays Mar. 1993 96 p

(AD-A263490) Avail: CASI HC A05/MF A01

Five hydrographic (CTD) and acoustic Doppler current profiler (ADCP) cruises were conducted in Feb., May, Aug., and late Oct./early Nov. 1991 and Feb. 1992 near the Farallon Islands off of central California in order to determine the seasonal variation of the circulation in the region. The timing of the study was such that the onset of the 1991-1992 El Nino/Southern Oscillation was directly observed in the data obtained. A detailed hydrographic analysis of the data showed single station temperature anomalies as great as 4.48 standard deviations warmer than the historical 40 year CalCOFI mean, and salinity anomalies 5.58 standard deviations fresher during Feb. 1992. The maximum anomalies for both temperature and salinity were between 100-150 m depth and within one Rossby radius (20 km) of the continental shelf break. A T-S analysis suggested that there were no large intrusions of different water mass types, and that, the anomalies resulted primarily from altered mixing processes due to thermocline/halocline depression. Strong positive sea level anomalies for the west coast of North and South America occurred simultaneously at the Equator and the far north (Gulf of Alaska) then spread from both directions towards central California. The broadening and strengthening of the Aleutian low caused onshore transport and downwelling at the Farallones site. Oceanic processes propagating northward may have occurred but could not be rigorously identified with this data set. DTIC

N93-29914# Hawaii Univ., Honolulu.

DYNAMICS OF SMALL-SCALE OCEANIC MOTIONS

Peter Muller 1992 4 p

(Contract N00014-90-J-1419)

(AD-A263582) Avail: CASI HC A01/MF A01

Goals of this research include a description and modeling of the kinematical structure and dynamical processes of oceanic motions that have horizontal scales from a few meters to a few kilometers; understanding the role that these small-scale motions play in the redistribution and mixing of the momentum, potential vorticity, heat, and salt; and to contribute to the construction of a global numerical model that will predict this redistribution and mixing. Objectives are to identify the processes that affect the kinematical and dynamical evolution of near-inertial internal gravity waves, especially those processes that can transfer energy out of near-inertial internal waves into the internal wave continuum and to simulate these processes in a numerical model. DTIC

N93-29977# Naval Postgraduate School, Monterey, CA.

ANALYSIS OF A SIMULATION OF THE SEASONAL CYCLE IN THE TROPICAL PACIFIC OCEAN IN AN EDDY-RESOLVING GLOBAL OCEAN MODEL M.S. Thesis

Lawrence J. Gordon Sep. 1992 81 p

(AD-A264007) Avail: CASI HC A05/MF A01

The multi-level, primitive equation, global ocean circulation model of Semtner and Chervin is examined for its ability to simulate the seasonal cycle in the tropical Pacific Ocean. The result of a 20-year integration of this model using annual mean wind forcing was reported in Semtner and Chervin. This was the first global eddy-resolving ocean calculation and it showed many realistic features of ocean circulation. The phase of the simulation analyzed incorporates seasonally varying wind forcing from the Hellerman and Rosenstein global data set. These wind stress values were defined on a grid with 2 deg spacing which were interpolated to the one-half degree grid points of the Semtner and Chervin model. There is no interannual variability in the wind fields of this data set. The results presented are from the fourth year of a 10-year seasonal cycle run. The upper oceanic circulation of the equatorial Pacific Ocean consists of alternating westward and eastward flows that vary seasonally in strength and extent. The eastward flows investigated are the Equatorial Undercurrent and North Equatorial Countercurrent; the westward currents are the North and South Equatorial Currents. The Equatorial Undercurrent is most intense late in the Northern Hemisphere spring and is weak in the late fall at which time the North Equatorial Countercurrent and the South Equatorial Current are most intense. This result is in agreement with observations and other model studies. DTIC

N93-30040# National Board of Waters and the Environment, Helsinki (Finland).

MODELLING THE DYNAMICS OF A LARGE SEA AREA

J. Koponen (Oulu Univ., Finland.), E. Alasaarela (Oulu Univ., Finland.), K. Lehtinen (Water and Environment District of Central Finland.), J. Sarkkula, P. Simbierowicz (Technical Research Centre of Finland, Helsinki.), Heimo Vepsa (Water and Environment District of Oulu, Finland.), and M. Viranen (Technical Research Centre of Finland, Helsinki.) 1992 91 p

(DE93-778330; VYH-Pub-7; ISBN-951-47-4284-2) Avail: CASI HC A05/MF A01

The dynamics of the Bothnian Bay was studied mainly by means of numerical models. The model results were supported by flow velocity measurements and by water quality components sampled for more than twenty years in the research area. Prior to the study an extensive review was made on the model usage abroad. The main tools of the project, 3-dimensional (3D) current and water quality models were developed in many aspects. An efficient 2D multigrid model for flow fields and an automatic grid generation program were developed for applications where good horizontal resolution is needed over large sea areas. The success in computing the surface currents was tested in several cases (oil accident, drifting of objects). As a local application of the models, the effects of different loading alternatives on the water quality off the town of Kemi was calculated. Based on model results and measurements a proposal was made to develop the water quality monitoring program. DOE

N93-30046 California Univ., San Diego.

SHEAR, STRAIN, AND THERMOHALINE VERTICAL FINE STRUCTURE IN THE UPPER OCEAN Ph.D. Thesis

Steven Paul Anderson 1992 187 p

Avail: Univ. Microfilms Order No. DA9307900

Observations of fine scale (1-100m) vertical shear, strain, and thermohaline structure are interpreted in terms of internal wave and frontal zone dynamics. The data were collected with the Marine Physical Laboratory 161 kHz Doppler sonar and a pair of CTD's. The two systems were operated from R/P FLIP for 18 days during February-March, 1990, as part of the SWAPP (35 deg N, 127 deg W) experiment. These simultaneous measurements of velocity and density provide an unique opportunity to study the vertical advection of shear layers. The observed shear variance is dominated by near inertial waves, with 35 m vertical wavelengths. These inertial waves propagate down from the mixed layer and are vertically advected by higher frequency waves. Vertical wavenumber-frequency spectra of shear and strain are examined in Eulerian (fixed depth) and semi-Lagrangian (isopycnal following) coordinates. The semi-Lagrangian shear and strain variances are more consistent with variances modeled by a linear superposition of internal waves. The p.d.f.'s of buoyancy frequency and Froude number (buoyancy normalized shear) are determined using the kinematic strain model of Pinkel and Anderson. The Froude number distribution shows good agreement with data presented and historical data. The advection of a frontal zone past the experiment site yielded detailed observations of frontal interleaving. Two vertical interleaving scales are observed. Five to fifteen meter scales appear to be double diffusively driven and are consistent with the laboratory model of Ruddick and Turner, 40 m to 60 m scales are likely determined by internal wave or sub-mesoscale frontal dynamics. The observed front appears to be in near geostrophic balance. Dissert. Abstr.

N93-30056# Woods Hole Oceanographic Inst., MA. Dept. of Marine Chemistry and Geochemistry.
FIBER OPTIC CHEMICAL SENSORS FOR CHARACTERIZING THE CARBON CYCLE IN OCEAN MARGIN REGIONS
M. D. DeGrandpre and F. L. Sayles 13 Apr. 1993 7 p
(Contract DE-FG02-92ER-61437)
(DE93-011442; DOE/ER-61437/1) Avail: CASI HC A02/MF A01

The overall objective of our DOE-Ocean Margins Programs grant is to develop a pCO2 sensor for long-term monitoring of pCO2 in the ocean margins and to establish a proving ground for the development of other chemical sensors for characterizing the carbon cycle in these regions. We have succeeded in keeping with the approximate timeline outlined in the original proposal, which, for year 1 included the following objectives: Continue sensor optimization, test response characteristics (reagent and sample flow rates, temperature), introduce position sensitive photodiode and photodiode array spectrophotometers and evaluate, develop reliable and reproducible fabrication techniques, develop sensor based on preliminary studies optimized for field measurements (minimize size and power requirements), test long-term stability of the sensor in the laboratory, determine susceptibility to fouling and corrosion. This work is summarized below along with a brief review of the sensor's operating principle. DOE

N93-30143# New South Wales Univ., Kensington (Australia).
THE IUTAM SYMPOSIUM ON BREAKING WAVES
M. L. Banner and R. H. Grimshaw 1991 402 p Symposium held in Sydney, Australia, 15-19 Jul. 1991
(Contract N00014-91-J-1538)
(AD-A264196) Avail: CASI HC A18/MF A04

The Symposium focused on water waves of all scales from capillary waves to ocean swell, but also considered internal waves and the filamentation of vorticity interfaces. Specific topics included were: (1) Fundamental theoretical studies, wave instabilities, routes to breaking; (2) Models of wave breaking; (3) Field observations, including statistical information; (4) Laboratory studies; (5) Shoaling waves, breaking waves on currents, breaking induced by the motion of a ship; (6) Consequences of waves breaking for oceanic studies, microwave remote sensing, role of breaking in air-sea fluxes, wind-wave prediction models, acoustics of wave breaking, and bubble formation; and (7) Wave breaking in industrial applications and wave forces on structures. DTIC

N93-30178 Naval Postgraduate School, Monterey, CA.
MEASUREMENTS OF OCEAN CURRENTS ACROSS THE CONTINENTAL MARGIN OFF POINT SUR, CALIFORNIA, DURING MARCH 1989 M.S. Thesis
Anthony J. Negron Mar. 1993 87 p Limited Reproducibility: More than 20% of this document may be affected by microfiche quality
(AD-A264853) Avail: CASI HC A05

Mean currents and density were measured off Point Sur, California in March 1989 using Pegasus and CTD instruments. Velocity, temperature, salinity, and density fields are examined to discern the structure of the California and Davidson currents. Velocities measured by Pegasus are compared to flow fields derived from geostrophy. The Davidson Current flows poleward at the surface in its winter configuration despite northerly winds and coastal upwelling which normally drive the flow subsurface in the summer months. DTIC

N93-30420# Naval Oceanographic Office, Bay Saint Louis, MS.
A CALIBRATION PROCEDURE FOR THE SBE 19 CONDUCTIVITY, TEMPERATURE, AND DEPTH (CTD) PROFILER
Peter A. Lessing Mar. 1993 12 p
(AD-A264435; NOO-TN-02-93) Avail: CASI HC A03/MF A01

A procedure for calibration of conductivity, temperature, and depth (CTD) sensors of SBE 19 CTD profilers is discussed. Pressure is calibrated using a linear model; temperature is calibrated using a third-order polynomial least-squares fit. A Levenberg-Marquardt nonlinear parameter estimation technique is used to model the conductivity sensor. DTIC

N93-30525# Naval Postgraduate School, Monterey, CA.
FINITE ELEMENT APPROXIMATION OF THE SHALLOW WATER EQUATIONS ON THE MASPAR
Beny Neta and Rex Thanakij 1 Apr. 1993 23 p
(AD-A264649; NPS-MA-93-014) Avail: CASI HC A03/MF A01

Here we report on development of a high order finite element code for the solution of the shallow water equations on the massively parallel computer MP-1104. We have compared the parallel code to the one available on the Amdahl serial computer. It is suggested that one uses a low order finite element to reap the benefit of the massive number of processors available. DTIC

N93-30603# Brown Univ., Providence, RI. Inst. for Brain and Neural Systems.
PRINCIPAL COMPONENTS OF NATURAL IMAGES: AN ANALYTICAL SOLUTION
Yong Liu and Harel Shouval 17 May 1993 9 p
(Contract N00014-91-J-1316)
(AD-A264800) Avail: CASI HC A02/MF A01

The structure of receptive fields in the visual cortex is believed to be shaped by unsupervised learning. A simple variant of unsupervised learning is the extraction of principal components. In this paper, we derived analytically the form of the principal components of natural images. This derivation relies on results about the covariance matrix of natural images. Our results predict both the shapes and the phases of the receptive fields. We also compared our results to numerical simulation results. Finally, the biological relevance of our results is discussed. DTIC

N93-30612# Office of Naval Research, Arlington, VA.
OCEANOGRAPHIC RESEARCH TOWERS IN EUROPEAN WATERS
Hans Dolezalek 1 Dec. 1992 27 p
(AD-A264795; ONREUR-92-7-R) Avail: CASI HC A03/MF A01

The author of this report discusses methods used to obtain in-situ measurements for scientific data in the various disciplines of oceanography and maritime meteorology. The author also points out the advantages of research towers and factors in the selection of a particular tower. Included in the report is a list of research towers which does not include temporary setups, anchored ships, oil towers temporarily used for research, and research installations on high rocks at the shore as they exist or existed near Stad in Norway and on the Crimea peninsula. DTIC

N93-30827# National Oceanic and Atmospheric Administration, Miami, FL. Atlantic Oceanographic and Meteorological Labs.
HYDROGRAPHIC OBSERVATIONS IN THE WESTERN TROPICAL AND SUBTROPICAL NORTH ATLANTIC OCEAN: ATLANTIC CLIMATE CHANGE PROGRAM (ACCP) AND WESTERN TROPICAL ATLANTIC EXPERIMENT (WESTRAX) DURING 1990
E. Johns and A. M. Wilburn Mar. 1993 109 p See also PB89-230825 and report for 1991, PB93-184778
(PB93-184760; NOAA-DR-ERL-AOML-22) Avail: CASI HC A06/MF A02

Data collected during the 1990 Atlantic Climate Change Program and the Western Tropical Atlantic Experiment were presented. The goals of the programs were to increase the understanding of the roles of the regional circulation and ocean circulation in global climate. Salinity, ocean temperature as a function of depth, and other hydrographic data were collected from shipborne platforms. NTIS

N93-30830# National Ocean Service, Rockville, MD. Coastal Monitoring and Bioeffects Div.
STANDARD AND REFERENCE MATERIALS FOR MARINE SCIENCE, THIRD EDITION

A. Y. Cantillo Aug. 1992 560 p See also PB90-172438
(PB93-185684; NOAA-TM-NOS-ORCA-68) Avail: CASI HC A24/MF A04

The third edition of the catalog of reference materials suited for use in marine science, originally compiled in 1986 for NOAA, IOC, and UNEP, is presented. The catalog lists close to 2,000 reference materials from sixteen producers and contains information about their proper use, sources, availability, and analyte concentrations. Indices are included for elements, isotopes, and organic compounds, as are cross references to CAS registry numbers, alternate names, and chemical structures of selected organic compounds. The catalog is being published independently by both NOAA and IOC/UNEP and is available from NOAA/NOS/ORCA in electronic form. NTIS

N93-30906# North Carolina State Univ., Raleigh. Dept. of Mechanical and Aerospace Engineering.
ICE-OCEAN FOUR DIMENSIONAL STRUCTURE AND DYNAMICS Annual Technical Report, 31 Mar. 1992 - 31 Mar. 1993
F. Y. Sorrell 29 Apr. 1993 4 p
(Contract N00014-90-J-4128)
(AD-A264850) Avail: CASI HC A01/MF A01

To understand the relationship among under ice morphology, ice thickness, and the structure of the oceanic boundary layer, an Autonomous Oceanographic Sampling Network is being developed. Each network consists of a base buoy and a number of Autonomous Oceanographic Vehicles (AOV's) at fixed levels. The base buoy serves as a navigation beacon, energy source, telemetry link and surface sensor platform. Each AVO functions as a subsurface sensor platform, short term data logger and programmable, navigable vessel. Development of system components capitalizes on advanced microprocessors, navigation, and communication systems developed by DoD and industry for buoy and vessel technology. The first step will be to produce an AVO that has acceptable performance as a subsurface platform and which can dock with the base buoy and conduct data exchange. DTIC

N93-31019# United Nations Educational, Scientific and Cultural Organization, Paris (France).
IOC-UNEP REVIEW MEETING ON OCEANOGRAPHIC PROCESSES OF TRANSPORT AND DISTRIBUTION OF POLLUTANTS IN THE SEA
1991 29 p Meeting of the Review IOC-United Nations Environment Programme held in Zagreb, Yugoslavia, 15 May 1991
(DE93-605070; INIS-mf-13371; CONF-9105381) Avail: CASI HC A03/MF A01 (US Sales Only)

The IOC-UNEP Review Meeting on Oceanographic Processes of Transfer and Distribution of Pollutants in the Sea was opened at the Ruder Boskovic Institute, Zagreb, Yugoslavia on Monday, 15 May 1989. Papers presented at the meeting dealt with physical and geochemical processes in sea-water and sediment in transport mixing and dispersal of pollutants. The importance of mesoscale eddies and gyres in the open sea, wind-driven currents and upwelling events in the coastal zone, and thermohaline processes in semi-enclosed bays and estuaries was recognized. There is strong evidence that non-local forcing can drive circulation in the coastal area. Concentrations, horizontal and vertical distributions, and transport of pollutants were investigated and presented for a number of coastal areas. Riverine and atmospheric inputs of different pollutants to the western Mediterranean were discussed. Reports on two on-going nationally/internationally coordinated projects (MEDMODEL, EROS 2000) were presented. Discussions during the meeting enabled an exchange of ideas between specialists in different disciplines to be made. It is expected that this will promote the future interdisciplinary approach in this field. The meeting recognized the importance of physical oceanographic studies in investigating the transfer and distribution of pollutants in the sea and in view of the importance of the interdisciplinary approach and bilateral and/or multilateral co-operation a number of recommendations were adopted. DOE

51 LIFE SCIENCES (GENERAL)

N93-28651# Massachusetts Inst. of Tech., Cambridge. Center for Environmental Health Sciences.
COMPARATIVE MUTAGENESIS OF HUMAN CELLS IN VIVO AND IN VITRO
W. G. Thilly May 1993 23 p
(Contract DE-FG02-86ER-60448)
(DE93-012269; DOE/ER-60448/T6) Avail: CASI HC A03/MF A01

This annual progress report describes advances made in combining denaturing gradient gel electrophoresis with high fidelity DNA amplification and with mismatch amplification (MAMA) along with advances in high efficiency restriction enzyme digestion of wild type sequences. Also, theoretical studies on gene mutations in oncogenesis are described. DOE

N93-28683# Joint Publications Research Service, Arlington, VA.
JPRS REPORT: SCIENCE AND TECHNOLOGY. CENTRAL EURASIA: LIFE SCIENCES
30 Mar. 1993 32 p Transl. into ENGLISH from various Russian articles
(JPRS-ULS-93-005) Avail: CASI HC A03/MF A01

Translated articles cover the following topics: aerospace medicine; agricultural science; biotechnology; environment; immunology; laser bioeffects; medicine; microbiology; physiology; public health; psychology; and radiation biology. CASI

N93-28684# Joint Publications Research Service, Arlington, VA.
JPRS REPORT: SCIENCE AND TECHNOLOGY. CENTRAL EURASIA: LIFE SCIENCES
30 Dec. 1992 65 p Transl. into ENGLISH from various Russian articles
(JPRS-ULS-92-027) Avail: CASI HC A04/MF A01

Translated articles cover the following topic: aerospace medicine; biochemistry; biotechnology; environment; epidemiology; genetics; medicine; pharmacology and toxicology; physiology; psychology; and radiation biology. CASI

N93-28848# Hunter Coll., New York, NY.
GENE TRANSCRIPTION AND ELECTROMAGNETIC FIELDS
A. S. Henderson 1992 7 p
(Contract DE-FG01-89CE-34023)
(DE93-010854; DOE/CE-34023/T1) Avail: CASI HC A02/MF A01

Our overall aim is to obtain sufficient information to allow us to ultimately determine whether ELF EM field exposure is an initiating factor in neoplastic transformation and/or if exposure can mimic characteristics of the second-step counterpart in neoplastic disease. This aim is based on our previous findings that levels of some transcripts are increased in cells exposed to EM fields. While the research is basic in nature, the ramifications have bearing on the general safety of exposure to EM fields in industrial and everyday life. A large array of diverse biological effects are reported to occur as the result of exposure to elf EM fields, suggesting that the cell response to EM fields is at a basic level, presumably initiated by molecular and/or biophysical events at the cell membrane. The hypothesized route is a signal transduction pathway involving membrane calcium fluxes. Information flow resulting from signal transduction can mediate the induction of regulatory factors in the cell, and directly affect how transcription is regulated. DOE

N93-28890# Oak Ridge National Lab., TN.
INTRODUCTIONS TO THE PROCEEDINGS OF THE FOURTEENTH SYMPOSIUM ON BIOTECHNOLOGY FOR FUELS AND CHEMICALS
J. Woodward, C. E. Wyman (Midwest Research Inst., Golden, CO.), and B. J. Goodman (Midwest Research Inst., Golden, CO.) 1992 9 p Symposium held in Gatlinburg, TN, 11-15 May 1992
(Contracts DE-AC05-84OR-21400; DE-AC02-83CH-10093)
(DE93-006235; CONF-920508-6) Avail: CASI HC A02/MF A01

This report is a collection of introductions to sessions made at the Fourteenth Symposium on Biotechnology for Fuels and Chemicals. DOE

N93-28952*# National Aeronautics and Space Administration. Marshall Space Flight Center, Huntsville, AL.
AMINO ACID SEQUENCES FOR THE BINDING REGIONS IN SERUM ALBUMIN PROTEINS Patent Application
Daniel C. Carter, inventor (to NASA) 1 Mar. 1993 17 p
(NASA-Case-MFS-28402-1; NAS 1.71:MFS-28402-1; US-Patent-Appl-SN-024547) Avail: CASI HC A03/MF A01

In accordance with the present invention, biologically active protein fragments can be constructed which contain only those specific portions of the serum albumin family of proteins such as regions known as subdomains IIA and IIIA which are primarily responsible for the binding properties of the serum albumins. The artificial serums that can be prepared from these biologically active protein fragments are advantageous in that they can be produced much more easily than serums containing the whole albumin, yet still retain all or most of the original binding potential of the full albumin proteins. In addition, since the protein fragment serums of the present invention can be made from non-natural sources using conventional recombinant DNA techniques, they are far safer than serums containing natural albumin because they do not carry the potentially harmful viruses and other contaminants that will be found in the natural substances.
NASA

N93-29174*# National Aeronautics and Space Administration. Marshall Space Flight Center, Huntsville, AL.
PROCESS FOR SELECTIVELY RECOVERING ALGAE AND PROTOZOA Patent Application
David A. Noever, inventor (to NASA) (Universities Space Research Association, Huntsville, AL.) 12 Apr. 1993 8 p
(NASA-Case-MFS-26124-1-NPO; NAS 1.71:MFS-26124-1-NPO; US-Patent-Appl-SN-045142) Avail: CASI HC A02/MF A01

A process is presented for selectively recovering swimming microorganisms from a liquid wherein the liquid is placed in a container and the container is rotated such that the coriolis force and the swimming activity of the microorganisms cause the microorganisms to concentrate in rings at different radii from the axis of rotation of the liquid. Liquid is withdrawn from the container at different distances from the axis of rotation of the container to selectively recover the microorganisms. NASA

N93-29181# Ohio State Univ., Columbus. Research Foundation.
REGULATION OF ALTERNATIVE CO2 FIXATION PATHWAYS IN PROCARYOTIC AND EUCARYOTIC PHOTOSYNTHETIC ORGANISMS
1992 3 p
(Contract DE-FG02-91ER-20033)
(DE93-012109; DOE/ER-20033/1) Avail: CASI HC A01/MF A01

The major goal of this project is to determine how microorganisms regulate the assimilation of CO2 via pathways alternative to the usual Calvin reductive pentose phosphate scheme. In particular, we are interested in the molecular basis for switches in CO2 metabolic paths. Several earlier studies had indicated that purple nonsulfur photosynthetic bacteria assimilate significant amounts of CO2 via alternative non-Calvin routes. We have deleted the gene that encodes. RubisCo (ribulose bisphosphate carboxylase/oxygenase) in both the Rhodobacter sphaeroids and Rhodospirillum rubrum. The R. sphaeroides RubisCO deletion strain (strain 16) could not grow under photoheterotrophic conditions with malate as electron donor and CO2 as the electron acceptor; however the R. rub RubisCO deletion strain (strain I-19) could. Over the past year we have sought to physiologically characterize strain 16PHC. We found that, 16PHC exhibited rates of whole-cell CO2 fixation which were significantly higher than strain 16. Strain 16PHC could not grow photolithoautotrophically in a CO2 atmosphere; however, CO2 fixation catalyzed by photoheterotrophically grown 16PHC was repressed by the addition of DMSO. Likewise, we found that cells initially grown in the presence of DMSO could induce the CO2 fixation system when DMSO was removed. Thus, these results suggested that both PHC and I-19 could be used to study alternative CO2 fixation reactions and their significance in R. sphaexoides and R. rubrum. DOE

N93-29216*# Texas A&M Univ., College Station. Research Foundation.
GROWING WHEAT TO MATURITY IN REDUCED GAS PRESSURES Final Report, 1 Apr. 1992 - 30 Jun. 1993
Edward J. Rykiel, Jr., Malcolm C. Drew, and Brad D. Etter 30 Jun. 1993 70 p
(Grant NAG9-582)
(NASA-CR-193245; NAS 1.26:193245) Avail: CASI HC A04/MF A01

The main objective of this project was to determine assimilation of CO2 and efficiency of water use in wheat grown to maturity in a low pressure total gas pressure environment. A functional test of the low pressure plant growth chamber system was accomplished in February and March of 1993 wherein this objective was partially achieved. Plants were grown to maturity in the chambers. Data were actively collected during the first 29 days. The plants were allowed to maintain themselves at the CO2 compensation point until day 45 of the study at which point active atmospheric regulation was resumed. This provided data at the vegetative and reproductive stages of the life cycle of the plants. However, this information may not be representative of the performance of the plants due to the loss of low pressure on a number of days during the study, which affected the plants by changing the pressure potential of the tissues. The performance of the system will be discussed on a component by component basis. The maintenance of the plants at the CO2 compensation point was driven by the failure of the computer program operating the system. The software problems that arose during the functional test have since been corrected. Results from the functional test also indicated that the plants were not receiving adequate light and nutrients. The growth chambers have been relocated and the growth room modified to compensate for these deficiencies. Derived from text

N93-29274# European Space Agency, Paris (France).
PHOTOBIOLOGICAL INVESTIGATIONS ON SPORES OF STREPTOMYCES GRISEUS
Birgit Keller (Deutsche Forschungsanstalt fuer Luft- und Raumfahrt, Cologne, Germany.) Nov. 1992 118 p Transl. into ENGLISH of Photobiologische Untersuchungen an Sporen von Streptomyces griseus (Cologne, Germany, DLR) Mar. 1991 p 1-111 Original language document was announced as N91-32748
(ESA-TT-1269; DLR-FB-91-14; ETN-93-93715) Avail: CASI HC A06/MF A02; Original German version available from DLR, Wissenschaftliches Berichtswesen, VB-PL-DO, Postfach 90 60 58, 5000 Cologne, Germany, HC

Ultraviolet action spectra of inactivation were compared between wet and dry state spores of the Streptomyces griseus. In vacuum, the spores are more resistant to UV by a factor of 2 than under wet conditions. Their photoreactivability is reduced. The cross sections for induction of DNA (Deoxyribonucleic Acid) double strand breaks and for inactivation show similar dependence on wavelengths. ESA

N93-29915# Cornell Univ., Ithaca, NY.
CENTER OF EXCELLENCE IN BIOTECHNOLOGY (RESEARCH) Final Report, 22 Dec. 1986 - 21 Dec. 1992
L. Jelinski and Milton Zaitlin Mar. 1993 32 p
(Contract DAAL03-87-K-0004)
(AD-A263598; ARO-24629.68-LS-UIR) Avail: CASI HC A03/MF A01

The ARO Center of Excellence in Biotechnology was established within the Cornell University Biotechnology Program in 1986. The research focus of the Center was protein structure and function, with special emphasis on enzymes and receptors. Research projects funded through the Center represented a multidisciplinary attack on the molecular basis of how proteins and enzymes work, how energy and enzymic processes are coupled through cell membranes, how membrane receptors are used to transmit signals to the cell, and how signals are transmitted in the nervous system. The final report summarizes the results of the research. DTIC

N93-30483# Sandia National Labs., Albuquerque, NM.
A ROBUST MODEL FOR FINDING OPTIMAL EVOLUTIONARY TREES
M. Farach (Rutgers - The State Univ., Piscataway, NJ.), S. Kannan (Arizona Univ., Tucson.), and T. Warnow 1993 13 p Presented at the Association for Computing Machinery Symposium on the Theory of Computing, San Diego, CA, May 1993
(Contract DE-AC04-76DP-00789)
(DE93-010682; SAND-93-0361C; CONF-9305153-2) Avail: CASI HC A03/MF A01

Constructing evolutionary trees for species sets is a fundamental problem in biology. One of the standard models assumes the ability to compute distances between every pair of species and seeks to find an edge-weighted tree T in which the distance d(sub ij)(exp T) in the tree between the leaves of T corresponding to the species i and j exactly equals the observed distance, d(exp ij). When such a tree exists, this is expressed in the biological literature by saying that the distance function or matrix is additive, and trees can be constructed from additive distance matrices in O(n(exp 2)) time. Real distance data is hardly ever additive, and we therefore need methods (such as approximation algorithms with guaranteed error bounds) for handling such data. In this paper, we present several natural and realistic ways of modeling the inaccuracies in the distance data. In one model, we assume that we have upper and lower bounds for the distances between pairs of species and try to find an additive distance matrix between these bounds. In a second model, we are given a partial matrix and asked to find if we can fill in the unspecified entries in order to make the entire matrix additive. For both of these models, we also consider a more restrictive problem of finding a matrix that fits a tree which is not only additive but also ultrametric. Ultrametric matrices correspond to trees which can be rooted so that the distance from the root to any leaf is the same. Ultrametric matrices are desirable in biology since the trees then indicate evolutionary time. We give polynomial time algorithms for some of the problems while showing others to be NP-Complete. We also consider various ways of 'fitting' a given distance matrix to a tree in order to minimize various criteria of error in the fit. For most criteria this optimization problem turns out to be NP-Hard, while we do get polynomial time algorithms for some. DOE

N93-30594# Wake Forest Univ., Winston-Salem, NC. Bowman Gray School of Medicine.

MULTIPLE NEURON RECORDING IN THE HIPPOCAMPUS OF FREELY MOVING ANIMALS Annual Report, 1 Dec. 1991 - 30 Nov. 1992

Sam A. Deadwyler 30 Mar. 1993 6 p
(Grant AF-AFOSR-0092-90)
(AD-A264807; BGSM-PP-92-001; AFOSR-93-0285TR) Avail: CASI HC A02/MF A01

Progress has been significant over the previous year on the development of multineuronal recording and systems for analysis of the multineuronal data. This was a primary objective of the three laboratory consortium, and it has been a principle focus of the research efforts. The multitasking computer system has been in operation in all three laboratories this past year, as well as the DSP-based multineuron spike-sorter and the associated software interface for neural spike discrimination. Much of the research effort in the past year has been directed toward implementing the spike-sorter system, collecting multineuron data, and developing the analysis strategies. In addition, studies using the multineuron data acquisition have revealed new relationships between the behavioral events in the DMTS and patterns of simultaneously active neurons in the hippocampus. The following report will summarize these and other accomplishments in the third year of the award. DTIC

N93-30665*# Woods Hole Oceanographic Inst., MA.

MARINE MICROBIAL PRODUCTION OF DIMETHYLSULFIDE FROM DISSOLVED DIMETHYLSULFONIOPROPIONATE Ph.D. Thesis

Kathleen M. Ledyard Feb. 1993 228 p
(Grants NAGw-606; NSF OCE-90-2532)
(NASA-CR-193278; NAS 1.26:193278; AD-A264794; WHOI-93-07) Avail: CASI HC A11/MF A03

Dimethylsulfide (DMS) plays a central role in the transfer of sulfur from the ocean to the atmosphere and ultimately to land. The most abundant volatile organosulfur compound in seawater, DMS is believed to account for the bulk of the sea-to-air biogenic sulfur flux. DMS has also been implicated as the major precursor of submicron-sized sulfate aerosol over the ocean. This aerosol acts as an effective site for cloud droplet condensation suggesting a possibly important role for DMS in marine cloud formation. In the ocean, the precursor of DMS is presumed to be the zwitterionic sulfonium compound dimethylsulfoniopropionate (DMSP), a common osmoticum in certain classes of marine algae. While some algae can cleave DMSP intracellularly to form DMS, correlation of DMS concentrations with indicators of algal productivity on a local scale is poor. This thesis focuses on an alternative pathway of DMS formation: microbial cleavage of dissolved (extracellular) DMSP. In laboratory studies, bacteria able to cleave DMSP to form DMS were isolated from seawater by a DMSP enrichment technique, and the kinetics of DMSP uptake and DMS production were examined closely in pure cultures of a bacterial isolate from the Sargasso Sea. The isolate could grow with both DMSP and acrylic acid, one of the products of DMSP cleavage, as the sole source of carbon and energy, and the enzyme catalyzing DMSP cleavage appeared to be induced by both of these compounds. Kinetic parameters were estimated for DMSP uptake and cleavage by whole cells. Comparison of the 16S rRNA sequence of this isolate with that of known eubacteria showed that it was most closely related to Erythrobacter longus, an aerobic, bacteriochlorophyll-containing member of the alpha proteobacteria. DTIC

N93-30818# Naval Medical Research Inst., Bethesda, MD.

AN ASSESSMENT OF PERIPHERAL NERVE DAMAGE IN THE RAT FOLLOWING NON-FREEZING COLD EXPOSURE: AN ELECTROPHYSIOLOGICAL AND HISTOPATHOLOGICAL EXAMINATION Technical Report, Jan. 1991 - Jan. 1992

David Shurtleff, Roger W. Gilliatt, John R. Thomas, and G. H. Pezeshkpour 20 Jan. 1993 19 p
(AD-A264293; NMRI-93-1) Avail: CASI HC A03/MF A01

The effect of exposure to non-freezing cold temperature on peripheral nerve was studied in vivo. Rats' tails and a portion of their lower backs were submerged in 1 C water for either 10 or 12 hours. Changes in evoked ascending nerve action potentials, and muscle action potentials in the rat tail and lumbar spine, were studied periodically over a three week period following cold exposure. In addition, ventral caudal nerves were excised 27 days following cold exposure and histopathology was performed. Electrophysiological analysis indicated initial nerve damage appeared to be just below the surface of the water, and later, in the first week after exposure, Wallerian degeneration occurred. Histopathological analysis revealed damage to the large myelinated fibers and capillaries within the fascicle following cold exposure. These results further validate the use of the rat tail as a model for non-freezing cold injury (NFCI) and suggest that the injury's etiology is multifaceted, which may require a variety of strategies and interventions to prevent its occurrence. DTIC

N93-29702*# Oklahoma State Univ., Stillwater.

FINAL RESULTS OF SPACE EXPOSED EXPERIMENT DEVELOPED FOR STUDENTS

Doris K. Grigsby *In* NASA. Langley Research Center, LDEF: 69 Months in Space. Part 4: Second Post-Retrieval Symposium Apr. 1993 p 1479-1492 (For primary document see N93-29682 11-99)
Avail: CASI HC A03/MF A03; 2 functional color pages

N93-29703*# Park Seed Co., Inc., Greenwood, SC.

CONTINUED RESULTS OF THE SEEDS IN SPACE EXPERIMENT

Jim A. Alston *In* NASA. Langley Research Center, LDEF: 69 Months in Space. Part 4: Second Post-Retrieval Symposium Apr. 1993 p 1493-1497 (For primary document see N93-29682 11-99)
Avail: CASI HC A01/MF A03; 2 functional color pages

52 AEROSPACE MEDICINE

Includes physiological factors; biological effects of radiation; and effects of weightlessness on man and animals.

N93-28469# Technische Univ., Berlin (Germany). Fachbereich Informatik.

DOKMA: A DOCUMENT ORIENTED COMMUNICATION MODEL FOR MEDICAL APPLICATIONS AS A BASIS OF A ROLE SYSTEM IN THE MEDICAL FIELD Ph.D. Thesis [DOKMA: EIN DOKUMENTENORIENTIERTES KOMMUNIKATIONSMODELL FUER MEDIZINISCHE ANWENDUNGEN ALS BASIS FUER EIN ROLLENSYSTEM IM MEDIZINISCHEN UMFELD]

Christian Gayda 1992 248 p In GERMAN
(ETN-93-93799) Avail: CASI HC A11/MF A03

Starting with an abstract communication model that examines communication aspects in general, the document oriented communication model for medical applications is developed. It relies on a transfer model. The requirements towards this transfer model are defined by means of the document oriented communication model for medical applications. The communication model itself has to fulfill three requirements. A specification phase has to be supported by this model. Furthermore, it should constitute a kind of reference model for discussion purposes and it must support a verification phase. In order to reach these goals within the communication model for medical applications, the related problems concerning document oriented communication are assigned to layers that are put in relation to each other. The integration and communication of patient data by means of computers imply special requirements on data security. Therefore, the document oriented communication model for medical applications takes these aspects into consideration within a security of roles. A second goal of this model is to support the flow of documents. The description of the role model and its implementation (the role system) constitutes the second focal point of this thesis. ESA

N93-28758# Chemical Warfare/Chemical and Biological Defense Information Analysis Center, Edgewood, MD.
EVALUATION AND OPTIMIZATION OF A FLEXIBLE FILTRATION SYSTEM FOR RESPIRATORY PROTECTION SYSTEM 21 Final Report
K. C. Hofacre, R. L. Markham, and V. M. Northrup Feb. 1993 43 p
(Contract DLA900-86-C-2045)
(AD-A262467; CBIAC-SS-373) Avail: CASI HC A03/MF A01

Current filter elements for the M40 series of respirators are housed in rigid, metal canisters that contain media for aerosol filtration, and adsorption of gases or vapors. The filtration media is often pleated for increased surface area. Certain harmful gases are removed by adsorption to activated carbon that has been treated with hexavalent chromium or zinc metal cations in a process known as whetlerization. Whetlerization provides active sites to chemisorb certain poison gases. The carbon is generally present as a coarse granular bed, but can also be present in a powder form incorporated in a fabric, as in the M13A2 filter element. DTIC

N93-28759# California Univ., San Diego, La Jolla. Dept. of Chemistry.
WOUND HEALING AND CONNECTIVE TISSUE METABOLISM: THE ROLE OF HYPERBARIC OXYGEN THERAPY Final Report, 1 Jul. 1991 - 30 Jun. 1992
Elvin Harper Jun. 1992 6 p
(Grant AF-AFOSR-0413-91)
(AD-A262483; AFOSR-93-0202TR) Avail: CASI HC A02/MF A01

The effect of hyperbaric oxygen on wound healing by the following growth promoting factors is discussed: Epidermal growth factor (EGF), platelet derived growth factor (PDGF), and transforming growth factor B (TGFB). These compounds are of particular interest since they have been reported to increase collagenase secretion. EGF when applied directly to skin increased the rate of healing by 100%. DTIC

N93-28835# Department of Energy, Washington, DC. Medical Applications and Biophysical Research Div.
PROCEEDINGS OF A WORKSHOP ON MOLECULAR NUCLEAR MEDICINE
R. C. Reba, ed. 1992 161 p Workshop held in Washington, DC, 22-23 Jan. 1992
(DE93-010828; CONF-920113-7) Avail: CASI HC A08/MF A02

The Office of Health and Environmental Research (OHER) of the Department of Energy (DOE) has increased the emphasis on research in structural biology and molecular biology. The department has increased support substantially in the area of basic molecular and structural biology research. To exploit the advances in these fields, OHER has sought to apply those advances in their other areas of responsibility, e.g., health effects research, environmental biology, and, in particular, nuclear medicine. The applications of biotechnology have contributed greatly to the productive research efforts of molecular biology. These techniques include gene manipulation for targeted gene delivery; characterization of molecular probes for hormone, tumor, and neuroreceptors; the receptor-agonist/antagonist binding interactions; studies of mechanisms of cellular communication; and the development of in vitro diagnostics such as molecular probes for studying the aging process and patients with mental disorders, cancer, and atherosclerosis. The importance of this work is the reasonable expectation that mainly, through an appreciation of the molecular basis of disease, will the most effective and rapid progress be made toward understanding, identifying, solving, and preventing specific disease processes. Critical questions arising before and during the workshop are how the following technologies can be applied in a practical clinical research or patient management setting: the recombinant DNA methodology, the technology of engineered monoclonal antibodies, the new methods for protein production and purification, and the production of transgenic animals. DOE

N93-28939# Defence and Civil Inst. of Environmental Medicine, Downsview (Ontario).
INFLUENCE OF THE COLD BUSTER (TM) SPORTS BAR ON HEAT DEBT, MOBILIZATION AND OXIDATION OF ENERGY SUBSTRATES
A. L. Vallerand, I. F. Schmegner, and I. Jacobs Dec. 1992 30 p
(AD-A262762; DCIEM-92-60) Avail: CASI HC A03/MF A01

In a recent study, we have shown that the commercially available Cold Buster(TM) Sports bar, purported to improve cold resistance, did not do so in our subjects exposed to a relatively severe cold test. One possible explanation for our conflicting results is that our metabolic rate (M) was too high for the possibly small thermogenic effect of the bar to be measurable. The goal of this study was therefore to re-evaluate, under milder conditions, the influence of the Cold Buster(TM) on heat balance (heat debt = heat production - heat losses) and body temperatures. Eight semi-nude fasted subjects were exposed to the cold (3h at rest, 10 C, less than 0.4 m/s wind) on two occasions following the ingestion of either a placebo (100 ml water) or a Cold Buster(TM) (all feedings at min 0 and 90). As a result of the cold, M, dry heat losses and heat debt (S) increased whereas mean skin temperature decreased (P less than 0.05). Rectal temperature remained unchanged due to the mild cold. In all of the above parameters, there were no differences between treatments. Ingestion of the Colt Buster(TM) significantly increased carbohydrate oxidation compared to the placebo. However, this was without impact on M, since it occurred entirely at the expense of fat oxidation. Interestingly, the Cold Buster(TM) increased plasma glucose and insulin levels 2h into the cold. This secretion of insulin seems to have blunted lipid mobilization since it significatly reduced plasma free fatty acids levels. The result confirm previous data where the ingestion of the Cold Buster(TM) Sports bar did not alter heat production, heat losses, heat debt or even body temperatures, and extended these observations to a mild cold stress. DTIC

N93-29041*# Mount Sinai School of Medicine, New York, NY. Dept. of Neurology.
NASA SUPPORTING STUDIES FOR MICROGRAVITY RESEARCH ON EYE MOVEMENTS Final Technical Report, 1 Jan. - 31 Dec. 1990
Bernard Cohen 31 Dec. 1990 6 p
(Grant NAGw-1998)
(NASA-CR-193233; NAS 1.26:193233) Avail: CASI HC A02/MF A01

The purpose of the work on this project was to provide support for ground-based studies on the effects of gravity on eye movements. The effects of microgravity on the optokinetic eye movements of humans are investigated. OKN was induced by having subjects watch 3.3 deg stripes moving at 35 deg/s for 45 s in a binocular, head-fixed apparatus. The field (hor., 88 deg; vert., 72 deg), was rotated about axes that were upright or tilted 45 deg or 90 deg. The head was upright or tilted 45 deg on the body. Head-horizontal (yaw axis) and head-vertical (pitch axis) components of OKN were recorded with electro-oculography (EOG). Slow phase velocity vectors were determined relative to gravity. With the head upright, the axis of eye rotation during yaw axis OKN was coincident with the stimulus axis and the spatial vertical. With the head tilted 45 deg on the body, a persistent vertical component of eye velocity developed during yaw axis stimulation, and there was an average shift of the axis of eye rotation toward the spatial vertical of approximately 18 deg in six subjects. During oblique optokinetic stimulation with the head upright, the axis of eye rotation shifted 12 deg toward the spatial vertical. When the head was tilted, the axis of eye rotation rotated to the other side of the spatial vertical by 5.4 deg during the same oblique stimulation. This counter-rotation of the axis of eye rotation is similar to the 'Muller (E) effect', in which the perception of the upright counter-rotates to the opposite side of the spatial vertical when subjects are tilted in darkness. The data were simulated by a model of OKN. Despite the short OKAN time constants, strong horizontal to vertical cross-coupling was produced if the horizontal and vertical time constants were in proper ratio, and there was no suppression of nystagmus orthogonal to the stimulus direction. This shows that the spatial orientation of OKN can be due to a restructuring of the system matrix of velocity storage as a function of gravity. It is concluded that although human OKAN is weak, velocity storage orients the slow phase velocity of OKN towards the spatial vertical. Author (revised)

N93-29199# Utah Univ., Salt Lake City. Ergonomics Lab.
SUDDEN LOADING AND FATIGUE EFFECTS ON THE HUMAN SPINE Final Report

Daniel R. Baker and Donald S. Bloswick 16 Nov. 1992 54 p
(Grant PHS-R03-OH0-2821-01)
(PB93-167526) Avail: CASI HC A04/MF A01

The effects of fatigue and load magnitude on the in vivo torso response of human subjects to a sudden load were analyzed in six individuals. Parameter identification of the human spine was performed within a sudden loading, short duration, high intensity fatigue paradigm. The findings indicated that fatigue is an important factor under conditions of sudden loading. The fatigued subject does not respond in the same way as he does when not tired. It is suggested that a higher degree of injury would be expected under conditions of fatigue. Most of the time the worker is not at the point of fatigue, and performance of certain tasks is usually practiced under conditions which are better than those prevalent under conditions of fatigue. Two reports are being produced from the data gathered in the study. The first will examine the electromyographic responses of the individual and compare them to the dynamics of the torso. The second study will mathematically study the compression levels expected as a result of earlier work. The authors suggest that their most important finding was the ability to mathematically model a complex response of the torso to a sudden load with a simple second order linear model. The study demonstrated that short duration, high intensity muscular fatigue changes the way in which the torso responds to a sudden load. NTIS

N93-29400# Air Force Systems Command, Wright-Patterson AFB, OH. Armstrong Lab.

A TUTORIAL ON EXIT PUPILS AND EYE ROTATION WITH VIRTUAL IMAGE OPTICAL DISPLAYS Interim Report, Aug. 1991 - Sep. 1992

Herschel C. Self Dec. 1992 37 p
(AD-A262399; AL-TR-1993-0010) Avail: CASI HC A03/MF A01

Exit pupils of virtual image optical displays and eye entrance pupils and how their sizes and relative positions influence light input to the eye are discussed. Equations based on simplifying assumptions about the eye and its rotational behavior are derived and graphed to describe the position of the center and edge of the eye entrance pupil after eye rotation and for the rotation angles at which exit pupil vignetting begins and at which vignetting is total. The graphs and equations are useful for descriptive purposes and for practical application in choosing, specifying or designing virtual image optical display devices. Worked out numerical examples are supplied to further aid in understanding pupils and eye rotation and how they interact. The reader is not required to have a background in optics or in college mathematics. DTIC

N93-29421# Massachusetts Inst. of Tech., Cambridge.

PROGRAMMABLE INTERACTIVE SYSTEM FOR COCHLEAR IMPLANT ELECTRODE STIMULATION Technical Report

Joseph Tierney, Marc A. Zissman, Donald K. Eddington, and William M. Rabinowitz 12 Jan. 1993 51 p
(Contract F19628-90-C-0002)
(AD-A262558; TR-970; ESC-TR-92-139) Avail: CASI HC A04/MF A01

The aim of this research, which was performed as a Lincoln Laboratory Innovative Research Program (IRP) project, was to apply advanced digital speech and signal-processing techniques toward improving cochlear implant electrode simulators. By providing a flexible stimulator whose function could be tuned depending on the subject's residual auditory nerves and the efficiency of the implant's coupling to those nerves, it was hypothesized that the subject's speech reception could be improved. The approach to providing these new and improved electrode stimulators included the design of a laboratory signal processor used for interactive testing of new algorithms with implant subjects. This Programmable Interactive System for Cochlear Implant Electrode Stimulation (PISCES) was designed, built, and tested at Lincoln Laboratory and then delivered to the Massachusetts Eye and Ear Infirmary (MEEI) Cochlear Implant Research Laboratory (CIRL). In collaboration with researchers at MEEI CIRL and MIT Research Laboratory of Electronics (RLE), new algorithms run on PISCES resulted in substantial improvements in subject speech reception relative to that with their current implant stimulators. These results were obtained as a result of interactive algorithm adjustment at the clinic, which demonstrated the importance of a flexible signal processor. DTIC

N93-29502*# National Aeronautics and Space Administration. Lyndon B. Johnson Space Center, Houston, TX.

PHARMACOKINETICS AND PHARMACODYNAMICS IN SPACE

Lakshmi Putcha and Nitza M. Cintron Apr. 1990 31 p Workshop held in Houston, TX, 29-30 Aug. 1988
(NASA-CP-10048; NAS 1.55:10048) Avail: CASI HC A03/MF A01

The Pharmacokinetics and Pharmacodynamics Panel met on 29-30 Aug. 1988 at the Lunar and Planetary Institute in Houston, Texas to discuss pharmacokinetic and pharmacodynamic implications of space flight and make recommendations for operational and research strategies. Based on the knowledge available on the physiological changes that occur during space flight, the dependence of pharmacokinetics on physiological factors, and the therapeutic requirements for future space missions, the panel made several recommendations for research. It was suggested that using medications available with a large (wide) therapeutic window will avoid unforeseen therapeutic consequences during flight. The sequence for conducting research was outlined as follows: (1) identify ground-based simulation models (e.g., antiorthostatic bed rest) for conducting pharmacokinetic and pharmacodynamic research; (2) estimate parametric changes in these models using pharmacologic agents that have different pharmacokinetic characteristics and a narrow therapeutic index; (3) verify these findings during flight; and (4) develop and identify appropriate and effective drug delivery systems, dosage forms, and regimens. The panel recommended gaining a thorough understanding of the pharmacokinetic deviations of medications that have a narrow therapeutic index (e.g. cardiovascular drugs and sedative hypnotics) in order to ensure safe and effective treatment during flight with these agents. It was also suggested that basic information on physiological factors such as organ blood flow, protein composition and binding, tissue distribution, and metabolism by hepatic enzymes must be accumulated by conducting ground-based animal and human studies using models of weightlessness. This information will be useful to construct and identify physiologically based pharmacokinetic models that can provide valuable information on the pharmacodynamic consequences of space flight and aid in identifying appropriate therapeutic regimens. Author (revised)

N93-29509# Biotronics Technologies, Inc., Waukesha, WI.

TRANSCUTANEOUS ANALYTE MEASURING METHODS Quarterly Progress Report No. 6, Jan. - Mar. 1993

Kenneth J. Schlager 2 Apr. 1993 15 p
(Contract N00014-91-C-0190)
(AD-A262861) Avail: CASI HC A03/MF A01

The major objective of this quarter was to complete all patient data collection at Froedtert Lutheran Memorial Hospital (Medical College of Wisconsin), finalize all TAMM algorithms, integrate the new diagnostic software into the NIR-800 Array Analyzer and deliver the instrument to the Naval Health Research Center (NHRC) in San Diego, California. All of the above work activities were completed, and the NIR-800 was shipped to NHRC on March 9, 1993. Prior to shipment, test set runs on all 9 of the analytes were completed with the results shown in Table 1. All of the electrolytes recorded average errors of less than 6% of mean value with all except bicarbonate less than 4%. The reliable operating range of the system for each analyte is also indicated in Table 1. This limited range results from the lack of sufficient extreme values for all analytes except glucose. Even glucose by these standards is marginal because only a few values over 150 mg/dl were obtained during preclinical testing. Extension of this range to include abnormal values for each analyte will require additional data collection in an Intensive Care Unit (ICU) where extreme analyte concentration values are common. Data on 531 patients have been collected of which 514 were acceptable. Best results were obtained using the final 73 patients for whom data collection instrumentation and procedures were optimized. A description of the preliminary field instrument design is included in this report. DTIC

N93-29620# East Carolina Univ., Greenville, NC. School of Medicine.

EVALUATION OF DRIED STORAGE OF PLATELETS FOR TRANSFUSION: PHYSIOLOGIC INTEGRITY AND HEMOSTATIC FUNCTIONALITY Annual Report No. 1, 1 Feb. 1992 - 31 Jan. 1993

Arthur P. Bode, Majorie S. Read, and Robert L. Reddick 31 Jan. 1993 9 p
(Contract N00014-92-J-1244)
(AD-A263240) Avail: CASI HC A02/MF A01

The intramural collaboration at East Carolina University to study metabolic activity of lyophilized platelets was cancelled after six months due to departure of the investigator. This study will now be carried out by colleagues at the American Red Cross Research Laboratory in Norfolk, VA. Samples of various platelet preparations were sent and analysis is underway. The major objectives achieved at ECU in the first year were initiation of long-term storage studies of the standard lyophilized platelet preparation, set-up of Baumgartner chamber methodology for assessment of platelet adhesiveness, and further development of permanganate-based stabilization protocols before platelet lyophilization. A long-term study of the stability of surface receptors on lyophilized platelets stored under various conditions (desiccated, at room temperature or 4 deg C, or frozen at -70 deg C) was initiated in June 1992, with a single large batch of paraformaldehyde-treated dried human platelets. At one month intervals, sample vials from each storage environment were reconstituted and assayed by flow cytometry with monoclonal antibody probes to the major surface glycoproteins. The only signigicant finding thus far is a decrease in binding of MoAb SZ-1 to the dried platelets stored at room temperature. DTIC

N93-29651*# National Aeronautics and Space Administration. Lyndon B. Johnson Space Center, Houston, TX.

ISSUES ON HUMAN ACCELERATION TOLERANCE AFTER LONG-DURATION SPACE FLIGHTS

K. Vasantha Kumar (Krug Life Sciences, Inc., Houston, TX.) and William T. Norfleet Oct. 1992 55 p

(Contract NAS9-18492)

(NASA-TM-104753; S-686; NAS 1.15:104753) Avail: CASI HC A04/MF A01

This report reviewed the literature on human tolerance to acceleration at 1 G and changes in tolerance after exposure to hypogravic fields. It was found that human tolerance decreased after exposure to hypokinetic and hypogravic fields, but the magnitude of such reduction ranged from 0 to 30 percent for plateau G forces and 30 to 70 percent for time tolerance on sustained G forces. A logistic regression model of the probability of individuals with 25 percent reduction in +Gz tolerance after 1 to 41 days of hypogravic exposures was constructed. The estimated values from the model showed a good correlation with the observed data. A brief review of the need for in-flight centrifuge during long-duration missions was also presented. Review of the available data showed that the use of countermeasures (such as anti-G suits, periodic acceleration, and exercise) reduced the decrement in acceleration tolerance after long-duration space flights. Areas of further research include quantification of the effect of countermeasures on tolerance, and methods to augment tolerance during and after exposures to hypogravic fields. Such data are essential for planning long-duration human missions. Author (revised)

N93-29820# Colorado Univ., Denver. School of Medicine.

BETA-ADRENERGIC BLOCKADE AND LACTATE METABOLISM DURING EXERCISE AT HIGH ALTITUDE Final Report, 10 Jun. 1991 - 9 Dec. 1992

John T. Reeves 28 Jan. 1993 6 p

(Contract DAMD17-91-C-1112; DA Proj. 3M1-61102-BS-15)

(AD-A263544) Avail: CASI HC A02/MF A01

The primary thrust of this contract was to perform high altitude research on Pikes Peak Colorado (with the sea level phase to be done in Palo Alto) in the summer of 1991. The work was to test the hypothesis that the adreno-sympathetic system mediated many of the adaptations to high altitude, particularly the metabolic changes. DTIC

N93-30153# Arizona Univ., Tucson.

THE CHRONIC EFFECTS OF JP-8 JET FUEL EXPOSURE ON THE LUNGS Annual Technical Report, 1 Apr. 1992 - 1 Apr. 1993

Mark L. Witten 13 Apr. 1993 12 p

(Grant AF-AFOSR-0199-91)

(AD-A264162; AFOSR-93-0302TR) Avail: CASI HC A03/MF A01

The second year of this project concentrated on using a 'high' dose of JP-8 jet fuel in our exposure regimen. We selected a target dose of approximately 1,000 mg/cu m based on a published epidemiological study conducted at NATO Air Force Bases that demonstrated jet fuel concentrations as high as 1,020 mg/cu m during refueling operations. The rats in the 'high' dose studies were exposed to an average of 813.8 Mg/cu m for one hour/day for 7 and 28 days. In our previous work, a 'low' dose concentration of JP-8 jet fuel (500 mg/cu m) for one hour/day for 7 and 28 days did not show any significant changes in lung structures by light microscopy. However, when light microscopy was performed on lung sections from rats exposed to JP-8 jet fuel for 7 and 28 days at the 'high' dose concentration, the evidence for injury to the alveolar-capillary barrier was overwhelming. In these rats, we observed red blood cells in the alveolar air spaces, distortion of the bronchial airways, and loss of epithelial cells in the alveoli. These findings were substantiated by electron microscopy which showed epithelial cells missing their basement membrane, airways devoid of cilia, and alterations of type 2 alveolar epithelial cells. DTIC

N93-30160# Vanderbilt Univ., Nashville, TN. Dept. of Physics and Astronomy.

THE AFOSR WORKSHOP ON THE FUTURE OF EEG AND MEG Final Report, 1 Apr. 1992 - 30 Sep. 1992

John Wikswo, Jr., Alan Gevins, and Samuel J. Williamson 2 Feb. 1993 41 p Workshop held in Virginia Beach, VA, 17-22 May 1992 Prepared in cooperation with EEG Systems Lab, San Francisco, CA

(Contract F49620-92-J-0214)

(AD-A264338; AFOSR-93-0256TR) Avail: CASI HC A03/MF A01

A workshop on the prospects of the electroencephalogram (EEG) and the magnetoencephalogram (MEG) for elucidating human brain function was held at Virginia Beach, Virginia from 17-22 May 1992. The purpose of the workshop was to discuss the EEG and the MEG in relation to other rapidly advancing imaging modalities such as PET, SPECT, and functional MRI (MRI), and in terms of the recognized research, medical, and personnel evaluation needs for advanced brain imaging. Medical areas where these and other advanced technologies will undoubtedly be utilized include the diagnosis and treatment of diseases of the brain such as epilepsy, Alzheimer's, and schizophrenia; the monitoring and facilitation of recovery of function from head trauma and stroke; and the quantitative assessment of the effect on the brain of toxins and other bioenvironmental hazards. Non-medical applications of these techniques include a furthering of our understanding of the factors that are limiting the development and full utilization of human intelligence, particularly in recognition of increasing demands that are being placed on the mental capacities of people who live and work in our modern, post-industrial society. DTIC

N93-30192# Harvard Univ., Cambridge, MA.

INTERMEDIATE LEVELS OF VISUAL PROCESSING Annual Report, 1 Oct. 1991 - 30 Sep. 1992

Ken Nakuyama 30 Sep. 1992 4 p

(Contract F49620-92-J-0016)

(AD-A264117; AFOSR-93-0308TR) Avail: CASI HC A01/MF A01

The following topics were discussed: (1) Developed a theory to explain perceived depth in untextured stereograms which relies on the principle of generic image sampling. (2) Conducted experiments on visual search and visual texture segregation which show that early filter outputs are not accessible to either of these two operations. (3) Discovered a new form of implicit memory which is uniquely shortlasting (approx 30 seconds) and which assists in enabling more speedy popout with repeated trials. (4) Developed a new theory of binocular vision which relies heavily on the importance identification of half-occlusions. DTIC

N93-30196# Army Natick Research and Development Command, MA.

THE ENVIRONMENTAL SYMPTOMS QUESTIONNAIRE (ESQ): DEVELOPMENT AND APPLICATION Final Report, Sep. 1990 - Jun. 1992

James B. Sampson, John L. Kobrick, and Richard F. Johnson Mar. 1993 27 p

(DA Proj. 1L1-62786-AH-98)

(AD-A264127; NATICK/TR-93/026) Avail: CASI HC A03/MF A01

The Environmental Symptoms Questionnaire (ESQ) was developed to help researchers quantify symptoms experienced by individuals exposed to extreme conditions. The ESQ has evolved into a general symptom questionnaire from earlier designs for capturing the symptoms of acute mountain sickness. Item have been added, removed and revised, and scale changes were made for greater reliability and ease of administration and completion. Factor analysis revealed significant symptom clusters and weights for scoring the ESQ. Discussion is given to these developments and to the application to a number of environmental studies. Recommendations are offered for its administration and scoring using either factor weights or nonfactored clusters. DTIC

N93-30382# Virginia Univ., Charlottesville. Dept. of Biology.
CONTROL AND CIRCADIAN BEHAVIOR BY TRANSPLANTED SUPRACHIASMATIC NUCLEI Final Report, 15 Nov. 1989 - 14 Nov. 1992
Michael Menaker 14 Nov. 1992 10 p
(Grant AF-AFOSR-0098-90)
(AD-A264553; AFOSR-93-0337TR) Avail: CASI HC A02/MF A01

Fetal SCN tissue transplanted into the third ventricle of hamsters bearing complete SCN lesions restores the circadian locomotor rhythm with a period that depends exclusively on the genetically determined period of the tissue donor. If the host is only partially lesioned and thus retains rhythmicity with its own genetically determined period, an implant from an animal of a different genotype can induce a second rhythm with a period determined by the donor genotype. Both rhythms can be present simultaneously in the record of such a temporal chimera, interacting only superficially (i.e., not at the level of the pacemaker). Our data support the interpretation that under such circumstances the graft is able to capture part of the locomotor output of the circadian system but does not make functional connections with the host SCN pacemaking system. DTIC

N93-30400# Krug Life Sciences, Inc., San Antonio, TX.
ACQUISITION OF PHYSIOLOGICAL DATA DURING G-INDUCED LOSS OF CONSCIOUSNESS (G-LOC) Final Report, Apr. 1991 - 1992
Paul M. Werchan, Sharon K. Garcia, Jemett L. Desmond, Samual Galindo, Jr., and Judy A. Barber Apr. 1993 9 p
(Contract F33615-89-C-0603)
(AD-A264492; AL-TP-1992-0053) Avail: CASI HC A02/MF A01

The objective of this study was to develop a data acquisition system for the small animal centrifuge (SAC) and the transcranial Doppler (TCD) and to perform required research into the hemodynamic/biochemical alterations during G-induced loss of consciousness (G-LOC). This effort was to include the daily operation and maintenance of the SAC and Waters High Performance Liquid Chromatography units. The original data were turned over to the Flight Motion Effects Branch. The results of this effort were published as the article and abstracts included in this technical paper. DTIC

N93-30421# Scripps Clinic and Research Foundation, La Jolla, CA.
MOLECULAR APPROACH TO HYPOTHALAMIC RHYTHMS Annual Report, 15 Mar. 1992 - 14 Mar. 1993
J. G. Sutcliffe 14 Mar. 1993 25 p
(Contract F49620-92-J-0188)
(AD-A264438; AFOSR-93-0280TR) Avail: CASI HC A03/MF A01

We have utilized polymerase chain reaction with primers corresponding to conserved amino acid sequences within membrane-spanning regions of known serotonin receptors to identify clones of 4 putative new indoleamine receptors. We have determined complete amino acid sequences of these 4 receptors which fall into 3 subfamilies; two of these subfamilies are novel. The sites of expression within the brain have been determined for each of the genes. Expression in mammalian cells demonstrates that each new protein is a receptor for serotonin and each has a distinct pharmacology when compared to known receptors. Two of the new receptors are coupled to CAMP, one negatively (G) and one positively (Gs). The latter is a candidate for the serotonin receptor that mediates phase advances in circadian rhythms of the SCN. DTIC

N93-30422# Drexel Univ., Philadelphia, PA. Environmental Studies Inst.
DEVELOPMENT OF NOVEL MODELS FOR DESCRIBING MULTIPLE TOXICITY EFFECTS Annual Report, 20 Sep. 1991 - 19 Sep. 1993
Charles N. Haas 19 Sep. 1992 3 p
(Grant AF-AFOSR-0428-91)
(AD-A264439; AFOSR-93-0242TR) Avail: CASI HC A01/MF A01

The project was initiated October 1, 1991. Major accomplishments during the first year of the project were: (1) refinement of data analysis software; (2) conduct of a literature review of binary and multicomponent toxic response data; (3) analysis of a sample of data sets using the developed software; and (4) refinement of the theory of copulas with respect to multicomponent dose-response relationships. Papers relating to the work have been submitted and/or presented in the following locations: International Association on Water Pollution Research and Control, Water Science and Technology, Eastern North American Regional Meeting of the Biometric Society, Environmental Toxicology and Chemistry. DTIC

N93-30494# Texas Univ., San Antonio. Nonlinear Signal Processing Lab.
ANALYSIS OF VISUAL LOSS FROM RETINAL LESIONS Final Report, 1 Sep. 1989 - 31 Oct. 1992
Harold Longbotham 31 Oct. 1992 5 p
(Grant AF-AFOSR-0490-89)
(AD-A264692; AFOSR-93-0270TR) Avail: CASI HC A01/MF A01

Progress was made during the course of the grant on the application of Order Statistics and Neural Network modeling to analysis of the onset of retinal lesions. Several medical applications of WMMR filters were initiated, leading to a number of publications and conference presentations by the PI and his co-workers. DTIC

N93-30515# Naval Command, Control and Ocean Surveillance Center, San Diego, CA.
A SIMPLE COMPUTATIONAL MODEL OF CENTER-SURROUND RECEPTIVE FIELDS IN THE RETINA
M. R. Blackburn Feb. 1993 17 p
(AD-A264723; NRAD-TD-2454) Avail: CASI HC A03/MF A01

This report discloses a simple computational model of the outer retinal layers. The algorithm incorporates both rectified on-center/off-surround and off-center/on-surround bipolar elements, and an increase in the convergence of receptors to output elements that accounts for resolution differences between central and peripheral vision. The phenomenon of even and odd symmetry observed in biological receptive fields can be reproduced by the response of the model system to a moving line. DTIC

N93-30588# Army Research Inst. of Environmental Medicine, Natick, MA.
MEDICAL ASPECTS OF COLD WEATHER OPERATIONS: A HANDBOOK FOR MEDICAL OFFICERS
Robert E. Burr Apr. 1993 66 p
(AD-A263559; TN-93-4) Avail: CASI HC A04/MF A01

Soldiers engaged in military operations in cold weather are at risk of cold weather injuries and illnesses. The physiology of cold exposure, the prevention of cold injuries, and the medical management of cold injuries are reviewed and briefing points for medical personnel to use in training are provided. Author (revised)

N93-30613# New York Medical Coll., NY. Dept. of Physiology.
BIOPHYSICAL AND BIOCHEMICAL MECHANISMS IN SYNAPTIC TRANSMITTER RELEASE Annual Technical Report, 1 Jun. 1992 - 31 May 1993
Rodolfo R. Llinas 2 Apr. 1992 4 p
(Contract F49620-92-J-0363)
(AD-A264829; AFOSR-93-0281TR) Avail: CASI HC A01/MF A01

Three areas of research were implemented experimentally in the summer of 1992. The areas are as follows: (1) further description of calcium microdomains and their role in synaptic transmission; (2) a morphological analysis of rat synaptic vesicles injected into presynaptic terminal of the squid; and (3) the effect of Brefilden A (BFA) on the distribution and size of synaptic vesicles. DTIC

N93-30659# Michigan Univ., Ann Arbor. Transportation Research Inst.
DISCOMFORT GLARE FROM HIGH-INTENSITY DISCHARGE HEADLAMPS: EFFECTS OF CONTEXT AND EXPERIENCE
M. J. Flannagan, M. Sivak, D. S. Battle, T. Sato, and E. C. Traube Mar. 1993 31 p Sponsored by Industry Affiliation Program for Human Factors in Transportation Safety, Ann Arbor, MI
(PB93-174720; UMTRI-93-10) Avail: CASI HC A03/MF A01

The study was designed to investigate a difference in the discomfort glare produced by tungsten-halogen (TH) and high-intensity discharge (HID) headlamps. In a static field setup, 36 subjects, 24 in a younger group and 12 in an older group, made de Boer ratings of discomfort glare for TH and HID lamps. The lighting conditions were similar to those seen while driving on a dark, two-lane road when glare from an oncoming car is encountered. The results replicated the difference between TH and HID lamps that the authors observed in the earlier study, and indicated that the difference is not reduced by several manipulations of context and experience that the authors introduced in the present study. Analysis of subjects' discomfort ratings indicated that when TH and HID lamps produce equal discomfort glare, the tungsten-halogen lamps produce more photooptic lux at the eye of the observer. The magnitude of the difference was not affected by the type of headlamp (TH or HID) used on the car in which observers sat while viewing the glare stimuli, nor by whether the TH and HID lamps were presented in the context of headlamps that had been filtered to produce strongly saturated colors. NTIS

N93-30882# Naval Medical Research Inst., Bethesda, MD.
HYDROGEN-RATED SYSTEM FOR IN VITRO STUDIES AT PRESSURE: OPERATING PROCEDURES AND EMERGENCY PROCEDURES
Technical Report, Jan. 1989 - Jun. 1992
Homer J. Moore, Joel S. Colton, Walt Long, Karen Miller, and Guy Imbert
Mar. 1993 60 p
(NR Proj. MR0-4101)
(AD-A264179; NMRI-93-14) Avail: CASI HC A04/MF A01

A special apparatus was constructed to study the neurophysiologic effect of high pressure and the pharmacology of various gaseous agents using the isolated nerve terminal (synaptosome) tissue preparation. Design features were incorporated to permit investigations using H2, among other gases. Detailed operating procedures and emergency procedures for the use of H2 were established. These procedures are memorialized by this report. The theory of operation of the device and a pertinent overview of safety considerations are covered. DTIC

N93-30890# Saint Louis Univ., MO. School of Medicine.
CARBON MONOXIDE EXPOSURE OF SUBJECTS WITH DOCUMENTED CARDIAC ARRHYTHMIAS Research Report, Aug. 1987 - Jul. 1991
B. R. Chaitman, T. E. Dahms, S. Byers, L. W. Carroll, and L. T. Younis
Sep. 1992 48 p Sponsored by Health Effects Inst.
(PB93-179943; HEI/RR-92/52) Copyright Avail: CASI HC A03/MF A01

The authors studied 30 subjects with well-documented coronary artery disease who had an average of at least 30 ventricular ectopic beats per hour over a 20-hour monitoring interval. Subjects were selected and enrolled in a randomized double-blind study; the carbon monoxide exposure was designed to result in 3% or 5% carboxyhemoglobin levels, as measured by gas chromatography. Total and repetitive ventricular arrhythmias were measured for four specific time intervals: (1) two hours before carbon monoxide exposure; (2) during the two-hour carbon monoxide exposure; (3) six hours after carbon monoxide exposure; and (4) approximately 10 hours after exposure, or the remaining recording interval on the Holter monitor. There was no increase in ventricular arrhythmia frequency after carbon monoxide exposure, regardless of the level of carboxyhemoglobin or the type of activity. During steady-state conditions at rest, the number of ventricular ectopic beats per hour was 115 +/- 153 (SD) for room air exposure (0.7% carboxyhemoglobin), 121 +/- 171 for the lower carbon monoxide exposure (3.2% carboxyhemoglobin), and 94 +/- 129 for the higher carbon monoxide exposure (5.1% carboxyhemoglobin). The frequency of complex ventricular ectopy was not altered at the levels of carbon monoxide studied. Secondary analysis of the impact of carbon monoxide on ventricular ectopic beat frequency stratified by baseline ejection fraction, baseline ventricular ectopic beat frequency, and exercise-induced ST-segment changes did not indicate an effect of carbon monoxide on ventricular arrhythmias. However, patients with symptomatic ventricular arrhythmias and symptomatic myocardial ischemia were excluded from the present study. NTIS

N93-30894# Army Research Inst. of Environmental Medicine, Natick, MA.
FIELD TRIAL OF CAFFEINE ON PHYSICAL PERFORMANCE AT ALTITUDE: AN ATTEMPT TO OVERCOME THE CHALLENGE
Nancy King, Charles S. Fulco, Carol J. Baker-Fulco, Stephen Muza, and Timothy Lyons May 1993 52 p
(AD-A264260) Avail: CASI HC A04/MF A01

This study was designed to determine if caffeine would enhance the physical performance of soldiers at altitude (Pikes Peak, Colo.). Eight male soldiers from the Special Forces (ages 22 to 35 years old) completed two ascents of a 22 km, mountain trail (hiking from 1800 m to 4300 m above sea level) after having resided for 8 and 17 days at the summit (4300 m). Soldiers were asked to refrain from caffeinated foods and beverages for two days prior to each ascent. The composition and timing of the pre-ascent breakfasts were controlled. Ninety minutes after breakfast (one hour prior to ascent) each soldier received either caffeine (4 mg/kg body weight) or placebo in a double-blind, cross-over design. Urine samples were collected prior to each ascent for 1-methylxanthine determination. Perceived exertion, oxygen saturation, symptomatology, and 'split times' were measured at selected points along the trail. None of the variables measured differed between placebo and caffeine ascents. The inability to demonstrate an improvement due to caffeine may have been due to unavoidable, confounding factors such as inclement weather on the second ascent, altitude acclimatization between ascents, and/or lack of compliance to a caffeine-free diet, as well as the small sample size. DTIC

N93-30897# Naval Command, Control and Ocean Surveillance Center, San Diego, CA. Research, Development, Test and Evaluation.
AN ALGORITHM FOR SIMPLE AND COMPLEX FEATURE DETECTION: FROM RETINA TO PRIMARY VISUAL CORTEX Final Report
M. R. Blackburn Feb. 1993 30 p
(AD-A264306; NRAD-TD-2456) Avail: CASI HC A03/MF A01

This report describes a hierarchy of functions for the processing of visual motion and pattern information culminating in descriptive sets of features. Processing elements that model simple feature detectors respond maximally only when a stimulus grating pattern with a specific orientation and spatial period is located in phase with the center and surround of the element's receptive field. Processing elements that model complex feature detectors respond maximally only when a stimulus grating pattern with a specific orientation and spatial period is moved in a specific direction through the element's receptive field. DTIC

N93-30904# Gordon Research Conferences, Inc., Kingston, RI.
THE GORDON RESEARCH CONFERENCE ON PINEAL CELL BIOLOGY Final Progress Report, 15 Jul. 1991 - 14 Jul. 1992
Martin Zatz 14 Jul. 1992 12 p Conference held in Andover, NH, 12-16 Aug. 1991
(Grant AF-AFOSR-0279-91)
(AD-A264840; AFOSR-93-0217TR) Avail: CASI HC A03/MF A01

The objective of the 1991 Gordon Research Conference on Pineal Cell Biology was to bring together scientists so they could exchange recent research results and the conference provided a mechanism for the development of close interactions between these scientists. The quality of all of the lectures was exceptionally high and considerable discussion followed each lecture. Many of the conferees expressed very favorable comments about the intellectual stimulation provided by this conference. DTIC

N93-30908# Virginia Univ., Charlottesville. Dept. of Biology.
PHOTORECEPTORS REGULATING CIRCADIAN BEHAVIOR: A MOUSE MODEL Annual Report, 15 Mar. 1992 - 14 Mar. 1993
Russell G. Foster 14 Mar. 1993 19 p
(Contract F49620-92-J-0205)
(AD-A264881; AFOSR-93-0352TR) Avail: CASI HC A03/MF A01

Recent studies examined circadian photoreception in mice with hereditary retinal disorders (rd/rd and rds/rds). Despite the loss of visual function in these mice, circadian responses to light remain unaffected. Using c-fos expression within the SCN as a marker of neural activation of the circadian entrainment pathway, identical levels of Fos in the SCN of rd/rd and +/+ mice in response to retinal illumination are found. On the basis of action spectrum studies, and measurements of photopigment retinoids using HPLC, it is believed the photopigment mediating circadian responses to light is based upon an opsin, and that 11-cis-retinaldehyde is the photopigment chromophore. Preliminary measurements of mouse rod opsin, blue cone, and green/red cone opsin mRNA in retinally degenerate mice suggest that none of these opsins are exclusively used to mediate circadian responses to light. Collectively our data suggest that circadian photoreception can be maintained by a very small number of rod or cone cells without outer segments, or alternatively, is performed by an unrecognized class of photoreceptive cell within the mammalian retina. DTIC

N93-28739*# Aerospace Medical Research Labs., Wright-Patterson AFB, OH. Visual Display Systems Branch.
ARMSTRONG LABORATORY SPACE VISUAL FUNCTION TESTER PROGRAM
Melvin R. ONeal, H. Lee Task, and Gerald A. Gleason *In* NASA, Washington, NASA/DOD Flight Experiments Technical Interchange Meeting

Proceedings 1992 6 p (For primary document see N93-28699 11-12)
Avail: CASI HC A02/MF A10

N93-28740*# Aerospace Medical Research Labs., Wright-Patterson AFB, OH. Visual Display Systems Branch.
EFFECT OF MICROGRAVITY ON SEVERAL VISUAL FUNCTIONS DURING STS SHUTTLE MISSIONS: VISUAL FUNCTION TESTER-MODEL 1 (VFT-1)
Melvin R. ONeal, H. Lee Task, and Louis V. Genco *In* NASA, Washington, NASA/DOD Flight Experiments Technical Interchange Meeting Proceedings 1992 14 p (For primary document see N93-28699 11-12)
Avail: CASI HC A03/MF A10

N93-28741*# Aerospace Medical Research Labs., Wright-Patterson AFB, OH. Visual Display Systems Branch.
EFFECT OF MICROGRAVITY ON VISUAL CONTRAST THRESHOLD DURING STS SHUTTLE MISSIONS: VISUAL FUNCTION TESTER-MODEL 2 (VFT-2)
Melvin R. ONeal, H. Lee Task, and Louis V. Genco *In* NASA, Washington, NASA/DOD Flight Experiments Technical Interchange Meeting Proceedings 1992 6 p (For primary document see N93-28699 11-12)
Avail: CASI HC A02/MF A10

N93-28742*# Aerospace Medical Research Labs., Wright-Patterson AFB, OH. Visual Display Systems Branch.
EFFECT OF MICROGRAVITY ON THE VISUAL NEAR POINT: VISUAL FUNCTION TESTER-MODEL 4 (VFT-4)
Gerald A. Gleason, H. Lee Task, and Melvin R. ONeal *In* NASA, Washington, NASA/DOD Flight Experiments Technical Interchange Meeting Proceedings 1992 8 p (For primary document see N93-28699 11-12)
Avail: CASI HC A02/MF A10

N93-29546*# Guelph Univ. (Ontario). Dept. of Computing and Information Science.
FUZZY NEURAL NETWORK METHODOLOGY APPLIED TO MEDICAL DIAGNOSIS
Marian B. Gorzalczany (Technical Univ. of Kielce, Poland.) and Mary Deutsch-McLeish *In* NASA. Johnson Space Center, North American Fuzzy Logic Processing Society (NAFIPS 1992), Volume 1 Dec. 1992 p 266-275 (For primary document see N93-29516 11-59)
Avail: CASI HC A02/MF A03

N93-30269 Simon Fraser Univ., Burnaby (British Columbia).
MODELLING AND SIMULATION OF HUMAN RETINAL VISION PROCESSING
Philip J. Scheltens, Andrew H. Rawicz, and Marek J. Syrzycki *In* Engineering Inst. of Canada, Canadian Conference on Electrical and Computer Engineering, Volumes 1 and 2 1990 4 p (For primary document see N93-30215 11-31)
Avail: Engineering Inst. of Canada, 2050 rue Mansfield, Suite 700, Montreal, Quebec H3A 1Z2 Canada

53 BEHAVIORAL SCIENCES

Includes psychological factors; individual and group behavior; crew training and evaluation; and psychiatric research.

N93-28622# Civil Aeromedical Inst., Oklahoma City, OK.
ACCIDENT PRONENESS: A RESEARCH REVIEW Final Report
Mark D. Rodgers and Robert E. Blanchard May 1993 6 p
(DOT/FAA/AM-93/9) Avail: CASI HC A02/MF A01

Accident proneness is a concept that refers to an enduring or stable personality characteristic that predisposes an individual toward having accidents. The concept is controversial and has sustained a lively debate in the literature over the past 75 years. For the most part, though, continual interest has been fueled by poor experimental procedures, misinterpretation of previously reported results, the need to assign blame to individuals, and a rather curious doggedness in attempting to establish a relationship between accidents and personality traits, despite the lack of supporting scientific evidence. The origins of the notion of accident proneness are reported and the studies that purport to support or refute it are reviewed.
Author (revised)

N93-28901# Georgia Univ., Athens. Dept. of Psychology.
EXPERTISE, TEXT COHERENCE, AND CONSTRAINT SATISFACTION: EFFECTS ON HARMONY AND SETTLING RATE Quarterly Report
Bruce K. Britton and F. J. Eisenhart 8 Mar. 1993 10 p
(AD-A262703) Avail: CASI HC A02/MF A01

This paper reports four experiments showing that 27 experts' mental representations had significantly higher harmony and faster settling rates than 652 novices when activation was spread through the representations in a simulation of thinking; that when coherent texts were read by novices, they produced mental representations with significantly higher harmony and faster settling rates than less coherent texts; and that novices whose representations matched the experts' mental representations had significantly higher harmony and faster settling rates. The results were found for declarative experts in history and procedural experts in literary interpretation, for Dutch and American experts, for novice groups including U.S. Air Force recruits and U.S. and Dutch undergraduates, and for both history texts and literary texts. These results were consistent with our hypothesis that the quality of a person's prior knowledge determines the harmony and settling rates of their representations and that these can be measured by simulating the spread of activation through the person's mental representation of a subject matter domain. Harmony may also be used as a metacognitive signal.
DTIC

N93-29481# Aerospace Medical Research Labs., Brooks AFB, TX.
PILOT CANDIDATE SELECTION METHOD (PCSM): WHAT MAKES IT WORK? Interim Report, Jan. - Dec. 1992
Thomas R. Carretta and Malcolm J. Rice Mar. 1993 17 p
(AF Proj. 7719)
(AD-A262871; AL-TP-1992-0063) Avail: CASI HC A03/MF A01

A sample of 678 Air Force pilot training candidates were tested with a paper-and-pencil aptitude battery and computer-administered tests of psychomotor skills, information processing, and attitude toward risk. A self report of flying experience was also collected. These data were used in regression analyses to determine which variables provided the best prediction of two flying criteria, passing-failing flying training and class ranking at the end of flying training. The paper-and-pencil tests were found to be the best predictors. The measures of flying experience, psychomotor skills, and attitude toward risk incremented the prediction of the criteria. Information processing was not found to be incremental to the other variables in the prediction of the criteria.
DTIC

N93-29610* National Aeronautics and Space Administration. Lyndon B. Johnson Space Center, Houston, TX.
AN ACCELERATED TRAINING METHOD FOR BACK PROPAGATION NETWORKS Patent
Robert O. Shelton, inventor (to NASA) 13 Jul. 1993 21 p Filed 17 Jun. 1991 Supersedes N91-28730 (29 - 20, p 3381)
(NASA-Case-MSC-21625-1; US-Patent-5,228,113;
US-Patent-Appl-SN-716182; US-Patent-Class-395-23;
Int-Patent-Class-G06F-15/18) Avail: US Patent and Trademark Office

The principal objective is to provide a training procedure for a feed forward, back propagation neural network which greatly accelerates the training process. A set of orthogonal singular vectors are determined from the input matrix such that the standard deviations of the projections of the input vectors along these singular vectors, as a set, are substantially maximized, thus providing an optimal means of presenting the input data. Novelty exists in the method of extracting from the set of input data, a set of features which can serve to represent the input data in a simplified manner, thus greatly reducing the time/expense to training the system.
Official Gazette of the U.S. Patent and Trademark Office

N93-30026# Aerospace Medical Research Labs., Brooks AFB, TX.
PREDICTING AIRCREW TRAINING PERFORMANCE WITH PSYCHOMETRIC g Interim Report, Jan. - Jun. 1992
Michele M. Olea and Malcolm J. Ree Apr. 1993 16 p
(AF Proj. 1121)
(AD-A264021; AL-TP-1993-0011) Avail: CASI HC A03/MF A01

A comparison of the validity of general cognitive ability, g, and specific ability, s, for predicting pilot and navigator training success revealed that g was the best predictor for all ten criteria and that s contributed little beyond g. The criteria included both academic performance, flying maneuvers, and airborne navigation. DTIC

N93-30027# Aerospace Medical Research Labs., Wright-Patterson AFB, OH.
HANDEDNESS AND MOTOR PROGRAMMING EFFECTS OF MANUAL CONTROL AND MOVEMENT Final Report, Sep. 1987 - May 1991
David Curry Sep. 1992 134 p
(AD-A264022; AL-TR-1992-0127) Avail: CASI HC A07/MF A02

Four studies with a unidimensional, cursor-positioning task, employing both response-priming and response-precuing techniques, were performed to evaluate differences in motor control between the preferred and nonpreferred hands. None of the major hypotheses proposed previously to explain these differences (e.g., ones based on practice, force variability, feedback-processing speed, hemispheric specialization, and sequential movement control) was supported. Instead, hand differences may stem from greater automaticity during the execution of motor programs for moving by the preferred hand. Furthermore, the present studies do not support the distinctive-features model of motor programming proposed by Rosenbaum and other investigators. Such programs appear to be hierarchically organized and serially executed, with information about movement direction required before movement information is used. This conclusion is consistent with results obtained during both the initial programming of aimed movements and their reprogramming when the original information for them turns out to be incorrect. DTIC

N93-30033# New York Univ. Medical Center.
COMPUTING WITH NEURAL MAPS: APPLICATION TO PERCEPTUAL AND COGNITIVE FUNCTION Annual Report, 1 Aug. 1990 - 30 Jul. 1991
Eric L. Schwartz 26 Mar. 1993 4 p
(Grant AF-AFOSR-0275-88)
(AD-A264056; AFOSR-93-0314TR) Avail: CASI HC A01/MF A01

Models for visual attention, based on the representation of an attentional space as a two dimensional map have led to a model of visual attention which has been successfully used in the application of a space-variant active vision system, described below. Also, it has been demonstrated that stereo fusion limits, such as Panum's fusional area, scale in a manner which is determined by the size of a cortical hypercolumn, and the local value of cortical magnification factor. This in turn supports the notion that stereo disparity is computed by a local correlational operator defined on the span of a single pair of ocular dominance columns. A generalized image warp technique has been developed, which we term the 'protocolumn algorithm', which provides image level models of the mapping of ocular dominance and orientation column systems at the level of primary visual cortex. Finally, many of the ideas developed in this project have reached fruition in the construction of a space-variant active vision system. An initial prototype system has been constructed under hardware support from DARPA, and a number of difficult algorithmic problems in motor control, attention, space-variant image processing, and space-variant pattern classification, have begun to be studied. DTIC

N93-30163# Yale Univ., New Haven, CT.
REPRESENTATIONS OF SHAPE IN OBJECT RECOGNITION AND LONG-TERM VISUAL MEMORY Annual Report, 15 Jan. 1992 - 14 Jan. 1993
Michael J. Tarr 11 Feb. 1993 31 p
(Contract F49620-92-J-0169)
(AD-A264342; AFOSR-93-0237TR) Avail: CASI HC A03/MF A01

A variety of studies examining the mechanisms and representations underlying human object recognition have been conducted. One track has investigated the role of view-based object representations in perception and recognition. Results indicate that certain classes of viewpoint-dependent features may be used to define boundaries between characteristic views of objects. A second track has investigated the interaction between orientation-dependent and orientation-independent recognition mechanisms. Results here indicate that humans learn both object-based, orientation-independent and view-based, orientation-dependent representations regardless of the initial learning context. Other results indicate that task conditions mediate whether structural descriptions or episodic representations of objects are used in performing an implicit memory task. Finally, a third track has investigated the nature of spatial relations between objects, as well as the relationship between perceptual and lexical representations of spatial relations. Results indicate that spatial prepositions (e.g., above, left) encode the relationship between figural and reference objects as a gradient that decreases with distance from the qualitative or veridical position. Moreover, results indicate that this may in part be a lexical effect, in that stronger qualitative effects are found when subjects have lexically encoded the relationship--although further results indicate that qualitative gradients are present in purely perceptual judgments. DTIC

N93-30425# Air Force Systems Command, Brooks AFB, TX. Armstrong Lab.
FIELD TEST OF A COMPUTER-DRIVEN TOOL TO MEASURE PSYCHOLOGICAL CHARACTERISTICS OF AIRCREW Final Technical Report, 15 Nov. 1991 - 15 Nov. 1992
Christopher F. Flynn, Walter E. Sipes, Milton J. Grosenbach, and Jon Ellsworth Mar. 1993 36 p
(AD-A264484; AL-TR-1992-0171) Avail: CASI HC A03/MF A01

Twenty-eight (80%) subjects from a squadron of 36 F-16 pilots voluntarily participated in a newly developed anonymous, self-administered, computerized testing protocol. The test battery consisted of two 2.5-hour blocks that measured personality (MMPI-2), cognitive capacity (MAB), crew coordination skills (PCI), and potential psychiatric diagnoses (C-DIS); it also gathered demographic information. A peer rating survey gathered information about the squadron's top performers and their personal qualities. This pilot project demonstrated the success of the battery to gather aircrew information in a field location. Results also indicated that aviators can agree who are top performers and what personal qualities are important in top performers. DTIC

N93-30426# Naval Submarine Medical Research Lab., Groton, CT.
CONSPICUITY OF AIDS TO NAVIGATION. PART 1: TEMPORAL PATTERNS FOR FLASHING LIGHTS
Kevin Laxar and Sandra L. Benoit 3 May 1993 15 p
(Contract MIPR-Z51100-1-E27A57)
(AD-A264626; NSMRL-1187) Avail: CASI HC A03/MF A01

Mariners frequently have trouble picking out lighted aids to navigation in harbors and other areas that have a high density of background lights. The U.S. Coast Guard is seeking ways to enhance the conspicuity, or likelihood of being noticed, of these aids. Literature has shown that a flashing light is more conspicuous than a light that is not flashing. This investigation sought to improve conspicuity by finding the optimal flash characteristics for a light on a background of steady lights. Twenty observers searched for a flashing point source of light among backgrounds of steady lights of various numerosities on a computer controlled CRT screen. They indicated which of the five screen sectors contained the flashing target, and the computer recorded the accuracy and response time. Targets were flashed at the rates of 1, 2, and 3.85 Hz, each at duty cycles of .3, .5, and .8 (proportion of total time on). After a brief practice period, each observer completed 360 trials in a single one-hour session. An ANOVA showed significant effects of frequency, duty cycle, and background light density. Search time increased as the number of background lights increased. Conspicuity improved as frequency increased and as duty cycle decreased. The flash pattern that provides the greatest conspicuity consumes the least amount of electrical energy, an important consideration for an aid to navigation. The results can be used as guidelines for the flash characteristics of lighted aids to navigation. DTIC

N93-30542# Dayton Univ., OH. Research Inst.
EFFECTS OF AREA-OF-INTEREST DISPLAY CHARACTERISTICS OF VISUAL SEARCH PERFORMANCE AND HEAD MOVEMENTS IN SIMULATED LOW-LEVEL FLIGHT Final Technical Report, Sep. 1989 - Jul. 1992
Harold D. Warner, Gary L. Serfoss, and David C. Hubbard Mar. 1993 37 p
(Contract F33615-90-C-0005)
(AD-A264661; AL-TR-1993-0023) Avail: CASI HC A03/MF A01

An investigation was conducted to evaluate the influence of area-of-interest (AOI) display characteristics on target detection performance and head movements. Two AOI display conditions were compared: a small

(26.44 by 21.51 deg horizontal and vertical), higher resolution AOI and a large (40.00 by 30.00 deg horizontal and vertical), lower resolution AOI. The observers viewed a computer-generated visual scene consisting of three-dimensional cylinder-shaped objects placed upright on a desert like terrain surface. Black bands were modeled on some of the cylinders, and the bands constituted the targets. Cylinders height and diameter were varied along with the position of the banded cylinders relative to the flight path of the simulated aircraft. Both pilots and nonpilots were used as observers. Results indicate that target detection distance varied as a function of AOI condition and the height and diameter of the cylinders on which the bands were placed, but not type of observer. Both horizontal and vertical head movements were sensitive to the differences between the AOI conditions, and the vertical movements were also influenced by type of observer. It is recommended that the small, higher resolution AOI be used in situations where greater target detection distance and higher image detail are required. DTIC

N93-30543# Pennsylvania Univ., Philadelphia.
THE DYNAMICS OF VISUAL REPRESENTATION, ATTENTION, ENCODING, AND RETRIEVAL PROCESSES Final Report, 1 Oct. 1990 - 30 Oct. 1992
Saul Sternberg 20 Apr. 1993 12 p
(AD-A264674; AFOSR-91-0015; AFOSR-93-0339TR) Avail: CASI HC A03/MF A01

The Final Technical Report on the dynamics of visual representation: attention, encoding, and retrieval processes is presented. After a section describing the objectives of the work, the report provides a synopsis of the principal accomplishments, in five categories: (1) investigation of the relation between location-probe and probed-reciting paradigms, to test whether the transformations that underlie performance changes with probe delay in the two paradigms are the same or different; (2) investigation of the transformation associated with the location-probe paradigm; (3) extensive work with the probed-reciting paradigm at zero probe delay, manipulating the legibility of the displayed characters as another approach to studying the transformation required for response; (4) application of variants of a traditional visual search paradigm to investigate effects of properties of the early representation on the order of search, again by manipulating legibility; (5) development of new tests of stage models of mental operations. DTIC

N93-30575# Air Force Systems Command, Brooks AFB, TX. Armstrong Lab.
DETERMINANTS OF PERFORMANCE RATING ACCURACY: A FIELD STUDY Interim Report, Jan. 1990 - Dec. 1992
Mark S. Teachout and Terry L. Dickinson Apr. 1993 93 p
(AD-A264726; AL-TP-1993-0010) Avail: CASI HC A05/MF A01

The purpose was to investigate the influence of rater and ratee characteristics, performance constraints, and rating system acceptability on the accuracy of supervisory performance ratings in a field setting. Participants were 212 raters and 405 ratees across three jobs in the United States Air Force. An hypothesized structural model of rating accuracy was tested using LISREL 7 to determine the relationships among nine latent variables. Although the goodness-of-fit statistics for the model were considered marginal, results indicated that motivation to rate accurately, trust in the appraisal process, rating form acceptability, rater cognitive ability, rater experience, and ratee experience were related to rating accuracy. Interpretations and suggestions for future research were discussed. DTIC

N93-29564*# Dayton Univ., OH. Dept. of Mathematics.
QUANTIFICATION OF HUMAN RESPONSES
R. C. Steinlage, T. E. Gantner, and P. Y. W. Lim (Boise Cascade Corp., Portland, OR.) *In* NASA. Johnson Space Center, North American Fuzzy Logic Processing Society (NAFIPS 1992), Volume 2 Dec. 1992 p 427-436 (For primary document see N93-29556 11-59)
Avail: CASI HC A02/MF A03

N93-30322 Hickling (James F.) Management Consultants Ltd., Ottawa (Ontario).
THE AIR TRAFFIC CONTROLLER'S MENTAL MODEL AND IT'S IMPLICATIONS FOR EQUIPMENT DESIGN AND TRAINEE SELECTION
Richard H. Mogford *In* Engineering Inst. of Canada, Canadian Conference on Electrical and Computer Engineering, Volumes 1 and 2 1990 4 p (For primary document see N93-30215 11-31)
Avail: Engineering Inst. of Canada, 2050 rue Mansfield, Suite 700, Montreal, Quebec H3A 1Z2 Canada

N93-30676*# National Aeronautics and Space Administration. Ames Research Center, Moffett Field, CA.
HELICOPTER SIMULATION: AN AIRCREW TRAINING AND QUALIFICATION PERSPECTIVE
Richard A. Birnbach and Thomas M. Longridge *In its* NASA/FAA Helicopter Simulator Workshop Apr. 1992 p 35-38 (For primary document see N93-30673 11-01)
Avail: CASI HC A01/MF A02

N93-30679*# National Aeronautics and Space Administration. Ames Research Center, Moffett Field, CA.
TRAINING EFFECTIVENESS ASSESSMENT: WHERE ARE WE?
Greg McGowan *In its* NASA/FAA Helicopter Simulator Workshop Apr. 1992 p 49-54 (For primary document see N93-30673 11-01)
Avail: CASI HC A02/MF A02

N93-30680*# National Aeronautics and Space Administration. Ames Research Center, Moffett Field, CA.
CURRENT TRAINING: WHERE ARE WE?
Gerald Golden *In its* NASA/FAA Helicopter Simulator Workshop Apr. 1992 p 55-59 (For primary document see N93-30673 11-01)
Avail: CASI HC A01/MF A02

N93-30684*# National Aeronautics and Space Administration. Ames Research Center, Moffett Field, CA.
TRAINING EFFECTIVENESS ASSESSMENT: METHODOLOGICAL PROBLEMS AND ISSUES
Kenneth D. Cross *In its* NASA/FAA Helicopter Simulator Workshop Apr. 1992 p 77-90 (For primary document see N93-30673 11-01)
Avail: CASI HC A03/MF A02

54 MAN/SYSTEM TECHNOLOGY AND LIFE SUPPORT

Includes human engineering; biotechnology; and space suits and protective clothing.

For related information see also *16 Space Transportation.*

N93-28464# Little (Arthur D.), Inc., Cambridge, MA.
HYBRID OXYGEN SYSTEM Final Report, Sep. 1986 - Dec. 1991
W. D. Lee Oct. 1992 197 p
(Contract F33615-86-C-4505)
(AD-A262417; Rept-56913-10; AL-TR-1992-0014) Avail: CASI HC A09/MF A03

Investigation of concepts for generating oxygen on-board combat aircraft and development of a bleed air-driven refrigeration, liquefaction, and cryogenic storage system for oxygen were undertaken in this study. A number of alternative approaches were examined while considering size, weight and power consumption. An open-loop bleed air-driven system was selected for design, development, and testing. The bleed air-driven refrigeration unit achieved oxygen liquefaction temperatures of 90 deg K and liquefied and stored oxygen generated from a molecular sieve oxygen generating system (MSOGS). The oxygen was stored in cryogenic dewars, vaporized, and withdrawn from the system to simulate aircrew consumption. A heat exchanger flow reversing valving system was used to sublime and blow out condensates (water vapor and carbon dioxide) which normally collect in an open-loop refrigeration cycle operating from ambient air. The collection of condensate in the cryogenic system represented the largest technological area to overcome, and the reverse cycle system overcame the problem. The laboratory demonstrator utilized a helium cycle cold head refrigeration unit in conjunction with a J-T valve to simulate a cryogenic expander to be used in the flight system. Further work to incorporate a cryogenic expander in place of the cold head and J-T valve is recommended. DTIC

N93-28479# General Electric Co., Gilbert, AZ. Government Services.
LOW-COST HELMET-MOUNTED DISPLAYS Final Technical Report, Apr. 1991 - Apr. 1992
Roger W. Leinenwever, Leonard G. Best, and Bryce J. Ericksen Feb. 1993 14 p
(Contract F33615-88-C-0014)
(AD-A262616; AL-TR-1993-0008) Avail: CASI HC A03/MF A01

This report contains two papers presented at the Helmet-Mounted Displays IV, International Symposium and Exhibition on Optical Engineering and Photonics, held at Orlando, FL on 20-24 April 1992. This symposium was sponsored by the Society of Photo-Optical Instrumentation Engineers (SPIE). The papers describe the development and demonstration of two helmet-mounted displays: a low-cost monochrome helmet display and a low-cost color helmet display, both with see-through optics. The present monochrome CRT display helmet design, through demonstrations and system measurements, provided positive data as a research device. The color LCD helmet display system was successfully completed and although the resolution of the LCD matrix structure is not suited for the application of small text in the presentation, the high contrast and vivid colors produced by the LCD, as well as the see-through function of the optics, provide the capability for a full field-of-regard visual simulation system which can be used in conjunction with low-cost cockpit training devices. DTIC

N93-28757# Chemical Warfare/Chemical and Biological Defense Information Analysis Center, Edgewood, MD.
EVALUATION OF TEST METHODS AND REQUIREMENTS FOR RESPIRATORY PROTECTION SYSTEMS 21 Final Report
T. L. Ramirez, K. M. Reed, M. R. Perry, C. M. Grove, and D. E. Molnar Nov. 1992 73 p
(Contract DLA900-86-C-2045)
(AD-A262466; CBIAC-SS-335) Avail: CASI HC A04/MF A01

The Joint Services Operational Requirements (JSOR) for vision, communications, respiration, thermal, personal support, compatibility, and psychological factors are presented in this summary. The body of the report provides the test methods used with other pertinent information. The test equipment and cost of equipment are provided with recommendations for selection of the test and the equipment. The recommendation section provides a synopsis of the findings and suggested equipment the advanced protective systems integration laboratory may want to evaluate for use with advanced mask design. DTIC

N93-28850# Advisory Group for Aerospace Research and Development, Neuilly-Sur-Seine (France). Flight Mechanics Panel.
COMBAT AUTOMATION FOR AIRBORNE WEAPON SYSTEMS: MAN/MACHINE INTERFACE TRENDS AND TECHNOLOGIES [L'AUTOMATISATION DU COMBAT AERIEN: TENDANCES ET TECHNOLOGIES POUR L'INTERFACE HOMME/MACHINE]
Apr. 1993 268 p Symposium held in Edinburgh, Scotland, 19-22 Oct. 1992
(AGARD-CP-520; ISBN-92-835-0706-1) Copyright Avail: CASI HC A12/MF A03

Recent advances in combat automation technologies offer significant potential for improving overall mission effectiveness. Development of advanced situational awareness display concepts, parallel distributed computer architecture, and tactical information fusion techniques have paved the way for new operational capabilities and weapon system employment tactics. Harnessing these innovative technologies is critically dependent upon establishing an effective and intuitive pilot vehicle interface. The symposium addressed changing and possible future operational scenarios, advanced technology concepts, application issues and experimental development efforts and included sessions on: fusion, situation awareness, human capabilities and limitations, and design and evaluation of integrated systems. For individual titles, see N93-28851 through N93-28872.

N93-28851# Defense Advanced Research Projects Agency, Arlington, VA.
X-31 DEMONSTRATION OF INTEGRATED FLIGHT AND PROPULSION CONTROL FOR EFFECTIVE COMBAT AT EXTREME ANGLES OF ATTACK c08
Michael S. Francis, E. DeVere Henderson (Spectra Research Systems, Inc., Arlington, VA.), Erwin Kunz (Messerschmitt-Boelkow-Blohm G.m.b.H., Munich, Germany.), Sid Powers (Rockwell International Corp., El Segundo, CA.), and Helmut Richter (Ministry of Defence, Germany.) *In* AGARD, Combat Automation for Airborne Weapon Systems: Man/Machine Interface Trends and Technologies Apr. 1993 14 p (For primary document see N93-28850 11-54)
Copyright Avail: CASI HC A03/MF A03

The X-31 Program is providing new options for conducting and winning close-in air combat in the future. Through the exploitation of the key EFM technologies - high thrust-to-weight ratio, multi-axis thrust vectoring, integrated flight-propulsion controls coupled with a 'pilot friendly' vehicle interface - the X-31 is pioneering dynamic post stall flight for a variety of combat applications. The key challenge to effective control in this arena is a compatible and properly tuned pilot-vehicle combination. The program's emphasis on control, simplicity, carefree handling, and situational awareness issues should help assure that its key objectives will be met. Various aspecs of the X-31 Program are discussed. Derived from text

N93-28852# GEC Ferranti, Edinburgh (Scotland). Radar Systems Div.
PLANNING FOR AIR TO AIR COMBAT c66
I. D. Gray *In* AGARD, Combat Automation for Airborne Weapon Systems: Man/Machine Interface Trends and Technologies Apr. 1993 13 p (For primary document see N93-28850 11-54)
Copyright Avail: CASI HC A03/MF A03

Air combat planning has always proven very difficult because of the dynamic environment, intelligent adversaries, group operations, and the incomplete nature of any information. Two approaches, those of 'expert systems' and classical adversary search are presented and compared. Searching is then described and developed in detail. The implications of such an approach are considered for the future of air combat. Derived from text

N93-28853# Elliott-Automation Space and Advanced Military Systems Ltd., Camberley (England). Aerospace Systems Div.
PILOT DECISION AIDING FOR WEAPON DELIVERY: A NOVEL APPROACH TO FIRE CONTROL CUEING USING PARALLEL COMPUTING
A. R. Buffett and R. M. Wimbush *In* AGARD, Combat Automation for Airborne Weapon Systems: Man/Machine Interface Trends and Technologies Apr. 1993 18 p (For primary document see N93-28850 11-54)
Copyright Avail: CASI HC A03/MF A03

This paper describes the application of advanced technology, both hardware and software, to provide improved pilot Man-Machine Interface (MMI) automation for the central function of an airborne weapon system, namely weapon release. The specific scenario addressed is that of providing the pilot with decision aiding, in the form of firing cues, for the use of air-to-air missiles. The paper gives an overview of the need for automation/decision aiding in air-to-air missile fire control, by illustrating the way in which missile performance can vary greatly with the changes of engagement parameters which occur rapidly in an air-to-air combat scenario. The high pilot workload in this type of scenario, and the future requirement for multiple simultaneous missile firings, further support the need for automation to provide pilots with simple, processed, predictive data on which to base their firing decisions. Derived from text

N93-28854# GEC Sensors Ltd., Basildon (England).
A NEW CLASS OF MISSION SUPPORT FOR COMBAT AIR-CREW c66
Harvey J. Pipe *In* AGARD, Combat Automation for Airborne Weapon Systems: Man/Machine Interface Trends and Technologies Apr. 1993 6 p (For primary document see N93-28850 11-54)
Copyright Avail: CASI HC A02/MF A03

In the next century, combat aircraft will be even more complex than those planned as current replacements; this is to counter increasingly competent aggressors, who may operate anywhere in the world. This paper covers the integration of a mission management aid (MMA) into future combat aircraft, its operation, the core topics of Sensor Fusion, Situation Assessment (including Dynamic Threat Assessment), Planning and Tactical Routing (with Defense/Attack Options Management). Evaluation of the MMA is showing that better situation awareness is obtained, increasing mission effectiveness and survivability, and that overall the MMA is a vital integral system for future aviation. Derived from text

N93-28855# Universitaet der Bundeswehr Muenchen, Neubiberg (Germany). Inst. fuer Systemdynamik und Flugmechanik.

PILOT INTENT AND ERROR RECOGNITION AS PART OF A KNOWLEDGE BASED COCKPIT ASSISTANT

T. Wittig and R. Onken *In* AGARD, Combat Automation for Airborne Weapon Systems: Man/Machine Interface Trends and Technologies Apr. 1993 10 p (For primary document see N93-28850 11-54)
Copyright Avail: CASI HC A02/MF A03

A Pilot Intent and Error Recognition module as part of a knowledge based Cockpit Assistant System is presented, which is being developed at the University of the Armed Forces in Munich in cooperation with the Dornier company and implemented in a flight simulator. The system mainly supports the pilot crew with regard to the monitoring and planning task and provides assistance for a number of plan execution functions for the civil flight operation under Instrument Flight Rules. During the whole flight, the Pilot Intent and Error Recognition module monitors pilot activities and the flight status in order to detect deviations from the actual flight plan immediately. In this case, the current flight situation is evaluated, the pilot behavior is analyzed over a certain time period and by use of both pilot intent or error is recognized. Pilot errors lead to warning messages, and recognized pilot intent to a modification of the flight plan. In this paper, a short survey is given of the concept and the function of the Cockpit Assistant System. After that the structure of the Pilot Intent and Error Recognition will be described in detail. At the end, the integration of this module into the Cockpit Assistant System and the evaluation in a flight simulator are presented. Derived from text

N93-28856# Defence Research Agency, Bedford (England). Flight Dynamics and Simulation Div.

THE DESIGN AND DEVELOPMENT OF THE NEW RAF STANDARD HUD FORMAT

J. R. Hall *In* AGARD, Combat Automation for Airborne Weapon Systems: Man/Machine Interface Trends and Technologies Apr. 1993 11 p Sponsored by RAF (For primary document see N93-28850 11-54)
Copyright Avail: CASI HC A03/MF A03

In poor weather and on instruments, the safe piloting of an aircraft requires the display of basic flight information to the pilot in a manner that is instinctive, immediate, and unambiguous. Head-up display formats have singularly failed in this regard over the years and are known to be a contributing factor in many incidents involving lack of spatial awareness by the pilot. This paper describes the theory, experimental development, and flight proving of the DRA Fast-Jet HUD Format (FJF). This format has been designed to keep the pilot spatially aware under the most dynamic of flight maneuvers while retaining the flight-path information so necessary for mission effectiveness during normal tactical maneuvering and steady flight conditions. These include low level night operations with FLIR and NVGs and highly dynamic, hard maneuvering flight in poor weather or on instruments either at low level or in the air-to-air role. Derived from text

N93-28857# Dornier Luftfahrt G.m.b.H., Friedrichshafen (Germany). Flight Simulation Dept.

SYMBOLOGY FOR HEAD UP AND HEAD DOWN APPLICATIONS FOR HIGHLY AGILE FIGHTER AIRCRAFT: TO IMPROVE SPATIAL AWARENESS, TRAJECTORY CONTROL, AND UNUSUAL ATTITUDE RECOVERY, PART 1

G. Fischer and W. Fuchs *In* AGARD, Combat Automation for Airborne Weapon Systems: Man/Machine Interface Trends and Technologies Apr. 1993 6 p (For primary document see N93-28850 11-54)
Copyright Avail: CASI HC A02/MF A03

The progressively increasing agility of modern fighter aircraft (a/c) with high onset and high sustained pitch and roll rates makes spatial orientation and awareness an even more demanding task for the operator. Pilots already complain about fast moving and twisting pitch bars in the HUD and the necessity to concentrate almost their entire attention on maintaining spatial orientation. Scaled and geared pitch bars relieved the problem to some extent but didn't solve it, at least according to our opinion. The above mentioned problems are aggravated with the introduction of advanced fighter a/c capable of even higher onset and angular rates and flying at higher angles of attack (AoA) or even in the post-stall regime where the actual flight path in space and the a/c attitude may deviate to a great extent. In order to overcome the problems mentioned above, a more stationary and more easily interpretable reference symbology, a circular arc segment, is used to indicate pitch (theta) or flight path angle (gamma), whereas the roll angle (phi) is given by the angular relation between a/c reference symbol and the center of the arc segment. Author (revised)

N93-28858# Rockwell International Corp., Los Angeles, CA.

VIRTUAL INTERFACE APPLICATIONS FOR AIRBORNE WEAPONS SYSTEMS

Emily Howard *In* AGARD, Combat Automation for Airborne Weapon Systems: Man/Machine Interface Trends and Technologies Apr. 1993 6 p (For primary document see N93-28850 11-54)
Copyright Avail: CASI HC A02/MF A03

This paper addresses a class of control and display technology that shall be referred to collectively as Virtual Interface (VI) technology. The contents of this paper are presented in three parts. Part 1 will describe what is meant by a 'virtual interface,' a suite of control and display technology being developed for future implementation in operational aircraft systems. The problem that will be discussed is how the transition process between development and operational status is particularly difficult for VI technology, given current applications. Part 2 will describe some new applications of VI technology, based upon several programs that utilize embedded simulation for operational test and evaluation and training purposes. A review of the benefits of VI technology shows promise for accelerating the transition process at least toward these operational activities. Part 3 then will describe a new display concept, based on virtual interface technology, that was designed for one of these embedded simulation applications and conclude with a discussion of plans for future development. Author (revised)

N93-28859# General Dynamics Corp., Fort Worth, TX.

HEAD-STEERED SENSOR FLIGHT TEST RESULTS AND IMPLICATIONS

L. N. Lydick *In* AGARD, Combat Automation for Airborne Weapon Systems: Man/Machine Interface Trends and Technologies Apr. 1993 7 p (For primary document see N93-28850 11-54)
Copyright Avail: CASI HC A02/MF A03

A comprehensive flight test program of a head-steered FLIR/HMD night attack system was conducted between Aug. 1987 and Jan. 1990. Seventy-five development and demonstration F-16B flights were flown. Approximately 90 percent of the flights were conducted in night visual meteorological conditions. The remainder were conducted in daytime with the pilot's vision obscured by an opaque visor cover to simulate night and to study laser eye protection. Because the new FLIR/HMD systems were fully integrated with the F-16B fire control, navigation, communication, and display system, it was possible to achieve a considerable degree of tactical relevance in the tests. The night attack portion of the testing was a subset of a broader series of tests to explore advanced techniques for close air support (CAS). The work was industry sponsored by a number of corporations in a cooperative effort of about thirty million dollars. The tests and demonstrations culminated in operational test by (then) Tactical Air Command pilots at Nellis Air Force Base, Nevada, and Fort Hood, Texas. The night CAS systems evaluations were quite favorable and were planned for production until the remarkable end of the cold war reoriented (or perhaps gave pause to) planned introduction of the concepts to the fleet. In this paper, the author provides a summary overview of the mission, a description of the systems, the lessons learned, and some thoughts about future system requirements. Author (revised)

N93-28860# Defence Research Agency, Farnborough (England). Flight Systems Dept.

THE QUEST FOR AN INTEGRATED FLYING HELMET

A. Karavis and D. N. Jarrett *In* AGARD, Combat Automation for Airborne Weapon Systems: Man/Machine Interface Trends and Technologies Apr. 1993 19 p (For primary document see N93-28850 11-54)
Copyright Avail: CASI HC A03/MF A03

The addition of vision enhancement, display, and control functions to aviator's headgear is operationally attractive. The jets and helicopters that are currently under development call for headgear with a combination of these novel facilities. This paper reviews the recent history of such helmet systems, which demonstrate admirably the inventiveness of the design teams. However, there are attendant perceptual and operational concerns and the addition of extra components invariably compromises basic ergonomic qualities. A new design philosophy, which emphasizes functional integration rather than the incorporation of compatible sub-systems, is emerging. This will be assisted significantly when key optical and electro-optical technologies become mature. Author (revised)

N93-28861# Royal Air Force Inst. of Aviation Medicine, Farnborough (England). Biodynamics Div.

THE PHYSIOLOGICAL LIMITATIONS OF MAN IN THE HIGH G ENVIRONMENT

N. D. C. Green *In* AGARD, Combat Automation for Airborne Weapon Systems: Man/Machine Interface Trends and Technologies Apr. 1993 8 p (For primary document see N93-28850 11-54)
Copyright Avail: CASI HC A02/MF A03

The physiological limitations imposed upon man by the high-G environment are discussed, with particular reference to the cardiovascular, respiratory, and musculo-skeletal systems. Anti-G technology has been developed specifically for agile fighter aircraft, but it is apparent that if man is to have the capacity to tolerate any further increases in aircraft agility, a radically different approach to G protection is required. The most effective physiological solution is to change the orientation of the pilot such that his long axis is no longer in the plane of greatest acceleration, entailing major cockpit redesign. This and other solutions are examined, and their acceptability to aviators is considered. Author (revised)

N93-28862# British Aerospace Public Ltd. Co., Bristol (England). Research Centre.

OCULO-MOTOR RESPONSES AND VIRTUAL IMAGE DISPLAYS

G. K. Edgar, C. Neary, I. Craig, and J. C. D. Pope *In* AGARD, Combat Automation for Airborne Weapon Systems: Man/Machine Interface Trends and Technologies Apr. 1993 8 p (For primary document see N93-28850 11-54)
Copyright Avail: CASI HC A02/MF A03

Virtual image displays are likely to become more prominent in the cockpit, the most common examples being the head-up display (HUD) and, more recently, the helmet-mounted display (HMD). This paper describes a series of experiments highlighting some of the advantages and disadvantages of displays of this type. The first experiments demonstrate that introducing perceived depth differences into displays may improve eye-tracking performance. The second series of experiments illustrates some of the problems with virtual image displays; namely that the eyes may be inappropriately accommodated (focused) when using virtual image displays. The possible consequences of these problems are discussed. Author

N93-28863# Texas Technological Univ., Lubbock. Dept. of Industrial Engineering.

HUMAN CAPABILITIES AND LIMITATIONS IN SITUATION AWARENESS

Mica R. Endsley and Cheryl A. Bolstad (Monterey Technologies, Inc., Cary, NC.) *In* AGARD, Combat Automation for Airborne Weapon Systems: Man/Machine Interface Trends and Technologies Apr. 1993 10 p (For primary document see N93-28850 11-54)
Copyright Avail: CASI HC A02/MF A03

Achieving high situation awareness (SA) is a major goal in the design of aircraft systems. Efforts are currently underway by a number of individuals who are attempting to address this need through improvements in avionics system design, automation, and the pilot-vehicle interface (PVI). These efforts can be greatly enhanced through an understanding of human capabilities and limitations in achieving SA. This paper presents an identification of those factors which underlie basic human SA capabilities, including key information processing mechanisms, critical human skills, and a discussion of external factors which act to hamper SA. The implications of each of these issues for the design of systems, including PVI and automation efforts, are discussed. Author

N93-28864# Royal Air Force Inst. of Aviation Medicine, Farnborough (England).

OPERATOR AND AUTOMATION CAPABILITY ANALYSIS: PICKING THE RIGHT TEAM

R. M. Taylor and S. J. Selcon *In* AGARD, Combat Automation for Airborne Weapon Systems: Man/Machine Interface Trends and Technologies Apr. 1993 17 p (For primary document see N93-28850 11-54)
Copyright Avail: CASI HC A03/MF A03

A review of the role of operator and automation capability analysis in aircrew systems design is provided. The changing perceptions of human and machine functionality with increasing machine capability, from early pilot-in-the-loop control, through to the division and sharing of responsibilities for systems management and mission problem solving, are charted. Concepts for the integration of human and machine resources in the performance of physical and cognitive tasks, including decision-making, are discussed in the context of developments in machine intelligence. Operator capability and task analysis, and the modeling of human performance, are seen to have developed from providing tools for system design, to giving critical support for real-time dynamic function allocation in advanced adaptive systems. A model of cooperative teamwork, with the machine conceived of as an electronic-crew teaming resource, is proposed as broad framework for thinking about future adaptive systems requirements. The results of a recent study of human-electronic crew teamwork with RAF Harrier and Tornado aircrew are reported. The results provide evidence for the validity of the teamwork model, and indicate directions for extending the capability for cooperative functioning in future aircrew adaptive systems. Author (revised)

N93-28865# Aerospace Medical Research Labs., Wright-Patterson AFB, OH. Human Engineering Div.

COGNITIVE INTERFACE CONSIDERATIONS FOR INTELLIGENT COCKPITS

Robert G. Eggleston *In* AGARD, Combat Automation for Airborne Weapon Systems: Man/Machine Interface Trends and Technologies Apr. 1993 16 p (For primary document see N93-28850 11-54)
Copyright Avail: CASI HC A03/MF A03

The concept of an Intelligent Cockpit as a knowledge-based aiding system is presented. It argues that, in order to maximally support the air crew, user aiding in two areas is required: mission task aiding and interface useability aiding. These areas of aiding are discussed in relation to four different forms of an intelligent cockpit. The central purpose, however, is to introduce the concept of a cognitive design requirement for aiding systems, and to suggest its importance to design solutions expected to achieve crew aiding in both the mission task and interface useability areas. Two arguments are made: (1) A deeper knowledge of human capabilities and limitations is needed to generate effective cognitive design requirements for an aiding system; and (2) more cognitive design requirements are needed for an intelligent cockpit in comparison with a conventional one. Illustrations of possible cognitive design requirements are presented in support of these arguments. Special attention is given to requirements that derive from human capabilities and limitations. Based on the general discussion, it is also concluded that an intelligent cockpit should be a separate module from the traditional systems avionics, since it requires a unique process architecture. Author (revised)

N93-28866# British Aerospace Public Ltd. Co., Kingston-upon-Thames (England). Military Aircraft Div.

ERGONOMIC DEVELOPMENT OF DIGITAL MAP DISPLAYS

Adrian Martel and George A. Ward *In* AGARD, Combat Automation for Airborne Weapon Systems: Man/Machine Interface Trends and Technologies Apr. 1993 8 p (For primary document see N93-28850 11-54)
Copyright Avail: CASI HC A02/MF A03

In the high workload environment of the cockpit, the importance of efficient transfer of information from visual displays to the pilot is of the highest priority. British Aerospace, Kingston, has developed a prototype Situational Awareness display which successfully combines tactical information with a digital map and aeronautical information. The interface in terms of presentation and functionality is designed to complement the process whereby visual information is cognitively integrated into mental models of Situational Awareness by the user. The development of the display involved a comprehensive literature search on perception and cognition, analysis of map representations, and an iterative evaluation whereby successive prototypes were developed and refined. The many visual design principles which were identified during this work which were successfully incorporated into this display and which may in addition be of great benefit to other displays are detailed. Where displays are being radically revised, a holistic redesign from first principles is preferable to simply adding new features. Author (revised)

N93-28867# Wright Lab., Wright-Patterson AFB, OH.

SYSTEM AUTOMATION AND PILOT-VEHICLE-INTERFACE FOR UNCONSTRAINED LOW-ALTITUDE NIGHT ATTACK

T. O. Church and W. S. Bennett, II (General Dynamics Corp., Fort Worth,

TX.) *In* AGARD, Combat Automation for Airborne Weapon Systems: Man/Machine Interface Trends and Technologies Apr. 1993 7 p (For primary document see N93-28850 11-54)
Copyright Avail: CASI HC A02/MF A03

Unconstrained low-altitude night attack is achievable today through automation and integration of current technologies. Many of these technologies are advanced avionic systems that still require additional development before they are production-ready. However, their performance and synergistic benefits have been demonstrated. Additional efforts are still warranted to increase system safety, improve situational awareness, decrease pilot workload, and provide a more effective weapon system. Author

N93-28868# Thomson-CSF, Trappes (France). Dept. Simulateurs.
COMPUTER ASSISTED EVALUATION FOR AIR CLOSE COMBAT BASED ON TIME INTERVAL CHARACTERIZATION [EVALUATION AUTOMATIQUE DE COMBATS AERIENS FONDEE SUR LES INTERVALLES CARACTERISTIQUES] **c66**
P. Poutignat and H. deFontenilles *In* AGARD, Combat Automation for Airborne Weapon Systems: Man/Machine Interface Trends and Technologies Apr. 1993 9 p In FRENCH (For primary document see N93-28850 11-54)
Copyright Avail: CASI HC A02/MF A03

The complexity of modern military simulations poses a formidable debriefing task. A study was therefore conducted to demonstrate feasibility of an evaluation aid system for close air-to-air combat analysis. This analysis is based on a new concept of Time Interval Characterization (TIC). This concept is an extension of the method of breaking down a combat sequence into individual maneuvers. The TIC concept is also generic enough to ensure that the proposed aid system is adequate for every type of mission, and not only in the very specific domain of aircraft close-in combat. The analysis system does principally: (1) a measurement of pilot performance; (2) an extraction of characteristical intervals; (3) a detection of good or bad behavior according to expertise rules of debriefing; and (4) an optional generation of alternative trajectories by an aircraft combat expert system. Results obtained during these stages can be fully exploited with the interactive Man Machine Interface (MMI) which forms a part of the aid system. Expertise rules and MMI were defined in consultation with relevant experts. Author (revised)

N93-28869*# National Aeronautics and Space Administration. Ames Research Center, Moffett Field, CA.
FLIGHT EVALUATION OF A COMPUTER AIDED LOW-ALTITUDE HELICOPTER FLIGHT GUIDANCE SYSTEM **c08**
Harry N. Swenson, Raymond D. Jones (Army Avionics Research and Development Activity, Fort Monmouth, NJ.), and Raymond Clark (Army Avionics Research and Development Activity, Fort Monmouth, NJ.) *In* AGARD, Combat Automation for Airborne Weapon Systems: Man/Machine Interface Trends and Technologies Apr. 1993 11 p (For primary document see N93-28850 11-54)
Copyright Avail: CASI HC A03/MF A03

The Flight Systems Development branch of the U.S. Army's Avionics Research and Development Activity (AVRADA) and NASA Ames Research Center have developed for flight testing a Computer Aided Low-Altitude Helicopter Flight (CALAHF) guidance system. The system includes a trajectory-generation algorithm which uses dynamic programming and a helmet-mounted display (HMD) presentation of a pathway-in-the-sky, a phantom aircraft, and flight-path vector/predictor guidance symbology. The trajectory-generation algorithm uses knowledge of the global mission requirements, a digital terrain map, aircraft performance capabilities, and precision navigation information to determine a trajectory between mission way points that seeks valleys to minimize threat exposure. This system was developed and evaluated through extensive use of piloted simulation and has demonstrated a 'pilot centered' concept of automated and integrated navigation and terrain mission planning flight guidance. This system has shown a significant improvement in pilot situational awareness, and mission effectiveness as well as a decrease in training and proficiency time required for a near terrain, nighttime, adverse weather system. AVRADA's NUH-60A STAR (Systems Testbed for Avionics Research) helicopter was specially modified, in house, for the flight evaluation of the CALAHF system. The near terrain trajectory generation algorithm runs on a multiprocessor flight computer. Global Positioning System (GPS) data are integrated with Inertial Navigation Unit (INU) data in the flight computer to provide a precise navigation solution. The near-terrain trajectory and the aircraft state information are passed to a Silicon Graphics computer to provide the graphical 'pilot centered' guidance, presented on a Honeywell Integrated Helmet And Display Sighting System (IHADSS). The system design, piloted simulation, and initial flight test results are presented. Author (revised)

N93-28870# Rockwell International Corp., Los Angeles, CA.
REQUIREMENTS FOR PILOT ASSISTANCE IN A THRUST-VECTORING COMBAT AIRCRAFT
Emily Howard and Robert E. Bitten *In* AGARD, Combat Automation for Airborne Weapon Systems: Man/Machine Interface Trends and Technologies Apr. 1993 15 p (For primary document see N93-28850 11-54)
(Contract N00019-88-C-0288)
Copyright Avail: CASI HC A03/MF A03

With the emergence of thrust-vectoring aircraft such as the X-31 and F-22, new questions arise regarding the maximum potential of this technology for increasing air-to-air combat effectiveness. Recent dome-to-dome (man-in-the-loop) simulations have demonstrated a significant increase in close-in air combat effectiveness with the addition of thrust vector capability. Much of this increased effectiveness can be attributed to the ability of the thrust-vectoring aircraft to continue maneuvering while operating well beyond conventional aircraft stall limits. Such poststall maneuvering (PST) can dramatically increase an aircraft's turn rate while simultaneously minimizing its turn radius, providing a significant tactical advantage in close in air combat. Comparisons with all-digital (computer-in- the-loop) simulations under the same test conditions, however, show that the combat effectiveness of PST is consistently greater within the all-digital analyses than within the all-manned analyses. These comparisons are summarized and whether pilots may require supplemental assistance in order to exploit the full potential of PST utility is considered. Through analysis of both man- and computer-in-the-loop combat simulations, requirements for pilot assistance were tentatively identified, along with some of the methods applicable to meeting these requirements. These methods include expanded training, improved displays, and increased automation. The results of this analysis, based upon the studies available to date, are presented. Plans for further analysis and validation studies are described. Author (revised)

N93-28871# Westinghouse Electric Corp., Baltimore, MD. Electro-Optical Systems Dept.
DESIGN CONSIDERATIONS FOR A NIGHT, AIR-TO-SURFACE ATTACK CAPABILITY ON A DUAL ROLE FIGHTER **c06**
Robert A. Hale, John J. Chino, L. Larkin Niemyer, John R. Jadik, and Barry E. Lightner *In* AGARD, Combat Automation for Airborne Weapon Systems: Man/Machine Interface Trends and Technologies Apr. 1993 8 p Prepared in cooperation with Westinghouse Electric Corp., Orlando, FL (For primary document see N93-28850 11-54)
Copyright Avail: CASI HC A02/MF A03

The Falcon Knight design objective was to achieve a compact lightweight and affordable night air-to-surface attack capability for a small single seat dual role fighter. The design constraints were cost, performance, physical size, weight, aerodynamic impact, and ease of retrofit. An analysis of the mission and the pilot's tasks and workload during the mission revealed the need for two electro-optical lines-of-sight (LOS's). The first LOS, pilot age, is required to provide an uninterrupted night vision, or pilot age, capability for a high level of situational awareness at all normal pilot viewing angles. The second LOS, targeting, is to provide a simultaneous independent targeting capability for cueing, search, detection, recognition, fire control tracking, and/or weapon hand-off leading to the delivery of weapons on the target. The Falcon Knight forward looking infrared (FLIR) sensor is a unique optically multiplexed dual line of sight (LOS) Head Steered FLIR (HSF) which provides both pilot age and targeting LOS's simultaneously within the design constraints cited above. The Falcon Knight FLIR is also integrated with the aircraft's Fire Control Radar (FCR) to create an integrated FLIR/Fire Control Radar Multisensor. Westinghouse built a company funded Falcon Knight FLIR/Fire Control Multisensor Radar prototype. The prototype was evaluated in flight on the Westinghouse BAC 1-11 Avionics Test Bed aircraft. The United States Air Force is currently evaluating the Falcon Knight FLIR/Fire Control Radar Multisensor on the Advanced Fighter Technology Integration (AFTI) F-16 test aircraft at Edwards Air Force Base (AFB) California. Author (revised)

N93-28872# National Aerospace Lab., Amsterdam (Netherlands).
OVERVIEW OF COCKPIT TECHNOLOGY RESEARCH AND DEVELOPMENT PROGRAMS FOR IMPROVEMENT OF THE MAN/MACHINE INTERFACE: REVIEW OF THE AGARD AVP SYMPOSIUM HELD IN MADRID, MAY 1992
P. J. M. Urlings and E. W. Pijpers *In* AGARD, Combat Automation for Airborne Weapon Systems: Man/Machine Interface Trends and Technologies Apr. 1993 12 p (For primary document see N93-28850 11-54)
Copyright Avail: CASI HC A03/MF A03

A review of the AGARD Avionics Panel (AVP) symposium on 'Advanced Aircraft Interfaces: The Machine Side of the Man-Machine Interface', held in May 1992 at Madrid is provided. The theme of this symposium was limited to the 'machine-side' since a subsequent AGARD symposium at Edinburgh, Scotland, later that year was scheduled to cover the 'man-side' of the subject. The main findings of the Madrid symposium were summarized for presentation in Edinburgh. The complete text of the papers of the AVP symposium can be found in AGARD Conference Proceedings CP-521. Author (revised)

N93-28884# Army Research Inst. of Environmental Medicine, Natick, MA.
BIOPHYSICAL MODEL FOR HANDWEAR INSULATION TESTING
W. R. Santee, L. A. Blanchard, S. K. Chang, and R. R. Gonzalez Mar. 1993 26 p
(AD-A262926; USARIEMT7-93) Avail: CASI HC A03/MF A01

Biophysical models of hands, feet, and full manikins are used for direct measurement of clothing insulation. Thermal resistance values (m(sup 2)K/W) were measured with a weather resistant and simplified 7 zone hand model with upgraded controls and then compared to values from a 22 zone articulated copper model. Insulation is calculated from the power demand required to maintain a selected surface temperature setpoint at known thermal gradient between the surface setpoint and the environment. For the new model, dry insulation values were 0.21 m(sup 2)K/W for the standard military trigger finger mitten and 0.12 m(sup 2)K/W for the light-duty shell. Values for the 22 section copper hand model were 0.23 and 0.14 m(sup 2)K/W, respectively. Both hand models provide replicable measurements of relative total handwear insulation. DTIC

N93-28897# Oxford Univ. (England). Robotics Research Group.
A MODULAR HEAD/EYE PLATFORM FOR REAL-TIME REACTIVE VISION
Ian D. Reid, Paul M. Sharkey, Philip F. Mclauchlan, and David W. Murray 1992 12 p
(OUEL-1941/92; ETN-93-93877) Avail: CASI HC A03/MF A01

The design and implementation of a high speed reactive system in which the primary sense is vision are presented. An architecture for visual processing based around a configurable network of general purpose processors is described. A purpose built, versatile, high quality engineered mount based on geared DC motors was developed to facilitate rapid redirection of gaze. Performance results for this device are presented. Results for a preliminary implementation of closed loop visual control using a brightest spot detector are given. ESA

N93-28941# Army Research Lab., Aberdeen Proving Ground, MD.
A STUDY OF THE EFFECTS OF LENS FOCAL LENGTH ON REMOTE DRIVER PERFORMANCE Final Report
Monica M. Glumm, Patricia W. Kilduff, and Amy S. Masley Nov. 1992 35 p
(DA Proj. 1L1-62716-AH-70)
(AD-A263191; ARL-TR-25) Avail: CASI HC A03/MF A01

The effects of three lens focal lengths on remote driving performance were measured. The three focal lengths and their corresponding horizontal fields of view (FOV's) were 12 mm (29 deg), 6 mm (55 deg), and 3.5 mm (94 deg). On-board driving performance (direct view) was also measured. The study was conducted on an indoor test course consisting of six segments: straightaways, right-hand turns, left-hand turns, serpentine, figure 8, and obstacle avoidance. The findings are presented. DTIC

N93-28942# Edgerton, Germeshausen and Grier, Inc., Idaho Falls, ID.
CRUCIAL ROLE OF DETAILED FUNCTION, TASK, TIMELINE, LINK, AND HUMAN VULNERABILITY ANALYSES IN HRA
T. G. Ryan, L. N. Haney, and L. T. Ostrom 1992 20 p Presented at the Reliability and Maintainability Symposium, Atlanta, GA, 26-28 Jun. 1993
(Contract DE-AC07-76ID-01570)
(DE93-001923; EGG-M-92402; CONF-930661-1) Avail: CASI HC A03/MF A01

This paper addresses one major cause for large uncertainties in human reliability analysis (HRA) results, that is, an absence of detailed function, task, timeline, link, and human vulnerability analyses. All too often this crucial step in the HRA process is done in a cursory fashion using word of mouth or written procedures which themselves may incompletely or inaccurately represent the human action sequences and human error vulnerabilities being analyzed. The paper examines the potential contributions these detailed analyses can make in achieving quantitative and qualitative HRA results which are as follows: (1) creditable, that is, minimize uncertainty; (2) auditable, that is, systematically linking quantitative results and qualitative information from which the results are derived; (3) capable of supporting root cause analyses on human reliability factors determined to be major contributors to risk; and (4) capable of repeated measures and being combined with similar results from other analyses to examine HRA issues transcending individual systems and facilities. Based on experience analyzing test and commercial nuclear reactors, and medical applications of nuclear technology, an iterative process is suggested for doing detailed function, task, timeline, link and human vulnerability analyses using documentation reviews, open-ended and structured interviews, direct observations, and group techniques. Finally, the paper concludes that detailed analyses done in this manner by knowledgeable human factors practitioners, can contribute significantly to the credibility, auditability, causal factor analysis, and combining goals of the HRA. DOE

N93-28977*# National Aeronautics and Space Administration. Marshall Space Flight Center, Huntsville, AL.
COMPUTERIZED ATMOSPHERIC TRACE CONTAMINANT CONTROL SIMULATION FOR MANNED SPACECRAFT
J. L. Perry Jun. 1993 171 p Sponsored by NASA, Washington
(NASA-TM-108409; NAS 1.15:108409) Avail: CASI HC A08/MF A02

Buildup of atmospheric trace contaminants in enclosed volumes such as a spacecraft may lead to potentially serious health problems for the crew members. For this reason, active control methods must be implemented to minimize the concentration of atmospheric contaminants to levels that are considered safe for prolonged, continuous exposure. Designing hardware to accomplish this has traditionally required extensive testing to characterize and select appropriate control technologies. Data collected since the Apollo project can now be used in a computerized performance simulation to predict the performance and life of contamination control hardware to allow for initial technology screening, performance prediction, and operations and contingency studies to determine the most suitable hardware approach before specific design and testing activities begin. The program, written in FORTRAN 77, provides contaminant removal rate, total mass removed, and per pass efficiency for each control device for discrete time intervals. In addition, projected cabin concentration is provided. Input and output data are manipulated using commercial spreadsheet and data graphing software. These results can then be used in analyzing hardware design parameters such as sizing and flow rate, overall process performance and program economics. Test performance may also be predicted to aid test design. Author

N93-29044*# National Aeronautics and Space Administration. Lyndon B. Johnson Space Center, Houston, TX.
ANTHROPOMETRIC DATA FROM LAUNCH AND ENTRY SUITED TEST SUBJECTS FOR THE DESIGN OF A RECUMBENT SEATING SYSTEM
Lara E. Stoycos (Lockheed Engineering and Sciences Co., Houston, TX.) and Glen K. Klute Jun. 1993 29 p
(Contract NAS9-17900)
(NASA-TM-104769; S-720; NAS 1.15:104769) Avail: CASI HC A03/MF A01

Returning space crews to Earth in a recumbent position requires the design of a new seating system. Current anthropometric data are based on measurements taken while the subjects were unsuited and sitting. To be most accurate, it is necessary to design by measurements of subjects in the launch and entry suit in a recumbent position. Since the design of the recumbent seating system must meet the requirements of both 5th percentile Japanese female and 95th percentile American male crew members, a delta is reported rather than absolute measurements of the test subjects. This delta is the difference in the measurements taken with the subjects unsuited and sitting and those taken with the subjects suited and recumbent. This delta, representative of the change due to the suit, can be added to the existing Man-Systems Integration Standards (NASA-STD-3000) anthropometric data to project the measurements for 5th percentile Japanese female and 95th percentile American male crew members. A delta accounting for the spinal elongation caused by prolonged exposures to microgravity is added as well. Both unpressurized and pressurized suit conditions are considered. Background information, the test protocol and procedure, analysis of the data, and recommendations are reported. Author (revised)

N93-29324*# National Aeronautics and Space Administration. Lyndon B. Johnson Space Center, Houston, TX.

ANTHROPOMETRIC SURVEY OF THE ASTRONAUT APPLICANTS AND ASTRONAUTS FROM 1985 TO 1991

Sudhakar L. Rajulu (Lockheed Engineering and Sciences Co., Houston, TX.) and Glenn K. Klute May 1993 96 p
(Contract NAS9-17900)
(NASA-RP-1304; S-718; NAS 1.61:1304) Avail: CASI HC A05/MF A01

The Anthropometry and Biomechanics Laboratory at the Johnson Space Center has been collecting anthropometric data from astronaut applicants since 1977. These anthropometric measurements had been taken from 473 applicants. Based on the position they applied for, these applicants were classified as either mission specialists, payload specialists, pilots, or observers. The main objective was to document the variations among these applicants and tabulate the percentile data for each anthropometric dimension. The percentile and the descriptive statistics data were tabulated and graphed for the whole astronaut candidate population; for the male and female groups; for each subject classification such as pilot, mission specialist, and payload specialist; and finally, for those who were selected as astronauts. Author (revised)

N93-29340# Mitre Corp., Bedford, MA.

HEAD MOUNTED DISPLAYS FOR VIRTUAL REALITY

Paul J. Hezel and Harry Veron Feb. 1993 49 p
(Contract F19628-89-C-0001)
(AD-A263498; MTR-93B0000015) Avail: CASI HC A03/MF A01

One of the goals in the development of Virtual Reality (VR) is to achieve total immersion where one sees and interacts with objects in a virtual world in the same way that one sees and interacts with the objects of the real world. One becomes immersed in another world through the sense of sight. Thus the technique of displaying a virtual environment determines, in part, the degree to which one can become transported out of the real world and into the virtual world. The developers of VR have utilized the head mounted display (HMD) as a means of displaying the virtual environment to the user. The HMD is not new but has seen widespread use as an information display in military aircraft. In an HMD, displays and imaging optics mounted on a headset provide a virtual image in front of the eyes. In the VR domain, this design provides the user with a view of the virtual environment while blocking out the user's real environment. A tracking device allows the computer to present a viewpoint corresponding to the user's head position and orientation, thus enabling freedom of movement for the user within the virtual environment. These and other characteristics enhance the total immersion capabilities of the HMB. DTIC

N93-29406# Army Air Mobility Research and Development Lab., Fort Eustis, VA.

SOUND ATTENUATION CHARACTERISTICS OF THE STANDARD DH-132A AND SPH-4 HELMETS WORN IN COMBINATION WITH STANDARD ISSUE EARPLUGS

Ben T. Mozo, Linda S. Barlow, and Barbara A. Murphy Jan. 1993 19 p
(AD-A263011; USAARL-93-10) Avail: CASI HC A03/MF A01

The Health Hazard Assessment (HHA) of Army systems usually requires a review of noise and hearing protection associated with the systems used. Hearing protection for crews in combat vehicles is specified to be the DH-132A and, in some cases where noise levels are extremely high, earplugs are worn in combination with the helmet in order to provide adequate protection. Hearing protection for Army helicopter crewmembers is the SPH-4 helmet with a few exceptions. The attenuation data used for the HHA are measured at this Laboratory. This report incorporates the results of attenuation measurements of the SPH-4 and DH-132A helmets worn in combination with the standard Army issue earplugs. Earplugs used in the study were the single flange, triple flange, and yellow/white foam plug. DTIC

N93-29444 Naval Postgraduate School, Monterey, CA.

PERFORMANCE MEASUREMENT SYSTEMS: A BEST PRACTICES STUDY M.S. Thesis

Sandra K. Chachula Dec. 1992 106 p Limited Reproducibility: More than 20% of this document may be affected by microfiche quality
(AD-A262180) Avail: CASI HC A06

The purpose of this cost management research was the identification and analysis of internal performance measurement best practices which can serve as a benchmark for companies who seek to improve their performance measurement systems and competitiveness. The study used data that were previously collected from eleven diverse, high performing companies. This study identified twenty-one characteristics of performance measurement systems across eleven companies and across levels of management. The twenty-one characteristics have previously been identified in the performance measurement literature as characteristics necessary for organizations to maintain their competitive edge. The study, therefore, is confirmatory. The summary of performance measurement best practices identified in this study, then, can be used as a benchmark by organizations who seek to improve their performance measurement systems and their competitiveness. DTIC

N93-29471# Defence and Civil Inst. of Environmental Medicine, Downsview (Ontario).

EVALUATION OF PERSONAL COOLING SYSTEMS IN CONJUNCTION WITH EXPLOSIVE ORDNANCE DISPOSAL SUITS

J. Frim and Andrew Morris Jun. 1992 71 p
(AD-A262862; DCIEM-92-31) Avail: CASI HC A04/MF A01

This study examined the capabilities of three technologies (a liquid cooled undergarment, a thickly-ribbed vest of hydrophylic nylon, and an air vest) to alleviate thermal strain in personnel working in Explosives Ordnance Disposal (EOD) clothing under environmental conditions of 18 C and 40% relative humidity (rh), 340 C and 40% rh, and 34 C and 80% rh. Simulated EOD tasks consisted of treadmill walking (10 min), unstacking/carrying/stacking weighted boxes (10 min), and a rest period (15 min) with the EOD helmet and jacket removed repeated for a target duration time of 90 min. Physiological data included rectal temperature, skin temperature, heart rate, sweat production and evaporation, metabolic rate, and subjective evaluations of thermal comfort and perceived exertion. The results indicated that wearing the EOD suit produces significant increases in thermal physiological strain over performing the same tasks in a standard station uniform. However, the liquid-cooled Exotemp personal cooling system was very effective in reducing that strain during heat exposure. Rectal temperatures, heart rates, and fluid losses (dehydration) were reduced back to values comparable to those when not wearing the EOD suit, while skin temperatures were actually lower with the cooling system than with only the station uniform. Subjects indicated reduced perceived exertion levels and improved thermal comfort when wearing the liquid-cooled garment with the EOD suit. In contrast, the ribbed vest and air vest showed no significant benefits with the EOD suit. It is concluded that the increase in thermal physiology strain, resulting from wearing the EOD suit during EOD work in hot environments can effectively be minimized by use of Exotemp personnel cooling system. DTIC

N93-29484# Science Applications International Corp., McLean, VA.

PREDICTING RADIATION INDUCED PERFORMANCE DECREMENTS OF AH-1 HELICOPTER CREWS. VOLUME 2: EVALUATION OF MODELING AND SIMULATION TECHNIQUES FOR PREDICTING RADIATION INDUCED PERFORMANCE DECREMENTS Technical Report, 25 Sep. 1986 - 30 Nov. 1991

William A. Perez, Vaughan W. Inman, Joseph I. Peters, Robert R. Sanchez, and Robert W. Young 1 Mar. 1993 118 p
(Contract DNA001-86-C-0308)
(AD-A262872; DNA-TR-92-54-V2-Vol-2) Avail: CASI HC A06/MF A02

The effects of intermediate doses of ionizing radiation on Army helicopter crew performance are investigated. The analysis of performance on the Walter Reed Performance Assessment Battery (WRPAB), and the development of an initial model for the WRPAB using Multidimensional Scaling (MDS) techniques is documented. The WRPAB was used in a study where 20 AH-1 pilots (1) predicted the effects of various symptom complexes on their performance, (2) went through a 36-hour protocol to induce symptoms similar to symptoms that follow exposure to intermediate doses of radiation, (3) performed a simulated AH-1 mission before and after symptom induction, and (4) were administered the WRPAB approximately every 2 hours throughout the 36-hour protocol. MicroSAINT models for AH-1 tank engagements were developed that used PAB performance to predict AH-1 performance degradation. The results indicate that the WRPAB (or some other test battery) has utility for the prediction of operator performance as affected by stressors such as ionizing radiation. DTIC

N93-29606 Department of the Navy, Washington, DC.
HELMET VISOR SUPPORT APPARATUS Patent
Daniel J. Schmidt, inventor (to Navy) and John D. Jacks, inventor (to Navy) 12 Jan. 1993 11 p Filed 10 Dec. 1991
(AD-D015684; US-Patent-5,177,816; US-Patent-Appl-SN-805281; US-Patent-Class-2-424) Avail: US Patent and Trademark Office

Helmet visor support apparatus is provided which can move the visor between a raised and a lowered position by the operation of one hand. The apparatus comprises a visor support arm pivotally attached to the helmet at a pivot point for moving the visor between the raised and lowered positions. A positioning means is attached to the helmet at the pivot point and has at least two bores corresponding to the raised and lowered visor positions. A locking pin retractably engages either one of the bores in the positioning means to lock the visor support arm in position. A spring coiled around the locking pin normally biases the locking pin in engagement with one of the bores. A manually activatable retracting means is attached to the locking pin for retracting the locking pin from the one of the bores upon being manually activated, thereby allowing the visor support arm to pivot. The retracting means is supported on the visor support arm between the two ends thereof and is positioned to be activated by manual movement away from the pivot point and towards the visor. DTIC

N93-29607 Department of the Navy, Washington, DC.
GOGGLES EMERGENCY RELEASE APPARATUS Patent
Daniel J. Schmidt, inventor (to Navy), Thomas J. Dillon, inventor (to Navy), and Ricky L. Greth, inventor (to Navy) 5 Jan. 1993 7 p Filed 30 Dec. 1991
(AD-D015685; US-Patent-5,176,342; US-Patent-Appl-SN-815294; US-Patent-Class-244-122) Avail: US Patent and Trademark Office

A goggles emergency release apparatus is disclosed wherein an actuator, positioned adjacent the goggles latching mechanism, drives a wedge into the mechanism to push a release pin into the open position and push the goggles away from the helmet. The actuator receives its initiation power when the ejection seat movement closes a microswitch. DTIC

N93-29675 IIT Research Inst., Chicago, IL.
ENGINEMAN STRESS AND FATIGUE: PILOT TESTS Final Report, Feb. 1991 - Jun. 1992
G. I. Kuehn Feb. 1993 74 p Sponsored by Federal Railroad Administration, Washington, DC, Office of Research and Development Limited Reproducibility: More than 20% of this document may be affected by microfiche quality
(Contract DTFR53-82-C-00254)
(PB93-175008; IITRI-E06641; FRA/ORD-92/17) Avail: CASI HC A04

In the pilot study, the effects of fatigue on the train handling performance and vigilance of four certified train service locomotive engineers was assessed while they operated the Federal Railroad Administration (FRA), Research and Locomotive Evaluator/Simulator (RALES). Subjects operated on an hourly cycle of 12 work-12 rest-8 work as a normal cycle followed by an hourly cycle of 12W-8R-8W the following week as a fatigue cycle. Subject activity diaries, scoring of various aspects of train handling, subject exit interviews, and observer's run observation notes were collected. Core body temperature and performance on a fitness for work measure were also recorded. The sleep records of the subjects were plotted and found to be atypical in comparison with those of non-engineer persons. The controlled, low interruption rest periods of the study may have been superior to the rest normally attained by the subjects, thus accounting for the failure to show differences between the two experimental conditions. The observed deterioration of performance regardless of schedule, coupled with the irregular sleep/work patterns of the subjects suggest continued research which focuses on sleep/work patterns and those performance related variables which were attendant on the decreases in performance in the pilot study. NTIS

N93-29845*# National Aeronautics and Space Administration. Marshall Space Flight Center, Huntsville, AL.
PLATFORM STAIR LIFT Patent Application
Bruce Weddendorf, inventor (to NASA) and Kosta Varnavas, inventor (to NASA) 22 Mar. 1993 21 p
(NASA-Case-MFS-28772-1; NAS 1.71:MFS-28772-1; US-Patent-Appl-SN-035345) Avail: CASI HC A03/MF A01

A motorized lift system for carrying a wheelchair user up or down a flight of stairs includes a platform sized to underlie and support a wheelchair and a person sitting thereon. The platform is driven upwardly or downwardly along one side of the stairway between the floors at the opposite ends thereof, in response to manual operation of a start/stop switch mounted on an upwardly projecting side rail portion of the platform, in a manner maintaining the platform in a horizontal orientation at all times. With the platform resting on the floor at the appropriate end of the stairs, a user simply rolls his wheelchair onto the platform and pushes the start button. This initiates the movement of the platform toward the opposite end of the stairs and also automatically closes guard rail structures at the opposite ends of the platform to retain the wheelchair thereon during platform movement. When the platform reaches the opposite end of the stairs, and is brought to rest on the floor adjacent thereto, the platform movement is automatically terminated and the guard rail structure opened. This permits the user to simply roll his wheelchair off the platform onto the floor and be on his way after comfortably and conveniently traversing the stairs on the platform. NASA

N93-29888# Aerospace Medical Research Labs., Wright-Patterson AFB, OH.
AN EVALUATION OF B-1B PILOT PERFORMANCE DURING SIMULATED INSTRUMENT APPROACHES WITH AND WITHOUT STATUS INFORMATION Final Report, Mar. 1991 - Jul. 1992
Bradley D. Purvis Sep. 1992 87 p
(AF Proj. 7184)
(AD-A263874; AL-TR-1992-0088) Avail: CASI HC A05/MF A01

The majority of aircraft incidents occur during the approach to landing phase of flight. Little research has been conducted that evaluates the efficiency of the instrument display format used by the pilots for the approach to landing. This research examined the effects of two Instrument Landing System display formats on the tracking performance of pilots in a B-1B simulator under varying crosswind and starting conditions. One display contained flight director command steering supplemented with raw glideslope and localizer data; the other display was the same minus the raw data. This research was based on the hypothesis that superior tracking performance would result with flight director and raw glideslope and localizer data on the Instrument Landing System display. The independent variables were as follows: display types, initial starting point, and wind. The dependent variables were as follows: glideslope deviation, localizer deviation, airspeed, roll rate variability, pitch rate variability, and altitude Above Ground Level. Twelve qualified B-1 pilots served as subjects in this simulation study, each subject flew a total of 16 Instrument Landing System approaches after practice. The two types of Instrument Landing System formats were evaluated under two wind conditions that began with two starting positions. DTIC

N93-29889# Aerospace Medical Research Labs., Wright-Patterson AFB, OH.
METHODS FOR CHARACTERIZING THE HUMAN HEAD FOR THE DESIGN OF HELMETS Final Report, Sep. 1990 - Apr. 1992
Kathleen M. Robinette and Jennifer J. Whitestone Apr. 1992 73 p
(AF Proj. 7184)
(AD-A263875; AL-TR-1992-0061) Avail: CASI HC A04/MF A01

For complex helmet systems that include optical displays and enhancements, as well as advanced sound attenuation, etc., the old methods for using anthropometry in design are inadequate. In this report, approaches for characterizing the human in the design process are described that provide, for the first time, shape and contour information. These methods have begun to revolutionize the helmet design process. DTIC

N93-29924# Dayton Univ. Research Inst., OH.
CATS EYES ADJUSTMENT PROCEDURES Final Report, Nov. 1992 - Jan. 1993
Joseph C. Antonio Apr. 1993 16 p
(Contract F33615-90-C-0005)
(AD-A264069; AL-TR-1993-0025) Avail: CASI HC A03/MF A01

Night vision goggles (NVGs) have been employed in a variety of aircraft for over 20 years; however, only recently has their application begun in fighter/attack aircraft. Research accomplished by the Night Vision Programs Office at the Aircrew Training Research Division of the USAF Armstrong Laboratory demonstrated the loss of NVG performance resulting from improper goggle adjustments. This report describes correct adjustment procedures for the CATS EYES NVG system currently being used by USAF, USN, and USMC fighter/attack pilots. The procedures described were developed so aircrews could take advantage of the adjustments available on the NVGs. Additionally, image descriptions are given to help aircrews evaluate NVG performance. Information on the necessary equipment/space needed for proper evaluation is also included. DTIC

N93-30167# Krug Life Sciences, Inc., San Antonio, TX. San Antonio Div.
UTILITY OF A GHOST HORIZON AND CLIMB/DIVE LADDER LINE TAPERING ON A HEAD-UP DISPLAY Final Report, Aug. 1991 - Aug. 1992
Lisa F. Weinstein and William R. Ercoline Apr. 1993 17 p
(DA Proj. 2930)
(AD-A264401; AL-TR-1992-0168) Avail: CASI HC A03/MF A01

As part of a United States Air Force (USAF) effort to standardize head-up display (HUD) symbology, an unusual attitude recovery task was employed to investigate the utility of a cue, the ghost horizon, that indicates the direction of the actual horizon when the climb/dive ladder (CDL) horizon line is not within the HUD field of view. Six HUD-experienced and 6 non-HUD-experienced military pilot subjects were used to determine whether there was improvement, with the ghost horizon, in ability to recover from nose-down unusual attitudes in a flight simulator. The ghost horizon was evaluated with 3 different CDL line configurations (tapered, nontapered, reverse tapered). In terms of accuracy of the initial stick input, the ghost-horizon configurations resulted in significantly better performance (about 11% better) than did the non-ghost-horizon configurations. The ghost horizon had no effect on initial stick input reaction time or total recovery time. The CDL line taper configuration did not affect accuracy, initial stick input reaction time, or total recovery time. Subjective data indicated that the pilots did not have a strong preference for any of the configurations. These findings suggest that the ghost horizon is a useful aid to unusual attitude recovery performance, and may reduce spatial disorientation. DTIC

N93-30204 Stanford Univ., CA.
VISUALIZATION TECHNIQUES FOR ANALYZING CONTROL OF HUMAN MOVEMENT: AFFINE MAPPINGS BETWEEN MULTI-DIMENSIONAL SPACES Ph.D. Thesis
Arthur Daniel Kuo 1993 124 p
Avail: Univ. Microfilms Order No. DA9309625

Control of human movement is difficult to study in part due to the number of muscles, joints, and degrees-of-freedom about the joints. Interpreting the commands generated by the central nervous system or the resultant motion generated by muscles is not possible without a method for reducing the number of variables examined. The goal is to develop and apply a method for understanding control of movement through visualization. This is made possible by examining the possible outputs of a system in terms of vectors composed of achievable accelerations and forces. The effect of many variables can then be seen in the final output, which is the summation of intermediate transformations. The visualization is predicated on a mathematical characteristic of the equations of motion, that they describe affine mappings. A theory of muscle function in terms of output vectors was developed and applied to the study of the action of muscles that cross more than one joint, a topic of contemporary interest in the biomechanics community. It was found that each muscle can be described in terms of its resultant output vector. Any presumed special qualities are due to the muscle's unique location rather than the number of joints it crosses, as had been previously thought. The theory of muscle function was also extended to encompass the set of all possible outputs. This set is useful to study when the actual command inputs or muscle forces are unknown, as is often the case in human movement. Movements made in response to postural perturbations were examined in light of the constraints acting upon this set. The constraints were found to greatly restrict the choices available to the central nervous system when forming a control. Sensitivity studies indicated that strengthening certain muscles can effect changes on the possible outputs. Finally, given the limited choices available, a model for central nervous system control showed that simple stability criteria are sufficient to approximate human behavior. Dissert. Abstr.

N93-30566*# National Aeronautics and Space Administration. Marshall Space Flight Center, Huntsville, AL.
PROSTHETIC ELBOW JOINT Patent Application
Bruce Weddendorf, inventor (to NASA) 8 Jul. 1992 19 p
(NASA-Case-MFS-28707-1; NAS 1.71:MFS-28707-1; US-Patent-Appl-SN-912953) Avail: CASI HC A03/MF A01

An artificial manually positionable elbow joint for use in an upper extremity, above-elbow, prosthetic which provides a locking feature that is easily controlled by the wearer is described. The instant elbow joint is very strong and durable to withstand the repeated heavy loadings encountered by a wearer who works in an industrial, construction, farming or similar environment. The elbow joint of the present invention comprises a turntable, a frame, a forearm, and a locking assembly. The frame generally includes a housing for the locking assembly and two protruding ears. The forearm includes an elongated beam having a cup-shaped cylindrical member at one end and a locking wheel having a plurality of holes along a circular arc on its other end with a central bore for pivotal attachment to the protruding ears of the frame. The locking assembly includes a collar having a central opening with a plurality of internal grooves, a plurality of internal cam members each having a chamfered surface at one end and a V-shaped slot at its other end; an elongated locking pin having a crown wheel with cam surfaces and locking lugs secured thereto; two coiled compression springs; and a flexible filament attached to one end of the elongated locking pin and extending from the locking assembly for extending and retracting the locking pin into the holes in the locking wheel to permit selective adjustment of the forearm relative to the frame. In use, the turntable is affixed to the upper arm part of the prosthetic in the conventional manner and the cup-shaped cylindrical member on one end of the forearm is affixed to the forearm piece of the prosthetic in the conventional manner. The elbow joint is easily adjusted and locked between maximum flex and extended positions. NASA

N93-30590 Anacapa Sciences, Inc., Fort Rucker, AL.
THE EFFECTS OF SUPERIMPOSING SYMBOLOGY ON A SIMULATED NIGHT VISION GOGGLE DISPLAY Interim Report
D. M. McAnulty, John W. Ruffner, and David B. Hamilton Feb. 1993 84 p Limited Reproducibility: More than 20% of this document may be affected by microfiche quality
(Contract MDA903-92-D-0025)
(AD-A263458; ARI-RR-1636) Avail: CASI HC A05

The U.S. Army is acquiring a system that superimposes instrument symbology on night vision goggle (NVG) imagery. However, previous research indicates that the symbology may distract a pilot's attention from obstacle detection, recognition, and avoidance and may interfere with proper scanning patterns. To test the effects of combining imager and symbology, 36 helicopter pilots were presented night-flight scenarios simulating NVG imagery only, symbology only, and imagery plus symbology. The aviators were required to monitor and respond to predefined scene and symbology targets. They detected and responded rapidly to a high percentage of targets when viewing the scene-only and symbology-only scenarios. Their performance decreased significantly when the two types of information were presented together, but the decrease was small when compared to the increased amount of information available in the display. Aviator performance improved with practice and was related to experience and eye dominance. The aviators suggested several modifications for the symbology suite. DTIC

N93-29727*# Colorado Univ., Boulder.
EARTH TO LUNAR CELSS EVOLUTION
In Universities Space Research Association, Houston, Proceedings of the Seventh Annual Summer Conference. NASA/USRA: University Advanced

Design Program 1991 p 123-132 (For primary document see N93-29712 11-01)
Avail: CASI HC A02/MF A03

N93-29728*# Florida Univ., Gainesville.
DESIGN OF BIOMASS MANAGEMENT SYSTEMS AND COMPONENTS FOR CLOSED LOOP LIFE SUPPORT SYSTEMS
In Universities Space Research Association, Houston, Proceedings of the Seventh Annual Summer Conference. NASA/USRA: University Advanced Design Program 1991 p 133-137 (For primary document see N93-29712 11-01)
Avail: CASI HC A01/MF A03

N93-29733*# Idaho Univ., Moscow.
EXERCISE/RECREATION FACILITY FOR A LUNAR OR MARS ANALOG
In Universities Space Research Association, Houston, Proceedings of the Seventh Annual Summer Conference. NASA/USRA: University Advanced Design Program 1991 p 155-158 (For primary document see N93-29712 11-01)
Avail: CASI HC A01/MF A03

N93-29734*# Kansas State Univ., Manhattan.
AUTOMATION OF CLOSED ENVIRONMENTS IN SPACE FOR HUMAN COMFORT AND SAFETY
In Universities Space Research Association, Houston, Proceedings of the Seventh Annual Summer Conference. NASA/USRA: University Advanced Design Program 1991 p 159-163 (For primary document see N93-29712 11-01)
Avail: CASI HC A01/MF A03

N93-29747*# Prairie View Agricultural and Mechanical Coll., TX.
MARS HABITAT
In Universities Space Research Association, Houston, Proceedings of the Seventh Annual Summer Conference. NASA/USRA: University Advanced Design Program 1991 p 253-263 (For primary document see N93-29712 11-01)
Avail: CASI HC A03/MF A03

N93-29748*# Puerto Rico Univ., Rio Piedras.
SELENIA: A HABITABILITY STUDY FOR THE DEVELOPMENT OF A THIRD GENERATION LUNAR BASE
In Universities Space Research Association, Houston, Proceedings of the Seventh Annual Summer Conference. NASA/USRA: University Advanced Design Program 1991 p 265-273 (For primary document see N93-29712 11-01)
Avail: CASI HC A02/MF A03

N93-29760*# Wisconsin Univ., Milwaukee.
GENESIS 2: ADVANCED LUNAR OUTPOST
Gary T. Moore *In* Universities Space Research Association, Houston, Proceedings of the Seventh Annual Summer Conference. NASA/USRA: University Advanced Design Program 1991 p 329-334 (For primary document see N93-29712 11-01)
(Contract NASw-4435)
Avail: CASI HC A02/MF A03

55 SPACE BIOLOGY

Includes exobiology; planetary biology; and extraterrestrial life.

N93-28895*# Harvard Univ., Cambridge, MA.
WIDE-BANDWIDTH HIGH-RESOLUTION SEARCH FOR EXTRATERRESTRIAL INTELLIGENCE Semiannual Status Report, 15 Dec. 1992 - 15 Jun. 1993
Paul Horowitz 15 Jun. 1993 26 p
(Grant NAGw-2872)
(NASA-CR-193137; NAS 1.26:193137) Avail: CASI HC A03/MF A01

Research accomplished during the third 6-month period is summarized. Research covered the following: dual-horn antenna performance; high electron mobility transistors (HEMT) low-noise amplifiers; downconverters; fast Fourier transform (FFT) array; and backend 'feature recognizer' array. CASI

59 MATHEMATICAL AND COMPUTER SCIENCES (GENERAL)

N93-28573# Argonne National Lab., IL.
RESEARCH IN MATHEMATICS AND COMPUTER SCIENCE, MARCH 1, 1991 - SEPTEMBER 30, 1992
G. W. Pieper Oct. 1992 56 p
(Contract W-31-109-eng-38)
(DE93-011492; ANL-92/37) Avail: CASI HC A04/MF A01

This report discusses the following topics in mathematics and computer science at Argonne National Laboratory: harnessing the power; modeling piezoelectric crystals; a two-way street; the challenge is on; a true molecular engineering capability; CHAMMPions attack climate issues; studying vortex dynamics; studying vortex structure; providing reliable and fast derivatives; automating reasoning for scientific problem solving; optimization and mathematical programming; scalable algorithms for linear algebra; reliable core software; computing phylogenetic trees; managing life-critical systems; interacting with fata through visualization; new tools for new technologies. DOE

N93-28841*# Institute for Computer Applications in Science and Engineering, Hampton, VA.
GODUNOV-TYPE SCHEMES APPLIED TO DETONATION FLOWS
James J. Quirk Washington Apr. 1993 92 p
(Contracts NAS1-19480; NAS1-18605; NAS1-18107; NAS1-17070; NAS1-17130; NAS1-15830; NAS1-16394; NAS1-14101; NAS1-14472; RTOP 505-90-52-01)
(NASA-CR-191447; NAS 1.26:191447; ICASE-93-15) Avail: CASI HC A05/MF A01

The Institute for Computer Applications in Science and Engineering (ICASE) is operated at the Langley Research Center of NASA by the Universities Space Research Association (USRA) under a contract with the Center. The Institute conducts research in applied mathematics, numerical analysis, fluid mechanics, and computer science in order to extend and improve problem solving capabilities in science and engineering, particularly in aeronautics and space. Current ICASE research programs are applied and numerical mathematics, including numerical analysis and algorithm development; theoretical and computational research in fluid mechanics in selected areas of interest to LaRC, including acoustics and combustion; experimental research in transition and turbulence and aerodynamics involving LaRC facilities and scientists; and computer science. A complete listing of ICASE reports for 1975 - 1991 are given. Derived from text

N93-29516*# National Aeronautics and Space Administration. Lyndon B. Johnson Space Center, Houston, TX.
NORTH AMERICAN FUZZY LOGIC PROCESSING SOCIETY (NAFIPS 1992), VOLUME 1
James A. Villarreal, comp. Dec. 1992 376 p Conference held in Puerto Vallarta, Mexico, 15-17 Dec. 1992 Sponsored in part by Inst. Tecnologico de Morelia; Indian Society for Fuzzy Mathematics and Information Processing; Inst. Technologico y de Estudios Superiores de Monterrey; International Fuzzy Systems Association; Japan Society for Fuzzy Theory and Systems; and Microelectronics and Computer Technology Corp.
(NASA-CP-10112-Vol-1; S-702-Vol-1; NAS 1.55:10112-Vol-1) Avail: CASI HC A17/MF A03

This document contains papers presented at the NAFIPS '92 North American Fuzzy Information Processing Society Conference. More than 75 papers were presented at this Conference, which was sponsored by NAFIPS in cooperation with NASA, the Instituto Tecnologico de Morelia, the Indian Society for Fuzzy Mathematics and Information Processing (ISFUMIP), the Instituto Tecnologico de Estudios Superiores de Monterrey (ITESM), the International Fuzzy Systems Association (IFSA), the Japan Society for Fuzzy Theory and Systems, and the Microelectronics and Computer Technology Corporation (MCC). The fuzzy set theory has led to a large number of diverse applications. Recently, interesting applications have been developed which involve the integration of fuzzy systems with adaptive processes such as neural networks and genetic algorithms. NAFIPS '92 was directed toward the advancement, commercialization, and engineering development of these technologies. For individual titles, see N93-29517 through N93-29555.

N93-29517*# Louisville Univ., KY. Dept. of Mathematics.
AN ANALYSIS OF POSSIBLE APPLICATIONS OF FUZZY SET THEORY TO THE ACTUARIAL CREDIBILITY THEORY **c67**
Krzysztof Ostaszewski and Waldemar Karwowski *In* NASA. Johnson Space Center, North American Fuzzy Logic Processing Society (NAFIPS 1992), Volume 1 Dec. 1992 p 1-6 (For primary document see N93-29516 11-59)
Avail: CASI HC A02/MF A03

In this work, we review the basic concepts of actuarial credibility theory from the point of view of introducing applications of the fuzzy set-theoretic method. We show how the concept of actuarial credibility can be modeled through the fuzzy set membership functions and how fuzzy set methods, especially fuzzy pattern recognition, can provide an alternative tool for estimating credibility. Author (revised)

N93-29518*# Toulouse Univ. (France).
ESTIMATIONS OF EXPECTEDNESS AND POTENTIAL SURPRISE IN POSSIBILITY THEORY **c65**
Henri Prade and Ronald R. Yager (Iona Coll., New Rochelle, NY.) *In* NASA. Johnson Space Center, North American Fuzzy Logic Processing Society (NAFIPS 1992), Volume 1 Dec. 1992 p 7-13 (For primary document see N93-29516 11-59)
Avail: CASI HC A02/MF A03

This note investigates how various ideas of 'expectedness' can be captured in the framework of possibility theory. Particularly, we are interested in trying to introduce estimates of the kind of lack of surprise expressed by people when saying 'I would not be surprised that...' before an event takes place, or by saying 'I knew it' after its realization. In possibility theory, a possibility distribution is supposed to model the relative levels of mutually exclusive alternatives in a set, or equivalently, the alternatives are assumed to be rank-ordered according to their level of possibility to take place. Four basic set-functions associated with a possibility distribution, including standard possibility and necessity measures, are discussed from the point of view of what they estimate when applied to potential events. Extensions of these estimates based on the notions of Q-projection or OWA operators are proposed when only significant parts of the possibility distribution are retained in the evaluation. The case of partially-known possibility distributions is also considered. Some potential applications are outlined. Author (revised)

N93-29519*# New South Wales Univ., Kensington (Australia). Dept. of Computer Science.
COMPARISON OF SPECIFICITY AND INFORMATION FOR FUZZY DOMAINS **c67**
Arthur Ramer *In* NASA. Johnson Space Center, North American Fuzzy Logic Processing Society (NAFIPS 1992), Volume 1 Dec. 1992 p 14-20 (For primary document see N93-29516 11-59)
Avail: CASI HC A01/MF A03

This paper demonstrates how an integrated theory can be built on the foundation of possibility theory. Information and uncertainty were considered in 'fuzzy' literature since 1982. Our departing point is the model proposed by Klir for the discrete case. It was elaborated axiomatically by Ramer, who also introduced the continuous model. Specificity as a numerical function was considered mostly within Dempster-Shafer evidence theory. An explicity definition was given first by Yager, who has also introduced it in the context of possibility theory. Axiomatic approach and the continuous model have been developed very recently by Ramer and Yager. They also establish a close analytical correspondence between specificity and information. In literature to date, specificity and uncertainty are defined only for the discrete finite domains, with a sole exception. Our presentation removes these limitations. We define specificity measures for arbitrary measurable domains. Author (revised)

N93-29520*# Soviet Association of Fuzzy Systems, Moscow (Russia).
THE AXIOMATIC DEFINITION OF A LINGUISTIC SCALE FUZZINESS DEGREE, ITS MAJOR PROPERTIES, AND APPLICATIONS **c67**
Alexander P. Ryjov *In* NASA. Johnson Space Center, North American Fuzzy Logic Processing Society (NAFIPS 1992), Volume 1 Dec. 1992 p 21-28 (For primary document see N93-29516 11-59)
Avail: CASI HC A02/MF A03

A model that makes use of fuzzy linguistic scales (FLS) is considered in this report. The definition of FLS fuzziness and its major properties are given in the report. Definitions that are concerned with information loss and noise are also presented. Author (revised)

N93-29521*# Toronto Univ. (Ontario). Dept. of Industrial Engineering.
HOW TO SELECT COMBINATION OPERATORS FOR FUZZY EXPERT SYSTEMS USING CRI **c67**
I. B. Turksen and Y. Tian *In* NASA. Johnson Space Center, North American Fuzzy Logic Processing Society (NAFIPS 1992), Volume 1 Dec. 1992 p 29-38 Sponsored in part by Natural Sciences and Engineering Research Council and Manufacturing Research Corp. (For primary document see N93-29516 11-59)
Avail: CASI HC A02/MF A03

A method to select combination operators for fuzzy expert systems using the Compositional Rule of Inference (CRI) is proposed. First, fuzzy inference processes based on CRI are classified into three categories in terms of their inference results: the Expansion Type Inference, the Reduction Type Inference, and Other Type Inferences. Further, implication operators under Sup-T composition are classified as the Expansion Type Operator, the Reduction Type Operator, and the Other Type Operators. Finally, the combination of rules or their consequences is investigated for inference processes based on CRI. Author (revised)

N93-29522*# Texas A&M Univ., College Station. Center for Fuzzy Logic and Intelligent Systems.
APPROXIMATE REASONING USING TERMINOLOGICAL MODELS **c63**
John Yen and Nitin Vaidya (Texas A&M Univ., Houston.) *In* NASA. Johnson Space Center, North American Fuzzy Logic Processing Society (NAFIPS 1992), Volume 1 Dec. 1992 p 39-48 (For primary document see N93-29516 11-59)
Avail: CASI HC A02/MF A03

Term Subsumption Systems (TSS) form a knowledge-representation scheme in AI that can express the defining characteristics of concepts through a formal language that has a well-defined semantics and incorporates a reasoning mechanism that can deduce whether one concept subsumes another. However, TSS's have very limited ability to deal with the issue of uncertainty in knowledge bases. The objective of this research is to address issues in combining approximate reasoning with term subsumption systems. To do this, we have extended an existing AI architecture (CLASP) that is built on the top of a term subsumption system (LOOM). First, the assertional component of LOOM has been extended for asserting and representing uncertain propositions. Second, we have extended the pattern matcher of CLASP for plausible rule-based inferences. Third, an approximate reasoning model has been added to facilitate various kinds of approximate reasoning. And finally, the issue of inconsistency in truth values due to inheritance is addressed using justification of those values. This architecture enhances the reasoning capabilities of expert systems by providing support for reasoning under uncertainty using knowledge captured in TSS. Also, as definitional knowledge is explicit and separate from heuristic knowledge for plausible inferences, the maintainability of expert systems could be improved. Author (revised)

N93-29523*# Missouri Univ., Columbia. Dept. of Electrical and Computer Engineering.
QUANTITATIVE ANALYSIS OF PROPERTIES AND SPATIAL RELATIONS OF FUZZY IMAGE REGIONS **c67**
Raghu Krishnapuram, James M. Keller, and Yibing Ma *In* NASA. Johnson Space Center, North American Fuzzy Logic Processing Society (NAFIPS 1992), Volume 1 Dec. 1992 p 49-58 (For primary document see N93-29516 11-59)
Avail: CASI HC A02/MF A03

Properties of objects and spatial relations between objects play an important role in rule-based approaches for high-level vision. The partial presence or absence of such properties and relationships can supply both positive and negative evidence for region labeling hypotheses. Similarly, fuzzy labeling of a region can generate new hypotheses pertaining to the properties of the region, its relation to the neighboring regions, and finally, the labels of the neighboring regions. In this paper, we present a unified methodology to characterize properties and spatial relationships of object regions in a digital image. The proposed methods can be used to arrive at more meaningful decisions about the contents of the scene. Author

N93-29524*# Missouri Univ., Columbia. Dept. of Electrical and Computer Engineering.

A FUZZY CLUSTERING ALGORITHM TO DETECT PLANAR AND QUADRIC SHAPES **c61**

Raghu Krishnapuram, Hichem Frigui, and Olfa Nasraoui *In* NASA. Johnson Space Center, North American Fuzzy Logic Processing Society (NAFIPS 1992), Volume 1 Dec. 1992 p 59-68 (For primary document see N93-29516 11-59)

Avail: CASI HC A02/MF A03

In this paper, we introduce a new fuzzy clustering algorithm to detect an unknown number of planar and quadric shapes in noisy data. The proposed algorithm is computationally and implementationally simple, and it overcomes many of the drawbacks of the existing algorithms that have been proposed for similar tasks. Since the clustering is performed in the original image space, and since no features need to be computed, this approach is particularly suited for sparse data. The algorithm may also be used in pattern recognition applications. Author (revised)

N93-29525*# National Aeronautics and Space Administration. Lyndon B. Johnson Space Center, Houston, TX.

A FUZZY MEASURE APPROACH TO MOTION FRAME ANALYSIS FOR SCENE DETECTION M.S. Thesis - Houston Univ. **c67**

Albert B. Leigh (McDonnell-Douglas Space Systems Co., Houston, TX.) and Sankar K. Pal (Indian Statistical Inst., Calcutta.) *In its* North American Fuzzy Logic Processing Society (NAFIPS 1992), Volume 1 Dec. 1992 p 69-80 (For primary document see N93-29516 11-59)

Avail: CASI HC A03/MF A03

This paper addresses a solution to the problem of scene estimation of motion video data in the fuzzy set theoretic framework. Using fuzzy image feature extractors, a new algorithm is developed to compute the change of information in each of two successive frames to classify scenes. This classification process of raw input visual data can be used to establish structure for correlation. The algorithm attempts to fulfill the need for nonlinear, frame-accurate access to video data for applications such as video editing and visual document archival/retrieval systems in multimedia environments. Author (revised)

N93-29526*# Missouri Univ., Columbia. Dept. of Electrical and Computer Engineering.

AUTOMATIC RULE GENERATION FOR HIGH-LEVEL VISION **c61**

Frank Chung-Hoon Rhee and Raghu Krishnapuram *In* NASA. Johnson Space Center, North American Fuzzy Logic Processing Society (NAFIPS 1992), Volume 1 Dec. 1992 p 81-88 (For primary document see N93-29516 11-59)

Avail: CASI HC A02/MF A03

Many high-level vision systems use rule-based approaches to solving problems such as autonomous navigation and image understanding. The rules are usually elaborated by experts. However, this procedure may be rather tedious. In this paper, we propose a method to generate such rules automatically from training data. The proposed method is also capable of filtering out irrelevant features and criteria from the rules. Author (revised)

N93-29527*# Toledo Univ., OH. Dept. of Electrical Engineering.

ENCODING SPATIAL IMAGES: A FUZZY SET THEORY APPROACH **c67**

Leszek M. Sztandera *In* NASA. Johnson Space Center, North American Fuzzy Logic Processing Society (NAFIPS 1992), Volume 1 Dec. 1992 p 89-97 (For primary document see N93-29516 11-59)

Avail: CASI HC A02/MF A03

As the use of fuzzy set theory continues to grow, there is an increased need for methodologies and formalisms to manipulate obtained fuzzy subsets. Concepts involving relative position of fuzzy patterns are acknowledged as being of high importance in many areas. In this paper, we present an approach based on the concept of dominance in fuzzy set theory for modelling relative positions among fuzzy subsets of a plane. In particular, we define the following spatial relations: to the left (right), in front of, behind, above, below, near, far from, and touching. This concept has been implemented to define spatial relationships among fuzzy subsets of the image plane. Spatial relationships based on fuzzy set theory, coupled with a fuzzy segmentation, should therefore yield realistic results in scene understanding. Author

N93-29528*# University of West Florida, Pensacola. Computer Science Div.

IMAGE SEGMENTATION USING FUZZY LVQ CLUSTERING NETWORKS **c67**

Eric Chen-Kuo Tsao, James C. Bezdek, and Nikhil R. Pal *In* NASA. Johnson Space Center, North American Fuzzy Logic Processing Society (NAFIPS 1992), Volume 1 Dec. 1992 p 98-107 (For primary document see N93-29516 11-59)

(Grant NSF IRI-90-03252)

Avail: CASI HC A02/MF A03

In this note we formulate image segmentation as a clustering problem. Feature vectors extracted from a raw image are clustered into subregions, thereby segmenting the image. A fuzzy generalization of a Kohonen learning vector quantization (LVQ) which integrates the Fuzzy c-Means (FCM) model with the learning rate and updating strategies of the LVQ is used for this task. This network, which segments images in an unsupervised manner, is thus related to the FCM optimization problem. Numerical examples on photographic and magnetic resonance images are given to illustrate this approach to image segmentation. Author (revised)

N93-29529*# Cincinnati Univ., OH. Dept. of Electrical and Computer Engineering.

A NEURO-FUZZY ARCHITECTURE FOR REAL-TIME APPLICATIONS **c67**

P. A. Ramamoorthy and Song Huang *In* NASA. Johnson Space Center, North American Fuzzy Logic Processing Society (NAFIPS 1992), Volume 1 Dec. 1992 p 108-117 (For primary document see N93-29516 11-59)

Avail: CASI HC A02/MF A03

Neural networks and fuzzy expert systems perform the same task of functional mapping using entirely different approaches. Each approach has certain unique features. The ability to learn specific input-output mappings from large input/output data possibly corrupted by noise and the ability to adapt or continue learning are some important features of neural networks. Fuzzy expert systems are known for their ability to deal with fuzzy information and incomplete/imprecise data in a structured, logical way. Since both of these techniques implement the same task (that of functional mapping--we regard 'inferencing' as one specific category under this class), a fusion of the two concepts that retains their unique features while overcoming their individual drawbacks will have excellent applications in the real world. In this paper, we arrive at a new architecture by fusing the two concepts. The architecture has the trainability/adaptibility (based on input/output observations) property of the neural networks and the architectural features that are unique to fuzzy expert systems. It also does not require specific information such as fuzzy rules, defuzzification procedure used, etc., though any such information can be integrated into the architecture. We show that this architecture can provide better performance than is possible from a single two or three layer feedforward neural network. Further, we show that this new architecture can be used as an efficient vehicle for hardware implementation of complex fuzzy expert systems for real-time applications. A numerical example is provided to show the potential of this approach. Author (revised)

N93-29530*# Missouri Univ., Columbia. Dept. of Mechanical and Aerospace Engineering.

A COMPOSITE SELF TUNING STRATEGY FOR FUZZY CONTROL OF DYNAMIC SYSTEMS **c67**

C.-Y. Shieh and Satish S. Nair *In* NASA. Johnson Space Center, North American Fuzzy Logic Processing Society (NAFIPS 1992), Volume 1 Dec. 1992 p 118-124 Sponsored in part by National Center for Supercomputing Applications (For primary document see N93-29516 11-59)

Avail: CASI HC A02/MF A03

The feature of self learning makes fuzzy logic controllers attractive in control applications. This paper proposes a strategy to tune the fuzzy logic controller on-line by tuning the data base as well as the rule base. The structure of the controller is outlined and preliminary results are presented using simulation studies. Author

N93-29531*# California Univ., Irvine. Dept. of Electrical and Computer Engineering.

A SELF-LEARNING RULE BASE FOR COMMAND FOLLOWING IN DYNAMICAL SYSTEMS c61

Wei K. Tsai, Hon-Mun Lee, and Alexander Parlos (Texas A&M Univ., College Station.) *In* NASA. Johnson Space Center, North American Fuzzy Logic Processing Society (NAFIPS 1992), Volume 1 Dec. 1992 p 125-134 (For primary document see N93-29516 11-59)
(Contract DE-FG07-89ER-12893)
Avail: CASI HC A02/MF A03

In this paper, a self-learning Rule Base for command following in dynamical systems is presented. The learning is accomplished though reinforcement learning using an associative memory called SAM. The main advantage of SAM is that it is a function approximator with explicit storage of training samples. A learning algorithm patterned after the dynamic programming is proposed. Two artificially created, unstable dynamical systems are used for testing, and the Rule Base was used to generate a feedback control to improve the command following ability of the otherwise uncontrolled systems. The numerical results are very encouraging. The controlled systems exhibit a more stable behavior and a better capability to follow reference commands. The rules resulting from the reinforcement learning are explicitly stored and they can be modified or augmented by human experts. Due to overlapping storage scheme of SAM, the stored rules are similar to fuzzy rules. Author (revised)

N93-29532*# Iona Coll., New Rochelle, NY. Machine Intelligence Inst.

ADAPTIVE DEFUZZIFICATION FOR FUZZY SYSTEMS MODELING c67

Ronald R. Yager and Dimitar P. Filev *In* NASA. Johnson Space Center, North American Fuzzy Logic Processing Society (NAFIPS 1992), Volume 1 Dec. 1992 p 135-142 (For primary document see N93-29516 11-59)
Avail: CASI HC A02/MF A03

We propose a new parameterized method for the defuzzification process based on the simple M-SLIDE transformation. We develop a computationally efficient algorithm for learning the relevant parameter as well as providing a computationally simple scheme for doing the defuzzification step in the fuzzy logic controllers. The M-SLIDE method results in a particularly simple linear form of the algorithm for learning the parameter which can be used both off- and on-line. Author (revised)

N93-29533*# Texas A&M Univ., College Station. Center for Fuzzy Logic and Intelligent Systems Research.

DESIGN ISSUES OF A REINFORCEMENT-BASED SELF-LEARNING FUZZY CONTROLLER FOR PETROCHEMICAL PROCESS CONTROL c67

John Yen, Haojin Wang, and Walter C. Daugherity *In* NASA. Johnson Space Center, North American Fuzzy Logic Processing Society (NAFIPS 1992), Volume 1 Dec. 1992 p 143-153 (For primary document see N93-29516 11-59)
Avail: CASI HC A03/MF A03

Fuzzy logic controllers have some often-cited advantages over conventional techniques such as PID control, including easier implementation, accommodation to natural language, and the ability to cover a wider range of operating conditions. One major obstacle that hinders the broader application of fuzzy logic controllers is the lack of a systematic way to develop and modify their rules; as a result the creation and modification of fuzzy rules often depends on trial and error or pure experimentation. One of the proposed approaches to address this issue is a self-learning fuzzy logic controller (SFLC) that uses reinforcement learning techniques to learn the desirability of states and to adjust the consequent part of its fuzzy control rules accordingly. Due to the different dynamics of the controlled processes, the performance of a self-learning fuzzy controller is highly contingent on its design. The design issue has not received sufficient attention. The issues related to the design of a SFLC for application to a petrochemical process are discussed, and its performance is compared with that of a PID and a self-tuning fuzzy logic controller. Author (revised)

N93-29534*# National Aeronautics and Space Administration. Lyndon B. Johnson Space Center, Houston, TX.

LEARNING CHARACTERISTICS OF A SPACE-TIME NEURAL NETWORK AS A TETHER SKIPROPE OBSERVER c63

Robert N. Lea, James A. Villarreal, Yashvant Jani (Togai InfraLogic, Inc., Houston, TX.), and Charles Copeland (Loral Space Information Systems, Houston, TX.) *In its* North American Fuzzy Logic Processing Society (NAFIPS 1992), Volume 1 Dec. 1992 p 154-165 (For primary document see N93-29516 11-59)
Avail: CASI HC A03/MF A03

The Software Technology Laboratory at JSC is testing a Space Time Neural Network (STNN) for observing tether oscillations present during retrieval of a tethered satellite. Proper identification of tether oscillations, known as 'skiprope' motion, is vital to safe retrieval of the tethered satellite. Our studies indicate that STNN has certain learning characteristics that must be understood properly to utilize this type of neural network for the tethered satellite problem. We present our findings on the learning characteristics including a learning rate versus momentum performance table. Author (revised)

N93-29535*# Texas Technological Univ., Lubbock. Dept. of Electrical Engineering.

CLUSTERING OF TETHERED SATELLITE SYSTEM SIMULATION DATA BY AN ADAPTIVE NEURO-FUZZY ALGORITHM c67

Sunanda Mitra and Surya Pemmaraju *In* NASA. Johnson Space Center, North American Fuzzy Logic Processing Society (NAFIPS 1992), Volume 1 Dec. 1992 p 166-174 Sponsored in part by Northrop Corp. and Texas Advanced Technology Program (For primary document see N93-29516 11-59)
(Grant NAG9-509)
Avail: CASI HC A02/MF A03

Recent developments in neuro-fuzzy systems indicate that the concepts of adaptive pattern recognition, when used to identify appropriate control actions corresponding to clusters of patterns representing system states in dynamic nonlinear control systems, may result in innovative designs. A modular, unsupervised neural network architecture, in which fuzzy learning rules have been embedded is used for on-line identification of similar states. The architecture and control rules involved in Adaptive Fuzzy Leader Clustering (AFLC) allow this system to be incorporated in control systems for identification of system states corresponding to specific control actions. We have used this algorithm to cluster the simulation data of Tethered Satellite System (TSS) to estimate the range of delta voltages necessary to maintain the desired length rate of the tether. The AFLC algorithm is capable of on-line estimation of the appropriate control voltages from the corresponding length error and length rate error without a priori knowledge of their membership functions and familarity with the behavior of the Tethered Satellite System. Author (revised)

N93-29536*# North Carolina Univ., Charlotte. Dept. of Computer Science.

CHARACTER RECOGNITION USING A NEURAL NETWORK MODEL WITH FUZZY REPRESENTATION c63

Nassrin Tavakoli and David Seniw *In* NASA. Johnson Space Center, North American Fuzzy Logic Processing Society (NAFIPS 1992), Volume 1 Dec. 1992 p 175-184 (For primary document see N93-29516 11-59)
Avail: CASI HC A02/MF A03

The degree to which digital images are recognized correctly by computerized algorithms is highly dependent upon the representation and the classification processes. Fuzzy techniques play an important role in both processes. In this paper, the role of fuzzy representation and classification on the recognition of digital characters is investigated. An experimental Neural Network model with application to character recognition was developed. Through a set of experiments, the effect of fuzzy representation on the recognition accuracy of this model is presented. Author (revised)

N93-29537*# Texas A&M Univ., College Station. Dept. of Computer Science.

DESIGNING A FUZZY SCHEDULER FOR HARD REAL-TIME SYSTEMS c67

John Yen, Jonathan Lee, Nathan Pfluger, and Swami Natarajan *In* NASA. Johnson Space Center, North American Fuzzy Logic Processing Society

(NAFIPS 1992), Volume 1 Dec. 1992 p 185-194 (For primary document see N93-29516 11-59)
Avail: CASI HC A02/MF A03

In hard real-time systems, tasks have to be performed not only correctly, but also in a timely fashion. If timing constraints are not met, there might be severe consequences. Task scheduling is the most important problem in designing a hard real-time system, because the scheduling algorithm ensures that tasks meet their deadlines. However, the inherent nature of uncertainty in dynamic hard real-time systems increases the problems inherent in scheduling. In an effort to alleviate these problems, we have developed a fuzzy scheduler to facilitate searching for a feasible schedule. A set of fuzzy rules are proposed to guide the search. The situation we are trying to address is the performance of the system when no feasible solution can be found, and therefore, certain tasks will not be executed. We wish to limit the number of important tasks that are not scheduled. Author (revised)

N93-29538*# SGS-Thomson Microelectronics, Inc., Agrate Brianza (Italy). Corporate Advanced System Architectures.
WARP: WEIGHT ASSOCIATIVE RULE PROCESSOR. A DEDICATED VLSI FUZZY LOGIC MEGACELL **c67**
A. Pagni, R. Poluzzi, and G. G. Rizzotto *In* NASA. Johnson Space Center, North American Fuzzy Logic Processing Society (NAFIPS 1992), Volume 1 Dec. 1992 p 195-204 (For primary document see N93-29516 11-59)
Avail: CASI HC A02/MF A03

During the last five years Fuzzy Logic has gained enormous popularity in the academic and industrial worlds. The success of this new methodology has led the microelectronics industry to create a new class of machines, called Fuzzy Machines, to overcome the limitations of traditional computing systems when utilized as Fuzzy Systems. This paper gives an overview of the methods by which Fuzzy Logic data structures are represented in the machines (each with its own advantages and inefficiencies). Next, the paper introduces WARP (Weight Associative Rule Processor) which is a dedicated VLSI megacell allowing the realization of a fuzzy controller suitable for a wide range of applications. WARP represents an innovative approach to VLSI Fuzzy controllers by utilizing different types of data structures for characterizing the membership functions during the various stages of the Fuzzy processing. WARP dedicated architecture has been designed in order to achieve high performance by exploiting the computational advantages offered by the different data representations. Author (revised)

N93-29539*# Loki Software, Inc., Liberty Corner, NJ.
EVALUATION OF FUZZY INFERENCE SYSTEMS USING FUZZY LEAST SQUARES **c67**
Joseph M. Barone *In* NASA. Johnson Space Center, North American Fuzzy Logic Processing Society (NAFIPS 1992), Volume 1 Dec. 1992 p 205-214 (For primary document see N93-29516 11-59)
Avail: CASI HC A02/MF A03

Efforts to develop evaluation methods for fuzzy inference systems which are not based on crisp, quantitative data or processes (i.e., where the phenomenon the system is built to describe or control is inherently fuzzy) are just beginning. This paper suggests that the method of fuzzy least squares can be used to perform such evaluations. Regressing the desired outputs onto the inferred outputs can provide both global and local measures of success. The global measures have some value in an absolute sense, but they are particularly useful when competing solutions (e.g., different numbers of rules, different fuzzy input partitions) are being compared. The local measure described here can be used to identify specific areas of poor fit where special measures (e.g., the use of emphatic or suppressive rules) can be applied. Several examples are discussed which illustrate the applicability of the method as an evaluation tool. Author (revised)

N93-29540*# California Univ., Berkeley. International Computer Science Inst.
A MODEL FOR AMALGAMATION IN GROUP DECISION MAKING **c81**
Vincenzo Cutello (Catania Univ., Italy.) and Javier Montero (Universidad Complutense, Madrid, Spain.) *In* NASA. Johnson Space Center, North American Fuzzy Logic Processing Society (NAFIPS 1992), Volume 1 Dec. 1992 p 215-223 Sponsored in part by Direccion General de Investigacion Cientifica y Tecnica (For primary document see N93-29516 11-59)
Avail: CASI HC A02/MF A03

In this paper we present a generalization of the model proposed by Montero, by allowing non-complete fuzzy binary relations for individuals. A degree of unsatisfaction can be defined in this case, suggesting that any democratic aggregation rule should take into account not only ethical conditions or some degree of rationality in the amalgamating procedure, but also a minimum support for the set of alternatives subject to the group analysis. Author (revised)

N93-29541*# Odessa Inst. of National Economy (Ukraine). Dept. of Computer Science.
FUZZY FORECASTING AND DECISION MAKING IN SHORT DYNAMIC TIME SERIES **c81**
Efim J. Karpovsky, comp. and Ibrahim Ohiokhoya Ozoya *In* NASA. Johnson Space Center, North American Fuzzy Logic Processing Society (NAFIPS 1992), Volume 1 Dec. 1992 p 224-228 (For primary document see N93-29516 11-59)
Avail: CASI HC A01/MF A03

This paper focuses on the usage of fuzzy set theory in forecasting and decision-making. The primary area of concern is on those decisions with dynamically short time series. Author (revised)

N93-29542*# Georgia State Univ., Atlanta. Dept. of Decision Sciences.
DECISION ANALYSIS WITH APPROXIMATE PROBABILITIES **c81**
Thomas Whalen *In* NASA. Johnson Space Center, North American Fuzzy Logic Processing Society (NAFIPS 1992), Volume 1 Dec. 1992 p 229-238 (For primary document see N93-29516 11-59)
Avail: CASI HC A02/MF A03

This paper concerns decisions under uncertainty in which the probabilities of the states of nature are only approximately known. Decision problems involving three states of nature are studied. This is due to the fact that some key issues do not arise in two-state problems, while probability spaces with more than three states of nature are essentially impossible to graph. The primary focus is on two levels of probabilistic information. In one level, the three probabilities are separately rounded to the nearest tenth. This can lead to sets of rounded probabilities which add up to 0.9, 1.0, or 1.1. In the other level, probabilities are rounded to the nearest tenth in such a way that the rounded probabilities are forced to sum to 1.0. For comparison, six additional levels of probabilistic information, previously analyzed, were also included in the present analysis. A simulation experiment compared four criteria for decisionmaking using linearly constrained probabilities (Maximin, Midpoint, Standard Laplace, and Extended Laplace) under the eight different levels of information about probability. The Extended Laplace criterion, which uses a second order maximum entropy principle, performed best overall. Author (revised)

N93-29543*# Rockwell International Science Center, Thousand Oaks, CA.
DISTRIBUTED TRAFFIC SIGNAL CONTROL USING FUZZY LOGIC **c67**
Stephen Chiu *In* NASA. Johnson Space Center, North American Fuzzy Logic Processing Society (NAFIPS 1992), Volume 1 Dec. 1992 p 239-247 (For primary document see N93-29516 11-59)
Avail: CASI HC A02/MF A03

We present a distributed approach to traffic signal control, where the signal timing parameters at a given intersection are adjusted as functions of the local traffic condition and of the signal timing parameters at adjacent intersections. Thus, the signal timing parameters evolve dynamically using only local information to improve traffic flow. This distributed approach provides for a fault-tolerant, highly responsive traffic management system. The signal timing at an intersection is defined by three parameters: cycle time, phase split, and offset. We use fuzzy decision rules to adjust these three parameters based only on local information. The amount of change in the timing parameters during each cycle is limited to a small fraction of the current parameters to ensure smooth transition. We show the effectiveness of this method through simulation of the traffic flow in a network of controlled intersections. Author

N93-29544*# George Mason Univ., Fairfax, VA. Center for Excellence.
INTELLIGENT VIRTUAL REALITY IN THE SETTING OF FUZZY SETS **c67**
John Dockery (Defense Information Systems Agency, Arlington, VA.) and David Littman *In* NASA. Johnson Space Center, North American Fuzzy

Logic Processing Society (NAFIPS 1992), Volume 1 Dec. 1992 p 248-256 (For primary document see N93-29516 11-59)
Avail: CASI HC A02/MF A03

The authors have previously introduced the concept of virtual reality worlds governed by artificial intelligence. Creation of an intelligent virtual reality was further proposed as a universal interface for the handicapped. This paper extends consideration of intelligent virtual realty to a context in which fuzzy set principles are explored as a major tool for implementing theory in the domain of applications to the disabled. Author

N93-29545*# Missouri Univ., Columbia. Dept. of Electrical and Computer Engineering.

COMPARISON OF CRISP AND FUZZY CHARACTER NETWORKS IN HANDWRITTEN WORD RECOGNITION c63

Paul Gader, Magdi Mohamed, and Jung-Hsien Chiang *In* NASA. Johnson Space Center, North American Fuzzy Logic Processing Society (NAFIPS 1992), Volume 1 Dec. 1992 p 257-265 Sponsored in part by Environmental Research Inst. of Michigan and Postal Service (For primary document see N93-29516 11-59)
Avail: CASI HC A02/MF A03

Experiments involving handwritten word recognition on words taken from images of handwritten address blocks from the United States Postal Service mailstream are described. The word recognition algorithm relies on the use of neural networks at the character level. The neural networks are trained using crisp and fuzzy desired outputs. The fuzzy outputs were defined using a fuzzy k-nearest neighbor algorithm. The crisp networks slightly outperformed the fuzzy networks at the character level but the fuzzy networks outperformed the crisp networks at the word level. Author (revised)

N93-29546*# Guelph Univ. (Ontario). Dept. of Computing and Information Science.

FUZZY NEURAL NETWORK METHODOLOGY APPLIED TO MEDICAL DIAGNOSIS c52

Marian B. Gorzalczany (Technical Univ. of Kielce, Poland.) and Mary Deutsch-McLeish *In* NASA. Johnson Space Center, North American Fuzzy Logic Processing Society (NAFIPS 1992), Volume 1 Dec. 1992 p 266-275 (For primary document see N93-29516 11-59)
Avail: CASI HC A02/MF A03

This paper presents a technique for building expert systems that combines the fuzzy-set approach with artificial neural network structures. This technique can effectively deal with two types of medical knowledge: a nonfuzzy one and a fuzzy one which usually contributes to the process of medical diagnosis. Nonfuzzy numerical data is obtained from medical tests. Fuzzy linguistic rules describing the diagnosis process are provided by a human expert. The proposed method has been successfully applied in veterinary medicine as a support system in the diagnosis of canine liver diseases. Author (revised)

N93-29547*# Toronto Univ. (Ontario).

AN EXPERIMENTAL METHODOLOGY FOR A FUZZY SET PREFERENCE MODEL c67

I. B. Turksen and Ian A. Willson *In* NASA. Johnson Space Center, North American Fuzzy Logic Processing Society (NAFIPS 1992), Volume 1 Dec. 1992 p 276-285 (For primary document see N93-29516 11-59)
Avail: CASI HC A02/MF A03

A flexible fuzzy set preference model first requires approximate methodologies for implementation. Fuzzy sets must be defined for each individual consumer using computer software, requiring a minimum of time and expertise on the part of the consumer. The amount of information needed in defining sets must also be established. The model itself must adapt fully to the subject's choice of attributes (vague or precise), attribute levels, and importance weights. The resulting individual-level model should be fully adapted to each consumer. The methodologies needed to develop this model will be equally useful in a new generation of intelligent systems which interact with ordinary consumers, controlling electronic devices through fuzzy expert systems or making recommendations based on a variety of inputs. The power of personal computers and their acceptance by consumers has yet to be fully utilized to create interactive knowledge systems that fully adapt their function to the user. Understanding individual consumer preferences is critical to the design of new products and the estimation of demand (market share) for existing products, which in turn is an input to management systems concerned with production and distribution. The question of what to make, for whom to make it and how much to make requires an understanding of the customer's preferences and the trade-offs that exist between alternatives. Conjoint analysis is a widely used methodology which de-composes an overall preference for an object into a combination of preferences for its constituent parts (attributes such as taste and price), which are combined using an appropriate combination function. Preferences are often expressed using linguistic terms which cannot be represented in conjoint models. Current models are also not implemented an individual level, making it difficult to reach meaningful conclusions about the cause of an individual's behavior from an aggregate model. The combination of complex aggregate models and vague linguistic preferences has greatly limited the usefulness and predictive validity of existing preference models. A fuzzy set preference model that uses linguistic variables and a fully interactive implementation should be able to simultaneously address these issues and substantially improve the accuracy of demand estimates. The parallel implementation of crisp and fuzzy conjoint models using identical data not only validates the fuzzy set model but also provides an opportunity to assess the impact of fuzzy set definitions and individual attribute choices implemented in the interactive methodology developed in this research. The generalized experimental tools needed for conjoint models can also be applied to many other types of intelligent systems. Author (revised)

N93-29548*# Toronto Univ. (Ontario).

A FUZZY SET PREFERENCE MODEL FOR MARKET SHARE ANALYSIS c67

I. B. Turksen and Ian A. Willson *In* NASA. Johnson Space Center, North American Fuzzy Logic Processing Society (NAFIPS 1992), Volume 1 Dec. 1992 p 286-295 (For primary document see N93-29516 11-59)
Avail: CASI HC A02/MF A03

Consumer preference models are widely used in new product design, marketing management, pricing, and market segmentation. The success of new products depends on accurate market share prediction and design decisions based on consumer preferences. The vague linguistic nature of consumer preferences and product attributes, combined with the substantial differences between individuals, creates a formidable challenge to marketing models. The most widely used methodology is conjoint analysis. Conjoint models, as currently implemented, represent linguistic preferences as ratio or interval-scaled numbers, use only numeric product attributes, and require aggregation of individuals for estimation purposes. It is not surprising that these models are costly to implement, are inflexible, and have a predictive validity that is not substantially better than chance. This affects the accuracy of market share estimates. A fuzzy set preference model can easily represent linguistic variables either in consumer preferences or product attributes with minimal measurement requirements (ordinal scales), while still estimating overall preferences suitable for market share prediction. This approach results in flexible individual-level conjoint models which can provide more accurate market share estimates from a smaller number of more meaningful consumer ratings. Fuzzy sets can be incorporated within existing preference model structures, such as a linear combination, using the techniques developed for conjoint analysis and market share estimation. The purpose of this article is to develop and fully test a fuzzy set preference model which can represent linguistic variables in individual-level models implemented in parallel with existing conjoint models. The potential improvements in market share prediction and predictive validity can substantially improve management decisions about what to make (product design), for whom to make it (market segmentation), and how much to make (market share prediction). Author

N93-29549*# Technische Univ., Brunswick (Germany). Dept. of Computer Science.

INFORMATION COMPRESSION IN THE CONTEXT MODEL c82

Joerg Gebhardt, Rudolf Kruse, and Detlef Nauck *In* NASA. Johnson Space Center, North American Fuzzy Logic Processing Society (NAFIPS 1992), Volume 1 Dec. 1992 p 296-303 (For primary document see N93-29516 11-59)
Avail: CASI HC A02/MF A03

The Context Model provides a formal framework for the representation, interpretation, and analysis of vague and uncertain data. The clear semantics of the underlying concepts make it feasible to compare well-known approaches to the modeling of imperfect knowledge like that given in Bayes Theory, Shafer's Evidence Theory, the Transferable Belief Model, and Possibility Theory. In this paper we present the basic ideas of the Context Model and show its applicability as an alternative foundation of Possibility Theory and the epistemic view of fuzzy sets. Author (revised)

N93-29550*# Universidad Nacional Autonoma de Mexico, Coyoacan. Inst. de Ingenieria.

FUZZY KNOWLEDGE BASE CONSTRUCTION THROUGH BELIEF NETWORKS BASED ON LUKASIEWICZ LOGIC c67

Felipe Lara-Rosano *In* NASA. Johnson Space Center, North American Fuzzy Logic Processing Society (NAFIPS 1992), Volume 1 Dec. 1992 p 304-311 (For primary document see N93-29516 11-59)
Avail: CASI HC A02/MF A03

In this paper, a procedure is proposed to build a fuzzy knowledge base founded on fuzzy belief networks and Lukasiewicz logic. Fuzzy procedures are developed to do the following: to assess the belief values of a consequent, in terms of the belief values of its logical antecedents and the belief value of the corresponding logical function; and to update belief values when new evidence is available. Author (revised)

N93-29551*# Minnesota Univ., Minneapolis. Dept. of Electrical Engineering.

INTELLIGENT FUZZY CONTROLLER FOR EVENT-DRIVEN REAL TIME SYSTEMS c67

Janos Grantner (Technical Univ. of Budapest, Hungary.), Marek Patyra (Minnesota Univ., Duluth.), and Marian S. Stachowicz (Minnesota Univ., Duluth.) *In* NASA. Johnson Space Center, North American Fuzzy Logic Processing Society (NAFIPS 1992), Volume 1 Dec. 1992 p 312-321 (For primary document see N93-29516 11-59)
Avail: CASI HC A02/MF A03

Most of the known linguistic models are essentially static, that is, time is not a parameter in describing the behavior of the object's model. In this paper we show a model for synchronous finite state machines based on fuzzy logic. Such finite state machines can be used to build both event-driven, time-varying, rule-based systems and the control unit section of a fuzzy logic computer. The architecture of a pipelined intelligent fuzzy controller is presented, and the linguistic model is represented by an overall fuzzy relation stored in a single rule memory. A VLSI integrated circuit implementation of the fuzzy controller is suggested. At a clock rate of 30 MHz, the controller can perform 3 MFLIPS on multi-dimensional fuzzy data. Author (revised)

N93-29552*# Manitoba Univ., Winnipeg. Dept. of Electrical and Computer Engineering.

FUZZY COORDINATOR IN CONTROL PROBLEMS c67

A. Rueda and W. Pedrycz *In* NASA. Johnson Space Center, North American Fuzzy Logic Processing Society (NAFIPS 1992), Volume 1 Dec. 1992 p 322-329 (For primary document see N93-29516 11-59)
(Grant CONACyT-60558)
Avail: CASI HC A02/MF A03

In this paper a hierarchical control structure using a fuzzy system for coordination of the control actions is studied. The architecture involves two levels of control: a coordination level and an execution level. Numerical experiments will be utilized to illustrate the behavior of the controller when it is applied to a nonlinear plant. Author

N93-29553*# Georgia State Univ., Atlanta.

TUNING A FUZZY CONTROLLER USING QUADRATIC RESPONSE SURFACES c67

Brian Schott and Thomas Whalen *In* NASA. Johnson Space Center, North American Fuzzy Logic Processing Society (NAFIPS 1992), Volume 1 Dec. 1992 p 330-339 (For primary document see N93-29516 11-59)
Avail: CASI HC A02/MF A03

Response surface methodology, an alternative method to traditional tuning of a fuzzy controller, is described. An example based on a simulated inverted pendulum 'plant' shows that with (only) 15 trial runs, the controller can be calibrated using a quadratic form to approximate the response surface. Author

N93-29554*# Mentalogic Systems, Inc., Markham (Ontario). Research and Development.

THE COGNITIVE BASES FOR THE DESIGN OF A NEW CLASS OF FUZZY LOGIC CONTROLLERS: THE CLEARNESS TRANSFORMATION FUZZY LOGIC CONTROLLER c67

Labib Sultan (York Univ., Toronto, Ontario.) and Talib Janabi *In* NASA. Johnson Space Center, North American Fuzzy Logic Processing Society (NAFIPS 1992), Volume 1 Dec. 1992 p 340-349 Sponsored in part by Natural Sciences and Engineering Research Council (For primary document see N93-29516 11-59)
Avail: CASI HC A02/MF A03

This paper analyses the internal operation of fuzzy logic controllers as referenced to the human cognitive tasks of control and decision making. Two goals are targeted. The first goal focuses on the cognitive interpretation of the mechanisms employed in the current design of fuzzy logic controllers. This analysis helps to create a ground to explore the potential of enhancing the functional intelligence of fuzzy controllers. The second goal is to outline the features of a new class of fuzzy controllers, the Clearness Transformation Fuzzy Logic Controller (CT-FLC), whereby some new concepts are advanced to qualify fuzzy controllers as 'cognitive devices' rather than 'expert system devices'. The operation of the CT-FLC, as a fuzzy pattern processing controller, is explored, simulated, and evaluated. Author (revised)

N93-29555*# Institutul Politehnic din Iasi (Romania). Center for Research in Fuzzy Systems and Artificial Intelligence.

A FUZZY CONTROL DESIGN CASE: THE FUZZY PLL c67

H. N. Teodorescu and I. Bogdan *In* NASA. Johnson Space Center, North American Fuzzy Logic Processing Society (NAFIPS 1992), Volume 1 Dec. 1992 p 350-359 (For primary document see N93-29516 11-59)
Avail: CASI HC A02/MF A03

The aim of this paper is to present a typical fuzzy control design case. The analyzed controlled systems are the phase-locked loops (PLL's)--classic systems realized in both analogic and digital technology. The crisp PLL devices are well known. Author (revised)

N93-29556*# National Aeronautics and Space Administration. Lyndon B. Johnson Space Center, Houston, TX.

NORTH AMERICAN FUZZY LOGIC PROCESSING SOCIETY (NAFIPS 1992), VOLUME 2

James A. Villarreal, comp. Dec. 1992 292 p Conference held in Puerto Vallarta, Mexico, 15-17 Dec. 1992 Sponsored in part by Inst. Tecnologico de Morelia; Indian Society for Fuzzy Mathematics and Information Processing; Inst. Technologico y de Estudios Superiores de Monterrey; International Fuzzy Systems Association; Japan Society for Fuzzy Theory and Systems; and Microelectronics and Computer Technology Corp.
(NASA-CP-10112-Vol-2; S-702-Vol-2; NAS 1.55:10112-Vol-2) Avail: CASI HC A13/MF A03

This document contains papers presented at the NAFIPS '92 North American Fuzzy Information Processing Society Conference. More than 75 papers were presented at this Conference, which was sponsored by NAFIPS in cooperation with NASA, the Instituto Tecnologico de Morelia, the Indian Society for Fuzzy Mathematics and Information Processing (ISFUMIP), the Instituto Tecnologico de Estudios Superiores de Monterrey (ITESM), the International Fuzzy Systems Association (IFSA), the Japan Society for Fuzzy Theory and Systems, and the Microelectronics and Computer Technology Corporation (MCC). The fuzzy set theory has led to a large number of diverse applications. Recently, interesting applications have been developed which involve the integration of fuzzy systems with adaptive processes such a neural networks and genetic algorithms. NAFIPS '92 was directed toward the advancement, commercialization, and engineering development of these technologies. For individual titles, see N93-29557 through N93-29585.

N93-29557*# Academia R. P. R., Bucharest. Inst. for Computer Science.

ADDING DYNAMIC RULES TO SELF-ORGANIZING FUZZY SYSTEMS c67

Catalin V. Buhusi *In* NASA. Johnson Space Center, North American Fuzzy Logic Processing Society (NAFIPS 1992), Volume 2 Dec. 1992 p 360-367 (For primary document see N93-29556 11-59)
Avail: CASI HC A02/MF A03

This paper develops a Dynamic Self-Organizing Fuzzy System (DSOFS) capable of adding, removing, and/or adapting the fuzzy rules and the fuzzy reference sets. The DSOFS background consists of a self-organizing neural structure with neuron relocation features which will develop a map of the input-output behavior. The relocation algorithm extends the topological ordering concept. Fuzzy rules (neurons) are dynamically added or released while the neural structure learns the pattern. The DSOFS advantages are the automatic synthesis and the possibility of parallel implementation. A high adaptation speed and a reduced number of neurons is needed in order to keep errors under some limits. The computer simulation results are presented in a nonlinear systems modelling application. Author

N93-29558*# Dynetics, Inc., Huntsville, AL.

FUZZY LEARNING UNDER AND ABOUT AN UNFAMILIAR FUZZY TEACHER **c67**

Belur V. Dasarathy *In* NASA. Johnson Space Center, North American Fuzzy Logic Processing Society (NAFIPS 1992), Volume 2 Dec. 1992 p 368-377 (For primary document see N93-29556 11-59)

Avail: CASI HC A02/MF A03

This study addresses the problem of optimal parametric learning in unfamiliar fuzzy environments. Prior studies in the domain of unfamiliar environments, which employed either crisp or fuzzy approaches to model the uncertainty or imperfectness of the learning environment, assumed that the training sample labels provided by the unfamiliar teacher were crisp, even if not perfect. Here, the more realistic problem of fuzzy learning under an unfamiliar teacher who provides only fuzzy (instead of crisp) labels, is tackled by expanding the previously defined fuzzy membership concepts to include an additional component representative of the fuzziness of the teacher. The previously studied scenarios, namely, crisp and fuzzy learning under (crisp) unfamiliar teacher, can be looked upon as special cases of this new methodology. As under the earlier studies, the estimated membership functions can then be deployed during the ensuing classification decision phase to judiciously take into account the imperfectness of the learning environment. The study also offers some insight into the properties of several of these fuzzy membership function estimators by examining their behavior under certain specific scenarios. Author

N93-29559*# NYNEX Science and Technology, Inc., White Plains, NY.

SOME PROBLEMS WITH THE DESIGN OF SELF-LEARNING MANAGEMENT SYSTEMS **c67**

Ziny Flikop *In* NASA. Johnson Space Center, North American Fuzzy Logic Processing Society (NAFIPS 1992), Volume 2 Dec. 1992 p 378-387 (For primary document see N93-29556 11-59)

Avail: CASI HC A02/MF A03

In this paper some problems in the design of management systems for complex objects are discussed. Considering the absence of adequate models and the fact that human expertise in the management of non-stationary objects becomes obsolete quickly, the use of self-learning together with a two-step optimization of on-line control rules is suggested. To prepare for the object analysis, a set of definitions has been proposed. Traditional and fuzzy sets approaches are used in the analysis. To decrease the reaction time of the control system, we propose the development of control rules without feedback. Author

N93-29560*# Technische Univ., Brunswick (Germany). Dept. of Computer Science.

A NEURAL FUZZY CONTROLLER LEARNING BY FUZZY ERROR PROPAGATION **c67**

Detlef Nauck and Rudolf Kruse *In* NASA. Johnson Space Center, North American Fuzzy Logic Processing Society (NAFIPS 1992), Volume 2 Dec. 1992 p 388-397 (For primary document see N93-29556 11-59)

Avail: CASI HC A02/MF A03

In this paper, we describe a procedure to integrate techniques for the adaptation of membership functions in a linguistic variable based fuzzy control environment by using neural network learning principles. This is an extension to our work. We solve this problem by defining a fuzzy error that is propagated back through the architecture of our fuzzy controller. According to this fuzzy error and the strength of its antecedent each fuzzy rule determines its amount of error. Depending on the current state of the controlled system and the control action derived from the conclusion, each rule tunes the membership functions of its antecedent and its conclusion. By this we get an unsupervised learning technique that enables a fuzzy controller to adapt to a control task by knowing just about the global state and the fuzzy error. Author (revised)

N93-29561*# National Aeronautics and Space Administration. Lyndon B. Johnson Space Center, Houston, TX.

DETERMINING RULES FOR CLOSING CUSTOMER SERVICE CENTERS: A PUBLIC UTILITY COMPANY'S FUZZY DECISION **c67**

Andre deKorvin (Houston Univ., TX.), Margaret F. Shipley (Houston Univ., TX.), and Robert N. Lea *In its* North American Fuzzy Logic Processing Society (NAFIPS 1992), Volume 2 Dec. 1992 p 398-407 (For primary document see N93-29556 11-59)

Avail: CASI HC A02/MF A03

In the present work, we consider the general problem of knowledge acquisition under uncertainty. Simply stated, the problem reduces to the following: how can we capture the knowledge of an expert when the expert is unable to clearly formulate how he or she arrives at a decision? A commonly used method is to learn by examples. We observe how the expert solves specific cases and from this infer some rules by which the decision may have been made. Unique to our work is the fuzzy set representation of the conditions or attributes upon which the expert may possibly base his fuzzy decision. From our examples, we infer certain and possible fuzzy rules for closing a customer service center and illustrate the importance of having the decision closely relate to the conditions under consideration. Author (revised)

N93-29562*# Lappeenranta Univ. of Technology (Finland). Dept. of Chemical Technology.

FUZZY SIMULATION IN CONCURRENT ENGINEERING **c67**

A. Kraslawski and L. Nystrom *In* NASA. Johnson Space Center, North American Fuzzy Logic Processing Society (NAFIPS 1992), Volume 2 Dec. 1992 p 408-417 (For primary document see N93-29556 11-59)

Avail: CASI HC A02/MF A03

Concurrent engineering is becoming a very important practice in manufacturing. A problem in concurrent engineering is the uncertainty associated with the values of the input variables and operating conditions. The problem discussed in this paper concerns the simulation of processes where the raw materials and the operational parameters possess fuzzy characteristics. The processing of fuzzy input information is performed by the vertex method and the commercial simulation packages POLYMATH and GEMS. The examples are presented to illustrate the usefulness of the method in the simulation of chemical engineering processes. Author (revised)

N93-29563*# Texas Univ., El Paso. Dept. of Computer Science.

INVERSE PROBLEMS: FUZZY REPRESENTATION OF UNCERTAINTY GENERATES A REGULARIZATION **c67**

V. Kreinovich, Ching-Chuang Chang, L. Reznik (Footscray Inst. of Tech., Australia.), and G. N. Solopchenko (Saint Petersburg Technical Univ., Russia.) *In* NASA. Johnson Space Center, North American Fuzzy Logic Processing Society (NAFIPS 1992), Volume 2 Dec. 1992 p 418-426 Sponsored in part by Inst. for Manufacturing and Materials Management (For primary document see N93-29556 11-59)

(Grants NAG9-482; NSF CDA-90-15006)

Avail: CASI HC A02/MF A03

In many applied problems (geophysics, medicine, and astronomy) we cannot directly measure the values x(t) of the desired physical quantity x in different moments of time, so we measure some related quantity y(t), and then we try to reconstruct the desired values x(t). This problem is often ill-posed in the sense that two essentially different functions x(t) are consistent with the same measurement results. So, in order to get a reasonable reconstruction, we must have some additional prior information about the desired function x(t). Methods that use this information to choose x(t) from the set of all possible solutions are called regularization methods. In some cases, we know the statistical characteristics both of x(t) and of the measurement errors, so we can apply statistical filtering methods (well-developed since the invention of a Wiener filter). In some situations, we know the properties of the desired process, e.g., we know that the derivative of x(t) is limited by some number delta, etc. In this case, we can apply standard regularization techniques (e.g., Tikhonov's regularization). In many cases, however, we have only uncertain knowledge about the values of x(t), about the rate with which the values of x(t) can change, and about the measurement errors. In these cases, usually one of the existing regularization methods is applied. There exist several heuristics that choose such a method. The problem with these heuristics is that they often lead to choosing different methods, and these methods lead to different functions x(t). Therefore, the results x(t) of applying these heuristic methods are often unreliable. We show that if we use fuzzy logic to describe this uncertainty, then we automatically arrive at a unique regularization method, whose parameters are uniquely determined by the experts knowledge. Although we start with the fuzzy description, but the resulting regularization turns out to be quite crisp. Author (revised)

N93-29564*# Dayton Univ., OH. Dept. of Mathematics.

QUANTIFICATION OF HUMAN RESPONSES **c53**

R. C. Steinlage, T. E. Gantner, and P. Y. W. Lim (Boise Cascade Corp., Portland, OR.) *In* NASA. Johnson Space Center, North American Fuzzy Logic Processing Society (NAFIPS 1992), Volume 2 Dec. 1992 p 427-436 (For primary document see N93-29556 11-59)
Avail: CASI HC A02/MF A03

Human perception is a complex phenomenon which is difficult to quantify with instruments. For this reason, large panels of people are often used to elicit and aggregate subjective judgments. Print quality, taste, smell, sound quality of a stereo system, softness, and grading Olympic divers and skaters are some examples of situations where subjective measurements or judgments are paramount. We usually express what is in our mind through language as a medium but languages are limited in available choices of vocabularies, and as a result, our verbalizations are only approximate expressions of what we really have in mind. For lack of better methods to quantify subjective judgments, it is customary to set up a numerical scale such as 1, 2, 3, 4, 5 or 1, 2, 3, ..., 9, 10 for characterizing human responses and subjective judgments with no valid justification except that these scales are easy to understand and convenient to use. But these numerical scales are arbitrary simplifications of the complex human mind; the human mind is not restricted to such simple numerical variations. In fact, human responses and subjective judgments are psychophysical phenomena that are fuzzy entities and therefore difficult to handle by conventional mathematics and probability theory. The fuzzy mathematical approach provides a more realistic insight into understanding and quantifying human responses. This paper presents a method for quantifying human responses and subjective judgments without assuming a pattern of linear or numerical variation for human responses. In particular, quantification and evaluation of linguistic judgments was investigated. Author (revised)

N93-29565*# Instituto Tecnologico de Morelia (Mexico).

NON-SCALAR UNCERTAINTY: UNCERTAINTY IN DYNAMIC SYSTEMS **c65**

Salvador Gutierrez Martinez *In* NASA. Johnson Space Center, North American Fuzzy Logic Processing Society (NAFIPS 1992), Volume 2 Dec. 1992 p 437-448 (For primary document see N93-29556 11-59)
Avail: CASI HC A03/MF A03

The following point is stated throughout the paper: dynamic systems are usually subject to uncertainty, be it the unavoidable quantic uncertainty when working with sufficiently small scales or when working in large scales uncertainty can be allowed by the researcher in order to simplify the problem, or it can be introduced by nonlinear interactions. Even though non-quantic uncertainty can generally be dealt with by using the ordinary probability formalisms, it can also be studied with the proposed non-scalar formalism. Thus, non-scalar uncertainty is a more general theoretical framework giving insight into the nature of uncertainty and providing a practical tool in those cases in which scalar uncertainty is not enough, such as when studying highly nonlinear dynamic systems. This paper's specific contribution is the general concept of non-scalar uncertainty and a first proposal for a methodology. Applications should be based upon this methodology. The advantage of this approach is to provide simpler mathematical models for prediction of the system states. Present conventional tools for dealing with uncertainty prove insufficient for an effective description of some dynamic systems. The main limitations are overcome abandoning ordinary scalar algebra in the real interval (0, 1) in favor of a tensor field with a much richer structure and generality. This approach gives insight into the interpretation of Quantum Mechanics and will have its most profound consequences in the fields of elementary particle physics and nonlinear dynamic systems. Concepts like 'interfering alternatives' and 'discrete states' have an elegant explanation in this framework in terms of properties of dynamic systems such as strange attractors and chaos. The tensor formalism proves especially useful to describe the mechanics of representing dynamic systems with models that are closer to reality and have relatively much simpler solutions. It was found to be wise to get an approximate solution to an accurate model than to get a precise solution to a model constrained by simplifying assumptions. Precision has a very heavy cost in present physical models, but this formalism allows the trade between uncertainty and simplicity. It was found that modeling reality sometimes requires that state transition probabilities should be manipulated as nonscalar quantities, finding at the end that there is always a transformation to get back to scalar probability. Author (revised)

N93-29566*# Mentalogic Systems, Inc., Markham (Ontario).

COMPARISON BETWEEN THE PERFORMANCE OF TWO CLASSES OF FUZZY CONTROLLERS **c67**

T. H. Janabi and L. H. Sultan (York Univ., Toronto, Ontario.) *In* NASA. Johnson Space Center, North American Fuzzy Logic Processing Society (NAFIPS 1992), Volume 2 Dec. 1992 p 449-457 (For primary document see N93-29556 11-59)
Avail: CASI HC A02/MF A03

This paper presents an application comparison between two classes of fuzzy controllers: the Clearness Transformation Fuzzy Controller (CTFC) and the CRI-based Fuzzy Controller. The comparison is performed by studying the application of the controllers to simulation examples of nonlinear systems. The CTFC is a new approach for the organization of fuzzy controllers based on a cognitive model of parameter driven control, the notion of fuzzy patterns to represent fuzzy knowledge and the Clearness Transformation Rule of Inference (CTRI) for approximate reasoning. The approach facilitates the implementation of the basic modules of the controller: the fuzzifier, defuzzifier, and the control protocol in a rule-based architecture. The CTRI scheme for approximate reasoning does not require the formation of fuzzy relation matrices yielding improved performance in comparison with the traditional organization of fuzzy controllers. Author (revised)

N93-29567*# State Univ. of New York, Binghamton. Dept. of Systems Science.

POSSIBILISTIC MEASUREMENT AND SET STATISTICS **c65**

Cliff Joslyn *In* NASA. Johnson Space Center, North American Fuzzy Logic Processing Society (NAFIPS 1992), Volume 2 Dec. 1992 p 458-467 (For primary document see N93-29556 11-59)
(Grant NGT-50757)
Avail: CASI HC A02/MF A03

Set-based statistics are necessary to generate possibility distributions from measured data. Methods by which physical measurements can generate statistical data on real intervals are considered, including the following: trials from multiple heterogeneous measurement devices rather than a single instrument at multiple times; classes of consistent intervals constructed from statistical data around a common point focus or interval core; and consonant intervals constructed from statistical data. Author (revised)

N93-29568*# Missouri Univ., Columbia. Dept. of Electrical and Computer Engineering.

THE FUSION OF INFORMATION VIA FUZZY INTEGRATION **c67**

James M. Keller and Hossein Tahani *In* NASA. Johnson Space Center, North American Fuzzy Logic Processing Society (NAFIPS 1992), Volume 2 Dec. 1992 p 468-477 (For primary document see N93-29556 11-59)
Avail: CASI HC A02/MF A03

Multisensor fusion is becoming increasingly important in intelligent computer vision systems. In this paper we present the generalized fuzzy integral with respect to an S-decomposable measure as a tool for fusing information from multiple sensors in an object recognition problem. Results from an experiment with automatic target recognition imagery are provided. Author (revised)

N93-29569*# Institut de Recherche en Informatique et Systemes Aleatoires, Lannion (France). ENSSAT.

ON THE EVALUATION OF FUZZY QUANTIFIED QUERIES IN A DATABASE MANAGEMENT SYSTEM **c82**

Patrick Bosc and Olivier Pivert *In* NASA. Johnson Space Center, North American Fuzzy Logic Processing Society (NAFIPS 1992), Volume 2 Dec.

1992 p 478-487 (For primary document see N93-29556 11-59)
Avail: CASI HC A02/MF A03

Many propositions to extend database management systems have been made in the last decade. Some of them aim at the support of a wider range of queries involving fuzzy predicates. Unfortunately, these queries are somewhat complex and the question of their efficiency is a subject under discussion. In this paper, we focus on a particular subset of queries, namely those using fuzzy quantified predicates. More precisely, we will consider the case where such predicates apply to individual elements as well as to sets of elements. Thanks to some interesting properties of alpha-cuts of fuzzy sets, we are able to show that the evaluation of these queries can be significantly improved with respect to a naive strategy based on exhaustive scans of sets or files. Author

N93-29570*# Cincinnati Univ., OH. Artificial Intelligence and Computer Vision Lab.

A FUZZY CASE BASED REASONING TOOL FOR MODEL BASED APPROACH TO ROCKET ENGINE HEALTH MONITORING c20

Srinivas Krovvidy, Adam Nolan, Yong-Lin Hu, and William G. Wee *In* NASA. Johnson Space Center, North American Fuzzy Logic Processing Society (NAFIPS 1992), Volume 2 Dec. 1992 p 488-495 (For primary document see N93-29556 11-59)
Avail: CASI HC A02/MF A03

In this system we develop a fuzzy case based reasoner that can build a case representation for several past anomalies detected, and we develop case retrieval methods that can be used to index a relevant case when a new problem (case) is presented using fuzzy sets. The choice of fuzzy sets is justified by the uncertain data. The new problem can be solved using knowledge of the model along with the old cases. This system can then be used to generalize the knowledge from previous cases and use this generalization to refine the existing model definition. This in turn can help to detect failures using the model based algorithms. Author (revised)

N93-29571*# Bell Communications Research, Inc., Livingston, NJ.

A HIGH PERFORMANCE, AD-HOC, FUZZY QUERY PROCESSING SYSTEM FOR RELATIONAL DATABASES c82

William H. Mansfield, Jr. and Robert M. Fleischman *In* NASA. Johnson Space Center, North American Fuzzy Logic Processing Society (NAFIPS 1992), Volume 2 Dec. 1992 p 496-505 (For primary document see N93-29556 11-59)
Avail: CASI HC A02/MF A03

Database queries involving imprecise or fuzzy predicates are currently an evolving area of academic and industrial research. Such queries place severe stress on the indexing and I/O subsystems of conventional database environments since they involve the search of large numbers of records. The Datacycle architecture and research prototype is a database environment that uses filtering technology to perform an efficient, exhaustive search of an entire database. It has recently been modified to include fuzzy predicates in its query processing. The approach obviates the need for complex index structures, provides unlimited query throughput, permits the use of ad-hoc fuzzy membership functions, and provides a deterministic response time largely independent of query complexity and load. This paper describes the Datacycle prototype implementation of fuzzy queries and some recent performance results. Author (revised)

N93-29572*# Bureau of Mines, Tuscaloosa, AL.

GENETIC ALGORITHMS IN ADAPTIVE FUZZY CONTROL c67

C. Lucas Karr and Tony R. Harper *In* NASA. Johnson Space Center, North American Fuzzy Logic Processing Society (NAFIPS 1992), Volume 2 Dec. 1992 p 506-514 (For primary document see N93-29556 11-59)
Avail: CASI HC A02/MF A03

Researchers at the U.S. Bureau of Mines have developed adaptive process control systems in which genetic algorithms (GA's) are used to augment fuzzy logic controllers (FLC's). GA's are search algorithms that rapidly locate near-optimum solutions to a wide spectrum of problems by modeling the search procedures of natural genetics. FLC's are rule based systems that efficiently manipulate a problem environment by modeling the 'rule-of-thumb' strategy used in human decision making. Together, GA's and FLC's possess the capabilities necessary to produce powerful, efficient, and robust adaptive control systems. To perform efficiently, such control systems require a control element to manipulate the problem environment, an analysis element to recognize changes in the problem environment, and a learning element to adjust fuzzy membership functions in response to the changes in the problem environment. Details of an overall adaptive control system are discussed. A specific computer-simulated chemical system is used to demonstrate the ideas presented. Author (revised)

N93-29573*# National Aeronautics and Space Administration. Lyndon B. Johnson Space Center, Houston, TX.

A GENETIC ALGORITHMS APPROACH FOR ALTERING THE MEMBERSHIP FUNCTIONS IN FUZZY LOGIC CONTROLLERS c67

Hana Shehadeh (LinCom Corp., Houston, TX.) and Robert N. Lea *In its* North American Fuzzy Logic Processing Society (NAFIPS 1992), Volume 2 Dec. 1992 p 515-523 (For primary document see N93-29556 11-59)
Avail: CASI HC A02/MF A03

Through previous work, a fuzzy control system was developed to perform translational and rotational control of a space vehicle. This problem was then re-examined to determine the effectiveness of genetic algorithms on fine tuning the controller. This paper explains the problems associated with the design of this fuzzy controller and offers a technique for tuning fuzzy logic controllers. A fuzzy logic controller is a rule-based system that uses fuzzy linguistic variables to model human rule-of-thumb approaches to control actions within a given system. This 'fuzzy expert system' features rules that direct the decision process and membership functions that convert the linguistic variables into the precise numeric values used for system control. Defining the fuzzy membership functions is the most time consuming aspect of the controller design. One single change in the membership functions could significantly alter the performance of the controller. This membership function definition can be accomplished by using a trial and error technique to alter the membership functions creating a highly tuned controller. This approach can be time consuming and requires a great deal of knowledge from human experts. In order to shorten development time, an iterative procedure for altering the membership functions to create a tuned set that used a minimal amount of fuel for velocity vector approach and station-keep maneuvers was developed. Genetic algorithms, search techniques used for optimization, were utilized to solve this problem. Author (revised)

N93-29574*# Clemson Univ., SC. Dept. of Civil Engineering.

FUZZY MULTIPLE LINEAR REGRESSION: A COMPUTATIONAL APPROACH c67

C. H. Juang, X. H. Huang, and J. W. Fleming *In* NASA. Johnson Space Center, North American Fuzzy Logic Processing Society (NAFIPS 1992), Volume 2 Dec. 1992 p 524-534 (For primary document see N93-29556 11-59)
(Grant NSF MSS-90-20252)
Avail: CASI HC A03/MF A03

This paper presents a new computational approach for performing fuzzy regression. In contrast to Bardossy's approach, the new approach, while dealing with fuzzy variables, closely follows the conventional regression technique. In this approach, treatment of fuzzy input is more 'computational' than 'symbolic.' The following sections first outline the formulation of the new approach, then deal with the implementation and computational scheme, and this is followed by examples to illustrate the new procedure. Author (revised)

N93-29575*# California State Univ., Fresno.

INCORPORATION OF VARYING TYPES OF TEMPORAL DATA IN A NEURAL NETWORK c63

M. E. Cohen and D. L. Hudson (California Univ., San Francisco.) *In* NASA. Johnson Space Center, North American Fuzzy Logic Processing Society (NAFIPS 1992), Volume 2 Dec. 1992 p 535-544 (For primary document see N93-29556 11-59)
Avail: CASI HC A02/MF A03

Most neural network models do not specifically deal with temporal data. Handling of these variables is complicated by the different uses to which temporal data are put, depending on the application. Even within the same application, temporal variables are often used in a number of different ways. In this paper, types of temporal data are discussed, along with their implications for approximate reasoning. Methods for integrating approximate temporal reasoning into existing neural network structures are presented. These methods are illustrated in a medical application for diagnosis of graft-versus-host disease which requires the use of several types of temporal data. Author (revised)

N93-29576*# Hungarian Academy of Sciences, Budapest. Dept. of Anatomy.
FUZZY OPERATORS AND CYCLIC BEHAVIOR IN FORMAL NEURONAL NETWORKS **c67**
E. Labos, A. V. Holden (Leeds Univ., England.), J. Laczko (Ludwig-Maximilians-Univ., Munich, Germany.), L. Orzo, and A. S. Labos *In* NASA. Johnson Space Center, North American Fuzzy Logic Processing Society (NAFIPS 1992), Volume 2 Dec. 1992 p 545-554 (For primary document see N93-29556 11-59)
(Grant OTKA-2621)
Avail: CASI HC A02/MF A03

Formal neuronal networks (FNN), which are comprised of threshold gates, make use of the unit step function. It is regarded as a degenerated distribution function (DDF) and will be referred to here as a non-fuzzy threshold operator (nFTO). Special networks of this kind generating long cycles of states are modified by introduction of fuzzy threshold operators (FTO), i.e., non-degenerated distribution functions (nDDF). The cyclic behavior of the new nets is compared with the original ones. The interconnection matrix and threshold values are not modified. It is concluded that the original long cycles change the fixed points and short cycles, and as the computer simulations demonstrate, the aperiodic motion that is associated with chaotic behavior appears. The emergence of the above changes depend on the steepness of the threshold operators. Author (revised)

N93-29577*# Moravian Coll., Bethlehem, PA. Dept. of Mathematics.
NEURAL NETWORKS: A SIMULATION TECHNIQUE UNDER UNCERTAINTY CONDITIONS **c63**
M. Luisa Nicosia McAllister *In* NASA. Johnson Space Center, North American Fuzzy Logic Processing Society (NAFIPS 1992), Volume 2 Dec. 1992 p 555-564 (For primary document see N93-29556 11-59)
Avail: CASI HC A02/MF A03

This paper proposes a new definition of fuzzy graphs and shows how transmission through a graph with linguistic expressions as labels provides an easy computational tool. These labels are represented by modified Kauffmann Fuzzy numbers. Author (revised)

N93-29578*# Minnesota Univ., Duluth. Dept. of Computer Engineering.
INCOMPLETE FUZZY DATA PROCESSING SYSTEMS USING ARTIFICIAL NEURAL NETWORK **c67**
Marek J. Patyra *In* NASA. Johnson Space Center, North American Fuzzy Logic Processing Society (NAFIPS 1992), Volume 2 Dec. 1992 p 565-574 (For primary document see N93-29556 11-59)
Avail: CASI HC A02/MF A03

In this paper, the implementation of a fuzzy data processing system using an artificial neural network (ANN) is discussed. The binary representation of fuzzy data is assumed, where the universe of discourse is decartelized into n equal intervals. The value of a membership function is represented by a binary number. It is proposed that incomplete fuzzy data processing be performed in two stages. The first stage performs the 'retrieval' of incomplete fuzzy data, and the second stage performs the desired operation on the retrieval data. The method of incomplete fuzzy data retrieval is proposed based on the linear approximation of missing values of the membership function. The ANN implementation of the proposed system is presented. The system was computationally verified and showed a relatively small total error. Author (revised)

N93-29579*# Institutul Politehnic din Iasi (Romania).
STOCHASTIC ARCHITECTURE FOR HOPFIELD NEURAL NETS **c63**
Sandy Pavel *In* NASA. Johnson Space Center, North American Fuzzy Logic Processing Society (NAFIPS 1992), Volume 2 Dec. 1992 p 575-580 (For primary document see N93-29556 11-59)
Avail: CASI HC A02/MF A03

An expandable stochastic digital architecture for recurrent (Hopfield like) neural networks is proposed. The main features and basic principles of stochastic processing are presented. The stochastic digital architecture is based on a chip with n full interconnected neurons with a pipeline, bit processing structure. For large applications, a flexible way to interconnect many such chips is provided. Author (revised)

N93-29580*# Manitoba Univ., Winnipeg. Dept. of Electrical and Computer Engineering.
HIERARCHICAL MODEL OF MATCHING **c67**
Witold Pedrycz and Eugene Roventa (York Univ., Toronto, Ontario.) *In* NASA. Johnson Space Center, North American Fuzzy Logic Processing Society (NAFIPS 1992), Volume 2 Dec. 1992 p 581-588 Sponsored in part by Natural Sciences and Engineering Research Council and MicroNet (For primary document see N93-29556 11-59)
Avail: CASI HC A02/MF A03

The issue of matching two fuzzy sets becomes an essential design aspect of many algorithms including fuzzy controllers, pattern classifiers, knowledge-based systems, etc. This paper introduces a new model of matching. Its principal features involve the following: (1) matching carried out with respect to the grades of membership of fuzzy sets as well as some functionals defined on them (like energy, entropy,transom); (2) concepts of hierarchies in the matching model leading to a straightforward distinction between 'local' and 'global' levels of matching; and (3) a distributed character of the model realized as a logic-based neural network. Author (revised)

N93-29581*# Rice Univ., Houston, TX. Dept. of Electrical and Computer Engineering.
A CONJUGATE GRADIENTS/TRUST REGIONS ALGORITHMS FOR TRAINING MULTILAYER PERCEPTRONS FOR NONLINEAR MAPPING **c61**
Raghavendra K. Madyastha, Behnaam Aazhang, Troy F. Henson (International Business Machines Corp., Houston, TX.), and Wendy L. Huxhold (International Business Machines Corp., Houston, TX.) *In* NASA. Johnson Space Center, North American Fuzzy Logic Processing Society (NAFIPS 1992), Volume 2 Dec. 1992 p 589-597 (For primary document see N93-29556 11-59)
Avail: CASI HC A02/MF A03

This paper addresses the issue of applying a globally convergent optimization algorithm to the training of multilayer perceptrons, a class of Artificial Neural Networks. The multilayer perceptrons are trained towards the solution of two highly nonlinear problems: (1) signal detection in a multi-user communication network, and (2) solving the inverse kinematics for a robotic manipulator. The research is motivated by the fact that a multilayer perceptron is theoretically capable of approximating any nonlinear function to within a specified accuracy. The algorithm that has been employed in this study combines the merits of two well known optimization algorithms, the Conjugate Gradients and the Trust Regions Algorithms. The performance is compared to a widely used algorithm, the Backpropagation Algorithm, that is basically a gradient-based algorithm, and hence, slow in converging. The performances of the two algorithms are compared with the convergence rate. Furthermore, in the case of the signal detection problem, performances are also benchmarked by the decision boundaries drawn as well as the probability of error obtained in either case. Author (revised)

N93-29582*# State Univ. of New York, Binghamton. Dept. of Systems Science.
ON PROBABILITY-POSSIBILITY TRANSFORMATIONS **c65**
George J. Klir and Behzad Parviz (California State Univ., Los Angeles.) *In* NASA. Johnson Space Center, North American Fuzzy Logic Processing Society (NAFIPS 1992), Volume 2 Dec. 1992 p 598-607 (For primary document see N93-29556 11-59)
(Grant NSF IRI-90-15675)
Avail: CASI HC A02/MF A03

Several probability-possibility transformations are compared in terms of the closeness of preserving second-order properties. The comparison is based on experimental results obtained by computer simulation. Two second-order properties are involved in this study: noninteraction of two distributions and projections of a joint distribution. Author

N93-29583*# Pohang Inst. of Science and Technology (Republic of Korea). Dept. of Computer Science.
INFERENCE IN FUZZY RULE BASES WITH CONFLICTING EVIDENCE **c67**
Laszlo T. Koczy (Technical Univ. of Budapest, Hungary.) *In* NASA. Johnson Space Center, North American Fuzzy Logic Processing Society (NAFIPS 1992), Volume 2 Dec. 1992 p 608-617 (For primary

document see N93-29556 11-59)
Avail: CASI HC A02/MF A03

Inference based on fuzzy 'If ... then' rules has played a very important role since when Zadeh proposed the Compositional Rule of Inference and, especially, since the first successful application presented by Mamdani. From the mid-1980's when the 'fuzzy boom' started in Japan, numerous industrial applications appeared, all using simplified techniques because of the high levels of computational complexity. Another feature is that antecedents in the rules are distributed densely in the input space, so the conclusion can be calculated by some weighted combination of the consequents of the matching (fired) rules. The CRI works in the following way: If R is a rule and A* is an observation, the conclusion is computed by B* = R o A* (o stands for the max-min composition). Algorithms implementing this idea directly have an exponential time complexity (maybe the problem is NP-hard) as the rules are relations in X x Y, a k1 x k2 dimensional space, if X is k1, Y is k2 dimensional. The simplified techniques usually decompose the relation into k1 projections in X(sub i) and measure in some way the degree of similarity between observation and antecedent by some parameter of the overlapping. These parameters are aggregated to a single value in (0,1) which is applied as a resulting weight for the given rule. The projections of rules in dimensions Y(sub i) are weighted by these aggregated values and then they are combined in order to obtain a resulting conclusion separately in every dimension. This method is unapplicable with sparse bases as there is no guarantee that an arbitrary observation matches with any of the antecedents. Then, the degree of similarity is 0 and all consequents are weighted by 0. Some considerations for such a situation are summarized in the next sections. Author (revised)

N93-29584*# Texas Univ., El Paso. Dept. of Computer Science.
GAUSSIAN MEMBERSHIP FUNCTIONS ARE MOST ADEQUATE IN REPRESENTING UNCERTAINTY IN MEASUREMENTS **c65**
V. Kreinovich, C. Quintana (Michigan Univ., Ann Arbor.), and L. Reznik (Footscray Inst. of Tech., Australia.) *In* NASA. Johnson Space Center, North American Fuzzy Logic Processing Society (NAFIPS 1992), Volume 2 Dec. 1992 p 618-624 (For primary document see N93-29556 11-59)
(Grants NAG9-482; NSF CDA-90-15006)
Avail: CASI HC A02/MF A03

In rare situations, like fundamental physics, we perform experiments without knowing what their results will be. In the majority of real-life measurement situations, we more or less know beforehand what kind of results we will get. Of course, this is not the precise knowledge of the type 'the result will be between alpha - beta and alpha + beta,' because in this case, we would not need any measurements at all. This is usually a knowledge that is best represented in uncertain terms, like 'perhaps (or 'most likely', etc.) the measured value x is between alpha - beta and alpha + beta.' Traditional statistical methods neglect this additional knowledge and process only the measurement results. So it is desirable to be able to process this uncertain knowledge as well. A natural way to process it is by using fuzzy logic. But, there is a problem; we can use different membership functions to represent the same uncertain statements, and different functions lead to different results. What membership function do we choose? In the present paper, we show that under some reasonable assumptions, Gaussian functions mu(x) = exp(-beta(x(exp 2))) are the most adequate choice of the membership functions for representing uncertainty in measurements. This representation was efficiently used in testing jet engines to airplanes and spaceships. Author (revised)

N93-29585*# Togai InfraLogic, Inc., Houston, TX.
LIFE INSURANCE RISK ASSESSMENT USING A FUZZY LOGIC EXPERT SYSTEM **c65**
Luis A. Carreno and Roy A. Steel *In* NASA. Johnson Space Center, North American Fuzzy Logic Processing Society (NAFIPS 1992), Volume 2 Dec. 1992 p 627-635 (For primary document see N93-29556 11-59)
Avail: CASI HC A02/MF A03

In this paper, we present a knowledge based system that combines fuzzy processing with rule-based processing to form an improved decision aid for evaluating risk for life insurance. This application illustrates the use of FuzzyCLIPS to build a knowledge based decision support system possessing fuzzy components to improve user interactions and KBS performance. The results employing FuzzyCLIPS are compared with the results obtained from the solution of the problem using traditional numerical equations. The design of the fuzzy solution consists of a CLIPS rule-based system for some factors combined with fuzzy logic rules for others. This paper describes the problem, proposes a solution, presents the results, and provides a sample output of the software product. Author

N93-29864*# Institute for Computer Applications in Science and Engineering, Hampton, VA.
ICASE Semiannual Report, 1 Apr. - 30 Sep. 1992
Dec. 1992 93 p
(Contracts NAS1-19480; NAS1-18605; RTOP 505-90-52-01)
(NASA-CR-193257; NAS 1.26:193257; AD-A263983) Avail: CASI HC A05/MF A01

This report summarizes research conducted at the Institute for Computer Applications in Science and Engineering in applied mathematics, numerical analysis, and computer science during the period April 1, 1992 through September 30, 1992. DTIC

60 COMPUTER OPERATIONS AND HARDWARE

Includes hardware for computer graphics, firmware, and data processing.

For components see *33 Electronics and Electrical Engineering.*

N93-29058# Lawrence Livermore National Lab., CA.
SEU TOLERANT COMPUTER BASED ON THE R3000
J. L. Kaschmitter, D. B. Butner, D. L. Shaeffer, N. J. Colella, C. L. McKnett (JAYCOR, Santa Monica, CA.), and P. G. Coakley (JAYCOR, Santa Monica, CA.) 30 Jan. 1993 5 p Presented at the IEEE Fault Tolerant Computing Symposium, Boston, MA, 6-10 Jul. 1992
(Contract W-7405-eng-48)
(DE93-009294; UCRL-JC-109575; CONF-9207187-1) Avail: CASI HC A01/MF A01

We have built and tested a Single Event Upset (SEU) tolerant computer (STC) based on the MIPS R3000 processor. Testing in a proton environment is ongoing. The design of this computer was postulated in previous work and based upon extensive radiation effects testing performed by Lawrence Livermore National Laboratory (LLNL). This computer is based entirely on commercially available parts. The purpose of these tests is to demonstrate the capability of using non-radiation hardened parts in an SEU environment, in this case Low Earth Orbit (LEO), with upset mitigation through fault tolerant hardware and software design methodologies. The hardware and software designs are described in detail, the test setup and test parameters are given, and test results are presented. DOE

N93-29070*# National Aeronautics and Space Administration. Langley Research Center, Hampton, VA.
PARALLEL SOFTWARE TOOLS AT LANGLEY RESEARCH CENTER
Stuti Moitra, Geoffrey M. Tennille, Christopher D. Lakeotes (Computer Sciences Corp., Hampton, VA.), Donald P. Randall, Jarvis J. Arthur (Computer Sciences Corp., Hampton, VA.), Dana P. Hammond (Computer Sciences Corp., Hampton, VA.), and Gerald H. Mall (Computer Sciences Corp., Hampton, VA.) Mar. 1993 82 p
(RTOP 505-90-53-02)
(NASA-TM-108995; NAS 1.15:108995) Avail: CASI HC A05/MF A01

This document gives a brief overview of parallel software tools available on the Intel iPSC/860 parallel computer at Langley Research Center. It is intended to provide a source of information that is somewhat more concise than vendor-supplied material on the purpose and use of various tools. Each of the chapters on tools is organized in a similar manner covering an overview of the functionality, access information, how to effectively use the tool, observations about the tool and how it compares to similar software, known problems or shortfalls with the software, and reference documentation. It is primarily intended for users of the iPSC/860 at Langley Research Center and is appropriate for both the experienced and novice user. Author (revised)

N93-29482# California Univ., San Diego, La Jolla. Dept. of Electrical and Computer Engineering.
ASSOCIATIVE MEMORIES FOR SUPERCOMPUTERS Final Report, Jul. 1989 - Jan. 1991
Sadik C. Esener, Philippe Marchand, and Ashok Krishnamoorthy Dec.

1992 57 p
(Contract F30602-89-C-0145)
(AD-A263142; RL-TR-92-295) Avail: CASI HC A04/MF A01

A motionless head 2-D parallel readout system for optical disks is presented. Its unique features are discussed and it is compared to various parallel access optical storage media. The motionless-head parallel read-out system for optical disks is shown to meet current and near-term future requirements for high performance secondary storage. In order to select a memory architecture compatible with the motionless-head disk, inner-product and outer-product associative memory algorithms are compared in terms of their storage requirements, search times, system complexities, and fault tolerance. Based on this comparison, the page serial, bit-parallel inner-product method is shown to be well suited to implementation with parallel readout optical disk, and opto-electronic XNOR gate arrays, using for instance the Si/PLZT technology. Finally, the associative memory system design is presented. DTIC

N93-29492# Colsa, Inc., Huntsville, AL.

DIGITAL HARDWARE ARCHITECTURE IMPLEMENTATION Annual Report

15 Feb. 1993 61 p
(Contract DASG60-91-C-0006)
(AD-A263219; CI-2071-93-0008) Avail: CASI HC A04/MF A01

During the past year's Ground-Based Radar (GBR) development cycle, COLSA supported the Project Office in many technical areas, which will be described in detail within the course of this annual report. The report is segmented into five sections: Section 1-Executive Overview, Section 2-Introduction, Section 3-Technical Evaluations, Section 4-Trips and Meetings, and Section 5-Conclusions and Recommendations. Section 3-Technical Evaluations is the principal focus of this report, describing in detail a number of subjects important to a sound GBR design. The report will describe in detail the probable hardware candidates that were assessed during the contract proposal period, along with the actual GBR configurations, which became evident upon contract award. The subjects to be covered will include descriptions of hardware communications; signal and data processors; workstations; and the latest results of up-to-date microprocessor designs, as advertised by the industry. DTIC

N93-29504* National Aeronautics and Space Administration. Pasadena Office, CA.

PARALLEL INFERENCING METHOD AND APPARATUS FOR RULE-BASED EXPERT SYSTEMS Patent

Ursula M. Schwuttke, inventor (to NASA), Dan Moldovan, inventor (to NASA), and Steve Kuo, inventor (to NASA) 6 Jul. 1993 9 p Filed 29 Mar. 1991
(NASA-Case-NPO-18004-1-CU; US-Patent-5,226,110;
US-Patent-Appl-SN-677059; US-Patent-Class-395-11;
US-Patent-Class-395-51; Int-Patent-Class-G06F-15/18) Avail: US Patent and Trademark Office

The invention analyzes areas of conditions with an expert knowledge base of rules using plural separate nodes which fire respective rules of said knowledge base, each of said rules upon being fired altering certain of said conditions predicated upon the existence of other said conditions. The invention operates by constructing a P representation of all pairs of said rules which are input dependent or output dependent; constructing a C representation of all pairs of said rules which are communication dependent or input dependent; determining which of the rules are ready to fire by matching the predicate conditions of each rule with the conditions of said set; enabling said node means to simultaneously fire those of the rules ready to fire which are defined by said P representation as being free of input and output dependencies; and communicating from each node enabled by said enabling step the alteration of conditions by the corresponding rule to other nodes whose rules are defined by said C matrix means as being input or communication dependent upon the rule of said enabled node. Official Gazette of the U.S. Patent and Trademark Office

N93-29608* National Aeronautics and Space Administration. Pasadena Office, CA.

SPECIAL PURPOSE PARALLEL COMPUTER ARCHITECTURE FOR REAL-TIME CONTROL AND SIMULATION IN ROBOTIC APPLICATIONS Patent

Amir Fijany, inventor (to NASA) (Jet Propulsion Lab., California Inst. of Tech., Pasadena.) and Antal K. Bejczy, inventor (to NASA) (Jet Propulsion Lab., California Inst. of Tech., Pasadena.) 8 Jun. 1993 10 p Filed 28 Dec. 1989 Supersedes N90-27268 (30 - 21, p 3038)
(NASA-Case-NPO-17629-1-CU; US-Patent-5,218,709;
US-Patent-Appl-SN-458280; US-Patent-Class-395-800;
US-Patent-Class-364-231.9; US-Patent-Class-364-DIG.1;
Int-Patent-Class-G06F-9/00; Int-Patent-Class-G06F-15/16) Avail: US Patent and Trademark Office

This is a real-time robotic controller and simulator which is a MIMD-SIMD parallel architecture for interfacing with an external host computer and providing a high degree of parallelism in computations for robotic control and simulation. It includes a host processor for receiving instructions from the external host computer and for transmitting answers to the external host computer. There are a plurality of SIMD microprocessors, each SIMD processor being a SIMD parallel processor capable of exploiting fine grain parallelism and further being able to operate asynchronously to form a MIMD architecture. Each SIMD processor comprises a SIMD architecture capable of performing two matrix-vector operations in parallel while fully exploiting parallelism in each operation. There is a system bus connecting the host processor to the plurality of SIMD microprocessors and a common clock providing a continuous sequence of clock pulses. There is also a ring structure interconnecting the plurality of SIMD microprocessors and connected to the clock for providing the clock pulses to the SIMD microprocessors and for providing a path for the flow of data and instructions between the SIMD microprocessors. The host processor includes logic for controlling the RRCS by interpreting instructions sent by the external host computer, decomposing the instructions into a series of computations to be performed by the SIMD microprocessors, using the system bus to distribute associated data among the SIMD microprocessors, and initiating activity of the SIMD microprocessors to perform the computations on the data by procedure call.
Official Gazette of the U.S. Patent and Trademark Office

N93-29662 National Inst. of Standards and Technology, Gaithersburg, MD.

COMPUTER SYSTEMS LABORATORY Annual Report, period ending 1992

E. B. Lennon, S. M. Radack, and R. K. Roach Feb. 1993 100 p See also report for 1991, PB92-172709 Limited Reproducibility: More than 20% of this document may be affected by microfiche quality
(PB93-181873; NISTIR-5127) Avail: CASI HC A05

The Computer Systems Laboratory (CSL) Annual Report-1992 describes the annual computer and related telecommunications activities and accomplishments of the Laboratory. Following the Director's Foreword, an overview of the Laboratory is presented, including a current CLS Organization Chart. Overviews of CSL's five technical divisions are featured next, followed by a section on Technology Transfer which details the vehicles CSL uses to disseminate research and information to the public and technical communities. A list of Federal Information Processing Standards (FIPS) and FIPS order information concludes the annual report. NTIS

N93-30104# European Space Agency, Paris (France).

THREE-DIMENSIONAL GRAPHICAL REPRESENTATION OF OBJECTS ACCORDING TO MOVEMENT DATA IN REALTIME

Klaus Alvermann (Deutsche Forschungsanstalt fuer Luft- und Raumfahrt, Brunswick, Germany.) Nov. 1991 48 p Transl. into ENGLISH of Dreidimensionale Darstellung von Objekten nach Bewegungsdaten in Echtzeit (Brunswick, Germany, DLR) 30 Oct. 1990 p 1-70 Original language document was announced as N91-23725
(ESA-TT-1258; DLR-FB-90-51; ETN-93-93713) Avail: CASI HC A03/MF A01; original German version available from DLR Wissenschaftliches Berichtswesen, VB-PL-DO, Postfach 90 60 58, 5000 Cologne, Germany, HC

A system capable of showing three dimensional images of flying objects is described. The objects are moved by flight data coming from several possible sources, that is, a (real time) simulation or telemetry. The system is implemented on a personal computer and a transputer network. The transputer network is capable of showing the movement in real time, that is, there are enough images per second to have a smooth movement. The basic concepts of three dimensional images are defined, the mathematical background is prepared, and both implementations are described. ESA

N93-30179 Texas Technological Univ., Lubbock. Dept. of Electrical Engineering.
ACCURACY ENHANCEMENT IN OPTICAL COMPUTING Annual Report, 1 Mar. 1992 - 28 Feb. 1993
John F. Walkup and Thomas F. Krile 25 Mar. 1993 38 p Limited Reproducibility: More than 20% of this document may be affected by microfiche quality
(Grant AF-AFOSR-0192-91)
(AD-A264872; AFOSR-93-0354TR) Avail: CASI HC A03

Investigations of techniques for describing and enhancing the accuracy of optical linear algebra processors have been conducted. Significant accomplishments include: (1) development and simulation of a system model incorporating device dynamic range for better quantitative assessment of error-correction code performance; (2) extension of earlier statistical models to include crosstalk, background, avalanche gain, flicker and generation-recombination noise effects; (3) construction of the Optical Analysis Simulation Interactive System (OASIS) software for the acquisition, analysis and manipulation of experimental data; and (4) identification of major noise sources of experimental concern using OASIS. DTIC

N93-30570# Congressional Budget Office, Washington, DC.
PROMOTING HIGH-PERFORMANCE COMPUTING AND COMMUNICATIONS
Jun. 1993 78 p
(ISBN-0-16-041828-3) Avail: CASI HC A05/MF A01

The High Performance Computing and Communications (HPCC) program embodies many concerns regarding federal technology policy: the role of the federal government in promoting new industries, building infrastructure, supporting joint federal-private efforts, and encouraging the transfer of technology. This report focuses on the first of these concerns--the federal role in promoting new industries. As requested by the Senate Committee on Commerce, Science, and Transportation, the report concentrates on the obstacles--mainly on the demand side--that might prevent the high-performance computing and data communications industries from growing and using the technology being developed under the HPCC program. In keeping with the Congressional Budget Office's (CBO's) mandate to provide nonpartisan analysis, no recommendations are made. Derived from text

N93-30832# National Inst. of Standards and Technology, Gaithersburg, MD.
MINIMUM SECURITY REQUIREMENTS FOR MULTI-USER OPERATING SYSTEMS
Mar. 1993 50 p
(PB93-185999; NISTIR-5153) Avail: CASI HC A03/MF A01

The Minimum Security Requirements for Multi-User Operating Systems (MSR) document provides basic commercial computer system security requirements applicable to both government and commercial organizations. These requirements include technical measures that can be incorporated into multi-user, remote-access, resource-sharing, and information-sharing computer systems. The MSR document was written from the prospective of protecting the confidentiality and integrity of an organization's resources and promoting the continual availability of these resources. The MSR presented in the document form the basis for the commercially oriented protection profiles in Volume 2 of the draft Federal Criteria for Information Technology Security document. The MSR document has been developed by the MSR Working Group of the Federal Criteria Project under National Institute of Standards and Technology (NIST) leadership with a high level of private sector participation. Its contents are based on the Trusted Computer System Evaluation Criteria (TCSEC) C2 criteria class, with additions from current computer industry practice and commercial security requirements specifications. NTIS

N93-30840# National Aerospace Lab., Amsterdam (Netherlands). Informatics Div.
TRANSPUTERS, PARALLEL PROCESSING IN EMBEDDED SYSTEMS FOR IMAGE COMPRESSION IN SPACE APPLICATIONS [TRANSPUTERS, PARALLEL REKENEN IN EMBEDDED SYSTEMEN TEN BEHOEVE VAN BEELDCOMPRESIE VOOR RUIMTEVAARTTOEPASSINGEN]
M. H. J. B. Versteeg 28 Jun. 1989 14 p In DUTCH Presented at Massief Rekenen, The Hague, Netherlands, 7 Jun. 1989
(NLR-TP-89242-U; ETN-93-93317) Avail: CASI HC A03/MF A01

A system was developed for ESOC (European Space Operations Center) in the framework of the METEODIS (Meteosat Dissemination) to demonstrate the use of data compression and encryption within the operational Meteosat dissemination system. The compression function was used to increase the amount of meteorological data (images) that can be disseminated to the users. Programmable units were used to perform the compression and decompression functions within the METEODIS system. A powerful multiprocessor system is required to perform these functions fast enough. In the METEODIS project the compression and decompression functions are realized with four transputers each. The transputer is a single chip microprocessor with a RISC (Reduced Instruction Set Computer) architecture specially suited for use in multiprocessor systems. ESA

N93-28813*# Southwest Research Inst., San Antonio, TX.
SPACECRAFT COMPUTER TECHNOLOGY AT SOUTHWEST RESEARCH INSTITUTE Abstract Only
D. J. Shirley *In* Lunar and Planetary Inst., Workshop on Advanced Technologies for Planetary Instruments, Part 1 1993 p 21 (For primary document see N93-28764 11-91)
Avail: CASI HC A01/MF A01

N93-30259 Manitoba Univ., Winnipeg.
GENERATION OF CONFIGURABLE SELF-SYNCHRONIZING SYNCHRONOUS CMOS STATIC RAMs
W. Kinsner *In* Engineering Inst. of Canada, Canadian Conference on Electrical and Computer Engineering, Volumes 1 and 2 1990 4 p (For primary document see N93-30215 11-31)
Avail: Engineering Inst. of Canada, 2050 rue Mansfield, Suite 700, Montreal, Quebec H3A 1Z2 Canada

N93-30327 National Research Council of Canada, Ottawa (Ontario). Inst. for Information Technology.
A MULTIPROCESSOR ARCHITECTURE FOR REALTIME ROBOT CONTROL
Shadia Elgazzar *In* Engineering Inst. of Canada, Canadian Conference on Electrical and Computer Engineering, Volumes 1 and 2 1990 5 p (For primary document see N93-30215 11-31)
Avail: Engineering Inst. of Canada, 2050 rue Mansfield, Suite 700, Montreal, Quebec H3A 1Z2 Canada

N93-30329 National Research Council of Canada, Ottawa (Ontario). Flight Research Lab.
AIRBORNE DATA ACQUISITION USING A FRONT-END PROCESSOR ARCHITECTURE
J. E. Jordan and K. K. Lum *In* Engineering Inst. of Canada, Canadian Conference on Electrical and Computer Engineering, Volumes 1 and 2 1990 4 p (For primary document see N93-30215 11-31)
Avail: Engineering Inst. of Canada, 2050 rue Mansfield, Suite 700, Montreal, Quebec H3A 1Z2 Canada

N93-30480*# Carnegie-Mellon Univ., Pittsburgh, PA.
USING TRANSPARENT INFORMED PREFETCHING (TIP) TO REDUCE FILE READ LATENCY
R. H. Patterson, G. A. Gibson, and M. Satyanarayanan *In* NASA. Goddard Space Flight Center, Goddard Conference on Mass Storage Systems and Technologies, Volume 1, 1993 p 329-342 (For primary document see N93-30449 11-82)
Avail: CASI HC A03/MF A03

61 COMPUTER PROGRAMMING AND SOFTWARE

Includes computer programs, routines, alogorithms, and specific applications, e.g., CAD/CAM.

N93-28482# Nijmegen Univ. (Netherlands). Dept. of Informatics.
CONCURRENT CLEAN LANGUAGE MANUAL, VERSION 0.8

Marko vanEekelen, Halbe Huitema, Eric Necker, Sjaak Smetsers, and Rinus Plasmeijer Aug. 1992 98 p
(TR-92-18; ETN-93-93872) Avail: CASI HC A05/MF A02

Concurrent Clean is an experimental purely lazy functional language suited for evaluation in different kinds of machine architectures varying from simple computers to highly parallel architectures. Concurrent Clean is introduced by a demonstration of how some functional programs are written down in this formalism. The basic semantics of Current Clean, the type system, the modules (exporting, importing, etc.), input/output handling, and annotations, are described. The description of Current Clean given corresponds to the Concurrent Clean System version 0.8. Changes and additions to the previous release (0.7) are documented. ESA

N93-28484# Nijmegen Univ. (Netherlands). Declarative Systems Research Inst.

THE CONCURRENT CLEAN SYSTEM USER'S MANUAL AND PABCSTAT USER'S MANUAL, VERSION 0.8

Halbe Huitema and Rinus Plasmeijer Aug. 1992 44 p
(TR-92-19; ETN-93-93873) Avail: CASI HC A03/MF A01

The user manual for the Concurrent Clean system, a programming environment for Concurrent Clean, an experimental functional programming language, is presented. Concurrent Clean can be used on a range of computer architectures varying from personal computers to parallel machine architectures. The user's manual for PABCstat, a graphical tool for the analysis of parallel Concurrent Clean programs, is also presented. PABCstat uses the statistic file produced by the PABC (Parallel ABC) simulator of the Concurrent Clean system version 0.8 to give a graphical representation of the parallel execution of a Concurrent Clean program. ESA

N93-28485# Oxford Univ. (England). Robotics Research Group.

COARSE IMAGE MOTION FOR SACCADE CONTROL

Philip F. Mclauchlan and David W. Murray Oct. 1991 17 p
(OUEL-1916/92; ETN-93-93874) Avail: CASI HC A03/MF A01

A two dimensional vision module that estimates the translational motion of moving objects for the purpose of driving saccadic camera motions to fixate them is described. Robustness and a fast reaction time are the main requirements of the module. The algorithm is designed for use with a head whose movements can be described to a first approximation as pure rotation. The apparently moving background is segmented from the moving objects on the scene using a prediction of the background flow obtained from head odometry. Subsequently the detected objects are analyzed to determine their velocity using a simple least square method to solve the aperture problem. The potential of the algorithm for parallelism and pipelining is described. ESA

N93-28486# Oxford Univ. (England). Robotics Research Group.

RECOGNIZING PARAMETERIZED OBJECTS FROM RANGE DATA

Ian David Reid 1991 129 p Sponsored by Rhodes Trust, and Sasakawa Fund
(OUEL-1918/92; ETN-93-93875) Avail: CASI HC A07/MF A02

Techniques for recognizing instances of 3D (three dimensional) object classes from sets of 3D feature observations are developed, motivated by the problem of pallet acquisition for a mobile vehicle equipped with a laser triangulation range finder. Recognition is structured as a depth first search of an interpretation tree. The combinatorial explosion of the number of interpretations is controlled by constraints on geometric measurements between pairs of sensed features, which are also used to determine upper and lower bounds on the model parameter values of the instance. A real valued constraint propagation network unifies the representations of the model parameters, model constraints and feature constraints, and provides a simple and effective mechanism for accessing and updating parameter values. Recognition of objects with multiple internal degrees of freedom, including non-uniform scaling and stretching, articulations, and subpart repetitions, is demonstrated for two different types of real range data: 3D fragments from a stereo vision system, and position/surface normal data derived from planar patches extracted from a range image. Although there is an increase in the computation required relative to fixed models, the added flexibility of the system is shown to more than compensate. Range data is obtained using a laser stripe triangulation range sensor, fitted to a mobile vehicle. The design of the range finder is discussed and an effective, accurate calibration procedure derived. Simple features are extracted from range images delivered by the sensor and used to compute the geometric measurements for recognition, providing a high level of robustness to occlusion. ESA

N93-28503# Nijmegen Univ. (Netherlands). Dept. of Information Systems.

FORMAL DEFINITION OF A CONCEPTUAL LANGUAGE FOR THE DESCRIPTION AND MANIPULATION OF INFORMATION MODELS

A. H. M. terHofstede (Utrecht State Univ., Netherlands.), H. A. Proper, and T. P. danderWeide Jul. 1992 58 p Sponsored in part by Software Engineering Research Center, Netherlands, and Netherlands Organization for Scientific Research
(TR-92-16; ETN-93-93870) Avail: CASI HC A04/MF A01

The redesign of strongly extended version of RIDL (Reference and IDea Language) is addressed. RIDL was developed for manipulating and querying an information structure. The resulting language is called LISA-D (Language for Information Structure and Access Descriptions), and is based on PSM (Predictor Set Modeling). An informal introduction to PSM and LISA-D is given and a summary of the formal definition of PSM is given. Path expressions, which form a primitive, yet powerful language for information manipulation, are introduced. The language LISA-D is introduced and formally defined by means of a translation to path expressions. Information descriptors form the basic syntactical construct of LISA-D, and they are used for the definition of constraints, queries and updates in LISA-D. ESA

N93-28504# Institut National de Recherche d'Informatique et d'Automatique, Valbonne (France). Programme 4: Robotique, Image et Vision.

JPDRAW USER'S MANUAL, VERSION 3.3 [NOTICE D'UTILISATION JPDRAW, VERSION 3.3]

Jean-Pierre Merlet Mar. 1992 111 p In FRENCH
(INRIA-RT-0139; ETN-93-93883) Avail: CASI HC A06/MF A02

The use of a graphic editor for the Sun workstation in the suntools environment or any workstations in the X-window environment is described. This editor generates 'LATEX' files for the text and Postcript files for the drawing which can be included in a 'LATEX' file. It enables the creation of various geometric primitives (lines, texts, boxes, polygons, ellipses, ovals and miscellaneous curves) and various tools to manipulate them. Two metalanguages for the description of graphics in an external file are understandable by this software, enabling the creation of drawings as results of various programs (for instance CAD (Computer Aided Design) system or image processing). ESA

N93-28526# Technische Hochschule, Darmstadt (Germany). Fachbereich Informatik.

DYNAMIC OBJECT ORIENTED INTERACTION AND ITS IMPLEMENTATION IN THE FRAMEWORK IN AN INTERFACE MANAGEMENT SYSTEM Ph.D. Thesis [DYNAMISCHE OBJEKTORIENTIERTE INTERAKTION UND IHRE IMPLEMENTIERUNG IM RAHMEN EINES SCHNITTSTELLENVERWALTUNGSSYSTEMS]

Hinrich Bruening 1990 109 p In GERMAN
(ETN-93-93795) Avail: CASI HC A06/MF A02

The final goal of the DIADES (Design tool for Interactive programs with provisions to Assess DESign decisions) project is the development of an integrated tool for the design, assessment, and generation of user interfaces. The communication of this tool with the user in different machines and operating systems shall be done through a uniform graphic interface. The interface shall realize an object oriented management of visualized communication parts with a mostly automatic dynamic control of the coherence in planning and timing. Requirements for such an interface are discussed. A balance between ideally desirable and realistically gainable capabilities must be found. An interface module is developed, which should demonstrate some new functionalities: automatic horizontal scrolling of text, to present longer text in small parts of the screen; the presentation and control of picture sequences as another kind of animation of graphic representations; automatic distribution of parts of the representation inside the limit resource of screen space, including the space sharing of specific parts; arranging representable parts in a time axis to make them appear at a specific moment for a specified time interval (including the possible rearrangement of other parts of the representation); and some means for the user to change the order (and logical grouping) of represented parts of the picture. The virtual interaction device, together with a (conventional) window manager, will adapt all input and output to a standard graphic interface. Different graphic interface systems with the requirements of the interaction device are considered and one is selected for the implementation. The reason for selecting X-Windows and the implementation of the virtual interaction device are described. ESA

N93-28531# Japan Atomic Energy Research Inst., Tokyo.
STUDY ON THE CONCURRENT CALCULATION WITH A MULTITRANSPUTER NETWORK
Shinji Inomata and Katsuo Suzuki Jun. 1992 86 p
(DE93-753191; JAERI-M-92-084) Avail: CASI HC A05/MF A01

A relation between the calculation processing time and the overhead of multitransputer network is studied in performing several concurrent calculations. The hardware configuration we used was a ring-type linked nine transputer network on an INMOS B008 mother board which was inserted into a slot of a personal computer compatible with IBM PC/AT. Further, we used the occam2 toolset of MS-DOS version to write the calculation programs in the occam2 language. On arithmetic operations, some trigonometric, and transcendental functions and numerical integrations, the calculation time and overhead were measured. The results show that the relative calculation speed is proportional to the number of transputers when the ratio of calculation time to overhead is much greater than 1.0. The overhead is consumed in intercommunicating among transputers for the parallel calculation set-up. DOE

N93-28537# Japan Atomic Energy Research Inst., Tokyo.
INSTALLATION OF A NEW FORTRAN COMPILER AND EFFECTIVE PROGRAMMING METHOD ON THE VECTOR SUPERCOMPUTER
Toshiyuki Nemoto, Koichiro Suzuki, Kenji Watanabe, Masahiko Machida, Seiji Osanai, Nobuo Isobe, Hiroo Harada, and Mitsuo Yokokawa (Japan Atomic Energy Research Inst., Ibaraki.) Jul. 1992 217 p
(DE93-753322; JAERI-M-92-105) Avail: CASI HC A10/MF A03

The Fortran compiler, version 10 has been replaced with the new one, version 12 (V12) on the Fujitsu Computer system at JAERI since May, 1992. The benchmark test for the performance of the V12 compiler is carried out with 16 representative nuclear codes in advance of the installation of the compiler. The performance of the compiler is achieved by the factor of 1.13 in average. The effect of the enhanced functions of the compiler and the compatibility to the nuclear codes are also examined. The assistant tool for vectorization TOP10EX is developed. In this report, the results of the evaluation of the V12 compiler and the usage of the tools for vectorization are presented. DOE

N93-28550# Lawrence Livermore National Lab., CA.
DIRECT VOLUME VISUALIZATION OF THREE-DIMENSIONAL VECTOR FIELDS
R. A. Crawfis and N. L. Max Apr. 1992 12 p Presented at the Visualization 1992, Boston, MA, 19-23 Oct. 1992
(Contract W-7405-eng-48)
(DE93-009233; UCRL-JC-109885; CONF-921079-4) Avail: CASI HC A03/MF A01

Current techniques for direct volume visualization offer only the ability to examine scalar fields. However, most scientific explorations require the examination of vector and possibly tensor fields as well as numerous scalar fields. An algorithm to directly render three-dimensional scalar and vector fields is described. The algorithm uses a combination of sampling and splatting techniques, that are extended to integrate display of vector field data within the image. DOE

N93-28577# Air Force Inst. of Tech., Wright-Patterson AFB, OH. School of Engineering.
TOWARD REUSABLE GRAPHICS COMPONENTS IN Ada M.S. Thesis
Sam-Kyu Lim Mar. 1993 119 p
(AD-A262568; AFIT/GCS/ENG/93M-03) Avail: CASI HC A06/MF A02

This thesis demonstrates and illustrates a way of developing reusable graphics software components in Ada associated with a C++/C library. The work was carried out using object-oriented software development techniques that were used to analyze, design and implement a partial flight simulator. The objective of this thesis was to present a way of building reusable software components with Ada in a graphics application environment. An object-oriented approach was taken in the development of a set of reusable graphics software components for a flight simulator domain. A selection of a set of reusable software components came from domain analysis. These components were analyzed in detail, then redesigned to demonstrate and illustrate the thesis objective. Examples from design and implementation demonstrate how Ada 83 was applied in building reusable graphics software components associated with C++ routines, the limitations of Ada 83, and how Ada9X addresses these limitations. DTIC

N93-28579# University of Southern California, Marina del Rey. Information Sciences Inst.
NATURAL LANGUAGE GENERATION Final Report, Mar. 1989 - Dec. 1991
Eduard H. Hovy Dec. 1992 87 p
(Contract F30602-89-C-0041)
(AD-A262578; RL-TR-92-273) Avail: CASI HC A05/MF A01

This document reports on research investigating the automatic planning and generation of multisentence text and multimodal presentations by computer. This work was performed from mid-1989 to late 1991 at the Information Services Institute of the University of Southern California (USC/ISI). The research consisted of three stages: development of the basic planning algorithms, collection and synthesis of subsidiary information required for text and multimedia presentations, and design and construction of a new type of communication planner architecture. DTIC

N93-28640# Los Alamos National Lab., NM.
HOW TO WRITE FAST AND CLEAR PARALLEL PROGRAMS USING ALGEBRA
L. Stiller 1992 21 p Presented at the Parallel Architectures and Languages Europa (PARLE), Munich, Germany, 14-28 Jun. 1993
(Contract W-7405-eng-36)
(DE93-000797; LA-UR-92-2924; CONF-930649-1) Avail: CASI HC A03/MF A01

An algebraic method for the design of efficient and easy to port codes for parallel machines is described. The method was applied to speed up and to clarify certain communication functions, n-body codes, a biomolecular analysis, and a chess problem. DOE

N93-28644# Argonne National Lab., IL.
BlockSolve v1.1: SCALABLE LIBRARY SOFTWARE FOR THE PARALLEL SOLUTION OF SPARSE LINEAR SYSTEMS
M. T. Jones and P. E. Plassmann Mar. 1993 15 p
(Contract W-31-109-eng-38)
(DE93-011391; ANL-92/46) Avail: CASI HC A03/MF A01

BlockSolve is a software library for solving large, sparse systems of linear equations on massively parallel computers. The matrices must be symmetric, but may have an arbitrary sparsity structure. BlockSolve is a portable package that is compatible with several different message-passing pardigms. This report gives detailed instructions on the use of BlockSolve in applications programs. DOE

N93-28755# Institut National de Recherche d'Informatique et d'Automatique, Valbonne (France). Programme 2: Calcul Symbolique, Programmation et Genie Logiciel.
THE GENERIC ARITHMETIC OF SISYPHE [L'ARITHMETIQUE GENERIQUE DE SISYPHE]
Jose Grimm Dec. 1991 44 p In FRENCH
(INRIA-RT-0136; ETN-93-93882) Avail: CASI HC A03/MF A01

The implementation of the arithmetics of the computer algebra system SISYPHE, based on the existence in LELISP of low level primitives (such as multiplication of two 16 bit integers yielding a 32 bit result) and a generic arithmetic (meant to be extended) are described. The primitives are used to implement undigned bignums of arbitrary size. An extension to signed integers and rational numbers is given using the generic arithmetic. Complex numbers and transcendental functions are defined and input/output functions are described. ESA

N93-28834# Edgerton, Germeshausen and Grier, Inc., Idaho Falls, ID.
BASIC OSF/MOTIF PROGRAMMING AND APPLICATIONS
D. Brooks and B. Novak (Westinghouse Idaho Nuclear Co., Inc., Idaho Falls.) 15 Sep. 1992 9 p Presented at the Idaho National Engineering Laboratory Computing Symposium, Idaho Falls, ID, 22-24 Sep. 1992

(Contract DE-AC07-76ID-01570)
(DE93-010800; EGG-M-92535; CONF-9209166-2) Avail: CASI HC A02/MF A01

When users refer to Motif, they are usually talking about mwm, the window manager. However, when programmers mention Motif they are usually discussing the programming toolkit. This toolkit is used to develop new or modify existing applications. In this presentation, the term Motif will refer to the toolkit. Motif comes with a number of features that help users effectively use the applications built with it. The term look and feel may be overused; nonetheless, a consistent and well designed look and feel assists the user in Teaming and using new applications. The term point and click generally refers to using a mouse to select program commands. While Motif supports point and click, the toolkit also supports using the keyboard as a substitute for many operations. This gives a good typist a distinct advantage when using a familiar application. We will give an overview of the toolkit, touching on the user interface features and general programming considerations. Since the source code for many useful Motif programs is readily available, we will explain how to get these sources and touch on derived benefits. We will also point to other sources of on-line help and documentation. Finally, we will present some practical experiences developing applications. DOE

N93-28877# Argonne National Lab., IL. Mathematics and Computer Science Div.
A SUMMARY OF BLOCK SCHEMES FOR REDUCING A GENERAL MATRIX TO HESSENBERG FORM
C. H. Bischof Feb. 1993 6 p
(Contract W-31-109-eng-38)
(DE93-010621; ANL/MCS-TM-175) Avail: CASI HC A02/MF A01

Various strategies have been proposed for arriving at block algorithms for reducing a general matrix to Hessenberg form by means of orthogonal similarity transformations. This paper reviews and systematically categorizes the various strategies and discusses their computational characteristics. DOE

N93-28934*# National Academy of Sciences - National Research Council, Washington, DC. Commission on Engineering and Technical Systems.
AN ASSESSMENT OF SPACE SHUTTLE FLIGHT SOFTWARE DEVELOPMENT PROCESSES
1993 184 p
(Contract NASw-4003)
(NASA-CR-193179; NAS 1.26:193179; ISBN-0-309-04880-X; LC-93-84549) Copyright Avail: CASI HC A09/MF A02

In early 1991, the National Aeronautics and Space Administration's (NASA's) Office of Space Flight commissioned the Aeronautics and Space Engineering Board (ASEB) of the National Research Council (NRC) to investigate the adequacy of the current process by which NASA develops and verifies changes and updates to the Space Shuttle flight software. The Committee for Review of Oversight Mechanisms for Space Shuttle Flight Software Processes was convened in Jan. 1992 to accomplish the following tasks: (1) review the entire flight software development process from the initial requirements definition phase to final implementation, including object code build and final machine loading; (2) review and critique NASA's independent verification and validation process and mechanisms, including NASA's established software development and testing standards; (3) determine the acceptability and adequacy of the complete flight software development process, including the embedded validation and verification processes through comparison with (1) generally accepted industry practices, and (2) generally accepted Department of Defense and/or other government practices (comparing NASA's program with organizations and projects having similar volumes of software development, software maturity, complexity, criticality, lines of code, and national standards); (4) consider whether independent verification and validation should continue. An overview of the study, independent verification and validation of critical software, and the Space Shuttle flight software development process are addressed. Findings and recommendations are presented. Derived from text

N93-28976*# Institute for Computer Applications in Science and Engineering, Hampton, VA.
A SIMPLE PARALLEL PREFIX ALGORITHM FOR COMPACT FINITE-DIFFERENCE SCHEMES Final Report
Xian-He Sun and Ronald D. Joslin Washington Apr. 1993 31 p Submitted for publication
(Contract NAS1-19480; RTOP 505-90-52-01)
(NASA-CR-191448; NAS 1.26:191448; ICASE-93-16) Avail: CASI HC A03/MF A01

A compact scheme is a discretization scheme that is advantageous in obtaining highly accurate solutions. However, the resulting systems from compact schemes are tridiagonal systems that are difficult to solve efficiently on parallel computers. Considering the almost symmetric Toeplitz structure, a parallel algorithm, simple parallel prefix (SPP), is proposed. The SPP algorithm requires less memory than the conventional LU decomposition and is highly efficient on parallel machines. It consists of a prefix communication pattern and AXPY operations. Both the computation and the communication can be truncated without degrading the accuracy when the system is diagonally dominant. A formal accuracy study was conducted to provide a simple truncation formula. Experimental results were measured on a MasPar MP-1 SIMD machine and on a Cray 2 vector machine. Experimental results show that the simple parallel prefix algorithm is a good algorithm for the compact scheme on high-performance computers. Author

N93-28978# Japan Atomic Energy Research Inst., Tokyo.
USERS MANUAL FOR FAULT TREE ANALYSIS CODE: CUT-TD
Norio Watanabe (Japan Atomic Energy Research Inst., Ibaraki.) and Mikio Kiyota Jun. 1992 57 p
(DE93-753272; JAERI-M-92-089) Avail: CASI HC A04/MF A01

The CUT-TD code was developed to find minimal cut sets for a given fault tree and to calculate the occurrence probability of its top event. This code uses an improved top-down algorithm which can enhance the efficiency in deriving minimal cut sets. The features in processing techniques incorporated into CUT-TD are as follows: (1) consecutive OR gates or consecutive AND gates can be coalesced into a single gate, as a result, this processing directly produces cut sets for the redefined single gate with each gate not being developed; (2) the independent subtrees are automatically identified and their respective cut sets are separately found to enhance the efficiency in processing; (3) the minimal cut sets can be obtained for the top event of a fault tree by combining their respective minimal cut sets for several gates of the fault tree; (4) the user can reduce the computing time for finding minimal cut sets and control the size and significance of cut sets by inputting a minimum probability cut off and/or a maximum order cut off; (5) the user can select events that need not to be further developed in the process of obtaining minimal cut sets (this option can reduce the number of minimal cut sets, save the computing time and assists the user in reviewing the result); (6) computing time is monitored by the CUT-TD code so that it can prevent the running job from abnormally ending due to excessive CPU time and produce an intermediate result. The CUT-TD code has the ability to restart the calculation with use of the intermediate result. A users' manual for the CUT-TD code. is provided. DOE

N93-28986# California Univ., Berkeley.
RESEARCH IN EFFICIENT SCIENTIFIC COMPUTATION Final Report, 1 Jan. 1990 - 31 Dec. 1992
B. N. Parlett 1992 4 p
(Contract N00014-90-J-1372)
(AD-A262084) Avail: CASI HC A01/MF A01

The more common obstacle, called curable breakdown, is handled by Look Ahead versions of the algorithm. This term was introduced earlier by Prof. Parlett and is now the generally accepted way to implement the Lanczos algorithm. Now that the algorithm is understood theoretically good implementations are being developed in many groups. Another long quest that Prof. Parlett completed in this period was to understand the phenomenon of Forward Instability in the symmetric tridiagonal QR algorithm. We now know when and only when this alarming phenomenon can occur. It is invariable associated with premature deflation of an eigenvalue. Through a series of delays the paper was not published until January 1993. In a completely different view Prof. Parlett, and a gifted student Wu-Liang Heng, developed a novel approach to the 2D Ising model problem that arises in Statistical Mechanics. The new method enables us to solve cases close to criticality for n = 30, and even up to 35. Other methods cannot get beyond n = 18 for reasonable costs. This work is only available in technical reports at present. The following lists show that a lot of other commendable work was either published or completed during this period. DTIC

N93-29026*# Research Inst. for Computing and Information Systems, Houston, TX.

TRANSFORMING AdaPT TO Ada9x

Stephen J. Goldsack (Imperial Coll. of Science and Technology, London, England.), A. A. Holzbach-Valero (Imperial Coll. of Science and Technology, London, England.), Richard A. Volz (Texas A&M Univ., Houston.), and Raymond S. Waldrop (Texas A&M Univ., Houston.) 8 Apr. 1993 35 p
(Contract NCC9-16; RICIS Proj. SE-35)
(NASA-CR-193117; NAS 1.26:193117) Avail: CASI HC A03/MF A01

How the concepts of AdaPT can be transformed into programs using the object oriented features proposed in the preliminary mapping for Ada9x are described. Emphasizing, as they do, the importance of data types as units of program, these features match well with the development of partitions as translations into Abstract Data Types which was exploited in the Ada83 translation covered in report R3. By providing a form of polymorphic type, the Ada83 version also gives support for the conformant partition idea which could be achieved in Ada83 only by using UNCHECKED CONVERSIONS. It is assumed that the reader understands AdaPT itself, but the translation into Ada83 is briefly reviewed, by applying it to a small example. This is then used to show how the same translation would be achieved in the 9x version. It is important to appreciate that the distribution features which are proposed in current mapping are not used or discussed in any detail, as those are not well matched to the AdaPT approach. Critical evaluation and comparison of these approaches is given in a separate report. Author (revised)

N93-29027*# Research Inst. for Computing and Information Systems, Houston, TX.

CONCEPT DOCUMENT OF THE REPOSITORY-BASED SOFTWARE ENGINEERING PROGRAM: A CONSTRUCTIVE APPRAISAL

20 Jan. 1992 21 p Prepared in cooperation with Applied Expertise, Inc., Houston, TX
(Contract NCC9-16; RICIS Proj. RB-04)
(NASA-CR-193125; NAS 1.26:193125) Avail: CASI HC A03/MF A01

A constructive appraisal of the Concept Document of the Repository-Based Software Engineering Program is provided. The Concept Document is designed to provide an overview of the Repository-Based Software Engineering (RBSE) Program. The Document should be brief and provide the context for reading subsequent requirements and product specifications. That is, all requirements to be developed should be traceable to the Concept Document. Applied Expertise's analysis of the Document was directed toward assuring that: (1) the Executive Summary provides a clear, concise, and comprehensive overview of the Concept (rewrite as necessary); (2) the sections of the Document make best use of the NASA 'Data Item Description' for concept documents; (3) the information contained in the Document provides a foundation for subsequent requirements; and (4) the document adequately: identifies the problem being addressed; articulates RBSE's specific role; specifies the unique aspects of the program; and identifies the nature and extent of the program's users. Author (revised)

N93-29028*# Software and Engineering Associates, Inc., Carson City, NV.

ADDITIONAL SUPPORT FOR THE TDK/MABL COMPUTER PROGRAM Final Report

G. R. Nickerson and Stuart S. Dunn 19 Mar. 1993 100 p
(Contract NAS8-39048)
(NASA-CR-193037; NAS 1.26:193037; SN-130; T93-0345) Avail: CASI HC A05/MF A02

An advanced version of the Two-Dimensional Kinetics (TDK) computer program was developed under contract and released to the propulsion community in early 1989. Exposure of the code to this community indicated a need for improvements in certain areas. In particular, the TDK code needed to be adapted to the special requirements imposed by the Space Transportation Main Engine (STME) development program. This engine utilizes injection of the gas generator exhaust into the primary nozzle by means of a set of slots. The subsequent mixing of this secondary stream with the primary stream with finite rate chemical reaction can have a major impact on the engine performance and the thermal protection of the nozzle wall. In attempting to calculate this reacting boundary layer problem, the Mass Addition Boundary Layer (MABL) module of TDK was found to be deficient in several respects. For example, when finite rate chemistry was used to determine gas properties, (MABL-K option) the program run times became excessive because extremely small step sizes were required to maintain numerical stability. A robust solution algorithm was required so that the MABL-K option could be viable as a rocket propulsion industry design tool. Solving this problem was a primary goal of the phase 1 work effort. Author (revised)

N93-29045# Aerospace Industries Association of America, Inc., Washington, DC. Superconductivity Committee.

A DETAILED TECHNOLOGY ROADMAP FOR SUPERCONDUCTIVITY

1 May 1992 60 p
Avail: CASI HC A04/MF A01

Superconductors are materials that conduct electricity without resistance and exhibit other unique electromagnetic properties. Because of these properties, they have potential application in the aerospace industry in such areas as very fast electronics, compact motors/generators/actuators, energy storage devices, and extremely sensitive sensors. A description of superconductors is given. Topics covered include: history of superconductors; superconductor properties; Josephson Effect; electrical effects; magnetic effects exclusion; applications to aerospace products; and magnetically levitated vehicles. CASI

N93-29127# Sandia National Labs., Albuquerque, NM. Parallel Computational Sciences Dept.

IMPLEMENTATION OF A SINGLE-MATERIAL VERSION OF PAGOSA ON MIMD HYPERCUBES

D. R. Gardner, D. D. Cline, and C. T. Vaughan Jun. 1992 27 p
Prepared in cooperation with Sandia National Labs., Livermore, CA
(Contract DE-AC04-76DP-00789)
(SAND-92-0640; UC-705) Avail: CASI HC A03/MF A01

A single-material version of the PAGOSA code has been implemented on two multiple-instruction, multiple-data (MIMD) hypercube massively parallel computers. PAGOSA is an explicit, Eulerian high-speed flow hydrodynamics code developed in CM Fortran by Los Alamos National Laboratory for the Thinking Machines Corporation Connection Machine-2 (CM-2). The CM-2 is a single-instruction, multiple-data (SIMD) computer. In the work described here, a version of PAGOSA which treats hydrodynamic flow of a single ideal gas was converted to Fortran 77, and domain decomposition and interprocessor communication routines were added to enable the code to run on the nCUBE 2 and Intel iPSC/860 hypercubes. In this report, the conversion process is described and a test problem illustrating the simulation of three-dimensional shock wave physics problems is displayed. We also present scaled speedup data which demonstrates the performance of the code on the two hypercubes. In particular, using the MIMD version of PAGOSA to simulate a simple blast wave we achieved grind times of 16.4 and 5.82 microseconds with corresponding scaled speedups of 55.3 and 43.6 on 64 nodes of nCUBE 2 and the Intel iPSC/860, respectively. A preliminary performance comparison of PAGOSA on the CM-2, the nCUBE 2, and the Intel iPSC/860 indicates that the unoptimized code runs at similar speeds on all three machines. Author (revised)

N93-29145# Air Force Inst. of Tech., Wright-Patterson AFB, OH.

MODELLING TEMPORAL ABDUCTIVE EXPLANATION

Eugene Santos, Jr. 11 Mar. 1993 24 p
(AD-A263096; AFIT/EN/TR-93-01) Avail: CASI HC A03/MF A01

Abductive reasoning and temporal reasoning have for the most part remained separate fields of study. Models for either tasks have made overly-simplistic assumptions about the other in order to concentrate on small highly-domain specific tasks. For example, existing abductive models have precluded any temporal information in their formulations whereas temporal models do not address abduction being only concerned with consistency issues. We present a unified approach to merging abductive and temporal reasoning. This approach properly subsumes existing abductive models as well as temporal ones and provides a precise framework for explanatory reasoning. Furthermore, effective algorithms for this new model are developed based on linear programming techniques. DTIC

N93-29169*# University of Southern California, Los Angeles. Information Sciences Inst.

DISTRIBUTED VIRTUAL SYSTEM (DIVIRS) PROJECT Semiannual Progress Report No. 10

Herbert Schorr and B. Clifford Neuman Jun. 1993 23 p
(Contract NCC2-539)
(NASA-CR-193234; NAS 1.26:193234) Avail: CASI HC A03/MF A01

As outlined in our continuation proposal 92-ISI-50R (revised) on contract NCC 2-539, we are (1) developing software, including a system manager and a job manager, that will manage available resources and that will enable programmers to program parallel applications in terms of a virtual configuration of processors, hiding the mapping to physical nodes; (2) developing communications routines that support the abstractions implemented in item one; (3) continuing the development of file and information systems based on the virtual system model; and (4) incorporating appropriate security measures to allow the mechanisms developed in items 1 through 3 to be used on an open network. The goal throughout our work is to provide a uniform model that can be applied to both parallel and distributed systems. We believe that multiprocessor systems should exist in the context of distributed systems, allowing them to be more easily shared by those that need them. Our work provides the mechanisms through which nodes on multiprocessors are allocated to jobs running within the distributed system and the mechanisms through which files needed by those jobs can be located and accessed. Author (revised)

N93-29170*# Illinois Univ., Urbana-Champaign. Center for Reliable and High-Performance Computing.

COMPILER-ASSISTED MULTIPLE INSTRUCTION ROLLBACK RECOVERY USING A READ BUFFER

N. J. Alewine, S.-K. Chen, W. K. Fuchs, and W.-M. Hwu May 1993 33 p
(Grant NAG1-613)
(NASA-CR-193175; NAS 1.26:193175; UILU-ENG-93-2220; CRHC-93-11)
Avail: CASI HC A03/MF A01

Multiple instruction rollback (MIR) is a technique that has been implemented in mainframe computers to provide rapid recovery from transient processor failures. Hardware-based MIR designs eliminate rollback data hazards by providing data redundancy implemented in hardware. Compiler-based MIR designs have also been developed which remove rollback data hazards directly with data-flow transformations. This paper focuses on compiler-assisted techniques to achieve multiple instruction rollback recovery. We observe that some data hazards resulting from instruction rollback can be resolved efficiently by providing an operand read buffer while others are resolved more efficiently with compiler transformations. A compiler-assisted multiple instruction rollback scheme is developed which combines hardware-implemented data redundancy with compiler-driven hazard removal transformations. Experimental performance evaluations indicate improved efficiency over previous hardware-based and compiler-based schemes. Author (revised)

N93-29171*# Old Dominion Univ., Norfolk, VA. Dept. of Electrical and Computer Engineering.

RESOURCE UTILIZATION MODEL FOR THE ALGORITHM TO ARCHITECTURE MAPPING MODEL Progress Report, period ending 30 Jun. 1993

John W. Stoughton and Rakesh R. Patel Jun. 1993 172 p
(Contract NCC1-136)
(NASA-CR-193122; NAS 1.26:193122) Avail: CASI HC A08/MF A02

The analytical model for resource utilization and the variable node time and conditional node model for the enhanced ATAMM model for a real-time data flow architecture are presented in this research. The Algorithm To Architecture Mapping Model, ATAMM, is a Petri net based graph theoretic model developed at Old Dominion University, and is capable of modeling the execution of large-grained algorithms on a real-time data flow architecture. Using the resource utilization model, the resource envelope may be obtained directly from a given graph and, consequently, the maximum number of required resources may be evaluated. The node timing diagram for one iteration period may be obtained using the analytical resource envelope. The variable node time model, which describes the change in resource requirement for the execution of an algorithm under node time variation, is useful to expand the applicability of the ATAMM model to heterogeneous architectures. The model also describes a method of detecting the presence of resource limited mode and its subsequent prevention. Graphs with conditional nodes are shown to be reduced to equivalent graphs with time varying nodes and, subsequently, may be analyzed using the variable node time model to determine resource requirements. Case studies are performed on three graphs for the illustration of applicability of the analytical theories. Author (revised)

N93-29212*# Research Inst. for Computing and Information Systems, Houston, TX.

RBSE: PRODUCT DEVELOPMENT TEAM RESEARCH ACTIVITY DELIVERABLES

1992 288 p Prepared in cooperation with GHG Corp., Houston, TX
(Contract NCC9-16; RICIS Proj. RB-05)
(NASA-CR-193115; NAS 1.26:193115) Avail: CASI HC A13/MF A03

The GHG Functions and Extensions to be added to the NASA Electronic Library System (NELS) 1.1 product are described. These functions will implement the 'output request' capability within the Object Browser. The functions will be implemented in two parts. The first part is a code to be added to the Object Browser (X version) to implement menus allowing the user to request that objects be copied to specific media, or that objects be downloaded to the user's system following a specific protocol, or that the object be printed to one of the printers attached to the host system. The second part is shell scripts which support the various menu selections. Additional scripts to support functions within the GHG shell (X version) will also be created along with the X version of the GHG Shell as initial capability for the 27 Mar. prototype. The scripts will be composed of C shell routines that will accept parameters (primary file pathways). Certain limitations in functionality will invoke Mail instead of Oracle Mail since that has yet to be delivered and the NELS invocation will default to the X-Windows version instead of the ASCII version. Derived from text

N93-29218*# Rensselaer Polytechnic Inst., Troy, NY. Center for Intelligent Robotic Systems for Space Exploration.

GRAPHICAL INTERFACE BETWEEN THE CIRSSE TESTBED AND CIMSTATION SOFTWARE WITH MCS/CTOS

Anna B. Hron Dec. 1992 126 p
(Grant NAGw-1333)
(NASA-CR-193276; NAS 1.26:193276; CIRSSE-131) Avail: CASI HC A07/MF A02

This research is concerned with developing a graphical simulation of the testbed at the Center for Intelligent Robotic Systems for Space Exploration (CIRSSE) and the interface which allows for communication between the two. Such an interface is useful in telerobotic operations, and as a functional interaction tool for testbed users. Creating a simulated model of a real world system, generates inevitable calibration discrepancies between them. This thesis gives a brief overview of the work done to date in the area of workcell representation and communication, describes the development of the CIRSSE interface, and gives a direction for future work in the area of system calibration. The CimStation software used for development of this interface, is a highly versatile robotic workcell simulation package which has been programmed for this application with a scale graphical model of the testbed, and supporting interface menu code. A need for this tool has been identified for the reasons of path previewing, as a window on teleoperation and for calibration of simulated vs. real world models. The interface allows information (i.e., joint angles) generated by CimStation to be sent as motion goal positions to the testbed robots. An option of the interface has been established such that joint angle information generated by supporting testbed algorithms (i.e., TG, collision avoidance) can be piped through CimStation as a visual preview of the path. Author (revised)

N93-29219*# Old Dominion Univ., Norfolk, VA. Dept. of Computer Science.

BUILDING A GENERALIZED DISTRIBUTED SYSTEM MODEL

R. Mukkamala Jun. 1993 62 p
(Grant NAG1-1114)
(NASA-CR-193239; NAS 1.26:193239) Avail: CASI HC A04/MF A01

The key elements in the 1992-93 period of the project are the following: (1) extensive use of the simulator to implement and test - concurrency control algorithms, interactive user interface, and replica control algorithms; and (2) investigations into the applicability of data and process replication in real-time systems. In the 1993-94 period of the project, we intend to accomplish the following: (1) concentrate on efforts to investigate the effects of data and process replication on hard and soft real-time systems - especially we will concentrate on the impact of semantic-based consistency control schemes on a distributed real-time system in terms of improved reliability, improved availability, better resource utilization, and reduced missed task deadlines; and (2) use the prototype to verify the theoretically predicted performance of locking protocols, etc. Author (revised)

N93-29294# New Mexico State Univ., Las Cruces. Dept. of Electrical and Computer Engineering.

MULTISENSOR IMAGE ANALYSIS SYSTEM Final Report, 1 Oct. 1987 - 28 Apr. 1993

Gerald M. Flachs, Michael Giles, Jay Jordan, Eric Johnson, and Ramon Parra 15 Apr. 1993 48 p
(Contract DAAL03-87-K-0106)
(AD-A263679; ARO-25173.44-EL-SAH) Avail: CASI HC A03/MF A01

The research sponsored by this grant is focused on the development of robust scene analysis algorithms to reliably analyze complex scenes with widely varying environmental and countermeasure conditions. Hybrid digital/optical processing architectures are developed to assimilate large quantities of multisensory information to locate and recognize targets in cluttered scenes. The major contribution of the research is the development of a theoretical and technological basis for designing robust multisensory vision systems. DTIC

N93-29345# Naval Postgraduate School, Monterey, CA. Dept. of Operations Research.

DYNAMIC FACTORIZATION IN LARGE-SCALE OPTIMIZATION

Gerald G. Brown and Michael P. Olson 12 Mar. 1993 38 p
(Contract AFOSR-MIPR-0007-92)
(AD-A263993; NPSOR-93-008) Avail: CASI HC A03/MF A01

Factorization of linear programming (LP) models enables a large portion of the LP tableau to be represented implicitly and generated from the remaining explicit part. Dynamic factorization admits algebraic elements which change in dimension during the course of solution. A unifying mathematical framework for dynamic row factorization is presented with three algorithms which derive from different LP model row structures: generalized upper bound rows, pure network rows, and generalized network rows. Each of these structures is a generalization of its predecessors, and each corresponding algorithm exhibits just enough additional richness to accommodate the structure at hand within the unified framework. Implementation and computational results are presented for a variety of real-world models. These results suggest that each of these algorithms is superior to the traditional, non-factorized approach, with the degree of improvement depending upon the size and quality of the row factorization identified. DTIC

N93-29418# Air Force Inst. of Tech., Wright-Patterson AFB, OH.

DEVELOPMENT OF A VISUAL SYSTEM INTERFACE TO SUPPORT A DOMAIN-ORIENTED APPLICATION COMPOSITION SYSTEM M.S. Thesis

Timothy L. Weide 23 Mar. 1993 152 p
(AD-A262489; AFIT/GCS/ENG/93M-05) Avail: CASI HC A08/MF A02

A visual system interface was designed and prototyped to generate, display, and modify domain-oriented application specifications. A visual system interface, called the Architect Visual System Interface (AVSI), supplements a text-based environment, called Architect, previously developed by two other students. Using canonical formal specifications of domain objects, Architect rapidly composes these specifications into a software application and executes a prototype of that application as a means to demonstrate its correctness before any programming language specific code is generated. Visual techniques for populating, manipulating, viewing, and composing these software application specifications within the formal object base scheme required by Architect are investigated. A Visual Specification Language (VSL) was developed to define the visual display characteristics of domain objects. AVSI provides automatic diagram layout, and also produces a textual display in a domain specific language. The Software Refinery environment, including its graphical interface tool INTERVISTA, was used to develop techniques for visualizing application data and for manipulating the formal object base. AVSI was validated with a well-understood domain, digital logic, and was found to significantly enhance Architect's application composition process. DTIC

N93-29463# Carnegie-Mellon Univ., Pittsburgh, PA. School of Computer Science.

APPLYING HIGH-LEVEL LANGUAGE PARADIGMS TO COMMUNICATIONS SOFTWARE FOR DISTRIBUTED SYSTEMS

Ellen H. Siegel Jan. 1993 131 p
(Contract F19628-91-C-0128)
(AD-A263001; CMU-CS-93-11) Avail: CASI HC A07/MF A02

Many traditional approaches to systems software do not adapt well to the complexity and scale of distributed systems, but realities of scale and the growing dependency on electronic communication and resource sharing nevertheless make some degree of distribution inescapable. Among other things, distributing systems software introduces complex failure modes and event orderings as well as issues related to heterogeneity and communication latency. Language designers have been investigating techniques for expressing complex systems more cleanly and effectively: various combinations of language mechanisms such as a parameterized module system, first-class functions, abstract types, exceptions, polymorphism, and a strong static type system can also be applied to great advantage in the design, implementation, and maintenance of distributed systems. The benefits of high-level language support in the design and implementation of communications software for distributed systems are evaluated. Three case studies illustrate the effects of distributed system design and implementation within the framework of a type-safe high-level language with advanced language mechanisms: a remote procedure call system, a distributed Linda system, and a protocol processing framework. The case studies are designed and implemented using Standard ML of New Jersey, which supports many of the relevant language features. Analysis of the design and implementation processes illustrates the benefits and drawbacks of using these advanced language features both individually and in combination to support distributed systems. DTIC

N93-29469*# Stanford Univ., CA. Dept. of Computer Science.

A TEMPORAL PROOF METHODOLOGY FOR REACTIVE SYSTEMS

Zohar Manna and Amir Pnueli Feb. 1993 39 p
(Grant NAG2-703)
(NASA-CR-193145; NAS 1.26:193145; AD-A262848; SU-STAN-CS-92-1463)
Avail: CASI HC A03/MF A01

The paper presents a minimal proof theory which is adequate for proving the main important temporal properties of reactive programs. The properties we consider consist of the classes of invariance, response, and precedence properties. For each of these classes we present a small set of rules that is complete for verifying properties belonging to this class. We illustrate the application of these rules on several examples. We discuss concise presentations of complex proofs using the devices of transition tables and proof diagrams. DTIC

N93-29473# Iowa State Univ. of Science and Technology, Ames. Center for Emerging Manufacturing Technology.

A VIRTUAL ENVIRONMENT FOR MANUFACTURING SYSTEMS Quarterly Progress Report No. 2, Jan. - Mar. 1993

J. H. Oliver, L. L. Chen, and M. J. Vanderploeg Mar. 1993 2 p
(Contract N00014-92-J-4092)
(AD-A263128) Avail: CASI HC A01/MF A01

This is the second quarterly progress report on the projects. Topics include the following: Assembly Planning Through Visualization; Off-line Programming and Visualization of Robots; and Simulation and Verification of Material Removal Processes. DTIC

N93-29483# Cambridge Hydrodynamics, Inc., Princeton, NJ.

DEVELOPMENT OF A NEW TECHNIQUE FOR IMAGE RECONSTRUCTION, ENHANCEMENT, AND VISUALIZATION Final Report, 15 Apr. 1990 - 14 Oct. 1992

Steven A. Orszag Feb. 1993 68 p
(Contract F49620-90-C-0028)
(AD-A263145; AFOSR-93-0255TR) Avail: CASI HC A04/MF A01

The problem of describing and reconstructing a surface, both analytically and visually, has been extensively addressed in this work. Various algorithms have been developed, tested, and compared and several conclusions have been reached. They are: (1) if the surface information is given on a uniform grid, the surface is best described by a set of contour plotting routines that exploit the GL graphics libraries both in a solid as well as a wire-mesh framework; and (2) if the surface information is given on a non-uniform grid, the surface can be described by Delaunay triangulation, a sophisticate graphics computer, or by interpolation back to a uniform grid. Numerous examples are given which show the advantages of these methods for specific applications. DTIC

N93-29486# Carnegie Inst. of Tech., Pittsburgh, PA. Dept. of Computer Science.
NONRESIDENT AND ENDANGERED VARIABLES: THE EFFECTS OF CODE GENERATION OPTIMIZATIONS ON SYMBOLIC DEBUGGING
Ali-Reza Adl-Tabatabai Dec. 1992 34 p
(Contract MDA972-90-C-0035)
(AD-A263149; CMU-CS-92-221) Avail: CASI HC A03/MF A01

Instruction scheduling and register allocation/assignment are two optimizations that are commonly used in the code generation phase of modern compilers. These optimizations are important for processors with exposed instruction-level parallelism and large register files. These optimizations, however, impact the task of the symbolic debugger which attempts to present to the user a source-level view of program execution. The debuggers for most systems today usually punt the issue of optimized code, either by turning optimizations off whenever the user asks for source level debugging, or by not detecting the effects of optimizations on the source-level state. To not mislead the user, the debugger must provide feedback of the effects of optimizations. In this paper, we investigate the effects of instruction scheduling and global register allocation/assignment on symbolic debugging and present approaches that a debugger can take. DTIC

N93-29488# Institut National de Recherche d'Informatique et d'Automatique, Valbonne (France). Programme 5: Traitement du Signal, Automatique et Productique.
AUTOMATED REASONING WITH FUNCTION EVALUATION FOR COCOLOG
Suning Wang (McGill Univ., Montreal, Quebec.) and Peter E. Caines (McGill Univ., Montreal, Quebec.) Jun. 1992 39 p Sponsored in part by INRIA, Sophia-Antipolis, France
(Grant NSERC-A1329)
(INRIA-RR-1713; ETN-93-93912) Avail: CASI HC A03/MF A01

A logic for the study of dynamical control systems, called a Conditional Observer and Controller Logic for finite machines (COCOLOG), is addressed. The properties of consistency and completeness for each first order logical theory in the tree of such theories in a COCOLOG were previously established, but the efficacy of automatic theorem proving is a crucial issue in the implementation of COCOLOG. A function evaluation based resolution for COCOLOG called FE (Function Evaluation) resolution is presented. The unique model property of COCOLOG is first proved via the complete axiomatization property and then the decidability property of any theory in a COCOLOG is deduced. Completeness and complexity reduction of FE resolution is discussed in terms of relative truthfulness and validity. ESA

N93-29493# General Electric Co., Schenectady, NY.
REPRESENTATION AND RECOGNITION WITH INVARIANTS AND GEOMETRIC CONSTRAINT MODELS Quarterly Progress Report, 1 Mar. - 1 Jun. 1992
3 Nov. 1992 4 p
(Contract MDA972-91-C-0053; ARPA Order 8228)
(AD-A263235) Avail: CASI HC A01/MF A01

A new approach to the recognition of solids of revolution has been developed and demonstrated. The technique involves the construction of bi-tangents to the outline curve of the occluding boundary of the object. The intersection of these bi-tangent lines corresponds to the image of a point on the axis of revolution of the object. An invariant index can then be computed from four or more such points by using the standard cross ratio. Several new projective invariants have been developed for 3D geometric features including, four 3D lines, 63D points, and 4 coplanar points with two additional points not on the plane. These invariants can be computed from two views of the object. DTIC

N93-29496# Duke Univ., Durham, NC.
IMPLEMENTATION OF PARALLEL ALGORITHMS Quarterly Report, 1 Jan. - 31 Mar. 1993
John H. Reif and Robert Wagner 31 Mar. 1993 19 p
(Contract N00014-91-J-1985)
(AD-A263126) Avail: CASI HC A03/MF A01

The topics covered include the following: Intermediate Representation for Parallel Implementation; Data Movement on Processor Arrays; Data-Parallel Implementations of Fast Multipole Algorithms for N-Body Interaction; Rate Control in Parallel Algorithms; Implementing Asynchronous Parallelism using Tagged-Memory; Implementations of Parallel Algorithms in Computational Geometry; and Parallel Sort Implementation. DTIC

N93-29497# Naval Postgraduate School, Monterey, CA. Dept. of Electrical and Computer Engineering.
FDDI INSTALLATION AND PERFORMANCE ANALYSIS M.S. Thesis
Gifford A. Hammar Dec. 1992 196 p
(AD-A263263) Avail: CASI HC A09/MF A03

This thesis discusses the theory behind collision based and noncollision based network protocols. From this basis, a complete theoretical performance analysis is performed on both Ethernet and FDDI. The CAPSnet FDDI installation is discussed and evaluated. Actual performance tests for both Ethernet and FDDI are provided and the results are discussed in detail. The test results are compared and analyzed. Actual performance is compared to theoretical performance. An explanation is provided to explain why actual performance does not match theoretical performance. DTIC

N93-29647# Mitre Corp., Bedford, MA.
NETSTAT: A PROBABILISTIC NETWORK CONNECTIVITY ANALYSIS TOOL
G. S. Marzot Feb. 1993 107 p
(AD-A262838; M-93B0000034) Avail: CASI HC A06/MF A02

This paper describes a computer program, NetStat, that is designed to analyze the connectivity of probabalistic networks. The program, which offers a full graphical user interface (GUI), allows the user to visually layout a network topology and specify the destruction probability, P(sub d), for each network element. A Monte-Carlo simulation is utilized to obtain estimates of various connectivity metrics. Some details of the implementation are discussed and an example application is illustrated. A user manual is provided. Source code is also provided, written in Symantec's Think Pascal for the Macintosh personal computer. DTIC

N93-29657# Wickersheimer Engineers, Inc., Champaign, IL.
CONCEPT DESIGN EXAMPLE, COMPUTER AIDED STRUCTURAL MODELING (CASM). SCHEME A Instruction Report No. 1
David Wickersheimer, Gene McDermott, Carl Roth, and Michael E. Pace Jun. 1992 184 p
(Contract DACA39-86-C-0024)
(AD-A264759; WES/IR/ITL-92-3) Avail: CASI HC A09/MF A02

This is one in a series of three manuals designed to instruct in the use of the Computer Aided Structural Modeling (CASM) computer program. The manuals are composed of flowcharts which show step-by-step procedures for executing a broad range of CASM capabilities. CASM is a computer program designed to aid the structural engineer in the preliminary design and evaluation of structural building systems by the use of three-dimensional (3-D) interactive graphics. This manual contains one of three different framing schemes for the same 1-2 story office building. The examples contain a complete range of capabilities to permit framing comparisons, including 3-D geometry modeling. criteria specifications, development of loads (snow, wind, seismic, dead, and live), drawing structural elements, preliminary analysis and design of structural elements, and quantity take-offs. DTIC

N93-29658# Wickersheimer Engineers, Inc., Champaign, IL.
CONCEPT DESIGN EXAMPLE, COMPUTER AIDED STRUCTURAL MODELING (CASM). SCHEME B Instruction Report No. 2
David Wickersheimer, Gene McDermott, Carl Roth, and Michael E. Pace Jun. 1992 164 p
(Contract DACA39-86-C-0024)
(AD-A264760; WES/IR/ITL-92-3) Avail: CASI HC A08/MF A02

This is one in a series of three manuals designed to instruct in the use of the Computer Aided Structural Modeling (CASM) computer program. The manuals are composed of flowcharts which show step-by-step procedures for executing a broad range of CASM capabilities. CASM is a computer program designed to aid the structural engineer in the preliminary design and evaluation of structural building systems by the use of three-dimensional (3-D) interactive graphics. This manual contains one of three different framing schemes for the same 1-2 story office building. The examples contain a complete range of capabilities to permit framing comparisons, including 3-D geometry modeling, criteria specifications, development of loads (snow, wind, seismic, dead, and live), drawing structural elements, preliminary analysis and design of structural elements, and quantity take-offs. DTIC

N93-29678 National Inst. of Standards and Technology, Gaithersburg, MD.
DATA PROBE USER'S GUIDE
D. A. Sauder Mar. 1993 61 p Sponsored by Assistant Secretary of Defense (Production and Logistics), Washington, DC, Computer-aided Acquisition and Logistic Support Program Limited Reproducibility: More than 20% of this document may be affected by microfiche quality
(PB93-178655; NISTIR-5141) Avail: CASI HC A04

Data Probes are software tools built using the emerging international Standard for the Exchange of Product Model Data (STEP). A Data Probe is created from an information model written in the Express modeling language. A Data Probe is used to create, edit, or view data that conforms to the specification found in the information model from which it is created. It is also used to conveniently view information from the information model. Data Probe was built at the National Institute of Standards and Technology (NIST) to assist in the development of STEP. A Data Probe may, however, be used by anyone that wishes to create and edit data corresponding to an information model. Data Probe is available as public domain software. The document explains what Data Probes are, discusses what is involved in creating a Data Probe, explains how to run a Data Probe, and provides a detailed explanation of the commands needed to use a Data Probe. NTIS

N93-29808# Sandia National Labs., Albuquerque, NM.
POLYNOMIAL SPACE POLYNOMIAL DELAY ALGORITHMS FOR LISTING FAMILIES OF GRAPHS
L. A. Goldberg 1992 8 p Presented at the ACM Symposium on the Theory of Computing, San Diego, CA, May 1993
(Contract DE-AC04-76DP-00789)
(DE93-010677; SAND-92-2483C; CONF-9305153-1) Avail: CASI HC A02/MF A01

The main result of this paper is a method that turns any almost sure sentence in the first order language of graphs into a deterministic polynomial space polynomial delay algorithm for listing the graphs that satisfy the sentence (our result is the first such method). Our work builds upon earlier work of Fagin. In particular, Fagin defined an infinite collection of combinatorial axioms and showed that for any fixed integer k almost every graph satisfies the kth axiom in his collection. DOE

N93-29821# Carnegie-Mellon Univ., Pittsburgh, PA. School of Computer Science.
FULL ABSTRACTION FOR A SHARED VARIABLE PARALLEL LANGUAGE
Stephen Brookes Apr. 1993 21 p
(Contract F33615-90-C-1465; ARPA Order 7597)
(AD-A263547; CMU-CS-93-141) Avail: CASI HC A03/MF A01

We give a new denotational semantics for a shared variable parallel programming language and prove full abstraction: the semantics gives identical meanings to commands if and only if they induce the same partial correctness behavior in all program contexts. The meaning of a command is a set of 'transition traces', which record the ways in which a command may interact with and be affected by its environment. We show how to modify the semantics to incorporate new program constructs, to allow for different levels of granularity or atomicity, and to model fair infinite computation, in each case achieving full abstraction with respect to an appropriate notion of program behavior. DTIC

N93-29822# Carnegie-Mellon Univ., Pittsburgh, PA. School of Computer Science.
NESL: A NESTED DATA-PARALLEL LANGUAGE (VERSION 2.6)
Guy E. Blelloch Apr. 1993 57 p
(Contract F33615-90-C-1465; ARPA Order 7597)
(AD-A263548; CMU-CS-93-129) Avail: CASI HC A04/MF A01

This report describes NESL, a strongly-typed, applicative, data-parallel language. NESL is intended to be used as a portable interface for programming a variety of parallel and vector supercomputers, and as a basis for teaching parallel algorithms. Parallelism is supplied through a simple set of data-parallel constructs based on sequences (ordered sets), including a mechanism for applying any function over the elements of a sequence in parallel and a rich set of parallel functions that manipulate sequences. NESL fully supports nested sequences and nested parallelism -the ability to take a parallel function and apply it over multiple instances in parallel. Nested parallelism is important for implementing algorithms with complex and dynamically changing data structures, such as required in many graph and sparse matrix algorithms. NESL also provides a mechanism for calculating the asymptotic running time for a program on various parallel machine models, including the parallel random access machine (PRAM). This is useful for estimating running times of algorithms on actual machines and, when teaching algorithms, for supplying a close correspondence between the code and the theoretical complexity. DTIC

N93-29823# Carnegie-Mellon Univ., Pittsburgh, PA. School of Computer Science.
CLASS NOTES: PROGRAMMING PARALLEL ALGORITHMS CS 15-840B (FALL 1992)
Guy E. Blelloch and Jonathan C. Hardwick Feb. 1993 142 p
(Contract F33615-90-C-1465; ARPA Order 7597)
(AD-A263549; CMU-CS-93-115) Avail: CASI HC A07/MF A02

These are the lecture notes for CS 15-840B, a hands-on class in programming parallel algorithms. The class was taught in the fall of 1992 by Guy Blelloch, using the programming language, NESL. It stressed the clean and concise expression of a variety of parallel algorithms. About 35 graduate students attended the class, of whom 28 took it for credit. These notes were written by students in the class, and were then reviewed and organized by Guy Blelloch and Jonathan Hardwick. The sample NESL code has been converted from the older LISP-style syntax into the new NIL-style syntax. These notes are not in a polished form, and probably contain several errors and omissions, particularly with respect to references in the literature. DTIC

N93-29852# Carnegie-Mellon Univ., Pittsburgh, PA. Software Engineering Inst.
CAPABILITY MATURITY MODEL FOR SOFTWARE, VERSION 1.1
Mark C. Paulk, Bill Curtis, Mary Beth Chrissis, and Charles V. Weber Feb. 1993 84 p
(AD-A263403; CMU/SEI-93-TR-24; ESC-TR-93-177) Avail: CASI HC A05/MF A01

A technical overview of the Capability Maturity Model for Software reflecting Version 1.1 is provided. Specifically, the process maturity framework of five maturity levels, the structural components that comprise the CMM, how the CMM is used in practice, and future directions of the CMM are described. This paper serves as one of the best sources for understanding the CMM, and it should clear up some of the misconceptions associated with software process maturity as advocated by the SEI. DTIC

N93-29865# California Univ., San Diego, La Jolla.
PERFORMANCE ANALYSIS OF SUBSPACE METHODS Final Report, 1 Apr. 1990 - 31 Mar. 1993
Bhaskar D. Rao 31 Mar. 1993 26 p
(Contract DAAL03-90-G-0095)
(AD-A263984; ARO-26802.20-MA-SDI) Avail: CASI HC A03/MF A01

The main focus of this research was determining the accuracy of subspace based methods for estimating the Direction of Arrival (DoA) of multiple sources from measurements obtained at the output of a sensor array. Subspace methods like MUSIC (MUltiple SIgnal Classification), ESPRIT (Estimation of Signal Parameters via Rotational Invariant Techniques), the Minimum-Norm methods have recently received much attention, and their estimation accuracy as well as a rigorous comparative study is of much interest. This was the goal of this research. Of particular interest was the affect of spatial smoothing on the performance of the subspace methods. Spatial smoothing is useful in dealing with coherent sources and for the possible enhancement of the performance of the methods. Also examined were the implementation issues associated with these methods. As opposed to implementing a single algorithm, implementing a signal processing task which consists of several stages on special purpose hardware gives prominence to the interesting issues of partitioning, and composite tasking, which are examined in this research. We believe our results have significantly improved the understanding of the performance of subspace methods, and have lead to interesting insights into the implementation issues. DTIC

N93-29866# Carnegie-Mellon Univ., Pittsburgh, PA. School of Computer Science.
REACTIVE INTEGRATION FOR TRADITIONAL PROGRAMMING LANGUAGES
David Garlan and Curtis Scott Dec. 1992 16 p
(Contract MDA972-92-J-1002)
(AD-A263986; CMU-CS-92-217) Avail: CASI HC A03/MF A01

Reactive integration based on event broadcast is an increasingly important technique for developing systems. However, the use of this technique has largely been confined to tool integration systems - in which tools exist as independent processes - and special-purpose languages - in which specialized forms of event broadcast are designed into the language from the start. This paper broadens the class of systems that can benefit from this approach by showing how to augment general-purpose programming languages with facilities for implicit invocation. We illustrate the approach in the context of the Ada language, and highlight the important design considerations that arise in extending such languages with facilities for reactive integration. DTIC

N93-29873*# Stanford Univ., CA. Dept. of Computer Science.
AUTOMATED MODELING OF PHYSICAL SYSTEMS
P. P. Nayak Sep. 1992 315 p
(Contract NCC2-537; NAG2-581; ARPA Order 6822)
(NASA-CR-193256; NAS 1.26:193256; AD-A263755; SU-STAN-CS-92-1443) Avail: CASI HC A14/MF A03

Effective reasoning about complex physical systems requires the use of models that are adequate for the task. Constructing such adequate models is often difficult. In this dissertation, we address this difficulty by developing efficient techniques for automatically selecting adequate models of physical systems. We focus on the important task of generating parsimonious causal explanations for phenomena of interest. Formally, we propose answers to the following: (1) what is a model and what is the space of possible models; (2) what is an adequate model; and (2) how do we find adequate models. We define a model as a set of model fragments, where a model fragment is a set of independent equations that partially describes some physical phenomenon. The space of possible models is defined implicitly by the set of applicable model fragments: different subsets of this set correspond to different models. An adequate model is defined as a simplest model that can explain the phenomenon of interest, and that satisfies any domain-independent and domain-dependent constraints on the structure and behavior of the physical system. We show that, in general, finding an adequate model is intractable (NP-hard). We address this intractability, by introducing a set of restrictions, and use these restrictions to develop an efficient algorithm for finding adequate models. The most significant restriction is that all the approximation relations between model fragments are required to be causal approximations. In practice this is not a serious restriction because most commonly used approximations are causal approximations. We also develop a novel order of magnitude reasoning technique, which strikes a balance between purely qualitative and purely quantitative methods. DTIC

N93-29874# Human Resources Research Organization, Alexandria, VA.
CONCEPT FORMULATION PROCESS AID FOR TRADE-OFF DETERMINATION: OPERATOR'S GUIDE Final Report, Apr. 1991 - Sep. 1992
Gary L. Page, H. R. Blacksten, B. L. Elder, Paul J. Sticha, and Michael J. Singer Mar. 1993 73 p
(Contract DAHC35-89-D-0046)
(AD-A263756; ARI-93-07) Avail: CASI HC A04/MF A01

This report describes the structure of the prototype concept formulation process aid for trade-off determination. The goal was to adapt previously developed models for use during a specific step in the development of a training device. This report identifies the hardware requirements and the necessary configuration and describes the installation procedures. A brief overview of the aiding system execution and use is presented. The report also describes the structure and function of the program files. The data elements, links between elements, and aiding functions are described in the context of the program routines. DTIC

N93-29916# Stevens Inst. of Tech., Hoboken, NJ. Dept. of Electrical Engineering and Computer Science.
EFFICIENT ALGORITHMS FOR THE EVALUATION OF PLANAR NETWORK RELIABILITY Final Report
A. Satyanarayana and R. Tindell 15 Mar. 1993 22 p
(Contract DAAL03-90-G-0078)
(AD-A263602; TR-9302; ARO-25706.10-MA) Avail: CASI HC A03/MF A01

Computation of the all-terminal reliability for general classes of networks is NP-hard. The problem of characterizing subclasses of networks and designing efficient algorithms to compute their reliability is a major area of current research in network reliability. Supported by the ARO grant DAAL03-90-G-0078, we have made significant progress in enlarging the class of planar networks for which there exists efficient all-terminal reliability algorithms. The importance of this work is enhanced by the recent proof of Vertigan that the all-terminal network reliability problem for the full class of planar networks is NP-hard. A important outgrowth of our work is the discovery of general techniques for developing O(n log n) algorithms for a greatly enlarged class of planar and nonplanar networks. DTIC

N93-29920# Mitre Corp., Bedford, MA.
A GUIDE TO TOTAL SOFTWARE QUALITY CONTROL, VOLUME 1 Final Report, Oct. 1989 - Sep. 1992
Judith A. Clapp and Saul F. Stanten Dec. 1992 110 p
(Contract F19628-89-C-0001)
(AD-A263881; MTR11284-Vol-1; RL-TR-92-316-Vol-1) Avail: CASI HC A06/MF A02

This is a guide for program offices that provides strategies and techniques for controlling the quality of software for mission-critical systems. It describes techniques to prevent, detect, and correct defects, and to make improvements in the processes and resources used to develop the software. It recommends use of a Total Software Quality Control Plan and shows how to create one prior to the start of system development. Volume 1 contains an overview of techniques and the planning process. Volume 2 is a compendium of descriptions of individual techniques. DTIC

N93-29921# Mitre Corp., Bedford, MA.
A GUIDE TO TOTAL SOFTWARE QUALITY CONTROL, VOLUME 2 Final Report, Oct. 1989 - Sep. 1992
Judith A. Clapp and Saul F. Stanten Dec. 1992 161 p
(Contract F19628-89-C-0001)
(AD-A263891; MTR-11284-Vol-2; RL-TR-92-316-Vol-2) Avail: CASI HC A08/MF A02

This is a guide for program offices that provides strategies and techniques for controlling the quality of software for mission-critical systems. It describes techniques to prevent, detect, and correct defects, and to make improvements in the processes and resources used to develop the software. It recommends use of a Total Software Quality Control Plan and shows how to create one prior to the start of system development. Volume 1 contains an overview of techniques and the planning process. Volume 2 is a compendium of descriptions of individual techniques. DTIC

N93-29976# Cornell Univ., Ithaca, NY. Dept. of Computer Science.
A REDESIGNED ISIS AND META SYSTEM UNDER MACH Quarterly Status Report No. 1
Kenneth P. Birman and Keith Marzullo 1 Jan. 1993 17 p
(Contract N00014-92-J-1866)
(AD-A263576) Avail: CASI HC A03/MF A01

This status report covers activities of the Isis project during the first quarter of 1992. This is our first progress report under ONR funding, but because these status reports are intended to be brief and our proposal was recently funded, we assume that the reader has some background regarding the goals and status of our effort, and focus instead on technical accomplishments during the report period and goals for the next three months. Readers unfamiliar with our work could start by reading some of the papers cited below, such as TR 1216. During the report period, the Isis effort has achieved a major milestone in its effort to redesign and reimplement the Isis system using Mach and Chorus as target operating system environments. In addition, we completed a number of publications that address issues raised in our prior work; some of these have recently appeared in print, while others are now being considered for publication in a variety of journals and conferences. DTIC

N93-29980# Memphis State Univ., TN.
ALGORITHMS FOR POINT SET CONGRUENCE Final Report, 15 Aug. 1992 - 14 Feb. 1993
Paul J. Heffernan 31 Mar. 1993 21 p
(Contract DAAL03-92-G-0378)
(AD-A264016; ARO-30778.3-MA) Avail: CASI HC A03/MF A01

The primary purpose of the project was to expand research in point matching, by applying the perturbation technique and the approximate algorithm paradigm to more complex problem formulations. The main results of this research are contained in the paper 'Generalized approximate algorithms for point set congruence'. This paper is still undergoing revisions, and a copy of the most recent draft is included. A device called the (e,k)-map, which is a more general measure of point set congruence than the one previously examined by the investigator is introduced. Ways to construct the (e,k)-map are discussed. While the investigator's previous work was limited to equal cardinality, planar point sets, this current work has expanded attention both to point sets of unequal cardinality and to point sets in higher dimensions. The investigator has even begun the study of projective congruence, in which one compares a 2-dimensional image with the family of projections of a 3-dimensional model. DTIC

N93-29997# Technical Research Centre of Finland, Espoo. Telecommunications Lab.
OSI TRANSACTION PROCESSING STANDARD: AN INTRODUCTION AND OUTLINES OF IMPLEMENTATION
Jarmo Harju, Esko Ojanpera, Henryka Siejka-Jormakka, and Kirsi Valtari May 1991 47 p
(VTT-TIED-1250; ISBN-951-38-3882-X; ETN-93-93773) Copyright Avail: CASI HC A03/MF A01

A general introduction to distributed transaction processing systems is given. OSI (Open Systems Interconnection) Transaction Processing (OSI TP) standard and IBM LU (Logical Units) 6.2 are described, and their properties are compared with each other. An implementation plan for OSI TP using the object oriented tools OTSO and CLASN is outlined. ESA

N93-30014# Colorado Univ., Boulder. Dept. of Electrical and Computer Engineering.
ACCELERATING THE TRANSFER OF TECHNOLOGY FOR IMPLEMENTING DOMAIN SPECIFIC SOFTWARE ARCHITECTURES Final Report
Vincent P. Heuring and William M. Waite 12 Apr. 1993 5 p
(Contract DAAL03-91-G-0203)
(AD-A264017; ARO-28950.1-MA) Avail: CASI HC A01/MF A01

The purpose of the research effort was to find one or more clients within the DoD community to help evaluate the Eli system when applied to problems of interest to the DoD. Information was solicited from a number of DoD agencies, and finally formed a relationship with a group at the Naval Postgraduate School (NPS). As a result of that relationship, a formal specification for the NPS language, PSDL, using the EH system was developed. That specification was subsequently modified by NPS personnel whom were trained in the use of the Eli system, and the resulting PSDL translator is being used by NPS personnel. The research also led to further modifications to the Eli system. A literate programming tool was added to Eli that has proven to be a significant aid in organizing and explaining specifications. DTIC

N93-30017# Center for Mathematics and Computer Science, Amsterdam (Netherlands). Dept. of Computer Science and Software Technology.
TURNING SOS RULES INTO EQUATIONS
Luca Aceto (Hewlett-Packard Labs., Pisa, Italy.), Bard Bloom (Cornell Univ., Ithaca, NY.), and Frits W. Vaandrager (Amsterdam Univ., Netherlands.) Jun. 1992 47 p
(Grant NSF CCR-90-03441)
(CWI-CS-R9218; ETN-93-93231) Copyright Avail: CASI HC A03/MF A01

Many process algebras are defined by Structural Operation Semantics (SOS). Most such definitions are structured and fit the GSOS format. A procedure for converting any GSOS language definition to a finite complete equational axiom system which characterizes strong bisimulation of processes, is given. The procedure introduces new operations. The method applies to almost all SOS systems for process algebras. The following is shown: how to express an arbitrary smooth operation as a sum of smooth distinctive operations; and how to introduce auxiliary smooth operations which do copying in the equation rather than in the operation. Completeness is discussed and variations of the method are studied. ESA

N93-30022# Mitre Corp., McLean, VA.
ESTIMATING Ada SYSTEM SIZE DURING DEVELOPMENT Interim Report, Oct. 1989 - Dec. 1991
W. M. Evanco, W. M. Thomas, and W. W. Agresti Dec. 1992 30 p
(Contract F19628-89-C-0001)
(AD-A263880; MTR-91W00132; RL-TR-92-318) Avail: CASI HC A03/MF A01

A set of four models is developed for estimating the size of Ada systems at intermediate points in a software development project. The motivation for the models is the need to take advantage of current information about the evolving Ada product to improve the estimate of system size. The models are based on successively more detailed design and implementation data. An empirical investigation using multivariate regression analysis was conducted on a set of twenty-one Ada subsystems. As more detail was incorporated into the models, a greater fraction of the variation in lines of code as measured by the coefficient of determination was explained. DTIC

N93-30023*# National Aeronautics and Space Administration. Goddard Space Flight Center, Greenbelt, MD.
XRONOS: A TIMING ANALYSIS SOFTWARE PACKAGE. USER'S GUIDE, VERSION 3.00
L. Stella (Osservatorio Astronomico, Brera, Milan, Italy.), L. Angelli (European Space Agency. European Space Research and Technology Center, ESTEC, Noordwijk, Netherlands.), and Chris Barron, ed. Paris ESA Sep. 1992 109 p
(NASA-TM-109222; NAS 1.15:109222; ESA-TM-165; ISBN-92-9092-221-4; ETN-93-93717) Copyright Avail: CASI HC A06/MF A02; ESA, EPD, ESTEC, Noordwijk, Netherlands, HC

XRONOS is a general purpose timing analysis package. Although it was designed mainly for x-ray astronomy, XRONOS is basically detector and wavelength independent. It has been used to analyze data from the Einstein Observatory, Exosat and Ginga, as well as optical photometry and helioseismology data. It includes programs for: light curve(s), hardness ratio and color-color plotting, epoch folding, power spectrum, autocorrelation, cross correlation, time skewness, and statistical analysis. An overview of XRONOS and walkthrough of a XRONOS session are presented. The QDP/PLT plotting and function fitting program used by XRONOS is outlined and the algorithm and features of XRONOS are detailed. ESA

N93-30034# Edgerton, Germeshausen and Grier, Inc., Idaho Falls, ID.
AHP VERSION 5.1 USER'S MANUAL
J. C. Watkins and L. S. Ghan Oct. 1992 115 p
(Contract DE-AC07-76ID-01570)
(DE93-007050; EGG-ERTP-10585) Avail: CASI HC A06/MF A02

As decisions become more and more complex, decision makers are faced with the challenge of sorting through many variables to arrive at a sound decision. The Analytical Hierarchy Process (AHP) is a tool, that allows a systematic, logical approach to reducing complex issues into manageable pieces. The decision maker can then sort through the variables and determine to what degree a particular variable should influence the final decision. The power of the AHP as a management tool comes from the fact that it reduces complex problems to many simple pairwise decisions. Only two items need be compared against one another - a much simpler task than comparing an item to all the others simultaneously. By arranging the items that influence a decision in the form of a matrix and comparing appropriate pairs in this matrix to each other, each item can be compared with every other item. Matrix algebra can then operate on this matrix and rank each item according to its importance to the final decision. DOE

N93-30050# Sandia National Labs., Albuquerque, NM.
SOFTWARE TESTING USING THE IEEE STANDARDS
J. Klamerus and J. Weeks 1992 23 p Presented at the STAR 1993: Software Testing Analysis and Review: INGRES World 1993 Conference,

Monterey, CA; Santa Clara, CA, 2-6 May 1993; 9-13 May 1993
(Contract DE-AC04-76DP-00789)
(DE93-009833; SAND-92-2521C; CONF-9305160-1; CONF-9305161-1)
Avail: CASI HC A03/MF A01

Testing is an important part of the software application development process. To achieve quality software deliverables and to avoid costly redevelopment of program code or repair of bad data, testing must be performed throughout the software development life cycle. A software engineering process to produce a software test plan based upon the 'IEEE (Institute of Electrical and Electronics Engineers) Software Engineering Standards Collection' guidelines and corporate guidelines is discussed. Demonstrated examples of the software testing process involving interactive graphical user interface and standard ASCII text forms-based software are provided. Sandia National Laboratories has a Software Quality Assurance Department which provides corporate guidelines, in addition to recommending the use of IEEE processes. Both corporate guidelines and a specific subset of the IEEE guidelines were applied to the software development projects discussed. The rationale for applying a specific subset of the IEEE guidelines for each of the software on development projects are given. The development of the test procedures in the INGRES/WINDOWS 4GL environment (graphical user interface) as well as in the INGRES/ABF environment (Applications-By-Forms, ASCII Text) are be presented and contrasted. The documentation of the testing process and results are explained. DOE

N93-30125# Carnegie-Mellon Univ., Pittsburgh, PA. School of Computer Science.

USING THE MACH COMMUNICATION PRIMITIVES IN X11

Michael Ginsberg (Microsoft Corp., Redmond, WA.), Robert V. Baron, and Brian N. Bershad Mar. 1993 10 p
(Contract MDA972-90-C-0035; ARPA Order 7330)
(AD-A264049; CMU-CS-93-121) Avail: CASI HC A02/MF A01

We have modified the X11 windowing system to use the native communication facilities of the Mach 3.0 microkernel. Our new implementation can rely on Mach's low-overhead IPC facility as a direct replacement for sockets, or it can use shared memory as a transport between X11 clients and the server. On conventional BSD UNIX systems, X11 communication is done through sockets. Because a user-level process implements UNIX functionality on top of Mach 3.0, a socket-based version of X11 performs substantially worse than when running a monolithic UNIX kernel. Using Mach IPC as the transport between X11 clients and the server, X11 performance is slightly better than that of a monolithic system in which sockets are implemented inside the kernel as opposed to within a user level process. Using Mach's shared memory facilities as the transport, we have measured performance improvements of over 40%. DTIC

N93-30202# General Accounting Office, Washington, DC. Information Management and Technology Div.

HIGH PERFORMANCE COMPUTING: ADVANCED RESEARCH PROJECTS AGENCY SHOULD DO MORE TO FOSTER PROGRAM GOALS. REPORT TO THE CHAIRMAN, COMMITTEE ON ARMED SERVICES, HOUSE OF REPRESENTATIVES

May 1993 42 p Original contains color illustrations
(GAO/IMTEC-93-24; B-252539) Avail: CASI HC A03/MF A01; GAO, PO Box 6015, Gaithersburg, MD 20877 HC

The federal High Performance Computing and Communications Initiative is a research and development effort that seeks to significantly accelerate the availability and utilization of high performance computers and networks in order to better address these challenges. At $275 million in fiscal year 1993, the Advanced Research Projects Agency (ARPA) has the largest budget of any single agency participating in the $800-million federal initiative. Given the importance of this initiative and ARPA'S dominant role in it, the House Armed Services Committee asked GAO to assess the program, particularly (1) the agency's distribution of advanced computers to research sites, (2) its interaction with the research community, and (3) the balance between hardware and software investments in the ARPA program. While ARPA has fostered significant advances in high-performance computing research and development for a decade, its current program has shortcomings in several areas. First, its placing of new computers at laboratories, while important to facilitating research, has focused on just a few massively parallel processing machines. Researchers need access to a broader range of new computing technologies to explore all promising alternatives. Second, the agency's limited interactions with the technical community may hinder the rapid progress needed to achieve its ambitious program goals. ARPA has been weak in disseminating program information, soliciting input from the research community, and publishing performance data. Finally, while much progress has been made in hardware development, software remains too primitive to make massively parallel processing systems useful. ARPA'S goal of achieving a thousand-fold increase in useful computing power by 1996 will likely not be met without greater emphasis on the development of system software. Derived from text

N93-30380*# ORA Corp., Ithaca, NY.

USING PENELOPE TO ASSESS THE CORRECTNESS OF NASA Ada SOFTWARE: A DEMONSTRATION OF FORMAL METHODS AS A COUNTERPART TO TESTING Final Report

Carl T. Eichenlaub, C. Douglas Harper, and Geoffrey Hird Washington May 1993 158 p
(Contract NAS1-18972; RTOP 505-64-10-05)
(NASA-CR-4509; NAS 1.26:4509) Avail: CASI HC A08/MF A02

Life-critical applications warrant a higher level of software reliability than has yet been achieved. Since it is not certain that traditional methods alone can provide the required ultra reliability, new methods should be examined as supplements or replacements. This paper describes a mathematical counterpart to the traditional process of empirical testing. ORA's Penelope verification system is demonstrated as a tool for evaluating the correctness of Ada software. Grady Booch's Ada calendar utility package, obtained through NASA, was specified in the Larch/Ada language. Formal verification in the Penelope environment established that many of the package's subprograms met their specifications. In other subprograms, failed attempts at verification revealed several errors that had escaped detection by testing. Author (revised)

N93-30383# Naval Command, Control and Ocean Surveillance Center, San Diego, CA.

AN APPLICATION PROTOCOL FOR CAD TO CAD TRANSFER OF ELECTRONIC INFORMATION

Charles C. Azu, Jr. Mar. 1993 13 p
(AD-A264554) Avail: CASI HC A03/MF A01

The exchange of Computer Aided Design (CAD) information between dissimilar CAD systems is a problem. This is especially true for transferring electronics CAD information such as multi-chip module (MCM), hybrid microcircuit assembly (HMA), and printed circuit board (PCB) designs. Currently, there exists several neutral data formats for transferring electronics CAD information. These include IGES, EDIF, and DXF formats. All these formats have limitations for use in exchanging electronic data. In an attempt to overcome these limitations, the Navy's MicroCIM program implemented a project to transfer hybrid microcircuit design information between dissimilar CAD systems. The IGES (Initial Graphics Exchange Specification) format is used since it is well established within the CAD industry. The goal of the project is to have a complete transfer of microelectronic CAD information, using IGES, without any data loss. An Application Protocol (AP) is being developed to specify how hybrid microcircuit CAD information will be represented by IGES entity constructs. The AP defines which IGES data items are appropriate for describing HMA geometry, connectivity, and processing as well as HMA material characteristics. DTIC

N93-30418# Maryland Univ., College Park. Center for Automation Research.

QUALITATIVE METHODS IN COMPUTER VISION Final Report, 1 Jun. 1991 - 30 Sep. 1992

Azriel Rosenfeld Jan. 1993 10 p
(Grant AF-AFOSR-0239-91)
(AD-A264335; AFOSR-93-0214TR) Avail: CASI HC A02/MF A01

Current object recognition systems can only recognize a limited class of objects. Objects having variable numbers of parts and only loosely constrained shapes cannot be modeled and recognized by these systems. The PI proposed the use of a data structure called the VAPOR (Variable APpearance Object Representation) model to represent objects with these kinds of variable appearances and develop a search procedure called MOSS (MOdel Space Search) to find instances of these models in two-dimensional image data. The VAPOR model is an idealization of the object; all instances of the model in the image are variations from ideal appearance. The variations are evaluated by the description length of the model, measured in information-theoretic bits. MOSS selects the best model for the given image data by choosing the minimal length description. It was demonstrated how the system performs in a simple domain of circles and polygons and in the complex domain of finding cloverleaf intersections in aerial images of roads. DTIC

N93-30495# Case Western Reserve Univ., Cleveland, OH. Dept. of Computer Engineering and Science.
MEMORY DRIVEN FEATURE-BASED DESIGN Interim Report, Feb. 1988 - Dec. 1992
Y. H. Pao, F. L. Merat, and G. M. Radack Jan. 1993 96 p
(Contract F33615-87-C-5250)
(AD-A264697; WL-TR-93-4021) Avail: CASI HC A05/MF A01

The act of design is a critical operation in the whole train of event's of manufacturing. Improvement of the efficiency and effectiveness of the design process would certainly have a major effect on the entire manufacturing operation as a whole. Engineering design seems to be an admixture of synthesis and analysis activities with synthesis dominating the conceptual design and embodiment design phases of the activity; and analysis dominating the problem definition and detailing phases of the activity. In addition, in nearly all phases of the design procedure, the designer often finds it helpful to be able to recollect many other previous designs or pertinent portions of such similar designs; and to be able to visualize or sketch variations on a theme and to be able to evaluate those comparatively. This is especially true for circumstances where the person has not had extensive personal experience in this matter. The research reported on in this document focuses on that aspect of design and planning. Namely, how stores of public (handbook type) knowledge and memory of private (episodic) knowledge can be and should be used effectively in combination with computer-based systems, in support of designers and fabricators. DTIC

N93-30523# Carnegie-Mellon Univ., Pittsburgh, PA. School of Computer Science.
THE MIDWAY DISTRIBUTED SHARED MEMORY SYSTEM
Brian N. Bershad, Matthew J. Zekauskas, and Wayne A. Sawdon Mar. 1993 13 p
(Contract MDA972-90-C-0035; ARPA Order 7330)
(AD-A264645; CMU-CS-93-119) Avail: CASI HC A03/MF A01

This paper describes the motivation, design and performance of Midway, a programming system for a distributed shared memory multicomputer (DSM) such as an ATM-based cluster, a CM-5, or a Paragon. Midway supports a new memory consistency model called entry consistency. Entry consistency guarantees that shared data becomes consistent at a processor when the processor acquires a synchronization object known to guard the data. Entry consistency is weaker than other models described in the literature, such as processor consistency and release consistency, but it makes possible higher performance implementations of the underlying consistency protocols. Midway programs are written in C, and the association between synchronization objects and data must be made with explicit annotations. As a result, pure entry consistent programs can require more annotations than programs written to other models. In addition to entry consistency, Midway also supports the stronger release consistent and processor consistent models at the granularity of individual data items. Consequently, the programmer can tradeoff potentially reduced performance for the additional programming complexity required to write an entry consistent parallel program. DTIC

N93-30544# Tennessee Univ., Knoxville.
EFFICIENT ALGORITHMS AND DATA STRUCTURES IN GEOMETRIC DESIGN Final Report, 1 Jun. 1991 - 31 Mar. 1993
Chandrajit L. Bajaj 31 Mar. 1993 4 p
(Grant AF-AFOSR-0276-91)
(AD-A264678; AFOSR-93-0328TR) Avail: CASI HC A01/MF A01

Research was conducted on the design of a numerically stable and topologically robust algorithm for boolean set operations between solids with algorithms surface patches of arbitrary degree. DTIC

N93-30546# Mitre Corp., McLean, VA. Washington C3 Div.
PROCEDURES FOR APPLYING Ada QUALITY PREDICTION MODELS Final Report, Oct. 1991 - Sep. 1992
D. D. Murphy, W. M. Thomas, W. M. Evanco, and W. W. Agresti Dec. 1992 86 p
(Contract F19628-89-C-0001)
(AD-A264730; MTR-90-W0000165; RL-TR-92-317) Avail: CASI HC A05/MF A01

Procedures for applying Ada software quality prediction models for purposes of model validation are described. The multivariate regression models predict metrics related to software reliability, maintainability, and flexibility. The procedures include the use of an Ada source code analysis tool and the Statistical Analysis System (SAS) to extract data from Ada source code and create data sets containing quantities needed for the models. DTIC

N93-30547# Mitre Corp., McLean, VA. Washington C3 Div.
AN APPROACH TO SOFTWARE QUALITY PREDICTION FROM Ada DESIGNS Final Report, Oct. 1989 - Sep. 1990
W. W. Agresti, W. M. Evanco, M. C. Smith, and D. R. Clarson Dec. 1992 62 p
(Contract F19628-89-C-0001)
(AD-A264731; MTR-90-W00135; RL-TR-92-315) Avail: CASI HC A04/MF A01

An ongoing research project on estimating software quality from Ada designs is discussed. The research is motivated by the need for technology to analyze designs, when they are first represented, for their likely effect on quality factors. The objective of this research is to build multivariate models relating design characteristics and environmental factors to reliability and maintainability. Early results of the research are discussed, including alternative definitions of reliability and maintainability, a representation of Ada design structure, characteristics of software project data used for analysis, and preliminary statistical results testing hypotheses concerning the effects of design structure on reliability and maintainability. DTIC

N93-30549# California Univ., Berkeley. Dept. of Electrical Engineering and Computer Science.
NONSMOOTH OPTIMIZATION ALGORITHMS, SYSTEM THEORY, AND SOFTWARE TOOLS Final Report, 1 Nov. 1989 - 31 Dec. 1992
Elijah Polak 13 Apr. 1993 10 p
(Grant AF-AFOSR-0068-90)
(AD-A264679; AFOSR-93-0327TR) Avail: CASI HC A02/MF A01

The research described in this report deals with the development of (1) efficient, consistent discretization techniques for use in semi-infinite optimization, optimal control algorithms that solve problems with dynamics governed by partial differential equations, (2) superlinearly converging semi-finite optimization algorithms, (3) various techniques for finding design parameters satisfying specifications, (4) optimal control algorithms for discrete and distributed systems with control, state and shape constraints, and (5) efficient numerical procedures for the integrated design of flexible structures and their control systems. DTIC

N93-30561# Massachusetts Univ., Amherst.
ADAPTIVE NETWORKS FOR SEQUENTIAL DECISION PROBLEMS Final Report, 30 Sep. 1989 - 29 Sep. 1992
Andrew Barto 29 Sep. 1992 14 p
(Grant AF-AFOSR-0526-89)
(AD-A264756; AFOSR-93-0208TR) Avail: CASI HC A03/MF A01

Considerable progress was made in developing artificial neural network methods for solving stochastic sequential decision problems. The research focused on reinforcement learning methods based on approximating dynamic programming (DP). They used problems in the domains of robot fine motion control, navigation, and steering control in order to develop and test learning algorithms and architectures. Although most of these problems were simulated, they also began to apply DP-based learning algorithms to actual robot control problems with considerable success. Progress was made on reinforcement learning methods using continuous actions, modular network architectures, and architectures using abstract actions. Theoretical progress was made in relating DP-based reinforcement learning algorithms to more conventional methods for solving stochastic sequential decision problems. As a result of this research there is an improved understanding of these algorithms and how they can be successfully used in applications. DTIC

N93-30577# Army Armament Research, Development and Engineering Center, Picatinny Arsenal, NJ.
ELECTRONICS MIXED-MODE SIMULATION

H. G. Niera May 1993 15 p
(AD-A264734; ARFSD-TR-93003) Avail: CASI HC A03/MF A01

Mixed-mode simulation is an engineering software tool that electrical engineers are now using to design and/or analyze and troubleshoot electronic circuits that have analog as well as digital circuitry and componentry together, and can run a simultaneous simulation of them under the same environment. The object is to give the reader a thumbnail sketch of this emerging technology's evolvement in the electronic industry, and to bring the reader up-to-date on the trends and methodologies popular in this industry. Mixed-mode simulation, the latest offshoot of the computer aided engineering industry, appears to have arrived, after many false starts, as a bona fide and practical engineering tool. DTIC

N93-30602# Carnegie-Mellon Univ., Pittsburgh, PA. Software Engineering Inst.

AN ANNOTATED BIBLIOGRAPHY ON INTEGRATION IN SOFTWARE ENGINEERING ENVIRONMENTS

Alan W. Brown and Maria H. Penedo May 1992 20 p
(Contract F19628-90-C-0003)
(AD-A264798) Avail: CASI HC A03/MF A01

This paper provides an annotated bibliography on integration in software engineering environments (SEE's). The aim is to provide readers with a source of information that can be used as the basis for more detailed studies in this area. DTIC

N93-30614# Stanford Univ., CA. Computer Systems Lab.

INTELLIGENT REAL-TIME PROBLEM SOLVING Final Report, 15 Mar. 1991 - 14 Sep. 1992

Yoav Shoham 14 Sep. 1992 6 p
(Grant AF-AFOSR-0205-91)
(AD-A264830; AFOSR-93-0268TR) Avail: CASI HC A02/MF A01

The researchers proposed to develop and test a framework for designing and analyzing complex control systems consisting of independent modules, called agents, that communicate through fixed channels. These agents possess and acquire knowledge and negotiate with one another regarding the use of their capabilities. The results were along the following dimensions: real-time, machine, and environments; agent-oriented programming; temporal data bases; anytime belief update; planning and control; and social rules, utilities, and organizations. DTIC

N93-30647# Argonne National Lab., IL.

NONLINEAR EXPLICIT TRANSIENT FINITE ELEMENT ANALYSIS ON THE INTEL DELTA

E. J. Plaskacz, M. R. Ramirez (Johns Hopkins Univ., Baltimore, MD.), and S. Gupta (Johns Hopkins Univ., Baltimore, MD.) 1993 20 p Presented at the 2nd Symposium on Parallel Computational Methods for Large-Scale Structural Analysis and Design, Norfolk, VA, 24-25 Feb. 1993
(Contract W-31-109-eng-38)
(DE93-009561; ANL/CTD/CP-78758; CONF-930286-1) Avail: CASI HC A03/MF A01

Many large scale finite element problems are intractable on current generation production supercomputers. High-performance computer architectures offer effective avenues to bridge the gap between computational needs and the power of computational hardware. The biggest challenge lies in the substitution of the key algorithms in an application program with redesigned algorithms which exploit the new architectures and use better or more appropriate numerical techniques. A methodology for implementing nonlinear finite element analysis on a homogeneous distributed processing network is discussed. The method can also be extended to heterogeneous networks comprised of different machine architectures provided that they have a mutual communication interface. This unique feature has greatly facilitated the port of the code to the 8-node Intel Touchstone Gamma and then the 512-node Intel Touchstone Delta. The domain is decomposed serially in a preprocessor. Separate input files are written for each subdomain. These files are read in by local copies of the program executable operating in parallel. Communication between processors is addressed utilizing asynchronous and synchronous message passing. The basic kernel of message passing is the internal force exchange which is analogous to the computed interactions between sections of physical bodies in static stress analysis. Benchmarks for the Intel Delta are presented. Performance exceeding 1 gigaflop was attained. Results for two large-scale finite element meshes are presented. DOE

N93-30787# Joint Inst. for Nuclear Research, Dubna (USSR). Lab. of Computing Techniques and Automation.

COMPUTER ALGEBRA TOOLS FOR HIGHER SYMMETRY ANALYSIS OF NONLINEAR EVOLUTION EQUATIONS

V. P. Gerdt 1991 10 p Presented at the Working Conference on Programming Environments for High-Level Scientific Problem Solving, Karlsruhe, Germany, 23-27 Sep. 1991
(DE93-606089; JINR-E-5-91-402) Avail: CASI HC A02/MF A01 (US Sales Only)

This paper presents a computer-aided approach and a software package for symbolic algebraic computation to solve the problem of verifying the existence of the canonical Lie-Backlund symmetries for multicomponent quasilinear evolution equations with polynomial-nonlinearity and computing a given order symmetry. In the presence of arbitrary numerical parameters, the problem is reduced to investigation and solution of nonlinear algebraic equations in those parameters. DOE

N93-30824# National Center for Atmospheric Research, Boulder, CO. Scientific Computing Div.

PARCELS WITH TAGS

J. L. Sloan Oct. 1992 23 p Sponsored by NSF, Washington, DC.
(PB93-181824; NCAR/TN-377+IA) Avail: CASI HC A03/MF A01

The National Center for Atmospheric Research (NCAR) Text And Graphics System (TAGS) is a graphics and text batch output production facility. It is distributed across several networked computers which run the UNIX operating system. The control function of TAGS is implemented as multiple processes which communicate via message passing. The TAGS message passing scheme allows processes to exchange a simple form of associative memory, called a parcel, in an architecture neutral fashion. The associative memory is implemented as a binary tree containing paris of keyword and value strings ordered by collating sequence. The underlying interprocess communication mechanism is based on Berkeley internet stream sockets. The message passing scheme provides information hiding inside the message, and allows new parameters to be added to messages without recompiling or relinking intermediate modules which handle the messages. NTIS

N93-30914# Joint Inst. for Nuclear Research, Dubna (USSR). Lab. of Computing Techniques and Automation.

ALGORITHM FOR THE SOLUTION OF THE FADDEEV EQUATION FOR A SYSTEM OF THREE IDENTICAL SPINLESS PARTICLES [ALGORITM RESHENIYA URANENIJ FADDEEVA DIYA SISTEMY TREKH TOZHDESTVENNYKH]

V. B. Belyaev, O. I. Kochkin, and O. I. Kartavtsev 1991 8 p In RUSSIAN
(DE92-644678; JINR-R-4-91-254) Avail: CASI HC A02/MF A01 (US Sales Only)

The homogeneous Faddeev equation for three identical spinless particles in numerically solved by means of Fortran program for finding the binding energy. The algorithm is based on the finite-dimensional approximation of the differential operator. Estimation of errors of this method has been analyzed. This task has a more methodical character, but can be applied to the solution of many specific problems of quantum mechanics for a few-body system. DOE

N93-30915# Joint Inst. for Nuclear Research, Dubna (USSR). Lab. of Computing Techniques and Automation.

ALGORITHM OF NUMERICAL CALCULATIONS OF DIFFERENTIAL YAKUBOVSKY EQUATIONS FOR THE (1 + 3) SCATTERING PROBLEM [ALGORITM CHISLENNOGO RESHENIYA DIFFERENTSIAL'NYKH URAVNENIJ YAKUBOVSKOGO DIYA ZADACHI RASSEYANIYA ODNOJ CHASTITSY NA SVYAZANNOM KOMPLEKSE TREKH CHASTITS]

V. B. Belyaev, V. I. Kochkin, and V. I. Kartavtsev 1991 10 p In RUSSIAN
(DE92-644679; JINR-R-4-91-261) Avail: CASI HC A02/MF A01 (US Sales Only)

This work is the continuation of the numerical calculations of the Yakubovsky equations for the scattering problem for four spinless identical particles. More exact wave function for the bound complex of three particles is used here as distinct from the foregoing calculations. This wave function is calculated by means of a FORTRAN program. The obtained scattering lengths are compared with the former calculations of the authors and with the available data. DOE

N93-30934# Harvard Univ., Boston, MA. Dept. of Genetics.
COMPUTER ASSISTED MULTIPLEX SEQUENCING Progress Report, 1 Aug. 1991 - 31 Jul. 1992
G. M. Church Aug. 1992 5 p
(Contract DE-FG02-87ER-60565)
(DE93-007144; DOE/ER-60565) Avail: CASI HC A01/MF A01

The objective of this project is automation and optimization of multiplex sequencing. This year, we have integrated direct transfer electrophoresis, automated multiplex hybridizations and automated film reading and applied this toward sequencing of three contiguous E. coli cosmids. Primers for the directed dideoxy sequence walking and sequence confirmation steps were synthesized with a 15 base tag complimentary to an alkaline phosphatase conjugate. A higher throughput synthesis device is well along in testing as are new automated hybridization devices. We have developed software for automatically annotating ORF's and databases of precise terminology of proteins and RNA. DOE

N93-31001# International Atomic Energy Agency, Vienna (Austria).
DEVELOPMENT OF A PC CODE PACKAGE FOR THE ANALYSIS OF RESEARCH AND POWER REACTORS
N. Urli (Institut Rudjer Boskovic, Zagreb, Yugoslavia.) Jun. 1992 19 p
(DE92-638517; IAEA-R-5132-F) Avail: CASI HC A03/MF A01 (US Sales Only)

Computer codes available for performing reactor physics calculations for nuclear research reactors and power reactors are normally suited for running on mainframe computers. With the fast development in speed and memory of the PCs and affordable prices, it became feasible to develop PC versions of commonly used codes. The present work performed under an IAEA sponsored research contract has successfully developed a code package for running on a PC. This package includes a cross-section generating code PSU-LEOPARD and 2D and 1D spatial diffusion codes, MCRAC and MCYC 1D. For adapting PSU-LEOPARD for a PC, the binary library has been reorganized to decimal form, upgraded to FORTRAN-77 standard and arrays and subroutines reorganized to conform to PC compiler. Similarly, PC version of MCRAC for FORTRAN-77 and 1D code MCYC 1D have been developed. Tests, verification and benchmark results show excellent agreement with the results obtained from mainframe calculations. The execution speeds are also very satisfactory. DOE

N93-31026# University of Southern California, Marina del Rey. Information Sciences Inst.
GIGABIT NETWORK COMMUNICATIONS RESEARCH Quarterly Research and Development Status Report No. 9, 1 Oct. - 31 Dec. 1992
31 Dec. 1992 13 p
(Contract DABT63-91-C-0001)
(AD-A264895) Avail: CASI HC A03/MF A01

The ATOMIC project utilizes inexpensive fine-grain multicomputer components to create a multi-gigabit per second local area network. This unique approach leverages recent DARPA supported research at Caltech by Prof. Charles Seitz and his students. That research produced dense and extremely fast Mosaic single-chip multicomputer nodes. ATOMIC is a unique example of network development that grows upwards from multicomputer machine networking into the domain of a LAN. The principal concerns for this quarter were performance improvement and testing of the SPARCstation ATOMIC SBus card and modification to allow multicast. DTIC

N93-29524*# Missouri Univ., Columbia. Dept. of Electrical and Computer Engineering.
A FUZZY CLUSTERING ALGORITHM TO DETECT PLANAR AND QUADRIC SHAPES
Raghu Krishnapuram, Hichem Frigui, and Olfa Nasraoui *In* NASA. Johnson Space Center, North American Fuzzy Logic Processing Society (NAFIPS 1992), Volume 1 Dec. 1992 p 59-68 (For primary document see N93-29516 11-59)
Avail: CASI HC A02/MF A03

N93-29526*# Missouri Univ., Columbia. Dept. of Electrical and Computer Engineering.
AUTOMATIC RULE GENERATION FOR HIGH-LEVEL VISION
Frank Chung-Hoon Rhee and Raghu Krishnapuram *In* NASA. Johnson Space Center, North American Fuzzy Logic Processing Society (NAFIPS 1992), Volume 1 Dec. 1992 p 81-88 (For primary document see N93-29516 11-59)
Avail: CASI HC A02/MF A03

N93-29531*# California Univ., Irvine. Dept. of Electrical and Computer Engineering.
A SELF-LEARNING RULE BASE FOR COMMAND FOLLOWING IN DYNAMICAL SYSTEMS
Wei K. Tsai, Hon-Mun Lee, and Alexander Parlos (Texas A&M Univ., College Station.) *In* NASA. Johnson Space Center, North American Fuzzy Logic Processing Society (NAFIPS 1992), Volume 1 Dec. 1992 p 125-134 (For primary document see N93-29516 11-59)
(Contract DE-FG07-89ER-12893)
Avail: CASI HC A02/MF A03

N93-29581*# Rice Univ., Houston, TX. Dept. of Electrical and Computer Engineering.
A CONJUGATE GRADIENTS/TRUST REGIONS ALGORITHMS FOR TRAINING MULTILAYER PERCEPTRONS FOR NONLINEAR MAPPING
Raghavendra K. Madyastha, Behnaam Aazhang, Troy F. Henson (International Business Machines Corp., Houston, TX.), and Wendy L. Huxhold (International Business Machines Corp., Houston, TX.) *In* NASA. Johnson Space Center, North American Fuzzy Logic Processing Society (NAFIPS 1992), Volume 2 Dec. 1992 p 589-597 (For primary document see N93-29556 11-59)
Avail: CASI HC A02/MF A03

N93-29595*# Jet Propulsion Lab., California Inst. of Tech., Pasadena.
THE GENERAL THEORY OF CONVOLUTIONAL CODES
R. J. McEliece (California Inst. of Tech., Pasadena.) and R. P. Stanley (California Inst. of Tech., Pasadena.) *In its* The Telecommunications and Data Acquisition Report 15 May 1993 p 89-98 (For primary document see N93-29586 11-32)
(RTOP 310-30-71-83-04)
Avail: CASI HC A02/MF A03

N93-30239 McMaster Univ., Hamilton (Ontario). Communications Research Lab.
QR DECOMPOSITION BASED LEAST SQUARES LATTICE ALGORITHM
Simon Haykin *In* Engineering Inst. of Canada, Canadian Conference on Electrical and Computer Engineering, Volumes 1 and 2 1990 3 p (For primary document see N93-30215 11-31)
Avail: Engineering Inst. of Canada, 2050 rue Mansfield, Suite 700, Montreal, Quebec H3A 1Z2 Canada

N93-30240 Alberta Telecommunications Research Centre, Edmonton.
ENHANCED RESOLUTION AND DE-ALIASING TECHNIQUES FOR FAST FOURIER TRANSFORMS
G. D. Cormack and J. N. McMullin *In* Engineering Inst. of Canada, Canadian Conference on Electrical and Computer Engineering, Volumes 1 and 2 1990 5 p (For primary document see N93-30215 11-31)
Avail: Engineering Inst. of Canada, 2050 rue Mansfield, Suite 700, Montreal, Quebec H3A 1Z2 Canada

N93-30243 Ottawa Univ. (Ontario). Dept. of Electrical Engineering.
FEATURE SEGMENTATION USING A MULTIPLE-STACK BASED CHAIN CODING ALGORITHM
Dan Ionescu and Michael A. Sasarman *In* Engineering Inst. of Canada, Canadian Conference on Electrical and Computer Engineering, Volumes 1 and 2 1990 4 p (For primary document see N93-30215 11-31)
Avail: Engineering Inst. of Canada, 2050 rue Mansfield, Suite 700, Montreal, Quebec H3A 1Z2 Canada

N93-30255 McMaster Univ., Hamilton (Ontario). Communications Research Lab.
AN ADAPTIVE ALGORITHM FOR LINEAR ASSOCIATIVE MEMORY PROBLEM

Sanzheng Qiao *In* Engineering Inst. of Canada, Canadian Conference on Electrical and Computer Engineering, Volumes 1 and 2 1990 4 p (For primary document see N93-30215 11-31)
Avail: Engineering Inst. of Canada, 2050 rue Mansfield, Suite 700, Montreal, Quebec H3A 1Z2 Canada

N93-30270 Simon Fraser Univ., Burnaby (British Columbia). School of Engineering Science.
QUANTIZATION EFFECTS IN SEGMENTATION OF RANGE IMAGES
Troy L. Yee and Kamal Kant Gupta *In* Engineering Inst. of Canada, Canadian Conference on Electrical and Computer Engineering, Volumes 1 and 2 1990 4 p (For primary document see N93-30215 11-31)
Avail: Engineering Inst. of Canada, 2050 rue Mansfield, Suite 700, Montreal, Quebec H3A 1Z2 Canada

N93-30273 Kansas State Univ., Manhattan. Dept. of Electrical and Computer Engineering.
A NEW WAY TO USE FUZZY SETS IN IMAGE SHARPENING
Yiming Yu and Eddie R. Fowler *In* Engineering Inst. of Canada, Canadian Conference on Electrical and Computer Engineering, Volumes 1 and 2 1990 4 p (For primary document see N93-30215 11-31)
Avail: Engineering Inst. of Canada, 2050 rue Mansfield, Suite 700, Montreal, Quebec H3A 1Z2 Canada

N93-30279 Carleton Univ., Ottawa (Ontario).
ON ANALYTICAL PERFORMANCE MODELLING OF SOFTWARE FOR DISTRIBUTED SYSTEMS
D. C. Petriu, C. M. Woodside, J. E. Neilson, and S. Majumdar *In* Engineering Inst. of Canada, Canadian Conference on Electrical and Computer Engineering, Volumes 1 and 2 1990 4 p (For primary document see N93-30215 11-31)
Avail: Engineering Inst. of Canada, 2050 rue Mansfield, Suite 700, Montreal, Quebec H3A 1Z2 Canada

N93-30287 National Research Council of Canada, Ottawa (Ontario).
APPLICATIONS OF DIGITAL 3-D IMAGING
M. Rioux *In* Engineering Inst. of Canada, Canadian Conference on Electrical and Computer Engineering, Volumes 1 and 2 1990 10 p (For primary document see N93-30215 11-31)
Avail: Engineering Inst. of Canada, 2050 rue Mansfield, Suite 700, Montreal, Quebec H3A 1Z2 Canada

N93-30288 Laval Univ. (Quebec). Lab. de Vision et Systemes Numeriques.
A ROBUST MULTI-OPERATOR 3-D EDGE DETECTION APPROACH FOR RANGE IMAGE SEGMENTATION
Marc Soucy and Denis Laurendeau *In* Engineering Inst. of Canada, Canadian Conference on Electrical and Computer Engineering, Volumes 1 and 2 1990 4 p (For primary document see N93-30215 11-31)
Avail: Engineering Inst. of Canada, 2050 rue Mansfield, Suite 700, Montreal, Quebec H3A 1Z2 Canada

N93-30289 Ottawa Univ. (Ontario).
RECOGNIZING PARTIALLY OVERLAPPING OBJECTS
Tayeb Damerji, Badreddine Karoui, and Dan Ionescu *In* Engineering Inst. of Canada, Canadian Conference on Electrical and Computer Engineering, Volumes 1 and 2 1990 4 p (For primary document see N93-30215 11-31)
Avail: Engineering Inst. of Canada, 2050 rue Mansfield, Suite 700, Montreal, Quebec H3A 1Z2 Canada

N93-30301 Carleton Univ., Ottawa (Ontario). Dept. of Systems and Computer Engineering.
MLOG: A LANGUAGE FOR PROTOTYPING CONCURRENT SYSTEMS
Gerald M. Karam and Jeff T. Wilson *In* Engineering Inst. of Canada, Canadian Conference on Electrical and Computer Engineering, Volumes 1 and 2 1990 6 p (For primary document see N93-30215 11-31)
Avail: Engineering Inst. of Canada, 2050 rue Mansfield, Suite 700, Montreal, Quebec H3A 1Z2 Canada

N93-30304 Bell-Northern Research Ltd., Ottawa (Ontario).
GENERALIZED OCTREES FOR CONSTRAINED OBJECT MODELING
David J. Brewer and Andrew K. C. Wong (Waterloo Univ., Ontario.) *In* Engineering Inst. of Canada, Canadian Conference on Electrical and Computer Engineering, Volumes 1 and 2 1990 4 p (For primary document see N93-30215 11-31)
Avail: Engineering Inst. of Canada, 2050 rue Mansfield, Suite 700, Montreal, Quebec H3A 1Z2 Canada

N93-30462*# AC Technology Systems and Storage Technology, McLean, VA.
RAID 7 DISK ARRAY
Lloyd Stout *In* NASA. Goddard Space Flight Center, Goddard Conference on Mass Storage Systems and Technologies, Volume 1, 1993 p 159-161 (For primary document see N93-30449 11-82)
Avail: CASI HC A01/MF A03

N93-30463*# Carnegie-Mellon Univ., Pittsburgh, PA. School of Computer Science.
TUTORIAL: PERFORMANCE AND RELIABILITY IN REDUNDANT DISK ARRAYS
Garth A. Gibson *In* NASA. Goddard Space Flight Center, Goddard Conference on Mass Storage Systems and Technologies, Volume 1, 1993 p 163-202 (For primary document see N93-30449 11-82)
Avail: CASI HC A03/MF A03

62 COMPUTER SYSTEMS

Includes computer networks and special application computer systems.

N93-28478# Air Force Inst. of Tech., Wright-Patterson AFB, OH. School of Engineering.
DESIGN OF A HARDWARE DISCRETE EVENT SIMULATION COPROCESSOR M.S. Thesis
David W. Daniel Mar. 1993 150 p
(AD-A262614; AFIT/GCE/ENG/93M-01) Avail: CASI HC A07/MF A02

A hardware discrete event simulation (DES) coprocessor was designed to eliminate synchronization overhead as a possible bottleneck. The target architecture is an eight node Intel iPSC/2 Hypercube, but this design has application to future CPU designs that wish to incorporate on-chip architectural features to better support parallel processor synchronization. A structural description of a general-purpose DES hardware coprocessor is given with approximately 90 percent of the components written at the gate level. The remaining components use low-level behavioral descriptions. While the DES coprocessor microcode implements the Chandy-Misra protocol, general-purpose support for a wide-range of protocols was a primary hardware design objective. DTIC

N93-28505# Institut National de Recherche d'Informatique et d'Automatique, Valbonne (France). Programme 2: Calcul Symbolique, Programmation et Genie Logiciel.
NETS OF REACTIVE PROCESSES [RESEAUX DE PROCESSUS REACTIFS]
Frederic Boussinot (Ecole Nationale Superieure des Mines, Valbonne, France.) Jan. 1992 16 p In FRENCH
(INRIA-RR-1588; ETN-93-93885) Avail: CASI HC A03/MF A01

The model of nets made of reactive processes is introduced. An implementation of these nets is described. A denotational semantics is given to them. The implementation of the synchronous languages LUSTRE and SIGNAL is studied, considering their programs as reactive nets. ESA

N93-28544# Lawrence Livermore National Lab., CA.
PARALLEL COMPUTATION AND THE BASIS SYSTEM
G. R. Smith 16 Dec. 1992 40 p
(Contract W-7405-eng-48)
(DE93-008755; UCRL-ID-112738) Avail: CASI HC A03/MF A01

A software package was written that can facilitate efforts to develop powerful, flexible, and easy-to-use programs that can run in single-processor, massively parallel, and distributed computing environments. Particular attention was given to the difficulties posed by a program consisting of many science packages that represent subsystems of a complicated, coupled system. Methods were found to maintain independence of the packages by hiding data structures without increasing the communication costs in a parallel computing environment. Concepts developed in this work are demonstrated by a prototype program that uses library routines from two existing software systems, Basis and Parallel Virtual Machine (PVM). Most of the details of these libraries were encapsulated in routines and macros that could be rewritten for alternative libraries that possess certain minimum capabilities. The prototype software uses a flexible master-and-slaves paradigm for parallel computation and supports domain decomposition with message passing for partitioning work among slaves. Facilities are provided for accessing variables that are distributed among the memories of slaves assigned to subdomains. The software is named PROTOPAR. DOE

N93-28628*# National Aeronautics and Space Administration. Lewis Research Center, Cleveland, OH.

A MULTIARCHITECTURE PARALLEL-PROCESSING DEVELOPMENT ENVIRONMENT

Scott Townsend (Sverdrup Technology, Inc., Brook Park, OH.), Richard Blech, and Gary Cole Apr. 1993 8 p Presented at the Seventh International Parallel Processing Symposium, Newport Beach, CA, 13-16 Apr. 1993; sponsored by IEEE Computer Society
(Contract NAS3-25266; RTOP 505-62-52)
(NASA-TM-106180; E-7744; NAS 1.15:106180) Avail: CASI HC A02/MF A01

A description is given of the hardware and software of a multiprocessor test bed - the second generation Hypercluster system. The Hypercluster architecture consists of a standard hypercube distributed-memory topology, with multiprocessor shared-memory nodes. By using standard, off-the-shelf hardware, the system can be upgraded to use rapidly improving computer technology. The Hypercluster's multiarchitecture nature makes it suitable for researching parallel algorithms in computational field simulation applications (e.g., computational fluid dynamics). The dedicated test-bed environment of the Hypercluster and its custom-built software allows experiments with various parallel-processing concepts such as message passing algorithms, debugging tools, and computational 'steering'. Such research would be difficult, if not impossible, to achieve on shared, commercial systems. Author (revised)

N93-28894# Oak Ridge National Lab., TN.

NEURAL NETWORK SIMULATIONS ON MASSIVELY PARALLEL COMPUTERS: APPLICATIONS IN CHEMICAL PHYSICS

B. G. Sumpter, C. Getino, D. W. Noid, R. E. Guenther (Nebraska Univ., Omaha.), and C. Halloy (Tennessee Univ., Knoxville.) 1993 5 p Presented at the International Neural Network Conference, Barcelona, Spain, 9-11 Jun. 1993
(Contract DE-AC05-84OR-21400)
(DE93-006739; CONF-9306101-1) Avail: CASI HC A01/MF A01

A fully connected feedforward neural network is simulated on a number of parallel computers (MasPar-1, Connection Machine CM5, Intel iPSC-2, and iPSC-860) and the performance is compared to that obtained on sequential vector computers (Cray YMP, Cray C90, IBM-3090) and to a scaler workstation (IBM RISC-6000). Peak performances of up to 342 million connections per second (MCPS) could be obtained on the Cray C90 using a single processor while the optimum performance obtained on the parallel computers was 90 MCPS using 4096 processors. Efficiency such as these has enabled neural network computations to be carried out for a number of chemical physics problems. Several examples are discussed: multi-dimensional function/surface fitting, coordinate transformations, and predictions of physical properties from chemical structure. DOE

N93-28937# Institut National de Recherche d'Informatique et d'Automatique, Valbonne (France). Programme 1: Architectures Paralleles, Bases de Donnees, Reseaux et Systemes Distribues.

PREEMPTIVE SCHEDULING WITH VARIABLE PROFILE, PRECEDENCE CONSTRAINTS AND DUE DATES

Zhen Liu and Eric Sanlaville (Paris VI Univ., France.) Feb. 1992 27 p
(INRIA-RR-1622; ETN-93-93894) Avail: CASI HC A03/MF A01

The problem of scheduling preemptive tasks subject to precedence constraints in order to minimize the maximum lateness and the makespan is addressed. The number of available parallel processors is allowed to vary in time. It is shown that when an earliest due date first algorithm provides an optimal nonpreemptive schedule for unit execution time tasks, then the preemptive priority scheduling algorithm, referred to as smallest laxity first, provides an optimal preemptive schedule for real execution time tasks. When the objective is to minimize the makespan, the same kind of result is obtained between highest level first schedules solving nonpreemptive tasks with unit execution time and the longest remaining path first schedule for the corresponding preemptive scheduling problem with real execution time tasks. These results are applied to four specific profile scheduling problems and new optimality results are obtained. ESA

N93-29030*# Computational Mechanics Co., Austin, TX.

PRE- AND POSTPROCESSING TECHNIQUES FOR DETERMINING GOODNESS OF COMPUTATIONAL MESHES Final Report, 11 Sep. 1990 - 23 Apr. 1993

J. Tinsley Oden, T. Westermann, and J. M. Bass 27 Apr. 1993 238 p
Original contains color illustrations
(Contract NAS8-38478)
(NASA-CR-192553; NAS 1.26:192553; TR-93-06) Avail: CASI HC A11/MF A03; 6 functional color pages

Research in error estimation, mesh conditioning, and solution enhancement for finite element, finite difference, and finite volume methods has been incorporated into AUDITOR, a modern, user-friendly code, which operates on 2D and 3D unstructured neutral files to improve the accuracy and reliability of computational results. Residual error estimation capabilities provide local and global estimates of solution error in the energy norm. Higher order results for derived quantities may be extracted from initial solutions. Within the X-MOTIF graphical user interface, extensive visualization capabilities support critical evaluation of results in linear elasticity, steady state heat transfer, and both compressible and incompressible fluid dynamics. Author

N93-29186# Sandia National Labs., Albuquerque, NM.

EFFICIENT WIRING OF RECONFIGURABLE PARALLEL PROCESSORS

D. S. Greenberg 28 Aug. 1992 11 p Presented at the 4th Annual ACM-SIAM Conference on Discrete Algorithms, Austin, TX, 25-27 Jan. 1993
(Contract DE-AC04-76DP-00789)
(DE93-009847; SAND-92-2011C; CONF-930194-2) Avail: CASI HC A03/MF A01

The advent of chips which include one or more CPU's, some local memory, and rudimentary communications and routing hardware has opened a new area in computer architecture design. What is the best way to connect these chips to solve particular problems? This paper defines the efficiency of a wiring scheme for a set of communication patterns. It then gives upper and lower bounds on the best efficiency achievable. It also presents simple wiring schemes for some stencil patterns used in mesh-based discrete simulations. DOE

N93-29487# Institut National de Recherche d'Informatique et d'Automatique, Valbonne (France). Programme 6: Calcul Scientifique, Modelisation et Logiciels Numeriques.

A C++ INTERFACE FOR PROGRAMMING ON THE CONNECTION MACHINE [UN INTERFACE C++ POUR PROGRAMMER SUR LA CONNECTION MACHINE]

Philippe R. B. Devloo (Instituto de Pesquisas Espaciais, Sao Jose dos Campos, Brazil.), Loula Fezoui, and Stephan Lacire May 1992 48 p
In FRENCH
(INRIA-RR-1698; ETN-93-93910) Avail: CASI HC A03/MF A01

A set of C++ classes which provide the Connection Machine (CM) programmer with a simplified interface to the PARIS (Parallel Instruction Set) library are described. Numerical test cases such as parallel arithmetic operations (scalar product, SAXPY), and a Jacobi iterative resolution, are used to perform a validation of the C++ interface. Performance results of the C++ interface are presented and compared to those obtained using the PARIS library or using high level languages of the CM-2 system such as C(star) or CM-FORTRAN. A classical example in numerical ecology is used for illustrating the performance in parallel computation with integers. ESA

N93-29490# Federal Aviation Administration, Atlantic City, NJ. Technical Center.

DATA MULTIPLEXING NETWORK (DMN) EQUIPMENT OPERATIONAL TEST AND EVALUATION (OT&E) INTEGRATION TEST REPORT

Wayne E. Bell and Phillip P. Hoang Mar. 1993 26 p
(AD-A263172; DOT/FAA/CT-TN9) Avail: CASI HC A03/MF A01

This test report contains the test results of the Operational Test and Evaluation (OT and E) Integration testing of Data Multiplexing Network (DMN) Phase 3B Commercial Off-The-Shelf (COTS) equipment. The OT and E Integration testing was accomplished by conducting unit level tests at the Federal Aviation Administration (FAA) Technical Center, and integration tests at the Air Route Traffic Control Center (ARTCC) in Minneapolis, Minnesota. Based on the test results, it is concluded that the Motorola Codex COTS equipment performed its function of providing data exchange between NAS facilities and is considered qualified for the NAS environment. DTIC

N93-29508# Stanford Univ., CA. Dept. of Computer Science.

EXPLOITING THE MEMORY HIERARCHY IN SEQUENTIAL AND PARALLEL SPARSE CHOLESKY FACTORIZATION

Edward Rothberg Nov. 1992 168 p
(Contracts N00039-91-C-0138; N00014-87-K-0828)
(AD-A262849; SU-Stan-CS-92-1459; CSL-TR-92-555) Avail: CASI HC A08/MF A02

Cholesky factorization of large sparse matrices is an extremely important computation, arising in a wide range of domains including linear programming, finite element analysis, and circuit simulation. This thesis investigates crucial issues for obtaining high performance for this computation on sequential and parallel machines with hierarchical memory systems. The thesis begins by providing the first thorough analysis of the interaction between sequential sparse Cholesky factorization methods and memory hierarchies. We look at popular existing methods and find that they produce relatively poor memory hierarchy performance. The methods are extended, using blocking techniques, to reuse data in the fast levels of the memory hierarchy. This increased reuse is shown to provide a three-fold speedup over popular existing approaches (e.g., SPARSPAK) on modem workstations. The thesis then considers the use of blocking techniques in parallel sparse factorization. We first describe parallel methods we have developed that are natural extensions of the sequential approach described above. These methods distribute panels (sets of contiguous columns with nearly identical non-zero structures) among the processors. The thesis shows that for small parallel machines, the resulting methods again produce substantial performance improvements over existing methods. A framework is provided for understanding the performance of these methods, and also for understanding the limitations inherent in them. Using this framework, the thesis shows that panel methods are inappropriate for large-scale parallel machines because they do not expose enough concurrency. DTIC

N93-29650# Office of Technology Assessment, Washington, DC.

ADVANCED NETWORK TECHNOLOGY: BACKGROUND PAPER

Jun. 1993 86 p Original contains color illustrations
(OTA-BP-TCT-101; ISBN-0-16-041805-4) Avail: CASI HC A05/MF A01; SOD HC

Computer networks are having dramatic impacts on our lives. What were once esoteric tools used only by scientists and engineers are becoming more widely used in schools, libraries, and businesses. At the same time, researchers are working to develop even more capable networks that promise to change fundamentally the way we communicate. This background paper analyzes technologies for tomorrow's information superhighways. Advanced networks will first be used to support scientists in their work, linking researchers to supercomputers, databases, and scientific instruments. As the new networks are deployed more widely, they will be used by a broader range of users for business, entertainment, health care, and education applications. The background paper also describes six test networks that are being funded as part of the High Performance Computing and Communications Program. Author (revised)

N93-29661 National Oceanic and Atmospheric Administration, Boulder, CO.

CONTEXT SWITCH TIME SCALABILITY: BENCHMARK RESULTS

J. L. Sloan Oct. 1992 42 p Sponsored by National Science Foundation, Washington, DC Limited Reproducibility: More than 20% of this document may be affected by microfiche quality
(PB93-181832; NCAR/TN-378+STR) Avail: CASI HC A03

The work a computer system performs to temporarily suspend execution of one process and resume execution of another process is called a context switch. The time it takes for a computer system to perform a context switch is often cited as an important performance metric. Lengthy context switch time can result in poor performance in process-intensive applications such as distributed servers or interactive systems. However, context switch time is usually assumed to be constant for a particular system. The document describes a benchmark program which shows that for many systems this is not the case. The program was run on a variety of UNIX-based systems at the National Center for Atmosphere Research (NCAR), and the results are given in both tabular and graphical form. They show that for many systems, context switch time increases, sometimes dramatically, with the number of concurrent processes running in the system. This non-scalability of context switch times leads to diminishing returns when, for example, upgrading to a faster processor in order to support more interactive users. NTIS

N93-29677 National Inst. of Standards and Technology, Gaithersburg, MD.

USING SYNTHETIC-PERTURBATION TECHNIQUES FOR TUNING SHARED MEMORY PROGRAMS

Robert Snelick, Joseph JaJa (Maryland Univ., College Park.), Raghu Kacker, and Gordon Lyon Mar. 1993 35 p See also PB93-161339 Sponsored in part by DARPA Limited Reproducibility: More than 20% of this document may be affected by microfiche quality
(PB93-178572; NISTIR-5139) Avail: CASI HC A03

The Synthetic Perturbation Tuning (SPT) methodology is based on an empirical approach that introduces artificial delays into the multiple-instruction stream, multiple-data stream (MIMD) program and captures the effects of such delays by using the modern branch of statistics called design of experiments. SPT provides the basis of a powerful tool for tuning MIMD programs that are portable across machines and architectures. The purpose of the paper is to explain the general approach and to extend it to address specific features that are the main source of poor performance on the shared memory programming model. These include performance degradation due to loan imbalance and insufficient parallelism, overhead introduced by synchronizations and by accessing shared data structures, and compute time bottlenecks. The authors illustrate its use on two very different case studies: a large image processing benchmark and a parallel quicksort. NTIS

N93-29782# Lawrence Livermore National Lab., CA.

DATA PARALLELISM

B. C. Gorda Sep. 1992 4 p Presented at the 26th Hawaiian International Conference on System Science: Biotechnology Computing Track, Kauai, HI, 5-8 Jan. 1993
(Contract W-7405-eng-48)
(DE93-009300; UCRL-JC-111827; CONF-930117-6) Avail: CASI HC A01/MF A01

Data locality is fundamental to performance on distributed memory parallel architectures. Application programmers know this well and go to great pains to arrange data for optimal performance. Data Parallelism, a model from the Single Instruction Multiple Data (SIMD) architecture, is finding a new home on the Multiple Instruction Multiple Data (MIMD) architectures. This style of programming, distinguished by taking the computation to the data, is what programmers have been doing by hand for a long time. Recent work in this area holds the promise of making the programmer's task easier. DOE

N93-30361# Oregon State Univ., Newport. Hatfield Marine Science Center.

PARALLEL PROCESSING AND LEARNING: VARIABILITY AND CHAOS IN SELF-ORGANIZATION OF ACTIVITY IN GROUPS OF NEURONS

Annual Report, 15 Jan. 1992 - 1 Feb. 1993

George J. Mpitsos 9 Mar. 1993 3 p
(Contract F49620-92-J-0140)
(AD-A264224; AFOSR-93-0238TR) Avail: CASI HC A01/MF A01

Results of computer simulations of catalytic networks were recently published, and the problem of the effect that catalytic error has in controlling system dynamics was addressed. Simulations of large networks are being designed in order to examine spatio-temporal dynamics in reaction-diffusion systems. The aim is to develop visualization and analysis methods to apply large networks composed of biologically realistic neurons. Immunohistochemical studies examined mammalian tissues that may be useful as model systems to examine distributed function in neurotransmission and neuromodulation. It is necessary, as these and other publications indicate, not only to understand neural organization in a simple animal, but also to examine the applicability of the findings to higher animals, and, if possible, to humans. Molecular biological studies of muscarinic receptors were performed. In previous AFOSR-published work, it was shown that brief pharmacologic blocking of these receptors enhances 1-Trial associative learning. Over the past year, cloning vectors for generating fusing proteins to all of the five known muscarinic receptor subtypes in humans were developed. Our next step is to obtaine immunofluorescent antisera to the fusion proteins in order to visually identify cells containing the different muscarinic receptors. The in-between step will be to determine the specificity of the antisera. The findings will be applicable not only to our experimental animal, but also to studies of learning and pathologies in humans. DTIC

N93-30364# Louisiana State Univ., Baton Rouge. Dept. of Electrical and Computer Engineering.
MULTIPROCESSING SYSTEMS: RELIABILITY MODELLING AND ANALYSIS USING MULTIMODE COMPONENTS AND DEPENDENT FAILURES Final Report, 1 Oct. 1990 - 31 Oct. 1992
Suresh Rai 31 Oct. 1992 109 p
(Grant AF-AFOSR-0025-91)
(AD-A264230; AFOSR-93-0251TR) Avail: CASI HC A06/MF A02

The researchers established simple and efficient algorithms for terminal reliability (TR) and broadcast reliability (BR) evaluation of the shuffle-exchange network with an extra stage (SENE). In the SENE, each input is connected to each output by a pair of complete binary trees such that the input is connected by a directed edge to each of the roots, ad the leaves of both trees are identical. These very regular paths from an input to the outputs offer the structure necessary to solve the TR BR problems efficiently. DTIC

N93-30633# Los Alamos National Lab., NM.
MULTIPROCESSING MCNP ON AN IBM RS/6000 CLUSTER
G. W. McKinney and J. T. West (International Business Machines Corp., Houston, TX.) 1993 7 p Presented at the American Nuclear Society (ANS) Annual Meeting, San Diego, CA, 20-24 Jun. 1993
(Contract W-7405-eng-36)
(DE93-008712; LA-UR-93-463; CONF-930601-8) Avail: CASI HC A02/MF A01

The advent of high-performance computer systems has brought to maturity programming concepts like vectorization, multiprocessing, and multitasking. While there are many schools of thought as to the most significant factor in obtaining order-of-magnitude increases in performance, such speedup can only be achieved by integrating the computer system and application code. Vectorization leads to faster manipulation of arrays by overlapping instruction CPU cycles. Discrete ordinates codes, which require the solving of large matrices, have proved to be major benefactors of vectorization. Monte Carlo transport, on the other hand, typically contains numerous logic statements and requires extensive redevelopment to benefit from vectorization. Multiprocessing and multitasking provide additional CPU cycles via multiple processors. Such systems are generally designed with either common memory access (multitasking) or distributed memory access. In both cases, theoretical speedup, as a function of the number of processors (P) and the fraction of task time that multiprocesses (f), can be formulated using Amdahl's Law $S(f,P) = 1/(1 - f + f/P)$. However, for most applications this theoretical limit cannot be achieved, due to additional terms not included in Amdahl's Law. Monte Carlo transport is a natural candidate for multiprocessing, since the particle tracks are generally independent and the precision of the result increases as the square root of the number of particles tracked. DOE

N93-30895# Sparta, Inc., Lexington, MA.
4D INTERCONNECT EXPERIMENTAL DEVELOPMENT Final Technical Report, 1 Oct. 1991 - 30 Sep. 1992
Philip D. Henshaw, Steven A. Lis, and Michael G. Cheifetz 29 Jun. 1993 46 p
(Contract F49620-91-C-0002)
(AD-A264298; LTR93-003; AFOSR-93-0289TR) Avail: CASI HC A03/MF A01

This report summarizes the work performed during a two-year program aimed at demonstrating the feasibility of constructing a 4-dimensional neural network based on the unique properties of spectral hole burning (SHB) materials. SHB materials were synthesized and excellent quality holograms were recorded and retrieved. Both wavelength and angle multiplexing were demonstrated with no apparent crosstalk. We assembled a demonstration holographic optical neural network and tested it as a bidirectional associative memory system. The results obtained clearly demonstrate the fundamental ability to fully connect two 2D planes of digital information. Expectations are that this architecture can be extended to capacities of 10(exp 12) interconnects or greater. DTIC

N93-30262 McGill Univ., Montreal (Quebec). Dept. of Biomedical Engineering.
A PARALLEL PROCESSING SYSTEM FOR INTENSIVE I/O
Sylvain Martel, Serge Lafontaine, and Ian Hunter *In* Engineering Inst. of Canada, Canadian Conference on Electrical and Computer Engineering, Volumes 1 and 2 1990 5 p (For primary document see N93-30215 11-31)
Avail: Engineering Inst. of Canada, 2050 rue Mansfield, Suite 700, Montreal, Quebec H3A 1Z2 Canada

N93-30263 McMaster Univ., Hamilton (Ontario). Dept. of Electrical and Computer Engineering.
A TRANSPUTER BASED PARALLEL PROCESSING ARCHITECTURE FOR ROBOTICS APPLICATIONS
Akilesh Parameswar and Naresh K. Sinha *In* Engineering Inst. of Canada, Canadian Conference on Electrical and Computer Engineering, Volumes 1 and 2 1990 4 p (For primary document see N93-30215 11-31)
Avail: Engineering Inst. of Canada, 2050 rue Mansfield, Suite 700, Montreal, Quebec H3A 1Z2 Canada

N93-30280 Concordia Univ., Montreal (Quebec). Faculty of Engineering and Computer Science.
OPTIMIZED PARTITIONING AND BALANCING FOR PARALLEL PROCESSING
Y. C. Zhao, L. Tao, K. Thulasiraman, and M. N. S. Swamy *In* Engineering Inst. of Canada, Canadian Conference on Electrical and Computer Engineering, Volumes 1 and 2 1990 4 p (For primary document see N93-30215 11-31)
Avail: Engineering Inst. of Canada, 2050 rue Mansfield, Suite 700, Montreal, Quebec H3A 1Z2 Canada

63 CYBERNETICS

Includes feedback and control theory, artificial intelligence, robotics and expert systems.

For related information see also *54 Man/System Technology and Life Support.*

N93-28480# Universiteit Twente, Enschede (Netherlands). Dept. of Computer Science.
RESOURCE LIMITED REASONING: A STUDY OF LITERATURE IN THE CONTEXT OF MODEL-BASED DIAGNOSIS
R. F. Riswick Sep. 1992 40 p Sponsored by Stichting Knowledge Based Systems, Netherlands
(Memo-INF-92-38; UT-KBS-92-40; SKBS-A1/92-19; ETN-93-93836)
Copyright Avail: CASI HC A03/MF A01

Model based diagnosis is concerned with finding defects in technical devices. The research in this field has concentrated on two main problems, a modeling problem and an efficiency problem. The modeling problem is to find a useful model to perform model based diagnosis. The efficiency problem is concerned with finding ways to reason about the obtained models in an efficient way. The requirement of putting model based diagnosis into practice produces an additional problem. In general, the diagnosis program to be built will not be able to use unlimited resources. The most important limitation is the costs, for example the cost of time, space, and computational power. But also, the costs of repairing a component in the system and the cost a breakdown of the system will cause. The study focuses on the cost of time. The most important question addresses how a system that provides an answer before a certain deadline can be built. Some literature from the field of real time systems and the field of metareasoning is discussed and preliminary areas about applying this theory to model based diagnosis are given. Anytime algorithms will turn out to be a possible solution to the problem of providing an answer within a particular time. In combination with metareasoning techniques, these algorithms could be used to construct a resource limited diagnostic system. ESA

N93-28494# Rome Lab., Griffiss AFB, NY.
THE DYNAMIC BEHAVIOR OF CONSTRAINED ADAPTIVE ARRAY SENSOR PROCESSORS
Jay S. Goldstein Dec. 1992 130 p
(AD-A262402; RL-TR-92-327) Avail: CASI HC A07/MF A02

The transient behavior of constrained wideband adaptive array sensors is examined with the goal of improving the convergence properties while simultaneously satisfying a requirement for limited computational complexity. The multichannel wideband adaptive filter is derived for the tapped-delay-line, frequency domain, lattice and Gram-Schmidt structures. The mean-square error for each structure is estimated and compared over varying degrees of difficulty with respect to the signal environment. A new multichannel wideband extension of the frequency domain structure is presented, and the performance is demonstrated to surpass that of the conventional tapped-delay line structure. It is shown via simulation that utilizing the Discrete Cosine Transform, the new structure is capable of converging at speeds which rival the more computationally expensive least square methods at no increase in the required number of adaptive coefficients. The multichannel wideband lattice structure is shown to perform better than the other structures and the least squares method of Sample Matrix Inversion. DTIC

N93-28498# Washington Univ., Saint Louis, MO. Dept. of Systems Science and Mathematics.
ARTIFICIAL INTELLIGENCE METHODOLOGIES IN FLIGHT RELATED DIFFERENTIAL GAME, CONTROL AND OPTIMIZATION PROBLEMS Final Report, 30 Sep. 1989 - 29 Dec. 1992
Ervin Y. Rodin 31 Jan. 1993 175 p
(Grant AF-AFOSR-0518-89)
(AD-A262405; AFOSR-93-0187TR) Avail: CASI HC A08/MF A02

Artificial intelligence methodologies have been applied to the modeling and implementation of control systems and differential games problems. To be more specific, artificial neural networks, a multiple instruction multiple data parallel processor tuned by connection weights, are used to model a control system or used as an identifier/controller which functions as a mapping between two information domains. Significant advances have been achieved in applying differential games theory to practical problems. DTIC

N93-28637# Institut National de Recherche d'Informatique et d'Automatique, Valbonne (France). Centre Sophia Antipolis.
OPTIMAL CONTROL OF THE M/G/1 QUEUE WITH REPEATED VACATIONS OF THE SERVER Programme 1: Architectures paralleles, bases de donnees, reseaux et systemes distribues
Eitan Altman and Philippe Nain Mar. 1992 20 p
(Grant FISCCSE-3321190)
(INRIA-RR-1637; ETN-93-93896) Avail: CASI HC A03/MF A01

An M/G/1 queue where the server may take repeated vacations is considered. Whenever a busy period terminates (that is, when the queue empties), the server takes a vacation of random duration. At the end of each vacation the server may either take a new vacation or resume service provided that the system is nonempty. The decision to turn the server on/off may depend on all the history of the process (which includes the number of customers and all past decisions). The optimization problem typically arises when imposing a cost structure that involves a holding cost per unit time and customer and a cost for turning the server on (a shut down cost may also be included in the latter cost). Restrictions to threshold policies where the server is turned on at the end of each vacation if and only if the queue length is greater than or equal to a fixed threshold may be desired. The study aims to establish the optimality of threshold policies over all policies for two long run average cost criteria. ESA

N93-28638# Institut National de Recherche d'Informatique et d'Automatique, Valbonne (France).
CLOSED-LOOP CONTROL WITH DELAYED INFORMATION Programme 1: Architectures paralleles, bases de donnees, reseaux et systemes distribues
Eitan Altman and Philippe Nain Mar. 1992 18 p
(Grant FISCCSE-3321190)
(INRIA-RR-1638; ETN-93-93897) Avail: CASI HC A03/MF A01

The theory of Markov Control Model with Perfect State Information, (MCM-PSI) requires that the current state of the system is known to the decision maker at decision instants. Otherwise, MCM with Imperfect SI (MCM-ISI) is extant. A class of MCM-ISI, where the information on the state of the system is delayed, is introduced. Such an information structure is encountered, for instance, in high speed data networks. By enlarging the state space so as to include the last known state as well as all the decisions made during the travel time of the information, it is shown that an MCM-ISI can be reduced to a MCM-PSI. This result is applied to a flow control problem. A discrete time queueing model with Bernoulli arrivals and geometric services, where the intensity of the arrival stream is controlled, is considered. At the beginning of slot $t + 1$, $t = 0, 1, 2, \ldots$, the decision maker has to select the probability of having one arrival in the current time slot from the set (p1, p2), p2 greater than 0 and less than p1 and p1 less than or equal to 1, only on the basis of the queue length and action histories in (0,t). The aim is to optimize a discounted throughout/delay criterion. An optimal policy of a threshold type, where the threshold is seen to depend on the last action, is shown to exist. ESA

N93-28898# Oxford Univ. (England). Dept. of Engineering Science.
STABILIZATION USING LOW-GAIN PI CONTROL: SISO CASE
Denis Mustafa 22 Jul. 1992 11 p Presented at the 1993 International Symposium on Mathematical Theory of Networks and Systems
(OUEL-1947/92; ETN-93-93878) Avail: CASI HC A03/MF A01

A characterization of a maximal class of stabilizing low gain proportional-integral (PI) controllers, in the SISO case, is given. Specifically, the following four cases are studied, where in each case a closed formula is derived for the largest gain tolerable before the controller ceases to be stabilizing: no integral gain, proportional gain increased from zero; no proportional gain, integral gain increased from zero; proportional gain increased from zero to some stabilizing value, then integral gain increased from zero; and integral gain increased from zero to some stabilizing value, then proportional gain increased from zero. The key analytical tool is a block structured guardian map that leads to closed eigenvalue formulae for the largest permissible gains. ESA

N93-28987# Anthropology Research Project, Yellow Springs, OH.
NEURAL NETWORK TECHNOLOGIES Final Report, Feb. 1992 - Feb. 1993
Randy B. Pollack Feb. 1993 21 p LIMITED REPRODUCIBILITY: More than 20% of this document may be affected by microfiche quality
(Contract F33615-89-C-0572)
(AD-A262576; AL-SR-1993-0002) Avail: Issuing Activity (Defense Technical Information Center (DTIC))

This work is a continuation of research performed under the 1990 AFOSR Research Initiator Program. In this report the architecture from the previous effort was improved to support easy modification and extension. The result is a system which can be used to automatically identify human landmarks from high density surface digital data. DTIC

N93-29047# Oak Ridge National Lab., TN.
ROBOTICS AND ARTIFICIAL INTELLIGENCE FOR HAZARDOUS ENVIRONMENTS
P. F. Spelt 1993 13 p Presented at the 17th Congress of Investigation Cientifica Universidad Interamericana De Puerto Rico, San Juan, Puerto Rico, 11-12 Feb. 1993
(Contract DE-AC05-84OR-21400)
(DE93-008271; CONF-930264-1) Avail: CASI HC A03/MF A01

In our technological society, hazardous materials including toxic chemicals, flammable, explosive, and radioactive substances, and biological agents, are used and handled routinely. Each year, many workers who handle these substances are accidently contaminated, in some cases resulting in injury, death, or chronic disabilities. If these hazardous materials could be handled remotely, either with a teleoperated robot (operated by a worker in a safe location) or by an autonomous robot, then human suffering and economic costs of accidental exposures could be dramatically reduced. At present, it is still difficult for commercial robotic technology to completely replace humans involved in performing complex work tasks in hazardous environments. The robotics efforts at the Center for Engineering Systems

Advanced Research represent a significant effort at contributing to the advancement of robotics for use in hazardous environments. While this effort is very broad-based, ranging from dextrous manipulation to mobility and integrated sensing, focus is on machine learning and the high-level decision making needed for autonomous robotics. DOE

N93-29079 Arizona State Univ., Tempe.

ROBUST FEEDFORWARD/FEEDBACK CONTROL SYNTHESIS FOR UNCERTAIN DYNAMICAL SYSTEMS Ph.D. Thesis

Qiang Liu 1992 218 p

Avail: Univ. Microfilms Order No. DA9307106

A robust H(sub infinity) control design method for dynamical systems with structured parametric uncertainty is developed. The proposed design methodology incorporates the internal model principle for persistent-disturbance rejection. A non-colocated control problem of flexible space structures subject to parameter variations is used to illustrate the design methodology and to address some important issues arising in robust control design. The infinity-norm parameter margin as well as the conventional gain/phase margins are employed as a stability robustness measure of a closed-loop system with structured multi-parameter variations. A proper implementation of a robust non-minimum-phase compensator for a non-zero set-point control problem is also proposed. The proposed robust control design methodology was successfully applied to the Hubble Space Telescope and the Space Station, resulting in significant improvement in system performance and stability robustness. Two approaches to robustified open-loop control of uncertain flexible systems are developed with the objective of achieving fast maneuvering and reduction of residual vibration. In the first approach, robust time-optimal control inputs are obtained by solving a parameter optimization problem subject to robustness constraints. In the second approach, a time-optimal control input is preshaped using a tapped delay filter. It is shown that new approaches provide near-minimum-time maneuvering and robust suppression of residual structural vibrations in the presence of model parameter variations. On-off reaction jet control logic for uncertain flexible spacecraft are also investigated from the viewpoint of minimizing the maneuver time, fuel consumption, and structural mode excitation. Dissert. Abstr.

N93-29176*# National Aeronautics and Space Administration. Pasadena Office, CA.

THREE-PARAMETER TUNABLE TILT-INTEGRAL-DERIVATIVE (TID) CONTROLLER Patent Application

Boris J. Lurie, inventor (to NASA) (Jet Propulsion Lab., California Inst. of Tech., Pasadena.) 1 Feb. 1993 24 p

(Contract NAS7-918)

(NASA-Case-NPO-18492-1-CU; NAS 1.71:NPO-18492-1-CU; US-Patent-Appl-SN-023253) Avail: CASI HC A03/MF A01

A feedback control system compensator of the PID type is provided, wherein the proportional component of the compensator is replaced with a tilted component having a transfer function s to the power of -1/n. The resulting transfer function of the entire compensator more closely approximates an optimal transfer function, thereby achieving improved feedback controller. Further, as compared to conventional PID compensators, the TID compensator allows for simpler tuning, better disturbance rejection ratio, and smaller effects of plant parameter variations on closed loop response. NASA

N93-29192*# Boeing Commercial Airplane Co., Seattle, WA. Flight Deck Research.

SPURIOUS SYMPTOM REDUCTION IN FAULT MONITORING

William D. Shontz, Roger M. Records, and Jai J. Choi Jun. 1993 108 p

(Contract NAS1-18027; RTOP 505-64-13-22)

(NASA-CR-191453; NAS 1.26:191453) Avail: CASI HC A06/MF A02

Previous work accomplished on NASA's Faultfinder concept suggested that the concept was jeopardized by spurious symptoms generated in the monitoring phase. The purpose of the present research was to investigate methods of reducing the generation of spurious symptoms during in-flight engine monitoring. Two approaches for reducing spurious symptoms were investigated. A knowledge base of rules was constructed to filter known spurious symptoms and a neural net was developed to improve the expectation values used in the monitoring process. Both approaches were effective in reducing spurious symptoms individually. However, the best results were obtained using a hybrid system combining the neural net capability to improve expectation values with the rule-based logic filter. Author (revised)

N93-29386*# National Aeronautics and Space Administration. Ames Research Center, Moffett Field, CA.

MoCog1: A COMPUTER SIMULATION OF RECOGNITION-PRIMED HUMAN DECISION MAKING

William B. Gevarter Oct. 1991 20 p

(RTOP 590-12-42)

(NASA-TM-103868; A-91160; NAS 1.15:103868) Avail: CASI HC A03/MF A01

The results of the first stage of a research effort to develop a 'sophisticated' computer model of human cognitive behavior are described. Most human decision making is an experience-based, relatively straight-forward, largely automatic response to internal goals and drives, utilizing cues and opportunities perceived from the current environment. The development of the architecture and computer program (MoCog1) associated with such 'recognition-primed' decision making is discussed. The resultant computer program was successfully utilized as a vehicle to simulate earlier findings that relate how an individual's implicit theories orient the individual toward particular goals, with resultant cognitions, affects, and behavior in response to their environment. Author (revised)

N93-29420# Air Force Inst. of Tech., Wright-Patterson AFB, OH. School of Engineering.

A FUZZY LOGIC OPTIMAL CONTROL LAW SOLUTION TO THE CMMCA TRACKING PROBLEM M.S. Thesis

Randy E. Nelson Mar. 1993 146 p

(AD-A262555; AFIT/GST/ENS/93M-10) Avail: CASI HC A07/MF A02

The Air Force uses the C-18 Cruise Missile Mission Control Aircraft (CMMCA) to radar track cruise missiles (CM) during test flights. Because of the complexity of the CM flight profiles, maintaining radar coverage at all times is very difficult. Optimal control theory is applied to construct a simulation providing 100% radar coverage. The simulation was divided into ten second intervals, and fuzzy logic was used at the start of each interval to determine the set point, i.e., that point in space where the CMMCA should be in ten seconds. The set point calculation's fuzzy logic balanced CMMCA maneuvering based on present and future CM positions. Three different future times were used: 60, 90, and 120 seconds ahead, and the performance for each time was compared. The simulation was performed on an IBM compatible PC with Matlab and Simulink (both by The MathWorks). The final form of the fuzzy logic provided varying radar coverage at each look ahead time for a complex CM flight path (CM in 20 degrees of bank) 1850 seconds long. At 120 seconds look ahead time, the coverage was 100%. When the same profile was performed with the CM in 30 degrees of bank, coverage was degraded, and 60 seconds look ahead performed best. DTIC

N93-29763 Carnegie-Mellon Univ., Pittsburgh, PA. School of Computer Science.

COMMUNICATIONS NEURAL NET PROCESSORS Final Technical Report

H. T. Kung Dec. 1992 30 p Limited Reproducibility: More than 20% of this document may be affected by microfiche quality

(Contract F30602-88-D-0028)

(AD-A263330; RL-TR-92-306) Avail: CASI HC A03

This report covers several neural net algorithms. The report describes the rationale for their developments and the details of their operation. The report also addresses the efficient implementation of the algorithms on the i WARP procession. Optimum architectures are also discussed. DTIC

N93-29771*# Rensselaer Polytechnic Inst., Troy, NY. Center for Intelligent Robotic Systems for Space Exploration.

PLANNING COLLISION FREE PATHS FOR TWO COOPERATING ROBOTS USING A DIVIDE-AND-CONQUER C-SPACE TRAVERSAL HEURISTIC

Johnathan M. Weaver May 1993 161 p

(Grant NAGw-1333)

(NASA-CR-193252; NAS 1.26:193252; CIRSSE-136) Avail: CASI HC A08/MF A02

A method was developed to plan feasible and obstacle-avoiding paths

for two spatial robots working cooperatively in a known static environment. Cooperating spatial robots as referred to herein are robots which work in 6D task space while simultaneously grasping and manipulating a common, rigid payload. The approach is configuration space (c-space) based and performs selective rather than exhaustive c-space mapping. No expensive precomputations are required. A novel, divide-and-conquer type of heuristic is used to guide the selective mapping process. The heuristic does not involve any robot, environment, or task specific assumptions. A technique was also developed which enables solution of the cooperating redundant robot path planning problem without requiring the use of inverse kinematics for a redundant robot. The path planning strategy involves first attempting to traverse along the configuration space vector from the start point towards the goal point. If an unsafe region is encountered, an intermediate via point is identified by conducting a systematic search in the hyperplane orthogonal to and bisecting the unsafe region of the vector. This process is repeatedly applied until a solution to the global path planning problem is obtained. The basic concept behind this strategy is that better local decisions at the beginning of the trouble region may be made if a possible way around the 'center' of the trouble region is known. Thus, rather than attempting paths which look promising locally (at the beginning of a trouble region) but which may not yield overall results, the heuristic attempts local strategies that appear promising for circumventing the unsafe region.
Author (revised)

N93-29791# Boston Univ., MA. Center for Adaptive Systems.
DEVELOPMENT OF NEURAL NETWORK ARCHITECTURES FOR SELF-ORGANIZING PATTERN RECOGNITION AND ROBOTICS Final Technical Report, 1 Oct. 1989 - 31 Dec. 1992
Gail A. Carpenter and Stephen Grossberg Mar. 1993 27 p
(Grant AF-AFOSR-0083-90)
(AD-A264831; AFOSR-93-0274TR) Avail: CASI HC A03/MF A01

During the DARPA ANNT Program contract, new neural network architectures were developed to carry out autonomous real-time preprocessing, segmentation, recognition, timing, and control of both spatial and temporal inputs. These architectures contribute to: (1) preprocessing of visual form and motion signals; (2) preprocessing of acoustic signals; (3) adaptive pattern recognition and categorization in an unsupervised learning context; (4) adaptive pattern recognition and prediction in a supervised learning context; (5) processing of temporal patterns using working memory networks, with applications to 3-D object recognition; (6) adaptive timing for task scheduling; (7) adaptive sensory-motor control using head-centered spatial representations of 3-D target position. DTIC

N93-29917# Massachusetts Inst. of Tech., Cambridge. Center for Intelligent Control Systems.
CENTER FOR THE STUDY OF INTELLIGENT CONTROL SYSTEMS (FELLOWSHIPS) Final Report, 1 Oct. 1986 - 31 Dec. 1992
Sanjoy K. Mitter Mar. 1993 7 p
(Contract DAAL03-86-G-0208)
(AD-A263604; ARO-24637.Z-MA-UIF) Avail: CASI HC A02/MF A01

Each institution of the Center for Intelligent Control Systems, Brown University, Harvard University and M.I.T., administered its own pre-doctoral fellowship program which attracted outstanding American graduate students. However, Brown University's Center Fellows were supported under a separate grant, DAAL03-89-G-0010. The criteria for selection was academic excellence and interest in the research of the Center. Continuance of fellowship support was contingent upon superior performance in the graduate program. DTIC

N93-29998# Technical Research Centre of Finland, Espoo. Information Processing Lab.
A NEURAL NETWORK BASED APPROACH FOR MACHINE FAULT DIAGNOSIS
Ari M. Vepsalainen Aug. 1991 30 p
(VTT-TIED-1274; ISBN-951-38-4007-7; ETN-93-93775) Copyright Avail: CASI HC A03/MF A01

An approach to classifying the state of a machine based on vibration measurements and the use of a dynamic neural network is presented. Some comparisons are made between the presented method, the linear classifier, the third order nonlinear classifier, the Markov model based classifier, and the recurrent backpropagation network. The proposed classifier can be considered as a spatiotemporal neural network. Spatiotemporal neural networks are used to transform input patterns into time varying class number output codes. Usually, time is assumed to move forward in small discrete steps. The recurrent backpropagation network and the Spatiotemporal Pattern Recognizer Neural Network (SPRNN) are other examples of spatiotemporal neural networks. The spatiotemporal neural network can effectively store much more information than most other types of neural networks with the same number of nodes. The presented approach is suited to machine maintenace for two reasons: it can model temporal relations, for example, it can describe the development of the symptoms of faults; and it can efficiently handle large amounts of data. Because the spectral signatures of faults may change significantly depending on environmental operating and physical conditions, the amount of training information is very large. ESA

N93-30012# Sandia National Labs., Albuquerque, NM.
APPLICATION OF SENSORS TO THE CONTROL OF ROBOTIC SYSTEMS
R. W. Harrigan 1993 8 p Presented at the 50th Anniversary Spring Conference on Experimental Mechanics, Dearborn, MI, 9 Jun. 1993
(Contract DE-AC04-76DP-00789)
(DE93-009837; SAND-93-0589C; CONF-9306127-1) Avail: CASI HC A02/MF A01

Hazardous operations which in the past have been completed by technicians are under increased scrutiny due to high costs and low productivity associated with providing protective clothing and environments. As a result, remote systems are needed to accomplish many hazardous materials handling tasks such as the clean up of waste sites in which the exposure of personnel to radiation, chemical, explosive, and other hazardous constituents is unacceptable. Traditional remote manual operations have proven to have very low productivity when compared with unencumbered humans. Computer models augmented by sensing and structured, modular computing environments are proving to be effective in automating many unstructured hazardous tasks. DOE

N93-30039*# Rensselaer Polytechnic Inst., Troy, NY. Center for Intelligent Robotic Systems for Space Exploration.
THE PLANNING COORDINATOR: A DESIGN ARCHITECTURE FOR AUTONOMOUS ERROR RECOVERY AND ON-LINE PLANNING OF INTELLIGENT TASKS
Jeffrey J. Farah Dec. 1992 132 p
(Grant NAGw-1333)
(NASA-CR-193250; NAS 1.26:193250; CIRSSE-134) Avail: CASI HC A07/MF A02

Developing a robust, task level, error recovery and on-line planning architecture is an open research area. There is previously published work on both error recovery and on-line planning; however, none incorporates error recovery and on-line planning into one integrated platform. The integration of these two functionalities requires an architecture that possesses the following characteristics. The architecture must provide for the inclusion of new information without the destruction of existing information. The architecture must provide for the relating of pieces of information, old and new, to one another in a non-trivial rather than trivial manner (e.g., object one is related to object two under the following constraints, versus, yes, they are related; no, they are not related). Finally, the architecture must be not only a stand alone architecture, but also one that can be easily integrated as a supplement to some existing architecture. This thesis proposal addresses architectural development. Its intent is to integrate error recovery and on-line planning onto a single, integrated, multi-processor platform. This intelligent x-autonomous platform, called the Planning Coordinator, will be used initially to supplement existing x-autonomous systems and eventually replace them. Derived from text

N93-30116# Institut National de Recherche d'Informatique et d'Automatique, Valbonne (France). Programme 4: Robotique, Image et Vision.
SOME RESULTS ON FEEDBACK STABILIZATION OF A ONE-LINK FLEXIBLE ARM
Sylvie Icart (I3S-LASSY, Valbonne, France.), Juliette Leblond, and Claude Samson May 1992 30 p
(INRIA-RR-1682; ETN-93-93903) Avail: CASI HC A03/MF A01

A report aimed at exhibiting a class of stabilizing feedback laws for a structurally undamped one link flexible arm with control applied at one extremity is presented. A finite dimensional model of the arm, corresponding to a discretization in space, is first considered. The arm is then modeled by a classical partial differential equation, no finite dimensional approximation being made in the control analysis. In both cases, stability of the closed loop system is proven, using a Lyapunov method and applying Lasalle's principle. The practical significance of the proposed results is commented upon and illustrated by simulation experiments. ESA

N93-30165# Johns Hopkins Univ., Baltimore, MD. Dept. of Psychology.
NEURAL MECHANISMS OF ATTENTION
David S. Olton 23 Mar. 1993 12 p
(Grant AF-AFOSR-0481-89)
(AD-A264345; AFOSR-93-0254TR) Avail: CASI HC A03/MF A01

This project attained its objectives of developing an animal model to examine the neural mechanisms of attention. The concepts and procedures were successfully produced and resulted in two publications describing the experimental strategy and the results. The last part of the project examined the role of the basal forebrain cholinergic system and its projections to the frontal cortex. This system is important for attention as assessed in the two-choice reaction time task. These results have implications for behavioral, cognitive, and neural descriptions of the mechanisms involved in attention. DTIC

N93-30529# Oak Ridge National Lab., TN.
A VIDEO TRANSMISSION SYSTEM FOR LOW-BANDWIDTH REMOTE DRIVING
F. W. DePiero, T. E. Noell, and T. F. Gee (Georgia Inst. of Tech., Atlanta.) 1993 6 p Presented at the 5th Topical Meeting on Robotics and Remote Systems, Knoxville, TN, 26-29 Apr. 1993
(Contract DE-AC05-84OR-21400)
(DE93-010275; CONF-930403-40) Avail: CASI HC A02/MF A01

Oak Ridge National Laboratory (ORNL) staff have developed a real-time video transmission system for low-bandwidth remote operations. The system supports both continuous transmission of video for remote driving and progressive transmission of still images. Inherent in the system design is a spatiotemporal limitation to the effects of channel errors. The average data rate of the system is 64,000 bits/s, a compression of approximately 1000:1 for the black-and-white National Television Standard Code video. The image quality of the transmissions is maintained at a level that supports the teleoperated driving of a High-Mobility Multipurpose Wheeled Vehicle at speeds of up to 15 mph on a moguled dirt tract. The system also provides video transmissions for a mission package on board the vehicle. The system supports dynamic image quality adjustments that allow the remote driver to adjust to changing scenery and viewing requirements. During driving, the system's nominal configuration had a frame rate of 4 Hz, a compression per frame of 125:1, and a resulting latency of approx. 1s. DOE

N93-30556# Navy Personnel Research and Development Center, San Diego, CA.
INDEPENDENT RESEARCH AND INDEPENDENT EXPLORATORY DEVELOPMENT PROGRAMS Annual Report, Oct. 1991 - Sep. 1992
William E. Montague Apr. 1993 85 p
(AD-A264735; NPRDC-AP-93-4) Avail: CASI HC A05/MF A01

This report documents research efforts conducted at the Navy Personnel Research and Development Center under the Independent Research/Independent Exploratory Development (IR/IED) program. The FY-92 IR program included the following: Brain Mechanisms and Cognition: Advanced Signal Analysis Using the Wavelet Transform; An Exploratory Examination of Artificial Neural Networks as an Alternative to Linear Regression, Artificial Neural Networks and Training; Individual Differences in Information Acquisition and Processing Style; Cognitive Resources, Performance Feedback, and Decision Processes in a Simulated Work Environment; and The Role of Feedback in Computer-Based Training: Follow-On Work. Progress reports on IED projects included: Effects of Administration Method and Anonymity/Identification on Survey Responses; Biodata and Personality: Are They Related?; and Optimal Enlisted Requisition Model. DTIC

N93-30591# SRI International Corp., Menlo Park, CA.
OCEANOGRAPHIC DATA PROCESSING PROGRAM
James F. Arnold and Scott W. Shaw Apr. 1993 35 p
(Contract N00014-92-C-0015)
(AD-A264801; SRI-3047) Avail: CASI HC A03/MF A01

The purpose of the FY92/93 effort was to investigate and, where appropriate, develop and deliver software tools to improve the productivity and quality of oceanographic data interpretation. Specifically, this effort comprised three tasks: Task (1) Research and Develop Methods for Improving the Performance of Automated Outlier Detection. Based on algorithms and software developed by SRI under a previous DMA program, several enhancements were carried out. Task (2) Implement, Document, and Deliver the Improved Outlier Detection Algorithms. Additional modifications were made to support generic multibeam format (GMF) data sets. Task (3) Identify and Evaluate More Advanced Oceanographic Data Analysis Tools. A study was made to determine the data automation needs of the oceanographic community, and then compare these needs to data analysis tools already developed for other scientific application areas. Research indicated that a significant body of relevant techniques has indeed been developed for applications such as robotics, image understanding, and various statistical analysis applications. DTIC

N93-30592# Naval Command, Control and Ocean Surveillance Center, San Diego, CA.
EVOLVING NEURAL NETWORK ARCHITECTURE
John R. McDonnell and Don Waagen Mar. 1993 14 p
(AD-A264802) Avail: CASI HC A03/MF A01

This work investigates the application of a stochastic search technique, evolutionary programming, for developing self-organizing neural networks. The chosen stochastic search method is capable of simultaneously evolving both network architecture and weights. The number of synapses and neurons are incorporated into an objective function so that network parameter optimization is done with respect to computational costs as well as mean pattern error. Experiments are conducted using feedforward networks for simple binary mapping problems. DTIC

N93-30886# Science Applications International Corp., Falls Church, VA.
CENTRALIZED MAINTENANCE EVALUATION Final Report, Aug. 1991 - Sep. 1992
Robert D. Lambert and David D. Sorensen Dec. 1992 72 p
(Contract F30602-91-D-0007)
(AD-A264400; RL-TR-92-329) Avail: CASI HC A04/MF A01

This report documents the Centralized Maintenance Evaluation (CME). The CME was a project to demonstrate and evaluate the generic concept of operations, procedures, requirements, and responsibilities for centralized maintenance support for AN/GYQ-21 (5) Intelligence Data Handling Systems (IDHS). The report documents the technical work accomplished and the information gained during the performance of the CME task. The report includes observations, the nature of problems, positive and negative results, procedures followed, processes developed, and 'lessons learned'. DTIC

N93-30893 Michigan Univ., Ann Arbor.
CONTROL OF NONLINEAR SYSTEMS WITH APPLICATIONS TO CONSTRAINED ROBOTS AND SPACECRAFT ATTITUDE STABILIZATION Ph.D. Thesis
Hariharan Krishnan 1992 217 p
Avail: Univ. Microfilms Order No. DA9308365

Control systems described by a class of nonlinear differential and algebraic equations are introduced. A procedure for local stabilization based on a local state realization is developed. An alternative approach to local stabilization is developed based on a classical linearization of the nonlinear differential-algebraic equations. A theoretical framework is established for solving a tracking problem associated with the differential-algebraic system. First, a simple procedure is developed for the design of a feedback control law which ensures, at least locally, that the tracking error in the closed loop system lies within any given bound if the reference inputs are sufficiently slowly varying. Next, by imposing additional assumptions a procedure is developed for the design of a feedback control law which ensures that the tracking error in the closed loop system approaches zero exponentially for reference inputs which are not necessarily slowly varying. The control design methodologies are used for simultaneous force and position control in constrained robot systems. The differential-algebraic equations are shown to characterize the slow dynamics of a certain nonlinear control system in nonstandard singularly perturbed form. The attitude stabilization (reorientation) of a rigid spacecraft using only two control torques is considered. First, the case of momentum wheel actuators is considered. The complete spacecraft dynamics are not controllable. However, the spacecraft dynamics are small time locally controllable in a reduced sense. The reduced spacecraft dynamics cannot be asymptotically stabilized using continuous feedback, but a discontinuous feedback control strategy is constructed. Next, the case of gas jet actuators is considered. If the uncontrolled principal axis is not an axis of symmetry, the complete spacecraft dynamics are small time locally controllable. However, the spacecraft attitude cannot be asymptotically stabilized using continuous feedback, but a discontinuous stabilizing feedback control strategy is constructed. If the uncontrolled principal axis is an axis of symmetry, the complete spacecraft dynamics cannot be stabilized. However, the spacecraft dynamics are small time locally controllable in a reduced sense. The reduced spacecraft dynamics cannot be asymptotically stabilized using continuous feedback, but again a discontinuous feedback control strategy is constructed. Dissert. Abstr.

N93-30903 Michigan Univ., Ann Arbor.
ADAPTIVE MOTION CONTROL OF MOBILE ROBOTS Ph.D. Thesis
Liqiang Feng 1992 172 p
Avail: Univ. Microfilms Order No. DA9308310

Three topics related to mobile robot motion control are discussed. A hybrid opto-electronic processor is developed to provide the absolute robot motion information. A cross-coupling controller is used to coordinate the motion of different control loops. An adaptive motion controller is used to compensate for the external motion errors. A method that determines the absolute position of a mobile robot with a hybrid opto-electronic processor was developed. Position estimates are based on an analysis of circular landmarks that are detected by a TV camera attached to a mobile robot. For robust operation, the parameters of the landmark image are extracted at high speeds using an optical Hough Transform processor. The coordinates of the mobile robot are then computed. Different sources of position estimation errors were also analyzed, and consequent algorithms to improve the navigation performance of the mobile robot were developed and evaluated by both computer simulation and experiments to provide good performance. Cross-coupling control is used to coordinate the motion of different drive loops, which results in only small position and orientation errors. The cross-coupling controller has excellent disturbance rejection and, therefore, is advantageous when the robot is not loaded symmetrically or travels at high speed. The cross-coupling controller is analyzed and experiments are conducted to evaluate its performance. The experimental results show accuracy improvements over conventional controllers, especially in compensating for orientation error caused by the internal error sources. A model reference adaptive motion controller is designed and built for a differential-drive mobile robot. The controller uses absolute robot motion information to modify the control parameters in real time and, in turn, to compensate for the motion errors. The cross-coupling control method is used to compensate for the internal errors that can be detected by the wheel encoders. The adaptive controller provides compensation for the external errors. The adaptive controller is analyzed, and the stability and convergence are discussed. Both computer simulation and experiments are conducted to evaluate the control system. The results show significant improvements over the conventional controller. Dissert. Abstr.

N93-31029 Notre Dame Univ., IN.
STRUCTURAL DESIGN USING NEURAL NETWORKS Ph.D. Thesis
Richard Alan Swift 1993 208 p
Avail: Univ. Microfilms Order No. DA9308230

At the early stages of design, it is necessary to obtain an understanding of the design space characteristics for the structural concepts under consideration. This involves developing a representation of the structural system's behavior to variations in the design variables of interest. The effort was to efficiently obtain both qualitative and quantitative structural design space mappings for use in preliminary design studies. Recent advances in finite element based structural optimization techniques provide the means to address this concern, but these approaches typically involve the determination of 'points' in the design space, rather than a mapping of the design space. Neural networks, mathematical models of biologically occurring neural systems, were employed to quantify the design space representations. The neural networks form the representation of the design space based on a set of optimal designs obtained from math-programming and fully-stressed design optimization programs. Feed-forward, back propagation neural networks were used to form the design space representation. The neural network representations were then used to ascertain trends in the design space, and the neural networks were also 'searched' using various optimization procedures to define those regions of the design space that showed the most promising design characteristics. Math-programming techniques and simulated annealing procedures were employed to perform the searches of the design spaces. Recursive learning was explored to minimize the amount of training data necessary (training data generation being the most computationally expensive part of the neural network procedure). Continuous as well as discrete design variables were examined. The continuous design variable cases involved configurations design, while the discrete design variable cases involved material selection. Planar trusses, a 3-D space truss, and three semi-monocoque wings were used to describe the implementation of the neural network procedure. The results obtained from these models show that the design spaces are effectively represented by the neural networks. The neural networks also provide the means to determine significantly improved designs, with reductions in objective function values of over 10 percent noted for several cases. The neural network approach to design space representation appears to hold promise to a wide range of structural design problems.
Dissert. Abstr.

N93-29522*# Texas A&M Univ., College Station. Center for Fuzzy Logic and Intelligent Systems.
APPROXIMATE REASONING USING TERMINOLOGICAL MODELS
John Yen and Nitin Vaidya (Texas A&M Univ., Houston.) *In* NASA. Johnson Space Center, North American Fuzzy Logic Processing Society (NAFIPS 1992), Volume 1 Dec. 1992 p 39-48 (For primary document see N93-29516 11-59)
Avail: CASI HC A02/MF A03

N93-29534*# National Aeronautics and Space Administration. Lyndon B. Johnson Space Center, Houston, TX.
LEARNING CHARACTERISTICS OF A SPACE-TIME NEURAL NETWORK AS A TETHER SKIPROPE OBSERVER
Robert N. Lea, James A. Villarreal, Yashvant Jani (Togai InfraLogic, Inc., Houston, TX.), and Charles Copeland (Loral Space Information Systems, Houston, TX.) *In its* North American Fuzzy Logic Processing Society (NAFIPS 1992), Volume 1 Dec. 1992 p 154-165 (For primary document see N93-29516 11-59)
Avail: CASI HC A03/MF A03

N93-29536*# North Carolina Univ., Charlotte. Dept. of Computer Science.
CHARACTER RECOGNITION USING A NEURAL NETWORK MODEL WITH FUZZY REPRESENTATION
Nassrin Tavakoli and David Seniw *In* NASA. Johnson Space Center, North American Fuzzy Logic Processing Society (NAFIPS 1992), Volume 1 Dec. 1992 p 175-184 (For primary document see N93-29516 11-59)
Avail: CASI HC A02/MF A03

N93-29545*# Missouri Univ., Columbia. Dept. of Electrical and Computer Engineering.
COMPARISON OF CRISP AND FUZZY CHARACTER NETWORKS IN HANDWRITTEN WORD RECOGNITION
Paul Gader, Magdi Mohamed, and Jung-Hsien Chiang *In* NASA. Johnson Space Center, North American Fuzzy Logic Processing Society (NAFIPS 1992), Volume 1 Dec. 1992 p 257-265 Sponsored in part by Environmental Research Inst. of Michigan and Postal Service (For primary document see N93-29516 11-59)
Avail: CASI HC A02/MF A03

N93-29575*# California State Univ., Fresno.
INCORPORATION OF VARYING TYPES OF TEMPORAL DATA IN A NEURAL NETWORK
M. E. Cohen and D. L. Hudson (California Univ., San Francisco.) *In* NASA. Johnson Space Center, North American Fuzzy Logic Processing Society (NAFIPS 1992), Volume 2 Dec. 1992 p 535-544 (For primary document see N93-29556 11-59)
Avail: CASI HC A02/MF A03

N93-29577*# Moravian Coll., Bethlehem, PA. Dept. of Mathematics.
NEURAL NETWORKS: A SIMULATION TECHNIQUE UNDER UNCERTAINTY CONDITIONS
M. Luisa Nicosia McAllister *In* NASA. Johnson Space Center, North American Fuzzy Logic Processing Society (NAFIPS 1992), Volume 2 Dec. 1992 p 555-564 (For primary document see N93-29556 11-59)
Avail: CASI HC A02/MF A03

N93-29579*# Institutul Politehnic din Iasi (Romania).
STOCHASTIC ARCHITECTURE FOR HOPFIELD NEURAL NETS
Sandy Pavel *In* NASA. Johnson Space Center, North American Fuzzy Logic Processing Society (NAFIPS 1992), Volume 2 Dec. 1992 p 575-580 (For primary document see N93-29556 11-59)
Avail: CASI HC A02/MF A03

N93-30216 Queens Univ., Kingston (Ontario). Dept. of Electrical Engineering.
ROBUST CONTROL VIA H-INFINITY OPTIMIZATION
J. R. Sveinsson and F. W. Fairman *In* Engineering Inst. of Canada, Canadian Conference on Electrical and Computer Engineering, Volumes 1 and 2 1990 3 p (For primary document see N93-30215 11-31)
Avail: Engineering Inst. of Canada, 2050 rue Mansfield, Suite 700, Montreal, Quebec H3A 1Z2 Canada

N93-30217 Quality Management Control, Inc., Ottawa (Ontario).
CONTROL SYSTEM DESIGN AND MULTIPARAMETER VARIATIONS
James Morris Overton *In* Engineering Inst. of Canada, Canadian Conference on Electrical and Computer Engineering, Volumes 1 and 2 1990 4 p (For primary document see N93-30215 11-31)
Avail: Engineering Inst. of Canada, 2050 rue Mansfield, Suite 700, Montreal, Quebec H3A 1Z2 Canada

N93-30218 Victoria Univ. (British Columbia). Dept. of Electrical and Computer Engineering.
A CLOSED-FORM FORMULA FOR THE MANIPULATOR REGRESSOR
W.-S. Lu and Q.-H. Meng *In* Engineering Inst. of Canada, Canadian Conference on Electrical and Computer Engineering, Volumes 1 and 2 1990 4 p (For primary document see N93-30215 11-31)
Avail: Engineering Inst. of Canada, 2050 rue Mansfield, Suite 700, Montreal, Quebec H3A 1Z2 Canada

N93-30233 McMaster Univ., Hamilton (Ontario). Dept. of Electrical and Computer Engineering.
DIVISION BY POLYNOMIAL MATRIX AND ITS APPLICATION TO MULTIVARIABLE LINEAR SYSTEMS
Jianguo Fu and N. K. Sinha *In* Engineering Inst. of Canada, Canadian Conference on Electrical and Computer Engineering, Volumes 1 and 2 1990 3 p (For primary document see N93-30215 11-31)
Avail: Engineering Inst. of Canada, 2050 rue Mansfield, Suite 700, Montreal, Quebec H3A 1Z2 Canada

N93-30247 Quebec Univ., Montreal. Dept. of Mathematics and Computer Science.
AN INFORMATION THEORETIC APPROACH TO STOCHASTIC ADAPTIVE CONTROL APPLICATION TO MANIPULATORS WITH ACTIVE INERTIA
Guy Jumarie *In* Engineering Inst. of Canada, Canadian Conference on Electrical and Computer Engineering, Volumes 1 and 2 1990 4 p (For primary document see N93-30215 11-31)
Avail: Engineering Inst. of Canada, 2050 rue Mansfield, Suite 700, Montreal, Quebec H3A 1Z2 Canada

N93-30248 Nova Scotia Technical Coll., Halifax.
AN ADAPTIVE CONTROLLER FOR A CLASS OF MIMO NON-MINIMUM PHASE SYSTEMS WITH DISTURBANCE REJECTION DESIGN
X. Li and C. R. Baird *In* Engineering Inst. of Canada, Canadian Conference on Electrical and Computer Engineering, Volumes 1 and 2 1990 4 p (For primary document see N93-30215 11-31)
Avail: Engineering Inst. of Canada, 2050 rue Mansfield, Suite 700, Montreal, Quebec H3A 1Z2 Canada

N93-30278 Queens Univ., Kingston (Ontario). Dept. of Electrical Engineering.
TASK ALLOCATION AND REAL-TIME CONSIDERATIONS FOR THE ROBOT CONTROLLER TEST STATION (RCTS)
R. Allard, M. A. Ramsay, and M. M. Bayoumi *In* Engineering Inst. of Canada, Canadian Conference on Electrical and Computer Engineering, Volumes 1 and 2 1990 4 p (For primary document see N93-30215 11-31)
Avail: Engineering Inst. of Canada, 2050 rue Mansfield, Suite 700, Montreal, Quebec H3A 1Z2 Canada

N93-30326 National Research Council of Canada, Ottawa (Ontario). Inst. for Information Technology.
SUPERVISED AUTONOMY IN TELEROBOTICS
N. Burtnyk and J. Basran (Ottawa Univ., Ontario.) *In* Engineering Inst. of Canada, Canadian Conference on Electrical and Computer Engineering, Volumes 1 and 2 1990 7 p (For primary document see N93-30215 11-31)
Avail: Engineering Inst. of Canada, 2050 rue Mansfield, Suite 700, Montreal, Quebec H3A 1Z2 Canada

64 NUMERICAL ANALYSIS

Includes iteration, difference equations, and numerical approximation.

N93-28466# Technische Hochschule, Darmstadt (Germany). Fachbereich Informatik.
TOPOLOGY OF HYBRID OBJECTS Ph.D. Thesis [TOPOLOGIE VON HYBRIDEN OBJEKTEN]
Shin-Ting Wu 1991 204 p In GERMAN Sponsored by Coordenacao de Aperfeicoamento de Pessoal de Nivel Superior, Brazil LIMITED REPRODUCIBILITY: More than 20% of this document may be affected by microfiche quality
(ETN-93-93594) Avail: CASI HC A10

The role of algebraic topology in geometric modeling is explored, with particular consideration to the uniform handling of both manifold and nonmanifold classes of geometrical objects in the boundary based modeling systems. A conceptual data model is achieved for depicting the structural relationships between the topological entities of geometrical objects. A set of basic operators is constructed to uniquely define these relationships, so that they insulate the application dependent functionalities from the underlying data structure. An underlying data structure for storing the complex boundary and adjacency relationships between the topological properties is designed. Basic algorithms are created for extracting useful topological properties of geometrical objects from the proposed data structure, such as determination of sectors separated by two oriented surfaces, estimation of a chain of topological primitives between two corners, estimation of the formation of a cyclic succession of surfaces by addition of a new surface, and demonstration of the orientability of an object. An example of implementation of operators, data structure and algorithms in the interactive, geometrical modeller Phoenix designed for graphic data processing, is presented. ESA

N93-28509# Institut National de Recherche d'Informatique et d'Automatique, Valbonne (France). Programme 6: Calcul Scientifique, Modelisation et Logiciels Numeriques par Ordinateur.
UPWIND FINITE ELEMENT SCHEMES FOR SOLVING THE MAXWELL EQUATIONS [APPROXIMATION DES EQUATIONS DE MAXWELL PAR DES SCHEMAS DECENTRES EN ELEMENTS FINIS]
Jean-Pierre Cioni, Loula Fezoui, and Herve Steve Feb. 1992 48 p In FRENCH
(INRIA-RR-1601; ETN-93-93889) Avail: CASI HC A03/MF A01

A finite volume/finite element mixed approach, largely used in computational fluid dynamics, is applied here to solve numerically the time dependent Maxwell system. The scheme used is third order accurate both in time and space. Particular concern is given to the simulation of bidimensional scattering problems, in the case of linear material and homogeneous media. ESA

N93-28511# Institut National de Recherche d'Informatique et d'Automatique, Valbonne (France). Programme 4: Robotique, Image et Vision.

ROBUST AND EFFICIENT IMPLEMENTATION OF THE DELAUNAY TREE

Olivier Devilliers Feb. 1992 14 p Sponsored by EEC
(INRIA-RR-1619; ETN-93-03891) Avail: CASI HC A03/MF A01

Some practical results concerning the implementation of the algorithm which computes dynamically the Delaunay triangulation of a set of sites in the plane in logarithmic expected update time are presented. More precisely, the hypotheses of non degenerate positions can be dropped and the problem of precisions can be treated correctly. ESA

N93-28512# Institut National de Recherche d'Informatique et d'Automatique, Valbonne (France). Programme 4: Robotique, Image et Vision.

THE SPACE OF SPHERES, A GEOMETRIC TOOL TO UNIFY DUALITY RESULTS IN VORONOI DIAGRAMS

Olivier Devilliers, Stefan Meiser (Max-Planck-Inst. fuer Informatik, Saarbruecken, Germany.), and Monique Teillaud Feb. 1992 34 p Sponsored in part by EEC
(INRIA-RR-1620; ETN-93-93892) Avail: CASI HC A03/MF A01

A framework that allows the easy derivation of transformations for various kinds of Voronoi and Power diagrams including kth order and weighted versions is presented. All proofs are essentially geometric and require no analytic calculations. Some new algorithms can be presented in special cases. ESA

N93-28513# Institut National de Recherche d'Informatique et d'Automatique, Valbonne (France). Programme 4: Robotique, Image et Vision.

POLYGONAL APPROXIMATION OVERVIEWS AND PERSPECTIVES [L'APPROXIMATION POLYGONALE BILANS ET PERSPECTIVES]

Philippe Garnesson and Gerard Giraudon Feb. 1992 61 p In FRENCH
(INRIA-RR-1621; ETN-93-93893) Avail: CASI HC A04/MF A01

Polygonal approximation is the transformation of linked edge point into a sequence of line segments. In computer vision, polygonal approximation is a standard task; it is even unavoidable if geometric characteristics of objects must be considered. Different criteria, sometimes inconsistent within themselves, which are used in polygonal approximation are presented and the field of present methods is reviewed. An approach based on the minimization of an energy along the linked edge points is proposed. This energy is based on the maximum distance between the line segments and the linked edge points and on the sum of these distances. Using many examples, the interest of the appproach is illustrated through objective tests (demonstrating for example invariance in rotation or with a mask) and through subjective tests showing geometric shape preservation (such as angles) and the influence of noise. ESA

N93-28524# Technische Hochschule, Darmstadt (Germany). Fachbereich Mathematik.

LIE GROUPS WHOSE SET OF COMPACT SUBGROUPS IS INDUCTIVE Ph.D. Thesis

Christian Terp 1991 73 p Sponsored by Studienstiftung des Deutschen Volkes
(ETN-93-93791) Avail: CASI HC A04/MF A01

A set k of compact subgroups of a locally compact group is addressed. Those groups which have inductive k, where k is partially ordered by set inclusion, are of interest. Characterizations for these groups are given. The classification of dicrete k inductive groups is addressed. ESA

N93-28527# Technische Univ., Berlin (Germany). Fachbereich Mathematik.

PACKING OF STEINER TREES: POLYHEDRIC STUDIES AND APPLICATION Ph.D. Thesis [PACKEN VON STEINERBAEUMEN: POLYEDRISCHE STUDIEN UND ANWENDUNG]

Alexander Martin 1992 196 p In GERMAN
(ETN-93-93796) Avail: CASI HC A09/MF A03

A formulation to solve the Steiner tree packing problem, by means of graph theory, linear algebra polyhedra theory, and linear programming is developed. The connectivity problem in very large scale integration design, and plane, Manhattan, and knock knee models are presented. Some algorithms for switch box connectivity, such as multicommodity flows in graphs are proposed. Canonic, facet based, and explicit formulation of arborescence polyhedra were examined. The chosen polyhedron was defined as the convex hull of all incidence vectors of Steiner tree packings of a given instance of the problem. A cutting plane algorithm to solve inequalities for polyhedron facet definition with a branch and cut process was developed. Partitioning procedures were realized to solve the separation problem inequalities. The method was applied to problems for the literature. ESA

N93-28615*# Institut National de Recherche d'Informatique et d'Automatique, Valbonne (France). Programme 6: Calcul Scientifique, Modelisation et Logiciels Numeriques par Ordinateur.

DESIGN OF AN ESSENTIALLY NON-OSCILLATORY RECONSTRUCTION PROCEDURE IN FINITE-ELEMENT TYPE MESHES

Remi Abgrall Jan. 1992 51 p
(Contract NAS1-8605)
(INRIA-RR-1584; ETN-93-93844) Avail: CASI HC A04/MF A01

An essentially non oscillatory reconstruction for functions defined on finite element type meshes is designed. Two related problems are studied: the interpolation of possibly unsmooth multivariate functions on arbitary meshes and the reconstruction of a function from its averages in the control volumes surrounding the nodes of the mesh. Concerning the first problem, the behavior of the highest coefficients of two polynomial interpolations of a function that may admit discontinuities of locally regular curves is studied: the Lagrange interpolation and an approximation such that the mean of the polynomial on any control volume is equal to that of the function to be approximated. This enables the best stencil for the approximation to be chosen. The choice of the smallest possible number of stencils is addressed. Concerning the reconstruction problem, two methods were studied: one based on an adaptation of the so called reconstruction via deconvolution method to irregular meshes and one that lies on the approximation on the mean as defined above. The first method is conservative up to a quadrature formula and the second one is exactly conservative. The two methods have the expected order of accuracy, but the second one is much less expensive than the first one. Some numerical examples are given which demonstrate the efficiency of the reconstruction. ESA

N93-28616# Institut National de Recherche d'Informatique et d'Automatique, Valbonne (France). Programme 4: Robotique, Image et Vision.

THREE DIMENSIONAL RECONSTRUCTION OF COMPLEX SHAPES BASED ON THE DELAUNAY TRIANGULATION

Jean-Daniel Boissonnat and Bernhard Geiger May 1992 23 p
(INRIA-RR-1697; ETN-93-93909) Avail: CASI HC A03/MF A01

A solution to the problem of three dimensional reconstruction from cross sections, based on Delaunay triangulation of object contours, is proposed. Its properties, especially the close relationship to the medial axis, enable a compact tetrahedrization resulting in a nearest neighbor connection to be carried out. The reconstruction of complex shapes is improved by adding vertices on and inside contours. ESA

N93-28648# California Univ., Berkeley. Dept. of Mathematics.

STABILITY, BIFURCATION, AND CONTROL OF HAMILTONIAN SYSTEMS

J. E. Marsden and T. S. Ratiu 1993 10 p
(Contract DE-FG03-92ER-25129)
(DE93-012103; DOE/ER-25129/T1) Avail: CASI HC A02/MF A01

Work is being done on dissipation-induced instabilities, gyroscopic stabilization, and its destruction by a small damping for both finite dimensional and certain infinite dimensional systems (such as rotating rods, strings), nonabelian and abelian cases, Euler-Lagrange-Poincare equations, the Routhian having a form of a Lagrangian with a gyroscopic term, Euler-Lagrange equations, etc. DOE

N93-28667# Universiteit Twente, Enschede (Netherlands). Dept. of Applied Mathematics.

DEFORMATIONS OF THE LIE ALGEBRAS L1(H(2)) AND L1(W(2))

Nico vandenHijligenberg, Youri Kotchetkov (Moscow Inst. of New Technologies, Russia.), and Gerhard Post May 1992 12 p
(MEMO-1056; ETN-93-93841) Avail: CASI HC A03/MF A01

For the Lie algebras L1(H(2)) and L1(W(2)), infinitesimal deformations and the corresponding global ones are studied. It is shown that, as in the case of L1(W(1)), all infinitesimal deformations of L1(H(2)) and L1(W(2)) that are extendable to global deformations can be extended by means of a trivial prolongation. It is also deduced that all deformations of L1(H(2)) arise as restrictions of deformations of L1(W(2)) to L1(H(2)). ESA

N93-28671 Syracuse Univ., NY.
AN ALGEBRAIC APPROACH TO THE QUANTIZATION OF CONSTRAINED SYSTEMS: FINITE DIMENSIONAL EXAMPLES Ph.D. Thesis
Ranjeet Shekhar Tate 1992 162 p
Avail: Univ. Microfilms Order No. DA9308943

General relativity has two features in particular, which make it difficult to apply to it existing schemes for the quantization of constrained systems. First, there is no background structure in the theory, which could be used, e.g., to regularize constraint operators, to identify a 'time', or to define an inner product on physical states. Second, in the Ashtekar formulation of general relativity, which is a promising avenue to quantum gravity, the natural variables for quantization are not canonical; and, classically, there are algebraic identities between them. Existing schemes are usually not concerned with such identities. Thus, from the point of view of canonical quantum gravity, it has become imperative to find a framework for quantization which provides a general prescription to find the physical inner product, and is flexible enough to accommodate non-canonical variables. I present an algebraic formulation of the Dirac approach to the quantization of constrained systems. The Dirac quantization program is augmented by a general principle to find the inner product on physical states. Essentially, the Hermiticity conditions on physical operators determine this inner product. I also clarify the role in quantum theory of possible algebraic identities between the elementary variables. I use this approach to quantize various finite dimensional systems. Some of these models test the new aspects of the algebraic framework. Others bear qualitative similarities to general relativity, and may give some insight into the pitfalls lurking in quantum gravity. The previous quantizations of one such model had many surprising features. When this model is quantized using the algebraic program, there is no longer any unexpected behavior. I also construct the complete quantum theory for a previously unsolved relativistic cosmology. All these models indicate that the algebraic formulation provides powerful new tools for quantizations. In (spatially compact) general relativity, the Hamiltonian is constrained to vanish. I present various approaches one can take to obtain an interpretation of the quantum theory of such 'dynamically constrained' systems. I apply some of these ideas to the Bianchi 1 cosmology, and analyze the issue of the initial singularity in quantum theory. Author (revised)

N93-28753# Groningen Rijksuniv. (Netherlands). Dept. of Mathematics.
A NORMALLY ELLIPTIC HAMILTONIAN BIFURCATION
Henk Broer, Shui-Nee Chow (Georgia Inst. of Tech., Atlanta.), and Yong-In Kim (Ulsan Univ., Republic of Korea.) 1992 30 p
(W-9201; ETN-93-93330) Avail: CASI HC A03/MF A01

A universal local bifurcation analysis is presented of an autonomous Hamiltonian system around a certain equilibrium point. This central equilibrium has a double zero eigenvalue; the other eigenvalues being in general position. Main emphasis is given to the two degrees of freedom case where these other eigenvalues are purely imaginary. By normal form techniques and singularity theory unfoldings are obtained, having 'integrable' approximations related to the elliptic and hyperbolic umbilic catastrophes. ESA

N93-28754# Oxford Univ. (England). Dept. of Engineering Science.
BALANCED APPROXIMATION CAN BE OPTIMAL
D. Mustafa and T. N. Davidson 1 Sep. 1992 11 p Submitted for publication Sponsored by Rhodes Trust
(OUEL-1950/92; ETN-93-93879) Avail: CASI HC A03/MF A01

A study showing that by example there exist systems whose balanced approximations are optimal is presented. Specifically, for various norms including the Hankel norm and the L2 norm, it is shown that the approximation error can achieve the minimum possible. ESA

N93-28891# Brookhaven National Lab., Upton, NY.
BENCHMARK EIGENVALUE SPECTRUM CALCULATIONS WITH ANISOTROPIC EFFECTS
P. Kohut 1993 6 p Presented at the 4th International Conference on Simulation Methods in Nuclear Engineering, Montreal, Quebec, 2-4 Jun. 1993
(Contract DE-AC02-76CH-00016)
(DE93-006387; BNL-48228; CONF-930651-1) Avail: CASI HC A02/MF A01

Complete eigenvalue spectrum calculations are usually performed for benchmark analysis to compare the accuracy of various approximate methods. In one-speed criticality studies the most accurate methods either rely on analytical techniques (singular eigenfunction) or high order spatial expansion (Carlvik's method). The extension of these techniques to calculate higher order anisotropy is somewhat cumbersome and rarely done in practice. In this paper, a low spatial order technique is examined for its capability to produce accurate benchmark results with higher order of anisotropy. In the past, the use of low order methods were generally discarded for this type of calculation due to the large computer memory and time requirements. With the recent development and availability of greatly improved computing power, these limitations are largely removed and low order spatial approximations may also produce accurate solutions. DOE

N93-28973*# Texas Univ., El Paso.
UNCERTAINTY REASONING IN EXPERT SYSTEMS Final Technical Report, 1 Sep. 1990 - 31 Mar. 1993
Vladik Kreinovich 31 Mar. 1993 19 p
(Grant NAG9-482)
(NASA-CR-193120; NAS 1.26:193120) Avail: CASI HC A03/MF A01

Intelligent control is a very successful way to transform the expert's knowledge of the type 'if the velocity is big and the distance from the object is small, hit the brakes and decelerate as fast as possible' into an actual control. To apply this transformation, one must choose appropriate methods for reasoning with uncertainty, i.e., one must: (1) choose the representation for words like 'small', 'big'; (2) choose operations corresponding to 'and' and 'or'; (3) choose a method that transforms the resulting uncertain control recommendations into a precise control strategy. The wrong choice can drastically affect the quality of the resulting control, so the problem of choosing the right procedure is very important. From a mathematical viewpoint these choice problems correspond to non-linear optimization and are therefore extremely difficult. In this project, a new mathematical formalism (based on group theory) is developed that allows us to solve the problem of optimal choice and thus: (1) explain why the existing choices are really the best (in some situations); (2) explain a rather mysterious fact that fuzzy control (i.e., control based on the experts' knowledge) is often better than the control by these same experts; and (3) give choice recommendations for the cases when traditional choices do not work. Author (revised)

N93-29024# Royal Inst. of Tech., Stockholm (Sweden). Dept. of Numerical Analysis and Computing Science.
A MULTIGRID EXTENSION OF THE FFT FOR THE NUMERICAL INVERSION OF FOURIER AND LAPLACE TRANSFORMS
Germund Dahlquist 1991 28 p
(TRITA-NA-9204) Avail: CASI HC A03/MF A01

An algorithm for accurate numerical inversion of slowly convergent Fourier and Laplace Transforms is studied. It makes use of several equidistant grids with the same number of points, covering different symmetric intervals of the time and frequency axes. Author

N93-29057# Society for Industrial and Applied Mathematics, Philadelphia, PA.
SIAM CONFERENCE ON APPLICATIONS OF DYNAMICAL SYSTEMS
1992 84 p Conference held in Snowbird, UT, 15-19 Oct. 1992
(Contract DE-FG02-92ER-25146)
(DE93-007969; DOE/ER-25146/1; CONF-9210317-Absts) Avail: CASI HC A05/MF A01

A conference (15-19 Oct. 1992, Snowbird, Utah; sponsored by SIAM (Society for Industrial and Applied Mathematics) Activity Group on Dynamical Systems) was held that highlighted recent developments in applied dynamical systems. The main lectures and minisymposia covered theory about chaotic motion, applications in high energy physics and heart fibrillations, turbulent motion, Henon map and attractor, integrable problems in classical physics, pattern formation in chemical reactions, etc. The conference fostered an exchange between mathematicians working on theoretical issues of modern dynamical systems and applied scientists. This two-part document contains abstracts, a conference program, and an author index. DOE

N93-29060# Lawrence Livermore National Lab., CA.
INDEX MAPPINGS FOR INTERACTIVE EDITING OF SYMBOLIC MATRICES
J. F. Painter May 1992 8 p Presented at the 7th International Association of Mathematics and Computer Simulation (IMACS) International Conference on Computer Methods for Partial Differential Equations, New Brunswick, NJ, 22-24 Jun. 1992
(Contract W-7405-eng-48)
(DE93-009316; UCRL-JC-110700; CONF-9206185-11) Avail: CASI HC A02/MF A01

ALPAL is a program which automatically generates code to solve nonlinear partial differential equations and other problems. The ALPAL user specifies the equations to be solved and their numerical methods at a very high level of abstraction. When equations are solved by implicit methods, the solution involves Jacobian matrices. The Matrix Editor is a graphical, interactive tool that lets the ALPAL user specify how the generated code should store matrices and solve linear equations. At the heart of the Matrix Editor lies a set of functions which map between symbolic expressions for different indices which represent a matrix in different ways. This paper discusses how the Matrix Editor constructs these functions. DOE

N93-29187# Sandia National Labs., Albuquerque, NM.
ABLATION PROBLEMS USING A FINITE CONTROL VOLUME TECHNIQUE
B. F. Blackwell, A. L. Thornton, and R. E. Hogan 1993 8 p Presented at the Moving Boundaries 1993: Computational Modeling of Free and Moving Boundary Problems, Milan, Italy, 23-25 Jun. 1993
(Contract DE-AC04-76DP-00789)
(DE93-009861; SAND-93-0284C; CONF-9306128-1) Avail: CASI HC A02/MF A01

An element based finite control volume procedure is applied to the solution of ablation problems for 2-D axisymmetric geometries. A mesh consisting of four node quadrilateral elements was used. The nodes are allowed to move in response to the surface recession rate. The computational domain is divided into a region with a structured mesh with moving nodes and a region with an unstructured mesh with stationary nodes. The mesh is constrained to move along spines associated with the original mesh. Example problems are presented for the ablation of a realistic nose tip geometry exposed to aerodynamic heating from a uniform free stream environment. DOE

N93-29413# Stanford Univ., CA. Dept. of Statistics.
PARAMETRIC LIKELIHOOD INFERENCE FOR RECORD BREAKING PROBLEMS Technical Report
Bradley P. Carlin and Alan E. Gelfand 9 Mar. 1993 28 p
(Contract N00014-92-J-1264)
(AD-A262546; TR-465) Avail: CASI HC A03/MF A01

In this paper we consider the analysis of record breaking datasets, where only observations that exceed the current extreme value are recorded. Examples of application areas leading to data of this type include industrial stress testing, meteorological analysis, sporting and athletic events, and oil and mining surveys. The inherent missing data structure present in such problems leads to likelihood functions that contain possibly high-dimensional integrals, thus rendering traditional maximum likelihood methods difficult or infeasible. Fortunately, we may obtain arbitrarily accurate approximations to the likelihood function by iteratively applying Monte Carlo integration methods. Subiteration using the Gibbs sampler may help to evaluate any multivariate integrals encountered during this process. This approach enables a far more sophisticated set of parametric models than have been applied previously in record breaking contexts. In particular, we illustrate the methodology for a wide array of discrete and continuous distributional settings, and for observations that may be correlated and subject to mean shifts over time. Related issues in model selection and prediction are also addressed. Finally, we present two numerical examples. The first uses a generated dataset exhibiting a high degree of autocorrelation, while the second involves records in the Olympic high jump competition. DTIC

N93-29769# Los Alamos National Lab., NM.
A FUNCTIONAL IMPLEMENTATION OF THE JACOBI EIGEN-SOLVER
A. P. W. Boehm (Colorado State Univ., Fort Collins.) and R. E. Hiromoto 1993 9 p Presented at the Conference on Functional Programming Language and Computer Architectures, Copenhagen, 9-11 Jun. 1993
(Contract W-7405-eng-36; NSF MIP-91-13268)
(DE93-007349; LA-UR-93-298; CONF-9306102-1) Avail: CASI HC A02/MF A01

The systematic development of two implementations of the Jacobi eigen-solver are described and performance results for the MIT/Motorola Monsoon dataflow machine are given. Our study is carried out using MINT, the MIT Monsoon simulator. The design of these implementations follows from the mathematics of the Jacobi method, and not from a translation of an existing sequential code. The functional semantics with respect to array updates, which cause excessive array copying, has lead us to a new implementation of a parallel 'group-rotations' algorithm first described by Sameh. Our version of this algorithm requires O(n(sup 3)) operations, whereas Sameh's original version requires O(n(sup 4)) operations. The implementations are programmed in the language Id, and although Id has non-functional features, the development of our eigen-solvers was restricted to the functional sub-set of the language. DOE

N93-29849# Center for Mathematics and Computer Science, Amsterdam (Netherlands). Dept. of Operations Research, Statistics, and System Theory.
PACKING ODD PATHS
A. Schrijver (Amsterdam Univ., Netherlands.) and P. D. Seymour (Bell Communications Research, Inc., Morristown, NJ.) Apr. 1992 14 p
(CWI-BS-R9207; ETN-93-93247) Copyright Avail: CASI HC A03/MF A01

Let (s,t) be vertices of a graph G, and let each edge e have a 'capacity' c(e) which belongs to the set R(sub +). It is demonstrated that for every k belonging to R(sub +) the following statements are equivalent: there is a 'fractional packing' of value k of the odd s-t paths, so that no edge is used more than its capacity; and for every subgraph Hof G with (s,t) pertaining to V(H) in which there no odd s-t path, summation sign (v belonging to V(H)) summation sign (c(e): e belongs to E(G)-E(H), and e is incident with v) greater than or equal to 2K. ESA

N93-29854# Florida State Univ., Tallahassee. Dept. of Statistics.
MIXED LIMIT THEOREMS FOR PATTERN ANALYSIS
Ulf Grenander and Jayaram Sethuraman Feb. 1993 17 p
(Contract DAAL03-90-G-0103)
(AD-A263735; FSU-R-885; ARO-27868.25-MA) Avail: CASI HC A03/MF A01

Limit theorems are derived for probability measures of random configurations over graphs which are used as prior distributions in pattern theory. For one-dimensional graphs, these limits can be viewed as distributions of certain stochastic processes, while in higher dimensions the limits will in some cases have to be interpreted as belonging to Schwartz distributions. Such limit distributions are easy to use in pattern analysis and greatly reduce the computing effort required in comparison with stochastic relaxation methods. DTIC

N93-29871# Brown Univ., Providence, RI. Inst. for Brain and Neural Systems.
COMPUTATION AND GENERALIZATION IN NEURAL NETWORKS Final Report, 1 Jul. 1988 - 30 Jun. 1991
Leon N. Cooper 5 May 1993 4 p
(Contract DAAL03-88-K-0116)
(AD-A263752; ARO-25515.3-LS) Avail: CASI HC A01/MF A01

During this contract period, our research into backward propagation has led to a number of new theoretical and empirical results. We have developed a generalized version of backward propagation. In our generalized network, both gains and synapses are modified by a backward propagation procedure. Synapses are modified in proportion to the negative gradient of the energy with respect to the synaptic weight as in ordinary backward propagation, and gains are modified in proportion to the negative partial derivative with respect to gain. Since the resulting error signals for the gain and synaptic weights are proportional to one another, the computational complexity of our generalized network is comparable to that of the original backward propagation model. DTIC

N93-29872# Stanford Univ., CA. Dept. of Operations Research.
A DIFFUSION APPROXIMATION FOR A NETWORK OF RESERVOIRS WITH POWER LAW RELEASE RULE
Peter W. Glynn and John E. Glynn Nov. 1992 21 p
(Contract DAAL03-91-G-0101)
(AD-A263753; SU-TR-92-20; ARO-28809.10-MA-SDI) Avail: CASI HC A03/MF A01

A diffusion approximation for a network of continuous time reservoirs with power law release rules is examined. Under a mild assumption on the inflow processes, we show that for physically reasonable values of the power law constants, the system of processes converges to a multi-dimensional Gaussian diffusion process. We also illustrate how the limiting Gaussian process may be used to compute approximations to the original system of processes. In addition, we study the quality of our approximations by comparing them to results obtained by simulations of the original watershed model. The simulations offer support for the use of the developed approximation. DTIC

N93-29876# Texas A&M Univ., College Station. Dept. of Electrical Engineering.
CONTINUATION OF: APPLICATIONS OF GAUGE THEORIES TO ENHANCE NUMERICAL SOLUTIONS OF MIXED POTENTIAL INTEGRAL EQUATIONS Final Report
Robert D. Nevels, Chenhong Huang, and Zuoguo Wo 12 Mar. 1993 107 p
(Contract N00012-90-J-1334)
(AD-A263763) Avail: CASI HC A06/MF A02

The intention of this research has been to investigate techniques for solving Maxwell's equations under scattering, radiation, and propagation conditions by adapting methods recently developed in mathematical physics. During the first few months of this contract we continued the work begun during the previous three years concerning the possibility of substituting the Coulomb gauge for the standard Lorentz gauge in mixed potential integral equation formulations. In this report, we present our investigations concerning conduction current invariance under gauge transformation and the implementation of the Coulomb gauge in time domain integral equation analysis. Although it is widely known that the electromagnetic field is invariant under a gauge transformation, to the authors' knowledge no previous proof existed showing current invariance. DTIC

N93-29978# Naval Postgraduate School, Monterey, CA.
A MULTILEVEL APPROACH TO MINIMUM COST NETWORK FLOWS M.S. Thesis
Kevin J. Cavanaugh Sep. 1992 104 p
(AD-A264008) Avail: CASI HC A06/MF A02

Multigrid/multilevel techniques were originally developed for numerically solving partial differential equations. The application of multilevel techniques to a non-geometric long transportation problem is explored. An introduction to multigrid is given, and specifics of how it is applied to this minimum cost network flow problem are explored. This research shows that multilevel techniques can be applied to network optimization problems. Further, since a previous restriction is removed by transferring the problem from a physical space to a cost space, the techniques can be applied to a broader range of problems. Both a multilevel V-cycle and a Full Multigrid (FMG) algorithm are implemented. Various strategies for restriction and local relaxation are discussed, and comparisons between the methods are made. Directions for future work include investigation of graph theoretic aspects of the problems, implementation of a regular grid overlay of the domain, exploration of a fast adaptive composite (FAC) grid algorithm, and development of a full approximation scheme (FAS) algorithm. DTIC

N93-30041# Pacific Northwest Lab., Richland, WA.
ADVANCES IN THE IDENTIFICATION OF ELECTROCHEMICAL TRANSFER FUNCTION MODELS USING PRONY ANALYSIS
D. J. Trudnowski, M. K. Donnelly (Control Technology, Inc., Bozeman, MT.), and J. F. Hauer (Bonneville Power Administration, Portland, OR.) Feb. 1993 7 p Presented at the IEEE Winter Power Meeting, Columbus, OH, Feb. 1993
(Contract DE-AC06-76RL-01830)
(DE93-009424; PNL-SA-21265; CONF-930279-2) Avail: CASI HC A02/MF A01

The usefulness and understanding of Prony analysis as a tool for identification of power system electromechanical oscillation models is further advanced. These linear models are developed by analyzing power system ring-down data. The presented results allow more generality in the assumed model formulation. In addition, a comparison is made between Prony analysis and autoregressive moving-average (KARMA) modeling, which was also proposed for analysis of system oscillations. Under the conditions investigated, the Prony algorithm performed more accurate identification. DOE

N93-30117# Institut National de Recherche d'Informatique et d'Automatique, Valbonne (France). Programme 6: Calcul Scientifique, Modelisation et Logiciels Numeriques.
ON HIGH RESOLUTION EXTENSIONS OF LAGRANGE-GALERKIN FINITE-ELEMENT SCHEMES
Alain Dervieux, Loula Fezoui, and Francoise Loriot (Simulog, Valbonne, France.) Jun. 1992 16 p
(INRIA-RR-1703; ETN-93-93911) Avail: CASI HC A03/MF A01

A study showing how two typical one dimensional finite volume high resolution schemes, like FCT (Flux Corrected Transport) or MUSCL can be introduced in the multidimensional background of a class of Lagrange-Galerkin finite element methods, is presented. For the sake of simplicity, bidimensional spatial discretization is considered, although most of the ideas presented can be extended to three dimensions. Schemes that apply to a class of partial differential equations involving, as in compressible CFD (Computational Fluid Dynamics) for instance, hyperbolic terms and parabolic (diffusion) terms, are concerned. The presented schemes are concluded to enjoy many of the interesting properties of their ingredients: easy and rational derivation of first and second derivatives, on possibly heterogeneous meshes (triangles combined with quadrilaterals), relaxing the constraint of node by node consistency through a variational point of view; positiveness preservation (at least for first order Godunov and scalar FCT) and, more generally, stabilization terms allowing discontinuity capturing (high Mach) and collocated meshes without spurious pressure nodes. ESA

N93-30136# Office National d'Etudes et de Recherches Aerospatiales, Paris (France).
DIFFERENCE METHODS FOR HYPERBOLIC PROBLEMS WITH EMPHASIS ON SPACE-CENTERED APPROXIMATIONS
Alain Lerat 1990 92 p Presented at VKI Lecture Series 1990-1993 on Computational Fluid Dynamics, Rhode Saint Genese, Belgium, 5-9 Mar. 1990 Previously announced as N90-27998
(ONERA-NT-1990-4; ETN-93-93724) Avail: CASI HC A05/MF A01

A general framework for the approximation of hyperbolic systems of conservation laws in one space dimension by explicit or implicit two level difference schemes is proposed. Under few natural assumptions, a general scheme is constructed. Its order of accuracy is characterized and a linear analysis is developed to obtain necessary and sufficient conditions for solvability, L(sub 2) stability, dissipation in the sense of Kreiss and good numerical solution of the algebraic systems associated to implicit approximations. A nonlinear analysis concerning the TVD property for a single conservation law and results on the discrete entropy inequality for systems is also presented. Various examples of schemes (mostly centered) are analyzed. These examples show that the general framework is useful to study a particular approximation easily or to systematically determine a new scheme satisfying some properties given in advance. ESA

N93-30140# Argonne National Lab., IL.
SIMPLIFIED LINEAR EQUATION SOLVERS: USER'S MANUAL
W. Gropp and B. Smith (California Univ., Los Angeles.) Feb. 1993 51 p
(Contract W-31-109-eng-38)
(DE93-011975; ANL-93/8) Avail: CASI HC A04/MF A01

The solution of large sparse systems of linear equations is at the heart of many algorithms in scientific computing. The Simplified Linear Equation Solvers (SLES) package is a set of easy-to-use yet powerful and extensible routines for solving large sparse linear systems. The design of the package allows new techniques to be used in existing applications without any source code changes in the applications. DOE

N93-30392# California Univ., Berkeley. Lawrence Berkeley Lab.
DIFFERENTIAL CALCULUS ON QUANTUM SPACES AND QUANTUM GROUPS
B. Zumino 10 Dec. 1992 19 p Presented at the 19th International Conference on Group Theoretic Methods in Physics, Salamanca, Spain, 10-14 Nov. 1992
(Contract DE-AC03-76SF-00098)
(DE93-010425; LBL-33249; CONF-9211219-1) Avail: CASI HC A03/MF A01

A review of recent developments in the quantum differential calculus is discussed. The quantum group GL(sub q)(n) is treated by considering it as a particular quantum space. Functions on SL(sub q) (n) are defined as a subclass of functions on GL(sub q)(n). The case of SO(sub q)(n) is also briefly considered. These notes cover part of a lecture given at the XIX International Conference on Group Theoretic Methods in Physics, Salamanca, Spain 1992. DOE

N93-30503# Naval Command, Control and Ocean Surveillance Center, San Diego, CA.
EXTRACTING INFINITE SYSTEM PROPERTIES FROM FINITE SIZE CLUSTERS: PHASE RANDOMIZATION/BOUNDARY CONDITION AVERAGING
J. T. Gammel, D. K. Campbell, and E. Y. Loh, Jr. Mar. 1993 7 p
(AD-A264712) Avail: CASI HC A02/MF A01

When electron-electron correlations are important, it is often necessary to use exact numerical methods, such as Lanczos diagonalization, to study the full many-body Hamiltonian. Unfortunately, such exact diagonalization methods are restricted to small system sizes. We show that if the Hubbard U term is replaced by a periodic Hubbard term, the full many body Hamiltonian may be exactly solved, even for very large systems, though for low fillings. However, for half-filled systems and large U, this approach is not only no longer exact, it no longer improves extrapolation to larger systems. We discuss how generalized randomized variable averaging (RVA) or phase randomization schemes can be reliably employed to improve extrapolation to large system sizes in this regime. This general approach can be combined with any many-body method and is thus of broad interest and applicability. DTIC

N93-30572# Technische Univ., Berlin (Germany). Fachbereich fuer Verkehrswesen.
A METHOD FOR INTERSECTION LINE CALCULATION BETWEEN PARAMETRIC SURFACES Ph.D. Thesis [EINE METHODE ZUR SCHNITTKURVENBERECHNUNG ZWISCHEN PARAMETRISCHEN FLAECHEN]
Hyung-Bae Jung 1992 93 p In GERMAN
(ETN-93-94178) Avail: CASI HC A05/MF A01

A method for intersection calculation between two parametric surfaces such as B splines, which uses an adaptive subdivision algorithm with a facet oriented model based on triangles, is presented. This method is used for examination of area refinement which eliminates empty mesh areas from the study domain. Numerous intersection points were obtained. These intersection points can accurately represent the intersection curve with a linear reliationship. Boundary box, linearization criterion, and connection technique were developed to guarante global precision. ESA

N93-30765# Joint Inst. for Nuclear Research, Dubna (USSR). Lab. of Theoretical Physics.
ON THE METHOD OF DETERMINING RELATIONS [O METODE OPREDEIYAYUSHCHIKH SOOTNOSHENIJ]
V. K. Melnikov 1991 8 p In RUSSIAN Presented at the 7th Conference on Nonlinear Evolution Equations and Dynamic Systems, Italy, Jun. 1991
(DE93-606041; JINR-R-2-91-403) Avail: CASI HC A02/MF A01 (US Sales Only)

It is shown that a multicomponent nonlinear Schroedinger equation with a source can be derived by the method of determining relations thus making it possible to apply the inverse scattering method to analyze this equation. However, the system of evolution equations for the scattering data turned out to be nonlinear. An operator relation of the Lax type is also derived which holds due to this equation. However, this operator relation does not uniquely determine this equation and does not guarantee independence of time of the discrete spectrum of the corresponding linear operator. DOE

N93-30809# International Centre for Theoretical Physics, Trieste (Italy).
POSITIVE ENERGY REPRESENTATIONS OF THE CONFORMAL QUANTUM ALGEBRA
L. Dabrowski (International School for Advanced Studies, Trieste, Italy.), V. K. Dobrev (International School for Advanced Studies, Trieste, Italy.), V. Husain, and R. Floreanini (Istituto Nazionale di Fisica Nucleare, Trieste, Italy.) Jul. 1992 13 p
(DE93-606064; IC-92/187; SISSA-137/92/FM; UTS-DFT-22-92) Avail: CASI HC A03/MF A01 (US Sales Only)

The positive-energy unitary irreducible representations of the q-deformed conformal algebra delta-C(sub q) = U(sub q)(su(2,2)) are obtained by appropriate deformation of the classical ones. When the deformation parameter q is Nth root of unity, all these unitary representations become finite-dimensional. For this case we discuss in some detail the massless representations, which are also irreducible representations of the q-deformed Poincare subalgebra of delta-C(sub q). Generically, their dimensions are smaller than the corresponding finite-dimensional non-unitary representation of su(2,2), except when N = 2 module h + 1, where h is the helicity of the representations. The latter cases include the fundamental representations with h = (+-)1/2. DOE

N93-30810# International Centre for Theoretical Physics, Trieste (Italy).
CONNECTIONS BETWEEN QUANTIZED AFFINE ALGEBRAS AND SUPERALGEBRAS
R. B. Zhang Aug. 1992 12 p
(DE93-606065; IC-92/190) Avail: CASI HC A03/MF A01 (US Sales Only)

Every affine superalgebra with a symmetrizable Cartan matrix is closely related to an ordinary affine algebra with the same Cartan matrix. It is shown that the quantum supergroup associated with the former is essentially isomorphic to the quantum group associated with the latter in an appropriate class of representations. At the classical level, each integrable irreducible highest weight representation of the affine superalgebra has a corresponding irreducible representation of the affine algebra, which has the same weight space decomposition. DOE

N93-30912# Joint Inst. for Nuclear Research, Dubna (USSR). Lab. of Theoretical Physics.
ON THE INVARIANT MEASURE FOR THE NONLINEAR SCHROEDINGER EQUATION
P. R. Zhidkov 1991 20 p
(DE92-644672; JINR-E-5-91-174) Avail: CASI HC A03/MF A01 (US Sales Only)

The invariant measure for the nonlinear Schroedinger equation is constructed. In fact, it is assumed that the nonlinearity in the equation is semilinear. The main aim of the paper is the explanation of the Fermi-Past-Ulam phenomenon. Poincare theorem gives the answer to this question. DOE

N93-30913# Joint Inst. for Nuclear Research, Dubna (USSR). Lab. of Computing Techniques and Automation.
A NUMERICAL SOLUTION OF THE TWO-CENTER PROBLEM [CHISLENNOE RESHENIE ZADACHI DVUKH TSENTROV]
T. Zhanlav, D. V. Pavlov, and I. V. Puzynin 1991 16 p In RUSSIAN
(DE92-644674; JINR-R-11-91-138) Avail: CASI HC A03/MF A01 (US Sales Only)

Two different statements of the two-center boundary problem are suggested. The problems stated are considered as a nonlinear functional equation which is solved by the continuous analog of Newton's method, and its modification. The differential equations are approximated by the finite-difference method and the method of spline with an accuracy of the order of O(h(exp 4)), where h is the step of a uniform mesh. DOE

N93-30929# International Centre for Theoretical Physics, Trieste (Italy).
NORMAL EQUIVARIANT FORMS OF VECTOR FIELDS [FORMES NORMALES EQUIVARIANTES DE CHAMPS DE CHAMPS DE VECTEURS]
F. SanchezBringas Jul. 1992 6 p In FRENCH

(DE92-644845; IC-92/140) Avail: CASI HC A02/MF A01 (US Sales Only)

We prove a theorem of linearization of type Siegel and a theorem of normal forms of type Poincare-Dulac for germs of holomorphic vector fields in the origin of C(sup 2), gamma -equivariants, where gamma is a finite subgroup of GL(2,C). DOE

N93-30942# International Centre for Theoretical Physics, Trieste (Italy).
FIXED POINT ITERATIONS FOR QUASI-CONTRACTIVE MAPS IN UNIFORMLY SMOOTH BANACH SPACES
C. E. Chidume (Nigeria Univ., Nsukka.) and M. O. Osilike (Nigeria Univ., Nsukka.) May 1992 12 p
(DE92-641348; IC-92/93) Avail: CASI HC A03/MF A01 (US Sales Only)

Two well-known fixed point iteration methods are applied to approximate fixed points of quasi-contractive maps in real uniformly smooth Banach spaces. While our theorems generalize important known results, our method is of independent interest. DOE

N93-30946# Joint Inst. for Nuclear Research, Dubna (USSR). Lab. of Theoretical Physics.
A REMARK ON THE INVARIANT MEASURE FOR THE NONLINEAR SCHROEDINGER EQUATION
P. E. Zhidkov 1992 11 p
(DE93-609840; JINR-E-5-92-23) Avail: CASI HC A03/MF A01 (US Sales Only)

The invariant measure for the nonlinear Schroedinger equation with the power nonlinearity is constructed. The proof is based on the earlier author's paper. Due to the result obtained, one can apply the Poincare recurrence theorem to the nonlinear Schroedinger equation. DOE

N93-30984# Joint Inst. for Nuclear Research, Dubna (USSR). Lab. of Theoretical Physics.
SCHROEDINGER EQUATIONS OF HIGHER (GREATER THAN 2) ORDER [URAVNENIYA SHREDINGERA VYSSHEGO (GREATER THAN GO) PORYADKA]
B. N. Zakharev 1991 15 p In RUSSIAN
(DE92-644677; JINR-R-4-91-127) Avail: CASI HC A03/MF A01 (US Sales Only)

A review of papers that are useful for understanding the 'Schroedinger equations of higher order' is presented. The papers should serve as a bridge to mastering the nonlocal potentials. Additionally, the following topics are also discussed: Different types of barriers--in coefficients at the derivatives of different order; Transformations of waves with one wave number into the waves with another wave number for fixed energy; Intensified tunnelling and violation of its symmetry; A crisis in nuclear physics; and an appendix--Bessel functions J(sub (alpha)) as bound states on the lattice (alpha) at the slope of the linear potential. DOE

N93-31012# Groningen Rijksuniv. (Netherlands). Computing Science Section.
MANIFOLD SHAPE: FROM DIFFERENTIAL GEOMETRY TO MATHEMATICAL MORPHOLOGY
J. B. T. M. Roerdink 1992 19 p
(CS-9204; ETN-93-94094) Avail: CASI HC A03/MF A01

Stimulated by developments in extending Euclidean mathematical morphology to complex structures such as complex lattices, the question of shape description of patterns on arbitary (smooth) surfaces based on mathematical morphology is studied. To outline the mathematical structure of this description is of primary interest. Some concepts of differential geometry, in particular, those of parallel transport and covariant differentiation, are used to replace the more restricted concept of invariance used so far in mathematical morphology. The corresponding morphological operators which leave the geometry on the surface invariant are then constructed. ESA

N93-31014# Groningen Rijksuniv. (Netherlands). Computing Science Section.
SHORT-CIRCUIT EVALUATION OF BOOLEAN EXPRESSIONS
C. Bron, E. J. Dijkstra, J. Jongejan, and B. Laverman 9 Oct. 1992 12 p
(CS-9205; ETN-93-94095) Avail: CASI HC A03/MF A01

Short circuit evaluation of boolean expressions is a form of evaluation in which the evaluation of subexpression may be suppressed of the boolean result if the expression as a whole is already known. The derivation of an algorithm for generating control structure code for boolean expressions is presented. The algorithm can create optimal branch code in a single pass over the expression without a need to store the intermediate information or to patch the code of previously generated branches. ESA

N93-30254 Naval Surface Warfare Center, Silver Spring, MD. Information and Mathematical Sciences Branch.
ZERO-CROSSING RATE OF SOME NON-GAUSSIAN PROCESSES
John Barnett and Benjamin Kedem (Maryland Univ., College Park.) *In* Engineering Inst. of Canada, Canadian Conference on Electrical and Computer Engineering, Volumes 1 and 2 1990 4 p (For primary document see N93-30215 11-31)
Avail: Engineering Inst. of Canada, 2050 rue Mansfield, Suite 700, Montreal, Quebec H3A 1Z2 Canada

N93-30260 Bell-Northern Research Ltd., Ottawa (Ontario).
A NUMERICAL SIMULATOR FOR TESTING SLIDING MODE CONTROLS IN STOCHASTIC SYSTEMS
P. Gauthier and R. P. Malhame (Ecole Polytechnique, Montreal, Quebec.) *In* Engineering Inst. of Canada, Canadian Conference on Electrical and Computer Engineering, Volumes 1 and 2 1990 4 p (For primary document see N93-30215 11-31)
Avail: Engineering Inst. of Canada, 2050 rue Mansfield, Suite 700, Montreal, Quebec H3A 1Z2 Canada

N93-30688*# National Aeronautics and Space Administration. Ames Research Center, Moffett Field, CA.
VALIDATION AND UPGRADING OF PHYSICALLY BASED MATHEMATICAL MODELS
Ronald DuVal *In its* NASA/FAA Helicopter Simulator Workshop Apr. 1992 p 123-129 (For primary document see N93-30673 11-01)
Avail: CASI HC A02/MF A02

65 STATISTICS AND PROBABILITY

Includes data sampling and smoothing; Monte Carlo method; and stochastic processes.

N93-28506# Institut National de Recherche d'Informatique et d'Automatique, Valbonne (France). Programme 1: Architectures Paralleles, Bases de Donnees, Reseaux et Systemes Distribues.
SOME QUALITATIVE PROPERTIES IN POLLING SYSTEMS
Eitan Altman, Panagiotis Konstantopoulos, and Zhen Liu Feb. 1992 32 p
(INRIA-RR-1596; ETN-93-93886) Avail: CASI HC A03/MF A01

A polling system with K greater than or equal to 1 queues and a single server that visits the queues in a cyclic order is considered. The polling discipline in each queue is of general gated type or exhaustive type. It is assumed that in each queue the arrival times form a Poisson process, and that the service times, the walking times as well as the set-up times form sequences of independent and identically distributed random variables. For such a system, sufficient conditions under which the vector of queue lengths is stable are provided. Several criterions for stability are treated: the ergodicity of the process, the geometric ergodicity, and the geometric rate of convergence of the first moment. The ergodicity implies the weak convergence of station times, intervisit times and cycle times. The queue lengths, station times, intervisit times and cycle times are shown to be stochastically increasing in arrival rates, in service times, in walking and in set-up times. The stability conditions and the stochastic monotonicity results are extended to the polling systems with additional customer routing between the queues, as well as bulk and correlated arrivals. For polling systems with mixed limited, gated and exhaustive service disciplines and without set up times, the weighted sum of mean waiting times is proved to increase in the arrival rate, in the first and second moments of the service times and in the variances of the walking times. The monotonicity also holds with respect to the mean walking times if they are deterministic or if there are 'many queues' or the system is heavily loaded. The mean cycle time, the mean intervisit time and the mean station times are proved to be invariant under general service disciplines and general stationary arrival and service processes. ESA

N93-28507# Institut National de Recherche d'Informatique et d'Automatique, Valbonne (France). Programme 1: Architectures Paralleles, Bases de Donnees, Reseaux et Systemes Distribues.

FLOW CONTROL USING THE THEORY OF ZERO SUM MARKOV GAMES

Eitan Altman Feb. 1992 19 p Sponsored by Chateaubriand Fellowship, Israel

(INRIA-RR-1597; ETN-93-93887) Avail: CASI HC A03/MF A01

The problem of dynamic flow control of arriving packets into an infinite buffer is considered. The service rate may depend on the state of the system, may change in time and is unknown to the controller. Tne goal of the controller is to design an efficient policy which guarantees the best performance under the worst service conditions. The cost is composed of a holding cost, a cost for rejecting customers (packets) and a cost that depends on the quality of the service. The problem is studied in the framework of zero sum Markov games, and a value iteration algorithm is used to solve it. An optimal stationary policy (such that the decisions depend only on the actual number of customers in the queue) is shown to exist: it is of a threshold type, and it uses randomization in at most one state. ESA

N93-28508# Institut National de Recherche d'Informatique et d'Automatique, Valbonne (France). Programme 1: Architectures Paralleles, Bases de Donnees, Reseaux et Systemes Distribues.

ASYMPTOTIC PROPERTIES OF CONSTRAINED MARKOV DECISION PROCESSES

Eitan Altman Feb. 1992 22 p Sponsored by Chateaubriand Fellowship, Israel

(INRIA-RR-1598; ETN-93-93888) Avail: CASI HC A03/MF A01

Several asymptotic properties of constrained Markov Decision Processes (MDP's) with a countable state space are presented. Both the discounted and the expected average cost, with unbounded cost, are addressed. The convergence of finite horizon MDP's to the infinite horizon MDP, convergence of MDP's with a truncated state space to the problem with infinite state space, and convergence of MDP's as the discount factor goes to a limit, are concerned. In all these cases, the convergence of optimal values and policies is established. Based on the optimal policy for the limiting problem, policies which are almost optimal for the other (approximating) problems are constructed. ESA

N93-28510# Institut National de Recherche d'Informatique et d'Automatique, Valbonne (France). Programme 4: Robotique, Image et Vision.

IMAGE CLASSIFICATION USING MARKOV RANDOM FIELDS WITH TWO NEW RELAXATION METHODS: DETERMINISTIC PSEUDO ANNEALING AND MODIFIED METROPOLIS DYNAMICS

Zoltan Kato, Josiane Zerubia, Marc Berthod, and Jean-Paul Stromboni (Nice Univ., France.) Feb. 1992 20 p

(INRIA-RR-1606; ETN-93-93890) Avail: CASI HC A03/MF A01

Two relaxation techniques are presented: deterministic Pseudo Annealing (DPA) and Modified Metropolis Dynamics (MMD) in order to do image classification using a Markov random field modelization. For the first algorithm (DPA), the a posteriori probability of a tentative labeling is generalized to continuous labeling. The merit function thus defined has the same maxima under constraints yielding probability vectors. Changing these contraints convexifies the merit function. The algorithm solves this unambiguous maximization problem and then tracks down the solution while the original constraints are restored yielding a good even if suboptimal solution to the original labeling assignment problem. The second method (MMD) is a modified version of the Metropolis algorithm: at each iteration the new state is chosen randomly but the decision to accept it is purely deterministic. This is of course also a suboptimal technique which gives faster results than stochastic relaxation. These two methods were implemented on a Connection Machine CM2 and simulation results are shown with a synthetic noisy image and a SPOT image. These results are compared to those obtained with the Metropolis algorithm, the Gibbs sampler and ICM (Iterated Conditional Mode). ESA

N93-28574# Air Force Inst. of Tech., Wright-Patterson AFB, OH. School of Engineering.

MODIFIED GOODNESS-OF-FIT TESTS FOR THE WEIBULL DISTRIBUTION M.S. Thesis

Erol Yucel Mar. 1993 91 p

(AD-A262552; AFIT/GOR/ENS/93M-25) Avail: CASI HC A05/MF A01

This research will produce a new modified Anderson-Darling and W* Goodness of fit statistics for the three parameter Weibull Distribution when all parameters unknown and estimated by Maximum Likelihood-Minimum Distance combination. The critical values for each statistic, sample size and levels 0.20, 0.15, 0.10, 0.05 and 0.01 are produced. The Monte Carlo Simulation used 5000 repetitions for sample sizes of 10, 15, 20, 25, 30, 40, and 50 with the Weibull shape equals to 3, scale equals to 4, and location equals to 10. The power study is made for the same sizes as above with the hypothesized Weibull Distribution against 8 other distributions. DTIC

N93-28575# Air Force Inst. of Tech., Wright-Patterson AFB, OH. School of Engineering.

MODIFIED ANDERSON-DARLING AND CRAMER-VON MISES GOODNESS-OF-FIT TESTS FOR THE NORMAL DISTRIBUTION M.S. Thesis

David A. Gwinn Mar. 1993 92 p

(AD-A262554; AFIT/GOR/ENS/93M-07) Avail: CASI HC A05/MF A01

New techniques for calculating goodness-of-fit statistics for normal distributions with parameters estimated from the sample are investigated. Samples are generated for a Normal(0,1) distribution. Critical values are calculated for five modifications to the Anderson-Darling statistic and five modifications to the Cramer-Von Mises statistic. An extensive power study is done to test the power of the new statistics versus the power of the unmodified statistics. Powers of six of the new statistics show minimal to no improvement; two of the new statistics show a marked decrease in power; two of the new statistics show an overall increase in power over the unmodified statistics. One of these two improved statistics was the obvious better of the two, and it was a modification to the Anderson-Darling statistic. Complete tables of critical values for sample sizes $n=4$ through $n=50$ are included for all Anderson-Darling and Cramer-Von Mises statistics, both modified and unmodified. DTIC

N93-28587# Air Force Inst. of Tech., Wright-Patterson AFB, OH. School of Engineering.

A NEW GOODNESS-OF-FIT TEST FOR THE WEIBULL DISTRIBUTION BASED ON SPACINGS M.S. Thesis

Mark C. Coppa Mar. 1993 115 p

(AD-A262615; AFIT/GST/ENS/93M-02) Avail: CASI HC A06/MF A02

The critical values for a new goodness-of-fit test based on spacings are generated for the Weibull distribution when the shape parameter is known. The critical values are used for testing whether a set of observations follow a Weibull distribution when the scale and location parameters are unknown. A Monte Carlo simulation with 10,000 iterations is used to generate the critical values for sample sizes 5(5)35 at shape parameters k equal to 0.5(0.5)1.5 and for sample sizes 5(5)20 at shape parameters k = 2.0(1.0)4.0. A Monte Carlo power study of the Z* test statistic using 5000 iterations is accomplished using nine alternate distributions H sub A. The power is good to excellent when the null hypothesis H(0) is from a skewed distribution (k less than 2.0). Power results at shape parameters k greater than 2.0 are poor for all sample sizes considered. A comparison is made, at shape parameter 1.0, against the prominent competing goodness-of-fit test statistics. Data is obtained from a prior AFIT thesis by Bush. Results indicate that the Z* test is more powerful than the competition at the available sample sizes of 5, 15 and 25 and alpha levels: 0.05 and 0.01. A relationship between the critical value and the sample size is investigated to allow for greater usage of the test statistic. Satisfactory values of fit are attained with a simple log-linear relationship. DTIC

N93-28760# Air Force Inst. of Tech., Wright-Patterson AFB, OH.

A MODIFIED ANDERSON DARLING GOODNESS-OF-FIT TEST FOR THE GAMMA DISTRIBUTION WITH UNKNOWN SCALE AND LOCATION PARAMETERS M.S. Thesis

Tamer Ozmen 8 Mar. 1993 122 p

(AD-A262486; AFIT/GOR/ENS/93M-24) Avail: CASI HC A06/MF A02

A new modified Anderson-Darling goodness-of-fit test is introduced for the three-parameter Gamma distribution when the location parameter is found by minimum distance estimation and scale parameter by maximum likelihood estimation. Monte Carlo simulation studies were performed to calculate the critical values for A-D test when A-D statistic is minimized. These critical values are then used for testing whether a set of observations follows a Gamma distribution when the scale and location parameters are unspecified and are estimated from the sample. Functional relationship between the critical values of A-D is also examined for each shape parameter by the variables, sample size and significance level. The power study is performed with the hypothesized gamma against alternate distributions. Comparison with the previous study which uses MLEs for location and scale showed that the modified test is better in most cases. DTIC

N93-28763# Los Alamos National Lab., NM.
INFORMATION-THEORETIC PERFORMANCE BOUNDING OF BAYESIAN IDENTIFIERS
S. D. Briles 1993 13 p Presented at the Automatic Object Recognition 3, Society of Photo-Optical Instrumentation Engineers (SPIE) OE/Aerospace Science and Sensing Meeting, Orlando, FL, 11-16 Apr. 1993
(Contract W-7405-eng-36)
(DE93-010705; LA-UR-93-919; CONF-930445-4) Avail: CASI HC A03/MF A01

Statistical target recognition techniques perform well when the 'true' target-signature data are deterministic. If the deterministic nature of the data exists and the probabilistic values of a given problem are known, then identifiers, based on Bayesian estimation theory, have great potential for solving the target identification problem. How well an identifier will perform is usually answered by Monte Carlo simulations or implementation experiments. An alternative to these performance analysis techniques is the use of information theory. Information theory has long been applied to the investigation of data compression, which deals with average distortional measures. The association of Bayes risk with distortion allows for information-theoretic tools to be applied to the statistical target identification problem. The rate-distortion function of data compression can be extended to the Bayes rate-distortion function. Derived from designer-specified risk and identifier structure, the theoretical Bayes rate-distortion function relates mutual information to the identifier performance. Mutual information is determined from the target-signature data used by the identifier and by the nature of the noise imposed upon the data. Computational efforts in determining mutual information values allow for identifier performance bounds to be extracted from the Bayes rate-distortion function. DOE

N93-28844# Air Force Inst. of Tech., Wright-Patterson AFB, OH. School of Engineering.
A MONTE CARLO STUDY OF THE RAW AND NORMAL VARIMAX ROTATION CRITERION IN FACTOR ANALYSIS M.S. Thesis
Willam M. Ibinson 23 Mar. 1993 112 p Limited Reproducibility: More than 20% of this document may be affected by microfiche quality
(AD-A262516; AFIT/GOR/ENS/93M-27) Avail: Issuing Activity (Defense Technical Information Center (DTIC)

Factor analysis is a multivariate statistical procedure for analyzing and reducing large data sets. Many factor analysis schemes and techniques are available that lead to strikingly different results from the same data. This research effort used a Monte Carlo approach to investigate the properties of two rotation methods for simple structure, Kaiser's raw and normal varimax criterion. Data sets were developed from a set of contrived experimental factor patterns by multiplying each factor pattern by its transpose to create a covariance matrix. Data sets of multivariate normal deviates were in turn generated from each covariance matrix via the Choleski algorithm. Rotated factor pattern matrices from each data set were compared to their respective experimental factor pattern on the basis of structure, loadings, and eigenvalues. These performance issues are addressed through regression analysis and separate factor analysis in which the grand mean of proposed measures of effectiveness are predicted. These measures of effectiveness include structure matching and root mean square error between the experimental and observed factor patterns. Several methods of characterizing factor pattern complexity and predicting rotation criterion performance are explored. DTIC

N93-28845# Air Force Inst. of Tech., Wright-Patterson AFB, OH. School of Engineering.
A MODIFIED CHI-SQUARED GOODNESS-OF-FIT TEST FOR THE THREE-PARAMETER GAMMA DISTRIBUTION WITH UNKNOWN PARAMETERS M.S. Thesis
Thomas J. Sterle Mar. 1993 61 p
(AD-A262553; AFIT/GOR/ENS/93M-21) Avail: CASI HC A04/MF A01

A modified chi-squared goodness-of-fit test was created for the gamma distribution in the case where all three parameters must be estimated from the sample. Critical values are generated using a Monte Carlo simulation procedure with 5000 repetitions each. Random samples of 8 different sizes are drawn from gamma distributions with shape parameters 1, 1.5, 2.0, and 2.5. The shape, scale, and location parameters were then estimated from each sample, using an iterative technique combining the maximum likelihood and minimum distance methods, enabling computation of the chi-squared statistics and critical values. The same process is used to generate random samples, parameter estimates, and chi-squared statistics from 10 alternate distributions as a check on the power of this chi-squared goodness-of-fit test. The goodness-of-fit tests were executed by comparing the chi-squared statistics from the alternate distributions with the gamma critical values, allowing the power to be calculated against each alternate distribution. DTIC

N93-29292# Stanford Univ., CA. Dept. of Operations Research.
ON THE VALUE OF FUNCTION EVALUATION LOCATION INFORMATION IN MONTE CARLO SIMULATION
Thomas J. DiCiccio and Peter W. Glynn Nov. 1992 11 p
(Contract DAAL03-91-G-0101)
(AD-A263662; TR-92-17; ARO-28809.11-MA-SDI) Avail: CASI HC A03/MF A01

The point estimator used in naive Monte Carlo sampling weights all the computed function evaluations equally, and it does not take into account the precise locations at which the function evaluations are made. In this note, we show for one-dimensional integration problems that if the weights are suitably modified to reflect the location information present in the sample, then the convergence rate of the Monte Carlo estimator can be dramatically improved from order n(-1/2) to order n(-2), where the number of function evaluations is computed. DTIC

N93-29385# Texas Univ., El Paso. Dept. of Mathematical Sciences.
EMPIRICAL QUANTILE FUNCTION NONPARAMETRIC INTEGRATED ANALYSES Final Report, 1 Sep. 1989 - 28 Feb. 1993
W. D. Kaigh 1 May 1993 15 p
(Contract DAAL03-89-G-0098)
(AD-A263704; ARO-27159.9-MA-SAH) Avail: CASI HC A03/MF A01

This three-year statistics research project addressed theoretical development, efficiency evaluation, and desktop computer implementation of an integrated nonparametric statistical data analysis approach based on Fourier analytic techniques applied to the empirical quantile function (EQF). New EQF statistical procedures were developed for data smoothing and reduction methods, nonparametric estimation of various functionals associated with the quantile function, composite goodness-of-fit tests for uniform and exponential models with applications to related stochastic processes, and nonparametric analysis of variance rank procedures for analysis of independent samples. These EQF methods exploit discrete Hahn polynomial orthogonal polynomial component representations to produce statistics for significance testing and interval estimation for both omnibus and directional alternative models. Performance evaluations of the proposed techniques included theoretical and Monte Carlo efficiency comparisons as well as numerical applications to challenging data sets. Interactive desktop computer and graphics routines utilizing symbolic programming languages were developed to facilitate implementation of EQF data analysis techniques by statistical users. Transl. by SCITRAN

N93-29411 California Univ., Riverside. Dept. of Statistics.
STUDY ON VARIOUS PROBLEMS IN STATISTICAL PLANNING AND INFERENCE Final Report, 15 Dec. 1990 - 14 Dec. 1992
Subir Ghosh 14 Dec. 1992 10 p Limited Reproducibility: More than 20% of this document may be affected by microfiche quality
(Grant AF-AFOSR-0115-91)
(AD-A262484; AFOSR-93-0200TR) Avail: CASI HC A02

The research done under this grant is (1) New main effect plus one plans and their robustness property against deletion of runs, and (2) Robust experimental plan and its role in determining robust design against noise factors. The researchers near completion are on (1) Incorrectness of orthogonality condition for main effect plans, and (2) Determination of robust design against noise factors and in presence of signal factors. DTIC

N93-29447# Air Force Inst. of Tech., Wright-Patterson AFB, OH.
AN ANALYSIS OF THE GENERALIZED LAMBDA DISTRIBUTION M.S. Thesis
Robert J. Bergevin Mar. 1993 82 p
(AD-A262485; AFIT/GST/ENS/93M-01) Avail: CASI HC A05/MF A01

The Generalized Lambda Distribution (GLD) is a four parameter function that is capable of mimicking the behavior of a wide range of probability density functions (pdfs). Unfortunately, the GLD presently cannot model every possible type of pdf. Since the reasons for this limitation are unknown, this thesis examines several potential problems in an attempt to expand the range of distributions the GLD can mimic. We first present a discussion of the behavior of the algorithm that is used to search for the appropriate GLD parameter values. In particular, we examine the effect of using an unconstrained search to find the parameters subject to a constraint that ensures that the resulting pdf is valid. We also develop a reparameterization of the GLD that creates an unconstrained search region. This does not expand the range of distributions the GLD can mimic. We then use an extensive numerical investigation to examine the set of distributions that can be obtained from combinations of the GLD parameters. This examination allows us to expand the range of pdfs that the GLD can model. We also inspect some pdfs that cannot be modeled using the GLD, as well as present an alternative to the method of moments for determining parameter values, using the concept of L-moments. DTIC

N93-29454# Texas Univ., Austin. Dept. of Electrical and Computer Engineering.
THEORY AND APPLICATIONS OF RANDOM FIELDS Final Report, 1 Apr. 1990 - 30 Sep. 1992
Gary L. Wise 31 Mar. 1993 45 p
(Contract N00014-90-J-1712)
(AD-A262829) Avail: CASI HC A03/MF A01

This Final Technical Report constitutes a summary of the research performed under Grant N00014-90-J-1712 during the period of April 1, 1990 through September 30, 1992. First, we present a list of the personnel involved in the research effort. Then, we present a brief summary of the research results that have been achieved. Each of these results is well documented in technical articles, and references to these articles are made in the summary of the research results. DTIC

N93-29857# Army Missile Command, Redstone Arsenal, AL. Guidance and Control Directorate.
MONTE CARLO SIMULATION OF MAGNITUDE-ANGLE ERROR SOURCES Final Report, Oct. - Nov. 1990
Philip N. Jenkins Feb. 1993 27 p
(AD-A263738; AD-E951985; AMSMI/TR-RD-GC-93-4) Avail: CASI HC A03/MF A01

A common error source in Monte Carlo simulations takes the form of a random magnitude at a random angle. This occurs with winds that may have a random angular misalignment oriented in a random direction. A common way of handling this type of error in Monte Carlo simulations is to obtain the magnitude from a gaussian distribution of zero mean and desired standard deviation and to obtain the direction from a uniform distribution. Another common method of handling this error source is to obtain two values from gaussian distribution with zero mean and equal standard deviation and calculate the magnitude and angle. To fully understand each method, the joint probability distribution functions are derived and shown as three-dimensional plots. Author (DTIC)

N93-29878# Stanford Univ., CA. Dept. of Operations Research.
GRADIENT ESTIMATION FOR REGENERATIVE PROCESSES
Paul Glasserman and Peter W. Glynn Aug. 1992 10 p
(Contract DAAL03-91-G-0101)
(AD-A263766; SU-TR-92-8; ARO-28809.8-MA-SDI) Avail: CASI HC A02/MF A01

This paper is concerned with gradient estimation techniques for steady-state performance measures associated with regenerative stochastic processes. The principal emphasis is on the discussion of conditions under which likelihood ratio methods and infinitesimal perturbation analysis techniques are valid. DTIC

N93-29923# Maryland Univ., Baltimore.
SOME STATISTICAL INFERENCE PROBLEMS IN LINEAR MODELS AND VARIANCE COMPONENTS MODELS AND THEIR APPLICATIONS Final Report, 1 Jan. 1989 - 31 Dec. 1992
Thomas Mathew 10 Mar. 1993 5 p
(Grant AF-AFOSR-0237-89)
(AD-A264062; AFOSR-93-0312TR) Avail: CASI HC A01/MF A01

The proposal dealt with several statistical inference problems in the context of univariate and multivariate linear models having effects, i.e., fixed effects as well as random effects. Most of the articles that were completed under the grant are on the following topics: (1) improved nonnegative estimation of variance components; (2) exact and/or optimum tests for the fixed effects; and (3) exact and/or optimum tests for variance components. The results have the potential for applications in all areas where the mixed model methodology is used and the applications are highlighted in most of the articles that were written based on the problems in the proposal. DTIC

N93-29979# Florida State Univ., Tallahassee. Dept. of Statistics.
EASY-TO-APPLY RESULTS FOR ESTABLISHING CONVERGENCE OF MARKOV CHAINS IN BAYESIAN ANALYSIS
Krishna B. Athreya (Iowa State Univ. of Science and Technology, Ames.), Hani Doss, and Jayaram Sethuraman Feb. 1993 9 p
(Contract DAAL03-90-G-0103; AF-AFOSR-0202-90; NSF DMS-92-04938)
(AD-A264015; FSU-TR-884; ARO-27868.26-MA) Avail: CASI HC A02/MF A01

The Markov chain simulation method has become a powerful computational method in Bayesian analysis. The success of this method depends on the convergence of the Markov chain to its stationary distribution. Two carefully stated theorems, whose conditions are easy to verify, that establish this convergence are given. Versions of our conditions which are simpler to verify for the Markov chains that arise most commonly in Bayesian analysis are given. DTIC

N93-30363# California Univ., Davis. Dept. of Mathematics.
PARAMETRIC AND COMBINATORIAL PROBLEMS IN CONSTRAINED OPTIMIZATION Final Report, 1 Mar. 1990 - 30 Sep. 1992
Roger D. Wets 17 Mar. 1993 5 p
(Grant AF-AFOSR-0050-91)
(AD-A264229; AFOSR-93-0296TR) Avail: CASI HC A01/MF A01

The aggregation principle in stochastic optimization was exploited to build an algorithmic, progressive hedging, for solving such problems. Relationships were developed between asymptotic results for statistical estimators and those for the solution of stochastic optimization problems. DTIC

N93-29518*# Toulouse Univ. (France).
ESTIMATIONS OF EXPECTEDNESS AND POTENTIAL SURPRISE IN POSSIBILITY THEORY
Henri Prade and Ronald R. Yager (Iona Coll., New Rochelle, NY.) *In* NASA. Johnson Space Center, North American Fuzzy Logic Processing Society (NAFIPS 1992), Volume 1 Dec. 1992 p 7-13 (For primary document see N93-29516 11-59)
Avail: CASI HC A02/MF A03

N93-29565*# Instituto Tecnologico de Morelia (Mexico).
NON-SCALAR UNCERTAINTY: UNCERTAINTY IN DYNAMIC SYSTEMS
Salvador Gutierrez Martinez *In* NASA. Johnson Space Center, North American Fuzzy Logic Processing Society (NAFIPS 1992), Volume 2 Dec. 1992 p 437-448 (For primary document see N93-29556 11-59)
Avail: CASI HC A03/MF A03

N93-29567*# State Univ. of New York, Binghamton. Dept. of Systems Science.
POSSIBILISTIC MEASUREMENT AND SET STATISTICS
Cliff Joslyn *In* NASA. Johnson Space Center, North American Fuzzy Logic Processing Society (NAFIPS 1992), Volume 2 Dec. 1992

p 458-467 (For primary document see N93-29556 11-59)
(Grant NGT-50757)
Avail: CASI HC A02/MF A03

N93-29582*# State Univ. of New York, Binghamton. Dept. of Systems Science.
ON PROBABILITY-POSSIBILITY TRANSFORMATIONS
George J. Klir and Behzad Parviz (California State Univ., Los Angeles.) *In* NASA. Johnson Space Center, North American Fuzzy Logic Processing Society (NAFIPS 1992), Volume 2 Dec. 1992 p 598-607 (For primary document see N93-29556 11-59)
(Grant NSF IRI-90-15675)
Avail: CASI HC A02/MF A03

N93-29584*# Texas Univ., El Paso. Dept. of Computer Science.
GAUSSIAN MEMBERSHIP FUNCTIONS ARE MOST ADEQUATE IN REPRESENTING UNCERTAINTY IN MEASUREMENTS
V. Kreinovich, C. Quintana (Michigan Univ., Ann Arbor.), and L. Reznik (Footscray Inst. of Tech., Australia.) *In* NASA. Johnson Space Center, North American Fuzzy Logic Processing Society (NAFIPS 1992), Volume 2 Dec. 1992 p 618-624 (For primary document see N93-29556 11-59)
(Grants NAG9-482; NSF CDA-90-15006)
Avail: CASI HC A02/MF A03

N93-29585*# Togai InfraLogic, Inc., Houston, TX.
LIFE INSURANCE RISK ASSESSMENT USING A FUZZY LOGIC EXPERT SYSTEM
Luis A. Carreno and Roy A. Steel *In* NASA. Johnson Space Center, North American Fuzzy Logic Processing Society (NAFIPS 1992), Volume 2 Dec. 1992 p 627-635 (For primary document see N93-29556 11-59)
Avail: CASI HC A02/MF A03

N93-30344 Bell-Northern Research Ltd., Ottawa (Ontario).
SEMI-BLIND RESTORATION OF IMAGES DISTORTED BY RANDOM TIME VARYING POINT SPREAD FUNCTIONS
Edward Lam and Rabab K. Ward (British Columbia Univ., Vancouver.) *In* Engineering Inst. of Canada, Canadian Conference on Electrical and Computer Engineering, Volumes 1 and 2 1990 4 p (For primary document see N93-30215 11-31)
Avail: Engineering Inst. of Canada, 2050 rue Mansfield, Suite 700, Montreal, Quebec H3A 1Z2 Canada

66 SYSTEMS ANALYSIS

Includes mathematical modeling; network analysis; and operations research.

N93-28572*# National Aeronautics and Space Administration, Washington, DC.
PROCEEDINGS OF THE NEAR-EARTH-OBJECT INTERCEPTION WORKSHOP
G. J. Canavan, ed. (Sandia National Labs., Albuquerque, NM.), J. C. Solem, ed. (Sandia National Labs., Albuquerque, NM.), and John D. G. Rather, ed. Feb. 1993 296 p Workshop held in Los Alamos, NM, 14-26 Jan. 1992
(Contract W-7405-eng-36)
(NASA-TM-108236; NAS 1.15:108236; DE93-011040; LA-12476-C; CONF-920180) Avail: CASI HC A13/MF A03

The National Aeronautics and Space Administration Headquarters sponsored the Near-Earth-Object Interception Workshop hosted by the Los Alamos National Laboratory on 14-16 Jan. 1992 at the J. Robert Oppenheimer Study Center in Los Alamos, New Mexico. The Workshop evaluated the issues involved in intercepting celestial objects that could hit the Earth. It covered the technologies for acquiring, tracking, and homing, as well as those for sending interceptors to inspect, rendezvous with, land on, irradiate, deflect, or destroy them. This report records the presentations and technical options reviewed. DOE

N93-28852# GEC Ferranti, Edinburgh (Scotland). Radar Systems Div.
PLANNING FOR AIR TO AIR COMBAT
I. D. Gray *In* AGARD, Combat Automation for Airborne Weapon Systems: Man/Machine Interface Trends and Technologies Apr. 1993 13 p (For primary document see N93-28850 11-54)
Copyright Avail: CASI HC A03/MF A03

N93-28854# GEC Sensors Ltd., Basildon (England).
A NEW CLASS OF MISSION SUPPORT FOR COMBAT AIR-CREW
Harvey J. Pipe *In* AGARD, Combat Automation for Airborne Weapon Systems: Man/Machine Interface Trends and Technologies Apr. 1993 6 p (For primary document see N93-28850 11-54)
Copyright Avail: CASI HC A02/MF A03

N93-28868# Thomson-CSF, Trappes (France). Dept. Simulateurs.
COMPUTER ASSISTED EVALUATION FOR AIR CLOSE COMBAT BASED ON TIME INTERVAL CHARACTERIZATION [EVALUATION AUTOMATIQUE DE COMBATS AERIENS FONDEE SUR LES INTERVALLES CARACTERISTIQUES]
P. Poutignat and H. deFontenilles *In* AGARD, Combat Automation for Airborne Weapon Systems: Man/Machine Interface Trends and Technologies Apr. 1993 9 p In FRENCH (For primary document see N93-28850 11-54)
Copyright Avail: CASI HC A02/MF A03

N93-29746*# Pennsylvania State Univ., University Park.
MARS SAMPLE RETURN MISSION: TWO ALTERNATE SCENARIOS
In Universities Space Research Association, Houston, Proceedings of the Seventh Annual Summer Conference. NASA/USRA: University Advanced Design Program 1991 p 249-252 (For primary document see N93-29712 11-01)
Avail: CASI HC A01/MF A03

N93-29756*# Naval Academy, Annapolis, MD.
MARS AQUARIUS MISSION AND TITAN EXPLORER
Brian Dulla, Christina Glaser, Jason Lopez, Jeffrey Lucas, Michelle Reyes, James Rimrodt, Stephen Philpott, Paul Diedrich, Terry Ladau, and David Lagassa et al *In* Universities Space Research Association, Houston, Proceedings of the Seventh Annual Summer Conference. NASA/USRA: University Advanced Design Program 1991 p 305-308 (For primary document see N93-29712 11-01)
Avail: CASI HC A01/MF A03

67 THEORETICAL MATHEMATICS

Includes topology and number theory.

N93-28601# Texas Univ., Austin. Center for Particle Physics.
CLASSIFICATION THEOREM FOR PRINCIPAL FIBRE BUNDLES, BERRY'S PHASE, AND EXACT CYCLE EVOLUTION
A. Bohm, L. J. Boya, A. Mostafazadeh, and G. Rudolph (Leipzig Univ., German D.R..) Mar. 1993 20 p
(Contract DE-FG03-93ER-40757)
(DE93-011114; DOE/ER-40757/005) Avail: CASI HC A03/MF A01

The relation between the two mathematical interpretations of the geometric (Berry) phase is discussed, using either the fiber bundle over parameter space or over projective Hilbert space. It turns out that these two geometric constructions are linked by the classification theorem for vector bundles. The classification theorem provides the means to classify the parameter space bundles for adiabatic evolution and for non-adiabatic cyclic evolution of the statevectors. DOE

N93-29423# Army Research Lab., Adelphi, MD.
ESTIMATING THE PARAMETERS OF CHAOTIC MAPS Final Report, Jan. - Apr. 1992
Scott Hayes Feb. 1993 28 p
(AD-A262574; ARL-TR-95) Avail: CASI HC A03/MF A01

The lowest mean square error (LMSE) parameter estimator for a chaotic map (a discrete-time dynamical system) is developed, its implementation is discussed, and the results of computer simulations evaluating its performance are presented. The estimator detects the control parameter of a one-dimensional chaotic map from observations of the output sequence in the presence of additive noise. This type of estimation problem is of interest for finding dynamical models of physical systems from measurements by estimating the return map for a Poincare surface of section in state space. Several common estimators for maps are first described. The Cramer-Rao LMSE bound for estimators of chaotic maps is then computed, and the optimal estimator is developed. It is shown that this estimator is efficient (attains the Cramer-Rao bound) and it converges exponentially to the correct parameter for certain trajectories. Because the estimator becomes impractical to use for very long data sequences, an alternative implementation for long data blocks is also described. The exponentially increasing accuracy of this estimator as a function of sample size indicates that the estimator extracts parameter information at a constant rate, unlike a typical estimator with inverse square root convergence, which has a decaying information rate. The information rate is shown to be given by a parameter entropy function formally similar to the Kolmogorov entropy for maps. The information rate is therefore quantitatively linked to the global chaos of the system through this parameter entropy. DTIC

N93-30048# Maryland Univ., College Park.
STUDY OF EFFECTS OF SMALL PERTURBATIONS ON CHAOTIC SYSTEMS
C. Grebogi and J. A. Yorke Jan. 1993 8 p
(Contract DE-FG05-87ER-25036)
(DE93-009762; DOE/ER-25036/6) Avail: CASI HC A02/MF A01

Very brief summaries are given of work on the following topics: prevalence, border crossing bifurcations, numerical procedure for computing the dimension, generalized saddle straddle trajectories methods, and finding typical trajectories numerically. DOE

N93-30917# International Centre for Theoretical Physics, Trieste (Italy).
NONLINEAR REALISATIONS OF OMEGA(1 + INFINITY)
E. Sezgin and K. S. Stelle (Imperial Coll. of Science and Technology, London, England.) Jun. 1992 20 p
(DE92-644721; IC-92/122; Imperial/TP-90-91/21; CTP-TAMU-26/91)
Avail: CASI HC A03/MF A01 (US Sales Only)

The nonlinear scalar-field realization of omega(sub 1 + infinity) symmetry in d = 2 dimensions is studied in analogy to the nonlinear realization of d = 4 conformal symmetry SO(4,2). The omega(sub 1 + infinity) realization is derived from a coset-space construction in which the divisor group is generated by the non-negative modes of the Virasoro algebra, with subsequent application of an infinite set of covariant constraints. The initial doubly-infinite set of Goldstone fields arising in this construction is reduced by the covariant constraints to a singly-infinite set corresponding to the Cartan-subalgebra generators upsilon(sup l)(sub -(l+1)). We derive the transformation rules of this surviving set of fields, finding a triangular structure in which fields transform into themselves or into lower members of the set only. This triangular structure gives rise to finite-component subrealizations, including the standard one for a single scalar. We derive the Maurer-Cartan form and discuss the construction of invariant actions. DOE

N93-30922# Joint Inst. for Nuclear Research, Dubna (USSR). Lab. of Theoretical Physics.
A NEW EXACT SOLUTION TO THE CLASSICAL EQUATIONS OF MOTION OF THE RELATIVISTIC STRING WITH MASSIVE ENDS
B. M. Barbashov and A. M. Chervyakov 1991 14 p
(DE92-644736; JINR-E-2-91-118) Avail: CASI HC A03/MF A01 (US Sales Only)

The classical histories of the relativistic string with massive ends in space-time are examined in terms of geometric invariants of both the string world surface and world lines of the point masses at the string ends. In this formulation, the string variables are completely defined by means of the constant curvatures and torsions of the endpoint trajectories which are subjected to a system of differential equations with a delayed argument that incorporates retardation effects of the interaction of two point masses through the string. The well-known example of the rotating straight-line string with massive ends corresponds to a particular solution of this system for the constant torsions. A new exact solution for the periodic torsions of the world trajectories of the massive string ends is found. In this case, the string coordinates are represented in terms of normal elliptic integrals and describe a more intricate motion including its transverse vibrations than rotation of a stretched string in a given plane. DOE

N93-30926# Joint Inst. for Nuclear Research, Dubna (USSR). Lab. of Theoretical Physics.
ON THE ENERGY-MOMENTUM TENSORS FOR FIELD THEORIES IN SPACES WITH AFFINE CONNECTION AND METRIC
S. Manoff 1991 16 p
(DE92-644743; JINR-E-2-91-77) Avail: CASI HC A03/MF A01 (US Sales Only)

Generalized covariant Bianchi type identities are obtained and investigated for Lagrangian densities, depending on co- and contravariant tensor fields and their first and second covariant derivatives in spaces with affine connection and metric (L(sub n)-space). The notions of canonical, generalized canonical, symmetric, and variational energy-momentum tensor are introduced and necessary and sufficient conditions for the existence of the symmetric energy-momentum tensor as a local conserved quantity are obtained. DOE

N93-30927# Joint Inst. for Nuclear Research, Dubna (USSR). Lab. of Theoretical Physics.
ON THE ENERGY-MOMENTUM TENSORS FOR FIELD THEORIES IN SPACES WITH AFFINE CONNECTION AND METRIC
S. Manoff 1991 15 p
(DE92-644744; JINR-E-2-91-78) Avail: CASI HC A03/MF A01 (US Sales Only)

It is shown that the Euler-Lagrange equations for a material system in L(sub n) space (in accordance with the case in U(sub n)-space in contrast to the case in V(sub n) space) cannot be used as sufficient conditions for the existence of the energy-momentum tensor as a local conserved quantity. The non-equivalent of Belinfante's and Hilbert's symmetric energy-momentum tensor for the general case is considered. It is shown from a more general point of view that Einstein's tensor in the general relativity is equal to the symmetric energy-momentum tensor for the gravitational field. DOE

N93-30928# International Centre for Theoretical Physics, Trieste (Italy).
BELTRAMI PARAMETRIZATION AND GAUGING OF VIRASORO AND w-INFINITY ALGEBRAS
L. Tatar (Academia R. P. R., Cluj.) Jul. 1992 20 p
(DE92-644844; IC-92/126) Avail: CASI HC A03/MF A01 (US Sales Only)

The gauging of the Virasoro and w-infinity algebras are discussed from the point of view of BRST symmetry. Both algebras are realized as 'Russian formulas' for the curvatures built from the generators of the Lie algebras and the corresponding gauge fields. The generalized curvatures are used to determine the gauge invariant Lagrangians as well as the anomaly structures of the conformal two dimensional theory and the w-gravity. DOE

N93-30981# International Centre for Theoretical Physics, Trieste (Italy).
EQUIVARIANT ELLIPTIC HOMOLOGY
J. A. Devoto May 1992 31 p
(DE92-641338; IC-92/72) Avail: CASI HC A03/MF A01 (US Sales Only)

In a previous paper, we studied the modular properties of indices of elliptic operators on twisted loop spaces of manifolds with finite group actions. This motivates the introduction of the universal twisted elliptic genus. This genus can be interpreted as a ring homomorphism from the equivariant bordism ring MU(sub *)(sup G) to a ring Ell(sub *)(sup G). It is shown that the factor X yields Ell(sub *)(sup G) = MU(sub *)(sup G)(X)(x)(sub MU(sub *))(sup G)Ell(sub *)(sup G) defines an equivariant homology theory, and that the associated cohomology theory satisfies a conjecture of Atiyah and Segal about generalized Lefchetz formulas. DOE

N93-30985# International Centre for Theoretical Physics, Trieste (Italy).
NTH ROOTS OF NORMAL CONTRACTIONS
B. P. Duggal Jul. 1992 14 p
(DE92-644725; IC-92/133) Avail: CASI HC A03/MF A01 (US Sales Only)

Given a complex separable Hilbert space H and a contraction A on H such that A(exp n), where n is greater than or equal to 2 some integer, is normal it is shown that if the defect operator D(sub A) = (1 - A(exp *)A)(exp 1/2) is of the Hilbert-Schmidt class, then A is similar to a normal contraction, either A or A(exp 2) is normal, and if A(exp 2) is normal (but A is not) then there is a normal contraction N and a positive definite contraction P of trace class such that (A - N)(sub 1) = 1/2(P + P)(sub 1). If T is a compact contraction such that its characteristic function admits a scalar factor, if T = A(exp n) for some integer n greater than o r equal to 2 and contraction A with simple eigenvalues, and if both T and A satisfy a 'reductive property', then A is a compact normal contraction. DOE

N93-30986# International Centre for Theoretical Physics, Trieste (Italy).
ON ONE-DIMENSIONAL TOPOLOGICAL AND CONFORMAL FIELD THEORIES
S. A. Bulgadaev Jul. 1992 11 p
(DE92-644726; IC-92/135) Avail: CASI HC A03/MF A01 (US Sales Only)

It is shown how starting from the one-dimensional topological field theory of Schwarz-type, with holomorphic differential l-form and using Hilbert reduction, one can construct one-dimensional conformal free scalar theory. This can be used to realize infinite-dimensional conformal symmetries of W(sub 1 + (infinity)) type as well as sl(2) Kac-Moody algebra. DOE

N93-30988# International Centre for Theoretical Physics, Trieste (Italy).
SPHERICALLY SYMMETRIC LINE ELEMENT AND KILLING VECTORS IN FIVE-DIMENSIONAL SPACE
G. Rcheulishvili Jun. 1992 9 p
(DE93-604132; IC-92/108) Avail: CASI HC A02/MF A01 (US Sales Only)

The series of Killing vectors for the line element are described. Their algebras and curvature are presented. The explicit expressions of metrics for higher symmetries are written down. DOE

N93-30989# International Centre for Theoretical Physics, Trieste (Italy).
SUPERCONFORMAL STRUCTURES AND HOLOMORPHIC 1/2-SUPERDIFFERENTIALS ON N = 1 SUPER RIEMANN SURFACES
H. Kachkachi and M. Kachkachi Jul. 1992 15 p
(DE93-604133; IC-92/146) Avail: CASI HC A03/MF A01 (US Sales Only)

Using the Super Riemann-Roch theorem we give a local expression for a holomorphic 1/2-superdifferential in a superconformal structure parametrized by special isothermal coordinates on an N = 1 Super Riemann Surface (SRS). This construction is done by choosing a suitable origin for these coordinates. The holomorphy of the latter with respect to super Beltrami differentials is proven. DOE

N93-29517*# Louisville Univ., KY. Dept. of Mathematics.
AN ANALYSIS OF POSSIBLE APPLICATIONS OF FUZZY SET THEORY TO THE ACTUARIAL CREDIBILITY THEORY
Krzysztof Ostaszewski and Waldemar Karwowski *In* NASA. Johnson Space Center, North American Fuzzy Logic Processing Society (NAFIPS 1992), Volume 1 Dec. 1992 p 1-6 (For primary document see N93-29516 11-59)
Avail: CASI HC A02/MF A03

N93-29519*# New South Wales Univ., Kensington (Australia). Dept. of Computer Science.
COMPARISON OF SPECIFICITY AND INFORMATION FOR FUZZY DOMAINS
Arthur Ramer *In* NASA. Johnson Space Center, North American Fuzzy Logic Processing Society (NAFIPS 1992), Volume 1 Dec. 1992 p 14-20 (For primary document see N93-29516 11-59)
Avail: CASI HC A01/MF A03

N93-29520*# Soviet Association of Fuzzy Systems, Moscow (Russia).
THE AXIOMATIC DEFINITION OF A LINGUISTIC SCALE FUZZINESS DEGREE, ITS MAJOR PROPERTIES, AND APPLICATIONS
Alexander P. Ryjov *In* NASA. Johnson Space Center, North American Fuzzy Logic Processing Society (NAFIPS 1992), Volume 1 Dec. 1992 p 21-28 (For primary document see N93-29516 11-59)
Avail: CASI HC A02/MF A03

N93-29521*# Toronto Univ. (Ontario). Dept. of Industrial Engineering.
HOW TO SELECT COMBINATION OPERATORS FOR FUZZY EXPERT SYSTEMS USING CRI
I. B. Turksen and Y. Tian *In* NASA. Johnson Space Center, North American Fuzzy Logic Processing Society (NAFIPS 1992), Volume 1 Dec. 1992 p 29-38 Sponsored in part by Natural Sciences and Engineering Research Council and Manufacturing Research Corp. (For primary document see N93-29516 11-59)
Avail: CASI HC A02/MF A03

N93-29523*# Missouri Univ., Columbia. Dept. of Electrical and Computer Engineering.
QUANTITATIVE ANALYSIS OF PROPERTIES AND SPATIAL RELATIONS OF FUZZY IMAGE REGIONS
Raghu Krishnapuram, James M. Keller, and Yibing Ma *In* NASA. Johnson Space Center, North American Fuzzy Logic Processing Society (NAFIPS 1992), Volume 1 Dec. 1992 p 49-58 (For primary document see N93-29516 11-59)
Avail: CASI HC A02/MF A03

N93-29525*# National Aeronautics and Space Administration. Lyndon B. Johnson Space Center, Houston, TX.
A FUZZY MEASURE APPROACH TO MOTION FRAME ANALYSIS FOR SCENE DETECTION M.S. Thesis - Houston Univ.
Albert B. Leigh (McDonnell-Douglas Space Systems Co., Houston, TX.) and Sankar K. Pal (Indian Statistical Inst., Calcutta.) *In its* North American Fuzzy Logic Processing Society (NAFIPS 1992), Volume 1 Dec. 1992 p 69-80 (For primary document see N93-29516 11-59)
Avail: CASI HC A03/MF A03

N93-29527*# Toledo Univ., OH. Dept. of Electrical Engineering.
ENCODING SPATIAL IMAGES: A FUZZY SET THEORY APPROACH
Leszek M. Sztandera *In* NASA. Johnson Space Center, North American Fuzzy Logic Processing Society (NAFIPS 1992), Volume 1 Dec. 1992 p 89-97 (For primary document see N93-29516 11-59)
Avail: CASI HC A02/MF A03

N93-29528*# University of West Florida, Pensacola. Computer Science Div.
IMAGE SEGMENTATION USING FUZZY LVQ CLUSTERING NETWORKS
Eric Chen-Kuo Tsao, James C. Bezdek, and Nikhil R. Pal *In* NASA. Johnson Space Center, North American Fuzzy Logic Processing Society (NAFIPS 1992), Volume 1 Dec. 1992 p 98-107 (For primary document see N93-29516 11-59)
(Grant NSF IRI-90-03252)
Avail: CASI HC A02/MF A03

N93-29529*# Cincinnati Univ., OH. Dept. of Electrical and Computer Engineering.
A NEURO-FUZZY ARCHITECTURE FOR REAL-TIME APPLICATIONS
P. A. Ramamoorthy and Song Huang *In* NASA. Johnson Space Center, North American Fuzzy Logic Processing Society (NAFIPS 1992), Volume 1 Dec. 1992 p 108-117 (For primary document see N93-29516 11-59)
Avail: CASI HC A02/MF A03

N93-29530*# Missouri Univ., Columbia. Dept. of Mechanical and Aerospace Engineering.
A COMPOSITE SELF TUNING STRATEGY FOR FUZZY CONTROL OF DYNAMIC SYSTEMS
C.-Y. Shieh and Satish S. Nair *In* NASA. Johnson Space Center, North American Fuzzy Logic Processing Society (NAFIPS 1992), Volume 1 Dec. 1992 p 118-124 Sponsored in part by National Center for Supercomputing Applications (For primary document see N93-29516 11-59)
Avail: CASI HC A02/MF A03

N93-29532*# Iona Coll., New Rochelle, NY. Machine Intelligence Inst.
ADAPTIVE DEFUZZIFICATION FOR FUZZY SYSTEMS MODELING
Ronald R. Yager and Dimitar P. Filev *In* NASA. Johnson Space Center, North American Fuzzy Logic Processing Society (NAFIPS 1992), Volume 1 Dec. 1992 p 135-142 (For primary document see N93-29516 11-59)
Avail: CASI HC A02/MF A03

N93-29533*# Texas A&M Univ., College Station. Center for Fuzzy Logic and Intelligent Systems Research.
DESIGN ISSUES OF A REINFORCEMENT-BASED SELF-LEARNING FUZZY CONTROLLER FOR PETROCHEMICAL PROCESS CONTROL

John Yen, Haojin Wang, and Walter C. Daugherity *In* NASA. Johnson Space Center, North American Fuzzy Logic Processing Society (NAFIPS 1992), Volume 1 Dec. 1992 p 143-153 (For primary document see N93-29516 11-59)
Avail: CASI HC A03/MF A03

N93-29535*# Texas Technological Univ., Lubbock. Dept. of Electrical Engineering.
CLUSTERING OF TETHERED SATELLITE SYSTEM SIMULATION DATA BY AN ADAPTIVE NEURO-FUZZY ALGORITHM
Sunanda Mitra and Surya Pemmaraju *In* NASA. Johnson Space Center, North American Fuzzy Logic Processing Society (NAFIPS 1992), Volume 1 Dec. 1992 p 166-174 Sponsored in part by Northrop Corp. and Texas Advanced Technology Program (For primary document see N93-29516 11-59)
(Grant NAG9-509)
Avail: CASI HC A02/MF A03

N93-29537*# Texas A&M Univ., College Station. Dept. of Computer Science.
DESIGNING A FUZZY SCHEDULER FOR HARD REAL-TIME SYSTEMS
John Yen, Jonathan Lee, Nathan Pfluger, and Swami Natarajan *In* NASA. Johnson Space Center, North American Fuzzy Logic Processing Society (NAFIPS 1992), Volume 1 Dec. 1992 p 185-194 (For primary document see N93-29516 11-59)
Avail: CASI HC A02/MF A03

N93-29538*# SGS-Thomson Microelectronics, Inc., Agrate Brianza (Italy). Corporate Advanced System Architectures.
WARP: WEIGHT ASSOCIATIVE RULE PROCESSOR. A DEDICATED VLSI FUZZY LOGIC MEGACELL
A. Pagni, R. Poluzzi, and G. G. Rizzotto *In* NASA. Johnson Space Center, North American Fuzzy Logic Processing Society (NAFIPS 1992), Volume 1 Dec. 1992 p 195-204 (For primary document see N93-29516 11-59)
Avail: CASI HC A02/MF A03

N93-29539*# Loki Software, Inc., Liberty Corner, NJ.
EVALUATION OF FUZZY INFERENCE SYSTEMS USING FUZZY LEAST SQUARES
Joseph M. Barone *In* NASA. Johnson Space Center, North American Fuzzy Logic Processing Society (NAFIPS 1992), Volume 1 Dec. 1992 p 205-214 (For primary document see N93-29516 11-59)
Avail: CASI HC A02/MF A03

N93-29543*# Rockwell International Science Center, Thousand Oaks, CA.
DISTRIBUTED TRAFFIC SIGNAL CONTROL USING FUZZY LOGIC
Stephen Chiu *In* NASA. Johnson Space Center, North American Fuzzy Logic Processing Society (NAFIPS 1992), Volume 1 Dec. 1992 p 239-247 (For primary document see N93-29516 11-59)
Avail: CASI HC A02/MF A03

N93-29544*# George Mason Univ., Fairfax, VA. Center for Excellence.
INTELLIGENT VIRTUAL REALITY IN THE SETTING OF FUZZY SETS
John Dockery (Defense Information Systems Agency, Arlington, VA.) and David Littman *In* NASA. Johnson Space Center, North American Fuzzy Logic Processing Society (NAFIPS 1992), Volume 1 Dec. 1992 p 248-256 (For primary document see N93-29516 11-59)
Avail: CASI HC A02/MF A03

N93-29547*# Toronto Univ. (Ontario).
AN EXPERIMENTAL METHODOLOGY FOR A FUZZY SET PREFERENCE MODEL
I. B. Turksen and Ian A. Willson *In* NASA. Johnson Space Center, North American Fuzzy Logic Processing Society (NAFIPS 1992), Volume 1 Dec. 1992 p 276-285 (For primary document see N93-29516 11-59)
Avail: CASI HC A02/MF A03

N93-29548*# Toronto Univ. (Ontario).
A FUZZY SET PREFERENCE MODEL FOR MARKET SHARE ANALYSIS
I. B. Turksen and Ian A. Willson *In* NASA. Johnson Space Center, North American Fuzzy Logic Processing Society (NAFIPS 1992), Volume 1 Dec. 1992 p 286-295 (For primary document see N93-29516 11-59)
Avail: CASI HC A02/MF A03

N93-29550*# Universidad Nacional Autonoma de Mexico, Coyoacan. Inst. de Ingenieria.
FUZZY KNOWLEDGE BASE CONSTRUCTION THROUGH BELIEF NETWORKS BASED ON LUKASIEWICZ LOGIC
Felipe Lara-Rosano *In* NASA. Johnson Space Center, North American Fuzzy Logic Processing Society (NAFIPS 1992), Volume 1 Dec. 1992 p 304-311 (For primary document see N93-29516 11-59)
Avail: CASI HC A02/MF A03

N93-29551*# Minnesota Univ., Minneapolis. Dept. of Electrical Engineering.
INTELLIGENT FUZZY CONTROLLER FOR EVENT-DRIVEN REAL TIME SYSTEMS
Janos Grantner (Technical Univ. of Budapest, Hungary.), Marek Patyra (Minnesota Univ., Duluth.), and Marian S. Stachowicz (Minnesota Univ., Duluth.) *In* NASA. Johnson Space Center, North American Fuzzy Logic Processing Society (NAFIPS 1992), Volume 1 Dec. 1992 p 312-321 (For primary document see N93-29516 11-59)
Avail: CASI HC A02/MF A03

N93-29552*# Manitoba Univ., Winnipeg. Dept. of Electrical and Computer Engineering.
FUZZY COORDINATOR IN CONTROL PROBLEMS
A. Rueda and W. Pedrycz *In* NASA. Johnson Space Center, North American Fuzzy Logic Processing Society (NAFIPS 1992), Volume 1 Dec. 1992 p 322-329 (For primary document see N93-29516 11-59)
(Grant CONACyT-60558)
Avail: CASI HC A02/MF A03

N93-29553*# Georgia State Univ., Atlanta.
TUNING A FUZZY CONTROLLER USING QUADRATIC RESPONSE SURFACES
Brian Schott and Thomas Whalen *In* NASA. Johnson Space Center, North American Fuzzy Logic Processing Society (NAFIPS 1992), Volume 1 Dec. 1992 p 330-339 (For primary document see N93-29516 11-59)
Avail: CASI HC A02/MF A03

N93-29554*# Mentalogic Systems, Inc., Markham (Ontario). Research and Development.
THE COGNITIVE BASES FOR THE DESIGN OF A NEW CLASS OF FUZZY LOGIC CONTROLLERS: THE CLEARNESS TRANSFORMATION FUZZY LOGIC CONTROLLER
Labib Sultan (York Univ., Toronto, Ontario.) and Talib Janabi *In* NASA. Johnson Space Center, North American Fuzzy Logic Processing Society (NAFIPS 1992), Volume 1 Dec. 1992 p 340-349 Sponsored in part by Natural Sciences and Engineering Research Council (For primary document see N93-29516 11-59)
Avail: CASI HC A02/MF A03

N93-29555*# Institutul Politehnic din Iasi (Romania). Center for Research in Fuzzy Systems and Artificial Intelligence.
A FUZZY CONTROL DESIGN CASE: THE FUZZY PLL
H. N. Teodorescu and I. Bogdan *In* NASA. Johnson Space Center, North American Fuzzy Logic Processing Society (NAFIPS 1992), Volume 1 Dec. 1992 p 350-359 (For primary document see N93-29516 11-59)
Avail: CASI HC A02/MF A03

N93-29557*# Academia R. P. R., Bucharest. Inst. for Computer Science.
ADDING DYNAMIC RULES TO SELF-ORGANIZING FUZZY SYSTEMS
Catalin V. Buhusi *In* NASA. Johnson Space Center, North American Fuzzy Logic Processing Society (NAFIPS 1992), Volume 2 Dec. 1992 p 360-367 (For primary document see N93-29556 11-59)
Avail: CASI HC A02/MF A03

N93-29558*# Dynetics, Inc., Huntsville, AL.
FUZZY LEARNING UNDER AND ABOUT AN UNFAMILIAR FUZZY TEACHER

Belur V. Dasarathy *In* NASA. Johnson Space Center, North American Fuzzy Logic Processing Society (NAFIPS 1992), Volume 2 Dec. 1992 p 368-377 (For primary document see N93-29556 11-59)
Avail: CASI HC A02/MF A03

N93-29559*# NYNEX Science and Technology, Inc., White Plains, NY.
SOME PROBLEMS WITH THE DESIGN OF SELF-LEARNING MANAGEMENT SYSTEMS
Ziny Flikop *In* NASA. Johnson Space Center, North American Fuzzy Logic Processing Society (NAFIPS 1992), Volume 2 Dec. 1992 p 378-387 (For primary document see N93-29556 11-59)
Avail: CASI HC A02/MF A03

N93-29560*# Technische Univ., Brunswick (Germany). Dept. of Computer Science.
A NEURAL FUZZY CONTROLLER LEARNING BY FUZZY ERROR PROPAGATION
Detlef Nauck and Rudolf Kruse *In* NASA. Johnson Space Center, North American Fuzzy Logic Processing Society (NAFIPS 1992), Volume 2 Dec. 1992 p 388-397 (For primary document see N93-29556 11-59)
Avail: CASI HC A02/MF A03

N93-29561*# National Aeronautics and Space Administration. Lyndon B. Johnson Space Center, Houston, TX.
DETERMINING RULES FOR CLOSING CUSTOMER SERVICE CENTERS: A PUBLIC UTILITY COMPANY'S FUZZY DECISION
Andre deKorvin (Houston Univ., TX.), Margaret F. Shipley (Houston Univ., TX.), and Robert N. Lea *In its* North American Fuzzy Logic Processing Society (NAFIPS 1992), Volume 2 Dec. 1992 p 398-407 (For primary document see N93-29556 11-59)
Avail: CASI HC A02/MF A03

N93-29562*# Lappeenranta Univ. of Technology (Finland). Dept. of Chemical Technology.
FUZZY SIMULATION IN CONCURRENT ENGINEERING
A. Kraslawski and L. Nystrom *In* NASA. Johnson Space Center, North American Fuzzy Logic Processing Society (NAFIPS 1992), Volume 2 Dec. 1992 p 408-417 (For primary document see N93-29556 11-59)
Avail: CASI HC A02/MF A03

N93-29563*# Texas Univ., El Paso. Dept. of Computer Science.
INVERSE PROBLEMS: FUZZY REPRESENTATION OF UNCERTAINTY GENERATES A REGULARIZATION
V. Kreinovich, Ching-Chuang Chang, L. Reznik (Footscray Inst. of Tech., Australia.), and G. N. Solopchenko (Saint Petersburg Technical Univ., Russia.) *In* NASA. Johnson Space Center, North American Fuzzy Logic Processing Society (NAFIPS 1992), Volume 2 Dec. 1992 p 418-426 Sponsored in part by Inst. for Manufacturing and Materials Management (For primary document see N93-29556 11-59)
(Grants NAG9-482; NSF CDA-90-15006)
Avail: CASI HC A02/MF A03

N93-29566*# Mentalogic Systems, Inc., Markham (Ontario).
COMPARISON BETWEEN THE PERFORMANCE OF TWO CLASSES OF FUZZY CONTROLLERS
T. H. Janabi and L. H. Sultan (York Univ., Toronto, Ontario.) *In* NASA. Johnson Space Center, North American Fuzzy Logic Processing Society (NAFIPS 1992), Volume 2 Dec. 1992 p 449-457 (For primary document see N93-29556 11-59)
Avail: CASI HC A02/MF A03

N93-29568*# Missouri Univ., Columbia. Dept. of Electrical and Computer Engineering.
THE FUSION OF INFORMATION VIA FUZZY INTEGRATION
James M. Keller and Hossein Tahani *In* NASA. Johnson Space Center, North American Fuzzy Logic Processing Society (NAFIPS 1992), Volume 2 Dec. 1992 p 468-477 (For primary document see N93-29556 11-59)
Avail: CASI HC A02/MF A03

N93-29572*# Bureau of Mines, Tuscaloosa, AL.
GENETIC ALGORITHMS IN ADAPTIVE FUZZY CONTROL
C. Lucas Karr and Tony R. Harper *In* NASA. Johnson Space Center, North American Fuzzy Logic Processing Society (NAFIPS 1992), Volume 2 Dec. 1992 p 506-514 (For primary document see N93-29556 11-59)
Avail: CASI HC A02/MF A03

N93-29573*# National Aeronautics and Space Administration. Lyndon B. Johnson Space Center, Houston, TX.
A GENETIC ALGORITHMS APPROACH FOR ALTERING THE MEMBERSHIP FUNCTIONS IN FUZZY LOGIC CONTROLLERS
Hana Shehadeh (LinCom Corp., Houston, TX.) and Robert N. Lea *In its* North American Fuzzy Logic Processing Society (NAFIPS 1992), Volume 2 Dec. 1992 p 515-523 (For primary document see N93-29556 11-59)
Avail: CASI HC A02/MF A03

N93-29574*# Clemson Univ., SC. Dept. of Civil Engineering.
FUZZY MULTIPLE LINEAR REGRESSION: A COMPUTATIONAL APPROACH
C. H. Juang, X. H. Huang, and J. W. Fleming *In* NASA. Johnson Space Center, North American Fuzzy Logic Processing Society (NAFIPS 1992), Volume 2 Dec. 1992 p 524-534 (For primary document see N93-29556 11-59)
(Grant NSF MSS-90-20252)
Avail: CASI HC A03/MF A03

N93-29576*# Hungarian Academy of Sciences, Budapest. Dept. of Anatomy.
FUZZY OPERATORS AND CYCLIC BEHAVIOR IN FORMAL NEURONAL NETWORKS
E. Labos, A. V. Holden (Leeds Univ., England.), J. Laczko (Ludwig-Maximilians-Univ., Munich, Germany.), L. Orzo, and A. S. Labos *In* NASA. Johnson Space Center, North American Fuzzy Logic Processing Society (NAFIPS 1992), Volume 2 Dec. 1992 p 545-554 (For primary document see N93-29556 11-59)
(Grant OTKA-2621)
Avail: CASI HC A02/MF A03

N93-29578*# Minnesota Univ., Duluth. Dept. of Computer Engineering.
INCOMPLETE FUZZY DATA PROCESSING SYSTEMS USING ARTIFICIAL NEURAL NETWORK
Marek J. Patyra *In* NASA. Johnson Space Center, North American Fuzzy Logic Processing Society (NAFIPS 1992), Volume 2 Dec. 1992 p 565-574 (For primary document see N93-29556 11-59)
Avail: CASI HC A02/MF A03

N93-29580*# Manitoba Univ., Winnipeg. Dept. of Electrical and Computer Engineering.
HIERARCHICAL MODEL OF MATCHING
Witold Pedrycz and Eugene Roventa (York Univ., Toronto, Ontario.) *In* NASA. Johnson Space Center, North American Fuzzy Logic Processing Society (NAFIPS 1992), Volume 2 Dec. 1992 p 581-588 Sponsored in part by Natural Sciences and Engineering Research Council and MicroNet (For primary document see N93-29556 11-59)
Avail: CASI HC A02/MF A03

N93-29583*# Pohang Inst. of Science and Technology (Republic of Korea). Dept. of Computer Science.
INFERENCE IN FUZZY RULE BASES WITH CONFLICTING EVIDENCE
Laszlo T. Koczy (Technical Univ. of Budapest, Hungary.) *In* NASA. Johnson Space Center, North American Fuzzy Logic Processing Society (NAFIPS 1992), Volume 2 Dec. 1992 p 608-617 (For primary document see N93-29556 11-59)
Avail: CASI HC A02/MF A03

70 PHYSICS (GENERAL)

For precision time and time interval (PTTI) see *35 Instrumentation and Photography;* for geophysics, astrophysics or solar physics see *46 Geophysics, 90 Astrophysics,* or *92 Solar Physics.*

N93-29022# Joint Publications Research Service, Arlington, VA.
JPRS REPORT: SCIENCE AND TECHNOLOGY. CENTRAL EURASIA:

PHYSICS AND MATHEMATICS
29 Apr. 1993 82 p Transl. into ENGLISH from various Russian articles
(JPRS-UPM-93-002) Avail: CASI HC A05/MF A01

Translated abstracts cover the following areas: acoustics, lasers, semiconductors, high temperature physics, magnetohydrodynamics and plasmas, optics, superconductivity, theoretical physics, numerical analysis, control theory, and differential equations. Some specific articles address the following topics: generation and transport of solar cosmic rays (survey); relative locations of a powerful flare, the heliospheric current sheet, and the earth fostering the onset of a strong geomagnetic storm; quiet and disturbed heliospheric streamers near earth; effect of vibrationally excited nitrogen on the formation of the main ionospheric trough of electron density in the ionospheric F region; effects of chemical modification of the ionosphere from shortwave doppler measurements over oblique radio communication lines; observation of electromagnetic VLF radiation of seismic origin from Interkosmos-24; anisotropy of electron distribution in ultrastrong microwave field; and effect of a rapid increase in plasma concentration on the propagation dynamics of an electromagnetic wave through it. CASI

N93-29189# Argonne National Lab., IL.
FORCES ON A MAGNET MOVING PAST FIGURE-EIGHT COILS
T. H. Mulcahy, Jianliang He, D. M. Rote, and T. D. Rossing (University of Northern Illinois, De Kalb.) 1993 4 p Presented at the International Magnetics Conference, Stockholm, Sweden, 13-16 Apr. 1993
(Contract W-31-109-eng-38)
(DE93-009965; ANL/MCT/CP-77846; CONF-930416-1) Avail: CASI HC A01/MF A01

For the first time, the lift, drag, and guidance forces acting on a permanent magnet are measured as the magnet passes over different arrays of figure-eight (null-flux) coils. The experimental results are in good agreement with the predictions of dynamic circuit theory, which is used to explain more optimal coil arrays. DOE

N93-29711# Naval Command, Control and Ocean Surveillance Center, San Diego, CA.
DYNAMICS AND PHOTOEXCITATION IN MX AND MXX' CHAIN SOLIDS
J. T. Gammel, A. Saxena, and A. R. Bishop Mar. 1993 6 p
(AD-A264823) Avail: CASI HC A02/MF A01

Nonlinear adiabatic dynamics associated with nonlinear excitations in MX and MXX chain materials are numerically studied within a discrete, 3/4-filled, two-band, tight-binding extended Peierls-Hubbard model. Both Hartree-Fock (HF) adiabatic molecular relaxation and molecular dynamics techniques are employed to investigate the time evolution of solitons, polarons, bipolarons in charge-density wave (CDW), bond order wave (BOW), and spin-density-wave (SDW) ground state materials. Photoexcitations are performed between (1) continuum levels, (2) localized levels, and (3) continuum and localized level. The subsequent formation and time evolution of excitons, defect pairs, breathers, and, for the MXX solids, charge separations are studied in terms of energy levels and distortion patterns. These results are compared with the dynamics of previously studied 1/2-filled, one band, SSH-type electron-photon models, used for studying polyenes and polyynes, and experimental data. DTIC

N93-30519# Stanford Univ., CA. Edward L. Ginzton Lab. of Physics.
THE ROAD TO ROOM TEMPERATURE SUPERCONDUCTIVITY WORKSHOP Final Report, 15 Oct. 1992 - 14 Jan. 1993
Theodore H. Geballe 14 Jan. 1993 8 p Workshop held in Bodega Bay, CA, 19-21 Oct. 1992
(Contract F49620-93-1-0038)
(AD-A264633; AFOSR-93-0257TR) Avail: CASI HC A02/MF A01

History shows right from the beginning that there has been no successful prediction of new families of superconductors. Discoveries in this field have been unexpected, even revolutionary, and not foreseen as simple and logical next steps in an ongoing scientific enterprise. The Bednorz-Muller discovery of superconductivity in the copper-oxide pervoskite family was just such a revolutionary jump. But evolutionary research aimed at the synthesis and characterization of new compositions can also give insightful and even unexpected results. To this end, a 2-day workshop was recently held in which a diverse group of researchers discussed the possibility of reaching substantially higher transition temperatures than are presently known. DTIC

N93-30888# National Inst. of Standards and Technology, Gaithersburg, MD.
PHYSICS LABORATORY TECHNICAL ACTIVITIES, 1992
Mar. 1993 219 p See also PB92-172824
(PB93-178648; NISTIR-5133) Avail: CASI HC A10/MF A03

The report summarizes research projects, measurement method development, calibration and testing, and data evaluation activities that were carried out during calendar year 1992 in the NIST Physics Laboratory. These activities were in the areas of electron and optical physics, atomic physics, molecular physics, radiometric physics, quantum metrology, ionizing radiation, time and frequency, quantum physics, and fundamental constants. NTIS

71 ACOUSTICS

Includes sound generation, transmission and attenuation.
For noise pollution see *45 Environmental Pollution.*

N93-28692*# National Aeronautics and Space Administration. Langley Research Center, Hampton, VA.
SUBJECTIVE RESPONSE TO SIMULATED SONIC BOOMS WITH GROUND REFLECTIONS
B. M. Sullivan (Lockheed Engineering and Sciences Co., Hampton, VA.) and J. D. Leatherwood Jun. 1993 35 p
(RTOP 537-03-21-03)
(NASA-TM-107764; NAS 1.15:107764) Avail: CASI HC A03/MF A01

The Sonic Boom Simulator at NASA LaRC was used for the following: (1) quantify subjective loudness of simulated composite sonic booms, each of which was comprised of a simulated direct (non-reflected) boom combined with a simulated reflection of the direct boom; and (2) evaluate several metrics as estimators of loudness for these composite booms. The direct booms consisted of selected N-wave and minimized signatures having front-shock rise times of 3, 6, and 9 milliseconds and durations of 300 milliseconds. Delay times of the reflected booms ranged from 0 to 12 milliseconds. Subjective loudness results indicated that composite booms formed using reflections with non-zero delay times were generally rated as being less loud than composite booms containing non-delayed reflections. The largest reductions in loudness occurred when delay times were equal to the front shock rise times of the direct booms and were, in some cases, equivalent to reductions in Perceived Level of 6 to 7 dB. Results also showed Perceived Level to be an effective metric for assessing subjective loudness effects for the composite signatures. This was confirmed by statistical analysis, which showed that, for equal Perceived Level, no significant differences existed between the subjective loudness responses to composite booms containing reflections with zero delay and those containing reflections with non-zero delays. Author (revised)

N93-28953*# National Aeronautics and Space Administration. Lewis Research Center, Cleveland, OH.
JET MIXER NOISE SUPPRESSOR USING ACOUSTIC FEEDBACK Patent Application
Edward J. Rice, inventor (to NASA) 14 Apr. 1993 20 p
(NASA-Case-LEW-15170-1; NAS 1.71:LEW-15170-1;
US-Patent-Appl-SN-046256) Avail: CASI HC A03/MF A01

The present invention generally relates to providing an improved jet mixer noise suppressor for high speed jets that rapidly mixes high speed air flow with a lower speed air flow, and more particularly, relates to an improved jet mixer noise suppressor that uses feedback of acoustic waves produced by the interaction of sheer flow instability waves with an obstacle downstream of the jet nozzle. NASA

N93-28995# Mississippi Univ., University. Physical Acoustics Research Lab.
THEORETICAL AND EXPERIMENTAL STUDY OF THERMOACOUSTIC ENGINES Final Report, 1 Jul. 1989 - 30 Sep. 1992
Richard Raspet, Henry E. Bass, and W. P. Arnott 31 Dec. 1992 98 p
(Contract N00014-89-J-3087)
(AD-A261934; PARGUM-92-03) Avail: CASI HC A05/MF A02

A three year study of thermoacoustic engines operating as prime movers and refrigerators was completed. The major thrust of this effort was the use and theoretical description of ceramic honeycomb structures as the active element in thermoacoustic engines. An air-filled demonstration prime mover was constructed and demonstrated at Acoustical Society of America and IEE meetings. A helium-filled test prime mover was designed and built an is being employed in studies of the threshold of oscillation as a function of temperature difference and pressure. In addition, acoustically based theories of the thermoacoustic engine have been developed and tested for a parallel plate stack at the Naval Postgraduate School and for a honeycomb stack at the University of Mississippi. Most of this work is described in detail in the attached publications. In this report we will give an overview of the research completed to date and its relationship to work performed at the Naval Postgraduate School and to future work at the University of Mississippi. DTIC

N93-29279 Department of the Navy, Washington, DC.
ACOUSTIC TRANSDUCER SYSTEM Patent
Edward J. Hilliard, Jr., inventor (to Navy) 16 Feb. 1993 6 p Filed 28 May 1992
(AD-D015713; US-Patent-5,187,690; US-Patent-Appl-SN-892063; US-Patent-Class-367-131) Avail: US Patent and Trademark Office

An acoustic transducer system employs a seawater return cable as a receiver element. The cable is either open ended or short circuited with the seawater. A carrier frequency is applied at one end of the cable. Acoustic-pressure waves impinging the cable, change the characteristic input impedance of the cable. The changes in the impedance amplitude and phase angle are processed to derive information descriptive of the acoustic source. DTIC

N93-29392# Naval Postgraduate School, Monterey, CA.
INVESTIGATION OF THERMOACOUSTIC MUFFLER M.S. Thesis
Chun-Hua Che Dec. 1992 40 p
(AD-A262009) Avail: CASI HC A03/MF A01

The design, construction, and testing of a thermoacoustic muffler is discussed. The performance of the muffler is characterized by measuring its ability to reduce the quality factor Q of an acoustic resonator. Measurements of the Q of a helium filled muffler were made for temperature differences ranging from 0 to -130 deg C. The measured Q-reduction, approximately 30%, agrees with predicted reductions. The predictions are based on a standing wave analysis of thermoacoustic engines. These results indicate that Q-reduction is possible. Future work should concentrate on optimization, to determine if a thermoacoustic muffler is, in fact, practical. DTIC

N93-29480# Army Test and Evaluation Command, Aberdeen Proving Ground, MD.
EXTERNAL ACOUSTICAL NOISE MEASUREMENTS FOR AVIATION SYSTEMS Final Report
5 Feb. 1993 14 p Supersedes TOP-7-3-5-526 dated 10 Jun. 1971
(AD-A263138; TOP-7-3-526) Avail: CASI HC A03/MF A01

This TOP describes procedures for measuring external acoustical noise of Army helicopters. It covers test procedures for the measurements of steady-state and impulse noise. DTIC

N93-29816# Naval Postgraduate School, Monterey, CA.
FEATURE BASED NEURAL NETWORK ACOUSTIC TRANSIENT SIGNAL CLASSIFICATION M.S. Thesis
Terry S. Wichert Mar. 1993 111 p
(AD-A263437) Avail: CASI HC A06/MF A02

Utilization of neural network techniques to recognize and classify acoustic signals has long been pursued and shows great promise as a robust application of neural network technology. Traditional techniques have proven effective but in some cases are quite computationally intensive, as the sampling rates necessary to capture the transient result in large input vectors and thus large neural networks. This thesis presents an alternative transient classification scheme which considerably reduces neural network size and thus computation time. Parameterization of the acoustic transient to a set of distinct characteristics (e.g., frequency, power spectral density) which capture the structure of the input signal is the key to this new approach. Testing methods and results are presented on networks for which computation time is a fraction of the necessary with traditional methods, yet classification reliability is maintained. Neural network acoustic classification systems utilizing the above techniques are compared to classic time domain classification networks. Lastly, a case study is presented which looks at these techniques applied to the acoustic intercept problem. DTIC

N93-30029# Materials Research Labs., Ascot Vale (Australia).
SOUND WAVE SCATTERING FROM AN ELASTIC SPHERICAL SHELL
C. J. Partridge Jan. 1993 54 p
(AD-A264039; MRL-TR-91-10; DODA-AR-006-357) Avail: CASI HC A04/MF A01

The Helmholtz integral equation may be formulated by combining the scalar wave equation and Euler's equation for motion within a fluid. The solution to this integral equation yields the radiated pressure from a submerged vibrating body. The solution obtained from applying Hamilton's variational principle governs the response to a given surface pressure excitation. These two solutions may be used in conjunction to investigate the scattering of incident sound waves from shell-like bodies. In this report, the scattering from a submerged steel spherical shell having a thickness to radius ratio of 0.01 is investigated for ka values up to 8. DTIC

N93-30110# Office National d'Etudes et de Recherches Aerospatiales, Paris (France).
COMPUTATION OF FAR-FIELD HELICOPTER ROTOR TONE NOISE Ph.D. Thesis - Univ. de Tech. de Compiegne, 1985 [CALCUL DU BRUIT DE RAIES EMIS PAR UN ROTOR D'HELICOPTERE EN CHAMP LOINTAIN]
Michel Caplot 1990 236 p In FRENCH
(ONERA-P-1990-5; ETN-93-93722) Avail: CASI HC A11/MF A03

The prediction of helicopter main rotor tone noise in subsonic regime is addressed. A synthesis of the different approaches to this problem is given and a method in the frequency domain is proposed, and compared to a more usual time domain method. For the velocities considered, it appears that the two main tone noise sources are the thickness noise of the monopolar type and the loading noise of the dipolar type. A noise prediction computation code was developed that allows the study of these two sources. For thickness noise, the important factors are the advancing blade and rotational top Mach numbers and the geometric characteristics of the rotor blade. For loading noise, the study is more complicated because the input data are issued from an aerodynamic code. Nevertheless, the use of the frequency method, associated with harmonic analysis of the rotor loads, has real advantages, especially for future developments in the case of blade-vortex interactions. To predict levels under acoustic certification conditions for helicopters, sound wave reflections on the ground and the Doppler effect were introduced in the calculation scheme. ESA

N93-30121 Pennsylvania State Univ., University Park. Materials Research Lab.
MATERIALS FOR ADAPTIVE STRUCTURAL ACOUSTIC CONTROL, VOLUME 1 Annual Report, 1 Feb. 1992 - 31 Jan. 1993
L. E. Cross 6 Apr. 1993 121 p Limited Reproducibility: More than 20% of this document may be affected by microfiche quality
(Contract N00014-92-J-1510)
(AD-A264619) Avail: CASI HC A06

This report documents work carried out in the Materials Research Laboratory of the Pennsylvania State University over the first year of a new ONR sponsored University Research Initiative (URI) entitled Materials for Adaptive Structural Acoustic Control. For this report the activities have been grouped under the following topic headings: (1) General Summary Papers; (2) Materials Studies; (3) Composite Sensors; (4) Actuator Studies; (5) Integration Issues; (6) Processing Studies; and (7) Thin Film Ferroelectrics. In material studies important advances have been made in the understanding of the evaluation of relaxor behavior in the PLZT's and of the order disorder behavior in lead scandium tantalate:lead titanate solid solutions and of the Morphotropic Phase Boundary in this system. DTIC

N93-30157# Materials Research Labs., Ascot Vale (Australia).
SOUND WAVE SCATTERING FROM A RIGID SPHERE
C. J. Partridge Jan. 1993 49 p
(AD-A264182; MRL-TR-91-9; DODA-R-006-356) Avail: CASI HC A03/MF A01

The Helmholtz integral equation may be formed by combining the scalar wave equation with Euler's equation for motion within a fluid. The solution of this integral equation yields the radiated pressure from a submerged, vibrating body and may be used to characterize the scattering of incident sound waves from bodies. In this report the scattering from underwater rigid spheres is investigated and results are presented for ka less than or equal to 8.0. DTIC

N93-30385# Pennsylvania State Univ., University Park. Materials Research Lab.
MATERIALS FOR ADAPTIVE STRUCTURAL ACOUSTIC CONTROL, VOLUME 2 Annual Report, 1 Feb. 1992 - 31 Jan. 1993
L. E. Cross 6 Apr. 1993 120 p
(Contract N00014-92-J-1510)
(AD-A264620) Avail: CASI HC A06/MF A02

This report documents work carried out in the Materials Research Laboratory of the Pennsylvania State University over the first year of a new ONR sponsored University Research Initiative (URI) entitled Materials for Adaptive Structural Acoustic Control. For this report the activities have been grouped under the following topic headings: (1) General Summary Papers; (2) Materials Studies; (3) Composite Sensors; (4) Actuator Studies; (5) Integration Issues; (6) Processing Studies; (7) Thin Film Ferroelectrics. In material studies important advances have been made in the understanding of the evaluation of relaxor behavior in the PLZT's and of the order disorder behavior in lead scandium tantalate:lead titanate solid solutions and of the Morphotropic Phase Boundary in this system. For both composite sensors and actuators we have continued to explore and exploit the remarkable versatility of the flextensional moonie type structure. Finite element (FEA) calculations have given a clear picture of the lower order resonant modes and permitted the evaluation of various end cap metals, cap geometries and load conditions. In actuator studies multilayer structures have been combined with flextensional moonie endcaps to yield high displacement (50 micrometers) compact structures. Electrically controlled shape memory has been demonstrated in lead zirconate stannate titanate compositions, and used for controlling a simple latching relay. DTIC

N93-30899# Naval Surface Warfare Center, Bethesda, MD.
EVALUATION OF THE SCATTERED PRESSURE DUE TO INFINITE RIGID CYLINDERS, INFINITE ELASTIC CYLINDRICAL SHELLS, AND RIGID SPHERES IN THE PRESENCE OF AN AMBIENT NOISE FIELD Final Report, Jan. - Sep. 1992
Rebecca L. Honeycutt and Steven J. Johnson Apr. 1993 64 p
(AD-A264835; CDNSWC-SIG-93/108-745) Avail: CASI HC A04/MF A01

The sound scattering due to an ambient noise field, approximated by a squared cosine function, is considered for infinite rigid and elastic cylinders and rigid spheres. For the cylinders, it is assumed that the acoustic wave front is parallel to the axis of the cylinder (informally incident). For this assumption, a closed form expression for the scattered sound field-to-incident ambient noise field (signal-to-noise) ratio is obtained not only for the cosine squared directivity, but for any arbitrary directivity which can be expressed in terms of a Fourier series. For the sphere, it is assumed that the noise is circumferentially symmetric which leads to a closed form expression for the signal-to-noise ratio due to a cosine squared directivity. DTIC

N93-30980 Stanford Univ., CA.
STRONG PARALLEL BLADE-VORTEX INTERACTION AND NOISE PROPAGATION IN HELICOPTER FLIGHT Ph.D. Thesis
Soogab Lee 1992 152 p
Avail: Univ. Microfilms Order No. DA9309693

Rotor impulsive noise is, of all the known sources of helicopter far-field noise radiation, the one which tends to dominate the acoustic spectrum generated by most helicopters. The helicopter generates a highly directional and rather unique form of impulsive noise which is thought to be generated by two source mechanisms: (1) high-speed impulsive noise due to formation of a shock on the advancing blade tip, and (2) Blade-Vortex Interaction (BVI) noise in low-powered descending flight or maneuvers, especially during an approach to a landing. As an experimental approach, a shock tube was built to generate a compressible viscous vortex which was being convected at a constant velocity in a quasi-uniform subsonic or transonic stream. The vortex then interacted with a target airfoil (NACA 0012 shape). In order to measure quantitatively the flow field, a DPHI (Dual Pulsed Holographic Interferometry) technique was utilized for both flow visualization and density field measurements, and fast-response Kulite transducers were used to obtain pressure histories at the surfaces of both the test section and the airfoil. Secondly, as a numerical approach, the Thin-Layer Navier-Stokes equations were solved not only to simulate the experimental measurements, but also to develop the fundamental understanding of flow field and sound generating mechanisms and, furthermore, to understand the effect of several important parameters on the sound generation due to blade-vortex interaction. The results indicate that the main noise generating mechanism in strong blade-vortex interactions is the severe pressure fluctuation near the leading-edge, caused by rapid oscillation of the stagnation point and formation of a suction peak. In strong parallel BVI, a secondary vortex may be generated by separation on the lower surface if the original vortex is clockwise. In that case, the induced vortex has an opposite rotation. The generated noise level is strongly dependent on Mach number, miss distance, angle of attack, and vortex structure (circulation and core size). The near-field acoustic behavior also depends on the leading-edge shape and thickness of the airfoil rather than the chord length. Results also indicate that transpiration on the leading-edge can suppress pressure fluctuation near the leading-edge and reduce the amplitude of propagating noise. Dissert. Abstr.

72 ATOMIC AND MOLECULAR PHYSICS

Includes atomic structure, electron properties, and molecular spectra.

N93-28521# Lawrence Livermore National Lab., CA.
MEASUREMENT OF 1S2S(SUP 3)S(SUB 1)-1S2P(SUP 3)P(SUB 2,0) INTERVALS IN HELIUM-LIKE NEON
W. A. Hallett, J. D. Silver, and D. D. Dietrich Apr. 1992 6 p Presented at the 10th International Colloquium on Ultra Violet and X Ray Spectroscopy of Astrophysical and Laboratory Plasmas, Berkeley, CA, 3-5 Feb. 1992
(Contract W-7405-eng-48)
(DE93-009243; UCRL-JC-110220; CONF-9202103-6) Avail: CASI HC A02/MF A01

The vacuum ultra-violet 1s2s(sup 3)S(sub 1)-1s2p(sup 3)P(sub 2,0) transition wavelengths in helium-like neon by photographic spectroscopy of a recoil ion source were measured. The results are 1248.01 +/- 0.01 A and 1277.74 +/- 0.04 A respectively and are a sensitive test of present relativistic and quantum electrodynamic calculations. DOE

N93-28542# Northeastern Univ., Boston, MA.
TOPICS IN GAUGE THEORIES AND THE UNIFICATION OF ELEMENTARY PARTICLE INTERACTIONS
Y. N. Srivastava and M. T. Vaughn Feb. 1993 14 p
(Contract DE-FG02-85ER-40233)
(DE93-009370; DOE/ER-40233/8) Avail: CASI HC A03/MF A01

Work done on the following topics is summarized: (1) Coulomb potential in QED on the lattice; (2) Weyl cosmic strings and their consequences; (3) Interference between past and future events in phi yields K(bar K); (4) Quantum effects of strong classical electromagnetic fields; (5) Application of computer algebra to calculations in supersymmetry and supergravity; (6) Numerical studies of classical scalar phi(exp 4) field theory and related nonlinear sigma-models; (7) Analysis of a cubic model field theory; and (8) Renormalization group analysis of unified gauge theories. DOE

N93-28546# Michigan Univ., Ann Arbor.
FAST NEUTRON CROSS SECTION MEASUREMENTS
G. F. Knoll 26 Oct. 1992 41 p
(Contract DE-FG02-87ER-40339)
(DE93-009053; DOE/ER-40339/6) Avail: CASI HC A03/MF A01

From its inception, the Nuclear Data Project at the University of Michigan has concentrated on two major objectives: (1) to carry out carefully controlled nuclear measurements of the highest possible reliability in support of the national nuclear data program, and (2) to provide an educational opportunity for students with interests in experimental nuclear science. The project has undergone a successful transition from a primary dependence on the photoneutron laboratory to one in which current research is entirely based on a unique pulsed 14 MeV fast neutron facility. The new experimental facility is unique in its ability to provide nanosecond bursts of 14 MeV neutrons under conditions that are 'clean' and as scatter-free as possible, and is the only one of its type currently in operation in the United States. It was designed and put into operation primarily by graduate students, and has met or exceeded all of its important initial performance goals. The point of its routine operation has been reached, and most of the data are now in hand that will serve as the basis for the first two doctoral dissertations to be written by participating graduate students. Our initial results on double differential neutron cross sections will be presented at the May 1993 Fusion Reactor Technology Workshop. After investing several years in equipment assembly and optimization, the project has now entered its 'data production' phase. DOE

N93-28549# Argonne National Lab., IL. High Energy Physics Div.
SPIN OBSERVABLES IN LARGE t ELASTIC N-N SCATTERING
G. P. Ramsey 11 Jan. 1993 13 p Presented at the 10th International Symposium on High-Energy Spin Physics, Nagoya, Japan, 9-14 Nov. 1992
(Contract W-31-109-eng-38)
(DE93-009211; ANL-HEP-CP-93-02; CONF-921131-8) Avail: CASI HC A03/MF A01

Model amplitudes for pp yields pp elastic scattering in the intermediate hard scattering kinematic regime: m(sub p)(sup 2) much less than absolute value of t much less than s are presented, and they are applied to the calculation of spin observables. In this region, the t-dependent Landshoff amplitudes have a significant contribution to the spin observables. Helicity non-conserving effects may also play a major role in this regime. Specific quantum chromodynamics (QCD) motivated predictions for the spin observables can be tested at polarized proton beam facilities. A program is suggested for elastic polarized proton scattering experiments in this kinematic region, which can be used to test the foundations of exclusive QCD. DOE

N93-28562# SRI International Corp., Menlo Park, CA.
SYNTHESIS OF CUBANE BASED ENERGETIC MOLECULES Final Report, Feb. 1986 - Mar. 1992
Robert J. Schmitt, Jeffrey C. Bottaro, and Paul E. Penwell 10 Feb. 1993 139 p
(Contract N00014-86-C-0699)
(AD-A263271) Avail: CASI HC A07/MF A02

The need to pack more power with less weight into less space in tomorrow's weapons drove this program for the synthesis of super energetic materials. Our original impetus was a program based solely on the energetic properties of cubane. However, in the course of our studies here and in a parallel ONR sponsored program, we discovered and developed an alternative oxidizer to cubyl based systems, the dinitramide salts. We will report on our developments in the synthesis of new oxidizers based on cubane and dinitramide. In this research, we developed new methods for the functionalization of the cubane nucleus and synthesized new energetic cubanes. We developed several new routes for the synthesis of the dinitramino group. Our work on the preparation of the dinitramide group led to the synthesis of the dinitramide ion, and as a consequence ammonium dinitramide. We have in turn used this synthesis to prepare cubane ammonium dinitramide salts. We synthesized cubane-1,4bis-(ammonium dinitramide) and cubane1,2,4,7-tetrakis(ammonium dinitramide) as well as several other dinitramide salts. DTIC

N93-28604# Oregon Univ., Eugene. Dept. of Chemistry.
DYNAMICAL ANALYSIS OF HIGHLY EXCITED MOLECULAR SPECTRA
M. E. Kellman 1992 5 p
(Contract DE-FG06-92ER-14236)
(DE93-010771; DOE/ER-14236/1) Avail: CASI HC A01/MF A01

Methods of spectral analysis, pattern recognition, and assignment are sought using nonlinear dynamics (bifurcation theory, phase space classification, and quantization of phase space structures) for the analysis of excited vibrational spectra of molecules with strong nonlinear resonances and classical chaos (normal mode analysis is inadequate). A vector method is being applied to excited C2H2. Analysis is being performed of standard fitting Hamiltonians for triatomics. DOE

N93-28611# Wyoming Univ., Laramie.
EXOTIC ATOMS
R. Kunselman 1993 12 p
(Contract DE-FG02-87ER-40333)
(DE93-010242; DOE/ER-40333/133; COO-2197-133) Avail: CASI HC A03/MF A01

The experiments use a solid hydrogen layer to form muonic hydrogen isotopes that escape into vacuum. The method relies on transfer of the muon from protium to either a deuteron or a triton. The resulting muonic deuterium or muonic tritium will not immediately thermalize because of the very low elastic cross sections, and may be emitted from the surface of the layer. Measurements which detect decay electrons, muonic x-rays, and fusion products were used to study the processes. A target was constructed which exploits muonic atom emission in order to learn more about the energy dependence of transfer and muon molecular formation. DOE

N93-28652# Rochester Univ., NY.
SPECTROSCOPIC PROBES OF VIBRATIONALLY EXCITED MOLECULES AT CHEMICALLY SIGNIFICANT ENERGIES
T. R. Rizzo Apr. 1993 6 p
(Contract DE-FG02-88ER-13965)
(DE93-012328; DOE/ER-13965/5) Avail: CASI HC A02/MF A01

Infrared-optical double resonance is being used to study the unimolecular dissociation dynamics of hydrazoic acid (HN3). The 6(nu)(sub NH) vibrational overtone excitation spectra are given for HN3. Work was begun to determine the feasibility of extending the infrared-optical double resonance photofragment spectroscopy to small free radicals, and to be able to monitor atomic dissociation fragments via laser induced fluorescence in the VUV spectrum. DOE

N93-28665# Tennessee Univ., Knoxville. Dept. of Physics.
THE PRODUCTION AND DESTRUCTION OF NEGATIVE IONS
D. J. Pegg 1993 12 p
(Contract DE-FG05-85ER-13456)
(DE93-010527; DOE/ER-13456/47) Avail: CASI HC A03/MF A01

Single photon absorption-single electron detachment from few-electron atomic negative ions was studied. A crossed beam apparatus is being used to perform energy- and angle-resolved photoelectron spectroscopic measurements following photodetachment. Forward-directed electrons were collected and energy analyzed. The kinetic energies and yields of the photoelectrons were obtained by fitting the spectral peaks to Gaussian functions. Electron affinities, asymmetry parameters, and cross sections are determined from these measurements. A ratio method in which the cross section for the ion of interest is measured relative to that of a reference ion was used. The study of the photodetachment of Li(-) was completed, and attention has turned to the photodetachment of the stable ion B(-) and the metastable ion Be(-). DOE

N93-28678# Pittsburgh Univ., PA. Dept. of Physics and Astronomy.
STUDIES OF RELATIVISTIC HEAVY ION COLLISIONS AT THE AGS (E814/E877)
W. E. Cleland 1993 45 p
(Contract DE-FG02-87ER-40363)
(DE93-008541; DOE/ER-40363/6) Avail: CASI HC A03/MF A01

Efforts have continued in the area of peripheral and central collisions of relativistic heavy ions. In the area of peripheral collisions, the analysis of the 1n and 2p decay channels has been completed. In the area of central collisions, the first measurement of the E(sub T) distributions in Au + Au collisions, through the use of the participant calorimeter, was completed, and the results were compared with those obtained in collisions with Si projectiles. In addition, a thorough study of two-particle correlation functions was carried out by use of the data from the silicon pad multiplicity detector. Differential cross sections for 14.6-GeV/c Si-28 on Al, Cu, and Pb, and 11.4-GeV/c Au-197 on Al, Cu, Au, and Pb are given. DOE

N93-28762# Lawrence Livermore National Lab., CA.
POLARIZATION DEPENDENCE OF THE IONIZATION OF HELIUM AND NEON BY 120 FEMTOSECOND PULSES AT 614 NM
D. N. Fittinghoff and P. R. Bolton 3 Mar. 1993 7 p Presented at the 5th Short Wavelength: Physics With Intense Laser Pulses, San Diego, CA, 29-31 Mar. 1993
(Contract W-7405-eng-48)
(DE93-010514; UCRL-JC-113259; CONF-9303119-1) Avail: CASI HC A02/MF A01

A strong polarization dependence is observed for the helium and neon ion yields for the higher charge states produced by 120-fs pulses of 614-nm light. DOE

N93-28831# Los Alamos National Lab., NM.
MESON-MESON INTERACTIONS AND PHI-ENHANCEMENT IN NUCLEUS COLLISIONS
M. Berenguer, H. Sorge, H. Stoecker (Johann-Wolfgang-Goethe-Univ., Frankfurt am Main, Germany.), and W. Greiner (Johann-Wolfgang-Goethe-Univ., Frankfurt am Main, Germany.) 1993 7 p Presented at the 9th Winter Workshop on Nuclear Dynamics, Key West, FL, 30 Jan. - 6 Feb. 1993
(Contract W-7405-eng-36)
(DE93-010725; LA-UR-93-1003; CONF-930197-1) Avail: CASI HC A02/MF A01

We present a novel approach for interactions between pseudoscalar and vector mesons. The parameters of the model are adjusted to pion-pion and pion-kaon data. The obtained cross sections are implemented into the Monte Carlo Code RQMD (Relativistic Quantum Molecular Dynamics) for heavy ion collisions. Phi production for S on U and pp collisions at 200 AGeV is calculated. A factor of 2 enhancement for the ratio (Phi/(w plus p))su/(Phi/(w plus p))(sub pp) is found in central AA collisions. DOE

N93-28833# Edgerton, Germeshausen and Grier, Inc., Idaho Falls, ID.
COMPARISON OF ANALYTICAL TRANSPORT AND STOCHASTIC SOLUTIONS FOR NEUTRON SLOWING DOWN IN AN INFINITE MEDIUM
S. N. Jahshan, C. A. Wemple, and B. D. Ganapol (Arizona Univ., Tucson.) 1993 10 p Presented at the International Topical Meeting on Mathematical Methods and Supercomputing in Nuclear Applications (M/C+SNA 1993), Karlsruhe, Germany, 19-23 Apr. 1993
(Contract DE-AC07-76ID-01570)
(DE93-010799; EGG-M-92468; CONF-930404-8) Avail: CASI HC A02/MF A01

A comparison of the numerical solutions of the transport equation describing the steady neutron slowing down in an infinite medium with constant cross sections is made with stochastic solutions obtained from tracking successive neutron histories in the same medium. The transport equation solution is obtained using a numerical Laplace transform inversion algorithm. The basis for the algorithm is an evaluation of the Bromwich integral without analytical continuation. Neither the transport nor the stochastic solution is limited in the number of scattering species allowed. The medium may contain an absorption component as well. DOE

N93-28849# Syracuse Univ., NY.
SPIN DEPENDENT PHENOMENA IN MEDIUM ENERGY PHYSICS
P. A. Souder Nov. 1992 42 p
(Contract DE-FG02-84ER-40146)
(DE93-010972; DOE/ER-40146/4) Avail: CASI HC A03/MF A01

The Syracuse University Medium Energy Physics Group was actively engaged in several research projects. A laser was used to polarize muonic atoms with the goal of measuring fundamental spin-dependent parameters in the reaction mu(-) + He-3 yields H-3 + nu. Time-averaged polarizations of 26.8 +/- 2.3% were achieved for the muon in muonic He-3. The new approach uses atomic spin-dependent reactions between laser polarized Rb vapor and muonic helium. To exploit these high polarizations in a muon capture experiment, we are developing an ion chamber which will detect the recoil tritons and also serve as a polarizing cell. Final data-taking will begin for an experiment to measure the spin-dependent structure functions of the neutron. A 288-element hodoscope system which features good timing and precise mechanical tolerances was constructed and evaluated. DOE

N93-28879# Wisconsin Univ., Madison.
THE PHOTODISSOCIATION AND REACTION DYNAMICS OF VIBRATIONALLY EXCITED MOLECULES
1993 9 p
(Contract DE-FG02-86ER-13500)
(DE93-010896; DOE/ER-13500/T3) Avail: CASI HC A02/MF A01

We have used combined vibrational overtone excitation and laser induced fluorescence detection to study dissociation dynamics of hydroxylamine (NH2OH), have performed our first laser induced grating experiments on water, and have begun assembling a new apparatus for preparing vibrationally excited molecules with simulated Raman excitation. We study role of vibrational excitation in photodissociation dynamics by using a vibrational state preparation technique, such as vibrational overtone excitation or stimulated Raman excitation, to create molecules with particular nuclear motions and then to excite that molecule to a dissociative electronic state. DOE

N93-28892# Argonne National Lab., IL.
QUANTUM DYNAMICS OF X2BC VAN DER WAALS CLUSTERS
S. K. Gray 1992 11 p Presented at the International Society for Optical Engineering (SPIE) Conference, Los Angeles, CA, 16-23 Jan. 1993
(Contract W-31-109-eng-38)
(DE93-006416; ANL/CHM/CP-78499; CONF-930159-4) Avail: CASI HC A03/MF A01

Wave packet calculations modeling vibrational predissociation in X(2)BC(v(')) van der Waals clusters are discussed. A model involving three active degrees of freedom is used. Cluster lifetimes and BC vibrational product distributions are obtained, and compared with available experimental results for He2Cl2, and Ne2Cl2. Some preliminary results for He2I2 and Ne2I2 are also discussed. Mechanistic issues, including the role of direct versus sequential mechanisms in leading to the production of 2X + BC are addressed, as well as the role of intramolecular vibrational relaxation (IVR). Higher dimension extensions of the model are suggested. DOE

N93-28914# Los Alamos National Lab., NM.
THE INVESTIGATION OF NONLINEAR EFFECTS ON QUASIPARTICLE TRANSPORT IN CONDENSED MATTER SYSTEMS
V. M. Kenkre and D. Campbell 1993 3 p Prepared in cooperation with New Mexico Univ., Albuquerque, NM
(Contract W-7405-eng-36)
(DE93-009582; LA-Sub-93-127) Avail: CASI HC A01/MF A01

This short communication summarizes a study to investigate nonlinear effects on quasiparticle transport in condensed matter systems. The specific direction of work was to study the quantum nonlinear dimer from a microscopic viewpoint. DOE

N93-28959# Massachusetts Inst. of Tech., Cambridge. Research Lab. of Electronics.
COHERENT AND SEMI-COHERENT NEUTRON TRANSFER REACTIONS
P. L. Hagelstein 1992 10 p Presented at the ICCF3 Conference, Nagoya, Japan, Oct. 1992
(Contract DE-FG02-89ER-14012)
(DE93-008336; CONF-9210321-1) Avail: CASI HC A02/MF A01

Neutron transfer reactions are proposed to account for anomalies reported in Pons-Fleischmann experiments. The prototypical reaction involves the transfer of a neutron (mediated by low frequency electric or magnetic fields) from a donor nucleus to virtual continuum states, followed by the capture of the virtual neutron by an acceptor nucleus. In this work, we summarize basic principles, recent results, and the ultimate goals of the theoretical effort. DOE

N93-28960# Minnesota Univ., Minneapolis. School of Physics and Astronomy.
RESEARCH IN THEORETICAL NUCLEAR PHYSICS
2 Mar. 1993 9 p
(Contract DE-FG02-87ER-40328)
(DE93-008380; DOE/ER-40328/1) Avail: CASI HC A02/MF A01

Research in progress and plans for future investigations are briefly summarized for the following areas: light-ion structure and reactions; nuclear structure; peripheral heavy-ion reactions at medium and high energy; medium-energy heavy-ion collisions and properties of highly excited nuclear matter; and high-energy heavy-ion collisions and QCD plasma. DOE

N93-29099# Lawrence Livermore National Lab., CA.
ION MOTION EFFECTS ON CHARGED RADIATORS
D. B. Boercker Jun. 1992 17 p Presented at the 11th International Conference on Spectra Line Shapes, Carry Le Rouet, France, 8-12 Jun. 1992
(Contract W-7405-eng-48)
(DE93-009257; UCRL-JC-110949; CONF-9206255-2) Avail: CASI HC A03/MF A01

Stark broadening of plasma line radiation results from the interaction of the internal degrees of freedom of the radiators with the electric microfields produced by the plasma. For the case of a charged radiator, the microfield is also responsible for the acceleration of the center-of-mass through its interaction with the net charge. This relationship between the radiative and transport properties of charged radiators has been exploited to obtain an accurate and practical description of ion motion effects on line shapes from simple, hydrogenic ions. In this paper, this model will be extended to include the edicts of fine structure in hydrogen. Comparisons with computer simulation results are also made. DOE

N93-29143# California Univ., Davis. Dept. of Chemistry.
A SIMPLE MODEL FOR ION SOLVATION WITH NON ADDITIVE CORES
W. R. Fawcett and Lesser Blum (Puerto Rico Univ., Rio Piedras.) 15 Apr. 1993 22 p
(Contract N00014-93-1-0351)
(AD-A263075) Avail: CASI HC A03/MF A01

The solvation of monoatomic ions at infinite dilution in polar solvents is considered within the context of the mean spherical approximation (MSA). The role of both ion-dipole and dipole-dipole interactions in determining the Gibbs energy and entropy of solvation is considered in detail for the alkali metal and halide ions in water. The significance of the MSA parameters with respect to local interactions of water molecules with the ions and each other is discussed. DTIC

N93-29183# Michigan Technological Univ., Houghton.
THEORETICAL HYPERFINE STRUCTURE CONSTANTS FOR TRANSITION METAL ATOMS AND IONS
D. R. Beck 23 Mar. 1993 3 p
(Contract DE-FG02-92ER-14282)
(DE93-012325; DOE/ER-14282/1) Avail: CASI HC A01/MF A01

Accurate calculation of hyperfine structure of (d+s)(sup n) states involves dealing with both relativistic and correlation effects in a multi-reference framework (all (d+s)(sup n) states of fixed n,J treated at once). The algorithms were improved (BCB and REDUCE methods) and applied to the hfs of Zr II for (d+s)(sup 3) states. The fs intervals were determined to within 0.075 eV, and the hfs was only 17% in error; this represents the first time that all of the (d+s)(sup n) fs levels have been accurately determined by ab initio theory. Calculations for Nb III, La I, and Hf II (J=1.5) will be published when the J=0.5 calculations are complete. DOE

N93-29184# North Carolina State Univ., Raleigh. Dept. of Physics.
NUCLEAR STRUCTURE RESEARCH AT THE TRIANGLE UNIVERSITIES NUCLEAR LABORATORY
G. E. Mitchell 1 Oct. 1992 199 p
(Contracts DE-FG05-88ER-40441; DE-AC05-76ER-01067; DE-FG05-88ER-40442)
(DE93-009756; DOE/ER-40441/5) Avail: CASI HC A09/MF A03

Studies of fundamental symmetries by the TRIPLE collaboration using the unique capabilities at LAMTF have found unexpected systematics in the parity-violating amplitudes for epithermal-neutron scattering. Tests to lower the present limits on time-reversal-invariance violation in the strong interaction are being made at in experiments on the scattering of polarized fast neutrons from aligned holmium targets. Studies of few-nucleon systems have received increasing emphasis over the past year, involving a broad program for testing the low- to medium-energy internucleon interactions, from the tensor component in n-p scattering and the n-n scattering lengths, through three-nucleon systems and the alpha particle, on up to Be-8. Of particular interest are three-nucleon systems, both in elastic scattering and in three-body breakup. Beam requirements range from production of intense and highly-polarized neutron beams to tensor-polarized beams for measurements at both very low energies (25-80 keV) and at tandem energies for definitive measurements of D-state components of the triton, He-3, and He-4 obtained from transfer reactions. The program in nuclear astrophysics expanded during 1991-1992. Several facets of the nuclear many-body problem and of excitation mechanisms of the nucleus are being elucidated, including measurements and analyses to elucidate the neutron-nucleus elastic-scattering interaction over a wide range of nuclei and energies. Several projects involved developments in electronuclear physics, instrumentation, RF-transition units, and low-temperature bolometric particle detectors. DOE

N93-29206# Lawrence Livermore National Lab., CA.
ELASTIC AND REACTIVE COLLISIONS OF ATOMS AND MOLECULES WITH NEUTRAL ALKALI CLUSTERS
A. Scheidemann (Washington Univ., Seattle.) and V. V. Kresin 14 Sep. 1992 7 p Presented at the 6th International Symposium on Small Particles and Inorganic Clusters, Chicago, IL, 16-22 Sep. 1992
(Contract W-7405-eng-48)
(DE93-009313; UCRL-JC-111650; CONF-920921-9) Avail: CASI HC A02/MF A01

We have measured absolute integral cross sections for low-energy collisions of atoms and molecules with neutral sodium clusters over a wide cluster size range (n = 2--40). The cross sections are exceptionally large, reaching values of thousands of square angstroms. Consequently, the scattering involves long-range interactions. The Van der Waals force, acting either along (Na(n) + N2) or in concert with the inelastic charge-transfer 'harpooning' channel (Na(n) + Cl2, Na(n) + O2) can describe the measurements. Using interaction parameters taken from spectroscopic studies of alkali clusters, we find very good agreement with the data. This provides a point of contact between beam scattering experiments and studies of cluster electromagnetic response properties. DOE

N93-29261# New Mexico Univ., Albuquerque. Dept. of Physics and Astronomy.
NEW MEXICO CENTER FOR PARTICLE PHYSICS: STUDIES OF FUNDAMENTAL INTERACTIONS
J. A. J. Matthews 1992 103 p
(Contract DE-FG03-92ER-40732)
(DE93-008302; DOE/ER-40732/T1) Avail: CASI HC A06/MF A02

The New Mexico Center/UNM group research program includes the CDF experiment at Fermilab and the SDC experiment at the SSC. In both experiments the UNM group research focuses on silicon strip tracking systems. The present research goals are to develop and utilize precision silicon tracking to increase significantly the physics reach of the Tevatron, and to make possible the study of high-P(sub t) physics at the SSC. The search for the t-quark in CDF is the primary goal of the upcoming Tevatron runs. This Progress Report summarizes our research accomplishments from the last year. DOE

N93-29313# Los Alamos National Lab., NM.
MEASUREMENT OF W-Z INTERFERENCE FROM NEUTRINO-ELECTRON SCATTERING
R. L. Burman, T. J. Bowles, R. D. Carlini, D. R. F. Cochran, P. J. Doe, J. S. Frank, M. E. Potter, V. D. Sandberg, D. A. Krakauer (Argonne National Lab., IL.), and R. L. Talaga (Argonne National Lab., IL.) 1993 7 p Presented at the International Symposium on 30 Years of Neutral Currents, Los Angeles, CA, 3-5 Feb. 1993
(Contracts W-7405-eng-36; DE-AC05-76ER-02504; W-31-109-eng-38)
(DE93-010724; LA-UR-93-1004; CONF-930293-1) Avail: CASI HC A02/MF A01

Neutrino-electron elastic scattering was observed at LAMPF with a 15-ton fine-grained tracking calorimeter exposed to electron-neutrinos from muon decay at rest. The measured nu(sub e)e(-) (yields) nu(sub e)e(-) elastic scattering cross section, 10.0 +/- 1.5(stat) +/- 0.9(syst) x 10(exp -45) sq cm x (E(sub nu)(MeV)), gives a model independent measurement of the strength of the destructive interference between the charged and neutral currents, I = -1.07 +/- 0.21, that agrees well with the standard model (SM) prediction I = -1.08. The agreement between the measured electroweak parameters and SM expectations is used to place limits on neutrino properties, such as neutrino flavor-changing neutral currents and neutrino electromagnetic moments and on the masses of hypothetical new bosons that would interact with leptons. DOE

N93-29315# Los Alamos National Lab., NM.
NEUTRINO MASS
T. J. Bowles 1993 11 p Presented at the Texas/PASCO 1992 International Conference, Berkeley, CA, 13-18 Dec. 1992
(Contract W-7405-eng-36)
(DE93-010735; LA-UR-93-1009; CONF-921266-1) Avail: CASI HC A03/MF A01

Neutrinos play a dominant role in both particle physics, astrophysics, and cosmology. In the our present understanding of the strong, weak, and electromagnetic forces, the group structure of the Standard Model is SU(3)(sub C) (circle times) SU(2)(sub L) (circle times) U(l)(sub EM). In the Weinberg-Salam-Glashow Standard Electroweak Model, left-handed neutrinos sit in a doublet, while right-handed neutrinos are in a singlet, and therefore do not interact with the other known particles. Also in this model, the neutrinos are intrinsically massless. However, while the W-S-G model provides an amazingly accurate picture of our present cold Universe, it has a number of deficits. The Standard Model does not explain the origin of the group structure, it does not reduce the number of coupling constants required, nor does it offer any prediction for the physical masses of the particles. Thus, it is generally assumed that the Standard Model is but a subset of some larger gauge theory. A wide variety of Grand Unified field Theories (GUT's), Super Symmetric Models (SUSY), and Superstring models have been proposed as the model for this larger structure. In general, these models predict nonzero neutrino masses and contain mechanisms that provide for lepton-number violation. Thus, a variety of new phenomena are predicted, including finite neutrino masses and the possibility that neutrinos can oscillate from one type to another. DOE

N93-29332# Pennsylvania State Univ., University Park. Dept. of Chemistry.
WHAT IS UNDERNEATH? MOVING ATOMS AND MOLECULES TO FIND OUT Technical Report, 1 Jun. 1992 - 31 May 1993
P. S. Weiss and D. M. Eigler 1 Dec. 1992 6 p
(Contract N00014-91-J-1630)
(AD-A263363; TR-5) Avail: CASI HC A02/MF A01

We have used the scanning tunneling microscope (STM) to move adsorbates such as benzene molecules and Xe clusters in order to determine their initial adsorption site. This has allowed us to image the initiation of the growth of a Xe surface overlayer, and to identify the sites at which this growth begins. This capability has also allowed us not only to examine the binding sites of the adsorbates, but also to learn the effect that these sites have on the STM images. DTIC

N93-29336# International Business Machines Corp., San Jose, CA. Almaden Research Center.
FAST MULTIPOLE METHOD IN SIMULATIONS OF AQUEOUS SYSTEMS
James N. Glosli and Michael R. Philpott 14 Apr. 1993 14 p
(Contract N00014-92-C-0173)
(AD-A263422; TR-03) Avail: CASI HC A03/MF A01

The fast multipole method (fmm) for calculating electric fields developed by Greengard and Rokhlin (J. Comp. Phys. 73, 325(1987)), has been implemented specifically for molecular dynamics simulations of electrochemical problems including boundary conditions associated with metal electrodes. This order N (number of charged particles) algorithm is known to be computationally much more efficient than direct or Ewald sum methods (order N 2) for systems with as few as one thousand charged particles (equivalent to 300 water molecules). Timings and accuracy estimates with system size N (16 less than or N less than or equal 16000) are given to illustrate the effectiveness and efficiency of the fmm. As an application of fmm, we describe it's use with constant temperature molecular dynamics to calculate the dielectric constant of the space water model in bulk at temperatures 298 and 361 K. System sizes of 27, 64, 125, and 216 water molecules were considered. Comparison with the Ewald and reaction field methods was made. At 298 K, the dielectric constant was calculated to be epsilon = 75.5 + or - 5% and at 361 K epsilon = 57.3 + or - 4%. Both values compare well with experiment and the reaction field theory simulations. DTIC

N93-29351# Fermi National Accelerator Lab., Batavia, IL.
NEW LIMITS ON GENERATION-1 LEPTOQUARKS
S. M. Moulding (Brandeis Univ., Waltham, MA.) Nov. 1992 5 p Presented at the Meeting of the Division of Particles and Fields of the American Physics Society, Batavia, IL, 10-14 Nov. 1992
(Contract DE-AC02-76CH-03000)
(DE93-008138; FNAL/C-92/341-E; CONF-921122-44) Avail: CASI HC A01/MF A01

With the turn-on of HERA there is currently considerable interest in the properties of first-generation leptoquarks. In this paper we present new results of a search for these particles at CDF. Our findings are based on an analysis of 4.1 pb(exp -1) of data collected at sq. root of s = 1.8 TeV during the 1988-89 Tevatron run. The leptoquarks are assumed to decay rapidly to first-generation leptons and quarks. We search for an excess of events containing two high energy electrons and two jets and find no events in our signal region. Events outside the signal region are consistent with Z(sup 0) + dijet production. Based on this, and assuming BR(LQ(sub 1) yields e + q) = 100 %, we exclude first-generation leptoquarks with masses M(LQ(sub 1)) less than 113 GeV at the 95% CL. At BR(LQ(sub 1) yields e + q) = 50 %, we exclude M(LQ(sub 1)) less than 82 GeV. DOE

N93-29403# Pennsylvania State Univ., University Park. Dept. of Materials Science and Engineering.
FI-STM INVESTIGATION OF ATOMIC HYDROGEN ADSORPTION ON THE Si(100)2X1 SURFACE
Xiangdong Wang, T. Hashizume, H. Lu, H. W. Pickering, and T. Sakurai Apr. 1993 27 p
(Contract N00014-91-J-1189)
(AD-A262748) Avail: CASI HC A03/MF A01

A field ion-scanning tunneling microscopy study on hydrogen chemisorption on the Si(100)2x1 surface is presented. At low coverages, hydrogen atoms reside singly on top of the dimerised Si atoms, and are imaged brightly. The hydrogen chemisorption induces the buckling of dimers, indicating the strong bonding between Si and H atoms. With increasing coverage, both the 2x1 monohydride and 1x1 dihydride phases were formed. The former is imaged dark compared with the unreacted Si dimers, due to the reduction of the density of electronic states near the Fermi level. Surface etching was also observed. It was found that the corrosion of the surface is modest in the monohydride phase, while during the formation of the dihydride phase, the corrosion becomes significant. The behavior of hydrogen desorption from the dihydride and monohydride phases was investigated as a function of annealing temperature. Our STM results support the mechanism that the desorbing H2 molecules are formed by combination of two hydrogen atoms forming the dihydride phase. Upon annealing at elevated temperatures, the Si overlayer stripes are formed by desorption of hydrogen from the etching products and the rearrangement of the Si atoms. DTIC

N93-29415# Air Force Inst. of Tech., Wright-Patterson AFB, OH. School of Engineering.
CONSTRUCTION AND TESTING OF A NEUTRON AND GAMMA SPECTROMETRY SYSTEM USING PULSE SHAPE DISCRIMINATION WITH AN ORGANIC SCINTILLATOR M.S. Thesis
Robert S. Pope Mar. 1993 207 p
(AD-A262550; AFIT/GNE/ENP/93M-6) Avail: CASI HC A10/MF A03

The goal of this thesis was to construct and test a neutron detector to measure the energy spectrum of 1 to 14-MeV neutrons in the presence of gammas. A spectrometer based on the process of pulse shape discrimination (PSD) was constructed, in which the scintillator NE-213 was used. The primary neutron/gamma sources used were 78-mCi and 4.7-Ci Pu-239Be sources, while 4.7-micro-Ci and 97.6-micro-Ci Na-22 gamma sources were used for energy calibration and additional testing of the detector. Proton recoil spectra and Compton electron spectra were unfolded with the neutron and gamma unfolding code FORIST to generate the incident neutron and gamma spectra, respectively. FORIST, which was written for a CDC computer, was modified to run on a VAX 6420. The experimental spectra were compared to those in the literature. The locations of the peaks in the Pu-239Be spectrum agreed with the literature to within 8.3%, the Pu-239Be gamma spectrum agreed to within 0.7%, while the Na-22 gamma spectrum agreed exactly. Uncertainties in the detection system and unfolding procedure are on the order of 5-10%. This thesis is intended to be a summary of the relevant literature and a user's guide to the PSD spectrometer. DTIC

N93-29416# Iowa State Univ. of Science and Technology, Ames.
THE PARALLEL IMPLEMENTATION OF A BACKPROPAGATION NEURAL NETWORK AND ITS APPLICABILITY TO SPECT IMAGE RECONSTRUCTION Ph.D. Thesis
J. P. Kerr 1992 54 p
(Contract DE-FG02-92ER-75700)
(DE93-010304; DOE/ER-75700/T3) Avail: CASI HC A04/MF A01

The objective of this study was to determine the feasibility of using an Artificial Neural Network (ANN), in particular a backpropagation ANN, to improve the speed and quality of the reconstruction of three-dimensional SPECT (single photon emission computed tomography) images. In addition, since the processing elements (PE)s in each layer of an ANN are independent of each other, the speed and efficiency of the neural network architecture could be better optimized by implementing the ANN on a massively parallel computer. The specific goals of this research were: to implement a fully interconnected backpropagation neural network on a serial computer and a SIMD parallel computer, to identify any reduction in the time required to train these networks on the parallel machine versus the serial machine, to determine if these neural networks can learn to recognize SPECT data by training them on a section of an actual SPECT image, and to determine from the knowledge obtained in this research if full SPECT image reconstruction by an ANN implemented on a parallel computer is feasible both in time required to train the network, and in quality of the images reconstructed. DOE

N93-29446# Florida Agricultural and Mechanical Univ., Tallahassee. Dept. of Physics.

ELECTRON INTERACTIONS WITH NON-LINEAR POLYATOMIC MOLECULES AND THEIR RADICALS AND IONS Interim Report, 7 Jun. 1991 - 6 Jun. 1992

Ashok K. Jain Jun. 1992 129 p
(Contract F33615-90-C-2032)
(AD-A262279; WL-TR-92-2079) Avail: CASI HC A07/MF A02

The low energy electron collisions with H2O and H2S have been studied for elastic and rotational excitation channels. A parameter-free ab initio approach is employed in which electron exchange interaction is treated exactly and the polarization effects via perturbation theory. The integro-differential coupled equations are solved iteratively to yield scattering parameters. Detailed results are obtained for differential, integral, and momentum transfer cross sections. The agreement with experimental data for all the parameters is very good. The intermediate and high energy electron scattering with a large number of diatomic and polyatomic molecules is studied between 20-5000 eV and results for total (elastic plus inelastic) cross sections are reported. DTIC

N93-29489# IBM Research Lab., San Jose, CA. Almaden Research Center.

MOLECULAR DYNAMICS MODELING OF ELECTRIC DOUBLE LAYERS WITH SPECTROSCOPIC APPLICATIONS Technical Report

M. R. Philpott and J. N. Glosli 14 Apr. 1993 8 p
(Contract N00014-92-C-0173)
(AD-A263168; TR-06) Avail: CASI HC A02/MF A01

Molecular dynamics is used to model the structure and dynamics of electric double layers at a charged metal surface and to ask questions of spectroscopic interest. In particular, what is the molecular basis for changing the position of the outer Helmholtz plane (OHP) thereby tuning the electric field across the inner layer? Another topic is the microscopic basis of modulation spectroscopies like SNIFTIRS. Our MD simulations of an immersed electrode show features corresponding to: compact layer, diffuse layer, highly oriented water layer next to the metal when the electrode is charged and ions are present; penetration of nominally diffuse layer species into inner layer; and ion pair formation between contact adsorbed ion and diffuse layer ion when the electrode is uncharged, poorly oriented surface water when the electrode is uncharged. All these properties arise from the model with the restriction that charge on the metal and aqueous phase sums to zero. DTIC

N93-29619# IBM Research Lab., San Jose, CA.

ADSORPTION OF HYDRATED HALIDE IONS ON CHARGED ELECTRODES: MOLECULAR DYNAMICS SIMULATION Technical Report

James N. Glosli and Michael R. Philpott 14 Apr. 1993 60 p
(Contract N00014-92-C-0173)
(AD-A263137) Avail: CASI HC A04/MF A01

Constant temperature molecular dynamics has been used to simulate the adsorption of hydrated halide ion X(-) = F(-), Cl(-), Br(-), and I(-), and lithium ion Li(+) on a flat uniformly charged surfaces. The simulations were done with either 214 water molecules and two ions (Li(+) and X(-)) in a box 2.362 nm deep or with 430 water molecules and the two ions in a box 4.320 nm deep. The boxes were periodically replicated in the xy directions. The magnitude of the surface charge on the box end was + or - 0.11 c/nm(sup 2), corresponding to an electric field of 2 x 10(exp 7) V/cm. The lateral dimensions of the simulation cell were 1.862 nm x 1.862 nm (x times y) in each case. All of the water molecules and ions interacted with the end walls via a weak 9 - 3 potential. The ST2 water model and parameters optimized for alkali halides interacting with the model ST2 water molecule were used in the calculations. Common practices of truncating the interactions at a finite distance (0.82 nm) and switching off Coulomb interactions at small distances were followed. The temperature was set at T = 2.411 kJ/mole (290 K). Some of the properties calculated were: distribution density profiles for ions and water across the gap important for comparisons iwth Gouy-Chapman theory, adsorbed ion-water pair correlation functions, the number of water molecules in the first and second hydration shells of the ions as a function of time. The time spent by a water molecule in the hydration shell was calculated to be approximately ten times longer for lithium than any other ion. The correlation between distance from the electrode and hydration number was studied and generally found to be pronounced for the larger anions. DTIC

N93-29764# Tennessee Univ., Knoxville. Dept. of Physics and Astronomy.

ELEMENTARY PARTICLE INTERACTIONS

W. M. Bugg, G. T. Condo, T. Handler, E. L. Hart, K. Read, and B. F. L. Ward Oct. 1992 277 p
(Contract DE-FG05-91ER-40627)
(DE93-005113; DOE/ER-40627/2) Avail: CASI HC A13/MF A03

Work continues on strange particle production in weak interactions using data from a high-energy neutrino exposure in a freon bubble chamber. Meson photoproduction has also consumed considerable effort. Detector research and development activities have been performed. DOE

N93-29784# Lawrence Livermore National Lab., CA.

NUCLEAR ISOMERS AS ULTRA-HIGH-ENERGY-DENSITY MATERIALS

C. H. Poppe, M. S. Weiss, and J. D. Anderson Apr. 1992 7 p
Presented at the 1992 Air Force High Energy Density Materials Contractors Meeting, Lancaster, CA, 12-14 Apr. 1992
(Contract W-7405-eng-48)
(DE93-009520; UCRL-JC-109928; CONF-9204235-1) Avail: CASI HC A02/MF A01

Nuclear isomers are metastable states of atomic nuclei which release their energy in a prompt burst of electromagnetic radiation. Two kinds of nuclear isomers are known to exist: spin isomers and shape isomers. There is evidence for at least 27 different fissionless shape isomers in isotopes of mercury, lead, and thallium, in agreement with theoretical predictions. Three potential mechanisms for releasing the stored isomeric energy are neutron catalysis, laser-electron-nuclear coupling, and Stark-shift-induced mixing. While shape isomers are believed to hold the most promise for radioactivity-free, ultra-high-energy-density materials, spin isomers can be used as surrogates for developing the release mechanisms. It is proposed to undertake shell-model calculations for the nuclear levels in vicinity of the (sup 178)Hf spin isomer, in order to estimate the efficacy of neutron catalysis. It is also proposed to use the toroidal electron spectrometer to measure the conversion electrons from laser-induced transitions in (sup 229)Th. The final mechanism, Stark-shift-induced mixing of atomic and nuclear levels, would also be studied theoretically. Finally, isomer production is considered briefly, including the possibility of shape isomers in fission products from radwaste or nuclear explosions. DOE

N93-29787# Arcon Corp., Waltham, MA.

ELECTRON TRANSPORT CALCULATIONS BETWEEN 1 MeV AND 1 eV Final Report, Sep. 1989 - Jul. 1992

Stanley Woolf Dec. 1992 50 p
(Contract F19628-89-C-0189)
(AD-A263412; RL-TR-92-311) Avail: CASI HC A03/MF A01

In this report, we describe mathematical analysis, physics research, and computer program development for the simulation of charged particle transport in irradiated and non-irradiated solids. The simulation techniques described were used to calculate energy deposition, charge, and current distributions in these solids. The scope of the work included: (1) discrete ordinates transport calculations of low energy (l eV to 20 eV) electrons in silicon dioxide with and without electric fields; (2) comparison testing of one-dimensional discrete ordinates transport codes for charged and neutral particles with analytical benchmark calculations; (3) Monte Carlo transport calculations for low energy electrons in the presence of strong electric fields in silicon dioxide; and (4) Monte Carlo transport calculations for high energy (MeV) electrons in insulating materials with internal electric fields. DTIC

N93-29805# California Univ., Berkeley. Lawrence Berkeley Lab.
NMR STUDIES OF MOLECULES IN LIQUID CRYSTALS AND GRAPHITE Ph.D. Thesis
M. E. Rosen Jun. 1992 174 p
(Contract DE-AC03-76SF-00098)
(DE93-010423; LBL-33520) Avail: CASI HC A08/MF A02

NMR experiments to measure proton dipole couplings were performed on a series of n-alkanes (n-hexane through n-decane) dissolved in nematic liquid crystals. Computer modeling of the experimental NMR-spectra was done using several different models for intermolecular interactions in these systems. The model of Photinos et al. was found to be best in describing the intermolecular interactions in these systems and can provide a statistical picture of the conformation and orientation of the alkane molecules in their partially-oriented environment. Order parameters and conformational distributions for the alkanes can be calculated from the modeling. The alkanes are found to have conformational distributions very much like those found in liquid alkanes. Proton NMR spectra of tetrahydrofuran (THF) intercalated in two graphite intercalation compounds were also measured. Computer simulations of these spectra provide a picture of THF in the constrained environment between the graphene layers where the THF is oriented at a particular angle, can translate and rotate freely, but does not appear to pseudorotate. DOE

N93-29807# Maryland Univ., College Park. Dept. of Chemistry and Biochemistry.
REACTION MECHANISM STUDIES OF HEAVY ION INDUCED NUCLEAR REACTIONS
A. C. Mignerey Feb. 1993 46 p
(Contract DE-FG05-87ER-40321)
(DE93-010496; DOE/ER-40321/12) Avail: CASI HC A03/MF A01

Completed work is summarized on the topics of excitation energy division in deep-inelastic reactions and the onset of multifragmentation in La-induced reactions at E/A = 45 MeV. Magnetic fields are being calculated for the PHOBOS detector system, a two-arm multiparticle spectrometer for studying low-transverse-momentum particles produced at the Relativistic Heavy Ion Collider. The Maryland Forward Array is being developed for detection of the reaction products from very peripheral collisions; it consists of two individual units of detectors: the annular silicon detector in front and the plastic phoswich detector at back. DOE

N93-29839# Pennsylvania State Univ., University Park. Dept. of Chemistry.
OBSERVATION OF PHASE-SEPARATED NANOMETER SCALE MOLECULAR DOMAINS IN MIXED SELF-ASSEMBLED MONOLAYERS Technical Report, 1 Jun. 1992 - 31 May 1993
S. J. Stranick, P. S. Weiss, A. N. Parikh, Y. T. Tao, and D. L. Allara 13 Apr. 1993 16 p
(Contract N00014-91-J-1630)
(AD-A263470; Rept-TR-8) Avail: CASI HC A03/MF A01

We demonstrate the phase separation, into nanometer scale domains, of two-component monolayers, prepared by self-assembly on gold, of CH3(CH2)15SH and CH3O2C(CH2)15SH, two similar, non-hydrogen bonding alkane thiols of identical alkyl chain length. By varying the fractions of the two components, we have learned to distinguish between domains of each molecule by scanning tunneling microscopy. These observations have important implications for both the scientific understanding of phase segregation in quasi-two-dimensional molecular mixtures and for applications of self-assembly in which the formation of spatially resolved mixed functional group surfaces is desired (targeted). Further, these observations provide a caveat with regard to the common assumption of complete mixing in multi-component self-assembled monolayers. DTIC

N93-29841# Oregon Univ., Eugene. Inst. of Theoretical Science.
TASK A: THEORY OF ELEMENTARY PARTICLES
N. G. Deshpande and D. E. Soper 16 Oct. 1992 12 p
(Contract DE-FG06-85ER-40224)
(DE93-010561; DOE/ER-40224/228) Avail: CASI HC A03/MF A01

Brief summaries of work are given in the following areas: grandunification, properties of neutrinos, rare decays of heavy quarks, jet production in hadron collisions (theory, structure, two-jet cross section, and null-plane field theory), neutrino physics, and QCD calculations of annihilation of e(+)e(-) into hadrons. DOE

N93-29860# California Univ., Berkeley. Lawrence Berkeley Lab.
REACTION AND REORIENTATION OF ELECTRONICALLY EXCITED H2(B) Ph.D. Thesis
C. D. Pibel Sep. 1992 227 p
(Contract DE-AC03-76SF-00098)
(DE93-010435; LBL-33473) Avail: CASI HC A11/MF A03

The room temperature rate (TR) constants for fluorescence quenching fluorescence of H2, HD, and D2 B (sup 1)Sigma(sub u)(sup +) by He-4 were measured as a function of the initially excited rotational and vibrational level of the hydrogen molecule, and the RT rate constants for molecular angular momentum reorientation of H2, HD and D2 (B (sup 1)Sigma(sub u)(sup +), v' = 0, J' = 1, M(sub J) = 0) in collisions with He, Ne, Ar and H2(X (sup 1)Sigma(sub g)(sup +)) were also measured. Vibrational state dependence of the quenching cross sections fits a vibrationally adiabatic model of the quenching process. From the vibrational state dependence of the quenching cross section, the barrier height for the quenching reaction is found to be 250 plus or minus 40 cm(sup -1), and the difference in the H-H stretching frequencies between H2(B) and the H2-He complex at the barrier to reaction is 140 plus or minus 80 cm(sup -1). The effective cross sections for angular momentum reorientation in collisions of H2, HD, and D2 with He and Ne were found to be about 30 A(sup 2) and were nearly the same for each isotope and with He and Ne as collision partners. Cross sections for reorientation of HD and D2 in collisions with Ar were 10.6 plus or minus 2.0 and 13.9(plus or minus) 3.0 A(sup 2), respectively. Reorientation of D2(B) in collisions with room temperature H2(X) occurs with a 7.6 plus or minus 3.4 A(sup 2) cross section. Calculated cross sections using semiclassical and quantum close coupled methods give cross sections for reorientation of H2(B) and D2(B) in collisions with He that agree quantitatively with experiment. Discrepancy between the calculated and experimental cross sections for HD(B)-He are likely due to rotational relaxation in HD. A Turbo PASCAL version of the data-taking program is included. DOE

N93-30128# State Univ. of New York, Albany. Research Foundation.
STUDY OF HEAVY-FLAVORED PARTICLES
1993 26 p
(Contract DE-FG02-91ER-40631)
(DE93-011535; DOE/ER-40631/2) Avail: CASI HC A03/MF A01

The program of physics analysis using CLEO II data is reported. A statistically significant measurement was made of the isospin mass splitting of the Sigma(sub c)(sup +) with respect to the Sigma(sub c)(sup o) and Sigma(sub c)(sup ++). This result is based on first observation of the Sigma(sub c)(sup +) in the decay mode Lambda(sub c)(sup +)pi(sup 0). Many new decay modes of the charmed baryon Lambda(sub c)(sup +) were studied. Several new decay modes of xi(sub c)'s were observed. Some preliminary results on 3 new modes of Omega(sub c)(sup 0) decay are reported. In the area of B-meson decay into baryons, the decays B yields Sigma(sub c)(sup 0) and Sigma(sub c)(sup ++) were observed conclusively. From about 1500 events corresponding to B yields Lambda(sub c)(sup +)X reconstruction of exclusive final states of the form Lambda(sub c)(sup +)(n(pi)) was started. A comprehensive investigation of particle identification using both the time-of-flight and dE/dx systems was made. Measurement of pion, kaon, and proton identification efficiencies were made, corresponding to several different selection criteria. Measurements of corresponding pion probabilities to fake kaons and protons were also made. DOE

N93-30130# Los Alamos National Lab., NM.
PARTIAL CROSS SECTIONS IN H(-) PHOTODETACHMENT Ph.D. Thesis
M. Halka Apr. 1993 172 p
(Contract W-7405-eng-36)
(DE93-011570; LA-12533-T) Avail: CASI HC A08/MF A02

Experimental measurements of partial decay cross sections in the H(-) photodetachment spectrum are reported. Observed decays of the (P(sub 0))-1 H(-)(sup **)(n) doubly-excited resonances to the H(N=2) continuum are reported for n=2, 3, and 4 from 1990 runs in which the author participated. A recent analysis of 1989 data revealing effects of static electric fields on the partial decay spectrum above 13.5 eV is also presented. The experiments were performed at the High Resolution Atomic Beam Facility (HIRAB), the Los Alamos Meson Physics Facility (LAMPF), with a relativistic H(-) beam (beta = 0.842) intersecting a ND:YAG laser. Variation of the intersection angle amounts to Doppler-shifting the photon energy, allowing continuous tuning of the laser energy as viewed from the moving ions' frame. DOE

N93-30366# Northwestern Univ., Evanston, IL.
CENTER FOR SURFACE RADIATION DAMAGE STUDIES Final Report, 15 Sep. 1989 - 30 Nov. 1992
Laurence D. Marks 28 Feb. 1993 29 p
(Grant AF-AFOSR-0045-90)
(AD-A264330; Rept-0650-350-W410; AFOSR-93-0273TR) Avail: CASI HC A03/MF A01

Research focussed around understanding surface damage processes at the atomistic microstructure level was performed using high resolution electron microscopy in ultra-high vacuum and by other techniques. Techniques for obtaining clean and well-ordered surfaces and understand the image obtained were developed and used to characterize damage processes. This data, combined with other high resolution electron microscopy data was combined with analytical and numerical models with a high degree of success. Attempts to produce a small atomic oxygen source based upon electron stimulated desorption of oxygen neutrals led to the conclusion that literature estimates are much too high for the neutral to ion ratio. A strong upper bound was placed on this ratio of greater than 10, whereas values in the literature are as high as 10. DTIC

N93-30448# Los Alamos National Lab., NM.
THE CALCULATION OF ELECTROSTATIC INTERACTIONS AND THEIR ROLE IN DETERMINING THE ENERGIES AND GEOMETRIES OF MOLECULAR HE CRYSTALS
E. M. Kober, A. S. Copenhaver, and J. P. Ritchie 1992 8 p Presented at the 10th Detonation Symposium, Boston, MA, 12-16 Jul. 1993
(Contract W-7405-eng-36)
(DE92-040374; LA-UR-92-2794; CONF-930713-4) Avail: CASI HC A02/MF A01

The properties (crystalline density, orientation, defects, H bonds) of high explosive (HE) single crystals affect the performance and sensitivity of the material. A computer code is being developed to model and predict the properties of molecular HE crystals. The intermolecular interaction energy is the sum of repulsion, dispersion, and electrostatic contributions. A more accurate electrostatic treatment was implemented by using multipole expansions. The formulations were implemented into the crystallographic packing code PCK/ME. The performance of this program was evaluated with a series of HE and other organic compounds. Crystal structures for a set of 15 molecules were optimized using the model with quadrupole level expansion for the electrostatics. The largest errors were for systems with strong hydrogen bonds; corrections were applied. The electrostatic interaction energy was equal to about half the total interaction energy for almost all the molecules. DOE

N93-30505# Notre Dame Univ., IN.
THEORETICAL STUDIES IN NUCLEAR STRUCTURE
E. R. Marshalek Dec. 1992 11 p
(Contract DE-FG02-91ER-40640)
(DE93-012290; DOE/ER-40640/2) Avail: CASI HC A03/MF A01

Two topics of current interest, strongly anharmonic collective vibrations and collective rotation about a tilted axis, have been related through a theorem. This theorem, which will be called the Bifurcation Theorem, states that if a system has an axis of rotational symmetry in a static mean-field approximation, then self-consistent cranking about this axis gives rise to symmetry-breaking bifurcations that occur for critical cranking frequencies (Omega)(sub c) given by Omega(sub c) = omega(sub mu)/K(sub mu), where omega(sub mu) is the small-oscillation (RPA) frequency of any normal mode carrying (h bar)K(sub mu) (not = 0) units of angular momentum along the symmetry axis. The bifurcations represent families of anharmonic oscillations built on the axially symmetric mean field. For certain values of K(sub mu), the solutions appear as rotations about an axis that is tilted with respect to the principal axis of the density distribution. The theorem has been tested on some simple models in preparation for more realistic calculations that are planned for the near future. DOE

N93-30540# California Univ., Santa Barbara. Dept. of Chemistry.
ORDERED MOLECULAR ARRAYS AS TEMPLATES: A NEW APPROACH TO SYNTHESIS OF MESOPOROUS MATERIALS Technical Report, 1 Jun. 1992 - 31 May 1993
P. Behrens and G. Stucky 1993 9 p
(Contract N00014-90-J-1159)
(AD-A264631) Avail: CASI HC A02/MF A01

There has been a growing interest in the extension of the microporous molecular sieve synthesis and applications to mesoscopic dimensions. Typical areas for the application of mesoscopic zeolite-type structures are in separation (e.g., protein separation and selective adsorption of large organic molecules from waste waters) and catalysis (e.g., processing of tar sand and of the high distillates of crude oils to valuable low-boiling products). Another is in the supramolecular assembly of molecular array and polymers for electronic and optical applications. In a new concept in the synthesis of porous material the templating agent is no longer a single, solvated, organic molecule or metal ion, but rather a self-assembled molecular array. This template leads to mesoporous materials with adjustable pore sizes between 16 and greater than 100 Angstrom, covering well the mesophorous range of greatest interest. The periodic arrangement of pores is very regular, and the pore size distribution measured by absorption is nearly as sharp as that of conventional zeolites. DTIC

N93-30558# Florida Univ., Gainesville.
DEVELOPMENT OF AN O ATOM GUN Final Report, 1 Sep. 1991 - 31 Aug. 1992
Gar B. Hoflund 29 Mar. 1993 24 p
(Contract F49620-91-C-0087)
(AD-A264753; AFOSR-93-0219TR) Avail: CASI HC A03/MF A01

The goal of this project was to produce a source which is compact, durable, and mounts on a standard UHV flange for the generation of hyperthermal oxygen atoms. This has been accomplished. In this source, oxygen atoms permeate through a Ag membrane held at 500 C and are then emitted toward the target from the vacuum side of the membrane by electron stimulated desorption (ESD). The current prototype model generates usable O-atom fluxes of about 10(exp 12) atoms/sq cm/s, and future modifications should increase this flux by 1 to 3 orders of magnitude. Based on the O+ energy distribution, the average O neutral energy is about 5 eV with a fairly broad distribution (FWHM approx. equal 3.6 eV). The information required for the development of this source and a design of the source are presented. DTIC

N93-30589 Polish Academy of Sciences, Warsaw.
EXPERIMENTAL AND THEORETICAL ASPECTS OF EXCITED STATE ELECTRON TRANSFER AND RELATED PHENOMENA
2 Oct. 1992 120 p Conference held in Pultusk, Poland, 27 Oct. - 2 Oct. 1992 Limited Reproducibility: More than 20% of this document may be affected by microfiche quality
(AD-A263457) Avail: Issuing Activity (Defense Technical Information Center (DTIC))

Abstracts of papers presented at the conference on experimental and theoretical aspects of excited state electron transfer and related phenomena are included. The conference was held on 27 Sep. - 2 Oct. 1992. DTIC

N93-30669# Sandia National Labs., Albuquerque, NM.
HARDNESS ASSURANCE AND TESTING ISSUES FOR BIPOLAR/BICMOS DEVICES
R. N. Nowlin (Arizona Univ., Tucson.), R. D. Schrimpf (Arizona Univ., Tucson.), D. M. Fleetwood, and R. L. Pease (Mission Research Corp., Albuquerque, NM.) 1993 5 p Presented at the Nuclear and Space Radiation Effects Conference, Snowbird, UT, 19-23 Jul. 1993
(Contract DE-AC04-76DP-00789)
(DE93-009623; SAND-93-0380C; CONF-930704-3) Avail: CASI HC A01/MF A01

The dose-rate dependence of the total-dose response of bipolar transistors is mapped for several dose rates. Comparisons are made between the total-dose response in x-ray and Co-60 irradiations. Implications for hardness assurance are discussed. DOE

N93-30670# Technische Hochschule, Darmstadt (Germany). Fachbereich Physik.
UNITARY APPROXIMATION OF BHABHA DIFFUSION BY HIGH ENERGIES AND ITS IMPLEMENTATION IN MONTE CARLO EVENT GENERATORS Ph.D. Thesis [UNITAERE NAEHERUNG ZUR BHABHA-STREUUNG BEI HOHEN ENERGIEN UND IHRE IMPLEMENTATION IN MONTE CARLO EVENTGENERATOREN]
Thorsten Ohl 1990 78 p In GERMAN
(ETN-93-93622) Avail: CASI HC A05/MF A01

Calculation methods are improved to evaluate precision data from large electron positron collider and hadron electron ring facility measurements, by considering electroweak interaction standard model and quantum chromodynamics as theory of the strong interaction. The electromagnetic radiation (bremsstrahlung) corrections for processing weak interaction at high energies were considered, with focus on Z(null) resonance neighboring. The Kulish-Fadeev form of Hamilton operator and the S matrix theory were used and degeneration singularities were taken into account with a highly energetic scatter process. Schroedinger equation was solved with the Magnus method. The calculated terms were taken into account with the desired order in the Baker Campbell Hausdorff identity. The method was applied to Bhabha scattering and a recursion relationship was obtained for the scattering amplitude, which was implemented in a Monte-Carlo event generator, which can produce a large number of photons. The simulated cross sections were found to be positive and the method is shown to be efficient for infrared and mass singularities handling. ESA

N93-30788# Academy of Sciences (USSR), Novosibirsk. Inst. Yadernoj Fiziki.
PARTON'S PICTURE OF THE ELECTROWEAK PROCESSES IN HIGH ENERGY E(+)E(-)-COLLISIONS
A. V. Ivkin, M. T. Nazirov, Wang Ping, and E. Kuraev 1991 16 p
(DE93-606107; IYaF-90-136) Avail: CASI HC A03/MF A01 (US Sales Only)

Regarding the initial e(+), e(-) as a source of partons (e(+), e(-), gamma), we obtain the distributions of the invariant mass of the system phi. The following processes occurred: e(+)e(-) yields e(+)'e(-)'(phi), e(+)'(gamma)(phi), and gamma(gamma)(phi). Radiative corrections are taken into account for all orders of perturbation theory. Polarized and unpolarized cases are considered. Estimations of the numbers of W(sup +-), W(sup +)W(sup -), and Z produced are given. DOE

N93-30789# International Centre for Theoretical Physics, Trieste (Italy).
NEUTRINO OSCILLATIONS AND A NEW FARADAY EFFECT
M. AnwarMughal and K. Ahmed Jul. 1992 18 p
(DE93-606111; IC-92/185) Avail: CASI HC A03/MF A01 (US Sales Only)

By analogy with the classical Faraday effect for electromagnetic waves, a Faraday effect for massive neutrinos is found to be a somewhat generic description of neutrino oscillations when the neutrinos traverse a dense medium with or without a magnetic field. We further plot the Faraday angle for the solar neutrino problem as an illustration of the fact that the Faraday effect may yield a conceptually convenient parameterization of various neutrino oscillation scenarios. DOE

N93-30790# Academy of Sciences (USSR), Novosibirsk. Inst. Yadernoj Fiziki.
PION PAIR PRODUCTION IN PHOTON-PHOTON COLLISIONS
A. E. Blinov, V. E. Blinov, and A. E. Bondar et al 1991 23 p
(DE93-606114; IYaF-91-71) Avail: CASI HC A03/MF A01 (US Sales Only)

The process gamma(gamma) yields pi(+)pi(-) was measured with the detector MD-1 at VEPP-4. The two-photon reactions of e(+)e(-), mu(+)mu(-), and pi(+)pi(-) pair production were separated using scintillation counters, Cherenkov counters, and shower-range chambers. The radiation width Gamma(sub (gamma)(gamma)) (f(sub 2)(1270)) = 3.1 +/- 0.35 +/- 0.35 keV was obtained. DOE

N93-30791# Joint Inst. for Nuclear Research, Dubna (USSR). Lab. of Theoretical Physics.
COUPLED-CHANNEL ANALYSIS OF LOW ENERGY NUCLEON-ANTINUCLEON INTERACTIONS
V. K. Henner (Moscow State Univ., Russia.) and V. A. Meshcheryakov 1991 20 p Presented at the Nucleon-Anti-Nucleon Conference (NAN 1991), Moscow, Russia, 10 Jul. 1991 Submitted for publication
(DE93-606115; JINR-E-2-91-360) Avail: CASI HC A03/MF A01 (US Sales Only)

The multichannel M-matrix method is applied to an N(bar-N)-system that takes into account elastic p(bar-p)-scattering, the charge-exchange p(bar-p) yields n(bar-n) reaction, and p(bar-p) annihilation. It is shown that, contrary to standard assumptions, the isotopic invariance due the large influence of the charge exchange channel very significantly affects the parameters of strong interactions. Contrary to previous descriptions, M-matrix elements are treated as real functions. The differential and total cross-sections for p(bar-p) yields p(bar-p) and p(bar-p) yields n(bar-n) processes, cross-section delta(sub tot)(p(bar-p)) and the real-to-imaginary ratio of the forward amplitude of elastic p(bar-p) scattering up to beam momenta p(sub lab) = 600 MeV/c are described. The fitting leads to a resonance in the s-wave at about p(sub lab) = 500 MeV/c and to bound states in p-wave near the pp-bar threshold. DOE

N93-30792# Joint Inst. for Nuclear Research, Dubna (USSR). Lab. of Theoretical Physics.
TOWARDS THE RESULTS OF GLOBAL ANALYSIS OF DATA ON NUCLEON ELECTROMAGNETIC STRUCTURE
S. I. Bilenkaya, S. Dubnicka, A. Z. Dubnickova, and P. Strizenec 1991 14 p
(DE93-606125; JINR-E-2-91-475) Avail: CASI HC A03/MF A01 (US Sales Only)

Peculiar features of the recent global analysis of data on the nucleon electromagnetic structure are discussed. This was done in order to reconsider the reliability of the predicted result that the electron-positron annihilation into a neutron-antineutron cross-section is considerably larger that the cross-section of the electron-positron annihilation into a proton-antiproton pair. DOE

N93-30793# International Centre for Theoretical Physics, Trieste (Italy).
PLANCK SCALE EFFECTS IN NEUTRINO PHYSICS
E. K. Akhmedov, G. Senjanovic, Zhi-Jan Tao, and Z. G. Berezhiani (Ludwig-Maximilians-Univ., Munich, Germany.) Aug. 1992 22 p
(DE93-606133; IC-92/196; SISSA-140/92/EP; LMU-09/92) Avail: CASI HC A03/MF A01 (US Sales Only)

We study the phenomenology and cosmology of the Majoron (flavon) models of one inert neutrino and three active ones. We pay special attention to the possible (almost) conserved generalization of the Zeldovich-Konopinski-Mahmoud lepton charge. Using Planck scale physics effects, which provide the breaking of the lepton charge, we show how, in this picture, one can incorporate the solutions to some of the central issues in neutrino physics, such as the solar and atmospheric neutrino puzzles, dark matter, and a 17 keV neutrino. These gravitation effects induce tiny Majorana mass terms for neutrinos and considerable masses for flavons. The cosmological demand for the sufficiently fast decay of flavons implies a lower limit on the electron neutrino mass in the range of 0.1-1 eV. DOE

N93-30800# Academy of Sciences (USSR), Novosibirsk. Inst. Yadernoj Fiziki.
ORBITAL MOTION CALCULATION USING LIE METHOD IN COLLIDER NONLINEAR MAGNETIC FIELD [RASCHET ORBITAL'NOGO DVIZHENIYA V NELINEJNOJ MAGNITNOJ SISTEME NAKOPITELYA S ISPOL,ZOVANIEM TEKHNIKI LI OPERATOROV]
Y. I. Ehjdelman and V. E. Yakimenko 1991 31 p In RUSSIAN
(DE93-605733; IYaF-91-6) Avail: CASI HC A03/MF A01 (US Sales Only)

The orbital motion calculation using Lie method in a nonlinear magnetic field is employed to solving the orbital motion equation of a charged particle in a nonlinear field of a collider. The first four orders of orbital motion Hamiltonian series are obtained. DOE

N93-30901# Scripps Clinic and Research Foundation, La Jolla, CA.
DEFINING PROTEIN ELECTROSTATIC RECOGNITION PROCESSES Final Report, 1 Dec. 1988 - 30 Nov. 1991
Elizabeth D. Getzoff and Victoria A. Roberts 1992 5 p
(Contract N00014-89-J-11745)
(AD-A264838) Avail: CASI HC A01/MF A01

The objective is to elucidate the nature of electrostatic forces controlling protein recognition processes by using a tightly coupled computational and interactive computer graphics approach. The TURNIP program was developed to determine the most favorable precollision orientations for two molecules by systematic search of all orientations and evaluation of the resulting electrostatic interactions. TURNIP was applied to the transient interaction between two electron transfer metalloproteins, plastocyanin and cytochrome c. The results suggest that the productive electron-transfer complex involves interaction of the positive region of cytochrome c with the negative patch of plastocyanin, consistent with experimental data. Application of TURNIP to the formation of the stable complex between the HyHEL-5 antibody and its protein antigen lysozyme showed that long-distance electrostatic forces guide lysozyme toward the HyHEL-5 binding site, but do not fine tune its orientation. Determination of docked antigen/antibody complexes requires including steric as well as electrostatic interactions, as was done for the U10 mutant of the anti-phosphorylcholine antibody S107. The graphics program Flex, a convenient desktop workstation program for visualizing molecular dynamics and normal mode motions, was enhanced. Flex now has a user interface and was rewritten to use standard graphics libraries, so as to run on most desktop workstations. DTIC

N93-30930# Gosudarstvennyi Komitet po Ispolzovaniyu Atomnoi Energii, Serpukhov (USSR). Inst. Fiziki Vysokikh Ehnergij.

SINGLE t-QUARK PRODUCTION IN HIGH ENERGY (GAMMA)e COLLISIONS

G. V. Jikia 1991 23 p
(DE92-644947; IHEP-OTF-91-33) Avail: CASI HC A03/MF A01 (US Sales Only)

The explicit formulae for the cross sections of single t-quark production in gamma-e collisions are presented. The contribution of the hadronic structure of the photon to the production cross sections is also calculated. Total t-quark and fourth generation b'-quark production rates and discuss theoretical uncertainties are evaluated. Assuming the luminosity of 10(exp 33) cm(exp -2)s(exp -1) in TeV energy range, we estimate that the Cabibbo-Kobayashi-Maskawa matrix element V(sub tb) can be probed to an accuracy of 3-5%. DOE

N93-30931# International Centre for Theoretical Physics, Trieste (Italy).

MASSIVE MAJORANA NEUTRINOS IN PRE-BOUNCE SUPERNOVAE

S. Goswami (Calcutta Univ., India.), K. Kar (Saha Inst. of Nuclear Physics, Calcutta, India.), and A. Raychaudhuri Jun. 1992 22 p
(DE92-642597; IC-92/92; CUPP-92/3) Avail: CASI HC A03/MF A01 (US Sales Only)

The currently accepted models of supernova collapse rely on the standard electroweak theory and massless left-handed neutrinos. We consider the effect of massive right-handed Majorana neutrinos on this scenario. In order that they do not upset the agreement of the usual treatment with observation, we require that in the pre-bounce stage either (1) these neutrinos are trapped, or (2) if they free stream they do not change the electron fraction to the extent that the explosion is prevented. From these constraints, we obtain upper and lower bounds on the right-handed interaction strengths as a function of the neutrino mass which can be translated to bounds on the right-handed gauge boson mass. DOE

N93-30944# Instituto de Fisica Teorica, Sao Paulo (Brazil).

LOW-ENERGY BEHAVIOUR OF FEW-PARTICLE SCATTERING AMPLITUDES IN TWO DIMENSIONS

S. K. Adhikari and W. L. Gibson (Sydney Univ., Australia.) Jun. 1992 29 p
(DE93-609834; IFT-P-024/92) Avail: CASI HC A03/MF A01 (US Sales Only)

A study of the analytic behavior of different few-particle scattering amplitudes at low energies in two space dimensions is presented. Such a study is of use in modeling and understanding different few-particle processes at low energies. A detailed discussion of the energy and the momentum dependence of the partial-wave on-the-energy-shell and off-the-energy-shell two-particle t matrices is given. These t matrix element tend to zero as the energy and momentum variables tend to zero. The multiple scattering series is used to show that the connected three-to-three amplitudes diverge in the low energy-momentum limit. Unitarity relations are used logarithmic singularities at the m particle breakup threshold. The subenergy singularity in the two-to-three amplitudes is also studied, and comments are made on some applications of the present study in different problems of physical interest. DOE

N93-31008# Nationaal Inst. voor Kernfysica en Hoge Energiefysica, Amsterdam (Netherlands).

BARYON NUMBER VIOLATION AND PARTICLE COLLIDER EXPERIMENTS

F. R. Klinkhamer Sep. 1992 11 p Submitted for publication
Sponsored by Royal Netherlands Academy of Arts and Sciences
(NIKHEF-H/92-14; ETN-93-94085) Avail: CASI HC A03/MF A01

Baryon number nonconservation, due to nonperturbative effects (sphalerons) in the standard model, may have been important in the early Universe. The possibility that similar effects could show up at future particle collider experiments is discussed. These would be multiparticle events with average transverse momenta of the order of p(sub t) approximately equal to M(sub W). A motivation to look for these effects in laboratory experiments is to be sure of the physics that goes into the early Universe. ESA

N93-29628*# Los Alamos National Lab., NM. Space Science and Technology Div.

RADIOACTIVITIES INDUCED IN SOME LDEF SAMPLES

Robert C. Reedy, Calvin E. Moss, S. George Bobias, and Jozef Masarik *In* NASA. Langley Research Center, LDEF: 69 Months in Space. Part 1: Second Post-Retrieval Symposium Apr. 1993 p 87-96 (For primary document see N93-29621 11-99)
Avail: CASI HC A02/MF A03

N93-29629*# California Univ., Berkeley. Lawrence Berkeley Lab. Engineering Div.

A PHOTON PHREAK DIGS THE LDEF HAPPENING

Alan R. Smith and Donna L. Hurley *In* NASA. Langley Research Center, LDEF: 69 Months in Space. Part 1: Second Post-Retrieval Symposium Apr. 1993 p 97-105 (For primary document see N93-29621 11-99)
(Contract NASA Order H-06815-D; DE-AC03-76SF-00098)
Avail: CASI HC A02/MF A03

N93-29630*# Massachusetts Inst. of Tech., Cambridge. Nuclear Reactor Lab.

CHARGED PARTICLE ACTIVATION STUDIES ON THE SURFACE OF LDEF SPACECRAFT

Ilhan Olmez, Forest Burns (Army Materials Technology Lab., Watertown, MA.), and Paul Sagalyn (Army Materials Technology Lab., Watertown, MA.) *In* NASA. Langley Research Center, LDEF: 69 Months in Space. Part 1: Second Post-Retrieval Symposium Apr. 1993 p 107-109 (For primary document see N93-29621 11-99)
Avail: CASI HC A01/MF A03

N93-29632*# National Aeronautics and Space Administration. Marshall Space Flight Center, Huntsville, AL.

INDUCED ACTIVATION STUDY OF LDEF

B. A. Harmon, G. J. Fishman, T. A. Parnell, and C. E. Laird (University of Eastern Kentucky, Richmond.) *In* NASA. Langley Research Center, LDEF: 69 Months in Space. Part 1: Second Post-Retrieval Symposium Apr. 1993 p 125-136 (For primary document see N93-29621 11-99)
Avail: CASI HC A03/MF A03

N93-29633*# National Aeronautics and Space Administration. Marshall Space Flight Center, Huntsville, AL.

REVISED PREDICTION OF LDEF EXPOSURE TO TRAPPED PROTONS

John W. Watts, T. W. Armstrong (Science Applications International Corp., Prospect, TN.), and B. L. Colborn (Science Applications International Corp., Prospect, TN.) *In* NASA. Langley Research Center, LDEF: 69 Months in Space. Part 1: Second Post-Retrieval Symposium Apr. 1993 p 137-145 (For primary document see N93-29621 11-99)
Avail: CASI HC A02/MF A03

N93-29634*# Aerospace Corp., Los Angeles, CA. Space and Environment Technology Center.

A MEASUREMENT OF THE RADIATION DOSE TO LDEF BY PASSIVE DOSIMETRY

J. B. Blake and S. S. Imamoto *In* NASA. Langley Research Center,

LDEF: 69 Months in Space. Part 1: Second Post-Retrieval Symposium Apr. 1993 p 147-155 (For primary document see N93-29621 11-99)
(Contract F04701-88-C-0089)
Avail: CASI HC A02/MF A03

N93-29635*# Departement d'Etudes et de Recherches en Technologie Spatiale, Toulouse (France).
LDEF: DOSIMETRIC MEASUREMENT RESULTS (AO 138-7 EXPERIMENT)
J. Bourrieau *In* NASA. Langley Research Center, LDEF: 69 Months in Space. Part 1: Second Post-Retrieval Symposium Apr. 1993 p 157-162 (For primary document see N93-29621 11-99)
Avail: CASI HC A02/MF A03

N93-29636*# Eril Research, Inc., San Rafael, CA.
ABSORBED DOSE MEASUREMENTS AND PREDICTIONS ON LDEF
A. L. Frank, E. V. Benton, T. W. Armstrong (Science Applications International Corp., Prospect, TN.), and B. L. Colborn (Science Applications International Corp., Prospect, TN.) *In* NASA. Langley Research Center, LDEF: 69 Months in Space. Part 1: Second Post-Retrieval Symposium Apr. 1993 p 163-170 (For primary document see N93-29621 11-99)
(Contract NAS8-38610)
Avail: CASI HC A02/MF A03

N93-29637*# National Aeronautics and Space Administration. Marshall Space Flight Center, Huntsville, AL.
LET SPECTRA MEASUREMENTS OF CHARGED PARTICLES IN THE P0006 EXPERIMENT ON LDEF
E. V. Benton (San Francisco Univ., CA.), I. Csige (San Francisco Univ., CA.), K. Oda (San Francisco Univ., CA.), R. P. Henke (San Francisco Univ., CA.), A. L. Frank (San Francisco Univ., CA.), E. R. Benton (San Francisco Univ., CA.), L. A. Frigo (San Francisco Univ., CA.), T. A. Parnell, J. W. Watts, Jr., and J. H. Derrickson *In* NASA. Langley Research Center, LDEF: 69 Months in Space. Part 1: Second Post-Retrieval Symposium Apr. 1993 p 171-180 (For primary document see N93-29621 11-99)
(Grant NAG8-168)
Avail: CASI HC A02/MF A03

N93-29638*# Eril Research, Inc., San Rafael, CA.
LIGHT-HEAVY ION MEASUREMENTS IN CR-39 LOCATED ON THE EARTH SIDE OF LDEF
I. Csige, E. V. Benton, S. Soundararajan, and E. R. Benton *In* NASA. Langley Research Center, LDEF: 69 Months in Space. Part 1: Second Post-Retrieval Symposium 181-186 (SEE N93-29621 11-99) Apr. 1993 (For primary document see N93-29621 11-99)
(Contract NAS8-38610)
Avail: CASI HC A03/MF A03

N93-29639*# National Aeronautics and Space Administration. Marshall Space Flight Center, Huntsville, AL.
THREE-DIMENSIONAL SHIELDING EFFECTS ON CHARGED PARTICLE FLUENCES MEASURED IN THE P0006 EXPERIMENT OF LDEF
I. Csige (San Francisco Univ., CA.), E. V. Benton (San Francisco Univ., CA.), L. Frigo (San Francisco Univ., CA.), T. A. Parnell, J. W. Watts, Jr., T. W. Armstrong (Science Applications International Corp., Prospect, TN.), and B. L. Colborn (Science Applications International Corp., Prospect, TN.) *In* NASA. Langley Research Center, LDEF: 69 Months in Space. Part 1: Second Post-Retrieval Symposium Apr. 1993 p 187-194 (For primary document see N93-29621 11-99)
(Grant NAG8-168)
Avail: CASI HC A02/MF A03

N93-29640*# Science Applications International Corp., Prospect, TN.
DEVELOPMENT AND APPLICATION OF A 3-D GEOMETRY/MASS MODEL FOR LDEF SATELLITE IONIZING RADIATION ASSESSMENTS
B. L. Colborn and T. W. Armstong *In* NASA. Langley Research Center, LDEF: 69 Months in Space. Part 1: Second Post-Retrieval Symposium Apr. 1993 p 195-205 (For primary document see N93-29621 11-99)
(Contracts NAS8-38121; NAS8-39386)
Avail: CASI HC A03/MF A03

N93-29641*# Science Applications International Corp., Prospect, TN.
RADIATION MODEL PREDICTIONS AND VALIDATION USING LDEF SATELLITE DATA
T. W. Armstrong and B. L. Colborn *In* NASA. Langley Research Center, LDEF: 69 Months in Space. Part 1: Second Post-Retrieval Symposium Apr. 1993 p 207-220 (For primary document see N93-29621 11-99)
(Contracts NAS8-38770; NAS8-39386)
Avail: CASI HC A03/MF A03

N93-29642*# Science Applications International Corp., Prospect, TN.
FUTURE DIRECTIONS FOR LDEF IONIZING RADIATION MODELING AND ASSESSMENTS
T. W. Armstrong and B. L. Colborn *In* NASA. Langley Research Center, LDEF: 69 Months in Space. Part 1: Second Post-Retrieval Symposium Apr. 1993 p 221-230 (For primary document see N93-29621 11-99)
(Contract NAS8-39386)
Avail: CASI HC A02/MF A03

N93-29643*# National Aeronautics and Space Administration. Marshall Space Flight Center, Huntsville, AL.
COSMOGENIC RADIONUCLIDES ON LDEF: AN UNEXPECTED Be-10 RESULT
J. C. Gregory (Alabama Univ., Huntsville.), A. Albrecht (Rutgers Univ., New Brunswick, NJ.), G. Herzog (Rutgers Univ., New Brunswick, NJ.), J. Klein (Pennsylvania Univ., Philadelphia.), R. Middleton (Pennsylvania Univ., Philadelphia.), B. Dezfouly-Arjomandy (Pennsylvania Univ., Philadelphia.), and B. A. Harmon *In* NASA. Langley Research Center, LDEF: 69 Months in Space. Part 1: Second Post-Retrieval Symposium Apr. 1993 p 231-237 (For primary document see N93-29621 11-99)
Avail: CASI HC A02/MF A03

N93-29644*# Kiel Univ. (Germany).
HEAVY ION MEASUREMENT ON LDEF
D. Jonathal, R. Beaujean, and W. Enge *In* NASA. Langley Research Center, LDEF: 69 Months in Space. Part 1: Second Post-Retrieval Symposium Apr. 1993 p 239-245 (For primary document see N93-29621 11-99)
Avail: CASI HC A02/MF A03

N93-29645*# Naval Research Lab., Washington, DC.
PROGRESS REPORT ON THE HEAVY IONS IN SPACE (HIIS) EXPERIMENT
James H. Adams, Jr., Lorraine P. Beahm, Paul R. Boberg, and Allan J. Tylka *In* NASA. Langley Research Center, LDEF: 69 Months in Space. Part 1: Second Post-Retrieval Symposium Apr. 1993 p 247-259 (For primary document see N93-29621 11-99)
Avail: CASI HC A03/MF A03

N93-30097 Naval Research Lab., Washington, DC.
MOLECULAR DYNAMICS OF DETONATION IN CRYSTALS WITH DEFECTS
Lee Phillips and Robert S. Sinkovits *In* JHU, ONR/LANL Workshop on the Fundamental Physics and Chemistry of Combustion, Initiation, and Detonation of Energetic Materials Mar. 1992 p 495-496 Sponsored in part by ONR (For primary document see N93-30061 11-28)
Avail: CPIA, 10630 Little Patuxent Pkwy., Suite 202, Columbia, MD 21044-3200 HC

73 NUCLEAR AND HIGH-ENERGY PHYSICS

Includes elementary and nuclear particles; and reactor theory.
For space radiation see *93 Space Radiation.*

N93-28522# Maryland Univ., College Park. Lab. for Plasma Research.
ACCELERATOR RESEARCH STUDIES
1993 95 p
(Contract DE-FG05-91ER-40642)
(DE93-009353; DOE/ER-40642/2) Avail: CASI HC A05/MF A01

The Accelerator Research Studies program at the University of Maryland, sponsored by the Department of Energy, is currently in the second year of a three-year funding cycle. The program consists of the following three tasks: (1) study of transport and longitudinal compression of intense, high-brightness beams; (2) study of collective ion acceleration by intense electron beams and pseudospark produced high brightness electron beams; and (3) study of a gyroklystron high-power microwave source for linear colliders. The progress that was made during the past year for each of the three tasks is reported. DOE

N93-28565# Illinois Univ., Chicago. Dept. of Physics.
STUDIES IN THEORETICAL HIGH ENERGY PARTICLE PHYSICS
H. Aratyn, L. Brekke, Wai-Yee Keung, and U. Sukhatme Jan. 1993 16 p
(Contract DE-FG02-84ER-40173)
(DE93-007990; DOE/ER-40173/8) Avail: CASI HC A03/MF A01

Theoretical work on the following topics is briefly summarized: symmetry structure of conformal affine Toda model and KP hierarchy; solitons in the affine Toda and conformal affine Toda models; classical r-matrices and Poisson bracket structures on infinite-dimensional groups; R-matrix formulation of KP hierarchies and their gauge equivalence; statistics of particles and solitons; charge quantization in the presence of an Alice string; knotting and linking of nonabelian flux; electric dipole moments; neutrino physics in gauge theories; CP violation in the high energy colliders; supersymmetric quantum mechanics; parton structure functions in nuclei; and a dual parton model. DOE

N93-28569# Yale Univ., New Haven, CT. Dept. of Physics.
MEASUREMENTS OF RARE COMPOSITE OBJECTS AND HIGH SENSITIVITY SEARCHES FOR NOVEL FORMS OF MATTER PRODUCED IN HIGH ENERGY HEAVY ION COLLISIONS
1993 10 p
(Contract DE-FG02-90ER-40562)
(DE93-009945; DOE/ER-40562/T1) Avail: CASI HC A02/MF A01

The program consists of two complementary parts. First, searches for new particles include strange quark matter, as well as strange chiral solitons and multistrange hypernuclei. These and other new phenomena may result from the extreme conditions present in relativistic heavy ion collisions, which is a regime that is still relatively new and untested. Second, measurements will be made of known particles, such as the coalescence production of nuclei and antinuclei. Knowledge of coalescence production is not only crucial to interpreting the limits in strange matter searches, but also is useful in probing the relativistic heavy ion collision process. While data analysis is proceeding efforts will focus on the construction, running, and analysis of a new more precise experiment. The heavy ion program at BNL's RHIC accelerator will continue. This will be a 'fixed-target' experiment using a gas jet or pellet target that would extend studies of new particles in the high energy regime offered by this new accelerator. DOE

N93-28969# South Carolina Univ., Columbia.
RESEARCH PROGRAMS FROM THE UNIVERSITY OF SOUTH CAROLINA ON HIGH ENERGY PHYSICS
C. Rosenfeld 1993 17 p
(Contract DE-FG02-92ER-40719)
(DE93-007829; DOE/ER-40719/1) Avail: CASI HC A03/MF A01

Work on three main experiments is summarized: (1) study of charm physics in a wide-band photon beam; (2) charmless two-body decays of b-flavored mesons and baryons studied with a ring imaging Cherenkov counter; and (3) the AMY Program, which studies e(+)e(-) interactions using the TRISTAN collider at KEK, with emphasis on trigger upgrades. Future work related to the existence of a 17-keV neutrino in beta decay and nu(sub mu)/nu(sub tau) oscillation is described. DOE

N93-28970# Argonne National Lab., IL.
A HIGH FIELD OPTICAL-PUMPING SPIN-EXCHANGE POLARIZED DEUTERIUM SOURCE
K. P. Coulter, R. J. Holt, E. R. Kinney, R. S. Kowalczyk, M. Poelker, D. H. Potterveld, L. Young, B. Zeidman, and D. Toporkov (Academy of Sciences, USSR, Novosibirsk.) 1992 5 p Presented at the 10th International Symposium on High-Energy Spin Physics, Nagoya, Japan, 9-14 Nov. 1992
(Contract W-31-109-eng-38)
(DE93-009208; ANL/PHY/CP-79003; CONF-921131-9) Avail: CASI HC A01/MF A01

Recent results from a prototype high field optical-pumping spin-exchange polarized deuterium source are presented. Atomic polarization as high as 62% have been observed with an intensity of 6.3 x 10(exp 17) atoms-sec(exp -1) and 65% dissociation fraction. DOE

N93-29062# Forschungszentrum Juelich G.m.b.H. (Germany). Inst. fuer Kernphysik.
MODERN MONTE CARLO PARTICLE TRANSPORT SIMULATION FOR SAFETY AND RADIATION PROTECTION APPLICATIONS IN ACCELEROMETER TECHNOLOGY AND IN SPACE SCIENCE [MODERNE MONTE CARLO TEILCHENTRANSPORT-SIMULATIONSVERFAHREN FUER SICHERHEITSTECHNISCHE ANWENDUNGEN UND FRAGESTELLUNGEN IN DER BESCHLEUNIGERTECHNIK UND IN DER RAUMFAHRT]
Detlef Filges Apr. 1992 208 p In GERMAN
(Juel-2609; ETN-93-93464) Avail: CASI HC A10/MF A03

The application potential of modern particle radiation transport simulations to solve safety and radiation protection problems in accelerator technology and in space science and technology is presented. It is shown to what extent Monte Carlo simulation is helpful in defining safety regulations, safety standards and in determining corresponding safety proofs. For this purpose the basic methods are described and their performance together with particular examples are assessed. The state of the art of the computational methods is described together with the existing computer codes. The details of the current three dimensional geometry packages are also given. Necessary nuclear transport data and reaction cross sections in respect to shielding and safety protection problems are investigated. The performance and flexibility of HERMES (High Energy Radiation Monte Carlo Elaborate System), and its utilization in solving safety protection problems are demonstrated. Examples of radiation protection and high energy source shielding for medium and high energy particle accelerators and for high current particle accelerator target systems are summarized. Radiation protection and shielding of space vehicles against cosmic ray radiation are compiled and assessed. Validations of experimental results are also given. ESA

N93-29103# Lawrence Livermore National Lab., CA.
MAXIMIZING THE LUMINOSITY OF HADRON, SUPERCOLLIDERS AT 10-100 TeV
W. A. Barletta (California Univ., Los Angeles.) Jul. 1992 38 p Presented at the 19th INFN Eloisation Project: Maximizing Luminosity of Hadron Colliders At 100 TeV, Erice, Italy, 13-19 Nov. 1991
(Contract W-7405-eng-48)
(DE93-009247; UCRL-JC-110768; CONF-9111208-4) Avail: CASI HC A03/MF A01

As physicists seek to build colliders of ever higher energy, they are generally faced with the task of simultaneously increasing the luminosity to compensate for the decrease in cross sections. Extending the physics reach and discovery potential of hadron supercolliders to the maximum extent will require accelerator designers Teaming how to achieve luminosities much greater than 10(exp 35) cm(exp -2)/s at energies of at least 100 TeV per beam. The application of the presently available accelerator technologies embodied in the designs of the LHC (at 8 TeV per beam and 10(exp 34)cm(exp -2)/s) and the SSC (20 TeV per beam at 10(exp 33) cm(exp -2)/s) to an ELOISATRON (ELN) operating at 100 TeV per beam would yield a collider design with a luminosity of 10(exp 34) cm(exp -2)/s. Yet higher energies and luminosities are clearly possible. This paper presents a general context for assessing the performance of future hadron colliders. It begins by illustrating machine trends and by defining of key collider characteristics. Descriptions of limiting beam physics and limiting accelerator technologies constitute the next two sections. These considerations have been folded into a simple spreadsheet-based computer code that allows one to perform self-consistent parameter searches to maximize luminosity. Section five presents some results from the parameter searches. The paper concludes with by sketching the characteristics of an ultimate hadron supercollider, i.e., an Ultra-ELOISATRON (UELN). DOE

N93-29137# Japan Atomic Energy Research Inst., Tokyo.
ANNUAL PROGRESS REPORT ON THE NSRR EXPERIMENTS, (21)
May 1992 210 p
(DE93-753190; JAERI-M-92-072) Avail: CASI HC A10/MF A03

Fuel behavior studies under simulated reactivity-initiated accident (RIA) conditions have been performed in the Nuclear Safety Research Reactor (NSRR) since 1975. This report gives the results of experiments performed from April, 1989 through March, 1990 and discussions of them. A total of 41 tests were carried out during this period. The tests are distinguished into pre-irradiated fuel tests and fresh fuel tests; the former includes 2 JMTR pre-irradiated fuel tests, 2 PWR pre-irradiated fuel tests, and 2 BWR pre-irradiated fuel tests, and the latter includes 6 standard fuel tests (6 SP(center dot)CP scoping tests), 7 power and cooling condition parameter tests (4 flow shrouded fuel tests, 1 bundle simulation test, 1 fully water-filled vessel test, 1 high pressure/high temperature loop test), 12 special fuel tests (3 stainless steel clad fuel tests, 3 improved PWR fuel tests, 6 improved BWR fuel tests), 3 severe fuel damage tests (1 high temperature flooding test, 1 flooding behavior observation test, 1 debris coolability test), 3 fast breeder reactor fuel tests (2 moderator material characteristic measurement tests, 1 fuel behavior observation test), and 2 miscellaneous tests (2 preliminary tests for pre-irradiated fuel tests). DOE

N93-29151# Sandia National Labs., Albuquerque, NM.

AN EXPERIMENTAL INVESTIGATION OF RADIOACTIVITY INDUCED BY IONS ASSOCIATED WITH THE OPERATION OF PULSED-POWER ACCELERATORS

S. K. Vosburg, C. L. Ruiz, G. W. Cooper (New Mexico Univ., Albuquerque.), and F. A. Schmidlapp (Ktech Corp., Albuquerque, NM.) Mar. 1993 91 p
(Contract DE-AC04-76DP-00789)
(DE93-011478; SAND-92-2075) Avail: CASI HC A05/MF A01

Energetic light ion beams are being studied in Sandia National Laboratories' Particle Beam Fusion Accelerator II (PBFA II) for the purpose of studying the physics of applied B-diodes with the hope that these beams can be applied to inertial confinement fusion. These beams induce nuclear reactions both in the diode itself and in the materials surrounding the diode. A series of experiments was conducted wherein samples of metals typically used in the diode/gas cell region of PBFA II were exposed to ion beams at energies expected to be achieved in PBFA II. The metals studied were aluminum alloys 2024 and 6061, brass, copper, Inconel alloys 625 and 718, Stainless Steel 304, tantalum, titanium, and tungsten. The ion beams studied consisted of protons at energies of 6, 12, and 19 MeV; deuterons at 6 MeV; Lithium-7 at energies of 10, 15, 20, and 30 MeV; Lithium-6 at 30 MeV; and Boron-10 and Boron-11 at 30 MeV. The induced activity of each sample was measured as a function of time with an ion chamber and was used to estimate the rate at which the initial short-lived activity of the sample decayed. In addition, the activity of each sample was periodically measured with a Geiger counter in contact with the irradiated surface of the sample, was normalized to the total amount of energy incident on the sample, and was used as a basis to compare the amount of activity generated per mega-joule of energy for each sample. Additionally, gamma-ray spectra of the activated samples were collected using a germanium detector, and these spectra were analyzed qualitatively to identify the long-lived radioisotopes present in the sample. DOE

N93-29302# California Univ., Berkeley. Lawrence Berkeley Lab.

AN RF DRIVEN H(-) SOURCE AND A LOW ENERGY BEAM INJECTION SYSTEM FOR RFQ OPERATION

K. N. Leung, D. A. Bachman, C. F. Chan, and D. S. McDonald 1992 4 p Presented at the International Conference on High Energy Accelerators, Hamburg, Germany, 20-24 Jul. 1992
(Contract DE-AC03-76SF-00098)
(DE93-010438; LBL-32593; CONF-920706-50) Avail: CASI HC A01/MF A01

An RF driven H(-) source has been developed at LBL for use in the Superconducting Super Collider (SSC). To date, an H(-) current of approximately 40 mA can be obtained from a 5.6-cm diam. aperture with the source operated at a pressure of about 12 m Torr and 50 kW of RF power. In order to match the accelerated H(-) beam into the SSC RFQ, a low-energy H(-) injection system has been designed. This injector produces an outgoing H(-) beam free of electron contamination, with small radius, large convergent angle, and small projectional emittance. DOE

N93-29317# Brookhaven National Lab., Upton, NY.

DESIGN AND TEST OF A SUPERCONDUCTING RFQ FOR HEAVY IONS

I. Ben-Zvi (State Univ. of New York, Stony Brook.), A. Jain (State Univ. of New York, Stony Brook.), J. W. Noe (State Univ. of New York, Stony Brook.), P. Paul (State Univ. of New York, Stony Brook.), and H. Wang (State Univ. of New York, Stony Brook.) 1992 7 p Presented at the 6th International Conference on Electrostatic Accelerators and Associated Boosters, Padua, Italy, 1-4 Jun. 1992
(Contract DE-AC02-76CH-00016)
(DE93-010862; BNL-48571; CONF-920656-5) Avail: CASI HC A02/MF A01

A prototype SRFQ resonator optimized for a velocity of (beta)=0.03 and a charge to mass ratio (q/M) of 1/6 was designed, fabricated, and tested. This is a short RFQ structure (only 2(beta)(lambda) long) operating at 57.4MHz. The resonator is made of copper, and a 1.5 micron thick layer of electroplated Pb-2 at.% Sn is used as the superconductor. The electrical characteristics of the resonator derived from detailed 3-D numerical simulations using the MAFIA codes and also from measurements on the actual resonator are described. The multipactoring levels could be processed away with ease. Quality factor (Q) is greater than 1(10)(exp 8) is obtained for E(sub a) up to 1 MV/m. Other parameters relevant to superconducting operation are also presented. DOE

N93-29809# Los Alamos National Lab., NM.

HIGH-CURRENT NEGATIVE-ION BEAM TRANSPORT

R. R. Stevens, Jr. 1993 11 p Presented at the 6th International Symposium on the Production and Neutralization of Negative Ions and Beams, Long Island, NY, 9-13 Nov. 1992
(Contract W-7405-eng-36)
(DE93-010732; LA-UR-93-1038; CONF-921145-6) Avail: CASI HC A03/MF A01

The requirements for transporting high-current, negative-ion beams are presented with particular emphasis on applications involving negative-hydrogen-ion beams. In addition to the usual matching and steering problems, particular attention must be paid to beam emittance growth in the transport system. Depending on the application, a number of approaches have been developed using both magnetic and electric lenses. I discuss the design considerations for transporting and matching these beams to radiofrequency quadrupole accelerators, and present a survey of the various types of beamlines now used for negative-ion beams. DOE

N93-29870# California Univ., Berkeley. Lawrence Berkeley Lab.

THREE-DIMENSIONAL SIMULATION ANALYSIS OF THE STANDING-WAVE FREE-ELECTRON LASER TWO-BEAM ACCELERATOR

C. Wang and A. Sessler Jan. 1993 5 p Presented at the OE/LASE International Society for Optical Engineering (SPIE) Conference, Los Angeles, CA, 16-23 Jan. 1993
(Contract DE-AC03-76SF-00098)
(DE93-010461; LBL-32481; ESG-199; CONF-930159-26) Avail: CASI HC A01/MF A01

We have modified a two-dimensional relativistic klystron code, developed by Ryne and Yu, to simulate both the standing-wave free-electron laser two-beam accelerator and the relativistic klystron two-beam accelerator. In this paper, the code is used to study a standing-wave free-electron laser with three cavities. The effect of the radius of the electron beam on the RF output power (a three-dimensional effect) is examined. DOE

N93-29996# Technical Research Centre of Finland, Espoo. Nuclear Engineering Lab.

TRAB: A TRANSIENT ANALYSIS PROGRAM FOR BWR. PART 2: USER'S MANUAL

Hanna Raty and Markku Rajamaeki May 1991 155 p
(VTT-TIED-1232-Pt-2; ISBN-951-38-3875-7; ETN-93-93771) Copyright Avail: CASI HC A08/MF A02

A user manual with documentation of the structure, contents, and preparation of input, for the TRAB (Transient Analysis) code for BWR's (Boiling Water Reactors) is presented. TRAB models the phenomena in the interior of the BWR pressure vessel and in related subsystems. The code model of TRAB can be used separately for LWR (Light) modeling. For PWR (Pressurized) modeling the core model of TRAB is connected to circuit model SMABRE to form the SMATRA code. The structure of TRAB input is very flexible, featuring input groups and subgroups identified with keywords and given in any order as well as data items in free format, freely mixed with explanatory texts. The user interface of the code can be used for modeling within input; through normal input it is possible to create new submodels. These may be functional or tabulated dependencies of the code variables, different types of delays, or ordinary linear differential equations (control systems). ESA

N93-30002 Tokyo Univ., Tanashi (Japan). Inst. for Nuclear Study.
RESEARCH AND EDUCATION BY SF CYCLOTRON FACILITY
Apr. 1992 51 p Limited Reproducibility: More than 20% of this document may be affected by microfiche quality
(DE93-753135; INS-T-507) Avail: CASI HC A04

This report represents the current activities in research and education using the cyclotron facility and related apparatus which are supported by Nuclear Physics Division and this is a continuation of INS-T-466 (1986, December). In this version, an iron-free beta-ray spectrometer and a cooler-synchrotron (TARN 2) are briefly described also in the first chapter. The second chapter explains experimental programs performed in the last 5 years. The third chapter gives the number of publications on researches performed in 1975-1991, and also gives twelve topics obtained from the cyclotron and the beta-ray spectrometer in recent 5 years. The last chapter provides the whole list of the works for Doctor and Master theses performed at the facility in the last 10 years. DOE

N93-30006 Japan Atomic Energy Research Inst., Tokai.
AIR OXIDATION BEHAVIOR OF FUEL FOR THE HIGH TEMPERATURE ENGINEERING TEST REACTOR (HTTR)
Hironobu Kikuchi, Kimio Hayashi, and Kousaku Fukuda Aug. 1992 26 p Limited Reproducibility: More than 20% of this document may be affected by microfiche quality
(DE93-753349; JAERI-M-92-114) Avail: CASI HC A03

The oxidation behavior of the HTTR fuel was studied with respect to the scenario of an air ingress accident which had been assessed in the HTTR safety analysis. The coated fuel particles were heated under a sufficient air flow in the temperature range of 900-1400 C for maximum duration of 600 h (at 1300 C). Failure fractions of the SiC coating layer after the heat treatments remained within the fraction at the fuel production. And the failure behavior of the SiC layer did not depend on such heating conditions as the temperature and the duration in the present experiment. It was confirmed by scanning electron microscopy (SEM), X-ray diffraction, and laser Raman spectroscopy that a thin oxide film was formed on the SiC layer by the heat treatments. DOE

N93-30019# Nationaal Inst. voor Kernfysica en Hoge Energiefysica, Amsterdam (Netherlands).
MECHANICAL BEHAVIOUR OF A CLOSED COLLAR MODEL FOR AN 11.5 T DIPOLE
W. vanEmden, C. Daum, J. Geerinck, A. denOuden (Universiteit Twente, Enschede, Netherlands.), H. H. J. tenKate (Universiteit Twente, Enschede, Netherlands.), D. terAvest (Universiteit Twente, Enschede, Netherlands.), S. Wessel (HOLEC, Inc., Ridderkerk, Netherlands.), and R. Dubbeldam Mar. 1992 20 p
(NIKHEF-H/92-03; LHC-Note-181; ETN-93-93298) Avail: CASI HC A03/MF A01

A 10 cm long model of an 11.5 T Nb3Sn accelerator dipole magnet, with a closed ring shaped collar was constructed. A new collar design in which the prestress in the coil is achieved by shrink fitting a closed ring shaped collar around the coil package of each aperture is studied. Measurements of the collar deformation and the prestress at the poles are discussed. The finite element analysis of an 11.5 T Nb3Sn Large Hadron Collider dipole magnet equipped with closed collars around each aperture showed the applicability of this collar system. The shrinking process of the collars around the coils were repeated many times with the short dummy model and is expected to cause no problems in the assembly of a 1 m magnet. A systematic study of stresses and deformations inside the structure could be used to define the manufacturing tolerances of the various components. Studies of the effects of friction in the structural behavior were performed. For reasonable values of the friction coefficient between 0 and 0.6 major problems arise. From measurements in a short dummy model of the coil system it is concluded that measured and calculated deformations and stresses agree within limits imposed by manufacturing tolerances. The beam type strain gauge transducers are suitable for monitoring transverse stresses in the system provided a proper calibration procedure precedes their final mounting. ESA

N93-30054# Tennessee Technological Univ., Cookeville. Dept. of Physics.
STUDIES OF FLUCTUATION PROCESSES IN NUCLEAR COLLISIONS
S. Ayik Feb. 1993 18 p
(Contract DE-FG05-89ER-40530)
(DE93-011263; DOE/ER-40530/4) Avail: CASI HC A03/MF A01

Investigations of various aspects of heavy-ion collisions were carried out in the framework of the Boltzmann-Langevin Model (BLM). In a previous work, by projection of the BLM onto a collective space, a memory-dependent collective transport model was reduced. This model was applied to thermal fission to investigate the influence of the memory effects on the fission dynamics. Some results of the calculations are presented. In addition, a reduction of the relativistic BLM to a two-fluid model was carried out, and transport coefficients associated with fluid dynamical variables were derived. Then this model was applied to investigate equilibration and fluctuation properties in a counter-streaming nuclear fluid. DOE

N93-30390# Lawrence Livermore National Lab., CA.
PULSE CONTROL IN AN ACCELERATOR FOR HEAVY-ION FUSION
W. M. Sharp, J. J. Barnard, and S. S. Yu 1 Oct. 1992 5 p Presented at the 16th International LINAC Conference, Ottawa, Canada, 23-28 Aug. 1992
(Contract W-7405-eng-48)
(DE93-009527; UCRL-JC-110221; CONF-9208109-78) Avail: CASI HC A01/MF A01

In induction accelerators proposed for heavy-ion fusion, the ion beam is usually confined longitudinally by an axial electric field tailored to balance the space-charge field. Since generating such electric field 'ears' is costly and imprecise, it is important to know how frequently the ears must be applied and what errors in the waveform are tolerable. For practical parameters, cell breakdown is found to impose the principal limit on the spacing of the acceleration modules applying the ear field. Also, it is demonstrated that ear fields may be approximated in several ways by discrete field steps with little impairment of the longitudinal confinement. DOE

N93-30488# Massachusetts Univ., Amherst.
HIGH-ENERGY ELECTRON-POSITRON INTERACTIONS
S. S. Hertzbach and R. R. Kofler Mar. 1993 33 p
(Contract DE-AC02-85ER-40194)
(DE93-011611; DOE/ER-40194/6) Avail: CASI HC A03/MF A01

The purpose of the research was the study of electron-positron interactions at high energies using the Time Projection Chamber (TPC) at the Positron Electron Project (PEP) at SLAC. The TPC detector had an initial data gathering from 1982 until 1986 and accumulated a data sample with an integrated luminosity of -150 pb(exp -1) at an electron-positron energy of 29 GeV. The data runs in the 1988-1990 time period (yielding approximately pb(exp -1)) were abbreviated, due to the need of the laboratory to give highest priority to the new Stanford Linear Collider (SLC). The TPC collaboration decided in 1991 to discontinue data taking, but has continued the collaboration for the purpose of completing the analysis of the data. When UMass joined the SLD project, it was being designed as a new state-of-the-art detector for studying electron-positron interactions at energies in the vicinity of 91 GeV, the Z(sup 0) mass. The detector was completed and installed at the interaction point of the SLC in 1991, at which time an initial, 'engineering run' allowed the debugging of detector components and provided a data sample of approximately 1,000 events with hadronic Z(sup 0) decays. In 1992 the SLC provided beams of polarized electrons and the SLD collected a data sample in excess of 11,000 hadronic Z(sup 0) events produced by polarized electrons, allowing unique measurements of some of the parameters of the standard model. This project is continuing to take data in 1993 with increased polarization and higher luminosity. This report reviews the research work performed under the contract, and survey's the physics results. DOE

N93-30527# Argonne National Lab., IL.
REQUIREMENTS FOR A SYSTEM TO ANALYZE HEP EVENTS USING DATABASE COMPUTING
E. May, D. Lifka, E. Lusk, L. E. Price, C. T. Day, S. Loken, J. F. MacFarlane, and A. Baden 1992 8 p Presented at the 12th IEEE Symposium on Mass Storage Systems, Monterey, CA, 25 Apr. 1993

(Contract W-31-109-eng-38)
(DE93-009960; ANL-HEP-CP-92-101; CONF-930461-3) Avail: CASI HC A02/MF A01

We describe the requirements for the design and prototyping of an object-oriented database designed to analyze data in high energy physics. Our goal is to satisfy the data processing and analysis needs of a generic high energy physics (HEP) experiment to be proposed for the Superconducting SuperCollider (SSC), and requires the collection and analysis of between 10 and 100 million sets of vectors (events), each approximately one megabyte in length. We sketch how this analysis would proceed using an object-oriented database which support the basic data types used in HEP. DOE

N93-30532# Oregon Univ., Eugene.
MULTIDIMENSIONAL INTERMITTENCY IN HADRONIC COLLISIONS
J. Pan and R. C. Hwa Jun. 1992 24 p
(Contracts DE-FG06-85ER-40224; DE-FG06-91ER-40637)
(DE93-010562; DOE/ER-40224/243; OITS-494) Avail: CASI HC A03/MF A01

The study of intermittency in high-energy hadronic collisions by the Monte Carlo code ECCO is extended to 3-dimensional phase space. Strong intermittency is found in agreement with the data. Fluctuation in the impact parameter is responsible for the intermittency in 1np(sub T), and the transverse-momentum conservation leads to negative intermittency slopes in the azimuthal angle (phi). The Ochs-Wosiek plots are linear in all dimensions having universal slopes. An exponent nu = 1.448 emerges to characterize multiparticle production in pp collisions. The properties of G moments are also examined, and the fractal dimensions determined. DOE

N93-30607 National Lab. for High Energy Physics, Tsukuba (Japan).
NON-PERTURBATIVE CALCULATION OF EQUILIBRIUM POLARIZATION OF STORED ELECTRON BEAMS
Kaoru Yokoya May 1992 22 p Limited Reproducibility: More than 20% of this document may be affected by microfiche quality
(DE93-764500; KEK-92-6) Avail: CASI HC A03

Stored electron/positron beams polarize spontaneously owing to the spin-flip synchrotron radiation. In the existing computer codes, the degree of the equilibrium polarization has been calculated using perturbation expansions in terms of the orbital oscillation amplitudes. In this paper a new numerical method is presented which does not employ the perturbation expansion. DOE

N93-30837# Nationaal Inst. voor Kernfysica en Hoge Energiefysica, Amsterdam (Netherlands).
CHARGE TO FREQUENCY CONVERTER FOR IONIZATION CHAMBERS BELONGING TO THE RADIATION PROTECTION SYSTEM OF AmPS/MEA [LADING NAAR FREQUENTIE CONVERTER VOOR DE IONISATIEKAMERS WELKE DEEL UITMAKEN VAN HET STRALING BEVEILIGINGS-SYSTEEM VAN AMPS/MEA]
J. T. vanEs and J. C. Boes 1991 12 p In DUTCH
(DIGEL-1991-6; ETN-93-93309) Avail: CASI HC A03/MF A01

A charge to frequency converter was developed to measure the radiation from the particle accelerator and AmPS (Amsterdam Pulse Stretcher) using an ionization chamber. The volume of the chamber is such that the electrons hitting the electrode of the ionization chamber produce a current of 1 pA at a radiation level of 20 mRem. This current is then converted in two frequencies which are a measure for the present radiation level. ESA

N93-30990# Institute of Nuclear Physics, Krakow (Poland).
FLUCTUATIONS AND INTERMITTENCY IN HIGH ENERGY NUCLEUS-NUCLEUS COLLISIONS
B. Wosiek Feb. 1991 96 p
(DE93-608481; INP-1533/PH) Avail: CASI HC A05/MF A01 (US Sales Only)

Fluctuations of the particle densities in semi-central collisions of O-16, Si-28, and S-32 nuclei with heavy components of nuclear emulsion at different primary energies are studied. Various methods of data analysis have been used ranging from the examination of the structure in individual events to the study of the average factorial moments and conventional correlation functions. Emphasis is put on the analysis of the average factorial moments which appear to be the most efficient tool in searching for dynamical fluctuations. Unquestionable evidence for non-statistical fluctuations is found in O-16 and S-32 interactions with Ag/Br targets at 200 GeV/nucleon. Specifically, I observed larger deviations of individual pseudo-rapidity distributions from a smooth spectrum and more frequent occurrence of narrow spikes than expected from Monte Carlo simulations based on independent emission of secondary particles. Clear intermittency signals are found in pseudo-rapidity and azimuthal angle distributions. The intermittency effect is also observed in two dimensions, where it has turned out to be stronger and cleaner than in one-dimensional distributions. Multiplicity distributions in the restricted phase space domains are well described by the negative binomial formula and consequently it was found that factorial moments can be equivalently obtained from the parameters of the negative binomial fits. On the other hand, investigation of the two-particle correlation functions in pseudorapidity provides no supporting evidence for pronounced non-statistical correlations. The occurrence of large particle-density fluctuations is expected in the presence of phase transition in ultrarelativistic nuclear collisions. Even though the obtained results can not be unambigously interpreted as an indication for quark-gluon plasma formation, they clearly show that some collective effects are present in high energy nucleus-nucleus collisions. DOE

N93-28733*# Army Strategic Defense Command, Huntsville, AL.
NPB CESIUM SPACE EXPERIMENT
George M. Parsons, III *In* NASA, Washington, NASA/DOD Flight Experiments Technical Interchange Meeting Proceedings 1992 11 p
(For primary document see N93-28699 11-12)
Avail: CASI HC A03/MF A10

74 OPTICS

Includes light phenomena; and optical devices.
For lasers see *36 Lasers and Masers.*

N93-28982# Central Research Inst. of Electric Power Industry, Tokyo (Japan). Energy and Environment Lab.
FUNDAMENTAL STUDY OF THE SIGNAL PROCESSING BY OPTICS
M. Kuribara and R. Ishino May 1992 22 p
(DE93-776265; CRIE-T-91044) Avail: CASI HC A03/MF A01

The result of discussing conversion of time sequential information (electric signals) into two-dimensional optical information, and optical computation using a Pockels readout optical modulator (PROM) is reported. The following is described: operation to polarize light beams by means of input electric signals using two ultrasonic beam polarizing elements and make two-dimensional patterns; operation to write information into the PROM using short wave length beams and read out the information using long wave length beams; and the principle of optical computation using a system with two PROM's and three polarizing elements arranged in front and rear of the system. An optical computation experimental equipment was used that comprises an optical system including the above elements, a writing light source, a reading out light source, and lenses, and a shutter and controls. The experiment verified that two-dimensional light patterns that correspond to time sequential information are written into the PROM, and the optical computation is executed with the readout beams that pass through the PROM. Additionally, the applicability of this optical computation to measuring and controlling systems is described. DOE

N93-29038# Department of the Navy, Washington, DC.
FIBER GRATING-BASED SENSING SYSTEM WITH INTERFEROMETRIC WAVELENGTH-SHIFT DETECTION Patent Application
Alan D. Kersey, inventor (to Navy) and T. A. Berkoff, inventor (to Navy) 4 Nov. 1992 32 p
(AD-D015697; US-Patent-Appl-SN-971117; Navy-Case-74106) Avail: CASI HC A03/MF A01

A typical fiber grating-based strain sensing system for sensing a measurand field according to the prior art comprises an optical source for providing broadband light to an array of serially coupled sensor elements. Each sensor element returns an optical signal having a narrow-band wavelength component, the wavelength depending by a known functional relation on the measurand field being sensed. The measurand field is a particular environmental condition or physical phenomenon under consideration. In other words, perturbation of that condition or phenomenon at element results in a change of the wavelength of optical signal. The array combines the individual signals, such as by wavelength-division or time-division multiplexing, to produce a composite return signal having a plurality of components, each uniquely corresponding to a signal from an individual sensor element. DTIC

N93-29086* National Aeronautics and Space Administration. Pasadena Office, CA.
IMPROVED REAL-TIME IMAGING SPECTROMETER Patent
James L. Lambert, inventor (to NASA) (Jet Propulsion Lab., California Inst. of Tech., Pasadena.), Tien-Hsin Chao, inventor (to NASA) (Jet Propulsion Lab., California Inst. of Tech., Pasadena.), Jeffrey W. Yu, inventor (to NASA) (Jet Propulsion Lab., California Inst. of Tech., Pasadena.), and Li-Jen Cheng, inventor (to NASA) (Jet Propulsion Lab., California Inst. of Tech., Pasadena.) 1 Jun. 1993 14 p Filed 9 Dec. 1991 Supersedes N92-29832 (30 - 20, p 3552)
(Contract NAS7-918)
(NASA-Case-NPO-18410-1-CU; US-Patent-5,216,484;
US-Patent-Appl-SN-805341; US-Patent-Class-356-326;
US-Patent-Class-356-51; US-Patent-Class-250-339;
US-Patent-Class-359-308; Int-Patent-Class-G01J-3/12) Avail: US Patent and Trademark Office

An improved AOTF-based imaging spectrometer that offers several advantages over prior art AOTF imaging spectrometers is presented. The ability to electronically set the bandpass wavelength provides observational flexibility. Various improvements in optical architecture provide simplified magnification variability, improved image resolution and light throughput efficiency and reduced sensitivity to ambient light. Two embodiments of the invention are: (1) operation in the visible/near-infrared domain of wavelength range 0.48 to 0.76 microns; and (2) infrared configuration which operates in the wavelength range of 1.2 to 2.5 microns.
Official Gazette of the U.S. Patent and Trademark Office

N93-29128*# Alabama Univ., Birmingham. Dept. of Physics.
ULTRA-HIGH RESOLUTION WATER WINDOW X RAY MICROSCOPE OPTICS DESIGN AND ANALYSIS Final Report, 18 Mar. 1992 - 17 Jun. 1993
David L. Shealy and C. Wang 25 Jun. 1993 36 p
(NASA Order H-13006-D)
(NASA-CR-193225; NAS 1.26:193225) Avail: CASI HC A03/MF A01

This project has been focused on the design and analysis of an ultra-high resolution water window soft-x-ray microscope. These activities have been accomplished by completing two tasks contained in the statement of work of this contract. The new results from this work confirm: (1) that in order to achieve resolutions greater than three times the wavelength of the incident radiation, it will be necessary to use spherical mirror surfaces and to use graded multilayer coatings on the secondary in order to accommodate the large variations of the angle of incidence over the secondary when operating the microscope at numerical apertures of 0.35 or greater; (2) that surface contour errors will have a significant effect on the optical performance of the microscope and must be controlled to a peak-to-valley variation of 50-100 A and a frequency of 8 periods over the surface of a mirror; and (3) that tolerance analysis of the spherical Schwarzschild microscope has been shown that the water window operations will require 2-3 times tighter tolerances to achieve a similar performance of operations with 130 A radiation. These results have been included in a manuscript included in the appendix. Author (revised)

N93-29139# Massachusetts Inst. of Tech., Lexington. Lincoln Lab.
SWAT 2 OVERVIEW Project Report
Ronald R. Parenti, Patrick N. Everett, Robert Kramer, and Daniel A. Page 10 Mar. 1993 102 p Revised
(Contract F19628-90-C-0002)
(AD-A262905; PR-SWP-3-Rev-1; ESC-TR-92-145-Rev-1) Avail: CASI HC A06/MF A02

All adaptive optics systems incorporate devices designed to measure and compensate phase distortions that accumulate over the propagation path of an optical beam. Measurement of the wavefront is accomplished with the aid of a bright source, or beacon, which must be accurately positioned along the beampath. In some scenarios of interest no physical beacon exists; for instance, the propagation of a laser beam to an exoatmospheric object moving at velocity upsilon requires that the beacon lead the target by an angle 2 v/c. In the early 1980's it was proposed that laser backscatter in the atmosphere might provide a suitable alternative source in such cases. Although a synthetic beacon generated in this manner can be placed arbitrarily in angle, any range discrepancy between the target and the beacon can lead to a form of measurement error known as focal anisoplanatism. Lincoln Laboratory's SWAT (Short-Wavelength Adaptive Techniques) program was initiated in 1983 to provide experimental verification of the most promising synthetic beacon concepts and to quantify the magnitude of the associated focal anisoplanatic errors. The test plan for this program includes passive imaging experiments using single and binary stars, as well as active experiments in which a scoring beam will be projected to rocket and satellite targets. DTIC

N93-29140# Massachusetts Inst. of Tech., Lexington. Lincoln Lab.
SWAT LABORATORY TEST RESULTS Project Report
Ronald R. Parenti and Daniel V. Murphy 10 Mar. 1993 46 p Revised
(Contract F19628-90-C-0002)
(AD-A262906; PR-SWP-6-Rev-1; ESC-TR-92-143-Rev-1) Avail: CASI HC A03/MF A01

The non-cooperative-target beam-control problem has been the subject of intense investigation since the synthetic-beacon concept was first introduced to the high-energy-laser community in 1982. While numerous analytical studies and computer simulations have been performed to evaluate the practical utility of this phase-measurement technique, prior to Lincoln Laboratory's SWAT (Short-Wavelength Adaptive Techniques) program, no experimental verification had been obtained. In the first phase of the SWAT investigation, completed in 1985, a high degree of correlation between differential-phase measurements from natural and artificial sources was demonstrated. The next phase of the SWAT program will be performed at the AMOS (Air Force Maui Optical Station) facility in Maui, where a 241-actuator adaptive-optics system and an array of six dye lasers will be integrated with the site's 60-cm beam director. Prior to shipment, the adaptive-optics subsystem was subjected to a thorough laboratory evaluation, which culminated in a series of compensation tests involving simulated beacon sources. The results of these measurements are in good agreement with theoretical predictions and provide strong evidence of the efficacy of the synthetic-beacon approach. DTIC

N93-29178 Notre Dame Univ., IN.
VISION-BASED CONTROL OF HOLONOMIC ROBOTS FOR 3-DIMENSIONAL RIGID-BODY POSITIONING USING CAMERA-SPACE MANIPULATION Ph.D. Thesis
Wenzong Chen 1993 164 p
Avail: Univ. Microfilms Order No. DA9308222

Camera-space manipulation was developed in this work for 3-dimensional 6-degree-of-freedom rigid-body positioning tasks with unknown work piece position and orientation. Using standard imaging devices and the very large GMF S-400 manipulator, highly precise manuever precision was achieved with negligible passive compliance. The maneuver succeeded consistently within a large range of work piece position and orientation provided the piece remained in the cameras' fields of view. The maneuver precision was further improved by accounting for the perspective effect in the camera-space locations of visually-detected cues painted on the objects to be positioned, using an iterative procedure that we devised in this work. The application of this procedure also increased the range of the work piece position and orientation within which the maneuver succeeded consistently. Also developed in this work was an iterative method for the estimation for grasp uncertainty in rigid-body positioning with camera-space manipulation. This added capability of camera-space manipulation allowed rigid-body positioning tasks to be accomplished with both unknown work piece position and orientation and unknown grasp. Dissert. Abstr.

N93-29270# Technische Univ., Eindhoven (Netherlands).
OPTICAL COHERENT PHASE DIVERSITY SYSTEMS Ph.D. Thesis
Willibrordus Hubertu deKrom 1992 191 p
(ISBN-90-9004897-9; ETN-93-93580) Copyright Avail: CASI HC A09/MF A02

The calculation and specification of necessary system parameters and component tolerances for an optical coherent phase diversity receiver was studied with respect to the development of receivers for broadband communications. By means of mathematical models, phase diversity receivers of interest were analyzed in terms of the bit error rate as a function of the signal to noise ratio. The application of phase diversity techniques has several advantages which are explained. Special attention was paid to the influence and reduction of different system imperfections. Restriction to the following most promising digital modulation formats was made: Amplitude Shift Keying (ASK); Differential Phase Shift Keying (DPSK); Frequency Shift Keying (FSK); and Continuous Phase Frequency Shift Keying (CPFSK). ESA

N93-29350# Los Alamos National Lab., NM.
FIBER-OPTIC CURRENTS MEASUREMENTS
P. R. Forman, L. D. Looney, and L. J. Tabaka 1993 13 p Presented at the OPTO 1993, Paris, France, 11-13 May 1993
(Contract W-7405-eng-36)
(DE93-007970; LA-UR-93-418; CONF-9305133-1) Avail: CASI HC A03/MF A01

Polarization maintaining pigtailed laser diodes have greatly increased the ease with which fiber-optic sensors for Faraday current measurements on large pulsed experiments can be deployed. 670, 830, and 1300 nm units are readily available. Such diode lasers can easily be mounted in an RF shielded box along with the simple electronics and batteries to power them. Our units measure 16.5 x 8 x 6 cm. and have a single external control; an on off switch. They use two 1.5 volt C cell batteries. By using an LT1073 chip in the electronics, the batteries are an energy source rather than a voltage source. These units can provide 100 mA drive to a LT015MD laser diode so that 1 mW of 830 nm light exits the fiber pigtail for up to 23 hours with no detectable droop in power. For the sensor element, twisted single mode low birefringence fibers are wrapped around the region of interest. The fiber pigtail is fused to the sensor section so changes in alignment are avoided. The light exiting the fiber sensor section is immediately analyzed by a compact, 3 x 3.5 x 5 cm, bulk optical unit which outputs quadrature optical signals into two multimode fibers leading to detectors in a screen room. The system is thus completely free of ground loops and is as immune to noise as the screen room. These sensors have the usual advantages claimed for them and the all dielectric feature was the original reason for their use on our experiments. The ease of deployment however is not usually cited. On our Pegasus 2 experiment, the need arose for a total current measurement at the main header of the capacitor banks. A single turn of optical fiber was easily strung in a 6.4 m diameter circle and attached to laser and analyzer in a few hours. DOE

N93-29470# Massachusetts Inst. of Tech., Lexington. Lincoln Lab.
SWAT SYSTEM PERFORMANCE PREDICTIONS Project Report
Ronald R. Parenti and Richard J. Sasiela 10 Mar. 1993 103 p Revised
(Contract F19628-90-C-0002)
(AD-A262857; PR-SWP-8-Rev-1; ESC-TR-92-144-Rev-1) Avail: CASI HC A06/MF A02

In the next phase of Lincoln Laboratory's SWAT (Short-Wavelength Adaptive Techniques) program, the performance of a 241-actuator adaptive-optics system will be measured using a variety of synthetic-beacon geometries. As an aid in this experimental investigation, a detailed set of theoretical predictions has also been assembled. The computational tools that have been applied in this study include a numerical approach in which Monte-Carlo ray-trace simulations of accumulated phase error are developed, and an analytical analysis of the expected system behavior. This report describes the basis of these two computational techniques and compares their estimates of overall system performance. Although their regions of applicability tend to be complementary rather than redundant, good agreement is usually obtained when both sets of results can be derived for the same engagement scenario. DTIC

N93-29656# Army Missile Command, Redstone Arsenal, AL. Weapons Science Directorate.
SPATIAL LIGHT MODULATORS (SLMs) SURFACE QUALITY Final Technical Report, 1 Jun. - 1 Sep. 1992
Tracy D. Hudson Mar. 1993 17 p
(AD-A263249; AD-E952004; AMSMI/TR-RD-WS-93-3) Avail: CASI HC A03/MF A01

The phase modulating properties of spatial light modulators (SLM's) were investigated for optical pattern recognition purposes for many years. An interferometric microscope was recently utilized to investigate the surface uniformity, and thus phase distortion, of several SLM's that are commercially available. These interferometric results are presented and verify that the optical uniformity of SLM's should be considered when phase modulating properties of the devices are to be applied in optical systems. DTIC

N93-29667# National Inst. of Standards and Technology, Gaithersburg, MD. Robot Systems Div.
BINOCULAR SPHERICAL DISPARITY: A STUDY IN REPRESENTATION FOR A FORWARD TRANSLATING CAMERA
D. J. Orser Jun. 1992 136 p
(PB93-184422; NISTIR-4865) Avail: CASI HC A07/MF A02

The problem of interpreting optical flow and binocular disparities for a forward translating camera is addressed. A solution is offered in the form of image remappings which convert the images to the analogous well understood case for a laterally translating camera. After reviewing this latter case, a binocular camera-retina imaging model utilizing spherical projection and foveal peripheral resolution is described for analyzing both binocular disparity and optical flow. The result provides the basis for analyzing both types of disparities within a single framework for the purpose of understanding how these 'orthogonal' sources of information can be exploited in a computational model. The process of image remapping, called 'normalization,' is then defined for four 1-D parameterizations of 3-D space: range, depth, looming and clearance. It is shown that normalization transforms optical flow into a form analogous to that for the laterally translating camera. In addition, it is shown how to obtain these same normalizations from standard planar projection images. A binocular wire frame scene simulator is used to experimentally verify the ideas. In addition a program for normalizing real iconic planar projection imagery is applied to several example images and the results demonstrated. NTIS

N93-29824# Carnegie-Mellon Univ., Pittsburgh, PA. School of Computer Science.
WHAT IS THE CENTER OF THE IMAGE?
Reg G. Willson and Steven A. Shafer Apr. 1993 27 p
(Contract F33615-90-C-1465; ARPA Order 7597)
(AD-A263550; CMU-CS-93-122) Avail: CASI HC A03/MF A01

People need to calibrate camera systems in order to determine the relationship between the positions of features in object space and their corresponding positions in the image. Part of camera calibration is the determination of image center. But, what is the image center? Ideally, the image center is considered to be the point of intersection of the camera's optical axis with the camera's sensing plane. In fact there are many possible definitions of image center, and in real lenses most do not have the same coordinates. In addition, the image centers move as lens parameters are changed. In this paper, we examine why image centers are not necessarily the same for different image properties and why they vary with lens parameter's. We then provide a taxonomy of 16 different image centers and describe procedures for measuring them. Finally, we examine the calibration of image center for a variable parameter lens. Several techniques are applied to a precision automated zoom lens and experimental results are shown. We conclude that the accuracy of the image center can be an important factor in the accuracy of the overall camera calibration, and that the large variation in the position of the image center across different definitions and different lens settings makes the calibration problem much more complex than is conventionally believed. With proper modeling, by using correct definitions for all image centers in a system, we can improve the accuracy of our camera calibration. DTIC

N93-29848*# National Aeronautics and Space Administration. Pasadena Office, CA.
WAVELENGTH-DIVISION MULTIPLEXED OPTICAL INTEGRATED CIRCUIT WITH VERTICAL DIFFRACTION GRATING Patent Application
Robert J. Lang, inventor (NASA) (Jet Propulsion Lab., California Inst. of Tech., Pasadena.) and Siamak Forouhar, inventor (to NASA) (Jet Propulsion Lab., California Inst. of Tech., Pasadena.) 17 Mar. 1993 35 p
(Contract NAS7-918)
(NASA-Case-NPO-18357-1-CU; NAS 1.71:NPO-18357-1-CU; US-Patent-Appl-SN-033512) Avail: CASI HC A03/MF A01

A semiconductor optical integrated circuit for wave division multiplexing has a semiconductor waveguide layer, a succession of diffraction grating points in the waveguide layer along a predetermined diffraction grating contour, a semiconductor diode array in the waveguide layer having plural optical ports facing the succession of diffraction grating points along a first direction, respective semiconductor diodes in the array corresponding to respective ones of a predetermined succession of wavelengths, an optical fiber having one end thereof terminated at the waveguide layer, the one end of the optical fiber facing the succession of diffraction grating points along a second direction, wherein the diffraction grating points are spatially distributed along the predetermined contour in such a manner that the succession of diffraction grating points diffracts light of respective ones of the succession of wavelengths between the one end of the optical fiber and corresponding ones of the optical ports. NASA

N93-29880# Wisconsin Univ., Madison. Engine Research Center.
APPLICATION OF SCHLIEREN OPTICAL TECHNIQUES FOR THE MEASUREMENT OF GAS TEMPERATURE AND TURBULENT DIFFUSIVITY IN A DIESEL ENGINE
Roberto P. Giangregorio, Yuanxian Zhu, and Rolf D. Reitz 5 Mar. 1993 17 p
(Contract DAAL03-86-K-0174)
(AD-A263810; ARO-24623.125-EG-UIR) Avail: CASI HC A03/MF A01

A new technique which is based on optoacoustic phenomena has been developed for measuring in-cylinder gas temperature and turbulent diffusivity. In the experiments, a high energy Nd:YAG pulsed laser beam was focused to cause local ionization of air at a point in the combustion chamber. This initiates a shock wave and creates a hot spot. The local temperature and turbulent diffusivity are determined by monitoring the shock propagation and the hot spot growth, respectively, with a Schlieren photography system. In order to assess the validity and accuracy of the measurements, the technique was also applied to a turbulent jet. The temperature measurements were found to be accurate to within 3 percent. Results from the turbulent jet measurements also showed that the growth rate of the hot spot diameter can be used to estimate the turbulent diffusivity. DTIC

N93-29887# Texas A&M Univ., College Station. Dept. of Physics.
MEASUREMENTS OF LIGHT SCATTERING BY SMALL PARTICLES AT AN ANGLE OF ZERO DEGREES Final Report, 1 Jul. - 30 Nov. 1992
Edward S. Fry 28 Jan. 1993 5 p
(Contract DAAL03-92-G-0296)
(AD-A263856; ARO-30495.3-GS) Avail: CASI HC A01/MF A01

We recently demonstrated an innovative new idea that permits light scattering measurements at an angle of 0 deg for the first time. The idea is based on the use of coherent beam coupling in a nonlinear, photorefractive crystal of BaTiO3 to separate the scattered light from the unscattered direct beam. The present problem is to extend these ideas to the following: (1) angular distribution measurements; (2) measurements of the phase as well as the amplitude (i.e. both real and imaginary parts) of the 0 deg scattering; and (3) determination of the effects of coherent scattering at 0 deg. We have successfully measured the angular distribution of forward light scattering from quartz fibers of radii from 15 mm to 30 mm. Data have been obtained in the angular range of 0 deg to 0.3 deg with an angular resolution of better than 0.01 deg. The results are in good agreement with theory. Finally, the existence of coherent scattering effects at zero degrees have been considered and analyzed theoretically. Experimental data were obtained that confirm these coherent scattering affects in suspensions of polystyrene spheres. DTIC

N93-29973# Honeywell, Inc., Minneapolis, MN. Systems and Research Center.
OPTOELECTRONIC TECHNOLOGY CONSORTIUM Quarterly Technical Report No. 2
Mary Hibbs-Brenner 31 Dec. 1992 9 p
(Contract MDA972-92-C-0071; ARPA Order 8351)
(AD-A263580) Avail: CASI HC A02/MF A01

The Optoelectronics Technology Consortium has been established to position U.S. industry as the world leader in optical interconnect technology by developing, fabricating, intergrating and demonstrating the producibility of optoelectronic components for high-density/high-data-rate processors and accelerating the insertion of this technology into military and commercial applications. This objective will be accomplished by a program focused in three areas. (1) Demonstrated performance: OETC will demonstrate an aggregate data transfer rate of 16 Gbit/s between single transmitter and receiver packages, as well as the expandability of this technology by combing four links in parallel to achieve a 64 Gbit/s link. (2) Accelerated development: By collaborating during precompetitive technology development stage, OTEC will advance the development of optical components and produce links for a multiboard processor testbed demonstration; and (3) Producibility: OETC's technology will achieve this performance by using components that are affordable, and reliable, with a line BER less than 10(exp -15) and MTTF greater than 10(exp 6) hours. DTIC

N93-30205# Colorado Univ., Boulder. Dept. of Physics and Astrophysics.
APPLICATIONS OF THE PHOTOREFRACTIVE EFFECT AND DAMAGE INDUCED EFFECTS IN FIBERS Final Report, 1 Mar. 1990 - 31 Oct. 1992
Dana Z. Anderson 31 Oct. 1992 34 p
(Grant AF-AFOSR-0198-90)
(AD-A264339; AFOSR-93-0247TR) Avail: CASI HC A03/MF A01

The focus of this report is two-fold. One aspect concerns photoinduced effects in fibers, especially the processes of self-organized second-harmonic generation in fibers. For the most part we have developed the microscopic theory of defect formation in glass. The basic physics involved in second-harmonic generation in fibers has to led to a number of other possible experiments and applications. For example it is known that a photogenerated current cannot be produced by a single optical beam illuminating a centrosymmetric medium but it is now recognized that a current can be generated in a centrosymmetric medium by illumination with two harmonically related optical fields. However, we have concluded that as an application, self-organized second-harmonic generation in fibers does not appear to be a practical means of frequency doubling conventional lasers. Thus until a conceptual or practical breakthrough occurs, we have brought to a close the experimental and theoretical work on this subject. DTIC

N93-30368# Arizona State Univ., Tempe. Dept. of Industrial and Management Systems Engineering.
STUDIES OF THE EFFECT OF IMAGE DEGRADATION AND RECOMBINATION ON VISUAL PERCEPTION Annual Report, 1 Mar. 1992 - 1 Mar. 1993
William R. Uttal 1 Apr. 1993 6 p
(Contract F49620-92-J-0176)
(AD-A264332; PERLAB-1; AFOSR-93-0263TR) Avail: CASI HC A02/MF A01

In the first year of this grant, progress was made on two major series of experiments. In the first, the effect of noise, brightness, contrast, and geometrical artifacts on a detection task simulating enhanced night vision devices in a series of 10 experiments were examined. An article was submitted based on this study. In the second, the effects of noise, Fourier filtering, reduced acuity (by means of blocking), and combinations thereof in a discrimination task were explored. Ten experiments also were carried out in this series and were analyzed and a publication is being prepared. DTIC

N93-30372*# Rensselaer Polytechnic Inst., Troy, NY. Dept. of Mechanical Engineering, Aeronautical Engineering and Mechanics.
POLARIZATION MODULATED ELLIPSOMETRY Final Report
James L. Lauer and Norbert Marxer Washington Sep. 1986 113 p
(Grant NAG3-222; RTOP 505-63-01)
(NASA-CR-4012; E-3173; NAS 1.26:4012) Avail: CASI HC A06/MF A02

For the investigation of the composition and thickness of thin nonuniform films on bearing and other tribological surfaces an automated ellipsometer was built, which is extremely sensitive to relative changes in thickness and composition of surface films. These changes can be seen by scanning across the surface with 20 micron lateral resolution. By measuring at different angles of incidence, one can determine the film thickness and identify the material of the film by its complex index of refraction. For the analysis of organic layers on top of several metallic layers, it was necessary to develop mathematical procedures to increase the absolute precision of the instrument. The ellipsometer is described in detail, and the precision is discussed. The actual performance of the ellipsometer was tested on three experiments. In the first one, the composition and thickness of patches of an oxide film inside a wear track were determined. In the third, the thickness of silicon oxide on top of a silicon substrate was found. Important features of this apparatus are (1) accurate settings of the polarization stages and the angle of incidence (both animated), (2) high precision in the determination of the ellipsometric parameters without calibration prior to an experiment, and (3) very accurate scanning modes with high spatial resolution. The instrumentation and the mathematical procedures were developed here for the first time. Author (revised)

N93-30410# Department of the Navy, Washington, DC.
METHOD AND APPARATUS FOR IMAGING AN OBJECT IN OR THROUGH A SCATTERING MEDIUM BY USING MULTIPLE-WAVE MIXING Patent Application
Mark Bashkansky, inventor (to Navy) and John F. Reintjes, inventor (to Navy) 30 Nov. 1992 24 p
(AD-D015707; US-Patent-Appl-SN-983334; Navy-Case-74287) Avail: CASI HC A03/MF A01

This patent application discloses a method and apparatus for imaging an object that is part of, embedded in, or view through a scattering medium. A broadband stochastic beam generator, such as a broadband laser, generates a broadband stochastic beam and a narrowband beam generator generates a narrowband beam. A non-linear mixing crystal receives the broadband stochastic beam and the narrowband beam and provides a signal light beam conjugate correlated with the broadband stochastic beam to scattering medium. A multiple-wave mixing call is disposed to receive the signal light beam from scattering medium. An adjustable delay path also illuminates the multiple-wave mixing cell with the broadband stochastic beam. A supplemental beam generator is also provided for also additionally illuminating the multiple-wave mixing cell with a supplemental beam having characteristics sufficient to satisfy phase matching with the material of the multiple-wave mixing cell. The multiple-wave mixing cell produces an image-bearing beam which contains an image of an object extracted from signal light beam emitted from the scattering medium. The apparatus can further include a detector to record the image of the object in the object in the image-bearing beam. DTIC

N93-30500# Georgia Inst. of Tech., Atlanta. School of Electrical Engineering.
INFRARED IMAGING ARRAY INTEGRATED IN THREE DIMENSIONS DIRECTLY ON TOP OF SILICON CIRCUITS
M. Brooke, N. Jokerst, M. Allen, and S. DeWeerth May 1993 24 p
(AD-A264707) Avail: CASI HC A03/MF A01

We have demonstrated the first three dimensional integration of a high quality compound semiconductor infrared imaging detector array directly on top of a foundry-produced silicon neuromorphic image processing circuit. There is great potential for this new technology in neuromorphic image processing applications. This new ability to construct complex locally connected neuromorphic focal-plane processors with direct massively parallel connections to high quality compound semiconductor imaging arrays will lead to new levels of sophistication in focal-plane processing. During this research, thin film p-i-n and metal-semiconductor-metal (MSM) detectors were fabricated and tested. A four-by-four array of detectors was integrated onto a metallized silicon substrate and directly on top of an array of silicon circuits. The yield of each of these arrays was 100%, i.e., every detector was functional, and, in the integration onto silicon circuitry, every circuit underneath the detectors was also functional. DTIC

N93-30520# Stanford Univ., CA. Edward L. Ginzton Lab. of Physics.
SUBPICOSECOND ELECTROOPTIC SAMPLING Interim Report, 1 Feb. 1992 - 31 Jan. 1993
David M. Bloom Jan. 1993 131 p
(Contract F49620-92-J-0099)
(AD-A264635; AFOSR-93-0258TR) Avail: CASI HC A07/MF A02

The electro-optic sampling system developed under AFOSR contract no. F49620-85-0016 has been the workhorse for high speed measurements made in this lab. This report documents the continuing effort to improve this tool and highlights its most recent uses. In addition, we report the development of a time-lens, a new tool that gives us electronic control of the shape of optical pulses. The development of a time-lens has opened up a new field of research. It is a tool to electronically control the temporal characteristics of optical pulses just like glass lenses control the spatial characteristics. Our results to date include the creation of 7 ps pulses from a CW laser, active focusing (compression) of 55 ps pulses down to 2 ps, and demonstration of the time-reversal properties of time-lenses. A Ph.D. thesis detailing the Stanford time-lens and pulse compression experiments is included as an appendix. DTIC

N93-30522# Institute of Electrical and Electronics Engineers, Piscataway, NJ.
TOPICAL MEETING OF BROADBAND ANALOG AND DIGITAL OPTOELECTRONICS Final Report, 1 May - 31 Dec. 1992
Robert Wangemann 1992 326 p
(Contract F49620-92-J-0199)
(AD-A264643; AFOSR-93-0318TR) Avail: CASI HC A15/MF A03

Partial Contents: Analog Systems; Multichannel Video Distribution; Digital Video and Compression Techniques; Digital Transmission Technology; Linearization and Harmonic Distortion. DTIC

N93-30609# Princeton Univ., NJ.
OPTICALLY POWERED, OPTOELECTRONIC SPATIAL LIGHT MODULATORS Annual Technical Report, 1 Aug. 1992 - 31 Jan. 1993
Stephen R. Forrest 26 Apr. 1993 110 p
(Contract F49620-92-J-0432)
(AD-A264765; AFOSR-93-0351TR) Avail: CASI HC A06/MF A02

We describe a program which endeavors to make significant progress towards the realization of very high density, fast, InP-based optoelectronic spatial light modulators (SLM's). The central concept of the devices is to eliminate as many contacts to the SLM as possible by supplying integral, local circuit power, and control via the connection of the active circuit to integrated photovoltaic (PV) cells. Power to the circuits is thereby supplied by a bright light source operating at a different wavelength than the optical data channel. The SLM will be fabricated in InP-based materials due to the ease of integration of photovoltaic cells (used in providing circuit power and control), with high bandwidth transceiver optoelectronic integrated circuits (OEIC's). Work includes materials and device fabrication, packaging and systems demonstrations. In addition to applications in optical interconnection and optical computing, such contactless circuit concepts can also be applied to many diverse systems such as for providing highly synchronous optical clock signals on VLSI chips, and for powering OEIC's placed at the end of remote probes where size, power, and environmental restrictions prohibit the placement of the power source adjacent to the active electronics. We are engaged in a broad program directed at investigating the fundamental limits confronting materials, devices, circuits, and systems which make use of the family of novel devices which are based on the optical powering concept. DTIC

N93-30666# Pennsylvania Univ., Philadelphia. Dept. of Physics.
NATO ADVANCED RESEARCH WORKSHOP ON FRONTIERS OF OPTICAL PHENOMENA IN SEMICONDUCTOR STRUCTURE OF REDUCED DIMENSION
Elias Burstein 31 Jul. 1992 9 p Workshop held in Yountville, CA, 27-31 Jul. 1992
(Contract N00014-92-J-1557)
(AD-A264813) Avail: CASI HC A02/MF A01

The NATO Advanced Research Workshop on Frontiers of Optical Phenomena in Semiconductor Structures of Reduced Dimensions provided a forum in which experimental and theoretical physicists discussed and evaluated recent developments in the optical research of the exciting new phenomena that occur in the electron systems of semiconductor nanostructures. The topics of principal interest to the participants included the integral and fractional quantum Hall effects, the nonlinear optics of low dimensional electron systems, the optical responses associated with electrons in quantum wires, and dots and the optical characterization of electron tunneling in ultra-small structures. We also had informative presentations on recent developments in the studies of optically active porous silicon and the optical properties of C60 molecules. DTIC

N93-30905# City Coll. of the City Univ. of New York, NY. Dept. of Electrical Engineering.
MASSIVELY PARALLEL SPATIAL LIGHT MODULATION-BASED OPTICAL SIGNAL PROCESSING Final Report, Jul. 1990 - Sep. 1992
Yao Li 21 Mar. 1993 5 p
(Grant AF-AFOSR-0260-88)
(AD-A264846; AFOSR-93-0350TR) Avail: CASI HC A01/MF A01

A new optical parallel arithmetic processing scheme using a nonholographic optoelectronic content-addressable memory (CAM) was proposed. The design of a four-bit CAM-based optical carry look-ahead adder was studied. Compared with existing optoelectronic binary addition approaches, this nonholographic CAM Scheme offers a number of practical advantages, such as faster processing speed and ease of optical implementation and alignment. For an addition of numbers longer than four bits, by incorporating the previous stage's carry, a number of four-bit CLA's can be cascaded. Experimental results were also demonstrated. One paper to the Optics Letters was published. DTIC

N93-31035*# Alabama Univ., Huntsville. Dept. of Physics.
OPTICAL SYSTEM ANALYSIS FOR THE GROUND BASED EXVM Final Report
L. W. Hillman, R. A. Chipman, and M. H. Smith 30 Jun. 1993 88 p
(Contract NAS8-38609)
(NASA-CR-192588; NAS 1.26:192588) Avail: CASI HC A05/MF A01

The MSFC's Experimental Vector Magnetograph (EXVM) is an instrument that observes a 4.4 x 8.8 arcmin field of the sun. The transverse and longitudinal components of the surface magnetic field and the line-of-sight velocities of the photospheric gases can be determined from polarimetric and spectral analysis of the 525.02 nm absorption line of Fe 1. The EXVM has been breadboarded and tested in the laboratory. The optics of the EXVM were tested with a point-diffraction (Smartt) interferometer. The 12 inch Cassegrain telescope was found to have 0.20 waves RMS (at 525.02 nm) of aberration. The post-telescope relay optics were nearly diffraction limited on-axis and had about one wave of primary coma as the predominant aberration at full-field. From theoretical modulation transfer function (MTF) curves of known aberrations, it was concluded that the EXVM should attain a maximum spatial resolution of about 0.5 arcseconds. A resolution test target indicated maximum angular resolutions better than 0.6 arcsec on-axis and 0.7 arcsec at full-field-of-view. A 20 inch heliostat (sun-tracking mirror) was used to direct sunlight into the lab and into the EXVM. Solar images obtained were limited by atmospheric seeing effects. During brief moments of good seeing, angular resolutions of about 1 arcsecond were realized with the EXVM. Author (revised)

N93-28786*# Wisconsin Univ., Madison. Space Astronomy Lab.
NEW TECHNOLOGIES FOR UV DETECTORS Abstract Only
C. L. Joseph *In* Lunar and Planetary Inst., Workshop on Advanced Technologies for Planetary Instruments, Part 1 1993 p 11 (For primary document see N93-28764 11-91)
Avail: CASI HC A01/MF A01

N93-28788*# National Aeronautics and Space Administration. Goddard Space Flight Center, Greenbelt, MD.
OPTICAL TECHNOLOGIES FOR UV REMOTE SENSING INSTRUMENTS Abstract Only
R. A. M. Keski-Kuha, J. F. Osantowski, D. B. Leviton, T. T. Saha, D. A. Content, R. A. Boucarut, J. S. Gum, G. A. Wright, C. M. Fleetwood, and T. J. Madison *In* Lunar and Planetary Inst., Workshop on Advanced Technologies for Planetary Instruments, Part 1 1993 p 12 (For primary document see N93-28764 11-91)
Avail: CASI HC A01/MF A01

N93-28789*# Texas Technological Univ., Lubbock. Computer Vision and Image Analysis Lab.
MULTISCALE MORPHOLOGICAL FILTERING FOR ANALYSIS OF NOISY AND COMPLEX IMAGES Abstract Only
A. Kher and S. Mitra *In* Lunar and Planetary Inst., Workshop on Advanced Technologies for Planetary Instruments, Part 1 1993 p 12-13 (For primary document see N93-28764 11-91)
Avail: CASI HC A01/MF A01

N93-28806*# Honeywell Corporate Research Center, Bloomington, MN.
HONEYWELL'S COMPACT, WIDE-ANGLE UV-VISIBLE IMAGING SENSOR Abstract Only
D. Pledger and J. Billing-Ross (Honeywell, Inc., Glendale, AZ.) *In* Lunar and Planetary Inst., Workshop on Advanced Technologies for Planetary Instruments, Part 1 1993 p 19 (For primary document see N93-28764 11-91)
Avail: CASI HC A01/MF A01

N93-28808*# Little (Arthur D.), Inc., Cambridge, MA.
INFRARED RUGATES BY MOLECULAR BEAM EPITAXY Abstract Only
M. Rona *In* Lunar and Planetary Inst., Workshop on Advanced Technologies for Planetary Instruments, Part 1 1993 p 20 (For primary document see N93-28764 11-91)
Avail: CASI HC A01/MF A01

N93-28810*# Johns Hopkins Univ., Laurel, MD. Applied Physics Lab.
A COMPACT IMAGING DETECTOR OF POLARIZATION AND SPECTRAL CONTENT Abstract Only
D. M. Rust, A. Kumar, and K. E. Thompson *In* Lunar and Planetary Inst., Workshop on Advanced Technologies for Planetary Instruments, Part 1 1993 p 20 (For primary document see N93-28764 11-91)
Avail: CASI HC A01/MF A01

N93-28827*# Alabama Univ., Birmingham. Dept. of Physics.
ULTRAVIOLET IMAGING SPECTROMETER Abstract Only
T. J. Wdowiak *In* Lunar and Planetary Inst., Workshop on Advanced Technologies for Planetary Instruments, Part 1 1993 p 27 (For primary document see N93-28764 11-91)
Avail: CASI HC A01/MF A01

N93-29689*# Georgia Tech Research Inst., Atlanta.
DEGRADATION OF ELECTRO-OPTIC COMPONENTS ABOARD LDEF
M. D. Blue *In* NASA. Langley Research Center, LDEF: 69 Months in Space. Part 4: Second Post-Retrieval Symposium Apr. 1993 p 1333-1342 (For primary document see N93-29682 11-99)
Avail: CASI HC A02/MF A03; 2 functional color pages

N93-29691*# Paris XI Univ., Orsay (France). Inst. d'Astrophysique Spatiale.
IN ORBIT DEGRADATION OF EUV OPTICAL COMPONENTS IN THE WAVELENGTH RANGE 10-40 nm AO 138-3
J. P. Delaboudiniere, C. Carabetian, and J. F. Hochedez *In* NASA. Langley Research Center, LDEF: 69 Months in Space. Part 4: Second Post-Retrieval Symposium Apr. 1993 p 1355-1360 Sponsored in part by CNES (For primary document see N93-29682 11-99)
Avail: CASI HC A02/MF A03; 2 functional color pages

N93-29692*# Phillips Lab., Kirtland AFB, NM.
DEGRADATION OF OPTICAL COMPONENTS IN A SPACE ENVIRONMENT
Linda L. DeHainaut, John R. Kenemuth, Cynthia E. Tidler, and David W. Seegmiller (Schafer, W. J. Associates, Inc., Albuquerque, NM.) *In* NASA. Langley Research Center, LDEF: 69 Months in Space. Part 4: Second Post-Retrieval Symposium Apr. 1993 p 1361-1373 (For primary document see N93-29682 11-99)
Avail: CASI HC A03/MF A03; 2 functional color pages

N93-29693*# National Aeronautics and Space Administration. Lewis Research Center, Cleveland, OH.
STUDIES OF EFFECTS ON OPTICAL COMPONENTS AND SENSORS: LDEF EXPERIMENTS AO-147 (ERB COMPONENTS) AND S-0014 (APEX)
John R. Hickey (Eppley Lab., Inc., Newport, RI.), David J. Brinker, and Philip Jenkins (Sverdrup Technology, Inc., Brook Park, OH.) *In* NASA. Langley Research Center, LDEF: 69 Months in Space. Part 4: Second Post-Retrieval Symposium Apr. 1993 p 1375-1388 (For primary document see N93-29682 11-99)
(Contracts NAS1-15350; NAS3-25958)
Avail: CASI HC A03/MF A03; 2 functional color pages

N93-29694*# Eastman Kodak Co., Rochester, NY.
EFFECTS OF LONG TERM SPACE ENVIRONMENT EXPOSURE ON OPTICAL SUBSTRATES AND COATINGS (S0050-2)
Keith Harvey, Arthur Mustico, and John Vallimont *In* NASA. Langley Research Center, LDEF: 69 Months in Space. Part 4: Second Post-Retrieval Symposium Apr. 1993 p 1389-1397 (For primary document see N93-29682 11-99)
Avail: CASI HC A02/MF A03; 2 functional color pages

N93-29695*# Science Applications International Corp., Santa Monica, CA.
LDEF SPACE OPTICS HANDBOOK Abstract Only
Robert J. Champetier, Dale R. Atkinson (POD Associates, Inc., Albuquerque,

NM.), and William T. Kemp (Phillips Lab., Kirtland AFB, NM.) *In* NASA. Langley Research Center, LDEF: 69 Months in Space. Part 4: Second Post-Retrieval Symposium Apr. 1993 p 1399 (For primary document see N93-29682 11-99)
Avail: CASI HC A01/MF A03; 2 functional color pages

N93-29698*# Phillips Lab., Kirtland AFB, NM. Directorate of Space and Missiles Technology.
CHARACTERIZATION OF A SPACE ORBITED INCOHERENT FIBER OPTIC BUNDLE
Stephen A. DeWalt and Edward W. Taylor *In* NASA. Langley Research Center, LDEF: 69 Months in Space. Part 4: Second Post-Retrieval Symposium Apr. 1993 p 1413-1423 (For primary document see N93-29682 11-99)
Avail: CASI HC A03/MF A03; 2 functional color pages

N93-29699*# Phillips Lab., Kirtland AFB, NM. Directorate of Space and Missiles Technology.
ANALYSES OF SPACE ENVIRONMENT EFFECTS ON ACTIVE FIBER OPTIC LINKS ORBITED ABOARD THE LDEF
Edward W. Taylor, T. W. Monarski, J. N. Berry, A. D. Sanchez, R. J. Padden, and S. P. Chapman *In* NASA. Langley Research Center, LDEF: 69 Months in Space. Part 4: Second Post-Retrieval Symposium Apr. 1993 p 1425-1437 (For primary document see N93-29682 11-99)
Avail: CASI HC A03/MF A03; 2 functional color pages

N93-29700*# Jet Propulsion Lab., California Inst. of Tech., Pasadena.
RADIATION AND TEMPERATURE EFFECTS ON LDEF FIBER OPTIC SAMPLES
A. R. Johnston, R. Hartmayer, and L. A. Bergman *In* NASA. Langley Research Center, LDEF: 69 Months in Space. Part 4: Second Post-Retrieval Symposium Apr. 1993 p 1439-1453 (For primary document see N93-29682 11-99)
Avail: CASI HC A03/MF A03; 2 functional color pages

N93-29706*# AZ Technology, Huntsville, AL.
NEXT GENERATION OPTICAL INSTRUMENTS AND SPACE EXPERIMENT BASED ON THE LDEF THERMAL CONTROL SURFACES EXPERIMENT (S0069)
Donald R. Wilkes *In* NASA. Langley Research Center, LDEF: 69 Months in Space. Part 4: Second Post-Retrieval Symposium Apr. 1993 p 1521-1533 (For primary document see N93-29682 11-99)
Avail: CASI HC A03/MF A03; 2 functional color pages

N93-30231 Carleton Univ., Ottawa (Ontario).
RIB ARROW INTEGRATED OPTIC POLARIZER
S. Yuen, B. Syrett, W. Jiang (Canadian Marconi Co. Ltd., Montreal, Quebec.), J. Chrostowski (National Research Council of Canada, Ottawa, Ontario.), and J. Wartak (National Research Council of Canada, Ottawa, Ontario.) *In* Engineering Inst. of Canada, Canadian Conference on Electrical and Computer Engineering, Volumes 1 and 2 1990 4 p (For primary document see N93-30215 11-31)
Avail: Engineering Inst. of Canada, 2050 rue Mansfield, Suite 700, Montreal, Quebec H3A 1Z2 Canada

N93-30253 Defence Research Establishment, Ottawa (Ontario).
ACOUSTO-OPTIC TIME-INTEGRATING CORRELATORS FOR PROCESSING WIDEBAND DIGITAL DATA
N. Brousseau and J. W. A. Salt *In* Engineering Inst. of Canada, Canadian Conference on Electrical and Computer Engineering, Volumes 1 and 2 1990 3 p (For primary document see N93-30215 11-31)
Avail: Engineering Inst. of Canada, 2050 rue Mansfield, Suite 700, Montreal, Quebec H3A 1Z2 Canada

N93-30271 Ecole Polytechnique, Montreal (Quebec).
RECURSIVE-BATCH ESTIMATION OF STRUCTURE AND MOTION FROM STEREO IMAGE SEQUENCES
Juyang Weng and Paul Cohen *In* Engineering Inst. of Canada, Canadian Conference on Electrical and Computer Engineering, Volumes 1 and 2 1990 4 p (For primary document see N93-30215 11-31)
Avail: Engineering Inst. of Canada, 2050 rue Mansfield, Suite 700, Montreal, Quebec H3A 1Z2 Canada

N93-30272 Laval Univ. (Quebec).
A SINGLE BAND PROCESSOR FOR THE COMPUTATION OF RANGE FROM OPTICAL ABSORBANCE
Paul Fortier, Denis Laurendeau, Stephane Morin, and Louis Begin *In* Engineering Inst. of Canada, Canadian Conference on Electrical and Computer Engineering, Volumes 1 and 2 1990 4 p (For primary document see N93-30215 11-31)
Avail: Engineering Inst. of Canada, 2050 rue Mansfield, Suite 700, Montreal, Quebec H3A 1Z2 Canada

N93-30286 National Research Council of Canada, Ottawa (Ontario). Inst. for Information Technology.
ON THE IMPLEMENTATION OF THE BIRIS RANGE SENSOR FOR APPLICATIONS IN ROBOTIC CONTROL AND AUTONOMOUS NAVIGATION
F. Blais, M. Rioux, J. Domey, and J. A. Beraldin *In* Engineering Inst. of Canada, Canadian Conference on Electrical and Computer Engineering, Volumes 1 and 2 1990 4 p (For primary document see N93-30215 11-31)
Avail: Engineering Inst. of Canada, 2050 rue Mansfield, Suite 700, Montreal, Quebec H3A 1Z2 Canada

75 PLASMA PHYSICS

Includes magnetohydrodynamics and plasma fusion.
For ionospheric plasmas see *46 Geophysics.* For space plasmas see *90 Astrophysics.*

N93-28530# Japan Atomic Energy Research Inst., Tokyo.
JT-60 UPGRADE VERTICAL STABILITY EXPERIMENTS AND ANALYSIS
D. A. Humphreys and Ryuji Yoshino May 1992 31 p
(DE93-753131; JAERI-M-92-069) Avail: CASI HC A03/MF A01

The JT-60 Upgrade tokamak (JT-60U), can produce plasmas with vertical elongation (kappa approximately = 1.6), and thus allows investigation of vertical instability phenomena. The present work describes investigation of the vertical stability characteristics of JT-60U plasmas through experimental results and simulation. Experiments described include feedback turnoff cases and high beta(sub p) unstable plasma cases. For purposes of simulation, the plasma is modeled as a rigid assembly of current-carrying axisymmetric loops. A nominal conductor model based on design geometry was modified to reproduce the results of a series of coil excitation experiments using a reduced order system identification approach. A two-coil model was used to fit the experimental coil excitation behavior, and the full order conductor model was modified to allow the dominant modes to reflect the low order dynamic response. The resulting plasma-conductor model is shown to reproduce the vertical stability behavior of JT-60U fairly well. Theoretical predictions of limits on the value of Shafranov (Lambda) achievable in JT-60U are made. DOE

N93-28532# Nagoya Univ. (Japan). Plasma Science Center.
EDGE PLASMA CONTROL BY RF ELECTRIC FIELD IN COMPACT HELICAL SYSTEM (CHS)
T. Shoji, A. Sagara, and N. Noda May 1992 19 p
(DE93-753242; PSC-18) Avail: CASI HC A03/MF A01

Reducing plasma heat flux on the material limiter and stabilizing fluctuations at the plasma boundary by the use of an RF ponderomotive potential barrier on the limiter (RF limiter) have been demonstrated in Compact Helical System (CHS) for ECH heated plasma. The RF current on a graphite limiter surface along magnetic field lines produces a ponderomotive potential barrier, which is large at the limiter edges. The high heat load on the limiter edges, which is measured using a infrared TV camera, has been shown to be reduced by an RF power of 1.4 kW at the frequency 10 MHz (omega(sub ci) less than omega much less than omega(sub ce)). Another remarkable effect of the ponderomotive potential barrier on the limiter that has been observed is the suppression of density fluctuations (less than 100 kHz) at the plasma boundary. DOE

N93-28533# Nagoya Univ. (Japan). Plasma Science Center.
OBSERVATION OF A BEAM ENERGY SHIFT CAUSED BY A PLASMA WAKEFIELD

A. Ogata, A. Enomoto, K. Nakajima, H. Nakanishi, Y. Suetsugu, T. Shoji, Y. Nishida, and N. Yugami Jun. 1992 15 p
(DE93-753243; PSC-20) Avail: CASI HC A03/MF A01

The energy shifts of linac electron beams caused by a plasma wakefield were measured in plasmas with a density on the order of 10(exp 12)/cc. The linac provided a sequence of several bunches which generated a wakefield in the plasma. The wakefield, in turn, caused an energy change in the bunches. Data processing took account of the finite bunch length, which was comparable or even longer than the plasma wavelength. It shows that the observed wakefield, if converted into the values at the bunch center, amounted to approx. 20 MeV/m in certain cases. The energy spectra were qualitatively consistent with the calculations. No buildup of the wakefield was obvious after the maximum bunch. DOE

N93-28535# Japan Atomic Energy Research Inst., Tokyo.
MEASUREMENTS OF BREAKAWAY REACTION BETWEEN BERYLLIUM AND WATER VAPOR FOR ITER BLANKET DESIGN
Hiroshi Yoshida, Mikio Enoeda, Kusuo Ashibe, and Kiyoshi Ono Jun. 1992 35 p
(DE93-753270; JAERI-M-92-083) Avail: CASI HC A03/MF A01

Beryllium will be utilized as the neutron multiplier in the ITER breeding blanket. As part of Japanese contribution of the water-cooled blanket design, preliminary study was performed to investigate beryllium breakaway reaction, which is one of safety issues of ITER under high temperature conditions. Thermogravimetric measurements in the temperature range 550 - 750 C were carried out under helium gas flow containing water vapor of 7.6 and 0.76 Torr. The test samples were prepared from commercially available hot-pressed and hot-rolled beryllium plates. Characterization of the surface reaction product was performed by macro and microscopic observations, and x-ray diffraction analysis. Linear and parabolic rate laws were found for the dominant reaction steps in the preceding period of the breakaway reaction. Microstructure of the surface reaction layer formed in all exposure conditions revealed brittle structure, which was composed of blister and microcracks. The rate equations were obtained for the preceding step of breakaway reaction. DOE

N93-28583# Oak Ridge National Lab., TN.
NEW REMOTE MAINTENANCE APPROACH FOR TPX
F. C. Davis, M. S. Walker, and T. G. Brown (Princeton Univ., NJ.) 1993 5 p Presented at the 5th Topical Meeting on Robotics and Remote Systems, Knoxville, TN, 26-29 Apr. 1993
(Contract DE-AC05-84OR-21400)
(DE93-007857; CONF-930403-23) Avail: CASI HC A01/MF A01

The Tokamak Physics Experiment (TPX), to be located at Princeton Plasma Physics Laboratory, will be a steady-state, high-performance fusion machine. It will use hydrogen fuel during its original operation, deuterium-deuterium (D-D) fuel for an extended intermediate period of time and then a limited number of runs using deuterium-tritium (D-T) fuel. The D-D operations will generate neutron fluxes that will activate materials of the vacuum vessel. From that point on, the resulting ionizing radiation, which will continue to increase, particularly during D-T operation, will prevent personnel access into the vessel to perform either scheduled or unscheduled maintenance activities. All activities performed within the vacuum vessel must be accomplished using remote means. TPX has taken a new approach for remote maintenance of the components within the vacuum vessel. This document describes the system that is being developed. DOE

N93-28598# Texas Univ., Austin. Inst. for Fusion Studies.
A FOKKER-PLANCK OPERATOR FOR THE EMISSION AND ABSORPTION OF ELECTRON PLASMA WAVES IN A MAGNETIZED PLASMA
A. A. Ware Mar. 1993 25 p
(Contract DE-FG05-80ET-53088)
(DE93-009579; DOE/ET-53088/590; IFSR-590) Avail: CASI HC A03/MF A01

For slab geometry the perturbation of the electrostatic wake of a superthermal test electron in a magnetized plasma (omega(sub ce) much greater than omega(sub pe)) due to moderate magnetic shear is determined. Allowing for the spherical symmetry of the surfaces of constant phase to the rear of the test electron, the 'resonant' field electrons causing the damping of the wave in a magnetic surface at a distance x from the test electron are those with parallel velocity upsilon'(parallel) = upsilon(parallel) cos(beta) / cos(beta + gamma). Here beta is the angle between the emitted ray and B(0), gamma is the angle between B(0) and B(x) and upsilon(parallel) is the velocity of the test electron. As a result the damping in the WKB approximation for the wave emission is a function of both the angle of emission and gamma. A Fokker-Planck equation is derived for the rate of change of the electron distribution function (f) due to the emission and absorption of the waves under these conditions. F is assumed approximately Maxwellian for upsilon(parallel) greater than upsilon(sub T). DOE

N93-28599# Texas Univ., Austin. Inst. for Fusion Studies.
SELF-CONSISTENT CHAOS IN THE BEAM-PLASMA INSTABILITY
J. L. Tennyson (Stanford Linear Accelerator Center, CA.), J. D. Meiss (Colorado Univ., Boulder.), and P. J. Morrison Feb. 1993 37 p
(Contract DE-FG05-80ET-53088)
(DE93-009581; DOE/ET-53088/587; IFSR-587) Avail: CASI HC A03/MF A01

The effect of self-consistency on Hamiltonian systems with a large number of degrees-of-freedom is investigated for the beam-plasma instability using the single-wave model of O'Neil, Winfrey, and Malmberg. The single-wave model is reviewed and then rederived within the Hamiltonian context, which leads naturally to canonical action-angle variables. Simulations are performed with a large (10(sup 4)) number of beam particles interacting with the single wave. It is observed that the system relaxes into a time asymptotic periodic state where only a few collective degrees are active; namely, a clump of trapped particles oscillating in a modulated wave, within a uniform chaotic sea with oscillating phase space boundaries. Thus self-consistency is seen to effectively reduce the number of degrees-of-freedom. A simple low degree-of-freedom model is derived that treats the clump as a single macroparticle, interacting with the wave and chaotic sea. The uniform chaotic sea is modeled by a fluid waterbag, where the waterbag boundaries correspond approximately to invariant tori. This low degree-of-freedom model is seen to compare well with the simulation. DOE

N93-28602# Wisconsin Univ., Madison.
NONLINEAR COUPLING OF TEARING FLUCTUATIONS IN THE MADISON SYMMETRIC TORUS
J. S. Sarff, A. F. Almagri, M. Cekic, D. J. DenHartog, G. Fiksel, S. A. Hokin, H. Ji, S. C. Prager, W. Shen, and M. R. Stoneking et al Nov. 1992 24 p Presented at the Meeting of the Division of Plasma Physics of the American Physical Society, Seattle, WA, 16-20 Nov. 1992
(Contract DE-FG02-85ER-53198)
(DE93-010131; DOE/ER-53198/211; CONF-921103-9) Avail: CASI HC A03/MF A01

Three-wave, nonlinear, tearing mode coupling has been measured in the Madison Symmetric Torus (MST) reversed-field pinch (RFP) using bispectral analysis of edge magnetic fluctuations resolved in 'k-space.' The strength of nonlinear three-wave interactions satisfying the sum rules m(sub 1) + m(sub 2) = m(sub 3) and n(sub 1) + n(sub 2) = n(sub 3) is measured by the bicoherency. In the RFP, m = 1, n approximately 2R/a (6 for MST) internally resonant modes are linearly unstable and grow to large amplitude. Large values of bicoherency occur for two m = 1 modes coupled to an m = 2 mode and the coupling of intermediate toroidal modes, e.g., n = 6 and 7 coupled to n = 13. These experimental bispectral features agree with predicted bispectral features derived from MHD computation. However, in the experiment, enhanced coupling occurs in the 'crash' phase of a sawtooth oscillation concomitant with a broadened mode spectrum suggesting the onset of a nonlinear cascade. DOE

N93-28649# MSE, Inc., Butte, MT.
MAGNETOHYDRODYNAMIC PROJECTS AT THE CDIF
1992 12 p
(Contract DE-AC22-88ID-12735)
(DE93-012195; DOE/ID-12735/T25) Avail: CASI HC A03/MF A01

This quarterly technical progress report presents the tasks accomplished at the Component Development and Integration Facility (CDIF) during the fourth quarter of FY92. Areas of technical progress this quarter included: coal system development; seed system development; test train/A-Bay modifications; channel power dissipation and distribution system development; integrated topping cycle current consolidators; solid suspension injection system upgrade; oxygen system storage upgrade; iron-core magnet repair/upgrade; TRW slag rejector/CDIF slag removal project; emission compliance project; air emissions monitoring support; coal-fired combustor support; 1A channels fabrication and assembly; support of Mississippi State University diagnostic testing; test operations and results; data analysis and modeling; technical papers; and projected activities. DOE

N93-28749# Maryland Univ., College Park. Lab. for Plasma Research.
NONLINEAR DYNAMICS AND PLASMA TRANSPORT
T. M. Antonsen, Jr., J. F. Drake, J. M. Finn, P. N. Guzdar, A. B. Hassam, and R. Z. Sageev 1993 15 p
(Contract DE-FG05-89ER-53301)
(DE93-012238; DOE/ER-53301/2) Avail: CASI HC A03/MF A01

This progress report details work done on a program in nonlinear dynamical aspects of plasma turbulence and transport funded by DOE since 1989. This program has been in cooperation with laboratories in the USSR (now Russia and the Confederation of Independent States (CIS)). The purpose of this program is as follows: To promote the utilization of recent pathbreaking developments in nonlinear science in plasma turbulence and transport; and to promote cooperative scientific investigations between the U.S. and CIS in the related areas of nonlinear science and plasma turbulence and transport. In the work reported in our progress report, we have studied simple models which are motivated by observation on actual fusion devices. The models focus on the important physical processes without incorporating the complexity of the geometry of real devices. This allows for a deeper analysis and understanding of the system both analytically and numerically. DOE

N93-28836# General Atomic Co., San Diego, CA.
INERTIAL CONFINEMENT FUSION TARGET COMPONENT FABRICATION AND TECHNOLOGY DEVELOPMENT SUPPORT Report, 1 Jan. 1991 - 30 Sep. 1992
D. Steinman, ed. Mar. 1993 114 p
(Contract DE-AC03-91SF-18601)
(DE93-010836; GA-A-21203) Avail: CASI HC A06/MF A02

On December 31, 1990, the U.S. Department of Energy entered into a contract with General Atomics (GA) to be the Inertial Confinement Fusion (ICF) Target Component Fabrication and Technology Development Support contractor. This report documents the technical activities of the period January 1, 1991 through September 30, 1992. During this period, GA was assigned 15 tasks in support of the Inertial Confinement Fusion program and its laboratories. These tasks included Facilities Activation, Staff Development, and Capabilities Validation to establish facilities and equipment, and demonstrate capability to perform ICF target fabrication research, development, and production activities. The capabilities developed and demonstrated are those needed for fabrication and precise characterization of polymer shells and polymer coatings. We made progress toward production capability for glass shells, barrier layer coatings, and gas idling of shells. We fabricated over 1000 beam diagnostic foil targets for Sandia National Laboratory Albuquerque and provided full-time on-site engineering support for target fabrication and characterization. We initiated development of methods to fabricate polymer shells by a controlled mass microencapsulation technique, and performed chemical syntheses of several chlorine- and silicon-doped polymer materials for the University of Rochester's Laboratory for Laser Energetics (UR/LLE). We performed the conceptual design of a cryogenic target handling system for UR/LLE that will fill, transport, layer, and characterize targets filled with cryogenic deuterium or deuterium-tritium fuel, and insert these cryogenic targets into the OMEGA-Upgrade target chamber for laser implosion experiments. This report summarizes and documents the technical progress made on these tasks. DOE

N93-28910# Texas Univ., Austin. Inst. for Fusion Studies.
SELF-ORGANIZED PROFILE RELAXATION BY ION TEMPERATURE GRADIENT INSTABILITY IN TOROIDAL PLASMAS
Y. Kishimoto, T. Tajima, M. J. LeBrun, M. G. Gray, J. Y. Kim, and W. Horton Feb. 1993 13 p
(Contract DE-FG05-80ET-53088)
(DE93-009580; DOE/ET-53088/589; IFSR-589) Avail: CASI HC A03/MF A01

Toroidal effects on the ion-temperature gradient mode are found to dictate the temperature evolution and the subsequent relaxed profile realization according to our toroidal particle simulation. Both in the strongly unstable fluid regime as well as in the near-marginal kinetic regime we observe that the plasma maintains an exponential temperature profile and forces the heat flux to be radially independent. The self-organized critical relaxed state is sustained slightly above the marginal stability, where the weak wave growth balances the wave decorrelation. DOE

N93-28912# Wisconsin Univ., Madison. Dept. of Physics.
THE FLUCTUATION INDUCED HALL EFFECT
W. Shen and S. C. Prager Feb. 1993 7 p
(Contract DE-FG02-85ER-53198)
(DE93-010130; DOE/ER-53198/216) Avail: CASI HC A02/MF A01

The fluctuation induced Hall term, (J' x B'), has been measured in the MST reversed field pinch. The term is of interest as a possible source of current self-generation (dynamo). It is found to be non-negligible, but small in that it can account for less than 25% of the dynamo driven current. DOE

N93-28913# Wisconsin Univ., Madison. Dept. of Physics.
NONCONSERVATIVE AND REVERSE SPECTRAL TRANSFER IN HASEGAWA-MIMA TURBULENCE
P. W. Terry and D. E. Newman Jan. 1993 22 p
(Contract DE-FG02-89ER-53291)
(DE93-010132; DOE/ER-53291/215) Avail: CASI HC A03/MF A01

The dual cascade is generally represented as a conservative cascade of enstrophy to short wavelengths through an enstrophy similarity range and an inverse cascade of energy to long wavelengths through an energy similarity range. This picture, based on a proof due to Kraichnan (Phys. Fluids 10, 1417 (1967)), is found to be significantly modified for a spectra of finite extent. Dimensional arguments and direct measurement of spectral flow in Hasegawa-Mima turbulence indicate that for both the energy and enstrophy cascades, transfer of the conserved quantity is accompanied by a nonconservative transfer of the other quantity. The decrease of a given invariant (energy or enstrophy) in the nonconservative transfer in one similarity range is balanced by the increase of that quantity in the other similarity range, thus maintaining net invariance. The increase or decrease of a given invariant quantity in one similarity range depends on the injection scale and is consistent with that quantity being carried in a self-similar transfer of the other invariant quantity. This leads, in an inertial range of finite size, to some energy being carried to small scales and some enstrophy being carried to large scales. DOE

N93-28979# Japan Atomic Energy Research Inst., Tokyo.
MOMENT APPROACH TO FAST ION NEOCLASSICAL TRANSPORT AND VISCOUS FORCES
Jian-Ping Wang, Masafumi Azumi, Keiji Tani (Japan Atomic Energy Research Inst., Ibaraki.), and J. D. Callen Jul. 1992 34 p
(DE93-753305; JAERI-M-92-107) Avail: CASI HC A03/MF A01

Fast ion drift kinetic equation is analytically solved in banana regime using a pitch-angle scattering eigenfunction expansion method. The analytical solution of this eigenfunction is made feasible by adopting Cordey's model where the flux-surface averaged pitch-angle (nu(sub parallel)/nu) is replaced by xi, the pitch-angle at the minimum magnetic field. Then, the flux-surface averaged parallel viscous and heat viscous forces, (B dot product del dot product Pi(sub parallel)) and (B dot product del dot product Theta(sub parallel)), are calculated from the drift-kinetic solution to provide the key closure moments which give rise to radial neoclassical transport and bootstrap current. In combination with the recently derived fast ion friction forces, a moment approach is schemed for fusion plasmas with significant fraction of fast ion component. A new orthogonal polynomial expansion method is presented for the fluid flow distortion from an isotropic distribution and applied to expressing the friction forces between fast ions and thermal ions. DOE

N93-28981# Japan Atomic Energy Research Inst., Tokyo.
A STUDY ON RADIATION SHIELDING ANALYSIS FOR TOROIDAL FIELD COILS OF A TOKAMAK-TYPE FUSION REACTOR
Sergei Zimin (Japan Atomic Energy Research Inst., Ibaraki.) Aug. 1992 226 p
(DE93-753398; JAERI-M-92-120) Avail: CASI HC A11/MF A03

A study on the radiation shield for toroidal field (TF) coils of a tokamak type fusion device is reported. The study was performed to provide the design data base for the radiation shielding analysis for TF coils which can be commonly used for other systems, and to produce some universal recommendation about the neutron flux attenuation in the shield of a fusion reactor. Some simple estimation procedure instead of difficult and expensive neutron calculation can be carried out in this case on the basis of the fundamental knowledge on neutron behavior. The present studies are composed of the fundamentals required for shield estimation, the analysis of shield effectiveness, the analysis of the shielding performance of blankets, the analysis of radiation permeating through the inhomogeneous blanket and shield of a fusion reactor, and the analysis of the TF coil shield of the International Thermonuclear Experimental Reactor (ITER) on the basis of the results of the ITER conceptual design activities for three years. The methodological recommendation was developed for the ANISN and the DOT3 codes. DOE

N93-29049# Lehigh Univ., Bethlehem, PA. Dept. of Physics.
ELECTRON CYCLOTRON HEATING AND CURRENT DRIVE IN TOROIDAL GEOMETRY
A. H. Kritz Mar. 1993 16 p
(Contract DE-FG02-92ER-54141)
(DE93-010400; DOE/ER-54141/1) Avail: CASI HC A03/MF A01

The Principal Investigator has continued to work on problems associated both with the deposition and with the emission of electron cyclotron heating power electron cyclotron heating in toroidal plasmas. In particular, the work has focused on the use of electron cyclotron heating to stabilize $q = 1$ and $q = 2$ instabilities in tokamaks and on the use of electron cyclotron emission as a plasma diagnostic. The research described in this report has been carried out in collaboration with scientists at Princeton, MIT and Livermore. The Principal Investigator is now employed at Lehigh University, and a small group effort on electron cyclotron heating in plasmas has begun to evolve at Lehigh involving undergraduate and graduate students. Work has also been done in support of the electron cyclotron heating and current drive program at the Center for Research in Plasma Physics in Lausanne, Switzerland. DOE

N93-29053# Lawrence Livermore National Lab., CA.
THE HYDRAULIC ANALYSIS OF CYLINDRICAL FLIBE JETS IN A HYLIFE-2 ICF REACTOR
X. M. Chen (California Univ., Berkeley.), V. E. Schrock (California Univ., Berkeley.), and P. F. Peterson (California Univ., Berkeley.) 10 Mar. 1992 14 p Presented at the 10th Topical Meeting on Technology of Fusion Energy, Boston, MA, 7-12 Jun. 1992
(Contract W-7405-eng-48)
(DE93-009234; UCRL-CR-109547; CONF-920607-20) Avail: CASI HC A03/MF A01

In HYLIFE, a conceptual design of inertial confinement fusion reactors, a liquid jet array is proposed to protect the reactor chamber from fusion radiation. During the pulse of fusion, the jets will sustain severe neutron and x-ray heating. Since the high energy neutrons can penetrate the material fairly well, they induce a nearly uniform and very large pressure rise within each jet. This energy is deposited within nanoseconds or much faster than the time scale for fluid dynamic relaxation. The analysis of the relaxation of the liquid jets in a HYLIFE reactor is important for understanding the configuration of the liquid blanket, which is directly related with the vapor and liquid impacts on the chamber wall. The correct estimation of these impacts will allow designers to optimize the cost and strength of the reactor. The calculations for the cylindrical lithium jets in the HYLIFE-I reactor were done previously by using a compressible flow mode and a soft sphere equation of state developed by Young. A similar equation of state model for Flibe, the HYLIFE-2 blanket material, was recently developed. This equation of state allows us to use the same compressible analysis code to calculate the pressure field in the Flibe jets and to estimate the upper bound of Flibe tension limit. With these results we can predict the possibility of the liquid breakup and the momentum distribution generated by relaxation and breakup. DOE

N93-29056# New York Univ., New York. Magneto-Fluid Dynamics Div.
A SURVEY OF PROBLEMS IN DIVERTOR AND EDGE PLASMA THEORY
A. Boozer (College of William and Mary, Williamsburg, VA.), B. Braams, H. Weitzner, and R. Cohen (Lawrence Livermore National Lab., CA.) 22 Dec. 1992 47 p
(Contract DE-FG02-86ER-53223)
(DE93-007531; DOE/ER-53223/196; MF-125) Avail: CASI HC A03/MF A01

Theoretical physics problems related to divertor design are presented, organized by the region in which they occur. Some of the open questions in edge physics are presented from a theoretician's point of view. After a cursory sketch of the fluid models of the edge plasma and their numerical realization, the following topics are taken up: time-dependent problems, non-axisymmetric effects, anomalous transport in the scrape-off layer, edge kinetic theory, sheath effects and boundary conditions in divertors, electric field effects, atomic and molecular data issues, impurity transport in the divertor region, poloidally localized power dissipation (MARFE's and dense gas targets), helium ash removal, and neutral transport. A summary of selected problems of particular significance and a brief bibliography of survey articles and related conference proceedings are included. DOE

N93-29081# Kernforschungszentrum G.m.b.H., Karlsruhe (Germany). Inst. fuer Neutronenphysik und Reaktortechnik.
NUMERICAL MODELLING OF THE COLD PLASMA WITH TIME-DEPENDENT, MAGNETOHYDRODYNAMIC METHODS [MODELLIERUNG DES KALTEN PLASMAS MIT HILFE ZEITABHAENGIGER MAGNETOHYDRODYNAMISCHER METHODEN]
R. Schneider and C.-D. Munz May 1992 70 p In GERMAN
(KfK-5053; ETN-93-93463) Copyright Avail: CASI HC A04/MF A01

A simple, one dimensional two phase model of the cold plasma is investigated with the aid of numerical methods playing an important role in compressible hydrodynamics, such as the particle in cell method and the boundary fitted coordinates concept. These methods were developed for the numerical solution of nonlinear hyperbolic conservation laws and are well known in this field as high resolution upwind schemes. On the basis of these methods a new code is developed which solves numerically the time dependent, one dimensional system of model Vlasov and Maxwell equations of the cold plasma. Numerical results obtained with the code for ion transport, electron branching and stationary case show the quality and the properties of the applied methods. ESA

N93-29093# Los Alamos National Lab., NM.
START BROADENED PROFILES WITH SELF-CONSISTENT RADIATION TRANSFER AND ATOMIC KINETICS IN PLASMAS PRODUCED BY HIGH INTENSITY LASERS
G. L. Olson, J. C. Comly, J. K. LaGattuta, and D. P. Kilcrease 1993 14 p Presented at the Radiative Properties of Hot Dense Matter Conference, Santa Barbara, CA, 2-6 Nov. 1992
(Contract W-7405-eng-36)
(DE93-008706; LA-UR-93-478; CONF-9211211-1) Avail: CASI HC A03/MF A01

Spectral line shapes and line strengths have long been used to diagnose plasma temperatures and densities. In dense plasmas, the additional broadening due to Stark effects give additional information about the plasma density. We present calculations that are self-consistent in that the radiation fields of the line transitions and the atomic kinetics are itegrated to convergence. Examples are given for simple plasmas with temperature gradients, density gradients, and velocity fields. Then, a more complex example of a laser produced plasma is presented. DOE

N93-29123 California Univ., San Diego.
THEORY OF TOKAMAK EDGE TURBULENCE: DRIFT-THERMAL INSTABILITY-INDUCED TURBULENCE AND IONIZATION-DRIVEN DRIFT WAVE TURBULENCE Ph.D. Thesis
Andrew Simon Ware 1992 133 p
Avail: Univ. Microfilms Order No. DA9307205

Two models of tokamak edge turbulence are examined: drift-thermal instability-induced turbulence and ionization driven drift wave turbulence. A simple model for drift-thermal instability-induced turbulence is derived and studied both analytically and numerically. Both nonlocal, nonlinear analytical calculations and three-dimensional computations are used. Potential and temperature fluctuation levels and radial correlation lengths are calculated and compared to numerical results. The saturation mechanism and the role of a fluctuation-generated shear flow are elucidated. The numerical calculations are used to obtain spectra and correlation lengths. A detailed comparison of analytical and numerical results is given. The theory of ionization-driven drift wave turbulence is presented in the context of a quasi-local model. Linear analysis reveals that ionization effects can destabilize collisional drift waves and can possibly induce parallel shear flow instabilities, as well. Nonlinear analysis indicates that energy is transferred from large to small stable scales and converted to ion kinetic energy. Results indicate mode coupling effects are dominant. Large fluctuation levels, in excess of mixing length expectations, are predicted. The ionization source drives a purely inward particle flux, which can explain the anomalously rapid up-take of particles which occurs in response to gas puffing. Finally, the development of a local model of ionization driven drift wave turbulence is extended to include the effects of magnetic shear and poloidal source asymmetry, as well as poloidal mode coupling arising from both magnetic drifts and the source asymmetry. Numerical and analytic investigation confirms that ionization effects can destabilize collisional toroidal drift waves. However, the mode structure is determined primarily by the ion curvature and del(B) drifts and is not overly affected by the poloidal source asymmetry. In addition, the role poloidal asymmetries in both the source and turbulent particle diffusion play in the generation of sheared mean parallel flow is considered. Predictions of sonic parallel shear flow (v(sub parallel)(r) is approximately c(sub s)) induced by poloidally asymmetric diffusion are an unphysical result of the assumption of purely parallel flow (i.e. v(sub perpendicular) = 0) and the neglect of turbulent parallel momentum transport. Results indicate that the flow produced is subcritical to the parallel shear flow instability when diamagnetic effects are poorly considered. Dissert. Abstr.

N93-29148# Texas Univ., Austin. Inst. for Fusion Studies.
COLLECTIVE TRANSPORT OF ALPHA PARTICLES DUE TO ALFVEN WAVE INSTABILITY
B. N. Breizman, H. L. Berk, and H. Ye Feb. 1993 32 p
(Contract DE-FG05-80ET-53088)
(DE93-009578; DOE/ET-53088/591; IFSR-591) Avail: CASI HC A03/MF A01

Recently a new point of view has developed for describing saturation of discrete modes excited by weak sources. The method applies to the evolution of energetic particles in the beam plasma instability as well as to the description of how (alpha) particles evolve when they destabilize Alfven waves under reactor conditions. Over a wide range of parameters the system produces pulsations, where there are relatively brief bursts of wave energy separated by longer intervals of quiescence. There are two types of pulsations; benign and explosive. In the benign phase, valid when particle motion is not stochastic, the distribution function is close to that predicted by classical transport theory, and the instability saturates when the wave trapping frequency equals the expected linear growth rate. If the field amplitude in a burst reaches the level where orbit stochasticity occurs, the quasilinear diffusion causes rapid transfer of particle energy to wave energy and rapid flattening of the particle distribution function. The bursting phase is followed by a relatively long quiescent time interval where the source provides the necessary free energy to regenerate the cycle. The critical issue is whether the instability develops to a high enough level to produce stochastic diffusion. In general this question can be assessed by using mapping methods to obtain criteria of overlapping of orbit resonance. DOE

N93-29190# Department of Energy, Washington, DC. Office of Fusion Energy.
COMPUTING FOR MAGNETIC FUSION ENERGY RESEARCH: AN UPDATED VISION
P. Henline, ed. 24 Feb. 1993 23 p
(DE93-010394; DOE/ER-0583T) Avail: CASI HC A03/MF A01

This Fusion Computing Council perspective is written to present the primary of the fusion computing community at the time of publication of the report necessarily as a summary of the information contained in the individual sections. These concerns reflect FCC discussions during final review of contributions from the various working groups and portray our latest information. This report itself should be considered as dynamic, requiring periodic updating in an attempt to track rapid evolution of the computer industry relevant to requirements for magnetic fusion research. The most significant common concern among the Fusion Computing Council working groups is networking capability. All groups see an increasing need for network services due to the use of workstations, distributed computing environments, increased use of graphic services, X-window usage, remote experimental collaborations, remote data access for specific projects and other collaborations. Other areas of concern include support for workstations, enhanced infrastructure to support collaborations, the User Service Centers, NERSC and future massively parallel computers, and FCC sponsored workshops. DOE

N93-29243# Japan Atomic Energy Research Inst., Tokyo.
STRUCTURAL DESIGN OF CRYOSTAT AND PORT PENETRATION OF INTERNATIONAL THERMONUCLEAR EXPERIMENTAL REACTOR (ITER)
Masafumi Sawa, Naokazu Kanamori, Katsuhiro Shimizu, Yukio Nomura, Yoshinao Ohkawa, Kiyoshi Shibanuma, and Eisuke Tada Jul. 1992 110 p
(DE93-753267; JAERI-M-92-094) Avail: CASI HC A06/MF A02

Preliminary structural design of the ITER cryostat and port penetration based on concrete cryostat was conducted and the structural concept compatible with remote handling and nuclear shielding is proposed. The ITER cryostat was mainly composed of side wall, upper cover, upper port, horizontal port, vacuum port, and cooling pipe penetration. The upper cover is designed to be fully detachable structure by remote handling for assembling/disassembling the poloidal field coils. In addition, the upper cover provides the biological shield for personal access for the blanket maintenance operation. The upper port is designed to meet the requirements of cooling pipe penetration, blanket maintenance and biological shield. The layout of the cooling pipe is defined by simple thermal stress analysis. There are 16 horizontal ports arranged around the cryostat to provide the access of heating and current drive system, fuel injection, blanket test modules, vacuum pumps and remote handling manipulators. Each port should have the biological shield and bellows to prevent an excessive thermal stress due to thermal expansion. These bellows are non-circular cross-section and the reinforced structure to prevent buckling is proposed. A partial model of the seal mechanism applicable to large gate valves connected to the horizontal ports was fabricated and the basic performance under cyclic loading was investigated. As a whole, the design concept of the cryostat and port penetration was successfully developed and more detailed analysis and critical technology development will be conducted in the Engineering Design Phase. DOE

N93-29299# Argonne National Lab., IL. Energy Systems Div.
TRANSIENT TESTS ON AN MHD THRUSTER
E. S. Pierson (Purdue Univ., Hammond, IN.), J. Libera, and M. Petrick 1993 29 p Presented at the 7th Beer-Sheva International Seminar on Magnetohydrodynamics, Jerusalem, Israel, 14-18 Feb. 1993
(Contract W-31-109-eng-38)
(DE93-008656; ANL/ES/CP-78904; CONF-930216-1) Avail: CASI HC A03/MF A01

Three different types of transient tests were made: coast downs to zero voltage and current under open circuit and short circuit conditions, reverses where the applied voltage was reversed to the same or a different value, and jumps where the voltage applied to the thruster was increased without a change in polarity. Most except the coast downs were done both quickly (voltage changes as fast as possible) and slowly (6 s to complete the voltage change). A few slower (12 s) transients were done. Transient runs were made for water conductivities of 16.2 and 5.09 S/m. In all cases steady-state conditions were established and several seconds of data taken before initiating the transients. Data were measured every 0.75 to 1 .5 second over the time interval of interest. Particular attention was paid to looking for evidence of gas bubbles, and to the chance of the voltage profiles between the electrodes. The data are interpreted based on the behavior of the power supply and the thruster. DOE

N93-29303# Lawrence Livermore National Lab., CA.
POLOIDAL FIELD MEASUREMENTS DURING TRANSIENT PHENOMENA ON MTX: SAWTOOTH PERTURBATIONS AND THE EFFECT OF ECH ON DISRUPTIONS
B. W. Rice and E. B. Hooper Jan. 1993 28 p Presented at the US-Japan Workshop on Transient Phenomena in Toroidal Plasmas, San Diego, CA, 20-22 Jan. 1993
(Contract W-7405-eng-48)
(DE93-010516; UCRL-JC-112718; CONF-930198-1) Avail: CASI HC A03/MF A01

A fifteen channel far-infrared polarimeter has been used to measure poloidal field (B(sub p)) profiles during transient events on MTX. Here we present experimental results on two separate phenomena. First, strong

B(sub p) perturbations are observed to be correlated with the sawtooth crash. The on-axis safety factor q(sub 0) approximately 0.8, is approximately constant before and after the crash. Although the perturbed field profile during the crash is too complex to invert unambiguously, several observations concerning existing sawtooth models can be made. The low value of q(sub 0) combined with the large amplitude and complex radial structure of the B(sub p) perturbations, is more consistent with the stochastic or the double-layer reconnection sawtooth models rather than other standard models such as Kadomtsev reconnection or quasi-interchange. In addition, poloidal field measurements were made prior to disruptions on MTX, both with and without electron cyclotron heating (ECH). The disruption studied here, is related to the buildup of heavy-metal impurities in the core, which is particularly prevalent at lower densities. The impurity radiation leads to a collapse of the T(sub e), and J profiles followed by a disruption. The application of on-axis ECH during the T(sub e) collapse but prior to the disruption can repeak the T(sub e) and J profiles thus preventing the disruption. Since the core impurity radiation depends quite sensitively on T(sub e) heating significantly effects the power balance in the core, leading to stability for this type of disruption. DOE

N93-29334# Lawrence Livermore National Lab., CA.
EFFECTS OF NEUTRAL GAS COLLISIONS ON THE POWER TRANSMISSION FACTOR AT THE DIVERTOR SHEATH
A. H. Futch, D. N. Hill, R. A. Jong, G. D. Porter, G. F. Matthews (Joint European Torus Project, Abingdon, England.), and D. Buchenauer (Sandia National Labs., Albuquerque, NM.) 23 Mar. 1992 12 p Presented at the 10th International Conference on Plasma-Surface Interactions in Controlled Fusion Devices, Monterey, CA, 30 Mar. - 3 Apr. 1992
(Contracts W-7405-eng-48; DE-AC03-89ER-51114; DE-AC04-76DP-00789)
(DE93-009320; UCRL-JC-109999; CONF-920311-27) Avail: CASI HC A03/MF A01

We show that charge-exchange and other ion-neutral collisions can reduce the power transmission factor of the plasma sheath, thereby lowering the ion impact energy and target plate sputtering. The power transmission factor relates the heat flux reaching the divertor target to the surface: Delta= Q(sub surf)/n(sub e)T(sub e)C(sub s). Experimental data from the D3-D tokamak suggest that Delta could be as low as 2-3 near the region of peak divertor particle flux, instead of the 7-8 expected from usual sheath theory. Several effects combine to allow ion-neutral interactions to be important in the divertor plasma sheath. The shallow angle of incidence of the magnetic field (1-3 degrees in D3-D) leads to the spatial extension of the sheath from approximately (pi)i approximately = 1 mm normal to the plate to several centimeters along the field lines. Ionization reduces the sheath potential, and collisions reduce the ion impact energy. DOE

N93-29382# Boston Coll., Chestnut Hill, MA. Dept. of Physics.
A NOVEL APPROACH FOR NEW RADIATION SOURCES BASED ON SOLID STATE PLASMA INSTABILITIES Final Report, Dec. 1989 - 1992
P. Bakshi and K. Kempa Feb. 1993 11 p
(Contract DAAL03-90-G-0015)
(AD-A263699; ARO-26682.12-PH) Avail: CASI HC A03/MF A01

A Novel Approach for New Radiation Sources based on current driven plasma instabilities (CDPI) in layered solid state systems was developed. The feasibility of generating CDPI in a variety of systems, and of conversion of the energy of the growing plasma waves to electromagnetic radiation is demonstrated. The most promising candidates for experimental verification and device applications within the class of uniform lower dimensional systems were identified. In addition, there are preliminary indications that modulated lower dimensional systems would significantly enhance these effects. Experimental efforts were stimulated to confirm the results of the investigations. DTIC

N93-29434# Nagoya Univ. (Japan). Plasma Science Center.
ELEMENTAL COMPOSITIONS OF HIGH-ENERGY IONS PRODUCED BY MAGNETOSONIC WAVES IN QUIESCENT PLASMAS
M. Toida, T. X. Zhang, and Y. Ohsawa May 1992 18 p
(DE93-753241; PSC-17) Avail: CASI HC A03/MF A01

The structure of a nonlinear magnetosonic wave in a multiple-ion-species plasma is analytically investigated, and the elemental composition of ions reflected by the magnetosonic wave is studied. Firstly, stationary solutions of magnetosonic waves propagating perpendicularly to a magnetic field in a plasma consisting of electrons and two-species ions are obtained from a fluid model. Secondly, on the basis of the solitary wave solution, conditions for ion reflection are discussed. Then, the fraction of high-energy ions produced by a magnetosonic wave is expressed in terms of the ion mass, charge, thermal speed, Alfven speed, and wave amplitude. It rapidly decreases with increasing mass. It is found that most of the light ions can be reflected in a multiple-ion-species plasma even for small-amplitude waves if the masses of the main component ions are sufficiently heavy. DOE

N93-29772# Lawrence Livermore National Lab., CA.
MODELING THE D3-D PLASMA BOUNDARY WITH THE LEDGE CODE
G. D. Porter, M. E. Rensink, T. D. Rognlien, R. A. Jong, and D. N. Hill Aug. 1992 6 p Presented at the 14th International Conference on Plasma and 19th European Physical Society (EPS) Conference on Controlled Fusion and Plasma Physics, Innsbruck, Austria, 29 Jun. - 3 Jul. 1992
(Contract W-7405-eng-48)
(DE93-009301; UCRL-JC-109538; CONF-920610-15) Avail: CASI HC A02/MF A01

The results of a determination of the radial transport coefficients in the boundary plasma of the DIII-D tokamak is reported. The boundary plasma is defined to be the plasma in the region immediately outside the last closed flux surface of a diverted plasma configuration. Values of the electron thermal diffusivity, chi(sub e), the particle diffusivity, D(sub perpendicular), and the radial convective velocity, v(sub perpendicular) are obtained by comparison between experimental data and a 2-D fluid model. The data are obtained from neutral beam heated ELMing H-mode discharges with 5.0 less than or equal to P(sub beam) less than or equal to 11.0 MW, and 1.0 less than or equal to I(sub P) less than or equal to 1.75 MA. The diffusion coefficients lie in the range 0.03 less than or equal to D(sub perpendicular) less than or equal to 0.25 sq m/s, and 0.2 less than or equal to chi(sub e) less than or equal to 0.5 sq m/s. The convective velocity is found to be zero for all data discussed. The 2-D fluid code and the data used for determination of the transport coefficients are described. The results of our analysis are described, and conclusions are presented. DOE

N93-29780# Lawrence Livermore National Lab., CA.
FUSION LASER OSCILLATOR AND PULSE-FORMING SYSTEM USING INTEGRATED OPTICS
R. B. Wilcox, W. Behrendt, D. F. Browning, D. R. Speck, and B. M. VanWonterghem Jan. 1993 13 p Presented at the International Symposium on Advanced Electronic and Optoelectronic Materials, Los Angeles, CA, 20-23 Jan. 1993
(Contract W-7405-eng-48)
(DE93-009286; UCRL-JC-111393; CONF-930135-1) Avail: CASI HC A03/MF A01

In order to demonstrate new technology for the proposed National Ignition Facility (NIF), we are currently building a 5-kilojoule laser called Beamlet. The oscillator and pulse shaping system for Beamlet represents a major technological improvement over previous designs. This is true of the laser systems being considered for a NIF in general, but the pulse-forming system is a particularly radical departure from the typical philosophy of master-oscillator design. Using integrated optics, fiber optics, and diode-pumped lasers instead of bulk optics and flashlamp-pumped lasers, this new master oscillator takes advantage of current technology to make a system with numerous advantages. The requirements for a NM for greater flexibility and reliability necessitate this new approach: the pulse-forming system for the Beamlet will demonstrate a subset of the capabilities required for a NIF. For the Beamlet we must produce a single 1-10 ns. shaped- and frequency-modulated pulse. The Beamlet needs only to generate square output pulses for technology demonstration purposes, but the input pulses must be shaped to compensate for gain saturation in the power amplifier. To prevent stimulated Brillouin scattering (SBS) from damaging the output optics, the output pulse must have some bandwidth, and thus the pulse-forming system phase modulates the input pulse. These requirements are very similar to those for the Nova master oscillator system, but Nova technology is not the best choice for the Beamlet. In developing an oscillator design for a fusion laser system, the system requirements are defined by the oscillator's place in the overall laser architecture. Both Nova and the Beamlet use a master oscillator-power amplifier (MOPA) architecture. In a MOPA-laser architecture, a low-power oscillator is followed by a high-gain, high-power amplifier. If the output signal is to have a high signal-to-noise ratio (SNR), the oscillator-signal power must be high above the amplifier noise power. DOE

N93-30000 Brown Univ., Providence, RI.
THE PRODUCTION AND EVOLUTION OF PLASMA AND ASSOCIATED MAGNETIC FIELDS DURING HYPERVELOCITY IMPACTS: IMPLICATIONS FOR PLANETARY PALEOMAGNETISM Ph.D. Thesis
David Allen Crawford 1992 217 p
Avail: Univ. Microfilms Order No. DA9308794

Magnetic fields generated within plasma produced by hypervelocity meteoroid impacts were proposed to explain the remanent magnetism of some lunar samples as well as broad areas of the lunar surface. The origin of the lunar remanent fields may be due to crustal remanence of a core dynamo field occurring early in lunar history prior to extensive modification by impact or remanence of transient fields, particularly associated with impacts, occurring on a local scale throughout lunar history. The presence of an early core dynamo field would have strong consequences for the formation and early evolution of the Moon, yet to deconvolve the role that an internally generated core dynamo field may have had, it is necessary to understand the important role that impact-induced magnetization may have on the magnetic state of the lunar surface. The production and evolution of plasma and associated magnetic fields during hypervelocity impacts through an iterative experimental and theoretical approach is addressed. The configuration and duration of spontaneous impact-generated magnetic field observed in the laboratory are dependent on projectile and target composition and have a strong dependence on impact angle. Self-similar, one-dimensional solutions for the evolution of the magnetic field within impact-generated plasma demonstrate that peak magnetic field strength probably increases with increasing crater size at the same diameter-scaled distance. Magnetic fields produced by highly oblique (less than 15 deg -30 deg from horizontal) impacts are particularly enhanced. Impact-generated magnetic fields, extrapolated from experimental data, are likely to be large enough to account for the magnetization of certain relatively young (less than 3 Ma-1.5 Ga) lunar sample and may help account for the lunar magnetic record during the last approximately 3.6 billion years. More generally, crater-related paleomagnetic fields on solid surface bodies in the solar system may be general compositional indicators (e.g. asteroidal vs. cometary impacts) and may yield a diagnostic signature of impact angle where other clues (shape, eject a pattern) are absent or ambiguous. Dissert. Abstr.

N93-30003 Japan Atomic Energy Research Inst., Tokyo.
BOOTSTRAP CURRENT PROFILES AND SCALING IN LARGE ASPECT RATIO TOKAMAKS
Noboru Fujisawa (Japan Atomic Energy Research Inst., Naka.) and Tomonori Takizuka (Japan Atomic Energy Research Inst., Naka.) May 1992 19 p Limited Reproducibility: More than 20% of this document may be affected by microfiche quality
(DE93-753158; JAERI-M-92-064) Avail: CASI HC A03

Recently, bootstrap currents, generated spontaneously in a tokamak plasma, have been observed in large tokamak devices. Those bootstrap currents are applied to designs of a next-generation experimental tokamak reactor like ITER and following tokamak power reactors. A simple expression for a bootstrap current of a tokamak with a large aspect ratio is proposed, which can easily evaluate the bootstrap current. Some empirical scalings for a bootstrap current with a finite aspect ratio have been proposed so far, and the applicability of them is briefly discussed. DOE

N93-30181# Edgerton, Germeshausen and Grier, Inc., Idaho Falls, ID.
PLASMA/PARTICLE INTERACTION IN SUBSONIC ARGON/HELIUM THERMAL PLASMA JETS
W. D. Swank, J. R. Fincke, and D. C. Haggard 1993 6 p Presented at the National Thermal Spray Conference, Anaheim, CA, 7-11 Jun. 1993
(Contract DE-AC07-76ID-01570)
(DE93-010808; EGG-M-92454; CONF-9306130-1) Avail: CASI HC A02/MF A01

Understanding the behavior of a particle and the interactions between a particle and the plasma surrounding it is important to the development and optimization of the plasma spray coating process. This is an experimental study of the interaction between a subsonic thermal plasma jet and injected nickel-aluminum particles. The velocity, temperature and composition of the gas flow field is mapped using an enthalpy probe/mass spectrometer system. The particle flow field is examined by simultaneously measuring the in-flight size, velocity, and temperature of individual particles. The complex interaction between the gas and particle flow fields is examined by combining the two sets of data. Particle and gas temperatures and velocities are compared in the vicinity of a nominal substrate standoff distance and axially along the median particle trajectory. The temperature and velocity difference is shown to vary substantially depending on the particle's trajectory. By the time a particle on the median trajectory reaches the nominal substrate stand off of 63.5 mm it is transferring it's heat and momentum to the plasma gas. DOE

N93-30189# Lodestar Research Corp., Boulder, CO.
FUNDAMENTAL STUDIES OF FUSION PLASMAS
R. E. Aamodt, P. J. Catto, D. A. Dippolito, J. R. Myra, and D. A. Russell 27 Apr. 1993 24 p
(Contract DE-FG02-88ER-53263)
(DE93-013144; DOE/ER-53263/28; LRC-93-41) Avail: CASI HC A03/MF A01

Work on ICRF interaction with the edge plasma is reported. ICRF generated convective cells have been established as an important mechanism for influencing edge transport and interaction with the H-mode, and for controlling profiles in the tokamak scrape-off-layer. Power dissipation by RF sheaths has been shown to be significant for some misaligned ICRF and IIBW antenna systems. Near-field antenna sheath work has been extended to the far-field case, important for experiments with low single pass absorption. Impurity modeling and Faraday screen design support has been provided for the ICRF community. In the area of core-ICRF physics, the kinetic theory of heating by applied ICRF waves has been extended to retain important geometrical effects relevant to modeling minority heated tokamak plasmas, thereby improving on the physics base that is standard in presently employed codes. Both the quasilinear theory of ion heating, and the plasma response function important in wave codes have been addressed. In separate studies, it has been shown that highly anisotropic minority heated plasmas can give rise to unstable field fluctuations in some situations. A completely separate series of studies have contributed to the understanding of tokamak confinement physics. Additionally, a diffraction formalism has been produced which will be used to access the focusability of lower hybrid, ECH, and gyrotron scattering antennas in dynamic plasma configurations. DOE

N93-30190# Japan Atomic Energy Research Inst., Ibaraki.
MEASUREMENT OF WORK FUNCTION OF A PLASMA GRID IN A CESIUM SEEDED NEGATIVE ION SOURCE
Yasuo Suzuki, Masaya Hanada, Yoshikazu Okumura, and Masanobu Tanaka Nov. 1992 22 p
(DE93-764153; JAERI-M-92-168) Avail: CASI HC A03/MF A01

Work function of a plasma grid in a cesium seeded negative ion source was measured by Las photo-emission technique. We have investigated the relation between the work function and the H(sup -) ion current as well as the temperature of the plasma grid. Changing the position of the Laser incidence, we found that a uniform cesium layer was formed over the plasma grid by continuous arc discharge. The work function was decreased with temperature rise of the plasma grid. The minimum work function was estimated to be 1.75 eV at 260 C. Dependence of the H(sup -) ion current on the work function was investigated in the JAERI Multi-Ampere H(sup -) ion source. As a result, it was confirmed that the H(sup -) ion current increased rapidly as the work function decreased. When the H(sup -) ion current was the maximum, the work function was found to be about 1.8 eV. These dependence agree with H(sup -) ion current rise induced by cesium seeding. DOE

N93-30397 Japan Atomic Energy Research Inst., Naka.
PRELIMINARY DESIGN STUDY OF A STEADY STATE TOKAMAK DEVICE
Naoyuki Miya, Shinji Nakajima, and Kenkichi Ushigusa Sep. 1992 162 p Limited Reproducibility: More than 20% of this document may be affected by microfiche quality
(DE93-764162; JAERI-M-92-140) Avail: CASI HC A08

Preliminary design study has been made for a steady tokamak with the plasma current of 10MA, as the next to the JT-60U experimental programs. The goal of the research program is the integrated study of steady state, high-power physics and technology. Present candidate design is to use superconducting TF and PF magnet systems and long pulse operation of 100's-1000's of sec with non inductive current drive mainly by 500keV negative ion beam injection of 60MW. Low activation material such as titanium alloy is chosen for the water tank type vacuum vessel, which is also the nuclear shield for the superconducting coils. The present preliminary design study shows that the device can meet the existing JT-60U facility capability. DOE

N93-30398 Japan Atomic Energy Research Inst., Naka.
OPERATION OF A 20-CHANNEL GRATING POLYCHROMATOR DIAGNOSTIC SYSTEM AND ITS APPLICATION TO SAWTOOTH OBSERVATIONS IN JT-60U
Shinichi Ishida, Nobuaki Isei, and Masayasu Sato Aug. 1992 24 p Limited Reproducibility: More than 20% of this document may be affected by microfiche quality
(DE93-764388; JAERI-M-92-111) Avail: CASI HC A03

In the JT-60U tokamak, the ECE measurements have been made by means of a twenty-channel grating polychromator diagnostic system (GPS) in which a newly developed detector system by the use of low-noise preamplifiers was installed. Operational performance of the GPS with respect to resolutions and noise level is described. The ECE measurements coupled with equilibrium analysis to calculate a local magnetic field strength show good internal-consistency between the equilibrium configuration and the sawtooth inversion locations. Based on the result, the dependence of the normalized inversion radius on the inverse safety factor and the observation of m = 1 mode oscillations are presented. A preliminary result from ECE reconstruction applied to a precursor oscillation represents the formation of a clear crescent m = 1 island, a hot spot and a narrow cold region. DOE

N93-30533# Nagoya Univ. (Japan). Plasma Science Center.
ION RING DISTRIBUTION PRODUCED BY A MAGNETOSONIC WAVE
M. Toida, T. X. Zhang, and Y. Ohsawa Jul. 1992 13 p
(DE93-754311; PSC-23) Avail: CASI HC A03/MF A01

Ion orbits reflected by a magnetosonic wave are theoretically analyzed, and the conditions for ion reflection are derived. In a low beta case, those reflected ions can form a ring distribution in the velocity space. The velocity and energy distribution functions of those particles are obtained. DOE

N93-30585# Utah State Univ., Logan.
USU CENTER OF EXCELLENCE IN THEORY AND ANALYSIS OF THE GEO-PLASMA ENVIRONMENT Final Report, 1 Oct. 1989 - 30 Sep. 1992
Robert W. Schunk 17 Feb. 1993 33 p
(Grant AF-AFOSR-0026-90)
(AD-A264750; AFOSR-93-0204TR) Avail: CASI HC A03/MF A01

A team of ten Ph.D. scientists and several graduate students was assembled at USU to work in close collaboration with scientists at the Air Force Geophysics Laboratory on a number of problems that are relevant to Air Force systems, including OTH radars, communications, and orbiting space structures. The overall goal of the research was to obtain a better understanding of the basic chemical and physical processes operating in the geoplasma environment, including the ionosphere, thermosphere, and magnetosphere. Some of the specific tasks included the following: (1) studies of ionospheric structure and irregularities; (2) study the feasibility of developing better operational ionospheric models; (3) conduct model/data comparisons in order to validate the ionospheric models; (4) study plasma electrodynamics in the high latitude ionosphere; (5) study magnetosphere-ionosphere coupling problems; (6) continue the development of a thermospheric circulation model; (7) study plasmasphere refilling problems; (8) study OTH ray tracing problems at high latitudes; and (9) study certain spacecraft-environment interaction problems, including those related to high-voltage power sources, spacecraft outgassing, artificial plasma cloud expansion, and spacecraft charging at LEO altitudes. DTIC

N93-30600# Cornell Univ., Ithaca, NY. Lab. of Plasma Studies.
NOVEL METHODS OF ACCELERATION Final Report, 1 Feb. 1992 - 31 Jan. 1993
John A. Nation 31 Jan. 1993 25 p
(Contract F49620-92-J-0153)
(AD-A264828; AFOSR-93-0276TR) Avail: CASI HC A03/MF A01

This report describes work carried out on AFOSR grant number F49620-92-J-0153DEF during the period February 1, 1992 to January 31, 1993. The report provides a brief description of the program objectives, summarizes the main accomplishments during the last year, and concludes with listings of conferences and referred publications, which have either been submitted for publications or published during the program year. DTIC

N93-30606 Japan Atomic Energy Research Inst., Tokyo.
HIGH DENSITY PLASMA PRODUCTION IN A MULTICUSP PLASMA GENERATOR WITH RF ANTENNA
Yasuo Suzuki, Masaya Hanada, Yoshikazu Okumura, and Masanobu Tanaka Oct. 1992 22 p Limited Reproducibility: More than 20% of this document may be affected by microfiche quality
(DE93-764493; JAERI-M-92-156) Avail: CASI HC A03

A high density plasma was produced by radio-frequency in a multicusp plasma generator. The generator is a cylindrical chamber of 200 mm in inner diameter and 270 mm in length with 1-3 turn copper tube antenna. By injecting a 2 MHz, 20 kW RF into the multicusp plasma generator, hydrogen plasma of an ion saturation current density of 120 mA/sq cm and a hydrogen plasma of a density of 6.0(10)(exp 11)/cu cm was produced at a pressure of 0.6 Pa in the generator. The ion saturation current density was uniform over the central area of 100 mm in diameter. Coating the antenna with an insulator, we proved that the efficiency of the plasma production was improved. DOE

N93-30649 Japan Atomic Energy Research Inst., Naka.
OPTIMIZATION FOR STEADY-STATE AND HYBRID OPERATIONS OF ITER BY USING SCALING MODELS OF DIVERTOR HEAT LOAD
Yoshiki Murakami, Kiyoshi Itami, Masayoshi Sugihara, and Hirobumi Fujieda Sep. 1992 54 p Limited Reproducibility: More than 20% of this document may be affected by microfiche quality
(DE93-764151; JAERI-M-92-145) Avail: CASI HC A04

Steady-state and hybrid mode operations of ITER are investigated by 0-D power balance calculations assuming no radiation and charge-exchange cooling in divertor region. Operation points are optimized with respect to divertor heat load which must be reduced to the level of ignition mode (approximately 5 MW/sq m). Dependence of the divertor heat load on the variety of the models, i.e., constant-(chi) model, Bohm-type-(chi) model, and JT-60U empirical scaling model, is also discussed. The divertor heat load increases linearly with the fusion power (P(sub FUS)) in all models. The possible highest fusion power greatly differs for each model with an allowable divertor heat load. The heat load evaluated by the constant-(chi) model is, for example, about 1.8 times larger than that by Bohm-type-(chi) model at P(sub FUS) = 750 MW. Effect of reduction of the helium accumulation, improvements of the confinement capability and the current-drive efficiency are also investigated aiming at lowering the divertor heat load. It is found that NBI power should be larger than about 60 MW to obtain a burn time longer than 2000 s. The optimized operation point, where the minimum divertor heat load is achieved, does not depend on the model and is the point with the minimum-P(sub FUS) and the maximum-P(sub NBI). When P(sub FUS) = 690 MW and P(sub NBI) = 110 MW, the divertor heat load can be reduced to the level of ignition mode without impurity seeding if H = 2.2 is achieved. Controllability of the current-profile is also discussed. DOE

N93-30768# Academy of Sciences (USSR), Novosibirsk. Inst. Yadernoj Fiziki.
MEASUREMENTS OF THE ENERGY SPECTRUM OF AN INTENSE MICROSECOND RELATIVISTIC ELECTRON BEAM IN THE BEAM-PLASMA EXPERIMENTS USING A MULTI-FOIL ANALYZER [IZMERENIE EHNERGETICHESKOGO SPEKTRA MOSHCHNOGO MIKROSEKUNDNOGO REHP PUCHKOVO-PLAZMENNYKH EHKSPERIMENTAKH MNOGOFOL'GOVYM ANALIZATOROM]
B. A. Knyazev, P. I. Melnikov, A. A. Nikiforov, and V. V. Chikunov 1991 37 p In RUSSIAN
(DE93-606271; IYaF-91-66) Avail: CASI HC A03/MF A01 (US Sales Only)

Energy spectra of a 1 MeV, 70 kA, 4(mu)s, 140 kJ relativistic electron beam (REB) on the U1-SPIN device are measured before and after passing through gas/plasma prefilled drift chamber using multifoil analyzer. The drift chamber is a 1-meter, 10 cm diameter stainless steel tube with 4T longitudinal magnetic field. The initial beam injected to the tube from the accelerator diode is monoenergetic. For high gas densities (approximately 10(exp 16)cm(sup -3)) the energy spectrum on the exit of the tube remains the same as it is the diode. If the gas/plasma density is less then 10(exp 15)cm(sup -3) the energy loss up to 20% is observed. At the initial gas density about 10(exp 13)cm(sup -3) appreciable fraction (approximately 10%) of the beam electrons with the energy more than initial one appears. Specific features of the diagnostic technique are discussed in detail. DOE

N93-30780# Academy of Sciences (USSR), Novosibirsk. Inst. Yadernoj Fiziki.
EXPERIMENTAL MHD STABILITY LIMIT IN THE GAS-DYNAMIC TRAP
P. A. Bagryanskij, A. A. Ivanov, and A. N. Karpushov et al 1991 14 p
(DE93-606218; IYaF-91-68) Avail: CASI HC A03/MF A01 (US Sales Only)

The results of extensive experimental investigations of a plasma magnetohydrodynamic (MHD) stability in gas-dynamic trap GDT, which were carried out over the past 3 years at Novosibirsk are summarized. The objective of the experiments reported was to give experimental evidence of plasma stability in GDT and compare the conditions under which it would be achieved, with the theoretical predictions. It was found that theoretical predictions generally agree with the measurements with only one notable exception, namely the limit in the mirror ratio for the plasma stability. This observation is discussed in detail. DOE

N93-30795# International Atomic Energy Agency, Vienna (Austria).
PLASMA PHYSICS NETWORK NEWSLETTER, NO. 5
Aug. 1992 5 p
(DE93-606216; INIS-MF-13361) Avail: CASI HC A01/MF A01 (US Sales Only)

The fifth Plasma Physics Network Newsletter (IAEA, Vienna, Aug. 1992) includes the following topics: (1) the availability of a list of the members of the Third World Plasma Research Network (TWPRN); (2) the announcement of the fourteenth IAEA International Conference on Plasma Physics and Controlled Nuclear Fusion Research to be held in Wuerzburg, Germany, from 30 Sep. to 7 Oct. 1992; (3) the announcement of a Technical Committee Meeting on research using small tokamaks, organized by the IAEA as a satellite meeting to the aforementioned fusion conference; (4) IAEA Fellowships and Scientific Visits for the use of workers in developing member states, and for which plasma researchers are encouraged to apply through Dr. D. Banner, Head, Physics Section, IAEA, P.O. Box 100, A-1400 Vienna, Austria; (5) the initiation in 1993 of a new Coordinated Research Programme (CRP) on 'Development of Software for Numerical Simulation and Data Processing in Fusion Energy Research', as well as a proposed CRP on 'Fusion Research in Developing Countries using Middle- and Small-Scale Plasma Devices'; (6) support from the International Centre for Theoretical Physics (ICTP) for meetings held in Third World countries; (7) a report by W. Usada on Fusion Research in Indonesia; (8) News on ITER; (9) the Technical Committee Meeting planned 8-12 Sep. 1992, Canada, on Tokamak Plasma Biasing; (10) software made available for the study of tokamak transport; (11) the electronic mail address of the TWPRN; (12) the FAX, e-mail, and postal address for contributions to this plasma physics network newsletter. DOE

N93-31007# Instituto de Pesquisas Espaciais, Sao Jose dos Campos (Brazil).
PLASMA DIFFUSION THROUGH MULTIDIPOLE MAGNETIC FIELDS
J. L. Ferreira Mar. 1992 26 p
(DE93-608548; INPE-5384; PRE-1750) Avail: CASI HC A03/MF A01 (US Sales Only)

The diffusion of a cold plasma through multidipole fields of a magnetic picket fence is presented. The ion diffusion and trapping is determined by electric potentials inside the multidipole fields. The electron diffusion is regulated by an anomalous transport process driven by low frequency fluctuations inside the magnetic sheath. Particles drifting with velocities above the ion acoustic speed generates high amplitude turbulent waves responsible for an anomalous diffusion process. DOE

76 SOLID-STATE PHYSICS

Includes superconductivity.

For related information, see also *33 Electronics and Electrical Engineering* and *36 Lasers and Masers.*

N93-28470# Technische Univ., Berlin (Germany). Fachbereich Elektrotechnik.
ANALYSIS OF ELECTROTHERMAL INTERACTIONS IN POWER SEMICONDUCTOR MODULES Ph.D. Thesis [EIN BEITRAG SUR ANALYSE DER ELEKTROTHERMISCHEN WECHSELWIRKUNGEN IN LEISTUNGSHALBLEITERMODULEN]
Peter Zwanziger 1992 258 p In GERMAN
(ETN-93-93800) Avail: CASI HC A12/MF A03

The electrothermal coupling through combination of an electrical and a thermal model based on physically phenomenological concepts is described. The models are developed for bipolar power transistors and IGBT (Insulated Gate Bipolar Transistors) and take into account nonhomogeneities and temperature variations. Electrical components and characteristics of choppers realized with semiconductor devices were analyzed: a linear model was developed for describing switching processes, and switching dissipation in diode was calculated by periodic impulses of switcher. Influence of inductive potential drop, intermediate circuit tension, and return current on power balance were characterized. Charge carrier lifetime, conduction voltage of diodes and several transistors were calculated by varying blocking layer temperature and conduction voltages of a transistor with three level Darlington configuration and of an IGBT were calculated. A stationary model of the temperature distribution in substrate with semiconductor modules cooled on one side was developed and the temperature of coupled semiconductors was calculated with dissipation dependent, equivalent thermal resistances. The electrothermal simulation was applied to both bridge arms of a pulse width modulation converter with voltage feed. ESA

N93-28471# Air Force Inst. of Tech., Wright-Patterson AFB, OH. School of Engineering.
LUMINESCENCE STUDY OF ION-IMPLANTED AND MBE-GROWN Er-DOPED GaAs AND Al(x)Ga(1-x)As Ph.D. Thesis
Jose E. Colon Mar. 1993 275 p
(AD-A262602; AFIT/DS/ENP/93-01) Avail: CASI HC A12/MF A03

The excitation and de-excitation mechanisms of the 1.54 microns emissions, from ion implanted and MBE grown GaAs:Er and Al(x)Ga(1-x)As:Er, were studied through luminescence experiments. Experimental techniques included photoluminescence, time resolved photoluminescence, and selective excitation photoluminescence. The Er(3+) emissions were studied as a function of Er concentration, aluminum mole fraction, n- and p-type doping level, and annealing temperature. In addition oxygen co-doping studies were done in order to determine the role played by oxygen in the Er(3+) luminescence. DTIC

N93-28496# Maryland Univ., College Park. Dept. of Electrical Engineering.
OPTICALLY CONTROLLED SOLID STATE OPENING SWITCHES Final Report, 1 Aug. 1988 - 31 May 1992
Chi H. Lee and M. J. Rhee 1992 234 p
(Grant AF-AFOSR-0246-88)
(AD-A262404; AFOSR-93-0197TR) Avail: CASI HC A11/MF A03

This is the final technical report for a research program to study optical controlled solid state opening switches. This program covers the period between August, 1988 and May, 1992 under the grant No. AFOSR-88-0246. The goal of the research is to study fundamental issues in a novel scheme to generate high power electrical pulsed power using optical controlled solid state opening switches. An optically controlled pulsed power system has been developed which is capable of delivering high power pulsed energy. This system employs a photoconductive semiconductor switch (PCSS) in an inductive energy storage pulsed power system (IESPPS). IESPPS offer advantage of small size with voltage and power step-up. However IESPPS imposes several stringent requirements on the switch. In fact, the switch must be nearly ideal with regard to fast opening time and low on-state resistance. Nevertheless, the PCSS performs quite well, yielding power gains of 50 with power output of nearly 100 KW. In this work, the pulse forming theories in the dual of the LC generator, the current charged transmission line (CCTL) and the dual of the Blumlein line DBL are studied for the first time. DTIC

N93-28568# EG and G Mound Applied Technologies, Miamisburg, OH.
POWDER X RAY DIFFRACTION PATTERNS OF ENERGETIC MATERIALS FOR USE AS REFERENCE STANDARDS
D. B. Sullenger (Miami Univ., Oxford, OH.), J. S. Cantrell (Miami Univ., Oxford, OH.), and T. A. Beiter (Miami Univ., Oxford, OH.) 18 Mar. 1993 128 p
(Contract DE-AC04-88DP-43495)
(DE93-009903; MLM-3774) Avail: CASI HC A07/MF A02

This report lists eighteen quality powder x-ray diffraction patterns produced at Mound for various explosives of recent and current interest. In each case the best possible experimental pattern, obtained from the substance in question via automated diffractometric step-scans, was compared with the corresponding pattern, calculated from the lattice and atomic positional parameters of the crystal structure, if known, and a reconciliation sought between the two was sought. In order to make these patterns more useful to various types of practitioners, previously published patterns for these substances have been included, together with a brief description of their crystallographies, some Chemical Abstracts reference information about them, and an evaluation of their quality via accepted powder diffraction criteria. Most of these patterns have been accepted by the International Center for Diffraction Data for inclusion in their Powder Data File; the others will be submitted in due course. DOE

N93-28582# California Univ., Berkeley. Lawrence Berkeley Lab.
THEORY OF NORMAL AND SUPERCONDUCTING PROPERTIES OF FULLERENE-BASED SOLIDS
M. L. Cohen Oct. 1992 23 p
(Contract DE-AC03-76SF-00098)
(DE93-007722; LBL-32955) Avail: CASI HC A03/MF A01

Recent experiments on the normal-state and superconducting properties of fullerene-based solids are used to constrain the proposal theories of the electronic nature of these materials. In general, models of superconductivity based on electron pairing induced by phonons are consistent with electronic band theory. The latter experiments also yield estimates of the parameters characterizing these type H superconductors. It is argued that, at this point, a 'standard model' of phonons interacting with itinerant electrons may be a good first approximation for explaining the properties of the metallic fullerenes. DOE

N93-28584# California Univ., Santa Barbara. Dept. of Chemistry.
Be3(AsO4)2 2H2O: A NEW BERYLLOARSENATE PHASE CONTAINING BRIDGED TETRAHEDRAL 3-RINGS Technical Report, 1 Jun. 1992 - 31 May 1993
William T. Harrison, Tina M. Nenoff, Thurman E. Gier, and Galen D. Stucky 15 Feb. 1993 22 p
(Contract N00014-90-J-1159)
(AD-A262518) Avail: CASI HC A03/MF A01

The high-temperature/high-pressure hydrothermal synthesis and x-ray single crystal structure of Be3(AsO4)2*2H2O is described: the title compound contains a three-dimensional network of BeO4 and AsO4 tetrahedra. The structural motif includes infinite layers of 'bridged' tetrahedral 3- and 4-rings. The 9Be MAS NMR data are consistent with the Be-atom environments in the crystal structure. DTIC

N93-28590# Honeywell, Inc., Bloomington, MN. Systems and Research Center.
OPTICALLY TILED FLAT PANEL DISPLAYS. A FEASIBILITY STUDY Final Report
Bernard S. Fritz Nov. 1992 18 p
(Contract MDA972-92-M-0007)
(AD-A262737) Avail: CASI HC A03/MF A01

This report presents the results of a study examining the feasibility of micro-optic arrays to eliminate the seams between tiling modules making up a large flat panel display. The individual modules consist of commercially-available liquid crystal displays (LCD). We have found that tiling seams can be removed with micro-optic arrays but only by compromising other important display attributes, most notably display luminance and spectral bandwidth. The assumed module edge gap of 17.5 mm is the dominant parameter limiting performance, and this gap must be less than approx. 1-10 mm in order to have acceptable performance with existing backlights and LCD modules. DTIC

N93-28642# California Univ., Berkeley. Lawrence Berkeley Lab.
EXCITED STATES IN ELECTRONIC STRUCTURE CALCULATIONS
S. G. Louie Jul. 1992 10 p Presented at the 10th International Conference on Vacuum Ultraviolet Radiation Physics, Paris, France, 27-31 Jul. 1992
(Contract DE-AC03-76SF-00098)
(DE93-007704; LBL-33356; CONF-920735-5) Avail: CASI HC A02/MF A01

A first-principles quasiparticle approach to the electronic excitation energies in crystals and at surfaces is described. The quasiparticle energies are calculated within the GW approximation for comparison with photoemission and other spectroscopic experiments. Applications of the method to bulk semiconductors and the Si(111)2x1, Ge(111)2x1, and H/Si(111) surfaces are presented. In both cases, significant self-energy corrections arising from many-electron effects to the excitation energies are found. Using atomic positions from total energy minimization, the calculated excitation energies explain quantitatively the experimental spectra. This approach provides an ab initio means for analyzing and predicting results from spectroscopic probes. DOE

N93-28643# Wisconsin Univ., Madison. Applied Superconductivity Center.
MICROSTRUCTURAL UNDERSTANDING AND CRITICAL CURRENT OPTIMIZATION OF ADVANCED HIGH FIELD SUPERCONDUCTORS
L. A. Bonney, T. C. Willis, and D. C. Larbalestier 1993 17 p
(Contract DE-FG02-86ER-52131)
(DE93-011046; DOE/ER-52131/13) Avail: CASI HC A03/MF A01

It is of great importance to improve critical current density, J(sub c) in A15 superconductors for high field magnet applications. Most current work to improve J(sub c) in A15 wires concentrates on increasing the overall J(sub c) by increasing the fraction of superconducting phase in the wire, by improving the uniformity of the superconductor cross section along the length of the wire, and by adjusting the strainstate of the A15 layer. The goal of the A15 work in this group was to investigate the intrinsic J(sub c) of the A15 layer itself. To do this, a better understanding of factors controlling the intrinsic J(sub c) of the Nb3Sn was pursued. DOE

N93-28647# West Virginia Univ., Morgantown.
PLANNING OF A WEST VIRGINIA UNIVERSITY RESEARCH CENTER IN THE BASIC MATERIALS SCIENCES
F. Calzonetti Mar. 1993 10 p
(Contract DE-FG02-91CH-10482)
(DE93-011731; DOE/CH-10482/1) Avail: CASI HC A02/MF A01

Research is being conducted on both structural and functional materials. The following research projects are being conducted: modeling of metallic alloy system for high-temperature structural applications, atomistic origins of embrittlement effects with alloy, high temperature crack growth, modeling of 2-6 semiconductor superlattices for electrooptic applications, and highly parallel computer science research for materials modeling. DOE

N93-28661# Argonne National Lab., IL. Materials and Components Technology Div.
ENHANCEMENTS OF THE CRITICAL CURRENTS OF YBaCuO SINGLE CRYSTALS BY NEUTRON (n) AND PROTON (p) IRRADIATION
B. M. Vlcek, M. C. Frischherz, H. K. Vishwanathan, U. Welp, G. W. Crabtree, and M. A. Kirk 1992 5 p Presented at the Applied Superconductivity Conference, Chicago, IL, 23-28 Aug. 1992
(Contract W-31-109-eng-38)
(DE93-007892; ANL/MSD/CP-78800; CONF-920802-51) Avail: CASI HC A01/MF A01

Results of magnetization hysteresis and T(sub c) measurements of neutron and proton irradiated YBaCuO single crystals are presented. The crystals used for comparison were irradiated to a fluence of 2 x 10(exp 17) n/sq cm (n,E is greater than 0.1 MeV) and 1 x 10(exp 16) p/sq cm (p,E = 3.5 MeV). The critical currents at 1T and 10K are enhanced by a factor of 5 for the neutron irradiated and a factor of 9 for the proton irradiated sample respectively. After irradiation the crystals were annealed at 100, 200, and 300 C for 8h each in air. Following each annealing step the critical temperature and the magnetization hysteresis at 10 and 70K was measured. Upon annealing, a decrease of the critical currents, which is more pronounced for the proton irradiated sample was observed. This decrease is related to the removal of point defects or their small clusters. Thus, their contribution to pinning can be studied. The critical temperature decreases after both types of irradiation by about 0.5K and is fully recovered after annealing. DOE

N93-28874# North Carolina State Univ., Raleigh.
GROWTH, CHARACTERIZATION AND DEVICE DEVELOPMENT IN MONOCRYSTALLINE DIAMOND FILMS Quarterly Letter Report, 1 Jan. - 31 Mar. 1993
R. F. Davis, J. T. Glass, R. J. Nemanich, and R. J. Trew 31 Mar. 1993 24 p
(Contract N00014-90-J-1604)
(AD-A263204) Avail: CASI HC A03/MF A01

Silicon-germanium films have been grown by electron-beam deposition on naturally occurring p-type semiconducting diamond (OO1) substrates. As evidenced by low-energy electron diffraction and scanning tunneling microscopy, the SiGe layers were polycrystalline. Corresponding current-voltage (I-V) measurements conducted at room temperature demonstrated the formation of a low-barrier rectifying contact. Consistent with the observed low-barrier height, the I-V measurements recorded at 300 C exhibited ohmic-behavior. In addition, subsequent post-growth annealing of the SiGe contacts at 850 C in ultra-high vacuum showed an apparent degradation in the I-V characteristics. Microwave performance of p-type diamond MESFET's is under investigation. A simulation program is being developed to enable a realistic evaluation of diamond MESFETs for high temperature and RF power applications. The program currently accounts for incomplete activation and will eventually account for all physical phenomena believed to be significant, including thermal and breakdown effects. DTIC

N93-28888# Fermi National Accelerator Lab., Batavia, IL.
SILICON CRYSTAL UNDER BENDING
Z. Tang 11 Feb. 1993 29 p
(Contract DE-AC02-76CH-03000)
(DE93-010522; FNAL-TM-1827) Avail: CASI HC A03/MF A01

The mechanical behavior of a silicon crystal under bending is investigated. For a crystal of length 30 mm and thickness 3 mm, to achieve the specified bend angle of 0.64 mrad, the appropriate angle of the aluminum punches is 0.96 mrad. DOE

N93-28956# Oak Ridge National Lab., TN.
NEUTRON SCATTERING STUDIES OF THE STRUCTURES AND LATTICE DYNAMICS OF THE ALKALI METALS
H. G. Smith, R. Berliner (Missouri Univ., Columbia.), and J. Trivisonno (John Carroll Univ., Cleveland, OH.) 1992 7 p Presented at the International Conference on Martensitic Transformations, Monterey, CA, 20-24 Jul. 1992
(Contract DE-AC05-84OR-21400)
(DE93-008272; CONF-920722-5) Avail: CASI HC A02/MF A01

The crystal structures, phonon behavior, and pre-martensitic behavior of Li, Na, K, Rb, and Cs as a function of temperature and pressure (Li, Na, Rb, and Cs) are reviewed. Li has been shown to partially transform to the 9R (Sm-type) structure in the vicinity of 75 K and then partially to fcc on annealing. Its (Tc) increases with applied pressure. Na, on the other hand, partially transforms to a mixture of 9R and nearly hexagonal R-polytypes, which approach hcp on annealing. Its (Tc) is rapidly suppressed by application of modest pressures. No martensitic or pre-martensitic phenomenon, or phonon anomaly, has been observed in K down to 5 K. Also, a search for CDW's in the vicinity of (110) has been inconclusive. Similar negative results have been obtained for Rb. DOE

N93-28966# Los Alamos National Lab., NM.
QUANTUM LATTICE FLUCTUATIONS IN A 1-DIMENSIONAL CHARGE-DENSITY-WAVE MATERIAL: LUMINESCENCE AND RESONANCE RAMAN STUDIES OF AN MX SOLID
F. H. Long, S. P. Love, and B. I. Swanson 1993 7 p Presented at the OE/LASE 1993: International Society for Optical Engineering (SPIE) Conference, Los Angeles, CA, 16-23 Jan. 1993
(Contract W-7405-eng-36)
(DE93-007362; LA-UR-93-0003; CONF-930159-10) Avail: CASI HC A02/MF A01

Luminescence spectra, both emission and excitation, and the excitation dependence of the resonance Raman (RR) spectra were measured for a 1-dimensional charge-density-wave solid, (Pt(L)2Cl2))(Pt(L)2)(ClO4))4; L = 1,2- diaminoethane. The luminescence experiments support the existence of tail states in the band gap region, which indicate the presence of disorder. In contrast, the RR measurements conclusively demonstrated that the effects of static structural disorder on the vibrational spectroscopy can be neglected. This apparently paradoxical result can be explained by considering the zero-point motion of the lattice. The experimental results are compared to recent theoretical models. DOE

N93-29094# Los Alamos National Lab., NM.
FLUX LATTICE RELAXATION, NOISE, AND SYMMETRY-BREAKING IN FRUSTRATED JOSEPHSON JUNCTION ARRAYS
N. Gronbech-Jensen, A. R. Bishop, and P. S. Lomdahl 1993 16 p Presented at the Field Theory and Collective Phenomena, Perugia, Italy, May 1992
(Contract W-7405-eng-36)
(DE93-008713; LA-UR-93-460; CONF-9205310-1) Avail: CASI HC A03/MF A01

The purpose of the present report is to study: (1) Relaxation from an initially random flux state. We wish to exhibit the multiple length and time scales involved in this relaxation, and the influence of thermal fluctuations. This noisy relaxation is controlled by the dynamics of various mesoscopic 'defect' structures defined with respect to the underlying ground-state flux structure. The defects, their mesoscopic collective patterns, and their dynamics control a complex macroscopic response, but are themselves microscopically controlled by the competitions producing the ground-state flux completely. Such multiscale-responses have been observed in other competing interaction systems e.g., spin glasses, random field magnets, and weakly pinned charge-density waves, as well as noisy responses in high-temperature superconductors. Various 'creep' and 'stretched-exponential' regimes have been proposed, as well as phenomenological scaling theories attempting to relate spatial domain sizes with temporal scales. (2) Noisy (i.e.,multitime-scale) voltages responses, and their relation to multilength scales, in current driven JJA's in the presence of a uniform extended magnetic field which frustrates the flux order. DOE

N93-29096# Rochester Univ., NY.
ULTRAFAST OPTICAL STUDIES OF SURFACE REACTION PROCESSES AT SEMICONDUCTOR INTERFACES
R. J. D. Miller Mar. 1993 6 p
(Contract DE-FG02-91ER-14185)
(DE93-009049; DOE/ER-14185/2) Avail: CASI HC A02/MF A01

Rectifying properties of semiconductor liquid junctions make them a simple system for converting and storing optical energy. However, interfacial electron or hole carrier transfer and competing non-radiative (energy loss) channels are not well understood at surfaces. This research has explored the use of three optical techniques, Surface Space Charge Electrooptic Sampling, Surface Restricted Transient Grating Spectroscopy, and Femtosecond Optical Kerr Spectroscopy (OKE) to obtain time evolution of the surface spatial distribution of photogenerated charge carriers, photocarrier population dynamics at semiconductor interfaces, and solvent modes responsible for charge localization and separation. These studies have shown that carriers arrive at GaAs(100) surfaces on the hundred femtosecond time scale. Improvements in time resolution, using surface grating spectroscopy, have shown interfacial hole transfer is occurring on the picosecond time scale. The OKE approach to solvent dynamics has determined that the response of water to a field is multiexpontential with a major relaxation component of 100 femtoseconds. The observed interfacial hole transfer to Se(-2) acceptors is occurring on this same time scale. This observation illustrates charge transfer processes can occur in the strong electronic coupling limit and can be competitive with carrier thermalization. DOE

N93-29138# California Univ., Santa Barbara. Dept. of Chemistry.
THE SYNTHESIS AND AB INITIO STRUCTURE DETERMINATION OF Zn4O(BO3)2: A MICROPOROUS ZINCOBORATE BUILT UP FROM FUSED 3-RING AND 5-RING SUB-UNITS Technical Report, 1 Jun. 1992 - 31 May 1993
William T. Harrison, Thurman E. Gier, and Galen D. Stucky 15 Feb. 1993 18 p
(Contract N00014-90-J-1159; NSF DMR-92-08511)
(AD-A262504; T-6) Avail: CASI HC A03/MF A01

The synthesis and structure of Zn4O(BO3)2, a new, neutral-framework, microporous zincoborate are reported. The crystal structure of Zn4O(BO3)2 has been solved ab initio from laboratory X-ray powder diffraction data, and consists of a network of vertex-sharing tetrahedral ZnO4 and triangular BO3 moieties enclosing interlinked, 'cigar'-shaped cages and a three-dimensional network of intersecting channels (minimum diameter approx. 3.5 A). The 'fused' 3-ring/5-ring connectivity of the Zn/B/O framework is novel. Crystal data: Zn4O(BO3)2, M sub r = 384.37, rhombohedral, space group R3c (No. 167), a = 9.9115(4) A, alpha = 48.602(1) deg, V = 502.61 A sup 3, Z = 3, R sub p = 10.9%, R sub wp = 14.2% for 4198 powder data (Cu K alpha radiation, lambda = 1.54178 A). DTIC

N93-29150# California Univ., Berkeley. Lawrence Berkeley Lab.
UNIAXIALLY STRESSED Ge:Ga AND Ge:Be Ph.D. Thesis
O. D. Dubon, Jr. Dec. 1992 97 p
(Contract DE-AC03-76SF-00098)
(DE93-010426; LBL-33454) Avail: CASI HC A05/MF A02

The application of a large uniaxial stress to p-type Ge single crystals changes the character of both the valence band and the energy levels associated with the acceptors. Changes include the splitting of the fourfold degeneracy of the valence band top and the reduction of the ionization energy of shallow acceptors. In order to study the effect of uniaxial stress on transport properties of photoexcited holes, a variable temperature photo-Hall effect system was built in which stressed Ge:Ga and Ge:Be could be characterized. Results indicate that stress increases the lifetime and Hall mobility of photoexcited holes. These observations may help further the understanding of fundamental physical processes that affect the performance of stressed Ge photoconductors including the capture of holes by shallow acceptors. DOE

N93-29188# Sandia National Labs., Albuquerque, NM.
SURFACE DIFFUSION: ATOMISTICS AND SURFACE MORPHOLOGY (SUMMARY OF MRS SYMPOSIUM B PANEL DISCUSSION)
M. H. Grabow, bj145143, G. H. Gilmer (Bell Telephone Labs., Inc., Murray Hill, NJ.), P. J. Feibelman, and B. H. Cooper (Cornell Univ., Ithaca, NY.) 1993 10 p Presented at the Materials Research Society (MRS) Symposium, Boston, MA, 2-6 Dec. 1992
(Contract DE-AC04-76DP-00789)
(DE93-009862; SAND-93-0341C; CONF-921206-12) Avail: CASI HC A02/MF A01

The paper gives some of the highlights of a panel discussion on surface diffusion held November 30, 1992 at the Fall MRS Meeting in Boston, Massachusetts. Four invited speakers discussed computer modeling techniques and scanning tunneling microscopy experiments that have been used to provide new understanding of the atomistic processes that occur at surfaces. We present a summary of each of the invited talks, indicate other presentations on surface diffusion in this proceedings, and provide a transcript of the two discussion sessions. DOE

N93-29214*# Virginia Polytechnic Inst. and State Univ., Blacksburg. Dept. of Civil Engineering.
A SPECTRAL METHOD DETERMINATION OF THE FIRST CRITICAL RAYLEIGH NUMBER FOR A LOW-PRANDTL NUMBER CRYSTAL MELT IN A CYLINDRICAL CONTAINER
C. M. Dietz, Jr. and P. Diplas Jul. 1993 133 p
(Grant NAG1-1084)
(NASA-CR-193238; NAS 1.26:193238) Avail: CASI HC A07/MF A02

The onset of laminar axisymmetric Rayleigh-Benard convection is investigated for a low-Prandtl number liquid metal in a cylindrical container. All surfaces are considered to be solid and no-slip. Two separate cases are examined for the thermal boundary conditions at the side wall, one with conducting and the other with insulated surface. The governing Boussinesq system is first perturbed and then simplified by introducing a Stokes stream function. Subsequently, a Chebyshev Galerkin spectral model is employed to reduce the simplified system to a system of first-order nonlinear ordinary differential equations. A local stability analysis determines the two values of the first critical Rayleigh number, Ra(sub cl), for the insulated and conducting side walls. As expected, the conducting Ra(sub cl) value of 2882.5 obtained from the present approach exceeded the corresponding insulated Ra(sub cl) value of 2331.6. For the insulated case, an earlier study using a different numerical approach suggests that Ra(sub cl) = 2261.9, while an experimental study measured Ra(sub cl) = 2700. Author

N93-29249# California Univ., Berkeley. Lawrence Berkeley Lab.
RESPONSE OF A Nb/Al2O3/Nb TUNNEL JUNCTION TO PICOSECOND ELECTRICAL PULSES
C. Karadi, S. Verghese, C. A. Mears, J. O. Orenstein, P. L. Richards, and A. T. Barfknecht (Conductus, Inc., Sunnyvale, CA.) Jan. 1993 4 p Presented at the Optical Society of America (OSA) Meeting on Ultrafast Optics and Optoelectronics, San Francisco, CA, 25-27 Jan. 1993 Revised
(Contract DE-AC03-76SF-00098)
(DE93-010416; LBL-32901-Rev; CONF-930150-Rev) Avail: CASI HC A01/MF A01

We have resolved the time domain response of the quasiparticle current in a superconducting tunnel junction to picosecond electrical pulses propagating in free space. DOE

N93-29293# Colorado Univ., Boulder. Dept. of Physics.
STRUCTURE AND SWITCHING DYNAMICS IN FERROELECTRIC CRYSTAL AND LIQUID CRYSTAL THIN FILMS Final Report, Dec. 1989 - 1992; Progress Report 1 Jul. - 31 Dec. 1992
Noel A. Clark and James F. Scott Mar. 1993 15 p
(Contract DAAL03-90-G-0002)
(AD-A263664) Avail: CASI HC A03/MF A01

The structure and switching dynamics of ferroelectric solid state and liquid crystal thin films were investigated experimentally using x-ray scattering, dielectric measurements, and optical microspectroscopy. Crystalline piezoelectric ferroelectric films, formed by sol-gel and sputter deposition, were developed and analyzed for application as high speed nonvolatile memories. Ferroelectric liquid crystal devices were studied for application as fast electro-optic light valves in spatial light modulator applications. A novel thermo-optical effect in ferroelectric lead magnesium niobate suitable for use in pressure sensing applications was discovered. DTIC

N93-29301# Lawrence Livermore National Lab., CA.
HIGH-DOSE IMPLANTATIONS OF Al INTO Si(111) AND Si(100)
R. S. Daley and R. G. Musket 14 Dec. 1992 14 p Presented at the 8th International Conference on Ion Beam Modification of Materials, Heidelberg, Germany, 7-11 Sep. 1992
(Contract W-7405-eng-48)
(DE93-009552; UCRL-JC-110338; CONF-9209200-8) Avail: CASI HC A03/MF A01

High dose implants of Al (0.5(10)(exp 18) to 2.0(10)(exp 18)/sq cm) at 200 keV into silicon substrates at 375 C were performed in an attempt to form a pure, monocrystalline buried layer of Al in silicon, upon post-implant annealing. Nuclear reaction analysis (NRA) and Auger electron spectroscopy (AES) were used to determine the Al concentration and morphology as a function of depth. Results show a peak Al concentration of 83 at.% at a depth of approximately 350 run for the highest dose, and the morphology of the Al is of an interconnected network of 100 at.% Al. Failure to form a continuous elemental layer is explained by the as-implanted morphology resulting thermally induced precipitate coarsening rate at 375 C. Formation of large, stable, individual Al precipitates was thermodynamically favored for the implant conditions and effectively precluded coalescence into a continuous layer. DOE

N93-29314# Los Alamos National Lab., NM.
INVESTIGATION OF ION BEAM MIXING OF IRON MARKER LAYERS IN ALUMINUM OXIDE BY RBS
E. A. Cooper, M. Nastasi, and K. E. Sickafus 1993 7 p Presented at the 16th Material Research Society International Symposium on the Scientific Basis for Nuclear Waste Management Fall Meeting, Boston, MA, 30 Nov. -

5 Dec. 1992
(Contract W-7405-eng-36)
(DE93-010727; LA-UR-93-985; CONF-921101-107) Avail: CASI HC A02/MF A01

Thin films made with a thin embedded marker layer of iron or iron oxide in amorphous alumina were ion mixed with 210 keV Ar over a temperature range of RT to 750 C in vacuum. The dose range was 5(10)(exp 15) - 7(10)(exp 16) ions/sq cm with an average dose rate of 4.5(10)(exp 12)ions/sq cm-sec. The resulting marker distributions were analyzed using RBS. Spreading of the iron RBS peak due to mixing into the alumina matrix was observed in the Fe2O3 marker samples and was clearly seen to be a function of temperature (greater than 400 C) and dose, whereas for the Fe marker sample, no such temperature dependence was observed. An activation energy for the thermally assisted ion mixing in the Fe2O3 marker sample was determined to be 0.69 eV in comparison to an activation energy of 1.77 eV for samples that underwent only a thermal treatment. DOE

N93-29331# Cornell Univ., Ithaca, NY.
IN-SITU X RAY STUDIES OF THE UNDERPOTENTIAL DEPOSITION OF COPPER ON PLATINUM (3)
Howell S. Yee and Hector D. Abruna 1992 51 p Sponsored in part by NSF, Offices of Naval and Army Research
(AD-A263361) Avail: CASI HC A04/MF A01

In-situ x-ray fluorescence detected surface EXAFS spectroscopy has been employed to elucidate the in-plane structure of copper underpotentially deposited on a clean and well ordered platinum (111) single crystal electrode. XANES and EXAFS analyses were made as function of applied potential (+O.2V, +O.1V, and O.OV) corresponding to coverages of approximately 0.5ML, 0.75ML, and 1ML, respectively. The charge derived from electrochemical measurements indicate that at the three potentials studied, the electrodeposited copper was not completely discharged. The XANES analysis revealed similarities between the electrodeposited copper and the Cu2O reference lending support to earlier findings of a partially discharged copper ad-layer. EXAFS results suggest two cluster phases at the most positive potential (+O.2V) studied and an epitaxial arrangement at the most negative potential (O.OV). DTIC

N93-29333# Naval Surface Warfare Center, Bethesda, MD.
PROCESSING AND PROPERTY EVALUATION OF SILVER OR ALUMINUM MATRIX YBa2Cu3O(6+x) SUPERCONDUCTING MATERIALS
A. S. Rao Mar. 1993 56 p
(AD-A263382; CARDEROCKDIV-SSM-61-93/05) Avail: CASI HC A04/MF A01

In order to **understand the physical behavior at the atomistic level of the superconducting metal matrix composites,** both aluminum/YBa2CU3O(6+x) and silver/YBa2CU3O(6+). composites have been investigated. The results suggest that silver forms superconducting composites in the concentration range 10-72 wt. %. The aluminum based composites showed the superconducting property only for composites containing 60 wt.% aluminum and 40 wt. % YBa2CU3O(6+x) In addition, it was found that the superconducting behavior of the aluminum YBa2CU3O(6+x) composites is very sensitive to the sintering temperature and the duration of sintering. DTIC

N93-29341# Technology Assessment and Transfer, Inc., Annapolis, MD.
REAL TIME SELF-DIRECTED MBE FLUX CONTROL INCORPORATION IN SITU ELLIPSOMETRY, PHASE 1 Final Report, 27 May - 27 Nov. 1992
David Palaith and Jeffrey J. Heyob Nov. 1992 141 p
(Contract F33615-92-C-5942)
(AD-A263501; APL-UW-TR-9212; WL-TR-93-4039) Avail: CASI HC A07/MF A02

The objective of this program was to achieve real-time control of thin film properties during deposition by the molecular beam epitaxy (MBE) method. Satisfying this objective required development of techniques that would permit rapid and accurate control of the beam fluxes of the chemical constituents of the growing film. This objective of precise flux control was to be achieved by the following means: (1) using self-directed temperature and shutter control, and (2) employing ellipsometry for direct monitoring and feedback over alloy composition and film thickness. DTIC

N93-29383# California Univ., Los Angeles. Dept. of Electrical Engineering.
QUANTUM DEVICES USING Si-BASED SUPERLATTICES AND STRUCTURES
Kang L. Wang and Gamani Karunasiri 4 Feb. 1993 26 p
(Contract DAAL03-89-K-0167)
(AD-A263700; ARO-26896.11-EL) Avail: CASI HC A03/MF A01

The purpose of the research was to perform scientific study and experimentation on potential new Si-based devices for future optical and electronic applications. The research areas included detectors, sources, new properties, and other quantum devices using Si molecular beam epitaxy (Si-MBE) based superlattices and superstructures. With the current ARO support, significant advances in the understanding of optical properties of intersubband transition of SiGe/Si multiple quantum wells, and the fabrication of multiple quantum well infrared detectors operating in the mid infrared range were made. Large many-body effects were observed in heavily doped Si and SiGe/Si quantum well structures. Normal incidence intersubband transitions were demonstrated for both n and p type SiGe/Si quantum well structures. For potential realization of Si-based light sources, the luminescence from monolayer superlattices and strained alloy layers was studied. In the area of quantum transport, a resonant tunneling transistor was demonstrated. DTIC

N93-29397# Materials and Electrochemical Research Corp., Tucson, AZ.
AMBIENT-ATMOSPHERE COMPATIBLE SUPERCONDUCTING FULLERENES
T. A. Miller 22 Feb. 1993 68 p
(Contract DASG60-92-C-0087)
(AD-A262025) Avail: CASI HC A04/MF A01

The goal of this phase 1 project was to evaluate different methods to produce ambient-atmosphere compatible superconducting fullerenes. Three approaches toward this goal were surveyed: (1) protective overlayers; (2) in-cage dopants; and (3) alternate dopants. A source of electrons for the conduction band derived from the lowest unoccupied molecular orbitals, other than reactive alkali metals, is desired. All three methods demonstrated interesting and tantalizing results. Potassium doped fullerene films were produced in our high vacuum (HV) deposition chamber. Difficulties in transporting potassium from the shipping container to the deposition chamber were solved by using a kerosene/isopropanol bath. Measuring electric resistivity proved to be an effective method of monitoring the doping process. Protective overlayers of doped fullerence films were formed with various combinations of electrical conductors and insulators. The electrically insulating layers could be tested immediately at MER, while the metallic layers required cryogenic measurements. DTIC

N93-29417# California Univ., Berkeley. Lawrence Berkeley Lab.
DEFECT STUDIES IN LOW-TEMPERATURE-GROWN GaAs Ph.D. Thesis
D. E. Bliss Nov. 1992 201 p
(Contract DE-AC03-76SF-00098)
(DE93-010405; LBL-33378) Avail: CASI HC A10/MF A03

High content of excess As is incorporated in GaAs grown by low-temperature molecular-beam-epitaxy (LTMBE). The excess As exists primarily as As antisite defects AsGa and a lesser extent of gallium vacancies V(sub Ga). The neutral AsGa-related defects were measured by infrared absorption at 1 micron. Gallium vacancies, V(sub Ga), was investigated by slow positron annihilation. Dependence of defect contents on doping was studied by Si and Be dopants. No free carriers are generated by n-type or p-type doping up to 10(exp 19)/cc Si or Be. Raman data indicate Be occupies Ga substitutional sites but Si atom is not substitutional. Si induces more As(sub Ga) in the layer. As As(sub Ga) increases, photoquenchable As(sub Ga) decreases. Fraction of photoquenchable defects correlates to defects within 3 nearest neighbor separations disrupting the metastability. Annealing reduces neutral As(sub Ga) content around 500 C, similar to irradiation damaged and plastically deformed Ga(sub As), as opposed to bulk grown GaAs in which As(sub Ga)-related defects are stable up to 1100 C. The lower temperature defect removal is due to V(sub Ga) enhanced diffusion of As(sub Ga) to As precipitates. The supersaturated V(sub Ga) and also decreases during annealing. Annealing kinetics for As(sub Ga)-related defects gives 2.0 +/- 0.3 eV and 1.5 +/- 0.3 eV migration enthalpies for the As(sub Ga) and V(sub Ga). This represents the difference between Ga and As atoms hopping into the vacancy. The non-photoquenchable As(sub Ga)-related defects anneal with an activation energy of 1.1 +/- 0.3 eV. Be acceptors can be activated by 800 C annealing. Temperature difference between defect annealing and Be activation formation of As(sub Ga)-Be(sub Ga) pairs. Si donors can only be partially activated. DOE

N93-29424 Air Force Inst. of Tech., Wright-Patterson AFB, OH. School of Engineering.

DESIGN AND PERFORMANCE EVALUATION OF A GAS CHROMATOGRAPH MICROMACHINED IN A SINGLE CRYSTAL SILICON SUBSTRATE Ph.D. Thesis

Rocky R. Reston Mar. 1993 365 p Limited Reproducibility: More than 20% of this document may be affected by microfiche quality
(AD-A262594; AFIT/DS/ENG/93M-01) Avail: Issuing Activity (Defense Technical Information Center (DTIC))

A miniature gas chromatograph (GC) using silicon micromachining techniques was designed and developed. The GC is composed of a miniature sample injector (10 micro-l sample loop); a 0.9 m long, rectangular-shaped (300 micrometers width and 10 micrometers height) capillary column coated with a 0.2 micrometer thick copper phthalocyanine (CuPc) stationary phase; and a dual-detector scheme incorporating a CuPc-coated chemiresistor and a 125 micrometer diameter thermal conductivity detector bead. Micromachining was employed to fabricate the sample injector interface, the GC column, and the dual-detector cavity. A processing technique was developed to sublime the CuPc stationary phase coating on the GC column walls. The miniature GC system was used to separate parts-per-million ammonia and nitrogen dioxide concentrations in less than 30 minutes (10 microliters sample injected at 40 psi). A secondary discovery was the heat of adsorption of nitrogen dioxide (0.38 eV) on a polycrystalline CuPc film (0.2 micrometer thick). This research demonstrated the utilization of a miniature GC to investigate the adsorptive properties of thin films. Also, the time-domain performance model of the miniature GC developed will facilitate the optimization of future miniature GC designs. DTIC

N93-29430# State Univ. of New York, Buffalo. Dept. of Chemistry.

CHARACTERIZATION OF COPPER IODIDE THIN FILMS FABRICATED VIA LASER ASSISTED MOLECULAR BEAM EPITAXY

W. M. Weijekoon, M. Y. Lyktey, P. N. Prasd, and James F. Garvey 3 Apr. 1993 24 p
(Contract N00014-88-K-0483)
(AD-A262823; TR-42) Avail: CASI HC A03/MF A01

For the first time the technique laser assisted molecular beam epitaxy (LAMBE) has been used to fabricate a molecular film by reaction in a molecular beam. Molecular iodine vapor entrained into a stream of helium carrier gas was introduced via a supersonic expansion into the plasma plume of laser evaporated copper to produce copper iodide. Films were deposited on substrates that were situated about 3 cm downstream on the path of the molecular beam. The surface morphology of films depends greatly on the fluence of the incident laser beam and expansion conditions. Films grown at low laser powers show small surface inhomogeneities in their electron micrographs compared to the films that were grown at higher laser powers. Copper in the LAMBE films is found to be mainly in the Cu(+) state as characterized by electron spectroscopy for chemical analysis (ESCA). A comparison of the surface and structural properties of LAMBE films with that of a vacuum evaporated film suggests both films have similar lattice structures and compositions. It seems that LAMBE can be a powerful technique to deposit novel molecular and composite films for electronics and photonics. DTIC

N93-29445 Minnesota Univ., Minneapolis. Dept. of Chemical Engineering and Materials Science.

ELECTRIC FIELD INDUCED PHENOMENA IN STM: TIP DEFORMATIONS AND Au(111)-SURFACE PHASE TRANSITIONS DURING TUNNELING SPECTROSCOPY EXPERIMENTS Technical Report, 30 Jun. 1992 - 31 Mar. 1993

Joachim H. Schott and Henry S. White 20 Mar. 1993 34 p Limited Reproducibility: More than 20% of this document may be affected by microfiche quality
(Contract N00014-91-J-1927)
(AD-A262208; TR-10) Avail: CASI HC A03

We report electric field induced phase transitions of Au(111) surfaces and electric field stress induced elongations of Pt-Ir and Au tips during current voltage measurements with an STM in air. Transitions between the reconstructed square root of 3 x 22 and the unreconstructed 1 x 1 phase of the Au(111) surface are attributed to changes in the electronic surface excess charge density induced by the electric field between tip and sample. Elongations of STM tips during tunneling spectroscopy give rise to a distinct nonlinear current-voltage response at tip-to-sample biases greater than approximately the absolute value of 0.5V. Similar behavior is observed during tunneling measurements on pyrolytic graphite and oxidized Ag surfaces. Extensive elongations can result in tip-sample point-contact and tip-fracture. Artificially low values of the apparent barrier height are shown to result from tip elongation. DTIC

N93-29796# Air Force Systems Command, Wright-Patterson AFB, OH. Foreign Aerospace Science and Technology Center.

ANELASTIC RELAXATIONS ASSOCIATED WITH LOCAL DISORDERING IN GRAIN BOUNDARIES

Bolin Cheng and Tingsui Ge 2 Apr. 1993 14 p Transl. into ENGLISH from Jinshu Xuebao (China), v. 26, no. 5, 1990 p 317-322
(AD-A263101; FASTC-ID(RS)T-0308-92) Avail: CASI HC A03/MF A01

Internal friction and micro-creep measurements were performed with high-purity Al bamboo-crystal specimens. The relaxation strength was found to decrease with the decrease of the temperature of measurement and became zero at about 0.4 T sub m, (T sub m being melting temperature). This reflects the occurrence of local disordering in the bamboo boundary region at this temperature. This result conforms to the picture of grain boundary disordering constructed by atomic simulation studies. DTIC

N93-29859# Stanford Univ., CA.

FERROELECTRIC LIQUID CRYSTAL OPTICAL INTERCONNECT SWITCHING SYSTEMS Final Report, 1 Jul. 1990 - 31 Dec. 1992

Joseph W. Goodman 26 Feb. 1993 7 p
(Contract DAAL03-89-K-0102)
(AD-A263751; ARO-26695.7-PH) Avail: CASI HC A02/MF A01

This grant explored the possible use of ferroelectric liquid crystals (FLC's) in the reamization of photonic switching fabrics. Problems addressed included device fabrication, switch architectures, and switch performance. Experimental versions of most architectures were constructed. The aim of the contract was to develop techniques for using ferroelectric liquid crystals (FLC's) for novel photonic switching architectures. Initial work was devoted to mastering the technology of making FLC polarization rotation shutters, which formed the basis for the switching architecture work to follow. Much of this work was performed using the facilities of Stanford's Center for Integrated Systems. We were able to build such shutters with respectable properties, including reasonable uniformity, insertion losses of the order X dB, and extinction ratios of the order of Y db. Switching speeds observed were on the order of ZZZ. Having mastered the basic shutter technology, we moved on to employing such shutters in novel architectures. DTIC

N93-29868# California Univ., Berkeley. Lawrence Berkeley Lab.

SUBMILLIMETER AND MICROWAVE RESIDUAL LOSSES IN EPITAXIAL FILMS OF Y-Ba-Cu-O AND Tl-Ca-Ba-Cu-O

D Miller, P. L. Richards, C. B. Eom (Stanford Univ., CA.), T. H. Geballe (Stanford Univ., CA.), S. M. Garrison (Conductus, Inc., Sunnyvale, CA.), N. Newman (Conductus, Inc., Sunnyvale, CA.), S. Etemad (Bell Communications Research, Inc., Red Bank, NJ.), A. Inam (Bell Communications Research, Inc., Red Bank, NJ.), T. Venkatesan (Bell Communications Research, Inc., Red Bank, NJ.), and J. S. Martens (IBM Research Lab., San Jose, CA.) Dec. 1992 2 p Presented at the 17th Annual Society of Photo-Optical Instrumentation Engineers (SPIE) International Conference on Infrared and Millimeter Wave Sources, Pasadena, CA, 14-18 Dec. 1992
(Contract DE-AC03-76SF-00098)
(DE93-010430; LBL-33557; CONF-921217-6) Avail: CASI HC A01/MF A01

We have used a novel bolometric technique and a resonant technique to obtain accurate submillimeter and microwave residual loss data for epitaxial thin films of YBa2Cu3O7, Tl2Ca2Ba2Cu3O10 and Tl2CaBa2Cu2O8. For all films we obtain good agreement between the submillimeter and microwave data, with the residual losses in both the Y-Ba-Cu-O and Tl-Ca-Ba-Cu-O films scaling approximately as frequency squared below approximately 1 THz. We are able to fit the losses in the Y-Ba-Cu-O films to a two fluid and a weakly coupled grain model for the a-b plane conductivity, in good agreement with results from a Kramers-Kronig analysis of the loss data. DOE

N93-29974# Commission of the European Communities (Luxembourg).
PROCEEDINGS OF SYMPOSIUM F ON NEW ASPECTS ON THE GROWTH, CHARACTERIZATION AND APPLICATIONS OF CdTe AND RELATED Cd RICH ALLOYS 5, 1992
R. Triboulet, W. R. Wilcox, and O. Oda 1992 333 p Symposium held in Strasbourg, France, 2 Jun. 1992
(Contract DAJA45-92-M-0260)
(AD-A263541; R/D-6882-EE-02) Avail: CASI HC A15/MF A03

This four-day Symposium has provided the opportunity to take stock of the research devoted to CdTe and related Cd-rich alloys (roughly in the band gap energy range 1-2 eV) during the last decade, since the encyclopedic and famous work of De Nobel (1960), the Strasbourg conferences of 1972 and 1977, both dedicated to CdTe, and the excellent monograph of K. Zanio (1977). CdTe exhibits numerous attractive features. It has a band gap of 1.5 eV, just in the middle of the solar spectrum, making it an ideal material for photovoltaic conversion. It also has a high average atomic number of 50, very convenient for nuclear detection. A high electro-optic coefficient is another feature (5.5 for CdTe:V to compare with 1.2 for GaAs:Cr or 1.34 for InP:Fe) allowing high performance electro-optic modulators and photorefractive devices. It can present both types of conductivity (n and p), which makes diode technology and field effect transistors possible, and it has a semi-insulating state as well. DTIC

N93-30120 Stanford Univ., CA. Electronics Lab.
FUNDAMENTAL STUDIES OF THE MORPHOLOGY, CHEMISTRY, AND ELECTRICAL PROPERTIES OF METALS ON GaAs AND OTHER III-V SEMICONDUCTOR COMPOUNDS Final Report, 1 Oct. 1988 - 30 Sep. 1991
W. E. Spicer and I. Lindau 30 Sep. 1992 19 p Limited Reproducibility: More than 20% of this document may be affected by microfiche quality
(Contract N00014-89-J-1083; DARPA Order 56743)
(AD-A264417) Avail: CASI HC A03

A large effort has been placed to understand and develop passivation for the III-V surfaces. Although the major objective of these studies, to develop practical passivation for III-V devices other than heterojunctions (e.g. AlGaAs), is still unresolved (due to chemical instability of coatings in atmosphere) large progress in the understanding of many basic phenomena has been made. Our studies concentrated on two avenues. Firstly we explored the use S based solutions (Na2S, (NH4)2S etc.) which markedly reduce surface recombination at the GaAs(100) surface. Secondly we studied the Sb interlayers on both GaAs and InP surfaces as an intermediate reaction barrier for the passivating layer. DTIC

N93-30141# California Univ., Los Angeles. Dept. of Physics.
APPLICATIONS OF MESOSCOPIC PHYSICS
Shechao Feng 1993 9 p
(Contract DE-FG03-88ER-45378)
(DE93-012104; DOE/ER-45378/T4) Avail: CASI HC A02/MF A01

Research activities in the area of applications of mesoscopic physics to novel correlations and fluctuations of speckle patterns: imaging and tomography with multiply scattered classical waves are briefly summarized. The main thrust in fundamental research is in the general areas of mesoscopic effects in disordered semiconductors and metals and the related field of applications of mesoscopic physics to the subject matter of classical wave propagation through disordered scattering media. Specific topics are Fabry-Perot interferometer with disorder: correlations and light localization; electron-phonon inelastic scattering rate and the temperature scaling exponent in integer quantum Hall effect; and transmission and reflection correlations of second harmonic waves in nonlinear random media. Research in applied physics centered on far infrared photon-assisted transport through quantum point contact devices and photon migration distributions in multiple scattering media. DOE

N93-30144# Rome Lab., Griffiss AFB, NY.
PHOTOREFRACTIVE INTEGRATORS AND CORRELATORS Technical Report, Oct. 1990 - Sep. 1992
George A. Brost Dec. 1992 85 p
(DA Proj. LDF-P)
(AD-A264200; RL-TR-92-340) Avail: CASI HC A05/MF A01

The use of photorefractive crystals as optically addressed time integrating spatial light modulators in acousto-optic signal processing applications was examined. Nonstationary recording techniques of alternating electric fields and moving fringe patterns were investigated in detail. A finite difference technique was used to model grating formation characteristics. Photorefractive Bi12SiO20 and BaTiO3 crystals were tested experimentally in an adaptive acousto-optic processor. These results demonstrated the feasibility of using photorefractives for such applications. DTIC

N93-30146# Minnesota Univ., Minneapolis. Dept. of Chemistry.
DESIGN OF ACENTRIC MATERIALS: X RAY STRUCTURES OF GUANIDINIUM P-NITRO- AND P-HYDROXYBENZENESULFONATE Technical Report, 1 Jun. 1992 - 31 May 1993
V. A. Russell, M. C. Etter, and M. D. Ward 22 Apr. 1993 7 p
(Contract N00014-89-J-1301; DA Proj. 4135)
(AD-A264220; TR-24) Avail: CASI HC A02/MF A01

Guanidinium p-nitro- and p-hydroxybenzenesulfonate crystallize in noncentros (acentric) space groups and exhibit second-harmonic generation. The engineering of these structures was accomplished using hydrogen bonding and the tendency to pack in centrosymmetric structures overcome by screening of the dipolar forces between arylsulfonates by charged layers of guanidinium ions. DTIC

N93-30161# California Univ., San Diego, La Jolla.
SENSITIVE DETECTION OF NEW SUPERCONDUCTORS CREATED AT ULTRA HIGH PRESSURES Final Report, 1 Aug. 1990 - 31 Jan. 1993
Sheldon Schultz 31 Jan. 1993 9 p
(Grant AF-AFOSR-0365-90)
(AD-A264340; AFOSR-93-0246TR) Avail: CASI HC A02/MF A01

In the original proposal we presented the evidence that by utilizing Low Field Modulated Microwave (LFMM) spectroscopy we could sensitively detect the onset of superconductivity in either films, pellets, or single crystals. The technique does not require leads, nor a percolation path, and is unperturbed by the presence of other non-superconducting phases. We suggested that by incorporating this technique in conjunction with the diamond anvil cell approach to high pressures, we could open up new opportunities for rapidly and sensitively studying the significant phase space corresponding to the pressure axis. The primary goal was to detect new normal metal to superconducting phase transitions, starting for example, with those copper compounds for which interesting transitory pressure effects had been reported many years prior to the discovery of the superconducting cuprates. DTIC

N93-30164# Purdue Univ., West Lafayette, IN. School of Electrical Engineering.
THE 2-6 SEMICONDUCTOR SUPERLATTICES Final Report, 1 Dec. 1989 - 30 Nov. 1992
R. L. Gunshor and N. Otsuka 1 Dec. 1992 25 p
(Grant AF-AFOSR-0438-89)
(AD-A264343; AFOSR-03-0245TR) Avail: CASI HC A03/MF A01

The first operational semiconductor diode lasers were demonstrated in the summer of 1991 independently by two U.S. groups, one at 3M and the other a team effort shared by Purdue and Brown Universities. As a result of the close collaboration between MBE and TEM groups within the grant, the structures for lasing and LED (as well as display device) operation were realized with the lowest defect concentrations ever reported for 2-6 structures grown on GaAs by MBE. The reduction of the dislocation levels resulted from an iterative process where the growth could be modified in response to the TEM analysis. The AFOSR funded interface studies have led to our appreciation of the electrical and microstructural considerations obtaining at 2-6/3-5 heterovalent interfaces. As a result the Purdue/Brown group has had equal success in making laser diodes with substrates of both doping types. The Purdue/Brown collaboration has obtained CW operations at 77 K as well as pulsed operation at room temperature using a Zn(S,Se)-based device configuration emitting in the blue (490 nm at room temperature). DTIC

N93-30175# Tristan Technologies, Inc., San Diego, CA.
ADVANCED MICROWAVE FREQUENCY SOURCES AND FILTERS BASED ON SUPERCONDUCTING PHOTONIC BAND GAP (PBG) STRUCTURES Final Report, 1 Jul. - 31 Dec. 1992
Duane Crum, Joseph Anderberg, and S. Schultz 16 Mar. 1993 16 p
(Contract F49620-92-C-0045)

(AD-A264404; Rept-92SBIRPBGFinal; AFOSR-93-0291TR) Avail: CASI HC A03/MF A01

The applicability of photonic band gap structures in high Q resonators has been studied. A review of numerical simulations, experiments, and system design studies are presented. These results confirmed the technical feasibility of utilizing, 2-D photonic band gap structures with high temperature superconducting end plates as high Q resonators for fabricating low phase noise oscillators. A particularly important result of the numerical simulations is that inverse structures (dielectric host with air holes) exhibited useful photonic band gap properties. Experiments performed at 10 GHz demonstrated two methods of modulating the defect mode frequency. A supplier of high temperature superconducting films, suitable for millimeter-wave photonic band gap resonators has agreed to collaborate with Tristan Technologies in a Phase 2 effort. Potential commercial and government applications for photonic band gap resonators with high temperature superconducting end plates have been identified. DTIC

N93-30393# California Univ., Berkeley. Lawrence Berkeley Lab.
A HIGH RESOLUTION 14-BIT ADC FOR GAMMASPHERE PROJECT
B. T. Turko, A. A. Arthur, J. E. Galvin, M. R. Maier, and G. J. Zizka Oct. 1992 5 p Presented at the IEEE Nuclear Science Symposium and Medical Imaging Conference, Orlando, FL, 26-31 Oct. 1992
(Contract DE-AC03-76SF-00098)
(DE93-010446; LBL-32246; CONF-921005-32) Avail: CASI HC A01/MF A01

A system of 110 high performance A/D converters, required for the Gammasphere Project at the Lawrence Berkeley Laboratory, is described. The ADC's are compact, linear plus/minus 0.006% integral, plus/minus 0.5% differential, with a conversion deadtime of 5.3 micro-s and channel profile flatness of 50% over a 13-bit range. The converter is based on a new low power (0.25 W), low cost, monolithic high speed sampling ADC, exibiting a very high stability and no missing codes over the entire 16-bit range. Differential linearity was achieved by applying the 'Gatti method', covering a 8-bit range. Measured data and methods of testing the ADC are also presented. DOE

N93-30407# California Univ., Santa Barbara. Dept. of Chemistry.
SYNTHESIS AND CHARACTERIZATION OF MIXED 3-5 AND 2-6 SEMICONDUCTOR MONOMERS INCLUDED IN THE BORATE SODALITE ANALOGUE Technical Report, 1 Jun. 1992 - 31 May 1993
K. L. Moran, T. E. Gier, W. T. Harrison, G. D. Stucky, and H. Eckert 30 Apr. 1993 27 p
(Contract N00014-90-J-1159)
(AD-A264523) Avail: CASI HC A03/MF A01

The synthesis of the solid solution series Ga(x)Zn(8-x)(BO2)12P(x)Se(2-x) (x = 0, 0.5, 1, 2) is reported and the local and average long-range structures are discussed based on x-ray diffraction data, UV/visible spectroscopic measurements and a variety of field-dependent static and magic angle spinning and solid state NMR experiments. Inclusion of GaP within the borate sodalite analogue results in the formation of an isolated 31p-69,71 Ga dipolar spin pair that exhibits resolved J-coupling in the 31P MAS NMR spectra. Theoretical analysis reveals that there are four different intracage structures distributed in small domains throughout the crystallographically single phase materials and these are identified as (Zn4Se)(6+), (GaZn3P)(6+), (Zn4 P)(5+) and, by inference, (Ga2Zn2P)(7+). DTIC

N93-30408# Northwestern Univ., Evanston, IL. Dept. of Materials Science and Engineering.
COMPLEX DIELECTRIC FUNCTION OF AMORPHOUS DIAMOND FILMS DEPOSITED BY PULSED EXCIMER (ArF) LASER ABLATION OF GRAPHITE
F. Xiong, Y. Y. Wang, and R. P. Chang May 1993 27 p
(Contract N00014-89-J-1848)
(AD-A264527; TR-13-ONR) Avail: CASI HC A03/MF A01

Amorphous diamond films have been synthesized by pulsed excimer (ArF) laser ablation of graphite at room temperature. Detailed studies of the energy-dependent complex dielectric function in the energy range up to 40 eV have been carried out by Kramers-Kronig dispersion analysis of transmission electron energy loss spectroscopy and spectroscopic ellipsometry. Distinct from those of graphitic amorphous carbon and diamond-like carbon, the optical constants of amorphous diamond films are closely related to that of crystalline diamond, but with a smooth band structure, a decrease in the magnitude strength, and band shift towards lower energies. The variation of dielectric function from crystalline diamond to amorphous diamond is analogue to those of crystalline and amorphous semiconductors such as Si and Ge. The extracted optical energy band gap reaches 2.6 eV, the highest value among the reported results of amorphous carbon films. The implication of dielectric function to the bond structure analysis of a-D films has also confirmed its diamond character. All of these provide further evidence of the existence of amorphous diamond. DTIC

N93-30445# Los Alamos National Lab., NM.
COMPUTATIONAL ANALYSIS OF SLIP IN PETN
J. P. Ritchie 1992 13 p Presented at the 10th Detonation Symposium, Boston, MA, 12-16 Jul. 1993
(Contract W-7405-eng-36)
(DE92-040222; LA-UR-92-2773; CONF-930713-1) Avail: CASI HC A03/MF A01

Analysis of slip over two entire planes in crystalline PETN was performed. It showed that slip on 100 must always result in contacts of 1.2 (Angstrom) or less. In contrast, slip on 110 can occur without such close approaches. Molecular modeling of slip supposed to be stimulated by shocks was also performed. It was found that slip was more difficult (that is costly in energy) and led to greater molecular distortions in the sensitive direction than the insensitive direction. Extensive molecular deformation occurred during slip along either of the directions examined. This information has contributed to our knowledge of the molecular distortions occurring during slip, and may be useful in trying to unravel reactivity patterns. Additional investigations are being performed to examine slip along other directions. Also, dynamical calculations simulating the shock and the motions it induces are in progress. DOE

N93-30501# Naval Command, Control and Ocean Surveillance Center, San Diego, CA.
PHOTOINDUCED CHARGE SEPARATION IN Q1D HETEROJUNCTION MATERIALS: EVIDENCE FOR ELECTRON-HOLE PAIR SEPARATION IN MIXED-HALIDE MX SOLIDS
L. A. Worl, S. C. Huckett, B. I. Swanson, A. Saxena, and A. R. Bishop Mar. 1993 5 p
(AD-A264711) Avail: CASI HC A01/MF A01

Resonance Raman experiments on doped and photoexcited single crystals of mixed-halide MX complexes (M = Pt; X = Cl, Br) clearly indicate charge separation; electron polarons preferentially locate on PtBr segments while hole polarons are trapped within PtCl segments. This polaron selectivity, potentially very useful for device applications, is demonstrated theoretically using a discrete, 3/4-filled, two-band, tight-binding, extended Peierls-Hubbard model. Strong hybridization of the PtCl and PtBr electronic bands is the driving force for separation. DTIC

N93-30511# Sandia National Labs., Albuquerque, NM.
UNEXPECTED INCREASE IN THE THERMAL GENERATION RATE OF BULK GaAs DUE TO ELECTRON-BEAM METALLIZATION
T. S. Mayer, M. R. Melloch, J. A. Cooper, Jr., D. M. Fleetwood, and D. E. Beutler 1993 5 p Presented at the Nuclear and Space Radiation Effects Conference, Snowbird, UT, 19-23 Jul. 1993
(Contract DE-AC04-76DP-00789)
(DE93-009829; SAND-93-0382C; CONF-930704-5) Avail: CASI HC A01/MF A01

Damage induced during electron-beam metallization results in a three-order-of-magnitude increase in the generation rate of bulk GaAs is discussed. The damage appears to be radiation induced, with low-energy electrons being the most likely from p(+)-i-n-i-p(+)-GaAs layers damaging mechanism. DOE

N93-30517# Sandia National Labs., Albuquerque, NM.
PHASE SEPARATION, ANTIFERROMAGNETISM, AND SUPERCONDUCTIVITY IN SUPERCONDUCTING-SUPEROXYGENATED La(2-x)Sr(x)CuO(4+(DELTA))
G. H. Kwei, J. A. Goldstone, A. C. Lawson (Los Alamos National Lab., NM.), J. E. Schirber, B. Morosin, E. L. Venturini, and J. A. Voigt 1993 17 p Presented at the Conference on Spectroscopies in Novel Superconductors, Santa Fe, NM, 17-19 Mar. 1993

(Contracts DE-AC04-76DP-00789; W-7405-eng-36)
(DE93-009852; SAND-93-0366C; CONF-930367-2) Avail: CASI HC A03/MF A01

La(2-x)Sr(x)CuO(4+(delta)) with x = 0.01, 0.025, 0.050, 0.10, and 0.16 and excess oxygen delta incorporated by high-pressure O(2) anneals is discussed. These compounds were examined using time-of-flight neutron diffraction data. Various models were fit by Rietveld least-squares refinement, with the maximum amount of delta being only of the order of 10 standard deviations. Delta is largest for x near 0, is zero for x = 0.10 and is intermediate for x = 0.16. Only the sample with x = 0.01 is found to phase separate distinctly into a nearly stoichiometric phase with delta approximately 0 and an oxygen-rich superconducting phase as the temperature is lowered. Coincidence of phase separation and Neel temperature strongly suggests that the phase separation is driven by free energy provided by long-range antiferromagnetic ordering in the nearly stoichiometric, weakly Sr-doped La(2-x)Sr(x)CuO4. The excess oxygen stoichiometry shows that at low values of x, hole doping is provided primarily by the excess oxygen, and is enhanced substantially by phase separation. At larger values of x, excess oxygen is no longer incorporated, and hole doping is provided by the substitution of Sr(+2) for La(+3). DOE

N93-30518# California Univ., Santa Barbara. Dept. of Chemistry.
TWO NEW TITANIUM PYROARSENATES: ALPHA-TiAs2O7 AND BETA-TiAs2O7 Technical Report, 1 Jun. 1992 - 31 May 1993
William T. Harrison, Thurman E. Gier, and Galen D. Stucky 20 Apr. 1993 14 p Prepared in cooperation with Houston Univ.
(Contract N00014-90-J-1159)
(AD-A264632) Avail: CASI HC A03/MF A01

Two new titanium pyroarsenate phases, alpha-TiAS2O7 and beta-TiAS2O7, have been prepared by high temperature hydrothermal methods and characterized by single crystal x-ray diffraction techniques. Both structures are based on different three-dimensional networks of vertex-sharing TiO6 octahedra and AsO4 tetrahedra. The TiO6 groups show little distortion from regular octahedral geometry, and the arsenate anions are linked in pairs via As-O-As bonds to form pyroarsenate (As2O7) groups. Alpha-TiAS2O7 is isostructural with a polymorph of SiP2O7; beta-TiAS2O7 is a new structure. DTIC

N93-30536# Florida Univ., Gainesville. Dept. of Electrical Engineering.
DEVELOPMENT OF ULTRA-LOW NOISE, HIGH SENSITIVITY PLANAR METAL GRATING COUPLED 3-5 MULTIQUANTUM WELL INFRARED DETECTORS FOR FOCAL PLANE ARRAY STARING IR SENSOR SYSTEMS Quarterly Progress Report No. 7, 1 Feb. 1993 - 30 Apr. 1993
Sheng S. Li 1 May 1993 71 p
(Contract N00014-91-J-1976)
(AD-A264465) Avail: CASI HC A04/MF A01

To develop ultra-low dark current and high detectivity planar metal grating coupled bound-to-miniband (BTM) III-V quantum well infrared photodetectors (QWIP's) for 8 to 12 micron focal plane arrays (FPA's) staring IR sensor systems. To develop novel type-I and type II III-V QWIP's with multicolor, broad and narrow band spectral response in the 8 to 14 micron wavelength range. The material systems to be studied include GaAS/AlGaAs, AlAs/AlGaAs, InGaP/GaAs (by MOCVD) grown on GaAs substrates and InAlAs/InGaAs (MBE) grown on InP substrate. To conduct theoretical and experimental studies of the planar metal grating coupled structures for normal incidence illumination on QWIP's. Different metal grating coupled structures using 1-D (line) and 2-D (square mesh and dot) metal gratings will be studied in order to achieve high coupling quantum efficiency under normal frontside and backside illuminations on QWIP's. To perform theoretical and experimental studies of dark current, photocurrent, optical absorption, spectral responsivity, noise, and detectivity in different types of QWIP's developed under this program. DTIC

N93-30548# Northwestern Univ., Evanston, IL. Dept. of Materials Science and Engineering.
DIAMOND NUCLEATION OF SURFACES USING CARBON CLUSTERS
R. J. Meilunas and R. P. Chang May 1993 60 p
(Contract N00014-89-J-1848)
(AD-A264634; TR-12) Avail: CASI HC A04/MF A01

Thin solid films of C(60) and C(70) have been used as nucleation layers for the growth of diamond thin films on a variety of substrate surfaces including metal, insulator, and semiconductors. Compared to other forms of carbon, such as graphite, amorphous carbon, soot, etc., it is found that the nucleation density on C(70) is equivalent to that of diamond seeds themselves. On the other hand, diamond nucleation of C(60) is less favorable. We argue from our experiments that the reason for C(70) to have such favorable nucleating properties is its chemical stability and geometry. A working model is proposed to explain the nucleation of diamond on solid C(70) films. Application of this work extending to the growth of diamond on a wide range of substrates is also discussed. DTIC

N93-30554# Rome Lab., Griffiss AFB, NY.
ENHANCED PHOTOREFRACTIVE EFFECTS IN BARIUM TITANATE
George A. Brost Dec. 1992 51 p
(AD-A264724; RL-TR-92-314) Avail: CASI HC A04/MF A01

This report documents investigations of characteristics of secondary centers (shallow traps) in BaTiO3, and the possible utilization of these traps for enhanced photorefractive effects at infrared wavelengths. Secondary centers were characterized by photoinduced absorption and two-beam coupling experiments. Two species were identified, with concentrations of approximately 1.5 x 10(exp 17)/cc and 2 x 10(exp 16)/cc. The effect of secondary centers on the sublinear intensity dependence and temperature dependent photorefractive effects were also examined. No enhancements of photorefractive effects were also examined. No enhancements of photorefractive effects from induced population of secondary centers by external pumping were observed. DTIC

N93-30560# North Carolina State Univ., Raleigh. Dept. of Electrical Engineering.
ATOMIC LAYER EPITAXY OF SEMICONDUCTOR HETEROSTRUCTURES Final Report, 15 Sep. 1991 - 14 Sep. 1992
Salah Bedair Nov. 1992 43 p
(Grant AF-AFOSR-0422-91)
(AD-A264755; AFOSR-93-0244TR) Avail: CASI HC A03/MF A01

AlGaP and GaP films were deposited on the (100) Si substrates by Atomic Layer Epitaxy (ALE) in the temperature range between 450 and 600 C. Under optimum growth conditions, the growth of GaP and AlGaP was observed to proceed in a two-dimensional (2-D) fashion in the initial growth stages. These ALE-grown films have better surface morphology when compared with the corresponding MOCVD-grown films. With an AlGaP buffer layer grown on Si, the subsequent growth of GaAs on the AlGaP-coated Si substrates tends to proceed 2-D growth. This avoids island growth and the two-step growth process currently used. DTIC

N93-30568# Massachusetts Inst. of Tech., Cambridge. Dept. of Chemistry.
1,2-DIMETHYL-1,2-DISILA-CLOSO-DODECABORANE(12), A SILICON ANALOG OF AN ORTHO-CARBORANE: SYNTHESIS; X RAY CRYSTAL STRUCTURE; NMR, VIBRATIONAL AND PHOTOELECTRON SPECTRA; BONDING
Dietmar Seyferth, Klaus D. Buechner, William S. Rees, Jr., Lars Wesemann, and William M. Davis 20 Apr. 1993 42 p
(Contract N00014-90-J-1590)
(AD-A264709; TR-40-ONR) Avail: CASI HC A03/MF A01

The reaction of (CH3)2Si(NMe2)2 with B1OH14 Yields a polymer, B1OH12 (dot) Me2NSi(CH3)2NMe2(sub n), whose pyrolysis in a stream of ammonia gives hexagonal boron nitride containing a little silicon nitride. In contrast, CH3(H)Si(NMe2)2 reacts with B1OH14 to give 1,2-dimethyl-1,2-disila-closo- dodecaborane(12) (DMSB), an air-sensitive solid, the structure of whose 1:1 benzene solvate was determined by X-ray diffraction. This compound crystallizes in the space group P ccn (56) with a = 10.081(1) A, b = 10.666(8) A, c = 16.130(5) A, V = 1734(2) cu A, and Z = 4. The final R is equal to 0.044 and RW = 0.058. The H-1, C-13, Si-29, and B-11 NMR spectra and mass spectrum of DMSB are reported. Its vibrational spectrum (Raman, 5-3600 /cm; IR, 200-3600 /cm) was measured and compared with that of ortho-carborane. A study of its He(1) photoelectron spectrum led to the conclusion that DMSB is the most electron-rich cluster of type XYB1OH1O with two adjacent main group element centers known. DTIC

N93-30569# Naval Command, Control and Ocean Surveillance Center, San Diego, CA.

PHOTOINDUCED ELECTRON-HOLE CHARGE SEPARATION, INTRINSIC SELF-DOPING AND NOVEL DEVICE APPLICATIONS OF Q1D HETEROJUNCTION MATERIALS: MIXED-HALIDE MX SOLIDS

A. Saxena, X. Z. Huang, J. T. Gammel, A. R. Bishop, and L. A. Worl
Mar. 1993 10 p
(AD-A264714) Avail: CASI HC A02/MF A01

We have extensively studied, both experimentally and theoretically, the following three mixed-halide systems: (1) PtCl(x)Br(1 - x); (2) PtCl(x)I(1 - x); and (3) PtBr(x)I(1 - x) for a variety of concentrations x. We have obtained direct spectroscopic evidence (vibrational modes) for charge separation from resonance raman (RR) experiments on doped and photoexcited single crystals of PtCl(x)Br(1 - x). In particular, electron polarons preferentially locate on the PtBr segment while hole polarons are trapped within PtCl segments. This polaron charge selectivity, which is potentially very useful for photovoltaic device applications, is demonstrated within theoretical calculations based on a discrete, 3/4-filled, two-band, tight-binding, extended Peierls-Hubbard model, showing strong hybridization of PtCl and PtBr electronic bands as the driving force for separation. In contrast to PtCl(x)Br(1 - x), we find that both the PtCl(x)I(1 - x) and the PtCl(x)Br(1 - x) systems exhibit qualitatively different behavior, such as intrinsic self doping. In other words, our simulations predict that electronic charge is spontaneously removed from the PtI segment and injected into the PtCl (or PtBr) segment, thus creating hole defects in PtI and electron defects (polarons/bipolarons) in PtCl (or PtBr). DTIC

N93-30668# Lawrence Livermore National Lab., CA.

RADIATION EFFECTS IN FCC METALS AND INTERMETALLIC COMPOUNDS: A MOLECULAR DYNAMICS COMPUTER SIMULATION STUDY

T. DiazdelaRubia, M. W. Guinan, and A. Caro (Paul Scherrer Inst., Villigen, Switzerland.) 16 Nov. 1992 35 p Presented at the Conference on Computer Simulations of Radiation Effects in Solids, Berlin, Germany, 23-28 Aug. 1992
(Contract W-7405-eng-48)
(DE93-009546; UCRL-JC-112059; CONF-9208146-2) Avail: CASI HC A03/MF A01

Recent results on atomic mixing, radiation-induced disordering, and defect production and clustering induced by displacement cascades in Cu, Ag, Cu3Au and Ni3Al are reviewed. Molecular dynamics computer simulation methods are employed with isotropic many body potentials and recoil energies near subcascade formation regime up the locally molten cascade core in the pure metals and intermetallics. Disordering of intermetallics takes place in the cascade core, but because of the short lifetime of the displacement cascade, chemical short range order is preserved in molten zone. Results reveal very large vacancy and interstitial type defect clusters at high recoil energy and cascade energy density. Vacancies agglomerate and collapse into Frank dislocation loops in quenching of the cascade molten core. Large interstitial clusters are directly produced in cascades and form prismatic dislocation loops. Fraction of defects in clusters for low temperature cascades increases with recoil energy and approaches approximately 70 and 60% for interstitials and vacancies, at recoil energies near threshold for subcascades. In the case of intermetallics the large energy required to produce and transport a superdislocation appears to inhibit interstitial prismatic loop punching and interstitials appear as isolated (100) dumbbells. DOE

N93-30766# Joint Inst. for Nuclear Research, Dubna (USSR). Lab. of Neutron Physics.

ENERGY SPECTRA AND PHOTOELECTRON WORK FUNCTION FROM YBa2Cu3O7 HIGH-T(SUB c) SUPERCONDUCTOR [EHNERGETICHESKIE SPEKTRY I RABOTA VYKHODA FOTOEHIEKTRONOV IZ VTSP YBA2CU3O7]

I. M. Matora, A. A. Bogdzel, and V. V. Zhuravlev et al 1991 10 p In RUSSIAN
(DE93-606329; JINR-R-13-91-158) Avail: CASI HC A02/MF A01 (US Sales Only)

The results are presented of the experiments on the JINR newly built instrument for the photoelectron spectroscopy by the time-of-flight method. The energy resolution achieved was 0.2-0.05 eV. The electron work function (phi) from three samples of polycrystalline high-T(sub c) superconductor YBa2Cu3O7 were measured to be phi = 5.5 +/- 0.2 eV. Spectra of photoelectrons in dependence on time and energy are given. DOE

N93-30769# International Centre for Theoretical Physics, Trieste (Italy).

ELECTRONIC STATES IN QUANTUM WELLS WITH PERIODICALLY STRUCTURED INTERFACES

Sun Hong Aug. 1992 20 p
(DE93-606295; IC-92/191) Avail: CASI HC A03/MF A01 (US Sales Only)

The electronic energy subbands and minigaps in Lateral-Surface-Superlattices (LSSL's) produced by deposition of AlAs and GaAs fractional layers on (001) vicinal GaAs substrates were predicated by variational calculations. A coordinate transformation was introduced in the calculation which transforms the LSSL's with periodically structured interfaces to quantum wells with planar interfaces so that the boundary conditions of the electronic wave functions on the LSSL interfaces can be satisfied exactly. The calculations showed that our theory gives lower subband energies than those predicated by other variational calculations. The dependence of the energy minigaps between the first and second subbands on the LSSL structural parameters, such as the average widths of the LSSL's and the periods of their interface structures, was investigated. In the calculation, the barrier between GaAs and AlAs was assumed to be finite (=1.06eV) and infinite. The infinitely high potential barrier approximation (IHPBA) overestimates the energy minigap by 50% when the average width of the LSSL is 100A, and it reduces to 25% when the width is 200A. IHPBA does not work well when the average widths of the LSSL's are less than 200A. DOE

N93-30770# Academy of Sciences (USSR), Novosibirsk. Inst. Yadernoj Fiziki.

HARD PHOTON EMISSION FROM HIGH ENERGY ELECTRONS AND POSITRONS IN SINGLE CRYSTALS

V. N. Bajer, V. M. Katkov, and V. M. Strakhovenko 1991 31 p
(DE93-606328; IYaF-91-111) Avail: CASI HC A03/MF A01 (US Sales Only)

A radiation of electrons and positrons in single crystals in coherent bremsstrahlung (CBS) region was considered for the case when CBS has the most hard spectrum. Under this condition a particle moves near a crystalline plane (in fcc(d) crystal for axis (001) this is the plane (110)) and influence of the continuous plane potential should be taken into account. This potential gives additional contribution in soft part of the spectrum and affects on hard photon emission. Observation of this phenomena at high energy is discussed. DOE

N93-30771# Joint Inst. for Nuclear Research, Dubna (USSR). Lab. of Nuclear Problems.

MEASUREMENT OF MAGNETIC FIELD PENETRATION DEPTH IN NIOBIUM POLYCRYSTALLINE FILMS BY POLARIZED NEUTRON REFLECTION METHOD

L. P. Chernenko, D. A. Korneev, A. V. Petrenko, N. I. Balalykin, and A. V. Skripnik 1991 4 p
(DE93-606390; JINR-E-3-91-330) Avail: CASI HC A01/MF A01 (US Sales Only)

The values of the superconducting penetration depth measured on thin and thick niobium films are presented. The obtained values of spd in our experiments at T = 4.9 K are 145 (+/-15) nm for a thin film and 90 (+/-) nm for a thick film. It is essentially different from that one for bulk niobium. DOE

N93-30772# Instituto de Pesquisas Energeticas e Nucleares, Sao Paulo (Brazil).

SUPERCONDUCTING FILMS OF YBaCuO M.S. Thesis [FILMES SUPERCONDUTORES DO SISTEMA YBACUO]

A. L. Coelho 1991 59 p In PORTUGESE
(DE93-606831; INIS-BR-2987) Avail: CASI HC A04/MF A01 (US Sales Only)

Thick films of YBa2Cu3O(7-x) were prepared on alumina and YSZ (Yttria-stabilized zirconia) substrates by the screen printing technique. Several experimental conditions were studied, for instance: sintering time, temperature, thickness, and atmosphere annealed. The resulting films were characterized by x ray diffraction, AC electrical resistance, AC susceptibility, and scanning electron microscopy. The surface and cross-section were observed with an optical microscope. The x ray diffraction patterns were compared with a typical pattern and that has indicated the good quality of the samples. AC resistance and its temperature dependence were measured in the standard four-probe configuration. Films thickness was estimated in the scanning electron microscope. This technique was suitable for production of high T(sub c) superconducting films being a simple and inexpensive method. DOE

N93-30776# Minas Gerais Univ., Belo Horizonte (Brazil). Dept. de Fisica.

EFFECT OF PLANAR MAGNETIC FIELD ON ELECTRON TRANSPORT PROPERTIES OF n-AlGaAs/GaAs HETEROJUNCTION AND PHOTOLUMINESCENCE MEASURES IN GaAs SAMPLES M.S. Thesis [EFEITO DO CAMPO MAGNETICO PLANAR SOBRE AS PROPRIEDADES DE TRANSPORTE ELETRICO NA HETEROJUNCAO N-ALGAAS/GAAS E MEDIDAS DE FOTOLUMINESCENCIA EM AMOSTRAS DE GAAS]

A. R. Alves 1991 104 p In PORTUGESE

(DE93-608739; INIS-BR-2992) Avail: CASI HC A06/MF A02 (US Sales Only)

The effects of magnetic fields applied parallel to the interface of an heterojunction n-AlGaAs/GaAs is studied. A qualitative analysis showed that this field modifies the Fermi surface of the two dimensional electron gas (2 DEG) confined on the heterojunction. It produces a strong asymmetry on the magnetoresistance of the 2 DEG relative to the two directions of the electric current. This interpretation is confirmed by a self-consistent numerical calculation involving a solution of the Schroedinger and Poisson equations. To verify this result, measurements with samples grown by Molecular Beam Epitaxy (MBE) under magnetic fields up to 13.0 T are performed and the results obtained confirm the asymmetry in the magnetoresistance. Also, a strong negative magnetoresistance attributed to the imperfections of the interface is seen. It can be used to evaluate the quality of the heterojunction interface. The details about the implantation of the photoluminescence measurement system are discussed. Spectra of an asymmetric quantum well and delta-doped GaAs:Si samples at 300 K and 55 K are shown. DOE

N93-30794# International Centre for Theoretical Physics, Trieste (Italy).

A TIGHT BINDING MODEL FOR THE ELECTRONIC STRUCTURE OF FCC AND SC C60

N. Tit and V. Kumar Jul. 1992 5 p

(DE93-606214; IC-92/168) Avail: CASI HC A01/MF A01 (US Sales Only)

Ab-initio calculations for K3C60 indicate that the general features of the energy bands within LDA remain nearly unchanged as compared to C60. In the electron-phonon pairing mechanism of superconductivity in these materials, the variation in T(sub c) has been attributed to changes in the lattice constant which affects N(E(sub F)). We have therefore, fitted the valence and conduction bands of the FCC C60, which were obtained by Troullier and Martins from an LDA plane wave basis calculations, with a tight binding model and studied the energy bands as a function of the lattice constant. As the overlap between orbitals on neighboring balls is small, the band width is found to decrease by about 30% in going from K3C60 to Rb2CsC60. The density of states, thus, obtained is used to estimate variation in T(sub c) from McMillian's formula. These results are in good agreement with experimental data. Calculations of the energy bands are also presented for the low temperature Pa3-bar structure. DOE

N93-30798# Joint Inst. for Nuclear Research, Dubna (USSR). Lab. of Computing Techniques and Automation.

HEAT GENERATION PRODUCED IN THIN LAYERS OF GaAs SUPERCONDUCTORS UNDER HIGH ENERGY PARTICLES IRRADIATION [EHNERGOVYDEIENIE V TONKIKH SLOYAKH ARSENIDA GALLIYA POD DEJSTVIEM VYSOKOEHNERGETICHESKIKH CHASTITS]

V. S. Barashenkov, A. N. Sosnin, S. Y. Shmakov, and A. Polanski 1991 3 p In RUSSIAN

(DE93-606332; JINR-R-2-91-333) Avail: CASI HC A01/MF A01 (US Sales Only)

Monte Carlo simulation of heat generation spectra in thin layers of GaAs is carried out basing on interactions of protons and C-12 ions at 3.65 GeV/c. These calculated results are compared to those for silicon. The most important from the point of view of radiation damages of semiconductor devices is mainly determined by macroscopic cross-section and the spectrum is weakly dependent on the type of bombarding particle and composition of the target. DOE

N93-30799# Joint Inst. for Nuclear Research, Dubna (USSR). Lab. of Neutron Physics.

A POSSIBILITY TO INVESTIGATE THE SUPERCONDUCTING GAP WITH THE HELP OF NEUTRONS [VOZMOZHNOSTI ISSLEDOVANIYA SVERKHPROVODYASHCEJ SHCHEII S POMOSHCH'YU NEJTRONOV]

V. K. Ignatovich and V. I. Lushchikov 1991 8 p In RUSSIAN

(DE93-606392; JINR-R-4-91-142) Avail: CASI HC A02/MF A01 (US Sales Only)

The neutron scattering on conduction electrons in normal metals and paired electrons in superconductors is theoretically considered. The contribution of conduction electrons of metals to heaving ultracold neutrons is also estimated (nu = 10(exp -12)). DOE

N93-30811 Florida Univ., Gainesville. Dept. of Materials Science and Engineering.

VISIBLE LIGHT EMITTING MATERIALS AND INJECTION DEVICES Progress Report, 1 Jan. - 28 Feb. 1993

Paul H. Holloway, Kevin Jones, Robert Park, Joe Simmons, Tim Anderson, Peter Zory (Colorado Univ., Boulder.), Jacques Pankove (Columbia Univ., New York, NY.), Gertrude Neumark (Oregon Graduate Inst. of Science and Technology, Beaverton.), and Reinhart Engelmann (Oregon Graduate Inst. of Science and Technology, Beaverton.) 28 Feb. 1993 27 p Limited Reproducibility: More than 20% of this document may be affected by microfiche quality

(Contract N00014-92-J-1895)

(AD-A263499) Avail: CASI HC A03

The following topics are discussed: molecular beam epitaxial growth; MOCVD growth; ohmic contact formation; microstructural characterization of column 3 nitride films; optical and electrical properties of ZnSe; diode laser fabrication and testing; theoretical calculations for dopants in ZnSe; and gain modeling in 2-6 strained-layer QW structures. DTIC

N93-30819# Martin Marietta Labs., Baltimore, MD.

TENSILE STUDY OF SINGLE-CRYSTAL TERNARY L1(2) TRIALUMINIDE Al66Ti25Mn(SUB g) Final Report, 1 Sep. 1991 - 31 Jan. 1993

S. A. Brown and K. S. Kumar 2 Mar. 1993 43 p

(Contract F49620-91-C-0099)

(AD-A264297; MML-TR-93-01; AFOSR-93-0287TR) Avail: CASI HC A03/MF A01

Single crystal Al66Ti25Mn9 has been produced and tested in compression as well as uniaxial tension. Yield strengths in compression for orientations near (001) and (111) continuously decrease with increasing temperature in a manner similar to other single crystal L1(sub 2) trialuminides and also to polycrystals of these materials. Slip was determined to occur on the (111) octahedral planes using two-surface analysis. Critical resolved shear stress (CRSS) variation with temperature, calculated for the (111) zone axes (1'01) slip system, overlaps closely for both orientations. Dislocation analysis confirmed the Burgers vectors to be of the type a group of zone axes (110) at both 298 and 1073 K. A few uniaxial tension tests were conducted near zone axes (001) at 1073 K; the HIPed specimens contained a small amount of residual porosity and second phases, which resulted in elastic failure even at this high temperature. Efforts to produce additional crystals with even better microstructures for tension testing are underway. DTIC

N93-30878# Gumbs (R.) Associates, East Brunswick, NJ.

ULTRAFAST, PASSIVE, BROAD-BAND, OPTICAL SHUTTER BASED ON NOVEL SEMICONDUCTOR/CONDUCTING POLYMER INTERFACES Final Report, 15 Jan. - 15 Dec. 1992

P. Chandrasekhar 18 Dec. 1992 9 p

(Contract F49620-92-C-0040)

(AD-A264098; AFOSR-93-0301TR) Avail: CASI HC A02/MF A01

The project is sought to implement new technology for a novel solid state optical shutter. The shutter was obtained by interfacing inorganic semiconductors to conducting polymers, which then switch on activation by a high intensity radiation source in the ultrafast regime. Se/P(DPA) interfaces were prepared and yielded switching efficiencies at 532 nm, calculated as Delta OD= OD(laser)-OD(rest), of between 0.3 and 0.6 at pulse energies as low as 0.1-1.0 mJ/pulse (7 mm beam). Tests with CdSe and AlSb yielded similar Delta OD values. Tests with single crystal CdSe did not yield promising results. The conclusion appears to be that much additional work is needed, especially on a scientific level probing the physical aspects of the phenomenon, before practical devices can become feasible. DTIC

N93-30998# International Centre for Theoretical Physics, Trieste (Italy).
GROWTH MODEL OF Au FILMS ON Ru(001)
E. Canessa and A. Calmetta Jun. 1992 13 p
(DE92-642126; IC-92/123) Avail: CASI HC A03/MF A01 (US Sales Only)

In an attempt to find generic features on the fractal growth of Au films deposited on Ru(001), a simple simulation model based on irreversible diffusion-limited aggregation (DLA) is discussed. Highly irregular two-dimensional dentritic islands of Au particles that gradually grow on a larger host lattice of Ru particles and have fractal dimension d(sub f) approximately 1.70 each, are generated via a multiple had-hoc version of the DLA algorithm for single aggregates. Annealing effects on the islands morphology are reproduced assuming different sticking probabilities at nearest-neighbor lattice sites of Au films on Ru(001). Using simulation data, islands growth are described in analogy to diffusion-limited, precipitate growth with soft impingement of precipities. This leads to analyze thin film island growth kinetics in such fractal systems and to predict a main peak in scattering intensity patterns due to interisland interference. DOE

N93-31025# Joint Inst. for Nuclear Research, Dubna (USSR). Lab. of Theoretical Physics.
A DYNAMICAL MODEL OF STRUCTURAL PHASE TRANSITION IN La2CuO4
N. M. Plakida and S. E. Krasavin 1991 10 p
(DE93-605325; JINR-E-17-91-159) Avail: CASI HC A02/MF A01 (US Sales Only)

A microscopical model of anharmonic lattice dynamics for La(2-x)M(x)CuO4 crystals is proposed to describe the soft tilting mode and its interaction with strains. The free energy for the model is calculated and the structural phase transition D(sub 4h)(sup 17) yields D(sub 2h)(sup 18) yields D(sub 4h)(sup 16) are considered. It is proposed a strong x-dependence of anharmonic constants especially for apical oxygen displacements. DOE

N93-31027# International Centre for Theoretical Physics, Trieste (Italy).
ROLE OF OXYGEN VACANCIES IN ANODIC TiO2 THIN FILMS
N. Tit (Minnesota Univ., Minneapolis.) and J. W. Halley (Minnesota Univ., Minneapolis.) May 1992 15 p
(DE92-642137; IC-92/88) Avail: CASI HC A03/MF A01 (US Sales Only)

Defects play an important role in the electronic and optical properties of amorphous solids in general. Both experimental and theoretical investigations on the nature and origin of defect states in anodic rutile TiO2 thin films (of thickness 5nm to 20nm) were presented. There is experimental evidence that the observed gap state at 0.7eV below the edge of conduction-band is due to an oxygen vacancy. For this reason, oxygen vacancies are used in our model. A comparison of the calculated bulk-photoconductivity to photospectroscopy experiment reveals that the films have bulk-like transport properties. On the other hand a fit of the surface density of states to the scanning tunneling microscopy (STM) on the (001) surfaces has suggested a surface defect density of 5% of oxygen vacancies. To resolve this discrepancy, the dc-conductivity where localization effects are included was calculated. Our results show an impurity band formation at about p(sub c) = 9% of oxygen vacancies. It was concluded that the gap states seen in STM are localized and the oxygen vacancies are playing the role of trapping centers (deep levels) in the studied films. DOE

N93-29381*# Technical Univ. of Denmark, Lyngby. Physics Lab.
FOLLOW UP ON THE CRYSTAL GROWTH EXPERIMENTS OF THE LDEF
K. F. Nielsen and M. D. Lind (Rockwell International Science Center, Thousand Oaks, CA.) *In* NASA. Langley Research Center, LDEF: 69 Months in Space. Second Post-Retrieval Symposium, Part 2 Apr. 1993 p 725-733 (For primary document see N93-29354 11-99)
Avail: CASI HC A02/MF A04

N93-29684*# Aerospace Corp., El Segundo, CA.
POST-FLIGHT ANALYSES OF THE CRYSTALS FROM THE M0003-14 QUARTZ CRYSTAL MICROBALANCE EXPERIMENT
W. K. Stuckey, G. Radhakrishnan, and D. Wallace (QCM Research, Laguna Beach, CA.) *In* NASA. Langley Research Center, LDEF: 69 Months in Space. Part 4: Second Post-Retrieval Symposium Apr. 1993 p 1269-1283 (For primary document see N93-29682 11-99)
Avail: CASI HC A03/MF A03; 2 functional color pages

N93-30229 Victoria Univ. (British Columbia). Dept. of Electrical and Computer Engineering.
MODELLING OF CHANNEL THICKNESS MODULATION EFFECT IN SI GaAs MESFET'S
H. L. Kwok *In* Engineering Inst. of Canada, Canadian Conference on Electrical and Computer Engineering, Volumes 1 and 2 1990 4 p (For primary document see N93-30215 11-31)
Avail: Engineering Inst. of Canada, 2050 rue Mansfield, Suite 700, Montreal, Quebec H3A 1Z2 Canada

N93-30230 Defence Research Establishment, Ottawa (Ontario).
SIMULATION OF TRANSIENT RADIATION EFFECTS ON SEMICONDUCTOR DEVICES USING A PULSED Q-SWITCHED Nd:YAG LASER
G. T. Pepper and S. M. Khanna *In* Engineering Inst. of Canada, Canadian Conference on Electrical and Computer Engineering, Volumes 1 and 2 1990 4 p (For primary document see N93-30215 11-31)
Avail: Engineering Inst. of Canada, 2050 rue Mansfield, Suite 700, Montreal, Quebec H3A 1Z2 Canada

N93-30959*# North Carolina Agricultural and Technical State Univ., Greensboro. Dept. of Manufacturing Systems.
IMPROVED MEASUREMENT OF THERMAL EFFECTS ON MICROSTRUCTURE
Mansur Rastani *In* NASA. Langley Research Center, National Educators' Workshop. Update 92: Standard Experiments in Engineering Materials Science and Technology Jun. 1993 p 197-207 (For primary document see N93-30948 11-23)
Avail: CASI HC A02/MF A04

N93-30968*# North Carolina State Univ., Raleigh. Dept. of Materials Science and Engineering.
THE CHARACTERIZATION OF MATERIALS USING X RAY DIFFRACTION
A. F. Sprecher, Jr., Harvey A. West, and A. A. Fahmy *In* NASA. Langley Research Center, National Educators' Workshop. Update 92: Standard Experiments in Engineering Materials Science and Technology Jun. 1993 p 337-349 (For primary document see N93-30948 11-23)
Avail: CASI HC A03/MF A04

N93-30970*# State Univ. of Southeast Missouri, Cape Girardeau.
PHASE TRANSITION STUDIES IN BARIUM AND STRONTIUM TITANATES AT MICROWAVE FREQUENCIES
Jai N. Dahiya *In* NASA. Langley Research Center, National Educators' Workshop. Update 92: Standard Experiments in Engineering Materials Science and Technology Jun. 1993 p 359-370 (For primary document see N93-30948 11-23)
Avail: CASI HC A03/MF A04

77 THERMODYNAMICS AND STATISTICAL PHYSICS

Includes quantum mechanics; theoretical physics; and Bose and Fermi statistics.

For related information see also *25 Inorganic and Physical Chemistry* and *34 Fluid Mechanics and Heat Transfer.*

N93-28472# Deutsches Elektronen-Synchrotron, Hamburg (Germany).
THE SEMICLASSICAL STABILITY OF DE SITTER SPACETIME
C. Busch (Technische Univ., Hanover, Germany.) Sep. 1992 23 p
(DESY-92-131; ITP-UH-9/92; ETN-93-93801) Copyright Avail: CASI HC A03/MF A01

The semiclassical Einstein-Schroedinger equations describing the evolution of spacetime geometry and a massive scalar quantum field with arbitrary coupling to curvature are linearized around their de Sitter-Bunch-Davies solution. The renormalized energy momentum tensor expectation value is calculated in linear order for a spatially homogeneous deviation from the Sitter-Bunch-Davies system. The momentum integrations are executed analytically. The linearized backreaction problem is completely solved via Laplace transformation and the general solution is analyzed with respect to instabilities. There are only two potential instabilities: a constant mode which is just a pure gauge and an instability on the Planck time scale which lies outside of the scope of the study's semiclassical theory. ESA

N93-28690 California Inst. of Tech., Pasadena.
TOPICS IN GENERAL RELATIVITY THEORY: GRAVITATIONAL-WAVE MEASUREMENTS OF BLACK-HOLE PARAMETERS; GRAVITATIONAL COLLAPSE OF A CYLINDRICAL BODY; AND CLASSICAL-PARTICLE EVOLUTION IN THE PRESENCE OF CLOSED, TIMELIKE CURVES Ph.D. Thesis
Fernando Echeverria 1993 95 p
Avail: Univ. Microfilms Order No. DA9307036

I study three different topics in general relativity. The first study investigates the accuracy with which the mass and angular momentum of a black hole can be determined by measurements of gravitational waves from the hole, using a gravitational-wave detector. The black hole is assumed to have been strongly perturbed and the detector measures the waves produced by its resulting vibration and ring-down. The uncertainties in the measured parameters arise from the noise present in the detector. It is found that the faster the hole rotates, the more accurate the measurements will be, with the uncertainty in the angular momentum decreasing rapidly with increasing rotation speed. The second study is an analysis of the gravitational collapse of an infinitely long, cylindrical dust shell, an idealization of more realistic, finite-length bodies. It is found that the collapse evolves into a naked singularity in finite time. Analytical expressions for the variables describing the collapse are found at late times, near the singularity. The collapse is also followed, with a numerical simulation, from the start until very close to the singularity. The singularity is found to be strong, in the sense that an observer riding on the shell will be infinitely stretched in one direction and infinitely compressed in another. The gravitational waves emitted from the collapse are also analyzed. The last study focuses on the consequences of the existence of closed time like curves in a worm hole space time. One might expect that such curves might cause a system with apparently well-posed initial conditions to have no self-consistent evolution. We study the case of a classical particle with a hard-sphere potential, focusing attention on initial conditions for which the evolution, if followed naively, is self-inconsistent: the ball travels to the past through the worm hole colliding with its younger self, preventing itself from entering the worm hole. We find, surprisingly, that for all such 'dangerous' initial conditions, there are an infinite number of self-consistent solutions. We also find that for many non-dangerous initial conditions, there also exist an infinity of possible evolutions. Author (revised)

N93-28747# IIT Research Inst., Bartlesville, OK.
THERMODYNAMIC PROPERTIES FOR POLYCYCLIC SYSTEMS BY NON-CALORIMETRIC METHODS
W. V. Steele, R. D. Chirico, and T. D. Klots Mar. 1993 15 p
(Contract DE-FG02-92ER-14288)
(DE93-011373; DOE/ER-14288/1) Avail: CASI HC A03/MF A01

A detailed vibrational spectroscopic study of furan, pyrrole, and thiophene has been completed. These compounds form part of the base of five-membered ring systems on which the rest of the research program will be built. Several methyl-substituted derivatives were also studied. The results will be used to confirm the model for alkyl-substitution in the ring systems. Gas-phase spectra and fundamental frequency assignments were completed for 2,3- and 2,5-dihydrofuran. Those compounds initiate work on ring-puckering within the research program. A paper describing the need for third virial estimation, when using the virial equation of state to derive thermodynamic properties at pressures greater than 1 bar was completed. DOE

N93-28933*# Eloret Corp., Palo Alto, CA.
PHOTODISSOCIATION OF HBr/LiF(001): A QUANTUM MECHANICAL MODEL
Tamar Seideman 1993 31 p
(Contract NCC2-737)
(NASA-CR-193119; NAS 1.26:193119) Avail: CASI HC A03/MF A01

The photodissociation dynamics of HBr adsorbed on a LiF(001) surface is studied using time-independent quantum mechanics. The photodissociation lineshape and the Br(P(sub 1/2)-2)/Br(P(sub 3/2)-2) yield ratio are computed and compared with the corresponding quantities for gas phase photodissociation. The angular distribution of the hydrogen photofragments following excitation of adsorbed HBr is computed and found to agree qualitatively with experimental data. The effect of polarization of the photon is illustrated and discussed. The field polarization is found to affect significantly the magnitude of the photodissociation signal but not the angular dependence of the photofragment distribution, in agreement with experiment and in accord with expectations for a strongly aligned adsorbed phase. Author (revised)

N93-28958# California Univ., Santa Barbara. Dept. of Physics.
NUMERICAL SIMULATION OF QUANTUM MANY-BODY SYSTEMS
D. J. Scalapino 1992 5 p
(Contract DE-FG03-85ER-45197)
(DE93-008300; DOE/ER-45197/T1) Avail: CASI HC A01/MF A01

Results for the single-particle density of states and the conductivity were obtained for both the attractive-and repulsive-U Hubbard models. At half-filling, the densities of states for both models are identical, but the gap for the attractive case arises from the formation of charge-density-wave and superconducting correlations, while for the repulsive-U Hubbard model the gap is the Mott-Hubbard gap and arises from the antiferromagnetic, Coulomb, correlations. Hubbard chains were studied by use of a generalization of Handscomb's quantum Monte Carlo scheme. Monte Carlo calculations of the two-particle vertex of the 2D repulsive-U Hubbard model were performed. Criteria for determining whether a system is insulating, metallic, or superconducting were investigated; it was found for lattice models (Hubbard, Holstein, etc.) that this is determined by the value of the current- function. DOE

N93-28961# Johns Hopkins Univ., Baltimore, MD. Dept. of Physics and Astronomy.
RESEARCH IN THEORETICAL PHYSICS
G. Domokos and S. Kovesi-Domokos Dec. 1992 52 p
(Contract DE-FG02-85ER-40211)
(DE93-008401; DOE/ER-40211/8) Avail: CASI HC A04/MF A01

Progress made in the following areas is summarized: simulation of extensive air showers induced by interactions existing beyond the currently accepted 'Standard Model' of elementary particle interactions; search for physics beyond the 'Standard Model' in gluonic inclusive decays of heavy quarks; obtaining limits on the applicability of the special theory of relativity; and an improved method of obtaining upper limits on the masses of primaries of extensive air showers associated with point sources in the sky. DOE

N93-28964# IIT Research Inst., Bartlesville, OK.
THE THERMODYNAMIC PROPERTIES OF THIANTHRENE AND PHENOXATHIIN
W. V. Steele, R. D. Chirico, S. E. Knipmeyer, and A. Nguyen Apr. 1993 47 p
(Contract DE-FC22-83FE-60149)
(DE93-000124; NIPER-659) Avail: CASI HC A03/MF A01

Measurements leading to the calculation of the ideal-gas thermodynamic properties are reported for thianthrene and phenoxathiin. Experimental methods included combustion calorimetry, adiabatic heat-capacity calorimetry, vibrating-tube densitometry, comparative ebulliometry, inclined-piston gauge manometry, and differential-scanning calorimetry (d.s.c.). Critical properties were estimated for both materials based on the measurement results. Entropies, enthalpies, and Gibbs energies of formation were derived for the ideal gas for both compounds for selected temperatures between 298.15 K and 700 K. The property-measurement results reported here for thianthrene and phenoxathiin provide the first experimental gas-phase Gibbs energies of formation for tricyclic diheteroatom-containing molecules. DOE

N93-29168*# Old Dominion Univ., Norfolk, VA. Dept. of Mechanical Engineering and Mechanics.

RADIATIVE INTERACTIONS IN MOLECULAR GASES UNDER LOCAL AND NONLOCAL THERMODYNAMIC EQUILIBRIUM CONDITIONS Progress Report, period ending 30 Apr. 1993

S. N. Tiwari and M. K. Jha Jun. 1993 257 p
(Grant NAG1-423)
(NASA-CR-193223; NAS 1.26:193223) Avail: CASI HC A12/MF A03

Basic formulations, analyses, and numerical procedures are presented to investigate radiative heat interactions in diatomic and polyatomic gases under local and nonlocal thermodynamic equilibrium conditions. Essential governing equations are presented for both gray and nongray gases. Information is provided on absorption models, relaxation times, and transfer equations. Radiative flux equations are developed which are applicable under local and nonlocal thermodynamic equilibrium conditions. The problem is solved for fully developed laminar incompressible flows between two parallel plates under the boundary condition of a uniform surface heat flux. For specific applications, three diatomic and three polyatomic gases are considered. The results are obtained numerically by employing the method of variation of parameters. The results are compared under local and nonlocal thermodynamic equilibrium conditions at different temperature and pressure conditions. Both gray and nongray studies are conducted extensively for all molecular gases considered. The particular gases selected for this investigation are CO, NO, OH, CO2, H2O, and CH4. The temperature and pressure range considered are 300-2000 K and 0.1-10 atmosphere, respectively. In general, results demonstrate that the gray gas approximation overestimates the effect of radiative interaction for all conditions. The conditions of NLTE, however, result in underestimation of radiative interactions. The method developed for this study can be extended to solve complex problems of radiative heat transfer involving nonequilibrium phenomena. Author (revised)

N93-29242# Tokyo Univ., Tanashi (Japan). Inst. for Nuclear Study.

BOREL SUM RULES FOR OCTET BARYONS IN NUCLEAR MEDIUM

Y. Kondo and O. Morimatsu Jun. 1992 13 p
(DE93-753245; INS-933) Avail: CASI HC A03/MF A01

Borel sum rules are examined for octet baryons in the nuclear medium. First, it is noticed that in the medium the dispersion relation is realized for the retarded correlation Pi(sup R)(omega, q(sup 2)) in the energy omega. Then, Pi(sup R)(omega, q(sup 2)) is split into even and odd parts of omega in order to apply the Borel transformation. The obtained Borel sum rules differ from those of previous works. The mass shifts of octet baryons are calculated in the leading order of the operator product expansion with linear density approximation for the condensates. It is found that both scalar and vector condensates of the quark field, (q-bar q) and (q(sup +)q), induce attraction to the octet baryons in the medium in contrast to the results of previous works. It is also found that absolute value of (delta)M(sub N) is greater than absolute value of (delta)M(sub Lambda) is greater than absolute value of (delta)M(sub Sigma) is approximately absolute value of (delta)M(sub Xi). The absolute values, however, turn out to be one order of magnitude larger than those empirically known if a Borel mass of around 1 GeV is used in the present approximation. DOE

N93-29384# Duke Univ., Durham, NC. Dept. of Mechanical Engineering and Materials Science.

CHAOS IN MECHANICAL SYSTEMS WITH ESPECIAL REFERENCE TO ROTORCRAFT AND MISSILES Final Report, 9 Feb. 1987 - 31 Aug. 1990

Earl H. Dowell Feb. 1993 5 p
(Contract DAAL03-87-K-0023)
(AD-A263703; ARO-23555.12-EG) Avail: CASI HC A01/MF A01

Work has focussed on the following topics using the buckled beam as prototypical generic system: (1) the effect of higher modes on the response of the buckled beam; (2) initial condition maps and their interpretation; (3) Lyapunov exponents (nonlinear eigenvalues) as a predictor of chaos; (4) necessary and sufficient conditions for chaos to occur; (5) systems with both positive and negative linear stiffness; (6) systems with nonlinear damping; (7) a (buckled) beam-tube with an internal flowing fluid; (8) a survey paper summarizing much of our work; (9) a buckled beam under a constant as well as oscillating transverse load; (10) a curved beam (or plate) held (on one side) against a rigid surface; (11) the development of'turbulence' in an aeroelastic system that is responding chaotically in many degrees of freedom; and (12) an experimental study of a simple prototypical system exhibiting sensitivity to initial conditions and chaos. Transl. by SCITRAN

N93-29428# Texas A&M Univ., College Station. Dept. of Chemical Engineering.

THERMODYNAMIC PROPERTIES OF NATURAL GAS MIXTURES Annual Report, 1 Jan. 1989 - 31 Dec. 1989

J. C. Holste and K. R. Hall Nov. 1992 22 p
(Contract GRI-5087-260-1449; RF Proj. 5696)
(PB93-162816) Avail: CASI HC A03/MF A01

The objective of the project is to provide PVT and calorimetric data for fluids and fluid mixtures which are components of natural gas or synthetic gas. Data collected on a pycnometer and a Burnett are presented. These data range from 225-350 K and from 0-70 MPa and include densities and virial coefficients. The fluids covered are a ternary mixture of methane, ethane and carbon dioxide; a binary mixture of methane and ethane; and two constructed standard reference gasses representative of natural gas in the USA. NTIS

N93-29794 Texas A&M Univ., College Station. Research Foundation.

THERMODYNAMIC PROPERTIES OF NATURAL GAS MIXTURES Final Report, 1 Feb. 1987 - 30 Sep. 1992

J. C. Holste and K. R. Hall Nov. 1992 149 p See also PB93-156818
Sponsored by Gas Research Inst. Limited Reproducibility: More than 20% of this document may be affected by microfiche quality
(Contract GRI-5087-260-1449)
(PB93-176162; GRI-93/0006) Avail: CASI HC A07

The development and application of high accuracy thermodynamic data and models for the natural gas industry is important in a number of applications. As better in situ fluid sensing technology develops, greater need will arise for high quality thermodynamic data to allow real time monitoring of changes occurring to the fluid. The application of the data in the gas industry covers a broad range and includes natural gas custody transfer, gas production and processing, compressed natural gas vehicles to name a few. Comprehensive data sets of high quality thermodynamic data covering the ranges of pressure and temperature required to meet all of the gas industry's applications are very rare. NTIS

N93-29806# California Univ., Berkeley. Lawrence Berkeley Lab.

UNDERSTANDING CONFORMAL FIELD THEORY THROUGH PARAFERMIONS AND CHERN SIMONS THEORY Ph.D. Thesis

S. A. Hotes 19 Nov. 1992 56 p
(Contract DE-AC03-76SF-00098)
(DE93-010452; LBL-33186) Avail: CASI HC A04/MF A01

Conformal field theories comprise a vast class of exactly solvable two dimensional quantum field theories. Conformal theories with an enlarged symmetry group, the current algebra symmetry, are a key ingredient to possible string compactification models. The following work explores a Lagrangian approach to these theories. In the first part of this thesis, a large class of conformal theories, the so-called coset models, are derived semi-classically from a gauged version of the Wess-Zumino-Witten functional. A non-local field transformation to the parafermionic field description is employed in the quantization procedure. Classically, these parafermionic fields satisfy non-trivial Poisson brackets, providing insight into the fractional spin nature of the conformal theory. The W-algebra symmetry is shown to appear naturally in this approach. In the second part of this thesis, the connection between the fusion algebra structure of Wess-Zumino-Witten models and the quantization of the Chern-Simons action on the torus is made explicit. The modular properties of the conformal model are also derived in this context, giving a natural demonstration of the Verlinde conjecture. The effects of background gauge fields and monopoles are also discussed. DOE

N93-30359 Waterloo Univ. (Ontario).
THERMODYNAMIC AND STRUCTURAL PROPERTIES OF METALLIC GLASSES AND SUPERCOOLED LIQUIDS Ph.D. Thesis
Dewei Qi 1991 177 p
(ISBN-0-315-72443-9) Avail: Univ. Microfilms Order No. DANN72443

It is demonstrated, both theoretically and numerically, that the Gibbs-Bogoliubov (GB) thermodynamic variational calculations, developed originally for equilibrium systems, can be applied to a metastable thermodynamic system provided the structure of the chosen reference system has the same main features as the metastable system under consideration. It appears that the Einstein model, which properly contains the basic glass characteristics, can be used as a reference system for metallic glasses and that the hard sphere model, which properly includes the basic liquid properties, can be used as a reference system for supercooled metallic liquids. The results for the thermodynamic quantities, calculated for the glass states of Mg3Ca7 and Al and for the supercooled liquid states of Mg3Ca7, Ti66V34, In, and V are in a good agreement with those of computer and laboratory experiments. Also, the investigation of the GB variational calculations for the behavior of the heat capacity at constant pressure for supercooled liquid Rb suggests that supercooled liquids can be divided into two regions: the undercooled region and the hypercooled region, in which the structure of the liquids may differ. Next, in order to study the topological structure of supercooled liquids and glasses, molecular-dynamics simulations with a damped force method are performed to model the liquids and glasses in a sample of 150 Mg atoms and 350 Ca atoms. The techniques of pair analysis and steepest descent minimization with the conjugate gradient method are used to analyze the structural properties for the supercooled liquids and glasses. Not only are the usual Frank-Kasper polyhedra with coordination number 14-16 and Bernal 'hole' polyhedra with coordination number 10 detected, but also fourteen other kinds of defective icosahedra are identified. Especially, the number of the defective icosahedra defined by eight 1551 pairs, two 1661 pairs and two 1441 pairs is greater than that of Frank-Kasper or that of Bernal polyhedra, and is next to the number of icosahedra. On average, 61 percent of the atoms are in icosahedra and 32 percent atoms are in defective icosahedra at T = 100 K. The correlation between the energies and populations of the different kinds of pairs is explained. These results strongly support the physical picture of liquids and glasses being a disordered, entangled array of +72 deg and -72 deg disclination lines in an icosahedral medium. Further, it is proved that W(sub 6). is a standard gauge of icosahedral order for a variety of defective icosahedra. Dissert. Abstr.

N93-30481# Washington Univ., Seattle. Dept. of Physics.
QUANTUM FIELD THEORY IN SPACES WITH CLOSED TIME-LIKE CURVES
D. G. Boulware 1992 51 p
(Contract DE-FG06-91ER-40614)
(DE93-010564; DOE/ER-40614/19) Avail: CASI HC A04/MF A01

Gott spacetime has closed timelike curves, but no locally anomalous stress-energy. A complete orthonormal set of eigenfunctions of the wave operator is found in the special case of a spacetime in which the total deficit angle is 27(pi). A scalar quantum field theory is constructed using these eigenfunctions. The resultant interacting quantum field theory is not unitary because the field operators can create real, on-shell, particles in the acausal region. These particles propagate for finite proper time accumulating an arbitrary phase before being annihilated at the same spacetime point as that at which they were created. As a result, the effective potential within the acausal region is complex, and probability is not conserved. The stress tensor of the scalar field is evaluated in the neighborhood of the Cauchy horizon; in the case of a sufficiently small Compton wavelength of the field, the stress tensor is regular and cannot prevent the formation of the Cauchy horizon. DOE

N93-30779# International Centre for Theoretical Physics, Trieste (Italy).
QUANTUM GROUP AND SYMMETRY OF THE HEAT EQUATION
P. K. Jha (Delhi Univ., India.) and K. C. Tripathy Jul. 1992 9 p
(DE93-607560; IC-92/163) Avail: CASI HC A02/MF A01 (US Sales Only)

The symmetry associated with the heat equation is re-examined using Lie's method. Under suitable choice of the arbitrary parameters in the Lie field, it is shown that the system exhibits SL(2,R) symmetry. On inspection of the q-analog of the principal solution, broadening of the Gaussian-flow curve when q is varied from 1 to 0.002 is found. The q-analog of the general solution predicts the existence of additional degeneracy. DOE

N93-30781# Joint Inst. for Nuclear Research, Dubna (USSR). Lab. of Computing Techniques and Automation.
APPROXIMATION FORMULAE FOR FUNCTIONAL INTEGRALS IN P(PHI)2-QUANTUM FIELD THEORY
Y. Y. Lobanov, O. V. Zejnalova, and E. P. Zhidkov 1991 22 p
(DE93-606067; JINR-E-11-91-352) Avail: CASI HC A03/MF A01 (US Sales Only)

The approximation formulas for functional integrals with Gaussian measure in P(Phi)(sub 2)-quantum field theory are constructed. The formulas are exact on a class of polynomial functionals. Under determined conditions, the convergence of approximations to the exact value of the integral is proved, and the speed of convergence is estimated. DOE

N93-30782# Joint Inst. for Nuclear Research, Dubna (USSR). Lab. of Theoretical Physics.
PHASE STRUCTURE OF THREE- AND FOUR-DIMENSIONAL PHI(EXP 4) FIELD THEORY
G. V. Efimov and S. N. Nedelko (Tomsk State Univ., USSR.) 1991 28 p
(DE93-606069; JINR-E-2-91-445) Avail: CASI HC A03/MF A01 (US Sales Only)

The strong coupling regime of g(phi)(exp 4) theory in space-time R(sup d), where d = 3 or 4, is investigated by the methods of canonical transformations and renormalization group theory. It is shown that the model describes a system symmetric under transformation phi approaches (-)phi both at small and large coupling constant g. Comparison with the case d = 2 shows a crucial influence of the renormalization structure on the theory of its phase structure. DOE

N93-30783# Joint Inst. for Nuclear Research, Dubna (USSR). Lab. of Theoretical Physics.
A COVARIANT FORM OF THE MAXWELL'S EQUATIONS IN FOUR-DIMENSIONAL SPACES WITH AN ARBITRARY SIGNATURE
I. Lukac 1991 22 p
(DE93-606070; JINR-E-2-91-448) Avail: CASI HC A03/MF A01 (US Sales Only)

The concept of duality in four-dimensional spaces with the arbitrary constant metric is strictly mathematically formulated. A covariant model for covariant and contravariant bivectors in this space, based on three four-dimensional vectors, is proposed. DOE

N93-30784# Joint Inst. for Nuclear Research, Dubna (USSR). Lab. of Theoretical Physics.
GEOMETRICAL APPROACH TO THE DYNAMICS OF A RELATIVISTIC STRING IN THE D-DIMENSIONAL MINKOWSKI SPACE
B. M. Barbashov and N. R. Shvetz (Moscow State Univ., Russia.) 1991 15 p
(DE93-606071; JINR-E-2-91-7) Avail: CASI HC A03/MF A01 (US Sales Only)

A geometrical method is considered for solving the boundary-value problem in the theory of a relativistic string with point masses at the ends in the D-dimensional pseudo-Euclidean space. The string world-surface is restricted by two curves, the world trajectories of the point masses, and is described in terms of the quadratic differential forms and the torsion vectors. The case D = 4 is considered in detail where the equations of the boundaries of the string surface become the Frenet equations. The choice of the constant second and third curvatures of the world trajectories, the latter being equal to zero, determines the world sheet of a relativistic string to be a helicoid, when appropriate transformations of global coordinates are made. The same result has been obtained in a space with D less than 4, but this requires a further estimate of the torsion vectors at the boundaries. DOE

N93-30786# Joint Inst. for Nuclear Research, Dubna (USSR). Lab. of Theoretical Physics.
BEYOND TWO DIMENSIONS
V. Tapia 1991 7 p
(DE93-606084; JINR-E-2-91-316) Avail: CASI HC A02/MF A01 (US Sales Only)

We show that the critical dimension, for which the symmetry group of a conformal field theory is infinite-dimensional, is equal to the rank of the metric of the base space. We prove our claim for fourth-rank metrics and show that the critical dimension is four. The symmetry group is Vir(+)Vir(+)Vir(+)Vir. DOE

N93-30796# Joint Inst. for Nuclear Research, Dubna (USSR). Lab. of Nuclear Problems.
QUANTUM-KINETIC GREEN FUNCTION AND MACROSCOPIC WAVE FUNCTION [KVANTOVO-KINETICHESKAYA FUNKTSIYA GRINA I MAKROSKOPICHESKAYA VOLNOVAYA FUNKTSIYA]
V. I. Lushchikov and A. E. Saveleva 1991 16 p In RUSSIAN
(DE93-606040; JINR-R-17-91-446) Avail: CASI HC A03/MF A01 (US Sales Only)

On the basis of Schroedinger equation, generalized to six-dimensional phase space and brought into correspondence with the hypothesis of the particle interaction with vacuum, the equations for quantum-kinetic Green function and macroscopic wave function are proposed. The quantum-kinetic Green function is found, which takes into account both the motion properties of a separate particle and the collective characteristics of the system. DOE

N93-30797# Joint Inst. for Nuclear Research, Dubna (USSR). Lab. of Theoretical Physics.
INTEGRALS OF MOTION ON THE GROUP OF INVARIANCE OF AN INTERVAL IN THREE-DIMENSIONAL SPACES [INTEGRALY DVIZHENIYA NA GRUPPE INVARIANTNOSTI INTERVALA TREKHMERNYKH PROSTRANSTV]
I. Lukac 1991 23 p In RUSSIAN
(DE93-606090; JINR-R-2-91-315) Avail: CASI HC A03/MF A01 (US Sales Only)

The six parametrical group of motion of three-dimensional spaces with arbitrary constant metric conserving the square of distance between two points (the group of invariance of an interval) is considered. The special attention is paid to the group of transformations of an arbitrary homogeneous three-dimensional quadric which is a subgroup of the group of invariance of an interval. The Riemann geometry of this group space is studied and its geometrical characteristics (metric, Riemann's and Ricci's tensors, curvature, etc.) are determined. The complete set of the integrals of motion on the group of invariance of an interval in three-dimensional spaces is found. The square of momentum, square of total angular momentum, helicity, and square of spin are induced in the set of observables. DOE

N93-30802# Academy of Sciences (USSR), Novosibirsk. Inst. Yadernoj Fiziki.
CHAOTIC QUANTUM SYSTEMS
B. V. Chirikov 1991 58 p Presented at the 10th International Congress on Mathematical Physics, Leipzig, Germany, 1991
(DE93-606030; IYaF-91-83) Avail: CASI HC A04/MF A01 (US Sales Only)

The overview of recent developments in the theory of quantum chaos is presented with the special emphasis on a number of unsolved problems and current apparent contradictions. The relation between dynamical quantum chaos and statistical random matrix theory is discussed. DOE

N93-30803# Academy of Sciences (USSR), Novosibirsk. Inst. Yadernoj Fiziki.
SCALING PROPERTIES OF LOCALIZED QUANTUM CHAOS
F. M. Izrailev 1991 23 p
(DE93-606031; IYaF-91-97) Avail: CASI HC A03/MF A01 (US Sales Only)

Statistical properties of spectra and eigenfunctions are studied for the model of quantum chaos in the presence of dynamical localization. Mainly, attention is paid to the scaling properties of localization length and level spacing distribution in the intermediate region between Poissonian and Wigner-Dyson statistics. It is shown that main features of such localized quantum chaos are well described by the introduced ensemble of band random matrices. DOE

N93-30804# Joint Inst. for Nuclear Research, Dubna (USSR). Lab. of High Energy.
MODERN APPROACH TO RELATIVITY THEORY (RADAR FORMULATION)
V. N. Streltsov 1991 7 p
(DE93-606032; JINR-D-2-91-436) Avail: CASI HC A02/MF A01 (US Sales Only)

The main peculiarities of the radar formulation of the relativity theory are presented. This formulation operates with the retarded (light) distances and relativistic or radar length introduced on their basis. DOE

N93-30805# Joint Inst. for Nuclear Research, Dubna (USSR). Lab. of Theoretical Physics.
ON TWO-DIMENSIONAL QUASICLASSICS
M. P. Balandin and L. G. Zastavenko 1991 11 p
(DE93-606034; JINR-E-2-91-133) Avail: CASI HC A03/MF A01 (US Sales Only)

Quasiclassical limit of the two-dimensional Schroedinger equation is studied. Potential is supposed to weakly depend on the azimuthal angle. Behavior of the quasiclassical wave function in a vicinity of the turning curve is considered. DOE

N93-30806# Joint Inst. for Nuclear Research, Dubna (USSR). Lab. of Nuclear Reactions.
ON THE IMPOSSIBILITY OF CREATING THE QUANTUM CORRELATIONS WITH COMPUTERS
M. Vinduska 1991 15 p
(DE93-606039; JINR-E-5-91-485) Avail: CASI HC A03/MF A01 (US Sales Only)

It is indicated that Feynman's proof about the impossibility of creating the quantum correlations with computers does not hold if the general transformations of the probability measure of the treated systems does not hold for a group. The consequences of this fact are considered in relation to the Bell inequalities and to the models of relative probability measure on the concave surfaces. DOE

N93-30807# International Centre for Theoretical Physics, Trieste (Italy).
ELECTRIC MAGNETIC DUALITY IN STRING THEORY
A. Sen Jul. 1992 16 p
(DE93-606061; IC-92/171; TIFR-TH-92-41) Avail: CASI HC A03/MF A01 (US Sales Only)

The electric-magnetic duality transformation in four dimensional heterotic string theory discussed by Shapere, Trivedi, and Wilczek is shown to be an exact symmetry of the equations of motion of low energy effective field theory even after including the scalar and the vector fields, arising due to compactification, in the effective field theory. Using this duality transformation we construct rotating black hole solutions in the effective field theory carrying both electric and magnetic charges. The spectrum of extreme magnetically charged black holes turn out to be similar to that of electrically charged elementary string excitations lying on the leading Regge trajectory. We also discuss the possibility that the duality symmetry is an exact symmetry of the full string theory under which electrically charged elementary string excitations get exchanged with magnetically charged soliton like solutions. This proposal might be made concrete following the suggestion of Dabholkar et. al. that fundamental strings may be regarded as soliton like classical solutions in the effective field theory. DOE

N93-30808# International Centre for Theoretical Physics, Trieste (Italy).
THE GROUND STATE WAVEFUNCTIONS OF A CONFORMALLY INVARIANT SCALAR FIELD IN DIFFERENT SPACETIME BACKGROUND
Y. Anini Jul. 1992 17 p
(DE93-606063; IC-92/184) Avail: CASI HC A03/MF A01 (US Sales Only)

We carefully construct the ground state wavefunction of a conformally invariant scalar field as an Euclidean path integral over real field configurations that vanish at the past end point of Euclidean time. We consider two Euclidean spacetime backgrounds. The compact without boundary, i.e., a 4-sphere, and the asymptotically flat, i.e., a wormhole spacetime. Finally, we show that the analytic continuation of these states to the corresponding Lorentzian spacetime satisfy the time-dependent Schroedinger equation with proper choice of the pre-factor for the wavefunction. DOE

N93-30884# California Univ., San Diego, La Jolla. Inst. for Pure and Applied Physical Sciences.

KNOT INVARIANTS AND CELLULAR AUTOMATA Final Technical Report, 1 Oct. 1990 - 30 Sep. 1991

David A. Meyer 4 May 1993 7 p

(Contract N00014-91-J-1512)

(AD-A264199) Avail: CASI HC A02/MF A01

The goal of this project was to build on an understanding of the connections between knot invariants, exactly solvable statistical mechanics models, and discrete dynamical systems toward an answer to the question of how early and robust thermodynamic behavior appears in lattice gas automata. Preliminary work focussed on developing an understanding of state models in knot theory and their relation to statistical mechanics models. Rather than considering the complicated and somewhat more difficult case of lattice gas hydrodynamics, the researcher began with a simpler model: a reversible cellular automaton in one dimension. This particular automaton has an additive conserved quantity which has been used to construct a one dimensional statistical mechanics model. He observes in simulations that the cellular automaton displays thermodynamic behavior which is well described by this one dimensional statistical mechanics model. In previous works it was shown that there is a naturally associated two dimensional statistical mechanics model as well, then examined the properties of this model, and suggested how these properties may relate to the behavior of the dynamical cellular automaton. DTIC

N93-30916# Moscow State Univ. (Russia). Nauchno-Issledovatel'skij Inst. Yadernoj Fiziki.

A SIMPLE FORMULA FOR REDUCING FEYNMAN DIAGRAMS TO SCALAR INTEGRALS

A. I. Davydychev 1991 12 p

(DE92-644717; INP-MSU-91-10-214; NIIYaF-MGU-91-10-214) Avail: CASI HC A03/MF A01 (US Sales Only)

An explicit general formula is obtained which makes it possible to reduce tensor Feynman integrals (corresponding to arbitrary one-loop N-point diagrams) to scalar integrals. DOE

N93-30920# International Centre for Theoretical Physics, Trieste (Italy).

QUANTUM GROUP GENERALIZATION OF THE HETEROTIC QFT

J. L. MatheusValle and M. A. R. Monteiro (Centro Brasileiro de Pesquisas Fisicas, Rio de Janeiro.) Jul. 1992 13 p

(DE92-644727; IC-92/138) Avail: CASI HC A03/MF A01 (US Sales Only)

Using the generalized Grassmann algebra provided by Quantum Groups, we introduce a new class of fields in two dimensions which have deformed commutation relations. We give the action involving this new class of fields and a bosonic scalar field and show that this action has a symmetry that resembles supersymmetry. We also construct the path-integral formalism for this new class of fields and compute the propagator for them in the context of the q-heterotic model. DOE

N93-30921# International Centre for Theoretical Physics, Trieste (Italy).

ABELIAN GAUGE THEORIES ON HOMOGENEOUS SPACES

D. V. Vassilevich Jul. 1992 9 p

(DE92-644730; IC-92/149) Avail: CASI HC A02/MF A01 (US Sales Only)

An algebraic technique of separation of gauge modes in Abelian gauge theories on homogeneous spaces is proposed. An effective potential for the Maxwell-Chern-Simons theory on S(sup 3) is calculated. A generalization of the Chern-Simons action is suggested and analyzed with the example of SU(3)/U(1) x U(1). DOE

N93-30924# Joint Inst. for Nuclear Research, Dubna (USSR). Lab. of Theoretical Physics.

INVARIANT STRUCTURES IN GAUGE THEORIES AND CONFINEMENT

L. V. Prokhorov (Leningrad State Univ., USSR.) and S. V. Shabanov 1991 20 p Submitted for publication

(DE92-644739; JINR-E-2-91-195) Avail: CASI HC A03/MF A01 (US Sales Only)

The problem of finding all gauge invariants is considered in connection with the problem of confinement. Polylocal gauge tensors are introduced and studied. It is shown (both in physical and pure geometrical approaches) that the path-ordered exponent is the only fundamental bilocal gauge tensor, which means that any irreducible polylocal gauge tensor is built of P-exponents and local tensors (matter fields). The simplest invariant structures in electrodynamics, chromodynamics, and a theory with the gauge group SU(2) are considered separately. DOE

N93-30925# Joint Inst. for Nuclear Research, Dubna (USSR). Lab. of Theoretical Physics.

INVARIANT STRUCTURES AND STATIC FORCES IN GAUGE THEORIES

L. V. Prokhorov (Leningrad State Univ., USSR.) and S. V. Shabanov 1991 12 p

(DE92-644740; JINR-E-2-91-266) Avail: CASI HC A03/MF A01 (US Sales Only)

The problem of finding all gauge invariants is considered in connection with confinement. It is shown that any gauge invariant may be built of the exponential line integrals (strings) and local gauge group tensors. The Coulomb field structure is analyzed from this point of view. In the pure SU(n) gauge theory (no matter), a potential of interacting static sources is found to be linearly rising with distance. DOE

N93-30932# Weizmann Inst. of Science, Rehovoth (Israel).

TOPOLOGY AND STATISTICS IN ZERO DIMENSIONS

Charilaos Aneziris May 1992 26 p

(DE93-604080; WIS-PH-92-38) Avail: CASI HC A03/MF A01 (US Sales Only)

It has been suggested that space-time may be intrinsically incontinuous, but discrete. We review some topological notions of discrete manifolds, in particular, ones made out of a final number of points. We also discuss the possibilities for statistics in such spaces. DOE

N93-30933# Weizmann Inst. of Science, Rehovoth (Israel).

REGULAR AND CHAOTIC MOTION OF TWO DIMENSIONAL ELECTRONS IN A STRONG MAGNETIC FIELD

Oded Bar-Lev and Shimon Levit May 1992 14 p

(DE93-604091; WIS-PH-92-45) Avail: CASI HC A03/MF A01 (US Sales Only)

For two dimensional system of electrons in a strong magnetic field, a standard approximation is the projection on a single Landau level. The resulting Hamiltonian is commonly treated semiclassically. An important element in applying the semiclassical approximation is the integrability of the corresponding classical system. We discuss the relevant integrability conditions and give a simple example of non-integrable system-two interacting electrons in the presence of two impurities-which exhibits a coexistence of regular and chaotic classical motions. Since the inverse of the magnetic field plays the role of the Planck constant in these problems, one has the opportunity to control the 'closeness' of chaotic physical systems to the classical limit. DOE

N93-30943# Instituto de Fisica Teorica, Sao Paulo (Brazil).

GENERAL METHOD FOR REDUCING THE TWO-BODY DIRAC EQUATION

A. P. Galeao and P. L. Ferreira 1992 27 p

(DE93-609833; IFT-P-004/92) Avail: CASI HC A03/MF A01 (US Sales Only)

A semirelativistic two-body Dirac equation with an enlarged set of phenomenological potentials, including Breit-type terms, is investigated for the general case of unequal masses. Solutions corresponding to definite total angular momentum and parity are shown to fall into two classes, each one being obtained by solving a system of four coupled first-order radial differential equations. The reduction of each of these systems to a pair of coupled Schroedinger-type equations is also discussed. DOE

N93-30945# Instituto de Fisica Teorica, Sao Paulo (Brazil).

A SQUEEZED STATE HOLOMORPHIC PHASE SPACE REPRESENTATION OF EQUATIONS OF MOTION

D. Galetti and J. S. Veiga Aug. 1992 21 p
(DE93-609835; IFT-P-031/92) Avail: CASI HC A03/MF A01 (US Sales Only)

A mapping scheme is presented which takes quantum operators associated to bosonic degrees of freedom into complex phase space integral kernel representatives. The procedure consists in using the Schroedinger equation sqeezed state as the starting point for the construction of the integral mapping kernel which, due to its inherent structure, is suited for the description of second quantized operators. Products and commutators of operators have their representatives explicitly written which reveal new details when compared to the usual q-p phase space description. The classical limit of the equations of motion for the canonical pair q-p is discussed in connection with the effect of sqeezing the quantum phase space cellular structure. DOE

N93-30983# Joint Inst. for Nuclear Research, Dubna (USSR). Lab. of High Energy.
RELATIVITY THEORY IN (2 + 2)-SPACE
V. N. Streltsov 1991 10 p
(DE92-644671; JINR-E-2-91-97) Avail: CASI HC A02/MF A01 (US Sales Only)

The formulation is discussed of relativity theory in noneuclidean space defined by the metric form d(tau)(sup 2) = dx(sup 1)dx(sup 2) + dx(sup 3)dx(sup 4). As is noted, in the particular case of (1+1) dimensions new variables x(sup 1) = t - z and x(sup 2) = t + z are quantities directly observed by the radar method which is used to define the concept of simultaneity and distance. The transition to them significantly simplifies (special) Lorentz transformations, the 'addition' theorem of velocities and so on. DOE

N93-30987# International Centre for Theoretical Physics, Trieste (Italy).
FORMULATION OF WAVE MECHANICS WITHOUT THE PLANCK CONSTANT h/2 PI
A. O. Barut Jul. 1992 4 p
(DE93-604083; IC-92/169) Avail: CASI HC A01/MF A01 (US Sales Only)

Quantum mechanics can be formulated without the parameters (h/2(pi)), m and e as a pure wave theory in terms of the frequencies alone. This is more directly related to experiments where one measures frequency differences rather than energies. Different quantum systems are then characterized by an intrinsic proper frequency omega(sub 0). DOE

N93-31003# International Centre for Theoretical Physics, Trieste (Italy).
THE GEOMETRY OF COMPLEX SPACE-TIMES WITH TORSION
G. Esposito May 1992 5 p
(DE92-641343; IC-92/80) Avail: CASI HC A01/MF A01 (US Sales Only)

The necessary and sufficient condition for the existence of alpha-surfaces in complex space-time manifolds with nonvanishing torsion is derived. For these manifolds, Lie brackets of vector fields with spinor Ricci identities contain explicitly the effects of torsion. This leads to an integrability condition for alpha-surfaces which does not involve just the self-dual Weyl spinor, as in complexified general relativity, but also the torsion spinor, in a nonlinear way, and its covariant derivative. A similar result also holds for four-dimensional, smooth real manifolds with a positive-definite metric. Interestingly, a particular solution of the integrability condition is given by right-flat and right-torsion-free space-times. DOE

80 SOCIAL SCIENCES (GENERAL)

Includes educational matters.

N93-29396# Research and Development Labs., Culver City, CA.
SUMMER RESEARCH PROGRAM (1992). HIGH SCHOOL APPRENTICESHIP PROGRAM (HSAP) REPORTS. VOLUME 16: ARNOLD ENGINEERING DEVELOPMENT CENTER CIVIL ENGINEERING LABORATORY Annual Report, 1 Sep. 1991 - 31 Aug. 1992
Gary Moore 28 Dec. 1992 227 p
(Contract F49620-90-C-0076)
(AD-A262024; AFOSR-93-0126TR-Vol-16) Avail: CASI HC A11/MF A03

The following reports were completed during the Air Force 1992 Summer Research Program: Graphics Library Routines for ETF Analysis Software; Visualization of Quantum Chemical Calculations for Molecules; Development of a Versatile Spreadsheet for Estimating Electrical Power and Operating Hours for AEDC's Tunnel 16T; Calibration and Application of a Spectrapro(Trademark)-275 Spectrometer; A Study of the Continuous Monitoring Station at Arnold Engineering Development Center; and Comparison of the HNU 311 Portable and Hewlett Packard 5890 Series 2 Gas Chromatographs. DTIC

N93-29440# Research and Development Labs., Culver City, CA.
SUMMER FACULTY RESEARCH PROGRAM (SFRP), VOLUME 1 Annual Report, 1 Sep. 1991 - 31 Aug. 1992
Gary Moore 28 Dec. 1992 578 p
(Contract F49620-90-C-0076)
(AD-A261988; AFOSR-93-0110TR-Vol-1) Avail: CASI HC A25/MF A06

The purpose of this program is to develop the basis for continuing research of interest to the Air Force at the institution of the faculty member; to stimulate continuing relations among faculty members and professional peers in the Air Force; to enhance the research interests and capabilities of scientific and engineering educators; and to provide follow-on funding for research of particular promise that was stated at an Air Force laboratory under the Summer Faculty Research Program. The following reports were submitted during the 1992 Air Force Summer Research program: Solar Detoxification of Contaminated Groundwater; Description of Weather Station and Its Datalogging Program; Computer Programs and Project Operations; Robotic Excavation: Lunar and Earth Based; and HSAP Summer Apprenticeship Program. DTIC

N93-30134*# National Aeronautics and Space Administration, Washington, DC.
THE 1992 TOWN MEETINGS: TOWARD A SHARED VISION
Apr. 1993 65 p
(NASA-NP-205; NAS 1.83:205) Avail: CASI HC A04/MF A01

With the goal of developing a shared vision for the future of NASA, the U.S. civil aeronautics and space agency conducted a series of town meetings across the country in Nov. and Dec. 1992. Specifically, NASA sought comment on the Agency's new vision statement and mission values, which were developed by the Agency's employees in an effort to redefine NASA's priorities and purpose for the 1990's and beyond. In practice, the meetings constituted a sort of nationwide brainstorming session on how to make aeronautics and space research more relevant to people's daily lives. Primary findings, NASA's action plan, town meeting proceedings, and conclusions are described. Derived from text

N93-30657# Office of Technology Assessment, Washington, DC.
PROFILES OF MAJOR FEDERAL LITERACY PROGRAMS
N. Kober Jul. 1992 79 p
(PB93-163863) Avail: CASI HC A05/MF A01

The bulk of Federal funding for adult literacy, as well as the most significant Federal policy guidance, comes from a group of programs that have the following characteristics: have adult literacy or basic skills education as their sole purpose or as one of a limited number of primary purposes; explicitly authorize literacy or basic skills education as a primary means of achieving a related purpose, such as job training or American citizenship; or through Departmental directive, have taken on significant new literacy missions, such as the Head Start family literacy programs. The programs constitute the core of the Federal role in adult education. Together they provide a starting point for understanding the nature, themes, and breadth of the Federal contribution to adult literacy education. NTIS

N93-30821# Department of Education, Washington, DC. Office of Educational Research and Improvement.
FILLING THE GAPS: AN OVERVIEW OF DATA ON EDUCATION IN GRADES K THROUGH 12
S. A. Bobbitt, P. Quinn, and P. Dabbs Nov. 1992 68 p
(PB93-176550; NCES-92-132) Avail: CASI HC A04/MF A01

The elementary/secondary education data collection system has undergone a major transformation over the course of the past decade. From a very limited universe data collection, supplemented with irregular and noncomparable sample surveys, it has developed into a coordinated, cohesive system with the following: (1) State, district, and public and private school universe components; (2) a regularly collected sample survey component with linkable data from districts, schools, principals, and teachers; (3) a student-based longitudinal studies component designed to explore the effects of school processes on student outcomes; (4) a household-based survey component, to address those issues such as early childhood and adult education which are difficult to assess through institution-based surveys; (5) a 'fast response' survey component, designed to provide timely data to inform current policy concerns; and (6) an assessment component in selected subjects at grades 4, 8, and 12. NTIS

N93-30958*# Norfolk State Univ., VA.
MATERIALS EDUCATION ACTIVITIES
Heidi R. Ries, Jonice Harris (National Inst. of Standards and Technology, Gaithersburg, MD.), Woodrow W. Leake (American Society for Engineering Education, Washington, DC.), L. Roy Bunnell (Battelle Pacific Northwest Labs., Richland, WA.), and Robert Berrettini (Materials Research Society, University Park, PA.) *In* NASA. Langley Research Center, National Educators' Workshop. Update 92: Standard Experiments in Engineering Materials Science and Technology Jun. 1993 p 193-196 (For primary document see N93-30948 11-23)
Avail: CASI HC A01/MF A04

N93-30971*# Loyola Coll., Baltimore, MD. Dept. of Engineering.
EXPERIMENTS IN MATERIALS SCIENCE FROM HOUSEHOLD ITEMS
F. Xavier Spiegel *In* NASA. Langley Research Center, National Educators' Workshop. Update 92: Standard Experiments in Engineering Materials Science and Technology Jun. 1993 p 371-375 (For primary document see N93-30948 11-23)
Avail: CASI HC A01/MF A04

N93-30975*# New Mexico Univ., Albuquerque. Dept. of Mechanical Engineering.
TAGUCHI METHOD OF EXPERIMENTAL DESIGN IN MATERIALS EDUCATION
Martin W. Weiser *In* NASA. Langley Research Center, National Educators' Workshop. Update 92: Standard Experiments in Engineering Materials Science and Technology Jun. 1993 p 403-414 (For primary document see N93-30948 11-23)
Avail: CASI HC A03/MF A04

81 ADMINISTRATION AND MANAGEMENT

Includes management planning and research.

N93-28985# Industrial Coll. of the Armed Forces, Washington, DC.
PRODUCTIVITY MEASUREMENT IN SCIENCE AND TECHNOLOGY CONTRACTING Research Report, Aug. 1991 - Apr. 1992
Thomas W. Mahler, Jr. Apr. 1992 29 p
(AD-A262077; NDU-ICAF-92-S60) Avail: CASI HC A03/MF A01

This paper demonstrates the feasibility of using traditional productivity measurement techniques to analyze the productivity of Science and Technology (S and T) contracting offices. S and T contracting offices are usually associated with the research laboratories of the Armed Services. It is important that these offices operate efficiently because current national security strategy emphasizes research as the primary means of maintaining technological superiority. The author argues that simple, partial measures of productivity are the only practical tools for measuring the productivity of S and T contracting offices. The author develops a simple productivity measurement technique that is based-on similar techniques used in industry. The technique is then demonstrated using real world data from the Air Force's Wright Laboratory contracting office. DTIC

N93-29142# Defense Systems Management School, Fort Belvoir, VA.
THE PROGRAM MANAGER'S NOTEBOOK
Jun. 1992 473 p
(AD-A263074) Avail: CASI HC A20/MF A04

This notebook is designed to provide system acquisition participants, particularly program managers, with a ready reference document which contains basic information and a reference list on selected subject areas of interest or concern to them. The fact sheets are designed to provide (1) Ready reference to quickly brush up on a topic without searching through lengthy reports, studies or articles; (2) Essential summarized guidance for performance of functions or preparation of documents in the selected subject areas; (3) Succinct summations of DOD and, if appropriate, service philosophy and policy regarding acquisition subject areas. DTIC

N93-29322*# National Aeronautics and Space Administration, Washington, DC.
THE NASA SBIR PRODUCT CATALOG
J. A. Gilman (Futron Corp., Bethesda, MD.), J. B. Paige (Futron Corp., Bethesda, MD.), and F. Carl Schwenk (Futron Corp., Bethesda, MD.) Oct. 1992 99 p
(NASA-TM-108242; NAS 1.15:108242) Avail: CASI HC A05/MF A02

The purpose of this catalog is to assist small business firms in making the community aware of products emerging from their efforts in the Small Business Innovation Research (SBIR) program. It contains descriptions of some products that have advanced into Phase 3 and others that are identified as prospective products. Both lists of products in this catalog are based on information supplied by NASA SBIR contractors in responding to an invitation to be represented in this document. Generally, all products suggested by the small firms were included in order to meet the goals of information exchange for SBIR results. Of the 444 SBIR contractors NASA queried, 137 provided information on 219 products. The catalog presents the product information in the technology areas listed in the table of contents. Within each area, the products are listed in alphabetical order by product name and are given identifying numbers. Also included is an alphabetical listing of the companies that have products described. This listing cross-references the product list and provides information on the business activity of each firm. In addition, there are three indexes: one a list of firms by states, one that lists the products according to NASA Centers that managed the SBIR projects, and one that lists the products by the relevant Technical Topics utilized in NASA's annual program solicitation under which each SBIR project was selected.
Derived from text

N93-29323*# National Aeronautics and Space Administration, Washington, DC.
NASA SBIR ABSTRACTS OF 1991 PHASE 1 PROJECTS
F. Carl Schwenk (Futron Corp., Bethesda, MD.), J. A. Gilman (Futron Corp., Bethesda, MD.), and J. B. Paige (Futron Corp., Bethesda, MD.) Sep. 1992 133 p
(NASA-TM-108240; SBIR-91-2; NAS 1.15:108240) Avail: CASI HC A07/MF A02

The objectives of 301 projects placed under contract by the Small Business Innovation Research (SBIR) program of the National Aeronautics and Space Administration (NASA) are described. These projects were selected competitively from among proposals submitted to NASA in response to the 1991 SBIR Program Solicitation. The basic document consists of edited, non-proprietary abstracts of the winning proposals submitted by small businesses. The abstracts are presented under the 15 technical topics within which Phase 1 proposals were solicited. Each project was assigned a sequential identifying number from 001 to 301, in order of its appearance in the body of the report. Appendixes to provide additional information about the SBIR program and permit cross-reference of the 1991 Phase 1 projects by company name, location by state, principal investigator, NASA Field Center responsible for management of each project, and NASA contract number are included. Author (revised)

N93-29433# Naval Postgraduate School, Monterey, CA.
THE IDENTIFICATION OF EARLY WARNING SIGNALS PRIOR TO CONTRACTOR DEFAULT M.S. Thesis
Roch A. Switlik 17 Dec. 1992 101 p
(AD-A262828) Avail: CASI HC A06/MF A02

The purpose of this thesis was to investigate the contract administration process, during contract performance, prior to the point at which a termination for default (TFD) decision is made. The objective of this thesis was to determine if there are systemic indicators that may provide early warning signals to contract administrators, during performance of the contract, that the contractor may fail in complying with the contractual obligations, thus being TFD. This research was limited to Fixed-Price Supply-type contracts. The data for this research were obtained through literature research, telephone interviews, and survey questionnaires conducted with various Defense Logistics Agency organizations. This thesis concluded by providing a Performance Indicator Management Model, developed by the researcher, based upon the data obtained from this research. This model focuses on the major areas of contract performance, monitored by contract administrators and provides the most effective indicators, which provide advance warning of contractor difficulty that may lead to default. DTIC

N93-29499# Institute for Defense Analyses, Alexandria, VA.
A PERSPECTIVE ON ACQUISITION OF NASA SPACE SYSTEMS Final Report, Oct. 1991 - Dec. 1992
J. R. Nelson, Karen W. Tyson, and Daniel M. Utech Dec. 1992 82 p
(AD-A263246; IDA-D-1224; IDA/HQ-92-42612) Avail: CASI HC A05/MF A01

The purpose of the work documented in this annotated briefing was for IDA to understand NASA's unique acquisition process (as opposed to DoD's), develop preliminary outcomes for space-related programs in terms of cost and schedule growth, and explore issues related to improving methods for estimating costs and schedules of space acquisition programs. IDA's initial findings concerning cost and schedule outcomes for NASA programs over the past thirty years show that manned programs generally show more cost growth then unmanned programs and high schedule growth is associated with high cost growth. Overall, NASA space programs have demonstrated enormous technical success; however, these successes take considerably more time and money than comparable DoD programs. DTIC

N93-29649# Office of Technology Assessment, Washington, DC.
DEFENSE CONVERSION: REDIRECTING RESEARCH AND DEVELOPMENT
May 1993 244 p Original contains color illustrations
(OTA-ITE-552; ISBN-0-16-041779-1) Avail: CASI HC A11/MF A03; SOD HC

Defense conversion means finding productive civilian uses for the resources and people formerly devoted to the Nation's defense. Channeling the savings from reduced defense R&D to civilian R&D is, of course, only one option for using the peace dividend. There are many others, including deficit reduction. This Report examines opportunities to advance civilian technologies and improve U.S. industrial competitiveness internationally by redirecting research and development from defense to dual-use or civilian purposes. The Report has two parts. Part One analyzes how R&D institutions currently pursuing defense missions could be more responsive and useful to civilian technology development. Part Two of the Report examines how proposals for new national missions might replace defense in contributing to the country's repository of technology, high-value-added jobs, and gross domestic product. Author (revised)

N93-29970# Carnegie-Mellon Univ., Pittsburgh, PA. Software Engineering Inst.
KEY PRACTICES OF THE CAPABILITY MATURITY MODEL, VERSION 1.1 Final Report
Mark C. Paulk, Charles V. Weber, Suzanne M. Garcia, Mary B. Chrissis, and Marilyn Bush Feb. 1993 499 p
(Contract F19628-90-C-0003)
(AD-A263432; CMU/SEI-93-TR-25; ESC-TR-93-178) Avail: CASI HC A21/MF A04

The key practices that correspond to each maturity level of the Capability Maturity Model (CMM) and information on how to interpret the key practices are provided. It is an elaboration of what is meant by maturity at each level of the CMM and a guide that can be used for software process improvement, software process assessments, and software capability evaluations. DTIC

N93-30124# Carnegie-Mellon Univ., Pittsburgh, PA.
INTELLIGENT SUPPORT FOR HUMAN COMPUTER INTERACTION AND DECISION-MAKING IN DISTRIBUTION PLANNING AND SCHEDULING SYSTEMS Final Report, 30 Sep. 1991 - 31 Dec. 1992
Steven F. Roth and Stephen F. Smith 28 Feb. 1993 12 p
(Contract DAAL03-90-G-0328)
(AD-A263985; ARO-29354.3-MA) Avail: CASI HC A03/MF A01

Research was conducted on two areas related to computer support for decision-making and analysis in complex domains, with a focus on distribution and transportation planning in the Army. The work addressed frameworks and tools for human-computer interaction in systems involving large amounts of diverse information and development of decision making models. Research on human-computer interaction involved: (1) dynamic display generation for information with more complex structure than previously addressed, including encoding new knowledge of graphic design for this data and more complex graphic styles, and (2) design and integration of new interactive data exploration and analysis tools. DTIC

N93-30158# Naval War Coll., Newport, RI.
MANAGING OPERATIONAL INTELLIGENCE OVERLOAD: GUIDELINES FOR AVOIDING DECISION PARALYSIS Final Report, 15 Nov. 1992 - 2 Feb. 1993
Wendy L. Lichtenstein 18 Jun. 1993 32 p
(AD-A264184) Avail: CASI HC A03/MF A01

This paper presents guidelines to help the operational commander reduce the risk of intelligence overload which can cause delays in making decisions. A brief review of history shows that technological advancements have increased the reliability and usefulness of intelligence. But technology has not replaced the human factor in intelligence work and command. In fact, technology is not a panacea. Instead, developments may actually contribute to intelligence overload. Additionally, certain factors in today's military planning and execution environment increase the risk of overload. Therefore, practical, management-oriented guidelines are presented which highlight the human factor and emphasize command, not dependence on technology. DTIC

N93-30177# RJO Enterprises, Inc., Dayton, OH.
AIR FORCE CALS BUSINESS PRACTICES
20 Apr. 1993 166 p
(Contract F33657-92-D-2171)
(AD-A264789; RJO-93-7091-ILS) Avail: CASI HC A08/MF A02

The purpose of this report is to document lessons learned as a result of the current budget cycle so that the business process for future budget cycles can be improved at the Air Force CALS Program Office. This effort was limited to an analysis of documentation previously prepared for various budget activities/exercises at the Air Force CALS Program Office. DTIC

N93-30644*# National Aeronautics and Space Administration, Washington, DC.
HOW TO COMPETE FOR NASA CONTRACTS
Aug. 1989 50 p Original contains color illustrations
(NASA-TM-109238; NAS 1.15:109238) Avail: CASI HC A03/MF A01; 1 functional color page

Various studies and NASA experience have found that business concerns can provide a vital and significant impetus to technological innovation, not only in the fields of space and aeronautics, but also in national technological growth. NASA personnel are determined to foster the development of small business capabilities in technical areas that will support future projects and establish a small business base for the development and production of flight hardware for future missions. The solicitation process for Federal contracts has grown quite complex over the years. Where possible, we continue to try to simplify and streamline procedures for obtaining and performing these contracts. This booklet is designed to help understand NASA solicitations, find the information needed in deciding whether to respond, and improve chances for success. The first section of this booklet will answer general questions concerning the various types of NASA solicitations. Your specific questions on how to prepare bids will be answered in the second section, which is followed by a third section on the unique features of construction contracting. A fourth section describes how to submit technical and cost proposals for the negotiated procurement process. Some tips or suggestions, called DO's and DONT's, are placed at the end of the second, third, and fourth sections. Then, in the fifth section, ways to seek business as a subcontractor are identified. Author (revised)

N93-30822# National Inst. of Standards and Technology, Gaithersburg, MD. Office of Standards Services.
PROCEEDINGS OF THE MEETING OF THE INTERGOVERNMENTAL US-RUSSIAN BUSINESS DEVELOPMENT COMMITTEE'S STANDARDS WORKING GROUP
S. I. Warshaw Apr. 1993 303 p Conference held in Gaithersburg, MD, 23-24 Mar. 1993
(PB93-179968; NISTIR-5166) Avail: CASI HC A14/MF A03

The 1992 U.S.-Russia Summit in Washington DC, marked the beginning of a new commercial relationship between the United States and Russia.

Additionally, the U.S. Secretary of Commerce and the Russian Minister of Foreign Economic Relations established an 'Intergovernmental U.S.-Russian Business Development Committee' to solve problems, promote trade development activities, and serve as the forum to assist in such trade related matters as standardization and conformity assessment matters. The Standards Working Group of the Committee held its first meeting in St. Petersburg, Russia, 8-9 Sep. 1992. The recommendations resulting from that first meeting are appended to the report. The second meeting of the Standards Working Group resulted in an exchange of information regarding the standards and conformity assessment practices of each country and an understanding of new standards related legislative initiatives within Russia. Of particular significance was the signing of a formal Memorandum of Understanding for cooperation on standards, certification, testing, and metrology matters between the United States (NIST) and Russia (GOSSTANDART). It was also the first public announcement of a new United States Department of Commerce initiative to provide financial support to Russians desiring to learn more about U.S. standardization practices within industrial and commercial enterprises. NTIS

N93-30936# Assistant Secretary of Defense (Comptroller), Washington, DC.

RESEARCH, DEVELOPMENT, TEST AND EVALUATION (R, D, T, AND E) PROGRAMS (R-1), DEPARTMENT OF DEFENSE BUDGET FOR FISCAL YEAR 1994

1993 77 p

(PB93-169878) Avail: CASI HC A05/MF A01

The report details the Department of Defense budget for fiscal year 1994 for research, development, test, and evaluation (RDT and E) programs NTIS

N93-29540*# California Univ., Berkeley. International Computer Science Inst.

A MODEL FOR AMALGAMATION IN GROUP DECISION MAKING

Vincenzo Cutello (Catania Univ., Italy.) and Javier Montero (Universidad Complutense, Madrid, Spain.) *In* NASA. Johnson Space Center, North American Fuzzy Logic Processing Society (NAFIPS 1992), Volume 1 Dec. 1992 p 215-223 Sponsored in part by Direccion General de Investigacion Cientifica y Tecnica (For primary document see N93-29516 11-59)

Avail: CASI HC A02/MF A03

N93-29541*# Odessa Inst. of National Economy (Ukraine). Dept. of Computer Science.

FUZZY FORECASTING AND DECISION MAKING IN SHORT DYNAMIC TIME SERIES

Efim J. Karpovsky, comp. and Ibrahim Ohiokhoya Ozoya *In* NASA. Johnson Space Center, North American Fuzzy Logic Processing Society (NAFIPS 1992), Volume 1 Dec. 1992 p 224-228 (For primary document see N93-29516 11-59)

Avail: CASI HC A01/MF A03

N93-29542*# Georgia State Univ., Atlanta. Dept. of Decision Sciences.

DECISION ANALYSIS WITH APPROXIMATE PROBABILITIES

Thomas Whalen *In* NASA. Johnson Space Center, North American Fuzzy Logic Processing Society (NAFIPS 1992), Volume 1 Dec. 1992 p 229-238 (For primary document see N93-29516 11-59)

Avail: CASI HC A02/MF A03

N93-29598*# Jet Propulsion Lab., California Inst. of Tech., Pasadena.

DSN SUPPORT OF MARS OBSERVER

M. R. Traxler *In its* The Telecommunications and Data Acquisition Report 15 May 1993 p 118-122 (For primary document see N93-29586 11-32)

(RTOP 314-40-22-30-01)

Avail: CASI HC A01/MF A03

82 DOCUMENTATION AND INFORMATION SCIENCE

Includes information management; information storage and retrieval technology; technical writing; graphic arts; and micrography.

For computer documentation see *61 Computer Programming and Software.*

N93-28481# Nijmegen Univ. (Netherlands). Dept. of Information Systems.

THE META MODEL HIERARCHY: A FRAMEWORK FOR INFORMATION SYSTEMS CONCEPTS AND TECHNIQUES

J. L. H. Oei, L. J. G. T. vanHemmen, E. D. Falkenberg, and S. Brinkkemper (Universiteit Twente, Enschede, Netherlands.) Jul. 1992 31 p Sponsored in part by Netherlands Organization for Scientific Research

(TR-92-17; ETN-93-93871) Avail: CASI HC A03/MF A01

The challenge of putting order into the chaos of modeling techniques on a formal basis is presented. The numerous information systems design methods and specification techniques being proposed can be compared on the basis of different criteria. A framework for ordering information systems modeling techniques based on meta models is proposed. This framework, called the meta model hierarchy, positions each technique according to an analysis of the distinctions between the basic concepts, and the set of constraints defined on these concepts. Relations between meta models are distinguished: partitioning, restriction, and degeneration. Each modeling technique is then positioned in the meta model hierarchy according to these order relations. The positioning of entity relationship modeling, NIAM, and Petri netsin the meta model hierarchy is discussed as an illustration of the use of the approach. ESA

N93-28525# Technische Hochschule, Darmstadt (Germany). Fachbereich Informatik.

ANTIRATIONAL TRANSDUCTIONS AND THEIR LANGUAGE FAMILIES Ph.D. Thesis [ANTIRATIONALE TRANSDUKTIONEN UND IHRE SPRACHFAMILIEN]

Juergen Schaefer 1991 258 p In GERMAN

(ETN-93-93794) Avail: CASI HC A12/MF A03

In the framework of the theory of formal languages and of context free grammar, the antirational transductions are introduced from a mathematical point of view. Concepts such as antidirect products of monoid form, Presburg arithmetics, and Kleene algebra were used for problem definition. Relationships between two band acceptors, linear grammar, and antirational transductions were examined. The inclusion problem in unsynchronous and synchronous cases was investigated. The section problem of a unary form is discussed and its internal structure is examined. ESA

N93-28528# Technische Univ., Berlin (Germany). Fachbereich Informatik.

A MODEL FOR PROCESSING THE SGML DOCUMENT IN VERSION ORIENTED HYPERTEXT SYSTEMS Ph.D. Thesis [ENTWURF EINES MODELLS DER VERARBEITUNG VON SGML-DOKUMENTEN IN VERSIONSORIENTIERTEN HYPERTEXT-SYSTEMEN DAS HYPERSGML-KONZEPT]

Hans-Walter Latz 1992 319 p In GERMAN

(ETN-93-93797) Avail: CASI HC A14/MF A03

The Hyper SGML concept, which combines the document model of hypertext and document architecture of SGML (Standard Generalized Markup Language) is presented. A general model for version conducting is discussed: the hypernet model allows the hypertext structure of HyperSGML documents to be defined and modules to be simultaneously used in several documents. Some characteristics of document processing with hypertext are given as examples: linear documents in macroliterary hypertext systems, coding of SGML documents and information losses by mixing, division, deletion, and compensation. The Hypertext Abstract Machine (HAM), a general data base system, and an interface in a distributed hypertext application which supplies basic objects such as modes, links, graphs, and attributes, is described. Some aspects of the unifying framework for version control in a computer aided design environment are depicted. ESA

N93-28580# Los Alamos National Lab., NM.

PREPROCESSING REMOTELY-SENSED DATA FOR EFFICIENT ANALYSIS AND CLASSIFICATION

P. M. Kelly and J. M. White 1993 8 p Presented at the Automatic Object Recognition 3, Society of Photo-Optical Instrumentation Engineers (SPIE) OE/Aerospace Science 8 Sensing Meeting, Orlando, FL, 11-16 Apr. 1993
(Contract W-7405-eng-36)
(DE93-007367; LA-UR-93-301; CONF-930445-2) Avail: CASI HC A02/MF A01

Interpreting remotely-sensed data typically requires expensive, specialized computing machinery capable of storing and manipulating large amounts of data quickly. In this paper, we present a method for accurately analyzing and categorizing remotely-sensed data on much smaller, less expensive platforms. Data size is reduced in such a way an efficient, interactive method of data classification. DOE

N93-28840# Oak Ridge K-25 Site, TN.
SECURITY CLASSIFICATION OF INFORMATION
A. S. Quist Apr. 1993 214 p
(Contract DE-AC05-84OT-21400)
(DE93-012416; K/CG-1077/V2) Avail: CASI HC A10/MF A03

This document is the second of a planned four-volume work that comprehensively discusses the security classification of information. The main focus of volume 2 is on the principles for classification of information. Included herein are descriptions of the two major types of information that governments classify for national security reasons (subjective and objective information), guidance to use when determining whether information under consideration for classification is controlled by the government (a necessary requirement for classification to be effective), information disclosure risks and benefits (the benefits and costs of classification), standards to use when balancing information disclosure risks and benefits, guidance for assigning classification levels (Top Secret, Secret, or Confidential) to classified information, guidance for determining how long information should be classified (classification duration), classification of associations of information, classification of compilations of information, and principles for declassifying and downgrading information. Rules or principles of certain areas of our legal system (e.g., trade secret law) are sometimes mentioned to provide added support to some of those classification principles. DOE

N93-28846# Air Force Inst. of Tech., Wright-Patterson AFB, OH. School of Engineering.
A DISTRIBUTED OBJECT-ORIENTED DATABASE APPLICATION DESIGN M.S. Thesis
Hsin-Feng Wu Mar. 1993 217 p
(AD-A262591; AFIT/GCS/ENG/93M-06) Avail: CASI HC A10/MF A03

The purpose of this study is to analyze and develop a distributed object-oriented database management system (DOODBMS) application to support parallel software development of the Parallel Algorithms and Applications Group (PAAG) at AFIT. By following the software lifecycle of object-oriented paradigm, this thesis investigation is intended to generate requirements analysis, design, implementation, user interface design and implementation, and integration of the database application with the user interface. ITASCA, an existing DOODBMS platform, has been chosen to prototype the application for its distribution functionalities and object-oriented modeling power. The user interface of the database application is based on x-window OSF/Motif front-end system for its efficiency. Various operations of this distributed database include: retrieving information in the database, modifying data at the local site, looking up information of publications of libraries, etc. The user may access each local computer through graphical user interface without knowing the query language constructs of the DOODBMS platform. DTIC

N93-28948*# National Aeronautics and Space Administration. Langley Research Center, Hampton, VA.
NASA/DOD AEROSPACE KNOWLEDGE DIFFUSION RESEARCH PROJECT. PAPER 28: THE TECHNICAL COMMUNICATION PRACTICES OF RUSSIAN AND US AEROSPACE ENGINEERS AND SCIENTISTS
Thomas E. Pinelli, Rebecca O. Barclay (Rensselaer Polytechnic Inst., Troy, NY.), Michael L. Keene (Tennessee Univ., Knoxville.), Madelyn Flammia (University of Central Florida, Orlando.), and John M. Kennedy (Indiana Univ., Bloomington.) 1993 11 p Repr. from IEEE Transactions on Professional Communication, v. 36, no. 2, Jun. 1993 p 95-104
(NASA-TM-108249; NAS 1.15:108249) Copyright Avail: CASI HC A03/MF A01

As part of Phase 4 of the NASA/DoD Aerospace Knowledge Diffusion Research Project, two studies were conducted that investigated the technical communication practices of Russian and U.S. aerospace engineers and scientists. Both studies had the same five objectives: first, to solicit the opinions of aerospace engineers and scientists regarding the importance of technical communication to their professions; second, to determine the use and production of technical communication by aerospace engineers and scientists; third, to seek their views about the appropriate content of the undergraduate course in technical communication; fourth, to determine aerospace engineers' and scientists' use of libraries, technical information centers, and on-line databases; and fifth, to determine the use and importance of computer and information technology to them. A self administered questionnaire was distributed to Russian aerospace engineers and scientists at the Central Aero-Hydrodynamic Institute (TsAGI) and to their U.S. counterparts at the NASA Ames Research Center and the NASA Langley Research Center. The completion rates for the Russian and U.S. surveys were 64 and 61 percent, respectively. Responses of the Russian and U.S. participants to selected questions are presented in this paper. Author

N93-29129 National Academy of Sciences - National Research Council, Washington, DC. Computer Science and Telecommunications Board.
NATIONAL COLLABORATORIES: APPLYING INFORMATION TECHNOLOGY FOR SCIENTIFIC RESEARCH
1993 114 p
(Grant NSF CDA-90-21110)
(LC-93-83795; ISBN-0-309-04848-6) Copyright Avail: Issuing Activity

To further explore the concept of a collaboratory as it was first articulated and discussed in 1989 (Towards a National Collaboratory, 1989), the Computer Science and Telecommunications Board of the National Research Council convened a committee in December 1991 to study the need for and benefits of collaboration in scientific research, factors determining the effectiveness of collaboration, and the ability of information technology--specifically of electronically integrated collaboratories--to support and enhance interactive scientific research. In addressing these issues, the committee focused on three discrete areas of scientific investigation--oceanography, in which the difficulty and expense of gathering data and the interdependence of modelers and experimentalists provide motivation for greater collaboration (Chapter 2); space physics, which has of necessity used extensive computational technology in the analysis of data collected by cooperatively fielded space- and ground-based instruments (Chapter 3); and gene mapping and sequencing research that has led to construction of and reliance on massive databases (Chapter 4). Research in these fields is sponsored by a variety of agencies, including the National Science Foundation, the National Institutes of Health, the National Aeronautics and Space Administration, the (Defense) Advanced Research Projects Agency, the Office of Naval Research, and the Department of Energy. The committee's investigations suggested technical requirements and social and practical issues (Chapter 5) that must be considered and dealt with as part of the process of initiating a national collaboratory program (Chapter 6) in support of scientific research. Derived from text

N93-29167*# National Aeronautics and Space Administration. Goddard Space Flight Center, Greenbelt, MD.
NSSDC DATA LISTING
Richard Horowitz and Joseph H. King Apr. 1993 150 p
(NASA-TM-108264; NSSDC/WDC-A-R/S-93-18; NAS 1.15:108264) Avail: CASI HC A07/MF A02

This document identifies, in a highly summarized way, all the data held at the NSSDC. These data cover astrophysics and astronomy, solar and space physics, planetary and lunar, and Earth science disciplines. They are primarily, but not exclusively, from past and ongoing NASA spaceflight missions. We first identify all the data electronically available through NSSDC's principal online (magnetic disk-based) and nearline (robotics jukebox-based) systems, and then those data available on CDROM's. Finally, we identify all NSSDC-held data, the majority of which are still offline on magnetic tape, film, etc., but including the electronically accessible and CD-ROM resident data of earlier sections. These comprehensive identifications are in the form of two listings, one for the majority of NSSDC-held data sets resulting from individual instruments flown on individual spacecraft, and the other listing for the remainder of NSSDC-held data sets which do not adhere to this spacecraft/experiment/dataset hierarchy. The latter listing is presented in two parts, one for the numerous source catalogs of the NSSDC-operated Astronomical Data Center, and the other for the remainder. Access paths to all these data, and to further information about each, are also given in the related sections of this Data Listing. Note that this document is a companion to the electronically accessible information files (in particular, the NASA Master Directory) at NSSDC which also identify NSSDC-resident (and other) data. Author (revised)

N93-29210# Defence Research Establishment, Ottawa (Ontario).
AN INVESTIGATION OF STEREOLITHOGRAPHY AS A MEANS OF PROTOTYPING FROM A CAD DATABASE
D. Hidson Jun. 1992 23 p
(AD-A263410; DREO-TN-92-25) Avail: CASI HC A03/MF A01

The Stereolithography (SLA) process was investigated to test its efficacy in producing three-dimensional parts from a Unigraphics CAD file. The method uses a photosensitive resin that is cured by means of a laser beam. The laser is directed to follow the CAD file and a model is built up with successive layers of resin between 0.127 and 0.508 mm (0.005 and 0.020 inch). Once the model is constructed, it is bathed in ultraviolet light for a postcuring process. It was found that the model undergoes various amounts of contraction and expansion, distorting its shape. A quantitative assessment of this is given. The process is very useful in producing a three-dimensional model from the CAD file, but the dimensional integrity is not sufficient for producing accurately dimensioned prototypes. DTIC

N93-29222* National Aeronautics and Space Administration, Washington, DC.
APPLIED INFORMATION SYSTEMS RESEARCH PROGRAM WORKSHOP
24 Jul. 1991 166 p Workshop held in Boulder, CO, 22-24 Jul. 1991
(NASA-TM-108773; NAS 1.15:108773) Avail: CASI HC A08

The first Applied Information Systems Research Program (AISRP) Workshop provided the impetus for several groups involved in information systems to review current activities. The objectives of the workshop included: (1) to provide an open forum for interaction and discussion of information systems; (2) to promote understanding by initiating a dialogue with the intended benefactors of the program, the scientific user community, and discuss options for improving their support; (3) create an advocacy in having science users and investigators of the program meet together and establish the basis for direction and growth; and (4) support the future of the program by building collaborations and interaction to encourage an investigator working group approach for conducting the program. For individual titles, see N93-29223 through N93-29241.

N93-29223*# National Aeronautics and Space Administration, Washington, DC.
APPLIED INFORMATION SYSTEMS RESEARCH PROGRAM WORKSHOP
Joe Bredekamp *In its* Applied Information Systems Research Program Workshop 24 Jul. 1991 50 p (For primary document see N93-29222 11-82)
Avail: CASI HC A03

Viewgraphs on Applied Information Systems Research Program Workshop are presented. Topics covered include: the Earth Observing System Data and Information System; the planetary data system; Astrophysics Data System project review; OAET Computer Science and Data Systems Programs; the Center of Excellence in Space Data and Information Sciences; and CASIS background. CASI

N93-29224*# Colorado Univ., Boulder. Colorado Space Grant Consortium.
PROGRAM PLAN FOR AN EXPERIMENTER'S LABORATORY FOR VISUALIZED INTERACTIVE SCIENCE
Elaine R. Hansen, Marjorie K. Klemp, Sally W. Lasater, Marti Szczur, and Joseph B. Klemp *In* NASA. Washington, Applied Information Systems Research Program Workshop 24 Jul. 1991 5 p (For primary document see N93-29222 11-82)
Avail: CASI HC A01

Viewgraphs on program plan for an experimenter's laboratory for visualized interactive science are presented. Goals and objectives, concept for accomplishing objectives, building blocks, and plans are addressed. CASI

N93-29225*# Maryland Univ., College Park. Dept. of Meteorology.
GRID ANALYSIS AND DISPLAY SYSTEM (GrADS): A PRACTICAL TOOL FOR EARTH SCIENCE VISUALIZATION
James L. Kinter, III and Brian E. Doty *In* NASA. Washington, Applied Information Systems Research Program Workshop 24 Jul. 1991 7 p (For primary document see N93-29222 11-82)
Avail: CASI HC A02

Viewgraphs on grid analysis and display system (GrADS): a practical tool for earth science visualization are presented. Topics covered include: GrADS design goals; data sets; and temperature profiles. CASI

N93-29226*# Jet Propulsion Lab., California Inst. of Tech., Pasadena.
A DISTRIBUTED SYSTEM FOR VISUALIZING AND ANALYZING MULTIVARIATE AND MULTIDISCIPLINARY DATA
Allan S. Jacobson, Mark A. Allen, Michael J. Bailey, Ronald G. Blom, Leo Blume, and Lee S. Elson *In* NASA. Washington, Applied Information Systems Research Program Workshop 24 Jul. 1991 3 p (For primary document see N93-29222 11-82)
Avail: CASI HC A01

Viewgraphs on a distributed system for visualizing and analyzing multivariate and multidisciplinary data are presented. Topics covered include: program objectives; and the linked windows interactive data system (LinkWinds). CASI

N93-29227*# Space Telescope Science Inst., Baltimore, MD.
DATA REDUCTION EXPERT ASSISTANT
Glenn E. Miller, Mark D. Johnston, and Robert J. Hanisch *In* NASA. Washington, Applied Information Systems Research Program Workshop 24 Jul. 1991 4 p (For primary document see N93-29222 11-82)
Avail: CASI HC A01

Viewgraphs on data reduction expert assistant are presented. Topics covered include: data analysis systems; philosophy of these systems; disadvantages; expert assistant; useful goals; and implementation considerations. CASI

N93-29228*# Canada Centre for Remote Sensing, Ottawa (Ontario).
OVERVIEW OF THE SYSTEM OF EXPERTS FOR INTELLIGENT DATA MANAGEMENT (SEIDAM)
David G. Goodenough, Ko Fung, and Joji Iisaka *In* NASA. Washington, Applied Information Systems Research Program Workshop 24 Jul. 1991 16 p (For primary document see N93-29222 11-82)
Avail: CASI HC A03

Viewgraphs on the system of experts for intelligent data management (SEIDAM) are presented. Topics covered include: multiple data sources integration; SEIDAM structure; machine learning; user interface; spatial knowledge expert system; digital terrain model (DTM) and segmentation expert systems; system validation; and tasks and plans. CASI

N93-29229*# National Aeronautics and Space Administration. Ames Research Center, Moffett Field, CA.
THE SCIENTIFIC MODELING ASSISTANT: AN ADVANCED SOFTWARE TOOL FOR SCIENTIFIC MODEL BUILDING
Richard M. Keller and Michael H. Sims *In its* Applied Information Systems Research Program Workshop 24 Jul. 1991 6 p (For primary document see N93-29222 11-82)
Avail: CASI HC A02

Viewgraphs on the scientific modeling assistant: an advanced software tool for scientific model building are presented. The objective is to build a specialized software tool to assist in scientific model-building. CASI

N93-29230*# Jet Propulsion Lab., California Inst. of Tech., Pasadena.
DATAHUB KNOWLEDGE BASED ASSISTANCE FOR SCIENCE VISUALIZATION AND ANALYSIS USING LARGE DISTRIBUTED DATABASES
Thomas H. Handley, Jr., Donald J. Collins, Richard J. Doyle, and Allan S. Jacobson *In* NASA. Washington, Applied Information Systems Research Program Workshop 24 Jul. 1991 11 p (For primary document see N93-29222 11-82)
Avail: CASI HC A03

Viewgraphs on DataHub knowledge based assistance for science visualization and analysis using large distributed databases. Topics covered include: DataHub functional architecture; data representation; logical access methods; preliminary software architecture; LinkWinds; data knowledge issues; expert systems; and data management. CASI

N93-29231*# Jet Propulsion Lab., California Inst. of Tech., Pasadena.
MULTI-CHANNEL HOLOGRAPHIC BIRFURCATIVE NEURAL NETWORK SYSTEM FOR REAL-TIME ADAPTIVE EOS DATA ANALYSIS
Hua-Kuang Liu, J. Diep, and K. Huang *In* NASA. Washington, Applied Information Systems Research Program Workshop 24 Jul. 1991 4 p (For primary document see N93-29222 11-82)
Avail: CASI HC A01

Viewgraphs on multi-channel holographic bifurcative neural network system for real-time adaptive Earth Observing System (EOS) data analysis are presented. The objective is to research and develop an optical bifurcating neuromorphic pattern recognition system for making optical data array comparisons and to evaluate the use of the system for EOS data classification, reduction, analysis, and other applications. CASI

N93-29232*# Illinois Univ., Urbana.
NATIONAL CENTER FOR SUPERCOMPUTER APPLICATIONS
Matthew Arrott *In* NASA. Washington, Applied Information Systems Research Program Workshop 24 Jul. 1991 4 p (For primary document see N93-29222 11-82)
Avail: CASI HC A01

Viewgraphs on the National Center for Supercomputer Applications are presented. The objective is to develop comprehensive computational research environments through the use of evolving software technology. CASI

N93-29233*# Colorado Univ., Boulder.
COLORADO CENTER FOR ASTRODYNAMICS RESEARCH (CCAR)
William Emery *In* NASA. Washington, Applied Information Systems Research Program Workshop 24 Jul. 1991 5 p (For primary document see N93-29222 11-82)
Avail: CASI HC A01

Viewgraphs on the Colorado Center for Astrodynamics Research (CCAR) are presented. Topics covered include: EOSDIS testbed: an Advanced Very High Resolution Radiometer (AVHRR) data system for snowpack and vegetation studies; satellite data processing software; satellite data analysis activities; mass storage systems; wide area network connections; and remote access. CASI

N93-29234*# Jet Propulsion Lab., California Inst. of Tech., Pasadena.
GEOGRAPHIC INFORMATION SYSTEM FOR FUSION AND ANALYSIS OF HIGH-RESOLUTION REMOTE SENSING AND GROUND TRUTH DATA
Anthony Freeman, Pascale Dubois, Franz Leberl, L. Norikane, and JoBea Way *In* NASA. Washington, Applied Information Systems Research Program Workshop 24 Jul. 1991 5 p (For primary document see N93-29222 11-82)
Avail: CASI HC A01

Viewgraphs on Geographic Information System for fusion and analysis of high-resolution remote sensing and ground truth data are presented. Topics covered include: scientific objectives; schedule; and Geographic Information System. CASI

N93-29235*# Science Applications International Corp., McLean, VA. Lab. for Atmospheric and Space Science.
SAVS: A SPACE DATA ANALYSIS AND VISUALIZATION SYSTEM
Edward Szuszczewicz, Charles C. Goodrich, and Alan Mankofsky *In* NASA. Washington, Applied Information Systems Research Program Workshop 24 Jul. 1991 5 p (For primary document see N93-29222 11-82)
Avail: CASI HC A01

Viewgraphs on a Space Data Analysis and Visualization System (SAVS) are presented. Topics covered include: SAVS - a data acquisition, manipulation, analysis and a visualization system; the SAVS focus; the NASA vision for the coming decade; statement of the problem; needs of the practicing scientist; projecting capabilities; and SAVS near term activities. CASI

N93-29236*# Wisconsin Univ., Madison.
A PLANETARY VERSION OF PC-McIDAS
Sanjay S. Limaye, Mike Martin, R. S. Saunders, and L. A. Sromovsky *In* NASA. Washington, Applied Information Systems Research Program Workshop 24 Jul. 1991 4 p (For primary document see N93-29222 11-82)
Avail: CASI HC A01

Viewgraphs on a planetary version of PC-McIDAS are presented. Topics covered include: McIDAS and PC-McIDAS; McIDAS hardware; real time data available; archived data available; McIDAS installed base; planetary McIDAS: and comparison of McIDAS and VICAR. CASI

N93-29237*# National Center for Atmospheric Research, Boulder, CO.
INTERACTIVE INTERFACE TO NCAR GRAPHICS
Robert Lackman *In* NASA. Washington, Applied Information Systems Research Program Workshop 24 Jul. 1991 4 p (For primary document see N93-29222 11-82)
Avail: CASI HC A01

Viewgraphs on interactive interface to NCAR graphics are presented. Topics covered include: NCAR graphics features; NCAR graphics components; NCAR graphics utilities; NCAR graphics programmatic interface; a typical application; and overview of NCAR interactive. CASI

N93-29238*# Maryland Univ., College Park.
VIEWCACHE: AN INCREMENTAL DATABASE ACCESS METHOD FOR AUTONOMOUS INTEROPERABLE DATABASES
Nick Roussopoulos and Timoleon Sellis *In* NASA. Washington, Applied Information Systems Research Program Workshop 24 Jul. 1991 6 p (For primary document see N93-29222 11-82)
Avail: CASI HC A02

The objective is to illustrate the concept of incremental access to distributed databases. An experimental database management system, ADMS, which has been developed at the University of Maryland, in College Park, uses VIEWCACHE, a database access method based on incremental search. VIEWCACHE is a pointer-based access method that provides a uniform interface for accessing distributed databases and catalogues. The compactness of the pointer structures formed during cross-referencing with no actual data movement between database sizes. Once the search is complete, the set of collected pointers pointing to the desired data are dereferenced. CASI

N93-29239*# Chicago Univ., IL.
SPATIAL ANALYSIS AND MODELING SYSTEMS (SAMS)
Charles Vermillion, Paul Chan, John Hill, Robert Jaske, Gilbert Rochon, and Fran Stetina *In* NASA. Washington, Applied Information Systems Research Program Workshop 24 Jul. 1991 2 p (For primary document see N93-29222 11-82)
Avail: CASI HC A01

The objective is to develop a uniform environmental data gathering and distribution system to support (1) emergency management for environmental disasters, and (2) the calibration and validation of remotely sensed data. Initial activities will be to select a data test site and to demonstrate multi-discipline applications using simulated or satellite data in a non real-time mode. Rainfall and flooding are chosen as the testbeds for the SAMS concept because of the abundance of data and the availability of models. The capability to display and process GOES data and analyze GOES generated rain-rate maps will be integrated into SAMS. Author (revised)

N93-29240*# National Aeronautics and Space Administration. Ames Research Center, Moffett Field, CA.
INTRODUCTION TO CADET CENTER FOR ADVANCED DATA EVALUATION TECHNOLOGY
Cathy Schulbach and C. Jorgensen *In its* Applied Information Systems Research Program Workshop 24 Jul. 1991 4 p (For primary document see N93-29222 11-82)
Avail: CASI HC A01

Viewgraphs on the Center for Advanced Data Evaluation Technology are presented. Topics covered include: technology problem; human problem; goals and objectives; key CADET focus; and elements of the modeling process. CASI

N93-29241*# Jet Propulsion Lab., California Inst. of Tech., Pasadena.
FLIGHT PROJECTS OFFICE INFORMATION SYSTEMS TESTBED (FIST)
Patricia Liggett *In* NASA. Washington, Applied Information Systems Research Program Workshop 24 Jul. 1991 4 p (For primary document see N93-29222 11-82)
Avail: CASI HC A01

Viewgraphs on the Flight Projects Office Information Systems Testbed (FIST) are presented. The goal is to perform technology evaluation and prototyping of information systems to support SFOC and JPL flight projects in order to reduce risk in the development of operational data systems for such projects. CASI

N93-29310# Lawrence Livermore National Lab., CA.
IMPLEMENTING ERROR-VALUED SEMANTICS FOR DATAFLOW LANGUAGES ON IMPERATIVE MACHINES
P. J. Miller 27 Aug. 1992 21 p Presented at the Working Conference on Architectures and Compilation Techniques for Fine and Medium Grain Parallelism, Orlando, FL, 20-22 Jan. 1993
(Contract W-7405-eng-48)
(DE93-009319; UCRL-JC-111550; CONF-930129-2) Avail: CASI HC A03/MF A01

Exception handling as presented by Goodenough and Liskov is based on the semantics of control flow. Dataflow languages, on the other hand, use value-oriented semantics to handle errors. Error values created by one operation flow to other operations. A naive implementation of these test-and-propagate semantics can be very slow. Here, we present a code space partitioning model for implementing error values on imperative architectures. Computation begins in a fast, error free partition. If errors do occur, then the computation moves to a slower, safer, test-and-propagate partition. The technique combines the speed of the error-detect model with the safety of the test-and-propagate model. If no errors occur, then the computation completes as fast as it would in error-detect only code. A prototype compiler for TMSAL (a powerful subset of SISAL) programs demonstrates the usefulness of the technique. DOE

N93-29431# Air Force Inst. of Tech., Wright-Patterson AFB, OH. Foreign Aerospace Science and Technology Center.
SELECTION AND TRANSMISSION OF INFORMATION. ISSUE 22: REPUBLIC INTERDEPARTMENTAL COLLECTION (SELECTED ARTICLES)
18 Mar. 1993 31 p Transl. into ENGLISH from Otbor i Peredacha Informatsii (Russia), no. 22, 22-33, 105 1969 p 1, 22-22, 105
(AD-A262825; FASTC-ID(RS)T-0962-92) Avail: CASI HC A03/MF A01

Analysis is given of representation of correlation functions of random processes and the processes themselves in the form of linear combinations of specific determined functions of time with random coefficients: general spectral, canonical, and orthogonal. It is shown that in contrast to the case of the commutative converters, analyzed in the terms of theory of C*-algebras and their Gelfand isomorphism, in the case of noncommutative converters, it is necessary to use operators of transformation of coordinates, composition of Volterra, and A-composition. The concept of T-representability, which generalizes the concept of harmonizability, is introduced. The examples examined are harmonic modulated oscillation/vibration, the periodically correlated processes, and sampling theorems. The problems of the linear theory of signal are solved within the framework of the covariance theory random process, which are represented in the form of the linear combination of the determined functions of time with the random coefficients. DTIC

N93-29439# Industrial Coll. of the Armed Forces, Washington, DC.
INFORMATION TECHNOLOGY: A FORCE FOR ORGANIZATIONAL CHANGE
William R. Bowen Apr. 1992 30 p
(AD-A261986; NDU-ICAF-92-S10) Avail: CASI HC A03/MF A01

Information Technology is changing the face of the world as we know it. Business use of technologies like Decision Support Systems and Electronic Data Interchange allow organizations to re-engineer their processes to eliminate unnecessary layers of management. New emerging technologies under the umbrella of Artificial Intelligence are helping us to replace the human being with computer technology that simulates expert advice or learns as it matures. To take advantage of these new technologies requires new organization structures and new ways of approaching problem solving. These new technologies are explored and related to organizational change. Author (revised)

N93-29459# Carnegie-Mellon Univ., Pittsburgh, PA. Dept. of Computer Science.
COLLECTION-ORIENTED MATCH: SCALING UP THE DATA IN PRODUCTION SYSTEMS
Anurag Acharya and Milind Tambe Dec. 1992 38 p
(Contract F33615-90-C-1465; ARPA Order 7597)
(AD-A262755; CMU/CS-92-218) Avail: CASI HC A03/MF A01

Match algorithms that are capable of handling large amounts of data, without giving up expressiveness are a key requirement for successful integration of relational database systems and powerful rule-based systems. Algorithms that have been used for database rule systems have usually been unable to support large and complex rule sets, while the algorithms that have been used for rule-based expert systems do not scale well with increasing amounts of data. Furthermore, these algorithms do not provide support for collection (or set) oriented production languages. A basic shift in the nature of match algorithms: from tuple-oriented to collection-oriented is proposed. A collection-oriented match algorithm matches each condition in a production with a collection of tuples and generates collection-oriented instantiations, i.e., instantiations that have collection of tuples corresponding to each condition in the production. This approach shows great promise for efficiently matching expressive productions against large amounts of data. In addition, it provides direct support for collection-oriented production languages. DTIC

N93-29709*# National Aeronautics and Space Administration. Langley Research Center, Hampton, VA.
NASA/DOD AEROSPACE KNOWLEDGE DIFFUSION RESEARCH PROJECT. PAPER 29: THE US GOVERNMENT TECHNICAL REPORT AND THE TRANSFER OF FEDERALLY FUNDED AEROSPACE R AND D
Thomas E. Pinelli, Rebecca O. Barclay (Rensselaer Polytechnic Inst., Troy, NY.), and John M. Kennedy (Indiana Univ., Bloomington.) 1993 20 p Repr. from Government Publications Review, v. 20, no. 3, Jul. - Aug. 1993 p 393-411
(Grant NAGw-1682)
(NASA-TM-109221; NAS 1.15:109221) Copyright Avail: CASI HC A03/MF A01

This article discusses the U.S. government technical report and the transfer of federally funded aerospace research and development in a conceptual framework of the federal government as a producer of scientific and technical information. The article summarizes current literature and research and discusses U.S. government technical report use and the importance of using data obtained from the NASA/DoD Aerospace Knowledge Diffusion Research Project. The authors make a case for changing existing U.S. technology policy and present a research agenda for the U.S. government technical report. Author

N93-29783# Lawrence Livermore National Lab., CA.
STORAGE SYSTEMS FOR NATIONAL INFORMATION ASSETS
R. A. Coyne (IBM Federal Systems Div., Houston, TX.), H. Hulen (IBM Federal Systems Div., Houston, TX.), and R. Watson 26 Aug. 1992 8 p Presented at the ACM/IEEE Supercomputing Conference, Minneapolis, MN, 14-21 Nov. 1992
(Contract W-7405-eng-48)
(DE93-009303; UCRL-JC-111558; CONF-921125-7) Avail: CASI HC A02/MF A01

An industry-led collaborative project, called the National Storage Laboratory, has been organized to investigate technology for storage systems that will be the future repositories for our national information assets. Lawrence Livermore National Laboratory through its National Energy Research Supercomputer Center (NERSC) is the operational site and the provider of applications. It is anticipated that the integrated testbed system will represent a significant advance in the technology for distributed storage systems capable of handling gigabyte class files at gigabit-per-second data rates. DOE

N93-30036*# National Aeronautics and Space Administration. Langley Research Center, Hampton, VA.

NASA/DOD AEROSPACE KNOWLEDGE DIFFUSION RESEARCH PROJECT. PAPER 30: THE ELECTRONIC TRANSFER OF INFORMATION AND AEROSPACE KNOWLEDGE DIFFUSION

Thomas E. Pinelli, Ann P. Bishop (Illinois Univ., Urbana-Champaign.), Rebecca O. Barclay (Rensselaer Polytechnic Inst., Troy, NY.), and John M. Kennedy (Indiana Univ., Bloomington.) Oct. 1992 10 p Repr. from the International Forum on Information and Documentation, v. 17, no. 4, Oct. 1992 p 8-16 Presented at the Annual Meeting of the American Association for the Advancement of Sciences, Chicago, IL, 8 Feb. 1992
(Grant NAGw-1682)
(NASA-TM-109223; NAS 1.15:109223) Avail: CASI HC A02/MF A01

Increasing reliance on and investment in information technology and electronic networking systems presupposes that computing and information technology will play a major role in the diffusion of aerospace knowledge. Little is known, however, about actual information technology needs, uses, and problems within the aerospace knowledge diffusion process. The authors state that the potential contributions of information technology to increased productivity and competitiveness will be diminished unless empirically derived knowledge regarding the information-seeking behavior of the members of the social system - those who are producing, transferring, and using scientific and technical information - is incorporated into a new technology policy framework. Research into the use of information technology and electronic networks by U.S. aerospace engineers and scientists, collected as part of a research project designed to study aerospace knowledge diffusion, is presented in support of this assertion. Author

N93-30037*# National Aeronautics and Space Administration. Langley Research Center, Hampton, VA.

NASA/DOD AEROSPACE KNOWLEDGE DIFFUSION RESEARCH PROJECT. PAPER 31: THE INFORMATION-SEEKING BEHAVIOR OF ENGINEERS

Thomas E. Pinelli, Ann P. Bishop (Illinois Univ., Urbana-Champaign.), Rebecca O. Barclay (Rensselaer Polytechnic Inst., Troy, NY.), and John M. Kennedy (Indiana Univ., Bloomington.) 1993 36 p Repr. from the Encyclopedia of Library and Information Science, v. 52, suppl. 15, 1993 p 167-201
(NASA-TM-109224; NAS 1.15:109224) Avail: CASI HC A03/MF A01

Engineers are an extraordinarily diverse group of professionals, but an attribute common to all engineers is their use of information. Engineering can be conceptualized as an information processing system that must deal with work-related uncertainty through patterns of technical communications. Throughout the process, data, information, and tacit knowledge are being acquired, produced, transferred, and utilized. While acknowledging that other models exist, we have chosen to view the information-seeking behavior of engineers within a conceptual framework of the engineer as an information processor. This article uses the chosen framework to discuss information-seeking behavior of engineers, reviewing selected literature and empirical studies from library and information science, management, communications, and sociology. The article concludes by proposing a research agenda designed to extend our current, limited knowledge of the way engineers process information. Derived from text

N93-30122# Adept IC Design, Oceanside, CA.

DESIGN OF A PIXEL CELL OPTIMIZED FOR A DATA PUSH ARCHITECTURE READOUT

E. L. Atlas, S. Shapiro (Stanford Univ., CA.), and D. Cords (Stanford Univ., CA.) Dec. 1992 14 p
(Contract DE-AC03-76SF-00515)
(DE93-011016; SLAC-TN-92-2) Avail: CASI HC A03/MF A01

A pixel cell has been designed which has been optimized for a data push architecture readout. It retains the features of preceding designs which allow time stamping, analog signal processing, XY address recording, ghost elimination and sparse data transmission. It eliminates a number of problems inherent in previous designs by use of sampled data techniques, destructive readout sampled data techniques, and current mode output drivers. This document examines the motivation for this new pixel and covers the theory of operation of the various blocks. A discussion of the tradeoffs affecting speed, power, device size, and radiation stability is included as well. DOE

N93-30123# Professional Analysis, Inc., Las Vegas, NV.

HANDBOOK OF FREQUENTLY USED ACRONYMS AND GLOSSARY OF TERMS

Nov. 1992 150 p
(DE93-011388; DOE/NV-360) Avail: CASI HC A07/MF A02

This handbook was compiled as a handy reference for acronyms and terms frequently used by DOE/NV organizations in the conduct of their day-to-day operations. Those acronyms and terms were selected from a wide variety of sources. The handbook is ordered alphabetically. DOE

N93-30193# Army War Coll., Carlisle Barracks, PA.

THE FUTURE ROLE OF THE DIRECTOR OF INFORMATION MANAGEMENT (DOIM) ORGANIZATION WITHIN THE DOD CORPORATE INFORMATION MANAGEMENT INITIATIVE Study Project

Archie M. Franks 15 Apr. 1993 41 p
(AD-A264118) Avail: CASI HC A03/MF A01

The Director of Information Management (DOIM) organization has the mission, with its duties and responsibilities, to satisfy installation users information management requirements. The DOIM's ability to carry out the automation or information management systems portion of that mission is being diminished by ongoing DOD initiatives and other factors (i.e., budget reductions, DOD drawdown, and antiquated infrastructure). Initiatives such as Corporate Information Management (CIM), Defense Business Operations Fund (DBOF), and Defense Management Report Decisions (DMRD) are aimed at improving service quality and organizational effectiveness and efficiency. They share common features like 'business process improvement'; yet may implement unique actions like personnel reductions or eliminations. Each impacts in some way on the DOIM's ability to accomplish its Information Mission Area (IMA) mission, along with above identified factors that operate within the information management environment. This study examines the DOIM organization within the framework of the CIM initiative, looking at the major factors which decrease organizational effectiveness. It attempts to find opportunities where the DOIM organization can eliminate duplication of effort and focus on an accomplishable mission, within today's constrained resource levels. DTIC

N93-30195# Electronics Research Lab., Adelaide (Australia).

DATA QUALITY STATEMENTS FOR SPATIAL DATABASES Research Note

R. J. Williams Jul. 1992 31 p
(AD-A264125; ERL-0632-RN; DODA-AR-006-971) Avail: CASI HC A03/MF A01

This paper overviews contemporary issues in incorporating data quality statements into spatial databases. The paper includes discussion of two approaches; one emanating from the Digital Chart of the World Project and one through a working party within the International Cartographic Association. DTIC

N93-30449*# National Aeronautics and Space Administration. Goddard Space Flight Center, Greenbelt, MD.

GODDARD CONFERENCE ON MASS STORAGE SYSTEMS AND TECHNOLOGIES, VOLUME 1

Ben Kobler, ed. and P. C. Hariharan, ed. (ST Systems Corp., Lanham, MD.) 1993 333 p Conference held in Greenbelt, MD, 22-24 Sep. 1992
(NASA-CP-3198; NAS 1.55:3198) Avail: CASI HC A15/MF A03

Copies of nearly all of the technical papers and viewgraphs presented at the Goddard Conference on Mass Storage Systems and Technologies held in Sep. 1992 are included. The conference served as an informational exchange forum for topics primarily relating to the ingestion and management of massive amounts of data and the attendant problems (data ingestion rates now approach the order of terabytes per day). Discussion topics include the IEEE Mass Storage System Reference Model, data archiving standards, high-performance storage devices, magnetic and magneto-optic storage systems, magnetic and optical recording technologies, high-performance helical scan recording systems, and low end helical scan tape drives. Additional topics addressed the evolution of the identifiable unit for processing purposes as data ingestion rates increase dramatically, and the present state of the art in mass storage technology. For individual titles, see N93-30450 through N93-30480.

N93-30450*# Lawrence Livermore National Lab., CA.
MASS STORAGE SYSTEM REFERENCE MODEL, VERSION 4
Sam Coleman, ed. and Steve Miller, ed. (SRI International Corp., La Jolla, CA.) *In* NASA. Goddard Space Flight Center, Goddard Conference on Mass Storage Systems and Technologies, Volume 1, 1993 p 1-72 (For primary document see N93-30449 11-82)
Avail: CASI HC A04/MF A03

The high-level abstractions that underlie modern storage systems are identified. The information to generate the model was collected from major practitioners who have built and operated large storage facilities, and represents a distillation of the wisdom they have acquired over the years. The model provides a common terminology and set of concepts to allow existing systems to be examined and new systems to be discussed and built. It is intended that the model and the interfaces identified from it will allow and encourage vendors to develop mutually-compatible storage components that can be combined to form integrated storage systems and services. The reference model presents an abstract view of the concepts and organization of storage systems. From this abstraction will come the identification of the interfaces and modules that will be used in IEEE storage system standards. The model is not yet suitable as a standard; it does not contain implementation decisions, such as how abstract objects should be broken up into software modules or how software modules should be mapped to hosts; it does not give policy specifications, such as when files should be migrated; does not describe how the abstract objects should be used or connected; and does not refer to specific hardware components. In particular, it does not fully specify the interfaces. Author (revised)

N93-30451*# Endl Associates, San Juan Capistrano, CA.
OPTICAL MEDIA STANDARDS FOR INDUSTRY
Kenneth J. Hallam *In* NASA. Goddard Space Flight Center, Goddard Conference on Mass Storage Systems and Technologies, Volume 1, 1993 p 73-76 (For primary document see N93-30449 11-82)
Avail: CASI HC A01/MF A03

Optical storage is a new and growing area of technology that can serve to meet some of the mass storage needs of the computer industry. Optical storage is characterized by information being stored and retrieved by means of diode lasers. When most people refer to optical storage, they mean rotating disk media, but there are 1 or 2 products that use lasers to read and write to tape. Optical media also usually means removable media. Because of its removability, there is a recognized need for standardization, both of the media and of the recording method. Industry standards can come about in one or more different ways. An industry supported body can sanction and publish a formal standard. A company may ship enough of a product that it so dominates an application or industry that it acquires 'standard' status without an official sanction. Such de facto standards are almost always copied by other companies with varying degrees of success. A governmental body can issue a rule or law that requires conformance to a standard. The standard may have been created by the government, or adopted from among many proposed by industry. These are often known as de jure standards. Standards are either open or proprietary. If approved by a government or sanctioning body, the standard is open. A de facto standard may be either open or proprietary. Optical media is too new to have de facto standards accepted by the marketplace yet. The proliferation of non-compatible media types in the last 5 years of optical market development have convinced many of the need for recognized media standards. Author (revised)

N93-30452*# IBM Federal Systems Div., Houston, TX.
TECHNOLOGY FOR NATIONAL ASSET STORAGE SYSTEMS
Robert A. Coyne, Harry Hulen, and Richard Watson (Lawrence Livermore National Lab., CA.) *In* NASA. Goddard Space Flight Center, Goddard Conference on Mass Storage Systems and Technologies, Volume 1, 1993 p 77-86 (For primary document see N93-30449 11-82)
Avail: CASI HC A02/MF A03

An industry-led collaborative project, called the National Storage Laboratory, was organized to investigate technology for storage systems that will be the future repositories for our national information assets. Industry participants are IBM Federal Systems Company, Ampex Recording Systems Corporation, General Atomics DISCOS Division, IBM ADSTAR, Maximum Strategy Corporation, Network Systems Corporation, and Zitel Corporation. Industry members of the collaborative project are funding their own participation. Lawrence Livermore National Laboratory through its National Energy Research Supercomputer Center (NERSC) will participate in the project as the operational site and the provider of applications. The expected result is an evaluation of a high performance storage architecture assembled from commercially available hardware and software, with some software enhancements to meet the project's goals. It is anticipated that the integrated testbed system will represent a significant advance in the technology for distributed storage systems capable of handling gigabyte class files at gigabit-per-second data rates. The National Storage Laboratory was officially launched on 27 May 1992. Author (revised)

N93-30453*# National Library of Medicine, Bethesda, MD.
THE VISIBLE HUMAN PROJECT OF THE NATIONAL LIBRARY OF MEDICINE: REMOTE ACCESS AND DISTRIBUTION OF A MULTI-GIGABYTE DATA SET
Michael J. Ackerman *In* NASA. Goddard Space Flight Center, Goddard Conference on Mass Storage Systems and Technologies, Volume 1, 1993 p 87-88 (For primary document see N93-30449 11-82)
Avail: CASI HC A01/MF A03

As part of the 1986 Long-Range Plan for the National Library of Medicine (NLM), the Planning Panel on Medical Education wrote that NLM should '...thoroughly and systematically investigate the technical requirements for and feasibility of instituting a biomedical images library.' The panel noted the increasing use of images in clinical practice and biomedical research. An image library would complement NLM's existing bibliographic and factual database services and would ideally be available through the same computer networks as are these current NLM services. Early in 1989, NLM's Board of Regents convened an ad hoc planning panel to explore possible roles for the NLM in the area of electronic image libraries. In its report to the Board of Regents, the NLM Planning Panel on Electronic Image Libraries recommended that 'NLM should undertake a first project building a digital image library of volumetric data representing a complete, normal adult male and female. This Visible Human Project will include digitized photographic images for cryosectioning, digital images derived from computerized tomography, and digital magnetic resonance images of cadavers.' The technologies needed to support digital high resolution image libraries, including rapid development; and that NLM encourage investigator-initiated research into methods for representing and linking spatial and textual information, structural informatics. The first part of the Visible Human Project is the acquisition of cross-sectional CT and MRI digital images and cross-sectional cryosectional photographic images of a representative male and female cadaver at an average of one millimeter intervals. The corresponding cross-sections in each of the three modalities are to be registerable with one another. Author (revised)

N93-30454*# National Environmental Satellite Service, Suitland, MD.
DATA MANAGEMENT IN NOAA
William M. Callicott *In* NASA. Goddard Space Flight Center, Goddard Conference on Mass Storage Systems and Technologies, Volume 1, 1993 p 89-98 (For primary document see N93-30449 11-82)
Avail: CASI HC A02/MF A03

The NOAA archives contain 150 terabytes of data in digital form, most of which are the high volume GOES satellite image data. There are 630 data bases containing 2,350 environmental variables. There are 375 million film records and 90 million paper records in addition to the digital data base. The current data accession rate is 10 percent per year and the number of users are increasing at a 10 percent annual rate. NOAA publishes 5,000 publications and distributes over one million copies to almost 41,000 paying customers. Each year, over six million records are key entered from manuscript documents and about 13,000 computer tapes and 40,000 satellite hardcopy images are entered into the archive. Early digital data were stored on punched cards and open reel computer tapes. In the late seventies, an advanced helical scan technology (AMPEX TBM) was implemented. Now, punched cards have disappeared, the TBM system was abandoned, most data stored on open reel tapes have been migrated to 3480 cartridges, many specialized data sets were distributed on CD ROM's, special archives are being copied to 12 inch optical WORM disks, 5 1/4 inch magneto-optical disks were employed for workstation applications, and 8 mm EXABYTE tapes are planned for major data collection programs. The rapid expansion of new data sets, some of which constitute large volumes of data, coupled with the need for vastly improved access

mechanisms, portability, and improved longevity are factors which will influence NOAA's future systems approaches for data management.
Author (revised)

N93-30455*# Geological Survey, Sioux Falls, SD.
INTERIM REPORT ON LANDSAT NATIONAL ARCHIVE ACTIVITIES Abstract Only
John E. Boyd *In* NASA. Goddard Space Flight Center, Goddard Conference on Mass Storage Systems and Technologies, Volume 1, 1993 p 99 (For primary document see N93-30449 11-82)
Avail: CASI HC A01/MF A03

The Department of the Interior (DOI) has the responsibility to preserve and to distribute most Landsat Thematic Mapper (TM) and Multispectral Scanner (MSS) data that have been acquired by the five Landsat satellites operational since July 1972. Data that are still covered by exclusive marketing rights, which were granted by the U.S. Government to the commercial Landsat operator, cannot be distributed by the DOI. As the designated national archive for Landsat data, the U.S. Geological Survey's EROS Data Center (EDC) has initiated two new programs to protect and make available any of the 625,000 MSS scenes currently archived and the 200,000 TM scenes to be archived at EDC by 1995. A specially configured system has begun converting Landsat MSS data from obsolete high density tapes (HDT's) to more dense digital cassette tapes. After transcription, continuous satellite swaths are (1) divided into standard scenes defined by a world reference system, (2) geographically located by latitude and longitude, and (3) assessed for overall quality. Digital browse images are created by subsampling the full-resolution swaths. Conversion of the TM HDT's will begin in the fourth quarter of 1992 and will be conducted concurrently with MSS conversion. Although the TM archive is three times larger than the entire MSS archive, conversion of data from both sensor systems and consolidation of the entire Landsat archive at EDC will be completed by the end of 1994. Some MSS HDT's have deteriorated, primarily as a result of hydrolysis of the pigment binder. Based on a small sample of the 11 terabytes of post-1978 MSS data and the 41 terabytes of TM data to be converted, it appears that to date, less than 2 percent of the data have been lost. The data loss occurs within small portions of some scenes; few scenes are lost entirely. Approximately 10,000 pre-1979 MSS HDT's have deteriorated to such an extent, as a result of hydrolysis, that the data cannot be recovered without special treatment of the tapes. An independent consulting division of a major tape manufacturer has analyzed affected tapes and is confident that restorative procedures can be applied to the HDT's to permit one pass to reproduce the data on another recording media. A system to distribute minimally processed Landsat data will be procured in 1992 and will be operational by mid-1994. Any TM or MSS data in the national archive that are not restricted by exclusive marketing rights will be reproduced directly from the archive media onto user specified computer-compatible media. TM data will be produced either at a raw level (radiometrically and geometrically uncorrected) or at an intermediate level (radiometrically corrected and geometrically indexed). MSS data will be produced to an intermediate level or to a fully corrected level (radiometrically corrected and geometrically transformed to an Oblique Mercator projection). The system will be capable of providing ordered scenes within 48 hours of receipt of order. Author (revised)

N93-30456*# National Aeronautics and Space Administration. Goddard Space Flight Center, Greenbelt, MD.
MR-CDF: MANAGING MULTI-RESOLUTION SCIENTIFIC DATA
Kenneth Salem (Maryland Univ., College Park.) *In its* Goddard Conference on Mass Storage Systems and Technologies, Volume 1, 1993 p 101-111 (For primary document see N93-30449 11-82)
Avail: CASI HC A03/MF A03

MR-CDF is a system for managing multi-resolution scientific data sets. It is an extension of the popular CDF (Common Data Format) system. MR-CDF provides a simple functional interface to client programs for storage and retrieval of data. Data is stored so that low resolution versions of the data can be provided quickly. Higher resolutions are also available, but not as quickly. By managing data with MR-CDF, an application can be relieved of the low-level details of data management, and can easily trade data resolution for improved access time. Author

N93-30457*# Loral AeroSys, Seabrook, MD.
HIGH-PERFORMANCE MASS STORAGE SYSTEM FOR WORKSTATIONS
T. Chiang, Y. Tang, L. Gupta, and S. Cooperman *In* NASA. Goddard Space Flight Center, Goddard Conference on Mass Storage Systems and Technologies, Volume 1, 1993 p 113-117 (For primary document see N93-30449 11-82)
Avail: CASI HC A01/MF A03

Reduced Instruction Set Computer (RISC) workstations and Personnel Computers (PC) are very popular tools for office automation, command and control, scientific analysis, database management, and many other applications. However, when using Input/Output (I/O) intensive applications, the RISC workstations and PC's are often overburdened with the tasks of collecting, staging, storing, and distributing data. Also, by using standard high-performance peripherals and storage devices, the I/O function can still be a common bottleneck process. Therefore, the high-performance mass storage system, developed by Loral AeroSys' Independent Research and Development (IR&D) engineers, can offload a RISC workstation of I/O related functions and provide high-performance I/O functions and external interfaces. The high-performance mass storage system has the capabilities to ingest high-speed real-time data, perform signal or image processing, and stage, archive, and distribute the data. This mass storage system uses a hierarchical storage structure, thus reducing the total data storage cost, while maintaining high-I/O performance. The high-performance mass storage system is a network of low-cost parallel processors and storage devices. The nodes in the network have special I/O functions such as: SCSI controller, Ethernet controller, gateway controller, RS232 controller, IEEE488 controller, and digital/analog converter. The nodes are interconnected through high-speed direct memory access links to form a network. The topology of the network is easily reconfigurable to maximize system throughput for various applications. This high-performance mass storage system takes advantage of a 'busless' architecture for maximum expandability. The mass storage system consists of magnetic disks, a WORM optical disk jukebox, and an 8mm helical scan tape to form a hierarchical storage structure. Commonly used files are kept in the magnetic disk for fast retrieval. The optical disks are used as archive media, and the tapes are used as backup media. The storage system is managed by the IEEE mass storage reference model-based UniTree software package. UniTree software will keep track of all files in the system, will automatically migrate the lesser used files to archive media, and will stage the files when needed by the system. The user can access the files without knowledge of their physical location. The high-performance mass storage system developed by Loral AeroSys will significantly boost the system I/O performance and reduce the overall data storage cost. This storage system provides a highly flexible and cost-effective architecture for a variety of applications (e.g., realtime data acquisition with a signal and image processing requirement, long-term data archiving and distribution, and image analysis and enhancement). Author (revised)

N93-30458*# General Electric Co., Camden, NJ. Government Communications Systems Dept.
GE NETWORKED MASS STORAGE SOLUTIONS SUPPORTING IEEE NETWORK MASS STORAGE MODEL
Donald Herzog *In* NASA. Goddard Space Flight Center, Goddard Conference on Mass Storage Systems and Technologies, Volume 1, 1993 p 119-121 (For primary document see N93-30449 11-82)
Avail: CASI HC A01/MF A03

The General Electric Government Communications Systems Department (GE/GCSD) has developed a near real time digital data storage and retrieval system that extends the capabilities currently available in today's marketplace. This system called DuraStore uses commercially available rotary tape drive technology with ANSI/IEEE standards for automated magnetic tape based data storage. It uses a nonproprietary approach to satisfy a wide range of data rates and storage capabilities requirements and is compliant with the IEEE Network Storage Model. Rotary tape drives, standard interfaces, application specific hardware/software, networked automated tape libraries, library administrator, write protection, volume/physical media linkages, and maximum resource utilization are addressed. Derived from text

N93-30459*# Exabyte Corp., Boulder, CO.
HIGH-SPEED DATA DUPLICATION/DATA DISTRIBUTION: AN ADJUNCT TO THE MASS STORAGE EQUATION
Kevin Howard *In* NASA. Goddard Space Flight Center, Goddard Conference on Mass Storage Systems and Technologies, Volume 1, 1993 p 123-133 (For primary document see N93-30449 11-82)
Avail: CASI HC A03/MF A03

The term 'mass storage' invokes the image of large on-site disk and tape farms which contain huge quantities of low- to medium-access data. Although the cost of such bulk storage is recognized, the cost of the bulk distribution of this data rarely is given much attention. Mass data distribution becomes an even more acute problem if the bulk data is part of a national or international system. If the bulk data distribution is to travel from one large data center to another large data center then fiber-optic cables or the use of satellite channels is feasible. However, if the distribution must be disseminated from a central site to a number of much smaller, and, perhaps varying sites, then cost prohibits the use of fiber-optic cable or satellite communication. Given these cost constraints much of the bulk distribution of data will continue to be disseminated via inexpensive magnetic tape using the various next day postal service options. For non-transmitted bulk data, our working hypotheses are that the desired duplication efficiency of the total bulk data should be established before selecting any particular data duplication system; and, that the data duplication algorithm should be determined before any bulk data duplication method is selected.
Author (revised)

N93-30460*# Strategic Management Resources Ltd., Bowie, MD.
THE FUNDAMENTALS AND FUTURES OF REMOVABLE MASS STORAGE ALTERNATIVES
Linda Kempster *In* NASA. Goddard Space Flight Center, Goddard Conference on Mass Storage Systems and Technologies, Volume 1, 1993 p 135-141 (For primary document see N93-30449 11-82)
Avail: CASI HC A02/MF A03

This article reflects my view of how the storage products have been introduced into the marketplace, where they came from, and where others will continue to come from in the future. My corporate goal is to be a resource for those searching for removable solutions to mass storage problems. My introduction to optical storage occurred a few months before signing a non-disclosure agreement with FileNet on 8 Aug. 1983. By 87 or 88, as the optical craze was getting more popular, I started looking for similar or complementary storage technologies. I am still looking and my research is constantly turning up new entrants into this field. Due to the scope of the coverage in this field, this article does not dwell on any single technology. The goal is to provide information that is not compiled in any other single source and focus on facts that are not commonly known. I have provided a few baseline assumptions to ensure the mathematical calculations remain consistent: (1) hard-copy 8.5 in x 11 in documents which are scanned at 200 dots per inch (dpi) and compressed at a ratio of 10:1 result in a document image which requires an average of 50 Kilobytes (KB) of storage; (2) an average ASCII page requires 2 KB of storage; (3) an average file cabinet drawer can hold 2500 pieces of paper; (4) one GB of storage can hold an average of 20,000 document images (a reel of 6250 tape holds 180 Megabytes (MB)). Author (revised)

N93-30461*# Sony Magnetic Products, Inc., Cypress, CA.
THE NT DIGITAL MICRO TAPE RECORDER c35
Toshikazu Sasaki, John Alstad, and Mike Younker *In* NASA. Goddard Space Flight Center, Goddard Conference on Mass Storage Systems and Technologies, Volume 1, 1993 p 143-157 (For primary document see N93-30449 11-82)
Avail: CASI HC A03/MF A03

The description of an audio recorder may at first glance seem out of place in a conference which has been dedicated to the discussion of the technology and requirements of mass data storage. However, there are several advanced features of the NT system which will be of interest to the mass storage technologist. Moreover, there are a sufficient number of data storage formats in current use which have evolved from their audio counterparts to recommend a close attention to major innovative introductions of audio storage formats. While the existing analog micro-cassette recorder has been (and will continue to be) adequate for various uses, there are significant benefits to be gained through the application of digital technology. The elimination of background tape hiss and the availability of two relatively wide band channels (for stereo recording), for example, would greatly enhance listenability and speech intelligibility. And with the use of advanced high-density recording and LSI circuit technologies, a digital micro recorder can realize unprecedented compactness with excellent energy efficiency. This is what was accomplished with the NT-1 Digital Micro Recorder. Its remarkably compact size contributes to its portability. The high-density NT format enables up to two hours of low-noise digital stereo recording on a cassette the size of a postage stamp. Its highly energy-efficient mechanical and electrical design results in low power consumption; the unit can be operated up to 7 hours (for continuous recording) on a single AA alkaline battery. Advanced user conveniences include a multifunction LCD readout. The unit's compactness and energy-efficiency, in particular, are attributes that cannot be matched by existing analog and digital audio formats. The size, performance, and features of the NT format are of benefit primarily to those who desire improved portability and audio quality in a personal memo product. The NT Recorder is the result of over ten years of intensive, multi-disciplinary research and development. What follows is a discussion of the technologies that have made the NT possible: (1) NT format mechanics, (2) NT media, (3) NT circuitry and board. Author (revised)

N93-30462*# AC Technology Systems and Storage Technology, McLean, VA.
RAID 7 DISK ARRAY c61
Lloyd Stout *In* NASA. Goddard Space Flight Center, Goddard Conference on Mass Storage Systems and Technologies, Volume 1, 1993 p 159-161 (For primary document see N93-30449 11-82)
Avail: CASI HC A01/MF A03

Each RAID level reflects a different design architecture. Associated with each is a backdrop of imposed limitations, as well as possibilities which may be exploited within the architectural constraints of that level. There are three unique features that differentiate RAID 7 from all other levels. RAID 7 is asynchronous with respect to usage of I/O data paths. Each I/O drive (includes all data and one parity drives) as well as each host interface (there may be multiple host interfaces) has independent control and data paths. This means that each can be accessed completely, independently, of the other. This is facilitated by a separate device cache for each device/interface as well. RAID 7 is asynchronous with respect to device hierarchy and data bus utilization. Each drive and each interface is connected to a high speed data bus controlled by the embedded operating system to make independent transfers to and from central cache. RAID 7 is asynchronous with respect to the operation of an embedded real time process oriented operating system. This means that exclusive and independent of the host, or multiple host paths, the embedded OS manages all I/O transfers asynchronously across the data and parity drives. A key factor to consider is that of the RAID 7's ability to anticipate and match host I/O usage patterns. This yields the following benefits over RAID's built around micro-code based architectures. RAID 7 appears to the host as a normally connected Big Fast Disk (BFD). RAID 7 appears, from the perspective of the individual disk devices, to minimize the total number of accesses and optimize read/write transfer requests. RAID 7 smoothly integrates the random demands of independent users with the principles of spatial and temporal locality. This optimizes small, large, and time sequenced I/O requests which results in users having an I/O performance which approaches performance to that of main memory. Author (revised)

N93-30463*# Carnegie-Mellon Univ., Pittsburgh, PA. School of Computer Science.
TUTORIAL: PERFORMANCE AND RELIABILITY IN REDUNDANT DISK ARRAYS c61
Garth A. Gibson *In* NASA. Goddard Space Flight Center, Goddard Conference on Mass Storage Systems and Technologies, Volume 1, 1993 p 163-202 (For primary document see N93-30449 11-82)
Avail: CASI HC A03/MF A03

A disk array is a collection of physically small magnetic disks that is packaged as a single unit but operates in parallel. Disk arrays capitalize on the availability of small-diameter disks from a price-competitive market to provide the cost, volume, and capacity of current disk systems but many times their performance. Unfortunately, relative to current disk systems, the larger number of components in disk arrays leads to higher rates of failure. To tolerate failures, redundant disk arrays devote a fraction of their capacity to an encoding of their information. This redundant information enables the contents of a failed disk to be recovered from the contents of non-failed disks. The simplest and least expensive encoding for this redundancy, known as N+1 parity is highlighted. In addition to compensating for the higher failure rates of disk arrays, redundancy allows highly reliable secondary storage systems to be built much more cost-effectively than is now achieved in conventional duplicated disks. Disk arrays that combine redundancy with the parallelism of many small-diameter disks are often called Redundant Arrays of Inexpensive Disks (RAID). This combination promises improvements to both the performance and the reliability of secondary storage. For example, IBM's premier disk product, the IBM 3390, is compared to a redundant disk array constructed of 84 IBM 0661 3 1/2-inch disks. The redundant disk array has comparable or superior values for each of the metrics given and appears likely to cost less. In the first section of this tutorial, I explain how disk arrays exploit the emergence of high performance, small magnetic disks to provide cost-effective disk parallelism that combats the access and transfer gap problems. The flexibility of disk-array configurations benefits manufacturer and consumer alike. In contrast, I describe in this tutorial's second half how parallelism, achieved through increasing numbers of components, causes overall failure rates to rise. Redundant disk arrays overcome this threat to data reliability by ensuring that data remains available during and after component failures. Author (revised)

N93-30464*# California Univ., Berkeley. Computer Science Dept.
STRIPED TERTIARY STORAGE ARRAYS
Ann L. Drapeau *In* NASA. Goddard Space Flight Center, Goddard Conference on Mass Storage Systems and Technologies, Volume 1, 1993 p 203-213 (For primary document see N93-30449 11-82)
Avail: CASI HC A03/MF A03

Data stripping is a technique for increasing the throughput and reducing the response time of large access to a storage system. In striped magnetic or optical disk arrays, a single file is striped or interleaved across several disks; in a striped tape system, files are interleaved across tape cartridges. Because a striped file can be accessed by several disk drives or tape recorders in parallel, the sustained bandwidth to the file is greater than in non-striped systems, where access to the file are restricted to a single device. It is argued that applying striping to tertiary storage systems will provide needed performance and reliability benefits. The performance benefits of striping for applications using large tertiary storage systems is discussed. It will introduce commonly available tape drives and libraries, and discuss their performance limitations, especially focusing on the long latency of tape accesses. This section will also describe an event-driven tertiary storage array simulator that is being used to understand the best ways of configuring these storage arrays. The reliability problems of magnetic tape devices are discussed, and plans for modeling the overall reliability of striped tertiary storage arrays to identify the amount of error correction required are described. Finally, work being done by other members of the Sequoia group to address latency of accesses, optimizing tertiary storage arrays that perform mostly writes, and compression is discussed. Author (revised)

N93-30465*# National Media Lab., Saint Paul, MN.
NATIONAL MEDIA LABORATORY MEDIA TESTING RESULTS Abstract Only
William Mularie *In* NASA. Goddard Space Flight Center, Goddard Conference on Mass Storage Systems and Technologies, Volume 1, 1993 p 215 (For primary document see N93-30449 11-82)
Avail: CASI HC A01/MF A03

The government faces a crisis in data storage, analysis, archive, and communication. The sheer quantity of data being poured into the government systems on a daily basis is overwhelming systems ability to capture, analyze, disseminate, and store critical information. Future systems requirements are even more formidable: with single government platforms having data rate of over 1 Gbit/sec, greater than Terabyte/day storage requirements, and with expected data archive lifetimes of over 10 years. The charter of the National Media Laboratory (NML) is to focus the resources of industry, government, and academia on government needs in the evaluation, development, and field support of advanced recording systems. Derived from text

N93-30466*# National Media Lab., Saint Paul, MN.
EVALUATION OF D-1 TAPE AND CASSETTE CHARACTERISTICS: MOISTURE CONTENT OF SONY AND AMPEX D-1 TAPES WHEN DELIVERED **c35**
Gary Ashton *In* NASA. Goddard Space Flight Center, Goddard Conference on Mass Storage Systems and Technologies, Volume 1, 1993 p 217-238 (For primary document see N93-30449 11-82)
Avail: CASI HC A03/MF A03

Commercial D-1 cassette tapes and their associated recorders were designed to operate in broadcast studios and record in accordance with the International Radio Consultative Committee (CCIR) 607 digital video standards. The D-1 recorder resulted in the Society of Motion Picture and Television Engineers (SMPTE) standards 224 to 228 and is the first digital video recorder to be standardized for the broadcast industry. The D-1 cassette and associated media are currently marketed for broadcast use. The recorder was redesigned for data applications and is in the early stages of being evaluated. The digital data formats used are specified in MIL-STD-2179 and the American National Standards Institute (ANSI) X3.175-190 standard. In early 1990, the National Media Laboratory (NML) was asked to study the effects of time, temperature, and relative humidity on commercial D-1 cassettes. The environmental range to be studied was the one selected for the Advanced Tactical Air Reconnaissance System (ATARS) program. Several discussions between NML personnel, ATARS representatives, recorder contractors, and other interested parties were held to decide upon the experimental plan to be implemented. Review meetings were held periodically during the course of the experiment. The experiments were designed to determine the dimensional stability of the media and cassette since this is one of the major limiting factors of helical recorders when the media or recorders are subjected to non-broadcasting environments. Measurements were also made to characterize each sample of cassettes to give preliminary information on which purchase specifications could be developed. The actual tests performed on the cassettes and media before and after aging fall into the general categories listed. Author (revised)

N93-30467*# Data Storage Technologies, Inc., Ridgewood, NJ.
GRAND CHALLENGES IN MASS STORAGE: A SYSTEMS INTEGRATORS PERSPECTIVE
Richard R. Lee and Daniel G. Mintz (Culver, W. J. Consulting, Inc., Vienna, VA.) *In* NASA. Goddard Space Flight Center, Goddard Conference on Mass Storage Systems and Technologies, Volume 1, 1993 p 239-243 (For primary document see N93-30449 11-82)
Avail: CASI HC A01/MF A03

Within today's much ballyhooed supercomputing environment, with its CFLOPS of CPU power, and Gigabit networks, there exists a major roadblock to computing success; that of Mass Storage. The solution to this mass storage problem is considered to be one of the 'Grand Challenges' facing the computer industry today, as well as long into the future. It has become obvious to us, as well as many others in the industry, that there is no clear single solution in sight. The Systems Integrator today is faced with a myriad of quandaries in approaching this challenge. He must first be innovative in approach, second choose hardware solutions that are volumetric efficient; high in signal bandwidth; available from multiple sources; competitively priced, and have forward growth extendibility. In addition he must also comply with a variety of mandated, and often conflicting software standards (GOSIP, POSIX, IEEE, MSRM 4.0, and others), and finally he must deliver a systems solution with the 'most bang for the buck' in terms of cost vs. performance factors. These quandaries challenge the Systems Integrator to 'push the envelope' in terms of his or her ingenuity and innovation on an almost daily basis. This dynamic is explored further, and an attempt to acquaint the audience with rational approaches to this 'Grand Challenge' is made. Author (revised)

N93-30468*# Penny and Giles Data Recorders Ltd. (England).
THE MODERN HIGH RATE DIGITAL CASSETTE RECORDER **c35**
Martin Clemow *In* NASA. Goddard Space Flight Center, Goddard Conference on Mass Storage Systems and Technologies, Volume 1, 1993 p 245-249 (For primary document see N93-30449 11-82)
Avail: CASI HC A03/MF A03

The magnetic tape recorder has played an essential role in the capture and storage of instrumentation data for more than thirty years. During this time, data recording technology has steadily progressed to meet user demands for more channels, wider bandwidths, and longer recording durations. When acquisition and processing moved from analog to digital techniques, so recorder design followed suit. Milestones marking the evolution of the data recorder through these various stages - multi-track analog, high density longitudinal digital, and more recently rotary digital - have often represented important breakthroughs in the handling of ever-greater quantities of data. Throughout this period there has been a very clear line of demarcation between data storage methods in the 'instrumentation world' on the one hand and the 'computer peripheral world' on the other. This is despite the fact that instrumentation data, whether analog or digital at the point of acquisition, is now likely to be processed on a digital computer at some stage. Regardless of whether the processing device is a small personal computer, a workstation, or the largest supercomputer, system integrators have traditionally been faced with the same basic problem - how to interface what is essentially a manually controlled, continuously running device (the tape recorder) into the fast start/stop computer environment without resorting to an excessive amount of complex custom interfacing and performance compromise. The increasing availability of affordable high power processing equipment throughout the scientific world is forcing recorder manufacturers to make their latest and perhaps most important breakthrough - the computer-friendly data recorder. The operating characteristics of such recorders are discussed and the resultant impact on both data acquisition and data analysis elements of system configuration are considered. Author (revised)

N93-30469*# Laboratoire Central de Recherches Thomson-CSF, Orsay (France).
TOWARDS A 1000 TRACKS DIGITAL TAPE RECORDER **c35**
J. M. Coutellier, J. P. Castera, J. Colineau, J. C. Lehureau, F. Maurice (Thomson Consumer Electronics, Illkirch, France.), and C. Hanna (Thomson Consumer Electronics, Illkirch, France.) *In* NASA. Goddard Space Flight Center, Goddard Conference on Mass Storage Systems and Technologies, Volume 1, 1993 p 251-252 (For primary document see N93-30449 11-82)
Avail: CASI HC A01/MF A03

As the demand for high data rate (up to 1 Gb/s), high density (down to 1 sq micron/bit) tape recorder increases, the main investigation trend is an improvement of the well known helical scan concept. The drawbacks of this technology are also well known; sophisticated mechanics, head to tape contact, and wear problems. In our fixed head approach, the recorder mechanics is made much more simple, but the complexity is turned towards the integrated magnetic components, which have to record and reproduce hundreds of tracks in parallel. Our multiplexed write inductive head and magneto-optical readout head will be described, and the global system performances evaluated. Author (revised)

N93-30470*# Datatape, Inc., Pasadena, CA.
EVOLUTION OF A HIGH-PERFORMANCE STORAGE SYSTEM BASED ON MAGNETIC TAPE INSTRUMENTATION RECORDERS **c35**
Bruce Peters *In* NASA. Goddard Space Flight Center, Goddard Conference on Mass Storage Systems and Technologies, Volume 1, 1993 p 253-256 (For primary document see N93-30449 11-82)
Avail: CASI HC A01/MF A03

In order to provide transparent access to data in network computing environments, high performance storage systems are getting smarter as well as faster. Magnetic tape instrumentation recorders contain an increasing amount of intelligence in the form of software and firmware that manages the processes of capturing input signals and data, putting them on media and then reproducing or playing them back. Such intelligence makes them better recorders, ideally suited for applications requiring the high-speed capture and playback of large streams of signals or data. In order to make recorders better storage systems, intelligence is also being added to provide appropriate computer and network interfaces along with services that enable them to interoperate with host computers or network client and server entities. Thus, recorders are evolving into high-performance storage systems that become an integral part of a shared information system. Data tape has embarked on a program with the Caltech sponsored Concurrent Supercomputer Consortium to develop a smart mass storage system. Working within the framework of the emerging IEEE Mass Storage System Reference Model, a high-performance storage system that works with the STX File Server to provide storage services for the Intel Touchstone Delta Supercomputer is being built. Our objective is to provide the required high storage capacity and transfer rate to support grand challenge applications, such as global climate modeling. Author (revised)

N93-30471*# LaserTape Systems, Inc., San Jose, CA.
MASS OPTICAL STORAGE-TAPE (MOST)
William S. Oakley *In* NASA. Goddard Space Flight Center, Goddard Conference on Mass Storage Systems and Technologies, Volume 1, 1993 p 257-264 (For primary document see N93-30449 11-82)
Avail: CASI HC A02/MF A03

In today's large mainframe and supercomputer environment there exists a continuous demand for increased performance in digital storage systems. The user need for near-line storage capacity is currently doubling every four years. In addition to higher capacity, a desire exists for higher data transfer rates, and longer term database archivability, at lower, and lower cost. Each component of this quartet of demands appears to be insatiable. Magnetic tape technology presently dominates the digital mass storage markets, but the continuous growth of requirements is drawing attention to the limitations of the technology as an archival mass storage medium. The lowest cost option currently available for long term data storage is to use magnetic tape, although it is not well suited to meeting the need for many tens of years of reliable storage. Today, the majority of magnetic tape mass storage systems are based on the IBM 3480/3490 (or compatible) tape drives. These drives offer only moderate transfer rates and relatively small increments of storage, both of which create a logistics problem due to the large numbers of cartridges necessary in a typical system and the time taken to transfer data. Both higher cartridge capacity and data transfer rates are available in some helical scan magnetic tape systems; however, these command a substantially higher price, exacerbating the cost problem, and are not compatible with most installed systems or tape databases. Author (revised)

N93-30472*# Imperial Chemical Industries Ltd., Brantham (England). Imagedata Div.
ICI OPTICAL DATA STORAGE TAPE: AN ARCHIVAL MASS STORAGE MEDIA
Andrew J. Ruddick *In* NASA. Goddard Space Flight Center, Goddard Conference on Mass Storage Systems and Technologies, Volume 1, 1993 p 265-273 (For primary document see N93-30449 11-82)
Avail: CASI HC A02/MF A03

At the 1991 Conference on Mass Storage Systems and Technologies, ICI Imagedata presented a paper which introduced ICI Optical Data Storage Tape. This paper placed specific emphasis on the media characteristics and initial data was presented which illustrated the archival stability of the media. More exhaustive analysis that was carried out on the chemical stability of the media is covered. Equally important, it also addresses archive management issues associated with, for example, the benefits of reduced rewind requirements to accommodate tape relaxation effects that result from careful tribology control in ICI Optical Tape media. ICI Optical Tape media was designed to meet the most demanding requirements of archival mass storage. It is envisaged that the volumetric data capacity, long term stability and low maintenance characteristics demonstrated will have major benefits in increasing reliability and reducing the costs associated with archival storage of large data volumes. Author (revised)

N93-30473*# Dow Chemical Co., Midland, MI. Central Research.
FLEXIBLE STORAGE MEDIUM FOR WRITE-ONCE OPTICAL TAPE
Andrew J. G. Strandjord, Steven P. Webb, Donald J. Perettie, and Robert A. Cipriano *In* NASA. Goddard Space Flight Center, Goddard Conference on Mass Storage Systems and Technologies, Volume 1, 1993 p 275-284 (For primary document see N93-30449 11-82)
Avail: CASI HC A02/MF A03

A write-once data storage media was developed which is suitable for optical tape applications. The media is manufactured using a continuous film process to deposit a ternary alloy of tin, bismuth, and copper. This laser sensitive layer is sputter deposited onto commercial plastic web as a single-layer thin film. A second layer is sequentially deposited on top of the alloy to enhance the media performance and act as an abrasion resistant hard overcoat. The media was observed to have laser write sensitivities of less than 2.0 njoules/bit, carrier-to-noise levels of greater than 50dB's, modulation depths of approximately 100 percent, read-margins of greater than 35, uniform grain sizes of less than 200 Angstroms, and a media lifetime that exceeds 10 years. Prototype tape media was produced for use in the CREO drive system. The active and overcoat materials are first sputter deposited onto three mil PET film in a single pass through the vacuum coating system, and then converted down into multiple reels of 35mm x 880m tape. One mil PET film was also coated in this manner and then slit and packaged into 3480 tape cartridges. Author (revised)

N93-30474*# Optex, Inc., Rockville, MD.
ELECTRON TRAPPING DATA STORAGE SYSTEM AND APPLICATIONS Abstract Only
Daniel Brower, Allen Earman, and M. H. Chaffin *In* NASA. Goddard Space Flight Center, Goddard Conference on Mass Storage Systems and Technologies, Volume 1, 1993 p 285 (For primary document see N93-30449 11-82)
Avail: CASI HC A01/MF A03

The advent of digital information storage and retrieval has led to explosive growth in data transmission techniques, data compression alternatives, and the need for high capacity random access data storage. Advances in data storage technologies are limiting the utilization of digitally based systems. New storage technologies will be required which can provide higher data capacities and faster transfer rates in a more compact format. Magnetic disk/tape and current optical data storage technologies do not provide these higher performance requirements for all digital data applications. A new technology developed at the Optex Corporation out-performs all other existing data storage technologies. The Electron Trapping Optical Memory (ETOM) media is capable of storing as much as 14 gigabytes of uncompressed data on a single, double-sided 54 inch disk with a data transfer rate of up to 12 megabits per second. The disk is removable, compact, lightweight, environmentally stable, and robust. Since the Write/Read/Erase (W/R/E) processes are carried out 100 percent photonically, no heating of the recording media is required. Therefore, the storage media suffers no deleterious effects from repeated Write/Read/Erase cycling. Author (revised)

N93-30475*# CONVEX Computer Corp., Richardson, TX.
THE STATE OF THE STATE OF THE ART IN MASS STORAGE TECHNOLOGY
Dale Lancaster *In* NASA. Goddard Space Flight Center, Goddard Conference on Mass Storage Systems and Technologies, Volume 1, 1993 p 287-293 (For primary document see N93-30449 11-82)
Avail: CASI HC A02/MF A03

In the last couple years, there has been an abnormal amount of interest and activity in the automated mass storage application area. At Convex we have been heavily involved in some of these efforts. Some of our experiences are described and the trends that are occurring in this industry are also discussed. Author (revised)

N93-30476*# Supercomputer Research Center, Bowie, MD.
MEASUREMENTS OVER DISTRIBUTED HIGH PERFORMANCE COMPUTING AND STORAGE SYSTEMS
Elizabeth Williams and Tom Myers (Department of Defense, Fort Meade, MD.) *In* NASA. Goddard Space Flight Center, Goddard Conference on Mass Storage Systems and Technologies, Volume 1, 1993 p 295-297 (For primary document see N93-30449 11-82)
Avail: CASI HC A01/MF A03

Requirements are carefully described in descriptions of systems to be acquired but often there is no requirement to provide measurements and performance monitoring to ensure that requirements are met over the long term after acceptance. A set of measurements for various UNIX-based systems will be available at the 1992 Goddard Conference on Mass Storage Systems and Technologies. The authors invite others to contribute to the set of measurements. The framework for presenting the measurements of supercomputers, workstations, file servers, mass storage systems, and the networks that interconnect them are given. Production control and database systems are also included. Though other applications and third party software systems are not addressed, it is important to measure them as well. The capability to integrate measurements from all these components from different vendors, and from the third party software systems was recognized and there are efforts to standardize a framework to do this. The measurement activity falls into the domain of management standards. Standards work is ongoing for Open Systems Interconnection (OSI) systems management; AT&T, Digital, and Hewlett-Packard are developing management systems based on this architecture even though it is not finished. Another effort is in the UNIX International Performance Management Working Group. In addition, there are the Open Systems Foundation's Distributed Management Environment and the Object Management Group. A paper comparing the OSI systems management model and the Object Management Group model has been written. The IBM world has had a capability for measurement for various IBM systems since the 1970's and different vendors were able to develop tools for analyzing and viewing these measurements. Since IBM was the only vendor, the user groups were able to lobby IBM for the kinds of measurements needed. In the UNIX world of multiple vendors, a common set of measurements will not be as easy to get.
Author (revised)

N93-30477*# Digital Equipment Corp., Maynard, MA.
ANALYSIS OF CACHE FOR STREAMING TAPE DRIVE **c35**
V. Chinnaswamy *In* NASA. Goddard Space Flight Center, Goddard Conference on Mass Storage Systems and Technologies, Volume 1, 1993 p 299-310 (For primary document see N93-30449 11-82)
Avail: CASI HC A03/MF A03

A tape subsystem consists of a controller and a tape drive. Tapes are used for backup, data interchange, and software distribution. The backup operation is addressed. During a backup operation, data is read from disk, processed in CPU, and then sent to tape. The processing speeds of a disk subsystem, CPU, and a tape subsystem are likely to be different. A powerful CPU can read data from a fast disk, process it, and supply the data to the tape subsystem at a faster rate than the tape subsystem can handle. On the other hand, a slow disk drive and a slow CPU may not be able to supply data fast enough to keep a tape drive busy all the time. The backup process may supply data to tape drive in bursts. Each burst may be followed by an idle period. Depending on the nature of the file distribution in the disk, the input stream to the tape subsystem may vary significantly during backup. To compensate for these differences and optimize the utilization of a tape subsystem, a cache or buffer is introduced in the tape controller. Most of the tape drives today are streaming tape drives. A streaming tape drive goes into reposition when there is no data from the controller. Once the drive goes into reposition, the controller can receive data, but it cannot supply data to the tape drive until the drive completes its reposition. A controller can also receive data from the host and send data to the tape drive at the same time. The relationship of cache size, host transfer rate, drive transfer rate, reposition, and ramp up times for optimal performance of the tape subsystem are investigated. Formulas developed will also show the advantages of cache watermarks to increase the streaming time of the tape drive, maximum loss due to insufficient cache, tradeoffs between cache and reposition times and the effectiveness of cache on a streaming tape drive due to idle times or interruptions due in host transfers. Several mathematical formulas are developed to predict the performance of the tape drive. Some examples are given illustrating the usefulness of these formulas. Finally, a summary and some conclusions are provided. Author (revised)

N93-30478*# Los Alamos National Lab., NM. Computer Systems Group.
LANL HIGH-PERFORMANCE DATA SYSTEM (HPDS)
M. William Collins, Danny Cook, Lynn Jones, Lynn Kluegel, and Cheryl Ramsey *In* NASA. Goddard Space Flight Center, Goddard Conference on Mass Storage Systems and Technologies, Volume 1, 1993 p 311-316 (For primary document see N93-30449 11-82)
Avail: CASI HC A02/MF A03

The Los Alamos High-Performance Data System (HPDS) is being developed to meet the very large data storage and data handling requirements of a high-performance computing environment. The HPDS will consist of fast, large-capacity storage devices that are directly connected to a high-speed network and managed by software distributed in workstations. The HPDS model, the HPDS implementation approach, and experiences with a prototype disk array storage system are presented.
Author (revised)

N93-30479*# Exabyte Corp., Boulder, CO.
OPTIMIZING DIGITAL 8MM DRIVE PERFORMANCE **c35**
Gerry Schadegg *In* NASA. Goddard Space Flight Center, Goddard Conference on Mass Storage Systems and Technologies, Volume 1,

1993 p 317-328 (For primary document see N93-30449 11-82)
Avail: CASI HC A03/MF A03

The experience of attaching over 350,000 digital 8mm drives to 85-plus system platforms has uncovered many factors which can reduce cartridge capacity or drive throughput, reduce reliability, affect cartridge archivability and actually shorten drive life. Some are unique to an installation. Others result from how the system is set up to talk to the drive. Many stem from how applications use the drive, the work load that's present, the kind of media used and, very important, the kind of cleaning program in place. Digital 8mm drives record data at densities that rival those of disk technology. Even with technology this advanced, they are extremely robust and, given proper usage, care and media, should reward the user with a long productive life. The 8mm drive will give its best performance using high-quality 'data grade' media. Even though it costs more, good 'data grade' media can sustain the reliability and rigorous needs of a data storage environment and, with proper care, give users an archival life of 30 years or more. Various factors, taken individually, may not necessarily produce performance or reliability problems. Taken in combination, their effects can compound, resulting in rapid reductions in a drive's serviceable life, cartridge capacity, or drive performance. The key to managing media is determining the importance one places upon their recorded data and, subsequently, setting media usage guidelines that can deliver data reliability. Various options one can implement to optimize digital 8mm drive performance are explored. Author (revised)

N93-30480*# Carnegie-Mellon Univ., Pittsburgh, PA.
USING TRANSPARENT INFORMED PREFETCHING (TIP) TO REDUCE FILE READ LATENCY **c60**
R. H. Patterson, G. A. Gibson, and M. Satyanarayanan *In* NASA. Goddard Space Flight Center, Goddard Conference on Mass Storage Systems and Technologies, Volume 1, 1993 p 329-342 (For primary document see N93-30449 11-82)
Avail: CASI HC A03/MF A03

As processor performance gains continue to outstrip Input/Output gains, I/O performance is becoming critical to overall system performance. File read latency is the most significant bottleneck for high performance I/O. Other aspects of I/O performance benefit from recent advances in disk bandwidth and throughput resulting from disk arrays, and in write performance derived from buffered write behind and the Log-structured File System. The access gap problem limiting improvements in read latency is exacerbated by distributed file systems operating over networks with diverse bandwidth. Focus is on extending the power of caching and prefetching to reduce file read latencies by exploiting hints from high-levels of a system. Such Transparent Informed Prefetching, TIP, and its benefits are described. It is argued that hints that disclose high level knowledge are a means for transferring optimization information across, without violating, module boundaries. How TIP can be used to convert the high throughput of new technologies such as disk arrays and log-structured file systems into low latency for applications is discussed. Our preliminary experiments show reductions in wall - clock execution time of 13 percent and 20 percent for a multiple module compilation tool (make) accessing data on a local disk and remote Coda file server, respectively, and a reduction of 30 percent for a text search (grep) remotely accessing many small files. Author (revised)

N93-30482# Sandia National Labs., Albuquerque, NM.
PROPOSAL FOR A NUMERICAL ARRAY LIBRARY
26 Feb. 1993 15 p Presented at the American National Standards Institute X3 Information Processing Systems Meeting, Portland, OR, 11 Mar. 1993
(Contract DE-AC04-76DP-00789)
(DE93-010678; SAND-93-0670C; CONF-9303100-2) Avail: CASI HC A03/MF A01

One of the most widely recognized inadequacies of C is its low-level treatment of arrays. Arrays are not first-class objects in C; an array name in an expression almost always decays into a pointer to the underlying type. This is unfortunate, especially since an increasing number of high-performance computers are optimized for calculations involving arrays of numbers. On such machines, double left square bracket-right square bracket may be regarded as an intrinsic data type comparable to double or int and quite distinct from double. This weakness of C is acknowledged in the ARM, where it is suggested that the inadequacies of the C array can be overcome in C++ by wrapping it in a class that supplies dynamic memory management bounds checking, operator syntax, and other useful features. Such 'smart arrays' can in fact supply the same functionality as the first-class arrays found in other high-level, general-purpose programming languages. Unfortunately, they are typically expensive in both time and memory and make poor use of advanced floating-point architectures. The reasons for these difficulties are discussed in X3JI6/92-0076//WG21/N0153, 'Optimization of Expressions Involving Array Classes'. Is there a better solution? The most obvious solution is to make arrays first-class objects and add the functionality mentioned in the previous paragraph. However, this would destroy C compatibility and significantly alter the C++ language. Major conflicts with existing practice would seem inevitable. I propose instead that a numerical array class be adopted as part of the C++ standard library. This class will have the functionality appropriate for the intrinsic arrays found on most high-performance computers, and the compilers written for these computers will be free to implement it as a built-in class. On other platforms, this class may be defined normally, and will provide users with basic array functionality without imposing an excessive burden on the implementor. DOE

N93-30559# Yale Univ., New Haven, CT. Dept. of Computer Science.
THE 1991 NEURAL INFORMATION PROCESSING SYSTEMS: NATURAL AND SYNTHETIC Final Report, 30 Sep. 1991 - 29 Sep. 1992
John Moody 4 Feb. 1993 24 p
(Grant AF-AFOSR-0438-91)
(AD-A264754; AFOSR-93-0271TR) Avail: CASI HC A03/MF A01

The 1991 'Neural Information Processing Systems-Natural and Synthetic' (NIPS) was held in Denver, CO, from 2-5 Dec. 1991. Since its inception in 1987, the NIPS conference has attracted researchers from many disciplines who are applying their expertise to problems in the field of neural networks. The conference and the following two day workshop have become a forum for presenting the latest research results and for leading researchers to gather and exchange ideas. The 1991 conference maintained the high level of excitement of its predecessors. Important new theoretical results were presented concerning the capability and generalization performance of networks. DTIC

N93-30907# Naval Postgraduate School, Monterey, CA.
A PROTOTYPE OF A FACULTY AND STAFF EXECUTIVE INFORMATION SYSTEM M.S. Thesis
Patricia D. Hutton Mar. 1993 86 p
(AD-A264852) Avail: CASI HC A05/MF A01

An alternative Naval Postgraduate School Facility and Staff Resume Book is prototyped. It designs and begins the development of a multimedia faculty and staff executive information system (EIS). This EIS is being developed using Asymetrix's Multimedia ToolBook authoring software. It uses computer graphics capability to display faculty and staff member photographs. In addition, the database component supports the manipulation and storage of large text fields. The hardware and software components of multimedia computing are also discussed. DTIC

N93-30994# Joint Inst. for Nuclear Research, Dubna (USSR). Lab. of Computing Techniques and Automation.
SOFTWARE CONCEPTION AND STRUCTURE OF AUTOMATED WORKSTATION FOR AN EXPERIMENTAL DATA PROCESSING [NAZNACHENIE I STRUKTURA PROGRAMMNOGO OBESPECHENIYA AVTOMATIZIROVANNOGO RABOCHEGO MESTA V RASPREDEIENNOJ SISTEME OBRABOTKI EHKSPERIMENTALNYKH DANNYKH]
V. G. Ivanov, F. F. Nodarse, and T. Ehrdehnehdehlgehr 1991 17 p
In RUSSIAN
(DE93-609815; JINR-R-10-91-105) Avail: CASI HC A03/MF A01 (US Sales Only)

In order to increase user efficiency and possibilities in the use of experimental data processing distributive systems, based on personal computers, the automated experimental data processing workstations are created. Basic principles including different kinds of users and their access attributes, operating regimes, the roll of the intelligent computer assistant, and software and hardware needed are analyzed. The software includes the following: knowledge bases, data bases, AI system building tools, intelligent system applications, general programs, and other service and teaching programs. DOE

N93-28803*# Geological Survey, Flagstaff, AZ.
SYSTEMATIC PROCESSING OF CLEMENTINE DATA FOR SCIENTIFIC ANALYSES Abstract Only
A. S. McEwen *In* Lunar and Planetary Inst., Workshop on Advanced Technologies for Planetary Instruments, Part 1 1993 p 17-18 (For primary document see N93-28764 11-91)
Avail: CASI HC A01/MF A01

N93-28811*# Consejo Superior de Investigaciones Cientificas, Tenerife (Spain). Inst. de Astrofisica de Canarias
DIGITAL IMAGE COMPRESSION USING ARTIFICIAL NEURAL NETWORKS Abstract Only
M. Serra-Ricart, L. Garrido (Barcelona Univ., Spain.), V. Gaitan (Barcelona Univ., Spain.), and A. Aloy (Digital Equipment Enterprise Espana S.A., Barcelona, Spain.) *In* Lunar and Planetary Inst., Workshop on Advanced Technologies for Planetary Instruments, Part 1 1993 p 20-21 (For primary document see N93-28764 11-91)
Avail: CASI HC A01/MF A01

N93-28814*# Naval Research Lab., Washington, DC.
THE BACKGROUNDS DATA CENTER Abstract Only
W. A. Snyder, H. Gursky, H. M. Heckathorn, R. L. Lucke, S. L. Berg (Computational Physics, Inc., Fairfax, VA.), E. G. Dombrowski (Sachs/Freeman Associates, Inc., Landover, MD.), and R. A. Kessel (Computational Physics, Inc., Fairfax, VA.) *In* Lunar and Planetary Inst., Workshop on Advanced Technologies for Planetary Instruments, Part 1 1993 p 21-22 (For primary document see N93-28764 11-91)
Avail: CASI HC A01/MF A01

N93-29549*# Technische Univ., Brunswick (Germany). Dept. of Computer Science.
INFORMATION COMPRESSION IN THE CONTEXT MODEL
Joerg Gebhardt, Rudolf Kruse, and Detlef Nauck *In* NASA. Johnson Space Center, North American Fuzzy Logic Processing Society (NAFIPS 1992), Volume 1 Dec. 1992 p 296-303 (For primary document see N93-29516 11-59)
Avail: CASI HC A02/MF A03

N93-29569*# Institut de Recherche en Informatique et Systemes Aleatoires, Lannion (France). ENSSAT.
ON THE EVALUATION OF FUZZY QUANTIFIED QUERIES IN A DATABASE MANAGEMENT SYSTEM
Patrick Bosc and Olivier Pivert *In* NASA. Johnson Space Center, North American Fuzzy Logic Processing Society (NAFIPS 1992), Volume 2 Dec. 1992 p 478-487 (For primary document see N93-29556 11-59)
Avail: CASI HC A02/MF A03

N93-29571*# Bell Communications Research, Inc., Livingston, NJ.
A HIGH PERFORMANCE, AD-HOC, FUZZY QUERY PROCESSING SYSTEM FOR RELATIONAL DATABASES
William H. Mansfield, Jr. and Robert M. Fleischman *In* NASA. Johnson Space Center, North American Fuzzy Logic Processing Society (NAFIPS 1992), Volume 2 Dec. 1992 p 496-505 (For primary document see N93-29556 11-59)
Avail: CASI HC A02/MF A03

N93-29625*# National Aeronautics and Space Administration. Goddard Space Flight Center, Greenbelt, MD.
EnviroNET: ON-LINE INFORMATION FOR LDEF
Michael Lauriente *In* NASA. Langley Research Center, LDEF: 69 Months in Space. Part 1: Second Post-Retrieval Symposium 51-67 (SEE N93-29621 11-99) Apr. 1993 (For primary document see N93-29621 11-99)
Avail: CASI HC A03/MF A03

N93-29631*# National Aeronautics and Space Administration. Marshall Space Flight Center, Huntsville, AL.
COLLECTION, ANALYSIS, AND ARCHIVAL OF LDEF ACTIVATION DATA
C. E. Laird (University of Eastern Kentucky, Richmond.), B. A. Harmon, G. J. Fishman, and T. A. Parnell *In* NASA. Langley Research Center, LDEF: 69 Months in Space. Part 1: Second Post-Retrieval Symposium Apr. 1993 p 111-124 (For primary document see N93-29621 11-99)
(NASA Order H-08071-D; NASA Order H-13029-D)
Avail: CASI HC A03/MF A03

N93-29704*# Schafer (W. J.) Associates, Inc., Hampton, VA.
LDEF ARCHIVAL SYSTEM PLAN
Brenda K. Wilson *In* NASA. Langley Research Center, LDEF: 69 months in Space. Part 4: Second Post-Retrieval Symposium Apr. 1993 p 1499-1509 (For primary document see N93-29682 11-99)
Avail: CASI HC A03/MF A03; 2 functional color pages

83 ECONOMICS AND COST ANALYSIS

Includes cost effectiveness studies.

N93-29100# California Univ., Berkeley.
PROPOSAL TO DEVELOP GUIDES FOR HIGH SCHOOL TEACHERS ON GLOBAL SYSTEMS SCIENCE
C. I. Sneider and R. Golden 16 Feb. 1993 4 p Prepared for California Univ., Davis
(Contract DE-FC03-90ER-61010)
(DE93-008759; DOE/ER-61010/T6) Avail: CASI HC A01/MF A01

The Lawrence Hall of Science requests funding for development of trial versions of five guides for high school teachers on the topic of Global Systems Science. The guides will reflect the guided-discovery approach for which the Lawrence Hall of Science has gained an international reputation. They will include a wealth of materials already developed as well as new materials, organized as a comprehensive program on global change. The guides could be used together for an entire one-semester course, or integrated individually into existing high school courses in the sciences and social studies. DOE

N93-29477# Naval Postgraduate School, Monterey, CA.
EVALUATING THE BIAS OF ALTERNATIVE COST PROGRESS MODELS: TESTS USING AEROSPACE INDUSTRY ACQUISITION PROGRAMS M.S. Thesis
David A. Tagg Dec. 1992 111 p
(AD-A262870) Avail: CASI HC A06/MF A02

The quality of cost estimates produced by each of four cost progress models - a random walk model, the traditional learning curve model, a production rate model (fixed-variable model), and a model incorporating both learning curve and production rate effects (Bemis production rate adjustment model) are evaluated. Emphasis is on assessing the level of bias associated with these models and determining the influence of various factors on model performance. Findings indicate, on average, the learning curve and Bemis models underestimate unit costs, while the random walk and fixed-variable models overestimate unit costs. Different factors are evaluated to determine their significance in explaining variations in the bias of unit cost predictions and relationships between the significant variables and model cost prediction bias are described. Findings indicate the Bemis model is superior to the other cost progress models because it exhibits the least bias and is not significantly influenced (in terms of bias) by variations in the factors considered. DTIC

N93-29668 Federal Library and Information Center Committee, Washington, DC.
THE 9TH FLICC FORUM ON FEDERAL INFORMATION POLICIES
C. Mulford, D. Dolan, A. K. Bohlin, R. Cermak, and J. Noble 1992 54 p Conference held in Washignton, DC, 17 Mar. 1992 See also PB92-147370 Limited Reproducibility: More than 20% of this document may be affected by microfiche quality
(PB93-184687) Copyright Avail: Issuing Activity

Contents: Current policy issues relating to government information; Case studies--problems, priorities and challenges; Changing information infostructure; Approaches and opportunities; Congressional policy initiatives regarding availability of federal government information and the role of the Joint Committee on Printing; A vision of the future; Keeping access to government-produced information open: The fallacy of information as a government profit center; Census data case study; The Patent and Trademark Office example: Managing massive amounts of data and delivering it to the public; State innovations in managing electronic information; The

European Community information policy program: establishing information priorities; Emerging roles for libraries and information centers; New linkages for library resources. NTIS

84 LAW, POLITICAL SCIENCE AND SPACE POLICY

Includes NASA appropriation hearings; aviation law; space law and policy; international law; international cooperation; and patent policy.

No abstracts in this category.

85 URBAN TECHNOLOGY AND TRANSPORTATION

Includes applications of space technology to urban problems; technology transfer; technology assessment; and surface and mass transportation.

For related information see also *03 Air Transportation and Safety, 16 Space Transportation,* and *44 Energy Production and Conversion.*

N93-28646# Los Alamos National Lab., NM.
APPLIED RESEARCH IN AMERICA
G. H. Canavan Mar. 1993 8 p
(Contract W-7405-eng-36)
(DE93-011725; LA-12448-MS) Avail: CASI HC A02/MF A01

There are structural problems in the execution of applied research in America which interfere with its competitiveness. They are hard to correct within the industrial sector itself. National Laboratories have the structure and talents to supply the missing stage of research that could improve the innovation process. That would require the laboratory to shift to a project orientation, serious involvement with industrial research, and attention to market discipline. If the process was successful, it would develop a mechanism for transferring much of the laboratory's activity to private sponsorship. Even if it was not, it would provide a mechanism for scaling back laboratory activities in accord with their actual worth. DOE

N93-29329# Pacific Northwest Lab., Richland, WA.
TECHNOLOGY TRANSFER PERSONNEL EXCHANGE AT THE BOEING COMPANY
Z. I. Antoniak Mar. 1993 68 p
(Contract DE-AC06-76RL-01830)
(DE93-010190; PNL-8549) Avail: CASI HC A04/MF A01

The objective of the exchange was to transfer Pacific Northwest Laboratory (PNL) technology and expertise in advanced ceramic fabric composites (ACFC) to the Boeing Defense & Space Group (Boeing Aerospace). Boeing Aerospace was especially interested in applying PNL-developed ACFC technology to its current and future spacecraft and space missions. Boeing has on-going independent research and development (R&D) programs on advanced radiators and heat pipes; therefore, PNL research in ceramic fabric heat pipes was of particular interest to Boeing. Thus, this exchange assisted in the transfer of PNL's ACFC heat pipe technology and other related research capabilities to private industrial application. The project was proposed as an initial step in building a long-term collaborative relationship between Boeing and PNL that may result in future Cooperative Research and Development Agreements (CRADA's) and/or other types of collaborative efforts. DOE

N93-30692*# National Aeronautics and Space Administration, Washington, DC.
TECHNOLOGY TRANSFER AND THE CIVIL SPACE PROGRAM. VOLUME 2: WORKSHOP PROCEEDINGS
1992 500 p Workshop held in McLean, VA, 17-19 Mar. 1992
(NASA-TM-108250; NAS 1.15:108250) Avail: CASI HC A21/MF A04

The objectives were to (1) provide a top-level review of the Integrated Technology Plan (ITP) and current civil space technology plans, including planning processes and technologies; (2) discuss and assess technology transfer (TT) experiences across a wide range of participants; (3) identify alternate categories/strategies for TT and define the objectives of transfer processes in each case; (4) identify the roles of various government 'stakeholders', aerospace industry, industries at large, and universities in civil space technology research, development, demonstration, and transfer; (5) identify potential barriers and/or opportunities to successful civil space TT; (6) identify specific needs for innovations in policy, programs, and/or procedures to facilitate TT; and (7) develop a plan of attack for the development of a workshop report. Papers from the workshop are presented. For individual titles, see N93-30693 through N93-30726.

N93-30693*# National Aeronautics and Space Administration, Washington, DC.
OAST SPACE RESEARCH AND TECHNOLOGY APPLICATIONS: TECHNOLOGY TRANSFER SUCCESSES
Gregory M. Reck *In its* Technology Transfer and the Civil Space Program. Volume 2: Workshop Proceedings 1992 26 p (For primary document see N93-30692 11-85)
Avail: CASI HC A03/MF A04

The ultimate measure of success in the Space Research and Technology Program is the incorporation of a technology into an operational mission. Charts are presented that describe technology products which OAST has helped support that (1) have been used in a space mission, (2) have been incorporated into the baseline design of a flight system in the development phase, or (3) have been picked up by a commercial or other non-NASA user. We hope that these examples will demonstrate the value of investment in technology. Pictured on the charts are illustrations of the technology product, the mission or user which has incorporated the technology, and where appropriate, results from the mission itself. Derived from text

N93-30694*# Department of Energy, Washington, DC. Office of Technology Analysis.
DEPARTMENTAL TECHNOLOGY TRANSFER UPDATE
Roger A. Lewis *In* NASA, Washington, Technology Transfer and the Civil Space Program. Volume 2: Workshop Proceedings 1992 21 p (For primary document see N93-30692 11-85)
Avail: CASI HC A03/MF A04

The objective is the following: to provide the perspective of the Department of Energy (DOE); emphasize new and emerging initiatives; and address unresolved issues that might impact successful program implementation. The approach is the following: to provide a brief overview of DOE, its R&D, and its technology transfer assets; to briefly describe the evolution of DOE's enhanced technology transfer program; to report on specific progress and achievements over the past year--as the spring board for our current and future plans; to present our near and longer term plans; and to survey the remaining issues and the resolution process. Derived from text

N93-30695*# Commerce Dept., Washington, DC. Office of Space Commerce.
US SPACE COMMERCE, 1991
Scott Pace *In* NASA, Washington, Technology Transfer and the Civil Space Program. Volume 2: Workshop Proceedings 1992 7 p (For primary document see N93-30692 11-85)
Avail: CASI HC A02/MF A04

The topics are presented in viewgraph form and include the following: the US share of commercial payloads in comparison with Ariane's share; world communications satellite orders; the US share of prime contracts for construction of commercial communications satellites; emerging markets; space activities at the Commerce Department (DOC); Office of Space Commerce (OSC) mission description; key drivers for commercial space; and general DOC space policy themes. CASI

N93-30696*# Office of Science and Technology, Washington, DC.
WHITE HOUSE/OSTP PERSPECTIVE
Donald Pryor *In* NASA, Washington, Technology Transfer and the Civil Space Program. Volume 2: Workshop Proceedings 1992 7 p (For primary document see N93-30692 11-85)
Avail: CASI HC A02/MF A04

Two aspects of the Office of Science and Technology Policy (OSTP) are discussed: (1) efforts to state the overarching technology policy in which technology transfer plays an important part; and (2) efforts to coordinate federal R&D contracts programs in several technology areas through the Federal Coordinating Council for Science, Engineering, and Technology (FCCSET) process. Derived from text

N93-30697*# National Center for Advanced Technologies, Washington, DC.
THE NCAT PROCESS
George Milburn *In* NASA, Washington, Technology Transfer and the Civil Space Program. Volume 2: Workshop Proceedings 1992 7 p (For primary document see N93-30692 11-85)
Avail: CASI HC A02/MF A04

The topics are presented in viewgraph form and include the following: National Center for Appropriate Technology (NCAT) history; technologies selection criteria; strategic plan status; implementation framework; forum composition; NCAT role as integrator; government/industry coordination; identification and selection process for demonstrations; criteria for demonstrations; criteria for non-selection; and future actions. CASI

N93-30698*# Massachusetts Inst. of Tech., Cambridge. Technology Licensing Office.
THE ROLE OF THE UNIVERSITY LICENSING OFFICE IN TRANSFERRING INTELLECTUAL PROPERTY TO INDUSTRY
John T. Preston *In* NASA, Washington, Technology Transfer and the Civil Space Program. Volume 2: Workshop Proceedings 1992 12 p (For primary document see N93-30692 11-85)
Avail: CASI HC A03/MF A04

Universities in the US have a significant impact on business through the transfer of technology. This transfer of technology takes various forms, including faculty communications, faculty consulting activities, and the direct transfer of technology through the licensing of patents, copyrights, and other intellectual property to industry. The topics discussed include the following: background of the MIT Technology Licensing Office (TLO), goals of the MIT TLO, MIT's technology transfer philosophy, and important factors for success in new company formation. CASI

N93-30699*# National Aeronautics and Space Administration, Washington, DC.
TECHNOLOGY TRANSFER
Frank E. Penaranda *In its* Technology Transfer and the Civil Space Program. Volume 2: Workshop Proceedings 1992 9 p (For primary document see N93-30692 11-85)
Avail: CASI HC A02/MF A04

The topics are presented in viewgraph form and include the following: international comparison of R&D expenditures in 1989; NASA Technology Transfer Program; NASA Technology Utilization Program thrusts for FY 1992 and FY 1993; National Technology Transfer Network; and NTTC roles. CASI

N93-30700*# Wheeling Coll., WV. National Technology Transfer Center.
NATIONAL TECHNOLOGY TRANSFER CENTER
Lee W. Rivers *In* NASA, Washington, Technology Transfer and the Civil Space Program. Volume 2: Workshop Proceedings 1992 8 p (For primary document see N93-30692 11-85)
Avail: CASI HC A02/MF A04

Viewgraphs on the National Technology Transfer Center (NTTC) are provided. The NTTC mission is to serve as a hub for the nationwide technology-transfer network to expedite the movement of federally developed technology into the stream of commerce. A description of the Center is provided. CASI

N93-30701*# Martin Marietta Corp., New Orleans, LA. Manned Space Systems.
TECHNOLOGY TRANSFER FROM THE VIEWPOINT OF A NASA PRIME CONTRACTOR
Gordon Dyer *In* NASA, Washington, Technology Transfer and the Civil Space Program. Volume 2: Workshop Proceedings 1992 4 p (For primary document see N93-30692 11-85)
Avail: CASI HC A01/MF A04

Viewgraphs on technology transfer from the viewpoint of a NASA prime contractor are provided. Technology Transfer Program for Manned Space Systems and the Technology Transfer Program status are addressed. CASI

N93-30702*# Department of Energy, Washington, DC.
SANDIA NATIONAL LABORATORIES
Laura R. Gilliom *In* NASA, Washington, Technology Transfer and the Civil Space Program. Volume 2: Workshop Proceedings 1992 7 p (For primary document see N93-30692 11-85)
Avail: CASI HC A02/MF A04

Sandia National Laboratories has identified technology transfer to U.S. industry as a laboratory mission which complements our national security mission and as a key component of the Laboratory's future. A number of technology transfer mechanisms - such as CRADA's, licenses, work-for-others, and consortia - are identified and specific examples are given. Sandia's experience with the Specialty Metals Processing Consortium is highlighted with a focus on the elements which have made it successful. A brief discussion of Sandia's potential interactions with NASA under the Space Exploration Initiative was included as an example of laboratory-to-NASA technology transfer. Viewgraphs are provided. CASI

N93-30703*# National Aeronautics and Space Administration. Ames Research Center, Moffett Field, CA.
TECHNOLOGY TRANSFER NEEDS AND EXPERIENCES: THE NASA RESEARCH CENTER PERSPECTIVE
Anthony R. Gross *In* NASA, Washington, Technology Transfer and the Civil Space Program. Volume 2: Workshop Proceedings 1992 4 p (For primary document see N93-30692 11-85)
Avail: CASI HC A01/MF A04

Viewgraphs on technology transfer needs and experiences - the NASA Research Center perspective are provided. Topics covered include: functions of NASA, incentives and benefits, technology transfer mechanisms, economics of technology commercialization, examples, and conclusions. CASI

N93-30704*# National Aeronautics and Space Administration. Goddard Space Flight Center, Greenbelt, MD.
TECHNOLOGY TRANSFER WITHIN THE NASA GODDARD SPACE FLIGHT CENTER
Henry H. Plotkin *In* NASA, Washington, Technology Transfer and the Civil Space Program. Volume 2: Workshop Proceedings 1992 4 p (For primary document see N93-30692 11-85)
Avail: CASI HC A01/MF A04

Viewgraphs on technology transfer within the NASA Goddard Space Flight Center presented to Civil Space Technology Development workshop on technology transfer and effectiveness are provided. Topics covered include: obstacles to technology transfer; technology transfer improvement program at GSFC: communication between technology developers and users; and user feedback to technologists. CASI

N93-30705*# National Aeronautics and Space Administration. Goddard Space Flight Center, Greenbelt, MD.
TECHNOLOGY TRANSFER AND SPACE SCIENCE MISSIONS
Mario Acuna *In* NASA, Washington, Technology Transfer and the Civil Space Program. Volume 2: Workshop Proceedings 1992 3 p (For primary document see N93-30692 11-85)
Avail: CASI HC A01/MF A04

Viewgraphs on technology transfer and space science missions are provided. Topics covered include: project scientist role within NASA; role of universities in technology transfer; role of government laboratories in research; and technology issues associated with science. CASI

N93-30706*# National Aeronautics and Space Administration, Washington, DC.
TECHNOLOGY COORDINATION
Steven Hartman *In its* Technology Transfer and the Civil Space Program. Volume 2: Workshop Proceedings 1992 4 p (For primary document see N93-30692 11-85)
Avail: CASI HC A01/MF A04

Viewgraphs on technology coordination are provided. Topics covered include: technology coordination process to date; goals; how the Office of

Aeronautics and Space Technology (OAST) can support the Office of Space Science and Applications (OSSA); how OSSA can support OAST; steps to technology transfer; and recommendations. CASI

N93-30707*# Jet Propulsion Lab., California Inst. of Tech., Pasadena.
TECHNOLOGY TRANSFER
Thomas Handley *In* NASA, Washington, Technology Transfer and the Civil Space Program. Volume 2: Workshop Proceedings 1992 39 p (For primary document see N93-30692 11-85)
Avail: CASI HC A03/MF A04

The requirements for a successful technology transfer program and what such a program would look like are discussed. In particular, the issues associated with technology transfer in general, and within the Jet Propulsion Laboratory (JPL) environment specifically are addressed. The section on background sets the stage, identifies the barriers to successful technology transfer, and suggests actions to address the barriers either generally or specifically. The section on technology transfer presents a process with its supporting management plan that is required to ensure a smooth transfer process. Viewgraphs are also included. CASI

N93-30708*# National Aeronautics and Space Administration. John C. Stennis Space Center, Bay Saint Louis, MS.
TECHNOLOGY TRANSFER WITHIN NASA
William St.Cyr *In* NASA, Washington, Technology Transfer and the Civil Space Program. Volume 2: Workshop Proceedings 1992 8 p (For primary document see N93-30692 11-85)
Avail: CASI HC A02/MF A04

Viewgraphs on technology transfer within NASA are provided. Assessment of technology transfer process, technology being transfered, issues and barriers, and observations and suggestions are addressed. Topics covered include: technology transfer within an organization (and across organization lines/codes) and space science/instrument technology and the role of universities in the technology development/transfer process. CASI

N93-30709*# Princeton Synergetics, Inc., NJ.
TECHNOLOGY TRANSFER WITHIN THE GOVERNMENT
Carissa Bryce Christensen *In* NASA, Washington, Technology Transfer and the Civil Space Program. Volume 2: Workshop Proceedings 1992 5 p (For primary document see N93-30692 11-85)
Avail: CASI HC A01/MF A04

The report of a workshop panel concerned with technology transfer within the government is presented. The suggested subtopics for the panel were as follows: (1) transfer from non-NASA U.S. government technology developers to NASA space missions/programs; and (2) transfer from NASA to other U.S. government civil space mission programs. Two presentations were made to the panel: Roles/Value of Early Strategic Planning Within the Space Exploration Initiative (SEI) to Facilitate Later Technology Transfer To and From Industry; and NOAA Satellite Programs and Technology Requirements. The panel discussion addresses the following major issues: DOD/NASA cooperation; alternative mechanisms for interagency communication and interactions; current technology transfer relationships among federal research agencies, and strategies for improving this transfer; technology transfer mechanisms appropriate to intragovernment transfer; the importance of industry as a technology transfer conduit; and measures of merit. Derived from text

N93-30710*# National Environmental Satellite Service, Washington, DC. Advanced Systems Planning Div.
NOAA SATELLITE PROGRAMS AND TECHNOLOGY REQUIREMENTS
Stanley R. Schneider *In* NASA, Washington, Technology Transfer and the Civil Space Program. Volume 2: Workshop Proceedings 1992 19 p (For primary document see N93-30692 11-85)
Avail: CASI HC A03/MF A04

Information concerning NOAA satellite programs is presented in vugraph form. The following topics are discussed: NOAA's space philosophy, the NESDIS FY-93 budget summary, LANDSAT program status, a history of geostationary satellites, the GOES program, current GOES instruments, improved GOES capabilities, polar orbiters, a history of TIROS R&D satellites, a history of ESSA operational satellites, a history of ITOS/NOAA satellites, and a history of TIROS-N/NOAA satellites. CASI

N93-30711*# Phillips Lab., Kirtland AFB, NM.
TECHNOLOGY TRANSFER WITHIN THE GOVERNMENT
John Russell *In* NASA, Washington, Technology Transfer and the Civil Space Program. Volume 2: Workshop Proceedings 1992 6 p (For primary document see N93-30692 11-85)
Avail: CASI HC A02/MF A04

The report of a workshop panel concerned with technology transfer within the government is presented. The presentation is made in vugraph form. The assigned subtopic for this panel are as follows: (1) transfer from non-NASA US government technology developers to NASA space missions/programs; and (2) transfer from NASA to other US government space mission programs. A specific area of inquiry was Technology Maturation Milestones. Three areas were investigated: technology development; advanced development; and flight hardware development. Derived from text

N93-30712*# Rockwell International Corp., Downey, CA.
[TECHNOLOGY TRANSFER AND ROCKWELL INTERNATIONAL]
Joseph Gernand *In* NASA, Washington, Technology Transfer and the Civil Space Program. Volume 2: Workshop Proceedings 1992 3 p (For primary document see N93-30692 11-85)
Avail: CASI HC A01/MF A04

Two technology partnership models are presented for consideration. The first model posits a government buyer of technology, and the second model posits that the customer is the consumer of the technology. These two models are concerned with methods of and impediments to technology transfer and information dissemination in government/contractor relationships. CASI

N93-30713*# National Aeronautics and Space Administration, Washington, DC.
NASP TECHNOLOGY TRANSFER
Charles Morris *In its* Technology Transfer and the Civil Space Program. Volume 2: Workshop Proceedings 1992 14 p (For primary document see N93-30692 11-85)
Avail: CASI HC A03/MF A04

It is the stated goal of this program, the National AeroSpace Plane (NASP) program, to develop and then demonstrate the technologies for single-stage-to-orbit flight and hypersonic cruise with airbreathing primary propulsion and horizontal takeoff and landing. This presentation is concerned with technology transfer in the context of the NASP program. Derived from text

N93-30714*# Jet Propulsion Lab., California Inst. of Tech., Pasadena.
ROBOTIC TECHNOLOGY EVOLUTION AND TRANSFER
Neville I. Marzwell *In* NASA, Washington, Technology Transfer and the Civil Space Program. Volume 2: Workshop Proceedings 1992 15 p (For primary document see N93-30692 11-85)
Avail: CASI HC A03/MF A04

A report concerning technology transfer in the area of robotics is presented in vugraph form. The following topics are discussed: definition of technology innovation and tech-transfer; concepts relevant for understanding tech-transfer; models advanced to portray tech-transfer process; factors identified as promoting tech-transfer; factors identified as impeding tech-transfer; what important roles do individuals fulfill in tech-transfer; federal infrastructure for promoting tech-transfer; federal infrastructure for promoting tech-transfer; robotic technology evolution; robotic technology transferred; and recommendations for successful robotics tech-transfer. Derived from text

N93-30715*# National Aeronautics and Space Administration, Washington, DC.
HIGH PERFORMANCE COMPUTING AND COMMUNICATIONS PROGRAM
Lee Holcomb *In its* Technology Transfer and the Civil Space Program. Volume 2: Workshop Proceedings 1992 6 p (For primary document see N93-30692 11-85)
Avail: CASI HC A02/MF A04

A review of the High Performance Computing and Communications (HPCC) program is provided in vugraph format. The goals and objectives of this federal program are as follows: extend U.S. leadership in high performance computing and computer communications; disseminate the technologies to speed innovation and to serve national goals; and spur gains in industrial competitiveness by making high performance computing integral to design and production. CASI

N93-30716*# TRW, Inc., Redondo Beach, CA.

TECHNOLOGY TRANSFER BETWEEN THE GOVERNMENT AND THE AEROSPACE INDUSTRY

Robert Sackheim and Dennis Dunbar *In* NASA, Washington, Technology Transfer and the Civil Space Program. Volume 2: Workshop Proceedings 1992 16 p Prepared in cooperation with General Dynamics Corp., San Diego, CA (For primary document see N93-30692 11-85)
Avail: CASI HC A03/MF A04

The object of this working group panel was to review questions and issues pertaining to technology transfer between the government and the aerospace industry for use on both government and commercial space customer applications. The results of this review are presented in vugraph form. Author (revised)

N93-30717*# National Media Lab., Saint Paul, MN.

NATIONAL MEDIA LABORATORY

Robert Clark *In* NASA, Washington, Technology Transfer and the Civil Space Program. Volume 2: Workshop Proceedings 1992 5 p (For primary document see N93-30692 11-85)
Avail: CASI HC A01/MF A04

A review of the National Media Laboratory (NML) is presented. The mission of the NML is to support current government user data storage needs and assist them in getting the most efficient 'commercial' solutions in the future. The motivation for a National Media Laboratory is as follows: recording systems are the major government image and data exploitation bottleneck; government data recording performance and storage requirements lead commercial practice by 3-5 years; the supporting commercial recorder industry is large but principally focused on video not data formats; lack of standards; and lack of transfer of commercial knowledge base to program offices and operational sites. Derived from text

N93-30718*# David Sarnoff Research Center, Princeton, NJ. National Information Display Lab.

INTRODUCTION TO THE NATIONAL INFORMATION DISPLAY LABORATORY

Curtis R. Carlson *In* NASA, Washington, Technology Transfer and the Civil Space Program. Volume 2: Workshop Proceedings 1992 9 p (For primary document see N93-30692 11-85)
Avail: CASI HC A02/MF A04

The goals of the National Information Display Laboratory (NIDL) are described in viewgraph form. The NIDL is a Center of Excellence in softcopy technology with the overall goal to develop new ways to satisfy government information needs through aggressive user support and the development of advanced technology. Government/industry/academia participation, standards development, and various display technologies are addressed. CASI

N93-30719*# Martin Marietta Corp., New Orleans, LA.

TECHNOLOGY TRANSFER TO THE BROADER ECONOMY

Gordon Dyer and Robert Clark *In* NASA, Washington, Technology Transfer and the Civil Space Program. Volume 2: Workshop Proceedings 1992 8 p Prepared in cooperation with National Media Lab., Saint Paul, MN (For primary document see N93-30692 11-85)
Avail: CASI HC A02/MF A04

Approaches to the transfer of government-funded civil space technology to the broader commercial economy were addressed by Working Panel no. 4. Some of the problems related to current strategies for technology transfer and recommendations for new approaches are described in outline form. CASI

N93-30720*# Jet Propulsion Lab., California Inst. of Tech., Pasadena.

STRATEGIC DIRECTIONS AND MECHANISMS IN TECHNOLOGY TRANSFER

Robert Mackin *In* NASA, Washington, Technology Transfer and the Civil Space Program. Volume 2: Workshop Proceedings 1992 5 p (For primary document see N93-30692 11-85)
Avail: CASI HC A01/MF A04

An outline summarizing the Working Panel discussion related to strategic directions for technology transfer is presented. Specific topics addressed include measuring success, management of technology, innovation and experimentation in the tech transfer process, integration of tech transfer into R&D planning, institutionalization of tech transfer, and policy/legislative resources. CASI

N93-30721*# National Aeronautics and Space Administration, Washington, DC.

WORKSHOP CONCLUSIONS: TECHNOLOGY TRANSFER AND THE CIVIL SPACE PROGRAM

John C. Mankins *In its* Technology Transfer and the Civil Space Program. Volume 2: Workshop Proceedings 1992 5 p (For primary document see N93-30692 11-85)
Avail: CASI HC A01/MF A04

Workshop objectives, participating organizations, results, and principal findings are presented in outline form. CASI

N93-30722*# National Aeronautics and Space Administration, Washington, DC.

NASA SPACE RESEARCH AND TECHNOLOGY OVERVIEW (ITP)

Gregory M. Reck *In its* Technology Transfer and the Civil Space Program. Volume 2: Workshop Proceedings 1992 23 p (For primary document see N93-30692 11-85)
Avail: CASI HC A03/MF A04

A series of viewgraphs summarizing NASA space research and technology is presented. Some of the specific topics covered include the organization and goals of the Office of Aeronautics and Space Technology, technology maturation strategy, integrated technology plan for the Civil Space Program, program selection and investment prioritization, and space technology benefits. CASI

N93-30723*# National Aeronautics and Space Administration, Washington, DC.

SPACE RESEARCH AND TECHNOLOGY OVERVIEW

Gregory M. Reck *In its* Technology Transfer and the Civil Space Program. Volume 2: Workshop Proceedings 1992 22 p (For primary document see N93-30692 11-85)
Avail: CASI HC A03/MF A04

A series of viewgraphs are presented that describe NASA's space research and technology activities. The following areas are covered: NASA organizational structure, overall program/mission objectives, program elements and milestones, planning and resources, accomplishments, and the role of NASA Centers. CASI

N93-30724*# National Aeronautics and Space Administration. Ames Research Center, Moffett Field, CA.

TECHNOLOGY TRANSFER IN THE NASA AMES ADVANCED LIFE SUPPORT DIVISION

Kathleen Connell (Bionetics Corp., Moffett Field, CA.), Nelson Schlater (Bionetics Corp., Moffett Field, CA.), Vincent Bilardo, and Paul Masson (Amtech, Inc., Newton, MA.) *In* NASA, Washington, Technology Transfer and the Civil Space Program. Volume 2: Workshop Proceedings 1992 20 p (For primary document see N93-30692 11-85)
Avail: CASI HC A03/MF A04

This paper summarizes a representative set of technology transfer activities which are currently underway in the Advanced Life Support Division of the Ames Research Center. Five specific NASA-funded research or technology development projects are synopsized that are resulting in transfer of technology in one or more of four main 'arenas:' (1) intra-NASA, (2) intra-Federal, (3) NASA - aerospace industry, and (4) aerospace industry - broader economy. Each project is summarized as a case history, specific issues are identified, and recommendations are formulated based on the lessons learned as a result of each project. Derived from text

N93-30725*# American Technology Initiative for Aerospace Research, Menlo Park, CA.

A RESEARCH EXPERIMENT ON FACILITATION AND FORMATION OF JOINT RESEARCH AND DEVELOPMENT PROGRAMS BETWEEN GOVERNMENT, INDUSTRY, AND UNIVERSITIES: OVERVIEW, PRELIMINARY FINDINGS, AND OBSERVATIONS

Syed Z. Shariq *In* NASA, Washington, Technology Transfer and the

Civil Space Program. Volume 2: Workshop Proceedings 1992 6 p
(For primary document see N93-30692 11-85)
Avail: CASI HC A02/MF A04

Presented is an overview of an experiment to explore the free-market approach to public-private collaboration through the development and implementation of a joint venture mechanism to enable formation of R&D projects between government, industry and academia. Some preliminary results related to time-to-commercialization and economic competitiveness are discussed. Derived from text

N93-30726*# National Aeronautics and Space Administration. Lyndon B. Johnson Space Center, Houston, TX.
EXPLORATION TECHNOLOGY PRIORITIZATION
Alex Dula *In* NASA, Washington, Technology Transfer and the Civil Space Program. Volume 2: Workshop Proceedings 1992 10 p (For primary document see N93-30692 11-85)
Avail: CASI HC A02/MF A04

A series of outlines and graphs describing NASA's Space Exploration Initiative (SEI) technology prioritization are presented. Prioritization criteria and preliminary critical technology priorities for a first lunar outpost and a Mars and permanently-manned lunar mission are addressed. CASI

88 SPACE SCIENCES (GENERAL)

N93-29453*# National Aeronautics and Space Administration. Ames Research Center, Moffett Field, CA.
FORMULATION OF AMES 24E2 IR-BLACK COATING
Sheldon M. Smith Jul. 1991 9 p
(RTOP 188-78-44)
(NASA-TM-102864; A-90280; NAS 1.15:102864) Avail: CASI HC A02/MF A01

The formulation of Ames 24E2 IR-black coating and a rationale for the selection of its components are given. The objective was to make a very rough, very thick, and highly absorbing coating to attenuate the specular reflectance of telescope baffles at far-IR wavelengths. Application and curing instructions are also given. Outgassing measurements are quite low following a 24-hour radiative cure. Author

89 ASTRONOMY

Includes radio, gamma-ray, and infrared astronomy, and astrometry.

N93-28608 Arizona Univ., Tucson.
SPECTROSCOPIC AND PHOTOMETRIC STUDIES OF MAIN SEQUENCE M STARS AND A SEARCH FOR LATE-TYPE DWARFS IN THE SOLAR VICINITY Ph.D. Thesis
Joseph Davy Kirkpatrick 1992 774 p
Avail: Univ. Microfilms Order No. DA9307644

As any introductory astronomy student knows, M dwarfs are the most common stars in the Galaxy and are the faintest of the core hydrogen burners. A comprehensive study of these faint objects is crucial to our understanding of the stellar composition of the Galaxy and necessary for a more complete knowledge of the transition between main sequence M stars and their slightly less massive counterparts, the brown dwarfs, which never achieve hydrogen burning in their cores. In this thesis, a spectroscopic catalog of 125 K and M dwarfs is first presented. This catalog covers the wavelength range from 6300 to 9000 A, near where these objects emit most of their light. Eight of these spectra, covering classes M2 through M9, are combined with infrared spectra from 0.9 to 1.5 micro meters to create a second catalog. The two sets of spectra are used to search for temperature-sensitive atomic lines and molecular bands, which are then used in fitting the observed spectra to a sequence of theoretical models. As a result, a new temperature scale for M dwarfs is determined, and this scale is more accurate than previous determinations which have depended on black body energy distributions. The sequence of spectra is also used to compare the spectrum of the brown dwarf candidate GD 165 B to known M dwarfs. Furthermore, the spectral catalog is used in an attempt to separate the spectra of faint companions from their M dwarf primaries in systems where the two objects are too close for conventional spectroscopy to resolve the individual components. A survey for faint M dwarfs is also launched using the data acquired through the CCD/Transit Instrument (CTI) on Kitt Peak, Arizona. Follow-up spectroscopy is presented for 133 of these objects, and several more very late M dwarfs are identified. This spectroscopy combined with photometric data from the CTI are used to construct a luminosity function for M dwarfs which is in excellent agreement with determinations from previous surveys. Finally, possible avenues for future work are discussed. These include spectroscopic follow-up of the reddest of Luyten's proper motion objects the first results from which have uncovered, in just twelve observations, two objects of type M7 and one of type M8, among the coolest objects yet recognized. Future searches, such as an all-sky survey for objects of extremely high proper motion, are also outlined. Dissert. Abstr.

N93-28634*# Washington Univ., Seattle. Dept. of Astronomy.
IUE OBSERVATIONS OF CATACLYSMIC VARIABLE Final Technical Report, 1979 - 1993
Paula Szkody 20 Jun. 1993 5 p
(Grant NsG-5395)
(NASA-CR-193188; NAS 1.26:193188) Avail: CASI HC A01/MF A01

Twenty two approved International Ultraviolet Explorer (IUE) programs were studied over a 14 year period. These programs are listed. The observations and subsequent analysis centered on cataclysmic variables (close binaries with a late main sequence star transferring material to a primary white dwarf via an accretion disk). The early studies highlighted the flux distribution of the accretion disk at outburst and quiescence, while later studies accomplished time-resolved observations throughout the orbital cycles, the study of the outflowing winds present at outburst, the study of the white dwarf in those systems with low accretion rate. There are 39 publications resulting from this work which are listed. These results include those for individual systems (Stepanian's star, Lanning 10, AM Her, MV Lyr, TV Col, VW Hyi, T Leo, IR Gem, TT Ari, Z Cam, BV Pup, IP Peg, PG1030+590, V1315 Aql, SW UMa, V426 Oph, WZ Sge, BY Cam, and U Gem) as well as review articles in journals and publications from reviews at meetings that summarize the impact of IUE on the study of accretion disks, white dwarfs, and hot spots resulting from stream impact as well as magnetic accretion columns. Author (revised)

N93-29008# Astronomische Gesellschaft, Hamburg (Germany).
ACTIVITIES REPORT OF THE ASTRONOMICAL SOCIETY [JAHRESBERICHTE ASTRONOMISCHER INSTITUT FUER 1991. TAGUNG IM BAMBERG. MITTEILUNGEN DES VORSTANDES]
1992 412 p In GERMAN
(Mitt-75; ETN-93-9345758) Avail: CASI HC A18/MF A04; Rendanten der Gesellschaft, Dr. H.-U. Keller, Planetarium Stuttgart, Neckarstr. 47, 7000 Stuttgart, Germany, HC

Activities, staff research results and publications of each German astronomical institute are presented. Projects are briefly described, in areas such as solar systems, galaxies, cataclismic variables, star atmospheres, extragalactic astronomy, white dwarf stars, stellar astronomy and double stars. ESA

N93-29156*# National Aeronautics and Space Administration. Goddard Space Flight Center, Greenbelt, MD.
FAR INFRARED SUPPLEMENT. THIRD EDITION: CATALOG OF INFRARED OBSERVATIONS (LAMBDA GREATER THAN OR EQUAL TO 4.6 MICROMETERS)
Daniel Y. Gezari, Marion Schmitz (Jet Propulsion Lab., California Inst. of Tech., Pasadena.), Patricia S. Pitts (Computer Sciences Corp., Calverton, MD.), and Jaylee M. Mead Washington Jun. 1993 375 p
(NASA-RP-1295; Rept-93A00689; NAS 1.61:1295) Avail: CASI HC A16/MF A03

The Far Infrared Supplement contains a subset of the data in the full Catalog of Infrared Observations (all observations at wavelengths greater than 4.6 microns). The Catalog of Infrared Observations (CIO), NASA RP-1294, is a compilation of infrared astronomical observational data obtained from an extensive literature search of scientific journals and major astronomical catalogs and surveys. The literature search is complete for years 1965 through 1990 in this third edition. The catalog contains about 210,000 observations of roughly 20,000 individual sources, and supporting appendices. The expanded third edition contains coded IRAS 4-band data for all CIO sources detected by IRAS. The appendices include an atlas of infrared source positions (also included in this volume), two bibliographies of catalog listings, and an atlas of infrared spectral ranges. The complete CIO database is available to qualified users in printed, microfiche, and magnetic tape formats. Author (revised)

N93-29163*# Smithsonian Astrophysical Observatory, Cambridge, MA.
PRECISION OPTICAL INTERFEROMETRY IN SPACE Final Report, 6 Feb. 1989 - 31 Jan. 1993
Robert D. Reasenberg Jul. 1993 68 p
(Grant NAGw-1647)
(NASA-CR-193264; NAS 1.26:193264) Avail: CASI HC A04/MF A01

POINTS, an astrometric Optical interferometer with a nominal measurement accuracy of 5 microarcseconds for the angle between a pair of stars separated by about 90 deg, is presently under consideration by two divisions of NASA-OSSA. It will be a powerful new multi-disciplinary tool for astronomical research. If chosen as the TOPS-1 (Toward Other Planetary Systems) instrument by the Solar-System Exploration Division, it will perform a definitive search for extra-solar planetary systems, either finding and characterizing a large number of them or showing that they are far less numerous than now believed. If chosen as the AIM (Astrometric Interferometry Mission) by the Astrophysics Division, POINTS will open new areas of astrophysical research and change the nature of the questions being asked in some old areas. In either case. it will be the first of a new class of powerful instruments in space and will prove the technology for the larger members of that class to follow. Based on a preliminary indication of the observational needs of the two missions, we find that a single POINTS mission will meet the science objectives of both TOPS-1 and AIM. The instrument detects dispersed fringe (channel led spectrum) and therefore can tolerate large pointing errors. Author (revised)

N93-29460# Visidyne, Inc., Burlington, MA.
A PROGRAM TO DETERMINE THE POINTING ANGLE TO A SPECULAR POINT
M. E. Gardner, T. S. Keneshea, and R. P. Pauliukonis 22 Oct. 1992 12 p
(Contract F19628-90-C-0187)
(AD-A262777; AD-E201426; PL-TR-92-2332; VI-1982; SR-2) Avail: CASI HC A03/MF A01

A method for determining the pointing angle to a specular point given attitude information to the Infrared Background Signature Survey/Shuttle Pallet Satellite (IBSS/SPAS) is described. The latitiude, longitude,inclination, yaw, and pitch of the IBSS/SPAS are given. DTIC

N93-29604*# Columbia Univ., New York, NY. Astrophysics Lab.
THE X RAY POPULATION IN GLOBULAR CLUSTERS AND THREE CRAB-LIKE SNR IN THE LARGE MAGELLANIC CLOUD Final Technical Report, period ending 31 May 1993
David J. Helfand Jun. 1993 5 p
(Grant NAG5-1557)
(NASA-CR-193172; NAS 1.26:193172; CAL-2115) Avail: CASI HC A01/MF A01

This document is to serve as the requisite Final Technical Report on grant NAG5-1557 which was awarded under the NASA ROSAT Guest Investigator Program to Columbia University. In response to the NASA Research Anouncement describing the first round of Guest Investigations to be carried out under the U.S.-German ROSAT Program (AO-1), the PI submitted several proposals, three of which were accepted in part: (1) the x-ray population of globular clusters; (2) three crab-like SNR in the Large Magellanic Cloud; and (3) x rays from nearby radio pulsars. The status of these three programs as of 31 May 1993, the termination date of the grant, is reported. Derived from text

N93-29785# Lawrence Livermore National Lab., CA.
SODIUM GUIDE STAR ADAPTIVE OPTICS SYSTEM FOR ASTRONOMICAL IMAGING IN THE VISIBLE AND NEAR-INFRARED
D. T. Gavel, J. R. Morris, and R. G. Vernon (Science Applications International Corp., Palm Beach Gardens, FL.) Mar. 1992 19 p Presented at the Laser Guide Star Adaptive Optics Workshop, Albuquerque, NM, 10-12 Mar. 1992
(Contract W-7405-eng-48)
(DE93-009543; UCRL-JC-109606; CONF-9203139-4) Avail: CASI HC A03/MF A01

We are building an adaptive-optic telescope system that is based on the use of an artificial guide star created by laser-induced fluorescence of the sodium mesospheric layer. This paper discusses the system design for mid-visible to near-infrared compensation of a one meter telescope at Livermore and near-infrared compensation of the ten meter Keck telescope at Mauna Kea. We calculate the expected Strehl ratio and resolution for a 69 channel deformable mirror system and also for a possible 241 channel system upgrade. With the 69 actuator system we expect near diffraction limited resolution, about 0.2 arcsec, with a Strehl ratio of about 0.5 at (lambda)=0.8,(mu)m on the 1m telescope, and resolution of about 0.05 arcsec with a Strehl ratio of about 0.5 at lambda = 2.0 microns on the 10 m telescope. Resolution will be limited by the performance of the tip/tilt correction loop, which uses an off-axis natural guide star as a reference. The effects which degrade tip/tilt correction are described in a companion paper. At Livermore, our design uses an existing high power (1 kW) laser source, which is expected to provide an approximately 6th magnitude artificial guide star. This strong beacon signal allows a short integration time in the wavefront sensor so that temporal changes in the atmospheric turbulence can be tracked accurately. For Mauna Kea, we explore how the system to be built for the Livermore site would perform in the infrared, assuming a 100 W laser source. DOE

N93-29811*# National Aeronautics and Space Administration. Goddard Space Flight Center, Greenbelt, MD.
BONNER DURCHMUSTERUNG (SOUTHERN DURCHMUSTERUNG)
Washington May 1993 382 p
(Contract NAS5-30960)
(NASA-RP-1298-Vol-3; NAS 1.61:1298-Vol-3; Rept-93B00049) Avail: CASI HC A17/MF A03

The Southern Durchmusterung (SD, Schoenfeld 1886, Becker 1949, Schmidt 1967) is a visual survey of stars in the declination zones -02 to -23 deg, completed as an extension to Argelander's (1859-62) monumental Bonner Durchmusterung (BD). Schoenfeld's survey was carried out using the same methods as had been used for the BD. The procedure consisted of allowing the telescope to drift along the mean declination of each zone and recording the positions and magnitudes of stars crossing the transit line of each field. The goal of the survey was to extend the BD to declination -23 deg (a plan originally adopted by Argelander) with approximately the same magnitude limits, although the primary instrument was of larger aperture (159 mm) than the 78-mm telescope used for the BD. Thus, whereas the BD magnitude estimates extend to 9.4 mag with all fainter stars assigned a magnitude of 9.5, the SD magnitude estimates extend to 9.9 mag with all fainter stars assigned a magnitude of 10. The SD contains a number of stars fainter than 10.0 mag and even some as faint as 11 mag. Lists of all corrections made to the original data as a result of published corrigenda, stars deleted according to overstriking in the printed catalogs or their inclusion in lists of 'missing' stars, and stars inserted in later editions are given. No other corrections or changes have been incorporated into the original data, e.g., from more modern positions and magnitudes or from comparison with other catalogs.
Derived from text

N93-30493 California Inst. of Tech., Pasadena.
THE FAINTEST STARS Ph.D. Thesis
Christopher Geoffrey Tinney 1993 250 p
Avail: Univ. Microfilms Order No. DA9307053

A 270 square degree photometric catalogue from plate material of the UKSRC and POSSII surveys was constructed. The procedures used and quality checks applied are described in detail, and should be considered as illustrative for those planning scientific programs with the forthcoming scans of these surveys. Infrared JHKLL photometry and low resolution infrared spectra (lambda is approximately equal to 1.0-2.5 microns) for a selection of the latest stars known are presented. The combined photometric and spectral data are used to evaluate bolometric corrections and bolometric magnitudes for late type M-dwarfs almost 2-magnitudes fainter than the faintest previously measured objects. Some of the current problems associated with the effective temperature scale for very low mass stars was examined. First results are presented from a CCD trigonometric parallax program at the Palomar 60 in telescope. The number of extremely late

M-dwarfs (M(sub bol) greater than 13) with directly measured distances was doubled. Structure in the main-sequences so constructed suggest that the faintest known stars may not be stably supported by nuclear burning. It is shown that sigma(pi) less than or equal to 0.004 in. can be obtained in a few years using standard CCD's on a common-user telescope. Infrared K-band photometry of complete samples of VLM candidates selected by our photographic catalogues are presented, and a bolometric luminosity function which extends to M(sub bol) = 13.75 was constructed. Significant evidence for a luminosity function decreasing towards these luminosities was found. The data are consistent with the results of studies based on the Nearby Star sample. The observed LF was converted into the form of a mass function which extends with reasonable statistics to 0.08 solar mass - the H-burning minimum mass. The mass function 'turns over' at approximately 0.25 solar mass, goes through a local minimum at approximately 0.15 solar mass, and seems to increase again below 0.1 solar mass - none of these features are predicted by any of the current theories of star formation. Lastly, the mass density observed just above the H-burning minimum mass makes it difficult to envisage brown dwarfs contributing significant quantities of missing mass without invoking either a mass function in this region significantly steeper than that seen for main sequence stars, or an extremely low cut-off mass to the mass function.
Dissert. Abstr.

N93-30578 Max-Planck-Inst. fuer Extraterrestrische Physik, Garching (Germany).
ROSAT DETECTION OF STELLAR X RAY SOURCES IN THE OLD OPEN CLUSTER M67
T. Belloni, F. Verbunt (Utrecht State Univ., Netherlands.), and J. H. M. M. Schmitt Aug. 1992 20 p Submitted for publication
(Grant NWO-PGS-78-277)
(MPE-Preprint-230; ETN-93-93941) Copyright Avail: Max-Planck-Inst. fuer Extraterrestrische Physik, D-8046 Garching, Germany

The observations of M67 with the Rosat satellite are discussed. The detected x-ray sources show a strong concentration towards the optical cluster which leads to the belief that most of the sources are actually associated with M67. In particular, the observation shows an x-ray counterpart for the cataclysmic variable recently discovered in M67. A larger fraction of the x-ray sources identified with M67 cluster members are binaries. It is shown that the x-ray properties of these stars make them good candidates for RS CVn systems in M67. ESA

N93-30615 Max-Planck-Inst. fuer Extraterrestrische Physik, Garching (Germany).
SUBMILLIMETER CO OBSERVATIONS OF WARM GAS AROUND T-TAURI STARS
K. F. Schuster (Hawaii Univ., Hilo.), A. I. Harris (Hawaii Univ., Hilo.), N. E. Anderson (Hawaii Univ., Hilo.), and A. P. G. Russell (Royal Observatory, Edinburgh, Scotland.) Oct. 1992 18 p Submitted for publication
(MPE-Preprint-232; ETN-93-93942) Copyright Avail: Fachinformationszentrum Karlsruhe, 7514 Leopoldshafen-Eggenstein 2, Germany

The first observations of T-Tauri stars in the (12)CO (6 to 5) line are reported. The observations trace the dynamics of warm and dense gas in a scale below 10 arcseconds. The CO submillimeter emission probably originates in the interaction of a stellar wind with a high column density of molecular material close to the stars. Additional CO data show that the emission extensions and line widths in T-Tau and HL-Tau are not consistent with Keplerian rotation or residual infall but can be explained by warm, dense, slowly outflowing material. The molecular outflow rate is at least 10 to the -6th power of the solar mass per year for T-Tau and 10 to the -7th power of the solar mass per year for HL-Tau, and may contribute to the dissipation of the clouds in which these stars formed. It is concluded that the dust associated with the warm molecular outflows accounts for a substantial fraction of T-Tau's and HL-Tau's far infrared continuum emission. ESA

N93-30629# Arizona Univ., Tucson. Lunar and Planetary Lab.
ADVANCED RESEARCH IN SKY SURVEILLANCE: A SEARCH FOR LOW-LUMINOSITY OBJECTS Annual Report, 1 Nov. 1991 - 31 Oct. 1992
Tom Gehrels 31 Oct. 1992 4 p
(Contract F49620-92-J-0051)
(AD-A264832; AFOSR-93-0284TR) Avail: CASI HC A01/MF A01

The new Charged Coupled Device (CCD) was installed. Improvements were made in the software and in the operation and the system is working well. All through the year the telescope was assigned for eighteen nights per month. Large numbers of main-belt asteroids were found. It was found that objects smaller than 2 meters occur two orders of magnitude more frequently that expected from extrapolation of the size-frequency relation of the larger near-Earth objects. The design of the new 1.8-meter Spacewatch Telescope began. DTIC

N93-30638# Laboratorium voor Ruimteonderzoek, Utrecht (Netherlands).
[ACTIVITIES REPORT FOR THE LABORATORY FOR SPACE RESEARCH GRONINGEN (NETHERLANDS)] [LABORATORIUM VOOR RUIMTE ONDERZOEK, GRONINGEN]
Sep. 1991 28 p In DUTCH
(ETN-93-93688) Avail: CASI HC A03/MF A01

The activities of the Laboratory of Space Research at Groningen are surveyed. This laboratory is a part of the Dutch Space Research Foundation. The 25 year history of space research at Groningen is summarized. Presently, the laboratory is building an infrared instrument (short wavelength spectrometer) for ISO (Infrared Space Observatory). The design and purposes of this instrument are described. SIS Detectors are developed for a submillimeter detector for ISO. ESA

N93-30641 Max-Planck-Inst. fuer Extraterrestrische Physik, Garching (Germany).
NEAR-INFRARED LINE IMAGING OF NGC 6240: GLOBAL SHOCK AND NUCLEAR STARBURST
P. P. vanderWerf, R. Genzel, A. Krabbe, M. Blietz, S. Drapatz, M. J. Ward (Oxford Univ., England.), and D. A. Forbes (Cambridge Univ., England.) Jun. 1992 52 p Submitted for publication Sponsored in part by Isaac Newton Studentship
(MPE-Preprint-226; ETN-93-93938) Copyright Avail: Max-Planck-Inst. fuer Extraterrestrische Physik.

Images of the luminous galaxy NGC 6240 in the H2 v = 1 to 0 S(1) 2.12 micrometers line and the (FeII) 1.64 micrometer line are presented. The images have an angular resolution of approximately = or less than 1 second, and for the H2 line, images in three adjacent 320 km/s wide velocity intervals are presented. The H2 emission extends over approximately 5 kpc and shows a complex morphology and chaotic velocity structure in its outer parts. It is concluded that the H2 emission is generated in large scale shocks resulting from the collision of the interstellar media of the merging galaxies. Line ratios indicate that the shock velocity is at most 40 km/s. It is shown that the shocks in NGC 6240 cannot account for the observed far-IR emission. In contrast to the H2 emission, the (FeII) emission comes from the nuclei of the galaxy and is generated in fast SNR shocks resulting from a nuclear starburst. The high (FeII)/Br-gamma ratio indicates a high iron abundance, probably resulting from efficient processing of the nuclear ISM in the starburst. Other aspects of this study are discussed.
ESA

N93-30642 Max-Planck-Inst. fuer Extraterrestrische Physik, Garching (Germany).
REJECTION OF ARCHIVAL PHOTOGRAPHIC OBJECTS AS OPTICAL COUNTERPARTS OF GAMMA RAY BURSTERS
J. Greiner Jul. 1992 20 p Submitted for publication
(MPE-Preprint-228; ETN-93-93939) Copyright Avail: Fachinformationszentrum Karlsruhe, 7514 Leopoldshafen-Eggenstein 2, Germany

The question of possible optical counterparts of gamma ray bursts from unique archival photographic plates is discussed. The photographic plates are evaluated under the reflected light microscopy, which is a valuable tool to detect plate defects. The analysis shows that two of the three objects found by Shaefer are plate defects, and serious doubts exist about the reality of the third. None of these three objects can be regarded as a candidate object for the optical counterpart of gamma ray bursts. There are still some possible candidates for possible optical counterparts of gamma ray bursts; however, it is still unproven that gamma ray bursts are accompanied by optical flashes. ESA

N93-30643 Max-Planck-Inst. fuer Extraterrestrische Physik, Garching (Germany).
INFRARED SPECTROSCOPY AND IMAGING OF STARBURST GALAXIES AND AGNs
R. Genzel, M. Cameron, and A. Krabbe Jul. 1992 29 p Submitted for publication
(MPE-Preprint-229; ETN-93-93940) Copyright Avail: Fachinformationszentrum Karlsruhe, 7514 Leopoldshafen-Eggenstein 2, Germany

High resolution data from infrared spectroscopy and imaging of starburst galaxies and Active Galactic Nuclei (AGN's) are discussed. Observations of starburst galaxies NGC 253, the interacting galaxy NGC 6240 and the Seyfert 2 galaxy NGC 1068 are emphasized. In the starburst galaxy NGC 253, the H2 emission comes from giant, circumnuclear star formation complexes assiciated with dense molecular clouds. In the merger NGC 6240, the H2 emission appears to originate in slow, large scale shocks of the two colliding interstellar media. In the Seyfert 2 galaxy NGC 1068, the H2 emission comes from molecular clouds in the narrow line region that are probably excited by radiation from the nuclear source. The large infrared obscuration of the nucleus of NGC 1068 may be due to intervening molecular clouds in the narrow line region. Strong near infrared (Fe(II)) emission appears to be associated with supernova shocks in starburst galaxies and with the interaction between nuclear outflow and narrow line clouds in NGC 1068. Coronal line emission from highly ionized species like Si(VI) may signify embedded AGN's. ESA

N93-28791*# National Aeronautics and Space Administration. Ames Research Center, Moffett Field, CA.
DETECTION OF OTHER PLANETARY SYSTEMS USING PHOTOMETRY Abstract Only
D. Koch, W. Borucki, and H. Reitsema (Ball Aerospace Systems Div., Boulder, CO.) *In* Lunar and Planetary Inst., Workshop on Advanced Technologies for Planetary Instruments, Part 1 1993 p 13 (For primary document see N93-28764 11-91)
Avail: CASI HC A01/MF A01

N93-30340 Calgary Univ. (Alberta). Dept. of Electrical Engineering.
AN AUTO-GUIDING SYSTEM FOR MID-SIZED TELESCOPES
J. W. Haslett, W. Gonnason, S. Balasubramanian, R. J. Condon, F. N. Trofimenkoff, and S. E. Nordquist *In* Engineering Inst. of Canada, Canadian Conference on Electrical and Computer Engineering, Volumes 1 and 2 1990 6 p (For primary document see N93-30215 11-31)
Avail: Engineering Inst. of Canada, 2050 rue Mansfield, Suite 700, Montreal, Quebec H3A 1Z2 Canada

90 ASTROPHYSICS

Includes cosmology; celestial mechanics; space plasmas; and interstellar and interplanetary gases and dust.

For related information see also *75 Plasma Physics.*

N93-28473# Bonn Univ. (Germany). Inst. fuer Physik.
DISTRIBUTION OF DARK MATTER IN THE GALAXY AND THE LOWER LIMITS FOR THE MASSES OF SUPERSYMMETRIC PARTICLES
V. S. Berezinsky (Laboratori Nazionali del Gran Sasso, Assergi, Italy.), A. V. Gurevich (Academy of Sciences, USSR, Moscow.), and K. P. Zybin (Academy of Sciences, USSR, Moscow.) Oct. 1992 15 p Sponsored in part by Alexander von Humbolt Foundation
(BONN-92-31; LNGS-92/40; ETN-93-93804) Avail: CASI HC A03/MF A01

An argument that the nonlinear stage of evolution of density fluctuations in a nondissipative gas results in the formation of a Nondissipative Gravitational Singularity (NGS) with density distribution rho(r) approximately r to the power of minus alpha where alpha is approximately equal to 1.8 is presented. This dependence holds from very small distance r(min) approximately 0.1 pc to very large distance r(max) approximately 5 Mpc. The predicted density distribution as well as the local density of the dark matter rho(stellar mass) is approximately equal to 0.3 GeV/cu cm are in good agreement with the observations. Dark matter particles have large space density in NGS and therefore, the rate of their annihilation is very high. This point like source of the radiation is the signature of NGS model. Assuming that dark matter in the Galaxy is composed mostly of neutralinos (approximately 70%) we calculate the flux of high energy gamma radiation and radio flux from the Galactic Center. ESA

N93-28547# Lawrence Livermore National Lab., CA.
MAGNETIC ACTIVITY IN LOW MASS STARS
S. L. Hawley 28 Dec. 1992 23 p Presented at the Hubble Fellows Symposium, Baltimore, MD, 9-11 Nov. 1992
(Contract W-7405-eng-48)
(DE93-009073; UCRL-JC-112640; CONF-9211209-1) Avail: CASI HC A03/MF A01

The manifestations of magnetic activity in low mass stars, particularly M dwarfs, can be used as a tool to study their evolution, the operation of the interior dynamo with changing interior conditions, and the structure of their outer atmospheres. Extensive background material on the current understanding of low mass stellar activity is presented. Two new surveys are described which will greatly increase the number of active low mass stars known in the field and in nearby open clusters. These surveys will define the characteristics of the activity on low mass stars, and how the activity changes with a number of parameters of interest, including mass, effective temperature, and age. The data will also allow a rigorous determination of a possible age-activity relation among the low mass M dwarfs. Theoretical models of M dwarf atmospheres, and their connection to the understanding of the observations, are also discussed. DOE

N93-28606 Harvard Univ., Cambridge, MA.
STELLAR ENCOUNTERS IN GLOBULAR CLUSTERS Ph.D. Thesis
Melvyn Barry Davies 1992 259 p
Avail: Univ. Microfilms Order No. DA9307541

This is a study of stellar encounters in globular clusters. I present 3D hydrodynamical simulations of collisions and close encounters between two single stars of various species. I show that the cross section for producing single, merged objects in such encounters is at least as large as that to produce detached binaries. I also consider encounters between binaries and a neutron star. The outcome of such encounters depends strongly on the separation of the components in the original binary. For extremely hard binaries, as may be formed from two single stars via tidal capture, a single merged object is the most likely outcome. In a small fraction of such encounters, the passing neutron star perturbs the two components of the binary such that their paths cross and they merge but remain unbound to the neutron star. Such encounters may be the mechanism to produce the high-velocity red giants observed in 47 Tuc. For primordial binaries, hardened to a separation of 0.2AU, clean exchanges seem the most likely outcome, though some 30 percent of exchange encounters lead to a merger between two of the stars, the coalesced object forming a binary with the third star. Applying King-Mitchie models to the globular clusters omega Cen, 47 Tuc, and NGC 6397, I compute the encounter rates between various stellar species and infer the production rates of objects of observational interest such as blue stragglers, millisecond pulsars (MSP's), and low-mass X-ray binaries (LMXB's). The production rate of merged objects containing neutron stars is also noted, as these systems may be a way to produce millisecond pulsars without passing through a precursor, X-ray emitting phase, as seems to be required by observations. I then consider the contribution of encounters between binaries and single stars, computing rates for reasonable binary populations in each of the three clusters. Such encounters may be the favored source of blue stragglers in globular clusters, in addition to producing merged objects that may later evolve into MSP's. A single population of hardened primordial binaries seems unable to boost the production rate of MSP's with respect to LMXB's by the factor of approx. 100 required by observations, although a more realistic binary population, with binaries having a range of separations and eccentricities, especially containing harder binaries, may be the solution. Dissert. Abstr.

N93-28607 Arizona Univ., Tucson.
NEAR-INFRARED SPECTROSCOPY AS AN ASTROPHYSICAL TOOL Ph.D. Thesis
Douglas Michael Kelly 1992 272 p
Avail: Univ. Microfilms Order No. DA9307648

Recent improvements in infrared detector arrays make it possible for the first time to conduct detailed spectroscopic studies of a complete range of objects in the 0.9-1.35 micron region. In this dissertation, I examine the 0.9-1.35 micron spectra of planetary and proto-planetary nebulae, M dwarfs, young stellar objects, Seyfert galaxies, an H II region, and a Wolf-Rayet star. Line identifications are made for each of these objects, and extensive line lists are presented. I also investigate what the lines can tell us about each object. The 0.9-1.35 spectrum of the proto-planetary nebula AFGL 618 is dominated by recombination lines, low-ionization, shock-excited lines, and thermal and fluorescent H2 lines. We use ratios of forbidden lines to show that there are two distinct physical regions in the lobes of AFGL 618, including one which must have been excited by shocks. We also show that the H2 lines in the 0.9-1.35 micron region are ideal for detecting low levels of fluorescent H2 emission, even when a strong thermal component is present. We present 0.6-1.5 micron spectra for M dwarfs ranging from M2 through M9. These spectra are compared with recent theoretical models, and a temperature scale is determined. In late-M dwarfs, the shape of the infrared spectrum and the depth of the 1.35 micron H2O feature are good temperature indicators. The temperatures we derive for the M dwarfs are higher than the temperatures found in earlier studies and are in closer agreement with theoretical tracks of the lower main sequence. We present 0.9-1.35 micron spectra for 7 young stellar objects. These objects exhibit a wide variety of behavior, including strong fluorescent emission. We show that the infrared spectra can be used to study all of the regions that are detected with visible and red spectra. As a result, 0.9-1.35 micron spectroscopy should be quite useful for studying heavily embedded sources. The 0.9-1.35 micron spectra of high-excitation objects include a number of distinctive features including He II lines, several high ionization lines, and very strong (S III) lines. We find that the excitation level of a source can be estimated based on these features alone. Dissert. Abstr.

N93-28672 North Carolina Univ., Chapel Hill.

THE USE OF OBJECTIVE PRISM RADIAL VELOCITIES FOR KINEMATIC STUDIES OF GALACTIC POPULATIONS Ph.D. Thesis

Rui Jorge L. S. Agostinho 1992 303 p
Avail: Univ. Microfilms Order No. DA9309837

Recent works do not agree about the number of Galactic populations and the solutions vary from models requiring two discrete populations, three discrete populations, to the continuous extended disk plus decoupled halo model. The objective prism survey by Rose has provided quantitative spectroscopic data for a kinematically unbiased study of Galactic populations in the magnitude range B is less than 12.5, i.e. up to a few hundred pc above the plane. In order to compute the velocity dispersion component sigma(sub zz) of these populations, the method of opposed dispersion plate pairs was used to obtain relative radial velocities of 956 stars in two fields at the SGP. Using the 4 deg + 6 deg prism combination in the Curtis Schmidt telescope (CTIO), the spectral resolution of 86.3 A/mm (at H(delta)) yields a radial velocity error distribution well described by a Gamma probability distribution function (pdf), which has final fitted parameters 15.5 +/- 7.0 km/s and 10.9 +/- 5.6 km/s (average +/- s.dev.) for the two fields. Since the velocity distribution seems to be well described by a gaussian, accurate (relative error of 1.5 percent G) velocity dispersions sigma(sub zz) for large samples, by curve fitting to both distributions were derived. For samples with less than 150 stars, Monte Carlo simulations using these two pdf's were run to estimate the error on sigma(sub zz). It was found that late-F stars have sigma(sub zz) = 21.8 +/- 3.7 km/s at B(sub mag) = 11 (50 stars), and sigma(sub zz) = 25.0 +/- 2.5 km/s at B(sub mag) = 12 (109 stars). The 112 G-dwarfs have sigma(sub zz) = 26.5 +/- 2.6 km/s at B(sub mag) = 12, almost identical to 27.5 +/- 2.5 km/s obtained by Gilmore & Wise (1987) to G-dwarfs at z = 200 pc. The 21 G-giants thick-disk candidates have sigma(sub zz) = 35.3 +/- 6.3 km/s comparable to the 37 km/s assigned by Carney et al (1989) to the thick-disk. The excellent agreement with higher resolution slit velocity dispersions shows that our very careful quantification of the errors translates into a reliable objective prism velocity dispersion, even for old thin disk typical values. Author (revised)

N93-28673 British Columbia Univ., Vancouver.

SPHERICALLY SYMMETRIC MODEL ATMOSPHERES FOR LATE-TYPE GIANT STARS Ph.D. Thesis

Philip Desmond Bennett 1991 256 p
(ISBN-0-315-72632-6) Avail: Univ. Microfilms Order No. DANN72632

The ATHENA computer code was developed to model the extended atmospheres of late-type giant and supergiant stars. The atmospheres are assumed to be static, spherically symmetric and in radiative and hydrostatic equilibrium. Molecular line blanketing (for now) is handled using the simplifying assumption of mean opacity. The complete linearization method of Auer and Mihalas, adapted to spherical geometry, is used to solve the model system. The radiative transfer is solved by using variable Eddington factors to close the system of moment transfer equations, and the entire system of transfer equations plus constraints is solved efficiently by arrangement into the Rybicki block matrix form. The variable Eddington factors are calculated from the full angle-dependent formal solution of the radiative transfer problem using the impact parameter method of Hummer, Kunas. We were guided by the work of Mihalas and Hummer in their development of extended models of O stars, but our method differs in the choice of the independent variable. The radius depth scale used by Mihals and Hummer was found to fail because of the strongly temperature-dependent opacities of late-type atmospheres. Instead, we were able to achieve an exact linearization of the radius. This permitted the use of the numerically well-behaved column mass or optical depth scales. The resulting formulation is analogous to the plane-parallel complete linearization method and reduces to this method in the compact atmosphere limit. Models of M giants were calculated for T(sub eff) = 3000K and 3500K with opacities of the CN, TiO, and H2O molecules included, and the results were in general agreement with other published spherical models. These models were calculated assuming radiative equilibrium. The importance of convective energy transport was estimated by calculating the convective flux that would result from the temperature structure of the models. The standard local mixing length theory was used for this purpose. Convection was found to be important only at depths with tau(sub RM) greater than 15 for the low gravity models with log g = O, but significant out to tau(sub RM) is approximately 1 at the most transparent frequencies for the higher gravity models with log g = 2. Thus, the temperature structure of the surface layers and the emergent flux for the log g = O models should be accurately modelled but the emergent flux for the log g = 2 models may be in error by up to 5 percent at the most transparent frequencies. Author (revised)

N93-28676# Fermi National Accelerator Lab., Batavia, IL.

DARK MATTER: THEORETICAL PERSPECTIVES

M. S. Turner Jan. 1993 26 p Presented at the NAS Special Colloquium on Physical Cosmology, Irvine, CA, Mar. 1992
(Contract DE-AC02-76CH-03000)
(DE93-008484; FNAL/C-92/382-A; CONF-9203232-1) Avail: CASI HC A03/MF A01

I both review and make the case for the current theoretical prejudice--a flat Universe whose dominant constituent is nonbaryonic dark matter--emphasizing that this is still a prejudice and not yet fact. The theoretical motivation for nonbaryonic dark matter is discussed in the context of current elementary-particle theory, and emphasis is placed on the following topics: (1) there are no dark matter candidates within the standard model of particle physics; (2) there are several compelling candidates within attractive extensions of the standard model of particle physics; and (3) the motivation for these compelling candidates comes from particle physics. The dark-matter problem is now a pressing issue in both cosmology and particle physics, and the detection of particle dark matter would provide evidence for a 'new physics.' The compelling candidates are: a very light axion (10(exp -6) eV - 10(exp -4) eV); a light neutrino (20 eV - 90 eV); and a heavy neutralino (10 GeV - 2 TeV). The production of these particles in the early Universe and the prospects for their detection are also discussed. I briefly mention more exotic possibilities for the dark matter, including a nonzero cosmological constant, superheavy magnetic monopoles, and decaying neutrinos. DOE

N93-28905# Los Alamos National Lab., NM.

WHY BLUE STRAGGLERS FORMED VIA COLLISIONS MAY NOT BE RAPID ROTATORS

Peter J. T. Leonard and Maurice J. Clement (Toronto Univ., Ontario.) 1993 4 p Presented at the Space Telescope Science Institute (STSI) Conference on Blue Stragglers, Baltimore, MD, 12-13 Oct. 1992
(Contract W-7405-eng-36)
(DE93-008708; LA-UR-93-472; CONF-9210324-3) Avail: CASI HC A01/MF A01

We propose that the blue stragglers formed via collisions may not be rapid rotators due to magnetic braking during a Hayashi phase as they approach the main sequence. It is conceivable that just the envelopes of the blue stragglers are spun down, while their cores remain rapidly rotating. This would greatly extend the main-sequence lifetimes of the blue stragglers produced by collisions. DOE

N93-28906# Los Alamos National Lab., NM.

DO THE POP 2 FIELD BLUE STRAGGLERS HAVE A COLLISIONAL ORIGIN?

Peter J. T. Leonard 1993 5 p Presented at the Space Telescope Science Institute (STSI) Conference on Blue Stragglers, Baltimore, MD, 12-13 Oct. 1992
(Contract W-7405-eng-36)
(DE93-008709; LA-UR-93-471; CONF-9210324-2) Avail: CASI HC A01/MF A01

The hypothesis that the Pop 2 field blue stragglers have a collisional origin is considered. It appears unlikely that the majority of these stragglers were formed via collisions, but it is difficult to rule out the possibility that a small, but observable, fraction of them were. DOE

N93-28907# Los Alamos National Lab., NM.

CAN PHYSICAL STELLAR COLLISIONS EXPLAIN THE BLUE STRAGGLERS IN THE DWARF SPHEROIDAL GALAXIES?

Peter J. T. Leonard 1993 4 p Presented at the Space Telescope Science Institute (STSI) Conference on Blue Stragglers, Baltimore, MD, 12-13 Oct. 1992
(Contract W-7405-eng-36)
(DE93-008711; LA-UR-93-467; CONF-9210324-1) Avail: CASI HC A01/MF A01

The hypothesis that the blue stragglers in the dwarf spheroidal galaxie have a collisional origin is considered. If all of the dark matter in these galaxies is in the form of low-mass stars and the binary frequency is (approx equal) 50%, then it is quite possible that (approx equal) 10% to 20% of their blue stragglers have been produced by physical stellar collisions. DOE

N93-28908# Los Alamos National Lab., NM.

THE HEATING AND COOLING OF WZ Sge

W. M. Sparks, E. M. Sion (Villanova Univ., PA.), S. G. Starrfield, and S. Austin (Arizona State Univ., Tempe.) 1993 5 p Presented at the 2nd Technion Haifa Conference on Cataclysmic Variables and Related Physics, Elat, Israel, 11-14 Jan. 1993
(Contract W-7405-eng-36)
(DE93-008720; LA-UR-93-731; CONF-930111-1) Avail: CASI HC A01/MF A01

The observations of WZ Sge provide us with the best test for computational codes trying to calculate the accretion process onto a white dwarf. We find that the accreted material on WZ Sge cannot spread over the whole star at least on a time scale of ten years. Numerical models which include the angular momentum of the accreted material provide the best fit to the observations. DOE

N93-28945 California Inst. of Tech., Pasadena.

THE MULTIPLICITY OF T TAURI STARS IN THE STAR FORMING REGIONS TAURUS-AURIGA AND OPHIUCHUS-SCORPIUS: A 2.2 MICRON SPECKLE IMAGING SURVEY Ph.D. Thesis

Andrea Ghez 1993 253 p
Avail: Univ. Microfilms Order No. DA9307038

The results of a magnitude limited (K is less than or equal to 8.5 mag) multiplicity survey of T Tauri stars (TTS) in two nearby star forming regions (SFR), Tauru-Auriga and Ophiuchus-Scorpius. Each of the 69 stars in the sample was observed at K(2.2 microns) with an infrared array camera on the Hale 5-m Telescope at Palomar Observatory and imaged using two-dimensional speckle interferometric techniques. Thirty-three companion stars were found, of which 15 were new detections. A subset of 64 observations was sensitive to all companion stars in the projected linear range 14 to 225 AU and the magnitude difference range 0.0 to 2.0 mag. This subset and region were used to study the multiplicity of TTS; the frequency of companion stars within this region is 34 +/- 9 percent, independent of SFR. A distinction between the classical TTS (CTTS) and the weak-lined TTS (WTTS) based on the binary star frequency as a function of separation was discovered; the WTTS dominate the binary star distribution at the closer separations and the CTTS populate the wider separations. The cross over occurred near 100 AU, the size typically quoted for a circumstellar disk. We suggest that all TTS begin as CTTS and become WTTS when accretion has ceased, and that the nearby companion stars act to shorten the accretion time scale in multiple star systems. Integrated over all magnitude differences the binary star frequency in the projected linear separation range 14 to 225 AU for TTS (59 +/- 16 percent) is a factor of 3.5 greater than that of the solar-type main sequence stars (17 +/- 3 percent). Given the limited angular separation range that we are sensitive to, i.e., both the spectroscopic and wide binaries are missed, the rate at which binaries are detected suggests that most, if not all, TTS stars have companions. We propose that the observed overabundance of companions to TTS with respect to their older counterparts on the main sequence is an evolutionary effect; in this scheme triple and higher order TTS, which are observed at higher frequencies than for the solar-type main sequence stars, are disrupted by close encounters with another star or system of stars. Dissert. Abstr.

N93-28963# Fermi National Accelerator Lab., Batavia, IL.

TESTS OF THE PARTICLE PHYSICS-PHYSICAL COSMOLOGY INTERFACE

D. N. Schramm (Chicago Univ., IL.) Jan. 1993 12 p Presented at the International Symposium on Neutrino Astrophysics, Kamioka, Japan, Oct. 1992
(Contract DE-AC02-76CH-03000)
(DE93-008483; FNAL/C-93/022-A; CONF-9210316-1) Avail: CASI HC A03/MF A01

Three interrelated interfaces of particle physics and physical cosmology are discussed: (1) inflation and other phase transitions; (2) Big Bang Nucleosynthesis (and also the quark-hadron transition); and (3) structure formation (including dark matter). Recent observations that affect each of these topics are discussed. Topic number 1 is shown to be consistent with the COBE observations but not proven and it may be having problems with some age-expansion data. Topic number 2 has now been well-tested and is an established 'pillar' of the Big Bang. Topic number 3 is the prime arena of current physical cosmological activity. Experiments to resolve the current exciting, but still ambiguous, situation following the COBE results are discussed. DOE

N93-29042*# Draper (Charles Stark) Lab., Inc., Cambridge, MA.

LUNAR GRAVITATIONAL FIELD ESTIMATION AND THE EFFECTS OF MISMODELING UPON LUNAR SATELLITE ORBIT PREDICTION M.S. Thesis

John H. Davis Jun. 1993 165 p
(Contract NAS9-18436)
(NASA-CR-188249; NAS 1.26:188249; CSDL-T-1180) Copyright Avail: CASI HC A08/MF A02

Lunar spherical harmonic gravity coefficients are estimated from simulated observations of a near-circular low altitude polar orbiter disturbed by lunar mascons. Lunar gravity sensing missions using earth-based nearside observations with and without satellite-based far-side observations are simulated and least squares maximum likelihood estimates are developed for spherical harmonic expansion fit models. Simulations and parameter estimations are performed by a modified version of the Smithsonian Astrophysical Observatory's Planetary Ephemeris Program. Two different lunar spacecraft mission phases are simulated to evaluate the estimated fit models. Results for predicting state covariances one orbit ahead are presented along with the state errors resulting from the mismodeled gravity field. The position errors from planning a lunar landing maneuver with a mismodeled gravity field are also presented. These simulations clearly demonstrate the need to include observations of satellite motion over the far side in estimating the lunar gravity field. The simulations also illustrate that the eighth degree and order expansions used in the simulated fits were unable to adequately model lunar mascons. Author

N93-29246# Los Alamos National Lab., NM.

SPACE OPTICAL AND LOW-FREQUENCY RADIO SEARCHES FOR EARTH-CROSSING ASTEROIDS AND COMETS

J. G. Hills and G. R. Gisler 1993 9 p Presented at the Hazards Due to Comets and Asteroids, Tucson, AZ, Jan. 1993
(Contract W-7405-eng-36)
(DE93-008716; LA-UR-93-599; CONF-930185-1) Avail: CASI HC A02/MF A01

Earth-crossing asteroids (ECA's) are small and backscatter strongly, so they are usually discovered near opposition during close approaches to Earth. This opposition effect produces strong biases in Earth-based searches for ECAS, particularly for Atens. An observing site much closer to the sun than the orbit of Earth, such as a satellite orbiting Venus or telescopes on Mercury, would not suffer this bias. All Atens that cross the orbit of Earth would be observable near opposition from these sites, so a survey from them would not systematically miss any large ECAS. A satellite at the Lagrangian point between the Earth and the sun would be effective in detecting objects in the final day before they hit Earth including asteroids and long-period comets that approach Earth from the sunward side. Outgassing comets present large cross sections to the solar wind. Spacecraft have observed low-frequency radio emission produced by the wiggling of the magnetic field in the solar wind as it sweeps past comets. Asteroids are expected to emit similar radio emission at lower power. This radiation may be observable by a radio array in space or on the moon. A satellite at the Lagrangian point could also detect the downstream solar wind wakes of comets and asteroids that approach Earth from the direction of the sun. Military surveillance satellites may be used to observe the fragmentation of large meteoroids in the atmosphere. Because it observes the entire atmosphere of Earth and is not affected by local weather conditions, such a surveillance network has a much larger cross section than a ground survey for observing the rare, large meteors that more closely approach the size of those that cause economic damage. DOE

N93-30053*# Columbia Univ., New York, NY. Dept. of Physics and Astronomy.
GRO: RED-SHIFTED ELECTRON-POSITRON ANNIHILATION GAMMA-RAYS FROM RADIOPULSARS Annual Status Report, 15 Jul. 1992 - 14 Jul. 1993
Malvin Ruderman Jul. 1993 7 p
(Grant NAG5-2016)
(NASA-CR-193243; NAS 1.26:193243; CAL-2118) Avail: CASI HC A02/MF A01

Reported red-shifted e(+) + e(-) yields gamma + gamma 511 keV gamma-rays from the Crab pulsar would, if ultimately confirmed, provide crucial clues about the structure of the powerful magnetospheric accelerator in that rapidly spinning gamma-ray pulsar. In an attempt to understand the origin of this component of the Crab pulsar's emission, we try to account for the following: (1) a flow of approximately 10 exp 40 e(+/-)/s into near the surface of the neutron star; (2) a relatively narrow annihilation line implying that the annihilating e(+/-) pairs probably had a velocity (along vector B) less than or approximately = 10(exp -1)c; and (3) a tentative light curve suggesting a doubly peaked structure different from that of the rest of the Crab pulsar's nonthermal radiation. Derived from text

N93-30148 Michigan Univ., Ann Arbor.
MODELS OF STAR FORMATION IN INTERACTING AND MERGING DISK GALAXIES Ph.D. Thesis
James Christopher Mihos 1992 133 p
Avail: Univ. Microfilms Order No. DA9308399

To better understand the role that interactions between galaxies plays in their overall evolution requires a clear picture of the types of interactions that trigger starburst events as well as an understanding of the specific star formation process in these starbursts. While the general occurrence of tidally triggered starbursts seems well demonstrated observationally, the specific response of star formation to a gravitational encounter is much less clear. In an effort to better understand the nature of the starburst trigger in interacting galaxies, numerical models of star forming interacting galaxies, which are then compared to observations of specific interacting systems, are constructed. The models show that in general, galaxy interactions trigger only mild increases in the global star formation rates (SRF's) of the participating galaxies. Starburst strengths for flyby interactions are a factor of a few at best and are strongest for prograde interactions. Mergers prove effective at triggering order-of-magnitude starbursts in the central regions of the merging galaxies; however, the relative scarcity of mergers ensures that very strong interaction-induced starbursts are rare. The starburst triggering mechanism is varied. The most intense starbursts are driven by gas inflow into the nuclear regions via a merger event or tidally-triggered bar formation. Less intense star formation may be induced through compressions of gas along the tidal arms, or direct collisions between the interacting ISM's. None of the mergers modeled were able to trigger starbursts much greater than an order of magnitude; this result makes it difficult to explain the emission from ultraluminous infrared galaxies through merger-induced star formation alone unless the merging galaxies were very gas rich. Furthermore, the merging process which produces such objects must occur rapidly; models of slow mergers depleted their ISM through star formation before developing the nuclear gas concentrations which could fuel an intense starburst. The models link these two criteria by showing that through a process of 'gas dynamical braking,' gas rich galaxies may merge more quickly than gas poor systems. Dissert. Abstr.

N93-30377 Boston Univ., MA.
YOUNG OPEN CLUSTERS AS PROBES OF THE STAR FORMATION PROCESS Ph.D. Thesis
Randy Lee Phelps 1993 363 p
Avail: Univ. Microfilms Order No. DA9306742

The star formation history of a region in the Perseus spiral arm of our Galaxy was explored using digital photometry, in the UBV system, of 23 open clusters. Magnitudes and colors of 35,788 stars were measured, making this the most comprehensive, homogeneous, single study of open cluster properties in one part of the Galaxy. The improved knowledge of the spatial distribution and formation sequence of the clusters, coupled with other studies of radial velocities, proper motions, and gas distribution in the region, strongly suggests that the majority of these clusters were formed during the impact of a high velocity cloud (HVC) with the Galactic disk. HVC's were detected in this region and predictions of a recently published theoretical model of an HVC impact with the disk agree with the observational data extremely well. While it was suggested that HVC impacts can trigger star formation, this is the first time that star formation can be directly connected to such an event. Mass functions for 8 of the clusters were calculated for stars more massive than the Sun, covering a region of the initial mass function (IMF) inaccessible through studies of field stars. These data indicate that, to about one solar mass, the mass functions of clusters, on average, are the same as the so-called 'Salpeter field star IMF'. Deviations do occur, however, with evidence for a deficiency of low mass stars in several clusters. A dip in the IMF at a mass about 1.4 times that of the Sun is detected, at various levels of statistical significance, in six of the clusters. Variations in binary content were seen, although no obvious correlation with cluster age, mass, or size is found. This result has implications for theories of the formation of binary stars. Other uses of this data base are discussed, including an improvement in the cluster age/gas-content relation, and potential improvement in the Cepheid star period-luminosity relation, since previous studies have associated Cepheids with 3 of the clusters in this survey. Dissert. Abstr.

N93-30411 Arizona Univ., Tucson.
CATASTROPHIC COLLISIONS: LABORATORY IMPACT EXPERIMENTS, HYDROCODE SIMULATIONS, AND THE SCALING PROBLEM Ph.D. Thesis
Eileen Valerie Cupta Ryan 1992 228 p
Avail: Univ. Microfilms Order No. DA9307670

The catastrophic fragmentation of finite targets is examined both in the laboratory and using a numerical hydrocode. The objective of the empirical study was to gain some insight into the collisional process, specifically, how impact conditions affect collisional outcome. The hydrocode allows us to investigate the fragmentation of large bodies, and to determine how target size influences the impact event. Nearly 150 experiments were performed. Impact velocities ranged from 50-5700 m/s; target material/structure as well as projectile type were varied, and the effect on fragment mass and velocity distributions was documented. Several factors were found to influence the result of a two-body collision: specific energy, momentum, target strength and internal structure, and projectile type. Velocity data showed that average fragment speeds are on the order of 10's of meters per second. Energy partitioned into ejecta kinetic energy is about 1.2 percent for high velocity collisions and more than 10 percent for low velocity impacts. Our two-dimensional hydrocode successfully reproduced fragment size distributions and mean ejecta velocities from laboratory impact experiments using basalt, and weak and strong mortar as target materials. It also reproduced size distributions from explosive disruption and applied external pressure experiments which used targets composed of weak mortar and weak basalt grout. Using this hydrocode, how target size influences the amount of energy (Q(sup *)) required for fracture is analyzed. Q(sup *) was found to decrease with increasing target size in the strength regime;

in the gravity regime where incoming stress waves must overcome both material bonds and self-compression, Q(sup *) increased with increasing target size. The Q(sup *) dependence on target size was found to be much stronger than predicted from scaling law theory. Dissert. Abstr.

N93-30412 Ohio State Univ., Columbus.
MULTIWAVELENGTH STUDIES OF CLASSICAL NOVA SHELLS Ph.D. Thesis
Pedro Saizar 1992 138 p
Avail: Univ. Microfilms Order No. DA9307846

Ground-based optical and satellite ultraviolet spectrophotometric observations are combined in order to study the shells of Classical Novae PW Vulpeculae 1984 and QU Vulpeculae 1984. First, the chemical composition of each shell is derived from emission line ratios carefully selected to minimize the effects of variations in the physical conditions within the shell, such as density in homogeneities. The results indicate that PW Vul has a nearly solar composition, with the exception of nitrogen, which is enhanced. QU Vul shows a strong enhancement of helium and several intermediate weight elements. These results are in qualitative agreement with current theories of nova outbursts, suggesting that PW and QU Vul's outbursts occurred in a carbon-oxygen and an oxygen-neon-magnesium white dwarf, respectively. Next, the source of ionizing radiation is investigated from the observed continuous spectrum, and from radiative-equilibrium photoionization modeling. A flat, featureless continuum indicates that the expanding shell is hotter than the temperature derived from emission-line diagnostics. Thus, a model is proposed in which the 'cold phase' has a temperature of 10(exp 4), and the 'hot phase' is in the range of 10(exp 5) to 10(exp 6) K. Methods are presented to constraint the temperature and density of the hot phase, and other properties of the shell, such as the mass, the energetics, and the geometry. The results suggest that the tenuous hot phase dominates the mass of the outburst, while the cold phase is denser, strongly inhomogeneous, and responsible for most of the emission line spectrum. These results bring new light and challenges to the fields of nova outbursts and galactic structure. The large ejected masses in combination with the enhanced abundances suggest that novae may be significant contributors to the chemical enrichment of the Galaxy. In particular, the observed mass of aluminum in the Galaxy can be explained as the result of nova outbursts similar to the QU Vul system, provided that these systems represent only 1-2 percent of the total nova rate. However, theoretical challenges now exist to explain the mechanisms that allow such large ejecta in oxygen-neon-magnesium novae. Dissert. Abstr.

N93-30502 Arizona Univ., Tucson.
DENSE GAS IN THE MONOCEROS OB1 DARK CLOUD AND ITS RELATIONSHIP TO STAR FORMATION Ph.D. Thesis
Grace Annamarie Wolf 1992 172 p
Avail: Univ. Microfilms Order No. DA9307668

A CS survey of the 10 outflows and 30 IRAS sources identified by Margulis in the Mon OB1 dark cloud was conducted to study the relationship between outflows, young stellar objects (YSO's), and dense cores in this cloud. It was found that the CS J = 2 approaches 1 transition traces a large portion of the dense, low-velocity components of the outflows in Mon OB1. The mass of this component is found to be nearly an order of magnitude greater than previous estimates of the outflow 'core' component. Little CS gas around the quiescent sources was detected in this cloud. CS 2 approaches 1 temperatures and integrated intensities are 2 to 7 and 2 to 14 times higher, respectively, in the vicinities of IRAS sources associated with outflow activity than about the quiescent sources. This implies CS abundances, temperatures, and/or densities are enhanced in regions where outflows impact the ambient cloud. The CS 2 approaches 1 emission is concentrated in two regions encompassing 6 of the 10 previously identified outflows in this cloud. Four of these six outflows are identifiable in CS. Two, previously identified as monopolar outflows, exhibit bipolar structure in CS. The CS J = 5 approaches 4 transition was detected in the vicinity of 4 of the 10 outflows in this cloud, and around none of the quiescent IRAS sources. The CS 5 approaches 4 emission is extended around two of the outflow sources and was mapped in these regions. CS J = 7 approaches 6 emission was mapped about the brightest outflow source in this cloud. The morphology of the 7 approaches 6 region suggests it may have been part of the collimating structure for the outflow associated with this source. The velocity structure and binding energies of the 5 approaches 4 and 7 approaches 6 cores suggest the outflows are disrupting these cores. The addition of the low-velocity CS outflow component to previous estimates of outflow energetics implies multiple generations of outflows need not be required to support this cloud against collapse. Our results neither support nor rule out the existence of fossil outflows in this cloud. A full-cloud, unbiased survey is required to search for such outflows. Dissert. Abstr.

N93-30528# Washington Univ., Seattle. Dept. of Physics.
PREDICTIONS OF A NON-GAUSSIAN MODEL FOR LARGE SCALE STRUCTURE
Z. H. Fan and J. M. Bardeen 26 Jun. 1992 41 p
(Contract DE-FG06-91ER-40614)
(DE93-010196; DOE/ER-40614/26) Avail: CASI HC A03/MF A01

A modified CDM model for the origin of structure in the universe based on an inflation model with two interacting scalar fields, is analyzed to make predictions for the statistical properties of the density and velocity fields and the microwave background anisotropy. The initial gauge-invariant potential zeta which is defined as zeta = (delta)rho/(rho + p) + 3(var phi), where (var phi) is the curvature perturbation amplitude and p is the pressure, is the sum of a Gaussian field phi(sub 1), and the square of a Gaussian field phi(sub 2). A Harrison-Zel'dovich scale-invariant power spectrum is assumed for phi(sub 1); and a log-normal 'peak' power spectrum for phi(sub 2). The location and the width of the peak are described by parameters k(sub c) and a. respectively. The model is motivated to some extent by inflation models with two interacting scalar fields, but is mainly interesting as an example of a model whose statistical properties change with scale. On small scales, it is almost identical to a standard scale-invariant Gaussian CDM model. On scales near the location of the peak of the non-Gaussian field, the distributions have long tails in high positive values of the density and velocity fields. Thus, it is easier to get large-scale streaming velocities than the standard CDM model. The quadrupole amplitude of fluctuations of the cosmic microwave background radiation and the rms variation of the temperature field smoothed with a 10 deg FWHM Gaussian are calculated; a reasonable agreement is found with the new COBE results. DOE

N93-30563 Boston Univ., MA.
A CHARACTERIZATION OF YOUNG STELLAR OBJECTS IN BOK GLOBULES: INFRARED IMAGING, SPECTRAL ENERGY DISTRIBUTIONS, AND MOLECULAR OUTFLOWS Ph.D. Thesis
Joao Lin Yun 1993 247 p
Avail: Univ. Microfilms Order No. DA9306747

A large-scale observational study of star formation in Bok globules is presented. A sample of 248 optically selected, small molecular clouds (mostly Bok globules) was probed using IRAS co-added images to search for associated young stellar objects (YSO's). Fifty-seven of the globules show evidence for a total of 72 point sources near locations of local dust heating. A sub-sample of 41 globules was observed, in the CO J = 1-0 line, to search for molecular outflows associated with the YSO's. Outflows were found in about one-third of the sample (14 of 41). The presence of an outflow was found to be correlated with the value of the IRAS-based spectral index (between 12 and 25 microns) of the YSO's. A near-infrared imaging survey of 34 globules containing YSO-candidates was conducted in the J, H, and K bands using infrared arrays. Eleven YSO-candidates displayed near-infrared nebulosities. This group of objects, when ordered by their values of the 12/25 microns spectral index, seems to form an evolutionary sequence, from younger objects with negative (red) indices and whose nebulosities are brighter in the K-band, to objects in later stages of pre-main-sequence evolution with positive (bluer) indices and whose nebular emission is brighter in the J-band. Comparison of the morphology of the infrared nebulae with the corresponding CO outflow morphology supports the idea that infrared reflection nebulae, seen at 2.2 microns, are good morphological tracers of CO mass outflow, and that CO outflows occur during the earliest YSO phases. Photometry of the near-infrared counterparts of the YSO-candidates was combined with their IRAS fluxes to yield broad-band spectral energy distributions (SED's). The broadness and steepness of the SED's indicated clear evidence of the evolutionary stage of the objects confirming their youth. Given all of the new information obtained, a firm conclusion emerged, namely that Bok globules are active sites of low-mass star formation. Dissert. Abstr.

N93-30579 Brown Univ., Providence, RI.
TOPICS IN INFLATIONARY UNIVERSE MEDELS AND COSMIC STRING THEORIES Ph.D. Thesis
Jong Hyun Kung 1992 137 p
Avail: Univ. Microfilms Order No. DA9308837

Few selected topics in the inflationary universe models and the cosmic string theories are studied. After the advent of inflationary universe models, questions were raised about the initial conditions of the scalar field which is necessary to give rise to inflation. At present, there are two viable inflationary models: New Inflation, and Linde's Chaotic Inflation. The time evolutions of single plane wave initial excitations of a real singlet scalar field with the potential V(phi) = lambda(phi)/2(phi(sup 2) - sigma(sup 2))(sup 2) was studied. The initial value of the scalar field energy density was bounded by the planck energy density. It is shown that even within this regime there are regions of the phase space for which the universe will enter into chaotic inflation and new inflation. The issue of the stability of chaotic inflation was also studied. Specifically, the possible interference effects of initially exciting another generic plane wave mode was investigated in addition to the mode which when evolved alone is known to give rise to chaotic inflation. The properties of the spectrum of gravitational radiation that was generated by a network of cosmic strings, which decayed by gravitational radiation in an expanding universe were studied. The network of cosmic strings that were used is an improvement of the network that was used in the literature. The conclusion is that the bounds on the gravitational energy density from the nucleosynthesis, the microwave anisotropy, and the pulsar timings arguments can not yet rule out cosmic string theories with G(sub mu) approximately 10(exp -6). The clustering of hot massive neutrinos by a cosmic string loop as a non-adiabatic perturbation is studied using Zel'dovich approximation in conjunction with the neutrino Jeans length. First, the results for a non-decaying loop using the Zel'dovich approximation are shown to exactly reproduce previous results using the Gilbert equation. Second, the analysis is extended to clustering by a decaying loop. It is shown that the effect of loop decay is to increase the radius and mass of the smallest structures that can be seeded by cosmic strings. In conclusion, with decaying loops, the smallest structures that can form by the present time via direct accretion onto loops have a mass of about M = 2.4 x 10(exp 8) solar mass (gamma/50)(sup 3/4)(G(sub mu)/10(exp -6))(sup 3/2)(v(sup eq)/0.04)(sup 3/4)(h(sup -5/2)) with a turn around radius of about r = 29Kpc(gamma/50)(sup 1/4)(G(sub m u)/10(exp -6))(sup 1/2)(v(sup eq)/0.04)(1/4)(h(sup -3/2)), which is to be compared to the present neutrino jeans mass of M = 2.8 x 10(exp 4) solar mass(v(sup eq)/0.04)(sup 3)(h(sup -7)) and its Jeans length of r = 2.9Kpc(v(sup eq)/0.04)h(sup -3). Dissert. Abstr.

N93-30639 Max-Planck-Inst. fuer Extraterrestrische Physik, Garching (Germany).
CO LINES TOWARD NGC 2024 AND OTHER STAR FORMING REGIONS: A CLOSER LOOK AT THE WARM GAS COMPONENT
U. U. Graf (Texas Univ., Austin.), A. Eckart, R. Genzel, A. I. Harris, A. Poglitsch, A. P. G. Russell (Royal Observatory, Edinburgh, Scotland.), and J. Stutzki (Cologne Univ., Germany.) Jun. 1992 56 p Submitted for publication
(MPE-Preprint-223; ETN-93-93935) Copyright Avail: Max-Planck-Inst. fuer Extraterrestrische Physik

Observations of the CO-13 J = 6 to 5 emission from a variety of galactic star forming regions are presented. Sources spanning a luminosity in the range of 1 to 10(exp 6) of the solar luminosity were investigated. The high line intensity confirms the presence of large column densities of warm molecular gas in typical regions of massive star formation. The CO-13/CO-12 J = 6 to 5 intensity ratio is typically much higher than the CO-13/CO-12 abundance ratio. Hence, even the mid-J transitions of the main CO isotope are very optically thick in most sources. The CO-13 6 to 5 emission is found to arise from quiescent gas. Strip maps of selected sources show that the CO-13 6 to 5 emitting gas is confined to narrow zones close to the H-2 regions in these star forming regions. A detailed multiline study of the molecular gas from NGC 2024 is presented. ESA

N93-30918# International Centre for Theoretical Physics, Trieste (Italy).
FOURTH-RANK GRAVITY AND COSMOLOGY
A. L. Marrakchi and V. Tapia Jul. 1992 40 p
(DE92-644722; IC-92/124) Avail: CASI HC A03/MF A01 (US Sales Only)

We consider the consequences of describing the metric properties of space-time through a quartic line element. The associated 'metric' is a fourth-rank tensor G(sub mu(upsilon)lambda(pi)). In order to recover a Riemannian behavior of the geometry, it is necessary to have G(sub mu(upsilon)lambda(pi)) = g (sub (mu(upsilon))g(sub lambda(pi))). We construct a theory for the gravitational field based on the fourth-rank metric G(sub mu(upsilon)lambda(pi)). In the absence of matter, the fourth-rank metric becomes separable and the theory coincides with General Relativity. In the presence of matter, we can maintain Riemmanianicity, but now gravitation couples, as compared to General Relativity, in a different way to matter. We develop a simple cosmological model based on a FRW metric with matter described by a perfect fluid. For the present time, the field equations are compatible with k(sub OBS) = O and Omega(sub OBS) less than 0.18, and they imply p/(rho) less than 0.038 which corresponds to an almost pressureless perfect fluid. Therefore, the flatness problem is solved. However, our approach is valid only for p/(rho) less than 0.236. Therefore, we consider an early universe in which the state equation of matter is p/(rho) = 0.236 rather than p/p = 1/3. There is no violation of causality, no horizon problem, for t greater than t(sub CLAS) approximately = 10(exp 20)t(sub PLANCK) approximately = 10(exp -23)s. Our final and most important result is the fact that the entropy is an increasing function of time. When interpreted at the light of General Relativity, the treatment is shown to be almost equivalent to that of the standard model of cosmology combined with the inflationary scenario. DOE

N93-30919# International Centre for Theoretical Physics, Trieste (Italy).
COMPENSATING FIELDS AND ANOMALIES IN SUPERGRAVITY
Y. Shamir Jul. 1992 24 p
(DE92-644724; IC-92/131) Avail: CASI HC A03/MF A01 (US Sales Only)

We discuss the quantization of theories which are formulated using compensating fields. In particular, we discuss the relation between the components formulation and the superspace formulation of supergravity theories. The requirement that the compensating field can be eliminated at the quantum level gives rise to on-shell constraints on the operators of the theory. In some cases, the constraints turn out to be physically unacceptable. Using these considerations, we show that new minimal supergravity is in general anomalous. DOE

N93-30997# International Centre for Theoretical Physics, Trieste (Italy).
FOURTH-RANK COSMOLOGY
A. E. L. Marrakchi and V. Tapia May 1992 27 p
(DE92-641346; IC-92/86) Avail: CASI HC A03/MF A01 (US Sales Only)

Some cosmological implications of the recently proposed fourth-rank theory of gravitation are studied. The model exhibits the possibility of being free from the horizon and flatness problems at the price of introducing a negative pressure. The field equations obtained are compatible with k(sub obs)=0 and Omega(sub obs) is less than 0.18 for our present day universe; they imply -p/rho is less than 0.055 which corresponds to an almost pressureless perfect fluid. Furthermore, there is no horizon problem for t is greater than t(sub clas) approximately 10(exp 20)t(sub Planck) approximately 10(exp -23)s. When interpreted at the light of General Relativity the treatment is shown to be almost equivalent to that of the standard model of cosmology combined with the inflationary scenario. Hence, an interpretation of the negative pressure hypothesis is provided. DOE

N93-31004# International Centre for Theoretical Physics, Trieste (Italy).
EFFECTS OF SPIRAL SHOCKS ON DISK EMISSION LINES
S. K. Chakrabarti and P. J. Wiita (Georgia State Univ., Atlanta.) May 1992 8 p
(DE92-641716; IC-92/82) Avail: CASI HC A02/MF A01 (US Sales Only)

We show that spiral shocks on stellar disks, induced by binary companions, can have significant effects upon observable emission lines. For an even number of shocks, the separations and heights of the two-horned emission lines will vary with binary phase, while for an odd number of shocks, red/blue asymmetries appear, with the red and the blue components alternating in brightness. DOE

N93-29355*# National Aeronautics and Space Administration. Lyndon B. Johnson Space Center, Houston, TX.
REPORT OF THE METEOROID AND DEBRIS SPECIAL INVESTIGATION GROUP Interim Report
Michael E. Zolensky, Herbert A. Zook, Fred Horz, Dale R. Atkinson (POD Associates, Inc., Albuquerque, NM.), Cassandra R. Coombs (POD Associates, Inc., Albuquerque, NM.), Alan J. Watts (POD Associates, Inc., Albuquerque, NM.), Claire B. Dardano (Lockheed Engineering and Sciences Co., Houston, TX.), Thomas H. See (Lockheed Engineering and Sciences Co., Houston, TX.), Charles G. Simon (Institute for Space Science and Technology, Inc., Gainesville, FL.), and William H. Kinard (National Aeronautics and Space Administration. Langley Research Center, Hampton, VA.) *In* NASA. Langley Research Center, LDEF: 69 Months in Space. Second Post-Retrieval Symposium, Part 2 Apr. 1993 p 277-302 (For primary document see N93-29354 11-99)
Avail: CASI HC A03/MF A04

N93-29356*# Departement d'Etudes et de Recherches en Technologie Spatiale, Toulouse (France).
MICROMETEOROIDS AND DEBRIS ON LDEF
Jean-Claude Mandeville *In* NASA. Langley Research Center, LDEF: 69 Months in Space. Second Post-Retrieval Symposium, Part 2 Apr. 1993 p 303-312 Sponsored by NASA and CNES (For primary document see N93-29354 11-99)
Avail: CASI HC A02/MF A04

N93-29358*# European Space Agency. European Space Research and Technology Center, ESTEC, Noordwijk (Netherlands).
PREDICTED AND OBSERVED DIRECTIONAL DEPENDENCE OF METEOROID/DEBRIS IMPACTS ON LDEF THERMAL BLANKETS
Gerhard Drolshagen *In* NASA. Langley Research Center, LDEF: 69 Months in Space. Second Post-Retrieval Symposium, Part 2 Apr. 1993 p 325-337 (For primary document see N93-29354 11-99)
Avail: CASI HC A03/MF A04

N93-29360*# National Aeronautics and Space Administration. Ames Research Center, Moffett Field, CA.
FURTHER ANALYSIS OF LDEF FRECOPA MICROMETEOROID REMNANTS
Janet Borg (Centre National de la Recherche Scientifique, Orsay, France.), Ted E. Bunch, Filippo RadicatidiBrozolo (Evans, Charles and Associates, Redwood City, CA.), and Jean Claude Mandeville (Departement d'Etudes et de Recherches en Technologie Spatiale, Toulouse, France.) *In* NASA. Langley Research Center, LDEF: 69 Months in Space. Second Post-Retrieval Symposium, Part 2 Apr. 1993 p 347-356 (For primary document see N93-29354 11-99)
(Contract NAS2-13178; RTOP 199-52-12; RTOP 506-48-00)
Avail: CASI HC A02/MF A04

N93-29361*# Aerospace Corp., El Segundo, CA. Mechanics and Materials Technology Center.
LONG DURATION EXPOSURE FACILITY (LDEF) EXPERIMENT M0003 METEOROID AND DEBRIS SURVEY
M. J. Meshishnek, S. R. Gyetvay, K. W. Paschen, and J. M. Coggi *In* NASA. Langley Research Center, LDEF: 69 Months in Space. Second Post-Retrieval Symposium, Part 2 Apr. 1993 p 357-415 Sponsored by the Strategic Defense Initiative Organization and AF Wright Lab. (For primary document see N93-29354 11-99)
Avail: CASI HC A04/MF A04

N93-29370*# National Aeronautics and Space Administration. Lyndon B. Johnson Space Center, Houston, TX.
PROJECTILE COMPOSITIONS AND MODAL FREQUENCIES ON THE CHEMISTRY OF MICROMETEOROIDS LDEF EXPERIMENT
Ronald P. Bernhard (Lockheed Engineering and Sciences Co., Houston, TX.), Thomas H. See (Lockheed Engineering and Sciences Co., Houston, TX.), and Friedrich Hoerz *In* NASA. Langley Research Center, LDEF: 69 Months in Space. Second Post-Retrieval Symposium, Part 2 Apr. 1993 p 551-573 (For primary document see N93-29354 11-99)
Avail: CASI HC A03/MF A04

N93-29371*# National Aeronautics and Space Administration. Lyndon B. Johnson Space Center, Houston, TX.
ASTEROIDAL VERSUS COMETARY METEOROID IMPACTS ON THE LONG DURATION EXPOSURE FACILITY (LDEF) Abstract Only
Herbert A. Zook *In* NASA. Langley Research Center, LDEF: 69 Months in Space. Second Post-Retrieval Symposium, Part 2 Apr. 1993 p 575 (For primary document see N93-29354 11-99)
Avail: CASI HC A01/MF A04

N93-29372*# National Aeronautics and Space Administration. Lyndon B. Johnson Space Center, Houston, TX.
INTERPLANETARY METEOROID DEBRIS IN LDEF METAL CRATERS
D. E. Brownlee (Washington Univ., Seattle.), D. Joswiak (Washington Univ., Seattle.), J. Bradley (MVA, Inc., Norcross, GA.), and Friedrich Hoerz *In* NASA. Langley Research Center, LDEF: 69 Months in Space. Second Post-Retrieval Symposium, Part 2 Apr. 1993 p 577-584 (For primary document see N93-29354 11-99)
Avail: CASI HC A02/MF A04

N93-29376*# Jet Propulsion Lab., California Inst. of Tech., Pasadena.
NEW METEOROID MODEL PREDICTIONS FOR DIRECTIONAL IMPACTS ON LDEF Abstract Only
Neil Divine and Rene C. Agueero *In* NASA. Langley Research Center, LDEF: 69 Months in Space. Second Post-Retrieval Symposium, Part 2 Apr. 1993 p 665 (For primary document see N93-29354 11-99)
Avail: CASI HC A01/MF A04

N93-29377*# National Aeronautics and Space Administration. Langley Research Center, Hampton, VA.
LONG DURATION EXPOSURE FACILITY (LDEF) ATTITUDE MEASUREMENTS OF THE INTERPLANETARY DUST EXPERIMENT
Philip C. Kassel, Jr., William R. Motley, III, S. Fred Singer (Institute for Space Science and Technology, Inc., Gainesville, FL.), J. Derral Mulholland (Institute for Space Science and Technology, Inc., Gainesville, FL.), John P. Oliver (Institute for Space Science and Technology, Inc., Gainesville, FL.), Jerry L. Weinberg (Institute for Space Science and Technology, Inc., Gainesville, FL.), William J. Cooke (Institute for Space Science and Technology, Inc., Gainesville, FL.), and Jim J. Wortman (North Carolina Univ., Raleigh.) *In its* LDEF: 69 Months in Space. Second Post-Retrieval Symposium, Part 2 Apr. 1993 p 667-675 (For primary document see N93-29354 11-99)
Avail: CASI HC A02/MF A04

N93-29378*# Institute for Space Science and Technology, Inc., Gainesville, FL.
ELEMENTAL ANALYSES OF HYPERVELOCITY MICROPARTICLE IMPACT SITES ON INTERPLANETARY DUST EXPERIMENT SENSOR SURFACES
Charles G. Simon, J. L. Hunter (North Carolina Univ., Raleigh.), D. P. Griffis (North Carolina Univ., Raleigh.), V. Misra (North Carolina Univ., Raleigh.), D. A. Ricks (North Carolina Univ., Raleigh.), Jim J. Wortman (North Carolina Univ., Raleigh.), and D. E. Brownlee (Washington Univ., Seattle.) *In* NASA. Langley Research Center, LDEF: 69 Months in Space. Second Post-Retrieval Symposium, Part 2 Apr. 1993 p 677-692 (For primary document see N93-29354 11-99)
Avail: CASI HC A03/MF A04

N93-29379*# National Aeronautics and Space Administration. Langley Research Center, Hampton, VA.
LONG-TERM MICROPARTICLE FLUX VARIABILITY INDICATED BY COMPARISON OF INTERPLANETARY DUST EXPERIMENT (IDE) TIMED IMPACTS FOR LDEF'S FIRST YEAR IN ORBIT WITH IMPACT DATA FOR THE ENTIRE 5.77-YEAR ORBITAL LIFETIME
Charles G. Simon (Institute for Space Science and Technology, Inc., Gainesville, FL.), J. Derral Mulholland (Institute for Space Science and Technology, Inc., Gainesville, FL.), John P. Oliver (Institute for Space Science and Technology, Inc., Gainesville, FL.), William J. Cooke (Institute for Space Science and Technology, Inc., Gainesville, FL.), and Philip C. Kassel, Jr. *In its* LDEF: 69 Months in Space. Second Post-Retrieval Symposium, Part 2 Apr. 1993 p 693-703 (For primary document see N93-29354 11-99)

(Grant NAG1-1218)
Avail: CASI HC A03/MF A04

N93-29380*# Bern Univ. (Switzerland). Physikalisches Inst.
THE INTERSTELLAR GAS EXPERIMENT: ANALYSIS IN PROGRESS
F. Buehler, D. L. Lind (Utah State Univ., Logan.), J. Geiss, and O. Eugster *In* NASA. Langley Research Center, LDEF: 69 Months in Space. Second Post-Retrieval Symposium, Part 2 Apr. 1993 p 705-723 (For primary document see N93-29354 11-99)
Avail: CASI HC A03/MF A04

91 LUNAR AND PLANETARY EXPLORATION

Includes planetology; and manned and unmanned flights.
For spacecraft design or space stations see *18 Spacecraft Design, Testing and Performance.*

N93-28764*# Lunar and Planetary Inst., Houston, TX.
WORKSHOP ON ADVANCED TECHNOLOGIES FOR PLANETARY INSTRUMENTS, PART 1 Abstracts Only
John F. Appleby, ed. 1993 46 p Workshop held in Fairfax, VA, 28-30 Apr. 1993; sponsored by Strategic Defense Initiative Organization
(Contract NASw-4574)
(NASA-CR-193015; NAS 1.26:193015; LPI-TR-93-02-Pt-1) Avail: CASI HC A03/MF A01

This meeting was conceived in response to new challenges facing NASA's robotic solar system exploration program. This volume contains papers presented at the Workshop on Advanced Technologies for Planetary Instruments on 28-30 Apr. 1993. This meeting was conceived in response to new challenges facing NASA's robotic solar system exploration program. Over the past several years, SDIO has sponsored a significant technology development program aimed, in part, at the production of instruments with these characteristics. This workshop provided an opportunity for specialists from the planetary science and DoD communities to establish contacts, to explore common technical ground in an open forum, and more specifically, to discuss the applicability of SDIO's technology base to planetary science instruments. For individual titles, see N93-28765 through N93-28829.

N93-28765*# Jet Propulsion Lab., California Inst. of Tech., Pasadena.
A MICROSEISMOMETER FOR TERRESTRIAL AND EXTRATERRESTRIAL APPLICATIONS Abstract Only c35
W. Banerdt, W. Kaiser, and T. VanZandt *In* Lunar and Planetary Inst., Workshop on Advanced Technologies for Planetary Instruments, Part 1 1993 p 1 (For primary document see N93-28764 11-91)
Avail: CASI HC A01/MF A01

The scientific and technical requirements of extraterrestrial seismology place severe demands on instrumentation. Performance in terms of sensitivity, stability, and frequency band must match that of the best terrestrial instruments, at a fraction of the size, mass, and power. In addition, this performance must be realized without operator intervention in harsh temperature, shock, and radiation environments. These constraints have forced us to examine some fundamental limits of accelerometer design in order to produce a small, rugged, sensitive seismometer. Silicon micromachined sensor technology offers techniques for the fabrication of monolithic, robust, compact, low-power and -mass accelerometers. However, currently available sensors offer inadequate sensitivity and bandwidth. Our implementation of an advanced silicon micro machined seismometer is based on principles developed at JPL for high-sensitivity position sensor technology. The use of silicon micro machining technology with these new principles should enable the fabrication of a 10(exp -11) g sensitivity seismometer with a bandwidth of at least 0.01 to 20 Hz. The low Q properties of pure single-crystal silicon are essential in order to minimize the Brownian thermal noise limitations generally characteristic of seismometers with small proof masses. A seismometer consists of a spring-supported proof mass and a transducer for measuring its motion. For long period motion a position sensor is generally used, for which the displacement is proportional to the ground acceleration. The mechanical sensitivity can be increased either by increasing the proof mass or decreasing the spring stiffness, neither of which is desirable for planetary applications. Our approach has been to use an ultra sensitive capacitive position sensor with a sensitivity of better than 10(exp -13) m/Hz(exp 1/2). This allows the use of a stiffer suspension and a smaller proof mass. We have built several prototypes using these principles, and tests show that these devices can exhibit performance comparable to state-of-the-art instruments.
Author (revised)

N93-28766*# Hughes Danbury Optical Systems, Inc., CT.
THE HYDICE INSTRUMENT DESIGN AND ITS APPLICATION TO PLANETARY INSTRUMENTS Abstract Only c35
R. Basedow, P. Silverglate, W. Rappoport, R. Rockwell, D. Rosenberg, K. Shu, R. Whittlesey, and E. Zalewski *In* Lunar and Planetary Inst., Workshop on Advanced Technologies for Planetary Instruments, Part 1 1993 p 1 (For primary document see N93-28764 11-91)
Avail: CASI HC A01/MF A01

The Hyperspectral Digital Imagery Collection Experiment (HYDICE) instrument represents a significant advance in the state of the art in hyperspectral sensors. It combines a higher signal-to-noise ratio (SNR) and significantly better spatial and spectral resolution and radio metric accuracy than systems flying on aircraft today. The need for 'clean' data, i.e., data free of sampling artifacts and excessive spatial or spectral noise, is a key driver behind the difficult combination of performance requirements laid out for HYDICE. Most of these involve the sensor optics and detector. This paper presents an optimized approach to those requirements, one that comprises push broom scanning, a single, mechanically cooled focal plane, a double-pass prism spectrometer, and an easily fabricated yet wide-field telescope. Central to the approach is a detector array that covers the entire spectrum from 0.4 to 2.5 microns. Among the major benefits conferred by such a design are optical and mechanical simplicity, low polarization sensitivity, and coverage of the entire spectrum without suffering the spectral gaps caused by beam splitters. The overall system minimizes interfaces to the C-141 aircraft on which it will be flown, can be calibrated on the ground and in flight to accuracies better than those required, and is designed for simple, push-button operation. Only unprocessed data are recorded during flight. A ground data processing station provides quick-look, calibration correction, and archiving capabilities, with a throughput better than the requirements. Overall performance of the system is expected to provide the solid database required to evaluate the potential of hyperspectral imagery in a wide variety of applications. HYDICE can be regarded as a test bed for future planetary instruments. The ability to spectrally image a wide field of view over multiple spectral octaves offers obvious advantages and is expected to maximize science return for the required cost and weight.
Author (revised)

N93-28767*# National Oceanic and Atmospheric Administration, Boulder, CO. Wave Propagation Lab.
RUGGED, NO-MOVING-PARTS WINDSPEED AND STATIC PRESSURE PROBE DESIGNS FOR MEASUREMENTS IN PLANETARY ATMOSPHERES Abstract Only c35
A. J. Bedard, Jr. and R. T. Nishiyama (Colorado Univ., Boulder.) *In* Lunar and Planetary Inst., Workshop on Advanced Technologies for Planetary Instruments, Part 1 1993 p 1-2 (For primary document see N93-28764 11-91)
Avail: CASI HC A01/MF A01

Instruments developed for making meteorological observations under adverse conditions on Earth can be applied to systems designed for other planetary atmospheres. Specifically, a wind sensor developed for making measurements within tornados is capable of detecting induced pressure differences proportional to wind speed. Adding strain gauges to the sensor would provide wind direction. The device can be constructed in a rugged form for measuring high wind speeds in the presence of blowing dust that would clog bearings and plug passages of conventional wind speed sensors. Sensing static pressure in the lower boundary layer required development of an omnidirectional, tilt-insensitive static pressure probe. The probe provides pressure inputs to a sensor with minimum error and is inherently weather-protected. The wind sensor and static pressure probes have been used in a variety of field programs and can be adapted for use in different planetary atmospheres.
Author (revised)

N93-28768*# Grumman Aerospace Corp., Bethpage, NY.
DESIGN OF A PARTICLE BEAM SATELLITE SYSTEM FOR LUNAR PROSPECTING Abstract Only c35
D. H. Berwald and P. Nordin *In* Lunar and Planetary Inst., Workshop on Advanced Technologies for Planetary Instruments, Part 1 1993 p 2

(For primary document see N93-28764 11-91)
(Contract DASG60-90-C-0103)
Avail: CASI HC A01/MF A01

One potential use for neutral particle beam (NPB) technology is as an active orbital probe to investigate the composition of selected locations on the lunar surface. Because the beam is narrow and can be precisely directed, the NPB probe offers possibilities for high resolution experiments that cannot be accomplished using passive techniques. Rather, the combination of both passive and active techniques can be used to provide both full-coverage mapping (passively) at low resolution (tens of kilometers) and high-resolution information for discrete locations of special interest. A preliminary study of NPB applicability for this dual-use application was recently conducted. The study was completed in Feb. 1993. A novel feature was the consideration of the use of a Russian launch vehicle (e.g., the Proton). The use of other Russian space hardware and capabilities was also encouraged. This paper describes the lunar prospector system design. Other researchers discuss the issues and opportunities involving lunar scientific experimentation using an NPB. The NPB lunar prospector utilizes a modified design of the Far Field Optics Experiment (FOX). Like the Earth-orbiting FOX, the core capability of the NPB lunar prospector will be a pulsed RF LINAC that produces a 5-MeV proton beam that is projected to the target with a 30-micro-r beam divergence and a 10-micro-r beam-pointing accuracy. Upon striking the lunar surface, the proton beam will excite characteristic radiation (e.g., X-rays) that can be sensed by one or more detectors on the NPB platform or on a separate detector satellite. Author (revised)

N93-28769*# Los Alamos National Lab., NM. Geology and Geochemistry Group.
LAER-INDUCED BREAKDOWN SPECTROSCOPY INSTRUMENT FOR ELEMENT ANALYSIS OF PLANETARY SURFACES Abstract Only c35
J. Blacic, D. Pettit, D. Cremers, and N. Roessler (McDonnell-Douglas Electronics Co., Saint Louis, MO.) *In* Lunar and Planetary Inst., Workshop on Advanced Technologies for Planetary Instruments, Part 1 1993 p 2-3 (For primary document see N93-28764 11-91)
Avail: CASI HC A01/MF A01

One of the most fundamental pieces of information about any planetary body is the elemental and mineralogical composition of its surface materials. We are developing an instrument to obtain such data at ranges of up to several hundreds of meters using the technique of Laser-Induced Breakdown Spectroscopy (LIBS). We envision our instrument being used from a spacecraft in close rendezvous with small bodies such as comets and asteroids, or deployed on surface-rover vehicles on large bodies such as Mars and the Moon. The elemental analysis is based on atomic emission spectroscopy of a laser-induced plasma or spark. A pulsed, diode pumped Nd:YAG laser of several hundred millijoules optical energy is used to vaporize and electronically excite the constituent elements of a rock surface remotely located from the laser. Light emitted from the excited plasma is collected and introduced to the entrance slit of a small grating spectrometer. The spectrally dispersed spark light is detected with either a linear photo diode array or area CCD array. When the latter detector is used, the optical and spectrometer components of the LIBS instrument can also be used in a passive imaging mode to collect and integrate reflected sunlight from the same rock surface. Absorption spectral analysis of this reflected light gives mineralogical information that provides a remote geochemical characterization of the rock surface. We performed laboratory calibrations in air and in vacuum on standard rock powders to quantify the LIBS analysis. We performed preliminary field tests using commercially available components to demonstrate remote LIBS analysis of terrestrial rock surfaces at ranges of over 25 m, and we have demonstrated compatibility with a six-wheeled Russian robotic rover vehicle. Based on these results, we believe that all major and most minor elements expected on planetary surfaces can be measured with absolute accuracy of 10-15 percent and much higher relative accuracy. We have performed preliminary systems analysis of a LIBS instrument to evaluate probable mass and power requirements; results of this analysis are summarized. Author (revised)

N93-28770*# Jet Propulsion Lab., California Inst. of Tech., Pasadena.
CLEMENTINE 2: A DOUBLE ASTEROID FLYBY AND IMPACTOR MISSION Abstract Only c12
R. J. Boain *In* Lunar and Planetary Inst., Workshop on Advanced Technologies for Planetary Instruments, Part 1 1993 p 3 (For primary document see N93-28764 11-91)
Avail: CASI HC A01/MF A01

Recently JPL was asked by SDIO to analyze and develop a preliminary design for a deep-space mission to fly by two near-Earth asteroids, Eros and Toutatis. As a part of this mission, JPL was also asked to assess the feasibility of deploying a probe on approach to impact Toutatis. This mission is a candidate for SDIO's Clementine 2. SDIO's motivations were to provide further demonstrations of precision, autonomous navigation for controlling the flight paths of both a spacecraft and a probe. NASA's interest in this mission is driven by the opportunity to obtain the first close-up images and other scientific measurements from a spacecraft of two important near-Earth objects. For Toutatis this is especially important since it was observed and imaged extensively just last Dec. using Earth-based radar; Clementine 2 will provide the opportunity to corroborate the radar data and validate the ultimate potential of the radar technique. Scientifically, the probe impact at Toutatis will allow the acquisition of data pertaining to the dynamic strength of surface material and data on the properties of the regolith and on stratification below the surface, and will potentially allow the measurement of thermal diffusivity between the interior and the surface. These determinations will be accomplished by means of high-resolution imagery of the impact crater and its surroundings in visible, ultraviolet, and infrared wave bands from the spacecraft flying by some 30 min. after the probe strike. In addition, if the spacecraft can be equipped with a lightweight mass spectrometer and dust analyzer, the potential also exists to measure the particle sizes and distribution and the composition of the eject a cloud. This mission is planned to be launched in Jul. 1995, with the Eros encounter on 13 Mar. 1996, and the Toutatis flyby on 4 Oct. 1996, some 440 days after launch. Author (revised)

N93-28771*# Massachusetts Inst. of Tech., Lexington. Lincoln Lab.
HIGH-PERFORMANCE VISIBLE/UV CCD FOCAL PLANE TECHNOLOGY FOR SPACEBASED APPLICATIONS Abstract Only c35
B. E. Burke, R. W. Mountain, J. A. Gregory, J. C. M. Huang, M. J. Cooper, E. D. Savoye, and B. B. Kosicki *In* Lunar and Planetary Inst., Workshop on Advanced Technologies for Planetary Instruments, Part 1 1993 p 3-4 Sponsored in part by AF (For primary document see N93-28764 11-91)
Avail: CASI HC A01/MF A01

We describe recent technology developments aimed at large CCD imagers for space based applications in the visible and UV. Some of the principal areas of effort include work on reducing device degradation in the natural space-radiation environment, improvements in quantum efficiency in the visible and UV, and larger-device formats. One of the most serious hazards for space based CCD's operating at low signal levels is the displacement damage resulting from bombardment by energetic protons. Such damage degrades charge-transfer efficiency and increases dark current. We have achieved improved hardness to proton-induced displacement damage by selective ion implants into the CCD channel and by reduced temperature of operation. To attain high quantum efficiency across the visible and UV we have developed a technology for back-illuminated CCD's. With suitable antireflection (AR) coatings such devices have quantum efficiencies near 90 percent in the 500-700-nm band. In the UV band from 200 to 400 nm, where it is difficult to find coatings that are sufficiently transparent and can provide good matching to the high refractive index of silicon, we have been able to substantially increase the quantum efficiency using a thin film of HfO2 as an AR coating. These technology efforts were applied to a 420 x 420-pixel frame-transfer imager, and future work will be extended to a 1024 x 1024-pixel device now under development. Author (revised)

N93-28772*# Hunter Coll., New York, NY. Dept. of Physics.
EVERY GOOD VIRTUE YOU EVER WANTED IN A Q-SWITCHED SOLID-STATE LASER AND MORE: MONOLITHIC, DIODE-PUMPED, SELF-Q-SWITCHED, HIGHLY REPRODUCIBLE, DIFFRACTION-LIMITED Nd:YAG LASER Abstract Only c36
Y. C. Chen and K. K. Lee (Colorado Univ., Colorado Springs.) *In* Lunar and Planetary Inst., Workshop on Advanced Technologies for Planetary Instruments, Part 1 1993 p 4 (For primary document see N93-28764 11-91)
Avail: CASI HC A01/MF A01

The applications of Q-switched lasers are well known, for example, laser radar, laser remote sensing, satellite orbit determination, Moon orbit and 'moon quake' determination, satellite laser communication, and many nonlinear optics applications. Most of the applications require additional properties of the Q-switched lasers, such as single-axial and/or single-transverse mode, high repetition rate, stable pulse shape and pulse width, or ultra compact and rugged oscillators. Furthermore, space based and airborne lasers for lidar and laser communication applications require efficient, compact, lightweight, long-lived, and stable-pulsed laser sources. Diode-pumped solid-state lasers (DPSSL) have recently shown the potential for satisfying all of these requirements. We will report on the operating characteristics of a diode-pumped, monolithic, self-Q-switched Cr,Nd:YAG laser where the chromium ions act as a saturable absorber for the laser emission at 1064 nm. The pulse duration is 3.5 ns and the output is highly polarized with an extinction ratio of 700:1. It is further shown that the output is single-longitudinal-mode with transform-limited spectral line width without pulse-to-pulse mode competition. Consequently, the pulse-to-pulse intensity fluctuation is less than the instrument resolution of 0.25 percent. This self-stabilization mechanism is because the lasing mode bleaches the distributed absorber and establishes a gain-loss grating similar to that used in the distributed feedback semiconductor lasers. A repetition rate above 5 KHz has also been demonstrated. For higher power, this laser can be used for injection seeding an amplifier (or amplifier chain) or injection locking of a power oscillator pumped by diode lasers. We will discuss some research directions on the master oscillator for higher output energy per pulse as well as how to scale the output power of the diode-pumped amplifier(s) to multi-kilowatt average power.

Author (revised)

N93-28773*# Lockheed Aircraft Corp., Palo Alto, CA. Research and Development Div.

PLANETARY AND SATELLITE X RAY SPECTROSCOPY: A NEW WINDOW ON SOLID-BODY COMPOSITION BY REMOTE SENSING Abstract Only

D. L. Chenette, R. W. Wolcott, and R. S. Selesnick (California Inst. of Tech., Pasadena.) *In* Lunar and Planetary Inst., Workshop on Advanced Technologies for Planetary Instruments, Part 1 1993 p 4 (For primary document see N93-28764 11-91)

Avail: CASI HC A01/MF A01

The rings and most of the satellites of the outer planets orbit within the radiation belts of their parent bodies. This is an environment with intense fluxes of energetic electrons. As a result, these objects are strong emitters of X-rays. The characteristic X-ray lines from these bodies depend on atomic composition, but they are not sensitive to how the material is arranged in compounds or mixtures. X-ray fluorescence spectral analysis has demonstrated its unique value in the laboratory as a qualitative and quantitative analysis tool. This technique has yet to be fully exploited in a planetary instrument for remote sensing. The characteristic X-ray emissions provide atomic relative abundances. These results are complementary to the molecular composition information obtained from IR, visible, and UV emission spectra. The atomic relative abundances are crucial to understanding the formation and evolution of these bodies. They are also crucial to the proper interpretation of the molecular composition results from the other sensors. The intensities of the characteristic X-ray emissions are sufficiently strong to be measured with an instrument of modest size. Recent developments in X-ray detector technologies and electronic miniaturization have made possible space-flight X-ray imaging and nonimaging spectrometers of high sensitivity and excellent energy resolution that are rugged enough to survive long-duration space missions. Depending on the application, such instruments are capable of resolving elemental abundances of elements from carbon through iron. At the same time, by measuring the bremsstrahlung intensity and energy spectrum, the characteristics of the source electron flux can be determined. We will discuss these concepts, including estimated source strengths, and will describe a small instrument capable of providing this unique channel of information for future planetary missions. We propose to build this instrument using innovative electronics packaging methods to minimize size and weight. Author (revised)

N93-28774*# Jet Propulsion Lab., California Inst. of Tech., Pasadena.

POLARIMETRIC MULTISPECTRAL IMAGING TECHNOLOGY Abstract Only c35

L.-J. Cheng, T.-H. Chao, M. Dowdy, C. Mahoney, and G. Reyes *In* Lunar and Planetary Inst., Workshop on Advanced Technologies for Planetary Instruments, Part 1 1993 p 4-5 (For primary document see N93-28764 11-91)

Avail: CASI HC A01/MF A01

The Jet Propulsion Laboratory is developing a remote sensing technology on which a new generation of compact, lightweight, high-resolution, low-power, reliable, versatile, programmable scientific polarimetric multispectral imaging instruments can be built to meet the challenge of future planetary exploration missions. The instrument is based on the fast programmable acousto-optic tunable filter (AOTF) of tellurium dioxide (TeO2) that operates in the wavelength range of 0.4-5 microns. Basically, the AOTF multispectral imaging instrument measures incoming light intensity as a function of spatial coordinates, wavelength, and polarization. Its operation can be in either sequential, random access, or multiwavelength mode as required. This provides observation flexibility, allowing real-time alternation among desired observations, collecting needed data only, minimizing data transmission, and permitting implementation of new experiments. These will result in optimization of the mission performance with minimal resources. Recently we completed a polarimetric multispectral imaging prototype instrument and performed outdoor field experiments for evaluating application potentials of the technology. We also investigated potential improvements on AOTF performance to strengthen technology readiness for applications. This paper will give a status report on the technology and a prospect toward future planetary exploration.

Author (revised)

N93-28775*# National Aeronautics and Space Administration. Langley Research Center, Hampton, VA.

A REMOTE LASER-MASS SPECTROMETER FOR DETERMINATION OF ELEMENTAL COMPOSITION Abstract Only c35

R. J. DeYoung and W. Situ (Hampton Univ., VA.) *In* Lunar and Planetary Inst., Workshop on Advanced Technologies for Planetary Instruments, Part 1 1993 p 5-6 (For primary document see N93-28764 11-91)

Avail: CASI HC A01/MF A01

Determination of the elemental composition of lunar, asteroid, and planetary surfaces is a major concern for science and resource utilization of space. The science associated with the development of a satellite or lunar rover laser-mass spectrometer instrument is presented here. The instrument would include a pulsed laser with sufficient energy to create a plasma on a remote surface. Ions ejected from this plasma travel back to the spacecraft or rover, where they are analyzed by a time-of-flight mass spectrometer, giving the elemental and isotope composition. This concept is based on the LIMA-D instrument on board the former Soviet Union Phobos-88 spacecraft sent to Mars. A laser-mass spectrometer placed on a rover or satellite would substantially improve the data return over alternative techniques. The spatial resolution would be centimeters, and a complete mass spectrum could be achieved in one laser shot. An experiment is described that demonstrates these features. A 400 mj Nd:YAG laser is focused, to an intensity of 10(exp 11) w/sq cm, onto a Al, Ag, Cu, Ge, or lunar simulant target. A plasma forms from which ions are ejected. Some of these ions travel down an 18-m evacuated flight tube to a microchannel plate detector. Alternatively, the ions are captured by an ion trap where they are stored until pulsed into a 1-m time-of-flight mass spectrometer, giving the elemental composition of the remote surface. A television camera monitors the plasma plume shape, and a photodiode monitors the temporal plasma emission . With this system, ions of Al, Ag, Cu, Ge, and lunar simulant have been detected at 18 m. The mass spectrum from the ion trap and 1-m time-of-flight tube will be presented. Author (revised)

N93-28776*# Laboratory for Astrophysics and Space Research, Chicago, IL.

THE APX SPECTROMETER FOR MARTIAN MISSIONS Abstract Only c35

T. Economou *In* Lunar and Planetary Inst., Workshop on Advanced Technologies for Planetary Instruments, Part 1 1993 p 6-7 (For primary document see N93-28764 11-91)

Avail: CASI HC A01/MF A01

Obtaining the chemical composition of any planetary body should be a prime science objective of each planetary mission. The APX spectrometer has been designed to provide a detailed and complete chemical composition of all major (except H) and minor elements with high accuracy, in situ and remotely. From such complete analyses a first-order mineralogy of analyzed samples can be deduced. Laboratory studies in the past have shown that rock types (e.g., dunites, basalts, Philippinate 300 sample) were a uniquely in blind test analyses. Such identification is more accurate than can be obtained from any other remote spectroscopic technique. The APX technique is based on three modes of nuclear and atomic interactions of alpha particles with matter resulting in three different energy spectra containing the compositional information. The instrument uses 50 to 100 mCi of Cm-242 or Cm-244 transuranium radioisotopes to provide a monoenergetic beam of alpha particles (6.01 MeV and 5.80 MeV respectively) and solid-state detectors for acquiring the energy spectra. Author (revised)

N93-28777*# Jet Propulsion Lab., California Inst. of Tech., Pasadena.
INVESTIGATION OF MARS ROTATIONAL DYNAMICS USING EARTH-BASED RADIO TRACKING OF MARS LANDERS Abstract Only
C. D. Edwards, Jr., W. M. Folkner, R. D. Kahn, and R. A. Preston *In* Lunar and Planetary Inst., Workshop on Advanced Technologies for Planetary Instruments, Part 1 1993 p 7 (For primary document see N93-28764 11-91)
Avail: CASI HC A01/MF A01

The development of space geodetic techniques over the past two decades has made it possible to measure the rotational dynamics of the Earth at the milliarcsecond level, improving our geophysical models of the Earth 's interior and the interactions between the solid Earth and its atmosphere. We have found that the rotational dynamics of Mars can be determined to nearly the same level of accuracy by acquiring Earth-based two-way radio tracking observations of three or more landers globally distributed on the surface of Mars. Our results indicate that the precession and long-term obliquity changes of the Mars pole direction can be determined to an angular accuracy corresponding to about 15 cm/yr at the planet's surface. In addition, periodic nutations of the pole and seasonal variations in the spin rate of the planet can be determined to 10 cm or less. Measuring the rotation of Mars at this accuracy would greatly improve the determination of the planet' s moment of inertia and would resolve the size of a planetary fluid core, providing a valuable constraint on Mars interior models. Detecting seasonal variations in the spin rate of Mars would provide global constraints on atmospheric angular momentum changes due to sublimation of the Mars CO2 polar ice caps. Finally, observation of quasisecular changes in Mars obliquity would have significant implications for understanding long-term climatic change. The key to achieving these accuracies is a globally distributed network of Mars landers with stable, phase-coherent radio transponders. By simultaneously acquiring coherent two-way carrier phase observations between a single Earth tracking station and multiple Mars landers, Earth media errors are essentially eliminated, providing an extremely sensitive measure of changes in the differential path lengths between the Earth tracking station and the Mars landers due to Mars rotation. Time variability of the instrumental phase delay through the radio transponder may represent the limiting error source for this technique. Calibration of the transponder stability to about 0.1 ns or less, over a single tracking arc of up to 12 hr, is sufficient to provide the decimeter-level determination of Mars orientation parameters quoted above. We will provide a detailed description of the multilander tracking technique and the requirements it imposes on both the lander radio system and the Earth-based ground-tracking system. This concept is currently part of the strawman science plan for the Mars Environmental Survey (MESUR) mission and complements many of the other MESUR science goals.
Author (revised)

N93-28778*# Innovative Concepts Co., McLean, VA.
CLEMENTINE SENSOR PROCESSING SYSTEM Abstract Only c19
A. A. Feldstein *In* Lunar and Planetary Inst., Workshop on Advanced Technologies for Planetary Instruments, Part 1 1993 p 7-8 (For primary document see N93-28764 11-91)
Avail: CASI HC A01/MF A01

The design of the DSPSE Satellite Controller (DSC) is baselined as a single-string satellite controller. The DSC performs two main functions: health and maintenance of the spacecraft; and image capture, storage, and playback. The DSC contains two processors: a radiation-hardened Mil-Std-1750, and a commercial R3000. The Mil-Std-1750 processor performs all housekeeping operations, while the R3000 is mainly used to perform the image processing functions associated with the navigation functions, as well as performing various experiments. The DSC also contains a data handling unit (DHU) used to interface to various spacecraft imaging sensors and to capture, compress, and store selected images onto the solid-state data recorder. The development of the DSC evolved from several key requirements; the DSPSE satellite was to do the following: (1) have a radiation-hardened spacecraft control system and be immune to single-event upsets (SEU's); (2) use an R3000-based processor to run the star tracker software that was developed by SDIO (due to schedule and cost constraints, there was no time to port the software to a radiation-hardened processor); and (3) fly a commercial processor to verify its suitability for use in a space environment. In order to enhance the DSC reliability, the system was designed with multiple processing paths. These multiple processing paths provide for greater tolerance to various component failures. The DSC was designed so that all housekeeping processing functions are performed by either the Mil-Std-1750 processor or the R3000 processor. The image capture and storage is performed either by the DHU or the R3000 processor. Author (revised)

N93-28779*# Arizona Univ., Tucson. Lunar and Planetary Lab.
DESIGN CONCEPT FOR AN IR MAPPING SPECTROMETER FOR THE PLUTO FAST FLYBY MISSION Abstract Only c19
U. Fink, F. Low, B. Hubbard, M. Rieke, G. Rieke, M. Mumma, S. Nozette, G. Neukum, H. Hamel, and M. DiSanti et al *In* Lunar and Planetary Inst., Workshop on Advanced Technologies for Planetary Instruments, Part 1 1993 p 8 (For primary document see N93-28764 11-91)
Avail: CASI HC A01/MF A01

The design of an IR mapping spectrometer that exceeds all the criteria of the Pluto Fast Flyby Mission will be presented. The instrument has a mass of approximately 1700 g and uses less than 4 W of power. The design concept is based on an f/3 spectrograph using an aberration-corrected concave holographic grating. Up to four spectral regions can be covered simultaneously by dividing the grating into two to four sections, each imaging the entrance slit on a different area of the array. The spectrography will be fed by a lightweight 5 in. f/3 telescope based on SDIO precepts. In order to provide spectroscopic access to the fundamental molecule frequencies, an extended-range NICMOS array to approximately 3.5 microns and an InSb array going to 5.8 microns will be considered. Author (revised)

N93-28780*# National Aeronautics and Space Administration. Goddard Space Flight Center, Greenbelt, MD.
MULTIBEAM LASER ALTIMETER FOR PLANETARY TOPOGRAPHIC MAPPING Abastract Only c36
J. B. Garvin, J. L. Bufton, and D. J. Harding *In* Lunar and Planetary Inst., Workshop on Advanced Technologies for Planetary Instruments, Part 1 1993 p 8 (For primary document see N93-28764 11-91)
Avail: CASI HC A01/MF A01

Laser altimetry provides an active, high-resolution, high-accuracy method for measurement of planetary and asteroid surface topography. The basis of the measurement is the timing of the roundtrip propagation of short-duration pulses of laser radiation between a spacecraft and the surface. Vertical, or elevation, resolution of the altimetry measurement is determined primarily by laser pulse width, surface-induced spreading in time of the reflected pulse, and the timing precision of the altimeter electronics. With conventional gain-switched pulses from solid-state lasers and nanosecond resolution timing electronics, submeter vertical range resolution is possible anywhere from orbital altitudes of approximately 1 km to altitudes of several hundred kilometers. Horizontal resolution is a function of laser beam footprint size at the surface and the spacing between successive laser pulses. Laser divergence angle and altimeter platform height above the surface determine the laser footprint size at the surface, while laser pulse repetition rate, laser transmitter beam configuration, and altimeter platform velocity determine the spacing between successive laser pulses. Multiple laser transmitters in a single laser altimeter instrument that is orbiting above a planetary or asteroid surface could provide across-track as well as along-track coverage that can be used to construct a range image (i.e., topographic map) of the surface. We are developing a pushbroom laser altimeter instrument concept that utilizes a linear array of laser transmitters to provide contiguous across-track and along-track data. The laser technology is based on the emerging monolithic combination of individual, 1-sq cm diode-pumped Nd:YAG laser pulse emitters. Details of the multi-emitter laser transmitter technology, the instrument configuration, and performance calculations for a realistic Discovery-class mission will be presented. Author (revised)

N93-28781*# National Aeronautics and Space Administration. Goddard Space Flight Center, Greenbelt, MD.

ACOUSTO-OPTIC INFRARED SPECTRAL IMAGER FOR PLUTO FAST FLYBY Abstract Only **c19**

D. A. Glenar and J. J. Hillman *In* Lunar and Planetary Inst., Workshop on Advanced Technologies for Planetary Instruments, Part 1 1993 p 8-9 (For primary document see N93-28764 11-91)

Avail: CASI HC A01/MF A01

Acousto-optic tunable filters (AOTF's) enable the design of compact, two-dimensional imaging spectrometers with high spectral and spatial resolution and with no moving parts. Tellurium dioxide AOTF's operate from about 400 nm to nearly 5 microns, and a single device will tune continuously over one octave by changing the RF acoustic frequency applied to the device. An infrared (1.2-2.5 micron) Acousto-Optic Imaging Spectrometer (AImS) was designed that closely conforms to the surface composition mapping objectives of the Pluto Fast Flyby. It features a 75-cm focal length telescope, infrared AOTF, and 256 x 256 NICMOS-3 focal plane array for acquiring narrowband images with a spectral resolving power (lambda/delta(lambda)) exceeding 250. We summarize the instrument design features and its expected performance at the Pluto-Charon encounter. Author (revised)

N93-28782*# National Aeronautics and Space Administration. Lyndon B. Johnson Space Center, Houston, TX.

THERMAL ANALYZER FOR PLANETARY SOIL (TAPS): AN IN SITU INSTRUMENT FOR MINERAL AND VOLATILE-ELEMENT MEASUREMENTS Abstract Only

J. L. Gooding, D. W. Ming, J. E. Gruener (Lockheed Engineering and Sciences Co., Houston, TX.), F. L. Gibbons (Lockheed Engineering and Sciences Co., Houston, TX.), and J. H. Allton (Lockheed Engineering and Sciences Co., Houston, TX.) *In* Lunar and Planetary Inst., Workshop on Advanced Technologies for Planetary Instruments, Part 1 1993 p 9 (For primary document see N93-28764 11-91)

Avail: CASI HC A01/MF A01

Thermal Analyzer for Planetary Soil (TAPS) offers a specific implementation for the generic thermal analyzer/evolved-gas analyzer (TA/EGA) function included in the Mars Environmental Survey (MESUR) strawman payload; applications to asteroids and comets are also possible. The baseline TAPS is a single-sample differential scanning calorimeter (DSC), backed by a capacitive-polymer humidity sensor, with an integrated sampling mechanism. After placement on a planetary surface, TAPS acquires 10-50 mg of soil or sediment and heats the sample from ambient temperature to 1000-1300 K. During heating, DSC data are taken for the solid and evolved gases are swept past the water sensor. Through ground based data analysis, multicomponent DSC data are deconvolved and correlated with the water release profile to quantitatively determine the types and relative proportions of volatile-bearing minerals such as clays and other hydrates, carbonates, and nitrates. The rapid-response humidity sensors also achieve quantitative analysis of total water. After conclusion of soil-analysis operations, the humidity sensors become available for meteorology. The baseline design fits within a circular-cylindrical volume less than 1000 cm(sup 3), occupies 1.2 kg mass, and consumes about 2 Whr of power per analysis. Enhanced designs would acquire and analyze multiple samples and employ additional microchemical sensors for analysis of CO2, SO2, NO(x), and other gaseous species. Atmospheric pumps are also being considered as alternatives to pressurized purge gas. Author (revised)

N93-28783*# Terra Systems, Inc., Kailua, HI.

IMAGING SPECTROMETERS USING CONCAVE HOLOGRAPHIC GRATINGS Abstract Only **c35**

J. Gradie and S. Wang (SETS Technology, Inc., Mililani, HI.) *In* Lunar and Planetary Inst., Workshop on Advanced Technologies for Planetary Instruments, Part 1 1993 p 9-10 (For primary document see N93-28764 11-91)

Avail: CASI HC A01/MF A01

Imaging spectroscopy combines the spatial attributes of imaging with the compositionally diagnostic attributes of spectroscopy. For spacebased remote sensing applications, mass, size, power, data rate, and application constrain the scanning approach. For the first three approaches, substantial savings in mass and size of the spectrometer can be achieved in some cases with a concave holographic grating and careful placement of an order-sorting filter. A hologram etched on the single concave surface contains the equivalent of the collimating, dispersing, and camera optics of a conventional grating spectrometer and provides substantial wavelength dependent corrections for spherical aberrations and a flat focal field. These gratings can be blazed to improve efficiency when used over a small wavelength range or left unblazed for broadband uniform efficiency when used over a wavelength range of up to 2 orders. More than 1 order can be imaged along the dispersion axis by placing an appropriately designed step order-sorting filter in front of the one- or two-dimensional detector. This filter can be shaped for additional aberration corrections. The VIRIS imaging spectrometer based on the broadband design provides simultaneous imaging of the entrance slit from lambda = 0.9 to 2.6 microns (1.5 orders) onto a 128 x 128 HgCdTe detector (at 77 K). The VIRIS spectrometer was used for lunar mapping with the UH 24.in telescope at Mauna Kea Observatory. The design is adaptable for small, low mass, space based imaging spectrometers. Author (revised)

N93-28784*# Naval Research Lab., Washington, DC. Naval Center for Space Technology.

THE ULTRAVIOLET PLUME INSTRUMENT (UVPI) Abstract Only **c19**

D. M. Horan *In* Lunar and Planetary Inst., Workshop on Advanced Technologies for Planetary Instruments, Part 1 1993 1 p (For primary document see N93-28764 11-91)

Avail: CASI HC A01/MF A01

The Ultraviolet Plume Instrument (UVPI) was launched aboard the Low-power Atmospheric Compensation Experiment (LACE) satellite on 14 Feb. 1990. Both the spacecraft and the UVPI were sponsored by the Directed Energy Office of the Strategic Defense Initiative Organization. The mission of the UVPI was to obtain radiometrically calibrated images of rocket plumes at high altitude and background image data of the Earth, Earth's limb, and celestial objects in the near- and middle-UV wave bands. The UVPI was designed for nighttime observations, i.e., to acquire and track relatively bright objects against a dark background. Author (revised)

N93-28785*# Spire Corp., Bedford, MA.

MICROTEXTURED METALS FOR STRAY-LIGHT SUPPRESSION IN THE CLEMENTINE STARTRACKER Abstract Only **c19**

E. A. Johnson *In* Lunar and Planetary Inst., Workshop on Advanced Technologies for Planetary Instruments, Part 1 1993 p 10-11 (For primary document see N93-28764 11-91)

Avail: CASI HC A01/MF A01

Anodized blacks for suppressing stray light in optical systems can now be replaced by microscopically textured metal surfaces. An application of these black surfaces to the Clementine star-tracker navigational system, which will be launched in early 1994 to examine the Moon, en route to intercept an asteroid, is detailed. Rugged black surfaces with Lambertian BRDF less than 10(exp -2) srad(sup -1) are critical for suppressing stray light in the star-tracker optical train. Previously available materials spall under launch vibrations to contaminate mirrors and lenses. Microtextured aluminum is nearly as dark, but much less fragile. It is made by differential ion beam sputtering, which generates light-trapping pores and cones slightly smaller than the wavelength to be absorbed. This leaves a sturdy but light-absorbing surface that can survive challenging conditions without generating debris or contaminants. Both seeded ion beams and plasma immersion (from ECR plasmas) extraction can produce these microscopic textures without fragile interfaces. Process parameters control feature size, spacing, and optical effects (THR, BRDF). Both broad and narrow absorption bands can be engineered with tuning for specific wavelengths and applications. Examples are presented characterized by FTIR in reflection librators (0.95 normal emissivity), heat rejection, and enhanced nucleate boiling. Author

N93-28786*# Wisconsin Univ., Madison. Space Astronomy Lab.

NEW TECHNOLOGIES FOR UV DETECTORS Abstract Only **c74**

C. L. Joseph *In* Lunar and Planetary Inst., Workshop on Advanced Technologies for Planetary Instruments, Part 1 1993 p 11 (For primary document see N93-28764 11-91)

Avail: CASI HC A01/MF A01

Several technologies are currently being developed, leading to substantial improvements in the performance of UV detectors or significant reductions in power or weight. Four technologies discussed are (1) thin-film coatings to enhance the UV sensitivity of CCD's, (2) highly innovative magnet assemblies that dramatically reduce weight and result in virtually no external flux, (3) new techniques for curving microchannel plates (MCP's) so that single plates can be used to prevent ion feedback and present highly localized charge clouds to an anode structure, and (4) high-performance alternatives to glass-based MCP's. In item (2), for example, very robust magnets are made out of rare earth materials such as samarium cobalt, and cladding magnets are employed to prevent flux from escaping from the detector into the external environment. These new ultralight magnet assemblies are able to create strong, exceptionally uniform magnetic fields for image intensification and focusing of photoelectrons. The principle advantage of such detectors is the quantum efficiencies of 70-80 percent obtained throughout ultraviolet wavelengths (900-2000 A), the highest of any device. Despite the improvements achieved under item (3), high-performance alternatives to conventional glass-based MCP's potentially offer three distinct new advantages that include (1) a 30-100-fold improvement in dynamic range resulting in correspondingly higher signal-to-noise ratios, (2) the use of pure dielectric and semiconductor materials that will not outgas contaminants that eventually destroy photocathodes, and (3) channels that have constant spacing providing long-ranged order since the plates are made using photolithography techniques from the semiconductor industry. The manufacturers of these advanced-technology MCP's, however, are a couple of years away from actually producing a functioning image intensifier. In contrast to the use of CCD's for optical, ground based observations, there is no single detector technology in the ultraviolet that dominates or is as universally suitable for all applications. Thus, several technological problems, recent advances, and the impact that these new enabling technologies represent for UV applications are addressed. Author (revised)

N93-28787*# Physical Sciences, Inc., Andover, MA.
LIGHTWEIGHT MODULAR INSTRUMENTATION FOR PLANETARY APPLICATIONS Abstract Only **c19**
P. B. Joshi *In* Lunar and Planetary Inst., Workshop on Advanced Technologies for Planetary Instruments, Part 1 1993 p 11-12 (For primary document see N93-28764 11-91)
Avail: CASI HC A01/MF A01

An instrumentation, called Space Active Modular Materials ExperimentS (SAMMES), is developed for monitoring the spacecraft environment and for accurately measuring the degradation of space materials in low earth orbit (LEO). The SAMMES architecture concept can be extended to instrumentation for planetary exploration, both on spacecraft and in situ. The operating environment for planetary application will be substantially different, with temperature extremes and harsh solar wind and cosmic ray flux on lunar surfaces and temperature extremes and high winds on venusian and Martian surfaces. Moreover, instruments for surface deployment, which will be packaged in a small lander/rover (as in MESUR, for example), must be extremely compact with ultralow power and weight. With these requirements in mind, the SAMMES concept was extended to a sensor/instrumentation scheme for the lunar and Martian surface environment. Author (revised)

N93-28788*# National Aeronautics and Space Administration. Goddard Space Flight Center, Greenbelt, MD.
OPTICAL TECHNOLOGIES FOR UV REMOTE SENSING INSTRUMENTS Abstract Only **c74**
R. A. M. Keski-Kuha, J. F. Osantowski, D. B. Leviton, T. T. Saha, D. A. Content, R. A. Boucarut, J. S. Gum, G. A. Wright, C. M. Fleetwood, and T. J. Madison *In* Lunar and Planetary Inst., Workshop on Advanced Technologies for Planetary Instruments, Part 1 1993 p 12 (For primary document see N93-28764 11-91)
Avail: CASI HC A01/MF A01

Over the last decade significant advances in technology have made possible development of instruments with substantially improved efficiency in the UV spectral region. In the area of optical coatings and materials, the importance of recent developments in chemical vapor deposited (CVD) silicon carbide (SiC) mirrors, SiC films, and multilayer coatings in the context of ultraviolet instrumentation design are discussed. For example, the development of chemically vapor deposited (CVD) silicon carbide (SiC) mirrors, with high ultraviolet (UV) reflectance and low scatter surfaces, provides the opportunity to extend higher spectral/spatial resolution capability into the 50-nm region. Optical coatings for normal incidence diffraction gratings are particularly important for the evolution of efficient extreme ultraviolet (EUV) spectrographs. SiC films are important for optimizing the spectrograph performance in the 90 nm spectral region. The performance evaluation of the flight optical components for the Solar Ultraviolet Measurements of Emitted Radiation (SUMER) instrument, a spectroscopic instrument to fly aboard the Solar and Heliospheric Observatory (SOHO) mission, designed to study dynamic processes, temperatures, and densities in the plasma of the upper atmosphere of the Sun in the wavelength range from 50 nm to 160 nm, is discussed. The optical components were evaluated for imaging and scatter in the UV. The performance evaluation of SOHO/CDS (Coronal Diagnostic Spectrometer) flight gratings tested for spectral resolution and scatter in the DGEF is reviewed and preliminary results on resolution and scatter testing of Space Telescope Imaging Spectrograph (STIS) technology development diffraction gratings are presented. Author (revised)

N93-28789*# Texas Technological Univ., Lubbock. Computer Vision and Image Analysis Lab.
MULTISCALE MORPHOLOGICAL FILTERING FOR ANALYSIS OF NOISY AND COMPLEX IMAGES Abstract Only **c74**
A. Kher and S. Mitra *In* Lunar and Planetary Inst., Workshop on Advanced Technologies for Planetary Instruments, Part 1 1993 p 12-13 (For primary document see N93-28764 11-91)
Avail: CASI HC A01/MF A01

Images acquired with passive sensing techniques suffer from illumination variations and poor local contrasts that create major difficulties in interpretation and identification tasks. On the other hand, images acquired with active sensing techniques based on monochromatic illumination are degraded with speckle noise. Mathematical morphology offers elegant techniques to handle a wide range of image degradation problems. Unlike linear filters, morphological filters do not blur the edges and hence maintain higher image resolution. Their rich mathematical framework facilitates the design and analysis of these filters as well as their hardware implementation. Morphological filters are easier to implement and are more cost effective and efficient than several conventional linear filters. Morphological filters to remove speckle noise while maintaining high resolution and preserving thin image regions that are particularly vulnerable to speckle noise were developed and applied to SAR imagery. These filters used combination of linear (one-dimensional) structuring elements in different (typically four) orientations. Although this approach preserves more details than the simple morphological filters using two-dimensional structuring elements, the limited orientations of one-dimensional elements approximate the fine details of the region boundaries. A more robust filter designed recently overcomes the limitation of the fixed orientations. This filter uses a combination of concave and convex structuring elements. Morphological operators are also useful in extracting features from visible and infrared imagery. A multiresolution image pyramid obtained with successive filtering and a subsampling process aids in the removal of the illumination variations and enhances local contrasts. A morphology-based interpolation scheme was also introduced to reduce intensity discontinuities created in any morphological filtering task. The generality of morphological filtering techniques in extracting information from a wide variety of images obtained with active and passive sensing techniques is discussed. Such techniques are particularly useful in obtaining more information from fusion of complex images by different sensors such as SAR, visible, and infrared. Author (revised)

N93-28790*# KET Canada, Inc., Winnipeg (Manitoba).
A UNIQUE PHOTON BOMBARDMENT SYSTEM FOR SPACE APPLICATIONS Abstract Only **c19**
E. J. Klein *In* Lunar and Planetary Inst., Workshop on Advanced Technologies for Planetary Instruments, Part 1 1993 p 13 Prepared in cooperation with Sol-RF Energy Systems, Inc., Winnipeg, Manitoba (For primary document see N93-28764 11-91)
Avail: CASI HC A01/MF A01

The innovative Electromagnetic Radiation Collection and Concentration System (EMRCCS) described is the foundation for the development of a multiplicity of space and terrestrial system formats. The system capability allows its use in the visual, infrared, and ultraviolet ranges of the spectrum for EM collection, concentration, source/receptor tracking, and targeting. The nonimaging modular optical system uses a physically static position aperture for EM radiation collection. Folded optics provide the concentration of the radiation and source autotracking. The collected and concentrated electromagnetic radiation is utilized in many applications, e.g., solar spectrum in thermal and associative photon bombardment applications for hazardous waste management, water purification, metal hardening, hydrogen generation, photovoltaics, etc., in both space and terrestrial segment utilization. Additionally, at the high end of the concentration capability range, i.e., 60,000+, a solar-pulsed laser system is possible. Author (revised)

N93-28791*# National Aeronautics and Space Administration. Ames Research Center, Moffett Field, CA.

DETECTION OF OTHER PLANETARY SYSTEMS USING PHOTOMETRY Abstract Only **c89**

D. Koch, W. Borucki, and H. Reitsema (Ball Aerospace Systems Div., Boulder, CO.) *In* Lunar and Planetary Inst., Workshop on Advanced Technologies for Planetary Instruments, Part 1 1993 p 13 (For primary document see N93-28764 11-91)

Avail: CASI HC A01/MF A01

Detection of extrasolar short-period planets, particularly if they are in the liquid-water zone, would be one of the most exciting discoveries of our lifetime. A well-planned space mission has the capability of making this discovery using the photometric method. An Earth-sized planet transiting a Sun-like star will cause a decrease in the apparent luminosity of the star by one part in 10,000 with a duration of about 12 hours and a period of about one year. Given a random orientation of orbital plane alignments with the line-of-sight to a star, and assuming our solar system to be typical, one would expect 1 percent of the stars monitored to exhibit planetary transits. A null result would also be significant and indicate that Earth-sized planets are rare. For the mission to be successful one needs a sensor system that can simultaneously monitor many thousands of stars with a photometric precision of one part in 30,000 per hour of integration. Confirmation of a detection will involve detection of a second transit that will yield a period and predict the time for a third and subsequent transits. The technology issues that need to be addressed are twofold: one is for an appropriate optical design; the other is for a detector system with the necessary photometric precision. Two candidates for the detector system are silicon diodes and CCD's. Author (revised)

N93-28792*# National Aeronautics and Space Administration. Ames Research Center, Moffett Field, CA.

AN INTEGRATED XRF/XRD INSTRUMENT FOR MARS EXOBIOLOGY AND GEOLOGY EXPERIMENTS Abstract Only

L. N. Koppel (ARACOR, Sunnyvale, CA.), E. D. Franco (ARACOR, Sunnyvale, CA.), J. A. Kerner (ARACOR, Sunnyvale, CA.), M. L. Fonda, D. E. Schwartz, and J. R. Marshall *In* Lunar and Planetary Inst., Workshop on Advanced Technologies for Planetary Instruments, Part 1 1993 p 13-14 (For primary document see N93-28764 11-91)

Avail: CASI HC A01/MF A01

By employing an integrated x-ray instrument on a future Mars mission, data obtained will greatly augment those returned by Viking; details characterizing the past and present environment on Mars and those relevant to the possibility of the origin and evolution of life will be acquired. A combined x-ray fluorescence/x-ray diffraction (XRF/XRD) instrument was breadboarded and demonstrated to accommodate important exobiology and geology experiment objectives outlined for MESUR and future Mars missions. Among others, primary objectives for the exploration of Mars include the intense study of local areas on Mars to establish the chemical, mineralogical, and petrological character of different components of the surface material; to determine the distribution, abundance, and sources and sinks of volatile materials, including an assessment of the biologic potential, now and during past epoches; and to establish the global chemical and physical characteristics of the Martian surface. The XRF/XRD breadboard instrument identifies and quantifies soil surface elemental, mineralogical, and petrological characteristics and acquires data necessary to address questions on volatile abundance and distribution. Additionally, the breadboard is able to characterize the biogenic element constituents of soil samples providing information on the biologic potential of the Mars environment. Preliminary breadboard experiments confirmed the fundamental instrument design approach and measurement performance. Author (revised)

N93-28793*# Howard Univ., Washington, DC. Dept. of Physics and Astronomy.

REMOTE MEASUREMENT OF PLANETARY MAGNETIC FIELDS BY THE HANLE EFFECT

C. K. Kumar, L. Klein, and M. Giraud (Provence Univ., Marseille, France.) *In* Lunar and Planetary Inst., Workshop on Advanced Technologies for Planetary Instruments, Part 1 1993 p 14 (For primary document see N93-28764 11-91)

Avail: CASI HC A01/MF A01

Resonance fluorescence lines in the spectra of planetary atmospheres are polarized. They will be depolarized by magnetic fields in the scattering medium (Hanle effect). The amount of depolarization was calculated for some atomic (FeI, CaI) lines and some molecular lines (NO gamma bands) seen in the Earth's day glow spectra. The results are presented and the potential advantages of LIDAR measurements for obtaining atmospheric magnetic fields are discussed. The depolarization of Na and Ca lines are suitable for measuring magnetic fields in and near Io. Author (revised)

N93-28794*# Lockheed Missiles and Space Co., Palo Alto, CA. Research Lab.

RESOLUTION-ENHANCED MAPPING SPECTROMETER Abstract Only **c35**

J. B. Kumer, J. N. Aubrun, W. J. Rosenberg, and A. E. Roche *In* Lunar and Planetary Inst., Workshop on Advanced Technologies for Planetary Instruments, Part 1 1993 p 14 (For primary document see N93-28764 11-91)

Avail: CASI HC A01/MF A01

A familiar mapping spectrometer implementation utilizes two dimensional detector arrays with spectral dispersion along one direction and spatial along the other. Spectral images are formed by spatially scanning across the scene (i.e., push-broom scanning). For imaging grating and prism spectrometers, the slit is perpendicular to the spatial scan direction. For spectrometers utilizing linearly variable focal-plane-mounted filters the spatial scan direction is perpendicular to the direction of spectral variation. These spectrometers share the common limitation that the number of spectral resolution elements is given by the number of pixels along the spectral (or dispersive) direction. Resolution enhancement by first passing the light input to the spectrometer through a scanned etalon or Michelson is discussed. Thus, while a detector element is scanned through a spatial resolution element of the scene, it is also temporally sampled. The analysis for all the pixels in the dispersive direction is addressed. Several specific examples are discussed. The alternate use of a Michelson for the same enhancement purpose is also discussed. Suitable for weight constrained deep space missions, hardware systems were developed including actuators, sensor, and electronics such that low-resolution etalons with performance required for implementation would weigh less than one pound. Author (revised)

N93-28795*# Johns Hopkins Univ., Laurel, MD. Applied Physics Lab.

PROPOSAL FOR A UNIVERSAL PARTICLE DETECTOR EXPERIMENT Abstract Only **c19**

J. C. Lesho, R. P Cain, and O. M. Uy *In* Lunar and Planetary Inst., Workshop on Advanced Technologies for Planetary Instruments, Part 1 1993 p 14-15 (For primary document see N93-28764 11-91)

Avail: CASI HC A01/MF A01

The Universal Particle Detector Experiment (UPDE), which consists of parallel planes of two diode laser beams of different wavelengths and a large surface metal oxide semiconductor (MOS) impact detector, is proposed. It will be used to perform real-time monitoring of contamination particles and meteoroids impacting the spacecraft surface with high resolution of time, position, direction, and velocity. The UPDE will discriminate between contaminants and meteoroids, and will determine their velocity and size distribution around the spacecraft environment. With two different color diode lasers, the contaminant and meteroid composition will also be determined based on laboratory calibration with different materials. Secondary particles dislodged from the top aluminum surface of the MOS detector will also be measured to determine the kinetic energy losses during energetic meteoroid impacts. The velocity range of this instrument is 0.1 m/s to more than 14 km/s, while its size sensitivity is from 0.2 microns to millimeter-sized particles. The particulate measurements in space of the kind proposed will be the first simultaneous multipurpose particulate experiment that includes velocities from very slow to hypervelocities, sizes from submicrometer- to pellet-sized diameters, chemical analysis of the particulate composition, and measurements of the kinetic energy losses after energetic impacts of meteroids. The experiment will provide contamination particles and orbital debris data that are critically needed for our present understanding of the space environment. The data will also be used to validate contamination and orbital debris models for predicting optimal configuration of future space sensors and for understanding their effects on sensitive surfaces such as mirrors, lenses, paints, and thermal blankets. Author (revised)

N93-28796*# Paris VI Univ. (France).

OPTIMISM EXPERIMENT AND DEVELOPMENT OF SPACE-QUALIFIED SEISMOMETERS IN FRANCE Abstract Only

P. Lognonne and J. F. Karczewski (Laboratoire de Geophysique Externe du CNRS, Saint Maur-des-Fosses, France.) *In* Lunar and Planetary Inst., Workshop on Advanced Technologies for Planetary Instruments, Part 1 1993 p 15 (For primary document see N93-28764 11-91)

Avail: CASI HC A01/MF A01

The OPTIMISM experiment will put two magnetometers and two seismometers on the Martian floor in 1995, within the framework of the Mars '94 mission. The seismometers are put within the two small surface stations. The seismometer sensitivity will be better than 10 exp -9 g at 1 Hz, 2 orders of magnitude higher than the Viking seismometer sensitivity. A priori waveform modeling for seismic signals on Mars shows that it will be sufficient to detect quakes with a seismic moment greater than 10 exp 15 Nm everywhere on Mars. Such events, according to the hypothesis of a thermoelastic cooling of the Martian lithosphere, are expected to occur at a rate close to one per week and may therefore be observed within the l-year lifetime of the experiment. Other aspects of the experiment are discussed. Author (revised)

N93-28797*# Naval Research Lab., Washington, DC.

FILTERING INTERPOLATORS FOR IMAGE COMPARISON ALGORITHMS Abstract Only c43

R. L. Lucke and A. D. Stocker (Space Computer Corp., Santa Monica, CA.) *In* Lunar and Planetary Inst., Workshop on Advanced Technologies for Planetary Instruments, Part 1 1993 p 15 (For primary document see N93-28764 11-91)

Avail: CASI HC A01/MF A01

Comparing two or more images, either by differencing or ratioing, is important to many remote sensing problems. Because the pixel sample points for the images are (almost) always separated by some nonzero shift, a resampling, or interpolation, process must be performed if one image is to be accurately compared to another. Considered in Fourier space, an interpolator acts as a filter that attenuates some frequencies (usually high) of the image. Thus, when the shifted and unshifted images are compared, the former has been filtered, while the latter has not; the effect of this difference is called interpolation error. The key idea of this paper is to apply a filter to the unshifted image that matches the filtering effect of applying the interpolator to the shifted image, thereby drastically reducing interpolation error. The resulting interpolators, called filtering interpolators, are derived and discussed in detail elsewhere. Basic results will be given in this presentation. Author (revised)

N93-28798*# National Aeronautics and Space Administration. Goddard Space Flight Center, Greenbelt, MD.

MASS SPECTROMETRIC MEASUREMENT OF MARTIAN KRYPTON AND XENON ISOTOPIC ABUNDANCE Abstract Only

P. Mahaffy and K. Mauersberger (Minnesota Univ., Minneapolis.) *In* Lunar and Planetary Inst., Workshop on Advanced Technologies for Planetary Instruments, Part 1 1993 p 15-16 (For primary document see N93-28764 11-91)

Avail: CASI HC A01/MF A01

The Viking gas chromatograph mass spectrometer experiment provided significant data on the atmospheric composition at the surface of Mars, including measurements of several isotope ratios. However, the limited dynamic range of this mass spectrometer resulted in marginal measurements for the important Kr and Xe isotopic abundance. The Xe-129 to Xe-132 ratio was measured with an uncertainty of 70%, but none of the other isotope ratios for these species were obtained. Accurate measurement of the Xe and Kr isotopic abundance in this atmosphere provides an important data point in testing theories of planetary formation and atmospheric evolution. The measurement is also essential for a stringent test for the Martian origin of the SNC meteorites, since the Kr and Xe fractionation pattern seen in gas trapped in glassy nodules of an SNC (EETA 79001) is unlike any other known solar system resevoir. Current flight mass spectrometer designs combined with the new technology of a high-performance vacuum pumping system show promise for a substantial increase in gas throughput and the dynamic range required to accurately measure these trace species. Various aspects of this new technology are discussed. Author (revised)

N93-28799*# Malin Space Science Systems, San Diego, CA.

VISIBLE IMAGING ON THE PLUTO FAST FLYBY MISSION Abstract Only

M. C. Malin *In* Lunar and Planetary Inst., Workshop on Advanced Technologies for Planetary Instruments, Part 1 1993 p 16 (For primary document see N93-28764 11-91)

Avail: CASI HC A01/MF A01

Objectives for visible imaging of the Pluto-Charon system, as prescribed by the Outer Planets Science Working Group, are to acquire (1) global observations (FOV of approximately 5000 IFOV's) at 1 km/line-pair for the purpose of characterizing surface morphology and geology, (2) global observations in 3-5 broadband colors at 5-10 km/line-pair for studies of surface properties and composition as it relates to morphology, and (3) selected observations at higher spatial resolution for study of surface processes. Several factors of the Pluto Fast Flyby mission make these difficult to achieve. These factors along with other aspects of the mission are discussed. Author (revised)

N93-28800*# National Aeronautics and Space Administration. Ames Research Center, Moffett Field, CA.

A DTA/GC FOR THE IN SITU IDENTIFICATION OF THE MARTIAN SURFACE MATERIAL Abstract Only

R. L. Mancinelli, M. R. White, and J. B. Orenberg (San Francisco State Univ., CA.) *In* Lunar and Planetary Inst., Workshop on Advanced Technologies for Planetary Instruments, Part 1 1993 p 16-17 (For primary document see N93-28764 11-91)

Avail: CASI HC A01/MF A01

The composition and mineralogy of the Martian surface material remain largely unknown. To determine its composition and mineralogy, several techniques are being considered for in situ analyses of the Martian surface material during missions to Mars. We have successfully developed, constructed, and tested a laboratory DTA/GC. The DTA is a Dupont model 1600 high temperature DTA coupled with a GC equipped with a MID detector. The system is operated by a Sun Sparc 11 workstation. When gas evolves during a thermal chemical event, it is shunted into the GC and the temperature is recorded in association with the specific thermal event. We have used this laboratory instrument to define experimental criteria necessary for determining the composition and mineralogy of the Martian surface in situ (e.g., heating of sample to 1100 C to distinguish clays). Our studies indicate that DTA/GC will provide a broad spectrum of mineralogical and evolved gas data pertinent to exobiology, geochemistry, and geology. Author (revised)

N93-28801*# San Jose State Univ., CA. Dept. of Electrical Engineering.

ONBOARD SIGNAL PROCESSING: WAVE OF THE FUTURE FOR PLANETARY RADIO SCIENCE? Abstract Only

E. A. Marouf *In* Lunar and Planetary Inst., Workshop on Advanced Technologies for Planetary Instruments, Part 1 1993 p 17 (For primary document see N93-28764 11-91)

Avail: CASI HC A01/MF A01

Future spacecraft-based radio observations of planetary surfaces, rings, and atmospheres could significantly benefit from recent technological advances in real-time digital signal processing (DSP) hardware. Traditionally, the radio observations have been carried out in a 'down link' configuration in which about 20-W spacecraft transmitted RF power illuminates the target of interest and the perturbed signal is collected at an Earth receiving station. The down link configuration was dictated by the large throughput of received data, corresponding to a relatively large recording band width (about 50 kHz) needed to capture the coherent and scattered signal components in the presence of trajectory, ephemeris, and measurement uncertainties. An alternative 'up link' configuration in which powerful Earth-based radio transmitters (20-200 kW) are used to illuminate the target and data are recorded on board a spacecraft could enhance the measurements' signal-to-noise ratio by a factor of about 1000, allowing a quantum leap in scientific capabilities. Various aspects of alternative signal processing technologies are discussed. Author (revised)

N93-28802*# Little (Arthur D.), Inc., Cambridge, MA.
SPACEBORNE PASSIVE RADIATIVE COOLER Abstract Only c31
S. Mathias *In* Lunar and Planetary Inst., Workshop on Advanced Technologies for Planetary Instruments, Part 1 1993 p 17 (For primary document see N93-28764 11-91)
Avail: CASI HC A01/MF A01

Radiative coolers are passive refrigeration devices for satellites and space probes that provide refrigeration for an infrared or other type of detector that operates at cryogenic temperatures. Typically a cooler can supply 20 mW of cooling at about 85 K, and over 500 mW of cooling at about 165 K. The exact cooler temperatures and heat loads are dependent upon the clear field of view of the cooler to space. Some features of the Arthur D. Little passive radiative cooler are given. Author (revised)

N93-28803*# Geological Survey, Flagstaff, AZ.
SYSTEMATIC PROCESSING OF CLEMENTINE DATA FOR SCIENTIFIC ANALYSES Abstract Only c82
A. S. McEwen *In* Lunar and Planetary Inst., Workshop on Advanced Technologies for Planetary Instruments, Part 1 1993 p 17-18 (For primary document see N93-28764 11-91)
Avail: CASI HC A01/MF A01

If fully successful, the Clementine mission will return about 3,000,000 lunar images and more than 5000 images of Geographos. Effective scientific analyses of such large datasets require systematic processing efforts. Concepts for two such efforts are described: glogal multispectral imaging of the moon; and videos of Geographos. Author (revised)

N93-28804*# National Aeronautics and Space Administration. Lyndon B. Johnson Space Center, Houston, TX.
SOURCES SOUGHT FOR INNOVATIVE SCIENTIFIC INSTRUMENTATION FOR SCIENTIFIC LUNAR ROVERS Abstract Only c35
C. Meyer *In* Lunar and Planetary Inst., Workshop on Advanced Technologies for Planetary Instruments, Part 1 1993 p 18 (For primary document see N93-28764 11-91)
Avail: CASI HC A01/MF A01

Lunar rovers should be designed as integrated scientific measurement systems that address scientific goals as their main objective. Scientific goals for lunar rovers are presented. Teleoperated robotic field geologists will allow the science team to make discoveries using a wide range of sensory data collected by electronic 'eyes' and sophisticated scientific instrumentation. rovers need to operate in geologically interesting terrain (rock outcrops) and to identify and closely examine interesting rock samples. Enough flight-ready instruments are available to fly on the first mission, but additional instrument development based on emerging technology is desirable. Various instruments that need to be developed for later missions are described. Author (revised)

N93-28805*# California Univ., Los Angeles. Dept. of Earth and Space Sciences.
DRILL/BORESCOPE SYSTEM FOR THE MARS POLAR PATHFINDER Abstract Only
D. A. Paige, S. E. Wood, and A. R. Vasavada *In* Lunar and Planetary Inst., Workshop on Advanced Technologies for Planetary Instruments, Part 1 1993 p 18-19 (For primary document see N93-28764 11-91)
Avail: CASI HC A01/MF A01

The primary goals of the Mars Polar Pathfinder (MPP) Discovery Mission are to characterize the composition and structure of Mars' north polar ice cap, and to determine whether a climate record may be preserved in layers of ice and dust. The MPP would land as close as possible to the geographic north pole of Mars and use a set of instruments similar to those used by glaciologists to study polar ice caps on Earth: a radar sounder, a drill/borescope system, and a thermal probe. The drill/borescope system will drill approximately 50 cm into the surface and image the sides of the hole at 10 micron resolution for compositional and stratigraphic analysis. Several uncertainties have guided the development of this instrument, and they are discussed. Author (revised)

N93-28806*# Honeywell Corporate Research Center, Bloomington, MN.
HONEYWELL'S COMPACT, WIDE-ANGLE UV-VISIBLE IMAGING SENSOR Abstract Only c74
D. Pledger and J. Billing-Ross (Honeywell, Inc., Glendale, AZ.) *In* Lunar and Planetary Inst., Workshop on Advanced Technologies for Planetary Instruments, Part 1 1993 p 19 (For primary document see N93-28764 11-91)
Avail: CASI HC A01/MF A01

Honeywell is currently developing the Earth Reference Attitude Determination System (ERADS). ERADS determines attitude by imaging the entire Earth's limb and a ring of the adjacent star field in the 2800-3000 A band of the ultraviolet. This is achieved through the use of a highly nonconventional optical system, an intensifier tube, and a mega-element CCD array. The optics image a 30 degree region in the center of the field, and an outer region typically from 128 to 148 degrees, which can be adjusted up to 180 degrees. Because of the design employed, the illumination at the outer edge of the field is only some 15 percent below that at the center, in contrast to the drastic rolloffs encountered in conventional wide-angle sensors. The outer diameter of the sensor is only 3 in; the volume and weight of the entire system, including processor, are 1000 cc and 6 kg, respectively. Author (revised)

N93-28807*# Los Alamos National Lab., NM.
GAMMA RAY/NEUTRON SPECTROMETERS FOR PLANETARY ELEMENTAL MAPPING Abstract Only
R. C. Reedy, G. F. Auchampaugh, B. L. Barraclough, W. W. Burt (TRW Space Technology Labs., Los Angeles, CA.), R. C. Byrd, D. M. Drake, B. C. Edwards, W. C. Feldman, R. A. Martin, and C. E. Moss et al *In* Lunar and Planetary Inst., Workshop on Advanced Technologies for Planetary Instruments, Part 1 1993 p 19 Sponsored in part by DOE (For primary document see N93-28764 11-91)
Avail: CASI HC A01/MF A01

Los Alamos has designed gamma ray and neutron spectrometers for Lunar Scout, two robotic missions to map the Moon from 100 km polar orbits. Knowledge of the elemental composition is desirable in identifying resources and for geochemical studies and can be obtained using gamma ray and neutron spectrometers. Measurements with gamma ray and neutron spectrometers complement each other in determining elemental abundances in a planet's surface. Various aspects of the instruments are discussed. Author (revised)

N93-28808*# Little (Arthur D.), Inc., Cambridge, MA.
INFRARED RUGATES BY MOLECULAR BEAM EPITAXY Abstract Only c74
M. Rona *In* Lunar and Planetary Inst., Workshop on Advanced Technologies for Planetary Instruments, Part 1 1993 p 20 (For primary document see N93-28764 11-91)
Avail: CASI HC A01/MF A01

Rugates are optical structures that have a sinusoidal index of refraction (harmonic gradient-index field). As their discrete high/ low index filter counterparts, they can be used as narrow rejection band filters. However, since rugates do not have abrupt interfaces, they tend to have a smaller absorption, hence deliver a higher in band reflectivity. The absence of sharp interfaces makes rugates even more desirable for high-energy narrow band reflectors. In this application, the lack of a sharp interface at the maximum internal standing wave electric field results in higher breakdown strengths. Our method involves fabricating rugates, with molecular beam epitaxy, on GaAs wafers as an Al(x)Ga(1-x)As single-crystal film. Author (revised)

N93-28809*# California Univ., Los Angeles. Inst. of Geophysics and Planetary Physics.
PLASMA, MAGNETIC, AND ELECTROMAGNETIC MEASUREMENTS AT NONMAGNETIC BODIES Abstract Only
C. T. Russell and J. G. Luhmann *In* Lunar and Planetary Inst., Workshop on Advanced Technologies for Planetary Instruments, Part 1 1993 p 20 (For primary document see N93-28764 11-91)
Avail: CASI HC A01/MF A01

The need to explore the magnetospheres of the Earth and the giant planets is widely recognized and is an integral part of our planetary exploration program. The equal need to explore the plasma, magnetic, and electromagnetic environments of the nonmagnetic bodies is not so widely appreciated. The previous, albeit incomplete, magnetic and electric field measurements at Venus, Mars, and comets have proven critical to our understanding of their atmospheres and ionospheres in areas ranging from planetary lightning to solar wind scavenging and accretion. In the cases of

Venus and Mars, the ionospheres can provide communication paths over the horizon for low-altitude probes and landers, but we know little about their lower boundaries. The expected varying magnetic fields below these planetary ionospheres penetrates the planetary crusts and can be used to sound the electrical conductivity and the thermal profiles of the interiors. However, we have no knowledge of the levels of such fields, let alone their morphology. Finally, we note that the absence of an atmosphere and an ionosphere does not make an object any less interesting for the purposes of electromagnetic exploration. Even weak remanent magnetism such as that found on the Moon during the Apollo program provides insight into the present and past states of planetary interiors. We have very intriguing data from our space probes during times of both close and distant passages of asteroids that suggest they may have coherent magnetization. If true, this observation will put important constraints on how the asteroids formed and have evolved. Our planetary exploration program must exploit its full range of exploration tools if it is to characterize the bodies of the solar system thoroughly. We should especially take advantage of those techniques that are proven and require low mass, low power, and low telemetry rates to undertake. Author (revised)

N93-28810*# Johns Hopkins Univ., Laurel, MD. Applied Physics Lab.
A COMPACT IMAGING DETECTOR OF POLARIZATION AND SPECTRAL CONTENT Abstract Only **c74**
D. M. Rust, A. Kumar, and K. E. Thompson *In* Lunar and Planetary Inst., Workshop on Advanced Technologies for Planetary Instruments, Part 1 1993 p 20 (For primary document see N93-28764 11-91)
Avail: CASI HC A01/MF A01

A new type of image detector will simultaneously analyze the polarization of light at all picture elements in a scene. The integrated Dual Imaging Detector (IDID) consists of a polarizing beam splitter bonded to a charge-coupled device (CCD), with signal-analysis circuitry and analog-to-digital converters, all integrated on a silicon chip. The polarizing beam splitter can be either a Ronchi ruling, or an array of cylindrical lenslets, bonded to a birefringent wafer. The wafer, in turn, is bonded to the CCD so that light in the two orthogonal planes of polarization falls on adjacent pairs of pixels. The use of a high-index birefringent material, e.g., rutile, allows the IDID to operate at f-numbers as high as f/3.5. Other aspects of the detector are discussed. Author (revised)

N93-28811*# Consejo Superior de Investigaciones Cientificas, Tenerife (Spain). Inst. de Astrofisica de Canarias
DIGITAL IMAGE COMPRESSION USING ARTIFICIAL NEURAL NETWORKS Abstract Only **c82**
M. Serra-Ricart, L. Garrido (Barcelona Univ., Spain.), V. Gaitan (Barcelona Univ., Spain.), and A. Aloy (Digital Equipment Enterprise Espana S.A., Barcelona, Spain.) *In* Lunar and Planetary Inst., Workshop on Advanced Technologies for Planetary Instruments, Part 1 1993 p 20-21 (For primary document see N93-28764 11-91)
Avail: CASI HC A01/MF A01

The problem of storing, transmitting, and manipulating digital images is considered. Because of the file sizes involved, large amounts of digitized image information are becoming common in modern projects. Our goal is to described an image compression transform coder based on artificial neural networks techniques (NNCTC). A comparison of the compression results obtained from digital astronomical images by the NNCTC and the method used in the compression of the digitized sky survey from the Space Telescope Science Institute based on the H-transform is performed in order to assess the reliability of the NNCTC. Author (revised)

N93-28812*# National Aeronautics and Space Administration. Lyndon B. Johnson Space Center, Houston, TX.
PROTOTYPE BACKSCATTER MOESSBAUER SPECTROMETER FOR MEASUREMENT OF MARTIAN SURFACE MINERALOGY Abstract Only
T. D. Shelfer, R. V. Morris, D. G. Agresti (Alabama Univ., Birmingham.), T. Nguyen (Lockheed Engineering and Sciences Co., Houston, TX.), E. L. Wills (Alabama Univ., Birmingham.), and M. H. Shen (Alabama Univ., Birmingham.) *In* Lunar and Planetary Inst., Workshop on Advanced Technologies for Planetary Instruments, Part 1 1993 p 21 (For primary document see N93-28764 11-91)
Avail: CASI HC A01/MF A01

We have designed and successfully tested a prototype of a backscatter Moessbauer spectrometer (BaMS) targeted for use on the Martian surface to (1) determine oxidation states of iron, and (2) identify and determine relative abundances of iron-bearing mineralogies. No sample preparation is required to perform measurements; it is only necessary to bring sample and instrument into physical contact. The prototype meets our projected specification for a flight instrument in terms of mass, power, and volume. A Moessbauer spectrometer on the Martian surface would provide wide variety of information about the current state of the Martian surface, and this information is described. Author (revised)

N93-28813*# Southwest Research Inst., San Antonio, TX.
SPACECRAFT COMPUTER TECHNOLOGY AT SOUTHWEST RESEARCH INSTITUTE Abstract Only **c60**
D. J. Shirley *In* Lunar and Planetary Inst., Workshop on Advanced Technologies for Planetary Instruments, Part 1 1993 p 21 (For primary document see N93-28764 11-91)
Avail: CASI HC A01/MF A01

Southwest Research Institute (SwRI) has developed and delivered spacecraft computers for a number of different near-Earth-orbit spacecraft including shuttle experiments and SDIO free-flyer experiments. We describe the evolution of the basic SwRI spacecraft computer design from those weighing in at 20 to 25 lb and using 20 to 30 W to newer models weighing less than 5 lb and using only about 5 W, yet delivering twice the processing throughput. Because of their reduced size, weight, and power, these newer designs are especially applicable to planetary instrument requirements. The basis of our design evolution has been the availability of more powerful processor chip sets and the development of higher density packaging technology, coupled with more aggressive design strategies in incorporating high-density FPGA technology and use of high-density memory chips. In addition to reductions in size, weight, and power, the newer designs also address the necessity of survival in the harsh radiation environment of space. Spurred by participation in such programs as MSTI, LACE, RME, Delta 181, Delta Star, and RADARSAT, our designs have evolved in response to program demands to be small, low-powered units, radiation tolerant enough to be suitable for both Earth-orbit microsats and for planetary instruments. Present designs already include MIL-STD-1750 and Multi-Chip Module (MCM) technology with near-term plans to include RISC processors and higher-density MCM's. Long term plans include development of whole-core processors on one or two MCM's. Author (revised)

N93-28814*# Naval Research Lab., Washington, DC.
THE BACKGROUNDS DATA CENTER Abstract Only **c82**
W. A. Snyder, H. Gursky, H. M. Heckathorn, R. L. Lucke, S. L. Berg (Computational Physics, Inc., Fairfax, VA.), E. G. Dombrowski (Sachs/Freeman Associates, Inc., Landover, MD.), and R. A. Kessel (Computational Physics, Inc., Fairfax, VA.) *In* Lunar and Planetary Inst., Workshop on Advanced Technologies for Planetary Instruments, Part 1 1993 p 21-22 (For primary document see N93-28764 11-91)
Avail: CASI HC A01/MF A01

The Strategic Defense Initiative Organization has created data centers for midcourse, plumes, and backgrounds phenomenologies. The Backgrounds Data Center (BDC) has been designated as the prime archive for data collected by SDIO programs. The BDC maintains a Summary Catalog that contains 'metadata,' that is, information about data, such as when the data were obtained, what the spectral range of the data is, and what region of the Earth or sky was observed. Queries to this catalog result in a listing of all data sets (from all experiments in the Summary Catalog) that satisfy the specified criteria. Thus, the user can identify different experiments that made similar observations and order them from the BDC for analysis. On-site users can use the Science Analysis Facility (SAFE for this purpose. For some programs, the BDC maintains a Program Catalog, which can classify data in as many ways as desired (rather than just by position, time, and spectral range as in the Summary Catalog). For example, data sets could be tagged with such diverse parameters as solar illumination angle, signal level, or the value of a particular spectral ratio, as long as these quantities can be read from the digital record or calculated from it by the ingest program. All unclassified catalogs and unclassified data will be remotely accessible. Author (revised)

N93-28815*# Boeing Defense and Space Group, Seattle, WA.
THE ENHANCED-MODEL LADAR WIND SENSOR AND ITS APPLICATION IN PLANETARY WIND VELOCITY MEASUREMENTS Abstract Only
D. C. Soreide, R. L. McGann, L. L. Erwin, and D. J. Morris *In* Lunar and Planetary Inst., Workshop on Advanced Technologies for Planetary Instruments, Part 1 1993 p 22 (For primary document see N93-28764 11-91)
Avail: CASI HC A01/MF A01

For several years we have been developing an optical air-speed sensor that has a clear application as a meteorological wind-speed sensor for the Mars landers. This sensor has been developed for aircraft use to replace the familiar, pressure-based Pitot probe. Our approach utilizes a new concept in the laser-based optical measurement of air velocity (the Enhanced-Mode Ladar), which allows us to make velocity measurements with significantly lower laser power than conventional methods. The application of the Enhanced-Mode Ladar to measuring wind speeds in the martian atmosphere is discussed. Author (revised)

N93-28816*# Cornell Univ., Ithaca, NY. Center for Radiophysics and Space Research.
THE MESUR MISSION Abstract Only
S. W. Squyres *In* Lunar and Planetary Inst., Workshop on Advanced Technologies for Planetary Instruments, Part 1 1993 p 22-23 (For primary document see N93-28764 11-91)
Avail: CASI HC A01/MF A01

The MESUR mission will place a network of small, robust landers on the Martian surface, making a coordinated set of observations for at least one Martian year. MESUR presents some major challenges for development of instruments, instrument deployment systems, and on board data processing techniques. The instrument payload has not yet been selected, but the straw man payload is (1) a three-axis seismometer; (2) a meteorology package that senses pressure, temperature, wind speed and direction, humidity, and sky brightness; (3) an alphaproton-X-ray spectrometer (APXS); (4) a thermal analysis/evolved gas analysis (TA/EGA) instrument; (5) a descent imager, (6) a panoramic surface imager; (7) an atmospheric structure instrument (ASI) that senses pressure, temperature, and acceleration during descent to the surface; and (8) radio science. Because of the large number of landers to be sent (about 16), all these instruments must be very lightweight. All but the descent imager and the ASI must survive landing loads that may approach 100 g. The meteorology package, seismometer, and surface imager must be able to survive on the surface for at least one Martian year. The seismometer requires deployment off the lander body. The panoramic imager and some components of the meteorology package require deployment above the lander body. The APXS must be placed directly against one or more rocks near the lander, prompting consideration of a micro rover for deployment of this instrument. The TA/EGA requires a system to acquire, contain, and heat a soil sample. Both the imagers and, especially, the seismometer will be capable of producing large volumes of data, and will require use of sophisticated data compression techniques. Author (revised)

N93-28817*# Jet Propulsion Lab., California Inst. of Tech., Pasadena.
A LOW-COST, LIGHTWEIGHT, AND MINIATURIZED TIME-OF-FLIGHT MASS SPECTROMETER (TOFMS) Abstract Only **c35**
S. K. Srivastava *In* Lunar and Planetary Inst., Workshop on Advanced Technologies for Planetary Instruments, Part 1 1993 p 23 (For primary document see N93-28764 11-91)
Avail: CASI HC A01/MF A01

Time-of-flight mass spectrometers (TOFMS) are commonly used for mass analysis and for the measurement of energy distributions of charged particles. For achieving high mass and energy resolution these instruments generally comprise long flight tubes, often as long as a few meters. This necessitates high voltages and a very clean environment. These requirements make them bulky and heavy. We have developed an instrument and calibration techniques that are based on the design principles of TOFMS. However, instead of one long flight tube it consists of a series of cylindrical electrostatic lenses that confine ions under study along the axis of the flight tube. Author (revised)

N93-28818*# Southwest Research Inst., San Antonio, TX. Space Science Dept.
PLUTO FAST FLYBY MISSION AND SCIENCE OVERVIEW Abstract Only
A. Stern *In* Lunar and Planetary Inst., Workshop on Advanced Technologies for Planetary Instruments, Part 1 1993 p 23 (For primary document see N93-28764 11-91)
Avail: CASI HC A01/MF A01

Planning for the Pluto Fast Flyby (PFF) mission centers on the launch of two small (110-160 kg) spacecraft late in the 1990s on fast, 6-8-year trajectories that do not require Jupiter flybys. The cost target of the two-spaceraft PFF mission is $40.0 million. Scientific payload definition by NASA's Outer Planets Science Working Group (OPSWG) and JPL design studies for the Pluto flyby spacecraft are now being completed, and the program is in Phase A development. Selection of a set of lightweight, low-power instrument demonstrations is planned for May 1993. According to plan, the completion of Phase A and then detailed Phase B spacecraft and payload design work will occur in FY94. The release of an instrument payload AO, followed by the selection of the flight payload, is also scheduled for FY94. Author (revised)

N93-28819*# National Aeronautics and Space Administration. Lewis Research Center, Cleveland, OH.
VENUS INTERIOR STRUCTURE MISSION (VISM): ESTABLISHING A SEISMIC NETWORK ON VENUS Abstract Only
E. R. Stofan (Jet Propulsion Lab., California Inst. of Tech., Pasadena.), R. S. Saunders (Jet Propulsion Lab., California Inst. of Tech., Pasadena.), D. Senske (Jet Propulsion Lab., California Inst. of Tech., Pasadena.), K. Nock (Jet Propulsion Lab., California Inst. of Tech., Pasadena.), D. Tralli (Jet Propulsion Lab., California Inst. of Tech., Pasadena.), P. Lundgren (Jet Propulsion Lab., California Inst. of Tech., Pasadena.), S. Smrekar (Jet Propulsion Lab., California Inst. of Tech., Pasadena.), B. Banerdt (Jet Propulsion Lab., California Inst. of Tech., Pasadena.), W. Kaiser (Jet Propulsion Lab., California Inst. of Tech., Pasadena.), and J. Dudenhoefer (Mechanical Technology, Inc., Latham, NY.) et al *In* Lunar and Planetary Inst., Workshop on Advanced Technologies for Planetary Instruments, Part 1 1993 p 23-24 (For primary document see N93-28764 11-91)
Avail: CASI HC A01/MF A01

Magellan radar data show the surface of Venus to contain a wide range of geologic features (large volcanoes, extensive rift valleys, etc.). Although networks of interconnecting zones of deformation are identified, a system of spreading ridges and subduction zones like those that dominate the tectonic style of the Earth do not appear to be present. In addition, the absence of a mantle low-viscosity zone suggests a strong link between mantle dynamics and the surface. As a natural follow-on to the Magellan mission, establishing a network of seismometers on Venus will provide detailed quantitative information on the large scale interior structure of the planet. When analyzed in conjunction with image, gravity, and topography information, these data will aid in constraining mechanisms that drive surface deformation. Author (revised)

N93-28820*# Utah State Univ., Logan. Space Dynamics Lab.
PLASMA DIAGNOSTICS BY ANTENNA IMPEDANCE MEASUREMENTS Abstract Only **c32**
C. M. Swenson, K. D. Baker, E. Pound, and M. D. Jensen *In* Lunar and Planetary Inst., Workshop on Advanced Technologies for Planetary Instruments, Part 1 1993 p 24 (For primary document see N93-28764 11-91)
Avail: CASI HC A01/MF A01

The impedance of an electrically short antenna immersed in a plasma provides an excellent in situ diagnostic tool for electron density and other plasma parameters. By electrically short we mean that the wavelength of the free-space electromagnetic wave that would be excited at the driving frequency is much longer than the physical size of the antenna. Probes using this impedance technique have had a long history with sounding rockets and satellites, stretching back to the early 1960s. This active technique could provide information on composition and temperature of plasmas for comet or planetary missions. Advantages of the impedance probe technique are discussed and two classes of instruments built and flown by SDL-USU for determining electron density (the capacitance and plasma frequency probes) are described. Author (revised)

N93-28821*# Hawaii Univ., Honolulu. Dept. of Geology and Geophysics.
LUNAR SCIENCE: USING THE MOON AS A TESTBED Abstract Only
G. J. Taylor *In* Lunar and Planetary Inst., Workshop on Advanced Technologies for Planetary Instruments, Part 1 1993 p 24-25 (For primary document see N93-28764 11-91)
Avail: CASI HC A01/MF A01

The Moon is an excellent test bed for innovative instruments and spacecraft. Excellent science can be done, the Moon has a convenient location, and previous measurements have calibrated many parts of it. I summarize these attributes and give some suggestions for the types of future measurements. The Lunar Scout missions planned by NASA's Office of Exploration will not make all the measurements needed. Thus, test missions to the Moon can also return significant scientific results, making them more than technology demonstrations. The Moon is close to Earth, so cruise time is insignificant, tracking is precise, and some operations can be controlled from Earth, but it is in the deep space environment, allowing full tests of instruments and spacecraft components. The existing database on the Moon allows tests of new instruments against known information. The most precise data come from lunar samples, where detailed analyses of samples from a few places on the Moon provide data on chemical and mineralogical composition and physical properties. Author (revised)

N93-28822*# Science Applications International Corp., Albuquerque, NM.
USE OF PARTICLE BEAMS FOR LUNAR PROSPECTING Abstract Only
A. J. Toepfer, D. Eppler, A. Friedlander, and R. Weitz *In* Lunar and Planetary Inst., Workshop on Advanced Technologies for Planetary Instruments, Part 1 1993 p 25 Prepared for Grumman Aerospace Corp., Bethpage, NY (For primary document see N93-28764 11-91)
(Contract DASG60-90-C-0103)
Avail: CASI HC A01/MF A01

A key issue in choosing the appropriate site for a manned lunar base is the availability of resources, particularly oxygen and hydrogen for the production of water, and ores for the production of fuels and building materials. NASA has proposed two Lunar Scout missions that would orbit the Moon and use, among other instruments, a hard X-ray spectrometer, a neutron spectrometer, and a Ge gamma ray spectrometer to map the lunar surface. This passive instrumentation will have low resolution (tens of kilometers) due to the low signal levels produced by natural radioactivity and the interaction of cosmic rays and the solar wind with the lunar surface. This paper presents the results of a concept definition effort for a neutral particle beam lunar mapper probe. The idea of using particle beam probes to survey asteroids was first proposed by Sagdeev et al., and an ion beam device was fielded on the 1988 Soviet probe to the Mars moon Phobos. During the past five years, significant advances in the technology of neutral particle beams (NPB) have led to a suborbital flight of a neutral hydrogen beam device in the SDIO-sponsored BEAR experiment. An orbital experiment, the Neutral Particle Beam Far Field Optics Experiment (NPB-FOX) is presently in the preliminary design phase. The development of NPB accelerators that are space-operable leads one to consider the utility of these devices for probing the surface of the Moon using gamma ray, X-ray, and optical/UV spectroscopy to locate various elements and compounds. We consider the utility of the NPB-FOX satellite containing a 5-MeV particle beam accelerator as a probe in lunar orbit. Irradiation of the lunar surface by the particle beam will induce secondary and back scattered radiation from the lunar surface to be detected by a sensor that may be co-orbital with or on the particle beam satellite platform, or may be in a separate orbit. The secondary radiation is characteristic of the make-up of the lunar surface. The size of the spot irradiated by the beam is less than 1 km wide along the ground track of the satellite, resulting in the potential for high resolution. The fact that the probe could be placed in polar orbit would result in global coverage of the lunar surface. The orbital particle beam probe could provide the basis for selection of sites for more detailed prospecting by surface rovers. Author (revised)

N93-28823*# Jet Propulsion Lab., California Inst. of Tech., Pasadena.
SUBNANORADIAN, GROUNDBASED TRACKING OF SPACEBORNE LASERS Abstract Only **c36**
R. N. Treuhaft *In* Lunar and Planetary Inst., Workshop on Advanced Technologies for Planetary Instruments, Part 1 1993 p 25-26 (For primary document see N93-28764 11-91)
Avail: CASI HC A01/MF A01

Over the next few decades groundbased tracking of lasers on planetary spacecraft will supplement or replace tracking of radio transponders. This paper describes research on two candidate technologies for groundbased, angular, laser tracking: the infrared interferometer and the optical filled-aperture telescope. The motivation for infrared and optical tracking will be followed by a description of the current (10-50 nanoradian) and future (subnanororadian) stellar tracking demonstrations with the University of California-Berkeley Infrared Spatial Interferometer (ISI) and the University of California-San Diego Optical Ronchi Telescope. Author (revised)

N93-28824*# National Aeronautics and Space Administration. Goddard Space Flight Center, Greenbelt, MD.
A TEAM APPROACH TO THE DEVELOPMENT OF GAMMA RAY AND X RAY REMOTE SENSING AND IN SITU SPECTROSCOPY FOR PLANETARY EXPLORATION MISSIONS Abstract Only
J. I. Trombka, S. Floyd, A. Ruitberg, L. Evans (Computer Sciences Corp., Calverton, MD.), R. Starr (Catholic Univ. of America, Washington, DC.), A. Metzger (Jet Propulsion Lab., California Inst. of Tech., Pasadena.), R. Reedy (Los Alamos Scientific Lab., NM.), D. Drake (Los Alamos Scientific Lab., NM.), C. Moss (Los Alamos Scientific Lab., NM.), and B. Edwards (Los Alamos Scientific Lab., NM.) *In* Lunar and Planetary Inst., Workshop on Advanced Technologies for Planetary Instruments, Part 1 1993 p 26 (For primary document see N93-28764 11-91)
Avail: CASI HC A01/MF A01

An important part of the investigation of planetary origin and evolution is the determination of the surface composition of planets, comets, and asteroids. Measurements of discrete line X-ray and gamma ray emissions from condensed bodies in space can be used to obtain both qualitative and quantitative elemental composition information. The Planetary Instrumentation Definition and Development Program (PIDDP) X-Ray/Gamma Ray Team has been established to develop remote sensing and in situ technologies for future planetary exploration missions. Author (revised)

N93-28825*# TRW, Inc., Redondo Beach, CA.
MINIATURE LONG-LIFE SPACE CRYOCOOLERS Abstract Only **c31**
E. Tward *In* Lunar and Planetary Inst., Workshop on Advanced Technologies for Planetary Instruments, Part 1 1993 p 26-27 (For primary document see N93-28764 11-91)
Avail: CASI HC A01/MF A01

TRW has designed, built, and tested a miniature integral Stirling cooler and a miniature pulse tube cooler intended for long-life space application. Both efficient, low-vibration coolers were developed for cooling IR sensors to temperatures as low as 50 K on lightsats. The vibrationally balanced nonwearing design Stirling cooler incorporates clearance seals maintained by flexure springs for both the compressor and the drive displacer. The design achieved its performance goal of 0.25 W at 65 K for an input power to the compressor of 12 W. The cooler recently passed launch vibration tests prior to its entry into an extended life test and its first scheduled flight in 1995. The vibrationally balanced, miniature pulse tube cooler intended for a 10-year long-life space application incorporates a flexure bearing compressor vibrationally balanced by a motor-controlled balancer and a completely passive pulse tube cold head. Author (revised)

N93-28826*# Johns Hopkins Univ., Laurel, MD. Applied Physics Lab.
ENVIRONMENTAL MONITORS IN THE MIDCOURSE SPACE EXPERIMENTS (MSX) Abstract Only **c19**
O. M. Uy *In* Lunar and Planetary Inst., Workshop on Advanced Technologies for Planetary Instruments, Part 1 1993 p 27 (For primary document see N93-28764 11-91)
Avail: CASI HC A01/MF A01

The Midcourse Space Experiment (MSX) is an SDIO sponsored space based sensor experiment with a full complement of optical sensors. Because of the possible deleterious effect of both molecular and particulate contamination on these sensors, a suite of environmental monitoring instruments are also being flown with the spacecraft. These instruments are the Total Pressure Sensor based on the cold-cathode gauge, a quadrupole mass spectrometer, a Bennett-type ion mass spectrometer, a cryogenic quartz crystal microbalance (QCM), four temperature-controlled QCM's, and a Xenon and Krypton Flash Lamp Experiment. These instruments have been fully space-qualified, are compact and low cost, and are possible candidate sensors for near-term planetary and atmospheric monitoring. The philosophy adopted during design and fabrication, calibration and ground testing, and modeling will be discussed . Author

N93-28827*# Alabama Univ., Birmingham. Dept. of Physics.
ULTRAVIOLET IMAGING SPECTROMETER Abstract Only c74
T. J. Wdowiak *In* Lunar and Planetary Inst., Workshop on Advanced Technologies for Planetary Instruments, Part 1 1993 p 27 (For primary document see N93-28764 11-91)
Avail: CASI HC A01/MF A01

Wide-field imaging systems equipped with objective prisms or gratings have had a long history of utility in groundbased observations of meteors and comets. Deployment of similar instruments from low Earth orbit would allow the first UV observations of meteors. This instrument can be used for comets and Lyman alpha coronae of Earth-orbit-crossing asteroids. A CaF2 prism imaging spectrograph designed for stellar observations was used aboard Skylab to observe Comet Kohoutek (1973f), but its 1300-A cut-off precluded Lyman alpha images and it was not used for observation of meteors. Because the observation of the UV spectrum of a meteor has never been attempted, researchers are denied the opportunity to obtain composition information from spectra at those wavelengths. We propose construction of a flight instrument functioning in the 1100-3200 A spectral range that is suitable for a dedicated satellite ('Quick Star') or as a space-station-attached payload. It can also be an autonomous package in the space shuttle cargo bay. Author (revised)

N93-28828*# Southwest Research Inst., San Antonio, TX. Instrumentation and Space Research Div.
DEVELOPMENT OF MINIATURIZED OPTIMIZED SMART SENSORS (MOSS) FOR SPACE PLASMAS Abstract Only c19
D. T. Young *In* Lunar and Planetary Inst., Workshop on Advanced Technologies for Planetary Instruments, Part 1 1993 p 27 (For primary document see N93-28764 11-91)
Avail: CASI HC A01/MF A01

The cost of space plasma sensors is high for several reasons: (1) Most are one-of-a-kind and state-of-the-art, (2) the cost of launch to orbit is high, (3) ruggedness and reliability requirements lead to costly development and test programs, and (4) overhead is added by overly elaborate or generalized spacecraft interface requirements. Possible approaches to reducing costs include development of small 'sensors' (defined as including all necessary optics, detectors, and related electronics) that will ultimately lead to cheaper missions by reducing (2), improving (3), and, through work with spacecraft designers, reducing (4). Despite this logical approach, there is no guarantee that smaller sensors are necessarily either better or cheaper. We have previously advocated applying analytical 'quality factors' to plasma sensors (and spacecraft) and have begun to develop miniaturized particle optical systems by applying quantitative optimization criteria. We are currently designing a Miniaturized Optimized Smart Sensor (MOSS) in which miniaturized electronics (e.g., employing new power supply topology and extensive us of gate arrays and hybrid circuits) are fully integrated with newly developed particle optics to give significant savings in volume and mass. The goal of the SwRI MOSS program is development of a fully self-contained and functional plasma sensor weighing 1 lb and requiring 1 W. MOSS will require only a typical spacecraft DC power source (e.g., 30 V) and command/data interfaces in order to be fully functional, and will provide measurement capabilities comparable in most ways to current sensors. Author (revised)

N93-28829*# Alabama Univ., Huntsville. Dept. of Physics.
X RAY, FAR, AND EXTREME ULTRAVIOLET COATINGS FOR SPACE APPLICATIONS Abstract Only c27
M. Zukic and D. G. Torr *In* Lunar and Planetary Inst., Workshop on Advanced Technologies for Planetary Instruments, Part 1 1993 p 27-28 (For primary document see N93-28764 11-91)
Avail: CASI HC A01/MF A01

The idea of utilizing imaging mirrors as narrow band filters constitutes the basis of the design of extreme ultraviolet imagers operating at 58.4 nm and 83.4 nm. The net throughput of both imaging-filtering systems is better than 20 percent. The superiority of the EUV self-filtering camera/telescope becomes apparent when compared to previously theoretically designed 83.4-nm filtering-imaging systems, which yielded transmissions of less than a few percent and therefore less than 0.1 percent throughput when combined with at least two imaging mirrors. Utilizing the self-filtering approach, instruments with similar performances are possible for imaging at other EUV wavelengths, such as 30.4 nm. The self-filtering concept is extended to the X-ray region where its application can result in the new generation of X-ray telescopes, which could replace current designs based on large and heavy collimators. Author (revised)

N93-29616 California Inst. of Tech., Pasadena.
THE THERMAL STRUCTURE, DUST LOADING, AND MERIDIONAL TRANSPORT IN THE MARTIAN ATMOSPHERE DURING LATE SOUTHERN SUMMER Ph.D. Thesis
Michelle Santee 1993 186 p
Avail: Univ. Microfilms Order No. DA9307049

The thermal structure, dust loading, and meridional transport in the Martian atmosphere are investigated using thermal emission spectra recorded by the Mariner 9 infrared interferometer spectrometer (IRIS). The analysis is restricted to a subset of the IRIS data consisting of approximately 2400 spectra spanning L(sub s) = 343 - 348 deg, corresponding to late southern summer on Mars. Simultaneous retrieval of the vertical distribution of both atmospheric temperature and dust optical depth is accomplished through an iterative procedure which is performed on each spectrum. Although atmospheric temperatures decrease from equator to pole at lower altitudes, both dayside and nightside temperatures above about 0.1 mbar (approximately 40 km) are warmer over the winter (north) polar region than over the equator or the summer (south) polar region. Zonal-mean zonal winds are derived from the atmospheric temperatures assuming gradient wind balance and zero surface zonal wind. Both hemispheres have intense mid-latitude westerly jets (with velocities of 80-90 m/s near 50 km); in the southern tropics the winds are strongly easterly (with velocities of 100 m/s near 50 km). A comprehensive radiative transfer model is used to compute solar heating and thermal cooling rates from the retrieved IRIS temperature and dust distributions. There are large net heating rates (up to 8 K/day) in the equatorial region and large net cooling rates (up to 20 K/day) in the polar regions. These net heating rates are used in a diagnostic stream function model which solves for the meridional and vertical components of the diabatic circulation simultaneously. The results show a vigorous two-cell circulation, with rising motion over the equatorial region (approximately 1.5 cm/s), poleward flow in both hemispheres (approximately 2 m/s), sinking motion over both polar regions (1-2 cm/s), and return flow in the lowest atmospheric levels. The meridional transport time scale is approximately 13 days. Water vapor desorbed from the low-latitude regolith during late northern winter/early northern spring may be transported upward by the ascending branch of this circulation, where it may be advected back to the polar regions by the high-altitude meridional winds. This process could provide a high-altitude source of water vapor for the formation and maintenance of the north polar hood. Dissert. Abstr.

N93-30214*# National Aeronautics and Space Administration. Ames Research Center, Moffett Field, CA.
PLANETARY PROTECTION ISSUES FOR THE MESUR MISSION: PROBABILITY OF GROWTH (Pg)
Harold P. Klein, ed. (Santa Clara Univ., CA.) Jul. 1993 129 p Workshop held in Palo Alto, CA, 3-4 Jun. 1991
(RTOP 186-58-01)
(NASA-CP-3167; A-92078; NAS 1.55:3167) Avail: CASI HC A07/MF A02

The purpose of the workshop was to re-evaluate the existing guidelines for the probability of growth of terrestrial organisms on Mars that were established by the National Academy of Sciences following the Viking Mission. A panel of specialists in microbiology and allied fields reviewed this issue in the light of current information about the physical and chemical environments expected on Mars. Their deliberations resulted in the virtually unanimous conclusion that the existing Pg guidelines were either appropriate or that the values for Pg should be further reduced. Individual assessments of this problem by each of the participants, together with those of additional invited experts are included. Author (revised)

N93-30635*# California Inst. of Tech., Pasadena. Div. of Geological and Planetary Sciences.
SPACECRAFT STUDIES OF PHOBOS AND MARS Final Technical Report, 1 Jun. 1988 - 31 Oct. 1990

Bruce C. Murray 1990 8 p
(Grant NAGw-1426)
(NASA-CR-193298; NAS 1.26:193298) Avail: CASI HC A02/MF A01

Utilizing the Termoskan data set of the Phobos '88 mission we have recognized a new feature on Mars: Ejecta blanket Distinct In the THermal infrared (EDITH). Virtually all of the more than one hundred of these features discovered in the Termoskan data are located on the plains near Valles Manneris. EDITH's have a startlingly clear dependence upon terrains of Hesperian age, implying a spatial or temporal dependence on Hesperian terrains. Almost no thermally distinct ejecta blankets are associated with any of the thousands of craters within the data set that occur on the older Noachian units. EDITH's also do not appear on the portions of the younger Tharsis Amazonian units seen in the data. The Hesperian terrain dependence cannot be explained by either atmospheric or impactor variations; Noachian and Hesperian terrains must have experienced identical atmospheric and impactor conditions during Hesperian times. Thermally distinct eject a blankets therefore reflect target material differences and/or secondary modification processes. A further discussion of EIDTH's is presented. Author (revised)

N93-31000 Michigan Univ., Ann Arbor.
ON SYMMETRIC CENTRAL CONFIGURATIONS WITH APPLICATION TO SATELLITE MOTION ABOUT RINGS Ph.D. Thesis
Daniel Jay Scheeres 1992 272 p
Avail: Univ. Microfilms Order No. DA9308439

The theory of planetary rings is the subject of much study recently, due to the discovery of rings around all the gas giant planets in the Solar System. Most of these studies focus on explaining the fine structure of rings and on modeling specific observed phenomenon. Starting from a classical model for rings, a new model for satellite motion is derived which accounts for the gravitational attraction of the ring. This model has application to spacecraft motion near a ring, mission planning considerations, and to the natural dynamics of ring growth and stability. Specifically, the use of symmetric central configurations to study selected issues of planetary ring dynamics was investigated. Classical stability results for symmetric central configurations are reconsidered and improved. The dynamics of satellites with infinitesimal mass attracted by a class of symmetric central configurations are investigated and a new and original dynamical model for satellite motion is derived. Fundamentals of this model are studied, including Hill stability, invariant transformations, equilibrium points and their stability, and periodic orbits. Rigorous approximations to this model are introduced for different geometries. When the satellite is far from the ring, the dynamical model may be reduced to a set of integrable equations. When the satellite is close to the ring, a simplified set of non-integrable equations are found, these equations are a generalization of Hill's equations of motion applied to the case of a planetary ring. A family of periodic orbits is also derived which describes the regular motion of a satellite about a ring. Several results from the new dynamical models are discussed. Among them are a self-limiting mechanism for a planetary ring to gain mass and a derivation of the general orbit of a satellite in the presence of a ring. Future applications of the dynamical models derived are discussed. These applications apply to artificial satellites, mission planning, and natural ring dynamics. Dissert. Abstr.

N93-29115*# Colorado Univ., Boulder.
LUNAR REGOLITH DENSIFICATION
Hon-Yim Ko and Stein Sture *In its* Space Construction Activities 1 Nov. 1991 p 28-30 (For primary document see N93-29108 11-18)
Avail: CASI HC A01/MF A01

N93-29116*# Colorado Univ., Boulder.
REGOLITH-STRUCTURE MODELING
Hon-Yim Ko and Stein Sture *In its* Space Construction Activities 1 Nov. 1991 p 31-35 (For primary document see N93-29108 11-18)
Avail: CASI HC A01/MF A01

N93-29117*# Colorado Univ., Boulder.
LUNAR REGOLITH PENETRATORS AND CUTTERS
Frank Barnes and Stein Sture *In its* Space Construction Activities 1 Nov. 1991 p 36-37 (For primary document see N93-29108 11-18)
Avail: CASI HC A01/MF A01

N93-29597*# Jet Propulsion Lab., California Inst. of Tech., Pasadena.
GALILEO POST-GASPRA CRUISE AND EARTH-2 ENCOUNTER
P. E. Beyer and M. M. Andrews *In its* The Telecommunications and Data Acquisition Report 15 May 1993 p 106-117 (For primary document see N93-29586 11-32)
(RTOP 314-40-22-37-01)
Avail: CASI HC A03/MF A03

92 SOLAR PHYSICS

Includes solar activity, solar flares, solar radiation and sunspots. For related information see *93 Space Radiation.*

N93-28585# Phillips Lab., Hanscom AFB, MA.
THE MECHANISMS OF SOLAR VARIABILITY (MSV) PROGRAM
John W. Leibacher, Robert W. Noyes, George W. Simon, and Donald F. Neidig 8 Mar. 1993 33 p
(AF Proj. 2311)
(AD-A262525; PL-TR-93-2054) Avail: CASI HC A03/MF A01

The Mechanisms of Solar Variability (MSV) Program aims toward understanding physical causes of variations in the radiative, magnetic, and particle emissions from the Sun. Solar particle and field variations influence the interplanetary medium and the magnetosphere; UV and X-ray variations affect the Earth's upper atmosphere; and total irradiance variations are a possibly significant perturber of tropospheric climate. Solar magnetic variability provides a close-up arena for studying important but otherwise unobservable astrophysical phenomena as well. The MSV program will advance our understanding of the causes of solar variability through high angular resolution observations of the interaction of solar surface magnetic fields and convective motions, as well as related x-ray, ultraviolet, and visible brightness variations. Through these high resolution studies, MSV will complement national programs aimed at monitoring integrated solar outputs, thus contributing to the better understanding and ultimate predictability of global solar variability. DTIC

N93-28605 Arizona Univ., Tucson.
THE DETECTION OF LOW-DEGREE SOLAR GRAVITY MODE OSCILLATIONS BY DIFFERENTIAL RADIUS OBSERVATIONS, 1986-1987 Ph. D. Thesis
Christopher Steven Cornuelle 1992 225 p
Avail: Univ. Microfilms Order No. DA9307677

Solar oscillations are observed by examination of time-varying properties of the photosphere. Over 800 hours of solar limb intensity profile observations in the equatorial region were collected during 1986 and 1987 at the SCLERA Mt. Bigelow site and an analysis using the FFTD was performed in an effort to detect low-degree g-mode oscillation signals in the solar photosphere. Fourier analysis of the data yielded power spectra whose peak frequencies and overall power were tested for the presence of g-mode signals at 245 classified low-degree g-mode eigenfrequencies of Hill and Gu (1990). Significant results arose from comparison of the detected eigenmode power in the 1979 data to the power density at those same classified eigenfrequencies in spectra from 1986-87 data. Also, significant correlation was found between the earlier and later mode power distributions using several different methods. Use of the parameter D(ij) to characterize the horizontal spatial behavior of eigenfunctions yielded significant results consistent with its known solar properties. Also, the observed relative signal power densities at those classified eigenfrequencies were found to be consistent with the theoretical development of Berthomieu and Provost (1990), and with previous SCLERA observations. It was noted that overall detected oscillation amplitudes in the photosphere are on average 4.0 x 0.6 times those observed in 1979, and the signal-to-noise ratio is substantially worse. The effects of instrumental defects, solar active regions, and terrestrial atmospheric noise were found to be minimal. Substantial agreement with the results of analysis of 1979 SCLERA data provides strong evidence of the correctness of the low-order g-mode classifications. The increase in g-mode signal power implied by these data, together with the other results, suggests that the photospheric behavior of these modes is variable, and perhaps solar-cycle dependent. Dissert. Abstr.

N93-28756 New York Univ., New York. Inst. of Mathematical Sciences.
SOLAR FLARE MDH Annual Report, 2 Jan. - 31 Dec. 1992

H. Strauss and E. Hameiri 26 Feb. 1993 8 p LIMITED REPRODUCIBILITY: Document partially illegible
(Grant AF-AFOSR-0044-91)
(AD-A262275; AFOSR-93-0162TR) Avail: Issuing Activity (Defense Technical Information Center (DTIC))

A new finite element time dependent, two dimensional magnetofluid code has been written. This code offers the possibility of localized mesh refinement to capture the development of current sheets, analogous to shocks by hydrodynamics. The finite difference MHD code was improved during the past year. The code is now robust, fast, and user friendly. Fast driven magnetic reconnection has been simulated in three dimensions and the reconnection time scale is consistent with one logarithmic in the plasma resistivity. A model has been found where a spontaneous discontinuous magnetic field develops from a continuous initial state, which phenomenon is believed to occur in the solar corona. Several theories of MHD and resistive MHD instabilities in the solar corona have been developed. DTIC

N93-28935*# Alabama Univ., Huntsville. Dept. of Mechanical Engineering.
A STUDY OF THE PHYSICAL MECHANISMS FOR FILAMENT ERUPTION AND CORONAL MASS EJECTION VIA NUMERICAL SIMULATION Progress Report, 1 Jan. - 31 Dec. 1992
S. T. Wu 31 Dec. 1992 31 p
(Grant NAGw-9)
(NASA-CR-193180; NAS 1.26:193180) Avail: CASI HC A03/MF A01

During this period of performance (1 Jan. 1992 - 31 Dec. 1992), the investigation of the following tasks was accomplished: (1) application of the Non-linear Force-free Field (NLFF) Model to study the active region evolution; (2) coronal dynamical responses due to emerging flux including the transition region; (3) loss of MHD equilibrium due to footpoint motions; and (4) two-dimensional MHD global coronal model: steady-state streamers. The detailed description of these studies are included. Derived from text

N93-29679 Space Environment Services Center, Boulder, CO.
SESC PRODUCTS AND SERVICES USER GUIDE
Jan. 1993 64 p See also PB92-185305 Limited Reproducibility: More than 20% of this document may be affected by microfiche quality
(PB93-178879) Avail: CASI HC A04

The Space Environment Services Center continuously monitors the Sun and the state of the near-Earth environment, acquiring data in real time from both ground-based and satellite-based sensors. Solar activity is monitored from satellites and observatories around the world on a 24-hour-a-day, 7-day-a-week basis. SESC forecasters issue alerts of significant solar and geomagnetic events. They also create products and provide services that summarize and predict space weather. Alerts and products are disseminated worldwide via a variety of delivery systems. The products and services are generally available to customers without cost. The document describes products, services, and delivery systems available to the customers on a range of time scales. The products include real-time alerts and warnings, daily products with summaries and forecasts, and a weekly publication of recent solar and geophysical activity. The publication is intended to allow customers already familiar with SESC to see at a glance the whole range of products and delivery systems. It does not address the needs of new customers who are not familiar with the data or how they might apply this information to their purposes. New customers are urged to contact SESC for more information. SESC collects data, in real time, to create the most timely and extensive space-weather data base in the world. Because of the urgency in collecting the data they are preliminary. Final data are available from the National Geophysical Data Center. NGDC publishes monthly reports and maintains long-term data sets for a wide range of stations and observations. NTIS

N93-30496 Alabama Univ., Huntsville.
TWO-DIMENSIONAL AND THREE-DIMENSIONAL TIME-DEPENDENT MHD MODEL OF EXTENDED CORONA Ph.D. Thesis
Ai-Hua Wang 1992 153 p
Avail: Univ. Microfilms Order No. DA9306604

A new time-dependent, numerical, magnetohydrodynamic (MHD) model for the simulation on two-dimensional and three-dimensional coronal streamers and coronal holes from the solar surface (r = 1 solar radius) to 15 solar radius is presented. For the two-dimensional coronal streamer simulation, three examples are given for dipole, quadrupole, and hexapole (Legendre polynomials P(sub 1), P(sub 2), and P(sub 3)) initial field topologies. For the two-dimensional coronal hole simulation, one example is given for a dipole initial field topology. For the three-dimensional coronal streamer simulation, one example is given for a spherical harmonic function (Y(sub 2))(sup 2) (spherical harmonical function) initial field topology. The computed physical variables are density, temperature, velocity, and magnetic field. The calculation is set up as an initial-boundary value problem wherein a relaxation in time produces the steady state solution. In the present cases, the initial flow field is a polytropic, hydrodynamic solution to the steady state radial flow equation superimposed on a potential magnetic field. For the two-dimensional coronal streamers, different sizes and shapes were obtained. Inside the streamer the velocity is very small and the density is high. For the two-dimensional coronal hole the highest solar wind comes from the center of the hole. At 15 solar radius the radial flow speed is about 412 km/s. With theoretical extrapolation, it shows that the radial flow speed is in the range between 512-800 km/s at 1AU. Also, at the center of the hole the number density is low with the order of 10(exp 5)/cu cm at 2 solar radius. For the three-dimensional numerical model, the preliminary coronal streamer results are presented. In addition to the properties of the solutions, their accuracy is discussed. Dissert. Abstr.

93 SPACE RADIATION

Includes cosmic radiation; and inner and outer earth's radiation belts.

For biological effects of radiation see *52 Aerospace Medicine.* For theory see *73 Nuclear and High-Energy Physics.*

N93-28962# Fermi National Accelerator Lab., Batavia, IL.
ON THE MEANING OF DELTA T/T
A. Stebbins Feb. 1993 4 p Presented at the 3rd Symposium on Particles, Strings and Cosmology and the 16th Texas Symposium on Relativistic Astrophysics Conference, Berkeley, CA, 13-18 Dec. 1992
(Contract DE-AC02-76CH-03000)
(DE93-008482; FNAL/C-93/014-A; CONF-921261-3) Avail: CASI HC A01/MF A01

One of the most interesting aspects of the discovery of Microwave Background Radiation (MBR) anisotropy by the COBE satellite is the ability to compare these anisotropies with the amplitude of density inhomogeneities we measure. Combining these two, we can get a 'unified' view of the inhomogeneities present in our universe on a broad range of scales. To make this comparison we must be able to translate (Delta)T/T into (delta)p/(bar p), the mass/density. This latter quantity we may try to determine from the distribution of galaxies and their velocities. DOE

N93-29164*# Chicago Univ., IL. Dept. of Astronomy and Astrophysics.
LIMITS ON NEUTRINO RADIATIVE DECAY FROM SN1987A
Andrew H. Jaffe, Ed Fenimore (Los Alamos National Lab., NM.), and Michael S. Turner 1993 6 p
(Grant NAG2-765)
(NASA-CR-193262; NAS 1.26:193262) Avail: CASI HC A02/MF A01

We calculate limits on the properties of neutrinos using data from gamma ray detectors on the Pioneer Venus Orbiter and Solar Max Mission satellites. A massive neutrino decaying in flight from the supernova would produce gamma rays detectable by these instruments. The lack of such a signal allows us to constrain the mass, radiative lifetime, and branching ratio to photons of a massive neutrino species produced in the supernova. Author

N93-30052*# New Hampshire Univ., Durham.
A SEARCH FOR RADIATIVE NEUTRINO DECAY FROM SUPERNOVAE
Richard S. Miller and Robert C. Svoboda (Louisiana State Univ., Baton Rouge.) [1993] 6 p
(Grant NAG5-2062)
(NASA-CR-193118; NAS 1.26:193118; LSU-HEPA-93-7) Avail: CASI HC A02/MF A01

This document presents the data analysis procedures proposed for use with the COMPTEL instrument aboard the Compton Gamma Ray Observatory (GRO) in the search for radiative neutrino decay from supernovae. The proposed analysis methodology is an extension of a standard procedure used by the COMPTEL team in searching for a variety of source types. We have applied the procedures to a set of simulated data to demonstrate the feasibility of the method to this project. Derived from text

N93-30419# Virginia Univ., Charlottesville. Dept. of Astronomy.
THE 12 UM CONTRIBUTION OF NEARBY GALAXIES TO THE INFRARED BACKGROUND Annual Report, 1 Oct. 1991 - 30 Sep. 1992
Trinh X. Thuan Apr. 1993 5 p
(Grant AF-AFOSR-0467-89)
(AD-A264336; AFOSR-93-0241TR) Avail: CASI HC A01/MF A01

The far infrared properties of normal non-infrared-bright galaxies were studied as a function of their morphological type using a sample of 1544 galaxies of magnitude less than 14.5. Most of the far infrared color trends as a function of galaxian morphological type can be reproduced by dust models with three components, combined with an appropriate dust heating spectral energy distribution. Work has been done on the use of far infrared luminosity as a star formation indicator in galaxies. The trends observed are consistent with a two-component model, with the citrus fraction as the second parameter and the star formation rate as the first parameter. Observations have been made and studies performed on dwarf and low surface brightness galaxies and starburst galaxies at intermediate red shifts. DTIC

N93-29626*# National Aeronautics and Space Administration. Marshall Space Flight Center, Huntsville, AL.
STATUS OF LDEF IONIZING RADIATION MEASUREMENTS AND ANALYSIS
Thomas A. Parnell *In* NASA. Langley Research Center, LDEF: 69 Months in Space. Part 1: Second Post-Retrieval Symposium Apr. 1993 p 69-78 (For primary document see N93-29621 11-99)
Avail: CASI HC A02/MF A03

N93-29646*# Dublin Inst. for Advanced Studies (Ireland).
PROGRESS REPORT ON THE ULTRA HEAVY COSMIC RAY EXPERIMENT (AO178)
A. Thompson, D. OSullivan, J. Bosch, R. Keegan (Dublin Inst. for Advanced Studies, Ireland.), K.-P. Wenzel (European Space Agency. European Space Research and Technology Center, ESTEC, Noordwijk, Netherlands.), F. Jansen (European Space Agency. European Space Research and Technology Center, ESTEC, Noordwijk, Netherlands.), and C. Domingo (Universidad Autonoma de Barcelona, Bellaterra, Spain.) *In* NASA. Langley Research Center, LDEF: 69 Months in Space. Part 1: Second Post-Retrieval Symposium Apr. 1993 p 261-268 (For primary document see N93-29621 11-99)
Avail: CASI HC A02/MF A03

N93-29708*# Naval Research Lab., Washington, DC.
FUTURE RADIATION MEASUREMENTS IN LOW EARTH ORBIT
James H. Adams, Jr. *In* NASA. Langley Research Center, LDEF: 69 Months in Space. Part 4: Second Post-Retrieval Symposium Apr. 1993 p 1551-1561 (For primary document see N93-29682 11-99)
Avail: CASI HC A03/MF A03; 2 functional color pages

99 GENERAL

N93-28477# Deutsche Forschungsgemeinschaft, Bonn (Germany).
SPACE RESEARCH IN GERMANY 1990-1991
1992 40 p
(ETN-93-93807) Avail: CASI HC A03/MF A01

The restructuring of space research in Germany after reunification is reflected in a report documenting the activities of institutes engaged in space astronomy, solar physics, the solar system, near Earth space, atmospheres and ionospheres, Earth observation, materials sciences, and life sciences. During the reported period, Rosat was launched and the first sky survey in x-rays was completed. Some 60,000 new x-ray sources, galactic and extragalactic, were found, many of them completely unexpected objects, and it is possible to determine the true diffuse x-ray background of the sky and to even see the Moon as a dark object against it. NASA's Gamma Ray Observatory (GRO), to which German scientists contributed, was launched. Some of the first results of this mission are the measurement of gamma rays from quasars and the identification of the Geminga source as a 237 msec pulsar. Other important launches were Ulysses, Galileo, CRRES, and the Texus rocket flights. A large fraction of the present activities are devoted to data reduction and the hardware development for missions like D2, Orfeus, Freja, Cluster, Soho, Mars 94/96, and more. ESA

N93-29258# Office of Naval Research, Arlington, VA.
COGNITIVE AND NEURAL SCIENCES DIVISION 1992 PROGRAMS Report, 1 Oct. 1991 - 30 Sep. 1992
Willard S. Vaughan Aug. 1992 245 p
(AD-A263400; OCNR-11492-17) Avail: CASI HC A11/MF A03

This report documents R and D performed by Principal Investigators under the sponsorship of the ONR Cognitive and Neural Sciences Division during fiscal year 1992. DTIC

N93-29354*# National Aeronautics and Space Administration. Langley Research Center, Hampton, VA.
LDEF: 69 MONTHS IN SPACE. SECOND POST-RETRIEVAL SYMPOSIUM, PART 2
Arlene S. Levine, ed. Washington Apr. 1993 460 p Symposium held in San Diego, CA, 1-5 Jun. 1992; sponsored by NASA and AIAA
(RTOP 506-48-91-11)
(NASA-CP-3194-Pt-2; L-17196-Pt-2; NAS 1.55:3194-Pt-2) Avail: CASI HC A20/MF A04

This document is a compilation of papers presented at the Second Long Duration Exposure Facility (LDEF) Post-Retrieval Symposium. The papers represent the data analysis of the 57 experiments flown on the LDEF. The experiments include materials, coatings, thermal systems, power and propulsion, science (cosmic ray, interstellar gas, heavy ions, micrometeoroid, etc.), electronics, optics, and life science. For individual titles, see N93-29355 through N93-29381.

N93-29355*# National Aeronautics and Space Administration. Lyndon B. Johnson Space Center, Houston, TX.
REPORT OF THE METEOROID AND DEBRIS SPECIAL INVESTIGATION GROUP Interim Report **c90**
Michael E. Zolensky, Herbert A. Zook, Fred Horz, Dale R. Atkinson (POD Associates, Inc., Albuquerque, NM.), Cassandra R. Coombs (POD Associates, Inc., Albuquerque, NM.), Alan J. Watts (POD Associates, Inc., Albuquerque, NM.), Claire B. Dardano (Lockheed Engineering and Sciences Co., Houston, TX.), Thomas H. See (Lockheed Engineering and Sciences Co., Houston, TX.), Charles G. Simon (Institute for Space Science and Technology, Inc., Gainesville, FL.), and William H. Kinard (National Aeronautics and Space Administration. Langley Research Center, Hampton, VA.) *In* NASA. Langley Research Center, LDEF: 69 Months in Space. Second Post-Retrieval Symposium, Part 2 Apr. 1993 p 277-302 (For primary document see N93-29354 11-99)
Avail: CASI HC A03/MF A04

The LDEF Meteoroid and Debris Special Investigation Group (hereafter M&D SIG) was formed to maximize the data harvest from LDEF by permitting the characterization of the meteoroid and space debris impact record of the entire satellite. Thus, our work is complementary to that of the various M&D PI's, all of whom are members of the SIG. This presentation will summarize recent results and discussions concerning five critical SIG goals: (1) classification of impactors based upon composition of residues, (2) small impact (microimpact) features, (3) impact cratering and penetration data to derive projectile sizes and masses, (4) particulate flux estimates in low-Earth orbit, and (5) the LDEF Meteoroid and Debris database. Author (revised)

N93-29356*# Departement d'Etudes et de Recherches en Technologie Spatiale, Toulouse (France).
MICROMETEOROIDS AND DEBRIS ON LDEF **c90**
Jean-Claude Mandeville *In* NASA. Langley Research Center, LDEF: 69 Months in Space. Second Post-Retrieval Symposium, Part 2 Apr. 1993 p 303-312 Sponsored by NASA and CNES (For primary document see N93-29354 11-99)
Avail: CASI HC A02/MF A04

Two experiments within the French Cooperative Payload (FRECOPA) and devoted to the detection of cosmic dust were flown on the Long

Duration Exposure Facility (LDEF). A variety of sensors and collecting devices have made possible the study of impact processes on dedicated sensors and on materials of technological interest. Examination of hypervelocity impact features on these experiments gives valuable information on the size distribution and nature of interplanetary dust particles in low-Earth orbit (LEO), within the 0.5-300 micrometer size range. However no crater smaller than 1.5 microns has been observed, thus suggesting a cut-off in the near Earth particle distribution. Chemical investigation of craters by EDX clearly shows evidence of elements (Na, Mg, Si, S, Ca, and Fe) consistent with cosmic origin. However, remnants of orbital debris have been found in a few craters; this can be the result of particles in eccentric orbits about the Earth and of the 8 deg offset in the orientation of LDEF. Crater size distribution is compared with results from other dust experiments flown on LDEF and with current models. Possible origin and orbital evolution of micrometeoroids is discussed. Use of thin foil detectors for the chemical study of particle remnants looks promising for future experiments. Author (revised)

N93-29357*# National Aeronautics and Space Administration. Lyndon B. Johnson Space Center, Houston, TX.

CONTINUED INVESTIGATION OF LDEF'S STRUCTURAL FRAME AND THERMAL BLANKETS BY THE METEOROID AND DEBRIS SPECIAL INVESTIGATION GROUP c18

Thomas H. See (Lockheed Engineering and Sciences Co., Houston, TX.), Kimberly S. Mack (Lockheed Engineering and Sciences Co., Houston, TX.), Jack L. Warren (Lockheed Engineering and Sciences Co., Houston, TX.), Michael E. Zolensky, and Herbert A. Zook *In* NASA. Langley Research Center, LDEF: 69 Months in Space. Second Post-Retrieval Symposium, Part 2 Apr. 1993 p 313-324 (For primary document see N93-29354 11-99)

Avail: CASI HC A03/MF A04

This report focuses on the data acquired by detailed examination of LDEF intercostals, 68 of which are now in possession of the Meteoroid and Debris Special Investigation Group (M&D SIG) at JSC. In addition, limited data will be presented for several small sections from the A0178 thermal control blankets that were examined/counted prior to being shipped to Principal Investigators (PI's) for scientific study. The data presented here are limited to measurements of crater and penetration-hole diameters and their frequency of occurrence which permits, yet also constrains, more model-dependent, interpretative efforts. Such efforts will focus on the conversion of crater and penetration-hole sizes to projectile diameters (and masses), on absolute particle fluxes, and on the distribution of particle-encounter velocities. These are all complex issues that presently cannot be pursued without making various assumptions which relate, in part, to crater-scaling relationships, and to assumed trajectories of natural and man-made particle populations in LEO that control the initial impact conditions. Author (revised)

N93-29358*# European Space Agency. European Space Research and Technology Center, ESTEC, Noordwijk (Netherlands).

PREDICTED AND OBSERVED DIRECTIONAL DEPENDENCE OF METEOROID/DEBRIS IMPACTS ON LDEF THERMAL BLANKETS c90

Gerhard Drolshagen *In* NASA. Langley Research Center, LDEF: 69 Months in Space. Second Post-Retrieval Symposium, Part 2 Apr. 1993 p 325-337 (For primary document see N93-29354 11-99)

Avail: CASI HC A03/MF A04

The number of impacts from meteoroids and space debris particles to the various LDEF rows is calculated using ESABASE/DEBRIS, a 3-D numerical analysis tool. It is based on recent reference environment flux models and includes geometrical and directional effects. A comparison of model predictions and actual observations is made for penetrations of the thermal blankets which covered the UHCR experiment. The thermal blankets were located on all LDEF rows, except 3, 9, and 12. Because of their uniform composition and thickness, these blankets allow a direct analysis of the directional dependence of impacts and provide a test case for the latest meteoroid and debris flux models. Author (revised)

N93-29359*# National Aeronautics and Space Administration. Lyndon B. Johnson Space Center, Houston, TX.

THREE-D CRATER ANALYSIS OF LDEF IMPACT FEATURES FROM STEREO IMAGERY c18

Clyde A. Sapp (Lockheed Engineering and Sciences Co., Houston, TX.), Thomas H. See (Lockheed Engineering and Sciences Co., Houston, TX.), and Michael E. Zolensky *In* NASA. Langley Research Center, LDEF: 69 Months in Space. Second Post-Retrieval Symposium, Part 2 Apr. 1993 p 339-345 (For primary document see N93-29354 11-99)

Avail: CASI HC A02/MF A04

The preliminary results from attempts to derive depth and diameter information from digitized stereo images of impact features on the LDEF are reported. Contrary to our prior assumption, we find that impact craters in the T6 A1 alloy are not paraboloid in cross section, but rather are better described by a 6th-order polynomial curve. We explore the implications of this discovery. Author (revised)

N93-29360*# National Aeronautics and Space Administration. Ames Research Center, Moffett Field, CA.

FURTHER ANALYSIS OF LDEF FRECOPA MICROMETEOROID REMNANTS c90

Janet Borg (Centre National de la Recherche Scientifique, Orsay, France.), Ted E. Bunch, Filippo RadicatidiBrozolo (Evans, Charles and Associates, Redwood City, CA.), and Jean Claude Mandeville (Departement d'Etudes et de Recherches en Technologie Spatiale, Toulouse, France.) *In* NASA. Langley Research Center, LDEF: 69 Months in Space. Second Post-Retrieval Symposium, Part 2 Apr. 1993 p 347-356 (For primary document see N93-29354 11-99)

(Contract NAS2-13178; RTOP 199-52-12; RTOP 506-48-00)

Avail: CASI HC A02/MF A04

In the Al collectors of experiment A0138-1 of the French Cooperative Payload (FRECOPA) payload, we identified a population of small craters (3-9 microns in diameter) induced by the impacts of micron-sized grains, mainly of extraterrestrial origin. Chemical analyses of the Interplanetary Dust Particle (IDP) remnants were made in the bottoms and on the rims of the craters, in addition to immediate off-rim areas. So far, the compositional investigation of the craters by Energy Dispersive Spectroscopy (EDS) has shown evidence of an extraterrestrial origin for the impacting grains. The systematic presence of C and O in the residues has been reported and may be compared with the existence of particles showing high proportions of biogenic light elements and detected in the close environment of P-Halley comet nucleus (called CHON particles). An analytical protocol has been established in order to extract molecular and possible isotopic information on these grains, a fraction of which could be of cometary origin. Although these very small craters may show crater features that are typical of the larger Long Duration Exposure Facility (LDEF) population (greater than 50 microns), some show unique morphologies that we have not previously observed. Our initial Laser Induced Mass Spectrometry (LIMS) analytical results show strong signals for nitrogen-bearing ions in craters characterized by high C and O contents; they also suggest that carbon contents in some craters could exceed that known for carbonaceous chondrites. Author (revised)

N93-29361*# Aerospace Corp., El Segundo, CA. Mechanics and Materials Technology Center.

LONG DURATION EXPOSURE FACILITY (LDEF) EXPERIMENT M0003 METEOROID AND DEBRIS SURVEY c90

M. J. Meshishnek, S. R. Gyetvay, K. W. Paschen, and J. M. Coggi *In* NASA. Langley Research Center, LDEF: 69 Months in Space. Second Post-Retrieval Symposium, Part 2 Apr. 1993 p 357-415 Sponsored by the Strategic Defense Initiative Organization and AF Wright Lab. (For primary document see N93-29354 11-99)

Avail: CASI HC A04/MF A04

A survey of the meteoroid and space debris impacts on LDEF experiment M0003 was performed. The purpose of this survey was to document significant impact phenomenology and to obtain impact crater data for comparison to current space debris and micrometeoroid models. The survey consists of the following: photomicrographs of significant impacts in a variety of material types; accurate measurements of impact crater coordinates and dimensions for selected experiment surfaces; and databasing of the crater data for reduction, manipulation, and comparison to models. Large area surfaces that were studied include the experiment power and data system (EPDS) sunshields, environment exposure control canister (EECC) sunshields, and the M0003 signal conditioning unit (SCU) covers. Crater diameters down to 25 microns were measured and cataloged. Both leading (D8) and trailing (D4) edge surfaces were studied and compared. The EPDS sunshields are aluminum panels painted with Chemglaze A-276 white thermal control paint, the EECC sunshields are chromic acid-anodized aluminum, and the SCU covers are aluminum painted with S13GLO white thermal control paint. Typical materials that have documented impacts are metals, glasses and ceramics, composites, polymers, electronic materials, and paints. The results of this survey demonstrate the different response of materials to hypervelocity impacts. Comparison of the survey data to curves derived from the Kessler debris model and the Cour-Palais micrometeoroid model indicates that these models overpredict small impacts (less than 100 micron) and may underpredict large impacts (greater than 1000 micron) while having fair to good agreement for the intermediate impacts. Comparison of the impact distributions among the various surfaces indicates significant variations, which may be a function of material response effects, or in some cases surface roughness. Representative photographs and summary graphs of the impact data are presented. Author (revised)

N93-29362*# Kent Univ., Canterbury (England). Physics Lab.
DERIVATION OF PARTICULATE DIRECTIONAL INFORMATION FROM ANALYSIS OF ELLIPTICAL IMPACT CRATERS ON LDEF **c18**
P. J. Newman, N. Mackay, S. P. Deshpande, S. F. Green, and J. A. M. McDonnell *In* NASA. Langley Research Center, LDEF: 69 Months in Space. Second Post-Retrieval Symposium, Part 2 Apr. 1993 p 417-429 Sponsored by the UK Science and Engineering Research Council (For primary document see N93-29354 11-99)
Avail: CASI HC A03/MF A04

The Long Duration Exposure Facility provided a gravity gradient stabilized platform which allowed limited directional information to be derived from particle impact experiments. The morphology of impact craters on semi-infinite materials contains information which may be used to determine the direction of impact much more accurately. We demonstrate the applicability of this technique and present preliminary results of measurements from LDEF and modelling of interplanetary dust and space debris. Author

N93-29363*# National Aeronautics and Space Administration. Lewis Research Center, Cleveland, OH.
CHARACTERISTICS OF HYPERVELOCITY IMPACT CRATERS ON LDEF EXPERIMENT S1003 AND IMPLICATIONS OF SMALL PARTICLE IMPACTS ON REFLECTIVE SURFACES **c18**
Michael J. Mirtich, Sharon K. Rutledge, Bruce A. Banks, Christopher DeVries (Cornell Univ., Ithaca, NY.), and James E. Merrow (Cleveland State Univ., OH.) *In* NASA. Langley Research Center, LDEF: 69 Months in Space. Second Post-Retrieval Symposium, Part 2 Apr. 1993 p 431-451 (For primary document see N93-29354 11-99)
Avail: CASI HC A03/MF A04

The Ion Beam textured and coated surfaces EXperiment (IBEX), designated S1003, was flown on LDEF at a location 98 deg in a north facing direction relative to the ram direction. Thirty-six diverse materials were exposed to the micrometeoroid (and some debris) environment for 5.8 years. Optical property measurements indicated no changes for almost all of the materials except S-13G, Kapton, and Kapton-coated surfaces, and these changes can be explained by other environmental effects. From the predicted micrometeoroid flux of NASA SP-8013, no significant changes in optical properties of the surfaces due to micrometeoroids were expected. There were hypervelocity impacts on the various diverse materials flown on IBEX, and the characteristics of these craters were documented using scanning electron microscopy (SEM). The S1003 alumigold-coated aluminum cover tray was sectioned into 2 cm x 2 cm pieces for crater documentation. The flux curve generated from this crater data fits well between the 1969 micrometeoroid model and the Kessler debris model for particles less than 10(exp -9) gm which were corrected for the S1003 positions (98 deg to ram). As the particle mass increases, the S1003 impact data is greater than that predicted by even the debris model. This, however, is consistent with data taken on intercostal F07 by the Micrometeoroid/Debris Special Investigating Group (M/D SIG). The mirrored surface micrometeoroid detector flown on IBEX showed no change in solar reflectance and corroborated the S1003 flux curve, as well as results of this surface flown on SERT 2 and OSO 3 for as long as 21 years. Author (revised)

N93-29364*# National Aeronautics and Space Administration. Ames Research Center, Moffett Field, CA.
HYPERVELOCITY IMPACT SURVIVABILITY EXPERIMENTS FOR CARBONACEOUS IMPACTORS **c18**
T. E. Bunch, Luann Becker (Scripps Institution of Oceanography, La Jolla, CA.), Jeffrey Bada (Scripps Institution of Oceanography, La Jolla, CA.), John Macklin (Washington Univ., Seattle.), Filippo RadicatidiBrozolo (Evans, Charles and Associates, Redwood City, CA.), R. H. Fleming (Evans, Charles and Associates, Redwood City, CA.), and Jozef Erlichman (TMA/Norcal, Richmond, CA.) *In* NASA. Langley Research Center, LDEF: 69 Months in Space. Second Post-Retrieval Symposium, Part 2 Apr. 1993 p 453-477 (For primary document see N93-29354 11-99)
(Contract NAS2-13178; RTOP 199-52-12; RTOP 506-48-00)
Avail: CASI HC A03/MF A04

We performed a series of hypervelocity impact experiments using carbon-bearing impactors (diamond, graphite, fullerenes, phthalic acid crystals, and Murchison meteorite) into Al plate at velocities between 4.2 and 6.1 km/s. These tests were made to do the following: (1) determine the survivability of carbon forms and organize molecules in low hypervelocity impact; (2) characterize carbonaceous impactor residues; and (3) determine whether or not fullerenes could form from carbonaceous impactors, under our experimental conditions, or survive as impactors. An analytical protocol of field emission SEM imagery, SEM-EDX, laser Raman spectroscopy, single and 2-stage laser mass spectrometry, and laser induced fluorescence (LIF) found the following: (1) diamonds did not survive impact at 4.8 km/s, but were transformed into various forms of disordered graphite; (2) intact, well-ordered graphite impactors did survive impact at 5.9 km/sec, but were only found in the crater bottom centers; the degree of impact-induced disorder in the graphite increases outward (walls, rims, ejecta); (3) phthalic acid crystals were destroyed on impact (at 4.2 km/s, although a large proportion of phthalic acid molecules did survive impact); (4) fullerenes did not form as products of carbonaceous impactors (5.9 - 6.1 km/s, fullerene impactor molecules mostly survived impact at 5.9 km/s; and (5) two Murchison meteorite samples (launched at 4.8 and 5.9 km/s) show preservation of some higher mass polycyclic aromatic hydrocarbons (PAHs) compared with the non-impacted sample. Each impactor type shows unique impactor residue morphologies produced at a given impact velocity. An expanded methodology is presented to announce relatively new analytical techniques together with innovative modifications to other methods that can be used to characterize small impact residues in LDEF craters, in addition to other acquired extraterrestrial samples. Author (revised)

N93-29365*# Auburn Univ., AL. Space Power Inst.
HYPERVELOCITY IMPACT FACILITY FOR SIMULATING MATERIALS EXPOSURE TO IMPACT BY SPACE DEBRIS **c18**
M. F. Rose, S. Best, T. Chaloupka, B. Stephens, and G. Crawford *In* NASA. Langley Research Center, LDEF: 69 Months in Space. Second Post-Retrieval Symposium, Part 2 Apr. 1993 p 479-492 Sponsored by NASA. Marshall Space Flight Center and NASA. Langley Research Center (For primary document see N93-29354 11-99)
Avail: CASI HC A03/MF A04

As a result of man's venturing into space, the local debris contributed by his presence exceeds, at some orbital altitudes, that of the natural component. Man's contribution ranges from fuel residue to large derelect satellites that weigh many kilograms. Current debris models are able to predict the growth of the problem and suggest that spacecraft must employ armor or bumper shields for some orbital altitudes now, and that, the problem will become worse as a function of time. The practical upper limit to the velocity distribution is on the order of 40 km/s and is associated with the natural environment. The maximum velocity of the man-made component is in the 14-16 km/s range. The Long Duration Exposure Facility (LDEF) has verified that the 'high probability of impact' particles are in the microgram to milligram range. These particles can have significant effects on coatings, insulators, and thin metallic layers. The surface of thick materials becomes pitted and the local debris component is enhanced by ejecta from the debris spectrum in a controlled environment. The facility capability is discussed in terms of drive geometry, energetics, velocity distribution, diagnostics, and projectile/debris loading. The facility is currently being used to study impact phenomena on Space Station Freedom's solar array structure, other solar array materials, potential structural materials for use in the station, electrical breakdown in the space environment, and as a means of clarifying or duplicating the impact phenomena on the LDEF surfaces. The results of these experiments are described in terms of the mass/velocity distribution incident on selected samples, crater dynamics, and sample geometry. Author (revised)

N93-29366*# Toronto Univ., North York (Ontario). Inst. for Aerospace Studies.
ANALYSIS OF LDEF MICROMETEOROID/DEBRIS DATA AND DAMAGE TO COMPOSITE MATERIALS **c24**
R. C. Tennyson and G. Manuelpillai *In* NASA. Langley Research Center, LDEF: 69 Months in Space. Second Post-Retrieval Symposium, Part 2 Apr. 1993 p 493-511 (For primary document see N93-29354 11-99)
Avail: CASI HC A03/MF A04

This report presented published LDEF micrometeoroid/debris impact data in a nomogram format useful for estimating the total number of hits that could be expected on a space structure as a function of time in orbit, angular location relative to ram, and exposed surface area. Correction factors accounting for different altitudes are given. These are normalized to the average LDEF altitude. Examples on how to use the nomograph are also included. In addition, impact data and damage areas observed on composite laminates (experiment AO 190) are discussed. Author (revised)

N93-29367*# Washington Univ., Saint Louis, MO. Center for Space Sciences.
SIMS CHEMICAL ANALYSIS OF EXTENDED IMPACTS ON THE LEADING AND TRAILING EDGES OF LDEF EXPERIMENT AO187-2 **c25**
S. Amari, J. Foote, P. Swan, R. M. Walker, E. Zinner, and G. Lange (Max-Planck-Inst. fuer Kernphysik, Heidelberg, Germany.) *In* NASA. Langley Research Center, LDEF: 69 Months in Space. Second Post-Retrieval Symposium, Part 2 Apr. 1993 p 513-528 (For primary document see N93-29354 11-99)
Avail: CASI HC A03/MF A04

Numerous 'extended impacts' found in both leading and trailing edge capture cells were successfully analyzed for the chemical composition of projectile residues by secondary ion mass spectrometry (SIMS). Most data were obtained from the trailing edge cells where 45 of 58 impacts were classified as 'probably natural' and the remainder as 'possibly man-made debris.' This is in striking contrast to leading edge cells where 9 of 11 impacts so far measured are definitely classified as orbital debris. Although all the leading edge cells had lost their plastic entrance foils during flight, the rate of foil failure was similar to that of the trailing edge cells, 10 percent of which were recovered intact. Ultraviolet embrittlement is suspected as the major cause of failure on both leading and trailing edges. The major impediment to the accurate determination of projectile chemistry is the fractionation of volatile and refractory elements in the hypervelocity impact and redeposition processes. This effect had been noted in a simulation experiment but is more pronounced in the LDEF capture cells, probably due to the higher average velocities of the space impacts. Surface contamination of the pure Ge surfaces with a substance rich in Si, but also containing Mg and Al, provides an additional problem for the accurate determination of impactor chemistry. The effect is variable, being much larger on surfaces that were exposed to space than in those cells that remained intact. Future work will concentrate on the analyses of more leading edge impacts and the development of new SIMS techniques for the measurement of elemental abundances in extended impacts. Author (revised)

N93-29368*# Vanderbilt Univ., Nashville, TN. Dept. of Materials Science and Engineering.
CRATERING IN GLASSES IMPACTED BY DEBRIS OR MICROMETEORITES **c27**
David E. Wiedlocher and Donald L. Kinser *In* NASA. Langley Research Center, LDEF: 69 Months in Space. Second Post-Retrieval Symposium, Part 2 Apr. 1993 p 529-539 (For primary document see N93-29354 11-99)
(Contracts NAS8-156; NAS8-32695; NASA Order L-17761-D)
Avail: CASI HC A03/MF A04

Mechanical strength measurements on five glasses and one glass-ceramic exposed on LDEF revealed no damage exceeding experimental limits of error. The measurement technique subjected less than 5 percent of the sample surface area to stresses above 90 percent of the failure strength. Seven micrometeorite or space debris impacts occurred at locations which were not in that portion of the sample subjected to greater than 90 percent of the applied stress. As a result of this, the impact events on the sample were not detected in the mechanical strength measurements. The physical form and structure of the impact sites was carefully examined to determine the influence of those events upon stress concentration associated with the impact and the resulting mechanical strength. The size of the impact site, insofar as it determines flaw size for fracture purposes, was examined. Surface topography of the impacts reveals that six of the seven sites display impact melting. The classical melt crater structure is surrounded by a zone of fractured glass. Residual stresses arising from shock compression and from cooling of the fused zone cannot be included in the fracture mechanics analyses based on simple flaw size measurements. Strategies for refining estimates of mechanical strength degradation by impact events are presented. Author (revised)

N93-29369*# National Aeronautics and Space Administration. Lyndon B. Johnson Space Center, Houston, TX.
SCANNING ELECTRON MICROSCOPE/ENERGY DISPERSIVE X RAY ANALYSIS OF IMPACT RESIDUES IN LDEF TRAY CLAMPS **c18**
Ronald P. Bernhard (Lockheed Engineering and Sciences Co., Houston, TX.), Christian Durin (Centre National d'Etudes Spatiales, Toulouse, France.), and Michael E. Zolensky *In* NASA. Langley Research Center, LDEF: 69 Months in Space. Second Post-Retrieval Symposium, Part 2 Apr. 1993 p 541-549 (For primary document see N93-29354 11-99)
Avail: CASI HC A02/MF A04

Detailed optical scanning of tray clamps is being conducted in the Facility for the Optical Inspection of Large Surfaces at JSC to locate and document impacts as small as 40 microns in diameter. Residues from selected impacts are then being characterized by Scanning Electron Microscopy/Energy Dispersive X-ray Analysis at CNES. Results from this analysis will be the initial step to classifying projectile residues into specific sources. Author (revised)

N93-29370*# National Aeronautics and Space Administration. Lyndon B. Johnson Space Center, Houston, TX.
PROJECTILE COMPOSITIONS AND MODAL FREQUENCIES ON THE CHEMISTRY OF MICROMETEOROIDS LDEF EXPERIMENT **c90**
Ronald P. Bernhard (Lockheed Engineering and Sciences Co., Houston, TX.), Thomas H. See (Lockheed Engineering and Sciences Co., Houston, TX.), and Friedrich Hoerz *In* NASA. Langley Research Center, LDEF: 69 Months in Space. Second Post-Retrieval Symposium, Part 2 Apr. 1993 p 551-573 (For primary document see N93-29354 11-99)
Avail: CASI HC A03/MF A04

The Chemistry of Micrometeoroids Experiment (LDEF instrument A0187-1) exposed witness plates of high-purity gold (greater than 99.99 percent Au) and commercial aluminum (greater than 99 percent Al) with the objective of analyzing the residues of cosmic-dust and orbital-debris particles associated with hypervelocity impact craters. The gold substrates were located approximately 8 deg off LDEF's trailing edge (Bay A03), while the aluminum surfaces resided in Bay A11, approximately 52 deg from LDEF's leading edge. SEM-EDX techniques were employed to analyze the residues associated with 199 impacts on the gold and 415 impacts on the aluminum surfaces. The residues that could be analyzed represent natural or man-made materials. The natural particles dominate at all particle sizes less than 5 micron. It is possible to subdivide both particle populations into subclasses. Chondritic compositions dominate the natural impactors (71 percent), followed by monomineralic, mafic-silicate compositions (26 percent), and by Fe-Ni rich sulfides (approximately 3 percent). Approximately 30 percent of all craters on the gold collectors were caused by man-made debris such as aluminum, paint flakes, and other disintegrated, structural and electronic components. Equations-of-state and associated calculations of shock stresses for typical LDEF impacts into the gold and aluminum substrates suggest that substantial vaporization may have occurred during many of the impacts and is the reason why approximately 50 percent of all craters did not contain sufficient residue to permit analysis by the SEM-EDX technique. After converting the crater diameters into projectile sizes using encounter speeds typical for the trailing-edge and forward-facing (Row 11) directions, and accounting for normalized exposure conditions of the CME collectors, we derived the absolute and relative fluxes of specific projectile classes. The natural impactors encounter all LDEF pointing directions with comparable, modal frequencies suggesting compositional (and dynamic) homogeneity of the interplanetary-dust environment in near-Earth orbit. Author (revised)

N93-29371*# National Aeronautics and Space Administration. Lyndon B. Johnson Space Center, Houston, TX.

ASTEROIDAL VERSUS COMETARY METEOROID IMPACTS ON THE LONG DURATION EXPOSURE FACILITY (LDEF) Abstract Only c90

Herbert A. Zook *In* NASA. Langley Research Center, LDEF: 69 Months in Space. Second Post-Retrieval Symposium, Part 2 Apr. 1993 p 575 (For primary document see N93-29354 11-99)

Avail: CASI HC A01/MF A04

Meteoroids that enter the Earth's atmosphere at low velocities will tend to impact the apex side (that surface facing the spacecraft direction of motion) of a spacecraft at a very high rate compared to the rate with which they will impact an antapex-facing surface. This ratio--apex to antapex impact rates--will become less as meteoroid entry velocities increase. The measured ration, apex to antapex, for 500 micron diameter impact craters in 6061-T6 aluminum on LDEF seems to be about 20 from the work of the meteoroid SIG group and others, that was presented at the first LDEF symposium. Such a ratio is more consistent with the meteoroid velocity distributions derived by Erickson and by Kessler, than it is with others that have been tested. These meteoroid velocity distributions have mean entry velocities into the Earth's atmosphere of 16.5 to 16.9 km/s. Others have numerically simulated the orbital evolution of small dust grains emitted from asteroids and comets. For those asteroidal grains small enough (below about 100 microns diameter) to drift from the asteroid belt to the orbit of the Earth, under P-R and solar wind drag, without suffering collisional destruction, the following results are found: as the ascending or descending nodes cross the Earth's orbit, their orbital eccentricities and inclinations are quite low (e less than 0.3, i less than 20 deg), and their mean velocity with respect to the Earth is about 5 or 6 km/s. When gravitational acceleration of the Earth is taken into account, the corresponding mean velocities relative to the top of the Earth's atmosphere are 12 to 13 km/s. This means that, at best, these small asteroidal particles cannot comprise more than 50 percent of the particles entering the Earth's atmosphere. When gravitational focusing is considered, they cannot comprise more than a few percent of those in heliocentric orbit at 1 AU. The rest are presumably of cometary origin. Author (revised)

N93-29372*# National Aeronautics and Space Administration. Lyndon B. Johnson Space Center, Houston, TX.

INTERPLANETARY METEOROID DEBRIS IN LDEF METAL CRATERS c90

D. E. Brownlee (Washington Univ., Seattle.), D. Joswiak (Washington Univ., Seattle.), J. Bradley (MVA, Inc., Norcross, GA.), and Friedrich Hoerz *In* NASA. Langley Research Center, LDEF: 69 Months in Space. Second Post-Retrieval Symposium, Part 2 Apr. 1993 p 577-584 (For primary document see N93-29354 11-99)

Avail: CASI HC A02/MF A04

We have examined craters in Al and Au LDEF surfaces to determine the nature of meteoroid residue in the rare cases where projectile material is abundantly preserved in the crater floor. Typical craters contain only small amounts of residue and we find that less than 10 percent of the craters in Al have retained abundant residue consistent with survival of a significant fraction (greater than 20 percent) of the projectile mass. The residue-rich craters can usually be distinguished optically because their interiors are darker than ones with little or no apparent projectile debris. The character of the meteoroid debris in these craters ranges from thin glass liners, to thick vesicular glass containing unmelted mineral fragments, to debris dominated by unmelted mineral fragments. In the best cases of meteoroid survival, unmelted mineral fragments preserve both information on projectile mineralogy as well as other properties such as nuclear tracks caused by solar flare irradiation. The wide range of the observed abundance and alteration state of projectile residue is most probably due to differences in impact velocity. The crater liners are being studied to determine the composition of meteoroids reaching the Earth. The compositional types most commonly seen in the craters are: (1) chondritic (Mg, Si, S, Fe in approximately solar proportions), (2) Mg silicate. amd (3) iron sulfide. These are also the most common compositional types of extraterrestrial particle types collected in the stratosphere. The correlation between these compositions indicates that vapor fractionation was not a major process influencing residue composition in these craters. Although the biases involved with finding analyzable meteoroid debris in metal craters differ from those for extraterrestrial particles collected in and below the atmosphere, there is a common bias favoring particles with low entry velocity. For craters this is very strong and probably all of the metal craters with abundant residue were caused by asteroidal dust impacting at minimum velocities. Author (revised)

N93-29373*# National Aeronautics and Space Administration. Lyndon B. Johnson Space Center, Houston, TX.

ORIGIN OF ORBITAL DEBRIS IMPACTS ON LDEF'S TRAILING SURFACES c18

Donald J. Kessler *In* NASA. Langley Research Center, LDEF: 69 Months in Space. Second Post-Retrieval Symposium, Part 2 Apr. 1993 p 585-593 (For primary document see N93-29354 11-99)

Avail: CASI HC A02/MF A04

A model was developed to determine the origin of orbital impacts measured on the training surfaces of LDEF. The model calculates the expected debris impact crater distribution around LDEF as a function of debris orbital parameters. The results show that only highly elliptical, low inclination orbits could be responsible for these impacts. The most common objects left in this type of orbit are orbital transfer stages used by the U.S. and ESA to place payloads into geosynchronous orbit. Objects in this type of orbit are difficult to catalog by the U.S. Space Command; consequently there are independent reasons to believe that the catalog does not adequately represent this population. This analysis concludes that the relative number of cataloged objects with highly elliptical, low inclination orbits must be increased by a factor of 20 to be consistent with the LDEF data. Author (revised)

N93-29374*# POD Associates, Inc., Albuquerque, NM.

DAMAGE AREAS ON SELECTED LDEF ALUMINUM SURFACES c18

Cassandra R. Coombs, Dale R. Atkinson, Martha K. Allbrooks, Alan J. Watts, Corey J. Hennessy, and John D. Wagner *In* NASA. Langley Research Center, LDEF: 69 Months in Space. Second Post-Retrieval Symposium, Part 2 Apr. 1993 p 595-618 Prepared for Schafer (W. J.) Associates, Inc., Arlington, VA (For primary document see N93-29354 11-99)

(Contracts SDIO-SC-89W-26-11; SDIO-89-C-0034; POD Proj. 019202)

Avail: CASI HC A03/MF A04

With the U.S. about to embark on a new space age, the effects of the space environment on a spacecraft during its mission lifetime become more relevant. Included among these potential effects are degradation and erosion due to micrometeoroid and debris impacts, atomic oxygen and ultraviolet light exposure as well as material alteration from thermal cycling, and electron and proton exposure. This paper focuses on the effects caused by micrometeoroid and debris impacts on several LDEF aluminum plates from four different bay locations: C-12, C-10, C-01, and E-09. Each plate was coated with either a white, black, or gray thermal paint. Since the plates were located at different orientations on the satellite, their responses to the hypervelocity impacts varied. Crater morphologies range from a series of craters, spall zones, domes, spaces, and rings to simple craters with little or no spall zones. In addition, each of these crater morphologies is associated with varying damage areas, which appear to be related to their respective bay locations and thus exposure angles. More than 5% of the exposed surface area examined was damaged by impact cratering and its coincident effects (i.e., spallation, delamination and blow-off). Thus, results from this analysis may be significant for mission and spacecraft planners and designers. Author (revised)

N93-29375*# POD Associates, Inc., Albuquerque, NM.

LDEF DATA: COMPARISONS WITH EXISTING MODELS c18

Cassandra R. Coombs, Alan J. Watts, John D. Wagner, and Dale R. Atkinson *In* NASA. Langley Research Center, LDEF: 69 Months in Space. Second Post-Retrieval Symposium, Part 2 Apr. 1993 p 619-664 Prepared for Lockheed Engineering and Sciences Co., Houston, TX (For primary document see N93-29354 11-99)

(Contract SDIO-SC-02N0165768; POD Proj. 019201)

Avail: CASI HC A03/MF A04

The relationship between the observed cratering impact damage on the Long Duration Exposure Facility (LDEF) versus the existing models for both the natural environment of micrometeoroids and the man-made debris was investigated. Experimental data was provided by several LDEF Principal Investigators, Meteoroid and Debris Special Investigation Group (M&D SIG) members, and by the Kennedy Space Center Analysis Team (KSC A-Team)

members. These data were collected from various aluminum materials around the LDEF satellite. A PC (personal computer) computer program, SPENV, was written which incorporates the existing models of the Low Earth Orbit (LEO) environment. This program calculates the expected number of impacts per unit area as functions of altitude, orbital inclination, time in orbit, and direction of the spacecraft surface relative to the velocity vector, for both micrometeoroids and man-made debris. Since both particle models are couched in terms of impact fluxes versus impactor particle size, and much of the LDEF data is in the form of crater production rates, scaling laws have been used to relate the two. Also many hydrodynamic impact computer simulations were conducted, using CTH, of various impact events, that identified certain modes of response, including simple metallic target cratering, perforations and delamination effects of coatings.
Author (revised)

N93-29376*# Jet Propulsion Lab., California Inst. of Tech., Pasadena.

NEW METEOROID MODEL PREDICTIONS FOR DIRECTIONAL IMPACTS ON LDEF Abstract Only

c90

Neil Divine and Rene C. Agueero *In* NASA. Langley Research Center, LDEF: 69 Months in Space. Second Post-Retrieval Symposium, Part 2 Apr. 1993 p 665 (For primary document see N93-29354 11-99)
Avail: CASI HC A01/MF A04

An extensive body of data, from meteors, zodiacal light, spacecraft-borne impact detectors (Helios, Pioneer, Galileo, Ulysses), and other sources, forms the basis of a new numerical model for the distributions of interplanetary meteoroids. For each of the five populations in this model it is possible to evaluate meteoroid concentration and flux for oriented surfaces or detectors having arbitrary position and velocity in interplanetary space. For a spacecraft in geocentric orbit the effects of gravitational focussing and shielding by the Earth have been newly derived with full attention to the directionality of the particles, both on approach (i.e., relative to a massless Earth) and at the target. This modeling approach was exercised to provide an estimate of meteoroid fluence for each of several oriented surfaces on LDEF.
Author (revised)

N93-29377*# National Aeronautics and Space Administration. Langley Research Center, Hampton, VA.

LONG DURATION EXPOSURE FACILITY (LDEF) ATTITUDE MEASUREMENTS OF THE INTERPLANETARY DUST EXPERIMENT

c90

Philip C. Kassel, Jr., William R. Motley, III, S. Fred Singer (Institute for Space Science and Technology, Inc., Gainesville, FL.), J. Derral Mulholland (Institute for Space Science and Technology, Inc., Gainesville, FL.), John P. Oliver (Institute for Space Science and Technology, Inc., Gainesville, FL.), Jerry L. Weinberg (Institute for Space Science and Technology, Inc., Gainesville, FL.), William J. Cooke (Institute for Space Science and Technology, Inc., Gainesville, FL.), and Jim J. Wortman (North Carolina Univ., Raleigh.) *In its* LDEF: 69 Months in Space. Second Post-Retrieval Symposium, Part 2 Apr. 1993 p 667-675 (For primary document see N93-29354 11-99)
Avail: CASI HC A02/MF A04

Analysis of the data from the Long Duration Exposure Facility (LDEF) Interplanetary Dust Experiment (IDE) sun sensors has allowed a confirmation of the attitude of LDEF during its first year in orbit. Eight observations of the yaw angle at specific times were made and are tabulated in this paper. These values range from 4.3 to 12.4 deg with maximum uncertainty of plus or minus 2.0 deg and an average of 7.9 deg. No specific measurements of pitch or roll were made but the data indicates that LDEF had an average pitch down attitude of less than 0.7 deg.
Author (revised)

N93-29378*# Institute for Space Science and Technology, Inc., Gainesville, FL.

ELEMENTAL ANALYSES OF HYPERVELOCITY MICROPARTICLE IMPACT SITES ON INTERPLANETARY DUST EXPERIMENT SENSOR SURFACES

c90

Charles G. Simon, J. L. Hunter (North Carolina Univ., Raleigh.), D. P. Griffis (North Carolina Univ., Raleigh.), V. Misra (North Carolina Univ., Raleigh.), D. A. Ricks (North Carolina Univ., Raleigh.), Jim J. Wortman (North Carolina Univ., Raleigh.), and D. E. Brownlee (Washington Univ., Seattle.) *In* NASA. Langley Research Center, LDEF: 69 Months in Space. Second Post-Retrieval Symposium, Part 2 Apr. 1993 p 677-692 (For primary document see N93-29354 11-99)
Avail: CASI HC A03/MF A04

The Interplanetary Dust Experiment (IDE) had over 450 electrically active ultra-high purity metal-oxide-silicon impact detectors located on the six primary sides of the Long Duration Exposure Facility (LDEF). Hypervelocity microparticles (approximately 0.2 to approximately 100 micron diameter) that struck the active sensors with enough energy to break down the 0.4 or 1.0 micron thick SIO2 insulator layer separating the silicon base (the negative electrode), and the 1000 A thick surface layer of aluminum (the positive electrode) caused electrical discharges that were recorded for the first year of orbit. The high purity Al-SiO2-Si substrates allowed detection of trace (ppm) amounts of hypervelocity impactor residues. After sputtering through a layer of surface contamination, secondary ion mass spectrometry (SIMS) was used to create two-dimensional elemental ion intensity maps of microparticle impact sites on the IDE sensors. The element intensities in the central craters of the impacts were corrected for relative ion yields and instrumental conditions and then normalized to silicon. The results were used to classify the particles' origins as 'manmade,' 'natural,' or 'indeterminate.' The last classification resulted from the presence of too little impactor residue, analytical interference from high background contamination, the lack of information on silicon and aluminum residues, or a combination of these circumstances. Several analytical 'blank' discharges were induced on flight sensors by pressing down on the sensor surface with a pure silicon shard. Analyses of these blank discharges showed that the discharge energy blasts away the layer of surface contamination. Only Si and Al were detected inside the discharge zones, including the central craters of these features. Thus far a total of 79 randomly selected microparticle impact sites from the six primary sides of the LDEF have been analyzed: 36 from tray C-9 (Leading (ram), or East, side), 18 from tray C-3 (Trailing (wake), or West, side), 12 from tray B-12 (North side), 4 from tray D-6 (South side), 3 from tray H-11 (Space end), and 6 from tray G-10 (Earth end). Residue from manmade debris was identified in craters on all trays. (Aluminum oxide particle residues were not detectable on the Al/Si substrates.) These results were consistent with the IDE impact record which showed highly variable long term microparticle impact flux rates on the West, Space and Earth sides of the LDEF which could not be ascribed to astronomical variability of micrometeorite density. The IDE record also showed episodic bursts of microparticle impacts on the East, North, and South sides of the satellite, denoting passage through orbital debris clouds or rings.
Author (revised)

N93-29379*# National Aeronautics and Space Administration. Langley Research Center, Hampton, VA.

LONG-TERM MICROPARTICLE FLUX VARIABILITY INDICATED BY COMPARISON OF INTERPLANETARY DUST EXPERIMENT (IDE) TIMED IMPACTS FOR LDEF'S FIRST YEAR IN ORBIT WITH IMPACT DATA FOR THE ENTIRE 5.77-YEAR ORBITAL LIFETIME

c90

Charles G. Simon (Institute for Space Science and Technology, Inc., Gainesville, FL.), J. Derral Mulholland (Institute for Space Science and Technology, Inc., Gainesville, FL.), John P. Oliver (Institute for Space Science and Technology, Inc., Gainesville, FL.), William J. Cooke (Institute for Space Science and Technology, Inc., Gainesville, FL.), and Philip C. Kassel, Jr. *In its* LDEF: 69 Months in Space. Second Post-Retrieval Symposium, Part 2 Apr. 1993 p 693-703 (For primary document see N93-29354 11-99)
(Grant NAG1-1218)
Avail: CASI HC A03/MF A04

The electronic sensors of the Interplanetary Dust Experiment (IDE) recorded precise impact times and approximate directions for submicron to approximately 100 micron size particles on all six primary sides of the spacecraft for the first 346 days of the LDEF orbital mission. Previously-reported analyses of the timed impact data have established their spatio-temporal features, including the demonstration that a preponderance of the particles in this regime are orbital debris and that a large fraction of the debris particles are encountered in megameter-size clouds. Short-term fluxes within such clouds can rise several orders of magnitude above the long-term average. These unexpectedly large short-term variations in debris flux raise the question of how representative an indication of the multi-year average flux is given by the nearly one year of timed data. One of the goals of the IDE was to conduct an optical survey of impact sites on detectors that remained active during the entire LDEF mission, to obtain full-mission fluxes. We present here the comparisons and contrasts among the new IDE optical survey impact data, the IDE first-year timed impact data, and impact data from other LDEF micrometeoroid and debris experiments. The following observations are reported: (1) the 5.77 year long-term integrated microparticle impact fluxes recorded by IDE detectors matched the integrated impact fluxes measured by other LDEF investigators for the same period; (2) IDE integrated microparticle impact fluxes varied by factors from 0.5 to 8.3 for LDEF days 1-346, 347-2106 and 1-2106 (5.77 years) on rows 3 (trailing edge, or West), 6 (South side), 12 (North side), and the Earth and Space ends; and (3) IDE integrated microparticle impact fluxes varied less than 3 percent for LDEF days 1-346, 347-2106 and 1-2106 (5.77 years) on row 9 (leading edge, or East). These results give further evidence of the accuracy and internal consistency of the recorded IDE impact data. This leads to the further conclusion that the utility of long-term ratios for impacts on various sides of a stabilized satellite in low Earth orbit (LEO) is extremely limited. These observations and their consequences highlight the need for continuous, real time monitoring of the dynamic microparticle environment in LEO. Author (revised)

N93-29380*# Bern Univ. (Switzerland). Physikalisches Inst.
THE INTERSTELLAR GAS EXPERIMENT: ANALYSIS IN PROGRESS **c90**
F. Buehler, D. L. Lind (Utah State Univ., Logan.), J. Geiss, and O. Eugster *In* NASA. Langley Research Center, LDEF: 69 Months in Space. Second Post-Retrieval Symposium, Part 2 Apr. 1993 p 705-723 (For primary document see N93-29354 11-99)
Avail: CASI HC A03/MF A04

The Interstellar Gas Experiment (IGE) exposed thin metallic foils aboard the LDEF spacecraft in low Earth orbit in order to collect neutral interstellar particles which penetrate the solar system due to their motion relative to the sun. By mechanical penetration these atoms were imbedded in the collecting foils along with precipitating magnetospheric ions and, possibly, with ambient atmospheric atoms. During the entire LDEF mission, seven of these foils collected particles arriving from seven different directions as seen from the spacecraft. After the foils were returned to Earth, a mass spectrometric analysis of the noble gas component of the trapped particles was begun. The isotopes of He-3, He-4, Ne-20, and Ne-22 were detected. We have given a first account of the experiment. In order to infer the isotopic ratios in the interstellar medium from the concentrations found in the foils, several lines of investigation had to be initiated. The flux of ambient atmospheric noble gas atoms moving toward the foils due to the orbital motion of LDEF was estimated by detailed calculations. Any of these particles which evaded the baffles in the IGE collector could be entrapped in the foils as a background flux. However, the calculations have shown that this flux is negligible, which was the intent of the experiment hardware design. This conclusion is supported by the measurements. However, both the concentration of trapped helium and its impact energy indicate that the flux of magnetospheric ions which was captured was larger than had been expected. In fact, it appears that the magnetospheric particles constitute the largest fraction of the particles in the foils. Since little is known about this particle flux, their presence in the IGE foils appears fortunate. The analysis of these particles provides information about their isotropic composition and average flux. Author (revised)

N93-29381*# Technical Univ. of Denmark, Lyngby. Physics Lab.
FOLLOW UP ON THE CRYSTAL GROWTH EXPERIMENTS OF THE LDEF **c76**
K. F. Nielsen and M. D. Lind (Rockwell International Science Center, Thousand Oaks, CA.) *In* NASA. Langley Research Center, LDEF: 69 Months in Space. Second Post-Retrieval Symposium, Part 2 Apr. 1993 p 725-733 (For primary document see N93-29354 11-99)
Avail: CASI HC A02/MF A04

The results of the 4 solution growth experiments on the LDEF have been published elsewhere. Both the crystals of CaCO3, which were large and well shaped, and the much smaller TTF-TCNQ crystals showed unusual morphological behavior. The follow up on these experiments was begun in 1981, when ESA initiated a 'Concept Definition Study' on a large, 150 kg, Solution Growth Facility (SGF) to be included in the payload of EURECA-1, the European Retrievable Carrier. This carrier was a continuation of the European Spacelab and at that time planned for launch in 1987. The long delay of the LDEF retrieval and of subsequent missions brought about reflections both on the concept of crystal growth in space and on the choice of crystallization materials that had been made for the LDEF. Already before the LDEF retrieval, research on TTF-TCNQ had been stopped, and a planned growth experiment with TTF-TCNQ on the SGF/EURECA had been cancelled. The target of the SGF investigation is now more fundamental in nature. None of the crystals to be grown here are, like TTF-TCNQ, in particular demand by science or industry, and the crystals only serve the purpose of model crystals. The real purpose of the investigation is to study the growth behavior. One of the experiments, the Soret Coefficient Measurement experiment is not growing crystals at all, but has it as its sole purpose to obtain accurate information on thermal diffusion, a process of importance in crystal growth from solution. Author (revised)

N93-29452*# National Aeronautics and Space Administration, Washington, DC.
RESEARCH AND TECHNOLOGY OBJECTIVES AND PLANS: SUMMARY FISCAL YEAR 1991
Mar. 1991 164 p
(NASA-TM-103086; NAS 1.15:103086) Avail: CASI HC A08/MF A02

This publication represents the NASA research and technology program for FY 1991. It is a compilation of the Summary portions of each of the RTOP's (Research and Technology Objectives and Plans) used for management review and control of research currently in progress throughout NASA. The RTOP Summary is designed to facilitate communication and coordination among concerned technical personnel in government, industry, and in universities. The first section contains citations and abstracts of the RTOP's and is followed by four indexes: Subject, Technical Monitor, Responsible NASA Organization, and RTOP Number. Author

N93-29500# European Space Agency, Paris (France).
THE PREHISTORY OF ESRO, 1959 - 1960
John Krige (European Univ. Inst., Florence, Italy.) Jul. 1992 35 p
(ESA-HSR-1) Avail: CASI HC A03/MF A01

The origins of a joint European space effort are generally traced back to a number of initiatives taken in 1959 and 1960 by a small group of scientists and science administrators, catalyzed by two friends, physicists and scientific statesmen, Edoardo Amaldi and Pierre Auger. Neither Amaldi nor Auger was a stranger to the cause of scientific collaboration on a European scale. Indeed it was they who, in the early 1950s, were key actors in the process which led to the setting up of CERN, the European Organization for Nuclear Research. Now, as the decade drew to a close, they turned their attention to space. Success was rapid. Within a year of the first formal discussions being held amongst scientists European governments had set up a preparatory commission to explore the possibilities for a joint space research effort. The most striking feature of the story presented here is the transformation of the scientist's original project into one which was more modest in scope- and over which they could hope to retain a large measure of control. Various aspects of the project transformation are presented. Author (revised)

N93-29621*# National Aeronautics and Space Administration. Langley Research Center, Hampton, VA.
LDEF: 69 MONTHS IN SPACE. PART 1: SECOND POST-RETRIEVAL SYMPOSIUM
Arlene S. Levine, ed. Apr. 1993 276 p Symposium held in San Diego, CA, 1-5 Jun. 1992; sponsored by NASA, and AIAA
(RTOP 506-48-91-11)
(NASA-CP-3194-Pt-1; L-17196-Pt-1; NAS 1.55:3194-Pt-1) Avail: CASI HC A13/MF A03

A compilation of papers presented at the Second Long Duration Exposure Facility (LDEF) Post-Retrieval Symposium is included. The papers represent the data analysis of the 57 experiments flown on the LDEF. The experiments include materials, coatings, thermal systems, power and propulsion, science (cosmic ray, interstellar gas, heavy ions, micrometeoroid, etc.), electronics, optics, and life sciences. For individual titles, see N93-29622 through N93-29646.

N93-29622*# National Aeronautics and Space Administration. Marshall Space Flight Center, Huntsville, AL.
REFINEMENTS ON THE PINHOLE CAMERA MEASUREMENTS OF THE LDEF ATTITUDE **c18**

Palmer N. Peters, Paul N. Whitehouse, and John C. Gregory (Alabama Univ., Huntsville.) *In* NASA. Langley Research Center, LDEF: 69 Months in Space. Part 1: Second Post-Retrieval Symposium Apr. 1993 p 3-12 (For primary document see N93-29621 11-99)
Avail: CASI HC A02/MF A03

The results from the University of Alabama in Huntsville (UAH) pinhole camera were reanalyzed to include the effects of corotation of the atmosphere with the Earth as well as satellite oscillation. Previous results from the instrument showed that the satellite had stable attitude offsets in yaw of 8.0 deg and 1.0 deg in pitch; these offsets are unchanged by the present analysis. The primary impact zone of oxygen, i.e., the directly exposed spot on a silver detector, had a ratio of major to minor axes equal to 1.05, which was interpreted as being caused by a small oscillation of plus or minus 0.35 degrees (with precision plus or minus 0.15 degrees). The present analysis shows that the observed effect can largely be accounted for by atmospheric corotation, but that an additional oscillation in yaw of the order of a degree cannot be excluded. The sensitivity of the pinhole camera to satellite oscillations is shown to decrease nonlinearly with decreasing magnitude of the oscillation and to vary inversely with the gas temperature. Author (revised)

N93-29623*# Boeing Defense and Space Group, Seattle, WA.
LDEF MICROENVIRONMENTS, OBSERVED AND PREDICTED c18
R. J. Bourassa, H. G. Pippin, and J. R. Gillis *In* NASA. Langley Research Center, LDEF: 69 Months in Space. Part 1: Second Post-Retrieval Symposium Apr. 1993 p 13-25 (For primary document see N93-29621 11-99)
(Contract NAS1-19247)
Avail: CASI HC A03/MF A03

A computer model for prediction of atomic oxygen exposure of spacecraft in low earth orbit, referred to as the primary atomic oxygen model, was originally described at the First Long Duration Exposure Facility (LDEF) Post-Retrieval Symposium. The primary atomic oxygen model accounts for variations in orbit parameters, the condition of the atmosphere, and for the orientation of exposed surfaces relative to the direction of spacecraft motion. The use of the primary atomic oxygen model to define average atomic oxygen exposure conditions for a spacecraft is discussed and a second microenvironments computer model is described that accounts for shadowing and scattering of atomic oxygen by complex surface protrusions and indentations. Comparisons of observed and predicted erosion of fluorinated ethylene propylene (FEP) thermal control blankets using the models are presented. Experimental and theoretical results are in excellent agreement. Work is in progress to expand modeling capability to include ultraviolet radiation exposure and to obtain more detailed information on reflecting and scattering characteristics of material surfaces. Author (revised)

N93-29624*# Lockheed Engineering and Sciences Co., Hampton, VA.
A GENERALIZED APPROACH TO THE THERMAL ANALYSIS OF THE LONG DURATION EXPOSURE FACILITY'S FLIGHT EXPERIMENTS c34
Thomas R. Sampair *In* NASA. Langley Research Center, LDEF: 69 Months in Space. Part 1: Second Post-Retrieval Symposium Apr. 1993 p 27-50 (For primary document see N93-29621 11-99)
Avail: CASI HC A03/MF A03

The generalized method employed in the thermal analysis of a Long Duration Exposure Facility (LDEF) flight experiment is presented. The method consists of thermal math model development, defining the orbital heating rates, and applying the appropriate temperature boundary conditions. This approach has proven to be an accurate method for predicting experiment component temperatures for the worst case orbital environments and calculating daily average component temperatures for any part or all time portions of the 5.8 year mission. The application of this method to the thermal analysis of the Ultra-Heavy Cosmic-Ray Nuclei experiment (UHCRE) is presented as an example of this approach. Author

N93-29625*# National Aeronautics and Space Administration. Goddard Space Flight Center, Greenbelt, MD.
EnviroNET: ON-LINE INFORMATION FOR LDEF c82
Michael Lauriente *In* NASA. Langley Research Center, LDEF: 69 Months in Space. Part 1: Second Post-Retrieval Symposium 51-67 (SEE N93-29621 11-99) Apr. 1993 (For primary document see N93-29621 11-99)
Avail: CASI HC A03/MF A03

EnviroNET is an on-line, free-form database intended to provide a centralized repository for a wide range of technical information on environmentally induced interactions of use to Space Shuttle customers and spacecraft designers. It provides a user-friendly, menu-driven format on networks that are connected globally and is available twenty-four hours a day - every day. The information, updated regularly, includes expository text, tabular numerical data, charts and graphs, and models. The system pools space data collected over the years by NASA, USAF, other government research facilities, industry, universities, and the European Space Agency. The models accept parameter input from the user, then calculate and display the derived values corresponding to that input. In addition to the archive, interactive graphics programs are also available on space debris, the neutral atmosphere, radiation, magnetic fields, and the ionosphere. A user-friendly, informative interface is standard for all the models and includes a pop-up help window with information on inputs, outputs, and caveats. The system will eventually simplify mission analysis with analytical tools and deliver solutions for computationally intense graphical applications to do 'What if...' scenarios. A proposed plan for developing a repository of information from the Long Duration Exposure Facility (LDEF) for a user group is presented. Author (revised)

N93-29626*# National Aeronautics and Space Administration. Marshall Space Flight Center, Huntsville, AL.
STATUS OF LDEF IONIZING RADIATION MEASUREMENTS AND ANALYSIS c93
Thomas A. Parnell *In* NASA. Langley Research Center, LDEF: 69 Months in Space. Part 1: Second Post-Retrieval Symposium Apr. 1993 p 69-78 (For primary document see N93-29621 11-99)
Avail: CASI HC A02/MF A03

At this symposium significant new data and analyses were reported in cosmic ray research, radiation dosimetry, induced radioactivity, and radiation environment modeling. Measurements of induced radioactivity and absorbed dose are nearly complete, but much analysis and modeling remains. Measurements and analyses of passive nuclear track detectors (PNTD), used to derive the cosmic ray composition and spectra, and linear energy transfer (LET) spectra, are only a few percent complete, but important results have already emerged. As one might expect at this stage of the research, some of the new information has produced questions rather than answers. Low-energy heavy nuclei detected by two experiments are not compatible with known solar or cosmic components. Various data sets on absorbed dose are not consistent, and a new trapped proton environment model does not match the absorbed dose data. A search for cosmogenic nuclei other than Be-7 on Long Duration Exposure Facility (LDEF) surfaces has produced an unexpected result, and some activation data relating to neutrons is not yet understood. Most of these issues will be resolved by the analysis of further experiment data, calibrations, or the application of the large LDEF data set that offers alternate data or analysis techniques bearing on the same problem. The scope of the papers at this symposium defy a compact technical summary. I have attempted to group the new information that I noted into the following groups: induced radioactivity; absorbed dose measurements; LET spectra and heavy ion dosimetry; environment modeling and three dimensional shielding effects; cosmogenic nuclei; and cosmic rays and other heavy ions. The papers generally are expository and have excellent illustrations, and I refer to their figures rather than reproduce them here. The general program and objectives of ionizing radiation measurements and analyses on LDEF has been described previously. Author (revised)

N93-29627*# Pacific Northwest Lab., Richland, WA.
SENSITIVITY OF LDEF FOIL ANALYSES USING ULTRA-LOW BACKGROUND GERMANIUM VS. LARGE NaI(Tl) MULTIDIMENSIONAL SPECTROMETERS c25
James H. Reeves, Richard J. Arthur, and Ronald L. Brodzinski *In* NASA. Langley Research Center, LDEF: 69 Months in Space. Part 1: Second Post-Retrieval Symposium Apr. 1993 p 79-86 (For primary document see N93-29621 11-99)
(Contract DE-AC06-76RL-01830)
Avail: CASI HC A02/MF A03

Cobalt foils and stainless steel samples were analyzed for induced Co-60 activity with both an ultra-low background germanium gamma-ray spectrometer and with a large NaI(Tl) multidimensional spectrometer, both of which use electronic anticoincidence shielding to reduce background counts resulting from cosmic rays. Aluminum samples were analyzed for Na-22. The results, in addition to the relative sensitivities and precisions afforded by the two methods, are presented. Author (revised)

N93-29628*# Los Alamos National Lab., NM. Space Science and Technology Div.
RADIOACTIVITIES INDUCED IN SOME LDEF SAMPLES c72
Robert C. Reedy, Calvin E. Moss, S. George Bobias, and Jozef Masarik *In* NASA. Langley Research Center, LDEF: 69 Months in Space. Part 1: Second Post-Retrieval Symposium Apr. 1993 p 87-96 (For primary document see N93-29621 11-99)
Avail: CASI HC A02/MF A03

Radioactivities induced in several Long Duration Exposure Facilities (LDEF) samples were measured by low-level counting at Los Alamos and elsewhere. These radionuclides have activities similar to those observed in meteorites and lunar samples. Some trends were observed in these measurements in terms of profiles in trunnion layers and as a function of radionuclide half-life. Several existing computer codes were used to model the production by the protons trapped in the Earth's radiation belts and by the galactic cosmic rays of some of these radionuclides, Mn-54 and Co-57 in steel, Sc-46 in titanium, and Na-22 in alloys of titanium and aluminum. Production rates were also calculated for radionuclides possibly implanted in LDEF, Be-7, Be-10, and C-14. Enhanced concentrations of induced isotopes in the surfaces of trunnion sections relative to their concentrations in the center are caused by the lower-energy protons in the trapped radiation. Secondary neutrons made by high-energy trapped protons and by galactic cosmic rays produce much of the observed radioactivities, especially deep in an object. Comparisons of the observed to calculated activities of several radionuclides with different half-lives indicate that the flux of trapped protons at LDEF decreased significantly at the end of the mission. Author (revised)

N93-29629*# California Univ., Berkeley. Lawrence Berkeley Lab. Engineering Div.
A PHOTON PHREAK DIGS THE LDEF HAPPENING c72
Alan R. Smith and Donna L. Hurley *In* NASA. Langley Research Center, LDEF: 69 Months in Space. Part 1: Second Post-Retrieval Symposium Apr. 1993 p 97-105 (For primary document see N93-29621 11-99)
(Contract NASA Order H-06815-D; DE-AC03-76SF-00098)
Avail: CASI HC A02/MF A03

A year ago at the First Long Duration Exposure Facility (LDEF) Post-Retrieval Symposium, detailed measurements on trunnion sections, as well as results from 'intentional' samples (Co, Ni, In, Ta, and V) and spacecraft parts were reported. For this year's Symposium, some of these findings are re-evaluated in combination with more recent results, to cast a longer perspective on the LDEF experience, and to sketch some promising avenues toward more effective participation in future missions. The LDEF analysis effort has been a superb training exercise, from which lessons learned need to be applied to future missions - right back to the early phases of mission planning. Author (revised)

N93-29630*# Massachusetts Inst. of Tech., Cambridge. Nuclear Reactor Lab.
CHARGED PARTICLE ACTIVATION STUDIES ON THE SURFACE OF LDEF SPACECRAFT c72
Ilhan Olmez, Forest Burns (Army Materials Technology Lab., Watertown, MA.), and Paul Sagalyn (Army Materials Technology Lab., Watertown, MA.) *In* NASA. Langley Research Center, LDEF: 69 Months in Space. Part 1: Second Post-Retrieval Symposium Apr. 1993 p 107-109 (For primary document see N93-29621 11-99)
Avail: CASI HC A01/MF A03

High energy proton induced nuclear reaction products are examined using seven elements, namely, Aluminum, Silicon, Nickel, Copper, Zirconium, Tantalum, and Tungsten. The samples were in the form of plates, 2 x 2 x 1/8 inches. Activities due to Na-22 from Al, Co-56 and Co-57 from Ni, Co-58 from Cu, and Y-88 from Zr targets were detected. No induced activity was observed in Si, Ta, and W, most probably due to the long cooling times. Only the Zr sample contained a weak Be-7 peak, although Ta and W were also located at the leading edge of the spacecraft. Gamma-rays of individual isotopes were measured using high-resolution Ge(Li) solid state detector coupled to 4096-multichannel analyzer. Activities were calculated for Co-56 (846 keV) and Co-57 (122 and 136 keV's) at the time of the entry of the spacecraft and found to be 0.014 plus or minus 0.005 c/sec. g, 0.018 plus or minus 0.002 c/sec. g, and 0.0024 plus or minus 0.0007 c/sec. g, respectively. Author (revised)

N93-29631*# National Aeronautics and Space Administration. Marshall Space Flight Center, Huntsville, AL.
COLLECTION, ANALYSIS, AND ARCHIVAL OF LDEF ACTIVATION DATA c82
C. E. Laird (University of Eastern Kentucky, Richmond.), B. A. Harmon, G. J. Fishman, and T. A. Parnell *In* NASA. Langley Research Center, LDEF: 69 Months in Space. Part 1: Second Post-Retrieval Symposium Apr. 1993 p 111-124 (For primary document see N93-29621 11-99)
(NASA Order H-08071-D; NASA Order H-13029-D)
Avail: CASI HC A03/MF A03

The study of the induced radioactivity of samples intentionally placed aboard the Long Duration Exposure Facility (LDEF) and samples obtained from the LDEF structure is reviewed. The eight laboratories involved in the gamma-ray counting are listed and the scientists and the associated counting facilities are described. Presently, most of the gamma-ray counting has been completed and the spectra are being analyzed and corrected for efficiency and self absorption. The acquired spectra are being collected at Eastern Kentucky University for future reference. The results of these analyses are being compiled and reviewed for possible inconsistencies as well as for comparison with model calculations. These model calculations are being revised to include the changes in trapped-proton flux caused by the onset of the period of maximum solar activity and the rapidly decreasing spacecraft orbit. Tentative plans are given for the storage of the approximately 1000 gamma-ray spectra acquired in this study and the related experimental data. Author

N93-29632*# National Aeronautics and Space Administration. Marshall Space Flight Center, Huntsville, AL.
INDUCED ACTIVATION STUDY OF LDEF c72
B. A. Harmon, G. J. Fishman, T. A. Parnell, and C. E. Laird (University of Eastern Kentucky, Richmond.) *In* NASA. Langley Research Center, LDEF: 69 Months in Space. Part 1: Second Post-Retrieval Symposium Apr. 1993 p 125-136 (For primary document see N93-29621 11-99)
Avail: CASI HC A03/MF A03

Analysis of the induced radioactivity of the Long Duration Exposure Facility (LDEF) is continuing with extraction of specific activities for various spacecraft materials. Data and results of activation measurements from eight facilities are being collected for interpretation at Eastern Kentucky University and NASA/Marshall Space Flight Center. The major activation mechanism in LDEF components is the proton flux in the South Atlantic Anomaly (SAA). This flux is highly anisotropic, and could be sampled by taking advantage of the gravity-gradient stabilization of the LDEF. The directionally-dependent activation due to these protons was clearly observed in the data from aluminum experiment tray clamps (reaction product Na-22), steel trunnions (reaction product Mn-54 and others) and is also indicated by the presence of a variety of nuclides in other materials. A secondary production mechanism, thermal neutron capture, was observed in cobalt, indium, and tantalum, which are known to have large capture cross sections. Experiments containing samples of these metals and significant amounts of thermalizing low atomic number (Z) material showed clear evidence of enhanced activation of Co-60, In-114m, and Ta-182. Other mechanisms which activate spacecraft material that are not as easily separable from SAA proton activation, such as galactic proton bombardment and secondary production by fast neutrons, are being investigated by comparison to radiation environmental calculations. Deviations from one-dimensional radiation models indicate that these mechanisms are more important at greater shielding depths. The current status of the induced radioactivity measurements as of mid-year 1992 are reviewed. Specific activities for a number of materials which show SAA effects and thermal neutron capture are presented. The results for consistency by combining data from the participating institutions is also examined. Author (revised)

N93-29633*# National Aeronautics and Space Administration. Marshall Space Flight Center, Huntsville, AL.
REVISED PREDICTION OF LDEF EXPOSURE TO TRAPPED PROTONS c72
John W. Watts, T. W. Armstrong (Science Applications International Corp., Prospect, TN.), and B. L. Colborn (Science Applications International Corp.,

Prospect, TN.) *In* NASA. Langley Research Center, LDEF: 69 Months in Space. Part 1: Second Post-Retrieval Symposium Apr. 1993 p 137-145 (For primary document see N93-29621 11-99)
Avail: CASI HC A02/MF A03

The Long Duration Exposure Facility (LDEF) spacecraft flew in a 28.5 deg inclination circular orbit with an altitude in the range from 319.4 to 478.7 km. For this orbital altitude and inclination, two components contribute most of the penetrating charge particle radiation encountered - the galactic cosmic rays and the geomagnetically trapped Van Allen protons. Where shielding is less than 1.0 g/sq cm geomagnetically trapped electrons make a significant contribution. The 'Vette' models together with the associated magnetic field models and the solar conditions were used to obtain the trapped electron and proton omnidirectional fluences reported previously. Results for directional proton spectra using the MSFC anisotropy model for solar minimum and 463 km altitude (representative for the LDEF mission) were also reported. The directional trapped proton flux as a function of mission time is presented considering altitude and solar activity variation during the mission. These additional results represent an extension of previous calculations to provide a more definitive description of the LDEF trapped proton exposure. Author (revised)

N93-29634*# Aerospace Corp., Los Angeles, CA. Space and Environment Technology Center.
A MEASUREMENT OF THE RADIATION DOSE TO LDEF BY PASSIVE DOSIMETRY **c72**
J. B. Blake and S. S. Imamoto *In* NASA. Langley Research Center, LDEF: 69 Months in Space. Part 1: Second Post-Retrieval Symposium Apr. 1993 p 147-155 (For primary document see N93-29621 11-99)
(Contract F04701-88-C-0089)
Avail: CASI HC A02/MF A03

The results from a pair of thermoluminescent dosimeter experiments flown aboard the Long Duration Exposure Facility (LDEF) show an integrated dose several times smaller than that predicted by the NASA environmental models for shielding thicknesses much greater than 0.10 gm/sq cm aluminum. For thicknesses between 0.01 and 0.1 gm/sq cm, the measured dose was in agreement with predictions. The Space and Environment Technology Center of The Aerospace Corporation fielded two related experiments on LDEF to measure the energetic radiation dose by means of passive dosimetry. The sensors were LiF thermoluminescent dosimeters mounted behind various thicknesses of shielding. The details of the experiment are described first, followed by the results of the observations. A comparison is made with the predictions based upon the NASA environmental models and the actual mission profile flown by LDEF; conclusions follow. Author (revised)

N93-29635*# Departement d'Etudes et de Recherches en Technologie Spatiale, Toulouse (France).
LDEF: DOSIMETRIC MEASUREMENT RESULTS (AO 138-7 EXPERIMENT) **c72**
J. Bourrieau *In* NASA. Langley Research Center, LDEF: 69 Months in Space. Part 1: Second Post-Retrieval Symposium Apr. 1993 p 157-162 (For primary document see N93-29621 11-99)
Avail: CASI HC A02/MF A03

One of the objectives of the AO 138-7 experiment on board the Long Duration Exposure Facility (LDEF) was a total dose measurement with Thermo Luminescent Detectors (TLD 100). Two identical packages, both of them including five TLD's inside various aluminum shields, are exposed to the space environment in order to obtain the absorbed dose profile. Radiation fluence received during the total mission length was computed, taking into account the trapped particles (AE8 and AP8 models during solar maximum and minimum periods) and the cosmic rays; due to the magnetospheric shielding the solar proton fluences are negligible on the LDEF orbit. The total dose induced by these radiations inside a semi infinite plane shield of aluminum are computed with the radiation transport codes available at DERTS. The dose profile obtained is in good agreement with the evaluation by E.V. Benton. TLD readings are performed after flight; due to the mission duration increase a post flight calibration was necessary in order to cover the range of the in flight induced dose. The results obtained, similar (plus or minus 30 percent) for both packages, are compared with the dose profile computation. For thick shields it seems that the measurements exceed the forecast (about 40 percent). That can be due to a cosmic ray and trapped proton contributions coming from the backside (assumed as perfectly shielded by the LDEF structure in the computation), or to an underestimate of the proton or cosmic ray fluences. A fine structural shielding analysis should be necessary in order to determine the origin of this slight discrepancy between forecast and in flight measurements. For the less shielded dosimeters, mainly exposed to the trapped electron flux, a slight overestimation of the dose (less than 40 percent) appears. Due to the dispersion of the TLD's response, this cannot be confirmed. In practice these results obtained on board LDEF, with less than a factor 1.4 between measurements and forecast, reinforce the validity of the computation methods and models used for the long term evaluation of the radiation levels (flux and dose) encountered in space on low inclination and altitude Earth orbits. Author (revised)

N93-29636*# Eril Research, Inc., San Rafael, CA.
ABSORBED DOSE MEASUREMENTS AND PREDICTIONS ON LDEF **c72**
A. L. Frank, E. V. Benton, T. W. Armstrong (Science Applications International Corp., Prospect, TN.), and B. L. Colborn (Science Applications International Corp., Prospect, TN.) *In* NASA. Langley Research Center, LDEF: 69 Months in Space. Part 1: Second Post-Retrieval Symposium Apr. 1993 p 163-170 (For primary document see N93-29621 11-99)
(Contract NAS8-38610)
Avail: CASI HC A02/MF A03

The overall radiation environment of the Long Duration Exposure Facility (LDEF) was determined in part through the use of thermoluminescent detectors (TLD's) which were included in several experiments. The results given are from four experiments (A0015 Biostack, M0004 Fiber Optics Data Link, P0004 Seeds in Space, and P0006 Linear Energy Transfer Spectrum Measurement) and represent a large fraction of existing absorbed dose data. The TLD's were located on the leading and the trailing edges and the Earth end of the spacecraft under various shielding depths (0.48 to 15.4 g/sq cm). The measured absorbed doses were found to reflect both directional dependence of incident trapped protons and shielding. At the leading edge, doses ranged from 2.10 to 2.58 Gy under shielding of 2.90 to 1.37 g/sq cm Al equivalent (M0004). At the trailing edge, doses varied from 3.04 to 4.49 Gy under shielding of 11.7 to 3.85 g/sq cm (A0015), doses varied from 2.91 to 6.64 Gy under shielding of 11.1 to 0.48 g/sq cm (P0004), and a dose range of 2.66 to 6.48 Gy was measured under shielding of 15.4 to 0.48 g/sq cm (P0006). At the Earth end of the spacecraft, doses from 2.41 to 3.93 Gy were found under shielding of 10.0 to 1.66 g/sq cm (A0015). The effect of the trapped proton anisotropy was such that the western side of LDEF received more than 2 times the dose of the eastern side at shielding depths of approximately 1 g/sq cm. Calculations utilizing a directional model of trapped proton spectra predict smaller doses than those measured, being about 50 percent of measured values at the trailing edge and Earth end, and about 80 percent near the leading edge. Author (revised)

N93-29637*# National Aeronautics and Space Administration. Marshall Space Flight Center, Huntsville, AL.
LET SPECTRA MEASUREMENTS OF CHARGED PARTICLES IN THE P0006 EXPERIMENT ON LDEF **c72**
E. V. Benton (San Francisco Univ., CA.), I. Csige (San Francisco Univ., CA.), K. Oda (San Francisco Univ., CA.), R. P. Henke (San Francisco Univ., CA.), A. L. Frank (San Francisco Univ., CA.), E. R. Benton (San Francisco Univ., CA.), L. A. Frigo (San Francisco Univ., CA.), T. A. Parnell, J. W. Watts, Jr., and J. H. Derrickson *In* NASA. Langley Research Center, LDEF: 69 Months in Space. Part 1: Second Post-Retrieval Symposium Apr. 1993 p 171-180 (For primary document see N93-29621 11-99)
(Grant NAG8-168)
Avail: CASI HC A02/MF A03

Measurements are under way of the charged particle radiation environment of the Long Duration Exposure Facility (LDEF) satellite using stacks of plastic nuclear track detectors (PNTD's) placed in different locations of the satellite. In the initial work the charge, energy, and linear energy transfer (LET) spectra of charged particles were measured with CR-39 double layer PNTD's located on the west side of the satellite (Experiment P0006). Primary and secondary stopping heavy ions were measured separately from the more energetic particles. Both trapped and galactic cosmic ray (GCR) particles are included, with the latter component being dominated by relativistic iron particles. The results from the P0006 experiment will be compared with similar measurements in other locations on LDEF with different orientation and shielding conditions. The remarkably detailed investigation of the charged particle radiation environment of the LDEF satellite will lead to a better understanding of the radiation environment of the Space Station Freedom. It will enable more accurate prediction of single event upsets (SEU's) in microelectronics and, especially, more accurate assessment of the risk - contributed by different components of the radiation field (GCR's, trapped protons, secondaries and heavy recoils, etc.) - to the health and safety of crew members. Author (revised)

N93-29638*# Eril Research, Inc., San Rafael, CA.
LIGHT-HEAVY ION MEASUREMENTS IN CR-39 LOCATED ON THE EARTH SIDE OF LDEF **c72**
I. Csige, E. V. Benton, S. Soundararajan, and E. R. Benton *In* NASA. Langley Research Center, LDEF: 69 Months in Space. Part 1: Second Post-Retrieval Symposium 181-186 (SEE N93-29621 11-99) Apr. 1993 (For primary document see N93-29621 11-99)
(Contract NAS8-38610)
Avail: CASI HC A03/MF A03

The azimuthal angle distribution and the charge and energy spectra of selected light-heavy (5 less than or equal to Z less than or equal to 8) stopping particles were measured in a single layer of CR-39 plastic nuclear track detector (PNTD) from the stack of the A0015 experiment located on the Earth-end of the LDEF satellite. The directional incidence of the trapped protons is studied by comparing the azimuthal angle distribution of selected recoils, obtained in the LDEF detectors, to that obtained through calibrations of PNTD's with exposures performed with 200 MeV proton beams from different directions. Author

N93-29639*# National Aeronautics and Space Administration. Marshall Space Flight Center, Huntsville, AL.
THREE-DIMENSIONAL SHIELDING EFFECTS ON CHARGED PARTICLE FLUENCES MEASURED IN THE P0006 EXPERIMENT OF LDEF **c72**
I. Csige (San Francisco Univ., CA.), E. V. Benton (San Francisco Univ., CA.), L. Frigo (San Francisco Univ., CA.), T. A. Parnell, J. W. Watts, Jr., T. W. Armstrong (Science Applications International Corp., Prospect, TN.), and B. L. Colborn (Science Applications International Corp., Prospect, TN.) *In* NASA. Langley Research Center, LDEF: 69 Months in Space. Part 1: Second Post-Retrieval Symposium Apr. 1993 p 187-194 (For primary document see N93-29621 11-99)
(Grant NAG8-168)
Avail: CASI HC A02/MF A03

Three-dimensional shielding effects on cosmic ray charged particle fluences were measured with plastic nuclear track detectors in the P0006 experiment on Long Duration Exposure Facility (LDEF). The azimuthal and polar angle distributions of the galactic cosmic ray particles (mostly relativistic iron) were measured in the main stack and in four side stacks of the P0006 experiment, located on the west end of the LDEF satellite. A shadowing effect of the shielding of the LDEF satellite is found. Total fluence of stopping protons was measured as a function of the position in the main and side stacks of the P0006 experiment. Location dependence of total track density is explained by the three-dimensional shielding model of the P0006 stack. These results can be used to validate 3D mass model and transport code calculations and also for predictions of the outer radiation environment for the Space Station Freedom. Author (revised)

N93-29640*# Science Applications International Corp., Prospect, TN.
DEVELOPMENT AND APPLICATION OF A 3-D GEOMETRY/MASS MODEL FOR LDEF SATELLITE IONIZING RADIATION ASSESSMENTS **c72**
B. L. Colborn and T. W. Armstong *In* NASA. Langley Research Center, LDEF: 69 Months in Space. Part 1: Second Post-Retrieval Symposium Apr. 1993 p 195-205 (For primary document see N93-29621 11-99)
(Contracts NAS8-38121; NAS8-39386)
Avail: CASI HC A03/MF A03

A three-dimensional geometry and mass model of the Long Duration Exposure Facility (LDEF) spacecraft and experiment trays was developed for use in predictions and data interpretation related to ionizing radiation measurements. The modeling approach, level of detail incorporated, example models for specific experiments and radiation dosimeters, and example applications of the model are described. Author (revised)

N93-29641*# Science Applications International Corp., Prospect, TN.
RADIATION MODEL PREDICTIONS AND VALIDATION USING LDEF SATELLITE DATA **c72**
T. W. Armstrong and B. L. Colborn *In* NASA. Langley Research Center, LDEF: 69 Months in Space. Part 1: Second Post-Retrieval Symposium Apr. 1993 p 207-220 (For primary document see N93-29621 11-99)
(Contracts NAS8-38770; NAS8-39386)
Avail: CASI HC A03/MF A03

Predictions and comparisons with the radiation dose measurements on Long Duration Exposure Facility (LDEF) by thermoluminescent dosimeters were made to evaluate the accuracy of models currently used in defining the ionizing radiation environment for low Earth orbit missions. The calculations include a detailed simulation of the radiation exposure (altitude and solar cycle variations, directional dependence) and shielding effects (three-dimensional LDEF geometry model) so that differences in the predicted and observed doses can be attributed to environment model uncertainties. The LDEF dose data are utilized to assess the accuracy of models describing the trapped proton flux, the trapped proton directionality, and the trapped electron flux. Author (revised)

N93-29642*# Science Applications International Corp., Prospect, TN.
FUTURE DIRECTIONS FOR LDEF IONIZING RADIATION MODELING AND ASSESSMENTS **c72**
T. W. Armstrong and B. L. Colborn *In* NASA. Langley Research Center, LDEF: 69 Months in Space. Part 1: Second Post-Retrieval Symposium Apr. 1993 p 221-230 (For primary document see N93-29621 11-99)
(Contract NAS8-39386)
Avail: CASI HC A02/MF A03

A calculational program utilizing data from radiation dosimetry measurements aboard the Long Duration Exposure Facility (LDEF) satellite to reduce the uncertainties in current models defining the ionizing radiation environment is in progress. Most of the effort to date has been on using LDEF radiation dose measurements to evaluate models defining the geomagnetically trapped radiation, which has provided results applicable to radiation design assessments being performed for Space Station Freedom. Plans for future data comparisons, model evaluations, and assessments using additional LDEF data sets (LET spectra, induced radioactivity, and particle spectra) are discussed. Author (revised)

N93-29643*# National Aeronautics and Space Administration. Marshall Space Flight Center, Huntsville, AL.
COSMOGENIC RADIONUCLIDES ON LDEF: AN UNEXPECTED Be-10 RESULT **c72**
J. C. Gregory (Alabama Univ., Huntsville.), A. Albrecht (Rutgers Univ., New Brunswick, NJ.), G. Herzog (Rutgers Univ., New Brunswick, NJ.), J. Klein (Pennsylvania Univ., Philadelphia.), R. Middleton (Pennsylvania Univ., Philadelphia.), B. Dezfouly-Arjomandy (Pennsylvania Univ., Philadelphia.), and B. A. Harmon *In* NASA. Langley Research Center, LDEF: 69 Months in Space. Part 1: Second Post-Retrieval Symposium Apr. 1993 p 231-237 (For primary document see N93-29621 11-99)
Avail: CASI HC A02/MF A03

Following the discovery of the atmospheric derived cosmogenic radionuclide Be-7 on the Long Duration Exposure Facility (LDEF), a search began for other known nuclides produced by similar mechanisms. None of the others have the narrow gamma-ray line emission of Be-7 decay which enabled its rapid detection and quantification. A search for Be-10 atoms on LDEF clamp plates using accelerator mass spectrometry is described. An unexpected result was obtained. Author (revised)

N93-29644*# Kiel Univ. (Germany).
HEAVY ION MEASUREMENT ON LDEF **c72**
D. Jonathal, R. Beaujean, and W. Enge *In* NASA. Langley Research Center, LDEF: 69 Months in Space. Part 1: Second Post-Retrieval Symposium Apr. 1993 p 239-245 (For primary document see N93-29621 11-99)
Avail: CASI HC A02/MF A03

Heavy ions with nuclear charge $Z = 6$ to $Z = 26$ are detected in a stack of plastic track detectors. The measured energies in the range of 10-240 MeV/nuc are well below the geomagnetic cut off value of the Long Duration Exposure Facility (LDEF) orbit. The arrival directions of the low energy particles ($Z = 6$-26, E less than 40 MeV/nuc) are consistent

with a trapped component incident in the South Atlantic Anomaly.
Author (revised)

N93-29645*# Naval Research Lab., Washington, DC.
PROGRESS REPORT ON THE HEAVY IONS IN SPACE (HIIS) EXPERIMENT **c72**
James H. Adams, Jr., Lorraine P. Beahm, Paul R. Boberg, and Allan J. Tylka *In* NASA. Langley Research Center, LDEF: 69 Months in Space. Part 1: Second Post-Retrieval Symposium Apr. 1993 p 247-259 (For primary document see N93-29621 11-99)
Avail: CASI HC A03/MF A03

One of the objectives of the Heavy Ions In Space (HIIS) experiment is to investigate heavy ions which appear at Long Duration Exposure Facility (LDEF) below the geomagnetic cutoff for fully-ionized galactic cosmic rays. Possible sources of such 'below-cutoff' particles are partially-ionized solar energetic particles, the anomalous component of cosmic rays, and magnetospherically-trapped particles. In recent years, there have also been reports of below-cutoff ions which do not appear to be from any known source. Although most of these observations are based on only a handful of ions, they have led to speculation about 'partially-ionized galactic cosmic rays' and 'near-by cosmic ray sources'. The collecting power of HIIS is order of magnitude larger than that of the instruments which reported these results, so HIIS should be able to confirm these observations and perhaps discover the source of these particles. Preliminary results on below-cutoff heavy-ions are reported. Observations to possible known sources of such ions are compared. A second objective of the HIIS experiment is to measure the elemental composition of ultraheavy galactic cosmic rays, beginning in the tin-barium region of the periodic table. A report on the status of this analysis is presented. Author (revised)

N93-29646*# Dublin Inst. for Advanced Studies (Ireland).
PROGRESS REPORT ON THE ULTRA HEAVY COSMIC RAY EXPERIMENT (AO178) **c93**
A. Thompson, D. OSullivan, J. Bosch, R. Keegan (Dublin Inst. for Advanced Studies, Ireland.), K.-P. Wenzel (European Space Agency. European Space Research and Technology Center, ESTEC, Noordwijk, Netherlands.), F. Jansen (European Space Agency. European Space Research and Technology Center, ESTEC, Noordwijk, Netherlands.), and C. Domingo (Universidad Autonoma de Barcelona, Bellaterra, Spain.) *In* NASA. Langley Research Center, LDEF: 69 Months in Space. Part 1: Second Post-Retrieval Symposium Apr. 1993 p 261-268 (For primary document see N93-29621 11-99)
Avail: CASI HC A02/MF A03

The Ultra Heavy Cosmic Ray Experiment (UHCRE) is based on a modular array of 192 side-viewing solid state nuclear track detector stacks. These stacks were mounted in sets of four in 48 pressure vessels employing sixteen peripheral Long Duration Exposure Facility (LDEF) trays. The extended duration of the LDEF mission has resulted in a greatly enhanced scientific yield from the UHCRE. The geometry factor for high energy cosmic ray nuclei, allowing for Earth shadowing, was 30 sq m-sr, giving a total exposure factor of 170 sq m-sr-y at an orbital inclination of 28.4 degrees. Scanning results indicate that about 3000 cosmic ray nuclei in the charge region with Z greater than 65 were collected. This sample is more than ten times the current world data in the field (taken to be the data set from the HEAO-3 mission plus that from the Ariel-6 mission) and is sufficient to provide the world's first statistically significant sample of actinide (Z greater than 88) cosmic rays. Results to date are presented including details of ultra-heavy cosmic ray nuclei, analysis of pre-flight and post-flight calibration events and details of track response in the context of detector temperature history. The integrated effect of all temperature and age related latent track variations cause a maximum charge shift of +/- 0.8 e for uranium and +/- 0.6 e for the platinum-lead group. The precision of charge assignment as a function of energy is derived and evidence for remarkably good charge resolution achieved in the UHCRE is considered. Astrophysical implications of the UHCRE charge spectrum are discussed. Author (revised)

N93-29682*# National Aeronautics and Space Administration. Langley Research Center, Hampton, VA.
LDEF: 69 MONTHS IN SPACE. PART 4: SECOND POST-RETRIEVAL SYMPOSIUM
Arlene S. Levine, ed. Washington Apr. 1993 309 p Symposium held in San Diego, CA, 1-5 Jun. 1992; sponsored by NASA, Washington and AIAA Original contains color illustrations
(RTOP 506-48-91-11)
(NASA-CP-3194-Pt-4; L-17196-Pt-4; NAS 1.55:3194-Pt-4) Avail: CASI HC A14/MF A03; 2 functional color pages

A compilation of papers presented at the Second Long Duration Exposure Facility (LDEF) Post-Retrieval Symposium are presented. The papers represent the data analysis of the 57 experiments flown on the LDEF. The experiments include materials, coatings, thermal systems, power and propulsion, science (cosmic ray, interstellar gas, heavy ions, micrometeoroid, etc.), electronics, optics, and life sciences. For individual titles, see N93-29683 through N93-29708.

N93-29683*# National Aeronautics and Space Administration. Goddard Space Flight Center, Greenbelt, MD.
OVERVIEW OF THE SYSTEMS SPECIAL INVESTIGATION GROUP INVESTIGATION **c25**
James B. Mason, Harry Dursch (Boeing Defense and Space Group, Seattle, WA.), and Joel Edelman (Long Duration Exposure Facility Newsletter, Silver Spring, MD.) *In* NASA. Langley Research Center, LDEF: 69 Months in Space. Part 4: Second Post-Retrieval Symposium Apr. 1993 p 1257-1268 (For primary document see N93-29682 11-99)
Avail: CASI HC A03/MF A03; 2 functional color pages

The Long Duration Exposure Facility (LDEF) carried a remarkable variety of electrical, mechanical, thermal, and optical systems, subsystems, and components. Nineteen of the fifty-seven experiments flown on LDEF contained functional systems that were active on-orbit. Almost all of the other experiments possessed at least a few specific components of interest to the Systems Special Investigation Group (Systems SIG), such as adhesives, seals, fasteners, optical components, and thermal blankets. Almost all top level functional testing of the active LDEF and experiment systems has been completed. Failure analysis of both LDEF hardware and individual experiments that failed to perform as designed has also been completed. Testing of system components and experimenter hardware of interest to the Systems SIG is ongoing. All available testing and analysis results were collected and integrated by the Systems SIG. An overview of our findings is provided. An LDEF Optical Experiment Database containing information for all 29 optical related experiments is also discussed.
Author

N93-29684*# Aerospace Corp., El Segundo, CA.
POST-FLIGHT ANALYSES OF THE CRYSTALS FROM THE M0003-14 QUARTZ CRYSTAL MICROBALANCE EXPERIMENT **c76**
W. K. Stuckey, G. Radhakrishnan, and D. Wallace (QCM Research, Laguna Beach, CA.) *In* NASA. Langley Research Center, LDEF: 69 Months in Space. Part 4: Second Post-Retrieval Symposium Apr. 1993 p 1269-1283 (For primary document see N93-29682 11-99)
Avail: CASI HC A03/MF A03; 2 functional color pages

Quartz Crystal Microbalances constructed by QCM Research were flown on the leading and trailing edges of LDEF as one of the sub-experiments of M0003. Response of the crystals coated with 150 A of In2O3 was recorded during the first 424 days of the mission. A second QCM with crystals coated with 150 A of ZnS was also flown but not monitored. After the flight, the QCM's were disassembled and analyzed in The Aerospace Corporation laboratories. The samples included the crystals from the leading and trailing edge samples of both types of coatings along with the reference crystals, which were inside the QCM housing. Analyses were performed by scanning electron microscopy, energy dispersive x-ray analyses, x-ray photoelectron spectroscopy, ion microprobe mass analysis, and reflectance spectroscopy in the infrared and UV/visible regions. The crystals are contaminated predominantly with silicone compounds. The contamination is higher on the leading edge than on the trailing edge and higher on the exposed crystals than on the reference crystals. Author (revised)

N93-29685*# Martin Marietta Labs., Baltimore, MD.
RADIATION SENSITIVITY OF QUARTZ CRYSTAL OSCILLATORS EXPERIMENT FOR THE LONG DURATION EXPOSURE FACILITY (LDEF), PART 2 **c33**
J. S. Ahearn and J. D. Venables *In* NASA. Langley Research Center, LDEF: 69 Months in Space. Part 4: Second Post-Retrieval Symposium Apr. 1993 p 1285-1289 (For primary document see N93-29682 11-99)
Avail: CASI HC A01/MF A03; 2 functional color pages

The stability of high precision quartz crystal oscillators exposed to the radiation environment of NASA's Long Duration Exposure Facility (LDEF) was studied. Comparisons between pre-flight and post-flight frequency drift rates indicate that oscillators made from swept premium Q quartz exhibited a significantly greater post-flight drift rate than before exposure, but that the effect annealed after five months aging at 75 C (the operating temperature). The result that six years worth of radiation damage annealed out in less than six months suggests that if the oscillators had been powered during the LDEF mission, no net change in drift rate beyond their normal baseline value would have occurred. Author (revised)

N93-29686*# National Aeronautics and Space Administration. Lewis Research Center, Cleveland, OH.

THE EFFECT OF THE LOW EARTH ORBIT ENVIRONMENT ON SPACE SOLAR CELLS: RESULTS OF THE ADVANCED PHOTOVOLTAIC EXPERIMENT (S0014) **c44**

David J. Brinker, John R. Hickey (Eppley Lab., Inc., Newport, RI.), and David A. Scheiman (Sverdrup Technology, Inc., Brook Park, OH.) *In* NASA. Langley Research Center, LDEF: 69 Months in Space. Part 4: Second Post-Retrieval Symposium Apr. 1993 p 1291-1302 (For primary document see N93-29682 11-99)
Avail: CASI HC A03/MF A03; 2 functional color pages

The results of post-flight performance testing of the solar cells flown on the Advanced Photovoltaic Experiment are reported. Comparison of post-flight current-voltage characteristics with similar pre-flight data revealed little or no change in solar cell conversion efficiency, confirming the reliability and endurance of space photovoltaic cells. This finding is in agreement with the lack of significant physical changes in the solar cells despite nearly six years in the low Earth orbit environment. Author

N93-29687*# Jet Propulsion Lab., California Inst. of Tech., Pasadena.

LEO EFFECTS ON CANDIDATE SOLAR CELL COVER MATERIALS **c44**

Paul M. Stella *In* NASA. Langley Research Center, LDEF: 69 Months in Space. Part 4: Second Post-Retrieval Symposium Apr. 1993 p 1303-1313 (For primary document see N93-29682 11-99)
Avail: CASI HC A03/MF A03; 2 functional color pages

In 1984, the LDEF (Long Duration Exposure Facility) was placed in LEO (Low Earth Orbit) for a mission planned to last approximately one year. Due to a number of factors, retrieval was delayed until 1990. An experiment, prepared under the direction of JPL, consisted of a test plate with thirty (30) individual thin silicon solar cell/cover samples. The covers consisted of conventional cerium doped microsheet platelets and potential candidate materials, such as FEP Teflon, silicon RTV's, glass resins, polyimides, and a silicone-polyimide copolymer encapsulant. The effects of the LDEF mission environment (micrometeorite/debris impacts, atomic oxygen, UV, and particulate radiation) on the samples are discussed. Author (revised)

N93-29688*# Centre National d'Etudes Spatiales, Toulouse (France).

NEW RESULTS FROM FRECOPA ANALYSIS **c37**

Christian Durin *In* NASA. Langley Research Center, LDEF: 69 Months in Space. Part 4: Second Post-Retrieval Symposium Apr. 1993 p 1315-1331 (For primary document see N93-29682 11-99)
Avail: CASI HC A03/MF A03; 2 functional color pages

New results from the ongoing analysis of the FRECOPA's (FREnch COoperative PAssive payload) system hardware are discussed. FRECOPA (AO138) was one of the 57 experiments flown on the LDEF satellite. The experiment was located on the trailing edge (Tray B3) and was exposed to UV radiation (11,100 equivalent sun hours), approximately equal to 34,000 thermal cycles, higher vacuum levels than the leading edge, a low atomic oxygen flux, and minor doses of protons and electrons. Due to LDEF's extended mission (5.8 years), CNES decided to set up a team to analyze the FRECOPA system. Initial results were presented at the First Post-Retrieval Conference, June, 1991. The results obtained since then are summarized. Author (revised)

N93-29689*# Georgia Tech Research Inst., Atlanta.

DEGRADATION OF ELECTRO-OPTIC COMPONENTS ABOARD LDEF **c74**

M. D. Blue *In* NASA. Langley Research Center, LDEF: 69 Months in Space. Part 4: Second Post-Retrieval Symposium Apr. 1993 p 1333-1342 (For primary document see N93-29682 11-99)
Avail: CASI HC A02/MF A03; 2 functional color pages

Remeasurement of the properties of a set of electro-optic components exposed to the low-earth environment aboard the Long Duration Exposure Facility (LDEF) indicates that most components survived quite well. Typical components showed some effects related to the space environment unless well protected. The effects were often small but significant. Results for semiconductor infrared detectors, lasers, and LED's, as well as filters, mirrors, and black paints are described. Semiconductor detectors and emitters were scarred but reproduced their original characteristics. Spectral characteristics of multi-layer dielectric filters and mirrors were found to be altered and degraded. Increased absorption in black paints indicates an increase in absorption sites, giving rise to enhanced performance as coatings for baffles and sunscreens. Author

N93-29690*# TRW Space Technology Labs., Redondo Beach, CA.

LDEF SPACE PLASMA-HIGH VOLTAGE DRAINAGE EXPERIMENT POST-FLIGHT RESULTS **c33**

J. Y. Yaung, B. K. Blakkolb, W. C. Wong, L. E. Ryan, H. J. Schurig, and W. W. L. Taylor *In* NASA. Langley Research Center, LDEF: 69 Months in Space. Part 4: Second Post-Retrieval Symposium Apr. 1993 p 1343-1354 (For primary document see N93-29682 11-99)
Avail: CASI HC A03/MF A03; 2 functional color pages

The Space Plasma-High Voltage Drainage Experiment (SP-HVDE) was comprised of two identical experimental trays. With one tray located on the leading (ram facing, B10) edge and the other located on the trailing (wake facing, D4) edge of the Long Duration Exposure Facility (LDEF), it was possible to directly compare the effects of ram and wake spacecraft environments on charged dielectric materials. Six arrays of Kapton dielectric samples of 2 mil, 3 mil, and 5 mil thicknesses maintained at +/- 300, +/- 500, and +/- 1000 voltage bias formed the experimental matrix of each tray. In addition, each tray carried two solar cell strings, one biased at +300 volts and the other at -300 volts, to study current leakage from High Voltage Solar Arrays (HVSA). The SP-HVDE provides the first direct, long-term, in-flight measurements of average leakage current through dielectric materials under electric stress. The experiment also yields information on the long term stability of the bulk dielectric properties of such materials. Data and findings of the SP-HVDE are an extension of those from shorter term flight experiments such as the PIX-1 (Plasma Interaction Experiment) and PIX-2 and are therefore valuable in the design and evaluation of long-lived space systems with high voltage systems exposed to the low earth orbital environment. A summary of the SP-HVDE post flight analysis final report delivered to the LDEF Project Office under contract to the National Aeronautics and Space Administration is presented. Author (revised)

N93-29691*# Paris XI Univ., Orsay (France). Inst. d'Astrophysique Spatiale.

IN ORBIT DEGRADATION OF EUV OPTICAL COMPONENTS IN THE WAVELENGTH RANGE 10-40 nm AO 138-3 **c74**

J. P. Delaboudiniere, C. Carabetian, and J. F. Hochedez *In* NASA. Langley Research Center, LDEF: 69 Months in Space. Part 4: Second Post-Retrieval Symposium Apr. 1993 p 1355-1360 Sponsored in part by CNES (For primary document see N93-29682 11-99)
Avail: CASI HC A02/MF A03; 2 functional color pages

A complement of EUV optical components, including mirrors and thin film filters, was flown as part of the Long Duration Exposure Facility (LDEF) AO 138-3. The most original amongst these components were multilayered interference reflectors for the 10-40 nm wavelength range. Very moderate degradation was observed for those components which were exposed to the sun. The degradation is compatible with the deposition of a few nanometers of absorbing material on the surface of the samples. Author

N93-29692*# Phillips Lab., Kirtland AFB, NM.

DEGRADATION OF OPTICAL COMPONENTS IN A SPACE ENVIRONMENT **c74**

Linda L. DeHainaut, John R. Kenemuth, Cynthia E. Tidler, and David W. Seegmiller (Schafer, W. J. Associates, Inc., Albuquerque, NM.) *In* NASA. Langley Research Center, LDEF: 69 Months in Space. Part 4: Second Post-Retrieval Symposium Apr. 1993 p 1361-1373 (For primary

document see N93-29682 11-99)
Avail: CASI HC A03/MF A03; 2 functional color pages

Phillips Laboratory's Long Duration Exposure Facility (LDEF) optical experiment is designed to determine the adverse effects of the natural space environment on laser optical component and coating materials. The experiment consists of 10 sample sets, each containing six different material samples. The materials were chosen because of their common use in laser optical components. Sample characterization is divided into three phases. Phase 1 testing is limited to visual and optical performance evaluation. Phase 2 tests investigate the fundamental causes of the performance degradation quantified in Phase 1. During Phase 3, selected samples will be cleaned and some Phase 1 measurements repeated to determine if acceptable optical performance can be restored, and laser damage testing will be performed on a small number of samples. Performance deteriorations will be correlated to exposure duration, sample location on the LDEF, atomic oxygen levels, and other space environment conditions. Preliminary results obtained on the optical samples are discussed. Author (revised)

N93-29693*# National Aeronautics and Space Administration. Lewis Research Center, Cleveland, OH.

STUDIES OF EFFECTS ON OPTICAL COMPONENTS AND SENSORS: LDEF EXPERIMENTS AO-147 (ERB COMPONENTS) AND S-0014 (APEX) **c74**

John R. Hickey (Eppley Lab., Inc., Newport, RI.), David J. Brinker, and Philip Jenkins (Sverdrup Technology, Inc., Brook Park, OH.) *In* NASA. Langley Research Center, LDEF: 69 Months in Space. Part 4: Second Post-Retrieval Symposium Apr. 1993 p 1375-1388 (For primary document see N93-29682 11-99)
(Contracts NAS1-15350; NAS3-25958)
Avail: CASI HC A03/MF A03; 2 functional color pages

Some additional results of testing of optical filters and window materials and thermopile sensors of the two experiments are included. The Advanced Photovoltaic Experiment (APEX) interference filters exhibited much greater degradation in space than the ERB filters. The adhesion of the Indium washers to the APEX interference filters is reported. Author (revised)

N93-29694*# Eastman Kodak Co., Rochester, NY.

EFFECTS OF LONG TERM SPACE ENVIRONMENT EXPOSURE ON OPTICAL SUBSTRATES AND COATINGS (S0050-2) **c74**

Keith Harvey, Arthur Mustico, and John Vallimont *In* NASA. Langley Research Center, LDEF: 69 Months in Space. Part 4: Second Post-Retrieval Symposium Apr. 1993 p 1389-1397 (For primary document see N93-29682 11-99)
Avail: CASI HC A02/MF A03; 2 functional color pages

Eastman Kodak Company included twelve substrate and coating samples on the Long Duration Exposure Facility (LDEF) structure. There were three Fused Silica and three Ultra Low Expansion (ULE) uncoated glass samples, two ULE samples with a high reflectance silver coating, two Fused Silica samples with an antireflectance coating, and two Fused silica samples with a solar rejection coating. A set of duplicate control samples was also manufactured and stored in a controlled environment for comparison purposes. Kodak's samples were included as a subset of the Georgia Institute of Technology tray, which was located on row 5-E, tray S0050-2. This placed the samples on the trailing edge of the structure, which protected them from the effects of atomic oxygen bombardment. An evaluation of the flight samples for effects from the 5 year mission showed that a contaminant was deposited on the samples, a micrometeoroid impact occurred on one of the samples, and the radiation darkening which was expected for the glass did not occur. The results are listed in more detail. Author

N93-29695*# Science Applications International Corp., Santa Monica, CA.

LDEF SPACE OPTICS HANDBOOK Abstract Only **c74**

Robert J. Champetier, Dale R. Atkinson (POD Associates, Inc., Albuquerque, NM.), and William T. Kemp (Phillips Lab., Kirtland AFB, NM.) *In* NASA. Langley Research Center, LDEF: 69 Months in Space. Part 4: Second Post-Retrieval Symposium Apr. 1993 p 1399 (For primary document see N93-29682 11-99)
Avail: CASI HC A01/MF A03; 2 functional color pages

There is a need to present design guidelines derived from the Long Duration Exposure Facility (LDEF) space optics experiments to hardware designers. In response to this need a small study program was just started by SAIC and POD Associates for the Phillips Laboratory. The objective is to prepare a top-level review of available results on the behavior of certain optical components in the LDEF space experiments. The optics interest centers on optical surfaces and coatings, and fabrication processes for laser windows and mirrors. The program has two main parts: the first phase, to be completed by the end of 1992, consists of identifying and acquiring data from the appropriate investigators. The second phase, ending in December 1993, comprises report preparation as well as selected, prioritized, additional characterization of certain samples, coordinated with the principal investigators and the Phillips Laboratory. This program is getting under way at the time of the Symposium and does not warrant more than the present summary at this time. Author (revised)

N93-29696*# Jobin et Yvon S.A., Longjumeau (France).

RULED AND HOLOGRAPHIC EXPERIMENT (AO 138-5) Abstract Only **c35**

Francis Bonnemason *In* NASA. Langley Research Center, LDEF: 69 Months in Space. Part 4: Second Post-Retrieval Symposium Apr. 1993 p 1401 (For primary document see N93-29682 11-99)
Avail: CASI HC A01/MF A03; 2 functional color pages

The AO 138-5 experiment was designed, via the FRECOPA (FRench COoperative PAyload) experiment with the aim to study the optical behavior of different diffraction gratings submitted to space vacuum long exposure and solar irradiation. Samples were ruled and holographic gratings, masters or replica, and some additional control mirrors with various coatings. The experiment was located on the B3, trailing edge of the LDEF and was protected against Atomic Oxygen flux. The experienced thermal cycling was evaluated from -23 C to 66 C during the flight, 34,000 orbits. The samples (two batches of four pieces) were located on a dedicated plate, by a pair of equivalent gratings or mirrors; optical faces were located on the external side. The plate was inside a canister, which had been opened in space for ten months. When the satellite returned to Kennedy Space Center, the remaining vacuum in the canister was still correct. The analysis focused on the triple point characterization including light efficiency, wavefront flatness quality and stray light level. Tests were conducted on control mirrors and gratings (rules and holographic master or replica) loaded but not exposed to cosmic dust or direct solar irradiations. They did not show any significant variations. Solar exposure had damaged the coating (aluminum and platinum) reflectivity in the Ultra-Violet region; the degradation is higher with the gratings, in terms of efficiency. However, wavefront flatness quality and stray light level tests revealed no additional changes. Author

N93-29697*# Georgia Inst. of Tech., Atlanta. School of Electrical Engineering.

HOLOGRAPHIC DATA STORAGE CRYSTALS FOR THE LDEF **c35**

W. Russell Callen and Thomas K. Gaylord *In* NASA. Langley Research Center, LDEF: 69 Months in Space. Part 4: Second Post-Retrieval Symposium Apr. 1993 p 1403-1411 (For primary document see N93-29682 11-99)
(Contract NAS1-15370)
Avail: CASI HC A02/MF A03; 2 functional color pages

Crystals of lithium niobate were passively exposed to the space environment of the Long Duration Exposure Facility (LDEF). Three of the four crystals contained volume holograms. Although the crystals suffered the surface damage characteristic of that suffered by other components on the Georgia Tech tray, the crystals remained suitable for the formation of volume holograms. Author (revised)

N93-29698*# Phillips Lab., Kirtland AFB, NM. Directorate of Space and Missiles Technology.

CHARACTERIZATION OF A SPACE ORBITED INCOHERENT FIBER OPTIC BUNDLE **c74**

Stephen A. DeWalt and Edward W. Taylor *In* NASA. Langley Research Center, LDEF: 69 Months in Space. Part 4: Second Post-Retrieval Symposium Apr. 1993 p 1413-1423 (For primary document see N93-29682 11-99)
Avail: CASI HC A03/MF A03; 2 functional color pages

The results of a study performed to determine the effects of adverse space environments on a bundle of over 1800 optical fibers orbited for 69 months are reported. Experimental results are presented on an incoherent fiber optic bundle oriented in low Earth orbit aboard the Long Duration Exposure Facility (LDEF) satellite as part of the Space Environment Effects Experiment (M0006). Measurements were performed to determine if space induced radiation effects changed the fiber bundle characteristics. Data demonstrating the success of light transmitting fibers to withstand the adverse space environment are presented. Author (revised)

N93-29699*# Phillips Lab., Kirtland AFB, NM. Directorate of Space and Missiles Technology.

ANALYSES OF SPACE ENVIRONMENT EFFECTS ON ACTIVE FIBER OPTIC LINKS ORBITED ABOARD THE LDEF c74

Edward W. Taylor, T. W. Monarski, J. N. Berry, A. D. Sanchez, R. J. Padden, and S. P. Chapman *In* NASA. Langley Research Center, LDEF: 69 Months in Space. Part 4: Second Post-Retrieval Symposium Apr. 1993 p 1425-1437 (For primary document see N93-29682 11-99)
Avail: CASI HC A03/MF A03; 2 functional color pages

The results of the 'Preliminary Analysis of WL Experiment no. 701, Space Environment Effects on Operating Fiber Optic Systems,' is correlated with space simulated post retrieval terrestrial studies performed on the M0004 experiment. Temperature cycling measurements were performed on the active optical data links for the purpose of assessing link signal to noise ratio and bit error rate performance some 69 months following the experiment deployment in low Earth orbit. The early results indicate a high correlation between pre-orbit, orbit, and post-orbit functionality of the first known and longest space demonstration of operating fiber optic systems. Author (revised)

N93-29700*# Jet Propulsion Lab., California Inst. of Tech., Pasadena.

RADIATION AND TEMPERATURE EFFECTS ON LDEF FIBER OPTIC SAMPLES c74

A. R. Johnston, R. Hartmayer, and L. A. Bergman *In* NASA. Langley Research Center, LDEF: 69 Months in Space. Part 4: Second Post-Retrieval Symposium Apr. 1993 p 1439-1453 (For primary document see N93-29682 11-99)
Avail: CASI HC A03/MF A03; 2 functional color pages

Results obtained from the JPL Fiber Optics Long Duration Exposure Facility (LDEF) Experiment since the June 1991 Experimenters' Workshop are addressed. Radiation darkening of laboratory control samples and the subsequent annealing was measured in the laboratory for the control samples. The long-time residual loss was compared to the LDEF flight samples and found to be in agreement. The results of laboratory temperature tests on the flight samples, extending over a period of about nine years, including the pre-flight and post-flight analysis periods, are described. The temperature response of the different cable samples varies widely, and appears in two samples to be affected by polymer aging. Conclusions to date are summarized. Author (revised)

N93-29701*# National Aeronautics and Space Administration. Goddard Space Flight Center, Greenbelt, MD.

LONG DURATION EXPOSURE FACILITY (LDEF) LOW TEMPERATURE HEAT PIPE EXPERIMENT PACKAGE (HEPP) FLIGHT RESULTS c34

Roy McIntosh, Craig McCreight (National Aeronautics and Space Administration. Ames Research Center, Moffett Field, CA.), and Patrick J. Brennan (OAO Corp., Greenbelt, MD.) *In* NASA. Langley Research Center, LDEF: 69 Months in Space. Part 4: Second Post-Retrieval Symposium Apr. 1993 p 1455-1475 (For primary document see N93-29682 11-99)
Avail: CASI HC A03/MF A03; 2 functional color pages

The Low Temperature Heat Pipe Flight Experiment (HEPP) is a fairly complicated thermal control experiment that was designed to evaluate the performance of two different low temperature ethane heat pipes and a low-temperature (182 K) phase change material. A total of 390 days of continuous operation with an axially grooved aluminum fixed conductance heat pipe and an axially grooved stainless steel heat pipe diode was demonstrated before the data acquisition system's batteries lost power. Each heat pipe had approximately 1 watt applied throughout this period. The HEPP was not able to cool below 188.6 K during the mission. As a result, the preprogrammed transport test sequence which initiates when the PCM temperature drops below 180 K was never exercised, and transport tests with both pipes and the diode reverse mode test could not be run in flight. Also, because the melt temperature of the n-heptane PCM is 182 K, its freeze/thaw behavior could not be tested. Post-flight thermal vacuum tests and thermal analyses have indicated that there was an apparent error in the original thermal analyses that led to this unfortunate result. Post-flight tests have demonstrated that the performance of both heat pipes and the PCM has not changed since being fabricated more than 14 years ago. A summary of HEPP's flight data and post-flight test results are presented. Author (revised)

N93-29702*# Oklahoma State Univ., Stillwater.

FINAL RESULTS OF SPACE EXPOSED EXPERIMENT DEVELOPED FOR STUDENTS c51

Doris K. Grigsby *In* NASA. Langley Research Center, LDEF: 69 Months in Space. Part 4: Second Post-Retrieval Symposium Apr. 1993 p 1479-1492 (For primary document see N93-29682 11-99)
Avail: CASI HC A03/MF A03; 2 functional color pages

SEEDS was a cooperative endeavor of NASA Headquarters, the NASA Langley Research Center, and the George W. Park Seed Company. Approximately 132,000 SEEDS kits containing Rutger's tomato seeds that had flown on LDEF, as well as similar seeds that had been stored in a climate-controlled warehouse for the same time period, were sent to schools in every state and 30 foreign countries. Student researchers from kindergarten through university compared germination and growth characteristics of the space-exposed and Earth-based seeds and returned data to NASA for analysis. Important scientific information was gained as students reported very little difference between the two seed groups. Author (revised)

N93-29703*# Park Seed Co., Inc., Greenwood, SC.

CONTINUED RESULTS OF THE SEEDS IN SPACE EXPERIMENT c51

Jim A. Alston *In* NASA. Langley Research Center, LDEF: 69 Months in Space. Part 4: Second Post-Retrieval Symposium Apr. 1993 p 1493-1497 (For primary document see N93-29682 11-99)
Avail: CASI HC A01/MF A03; 2 functional color pages

Two million seeds of 120 different varieties representing 106 species, 97 genera, and 55 plant families were flown aboard the Long Duration Exposure Facility (LDEF). The seed were housed on the Space Exposed Experiment Developed for Students (SEEDS) tray in the sealed canister number 6 and in two small vented canisters. The tray was in the F-2 position. The seed were germinated and the germination rates and the development of the resulting plants were compared to the performance of the control seed that stayed in Park Seed's seed storage facility. The initial results were presented in a paper at the First LDEF Post-Retrieval Symposium. There was a better survival rate of the seed in the sealed canister in space than in the storage facility at Park Seed. At least some of the seed in each of the vented canisters survived the exposure to vacuum for almost six years. The number of observed apparent mutations was very low. In the initial testing, the small seeded crops were not grown to maturity to check for mutations and obtain second generation seed. These small seeded crops have now been grown for evaluation and second generation seed collected. Author

N93-29704*# Schafer (W. J.) Associates, Inc., Hampton, VA.

LDEF ARCHIVAL SYSTEM PLAN c82

Brenda K. Wilson *In* NASA. Langley Research Center, LDEF: 69 months in Space. Part 4: Second Post-Retrieval Symposium Apr. 1993 p 1499-1509 (For primary document see N93-29682 11-99)
Avail: CASI HC A03/MF A03; 2 functional color pages

The Long Duration Exposure Facility (LDEF) has provided the first significant opportunity to extensively study the space environment and its effects upon spacecraft systems and materials. The long-term value of the data obtained from LDEF, which is applicable to a wide range of areas including space environment definition, space environmental effects, and spacecraft design, will depend upon the system developed to archive and retrieve the data. Therefore, in addition to the large effort undertaken to analyze LDEF data, a substantial effort is also necessary in order to retain and disseminate LDEF resources for future research and design. W. J. Schafer Associates, Inc., has a task subcontract to develop the LDEF archival system. The LDEF resources include data, hardware, photographic records, and publications which cover the 20-year history of LDEF from concept design through data analysis. Chronologically, prelaunch resources include documentation of facility and experiment development, testing integration, and operation. Post-retrieval resources are the observations, testing, analysis, and publications since the January 1990 retrieval of LDEF. A third set of resources is the experiment and facility hardware and specimens, including more than 10,000 test specimens flown on LDEF and subsequently divided and distributed among investigators at numerous laboratories. Many valuable science and technology investigations were undertaken with LDEF experiments and hardware, and many more investigations are being identified in areas not yet explored. LDEF data applications encompass primarily low-Earth orbit spacecraft and structures. The nearly six-year space exposure of LDEF has provided data to evaluate materials, systems, and living specimens exposed to radiation, meteoroids, debris, and other constituents of the low-Earth environment. Structural, mechanical, electrical, optical, and thermal systems were studied, and materials with applications in all aspects of space systems were exposed to the space environment. The objectives of the LDEF archival system are to maintain the existing LDEF hardware, data, analysis, publications, and photographs as a long term resource, and to provide a quick and simple mechanism by which LDEF resources can be identified, located, and applied. Author (revised)

N93-29705*# American Space Technology, Inc., Santa Monica, CA.

RETRIEVABLE PAYLOAD CARRIER, NEXT GENERATION LONG DURATION EXPOSURE FACILITY: UPDATE 1992 **c18**

A. T. Perry, J. A. Cagle, and S. C. Newman *In* NASA. Langley Research Center, LDEF: 69 Months in Space. Part 4: Second Post-Retrieval Symposium Apr. 1993 p 1511-1520 (For primary document see N93-29682 11-99)

Avail: CASI HC A02/MF A03; 2 functional color pages

Access to space and cost have been two major inhibitors of low Earth orbit research. The Retrievable Payload Carrier (RPC) Program is a commercial space program which strives to overcome these two barriers to space experimentation. The RPC Program's fleet of spacecraft, ground communications station, payload processing facility, and experienced integration and operations team will provide a convenient 'one-stop shop' for investigators seeking to use the unique vantage point and environment of low Earth orbit for research. The RPC is a regularly launched and retrieved, free-flying spacecraft providing resources adequate to meet modest payload/experiment requirements, and presenting ample surface area, volume, mass, and growth capacity for investigator usage. Enhanced capabilities of ground communications, solar-array-supplied electrical power, central computing, and on-board data storage pick up on the path where NASA's Long Duration Exposure Facility (LDEF) blazed the original technology trail. Mission lengths of 6-18 months, or longer, are envisioned. The year 1992 was designated as the 'International Space Year' and coincides with the 500th anniversary of Christopher Columbus's voyage to the New World. This is a fitting year in which to launch the full scale development of our unique shop of discovery whose intent is to facilitate retrieving technological rewards from another new world: space. Presented is an update on progress made on the RPC Program's development since the November 1991 LDEF Materials Workshop. Author (revised)

N93-29706*# AZ Technology, Huntsville, AL.

NEXT GENERATION OPTICAL INSTRUMENTS AND SPACE EXPERIMENT BASED ON THE LDEF THERMAL CONTROL SURFACES EXPERIMENT (S0069) **c74**

Donald R. Wilkes *In* NASA. Langley Research Center, LDEF: 69 Months in Space. Part 4: Second Post-Retrieval Symposium Apr. 1993 p 1521-1533 (For primary document see N93-29682 11-99)

Avail: CASI HC A03/MF A03; 2 functional color pages

The Thermal Control Surfaces Experiment (TCSE) was a successful experiment to study the effects of the space environment on thermal control surfaces using in-space optical properties measurements combined with post-flight analyses. The TCSE reflectometer performed well on the LDEF mission demonstrating that a portable compact integrating sphere spectroreflectometer can be built that is rugged and space rated. Since the retrieval of the TCSE package from space, several other instruments have evolved from its pioneering technologies. These are the Optical Properties Monitor (OPM), the Laboratory Portable SpectroReflectometer (LPSR), and the Space Portable SpectroReflectometer (SPSR). These instruments and experiment packages are described. Author (revised)

N93-29707*# Chicago Univ., IL. Lab. for Astrophysics and Space Research.

AN LDEF 2 DUST INSTRUMENT FOR DISCRIMINATION BETWEEN ORBITAL DEBRIS AND NATURAL PARTICLES IN NEAR-EARTH SPACE **c19**

A. J. Tuzzolino, J. A. Simpson, R. B. McKibben, H. D. Voss (Lockheed Missiles and Space Co., Palo Alto, CA.), and H. Gursky (Naval Research Lab., Washington, DC.) *In* NASA. Langley Research Center, LDEF: 69 Months in Space. Part 4: Second Post-Retrieval Symposium Apr. 1993 p 1535-1549 Sponsored in part by Lockheed Missiles and Space Co. (For primary document see N93-29682 11-99)

(Contract NAGw-3078; N00014-91-J-1716)

Avail: CASI HC A03/MF A03; 2 functional color pages

The characteristics of a space dust instrument which would be ideally suited to carry out near-Earth dust measurements on a possible Long Duraction Exposure Facility reflight mission (LDEF 2) is discussed. As a model for the trajectory portion of the instrument proposed for LDEF 2, the characteristics of a SPAce DUSt instrument (SPADUS) currently under development for flight on the USA ARGOS mission to measure the flux, mass, velocity, and trajectory of near-Earth dust is summarized. Since natural (cosmic) dust and man-made dust particles (orbital debris) have different velocity and trajectory distributions, they are distinguished by means of the SPADUS velocity/trajectory information. The SPADUS measurements will cover the dust mass range approximately 5 x 10(exp -12) g (2 microns diameter) to approximately 1 x 10(exp -5) g (200 microns diameter), with an expected mean error in particle trajectory of approximately 7 deg (isotropic flux). Arrays of capture cell devices positioned behind the trajectory instrumentation would provide for Earth-based chemical and isotopic analysis of captured dust. The SPADUS measurement principles, characteristics, its role in the ARGOS mission, and its application to an LDEF 2 mission are summarized. Author (revised)

N93-29708*# Naval Research Lab., Washington, DC.

FUTURE RADIATION MEASUREMENTS IN LOW EARTH ORBIT **c93**

James H. Adams, Jr. *In* NASA. Langley Research Center, LDEF: 69 Months in Space. Part 4: Second Post-Retrieval Symposium Apr. 1993 p 1551-1561 (For primary document see N93-29682 11-99)

Avail: CASI HC A03/MF A03; 2 functional color pages

The first Long Duration Exposure Facility (LDEF) mission has demonstrated the value of the LDEF concept for deep surveys of the space radiation environment. The kinds of measurements that could be done on a second LDEF mission are discussed. Ideas are discussed for experiments which: (1) capitalize on the discoveries from LDEF 1; (2) take advantage of LDEF's unique capabilities; and (3) extend the investigations begun on LDEF 1. These ideas have been gleaned from investigators on LDEF 1 and others interested in the space radiation environment. They include new approaches to the investigation of Be-7 that was discovered on LDEF 1, concepts to obtain further information on the ionic charge state of cosmic rays and other energetic particles in space and other ideas to extend the investigations begun on LDEF 1. Author (revised)

N93-29710# Anser Analytic Services, Inc., Arlington, VA.

DECISION MAKER'S GUIDE TO INTERNATIONAL SPACE

Robert Usher and Donald Blersch 1993 159 p

(Anser-STDN-93-4) Avail: CASI HC A08/MF A02

ANSER maintains an extensive knowledge base on international space activities. As part of its Independent Research and Development activities (IR&D), ANSER has developed an infrastructure that tracks the space development activities of more than 60 countries. Direct contact with foreign space officials and organizations provides a unique, steady flow of primary source data that is used in conjunction with data from open sources. The Decision Maker's Guide to International Space documents the highlights of ANSER's knowledge base in an easy-to-use reference book that provides top-level data in a uniform structure. The Guide is intended as a resource for senior-level US Government officials. As such, the format is kept concise for quick information retrieval and comparisons. Overall sources of information are cited at the end of the book, and current year budget figures are cited in individual country sections. While a rigorous footnoting system was not adopted, ANSER maintains this detailed level of data tracking as a feature within the International Space Capabilities Information System (ISCIS) database that supports publication of the Guide. The goal of this reference is to provide an accurate, standardized, functional guide to international space activities. For more rigorous investigations, ANSER currently uses its established knowledge base to perform in-depth analyses in a variety of international space areas and stands ready to meet additional needs of the US Government. Author (revised)

N93-30212# Horizon Data Corp., Reston, VA. Power Information Center.

INTERAGENCY ADVANCED POWER GROUP (IAPG) MEETING COMPENDIUM

Jan. 1993 130 p Symposium held in Alexandria, VA, 31 Mar. - 2 Apr. 1992

(Contract DE-AC01-90CE-90053)

(DE93-006189; CONF-920384-Summ) Avail: CASI HC A07/MF A02

Under the direction of the Interagency Advanced Power Group (IAPG), the Power Information Center (PIC) provides support services for each IAPG information exchange session. IAPG members meet a minimum of once each year to share programmatic and technical information on federally funded research and development (R&D) projects in the area of advanced power. This R&D is directed by one of the five IAPG member agencies-the US Army, US Navy, US Air Force, US Department of Energy, and the National Aeronautics and Space Administration. Affiliated federal groups and federally funded research and development centers can also participate. To enhance the exchange of information between government researchers, this 1992 IAPG Meeting Compendium has been assembled. This publication is a re-printing of abstracts of each IAPG presentation offered during 1991-1992. The information is arranged chronologically by IAPG meeting. During the 1992 IAPG meeting year, there were presentations restricted to government audiences only. These 'restricted' minutes have not been included in this compilation. DOE

N93-30513# Air Force Office of Scientific Research, Bolling AFB, Washington, DC.

AFOSR STATUS REPORT Quarterly Status Report, Jan. - Mar. 1993

Apr. 1993 92 p

(AD-A264720; AFOSR-93-0340TR) Avail: CASI HC A05/MF A01

The Research Proposal Quarterly Status Report is published in March, June, September, and December by the Air Force Office of Scientific Research (AFOSR). It lists all the research proposals received by AFOSR in the previous six months along with the action taken (Initiated, Declined, or Withdrawn) on each report. The report is divided into two parts. The Institution index lists proposals alphabetically by institution. This is followed by a more detailed listing by Directorate, and by Program Manager within the Directorate. This report is designed to inform other government sponsoring agencies of the proposals received by the AFOSR and the action taken on these proposals. Readers must keep in mind that declined proposals should not necessarily be special programmatic emphasis. DTIC

N93-30911# National Science Council, Taipei (Taiwan). Science and Technology Information Center.

SCIENTIFIC RESEARCH ABSTRACTS IN THE REPUBLIC OF CHINA, 1991 (SCIENCE AND TECHNOLOGY)

Dec. 1992 1823 p

Avail: CASI HC A99/MF A10

In order to meet the information needs of science and technology research in the country, reduce unwarranted repetition of research projects, and introduce the country's R&D activities to the international science and technology community, Science and Technology Information Center (STIC) compiles annually a set of abstracts as an effort to enlist all research projects completed in the year of interest. For the information to be comprehensive in scope, STIC collects data from all possible sources within the Republic of China, including research institutions, universities, and privately-funded laboratories. For the calendar year of 1991, entries covering all fields of Science and Technology are provided. Derived from text

SUBJECT INDEX

SCIENTIFIC AND TECHNICAL AEROSPACE REPORTS VOLUME 31 NUMBER 11

Typical Subject Index Listing

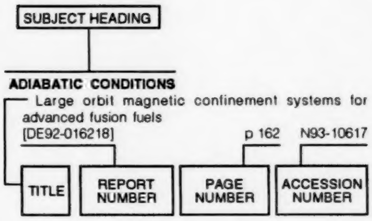
SUBJECT HEADING
ADIABATIC CONDITIONS
Large orbit magnetic confinement systems for advanced fusion fuels
[DE92-016218] p 162 N93-10617
TITLE
REPORT NUMBER
PAGE NUMBER
ACCESSION NUMBER

The subject heading is a key to the subject content of the document. Titles, report numbers, and accession numbers of pertinent documents are provided under each subject heading. When the title is insufficiently descriptive of the document content, a title extension is added, separated from the title by three hyphens. The report number helps to indicate the type of document cited (e.g., NASA report, NASA translation, NASA contractor report). The accession number is the number by which the document abstracts are arranged in this journal and by which the document is sold or requested. The page number helps you locate the citation in the abstract section. The titles, with title extensions if present, are arranged under each subject heading in ascending accession number order. The subject headings have been selected from the latest revision of the *NASA Thesaurus*.

A

A STARS
Precision optical interferometry in space
[NASA-CR-193264] p 3630 N93-29163

ABLATION
Altitude compensating ablative stiffening band for rocket motor nozzles
[NASA-CASE-MFS-28728-1] p 3288 N93-28950
Ablative shielding for hypervelocity projectiles
[NASA-CASE-MSC-21884-1] p 3331 N93-29088
Ablation problems using a finite control volume technique
[DE93-009861] p 3549 N93-29187

ABNORMALITIES
Energetic material response to abnormal environments p 3350 N93-30095

ABSORBENTS
Be3(AsO4)2 2H2O: A new berylloarsenate phase containing bridged tetrahedral 3-rings
[AD-A262518] p 3592 N93-28584
The synthesis and ab initio structure determination of Zn4O(BO3)2: A microporous zincoborate built up from fused 3-ring and 5-ring sub-units
[AD-A262504] p 3594 N93-29138
Ordered molecular arrays as templates: A new approach to synthesis of mesoporous materials
[AD-A264631] p 3570 N93-30540

ABSORBERS (MATERIALS)
Formulation of Ames 24E2 IR-black coating
[NASA-TM-102864] p 3629 N93-29453

ABSORPTION
A Fokker-Planck operator for the emission and absorption of electron plasma waves in a magnetized plasma
[DE93-009579] p 3584 N93-28598
Acid gas treating by aqueous alkanolamines
[PB93-176188] p 3471 N93-29676

ABSORPTION SPECTRA
Tomographic analysis of line-of-sight infrared spectra of low-pressure flames
[AD-A263185] p 3309 N93-28514
Microtextured metals for stray-light suppression in the Clementine startracker p 3286 N93-28785
Examination of shock induced chemical reactions in liquids using time-resolved optical spectroscopy
p 3318 N93-30073
Condensed phase diagnostics of nitramine propellant combustion p 3320 N93-30102
A novel flame thermometer based on the doppler width of ro-vibrational transitions
[AD-A264515] p 3315 N93-30405
A correlated k-distribution model of the atmospheric heating rates for overlapping spectra of CO2 and H2O
[DE93-007391] p 3474 N93-30504
Pulsed laser photoacoustic spectrometer for study of solid materials
[DE93-605290] p 3441 N93-31023

ABSORPTION SPECTROSCOPY
Development of ultraviolet absorption photometer for atmospheric ozone measurements and results from mid-latitude investigations p 3468 N93-28949
Femtosecond laser studies of excited state dynamics
[AD-A263708] p 3439 N93-29918
Experimental and theoretical aspects of excited state electron transfer and related phenomena
[AD-A263457] p 3570 N93-30589

ABSTRACTS
NASA SBIR abstracts of 1991 phase 1 projects
[NASA-TM-108240] p 3609 N93-29323
The 2nd International symposium on electrochemical impedance spectroscopy (extended abstracts)
[AD-A262994] p 3312 N93-29462
ONR/LANL Workshop on the Fundamental Physics and Chemistry of Combustion, Initiation, and Detonation of Energetic Materials
[CPIA-PUBL-589] p 3343 N93-30061
Scientific research abstracts in the Republic of China, 1991 (science and technology) p 3670 N93-30911

ABUNDANCE
Multiwavelength studies of classical nova shells
p 3636 N93-30412

ACCELERATION (PHYSICS)
Enhanced reduction of velocity data obtained during CETA flight experiment
[NASA-TM-4460] p 3431 N93-29209
Testing in combined dynamic environments
[DE93-010679] p 3278 N93-29250
Residual acceleration data on IML-1: Development of a data reduction and dissemination plan
[NASA-CR-193224] p 3281 N93-30038
GRO: Red-shifted electron-positron annihilation gamma-rays from radiopulsars
[NASA-CR-193243] p 3635 N93-30053

ACCELERATION STRESSES (PHYSIOLOGY)
Acquisition of physiological data during G-induced Loss of Consciousness (G-LOC)
[AD-A264492] p 3496 N93-30400

ACCELERATION TOLERANCE
Issues on human acceleration tolerance after long-duration space flights
[NASA-TM-104753] p 3495 N93-29651

ACCELERATORS
Low-frequency vibration environment for five Shuttle missions
[NASA-TM-106059] p 3285 N93-28554

ACCELEROMETERS
A microseismometer for terrestrial and extraterrestrial applications p 3434 N93-28765

ACCEPTOR MATERIALS
Growth, characterization and device development in monocrystalline diamond films
[AD-A263204] p 3593 N93-28874
Coherent and semi-coherent neutron transfer reactions
[DE93-008336] p 3565 N93-28959
Uniaxially stressed Ge:Ga and Ge:Be
[DE93-010426] p 3594 N93-29150
Defect studies in low-temperature-grown GaAs
[DE93-010405] p 3595 N93-29417
Experimental and theoretical aspects of excited state electron transfer and related phenomena
[AD-A263457] p 3570 N93-30589

ACCESS CONTROL
Minimum security requirements for multi-user operating systems
[PB93-185999] p 3522 N93-30832

ACCIDENT INVESTIGATION
Vehicle dynamic stability and rollover
[PB93-185437] p 3447 N93-30828

ACCIDENT PRONENESS
Accident proneness: A research review
[DOT/FAA/AM-93/9] p 3498 N93-28622

ACCOMMODATION COEFFICIENT
In-situ temperature and concentration measurements of organosilicon decomposition in a chemical vapor deposition reactor
[ONERA-P-1990-3] p 3313 N93-30109

ACCRETION DISKS
IUE observations of cataclysmic variable
[NASA-CR-193188] p 3629 N93-28634
Effects of spiral shocks on disk emission lines
[DE92-641716] p 3637 N93-31004

ACCUMULATIONS
SWAT system performance predictions
[AD-A262857] p 3579 N93-29470

ACCUMULATORS
From orbital debris capture systems through internal combustion engines on Mars p 3232 N93-29745

ACCURACY
The effect of clock, media, and station location errors on Doppler measurement accuracy
p 3246 N93-29588
Issues, concepts, and standard techniques in assessing accuracy of coordinate measuring machines
[PB93-184331] p 3354 N93-29666
Performance analysis of subspace methods
[AD-A263984] p 3530 N93-29865
Determinants of performance rating accuracy: A field study
[AD-A264726] p 3500 N93-30575

ACETALDEHYDE
Distribution of C1-C2 aldehydes in the free troposphere
[JUEL-2650] p 3475 N93-28475

ACETONE
Surface chemistry of hydrogen-passivated porous silicon-oxidation of surface Si-H groups by acetone
[AD-A264655] p 3315 N93-30526

ACETYLENE
Conjugated substituted ionic polyacetylenes
[AD-A264702] p 3337 N93-30497

ACID BASE EQUILIBRIUM
Coordination compounds of aluminum as precursors to aluminum nitride
[AD-A264700] p 3327 N93-30574

ACID RAIN
Emission inventories: A global modeling perspective
[DE93-005817] p 3469 N93-28965

ACIDITY
High octane ethers from synthesis gas-derived alcohols
[DE93-012470] p 3341 N93-28752

ACIDS
Studies in Lewis acid and superacid ionic liquids
[AD-A264683] p 3316 N93-30551

ACOUSTIC ATTENUATION
Sound attenuation characteristics of the standard DH-132A and SPH-4 helmets worn in combination with standard issue earplugs
[AD-A263011] p 3506 N93-29406
Sound wave scattering from a rigid sphere
[AD-A264182] p 3562 N93-30157

ACOUSTIC COUPLING
Theoretical and experimental study of thermoacoustic engines
[AD-A261934] p 3561 N93-28995

ACOUSTIC EXCITATION
Quiet by design: Numerical acousto-elastic analysis of aircraft structures
[ISBN-90-386-0042-9] p 3248 N93-29268

ACOUSTIC FATIGUE
Nonlinear analyses of composite aerospace structures in sonic fatigue
[NASA-CR-193124] p 3451 N93-29154

ACOUSTIC MEASUREMENT
Inservice diagnostic methods for solenoid-operated valves
[DE93-007823] p 3443 N93-28968
Acousto-Ultrasonic analysis of failure in ceramic matrix composite tensile specimens
[NASA-TM-106219] p 3449 N93-29073
Constant frequency pulsed phase-locked loop measuring device
[NASA-CASE-LAR-13823-1] p 3431 N93-29084
External acoustical noise measurements for aviation systems
[AD-A263138] p 3562 N93-29480

ACOUSTIC PROPAGATION
Sonic boom problem for future highspeed aircraft
[ONERA-NT-1990-3] p 3241 N93-30020

ACOUSTIC PROPERTIES
An integrated optimum design approach for high speed prop-rotors including acoustic constraints
[NASA-CR-193222] p 3248 N93-29153
Unsteady vortex loop/dipole theory applied to the work and acoustics of an ideal low speed propeller
[AD-A264057] p 3241 N93-29891

ACOUSTIC SCATTERING
The wave, the cylinder, and the plate
[DE93-009458] p 3450 N93-28596
Sound wave scattering from an elastic spherical shell
[AD-A264039] p 3562 N93-30029
Sound wave scattering from a rigid sphere
[AD-A264182] p 3562 N93-30157
Evaluation of the scattered pressure due to infinite rigid cylinders, infinite elastic cylindrical shells, and rigid spheres in the presence of an ambient noise field
[AD-A264835] p 3563 N93-30899

ACOUSTIC SOUNDING
Remote sensing survey of Mississippi River-Gulf Outlet, Breton Sound disposal area, Plaquemines Parish, Louisiana
[AD-A263097] p 3459 N93-29146

ACOUSTIC VELOCITY
Sound wave scattering from a rigid sphere
[AD-A264182] p 3562 N93-30157

ACOUSTICS
JPRS report: Science and technology. Central Eurasia: Physics and mathematics
[JPRS-UPM-93-002] p 3560 N93-29022
Acoustic charge transport technology investigation for advanced development transponder
p 3386 N93-29602
Unsteady vortex loop/dipole theory applied to the work and acoustics of an ideal low speed propeller
[AD-A264057] p 3241 N93-29891
The IUTAM Symposium on Breaking Waves
[AD-A264196] p 3489 N93-30143
Reception at Ascension Island, South Atlantic, of the transmissions from the Heard Island feasibility test
[PB93-176261] p 3394 N93-30662

ACOUSTO-OPTICS
Polarimetric multispectral imaging technology
p 3434 N93-28774
Acousto-optic infrared spectral imager for Pluto fast flyby p 3285 N93-28781
Modified Acousto-Optic Adaptive Processor (Mod-AOAP)
[AD-A261983] p 3381 N93-28997
Application of Schlieren optical techniques for the measurement of gas temperature and turbulent diffusivity in a diesel engine
[AD-A263810] p 3580 N93-29880
Photorefractive integrators and correlators
[AD-A264200] p 3597 N93-30144
Acousto-optic time-integrating correlators for processing wideband digital data p 3360 N93-30253

ACTIVATED CARBON
Fluids in porous media.
[PB93-175198] p 3428 N93-30759

ACTIVATION
Photobiological investigations on spores of streptomyces griseus
[ESA-TT-1269] p 3491 N93-29274

ACTIVATION ENERGY
Investigation of ion beam mixing of iron marker layers in aluminum oxide by RBS
[DE93-010727] p 3594 N93-29314
Applications of density functional theory to calculation of reaction energetics p 3351 N93-30098
Characterization of slow chromophore reorientation in nonlinear optical polymers by two-dimensional MAS NMR
[AD-A264809] p 3338 N93-30596

ACTIVE CONTROL
Low-cost Active Structural Control space experiment (LASC) p 3263 N93-28700
NASA instep/MDMSC jitter suppression experiment (JITTER) p 3263 N93-28702
Computerized atmospheric trace contaminant control simulation for manned spacecraft
[NASA-TM-108409] p 3505 N93-28977
Noise transmission properties and control strategies for composite structures p 3301 N93-30436
A theoretical and computational study on active wake control p 3243 N93-30892

ACTIVE GALACTIC NUCLEI
Infrared spectroscopy and imaging of starburst galaxies and AGNs
[MPE-PREPRINT-229] p 3632 N93-30643

ACTS
Design and construction of a prototype ACTS propagation terminal
[NASA-CR-193071] p 3404 N93-28539
System overview on electromagnetic compensation for reflector antenna surface distortion
[NASA-TM-106217] p 3273 N93-29195

ACTUATORS
Research programs from the University of South Carolina on high energy physics
[DE93-007829] p 3574 N93-28969
Evaluation of actuator energy storage and power sources for spacecraft applications
[NASA-CR-193226] p 3288 N93-29091
Single acting translation/rotational brake
[NASA-CASE-LAR-14738-1] p 3443 N93-29175
The design and modelling of a comb-drive-based microengine for mechanism drive applications
[DE93-009826] p 3443 N93-29185
Strategic avionics technology definition studies. Subtask 3-1A: Electrical Actuation (ELA) systems
[NASA-CR-193237] p 3271 N93-29215
Articulated fin/wing control system
[AD-D015712] p 3259 N93-29278
DSS-14 subreflector actuator dynamics during the Landers earthquake p 3386 N93-29600
An experimental/analytical evaluation of biaxial sheet failure
[DE93-010620] p 3453 N93-29843
Attitude stabilization of a rigid spacecraft using two momentum wheel actuators p 3280 N93-29990
Attitude stabilization of a rigid spacecraft using gas jet actuators operating in a failure mode
p 3280 N93-29992
Efficient reorientation of a deformable body in space: A free-free beam example p 3280 N93-29994
Materials for adaptive structural acoustic control, volume 1
[AD-A264619] p 3562 N93-30121
Materials for adaptive structural acoustic control, volume 2
[AD-A264620] p 3563 N93-30385

ADA (PROGRAMMING LANGUAGE)
Toward reusable graphics components in Ada
[AD-A262568] p 3524 N93-28577
Transforming AdaPT to Ada9x
[NASA-CR-193117] p 3526 N93-29026
Reactive integration for traditional programming languages
[AD-A263986] p 3531 N93-29866
Estimating Ada system size during development
[AD-A263880] p 3532 N93-30022
Using Penelope to assess the correctness of NASA Ada software: A demonstration of formal methods as a counterpart to testing
[NASA-CR-4509] p 3533 N93-30380
Procedures for applying Ada quality prediction models
[AD-A264730] p 3534 N93-30546
An approach to software quality prediction from Ada designs
[AD-A264731] p 3534 N93-30547

ADAPTATION
Adaptive defuzzification for fuzzy systems modeling
p 3512 N93-29532
Beta-adrenergic blockade and lactate metabolism during exercise at high altitude
[AD-A263544] p 3495 N93-29820
Enhanced convergence adaptive detection
[AD-A264100] p 3399 N93-30879

ADAPTIVE CONTROL
The dynamic behavior of constrained adaptive array sensor processors
[AD-A262402] p 3541 N93-28494
Description of the Joint Damping Experiment (JDX)
p 3263 N93-28703
Adaptive structures flight experiments
p 3263 N93-28704
Clustering of tethered satellite system simulation data by an adaptive neuro-fuzzy algorithm
p 3512 N93-29535
Genetic algorithms in adaptive fuzzy control
p 3518 N93-29572
Materials for adaptive structural acoustic control, volume 1
[AD-A264619] p 3562 N93-30121
Division by polynomial matrix and its application to multivariable linear systems p 3357 N93-30233
An information theoretic approach to stochastic adaptive control application to manipulators with active inertia
p 3359 N93-30247
An adaptive controller for a class of MIMO non-minimum phase systems with disturbance rejection design
p 3359 N93-30248
Materials for adaptive structural acoustic control, volume 2
[AD-A264620] p 3563 N93-30385

ADAPTIVE FILTERS
The dynamic behavior of constrained adaptive array sensor processors
[AD-A262402] p 3541 N93-28494
Realization of high speed adaptive FIR digital filters
p 3355 N93-30222
Synchronization of the LAPTV adative filter with input statistics p 3358 N93-30242
Adaptive filtering for clutter suppression in high frequency radar p 3377 N93-30355
Adaptive airborne radar simulation with equalization filter taps
[AD-A264722] p 3393 N93-30514
Enhanced convergence adaptive detection
[AD-A264100] p 3399 N93-30879

ADAPTIVE OPTICS
Characterization of laboratory generated turbulence by optical phase measurements
[AD-A262596] p 3480 N93-28465
SWAT 2 overview
[AD-A262905] p 3578 N93-29139
SWAT laboratory test results
[AD-A262906] p 3578 N93-29140
SWAT system performance predictions
[AD-A262857] p 3579 N93-29470
Sodium guide star adaptive optics system for astronomical imaging in the visible and near-infrared
[DE93-009543] p 3630 N93-29785

ADDITIVES
Process optimization of Hexoloy SX-SiC towards improved mechanical properties
[DE93-007913] p 3320 N93-28564
Ambient-atmosphere compatible superconducting fullerenes
[AD-A262025] p 3595 N93-29397
The 2-6 semiconductor superlattices
[AD-A264343] p 3597 N93-30164
Study on diamond semiconductor
[DE92-531076] p 3413 N93-30622

ADHESION
Evaluation of polyaryl adhesives in elastomer-stainless steel joints
[DE93-009794] p 3329 N93-28551
A study of the chemical mechanism in lubrication
[DE93-012230] p 3330 N93-28650
Effect of metallic-coating properties on the tribology of coated and oil-lubricated ceramics
[DE93-010663] p 3330 N93-28666
The mechanical response of gold substrates modified with self-assembling monolayer films
[AD-A262997] p 3452 N93-29515
Effect of water immersion on fiber/matrix adhesion in thermoplastic composites
[AD-A263646] p 3299 N93-29984
Structure, adhesion, and stability of metal/oxide and oxide/oxide interfaces
[DE93-012930] p 3325 N93-30060
Adhesion of thick film Au to alumina ceramics
[DE93-009802] p 3339 N93-30656
Studies of fiber-matrix adhesion on compression strength p 3304 N93-30846

ADHESION TESTS
Design and evaluation of a uniaxial pull test for lithium hydride/deuteride
[DE93-010760] p 3451 N93-28832

ADHESIVE BONDING
Evaluation of polyaryl adhesives in elastomer-stainless steel joints
[DE93-009794] p 3329 N93-28551
A study of the chemical mechanism in lubrication
[DE93-012230] p 3330 N93-28650
The adhesion of AgI molecules to gaseous metallic silver cluster cations
[AD-A264820] p 3338 N93-30628

ADHESIVES
Evaluation of polyaryl adhesives in elastomer-stainless steel joints
[DE93-009794] p 3329 N93-28551
Preliminary properties of a resin from ethynyl terminated materials p 3303 N93-30842

Performance of thermal adhesives in forced convection p 3293 N93-30974

ADIABATIC CONDITIONS
Dynamics and photoexcitation in MX and MXX' chain solids
[AD-A264823] p 3561 N93-29711

ADIABATIC EQUATIONS
Classification theorem for principal fibre bundles, Berry's phase, and exact cycle evolution
[DE93-011114] p 3556 N93-28601

ADJUSTING
CATS EYES adjustment procedures
[AD-A264069] p 3508 N93-29924

ADRENERGICS
Beta-adrenergic blockade and lactate metabolism during exercise at high altitude
[AD-A263544] p 3495 N93-29820

ADSORBENTS
Fluids in porous media.
[PB93-175198] p 3428 N93-30759

ADSORPTION
Adsorption of sulfate on metal electrodes
[AD-A263192] p 3309 N93-28540
Photodissociation of HBr/LiF(001): A quantum mechanical model
[NASA-CR-193119] p 3603 N93-28933
In situ Fourier transform infrared spectroscopic study of bisulfate and sulfate adsorption on gold, with and without the underpotential deposition of copper
[AD-A263421] p 3323 N93-29259
What is underneath? Moving atoms and molecules to find out
[AD-A263363] p 3567 N93-29332
FI-STM investigation of atomic hydrogen adsorption on the Si(100)2x1 surface
[AD-A262748] p 3567 N93-29403
Adsorption of hydrated halide ions on charged electrodes: Molecular dynamics simulation
[AD-A263137] p 3568 N93-29619
Interfacial viscosity measurements of adsorbed monolayers on metal surfaces
[AD-A263288] p 3324 N93-29803
Kinetics and dynamics of reacting systems
[AD-A264046] p 3313 N93-30030
Surface chemistry of N2H4 on Si(100)-2x1
[AD-A264819] p 3316 N93-30627
Fluids in porous media.
[PB93-175198] p 3428 N93-30759
Change of solar cell element properties influenced by adsorbed atoms
[DE93-606694] p 3466 N93-30777
Complex-compound heat pump: Topical report on phase 1 results
[PB93-185460] p 3466 N93-30814

ADVANCED VERY HIGH RESOLUTION RADIOMETER
Utilization of NOAA/AVHRR data for energy balance of Lake Constance (Switzerland) p 3458 N93-28926
Derivation of conductive heat transfer in mountains from AVHRR data p 3458 N93-28927

ADVECTION
Shear, strain, and thermohaline vertical fine structure in the upper ocean p 3488 N93-30046

AERIAL RECONNAISSANCE
Contributions to the American Meteorological Society's 26th International Conference on Radar Meteorology
[AD-A263385] p 3481 N93-29257

AEROACOUSTICS
Some aspects of the aeroacoustics of high-speed jets
[NASA-CR-191458] p 3418 N93-28975
Contribution to the study of the interaction between acoustic waves and coherent structures induced by a prismatic cylinder in a rectangular cavity
[ONERA-NT-1990-10] p 3314 N93-30203

AEROASSIST
Hypersonic lateral and directional stability characteristics of aeroassist flight experiment configuration in air and CF4
[NASA-TM-4435] p 3239 N93-29166

AERODYNAMIC CHARACTERISTICS
Effect of canard wing positions on aerodynamic characteristics of swept-forward wing
[AD-A262373] p 3238 N93-28493
International aviation (Selected articles)
[AD-A262566] p 3227 N93-28576
Experimental evaluation of a cooled radial-inflow turbine
[NASA-TM-106230] p 3251 N93-28697
An integrated optimum design approach for high speed prop-rotors including acoustic constraints
[NASA-CR-193222] p 3248 N93-29153
High Reynolds number and turbulence effects on aerodynamics and heat transfer in a turbine cascade
[NASA-TM-106187] p 3420 N93-29157
Recent applications of CFD to the aerodynamics of Army projectiles
[AD-A262953] p 3240 N93-29512
The application of concentric vortex simulation to calculating the aerodynamic characteristics of bodies of revolution at high angles of attack
[AD-A263879] p 3241 N93-29919
Heat transfer and aerodynamics of a 3D design nozzle guide vane tested in the Pyestock Isentropic Light Piston Facility p 3252 N93-29928
Experimental study of heat transfer close to a plane wall heated in the presence of multiple injections (subsonic flow) p 3253 N93-29931
The aerodynamic effect of coolant ejection in the leading edge region of a film-cooled turbine blade
p 3258 N93-29958
A computational model that couples aerodynamic and structural dynamic behavior of parachutes during the opening process
[AD-A264115] p 3241 N93-30119

AERODYNAMIC COEFFICIENTS
Hypersonic lateral and directional stability characteristics of aeroassist flight experiment configuration in air and CF4
[NASA-TM-4435] p 3239 N93-29166

AERODYNAMIC CONFIGURATIONS
Recent applications of CFD to the aerodynamics of Army projectiles
[AD-A262953] p 3240 N93-29512

AERODYNAMIC DRAG
Modeling the effects of drop drag and breakup on fuel sprays
[AD-A263650] p 3445 N93-29388
Construction, wind tunnel testing and data analysis for a 1/5 scale ultra-light wing model p 3243 N93-29778
Vortex shedding by blunt/bluff bodies at high Reynolds numbers. Volume 4: Rectangles
[AD-A264154] p 3241 N93-30151

AERODYNAMIC FORCES
Vortex shedding by blunt/bluff bodies at high Reynolds numbers. Volume 4: Rectangles
[AD-A264154] p 3241 N93-30151

AERODYNAMIC HEAT TRANSFER
The effect of orthogonal-mode rotation on forced convection in a circular-sectioned tube fitted with full circumferential transverse ribs p 3254 N93-29937

AERODYNAMIC HEATING
The infrared measurement for the reentry-body-translation
[AD-A263100] p 3278 N93-29134
Ablation problems using a finite control volume technique
[DE93-009861] p 3549 N93-29187

AERODYNAMIC LOADS
Evaluation of four advanced nozzle concepts for short takeoff and landing performance
[NASA-TP-3314] p 3239 N93-29165
Report on the test set-up for the structural testing of the Airmass Sunburst Ultralight Aircraft
p 3249 N93-29775
NASTRAN analysis for the Airmass Sunburst model 'C' Ultralight Aircraft p 3249 N93-29777
Construction, wind tunnel testing and data analysis for a 1/5 scale ultra-light wing model p 3243 N93-29778
Selection and static calibration of the Marsh J1678 pressure gauge p 3249 N93-29779

AERODYNAMIC NOISE
Subjective response to simulated sonic booms with ground reflections
[NASA-TM-107764] p 3561 N93-28692
Computation of far-field helicopter rotor tone noise
[ONERA-P-1990-5] p 3562 N93-30110

AERODYNAMIC STALLING
X-31 demonstration of integrated flight and propulsion control for effective combat at extreme angles of attack
p 3260 N93-28851
Requirements for pilot assistance in a thrust-vectoring combat aircraft p 3504 N93-28870
Simulation, characterization and control of forced unsteady viscous flows using Navier-Stokes equations
[AD-A264333] p 3425 N93-30369

AERODYNAMICS
International aviation (Selected articles)
[AD-A262566] p 3227 N93-28576
Construction, wind tunnel testing and data analysis for a 1/5 scale ultra-light wing model p 3243 N93-29778

AEROELASTICITY
The natural excitation technique (NExT) for modal parameter extraction from operating wind turbines
[DE93-010611] p 3463 N93-28603
Transonic flows on an oscillating airfoil and their effect on the flutter-boundary
[DLR-FB-92-08] p 3238 N93-29006
An integrated optimum design approach for high speed prop-rotors including acoustic constraints
[NASA-CR-193222] p 3248 N93-29153

AEROGELS
Thermal properties of organic and modified inorganic aerogels
[DE93-009230] p 3311 N93-29263

AERONAUTICAL ENGINEERING
JPRS report: Science and technology. Central Eurasia: Engineering and equipment
[JPRS-UEQ-92-007] p 3353 N93-28635
JPRS report: Science and technology. Central Eurasia: Engineering and equipment
[JPRS-UEQ-92-006] p 3353 N93-28636
JPRS report: Science and technology. Central Eurasia: Engineering and equipment
[JPRS-UEQ-92-010] p 3353 N93-28674
JPRS report: Science and technology. Central Eurasia: Engineering and equipment
[JPRS-UEQ-92-008] p 3353 N93-28675
JPRS report: Science and technology. Central Eurasia: Engineering and equipment
[JPRS-UEQ-93-003] p 3353 N93-28691
Proceedings of the Seventh Annual Summer Conference. NASA/USRA: University Advanced Design Program
[NASA-CR-192962] p 3227 N93-29712
Project summary p 3227 N93-29714
Preliminary design studies of an advanced general aviation aircraft p 3228 N93-29717

AERONAUTICS
Research and technology objectives and plans: Summary fiscal year 1991
[NASA-TM-103086] p 3660 N93-29452

AEROSOLS
Activities report of the International Meteorological Institute, Stockholm (Sweden)
[ETN-93-93768] p 3480 N93-28519
Aerosol particle analysis by Raman scattering technique
[DE93-005587] p 3309 N93-28880
Development of a 9.3 micrometer CW LIDAR for the study of atmospheric aerosol
[NASA-CR-193227] p 3381 N93-29105
Ocean aerosol measurements and models in the straits of Florida (The KEY-90 experiment)
[AD-A264777] p 3487 N93-29659
Quantifying and minimizing uncertainty of climate forcing by anthropogenic aerosols
[NASA-TM-108259] p 3472 N93-30043
Simulation and calculation of diffusive aerosol deposition
[DE93-007518] p 3474 N93-30506
Marine microbial production of dimethylsulfide from dissolved dimethylsulfoniopropionate
[NASA-CR-193278] p 3492 N93-30665

AEROSPACE ENGINEERING
International aviation (Selected articles)
[AD-A262566] p 3227 N93-28576
JPRS report: Science and technology. Central Eurasia: Engineering and equipment
[JPRS-UEQ-92-007] p 3353 N93-28635
JPRS report: Science and technology. Central Eurasia: Engineering and equipment
[JPRS-UEQ-92-006] p 3353 N93-28636
JPRS report: Science and technology. Central Eurasia: Engineering and equipment
[JPRS-UEQ-92-010] p 3353 N93-28674
JPRS report: Science and technology. Central Eurasia: Engineering and equipment
[JPRS-UEQ-92-008] p 3353 N93-28675
JPRS report: Science and technology. Central Eurasia: Engineering and equipment
[JPRS-UEQ-93-003] p 3353 N93-28691
Low-cost Active Structural Control space experiment (LASC) p 3263 N93-28700
Godunov-type schemes applied to detonation flows
[NASA-CR-191447] p 3509 N93-28841
NASA/DOD Aerospace Knowledge Diffusion Research Project. Paper 28: The technical communication practices of Russian and US aerospace engineers and scientists
[NASA-TM-108249] p 3612 N93-28948
Research and technology objectives and plans: Summary fiscal year 1991
[NASA-TM-103086] p 3660 N93-29452
A perspective on acquisition of NASA space systems
[AD-A263246] p 3610 N93-29499
Proceedings of the Seventh Annual Summer Conference. NASA/USRA: University Advanced Design Program
[NASA-CR-192962] p 3227 N93-29712
Design study to simulate the development of a commercial transportation system p 3228 N93-29718
An overview of DARPA's advanced space technology program p 3269 N93-29908
NASA/DoD Aerospace Knowledge Diffusion Research Project. Paper 30: The electronic transfer of information and aerospace knowledge diffusion
[NASA-TM-109223] p 3616 N93-30036

Technology Transfer and the Civil Space Program. Volume 2: Workshop proceedings [NASA-TM-108250] p 3625 N93-30692
OAST space research and technology applications: Technology transfer successes p 3625 N93-30693
Technology coordination p 3626 N93-30706
NASA space research and technology overview (ITP) p 3628 N93-30722
Space research and technology overview p 3628 N93-30723

AEROSPACE ENVIRONMENTS
Low-frequency vibration environment for five Shuttle missions [NASA-TM-106059] p 3285 N93-28554
The Optical Properties Monitor (OPM): A multipurpose optical laboratory in space p 3266 N93-28729
Low Earth orbital mission aboard the Space Test Experiments Platform (STEP-3) p 3267 N93-28732
High-performance visible/UV CCD focal plane technology for spacebased applications p 3434 N93-28771
Advanced engine study program [NASA-CR-187217] p 3287 N93-28946
Natural environmental service support to NASA vehicle, technology, and sensor development programs [NASA-CR-192554] p 3469 N93-29029
Enhanced reduction of velocity data obtained during CETA flight experiment [NASA-TM-4460] p 3431 N93-29209
LDEF: 69 Months in Space. Part 1: Second Post-Retrieval Symposium [NASA-CP-3194-PT-1] p 3660 N93-29621
LDEF: Dosimetric measurement results (AO 138-7 experiment) p 3573 N93-29635
LDEF: 69 Months in Space. Part 4: Second Post-Retrieval Symposium [NASA-CP-3194-PT-4] p 3665 N93-29682
Degradation of optical components in a space environment p 3582 N93-29692
Effects of long term space environment exposure on optical substrates and coatings (S0050-2) p 3582 N93-29694
LDEF space optics handbook p 3582 N93-29695
Holographic data storage crystals for the LDEF p 3435 N93-29697
Analyses of space environment effects on active fiber optic links orbited aboard the LDEF p 3583 N93-29699
Final results of space exposed experiment developed for students p 3492 N93-29702
Continued results of the seeds in space experiment p 3492 N93-29703
LDEF archival system plan p 3624 N93-29704
Next generation optical instruments and space experiment based on the LDEF thermal control surfaces experiment (S0069) p 3583 N93-29706
Future radiation measurements in low Earth orbit p 3654 N93-29708
Effects of device scaling and geometry on MOS radiation hardness assurance [DE93-009832] p 3413 N93-30516

AEROSPACE INDUSTRY
Technology Transfer and the Civil Space Program. Volume 2: Workshop proceedings [NASA-TM-108250] p 3625 N93-30692
NASP technology transfer p 3627 N93-30713
Technology transfer between the government and the aerospace industry p 3628 N93-30716

AEROSPACE MEDICINE
Acquisition of physiological data during G-induced Loss of Consciousness (G-LOC) [AD-A264492] p 3496 N93-30400

AEROSPACE SAFETY
Risk-based spacecraft fire safety experiments p 3267 N93-28738
SPECS: Orbital debris removal p 3234 N93-29754

AEROSPACE SCIENCES
Research and technology objectives and plans: Summary fiscal year 1991 [NASA-TM-103086] p 3660 N93-29452
The prehistory of ESRO, 1959 - 1960 [ESA-HSR-1] p 3660 N93-29500
Technology coordination p 3626 N93-30706

AEROSPACE SYSTEMS
Lightweight flexible composite tent materials [AD-A263021] p 3295 N93-28660
Low-cost Active Structural Control space experiment (LASC) p 3263 N93-28700
Graphical interface between the CIRSSE testbed and CimStation software with MCS/CTOS [NASA-CR-193276] p 3527 N93-29218
Spacecraft surface charging handbook [AD-A262778] p 3279 N93-29305
A perspective on acquisition of NASA space systems [AD-A263246] p 3610 N93-29499
Tactical satellites p 3284 N93-29893
Spacecraft and launch systems for TACSAT applications p 3284 N93-29904
An overview of DARPA's advanced space technology program p 3269 N93-29908
The planning coordinator: A design architecture for autonomous error recovery and on-line planning of intelligent tasks [NASA-CR-193250] p 3543 N93-30039
Consultative Committee for Space Data Systems recommendation for space data system standards: Telecommand. Part 2.1: Command operation procedures [NASA-TM-108158] p 3393 N93-30371
OAST space research and technology applications: Technology transfer successes p 3625 N93-30693
Technology transfer from the viewpoint of a NASA prime contractor p 3626 N93-30701
A representative survey of US space systems and methods for estimating their costs [AD-A264159] p 3272 N93-30881

AEROSPACE TECHNOLOGY TRANSFER
Technology Transfer and the Civil Space Program. Volume 2: Workshop proceedings [NASA-TM-108250] p 3625 N93-30692
OAST space research and technology applications: Technology transfer successes p 3625 N93-30693
White House/OSTP perspective p 3625 N93-30696
Technology transfer p 3626 N93-30699
Technology transfer to the broader economy p 3628 N93-30719
Strategic directions and mechanisms in technology transfer p 3628 N93-30720
Workshop conclusions: Technology transfer and the civil space program p 3628 N93-30721
Technology transfer in the NASA Ames Advanced Life Support Division p 3628 N93-30724
A research experiment on facilitation and formation of joint research and development programs between government, industry, and universities: Overview, preliminary findings, and observations p 3628 N93-30725

AEROSPACE VEHICLES
Preliminary properties of a resin from ethynyl terminated materials p 3303 N93-30842
Advanced electromagnetic methods for aerospace vehicles [NASA-CR-193468] p 3400 N93-31036

AEROTHERMODYNAMICS
Heat transfer in high turbulence flows: A 2-D planar wall jet p 3254 N93-29935
Aerothermic calculations of flows in interdisc cavities of turbines p 3256 N93-29947
Aero-thermal design of a cooled transonic NGV and comparison with experimental results p 3257 N93-29957

AFTERBODIES
Fabrication of the V-22 composite AFT fuselage using automated fiber placement p 3302 N93-30443

AFTERBURNING
Thrust augmentation system for low-cost-expendable turbojet engine [AD-A263727] p 3259 N93-30877

AGGREGATES
Growth model of Au films on Ru(001) [DE92-642126] p 3602 N93-30998

AGING (MATERIALS)
Molecular dynamics of physical aging processes in polymer glasses [AD-A263737] p 3334 N93-29856

AGING (METALLURGY)
The temperature dependence of the deformation and oxidation behavior of an age-hardenable beta + alpha-two titanium alloy [AD-A262232] p 3320 N93-28491
Molecular dynamics of physical aging processes in polymer glasses [AD-A263737] p 3334 N93-29856

AGRICULTURE
Remote sensing of agricultural vegetation: Status and perspectives p 3458 N93-28922
The MAESTRO-1 campaign: Analyses of polarimetric SAR data of agricultural fields and forests [BCRS-92-06] p 3460 N93-29320

AGROMETEOROLOGY
National remote sensing programme 2 ACMS project. Phase 1: Validation. Part 1: Definition of validation experiment [BCRS-92-10-PHASE-1-PT-1] p 3461 N93-29465

AIR
Methods for preparation of mixtures of gases in air at the parts-per-billion to parts-per-million concentration range for calibration of monitors [DE92-642433] p 3317 N93-30982

AIR BREATHING ENGINES
Conceptual design of a two-stage-to-orbit vehicle p 3228 N93-29716

AIR CARGO
The development of a parachute system for aerial delivery from high speed cargo aircraft [DE93-008339] p 3239 N93-29035

AIR CONDITIONING
Complex-compound heat pump: Topical report on phase 1 results [PB93-185460] p 3466 N93-30814

AIR CONDITIONING EQUIPMENT
Study of parameters affecting the performance of solar desiccant cooling systems [DE93-000088] p 3465 N93-30206

AIR COOLING
Experimental evaluation of a cooled radial-inflow turbine [NASA-TM-106230] p 3251 N93-28697
Transient thermal behaviour of a compressor rotor with axial cooling air flow and co-rotating or contra-rotating shaft p 3255 N93-29946
Impingement/effusion cooling p 3257 N93-29954

AIR DATA SYSTEMS
The Orbiter Experiments (OEX) program p 3266 N93-28731

AIR DEFENSE
Planning for air to air combat p 3501 N93-28852
Computer assisted evaluation for air close combat based on time interval characterization p 3504 N93-28868
Requirements for pilot assistance in a thrust-vectoring combat aircraft p 3504 N93-28870

AIR FILTERS
Evaluation and optimization of a flexible filtration system for respiratory protection system 21 [AD-A262467] p 3493 N93-28758

AIR FLOW
Jet mixer noise suppressor using acoustic feedback [NASA-CASE-LEW-15170-1] p 3561 N93-28953
The 3-D viscous flow CFD analysis of the propeller effect on an advanced ducted propeller subsonic inlet [NASA-TM-106240] p 3252 N93-29162
Aerothermic calculations of flows in interdisc cavities of turbines p 3256 N93-29947
Air oxidation behavior of fuel for the High Temperature Engineering Test Reactor (HTTR) [DE93-753349] p 3576 N93-30006

AIR LAND INTERACTIONS
Modeling land-surface/atmosphere dynamics for CHAMMP [DE93-008520] p 3476 N93-28677

AIR NAVIGATION
Advanced Transport Operating System (ATOPS) Flight Management/Flight Controls (FM/FC) software description [NASA-CR-191457] p 3250 N93-28621
Engineering management consideration for an integrated aeronautical mobile satellite service p 3374 N93-30337
Adapting system engineering principles to the Canadian Airspace System p 3247 N93-30338

AIR PIRACY
Air piracy and terrorism directed against U.S. Air carriers [AD-A264120] p 3244 N93-30194

AIR POLLUTION
Fugitive hydrocarbon emissions from Pacific OCS facilities, volume 1 [PB93-173797] p 3468 N93-28899
Atmospheric and Geophysical Sciences Division: G-Division did you know? [DE93-007412] p 3469 N93-28967
Global warming potential for SF6 [DE93-007394] p 3469 N93-28972
Summer 1990 Atlanta ozone precursor study (January 1993) [PB93-167203] p 3470 N93-29200
Analysis of protocol gases: An on-going quality assurance audit [PB93-168839] p 3311 N93-29204
The ANL electric vehicle battery R/D program for DOE-EHP [DE93-010658] p 3408 N93-29311
Study to determine the nature and extent of ozone and ozone precursor transport in selected areas of California [PB93-184828] p 3470 N93-29669
Potential effects of HFC-152a on global ozone and climate [DE93-008018] p 3471 N93-29792
Fugitive hydrocarbon emissions from Pacific OCS facilities. Volume 2: Executive summary and user's guide [PB93-173805-VOL-2] p 3471 N93-29861
Multi-Attribute Decision Theory methodology for pollution control measure analysis [DE93-005444] p 3472 N93-30008

AIR QUALITY
Analysis of protocol gases: An on-going quality assurance audit [PB93-168839] p 3311 N93-29204

Multi-Attribute Decision Theory methodology for pollution control measure analysis
[DE93-005444] p 3472 N93-30008
Case study of Frontal Boundary Study Mission 03
[DE93-007176] p 3473 N93-30183

AIR TO AIR MISSILES
Pilot decision aiding for weapon delivery: A novel approach to fire control cueing using parallel computing
p 3501 N93-28853

AIR TRAFFIC
Two simulation studies of precision runway monitoring of independent approaches to closely spaced parallel runways
[AD-A263433] p 3261 N93-29815

AIR TRAFFIC CONTROL
Results of DATAS investigation of ATCRBS environment at the Los Angeles International Airport
[DOT/FAA/CT-93/6] p 3245 N93-28625
Data Multiplexing Network (DMN) equipment Operational Test and Evaluation (OT&E) integration test report
[AD-A263172] p 3538 N93-29490
The 1991-1992 aviation system capacity plan
[AD-A263436] p 3261 N93-29788
Two simulation studies of precision runway monitoring of independent approaches to closely spaced parallel runways
[AD-A263433] p 3261 N93-29815
Classification of radar clutter in an air traffic control environment p 3246 N93-30299
Evolution of radar data processing in the French air traffic control system p 3247 N93-30325
Engineering management consideration for an integrated aeronautical mobile satellite service
p 3374 N93-30337
Adapting system engineering principles to the Canadian Airspace System p 3247 N93-30338
Issues of ATC conflict resolution under real-time constraints p 3247 N93-30350
National Airspace System Performance Analysis Capability (NASPAC) simulation model
p 3247 N93-30351
Enhancing availability, performance, and flexibility of air traffic control air-ground services p 3247 N93-30353
Changing role of telecommunications management in air traffic control in the FAA p 3247 N93-30354
Airspace Design Expert System (ADES), a 2D/3D mapping and modelling tool incorporating an expert system for use in instrument approach design
p 3247 N93-30357
An analysis of en route controller-pilot voice communications
[AD-A264784] p 3394 N93-30611

AIR TRAFFIC CONTROLLERS (PERSONNEL)
Two simulation studies of precision runway monitoring of independent approaches to closely spaced parallel runways
[AD-A263433] p 3261 N93-29815
The air traffic controller's mental model and it's implications for equipment design and trainee selection
p 3372 N93-30322
An analysis of en route controller-pilot voice communications
[AD-A264784] p 3394 N93-30611

AIR TRANSPORTATION
Design study to simulate the development of a commercial transportation system p 3228 N93-29718
The 1991-1992 aviation system capacity plan
[AD-A263436] p 3261 N93-29788
Air piracy and terrorism directed against U.S. Air carriers
[AD-A264120] p 3244 N93-30194

AIR WATER INTERACTIONS
Optical measurements of ripples using a scanning laser slope gauge. Part 1: Instrumentation and preliminary results
[AD-A261939] p 3486 N93-28996
Upper ocean model of dissolved atmospheric gases
[DE93-010151] p 3487 N93-29327
Optical slope/height measurements of small scale waves within the SAXON-FPN experiment
[AD-A262572] p 3487 N93-29422
The 17th Annual Climate Diagnostics Workshop
[PB93-183895] p 3483 N93-29664
A preliminary review of global CO2 exchange between ocean and atmosphere
[AD-A264019] p 3472 N93-30015
Marine microbial production of dimethylsulfide from dissolved dimethylsulfoniopropionate
[NASA-CR-193278] p 3492 N93-30665
Hydrographic observations in the western tropical and subtropical north Atlantic Ocean: Atlantic Climate Change Program (ACCP) and Western Tropical Atlantic Experiment (WESTRAX) during 1990
[PB93-184760] p 3489 N93-30827
IOC-UNEP review meeting on oceanographic processes of transport and distribution of pollutants in the sea
[DE93-605070] p 3490 N93-31019

AIRBORNE EQUIPMENT
Research and development of an airborne multispectral scanner to measure fire, terrestrial and atmospheric characteristics (50 channel)
[NASA-CR-193121] p 3456 N93-28620
A concluding study of the altitude determination deficiencies of the Service Aircraft Instrumentation Package (SAIP)
[AD-A263515] p 3250 N93-29971

AIRBORNE LASERS
Every good virtue you ever wanted in a Q-switched solid-state laser and more: Monolithic, diode-pumped, self-Q-switched, highly reproducible, diffraction-limited Nd:YAG laser p 3442 N93-28772

AIRBORNE RADAR
Development of an airborne MMW FM-CW radar for mapping river ice
[AD-A262655] p 3379 N93-28588
Adaptive airborne radar simulation with equalization filter taps
[AD-A264722] p 3393 N93-30514

AIRBORNE SURVEILLANCE RADAR
Radar beam effects for a flight simulator using signal processor based hardware p 3373 N93-30328

AIRBORNE/SPACEBORNE COMPUTERS
Spacecraft computer technology at Southwest Research Institute p 3522 N93-28813
SEU tolerant computer based on the R3000
[DE93-009294] p 3520 N93-29058
A real-time, hardware-in-the-loop simulation of an unmanned aerial research vehicle
[AD-A262477] p 3248 N93-29409
Airborne data acquisition using a front-end processor architecture p 3373 N93-30329
Space Generic Open Avionics Architecture (SGOAA) reference model technical guide
[NASA-CR-188246] p 3285 N93-31032

AIRCRAFT ACCIDENTS
World commercial aircraft accidents
[DE93-010892] p 3243 N93-28571
An evaluation of B-1B pilot performance during simulated instrument approaches with and without status information
[AD-A263874] p 3507 N93-29888

AIRCRAFT ANTENNAS
Models for performance assessment of HF antennas on the CH-135/Twin Huey helicopter
p 3366 N93-30291
Coupling gain computation between antennas on circular cylinders at SHF/EHF frequencies p 3369 N93-30309

AIRCRAFT APPROACH SPACING
Developing automation for terminal air traffic control: Case study of the imaging aid p 3247 N93-30356

AIRCRAFT COMMUNICATION
Tactical satellites for air command and control
p 3284 N93-29898
Design issues and initial performance of an adaptive air/ground/air HF communication system
p 3375 N93-30342
Enhancing availability, performance, and flexibility of air traffic control air-ground services p 3247 N93-30353

AIRCRAFT CONFIGURATIONS
High-altitude reconnaissance aircraft
p 3227 N93-29713

AIRCRAFT CONSTRUCTION MATERIALS
A demonstration of simple airfoils: Structural design and materials choices
[DE93-007882] p 3238 N93-28662
Nonlinear analyses of composite aerospace structures in sonic fatigue
[NASA-CR-193124] p 3451 N93-29154
Advanced technology composite aircraft structures
[NASA-CR-190420] p 3248 N93-29498
Static and dynamic large deflection flexural response of graphite-epoxy beams
[NASA-CR-4118] p 3454 N93-30374
Composites: A viable option p 3300 N93-30429
Advanced composite structural concepts and material technologies for primary aircraft structures
p 3300 N93-30430
Structural evaluation of curved stiffened composite panels fabricated using a THERM-Xsm process
p 3301 N93-30435
Lessons learned for composite structures
p 3302 N93-30444
First NASA Advanced Composites Technology Conference, part 2
[NASA-CP-3104-PT-2] p 3303 N93-30841
Characterization of multiaxial warp knit composites
p 3304 N93-30851
Development of resins for composites by resin transfer molding p 3305 N93-30853
Advanced fiber/matrix material systems
p 3305 N93-30854
Mechanical and analytical screening of braided composites for transport fuselage applications
p 3305 N93-30855
Construction and testing of simple airfoils to demonstrate structural design, materials choice, and composite concepts p 3243 N93-30979

AIRCRAFT CONTROL
Artificial intelligence methodologies in flight related differential game, control and optimization problems
[AD-A262405] p 3541 N93-28498
X-31 demonstration of integrated flight and propulsion control for effective combat at extreme angles of attack
p 3260 N93-28851

AIRCRAFT DESIGN
International aviation (Selected articles)
[AD-A262566] p 3227 N93-28576
Reliability assessment at airline inspection facilities. Volume 2: Protocol for an eddy current inspection reliability experiment
[DOT/FAA/CT-92/12-VOL-2] p 3449 N93-28685
Design considerations for a night, air-to-surface attack capability on a dual role fighter p 3251 N93-28871
An integrated optimum design approach for high speed prop-rotors including acoustic constraints
[NASA-CR-193222] p 3248 N93-29153
Quiet by design: Numerical acousto-elastic analysis of aircraft structures
[ISBN-90-386-0042-9] p 3248 N93-29268
High-altitude reconnaissance aircraft
p 3227 N93-29713
Project summary p 3227 N93-29714
Project ARES 2: High-altitude battery-powered aircraft
p 3227 N93-29715
Preliminary design studies of an advanced general aviation aircraft p 3228 N93-29717
Design study to simulate the development of a commercial transportation system p 3228 N93-29718
Design of a turbofan powered regional transport aircraft p 3228 N93-29721
Solar powered multipurpose remotely powered aircraft
p 3229 N93-29722
Preliminary development of a VTOL unmanned air vehicle for the close-range mission
[AD-A263514] p 3354 N93-29969
Sonic boom problem for future highspeed aircraft
[ONERA-NT-1990-3] p 3241 N93-30020
Cost studies for commercial fuselage crown designs
p 3302 N93-30440
A unified approach for composite cost reporting and prediction in the ACT program p 3302 N93-30441
Lessons learned for composite structures
p 3302 N93-30444
First NASA Advanced Composites Technology Conference, part 2
[NASA-CP-3104-PT-2] p 3303 N93-30841
Multi-parameter optimization tool for low-cost commercial fuselage crown designs
p 3305 N93-30858
Design and analysis of grid stiffened concepts for aircraft composite primary structural applications
p 3306 N93-30861
A comparison of classical mechanics models and finite element simulation of elastically tailored wing boxes
p 3306 N93-30863
Tailored composite wings with elastically produced chordwise camber p 3308 N93-30876

AIRCRAFT ENGINES
An analysis of the correlation between the J52 engine component improvement program and improved maintenance parameters
[AD-A262062] p 3251 N93-28984
The design of two-stage-to-orbit vehicles
p 3228 N93-29719

AIRCRAFT EQUIPMENT
Hybrid oxygen system
[AD-A262417] p 3500 N93-28464
A new class of mission support for combat air-crew
p 3501 N93-28854
The design and development of the new RAF standard HUD format p 3502 N93-28856
Standardization of automatic test equipment in the US Air force
[AD-A262076] p 3250 N93-29004
The NASA SBIR product catalog
[NASA-TM-108242] p 3609 N93-29322
High reliability, maintenance-free INS battery development
[AD-A264521] p 3412 N93-30406

AIRCRAFT FUELS
Advanced thermally-stable, coal-derived, jet fuels program: Experiment system and model development
[AD-A262747] p 3342 N93-29402

AIRCRAFT GUIDANCE
Advanced Transport Operating System (ATOPS) Flight Management/Flight Controls (FM/FC) software description
[NASA-CR-191457] p 3250 N93-28621
Head-steered sensor flight test results and implications p 3502 N93-28859
The quest for an integrated flying helmet
p 3502 N93-28860
Human capabilities and limitations in situation awareness p 3503 N93-28863
Tactical satellites for air command and control
p 3284 N93-29898
Evaluation of category 3 MLS designs
p 3247 N93-30358
Aircraft guidance for wind shear avoidance: Decision-making under uncertainty p 3246 N93-31005
AIRCRAFT ICING
A passive infrared ice detection technique for helicopter applications
[NASA-CR-193187] p 3244 N93-29152
FAA international conference on airplane ground deicing
[AD-A263617] p 3244 N93-29286
AIRCRAFT INSTRUMENTS
The design and development of the new RAF standard HUD format p 3502 N93-28856
Cognitive interface considerations for intelligent cockpits p 3503 N93-28865
A concluding study of the altitude determination deficiencies of the Service Aircraft Instrumentation Package (SAIP)
[AD-A263515] p 3250 N93-29971
AIRCRAFT LANDING
Helicopter approach capability using the differential global positioning system
[NASA-CR-193183] p 3245 N93-28936
Evaluation of four advanced nozzle concepts for short takeoff and landing performance
[NASA-TP-3314] p 3239 N93-29165
AIRCRAFT MAINTENANCE
Reliability assessment at airline inspection facilities. Volume 2: Protocol for an eddy current inspection reliability experiment
[DOT/FAA/CT-92/12-VOL-2] p 3449 N93-28685
Aircraft and refueler bonding and grounding study
[AD-A262027] p 3261 N93-29398
AIRCRAFT MANEUVERS
X-31 demonstration of integrated flight and propulsion control for effective combat at extreme angles of attack
p 3260 N93-28851
Planning for air to air combat p 3501 N93-28852
The design and development of the new RAF standard HUD format p 3502 N93-28856
Computation of a delta-wing roll-and-hold maneuver
[AD-A264704] p 3260 N93-30498
AIRCRAFT MODELS
A demonstration of simple airfoils: Structural design and materials choices
[DE93-007882] p 3238 N93-28662
Modal survey of a full-scale F-18 wind tunnel model
[AD-A262482] p 3240 N93-29410
Solution of Euler equations for forebody-inlet ensemble of aircraft at high angle of attack
[AD-A263905] p 3240 N93-29862
RCS of fundamental scatterers in the HF band by wire-grid modelling p 3371 N93-30320
AIRCRAFT NOISE
External acoustical noise measurements for aviation systems
[AD-A263138] p 3562 N93-29480
AIRCRAFT PERFORMANCE
Evaluation of four advanced nozzle concepts for short takeoff and landing performance
[NASA-TP-3314] p 3239 N93-29165
Flight mechanical model for performance calculations and interactions between flight vehicle and ramjet in regard to the flight orbit
[ESA-TT-1267] p 3248 N93-29464
AIRCRAFT PILOTS
Head-steered sensor flight test results and implications p 3502 N93-28859
The quest for an integrated flying helmet
p 3502 N93-28860
The physiological limitations of man in the high G environment p 3503 N93-28861
Field test of a computer-driven tool to measure psychological characteristics of aircrew
[AD-A264484] p 3499 N93-30425
AIRCRAFT SAFETY
FAA international conference on airplane ground deicing
[AD-A263617] p 3244 N93-29286
Progress through precedent: Going where no helicopter simulator has gone before p 3237 N93-30686
Aircraft guidance for wind shear avoidance: Decision-making under uncertainty p 3246 N93-31005
AIRCRAFT STRUCTURES
Reliability assessment at airline inspection facilities. Volume 2: Protocol for an eddy current inspection reliability experiment
[DOT/FAA/CT-92/12-VOL-2] p 3449 N93-28685
Nonlinear analyses of composite aerospace structures in sonic fatigue
[NASA-CR-193124] p 3451 N93-29154
Advanced technology composite aircraft structures
[NASA-CR-190420] p 3248 N93-29498
The Ultra Light Aircraft Testing
[NASA-CR-193043] p 3249 N93-29774
Report on the test set-up for the structural testing of the Airmass Sunburst Ultralight Aircraft
p 3249 N93-29775
Static and dynamic large deflection flexural response of graphite-epoxy beams
[NASA-CR-4118] p 3454 N93-30374
Composites: A viable option p 3300 N93-30429
Advanced composite structural concepts and material technologies for primary aircraft structures
p 3300 N93-30430
Composites technology for transport primary structure
p 3300 N93-30431
Design, analysis, and fabrication of the technology integration box beam p 3300 N93-30433
Structural evaluation of curved stiffened composite panels fabricated using a THERM-Xsm process
p 3301 N93-30435
Resin transfer molding for advanced composite primary aircraft structures p 3301 N93-30438
Consolidation of graphite thermoplastic textile preforms for primary aircraft structure p 3302 N93-30439
F-15 composite engine access door
p 3302 N93-30442
First NASA Advanced Composites Technology Conference, part 2
[NASA-CP-3104-PT-2] p 3303 N93-30841
Advanced fiber/matrix material systems
p 3305 N93-30854
Multi-parameter optimization tool for low-cost commercial fuselage crown designs
p 3305 N93-30858
Design and analysis of grid stiffened concepts for aircraft composite primary structural applications
p 3306 N93-30861
Optimization of composite sandwich cover panels subjected to compressive loadings p 3306 N93-30862
Advanced fiber placement of composite fuselage structures p 3306 N93-30864
Structural response of bead-stiffened thermoplastic shear webs p 3308 N93-30873
An overview of the crash dynamics failure behavior of metal and composite aircraft structures
p 3308 N93-30875
Construction and testing of simple airfoils to demonstrate structural design, materials choice, and composite concepts p 3243 N93-30979
AIRCRAFT WAKES
Determination of surface heat transfer and film cooling effectiveness in unsteady wake flow conditions
p 3253 N93-29933
Vortex wake characteristics of B757-200 and B767-200 aircraft using the tower fly-by technique
[PB93-180255] p 3242 N93-30387
Vortex wake characteristics of B757-200 and B767-200 aircraft using the tower fly-by technique
[PB93-180263] p 3242 N93-30388
AIRFOILS
Development and testing of the Perseus proof-of-concept aircraft
[DE93-010121] p 3247 N93-28586
A demonstration of simple airfoils: Structural design and materials choices
[DE93-007882] p 3238 N93-28662
Development of an unstructured solution adaptive method for the quasi-three-dimensional Euler and Navier-Stokes equations
[NASA-CR-193241] p 3421 N93-29213
A parallel implicit incompressible flow solver using unstructured meshes
[AD-A263395] p 3424 N93-29851
Keynote address: Unsteady, multimode transition in gas turbine engines p 3252 N93-29927
Determination of surface heat transfer and film cooling effectiveness in unsteady wake flow conditions
p 3253 N93-29933
Prediction of jet impingement cooling scheme characteristics (airfoil leading edge application)
p 3255 N93-29941
Construction and testing of simple airfoils to demonstrate structural design, materials choice, and composite concepts p 3243 N93-30979
AIRFRAMES
Development and testing of the Perseus proof-of-concept aircraft
[DE93-010121] p 3247 N93-28586
A unified approach for composite cost reporting and prediction in the ACT program p 3302 N93-30441
Fabrication of the V-22 composite AFT fuselage using automated fiber placement p 3302 N93-30443
AIRLINE OPERATIONS
The 1991-1992 aviation system capacity plan
[AD-A263436] p 3261 N93-29788
AIRPORT SECURITY
Future directions in aviation security
p 3244 N93-30274
AIRPORTS
The 1991-1992 aviation system capacity plan
[AD-A263436] p 3261 N93-29788
AIRSHIPS
Tethered aerostat VLF/LF transmitter system design considerations p 3399 N93-30753
AIRSPACE
The 1991-1992 aviation system capacity plan
[AD-A263436] p 3261 N93-29788
Airspace Design Expert System (ADES), a 2D/3D mapping and modelling tool incorporating an expert system for use in instrument approach design
p 3247 N93-30357
ALBEDO
Atmospheric correction of LANDSAT-TM-data for forest inventory p 3459 N93-28929
Modeling the bidirectional reflectance and spectra
[AD-A263570] p 3462 N93-29830
ALBUMINS
Amino acid sequences for the binding regions in serum albumin proteins
[NASA-CASE-MFS-28402-1] p 3491 N93-28952
ALCOHOLS
Design of a high activity and selectivity alcohol catalyst
[DE93-012277] p 3309 N93-28750
Mass spectrometric investigation of 2-methoxyethanol and 2-ethoxyethanol clusters: Magic numbers and structural implications
[AD-A262822] p 3312 N93-29429
ALDEHYDES
Distribution of C1-C2 aldehydes in the free troposphere
[JUEL-2650] p 3475 N93-28475
ALGAE
Process for selectively recovering algae and protozoa
[NASA-CASE-MFS-26124-1-NPO] p 3491 N93-29174
Marine microbial production of dimethylsulfide from dissolved dimethylsulfoniopropionate
[NASA-CR-193278] p 3492 N93-30665
ALGEBRA
Antirational transductions and their language families
[ETN-93-93794] p 3611 N93-28525
Research in mathematics and computer science, March 1, 1991 - September 30, 1992
[DE93-011492] p 3509 N93-28573
How to write fast and clear parallel programs using algebra
[DE93-000797] p 3524 N93-28640
Deformations of the Lie algebras L1(H(2)) and L1(W(2))
[MEMO-1056] p 3547 N93-28667
An algebraic approach to the quantization of constrained systems: Finite dimensional examples
p 3548 N93-28671
The generic arithmetic of SISYPHE
[INRIA-RT-0136] p 3524 N93-28755
Dynamic factorization in large-scale optimization
[AD-A263993] p 3528 N93-29345
The general theory of convolutional codes
p 3385 N93-29595
Turning SOS rules into equations
[CWI-CS-R9218] p 3532 N93-30017
Positive energy representations of the conformal quantum algebra
[DE93-606064] p 3551 N93-30809
Connections between quantized affine algebras and superalgebras
[DE93-606065] p 3551 N93-30810
Abelian gauge theories on homogeneous spaces
[DE92-644730] p 3607 N93-30921
Beltrami parametrization and gauging of Virasoro and w-infinity algebras
[DE92-644844] p 3557 N93-30928
On one-dimensional topological and conformal field theories
[DE92-644726] p 3558 N93-30986
ALGORITHMS
Resource limited reasoning: A study of literature in the context of model-based diagnosis
[MEMO-INF-92-38] p 3540 N93-28480

Coarse image motion for saccade control
[OUEL-1916/92] p 3523 N93-28485
Research in mathematics and computer science, March 1, 1991 - September 30, 1992
[DE93-011492] p 3509 N93-28573
Filtering interpolators for image comparison algorithms
p 3463 N93-28797
Planning for air to air combat p 3501 N93-28852
A summary of block schemes for reducing a general matrix to Hessenberg form
[DE93-010621] p 3525 N93-28877
A simple parallel prefix algorithm for compact finite-difference schemes
[NASA-CR-191448] p 3525 N93-28976
Research in efficient scientific computation
[AD-A262084] p 3525 N93-28986
Implementation of a multidomain Navier-Stokes code on the Intel iPSC2 hypercube
[FFA-TN-1992-37] p 3418 N93-28994
An autonomous vision-based mobile robot
p 3443 N93-29082
Resource utilization model for the algorithm to architecture mapping model
[NASA-CR-193122] p 3527 N93-29171
Speech recognition by recursive stochastic modelling
[ISBN-90-9005038-8] p 3382 N93-29266
Iterative encoding methods for computer generated holograms
[AD-A263705] p 3431 N93-29297
Fast multipole method in simulations of aqueous systems
[AD-A263422] p 3567 N93-29336
Collection-oriented match: Scaling up the data in production systems
[AD-A262755] p 3615 N93-29459
Implementation of parallel algorithms
[AD-A263126] p 3529 N93-29496
A fuzzy clustering algorithm to detect planar and quadric shapes p 3511 N93-29524
A fuzzy measure approach to motion frame analysis for scene detection p 3511 N93-29525
Adaptive defuzzification for fuzzy systems modeling
p 3512 N93-29532
A model for amalgamation in group decision making
p 3513 N93-29540
A conjugate gradients/trust regions algorithms for training multilayer perceptrons for nonlinear mapping
p 3519 N93-29581
Inference in fuzzy rule bases with conflicting evidence
p 3519 N93-29583
Reference equations of motion for automatic rendezvous and capture
[NASA-CR-185676] p 3269 N93-29652
Communications neural net processors
[AD-A263330] p 3542 N93-29763
A functional implementation of the Jacobi eigen-solver
[DE93-007349] p 3549 N93-29769
Polynomial space polynomial delay algorithms for listing families of graphs
[DE93-010677] p 3530 N93-29808
NESL: A nested data-parallel language (Version 2.6)
[AD-A263548] p 3530 N93-29822
Class notes: Programming parallel algorithms CS 15-840B (Fall 1992)
[AD-A263549] p 3530 N93-29823
Performance analysis of subspace methods
[AD-A263984] p 3530 N93-29865
Efficient algorithms for the evaluation of planar network reliability
[AD-A263602] p 3531 N93-29916
Turning SOS rules into equations
[CWI-CS-R9218] p 3532 N93-30017
Simplified Linear Equation Solvers: User's manual
[DE93-011975] p 3550 N93-30140
QR decomposition based least squares lattice algorithm p 3358 N93-30239
Feature segmentation using a multiple-stack based chain coding algorithm p 3359 N93-30243
Computation of a delta-wing roll-and-hold maneuver
[AD-A264704] p 3260 N93-30498
Efficient algorithms and data structures in geometric design
[AD-A264678] p 3534 N93-30544
Nonsmooth optimization algorithms, system theory, and software tools
[AD-A264679] p 3534 N93-30549
The 1991 neural information processing systems: Natural and synthetic
[AD-A264754] p 3623 N93-30559
Adaptive networks for sequential decision problems
[AD-A264756] p 3534 N93-30561
A method for intersection line calculation between parametric surfaces
[ETN-93-94178] p 3551 N93-30572
An algorithm for simple and complex feature detection: From retina to primary visual cortex
[AD-A264306] p 3497 N93-30897
Algorithm for the solution of the Faddeev equation for a system of three identical spinless particles
[DE92-644678] p 3535 N93-30914
Algorithm of numerical calculations of differential Yakubovsky equations for the (1 + 3) scattering problem
[DE92-644679] p 3535 N93-30915
Bayesian linear analysis with application to removal of atmospheric influences on optical remote sensing images
[BCRS-92-19] p 3463 N93-31011

ALKALI HALIDES
Adsorption of hydrated halide ions on charged electrodes: Molecular dynamics simulation
[AD-A263137] p 3568 N93-29619

ALKALI METALS
Neutron scattering studies of the structures and lattice dynamics of the alkali metals
[DE93-008272] p 3593 N93-28956
A simple model for ion solvation with non additive cores
[AD-A263075] p 3566 N93-29143
Elastic and reactive collisions of atoms and molecules with neutral alkali clusters
[DE93-009313] p 3566 N93-29206
Change of solar cell element properties influenced by adsorbed atoms
[DE93-606694] p 3466 N93-30777

ALKALINE EARTH METALS
Change of solar cell element properties influenced by adsorbed atoms
[DE93-606694] p 3466 N93-30777

ALKANES
Selective nitrations. Volume 2: The laser-induced nitration of three cycloalkanes
[AD-A263250] p 3438 N93-29800
NMR studies of molecules in liquid crystals and graphite
[DE93-010423] p 3569 N93-29805
Observation of phase-separated nanometer scale molecular domains in mixed self-assembled monolayers
[AD-A263470] p 3569 N93-29839

ALKYL COMPOUNDS
Catalytic synthesis of silicon carbide preceramic polymers: Polycarbosilanes
[DE93-008634] p 3329 N93-28541
Observation of phase-separated nanometer scale molecular domains in mixed self-assembled monolayers
[AD-A263470] p 3569 N93-29839

ALLOYING
Fundamental aspects in the design of passive alloys
[DE93-009028] p 3320 N93-28545
High temperature creep and oxidation resistant chromium silicide matrix alloy containing molybdenum
[NASA-CASE-LEW-15697-1] p 3323 N93-29172
Aluminium-high strength material by mechanical alloying and reaction milling: Basics of processing and characterisation of material
[ESA-TT-1249] p 3324 N93-29272
Eutectic solidification of Al-U at slowly cooling rates (10 C per second)
[DE92-640082] p 3328 N93-30941
Powder metallurgy: Solid and liquid phase sintering of copper p 3294 N93-30976

ALLOYS
JPRS report: Science and technology. Central Eurasia: Materials science
[JPRS-UMS-92-008] p 3322 N93-29012
JPRS report: Science and technology. Central Eurasia: Materials science
[JPRS-UMS-92-007] p 3322 N93-29013
JPRS report: Science and technology. Central Eurasia: Materials science
[JPRS-UMS-92-009] p 3322 N93-29015
JPRS report: Science and technology. Central Eurasia: Materials science
[JPRS-UMS-92-012] p 3296 N93-29016
JPRS report: Science and technology. Central Eurasia: Materials science
[JPRS-UMS-92-013] p 3296 N93-29017
JPRS report: Science and technology. Central Eurasia: Materials science
[JPRS-UMS-92-016] p 3296 N93-29018
JPRS report: Science and technology. Central Eurasia: Materials science
[JPRS-UMS-92-014] p 3322 N93-29019
JPRS report: Science and technology. Central Eurasia: Materials science
[JPRS-UMS-92-015] p 3322 N93-29020
JPRS report: Science and technology. Central Eurasia: Materials science
[JPRS-UMS-93-001] p 3296 N93-29021
DOE fundamentals handbook: Material science
[DE93-012224] p 3314 N93-30199
Tool grinding and spark testing p 3291 N93-30954

ALOHA SYSTEM
A slotted Aloha satellite channel simulator
p 3360 N93-30250
Comparison of two random access techniques for the North American MSAT system p 3370 N93-30315

ALPHA PARTICLES
Collective transport of alpha particles due to Alfven wave instability
[DE93-009578] p 3587 N93-29148

ALPINE METEOROLOGY
Fog studies in the Alpine region with digital NOAA/AVHRR data p 3458 N93-28925

ALPS MOUNTAINS (EUROPE)
SAR shape-from-shading for a populated alpine area
p 3458 N93-28923

ALTERNATIVES
An experimental methodology for a fuzzy set preference model p 3514 N93-29547

ALTIMETRY
Multibeam laser altimeter for planetary topographic mapping p 3442 N93-28780
Charting the remote southern oceans with geosat altimetry
[AD-A263452] p 3461 N93-29817

ALTITUDE
The cone structure and focusing of the electric field of VLF and LF waves at high altitudes of the ionosphere
p 3395 N93-30731

ALTITUDE ACCLIMATIZATION
Beta-adrenergic blockade and lactate metabolism during exercise at high altitude
[AD-A263544] p 3495 N93-29820
Field trial of caffeine on physical performance at altitude: An attempt to overcome the challenge
[AD-A264260] p 3497 N93-30894

ALTITUDE SICKNESS
The Environmental Symptoms Questionnaire (ESQ): Development and application
[AD-A264127] p 3495 N93-30196

ALUMINATES
Studies in Lewis acid and superacid ionic liquids
[AD-A264683] p 3316 N93-30551

ALUMINIDES
Microstructural effects on the deformation and fracture of the alloy Ti-25Al-10Nb-3B-1Mo
[AD-A263095] p 3323 N93-29144
Low temperature environmental embrittlement in ordered intermetallics
[DE93-009711] p 3324 N93-29786
Platinum-modified diffusion aluminide coatings on nickel-base superalloys
[AD-A263597] p 3325 N93-29981
Improvement in ductility of the intermetallic compound Ti3Al
[ESA-TT-1276] p 3325 N93-30105
Order-disorder transformations in Ni-Al alloys
[DE93-009293] p 3326 N93-30389

ALUMINUM
Microtextured metals for stray-light suppression in the Clementine startracker p 3286 N93-28785
Transient response of embedded thermocouples
[DE93-009889] p 3431 N93-29325
Processing and property evaluation of silver or aluminum matrix YBa2Cu3O(6+x) superconducting materials
[AD-A263382] p 3595 N93-29333
Damage areas on selected LDEF aluminum surfaces
p 3283 N93-29374
Boron carbide aluminum cermets for external pressure housing applications
[AD-A262749] p 3333 N93-29404
An experimental/analytical evaluation of biaxial sheet failure
[DE93-010620] p 3453 N93-29843

ALUMINUM ALLOYS
Electrochemical behavior and surface chemistry of aluminum alloys: Solute-rich interphase model
[AD-A262061] p 3322 N93-29002
The growth of small corrosion fatigue cracks in alloy 2024
[NASA-TM-107755] p 3451 N93-29069
An experimental investigation of radioactivity induced by ions associated with the operation of pulsed-power accelerators
[DE93-011478] p 3575 N93-29151
Oxidation behavior in reaction-bonded aluminum-silicon alloy/alumina powder compacts
[DE93-010407] p 3298 N93-29191
Aluminium-high strength material by mechanical alloying and reaction milling: Basics of processing and characterisation of material
[ESA-TT-1249] p 3324 N93-29272
Mechanisms of fracture and creep of structural alloys
[AD-A263108] p 3324 N93-29799

Mechanical properties of several magnesium and aluminum composites
[AD-A262481] p 3299 N93-30137
Two-parameter crack tip field associated with stable crack growth in a thin plate: A hybrid analysis
[AD-A264221] p 3453 N93-30147
Order-disorder transformations in Ni-Al alloys
[DE93-009293] p 3326 N93-30389
Constitutive laws for deformation and dynamic recrystallization in cubic metals
[DE93-010740] p 3326 N93-30486
Reactive sintering of Ni3Al intermetallic alloys under compressive stress
[DE93-009729] p 3327 N93-30652
Eutectic solidification of Al-U at slowly cooling rates (10 C per second)
[DE92-640082] p 3328 N93-30941

ALUMINUM ARSENIDES
Low-cost, high-efficiency solar cells utilizing GaAs-on-Si technology
[DE93-000096] p 3464 N93-29965

ALUMINUM CHLORIDES
Studies in Lewis acid and superacid ionic liquids
[AD-A264683] p 3316 N93-30551

ALUMINUM COMPOUNDS
Process optimization of Hexoloy SX-SiC towards improved mechanical properties
[DE93-007913] p 3320 N93-28564

ALUMINUM GALLIUM ARSENIDES
Luminescence study of ion-implanted and MBE-grown Er-doped GaAs and Al(x)Ga(1-x)As
[AD-A262602] p 3591 N93-28471
Infrared rugates by molecular beam epitaxy
p 3582 N93-28808
Optoelectronic technology consortium
[AD-A263580] p 3580 N93-29973
Growth and development of GaInAsP for use in high-efficiency solar cells
[DE93-000098] p 3465 N93-30208
Development of ultra-low noise, high sensitivity planar metal grating coupled 3-5 multiquantum well infrared detectors for focal plane array staring IR sensor systems
[AD-A264465] p 3599 N93-30536

ALUMINUM NITRIDES
Coordination compounds of aluminum as precursors to aluminum nitride
[AD-A264700] p 3327 N93-30574

ALUMINUM OXIDES
Oxidation behavior in reaction-bonded aluminum-silicon alloy/alumina powder compacts
[DE93-010407] p 3298 N93-29191
A transient FGM interlayer based approach to joining ceramics
[DE93-010415] p 3331 N93-29248
Investigation of ion beam mixing of iron marker layers in aluminum oxide by RBS
[DE93-010727] p 3594 N93-29314
Adhesion of thick film Au to alumina ceramics
[DE93-009802] p 3339 N93-30656
Tensile creep behavior of polycrystalline alumina fibers
[NASA-TM-106269] p 3340 N93-30938

ALUMINUM SILICATES
The effect of oxidation embrittlement on the impact behavior of nicalon reinforced CAS 2 ceramic matrix composites
[AD-A263567] p 3334 N93-29829

ALVEOLI
The chronic effects of jP-8 jet fuel exposure on the lungs
[AD-A264162] p 3495 N93-30153

AMBIENT TEMPERATURE
Ambient-atmosphere compatible superconducting fullerenes
[AD-A262025] p 3595 N93-29397

AMINES
Synthesis of cubane based energetic molecules
[AD-A263271] p 3564 N93-28562
Acid gas treating by aqueous alkanolamines
[PB93-176188] p 3471 N93-29676
Diffusion coefficients and heats of mixing in aqueous alkanolamines
[PB93-176212] p 3316 N93-30661

AMINO ACIDS
Amino acid sequences for the binding regions in serum albumin proteins
[NASA-CASE-MFS-28402-1] p 3491 N93-28952

AMINO RADICAL
NOx chemistry in natural gas flames
[PB93-175263] p 3317 N93-30760

AMMETERS
Investigation of methods for the measurement of small electron bundle currents
[DIGEL-1992-4] p 3413 N93-30763
A 250 mA toroid monitor for the measurement of the bundle current in the stretcher mode of AmPS
[DIGEL-1992-1] p 3413 N93-30835

AMMONIA
Complex-compound heat pump: Topical report on phase 1 results
[PB93-185460] p 3466 N93-30814

AMMONIUM COMPOUNDS
Synthesis of cubane based energetic molecules
[AD-A263271] p 3564 N93-28562
Ion emission during high-energy sputtering of ammonium dinitramide and ammonium nitrate crystals and the determination of ion decomposition pathways using tandem mass spectrometry p 3318 N93-30066

AMMONIUM NITRATES
Ion emission during high-energy sputtering of ammonium dinitramide and ammonium nitrate crystals and the determination of ion decomposition pathways using tandem mass spectrometry p 3318 N93-30066
Detonation shock dynamics of composite energetic materials p 3350 N93-30096
Isothermal and shock compression of high density ammonium nitrate and ammonium perchlorate
[DE93-000682] p 3315 N93-30209

AMMONIUM PERCHLORATES
Atomic force microscopy of ammmonium perchlorate
p 3349 N93-30091
Microstructural basis for enhanced shock-induced chemistry in single crystals of ammonium perchlorate
p 3319 N93-30092
Defect density measurements in a shocked single crystal of ammonium perchlorate p 3319 N93-30093
Comparison of deformation and shock reactivity for single crystals of RDX and ammonium perchlorate
p 3350 N93-30094
Isothermal and shock compression of high density ammonium nitrate and ammonium perchlorate
[DE93-000682] p 3315 N93-30209

AMORPHOUS MATERIALS
Polar order and relaxation of second order nonlinear optical susceptibility in an electric field polarized amorphous polymer
[AD-A262189] p 3329 N93-28489
High pressure studies of hydrated nafion membranes: Dielectric relaxation and deuteron NMR
[AD-A263511] p 3332 N93-29342
Dipolar orientational relaxation in guest/host amorphous polymer probed by second harmonic generation
[AD-A262006] p 3333 N93-29441
Complex dielectric function of amorphous diamond films deposited by pulsed excimer (ArF) laser ablation of graphite
[AD-A264527] p 3598 N93-30408
Role of oxygen vacancies in anodic TiO2 thin films
[DE92-642137] p 3602 N93-31027

AMPLIFIER DESIGN
Upgrading the LAMPF 201 MHz RF generators
[DE93-010715] p 3406 N93-28830

AMPLITUDE MODULATION
Results of the joint HIPAS/NUWC campaigns to investigate ELF generated by auroral electrojet modulation p 3398 N93-30746

ANALOG CIRCUITS
Analog CMOS circuits for neural networks
p 3355 N93-30223
An architecture for an analog VLSI neural network for early computer vision processing p 3359 N93-30244
Electronics mixed-mode simulation
[AD-A264734] p 3534 N93-30577

ANALOG COMPUTERS
Stochastic architecture for Hopfield neural nets
p 3519 N93-29579

ANALOG DATA
An architecture for an analog VLSI neural network for early computer vision processing p 3359 N93-30244

ANALOG TO DIGITAL CONVERTERS
A compact imaging detector of polarization and spectral content p 3582 N93-28810
Optical antenna beam steering using digital phase shifter control
[AD-D015688] p 3383 N93-29455
A high resolution 14-bit ADC for Gammasphere Project
[DE93-010446] p 3598 N93-30393
Low cost instrumentation: Parallel port analog to digital converter
[AD-A263468] p 3433 N93-30584
The use of DFT windows in signal-to-noise ratio and harmonic distortion computations
[DE93-009800] p 3433 N93-30655
An automated data collection system for a Charpy impact tester p 3293 N93-30972

ANALOGS
Visualizing weld metal solidification using organic analogs p 3293 N93-30973

ANALYSIS (MATHEMATICS)
Environmental studies: Mathematical, computational and statistical analyses
[AD-A264223] p 3473 N93-30360

ANALYTIC FUNCTIONS
Comparison of analytical transport and stochastic solutions for neutron slowing down in an infinite medium
[DE93-010799] p 3565 N93-28833

ANALYTICAL CHEMISTRY
Kinetic studies on gas-phase reaction mechanisms important to the combustion of energetic materials: The CO/N2O reaction p 3347 N93-30084

ANELASTICITY
Anelastic relaxations associated with local disordering in grain boundaries
[AD-A263101] p 3596 N93-29796

ANGLE OF ATTACK
X-31 demonstration of integrated flight and propulsion control for effective combat at extreme angles of attack
p 3260 N93-28851
An experimental study of flow over a 6 to 1 prolate spheroid at incidence p 3239 N93-29124
NASTRAN analysis for the Airmass Sunburst model 'C' Ultralight Aircraft p 3249 N93-29777
Solution of Euler equations for forebody-inlet ensemble of aircraft at high angle of attack
[AD-A263905] p 3240 N93-29862
The application of concentric vortex simulation to calculating the aerodynamic characteristics of bodies of revolution at high angles of attack
[AD-A263879] p 3241 N93-29919
Flight control system design factors for applying automated testing techniques
[NASA-TM-4242] p 3260 N93-30764

ANGULAR DISTRIBUTION
Measurements of light scattering by small particles at an angle of zero degrees
[AD-A263856] p 3580 N93-29887
Analysis of possibilities for using laser scattering for MeV electron beam diagnostics
[DE93-606223] p 3441 N93-30767

ANGULAR MOMENTUM
Investigation of Mars rotational dynamics using Earth-based radio tracking of Mars landers
p 3642 N93-28777
Nonlinear attitude control of planar structures in space using only internal controls p 3280 N93-29991
Planar reorientation of a free-free beam in space using embedded electromechanical actuators
p 3280 N93-29993
Space station attitude disturbance arising from internal motions p 3280 N93-29995
Theoretical studies in nuclear structure
[DE93-012290] p 3570 N93-30505
Integrals of motion on the group of invariance of an interval in three-dimensional spaces
[DE93-606090] p 3606 N93-30797

ANGULAR RESOLUTION
Smart skin structures for identifying and locating laser irradiation
[DE93-005464] p 3436 N93-28887
Measurements of light scattering by small particles at an angle of zero degrees
[AD-A263856] p 3580 N93-29887

ANGULAR VELOCITY
Symbology for head up and head down applications for highly agile fighter aircraft: To improve spatial awareness, trajectory control, and unusual attitude recovery, part 1
p 3502 N93-28857

ANHYDRIDES
Diphenylmethane-containing dianhydride and polyimides prepared therefrom
[NASA-CASE-LAR-14487-1] p 3331 N93-29085
Process to prepare 1,3-diamino-5-pentafluorosulfanylbenzene
[NASA-CASE-LAR-14773-2-CU] p 3312 N93-29506

ANIK SATELLITES
Security of the remote control link of Anik E satellites
p 3365 N93-30282

ANIMALS
Neural mechanisms of attention
[AD-A264345] p 3544 N93-30165
Multiple neuron recording in the hippocampus of freely moving animals
[AD-A264807] p 3492 N93-30594

ANIONS
Synthesis of oligoimides and oligoimide anion radicals
[AD-A263129] p 3290 N93-29474
High-current negative-ion beam transport
[DE93-010732] p 3575 N93-29809

ANISOTROPIC SHELLS
Application of integral and differential equation methods for various EM interaction problems
[AD-A264821] p 3394 N93-30597

ANISOTROPY
Benchmark eigenvalue spectrum calculations with anisotropic effects
[DE93-006387] p 3548 N93-28891
On the meaning of delta T/T
[DE93-008482] p 3653 N93-28962
Hydrodynamic interactions among fibers in high efficiency filters
[DE93-007117] p 3424 N93-30035
Application of integral and differential equation methods for various EM interaction problems
[AD-A264821] p 3394 N93-30597

ANNEALING
Neutron scattering studies of the structures and lattice dynamics of the alkali metals
[DE93-008272] p 3593 N93-28956
Bainitic stabilization of austenite in low alloy steels
[DE93-008275] p 3321 N93-28957
Effects of internal helium on mechanical properties of Nitronic (tm) 40 stainless steel
[DE93-009902] p 3324 N93-29265
Defect studies in low-temperature-grown GaAs
[DE93-010405] p 3595 N93-29417
Isothermal annealing and relaxation of the second harmonic generation signal from a nonlinear optical polymer
[AD-A262007] p 3333 N93-29442
Surface chemistry of N2H4 on Si(100)-2x1
[AD-A264819] p 3316 N93-30627
Superconducting films of YBaCuO
[DE93-606831] p 3600 N93-30772
Processing of novel nanoparticle dispersion strengthened ceramics for improved mechanical performance
[AD-A264191] p 3339 N93-30883

ANNIHILATION REACTIONS
Coupled-channel analysis of low energy nucleon-antinucleon interactions
[DE93-606115] p 3571 N93-30791

ANNOTATIONS
An annotated bibliography on integration in software engineering environments
[AD-A264798] p 3535 N93-30602

ANNUAL VARIATIONS
Investigation of Mars rotational dynamics using Earth-based radio tracking of Mars landers
p 3642 N93-28777
Convective and stratiform rain: Multichannel microwave sensing over oceans
[NASA-TM-104586] p 3482 N93-29448
The distribution of the annual and semiannual cycles in the tropics
[DE92-642213] p 3485 N93-31006

ANNULAR DUCTS
Fluid flow and heat transfer in the entrance region of an annulus between independently rotating tubes with a turbulent axial flow p 3256 N93-29952

ANODES
Alkali metal carbon dioxide electrochemical system for energy storage and/or conversion of carbon dioxide to oxygen
[NASA-CASE-LEW-14973-1] p 3464 N93-28974
Operational results of pilot cell test with cermet inert anodes
[DE93-009338] p 3322 N93-29061

ANOMALIES
A water mass analysis of the 1991-1992 El Nino signal in the Farallon Islands region
[AD-A263490] p 3488 N93-29819
On the photonic chiral anomaly in an external gravitational field
[DE93-606082] p 3479 N93-30785
Compensating fields and anomalies in supergravity
[DE92-644724] p 3637 N93-30919

ANTARCTIC REGIONS
The German satellite ground station in Antarctica: Realization and first results p 3458 N93-28924
A field investigation of water and salt movement in permafrost and the active layer
[AD-A263706] p 3487 N93-29298
Transient (approximately equals 10 s) VLF amplitude and phase perturbations due to lightning-induced electron precipitation into the ionosphere (the Trimpi effect)
p 3396 N93-30736

ANTENNA ARRAYS
Optical antenna beam steering using digital phase shifter control
[AD-D015688] p 3383 N93-29455
Planar microstrip YAGI antenna array
[NASA-CASE-NPO-17873-2-CU] p 3384 N93-29507
Tolerance theory of phased array antennas: A statistical approach p 3369 N93-30307
Results of the joint HIPAS/NUWC campaigns to investigate ELF generated by auroral electrojet modulation p 3398 N93-30746
Study of a VLF distributed antenna array
p 3398 N93-30749

ANTENNA COMPONENTS
DSS-14 subreflector actuator dynamics during the Landers earthquake p 3386 N93-29600
Durability of Quick Reaction Satellite Antenna (QRSA) trunnion castings
[AD-A264095] p 3281 N93-30813

ANTENNA DESIGN
A satellite-tracking millimeter-wave reflector antenna system for mobile satellite-tracking
[NASA-CASE-NPO-18772-1-CU] p 3381 N93-28955
System overview on electromagnetic compensation for reflector antenna surface distortion
[NASA-TM-106217] p 3273 N93-29195
Planar microstrip YAGI antenna array
[NASA-CASE-NPO-17873-2-CU] p 3384 N93-29507
Gravity referenced elevation encoder development
p 3385 N93-29592
DSS-14 subreflector actuator dynamics during the Landers earthquake p 3386 N93-29600
An analysis of the 70-meter antenna hydrostatic bearing by means of computer simulation p 3386 N93-29601
Widebanding techniques for VHF antennas 2
[AD-A263998] p 3387 N93-29882
Fundamental studies of fusion plasmas
[DE93-013144] p 3589 N93-30189
Status of the Canadian military Multibeam Antenna (MBA) development for EHF SATCOM
p 3374 N93-30334
Comparison and design of multiple beam antenna feed networks p 3374 N93-30335
Recent advances in bootlace lens design
p 3374 N93-30336
VLF/LF transmitting antennas p 3398 N93-30747
Application of the Fourier transform to short antennas
p 3398 N93-30750
Antenna modeling and analysis for ELF/VLF/LF applications p 3398 N93-30751

ANTENNA FEEDS
A dual polarized broadband multifrequency Earth station feed p 3371 N93-30319
Comparison and design of multiple beam antenna feed networks p 3374 N93-30335
Recent advances in bootlace lens design
p 3374 N93-30336

ANTENNA RADIATION PATTERNS
Predicting radiation characteristics from antenna physical dimensions
[AD-A262462] p 3379 N93-28654
System overview on electromagnetic compensation for reflector antenna surface distortion
[NASA-TM-106217] p 3273 N93-29195
Optical antenna beam steering using digital phase shifter control
[AD-D015688] p 3383 N93-29455
Propagation channel modeling for angle-diversity combining simulation p 3360 N93-30252
Models for performance assessment of HF antennas on the CH-135/Twin Huey helicopter
p 3366 N93-30291
Computer-aided modeling for analysis of arbitrary scatterers and feeds p 3367 N93-30293
Development of an antenna measurement facility operating in the 2 GHz - 100 GHz frequency range
p 3369 N93-30308
Application of the Fourier transform to short antennas
p 3398 N93-30750
Antenna modeling and analysis for ELF/VLF/LF applications p 3398 N93-30751
Pattern measurements of US Navy ELF antennas
p 3399 N93-30752
Advanced electromagnetic methods for aerospace vehicles
[NASA-CR-193468] p 3400 N93-31036

ANTHROPOMETRY
Neural network technologies
[AD-A262576] p 3541 N93-28987
Anthropometric data from launch and entry suited test subjects for the design of a recumbent seating system
[NASA-TM-104769] p 3505 N93-29044
Anthropometric survey of the astronaut applicants and astronauts from 1985 to 1991
[NASA-RP-1304] p 3506 N93-29324
Methods for characterizing the human head for the design of helmets
[AD-A263875] p 3507 N93-29889

ANTIADRENERGICS
Beta-adrenergic blockade and lactate metabolism during exercise at high altitude
[AD-A263544] p 3495 N93-29820

ANTIBODIES
Evaluation of dried storage of platelets for transfusion: Physiologic integrity and hemostatic functionality
[AD-A263240] p 3494 N93-29620

ANTIFERROMAGNETISM
Numerical simulation of quantum many-body systems
[DE93-008300] p 3603 N93-28958
Phase separation, antiferromagnetism, and superconductivity in superconducting-superoxygenated La(2-x)Sr(x)CuO(4+(delta))
[DE93-009852] p 3598 N93-30517

ANTIMISSILE DEFENSE
Magnetic field measurements of the CEBAF (NIST) wiggler using the pulsed wire method
[AD-A263997] p 3439 N93-29867

ANTINUCLEONS
Towards the results of global analysis of data on nucleon electromagnetic structure
[DE93-606125] p 3571 N93-30792

ANTIREFLECTION COATINGS
High-performance visible/UV CCD focal plane technology for spacebased applications
p 3434 N93-28771
Effects of long term space environment exposure on optical substrates and coatings (S0050-2)
p 3582 N93-29694

ANTISUBMARINE WARFARE
Feature based neural network acoustic transient signal classification
[AD-A263437] p 3562 N93-29816

APERTURES
Electro-optic characterisation of extremely wide bandwidth electrical signals
[AD-A264202] p 3392 N93-30145
Application of the Fourier transform to short antennas
p 3398 N93-30750

APPLICATIONS OF MATHEMATICS
Godunov-type schemes applied to detonation flows
[NASA-CR-191447] p 3509 N93-28841
SIAM Conference on Applications of Dynamical Systems
[DE93-007969] p 3548 N93-29057

APPLICATIONS PROGRAMS (COMPUTERS)
Parallel computation and the basis system
[DE93-008755] p 3537 N93-28544
Minimum Hamiltonian ascent trajectory evaluation (MASTRE) program (update to automatic flight trajectory design, performance prediction, and vehicle sizing for support of shuttle and shuttle derived vehicles) users manual
[NASA-CR-192556] p 3269 N93-28558
Basic OSF/Motif programming and applications
[DE93-010800] p 3524 N93-28834
A distributed object-oriented database application design
[AD-A262591] p 3612 N93-28846
A proposed approach for developing next-generation computational electromagnetics software
[DE93-007326] p 3380 N93-28900
Index mappings for interactive editing of symbolic matrices
[DE93-009316] p 3549 N93-29060
Summer research program (1992). High School Apprenticeship Program (HSAP) reports. Volume 16: Arnold Engineering Development Center Civil Engineering Laboratory
[AD-A262024] p 3608 N93-29396
RTE: A UNIX library with on-line documentation and sample programs for microwave radiative transfer calculations
[PB93-180248] p 3386 N93-29680
TRAB: A transient analysis program for BWR. Part 2: User's manual
[VTT-TIED-1232-PT-2] p 3575 N93-29996
The wake software suite: User's guide
[AD-A264181] p 3425 N93-30156
The First NASA Advanced Composites Technology Conference, part 1
[NASA-CP-3104-PT-1] p 3300 N93-30428
Development of a CFD code for casting simulation
[NASA-CR-192577] p 3427 N93-30492
Computer algebra tools for higher symmetry analysis of nonlinear evolution equations
[DE93-606089] p 3535 N93-30787
Algorithm for the solution of the Faddeev equation for a system of three identical spinless particles
[DE92-644678] p 3535 N93-30914
Algorithm of numerical calculations of differential Yakubovsky equations for the (1 + 3) scattering problem
[DE92-644679] p 3535 N93-30915

APPROACH CONTROL
Developing automation for terminal air traffic control: Case study of the imaging aid p 3247 N93-30356

APPROACH INDICATORS
Developing automation for terminal air traffic control: Case study of the imaging aid p 3247 N93-30356

APPROXIMATION
Polygonal approximation overviews and perspectives
[INRIA-RR-1621] p 3547 N93-28513

A diffusion approximation for a network of reservoirs with power law release rule
[AD-A263753] p 3550 N93-29872

Effect of design selection on response surface performance
[NASA-CR-4520] p 3249 N93-29885

Approximation formulae for functional integrals in P(phi)2-quantum field theory
[DE93-606067] p 3605 N93-30781

Algorithm for the solution of the Faddeev equation for a system of three identical spinless particles
[DE92-644678] p 3535 N93-30914

Fixed point iterations for quasi-contractive maps in uniformly smooth Banach spaces
[DE92-641348] p 3552 N93-30942

AQUEOUS SOLUTIONS

Acid solution absorption of extruded polyethylene foam
[DE93-011701] p 3330 N93-28839

The growth of small corrosion fatigue cracks in alloy 2024
[NASA-TM-107755] p 3451 N93-29069

A field investigation of water and salt movement in permafrost and the active layer
[AD-A263706] p 3487 N93-29298

Fast multipole method in simulations of aqueous systems
[AD-A263422] p 3567 N93-29336

Acid gas treating by aqueous alkanolamines
[PB93-176188] p 3471 N93-29676

Diffusion coefficients and heats of mixing in aqueous alkanolamines
[PB93-176212] p 3316 N93-30661

AQUIFERS

Performance and cost evaluation of bioremediation techniques for fuel spills
[PB93-175545] p 3474 N93-30762

ARC JET ENGINES

Measurements of magnetic fields produced by a 30 kWe class Arcjet Power Conditioning Unit
[AD-A262786] p 3287 N93-28658

ARC WELDING

Welding wire pressure sensor assembly
[NASA-CASE-MFS-26216-1] p 3442 N93-28951

ARCHAEOLOGY

Remote sensing survey of Mississippi River-Gulf Outlet, Breton Sound disposal area, Plaquemines Parish, Louisiana
[AD-A263097] p 3459 N93-29146

ARCHITECTURE

Mars habitat p 3233 N93-29747

Selenia: A habitability study for the development of a third generation lunar base p 3233 N93-29748

ARCHITECTURE (COMPUTERS)

Design of a hardware discrete event simulation coprocessor
[AD-A262614] p 3537 N93-28478

A model for processing the SGML document in version oriented hypertext systems
[ETN-93-93797] p 3611 N93-28528

A multiarchitecture parallel-processing development environment
[NASA-TM-106180] p 3538 N93-28628

Combat Automation for Airborne Weapon Systems: Man/Machine Interface Trends and Technologies
[AGARD-CP-520] p 3501 N93-28850

Efficient wiring of reconfigurable parallel processors
[DE93-009847] p 3538 N93-29186

Using today's technology to improve mobile C4I for the operational commander
[AD-A263613] p 3245 N93-29285

Multisensor image analysis system
[AD-A263679] p 3528 N93-29294

An architecture for robotic system integration
[DE93-010829] p 3444 N93-29316

The parallel implementation of a backpropagation neural network and its applicability to SPECT image reconstruction
[DE93-010304] p 3567 N93-29416

Development of a visual system interface to support a domain-oriented application composition system
[AD-A262489] p 3528 N93-29418

Associative memories for supercomputers
[AD-A263142] p 3520 N93-29482

Digital hardware architecture implementation
[AD-A263219] p 3521 N93-29492

Stochastic architecture for Hopfield neural nets
p 3519 N93-29579

Special purpose parallel computer architecture for real-time control and simulation in robotic applications
[NASA-CASE-NPO-17629-1-CU] p 3521 N93-29608

Synthesis techniques and analysis tools for on-chip fault-tolerance
[AD-A263167] p 3409 N93-29654

Communications neural net processors
[AD-A263330] p 3542 N93-29763

Development of neural network architectures for self-organizing pattern recognition and robotics
[AD-A264831] p 3543 N93-29791

Accelerating the transfer of technology for implementing domain specific software architectures
[AD-A264017] p 3532 N93-30014

The planning coordinator: A design architecture for autonomous error recovery and on-line planning of intelligent tasks
[NASA-CR-193250] p 3543 N93-30039

Canadian Conference on Electrical and Computer Engineering, volumes 1 and 2
[ISBN-0-9694170-1-2] p 3354 N93-30215

A parallel processing system for intensive I/O
p 3362 N93-30262

A transputer based parallel processing architecture for robotics applications p 3362 N93-30263

Technology for national asset storage systems
p 3617 N93-30452

Evolving neural network architecture
[AD-A264802] p 3544 N93-30592

Nonlinear explicit transient finite element analysis on the Intel Delta
[DE93-009561] p 3535 N93-30647

Space Generic Open Avionics Architecture (SGOAA) reference model technical guide
[NASA-CR-188246] p 3285 N93-31032

ARCTIC REGIONS

A field investigation of water and salt movement in permafrost and the active layer
[AD-A263706] p 3487 N93-29298

Design issues and initial performance of an adaptive air/ground/air HF communication system
p 3375 N93-30342

VLF propagation measurements in the Canadian Arctic p 3396 N93-30733

AREA NAVIGATION

Design and implementation of a Global Positioning System (GPS) supported area navigation system with electronic aircraft
[ILR-MITT-275(1992)] p 3246 N93-30671

ARGON

Upper ocean model of dissolved atmospheric gases
[DE93-010151] p 3487 N93-29327

ARID LANDS

A field investigation of water and salt movement in permafrost and the active layer
[AD-A263706] p 3487 N93-29298

Environmental Monitoring and Assessment Program. EMAP: Arid Colorado plateau pilot study
[PB93-181618] p 3474 N93-30823

ARITHMETIC

The generic arithmetic of SISYPHE
[INRIA-RT-0136] p 3524 N93-28755

ARMATURES

Two-dimensional model for current and heat transport in solid-armature railguns
[AD-A262014] p 3271 N93-29394

ARMED FORCES (UNITED STATES)

Summer Faculty Research Program (SFRP), volume 1
[AD-A261988] p 3608 N93-29440

Air Force CALS business practices
[AD-A264789] p 3610 N93-30177

Interagency Advancéd Power Group (IAPG) Meeting Compendium
[DE93-006189] p 3670 N93-30212

ARMOR

The effect of material strength on segment penetration behavior
[AD-A263262] p 3453 N93-29801

ARRAYS

The dynamic behavior of constrained adaptive array sensor processors
[AD-A262402] p 3541 N93-28494

Proposal for a numerical array library
[DE93-010678] p 3623 N93-30482

ARRHYTHMIA

Carbon monoxide exposure of subjects with documented cardiac arrhythmias
[PB93-179943] p 3497 N93-30890

ARSENATES

Two new titanium pyroarsenates: Alpha-TiAs2O7 and Beta-TiAs2O7
[AD-A264632] p 3599 N93-30518

ARSENIC COMPOUNDS

Be3(AsO4)2 2H2O: A new berylloarsenate phase containing bridged tetrahedral 3-rings
[AD-A262518] p 3592 N93-28584

ARTIFICIAL INTELLIGENCE

Artificial intelligence methodologies in flight related differential game, control and optimization problems
[AD-A262405] p 3541 N93-28498

Natural language generation
[AD-A262578] p 3524 N93-28579

Operator and automation capability analysis: Picking the right team p 3503 N93-28864

Cognitive interface considerations for intelligent cockpits p 3503 N93-28865

Uncertainty reasoning in expert systems
[NASA-CR-193120] p 3548 N93-28973

Modelling temporal abductive explanation
[AD-A263096] p 3526 N93-29145

MoCog1: A computer simulation of recognition-primed human decision making
[NASA-TM-103868] p 3542 N93-29386

Information technology: A force for organizational change
[AD-A261986] p 3615 N93-29439

Intelligent virtual reality in the setting of fuzzy sets
p 3513 N93-29544

Automated modeling of physical systems
[NASA-CR-193256] p 3531 N93-29873

Center for the Study of Intelligent Control Systems (Fellowships)
[AD-A263604] p 3543 N93-29917

The planning coordinator: A design architecture for autonomous error recovery and on-line planning of intelligent tasks
[NASA-CR-193250] p 3543 N93-30039

Evolution of a high-performance storage system based on magnetic tape instrumentation recorders
p 3435 N93-30470

Independent research and independent exploratory development programs
[AD-A264735] p 3544 N93-30556

Optimal trajectories for aircraft terrain following and terrain avoidance: A literature review update
[AD-A264075] p 3260 N93-30604

Intelligent real-time problem solving
[AD-A264830] p 3535 N93-30614

ARTIFICIAL SATELLITES

Automating the satellite range scheduling process
[AD-A262601] p 3270 N93-28468

STRV1-b flight experiment p 3265 N93-28723

NEP space test program objective
p 3265 N93-28724

Electric propulsion for lightsats: A review of applications and advantages p 3290 N93-29907

Satellite calibration requirements
[AD-A264279] p 3281 N93-30817

ASCENT TRAJECTORIES

Minimum Hamiltonian ascent trajectory evaluation (MASTRE) program (update to automatic flight trajectory design, performance prediction, and vehicle sizing for support of shuttle and shuttle derived vehicles) users manual
[NASA-CR-192556] p 3269 N93-28558

ASPECT RATIO

Bootstrap current profiles and scaling in large aspect ratio tokamaks
[DE93-753158] p 3589 N93-30003

ASSAYING

Analysis of protocol gases: An on-going quality assurance audit
[PB93-168839] p 3311 N93-29204

Thermal cycler temperature variation and its effect on the polymerase chain reaction
[AD-A264660] p 3337 N93-30541

ASSEMBLING

Spline screw autochanger
[NASA-CASE-GSC-13435-1] p 3445 N93-29505

ASSEMBLY

Spline screw autochanger
[NASA-CASE-GSC-13435-1] p 3445 N93-29505

ASSESSMENTS

Life insurance risk assessment using a fuzzy logic expert system p 3520 N93-29585

ASSOCIATIVE PROCESSING (COMPUTERS)

An adaptive algorithm for linear associative memory problem p 3360 N93-30255

ASTEROID MISSIONS

Clementine 2: A double asteroid flyby and impactor mission p 3268 N93-28770

ASTEROIDS

Proceedings of the Near-Earth-Object Interception Workshop
[NASA-TM-108236] p 3556 N93-28572

Clementine 2: A double asteroid flyby and impactor mission p 3268 N93-28770

A remote laser-mass spectrometer for determination of elemental composition p 3434 N93-28775

Multibeam laser altimeter for planetary topographic mapping p 3442 N93-28780

Systematic processing of Clementine data for scientific analyses p 3624 N93-28803

Space optical and low-frequency radio searches for Earth-crossing asteroids and comets
[DE93-008716] p 3634 N93-29246

Asteroidal versus cometary meteoroid impacts on the Long Duration Exposure Facility (LDEF)
p 3638 N93-29371

Galileo post-Gaspra cruise and Earth-2 encounter
p 3385 N93-29597
ASTRODYNAMICS
Colorado Center for Astrodynamics Research (CCAR)
p 3614 N93-29233
ASTROMETRY
Precision optical interferometry in space
[NASA-CR-193264] p 3630 N93-29163
ASTRONAUTS
Anthropometric survey of the astronaut applicants and astronauts from 1985 to 1991
[NASA-RP-1304] p 3506 N93-29324
ASTRONOMICAL CATALOGS
Far infrared supplement. Third edition: Catalog of infrared observations (lambda greater than or equal to 4.6 micrometers)
[NASA-RP-1295] p 3629 N93-29156
Bonner Durchmusterung (Southern Durchmusterung)
[NASA-RP-1298-VOL-3] p 3630 N93-29811
The faintest stars p 3630 N93-30493
ASTRONOMICAL MODELS
Dark matter: Theoretical perspectives
[DE93-008484] p 3633 N93-28676
Tests of the particle physics-physical cosmology interface
[DE93-008483] p 3634 N93-28963
Fourth-rank gravity and cosmology
[DE92-644722] p 3637 N93-30918
ASTRONOMICAL PHOTOMETRY
Spectroscopic and photometric studies of main sequence M stars and a search for late-type dwarfs in the solar vicinity p 3629 N93-28608
Detection of other planetary systems using photometry p 3632 N93-28791
XRONOS: A timing analysis software package. User's guide, version 3.00
[NASA-TM-109222] p 3532 N93-30023
ASTRONOMICAL SPECTROSCOPY
Spectroscopic and photometric studies of main sequence M stars and a search for late-type dwarfs in the solar vicinity p 3629 N93-28608
ASTRONOMY
Digital image compression using artificial neural networks p 3624 N93-28811
Activities report of the Astronomical Society
[MITT-75] p 3629 N93-29008
Far infrared supplement. Third edition: Catalog of infrared observations (lambda greater than or equal to 4.6 micrometers)
[NASA-RP-1295] p 3629 N93-29156
NSSDC data listing
[NASA-TM-108264] p 3612 N93-29167
ASTROPHYSICS
Near-infrared spectroscopy as an astrophysical tool
p 3632 N93-28607
On the meaning of delta T/T
[DE93-008482] p 3653 N93-28962
Activities report of the Astronomical Society
[MITT-75] p 3629 N93-29008
National collaboratories: Applying information technology for scientific research
[LC-93-83795] p 3612 N93-29129
NSSDC data listing
[NASA-TM-108264] p 3612 N93-29167
ASYMPTOTIC METHODS
Algorithm of numerical calculations of differential Yakubovsky equations for the (1 + 3) scattering problem
[DE92-644679] p 3535 N93-30915
ASYMPTOTIC PROPERTIES
Asymptotic properties of constrained Markov decision processes
[INRIA-RR-1598] p 3553 N93-28508
ASYMPTOTIC SERIES
Errors when shock waves interact due to numerical shock width
[DE93-010699] p 3426 N93-30484
ATLANTIC OCEAN
Steady-state and transient modeling of tracer and nutrient distributions in the global ocean
[DE93-011043] p 3486 N93-28670
Convective and stratiform rain: Multichannel microwave sensing over oceans
[NASA-TM-104586] p 3482 N93-29448
Hydrographic observations in the western tropical and subtropical north Atlantic Ocean: Atlantic Climate Change Program (ACCP) and Western Tropical Atlantic Experiment (WESTRAX) during 1990
[PB93-184760] p 3489 N93-30827
ATMOSPHERIC ATTENUATION
Tunable CW diode-pumped Tm,Ho:YLiF4 laser operating at or near room temperature
[NASA-CASE-NPO-18611-1-CU] p 3440 N93-30415
ATMOSPHERIC BOUNDARY LAYER
Wind loads on canopy roofs
[RR-CE132] p 3451 N93-29106
Surface shear stress estimates from geostrophic winds for use in sensible and latent heat flux formulations
p 3483 N93-30044
ATMOSPHERIC CHEMISTRY
Distribution of C1-C2 aldehydes in the free troposphere
[JUEL-2650] p 3475 N93-28475
Proceedings of the Second Atmospheric Radiation Measurement (ARM) Science Team Meeting
[DE93-005886] p 3476 N93-28889
Emission inventories: A global modeling perspective
[DE93-005817] p 3469 N93-28965
Atmospheric and Geophysical Sciences Division: G-Division did you know?
[DE93-007412] p 3469 N93-28967
Atmospheric and Geophysical Sciences Program report, 1990-1991
[DE93-007390] p 3470 N93-29055
Chemistry of the atmosphere: Its impact on global change. CHEMRAWN 7: Perspectives and recommendations
[PB93-180644] p 3488 N93-29670
Overview of the DOE Atmospheric Chemistry Program's Ozone Project
[DE93-007416] p 3471 N93-29770
Potential effects of HFC-152a on global ozone and climate
[DE93-008018] p 3471 N93-29792
Acoustic-gravity waves from low-altitude localized disturbances
[AD-A264804] p 3479 N93-30593
ATMOSPHERIC CIRCULATION
High performance dispersion model PHYSIC
[DE93-753303] p 3467 N93-28536
The Mechanisms of Solar Variability (MSV) program
[AD-A262525] p 3652 N93-28585
Modeling land-surface/atmosphere dynamics for CHAMMP
[DE93-008520] p 3476 N93-28677
The sensitivity of ageostrophic circulations to model resolution: A case study using NGM forecasts of ERICA IOP-4
[AD-A262011] p 3482 N93-29393
Evaluation of atmospheric wind field and dispersion models for fog-oil smoke dispersion in complex terrain: Field measurement and model evaluation program for assessment of the environmental effects of military smokes
[AD-A262051] p 3482 N93-29399
SWAT system performance predictions
[AD-A262857] p 3579 N93-29470
Wind measurement accuracy of a loran radiosonde
[AD-A263572] p 3483 N93-29832
USU center of excellence in theory and analysis of the geo-plasma environment
[AD-A264750] p 3590 N93-30585
Case study of the operational usefulness of the sharp workstation in forecasting a mesocyclone-induced cold sector tornado event in California
[PB93-178697] p 3485 N93-30889
ATMOSPHERIC COMPOSITION
Predicting the response of a temperate forest ecosystem to atmospheric CO2 increase
[DE93-010081] p 3467 N93-28543
Steady-state and transient modeling of tracer and nutrient distributions in the global ocean
[DE93-011043] p 3486 N93-28670
Mass spectrometric measurement of Martian krypton and xenon isotopic abundance p 3646 N93-28798
Development of ultraviolet absorption photometer for atmospheric ozone measurements and results from mid-latitude investigations p 3468 N93-28949
Emission inventories: A global modeling perspective
[DE93-005817] p 3469 N93-28965
Global warming potential for SF6
[DE93-007394] p 3469 N93-28972
Analysis of protocol gases: An on-going quality assurance audit
[PB93-168839] p 3311 N93-29204
Study to determine the nature and extent of ozone and ozone precursor transport in selected areas of California
[PB93-184828] p 3470 N93-29669
Potential effects of HFC-152a on global ozone and climate
[DE93-008018] p 3471 N93-29792
A preliminary review of global CO2 exchange between ocean and atmosphere
[AD-A264019] p 3472 N93-30015
Case study of Frontal Boundary Study Mission 03
[DE93-007176] p 3473 N93-30183
ATMOSPHERIC CORRECTION
Atmospheric correction of LANDSAT-TM-data for forest inventory p 3459 N93-28929
Bayesian linear analysis with application to removal of atmospheric influences on optical remote sensing images
[BCRS-92-19] p 3463 N93-31011
ATMOSPHERIC EFFECTS
Characterization of laboratory generated turbulence by optical phase measurements
[AD-A262596] p 3480 N93-28465
Results from the US/Russian Meteor-3/Total Ozone Mapping Spectrometer
[NASA-TM-104576] p 3467 N93-28682
Cloud Impacts on DOD Operations and Systems Conference (CIDOS-91)
[AD-A264463] p 3484 N93-30535
ATMOSPHERIC ENTRY
The infrared measurement for the reentry-body-translation
[AD-A263100] p 3278 N93-29134
ATMOSPHERIC GENERAL CIRCULATION MODELS
Modeling land-surface/atmosphere dynamics for CHAMMP
[DE93-008520] p 3476 N93-28677
Proceedings of the Second Atmospheric Radiation Measurement (ARM) Science Team Meeting
[DE93-005886] p 3476 N93-28889
Prognostic cloud water in the Los Alamos general circulation model
[DE93-007381] p 3482 N93-29347
Spectral energetics of the lower thermosphere
p 3477 N93-29467
ATMOSPHERIC HEATING
A correlated k-distribution model of the atmospheric heating rates for overlapping spectra of CO2 and H2O
[DE93-007391] p 3474 N93-30504
ATMOSPHERIC IONIZATION
Discharge of electrically charged clouds
[AD-A263212] p 3480 N93-28518
A computer simulation of the production of an artificially ionized layer using the Arecibo facility
[DE93-010817] p 3478 N93-30487
ATMOSPHERIC MODELS
High performance dispersion model PHYSIC
[DE93-753303] p 3467 N93-28536
Direct volume visualization of three-dimensional vector fields
[DE93-009233] p 3524 N93-28550
Steady-state and transient modeling of tracer and nutrient distributions in the global ocean
[DE93-011043] p 3486 N93-28670
Spherically symmetric model atmospheres for late-type giant stars
[ISBN-0-315-72632-6] p 3633 N93-28673
Emission inventories: A global modeling perspective
[DE93-005817] p 3469 N93-28965
Global warming potential for SF6
[DE93-007394] p 3469 N93-28972
The meteorological database
[DE93-007289] p 3481 N93-29054
Atmospheric and Geophysical Sciences Program report, 1990-1991
[DE93-007390] p 3470 N93-29055
National Center for Supercomputer Applications
p 3614 N93-29232
Exploitation of parallelism in climate models
[DE93-011259] p 3470 N93-29318
Upper ocean model of dissolved atmospheric gases
[DE93-010151] p 3487 N93-29327
The sensitivity of ageostrophic circulations to model resolution: A case study using NGM forecasts of ERICA IOP-4
[AD-A262011] p 3482 N93-29393
Evaluation of atmospheric wind field and dispersion models for fog-oil smoke dispersion in complex terrain: Field measurement and model evaluation program for assessment of the environmental effects of military smokes
[AD-A262051] p 3482 N93-29399
Ocean aerosol measurements and models in the straits of Florida (The KEY-90 experiment)
[AD-A264777] p 3487 N93-29659
The basics of weather models
[AD-A263386] p 3483 N93-29850
Quantifying and minimizing uncertainty of climate forcing by anthropogenic aerosols
[NASA-TM-108259] p 3472 N93-30043
Numerical modeling and parameterization of gravity wave processes and effects in the atmosphere
[AD-A264331] p 3478 N93-30367
A correlated k-distribution model of the atmospheric heating rates for overlapping spectra of CO2 and H2O
[DE93-007391] p 3474 N93-30504
Graphical comparison of U.S. standard atmospheres and military standard climatic extremes
[AD-A264639] p 3484 N93-30521

USU center of excellence in theory and analysis of the geo-plasma environment
[AD-A264750] p 3590 N93-30585
ATMOSPHERIC PHYSICS
JPRS report: Science and technology. Central Eurasia: Earth science
[JPRS-UES-93-003] p 3456 N93-29089
National collaboratories: Applying information technology for scientific research
[LC-93-83795] p 3612 N93-29129
NSSDC data listing
[NASA-TM-108264] p 3612 N93-29167
Analysis of mass transport and potential vorticity budget in a simulated tropopause folding
[PB93-156792] p 3476 N93-29197
Syllabus physical meteorology, part 1
[KNMI-TR-140-PT-1] p 3484 N93-30114
ATMOSPHERIC PRESSURE
Discharge of electrically charged clouds
[AD-A263212] p 3480 N93-28518
Surface shear stress estimates from geostrophic winds for use in sensible and latent heat flux formulations
p 3483 N93-30044
NOx chemistry in natural gas flames
[PB93-175263] p 3317 N93-30760
ATMOSPHERIC RADIATION
Proceedings of the Second Atmospheric Radiation Measurement (ARM) Science Team Meeting
[DE93-005886] p 3476 N93-28889
Clouds and radiation: A primier
[AD-A263136] p 3482 N93-29479
The possible direct use of satellite radiance measurements by the Atmospheric Radiation Measurement Program
[DE93-009819] p 3462 N93-30049
ATMOSPHERIC REFRACTION
Propagation channel modeling for angle-diversity combining simulation p 3360 N93-30252
ATMOSPHERIC SOUNDING
Case study of the operational usefulness of the sharp workstation in forecasting a mesocyclone-induced cold sector tornado event in California
[PB93-178697] p 3485 N93-30889
ATMOSPHERIC STRATIFICATION
Laboratory studies of gravity wave/mean flow interactions
[AD-A264226] p 3478 N93-30174
ATMOSPHERIC TURBULENCE
Characterization of laboratory generated turbulence by optical phase measurements
[AD-A262596] p 3480 N93-28465
SWAT system performance predictions
[AD-A262857] p 3579 N93-29470
Atmospheric transverse coherence length measurement system for laser communications
[AD-A263563] p 3439 N93-29827
ATOM CONCENTRATION
Planetary and satellite x ray spectroscopy: A new window on solid-body composition by remote sensing
p 3641 N93-28773
ATOMIC BEAMS
Surface modification of tribological components in transportation
[DE93-008647] p 3442 N93-28903
ATOMIC COLLISIONS
Elastic and reactive collisions of atoms and molecules with neutral alkali clusters
[DE93-009313] p 3566 N93-29206
ATOMIC EXCITATIONS
Excited states in electronic structure calculations
[DE93-007704] p 3592 N93-28642
Inner-shell photo-ionized x ray laser schemes
[DE93-009285] p 3438 N93-29309
ATOMIC INTERACTIONS
The APX spectrometer for Martian missions
p 3434 N93-28776
Radiation effects in FCC metals and intermetallic compounds: A molecular dynamics computer simulation study
[DE93-009546] p 3600 N93-30668
ATOMIC PHYSICS
Start broadened profiles with self-consistent radiation transfer and atomic kinetics in plasmas produced by high intensity lasers
[DE93-008706] p 3586 N93-29093
The 26th International Quantum Chemistry Symposium on Atomic, Molecular, and Condensed Matter Theory and Computational Methods
[AD-A264206] p 3315 N93-30534
Physics laboratory technical activities, 1992
[PB93-178648] p 3561 N93-30888
ATOMIC STRUCTURE
Powder x ray diffraction patterns of energetic materials for use as reference standards
[DE93-009903] p 3592 N93-28568
Theory of normal and superconducting properties of fullerene-based solids
[DE93-007722] p 3592 N93-28582
Excited states in electronic structure calculations
[DE93-007704] p 3592 N93-28642
Spectroscopic probes of vibrationally excited molecules at chemically significant energies
[DE93-012328] p 3564 N93-28652
Planetary and satellite x ray spectroscopy: A new window on solid-body composition by remote sensing
p 3641 N93-28773
Structure, adhesion, and stability of metal/oxide and oxide/oxide interfaces
[DE93-012930] p 3325 N93-30060
Center for surface radiation damage studies
[AD-A264330] p 3570 N93-30366
Atomic layer epitaxy of semiconductor heterostructures
[AD-A264755] p 3599 N93-30560
A tight binding model for the electronic structure of FCC and SC C60
[DE93-606214] p 3601 N93-30794
Role of oxygen vacancies in anodic TiO2 thin films
[DE92-642137] p 3602 N93-31027
ATOMIZING
Estimation of droplet collision frequency in a spray
[DE93-007991] p 3416 N93-28566
Aluminium-high strength material by mechanical alloying and reaction milling: Basics of processing and characterisation of material
[ESA-TT-1249] p 3324 N93-29272
Pulse mitigation and heat transfer enhancement techniques. Volume 2: Effect of surface wettability and roughness in evaporative spray cooling
[AD-A264174] p 3425 N93-30155
ATOMS
Atomic layer epitaxy of semiconductor heterostructures
[AD-A264755] p 3599 N93-30560
ATTENUATORS
Formulation of Ames 24E2 IR-black coating
[NASA-TM-102864] p 3629 N93-29453
ATTITUDE (INCLINATION)
Symbology for head up and head down applications for highly agile fighter aircraft: To improve spatial awareness, trajectory control, and unusual attitude recovery, part 1
p 3502 N93-28857
Long Duration Exposure Facility (LDEF) attitude measurements of the Interplanetary Dust Experiment
p 3638 N93-29377
Utility of a ghost horizon and climb/dive ladder line tapering on a head-up display
[AD-A264401] p 3508 N93-30167
Attitude determination using GPS: Development of an all solid-state guidance, navigation, and control sensor for air and space vehicles based on the global positioning system p 3246 N93-30605
ATTITUDE CONTROL
Reference equations of motion for automatic rendezvous and capture
[NASA-CR-185676] p 3269 N93-29652
Project MEDSAT p 3231 N93-29739
Efficient Reorientation Maneuvers for Spacecraft with Multiple Articulated Payloads
[NASA-CR-193142] p 3279 N93-29988
Control of nonlinear systems with applications to constrained robots and spacecraft attitude stabilization
p 3279 N93-29989
Attitude stabilization of a rigid spacecraft using two momentum wheel actuators p 3280 N93-29990
Nonlinear attitude control of planar structures in space using only internal controls p 3280 N93-29991
Attitude stabilization of a rigid spacecraft using gas jet actuators operating in a failure mode
p 3280 N93-29992
Utility of a ghost horizon and climb/dive ladder line tapering on a head-up display
[AD-A264401] p 3508 N93-30167
ATTITUDE INDICATORS
Honeywell's compact, wide-angle UV-visible imaging sensor p 3582 N93-28806
Symbology for head up and head down applications for highly agile fighter aircraft: To improve spatial awareness, trajectory control, and unusual attitude recovery, part 1
p 3502 N93-28857
ATTITUDE STABILITY
Refinements on the pinhole camera measurements of the LDEF attitude p 3283 N93-29622
Control of nonlinear systems with applications to constrained robots and spacecraft attitude stabilization
p 3279 N93-29989
Attitude stabilization of a rigid spacecraft using two momentum wheel actuators p 3280 N93-29990
Attitude stabilization of a rigid spacecraft using gas jet actuators operating in a failure mode
p 3280 N93-29992
Space station attitude disturbance arising from internal motions p 3280 N93-29995
AUDIO FREQUENCIES
High pressure studies of hydrated nafion membranes: Dielectric relaxation and deuteron NMR
[AD-A263511] p 3332 N93-29342
AUGER EFFECT
Research studies on short wavelength by selective auger processes
[AD-A264493] p 3440 N93-30401
AURORAL ABSORPTION
Performance statistics bulletin. High latitude meteor scatter propagation, May, June, July 1989
[AD-A264003] p 3399 N93-30757
AURORAL ARCS
Laboratory simulation of field-aligned currents
[NASA-CR-193091] p 3476 N93-28538
AURORAL ELECTROJETS
Results of the joint HIPAS/NUWC campaigns to investigate ELF generated by auroral electrojet modulation p 3398 N93-30746
AURORAS
Electrodynamics of the dayside cleft region based on ground observations at Svalbard
[AD-A263571] p 3477 N93-29831
AUSTENITE
Bainitic stabilization of austenite in low alloy steels
[DE93-008275] p 3321 N93-28957
AUSTENITIC STAINLESS STEELS
Preliminary test of liquid metal induced embrittlement in liquid LiPb and stainless-steel systems
[DE93-753130] p 3320 N93-28529
Transformation plasticity in ductile solids
[DE93-008636] p 3321 N93-28902
Interim fatigue design curves for carbon, low-alloy, and austenitic stainless steels in LWR environments
[DE93-009202] p 3323 N93-29102
A review of hot cracking in austenitic stainless steel weldments
[DE93-605280] p 3328 N93-31021
AUTOCORRELATION
A technique for single-pulse spectrum and pulse width measurements for an IR-FEL
[DE93-007732] p 3436 N93-28847
Operating manual for single-shot autocorrelator
[AD-A262016] p 3438 N93-29395
Parametric likelihood inference for record breaking problems
[AD-A262546] p 3549 N93-29413
Characterization of slow chromophore reorientation in nonlinear optical polymers by two-dimensional MAS NMR
[AD-A264809] p 3338 N93-30596
AUTOIONIZATION
Partial cross sections in H(-) photodetachment
[DE93-011570] p 3569 N93-30130
Research studies on short wavelength by selective auger processes
[AD-A264493] p 3440 N93-30401
AUTOMATA THEORY
Antirational transductions and their language families
[ETN-93-93794] p 3611 N93-28525
Knot invariants and cellular automata
[AD-A264199] p 3607 N93-30884
AUTOMATED EN ROUTE ATC
The Canadian Automated Air Traffic System
p 3246 N93-30323
Procedural development prototype in Automated En Route Air Traffic Control p 3247 N93-30352
AUTOMATIC CONTROL
Natural language generation
[AD-A262578] p 3524 N93-28579
Combat Automation for Airborne Weapon Systems: Man/Machine Interface Trends and Technologies
[AGARD-CP-520] p 3501 N93-28850
Operator and automation capability analysis: Picking the right team p 3503 N93-28864
System automation and pilot-vehicle-interface for unconstrained low-altitude night attack
p 3503 N93-28867
Welding wire pressure sensor assembly
[NASA-CASE-MFS-26216-1] p 3442 N93-28951
An autonomous vision-based mobile robot
p 3443 N93-29082
Lunar crane system p 3277 N93-29118
Remote vehicle survey tool
[DE93-010822] p 3460 N93-29255
Spline screw autochanger
[NASA-CASE-GSC-13435-1] p 3445 N93-29505
Automated modeling of physical systems
[NASA-CR-193256] p 3531 N93-29873
The planning coordinator: A design architecture for autonomous error recovery and on-line planning of intelligent tasks
[NASA-CR-193250] p 3543 N93-30039

A functional system architecture for fully autonomous robot p 3370 N93-30311
Supervised autonomy in telerobotics
p 3372 N93-30326
A multiprocessor architecture for realtime robot control p 3372 N93-30327
Graphical programming: On-line robot simulation for telerobotic control
[DE93-009796] p 3447 N93-30654
An automated data collection system for a Charpy impact tester p 3293 N93-30972

AUTOMATIC LANDING CONTROL
Advanced Transport Operating System (ATOPS) Flight Management/Flight Controls (FM/FC) software description
[NASA-CR-191457] p 3250 N93-28621

AUTOMATIC PILOTS
Analytical foundations of gain scheduling
[AD-A264682] p 3260 N93-30550

AUTOMATIC TEST EQUIPMENT
Standardization of automatic test equipment in the US Air force
[AD-A262076] p 3250 N93-29004
Flight control system design factors for applying automated testing techniques
[NASA-TM-4242] p 3260 N93-30764

AUTOMATION
Radiometric calibration system for IR cameras
[DE93-009237] p 3430 N93-28520
The future role of the Director of Information Management (DOIM) organization within the DOD corporate information management initiative
[AD-A264118] p 3616 N93-30193
Developing automation for terminal air traffic control: Case study of the imaging aid p 3247 N93-30356

AUTOMOBILE ENGINES
The drive to cost-effective structural ceramics
[DE93-009722] p 3335 N93-30047

AUTONOMOUS NAVIGATION
Clementine 2: A double asteroid flyby and impactor mission p 3268 N93-28770
An autonomous vision-based mobile robot
p 3443 N93-29082
On the implementation of the BIRIS range sensor for applications in robotic control and autonomous navigation p 3366 N93-30286

AUTONOMY
Robotics and artificial intelligence for hazardous environments
[DE93-008271] p 3541 N93-29047
Supervised autonomy in telerobotics
p 3372 N93-30326
A multiprocessor architecture for realtime robot control p 3372 N93-30327

AUTOREGRESSIVE PROCESSES
Parameter identification of time-varying systems using neural networks p 3356 N93-30226
Recognizing partially overlapping objects
p 3366 N93-30289

AUXILIARY POWER SOURCES
APU diaphragm testing. Test plan
[NASA-TM-108251] p 3271 N93-29387
APU diaphragm testing
[NASA-TM-108254] p 3272 N93-29501

AVIATION METEOROLOGY
STRATUS: A prototype expert advisory system for terminal weather forecasting p 3367 N93-30296
Meteorological information for aviation: A systems approach p 3367 N93-30298

AVIATION PSYCHOLOGY
Field test of a computer-driven tool to measure psychological characteristics of aircrew
[AD-A264484] p 3499 N93-30425

AVIONICS
A new class of mission support for combat air-crew
p 3501 N93-28854
Standardization of automatic test equipment in the US Air force
[AD-A262076] p 3250 N93-29004
Strategic avionics technology definition studies. Subtask 3-1A: Electrical Actuation (ELA) systems
[NASA-CR-193237] p 3271 N93-29215
Space Generic Open Avionics Architecture (SGOAA) reference model technical guide
[NASA-CR-188246] p 3285 N93-31032

AXIAL FLOW
Fluid flow and heat transfer in the entrance region of an annulus between independently rotating tubes with a turbulent axial flow p 3256 N93-29952

AXIAL FLOW TURBINES
Aero-thermal design of a cooled transonic NGV and comparison with experimental results
p 3257 N93-29957

AXIAL LOADS
Vibration localization in rotating shafts
p 3454 N93-30626
Development of an experimental method to determine the axial rigidity of a strut-node joint
p 3290 N93-30950

AXIAL STRAIN
Stress-intensity-factor influence coefficients for axial and circumferential flaws in reactor pressure vessels
[DE93-006206] p 3454 N93-30213

AXIAL STRESS
Uniaxially stressed Ge:Ga and Ge:Be
[DE93-010426] p 3594 N93-29150
An experimental/analytical evaluation of biaxial sheet failure
[DE93-010620] p 3453 N93-29843

AXISYMMETRIC BODIES
Axial impact of composites p 3297 N93-29078
Numerical computation of inviscid flow around nose tip of Space Shuttle with NND scheme
[AD-A264012] p 3421 N93-29260

AXISYMMETRIC FLOW
Large amplitude striations in an RF discharge
[DE93-753244] p 3379 N93-28534
Accelerated motion of rigid spheres in unsteady flows at low to moderate Reynolds numbers
p 3416 N93-28612
Turbulence characteristics of an axisymmetric reacting flow
[NASA-CR-4110] p 3242 N93-30373
Theoretical studies in nuclear structure
[DE93-012290] p 3570 N93-30505

B

B-1 AIRCRAFT
An evaluation of B-1B pilot performance during simulated instrument approaches with and without status information
[AD-A263874] p 3507 N93-29888

BACKGROUND RADIATION
Spectroscopic probes of vibrationally excited molecules at chemically significant energies
[DE93-012328] p 3564 N93-28652
The emulsion chamber technology experiment
p 3268 N93-28743
The Backgrounds Data Center p 3624 N93-28814
On the meaning of delta T/T
[DE93-008482] p 3653 N93-28962
A program to determine the pointing angle to a specular point
[AD-A262777] p 3630 N93-29460
The 12 UM contribution of nearby galaxies to the infrared background
[AD-A264336] p 3654 N93-30419
Predictions of a non-Gaussian model for large scale structure
[DE93-010196] p 3636 N93-30528

BACKSCATTERING
Ground clutter measurements for surface-sited radar
[AD-A262472] p 3379 N93-28655
Prototype backscatter Moessbauer spectrometer for measurement of Martian surface mineralogy
p 3648 N93-28812
Development of a 9.3 micrometer CW LIDAR for the study of atmospheric aerosol
[NASA-CR-193227] p 3381 N93-29105
Convective and stratiform rain: Multichannel microwave sensing over oceans
[NASA-TM-104586] p 3482 N93-29448
Polarization experiments with hadronic and electromagnetic probes
[DE93-011375] p 3392 N93-30126

BACKWARD FACING STEPS
A grid refinement study of two-dimensional transient flow over a backward-facing step using a spectral-element method
[DE92-018262] p 3417 N93-28639

BACTERIA
Regulation of alternative CO2 fixation pathways in procaryotic and eucaryotic photosynthetic organisms
[DE93-012109] p 3491 N93-29181
Marine microbial production of dimethylsulfide from dissolved dimethylsulfoniopropionate
[NASA-CR-193278] p 3492 N93-30665

BAFFLES
Formulation of Ames 24E2 IR-black coating
[NASA-TM-102864] p 3629 N93-29453

BAINITE
Bainitic stabilization of austenite in low alloy steels
[DE93-008275] p 3321 N93-28957

BALLISTIC MISSILES
Magnetic field measurements of the CEBAF (NIST) wiggler using the pulsed wire method
[AD-A263997] p 3439 N93-29867
Launch vehicles for lightweight TACSAT deployment
p 3271 N93-29903

BALLOON SOUNDING
Stabilized platform for tethered balloon soundings of broadband long- and short-wave radiation
[DE93-007876] p 3383 N93-29308

BALLOON-BORNE INSTRUMENTS
Aerospace payload design and development
[AD-A264502] p 3289 N93-30402

BANACH SPACE
Fixed point iterations for quasi-contractive maps in uniformly smooth Banach spaces
[DE92-641348] p 3552 N93-30942

BANDPASS FILTERS
Improved real-time imaging spectrometer
[NASA-CASE-NPO-18410-1-CU] p 3578 N93-29086
Optically controlled active impedance element particularly suited for a microwave oscillator
[AD-D015723] p 3408 N93-29281
Electro-optic characterisation of extremely wide bandwidth electrical signals
[AD-A264202] p 3392 N93-30145
Characterizing transient vibrations using band limited temporal moments
[DE93-009639] p 3453 N93-30185
Nonlinear processing of phase vocoded speech
p 3355 N93-30219

BANDWIDTH
A microseismometer for terrestrial and extraterrestrial applications p 3434 N93-28765
A comparison of high-speed links, their commercial support and ongoing R/D activities
[DE93-008134] p 3382 N93-29245
Characteristics of high-frequency signals, noise, availability, and duration of bandwidths based on ROTHR Amchitka spectrum measurements
[AD-A264480] p 3393 N93-30423
Bandwidth and SIMDUCE as simulator fidelity criteria
p 3238 N93-30690
A dynamic bandwidth and phase linearity measurement technique for 4-channel MSK VLF antenna systems
p 3398 N93-30748

BARIUM TITANATES
Investigations of self-pumped phase conjugate laser beams and coherence length
[AD-A263438] p 3438 N93-29789
Photorefractive integrators and correlators
[AD-A264200] p 3597 N93-30144
Enhanced photorefractive effects in barium titanate
[AD-A264724] p 3599 N93-30554
Phase transition studies in barium and strontium titanates at microwave frequencies p 3293 N93-30970

BARRIER LAYERS
Inertial confinement fusion target component fabrication and technology development support
[DE93-010836] p 3585 N93-28836

BARYONS
Research programs from the University of South Carolina on high energy physics
[DE93-007829] p 3574 N93-28969
Borel sum rules for octet baryons in nuclear medium
[DE93-753245] p 3604 N93-29242
Baryon number violation and particle collider experiments
[NIKHEF-H/92-14] p 3572 N93-31008

BASE FLOW
Tank issues: Site characterization for external leak monitoring
[PB93-161156] p 3469 N93-29034

BATHYMETERS
Charting the remote southern oceans with geosat altimetry
[AD-A263452] p 3461 N93-29817
A calibration procedure for the SBE 19 Conductivity, Temperature, and Depth (CTD) profiler
[AD-A264435] p 3489 N93-30420

BAYES THEOREM
Information-theoretic performance bounding of Bayesian identifiers
[DE93-010705] p 3554 N93-28763
Information compression in the context model
p 3514 N93-29549
Mixed limit theorems for pattern analysis
[AD-A263735] p 3549 N93-29854
Easy-to-apply results for establishing convergence of Markov chains in Bayesian analysis
[AD-A264015] p 3555 N93-29979
Bayesian linear analysis with application to removal of atmospheric influences on optical remote sensing images
[BCRS-92-19] p 3463 N93-31011

BEACONS
SWAT system performance predictions
[AD-A262857] p 3579 N93-29470
A satellite downlink spread spectrum timing beacon
p 3362 N93-30267

BEAM CURRENTS
Investigation of methods for the measurement of small electron bundle currents
[DIGEL-1992-4] p 3413 N93-30763
A 250 mA toroid monitor for the measurement of the bundle current in the stretcher mode of AmPS
[DIGEL-1992-1] p 3413 N93-30835
Microsecond ribbon relativistic electron beam in a plane undulator and generation of microwave radiation
[DE93-605693] p 3400 N93-30993

BEAM INJECTION
An RF driven H(-) source and a low energy beam injection system for RFQ operation
[DE93-010438] p 3575 N93-29302
High-current negative-ion beam transport
[DE93-010732] p 3575 N93-29809
Measurements of the energy spectrum of an intense microsecond relativistic electron beam in the beam-plasma experiments using a multi-foil analyzer
[DE93-606271] p 3590 N93-30768
Visible light emitting materials and injection devices
[AD-A263499] p 3601 N93-30811
Complex apparatus and results of active experiment Electron-1 with injection of electronic beam in the ionosphere
[DE93-605452] p 3480 N93-30991

BEAM INTERACTIONS
Complex apparatus and results of active experiment Electron-1 with injection of electronic beam in the ionosphere
[DE93-605452] p 3480 N93-30991

BEAM SPLITTERS
Measurement of a Michelson interferometer mirror velocity with a time interval analyzer
[AD-A263009] p 3430 N93-28659
The HYDICE instrument design and its application to planetary instruments p 3434 N93-28766
A compact imaging detector of polarization and spectral content p 3582 N93-28810
Operating manual for single-shot autocorrelator
[AD-A262016] p 3438 N93-29395

BEAMFORMING
Time-interpolation method for digital beamformers
[AD-D015709] p 3383 N93-29275
Recent advances in bootlace lens design
p 3374 N93-30336

BEAMS (SUPPORTS)
Interaction dynamics of on-orbit construction
p 3274 N93-29109
Evaluation of some scale effects in the response and failure of composite beams p 3308 N93-30874

BEARINGS
An analysis of the 70-meter antenna hydrostatic bearing by means of computer simulation p 3386 N93-29601
System for testing bearings
[NASA-CASE-MFS-28589-1] p 3445 N93-29618
Orbital transfer vehicle oxygen turbopump technology. Volume 3: Hot oxygen testing
[NASA-CR-191036] p 3448 N93-31039

BEAT FREQUENCIES
Carbon monoxide exposure of subjects with documented cardiac arrhythmias
[PB93-179943] p 3497 N93-30890

BEAUFORT SEA (NORTH AMERICA)
Leadex data report. Part 2: Rawinsonde and ice station data
[AD-A263218] p 3483 N93-29491

BELL AIRCRAFT
Models for performance assessment of HF antennas on the CH-135/Twin Huey helicopter
p 3366 N93-30291

BEND TESTS
Design and evaluation of a uniaxial pull test for lithium hydride/deuteride
[DE93-010760] p 3451 N93-28832

BENDING
A complete set of field equations for the dynamic simulation of a towed cable system
[AD-A262570] p 3442 N93-28578
Silicon crystal under bending
[DE93-010522] p 3593 N93-28888
Fracture of glass p 3293 N93-30969

BENDING FATIGUE
The effect of temperature on the impact behavior of TiB2 reinforced XDTM-TiAl intermetallic matrix composites
[AD-A262924] p 3296 N93-28886

BENZENE
What is underneath? Moving atoms and molecules to find out
[AD-A263363] p 3567 N93-29332
Performance and cost evaluation of bioremediation techniques for fuel spills
[PB93-175545] p 3474 N93-30762

BERYLLIUM
Measurements of breakaway reaction between beryllium and water vapor for ITER blanket design
[DE93-753270] p 3584 N93-28535
Uniaxially stressed Ge:Ga and Ge:Be
[DE93-010426] p 3594 N93-29150

BERYLLIUM ALLOYS
Deformation mechanisms in Be(sub 12)X compounds
[DE93-009080] p 3320 N93-28548

BERYLLIUM COMPOUNDS
Be3(AsO4)2 2H2O: A new berylloarsenate phase containing bridged tetrahedral 3-rings
[AD-A262518] p 3592 N93-28584

BERYLLIUM 10
Cosmogenic radionuclides on LDEF: An unexpected Be-10 result p 3573 N93-29643

BETA PARTICLES
Neutrino mass
[DE93-010735] p 3566 N93-29315

BETHE-SALPETER EQUATION
General method for reducing the two-body Dirac equation
[DE93-609833] p 3607 N93-30943

BEVERAGES
Field trial of caffeine on physical performance at altitude: An attempt to overcome the challenge
[AD-A264260] p 3497 N93-30894

BIAS
Measurement of the relative and absolute microgravity environment of space platforms, recent flight results, and determination of the spatial microgravity field
p 3266 N93-28725
Growth, characterization and device development in monocrystalline diamond films
[AD-A263204] p 3593 N93-28874
Evaluating the bias of alternative cost progress models: Tests using aerospace industry acquisition programs
[AD-A262870] p 3624 N93-29477

BIBLIOGRAPHIES
Energy efficient drivepower, volume 2
[DE93-012437] p 3410 N93-29814
Energy efficient drivepower
[DE93-012436] p 3411 N93-30058
An annotated bibliography on integration in software engineering environments
[AD-A264798] p 3535 N93-30602

BIDIRECTIONAL REFLECTANCE
Modeling the bidirectional reflectance and spectra
[AD-A263570] p 3462 N93-29830

BIG BANG COSMOLOGY
Tests of the particle physics-physical cosmology interface
[DE93-008483] p 3634 N93-28963

BINARY ALLOYS
Some effects of composition and microstructure on the B2 in equilibrium to DO3 ordered phase transition in Fe3Al alloys
[DE93-009724] p 3325 N93-29813
Effective interactions between concentration fluctuations and charge transfer in chemically ordering liquid alloys
[DE93-606724] p 3327 N93-30778

BINARY DATA
Wideband propagation measurements for wireless indoor communication
[PB93-175123] p 3382 N93-29202
Incomplete fuzzy data processing systems using artificial neural network p 3519 N93-29578
Massively parallel spatial light modulation-based optical signal processing
[AD-A264846] p 3581 N93-30905

BINARY FLUIDS
Loading and testing a light scattering cell with a binary fluid mixture near its critical composition
[NASA-CR-193147] p 3415 N93-28557

BINARY PHASE SHIFT KEYING
Wideband propagation measurements for wireless indoor communication
[PB93-175123] p 3382 N93-29202

BINARY STARS
Stellar encounters in globular clusters
p 3632 N93-28606
The multiplicity of T Tauri stars in the star forming regions Taurus-Auriga and Ophiuchus-Scorpius: A 2.2 micron speckle imaging survey p 3634 N93-28945
Effects of spiral shocks on disk emission lines
[DE92-641716] p 3637 N93-31004

BINDERS (MATERIALS)
Thermal control paints on LDEF: Results of M0003 sub-experiment 18
[AD-A263252] p 3329 N93-28561
An evaluation of factors affecting the solidification/stabilization of heavy metal sludge
[AD-A264128] p 3473 N93-30197

BINOCULAR VISION
Binocular spherical disparity: A study in representation for a forward translating camera
[PB93-184422] p 3579 N93-29667
Intermediate levels of visual processing
[AD-A264117] p 3495 N93-30192

BINOMIALS
Fluctuations and intermittency in high energy nucleus-nucleus collisions
[DE93-608481] p 3577 N93-30990

BIOCHEMISTRY
Clouds and radiation: A primier
[AD-A263136] p 3482 N93-29479
Solar world congress: Proceedings of the biennial congress of the international solar energy society, volume 1, part 2
[PB93-174779] p 3465 N93-30001
Biophysical and biochemical mechanisms in synaptic transmitter release
[AD-A264829] p 3496 N93-30613

BIOCONTROL SYSTEMS
Cognitive and Neural Sciences Division 1992 programs
[AD-A263400] p 3654 N93-29258

BIOCONVERSION
Introductions to the Proceedings of the Fourteenth Symposium on Biotechnology for Fuels and Chemicals
[DE93-006235] p 3490 N93-28890

BIODYNAMICS
Anthropometric survey of the astronaut applicants and astronauts from 1985 to 1991
[NASA-RP-1304] p 3506 N93-29324
Visualization techniques for analyzing control of human movement: Affine mappings between multi-dimensional spaces p 3508 N93-30204

BIOELECTRIC POTENTIAL
An assessment of peripheral nerve damage in the rat following non-freezing cold exposure: An electrophysiological and histopathological examination
[AD-A264293] p 3492 N93-30818

BIOINSTRUMENTATION
Transcutaneous analyte measuring methods
[AD-A262861] p 3494 N93-29509
Acquisition of physiological data during G-induced Loss of Consciousness (G-LOC)
[AD-A264492] p 3496 N93-30400

BIOLOGICAL EFFECTS
Predicting the response of a temperate forest ecosystem to atmospheric CO2 increase
[DE93-010081] p 3467 N93-28543
Gene transcription and electromagnetic fields
[DE93-010854] p 3490 N93-28848
State of the art: Ecological biomarkers
[DE93-006621] p 3469 N93-28992
Theoretical-experimental study of the non-thermal effects of the polarized laser radiation in living tissues
[DE93-607212] p 3441 N93-30775

BIOLOGICAL EVOLUTION
A robust model for finding optimal evolutionary trees
[DE93-010682] p 3491 N93-30483

BIOLOGICAL MODELS (MATHEMATICS)
Comparative mutagenesis of human cells in vivo and in vitro
[DE93-012269] p 3490 N93-28651
Sudden loading and fatigue effects on the human spine
[PB93-167526] p 3493 N93-29199
Modelling and simulation of human retinal vision processing p 3363 N93-30269
Parallel processing and learning: Variability and chaos in self-organization of activity in groups of neurons
[AD-A264224] p 3539 N93-30361
A robust model for finding optimal evolutionary trees
[DE93-010682] p 3491 N93-30483
A simple computational model of center-surround receptive fields in the retina
[AD-A264723] p 3496 N93-30515
Principal components of natural images: An analytical solution
[AD-A264800] p 3489 N93-30603

BIOMASS
Introductions to the Proceedings of the Fourteenth Symposium on Biotechnology for Fuels and Chemicals
[DE93-006235] p 3490 N93-28890
Design of biomass management systems and components for closed loop life support systems
p 3230 N93-29728

BIOMEDICAL DATA
The Visible Human Project of the National Library of Medicine: Remote access and distribution of a multi-gigabyte data set p 3617 N93-30453

BIOPHYSICS
Gene transcription and electromagnetic fields
[DE93-010854] p 3490 N93-28848
Biophysical model for handwear insulation testing
[AD-A262926] p 3505 N93-28884

Biophysical and biochemical mechanisms in synaptic transmitter release
[AD-A264829] p 3496 N93-30613

BIOTECHNOLOGY
Proceedings of a Workshop on Molecular Nuclear Medicine
[DE93-010828] p 3493 N93-28835
Center of Excellence in Biotechnology (Research)
[AD-A263598] p 3491 N93-29915
Solar world congress: Proceedings of the biennial congress of the international solar energy society, volume 1, part 2
[PB93-174779] p 3465 N93-30001

BIPOLAR TRANSISTORS
Analysis of electrothermal interactions in power semiconductor modules
[ETN-93-93800] p 3591 N93-28470
Charge separation in bipolar transistors
[DE93-009624] p 3413 N93-30650
Hardness assurance and testing issues for bipolar/BiCMOS devices
[DE93-009623] p 3570 N93-30669

BIPOLARITY
A simple computational model of center-surround receptive fields in the retina
[AD-A264723] p 3496 N93-30515

BIREFRINGENCE
A compact imaging detector of polarization and spectral content p 3582 N93-28810

BISMUTH OXIDES
The effect of Bi2 O3 on the electrical properties of Zr O2: 3 percent Mg O ceramic solid electrolytes
[DE93-607029] p 3339 N93-30774

BIT ERROR RATE
Theoretical bit error rate performance of the Kalman filter excisor for FM interference
[AD-A263018] p 3383 N93-29407
Signal-to-noise ratio losses in full spectrum combining of signals with a downconverted subcarrier
p 3386 N93-29599

BLACK HOLES (ASTRONOMY)
Topics in General Relativity theory: Gravitational-wave measurements of black-hole parameters; gravitational collapse of a cylindrical body; and classical-particle evolution in the presence of closed, timelike curves
p 3603 N93-28690
Electric magnetic duality in string theory
[DE93-606061] p 3606 N93-30807
Effects of spiral shocks on disk emission lines
[DE92-641716] p 3637 N93-31004

BLADE SLAP NOISE
Strong parallel blade-vortex interaction and noise propagation in helicopter flight p 3563 N93-30980

BLADE TIPS
Aerodynamic characteristics of a rotorcraft airfoil designed for the tip region of a main rotor blade
[NASA-TM-4264] p 3240 N93-29450

BLADE-VORTEX INTERACTION
Computation of far-field helicopter rotor tone noise
[ONERA-P-1990-5] p 3562 N93-30110
Strong parallel blade-vortex interaction and noise propagation in helicopter flight p 3563 N93-30980

BLANKETS (FUSION REACTORS)
Measurements of breakaway reaction between beryllium and water vapor for ITER blanket design
[DE93-753270] p 3584 N93-28535

BLAST LOADS
Mitigation of shock waves in a cylindrical tunnel by foam
[AD-A262491] p 3423 N93-29419

BLOCK COPOLYMERS
Gas permeability of E/EP semicrystalline diblock copolymers
[AD-A263241] p 3329 N93-28560

BLOCK DIAGRAMS
Technical examination and simulation of a photovoltaic system: Solar generator, battery, download
[ETN-93-94179] p 3466 N93-30573

BLOOD
Transcutaneous analyte measuring methods
[AD-A262861] p 3494 N93-29509

BLOOD FLOW
Pharmacokinetics and Pharmacodynamics in Space
[NASA-CP-10048] p 3494 N93-29502

BLUE STARS
Why Blue stragglers formed via collisions may not be rapid rotators
[DE93-008708] p 3633 N93-28905
Do the Pop 2 field blue stragglers have a collisional origin?
[DE93-008709] p 3634 N93-28906
Can physical stellar collisions explain the blue stragglers in the dwarf spheroidal galaxies?
[DE93-008711] p 3634 N93-28907

BLUFF BODIES
Vortex shedding by blunt/bluff bodies at high reynolds numbers. Volume 1: Data analysis
[AD-A264151] p 3241 N93-30171
Vortex shedding by Blunt/Bluff bodies at high reynolds numbers. Volume 2: Cylinders, octagon, hexagon
[AD-A264152] p 3241 N93-30172
Vortex shedding by blunt/bluff bodies at high reynolds numbers. Volume 3. Cubes
[AD-A264153] p 3242 N93-30173

BLUNT BODIES
Hypersonic lateral and directional stability characteristics of aeroassist flight experiment configuration in air and CF4
[NASA-TM-4435] p 3239 N93-29166
Vortex shedding by blunt/bluff bodies at high reynolds numbers. Volume 1: Data analysis
[AD-A264151] p 3241 N93-30171
Vortex shedding by Blunt/Bluff bodies at high reynolds numbers. Volume 2: Cylinders, octagon, hexagon
[AD-A264152] p 3241 N93-30172
Vortex shedding by blunt/bluff bodies at high reynolds numbers. Volume 3. Cubes
[AD-A264153] p 3242 N93-30173

BOATS
Development of a test program to evaluate structural defects in Glass-Reinforced Plastic (GRP), volume 2
[AD-A263814] p 3335 N93-29881

BODIES OF REVOLUTION
Axial impact of composites p 3297 N93-29078
Representation and recognition with invariants and geometric constraint models
[AD-A263235] p 3529 N93-29493
The application of concentric vortex simulation to calculating the aerodynamic characteristics of bodies of revolution at high angles of attack
[AD-A263879] p 3241 N93-29919

BODY CENTERED CUBIC LATTICES
The role of grain boundaries in hydrogen diffusion in metals at 25 C
[NASA-TM-108407] p 3322 N93-29043
Order-disorder transformations in Ni-Al alloys
[DE93-009293] p 3326 N93-30389

BODY TEMPERATURE
Influence of the Cold Buster (tm) sports bar on heat debt, mobilization and oxidation of energy substrates
[AD-A262762] p 3493 N93-28939
Evaluation of personal cooling systems in conjunction with explosive ordnance disposal suits
[AD-A262862] p 3506 N93-29471

BODY WEIGHT
Field trial of caffeine on physical performance at altitude: An attempt to overcome the challenge
[AD-A264260] p 3497 N93-30894

BOEING 757 AIRCRAFT
Vortex wake characteristics of B757-200 and B767-200 aircraft using the tower fly-by technique
[PB93-180255] p 3242 N93-30387
Vortex wake characteristics of B757-200 and B767-200 aircraft using the tower fly-by technique
[PB93-180263] p 3242 N93-30388

BOEING 767 AIRCRAFT
Vortex wake characteristics of B757-200 and B767-200 aircraft using the tower fly-by technique
[PB93-180255] p 3242 N93-30387
Vortex wake characteristics of B757-200 and B767-200 aircraft using the tower fly-by technique
[PB93-180263] p 3242 N93-30388

BOILING WATER REACTORS
Annual progress report on the NSRR experiments, (21)
[DE93-753190] p 3574 N93-29137
TRAB: A transient analysis program for BWR. Part 2: User's manual
[VTT-TIED-1232-PT-2] p 3575 N93-29996

BOLOMETERS
Novel low temperature superconducting bolometers
[DE93-010433] p 3430 N93-28664
Superconducting submillimeter and millimeter wave detectors
[DE93-007656] p 3431 N93-29149
Submillimeter and microwave residual losses in epitaxial films of Y-Ba-Cu-O and Tl-Ca-Ba-Cu-O
[DE93-010430] p 3596 N93-29868

BOLTS
The design and lifetime calculation of MHD generator walls based on subcritical crack growth in ceramics
[ISBN-90-9004009-9] p 3332 N93-29267
Mold bolt and means for achieving close tolerances between bolts and bolt holes
[NASA-CASE-MFS-28720-1] p 3447 N93-30567
Effects of bolt-hole contact on bearing-bypass damage-onset strength p 3307 N93-30870

BOLTZMANN TRANSPORT EQUATION
Optimization of HPM device parameters for maximum air transmission
[DE93-007332] p 3386 N93-29765

BOLTZMANN-VLASOV EQUATION
Numerical modelling of the cold plasma with time-dependent, magnetohydrodynamic methods
[KFK-5053] p 3586 N93-29081

BOMBARDMENT
A unique photon bombardment system for space applications p 3286 N93-28790

BONDED JOINTS
Diffusion bonding
[DE93-011480] p 3442 N93-28837

BONDING
Tailored interfaces for metal-matrix composites-fundamental considerations
[AD-A263048] p 3298 N93-29130
Observation of phase-separated nanometer scale molecular domains in mixed self-assembled monolayers
[AD-A263470] p 3569 N93-29839
Structure, adhesion, and stability of metal/oxide and oxide/oxide interfaces
[DE93-012930] p 3325 N93-30060
Applications of density functional theory to calculation of reaction energetics p 3351 N93-30098

BOOLEAN ALGEBRA
Modeling the bidirectional reflectance and spectra
[AD-A263570] p 3462 N93-29830
Efficient algorithms and data structures in geometric design
[AD-A264678] p 3534 N93-30544
Manifold shape: From differential geometry to mathematical morphology
[CS-9204] p 3552 N93-31012
Short-circuit evaluation of Boolean expressions
[CS-9205] p 3552 N93-31014

BORATES
The synthesis and ab initio structure determination of Zn4O(BO3)2: A microporous zincoborate built up from fused 3-ring and 5-ring sub-units
[AD-A262504] p 3594 N93-29138
Synthesis and characterization of mixed 3-5 and 2-6 semiconductor monomers included in the borate sodalite analogue
[AD-A264523] p 3598 N93-30407

BORESIGHT ERROR
Gravity referenced elevation encoder development
p 3385 N93-29592

BORESIGHTS
Cryogenic magnetic bearing
[AD-A264716] p 3446 N93-30512

BORON CARBIDES
Boron carbide aluminum cermets for external pressure housing applications
[AD-A262749] p 3333 N93-29404

BORON FLUORIDES
Efficient laser action from two CW laser pumped pyrromethene-BF2 complexes
[AD-A264887] p 3441 N93-30910

BORON REINFORCED MATERIALS
SESAME equation of state number 8010: Boron loaded silicone potting material
[DE93-012083] p 3300 N93-30395

BOROSILICATE GLASS
Large amplitude striations in an RF discharge
[DE93-753244] p 3379 N93-28534
Healing of lithographically introduced flaws in glass and glass containing ceramics
[DE93-010453] p 3330 N93-28761
Thermal certification tests of Orbiter Thermal Protection System tiles coated with KSC coating slurries
[NASA-TM-104766] p 3278 N93-29221

BOSONS
Massive Majorana neutrinos in pre-bounce supernovae
[DE92-642597] p 3572 N93-30931

BOUNDARIES
Information-theoretic performance bounding of Bayesian identifiers
[DE93-010705] p 3554 N93-28763
Detecting residue on a printed circuit board: An application of the Boundary Contour/Feature Contour System
[DE93-006283] p 3412 N93-30370

BOUNDARY CONDITIONS
Dense inclined flows: Theory and experiments
[DE93-011452] p 3417 N93-28630
Design optimization of space structures
p 3278 N93-29122
Fundamental studies of impingement cooling thermal boundary conditions p 3254 N93-29940
Geometrical approach to the dynamics of a relativistic string in the D-dimensional Minkowski space
[DE93-606071] p 3605 N93-30784

Numerical wave propagation and steady-state solutions p 3428 N93-30999

BOUNDARY ELEMENT METHOD
Nonlinear analyses of composite aerospace structures in sonic fatigue [NASA-CR-193124] p 3451 N93-29154

BOUNDARY INTEGRAL METHOD
Analysis of thermal bar using boundary-layer integral equations gradients [MATHS-REPT-A-177] p 3462 N93-30107

BOUNDARY LAYER CONTROL
The numerical simulation of circulation controlled airfoil flowfields p 3243 N93-30947

BOUNDARY LAYER FLOW
State vector splitting: A numerical scheme for the Euler equations p 3419 N93-29039
Flow visualization on helicopter blades using acenaphthen [ESA-TT-1255] p 3422 N93-29273
Experimental study of heat transfer close to a plane wall heated in the presence of multiple injections (subsonic flow) p 3253 N93-29931
Measurement of turbulent spots and intermittency modelling at gas-turbine conditions p 3253 N93-29934
Heat transfer in high turbulence flows: A 2-D planar wall jet p 3254 N93-29935
Analytical and experimental study of laminar free convective heat transfer from isothermal convex bodies of arbitrary shape [ISBN-0-315-72512-5] p 3426 N93-30379

BOUNDARY LAYER PLASMAS
Modeling the D3-D plasma boundary with the LEDGE code [DE93-009301] p 3588 N93-29772

BOUNDARY LAYER SEPARATION
Measurements of breakaway reaction between beryllium and water vapor for ITER blanket design [DE93-753270] p 3584 N93-28535
An experimental study of flow over a 6 to 1 prolate spheroid at incidence p 3239 N93-29124
The 3-D viscous flow CFD analysis of the propeller effect on an advanced ducted propeller subsonic inlet [NASA-TM-106240] p 3252 N93-29162
High-Reynolds-number test of a 5-percent-thick low-aspect-ratio semispan wing in the Langley 0.3-meter transonic cryogenic tunnel: Wing pressure distributions [NASA-TM-4227] p 3240 N93-29449
Vortex structure and mass transfer near the base of a cylinder and a turbine blade p 3253 N93-29929

BOUNDARY LAYER TRANSITION
Keynote address: Unsteady, multimode transition in gas turbine engines p 3252 N93-29927
Determination of surface heat transfer and film cooling effectiveness in unsteady wake flow conditions p 3253 N93-29933
Measurement of turbulent spots and intermittency modelling at gas-turbine conditions p 3253 N93-29934

BOUNDARY LAYERS
Thermal and mechanical analysis of flip-chips on a liquid cooled multichip module [DE93-007609] p 3405 N93-28641
Development of an unstructured solution adaptive method for the quasi-three-dimensional Euler and Navier-Stokes equations [NASA-CR-193241] p 3421 N93-29213
Heat transfer with moderate free stream turbulence p 3254 N93-29936
Analysis of thermal bar using boundary-layer integral equations gradients [MATHS-REPT-A-177] p 3462 N93-30107

BOUNDARY LUBRICATION
A study of the chemical mechanism in lubrication [DE93-012230] p 3330 N93-28650

BOUNDARY VALUE PROBLEMS
The wave, the cylinder, and the plate [DE93-009458] p 3450 N93-28596
Representation and recognition with invariants and geometric constraint models [AD-A263235] p 3529 N93-29493
Algorithms for point set congruence [AD-A264016] p 3532 N93-29980
Geometrical approach to the dynamics of a relativistic string in the D-dimensional Minkowski space [DE93-606071] p 3605 N93-30784
On the invariant measure for the nonlinear Schroedinger equation [DE92-644672] p 3551 N93-30912
A numerical solution of the two-center problem [DE92-644674] p 3551 N93-30913

BOUSSINESQ APPROXIMATION
High performance dispersion model PHYSIC [DE93-753303] p 3467 N93-28536

BOW WAVES
Kinetics and energy transfer in nonequilibrium fluid flows [AD-A263612] p 3240 N93-29284

BOX BEAMS
Design, analysis, and fabrication of the technology integration box beam p 3300 N93-30433

BRAIDED COMPOSITES
Environmental effects on stitched RTM composites [NASA-CR-193221] p 3297 N93-29107

BRAIN
The AFOSR Workshop on the Future of EEG and MEG [AD-A264338] p 3495 N93-30160

BRAIN CIRCULATION
Acquisition of physiological data during G-induced Loss of Consciousness (G-LOC) [AD-A264492] p 3496 N93-30400

BRAIN DAMAGE
The AFOSR Workshop on the Future of EEG and MEG [AD-A264338] p 3495 N93-30160

BRAKES (FOR ARRESTING MOTION)
Single acting translation/rotational brake [NASA-CASE-LAR-14738-1] p 3443 N93-29175

BRANCHING (MATHEMATICS)
A normally elliptic Hamiltonian bifurcation [W-9201] p 3548 N93-28753
Bifurcations phenomena in a nonlinear oscillator: Approximate analytical studies versus computer simulation results p 3407 N93-29037
Short-circuit evaluation of Boolean expressions [CS-9205] p 3552 N93-31014

BRASSES
An experimental investigation of radioactivity induced by ions associated with the operation of pulsed-power accelerators [DE93-011478] p 3575 N93-29151

BRAZING
A transient FGM interlayer based approach to joining ceramics [DE93-010415] p 3331 N93-29248
Direct use geothermal applications for brazed plate heat exchangers [DE93-008559] p 3465 N93-30011

BREEDER REACTORS
Annual progress report on the NSRR experiments, (21) [DE93-753190] p 3574 N93-29137

BREEDING (REPRODUCTION)
Preliminary test of liquid metal induced embrittlement in liquid LiPb and stainless-steel systems [DE93-753130] p 3320 N93-28529
Measurements of breakaway reaction between beryllium and water vapor for ITER blanket design [DE93-753270] p 3584 N93-28535

BREMSSTRAHLUNG
Hard photon emission from high energy electrons and positrons in single crystals [DE93-606328] p 3600 N93-30770

BRIGHTNESS
Discomfort glare from high-intensity discharge headlamps: Effects of context and experience [PB93-174720] p 3496 N93-30659

BRITTLE MATERIALS
Three-dimensional elastic stress analysis in materials with many inhomogeneities [AD-A263736] p 3453 N93-29855
Fracture of glass p 3293 N93-30969

BRITTLENESS
Environmental embrittlement of binary and Zr-doped Ni3Al [DE93-008575] p 3321 N93-28679
Materials characterization of cermet anodes tested in a pilot cell [DE93-008924] p 3323 N93-29101
Preliminary properties of a resin from ethynyl terminated materials p 3303 N93-30842

BROADBAND
Wideband propagation measurements for wireless indoor communication [PB93-175123] p 3382 N93-29202
Electro-optic characterisation of extremely wide bandwidth electrical signals [AD-A264202] p 3392 N93-30145
Topical meeting of broadband analog and digital optoelectronics [AD-A264643] p 3581 N93-30522
Ultrafast, passive, broad-band, optical shutter based on novel semiconductor/conducting polymer interfaces [AD-A264098] p 3601 N93-30878

BROADBAND AMPLIFIERS
Wide-bandwidth high-resolution search for extraterrestrial intelligence [NASA-CR-193137] p 3509 N93-28895

BROKEN SYMMETRY
Flux lattice relaxation, noise, and symmetry-breaking in frustrated Josephson junction arrays [DE93-008713] p 3593 N93-29094
Theoretical studies in nuclear structure [DE93-012290] p 3570 N93-30505
Phase structure of three- and four-dimensional phi(exp 4) field theory [DE93-606069] p 3605 N93-30782
Schroedinger equations of higher (greater than 2) order [DE92-644677] p 3552 N93-30984

BROMINE
Photodissociation of HBr/LiF(001): A quantum mechanical model [NASA-CR-193119] p 3603 N93-28933

BRONCHI
The chronic effects of jP-8 jet fuel exposure on the lungs [AD-A264162] p 3495 N93-30153

BROWNIAN MOVEMENTS
A microseismometer for terrestrial and extraterrestrial applications p 3434 N93-28765
Simulation and calculation of diffusive aerosol deposition [DE93-007518] p 3474 N93-30506

BRUSH SEALS
Preliminary experimental results for a cryogenic brush seal configuration [NASA-TM-106236] p 3416 N93-28627

BSCCO SUPERCONDUCTORS
Effect of lead addition on the formation of superconducting phases in Bi-Sr-Ca-Cu-O ceramics [DE93-606893] p 3339 N93-30773

BUBBLES
A four-field approach towards developing a mechanistic model for multiphase flow [DE93-006572] p 3420 N93-29126
Horizontal nucleate flow boiling heat transfer coefficient measurements and visual observations for R12, R134a, and R134a/ester lubricant mixtures [PB93-178598] p 3475 N93-30887

BUCKLING
Integrated approaches to parallelism in optimization and solution of inverse problems [AD-A262259] p 3452 N93-29349
Design and analysis of grid stiffened concepts for aircraft composite primary structural applications p 3306 N93-30861
Experimental behavior of graphite-epoxy Y-stiffened specimens loaded in compression p 3307 N93-30872

BUDGETING
A perspective on acquisition of NASA space systems [AD-A263246] p 3610 N93-29499
Air Force CALS business practices [AD-A264789] p 3610 N93-30177

BUFFER STORAGE
Compiler-assisted multiple instruction rollback recovery using a read buffer [NASA-CR-193175] p 3527 N93-29170

BUILDINGS
Concept design example, Computer Aided Structural Modeling (CASM). Scheme A [AD-A264759] p 3529 N93-29657
Concept design example, Computer Aided Structural Modeling (CASM). Scheme B [AD-A264760] p 3529 N93-29658
Rocket-triggered lightning studies for the protection of critical assets [DE93-009633] p 3484 N93-30651
ELF/VLF spectrum measurements p 3398 N93-30745

BUNDLES
Characterization of a space orbited incoherent fiber optic bundle p 3583 N93-29698
Powder towpreg process development p 3303 N93-30844

BUOYANCY
Macrostatistical hydrodynamics [DE93-012289] p 3417 N93-28751
Turbulent flow and heat transfer in idealized blade cooling passages p 3254 N93-29938
Effects of buoyancy on gas jet diffusion flames [NASA-CR-191109] p 3352 N93-31031

BYPASSES
Valve malfunction detection apparatus [NASA-CASE-MFS-29904-1] p 3432 N93-29503

C

C (PROGRAMMING LANGUAGE)
Proposal for a numerical array library [DE93-010678] p 3623 N93-30482

C BAND

Study of gain in C-band deflection cavities for a frequency-doubling magnicon amplifier
[AD-A263132] p 3409 N93-29478

C++ (PROGRAMMING LANGUAGE)

A C++ interface for programming on the Connection Machine
[INRIA-RR-1698] p 3538 N93-29487

Proposal for a numerical array library
[DE93-010678] p 3623 N93-30482

CABLES (ROPES)

Theoretical and experimental investigation of slack cable/mass system dynamics p 3455 N93-31028

CADMIUM ALLOYS

Proceedings of Symposium F on New Aspects on the Growth, Characterization and Applications of CdTe and related Cd rich alloys 5, 1992
[AD-A263541] p 3597 N93-29974

CADMIUM SELENIDES

Electrochemical fabrication of cadmium chalcogenide microdiode arrays
[AD-A263169] p 3310 N93-28988

Nonequilibrium screening and exciton dynamics probed by femtosecond laser pulses
[AD-A263603] p 3439 N93-29983

CADMIUM TELLURIDES

Electrochemical fabrication of cadmium chalcogenide microdiode arrays
[AD-A263169] p 3310 N93-28988

Proceedings of Symposium F on New Aspects on the Growth, Characterization and Applications of CdTe and related Cd rich alloys 5, 1992
[AD-A263541] p 3597 N93-29974

CAFFEINE

Field trial of caffeine on physical performance at altitude: An attempt to overcome the challenge
[AD-A264260] p 3497 N93-30894

CALCIUM COMPOUNDS

The effect of oxidation embrittlement on the impact behavior of nicalon reinforced CAS 2 ceramic matrix composites
[AD-A263567] p 3334 N93-29829

CALIBRATING

Radiometric calibration system for IR cameras
[DE93-009237] p 3430 N93-28520

The HYDICE instrument design and its application to planetary instruments p 3434 N93-28766

Program for an improved hypersonic temperature-sensing probe
[NASA-CR-186025] p 3431 N93-29066

Enhanced reduction of velocity data obtained during CETA flight experiment
[NASA-TM-4460] p 3431 N93-29209

Graphical interface between the CIRSSE testbed and CimStation software with MCS/CTOS
[NASA-CR-193276] p 3527 N93-29218

Preprocessing airborne remote sensing PARES calibration maintenance functional design document
[BCRS-92-07] p 3460 N93-29321

Transient response of embedded thermocouples
[DE93-009889] p 3431 N93-29325

Selection and static calibration of the Marsh J1678 pressure gauge p 3249 N93-29779

What is the center of the image?
[AD-A263550] p 3579 N93-29824

The possible direct use of satellite radiance measurements by the Atmospheric Radiation Measurement Program
[DE93-009819] p 3462 N93-30049

A calibration procedure for the SBE 19 Conductivity, Temperature, and Depth (CTD) profiler
[AD-A264435] p 3489 N93-30420

VLF/LF propagation measurements
p 3395 N93-30732

Satellite calibration requirements
[AD-A264279] p 3281 N93-30817

Physics laboratory technical activities, 1992
[PB93-178648] p 3561 N93-30888

ERS-1 directional wave spectra validation with the airborne SAR PHARS
[BCRS-92-18] p 3463 N93-31010

CALIFORNIA

Tidal and lunar data for Point Mugu, San Nicolas island, and the Barking Sands area during 1993
[AD-A262725] p 3477 N93-29401

Fugitive hydrocarbon emissions from Pacific OCS facilities. Volume 2: Executive summary and user's guide
[PB93-173805-VOL-2] p 3471 N93-29861

CALORIMETERS

Studies of relativistic heavy ion collisions at the AGS (E814/E877)
[DE93-008541] p 3564 N93-28678

The emulsion chamber technology experiment
p 3268 N93-28743

Measurement of W-Z interference from neutrino-electron scattering
[DE93-010724] p 3566 N93-29313

CAMBER

A comparison of classical mechanics models and finite element simulation of elastically tailored wing boxes
p 3306 N93-30863

CAMERAS

Radiometric calibration system for IR cameras
[DE93-009237] p 3430 N93-28520

Vision-based control of holonomic robots for 3-dimensional rigid-body positioning using camera-space manipulation p 3578 N93-29178

Binocular spherical disparity: A study in representation for a forward translating camera
[PB93-184422] p 3579 N93-29667

What is the center of the image?
[AD-A263550] p 3579 N93-29824

CAMS

Experimental and analytical investigation of finger-follower cam systems p 3446 N93-30378

CANADA

Canadian Conference on Electrical and Computer Engineering, volumes 1 and 2
[ISBN-0-9694170-1-2] p 3354 N93-30215

VLF propagation measurements in the Canadian Arctic p 3396 N93-30733

CANADIAN SPACECRAFT

Canadian EHF MILSATCOM research and development project p 3362 N93-30264

FASSET: A development model for a Canadian EHF MILSATCOM system p 3363 N93-30268

CANARD CONFIGURATIONS

Effect of canard wing positions on aerodynamic characteristics of swept-forward wing
[AD-A262373] p 3238 N93-28493

CANOPIES

Wind loads on canopy roofs
[RR-CE132] p 3451 N93-29106

CANOPIES (VEGETATION)

Remote sensing of agricultural vegetation: Status and perspectives p 3458 N93-28922

Modeling the bidirectional reflectance and spectra
[AD-A263570] p 3462 N93-29830

CAPACITORS

Adhesion of thick film Au to alumina ceramics
[DE93-009802] p 3339 N93-30656

CAPE KENNEDY LAUNCH COMPLEX

Guide for certifying pressure vessels and systems
[NASA-TM-107549] p 3449 N93-29220

CAPILLARY FLOW

Pulse mitigation and heat transfer enhancement techniques. Volume 5: Transient liquid movement in heat pipe wicks
[AD-A264513] p 3426 N93-30403

CAPILLARY TUBES

Velocity measurements of low Reynolds number tube flow using fiber-optic technology
[DE93-009865] p 3422 N93-29335

Improved heat removal by microscopic surface texturing of capillaries
[AD-A263483] p 3424 N93-29966

CAPILLARY WAVES

Optical measurements of ripples using a scanning laser slope gauge. Part 1: Instrumentation and preliminary results
[AD-A261939] p 3486 N93-28996

The IUTAM Symposium on Breaking Waves
[AD-A264196] p 3489 N93-30143

CARBENES

Laser spectroscopy of hydrocarbon radicals
[DE93-012555] p 3436 N93-28653

CARBOHYDRATE METABOLISM

Influence of the Cold Buster (tm) sports bar on heat debt, mobilization and oxidation of energy substrates
[AD-A262762] p 3493 N93-28939

CARBON

The design and testing of a high-temperature graphite dilatometer
[AD-A262185] p 3430 N93-28488

Research and development of carbon black anodes for lithium secondary cells
[DE93-781331] p 3406 N93-28746

Ocean Margins Program
[DE93-008937] p 3470 N93-29262

Hypervelocity impact survivability experiments for carbonaceous impactors p 3283 N93-29364

Experiment and analysis on elastic deformation properties of graphite and carbon materials for HTTR core components
[DE93-753271] p 3299 N93-30004

Diamond nucleation of surfaces using carbon clusters
[AD-A264634] p 3599 N93-30548

Study on diamond semiconductor
[DE92-531076] p 3413 N93-30622

CARBON CYCLE

Activities report of the International Meteorological Institute, Stockholm (Sweden)
[ETN-93-93768] p 3480 N93-28519

Steady-state and transient modeling of tracer and nutrient distributions in the global ocean
[DE93-011043] p 3486 N93-28670

Ocean Margins Program
[DE93-008937] p 3470 N93-29262

Fiber optic chemical sensors for characterizing the carbon cycle in ocean margin regions
[DE93-011442] p 3489 N93-30056

CARBON DIOXIDE

Predicting the response of a temperate forest ecosystem to atmospheric CO2 increase
[DE93-010081] p 3467 N93-28543

Steady-state and transient modeling of tracer and nutrient distributions in the global ocean
[DE93-011043] p 3486 N93-28670

Alkali metal carbon dioxide electrochemical system for energy storage and/or conversion of carbon dioxide to oxygen
[NASA-CASE-LEW-14973-1] p 3464 N93-28974

Regulation of alternative CO2 fixation pathways in procaryotic and eucaryotic photosynthetic organisms
[DE93-012109] p 3491 N93-29181

Growing wheat to maturity in reduced gas pressures
[NASA-CR-193245] p 3491 N93-29216

Acid gas treating by aqueous alkanolamines
[PB93-176188] p 3471 N93-29676

A preliminary review of global CO2 exchange between ocean and atmosphere
[AD-A264019] p 3472 N93-30015

Fiber optic chemical sensors for characterizing the carbon cycle in ocean margin regions
[DE93-011442] p 3489 N93-30056

Hydrogen sulfide decomposition into hydrogen and sulfur by quinone cycles, part 1
[PB93-175297] p 3317 N93-30761

CARBON DIOXIDE CONCENTRATION

Predicting the response of a temperate forest ecosystem to atmospheric CO2 increase
[DE93-010081] p 3467 N93-28543

CARBON DIOXIDE LASERS

Construction and operation of a gas transport CO2 laser
[AD-A263102] p 3438 N93-29797

CARBON DIOXIDE REMOVAL

Global warming issue and global economic model
[DE93-781334] p 3468 N93-28881

Study on technology for effective utilization of carbon dioxide in view of global environment
[DE93-781440] p 3468 N93-28883

CARBON DISULFIDE

Examination of shock induced chemical reactions in liquids using time-resolved optical spectroscopy
p 3318 N93-30073

Gas electron diffraction employing a pulsed electron beam synchronous with photoexcitation
p 3319 N93-30101

CARBON FIBER REINFORCED PLASTICS

Ultrasonic detection and identification of fabrication defects in composites p 3305 N93-30856

CARBON FIBERS

Apparatus for intercalating large quantities of fibrous structures
[NASA-CASE-LEW-15077-2] p 3298 N93-29609

Powder towpreg process development
p 3303 N93-30844

Studies of fiber-matrix adhesion on compression strength p 3304 N93-30846

The initiation, propagation, and effect of matrix microcracks in cross-ply and related laminates
p 3304 N93-30847

Characterization of multiaxial warp knit composites
p 3304 N93-30851

CARBON MONOXIDE

Generation of carbon monoxide in compartment fires
[PB93-146702] p 3244 N93-29211

Vibrational spectroscopy of shock-compressed fluids
p 3318 N93-30072

Submillimeter CO observations of warm gas around T-Tauri stars
[MPE-PREPRINT-232] p 3631 N93-30615

CO lines toward NGC 2024 and other star forming regions: A closer look at the warm gas component
[MPE-PREPRINT-223] p 3637 N93-30639

Carbon monoxide exposure of subjects with documented cardiac arrhythmias
[PB93-179943] p 3497 N93-30890

CARBON STEELS

Interim fatigue design curves for carbon, low-alloy, and austenitic stainless steels in LWR environments
[DE93-009202] p 3323 N93-29102

CARBON 13
1,2-Dimethyl-1,2-Disila-Closo-Dodecaborane(12), A silicon analog of an ortho-carborane: Synthesis; x ray crystal structure; NMR, vibrational and photoelectron spectra; bonding
[AD-A264709] p 3599 N93-30568

CARBONACEOUS CHONDRITES
Further analysis of LDEF FRECOPA micrometeoroid remnants p 3638 N93-29360

CARBOXYHEMOGLOBIN
Carbon monoxide exposure of subjects with documented cardiac arrhythmias
[PB93-179943] p 3497 N93-30890

CARBOXYLATION
A novel process for methanol synthesis
[DE93-013070] p 3314 N93-30188

CARCINOGENS
Gene transcription and electromagnetic fields
[DE93-010854] p 3490 N93-28848

CARDIOVASCULAR SYSTEM
The physiological limitations of man in the high G environment p 3503 N93-28861

CARGO AIRCRAFT
The development of a parachute system for aerial delivery from high speed cargo aircraft
[DE93-008339] p 3239 N93-29035

CARGO SPACECRAFT
Solar electric propulsion cargo spacecraft for Mars missions p 3235 N93-29758

CARRIER FREQUENCIES
Acoustic transducer system
[AD-D015713] p 3562 N93-29279

CARRIER MOBILITY
Femtosecond carrier processes in compound semiconductors and real time signal processing
[AD-A262966] p 3384 N93-29514

CARRIER WAVES
Signal-to-noise ratio losses in full spectrum combining of signals with a downconverted subcarrier
p 3386 N93-29599

CARTAN SPACE
Connections between quantized affine algebras and superalgebras
[DE93-606065] p 3551 N93-30810

CASCADE FLOW
Three-dimensional fiber-optic LDV measurements in the endwall region of a linear cascade of controlled-diffusion stator blades
[AD-A263513] p 3424 N93-29968

CASE HISTORIES
A fuzzy case based reasoning tool for model based approach to rocket engine health monitoring
p 3289 N93-29570
Technology transfer in the NASA Ames Advanced Life Support Division p 3628 N93-30724

CASSEGRAIN ANTENNAS
A note on the computation of antenna-blocking shadows p 3385 N93-29593
A dual polarized broadband multifrequency Earth station feed p 3371 N93-30319

CASSEGRAIN OPTICS
Optical system analysis for the ground based EXVM
[NASA-CR-192588] p 3582 N93-31035

CASTING
Infiltration/cure modeling of resin transfer molded composite materials using advanced fiber architectures
p 3303 N93-30843
Development of stitching reinforcement for transport wing panels p 3304 N93-30852
Development of resins for composites by resin transfer molding p 3305 N93-30853
Mechanical and analytical screening of braided composites for transport fuselage applications
p 3305 N93-30855

CASTINGS
Development of a CFD code for casting simulation
[NASA-CR-192577] p 3427 N93-30492
Durability of Quick Reaction Satellite Antenna (QRSA) trunnion castings
[AD-A264095] p 3281 N93-30813

CATACLYSMIC VARIABLES
IUE observations of cataclysmic variable
[NASA-CR-193188] p 3629 N93-28634

CATALOGS (PUBLICATIONS)
The NASA SBIR product catalog
[NASA-TM-108242] p 3609 N93-29322
Origin of orbital debris impacts on LDEF's trailing surfaces p 3283 N93-29373
Air weather service master station catalog USAFETAC climatic database users handbook no. 6
[AD-A264761] p 3484 N93-30608
Standard and reference materials for marine science, third edition
[PB93-185684] p 3489 N93-30830

CATALYSIS
Catalytic synthesis of silicon carbide preceramic polymers: Polycarbosilanes
[DE93-008634] p 3329 N93-28541
Supported organometallic complexes, surface chemistry, spectroscopy, and catalysis
[DE93-011930] p 3309 N93-28688
Kinetics and dynamics of reacting systems
[AD-A264046] p 3313 N93-30030
Organometallic and surface chemistry of mixed-metal systems
[DE93-012686] p 3325 N93-30059
Decomposition of hydrogen sulfide for small scale gas processing.
[PB93-174704] p 3316 N93-30658
Gordon Research Conferences, 1991
[AD-A264275] p 3317 N93-30816

CATALYSTS
Catalytic synthesis of silicon carbide preceramic polymers: Polycarbosilanes
[DE93-008634] p 3329 N93-28541
Design of a high activity and selectivity alcohol catalyst
[DE93-012277] p 3309 N93-28750
High octane ethers from synthesis gas-derived alcohols
[DE93-012470] p 3341 N93-28752
Applications of transition metal compounds in the preparation of useful silicon-containing ceramics
[AD-A264028] p 3335 N93-30028
Synthesis of chiral molybdenum ROMP initiators and all-cis highly tactic Poly-2,3-R2Norbornadiene (R = CF3 or CO2Me)
[AD-A264133] p 3336 N93-30169
A novel process for methanol synthesis
[DE93-013070] p 3314 N93-30188
Magnetic character investigation of higher alcohol synthesis Cu-Co-Cr catalysts
[DE93-009732] p 3316 N93-30653
Conjugated polymers from cyclohexadienediol monomers
[AD-A264837] p 3340 N93-30900

CATALYTIC ACTIVITY
Supported organometallic complexes, surface chemistry, spectroscopy, and catalysis
[DE93-011930] p 3309 N93-28688
Hydrogen sulfide decomposition into hydrogen and sulfur by quinone cycles, part 1
[PB93-175297] p 3317 N93-30761

CATHODE RAY TUBES
Low-cost helmet-mounted displays
[AD-A262616] p 3501 N93-28479

CATHODES
Field-emitter arrays for RF vacuum microelectronics
[AD-A262677] p 3404 N93-28483
Alkali metal carbon dioxide electrochemical system for energy storage and/or conversion of carbon dioxide to oxygen
[NASA-CASE-LEW-14973-1] p 3464 N93-28974

CATIONS
Synthesis and properties of a cation-conducting, high temperature polymer electrolyte
[AD-A263557] p 3334 N93-29825

CAUCHY PROBLEM
A Riemann problem for an elastic bar that changes phase
[AD-A262827] p 3452 N93-29432
Quantum field theory in spaces with closed time-like curves
[DE93-010564] p 3605 N93-30481

CAVITIES
Aerothermic calculations of flows in interdisc cavities of turbines p 3256 N93-29947
Study of flow structure in rotating cavities: Numerical predictions of laminar and turbulent, steady, and unsteady flows p 3256 N93-29948
Development of a CFD code for casting simulation
[NASA-CR-192577] p 3427 N93-30492

CAVITY RESONATORS
High-efficiency high-reliability optical components for a large, high-average-power visible laser system
[DE93-009225] p 3437 N93-29098
Study of gain in C-band deflection cavities for a frequency-doubling magnicon amplifier
[AD-A263132] p 3409 N93-29478
Experimental test of hole-coupled FEL resonator designs using a CW-HeNe laser
[DE93-010439] p 3440 N93-30530
Phase transition studies in barium and strontium titanates at microwave frequencies p 3293 N93-30970

CELL ANODES
Research and development of carbon black anodes for lithium secondary cells
[DE93-781331] p 3406 N93-28746
Materials characterization of cermet anodes tested in a pilot cell
[DE93-008924] p 3323 N93-29101

CELL MEMBRANES (BIOLOGY)
Micropipet manipulation of lipid membranes: Direct measurement of the material properties of a cohesive structure that is only two molecules thick
p 3291 N93-30953

CELLS (BIOLOGY)
Comparative mutagenesis of human cells in vivo and in vitro
[DE93-012269] p 3490 N93-28651
Biophysical and biochemical mechanisms in synaptic transmitter release
[AD-A264829] p 3496 N93-30613
The Gordon Research Conference on Pineal Cell Biology
[AD-A264840] p 3497 N93-30904

CENTER OF GRAVITY
Vehicle dynamic stability and rollover
[PB93-185437] p 3447 N93-30828

CENTRAL NERVOUS SYSTEM
Hydrogen-rated system for in vitro studies at pressure: Operating procedures and emergency procedures
[AD-A264179] p 3497 N93-30882

CENTRAL PROCESSING UNITS
Development of a PC code package for the analysis of research and power reactors
[DE92-638517] p 3536 N93-31001

CENTRIFUGAL FORCE
Combined centrifugal force/gravity gas/liquid separator system
[AD-D015726] p 3444 N93-29288

CENTRIFUGES
Testing in combined dynamic environments
[DE93-010679] p 3278 N93-29250
Combined centrifugal force/gravity gas/liquid separator system
[AD-D015726] p 3444 N93-29288
Acquisition of physiological data during G-induced Loss of Consciousness (G-LOC)
[AD-A264492] p 3496 N93-30400

CENTRIPETAL FORCE
Three-dimensional numerical simulation of gradual opening in a wave rotor passage
[NASA-CR-191157] p 3252 N93-29072

CEPSTRAL ANALYSIS
Examinations of perturbation reduction by automatic speech dependent recognition of separately spoken single words
[ETN-93-94180] p 3394 N93-30672

CERAMIC COATINGS
Laser gas alloying of titanium materials
[ETN-93-93805] p 3325 N93-30115
Development of adherent ceramic coatings to reduce contact stress damage of ceramics
[DE93-012518] p 3336 N93-30182
Colloid and interface chemistry aspects of ceramics
[AD-A264685] p 3337 N93-30552

CERAMIC FIBERS
Interfacial studies of refractory glass-ceramic matrix/advanced SiC fiber reinforced composites
[AD-A263264] p 3299 N93-29802
The effect of oxidation embrittlement on the impact behavior of nicalon reinforced CAS 2 ceramic matrix composites
[AD-A263567] p 3334 N93-29829

CERAMIC HONEYCOMBS
Theoretical and experimental study of thermoacoustic engines
[AD-A261934] p 3561 N93-28995

CERAMIC MATRIX COMPOSITES
Mechanics of elevated temperature fatigue damage in fiber-reinforced ceramics
[AD-A262403] p 3329 N93-28495
Ultrahigh temperature assessment study: Ceramic matrix composites
[AD-A262740] p 3295 N93-28592
Ceramic matrix composites properties/microstresses with complete and partial interphase bond
[NASA-TM-106136] p 3297 N93-29071
Acousto-Ultrasonic analysis of failure in ceramic matrix composite tensile specimens
[NASA-TM-106219] p 3449 N93-29073
Technology transfer personnel exchange at the Boeing Company
[DE93-010190] p 3625 N93-29329
Interfacial studies of refractory glass-ceramic matrix/advanced SiC fiber reinforced composites
[AD-A263264] p 3299 N93-29802
The effect of oxidation embrittlement on the impact behavior of nicalon reinforced CAS 2 ceramic matrix composites
[AD-A263567] p 3334 N93-29829
Whisker toughening of ceramic materials: A review
[DE93-011565] p 3336 N93-30129

Characterization of ceramic composite materials for gas turbine applications
[DE93-009719] p 3259 N93-30168
Wetting and dispersion in ceramic/polymer melt injection molding systems
[DE93-013240] p 3338 N93-30601
Design, synthesis, and chemical processing of hierarchical ceramic structures for aerospace applications
[AD-A264227] p 3339 N93-30885
Damage of multi-directionally reinforced ceramic-matrix composites p 3308 N93-30937

CERAMICS
Refractory metal disilicides research
[AD-A262416] p 3320 N93-28499
Catalytic synthesis of silicon carbide preceramic polymers: Polycarbosilanes
[DE93-008634] p 3329 N93-28541
Ultrahigh temperature assessment study: Ceramic matrix composites
[AD-A262740] p 3295 N93-28592
Soft computing in design and manufacturing of advanced materials
[NASA-TM-106032] p 3295 N93-28624
A study of the chemical mechanism in lubrication
[DE93-012230] p 3330 N93-28650
Effect of metallic-coating properties on the tribology of coated and oil-lubricated ceramics
[DE93-010663] p 3330 N93-28666
Healing of lithographically introduced flaws in glass and glass containing ceramics
[DE93-010453] p 3330 N93-28761
Use of local x ray computerized tomography for high-resolution, region-of-interest inspection of large ceramic components for engines
[DE93-005564] p 3449 N93-28943
JPRS report: Science and technology. Central Eurasia: Materials science
[JPRS-UMS-92-008] p 3322 N93-29012
JPRS report: Science and technology. Central Eurasia: Materials science
[JPRS-UMS-92-007] p 3322 N93-29013
JPRS report: Science and technology. Central Eurasia: Materials science
[JPRS-UMS-92-009] p 3322 N93-29015
JPRS report: Science and technology. Central Eurasia: Materials science
[JPRS-UMS-92-012] p 3296 N93-29016
JPRS report: Science and technology. Central Eurasia: Materials science
[JPRS-UMS-92-016] p 3296 N93-29018
JPRS report: Science and technology. Central Eurasia: Materials science
[JPRS-UMS-92-015] p 3322 N93-29020
JPRS report: Science and technology. Central Eurasia: Materials science
[JPRS-UMS-93-001] p 3296 N93-29021
Operational results of pilot cell test with cermet inert anodes
[DE93-009338] p 3322 N93-29061
Oxidation behavior in reaction-bonded aluminum-silicon alloy/alumina powder compacts
[DE93-010407] p 3298 N93-29191
A transient FGM interlayer based approach to joining ceramics
[DE93-010415] p 3331 N93-29248
Microwave processing of ceramics
[DE93-010708] p 3332 N93-29252
The design and lifetime calculation of MHD generator walls based on subcritical crack growth in ceramics
[ISBN-90-9004009-9] p 3332 N93-29267
Technology transfer personnel exchange at the Boeing Company
[DE93-010190] p 3625 N93-29329
Proceedings of the 25th European Conference on the Application of Polar Dielectrics to celebrate the 25th anniversary of the Dielectric Society, incorporating the 1st International Workshop on Integrated Ferroelectrics
[AD-A263427] p 3332 N93-29337
Boron carbide aluminum cermets for external pressure housing applications
[AD-A262749] p 3333 N93-29404
Crystallization of nanocomposite glasses made by the SSG process
[AD-A262892] p 3333 N93-29511
Properties of superconducting YBa2Cu3O(6+4) ceramic materials: Effect of processing parameters
[AD-A263441] p 3334 N93-29790
Balanced technology initiative on computational mechanics of materials
[AD-A263906] p 3453 N93-29863
Applications of transition metal compounds in the preparation of useful silicon-containing ceramics
[AD-A264028] p 3335 N93-30028
The drive to cost-effective structural ceramics
[DE93-009722] p 3335 N93-30047
Materials for adaptive structural acoustic control, volume 1
[AD-A264619] p 3562 N93-30121
Characterization of ceramic composite materials for gas turbine applications
[DE93-009719] p 3259 N93-30168
Methylhydridopolysilazane and its pyrolytic conversion to Si3N4/SiC ceramics
[AD-A264150] p 3336 N93-30170
Development of adherent ceramic coatings to reduce contact stress damage of ceramics
[DE93-012518] p 3336 N93-30182
Materials for adaptive structural acoustic control, volume 2
[AD-A264620] p 3563 N93-30385
A ceramic fracture model for high velocity impact
[AD-A264728] p 3454 N93-30545
Colloid and interface chemistry aspects of ceramics
[AD-A264685] p 3337 N93-30552
Mold bolt and means for achieving close tolerances between bolts and bolt holes
[NASA-CASE-MFS-28720-1] p 3447 N93-30567
Elastic stability considerations for deep submergence ceramic pressure housing
[AD-A264824] p 3454 N93-30598
Adhesion of thick film Au to alumina ceramics
[DE93-009802] p 3339 N93-30656
Decomposition of hydrogen sulfide for small scale gas processing.
[PB93-174704] p 3316 N93-30658
Effect of lead addition on the formation of superconducting phases in Bi-Sr-Ca-Cu-O ceramics
[DE93-606893] p 3339 N93-30773
The effect of Bi2 O3 on the electrical properties of Zr O2: 3 percent Mg O ceramic solid electrolytes
[DE93-607029] p 3339 N93-30774
Guideway structural design and power/propulsion/braking in relation to guideways, volume 1
[PB93-169902] p 3447 N93-30820
Processing of novel nanoparticle dispersion strengthened ceramics for improved mechanical performance
[AD-A264191] p 3339 N93-30883
Design, synthesis, and chemical processing of hierarchical ceramic structures for aerospace applications
[AD-A264227] p 3339 N93-30885
New materials: Fountainhead for new technologies and new science p 3291 N93-30952
Temperature-dependent electrical conductivity of soda-lime glass p 3294 N93-30978

CEREBRAL CORTEX
Principal components of natural images: An analytical solution
[AD-A264800] p 3489 N93-30603

CERMETS
Operational results of pilot cell test with cermet inert anodes
[DE93-009338] p 3322 N93-29061
Materials characterization of cermet anodes tested in a pilot cell
[DE93-008924] p 3323 N93-29101
Boron carbide aluminum cermets for external pressure housing applications
[AD-A262749] p 3333 N93-29404

CERTIFICATION
Building a generalized distributed system model
[NASA-CR-193239] p 3527 N93-29219
Guide for certifying pressure vessels and systems
[NASA-TM-107549] p 3449 N93-29220
Report on the test set-up for the structural testing of the Airmass Sunburst Ultralight Aircraft
p 3249 N93-29775
Helicopter simulator standards p 3236 N93-30675
Helicopter simulation: An aircrew training and qualification perspective p 3236 N93-30676

CESIUM IONS
NPB cesium space experiment p 3267 N93-28733
Measurement of work function of a plasma grid in a cesium seeded negative ion source
[DE93-764153] p 3589 N93-30190

CHALCOGENIDES
Electrochemical fabrication of cadmium chalcogenide microdiode arrays
[AD-A263169] p 3310 N93-28988

CHANNEL CAPACITY
A slotted Aloha satellite channel simulator
p 3360 N93-30250

CHANNEL FLOW
Analysis of unsteady wave processes in a rotating channel
[NASA-CR-191154] p 3251 N93-28617
A new flux conserving Newton's method scheme for the two-dimensional, steady Navier-Stokes equations
[NASA-TM-106160] p 3416 N93-28626
An efficient spectral integration method for the solution of the Navier-Stokes equations
[FFA-TN-1992-28] p 3418 N93-29009

CHANNELS (DATA TRANSMISSION)
A comparison of high-speed links, their commercial support and ongoing R/D activities
[DE93-008134] p 3382 N93-29245
T(lc2)acS(lc3)ats for Surveillance Verification and C3I
[AGARD-CP-522] p 3387 N93-29892
Tactical satellites p 3284 N93-29893
TACSAT-spacecraft bus concept and design: Application of a multimission bus for TACSAT in LEO
p 3284 N93-29896
Propagation channel modeling for angle-diversity combining simulation p 3360 N93-30252
Characteristics of high-frequency signals, noise, availability, and duration of bandwidths based on ROTHR Amchitka spectrum measurements
[AD-A264480] p 3393 N93-30423
Optically powered, optoelectronic spatial light modulators
[AD-A264765] p 3581 N93-30609

CHAOS
Self-consistent chaos in the beam-plasma instability
[DE93-009581] p 3584 N93-28599
Dynamical analysis of highly excited molecular spectra
[DE93-010771] p 3564 N93-28604
Bifurcations phenomena in a nonlinear oscillator: Approximate analytical studies versus computer simulation results p 3407 N93-29037
Chaos in mechanical systems with especial reference to rotorcraft and missiles
[AD-A263703] p 3604 N93-29384
Estimating the parameters of chaotic maps
[AD-A262574] p 3556 N93-29423
Non-scalar uncertainty: Uncertainty in dynamic systems p 3517 N93-29565
Study of effects of small perturbations on chaotic systems
[DE93-009762] p 3557 N93-30048
Chaotic quantum systems
[DE93-606030] p 3606 N93-30802
Scaling properties of localized quantum chaos
[DE93-606031] p 3606 N93-30803
General scalar-tensor theories for induced gravity inflation
[DE93-602505] p 3479 N93-30940

CHARACTER RECOGNITION
Character recognition using a neural network model with fuzzy representation p 3512 N93-29536
Comparison of crisp and fuzzy character networks in handwritten word recognition p 3514 N93-29545

CHARACTERIZATION
Growth, characterization and device development in monocrystalline diamond films
[AD-A263204] p 3593 N93-28874
Tank issues: Site characterization for external leak monitoring
[PB93-161156] p 3469 N93-29034
Characterization and optimization of a Hot Air Solder-Leveling System
[DE93-010188] p 3332 N93-29328
Applications of laser light scattering in polymer dilute solution characterization
[AD-A263110] p 3335 N93-30007
Electro-optic characterisation of extremely wide bandwidth electrical signals
[AD-A264202] p 3392 N93-30145
Measurements and Characterization Branch
[DE93-000094] p 3465 N93-30207
Application of non-standard signal processing to ELF noise characterization for the TSS1-OESEE programme
p 3397 N93-30743

CHARGE CARRIERS
New III-V cell design approaches for very high efficiency
[DE93-000097] p 3464 N93-28971
Ultrafast optical studies of surface reaction processes at semiconductor interfaces
[DE93-009049] p 3593 N93-29096
Charge separation in bipolar transistors
[DE93-009624] p 3413 N93-30650

CHARGE COUPLED DEVICES
High-performance visible/UV CCD focal plane technology for spacebased applications
p 3434 N93-28771
Honeywell's compact, wide-angle UV-visible imaging sensor p 3582 N93-28806
A compact imaging detector of polarization and spectral content p 3582 N93-28810
Operating manual for single-shot autocorrelator
[AD-A262016] p 3438 N93-29395
A new tubeless nanosecond streak camera based on optical deflection and direct CCD imaging
[DE93-011893] p 3433 N93-30491

Advanced research in sky surveillance: A search for low-luminosity objects
[AD-A264832] p 3631 N93-30629
CAESAR development plan 1992-1995
[BCRS-92-17] p 3463 N93-31009

CHARGE DISTRIBUTION
Antenna modeling and analysis for ELF/VLF/LF applications p 3398 N93-30751

CHARGE EXCHANGE
Coupled-channel analysis of low energy nucleon-antinucleon interactions
[DE93-606115] p 3571 N93-30791

CHARGE TRANSFER
High-performance visible/UV CCD focal plane technology for spacebased applications
p 3434 N93-28771
Analytical applications of electrified interfaces between two immiscible solutions
[AD-A263085] p 3311 N93-29132
Elastic and reactive collisions of atoms and molecules with neutral alkali clusters
[DE93-009313] p 3566 N93-29206
Effects of neutral gas collisions on the power transmission factor at the divertor sheath
[DE93-009320] p 3588 N93-29334
Experimental and theoretical aspects of excited state electron transfer and related phenomena
[AD-A263457] p 3570 N93-30589
Optimization for steady-state and hybrid operations of ITER by using scaling models of divertor heat load
[DE93-764151] p 3590 N93-30649
Charge separation in bipolar transistors
[DE93-009624] p 3413 N93-30650
Effective interactions between concentration fluctuations and charge transfer in chemically ordering liquid alloys
[DE93-606724] p 3327 N93-30778
Coupled-channel analysis of low energy nucleon-antinucleon interactions
[DE93-606115] p 3571 N93-30791

CHARGE TRANSFER DEVICES
Analyses of data from fine structure and circulation studies in the Gulf of California
[AD-A262910] p 3486 N93-28885

CHARGED PARTICLES
Transfer Orbit Plasma Interaction Experiment (TROPIX) p 3267 N93-28734
Nonlinear dynamics and plasma transport
[DE93-012238] p 3585 N93-28749
Ion motion effects on charged radiators
[DE93-009257] p 3565 N93-29099
Molecular dynamics modeling of electric double layers with spectroscopic applications
[AD-A263168] p 3568 N93-29489
Charged particle activation studies on the surface of LDEF spacecraft p 3572 N93-29630
LET spectra measurements of charged particles in the P0006 experiment on LDEF p 3573 N93-29637
Three-dimensional shielding effects on charged particle fluences measured in the P0006 experiment of LDEF
p 3573 N93-29639
Electron transport calculations between 1 MeV and 1 eV
[AD-A263412] p 3568 N93-29787
Design of acentric materials: X ray structures of guanidinium p-nitro- and p-hydroxybenzenesulfonate
[AD-A264220] p 3597 N93-30146

CHARM (PARTICLE PHYSICS)
Study of heavy-flavored particles
[DE93-011535] p 3569 N93-30128

CHARON
Visible imaging on the Pluto fast flyby mission
p 3646 N93-28799

CHARPY IMPACT TEST
An automated data collection system for a Charpy impact tester p 3293 N93-30972

CHEBYSHEV APPROXIMATION
A spectral method determination of the first critical Rayleigh number for a low-Prandtl number crystal melt in a cylindrical container
[NASA-CR-193238] p 3594 N93-29214

CHECKOUT
Nonresident and endangered variables: The effects of code generation optimizations on symbolic debugging
[AD-A263149] p 3529 N93-29486

CHELATES
Synthetic lubricating oil greases containing metal chelates of Schiff bases
[AD-D015694] p 3333 N93-29458
Rates and mechanisms of reaction of hydrogen sulfide with iron chelates
[PB93-184299] p 3312 N93-29665

CHEMICAL ANALYSIS
Evaluation of polyaryl adhesives in elastomer-stainless steel joints
[DE93-009794] p 3329 N93-28551
Laer-induced breakdown spectroscopy instrument for element analysis of planetary surfaces
p 3434 N93-28769
Further analysis of LDEF FRECOPA micrometeoroid remnants p 3638 N93-29360
SIMS chemical analysis of extended impacts on the leading and trailing edges of LDEF experiment AO187-2
p 3318 N93-29367
Transcutaneous analyte measuring methods
[AD-A262861] p 3494 N93-29509
Thermal cycler temperature variation and its effect on the polymerase chain reaction
[AD-A264660] p 3337 N93-30541
Hydrogeology and ground-water-quality conditions at the Reno County Landfill, South-Central Kansas, 1990-1991
[PB93-183085] p 3474 N93-30826

CHEMICAL BONDS
Adsorption of sulfate on metal electrodes
[AD-A263192] p 3309 N93-28540
What is underneath? Moving atoms and molecules to find out
[AD-A263363] p 3567 N93-29332
Synthesis of oligoimides and oligoimide anion radicals
[AD-A263129] p 3290 N93-29474
Molecular dynamics of detonation in crystals with defects p 3350 N93-30097
Applications of density functional theory to calculation of reaction energetics p 3351 N93-30098
Conjugated substituted ionic polyacetylenes
[AD-A264702] p 3337 N93-30497
Surface chemistry of N2H4 on Si(100)-2x1
[AD-A264819] p 3316 N93-30627
Defining protein electrostatic recognition processes
[AD-A264838] p 3571 N93-30901

CHEMICAL COMPOSITION
Laer-induced breakdown spectroscopy instrument for element analysis of planetary surfaces
p 3434 N93-28769
Planetary and satellite x ray spectroscopy: A new window on solid-body composition by remote sensing
p 3641 N93-28773
A remote laser-mass spectrometer for determination of elemental composition p 3434 N93-28775
The APX spectrometer for Martian missions
p 3434 N93-28776
Bainitic stabilization of austenite in low alloy steels
[DE93-008275] p 3321 N93-28957
Materials characterization of cermet anodes tested in a pilot cell
[DE93-008924] p 3323 N93-29101
Novel polymer compositions for high-temperature membrane applications, phase 1
[PB93-174126] p 3331 N93-29201
Real time self-directed MBE flux control incorporation in situ ellipsometry, phase 1
[AD-A263501] p 3595 N93-29341
SIMS chemical analysis of extended impacts on the leading and trailing edges of LDEF experiment AO187-2
p 3318 N93-29367
Geochemical and fluid dynamic investigations into the nature of chemical heterogeneity in the Earth's mantle
[AD-A262753] p 3477 N93-29405
Elemental compositions of high-energy ions produced by magnetosonic waves in quiescent plasmas
[DE93-753241] p 3588 N93-29434
Progress report on the Heavy Ions in Space (HIIS) experiment p 3573 N93-29645
Multiwavelength studies of classical nova shells
p 3636 N93-30412
Colloid and interface chemistry aspects of ceramics
[AD-A264685] p 3337 N93-30552
Study on diamond semiconductor
[DE92-531076] p 3413 N93-30622
Standard and reference materials for marine science, third edition
[PB93-185684] p 3489 N93-30830
Physical chemical studies on molecular composite compositions
[AD-A264834] p 3339 N93-30898

CHEMICAL ENERGY
Kinetics and energy transfer in nonequilibrium fluid flows
[AD-A263612] p 3240 N93-29284
Molecular dynamics of detonation in crystals with defects p 3350 N93-30097

CHEMICAL ENGINEERING
The use of quantum chemistry to estimate the performance and properties of explosives
[DE92-040369] p 3352 N93-30446

CHEMICAL EQUILIBRIUM
Synthesis of new high performance lubricants and solid lubricants
[DE93-012237] p 3330 N93-28748
Direct Monte Carlo simulation of the chemical equilibrium composition of detonation products
[DE92-040372] p 3315 N93-30447

CHEMICAL EXPLOSIONS
A simple model for explosives formulation
[DE93-010703] p 3341 N93-29251
Weakly nonlinear dynamics of near-CJ detonation waves
[DE93-007344] p 3424 N93-29836
Strategies for understanding the deflagration-to-detonation transition
p 3319 N93-30077
Pressure dependence of the reaction propagation rate of TATB to 40 GPa p 3319 N93-30082
Detonation shock dynamics of composite energetic materials p 3350 N93-30096
The use of quantum chemistry to estimate the performance and properties of explosives
[DE92-040369] p 3352 N93-30446
Direct Monte Carlo simulation of the chemical equilibrium composition of detonation products
[DE92-040372] p 3315 N93-30447
The calculation of electrostatic interactions and their role in determining the energies and geometries of molecular HE crystals
[DE92-040374] p 3570 N93-30448

CHEMICAL PROPERTIES
Structure, adhesion, and stability of metal/oxide and oxide/oxide interfaces
[DE93-012930] p 3325 N93-30060
Use of statistics in computational chemistry
[AD-A264307] p 3315 N93-30365

CHEMICAL REACTIONS
A study of the chemical mechanism in lubrication
[DE93-012230] p 3330 N93-28650
The onset of vortex turbulence
[DE93-010424] p 3417 N93-28663
Effect of metallic-coating properties on the tribology of coated and oil-lubricated ceramics
[DE93-010663] p 3330 N93-28666
Additional support for the TDK/MABL computer program
[NASA-CR-193037] p 3526 N93-29028
Report on the sintering and properties of MgO and MgO-5 percent TiC
[DE93-008676] p 3323 N93-29092
Tailored interfaces for metal-matrix composites-fundamental considerations
[AD-A263048] p 3298 N93-29130
A simple model for explosives formulation
[DE93-010703] p 3341 N93-29251
Weakly nonlinear dynamics of near-CJ detonation waves
[DE93-007344] p 3424 N93-29836
ONR/LANL Workshop on the Fundamental Physics and Chemistry of Combustion, Initiation, and Detonation of Energetic Materials
[CPIA-PUBL-589] p 3343 N93-30061
The thermochemistry and reaction pathways of the decomposition and combustion of energetic materials
p 3343 N93-30063
Examination of shock induced chemical reactions in liquids using time-resolved optical spectroscopy
p 3318 N93-30073
Single-shot femtosecond spectroscopy: A methodology for observation of solid-state chemical reactions
p 3319 N93-30075
Determination of gas phase species and temperature profiles above solid propellants p 3346 N93-30080
Metallization at detonation fronts in solids
p 3319 N93-30087
Microstructural basis for enhanced shock-induced chemistry in single crystals of ammonium perchlorate
p 3319 N93-30092
Rate constant determinations of reactions H + HNO from ab initio reaction path calculations
p 3319 N93-30099
Atomic layer epitaxy of semiconductor heterostructures
[AD-A264755] p 3599 N93-30560
Hydrogen sulfide decomposition into hydrogen and sulfur by quinone cycles, part 1
[PB93-175297] p 3317 N93-30761

CHEMICAL REACTORS
A novel process for methanol synthesis
[DE93-013070] p 3314 N93-30188

CHEMICAL RELEASE MODULES
FNAS CRRES program completion
[NASA-CR-192468] p 3476 N93-29032

CHEMISORPTION
FI-STM investigation of atomic hydrogen adsorption on the Si(100)2x1 surface
[AD-A262748] p 3567 N93-29403
Complex-compound heat pump: Topical report on phase 1 results
[PB93-185460] p 3466 N93-30814

CHEMISTRY
DOE fundamentals handbook: Chemistry
[DE93-012222] p 3314 N93-30198

CHINA
International aviation (Selected articles)
[AD-A262566] p 3227 N93-28576

CHIPS (ELECTRONICS)
Thermal and mechanical analysis of flip-chips on a liquid cooled multichip module
[DE93-007609] p 3405 N93-28641
Efficient wiring of reconfigurable parallel processors
[DE93-009847] p 3538 N93-29186
Department of defense advisory group on electron devices: Appendix to special technology area review on microwave packaging technology
[AD-A262136] p 3408 N93-29408
Multichip module high speed testing
[AD-A262989] p 3408 N93-29427
An MCM/chip concurrent engineering validation
[AD-A262959] p 3409 N93-29513
Design of a pixel cell optimized for a data push architecture readout
[DE93-011016] p 3616 N93-30122
A single chip high-speed CMOS Viterbi decoder
p 3358 N93-30238
Placement of cells: Theory and solution of a quadratic 0/1 optimization problem
[ETN-93-94182] p 3413 N93-30616

CHIPS (MEMORY DEVICES)
Spacecraft computer technology at Southwest Research Institute p 3522 N93-28813

CHIRAL DYNAMICS
On the photonic chiral anomaly in an external gravitational field
[DE93-606082] p 3479 N93-30785
Compensating fields and anomalies in supergravity
[DE92-644724] p 3637 N93-30919

CHLORINE
Studies in Lewis acid and superacid ionic liquids
[AD-A264683] p 3316 N93-30551

CHLOROFLUOROCARBONS
Potential effects of HFC-152a on global ozone and climate
[DE93-008018] p 3471 N93-29792

CHLOROPHYLLS
Remote sensing for water quality monitoring in the Tennessee Valley: Field tests of two systems
[DE93-008997] p 3462 N93-30637

CHOKED FLOW
Preliminary experimental results for a cryogenic brush seal configuration
[NASA-TM-106236] p 3416 N93-28627

CHOLESKY FACTORIZATION
Exploiting the memory hierarchy in sequential and parallel sparse Cholesky factorization
[AD-A262849] p 3539 N93-29508

CHOLINERGICS
Neural mechanisms of attention
[AD-A264345] p 3544 N93-30165

CHROMATOGRAPHY
Chromatographic and solvatochromic measurements on butyl rubbers
[AD-A263088] p 3334 N93-29795

CHROMIUM
The electrodeposition of low contraction chromium using high/low current pulsing
[AD-A264475] p 3327 N93-30538
Magnetic character investigation of higher alcohol synthesis Cu-Co-Cr catalysts
[DE93-009732] p 3316 N93-30653

CHROMIUM ALLOYS
High temperature creep and oxidation resistant chromium silicide matrix alloy containing molybdenum
[NASA-CASE-LEW-15697-1] p 3323 N93-29172
Effects of internal helium on mechanical properties of Nitronic (tm) 40 stainless steel
[DE93-009902] p 3324 N93-29265
Examination of formability to seamless tubes on Ni-Cr-W superalloy
[DE93-764158] p 3326 N93-30396
Development of Ni-Cr-W superalloys for high temperature components in high temperature gas-cooled reactors, part 2
[DE93-764469] p 3326 N93-30399

CHROMIUM STEELS
Preliminary test of liquid metal induced embrittlement in liquid LiPb and stainless-steel systems
[DE93-753130] p 3320 N93-28529

CIRCADIAN RHYTHMS
Control and circadian behavior by transplanted suprachiasmatic nuclei
[AD-A264553] p 3496 N93-30382
Molecular approach to hypothalamic rhythms
[AD-A264438] p 3496 N93-30421
Photoreceptors regulating circadian behavior: A mouse model
[AD-A264881] p 3497 N93-30908

CIRCUIT BOARDS
Prototype and short-run printed circuit board creation
[AD-A263245] p 3409 N93-29655
Detecting residue on a printed circuit board: An application of the Boundary Contour/Feature Contour System
[DE93-006283] p 3412 N93-30370

CIRCUIT PROTECTION
Characteristic and development report SA3581/MC4196 Lightning Arrestor Connector (LAC)
[DE93-010610] p 3412 N93-30118

CIRCUITS
Initial graphics exchange specification hybrid microcircuit application protocol
[PB93-175404] p 3407 N93-29203
An MCM/chip concurrent engineering validation
[AD-A262959] p 3409 N93-29513

CIRCULAR CYLINDERS
Direct numerical simulations of unsteady separated flows using vortex methods p 3419 N93-29077

CIRCULAR TUBES
The effect of orthogonal-mode rotation on forced convection in a circular-sectioned tube fitted with full circumferential transverse ribs p 3254 N93-29937

CIRCULATION CONTROL AIRFOILS
The numerical simulation of circulation controlled airfoil flowfields p 3243 N93-30947

CISLUNAR SPACE
Analysis of orbital system logistics in the cis-lunar space with particular consideration of life cycle costs
[ETN-93-93484] p 3268 N93-29063

CITIES
Summer 1990 Atlanta ozone precursor study (January 1993)
[PB93-167203] p 3470 N93-29200
Multi-Attribute Decision Theory methodology for pollution control measure analysis
[DE93-005444] p 3472 N93-30008

CIVIL AVIATION
Helicopter approach capability using the differential global positioning system
[NASA-CR-193183] p 3245 N93-28936
The 1991-1992 aviation system capacity plan
[AD-A263436] p 3261 N93-29788
Rotorcraft master plan p 3236 N93-30677
Sandia National Laboratories p 3626 N93-30702
The HSCT mission analysis of waverider designs
[NASA-CR-193467] p 3243 N93-31037

CLAMPS
Scanning electron microscope/energy dispersive x ray analysis of impact residues in LDEF tray clamps
p 3283 N93-29369
Spline screw autochanger
[NASA-CASE-GSC-13435-1] p 3445 N93-29505

CLASSICAL MECHANICS
A comparison of classical mechanics models and finite element simulation of elastically tailored wing boxes
p 3306 N93-30863

CLASSIFICATIONS
Image classification using Markov random fields with two new relaxation methods: Deterministic pseudo annealing and modified metropolis dynamics
[INRIA-RR-1606] p 3553 N93-28510
Preprocessing remotely-sensed data for efficient analysis and classification
[DE93-007367] p 3611 N93-28580
Classification theorem for principal fibre bundles, Berry's phase, and exact cycle evolution
[DE93-011114] p 3556 N93-28601
Security classification of information
[DE93-012416] p 3612 N93-28840
Evidence-based classification of satellite image data
p 3459 N93-28931
New classification methods p 3459 N93-28932
A fuzzy measure approach to motion frame analysis for scene detection p 3511 N93-29525
Feature based neural network acoustic transient signal classification
[AD-A263437] p 3562 N93-29816
A neural network based approach for machine fault diagnosis
[VTT-TIED-1274] p 3543 N93-29998
Computing with neural maps: Application to perceptual and cognitive function
[AD-A264056] p 3499 N93-30033

CLASSIFYING
Neural network cloud classification research
[AD-A264628] p 3484 N93-30176

CLEANING
Detecting residue on a printed circuit board: An application of the Boundary Contour/Feature Contour System
[DE93-006283] p 3412 N93-30370

CLEARANCES
An analysis of en route controller-pilot voice communications
[AD-A264784] p 3394 N93-30611

CLEAVAGE
The effect of temperature on the impact behavior of TiB2 reinforced XDTM-TiAl intermetallic matrix composites
[AD-A262924] p 3296 N93-28886

CLIMATE
Direct volume visualization of three-dimensional vector fields
[DE93-009233] p 3524 N93-28550
The Mechanisms of Solar Variability (MSV) program
[AD-A262525] p 3652 N93-28585
Atmospheric and Geophysical Sciences Division: G-Division did you know?
[DE93-007412] p 3469 N93-28967
Exploitation of parallelism in climate models
[DE93-011259] p 3470 N93-29318
The 17th Annual Climate Diagnostics Workshop
[PB93-183895] p 3483 N93-29664
Quantifying and minimizing uncertainty of climate forcing by anthropogenic aerosols
[NASA-TM-108259] p 3472 N93-30043

CLIMATE CHANGE
Development and testing of the Perseus proof-of-concept aircraft
[DE93-010121] p 3247 N93-28586
Modeling land-surface/atmosphere dynamics for CHAMMP
[DE93-008520] p 3476 N93-28677
Ocean Margins Program
[DE93-008937] p 3470 N93-29262
Stabilized platform for tethered balloon soundings of broadband long- and short-wave radiation
[DE93-007876] p 3383 N93-29308
Exploitation of parallelism in climate models
[DE93-011259] p 3470 N93-29318
Clouds and radiation: A primier
[AD-A263136] p 3482 N93-29479
Chemistry of the atmosphere: Its impact on global change. CHEMRAWN 7: Perspectives and recommendations
[PB93-180644] p 3488 N93-29670
Trend survey on the elucidation of the global warming mechanism by the governments of major industrialized nations
[DE93-776427] p 3470 N93-29672
Simulation of landscape disturbances and the effect of climatic change
[DE93-011615] p 3472 N93-30131

CLIMATOLOGY
Development and testing of the Perseus proof-of-concept aircraft
[DE93-010121] p 3247 N93-28586
Ocean Margins Program
[DE93-008937] p 3470 N93-29262
Exploitation of parallelism in climate models
[DE93-011259] p 3470 N93-29318
Clouds and radiation: A primier
[AD-A263136] p 3482 N93-29479
Advanced Earth Observing Satellite (ADEOS)
p 3279 N93-29648
The 17th Annual Climate Diagnostics Workshop
[PB93-183895] p 3483 N93-29664
Potential effects of HFC-152a on global ozone and climate
[DE93-008018] p 3471 N93-29792
Air weather service master station catalog USAFETAC climatic database users handbook no. 6
[AD-A264761] p 3484 N93-30608
Oceanographic research towers in european waters
[AD-A264795] p 3489 N93-30612
Deadliest, costliest, and most intense US hurricanes of this century (and other frequently requested hurricane facts)
[PB93-174993] p 3485 N93-30758
Shuttle landing facility cloud cover study: Climatological analysis and two tenths cloud cover rule evaluation
[NASA-CR-193016] p 3272 N93-31033

CLINICAL MEDICINE
DOKMA: A document oriented communication model for medical applications as a basis of a role system in the medical field
[ETN-93-93799] p 3492 N93-28469
Proceedings of a Workshop on Molecular Nuclear Medicine
[DE93-010828] p 3493 N93-28835
The Visible Human Project of the National Library of Medicine: Remote access and distribution of a multi-gigabyte data set p 3617 N93-30453

CLOCKS
The effect of clock, media, and station location errors on Doppler measurement accuracy
p 3246 N93-29588

Foreign technology assessment: Environmental evaluation of a radiation-hard oscillator/divider
[DE93-011481] p 3412 N93-30127

CLOSED ECOLOGICAL SYSTEMS
Earth to lunar CELSS evolution p 3229 N93-29727
Design of biomass management systems and components for closed loop life support systems
p 3230 N93-29728
Automation of closed environments in space for human comfort and safety p 3230 N93-29734

CLOUD COVER
An automated observing system for passive evaluation of cloud cover and visibility
[AD-A263207] p 3481 N93-28875
Sensitivity study of cloud/radiation interaction using a second order turbulence radiative-convective model
[DE93-007365] p 3477 N93-29346
Prognostic cloud water in the Los Alamos general circulation model
[DE93-007381] p 3482 N93-29347
Cloudiest year study: An analysis of the 3DNEPH and RTNEPH databases
[AD-A263409] p 3483 N93-29967
Daily sum of the global radiation: Calculation method and verification of forecast
[KNMI-TR-138] p 3478 N93-30113
STRATUS: A prototype expert advisory system for terminal weather forecasting p 3367 N93-30296
Shuttle landing facility cloud cover study: Climatological analysis and two tenths cloud cover rule evaluation
[NASA-CR-193016] p 3272 N93-31033

CLOUD HEIGHT INDICATORS
Sensitivity study of cloud/radiation interaction using a second order turbulence radiative-convective model
[DE93-007365] p 3477 N93-29346

CLOUD PHYSICS
Activities report of the International Meteorological Institute, Stockholm (Sweden)
[ETN-93-93768] p 3480 N93-28519
A stochastic formation of radiative transfer in clouds
[DE93-011372] p 3484 N93-30055

CLOUDS (METEOROLOGY)
Prognostic cloud water in the Los Alamos general circulation model
[DE93-007381] p 3482 N93-29347
Clouds and radiation: A primer
[AD-A263136] p 3482 N93-29479
Neural network cloud classification research
[AD-A264628] p 3484 N93-30176
Cloud classification from satellite imagery using neural computing p 3367 N93-30297
Cloud Impacts on DOD Operations and Systems Conference (CIDOS-91)
[AD-A264463] p 3484 N93-30535
Uplink laser propagation measurements through the sea surface, haze and clouds
[AD-A264687] p 3440 N93-30553

CLUSTER ANALYSIS
A fuzzy clustering algorithm to detect planar and quadric shapes p 3511 N93-29524
Image segmentation using fuzzy LVQ clustering networks p 3511 N93-29528
Clustering of tethered satellite system simulation data by an adaptive neuro-fuzzy algorithm
p 3512 N93-29535

CLUSTERS
Quantum dynamics of X2BC van der Waals clusters
[DE93-006416] p 3565 N93-28892
Mass spectrometric investigation of 2-methoxyethanol and 2-ethoxyethanol clusters: Magic numbers and structural implications
[AD-A262622] p 3312 N93-29429

CLUTTER
Ground clutter measurements for surface-sited radar
[AD-A262472] p 3379 N93-28655
Multichannel detection of partially correlated signals in clutter
[AD-A261984] p 3381 N93-28998
Classification of radar clutter in an air traffic control environment p 3246 N93-30299
Adaptive filtering for clutter suppression in high frequency radar p 3377 N93-30355
Adaptive airborne radar simulation with equalization filter taps
[AD-A264722] p 3393 N93-30514

CMOS
Analog CMOS circuits for neural networks
p 3355 N93-30223
A single chip high-speed CMOS Viterbi decoder
p 3358 N93-30238
High-speed, CMOS dual modulus frequency divider for RF frequency synthesis p 3359 N93-30245
Performance enhancement of dynamic CMOS logic circuits p 3361 N93-30257
Generation of configurable self-synchronizing synchronous CMOS static RAMs p 3361 N93-30259

Hardness assurance and testing issues for bipolar/BiCMOS devices
[DE93-009623] p 3570 N93-30669

COAL
Magnetohydrodynamic projects at the CDIF
[DE93-012195] p 3584 N93-28649

COAL DERIVED GASES
Development of alternative fuels from coal-derived syngas
[DE93-011629] p 3341 N93-28668

COAL DERIVED LIQUIDS
Advanced thermally-stable, coal-derived, jet fuels program: Experiment system and model development
[AD-A262747] p 3342 N93-29402

COAL GASIFICATION
Development of alternative fuels from coal-derived syngas
[DE93-011629] p 3341 N93-28668
High octane ethers from synthesis gas-derived alcohols
[DE93-012470] p 3341 N93-28752

COASTAL ECOLOGY
Building alliances to restore coastal environments: A coastal America progress report
[PB93-169464] p 3470 N93-29674

COASTAL WATER
Ocean Margins Program
[DE93-008937] p 3470 N93-29262

COASTS
Building alliances to restore coastal environments: A coastal America progress report
[PB93-169464] p 3470 N93-29674
A water mass analysis of the 1991-1992 El Nino signal in the Farallon Islands region
[AD-A263490] p 3488 N93-29819
Deadliest, costliest, and most intense US hurricanes of this century (and other frequently requested hurricane facts)
[PB93-174993] p 3485 N93-30758

COATING
Characterization and optimization of a Hot Air Solder-Leveling System
[DE93-010188] p 3332 N93-29328
Development of adherent ceramic coatings to reduce contact stress damage of ceramics
[DE93-012518] p 3336 N93-30182

COATINGS
Ion-beam-assisted deposition of wear-resistant coatings
[DE93-011529] p 3330 N93-28687
X ray, far, and extreme ultraviolet coatings for space applications p 3340 N93-28829
Effects of vacuum exposure on stress and spectral shift of high reflective coatings
[DE93-009318] p 3437 N93-29207
A simple model for explosives formulation
[DE93-010703] p 3341 N93-29251
Formulation of Ames 24E2 IR-black coating
[NASA-TM-102864] p 3629 N93-29453
Process to prepare 1,3-diamino-5-pentafluorosulfanylbenzene
[NASA-CASE-LAR-14773-2-CU] p 3312 N93-29506
Study of codeposition of aluminum-haffnium and deposition of yttrium by the cementation technique: Elaboration of Ni-Cr-Al and Ni-Cr-Al-Hf felt materials
[ONERA-NT-1990-9] p 3336 N93-30112

COAXIAL CABLES
Leaky coaxial cable signal transmission for remote facilities
[DE93-007916] p 3383 N93-29348

COBALT
Magnetic character investigation of higher alcohol synthesis Cu-Co-Cr catalysts
[DE93-009732] p 3316 N93-30653

COCKPIT SIMULATORS
An evaluation of B-1B pilot performance during simulated instrument approaches with and without status information
[AD-A263874] p 3507 N93-29888
Utility of a ghost horizon and climb/dive ladder line tapering on a head-up display
[AD-A264401] p 3508 N93-30167
NASA/FAA helicopter simulator workshop
[NASA-CP-3156] p 3236 N93-30673
Part 1: Executive summary p 3236 N93-30674
Helicopter simulator standards p 3236 N93-30675

COCKPITS
Oculo-motor responses and virtual image displays
p 3503 N93-28862
Cognitive interface considerations for intelligent cockpits p 3503 N93-28865
Ergonomic development of digital map displays
p 3503 N93-28866
Overview of cockpit technology research and development programs for improvement of the man/machine interface: Review of the AGARD AVP Symposium held in Madrid, May 1992
p 3505 N93-28872

CODE DIVISION MULTIPLE ACCESS
Comparison of multiple access techniques for bandwidth limited land-mobile satellite communications
p 3370 N93-30314

CODERS
Gravity referenced elevation encoder development
p 3385 N93-29592
Robot arm with positional absolute encoded joints
p 3370 N93-30312

CODING
Iterative encoding methods for computer generated holograms
[AD-A263705] p 3431 N93-29297
Nonresident and endangered variables: The effects of code generation optimizations on symbolic debugging
[AD-A263149] p 3529 N93-29486
The general theory of convolutional codes
p 3385 N93-29595
Activities report of PTT Research
[ISBN-9-07-212514-2] p 3392 N93-30025
Feature segmentation using a multiple-stack based chain coding algorithm p 3359 N93-30243
Short-circuit evaluation of Boolean expressions
[CS-9205] p 3552 N93-31014

COEFFICIENT OF FRICTION
Interfacial viscosity measurements of adsorbed monolayers on metal surfaces
[AD-A263288] p 3324 N93-29803
Vehicle dynamic stability and rollover
[PB93-185437] p 3447 N93-30828

COEFFICIENTS
Gas permeability of E/EP semicrystalline diblock copolymers
[AD-A263241] p 3329 N93-28560
Stress-intensity-factor influence coefficients for axial and circumferential flaws in reactor pressure vessels
[DE93-006206] p 3454 N93-30213

COGENERATION
Power generation and transportation systems research department
[PB93-178309] p 3352 N93-30663

COGNITION
Expertise, text coherence, and constraint satisfaction: Effects on harmony and settling rate — mental representations
[AD-A262703] p 3498 N93-28901
Cognitive and Neural Sciences Division 1992 programs
[AD-A263400] p 3654 N93-29258
MoCog1: A computer simulation of recognition-primed human decision making
[NASA-TM-103868] p 3542 N93-29386
Predicting aircrew training performance with psychometric g
[AD-A264021] p 3498 N93-30026
Computing with neural maps: Application to perceptual and cognitive function
[AD-A264056] p 3499 N93-30033
The AFOSR Workshop on the Future of EEG and MEG
[AD-A264338] p 3495 N93-30160
Representations of shape in object recognition and long-term visual memory
[AD-A264342] p 3499 N93-30163
Determinants of performance rating accuracy: A field study
[AD-A264726] p 3500 N93-30575

COGNITIVE PSYCHOLOGY
Expertise, text coherence, and constraint satisfaction: Effects on harmony and settling rate — mental representations
[AD-A262703] p 3498 N93-28901
Representations of shape in object recognition and long-term visual memory
[AD-A264342] p 3499 N93-30163
Neural mechanisms of attention
[AD-A264345] p 3544 N93-30165

COHERENT RADIATION
Undulator Spectromicroscopy Facility at the Advanced Light Source
[DE93-007964] p 3261 N93-28490
Development of coherent x ray lasers
[DE93-009288] p 3437 N93-29104
Optical coherent phase diversity systems
[ISBN-90-9004897-9] p 3578 N93-29270
Microwave emission from relativistic electron beams
[AD-A264102] p 3400 N93-30880

COHERENT SCATTERING
Measurements of light scattering by small particles at an angle of zero degrees
[AD-A263856] p 3580 N93-29887

In-situ temperature and concentration measurements of organosilicon decomposition in a chemical vapor deposition reactor
[ONERA-P-1990-3] p 3313 N93-30109

COHESION
Micropipet manipulation of lipid membranes: Direct measurement of the material properties of a cohesive structure that is only two molecules thick
p 3291 N93-30953

COLD PLASMAS
Numerical modelling of the cold plasma with time-dependent, magnetohydrodynamic methods
[KFK-5053] p 3586 N93-29081
Application of non-standard signal processing to ELF noise characterization for the TSS1-OESEE programme
p 3397 N93-30743
Plasma diffusion through multidipole magnetic fields
[DE93-608548] p 3591 N93-31007

COLD ROLLING
Environmental embrittlement of binary and Zr-doped Ni3Al
[DE93-008575] p 3321 N93-28679

COLD TOLERANCE
Influence of the Cold Buster (tm) sports bar on heat debt, mobilization and oxidation of energy substrates
[AD-A262762] p 3493 N93-28939
Medical aspects of cold weather operations: A handbook for medical officers
[AD-A263559] p 3496 N93-30588
An assessment of peripheral nerve damage in the rat following non-freezing cold exposure: An electrophysiological and histopathological examination
[AD-A264293] p 3492 N93-30818

COLD WEATHER
Medical aspects of cold weather operations: A handbook for medical officers
[AD-A263559] p 3496 N93-30588

COLD WEATHER TESTS
Biophysical model for handwear insulation testing
[AD-A262926] p 3505 N93-28884

COLD WORKING
Examination of formability to seamless tubes on Ni-Cr-W superalloy
[DE93-764158] p 3326 N93-30396

COLLAPSE
Advanced collapsible tank for liquid containment
[NASA-CR-188247] p 3353 N93-28698

COLLISION AVOIDANCE
Results of DATAS investigation of ATCRBS environment at the Los Angeles International Airport
[DOT/FAA/CT-93/6] p 3245 N93-28625
Sensor systems for monitoring Maglev guideway structures
[PB93-154821] p 3444 N93-29205
Graphical interface between the CIRSSE testbed and CimStation software with MCS/CTOS
[NASA-CR-193276] p 3527 N93-29218
Planning collision free paths for two cooperating robots using a divide-and-conquer C-space traversal heuristic
[NASA-CR-193252] p 3542 N93-29771
Optimal geometric design of robots for environments with obstacles p 3445 N93-30149
Issues of ATC conflict resolution under real-time constraints p 3247 N93-30350

COLLISION PARAMETERS
A possibility to investigate the superconducting gap with the help of neutrons
[DE93-606392] p 3601 N93-30799
Single t-quark production in high energy (gamma)e collisions
[DE92-644947] p 3572 N93-30930

COLLISION RATES
Estimation of droplet collision frequency in a spray
[DE93-007991] p 3416 N93-28566

COLLISIONS
Proceedings of the Near-Earth-Object Interception Workshop
[NASA-TM-108236] p 3556 N93-28572
Stellar encounters in globular clusters
p 3632 N93-28606
Why Blue stragglers formed via collisions may not be rapid rotators
[DE93-008708] p 3633 N93-28905
Do the Pop 2 field blue stragglers have a collisional origin?
[DE93-008709] p 3634 N93-28906
Can physical stellar collisions explain the blue stragglers in the dwarf spheroidal galaxies?
[DE93-008711] p 3634 N93-28907
Catastrophic collisions: Laboratory impact experiments, hydrocode simulations, and the scaling problem
p 3635 N93-30411

COLLOIDS
Colloid and interface chemistry aspects of ceramics
[AD-A264685] p 3337 N93-30552

COLORADO PLATEAU (US)
Environmental Monitoring and Assessment Program. EMAP: Arid Colorado plateau pilot study
[PB93-181618] p 3474 N93-30823

COLUMBIA (ORBITER)
APU diaphragm testing
[NASA-TM-108254] p 3272 N93-29501

COLUMBUS SPACE STATION
Assessment of Columbus payload operations capabilities by scheduling with the MARS system
[ESA-STR-235] p 3281 N93-30106

COMBAT
Combat Automation for Airborne Weapon Systems: Man/Machine Interface Trends and Technologies
[AGARD-CP-520] p 3501 N93-28850
X-31 demonstration of integrated flight and propulsion control for effective combat at extreme angles of attack
p 3260 N93-28851
Planning for air to air combat p 3501 N93-28852
Computer assisted evaluation for air close combat based on time interval characterization p 3504 N93-28868
Sound attenuation characteristics of the standard DH-132A and SPH-4 helmets worn in combination with standard issue earplugs
[AD-A263011] p 3506 N93-29406

COMBINATORIAL ANALYSIS
How to select combination operators for fuzzy expert systems using CRI p 3510 N93-29521
Polynomial space polynomial delay algorithms for listing families of graphs
[DE93-010677] p 3530 N93-29808
Parametric and combinatorial problems in constrained optimization
[AD-A264229] p 3555 N93-30363

COMBUSTIBLE FLOW
Turbulence characteristics of an axisymmetric reacting flow
[NASA-CR-4110] p 3242 N93-30373

COMBUSTION
Programmer's reference guide to FDMS file formats
[PB93-182038] p 3354 N93-29663
ONR/LANL Workshop on the Fundamental Physics and Chemistry of Combustion, Initiation, and Detonation of Energetic Materials
[CPIA-PUBL-589] p 3343 N93-30061
Energetic material response to abnormal environments p 3350 N93-30095

COMBUSTION CHAMBERS
Magnetohydrodynamic projects at the CDIF
[DE93-012195] p 3584 N93-28649
Application of Schlieren optical techniques for the measurement of gas temperature and turbulent diffusivity in a diesel engine
[AD-A263810] p 3580 N93-29880
Heat Transfer and Cooling in Gas Turbines
[AGARD-CP-527] p 3252 N93-29926
The effect of main stream flow angle on flame tube film cooling p 3257 N93-29953
Impingement/effusion cooling p 3257 N93-29954
Evaluation of multi-dimensional flux models for radiative transfer in cylindrical combustion chambers
p 3257 N93-29955
Calculations of reactive turbulent flows in aeronautical chambers p 3257 N93-29956
Method of fabricating a rocket engine combustion chamber
[NASA-CASE-MFS-28569-1] p 3338 N93-30565
Thrust augmentation system for low-cost-expendable turbojet engine
[AD-A263727] p 3259 N93-30877

COMBUSTION CHEMISTRY
Generation of carbon monoxide in compartment fires
[PB93-146702] p 3244 N93-29211
Response of energetic solids to light, heat and shock pulses
[AD-A263702] p 3342 N93-29296
Calculations of reactive turbulent flows in aeronautical chambers p 3257 N93-29956
Combustion/explosion chemistry of bulk materials
p 3343 N93-30062
The thermochemistry and reaction pathways of the decomposition and combustion of energetic materials
p 3343 N93-30063
Determination of gas phase species and temperature profiles above solid propellants p 3346 N93-30080
Thermal decomposition pathways of RDX in the condensed phase p 3347 N93-30083
Unsteady combustion of energetic materials using laser-recoil p 3319 N93-30085
Rate constant determinations of reactions H + HNO from ab initio reaction path calculations
p 3319 N93-30099

COMBUSTION PHYSICS
Weakly nonlinear dynamics of near-CJ detonation waves
[DE93-007344] p 3424 N93-29836
ONR/LANL Workshop on the Fundamental Physics and Chemistry of Combustion, Initiation, and Detonation of Energetic Materials
[CPIA-PUBL-589] p 3343 N93-30061
Combustion/explosion chemistry of bulk materials
p 3343 N93-30062
Propulsion and detonics research in France
p 3344 N93-30070
The outlook for understanding the combustion of solid propellants and what it will take p 3346 N93-30078
Dislocation roles in energetic crystal responses
p 3348 N93-30086
Homogeneous gas phase kinetic model with gradient sensitivity analysis for high temperature particulate boron combustion in fluorine enriched environments
p 3319 N93-30090
NOx chemistry in natural gas flames
[PB93-175263] p 3317 N93-30760
Thrust augmentation system for low-cost-expendable turbojet engine
[AD-A263727] p 3259 N93-30877

COMBUSTION PRODUCTS
Generation of carbon monoxide in compartment fires
[PB93-146702] p 3244 N93-29211
Multi-Attribute Decision Theory methodology for pollution control measure analysis
[DE93-005444] p 3472 N93-30008
Kinetic studies on gas-phase reaction mechanisms important to the combustion of energetic materials: The CO/N2O reaction p 3347 N93-30084
Unsteady combustion of energetic materials using laser-recoil p 3319 N93-30085
Direct Monte Carlo simulation of the chemical equilibrium composition of detonation products
[DE92-040372] p 3315 N93-30447
Detailed studies of soot formation in laminar diffusion flames for application to modeling studies
[AD-A264827] p 3317 N93-30667

COMBUSTION STABILITY
Weakly nonlinear dynamics of near-CJ detonation waves
[DE93-007344] p 3424 N93-29836
Contribution to the study of the interaction between acoustic waves and coherent structures induced by a prismatic cylinder in a rectangular cavity
[ONERA-NT-1990-10] p 3314 N93-30203
Detailed studies of soot formation in laminar diffusion flames for application to modeling studies
[AD-A264827] p 3317 N93-30667

COMBUSTION SYNTHESIS
Explosive consolidation of combustion synthesized TiC and TiB2: Precursor morphology effects
[AD-A263186] p 3341 N93-28515
Methylhydridopolysilazane and its pyrolytic conversion to Si3N4/SiC ceramics
[AD-A264150] p 3336 N93-30170

COMETS
Space optical and low-frequency radio searches for Earth-crossing asteroids and comets
[DE93-008716] p 3634 N93-29246
Asteroidal versus cometary meteoroid impacts on the Long Duration Exposure Facility (LDEF)
p 3638 N93-29371

COMFORT
Discomfort glare from high-intensity discharge headlamps: Effects of context and experience
[PB93-174720] p 3496 N93-30659

COMMAND AND CONTROL
Advanced Unmanned Search System (AUSS) supervisory command, control and navigation
[AD-A263171] p 3245 N93-28990
Using today's technology to improve mobile C4I for the operational commander
[AD-A263613] p 3245 N93-29285
T(lc2)acS(lc3)ats for Surveillance Verification and C3I
[AGARD-CP-522] p 3387 N93-29892
TACSAT ground control and data collection
p 3388 N93-29895
TACSAT-spacecraft bus concept and design: Application of a multimission bus for TACSAT in LEO
p 3284 N93-29896
Tactical satellites for air command and control
p 3284 N93-29898
Consultative Committee for Space Data Systems recommendation for space data system standards: Telecommand. Part 2.1: Command operation procedures
[NASA-TM-108158] p 3393 N93-30371
VLF/LF propagation measurements
p 3395 N93-30732

COMMERCE
Defense conversion: Redirecting research and development
[OTA-ITE-552] p 3610 N93-29649
Advanced network technology: Background paper
[OTA-BP-TCT-101] p 3539 N93-29650

The 1992 World Administrative Radio Conference: Technology and Policy Implications
[OTA-TCT-549] p 3392 N93-30150
US space commerce, 1991 p 3625 N93-30695
The role of the University Licensing Office in transferring intellectual property to industry p 3626 N93-30698
National Technology Transfer Center
p 3626 N93-30700
Proceedings of the meeting of the Intergovernmental US-Russian Business Development Committee's Standards Working Group
[PB93-179968] p 3610 N93-30822

COMMERCIAL AIRCRAFT
World commercial aircraft accidents
[DE93-010892] p 3243 N93-28571
Effects of intra- and inter-laminar resin content on the mechanical properties of toughened composite materials
p 3303 N93-30845
Process and assembly plans for low cost commercial fuselage structure p 3306 N93-30865

COMMERCIAL SPACECRAFT
US space commerce, 1991 p 3625 N93-30695

COMMUNICATION EQUIPMENT
Time delay measurements of current primary FAA air/ground transmitters and receivers
[DOT/FAA/CT-TN93/14] p 3379 N93-28555
Evaluation of test methods and requirements for respiratory protection systems 21
[AD-A262466] p 3501 N93-28757
The NASA SBIR product catalog
[NASA-TM-108242] p 3609 N93-29322
The 1992 World Administrative Radio Conference: Technology and Policy Implications
[OTA-TCT-549] p 3392 N93-30150

COMMUNICATION NETWORKS
A survey of network interface designs
[MEMO-INF-92-59] p 3379 N93-28502
National collaboratories: Applying information technology for scientific research
[LC-93-83795] p 3612 N93-29129
A comparison of high-speed links, their commercial support and ongoing R/D activities
[DE93-008134] p 3382 N93-29245
Communications neural net processors
[AD-A263330] p 3542 N93-29763
Ethernet performance of the Motorola Altair WIN system
[AD-A263877] p 3387 N93-29890
T(lc2)acS(lc3)ats for Surveillance Verification and C3I
[AGARD-CP-522] p 3387 N93-29892
TACSAT-spacecraft bus concept and design: Application of a multimission bus for TACSAT in LEO
p 3284 N93-29896
Advanced HF digital networks p 3375 N93-30343
Changing role of telecommunications management in air traffic control in the FAA p 3247 N93-30354
High performance computing and communications program p 3627 N93-30715
ELF/VLF/LF Radio Propagation and Systems Aspects
[AGARD-CP-529] p 3394 N93-30727
VLF/LF propagation measurements
p 3395 N93-30732
Viability assessment for reliable long-wave communication links p 3399 N93-30754
Orbiting transmitter and antenna for spaceborne communications at ELF/VLF to submerged submarines
p 3399 N93-30755

COMMUNICATION SATELLITES
Power beaming to communication satellites in GEO
[DE93-007608] p 3279 N93-29840
On-board B-ISDN fast packet switching architectures. Phase 2: Development. Proof-of-concept architecture definition report
[NASA-CR-191151] p 3273 N93-29884
T(lc2)acS(lc3)ats for Surveillance Verification and C3I
[AGARD-CP-522] p 3387 N93-29892
Tactical satellites p 3284 N93-29893
Evolution or revolution: The Catch 22 of TACSATs
p 3269 N93-29894
TACSAT-spacecraft bus concept and design: Application of a multimission bus for TACSAT in LEO
p 3284 N93-29896
Tactical satellites for air command and control
p 3284 N93-29898
Considerations for NATO satellite communications in the post-2000 era p 3388 N93-29899
Advanced technologies for lightweight EHF tactical communications satellites p 3389 N93-29900
Synchronization techniques for medium data rate EHF MILSATCOM systems p 3389 N93-29901
Terrain and coverage prediction analyses for non-geostationary orbit EHF satellite communications
p 3389 N93-29902
Launch vehicles for lightweight TACSAT deployment
p 3271 N93-29903
Spacecraft and launch systems for TACSAT applications p 3284 N93-29904
Attitude- and Orbit Control Subsystem concepts for TACSATS p 3284 N93-29906
Cost effective TacSats for military support
p 3285 N93-29912
Canadian EHF MILSATCOM research and development project p 3362 N93-30264
SAW technology for on-board processing in military satellite communications p 3362 N93-30265
FASSET: A development model for a Canadian EHF MILSATCOM system p 3363 N93-30268
Adaptive jammer nulling in EHF communications satellites p 3365 N93-30284
A dual polarized broadband multifrequency Earth station feed p 3371 N93-30319
US space commerce, 1991 p 3625 N93-30695

COMMUNICATION THEORY
Uncorrectable sequences and telecommand
p 3385 N93-29596

COMPACTING
Colloid and interface chemistry aspects of ceramics
[AD-A264685] p 3337 N93-30552

COMPANION STARS
The multiplicity of T Tauri stars in the star forming regions Taurus-Auriga and Ophiuchus-Scorpius: A 2.2 micron speckle imaging survey p 3634 N93-28945
Effects of spiral shocks on disk emission lines
[DE92-641716] p 3637 N93-31004

COMPARISON
Filtering interpolators for image comparison algorithms
p 3463 N93-28797
ERS-1 directional wave spectra validation with the airborne SAR PHARS
[BCRS-92-18] p 3463 N93-31010

COMPARTMENTS
Generation of carbon monoxide in compartment fires
[PB93-146702] p 3244 N93-29211

COMPATIBILITY
APU diaphragm testing
[NASA-TM-108254] p 3272 N93-29501
Compatibility studies of AISI type 316 stainless steel with lead-lithium eutectic alloy
[DE93-605281] p 3328 N93-31022

COMPENSATORS
Robust feedforward/feedback control synthesis for uncertain dynamical systems p 3542 N93-29079
Three-parameter tunable Tilt-Integral-Derivative (TID) controller
[NASA-CASE-NPO-18492-1-CU] p 3542 N93-29176
Division by polynomial matrix and its application to multivariable linear systems p 3357 N93-30233

COMPILERS
Installation of a new Fortran compiler and effective programming method on the vector supercomputer
[DE93-753322] p 3524 N93-28537
Compiler-assisted multiple instruction rollback recovery using a read buffer
[NASA-CR-193175] p 3527 N93-29170
Implementing error-valued semantics for dataflow languages on imperative machines
[DE93-009319] p 3615 N93-29310
Nonresident and endangered variables: The effects of code generation optimizations on symbolic debugging
[AD-A263149] p 3529 N93-29486
Development of a PC code package for the analysis of research and power reactors
[DE92-638517] p 3536 N93-31001

COMPLEX COMPOUNDS
Applications of transition metal compounds in the preparation of useful silicon-containing ceramics
[AD-A264028] p 3335 N93-30028
Applications of density functional theory to calculation of reaction energetics p 3351 N93-30098
Complex-compound heat pump: Topical report on phase 1 results
[PB93-185460] p 3466 N93-30814

COMPLEX SYSTEMS
A neuro-fuzzy architecture for real-time applications
p 3511 N93-29529
Some problems with the design of self-learning management systems p 3516 N93-29559
Fuzzy simulation in concurrent engineering
p 3516 N93-29562
Automated modeling of physical systems
[NASA-CR-193256] p 3531 N93-29873
Intelligent real-time problem solving
[AD-A264830] p 3535 N93-30614
Graphical programming: On-line robot simulation for telerobotic control
[DE93-009796] p 3447 N93-30654

COMPONENT RELIABILITY
High-efficiency high-reliability optical components for a large, high-average-power visible laser system
[DE93-009225] p 3437 N93-29098
Research on reconfigurable and reliable manipulators
[DE93-010244] p 3444 N93-29330
NetStat: A probabilistic network connectivity analysis tool
[AD-A262838] p 3529 N93-29647
Fault tolerance and testing for WSI systems
p 3361 N93-30258

COMPOSITE MATERIALS
JPRS report: Science and technology. Central Eurasia: Materials science
[JPRS-UMS-92-009] p 3322 N93-29015
JPRS report: Science and technology. Central Eurasia: Materials science
[JPRS-UMS-92-012] p 3296 N93-29016
JPRS report: Science and technology. Central Eurasia: Materials science
[JPRS-UMS-92-013] p 3296 N93-29017
JPRS report: Science and technology. Central Eurasia: Materials science
[JPRS-UMS-92-016] p 3296 N93-29018
JPRS report: Science and technology. Central Eurasia: Materials science
[JPRS-UMS-92-014] p 3322 N93-29019
JPRS report: Science and technology. Central Eurasia: Materials science
[JPRS-UMS-92-015] p 3322 N93-29020
JPRS report: Science and technology. Central Eurasia: Materials science
[JPRS-UMS-93-001] p 3296 N93-29021
Sensor systems for monitoring Maglev guideway structures
[PB93-154821] p 3444 N93-29205
Advanced technology composite aircraft structures
[NASA-CR-190420] p 3248 N93-29498
Semiconductor cooling apparatus
[NASA-CASE-LEW-14162-3] p 3299 N93-29614
Scattering through apertures and by three-dimensional structures. Application to the measurement of the surface impedance of conductive materials
[ONERA-P-1990-2] p 3392 N93-30018
The First NASA Advanced Composites Technology Conference, part 1
[NASA-CP-3104-PT-1] p 3300 N93-30428
Composites: A viable option p 3300 N93-30429
Advanced composite structural concepts and material technologies for primary aircraft structures
p 3300 N93-30430
Composites technology for transport primary structure
p 3300 N93-30431
Advanced technology commercial fuselage structure
p 3300 N93-30432
Design and manufacturing concepts for thermoplastic structures p 3301 N93-30434
Resin transfer molding for advanced composite primary aircraft structures p 3301 N93-30438
Lessons learned for composite structures
p 3302 N93-30444
Measurement of electromagnetic properties of composite materials
[AD-A264725] p 3303 N93-30555
Infiltration/cure modeling of resin transfer molded composite materials using advanced fiber architectures
p 3303 N93-30843
Powder towpreg process development
p 3303 N93-30844
Development of resins for composites by resin transfer molding p 3305 N93-30853
An overview of the crash dynamics failure behavior of metal and composite aircraft structures
p 3308 N93-30875
New materials: Fountainhead for new technologies and new science p 3291 N93-30952
Introduction to high performance composites
p 3291 N93-30957
Construction and testing of simple airfoils to demonstrate structural design, materials choice, and composite concepts p 3243 N93-30979
Advanced electromagnetic methods for aerospace vehicles
[NASA-CR-193468] p 3400 N93-31036

COMPOSITE PROPELLANTS
Damage growth in composite propellants
p 3348 N93-30088

COMPOSITE STRUCTURES
Influence of ply waviness on stiffness and strength reduction of composite laminates
[AD-A263224] p 3294 N93-28559
A thermal stress solution for multilayered composite cylinders
[AD-A262579] p 3295 N93-28657
Analysis for thermo-chemical decomposition of composite structures
[NASA-CR-193185] p 3295 N93-28843
Nonlinear analyses of composite aerospace structures in sonic fatigue
[NASA-CR-193124] p 3451 N93-29154

Technology transfer personnel exchange at the Boeing Company
[DE93-010190] p 3625 N93-29329

Advanced technology composite aircraft structures
[NASA-CR-190420] p 3248 N93-29498

Static and dynamic large deflection flexural response of graphite-epoxy beams
[NASA-CR-4118] p 3454 N93-30374

The First NASA Advanced Composites Technology Conference, part 1
[NASA-CP-3104-PT-1] p 3300 N93-30428

Composites: A viable option p 3300 N93-30429

Advanced composite structural concepts and material technologies for primary aircraft structures
p 3300 N93-30430

Composites technology for transport primary structure
p 3300 N93-30431

Advanced technology commercial fuselage structure
p 3300 N93-30432

Design, analysis, and fabrication of the technology integration box beam p 3300 N93-30433

Design and manufacturing concepts for thermoplastic structures p 3301 N93-30434

Structural evaluation of curved stiffened composite panels fabricated using a THERM-Xsm process
p 3301 N93-30435

Noise transmission properties and control strategies for composite structures p 3301 N93-30436

Long discontinuous fiber composite structure: Forming and structural mechanics p 3301 N93-30437

Resin transfer molding for advanced composite primary aircraft structures p 3301 N93-30438

Consolidation of graphite thermoplastic textile preforms for primary aircraft structure p 3302 N93-30439

Cost studies for commercial fuselage crown designs
p 3302 N93-30440

A unified approach for composite cost reporting and prediction in the ACT program p 3302 N93-30441

F-15 composite engine access door
p 3302 N93-30442

Fabrication of the V-22 composite AFT fuselage using automated fiber placement p 3302 N93-30443

Lessons learned for composite structures
p 3302 N93-30444

Development of stitching reinforcement for transport wing panels p 3304 N93-30852

Advanced fiber/matrix material systems
p 3305 N93-30854

Mechanical and analytical screening of braided composites for transport fuselage applications
p 3305 N93-30855

Ultrasonic detection and identification of fabrication defects in composites p 3305 N93-30856

Multi-parameter optimization tool for low-cost commercial fuselage crown designs
p 3305 N93-30858

Comparison of hand laid-up tape and filament wound composite cylinders and panels with and without impact damage p 3306 N93-30859

Effects of scale in predicting global structural response p 3306 N93-30860

Optimization of composite sandwich cover panels subjected to compressive loadings p 3306 N93-30862

Process and assembly plans for low cost commercial fuselage structure p 3306 N93-30865

Probabilistic composite analysis p 3307 N93-30868

A Rayleigh-Ritz analysis methodology for cutouts in composite structures p 3307 N93-30869

Prediction of stiffener-skin separation in composite panels p 3307 N93-30871

Evaluation of some scale effects in the response and failure of composite beams p 3308 N93-30874

An overview of the crash dynamics failure behavior of metal and composite aircraft structures
p 3308 N93-30875

COMPOUND A

Marine microbial production of dimethylsulfide from dissolved dimethylsulfoniopropionate
[NASA-CR-193278] p 3492 N93-30665

COMPOUNDING

Aluminium-high strength material by mechanical alloying and reaction milling: Basics of processing and characterisation of material
[ESA-TT-1249] p 3324 N93-29272

COMPRESSED AIR

Prefeasibility study on compressed air energy storage systems
[VTT-TIED-1267] p 3465 N93-30111

COMPRESSIBILITY EFFECTS

Studies of hydrogen-air diffusion flames and of compressibility effects related to high-speed propulsion
p 3310 N93-29125

COMPRESSIBLE FLOW

Analysis of unsteady wave processes in a rotating channel
[NASA-CR-191154] p 3251 N93-28617

The hydraulic analysis of cylindrical Flibe jets in a HYLIFE-2 ICF reactor
[DE93-009234] p 3586 N93-29053

Nonlinear relaxation algorithms for the compressible Navier-Stokes equations in two and three dimensions
p 3421 N93-29177

Heat transfer and leakage in high-speed rotating stepped labyrinth seals p 3256 N93-29951

Compressible turbulence in a high-speed high Reynolds number mixing layer p 3242 N93-30583

COMPRESSIBLE FLUIDS

Godunov-type methods for the equations of compressible fluid mechanics
[KFK-5058] p 3428 N93-31020

COMPRESSING

Dual arm generalized compliant motion with shared control
[NASA-CASE-NPO-18738-1-CU] p 3443 N93-28954

COMPRESSION LOADS

Isothermal and shock compression of high density ammonium nitrate and ammonium perchlorate
[DE93-000682] p 3315 N93-30209

Reactive sintering of Ni3Al intermetallic alloys under compressive stress
[DE93-009729] p 3327 N93-30652

Comparison of hand laid-up tape and filament wound composite cylinders and panels with and without impact damage p 3306 N93-30859

Optimization of composite sandwich cover panels subjected to compressive loadings p 3306 N93-30862

Prediction of stiffener-skin separation in composite panels p 3307 N93-30871

Experimental behavior of graphite-epoxy Y-stiffened specimens loaded in compression p 3307 N93-30872

COMPRESSION RATIO

High resolution free-electron laser spectroscopy
[AD-A263734] p 3439 N93-29853

Elastic stability considerations for deep submergence ceramic pressure housing
[AD-A264824] p 3454 N93-30598

COMPRESSION WAVES

Three-dimensional numerical simulation of gradual opening in a wave rotor passage
[NASA-CR-191157] p 3252 N93-29072

Shock waves and polymorphic phase transitions in energetic materials p 3351 N93-30100

COMPRESSIVE STRENGTH

Environmental effects on stitched RTM composites
[NASA-CR-193221] p 3297 N93-29107

Studies of fiber-matrix adhesion on compression strength p 3304 N93-30846

Comparison of impact results for several polymeric composites over a wide range of low impact velocities
p 3304 N93-30848

Effects of bolt-hole contact on bearing-bypass damage-onset strength p 3307 N93-30870

COMPRESSOR BLADES

Three-dimensional fiber-optic LDV measurements in the endwall region of a linear cascade of controlled-diffusion stator blades
[AD-A263513] p 3424 N93-29968

COMPRESSOR ROTORS

Transient thermal behaviour of a compressor rotor with axial cooling air flow and co-rotating or contra-rotating shaft p 3255 N93-29946

Flow and heat transfer between gas-turbine discs
p 3256 N93-29950

COMPRESSORS

Thrust augmentation system for low-cost-expendable turbojet engine
[AD-A263727] p 3259 N93-30877

COMPTON EFFECT

Construction and testing of a neutron and gamma spectrometry system using pulse shape discrimination with an organic scintillator
[AD-A262550] p 3567 N93-29415

Quantum field theory in spaces with closed time-like curves
[DE93-010564] p 3605 N93-30481

COMPUTATION

A proposed approach for developing next-generation computational electromagnetics software
[DE93-007326] p 3380 N93-28900

Research in efficient scientific computation
[AD-A262084] p 3525 N93-28986

Exploiting the memory hierarchy in sequential and parallel sparse Cholesky factorization
[AD-A262849] p 3539 N93-29508

Fuzzy multiple linear regression: A computational approach p 3518 N93-29574

Computation and generalization in neural networks
[AD-A263752] p 3549 N93-29871

Analysis and computation for vortex dynamics and rarefied gases
[AD-A264705] p 3427 N93-30499

COMPUTATIONAL CHEMISTRY

Applications of density functional theory to calculation of reaction energetics p 3351 N93-30098

Rate constant determinations of reactions H + HNO from ab initio reaction path calculations
p 3319 N93-30099

Shock waves and polymorphic phase transitions in energetic materials p 3351 N93-30100

Use of statistics in computational chemistry
[AD-A264307] p 3315 N93-30365

The 26th International Quantum Chemistry Symposium on Atomic, Molecular, and Condensed Matter Theory and Computational Methods
[AD-A264206] p 3315 N93-30534

COMPUTATIONAL FLUID DYNAMICS

Navier-Stokes analysis of radial turbine rotor performance
[NASA-CR-191153] p 3251 N93-28609

Accelerated motion of rigid spheres in unsteady flows at low to moderate Reynolds numbers
p 3416 N93-28612

Analysis of unsteady wave processes in a rotating channel
[NASA-CR-191154] p 3251 N93-28617

A new flux conserving Newton's method scheme for the two-dimensional, steady Navier-Stokes equations
[NASA-TM-106160] p 3416 N93-28626

A grid refinement study of two-dimensional transient flow over a backward-facing step using a spectral-element method
[DE92-018262] p 3417 N93-28639

Numerical simulation of perfect fluid flows around complex 3D configurations by a multidomain solver using the MUSCL approach p 3417 N93-28745

The development of a mixing layer under the action of weak streamwise vortices
[NASA-TM-106089] p 3418 N93-28947

Inviscid quasi one-dimensional nonequilibrium flow
[FFA-TN-1992-35] p 3418 N93-28993

Implementation of a multidomain Navier-Stokes code on the Intel iPSC2 hypercube
[FFA-TN-1992-37] p 3418 N93-28994

The numerical solution of low Mach number flow in confined regions by Richardson extrapolation
[TRITA-NA-9207] p 3238 N93-29005

An efficient spectral integration method for the solution of the Navier-Stokes equations
[FFA-TN-1992-28] p 3418 N93-29009

Pre- and postprocessing techniques for determining goodness of computational meshes
[NASA-CR-192553] p 3538 N93-29030

State vector splitting: A numerical scheme for the Euler equations p 3419 N93-29039

Stabilized space-time finite element formulations for unsteady incompressible flows involving fluid-body interactions p 3419 N93-29040

Studies of hydrogen-air diffusion flames and of compressibility effects related to high-speed propulsion
p 3310 N93-29125

The 3-D viscous flow CFD analysis of the propeller effect on an advanced ducted propeller subsonic inlet
[NASA-TM-106240] p 3252 N93-29162

Accuracy of least-squares methods for the Navier-Stokes equations
[NASA-TM-106209] p 3421 N93-29208

Numerical computation of inviscid flow around nose tip of Space Shuttle with NND scheme
[AD-A264012] p 3421 N93-29260

An upwind method for the solution of the 3D Euler and Navier-Stokes equations on adaptively refined meshes
[AD-A262863] p 3423 N93-29472

Recent applications of CFD to the aerodynamics of Army projectiles
[AD-A262953] p 3240 N93-29512

A parallel implicit incompressible flow solver using unstructured meshes
[AD-A263395] p 3424 N93-29851

Solution of Euler equations for forebody-inlet ensemble of aircraft at high angle of attack
[AD-A263905] p 3240 N93-29862

The application of concentric vortex simulation to calculating the aerodynamic characteristics of bodies of revolution at high angles of attack
[AD-A263879] p 3241 N93-29919

Aerothermic calculations of flows in interdisc cavities of turbines p 3256 N93-29947

Study of flow structure in rotating cavities: Numerical predictions of laminar and turbulent, steady, and unsteady flows p 3256 N93-29948

Modelling thermal behaviour of turbomachinery discs and casings p 3256 N93-29949

Flow and heat transfer between gas-turbine discs
p 3256 N93-29950

Aero-thermal design of a cooled transonic NGV and comparison with experimental results
p 3257 N93-29957

The aerodynamic effect of coolant ejection in the leading edge region of a film-cooled turbine blade p 3258 N93-29958

Coupling of 3D-Navier-Stokes external flow calculations and internal 3D-heat conduction calculations for cooled turbine blades p 3258 N93-29961

A Navier-Stokes solver with different turbulence models applied to film-cooled turbine cascades p 3258 N93-29962

Navier-Stokes analysis of three-dimensional flow and heat transfer inside turbine blade rows p 3259 N93-29963

On high resolution extensions of Lagrange-Galerkin finite-element schemes [INRIA-RR-1703] p 3550 N93-30117

A computational model that couples aerodynamic and structural dynamic behavior of parachutes during the opening process [AD-A264115] p 3241 N93-30119

Difference methods for hyperbolic problems with emphasis on space-centered approximations [ONERA-NT-1990-4] p 3550 N93-30136

Use of a genetic algorithm to solve two-fluid flow problems on an NCUBE multiprocessor computer [DE93-009630] p 3425 N93-30184

Simulation, characterization and control of forced unsteady viscous flows using Navier-Stokes equations [AD-A264333] p 3425 N93-30369

Topology and grid adaption for high-speed flow computations [NASA-CR-4216] p 3426 N93-30375

Development of a CFD code for casting simulation [NASA-CR-192577] p 3427 N93-30492

Computational fluid dynamics research on dynamically adaptive mesh methods for transonic flows [AD-A264833] p 3428 N93-30630

Turbulent drag reduction: Studies of feedback control and flow over riblets p 3242 N93-30645

An adaptive Lagrangian method for computing 1-D reacting flows and the theory of Riemann invariant manifolds for the compressible Euler equations p 3428 N93-30902

The numerical simulation of circulation controlled airfoil flowfields p 3243 N93-30947

Godunov-type methods for the equations of compressible fluid mechanics [KFK-5058] p 3428 N93-31020

The HSCT mission analysis of waverider designs [NASA-CR-193467] p 3243 N93-31037

COMPUTATIONAL GEOMETRY

Robust and efficient implementation of the Delaunay tree [INRIA-RR-1619] p 3547 N93-28511

The space of spheres, a geometric tool to unify duality results in Voronoi diagrams [INRIA-RR-1620] p 3547 N93-28512

Implementation of parallel algorithms [AD-A263126] p 3529 N93-29496

COMPUTATIONAL GRIDS

Design of an essentially non-oscillatory reconstruction procedure in finite-element type meshes [INRIA-RR-1584] p 3547 N93-28615

A grid refinement study of two-dimensional transient flow over a backward-facing step using a spectral-element method [DE92-018262] p 3417 N93-28639

Pre- and postprocessing techniques for determining goodness of computational meshes [NASA-CR-192553] p 3538 N93-29030

Design optimization of space structures p 3278 N93-29122

The three-dimensional Multi-Block Advanced Grid Generation System (3DMAGGS) [NASA-TM-108985] p 3420 N93-29155

Nonlinear relaxation algorithms for the compressible Navier-Stokes equations in two and three dimensions p 3421 N93-29177

Ablation problems using a finite control volume technique [DE93-009861] p 3549 N93-29187

Development of a new technique for image reconstruction, enhancement, and visualization [AD-A263145] p 3528 N93-29483

On high resolution extensions of Lagrange-Galerkin finite-element schemes [INRIA-RR-1703] p 3550 N93-30117

Simulation, characterization and control of forced unsteady viscous flows using Navier-Stokes equations [AD-A264333] p 3425 N93-30369

Topology and grid adaption for high-speed flow computations [NASA-CR-4216] p 3426 N93-30375

A method for intersection line calculation between parametric surfaces [ETN-93-94178] p 3551 N93-30572

Computational fluid dynamics research on dynamically adaptive mesh methods for transonic flows [AD-A264833] p 3428 N93-30630

An adaptive Lagrangian method for computing 1-D reacting flows and the theory of Riemann invariant manifolds for the compressible Euler equations p 3428 N93-30902

COMPUTER AIDED DESIGN

An investigation of stereolithography as a means of prototyping from a cad database [AD-A263410] p 3613 N93-29210

Iterative encoding methods for computer generated holograms [AD-A263705] p 3431 N93-29297

Advanced Construction Technology Center research [AD-A263654] p 3432 N93-29390

An MCM/chip concurrent engineering validation [AD-A262959] p 3409 N93-29513

Concept design example, Computer Aided Structural Modeling (CASM). Scheme A [AD-A264759] p 3529 N93-29657

Concept design example, Computer Aided Structural Modeling (CASM). Scheme B [AD-A264760] p 3529 N93-29658

Effect of design selection on response surface performance [NASA-CR-4520] p 3249 N93-29885

Robust control of intelligent rotor [AD-A263707] p 3259 N93-29985

Airspace Design Expert System (ADES), a 2D/3D mapping and modelling tool incorporating an expert system for use in instrument approach design p 3247 N93-30357

An application protocol for CAD to CAD transfer of electronic information [AD-A264554] p 3533 N93-30383

A unified approach for composite cost reporting and prediction in the ACT program p 3302 N93-30441

Memory driven feature-based design [AD-A264697] p 3534 N93-30495

Electronics mixed-mode simulation [AD-A264734] p 3534 N93-30577

Multi-parameter optimization tool for low-cost commercial fuselage crown designs p 3305 N93-30858

4D interconnect experimental development [AD-A264298] p 3540 N93-30895

COMPUTER AIDED MANUFACTURING

Soft computing in design and manufacturing of advanced materials [NASA-TM-106032] p 3295 N93-28624

A virtual environment for manufacturing systems [AD-A263128] p 3528 N93-29473

Memory driven feature-based design [AD-A264697] p 3534 N93-30495

COMPUTER AIDED TOMOGRAPHY

Use of local x ray computerized tomography for high-resolution, region-of-interest inspection of large ceramic components for engines [DE93-005564] p 3449 N93-28943

The parallel implementation of a backpropagation neural network and its applicability to SPECT image reconstruction [DE93-010304] p 3567 N93-29416

COMPUTER ASSISTED INSTRUCTION

Development of a concept formulation process aid for analyzing training requirements and developing training devices [AD-A263579] p 3261 N93-29972

Review of the effectiveness of video media in instruction [AD-A264228] p 3392 N93-30362

COMPUTER COMPATIBLE TAPES

ICI optical data storage tape: An archival mass storage media p 3621 N93-30472

Flexible storage medium for write-once optical tape p 3621 N93-30473

Analysis of cache for streaming tape drive p 3435 N93-30477

COMPUTER DESIGN

Spacecraft computer technology at Southwest Research Institute p 3522 N93-28813

SEU tolerant computer based on the R3000 [DE93-009294] p 3520 N93-29058

Efficient wiring of reconfigurable parallel processors [DE93-009847] p 3538 N93-29186

Using today's technology to improve mobile C4I for the operational commander [AD-A263613] p 3245 N93-29285

Canadian Conference on Electrical and Computer Engineering, volumes 1 and 2 [ISBN-0-9694170-1-2] p 3354 N93-30215

High performance computing and communications program p 3627 N93-30715

COMPUTER GRAPHICS

Rendering the out-the-window view for the AFIT virtual cockpit [AD-A262599] p 3260 N93-28467

JPDRAW user's manual, version 3.3 [INRIA-RT-0139] p 3523 N93-28504

Dynamic object oriented interaction and its implementation in the framework in an interface management system [ETN-93-93795] p 3523 N93-28526

Toward reusable graphics components in Ada [AD-A262568] p 3524 N93-28577

Ergonomic development of digital map displays p 3503 N93-28866

Initial graphics exchange specification hybrid microcircuit application protocol [PB93-175404] p 3407 N93-29203

A distributed system for visualizing and analyzing multivariate and multidisciplinary data p 3613 N93-29226

The scientific modeling assistant: An advanced software tool for scientific model building p 3613 N93-29229

DataHub knowledge based assistance for science visualization and analysis using large distributed databases p 3613 N93-29230

A planetary version of PC-McIDAS p 3614 N93-29236

Interactive interface to NCAR graphics p 3614 N93-29237

Remote vehicle survey tool [DE93-010822] p 3460 N93-29255

SPREE Interactive Data Analysis Tool (SIDAT) [AD-A262782] p 3273 N93-29306

Summer research program (1992). High School Apprenticeship Program (HSAP) reports. Volume 16: Arnold Engineering Development Center Civil Engineering Laboratory [AD-A262024] p 3608 N93-29396

Development of a visual system interface to support a domain-oriented application composition system [AD-A262489] p 3528 N93-29418

A virtual environment for manufacturing systems [AD-A263128] p 3528 N93-29473

Development of a new technique for image reconstruction, enhancement, and visualization [AD-A263145] p 3528 N93-29483

EnviroNET: On-line information for LDEF p 3624 N93-29625

Three-dimensional graphical representation of objects according to movement data in realtime [ESA-TT-1258] p 3521 N93-30104

An improved model-creation program for EM interaction analysis p 3367 N93-30294

Review of the effectiveness of video media in instruction [AD-A264228] p 3392 N93-30362

Introduction to the National Information Display Laboratory p 3628 N93-30718

Parcels with TAGS [PB93-181824] p 3535 N93-30824

Defining protein electrostatic recognition processes [AD-A264838] p 3571 N93-30901

A prototype of a faculty and staff executive information system [AD-A264852] p 3623 N93-30907

COMPUTER INFORMATION SECURITY

Minimum security requirements for multi-user operating systems [PB93-185999] p 3522 N93-30832

COMPUTER NETWORKS

Nets of reactive processes [INRIA-RR-1588] p 3537 N93-28505

Study on the concurrent calculation with a multitransputer network [DE93-753191] p 3524 N93-28531

National collaboratories: Applying information technology for scientific research [LC-93-83795] p 3612 N93-29129

RBSE: Product development team research activity deliverables [NASA-CR-193115] p 3527 N93-29212

A distributed system for visualizing and analyzing multivariate and multidisciplinary data p 3613 N93-29226

A comparison of high-speed links, their commercial support and ongoing R/D activities [DE93-008134] p 3382 N93-29245

Dynamic factorization in large-scale optimization [AD-A263993] p 3528 N93-29345

The parallel implementation of a backpropagation neural network and its applicability to SPECT image reconstruction [DE93-010304] p 3567 N93-29416

Data Multiplexing Network (DMN) equipment Operational Test and Evaluation (OT&E) integration test report
[AD-A263172] p 3538 N93-29490
Incorporation of varying types of temporal data in a neural network p 3518 N93-29575
NetStat: A probabilistic network connectivity analysis tool
[AD-A262838] p 3529 N93-29647
Advanced network technology: Background paper
[OTA-BP-TCT-101] p 3539 N93-29650
Communications neural net processors
[AD-A263330] p 3542 N93-29763
Storage systems for national information assets
[DE93-009303] p 3615 N93-29783
Ethernet performance of the Motorola Altair WIN system
[AD-A263877] p 3387 N93-29890
The planning coordinator: A design architecture for autonomous error recovery and on-line planning of intelligent tasks
[NASA-CR-193250] p 3543 N93-30039
Canadian Conference on Electrical and Computer Engineering, volumes 1 and 2
[ISBN-0-9694170-1-2] p 3354 N93-30215
Multiprocessing systems: Reliability modelling and analysis using multimode components and dependent failures
[AD-A264230] p 3540 N93-30364
Evolution of a high-performance storage system based on magnetic tape instrumentation recorders
p 3435 N93-30470
LANL High-Performance Data System (HPDS)
p 3622 N93-30478
Memory driven feature-based design
[AD-A264697] p 3534 N93-30495
High performance computing and communications program p 3627 N93-30715
Parcels with TAGS
[PB93-181824] p 3535 N93-30824
4D interconnect experimental development
[AD-A264298] p 3540 N93-30895

COMPUTER PROGRAMMING

Concurrent clean language manual, version 0.8
[TR-92-18] p 3522 N93-28482
Installation of a new Fortran compiler and effective programming method on the vector supercomputer
[DE93-753322] p 3524 N93-28537
Basic OSF/Motif programming and applications
[DE93-010800] p 3524 N93-28834
An assessment of space shuttle flight software development processes
[NASA-CR-193179] p 3525 N93-28934
Concept document of the repository-based software engineering program: A constructive appraisal
[NASA-CR-193125] p 3526 N93-29027
RBSE: Product development team research activity deliverables
[NASA-CR-193115] p 3527 N93-29212
Development of a visual system interface to support a domain-oriented application composition system
[AD-A262489] p 3528 N93-29418
A C++ interface for programming on the Connection Machine
[INRIA-RR-1698] p 3538 N93-29487
Using synthetic-perturbation techniques for tuning shared memory programs
[PB93-178572] p 3539 N93-29677
Electron transport calculations between 1 MeV and 1 eV
[AD-A263412] p 3568 N93-29787
NESL: A nested data-parallel language (Version 2.6)
[AD-A263548] p 3530 N93-29822
Capability maturity model for software, version 1.1
[AD-A263403] p 3530 N93-29852
ICASE
[NASA-CR-193257] p 3520 N93-29864
Automated modeling of physical systems
[NASA-CR-193256] p 3531 N93-29873
A guide to total software quality control, volume 1
[AD-A263881] p 3531 N93-29920
A guide to total software quality control, volume 2
[AD-A263891] p 3531 N93-29921
Key practices of the capability maturity model, version 1.1
[AD-A263432] p 3610 N93-29970
Estimating Ada system size during development
[AD-A263880] p 3532 N93-30022
Software testing using the IEEE standards
[DE93-009833] p 3532 N93-30050
Test structure to microcircuit correlation
[AD-A264157] p 3412 N93-30152
Canadian Conference on Electrical and Computer Engineering, volumes 1 and 2
[ISBN-0-9694170-1-2] p 3354 N93-30215
Proposal for a numerical array library
[DE93-010678] p 3623 N93-30482
The midway distributed shared memory system
[AD-A264645] p 3534 N93-30523
An approach to software quality prediction from Ada designs
[AD-A264731] p 3534 N93-30547
Nonsmooth optimization algorithms, system theory, and software tools
[AD-A264679] p 3534 N93-30549
Intelligent real-time problem solving
[AD-A264830] p 3535 N93-30614
Graphical programming: On-line robot simulation for telerobotic control
[DE93-009796] p 3447 N93-30654

COMPUTER PROGRAMS

The concurrent clean system user's manual and PABCstat user's manual, version 0.8
[TR-92-19] p 3523 N93-28484
High performance dispersion model PHYSIC
[DE93-753303] p 3467 N93-28536
Research in mathematics and computer science, March 1, 1991 - September 30, 1992
[DE93-011492] p 3509 N93-28573
Toward reusable graphics components in Ada
[AD-A262568] p 3524 N93-28577
BlockSolve v1.1: Scalable library software for the parallel solution of sparse linear systems
[DE93-011391] p 3524 N93-28644
The generic arithmetic of SISYPHE
[INRIA-RT-0136] p 3524 N93-28755
Solar flare MDH
[AD-A262275] p 3652 N93-28756
A modified Anderson Darling goodness-of-fit test for the gamma distribution with unknown scale and location parameters
[AD-A262486] p 3553 N93-28760
Implementation of a multidomain Navier-Stokes code on the Intel iPSC2 hypercube
[FFA-TN-1992-37] p 3418 N93-28994
Additional support for the TDK/MABL computer program
[NASA-CR-193037] p 3526 N93-29028
LDEF materials data bases
[NASA-TM-107757] p 3290 N93-29067
Parallel software tools at Langley Research Center
[NASA-TM-108995] p 3520 N93-29070
Ceramic matrix composites properties/microstresses with complete and partial interphase bond
[NASA-TM-106136] p 3297 N93-29071
The three-dimensional Multi-Block Advanced Grid Generation System (3DMAGGS)
[NASA-TM-108985] p 3420 N93-29155
Distributed Virtual System (DIVIRS) Project
[NASA-CR-193234] p 3526 N93-29169
Graphical interface between the CIRSSE testbed and CimStation software with MCS/CTOS
[NASA-CR-193276] p 3527 N93-29218
A planetary version of PC-McIDAS
p 3614 N93-29236
SWAT system performance predictions
[AD-A262857] p 3579 N93-29470
An analysis of the 70-meter antenna hydrostatic bearing by means of computer simulation p 3386 N93-29601
NetStat: A probabilistic network connectivity analysis tool
[AD-A262838] p 3529 N93-29647
Concept design example, Computer Aided Structural Modeling (CASM). Scheme A
[AD-A264759] p 3529 N93-29657
Concept design example, Computer Aided Structural Modeling (CASM). Scheme B
[AD-A264760] p 3529 N93-29658
Computer systems laboratory
[PB93-181873] p 3521 N93-29662
Using synthetic-perturbation techniques for tuning shared memory programs
[PB93-178572] p 3539 N93-29677
Data probe user's guide
[PB93-178655] p 3530 N93-29678
Key practices of the capability maturity model, version 1.1
[AD-A263432] p 3610 N93-29970
ARSRP signal processing software
[AD-A263543] p 3391 N93-29975
XRONOS: A timing analysis software package. User's guide, version 3.00
[NASA-TM-109222] p 3532 N93-30023
Assessment of Columbus payload operations capabilities by scheduling with the MARS system
[ESA-STR-235] p 3281 N93-30106
Test structure to microcircuit correlation
[AD-A264157] p 3412 N93-30152
On analytical performance modelling of software for distributed systems p 3364 N93-30279
Using Penelope to assess the correctness of NASA Ada software: A demonstration of formal methods as a counterpart to testing
[NASA-CR-4509] p 3533 N93-30380
SESAME equation of state number 8010: Boron loaded silicone potting material
[DE93-012083] p 3300 N93-30395
Oceanographic data processing program
[AD-A264801] p 3544 N93-30591
Acoustic-gravity waves from low-altitude localized disturbances
[AD-A264804] p 3479 N93-30593
Non-perturbative calculation of equilibrium polarization of stored electron beams
[DE93-764500] p 3577 N93-30607
Guide to Federal Water Quality Programs and Information: A Guide with Computer Software Developed by the Interagency Working Group on Water Quality
[PB93-186245] p 3475 N93-30834
Delaminations in composite plates under impact loads
p 3304 N93-30849
Software conception and structure of automated workstation for an experimental data processing
[DE93-609815] p 3623 N93-30994
Development of a PC code package for the analysis of research and power reactors
[DE92-638517] p 3536 N93-31001

COMPUTER STORAGE DEVICES

DOKMA: A document oriented communication model for medical applications as a basis of a role system in the medical field
[ETN-93-93799] p 3492 N93-28469
Structure and switching dynamics in ferroelectric crystal and liquid crystal thin films
[AD-A263664] p 3594 N93-29293
Associative memories for supercomputers
[AD-A263142] p 3520 N93-29482
Storage systems for national information assets
[DE93-009303] p 3615 N93-29783
Mass storage system reference model, Version 4
p 3617 N93-30450
The fundamentals and futures of removable mass storage alternatives p 3619 N93-30460
The NT digital micro tape recorder
p 3435 N93-30461
The state of the state of the art in mass storage technology p 3622 N93-30475
4D interconnect experimental development
[AD-A264298] p 3540 N93-30895

COMPUTER SYSTEMS DESIGN

Design of a hardware discrete event simulation coprocessor
[AD-A262614] p 3537 N93-28478
A multiarchitecture parallel-processing development environment
[NASA-TM-106180] p 3538 N93-28628
Spacecraft computer technology at Southwest Research Institute p 3522 N93-28813
A distributed object-oriented database application design
[AD-A262591] p 3612 N93-28846
LDEF materials data bases
[NASA-TM-107757] p 3290 N93-29067
Using today's technology to improve mobile C4I for the operational commander
[AD-A263613] p 3245 N93-29285
On analytical performance modelling of software for distributed systems p 3364 N93-30279
MLog: A language for prototyping concurrent systems
p 3368 N93-30301
Optimal trajectories for aircraft terrain following and terrain avoidance: A literature review update
[AD-A264075] p 3260 N93-30604
Multiprocessing MCNP on an IBM RS/6000 cluster
[DE93-008712] p 3540 N93-30633
Centralized maintenance evaluation
[AD-A264400] p 3544 N93-30886

COMPUTER SYSTEMS PERFORMANCE

Context switch time scalability: Benchmark results
[PB93-181832] p 3539 N93-29661
Accuracy enhancement in optical computing
[AD-A264872] p 3522 N93-30179

COMPUTER SYSTEMS PROGRAMS

A multiarchitecture parallel-processing development environment
[NASA-TM-106180] p 3538 N93-28628
RBSE: Product development team research activity deliverables
[NASA-CR-193115] p 3527 N93-29212
Applying high-level language paradigms to communications software for distributed systems
[AD-A263001] p 3528 N93-29463

COMPUTER TECHNIQUES

Godunov-type schemes applied to detonation flows
[NASA-CR-191447] p 3509 N93-28841

Computer assisted evaluation for air close combat based on time interval characterization p 3504 N93-28868

Flight evaluation of a computer aided low-altitude helicopter flight guidance system p 3260 N93-28869

Ceramic matrix composites properties/microstresses with complete and partial interphase bond [NASA-TM-106136] p 3297 N93-29071

Communications neural net processors [AD-A263330] p 3542 N93-29763

Capability maturity model for software, version 1.1 [AD-A263403] p 3530 N93-29852

Balanced technology initiative on computational mechanics of materials [AD-A263906] p 3453 N93-29863

ICASE [NASA-CR-193257] p 3520 N93-29864

Computer-controlled alignment for a 2000-line color monitor p 3247 N93-30324

Multiparticle imaging technique for two-phase fluid flows using pulsed laser speckle velocimetry [DE93-011734] p 3427 N93-30489

Computer algebra tools for higher symmetry analysis of nonlinear evolution equations [DE93-606089] p 3535 N93-30787

Computer assisted multiplex sequencing [DE93-007144] p 3536 N93-30934

An automated data collection system for a Charpy impact tester p 3293 N93-30972

COMPUTER VISION

Coarse image motion for saccade control [OUEL-1916/92] p 3523 N93-28485

Recognizing parameterized objects from range data [OUEL-1918/92] p 3523 N93-28486

Polygonal approximation overviews and perspectives [INRIA-RR-1621] p 3547 N93-28513

A modular head/eye platform for real-time reactive vision [OUEL-1941/92] p 3505 N93-28897

An autonomous vision-based mobile robot p 3443 N93-29082

A tutorial on exit pupils and eye rotation with virtual image optical displays [AD-A262399] p 3494 N93-29400

Representation and recognition with invariants and geometric constraint models [AD-A263235] p 3529 N93-29493

Automatic rule generation for high-level vision p 3511 N93-29526

Encoding spatial images: A fuzzy set theory approach p 3511 N93-29527

The fusion of information via fuzzy integration p 3517 N93-29568

Binocular spherical disparity: A study in representation for a forward translating camera [PB93-184422] p 3579 N93-29667

What is the center of the image? [AD-A263550] p 3579 N93-29824

An architecture for an analog VLSI neural network for early computer vision processing p 3359 N93-30244

Modelling and simulation of human retinal vision processing p 3363 N93-30269

Quantization effects in segmentation of range images p 3363 N93-30270

On the implementation of the BIRIS range sensor for applications in robotic control and autonomous navigation p 3366 N93-30286

Applications of digital 3-D imaging p 3366 N93-30287

Recognizing partially overlapping objects p 3366 N93-30289

Generalized octrees for constrained object modeling p 3369 N93-30304

Design and implementation of an interactive isochromatic fringe-analysis system using machine-vision techniques p 3369 N93-30305

Qualitative methods in computer vision [AD-A264335] p 3533 N93-30418

The 1991 neural information processing systems: Natural and synthetic [AD-A264754] p 3623 N93-30559

COMPUTERIZED SIMULATION

Rendering the out-the-window view for the AFIT virtual cockpit [AD-A262599] p 3260 N93-28467

High performance dispersion model PHYSIC [DE93-753303] p 3467 N93-28536

Advanced insulations for refrigerator/freezers: The potential for new shell designs incorporating polymer barrier construction [DE93-010600] p 3353 N93-28570

Probabilistic simulation of multi-scale composite behavior [NASA-TM-106196] p 3451 N93-28633

A grid refinement study of two-dimensional transient flow over a backward-facing step using a spectral-element method [DE92-018262] p 3417 N93-28639

Predicting radiation characteristics from antenna physical dimensions [AD-A262462] p 3379 N93-28654

Analysis for thermo-chemical decomposition of composite structures [NASA-CR-193185] p 3295 N93-28843

Neural network simulations on massively parallel computers: Applications in chemical physics [DE93-006739] p 3538 N93-28894

A proposed approach for developing next-generation computational electromagnetics software [DE93-007326] p 3380 N93-28900

Photodissociation of HBr/LiF(001): A quantum mechanical model [NASA-CR-193119] p 3603 N93-28933

Numerical simulation of quantum many-body systems [DE93-008300] p 3603 N93-28958

Computerized atmospheric trace contaminant control simulation for manned spacecraft [NASA-TM-108409] p 3505 N93-28977

Study on decreasing torque noise resulting from feedback noise for the modified bang-bang controller [AD-A263178] p 3407 N93-29010

Pre- and postprocessing techniques for determining goodness of computational meshes [NASA-CR-192553] p 3538 N93-29030

Large eddy simulations of shockwave passage through turbulence [DE92-019503] p 3419 N93-29050

Ceramic matrix composites properties/microstresses with complete and partial interphase bond [NASA-TM-106136] p 3297 N93-29071

Three-dimensional numerical simulation of gradual opening in a wave rotor passage [NASA-CR-191157] p 3252 N93-29072

Surface diffusion: Atomistics and surface morphology (summary of MRS Symposium B panel discussion) [DE93-009862] p 3594 N93-29188

Graphical interface between the CIRSSE testbed and CimStation software with MCS/CTOS [NASA-CR-193276] p 3527 N93-29218

Building a generalized distributed system model [NASA-CR-193239] p 3527 N93-29219

Computational simulations of a soft x ray projection lithography laser plasma source [DE93-009625] p 3437 N93-29264

On the value of function evaluation location information in Monte Carlo simulation [AD-A263662] p 3554 N93-29292

Fast multipole method in simulations of aqueous systems [AD-A263422] p 3567 N93-29336

MoCog1: A computer simulation of recognition-primed human decision making [NASA-TM-103868] p 3542 N93-29386

Experimental study of location and identification of ferrous spheroids using a smart total field magnetometer [AD-A263661] p 3324 N93-29391

A real-time, hardware-in-the-loop simulation of an unmanned aerial research vehicle [AD-A262477] p 3248 N93-29409

Estimating the parameters of chaotic maps [AD-A262574] p 3556 N93-29423

A virtual environment for manufacturing systems [AD-A263128] p 3528 N93-29473

An analysis of the 70-meter antenna hydrostatic bearing by means of computer simulation p 3386 N93-29601

Special purpose parallel computer architecture for real-time control and simulation in robotic applications [NASA-CASE-NPO-17629-1-CU] p 3521 N93-29608

LDEF microenvironments, observed and predicted p 3283 N93-29623

RTE: A UNIX library with on-line documentation and sample programs for microwave radiative transfer calculations [PB93-180248] p 3386 N93-29680

Electron transport calculations between 1 MeV and 1 eV [AD-A263412] p 3568 N93-29787

Two simulation studies of precision runway monitoring of independent approaches to closely spaced parallel runways [AD-A263433] p 3261 N93-29815

A search for radiative neutrino decay from supernovae [NASA-CR-193118] p 3653 N93-30052

Molecular dynamics of detonation in crystals with defects p 3350 N93-30097

Shock waves and polymorphic phase transitions in energetic materials p 3351 N93-30100

Three-dimensional graphical representation of objects according to movement data in realtime [ESA-TT-1258] p 3521 N93-30104

Simulation of landscape disturbances and the effect of climatic change [DE93-011615] p 3472 N93-30131

Annual report on monitoring of the unsaturated zone and recharge areas at INEL to the state of Idaho INLEL oversight committee [DE93-012947] p 3473 N93-30187

Analysis and simulation of a two degrees-of-freedom one-link flexible forearm p 3361 N93-30261

Modelling and simulation of human retinal vision processing p 3363 N93-30269

Coupling gain computation between antennas on circular cylinders at SHF/EHF frequencies p 3369 N93-30309

National Airspace System Performance Analysis Capability (NASPAC) simulation model p 3247 N93-30351

Procedural development prototype in Automated En Route Air Traffic Control p 3247 N93-30352

Parallel processing and learning: Variability and chaos in self-organization of activity in groups of neurons [AD-A264224] p 3539 N93-30361

Computational analysis of slip in PETN [DE92-040222] p 3598 N93-30445

The calculation of electrostatic interactions and their role in determining the energies and geometries of molecular HE crystals [DE92-040374] p 3570 N93-30448

A computer simulation of the production of an artificially ionized layer using the Arecibo facility [DE93-010817] p 3478 N93-30487

Development of a CFD code for casting simulation [NASA-CR-192577] p 3427 N93-30492

Analysis and computation for vortex dynamics and rarefied gases [AD-A264705] p 3427 N93-30499

Simulation and calculation of diffusive aerosol deposition [DE93-007518] p 3474 N93-30506

Adaptive airborne radar simulation with equalization filter taps [AD-A264722] p 3393 N93-30514

The structure and dynamics of the vorticity and passive scalar fields at small scales in homogeneous isotropic turbulence p 3427 N93-30625

Radiation effects in FCC metals and intermetallic compounds: A molecular dynamics computer simulation study [DE93-009546] p 3600 N93-30668

Validation and upgrading of physically based mathematical models p 3237 N93-30688

On the impossibility of creating the quantum correlations with computers [DE93-606039] p 3606 N93-30806

Vehicle dynamic stability and rollover [PB93-185437] p 3447 N93-30828

Environmental characteristics of EPA, NRC, and DOE sites contaminated with radioactive substances [PB93-185551] p 3475 N93-30829

Probabilistic composite analysis p 3307 N93-30868

Adaptive motion control of mobile robots p 3545 N93-30903

COMPUTERS

Computer systems laboratory [PB93-181873] p 3521 N93-29662

High performance computing: Advanced Research Projects Agency should do more to foster program goals. Report to the Chairman, Committee on Armed Services, House of Representatives [GAO/IMTEC-93-24] p 3533 N93-30202

CONCENTRATION (COMPOSITION)

In-situ temperature and concentration measurements of organosilicon decomposition in a chemical vapor deposition reactor [ONERA-P-1990-3] p 3313 N93-30109

CONCENTRATORS

Modification of flux profiles using a faceted concentrator [DE93-000087] p 3464 N93-29925

CONCRETE STRUCTURES

Sensor systems for monitoring Maglev guideway structures [PB93-154821] p 3444 N93-29205

CONCURRENT PROCESSING

Concurrent clean language manual, version 0.8 [TR-92-18] p 3522 N93-28482

The concurrent clean system user's manual and PABCstat user's manual, version 0.8 [TR-92-19] p 3523 N93-28484

Study on the concurrent calculation with a multitransputer network [DE93-753191] p 3524 N93-28531

Context switch time scalability: Benchmark results [PB93-181832] p 3539 N93-29661

MLog: A language for prototyping concurrent systems p 3368 N93-30301

CONDENSATION NUCLEI
Clouds and radiation: A primer
[AD-A263136] p 3482 N93-29479
Quantifying and minimizing uncertainty of climate forcing by anthropogenic aerosols
[NASA-TM-108259] p 3472 N93-30043
CONDENSED MATTER PHYSICS
The investigation of nonlinear effects on quasiparticle transport in condensed matter systems
[DE93-009582] p 3565 N93-28914
The 26th International Quantum Chemistry Symposium on Atomic, Molecular, and Condensed Matter Theory and Computational Methods
[AD-A264206] p 3315 N93-30534
CONDENSERS (LIQUEFIERS)
Pulse mitigation and heat transfer enhancement techniques. Volume 4: Transient behavior of heat pipe with thermal energy storage under pulse heat loads
[AD-A263497] p 3423 N93-29339
CONDENSING
Materials studies for preventing corrosion in condensing environments
[PB93-185478] p 3327 N93-30815
CONDUCTING POLYMERS
Synthesis of conducting polymer composite fibers in electrochemical flow cells
[AD-A262233] p 3294 N93-28492
Polymers with electrical and nonlinear optical properties
[AD-D015691] p 3333 N93-29457
Method of continuously determining crack length
[NASA-CASE-LAR-14480-1-CU] p 3452 N93-29612
Synthesis and properties of a cation-conducting, high temperature polymer electrolyte
[AD-A263557] p 3334 N93-29825
Triplet states and optical absorptions in finite polyenes and conjugated polymers
[AD-A264552] p 3337 N93-30381
Optically switchable conductive polymers
[AD-A264751] p 3337 N93-30557
Ultrafast, passive, broad-band, optical shutter based on novel semiconductor/conducting polymer interfaces
[AD-A264098] p 3601 N93-30878
CONDUCTION BANDS
A tight binding model for the electronic structure of FCC and SC C60
[DE93-606214] p 3601 N93-30794
CONDUCTION ELECTRONS
A possibility to investigate the superconducting gap with the help of neutrons
[DE93-606392] p 3601 N93-30799
CONDUCTIVE HEAT TRANSFER
Derivation of conductive heat transfer in mountains from AVHRR data p 3458 N93-28927
Pulse mitigation and heat transfer enhancement techniques. Volume 4: Transient behavior of heat pipe with thermal energy storage under pulse heat loads
[AD-A263497] p 3423 N93-29339
Modelling thermal behaviour of turbomachinery discs and casings p 3256 N93-29949
On the ideality of using a step-function current in a metallic foil to simulate a step-function heat-flux source
[AD-A264627] p 3413 N93-30539
CONDUCTORS
New III-V cell design approaches for very high efficiency
[DE93-000097] p 3464 N93-28971
Adhesion of thick film Au to alumina ceramics
[DE93-009802] p 3339 N93-30656
Some problems of relativistic electrodynamics
[DE92-644738] p 3400 N93-30923
CONFERENCES
Proceedings of the Near-Earth-Object Interception Workshop
[NASA-TM-108236] p 3556 N93-28572
International Conference on Martensitic Transformations (ICOMAT 92)
[AD-A262739] p 3321 N93-28591
NASA/DOD Flight Experiments Technical Interchange Meeting Proceedings
[NASA-TM-108721] p 3262 N93-28699
Workshop on Advanced Technologies for Planetary Instruments, part 1
[NASA-CR-193015] p 3639 N93-28764
Proceedings of a Workshop on Molecular Nuclear Medicine
[DE93-010828] p 3493 N93-28835
Combat Automation for Airborne Weapon Systems: Man/Machine Interface Trends and Technologies
[AGARD-CP-520] p 3501 N93-28850
Proceedings of the Second Atmospheric Radiation Measurement (ARM) Science Team Meeting
[DE93-005886] p 3476 N93-28889
Introductions to the Proceedings of the Fourteenth Symposium on Biotechnology for Fuels and Chemicals
[DE93-006235] p 3490 N93-28890
FNAS CRRES program completion
[NASA-CR-192468] p 3476 N93-29032
Contributions to the American Meteorological Society's 26th International Conference on Radar Meteorology
[AD-A263385] p 3481 N93-29257
Low temperature (LT) GaAs and related materials
[AD-A263607] p 3298 N93-29282
FAA international conference on airplane ground deicing
[AD-A263617] p 3244 N93-29286
Proceedings of the 25th European Conference on the Application of Polar Dielectrics to celebrate the 25th anniversary of the Dielectric Society, incorporating the 1st International Workshop on Integrated Ferroelectrics
[AD-A263427] p 3332 N93-29337
LDEF: 69 Months in Space. Second Post-Retrieval Symposium, part 2
[NASA-CP-3194-PT-2] p 3654 N93-29354
Symposium on high temperature superconductors: Materials research for emerging technologies
[AD-A263120] p 3409 N93-29495
North American Fuzzy Logic Processing Society (NAFIPS 1992), volume 1
[NASA-CP-10112-VOL-1] p 3509 N93-29516
North American Fuzzy Logic Processing Society (NAFIPS 1992), volume 2
[NASA-CP-10112-VOL-2] p 3515 N93-29556
LDEF: 69 Months in Space. Part 1: Second Post-Retrieval Symposium
[NASA-CP-3194-PT-1] p 3660 N93-29621
The 17th Annual Climate Diagnostics Workshop
[PB93-183895] p 3483 N93-29664
The 9th FLICC Forum on Federal Information Policies
[PB93-184687] p 3624 N93-29668
LDEF: 69 Months in Space. Part 4: Second Post-Retrieval Symposium
[NASA-CP-3194-PT-4] p 3665 N93-29682
Proceedings of the Seventh Annual Summer Conference. NASA/USRA: University Advanced Design Program
[NASA-CR-192962] p 3227 N93-29712
T(lc2)acS(lc3)ats for Surveillance Verification and C3I
[AGARD-CP-522] p 3387 N93-29892
Heat Transfer and Cooling in Gas Turbines
[AGARD-CP-527] p 3252 N93-29926
Proceedings of Symposium F on New Aspects on the Growth, Characterization and Applications of CdTe and related Cd rich alloys 5, 1992
[AD-A263541] p 3597 N93-29974
Solar world congress: Proceedings of the biennial congress of the international solar energy society, volume 1, part 2
[PB93-174779] p 3465 N93-30001
ONR/LANL Workshop on the Fundamental Physics and Chemistry of Combustion, Initiation, and Detonation of Energetic Materials
[CPIA-PUBL-589] p 3343 N93-30061
The IUTAM Symposium on Breaking Waves
[AD-A264196] p 3489 N93-30143
The 1992 World Administrative Radio Conference: Technology and Policy Implications
[OTA-TCT-549] p 3392 N93-30150
Canadian Conference on Electrical and Computer Engineering, volumes 1 and 2
[ISBN-0-9694170-1-2] p 3354 N93-30215
The First NASA Advanced Composites Technology Conference, part 1
[NASA-CP-3104-PT-1] p 3300 N93-30428
Topical meeting of broadband analog and digital optoelectronics
[AD-A264643] p 3581 N93-30522
The 26th International Quantum Chemistry Symposium on Atomic, Molecular, and Condensed Matter Theory and Computational Methods
[AD-A264206] p 3315 N93-30534
Cloud Impacts on DOD Operations and Systems Conference (CIDOS-91)
[AD-A264463] p 3484 N93-30535
The 1991 neural information processing systems: Natural and synthetic
[AD-A264754] p 3623 N93-30559
Technology Transfer and the Civil Space Program. Volume 2: Workshop proceedings
[NASA-TM-108250] p 3625 N93-30692
ELF/VLF/LF Radio Propagation and Systems Aspects
[AGARD-CP-529] p 3394 N93-30727
Introduction p 3395 N93-30728
Plasma Physics Network Newsletter, no. 5
[DE93-606216] p 3591 N93-30795
Gordon Research Conferences, 1991
[AD-A264275] p 3317 N93-30816
Proceedings of the meeting of the Intergovernmental US-Russian Business Development Committee's Standards Working Group
[PB93-179968] p 3610 N93-30822
First NASA Advanced Composites Technology Conference, part 2
[NASA-CP-3104-PT-2] p 3303 N93-30841
Solar World Congress: Proceedings of the Biennial Congress of the International Solar Energy Society, volume 2, part 2
[PB93-174795] p 3466 N93-30935
Advanced electromagnetic methods for aerospace vehicles
[NASA-CR-193468] p 3400 N93-31036
CONFIGURATION INTERACTION
Theoretical hyperfine structure constants for transition metal atoms and ions
[DE93-012325] p 3566 N93-29183
Applications of density functional theory to calculation of reaction energetics p 3351 N93-30098
Rate constant determinations of reactions H + HNO from ab initio reaction path calculations
p 3319 N93-30099
CONFINEMENT
A numerical study of confined turbulent jets
[NASA-TM-106197] p 3420 N93-29161
Optimization for steady-state and hybrid operations of ITER by using scaling models of divertor heat load
[DE93-764151] p 3590 N93-30649
CONFORMAL MAPPING
Understanding conformal field theory through parafermions and Chern Simons theory
[DE93-010452] p 3604 N93-29806
Positive energy representations of the conformal quantum algebra
[DE93-606064] p 3551 N93-30809
Superconformal structures and holomorphic 1/2-superdifferentials on N = 1 super Riemann surfaces
[DE93-604133] p 3558 N93-30989
CONGRESSIONAL REPORTS
Tropical forests and biological diversity: USAID report to Congress 1990-1991
[PB93-180453] p 3471 N93-29681
High performance computing: Advanced Research Projects Agency should do more to foster program goals. Report to the Chairman, Committee on Armed Services, House of Representatives
[GAO/IMTEC-93-24] p 3533 N93-30202
Promoting high-performance computing and communications
[ISBN-0-16-041828-3] p 3522 N93-30570
CONGRUENCES
Algorithms for point set congruence
[AD-A264016] p 3532 N93-29980
CONIFERS
Generation of carbon monoxide in compartment fires
[PB93-146702] p 3244 N93-29211
Modeling the bidirectional reflectance and spectra
[AD-A263570] p 3462 N93-29830
CONJUGATE GRADIENT METHOD
A conjugate gradients/trust regions algorithms for training multilayer perceptrons for nonlinear mapping
p 3519 N93-29581
CONJUGATION
Conjugated substituted ionic polyacetylenes
[AD-A264702] p 3337 N93-30497
CONNECTION MACHINE
Neural network simulations on massively parallel computers: Applications in chemical physics
[DE93-006739] p 3538 N93-28894
A C++ interface for programming on the Connection Machine
[INRIA-RR-1698] p 3538 N93-29487
Multiresolution analysis of SAR data
[AD-A264727] p 3393 N93-30576
CONNECTIVE TISSUE
Wound healing and connective tissue metabolism: The role of hyperbaric oxygen therapy
[AD-A262483] p 3493 N93-28759
CONNECTORS
Leaky coaxial cable signal transmission for remote facilities
[DE93-007916] p 3383 N93-29348
Quick connect fastener
[NASA-CASE-MFS-28833-1] p 3445 N93-29846
Optimal geometric design of robots for environments with obstacles p 3445 N93-30149
CONSERVATION
Building alliances to restore coastal environments: A coastal America progress report
[PB93-169464] p 3470 N93-29674
Tropical forests and biological diversity: USAID report to Congress 1990-1991
[PB93-180453] p 3471 N93-29681
CONSERVATION LAWS
A new flux conserving Newton's method scheme for the two-dimensional, steady Navier-Stokes equations
[NASA-TM-106160] p 3416 N93-28626
Nonlinear stability of viscous shock waves
[TRITA-NA-9205] p 3419 N93-29025

Integrals of motion on the group of invariance of an interval in three-dimensional spaces [DE93-606090] p 3606 N93-30797

CONSOLIDATION

Explosive consolidation of combustion synthesized TiC and TiB2: Precursor morphology effects [AD-A263186] p 3341 N93-28515

Consolidation of graphite thermoplastic textile preforms for primary aircraft structure p 3302 N93-30439

CONSTANTS

Rate constant determinations of reactions H + HNO from ab initio reaction path calculations p 3319 N93-30099

CONSTITUTIVE EQUATIONS

Constitutive laws for deformation and dynamic recrystallization in cubic metals [DE93-010740] p 3326 N93-30486

CONSTRUCTION

Measurement of a Michelson interferometer mirror velocity with a time interval analyzer [AD-A263009] p 3430 N93-28659

Lightweight flexible composite tent materials [AD-A263021] p 3295 N93-28660

Space construction activities [NASA-CR-192690] p 3274 N93-29108

Interaction dynamics of on-orbit construction p 3274 N93-29109

Hybrid CMS methods with model reduction for assembly of structures p 3274 N93-29110

Structural load control during construction p 3275 N93-29113

Systems engineering studies of on-orbit assembly operation p 3275 N93-29114

Lunar regolith densification p 3276 N93-29115

Lunar rovers and local positioning system p 3277 N93-29119

Systems engineering studies of lunar base construction p 3277 N93-29121

Advanced Construction Technology Center research [AD-A263654] p 3432 N93-29390

Construction and testing of simple airfoils to demonstrate structural design, materials choice, and composite concepts p 3243 N93-30979

CONSTRUCTION MATERIALS

Indigenous lunar construction materials p 3277 N93-29120

Systems engineering studies of lunar base construction p 3277 N93-29121

CONSUMERS

An experimental methodology for a fuzzy set preference model p 3514 N93-29547

A fuzzy set preference model for market share analysis p 3514 N93-29548

Evaluation of environmental marketing terms in the United States [PB93-175784] p 3474 N93-30660

CONTAINERS

Solving a product safety problem using a recycled high density polyethylene container p 3292 N93-30964

CONTAINMENT

Advanced collapsible tank for liquid containment [NASA-CR-188247] p 3353 N93-28698

Containment of explosions in spherical vessels [DE93-005445] p 3446 N93-30211

CONTAMINANTS

State of the art: Ecological biomarkers [DE93-006621] p 3469 N93-28992

Study to determine the nature and extent of ozone and ozone precursor transport in selected areas of California [PB93-184828] p 3470 N93-29669

Annual report on monitoring of the unsaturated zone and recharge areas at INEL to the state of Idaho INLEL oversight committee [DE93-012947] p 3473 N93-30187

An evaluation of factors affecting the solidification/stabilization of heavy metal sludge [AD-A264128] p 3473 N93-30197

Development of novel models for describing multiple toxicity effects [AD-A264439] p 3496 N93-30422

Guide to Federal Water Quality Programs and Information: A Guide with Computer Software Developed by the Interagency Working Group on Water Quality [PB93-186245] p 3475 N93-30834

CONTAMINATION

Environmental monitors in the Midcourse Space Experiments (MSX) p 3286 N93-28826

Post-flight analyses of the crystals from the M0003-14 quartz crystal microbalance experiment p 3602 N93-29684

Annual report on monitoring of the unsaturated zone and recharge areas at INEL to the state of Idaho INLEL oversight committee [DE93-012947] p 3473 N93-30187

Contamination of soil, soil gas, and ground water by hydrocarbon compounds near Greear, Morgan County, Kentucky [PB93-182244] p 3474 N93-30825

Environmental characteristics of EPA, NRC, and DOE sites contaminated with radioactive substances [PB93-185551] p 3475 N93-30829

CONTINENTAL SHELVES

A water mass analysis of the 1991-1992 El Nino signal in the Farallon Islands region [AD-A263490] p 3488 N93-29819

CONTINUITY (MATHEMATICS)

Comparison of analytical transport and stochastic solutions for neutron slowing down in an infinite medium [DE93-010799] p 3565 N93-28833

CONTINUOUS RADIATION

Development of a 9.3 micrometer CW LIDAR for the study of atmospheric aerosol [NASA-CR-193227] p 3381 N93-29105

The 2-6 semiconductor superlattices [AD-A264343] p 3597 N93-30164

CONTINUOUS WAVE LASERS

Tunable CW diode-pumped Tm,Ho:YLiF4 laser operating at or near room temperature [NASA-CASE-NPO-18611-1-CU] p 3440 N93-30415

Efficient laser action from two CW laser pumped pyrromethene-BF2 complexes [AD-A264887] p 3441 N93-30910

CONTINUOUS WAVE RADAR

Development of an airborne MMW FM-CW radar for mapping river ice [AD-A262655] p 3379 N93-28588

CONTINUUM MECHANICS

A continuum code investigation of stress integration using exact and approximate material rotation [DE93-001892] p 3454 N93-31013

CONTINUUM MODELING

A one-dimensional continuum model for shape-memory alloys [AD-A262505] p 3321 N93-28656

Progressive failure methodologies for predicting residual strength and life of laminated composites p 3307 N93-30866

CONTINUUMS

Coherent and semi-coherent neutron transfer reactions [DE93-008336] p 3565 N93-28959

Chemical dynamics simulations as a probe to the initiation and propagation of condensed phase detonations p 3318 N93-30071

CONTOURS

Methods for characterizing the human head for the design of helmets [AD-A263875] p 3507 N93-29889

Detecting residue on a printed circuit board: An application of the Boundary Contour/Feature Contour System [DE93-006283] p 3412 N93-30370

CONTRACT MANAGEMENT

The program manager's notebook [AD-A263074] p 3609 N93-29142

The identification of early warning signals prior to contractor default [AD-A262828] p 3609 N93-29433

CONTRACTION

Nth roots of normal contractions [DE92-644725] p 3557 N93-30985

CONTRACTORS

The identification of early warning signals prior to contractor default [AD-A262828] p 3609 N93-29433

Technology transfer and Rockwell International p 3627 N93-30712

CONTRACTS

How to compete for NASA contracts [NASA-TM-109238] p 3610 N93-30644

CONTROL EQUIPMENT

Sources sought for innovative scientific instrumentation for scientific lunar rovers p 3434 N93-28804

Strategic avionics technology definition studies. Subtask 3-1A: Electrical Actuation (ELA) systems [NASA-CR-193237] p 3271 N93-29215

Articulated fin/wing control system [AD-D015712] p 3259 N93-29278

Intelligent fuzzy controller for event-driven real time systems p 3515 N93-29551

Siphon breaker design requirements [DE93-011799] p 3425 N93-30132

CONTROL SIMULATION

Virtual interface applications for airborne weapons systems p 3502 N93-28858

Computerized atmospheric trace contaminant control simulation for manned spacecraft [NASA-TM-108409] p 3505 N93-28977

Building a generalized distributed system model [NASA-CR-193239] p 3527 N93-29219

A numerical simulator for testing sliding mode controls in stochastic systems p 3361 N93-30260

CONTROL STABILITY

Robust feedforward/feedback control synthesis for uncertain dynamical systems p 3542 N93-29079

Hybrid CMS methods with model reduction for assembly of structures p 3274 N93-29110

Controls for space structures p 3275 N93-29112

Some results on feedback stabilization of a one-link flexible arm [INRIA-RR-1682] p 3543 N93-30116

Robust control via H-infinity optimization p 3354 N93-30216

CONTROL SURFACES

Articulated fin/wing control system [AD-D015712] p 3259 N93-29278

CONTROL SYSTEMS DESIGN

NASA instep/MDMSC jitter suppression experiment (JITTER) p 3263 N93-28702

Control-structures interaction test of the LACE satellite p 3263 N93-28706

CSI-Star: A low-cost CSI orbital testbed p 3263 N93-28707

Multivariable control of the Space Shuttle Remote Manipulator System using linearization by state feedback [NASA-CR-188248] p 3443 N93-29080

Three-parameter tunable Tilt-Integral-Derivative (TID) controller [NASA-CASE-NPO-18492-1-CU] p 3542 N93-29176

Optically controlled active impedance element particularly suited for a microwave oscillator [AD-D015723] p 3408 N93-29281

A self-learning rule base for command following in dynamical systems p 3512 N93-29531

Evaluation of fuzzy inference systems using fuzzy least squares p 3513 N93-29539

The cognitive bases for the design of a new class of fuzzy logic controllers: The clearness transformation fuzzy logic controller p 3515 N93-29554

A fuzzy control design case: The fuzzy PLL p 3515 N93-29555

Genetic algorithms in adaptive fuzzy control p 3518 N93-29572

Automation of closed environments in space for human comfort and safety p 3230 N93-29734

Attitude- and Orbit Control Subsystem concepts for TACSATS p 3284 N93-29906

Control of nonlinear systems with applications to constrained robots and spacecraft attitude stabilization p 3279 N93-29989

Input relegation control for gross motion of a kinematically redundant manipulator [DE93-005301] p 3446 N93-30210

Control system design and multiparameter variations p 3355 N93-30217

Optimal filtering and LQR theory with constraints on system and control matrices p 3357 N93-30234

An adaptive controller for a class of MIMO non-minimum phase systems with disturbance rejection design p 3359 N93-30248

Noise transmission properties and control strategies for composite structures p 3301 N93-30436

Flight control system design factors for applying automated testing techniques [NASA-TM-4242] p 3260 N93-30764

Control of nonlinear systems with applications to constrained robots and spacecraft attitude stabilization p 3544 N93-30893

CONTROL THEORY

Resource limited reasoning: A study of literature in the context of model-based diagnosis [MEMO-INF-92-38] p 3540 N93-28480

Artificial intelligence methodologies in flight related differential game, control and optimization problems [AD-A262405] p 3541 N93-28498

The dynamics and control of space tethers p 3274 N93-28629

Stabilization using low-gain PI control: SISO case [OUEL-1947/92] p 3541 N93-28898

JPRS report: Science and technology. Central Eurasia: Physics and mathematics [JPRS-UPM-93-002] p 3560 N93-29022

Mathematical modeling and control law development for the atmospheric monitoring and control system of the Controlled Environment Research Chamber (CERC) at NASA Ames Research Center [AD-A261978] p 3261 N93-29436

Design issues of a reinforcement-based self-learning fuzzy controller for petrochemical process control p 3512 N93-29533

Fuzzy coordinator in control problems p 3515 N93-29552

Tuning a fuzzy controller using quadratic response surfaces p 3515 N93-29553

The cognitive bases for the design of a new class of fuzzy logic controllers: The clearness transformation fuzzy logic controller p 3515 N93-29554
A fuzzy control design case: The fuzzy PLL p 3515 N93-29555
Some problems with the design of self-learning management systems p 3516 N93-29559
A neural fuzzy controller learning by fuzzy error propagation p 3516 N93-29560
Center for the Study of Intelligent Control Systems (Fellowships) [AD-A263604] p 3543 N93-29917
Efficient Reorientation Maneuvers for Spacecraft with Multiple Articulated Payloads [NASA-CR-193142] p 3279 N93-29988
Optimal filtering and LQR theory with constraints on system and control matrices p 3357 N93-30234
Turbulent drag reduction: Studies of feedback control and flow over riblets p 3242 N93-30645

CONTROL VALVES
Magnetically operated check valve [NASA-CASE-MSC-22046-1] p 3442 N93-28501
Inservice diagnostic methods for solenoid-operated valves [DE93-007823] p 3443 N93-28968

CONTROLLABILITY
Structural load control during construction p 3275 N93-29113

CONTROLLED ATMOSPHERES
Mathematical modeling and control law development for the atmospheric monitoring and control system of the Controlled Environment Research Chamber (CERC) at NASA Ames Research Center [AD-A261978] p 3261 N93-29436

CONTROLLED FUSION
JT-60 Upgrade vertical stability experiments and analysis [DE93-753131] p 3583 N93-28530
Measurements of breakaway reaction between beryllium and water vapor for ITER blanket design [DE93-753270] p 3584 N93-28535
Effects of neutral gas collisions on the power transmission factor at the divertor sheath [DE93-009320] p 3588 N93-29334
Optimization for steady-state and hybrid operations of ITER by using scaling models of divertor heat load [DE93-764151] p 3590 N93-30649
Plasma Physics Network Newsletter, no. 5 [DE93-606216] p 3591 N93-30795

CONTROLLERS
Clementine sensor processing system p 3285 N93-28778
A modular head/eye platform for real-time reactive vision [OUEL-1941/92] p 3505 N93-28897
Study on decreasing torque noise resulting from feedback noise for the modified bang-bang controller [AD-A263178] p 3407 N93-29010
Three-parameter tunable Tilt-Integral-Derivative (TID) controller [NASA-CASE-NPO-18492-1-CU] p 3542 N93-29176
A composite self tuning strategy for fuzzy control of dynamic systems p 3511 N93-29530
Design issues of a reinforcement-based self-learning fuzzy controller for petrochemical process control p 3512 N93-29533
WARP: Weight Associative Rule Processor. A dedicated VLSI fuzzy logic megacell p 3513 N93-29538
Intelligent fuzzy controller for event-driven real time systems p 3515 N93-29551
Fuzzy coordinator in control problems p 3515 N93-29552
Tuning a fuzzy controller using quadratic response surfaces p 3515 N93-29553
The cognitive bases for the design of a new class of fuzzy logic controllers: The clearness transformation fuzzy logic controller p 3515 N93-29554
A fuzzy control design case: The fuzzy PLL p 3515 N93-29555
A neural fuzzy controller learning by fuzzy error propagation p 3516 N93-29560
Comparison between the performance of two classes of fuzzy controllers p 3517 N93-29566
Genetic algorithms in adaptive fuzzy control p 3518 N93-29572
A genetic algorithms approach for altering the membership functions in fuzzy logic controllers p 3518 N93-29573
Hierarchical model of matching p 3519 N93-29580
Acoustic charge transport technology investigation for advanced development transponder p 3386 N93-29602
Robust control of intelligent rotor [AD-A263707] p 3259 N93-29985
Dynamics and robust control of sampled data systems for large space structures [AD-A264192] p 3281 N93-30142
An adaptive controller for a class of MIMO non-minimum phase systems with disturbance rejection design p 3359 N93-30248
Robust boundary control of flexible structures governed by hybrid dynamics p 3285 N93-30249
A numerical simulator for testing sliding mode controls in stochastic systems p 3361 N93-30260
Task allocation and real-time considerations for the Robot Controller Test Station (RCTS) p 3364 N93-30278
Analysis of cache for streaming tape drive p 3435 N93-30477

CONVECTION
Prognostic cloud water in the Los Alamos general circulation model [DE93-007381] p 3482 N93-29347
Convective and stratiform rain: Multichannel microwave sensing over oceans [NASA-TM-104586] p 3482 N93-29448
An upwind method for the solution of the 3D Euler and Navier-Stokes equations on adaptively refined meshes [AD-A262863] p 3423 N93-29472
Vertical slot convection: A linear study [DE93-007643] p 3423 N93-29804
Observing and modelling F-region ionospheric dynamics using the OII 7320A emission p 3479 N93-30564

CONVECTION CURRENTS
The Mechanisms of Solar Variability (MSV) program [AD-A262525] p 3652 N93-28585

CONVECTIVE FLOW
A numerical study of confined turbulent jets [NASA-TM-106197] p 3420 N93-29161

CONVECTIVE HEAT TRANSFER
Spherically symmetric model atmospheres for late-type giant stars [ISBN-0-315-72632-6] p 3633 N93-28673
Thermal certification tests of Orbiter Thermal Protection System tiles coated with KSC coating slurries [NASA-TM-104766] p 3278 N93-29221
Thermal effects of a coolant film along the suction side of a high pressure turbine nozzle guide vane p 3253 N93-29930
Modelling thermal behaviour of turbomachinery discs and casings p 3256 N93-29949
Analytical and experimental study of laminar free convective heat transfer from isothermal convex bodies of arbitrary shape [ISBN-0-315-72512-5] p 3426 N93-30379
Performance of thermal adhesives in forced convection p 3293 N93-30974
High thermal conductivity of diamond p 3294 N93-30977

CONVERGENCE
Nonlinear relaxation algorithms for the compressible Navier-Stokes equations in two and three dimensions p 3421 N93-29177
A conjugate gradients/trust regions algorithms for training multilayer perceptrons for nonlinear mapping p 3519 N93-29581
Enhanced convergence adaptive detection [AD-A264100] p 3399 N93-30879

CONVERGENT NOZZLES
Performance characteristics of two multiaxis thrust-vectoring nozzles at Mach numbers up to 1.28 [NASA-TP-3313] p 3239 N93-29160

CONVERGENT-DIVERGENT NOZZLES
Cooling predictions in turbofan engine components p 3259 N93-29964

CONVOLUTION INTEGRALS
The general theory of convolutional codes p 3385 N93-29595

COOLANTS
Thermal effects of a coolant film along the suction side of a high pressure turbine nozzle guide vane p 3253 N93-29930

COOLERS
Spaceborne passive radiative cooler p 3378 N93-28802
Study of parameters affecting the performance of solar desiccant cooling systems [DE93-000088] p 3465 N93-30206

COOLING
The microchannel heatsink with liquid nitrogen cooling [DE93-009258] p 3422 N93-29300
Pulse mitigation and heat transfer enhancement techniques. Volume 1: Spray cooling [AD-A263495] p 3423 N93-29352
Semiconductor cooling apparatus [NASA-CASE-LEW-14162-3] p 3299 N93-29614
Heat Transfer and Cooling in Gas Turbines [AGARD-CP-527] p 3252 N93-29926
Turbulent flow and heat transfer in idealized blade cooling passages p 3254 N93-29938
Cooling geometry optimization using liquid crystal technique p 3254 N93-29939
Fundamental studies of impingement cooling thermal boundary conditions p 3254 N93-29940
Prediction of jet impingement cooling scheme characteristics (airfoil leading edge application) p 3255 N93-29941
An L2F-measurement device with image rotator prism for flow velocity analysis in rotating coolant channels p 3255 N93-29942
Local heat transfer measurement with liquid crystals on rotating surfaces including non-axisymmetric cases p 3255 N93-29943
Study of parameters affecting the performance of solar desiccant cooling systems [DE93-000088] p 3465 N93-30206
Complex-compound heat pump: Topical report on phase 1 results [PB93-185460] p 3466 N93-30814
Performance of thermal adhesives in forced convection p 3293 N93-30974

COOLING SYSTEMS
Inservice diagnostic methods for solenoid-operated valves [DE93-007823] p 3443 N93-28968
Reliability assessment of thrust chamber cooling concepts using probabilistic analysis techniques [NASA-CR-190785] p 3288 N93-29068
Evaluation of personal cooling systems in conjunction with explosive ordnance disposal suits [AD-A262862] p 3506 N93-29471
The effect of orthogonal-mode rotation on forced convection in a circular-sectioned tube fitted with full circumferential transverse ribs p 3254 N93-29937
The effect of main stream flow angle on flame tube film cooling p 3257 N93-29953
Impingement/effusion cooling p 3257 N93-29954
Study of parameters affecting the performance of solar desiccant cooling systems [DE93-000088] p 3465 N93-30206

COORDINATION
Fuzzy coordinator in control problems p 3515 N93-29552

COORDINATION POLYMERS
Organometallic compounds and polymers with second and third order nonlinear optical properties [AD-A264774] p 3338 N93-30610

COPOLYMERS
Thermodynamics of swelling and collapse of polyelectrolytic gels [ETN-93-93485] p 3331 N93-29064
Multichip module high speed testing [AD-A262989] p 3408 N93-29427

COPPER
Adsorption of sulfate on metal electrodes [AD-A263192] p 3309 N93-28540
In-situ x ray studies of the underpotential deposition of copper on platinum (3) [AD-A263361] p 3595 N93-29331
Magnetic character investigation of higher alcohol synthesis Cu-Co-Cr catalysts [DE93-009732] p 3316 N93-30653
Powder metallurgy: Solid and liquid phase sintering of copper p 3294 N93-30976
High thermal conductivity of diamond p 3294 N93-30977

COPPER ALLOYS
International Conference on Martensitic Transformations (ICOMAT 92) [AD-A262739] p 3321 N93-28591
An experimental investigation of radioactivity induced by ions associated with the operation of pulsed-power accelerators [DE93-011478] p 3575 N93-29151
Photo-desorption from copper alloys [DE93-011872] p 3326 N93-30490
Method of fabricating a rocket engine combustion chamber [NASA-CASE-MFS-28569-1] p 3338 N93-30565

COPPER COMPOUNDS
Characterization of copper iodide thin films fabricated via laser assisted molecular beam epitaxy [AD-A262823] p 3596 N93-29430
Sensitive detection of new superconductors created at ultra high pressures [AD-A264340] p 3597 N93-30161

COPPER OXIDES
In-situ x ray studies of the underpotential deposition of copper on platinum (3) [AD-A263361] p 3595 N93-29331

CORIOLIS EFFECT
Three-dimensional numerical simulation of gradual opening in a wave rotor passage [NASA-CR-191157] p 3252 N93-29072
Process for selectively recovering algae and protozoa [NASA-CASE-MFS-26124-1-NPO] p 3491 N93-29174

The effect of orthogonal-mode rotation on forced convection in a circular-sectioned tube fitted with full circumferential transverse ribs p 3254 N93-29937
Turbulent flow and heat transfer in idealized blade cooling passages p 3254 N93-29938
Some implications of a differential turbomachinery equation with viscous correction
[AD-A264693] p 3427 N93-30571
CORNERS
A corner matching and tracking strategy applied to videophony
[OUEL-1933/92] p 3380 N93-28896
CORONAL HOLES
Two-dimensional and three-dimensional time-dependent MHD model of extended corona
p 3653 N93-30496
CORONARY ARTERY DISEASE
Carbon monoxide exposure of subjects with documented cardiac arrhythmias
[PB93-179943] p 3497 N93-30890
COROTATION
Transient thermal behaviour of a compressor rotor with axial cooling air flow and co-rotating or contra-rotating shaft p 3255 N93-29946
CORRELATION
Studies of relativistic heavy ion collisions at the AGS (E814/E877)
[DE93-008541] p 3564 N93-28678
Selection and transmission of information. Issue 22: Republic interdepartmental collection (selected articles)
[AD-A262825] p 3615 N93-29431
Extracting infinite system properties from finite size clusters: Phase randomization/boundary condition averaging
[AD-A264712] p 3551 N93-30503
CORRELATORS
Photorefractive integrators and correlators
[AD-A264200] p 3597 N93-30144
Acousto-optic time-integrating correlators for processing wideband digital data p 3360 N93-30253
CORROSION
Preliminary test of liquid metal induced embrittlement in liquid LiPb and stainless-steel systems
[DE93-753130] p 3320 N93-28529
Polymeric materials for use in wet hydrochloric acid environments
[DE93-010881] p 3330 N93-28600
Operational results of pilot cell test with cermet inert anodes
[DE93-009338] p 3322 N93-29061
Direct use geothermal applications for brazed plate heat exchangers
[DE93-008559] p 3465 N93-30011
Materials studies for preventing corrosion in condensing environments
[PB93-185478] p 3327 N93-30815
CORROSION PREVENTION
Materials studies for preventing corrosion in condensing environments
[PB93-185478] p 3327 N93-30815
CORROSION RESISTANCE
Polymeric materials for use in wet hydrochloric acid environments
[DE93-010881] p 3330 N93-28600
Chromate-free corrosion resistant conversion coatings for aluminum
[DE93-009835] p 3336 N93-30051
Oxidation and hot corrosion of superalloys Rene 100 and X-40 at temperatures of 1475 F to 2000 F
[AD-A263747] p 3327 N93-30812
Materials studies for preventing corrosion in condensing environments
[PB93-185478] p 3327 N93-30815
CORROSION TESTS
The growth of small corrosion fatigue cracks in alloy 2024
[NASA-TM-107755] p 3451 N93-29069
APU diaphragm testing
[NASA-TM-108254] p 3272 N93-29501
Chromate-free corrosion resistant conversion coatings for aluminum
[DE93-009835] p 3336 N93-30051
Oxidation and hot corrosion of superalloys Rene 100 and X-40 at temperatures of 1475 F to 2000 F
[AD-A263747] p 3327 N93-30812
COSMIC BACKGROUND EXPLORER SATELLITE
On the meaning of delta T/T
[DE93-008482] p 3653 N93-28962
Tests of the particle physics-physical cosmology interface
[DE93-008483] p 3634 N93-28963
COSMIC DUST
Micrometeoroids and debris on LDEF
p 3638 N93-29356
An LDEF 2 dust instrument for discrimination between orbital debris and natural particles in near-Earth space
p 3286 N93-29707
COSMIC RAY SHOWERS
Research in theoretical physics
[DE93-008401] p 3603 N93-28961
COSMIC RAYS
Research in theoretical physics
[DE93-008401] p 3603 N93-28961
Status of LDEF ionizing radiation measurements and analysis p 3654 N93-29626
LDEF: Dosimetric measurement results (AO 138-7 experiment) p 3573 N93-29635
Progress report on the ultra heavy cosmic ray experiment (AO178) p 3654 N93-29646
Mathematical simulation of the induced (gamma)-radiation in structural materials of spaceships. Time dependence
[DE93-605312] p 3281 N93-31024
COSMOCHEMISTRY
Activities report of the Astronomical Society
[MITT-75] p 3629 N93-29008
COSMOLOGY
Topics in gauge theories and the unification of elementary particle interactions
[DE93-009370] p 3563 N93-28542
Dark matter: Theoretical perspectives
[DE93-008484] p 3633 N93-28676
Tests of the particle physics-physical cosmology interface
[DE93-008483] p 3634 N93-28963
Activities report of the Astronomical Society
[MITT-75] p 3629 N93-29008
Predictions of a non-Gaussian model for large scale structure
[DE93-010196] p 3636 N93-30528
Topics in inflationary universe medels and cosmic string theories p 3637 N93-30579
Fourth-rank gravity and cosmology
[DE92-644722] p 3637 N93-30918
General scalar-tensor theories for induced gravity inflation
[DE93-602505] p 3479 N93-30940
Fourth-rank cosmology
[DE92-641346] p 3637 N93-30997
COST ANALYSIS
Performance measurement systems: A best practices study
[AD-A262180] p 3506 N93-29444
Evaluating the bias of alternative cost progress models: Tests using aerospace industry acquisition programs
[AD-A262870] p 3624 N93-29477
A multilevel approach to minimum cost network flows
[AD-A264008] p 3550 N93-29978
Cost studies for commercial fuselage crown designs
p 3302 N93-30440
A unified approach for composite cost reporting and prediction in the ACT program p 3302 N93-30441
Performance and cost evaluation of bioremediation techniques for fuel spills
[PB93-175545] p 3474 N93-30762
Guideway structural design and power/propulsion/braking in relation to guideways, volume 1
[PB93-169902] p 3447 N93-30820
Process and assembly plans for low cost commercial fuselage structure p 3306 N93-30865
A representative survey of US space systems and methods for estimating their costs
[AD-A264159] p 3272 N93-30881
COST EFFECTIVENESS
Study on technology for effective utilization of carbon dioxide in view of global environment
[DE93-781440] p 3468 N93-28883
Spacecraft and launch systems for TACSAT applications p 3284 N93-29904
Cost effective TacSats for military support
p 3285 N93-29912
A multilevel approach to minimum cost network flows
[AD-A264008] p 3550 N93-29978
The First NASA Advanced Composites Technology Conference, part 1
[NASA-CP-3104-PT-1] p 3300 N93-30428
COST ESTIMATES
Evaluating the bias of alternative cost progress models: Tests using aerospace industry acquisition programs
[AD-A262870] p 3624 N93-29477
A perspective on acquisition of NASA space systems
[AD-A263246] p 3610 N93-29499
A representative survey of US space systems and methods for estimating their costs
[AD-A264159] p 3272 N93-30881
COST REDUCTION
Small Stirling dynamic isotope power system for robotic space missions
[NASA-TM-105785] p 3287 N93-28686
Low cost TACSAT for NATO surveillance
p 3285 N93-29911
The drive to cost-effective structural ceramics
[DE93-009722] p 3335 N93-30047
Advanced composite structural concepts and material technologies for primary aircraft structures
p 3300 N93-30430
Composites technology for transport primary structure
p 3300 N93-30431
Advanced technology commercial fuselage structure
p 3300 N93-30432
Design and manufacturing concepts for thermoplastic structures p 3301 N93-30434
Resin transfer molding for advanced composite primary aircraft structures p 3301 N93-30438
Consolidation of graphite thermoplastic textile preforms for primary aircraft structure p 3302 N93-30439
COUETTE FLOW
Stabilized space-time finite element formulations for unsteady incompressible flows involving fluid-body interactions p 3419 N93-29040
COULOMB POTENTIAL
Topics in gauge theories and the unification of elementary particle interactions
[DE93-009370] p 3563 N93-28542
Fast multipole method in simulations of aqueous systems
[AD-A263422] p 3567 N93-29336
COUNTER ROTATION
Transient thermal behaviour of a compressor rotor with axial cooling air flow and co-rotating or contra-rotating shaft p 3255 N93-29946
Flow and heat transfer between gas-turbine discs
p 3256 N93-29950
Numerical modeling and parameterization of gravity wave processes and effects in the atmosphere
[AD-A264331] p 3478 N93-30367
COUNTERMEASURES
Issues on human acceleration tolerance after long-duration space flights
[NASA-TM-104753] p 3495 N93-29651
Electro-optic characterisation of extremely wide bandwidth electrical signals
[AD-A264202] p 3392 N93-30145
COUNTERS
Measurement of a Michelson interferometer mirror velocity with a time interval analyzer
[AD-A263009] p 3430 N93-28659
COUPLED MODES
Nonlinear coupling of tearing fluctuations in the Madison Symmetric Torus
[DE93-010131] p 3584 N93-28602
Nonlinear mode coupling in free electron lasers
[AD-A263999] p 3439 N93-29883
COUPLINGS
Quick connect fastener
[NASA-CASE-MFS-28833-1] p 3445 N93-29846
COVALENT BONDS
Optically switchable conductive polymers
[AD-A264751] p 3337 N93-30557
COVARIANCE
A Monte Carlo study of the raw and normal varimax rotation criterion in factor analysis
[AD-A262516] p 3554 N93-28844
Investigation of a geodesy coexperiment to the Gravity Probe B relativity gyroscope program
[NASA-CR-193263] p 3460 N93-29179
Selection and transmission of information. Issue 22: Republic interdepartmental collection (selected articles)
[AD-A262825] p 3615 N93-29431
Determination of low frequency reference slipping for high frequency unstationary motion processes
[ILR-MITT-273(1992)] p 3455 N93-31017
CRAB NEBULA
GRO: Red-shifted electron-positron annihilation gamma-rays from radiopulsars
[NASA-CR-193243] p 3635 N93-30053
CRACK GEOMETRY
Method of continuously determining crack length
[NASA-CASE-LAR-14480-1-CU] p 3452 N93-29612
CRACK INITIATION
The growth of small corrosion fatigue cracks in alloy 2024
[NASA-TM-107755] p 3451 N93-29069
The initiation, propagation, and effect of matrix microcracks in cross-ply and related laminates
p 3304 N93-30847
Delaminations in composite plates under impact loads
p 3304 N93-30849
CRACK PROPAGATION
Crack length determination by ultrasonic methods
[DE93-008075] p 3450 N93-28567
Planning of a West Virginia University Research Center in the basic materials sciences
[DE93-011731] p 3592 N93-28647

The growth of small corrosion fatigue cracks in alloy 2024
[NASA-TM-107755] p 3451 N93-29069
The design and lifetime calculation of MHD generator walls based on subcritical crack growth in ceramics
[ISBN-90-9004009-9] p 3332 N93-29267
Damage growth in composite propellants
p 3348 N93-30088
Two-parameter crack tip field associated with stable crack growth in a thin plate: A hybrid analysis
[AD-A264221] p 3453 N93-30147
Stress-intensity-factor influence coefficients for axial and circumferential flaws in reactor pressure vessels
[DE93-006206] p 3454 N93-30213
The initiation, propagation, and effect of matrix microcracks in cross-ply and related laminates
p 3304 N93-30847
Micromechanics of fatigue in woven and stitched composites p 3304 N93-30850

CRACK TIPS
Crack length determination by ultrasonic methods
[DE93-008075] p 3450 N93-28567
Transformation toughening
[DE93-011805] p 3321 N93-28631
Two-parameter crack tip field associated with stable crack growth in a thin plate: A hybrid analysis
[AD-A264221] p 3453 N93-30147

CRACKING (CHEMICAL ENGINEERING)
A review of hot cracking in austenitic stainless steel weldments
[DE93-605280] p 3328 N93-31021

CRACKING (FRACTURING)
Whisker toughening of ceramic materials: A review
[DE93-011565] p 3336 N93-30129
Two-parameter crack tip field associated with stable crack growth in a thin plate: A hybrid analysis
[AD-A264221] p 3453 N93-30147
Durability of Quick Reaction Satellite Antenna (QRSA) trunnion castings
[AD-A264095] p 3281 N93-30813
Damage of multi-directionally reinforced ceramic-matrix composites p 3308 N93-30937

CRACKS
Crack length determination by ultrasonic methods
[DE93-008075] p 3450 N93-28567
Transformation toughening
[DE93-011805] p 3321 N93-28631
Environmental embrittlement of binary and Zr-doped Ni3Al
[DE93-008575] p 3321 N93-28679
Healing of lithographically introduced flaws in glass and glass containing ceramics
[DE93-010453] p 3330 N93-28761
The growth of small corrosion fatigue cracks in alloy 2024
[NASA-TM-107755] p 3451 N93-29069
Factors influencing the interlaminar fracture toughness and its evaluation in composites
[FFA-TN-1991-34] p 3451 N93-29076
Environmental effects on stitched RTM composites
[NASA-CR-193221] p 3297 N93-29107
Method of continuously determining crack length
[NASA-CASE-LAR-14480-1-CU] p 3452 N93-29612
Three-dimensional elastic stress analysis in materials with many inhomogeneities
[AD-A263736] p 3453 N93-29855
Interfacial melting in cracked explosives
p 3349 N93-30089
Two-parameter crack tip field associated with stable crack growth in a thin plate: A hybrid analysis
[AD-A264221] p 3453 N93-30147

CRANES
Lunar crane system p 3277 N93-29118
Leaky coaxial cable signal transmission for remote facilities
[DE93-007916] p 3383 N93-29348

CRASHWORTHINESS
Static and dynamic large deflection flexural response of graphite-epoxy beams
[NASA-CR-4118] p 3454 N93-30374

CRATERING
Report of the Meteoroid and Debris Special Investigation Group p 3638 N93-29355
Cratering in glasses impacted by debris or micrometeorites p 3340 N93-29368

CRATERS
Continued investigation of LDEF's structural frame and thermal blankets by the Meteoroid and Debris Special Investigation Group p 3282 N93-29357

CRAY COMPUTERS
Neural network simulations on massively parallel computers: Applications in chemical physics
[DE93-006739] p 3538 N93-28894

CREEP PROPERTIES
Ultrahigh temperature assessment study: Ceramic matrix composites
[AD-A262740] p 3295 N93-28592
Flux lattice relaxation, noise, and symmetry-breaking in frustrated Josephson junction arrays
[DE93-008713] p 3593 N93-29094
Bounds on internal state variables in viscoplasticity
[NASA-TM-106215] p 3451 N93-29196
Mechanisms of fracture and creep of structural alloys
[AD-A263108] p 3324 N93-29799
Hydrodynamic interactions among fibers in high efficiency filters
[DE93-007117] p 3424 N93-30035
Plastic deformation behaviour of oxide dispersion strengthened titanium alloys
[ONERA-NT-1990-6] p 3326 N93-30138

CREEP STRENGTH
High temperature creep and oxidation resistant chromium silicide matrix alloy containing molybdenum
[NASA-CASE-LEW-15697-1] p 3323 N93-29172
Tensile creep behavior of polycrystalline alumina fibers
[NASA-TM-106269] p 3340 N93-30938

CREEP TESTS
Tensile creep behavior of polycrystalline alumina fibers
[NASA-TM-106269] p 3340 N93-30938

CREWS
Sound attenuation characteristics of the standard DH-132A and SPH-4 helmets worn in combination with standard issue earplugs
[AD-A263011] p 3506 N93-29406

CRITERIA
A Monte Carlo study of the raw and normal varimax rotation criterion in factor analysis
[AD-A262516] p 3554 N93-28844

CRITICAL EXPERIMENTS
Loading and testing a light scattering cell with a binary fluid mixture near its critical composition
[NASA-CR-193147] p 3415 N93-28557

CRITICAL LOADING
Ion-beam-assisted deposition of wear-resistant coatings
[DE93-011529] p 3330 N93-28687
Tensile study of single-crystal ternary L1(2) trialuminide Al66Ti25Mn(sub g)
[AD-A264297] p 3601 N93-30819

CRITICAL PRESSURE
Super critical water oxidation on energetic materials
[DE93-010704] p 3342 N93-29312

CRITICAL TEMPERATURE
Super critical water oxidation on energetic materials
[DE93-010704] p 3342 N93-29312
Effect of lead addition on the formation of superconducting phases in Bi-Sr-Ca-Cu-O ceramics
[DE93-606893] p 3339 N93-30773

CROP GROWTH
National remote sensing programme 2 ACMS project. Phase 1: Validation. Part 1: Definition of validation experiment
[BCRS-92-10-PHASE-1-PT-1] p 3461 N93-29465

CROP INVENTORIES
National remote sensing programme 2 ACMS project. Phase 1: Validation. Part 1: Definition of validation experiment
[BCRS-92-10-PHASE-1-PT-1] p 3461 N93-29465

CROSS CORRELATION
Theoretical bit error rate performance of the Kalman filter excisor for FM interference
[AD-A263018] p 3383 N93-29407
Automated satellite image navigation
[AD-A262868] p 3269 N93-29475

CROSS COUPLING
Adaptive motion control of mobile robots
p 3545 N93-30903

CROSS FLOW
Experimental study of heat transfer close to a plane wall heated in the presence of multiple injections (subsonic flow) p 3253 N93-29931

CROSSLINKING
Characterization of slow chromophore reorientation in nonlinear optical polymers by two-dimensional MAS NMR
[AD-A264809] p 3338 N93-30596
Water-soluble polyphosphazenes and their hydrogels
[AD-A264883] p 3340 N93-30909

CRUDE OIL
The thermodynamic properties of thianthrene and phenoxathiin
[DE93-000124] p 3603 N93-28964
Fugitive hydrocarbon emissions from Pacific OCS facilities. Volume 2: Executive summary and user's guide
[PB93-173805-VOL-2] p 3471 N93-29861

CRYOGENIC COOLING
Miniature long-life space cryocoolers
p 3378 N93-28825

CRYOGENIC EQUIPMENT
Preliminary experimental results for a cryogenic brush seal configuration
[NASA-TM-106236] p 3416 N93-28627
Cryogenic Heat Pipe Experiment (CRYOHP)
p 3265 N93-28721
Spaceborne passive radiative cooler
p 3378 N93-28802
Miniature long-life space cryocoolers
p 3378 N93-28825
Cryogenic magnetic bearing
[AD-A264716] p 3446 N93-30512

CRYOGENIC FLUID STORAGE
Tank Pressure Control Experiment (TPCE)
p 3264 N93-28712
Tank Pressure Control Experiment/Thermal Phenomena (TPCE/TP) p 3264 N93-28713

CRYOGENIC FLUIDS
Tank Pressure Control Experiment (TPCE)
p 3264 N93-28712
Tank Pressure Control Experiment/Thermal Phenomena (TPCE/TP) p 3264 N93-28713
Cryogenic Heat Pipe Experiment (CRYOHP)
p 3265 N93-28721

CRYOGENIC ROCKET PROPELLANTS
Specific impulse calculations of high energy density solid cryogenic rocket propellants. 1. Atoms in solid H2
[AD-A263208] p 3341 N93-28517

CRYOGENICS
Inertial confinement fusion target component fabrication and technology development support
[DE93-010836] p 3585 N93-28836

CRYOSTATS
TESLA test cell cryostat support post thermal and structural analysis
[DE93-008365] p 3407 N93-29048
Structural design of cryostat and port penetration of International Thermonuclear Experimental Reactor (ITER)
[DE93-753267] p 3587 N93-29243

CRYSTAL DEFECTS
Deformation mechanisms in Be(sub 12)X compounds
[DE93-009080] p 3320 N93-28548
Flux lattice relaxation, noise, and symmetry-breaking in frustrated Josephson junction arrays
[DE93-008713] p 3593 N93-29094
Defect studies in low-temperature-grown GaAs
[DE93-010405] p 3595 N93-29417
Balanced technology initiative on computational mechanics of materials
[AD-A263906] p 3453 N93-29863
Low-cost, high-efficiency solar cells utilizing GaAs-on-Si technology
[DE93-000096] p 3464 N93-29965
Microstructural basis for enhanced shock-induced chemistry in single crystals of ammonium perchlorate
p 3319 N93-30092
Defect density measurements in a shocked single crystal of ammonium perchlorate p 3319 N93-30093
Molecular dynamics of detonation in crystals with defects p 3350 N93-30097
The 2-6 semiconductor superlattices
[AD-A264343] p 3597 N93-30164
Computational analysis of slip in PETN
[DE92-040222] p 3598 N93-30445
The calculation of electrostatic interactions and their role in determining the energies and geometries of molecular HE crystals
[DE92-040374] p 3570 N93-30448
Radiation effects in FCC metals and intermetallic compounds: A molecular dynamics computer simulation study
[DE93-009546] p 3600 N93-30668

CRYSTAL DISLOCATIONS
Deformation mechanisms in Be(sub 12)X compounds
[DE93-009080] p 3320 N93-28548
Plastic deformation behaviour of oxide dispersion strengthened titanium alloys
[ONERA-NT-1990-6] p 3326 N93-30138

CRYSTAL GROWTH
Measurement of the relative and absolute microgravity environment of space platforms, recent flight results, and determination of the spatial microgravity field
p 3266 N93-28725
Growth, characterization and device development in monocrystalline diamond films
[AD-A263204] p 3593 N93-28874
Follow up on the crystal growth experiments of the LDEF p 3602 N93-29381
Flame or plasma synthesis of diamond under turbulent and transition flow conditions
[AD-D015689] p 3333 N93-29456

Growth and development of GaInAsP for use in high-efficiency solar cells
[DE93-000098] p 3465 N93-30208
Study on diamond semiconductor
[DE92-531076] p 3413 N93-30622
Visible light emitting materials and injection devices
[AD-A263499] p 3601 N93-30811
Growth model of Au films on Ru(001)
[DE92-642126] p 3602 N93-30998

CRYSTAL LATTICES
Neutron scattering studies of the structures and lattice dynamics of the alkali metals
[DE93-008272] p 3593 N93-28956
Characterization of copper iodide thin films fabricated via laser assisted molecular beam epitaxy
[AD-A262823] p 3596 N93-29430
Integrals of motion on the group of invariance of an interval in three-dimensional spaces
[DE93-606090] p 3606 N93-30797
Growth model of Au films on Ru(001)
[DE92-642126] p 3602 N93-30998

CRYSTAL OPTICS
Photorefractive integrators and correlators
[AD-A264200] p 3597 N93-30144

CRYSTAL OSCILLATORS
Radiation sensitivity of quartz crystal oscillators experiment for the Long Duration Exposure Facility (LDEF), part 2 p 3414 N93-29685

CRYSTAL STRUCTURE
Powder x ray diffraction patterns of energetic materials for use as reference standards
[DE93-009903] p 3592 N93-28568
Be3(AsO4)2 2H2O: A new berylloarsenate phase containing bridged tetrahedral 3-rings
[AD-A262518] p 3592 N93-28584
Neutron scattering studies of the structures and lattice dynamics of the alkali metals
[DE93-008272] p 3593 N93-28956
The synthesis and ab initio structure determination of Zn4O(BO3)2: A microporous zincoborate built up from fused 3-ring and 5-ring sub-units
[AD-A262504] p 3594 N93-29138
Structure and switching dynamics in ferroelectric crystal and liquid crystal thin films
[AD-A263664] p 3594 N93-29293
Properties of superconducting YBa2Cu3O(6+4) ceramic materials: Effect of processing parameters
[AD-A263441] p 3334 N93-29790
Anelastic relaxations associated with local disordering in grain boundaries
[AD-A263101] p 3596 N93-29796
Improved field emitter current densities and stability through the application of a proprietary process
[AD-A264048] p 3411 N93-30031
A steric hindrance model for the crystal orientation dependence of the shock initiation sensitivity of PETN explosive
[LA-UR-92-1427] p 3345 N93-30074
Atomic force microscopy of ammmonium perchlorate
p 3349 N93-30091
Design of acentric materials: X ray structures of guanidinium p-nitro- and p-hydroxybenzenesulfonate
[AD-A264220] p 3597 N93-30146
Two new titanium pyroarsenates: Alpha-TiAs2O7 and Beta-TiAs2O7
[AD-A264632] p 3599 N93-30518
1,2-Dimethyl-1,2-Disila-Closo-Dodecaborane(12), A silicon analog of an ortho-carborane: Synthesis; x ray crystal structure; NMR, vibrational and photoelectron spectra; bonding
[AD-A264709] p 3599 N93-30568
Study on diamond semiconductor
[DE92-531076] p 3413 N93-30622
The characterization of materials using x ray diffraction p 3293 N93-30968
A dynamical model of structural phase transition in La2CuO4
[DE93-605325] p 3602 N93-31025

CRYSTAL SURFACES
Structure, adhesion, and stability of metal/oxide and oxide/oxide interfaces
[DE93-012930] p 3325 N93-30060
Molecular dynamics of detonation in crystals with defects p 3350 N93-30097

CRYSTALLINITY
Observation of reaction intermediates in crystalline RDX p 3318 N93-30067

CRYSTALLIZATION
Crystallization of nanocomposite glasses made by the SSG process
[AD-A262892] p 3333 N93-29511
An extension of a kinetic theory of polymer crystallization through the exclusion of negative barriers
[AD-A264810] p 3334 N93-29660

CRYSTALLOGRAPHY
Two new titanium pyroarsenates: Alpha-TiAs2O7 and Beta-TiAs2O7
[AD-A264632] p 3599 N93-30518

CRYSTALS
Excited states in electronic structure calculations
[DE93-007704] p 3592 N93-28642
A technique for single-pulse spectrum and pulse width measurements for an IR-FEL
[DE93-007732] p 3436 N93-28847
Silicon crystal under bending
[DE93-010522] p 3593 N93-28888
Modification of spectral distributions by multilayer structures
[DE93-009308] p 3310 N93-29059
Structure and switching dynamics in ferroelectric crystal and liquid crystal thin films
[AD-A263664] p 3594 N93-29293
Proceedings of the 25th European Conference on the Application of Polar Dielectrics to celebrate the 25th anniversary of the Dielectric Society, incorporating the 1st International Workshop on Integrated Ferroelectrics
[AD-A263427] p 3332 N93-29337
Follow up on the crystal growth experiments of the LDEF p 3602 N93-29381
Measurements of light scattering by small particles at an angle of zero degrees
[AD-A263856] p 3580 N93-29887
Ion emission during high-energy sputtering of ammonium dinitramide and ammonium nitrate crystals and the determination of ion decomposition pathways using tandem mass spectrometry p 3318 N93-30066
Dislocation roles in energetic crystal responses
p 3348 N93-30086
Photorefractive integrators and correlators
[AD-A264200] p 3597 N93-30144
Tunable CW diode-pumped Tm,Ho:YLiF4 laser operating at or near room temperature
[NASA-CASE-NPO-18611-1-CU] p 3440 N93-30415
Computational analysis of slip in PETN
[DE92-040222] p 3598 N93-30445
Intracavity-pumped 2.1 micrometer Ho(3+): YAG laser
[AD-D015728] p 3441 N93-30587
Phase transition studies in barium and strontium titanates at microwave frequencies p 3293 N93-30970

CUBANE
Synthesis of cubane based energetic molecules
[AD-A263271] p 3564 N93-28562

CUBIC LATTICES
Constitutive laws for deformation and dynamic recrystallization in cubic metals
[DE93-010740] p 3326 N93-30486

CUES
Pilot decision aiding for weapon delivery: A novel approach to fire control cueing using parallel computing
p 3501 N93-28853
An evaluation of B-1B pilot performance during simulated instrument approaches with and without status information
[AD-A263874] p 3507 N93-29888
Utility of a ghost horizon and climb/dive ladder line tapering on a head-up display
[AD-A264401] p 3508 N93-30167

CULTURAL RESOURCES
Remote sensing survey of Mississippi River-Gulf Outlet, Breton Sound disposal area, Plaquemines Parish, Louisiana
[AD-A263097] p 3459 N93-29146

CULTURE TECHNIQUES
Wound healing and connective tissue metabolism: The role of hyperbaric oxygen therapy
[AD-A262483] p 3493 N93-28759

CURING
An investigation of stereolithography as a means of prototyping from a cad database
[AD-A263410] p 3613 N93-29210

CURRENT DENSITY
Microstructural understanding and critical current optimization of advanced high field superconductors
[DE93-011046] p 3592 N93-28643
Operational results of pilot cell test with cermet inert anodes
[DE93-009338] p 3322 N93-29061
Improved field emitter current densities and stability through the application of a proprietary process
[AD-A263464] p 3411 N93-29833
Improved field emitter current densities and stability through the application of a proprietary process
[AD-A264048] p 3411 N93-30031

CURRENT DISTRIBUTION
Operational results of pilot cell test with cermet inert anodes
[DE93-009338] p 3322 N93-29061
Electron transport calculations between 1 MeV and 1 eV
[AD-A263412] p 3568 N93-29787

CURRENT SHEETS
Solar flare MDH
[AD-A262275] p 3652 N93-28756

CURVATURE
The curvature of plane elastic curves
[AD-A263198] p 3450 N93-28516

CURVE FITTING
Molecular dynamics of physical aging processes in polymer glasses
[AD-A263737] p 3334 N93-29856

CURVED BEAMS
Chaos in mechanical systems with especial reference to rotorcraft and missiles
[AD-A263703] p 3604 N93-29384

CURVED PANELS
Structural evaluation of curved stiffened composite panels fabricated using a THERM-Xsm process
p 3301 N93-30435
Prediction of stiffener-skin separation in composite panels p 3307 N93-30871

CURVES (GEOMETRY)
The curvature of plane elastic curves
[AD-A263198] p 3450 N93-28516
Packing odd paths
[CWI-BS-R9207] p 3549 N93-29849
A method for intersection line calculation between parametric surfaces
[ETN-93-94178] p 3551 N93-30572

CYANO COMPOUNDS
Synthesis and polymerization of azaethylenes and aza-1,3-dienes
[AD-A263651] p 3332 N93-29290

CYCLES
Development of nickel/metal hydride secondary battery
[DE93-781330] p 3406 N93-28669
Fuzzy operators and cyclic behavior in formal neuronal networks p 3519 N93-29576

CYCLIC COMPOUNDS
Applications of transition metal compounds in the preparation of useful silicon-containing ceramics
[AD-A264028] p 3335 N93-30028

CYCLIC HYDROCARBONS
Selective nitrations. Volume 2: The laser-induced nitration of three cycloalkanes
[AD-A263250] p 3438 N93-29800

CYCLOBUTANE
Selective nitrations. Volume 2: The laser-induced nitration of three cycloalkanes
[AD-A263250] p 3438 N93-29800

CYCLONES
Rhode Island hurricanes and tropical storms: A fifty-six year summary, 1936-1991
[PB93-162006] p 3481 N93-29198
The sensitivity of ageostrophic circulations to model resolution: A case study using NGM forecasts of ERICA IOP-4
[AD-A262011] p 3482 N93-29393

CYCLOPROPANE
Selective nitrations. Volume 2: The laser-induced nitration of three cycloalkanes
[AD-A263250] p 3438 N93-29800

CYCLOTRON RESONANCE
High mass resolution glow discharge mass spectrometry using an external ion source FT-ICR mass spectrometer
[AD-A264347] p 3314 N93-30166

CYCLOTRON RESONANCE DEVICES
Development of high power microwave source
[DE93-753316] p 3436 N93-28980
High-power Ka-band amplifier p 3385 N93-29590
Improved design concepts for millimeter wave power sources
[AD-A264060] p 3411 N93-29922

CYCLOTRONS
Research and education by SF cyclotron facility
[DE93-753135] p 3576 N93-30002

CYLINDERS
Vortex structure and mass transfer near the base of a cylinder and a turbine blade p 3253 N93-29929

CYLINDRICAL BODIES
The wave, the cylinder, and the plate
[DE93-009458] p 3450 N93-28596
A thermal stress solution for multilayered composite cylinders
[AD-A262579] p 3295 N93-28657
Topics in General Relativity theory: Gravitational-wave measurements of black-hole parameters; gravitational collapse of a cylindrical body; and classical-particle evolution in the presence of closed, timelike curves
p 3603 N93-28690
The hydraulic analysis of cylindrical Flibe jets in a HYLIFE-2 ICF reactor
[DE93-009234] p 3586 N93-29053
A numerical study of confined turbulent jets
[NASA-TM-106197] p 3420 N93-29161

A spectral method determination of the first critical Rayleigh number for a low-Prandtl number crystal melt in a cylindrical container
[NASA-CR-193238] p 3594 N93-29214
The equivalent flat nose diameter of hemispherical nose cylindrical projectiles for impact induced detonation of energetic materials
[AD-A263244] p 3342 N93-29494
Elastic stability considerations for deep submergence ceramic pressure housing
[AD-A264824] p 3454 N93-30598

CYLINDRICAL CHAMBERS
Evaluation of multi-dimensional flux models for radiative transfer in cylindrical combustion chambers
p 3257 N93-29955
High density plasma production in a multicusp plasma generator with RF antenna
[DE93-764493] p 3590 N93-30606

CYLINDRICAL TANKS
Liquid Motion in a rotating tank Experiment (LME)
p 3264 N93-28710
Combined centrifugal force/gravity gas/liquid separator system
[AD-D015726] p 3444 N93-29288

CYTOMETRY
Evaluation of dried storage of platelets for transfusion: Physiologic integrity and hemostatic functionality
[AD-A263240] p 3494 N93-29620

CZECHOSLOVAKIA
Remote sensing in Czechoslovakia and Hungary: An analysis of the possible co-operation of The Netherlands with Czechoslovakia and Hungary in the field of remote sensing
[BCRS-92-12] p 3461 N93-29466

D

D REGION
Investigations of equatorial ionosphere nighttime mode conversion at VLF p 3396 N93-30735

DAMAGE
High-performance visible/UV CCD focal plane technology for spacebased applications
p 3434 N93-28771
Novel polymer compositions for high-temperature membrane applications, phase 1
[PB93-174126] p 3331 N93-29201
Energetic material response to abnormal environments p 3350 N93-30095
The environment as an operational center of gravity
[AD-A264170] p 3472 N93-30154
Damage mechanics in 2-D and 3-D microstructures
[AD-A264337] p 3453 N93-30159
Applications of the photorefractive effect and damage induced effects in fibers
[AD-A264339] p 3580 N93-30205
Deadliest, costliest, and most intense US hurricanes of this century (and other frequently requested hurricane facts)
[PB93-174993] p 3485 N93-30758
Characterization of multiaxial warp knit composites
p 3304 N93-30851
Progressive failure methodologies for predicting residual strength and life of laminated composites
p 3307 N93-30866

DAMAGE ASSESSMENT
Defect density measurements in a shocked single crystal of ammonium perchlorate p 3319 N93-30093
Energetic material response to abnormal environments p 3350 N93-30095
Center for surface radiation damage studies
[AD-A264330] p 3570 N93-30366
An assessment of peripheral nerve damage in the rat following non-freezing cold exposure: An electrophysiological and histopathological examination
[AD-A264293] p 3492 N93-30818
Effects of bolt-hole contact on bearing-bypass damage-onset strength p 3307 N93-30870

DARK MATTER
Distribution of dark matter in the galaxy and the lower limits for the masses of supersymmetric particles
[BONN-92-31] p 3632 N93-28473
Dark matter: Theoretical perspectives
[DE93-008484] p 3633 N93-28676
Tests of the particle physics-physical cosmology interface
[DE93-008483] p 3634 N93-28963
Predictions of a non-Gaussian model for large scale structure
[DE93-010196] p 3636 N93-30528
Planck scale effects in neutrino physics
[DE93-606133] p 3571 N93-30793

DATA ACQUISITION
Radiometric calibration system for IR cameras
[DE93-009237] p 3430 N93-28520
Enhanced reduction of velocity data obtained during CETA flight experiment
[NASA-TM-4460] p 3431 N93-29209
A comparison of high-speed links, their commercial support and ongoing R/D activities
[DE93-008134] p 3382 N93-29245
Remote vehicle survey tool
[DE93-010822] p 3460 N93-29255
SPREE Interactive Data Analysis Tool (SIDAT)
[AD-A262782] p 3273 N93-29306
Advanced thermally-stable, coal-derived, jet fuels program: Experiment system and model development
[AD-A262747] p 3342 N93-29402
The Telecommunications and Data Acquisition Report
[NASA-CR-193144] p 3384 N93-29586
Collection, analysis, and archival of LDEF activation data p 3624 N93-29631
Project Copernicus: An Earth observing system
p 3231 N93-29738
TACSAT ground control and data collection
p 3388 N93-29895
Airborne data acquisition using a front-end processor architecture p 3373 N93-30329
Acquisition of physiological data during G-induced Loss of Consciousness (G-LOC)
[AD-A264492] p 3496 N93-30400
Data management in NOAA p 3617 N93-30454
High-energy electron-positron interactions
[DE93-011611] p 3576 N93-30488
Filling the gaps: An overview of data on education in grades K through 12
[PB93-176550] p 3608 N93-30821
An automated data collection system for a Charpy impact tester p 3293 N93-30972

DATA BASE MANAGEMENT SYSTEMS
A distributed object-oriented database application design
[AD-A262591] p 3612 N93-28846
VIEWCACHE: An incremental database access method for autonomous interoperable databases
p 3614 N93-29238
On the evaluation of fuzzy quantified queries in a database management system p 3517 N93-29569
A high performance, ad-hoc, fuzzy query processing system for relational databases p 3518 N93-29571
Data management in NOAA p 3617 N93-30454
High-performance mass storage system for workstations p 3618 N93-30457

DATA BASES
DOKMA: A document oriented communication model for medical applications as a basis of a role system in the medical field
[ETN-93-93799] p 3492 N93-28469
A model for processing the SGML document in version oriented hypertext systems
[ETN-93-93797] p 3611 N93-28528
Modeling land-surface/atmosphere dynamics for CHAMMP
[DE93-008520] p 3476 N93-28677
The Backgrounds Data Center p 3624 N93-28814
Design and evaluation of a uniaxial pull test for lithium hydride/deuteride
[DE93-010760] p 3451 N93-28832
A distributed object-oriented database application design
[AD-A262591] p 3612 N93-28846
The meteorological database
[DE93-007289] p 3481 N93-29054
LDEF materials data bases
[NASA-TM-107757] p 3290 N93-29067
National collaboratories: Applying information technology for scientific research
[LC-93-83795] p 3612 N93-29129
Hanford Environmental Information System (HEIS) user's manual, volume 1
[DE93-007465] p 3470 N93-29135
NSSDC data listing
[NASA-TM-108264] p 3612 N93-29167
Summer 1990 Atlanta ozone precursor study (January 1993)
[PB93-167203] p 3470 N93-29200
An investigation of stereolithography as a means of prototyping from a cad database
[AD-A263410] p 3613 N93-29210
RBSE: Product development team research activity deliverables
[NASA-CR-193115] p 3527 N93-29212
Program plan for an experimenter's laboratory for visualized interactive science p 3613 N93-29224
DataHub knowledge based assistance for science visualization and analysis using large distributed databases p 3613 N93-29230
Collection-oriented match: Scaling up the data in production systems
[AD-A262755] p 3615 N93-29459
A composite self tuning strategy for fuzzy control of dynamic systems p 3511 N93-29530
A high performance, ad-hoc, fuzzy query processing system for relational databases p 3518 N93-29571
EnviroNET: On-line information for LDEF
p 3624 N93-29625
Programmer's reference guide to FDMS file formats
[PB93-182038] p 3354 N93-29663
Decision maker's guide to international space
[ANSER-STDN-93-4] p 3669 N93-29710
Thunderstorm forecast study for Eglin AFB, Florida
[AD-A263423] p 3483 N93-29810
Charting the remote southern oceans with geosat altimetry
[AD-A263452] p 3461 N93-29817
On the development of a film cooling layer
p 3258 N93-29959
Cloudiest year study: An analysis of the 3DNEPH and RTNEPH databases
[AD-A263409] p 3483 N93-29967
Residual acceleration data on IML-1: Development of a data reduction and dissemination plan
[NASA-CR-193224] p 3281 N93-30038
Data quality statements for spatial databases
[AD-A264125] p 3616 N93-30195
The Visible Human Project of the National Library of Medicine: Remote access and distribution of a multi-gigabyte data set p 3617 N93-30453
Data management in NOAA p 3617 N93-30454
Interim report on Landsat national archive activities
p 3618 N93-30455
Requirements for a system to analyze HEP events using database computing
[DE93-009960] p 3576 N93-30527
Air weather service master station catalog USAFETAC climatic database users handbook no. 6
[AD-A264761] p 3484 N93-30608
Intelligent real-time problem solving
[AD-A264830] p 3535 N93-30614
Toward a coordinated spatial data infrastructure for the nation
[B-149] p 3456 N93-30634
Office of Water Environmental and Program Information Systems Compendium, FY 1992
[PB93-186203] p 3462 N93-30833
Land use database for the Netherlands using LANDSAT Thematic Mapper pictures
[BCRS-91-32] p 3463 N93-30839
A representative survey of US space systems and methods for estimating their costs
[AD-A264159] p 3272 N93-30881
A prototype of a faculty and staff executive information system
[AD-A264852] p 3623 N93-30907
Software conception and structure of automated workstation for an experimental data processing
[DE93-609815] p 3623 N93-30994
Shuttle landing facility cloud cover study: Climatological analysis and two tenths cloud cover rule evaluation
[NASA-CR-193016] p 3272 N93-31033

DATA COMPRESSION
Frequency domain speech compression using the Karhunen-Loeve Transform
[AD-A262613] p 3379 N93-28476
Information-theoretic performance bounding of Bayesian identifiers
[DE93-010705] p 3554 N93-28763
Digital image compression using artificial neural networks p 3624 N93-28811
Analysis and computation for vortex dynamics and rarefied gases
[AD-A264705] p 3427 N93-30499
Transputers, parallel processing in embedded systems for image compression in space applications
[NLR-TP-89242-U] p 3522 N93-30840

DATA CONVERTERS
Interim report on Landsat national archive activities
p 3618 N93-30455

DATA FLOW ANALYSIS
Flow control using the theory of zero sum Markov games
[INRIA-RR-1597] p 3553 N93-28507
Data Multiplexing Network (DMN) equipment Operational Test and Evaluation (OT&E) integration test report
[AD-A263172] p 3538 N93-29490
The modern high rate digital cassette recorder
p 3435 N93-30468

DATA INTEGRATION
Overview of the System of Experts for Intelligent Data Management (SEIDAM) p 3613 N93-29228
Multi-channel holographic birfurcative neural network system for real-time adaptive EOS data analysis
p 3614 N93-29231
An MCM/chip concurrent engineering validation
[AD-A262959] p 3409 N93-29513

The fusion of information via fuzzy integration
p 3517 N93-29568
Incorporation of varying types of temporal data in a neural network p 3518 N93-29575

DATA LINKS
Results of DATAS investigation of ATCRBS environment at the Los Angeles International Airport
[DOT/FAA/CT-93/6] p 3245 N93-28625
A comparison of high-speed links, their commercial support and ongoing R/D activities
[DE93-008134] p 3382 N93-29245
Hybrid data link
[AD-D015714] p 3383 N93-29280
Advanced Earth Observing Satellite (ADEOS)
p 3279 N93-29648
Ethernet performance of the Motorola Altair WIN system
[AD-A263877] p 3387 N93-29890
Optoelectronic technology consortium
[AD-A263580] p 3580 N93-29973
Security of the remote control link of Anik E satellites
p 3365 N93-30282
Orbiting transmitter and antenna for spaceborne communications at ELF/VLF to submerged submarines
p 3399 N93-30755

DATA MANAGEMENT
National collaboratories: Applying information technology for scientific research
[LC-93-83795] p 3612 N93-29129
Applied Information Systems Research Program Workshop p 3613 N93-29223
Overview of the System of Experts for Intelligent Data Management (SEIDAM) p 3613 N93-29228
DataHub knowledge based assistance for science visualization and analysis using large distributed databases p 3613 N93-29230
Flight Projects Office Information Systems Testbed (FIST) p 3615 N93-29241
Programmer's reference guide to FDMS file formats
[PB93-182038] p 3354 N93-29663
Storage systems for national information assets
[DE93-009303] p 3615 N93-29783
What's past is prologue: Supporting global change research with historical data
[DE93-005777] p 3472 N93-30009
Managing operational intelligence overload: Guidelines for avoiding decision paralysis
[AD-A264184] p 3610 N93-30158
The future role of the Director of Information Management (DOIM) organization within the DOD corporate information management initiative
[AD-A264118] p 3616 N93-30193
Consultative Committee for Space Data Systems recommendation for space data system standards: Telecommand. Part 2.1: Command operation procedures
[NASA-TM-108158] p 3393 N93-30371
Data management in NOAA p 3617 N93-30454
MR-CDF: Managing multi-resolution scientific data
p 3618 N93-30456
The state of the state of the art in mass storage technology p 3622 N93-30475
Toward a coordinated spatial data infrastructure for the nation
[B-149] p 3456 N93-30634

DATA PROCESSING
DOKMA: A document oriented communication model for medical applications as a basis of a role system in the medical field
[ETN-93-93799] p 3492 N93-28469
A survey of network interface designs
[MEMO-INF-92-59] p 3379 N93-28502
Dynamic object oriented interaction and its implementation in the framework in an interface management system
[ETN-93-93795] p 3523 N93-28526
A model for processing the SGML document in version oriented hypertext systems
[ETN-93-93797] p 3611 N93-28528
Research in mathematics and computer science, March 1, 1991 - September 30, 1992
[DE93-011492] p 3509 N93-28573
Preprocessing remotely-sensed data for efficient analysis and classification
[DE93-007367] p 3611 N93-28580
Exact trajectory determinator for ERS-1
p 3457 N93-28918
Users manual for fault tree analysis code: CUT-TD
[DE93-753272] p 3525 N93-28978
Fundamental study of the signal processing by optics
[DE93-776265] p 3577 N93-28982
Initial graphics exchange specification hybrid microcircuit application protocol
[PB93-175404] p 3407 N93-29203
Colorado Center for Astrodynamics Research (CCAR)
p 3614 N93-29233
SAVS: A Space Data Analysis and Visualization System p 3614 N93-29235
Spatial Analysis and Modeling Systems (SAMS)
p 3614 N93-29239
Introduction to cadet center for advanced data evaluation technology p 3614 N93-29240
Using today's technology to improve mobile C4I for the operational commander
[AD-A263613] p 3245 N93-29285
Software development and analysis for experimental high frequency surface wave radar data
[AD-A261982] p 3383 N93-29438
North American Fuzzy Logic Processing Society (NAFIPS 1992), volume 1
[NASA-CP-10112-VOL-1] p 3509 N93-29516
North American Fuzzy Logic Processing Society (NAFIPS 1992), volume 2
[NASA-CP-10112-VOL-2] p 3515 N93-29556
Incomplete fuzzy data processing systems using artificial neural network p 3519 N93-29578
Collection, analysis, and archival of LDEF activation data p 3624 N93-29631
Computer systems laboratory
[PB93-181873] p 3521 N93-29662
Capability maturity model for software, version 1.1
[AD-A263403] p 3530 N93-29852
ARSRP signal processing software
[AD-A263543] p 3391 N93-29975
OSI transaction processing standard: An introduction and outlines of implementation
[VTT-TIED-1250] p 3532 N93-29997
XRONOS: A timing analysis software package. User's guide, version 3.00
[NASA-TM-109222] p 3532 N93-30023
Generalized octrees for constrained object modeling
p 3369 N93-30304
High-energy electron-positron interactions
[DE93-011611] p 3576 N93-30488
Requirements for a system to analyze HEP events using database computing
[DE93-009960] p 3576 N93-30527
Efficient algorithms and data structures in geometric design
[AD-A264678] p 3534 N93-30544
Independent research and independent exploratory development programs
[AD-A264735] p 3544 N93-30556
The 1991 neural information processing systems: Natural and synthetic
[AD-A264754] p 3623 N93-30559
Oceanographic data processing program
[AD-A264801] p 3544 N93-30591
Solving a product safety problem using a recycled high density polyethylene container p 3292 N93-30964
Software conception and structure of automated workstation for an experimental data processing
[DE93-609815] p 3623 N93-30994

DATA PROCESSING EQUIPMENT
Digital hardware architecture implementation
[AD-A263219] p 3521 N93-29492
Implementation of parallel algorithms
[AD-A263126] p 3529 N93-29496
Incomplete fuzzy data processing systems using artificial neural network p 3519 N93-29578
Software conception and structure of automated workstation for an experimental data processing
[DE93-609815] p 3623 N93-30994

DATA RECORDERS
Clementine sensor processing system
p 3285 N93-28778

DATA RECORDING
The NT digital micro tape recorder
p 3435 N93-30461
The modern high rate digital cassette recorder
p 3435 N93-30468
Optimizing digital 8mm drive performance
p 3435 N93-30479
National Media Laboratory p 3628 N93-30717

DATA REDUCTION
A Monte Carlo study of the raw and normal varimax rotation criterion in factor analysis
[AD-A262516] p 3554 N93-28844
Enhanced reduction of velocity data obtained during CETA flight experiment
[NASA-TM-4460] p 3431 N93-29209
Data reduction expert assistant p 3613 N93-29227
Multi-channel holographic birfurcative neural network system for real-time adaptive EOS data analysis
p 3614 N93-29231
SAVS: A Space Data Analysis and Visualization System p 3614 N93-29235
Spatial Analysis and Modeling Systems (SAMS)
p 3614 N93-29239
Introduction to cadet center for advanced data evaluation technology p 3614 N93-29240
Empirical quantile function nonparametric integrated analyses
[AD-A263704] p 3554 N93-29385
Fuzzy multiple linear regression: A computational approach p 3518 N93-29574
Residual acceleration data on IML-1: Development of a data reduction and dissemination plan
[NASA-CR-193224] p 3281 N93-30038
Towards the results of global analysis of data on nucleon electromagnetic structure
[DE93-606125] p 3571 N93-30792
A miniature fatigue test machine p 3291 N93-30956

DATA RETRIEVAL
VIEWCACHE: An incremental database access method for autonomous interoperable databases
p 3614 N93-29238
LDEF archival system plan p 3624 N93-29704
MR-CDF: Managing multi-resolution scientific data
p 3618 N93-30456
High-performance mass storage system for workstations p 3618 N93-30457
GE networked mass storage solutions supporting IEEE network mass storage model p 3618 N93-30458

DATA SAMPLING
The HYDICE instrument design and its application to planetary instruments p 3434 N93-28766
Enhanced resolution and de-aliasing techniques for fast Fourier transforms p 3358 N93-30240

DATA SIMULATION
Numerical simulation of perfect fluid flows around complex 3D configurations by a multidomain solver using the MUSCL approach p 3417 N93-28745

DATA SMOOTHING
Empirical quantile function nonparametric integrated analyses
[AD-A263704] p 3554 N93-29385

DATA STORAGE
Colorado Center for Astrodynamics Research (CCAR)
p 3614 N93-29233
A planetary version of PC-McIDAS
p 3614 N93-29236
Holographic data storage crystals for the LDEF
p 3435 N93-29697
LDEF archival system plan p 3624 N93-29704
Storage systems for national information assets
[DE93-009303] p 3615 N93-29783
Goddard Conference on Mass Storage Systems and Technologies, Volume 1
[NASA-CP-3198] p 3616 N93-30449
Mass storage system reference model, Version 4
p 3617 N93-30450
Optical media standards for industry
p 3617 N93-30451
Technology for national asset storage systems
p 3617 N93-30452
The Visible Human Project of the National Library of Medicine: Remote access and distribution of a multi-gigabyte data set p 3617 N93-30453
Data management in NOAA p 3617 N93-30454
Interim report on Landsat national archive activities
p 3618 N93-30455
MR-CDF: Managing multi-resolution scientific data
p 3618 N93-30456
High-performance mass storage system for workstations p 3618 N93-30457
GE networked mass storage solutions supporting IEEE network mass storage model p 3618 N93-30458
High-speed data duplication/data distribution: An adjunct to the mass storage equation
p 3619 N93-30459
The fundamentals and futures of removable mass storage alternatives p 3619 N93-30460
The NT digital micro tape recorder
p 3435 N93-30461
RAID 7 disk array p 3537 N93-30462
Tutorial: Performance and reliability in redundant disk arrays p 3537 N93-30463
Striped tertiary storage arrays p 3620 N93-30464
National Media Laboratory media testing results
p 3620 N93-30465
Evaluation of D-1 tape and cassette characteristics: Moisture content of Sony and Ampex D-1 tapes when delivered p 3435 N93-30466
Grand challenges in mass storage: A systems integrators perspective p 3620 N93-30467
The modern high rate digital cassette recorder
p 3435 N93-30468
Evolution of a high-performance storage system based on magnetic tape instrumentation recorders
p 3435 N93-30470
Mass optical storage-tape (MOST)
p 3621 N93-30471
ICI optical data storage tape: An archival mass storage media p 3621 N93-30472
Flexible storage medium for write-once optical tape
p 3621 N93-30473

Electron trapping data storage system and applications p 3622 N93-30474
The state of the state of the art in mass storage technology p 3622 N93-30475
Measurements over distributed high performance computing and storage systems p 3622 N93-30476
Analysis of cache for streaming tape drive
p 3435 N93-30477
LANL High-Performance Data System (HPDS)
p 3622 N93-30478
Optimizing digital 8mm drive performance
p 3435 N93-30479
Using Transparent Informed Prefetching (TIP) to reduce file read latency p 3522 N93-30480
National Media Laboratory p 3628 N93-30717

DATA STRUCTURES
Topology of hybrid objects
[ETN-93-93594] p 3546 N93-28466
Formal definition of a conceptual language for the description and manipulation of information models
[TR-92-16] p 3523 N93-28503
Robust and efficient implementation of the Delaunay tree
[INRIA-RR-1619] p 3547 N93-28511
Parallel computation and the basis system
[DE93-008755] p 3537 N93-28544
Parametric likelihood inference for record breaking problems
[AD-A262546] p 3549 N93-29413
WARP: Weight Associative Rule Processor. A dedicated VLSI fuzzy logic megacell p 3513 N93-29538
NESL: A nested data-parallel language (Version 2.6)
[AD-A263548] p 3530 N93-29822
Consultative Committee for Space Data Systems recommendation for space data system standards: Telecommand. Part 2.1: Command operation procedures
[NASA-TM-108158] p 3393 N93-30371
Qualitative methods in computer vision
[AD-A264335] p 3533 N93-30418
Efficient algorithms and data structures in geometric design
[AD-A264678] p 3534 N93-30544

DATA SYSTEMS
NSSDC data listing
[NASA-TM-108264] p 3612 N93-29167
Applied Information Systems Research Program Workshop p 3613 N93-29223
A distributed system for visualizing and analyzing multivariate and multidisciplinary data
p 3613 N93-29226
Colorado Center for Astrodynamics Research (CCAR)
p 3614 N93-29233
Spatial Analysis and Modeling Systems (SAMS)
p 3614 N93-29239
Flight Projects Office Information Systems Testbed (FIST) p 3615 N93-29241
Collection-oriented match: Scaling up the data in production systems
[AD-A262755] p 3615 N93-29459
Consultative Committee for Space Data Systems recommendation for space data system standards: Telecommand. Part 2.1: Command operation procedures
[NASA-TM-108158] p 3393 N93-30371
LANL High-Performance Data System (HPDS)
p 3622 N93-30478
Using Transparent Informed Prefetching (TIP) to reduce file read latency p 3522 N93-30480
Centralized maintenance evaluation
[AD-A264400] p 3544 N93-30886

DATA TRANSFER (COMPUTERS)
OSI transaction processing standard: An introduction and outlines of implementation
[VTT-TIED-1250] p 3532 N93-29997
An application protocol for CAD to CAD transfer of electronic information
[AD-A264554] p 3533 N93-30383
High-speed data duplication/data distribution: An adjunct to the mass storage equation
p 3619 N93-30459
The modern high rate digital cassette recorder
p 3435 N93-30468
Mass optical storage-tape (MOST)
p 3621 N93-30471

DATA TRANSMISSION
Polarimetric multispectral imaging technology
p 3434 N93-28774
Selection and transmission of information. Issue 22: Republic interdepartmental collection (selected articles)
[AD-A262825] p 3615 N93-29431
Data Multiplexing Network (DMN) equipment Operational Test and Evaluation (OT&E) integration test report
[AD-A263172] p 3538 N93-29490
Galileo post-Gaspra cruise and Earth-2 encounter
p 3385 N93-29597
DSN support of Mars Observer p 3385 N93-29598
Signal-to-noise ratio losses in full spectrum combining of signals with a downconverted subcarrier
p 3386 N93-29599
Performance analysis of communication protocols using D-timed Petri net p 3356 N93-30227
Automatic synthesis of protocol specifications
p 3356 N93-30228
Consultative Committee for Space Data Systems recommendation for space data system standards: Telecommand. Part 2.1: Command operation procedures
[NASA-TM-108158] p 3393 N93-30371
RAID 7 disk array p 3537 N93-30462

DEAD RECKONING
Advanced Unmanned Search System (AUSS) supervisory command, control and navigation
[AD-A263171] p 3245 N93-28990

DEATH
World commercial aircraft accidents
[DE93-010892] p 3243 N93-28571

DEBONDING (MATERIALS)
Damage of multi-directionally reinforced ceramic-matrix composites p 3308 N93-30937

DEBRIS
Debris/ice/TPS assessment and integrated photographic analysis for Shuttle Mission STS-55
[NASA-TM-107559] p 3271 N93-29136

DECISION MAKING
Pilot decision aiding for weapon delivery: A novel approach to fire control cueing using parallel computing
p 3501 N93-28853
A new class of mission support for combat air-crew
p 3501 N93-28854
Crucial role of detailed function, task, timeline, link, and human vulnerability analyses in HRA
[DE93-001923] p 3505 N93-28942
Robotics and artificial intelligence for hazardous environments
[DE93-008271] p 3541 N93-29047
MoCog1: A computer simulation of recognition-primed human decision making
[NASA-TM-103868] p 3542 N93-29386
Information technology: A force for organizational change
[AD-A261986] p 3615 N93-29439
A perspective on acquisition of NASA space systems
[AD-A263246] p 3610 N93-29499
Estimations of expectedness and potential surprise in possibility theory p 3510 N93-29518
A model for amalgamation in group decision making
p 3513 N93-29540
Fuzzy forecasting and decision making in short dynamic time series p 3513 N93-29541
Decision analysis with approximate probabilities
p 3513 N93-29542
An experimental methodology for a fuzzy set preference model p 3514 N93-29547
A fuzzy set preference model for market share analysis p 3514 N93-29548
The cognitive bases for the design of a new class of fuzzy logic controllers: The clearness transformation fuzzy logic controller p 3515 N93-29554
Determining rules for closing customer service centers: A public utility company's fuzzy decision
p 3516 N93-29561
A fuzzy case based reasoning tool for model based approach to rocket engine health monitoring
p 3289 N93-29570
AHP version 5.1 user's manual
[DE93-007050] p 3532 N93-30034
Intelligent support for human computer interaction and decision-making in distribution planning and scheduling systems
[AD-A263985] p 3610 N93-30124
The environment as an operational center of gravity
[AD-A264170] p 3472 N93-30154
Managing operational intelligence overload: Guidelines for avoiding decision paralysis
[AD-A264184] p 3610 N93-30158
Hidden Markov models for fault detection in dynamic systems
[NASA-CASE-NPO-18982-1-CU] p 3449 N93-30413
Aircraft guidance for wind shear avoidance: Decision-making under uncertainty p 3246 N93-31005

DECISION THEORY
Resource limited reasoning: A study of literature in the context of model-based diagnosis
[MEMO-INF-92-38] p 3540 N93-28480
Asymptotic properties of constrained Markov decision processes
[INRIA-RR-1598] p 3553 N93-28508
Optimal control of the M/G/1 queue with repeated vacations of the server
[INRIA-RR-1637] p 3541 N93-28637
Closed-loop control with delayed information
[INRIA-RR-1638] p 3541 N93-28638
Determining rules for closing customer service centers: A public utility company's fuzzy decision
p 3516 N93-29561
Multi-Attribute Decision Theory methodology for pollution control measure analysis
[DE93-005444] p 3472 N93-30008

DECODERS
Uncorrectable sequences and telecommand
p 3385 N93-29596

DECODING
A systolic-array structure for MTCM receivers
p 3357 N93-30236
An error control protocol based on trellis coded modulations p 3358 N93-30237
Comparison of diversity combining, interleaving, and decoding techniques of a scintillated channel
p 3362 N93-30266

DECOMPOSITION
The thermochemistry and reaction pathways of the decomposition and combustion of energetic materials
p 3343 N93-30063
Thermal oxidation of HCN by NO2 in shock waves
p 3318 N93-30064
Ion emission during high-energy sputtering of ammonium dinitramide and ammonium nitrate crystals and the determination of ion decomposition pathways using tandem mass spectrometry p 3318 N93-30066
NO2 unimolecular decomposition: Step-like variation of k(sub uni)(E) p 3318 N93-30068
Thermal decomposition chemistry and shock sensitivity of thermally aged explosives p 3344 N93-30069
QR decomposition based least squares lattice algorithm p 3358 N93-30239
Decomposition of hydrogen sulfide for small scale gas processing.
[PB93-174704] p 3316 N93-30658
Hydrogen sulfide decomposition into hydrogen and sulfur by quinone cycles, part 1
[PB93-175297] p 3317 N93-30761

DEEP SPACE
Clementine 2: A double asteroid flyby and impactor mission p 3268 N93-28770

DEEP SPACE NETWORK
The Telecommunications and Data Acquisition Report
[NASA-CR-193144] p 3384 N93-29586
The effect of clock, media, and station location errors on Doppler measurement accuracy
p 3246 N93-29588
Gravity referenced elevation encoder development
p 3385 N93-29592
Maximum and minimum return losses from a passive two-port network terminated with a mismatched load
p 3385 N93-29594
Galileo post-Gaspra cruise and Earth-2 encounter
p 3385 N93-29597
DSN support of Mars Observer p 3385 N93-29598
An analysis of the 70-meter antenna hydrostatic bearing by means of computer simulation p 3386 N93-29601
The flight performance of the Galileo orbiter USO
p 3386 N93-29603

DEEP WATER
ELF propagation in deep and shallow sea water
p 3397 N93-30739

DEFECTS
Healing of lithographically introduced flaws in glass and glass containing ceramics
[DE93-010453] p 3330 N93-28761
Use of local x ray computerized tomography for high-resolution, region-of-interest inspection of large ceramic components for engines
[DE93-005564] p 3449 N93-28943
Characterization and optimization of a Hot Air Solder-Leveling System
[DE93-010188] p 3332 N93-29328
Three-dimensional elastic stress analysis in materials with many inhomogeneities
[AD-A263736] p 3453 N93-29855
Development of a test program to evaluate structural defects in Glass-Reinforced Plastic (GRP), volume 2
[AD-A263814] p 3335 N93-29881
Development of a test program to evaluate structural defects in Glass-Reinforced Plastic (GRP), volume 1
[AD-A263813] p 3335 N93-29886
Applications of the photorefractive effect and damage induced effects in fibers
[AD-A264339] p 3580 N93-30205
Stress-intensity-factor influence coefficients for axial and circumferential flaws in reactor pressure vessels
[DE93-006206] p 3454 N93-30213
Photoinduced electron-hole charge separation, intrinsic self-doping and novel device applications of Q1D heterojunction materials: Mixed-halide MX solids
[AD-A264714] p 3600 N93-30569

DEFENSE PROGRAM
Proceedings of the Near-Earth-Object Interception Workshop
[NASA-TM-108236] p 3556 N93-28572
International aviation (Selected articles)
[AD-A262566] p 3227 N93-28576
Workshop on Advanced Technologies for Planetary Instruments, part 1
[NASA-CR-193015] p 3639 N93-28764
Defense conversion: Redirecting research and development
[OTA-ITE-552] p 3610 N93-29649
The future role of the Director of Information Management (DOIM) organization within the DOD corporate information management initiative
[AD-A264118] p 3616 N93-30193
Technology transfer within the government
p 3627 N93-30709
First NASA Advanced Composites Technology Conference, part 2
[NASA-CP-3104-PT-2] p 3303 N93-30841
Research, Development, Test and Evaluation (R, D, T, and E) programs (R-1), Department of Defense budget for fiscal year 1994
[PB93-169878] p 3611 N93-30936

DEFLAGRATION
Strategies for understanding the deflagration-to-detonation transition
p 3319 N93-30077
Energetic material response to abnormal environments p 3350 N93-30095

DEFLECTION
Study of gain in C-band deflection cavities for a frequency-doubling magnicon amplifier
[AD-A263132] p 3409 N93-29478
Static and dynamic large deflection flexural response of graphite-epoxy beams
[NASA-CR-4118] p 3454 N93-30374
A new tubeless nanosecond streak camera based on optical deflection and direct CCD imaging
[DE93-011893] p 3433 N93-30491

DEFORESTATION
Advanced Earth Observing Satellite (ADEOS)
p 3279 N93-29648

DEFORMATION
The temperature dependence of the deformation and oxidation behavior of an age-hardenable beta + alpha-two titanium alloy
[AD-A262232] p 3320 N93-28491
Deformations of the Lie algebras L1(H(2)) and L1(W(2))
[MEMO-1056] p 3547 N93-28667
Silicon crystal under bending
[DE93-010522] p 3593 N93-28888
Microstructural effects on the deformation and fracture of the alloy Ti-25Al-10Nb-3B-1Mo
[AD-A263095] p 3323 N93-29144
Electric field induced phenomena in STM: Tip deformations and Au(111)-surface phase transitions during tunneling spectroscopy experiments
[AD-A262208] p 3596 N93-29445
Gravity referenced elevation encoder development
p 3385 N93-29592
Comparison of deformation and shock reactivity for single crystals of RDX and ammonium perchlorate
p 3350 N93-30094
Constitutive laws for deformation and dynamic recrystallization in cubic metals
[DE93-010740] p 3326 N93-30486

DEGASSING
Aluminium-high strength material by mechanical alloying and reaction milling: Basics of processing and characterisation of material
[ESA-TT-1249] p 3324 N93-29272

DEGENERATION
An assessment of peripheral nerve damage in the rat following non-freezing cold exposure: An electrophysiological and histopathological examination
[AD-A264293] p 3492 N93-30818

DEGRADATION
Thermal control paints on LDEF: Results of M0003 sub-experiment 18
[AD-A263252] p 3329 N93-28561
Neutron radiation induced degradation of diode characteristics
[AD-A263277] p 3405 N93-28563
High-performance visible/UV CCD focal plane technology for spacebased applications
p 3434 N93-28771
APU diaphragm testing. Test plan
[NASA-TM-108251] p 3271 N93-29387
Degradation of electro-optic components aboard LDEF p 3582 N93-29689
Degradation of optical components in a space environment p 3582 N93-29692

DEGREES OF FREEDOM
Quantum dynamics of X2BC van der Waals clusters
[DE93-006416] p 3565 N93-28892
Ion motion effects on charged radiators
[DE93-009257] p 3565 N93-29099
Input relegation control for gross motion of a kinematically redundant manipulator
[DE93-005301] p 3446 N93-30210
Analysis and simulation of a two degrees-of-freedom one-link flexible forearm p 3361 N93-30261

DEHUMIDIFICATION
Study of parameters affecting the performance of solar desiccant cooling systems
[DE93-000088] p 3465 N93-30206

DEHYDRATION
High octane ethers from synthesis gas-derived alcohols
[DE93-012470] p 3341 N93-28752

DEICERS
FAA international conference on airplane ground deicing
[AD-A263617] p 3244 N93-29286

DEICING
FAA international conference on airplane ground deicing
[AD-A263617] p 3244 N93-29286

DELAMINATING
Factors influencing the interlaminar fracture toughness and its evaluation in composites
[FFA-TN-1991-34] p 3451 N93-29076
Effects of freeze/thaw cycles on hydrostatically conditioned E-glass/J-2 composite
[AD-A262980] p 3298 N93-29425
The initiation, propagation, and effect of matrix microcracks in cross-ply and related laminates
p 3304 N93-30847
Delaminations in composite plates under impact loads
p 3304 N93-30849
Micromechanics of fatigue in woven and stitched composites p 3304 N93-30850
Progressive failure methodologies for predicting residual strength and life of laminated composites
p 3307 N93-30866

DELAY
Potential transmission and transients during corrosion: Applications to corrosion monitoring
[DE93-010863] p 3323 N93-29256

DELAY LINES
Acoustic charge transport technology investigation for advanced development transponder
p 3386 N93-29602

DELIVERY
The development of a parachute system for aerial delivery from high speed cargo aircraft
[DE93-008339] p 3239 N93-29035

DELTA WINGS
Computation of a delta-wing roll-and-hold maneuver
[AD-A264704] p 3260 N93-30498

DEMODULATION
Effects of imbalances and DC offsets on I/Q demodulation
[AD-A264466] p 3393 N93-30537

DEMOGRAPHY
Guide to Federal Water Quality Programs and Information: A Guide with Computer Software Developed by the Interagency Working Group on Water Quality
[PB93-186245] p 3475 N93-30834

DENSE PLASMAS
Start broadened profiles with self-consistent radiation transfer and atomic kinetics in plasmas produced by high intensity lasers
[DE93-008706] p 3586 N93-29093
Engineering consideration for the self-energizing magnetoplasmadynamic (MPD): Type fusion plasma thruster
[AD-A262785] p 3288 N93-29289

DENSIFICATION
Lunar regolith densification p 3276 N93-29115
Lunar regolith penetrators and cutters
p 3276 N93-29117
Reactive sintering of Ni3Al intermetallic alloys under compressive stress
[DE93-009729] p 3327 N93-30652
The effect of Bi2 O3 on the electrical properties of Zr O2: 3 percent Mg O ceramic solid electrolytes
[DE93-607029] p 3339 N93-30774

DENSITY DISTRIBUTION
Distribution of dark matter in the galaxy and the lower limits for the masses of supersymmetric particles
[BONN-92-31] p 3632 N93-28473
Using C-vector method to derive the three-dimensional circulation pattern near the East Greenland Polar Front
[AD-A261979] p 3487 N93-29437
Fluids in porous media.
[PB93-175198] p 3428 N93-30759

DENSITY MEASUREMENT
The XNOVAKTC rheological model
[AD-A263298] p 3342 N93-29762
Shear, strain, and thermohaline vertical fine structure in the upper ocean p 3488 N93-30046
Defect density measurements in a shocked single crystal of ammonium perchlorate p 3319 N93-30093

DEOXYRIBONUCLEIC ACID
Comparative mutagenesis of human cells in vivo and in vitro
[DE93-012269] p 3490 N93-28651
Computer assisted multiplex sequencing
[DE93-007144] p 3536 N93-30934

DEPOSITION
Ion-beam-assisted deposition of wear-resistant coatings
[DE93-011529] p 3330 N93-28687
Study of codeposition of aluminum-haffnium and deposition of yttrium by the cementation technique: Elaboration of Ni-Cr-Al and Ni-Cr-Al-Hf felt materials
[ONERA-NT-1990-9] p 3336 N93-30112
Simulation and calculation of diffusive aerosol deposition
[DE93-007518] p 3474 N93-30506

DEPTH
A methodology and tool for the prediction of depth of reception in the sea for a VLF/LF communications system p 3397 N93-30741

DEPTH MEASUREMENT
A calibration procedure for the SBE 19 Conductivity, Temperature, and Depth (CTD) profiler
[AD-A264435] p 3489 N93-30420

DERIVATION
Research in mathematics and computer science, March 1, 1991 - September 30, 1992
[DE93-011492] p 3509 N93-28573

DESICCANTS
Study of parameters affecting the performance of solar desiccant cooling systems
[DE93-000088] p 3465 N93-30206

DESIGN ANALYSIS
The meta model hierarchy: A framework for information systems concepts and techniques
[TR-92-17] p 3611 N93-28481
Formal definition of a conceptual language for the description and manipulation of information models
[TR-92-16] p 3523 N93-28503
Design and construction of a prototype ACTS propagation terminal
[NASA-CR-193071] p 3404 N93-28539
Ergonomic development of digital map displays
p 3503 N93-28866
Natural environmental service support to NASA vehicle, technology, and sensor development programs
[NASA-CR-192554] p 3469 N93-29029
Reliability assessment of thrust chamber cooling concepts using probabilistic analysis techniques
[NASA-CR-190785] p 3288 N93-29068
Lunar rovers and local positioning system
p 3277 N93-29119
Design optimization of space structures
p 3278 N93-29122
Ultra-high resolution water window x ray microscope optics design and analysis
[NASA-CR-193225] p 3578 N93-29128
Guide for certifying pressure vessels and systems
[NASA-TM-107549] p 3449 N93-29220
Velocity measurements of low Reynolds number tube flow using fiber-optic technology
[DE93-009865] p 3422 N93-29335
Integrated approaches to parallelism in optimization and solution of inverse problems
[AD-A262259] p 3452 N93-29349
Department of defense advisory group on electron devices: Appendix to special technology area review on microwave packaging technology
[AD-A262136] p 3408 N93-29408
Aerodynamic characteristics of a rotorcraft airfoil designed for the tip region of a main rotor blade
[NASA-TM-4264] p 3240 N93-29450
Effect of design selection on response surface performance
[NASA-CR-4520] p 3249 N93-29885
SAR sensors on TACSATS: A feasibility assessment
p 3286 N93-29909
Improved design concepts for millimeter wave power sources
[AD-A264060] p 3411 N93-29922
Mathematical model of frost heave and thaw settlement in pavements
[CRREL-REPT-93-2] p 3262 N93-30103
Communications systems design for testability: Grey-box testing p 3368 N93-30302
Structural design, analysis, and code evaluation of an odd-shaped pressure vessel
[DE93-008182] p 3447 N93-30632

Multi-parameter optimization tool for low-cost commercial fuselage crown designs p 3305 N93-30858
Process and assembly plans for low cost commercial fuselage structure p 3306 N93-30865
Multiple methods integration for structural mechanics analysis and design p 3307 N93-30867
Optimum design of multiwire cages for high-voltage applications [AD-A264310] p 3400 N93-30995
Structural design using neural networks p 3545 N93-31029

DESIGN TO COST
Process and assembly plans for low cost commercial fuselage structure p 3306 N93-30865

DESORPTION
Acid gas treating by aqueous alkanolamines [PB93-176188] p 3471 N93-29676
Photo-desorption from copper alloys [DE93-011872] p 3326 N93-30490
Development of an O atom gun [AD-A264753] p 3570 N93-30558
Surface chemistry of N2H4 on Si(100)-2x1 [AD-A264819] p 3316 N93-30627
Complex-compound heat pump: Topical report on phase 1 results [PB93-185460] p 3466 N93-30814

DESTRUCTIVE TESTS
Report on the test set-up for the structural testing of the Airmass Sunburst Ultralight Aircraft p 3249 N93-29775
Load test set-up for the Airmass Sunburst Ultra-Light Aircraft p 3249 N93-29776

DESULFURIZING
The thermodynamic properties of thianthrene and phenoxathiin [DE93-000124] p 3603 N93-28964
Rates and mechanisms of reaction of hydrogen sulfide with iron chelates [PB93-184299] p 3312 N93-29665

DETECTION
Valve malfunction detection apparatus [NASA-CASE-MFS-29904-1] p 3432 N93-29503
Advanced signal processing requirement in an ion mobility explosives detector p 3320 N93-30277
Detecting residue on a printed circuit board: An application of the Boundary Contour/Feature Contour System [DE93-006283] p 3412 N93-30370

DETECTORS
Sensor systems for monitoring Maglev guideway structures [PB93-154821] p 3444 N93-29205
A high resolution 14-bit ADC for Gammasphere Project [DE93-010446] p 3598 N93-30393

DETONATION
The equivalent flat nose diameter of hemispherical nose cylindrical projectiles for impact induced detonation of energetic materials [AD-A263244] p 3342 N93-29494
ONR/LANL Workshop on the Fundamental Physics and Chemistry of Combustion, Initiation, and Detonation of Energetic Materials [CPIA-PUBL-589] p 3343 N93-30061
Propulsion and detonics research in France p 3344 N93-30070
Chemical dynamics simulations as a probe to the initiation and propagation of condensed phase detonations p 3318 N93-30071
A steric hindrance model for the crystal orientation dependence of the shock initiation sensitivity of PETN explosive [LA-UR-92-1427] p 3345 N93-30074
Detonation mass spectrometry p 3319 N93-30076
Strategies for understanding the deflagration-to-detonation transition p 3319 N93-30077
Energetic material response to abnormal environments p 3350 N93-30095
Detonation shock dynamics of composite energetic materials p 3350 N93-30096
Molecular dynamics of detonation in crystals with defects p 3350 N93-30097
Shock waves and polymorphic phase transitions in energetic materials p 3351 N93-30100
The measurement of electrical conductivity in detonating condensed explosives [AD-A264482] p 3352 N93-30424
The use of quantum chemistry to estimate the performance and properties of explosives [DE92-040369] p 3352 N93-30446

DETONATION WAVES
Implementation of a single-material version of PAGOSA on MIMD hypercubes [SAND-92-0640] p 3526 N93-29127
Response of energetic solids to light, heat and shock pulses [AD-A263702] p 3342 N93-29296
Weakly nonlinear dynamics of near-CJ detonation waves [DE93-007344] p 3424 N93-29836
Metallization at detonation fronts in solids p 3319 N93-30087
Towards a better hydro for dynamic mix calculations [DE93-010702] p 3426 N93-30485

DETONATORS
Rocket-triggered lightning studies for the protection of critical assets [DE93-009633] p 3484 N93-30651

DEUTERIDES
Design and evaluation of a uniaxial pull test for lithium hydride/deuteride [DE93-010760] p 3451 N93-28832

DEUTERIUM
Exotic atoms [DE93-010242] p 3564 N93-28611
Inertial confinement fusion target component fabrication and technology development support [DE93-010836] p 3585 N93-28836
A high field optical-pumping spin-exchange polarized deuterium source [DE93-009208] p 3574 N93-28970
Reaction and reorientation of electronically excited H2(B) [DE93-010435] p 3569 N93-29860

DEUTERIUM COMPOUNDS
Laser spectroscopy of hydrocarbon radicals [DE93-012555] p 3436 N93-28653

DEUTERONS
Coherent and semi-coherent neutron transfer reactions [DE93-008336] p 3565 N93-28959

DIAGNOSIS
Resource limited reasoning: A study of literature in the context of model-based diagnosis [MEMO-INF-92-38] p 3540 N93-28480
Proceedings of a Workshop on Molecular Nuclear Medicine [DE93-010828] p 3493 N93-28835
Fuzzy neural network methodology applied to medical diagnosis p 3498 N93-29546
A neural network based approach for machine fault diagnosis [VTT-TIED-1274] p 3543 N93-29998
Centralized maintenance evaluation [AD-A264400] p 3544 N93-30886

DIAMETERS
Long Duration Exposure Facility (LDEF) experiment M0003 meteoroid and debris survey p 3638 N93-29361
Horizontal nucleate flow boiling heat transfer coefficient measurements and visual observations for R12, R134a, and R134a/ester lubricant mixtures [PB93-178598] p 3475 N93-30887
Application of hardness testing in foundry processing operations: A university and industry partnership p 3292 N93-30961

DIAMINES
Polyimides prepared from 3,5-diamino benzo trifluoride [NASA-CASE-LAR-14206-1] p 3331 N93-29083
Diphenylmethane-containing dianhydride and polyimides prepared therefrom [NASA-CASE-LAR-14487-1] p 3331 N93-29085
Process to prepare 1,3-diamino-5-pentafluorosulfanylbenzene [NASA-CASE-LAR-14773-2-CU] p 3312 N93-29506

DIAMOND FILMS
Growth, characterization and device development in monocrystalline diamond films [AD-A263204] p 3593 N93-28874
Complex dielectric function of amorphous diamond films deposited by pulsed excimer (ArF) laser ablation of graphite [AD-A264527] p 3598 N93-30408
Diamond nucleation of surfaces using carbon clusters [AD-A264634] p 3599 N93-30548
Study on diamond semiconductor [DE92-531076] p 3413 N93-30622

DIAMONDS
Hypervelocity impact survivability experiments for carbonaceous impactors p 3283 N93-29364
Flame or plasma synthesis of diamond under turbulent and transition flow conditions [AD-D015689] p 3333 N93-29456
Defect density measurements in a shocked single crystal of ammonium perchlorate p 3319 N93-30093
Sensitive detection of new superconductors created at ultra high pressures [AD-A264340] p 3597 N93-30161
Diamond nucleation of surfaces using carbon clusters [AD-A264634] p 3599 N93-30548
High thermal conductivity of diamond p 3294 N93-30977

DIAPHRAGMS (MECHANICS)
APU diaphragm testing [NASA-TM-108254] p 3272 N93-29501
Valve malfunction detection apparatus [NASA-CASE-MFS-29904-1] p 3432 N93-29503

DIATOMIC GASES
Radiative interactions in molecular gases under local and nonlocal thermodynamic equilibrium conditions [NASA-CR-193223] p 3604 N93-29168

DICHROISM
Experimental and modal verification of an integral equation solution for a thin-walled dichroic plate with cross-shaped holes p 3385 N93-29591

DICTIONARIES
Handbook of frequently used acronyms and glossary of terms [DE93-011388] p 3616 N93-30123

DIELECTRIC PROPERTIES
LDEF Space Plasma-High Voltage Drainage Experiment post-flight results p 3414 N93-29690
Complex dielectric function of amorphous diamond films deposited by pulsed excimer (ArF) laser ablation of graphite [AD-A264527] p 3598 N93-30408
Phase transition studies in barium and strontium titanates at microwave frequencies p 3293 N93-30970

DIELECTRICS
Improving the jitter of the 150 kJ experiments solid dielectric switches [DE93-009459] p 3405 N93-28597
Structure and switching dynamics in ferroelectric crystal and liquid crystal thin films [AD-A263664] p 3594 N93-29293
Proceedings of the 25th European Conference on the Application of Polar Dielectrics to celebrate the 25th anniversary of the Dielectric Society, incorporating the 1st International Workshop on Integrated Ferroelectrics [AD-A263427] p 3332 N93-29337
High pressure studies of hydrated nafion membranes: Dielectric relaxation and deuteron NMR [AD-A263511] p 3332 N93-29342
LDEF Space Plasma-High Voltage Drainage Experiment post-flight results p 3414 N93-29690
Phase transition studies in barium and strontium titanates at microwave frequencies p 3293 N93-30970
Advanced electromagnetic methods for aerospace vehicles [NASA-CR-193468] p 3400 N93-31036

DIENES
Synthesis and polymerization of azaethylenes and aza-1,3-dienes [AD-A263651] p 3332 N93-29290

DIESEL ENGINES
Application of Schlieren optical techniques for the measurement of gas temperature and turbulent diffusivity in a diesel engine [AD-A263810] p 3580 N93-29880

DIESEL FUELS
Limitations of the ideal phase-Doppler system: Extension to spatially and temporally inhomogeneous particle flows with an application to diesel sprays [DE93-009447] p 3416 N93-28595

DIETS
Field trial of caffeine on physical performance at altitude: An attempt to overcome the challenge [AD-A264260] p 3497 N93-30894

DIFFERENCE EQUATIONS
Towards a better hydro for dynamic mix calculations [DE93-010702] p 3426 N93-30485

DIFFERENTIAL CALCULUS
Differential calculus on quantum spaces and quantum groups [DE93-010425] p 3551 N93-30392

DIFFERENTIAL EQUATIONS
JPRS report: Science and technology. Central Eurasia: Physics and mathematics [JPRS-UPM-93-002] p 3560 N93-29022
Development of an unstructured solution adaptive method for the quasi-three-dimensional Euler and Navier-Stokes equations [NASA-CR-193241] p 3421 N93-29213
An upwind method for the solution of the 3D Euler and Navier-Stokes equations on adaptively refined meshes [AD-A262863] p 3423 N93-29472
Some implications of a differential turbomachinery equation with viscous correction [AD-A264693] p 3427 N93-30571
Application of integral and differential equation methods for various EM interaction problems [AD-A264821] p 3394 N93-30597
Determination of low frequency reference slipping for high frequency unstationary motion processes [ILR-MITT-273(1992)] p 3455 N93-31017

DIFFERENTIAL GEOMETRY
Manifold shape: From differential geometry to mathematical morphology
[CS-9204] p 3552 N93-31012

DIFFRACTION PATTERNS
Powder x ray diffraction patterns of energetic materials for use as reference standards
[DE93-009903] p 3592 N93-28568
Design of a high resolution spatial heterodyne interferometer
[AD-A262867] p 3285 N93-29461
The swollen polymer technique and its use for heat transfer investigations on film cooled surfaces
p 3255 N93-29944
Photorefractive integrators and correlators
[AD-A264200] p 3597 N93-30144
The characterization of materials using x ray diffraction p 3293 N93-30968

DIFFUSION
Applications of laser light scattering in polymer dilute solution characterization
[AD-A263110] p 3335 N93-30007
Studies of curvature, strain, and unsteady effects on premixed flames p 3316 N93-30646
Laboratory experiments in integrated circuit fabrication
p 3292 N93-30962

DIFFUSION COEFFICIENT
Diffusion coefficients and heats of mixing in aqueous alkanolamines
[PB93-176212] p 3316 N93-30661

DIFFUSION FLAMES
Studies of hydrogen-air diffusion flames and of compressibility effects related to high-speed propulsion
p 3310 N93-29125
Numerical modeling of multidimensional flames with application to energetic materials p 3319 N93-30079
Detailed studies of soot formation in laminar diffusion flames for application to modeling studies
[AD-A264827] p 3317 N93-30667
Effects of buoyancy on gas jet diffusion flames
[NASA-CR-191109] p 3352 N93-31031

DIFFUSION THEORY
The onset of vortex turbulence
[DE93-010424] p 3417 N93-28663
The role of grain boundaries in hydrogen diffusion in metals at 25 C
[NASA-TM-108407] p 3322 N93-29043

DIFFUSION WAVES
Nonlinear stability of viscous shock waves
[TRITA-NA-9205] p 3419 N93-29025

DIFFUSION WELDING
Healing of lithographically introduced flaws in glass and glass containing ceramics
[DE93-010453] p 3330 N93-28761
Diffusion bonding
[DE93-011480] p 3442 N93-28837

DIFFUSIVITY
Simulation and calculation of diffusive aerosol deposition
[DE93-007518] p 3474 N93-30506

DIGESTING
Comparative mutagenesis of human cells in vivo and in vitro
[DE93-012269] p 3490 N93-28651

DIGITAL COMPUTERS
Digital hardware architecture implementation
[AD-A263219] p 3521 N93-29492

DIGITAL DATA
Multiple image multipoint matching for automatic aerotriangulation p 3461 N93-29615
Acousto-optic time-integrating correlators for processing wideband digital data p 3360 N93-30253
Applications of digital 3-D imaging
p 3366 N93-30287
The Visible Human Project of the National Library of Medicine: Remote access and distribution of a multi-gigabyte data set p 3617 N93-30453
GE networked mass storage solutions supporting IEEE network mass storage model p 3618 N93-30458
Evaluation of D-1 tape and cassette characteristics: Moisture content of Sony and Ampex D-1 tapes when delivered p 3435 N93-30466
Towards a 1000 tracks digital tape recorder
p 3435 N93-30469
Mass optical storage-tape (MOST)
p 3621 N93-30471
Electron trapping data storage system and applications p 3622 N93-30474
Toward a coordinated spatial data infrastructure for the nation
[B-149] p 3456 N93-30634

DIGITAL ELECTRONICS
Electronics mixed-mode simulation
[AD-A264734] p 3534 N93-30577

DIGITAL FILTERS
Theoretical bit error rate performance of the Kalman filter excisor for FM interference
[AD-A263018] p 3383 N93-29407
International Journal of Numerical Modeling: Electronic Networks, Devices, and Fields, volume 5, number 3, August 1992
[AD-A263765] p 3387 N93-29877

DIGITAL INTEGRATORS
Acousto-optic time-integrating correlators for processing wideband digital data p 3360 N93-30253

DIGITAL SYSTEMS
Digital image compression using artificial neural networks p 3624 N93-28811
Time-interpolation method for digital beamformers
[AD-D015709] p 3383 N93-29275
Multisensor image analysis system
[AD-A263679] p 3528 N93-29294
Optical antenna beam steering using digital phase shifter control
[AD-D015688] p 3383 N93-29455
Dynamics and robust control of sampled data systems for large space structures
[AD-A264192] p 3281 N93-30142
A new way to use fuzzy sets in image sharpening
p 3363 N93-30273
The NT digital micro tape recorder
p 3435 N93-30461
Towards a 1000 tracks digital tape recorder
p 3435 N93-30469
Topical meeting of broadband analog and digital optoelectronics
[AD-A264643] p 3581 N93-30522
ELF/VLF spectrum measurements
p 3398 N93-30745

DIGITAL TECHNIQUES
Digital image compression using artificial neural networks p 3624 N93-28811
Digital image processing of descanned terrestrial ground photographs p 3459 N93-28928
Multisensor image analysis system
[AD-A263679] p 3528 N93-29294
The modern high rate digital cassette recorder
p 3435 N93-30468

DILATOMETRY
The design and testing of a high-temperature graphite dilatometer
[AD-A262185] p 3430 N93-28488

DIMENSIONAL ANALYSIS
Quantum group generalization of the heterotic QFT
[DE92-644727] p 3607 N93-30920

DIMENSIONAL MEASUREMENT
Possibilistic measurement and set statistics
p 3517 N93-29567
Method of continuously determining crack length
[NASA-CASE-LAR-14480-1-CU] p 3452 N93-29612
Issues, concepts, and standard techniques in assessing accuracy of coordinate measuring machines
[PB93-184331] p 3354 N93-29666
Atmospheric transverse coherence length measurement system for laser communications
[AD-A263563] p 3439 N93-29827
Application of hardness testing in foundry processing operations: A university and industry partnership
p 3292 N93-30961

DIMERS
Be3(AsO4)2 2H2O: A new berylloarsenate phase containing bridged tetrahedral 3-rings
[AD-A262518] p 3592 N93-28584

DIODES
Analysis of electrothermal interactions in power semiconductor modules
[ETN-93-93800] p 3591 N93-28470
Influence of optical feedback on the pulse behavior of semiconductor lasers
[ETN-93-93798] p 3436 N93-28614
Electrochemical fabrication of cadmium chalcogenide microdiode arrays
[AD-A263169] p 3310 N93-28988
ND laser with co-doped ion(s) pumped by visible laser diodes
[AD-D015711] p 3437 N93-29277

DIPHENYL COMPOUNDS
The thermodynamic properties of thianthrene and phenoxathiin
[DE93-000124] p 3603 N93-28964

DIPOLE ANTENNAS
Coupling gain computation between antennas on circular cylinders at SHF/EHF frequencies p 3369 N93-30309
Orbiting transmitter and antenna for spaceborne communications at ELF/VLF to submerged submarines
p 3399 N93-30755

DIPOLE MOMENTS
Experimental study of location and identification of ferrous spheroids using a smart total field magnetometer
[AD-A263661] p 3324 N93-29391

DIPOLES
Computation of far-field helicopter rotor tone noise
[ONERA-P-1990-5] p 3562 N93-30110

DIRAC EQUATION
General method for reducing the two-body Dirac equation
[DE93-609833] p 3607 N93-30943
Relativity theory in (2 + 2)-space
[DE92-644671] p 3608 N93-30983

DIRECTIONAL ANTENNAS
A satellite-tracking millimeter-wave reflector antenna system for mobile satellite-tracking
[NASA-CASE-NPO-18772-1-CU] p 3381 N93-28955
Planar microstrip YAGI antenna array
[NASA-CASE-NPO-17873-2-CU] p 3384 N93-29507

DIRECTIONAL STABILITY
Hypersonic lateral and directional stability characteristics of aeroassist flight experiment configuration in air and CF4
[NASA-TM-4435] p 3239 N93-29166
Vehicle dynamic stability and rollover
[PB93-185437] p 3447 N93-30828

DIRECTIVITY
Evaluation of the scattered pressure due to infinite rigid cylinders, infinite elastic cylindrical shells, and rigid spheres in the presence of an ambient noise field
[AD-A264835] p 3563 N93-30899

DISABILITIES
Intelligent virtual reality in the setting of fuzzy sets
p 3513 N93-29544

DISCONTINUITY
An investigation of graphite peek composite under compression with a centrally located circular discontinuity
[AD-A262549] p 3298 N93-29414

DISCRETE FUNCTIONS
Topology and statistics in zero dimensions
[DE93-604080] p 3607 N93-30932

DISCRIMINANT ANALYSIS (STATISTICS)
Thunderstorm forecast study for Eglin AFB, Florida
[AD-A263423] p 3483 N93-29810

DISEASES
Wound healing and connective tissue metabolism: The role of hyperbaric oxygen therapy
[AD-A262483] p 3493 N93-28759
Proceedings of a Workshop on Molecular Nuclear Medicine
[DE93-010828] p 3493 N93-28835
Gene transcription and electromagnetic fields
[DE93-010854] p 3490 N93-28848
Incorporation of varying types of temporal data in a neural network p 3518 N93-29575
The AFOSR Workshop on the Future of EEG and MEG
[AD-A264338] p 3495 N93-30160

DISILICIDES
Refractory metal disilicides research
[AD-A262416] p 3320 N93-28499

DISK OPERATING SYSTEM (DOS)
Study on the concurrent calculation with a multitransputer network
[DE93-753191] p 3524 N93-28531

DISLOCATIONS (MATERIALS)
Fundamental studies of the mechanical behavior of microelectronics thin film materials
[AD-A264334] p 3337 N93-30417

DISPLACEMENT MEASUREMENT
Issues, concepts, and standard techniques in assessing accuracy of coordinate measuring machines
[PB93-184331] p 3354 N93-29666
Portable fiber optic coupled Doppler interferometer system for detonation and shock wave diagnostics
[DE93-009827] p 3433 N93-30510

DISPLAY DEVICES
Optically tiled flat panel displays. A feasibility study
[AD-A262737] p 3592 N93-28590
Combat Automation for Airborne Weapon Systems: Man/Machine Interface Trends and Technologies
[AGARD-CP-520] p 3501 N93-28850
Pilot intent and error recognition as part of a knowledge based cockpit assistant p 3502 N93-28855
The design and development of the new RAF standard HUD format p 3502 N93-28856
Symbology for head up and head down applications for highly agile fighter aircraft: To improve spatial awareness, trajectory control, and unusual attitude recovery, part 1
p 3502 N93-28857
Head-steered sensor flight test results and implications p 3502 N93-28859
Oculo-motor responses and virtual image displays
p 3503 N93-28862
Ergonomic development of digital map displays
p 3503 N93-28866
Application of ray tracing in radiation heat transfer
[NASA-TM-106206] p 3419 N93-29075

Grid Analysis and Display System (GrADS): A practical tool for earth science visualization p 3613 N93-29225
Remote vehicle survey tool
[DE93-010822] p 3460 N93-29255
Head mounted displays for virtual reality
[AD-A263498] p 3506 N93-29340
A tutorial on exit pupils and eye rotation with virtual image optical displays
[AD-A262399] p 3494 N93-29400
A comparison of simulated parallax and single-station range aids to navigation
[AD-A263460] p 3246 N93-29818
Virtual reality flight control display with six-degree-of-freedom controller and spherical orientation overlay
[NASA-CASE-NPO-18733-1-CU] p 3251 N93-30416
The effects of superimposing symbology on a simulated night vision goggle display
[AD-A263458] p 3508 N93-30590
Laser based 3D volumetric display system
[AD-A264825] p 3441 N93-30599
Introduction to the National Information Display Laboratory p 3628 N93-30718

DISSOCIATION
Kinetics of nitric oxide formation behind 3 to 4 KM/S shock waves
[AD-A263653] p 3312 N93-29389
Ion emission during high-energy sputtering of ammonium dinitramide and ammonium nitrate crystals and the determination of ion decomposition pathways using tandem mass spectrometry p 3318 N93-30066

DISSOLVED GASES
Interim fatigue design curves for carbon, low-alloy, and austenitic stainless steels in LWR environments
[DE93-009202] p 3323 N93-29102
Upper ocean model of dissolved atmospheric gases
[DE93-010151] p 3487 N93-29327

DISTRIBUTED FEEDBACK LASERS
Every good virtue you ever wanted in a Q-switched solid-state laser and more: Monolithic, diode-pumped, self-Q-switched, highly reproducible, diffraction-limited Nd:YAG laser p 3442 N93-28772

DISTRIBUTED PARAMETER SYSTEMS
Distributed traffic signal control using fuzzy logic
p 3513 N93-29543

DISTRIBUTED PROCESSING
A distributed object-oriented database application design
[AD-A262591] p 3612 N93-28846
Distributed Virtual System (DIVIRS) Project
[NASA-CR-193234] p 3526 N93-29169
Applying high-level language paradigms to communications software for distributed systems
[AD-A263001] p 3528 N93-29463
Data parallelism
[DE93-009300] p 3539 N93-29782
A redesigned Isis and Meta system under Mach
[AD-A263576] p 3531 N93-29976
OSI transaction processing standard: An introduction and outlines of implementation
[VTT-TIED-1250] p 3532 N93-29997
On analytical performance modelling of software for distributed systems p 3364 N93-30279
Mass storage system reference model, Version 4
p 3617 N93-30450
Technology for national asset storage systems
p 3617 N93-30452
Measurements over distributed high performance computing and storage systems p 3622 N93-30476
Nonlinear explicit transient finite element analysis on the Intel Delta
[DE93-009561] p 3535 N93-30647

DISTRIBUTION (PROPERTY)
Distribution of C1-C2 aldehydes in the free troposphere
[JUEL-2650] p 3475 N93-28475

DISTRIBUTION FUNCTIONS
Evidence-based classification of satellite image data
p 3459 N93-28931
Possibilistic measurement and set statistics
p 3517 N93-29567

DISULFIDES
The thermodynamic properties of thianthrene and phenoxathiin
[DE93-000124] p 3603 N93-28964

DIURNAL VARIATIONS
Sensitivity study of cloud/radiation interaction using a second order turbulence radiative-convective model
[DE93-007365] p 3477 N93-29346
Spectral energetics of the lower thermosphere
p 3477 N93-29467
ELF/VLF spectrum measurements
p 3398 N93-30745
Atmospheric studies with SODAR at Kalpakkam
[DE93-605544] p 3480 N93-30992

DIVERGENCE
Design of a particle beam satellite system for lunar prospecting p 3434 N93-28768

DIVERTERS
A survey of problems in divertor and edge plasma theory
[DE93-007531] p 3586 N93-29056
Effects of neutral gas collisions on the power transmission factor at the divertor sheath
[DE93-009320] p 3588 N93-29334
Modeling the D3-D plasma boundary with the LEDGE code
[DE93-009301] p 3588 N93-29772
Optimization for steady-state and hybrid operations of ITER by using scaling models of divertor heat load
[DE93-764151] p 3590 N93-30649

DIVING (UNDERWATER)
Elastic stability considerations for deep submergence ceramic pressure housing
[AD-A264824] p 3454 N93-30598

DMSP SATELLITES
Electrodynamics of the dayside cleft region based on ground observations at Svalbard
[AD-A263571] p 3477 N93-29831
TACSAT meteorological payloads
p 3391 N93-29913

DOCUMENTATION
A model for processing the SGML document in version oriented hypertext systems
[ETN-93-93797] p 3611 N93-28528

DOCUMENTS
A model for processing the SGML document in version oriented hypertext systems
[ETN-93-93797] p 3611 N93-28528

DOMAINS
Comparison of specificity and information for fuzzy domains p 3510 N93-29519
Automated modeling of physical systems
[NASA-CR-193256] p 3531 N93-29873

DONOR MATERIALS
Optically switchable conductive polymers
[AD-A264751] p 3337 N93-30557
Experimental and theoretical aspects of excited state electron transfer and related phenomena
[AD-A263457] p 3570 N93-30589

DOORS
F-15 composite engine access door
p 3302 N93-30442

DOPED CRYSTALS
Theory of normal and superconducting properties of fullerene-based solids
[DE93-007722] p 3592 N93-28582
Texturing of InP surfaces for device applications
[NASA-TM-106061] p 3321 N93-28618
High octane ethers from synthesis gas-derived alcohols
[DE93-012470] p 3341 N93-28752
Subnanosecond high power performance of a bistable optically-controlled GaAs switch
[DE93-006285] p 3406 N93-28944
Uniaxially stressed Ge:Ga and Ge:Be
[DE93-010426] p 3594 N93-29150
Method of emitting on a specific wavelength fraunhofer line using a neodymium doped laser transmitter
[AD-D015710] p 3437 N93-29276
Quantum devices using Si-based superlattices and structures
[AD-A263700] p 3595 N93-29383
Ambient-atmosphere compatible superconducting fullerenes
[AD-A262025] p 3595 N93-29397
Defect studies in low-temperature-grown GaAs
[DE93-010405] p 3595 N93-29417
LEO effects on candidate solar cell cover materials
p 3467 N93-29687
Photoinduced charge separation in Q1D heterojunction materials: Evidence for electron-hole pair separation in mixed-halide MX solids
[AD-A264711] p 3598 N93-30501
Photoinduced electron-hole charge separation, intrinsic self-doping and novel device applications of Q1D heterojunction materials: Mixed-halide MX solids
[AD-A264714] p 3600 N93-30569
A tight binding model for the electronic structure of FCC and SC C60
[DE93-606214] p 3601 N93-30794

DOPPLER EFFECT
Some aspects of the aeroacoustics of high-speed jets
[NASA-CR-191458] p 3418 N93-28975
Acquisition of physiological data during G-induced Loss of Consciousness (G-LOC)
[AD-A264492] p 3496 N93-30400

DOPPLER NAVIGATION
Advanced Unmanned Search System (AUSS) supervisory command, control and navigation
[AD-A263171] p 3245 N93-28990

DOPPLER RADAR
Control-structures interaction test of the LACE satellite
p 3263 N93-28706
Doppler-radar wind-speed measurements in tornadoes: A comparison of real and simulated spectra
[DE93-008734] p 3481 N93-29095
Contributions to the American Meteorological Society's 26th International Conference on Radar Meteorology
[AD-A263385] p 3481 N93-29257
The effect of clock, media, and station location errors on Doppler measurement accuracy
p 3246 N93-29588

DOSAGE
The chronic effects of jP-8 jet fuel exposure on the lungs
[AD-A264162] p 3495 N93-30153

DOSIMETERS
Radiation monitoring equipment dosimeter experiment
p 3266 N93-28730
The emulsion chamber technology experiment
p 3268 N93-28743
Status of LDEF ionizing radiation measurements and analysis p 3654 N93-29626
A measurement of the radiation dose to LDEF by passive dosimetry p 3572 N93-29634
LDEF: Dosimetric measurement results (AO 138-7 experiment) p 3573 N93-29635
Development and application of a 3-D geometry/mass model for LDEF satellite ionizing radiation assessments
p 3573 N93-29640
Radiation model predictions and validation using LDEF satellite data p 3573 N93-29641

DOWN-CONVERTERS
Wide-bandwidth high-resolution search for extraterrestrial intelligence
[NASA-CR-193137] p 3509 N93-28895
Technical examination and simulation of a photovoltaic system: Solar generator, battery, download
[ETN-93-94179] p 3466 N93-30573

DOWNLINKING
Onboard signal processing: Wave of the future for planetary radio science? p 3646 N93-28801
Experimental and modal verification of an integral equation solution for a thin-walled dichroic plate with cross-shaped holes p 3385 N93-29591
A satellite downlink spread spectrum timing beacon
p 3362 N93-30267

DRAG
Bounds on internal state variables in viscoplasticity
[NASA-TM-106215] p 3451 N93-29196

DRAG REDUCTION
Flow visualization on helicopter blades using acenaphthen
[ESA-TT-1255] p 3422 N93-29273
Turbulent drag reduction: Studies of feedback control and flow over riblets p 3242 N93-30645

DREDGING
System analysis for a kinematic positioning system based on the global positioning system
[AD-A262830] p 3245 N93-29468

DRIFT RATE
Radiation sensitivity of quartz crystal oscillators experiment for the Long Duration Exposure Facility (LDEF), part 2 p 3414 N93-29685

DRILLING
Drill/borescope system for the Mars Polar Pathfinder
p 3647 N93-28805
Fugitive hydrocarbon emissions from Pacific OCS facilities, volume 1
[PB93-173797] p 3468 N93-28899
Fugitive hydrocarbon emissions from Pacific OCS facilities. Volume 2: Executive summary and user's guide
[PB93-173805-VOL-2] p 3471 N93-29861

DROP SIZE
Limitations of the ideal phase-Doppler system: Extension to spatially and temporally inhomogeneous particle flows with an application to diesel sprays
[DE93-009447] p 3416 N93-28595
Modeling the effects of drop drag and breakup on fuel sprays
[AD-A263650] p 3445 N93-29388
Nonlinear spectroscopy of multicomponent droplets and two- and three-dimensional measurements in flames
[AD-A264341] p 3425 N93-30162

DROPS (LIQUIDS)
Estimation of droplet collision frequency in a spray
[DE93-007991] p 3416 N93-28566
Studies of complexity in fluid systems
[DE93-010776] p 3418 N93-28878
A four-field approach towards developing a mechanistic model for multiphase flow
[DE93-006572] p 3420 N93-29126
Pulse mitigation and heat transfer enhancement techniques. Volume 1: Spray cooling
[AD-A263495] p 3423 N93-29352

Nonlinear spectroscopy of multicomponent droplets and two- and three-dimensional measurements in flames
[AD-A264341] p 3425 N93-30162

DROUGHT

Atmospheric and Geophysical Sciences Division: G-Division did you know?
[DE93-007412] p 3469 N93-28967

DRUGS

Pharmacokinetics and Pharmacodynamics in Space
[NASA-CP-10048] p 3494 N93-29502

DUALITY THEOREM

The space of spheres, a geometric tool to unify duality results in Voronoi diagrams
[INRIA-RR-1620] p 3547 N93-28512

DUCTED FLOW

A numerical study of confined turbulent jets
[NASA-TM-106197] p 3420 N93-29161

DUCTILITY

Environmental embrittlement of binary and Zr-doped Ni3Al
[DE93-008575] p 3321 N93-28679

The effect of temperature on the impact behavior of TiB2 reinforced XDTM-TiAl intermetallic matrix composites
[AD-A262924] p 3296 N93-28886

Transformation plasticity in ductile solids
[DE93-008636] p 3321 N93-28902

Materials characterization of cermet anodes tested in a pilot cell
[DE93-008924] p 3323 N93-29101

Tailored interfaces for metal-matrix composites-fundamental considerations
[AD-A263048] p 3298 N93-29130

Effects of internal helium on mechanical properties of Nitronic (tm) 40 stainless steel
[DE93-009902] p 3324 N93-29265

Low temperature environmental embrittlement in ordered intermetallics
[DE93-009711] p 3324 N93-29786

Balanced technology initiative on computational mechanics of materials
[AD-A263906] p 3453 N93-29863

Improvement in ductility of the intermetallic compound Ti3Al
[ESA-TT-1276] p 3325 N93-30105

Two-parameter crack tip field associated with stable crack growth in a thin plate: A hybrid analysis
[AD-A264221] p 3453 N93-30147

Durability of Quick Reaction Satellite Antenna (QRSA) trunnion castings
[AD-A264095] p 3281 N93-30813

DUCTS

Turbulent flow and heat transfer in idealized blade cooling passages p 3254 N93-29938

An L2F-measurement device with image rotator prism for flow velocity analysis in rotating coolant channels
p 3255 N93-29942

DUMP COMBUSTORS

Thrust augmentation system for low-cost-expendable turbojet engine
[AD-A263727] p 3259 N93-30877

DUNITE

Frequency dependent electrical properties of minerals and partial-melts
[DE93-009254] p 3410 N93-29793

DURABILITY

Durability of Quick Reaction Satellite Antenna (QRSA) trunnion castings
[AD-A264095] p 3281 N93-30813

DUST

Drill/borescope system for the Mars Polar Pathfinder
p 3647 N93-28805

DWARF GALAXIES

Can physical stellar collisions explain the blue stragglers in the dwarf spheroidal galaxies?
[DE93-008711] p 3634 N93-28907

The 12 UM contribution of nearby galaxies to the infrared background
[AD-A264336] p 3654 N93-30419

DWARF NOVAE

Multiwavelength studies of classical nova shells
p 3636 N93-30412

DWARF STARS

Magnetic activity in low mass stars
[DE93-009073] p 3632 N93-28547

Spectroscopic and photometric studies of main sequence M stars and a search for late-type dwarfs in the solar vicinity p 3629 N93-28608

DYE LASERS

Effects of vacuum exposure on stress and spectral shift of high reflective coatings
[DE93-009318] p 3437 N93-29207

Computer control of pulsed tunable dye lasers
[DE93-605896] p 3441 N93-30801

Efficient laser action from two CW laser pumped pyrromethene-BF2 complexes
[AD-A264887] p 3441 N93-30910

DYES

Characterization of slow chromophore reorientation in nonlinear optical polymers by two-dimensional MAS NMR
[AD-A264809] p 3338 N93-30596

DYNAMIC CHARACTERISTICS

A complete set of field equations for the dynamic simulation of a towed cable system
[AD-A262570] p 3442 N93-28578

Interaction dynamics of on-orbit construction
p 3274 N93-29109

Hybrid CMS methods with model reduction for assembly of structures p 3274 N93-29110

Molecular dynamics of detonation in crystals with defects p 3350 N93-30097

A computational model that couples aerodynamic and structural dynamic behavior of parachutes during the opening process
[AD-A264115] p 3241 N93-30119

DYNAMIC CONTROL

Controls of interaction dynamics of orbital assembly
p 3275 N93-29111

Articulated fin/wing control system
[AD-D015712] p 3259 N93-29278

Automated reasoning with function evaluation for COCOLOG
[INRIA-RR-1713] p 3529 N93-29488

Clustering of tethered satellite system simulation data by an adaptive neuro-fuzzy algorithm
p 3512 N93-29535

Dynamics and robust control of sampled data systems for large space structures
[AD-A264192] p 3281 N93-30142

DYNAMIC LOADS

Dynamic ice structure interaction: Theory and applications
[VTT-PUBS-90] p 3353 N93-28632

Structural load control during construction
p 3275 N93-29113

Sudden loading and fatigue effects on the human spine
[PB93-167526] p 3493 N93-29199

DYNAMIC MODELS

A complete set of field equations for the dynamic simulation of a towed cable system
[AD-A262570] p 3442 N93-28578

Interaction dynamics of on-orbit construction
p 3274 N93-29109

Lunar crane system p 3277 N93-29118

Vibration control of flexible space structures in noisy environment p 3285 N93-30235

Trajectory generation for dual-arm robots using artificial impedance approach p 3370 N93-30310

Experimental and analytical investigation of finger-follower cam systems p 3446 N93-30378

On symmetric central configurations with application to satellite motion about rings p 3652 N93-31000

A dynamical model of structural phase transition in La2CuO4
[DE93-605325] p 3602 N93-31025

DYNAMIC PROGRAMMING

Flow control using the theory of zero sum Markov games
[INRIA-RR-1597] p 3553 N93-28507

Robust and efficient implementation of the Delaunay tree
[INRIA-RR-1619] p 3547 N93-28511

A self-learning rule base for command following in dynamical systems p 3512 N93-29531

Adaptive networks for sequential decision problems
[AD-A264756] p 3534 N93-30561

Examinations of perturbation reduction by automatic speech dependent recognition of separately spoken single words
[ETN-93-94180] p 3394 N93-30672

DYNAMIC RANGE

Processing, fabrication, and demonstration of HTS integrated microwave circuits
[AD-A263161] p 3406 N93-28940

ELF/VLF spectrum measurements
p 3398 N93-30745

DYNAMIC RESPONSE

Control-structures interaction test of the LACE satellite
p 3263 N93-28706

A computational model that couples aerodynamic and structural dynamic behavior of parachutes during the opening process
[AD-A264115] p 3241 N93-30119

Containment of explosions in spherical vessels
[DE93-005445] p 3446 N93-30211

Static and dynamic large deflection flexural response of graphite-epoxy beams
[NASA-CR-4118] p 3454 N93-30374

Experimental and analytical investigation of finger-follower cam systems p 3446 N93-30378

DYNAMIC STABILITY

Vehicle dynamic stability and rollover
[PB93-185437] p 3447 N93-30828

DYNAMIC STRUCTURAL ANALYSIS

The dynamics and control of space tethers
p 3274 N93-28629

Dynamic ice structure interaction: Theory and applications
[VTT-PUBS-90] p 3353 N93-28632

NASA instep/MDMSC jitter suppression experiment (JITTER) p 3263 N93-28702

Description of the Joint Damping Experiment (JDX)
p 3263 N93-28703

Control-structures interaction test of the LACE satellite
p 3263 N93-28706

Upper atmosphere research satellite jitter study
p 3264 N93-28708

Controls of interaction dynamics of orbital assembly
p 3275 N93-29111

An integrated optimum design approach for high speed prop-rotors including acoustic constraints
[NASA-CR-193222] p 3248 N93-29153

Testing in combined dynamic environments
[DE93-010679] p 3278 N93-29250

Modal survey of a full-scale F-18 wind tunnel model
[AD-A262482] p 3240 N93-29410

Containment of explosions in spherical vessels
[DE93-005445] p 3446 N93-30211

Static and dynamic large deflection flexural response of graphite-epoxy beams
[NASA-CR-4118] p 3454 N93-30374

The middeck 0-gravity dynamics experiment
[NASA-CR-4500] p 3281 N93-30376

Theoretical and experimental investigation of slack cable/mass system dynamics p 3455 N93-31028

DYNAMIC TESTS

The middeck 0-gravity dynamics experiment
[NASA-CR-4500] p 3281 N93-30376

DYNAMICAL SYSTEMS

Nonlinear dynamics and plasma transport
[DE93-012238] p 3585 N93-28749

SIAM Conference on Applications of Dynamical Systems
[DE93-007969] p 3548 N93-29057

Robust feedforward/feedback control synthesis for uncertain dynamical systems p 3542 N93-29079

Estimating the parameters of chaotic maps
[AD-A262574] p 3556 N93-29423

A composite self tuning strategy for fuzzy control of dynamic systems p 3511 N93-29530

A self-learning rule base for command following in dynamical systems p 3512 N93-29531

Learning characteristics of a space-time neural network as a tether skiprope observer p 3512 N93-29534

Designing a fuzzy scheduler for hard real-time systems p 3512 N93-29537

Non-scalar uncertainty: Uncertainty in dynamic systems p 3517 N93-29565

Knot invariants and cellular automata
[AD-A264199] p 3607 N93-30884

On symmetric central configurations with application to satellite motion about rings p 3652 N93-31000

On neural networks in identification and control of dynamic systems
[NASA-TM-107702] p 3455 N93-31038

DYNAMO THEORY

The production and evolution of plasma and associated magnetic fields during hypervelocity impacts: Implications for planetary paleomagnetism p 3589 N93-30000

E

EAR PROTECTORS

Sound attenuation characteristics of the standard DH-132A and SPH-4 helmets worn in combination with standard issue earplugs
[AD-A263011] p 3506 N93-29406

EARTH (PLANET)

Proceedings of the Near-Earth-Object Interception Workshop
[NASA-TM-108236] p 3556 N93-28572

EARTH ATMOSPHERE

Prognostic cloud water in the Los Alamos general circulation model
[DE93-007381] p 3482 N93-29347

EARTH CORE

Modern seismic travel time tables and station corrections for P and S waves
[AD-A262536] p 3477 N93-29412

EARTH GRAVITATION

Investigation of a geodesy coexperiment to the Gravity Probe B relativity gyroscope program
[NASA-CR-193263] p 3460 N93-29179

EARTH IONOSPHERE
Ionospheric structure specifications and systems effects
[AD-A263573] p 3476 N93-29343
Electrodynamics of the dayside cleft region based on ground observations at Svalbard
[AD-A263571] p 3477 N93-29831
Variability of the electric field strength in the earth-ionosphere waveguide due to variations in the electron density profile
[AD-A264808] p 3394 N93-30595
The cone structure and focusing of the electric field of VLF and LF waves at high altitudes of the ionosphere
p 3395 N93-30731
Transient (approximately equals 10 s) VLF amplitude and phase perturbations due to lightning-induced electron precipitation into the ionosphere (the Trimpi effect)
p 3396 N93-30736
Studies of the propagation of Low Frequency (LF) radio waves p 3396 N93-30738

EARTH LIMB
Honeywell's compact, wide-angle UV-visible imaging sensor p 3582 N93-28806

EARTH MAGNETOSPHERE
Transfer Orbit Plasma Interaction Experiment (TROPIX) p 3267 N93-28734
Plasma, magnetic, and electromagnetic measurements at nonmagnetic bodies p 3647 N93-28809
The dynamic cusp at low altitudes: A case study combining Viking, DMSP, and Sondrestrom incoherent scatter radar observations
[NASA-CR-193152] p 3476 N93-28842
FNAS CRRES program completion
[NASA-CR-192468] p 3476 N93-29032

EARTH MANTLE
Geochemical and fluid dynamic investigations into the nature of chemical heterogeneity in the Earth's mantle
[AD-A262753] p 3477 N93-29405
Modern seismic travel time tables and station corrections for P and S waves
[AD-A262536] p 3477 N93-29412

EARTH OBSERVATIONS (FROM SPACE)
Space research in Germany 1990-1991
[ETN-93-93807] p 3654 N93-28477
Advanced Earth Observing Satellite (ADEOS)
p 3279 N93-29648
The 1990-1991 project summaries
p 3234 N93-29755
Evolution or revolution: The Catch 22 of TACSATs
p 3269 N93-29894
NOAA satellite programs and technology requirements
p 3627 N93-30710

EARTH OBSERVING SYSTEM (EOS)
Multi-channel holographic birfurcative neural network system for real-time adaptive EOS data analysis
p 3614 N93-29231

EARTH ORBITAL ENVIRONMENTS
Thermal control paints on LDEF: Results of M0003 sub-experiment 18
[AD-A263252] p 3329 N93-28561
Solar Array Module Plasma Interaction Experiment (SAMPIE) p 3265 N93-28716
The Photovoltaic Array Space Power Plus diagnostics (PASP Plus) flight experiment p 3265 N93-28717
Return flux experiment p 3266 N93-28727
Radiation monitoring equipment dosimeter experiment
p 3266 N93-28730
LDEF materials data bases
[NASA-TM-107757] p 3290 N93-29067
Effects of atomic oxygen and ultraviolet radiation on candidate elastomeric materials for long duration missions. Test series no.1
[NASA-TM-108408] p 3331 N93-29193
Hypervelocity impact facility for simulating materials exposure to impact by space debris
p 3283 N93-29365
Analysis of LDEF micrometeoroid/debris data and damage to composite materials p 3309 N93-29366
LDEF data: Comparisons with existing models
p 3283 N93-29375
The Interstellar Gas Experiment: Analysis in progress
p 3639 N93-29380
LDEF microenvironments, observed and predicted
p 3283 N93-29623
A generalized approach to the thermal analysis of the Long Duration Exposure Facility's flight experiments
p 3428 N93-29624
The effect of the low Earth orbit environment on space solar cells: Results of the Advanced Photovoltaic Experiment (S0014) p 3467 N93-29686
LEO effects on candidate solar cell cover materials
p 3467 N93-29687
New results from FRECOPA analysis
p 3448 N93-29688
Degradation of electro-optic components aboard LDEF p 3582 N93-29689
Characterization of a space orbited incoherent fiber optic bundle p 3583 N93-29698
Future radiation measurements in low Earth orbit
p 3654 N93-29708
Advanced research in sky surveillance: A search for low-luminosity objects
[AD-A264832] p 3631 N93-30629

EARTH ORBITS
SEU tolerant computer based on the R3000
[DE93-009294] p 3520 N93-29058

EARTH RADIATION BUDGET
Prognostic cloud water in the Los Alamos general circulation model
[DE93-007381] p 3482 N93-29347

EARTH RESOURCES
Tropical forests and biological diversity: USAID report to Congress 1990-1991
[PB93-180453] p 3471 N93-29681
Geoscience center research
[AD-A263465] p 3462 N93-29834
What's past is prologue: Supporting global change research with historical data
[DE93-005777] p 3472 N93-30009

EARTH ROTATION
Refinements on the pinhole camera measurements of the LDEF attitude p 3283 N93-29622

EARTH SCIENCES
JPRS report: Science and technology. Central Eurasia: Earth science
[JPRS-UES-93-003] p 3456 N93-29089
NSSDC data listing
[NASA-TM-108264] p 3612 N93-29167
Grid Analysis and Display System (GrADS): A practical tool for earth science visualization p 3613 N93-29225
JPRS report: Science and technology. Central Eurasia: Earth sciences
[JPRS-UES-93-002] p 3456 N93-30624

EARTH SURFACE
SAR shape-from-shading for a populated alpine area
p 3458 N93-28923

EARTH TERMINALS
Terrain and coverage prediction analyses for non-geostationary orbit EHF satellite communications
p 3389 N93-29902
Teleglobe's international Mobile Earth Terminal service p 3371 N93-30317

EARTH TIDES
Tidal and lunar data for Point Mugu, San Nicolas island, and the Barking Sanda area during 1993
[AD-A262725] p 3477 N93-29401

EARTH-IONOSPHERE WAVEGUIDE
Variability of the electric field strength in the earth-ionosphere waveguide due to variations in the electron density profile
[AD-A264808] p 3394 N93-30595
A long wave TE/TM noise prediction model
p 3397 N93-30742

EARTH-MOON SYSTEM
Double swingby at Earth-Moon for increase of excess velocity
[ETN-93-94177] p 3270 N93-30582

EARTHQUAKES
DSS-14 subreflector actuator dynamics during the Landers earthquake p 3386 N93-29600
Modeling earthquakes with local and regional broadband data p 3478 N93-30005

ECOLOGY
JPRS report: Science and technology. Central Eurasia: Earth science
[JPRS-UES-93-003] p 3456 N93-29089
Tropical forests and biological diversity: USAID report to Congress 1990-1991
[PB93-180453] p 3471 N93-29681
The environment as an operational center of gravity
[AD-A264170] p 3472 N93-30154

ECONOMIC ANALYSIS
Multi-Attribute Decision Theory methodology for pollution control measure analysis
[DE93-005444] p 3472 N93-30008
Prefeasibility study on compressed air energy storage systems
[VTT-TIED-1267] p 3465 N93-30111
Viability assessment for reliable long-wave communication links p 3399 N93-30754

ECONOMIC FACTORS
Global warming issue and global economic model
[DE93-781334] p 3468 N93-28881

ECONOMIC IMPACT
Using a neural network to estimate solvent consumption
[PB93-173110] p 3467 N93-28873

ECOSYSTEMS
Predicting the response of a temperate forest ecosystem to atmospheric CO2 increase
[DE93-010081] p 3467 N93-28543
State of the art: Ecological biomarkers
[DE93-006621] p 3469 N93-28992
Proposal to develop guides for high school teachers on global systems science
[DE93-008759] p 3624 N93-29100
Tropical forests and biological diversity: USAID report to Congress 1990-1991
[PB93-180453] p 3471 N93-29681
Environmental Monitoring and Assessment Program. EMAP: Arid Colorado plateau pilot study
[PB93-181618] p 3474 N93-30823

EDDY CURRENTS
Reliability assessment at airline inspection facilities. Volume 2: Protocol for an eddy current inspection reliability experiment
[DOT/FAA/CT-92/12-VOL-2] p 3449 N93-28685

EDDY VISCOSITY
Large eddy simulations of shockwave passage through turbulence
[DE92-019503] p 3419 N93-29050

EDGE DETECTION
A robust multi-operator 3-D edge detection approach for range image segmentation p 3366 N93-30288

EDGE DISLOCATIONS
Dislocation roles in energetic crystal responses
p 3348 N93-30086

EDUCATION
A demonstration of simple airfoils: Structural design and materials choices
[DE93-007882] p 3238 N93-28662
Proposal to develop guides for high school teachers on global systems science
[DE93-008759] p 3624 N93-29100
Advanced network technology: Background paper
[OTA-BP-TCT-101] p 3539 N93-29650
Concept formulation process aid for trade-off determination: Operator's guide
[AD-A263756] p 3531 N93-29874
Research and education by SF cyclotron facility
[DE93-753135] p 3576 N93-30002
Profiles of major federal literacy programs
[PB93-163863] p 3608 N93-30657
Filling the gaps: An overview of data on education in grades K through 12
[PB93-176550] p 3608 N93-30821
National Educators' Workshop. Update 92: Standard Experiments in Engineering Materials Science and Technology
[NASA-CP-3201] p 3290 N93-30948
Experiments in corrosion for younger students by and for older students p 3291 N93-30955
Introduction to high performance composites
p 3291 N93-30957
Materials education activities p 3291 N93-30958
Experiments in materials science from household items p 3293 N93-30971
An automated data collection system for a Charpy impact tester p 3293 N93-30972
Visualizing weld metal solidification using organic analogs p 3293 N93-30973
Taguchi method of experimental design in materials education p 3294 N93-30975
Powder metallurgy: Solid and liquid phase sintering of copper p 3294 N93-30976
High thermal conductivity of diamond
p 3294 N93-30977
Temperature-dependent electrical conductivity of soda-lime glass p 3294 N93-30978
Construction and testing of simple airfoils to demonstrate structural design, materials choice, and composite concepts p 3243 N93-30979

EDUCATIONAL TELEVISION
Review of the effectiveness of video media in instruction
[AD-A264226] p 3392 N93-30362

EFFERENT NERVOUS SYSTEMS
Evolving neural network architecture
[AD-A264802] p 3544 N93-30592

EFFLUENTS
Analysis of mass transport and potential vorticity budget in a simulated tropopause folding
[PB93-156792] p 3476 N93-29197

EIGENVALUES
Classification theorem for principal fibre bundles, Berry's phase, and exact cycle evolution
[DE93-011114] p 3556 N93-28601
A normally elliptic Hamiltonian bifurcation
[W-9201] p 3548 N93-28753
A summary of block schemes for reducing a general matrix to Hessenberg form
[DE93-010621] p 3525 N93-28877
Benchmark eigenvalue spectrum calculations with anisotropic effects
[DE93-006387] p 3548 N93-28891
Stabilization using low-gain PI control: SISO case
[OUEL-1947/92] p 3541 N93-28898

Vertical slot convection: A linear study
[DE93-007643] p 3423 N93-29804

EIGENVECTORS
Classification theorem for principal fibre bundles, Berry's phase, and exact cycle evolution
[DE93-011114] p 3556 N93-28601
A summary of block schemes for reducing a general matrix to Hessenberg form
[DE93-010621] p 3525 N93-28877
Benchmark eigenvalue spectrum calculations with anisotropic effects
[DE93-006387] p 3548 N93-28891

EINSTEIN EQUATIONS
The semiclassical stability of de Sitter spacetime
[DESY-92-131] p 3603 N93-28472

EISCAT RADAR SYSTEM (EUROPE)
Electrodynamics of the dayside cleft region based on ground observations at Svalbard
[AD-A263571] p 3477 N93-29831

EJECTA
Hypervelocity impact facility for simulating materials exposure to impact by space debris
p 3283 N93-29365
Multiwavelength studies of classical nova shells
p 3636 N93-30412
Spacecraft studies of Phobos and Mars
[NASA-CR-193298] p 3651 N93-30635

EL NINO
Atmospheric and Geophysical Sciences Division: G-Division did you know?
[DE93-007412] p 3469 N93-28967
A water mass analysis of the 1991-1992 El Nino signal in the Farallon Islands region
[AD-A263490] p 3488 N93-29819

ELASTIC BARS
A Riemann problem for an elastic bar that changes phase
[AD-A262827] p 3452 N93-29432

ELASTIC CYLINDERS
The wave, the cylinder, and the plate
[DE93-009458] p 3450 N93-28596
Evaluation of the scattered pressure due to infinite rigid cylinders, infinite elastic cylindrical shells, and rigid spheres in the presence of an ambient noise field
[AD-A264835] p 3563 N93-30899

ELASTIC DEFORMATION
Experiment and analysis on elastic deformation properties of graphite and carbon materials for HTTR core components
[DE93-753271] p 3299 N93-30004

ELASTIC PROPERTIES
The curvature of plane elastic curves
[AD-A263198] p 3450 N93-28516
Influence of ply waviness on stiffness and strength reduction of composite laminates
[AD-A263224] p 3294 N93-28559
Quiet by design: Numerical acousto-elastic analysis of aircraft structures
[ISBN-90-386-0042-9] p 3248 N93-29268
Some problems in the mechanics of solids with phase mixtures
[AD-A263652] p 3311 N93-29291
Electron interactions with non-linear polyatomic molecules and their radicals and ions
[AD-A262279] p 3568 N93-29446
Three-dimensional elastic stress analysis in materials with many inhomogeneities
[AD-A263736] p 3453 N93-29855
Balanced technology initiative on computational mechanics of materials
[AD-A263906] p 3453 N93-29863
Experiment and analysis on elastic deformation properties of graphite and carbon materials for HTTR core components
[DE93-753271] p 3299 N93-30004
Damage mechanics in 2-D and 3-D microstructures
[AD-A264337] p 3453 N93-30159
Elastic stability considerations for deep submergence ceramic pressure housing
[AD-A264824] p 3454 N93-30598
Micropipet manipulation of lipid membranes: Direct measurement of the material properties of a cohesive structure that is only two molecules thick
p 3291 N93-30953

ELASTIC SCATTERING
Spin observables in large t elastic N-N scattering
[DE93-009211] p 3564 N93-28549
The wave, the cylinder, and the plate
[DE93-009458] p 3450 N93-28596
Elastic and reactive collisions of atoms and molecules with neutral alkali clusters
[DE93-009313] p 3566 N93-29206
Measurement of W-Z interference from neutrino-electron scattering
[DE93-010724] p 3566 N93-29313
Coupled-channel analysis of low energy nucleon-antinucleon interactions
[DE93-606115] p 3571 N93-30791

ELASTIC SHELLS
Sound wave scattering from an elastic spherical shell
[AD-A264039] p 3562 N93-30029

ELASTIC WAVES
Determination of the space charge distribution within an e-irradiated polymer using the pressure wave propagation method
[ONERA-P-1990-4] p 3335 N93-30024

ELASTOMERS
Evaluation of polyaryl adhesives in elastomer-stainless steel joints
[DE93-009794] p 3329 N93-28551
Effects of atomic oxygen and ultraviolet radiation on candidate elastomeric materials for long duration missions. Test series no.1
[NASA-TM-108408] p 3331 N93-29193

ELBOW (ANATOMY)
Prosthetic elbow joint
[NASA-CASE-MFS-28707-1] p 3508 N93-30566

ELECTRETS
Determination of the space charge distribution within an e-irradiated polymer using the pressure wave propagation method
[ONERA-P-1990-4] p 3335 N93-30024

ELECTRIC AUTOMOBILES
Technical examination and simulation of a photovoltaic system: Solar generator, battery, download
[ETN-93-94179] p 3466 N93-30573

ELECTRIC BATTERIES
In situ characterization of interfacial and bulk properties of lithium polymer batteries using 4-probe DC techniques
[DE93-007699] p 3405 N93-28581
Approach to extending the cycle life of lithium secondary battery
[DE93-776266] p 3406 N93-28983
Evaluation of actuator energy storage and power sources for spacecraft applications
[NASA-CR-193226] p 3288 N93-29091
The ANL electric vehicle battery R/D program for DOE-EHP
[DE93-010658] p 3408 N93-29311
Temperature compensated lithium battery energy monitor
[AD-D015680] p 3409 N93-29605
Synthesis and properties of a cation-conducting, high temperature polymer electrolyte
[AD-A263557] p 3334 N93-29825

ELECTRIC CHARGE
Research and development of carbon black anodes for lithium secondary cells
[DE93-781331] p 3406 N93-28746
Dynamics and photoexcitation in MX and MXX' chain solids
[AD-A264823] p 3561 N93-29711
Some problems of relativistic electrodynamics
[DE92-644738] p 3400 N93-30923

ELECTRIC CONDUCTORS
Apparatus for intercalating large quantities of fibrous structures
[NASA-CASE-LEW-15077-2] p 3298 N93-29609

ELECTRIC CONNECTORS
Characteristic and development report SA3581/MC4196 Lightning Arrestor Connector (LAC)
[DE93-010610] p 3412 N93-30118

ELECTRIC CURRENT
Fiber-optic currents measurements
[DE93-007970] p 3579 N93-29350
Two-dimensional model for current and heat transport in solid-armature railguns
[AD-A262014] p 3271 N93-29394
Some problems of relativistic electrodynamics
[DE92-644738] p 3400 N93-30923

ELECTRIC DIPOLES
The cone structure and focusing of the electric field of VLF and LF waves at high altitudes of the ionosphere
p 3395 N93-30731
ELF propagation in deep and shallow sea water
p 3397 N93-30739
Comparative study of undersea fields produced by various dipoles p 3397 N93-30740

ELECTRIC DISCHARGES
Discharge of electrically charged clouds
[AD-A263212] p 3480 N93-28518
Research and development of carbon black anodes for lithium secondary cells
[DE93-781331] p 3406 N93-28746
Approach to extending the cycle life of lithium secondary battery
[DE93-776266] p 3406 N93-28983
Aircraft and refueler bonding and grounding study
[AD-A262027] p 3261 N93-29398
Determination of the space charge distribution within an e-irradiated polymer using the pressure wave propagation method
[ONERA-P-1990-4] p 3335 N93-30024

ELECTRIC ENERGY STORAGE
Alkali metal carbon dioxide electrochemical system for energy storage and/or conversion of carbon dioxide to oxygen
[NASA-CASE-LEW-14973-1] p 3464 N93-28974

ELECTRIC EQUIPMENT TESTS
Total dose tests for the PROMICS-3 instrument
[VTT-TIED-1203] p 3411 N93-30108

ELECTRIC FIELD STRENGTH
Mithras studies of the boundary between open and closed field lines
[AD-A264758] p 3479 N93-30562
Variability of the electric field strength in the earth-ionosphere waveguide due to variations in the electron density profile
[AD-A264808] p 3394 N93-30595

ELECTRIC FIELDS
Polar order and relaxation of second order nonlinear optical susceptibility in an electric field polarized amorphous polymer
[AD-A262189] p 3329 N93-28489
Observation of a beam energy shift caused by a plasma wakefield
[DE93-753243] p 3583 N93-28533
Plasma, magnetic, and electromagnetic measurements at nonmagnetic bodies p 3647 N93-28809
Coherent and semi-coherent neutron transfer reactions
[DE93-008336] p 3565 N93-28959
Proceedings of the Thunder and Lighting Seminar and the 3D Lightning Warning Workshop
[AD-A262766] p 3482 N93-29304
Fast multipole method in simulations of aqueous systems
[AD-A263422] p 3567 N93-29336
Electric field induced phenomena in STM: Tip deformations and Au(111)-surface phase transitions during tunneling spectroscopy experiments
[AD-A262208] p 3596 N93-29445
Molecular dynamics modeling of electric double layers with spectroscopic applications
[AD-A263168] p 3568 N93-29489
Electron transport calculations between 1 MeV and 1 eV
[AD-A263412] p 3568 N93-29787
Partial cross sections in H(-) photodetachment
[DE93-011570] p 3569 N93-30130
Progress in the development of broadband electric-field sensors for transient fields p 3369 N93-30306
Pulse control in an accelerator for heavy-ion fusion
[DE93-009527] p 3576 N93-30390
Variability of the electric field strength in the earth-ionosphere waveguide due to variations in the electron density profile
[AD-A264808] p 3394 N93-30595
The cone structure and focusing of the electric field of VLF and LF waves at high altitudes of the ionosphere
p 3395 N93-30731
Antenna modeling and analysis for ELF/VLF/LF applications p 3398 N93-30751
A covariant form of the Maxwell's equations in four-dimensional spaces with an arbitrary signature
[DE93-606070] p 3605 N93-30783
Electric magnetic duality in string theory
[DE93-606061] p 3606 N93-30807
Invariant structures and static forces in gauge theories
[DE92-644740] p 3607 N93-30925
Optimum design of multiwire cages for high-voltage applications
[AD-A264310] p 3400 N93-30995

ELECTRIC FURNACES
A high-temperature furnace for applications in microgravity p 3229 N93-29723

ELECTRIC GENERATORS
Design of the Nova Upgrade laser system for ignition fusion experiments
[DE93-009077] p 3436 N93-29097
Power generation and transportation systems research department
[PB93-178309] p 3352 N93-30663

ELECTRIC MOTOR VEHICLES
Polymer electrolyte fuel cells for transportation applications
[DE93-008721] p 3464 N93-29147
The ANL electric vehicle battery R/D program for DOE-EHP
[DE93-010658] p 3408 N93-29311

ELECTRIC MOTORS
Study on decreasing torque noise resulting from feedback noise for the modified bang-bang controller
[AD-A263178] p 3407 N93-29010

Energy efficient drivepower: An overview
[DE93-012435] p 3411 N93-30057
Energy efficient drivepower
[DE93-012436] p 3411 N93-30058

ELECTRIC NETWORKS
Widebanding techniques for VHF antennas 2
[AD-A263998] p 3387 N93-29882

ELECTRIC POTENTIAL
Potential transmission and transients during corrosion: Applications to corrosion monitoring
[DE93-010863] p 3323 N93-29256
Transient tests on an MHD thruster
[DE93-008656] p 3587 N93-29299
An improved linear ion trap physics package
p 3384 N93-29587
Microwave emission from relativistic electron beams
[AD-A264102] p 3400 N93-30880
Experiments in corrosion for younger students by and for older students p 3291 N93-30955

ELECTRIC PROPULSION
Measurements of magnetic fields produced by a 30 kWe class Arcjet Power Conditioning Unit
[AD-A262786] p 3287 N93-28658
Battery testing at Argonne National Laboratory
[DE93-009204] p 3407 N93-29036
Preliminary investigation of high power microwave plasmas for electrothermal thruster use
[NASA-TM-106207] p 3288 N93-29158
The ANL electric vehicle battery R/D program for DOE-EHP
[DE93-010658] p 3408 N93-29311
Electric propulsion for lightsats: A review of applications and advantages p 3290 N93-29907

ELECTRIC PULSES
Optically controlled solid state opening switches
[AD-A262404] p 3591 N93-28496
Response of a Nb/Al2O3/Nb tunnel junction to picosecond electrical pulses
[DE93-010416] p 3594 N93-29249

ELECTRIC ROCKET ENGINES
Engineering consideration for the self-energizing magnetoplasmadynamic (MPD): Type fusion plasma thruster
[AD-A262785] p 3288 N93-29289

ELECTRIC SWITCHES
Optically controlled solid state opening switches
[AD-A262404] p 3591 N93-28496
Improving the jitter of the 150 kJ experiments solid dielectric switches
[DE93-009459] p 3405 N93-28597
An explosively actuated electrical switch using Kapton insulation
[AD-A263835] p 3411 N93-30021

ELECTRIC WIRE
Microstructural understanding and critical current optimization of advanced high field superconductors
[DE93-011046] p 3592 N93-28643
Aircraft and refueler bonding and grounding study
[AD-A262027] p 3261 N93-29398
Widebanding techniques for VHF antennas 2
[AD-A263998] p 3387 N93-29882
Improved measurement of thermal effects on microstructure p 3292 N93-30959
Optimum design of multiwire cages for high-voltage applications
[AD-A264310] p 3400 N93-30995

ELECTRICAL ENGINEERING
Geoscience center research
[AD-A263465] p 3462 N93-29834
Canadian Conference on Electrical and Computer Engineering, volumes 1 and 2
[ISBN-0-9694170-1-2] p 3354 N93-30215
Novel methods of acceleration
[AD-A264828] p 3590 N93-30600

ELECTRICAL FAULTS
Microstructural modeling of electrical breakdown in solid fuel propellants
[AD-A263466] p 3342 N93-29835

ELECTRICAL GROUNDING
Aircraft and refueler bonding and grounding study
[AD-A262027] p 3261 N93-29398

ELECTRICAL IMPEDANCE
Acoustic transducer system
[AD-D015713] p 3562 N93-29279
Optically controlled active impedance element particularly suited for a microwave oscillator
[AD-D015723] p 3408 N93-29281
The 2nd International symposium on electrochemical impedance spectroscopy (extended abstracts)
[AD-A262994] p 3312 N93-29462
Frequency dependent electrical properties of minerals and partial-melts
[DE93-009254] p 3410 N93-29793
Widebanding techniques for VHF antennas 2
[AD-A263998] p 3387 N93-29882
Scattering through apertures and by three-dimensional structures. Application to the measurement of the surface impedance of conductive materials
[ONERA-P-1990-2] p 3392 N93-30018

ELECTRICAL INSULATION
Numerical simulation of quantum many-body systems
[DE93-008300] p 3603 N93-28958
An explosively actuated electrical switch using Kapton insulation
[AD-A263835] p 3411 N93-30021
Diamond nucleation of surfaces using carbon clusters
[AD-A264634] p 3599 N93-30548

ELECTRICAL MEASUREMENT
Plasma, magnetic, and electromagnetic measurements at nonmagnetic bodies p 3647 N93-28809
Constant frequency pulsed phase-locked loop measuring device
[NASA-CASE-LAR-13823-1] p 3431 N93-29084
Fiber-optic currents measurements
[DE93-007970] p 3579 N93-29350
The measurement of electrical conductivity in detonating condensed explosives
[AD-A264482] p 3352 N93-30424
Investigation of methods for the measurement of small electron bundle currents
[DIGEL-1992-4] p 3413 N93-30763
Analysis of possibilities for using laser scattering for MeV electron beam diagnostics
[DE93-606223] p 3441 N93-30767
Measurements of the energy spectrum of an intense microsecond relativistic electron beam in the beam-plasma experiments using a multi-foil analyzer
[DE93-606271] p 3590 N93-30768
Coupled-channel analysis of low energy nucleon-antinucleon interactions
[DE93-606115] p 3571 N93-30791

ELECTRICAL PROPERTIES
A detailed technology roadmap for superconductivity
p 3526 N93-29045
Polymers with electrical and nonlinear optical properties
[AD-D015691] p 3333 N93-29457
Frequency dependent electrical properties of minerals and partial-melts
[DE93-009254] p 3410 N93-29793
Synthesis and properties of a cation-conducting, high temperature polymer electrolyte
[AD-A263557] p 3334 N93-29825
Electrical relaxation in acid-form nafion
[AD-A263558] p 3410 N93-29826
Fundamental studies of the morphology, chemistry, and electrical properties of metals on GaAs and other III-V semiconductor compounds
[AD-A264417] p 3597 N93-30120

ELECTRICAL RESISTIVITY
Numerical simulation of quantum many-body systems
[DE93-008300] p 3603 N93-28958
High pressure studies of hydrated nafion membranes: Dielectric relaxation and deuteron NMR
[AD-A263511] p 3332 N93-29342
Electrical relaxation in acid-form nafion
[AD-A263558] p 3410 N93-29826
A calibration procedure for the SBE 19 Conductivity, Temperature, and Depth (CTD) profiler
[AD-A264435] p 3489 N93-30420
The measurement of electrical conductivity in detonating condensed explosives
[AD-A264482] p 3352 N93-30424
The effect of Bi2 O3 on the electrical properties of Zr O2: 3 percent Mg O ceramic solid electrolytes
[DE93-607029] p 3339 N93-30774
Temperature-dependent electrical conductivity of soda-lime glass p 3294 N93-30978

ELECTRO-OPTICAL EFFECT
Measurements and Characterization Branch
[DE93-000094] p 3465 N93-30207

ELECTRO-OPTICS
Planning of a West Virginia University Research Center in the basic materials sciences
[DE93-011731] p 3592 N93-28647
The quest for an integrated flying helmet
p 3502 N93-28860
Ultrafast optical studies of surface reaction processes at semiconductor interfaces
[DE93-009049] p 3593 N93-29096
Proceedings of the 25th European Conference on the Application of Polar Dielectrics to celebrate the 25th anniversary of the Dielectric Society, incorporating the 1st International Workshop on Integrated Ferroelectrics
[AD-A263427] p 3332 N93-29337
Multichip module high speed testing
[AD-A262989] p 3408 N93-29427
Degradation of electro-optic components aboard LDEF p 3582 N93-29689
Optoelectronic technology consortium
[AD-A263580] p 3580 N93-29973
Electro-optic characterisation of extremely wide bandwidth electrical signals
[AD-A264202] p 3392 N93-30145
Subpicosecond electrooptic sampling
[AD-A264635] p 3581 N93-30520
Topical meeting of broadband analog and digital optoelectronics
[AD-A264643] p 3581 N93-30522

ELECTROACOUSTIC TRANSDUCERS
Acoustic transducer system
[AD-D015713] p 3562 N93-29279

ELECTROCATALYSTS
The electrolyte factor in O2 reduction electrocatalysis
[AD-A263565] p 3313 N93-29828

ELECTROCHEMICAL CELLS
In situ characterization of interfacial and bulk properties of lithium polymer batteries using 4-probe DC techniques
[DE93-007699] p 3405 N93-28581
Research and development of carbon black anodes for lithium secondary cells
[DE93-781331] p 3406 N93-28746
Alkali metal carbon dioxide electrochemical system for energy storage and/or conversion of carbon dioxide to oxygen
[NASA-CASE-LEW-14973-1] p 3464 N93-28974

ELECTROCHEMICAL CORROSION
The growth of small corrosion fatigue cracks in alloy 2024
[NASA-TM-107755] p 3451 N93-29069
Potential transmission and transients during corrosion: Applications to corrosion monitoring
[DE93-010863] p 3323 N93-29256
Experiments in corrosion for younger students by and for older students p 3291 N93-30955

ELECTROCHEMISTRY
Synthesis of conducting polymer composite fibers in electrochemical flow cells
[AD-A262233] p 3294 N93-28492
Electrochemical behavior and surface chemistry of aluminum alloys: Solute-rich interphase model
[AD-A262061] p 3322 N93-29002
Analytical applications of electrified interfaces between two immiscible solutions
[AD-A263085] p 3311 N93-29132
Effect of zinc and iron ions on the electrochemistry of nickel oxide electrode: Slow cyclic voltammetry
[AD-A263098] p 3311 N93-29133
In situ Fourier transform infrared spectroscopic study of bisulfate and sulfate adsorption on gold, with and without the underpotential deposition of copper
[AD-A263421] p 3323 N93-29259
Fast multipole method in simulations of aqueous systems
[AD-A263422] p 3567 N93-29336
The 2nd International symposium on electrochemical impedance spectroscopy (extended abstracts)
[AD-A262994] p 3312 N93-29462
Characterization of lithium electrode surface in lithium secondary batteries by in situ Raman spectroscopic methods
[AD-A263728] p 3411 N93-29986
Studies in Lewis acid and superacid ionic liquids
[AD-A264683] p 3316 N93-30551
Gordon Research Conferences, 1991
[AD-A264275] p 3317 N93-30816
Experiments in corrosion for younger students by and for older students p 3291 N93-30955

ELECTRODE MATERIALS
Adsorption of sulfate on metal electrodes
[AD-A263192] p 3309 N93-28540

ELECTRODEPOSITION
Electrochemical fabrication of cadmium chalcogenide microdiode arrays
[AD-A263169] p 3310 N93-28988
In-situ x ray studies of the underpotential deposition of copper on platinum (3)
[AD-A263361] p 3595 N93-29331
The electrodeposition of low contraction chromium using high/low current pulsing
[AD-A264475] p 3327 N93-30538

ELECTRODES
Large amplitude striations in an RF discharge
[DE93-753244] p 3379 N93-28534
Adsorption of sulfate on metal electrodes
[AD-A263192] p 3309 N93-28540
Development of an updated pinch-welding capability
[DE93-009823] p 3442 N93-28552
Effect of zinc and iron ions on the electrochemistry of nickel oxide electrode: Slow cyclic voltammetry
[AD-A263098] p 3311 N93-29133
Transient tests on an MHD thruster
[DE93-008656] p 3587 N93-29299
Adsorption of hydrated halide ions on charged electrodes: Molecular dynamics simulation
[AD-A263137] p 3568 N93-29619

Characterization of lithium electrode surface in lithium secondary batteries by in situ Raman spectroscopic methods
[AD-A263728] p 3411 N93-29986
ELECTRODYNAMICS
Measurements of magnetic fields produced by a 30 kWe class Arcjet Power Conditioning Unit
[AD-A262786] p 3287 N93-28658
Electrodynamics of the dayside cleft region based on ground observations at Svalbard
[AD-A263571] p 3477 N93-29831
Some problems of relativistic electrodynamics
[DE92-644738] p 3400 N93-30923
ELECTROENCEPHALOGRAPHY
The AFOSR Workshop on the Future of EEG and MEG
[AD-A264338] p 3495 N93-30160
ELECTROLYSIS
Electrolysis performance improvement and validation experiment p 3267 N93-28737
Method for producing oxygen from lunar materials
[NASA-CASE-MSC-21759-1] p 3312 N93-29617
ELECTROLYTES
Analytical applications of electrified interfaces between two immiscible solutions
[AD-A263085] p 3311 N93-29132
Potential transmission and transients during corrosion: Applications to corrosion monitoring
[DE93-010863] p 3323 N93-29256
Transcutaneous analyte measuring methods
[AD-A262861] p 3494 N93-29509
The electrolyte factor in O2 reduction electrocatalysis
[AD-A263565] p 3313 N93-29828
Dioxygen reduction in various acid electrolytes
[AD-A263564] p 3317 N93-30664
Experiments in corrosion for younger students by and for older students p 3291 N93-30955
ELECTROLYTIC CELLS
Electrolysis performance improvement and validation experiment p 3267 N93-28737
Polymer electrolyte fuel cells for transportation applications
[DE93-008721] p 3464 N93-29147
Experiments in corrosion for younger students by and for older students p 3291 N93-30955
ELECTROMAGNETIC ABSORPTION
Microtextured metals for stray-light suppression in the Clementine startracker p 3286 N93-28785
A unique photon bombardment system for space applications p 3286 N93-28790
A single band processor for the computation of range from optical absorbance p 3363 N93-30272
Triplet states and optical absorptions in finite polyenes and conjugated polymers
[AD-A264552] p 3337 N93-30381
Optically switchable conductive polymers
[AD-A264751] p 3337 N93-30557
ELECTROMAGNETIC COMPATIBILITY
Coupling gain computation between antennas on circular cylinders at SHF/EHF frequencies p 3369 N93-30309
ELECTROMAGNETIC COUPLING
Electromagnetic diffusion and wire coupling
[AD-A263183] p 3381 N93-29011
ELECTROMAGNETIC FIELDS
Edge plasma control by RF electric field in Compact Helical System (CHS)
[DE93-753242] p 3583 N93-28532
Finite element analysis of time-independent superconductivity
[NASA-CR-191140] p 3450 N93-28556
Predicting radiation characteristics from antenna physical dimensions
[AD-A262462] p 3379 N93-28654
Gene transcription and electromagnetic fields
[DE93-010854] p 3490 N93-28848
Continuation of: Applications of gauge theories to enhance numerical solutions of mixed potential integral equations
[AD-A263763] p 3550 N93-29876
International Journal of Numerical Modeling: Electronic Networks, Devices, and Fields, volume 5, number 3, August 1992
[AD-A263765] p 3387 N93-29877
Applications of three-dimensional modeling in electromagnetic exploration p 3391 N93-30010
Quantification of thermographic mapping techniques
[AD-A264020] p 3391 N93-30016
Transient field computations within or proximity of complex structures: FD-TD approach
p 3366 N93-30292
Application of integral and differential equation methods for various EM interaction problems
[AD-A264821] p 3394 N93-30597
Rocket-triggered lightning studies for the protection of critical assets
[DE93-009633] p 3484 N93-30651
Modern approach to relativity theory (radar formulation)
[DE93-606032] p 3606 N93-30804
Some problems of relativistic electrodynamics
[DE92-644738] p 3400 N93-30923
ELECTROMAGNETIC INTERACTIONS
Finite element analysis of time-independent superconductivity
[NASA-CR-191140] p 3450 N93-28556
Measurement of W-Z interference from neutrino-electron scattering
[DE93-010724] p 3566 N93-29313
Neutrino mass
[DE93-010735] p 3566 N93-29315
An improved model-creation program for EM interaction analysis p 3367 N93-30294
Application of integral and differential equation methods for various EM interaction problems
[AD-A264821] p 3394 N93-30597
Parton's picture of the electroweak processes in high energy e(+)e(-)-collisions
[DE93-606107] p 3571 N93-30788
Massive Majorana neutrinos in pre-bounce supernovae
[DE92-642597] p 3572 N93-30931
ELECTROMAGNETIC INTERFERENCE
Electromagnetic diffusion and wire coupling
[AD-A263183] p 3381 N93-29011
ELECTROMAGNETIC MEASUREMENT
Plasma, magnetic, and electromagnetic measurements at nonmagnetic bodies p 3647 N93-28809
Progress in the development of broadband electric-field sensors for transient fields p 3369 N93-30306
Measurement of electromagnetic properties of composite materials
[AD-A264725] p 3303 N93-30555
ELECTROMAGNETIC NOISE
Influence of optical feedback on the pulse behavior of semiconductor lasers
[ETN-93-93798] p 3436 N93-28614
Analytical predictions of the intermodulation noise of semiconductor laser diode p 3361 N93-30256
ELF/VLF/LF Radio Propagation and Systems Aspects
[AGARD-CP-529] p 3394 N93-30727
A long wave TE/TM noise prediction model
p 3397 N93-30742
Application of non-standard signal processing to ELF noise characterization for the TSS1-OESEE programme
p 3397 N93-30743
ELF/VLF radio noise measurements at high latitudes during solar particle events p 3397 N93-30744
ELECTROMAGNETIC PROPERTIES
A detailed technology roadmap for superconductivity
p 3526 N93-29045
Elastic and reactive collisions of atoms and molecules with neutral alkali clusters
[DE93-009313] p 3566 N93-29206
Measurement of electromagnetic properties of composite materials
[AD-A264725] p 3303 N93-30555
ELECTROMAGNETIC PULSES
Measurements of magnetic fields produced by a 30 kWe class Arcjet Power Conditioning Unit
[AD-A262786] p 3287 N93-28658
Electromagnetic diffusion and wire coupling
[AD-A263183] p 3381 N93-29011
Optimization of HPM device parameters for maximum air transmission
[DE93-007332] p 3386 N93-29765
High resolution free-electron laser spectroscopy
[AD-A263734] p 3439 N93-29853
Nonequilibrium screening and exciton dynamics probed by femtosecond laser pulses
[AD-A263603] p 3439 N93-29983
Radiated fields from an electromagnetic pulse simulator p 3366 N93-30290
Transient field computations within or proximity of complex structures: FD-TD approach
p 3366 N93-30292
A computer simulation of the production of an artificially ionized layer using the Arecibo facility
[DE93-010817] p 3478 N93-30487
Subpicosecond electrooptic sampling
[AD-A264635] p 3581 N93-30520
ELECTROMAGNETIC RADIATION
Predicting radiation characteristics from antenna physical dimensions
[AD-A262462] p 3379 N93-28654
Gene transcription and electromagnetic fields
[DE93-010854] p 3490 N93-28848
An improved model-creation program for EM interaction analysis p 3367 N93-30294
Neutrino oscillations and a new Faraday effect
[DE93-606111] p 3571 N93-30789
ELECTROMAGNETIC SCATTERING
Continuation of: Applications of gauge theories to enhance numerical solutions of mixed potential integral equations
[AD-A263763] p 3550 N93-29876
International Journal of Numerical Modeling: Electronic Networks, Devices, and Fields, volume 5, number 3, August 1992
[AD-A263765] p 3387 N93-29877
Application of integral and differential equation methods for various EM interaction problems
[AD-A264821] p 3394 N93-30597
ELECTROMAGNETIC SHIELDING
Electromagnetic diffusion and wire coupling
[AD-A263183] p 3381 N93-29011
ELECTROMAGNETIC SPECTRA
ELF/VLF spectrum measurements
p 3398 N93-30745
ELECTROMAGNETIC WAVE TRANSMISSION
A computer simulation of the production of an artificially ionized layer using the Arecibo facility
[DE93-010817] p 3478 N93-30487
ELF/VLF/LF Radio Propagation and Systems Aspects
[AGARD-CP-529] p 3394 N93-30727
Introduction p 3395 N93-30728
ELF propagation in deep and shallow sea water
p 3397 N93-30739
Comparative study of undersea fields produced by various dipoles p 3397 N93-30740
ELECTROMAGNETISM
A proposed approach for developing next-generation computational electromagnetics software
[DE93-007326] p 3380 N93-28900
Electronics research at the University of Texas at Austin. Appendix: JSEP sponsored publications
[AD-A262993] p 3409 N93-29485
Advanced electromagnetic methods for aerospace vehicles
[NASA-CR-193468] p 3400 N93-31036
ELECTROMAGNETS
Cryogenic magnetic bearing
[AD-A264716] p 3446 N93-30512
ELECTROMECHANICAL DEVICES
The NASA SBIR product catalog
[NASA-TM-108242] p 3609 N93-29322
Automated modeling of physical systems
[NASA-CR-193256] p 3531 N93-29873
Efficient reorientation of a deformable body in space: A free-free beam example p 3280 N93-29994
Advances in the identification of electrochemical transfer function models using Prony analysis
[DE93-009424] p 3550 N93-30041
ELECTROMOTIVE FORCES
Research and development of carbon black anodes for lithium secondary cells
[DE93-781331] p 3406 N93-28746
Change of solar cell element properties influenced by adsorbed atoms
[DE93-606694] p 3466 N93-30777
ELECTROMYOGRAPHY
Sudden loading and fatigue effects on the human spine
[PB93-167526] p 3493 N93-29199
ELECTRON ACCELERATORS
Three-dimensional simulation analysis of the standing-wave free-electron laser two-beam accelerator
[DE93-010461] p 3575 N93-29870
Novel methods of acceleration
[AD-A264828] p 3590 N93-30600
Investigation of methods for the measurement of small electron bundle currents
[DIGEL-1992-4] p 3413 N93-30763
Microwave emission from relativistic electron beams
[AD-A264102] p 3400 N93-30880
ELECTRON BEAMS
Accelerator research studies
[DE93-009353] p 3573 N93-28522
Observation of a beam energy shift caused by a plasma wakefield
[DE93-753243] p 3583 N93-28533
Low-pump-rate multi-millisecond atomic xenon laser
[DE93-011484] p 3437 N93-29180
High-power Ka-band amplifier p 3385 N93-29590
Magnetic field measurements of the CEBAF (NIST) wiggler using the pulsed wire method
[AD-A263997] p 3439 N93-29867
Three-dimensional simulation analysis of the standing-wave free-electron laser two-beam accelerator
[DE93-010461] p 3575 N93-29870
Gas electron diffraction employing a pulsed electron beam synchronous with photoexcitation
p 3319 N93-30101
High-energy electron-positron interactions
[DE93-011611] p 3576 N93-30488

Unexpected increase in the thermal generation rate of bulk GaAs due to electron-beam metallization
[DE93-009829] p 3598 N93-30511

Non-perturbative calculation of equilibrium polarization of stored electron beams
[DE93-764500] p 3577 N93-30607

Complex apparatus and results of active experiment Electron-1 with injection of electronic beam in the ionosphere
[DE93-605452] p 3480 N93-30991

Microsecond ribbon relativistic electron beam in a plane undulator and generation of microwave radiation
[DE93-605693] p 3400 N93-30993

ELECTRON CYCLOTRON HEATING

Edge plasma control by RF electric field in Compact Helical System (CHS)
[DE93-753242] p 3583 N93-28532

Electron cyclotron heating and current drive in toroidal geometry
[DE93-010400] p 3586 N93-29049

Poloidal field measurements during transient phenomena on MTX: Sawtooth perturbations and the effect of ECH on disruptions
[DE93-010516] p 3587 N93-29303

ELECTRON DENSITY (CONCENTRATION)

Plasma diagnostics by antenna impedance measurements p 3400 N93-28820

Applications of density functional theory to calculation of reaction energetics p 3351 N93-30098

Variability of the electric field strength in the earth-ionosphere waveguide due to variations in the electron density profile
[AD-A264808] p 3394 N93-30595

ELECTRON DENSITY PROFILES

Variability of the electric field strength in the earth-ionosphere waveguide due to variations in the electron density profile
[AD-A264808] p 3394 N93-30595

ELECTRON DIFFRACTION

Diffraction and holography with photoelectrons and Auger electrons: Some new directions
[DE93-007664] p 3313 N93-29766

Gas electron diffraction employing a pulsed electron beam synchronous with photoexcitation
p 3319 N93-30101

ELECTRON DIFFUSION

Plasma diffusion through multidipole magnetic fields
[DE93-608548] p 3591 N93-31007

ELECTRON ENERGY

Construction and testing of a neutron and gamma spectrometry system using pulse shape discrimination with an organic scintillator
[AD-A262550] p 3567 N93-29415

ELECTRON GAS

Effect of planar magnetic field on electron transport properties of n-AlGaAs/GaAs heterojunction and photoluminescence measures in GaAs samples
[DE93-608739] p 3601 N93-30776

ELECTRON GUNS

Gas electron diffraction employing a pulsed electron beam synchronous with photoexcitation
p 3319 N93-30101

Microwave emission from relativistic electron beams
[AD-A264102] p 3400 N93-30880

ELECTRON MASS

Planck scale effects in neutrino physics
[DE93-606133] p 3571 N93-30793

ELECTRON MICROSCOPES

What is underneath? Moving atoms and molecules to find out
[AD-A263363] p 3567 N93-29332

Scanning electron microscope/energy dispersive x ray analysis of impact residues in LDEF tray clamps
p 3283 N93-29369

Scanning probe lithography. Part 1: Scanning tunneling microscope-induced lithography of self-assembled n-alkanethiol monolayer resists
[AD-A263130] p 3432 N93-29476

ELECTRON MICROSCOPY

Undulator Spectromicroscopy Facility at the Advanced Light Source
[DE93-007964] p 3261 N93-28490

Tailored interfaces for metal-matrix composites-fundamental considerations
[AD-A263048] p 3298 N93-29130

Scanning ionic microscopy with high spatial resolution: Parallel acquisition of elementary images by high resolution mass spectrometry
[ONERA-NT-1990-7] p 3314 N93-30139

Center for surface radiation damage studies
[AD-A264330] p 3570 N93-30366

ELECTRON MOBILITY

Wide-bandwidth high-resolution search for extraterrestrial intelligence
[NASA-CR-193137] p 3509 N93-28895

ELECTRON PARAMAGNETIC RESONANCE

Magnetic resonance studies of photo-induced electron transfer reactions
[DE93-012239] p 3311 N93-29182

ELECTRON PHONON INTERACTIONS

Electron transport calculations between 1 MeV and 1 eV
[AD-A263412] p 3568 N93-29787

Applications of mesoscopic physics
[DE93-012104] p 3597 N93-30141

ELECTRON PHOTON CASCADES

Beta/gamma Monte Carlo transport in repetitive structures of satellite systems
[DE93-007610] p 3281 N93-30509

ELECTRON PLASMA

Observation of a beam energy shift caused by a plasma wakefield
[DE93-753243] p 3583 N93-28533

A Fokker-Planck operator for the emission and absorption of electron plasma waves in a magnetized plasma
[DE93-009579] p 3584 N93-28598

ELECTRON PRECIPITATION

Transient (approximately equals 10 s) VLF amplitude and phase perturbations due to lightning-induced electron precipitation into the ionosphere (the Trimpi effect)
p 3396 N93-30736

Lightning-induced effects on VLF/LF radio propagation p 3396 N93-30737

ELECTRON SCATTERING

Electron interactions with non-linear polyatomic molecules and their radicals and ions
[AD-A262279] p 3568 N93-29446

Extracting infinite system properties from finite size clusters: Phase randomization/boundary condition averaging
[AD-A264712] p 3551 N93-30503

ELECTRON STATES

NO2 unimolecular decomposition: Step-like variation of k(sub uni)(E) p 3318 N93-30068

Triplet states and optical absorptions in finite polyenes and conjugated polymers
[AD-A264552] p 3337 N93-30381

Experimental and theoretical aspects of excited state electron transfer and related phenomena
[AD-A263457] p 3570 N93-30589

Electronic states in quantum wells with periodically structured interfaces
[DE93-606295] p 3600 N93-30769

ELECTRON TRAJECTORIES

Microwave emission from relativistic electron beams
[AD-A264102] p 3400 N93-30880

ELECTRON TRANSFER

Ultrafast optical studies of surface reaction processes at semiconductor interfaces
[DE93-009049] p 3593 N93-29096

Magnetic resonance studies of photo-induced electron transfer reactions
[DE93-012239] p 3311 N93-29182

Electron interactions with non-linear polyatomic molecules and their radicals and ions
[AD-A262279] p 3568 N93-29446

Scanning probe lithography. Part 1: Scanning tunneling microscope-induced lithography of self-assembled n-alkanethiol monolayer resists
[AD-A263130] p 3432 N93-29476

Electronics research at the University of Texas at Austin. Appendix: JSEP sponsored publications
[AD-A262993] p 3409 N93-29485

Electron transport calculations between 1 MeV and 1 eV
[AD-A263412] p 3568 N93-29787

Optically switchable conductive polymers
[AD-A264751] p 3337 N93-30557

Experimental and theoretical aspects of excited state electron transfer and related phenomena
[AD-A263457] p 3570 N93-30589

Effect of planar magnetic field on electron transport properties of n-AlGaAs/GaAs heterojunction and photoluminescence measures in GaAs samples
[DE93-608739] p 3601 N93-30776

ELECTRON TRANSITIONS

An improved linear ion trap physics package
p 3384 N93-29587

ELECTRON TUNNELING

What is underneath? Moving atoms and molecules to find out
[AD-A263363] p 3567 N93-29332

Scanning probe lithography. Part 1: Scanning tunneling microscope-induced lithography of self-assembled n-alkanethiol monolayer resists
[AD-A263130] p 3432 N93-29476

NATO Advanced Research Workshop on Frontiers of Optical Phenomena in Semiconductor Structure of Reduced Dimension
[AD-A264813] p 3581 N93-30666

ELECTRON-POSITRON PAIRS

New limits on generation-1 leptoquarks
[DE93-008138] p 3567 N93-29351

Towards the results of global analysis of data on nucleon electromagnetic structure
[DE93-606125] p 3571 N93-30792

ELECTRONIC CONTROL

Strategic avionics technology definition studies. Subtask 3-1A: Electrical Actuation (ELA) systems
[NASA-CR-193237] p 3271 N93-29215

Subpicosecond electrooptic sampling
[AD-A264635] p 3581 N93-30520

ELECTRONIC COUNTERMEASURES

Modified Acousto-Optic Adaptive Processor (Mod-AOAP)
[AD-A261983] p 3381 N93-28997

ELECTRONIC EQUIPMENT

Department of defense advisory group on electron devices: Appendix to special technology area review on microwave packaging technology
[AD-A262136] p 3408 N93-29408

Low cost instrumentation: Parallel port analog to digital converter
[AD-A263468] p 3433 N93-30584

Electronics for a neutron detector and a Geiger-Mueller detector for the radiation protection around MEA and AmPS
[DIGEL-1992-6] p 3413 N93-30838

Performance of thermal adhesives in forced convection p 3293 N93-30974

ELECTRONIC EQUIPMENT TESTS

Standardization of automatic test equipment in the US Air force
[AD-A262076] p 3250 N93-29004

ELECTRONIC MODULES

Thermal and mechanical analysis of flip-chips on a liquid cooled multichip module
[DE93-007609] p 3405 N93-28641

Department of defense advisory group on electron devices: Appendix to special technology area review on microwave packaging technology
[AD-A262136] p 3408 N93-29408

ELECTRONIC PACKAGING

Department of defense advisory group on electron devices: Appendix to special technology area review on microwave packaging technology
[AD-A262136] p 3408 N93-29408

Multichip module high speed testing
[AD-A262989] p 3408 N93-29427

ELECTRONS

High-energy electron-positron interactions
[DE93-011611] p 3576 N93-30488

Photoinduced charge separation in Q1D heterojunction materials: Evidence for electron-hole pair separation in mixed-halide MX solids
[AD-A264711] p 3598 N93-30501

Extracting infinite system properties from finite size clusters: Phase randomization/boundary condition averaging
[AD-A264712] p 3551 N93-30503

Unitary approximation of Bhabha diffusion by high energies and its implementation in Monte Carlo event generators
[ETN-93-93622] p 3571 N93-30670

ELECTROPHORESIS

Comparative mutagenesis of human cells in vivo and in vitro
[DE93-012269] p 3490 N93-28651

Computer assisted multiplex sequencing
[DE93-007144] p 3536 N93-30934

ELECTROPHYSIOLOGY

An assessment of peripheral nerve damage in the rat following non-freezing cold exposure: An electrophysiological and histopathological examination
[AD-A264293] p 3492 N93-30818

ELECTROPLATING

The electrodeposition of low contraction chromium using high/low current pulsing
[AD-A264475] p 3327 N93-30538

ELECTROSTATIC CHARGE

Spacecraft surface charging handbook
[AD-A262778] p 3279 N93-29305

Aircraft and refueler bonding and grounding study
[AD-A262027] p 3261 N93-29398

ELECTROSTATICS

Microstructural modeling of electrical breakdown in solid fuel propellants
[AD-A263466] p 3342 N93-29835

Antenna modeling and analysis for ELF/VLF/LF applications p 3398 N93-30751

Defining protein electrostatic recognition processes
[AD-A264838] p 3571 N93-30901

ELEMENTARY EXCITATIONS

Excited states in electronic structure calculations
[DE93-007704] p 3592 N93-28642

Response of a Nb/Al2O3/Nb tunnel junction to picosecond electrical pulses
[DE93-010416] p 3594 N93-29249
On the method of determining relations
[DE93-606041] p 3551 N93-30765
On the invariant measure for the nonlinear Schroedinger equation
[DE92-644672] p 3551 N93-30912

ELEMENTARY PARTICLE INTERACTIONS
Topics in gauge theories and the unification of elementary particle interactions
[DE93-009370] p 3563 N93-28542
Research in theoretical physics
[DE93-008401] p 3603 N93-28961
New Mexico Center for Particle Physics: Studies of fundamental interactions
[DE93-008302] p 3566 N93-29261
New limits on generation-1 leptoquarks
[DE93-008138] p 3567 N93-29351
Elementary particle interactions
[DE93-005113] p 3568 N93-29764
Task A: Theory of elementary particles
[DE93-010561] p 3569 N93-29841
High-energy electron-positron interactions
[DE93-011611] p 3576 N93-30488
Massive Majorana neutrinos in pre-bounce supernovae
[DE92-642597] p 3572 N93-30931

ELEMENTARY PARTICLES
Spectroscopic probes of vibrationally excited molecules at chemically significant energies
[DE93-012328] p 3564 N93-28652
Research in theoretical nuclear physics
[DE93-008380] p 3565 N93-28960
Modern Monte Carlo particle transport simulation for safety and radiation protection applications in accelerometer technology and in space science
[JUEL-2609] p 3574 N93-29062
Quantum-kinetic Green function and macroscopic wave function
[DE93-606040] p 3606 N93-30796
On the invariant measure for the nonlinear Schroedinger equation
[DE92-644672] p 3551 N93-30912
A squeezed state holomorphic phase space representation of equations of motion
[DE93-609835] p 3607 N93-30945

ELEVATION
Gravity referenced elevation encoder development
p 3385 N93-29592

ELEVATORS (LIFTS)
Platform stair lift
[NASA-CASE-MFS-28772-1] p 3507 N93-29845

ELLIPSOIDS
Hypersonic lateral and directional stability characteristics of aeroassist flight experiment configuration in air and CF4
[NASA-TM-4435] p 3239 N93-29166
Some problems of relativistic electrodynamics
[DE92-644738] p 3400 N93-30923

ELLIPSOMETERS
Polarization modulated ellipsometry
[NASA-CR-4012] p 3580 N93-30372

ELLIPSOMETRY
Real time self-directed MBE flux control incorporation in situ ellipsometry, phase 1
[AD-A263501] p 3595 N93-29341
Polarization modulated ellipsometry
[NASA-CR-4012] p 3580 N93-30372

ELONGATION
Electric field induced phenomena in STM: Tip deformations and Au(111)-surface phase transitions during tunneling spectroscopy experiments
[AD-A262208] p 3596 N93-29445

EMBEDDED COMPUTER SYSTEMS
Transputers, parallel processing in embedded systems for image compression in space applications
[NLR-TP-89242-U] p 3522 N93-30840

EMBEDDING
Virtual interface applications for airborne weapons systems p 3502 N93-28858
Transient response of embedded thermocouples
[DE93-009889] p 3431 N93-29325

EMBRITTLEMENT
Preliminary test of liquid metal induced embrittlement in liquid LiPb and stainless-steel systems
[DE93-753130] p 3320 N93-28529
Planning of a West Virginia University Research Center in the basic materials sciences
[DE93-011731] p 3592 N93-28647
Environmental embrittlement of binary and Zr-doped Ni3Al
[DE93-008575] p 3321 N93-28679
SIMS chemical analysis of extended impacts on the leading and trailing edges of LDEF experiment AO187-2
p 3318 N93-29367
The effect of oxidation embrittlement on the impact behavior of nicalon reinforced CAS 2 ceramic matrix composites
[AD-A263567] p 3334 N93-29829

EMISSION SPECTRA
Luminescence study of ion-implanted and MBE-grown Er-doped GaAs and Al(x)Ga(1-x)As
[AD-A262602] p 3591 N93-28471
Multifractal analysis of radio lobes
p 3380 N93-28689
The Backgrounds Data Center p 3624 N93-28814
Quantum lattice fluctuations in a 1-dimensional charge-density-wave material: Luminescence and resonance Raman studies of an MX solid
[DE93-007362] p 3593 N93-28966
A search for radiative neutrino decay from supernovae
[NASA-CR-193118] p 3653 N93-30052
Multiwavelength studies of classical nova shells
p 3636 N93-30412
Tunable CW diode-pumped Tm,Ho:YLiF4 laser operating at or near room temperature
[NASA-CASE-NPO-18611-1-CU] p 3440 N93-30415
Observing and modelling F-region ionospheric dynamics using the OII 7320A emission p 3479 N93-30564
Effects of spiral shocks on disk emission lines
[DE92-641716] p 3637 N93-31004

EMITTANCE
Development of an O atom gun
[AD-A264753] p 3570 N93-30558

EMITTERS
Field-emitter arrays for RF vacuum microelectronics
[AD-A262677] p 3404 N93-28483
Improved field emitter current densities and stability through the application of a proprietary process
[AD-A263464] p 3411 N93-29833
Improved field emitter current densities and stability through the application of a proprietary process
[AD-A264048] p 3411 N93-30031
RF vacuum microelectronics
[AD-A264528] p 3412 N93-30409

EMULSIONS
Detonation shock dynamics of composite energetic materials p 3350 N93-30096

END EFFECTORS
Spline screw autochanger
[NASA-CASE-GSC-13435-1] p 3445 N93-29505
Robot arm with positional absolute encoded joints
p 3370 N93-30312
A testbed for autonomous reflexive grasping
[AD-A264557] p 3446 N93-30384

ENDOSCOPES
Drill/borescope system for the Mars Polar Pathfinder
p 3647 N93-28805

ENERGY ABSORPTION
An automated data collection system for a Charpy impact tester p 3293 N93-30972

ENERGY BANDS
A tight binding model for the electronic structure of FCC and SC C60
[DE93-606214] p 3601 N93-30794

ENERGY BUDGETS
Steady-state and transient modeling of tracer and nutrient distributions in the global ocean
[DE93-011043] p 3486 N93-28670
Spectral energetics of the lower thermosphere
p 3477 N93-29467
The estimation and scaling of land-surface fluxes of latent and sensible heat with remotely sensed data over a grassland site p 3462 N93-30045

ENERGY CONSERVATION
Assessment of energy technologies contributing to environmental conservation
[DE93-781439] p 3468 N93-28882
Study on technology for effective utilization of carbon dioxide in view of global environment
[DE93-781440] p 3468 N93-28883
Energy efficient drivepower: An overview
[DE93-012435] p 3411 N93-30057
Energy efficient drivepower
[DE93-012436] p 3411 N93-30058

ENERGY CONSUMPTION
Assessment of energy technologies contributing to environmental conservation
[DE93-781439] p 3468 N93-28882
Summer research program (1992). High School Apprenticeship Program (HSAP) reports. Volume 16: Arnold Engineering Development Center Civil Engineering Laboratory
[AD-A262024] p 3608 N93-29396

ENERGY CONVERSION
Solar energy emplacement developer
p 3230 N93-29732

ENERGY CONVERSION EFFICIENCY
New III-V cell design approaches for very high efficiency
[DE93-000097] p 3464 N93-28971
The effect of the low Earth orbit environment on space solar cells: Results of the Advanced Photovoltaic Experiment (S0014) p 3467 N93-29686
Low-cost, high-efficiency solar cells utilizing GaAs-on-Si technology
[DE93-000096] p 3464 N93-29965
Magnetic character investigation of higher alcohol synthesis Cu-Co-Cr catalysts
[DE93-009732] p 3316 N93-30653

ENERGY DISSIPATION
Ultrafast optical studies of surface reaction processes at semiconductor interfaces
[DE93-009049] p 3593 N93-29096

ENERGY GAPS (SOLID STATE)
Role of oxygen vacancies in anodic TiO2 thin films
[DE92-642137] p 3602 N93-31027

ENERGY LEVELS
Numerical simulation of quantum many-body systems
[DE93-008300] p 3603 N93-28958
Inner-shell photo-ionized x ray laser schemes
[DE93-009285] p 3438 N93-29309
Electronic states in quantum wells with periodically structured interfaces
[DE93-606295] p 3600 N93-30769
Schroedinger equations of higher (greater than 2) order
[DE92-644677] p 3552 N93-30984

ENERGY METHODS
An investigation of graphite peek composite under compression with a centrally located circular discontinuity
[AD-A262549] p 3298 N93-29414

ENERGY OF FORMATION
The thermochemistry and reaction pathways of the decomposition and combustion of energetic materials
p 3343 N93-30063

ENERGY POLICY
Development of alternative fuels from coal-derived syngas
[DE93-011629] p 3341 N93-28668
Overview of the DOE Atmospheric Chemistry Program's Ozone Project
[DE93-007416] p 3471 N93-29770
Strategic Environmental Research and Development Program (SERDP)
[AD-A263745] p 3471 N93-29858

ENERGY REQUIREMENTS
Strategic avionics technology definition studies. Subtask 3-1A: Electrical Actuation (ELA) systems
[NASA-CR-193237] p 3271 N93-29215
Optimization of HPM device parameters for maximum air transmission
[DE93-007332] p 3386 N93-29765

ENERGY SPECTRA
Observation of a beam energy shift caused by a plasma wakefield
[DE93-753243] p 3583 N93-28533
Nonconservative and reverse spectral transfer in Hasegawa-Mima turbulence
[DE93-010132] p 3585 N93-28913
Construction and testing of a neutron and gamma spectrometry system using pulse shape discrimination with an organic scintillator
[AD-A262550] p 3567 N93-29415
Spectral energetics of the lower thermosphere
p 3477 N93-29467
LET spectra measurements of charged particles in the P0006 experiment on LDEF p 3573 N93-29637
Light-heavy ion measurements in CR-39 located on the Earth side of LDEF p 3573 N93-29638
A search for radiative neutrino decay from supernovae
[NASA-CR-193118] p 3653 N93-30052
Characterizing transient vibrations using band limited temporal moments
[DE93-009639] p 3453 N93-30185
Energy spectra and photoelectron work function from YBa2Cu3O7 high-T(sub c) superconductor
[DE93-606329] p 3600 N93-30766
Measurements of the energy spectrum of an intense microsecond relativistic electron beam in the beam-plasma experiments using a multi-foil analyzer
[DE93-606271] p 3590 N93-30768
Complex apparatus and results of active experiment Electron-1 with injection of electronic beam in the ionosphere
[DE93-605452] p 3480 N93-30991

ENERGY STORAGE
Sodium-Sulfur Cell Technology flight experiment (SSCT) p 3264 N93-28715
Evaluation of actuator energy storage and power sources for spacecraft applications
[NASA-CR-193226] p 3288 N93-29091
Research and development of lithium secondary batteries for load conditioner use, volume 2
[DE93-781329] p 3410 N93-29673

Nuclear isomers as ultra-high-energy-density materials [DE93-009520] p 3568 N93-29784

New hydrogen technologies [DE93-778353] p 3343 N93-30042

Prefeasibility study on compressed air energy storage systems [VTT-TIED-1267] p 3465 N93-30111

ENERGY TECHNOLOGY

Development of alternative fuels from coal-derived syngas [DE93-011629] p 3341 N93-28668

JPRS report: Science and technology. Central Eurasia: Engineering and equipment [JPRS-UEQ-93-003] p 3353 N93-28691

Assessment of energy technologies contributing to environmental conservation [DE93-781439] p 3468 N93-28882

JPRS report: Science and technology. Central Eurasia: Engineering and equipment [JPRS-UEQ-93-001] p 3274 N93-29014

Solar energy emplacement developer p 3230 N93-29732

Strategic Environmental Research and Development Program (SERDP) [AD-A263745] p 3471 N93-29858

Solar world congress: Proceedings of the biennial congress of the international solar energy society, volume 1, part 2 [PB93-174779] p 3465 N93-30001

Energy efficient drivepower: An overview [DE93-012435] p 3411 N93-30057

Energy efficient drivepower [DE93-012436] p 3411 N93-30058

Power generation and transportation systems research department [PB93-178309] p 3352 N93-30663

Departmental technology transfer update p 3625 N93-30694

Plasma Physics Network Newsletter, no. 5 [DE93-606216] p 3591 N93-30795

Solar World Congress: Proceedings of the Biennial Congress of the International Solar Energy Society, volume 2, part 2 [PB93-174795] p 3466 N93-30935

ENERGY TRANSFER

Observation of a beam energy shift caused by a plasma wakefield [DE93-753243] p 3583 N93-28533

Nonconservative and reverse spectral transfer in Hasegawa-Mima turbulence [DE93-010132] p 3585 N93-28913

Kinetics and energy transfer in nonequilibrium fluid flows [AD-A263612] p 3240 N93-29284

Response of energetic solids to light, heat and shock pulses [AD-A263702] p 3342 N93-29296

New hydrogen technologies [DE93-778353] p 3343 N93-30042

Vibrational spectroscopy of shock-compressed fluids p 3318 N93-30072

Some implications of a differential turbomachinery equation with viscous correction [AD-A264693] p 3427 N93-30571

ENGINE DESIGN

Small Stirling dynamic isotope power system for robotic space missions [NASA-TM-105785] p 3287 N93-28686

Experimental evaluation of a cooled radial-inflow turbine [NASA-TM-106230] p 3251 N93-28697

Use of local x ray computerized tomography for high-resolution, region-of-interest inspection of large ceramic components for engines [DE93-005564] p 3449 N93-28943

Advanced engine study program [NASA-CR-187217] p 3287 N93-28946

Additional support for the TDK/MABL computer program [NASA-CR-193037] p 3526 N93-29028

Investigation of thermoacoustic muffler [AD-A262009] p 3562 N93-29392

Heat transfer and aerodynamics of a 3D design nozzle guide vane tested in the Pyestock Isentropic Light Piston Facility p 3252 N93-29928

Aero-thermal design of a cooled transonic NGV and comparison with experimental results p 3257 N93-29957

ENGINE INLETS

The 3-D viscous flow CFD analysis of the propeller effect on an advanced ducted propeller subsonic inlet [NASA-TM-106240] p 3252 N93-29162

Solution of Euler equations for forebody-inlet ensemble of aircraft at high angle of attack [AD-A263905] p 3240 N93-29862

The influence of non-uniform spanwise inlet temperature on turbine rotor heat transfer p 3253 N93-29932

ENGINE PARTS

Surface modification of tribological components in transportation [DE93-008647] p 3442 N93-28903

An analysis of the correlation between the J52 engine component improvement program and improved maintenance parameters [AD-A262062] p 3251 N93-28984

Investigation of thermoacoustic muffler [AD-A262009] p 3562 N93-29392

Improved silicon nitride for advanced heat engines [NASA-CR-182193] p 3298 N93-29451

Heat transfer and aerodynamics of a 3D design nozzle guide vane tested in the Pyestock Isentropic Light Piston Facility p 3252 N93-29928

Thermal effects of a coolant film along the suction side of a high pressure turbine nozzle guide vane p 3253 N93-29930

Characterization of ceramic composite materials for gas turbine applications [DE93-009719] p 3259 N93-30168

ENGINE TESTING LABORATORIES

The USAF Advanced Turbine Aerothermal Research Rig (ATARR) p 3255 N93-29945

ENGINE TESTS

Heat transfer and aerodynamics of a 3D design nozzle guide vane tested in the Pyestock Isentropic Light Piston Facility p 3252 N93-29928

Thermal effects of a coolant film along the suction side of a high pressure turbine nozzle guide vane p 3253 N93-29930

The influence of non-uniform spanwise inlet temperature on turbine rotor heat transfer p 3253 N93-29932

Measurement of turbulent spots and intermittency modelling at gas-turbine conditions p 3253 N93-29934

Orbital transfer vehicle oxygen turbopump technology. Volume 3: Hot oxygen testing [NASA-CR-191036] p 3448 N93-31039

ENGINEERING

JPRS report: Science and technology. Central Eurasia: Engineering and equipment [JPRS-UEQ-93-001] p 3274 N93-29014

JPRS report: Science and technology. Central Eurasia: Engineering and equipment [JPRS-UEQ-93-004] p 3354 N93-29090

NASA/DoD Aerospace Knowledge Diffusion Research Project. Paper 31: The information-seeking behavior of engineers [NASA-TM-109224] p 3616 N93-30037

National Educators' Workshop. Update 92: Standard Experiments in Engineering Materials Science and Technology [NASA-CP-3201] p 3290 N93-30948

Materials education activities p 3291 N93-30958

ENGINEERING TEST REACTORS

Air oxidation behavior of fuel for the High Temperature Engineering Test Reactor (HTTR) [DE93-753349] p 3576 N93-30006

ENGINEERS

NASA/DOD Aerospace Knowledge Diffusion Research Project. Paper 28: The technical communication practices of Russian and US aerospace engineers and scientists [NASA-TM-108249] p 3612 N93-28948

Advanced network technology: Background paper [OTA-BP-TCT-101] p 3539 N93-29650

NASA/DoD Aerospace Knowledge Diffusion Research Project. Paper 31: The information-seeking behavior of engineers [NASA-TM-109224] p 3616 N93-30037

ENTHALPY

Some implications of a differential turbomachinery equation with viscous correction [AD-A264693] p 3427 N93-30571

ENTROPY

Thermodynamic properties for polycyclic systems by non-calorimetric methods [DE93-011373] p 3603 N93-28747

ENVIRONMENT EFFECTS

Environmental embrittlement of binary and Zr-doped Ni3Al [DE93-008575] p 3321 N93-28679

Low Earth orbital mission aboard the Space Test Experiments Platform (STEP-3) p 3267 N93-28732

Emission inventories: A global modeling perspective [DE93-005817] p 3469 N93-28965

Atmospheric and Geophysical Sciences Division: G-Division did you know? [DE93-007412] p 3469 N93-28967

State of the art: Ecological biomarkers [DE93-006621] p 3469 N93-28992

Proposal to develop guides for high school teachers on global systems science [DE93-008759] p 3624 N93-29100

Interim fatigue design curves for carbon, low-alloy, and austenitic stainless steels in LWR environments [DE93-009202] p 3323 N93-29102

Environmental effects on stitched RTM composites [NASA-CR-193221] p 3297 N93-29107

Ocean Margins Program [DE93-008937] p 3470 N93-29262

Characteristics of hypervelocity impact craters on LDEF experiment S1003 and implications of small particle impacts on reflective surfaces p 3283 N93-29363

Analyses of space environment effects on active fiber optic links orbited aboard the LDEF p 3583 N93-29699

Potential effects of HFC-152a on global ozone and climate [DE93-008018] p 3471 N93-29792

Quantifying and minimizing uncertainty of climate forcing by anthropogenic aerosols [NASA-TM-108259] p 3472 N93-30043

Foreign technology assessment: Environmental evaluation of a radiation-hard oscillator/divider [DE93-011481] p 3412 N93-30127

Simulation of landscape disturbances and the effect of climatic change [DE93-011615] p 3472 N93-30131

VLF/LF propagation measurements p 3395 N93-30732

Statement on the United Nations Conference on Environment and Development [DE93-601878] p 3475 N93-30996

ENVIRONMENT MANAGEMENT

Hanford Environmental Information System (HEIS) user's manual, volume 1 [DE93-007465] p 3470 N93-29135

Remote vehicle survey tool [DE93-010822] p 3460 N93-29255

An architecture for robotic system integration [DE93-010829] p 3444 N93-29316

Building alliances to restore coastal environments: A coastal America progress report [PB93-169464] p 3470 N93-29674

Strategic Environmental Research and Development Program (SERDP) [AD-A263745] p 3471 N93-29858

The environment as an operational center of gravity [AD-A264170] p 3472 N93-30154

Environmental Monitoring and Assessment Program. EMAP: Arid Colorado plateau pilot study [PB93-181618] p 3474 N93-30823

Environmental characteristics of EPA, NRC, and DOE sites contaminated with radioactive substances [PB93-185551] p 3475 N93-30829

ENVIRONMENT MODELS

Predicted and observed directional dependence of meteoroid/debris impacts on LDEF thermal blankets p 3638 N93-29358

Status of LDEF ionizing radiation measurements and analysis p 3654 N93-29626

A measurement of the radiation dose to LDEF by passive dosimetry p 3572 N93-29634

Environmental studies: Mathematical, computational and statistical analyses [AD-A264223] p 3473 N93-30360

ENVIRONMENT POLLUTION

Using a neural network to estimate solvent consumption [PB93-173110] p 3467 N93-28873

Global warming issue and global economic model [DE93-781334] p 3468 N93-28881

State of the art: Ecological biomarkers [DE93-006621] p 3469 N93-28992

Statement on the United Nations Conference on Environment and Development [DE93-601878] p 3475 N93-30996

ENVIRONMENT PROTECTION

Summer 1990 Atlanta ozone precursor study (January 1993) [PB93-167203] p 3470 N93-29200

Analysis of protocol gases: An on-going quality assurance audit [PB93-168839] p 3311 N93-29204

Tropical forests and biological diversity: USAID report to Congress 1990-1991 [PB93-180453] p 3471 N93-29681

Pollution prevention: A regulatory update [DE93-009727] p 3472 N93-30180

An evaluation of factors affecting the solidification/stabilization of heavy metal sludge [AD-A264128] p 3473 N93-30197

Planetary protection issues for the MESUR mission: Probability of growth (Pg) [NASA-CP-3167] p 3651 N93-30214

Environmental studies: Mathematical, computational and statistical analyses [AD-A264223] p 3473 N93-30360

Evaluation of environmental marketing terms in the United States
[PB93-175784] p 3474 N93-30660

ENVIRONMENTAL CONTROL
Automation of closed environments in space for human comfort and safety p 3230 N93-29734

ENVIRONMENTAL ENGINEERING
Assessment of energy technologies contributing to environmental conservation
[DE93-781439] p 3468 N93-28882

ENVIRONMENTAL MONITORING
Magnetohydrodynamic projects at the CDIF
[DE93-012195] p 3584 N93-28649
Orbital Debris Environment Monitor (ODEM)
p 3267 N93-28735
Lightweight modular instrumentation for planetary applications p 3286 N93-28787
Environmental monitors in the Midcourse Space Experiments (MSX) p 3286 N93-28826
Hanford Environmental Information System (HEIS) user's manual, volume 1
[DE93-007465] p 3470 N93-29135
Summer 1990 Atlanta ozone precursor study (January 1993)
[PB93-167203] p 3470 N93-29200
Mathematical modeling and control law development for the atmospheric monitoring and control system of the Controlled Environment Research Chamber (CERC) at NASA Ames Research Center
[AD-A261978] p 3261 N93-29436
Convective and stratiform rain: Multichannel microwave sensing over oceans
[NASA-TM-104586] p 3482 N93-29448
Advanced Earth Observing Satellite (ADEOS)
p 3279 N93-29648
What's past is prologue: Supporting global change research with historical data
[DE93-005777] p 3472 N93-30009
The environment as an operational center of gravity
[AD-A264170] p 3472 N93-30154
Case study of Frontal Boundary Study Mission 03
[DE93-007176] p 3473 N93-30183
Remote sensing for water quality monitoring in the Tennessee Valley: Field tests of two systems
[DE93-008997] p 3462 N93-30637
Environmental Monitoring and Assessment Program. EMAP: Arid Colorado plateau pilot study
[PB93-181618] p 3474 N93-30823
Planning and progress of EPA's pollution prevention research program
[PB93-185767] p 3475 N93-30831
Office of Water Environmental and Program Information Systems Compendium, FY 1992
[PB93-186203] p 3462 N93-30833

ENVIRONMENTAL QUALITY
Trend survey on the elucidation of the global warming mechanism by the governments of major industrialized nations
[DE93-776427] p 3470 N93-29672

ENVIRONMENTAL SURVEYS
Thermal Analyzer for Planetary Soil (TAPS): An in situ instrument for mineral and volatile-element measurements p 3643 N93-28782
Planetary protection issues for the MESUR mission: Probability of growth (Pg)
[NASA-CP-3167] p 3651 N93-30214
Environmental Monitoring and Assessment Program. EMAP: Arid Colorado plateau pilot study
[PB93-181618] p 3474 N93-30823

ENVIRONMENTAL TESTS
LDEF materials data bases
[NASA-TM-107757] p 3290 N93-29067

ENZYME ACTIVITY
Comparative mutagenesis of human cells in vivo and in vitro
[DE93-012269] p 3490 N93-28651

ENZYMES
Comparative mutagenesis of human cells in vivo and in vitro
[DE93-012269] p 3490 N93-28651
Introductions to the Proceedings of the Fourteenth Symposium on Biotechnology for Fuels and Chemicals
[DE93-006235] p 3490 N93-28890
Center of Excellence in Biotechnology (Research)
[AD-A263598] p 3491 N93-29915

EPHEMERIDES
Onboard signal processing: Wave of the future for planetary radio science? p 3646 N93-28801

EPIDEMIOLOGY
The chronic effects of jP-8 jet fuel exposure on the lungs
[AD-A264162] p 3495 N93-30153

EPITAXY
Low temperature (LT) GaAs and related materials
[AD-A263607] p 3298 N93-29282
In-situ x ray studies of the underpotential deposition of copper on platinum (3)
[AD-A263361] p 3595 N93-29331
Crystallization of nanocomposite glasses made by the SSG process
[AD-A262892] p 3333 N93-29511
Submillimeter and microwave residual losses in epitaxial films of Y-Ba-Cu-O and Tl-Ca-Ba-Cu-O
[DE93-010430] p 3596 N93-29868
Low-cost, high-efficiency solar cells utilizing GaAs-on-Si technology
[DE93-000096] p 3464 N93-29965
Atomic layer epitaxy of semiconductor heterostructures
[AD-A264755] p 3599 N93-30560
Design, synthesis, and chemical processing of hierarchical ceramic structures for aerospace applications
[AD-A264227] p 3339 N93-30885

EPOXY MATRIX COMPOSITES
Effects of intra- and inter-laminar resin content on the mechanical properties of toughened composite materials
p 3303 N93-30845
The initiation, propagation, and effect of matrix microcracks in cross-ply and related laminates
p 3304 N93-30847
Ultrasonic detection and identification of fabrication defects in composites p 3305 N93-30856

EPOXY RESINS
Synthesis of new high performance lubricants and solid lubricants
[DE93-012237] p 3330 N93-28748
Process to prepare 1,3-diamino-5-pentafluorosulfanylbenzene
[NASA-CASE-LAR-14773-2-CU] p 3312 N93-29506
Comparison of impact results for several polymeric composites over a wide range of low impact velocities
p 3304 N93-30848
Delaminations in composite plates under impact loads
p 3304 N93-30849
Characterization of multiaxial warp knit composites
p 3304 N93-30851
Ultrasonic detection and identification of fabrication defects in composites p 3305 N93-30856

EQUATIONS OF MOTION
Coarse image motion for saccade control
[OUEL-1916/92] p 3523 N93-28485
Reference equations of motion for automatic rendezvous and capture
[NASA-CR-185676] p 3269 N93-29652
Visualization techniques for analyzing control of human movement: Affine mappings between multi-dimensional spaces p 3508 N93-30204
Input relegation control for gross motion of a kinematically redundant manipulator
[DE93-005301] p 3446 N93-30210
A closed-form formula for the manipulator regressor
p 3355 N93-30218
Orbital motion calculation using Lie method in collider nonlinear magnetic field
[DE93-605733] p 3571 N93-30800
Electric magnetic duality in string theory
[DE93-606061] p 3606 N93-30807
A new exact solution to the classical equations of motion of the relativistic string with massive ends
[DE92-644736] p 3557 N93-30922
Some problems of relativistic electrodynamics
[DE92-644738] p 3400 N93-30923
On symmetric central configurations with application to satellite motion about rings p 3652 N93-31000
A non degenerate semi-classical Lagrangian for dilaton-gravity in two dimensions
[DE92-641339] p 3480 N93-31002
Theoretical and experimental investigation of slack cable/mass system dynamics p 3455 N93-31028

EQUATIONS OF STATE
Thermodynamic properties for polycyclic systems by non-calorimetric methods
[DE93-011373] p 3603 N93-28747
Tables of experimental data used for the correlation of the thermophysical properties of ethane
[PB93-173417] p 3313 N93-29768
SESAME equation of state number 8010: Boron loaded silicone potting material
[DE93-012083] p 3300 N93-30395
Direct Monte Carlo simulation of the chemical equilibrium composition of detonation products
[DE92-040372] p 3315 N93-30447
Fourth-rank gravity and cosmology
[DE92-644722] p 3637 N93-30918

EQUATORIAL REGIONS
A comparison of trans-equatorial ionosphere propagation predictions from AMBCOM with measured data
[AD-A264006] p 3391 N93-29987

EQUILIBRIUM EQUATIONS
A normally elliptic Hamiltonian bifurcation
[W-9201] p 3548 N93-28753

EQUIPMENT
JPRS report: Science and technology. Central Eurasia: Engineering and equipment
[JPRS-UEQ-93-001] p 3274 N93-29014
JPRS report: Science and technology. Central Eurasia: Engineering and equipment
[JPRS-UEQ-93-004] p 3354 N93-29090

EQUIPOTENTIALS
Some problems of relativistic electrodynamics
[DE92-644738] p 3400 N93-30923

EQUIVALENT CIRCUITS
Potential transmission and transients during corrosion: Applications to corrosion monitoring
[DE93-010863] p 3323 N93-29256
Antenna modeling and analysis for ELF/VLF/LF applications p 3398 N93-30751

ERGODIC PROCESS
Some qualitative properties in polling systems
[INRIA-RR-1596] p 3552 N93-28506

ERROR ANALYSIS
The use of objective prism radial velocities for kinematic studies of galactic populations p 3633 N93-28672
Pre- and postprocessing techniques for determining goodness of computational meshes
[NASA-CR-192553] p 3538 N93-29030
Lunar gravitational field estimation and the effects of mismodeling upon lunar satellite orbit prediction
[NASA-CR-188249] p 3634 N93-29042
Reliability assessment of thrust chamber cooling concepts using probabilistic analysis techniques
[NASA-CR-190785] p 3288 N93-29068
Thermoviscoplastic analysis of fibrous periodic composites using triangular subvolumes
[NASA-TM-106076] p 3297 N93-29074
Errors when shock waves interact due to numerical shock width
[DE93-010699] p 3426 N93-30484
Algorithm for the solution of the Faddeev equation for a system of three identical spinless particles
[DE92-644678] p 3535 N93-30914
Bayesian linear analysis with application to removal of atmospheric influences on optical remote sensing images
[BCRS-92-19] p 3463 N93-31011
A continuum code investigation of stress integration using exact and approximate material rotation
[DE93-001892] p 3454 N93-31013

ERROR CORRECTING CODES
Accuracy enhancement in optical computing
[AD-A264872] p 3522 N93-30179
An error control protocol based on trellis coded modulations p 3358 N93-30237
A single chip high-speed CMOS Viterbi decoder
p 3358 N93-30238

ERROR DETECTION CODES
Hidden Markov models for fault detection in dynamic systems
[NASA-CASE-NPO-18982-1-CU] p 3449 N93-30413

ERROR SIGNALS
Computation and generalization in neural networks
[AD-A263752] p 3549 N93-29871

ERRORS
Measurement of the relative and absolute microgravity environment of space platforms, recent flight results, and determination of the spatial microgravity field
p 3266 N93-28725
Implementing error-valued semantics for dataflow languages on imperative machines
[DE93-009319] p 3615 N93-29310
A neural fuzzy controller learning by fuzzy error propagation p 3516 N93-29560
Inverse problems: Fuzzy representation of uncertainty generates a regularization p 3516 N93-29563
The effect of clock, media, and station location errors on Doppler measurement accuracy
p 3246 N93-29588
Uncorrectable sequences and telecommand
p 3385 N93-29596
Monte Carlo simulation of magnitude-angle error sources
[AD-A263738] p 3555 N93-29857
A neural network based approach for machine fault diagnosis
[VTT-TIED-1274] p 3543 N93-29998
The planning coordinator: A design architecture for autonomous error recovery and on-line planning of intelligent tasks
[NASA-CR-193250] p 3543 N93-30039
Errors when shock waves interact due to numerical shock width
[DE93-010699] p 3426 N93-30484

An analysis of en route controller-pilot voice communications
[AD-A264784] p 3394 N93-30611

ERS-1 (ESA SATELLITE)

Proceedings of the 8th User Seminar of the German Remote Sensing Data Center of the German Aerospace Establishment (DLR)
[DLR-MITT-92-09] p 3456 N93-28915

The German PAF (Processing and Archiving Facilities) for ERS-1 p 3457 N93-28916

Processing of altimeter data by the German ERS-1 Processing and Archiving Facility (D-PAF)
p 3457 N93-28917

Exact trajectory determinator for ERS-1
p 3457 N93-28918

The interferometric SAR technology and its usability in the framework of ERS-1 p 3457 N93-28919

The German satellite ground station in Antarctica: Realization and first results p 3458 N93-28924

ERS-1 directional wave spectra validation with the airborne SAR PHARS
[BCRS-92-18] p 3463 N93-31010

ESCALATORS

Platform stair lift
[NASA-CASE-MFS-28772-1] p 3507 N93-29845

ESCHERICHIA

Computer assisted multiplex sequencing
[DE93-007144] p 3536 N93-30934

ESTERS

The swollen polymer technique and its use for heat transfer investigations on film cooled surfaces
p 3255 N93-29944

ESTIMATES

A modified chi-squared goodness-of-fit test for the three-parameter gamma distribution with unknown parameters
[AD-A262553] p 3554 N93-28845

Estimations of expectedness and potential surprise in possibility theory p 3510 N93-29518

A fuzzy set preference model for market share analysis p 3514 N93-29548

ESTIMATING

Subjective response to simulated sonic booms with ground reflections
[NASA-TM-107764] p 3561 N93-28692

Information-theoretic performance bounding of Bayesian identifiers
[DE93-010705] p 3554 N93-28763

Estimating test range capacity
[AD-A262493] p 3270 N93-28938

Theory and applications of random fields
[AD-A262829] p 3555 N93-29454

An analysis of possible applications of fuzzy set theory to the actuarial credibility theory p 3510 N93-29517

Performance analysis of subspace methods
[AD-A263984] p 3530 N93-29865

Gradient estimation for regenerative processes
[AD-A263766] p 3555 N93-29878

ETALONS

Tunable CW diode-pumped Tm,Ho:YLiF4 laser operating at or near room temperature
[NASA-CASE-NPO-18611-1-CU] p 3440 N93-30415

ETCHING

Texturing of InP surfaces for device applications
[NASA-TM-106061] p 3321 N93-28618

ETHANE

Tables of experimental data used for the correlation of the thermophysical properties of ethane
[PB93-173417] p 3313 N93-29768

ETHERS

High octane ethers from synthesis gas-derived alcohols
[DE93-012470] p 3341 N93-28752

Preliminary properties of a resin from ethynyl terminated materials p 3303 N93-30842

ETHYL ALCOHOL

Mass spectrometric investigation of 2-methoxyethanol and 2-ethoxyethanol clusters: Magic numbers and structural implications
[AD-A262822] p 3312 N93-29429

ETHYL COMPOUNDS

Studies in Lewis acid and superacid ionic liquids
[AD-A264683] p 3316 N93-30551

ETHYLENE

APU diaphragm testing. Test plan
[NASA-TM-108251] p 3271 N93-29387

EUCLIDEAN GEOMETRY

Input relegation control for gross motion of a kinematically redundant manipulator
[DE93-005301] p 3446 N93-30210

The ground state wavefunctions of a conformally invariant scalar field in different spacetime background
[DE93-606063] p 3606 N93-30808

EUKARYOTES

Regulation of alternative CO2 fixation pathways in procaryotic and eucaryotic photosynthetic organisms
[DE93-012109] p 3491 N93-29181

EULER EQUATIONS OF MOTION

Development of a 3-D Implicit Euler Code for Hypersonic and High Supersonic Flows
[ONERA-RSF-23/1123-AY-230A] p 3417 N93-28744

State vector splitting: A numerical scheme for the Euler equations p 3419 N93-29039

EULER-CAUCHY EQUATIONS

Numerical modelling of the cold plasma with time-dependent, magnetohydrodynamic methods
[KFK-5053] p 3586 N93-29081

EULER-LAGRANGE EQUATION

Stability, bifurcation, and control of Hamiltonian systems
[DE93-012103] p 3547 N93-28648

On the energy-momentum tensors for field theories in spaces with affine connection and metric
[DE92-644744] p 3557 N93-30927

EURECA (ESA)

The Optical Properties Monitor (OPM): A multipurpose optical laboratory in space p 3266 N93-28729

EUROPE

System of navigation by satellites with European coverage p 3284 N93-29897

EUROPEAN SPACE PROGRAMS

The prehistory of ESRO, 1959 - 1960
[ESA-HSR-1] p 3660 N93-29500

EUTECTIC ALLOYS

Compatibility studies of AISI type 316 stainless steel with lead-lithium eutectic alloy
[DE93-605281] p 3328 N93-31022

EUTECTICS

Preliminary test of liquid metal induced embrittlement in liquid LiPb and stainless-steel systems
[DE93-753130] p 3320 N93-28529

Eutectic solidification of Al-U at slowly cooling rates (10 C per second)
[DE92-640082] p 3328 N93-30941

A review of hot cracking in austenitic stainless steel weldments
[DE93-605280] p 3328 N93-31021

EVALUATION

Battery testing at Argonne National Laboratory
[DE93-009204] p 3407 N93-29036

Design and performance evaluation of a gas chromatograph micromachined in a single crystal silicon substrate
[AD-A262594] p 3596 N93-29424

Postflight hardware evaluation 360T025 (RSRM-25, STS-46). Appendix C: Nozzle PFORs
[NASA-CR-192565] p 3272 N93-30620

EVAPORATION

Prognostic cloud water in the Los Alamos general circulation model
[DE93-007381] p 3482 N93-29347

Pulse mitigation and heat transfer enhancement techniques. Volume 1: Spray cooling
[AD-A263495] p 3423 N93-29352

Unexpected increase in the thermal generation rate of bulk GaAs due to electron-beam metallization
[DE93-009829] p 3598 N93-30511

The adhesion of AgI molecules to gaseous metallic silver cluster cations
[AD-A264820] p 3338 N93-30628

EVAPORATIVE COOLING

Pulse mitigation and heat transfer enhancement techniques. Volume 2: Effect of surface wettability and roughness in evaporative spray cooling
[AD-A264174] p 3425 N93-30155

EVAPORATORS

Pulse mitigation and heat transfer enhancement techniques. Volume 4: Transient behavior of heat pipe with thermal energy storage under pulse heat loads
[AD-A263497] p 3423 N93-29339

EVAPOTRANSPIRATION

National remote sensing programme 2 ACMS project. Phase 1: Validation. Part 1: Definition of validation experiment
[BCRS-92-10-PHASE-1-PT-1] p 3461 N93-29465

EVOKED RESPONSE (PSYCHOPHYSIOLOGY)

An assessment of peripheral nerve damage in the rat following non-freezing cold exposure: An electrophysiological and histopathological examination
[AD-A264293] p 3492 N93-30818

EXCIMER LASERS

Gas electron diffraction employing a pulsed electron beam synchronous with photoexcitation
p 3319 N93-30101

EXCITATION

The natural excitation technique (NExT) for modal parameter extraction from operating wind turbines
[DE93-010611] p 3463 N93-28603

Femtosecond laser studies of excited state dynamics
[AD-A263708] p 3439 N93-29918

Nonequilibrium screening and exciton dynamics probed by femtosecond laser pulses
[AD-A263603] p 3439 N93-29983

Experimental and theoretical aspects of excited state electron transfer and related phenomena
[AD-A263457] p 3570 N93-30589

EXCITONS

Nonequilibrium screening and exciton dynamics probed by femtosecond laser pulses
[AD-A263603] p 3439 N93-29983

EXERCISE PHYSIOLOGY

Beta-adrenergic blockade and lactate metabolism during exercise at high altitude
[AD-A263544] p 3495 N93-29820

Field trial of caffeine on physical performance at altitude: An attempt to overcome the challenge
[AD-A264260] p 3497 N93-30894

EXHAUST DIFFUSERS

Cooling predictions in turbofan engine components
p 3259 N93-29964

EXHAUST EMISSION

Assessment of energy technologies contributing to environmental conservation
[DE93-781439] p 3468 N93-28882

Study on technology for effective utilization of carbon dioxide in view of global environment
[DE93-781440] p 3468 N93-28883

EXHAUST FLOW SIMULATION

Numerical simulation of perfect fluid flows around complex 3D configurations by a multidomain solver using the MUSCL approach p 3417 N93-28745

Effects of flow-path variations on internal reversing flow in a tailpipe offtake configuration for ASTOVL aircraft
[NASA-TM-106149] p 3252 N93-29065

EXHAUST GASES

Generation of carbon monoxide in compartment fires
[PB93-146702] p 3244 N93-29211

EXHAUST NOZZLES

Effects of flow-path variations on internal reversing flow in a tailpipe offtake configuration for ASTOVL aircraft
[NASA-TM-106149] p 3252 N93-29065

Evaluation of four advanced nozzle concepts for short takeoff and landing performance
[NASA-TP-3314] p 3239 N93-29165

EXHAUST SYSTEMS

Effects of flow-path variations on internal reversing flow in a tailpipe offtake configuration for ASTOVL aircraft
[NASA-TM-106149] p 3252 N93-29065

EXOBIOLOGY

Planetary protection issues for the MESUR mission: Probability of growth (Pg)
[NASA-CP-3167] p 3651 N93-30214

EXOTHERMIC REACTIONS

Chemical dynamics simulations as a probe to the initiation and propagation of condensed phase detonations p 3318 N93-30071

Rate constant determinations of reactions H + HNO from ab initio reaction path calculations
p 3319 N93-30099

EXPANDABLE STRUCTURES

Advanced collapsible tank for liquid containment
[NASA-CR-188247] p 3353 N93-28698

EXPERIMENT DESIGN

NASA instep/MDMSC jitter suppression experiment (JITTER) p 3263 N93-28702

CSI-Star: A low-cost CSI orbital testbed
p 3263 N93-28707

NASA in-step: Permeable membrane experiment
p 3267 N93-28736

Experiments in corrosion for younger students by and for older students p 3291 N93-30955

Improved measurement of thermal effects on microstructure p 3292 N93-30959

Direct tension experiments on compacted granular materials p 3292 N93-30960

Application of hardness testing in foundry processing operations: A university and industry partnership
p 3292 N93-30961

Laboratory experiments in integrated circuit fabrication
p 3292 N93-30962

A 69 cent look at thermoplastic softening
p 3292 N93-30963

Solving a product safety problem using a recycled high density polyethylene container p 3292 N93-30964

Walkway friction: Experiment and analysis
p 3293 N93-30966

Thermoforming from a systems viewpoint
p 3293 N93-30967

Fracture of glass p 3293 N93-30969

Experiments in materials science from household items p 3293 N93-30971

An automated data collection system for a Charpy impact tester p 3293 N93-30972

Visualizing weld metal solidification using organic analogs p 3293 N93-30973
Taguchi method of experimental design in materials education p 3294 N93-30975
Powder metallurgy: Solid and liquid phase sintering of copper p 3294 N93-30976
High thermal conductivity of diamond p 3294 N93-30977
Temperature-dependent electrical conductivity of soda-lime glass p 3294 N93-30978
Construction and testing of simple airfoils to demonstrate structural design, materials choice, and composite concepts p 3243 N93-30979

EXPERT SYSTEMS
Planning for air to air combat p 3501 N93-28852
Uncertainty reasoning in expert systems [NASA-CR-193120] p 3548 N93-28973
Neural network technologies [AD-A262576] p 3541 N93-28987
Systems engineering studies of on-orbit assembly operation p 3275 N93-29114
Spurious symptom reduction in fault monitoring [NASA-CR-191453] p 3542 N93-29192
Data reduction expert assistant p 3613 N93-29227
Overview of the System of Experts for Intelligent Data Management (SEIDAM) p 3613 N93-29228
DataHub knowledge based assistance for science visualization and analysis using large distributed databases p 3613 N93-29230
Collection-oriented match: Scaling up the data in production systems [AD-A262755] p 3615 N93-29459
Parallel inferencing method and apparatus for rule-based expert systems [NASA-CASE-NPO-18004-1-CU] p 3521 N93-29504
How to select combination operators for fuzzy expert systems using CRI p 3510 N93-29521
Approximate reasoning using terminological models p 3510 N93-29522
A neuro-fuzzy architecture for real-time applications p 3511 N93-29529
Fuzzy neural network methodology applied to medical diagnosis p 3498 N93-29546
An experimental methodology for a fuzzy set preference model p 3514 N93-29547
A genetic algorithms approach for altering the membership functions in fuzzy logic controllers p 3518 N93-29573
Life insurance risk assessment using a fuzzy logic expert system p 3520 N93-29585
Development of a concept formulation process aid for analyzing training requirements and developing training devices [AD-A263579] p 3261 N93-29972
Systems description of MIVOS (mist forecast system), part 1 [KNMI-TR-141-PT-1] p 3483 N93-30013
STRATUS: A prototype expert advisory system for terminal weather forecasting p 3367 N93-30296
An expert system for identification of the task status from tactile sensor data p 3368 N93-30300
Airspace Design Expert System (ADES), a 2D/3D mapping and modelling tool incorporating an expert system for use in instrument approach design p 3247 N93-30357

EXPLODING WIRES
Improving the jitter of the 150 kJ experiments solid dielectric switches [DE93-009459] p 3405 N93-28597
High-voltage pulse generator capable of 2000 J at 10 kV [AD-A262034] p 3407 N93-28999

EXPLOSIONS
Mitigation of shock waves in a cylindrical tunnel by foam [AD-A262491] p 3423 N93-29419
Combustion/explosion chemistry of bulk materials p 3343 N93-30062
Containment of explosions in spherical vessels [DE93-005445] p 3446 N93-30211
Acoustic-gravity waves from low-altitude localized disturbances [AD-A264804] p 3479 N93-30593
Tool grinding and spark testing p 3291 N93-30954

EXPLOSIVES
Synthesis of cubane based energetic molecules [AD-A263271] p 3564 N93-28562
Powder x ray diffraction patterns of energetic materials for use as reference standards [DE93-009903] p 3592 N93-28568
A simple model for explosives formulation [DE93-010703] p 3341 N93-29251
Response of energetic solids to light, heat and shock pulses [AD-A263702] p 3342 N93-29296
Evaluation of personal cooling systems in conjunction with explosive ordnance disposal suits [AD-A262862] p 3506 N93-29471
The equivalent flat nose diameter of hemispherical nose cylindrical projectiles for impact induced detonation of energetic materials [AD-A263244] p 3342 N93-29494
Selective nitrations. Volume 2: The laser-induced nitration of three cycloalkanes [AD-A263250] p 3438 N93-29800
An explosively actuated electrical switch using Kapton insulation [AD-A263835] p 3411 N93-30021
Combustion/explosion chemistry of bulk materials p 3343 N93-30062
Propulsion and detonics research in France p 3344 N93-30070
Chemical dynamics simulations as a probe to the initiation and propagation of condensed phase detonations p 3318 N93-30071
A steric hindrance model for the crystal orientation dependence of the shock initiation sensitivity of PETN explosive [LA-UR-92-1427] p 3345 N93-30074
Detonation mass spectrometry p 3319 N93-30076
Strategies for understanding the deflagration-to-detonation transition p 3319 N93-30077
Detonation shock dynamics of composite energetic materials p 3350 N93-30096
Shock waves and polymorphic phase transitions in energetic materials p 3351 N93-30100
Automatic detection of explosives using x ray imaging p 3244 N93-30275
Explosives detection systems for airport security gas chromatographic based devices p 3244 N93-30276
Advanced signal processing requirement in an ion mobility explosives detector p 3320 N93-30277
The measurement of electrical conductivity in detonating condensed explosives [AD-A264482] p 3352 N93-30424
Conjugated substituted ionic polyacetylenes [AD-A264702] p 3337 N93-30497
Rocket-triggered lightning studies for the protection of critical assets [DE93-009633] p 3484 N93-30651

EXPONENTIAL FUNCTIONS
Dipolar orientational relaxation in guest/host amorphous polymer probed by second harmonic generation [AD-A262006] p 3333 N93-29441

EXPOSURE
Issues on human acceleration tolerance after long-duration space flights [NASA-TM-104753] p 3495 N93-29651
The chronic effects of jP-8 jet fuel exposure on the lungs [AD-A264162] p 3495 N93-30153
An assessment of peripheral nerve damage in the rat following non-freezing cold exposure: An electrophysiological and histopathological examination [AD-A264293] p 3492 N93-30818
Carbon monoxide exposure of subjects with documented cardiac arrhythmias [PB93-179943] p 3497 N93-30890

EXTENSOMETERS
The design and testing of a high-temperature graphite dilatometer [AD-A262185] p 3430 N93-28488
Enhanced noncontacting laser extensometer for biaxial strain measurements [AD-A263170] p 3430 N93-28989

EXTERNAL SURFACE CURRENTS
Computer-aided modeling for analysis of arbitrary scatterers and feeds p 3367 N93-30293

EXTRAPOLATION
The numerical solution of low Mach number flow in confined regions by Richardson extrapolation [TRITA-NA-9207] p 3238 N93-29005

EXTRASOLAR PLANETS
Detection of other planetary systems using photometry p 3632 N93-28791

EXTRATERRESTRIAL RADIATION
The emulsion chamber technology experiment p 3268 N93-28743
High-performance visible/UV CCD focal plane technology for spacebased applications p 3434 N93-28771
Future radiation measurements in low Earth orbit p 3654 N93-29708

EXTREME ULTRAVIOLET RADIATION
In orbit degradation of EUV optical components in the wavelength range 10-40 nm AO 138-3 p 3582 N93-29691
Research studies on short wavelength by selective auger processes [AD-A264493] p 3440 N93-30401

EXTREMELY HIGH FREQUENCIES
High-power Ka-band amplifier p 3385 N93-29590
Advanced technologies for lightweight EHF tactical communications satellites p 3389 N93-29900
Synchronization techniques for medium data rate EHF MILSATCOM systems p 3389 N93-29901
Terrain and coverage prediction analyses for non-geostationary orbit EHF satellite communications p 3389 N93-29902
Coarse synchronization in an EHF frequency-hopped satellite communications system p 3365 N93-30281
Adaptive jammer nulling in EHF communications satellites p 3365 N93-30284

EXTREMELY LOW FREQUENCIES
Gene transcription and electromagnetic fields [DE93-010854] p 3490 N93-28848
ELF/VLF/LF Radio Propagation and Systems Aspects [AGARD-CP-529] p 3394 N93-30727
ELF propagation highlights p 3395 N93-30730
ELF propagation in deep and shallow sea water p 3397 N93-30739
A long wave TE/TM noise prediction model p 3397 N93-30742
Application of non-standard signal processing to ELF noise characterization for the TSS1-OESEE programme p 3397 N93-30743
ELF/VLF radio noise measurements at high latitudes during solar particle events p 3397 N93-30744
ELF/VLF spectrum measurements p 3398 N93-30745
Results of the joint HIPAS/NUWC campaigns to investigate ELF generated by auroral electrojet modulation p 3398 N93-30746
Pattern measurements of US Navy ELF antennas p 3399 N93-30752
Orbiting transmitter and antenna for spaceborne communications at ELF/VLF to submerged submarines p 3399 N93-30755

EXTREMELY LOW RADIO FREQUENCIES
Application of non-standard signal processing to ELF noise characterization for the TSS1-OESEE programme p 3397 N93-30743
Results of the joint HIPAS/NUWC campaigns to investigate ELF generated by auroral electrojet modulation p 3398 N93-30746
Pattern measurements of US Navy ELF antennas p 3399 N93-30752

EXTRUDING
Acid solution absorption of extruded polyethylene foam [DE93-011701] p 3330 N93-28839

EYE (ANATOMY)
Discomfort glare from high-intensity discharge headlamps: Effects of context and experience [PB93-174720] p 3496 N93-30659

EYE DOMINANCE
The effects of superimposing symbology on a simulated night vision goggle display [AD-A263458] p 3508 N93-30590

EYE MOVEMENTS
NASA supporting studies for microgravity research on eye movements [NASA-CR-193233] p 3493 N93-29041
Head mounted displays for virtual reality [AD-A263498] p 3506 N93-29340
A tutorial on exit pupils and eye rotation with virtual image optical displays [AD-A262399] p 3494 N93-29400
A simple computational model of center-surround receptive fields in the retina [AD-A264723] p 3496 N93-30515
An algorithm for simple and complex feature detection: From retina to primary visual cortex [AD-A264306] p 3497 N93-30897

F

F REGION
Mithras studies of the boundary between open and closed field lines [AD-A264758] p 3479 N93-30562
Observing and modelling F-region ionospheric dynamics using the OII 7320A emission p 3479 N93-30564

F-15 AIRCRAFT
F-15 composite engine access door p 3302 N93-30442

F-16 AIRCRAFT
Head-steered sensor flight test results and implications p 3502 N93-28859

F-18 AIRCRAFT
Modal survey of a full-scale F-18 wind tunnel model [AD-A262482] p 3240 N93-29410
Flight control system design factors for applying automated testing techniques [NASA-TM-4242] p 3260 N93-30764

FABRICATION
Lightweight flexible composite tent materials
[AD-A263021] p 3295 N93-28660
Novel low temperature superconducting bolometers
[DE93-010433] p 3430 N93-28664
Inertial confinement fusion target component fabrication and technology development support
[DE93-010836] p 3585 N93-28836
Processing, fabrication, and demonstration of HTS integrated microwave circuits
[AD-A263161] p 3406 N93-28940
Electrochemical fabrication of cadmium chalcogenide microdiode arrays
[AD-A263169] p 3310 N93-28988
Oxidation behavior in reaction-bonded aluminum-silicon alloy/alumina powder compacts
[DE93-010407] p 3298 N93-29191
Characterization and optimization of a Hot Air Solder-Leveling System
[DE93-010188] p 3332 N93-29328
Method and apparatus for weaving a woven angle ply fabric
[NASA-CASE-LAR-14048-1] p 3354 N93-29611
NSF Tokyo reports: Japanese R and D projects on micro- and nanofabrication and related basic research projects
[PB93-181261] p 3410 N93-29671
Ferroelectric liquid crystal optical interconnect switching systems
[AD-A263751] p 3596 N93-29859
A unified approach for composite cost reporting and prediction in the ACT program p 3302 N93-30441
Mold bolt and means for achieving close tolerances between bolts and bolt holes
[NASA-CASE-MFS-28720-1] p 3447 N93-30567
Infiltration/cure modeling of resin transfer molded composite materials using advanced fiber architectures
p 3303 N93-30843
Advanced fiber placement of composite fuselage structures p 3306 N93-30864
Near net shape processing: A necessity for advanced materials applications p 3290 N93-30949
New materials: Fountainhead for new technologies and new science p 3291 N93-30952
Introduction to high performance composites
p 3291 N93-30957
Laboratory experiments in integrated circuit fabrication
p 3292 N93-30962

FABRICS
Lightweight flexible composite tent materials
[AD-A263021] p 3295 N93-28660
Technology transfer personnel exchange at the Boeing Company
[DE93-010190] p 3625 N93-29329
Method and apparatus for weaving a woven angle ply fabric
[NASA-CASE-LAR-14048-1] p 3354 N93-29611
Characterization of multiaxial warp knit composites
p 3304 N93-30851
Ultrasonic detection and identification of fabrication defects in composites p 3305 N93-30856

FACE (ANATOMY)
Methods for characterizing the human head for the design of helmets
[AD-A263875] p 3507 N93-29889

FACE CENTERED CUBIC LATTICES
Neutron scattering studies of the structures and lattice dynamics of the alkali metals
[DE93-008272] p 3593 N93-28956
The role of grain boundaries in hydrogen diffusion in metals at 25 C
[NASA-TM-108407] p 3322 N93-29043
Order-disorder transformations in Ni-Al alloys
[DE93-009293] p 3326 N93-30389
A tight binding model for the electronic structure of FCC and SC C60
[DE93-606214] p 3601 N93-30794

FACTOR ANALYSIS
A Monte Carlo study of the raw and normal varimax rotation criterion in factor analysis
[AD-A262516] p 3554 N93-28844
Crucial role of detailed function, task, timeline, link, and human vulnerability analyses in HRA
[DE93-001923] p 3505 N93-28942
Dynamic factorization in large-scale optimization
[AD-A263993] p 3528 N93-29345

FACTORIAL DESIGN
Study on various problems in statistical planning and inference
[AD-A262484] p 3554 N93-29411

FACTORIALS
Fluctuations and intermittency in high energy nucleus-nucleus collisions
[DE93-608481] p 3577 N93-30990

FACTORIZATION
Dynamic factorization in large-scale optimization
[AD-A263993] p 3528 N93-29345

FADDEEV EQUATIONS
Algorithm for the solution of the Faddeev equation for a system of three identical spinless particles
[DE92-644678] p 3535 N93-30914
Algorithm of numerical calculations of differential Yakubovsky equations for the (1 + 3) scattering problem
[DE92-644679] p 3535 N93-30915

FAILURE
Overview of piping issues and trends
[DE93-006628] p 3354 N93-28893
An investigation of graphite peek composite under compression with a centrally located circular discontinuity
[AD-A262549] p 3298 N93-29414
Uncorrectable sequences and telecommand
p 3385 N93-29596
Tutorial: Performance and reliability in redundant disk arrays p 3537 N93-30463
Delaminations in composite plates under impact loads
p 3304 N93-30849
Micromechanics of fatigue in woven and stitched composites p 3304 N93-30850
Multi-parameter optimization tool for low-cost commercial fuselage crown designs
p 3305 N93-30858
Comparison of hand laid-up tape and filament wound composite cylinders and panels with and without impact damage p 3306 N93-30859
Effects of scale in predicting global structural response p 3306 N93-30860

FAILURE ANALYSIS
Inservice diagnostic methods for solenoid-operated valves
[DE93-007823] p 3443 N93-28968
Reliability assessment of thrust chamber cooling concepts using probabilistic analysis techniques
[NASA-CR-190785] p 3288 N93-29068
Acousto-Ultrasonic analysis of failure in ceramic matrix composite tensile specimens
[NASA-TM-106219] p 3449 N93-29073
Sensor systems for monitoring Maglev guideway structures
[PB93-154821] p 3444 N93-29205
A fuzzy case based reasoning tool for model based approach to rocket engine health monitoring
p 3289 N93-29570
Overview of the Systems Special Investigation Group investigation p 3318 N93-29683
An experimental/analytical evaluation of biaxial sheet failure
[DE93-010620] p 3453 N93-29843
Air oxidation behavior of fuel for the High Temperature Engineering Test Reactor (HTTR)
[DE93-753349] p 3576 N93-30006
Evaluation of category 3 MLS designs
p 3247 N93-30358
A ceramic fracture model for high velocity impact
[AD-A264728] p 3454 N93-30545
Elastic stability considerations for deep submergence ceramic pressure housing
[AD-A264824] p 3454 N93-30598
Durability of Quick Reaction Satellite Antenna (QRSA) trunnion castings
[AD-A264095] p 3281 N93-30813
Structural response of bead-stiffened thermoplastic shear webs p 3308 N93-30873
An overview of the crash dynamics failure behavior of metal and composite aircraft structures
p 3308 N93-30875
Direct tension experiments on compacted granular materials p 3292 N93-30960

FAILURE MODES
Inservice diagnostic methods for solenoid-operated valves
[DE93-007823] p 3443 N93-28968
An investigation of graphite peek composite under compression with a centrally located circular discontinuity
[AD-A262549] p 3298 N93-29414
An experimental/analytical evaluation of biaxial sheet failure
[DE93-010620] p 3453 N93-29843
Foreign technology assessment: Environmental evaluation of a radiation-hard oscillator/divider
[DE93-011481] p 3412 N93-30127
The initiation, propagation, and effect of matrix microcracks in cross-ply and related laminates
p 3304 N93-30847
Comparison of hand laid-up tape and filament wound composite cylinders and panels with and without impact damage p 3306 N93-30859
Prediction of stiffener-skin separation in composite panels p 3307 N93-30871
Experimental behavior of graphite-epoxy Y-stiffened specimens loaded in compression p 3307 N93-30872
Evaluation of some scale effects in the response and failure of composite beams p 3308 N93-30874

FALLING SPHERES
Macrostatistical hydrodynamics
[DE93-012289] p 3417 N93-28751

FAR FIELDS
Comparative study of undersea fields produced by various dipoles p 3397 N93-30740
Application of the Fourier transform to short antennas
p 3398 N93-30750

FAR INFRARED RADIATION
Far infrared supplement. Third edition: Catalog of infrared observations (lambda greater than or equal to 4.6 micrometers)
[NASA-RP-1295] p 3629 N93-29156
Formulation of Ames 24E2 IR-black coating
[NASA-TM-102864] p 3629 N93-29453
The 12 UM contribution of nearby galaxies to the infrared background
[AD-A264336] p 3654 N93-30419
A variable reflectivity output coupler for optically pumped far infrared lasers
[MPE-PREPRINT-225] p 3441 N93-30640

FAR ULTRAVIOLET RADIATION
Spectroscopic probes of vibrationally excited molecules at chemically significant energies
[DE93-012328] p 3564 N93-28652
Research studies on short wavelength by selective auger processes
[AD-A264493] p 3440 N93-30401

FARADAY EFFECT
Fiber-optic currents measurements
[DE93-007970] p 3579 N93-29350
Neutrino oscillations and a new Faraday effect
[DE93-606111] p 3571 N93-30789

FARM CROPS
Continued results of the seeds in space experiment
p 3492 N93-29703

FAST FOURIER TRANSFORMATIONS
A multigrid extension of the FFT for the numerical inversion of Fourier and LaPlace transforms
[TRITA-NA-9204] p 3548 N93-29024
Enhanced resolution and de-aliasing techniques for fast Fourier transforms p 3358 N93-30240
The use of data turning in airborne radars
p 3358 N93-30241

FAST NEUTRONS
Fast neutron cross section measurements
[DE93-009053] p 3563 N93-28546
Subnanosecond high power performance of a bistable optically-controlled GaAs switch
[DE93-006285] p 3406 N93-28944

FAST NUCLEAR REACTORS
Annual progress report on the NSRR experiments, (21)
[DE93-753190] p 3574 N93-29137
Compatibility studies of AISI type 316 stainless steel with lead-lithium eutectic alloy
[DE93-605281] p 3328 N93-31022

FASTENERS
Quick connect fastener
[NASA-CASE-MFS-28833-1] p 3445 N93-29846

FATIGUE (MATERIALS)
Mechanics of elevated temperature fatigue damage in fiber-reinforced ceramics
[AD-A262403] p 3329 N93-28495
Crack length determination by ultrasonic methods
[DE93-008075] p 3450 N93-28567
Ultrahigh temperature assessment study: Ceramic matrix composites
[AD-A262740] p 3295 N93-28592
Micromechanics of fatigue in woven and stitched composites p 3304 N93-30850

FATIGUE LIFE
Mechanics of elevated temperature fatigue damage in fiber-reinforced ceramics
[AD-A262403] p 3329 N93-28495
Reliability assessment of thrust chamber cooling concepts using probabilistic analysis techniques
[NASA-CR-190785] p 3288 N93-29068
Interim fatigue design curves for carbon, low-alloy, and austenitic stainless steels in LWR environments
[DE93-009202] p 3323 N93-29102

FATIGUE TESTS
A miniature fatigue test machine p 3291 N93-30956

FAULT TOLERANCE
SEU tolerant computer based on the R3000
[DE93-009294] p 3520 N93-29058
Femtosecond carrier processes in compound semiconductors and real time signal processing
[AD-A263076] p 3382 N93-29131
Compiler-assisted multiple instruction rollback recovery using a read buffer
[NASA-CR-193175] p 3527 N93-29170
Spurious symptom reduction in fault monitoring
[NASA-CR-191453] p 3542 N93-29192

Research on reconfigurable and reliable manipulators [DE93-010244] p 3444 N93-29330
Associative memories for supercomputers [AD-A263142] p 3520 N93-29482
Synthesis techniques and analysis tools for on-chip fault-tolerance [AD-A263167] p 3409 N93-29654
A redesigned Isis and Meta system under Mach [AD-A263576] p 3531 N93-29976
The planning coordinator: A design architecture for autonomous error recovery and on-line planning of intelligent tasks [NASA-CR-193250] p 3543 N93-30039
An artificial neural network model for periodic trajectory generation p 3356 N93-30225
Fault tolerance and testing for WSI systems p 3361 N93-30258

FAULT TREES
Users manual for fault tree analysis code: CUT-TD [DE93-753272] p 3525 N93-28978

FEASIBILITY
Study on technology for effective utilization of carbon dioxide in view of global environment [DE93-781440] p 3468 N93-28883
Reception at Ascension Island, South Atlantic, of the transmissions from the Heard Island feasibility test [PB93-176261] p 3394 N93-30662
CAESAR development plan 1992-1995 [BCRS-92-17] p 3463 N93-31009

FEASIBILITY ANALYSIS
Optically tiled flat panel displays. A feasibility study [AD-A262737] p 3592 N93-28590
Clustered Lance Booster (CLB) feasibility study [AD-A262746] p 3286 N93-28593
Information system for co-registration of CAESAR sea-images based on two dimensional image matching techniques (SCORE). Part 1: Introduction, user requirements, and feasibility tests [BCRS-90-40A-PT-1] p 3460 N93-29307
Solid oxide fuel cells for transportation: A clean, efficient alternative for propulsion [DE93-010662] p 3464 N93-29844
SAR sensors on TACSATS: A feasibility assessment p 3286 N93-29909
Prefeasibility study on compressed air energy storage systems [VTT-TIED-1267] p 3465 N93-30111

FEDERAL BUDGETS
A perspective on acquisition of NASA space systems [AD-A263246] p 3610 N93-29499
Research, Development, Test and Evaluation (R, D, T, and E) programs (R-1), Department of Defense budget for fiscal year 1994 [PB93-169878] p 3611 N93-30936

FEEDBACK
Influence of optical feedback on the pulse behavior of semiconductor lasers [ETN-93-93798] p 3436 N93-28614
Study on decreasing torque noise resulting from feedback noise for the modified bang-bang controller [AD-A263178] p 3407 N93-29010
Optimal filtering and LQR theory with constraints on system and control matrices p 3357 N93-30234

FEEDBACK CONTROL
Closed-loop control with delayed information [INRIA-RR-1638] p 3541 N93-28638
Stabilization using low-gain PI control: SISO case [OUEL-1947/92] p 3541 N93-28898
Robust feedforward/feedback control synthesis for uncertain dynamical systems p 3542 N93-29079
Multivariable control of the Space Shuttle Remote Manipulator System using linearization by state feedback [NASA-CR-188248] p 3443 N93-29080
An autonomous vision-based mobile robot p 3443 N93-29082
Three-parameter tunable Tilt-Integral-Derivative (TID) controller [NASA-CASE-NPO-18492-1-CU] p 3542 N93-29176
A self-learning rule base for command following in dynamical systems p 3512 N93-29531
Robust control of intelligent rotor [AD-A263707] p 3259 N93-29985
Control of nonlinear systems with applications to constrained robots and spacecraft attitude stabilization p 3279 N93-29989
Attitude stabilization of a rigid spacecraft using two momentum wheel actuators p 3280 N93-29990
Attitude stabilization of a rigid spacecraft using gas jet actuators operating in a failure mode p 3280 N93-29992
Planar reorientation of a free-free beam in space using embedded electromechanical actuators p 3280 N93-29993
Some results on feedback stabilization of a one-link flexible arm [INRIA-RR-1682] p 3543 N93-30116
Robust control via H-infinity optimization p 3354 N93-30216
Control system design and multiparameter variations p 3355 N93-30217
Robust boundary control of flexible structures governed by hybrid dynamics p 3285 N93-30249
Turbulent drag reduction: Studies of feedback control and flow over riblets p 3242 N93-30645
Control of nonlinear systems with applications to constrained robots and spacecraft attitude stabilization p 3544 N93-30893

FEEDFORWARD CONTROL
Neural network simulations on massively parallel computers: Applications in chemical physics [DE93-006739] p 3538 N93-28894
Evolving neural network architecture [AD-A264802] p 3544 N93-30592

FEMALES
Materials education activities p 3291 N93-30958

FERMI SURFACES
Effect of planar magnetic field on electron transport properties of n-AlGaAs/GaAs heterojunction and photoluminescence measures in GaAs samples [DE93-608739] p 3601 N93-30776

FERMIONS
Understanding conformal field theory through parafermions and Chern Simons theory [DE93-010452] p 3604 N93-29806

FERROELECTRICITY
Structure and switching dynamics in ferroelectric crystal and liquid crystal thin films [AD-A263664] p 3594 N93-29293
Proceedings of the 25th European Conference on the Application of Polar Dielectrics to celebrate the 25th anniversary of the Dielectric Society, incorporating the 1st International Workshop on Integrated Ferroelectrics [AD-A263427] p 3332 N93-29337
Ferroelectric liquid crystal optical interconnect switching systems [AD-A263751] p 3596 N93-29859
Materials for adaptive structural acoustic control, volume 1 [AD-A264619] p 3562 N93-30121
Materials for adaptive structural acoustic control, volume 2 [AD-A264620] p 3563 N93-30385

FERROUS METALS
JPRS report: Science and technology. Central Eurasia: Materials science [JPRS-UMS-92-008] p 3322 N93-29012
JPRS report: Science and technology. Central Eurasia: Materials science [JPRS-UMS-92-007] p 3322 N93-29013
JPRS report: Science and technology. Central Eurasia: Materials science [JPRS-UMS-92-009] p 3322 N93-29015
JPRS report: Science and technology. Central Eurasia: Materials science [JPRS-UMS-92-012] p 3296 N93-29016
JPRS report: Science and technology. Central Eurasia: Materials science [JPRS-UMS-92-013] p 3296 N93-29017
JPRS report: Science and technology. Central Eurasia: Materials science [JPRS-UMS-92-014] p 3322 N93-29019
JPRS report: Science and technology. Central Eurasia: Materials science [JPRS-UMS-92-015] p 3322 N93-29020
JPRS report: Science and technology. Central Eurasia: Materials science [JPRS-UMS-93-001] p 3296 N93-29021

FEYNMAN DIAGRAMS
A simple formula for reducing Feynman diagrams to scalar integrals [DE92-644717] p 3607 N93-30916
Invariant structures in gauge theories and confinement [DE92-644739] p 3607 N93-30924
Invariant structures and static forces in gauge theories [DE92-644740] p 3607 N93-30925

FIBER COMPOSITES
Mechanics of elevated temperature fatigue damage in fiber-reinforced ceramics [AD-A262403] p 3329 N93-28495
Probabilistic simulation of multi-scale composite behavior [NASA-TM-106196] p 3451 N93-28633
Aligned, short-fiber composites by novel flow processing methods [DE93-008701] p 3296 N93-28904
Ceramic matrix composites properties/microstresses with complete and partial interphase bond [NASA-TM-106136] p 3297 N93-29071
Thermoviscoplastic analysis of fibrous periodic composites using triangular subvolumes [NASA-TM-106076] p 3297 N93-29074
Factors influencing the interlaminar fracture toughness and its evaluation in composites [FFA-TN-1991-34] p 3451 N93-29076
Axial impact of composites p 3297 N93-29078
Method and apparatus for weaving a woven angle ply fabric [NASA-CASE-LAR-14048-1] p 3354 N93-29611
Interfacial studies of refractory glass-ceramic matrix/advanced SiC fiber reinforced composites [AD-A263264] p 3299 N93-29802
Effect of water immersion on fiber/matrix adhesion in thermoplastic composites [AD-A263646] p 3299 N93-29984
Mechanical properties of several magnesium and aluminum composites [AD-A262481] p 3299 N93-30137
Characterization of ceramic composite materials for gas turbine applications [DE93-009719] p 3259 N93-30168
Long discontinuous fiber composite structure: Forming and structural mechanics p 3301 N93-30437
First NASA Advanced Composites Technology Conference, part 2 [NASA-CP-3104-PT-2] p 3303 N93-30841
Studies of fiber-matrix adhesion on compression strength p 3304 N93-30846
The initiation, propagation, and effect of matrix microcracks in cross-ply and related laminates p 3304 N93-30847
Advanced fiber placement of composite fuselage structures p 3306 N93-30864
Tensile creep behavior of polycrystalline alumina fibers [NASA-TM-106269] p 3340 N93-30938
Mechanical properties of composite materials p 3290 N93-30951
Introduction to high performance composites p 3291 N93-30957

FIBER OPTICS
Gyroscope with excess noise subtraction [AD-D015698] p 3431 N93-29046
Hybrid data link [AD-D015714] p 3383 N93-29280
Velocity measurements of low Reynolds number tube flow using fiber-optic technology [DE93-009865] p 3422 N93-29335
Leaky coaxial cable signal transmission for remote facilities [DE93-007916] p 3383 N93-29348
Fiber-optic currents measurements [DE93-007970] p 3579 N93-29350
Characterization of a space orbited incoherent fiber optic bundle p 3583 N93-29698
Analyses of space environment effects on active fiber optic links orbited aboard the LDEF p 3583 N93-29699
Radiation and temperature effects on LDEF fiber optic samples p 3583 N93-29700
Wavelength-division multiplexed optical integrated circuit with vertical diffraction grating [NASA-CASE-NPO-18357-1-CU] p 3579 N93-29848
Fiber optic chemical sensors for characterizing the carbon cycle in ocean margin regions [DE93-011442] p 3489 N93-30056
Condensed phase diagnostics of nitramine propellant combustion p 3320 N93-30102
Applications of the photorefractive effect and damage induced effects in fibers [AD-A264339] p 3580 N93-30205
Fiber-optic polarimetric strain gauge p 3375 N93-30341
Portable fiber optic coupled Doppler interferometer system for detonation and shock wave diagnostics [DE93-009827] p 3433 N93-30510
Topical meeting of broadband analog and digital optoelectronics [AD-A264643] p 3581 N93-30522

FIBER ORIENTATION
Aligned, short-fiber composites by novel flow processing methods [DE93-008701] p 3296 N93-28904
Acousto-Ultrasonic analysis of failure in ceramic matrix composite tensile specimens [NASA-TM-106219] p 3449 N93-29073
Long discontinuous fiber composite structure: Forming and structural mechanics p 3301 N93-30437

FIBER STRENGTH
Studies of fiber-matrix adhesion on compression strength p 3304 N93-30846

FIBERS
Hydrodynamic interactions among fibers in high efficiency filters [DE93-007117] p 3424 N93-30035

FIELD ALIGNED CURRENTS
Laboratory simulation of field-aligned currents [NASA-CR-193091] p 3476 N93-28538

FIELD EFFECT TRANSISTORS

Optically controlled active impedance element particularly suited for a microwave oscillator
[AD-D015723] p 3408 N93-29281

Low temperature (LT) GaAs and related materials
[AD-A263607] p 3298 N93-29282

Acoustic charge transport technology investigation for advanced development transponder
p 3386 N93-29602

Planar active antennas and quasi-optical power combining arrays using FET's and slots
[AD-A263759] p 3387 N93-29875

Test structure to microcircuit correlation
[AD-A264157] p 3412 N93-30152

Analog CMOS circuits for neural networks
p 3355 N93-30223

Modelling of channel thickness modulation effect in SI GaAs MESFET's p 3356 N93-30229

Laboratory experiments in integrated circuit fabrication
p 3292 N93-30962

FIELD EMISSION

Improved field emitter current densities and stability through the application of a proprietary process
[AD-A263464] p 3411 N93-29833

Improved field emitter current densities and stability through the application of a proprietary process
[AD-A264048] p 3411 N93-30031

FIELD OF VIEW

Effects of area-of-interest display characteristics of visual search performance and head movements in simulated low-level flight
[AD-A264661] p 3499 N93-30542

FIELD STRENGTH

Variability of the electric field strength in the earth-ionosphere waveguide due to variations in the electron density profile
[AD-A264808] p 3394 N93-30595

ELF propagation highlights p 3395 N93-30730

VLF/LF propagation measurements
p 3395 N93-30732

Theoretical and experimental coverage analysis of a VLF transmitter p 3396 N93-30734

FIELD THEORY (PHYSICS)

Applications of unitarity in the standard model
p 3416 N93-28613

Understanding conformal field theory through parafermions and Chern Simons theory
[DE93-010452] p 3604 N93-29806

Task A: Theory of elementary particles
[DE93-010561] p 3569 N93-29841

Quantum field theory in spaces with closed time-like curves
[DE93-010564] p 3605 N93-30481

Approximation formulae for functional integrals in P(phi)2-quantum field theory
[DE93-606067] p 3605 N93-30781

Phase structure of three- and four-dimensional phi(exp 4) field theory
[DE93-606069] p 3605 N93-30782

A covariant form of the Maxwell's equations in four-dimensional spaces with an arbitrary signature
[DE93-606070] p 3605 N93-30783

On the photonic chiral anomaly in an external gravitational field
[DE93-606082] p 3479 N93-30785

Beyond two dimensions
[DE93-606084] p 3606 N93-30786

Quantum-kinetic Green function and macroscopic wave function
[DE93-606040] p 3606 N93-30796

Modern approach to relativity theory (radar formulation)
[DE93-606032] p 3606 N93-30804

Nonlinear realisations of omega(1 + infinity)
[DE92-644721] p 3557 N93-30917

Compensating fields and anomalies in supergravity
[DE92-644724] p 3637 N93-30919

Quantum group generalization of the heterotic QFT
[DE92-644727] p 3607 N93-30920

Abelian gauge theories on homogeneous spaces
[DE92-644730] p 3607 N93-30921

Invariant structures in gauge theories and confinement
[DE92-644739] p 3607 N93-30924

Invariant structures and static forces in gauge theories
[DE92-644740] p 3607 N93-30925

On the energy-momentum tensors for field theories in spaces with affine connection and metric
[DE92-644743] p 3557 N93-30926

On the energy-momentum tensors for field theories in spaces with affine connection and metric
[DE92-644744] p 3557 N93-30927

Beltrami parametrization and gauging of Virasoro and w-infinity algebras
[DE92-644844] p 3557 N93-30928

On one-dimensional topological and conformal field theories
[DE92-644726] p 3558 N93-30986

Spherically symmetric line element and Killing vectors in five-dimensional space
[DE93-604132] p 3558 N93-30988

Superconformal structures and holomorphic 1/2-superdifferentials on N = 1 super Riemann surfaces
[DE93-604133] p 3558 N93-30989

A non degenerate semi-classical Lagrangian for dilaton-gravity in two dimensions
[DE92-641339] p 3480 N93-31002

The geometry of complex space-times with torsion
[DE92-641343] p 3608 N93-31003

FIGHTER AIRCRAFT

X-31 demonstration of integrated flight and propulsion control for effective combat at extreme angles of attack
p 3260 N93-28851

Planning for air to air combat p 3501 N93-28852

A new class of mission support for combat air-crew
p 3501 N93-28854

Symbology for head up and head down applications for highly agile fighter aircraft: To improve spatial awareness, trajectory control, and unusual attitude recovery, part 1
p 3502 N93-28857

The physiological limitations of man in the high G environment p 3503 N93-28861

Requirements for pilot assistance in a thrust-vectoring combat aircraft p 3504 N93-28870

Design considerations for a night, air-to-surface attack capability on a dual role fighter p 3251 N93-28871

FILAMENT WINDING

Comparison of hand laid-up tape and filament wound composite cylinders and panels with and without impact damage p 3306 N93-30859

FILAMENTS

Improved measurement of thermal effects on microstructure p 3292 N93-30959

FILES

Programmer's reference guide to FDMS file formats
[PB93-182038] p 3354 N93-29663

FILLERS

Acid solution absorption of extruded polyethylene foam
[DE93-011701] p 3330 N93-28839

Welding wire pressure sensor assembly
[NASA-CASE-MFS-26216-1] p 3442 N93-28951

FILM BOILING

Horizontal nucleate flow boiling heat transfer coefficient measurements and visual observations for R12, R134a, and R134a/ester lubricant mixtures
[PB93-178598] p 3475 N93-30887

FILM COOLING

Small hydrogen/oxygen rocket flowfield behavior from heat flux measurements
[NASA-TM-106233] p 3286 N93-28619

Determination of surface heat transfer and film cooling effectiveness in unsteady wake flow conditions
p 3253 N93-29933

The effect of main stream flow angle on flame tube film cooling p 3257 N93-29953

Impingement/effusion cooling p 3257 N93-29954

The aerodynamic effect of coolant ejection in the leading edge region of a film-cooled turbine blade
p 3258 N93-29958

On the development of a film cooling layer
p 3258 N93-29959

Modeling of a turbulent flow in the presence of discrete parietal cooling jets p 3258 N93-29960

A Navier-Stokes solver with different turbulence models applied to film-cooled turbine cascades
p 3258 N93-29962

Cooling predictions in turbofan engine components
p 3259 N93-29964

Pulse mitigation and heat transfer enhancement techniques. Volume 2: Effect of surface wettability and roughness in evaporative spray cooling
[AD-A264174] p 3425 N93-30155

FILM THICKNESS

An analysis of the 70-meter antenna hydrostatic bearing by means of computer simulation p 3386 N93-29601

Polarization modulated ellipsometry
[NASA-CR-4012] p 3580 N93-30372

FILTERS

Hydrodynamic interactions among fibers in high efficiency filters
[DE93-007117] p 3424 N93-30035

FILTRATION

Evaluation and optimization of a flexible filtration system for respiratory protection system 21
[AD-A262467] p 3493 N93-28758

FINANCIAL MANAGEMENT

The program manager's notebook
[AD-A263074] p 3609 N93-29142

FINE STRUCTURE

Analyses of data from fine structure and circulation studies in the Gulf of California
[AD-A262910] p 3486 N93-28885

Ion motion effects on charged radiators
[DE93-009257] p 3565 N93-29099

Shear, strain, and thermohaline vertical fine structure in the upper ocean p 3488 N93-30046

FINITE DIFFERENCE THEORY

High performance dispersion model PHYSIC
[DE93-753303] p 3467 N93-28536

Advanced insulations for refrigerator/freezers: The potential for new shell designs incorporating polymer barrier construction
[DE93-010600] p 3353 N93-28570

Balanced approximation can be optimal
[OUEL-1950/92] p 3548 N93-28754

Solar flare MDH
[AD-A262275] p 3652 N93-28756

Filtering interpolators for image comparison algorithms
p 3463 N93-28797

A simple parallel prefix algorithm for compact finite-difference schemes
[NASA-CR-191448] p 3525 N93-28976

Pre- and postprocessing techniques for determining goodness of computational meshes
[NASA-CR-192553] p 3538 N93-29030

International Journal of Numerical Modeling: Electronic Networks, Devices, and Fields, volume 5, number 3, August 1992
[AD-A263765] p 3387 N93-29877

Difference methods for hyperbolic problems with emphasis on space-centered approximations
[ONERA-NT-1990-4] p 3550 N93-30136

Errors when shock waves interact due to numerical shock width
[DE93-010699] p 3426 N93-30484

Rocket-triggered lightning studies for the protection of critical assets
[DE93-009633] p 3484 N93-30651

A numerical solution of the two-center problem
[DE92-644674] p 3551 N93-30913

Numerical wave propagation and steady-state solutions p 3428 N93-30999

FINITE ELEMENT METHOD

Upwind finite element schemes for solving the Maxwell equations
[INRIA-RR-1601] p 3546 N93-28509

Finite element analysis of time-independent superconductivity
[NASA-CR-191140] p 3450 N93-28556

Design of an essentially non-oscillatory reconstruction procedure in finite-element type meshes
[INRIA-RR-1584] p 3547 N93-28615

Small hydrogen/oxygen rocket flowfield behavior from heat flux measurements
[NASA-TM-106233] p 3286 N93-28619

Thermal and mechanical analysis of flip-chips on a liquid cooled multichip module
[DE93-007609] p 3405 N93-28641

Solar flare MDH
[AD-A262275] p 3652 N93-28756

Design and evaluation of a uniaxial pull test for lithium hydride/deuteride
[DE93-010760] p 3451 N93-28832

Analysis for thermo-chemical decomposition of composite structures
[NASA-CR-193185] p 3295 N93-28843

Pre- and postprocessing techniques for determining goodness of computational meshes
[NASA-CR-192553] p 3538 N93-29030

Stabilized space-time finite element formulations for unsteady incompressible flows involving fluid-body interactions p 3419 N93-29040

Axial impact of composites p 3297 N93-29078

Design optimization of space structures
p 3278 N93-29122

Nonlinear analyses of composite aerospace structures in sonic fatigue
[NASA-CR-193124] p 3451 N93-29154

Accuracy of least-squares methods for the Navier-Stokes equations
[NASA-TM-106209] p 3421 N93-29208

Quiet by design: Numerical acousto-elastic analysis of aircraft structures
[ISBN-90-386-0042-9] p 3248 N93-29268

Some problems in the mechanics of solids with phase mixtures
[AD-A263652] p 3311 N93-29291

An experimental/analytical evaluation of biaxial sheet failure
[DE93-010620] p 3453 N93-29843

Mechanical behaviour of a closed collar model for an 11.5 T dipole
[NIKHEF-H/92-03] p 3576 N93-30019

On high resolution extensions of Lagrange-Galerkin finite-element schemes
[INRIA-RR-1703] p 3550 N93-30117
Two-parameter crack tip field associated with stable crack growth in a thin plate: A hybrid analysis
[AD-A264221] p 3453 N93-30147
Containment of explosions in spherical vessels
[DE93-005445] p 3446 N93-30211
Stress-intensity-factor influence coefficients for axial and circumferential flaws in reactor pressure vessels
[DE93-006206] p 3454 N93-30213
Static and dynamic large deflection flexural response of graphite-epoxy beams
[NASA-CR-4118] p 3454 N93-30374
Finite element approximation of the shallow water equations on the MASPAR
[AD-A264649] p 3489 N93-30525
Structural design, analysis, and code evaluation of an odd-shaped pressure vessel
[DE93-008182] p 3447 N93-30632
Nonlinear explicit transient finite element analysis on the Intel Delta
[DE93-009561] p 3535 N93-30647
Delaminations in composite plates under impact loads p 3304 N93-30849
Design and analysis of grid stiffened concepts for aircraft composite primary structural applications p 3306 N93-30861
A comparison of classical mechanics models and finite element simulation of elastically tailored wing boxes p 3306 N93-30863
Multiple methods integration for structural mechanics analysis and design p 3307 N93-30867
Structural design using neural networks p 3545 N93-31029

FINITE VOLUME METHOD
Upwind finite element schemes for solving the Maxwell equations
[INRIA-RR-1601] p 3546 N93-28509
Pre- and postprocessing techniques for determining goodness of computational meshes
[NASA-CR-192553] p 3538 N93-29030
Ablation problems using a finite control volume technique
[DE93-009861] p 3549 N93-29187
Study of flow structure in rotating cavities: Numerical predictions of laminar and turbulent, steady, and unsteady flows p 3256 N93-29948
On high resolution extensions of Lagrange-Galerkin finite-element schemes
[INRIA-RR-1703] p 3550 N93-30117

FINNED BODIES
Recent applications of CFD to the aerodynamics of Army projectiles
[AD-A262953] p 3240 N93-29512
The effect of orthogonal-mode rotation on forced convection in a circular-sectioned tube fitted with full circumferential transverse ribs p 3254 N93-29937

FINS
Articulated fin/wing control system
[AD-D015712] p 3259 N93-29278

FIR FILTERS
Realization of high speed adaptive FIR digital filters p 3355 N93-30222

FIRE CONTROL
Research and development of an airborne multispectral scanner to measure fire, terrestrial and atmospheric characteristics (50 channel)
[NASA-CR-193121] p 3456 N93-28620
Pilot decision aiding for weapon delivery: A novel approach to fire control cueing using parallel computing p 3501 N93-28853
Head-steered sensor flight test results and implications p 3502 N93-28859
Design considerations for a night, air-to-surface attack capability on a dual role fighter p 3251 N93-28871

FIRE PREVENTION
Risk-based spacecraft fire safety experiments p 3267 N93-28738

FIRES
Risk-based spacecraft fire safety experiments p 3267 N93-28738
Atmospheric and Geophysical Sciences Division: G-Division did you know?
[DE93-007412] p 3469 N93-28967
Generation of carbon monoxide in compartment fires
[PB93-146702] p 3244 N93-29211
Programmer's reference guide to FDMS file formats
[PB93-182038] p 3354 N93-29663

FISCHER-TROPSCH PROCESS
Development of alternative fuels from coal-derived syngas
[DE93-011629] p 3341 N93-28668
Design of a high activity and selectivity alcohol catalyst
[DE93-012277] p 3309 N93-28750

FISSION
Studies of fluctuation processes in nuclear collisions
[DE93-011263] p 3576 N93-30054

FISSION PRODUCTS
Air oxidation behavior of fuel for the High Temperature Engineering Test Reactor (HTTR)
[DE93-753349] p 3576 N93-30006

FLAME PROBES
Flame structure studies of propellant like low pressure flames using optical and mass spectrometric means p 3319 N93-30081

FLAME PROPAGATION
Studies in premixed combustion
[DE93-007955] p 3310 N93-29051
Numerical modeling of multidimensional flames with application to energetic materials p 3319 N93-30079
Studies of curvature, strain, and unsteady effects on premixed flames p 3316 N93-30646
NOx chemistry in natural gas flames
[PB93-175263] p 3317 N93-30760
Effects of buoyancy on gas jet diffusion flames
[NASA-CR-191109] p 3352 N93-31031

FLAME SPECTROSCOPY
Flame structure studies of propellant like low pressure flames using optical and mass spectrometric means p 3319 N93-30081

FLAME TEMPERATURE
A novel flame thermometer based on the doppler width of ro-vibrational transitions
[AD-A264515] p 3315 N93-30405

FLAMES
Tomographic analysis of line-of-sight infrared spectra of low-pressure flames
[AD-A263185] p 3309 N93-28514
Flame structure studies of propellant like low pressure flames using optical and mass spectrometric means p 3319 N93-30081
NOx chemistry in natural gas flames
[PB93-175263] p 3317 N93-30760

FLANGES
Development of an O atom gun
[AD-A264753] p 3570 N93-30558

FLASH
Conspicuity of aids to navigation. Part 1: Temporal patterns for flashing lights
[AD-A264626] p 3499 N93-30426

FLASH LAMPS
High-voltage pulse generator capable of 2000 J at 10 kV
[AD-A262034] p 3407 N93-28999
ND laser with co-doped ion(s) pumped by visible laser diodes
[AD-D015711] p 3437 N93-29277

FLASHOVER
Determination of the space charge distribution within an e-irradiated polymer using the pressure wave propagation method
[ONERA-P-1990-4] p 3335 N93-30024

FLAT PLATES
Vortex structure and mass transfer near the base of a cylinder and a turbine blade p 3253 N93-29929
Fundamental studies of impingement cooling thermal boundary conditions p 3254 N93-29940
Modeling of a turbulent flow in the presence of discrete parietal cooling jets p 3258 N93-29960
Design and analysis of grid stiffened concepts for aircraft composite primary structural applications p 3306 N93-30861

FLEXIBILITY
Lightweight flexible composite tent materials
[AD-A263021] p 3295 N93-28660

FLEXIBLE BODIES
Low-cost Active Structural Control space experiment (LASC) p 3263 N93-28700
Analysis and simulation of a two degrees-of-freedom one-link flexible forearm p 3361 N93-30261
Vibration localization in rotating shafts p 3454 N93-30626

FLEXIBLE SPACECRAFT
Low-cost Active Structural Control space experiment (LASC) p 3263 N93-28700
Control-structures interaction test of the LACE satellite p 3263 N93-28706
CSI-Star: A low-cost CSI orbital testbed p 3263 N93-28707
Robust feedforward/feedback control synthesis for uncertain dynamical systems p 3542 N93-29079
Efficient reorientation of a deformable body in space: A free-free beam example p 3280 N93-29994
Robust boundary control of flexible structures governed by hybrid dynamics p 3285 N93-30249

FLIGHT ALTITUDE
A concluding study of the altitude determination deficiencies of the Service Aircraft Instrumentation Package (SAIP)
[AD-A263515] p 3250 N93-29971

FLIGHT CHARACTERISTICS
The flight performance of the Galileo orbiter USO p 3386 N93-29603
Project ARES 2: High-altitude battery-powered aircraft p 3227 N93-29715

FLIGHT CLOTHING
Goggles emergency release apparatus
[AD-D015685] p 3507 N93-29607
CATS EYES adjustment procedures
[AD-A264069] p 3508 N93-29924

FLIGHT CONDITIONS
An automated observing system for passive evaluation of cloud cover and visibility
[AD-A263207] p 3481 N93-28875

FLIGHT CONTROL
Advanced Transport Operating System (ATOPS) Flight Management/Flight Controls (FM/FC) software description
[NASA-CR-191457] p 3250 N93-28621
Combat Automation for Airborne Weapon Systems: Man/Machine Interface Trends and Technologies
[AGARD-CP-520] p 3501 N93-28850
X-31 demonstration of integrated flight and propulsion control for effective combat at extreme angles of attack p 3260 N93-28851
Virtual interface applications for airborne weapons systems p 3502 N93-28858
Head-steered sensor flight test results and implications p 3502 N93-28859
Overview of cockpit technology research and development programs for improvement of the man/machine interface: Review of the AGARD AVP Symposium held in Madrid, May 1992 p 3505 N93-28872
A real-time, hardware-in-the-loop simulation of an unmanned aerial research vehicle
[AD-A262477] p 3248 N93-29409
Reference equations of motion for automatic rendezvous and capture
[NASA-CR-185676] p 3269 N93-29652
An evaluation of B-1B pilot performance during simulated instrument approaches with and without status information
[AD-A263874] p 3507 N93-29888
Handedness and motor programming effects of manual control and movement
[AD-A264022] p 3499 N93-30027
Virtual reality flight control display with six-degree-of-freedom controller and spherical orientation overlay
[NASA-CASE-NPO-18733-1-CU] p 3251 N93-30416
Analytical foundations of gain scheduling
[AD-A264682] p 3260 N93-30550
Flight control system design factors for applying automated testing techniques
[NASA-TM-4242] p 3260 N93-30764

FLIGHT CREWS
Predicting radiation induced performance decrements of AH-1 helicopter crews. Volume 2: Evaluation of modeling and simulation techniques for predicting radiation induced performance decrements
[AD-A262872] p 3506 N93-29484
Field test of a computer-driven tool to measure psychological characteristics of aircrew
[AD-A264484] p 3499 N93-30425
Part 1: Executive summary p 3236 N93-30674
Helicopter simulation: An aircrew training and qualification perspective p 3236 N93-30676

FLIGHT INSTRUMENTS
Optical technologies for UV remote sensing instruments p 3582 N93-28788
Prototype backscatter Moessbauer spectrometer for measurement of Martian surface mineralogy p 3648 N93-28812
Pilot intent and error recognition as part of a knowledge based cockpit assistant p 3502 N93-28855

FLIGHT MANAGEMENT SYSTEMS
Advanced Transport Operating System (ATOPS) Flight Management/Flight Controls (FM/FC) software description
[NASA-CR-191457] p 3250 N93-28621

FLIGHT MECHANICS
Flight mechanical model for performance calculations and interactions between flight vehicle and ramjet in regard to the flight orbit
[ESA-TT-1267] p 3248 N93-29464

FLIGHT PATHS
Minimum Hamiltonian ascent trajectory evaluation (MASTRE) program (update to automatic flight trajectory design, performance prediction, and vehicle sizing for support of shuttle and shuttle derived vehicles) users manual
[NASA-CR-192556] p 3269 N93-28558

Symbology for head up and head down applications for highly agile fighter aircraft: To improve spatial awareness, trajectory control, and unusual attitude recovery, part 1 p 3502 N93-28857
Flight mechanical model for performance calculations and interactions between flight vehicle and ramjet in regard to the flight orbit
[ESA-TT-1267] p 3248 N93-29464
Two simulation studies of precision runway monitoring of independent approaches to closely spaced parallel runways
[AD-A263433] p 3261 N93-29815

FLIGHT PLANS
Pilot intent and error recognition as part of a knowledge based cockpit assistant p 3502 N93-28855
Application and integration of diverse technology in an aviation system: The National Aeronautical Information Processing System p 3247 N93-30339

FLIGHT SAFETY
FAA international conference on airplane ground deicing
[AD-A263617] p 3244 N93-29286

FLIGHT SIMULATION
Virtual interface applications for airborne weapons systems p 3502 N93-28858
Requirements for pilot assistance in a thrust-vectoring combat aircraft p 3504 N93-28870
A real-time, hardware-in-the-loop simulation of an unmanned aerial research vehicle
[AD-A262477] p 3248 N93-29409
A fuzzy logic optimal control law solution to the CMMCA tracking problem
[AD-A262555] p 3542 N93-29420
Predicting radiation induced performance decrements of AH-1 helicopter crews. Volume 2: Evaluation of modeling and simulation techniques for predicting radiation induced performance decrements
[AD-A262872] p 3506 N93-29484
An evaluation of B-1B pilot performance during simulated instrument approaches with and without status information
[AD-A263874] p 3507 N93-29888
Three-dimensional graphical representation of objects according to movement data in realtime
[ESA-TT-1258] p 3521 N93-30104
Virtual reality flight control display with six-degree-of-freedom controller and spherical orientation overlay
[NASA-CASE-NPO-18733-1-CU] p 3251 N93-30416
Helicopter simulation: An aircrew training and qualification perspective p 3236 N93-30676
Simulators for corporate pilot training and evaluation p 3236 N93-30678
Training effectiveness assessment: Where are we? p 3236 N93-30679
Current training: Where are we? p 3236 N93-30680
Helicopter simulator qualification p 3237 N93-30681
Helicopter simulation: Making it work p 3237 N93-30682
Helicopter training simulators: Key market factors p 3237 N93-30683
Validation and upgrading of physically based mathematical models p 3237 N93-30688
Frequency-response techniques for documentation and improvement of rotorcraft simulators p 3237 N93-30689
Bandwidth and SIMDUCE as simulator fidelity criteria p 3238 N93-30690
Methodology development for evaluation of selective-fidelity rotorcraft simulation p 3238 N93-30691

FLIGHT SIMULATORS
Rendering the out-the-window view for the AFIT virtual cockpit
[AD-A262599] p 3260 N93-28467
Toward reusable graphics components in Ada
[AD-A262568] p 3524 N93-28577
Pilot intent and error recognition as part of a knowledge based cockpit assistant p 3502 N93-28855
Utility of a ghost horizon and climb/dive ladder line tapering on a head-up display
[AD-A264401] p 3508 N93-30167
Effects of area-of-interest display characteristics of visual search performance and head movements in simulated low-level flight
[AD-A264661] p 3499 N93-30542
Part 1: Executive summary p 3236 N93-30674
Helicopter simulator standards p 3236 N93-30675
Simulators for corporate pilot training and evaluation p 3236 N93-30678
Training effectiveness assessment: Where are we? p 3236 N93-30679
Current training: Where are we? p 3236 N93-30680
Helicopter simulator qualification p 3237 N93-30681
Helicopter simulation: Making it work p 3237 N93-30682
Training effectiveness assessment: Methodological problems and issues p 3237 N93-30684
Determining the transferability of flight simulator data p 3237 N93-30685
Progress through precedent: Going where no helicopter simulator has gone before p 3237 N93-30686
Transfer of training and simulator qualification or myth and folklore in helicopter simulation p 3237 N93-30687
Frequency-response techniques for documentation and improvement of rotorcraft simulators p 3237 N93-30689
Bandwidth and SIMDUCE as simulator fidelity criteria p 3238 N93-30690
Methodology development for evaluation of selective-fidelity rotorcraft simulation p 3238 N93-30691

FLIGHT TESTS
X-31 demonstration of integrated flight and propulsion control for effective combat at extreme angles of attack p 3260 N93-28851
Head-steered sensor flight test results and implications p 3502 N93-28859
Flight evaluation of a computer aided low-altitude helicopter flight guidance system p 3260 N93-28869
Helicopter approach capability using the differential global positioning system
[NASA-CR-193183] p 3245 N93-28936
Design study to simulate the development of a commercial transportation system p 3228 N93-29718
A concluding study of the altitude determination deficiencies of the Service Aircraft Instrumentation Package (SAIP)
[AD-A263515] p 3250 N93-29971
Vortex wake characteristics of B757-200 and B767-200 aircraft using the tower fly-by technique
[PB93-180255] p 3242 N93-30387
Vortex wake characteristics of B757-200 and B767-200 aircraft using the tower fly-by technique
[PB93-180263] p 3242 N93-30388
Postflight hardware evaluation 360T025 (RSRM-25, STS-46)
[NASA-CR-192562] p 3272 N93-30617
Postflight hardware evaluation 360T025 (RSRM-25, STS-46). Appendix C: Nozzle PFORs
[NASA-CR-192565] p 3272 N93-30620
Postflight hardware evaluation 360T025 (RSRM-25, STS-46). Appendix D: Nozzle postfire data
[NASA-CR-192580] p 3289 N93-30648
Determining the transferability of flight simulator data p 3237 N93-30685

FLIR DETECTORS
The design and development of the new RAF standard HUD format p 3502 N93-28856
Head-steered sensor flight test results and implications p 3502 N93-28859
Design considerations for a night, air-to-surface attack capability on a dual role fighter p 3251 N93-28871

FLOODS
Spatial Analysis and Modeling Systems (SAMS) p 3614 N93-29239

FLOW CHARACTERISTICS
Effects of flow-path variations on internal reversing flow in a tailpipe offtake configuration for ASTOVL aircraft
[NASA-TM-106149] p 3252 N93-29065
Flow phenomena in turbomachines
[AD-A263049] p 3420 N93-29141
Experimental study of instability growth patterns of a shock-accelerated, thin fluid layer
[DE93-010741] p 3421 N93-29253
Cooling geometry optimization using liquid crystal technique p 3254 N93-29939
Flow and heat transfer between gas-turbine discs p 3256 N93-29950
Three-dimensional fiber-optic LDV measurements in the endwall region of a linear cascade of controlled-diffusion stator blades
[AD-A263513] p 3424 N93-29968
Laboratory studies of gravity wave/mean flow interactions
[AD-A264226] p 3478 N93-30174
Vortex wake characteristics of B757-200 and B767-200 aircraft using the tower fly-by technique
[PB93-180255] p 3242 N93-30387
Vortex wake characteristics of B757-200 and B767-200 aircraft using the tower fly-by technique
[PB93-180263] p 3242 N93-30388

FLOW COEFFICIENTS
Horizontal nucleate flow boiling heat transfer coefficient measurements and visual observations for R12, R134a, and R134a/ester lubricant mixtures
[PB93-178598] p 3475 N93-30887

FLOW DISTORTION
Moment approach to fast ion neoclassical transport and viscous forces
[DE93-753305] p 3585 N93-28979
Methods for reducing turbulent flow aero-optical distortion
[AD-A263698] p 3423 N93-29353

FLOW DISTRIBUTION
Navier-Stokes analysis of radial turbine rotor performance
[NASA-CR-191153] p 3251 N93-28609
Small hydrogen/oxygen rocket flowfield behavior from heat flux measurements
[NASA-TM-106233] p 3286 N93-28619
Preliminary design of an intermittent smoke flow visualization system
[NASA-CR-186027] p 3248 N93-28693
Stabilized space-time finite element formulations for unsteady incompressible flows involving fluid-body interactions p 3419 N93-29040
Studies in premixed combustion
[DE93-007955] p 3310 N93-29051
Three-dimensional numerical simulation of gradual opening in a wave rotor passage
[NASA-CR-191157] p 3252 N93-29072
An experimental study of flow over a 6 to 1 prolate spheroid at incidence p 3239 N93-29124
Development of an unstructured solution adaptive method for the quasi-three-dimensional Euler and Navier-Stokes equations
[NASA-CR-193241] p 3421 N93-29213
Experimental study of instability growth patterns of a shock-accelerated, thin fluid layer
[DE93-010741] p 3421 N93-29253
Vortex structure and mass transfer near the base of a cylinder and a turbine blade p 3253 N93-29929
Fluid flow and heat transfer in the entrance region of an annulus between independently rotating tubes with a turbulent axial flow p 3256 N93-29952
The effect of main stream flow angle on flame tube film cooling p 3257 N93-29953
The aerodynamic effect of coolant ejection in the leading edge region of a film-cooled turbine blade p 3258 N93-29958
On the development of a film cooling layer p 3258 N93-29959
Turbulence characteristics of an axisymmetric reacting flow
[NASA-CR-4110] p 3242 N93-30373
Topology and grid adaption for high-speed flow computations
[NASA-CR-4216] p 3426 N93-30375
Two-dimensional and three-dimensional time-dependent MHD model of extended corona p 3653 N93-30496
Computation of a delta-wing roll-and-hold maneuver
[AD-A264704] p 3260 N93-30498
Strong parallel blade-vortex interaction and noise propagation in helicopter flight p 3563 N93-30980

FLOW EQUATIONS
Preliminary experimental results for a cryogenic brush seal configuration
[NASA-TM-106236] p 3416 N93-28627

FLOW GEOMETRY
An efficient spectral integration method for the solution of the Navier-Stokes equations
[FFA-TN-1992-28] p 3418 N93-29009

FLOW MEASUREMENT
Limitations of the ideal phase-Doppler system: Extension to spatially and temporally inhomogeneous particle flows with an application to diesel sprays
[DE93-009447] p 3416 N93-28595
Experimental study of heat transfer close to a plane wall heated in the presence of multiple injections (subsonic flow) p 3253 N93-29931
Turbulence characteristics of an axisymmetric reacting flow
[NASA-CR-4110] p 3242 N93-30373
Compressible turbulence in a high-speed high Reynolds number mixing layer p 3242 N93-30583

FLOW STABILITY
Theory of tokamak edge turbulence: Drift-thermal instability-induced turbulence and ionization-driven drift wave turbulence p 3586 N93-29123
Experimental study of instability growth patterns of a shock-accelerated, thin fluid layer
[DE93-010741] p 3421 N93-29253
Evolution of flow disturbances in cocurrent gas-liquid flows
[DE93-010083] p 3422 N93-29326
Vertical slot convection: A linear study
[DE93-007643] p 3423 N93-29804

FLOW THEORY
Interfacial melting in cracked explosives p 3349 N93-30089

FLOW VELOCITY
A four-field approach towards developing a mechanistic model for multiphase flow [DE93-006572] p 3420 N93-29126
Gravity sensitivity of a resistojet water vaporizer [NASA-TM-106220] p 3288 N93-29194
Velocity measurements of low Reynolds number tube flow using fiber-optic technology [DE93-009865] p 3422 N93-29335
Pulse mitigation and heat transfer enhancement techniques. Volume 3: Liquid sodium heat transfer facility and transient response of sodium heat pipe to pulse forward and reverse heat load [AD-A263496] p 3422 N93-29338
An L2F-measurement device with image rotator prism for flow velocity analysis in rotating coolant channels p 3255 N93-29942
Modelling the dynamics of a large sea area [DE93-778330] p 3488 N93-30040
Fiber optic chemical sensors for characterizing the carbon cycle in ocean margin regions [DE93-011442] p 3489 N93-30056
Turbulence characteristics of an axisymmetric reacting flow [NASA-CR-4110] p 3242 N93-30373

FLOW VISUALIZATION
Preliminary design of an intermittent smoke flow visualization system [NASA-CR-186027] p 3248 N93-28693
Flow visualization on helicopter blades using acenaphthen [ESA-TT-1255] p 3422 N93-29273
Shear sensitive monomer-polymer laminate structure and method of using same [NASA-CASE-LAR-14654-1-CU] p 3452 N93-29613
Vortex structure and mass transfer near the base of a cylinder and a turbine blade p 3253 N93-29929
The aerodynamic effect of coolant ejection in the leading edge region of a film-cooled turbine blade p 3258 N93-29958
Nonlinear spectroscopy of multicomponent droplets and two- and three-dimensional measurements in flames [AD-A264341] p 3425 N93-30162
Contribution to the study of the interaction between acoustic waves and coherent structures induced by a prismatic cylinder in a rectangular cavity [ONERA-NT-1990-10] p 3314 N93-30203

FLUENCE
Neutron radiation induced degradation of diode characteristics [AD-A263277] p 3405 N93-28563

FLUID DYNAMICS
The MODE family of facility class experiments p 3263 N93-28705
Liquid Motion in a rotating tank Experiment (LME) p 3264 N93-28710
JPRS report: Science and technology. Central Eurasia: Engineering and equipment [JPRS-UEQ-93-004] p 3354 N93-29090
Generation of carbon monoxide in compartment fires [PB93-146702] p 3244 N93-29211
Geochemical and fluid dynamic investigations into the nature of chemical heterogeneity in the Earth's mantle [AD-A262753] p 3477 N93-29405
Weakly nonlinear dynamics of near-CJ detonation waves [DE93-007344] p 3424 N93-29836
Hamiltonian dynamics of coupled potential vorticity and internal wave motion: 1. Linear modes [AD-A263469] p 3424 N93-29838
Measurement of turbulent spots and intermittency modelling at gas-turbine conditions p 3253 N93-29934
The middeck 0-gravity dynamics experiment [NASA-CR-4500] p 3281 N93-30376

FLUID FILMS
Pulse mitigation and heat transfer enhancement techniques. Volume 1: Spray cooling [AD-A263495] p 3423 N93-29352
Pulse mitigation and heat transfer enhancement techniques. Volume 2: Effect of surface wettability and roughness in evaporative spray cooling [AD-A264174] p 3425 N93-30155

FLUID FLOW
A grid refinement study of two-dimensional transient flow over a backward-facing step using a spectral-element method [DE92-018262] p 3417 N93-28639
Studies of complexity in fluid systems [DE93-010776] p 3418 N93-28878
A four-field approach towards developing a mechanistic model for multiphase flow [DE93-006572] p 3420 N93-29126
Experimental study of instability growth patterns of a shock-accelerated, thin fluid layer [DE93-010741] p 3421 N93-29253
Kinetics and energy transfer in nonequilibrium fluid flows [AD-A263612] p 3240 N93-29284
Velocity measurements of low Reynolds number tube flow using fiber-optic technology [DE93-009865] p 3422 N93-29335
Rotational fluid flow experiment p 3235 N93-29761
Vertical slot convection: A linear study [DE93-007643] p 3423 N93-29804
Fluid flow and heat transfer in the entrance region of an annulus between independently rotating tubes with a turbulent axial flow p 3256 N93-29952
Siphon breaker design requirements [DE93-011799] p 3425 N93-30132
Multiparticle imaging technique for two-phase fluid flows using pulsed laser speckle velocimetry [DE93-011734] p 3427 N93-30489

FLUID INJECTION
Modeling of a turbulent flow in the presence of discrete parietal cooling jets p 3258 N93-29960
A Navier-Stokes solver with different turbulence models applied to film-cooled turbine cascades p 3258 N93-29962

FLUID JETS
The hydraulic analysis of cylindrical Flibe jets in a HYLIFE-2 ICF reactor [DE93-009234] p 3586 N93-29053

FLUID MANAGEMENT
Vented Tank Resupply Experiment (VTRE) for In-Space Technology Experiment Program (IN-STEP) p 3264 N93-28711
Tank Pressure Control Experiment (TPCE) p 3264 N93-28712

FLUID MECHANICS
Estimation of droplet collision frequency in a spray [DE93-007991] p 3416 N93-28566
A grid refinement study of two-dimensional transient flow over a backward-facing step using a spectral-element method [DE92-018262] p 3417 N93-28639
Godunov-type schemes applied to detonation flows [NASA-CR-191447] p 3509 N93-28841
Methods for reducing turbulent flow aero-optical distortion [AD-A263698] p 3423 N93-29353
ICASE [NASA-CR-193257] p 3520 N93-29864
Unsteady vortex loop/dipole theory applied to the work and acoustics of an ideal low speed propeller [AD-A264057] p 3241 N93-29891

FLUID PRESSURE
Tank Pressure Control Experiment (TPCE) p 3264 N93-28712

FLUID-SOLID INTERACTIONS
The middeck 0-gravity dynamics experiment [NASA-CR-4500] p 3281 N93-30376

FLUIDS
Program for an improved hypersonic temperature-sensing probe [NASA-CR-186025] p 3431 N93-29066

FLUORIDES
Polyimides prepared from 3,5-diamino benzo trifluoride [NASA-CASE-LAR-14206-1] p 3331 N93-29083

FLUORINE ISOTOPES
Synthesis of new high performance lubricants and solid lubricants [DE93-012237] p 3330 N93-28748

FLUORINE ORGANIC COMPOUNDS
Synthesis of new high performance lubricants and solid lubricants [DE93-012237] p 3330 N93-28748
Process to prepare 1,3-diamino-5-pentafluorosulfanylbenzene [NASA-CASE-LAR-14773-2-CU] p 3312 N93-29506

FLUOROCARBONS
Synthesis of new high performance lubricants and solid lubricants [DE93-012237] p 3330 N93-28748

FLUX (RATE)
A new flux conserving Newton's method scheme for the two-dimensional, steady Navier-Stokes equations [NASA-TM-106160] p 3416 N93-28626
Utilization of NOAA/AVHRR data for energy balance of Lake Constance (Switzerland) p 3458 N93-28926
Radiation model predictions and validation using LDEF satellite data p 3573 N93-29641

FLUX DENSITY
Flux lattice relaxation, noise, and symmetry-breaking in frustrated Josephson junction arrays [DE93-008713] p 3593 N93-29094
Evaluation of multi-dimensional flux models for radiative transfer in cylindrical combustion chambers p 3257 N93-29955
Topics in inflationary universe medels and cosmic string theories p 3637 N93-30579
Fluids in porous media. [PB93-175198] p 3428 N93-30759

FLUX QUANTIZATION
Report of the Meteoroid and Debris Special Investigation Group p 3638 N93-29355

FLUX VECTOR SPLITTING
Nonlinear relaxation algorithms for the compressible Navier-Stokes equations in two and three dimensions p 3421 N93-29177

FLY BY WIRE CONTROL
Project ARES 2: High-altitude battery-powered aircraft p 3227 N93-29715

FLYBY MISSIONS
Clementine 2: A double asteroid flyby and impactor mission p 3268 N93-28770
Design concept for an IR mapping spectrometer for the Pluto fast flyby mission p 3285 N93-28779
Acousto-optic infrared spectral imager for Pluto fast flyby p 3285 N93-28781
Visible imaging on the Pluto fast flyby mission p 3646 N93-28799
Systematic processing of Clementine data for scientific analyses p 3624 N93-28803
Pluto fast flyby mission and science overview p 3649 N93-28818
Double swingby at Earth-Moon for increase of excess velocity [ETN-93-94177] p 3270 N93-30582

FLYING PLATFORMS
Hybrid data link [AD-D015714] p 3383 N93-29280

FOAMS
Acid solution absorption of extruded polyethylene foam [DE93-011701] p 3330 N93-28839
Thermal properties of organic and modified inorganic aerogels [DE93-009230] p 3311 N93-29263

FOCAL PLANE DEVICES
Polarization experiments with hadronic and electromagnetic probes [DE93-011375] p 3392 N93-30126
Development of ultra-low noise, high sensitivity planar metal grating coupled 3-5 multiquantum well infrared detectors for focal plane array staring IR sensor systems [AD-A264465] p 3599 N93-30536

FOCUSING
New meteoroid model predictions for directional impacts on LDEF p 3638 N93-29376

FOG
Fog studies in the Alpine region with digital NOAA/AVHRR data p 3458 N93-28925

FOILS (MATERIALS)
Micrometeoroids and debris on LDEF p 3638 N93-29356
SIMS chemical analysis of extended impacts on the leading and trailing edges of LDEF experiment AO187-2 p 3318 N93-29367

FOKKER-PLANCK EQUATION
A Fokker-Planck operator for the emission and absorption of electron plasma waves in a magnetized plasma [DE93-009579] p 3584 N93-28598
An information theoretic approach to stochastic adaptive control application to manipulators with active inertia p 3359 N93-30247

FOLDING STRUCTURES
Optimal geometric design of robots for environments with obstacles p 3445 N93-30149

FOLIAGE
Predicting the response of a temperate forest ecosystem to atmospheric CO2 increase [DE93-010081] p 3467 N93-28543

FORCE-FREE MAGNETIC FIELDS
A study of the physical mechanisms for filament eruption and coronal mass ejection via numerical simulation [NASA-CR-193180] p 3653 N93-28935

FORCED CONVECTION
Thermal and mechanical analysis of flip-chips on a liquid cooled multichip module [DE93-007609] p 3405 N93-28641
The effect of orthogonal-mode rotation on forced convection in a circular-sectioned tube fitted with full circumferential transverse ribs p 3254 N93-29937
Turbulent flow and heat transfer in idealized blade cooling passages p 3254 N93-29938
Performance of thermal adhesives in forced convection p 3293 N93-30974

FOREARM
Analysis and simulation of a two degrees-of-freedom one-link flexible forearm p 3361 N93-30261
Prosthetic elbow joint [NASA-CASE-MFS-28707-1] p 3508 N93-30566

FOREBODIES
Solution of Euler equations for forebody-inlet ensemble of aircraft at high angle of attack
[AD-A263905] p 3240 N93-29862
FORECASTING
Using a neural network to estimate solvent consumption
[PB93-173110] p 3467 N93-28873
Fuzzy forecasting and decision making in short dynamic time series p 3513 N93-29541
FOREST MANAGEMENT
The MAESTRO-1 campaign: Analyses of polarimetric SAR data of agricultural fields and forests
[BCRS-92-06] p 3460 N93-29320
Tropical forests and biological diversity: USAID report to Congress 1990-1991
[PB93-180453] p 3471 N93-29681
FORESTS
Predicting the response of a temperate forest ecosystem to atmospheric CO2 increase
[DE93-010081] p 3467 N93-28543
Recording of forest surface in SAR-images with statistical methods in areas of pronounced relief
p 3457 N93-28920
Forest examination with polarimetric radar image data
p 3457 N93-28921
Atmospheric correction of LANDSAT-TM-data for forest inventory p 3459 N93-28929
Tropical forests and biological diversity: USAID report to Congress 1990-1991
[PB93-180453] p 3471 N93-29681
Modeling the bidirectional reflectance and spectra
[AD-A263570] p 3462 N93-29830
FORMALDEHYDE
Distribution of C1-C2 aldehydes in the free troposphere
[JUEL-2650] p 3475 N93-28475
FORMALISM
Non-scalar uncertainty: Uncertainty in dynamic systems p 3517 N93-29565
FORMING TECHNIQUES
Long discontinuous fiber composite structure: Forming and structural mechanics p 3301 N93-30437
Consolidation of graphite thermoplastic textile preforms for primary aircraft structure p 3302 N93-30439
Near net shape processing: A necessity for advanced materials applications p 3290 N93-30949
Thermoforming from a systems viewpoint
p 3293 N93-30967
FORTRAN
Installation of a new Fortran compiler and effective programming method on the vector supercomputer
[DE93-753322] p 3524 N93-28537
RTE: A UNIX library with on-line documentation and sample programs for microwave radiative transfer calculations
[PB93-180248] p 3386 N93-29680
FORWARD SCATTERING
Diffraction and holography with photoelectrons and Auger electrons: Some new directions
[DE93-007664] p 3313 N93-29766
Measurements of light scattering by small particles at an angle of zero degrees
[AD-A263856] p 3580 N93-29887
FOUNDRIES
Application of hardness testing in foundry processing operations: A university and industry partnership
p 3292 N93-30961
FOUR BODY PROBLEM
Algorithm of numerical calculations of differential Yakubovsky equations for the (1 + 3) scattering problem
[DE92-644679] p 3535 N93-30915
FOURIER TRANSFORMATION
Tomographic analysis of line-of-sight infrared spectra of low-pressure flames
[AD-A263185] p 3309 N93-28514
Wavelet transform techniques and signal analysis
[DE93-007919] p 3382 N93-29244
In situ Fourier transform infrared spectroscopic study of bisulfate and sulfate adsorption on gold, with and without the underpotential deposition of copper
[AD-A263421] p 3323 N93-29259
High mass resolution glow discharge mass spectrometry using an external ion source FT-ICR mass spectrometer
[AD-A264347] p 3314 N93-30166
The use of DFT windows in signal-to-noise ratio and harmonic distortion computations
[DE93-009800] p 3433 N93-30655
Application of the Fourier transform to short antennas
p 3398 N93-30750
FRACTALS
Multifractal analysis of radio lobes
p 3380 N93-28689
FRACTURE MECHANICS
The growth of small corrosion fatigue cracks in alloy 2024
[NASA-TM-107755] p 3451 N93-29069
Interim fatigue design curves for carbon, low-alloy, and austenitic stainless steels in LWR environments
[DE93-009202] p 3323 N93-29102
Mechanisms of fracture and creep of structural alloys
[AD-A263108] p 3324 N93-29799
The effect of oxidation embrittlement on the impact behavior of nicalon reinforced CAS 2 ceramic matrix composites
[AD-A263567] p 3334 N93-29829
Balanced technology initiative on computational mechanics of materials
[AD-A263906] p 3453 N93-29863
Dislocation roles in energetic crystal responses
p 3348 N93-30086
Damage growth in composite propellants
p 3348 N93-30088
Interfacial melting in cracked explosives
p 3349 N93-30089
DOE fundamentals handbook: Material science
[DE93-012225] p 3314 N93-30200
Stress-intensity-factor influence coefficients for axial and circumferential flaws in reactor pressure vessels
[DE93-006206] p 3454 N93-30213
A ceramic fracture model for high velocity impact
[AD-A264728] p 3454 N93-30545
Evaluation of some scale effects in the response and failure of composite beams p 3308 N93-30874
Fracture of glass p 3293 N93-30969
FRACTURE STRENGTH
Factors influencing the interlaminar fracture toughness and its evaluation in composites
[FFA-TN-1991-34] p 3451 N93-29076
Materials characterization of cermet anodes tested in a pilot cell
[DE93-008924] p 3323 N93-29101
Microstructural effects on the deformation and fracture of the alloy Ti-25Al-10Nb-3B-1Mo
[AD-A263095] p 3323 N93-29144
Improved silicon nitride for advanced heat engines
[NASA-CR-182193] p 3298 N93-29451
The effect of oxidation embrittlement on the impact behavior of nicalon reinforced CAS 2 ceramic matrix composites
[AD-A263567] p 3334 N93-29829
Effects of intra- and inter-laminar resin content on the mechanical properties of toughened composite materials
p 3303 N93-30845
Studies of fiber-matrix adhesion on compression strength p 3304 N93-30846
A miniature fatigue test machine p 3291 N93-30956
FRACTURES (MATERIALS)
Environmental embrittlement of binary and Zr-doped Ni3Al
[DE93-008575] p 3321 N93-28679
Stress-intensity-factor influence coefficients for axial and circumferential flaws in reactor pressure vessels
[DE93-006206] p 3454 N93-30213
FRACTURING
Transformation plasticity in ductile solids
[DE93-008636] p 3321 N93-28902
Factors influencing the interlaminar fracture toughness and its evaluation in composites
[FFA-TN-1991-34] p 3451 N93-29076
Mechanisms of fracture and creep of structural alloys
[AD-A263108] p 3324 N93-29799
Three-dimensional elastic stress analysis in materials with many inhomogeneities
[AD-A263736] p 3453 N93-29855
A ceramic fracture model for high velocity impact
[AD-A264728] p 3454 N93-30545
Fracture of glass p 3293 N93-30969
FRAGMENTATION
Catastrophic collisions: Laboratory impact experiments, hydrocode simulations, and the scaling problem
p 3635 N93-30411
FRAGMENTS
Amino acid sequences for the binding regions in serum albumin proteins
[NASA-CASE-MFS-28402-1] p 3491 N93-28952
FRAMES
Continued investigation of LDEF's structural frame and thermal blankets by the Meteoroid and Debris Special Investigation Group p 3282 N93-29357
FRAMING CAMERAS
A new multichannel soft x ray framing camera for fusion experiments
[DE93-009302] p 3432 N93-29773
FRANCE
Propulsion and detonics research in France
p 3344 N93-30070
FRAUNHOFER LINES
Method of emitting on a specific wavelength fraunhofer line using a neodymium doped laser transmitter
[AD-D015710] p 3437 N93-29276
FREE BOUNDARIES
Planar reorientation of a free-free beam in space using embedded electromechanical actuators
p 3280 N93-29993
FREE CONVECTION
Analytical and experimental study of laminar free convective heat transfer from isothermal convex bodies of arbitrary shape
[ISBN-0-315-72512-5] p 3426 N93-30379
Performance of thermal adhesives in forced convection p 3293 N93-30974
FREE ELECTRON LASERS
Ultraviolet free electron laser facility preliminary design report
[DE93-009360] p 3435 N93-28594
A technique for single-pulse spectrum and pulse width measurements for an IR-FEL
[DE93-007732] p 3436 N93-28847
High resolution free-electron laser spectroscopy
[AD-A263734] p 3439 N93-29853
Magnetic field measurements of the CEBAF (NIST) wiggler using the pulsed wire method
[AD-A263997] p 3439 N93-29867
Three-dimensional simulation analysis of the standing-wave free-electron laser two-beam accelerator
[DE93-010461] p 3575 N93-29870
Nonlinear mode coupling in free electron lasers
[AD-A263999] p 3439 N93-29883
Experimental test of hole-coupled FEL resonator designs using a CW-HeNe laser
[DE93-010439] p 3440 N93-30530
FREE ENERGY
Transformation toughening
[DE93-011805] p 3321 N93-28631
A one-dimensional continuum model for shape-memory alloys
[AD-A262505] p 3321 N93-28656
Phase separation, antiferromagnetism, and superconductivity in superconducting-superoxygenated La(2-x)Sr(x)CuO(4+(delta))
[DE93-009852] p 3598 N93-30517
Effective interactions between concentration fluctuations and charge transfer in chemically ordering liquid alloys
[DE93-606724] p 3327 N93-30778
FREE FLOW
Heat transfer with moderate free stream turbulence
p 3254 N93-29936
FREE RADICALS
Spectroscopic probes of vibrationally excited molecules at chemically significant energies
[DE93-012328] p 3564 N93-28652
Rate constant determinations of reactions H + HNO from ab initio reaction path calculations
p 3319 N93-30099
FREE-PISTON ENGINES
Small Stirling dynamic isotope power system for robotic space missions
[NASA-TM-105785] p 3287 N93-28686
FREEZE DRYING
Evaluation of dried storage of platelets for transfusion: Physiologic integrity and hemostatic functionality
[AD-A263240] p 3494 N93-29620
FREEZING
Advanced insulations for refrigerator/freezers: The potential for new shell designs incorporating polymer barrier construction
[DE93-010600] p 3353 N93-28570
Effects of freeze/thaw cycles on hydrostatically conditioned E-glass/J-2 composite
[AD-A262980] p 3298 N93-29425
Mathematical model of frost heave and thaw settlement in pavements
[CRREL-REPT-93-2] p 3262 N93-30103
FREQUENCIES
The flight performance of the Galileo orbiter USO
p 3386 N93-29603
FREQUENCY CONTROL
Two-stage Doppler phasor corrected TCM/DMPSK for shadowed mobile satellite channels
p 3373 N93-30333
FREQUENCY CONVERTERS
Charge to frequency converter for ionization chambers belonging to the radiation protection system of AmPS/MEA
[DIGEL-1991-6] p 3577 N93-30837
FREQUENCY DISTRIBUTION
System overview on electromagnetic compensation for reflector antenna surface distortion
[NASA-TM-106217] p 3273 N93-29195

FREQUENCY DIVIDERS
High-speed, CMOS dual modulus frequency divider for RF frequency synthesis p 3359 N93-30245
FREQUENCY DIVISION MULTIPLE ACCESS
Comparison of multiple access techniques for bandwidth limited land-mobile satellite communications p 3370 N93-30314
FREQUENCY HOPPING
Widebanding techniques for VHF antennas 2 [AD-A263998] p 3387 N93-29882
Comparison of diversity combining, interleaving, and decoding techniques of a scintillated channel p 3362 N93-30266
Coarse synchronization in an EHF frequency-hopped satellite communications system p 3365 N93-30281
Coding for frequency hopped spread spectrum satellite communications p 3365 N93-30283
Temporal synchronization of frequency hopped DPSK p 3365 N93-30285
Performance of frequency hopped M-ary FSK in Rayleigh fading and partial-band jamming p 3368 N93-30303
FREQUENCY MEASUREMENT
Constant frequency pulsed phase-locked loop measuring device [NASA-CASE-LAR-13823-1] p 3431 N93-29084
FREQUENCY MODULATION
Laser radiation detection system [AD-D015724] p 3438 N93-29287
Theoretical bit error rate performance of the Kalman filter excisor for FM interference [AD-A263018] p 3383 N93-29407
FREQUENCY MULTIPLIERS
Method of emitting on a specific wavelength fraunhofer line using a neodymium doped laser transmitter [AD-D015710] p 3437 N93-29276
FREQUENCY RANGES
Comparative study of undersea fields produced by various dipoles p 3397 N93-30740
Tethered aerostat VLF/LF transmitter system design considerations p 3399 N93-30753
FREQUENCY RESPONSE
Frequency-response techniques for documentation and improvement of rotorcraft simulators p 3237 N93-30689
FREQUENCY SHIFT
Study of gain in C-band deflection cavities for a frequency-doubling magnicon amplifier [AD-A263132] p 3409 N93-29478
FREQUENCY SHIFT KEYING
Comparison of diversity combining, interleaving, and decoding techniques of a scintillated channel p 3362 N93-30266
Coding for frequency hopped spread spectrum satellite communications p 3365 N93-30283
Performance of frequency hopped M-ary FSK in Rayleigh fading and partial-band jamming p 3368 N93-30303
A dynamic bandwidth and phase linearity measurement technique for 4-channel MSK VLF antenna systems p 3398 N93-30748
FREQUENCY STABILITY
The flight performance of the Galileo orbiter USO p 3386 N93-29603
Improved field emitter current densities and stability through the application of a proprietary process [AD-A264048] p 3411 N93-30031
FREQUENCY STANDARDS
An improved linear ion trap physics package p 3384 N93-29587
Physics laboratory technical activities, 1992 [PB93-178648] p 3561 N93-30888
FREQUENCY SYNTHESIZERS
Advanced technologies for lightweight EHF tactical communications satellites p 3389 N93-29900
High-speed, CMOS dual modulus frequency divider for RF frequency synthesis p 3359 N93-30245
FRICTION
Fundamental studies of friction, lubrication, and wear by atomic force microscopy [AD-A264647] p 3446 N93-30524
Tribology: Friction, lubrication, and wear technology p 3292 N93-30965
Walkway friction: Experiment and analysis p 3293 N93-30966
FRICTION FACTOR
Dense inclined flows: Theory and experiments [DE93-011452] p 3417 N93-28630
Direct tension experiments on compacted granular materials p 3292 N93-30960
FRICTION REDUCTION
Effect of metallic-coating properties on the tribology of coated and oil-lubricated ceramics [DE93-010663] p 3330 N93-28666
FROST
Mathematical model of frost heave and thaw settlement in pavements [CRREL-REPT-93-2] p 3262 N93-30103
FUEL CELLS
Benchmark eigenvalue spectrum calculations with anisotropic effects [DE93-006387] p 3548 N93-28891
Polymer electrolyte fuel cells for transportation applications [DE93-008721] p 3464 N93-29147
Electrical relaxation in acid-form nafion [AD-A263558] p 3410 N93-29826
The electrolyte factor in O2 reduction electrocatalysis [AD-A263565] p 3313 N93-29828
Solid oxide fuel cells for transportation: A clean, efficient alternative for propulsion [DE93-010662] p 3464 N93-29844
Power generation and transportation systems research department [PB93-178309] p 3352 N93-30663
FUEL COMBUSTION
Generation of carbon monoxide in compartment fires [PB93-146702] p 3244 N93-29211
High pressure preignition chemistry of hydrocarbons and hydrocarbon mixtures [AD-A263611] p 3311 N93-29283
Kinetic studies on gas-phase reaction mechanisms important to the combustion of energetic materials: The CO/N2O reaction p 3347 N93-30084
FUEL CONTAMINATION
Performance and cost evaluation of bioremediation techniques for fuel spills [PB93-175545] p 3474 N93-30762
FUEL INJECTION
Liquid fuel injection elements for rocket engines [NASA-CASE-MFS-28547-1] p 3289 N93-29847
FUEL PRODUCTION
A novel process for methanol synthesis [DE93-013070] p 3314 N93-30188
FUEL SPRAYS
Estimation of droplet collision frequency in a spray [DE93-007991] p 3416 N93-28566
Limitations of the ideal phase-Doppler system: Extension to spatially and temporally inhomogeneous particle flows with an application to diesel sprays [DE93-009447] p 3416 N93-28595
Modeling the effects of drop drag and breakup on fuel sprays [AD-A263650] p 3445 N93-29388
FUEL TANKS
APU diaphragm testing [NASA-TM-108254] p 3272 N93-29501
FUEL TESTS
Development of alternative fuels from coal-derived syngas [DE93-011629] p 3341 N93-28668
FUEL-AIR RATIO
Turbulence characteristics of an axisymmetric reacting flow [NASA-CR-4110] p 3242 N93-30373
FUELS
Tank issues: Design and placement of floating liquid monitoring wells [PB93-161149] p 3469 N93-29033
FULL SCALE TESTS
Modal survey of a full-scale F-18 wind tunnel model [AD-A262482] p 3240 N93-29410
FULLERENES
Theory of normal and superconducting properties of fullerene-based solids [DE93-007722] p 3592 N93-28582
Ambient-atmosphere compatible superconducting fullerenes [AD-A262025] p 3595 N93-29397
A tight binding model for the electronic structure of FCC and SC C60 [DE93-606214] p 3601 N93-30794
FUNCTION SPACE
On the energy-momentum tensors for field theories in spaces with affine connection and metric [DE92-644743] p 3557 N93-30926
Equivariant elliptic homology [DE92-641338] p 3557 N93-30981
FUNCTIONAL INTEGRATION
The quest for an integrated flying helmet p 3502 N93-28860
FUNCTIONALLY GRADIENT MATERIALS
A transient FGM interlayer based approach to joining ceramics [DE93-010415] p 3331 N93-29248
FUNCTIONALS
Hierarchical model of matching p 3519 N93-29580
Approximation formulae for functional integrals in P(phi)2-quantum field theory [DE93-606067] p 3605 N93-30781
FUSELAGES
Quiet by design: Numerical acousto-elastic analysis of aircraft structures [ISBN-90-386-0042-9] p 3248 N93-29268
Advanced technology commercial fuselage structure p 3300 N93-30432
Design and manufacturing concepts for thermoplastic structures p 3301 N93-30434
Structural evaluation of curved stiffened composite panels fabricated using a THERM-Xsm process p 3301 N93-30435
Noise transmission properties and control strategies for composite structures p 3301 N93-30436
Cost studies for commercial fuselage crown designs p 3302 N93-30440
Fabrication of the V-22 composite AFT fuselage using automated fiber placement p 3302 N93-30443
Effects of intra- and inter-laminar resin content on the mechanical properties of toughened composite materials p 3303 N93-30845
Mechanical and analytical screening of braided composites for transport fuselage applications p 3305 N93-30855
Developments in impact damage modeling for laminated composite structures p 3305 N93-30857
Multi-parameter optimization tool for low-cost commercial fuselage crown designs p 3305 N93-30858
Design and analysis of grid stiffened concepts for aircraft composite primary structural applications p 3306 N93-30861
Advanced fiber placement of composite fuselage structures p 3306 N93-30864
Process and assembly plans for low cost commercial fuselage structure p 3306 N93-30865
FUSES (ORDNANCE)
Analysis of an MCG/fuse/PFS experiment [DE93-007355] p 3410 N93-29812
FUSION REACTORS
Fast neutron cross section measurements [DE93-009053] p 3563 N93-28546
A study on radiation shielding analysis for toroidal field coils of a tokamak-type fusion reactor [DE93-753398] p 3585 N93-28981
The hydraulic analysis of cylindrical Flibe jets in a HYLIFE-2 ICF reactor [DE93-009234] p 3586 N93-29053
SIRIUS-P: An inertially confined direct drive laser fusion power reactor [DE93-012433] p 3439 N93-30186
Preliminary design study of a steady state tokamak device [DE93-764162] p 3589 N93-30397
FUZZY SETS
Soft computing in design and manufacturing of advanced materials [NASA-TM-106032] p 3295 N93-28624
North American Fuzzy Logic Processing Society (NAFIPS 1992), volume 1 [NASA-CP-10112-VOL-1] p 3509 N93-29516
An analysis of possible applications of fuzzy set theory to the actuarial credibility theory p 3510 N93-29517
Estimations of expectedness and potential surprise in possibility theory p 3510 N93-29518
Comparison of specificity and information for fuzzy domains p 3510 N93-29519
The axiomatic definition of a linguistic scale fuzziness degree, its major properties, and applications p 3510 N93-29520
Approximate reasoning using terminological models p 3510 N93-29522
A fuzzy clustering algorithm to detect planar and quadric shapes p 3511 N93-29524
A fuzzy measure approach to motion frame analysis for scene detection p 3511 N93-29525
Automatic rule generation for high-level vision p 3511 N93-29526
Encoding spatial images: A fuzzy set theory approach p 3511 N93-29527
Fuzzy forecasting and decision making in short dynamic time series p 3513 N93-29541
Intelligent virtual reality in the setting of fuzzy sets p 3513 N93-29544
An experimental methodology for a fuzzy set preference model p 3514 N93-29547
A fuzzy set preference model for market share analysis p 3514 N93-29548
Information compression in the context model p 3514 N93-29549
Intelligent fuzzy controller for event-driven real time systems p 3515 N93-29551
North American Fuzzy Logic Processing Society (NAFIPS 1992), volume 2 [NASA-CP-10112-VOL-2] p 3515 N93-29556
Adding dynamic rules to self-organizing fuzzy systems p 3515 N93-29557
Fuzzy learning under and about an unfamiliar fuzzy teacher p 3516 N93-29558
Some problems with the design of self-learning management systems p 3516 N93-29559

A neural fuzzy controller learning by fuzzy error propagation p 3516 N93-29560
Determining rules for closing customer service centers: A public utility company's fuzzy decision p 3516 N93-29561
The fusion of information via fuzzy integration p 3517 N93-29568
On the evaluation of fuzzy quantified queries in a database management system p 3517 N93-29569
A fuzzy case based reasoning tool for model based approach to rocket engine health monitoring p 3289 N93-29570
Genetic algorithms in adaptive fuzzy control p 3518 N93-29572
Fuzzy multiple linear regression: A computational approach p 3518 N93-29574
Incorporation of varying types of temporal data in a neural network p 3518 N93-29575
Fuzzy operators and cyclic behavior in formal neuronal networks p 3519 N93-29576
Neural networks: A simulation technique under uncertainty conditions p 3519 N93-29577
Hierarchical model of matching p 3519 N93-29580
On probability-possibility transformations p 3519 N93-29582
Inference in fuzzy rule bases with conflicting evidence p 3519 N93-29583
Gaussian membership functions are most adequate in representing uncertainty in measurements p 3520 N93-29584
A new way to use fuzzy sets in image sharpening p 3363 N93-30273

FUZZY SYSTEMS
New classification methods p 3459 N93-28932
A fuzzy logic optimal control law solution to the CMMCA tracking problem [AD-A262555] p 3542 N93-29420
North American Fuzzy Logic Processing Society (NAFIPS 1992), volume 1 [NASA-CP-10112-VOL-1] p 3509 N93-29516
The axiomatic definition of a linguistic scale fuzziness degree, its major properties, and applications p 3510 N93-29520
How to select combination operators for fuzzy expert systems using CRI p 3510 N93-29521
Quantitative analysis of properties and spatial relations of fuzzy image regions p 3510 N93-29523
A fuzzy clustering algorithm to detect planar and quadric shapes p 3511 N93-29524
A neuro-fuzzy architecture for real-time applications p 3511 N93-29529
A composite self tuning strategy for fuzzy control of dynamic systems p 3511 N93-29530
A self-learning rule base for command following in dynamical systems p 3512 N93-29531
Adaptive defuzzification for fuzzy systems modeling p 3512 N93-29532
Design issues of a reinforcement-based self-learning fuzzy controller for petrochemical process control p 3512 N93-29533
Character recognition using a neural network model with fuzzy representation p 3512 N93-29536
Designing a fuzzy scheduler for hard real-time systems p 3512 N93-29537
WARP: Weight Associative Rule Processor. A dedicated VLSI fuzzy logic megacell p 3513 N93-29538
Evaluation of fuzzy inference systems using fuzzy least squares p 3513 N93-29539
A model for amalgamation in group decision making p 3513 N93-29540
Distributed traffic signal control using fuzzy logic p 3513 N93-29543
Intelligent virtual reality in the setting of fuzzy sets p 3513 N93-29544
Fuzzy neural network methodology applied to medical diagnosis p 3498 N93-29546
An experimental methodology for a fuzzy set preference model p 3514 N93-29547
Fuzzy knowledge base construction through belief networks based on Lukasiewicz logic p 3515 N93-29550
Intelligent fuzzy controller for event-driven real time systems p 3515 N93-29551
Fuzzy coordinator in control problems p 3515 N93-29552
Tuning a fuzzy controller using quadratic response surfaces p 3515 N93-29553
The cognitive bases for the design of a new class of fuzzy logic controllers: The clearness transformation fuzzy logic controller p 3515 N93-29554
A fuzzy control design case: The fuzzy PLL p 3515 N93-29555
North American Fuzzy Logic Processing Society (NAFIPS 1992), volume 2 [NASA-CP-10112-VOL-2] p 3515 N93-29556
Adding dynamic rules to self-organizing fuzzy systems p 3515 N93-29557
Fuzzy learning under and about an unfamiliar fuzzy teacher p 3516 N93-29558
Fuzzy simulation in concurrent engineering p 3516 N93-29562
Inverse problems: Fuzzy representation of uncertainty generates a regularization p 3516 N93-29563
Quantification of human responses p 3500 N93-29564
A high performance, ad-hoc, fuzzy query processing system for relational databases p 3518 N93-29571
Genetic algorithms in adaptive fuzzy control p 3518 N93-29572
A genetic algorithms approach for altering the membership functions in fuzzy logic controllers p 3518 N93-29573
Fuzzy multiple linear regression: A computational approach p 3518 N93-29574
Incomplete fuzzy data processing systems using artificial neural network p 3519 N93-29578
Inference in fuzzy rule bases with conflicting evidence p 3519 N93-29583
Gaussian membership functions are most adequate in representing uncertainty in measurements p 3520 N93-29584
Life insurance risk assessment using a fuzzy logic expert system p 3520 N93-29585

G

GALACTIC COSMIC RAYS
Radioactivities induced in some LDEF samples p 3572 N93-29628
Revised prediction of LDEF exposure to trapped protons p 3572 N93-29633
LET spectra measurements of charged particles in the P0006 experiment on LDEF p 3573 N93-29637
Three-dimensional shielding effects on charged particle fluences measured in the P0006 experiment of LDEF p 3573 N93-29639
Progress report on the Heavy Ions in Space (HIIS) experiment p 3573 N93-29645

GALACTIC EVOLUTION
Distribution of dark matter in the galaxy and the lower limits for the masses of supersymmetric particles [BONN-92-31] p 3632 N93-28473

GALACTIC RADIATION
The 12 UM contribution of nearby galaxies to the infrared background [AD-A264336] p 3654 N93-30419

GALACTIC STRUCTURE
Multiwavelength studies of classical nova shells p 3636 N93-30412

GALAXIES
On the meaning of delta T/T [DE93-008482] p 3653 N93-28962

GALERKIN METHOD
A spectral method determination of the first critical Rayleigh number for a low-Prandtl number crystal melt in a cylindrical container [NASA-CR-193238] p 3594 N93-29214
On high resolution extensions of Lagrange-Galerkin finite-element schemes [INRIA-RR-1703] p 3550 N93-30117
Vibration localization in rotating shafts p 3454 N93-30626
Multiple methods integration for structural mechanics analysis and design p 3307 N93-30867

GALILEO SPACECRAFT
Galileo post-Gaspra cruise and Earth-2 encounter p 3385 N93-29597
The flight performance of the Galileo orbiter USO p 3386 N93-29603

GALLIUM
Uniaxially stressed Ge:Ga and Ge:Be [DE93-010426] p 3594 N93-29150

GALLIUM ARSENIDES
Luminescence study of ion-implanted and MBE-grown Er-doped GaAs and Al(x)Ga(1-x)As [AD-A262602] p 3591 N93-28471
Infrared rugates by molecular beam epitaxy p 3582 N93-28808
New III-V cell design approaches for very high efficiency [DE93-000097] p 3464 N93-28971
Ultrafast optical studies of surface reaction processes at semiconductor interfaces [DE93-009049] p 3593 N93-29096
Low temperature (LT) GaAs and related materials [AD-A263607] p 3298 N93-29282
Defect studies in low-temperature-grown GaAs [DE93-010405] p 3595 N93-29417
Low-cost, high-efficiency solar cells utilizing GaAs-on-Si technology [DE93-000096] p 3464 N93-29965
Fundamental studies of the morphology, chemistry, and electrical properties of metals on GaAs and other III-V semiconductor compounds [AD-A264417] p 3597 N93-30120
Growth and development of GaInAsP for use in high-efficiency solar cells [DE93-000098] p 3465 N93-30208
Modelling of channel thickness modulation effect in SI GaAs MESFET's p 3356 N93-30229
Unexpected increase in the thermal generation rate of bulk GaAs due to electron-beam metallization [DE93-009829] p 3598 N93-30511
Development of ultra-low noise, high sensitivity planar metal grating coupled 3-5 multiquantum well infrared detectors for focal plane array staring IR sensor systems [AD-A264465] p 3599 N93-30536
Heat generation produced in thin layers of GaAs superconductors under high energy particles irradiation [DE93-606332] p 3601 N93-30798

GALLIUM PHOSPHIDES
Growth and development of GaInAsP for use in high-efficiency solar cells [DE93-000098] p 3465 N93-30208
Synthesis and characterization of mixed 3-5 and 2-6 semiconductor monomers included in the borate sodalite analogue [AD-A264523] p 3598 N93-30407

GAME THEORY
Artificial intelligence methodologies in flight related differential game, control and optimization problems [AD-A262405] p 3541 N93-28498

GAMMA RAY ASTRONOMY
A search for radiative neutrino decay from supernovae [NASA-CR-193118] p 3653 N93-30052
Rejection of archival photographic objects as optical counterparts of gamma ray bursters [MPE-PREPRINT-228] p 3631 N93-30642

GAMMA RAY SPECTRA
Collection, analysis, and archival of LDEF activation data p 3624 N93-29631

GAMMA RAY SPECTROMETERS
Gamma ray/neutron spectrometers for planetary elemental mapping p 3647 N93-28807
A team approach to the development of gamma ray and x ray remote sensing and in situ spectroscopy for planetary exploration missions p 3650 N93-28824
Instrumental neutron activation analysis developed for silicon integrated circuit technology [ETN-93-93581] p 3408 N93-29271
Sensitivity of LDEF foil analyses using ultra-low background germanium vs. large NaI(Tl) multidimensional spectrometers p 3318 N93-29627
A photon phreak digs the LDEF happening p 3572 N93-29629

GAMMA RAYS
Distribution of dark matter in the galaxy and the lower limits for the masses of supersymmetric particles [BONN-92-31] p 3632 N93-28473
Modern Monte Carlo particle transport simulation for safety and radiation protection applications in accelerometer technology and in space science [JUEL-2609] p 3574 N93-29062
Limits on neutrino radiative decay from SN1987A [NASA-CR-193262] p 3653 N93-29164
Charged particle activation studies on the surface of LDEF spacecraft p 3572 N93-29630
A search for radiative neutrino decay from supernovae [NASA-CR-193118] p 3653 N93-30052
GRO: Red-shifted electron-positron annihilation gamma-rays from radiopulsars [NASA-CR-193243] p 3635 N93-30053
A high resolution 14-bit ADC for Gammasphere Project [DE93-010446] p 3598 N93-30393
Mathematical simulation of the induced (gamma)-radiation in structural materials of spaceships. Time dependence [DE93-605312] p 3281 N93-31024

GARMENTS
Evaluation of personal cooling systems in conjunction with explosive ordnance disposal suits [AD-A262862] p 3506 N93-29471

GAS ANALYSIS
Analysis of protocol gases: An on-going quality assurance audit [PB93-168839] p 3311 N93-29204
Contamination of soil, soil gas, and ground water by hydrocarbon compounds near Greear, Morgan County, Kentucky [PB93-182244] p 3474 N93-30825

GAS CHROMATOGRAPHY
Mass spectrometric measurement of Martian krypton and xenon isotopic abundance p 3646 N93-28798

A DTA/GC for the in situ identification of the Martian surface material p 3646 N93-28800

High pressure preignition chemistry of hydrocarbons and hydrocarbon mixtures
[AD-A263611] p 3311 N93-29283

Summer research program (1992). High School Apprenticeship Program (HSAP) reports. Volume 16: Arnold Engineering Development Center Civil Engineering Laboratory
[AD-A262024] p 3608 N93-29396

Design and performance evaluation of a gas chromatograph micromachined in a single crystal silicon substrate
[AD-A262594] p 3596 N93-29424

An investigation of resolution as encountered in various chromatographic operational modes
[AD-A262883] p 3312 N93-29510

Explosives detection systems for airport security gas chromatographic based devices p 3244 N93-30276

Carbon monoxide exposure of subjects with documented cardiac arrhythmias
[PB93-179943] p 3497 N93-30890

GAS COOLING

Coupling of 3D-Navier-Stokes external flow calculations and internal 3D-heat conduction calculations for cooled turbine blades p 3258 N93-29961

GAS DENSITY

Distribution of dark matter in the galaxy and the lower limits for the masses of supersymmetric particles
[BONN-92-31] p 3632 N93-28473

Dense gas in the monoceros OB1 dark cloud and its relationship to star formation p 3636 N93-30502

Measurements of the energy spectrum of an intense microsecond relativistic electron beam in the beam-plasma experiments using a multi-foil analyzer
[DE93-606271] p 3590 N93-30768

GAS DETECTORS

Tank issues: Site characterization for external leak monitoring
[PB93-161156] p 3469 N93-29034

Explosives detection systems for airport security gas chromatographic based devices p 3244 N93-30276

Advanced signal processing requirement in an ion mobility explosives detector p 3320 N93-30277

Hydrogen-rated system for in vitro studies at pressure: Operating procedures and emergency procedures
[AD-A264179] p 3497 N93-30882

GAS DISCHARGE TUBES

Preliminary investigation of high power microwave plasmas for electrothermal thruster use
[NASA-TM-106207] p 3288 N93-29158

GAS DISSOCIATION

A computer simulation of the production of an artificially ionized layer using the Arecibo facility
[DE93-010817] p 3478 N93-30487

GAS DYNAMICS

Analysis of unsteady wave processes in a rotating channel
[NASA-CR-191154] p 3251 N93-28617

Three-dimensional numerical simulation of gradual opening in a wave rotor passage
[NASA-CR-191157] p 3252 N93-29072

Non-linear wave phenomena in a gas-vapour mixture with phase transition
[ETN-93-93582] p 3422 N93-29319

Experimental MHD stability limit in the gas-dynamic trap
[DE93-606218] p 3591 N93-30780

Knot invariants and cellular automata
[AD-A264199] p 3607 N93-30884

GAS EXCHANGE

Upper ocean model of dissolved atmospheric gases
[DE93-010151] p 3487 N93-29327

A preliminary review of global CO2 exchange between ocean and atmosphere
[AD-A264019] p 3472 N93-30015

GAS EXPANSION

Laser spectroscopy of hydrocarbon radicals
[DE93-012555] p 3436 N93-28653

GAS EXPLOSIONS

Weakly nonlinear dynamics of near-CJ detonation waves
[DE93-007344] p 3424 N93-29836

GAS FLOW

Preliminary investigation of high power microwave plasmas for electrothermal thruster use
[NASA-TM-106207] p 3288 N93-29158

Non-linear wave phenomena in a gas-vapour mixture with phase transition
[ETN-93-93582] p 3422 N93-29319

Evolution of flow disturbances in cocurrent gas-liquid flows
[DE93-010083] p 3422 N93-29326

Pulse mitigation and heat transfer enhancement techniques. Volume 4: Transient behavior of heat pipe with thermal energy storage under pulse heat loads
[AD-A263497] p 3423 N93-29339

Modeling the effects of drop drag and breakup on fuel sprays
[AD-A263650] p 3445 N93-29388

Flame or plasma synthesis of diamond under turbulent and transition flow conditions
[AD-D015689] p 3333 N93-29456

Heat transfer with moderate free stream turbulence
p 3254 N93-29936

Atmospheric studies with SODAR at Kalpakkam
[DE93-605544] p 3480 N93-30992

GAS GENERATORS

Additional support for the TDK/MABL computer program
[NASA-CR-193037] p 3526 N93-29028

GAS GIANT PLANETS

Planetary and satellite x ray spectroscopy: A new window on solid-body composition by remote sensing
p 3641 N93-28773

Plasma, magnetic, and electromagnetic measurements at nonmagnetic bodies p 3647 N93-28809

On symmetric central configurations with application to satellite motion about rings p 3652 N93-31000

GAS INJECTION

Additional support for the TDK/MABL computer program
[NASA-CR-193037] p 3526 N93-29028

GAS IONIZATION

Polarization dependence of the ionization of helium and neon by 120 femtosecond pulses at 614 nm
[DE93-010514] p 3564 N93-28762

Inner-shell photo-ionized x ray laser schemes
[DE93-009285] p 3438 N93-29309

Application of Schlieren optical techniques for the measurement of gas temperature and turbulent diffusivity in a diesel engine
[AD-A263810] p 3580 N93-29880

GAS JETS

Measurements of rare composite objects and high sensitivity searches for novel forms of matter produced in high energy heavy ion collisions
[DE93-009945] p 3574 N93-28569

Attitude stabilization of a rigid spacecraft using gas jet actuators operating in a failure mode
p 3280 N93-29992

Effects of buoyancy on gas jet diffusion flames
[NASA-CR-191109] p 3352 N93-31031

GAS LASERS

Low-pump-rate multi-millisecond atomic xenon laser
[DE93-011484] p 3437 N93-29180

GAS MIXTURES

Thermodynamic properties of natural gas mixtures
[PB93-162816] p 3604 N93-29428

Thermodynamic properties of natural gas mixtures
[PB93-176162] p 3604 N93-29794

Hydrogen-rated system for in vitro studies at pressure: Operating procedures and emergency procedures
[AD-A264179] p 3497 N93-30882

Methods for preparation of mixtures of gases in air at the parts-per-billion to parts-per-million concentration range for calibration of monitors
[DE92-642433] p 3317 N93-30982

GAS PRESSURE

Large amplitude striations in an RF discharge
[DE93-753244] p 3379 N93-28534

Growing wheat to maturity in reduced gas pressures
[NASA-CR-193245] p 3491 N93-29216

GAS SPECTROSCOPY

Advanced signal processing requirement in an ion mobility explosives detector p 3320 N93-30277

GAS TEMPERATURE

Application of Schlieren optical techniques for the measurement of gas temperature and turbulent diffusivity in a diesel engine
[AD-A263810] p 3580 N93-29880

GAS TRANSPORT

Gas permeability of E/EP semicrystalline diblock copolymers
[AD-A263241] p 3329 N93-28560

Analysis of mass transport and potential vorticity budget in a simulated tropopause folding
[PB93-156792] p 3476 N93-29197

Study of codeposition of aluminum-haffnium and deposition of yttrium by the cementation technique: Elaboration of Ni-Cr-Al and Ni-Cr-Al-Hf felt materials
[ONERA-NT-1990-9] p 3336 N93-30112

GAS TURBINE ENGINES

Effects of flow-path variations on internal reversing flow in a tailpipe offtake configuration for ASTOVL aircraft
[NASA-TM-106149] p 3252 N93-29065

Spurious symptom reduction in fault monitoring
[NASA-CR-191453] p 3542 N93-29192

Microwave processing of silicon nitride for advanced gas turbine applications
[DE93-007910] p 3334 N93-29767

Keynote address: Unsteady, multimode transition in gas turbine engines p 3252 N93-29927

Heat transfer and aerodynamics of a 3D design nozzle guide vane tested in the Pyestock Isentropic Light Piston Facility p 3252 N93-29928

Thermal effects of a coolant film along the suction side of a high pressure turbine nozzle guide vane
p 3253 N93-29930

The influence of non-uniform spanwise inlet temperature on turbine rotor heat transfer p 3253 N93-29932

Measurement of turbulent spots and intermittency modelling at gas-turbine conditions
p 3253 N93-29934

Heat transfer in high turbulence flows: A 2-D planar wall jet p 3254 N93-29935

Heat transfer with moderate free stream turbulence
p 3254 N93-29936

Prediction of jet impingement cooling scheme characteristics (airfoil leading edge application)
p 3255 N93-29941

Local heat transfer measurement with liquid crystals on rotating surfaces including non-axisymmetric cases
p 3255 N93-29943

The USAF Advanced Turbine Aerothermal Research Rig (ATARR) p 3255 N93-29945

Aerothermic calculations of flows in interdisc cavities of turbines p 3256 N93-29947

Modelling thermal behaviour of turbomachinery discs and casings p 3256 N93-29949

Flow and heat transfer between gas-turbine discs
p 3256 N93-29950

Heat transfer and leakage in high-speed rotating stepped labyrinth seals p 3256 N93-29951

The effect of main stream flow angle on flame tube film cooling p 3257 N93-29953

Impingement/effusion cooling p 3257 N93-29954

Characterization of ceramic composite materials for gas turbine applications
[DE93-009719] p 3259 N93-30168

GAS TURBINES

Use of local x ray computerized tomography for high-resolution, region-of-interest inspection of large ceramic components for engines
[DE93-005564] p 3449 N93-28943

Flow phenomena in turbomachines
[AD-A263049] p 3420 N93-29141

The effect of high temperature on wall shear in a two dimensional wall jet
[AD-A262982] p 3423 N93-29426

Heat Transfer and Cooling in Gas Turbines
[AGARD-CP-527] p 3252 N93-29926

The effect of orthogonal-mode rotation on forced convection in a circular-sectioned tube fitted with full circumferential transverse ribs p 3254 N93-29937

Coupling of 3D-Navier-Stokes external flow calculations and internal 3D-heat conduction calculations for cooled turbine blades p 3258 N93-29961

Orbital transfer vehicle oxygen turbopump technology. Volume 3: Hot oxygen testing
[NASA-CR-191036] p 3448 N93-31039

GAS-GAS INTERACTIONS

Non-linear wave phenomena in a gas-vapour mixture with phase transition
[ETN-93-93582] p 3422 N93-29319

GAS-LIQUID INTERACTIONS

NASA in-step: Permeable membrane experiment
p 3267 N93-28736

GASEOUS DIFFUSION

Fiber optic chemical sensors for characterizing the carbon cycle in ocean margin regions
[DE93-011442] p 3489 N93-30056

GASEOUS ROCKET PROPELLANTS

A new facility for advanced rocket propulsion research
[NASA-TM-106193] p 3270 N93-28696

GAUGE INVARIANCE

Topics in gauge theories and the unification of elementary particle interactions
[DE93-009370] p 3563 N93-28542

Continuation of: Applications of gauge theories to enhance numerical solutions of mixed potential integral equations
[AD-A263763] p 3550 N93-29876

Beyond two dimensions
[DE93-606084] p 3606 N93-30786

Abelian gauge theories on homogeneous spaces
[DE92-644730] p 3607 N93-30921

Invariant structures in gauge theories and confinement
[DE92-644739] p 3607 N93-30924

Invariant structures and static forces in gauge theories
[DE92-644740] p 3607 N93-30925

Beltrami parametrization and gauging of Virasoro and w-infinity algebras
[DE92-644844] p 3557 N93-30928

Normal equivariant forms of vector fields
[DE92-644845] p 3551 N93-30929
Superconformal structures and holomorphic 1/2-superdifferentials on N = 1 super Riemann surfaces
[DE93-604133] p 3558 N93-30989
A non degenerate semi-classical Lagrangian for dilaton-gravity in two dimensions
[DE92-641339] p 3480 N93-31002

GAUGE THEORY
Topics in gauge theories and the unification of elementary particle interactions
[DE93-009370] p 3563 N93-28542
Studies in theoretical high energy particle physics
[DE93-007990] p 3574 N93-28565
Neutrino mass
[DE93-010735] p 3566 N93-29315
Understanding conformal field theory through parafermions and Chern Simons theory
[DE93-010452] p 3604 N93-29806
Continuation of: Applications of gauge theories to enhance numerical solutions of mixed potential integral equations
[AD-A263763] p 3550 N93-29876
On the photonic chiral anomaly in an external gravitational field
[DE93-606082] p 3479 N93-30785
Abelian gauge theories on homogeneous spaces
[DE92-644730] p 3607 N93-30921
Invariant structures in gauge theories and confinement
[DE92-644739] p 3607 N93-30924
Invariant structures and static forces in gauge theories
[DE92-644740] p 3607 N93-30925

GAUSS EQUATION
Gaussian membership functions are most adequate in representing uncertainty in measurements
p 3520 N93-29584

GEIGER COUNTERS
Electronics for a neutron detector and a Geiger-Mueller detector for the radiation protection around MEA and AmPS
[DIGEL-1992-6] p 3413 N93-30838

GELS
Comparative mutagenesis of human cells in vivo and in vitro
[DE93-012269] p 3490 N93-28651
Thermodynamics of swelling and collapse of polyelectrolytic gels
[ETN-93-93485] p 3331 N93-29064
Thermal properties of organic and modified inorganic aerogels
[DE93-009230] p 3311 N93-29263
Crystallization of nanocomposite glasses made by the SSG process
[AD-A262892] p 3333 N93-29511

GENE EXPRESSION
Gene transcription and electromagnetic fields
[DE93-010854] p 3490 N93-28848

GENERAL AVIATION AIRCRAFT
Preliminary design studies of an advanced general aviation aircraft p 3228 N93-29717

GENERAL OVERVIEWS
Computer systems laboratory
[PB93-181873] p 3521 N93-29662

GENES
Molecular approach to hypothalamic rhythms
[AD-A264438] p 3496 N93-30421

GENETIC ALGORITHMS
Genetic algorithms in adaptive fuzzy control
p 3518 N93-29572
A genetic algorithms approach for altering the membership functions in fuzzy logic controllers
p 3518 N93-29573
Intelligent support for human computer interaction and decision-making in distribution planning and scheduling systems
[AD-A263985] p 3610 N93-30124
Use of a genetic algorithm to solve two-fluid flow problems on an NCUBE multiprocessor computer
[DE93-009630] p 3425 N93-30184

GENETIC CODE
Comparative mutagenesis of human cells in vivo and in vitro
[DE93-012269] p 3490 N93-28651
Computer assisted multiplex sequencing
[DE93-007144] p 3536 N93-30934

GENETIC ENGINEERING
National collaboratories: Applying information technology for scientific research
[LC-93-83795] p 3612 N93-29129
Computer assisted multiplex sequencing
[DE93-007144] p 3536 N93-30934

GENETICS
Comparative mutagenesis of human cells in vivo and in vitro
[DE93-012269] p 3490 N93-28651
Gene transcription and electromagnetic fields
[DE93-010854] p 3490 N93-28848
Computer assisted multiplex sequencing
[DE93-007144] p 3536 N93-30934

GEOCHEMISTRY
Laer-induced breakdown spectroscopy instrument for element analysis of planetary surfaces
p 3434 N93-28769
A DTA/GC for the in situ identification of the Martian surface material p 3646 N93-28800
Gamma ray/neutron spectrometers for planetary elemental mapping p 3647 N93-28807
Upper ocean model of dissolved atmospheric gases
[DE93-010151] p 3487 N93-29327
Geochemical and fluid dynamic investigations into the nature of chemical heterogeneity in the Earth's mantle
[AD-A262753] p 3477 N93-29405
IOC-UNEP review meeting on oceanographic processes of transport and distribution of pollutants in the sea
[DE93-605070] p 3490 N93-31019

GEOCHRONOLOGY
Drill/borescope system for the Mars Polar Pathfinder
p 3647 N93-28805

GEODESY
Investigation of Mars rotational dynamics using Earth-based radio tracking of Mars landers
p 3642 N93-28777
Investigation of a geodesy coexperiment to the Gravity Probe B relativity gyroscope program
[NASA-CR-193263] p 3460 N93-29179

GEODETIC ACCURACY
Exact trajectory determinator for ERS-1
p 3457 N93-28918

GEOGRAPHIC INFORMATION SYSTEMS
Near real-time GIS in deep-ocean exploration
[AD-A262073] p 3487 N93-29003
Geographic information system for fusion and analysis of high-resolution remote sensing and ground truth data
p 3614 N93-29234
National remote sensing programme 2 ACMS project. Phase 1: Validation. Part 1: Definition of validation experiment
[BCRS-92-10-PHASE-1-PT-1] p 3461 N93-29465
Data quality statements for spatial databases
[AD-A264125] p 3616 N93-30195
Toward a coordinated spatial data infrastructure for the nation
[B-149] p 3456 N93-30634

GEOGRAPHY
What's past is prologue: Supporting global change research with historical data
[DE93-005777] p 3472 N93-30009

GEOIDS
Charting the remote southern oceans with geosat altimetry
[AD-A263452] p 3461 N93-29817

GEOLOGICAL FAULTS
Modeling earthquakes with local and regional broadband data p 3478 N93-30005

GEOLOGICAL SURVEYS
Visible imaging on the Pluto fast flyby mission
p 3646 N93-28799
Applications of three-dimensional modeling in electromagnetic exploration p 3391 N93-30010
Toward a coordinated spatial data infrastructure for the nation
[B-149] p 3456 N93-30634

GEOLOGY
JPRS report: Science and technology. Central Eurasia: Earth science
[JPRS-UES-93-003] p 3456 N93-29089
Geoscience center research
[AD-A263465] p 3462 N93-29834
Hydrogeology and ground-water-quality conditions at the Reno County Landfill, South-Central Kansas, 1990-1991
[PB93-183085] p 3474 N93-30826

GEOMAGNETISM
SESC products and services user guide
[PB93-178879] p 3653 N93-29679
The cone structure and focusing of the electric field of VLF and LF waves at high altitudes of the ionosphere
p 3395 N93-30731

GEOMETRIC RECTIFICATION (IMAGERY)
Model-oriented correction of thematic mapper raw data p 3459 N93-28930
Preprocessing airborne remote sensing PARES calibration maintenance functional design document
[BCRS-92-07] p 3460 N93-29321

GEOMETRICAL OPTICS
Ultra-high resolution water window x ray microscope optics design and analysis
[NASA-CR-193225] p 3578 N93-29128
What is the center of the image?
[AD-A263550] p 3579 N93-29824
Modeling the bidirectional reflectance and spectra
[AD-A263570] p 3462 N93-29830

GEOMETRY
Topology of hybrid objects
[ETN-93-93594] p 3546 N93-28466
Representation and recognition with invariants and geometric constraint models
[AD-A263235] p 3529 N93-29493

GEOMORPHOLOGY
Visible imaging on the Pluto fast flyby mission
p 3646 N93-28799
Geoscience center research
[AD-A263465] p 3462 N93-29834
Spacecraft studies of Phobos and Mars
[NASA-CR-193298] p 3651 N93-30635

GEOPHYSICS
Investigation of Mars rotational dynamics using Earth-based radio tracking of Mars landers
p 3642 N93-28777
Atmospheric and Geophysical Sciences Program report, 1990-1991
[DE93-007390] p 3470 N93-29055
Geoscience center research
[AD-A263465] p 3462 N93-29834
Hamiltonian dynamics of coupled potential vorticity and internal wave motion: 1. Linear modes
[AD-A263469] p 3424 N93-29838
Applications of three-dimensional modeling in electromagnetic exploration p 3391 N93-30010

GEOPOTENTIAL
Investigation of a geodesy coexperiment to the Gravity Probe B relativity gyroscope program
[NASA-CR-193263] p 3460 N93-29179

GEORGIA
Summer 1990 Atlanta ozone precursor study (January 1993)
[PB93-167203] p 3470 N93-29200

GEOSAT SATELLITES
Charting the remote southern oceans with geosat altimetry
[AD-A263452] p 3461 N93-29817

GEOSTROPHIC WIND
Using C-vector method to derive the three-dimensional circulation pattern near the East Greenland Polar Front
[AD-A261979] p 3487 N93-29437
Surface shear stress estimates from geostrophic winds for use in sensible and latent heat flux formulations
p 3483 N93-30044

GEOSYNCHRONOUS ORBITS
Origin of orbital debris impacts on LDEF's trailing surfaces p 3283 N93-29373
NOAA satellite programs and technology requirements
p 3627 N93-30710

GEOTECHNICAL ENGINEERING
Lunar regolith densification p 3276 N93-29115
Regolith-structure modeling p 3276 N93-29116
Systems engineering studies of lunar base construction p 3277 N93-29121
A field investigation of water and salt movement in permafrost and the active layer
[AD-A263706] p 3487 N93-29298

GEOTHERMAL TECHNOLOGY
Direct use geothermal applications for brazed plate heat exchangers
[DE93-008559] p 3465 N93-30011

GERMANIUM
Uniaxially stressed Ge:Ga and Ge:Be
[DE93-010426] p 3594 N93-29150

GERMANIUM COMPOUNDS
Development of Si(1-x)Ge(x) technology for microwave sensing applications
[NASA-TM-106157] p 3405 N93-28610
Fundamental studies of the mechanical behavior of microelectronics thin film materials
[AD-A264334] p 3337 N93-30417

GERMINATION
Final results of space exposed experiment developed for students p 3492 N93-29702
Continued results of the seeds in space experiment
p 3492 N93-29703

GET AWAY SPECIALS (STS)
Description of the Joint Damping Experiment (JDX)
p 3263 N93-28703

GIBBS FREE ENERGY
A simple model for ion solvation with non additive cores
[AD-A263075] p 3566 N93-29143

GIMBALS
Gravity referenced elevation encoder development
p 3385 N93-29592
Cryogenic magnetic bearing
[AD-A264716] p 3446 N93-30512

GLACIOLOGY
The German satellite ground station in Antarctica: Realization and first results p 3458 N93-28924

GLARE
Discomfort glare from high-intensity discharge headlamps: Effects of context and experience
[PB93-174720] p 3496 N93-30659
GLASS
Healing of lithographically introduced flaws in glass and glass containing ceramics
[DE93-010453] p 3330 N93-28761
Cratering in glasses impacted by debris or micrometeorites p 3340 N93-29368
Crystallization of nanocomposite glasses made by the SSG process
[AD-A262892] p 3333 N93-29511
Molecular dynamics of physical aging processes in polymer glasses
[AD-A263737] p 3334 N93-29856
Whisker toughening of ceramic materials: A review
[DE93-011565] p 3336 N93-30129
Applications of the photorefractive effect and damage induced effects in fibers
[AD-A264339] p 3580 N93-30205
Fracture of glass p 3293 N93-30969
Temperature-dependent electrical conductivity of soda-lime glass p 3294 N93-30978
GLASS COATINGS
Inertial confinement fusion target component fabrication and technology development support
[DE93-010836] p 3585 N93-28836
GLASS FIBER REINFORCED PLASTICS
Development of a test program to evaluate structural defects in Glass-Reinforced Plastic (GRP), volume 2
[AD-A263814] p 3335 N93-29881
Development of a test program to evaluate structural defects in Glass-Reinforced Plastic (GRP), volume 1
[AD-A263813] p 3335 N93-29886
GLASS FIBERS
Effects of freeze/thaw cycles on hydrostatically conditioned E-glass/J-2 composite
[AD-A262980] p 3298 N93-29425
Applications of the photorefractive effect and damage induced effects in fibers
[AD-A264339] p 3580 N93-30205
GLASS LASERS
Design of the Nova Upgrade laser system for ignition fusion experiments
[DE93-009077] p 3436 N93-29097
GLASS TRANSITION TEMPERATURE
A 69 cent look at thermoplastic softening
p 3292 N93-30963
GLASSY CARBON
The design and testing of a high-temperature graphite dilatometer
[AD-A262185] p 3430 N93-28488
GLIDE PATHS
Evaluation of four advanced nozzle concepts for short takeoff and landing performance
[NASA-TP-3314] p 3239 N93-29165
GLOBAL AIR POLLUTION
Chemistry of the atmosphere: Its impact on global change. CHEMRAWN 7: Perspectives and recommendations
[PB93-180644] p 3488 N93-29670
GLOBAL ATMOSPHERIC RESEARCH PROGRAM
The distribution of the annual and semiannual cycles in the tropics
[DE92-642213] p 3485 N93-31006
GLOBAL POSITIONING SYSTEM
Flight evaluation of a computer aided low-altitude helicopter flight guidance system p 3260 N93-28869
Helicopter approach capability using the differential global positioning system
[NASA-CR-193183] p 3245 N93-28936
Investigation of a geodesy coexperiment to the Gravity Probe B relativity gyroscope program
[NASA-CR-193263] p 3460 N93-29179
System analysis for a kinematic positioning system based on the global positioning system
[AD-A262830] p 3245 N93-29468
Embedded GPS: The Canadian Marconi approach
p 3247 N93-30330
Attitude determination using GPS: Development of an all solid-state guidance, navigation, and control sensor for air and space vehicles based on the global positioning system p 3246 N93-30605
Design and implementation of a Global Positioning System (GPS) supported area navigation system with electronic aircraft
[ILR-MITT-275(1992)] p 3246 N93-30671
Satellite calibration requirements
[AD-A264279] p 3281 N93-30817
GLOBAL WARMING
Global warming issue and global economic model
[DE93-781334] p 3468 N93-28881
Emission inventories: A global modeling perspective
[DE93-005817] p 3469 N93-28965
Atmospheric and Geophysical Sciences Division: G-Division did you know?
[DE93-007412] p 3469 N93-28967
Global warming potential for SF6
[DE93-007394] p 3469 N93-28972
Trend survey on the elucidation of the global warming mechanism by the governments of major industrialized nations
[DE93-776427] p 3470 N93-29672
GLOBULAR CLUSTERS
Stellar encounters in globular clusters
p 3632 N93-28606
The x ray population in globular clusters and three crab-like SNR in the large Magellanic cloud
[NASA-CR-193172] p 3630 N93-29604
GLOVES
Biophysical model for handwear insulation testing
[AD-A262926] p 3505 N93-28884
GLOW DISCHARGES
High mass resolution glow discharge mass spectrometry using an external ion source FT-ICR mass spectrometer
[AD-A264347] p 3314 N93-30166
GOGGLES
Goggles emergency release apparatus
[AD-D015685] p 3507 N93-29607
CATS EYES adjustment procedures
[AD-A264069] p 3508 N93-29924
The effects of superimposing symbology on a simulated night vision goggle display
[AD-A263458] p 3508 N93-30590
GOLD
In situ Fourier transform infrared spectroscopic study of bisulfate and sulfate adsorption on gold, with and without the underpotential deposition of copper
[AD-A263421] p 3323 N93-29259
Electric field induced phenomena in STM: Tip deformations and Au(111)-surface phase transitions during tunneling spectroscopy experiments
[AD-A262208] p 3596 N93-29445
The mechanical response of gold substrates modified with self-assembling monolayer films
[AD-A262997] p 3452 N93-29515
Growth model of Au films on Ru(001)
[DE92-642126] p 3602 N93-30998
GOODNESS OF FIT
Modified goodness-of-fit tests for the Weibull distribution
[AD-A262552] p 3553 N93-28574
Modified Anderson-Darling and Cramer-Von Mises goodness-of-fit tests for the normal distribution
[AD-A262554] p 3553 N93-28575
A new goodness-of-fit test for the Weibull distribution based on spacings
[AD-A262615] p 3553 N93-28587
A modified Anderson Darling goodness-of-fit test for the gamma distribution with unknown scale and location parameters
[AD-A262486] p 3553 N93-28760
A modified chi-squared goodness-of-fit test for the three-parameter gamma distribution with unknown parameters
[AD-A262553] p 3554 N93-28845
GOVERNMENT PROCUREMENT
How to compete for NASA contracts
[NASA-TM-109238] p 3610 N93-30644
GOVERNMENT/INDUSTRY RELATIONS
Defense conversion: Redirecting research and development
[OTA-ITE-552] p 3610 N93-29649
Technology Transfer and the Civil Space Program. Volume 2: Workshop proceedings
[NASA-TM-108250] p 3625 N93-30692
The NCAT process p 3626 N93-30697
National Technology Transfer Center
p 3626 N93-30700
Technology transfer within the government
p 3627 N93-30711
Technology transfer and Rockwell International
p 3627 N93-30712
NASP technology transfer p 3627 N93-30713
High performance computing and communications program p 3627 N93-30715
Technology transfer between the government and the aerospace industry p 3628 N93-30716
National Media Laboratory p 3628 N93-30717
Technology transfer to the broader economy
p 3628 N93-30719
A research experiment on facilitation and formation of joint research and development programs between government, industry, and universities: Overview, preliminary findings, and observations
p 3628 N93-30725
GOVERNMENTS
Trend survey on the elucidation of the global warming mechanism by the governments of major industrialized nations
[DE93-776427] p 3470 N93-29672
The 1992 World Administrative Radio Conference: Technology and Policy Implications
[OTA-TCT-549] p 3392 N93-30150
Interagency Advanced Power Group (IAPG) Meeting Compendium
[DE93-006189] p 3670 N93-30212
Profiles of major federal literacy programs
[PB93-163863] p 3608 N93-30657
GRADIENTS
Gradient estimation for regenerative processes
[AD-A263766] p 3555 N93-29878
The structure and dynamics of the vorticity and passive scalar fields at small scales in homogeneous isotropic turbulence p 3427 N93-30625
GRAIN BOUNDARIES
Environmental embrittlement of binary and Zr-doped Ni3Al
[DE93-008575] p 3321 N93-28679
The role of grain boundaries in hydrogen diffusion in metals at 25 C
[NASA-TM-108407] p 3322 N93-29043
Anelastic relaxations associated with local disordering in grain boundaries
[AD-A263101] p 3596 N93-29796
GRAIN SIZE
Processing of novel nanoparticle dispersion strengthened ceramics for improved mechanical performance
[AD-A264191] p 3339 N93-30883
Tensile creep behavior of polycrystalline alumina fibers
[NASA-TM-106269] p 3340 N93-30938
GRAMMARS
Antirational transductions and their language families
[ETN-93-93794] p 3611 N93-28525
GRAND UNIFIED THEORY
Neutrino mass
[DE93-010735] p 3566 N93-29315
Task A: Theory of elementary particles
[DE93-010561] p 3569 N93-29841
GRANULAR MATERIALS
Dense inclined flows: Theory and experiments
[DE93-011452] p 3417 N93-28630
Studies of complexity in fluid systems
[DE93-010776] p 3418 N93-28878
Direct tension experiments on compacted granular materials p 3292 N93-30960
GRAPH THEORY
Packing of Steiner trees: Polyhedric studies and application
[ETN-93-93796] p 3547 N93-28527
Resource utilization model for the algorithm to architecture mapping model
[NASA-CR-193122] p 3527 N93-29171
Neural networks: A simulation technique under uncertainty conditions p 3519 N93-29577
Polynomial space polynomial delay algorithms for listing families of graphs
[DE93-010677] p 3530 N93-29808
Placement of cells: Theory and solution of a quadratic 0/1 optimization problem
[ETN-93-94182] p 3413 N93-30616
GRAPHICAL USER INTERFACE
A new class of mission support for combat air-crew
p 3501 N93-28854
Index mappings for interactive editing of symbolic matrices
[DE93-009316] p 3549 N93-29060
RBSE: Product development team research activity deliverables
[NASA-CR-193115] p 3527 N93-29212
Graphical interface between the CIRSSE testbed and CimStation software with MCS/CTOS
[NASA-CR-193276] p 3527 N93-29218
Building a generalized distributed system model
[NASA-CR-193239] p 3527 N93-29219
Intelligent support for human computer interaction and decision-making in distribution planning and scheduling systems
[AD-A263985] p 3610 N93-30124
GRAPHITE
The design and testing of a high-temperature graphite dilatometer
[AD-A262185] p 3430 N93-28488
Hypervelocity impact survivability experiments for carbonaceous impactors p 3283 N93-29364
An investigation of graphite peek composite under compression with a centrally located circular discontinuity
[AD-A262549] p 3298 N93-29414

Apparatus for intercalating large quantities of fibrous structures
[NASA-CASE-LEW-15077-2] p 3298 N93-29609

NMR studies of molecules in liquid crystals and graphite
[DE93-010423] p 3569 N93-29805

Experiment and analysis on elastic deformation properties of graphite and carbon materials for HTTR core components
[DE93-753271] p 3299 N93-30004

Complex dielectric function of amorphous diamond films deposited by pulsed excimer (ArF) laser ablation of graphite
[AD-A264527] p 3598 N93-30408

Consolidation of graphite thermoplastic textile preforms for primary aircraft structure p 3302 N93-30439

Diamond nucleation of surfaces using carbon clusters
[AD-A264634] p 3599 N93-30548

GRAPHITE-EPOXY COMPOSITES

Static and dynamic large deflection flexural response of graphite-epoxy beams
[NASA-CR-4118] p 3454 N93-30374

Delaminations in composite plates under impact loads
p 3304 N93-30849

Mechanical and analytical screening of braided composites for transport fuselage applications
p 3305 N93-30855

Comparison of hand laid-up tape and filament wound composite cylinders and panels with and without impact damage p 3306 N93-30859

Effects of bolt-hole contact on bearing-bypass damage-onset strength p 3307 N93-30870

Experimental behavior of graphite-epoxy Y-stiffened specimens loaded in compression p 3307 N93-30872

Evaluation of some scale effects in the response and failure of composite beams p 3308 N93-30874

GRAPHS (CHARTS)

Resource utilization model for the algorithm to architecture mapping model
[NASA-CR-193122] p 3527 N93-29171

Polynomial space polynomial delay algorithms for listing families of graphs
[DE93-010677] p 3530 N93-29808

Packing odd paths
[CWI-BS-R9207] p 3549 N93-29849

Thermoforming from a systems viewpoint
p 3293 N93-30967

GRASSLANDS

The estimation and scaling of land-surface fluxes of latent and sensible heat with remotely sensed data over a grassland site p 3462 N93-30045

GRATINGS (SPECTRA)

Ruled and holographic experiment (AO 138-5)
p 3434 N93-29696

Wavelength-division multiplexed optical integrated circuit with vertical diffraction grating
[NASA-CASE-NPO-18357-1-CU] p 3579 N93-29848

GRAVITATION

An algebraic approach to the quantization of constrained systems: Finite dimensional examples
p 3548 N93-28671

Dark matter: Theoretical perspectives
[DE93-008484] p 3633 N93-28676

The physiological limitations of man in the high G environment p 3503 N93-28861

On the meaning of delta T/T
[DE93-008482] p 3653 N93-28962

Gravity sensitivity of a resistojet water vaporizer
[NASA-TM-106220] p 3288 N93-29194

Gravity referenced elevation encoder development
p 3385 N93-29592

Fourth-rank gravity and cosmology
[DE92-644722] p 3637 N93-30918

General scalar-tensor theories for induced gravity inflation
[DE93-602505] p 3479 N93-30940

Fourth-rank cosmology
[DE92-641346] p 3637 N93-30997

A non degenerate semi-classical Lagrangian for dilaton-gravity in two dimensions
[DE92-641339] p 3480 N93-31002

GRAVITATION THEORY

Fourth-rank gravity and cosmology
[DE92-644722] p 3637 N93-30918

Compensating fields and anomalies in supergravity
[DE92-644724] p 3637 N93-30919

Beltrami parametrization and gauging of Virasoro and w-infinity algebras
[DE92-644844] p 3557 N93-30928

A non degenerate semi-classical Lagrangian for dilaton-gravity in two dimensions
[DE92-641339] p 3480 N93-31002

GRAVITATIONAL COLLAPSE

Topics in General Relativity theory: Gravitational-wave measurements of black-hole parameters; gravitational collapse of a cylindrical body; and classical-particle evolution in the presence of closed, timelike curves
p 3603 N93-28690

Massive Majorana neutrinos in pre-bounce supernovae
[DE92-642597] p 3572 N93-30931

A non degenerate semi-classical Lagrangian for dilaton-gravity in two dimensions
[DE92-641339] p 3480 N93-31002

Effects of spiral shocks on disk emission lines
[DE92-641716] p 3637 N93-31004

GRAVITATIONAL EFFECTS

Low-frequency vibration environment for five Shuttle missions
[NASA-TM-106059] p 3285 N93-28554

Dense inclined flows: Theory and experiments
[DE93-011452] p 3417 N93-28630

Sodium-Sulfur Cell Technology flight experiment (SSCT) p 3264 N93-28715

Heat pipe performance experiment
p 3265 N93-28722

NASA supporting studies for microgravity research on eye movements
[NASA-CR-193233] p 3493 N93-29041

Investigation of a geodesy coexperiment to the Gravity Probe B relativity gyroscope program
[NASA-CR-193263] p 3460 N93-29179

Gravity sensitivity of a resistojet water vaporizer
[NASA-TM-106220] p 3288 N93-29194

Acquisition of physiological data during G-induced Loss of Consciousness (G-LOC)
[AD-A264492] p 3496 N93-30400

GRAVITATIONAL FIELDS

Lunar gravitational field estimation and the effects of mismodeling upon lunar satellite orbit prediction
[NASA-CR-188249] p 3634 N93-29042

Investigation of a geodesy coexperiment to the Gravity Probe B relativity gyroscope program
[NASA-CR-193263] p 3460 N93-29179

Charting the remote southern oceans with geosat altimetry
[AD-A263452] p 3461 N93-29817

On the photonic chiral anomaly in an external gravitational field
[DE93-606082] p 3479 N93-30785

Fourth-rank gravity and cosmology
[DE92-644722] p 3637 N93-30918

On the energy-momentum tensors for field theories in spaces with affine connection and metric
[DE92-644744] p 3557 N93-30927

A non degenerate semi-classical Lagrangian for dilaton-gravity in two dimensions
[DE92-641339] p 3480 N93-31002

GRAVITATIONAL LENSES

New meteoroid model predictions for directional impacts on LDEF p 3638 N93-29376

GRAVITATIONAL PHYSIOLOGY

The physiological limitations of man in the high G environment p 3503 N93-28861

Issues on human acceleration tolerance after long-duration space flights
[NASA-TM-104753] p 3495 N93-29651

GRAVITATIONAL WAVES

Topics in General Relativity theory: Gravitational-wave measurements of black-hole parameters; gravitational collapse of a cylindrical body; and classical-particle evolution in the presence of closed, timelike curves
p 3603 N93-28690

Topics in inflationary universe medels and cosmic string theories p 3637 N93-30579

GRAVITY ANOMALIES

Charting the remote southern oceans with geosat altimetry
[AD-A263452] p 3461 N93-29817

GRAVITY PROBE B

Investigation of a geodesy coexperiment to the Gravity Probe B relativity gyroscope program
[NASA-CR-193263] p 3460 N93-29179

GRAVITY WAVES

Ocean waves in SAMSON/SWADE
[AD-A263681] p 3487 N93-29295

ARI: Internal gravity waves at abrupt topography
[AD-A263795] p 3477 N93-29879

Dynamics of small-scale oceanic motions
[AD-A263582] p 3488 N93-29914

Laboratory studies of gravity wave/mean flow interactions
[AD-A264226] p 3478 N93-30174

Numerical modeling and parameterization of gravity wave processes and effects in the atmosphere
[AD-A264331] p 3478 N93-30367

Acoustic-gravity waves from low-altitude localized disturbances
[AD-A264804] p 3479 N93-30593

GRAY GAS

Radiative interactions in molecular gases under local and nonlocal thermodynamic equilibrium conditions
[NASA-CR-193223] p 3604 N93-29168

GREASES

Synthetic lubricating oil greases containing metal chelates of Schiff bases
[AD-D015694] p 3333 N93-29458

GREEN'S FUNCTIONS

Excited states in electronic structure calculations
[DE93-007704] p 3592 N93-28642

Coherent and semi-coherent neutron transfer reactions
[DE93-008336] p 3565 N93-28959

Quantum-kinetic Green function and macroscopic wave function
[DE93-606040] p 3606 N93-30796

A possibility to investigate the superconducting gap with the help of neutrons
[DE93-606392] p 3601 N93-30799

Algorithm of numerical calculations of differential Yakubovsky equations for the (1 + 3) scattering problem
[DE92-644679] p 3535 N93-30915

GREENHOUSE EFFECT

Assessment of energy technologies contributing to environmental conservation
[DE93-781439] p 3468 N93-28882

Atmospheric and Geophysical Sciences Division: G-Division did you know?
[DE93-007412] p 3469 N93-28967

Global warming potential for SF6
[DE93-007394] p 3469 N93-28972

Clouds and radiation: A primier
[AD-A263136] p 3482 N93-29479

Quantifying and minimizing uncertainty of climate forcing by anthropogenic aerosols
[NASA-TM-108259] p 3472 N93-30043

Reception at Ascension Island, South Atlantic, of the transmissions from the Heard Island feasibility test
[PB93-176261] p 3394 N93-30662

GRID GENERATION (MATHEMATICS)

Design of an essentially non-oscillatory reconstruction procedure in finite-element type meshes
[INRIA-RR-1584] p 3547 N93-28615

A grid refinement study of two-dimensional transient flow over a backward-facing step using a spectral-element method
[DE92-018262] p 3417 N93-28639

Solar flare MDH
[AD-A262275] p 3652 N93-28756

The three-dimensional Multi-Block Advanced Grid Generation System (3DMAGGS)
[NASA-TM-108985] p 3420 N93-29155

Grid Analysis and Display System (GrADS): A practical tool for earth science visualization p 3613 N93-29225

Topology and grid adaption for high-speed flow computations
[NASA-CR-4216] p 3426 N93-30375

Computational fluid dynamics research on dynamically adaptive mesh methods for transonic flows
[AD-A264833] p 3428 N93-30630

Nonlinear explicit transient finite element analysis on the Intel Delta
[DE93-009561] p 3535 N93-30647

GRINDING (MATERIAL REMOVAL)

Tool grinding and spark testing p 3291 N93-30954

GROUND BASED CONTROL

TACSAT ground control and data collection
p 3388 N93-29895

GROUND EFFECT (COMMUNICATIONS)

Ground clutter measurements for surface-sited radar
[AD-A262472] p 3379 N93-28655

GROUND OPERATIONAL SUPPORT SYSTEM

TACSAT ground control and data collection
p 3388 N93-29895

GROUND SPEED

The 1990/1991 project summaries
p 3229 N93-29725

GROUND STATE

NO2 unimolecular decomposition: Step-like variation of k(sub uni)(E) p 3318 N93-30068

The ground state wavefunctions of a conformally invariant scalar field in different spacetime background
[DE93-606063] p 3606 N93-30808

GROUND STATIONS

QuickStar: System design, capabilities, and tactical applications of a small, smart space system
p 3284 N93-29905

VLF/LF propagation measurements
p 3395 N93-30732

GROUND SUPPORT SYSTEMS

DSN support of Mars Observer p 3385 N93-29598

Lunar lander ground support system
p 3230 N93-29729

GROUND TESTS

Heat pipe performance experiment
p 3265 N93-28722

The HYDICE instrument design and its application to planetary instruments p 3434 N93-28766

TACSAT ground control and data collection
p 3388 N93-29895

GROUND TRUTH

Geographic information system for fusion and analysis of high-resolution remote sensing and ground truth data
p 3614 N93-29234

GROUND WATER

Tank issues: Design and placement of floating liquid monitoring wells
[PB93-161149] p 3469 N93-29033

Tank issues: Site characterization for external leak monitoring
[PB93-161156] p 3469 N93-29034

Annual report on monitoring of the unsaturated zone and recharge areas at INEL to the state of Idaho INLEL oversight committee
[DE93-012947] p 3473 N93-30187

Performance and cost evaluation of bioremediation techniques for fuel spills
[PB93-175545] p 3474 N93-30762

Contamination of soil, soil gas, and ground water by hydrocarbon compounds near Greear, Morgan County, Kentucky
[PB93-182244] p 3474 N93-30825

Hydrogeology and ground-water-quality conditions at the Reno County Landfill, South-Central Kansas, 1990-1991
[PB93-183085] p 3474 N93-30826

GROUND WAVE PROPAGATION

Portable fiber optic coupled Doppler interferometer system for detonation and shock wave diagnostics
[DE93-009827] p 3433 N93-30510

GROUND-AIR-GROUND COMMUNICATION

Enhancing availability, performance, and flexibility of air traffic control air-ground services p 3247 N93-30353

GROUP THEORY

Lie groups whose set of compact subgroups is inductive
[ETN-93-93791] p 3547 N93-28524

Differential calculus on quantum spaces and quantum groups
[DE93-010425] p 3551 N93-30392

Integrals of motion on the group of invariance of an interval in three-dimensional spaces
[DE93-606090] p 3606 N93-30797

On one-dimensional topological and conformal field theories
[DE92-644726] p 3558 N93-30986

GUIDANCE SENSORS

An auto-guiding system for mid-sized telescopes
p 3375 N93-30340

GUIDE VANES

Heat transfer and aerodynamics of a 3D design nozzle guide vane tested in the Pyestock Isentropic Light Piston Facility p 3252 N93-29928

Thermal effects of a coolant film along the suction side of a high pressure turbine nozzle guide vane
p 3253 N93-29930

Aero-thermal design of a cooled transonic NGV and comparison with experimental results
p 3257 N93-29957

Coupling of 3D-Navier-Stokes external flow calculations and internal 3D-heat conduction calculations for cooled turbine blades p 3258 N93-29961

GULF OF CALIFORNIA (MEXICO)

Analyses of data from fine structure and circulation studies in the Gulf of California
[AD-A262910] p 3486 N93-28885

GULF OF MEXICO

Remote sensing survey of Mississippi River-Gulf Outlet, Breton Sound disposal area, Plaquemines Parish, Louisiana
[AD-A263097] p 3459 N93-29146

GYROSCOPES

Gyroscope with excess noise subtraction
[AD-D015698] p 3431 N93-29046

Investigation of a geodesy coexperiment to the Gravity Probe B relativity gyroscope program
[NASA-CR-193263] p 3460 N93-29179

Improved design concepts for millimeter wave power sources
[AD-A264060] p 3411 N93-29922

GYROSCOPIC STABILITY

Stability, bifurcation, and control of Hamiltonian systems
[DE93-012103] p 3547 N93-28648

GYROSTABILIZERS

Stability, bifurcation, and control of Hamiltonian systems
[DE93-012103] p 3547 N93-28648

H

H-INFINITY CONTROL

Robust control via H-infinity optimization
p 3354 N93-30216

HADRONS

Maximizing the luminosity of hadron, supercolliders at 10-100 TeV
[DE93-009247] p 3574 N93-29103

Polarization experiments with hadronic and electromagnetic probes
[DE93-011375] p 3392 N93-30126

Multidimensional intermittency in hadronic collisions
[DE93-010562] p 3577 N93-30532

Single t-quark production in high energy (gamma)e collisions
[DE92-644947] p 3572 N93-30930

HALIDES

A simple model for ion solvation with non additive cores
[AD-A263075] p 3566 N93-29143

Study of codeposition of aluminum-haffnium and deposition of yttrium by the cementation technique: Elaboration of Ni-Cr-Al and Ni-Cr-Al-Hf felt materials
[ONERA-NT-1990-9] p 3336 N93-30112

HALL EFFECT

The fluctuation induced Hall effect
[DE93-010130] p 3585 N93-28912

Uniaxially stressed Ge:Ga and Ge:Be
[DE93-010426] p 3594 N93-29150

NATO Advanced Research Workshop on Frontiers of Optical Phenomena in Semiconductor Structure of Reduced Dimension
[AD-A264813] p 3581 N93-30666

Regular and chaotic motion of two dimensional electrons in a strong magnetic field
[DE93-604091] p 3607 N93-30933

HAMILTONIAN FUNCTIONS

Self-consistent chaos in the beam-plasma instability
[DE93-009581] p 3584 N93-28599

Stability, bifurcation, and control of Hamiltonian systems
[DE93-012103] p 3547 N93-28648

A normally elliptic Hamiltonian bifurcation
[W-9201] p 3548 N93-28753

Balanced approximation can be optimal
[OUEL-1950/92] p 3548 N93-28754

Coherent and semi-coherent neutron transfer reactions
[DE93-008336] p 3565 N93-28959

Flux lattice relaxation, noise, and symmetry-breaking in frustrated Josephson junction arrays
[DE93-008713] p 3593 N93-29094

Hamiltonian dynamics of coupled potential vorticity and internal wave motion: 1. Linear modes
[AD-A263469] p 3424 N93-29838

Extracting infinite system properties from finite size clusters: Phase randomization/boundary condition averaging
[AD-A264712] p 3551 N93-30503

Orbital motion calculation using Lie method in collider nonlinear magnetic field
[DE93-605733] p 3571 N93-30800

HANDBOOKS

The program manager's notebook
[AD-A263074] p 3609 N93-29142

LDEF space optics handbook p 3582 N93-29695

Handbook of frequently used acronyms and glossary of terms
[DE93-011388] p 3616 N93-30123

DOE fundamentals handbook: Chemistry
[DE93-012222] p 3314 N93-30198

DOE fundamentals handbook: Material science
[DE93-012224] p 3314 N93-30199

DOE fundamentals handbook: Material science
[DE93-012225] p 3314 N93-30200

Medical aspects of cold weather operations: A handbook for medical officers
[AD-A263559] p 3496 N93-30588

Air weather service master station catalog USAFETAC climatic database users handbook no. 6
[AD-A264761] p 3484 N93-30608

HANDEDNESS

Handedness and motor programming effects of manual control and movement
[AD-A264022] p 3499 N93-30027

HANDLING EQUIPMENT

New remote maintenance approach for TPX
[DE93-007857] p 3584 N93-28583

Leaky coaxial cable signal transmission for remote facilities
[DE93-007916] p 3383 N93-29348

Application of sensors to the control of robotic systems
[DE93-009837] p 3543 N93-30012

HANDWRITING

Comparison of crisp and fuzzy character networks in handwritten word recognition p 3514 N93-29545

HANKEL FUNCTIONS

Balanced approximation can be optimal
[OUEL-1950/92] p 3548 N93-28754

HARDNESS

Tailored interfaces for metal-matrix composites-fundamental considerations
[AD-A263048] p 3298 N93-29130

Effects of atomic oxygen and ultraviolet radiation on candidate elastomeric materials for long duration missions. Test series no.1
[NASA-TM-108408] p 3331 N93-29193

Damage mechanics in 2-D and 3-D microstructures
[AD-A264337] p 3453 N93-30159

HARDNESS TESTS

Application of hardness testing in foundry processing operations: A university and industry partnership
p 3292 N93-30961

HARMONIC GENERATIONS

Polar order and relaxation of second order nonlinear optical susceptibility in an electric field polarized amorphous polymer
[AD-A262189] p 3329 N93-28489

Dipolar orientational relaxation in guest/host amorphous polymer probed by second harmonic generation
[AD-A262006] p 3333 N93-29441

Isothermal annealing and relaxation of the second harmonic generation signal from a nonlinear optical polymer
[AD-A262007] p 3333 N93-29442

Improved design concepts for millimeter wave power sources
[AD-A264060] p 3411 N93-29922

Design of acentric materials: X ray structures of guanidinium p-nitro- and p-hydroxybenzenesulfonate
[AD-A264220] p 3597 N93-30146

Applications of the photorefractive effect and damage induced effects in fibers
[AD-A264339] p 3580 N93-30205

HARMONIC OSCILLATION

Bifurcations phenomena in a nonlinear oscillator: Approximate analytical studies versus computer simulation results p 3407 N93-29037

HARMONICS

The use of DFT windows in signal-to-noise ratio and harmonic distortion computations
[DE93-009800] p 3433 N93-30655

The distribution of the annual and semiannual cycles in the tropics
[DE92-642213] p 3485 N93-31006

HARTREE APPROXIMATION

Dynamics and photoexcitation in MX and MXX' chain solids
[AD-A264823] p 3561 N93-29711

HAWAII

Tidal and lunar data for Point Mugu, San Nicolas island, and the Barking Sanda area during 1993
[AD-A262725] p 3477 N93-29401

Deadliest, costliest, and most intense US hurricanes of this century (and other frequently requested hurricane facts)
[PB93-174993] p 3485 N93-30758

HAZARDS

Super critical water oxidation on energetic materials
[DE93-010704] p 3342 N93-29312

Sound attenuation characteristics of the standard DH-132A and SPH-4 helmets worn in combination with standard issue earplugs
[AD-A263011] p 3506 N93-29406

Microstructural modeling of electrical breakdown in solid fuel propellants
[AD-A263466] p 3342 N93-29835

DOE fundamentals handbook: Chemistry
[DE93-012222] p 3314 N93-30198

HAZE

Uplink laser propagation measurements through the sea surface, haze and clouds
[AD-A264687] p 3440 N93-30553

HEAD (ANATOMY)

Methods for characterizing the human head for the design of helmets
[AD-A263875] p 3507 N93-29889

HEAD MOVEMENT

Effects of area-of-interest display characteristics of visual search performance and head movements in simulated low-level flight
[AD-A264661] p 3499 N93-30542

HEAD-UP DISPLAYS

Oculo-motor responses and virtual image displays
p 3503 N93-28862

Utility of a ghost horizon and climb/dive ladder line tapering on a head-up display
[AD-A264401] p 3508 N93-30167

HEARING
Programmable interactive system for cochlear implant electrode stimulation [AD-A262558] p 3494 N93-29421
HEAT AFFECTED ZONE
A review of hot cracking in austenitic stainless steel weldments [DE93-605280] p 3328 N93-31021
HEAT BALANCE
Influence of the Cold Buster (tm) sports bar on heat debt, mobilization and oxidation of energy substrates [AD-A262762] p 3493 N93-28939
HEAT ENGINES
Process optimization of Hexoloy SX-SiC towards improved mechanical properties [DE93-007913] p 3320 N93-28564
Theoretical and experimental study of thermoacoustic engines [AD-A261934] p 3561 N93-28995
Investigation of thermoacoustic muffler [AD-A262009] p 3562 N93-29392
The drive to cost-effective structural ceramics [DE93-009722] p 3335 N93-30047
HEAT EXCHANGERS
Preliminary endurance tests of water vaporizers for resistojet applications [NASA-TM-106222] p 3287 N93-28694
In-STEP Two-Phase Flow (TPF) thermal control experiment p 3265 N93-28719
Pulse mitigation and heat transfer enhancement techniques. Volume 3: Liquid sodium heat transfer facility and transient response of sodium heat pipe to pulse forward and reverse heat load [AD-A263496] p 3422 N93-29338
Investigation of thermoacoustic muffler [AD-A262009] p 3562 N93-29392
Direct use geothermal applications for brazed plate heat exchangers [DE93-008559] p 3465 N93-30011
Materials studies for preventing corrosion in condensing environments [PB93-185478] p 3327 N93-30815
HEAT FLUX
Small hydrogen/oxygen rocket flowfield behavior from heat flux measurements [NASA-TM-106233] p 3286 N93-28619
Radiative interactions in molecular gases under local and nonlocal thermodynamic equilibrium conditions [NASA-CR-193223] p 3604 N93-29168
Pulse mitigation and heat transfer enhancement techniques. Volume 1: Spray cooling [AD-A263495] p 3423 N93-29352
A generalized approach to the thermal analysis of the Long Duration Exposure Facility's flight experiments p 3428 N93-29624
Surface shear stress estimates from geostrophic winds for use in sensible and latent heat flux formulations p 3483 N93-30044
The estimation and scaling of land-surface fluxes of latent and sensible heat with remotely sensed data over a grassland site p 3462 N93-30045
Pulse mitigation and heat transfer enhancement techniques. Volume 2: Effect of surface wettability and roughness in evaporative spray cooling [AD-A264174] p 3425 N93-30155
On the ideality of using a step-function current in a metallic foil to simulate a step-function heat-flux source [AD-A264627] p 3413 N93-30539
Optimization for steady-state and hybrid operations of ITER by using scaling models of divertor heat load [DE93-764151] p 3590 N93-30649
HEAT GENERATION
Heat generation produced in thin layers of GaAs superconductors under high energy particles irradiation [DE93-606332] p 3601 N93-30798
HEAT MEASUREMENT
The swollen polymer technique and its use for heat transfer investigations on film cooled surfaces p 3255 N93-29944
Analytical and experimental study of laminar free convective heat transfer from isothermal convex bodies of arbitrary shape [ISBN-0-315-72512-5] p 3426 N93-30379
HEAT OF FORMATION
Laser spectroscopy of hydrocarbon radicals [DE93-012555] p 3436 N93-28653
HEAT PIPES
Cryogenic Heat Pipe Experiment (CRYOHP) p 3265 N93-28721
Heat pipe performance experiment p 3265 N93-28722
Technology transfer personnel exchange at the Boeing Company [DE93-010190] p 3625 N93-29329
Pulse mitigation and heat transfer enhancement techniques. Volume 3: Liquid sodium heat transfer facility and transient response of sodium heat pipe to pulse forward and reverse heat load [AD-A263496] p 3422 N93-29338
Pulse mitigation and heat transfer enhancement techniques. Volume 4: Transient behavior of heat pipe with thermal energy storage under pulse heat loads [AD-A263497] p 3423 N93-29339
Long Duration Exposure Facility (LDEF) low temperature Heat Pipe Experiment Package (HEPP) flight results p 3429 N93-29701
Thermion: Verification of a thermionic heat pipe in microgravity p 3235 N93-29757
Improved heat removal by microscopic surface texturing of capillaries [AD-A263483] p 3424 N93-29966
Pulse mitigation and heat transfer enhancement techniques. Volume 5: Transient liquid movement in heat pipe wicks [AD-A264513] p 3426 N93-30403
HEAT PUMPS
Investigation of thermoacoustic muffler [AD-A262009] p 3562 N93-29392
Complex-compound heat pump: Topical report on phase 1 results [PB93-185460] p 3466 N93-30814
HEAT RESISTANT ALLOYS
Fundamental aspects in the design of passive alloys [DE93-009028] p 3320 N93-28545
Planning of a West Virginia University Research Center in the basic materials sciences [DE93-011731] p 3592 N93-28647
High temperature creep and oxidation resistant chromium silicide matrix alloy containing molybdenum [NASA-CASE-LEW-15697-1] p 3323 N93-29172
Platinum-modified diffusion aluminide coatings on nickel-base superalloys [AD-A263597] p 3325 N93-29981
Examination of formability to seamless tubes on Ni-Cr-W superalloy [DE93-764158] p 3326 N93-30396
Development of Ni-Cr-W superalloys for high temperature components in high temperature gas-cooled reactors, part 2 [DE93-764469] p 3326 N93-30399
Oxidation and hot corrosion of superalloys Rene 100 and X-40 at temperatures of 1475 F to 2000 F [AD-A263747] p 3327 N93-30812
HEAT SINKS
The microchannel heatsink with liquid nitrogen cooling [DE93-009258] p 3422 N93-29300
Semiconductor cooling apparatus [NASA-CASE-LEW-14162-3] p 3299 N93-29614
Performance of thermal adhesives in forced convection p 3293 N93-30974
HEAT STORAGE
Thermal energy storage flight experiment in microgravity p 3265 N93-28720
Pulse mitigation and heat transfer enhancement techniques. Volume 4: Transient behavior of heat pipe with thermal energy storage under pulse heat loads [AD-A263497] p 3423 N93-29339
HEAT TOLERANCE
Evaluation of personal cooling systems in conjunction with explosive ordnance disposal suits [AD-A262862] p 3506 N93-29471
HEAT TRANSFER
Analysis of electrothermal interactions in power semiconductor modules [ETN-93-93800] p 3591 N93-28470
Small hydrogen/oxygen rocket flowfield behavior from heat flux measurements [NASA-TM-106233] p 3286 N93-28619
Theoretical and experimental study of thermoacoustic engines [AD-A261934] p 3561 N93-28995
Flow phenomena in turbomachines [AD-A263049] p 3420 N93-29141
High Reynolds number and turbulence effects on aerodynamics and heat transfer in a turbine cascade [NASA-TM-106187] p 3420 N93-29157
A manipulator kinematic design for high-vacuum operation [DE93-010264] p 3444 N93-29247
Transient response of embedded thermocouples [DE93-009889] p 3431 N93-29325
Technology transfer personnel exchange at the Boeing Company [DE93-010190] p 3625 N93-29329
Pulse mitigation and heat transfer enhancement techniques. Volume 3: Liquid sodium heat transfer facility and transient response of sodium heat pipe to pulse forward and reverse heat load [AD-A263496] p 3422 N93-29338
Pulse mitigation and heat transfer enhancement techniques. Volume 4: Transient behavior of heat pipe with thermal energy storage under pulse heat loads [AD-A263497] p 3423 N93-29339
Pulse mitigation and heat transfer enhancement techniques. Volume 1: Spray cooling [AD-A263495] p 3423 N93-29352
Investigation of thermoacoustic muffler [AD-A262009] p 3562 N93-29392
Two-dimensional model for current and heat transport in solid-armature railguns [AD-A262014] p 3271 N93-29394
Semiconductor cooling apparatus [NASA-CASE-LEW-14162-3] p 3299 N93-29614
Heat Transfer and Cooling in Gas Turbines [AGARD-CP-527] p 3252 N93-29926
Heat transfer and aerodynamics of a 3D design nozzle guide vane tested in the Pyestock Isentropic Light Piston Facility p 3252 N93-29928
Experimental study of heat transfer close to a plane wall heated in the presence of multiple injections (subsonic flow) p 3253 N93-29931
The influence of non-uniform spanwise inlet temperature on turbine rotor heat transfer p 3253 N93-29932
Determination of surface heat transfer and film cooling effectiveness in unsteady wake flow conditions p 3253 N93-29933
Measurement of turbulent spots and intermittency modelling at gas-turbine conditions p 3253 N93-29934
Heat transfer in high turbulence flows: A 2-D planar wall jet p 3254 N93-29935
Heat transfer with moderate free stream turbulence p 3254 N93-29936
Cooling geometry optimization using liquid crystal technique p 3254 N93-29939
Fundamental studies of impingement cooling thermal boundary conditions p 3254 N93-29940
Prediction of jet impingement cooling scheme characteristics (airfoil leading edge application) p 3255 N93-29941
An L2F-measurement device with image rotator prism for flow velocity analysis in rotating coolant channels p 3255 N93-29942
Local heat transfer measurement with liquid crystals on rotating surfaces including non-axisymmetric cases p 3255 N93-29943
The swollen polymer technique and its use for heat transfer investigations on film cooled surfaces p 3255 N93-29944
Transient thermal behaviour of a compressor rotor with axial cooling air flow and co-rotating or contra-rotating shaft p 3255 N93-29946
Flow and heat transfer between gas-turbine discs p 3256 N93-29950
Heat transfer and leakage in high-speed rotating stepped labyrinth seals p 3256 N93-29951
Fluid flow and heat transfer in the entrance region of an annulus between independently rotating tubes with a turbulent axial flow p 3256 N93-29952
Impingement/effusion cooling p 3257 N93-29954
Coupling of 3D-Navier-Stokes external flow calculations and internal 3D-heat conduction calculations for cooled turbine blades p 3258 N93-29961
Navier-Stokes analysis of three-dimensional flow and heat transfer inside turbine blade rows p 3259 N93-29963
Improved heat removal by microscopic surface texturing of capillaries [AD-A263483] p 3424 N93-29966
Direct use geothermal applications for brazed plate heat exchangers [DE93-008559] p 3465 N93-30011
Analysis of thermal bar using boundary-layer integral equations gradients [MATHS-REPT-A-177] p 3462 N93-30107
Pulse mitigation and heat transfer enhancement techniques. Volume 2: Effect of surface wettability and roughness in evaporative spray cooling [AD-A264174] p 3425 N93-30155
Pulse mitigation and heat transfer enhancement techniques. Volume 5: Transient liquid movement in heat pipe wicks [AD-A264513] p 3426 N93-30403
Quantum group and symmetry of the heat equation [DE93-607560] p 3605 N93-30779
Horizontal nucleate flow boiling heat transfer coefficient measurements and visual observations for R12, R134a, and R134a/ester lubricant mixtures [PB93-178598] p 3475 N93-30887
HEAT TRANSFER COEFFICIENTS
Thermal effects of a coolant film along the suction side of a high pressure turbine nozzle guide vane p 3253 N93-29930
Cooling geometry optimization using liquid crystal technique p 3254 N93-29939

Prediction of jet impingement cooling scheme characteristics (airfoil leading edge application)
p 3255 N93-29941
The swollen polymer technique and its use for heat transfer investigations on film cooled surfaces
p 3255 N93-29944
Horizontal nucleate flow boiling heat transfer coefficient measurements and visual observations for R12, R134a, and R134a/ester lubricant mixtures
[PB93-178598] p 3475 N93-30887

HEAT TRANSMISSION
Preliminary investigation of high power microwave plasmas for electrothermal thruster use
[NASA-TM-106207] p 3288 N93-29158
Investigation of thermoacoustic muffler
[AD-A262009] p 3562 N93-29392

HEAT TREATMENT
Oxidation behavior in reaction-bonded aluminum-silicon alloy/alumina powder compacts
[DE93-010407] p 3298 N93-29191
Effect of lead addition on the formation of superconducting phases in Bi-Sr-Ca-Cu-O ceramics
[DE93-606893] p 3339 N93-30773
Thermoforming from a systems viewpoint
p 3293 N93-30967

HEATERS
Heating head for induction heating apparatus
[NASA-CASE-LAR-14429-1] p 3407 N93-29173
Performance of thermal adhesives in forced convection p 3293 N93-30974

HEATING
Errors when shock waves interact due to numerical shock width
[DE93-010699] p 3426 N93-30484

HEAVING
Mathematical model of frost heave and thaw settlement in pavements
[CRREL-REPT-93-2] p 3262 N93-30103

HEAVY IONS
Measurements of rare composite objects and high sensitivity searches for novel forms of matter produced in high energy heavy ion collisions
[DE93-009945] p 3574 N93-28569
Studies of relativistic heavy ion collisions at the AGS (E814/E877)
[DE93-008541] p 3564 N93-28678
Design and test of a superconducting RFQ for heavy ions
[DE93-010862] p 3575 N93-29317
Heavy ion measurement on LDEF
p 3573 N93-29644
Progress report on the Heavy Ions in Space (HIIS) experiment p 3573 N93-29645
Reaction mechanism studies of heavy ion induced nuclear reactions
[DE93-010496] p 3569 N93-29807
Research and education by SF cyclotron facility
[DE93-753135] p 3576 N93-30002
Studies of fluctuation processes in nuclear collisions
[DE93-011263] p 3576 N93-30054
Pulse control in an accelerator for heavy-ion fusion
[DE93-009527] p 3576 N93-30390

HEAVY LIFT LAUNCH VEHICLES
Spacely's rockets: Personnel launch system/family of heavy lift launch vehicles p 3234 N93-29752

HEAVY NUCLEI
Status of LDEF ionizing radiation measurements and analysis p 3654 N93-29626
Progress report on the ultra heavy cosmic ray experiment (AO178) p 3654 N93-29646

HELICOPTERS
Flight evaluation of a computer aided low-altitude helicopter flight guidance system p 3260 N93-28869
Helicopter approach capability using the differential global positioning system
[NASA-CR-193183] p 3245 N93-28936
A passive infrared ice detection technique for helicopter applications
[NASA-CR-193187] p 3244 N93-29152
Aerodynamic characteristics of a rotorcraft airfoil designed for the tip region of a main rotor blade
[NASA-TM-4264] p 3240 N93-29450
External acoustical noise measurements for aviation systems
[AD-A263138] p 3562 N93-29480
Models for performance assessment of HF antennas on the CH-135/Twin Huey helicopter
p 3366 N93-30291
NASA/FAA helicopter simulator workshop
[NASA-CP-3156] p 3236 N93-30673
Part 1: Executive summary p 3236 N93-30674
Helicopter simulator standards p 3236 N93-30675
Helicopter simulation: An aircrew training and qualification perspective p 3236 N93-30676
Training effectiveness assessment: Where are we?
p 3236 N93-30679
Current training: Where are we? p 3236 N93-30680
Helicopter simulator qualification
p 3237 N93-30681
Helicopter simulation: Making it work
p 3237 N93-30682
Helicopter training simulators: Key market factors
p 3237 N93-30683
Training effectiveness assessment: Methodological problems and issues p 3237 N93-30684
Progress through precedent: Going where no helicopter simulator has gone before p 3237 N93-30686
Transfer of training and simulator qualification or myth and folklore in helicopter simulation
p 3237 N93-30687
Validation and upgrading of physically based mathematical models p 3237 N93-30688
Frequency-response techniques for documentation and improvement of rotorcraft simulators
p 3237 N93-30689
Bandwidth and SIMDUCE as simulator fidelity criteria
p 3238 N93-30690
Methodology development for evaluation of selective-fidelity rotorcraft simulation
p 3238 N93-30691
Strong parallel blade-vortex interaction and noise propagation in helicopter flight p 3563 N93-30980
Advanced electromagnetic methods for aerospace vehicles
[NASA-CR-193468] p 3400 N93-31036

HELIOSEISMOLOGY
XRONOS: A timing analysis software package. User's guide, version 3.00
[NASA-TM-109222] p 3532 N93-30023

HELIOSTATS
Thermal effects testing at the National Solar Thermal Test Facility
[DE93-009825] p 3465 N93-30391
Optical system analysis for the ground based EXVM
[NASA-CR-192588] p 3582 N93-31035

HELIUM
Polarization dependence of the ionization of helium and neon by 120 femtosecond pulses at 614 nm
[DE93-010514] p 3564 N93-28762
Spin dependent phenomena in medium energy physics
[DE93-010972] p 3565 N93-28849

HELIUM ISOTOPES
Effects of internal helium on mechanical properties of Nitronic (tm) 40 stainless steel
[DE93-009902] p 3324 N93-29265
Reaction and reorientation of electronically excited H2(B)
[DE93-010435] p 3569 N93-29860

HELIUM-NEON LASERS
Measurement of a Michelson interferometer mirror velocity with a time interval analyzer
[AD-A263009] p 3430 N93-28659
Experimental test of hole-coupled FEL resonator designs using a CW-HeNe laser
[DE93-010439] p 3440 N93-30530

HELMET MOUNTED DISPLAYS
Low-cost helmet-mounted displays
[AD-A262616] p 3501 N93-28479
Head-steered sensor flight test results and implications p 3502 N93-28859
The quest for an integrated flying helmet
p 3502 N93-28860
Oculo-motor responses and virtual image displays
p 3503 N93-28862
Head mounted displays for virtual reality
[AD-A263498] p 3506 N93-29340

HELMETS
The quest for an integrated flying helmet
p 3502 N93-28860
Sound attenuation characteristics of the standard DH-132A and SPH-4 helmets worn in combination with standard issue earplugs
[AD-A263011] p 3506 N93-29406
Helmet visor support apparatus
[AD-D015684] p 3507 N93-29606
Methods for characterizing the human head for the design of helmets
[AD-A263875] p 3507 N93-29889

HEMODYNAMICS
Acquisition of physiological data during G-induced Loss of Consciousness (G-LOC)
[AD-A264492] p 3496 N93-30400

HEPTANES
NMR studies of molecules in liquid crystals and graphite
[DE93-010423] p 3569 N93-29805

HERMITIAN POLYNOMIAL
A diffusion approximation for a network of reservoirs with power law release rule
[AD-A263753] p 3550 N93-29872

HETEROCYCLIC COMPOUNDS
Thermodynamic properties for polycyclic systems by non-calorimetric methods
[DE93-011373] p 3603 N93-28747

HETERODYNING
Development of a 9.3 micrometer CW LIDAR for the study of atmospheric aerosol
[NASA-CR-193227] p 3381 N93-29105
Design of a high resolution spatial heterodyne interferometer
[AD-A262867] p 3285 N93-29461

HETEROGENEITY
Possibilistic measurement and set statistics
p 3517 N93-29567
Applications of transition metal compounds in the preparation of useful silicon-containing ceramics
[AD-A264028] p 3335 N93-30028
Organometallic and surface chemistry of mixed-metal systems
[DE93-012686] p 3325 N93-30059

HETEROJUNCTIONS
Photoinduced charge separation in Q1D heterojunction materials: Evidence for electron-hole pair separation in mixed-halide MX solids
[AD-A264711] p 3598 N93-30501
Photoinduced electron-hole charge separation, intrinsic self-doping and novel device applications of Q1D heterojunction materials: Mixed-halide MX solids
[AD-A264714] p 3600 N93-30569
Effect of planar magnetic field on electron transport properties of n-AlGaAs/GaAs heterojunction and photoluminescence measures in GaAs samples
[DE93-608739] p 3601 N93-30776

HEURISTIC METHODS
Inverse problems: Fuzzy representation of uncertainty generates a regularization p 3516 N93-29563
Planning collision free paths for two cooperating robots using a divide-and-conquer C-space traversal heuristic
[NASA-CR-193252] p 3542 N93-29771
Evolving neural network architecture
[AD-A264802] p 3544 N93-30592

HEXANITROSTILBENE
Thermal decomposition chemistry and shock sensitivity of thermally aged explosives p 3344 N93-30069

HIERARCHIES
The meta model hierarchy: A framework for information systems concepts and techniques
[TR-92-17] p 3611 N93-28481
Fuzzy coordinator in control problems
p 3515 N93-29552
Hierarchical model of matching p 3519 N93-29580
AHP version 5.1 user's manual
[DE93-007050] p 3532 N93-30034

HIGH ALTITUDE
Beta-adrenergic blockade and lactate metabolism during exercise at high altitude
[AD-A263544] p 3495 N93-29820

HIGH ALTITUDE ENVIRONMENTS
The Environmental Symptoms Questionnaire (ESQ): Development and application
[AD-A264127] p 3495 N93-30196

HIGH CURRENT
High-current negative-ion beam transport
[DE93-010732] p 3575 N93-29809

HIGH ELECTRON MOBILITY TRANSISTORS
Development of Si(1-x)Ge(x) technology for microwave sensing applications
[NASA-TM-106157] p 3405 N93-28610
Wide-bandwidth high-resolution search for extraterrestrial intelligence
[NASA-CR-193137] p 3509 N93-28895

HIGH ENERGY ELECTRONS
Electron interactions with non-linear polyatomic molecules and their radicals and ions
[AD-A262279] p 3568 N93-29446
Electron transport calculations between 1 MeV and 1 eV
[AD-A263412] p 3568 N93-29787
Hard photon emission from high energy electrons and positrons in single crystals
[DE93-606328] p 3600 N93-30770

HIGH ENERGY FUELS
Nuclear isomers as ultra-high-energy-density materials
[DE93-009520] p 3568 N93-29784

HIGH ENERGY INTERACTIONS
Studies in theoretical high energy particle physics
[DE93-007990] p 3574 N93-28565
Research programs from the University of South Carolina on high energy physics
[DE93-007829] p 3574 N93-28969
Maximizing the luminosity of hadron, supercolliders at 10-100 TeV
[DE93-009247] p 3574 N93-29103
Elementary particle interactions
[DE93-005113] p 3568 N93-29764

Study of heavy-flavored particles [DE93-011535] p 3569 N93-30128

Requirements for a system to analyze HEP events using database computing [DE93-009960] p 3576 N93-30527

HIGH FIELD MAGNETS

Microstructural understanding and critical current optimization of advanced high field superconductors [DE93-011046] p 3592 N93-28643

HIGH LEVEL LANGUAGES

Applying high-level language paradigms to communications software for distributed systems [AD-A263001] p 3528 N93-29463

A C++ interface for programming on the Connection Machine [INRIA-RR-1698] p 3538 N93-29487

Implementation of parallel algorithms [AD-A263126] p 3529 N93-29496

NESL: A nested data-parallel language (Version 2.6) [AD-A263548] p 3530 N93-29822

HIGH POWER LASERS

All solid-state high power visible laser [NASA-CR-193163] p 3436 N93-28623

Start broadened profiles with self-consistent radiation transfer and atomic kinetics in plasmas produced by high intensity lasers [DE93-008706] p 3586 N93-29093

Fusion laser oscillator and pulse-forming system using integrated optics [DE93-009286] p 3588 N93-29780

Magnetic field measurements of the CEBAF (NIST) wiggler using the pulsed wire method [AD-A263997] p 3439 N93-29867

HIGH PRESSURE

High pressure preignition chemistry of hydrocarbons and hydrocarbon mixtures [AD-A263611] p 3311 N93-29283

Heat transfer and aerodynamics of a 3D design nozzle guide vane tested in the Pyestock Isentropic Light Piston Facility p 3252 N93-29928

Sensitive detection of new superconductors created at ultra high pressures [AD-A264340] p 3597 N93-30161

Hydrogen-rated system for in vitro studies at pressure: Operating procedures and emergency procedures [AD-A264179] p 3497 N93-30882

HIGH PRESSURE OXYGEN

Orbital transfer vehicle oxygen turbopump technology. Volume 3: Hot oxygen testing [NASA-CR-191036] p 3448 N93-31039

HIGH RESOLUTION

Ultra-high resolution water window x ray microscope optics design and analysis [NASA-CR-193225] p 3578 N93-29128

Geographic information system for fusion and analysis of high-resolution remote sensing and ground truth data p 3614 N93-29234

Design of a high resolution spatial heterodyne interferometer [AD-A262867] p 3285 N93-29461

High resolution free-electron laser spectroscopy [AD-A263734] p 3439 N93-29853

HIGH REYNOLDS NUMBER

The development of a mixing layer under the action of weak streamwise vortices [NASA-TM-106089] p 3418 N93-28947

High Reynolds number and turbulence effects on aerodynamics and heat transfer in a turbine cascade [NASA-TM-106187] p 3420 N93-29157

High-Reynolds-number test of a 5-percent-thick low-aspect-ratio semispan wing in the Langley 0.3-meter transonic cryogenic tunnel: Wing pressure distributions [NASA-TM-4227] p 3240 N93-29449

Vortex shedding by blunt/bluff bodies at high Reynolds numbers. Volume 4: Rectangles [AD-A264154] p 3241 N93-30151

Vortex shedding by blunt/bluff bodies at high reynolds numbers. Volume 1: Data analysis [AD-A264151] p 3241 N93-30171

Vortex shedding by Blunt/Bluff bodies at high reynolds numbers. Volume 2: Cylinders, octagon, hexagon [AD-A264152] p 3241 N93-30172

Vortex shedding by blunt/bluff bodies at high reynolds numbers. Volume 3. Cubes [AD-A264153] p 3242 N93-30173

Compressible turbulence in a high-speed high Reynolds number mixing layer p 3242 N93-30583

HIGH SPEED

Flash x ray system: Techniques and applications [DE93-011477] p 3430 N93-28645

The development of a parachute system for aerial delivery from high speed cargo aircraft [DE93-008339] p 3239 N93-29035

Weakly nonlinear dynamics of near-CJ detonation waves [DE93-007344] p 3424 N93-29836

The HSCT mission analysis of waverider designs [NASA-CR-193467] p 3243 N93-31037

HIGH SPEED PHOTOGRAPHY

High-voltage pulse generator capable of 2000 J at 10 kV [AD-A262034] p 3407 N93-28999

Debris/ice/TPS assessment and integrated photographic analysis for Shuttle Mission STS-55 [NASA-TM-107559] p 3271 N93-29136

HIGH STRENGTH

Lightweight flexible composite tent materials [AD-A263021] p 3295 N93-28660

HIGH STRENGTH ALLOYS

Fundamental aspects in the design of passive alloys [DE93-009028] p 3320 N93-28545

Mechanisms of fracture and creep of structural alloys [AD-A263108] p 3324 N93-29799

HIGH STRENGTH STEELS

Transformation plasticity in ductile solids [DE93-008636] p 3321 N93-28902

Bainitic stabilization of austenite in low alloy steels [DE93-008275] p 3321 N93-28957

The growth of small corrosion fatigue cracks in alloy 2024 [NASA-TM-107755] p 3451 N93-29069

HIGH TEMPERATURE

Mechanics of elevated temperature fatigue damage in fiber-reinforced ceramics [AD-A262403] p 3329 N93-28495

Healing of lithographically introduced flaws in glass and glass containing ceramics [DE93-010453] p 3330 N93-28761

A DTA/GC for the in situ identification of the Martian surface material p 3646 N93-28800

Program for an improved hypersonic temperature-sensing probe [NASA-CR-186025] p 3431 N93-29066

High temperature creep and oxidation resistant chromium silicide matrix alloy containing molybdenum [NASA-CASE-LEW-15697-1] p 3323 N93-29172

Novel polymer compositions for high-temperature membrane applications, phase 1 [PB93-174126] p 3331 N93-29201

Aluminium-high strength material by mechanical alloying and reaction milling: Basics of processing and characterisation of material [ESA-TT-1249] p 3324 N93-29272

Synthesis and properties of a cation-conducting, high temperature polymer electrolyte [AD-A263557] p 3334 N93-29825

Study of codeposition of aluminum-haffnium and deposition of yttrium by the cementation technique: Elaboration of Ni-Cr-Al and Ni-Cr-Al-Hf felt materials [ONERA-NT-1990-9] p 3336 N93-30112

Constitutive laws for deformation and dynamic recrystallization in cubic metals [DE93-010740] p 3326 N93-30486

Tensile study of single-crystal ternary L1(2) trialuminide Al66Ti25Mn(sub g) [AD-A264297] p 3601 N93-30819

Design, synthesis, and chemical processing of hierarchical ceramic structures for aerospace applications [AD-A264227] p 3339 N93-30885

HIGH TEMPERATURE AIR

Characterization and optimization of a Hot Air Solder-Leveling System [DE93-010188] p 3332 N93-29328

Experimental study of heat transfer close to a plane wall heated in the presence of multiple injections (subsonic flow) p 3253 N93-29931

HIGH TEMPERATURE ENVIRONMENTS

Oxidation and hot corrosion of superalloys Rene 100 and X-40 at temperatures of 1475 F to 2000 F [AD-A263747] p 3327 N93-30812

HIGH TEMPERATURE FLUIDS

Vibrational spectroscopy of shock-compressed fluids p 3318 N93-30072

HIGH TEMPERATURE GASES

Kinetic studies on gas-phase reaction mechanisms important to the combustion of energetic materials: The CO/N2O reaction p 3347 N93-30084

Orbital transfer vehicle oxygen turbopump technology. Volume 3: Hot oxygen testing [NASA-CR-191036] p 3448 N93-31039

HIGH TEMPERATURE PLASMAS

Edge plasma control by RF electric field in Compact Helical System (CHS) [DE93-753242] p 3583 N93-28532

Development of coherent x ray lasers [DE93-009288] p 3437 N93-29104

Inner-shell photo-ionized x ray laser schemes [DE93-009285] p 3438 N93-29309

A new multichannel soft x ray framing camera for fusion experiments [DE93-009302] p 3432 N93-29773

HIGH TEMPERATURE RESEARCH

Research and development of an airborne multispectral scanner to measure fire, terrestrial and atmospheric characteristics (50 channel) [NASA-CR-193121] p 3456 N93-28620

A high-temperature furnace for applications in microgravity p 3229 N93-29723

HIGH TEMPERATURE SUPERCONDUCTORS

ORNL superconducting technology program for electric energy systems [DE93-009588] p 3404 N93-28523

Processing, fabrication, and demonstration of HTS integrated microwave circuits [AD-A263161] p 3406 N93-28940

Flux lattice relaxation, noise, and symmetry-breaking in frustrated Josephson junction arrays [DE93-008713] p 3593 N93-29094

Symposium on high temperature superconductors: Materials research for emerging technologies [AD-A263120] p 3409 N93-29495

Submillimeter and microwave residual losses in epitaxial films of Y-Ba-Cu-O and Tl-Ca-Ba-Cu-O [DE93-010430] p 3596 N93-29868

Sensitive detection of new superconductors created at ultra high pressures [AD-A264340] p 3597 N93-30161

The Road to Room Temperature Superconductivity Workshop [AD-A264633] p 3561 N93-30519

Guideway structural design and power/propulsion/braking in relation to guideways, volume 1 [PB93-169902] p 3447 N93-30820

A dynamical model of structural phase transition in La2CuO4 [DE93-605325] p 3602 N93-31025

HIGH TEMPERATURE TESTS

Ion-beam-assisted deposition of wear-resistant coatings [DE93-011529] p 3330 N93-28687

Experiment and analysis on elastic deformation properties of graphite and carbon materials for HTTR core components [DE93-753271] p 3299 N93-30004

HIGH VACUUM

A manipulator kinematic design for high-vacuum operation [DE93-010264] p 3444 N93-29247

HIGH VOLTAGES

LDEF Space Plasma-High Voltage Drainage Experiment post-flight results p 3414 N93-29690

Optimum design of multiwire cages for high-voltage applications [AD-A264310] p 3400 N93-30995

HILBERT SPACE

Classification theorem for principal fibre bundles, Berry's phase, and exact cycle evolution [DE93-011114] p 3556 N93-28601

Nth roots of normal contractions [DE92-644725] p 3557 N93-30985

HILBERT TRANSFORMATION

The general theory of convolutional codes p 3385 N93-29595

HILSCH TUBES

The structure and dynamics of the vorticity and passive scalar fields at small scales in homogeneous isotropic turbulence p 3427 N93-30625

HIPPOCAMPUS

Multiple neuron recording in the hippocampus of freely moving animals [AD-A264807] p 3492 N93-30594

HISTORIES

The prehistory of ESRO, 1959 - 1960 [ESA-HSR-1] p 3660 N93-29500

What's past is prologue: Supporting global change research with historical data [DE93-005777] p 3472 N93-30009

HMX

Thermal decomposition of nitramines p 3318 N93-30065

Thermal decomposition chemistry and shock sensitivity of thermally aged explosives p 3344 N93-30069

HODOGRAPHS

Case study of the operational usefulness of the sharp workstation in forecasting a mesocyclone-induced cold sector tornado event in California [PB93-178697] p 3485 N93-30889

HODOSCOPES

Spin dependent phenomena in medium energy physics [DE93-010972] p 3565 N93-28849

HOLDERS

System for testing bearings [NASA-CASE-MFS-28589-1] p 3445 N93-29618

HOLE BURNING

4D interconnect experimental development [AD-A264298] p 3540 N93-30895

HOLE GEOMETRY (MECHANICS)

Experimental and modal verification of an integral equation solution for a thin-walled dichroic plate with cross-shaped holes p 3385 N93-29591

HOLE MOBILITY

Uniaxially stressed Ge:Ga and Ge:Be [DE93-010426] p 3594 N93-29150

HOLES (ELECTRON DEFICIENCIES)

Photoinduced charge separation in Q1D heterojunction materials: Evidence for electron-hole pair separation in mixed-halide MX solids [AD-A264711] p 3598 N93-30501

Photoinduced electron-hole charge separation, intrinsic self-doping and novel device applications of Q1D heterojunction materials: Mixed-halide MX solids [AD-A264714] p 3600 N93-30569

HOLES (MECHANICS)

Experimental and modal verification of an integral equation solution for a thin-walled dichroic plate with cross-shaped holes p 3385 N93-29591

Mold bolt and means for achieving close tolerances between bolts and bolt holes [NASA-CASE-MFS-28720-1] p 3447 N93-30567

HOLMIUM

Holmium quasi-two level laser [AD-D015706] p 3440 N93-30427

HOLOGRAPHIC INTERFEROMETRY

The swollen polymer technique and its use for heat transfer investigations on film cooled surfaces p 3255 N93-29944

HOLOGRAPHIC SPECTROSCOPY

Imaging spectrometers using concave holographic gratings p 3434 N93-28783

HOLOGRAPHY

Design concept for an IR mapping spectrometer for the Pluto fast flyby mission p 3285 N93-28779

Development of coherent x ray lasers [DE93-009288] p 3437 N93-29104

Iterative encoding methods for computer generated holograms [AD-A263705] p 3431 N93-29297

Diffraction and holography with photoelectrons and Auger electrons: Some new directions [DE93-007664] p 3313 N93-29766

4D interconnect experimental development [AD-A264298] p 3540 N93-30895

HOMOGENEITY

Abelian gauge theories on homogeneous spaces [DE92-644730] p 3607 N93-30921

HOMOGENEOUS TURBULENCE

The structure and dynamics of the vorticity and passive scalar fields at small scales in homogeneous isotropic turbulence p 3427 N93-30625

HOMOLOGY

Equivariant elliptic homology [DE92-641338] p 3557 N93-30981

HOMOMORPHISMS

Equivariant elliptic homology [DE92-641338] p 3557 N93-30981

HONEYCOMB STRUCTURES

Beta/gamma Monte Carlo transport in repetitive structures of satellite systems [DE93-007610] p 3281 N93-30509

HORIZON

Utility of a ghost horizon and climb/dive ladder line tapering on a head-up display [AD-A264401] p 3508 N93-30167

HORMONES

Molecular approach to hypothalamic rhythms [AD-A264438] p 3496 N93-30421

HORN ANTENNAS

Wide-bandwidth high-resolution search for extraterrestrial intelligence [NASA-CR-193137] p 3509 N93-28895

HOT CORROSION

Platinum-modified diffusion aluminide coatings on nickel-base superalloys [AD-A263597] p 3325 N93-29981

Oxidation and hot corrosion of superalloys Rene 100 and X-40 at temperatures of 1475 F to 2000 F [AD-A263747] p 3327 N93-30812

HOT ISOSTATIC PRESSING

Development of adherent ceramic coatings to reduce contact stress damage of ceramics [DE93-012518] p 3336 N93-30182

Tensile study of single-crystal ternary L1(2) trialuminide Al66Ti25Mn(sub g) [AD-A264297] p 3601 N93-30819

HOT WORKING

Examination of formability to seamless tubes on Ni-Cr-W superalloy [DE93-764158] p 3326 N93-30396

HOUSINGS

Boron carbide aluminum cermets for external pressure housing applications [AD-A262749] p 3333 N93-29404

Elastic stability considerations for deep submergence ceramic pressure housing [AD-A264824] p 3454 N93-30598

HTPB PROPELLANTS

Determination of gas phase species and temperature profiles above solid propellants p 3346 N93-30080

HUBBLE SPACE TELESCOPE

Digital image compression using artificial neural networks p 3624 N93-28811

HULLS (STRUCTURES)

Development of a test program to evaluate structural defects in Glass-Reinforced Plastic (GRP), volume 2 [AD-A263814] p 3335 N93-29881

Development of a test program to evaluate structural defects in Glass-Reinforced Plastic (GRP), volume 1 [AD-A263813] p 3335 N93-29886

HUMAN BEHAVIOR

Visualization techniques for analyzing control of human movement: Affine mappings between multi-dimensional spaces p 3508 N93-30204

HUMAN BEINGS

Comparative mutagenesis of human cells in vivo and in vitro [DE93-012269] p 3490 N93-28651

Sudden loading and fatigue effects on the human spine [PB93-167526] p 3493 N93-29199

HUMAN FACTORS ENGINEERING

Combat Automation for Airborne Weapon Systems: Man/Machine Interface Trends and Technologies [AGARD-CP-520] p 3501 N93-28850

A new class of mission support for combat air-crew p 3501 N93-28854

The design and development of the new RAF standard HUD format p 3502 N93-28856

Operator and automation capability analysis: Picking the right team p 3503 N93-28864

Ergonomic development of digital map displays p 3503 N93-28866

System automation and pilot-vehicle-interface for unconstrained low-altitude night attack p 3503 N93-28867

Crucial role of detailed function, task, timeline, link, and human vulnerability analyses in HRA [DE93-001923] p 3505 N93-28942

NASA supporting studies for microgravity research on eye movements [NASA-CR-193233] p 3493 N93-29041

Anthropometric data from launch and entry suited test subjects for the design of a recumbent seating system [NASA-TM-104769] p 3505 N93-29044

Exercise/recreation facility for a lunar or Mars analog p 3230 N93-29733

Mars habitat p 3233 N93-29747

Selenia: A habitability study for the development of a third generation lunar base p 3233 N93-29748

An evaluation of B-1B pilot performance during simulated instrument approaches with and without status information [AD-A263874] p 3507 N93-29888

Handedness and motor programming effects of manual control and movement [AD-A264022] p 3499 N93-30027

Managing operational intelligence overload: Guidelines for avoiding decision paralysis [AD-A264184] p 3610 N93-30158

Discomfort glare from high-intensity discharge headlamps: Effects of context and experience [PB93-174720] p 3496 N93-30659

HUMAN PERFORMANCE

Human capabilities and limitations in situation awareness p 3503 N93-28863

Crucial role of detailed function, task, timeline, link, and human vulnerability analyses in HRA [DE93-001923] p 3505 N93-28942

The dynamics of visual representation, attention, encoding, and retrieval processes [AD-A264674] p 3500 N93-30543

Determinants of performance rating accuracy: A field study [AD-A264726] p 3500 N93-30575

The quality assurance liaison: Combined technical and quality assurance support [DE93-008725] p 3450 N93-30636

HUMAN REACTIONS

Armstrong Laboratory space visual function tester program p 3267 N93-28739

The meteorological database [DE93-007289] p 3481 N93-29054

HUMAN TOLERANCES

Issues on human acceleration tolerance after long-duration space flights [NASA-TM-104753] p 3495 N93-29651

HUMIDITY

Environmental effects on stitched RTM composites [NASA-CR-193221] p 3297 N93-29107

Evaluation of personal cooling systems in conjunction with explosive ordnance disposal suits [AD-A262862] p 3506 N93-29471

HUNGARY

Remote sensing in Czechoslovakia and Hungary: An analysis of the possible co-operation of The Netherlands with Czechoslovakia and Hungary in the field of remote sensing [BCRS-92-12] p 3461 N93-29466

HURRICANES

Rhode Island hurricanes and tropical storms: A fifty-six year summary, 1936-1991 [PB93-162006] p 3481 N93-29198

Deadliest, costliest, and most intense US hurricanes of this century (and other frequently requested hurricane facts) [PB93-174993] p 3485 N93-30758

HYBRID CIRCUITS

Analysis of electrothermal interactions in power semiconductor modules [ETN-93-93800] p 3591 N93-28470

HYBRID COMPOSITES

Nonlinear analyses of composite aerospace structures in sonic fatigue [NASA-CR-193124] p 3451 N93-29154

HYBRID PROPULSION

Battery testing at Argonne National Laboratory [DE93-009204] p 3407 N93-29036

The ANL electric vehicle battery R/D program for DOE-EHP [DE93-010658] p 3408 N93-29311

HYDRAULIC EQUIPMENT

Siphon breaker design requirements [DE93-011799] p 3425 N93-30132

Experimental and analytical investigation of finger-follower cam systems p 3446 N93-30378

HYDRAULICS

The hydraulic analysis of cylindrical Flibe jets in a HYLIFE-2 ICF reactor [DE93-009234] p 3586 N93-29053

HYDRAZINES

APU diaphragm testing. Test plan [NASA-TM-108251] p 3271 N93-29387

APU diaphragm testing [NASA-TM-108254] p 3272 N93-29501

HYDRAZOIC ACID

Spectroscopic probes of vibrationally excited molecules at chemically significant energies [DE93-012328] p 3564 N93-28652

HYDRIDES

A study of the chemical mechanism in lubrication [DE93-012230] p 3330 N93-28650

HYDROCARBON COMBUSTION

Rate constant determinations of reactions H + HNO from ab initio reaction path calculations p 3319 N93-30099

HYDROCARBON FUELS

High pressure preignition chemistry of hydrocarbons and hydrocarbon mixtures [AD-A263611] p 3311 N93-29283

HYDROCARBONS

Laser spectroscopy of hydrocarbon radicals [DE93-012555] p 3436 N93-28653

Fugitive hydrocarbon emissions from Pacific OCS facilities, volume 1 [PB93-173797] p 3468 N93-28899

High pressure preignition chemistry of hydrocarbons and hydrocarbon mixtures [AD-A263611] p 3311 N93-29283

Fugitive hydrocarbon emissions from Pacific OCS facilities. Volume 2: Executive summary and user's guide [PB93-173805-VOL-2] p 3471 N93-29861

Carborane-(silane or siloxane)-unsaturated hydrocarbon based thermosetting polymers [AD-D015718] p 3338 N93-30580

Carborane-(siloxane or silane)-unsaturated hydrocarbon based polymers [AD-D015717] p 3338 N93-30586

Contamination of soil, soil gas, and ground water by hydrocarbon compounds near Greear, Morgan County, Kentucky [PB93-182244] p 3474 N93-30825

HYDROCHLORIC ACID

Polymeric materials for use in wet hydrochloric acid environments [DE93-010881] p 3330 N93-28600

HYDROCYANIC ACID

Thermal oxidation of HCN by NO2 in shock waves p 3318 N93-30064

Thermal decomposition chemistry and shock sensitivity of thermally aged explosives p 3344 N93-30069

HYDRODYNAMIC EQUATIONS

The basics of weather models
[AD-A263386] p 3483 N93-29850

HYDRODYNAMICS

A complete set of field equations for the dynamic simulation of a towed cable system
[AD-A262570] p 3442 N93-28578

Macrostatistical hydrodynamics
[DE93-012289] p 3417 N93-28751

Numerical modelling of the cold plasma with time-dependent, magnetohydrodynamic methods
[KFK-5053] p 3586 N93-29081

Implementation of a single-material version of PAGOSA on MIMD hypercubes
[SAND-92-0640] p 3526 N93-29127

Computational simulations of a soft x ray projection lithography laser plasma source
[DE93-009625] p 3437 N93-29264

Articulated fin/wing control system
[AD-D015712] p 3259 N93-29278

Hydrodynamic interactions among fibers in high efficiency filters
[DE93-007117] p 3424 N93-30035

Chemical dynamics simulations as a probe to the initiation and propagation of condensed phase detonations p 3318 N93-30071

Towards a better hydro for dynamic mix calculations
[DE93-010702] p 3426 N93-30485

Godunov-type methods for the equations of compressible fluid mechanics
[KFK-5058] p 3428 N93-31020

HYDROELECTRIC POWER STATIONS

Solar world congress: Proceedings of the biennial congress of the international solar energy society, volume 1, part 2
[PB93-174779] p 3465 N93-30001

HYDROELECTRICITY

Solar world congress: Proceedings of the biennial congress of the international solar energy society, volume 1, part 2
[PB93-174779] p 3465 N93-30001

New hydrogen technologies
[DE93-778353] p 3343 N93-30042

HYDROGEN

Photodissociation of HBr/LiF(001): A quantum mechanical model
[NASA-CR-193119] p 3603 N93-28933

FI-STM investigation of atomic hydrogen adsorption on the Si(100)2x1 surface
[AD-A262748] p 3567 N93-29403

Rate constant determinations of reactions H + HNO from ab initio reaction path calculations
p 3319 N93-30099

HYDROGEN ATOMS

Exotic atoms
[DE93-010242] p 3564 N93-28611

HYDROGEN BONDS

Design of acentric materials: X ray structures of guanidinium p-nitro- and p-hydroxybenzenesulfonate
[AD-A264220] p 3597 N93-30146

HYDROGEN EMBRITTLEMENT

Low temperature environmental embrittlement in ordered intermetallics
[DE93-009711] p 3324 N93-29786

HYDROGEN FUELS

New hydrogen technologies
[DE93-778353] p 3343 N93-30042

HYDROGEN IONS

High-current negative-ion beam transport
[DE93-010732] p 3575 N93-29809

Partial cross sections in H(-) photodetachment
[DE93-011570] p 3569 N93-30130

HYDROGEN OXYGEN ENGINES

Small hydrogen/oxygen rocket flowfield behavior from heat flux measurements
[NASA-TM-106233] p 3286 N93-28619

Advanced Earth-to-orbit propulsion technology information, dissemination and research
[NASA-CR-192561] p 3287 N93-28680

Advanced engine study program
[NASA-CR-187217] p 3287 N93-28946

HYDROGEN PLASMA

High density plasma production in a multicusp plasma generator with RF antenna
[DE93-764493] p 3590 N93-30606

HYDROGEN PRODUCTION

Hydrogen and sulfur production from hydrogen sulfide wastes
[DE93-008658] p 3310 N93-29052

New hydrogen technologies
[DE93-778353] p 3343 N93-30042

HYDROGEN SULFIDE

Hydrogen and sulfur production from hydrogen sulfide wastes
[DE93-008658] p 3310 N93-29052

Electron interactions with non-linear polyatomic molecules and their radicals and ions
[AD-A262279] p 3568 N93-29446

Rates and mechanisms of reaction of hydrogen sulfide with iron chelates
[PB93-184299] p 3312 N93-29665

Acid gas treating by aqueous alkanolamines
[PB93-176188] p 3471 N93-29676

Direct use geothermal applications for brazed plate heat exchangers
[DE93-008559] p 3465 N93-30011

Decomposition of hydrogen sulfide for small scale gas processing.
[PB93-174704] p 3316 N93-30658

Hydrogen sulfide decomposition into hydrogen and sulfur by quinone cycles, part 1
[PB93-175297] p 3317 N93-30761

HYDROGENATION

Design of a high activity and selectivity alcohol catalyst
[DE93-012277] p 3309 N93-28750

HYDROGENOLYSIS

A novel process for methanol synthesis
[DE93-013070] p 3314 N93-30188

HYDROGEOLOGY

Contamination of soil, soil gas, and ground water by hydrocarbon compounds near Greear, Morgan County, Kentucky
[PB93-182244] p 3474 N93-30825

Hydrogeology and ground-water-quality conditions at the Reno County Landfill, South-Central Kansas, 1990-1991
[PB93-183085] p 3474 N93-30826

HYDROGRAPHY

System analysis for a kinematic positioning system based on the global positioning system
[AD-A262830] p 3245 N93-29468

A water mass analysis of the 1991-1992 El Nino signal in the Farallon Islands region
[AD-A263490] p 3488 N93-29819

Reception at Ascension Island, South Atlantic, of the transmissions from the Heard Island feasibility test
[PB93-176261] p 3394 N93-30662

Hydrographic observations in the western tropical and subtropical north Atlantic Ocean: Atlantic Climate Change Program (ACCP) and Western Tropical Atlantic Experiment (WESTRAX) during 1990
[PB93-184760] p 3489 N93-30827

HYDROLOGICAL CYCLE

Steady-state and transient modeling of tracer and nutrient distributions in the global ocean
[DE93-011043] p 3486 N93-28670

HYDROLOGY

Tank issues: Site characterization for external leak monitoring
[PB93-161156] p 3469 N93-29034

A diffusion approximation for a network of reservoirs with power law release rule
[AD-A263753] p 3550 N93-29872

HYDROLOGY MODELS

Geoscience center research
[AD-A263465] p 3462 N93-29834

A diffusion approximation for a network of reservoirs with power law release rule
[AD-A263753] p 3550 N93-29872

Annual report on monitoring of the unsaturated zone and recharge areas at INEL to the state of Idaho INLEL oversight committee
[DE93-012947] p 3473 N93-30187

HYDROLYSIS

Technical bases for precipitate hydrolysis process operating parameters, revision 1
[DE93-009894] p 3309 N93-28553

HYDROSTATIC PRESSURE

Hydrostatic and uniaxial behavior of a high density polyurethane foam (FR-3720) at various temperatures
[DE93-011486] p 3330 N93-28838

An analysis of the 70-meter antenna hydrostatic bearing by means of computer simulation p 3386 N93-29601

Elastic stability considerations for deep submergence ceramic pressure housing
[AD-A264824] p 3454 N93-30598

HYDROSTATICS

Hydrostatic and uniaxial behavior of a high density polyurethane foam (FR-3720) at various temperatures
[DE93-011486] p 3330 N93-28838

Elastic stability considerations for deep submergence ceramic pressure housing
[AD-A264824] p 3454 N93-30598

HYDROXYL RADICALS

Design of acentric materials: X ray structures of guanidinium p-nitro- and p-hydroxybenzenesulfonate
[AD-A264220] p 3597 N93-30146

HYGRAL PROPERTIES

Factors influencing the interlaminar fracture toughness and its evaluation in composites
[FFA-TN-1991-34] p 3451 N93-29076

HYPERBOLIC DIFFERENTIAL EQUATIONS

Numerical modelling of the cold plasma with time-dependent, magnetohydrodynamic methods
[KFK-5053] p 3586 N93-29081

Finite element approximation of the shallow water equations on the MASPAR
[AD-A264649] p 3489 N93-30525

HYPERBOLIC FUNCTIONS

Difference methods for hyperbolic problems with emphasis on space-centered approximations
[ONERA-NT-1990-4] p 3550 N93-30136

HYPERCUBE MULTIPROCESSORS

Design of a hardware discrete event simulation coprocessor
[AD-A262614] p 3537 N93-28478

A multiarchitecture parallel-processing development environment
[NASA-TM-106180] p 3538 N93-28628

Implementation of a multidomain Navier-Stokes code on the Intel iPSC2 hypercube
[FFA-TN-1992-37] p 3418 N93-28994

Implementation of a single-material version of PAGOSA on MIMD hypercubes
[SAND-92-0640] p 3526 N93-29127

Multiprocessing systems: Reliability modelling and analysis using multimode components and dependent failures
[AD-A264230] p 3540 N93-30364

HYPERFINE STRUCTURE

Theoretical hyperfine structure constants for transition metal atoms and ions
[DE93-012325] p 3566 N93-29183

HYPERNUCLEI

Measurements of rare composite objects and high sensitivity searches for novel forms of matter produced in high energy heavy ion collisions
[DE93-009945] p 3574 N93-28569

HYPERSONIC AIRCRAFT

ASUR p 3228 N93-29720

HYPERSONIC FLOW

Development of a 3-D Implicit Euler Code for Hypersonic and High Supersonic Flows
[ONERA-RSF-23/1123-AY-230A] p 3417 N93-28744

Inviscid quasi one-dimensional nonequilibrium flow
[FFA-TN-1992-35] p 3418 N93-28993

Topology and grid adaption for high-speed flow computations
[NASA-CR-4216] p 3426 N93-30375

HYPERSONIC SPEED

Hypersonic lateral and directional stability characteristics of aeroassist flight experiment configuration in air and CF4
[NASA-TM-4435] p 3239 N93-29166

HYPERSONICS

Program for an improved hypersonic temperature-sensing probe
[NASA-CR-186025] p 3431 N93-29066

Hypersonic lateral and directional stability characteristics of aeroassist flight experiment configuration in air and CF4
[NASA-TM-4435] p 3239 N93-29166

HYPERVELOCITY IMPACT

Report of the Meteoroid and Debris Special Investigation Group p 3638 N93-29355

Micrometeoroids and debris on LDEF
p 3638 N93-29356

Three-D crater analysis of LDEF impact features from stereo imagery p 3283 N93-29359

Long Duration Exposure Facility (LDEF) experiment M0003 meteoroid and debris survey
p 3638 N93-29361

Characteristics of hypervelocity impact craters on LDEF experiment S1003 and implications of small particle impacts on reflective surfaces p 3283 N93-29363

Hypervelocity impact survivability experiments for carbonaceous impactors p 3283 N93-29364

Hypervelocity impact facility for simulating materials exposure to impact by space debris
p 3283 N93-29365

SIMS chemical analysis of extended impacts on the leading and trailing edges of LDEF experiment AO187-2
p 3318 N93-29367

Cratering in glasses impacted by debris or micrometeorites p 3340 N93-29368

Projectile compositions and modal frequencies on the chemistry of micrometeoroids LDEF experiment
p 3638 N93-29370

Asteroidal versus cometary meteoroid impacts on the Long Duration Exposure Facility (LDEF)
p 3638 N93-29371

Elemental analyses of hypervelocity microparticle impact sites on Interplanetary Dust Experiment sensor surfaces p 3638 N93-29378
The production and evolution of plasma and associated magnetic fields during hypervelocity impacts: Implications for planetary paleomagnetism p 3589 N93-30000
Hypervelocity impact testing of the Space Station utility distribution system carrier [NASA-TM-104771] p 3289 N93-30507

HYPERVELOCITY LAUNCHERS
ASUR p 3228 N93-29720

HYPERVELOCITY PROJECTILES
Ablative shielding for hypervelocity projectiles [NASA-CASE-MSC-21884-1] p 3331 N93-29088
SIMS chemical analysis of extended impacts on the leading and trailing edges of LDEF experiment AO187-2 p 3318 N93-29367
Interplanetary meteoroid debris in LDEF metal craters p 3638 N93-29372

HYPOKINESIA
Issues on human acceleration tolerance after long-duration space flights [NASA-TM-104753] p 3495 N93-29651

HYPOTHALAMUS
Control and circadian behavior by transplanted suprachiasmatic nuclei [AD-A264553] p 3496 N93-30382
Molecular approach to hypothalamic rhythms [AD-A264438] p 3496 N93-30421

HYPOTHESES
Handedness and motor programming effects of manual control and movement [AD-A264022] p 3499 N93-30027

I

ICE
Development of an airborne MMW FM-CW radar for mapping river ice [AD-A262655] p 3379 N93-28588
Dynamic ice structure interaction: Theory and applications [VTT-PUBS-90] p 3353 N93-28632
Drill/borescope system for the Mars Polar Pathfinder p 3647 N93-28805
Debris/ice/TPS assessment and integrated photographic analysis for Shuttle Mission STS-55 [NASA-TM-107559] p 3271 N93-29136
A passive infrared ice detection technique for helicopter applications [NASA-CR-193187] p 3244 N93-29152

ICE ENVIRONMENTS
The German satellite ground station in Antarctica: Realization and first results p 3458 N93-28924

ICE FORMATION
A passive infrared ice detection technique for helicopter applications [NASA-CR-193187] p 3244 N93-29152

ICE MAPPING
Development of an airborne MMW FM-CW radar for mapping river ice [AD-A262655] p 3379 N93-28588

ICE PREVENTION
FAA international conference on airplane ground deicing [AD-A263617] p 3244 N93-29286

ICE REPORTING
Leadex data report. Part 2: Rawinsonde and ice station data [AD-A263218] p 3483 N93-29491

IDEAL FLUIDS
Fourth-rank cosmology [DE92-641346] p 3637 N93-30997

IDEAL GAS
The thermodynamic properties of thianthrene and phenoxathiin [DE93-000124] p 3603 N93-28964
Tables of experimental data used for the correlation of the thermophysical properties of ethane [PB93-173417] p 3313 N93-29768

IGNITION
Design of the Nova Upgrade laser system for ignition fusion experiments [DE93-009077] p 3436 N93-29097
High pressure preignition chemistry of hydrocarbons and hydrocarbon mixtures [AD-A263611] p 3311 N93-29283
Fusion laser oscillator and pulse-forming system using integrated optics [DE93-009286] p 3588 N93-29780
Microstructural modeling of electrical breakdown in solid fuel propellants [AD-A263466] p 3342 N93-29835
Combustion/explosion chemistry of bulk materials p 3343 N93-30062
Strategies for understanding the deflagration-to-detonation transition p 3319 N93-30077
Pressure dependence of the reaction propagation rate of TATB to 40 GPa p 3319 N93-30082

IMAGE ANALYSIS
Multiscale morphological filtering for analysis of noisy and complex images p 3582 N93-28789
A planetary version of PC-McIDAS p 3614 N93-29236
Multisensor image analysis system [AD-A263679] p 3528 N93-29294
Quantitative analysis of properties and spatial relations of fuzzy image regions p 3510 N93-29523
A fuzzy clustering algorithm to detect planar and quadric shapes p 3511 N93-29524
Automatic rule generation for high-level vision p 3511 N93-29526
Encoding spatial images: A fuzzy set theory approach p 3511 N93-29527
Image segmentation using fuzzy LVQ clustering networks p 3511 N93-29528
Character recognition using a neural network model with fuzzy representation p 3512 N93-29536
Comparison of crisp and fuzzy character networks in handwritten word recognition p 3514 N93-29545
Modeling the bidirectional reflectance and spectra [AD-A263570] p 3462 N93-29830
Mixed limit theorems for pattern analysis [AD-A263735] p 3549 N93-29854
Neural network cloud classification research [AD-A264628] p 3484 N93-30176
Quantization effects in segmentation of range images p 3363 N93-30270
Recursive-batch estimation of structure and motion from stereo image sequences p 3363 N93-30271
Automatic detection of explosives using x ray imaging p 3244 N93-30275
Design and implementation of an interactive isochromatic fringe-analysis system using machine-vision techniques p 3369 N93-30305
Morphological and order statistic filters: A comparative study p 3375 N93-30345
Qualitative methods in computer vision [AD-A264335] p 3533 N93-30418

IMAGE CLASSIFICATION
Image classification using Markov random fields with two new relaxation methods: Deterministic pseudo annealing and modified metropolis dynamics [INRIA-RR-1606] p 3553 N93-28510

IMAGE CONTRAST
Digital image processing of descanned terrestrial ground photographs p 3459 N93-28928
Image enhancement using an analog device neural network p 3376 N93-30346

IMAGE ENHANCEMENT
Characterization of laboratory generated turbulence by optical phase measurements [AD-A262596] p 3480 N93-28465
Resolution-enhanced mapping spectrometer p 3434 N93-28794
Development of a new technique for image reconstruction, enhancement, and visualization [AD-A263145] p 3528 N93-29483
A new way to use fuzzy sets in image sharpening p 3363 N93-30273
Image enhancement using an analog device neural network p 3376 N93-30346

IMAGE FILTERS
Multiscale morphological filtering for analysis of noisy and complex images p 3582 N93-28789
Filtering interpolators for image comparison algorithms p 3463 N93-28797
Cloud classification from satellite imagery using neural computing p 3367 N93-30297
Semi-blind restoration of images distorted by random time varying point spread functions p 3375 N93-30344
Morphological and order statistic filters: A comparative study p 3375 N93-30345
Segmentation of SAR images p 3376 N93-30348

IMAGE INTENSIFIERS
Honeywell's compact, wide-angle UV-visible imaging sensor p 3582 N93-28806
Development of a new technique for image reconstruction, enhancement, and visualization [AD-A263145] p 3528 N93-29483

IMAGE PROCESSING
Coarse image motion for saccade control [OUEL-1916/92] p 3523 N93-28485
Image classification using Markov random fields with two new relaxation methods: Deterministic pseudo annealing and modified metropolis dynamics [INRIA-RR-1606] p 3553 N93-28510
Clementine sensor processing system p 3285 N93-28778
Filtering interpolators for image comparison algorithms p 3463 N93-28797
Systematic processing of Clementine data for scientific analyses p 3624 N93-28803
Digital image compression using artificial neural networks p 3624 N93-28811
A corner matching and tracking strategy applied to videophony [OUEL-1933/92] p 3380 N93-28896
A modular head/eye platform for real-time reactive vision [OUEL-1941/92] p 3505 N93-28897
Proceedings of the 8th User Seminar of the German Remote Sensing Data Center of the German Aerospace Establishment (DLR) [DLR-MITT-92-09] p 3456 N93-28915
The German PAF (Processing and Archiving Facilities) for ERS-1 p 3457 N93-28916
The interferometric SAR technology and its usability in the framework of ERS-1 p 3457 N93-28919
Forest examination with polarimetric radar image data p 3457 N93-28921
Digital image processing of descanned terrestrial ground photographs p 3459 N93-28928
Atmospheric correction of LANDSAT-TM-data for forest inventory p 3459 N93-28929
Model-oriented correction of thematic mapper raw data p 3459 N93-28930
Evidence-based classification of satellite image data p 3459 N93-28931
SAVS: A Space Data Analysis and Visualization System p 3614 N93-29235
Multisensor image analysis system [AD-A263679] p 3528 N93-29294
Information system for co-registration of CAESAR sea-images based on two dimensional image matching techniques (SCORE). Part 1: Introduction, user requirements, and feasibility tests [BCRS-90-40A-PT-1] p 3460 N93-29307
Preprocessing airborne remote sensing PARES calibration maintenance functional design document [BCRS-92-07] p 3460 N93-29321
The parallel implementation of a backpropagation neural network and its applicability to SPECT image reconstruction [DE93-010304] p 3567 N93-29416
Automated satellite image navigation [AD-A262868] p 3269 N93-29475
Automatic rule generation for high-level vision p 3511 N93-29526
Multiple image multipoint matching for automatic aerotriangulation p 3461 N93-29615
A new multichannel soft x ray framing camera for fusion experiments [DE93-009302] p 3432 N93-29773
What's past is prologue: Supporting global change research with historical data [DE93-005777] p 3472 N93-30009
Computing with neural maps: Application to perceptual and cognitive function [AD-A264056] p 3499 N93-30033
Canadian Conference on Electrical and Computer Engineering, volumes 1 and 2 [ISBN-0-9694170-1-2] p 3354 N93-30215
Feature segmentation using a multiple-stack based chain coding algorithm p 3359 N93-30243
An architecture for an analog VLSI neural network for early computer vision processing p 3359 N93-30244
Modelling and simulation of human retinal vision processing p 3363 N93-30269
A single band processor for the computation of range from optical absorbance p 3363 N93-30272
A new way to use fuzzy sets in image sharpening p 3363 N93-30273
On the implementation of the BIRIS range sensor for applications in robotic control and autonomous navigation p 3366 N93-30286
Applications of digital 3-D imaging p 3366 N93-30287
A robust multi-operator 3-D edge detection approach for range image segmentation p 3366 N93-30288
Recognizing partially overlapping objects p 3366 N93-30289
Segmentation of SAR images p 3376 N93-30348
Detecting residue on a printed circuit board: An application of the Boundary Contour/Feature Contour System [DE93-006283] p 3412 N93-30370
Multiscale and multigrid information representation, extraction and fusion [AD-A264623] p 3393 N93-30386
Analysis and computation for vortex dynamics and rarefied gases [AD-A264705] p 3427 N93-30499

Infrared imaging array integrated in three dimensions directly on top of silicon circuits
[AD-A264707] p 3581 N93-30500
Laser based 3D volumetric display system
[AD-A264825] p 3441 N93-30599
Principal components of natural images: An analytical solution
[AD-A264800] p 3489 N93-30603
Transputers, parallel processing in embedded systems for image compression in space applications
[NLR-TP-89242-U] p 3522 N93-30840
An algorithm for simple and complex feature detection: From retina to primary visual cortex
[AD-A264306] p 3497 N93-30897

IMAGE RECONSTRUCTION
Three dimensional reconstruction of complex shapes based on the Delaunay triangulation
[INRIA-RR-1697] p 3547 N93-28616
The parallel implementation of a backpropagation neural network and its applicability to SPECT image reconstruction
[DE93-010304] p 3567 N93-29416
Development of a new technique for image reconstruction, enhancement, and visualization
[AD-A263145] p 3528 N93-29483
Quantization effects in segmentation of range images
p 3363 N93-30270
Recursive-batch estimation of structure and motion from stereo image sequences p 3363 N93-30271
Semi-blind restoration of images distorted by random time varying point spread functions
p 3375 N93-30344

IMAGE RESOLUTION
Characterization of laboratory generated turbulence by optical phase measurements
[AD-A262596] p 3480 N93-28465
Improved real-time imaging spectrometer
[NASA-CASE-NPO-18410-1-CU] p 3578 N93-29086
X ray microscopy resource center at the Advanced Light Source
[DE93-010449] p 3261 N93-29869
Method and apparatus for imaging an object in or through a scattering medium by using multiple-wave mixing
[AD-D015707] p 3581 N93-30410
MR-CDF: Managing multi-resolution scientific data
p 3618 N93-30456
Effects of area-of-interest display characteristics of visual search performance and head movements in simulated low-level flight
[AD-A264661] p 3499 N93-30542
Multiresolution analysis of SAR data
[AD-A264727] p 3393 N93-30576
Laser based 3D volumetric display system
[AD-A264825] p 3441 N93-30599

IMAGERY
The HYDICE instrument design and its application to planetary instruments p 3434 N93-28766

IMAGES
A tutorial on exit pupils and eye rotation with virtual image optical displays
[AD-A262399] p 3494 N93-29400
What is the center of the image?
[AD-A263550] p 3579 N93-29824
The Visible Human Project of the National Library of Medicine: Remote access and distribution of a multi-gigabyte data set p 3617 N93-30453

IMAGING RADAR
Similarities between synthetic aperature radar and ground probing radar imaging p 3376 N93-30347

IMAGING SPECTROMETERS
Acousto-optic infrared spectral imager for Pluto fast flyby p 3285 N93-28781
Imaging spectrometers using concave holographic gratings p 3434 N93-28783
Resolution-enhanced mapping spectrometer
p 3434 N93-28794
Ultraviolet imaging spectrometer p 3582 N93-28827
Improved real-time imaging spectrometer
[NASA-CASE-NPO-18410-1-CU] p 3578 N93-29086

IMAGING TECHNIQUES
Low-cost helmet-mounted displays
[AD-A262616] p 3501 N93-28479
Coarse image motion for saccade control
[OUEL-1916/92] p 3523 N93-28485
Recognizing parameterized objects from range data
[OUEL-1918/92] p 3523 N93-28486
Three dimensional reconstruction of complex shapes based on the Delaunay triangulation
[INRIA-RR-1697] p 3547 N93-28616
Preliminary design of an intermittent smoke flow visualization system
[NASA-CR-186027] p 3248 N93-28693
Polarimetric multispectral imaging technology
p 3434 N93-28774
Clementine sensor processing system
p 3285 N93-28778
Imaging spectrometers using concave holographic gratings p 3434 N93-28783
The Ultraviolet Plume Instrument (UVPI)
p 3285 N93-28784
Visible imaging on the Pluto fast flyby mission
p 3646 N93-28799
Systematic processing of Clementine data for scientific analyses p 3624 N93-28803
Honeywell's compact, wide-angle UV-visible imaging sensor p 3582 N93-28806
A compact imaging detector of polarization and spectral content p 3582 N93-28810
Diffusion bonding
[DE93-011480] p 3442 N93-28837
A technique for single-pulse spectrum and pulse width measurements for an IR-FEL
[DE93-007732] p 3436 N93-28847
The multiplicity of T Tauri stars in the star forming regions Taurus-Auriga and Ophiuchus-Scorpius: A 2.2 micron speckle imaging survey p 3634 N93-28945
Research programs from the University of South Carolina on high energy physics
[DE93-007829] p 3574 N93-28969
What is underneath? Moving atoms and molecules to find out
[AD-A263363] p 3567 N93-29332
Optical slope/height measurements of small scale waves within the SAXON-FPN experiment
[AD-A262572] p 3487 N93-29422
Image segmentation using fuzzy LVQ clustering networks p 3511 N93-29528
Quantification of thermographic mapping techniques
[AD-A264020] p 3391 N93-30016
Applications of mesoscopic physics
[DE93-012104] p 3597 N93-30141
The AFOSR Workshop on the Future of EEG and MEG
[AD-A264338] p 3495 N93-30160
Method and apparatus for imaging an object in or through a scattering medium by using multiple-wave mixing
[AD-D015707] p 3581 N93-30410
Multiparticle imaging technique for two-phase fluid flows using pulsed laser speckle velocimetry
[DE93-011734] p 3427 N93-30489
A new tubeless nanosecond streak camera based on optical deflection and direct CCD imaging
[DE93-011893] p 3433 N93-30491
Infrared imaging array integrated in three dimensions directly on top of silicon circuits
[AD-A264707] p 3581 N93-30500
Observing and modelling F-region ionospheric dynamics using the OII 7320A emission p 3479 N93-30564

IMIDES
Synthesis of oligoimides and oligoimide anion radicals
[AD-A263129] p 3290 N93-29474

IMINES
Synthesis and polymerization of azaethylenes and aza-1,3-dienes
[AD-A263651] p 3332 N93-29290
Synthetic lubricating oil greases containing metal chelates of Schiff bases
[AD-D015694] p 3333 N93-29458

IMPACT
Comparison of impact results for several polymeric composites over a wide range of low impact velocities
p 3304 N93-30848

IMPACT DAMAGE
Cratering in glasses impacted by debris or micrometeorites p 3340 N93-29368
LDEF data: Comparisons with existing models
p 3283 N93-29375
Developments in impact damage modeling for laminated composite structures p 3305 N93-30857
Comparison of hand laid-up tape and filament wound composite cylinders and panels with and without impact damage p 3306 N93-30859
Experimental behavior of graphite-epoxy Y-stiffened specimens loaded in compression p 3307 N93-30872

IMPACT LOADS
The equivalent flat nose diameter of hemispherical nose cylindrical projectiles for impact induced detonation of energetic materials
[AD-A263244] p 3342 N93-29494
Molecular dynamics of detonation in crystals with defects p 3350 N93-30097
Static and dynamic large deflection flexural response of graphite-epoxy beams
[NASA-CR-4118] p 3454 N93-30374
A ceramic fracture model for high velocity impact
[AD-A264728] p 3454 N93-30545
Delaminations in composite plates under impact loads
p 3304 N93-30849

IMPACT MELTS
Cratering in glasses impacted by debris or micrometeorites p 3340 N93-29368

IMPACT RESISTANCE
The equivalent flat nose diameter of hemispherical nose cylindrical projectiles for impact induced detonation of energetic materials
[AD-A263244] p 3342 N93-29494

IMPACT STRENGTH
The effect of material strength on segment penetration behavior
[AD-A263262] p 3453 N93-29801
The effect of oxidation embrittlement on the impact behavior of nicalon reinforced CAS 2 ceramic matrix composites
[AD-A263567] p 3334 N93-29829

IMPACT TESTS
The effect of temperature on the impact behavior of TiB2 reinforced XDTM-TiAl intermetallic matrix composites
[AD-A262924] p 3296 N93-28886
Axial impact of composites p 3297 N93-29078
The effect of material strength on segment penetration behavior
[AD-A263262] p 3453 N93-29801
Dislocation roles in energetic crystal responses
p 3348 N93-30086
Catastrophic collisions: Laboratory impact experiments, hydrocode simulations, and the scaling problem
p 3635 N93-30411
Hypervelocity impact testing of the Space Station utility distribution system carrier
[NASA-TM-104771] p 3289 N93-30507
Comparison of impact results for several polymeric composites over a wide range of low impact velocities
p 3304 N93-30848

IMPACT TOLERANCES
The equivalent flat nose diameter of hemispherical nose cylindrical projectiles for impact induced detonation of energetic materials
[AD-A263244] p 3342 N93-29494

IMPACTORS
Clementine 2: A double asteroid flyby and impactor mission p 3268 N93-28770
Axial impact of composites p 3297 N93-29078
Report of the Meteoroid and Debris Special Investigation Group p 3638 N93-29355
Hypervelocity impact survivability experiments for carbonaceous impactors p 3283 N93-29364
LDEF data: Comparisons with existing models
p 3283 N93-29375
Elemental analyses of hypervelocity microparticle impact sites on Interplanetary Dust Experiment sensor surfaces
p 3638 N93-29378

IMPEDANCE
Planar active antennas and quasi-optical power combining arrays using FET's and slots
[AD-A263759] p 3387 N93-29875

IMPEDANCE MEASUREMENT
Plasma diagnostics by antenna impedance measurements p 3400 N93-28820

IMPEDANCE PROBES
Plasma diagnostics by antenna impedance measurements p 3400 N93-28820

IMPINGEMENT
Local heat transfer measurement with liquid crystals on rotating surfaces including non-axisymmetric cases
p 3255 N93-29943

IMPLANTED ELECTRODES (BIOLOGY)
Programmable interactive system for cochlear implant electrode stimulation
[AD-A262558] p 3494 N93-29421

IMPLOSIONS
Analysis of an MCG/fuse/PFS experiment
[DE93-007355] p 3410 N93-29812

IMPULSES
Wideband propagation measurements for wireless indoor communication
[PB93-175123] p 3382 N93-29202

IMPURITIES
Operational results of pilot cell test with cermet inert anodes
[DE93-009338] p 3322 N93-29061

IN SITU MEASUREMENT
In situ characterization of interfacial and bulk properties of lithium polymer batteries using 4-probe DC techniques
[DE93-007699] p 3405 N93-28581
A DTA/GC for the in situ identification of the Martian surface material p 3646 N93-28800
A team approach to the development of gamma ray and x ray remote sensing and in situ spectroscopy for planetary exploration missions p 3650 N93-28824
In situ Fourier transform infrared spectroscopic study of bisulfate and sulfate adsorption on gold, with and without the underpotential deposition of copper
[AD-A263421] p 3323 N93-29259
In-situ x ray studies of the underpotential deposition of copper on platinum (3)
[AD-A263361] p 3595 N93-29331

In-situ temperature and concentration measurements of organosilicon decomposition in a chemical vapor deposition reactor
[ONERA-P-1990-3] p 3313 N93-30109
Oceanographic research towers in european waters
[AD-A264795] p 3489 N93-30612

IN-FLIGHT MONITORING
Spurious symptom reduction in fault monitoring
[NASA-CR-191453] p 3542 N93-29192

INCIDENT RADIATION
Measurement of projectile surface temperature by means of its infrared radiation: A preliminary study
[AD-A264053] p 3432 N93-30032

INCOHERENT SCATTER RADAR
The dynamic cusp at low altitudes: A case study combining Viking, DMSP, and Sondrestrom incoherent scatter radar observations
[NASA-CR-193152] p 3476 N93-28842
Observing and modelling F-region ionospheric dynamics using the OII 7320A emission p 3479 N93-30564

INCOMPRESSIBLE FLOW
The numerical solution of low Mach number flow in confined regions by Richardson extrapolation
[TRITA-NA-9207] p 3238 N93-29005
An efficient spectral integration method for the solution of the Navier-Stokes equations
[FFA-TN-1992-28] p 3418 N93-29009
Stabilized space-time finite element formulations for unsteady incompressible flows involving fluid-body interactions p 3419 N93-29040
Accuracy of least-squares methods for the Navier-Stokes equations
[NASA-TM-106209] p 3421 N93-29208
Hamiltonian dynamics of coupled potential vorticity and internal wave motion: 1. Linear modes
[AD-A263469] p 3424 N93-29838
A parallel implicit incompressible flow solver using unstructured meshes
[AD-A263395] p 3424 N93-29851

INCOMPRESSIBLE FLUIDS
Hamiltonian dynamics of coupled potential vorticity and internal wave motion: 1. Linear modes
[AD-A263469] p 3424 N93-29838

INCONEL (TRADEMARK)
An experimental investigation of radioactivity induced by ions associated with the operation of pulsed-power accelerators
[DE93-011478] p 3575 N93-29151

INDENTATION
Comparison of impact results for several polymeric composites over a wide range of low impact velocities
p 3304 N93-30848

INDEPENDENT VARIABLES
A closed-form formula for the manipulator regressor
p 3355 N93-30218

INDIUM ARSENIDES
Growth and development of GaInAsP for use in high-efficiency solar cells
[DE93-000098] p 3465 N93-30208

INDIUM PHOSPHIDES
Texturing of InP surfaces for device applications
[NASA-TM-106061] p 3321 N93-28618
Low temperature (LT) GaAs and related materials
[AD-A263607] p 3298 N93-29282
Fundamental studies of the morphology, chemistry, and electrical properties of metals on GaAs and other III-V semiconductor compounds
[AD-A264417] p 3597 N93-30120
Growth and development of GaInAsP for use in high-efficiency solar cells
[DE93-000098] p 3465 N93-30208

INDUCTION HEATING
Heating head for induction heating apparatus
[NASA-CASE-LAR-14429-1] p 3407 N93-29173

INDUSTRIAL PLANTS
Application of hardness testing in foundry processing operations: A university and industry partnership
p 3292 N93-30961

INDUSTRIAL WASTES
Fugitive hydrocarbon emissions from Pacific OCS facilities, volume 1
[PB93-173797] p 3468 N93-28899
Hydrogen and sulfur production from hydrogen sulfide wastes
[DE93-008658] p 3310 N93-29052
Application of sensors to the control of robotic systems
[DE93-009837] p 3543 N93-30012

INDUSTRIES
ORNL superconducting technology program for electric energy systems
[DE93-009588] p 3404 N93-28523
The ANL electric vehicle battery R/D program for DOE-EHP
[DE93-010658] p 3408 N93-29311
The role of the University Licensing Office in transferring intellectual property to industry p 3626 N93-30698
High performance computing and communications program p 3627 N93-30715
National Media Laboratory p 3628 N93-30717
A research experiment on facilitation and formation of joint research and development programs between government, industry, and universities: Overview, preliminary findings, and observations
p 3628 N93-30725

INELASTIC SCATTERING
Neutron scattering studies of the structures and lattice dynamics of the alkali metals
[DE93-008272] p 3593 N93-28956
Applications of mesoscopic physics
[DE93-012104] p 3597 N93-30141
A possibility to investigate the superconducting gap with the help of neutrons
[DE93-606392] p 3601 N93-30799

INERTIAL CONFINEMENT FUSION
Inertial confinement fusion target component fabrication and technology development support
[DE93-010836] p 3585 N93-28836
The hydraulic analysis of cylindrical Flibe jets in a HYLIFE-2 ICF reactor
[DE93-009234] p 3586 N93-29053
SIRIUS-P: An inertially confined direct drive laser fusion power reactor
[DE93-012433] p 3439 N93-30186

INERTIAL NAVIGATION
Flight evaluation of a computer aided low-altitude helicopter flight guidance system p 3260 N93-28869
System analysis for a kinematic positioning system based on the global positioning system
[AD-A262830] p 3245 N93-29468
High reliability, maintenance-free INS battery development
[AD-A264521] p 3412 N93-30406

INFERENCE
Study on various problems in statistical planning and inference
[AD-A262484] p 3554 N93-29411
Parametric likelihood inference for record breaking problems
[AD-A262546] p 3549 N93-29413
How to select combination operators for fuzzy expert systems using CRI p 3510 N93-29521
Evaluation of fuzzy inference systems using fuzzy least squares p 3513 N93-29539
Comparison between the performance of two classes of fuzzy controllers p 3517 N93-29566
Inference in fuzzy rule bases with conflicting evidence
p 3519 N93-29583
Some statistical inference problems in linear models and variance components models and their applications
[AD-A264062] p 3555 N93-29923

INFILTRATION
Infiltration/cure modeling of resin transfer molded composite materials using advanced fiber architectures
p 3303 N93-30843

INFLATABLE STRUCTURES
In-step inflatable antenna experiment
p 3263 N93-28701
Developing an inflatable solar array
p 3264 N93-28714

INFLATING
A computational model that couples aerodynamic and structural dynamic behavior of parachutes during the opening process
[AD-A264115] p 3241 N93-30119

INFORMATION
Formal definition of a conceptual language for the description and manipulation of information models
[TR-92-16] p 3523 N93-28503
Comparison of specificity and information for fuzzy domains p 3510 N93-29519
The axiomatic definition of a linguistic scale fuzziness degree, its major properties, and applications
p 3510 N93-29520
Automatic rule generation for high-level vision
p 3511 N93-29526
Information compression in the context model
p 3514 N93-29549
Managing operational intelligence overload: Guidelines for avoiding decision paralysis
[AD-A264184] p 3610 N93-30158

INFORMATION DISSEMINATION
NASA/DOD Aerospace Knowledge Diffusion Research Project. Paper 28: The technical communication practices of Russian and US aerospace engineers and scientists
[NASA-TM-108249] p 3612 N93-28948
National collaboratories: Applying information technology for scientific research
[LC-93-83795] p 3612 N93-29129
The 9th FLICC Forum on Federal Information Policies
[PB93-184687] p 3624 N93-29668
LDEF archival system plan p 3624 N93-29704
NASA/DoD Aerospace Knowledge Diffusion Research Project. Paper 29: The US government technical report and the transfer of federally funded aerospace R and D
[NASA-TM-109221] p 3615 N93-29709
NASA/DoD Aerospace Knowledge Diffusion Research Project. Paper 30: The electronic transfer of information and aerospace knowledge diffusion
[NASA-TM-109223] p 3616 N93-30036
NASA/DoD Aerospace Knowledge Diffusion Research Project. Paper 31: The information-seeking behavior of engineers
[NASA-TM-109224] p 3616 N93-30037
Residual acceleration data on IML-1: Development of a data reduction and dissemination plan
[NASA-CR-193224] p 3281 N93-30038
Interagency Advanced Power Group (IAPG) Meeting Compendium
[DE93-006189] p 3670 N93-30212
High-speed data duplication/data distribution: An adjunct to the mass storage equation
p 3619 N93-30459
National Media Laboratory media testing results
p 3620 N93-30465
Technology Transfer and the Civil Space Program. Volume 2: Workshop proceedings
[NASA-TM-108250] p 3625 N93-30692
Technology transfer p 3626 N93-30699
Technology transfer needs and experiences: The NASA Research Center perspective p 3626 N93-30703
Technology transfer and space science missions
p 3626 N93-30705
Technology transfer within NASA
p 3627 N93-30708
Technology transfer and Rockwell International
p 3627 N93-30712
Plasma Physics Network Newsletter, no. 5
[DE93-606216] p 3591 N93-30795

INFORMATION FLOW
Resource utilization model for the algorithm to architecture mapping model
[NASA-CR-193122] p 3527 N93-29171
Hidden Markov models for fault detection in dynamic systems
[NASA-CASE-NPO-18982-1-CU] p 3449 N93-30413

INFORMATION MANAGEMENT
Security classification of information
[DE93-012416] p 3612 N93-28840
The 9th FLICC Forum on Federal Information Policies
[PB93-184687] p 3624 N93-29668
Storage systems for national information assets
[DE93-009303] p 3615 N93-29783
The future role of the Director of Information Management (DOIM) organization within the DOD corporate information management initiative
[AD-A264118] p 3616 N93-30193

INFORMATION PROCESSING (BIOLOGY)
Cognitive and Neural Sciences Division 1992 programs
[AD-A263400] p 3654 N93-29258
Quantification of human responses
p 3500 N93-29564
The dynamics of visual representation, attention, encoding, and retrieval processes
[AD-A264674] p 3500 N93-30543
Multiple neuron recording in the hippocampus of freely moving animals
[AD-A264807] p 3492 N93-30594
Principal components of natural images: An analytical solution
[AD-A264800] p 3489 N93-30603

INFORMATION RETRIEVAL
On the evaluation of fuzzy quantified queries in a database management system p 3517 N93-29569
Geoscience center research
[AD-A263465] p 3462 N93-29834
Electron trapping data storage system and applications p 3622 N93-30474

INFORMATION SYSTEMS
The meta model hierarchy: A framework for information systems concepts and techniques
[TR-92-17] p 3611 N93-28481
Natural language generation
[AD-A262578] p 3524 N93-28579
The Backgrounds Data Center p 3624 N93-28814
National collaboratories: Applying information technology for scientific research
[LC-93-83795] p 3612 N93-29129
Hanford Environmental Information System (HEIS) user's manual, volume 1
[DE93-007465] p 3470 N93-29135
NSSDC data listing
[NASA-TM-108264] p 3612 N93-29167
Distributed Virtual System (DIVIRS) Project
[NASA-CR-193234] p 3526 N93-29169

Summer 1990 Atlanta ozone precursor study (January 1993) [PB93-167203] p 3470 N93-29200

Initial graphics exchange specification hybrid microcircuit application protocol [PB93-175404] p 3407 N93-29203

Applied Information Systems Research Program Workshop [NASA-TM-108773] p 3613 N93-29222

Applied Information Systems Research Program Workshop p 3613 N93-29223

Program plan for an experimenter's laboratory for visualized interactive science p 3613 N93-29224

A distributed system for visualizing and analyzing multivariate and multidisciplinary data p 3613 N93-29226

Data reduction expert assistant p 3613 N93-29227

Overview of the System of Experts for Intelligent Data Management (SEIDAM) p 3613 N93-29228

The scientific modeling assistant: An advanced software tool for scientific model building p 3613 N93-29229

National Center for Supercomputer Applications p 3614 N93-29232

Colorado Center for Astrodynamics Research (CCAR) p 3614 N93-29233

SAVS: A Space Data Analysis and Visualization System p 3614 N93-29235

A planetary version of PC-McIDAS p 3614 N93-29236

Interactive interface to NCAR graphics p 3614 N93-29237

VIEWCACHE: An incremental database access method for autonomous interoperable databases p 3614 N93-29238

Introduction to cadet center for advanced data evaluation technology p 3614 N93-29240

Flight Projects Office Information Systems Testbed (FIST) p 3615 N93-29241

Information system for co-registration of CAESAR sea-images based on two dimensional image matching techniques (SCORE). Part 1: Introduction, user requirements, and feasibility tests [BCRS-90-40A-PT-1] p 3460 N93-29307

Preprocessing airborne remote sensing PARES calibration maintenance functional design document [BCRS-92-07] p 3460 N93-29321

Head mounted displays for virtual reality [AD-A263498] p 3506 N93-29340

Information technology: A force for organizational change [AD-A261986] p 3615 N93-29439

National remote sensing programme 2 ACMS project. Phase 1: Validation. Part 1: Definition of validation experiment [BCRS-92-10-PHASE-1-PT-1] p 3461 N93-29465

EnviroNET: On-line information for LDEF p 3624 N93-29625

Programmer's reference guide to FDMS file formats [PB93-182038] p 3354 N93-29663

The 9th FLICC Forum on Federal Information Policies [PB93-184687] p 3624 N93-29668

Decision maker's guide to international space [ANSER-STDN-93-4] p 3669 N93-29710

Storage systems for national information assets [DE93-009303] p 3615 N93-29783

Energy efficient drivepower, volume 2 [DE93-012437] p 3410 N93-29814

Activities report of PTT Research [ISBN-9-07-212514-2] p 3392 N93-30025

NASA/DoD Aerospace Knowledge Diffusion Research Project. Paper 30: The electronic transfer of information and aerospace knowledge diffusion [NASA-TM-109223] p 3616 N93-30036

Meteorological information for aviation: A systems approach p 3367 N93-30298

Application and integration of diverse technology in an aviation system: The National Aeronautical Information Processing System p 3247 N93-30339

Introduction to the National Information Display Laboratory p 3628 N93-30718

Minimum security requirements for multi-user operating systems [PB93-185999] p 3522 N93-30832

Office of Water Environmental and Program Information Systems Compendium, FY 1992 [PB93-186203] p 3462 N93-30833

A prototype of a faculty and staff executive information system [AD-A264852] p 3623 N93-30907

Scientific research abstracts in the Republic of China, 1991 (science and technology) p 3670 N93-30911

INFORMATION THEORY

Information-theoretic performance bounding of Bayesian identifiers [DE93-010705] p 3554 N93-28763

Theory and applications of random fields [AD-A262829] p 3555 N93-29454

Multiscale and multigrid information representation, extraction and fusion [AD-A264623] p 3393 N93-30386

INFORMATION TRANSFER

NASA/DOD Aerospace Knowledge Diffusion Research Project. Paper 28: The technical communication practices of Russian and US aerospace engineers and scientists [NASA-TM-108249] p 3612 N93-28948

NASA/DoD Aerospace Knowledge Diffusion Research Project. Paper 29: The US government technical report and the transfer of federally funded aerospace R and D [NASA-TM-109221] p 3615 N93-29709

NASA/DoD Aerospace Knowledge Diffusion Research Project. Paper 30: The electronic transfer of information and aerospace knowledge diffusion [NASA-TM-109223] p 3616 N93-30036

NASA/DoD Aerospace Knowledge Diffusion Research Project. Paper 31: The information-seeking behavior of engineers [NASA-TM-109224] p 3616 N93-30037

INFRARED ASTRONOMY

Near-infrared spectroscopy as an astrophysical tool p 3632 N93-28607

Far infrared supplement. Third edition: Catalog of infrared observations (lambda greater than or equal to 4.6 micrometers) [NASA-RP-1295] p 3629 N93-29156

The 12 UM contribution of nearby galaxies to the infrared background [AD-A264336] p 3654 N93-30419

Activities report for the Laboratory for Space Research Groningen (Netherlands) [ETN-93-93688] p 3631 N93-30638

Near-infrared line imaging of NGC 6240: Global shock and nuclear starburst [MPE-PREPRINT-226] p 3631 N93-30641

Infrared spectroscopy and imaging of starburst galaxies and AGNs [MPE-PREPRINT-229] p 3632 N93-30643

INFRARED ASTRONOMY SATELLITE

A characterization of young stellar objects in Bok globules: Infrared imaging, spectral energy distributions, and molecular outflows p 3636 N93-30563

INFRARED DETECTORS

Miniature long-life space cryocoolers p 3378 N93-28825

The infrared measurement for the reentry-body-translation [AD-A263100] p 3278 N93-29134

A passive infrared ice detection technique for helicopter applications [NASA-CR-193187] p 3244 N93-29152

Measurement of projectile surface temperature by means of its infrared radiation: A preliminary study [AD-A264053] p 3432 N93-30032

Condensed phase diagnostics of nitramine propellant combustion p 3320 N93-30102

Infrared imaging array integrated in three dimensions directly on top of silicon circuits [AD-A264707] p 3581 N93-30500

Development of ultra-low noise, high sensitivity planar metal grating coupled 3-5 multiquantum well infrared detectors for focal plane array staring IR sensor systems [AD-A264465] p 3599 N93-30536

INFRARED IMAGERY

Design concept for an IR mapping spectrometer for the Pluto fast flyby mission p 3285 N93-28779

Acousto-optic infrared spectral imager for Pluto fast flyby p 3285 N93-28781

Multiscale morphological filtering for analysis of noisy and complex images p 3582 N93-28789

Quantification of thermographic mapping techniques [AD-A264020] p 3391 N93-30016

Infrared imaging array integrated in three dimensions directly on top of silicon circuits [AD-A264707] p 3581 N93-30500

A characterization of young stellar objects in Bok globules: Infrared imaging, spectral energy distributions, and molecular outflows p 3636 N93-30563

INFRARED INSPECTION

Logarithmic time scale in thermographic Non Destructive Evaluation (NDE) of materials p 3359 N93-30246

INFRARED LASERS

Experimental test of hole-coupled FEL resonator designs using a CW-HeNe laser [DE93-010439] p 3440 N93-30530

INFRARED PHOTOMETRY

The faintest stars p 3630 N93-30493

INFRARED RADIATION

Acousto-optic infrared spectral imager for Pluto fast flyby p 3285 N93-28781

Infrared rugates by molecular beam epitaxy p 3582 N93-28808

A technique for single-pulse spectrum and pulse width measurements for an IR-FEL [DE93-007732] p 3436 N93-28847

Leadex data report. Part 1: Weather analysis and satellite images [AD-A263217] p 3481 N93-28876

The infrared measurement for the reentry-body-translation [AD-A263100] p 3278 N93-29134

Far infrared supplement. Third edition: Catalog of infrared observations (lambda greater than or equal to 4.6 micrometers) [NASA-RP-1295] p 3629 N93-29156

A program to determine the pointing angle to a specular point [AD-A262777] p 3630 N93-29460

Condensed phase diagnostics of nitramine propellant combustion p 3320 N93-30102

On the photonic chiral anomaly in an external gravitational field [DE93-606082] p 3479 N93-30785

INFRARED SIGNATURES

A passive infrared ice detection technique for helicopter applications [NASA-CR-193187] p 3244 N93-29152

A program to determine the pointing angle to a specular point [AD-A262777] p 3630 N93-29460

INFRARED SPACE OBSERVATORY (ISO)

Activities report for the Laboratory for Space Research Groningen (Netherlands) [ETN-93-93688] p 3631 N93-30638

INFRARED SPECTRA

Tomographic analysis of line-of-sight infrared spectra of low-pressure flames [AD-A263185] p 3309 N93-28514

Spectroscopic probes of vibrationally excited molecules at chemically significant energies [DE93-012328] p 3564 N93-28652

Acousto-optic infrared spectral imager for Pluto fast flyby p 3285 N93-28781

Far infrared supplement. Third edition: Catalog of infrared observations (lambda greater than or equal to 4.6 micrometers) [NASA-RP-1295] p 3629 N93-29156

In situ Fourier transform infrared spectroscopic study of bisulfate and sulfate adsorption on gold, with and without the underpotential deposition of copper [AD-A263421] p 3323 N93-29259

Condensed phase diagnostics of nitramine propellant combustion p 3320 N93-30102

The faintest stars p 3630 N93-30493

INFRARED SPECTROMETERS

Measurement of a Michelson interferometer mirror velocity with a time interval analyzer [AD-A263009] p 3430 N93-28659

Design concept for an IR mapping spectrometer for the Pluto fast flyby mission p 3285 N93-28779

Transcutaneous analyte measuring methods [AD-A262861] p 3494 N93-29509

INFRARED SPECTROSCOPY

Tomographic analysis of line-of-sight infrared spectra of low-pressure flames [AD-A263185] p 3309 N93-28514

Near-infrared spectroscopy as an astrophysical tool p 3632 N93-28607

In situ Fourier transform infrared spectroscopic study of bisulfate and sulfate adsorption on gold, with and without the underpotential deposition of copper [AD-A263421] p 3323 N93-29259

High pressure preignition chemistry of hydrocarbons and hydrocarbon mixtures [AD-A263611] p 3311 N93-29283

A novel flame thermometer based on the doppler width of ro-vibrational transitions [AD-A264515] p 3315 N93-30405

Surface chemistry of hydrogen-passivated porous silicon-oxidation of surface Si-H groups by acetone [AD-A264655] p 3315 N93-30526

Activities report for the Laboratory for Space Research Groningen (Netherlands) [ETN-93-93688] p 3631 N93-30638

INFRARED TELESCOPES

Sodium guide star adaptive optics system for astronomical imaging in the visible and near-infrared [DE93-009543] p 3630 N93-29785

An auto-guiding system for mid-sized telescopes p 3375 N93-30340

INFRARED TRACKING

Subnanoradian, groundbased tracking of spaceborne lasers p 3442 N93-28823

INITIATORS

Synthesis of chiral molybdenum ROMP initiators and all-cis highly tactic Poly-2,3-R2Norbornadiene (R = CF3 or CO2Me) [AD-A264133] p 3336 N93-30169

INJECTION
Experimental study of heat transfer close to a plane wall heated in the presence of multiple injections (subsonic flow) p 3253 N93-29931
INJECTION LOCKING
Every good virtue you ever wanted in a Q-switched solid-state laser and more: Monolithic, diode-pumped, self-Q-switched, highly reproducible, diffraction-limited Nd:YAG laser p 3442 N93-28772
INJECTION MOLDING
Improved silicon nitride for advanced heat engines [NASA-CR-182193] p 3298 N93-29451
Resin transfer molding for advanced composite primary aircraft structures p 3301 N93-30438
Wetting and dispersion in ceramic/polymer melt injection molding systems [DE93-013240] p 3338 N93-30601
INJECTORS
Liquid fuel injection elements for rocket engines [NASA-CASE-MFS-28547-1] p 3289 N93-29847
INJURIES
Wound healing and connective tissue metabolism: The role of hyperbaric oxygen therapy [AD-A262483] p 3493 N93-28759
Sudden loading and fatigue effects on the human spine [PB93-167526] p 3493 N93-29199
INLET AIRFRAME CONFIGURATIONS
Solution of Euler equations for forebody-inlet ensemble of aircraft at high angle of attack [AD-A263905] p 3240 N93-29862
INLET FLOW
The 3-D viscous flow CFD analysis of the propeller effect on an advanced ducted propeller subsonic inlet [NASA-TM-106240] p 3252 N93-29162
Nonlinear relaxation algorithms for the compressible Navier-Stokes equations in two and three dimensions p 3421 N93-29177
Solution of Euler equations for forebody-inlet ensemble of aircraft at high angle of attack [AD-A263905] p 3240 N93-29862
INLET TEMPERATURE
Flow phenomena in turbomachines [AD-A263049] p 3420 N93-29141
The influence of non-uniform spanwise inlet temperature on turbine rotor heat transfer p 3253 N93-29932
INORGANIC CHEMISTRY
Gordon Research Conferences, 1991 [AD-A264275] p 3317 N93-30816
INORGANIC COMPOUNDS
Thermal properties of organic and modified inorganic aerogels [DE93-009230] p 3311 N93-29263
Studies in Lewis acid and superacid ionic liquids [AD-A264683] p 3316 N93-30551
Carborane-(silane or siloxane)-unsaturated hydrocarbon based thermosetting polymers [AD-D015718] p 3338 N93-30580
Carborane-(siloxane or silane)-unsaturated hydrocarbon based polymers [AD-D015717] p 3338 N93-30586
Standard and reference materials for marine science, third edition [PB93-185684] p 3489 N93-30830
INPUT/OUTPUT ROUTINES
Concurrent clean language manual, version 0.8 [TR-92-18] p 3522 N93-28482
A parallel processing system for intensive I/O p 3362 N93-30262
RAID 7 disk array p 3537 N93-30462
Using Transparent Informed Prefetching (TIP) to reduce file read latency p 3522 N93-30480
INSPECTION
Reliability assessment at airline inspection facilities. Volume 2: Protocol for an eddy current inspection reliability experiment [DOT/FAA/CT-92/12-VOL-2] p 3449 N93-28685
Inservice diagnostic methods for solenoid-operated valves [DE93-007823] p 3443 N93-28968
Debris/ice/TPS assessment and integrated photographic analysis for Shuttle Mission STS-55 [NASA-TM-107559] p 3271 N93-29136
INSTALLING
Installation of a new Fortran compiler and effective programming method on the vector supercomputer [DE93-753322] p 3524 N93-28537
Transient response of embedded thermocouples [DE93-009889] p 3431 N93-29325
FDDI installation and performance analysis [AD-A263263] p 3529 N93-29497
Atmospheric studies with SODAR at Kalpakkam [DE93-605544] p 3480 N93-30992
INSTRUCTORS
Proposal to develop guides for high school teachers on global systems science [DE93-008759] p 3624 N93-29100
Summer Faculty Research Program (SFRP), volume 1 [AD-A261988] p 3608 N93-29440
Filling the gaps: An overview of data on education in grades K through 12 [PB93-176550] p 3608 N93-30821
INSTRUMENT APPROACH
An evaluation of B-1B pilot performance during simulated instrument approaches with and without status information [AD-A263874] p 3507 N93-29888
INSTRUMENT FLIGHT RULES
Pilot intent and error recognition as part of a knowledge based cockpit assistant p 3502 N93-28855
INSTRUMENT LANDING SYSTEMS
Two simulation studies of precision runway monitoring of independent approaches to closely spaced parallel runways [AD-A263433] p 3261 N93-29815
An evaluation of B-1B pilot performance during simulated instrument approaches with and without status information [AD-A263874] p 3507 N93-29888
INSTRUMENTS
Sources sought for innovative scientific instrumentation for scientific lunar rovers p 3434 N93-28804
INSULATION
Lightweight flexible composite tent materials [AD-A263021] p 3295 N93-28660
Spacecraft glow and the EISG/skirt experiment p 3266 N93-28728
Thermal properties of organic and modified inorganic aerogels [DE93-009230] p 3311 N93-29263
Postflight hardware evaluation 360T025 (RSRM-25, STS-46) [NASA-CR-192562] p 3272 N93-30617
Postflight hardware evaluation 360T025 (RSRM-25, STS-46). Appendix A: Insulation PFORs [NASA-CR-192563] p 3272 N93-30618
Postflight hardware evaluation 360T025 (RSRM-25, STS-46). Appendix E: Insulation postfire data [NASA-CR-192566] p 3272 N93-30621
INTEGERS
Packing odd paths [CWI-BS-R9207] p 3549 N93-29849
Nth roots of normal contractions [DE92-644725] p 3557 N93-30985
INTEGRAL EQUATIONS
Experimental and modal verification of an integral equation solution for a thin-walled dichroic plate with cross-shaped holes p 3385 N93-29591
Continuation of: Applications of gauge theories to enhance numerical solutions of mixed potential integral equations [AD-A263763] p 3550 N93-29876
Scattering through apertures and by three-dimensional structures. Application to the measurement of the surface impedance of conductive materials [ONERA-P-1990-2] p 3392 N93-30018
Sound wave scattering from an elastic spherical shell [AD-A264039] p 3562 N93-30029
Application of integral and differential equation methods for various EM interaction problems [AD-A264821] p 3394 N93-30597
INTEGRALS
Approximation formulae for functional integrals in P(phi)2-quantum field theory [DE93-606067] p 3605 N93-30781
Integrals of motion on the group of invariance of an interval in three-dimensional spaces [DE93-606090] p 3606 N93-30797
A simple formula for reducing Feynman diagrams to scalar integrals [DE92-644717] p 3607 N93-30916
Quantum group generalization of the heterotic QFT [DE92-644727] p 3607 N93-30920
INTEGRATED CIRCUITS
Packing of Steiner trees: Polyhedric studies and application [ETN-93-93796] p 3547 N93-28527
Measurement of a Michelson interferometer mirror velocity with a time interval analyzer [AD-A263009] p 3430 N93-28659
Processing, fabrication, and demonstration of HTS integrated microwave circuits [AD-A263161] p 3406 N93-28940
Handshake circuits: An intermediary between communicating processes and VLSI [ETN-93-93579] p 3408 N93-29269
Instrumental neutron activation analysis developed for silicon integrated circuit technology [ETN-93-93581] p 3408 N93-29271
Optically controlled active impedance element particularly suited for a microwave oscillator [AD-D015723] p 3408 N93-29281
New developments in vacuum microelectronics [AD-A263103] p 3410 N93-29798
Wavelength-division multiplexed optical integrated circuit with vertical diffraction grating [NASA-CASE-NPO-18357-1-CU] p 3579 N93-29848
Total dose tests for the PROMICS-3 instrument [VTT-TIED-1203] p 3411 N93-30108
Test structure to microcircuit correlation [AD-A264157] p 3412 N93-30152
A single chip high-speed CMOS Viterbi decoder p 3358 N93-30238
Fault tolerance and testing for WSI systems p 3361 N93-30258
Generation of configurable self-synchronizing synchronous CMOS static RAMs p 3361 N93-30259
Infrared imaging array integrated in three dimensions directly on top of silicon circuits [AD-A264707] p 3581 N93-30500
Effects of device scaling and geometry on MOS radiation hardness assurance [DE93-009832] p 3413 N93-30516
Laboratory experiments in integrated circuit fabrication p 3292 N93-30962
Design and integration of high bit rate four phase monolithic demodulators and modulators at X band [LAAS-92354] p 3414 N93-31030
INTEGRATED OPTICS
Fusion laser oscillator and pulse-forming system using integrated optics [DE93-009286] p 3588 N93-29780
Wavelength-division multiplexed optical integrated circuit with vertical diffraction grating [NASA-CASE-NPO-18357-1-CU] p 3579 N93-29848
INTEGRATORS
Photorefractive integrators and correlators [AD-A264200] p 3597 N93-30144
INTELLIGENCE
The AFOSR Workshop on the Future of EEG and MEG [AD-A264338] p 3495 N93-30160
Centralized maintenance evaluation [AD-A264400] p 3544 N93-30886
INTERACTING GALAXIES
Models of star formation in interacting and merging disk galaxies p 3635 N93-30148
INTERACTIONS
Dynamic ice structure interaction: Theory and applications [VTT-PUBS-90] p 3353 N93-28632
INTERACTIVE CONTROL
Controls of interaction dynamics of orbital assembly p 3275 N93-29111
INTERCALATION
Apparatus for intercalating large quantities of fibrous structures [NASA-CASE-LEW-15077-2] p 3298 N93-29609
INTERFACES
DOKMA: A document oriented communication model for medical applications as a basis of a role system in the medical field [ETN-93-93799] p 3492 N93-28469
A survey of network interface designs [MEMO-INF-92-59] p 3379 N93-28502
Handshake circuits: An intermediary between communicating processes and VLSI [ETN-93-93579] p 3408 N93-29269
INTERFACIAL TENSION
Heat pipe performance experiment p 3265 N93-28722
INTERFEROMETERS
Precision optical interferometry in space [NASA-CR-193264] p 3630 N93-29163
Design of a high resolution spatial heterodyne interferometer [AD-A262867] p 3285 N93-29461
Investigations of self-pumped phase conjugate laser beams and coherence length [AD-A263438] p 3438 N93-29789
Portable fiber optic coupled Doppler interferometer system for detonation and shock wave diagnostics [DE93-009827] p 3433 N93-30510
INTERFEROMETRY
Limitations of the ideal phase-Doppler system: Extension to spatially and temporally inhomogeneous particle flows with an application to diesel sprays [DE93-009447] p 3416 N93-28595
The interferometric SAR technology and its usability in the framework of ERS-1 p 3457 N93-28919
Development of coherent x ray lasers [DE93-009288] p 3437 N93-29104
Precision optical interferometry in space [NASA-CR-193264] p 3630 N93-29163

Interferometric tracking system for the tracking and data relay satellite
[NASA-CR-193274] p 3382 N93-29217

Precise tracking of the Magellan and Pioneer Venus orbiters by Same-Beam Interferometry. Part 2: Orbit determination analysis p 3270 N93-29589

INTERGRANULAR CORROSION

Overview of piping issues and trends
[DE93-006628] p 3354 N93-28893

INTERIOR BALLISTICS

The XNOVAKTC rheological model
[AD-A263298] p 3342 N93-29762

INTERLAMINAR STRESS

Influence of ply waviness on stiffness and strength reduction of composite laminates
[AD-A263224] p 3294 N93-28559

Factors influencing the interlaminar fracture toughness and its evaluation in composites
[FFA-TN-1991-34] p 3451 N93-29076

INTERLAYERS

A transient FGM interlayer based approach to joining ceramics
[DE93-010415] p 3331 N93-29248

INTERMETALLICS

Refractory metal disilicides research
[AD-A262416] p 3320 N93-28499

Transformation toughening
[DE93-011805] p 3321 N93-28631

The effect of temperature on the impact behavior of TiB2 reinforced XDTM-TiAl intermetallic matrix composites
[AD-A262924] p 3296 N93-28886

Microstructural effects on the deformation and fracture of the alloy Ti-25Al-10Nb-3B-1Mo
[AD-A263095] p 3323 N93-29144

Low temperature environmental embrittlement in ordered intermetallics
[DE93-009711] p 3324 N93-29786

Improvement in ductility of the intermetallic compound Ti3Al
[ESA-TT-1276] p 3325 N93-30105

Reactive sintering of Ni3Al intermetallic alloys under compressive stress
[DE93-009729] p 3327 N93-30652

Magnetic character investigation of higher alcohol synthesis Cu-Co-Cr catalysts
[DE93-009732] p 3316 N93-30653

Radiation effects in FCC metals and intermetallic compounds: A molecular dynamics computer simulation study
[DE93-009546] p 3600 N93-30668

INTERMITTENCY

Measurement of turbulent spots and intermittency modelling at gas-turbine conditions
p 3253 N93-29934

Fluctuations and intermittency in high energy nucleus-nucleus collisions
[DE93-608481] p 3577 N93-30990

INTERMODULATION

Analytical predictions of the intermodulation noise of semiconductor laser diode p 3361 N93-30256

INTERMOLECULAR FORCES

Molecular dynamics of detonation in crystals with defects p 3350 N93-30097

The calculation of electrostatic interactions and their role in determining the energies and geometries of molecular HE crystals
[DE92-040374] p 3570 N93-30448

INTERNAL FRICTION

Anelastic relaxations associated with local disordering in grain boundaries
[AD-A263101] p 3596 N93-29796

INTERNAL PRESSURE

Research and development of carbon black anodes for lithium secondary cells
[DE93-781331] p 3406 N93-28746

INTERNAL WAVES

Hamiltonian dynamics of coupled potential vorticity and internal wave motion: 1. Linear modes
[AD-A263469] p 3424 N93-29838

ARI: Internal gravity waves at abrupt topography
[AD-A263795] p 3477 N93-29879

Dynamics of small-scale oceanic motions
[AD-A263582] p 3488 N93-29914

The IUTAM Symposium on Breaking Waves
[AD-A264196] p 3489 N93-30143

The wake software suite: User's guide
[AD-A264181] p 3425 N93-30156

Laboratory studies of gravity wave/mean flow interactions
[AD-A264226] p 3478 N93-30174

INTERNATIONAL COOPERATION

Earth observation from space: Competition or cooperation?
[AD-A262044] p 3459 N93-29000

Contributions to the American Meteorological Society's 26th International Conference on Radar Meteorology
[AD-A263385] p 3481 N93-29257

Remote sensing in Czechoslovakia and Hungary: An analysis of the possible co-operation of The Netherlands with Czechoslovakia and Hungary in the field of remote sensing
[BCRS-92-12] p 3461 N93-29466

Decision maker's guide to international space
[ANSER-STDN-93-4] p 3669 N93-29710

Proceedings of the meeting of the Intergovernmental US-Russian Business Development Committee's Standards Working Group
[PB93-179968] p 3610 N93-30822

INTERNATIONAL LAW

The environment as an operational center of gravity
[AD-A264170] p 3472 N93-30154

INTERNATIONAL TRADE

Proceedings of the meeting of the Intergovernmental US-Russian Business Development Committee's Standards Working Group
[PB93-179968] p 3610 N93-30822

INTERPLANETARY DUST

Further analysis of LDEF FRECOPA micrometeoroid remnants p 3638 N93-29360

Derivation of particulate directional information from analysis of elliptical impact craters on LDEF
p 3283 N93-29362

Asteroidal versus cometary meteoroid impacts on the Long Duration Exposure Facility (LDEF)
p 3638 N93-29371

Interplanetary meteoroid debris in LDEF metal craters
p 3638 N93-29372

Long Duration Exposure Facility (LDEF) attitude measurements of the Interplanetary Dust Experiment
p 3638 N93-29377

Elemental analyses of hypervelocity microparticle impact sites on Interplanetary Dust Experiment sensor surfaces
p 3638 N93-29378

Long-term microparticle flux variability indicated by comparison of Interplanetary Dust Experiment (IDE) timed impacts for LDEF's first year in orbit with impact data for the entire 5.77-year orbital lifetime p 3638 N93-29379

INTERPLANETARY MAGNETIC FIELDS

Mithras studies of the boundary between open and closed field lines
[AD-A264758] p 3479 N93-30562

INTERPLANETARY SPACE

Project WISH: The Emerald City p 3232 N93-29744

INTERPLANETARY SPACECRAFT

Subnanoradian, groundbased tracking of spaceborne lasers p 3442 N93-28823

Space transfer concepts and analyses for exploration missions, phase 3
[NASA-CR-192584] p 3268 N93-31034

INTERPOLATION

Filtering interpolators for image comparison algorithms
p 3463 N93-28797

Time-interpolation method for digital beamformers
[AD-D015709] p 3383 N93-29275

INTERPRETATION

Quantification of human responses
p 3500 N93-29564

INTERPROCESSOR COMMUNICATION

A survey of network interface designs
[MEMO-INF-92-59] p 3379 N93-28502

Implementation of a single-material version of PAGOSA on MIMD hypercubes
[SAND-92-0640] p 3526 N93-29127

Efficient wiring of reconfigurable parallel processors
[DE93-009847] p 3538 N93-29186

A parallel processing system for intensive I/O
p 3362 N93-30262

Task allocation and real-time considerations for the Robot Controller Test Station (RCTS)
p 3364 N93-30278

On analytical performance modelling of software for distributed systems p 3364 N93-30279

Parcels with TAGS
[PB93-181824] p 3535 N93-30824

INTERSECTIONS

Distributed traffic signal control using fuzzy logic
p 3513 N93-29543

The global potential energy surfaces of the lowest two 1A-prime states of the ozone molecule: Theoretical determination and analysis
[DE93-007537] p 3313 N93-29837

A method for intersection line calculation between parametric surfaces
[ETN-93-94178] p 3551 N93-30572

INTERSTELLAR GAS

The Interstellar Gas Experiment: Analysis in progress
p 3639 N93-29380

INTERSTELLAR MATTER

The Interstellar Gas Experiment: Analysis in progress
p 3639 N93-29380

CO lines toward NGC 2024 and other star forming regions: A closer look at the warm gas component
[MPE-PREPRINT-223] p 3637 N93-30639

INTERSTITIALS

Method for preparation of a microporous structure with layered interstitial surface treatment
[NASA-CASE-MSC-21487-2] p 3296 N93-29023

INVARIANCE

Representation and recognition with invariants and geometric constraint models
[AD-A263235] p 3529 N93-29493

Integrals of motion on the group of invariance of an interval in three-dimensional spaces
[DE93-606090] p 3606 N93-30797

Scaling properties of localized quantum chaos
[DE93-606031] p 3606 N93-30803

The ground state wavefunctions of a conformally invariant scalar field in different spacetime background
[DE93-606063] p 3606 N93-30808

Enhanced convergence adaptive detection
[AD-A264100] p 3399 N93-30879

Nonlinear realisations of omega(1 + infinity)
[DE92-644721] p 3557 N93-30917

On one-dimensional topological and conformal field theories
[DE92-644726] p 3558 N93-30986

INVENTORIES

World commercial aircraft accidents
[DE93-010892] p 3243 N93-28571

INVERSE KINEMATICS

Dual arm generalized compliant motion with shared control
[NASA-CASE-NPO-18738-1-CU] p 3443 N93-28954

Planning collision free paths for two cooperating robots using a divide-and-conquer C-space traversal heuristic
[NASA-CR-193252] p 3542 N93-29771

INVERSE SCATTERING

On the method of determining relations
[DE93-606041] p 3551 N93-30765

INVESTMENT CASTING

Development of a CFD code for casting simulation
[NASA-CR-192577] p 3427 N93-30492

INVISCID FLOW

Inviscid quasi one-dimensional nonequilibrium flow
[FFA-TN-1992-35] p 3418 N93-28993

Three-dimensional numerical simulation of gradual opening in a wave rotor passage
[NASA-CR-191157] p 3252 N93-29072

Direct numerical simulations of unsteady separated flows using vortex methods p 3419 N93-29077

Nonlinear relaxation algorithms for the compressible Navier-Stokes equations in two and three dimensions
p 3421 N93-29177

Development of an unstructured solution adaptive method for the quasi-three-dimensional Euler and Navier-Stokes equations
[NASA-CR-193241] p 3421 N93-29213

Numerical computation of inviscid flow around nose tip of Space Shuttle with NND scheme
[AD-A264012] p 3421 N93-29260

An upwind method for the solution of the 3D Euler and Navier-Stokes equations on adaptively refined meshes
[AD-A262863] p 3423 N93-29472

Solution of Euler equations for forebody-inlet ensemble of aircraft at high angle of attack
[AD-A263905] p 3240 N93-29862

Hydrodynamic interactions among fibers in high efficiency filters
[DE93-007117] p 3424 N93-30035

IO

Remote measurement of planetary magnetic fields by the Hanle effect p 3645 N93-28793

IODIDES

Characterization of copper iodide thin films fabricated via laser assisted molecular beam epitaxy
[AD-A262823] p 3596 N93-29430

ION ACCELERATORS

Accelerator research studies
[DE93-009353] p 3573 N93-28522

Design and test of a superconducting RFQ for heavy ions
[DE93-010862] p 3575 N93-29317

Research and education by SF cyclotron facility
[DE93-753135] p 3576 N93-30002

ION ACOUSTIC WAVES

Plasma diffusion through multidipole magnetic fields
[DE93-608548] p 3591 N93-31007

ION BEAMS

An experimental investigation of radioactivity induced by ions associated with the operation of pulsed-power accelerators
[DE93-011478] p 3575 N93-29151

High-dose implantations of Al into Si(111) and Si(100)
[DE93-009552] p 3594 N93-29301

Investigation of ion beam mixing of iron marker layers in aluminum oxide by RBS
[DE93-010727] p 3594 N93-29314
Characteristics of hypervelocity impact craters on LDEF experiment S1003 and implications of small particle impacts on reflective surfaces p 3283 N93-29363
High-current negative-ion beam transport
[DE93-010732] p 3575 N93-29809
Improved heat removal by microscopic surface texturing of capillaries
[AD-A263483] p 3424 N93-29966
Research and education by SF cyclotron facility
[DE93-753135] p 3576 N93-30002
Pulse control in an accelerator for heavy-ion fusion
[DE93-009527] p 3576 N93-30390
Heat generation produced in thin layers of GaAs superconductors under high energy particles irradiation
[DE93-606332] p 3601 N93-30798

ION CURRENTS
NPB cesium space experiment p 3267 N93-28733

ION CYCLOTRON RADIATION
High mass resolution glow discharge mass spectrometry using an external ion source FT-ICR mass spectrometer
[AD-A264347] p 3314 N93-30166
Fundamental studies of fusion plasmas
[DE93-013144] p 3589 N93-30189

ION DISTRIBUTION
Ion ring distribution produced by a magnetosonic wave
[DE93-754311] p 3590 N93-30533

ION EMISSION
Ion emission during high-energy sputtering of ammonium dinitramide and ammonium nitrate crystals and the determination of ion decomposition pathways using tandem mass spectrometry p 3318 N93-30066
Scanning ionic microscopy with high spatial resolution: Parallel acquisition of elementary images by high resolution mass spectrometry
[ONERA-NT-1990-7] p 3314 N93-30139

ION EXCHANGE MEMBRANE ELECTROLYTES
Thermodynamics of swelling and collapse of polyelectrolytic gels
[ETN-93-93485] p 3331 N93-29064
Electrical relaxation in acid-form nafion
[AD-A263558] p 3410 N93-29826
The electrolyte factor in O2 reduction electrocatalysis
[AD-A263565] p 3313 N93-29828

ION EXCHANGING
Acid solution absorption of extruded polyethylene foam
[DE93-011701] p 3330 N93-28839

ION IMPACT
Effects of neutral gas collisions on the power transmission factor at the divertor sheath
[DE93-009320] p 3588 N93-29334

ION IMPLANTATION
Luminescence study of ion-implanted and MBE-grown Er-doped GaAs and Al(x)Ga(1-x)As
[AD-A262602] p 3591 N93-28471
Surface modification of tribological components in transportation
[DE93-008647] p 3442 N93-28903
High-dose implantations of Al into Si(111) and Si(100)
[DE93-009552] p 3594 N93-29301

ION IRRADIATION
An experimental investigation of radioactivity induced by ions associated with the operation of pulsed-power accelerators
[DE93-011478] p 3575 N93-29151

ION MICROSCOPES
Scanning ionic microscopy with high spatial resolution: Parallel acquisition of elementary images by high resolution mass spectrometry
[ONERA-NT-1990-7] p 3314 N93-30139

ION MOTION
Ion motion effects on charged radiators
[DE93-009257] p 3565 N93-29099

ION SCATTERING
Diffraction and holography with photoelectrons and Auger electrons: Some new directions
[DE93-007664] p 3313 N93-29766

ION SOURCES
NPB cesium space experiment p 3267 N93-28733
A high field optical-pumping spin-exchange polarized deuterium source
[DE93-009208] p 3574 N93-28970
An RF driven H(-) source and a low energy beam injection system for RFQ operation
[DE93-010438] p 3575 N93-29302
High mass resolution glow discharge mass spectrometry using an external ion source FT-ICR mass spectrometer
[AD-A264347] p 3314 N93-30166
Measurement of work function of a plasma grid in a cesium seeded negative ion source
[DE93-764153] p 3589 N93-30190

ION TEMPERATURE
Self-organized profile relaxation by ion temperature gradient instability in toroidal plasmas
[DE93-009580] p 3585 N93-28910

ION TRAPS (INSTRUMENTATION)
An improved linear ion trap physics package
p 3384 N93-29587

IONIC COLLISIONS
Studies of relativistic heavy ion collisions at the AGS (E814/E877)
[DE93-008541] p 3564 N93-28678

IONIC MOBILITY
Advanced signal processing requirement in an ion mobility explosives detector p 3320 N93-30277

IONIC REACTIONS
A simple model for ion solvation with non additive cores
[AD-A263075] p 3566 N93-29143

IONIZATION
Large amplitude striations in an RF discharge
[DE93-753244] p 3379 N93-28534
Laser spectroscopy of hydrocarbon radicals
[DE93-012555] p 3436 N93-28653
The emulsion chamber technology experiment
p 3268 N93-28743

IONIZATION CHAMBERS
Spin dependent phenomena in medium energy physics
[DE93-010972] p 3565 N93-28849
Charge to frequency converter for ionization chambers belonging to the radiation protection system of AmPS/MEA
[DIGEL-1991-6] p 3577 N93-30837

IONIZATION CROSS SECTIONS
The production and destruction of negative ions
[DE93-010527] p 3564 N93-28665

IONIZED GASES
Large amplitude striations in an RF discharge
[DE93-753244] p 3379 N93-28534

IONIZING RADIATION
New remote maintenance approach for TPX
[DE93-007857] p 3584 N93-28583
Radiation monitoring equipment dosimeter experiment
p 3266 N93-28730
Status of LDEF ionizing radiation measurements and analysis p 3654 N93-29626
Development and application of a 3-D geometry/mass model for LDEF satellite ionizing radiation assessments
p 3573 N93-29640
Radiation model predictions and validation using LDEF satellite data p 3573 N93-29641
Future directions for LDEF ionizing radiation modeling and assessments p 3573 N93-29642

IONOSPHERIC CONDUCTIVITY
ELF propagation highlights p 3395 N93-30730
Studies of the propagation of Low Frequency (LF) radio waves p 3396 N93-30738

IONOSPHERIC DISTURBANCES
USU center of excellence in theory and analysis of the geo-plasma environment
[AD-A264750] p 3590 N93-30585
Acoustic-gravity waves from low-altitude localized disturbances
[AD-A264804] p 3479 N93-30593
Numerical modeling of the propagation medium at VLF/LF p 3395 N93-30729
A long wave TE/TM noise prediction model
p 3397 N93-30742
Performance statistics bulletin. High latitude meteor scatter propagation, May, June, July 1989
[AD-A264003] p 3399 N93-30757

IONOSPHERIC ELECTRON DENSITY
Ionospheric structure specifications and systems effects
[AD-A263573] p 3476 N93-29343

IONOSPHERIC HEATING
Results of the joint HIPAS/NUWC campaigns to investigate ELF generated by auroral electrojet modulation p 3398 N93-30746

IONOSPHERIC PROPAGATION
A comparison of trans-equatorial ionosphere propagation predictions from AMBCOM with measured data
[AD-A264006] p 3391 N93-29987
Numerical modeling of the propagation medium at VLF/LF p 3395 N93-30729
Theoretical and experimental coverage analysis of a VLF transmitter p 3396 N93-30734
Studies of the propagation of Low Frequency (LF) radio waves p 3396 N93-30738
A long wave TE/TM noise prediction model
p 3397 N93-30742

IONS
Moment approach to fast ion neoclassical transport and viscous forces
[DE93-753305] p 3585 N93-28979
In situ Fourier transform infrared spectroscopic study of bisulfate and sulfate adsorption on gold, with and without the underpotential deposition of copper
[AD-A263421] p 3323 N93-29259
Molecular dynamics modeling of electric double layers with spectroscopic applications
[AD-A263168] p 3568 N93-29489
Design of acentric materials: X ray structures of guanidinium p-nitro- and p-hydroxybenzenesulfonate
[AD-A264220] p 3597 N93-30146
Conjugated substituted ionic polyacetylenes
[AD-A264702] p 3337 N93-30497
Studies in Lewis acid and superacid ionic liquids
[AD-A264683] p 3316 N93-30551

IRON
Prototype backscatter Moessbauer spectrometer for measurement of Martian surface mineralogy
p 3648 N93-28812
Effect of zinc and iron ions on the electrochemistry of nickel oxide electrode: Slow cyclic voltammetry
[AD-A263098] p 3311 N93-29133
Investigation of ion beam mixing of iron marker layers in aluminum oxide by RBS
[DE93-010727] p 3594 N93-29314

IRON ALLOYS
Effects of internal helium on mechanical properties of Nitronic (tm) 40 stainless steel
[DE93-009902] p 3324 N93-29265

IRON COMPOUNDS
Rates and mechanisms of reaction of hydrogen sulfide with iron chelates
[PB93-184299] p 3312 N93-29665

IRON ISOTOPES
Reaction mechanism studies of heavy ion induced nuclear reactions
[DE93-010496] p 3569 N93-29807

IRRADIATION
Smart skin structures for identifying and locating laser irradiation
[DE93-005464] p 3436 N93-28887
Defect studies in low-temperature-grown GaAs
[DE93-010405] p 3595 N93-29417
Charged particle activation studies on the surface of LDEF spacecraft p 3572 N93-29630

ISCCP PROJECT
Sensitivity study of cloud/radiation interaction using a second order turbulence radiative-convective model
[DE93-007365] p 3477 N93-29346

ISLANDS
Reception at Ascension Island, South Atlantic, of the transmissions from the Heard Island feasibility test
[PB93-176261] p 3394 N93-30662

ISOMERIZATION
Applications of density functional theory to calculation of reaction energetics p 3351 N93-30098

ISOMERS
Nuclear isomers as ultra-high-energy-density materials
[DE93-009520] p 3568 N93-29784

ISOTHERMAL PROCESSES
Isothermal and shock compression of high density ammonium nitrate and ammonium perchlorate
[DE93-000682] p 3315 N93-30209

ISOTHERMS
Analysis of thermal bar using boundary-layer integral equations gradients
[MATHS-REPT-A-177] p 3462 N93-30107
Fluids in porous media.
[PB93-175198] p 3428 N93-30759

ISOTOPE SEPARATION
High-efficiency high-reliability optical components for a large, high-average-power visible laser system
[DE93-009225] p 3437 N93-29098
Effects of vacuum exposure on stress and spectral shift of high reflective coatings
[DE93-009318] p 3437 N93-29207

ISOTOPES
Mass spectrometric measurement of Martian krypton and xenon isotopic abundance p 3646 N93-28798
Geochemical and fluid dynamic investigations into the nature of chemical heterogeneity in the Earth's mantle
[AD-A262753] p 3477 N93-29405
Standard and reference materials for marine science, third edition
[PB93-185684] p 3489 N93-30830

ISOTOPIC SPIN
Study of heavy-flavored particles
[DE93-011535] p 3569 N93-30128

ISOTROPIC TURBULENCE
The structure and dynamics of the vorticity and passive scalar fields at small scales in homogeneous isotropic turbulence p 3427 N93-30625

ITERATION
A genetic algorithms approach for altering the membership functions in fuzzy logic controllers
p 3518 N93-29573

ITERATIVE SOLUTION

BlockSolve v1.1: Scalable library software for the parallel solution of sparse linear systems [DE93-011391] p 3524 N93-28644

Iterative encoding methods for computer generated holograms [AD-A263705] p 3431 N93-29297

A numerical solution of the two-center problem [DE92-644674] p 3551 N93-30913

Fixed point iterations for quasi-contractive maps in uniformly smooth Banach spaces [DE92-641348] p 3552 N93-30942

IUE

IUE observations of cataclysmic variable [NASA-CR-193188] p 3629 N93-28634

J

J INTEGRAL

Two-parameter crack tip field associated with stable crack growth in a thin plate: A hybrid analysis [AD-A264221] p 3453 N93-30147

J-52 ENGINE

An analysis of the correlation between the J52 engine component improvement program and improved maintenance parameters [AD-A262062] p 3251 N93-28984

JACOBI MATRIX METHOD

A functional implementation of the Jacobi eigen-solver [DE93-007349] p 3549 N93-29769

JAMMING

Modified Acousto-Optic Adaptive Processor (Mod-AOAP) [AD-A261983] p 3381 N93-28997

Coarse synchronization in an EHF frequency-hopped satellite communications system p 3365 N93-30281

Adaptive jammer nulling in EHF communications satellites p 3365 N93-30284

Performance of frequency hopped M-ary FSK in Rayleigh fading and partial-band jamming p 3368 N93-30303

Adaptive airborne radar simulation with equalization filter taps [AD-A264722] p 3393 N93-30514

JAPAN

NSF Tokyo reports: Japanese R and D projects on micro- and nanofabrication and related basic research projects [PB93-181261] p 3410 N93-29671

JET AIRCRAFT NOISE

Jet mixer noise suppressor using acoustic feedback [NASA-CASE-LEW-15170-1] p 3561 N93-28953

Some aspects of the aeroacoustics of high-speed jets [NASA-CR-191458] p 3418 N93-28975

JET CONTROL

Robust feedforward/feedback control synthesis for uncertain dynamical systems p 3542 N93-29079

JET ENGINE FUELS

Advanced thermally-stable, coal-derived, jet fuels program: Experiment system and model development [AD-A262747] p 3342 N93-29402

JET FLOW

A numerical study of confined turbulent jets [NASA-TM-106197] p 3420 N93-29161

Experimental study of heat transfer close to a plane wall heated in the presence of multiple injections (subsonic flow) p 3253 N93-29931

Heat transfer in high turbulence flows: A 2-D planar wall jet p 3254 N93-29935

Modeling of a turbulent flow in the presence of discrete parietal cooling jets p 3258 N93-29960

Plasma/particle interaction in subsonic argon/helium thermal plasma jets [DE93-010808] p 3589 N93-30181

Effects of buoyancy on gas jet diffusion flames [NASA-CR-191109] p 3352 N93-31031

JET IMPINGEMENT

Fundamental studies of impingement cooling thermal boundary conditions p 3254 N93-29940

Prediction of jet impingement cooling scheme characteristics (airfoil leading edge application) p 3255 N93-29941

The +vbar breakout during approach to Space Station Freedom [NASA-TM-104772] p 3269 N93-30135

JET MIXING FLOW

On the development of a film cooling layer p 3258 N93-29959

JFET

Growth, characterization and device development in monocrystalline diamond films [AD-A263204] p 3593 N93-28874

JOINTS (JUNCTIONS)

Ceramic matrix composites properties/microstresses with complete and partial interphase bond [NASA-TM-106136] p 3297 N93-29071

Postflight hardware evaluation 360T025 (RSRM-25, STS-46). Appendix B: Case, seals, and joints PFORs [NASA-CR-192564] p 3272 N93-30619

Development of an experimental method to determine the axial rigidity of a strut-node joint p 3290 N93-30950

JOSEPHSON JUNCTIONS

Flux lattice relaxation, noise, and symmetry-breaking in frustrated Josephson junction arrays [DE93-008713] p 3593 N93-29094

Response of a Nb/Al2O3/Nb tunnel junction to picosecond electrical pulses [DE93-010416] p 3594 N93-29249

JP-4 JET FUEL

Performance and cost evaluation of bioremediation techniques for fuel spills [PB93-175545] p 3474 N93-30762

JP-8 JET FUEL

The chronic effects of jP-8 jet fuel exposure on the lungs [AD-A264162] p 3495 N93-30153

JUDGMENTS

Quantification of human responses p 3500 N93-29564

JUNCTION DIODES

Neutron radiation induced degradation of diode characteristics [AD-A263277] p 3405 N93-28563

Widebanding techniques for VHF antennas 2 [AD-A263998] p 3387 N93-29882

Laboratory experiments in integrated circuit fabrication p 3292 N93-30962

K

K-EPSILON TURBULENCE MODEL

A numerical study of confined turbulent jets [NASA-TM-106197] p 3420 N93-29161

Turbulent flow and heat transfer in idealized blade cooling passages p 3254 N93-29938

Modeling of a turbulent flow in the presence of discrete parietal cooling jets p 3258 N93-29960

Turbulence characteristics of an axisymmetric reacting flow [NASA-CR-4110] p 3242 N93-30373

The numerical simulation of circulation controlled airfoil flowfields p 3243 N93-30947

KALMAN FILTERS

An autonomous vision-based mobile robot p 3443 N93-29082

Theoretical bit error rate performance of the Kalman filter excisor for FM interference [AD-A263018] p 3383 N93-29407

Optimal filtering and LQR theory with constraints on system and control matrices p 3357 N93-30234

KAPTON (TRADEMARK)

An explosively actuated electrical switch using Kapton insulation [AD-A263835] p 3411 N93-30021

KARHUNEN-LOEVE EXPANSION

Frequency domain speech compression using the Karhunen-Loeve Transform [AD-A262613] p 3379 N93-28476

KEELS

Effects of intra- and inter-laminar resin content on the mechanical properties of toughened composite materials p 3303 N93-30845

KELVIN-HELMHOLTZ INSTABILITY

Electrodynamics of the dayside cleft region based on ground observations at Svalbard [AD-A263571] p 3477 N93-29831

KINEMATIC EQUATIONS

Attitude stabilization of a rigid spacecraft using gas jet actuators operating in a failure mode p 3280 N93-29992

KINEMATICS

The use of objective prism radial velocities for kinematic studies of galactic populations p 3633 N93-28672

A manipulator kinematic design for high-vacuum operation [DE93-010264] p 3444 N93-29247

Research on reconfigurable and reliable manipulators [DE93-010244] p 3444 N93-29330

System analysis for a kinematic positioning system based on the global positioning system [AD-A262830] p 3245 N93-29468

Input relegation control for gross motion of a kinematically redundant manipulator [DE93-005301] p 3446 N93-30210

KINETIC ENERGY

Dense inclined flows: Theory and experiments [DE93-011452] p 3417 N93-28630

Spectral energetics of the lower thermosphere p 3477 N93-29467

Applications of density functional theory to calculation of reaction energetics p 3351 N93-30098

KINETIC EQUATIONS

Moment approach to fast ion neoclassical transport and viscous forces [DE93-753305] p 3585 N93-28979

Bounds on internal state variables in viscoplasticity [NASA-TM-106215] p 3451 N93-29196

KINETIC THEORY

An extension of a kinetic theory of polymer crystallization through the exclusion of negative barriers [AD-A264810] p 3334 N93-29660

A computer simulation of the production of an artificially ionized layer using the Arecibo facility [DE93-010817] p 3478 N93-30487

Quantum-kinetic Green function and macroscopic wave function [DE93-606040] p 3606 N93-30796

KINETICS

Additional support for the TDK/MABL computer program [NASA-CR-193037] p 3526 N93-29028

Start broadened profiles with self-consistent radiation transfer and atomic kinetics in plasmas produced by high intensity lasers [DE93-008706] p 3586 N93-29093

Constitutive laws for deformation and dynamic recrystallization in cubic metals [DE93-010740] p 3326 N93-30486

Growth model of Au films on Ru(001) [DE92-642126] p 3602 N93-30998

KLYSTRONS

Accelerator research studies [DE93-009353] p 3573 N93-28522

Development of high power microwave source [DE93-753316] p 3436 N93-28980

Three-dimensional simulation analysis of the standing-wave free-electron laser two-beam accelerator [DE93-010461] p 3575 N93-29870

Improved design concepts for millimeter wave power sources [AD-A264060] p 3411 N93-29922

Microwave emission from relativistic electron beams [AD-A264102] p 3400 N93-30880

KNOWLEDGE BASED SYSTEMS

Pilot intent and error recognition as part of a knowledge based cockpit assistant p 3502 N93-28855

Cognitive interface considerations for intelligent cockpits p 3503 N93-28865

DataHub knowledge based assistance for science visualization and analysis using large distributed databases p 3613 N93-29230

The axiomatic definition of a linguistic scale fuzziness degree, its major properties, and applications p 3510 N93-29520

Fuzzy knowledge base construction through belief networks based on Lukasiewicz logic p 3515 N93-29550

Life insurance risk assessment using a fuzzy logic expert system p 3520 N93-29585

KNOWLEDGE BASES (ARTIFICIAL INTELLIGENCE)

Introduction to cadet center for advanced data evaluation technology p 3614 N93-29240

Parallel inferencing method and apparatus for rule-based expert systems [NASA-CASE-NPO-18004-1-CU] p 3521 N93-29504

Approximate reasoning using terminological models p 3510 N93-29522

Fuzzy knowledge base construction through belief networks based on Lukasiewicz logic p 3515 N93-29550

KNOWLEDGE REPRESENTATION

The axiomatic definition of a linguistic scale fuzziness degree, its major properties, and applications p 3510 N93-29520

Approximate reasoning using terminological models p 3510 N93-29522

Quantitative analysis of properties and spatial relations of fuzzy image regions p 3510 N93-29523

Fuzzy knowledge base construction through belief networks based on Lukasiewicz logic p 3515 N93-29550

Determining rules for closing customer service centers: A public utility company's fuzzy decision p 3516 N93-29561

Inverse problems: Fuzzy representation of uncertainty generates a regularization p 3516 N93-29563

KRYPTON

Mass spectrometric measurement of Martian krypton and xenon isotopic abundance p 3646 N93-28798

KUWAIT

Atmospheric and Geophysical Sciences Division: G-Division did you know? [DE93-007412] p 3469 N93-28967

L

LABORATORIES

Applied research in America [DE93-011725] p 3625 N93-28646

National collaboratories: Applying information technology for scientific research [LC-93-83795] p 3612 N93-29129

Testing in combined dynamic environments [DE93-010679] p 3278 N93-29250

Thermal effects testing at the National Solar Thermal Test Facility [DE93-009825] p 3465 N93-30391

Introduction to the National Information Display Laboratory p 3628 N93-30718

Physics laboratory technical activities, 1992 [PB93-178648] p 3561 N93-30888

LABYRINTH SEALS

Heat Transfer and Cooling in Gas Turbines [AGARD-CP-527] p 3252 N93-29926

Heat transfer and leakage in high-speed rotating stepped labyrinth seals p 3256 N93-29951

LACTATES

Beta-adrenergic blockade and lactate metabolism during exercise at high altitude [AD-A263544] p 3495 N93-29820

LAGRANGE COORDINATES

Godunov-type methods for the equations of compressible fluid mechanics [KFK-5058] p 3428 N93-31020

LAGRANGIAN FUNCTION

Stability, bifurcation, and control of Hamiltonian systems [DE93-012103] p 3547 N93-28648

Towards a better hydro for dynamic mix calculations [DE93-010702] p 3426 N93-30485

An adaptive Lagrangian method for computing 1-D reacting flows and the theory of Riemann invariant manifolds for the compressible Euler equations p 3428 N93-30902

On the energy-momentum tensors for field theories in spaces with affine connection and metric [DE92-644743] p 3557 N93-30926

Beltrami parametrization and gauging of Virasoro and w-infinity algebras [DE92-644844] p 3557 N93-30928

A non degenerate semi-classical Lagrangian for dilaton-gravity in two dimensions [DE92-641339] p 3480 N93-31002

LAMINAR BOUNDARY LAYER

Keynote address: Unsteady, multimode transition in gas turbine engines p 3252 N93-29927

Measurement of turbulent spots and intermittency modelling at gas-turbine conditions p 3253 N93-29934

Analytical and experimental study of laminar free convective heat transfer from isothermal convex bodies of arbitrary shape [ISBN-0-315-72512-5] p 3426 N93-30379

LAMINAR FLOW

A grid refinement study of two-dimensional transient flow over a backward-facing step using a spectral-element method [DE92-018262] p 3417 N93-28639

High Reynolds number and turbulence effects on aerodynamics and heat transfer in a turbine cascade [NASA-TM-106187] p 3420 N93-29157

Flow visualization on helicopter blades using acenaphthen [ESA-TT-1255] p 3422 N93-29273

Evolution of flow disturbances in cocurrent gas-liquid flows [DE93-010083] p 3422 N93-29326

Study of flow structure in rotating cavities: Numerical predictions of laminar and turbulent, steady, and unsteady flows p 3256 N93-29948

Detailed studies of soot formation in laminar diffusion flames for application to modeling studies [AD-A264827] p 3317 N93-30667

Effects of buoyancy on gas jet diffusion flames [NASA-CR-191109] p 3352 N93-31031

LAMINAR HEAT TRANSFER

Analytical and experimental study of laminar free convective heat transfer from isothermal convex bodies of arbitrary shape [ISBN-0-315-72512-5] p 3426 N93-30379

LAMINATES

Influence of ply waviness on stiffness and strength reduction of composite laminates [AD-A263224] p 3294 N93-28559

A thermal stress solution for multilayered composite cylinders [AD-A262579] p 3295 N93-28657

Metal Matrix Laminate Tailoring (MMLT) code: User's manual [NASA-TM-106052] p 3295 N93-28681

Composite laminate stiffnesses and their sensitivities [DLR-FB-92-16] p 3296 N93-29007

Modification of spectral distributions by multilayer structures [DE93-009308] p 3310 N93-29059

Ceramic matrix composites properties/microstresses with complete and partial interphase bond [NASA-TM-106136] p 3297 N93-29071

Axial impact of composites p 3297 N93-29078

Environmental effects on stitched RTM composites [NASA-CR-193221] p 3297 N93-29107

A transient FGM interlayer based approach to joining ceramics [DE93-010415] p 3331 N93-29248

Analysis of LDEF micrometeoroid/debris data and damage to composite materials p 3309 N93-29366

An investigation of graphite peek composite under compression with a centrally located circular discontinuity [AD-A262549] p 3298 N93-29414

Shear sensitive monomer-polymer laminate structure and method of using same [NASA-CASE-LAR-14654-1-CU] p 3452 N93-29613

First NASA Advanced Composites Technology Conference, part 2 [NASA-CP-3104-PT-2] p 3303 N93-30841

Effects of intra- and inter-laminar resin content on the mechanical properties of toughened composite materials p 3303 N93-30845

Comparison of impact results for several polymeric composites over a wide range of low impact velocities p 3304 N93-30848

Micromechanics of fatigue in woven and stitched composites p 3304 N93-30850

Characterization of multiaxial warp knit composites p 3304 N93-30851

Developments in impact damage modeling for laminated composite structures p 3305 N93-30857

Advanced fiber placement of composite fuselage structures p 3306 N93-30864

Progressive failure methodologies for predicting residual strength and life of laminated composites p 3307 N93-30866

Effects of bolt-hole contact on bearing-bypass damage-onset strength p 3307 N93-30870

Mechanical properties of composite materials p 3290 N93-30951

LANCE MISSILE

Clustered Lance Booster (CLB) feasibility study [AD-A262746] p 3286 N93-28593

LAND MOBILE SATELLITE SERVICE

Comparison of multiple access techniques for bandwidth limited land-mobile satellite communications p 3370 N93-30314

LAND USE

Land use database for the Netherlands using LANDSAT Thematic Mapper pictures [BCRS-91-32] p 3463 N93-30839

LANDAU-GINZBURG EQUATIONS

The onset of vortex turbulence [DE93-010424] p 3417 N93-28663

LANDFILLS

Hydrogeology and ground-water-quality conditions at the Reno County Landfill, South-Central Kansas, 1990-1991 [PB93-183085] p 3474 N93-30826

LANDING

An evaluation of B-1B pilot performance during simulated instrument approaches with and without status information [AD-A263874] p 3507 N93-29888

LANDSAT SATELLITES

Proceedings of the 8th User Seminar of the German Remote Sensing Data Center of the German Aerospace Establishment (DLR) [DLR-MITT-92-09] p 3456 N93-28915

Atmospheric correction of LANDSAT-TM-data for forest inventory p 3459 N93-28929

Interim report on Landsat national archive activities p 3618 N93-30455

LANGUAGE PROGRAMMING

The concurrent clean system user's manual and PABCstat user's manual, version 0.8 [TR-92-19] p 3523 N93-28484

LANGUAGES

Antirational transductions and their language families [ETN-93-93794] p 3611 N93-28525

The 1991 neural information processing systems: Natural and synthetic [AD-A264754] p 3623 N93-30559

LANTHANUM ISOTOPES

Reaction mechanism studies of heavy ion induced nuclear reactions [DE93-010496] p 3569 N93-29807

LAPLACE TRANSFORMATION

Comparison of analytical transport and stochastic solutions for neutron slowing down in an infinite medium [DE93-010799] p 3565 N93-28833

A multigrid extension of the FFT for the numerical inversion of Fourier and LaPlace transforms [TRITA-NA-9204] p 3548 N93-29024

LARGE SCALE INTEGRATION

On-board B-ISDN fast packet switching architectures. Phase 2: Development. Proof-of-concept architecture definition report [NASA-CR-191151] p 3273 N93-29884

LARGE SPACE STRUCTURES

Low-cost Active Structural Control space experiment (LASC) p 3263 N93-28700

Description of the Joint Damping Experiment (JDX) p 3263 N93-28703

Robust feedforward/feedback control synthesis for uncertain dynamical systems p 3542 N93-29079

Space construction activities [NASA-CR-192690] p 3274 N93-29108

Interaction dynamics of on-orbit construction p 3274 N93-29109

Controls of interaction dynamics of orbital assembly p 3275 N93-29111

Structural load control during construction p 3275 N93-29113

Systems engineering studies of on-orbit assembly operation p 3275 N93-29114

Dynamics and robust control of sampled data systems for large space structures [AD-A264192] p 3281 N93-30142

LARVAE

Predicting the response of a temperate forest ecosystem to atmospheric CO2 increase [DE93-010081] p 3467 N93-28543

LASER ABLATION

Complex dielectric function of amorphous diamond films deposited by pulsed excimer (ArF) laser ablation of graphite [AD-A264527] p 3598 N93-30408

LASER ALTIMETERS

Multibeam laser altimeter for planetary topographic mapping p 3442 N93-28780

LASER APPLICATIONS

Discharge of electrically charged clouds [AD-A263212] p 3480 N93-28518

Polarization dependence of the ionization of helium and neon by 120 femtosecond pulses at 614 nm [DE93-010514] p 3564 N93-28762

Spin dependent phenomena in medium energy physics [DE93-010972] p 3565 N93-28849

Enhanced noncontacting laser extensometer for biaxial strain measurements [AD-A263170] p 3430 N93-28989

Optical measurements of ripples using a scanning laser slope gauge. Part 1: Instrumentation and preliminary results [AD-A261939] p 3486 N93-28996

High-efficiency high-reliability optical components for a large, high-average-power visible laser system [DE93-009225] p 3437 N93-29098

An investigation of stereolithography as a means of prototyping from a cad database [AD-A263410] p 3613 N93-29210

Characterization of copper iodide thin films fabricated via laser assisted molecular beam epitaxy [AD-A262823] p 3596 N93-29430

SWAT system performance predictions [AD-A262857] p 3579 N93-29470

Selective nitrations. Volume 2: The laser-induced nitration of three cycloalkanes [AD-A263250] p 3438 N93-29800

Atmospheric transverse coherence length measurement system for laser communications [AD-A263563] p 3439 N93-29827

Advanced coordinate measuring machine at Sandia National Laboratories [DE93-010618] p 3432 N93-29842

Electro-optic characterisation of extremely wide bandwidth electrical signals [AD-A264202] p 3392 N93-30145

Method and apparatus for imaging an object in or through a scattering medium by using multiple-wave mixing [AD-D015707] p 3581 N93-30410

Uplink laser propagation measurements through the sea surface, haze and clouds [AD-A264687] p 3440 N93-30553

Laser based 3D volumetric display system [AD-A264825] p 3441 N93-30599

LASER BEAMS

Proposal for a universal particle detector experiment p 3286 N93-28795

SWAT 2 overview [AD-A262905] p 3578 N93-29139

SWAT laboratory test results
[AD-A262906] p 3578 N93-29140
Effects of vacuum exposure on stress and spectral shift of high reflective coatings
[DE93-009318] p 3437 N93-29207
An investigation of stereolithography as a means of prototyping from a cad database
[AD-A263410] p 3613 N93-29210
Laser radiation detection system
[AD-D015724] p 3438 N93-29287
Investigations of self-pumped phase conjugate laser beams and coherence length
[AD-A263438] p 3438 N93-29789
Three-dimensional simulation analysis of the standing-wave free-electron laser two-beam accelerator
[DE93-010461] p 3575 N93-29870
Analysis of possibilities for using laser scattering for MeV electron beam diagnostics
[DE93-606223] p 3441 N93-30767
Theoretical-experimental study of the non-thermal effects of the polarized laser radiation in living tissues
[DE93-607212] p 3441 N93-30775

LASER CAVITIES
Problems in the implementation of x ray optics with x ray lasers
[DE93-009297] p 3438 N93-29781
Investigations of self-pumped phase conjugate laser beams and coherence length
[AD-A263438] p 3438 N93-29789
Intracavity-pumped 2.1 micrometer Ho(3+): YAG laser
[AD-D015728] p 3441 N93-30587

LASER DOPPLER VELOCIMETERS
Three-dimensional fiber-optic LDV measurements in the endwall region of a linear cascade of controlled-diffusion stator blades
[AD-A263513] p 3424 N93-29968
Multiparticle imaging technique for two-phase fluid flows using pulsed laser speckle velocimetry
[DE93-011734] p 3427 N93-30489

LASER FUSION
Inertial confinement fusion target component fabrication and technology development support
[DE93-010836] p 3585 N93-28836
Design of the Nova Upgrade laser system for ignition fusion experiments
[DE93-009077] p 3436 N93-29097
Fusion laser oscillator and pulse-forming system using integrated optics
[DE93-009286] p 3588 N93-29780
SIRIUS-P: An inertially confined direct drive laser fusion power reactor
[DE93-012433] p 3439 N93-30186

LASER GUIDANCE
Sodium guide star adaptive optics system for astronomical imaging in the visible and near-infrared
[DE93-009543] p 3630 N93-29785

LASER HEATING
Selective nitrations. Volume 2: The laser-induced nitration of three cycloalkanes
[AD-A263250] p 3438 N93-29800
Determination of gas phase species and temperature profiles above solid propellants p 3346 N93-30080
Laser gas alloying of titanium materials
[ETN-93-93805] p 3325 N93-30115

LASER INDUCED FLUORESCENCE
Spectroscopic probes of vibrationally excited molecules at chemically significant energies
[DE93-012328] p 3564 N93-28652
The photodissociation and reaction dynamics of vibrationally excited molecules
[DE93-010896] p 3565 N93-28879
Experimental study of instability growth patterns of a shock-accelerated, thin fluid layer
[DE93-010741] p 3421 N93-29253
Sodium guide star adaptive optics system for astronomical imaging in the visible and near-infrared
[DE93-009543] p 3630 N93-29785
Flame structure studies of propellant like low pressure flames using optical and mass spectrometric means
p 3319 N93-30081
Detailed studies of soot formation in laminar diffusion flames for application to modeling studies
[AD-A264827] p 3317 N93-30667

LASER MATERIALS
Development of coherent x ray lasers
[DE93-009288] p 3437 N93-29104
Method of emitting on a specific wavelength fraunhofer line using a neodymium doped laser transmitter
[AD-D015710] p 3437 N93-29276

LASER OUTPUTS
Smart skin structures for identifying and locating laser irradiation
[DE93-005464] p 3436 N93-28887
High-efficiency high-reliability optical components for a large, high-average-power visible laser system
[DE93-009225] p 3437 N93-29098
Low-pump-rate multi-millisecond atomic xenon laser
[DE93-011484] p 3437 N93-29180
Operating manual for single-shot autocorrelator
[AD-A262016] p 3438 N93-29395
Construction and operation of a gas transport CO2 laser
[AD-A263102] p 3438 N93-29797
Applications of laser light scattering in polymer dilute solution characterization
[AD-A263110] p 3335 N93-30007
High-repetition rate x ray lasers and applications
[DE93-011882] p 3440 N93-30394
Research studies on short wavelength by selective auger processes
[AD-A264493] p 3440 N93-30401
Holmium quasi-two level laser
[AD-D015706] p 3440 N93-30427
Uplink laser propagation measurements through the sea surface, haze and clouds
[AD-A264687] p 3440 N93-30553
A variable reflectivity output coupler for optically pumped far infrared lasers
[MPE-PREPRINT-225] p 3441 N93-30640
Analysis of possibilities for using laser scattering for MeV electron beam diagnostics
[DE93-606223] p 3441 N93-30767

LASER PLASMA INTERACTIONS
A remote laser-mass spectrometer for determination of elemental composition p 3434 N93-28775
Development of coherent x ray lasers
[DE93-009288] p 3437 N93-29104

LASER PLASMAS
Computational simulations of a soft x ray projection lithography laser plasma source
[DE93-009625] p 3437 N93-29264

LASER POWER BEAMING
The lightcraft project p 3233 N93-29749
ASPEC: Solar power satellite p 3233 N93-29750
Power beaming to communication satellites in GEO
[DE93-007608] p 3279 N93-29840

LASER PROPULSION
The lightcraft project p 3233 N93-29749

LASER PUMPING
Low-pump-rate multi-millisecond atomic xenon laser
[DE93-011484] p 3437 N93-29180
ND laser with co-doped ion(s) pumped by visible laser diodes
[AD-D015711] p 3437 N93-29277
Research studies on short wavelength by selective auger processes
[AD-A264493] p 3440 N93-30401
Tunable CW diode-pumped Tm,Ho:YLiF4 laser operating at or near room temperature
[NASA-CASE-NPO-18611-1-CU] p 3440 N93-30415
Holmium quasi-two level laser
[AD-D015706] p 3440 N93-30427
Intracavity-pumped 2.1 micrometer Ho(3+): YAG laser
[AD-D015728] p 3441 N93-30587
A variable reflectivity output coupler for optically pumped far infrared lasers
[MPE-PREPRINT-225] p 3441 N93-30640

LASER RANGE FINDERS
Recognizing parameterized objects from range data
[OUEL-1918/92] p 3523 N93-28486

LASER SPECTROMETERS
Measurement of the rotation Raman spectra of nitrogen, oxygen, and water vapor under conditions of a temperature humidity lidar
[GKSS-92/E/32] p 3485 N93-31018

LASER SPECTROSCOPY
Spectroscopic probes of vibrationally excited molecules at chemically significant energies
[DE93-012328] p 3564 N93-28652
Laser spectroscopy of hydrocarbon radicals
[DE93-012555] p 3436 N93-28653
Laer-induced breakdown spectroscopy instrument for element analysis of planetary surfaces
p 3434 N93-28769
Aerosol particle analysis by Raman scattering technique
[DE93-005587] p 3309 N93-28880
High resolution free-electron laser spectroscopy
[AD-A263734] p 3439 N93-29853
Applications of laser light scattering in polymer dilute solution characterization
[AD-A263110] p 3335 N93-30007
Single-shot femtosecond spectroscopy: A methodology for observation of solid-state chemical reactions
p 3319 N93-30075
Flame structure studies of propellant like low pressure flames using optical and mass spectrometric means
p 3319 N93-30081
Computer control of pulsed tunable dye lasers
[DE93-605896] p 3441 N93-30801
Pulsed laser photoacoustic spectrometer for study of solid materials
[DE93-605290] p 3441 N93-31023

LASER TARGETS
Inertial confinement fusion target component fabrication and technology development support
[DE93-010836] p 3585 N93-28836
A new multichannel soft x ray framing camera for fusion experiments
[DE93-009302] p 3432 N93-29773
Gas electron diffraction employing a pulsed electron beam synchronous with photoexcitation
p 3319 N93-30101

LASER WEAPONS
Magnetic field measurements of the CEBAF (NIST) wiggler using the pulsed wire method
[AD-A263997] p 3439 N93-29867

LASERS
Laser based 3D volumetric display system
[AD-A264825] p 3441 N93-30599

LATE STARS
Spherically symmetric model atmospheres for late-type giant stars
[ISBN-0-315-72632-6] p 3633 N93-28673

LATENT HEAT
A passive infrared ice detection technique for helicopter applications
[NASA-CR-193187] p 3244 N93-29152
Surface shear stress estimates from geostrophic winds for use in sensible and latent heat flux formulations
p 3483 N93-30044
The estimation and scaling of land-surface fluxes of latent and sensible heat with remotely sensed data over a grassland site p 3462 N93-30045

LATERAL STABILITY
Hypersonic lateral and directional stability characteristics of aeroassist flight experiment configuration in air and CF4
[NASA-TM-4435] p 3239 N93-29166
Vehicle dynamic stability and rollover
[PB93-185437] p 3447 N93-30828

LATTICE PARAMETERS
Bainitic stabilization of austenite in low alloy steels
[DE93-008275] p 3321 N93-28957

LATTICE VIBRATIONS
Neutron scattering studies of the structures and lattice dynamics of the alkali metals
[DE93-008272] p 3593 N93-28956
High pressure studies of hydrated nafion membranes: Dielectric relaxation and deuteron NMR
[AD-A263511] p 3332 N93-29342
Knot invariants and cellular automata
[AD-A264199] p 3607 N93-30884
A dynamical model of structural phase transition in La2CuO4
[DE93-605325] p 3602 N93-31025

LAUNCH DATES
Payload flight assignments. NASA mixed fleet
[NASA-TM-108255] p 3268 N93-30133

LAUNCH VEHICLE CONFIGURATIONS
ASUR p 3228 N93-29720

LAUNCH VEHICLES
Space transportation analysis and design (Reissue A)
[AD-A262752] p 3271 N93-28487
Natural environmental service support to NASA vehicle, technology, and sensor development programs
[NASA-CR-192554] p 3469 N93-29029
Launch vehicles for lightweight TACSAT deployment
p 3271 N93-29903
An overview of DARPA's advanced space technology program p 3269 N93-29908
Payload flight assignments. NASA mixed fleet
[NASA-TM-108255] p 3268 N93-30133
A representative survey of US space systems and methods for estimating their costs
[AD-A264159] p 3272 N93-30881

LAUNCH WINDOWS
SeaWiFS technical report series. Volume 2: Analysis of orbit selection for SeaWiFS: Ascending versus descending node
[NASA-TM-104566-VOL-2] p 3486 N93-28497

LAUNCHING SITES
Shuttle landing facility cloud cover study: Climatological analysis and two tenths cloud cover rule evaluation
[NASA-CR-193016] p 3272 N93-31033

LAWS
Pollution prevention: A regulatory update
[DE93-009727] p 3472 N93-30180

LAY-UP
Advanced fiber placement of composite fuselage structures p 3306 N93-30864

LEAD ACID BATTERIES
High reliability, maintenance-free INS battery development
[AD-A264521] p 3412 N93-30406

Technical examination and simulation of a photovoltaic system: Solar generator, battery, download
[ETN-93-94179] p 3466 N93-30573

LEAD ALLOYS
Preliminary test of liquid metal induced embrittlement in liquid LiPb and stainless-steel systems
[DE93-753130] p 3320 N93-28529

LEAD TITANATES
Materials for adaptive structural acoustic control, volume 2
[AD-A264620] p 3563 N93-30385

LEAD ZIRCONATE TITANATES
Materials for adaptive structural acoustic control, volume 1
[AD-A264619] p 3562 N93-30121
Materials for adaptive structural acoustic control, volume 2
[AD-A264620] p 3563 N93-30385

LEADING EDGES
SIMS chemical analysis of extended impacts on the leading and trailing edges of LDEF experiment AO187-2
p 3318 N93-29367
Projectile compositions and modal frequencies on the chemistry of micrometeoroids LDEF experiment
p 3638 N93-29370
Long-term microparticle flux variability indicated by comparison of Interplanetary Dust Experiment (IDE) timed impacts for LDEF's first year in orbit with impact data for the entire 5.77-year orbital lifetime p 3638 N93-29379
Prediction of jet impingement cooling scheme characteristics (airfoil leading edge application)
p 3255 N93-29941
Topology and grid adaption for high-speed flow computations
[NASA-CR-4216] p 3426 N93-30375

LEAKAGE
Tank issues: Design and placement of floating liquid monitoring wells
[PB93-161149] p 3469 N93-29033
Tank issues: Site characterization for external leak monitoring
[PB93-161156] p 3469 N93-29034
Valve malfunction detection apparatus
[NASA-CASE-MFS-29904-1] p 3432 N93-29503
Heat transfer and leakage in high-speed rotating stepped labyrinth seals p 3256 N93-29951

LEARNING
Cognitive and Neural Sciences Division 1992 programs
[AD-A263400] p 3654 N93-29258
Parallel processing and learning: Variability and chaos in self-organization of activity in groups of neurons
[AD-A264224] p 3539 N93-30361
Profiles of major federal literacy programs
[PB93-163863] p 3608 N93-30657

LEAST SQUARES METHOD
Investigation of a geodesy coexperiment to the Gravity Probe B relativity gyroscope program
[NASA-CR-193263] p 3460 N93-29179
Enhanced reduction of velocity data obtained during CETA flight experiment
[NASA-TM-4460] p 3431 N93-29209
Evaluation of fuzzy inference systems using fuzzy least squares p 3513 N93-29539
QR decomposition based least squares lattice algorithm p 3358 N93-30239

LENGTH
Crack length determination by ultrasonic methods
[DE93-008075] p 3450 N93-28567
Atmospheric transverse coherence length measurement system for laser communications
[AD-A263563] p 3439 N93-29827

LENNARD-JONES POTENTIAL
Molecular dynamics of detonation in crystals with defects p 3350 N93-30097

LENS ANTENNAS
Recent advances in bootlace lens design
p 3374 N93-30336

LENS DESIGN
Development of a 9.3 micrometer CW LIDAR for the study of atmospheric aerosol
[NASA-CR-193227] p 3381 N93-29105

LENSES
A compact imaging detector of polarization and spectral content p 3582 N93-28810
A study of the effects of lens focal length on remote driver performance
[AD-A263191] p 3505 N93-28941
Ultra-high resolution water window x ray microscope optics design and analysis
[NASA-CR-193225] p 3578 N93-29128

LEPTONS
New limits on generation-1 leptoquarks
[DE93-008138] p 3567 N93-29351
Planck scale effects in neutrino physics
[DE93-606133] p 3571 N93-30793

LESIONS
Analysis of visual loss from retinal lesions
[AD-A264692] p 3496 N93-30494

LEVITATION
Forces on a magnet moving past figure-eight coils
[DE93-009965] p 3561 N93-29189

LEWIS BASE
Coordination compounds of aluminum as precursors to aluminum nitride
[AD-A264700] p 3327 N93-30574

LEWIS NUMBERS
Studies in premixed combustion
[DE93-007955] p 3310 N93-29051

LIBRARIES
BlockSolve v1.1: Scalable library software for the parallel solution of sparse linear systems
[DE93-011391] p 3524 N93-28644
A distributed object-oriented database application design
[AD-A262591] p 3612 N93-28846
RBSE: Product development team research activity deliverables
[NASA-CR-193115] p 3527 N93-29212
Summer research program (1992). High School Apprenticeship Program (HSAP) reports. Volume 16: Arnold Engineering Development Center Civil Engineering Laboratory
[AD-A262024] p 3608 N93-29396
The 9th FLICC Forum on Federal Information Policies
[PB93-184687] p 3624 N93-29668
Proposal for a numerical array library
[DE93-010678] p 3623 N93-30482

LIBRATIONAL MOTION
The dynamics and control of space tethers
p 3274 N93-28629

LICENSING
The role of the University Licensing Office in transferring intellectual property to industry p 3626 N93-30698

LIE GROUPS
Lie groups whose set of compact subgroups is inductive
[ETN-93-93791] p 3547 N93-28524
Deformations of the Lie algebras L1(H(2)) and L1(W(2))
[MEMO-1056] p 3547 N93-28667
Computer algebra tools for higher symmetry analysis of nonlinear evolution equations
[DE93-606089] p 3535 N93-30787
Orbital motion calculation using Lie method in collider nonlinear magnetic field
[DE93-605733] p 3571 N93-30800
Positive energy representations of the conformal quantum algebra
[DE93-606064] p 3551 N93-30809
Connections between quantized affine algebras and superalgebras
[DE93-606065] p 3551 N93-30810
Nonlinear realisations of omega(1 + infinity)
[DE92-644721] p 3557 N93-30917
Abelian gauge theories on homogeneous spaces
[DE92-644730] p 3607 N93-30921
Invariant structures in gauge theories and confinement
[DE92-644739] p 3607 N93-30924
Invariant structures and static forces in gauge theories
[DE92-644740] p 3607 N93-30925
Beltrami parametrization and gauging of Virasoro and w-infinity algebras
[DE92-644844] p 3557 N93-30928
Normal equivariant forms of vector fields
[DE92-644845] p 3551 N93-30929
The geometry of complex space-times with torsion
[DE92-641343] p 3608 N93-31003

LIFE (DURABILITY)
Development of nickel/metal hydride secondary battery
[DE93-781330] p 3406 N93-28669
The design and lifetime calculation of MHD generator walls based on subcritical crack growth in ceramics
[ISBN-90-9004009-9] p 3332 N93-29267

LIFE SCIENCES
Space research in Germany 1990-1991
[ETN-93-93807] p 3654 N93-28477
JPRS report: Science and technology. Central Eurasia: Life sciences
[JPRS-ULS-93-005] p 3490 N93-28683
JPRS report: Science and technology. Central Eurasia: Life sciences
[JPRS-ULS-92-027] p 3490 N93-28684

LIFE SUPPORT SYSTEMS
Evaluation of test methods and requirements for respiratory protection systems 21
[AD-A262466] p 3501 N93-28757
Mathematical modeling and control law development for the atmospheric monitoring and control system of the Controlled Environment Research Chamber (CERC) at NASA Ames Research Center
[AD-A261978] p 3261 N93-29436
Selenia: A habitability study for the development of a third generation lunar base p 3233 N93-29748
Technology transfer in the NASA Ames Advanced Life Support Division p 3628 N93-30724

LIFT
Unsteady vortex loop/dipole theory applied to the work and acoustics of an ideal low speed propeller
[AD-A264057] p 3241 N93-29891

LIFT AUGMENTATION
Tailored composite wings with elastically produced chordwise camber p 3308 N93-30876
The numerical simulation of circulation controlled airfoil flowfields p 3243 N93-30947

LIGANDS
Organometallic and surface chemistry of mixed-metal systems
[DE93-012686] p 3325 N93-30059
Organometallic compounds and polymers with second and third order nonlinear optical properties
[AD-A264774] p 3338 N93-30610
Gordon Research Conferences, 1991
[AD-A264275] p 3317 N93-30816

LIGHT (VISIBLE RADIATION)
Response of energetic solids to light, heat and shock pulses
[AD-A263702] p 3342 N93-29296
Conspicuity of aids to navigation. Part 1: Temporal patterns for flashing lights
[AD-A264626] p 3499 N93-30426

LIGHT AMPLIFIERS
All solid-state high power visible laser
[NASA-CR-193163] p 3436 N93-28623

LIGHT BEAMS
SWAT 2 overview
[AD-A262905] p 3578 N93-29139
SWAT laboratory test results
[AD-A262906] p 3578 N93-29140
Optical antenna beam steering using digital phase shifter control
[AD-D015688] p 3383 N93-29455
Applications of laser light scattering in polymer dilute solution characterization
[AD-A263110] p 3335 N93-30007

LIGHT ELEMENTS
A compact imaging detector of polarization and spectral content p 3582 N93-28810
Further analysis of LDEF FRECOPA micrometeoroid remnants p 3638 N93-29360

LIGHT EMITTING DIODES
Fiber-optic currents measurements
[DE93-007970] p 3579 N93-29350
Optical antenna beam steering using digital phase shifter control
[AD-D015688] p 3383 N93-29455
Visible light emitting materials and injection devices
[AD-A263499] p 3601 N93-30811

LIGHT MODULATION
Spatial Light Modulators (SLMs) surface quality
[AD-A263249] p 3579 N93-29656
Electro-optic characterisation of extremely wide bandwidth electrical signals
[AD-A264202] p 3392 N93-30145
Polarization modulated ellipsometry
[NASA-CR-4012] p 3580 N93-30372
Subpicosecond electrooptic sampling
[AD-A264635] p 3581 N93-30520
Optically powered, optoelectronic spatial light modulators
[AD-A264765] p 3581 N93-30609

LIGHT SCATTERING
Loading and testing a light scattering cell with a binary fluid mixture near its critical composition
[NASA-CR-193147] p 3415 N93-28557
Measurements of light scattering by small particles at an angle of zero degrees
[AD-A263856] p 3580 N93-29887
Applications of laser light scattering in polymer dilute solution characterization
[AD-A263110] p 3335 N93-30007
Detailed studies of soot formation in laminar diffusion flames for application to modeling studies
[AD-A264827] p 3317 N93-30667
Analysis of possibilities for using laser scattering for MeV electron beam diagnostics
[DE93-606223] p 3441 N93-30767

LIGHT SOURCES
Undulator Spectromicroscopy Facility at the Advanced Light Source
[DE93-007964] p 3261 N93-28490

X ray microscopy resource center at the Advanced Light Source
[DE93-010449] p 3261 N93-29869

A quality monitor and monitoring technique employing optically stimulated electron emission
[NASA-CASE-LAR-15063-1] p 3449 N93-30414

Optically powered, optoelectronic spatial light modulators
[AD-A264765] p 3581 N93-30609

LIGHTNING

Discharge of electrically charged clouds
[AD-A263212] p 3480 N93-28518

Proceedings of the Thunder and Lighting Seminar and the 3D Lightning Warning Workshop
[AD-A262766] p 3482 N93-29304

Thunderstorm forecast study for Eglin AFB, Florida
[AD-A263423] p 3483 N93-29810

Stand alone lightning detection equipment used at Canadian Forces air bases p 3367 N93-30295

Rocket-triggered lightning studies for the protection of critical assets
[DE93-009633] p 3484 N93-30651

Lightning-induced effects on VLF/LF radio propagation p 3396 N93-30737

A long wave TE/TM noise prediction model
p 3397 N93-30742

LIGHTNING SUPPRESSION

Characteristic and development report SA3581/MC4196 Lightning Arrestor Connector (LAC)
[DE93-010610] p 3412 N93-30118

LINE OF SIGHT

Tomographic analysis of line-of-sight infrared spectra of low-pressure flames
[AD-A263185] p 3309 N93-28514

Design considerations for a night, air-to-surface attack capability on a dual role fighter p 3251 N93-28871

An automated observing system for passive evaluation of cloud cover and visibility
[AD-A263207] p 3481 N93-28875

LINE SPECTRA

Start broadened profiles with self-consistent radiation transfer and atomic kinetics in plasmas produced by high intensity lasers
[DE93-008706] p 3586 N93-29093

CO lines toward NGC 2024 and other star forming regions: A closer look at the warm gas component
[MPE-PREPRINT-223] p 3637 N93-30639

Effects of spiral shocks on disk emission lines
[DE92-641716] p 3637 N93-31004

Optical system analysis for the ground based EXVM
[NASA-CR-192588] p 3582 N93-31035

LINEAR ACCELERATORS

Observation of a beam energy shift caused by a plasma wakefield
[DE93-753243] p 3583 N93-28533

Ultraviolet free electron laser facility preliminary design report
[DE93-009360] p 3435 N93-28594

NPB cesium space experiment p 3267 N93-28733

Design of a particle beam satellite system for lunar prospecting p 3434 N93-28768

Upgrading the LAMPF 201 MHz RF generators
[DE93-010715] p 3406 N93-28830

TESLA test cell cryostat support post thermal and structural analysis
[DE93-008365] p 3407 N93-29048

Study of gain in C-band deflection cavities for a frequency-doubling magnicon amplifier
[AD-A263132] p 3409 N93-29478

Magnetic field measurements of the CEBAF (NIST) wiggler using the pulsed wire method
[AD-A263997] p 3439 N93-29867

Pulse control in an accelerator for heavy-ion fusion
[DE93-009527] p 3576 N93-30390

LINEAR ARRAYS

Planar active antennas and quasi-optical power combining arrays using FET's and slots
[AD-A263759] p 3387 N93-29875

Tolerance theory of phased array antennas: A statistical approach p 3369 N93-30307

LINEAR ENERGY TRANSFER (LET)

LET spectra measurements of charged particles in the P0006 experiment on LDEF p 3573 N93-29637

LINEAR EQUATIONS

BlockSolve v1.1: Scalable library software for the parallel solution of sparse linear systems
[DE93-011391] p 3524 N93-28644

Simplified Linear Equation Solvers: User's manual
[DE93-011975] p 3550 N93-30140

LINEAR FILTERS

Synchronization of the LAPTV adative filter with input statistics p 3358 N93-30242

LINEAR PROGRAMMING

Packing of Steiner trees: Polyhedric studies and application
[ETN-93-93796] p 3547 N93-28527

Estimating test range capacity
[AD-A262493] p 3270 N93-28938

Modelling temporal abductive explanation
[AD-A263096] p 3526 N93-29145

Dynamic factorization in large-scale optimization
[AD-A263993] p 3528 N93-29345

Automated modeling of physical systems
[NASA-CR-193256] p 3531 N93-29873

LINEAR QUADRATIC REGULATOR

Dynamics and robust control of sampled data systems for large space structures
[AD-A264192] p 3281 N93-30142

Optimal filtering and LQR theory with constraints on system and control matrices p 3357 N93-30234

LINEAR SYSTEMS

BlockSolve v1.1: Scalable library software for the parallel solution of sparse linear systems
[DE93-011391] p 3524 N93-28644

Division by polynomial matrix and its application to multivariable linear systems p 3357 N93-30233

LINEARITY

A dynamic bandwidth and phase linearity measurement technique for 4-channel MSK VLF antenna systems
p 3398 N93-30748

LINEARIZATION

The semiclassical stability of de Sitter spacetime
[DESY-92-131] p 3603 N93-28472

Multivariable control of the Space Shuttle Remote Manipulator System using linearization by state feedback
[NASA-CR-188248] p 3443 N93-29080

LINGUISTICS

Antirational transductions and their language families
[ETN-93-93794] p 3611 N93-28525

The axiomatic definition of a linguistic scale fuzziness degree, its major properties, and applications
p 3510 N93-29520

Fuzzy neural network methodology applied to medical diagnosis p 3498 N93-29546

An experimental methodology for a fuzzy set preference model p 3514 N93-29547

A fuzzy set preference model for market share analysis p 3514 N93-29548

Intelligent fuzzy controller for event-driven real time systems p 3515 N93-29551

A neural fuzzy controller learning by fuzzy error propagation p 3516 N93-29560

Quantification of human responses
p 3500 N93-29564

Neural networks: A simulation technique under uncertainty conditions p 3519 N93-29577

LINKAGES

Joint drive development for the Space Station Remote Manipulator System p 3370 N93-30313

LIPIDS

Micropipet manipulation of lipid membranes: Direct measurement of the material properties of a cohesive structure that is only two molecules thick
p 3291 N93-30953

LIQUEFACTION

Hybrid oxygen system
[AD-A262417] p 3500 N93-28464

LIQUID ALLOYS

Effective interactions between concentration fluctuations and charge transfer in chemically ordering liquid alloys
[DE93-606724] p 3327 N93-30778

LIQUID COOLING

Thermal and mechanical analysis of flip-chips on a liquid cooled multichip module
[DE93-007609] p 3405 N93-28641

Evaluation of personal cooling systems in conjunction with explosive ordnance disposal suits
[AD-A262862] p 3506 N93-29471

Pulse mitigation and heat transfer enhancement techniques. Volume 2: Effect of surface wettability and roughness in evaporative spray cooling
[AD-A264174] p 3425 N93-30155

LIQUID CRYSTALS

Low-cost helmet-mounted displays
[AD-A262616] p 3501 N93-28479

Optically tiled flat panel displays. A feasibility study
[AD-A262737] p 3592 N93-28590

Structure and switching dynamics in ferroelectric crystal and liquid crystal thin films
[AD-A263664] p 3594 N93-29293

Shear sensitive monomer-polymer laminate structure and method of using same
[NASA-CASE-LAR-14654-1-CU] p 3452 N93-29613

NMR studies of molecules in liquid crystals and graphite
[DE93-010423] p 3569 N93-29805

Ferroelectric liquid crystal optical interconnect switching systems
[AD-A263751] p 3596 N93-29859

Cooling geometry optimization using liquid crystal technique p 3254 N93-29939

Local heat transfer measurement with liquid crystals on rotating surfaces including non-axisymmetric cases
p 3255 N93-29943

Characterization of slow chromophore reorientation in nonlinear optical polymers by two-dimensional MAS NMR
[AD-A264809] p 3338 N93-30596

Physical chemical studies on molecular composite compositions
[AD-A264834] p 3339 N93-30898

LIQUID FLOW

A four-field approach towards developing a mechanistic model for multiphase flow
[DE93-006572] p 3420 N93-29126

Evolution of flow disturbances in cocurrent gas-liquid flows
[DE93-010083] p 3422 N93-29326

Pulse mitigation and heat transfer enhancement techniques. Volume 5: Transient liquid movement in heat pipe wicks
[AD-A264513] p 3426 N93-30403

LIQUID METAL FAST BREEDER REACTORS

Compatibility studies of AISI type 316 stainless steel with lead-lithium eutectic alloy
[DE93-605281] p 3328 N93-31022

LIQUID METALS

Preliminary test of liquid metal induced embrittlement in liquid LiPb and stainless-steel systems
[DE93-753130] p 3320 N93-28529

A spectral method determination of the first critical Rayleigh number for a low-Prandtl number crystal melt in a cylindrical container
[NASA-CR-193238] p 3594 N93-29214

LIQUID NITROGEN

The microchannel heatsink with liquid nitrogen cooling
[DE93-009258] p 3422 N93-29300

Cryogenic magnetic bearing
[AD-A264716] p 3446 N93-30512

LIQUID OXYGEN

Hybrid oxygen system
[AD-A262417] p 3500 N93-28464

LIQUID PHASE SINTERING

Powder metallurgy: Solid and liquid phase sintering of copper p 3294 N93-30976

LIQUID PROPELLANT ROCKET ENGINES

Liquid fuel injection elements for rocket engines
[NASA-CASE-MFS-28547-1] p 3289 N93-29847

Method of fabricating a rocket engine combustion chamber
[NASA-CASE-MFS-28569-1] p 3338 N93-30565

Orbital transfer vehicle oxygen turbopump technology. Volume 3: Hot oxygen testing
[NASA-CR-191036] p 3448 N93-31039

LIQUID ROCKET PROPELLANTS

A new facility for advanced rocket propulsion research
[NASA-TM-106193] p 3270 N93-28696

LIQUID SLOSHING

The MODE family of facility class experiments
p 3263 N93-28705

Liquid Motion in a rotating tank Experiment (LME)
p 3264 N93-28710

The middeck 0-gravity dynamics experiment
[NASA-CR-4500] p 3281 N93-30376

LIQUID SODIUM

Pulse mitigation and heat transfer enhancement techniques. Volume 3: Liquid sodium heat transfer facility and transient response of sodium heat pipe to pulse forward and reverse heat load
[AD-A263496] p 3422 N93-29338

LIQUID-GAS MIXTURES

Combined centrifugal force/gravity gas/liquid separator system
[AD-D015726] p 3444 N93-29288

Evolution of flow disturbances in cocurrent gas-liquid flows
[DE93-010083] p 3422 N93-29326

Prediction of gas-liquid two-phase flow regime in microgravity
[NASA-TM-106274] p 3352 N93-30939

LIQUID-SOLID INTERFACES

Analytical applications of electrified interfaces between two immiscible solutions
[AD-A263085] p 3311 N93-29132

Potential transmission and transients during corrosion: Applications to corrosion monitoring
[DE93-010863] p 3323 N93-29256

LIQUIDS

Examination of shock induced chemical reactions in liquids using time-resolved optical spectroscopy
p 3318 N93-30073

Thermodynamic and structural properties of metallic glasses and supercooled liquids
[ISBN-0-315-72443-9] p 3605 N93-30359

Studies in Lewis acid and superacid ionic liquids
[AD-A264683] p 3316 N93-30551

LITHIUM

In situ characterization of interfacial and bulk properties of lithium polymer batteries using 4-probe DC techniques [DE93-007699] p 3405 N93-28581

Research and development of carbon black anodes for lithium secondary cells [DE93-781331] p 3406 N93-28746

Design and evaluation of a uniaxial pull test for lithium hydride/deuteride [DE93-010760] p 3451 N93-28832

Alkali metal carbon dioxide electrochemical system for energy storage and/or conversion of carbon dioxide to oxygen [NASA-CASE-LEW-14973-1] p 3464 N93-28974

Effect of zinc and iron ions on the electrochemistry of nickel oxide electrode: Slow cyclic voltammetry [AD-A263098] p 3311 N93-29133

Research and development of lithium secondary batteries for load conditioner use, volume 2 [DE93-781329] p 3410 N93-29673

Characterization of lithium electrode surface in lithium secondary batteries by in situ Raman spectroscopic methods [AD-A263728] p 3411 N93-29986

LITHIUM ALLOYS

Preliminary test of liquid metal induced embrittlement in liquid LiPb and stainless-steel systems [DE93-753130] p 3320 N93-28529

LITHIUM HYDRIDES

Design and evaluation of a uniaxial pull test for lithium hydride/deuteride [DE93-010760] p 3451 N93-28832

LITHIUM NIOBATES

Holographic data storage crystals for the LDEF p 3435 N93-29697

LITHIUM SULFUR BATTERIES

Approach to extending the cycle life of lithium secondary battery [DE93-776266] p 3406 N93-28983

Battery testing at Argonne National Laboratory [DE93-009204] p 3407 N93-29036

Temperature compensated lithium battery energy monitor [AD-D015680] p 3409 N93-29605

LITHOGRAPHY

Healing of lithographically introduced flaws in glass and glass containing ceramics [DE93-010453] p 3330 N93-28761

An investigation of stereolithography as a means of prototyping from a cad database [AD-A263410] p 3613 N93-29210

Computational simulations of a soft x ray projection lithography laser plasma source [DE93-009625] p 3437 N93-29264

Scanning probe lithography. Part 1: Scanning tunneling microscope-induced lithography of self-assembled n-alkanethiol monolayer resists [AD-A263130] p 3432 N93-29476

LITHOSPHERE

Optimism experiment and development of space-qualified seismometers in France p 3646 N93-28796

LOAD TESTING MACHINES

System for testing bearings [NASA-CASE-MFS-28589-1] p 3445 N93-29618

LOAD TESTS

Wind loads on canopy roofs [RR-CE132] p 3451 N93-29106

Load test set-up for the Airmass Sunburst Ultra-Light Aircraft p 3249 N93-29776

Comparison of deformation and shock reactivity for single crystals of RDX and ammonium perchlorate p 3350 N93-30094

Development of an experimental method to determine the axial rigidity of a strut-node joint p 3290 N93-30950

LOADS (FORCES)

Dynamic ice structure interaction: Theory and applications [VTT-PUBS-90] p 3353 N93-28632

Wind loads on canopy roofs [RR-CE132] p 3451 N93-29106

DSS-14 subreflector actuator dynamics during the Landers earthquake p 3386 N93-29600

Energy efficient drivepower [DE93-012436] p 3411 N93-30058

LOCAL AREA NETWORKS

FDDI installation and performance analysis [AD-A263263] p 3529 N93-29497

Gigabit network communications research [AD-A264895] p 3536 N93-31026

LOCKING

Prosthetic elbow joint [NASA-CASE-MFS-28707-1] p 3508 N93-30566

LOCOMOTIVES

Engineman stress and fatigue: Pilot tests [PB93-175008] p 3507 N93-29675

LOGARITHMS

Logarithmic time scale in thermographic Non Destructive Evaluation (NDE) of materials p 3359 N93-30246

LOGIC

Modelling temporal abductive explanation [AD-A263096] p 3526 N93-29145

LOGIC CIRCUITS

Hierarchical model of matching p 3519 N93-29580

Performance enhancement of dynamic CMOS logic circuits p 3361 N93-30257

Electronics mixed-mode simulation [AD-A264734] p 3534 N93-30577

LOGIC DESIGN

Intelligent fuzzy controller for event-driven real time systems p 3515 N93-29551

LOGIC PROGRAMMING

Automated reasoning with function evaluation for COCOLOG [INRIA-RR-1713] p 3529 N93-29488

LOGISTICS MANAGEMENT

The program manager's notebook [AD-A263074] p 3609 N93-29142

Intelligent support for human computer interaction and decision-making in distribution planning and scheduling systems [AD-A263985] p 3610 N93-30124

LONG DURATION EXPOSURE FACILITY

Thermal control paints on LDEF: Results of M0003 sub-experiment 18 [AD-A263252] p 3329 N93-28561

LDEF materials data bases [NASA-TM-107757] p 3290 N93-29067

LDEF: 69 Months in Space. Second Post-Retrieval Symposium, part 2 [NASA-CP-3194-PT-2] p 3654 N93-29354

Report of the Meteoroid and Debris Special Investigation Group p 3638 N93-29355

Micrometeoroids and debris on LDEF p 3638 N93-29356

Continued investigation of LDEF's structural frame and thermal blankets by the Meteoroid and Debris Special Investigation Group p 3282 N93-29357

Predicted and observed directional dependence of meteoroid/debris impacts on LDEF thermal blankets p 3638 N93-29358

Three-D crater analysis of LDEF impact features from stereo imagery p 3283 N93-29359

Further analysis of LDEF FRECOPA micrometeoroid remnants p 3638 N93-29360

Long Duration Exposure Facility (LDEF) experiment M0003 meteoroid and debris survey p 3638 N93-29361

Derivation of particulate directional information from analysis of elliptical impact craters on LDEF p 3283 N93-29362

Characteristics of hypervelocity impact craters on LDEF experiment S1003 and implications of small particle impacts on reflective surfaces p 3283 N93-29363

Hypervelocity impact survivability experiments for carbonaceous impactors p 3283 N93-29364

Hypervelocity impact facility for simulating materials exposure to impact by space debris p 3283 N93-29365

Analysis of LDEF micrometeoroid/debris data and damage to composite materials p 3309 N93-29366

SIMS chemical analysis of extended impacts on the leading and trailing edges of LDEF experiment AO187-2 p 3318 N93-29367

Cratering in glasses impacted by debris or micrometeorites p 3340 N93-29368

Scanning electron microscope/energy dispersive x ray analysis of impact residues in LDEF tray clamps p 3283 N93-29369

Projectile compositions and modal frequencies on the chemistry of micrometeoroids LDEF experiment p 3638 N93-29370

Asteroidal versus cometary meteoroid impacts on the Long Duration Exposure Facility (LDEF) p 3638 N93-29371

Interplanetary meteoroid debris in LDEF metal craters p 3638 N93-29372

Origin of orbital debris impacts on LDEF's trailing surfaces p 3283 N93-29373

Damage areas on selected LDEF aluminum surfaces p 3283 N93-29374

LDEF data: Comparisons with existing models p 3283 N93-29375

New meteoroid model predictions for directional impacts on LDEF p 3638 N93-29376

Long Duration Exposure Facility (LDEF) attitude measurements of the Interplanetary Dust Experiment p 3638 N93-29377

Elemental analyses of hypervelocity microparticle impact sites on Interplanetary Dust Experiment sensor surfaces p 3638 N93-29378

Long-term microparticle flux variability indicated by comparison of Interplanetary Dust Experiment (IDE) timed impacts for LDEF's first year in orbit with impact data for the entire 5.77-year orbital lifetime p 3638 N93-29379

The Interstellar Gas Experiment: Analysis in progress p 3639 N93-29380

Follow up on the crystal growth experiments of the LDEF p 3602 N93-29381

LDEF: 69 Months in Space. Part 1: Second Post-Retrieval Symposium [NASA-CP-3194-PT-1] p 3660 N93-29621

Refinements on the pinhole camera measurements of the LDEF attitude p 3283 N93-29622

LDEF microenvironments, observed and predicted p 3283 N93-29623

A generalized approach to the thermal analysis of the Long Duration Exposure Facility's flight experiments p 3428 N93-29624

EnviroNET: On-line information for LDEF p 3624 N93-29625

Status of LDEF ionizing radiation measurements and analysis p 3654 N93-29626

Sensitivity of LDEF foil analyses using ultra-low background germanium vs. large NaI(Tl) multidimensional spectrometers p 3318 N93-29627

Radioactivities induced in some LDEF samples p 3572 N93-29628

A photon phreak digs the LDEF happening p 3572 N93-29629

Charged particle activation studies on the surface of LDEF spacecraft p 3572 N93-29630

Collection, analysis, and archival of LDEF activation data p 3624 N93-29631

Induced activation study of LDEF p 3572 N93-29632

Revised prediction of LDEF exposure to trapped protons p 3572 N93-29633

A measurement of the radiation dose to LDEF by passive dosimetry p 3572 N93-29634

LDEF: Dosimetric measurement results (AO 138-7 experiment) p 3573 N93-29635

Absorbed dose measurements and predictions on LDEF p 3573 N93-29636

LET spectra measurements of charged particles in the P0006 experiment on LDEF p 3573 N93-29637

Light-heavy ion measurements in CR-39 located on the Earth side of LDEF p 3573 N93-29638

Three-dimensional shielding effects on charged particle fluences measured in the P0006 experiment of LDEF p 3573 N93-29639

Development and application of a 3-D geometry/mass model for LDEF satellite ionizing radiation assessments p 3573 N93-29640

Radiation model predictions and validation using LDEF satellite data p 3573 N93-29641

Future directions for LDEF ionizing radiation modeling and assessments p 3573 N93-29642

Cosmogenic radionuclides on LDEF: An unexpected Be-10 result p 3573 N93-29643

Heavy ion measurement on LDEF p 3573 N93-29644

Progress report on the Heavy Ions in Space (HIIS) experiment p 3573 N93-29645

Progress report on the ultra heavy cosmic ray experiment (AO178) p 3654 N93-29646

LDEF: 69 Months in Space. Part 4: Second Post-Retrieval Symposium [NASA-CP-3194-PT-4] p 3665 N93-29682

Overview of the Systems Special Investigation Group investigation p 3318 N93-29683

Post-flight analyses of the crystals from the M0003-14 quartz crystal microbalance experiment p 3602 N93-29684

Radiation sensitivity of quartz crystal oscillators experiment for the Long Duration Exposure Facility (LDEF), part 2 p 3414 N93-29685

LEO effects on candidate solar cell cover materials p 3467 N93-29687

New results from FRECOPA analysis p 3448 N93-29688

Degradation of electro-optic components aboard LDEF p 3582 N93-29689

LDEF Space Plasma-High Voltage Drainage Experiment post-flight results p 3414 N93-29690

In orbit degradation of EUV optical components in the wavelength range 10-40 nm AO 138-3 p 3582 N93-29691

Degradation of optical components in a space environment p 3582 N93-29692

Studies of effects on optical components and sensors: LDEF experiments AO-147 (ERB components) and S-0014 (APEX) p 3582 N93-29693

Effects of long term space environment exposure on optical substrates and coatings (S0050-2) p 3582 N93-29694

LDEF space optics handbook p 3582 N93-29695

Ruled and holographic experiment (AO 138-5) p 3434 N93-29696

Holographic data storage crystals for the LDEF p 3435 N93-29697

Characterization of a space orbited incoherent fiber optic bundle p 3583 N93-29698

Analyses of space environment effects on active fiber optic links orbited aboard the LDEF p 3583 N93-29699

Radiation and temperature effects on LDEF fiber optic samples p 3583 N93-29700

Long Duration Exposure Facility (LDEF) low temperature Heat Pipe Experiment Package (HEPP) flight results p 3429 N93-29701

Final results of space exposed experiment developed for students p 3492 N93-29702

Continued results of the seeds in space experiment p 3492 N93-29703

LDEF archival system plan p 3624 N93-29704

Retrievable payload carrier, next generation Long Duration Exposure Facility: Update 1992 p 3283 N93-29705

Next generation optical instruments and space experiment based on the LDEF thermal control surfaces experiment (S0069) p 3583 N93-29706

An LDEF 2 dust instrument for discrimination between orbital debris and natural particles in near-Earth space p 3286 N93-29707

Future radiation measurements in low Earth orbit p 3654 N93-29708

LONG DURATION SPACE FLIGHT

Effects of atomic oxygen and ultraviolet radiation on candidate elastomeric materials for long duration missions. Test series no.1 [NASA-TM-108408] p 3331 N93-29193

Issues on human acceleration tolerance after long-duration space flights [NASA-TM-104753] p 3495 N93-29651

LONG TERM EFFECTS

Degradation of electro-optic components aboard LDEF p 3582 N93-29689

Environmental Monitoring and Assessment Program. EMAP: Arid Colorado plateau pilot study [PB93-181618] p 3474 N93-30823

LONG WAVE RADIATION

The distribution of the annual and semiannual cycles in the tropics [DE92-642213] p 3485 N93-31006

LORAN

Wind measurement accuracy of a loran radiosonde [AD-A263572] p 3483 N93-29832

LORENTZ FORCE

Some problems of relativistic electrodynamics [DE92-644738] p 3400 N93-30923

LORENTZ TRANSFORMATIONS

A new exact solution to the classical equations of motion of the relativistic string with massive ends [DE92-644736] p 3557 N93-30922

Relativity theory in (2 + 2)-space [DE92-644671] p 3608 N93-30983

LOSSES

World commercial aircraft accidents [DE93-010892] p 3243 N93-28571

Signal-to-noise ratio losses in full spectrum combining of signals with a downconverted subcarrier p 3386 N93-29599

Analysis of visual loss from retinal lesions [AD-A264692] p 3496 N93-30494

LOUDNESS

Subjective response to simulated sonic booms with ground reflections [NASA-TM-107764] p 3561 N93-28692

LOW ALTITUDE

Acoustic-gravity waves from low-altitude localized disturbances [AD-A264804] p 3479 N93-30593

LOW ASPECT RATIO WINGS

High-Reynolds-number test of a 5-percent-thick low-aspect-ratio semispan wing in the Langley 0.3-meter transonic cryogenic tunnel: Wing pressure distributions [NASA-TM-4227] p 3240 N93-29449

LOW COST

Low-cost Active Structural Control space experiment (LASC) p 3263 N93-28700

Selection and static calibration of the Marsh J1678 pressure gauge p 3249 N93-29779

Planar active antennas and quasi-optical power combining arrays using FET's and slots [AD-A263759] p 3387 N93-29875

QuickStar: System design, capabilities, and tactical applications of a small, smart space system p 3284 N93-29905

LOW FREQUENCIES

The cone structure and focusing of the electric field of VLF and LF waves at high altitudes of the ionosphere p 3395 N93-30731

Studies of the propagation of Low Frequency (LF) radio waves p 3396 N93-30738

Comparative study of undersea fields produced by various dipoles p 3397 N93-30740

LOW PASS FILTERS

Theoretical bit error rate performance of the Kalman filter excisor for FM interference [AD-A263018] p 3383 N93-29407

LOW PRESSURE

Tomographic analysis of line-of-sight infrared spectra of low-pressure flames [AD-A263185] p 3309 N93-28514

Growing wheat to maturity in reduced gas pressures [NASA-CR-193245] p 3491 N93-29216

NOx chemistry in natural gas flames [PB93-175263] p 3317 N93-30760

LOW REYNOLDS NUMBER

Accelerated motion of rigid spheres in unsteady flows at low to moderate Reynolds numbers p 3416 N93-28612

A new flux conserving Newton's method scheme for the two-dimensional, steady Navier-Stokes equations [NASA-TM-106160] p 3416 N93-28626

Velocity measurements of low Reynolds number tube flow using fiber-optic technology [DE93-009865] p 3422 N93-29335

LOW SPEED

Unsteady vortex loop/dipole theory applied to the work and acoustics of an ideal low speed propeller [AD-A264057] p 3241 N93-29891

LOW SPEED WIND TUNNELS

Determination of surface heat transfer and film cooling effectiveness in unsteady wake flow conditions p 3253 N93-29933

On the development of a film cooling layer p 3258 N93-29959

LOW TEMPERATURE

Low temperature (LT) GaAs and related materials [AD-A263607] p 3298 N93-29282

Defect studies in low-temperature-grown GaAs [DE93-010405] p 3595 N93-29417

An assessment of peripheral nerve damage in the rat following non-freezing cold exposure: An electrophysiological and histopathological examination [AD-A264293] p 3492 N93-30818

LOW TEMPERATURE ENVIRONMENTS

Novel low temperature superconducting bolometers [DE93-010433] p 3430 N93-28664

A field investigation of water and salt movement in permafrost and the active layer [AD-A263706] p 3487 N93-29298

Microwave processing of silicon nitride for advanced gas turbine applications [DE93-007910] p 3334 N93-29767

LOWER IONOSPHERE

Lightning-induced effects on VLF/LF radio propagation p 3396 N93-30737

LUBRICANTS

A study of the chemical mechanism in lubrication [DE93-012230] p 3330 N93-28650

LUBRICATING OILS

Synthetic lubricating oil greases containing metal chelates of Schiff bases [AD-D015694] p 3333 N93-29458

LUBRICATION

Fundamental studies of friction, lubrication, and wear by atomic force microscopy [AD-A264647] p 3446 N93-30524

Tribology: Friction, lubrication, and wear technology p 3292 N93-30965

LUMINAIRES

Discomfort glare from high-intensity discharge headlamps: Effects of context and experience [PB93-174720] p 3496 N93-30659

Improved measurement of thermal effects on microstructure p 3292 N93-30959

LUMINESCENCE

Quantum lattice fluctuations in a 1-dimensional charge-density-wave material: Luminescence and resonance Raman studies of an MX solid [DE93-007362] p 3593 N93-28966

LUMINOSITY

Maximizing the luminosity of hadron, supercolliders at 10-100 TeV [DE93-009247] p 3574 N93-29103

The 12 UM contribution of nearby galaxies to the infrared background [AD-A264336] p 3654 N93-30419

LUMINOUS INTENSITY

Large amplitude striations in an RF discharge [DE93-753244] p 3379 N93-28534

Polarimetric multispectral imaging technology p 3434 N93-28774

Near-infrared line imaging of NGC 6240: Global shock and nuclear starburst [MPE-PREPRINT-226] p 3631 N93-30641

LUNAR BASED EQUIPMENT

Lunar science: Using the Moon as a testbed p 3650 N93-28821

The 1990-1991 project summaries p 3230 N93-29730

LUNAR BASES

Indigenous lunar construction materials p 3277 N93-29120

Systems engineering studies of lunar base construction p 3277 N93-29121

Earth to lunar CELSS evolution p 3229 N93-29727

Selenia: A habitability study for the development of a third generation lunar base p 3233 N93-29748

The 1990-1991 project summaries p 3234 N93-29755

GENESIS 2: Advanced lunar outpost p 3235 N93-29760

LUNAR CONSTRUCTION EQUIPMENT

Space construction activities [NASA-CR-192690] p 3274 N93-29108

Lunar crane system p 3277 N93-29118

Indigenous lunar construction materials p 3277 N93-29120

Systems engineering studies of lunar base construction p 3277 N93-29121

LUNAR ENVIRONMENT

Lunar science: Using the Moon as a testbed p 3650 N93-28821

LUNAR EXPLORATION

Design of a particle beam satellite system for lunar prospecting p 3434 N93-28768

LUNAR GRAVITATION

Lunar gravitational field estimation and the effects of mismodeling upon lunar satellite orbit prediction [NASA-CR-188249] p 3634 N93-29042

LUNAR LANDING MODULES

The 1990/1991 project summaries p 3229 N93-29725

Lunar lander ground support system p 3230 N93-29729

Project UM-HAUL: A self-unloading reusable lunar lander p 3232 N93-29740

B and T: Lunar landers p 3234 N93-29751

RS Landers: Lunar lander p 3234 N93-29753

LUNAR MAGNETIC FIELDS

The production and evolution of plasma and associated magnetic fields during hypervelocity impacts: Implications for planetary paleomagnetism p 3589 N93-30000

LUNAR MAPS

Imaging spectrometers using concave holographic gratings p 3434 N93-28783

LUNAR PHASES

Tidal and lunar data for Point Mugu, San Nicolas island, and the Barking Sanda area during 1993 [AD-A262725] p 3477 N93-29401

LUNAR PHOTOGRAPHS

Systematic processing of Clementine data for scientific analyses p 3624 N93-28803

LUNAR RESOURCES

Use of particle beams for lunar prospecting p 3650 N93-28822

Method for producing oxygen from lunar materials [NASA-CASE-MSC-21759-1] p 3312 N93-29617

LUNAR ROCKS

Regolith-structure modeling p 3276 N93-29116

Lunar regolith penetrators and cutters p 3276 N93-29117

Indigenous lunar construction materials p 3277 N93-29120

Method for producing oxygen from lunar materials [NASA-CASE-MSC-21759-1] p 3312 N93-29617

LUNAR ROVING VEHICLES

Sources sought for innovative scientific instrumentation for scientific lunar rovers p 3434 N93-28804

Lunar rovers and local positioning system p 3277 N93-29119

LUNAR SHELTERS

Indigenous lunar construction materials p 3277 N93-29120

LUNAR SOIL

Method for producing oxygen from lunar materials [NASA-CASE-MSC-21759-1] p 3312 N93-29617

LUNAR SPACECRAFT

Lunar gravitational field estimation and the effects of mismodeling upon lunar satellite orbit prediction [NASA-CR-188249] p 3634 N93-29042

LUNAR SURFACE

Design of a particle beam satellite system for lunar prospecting p 3434 N93-28768

Laer-induced breakdown spectroscopy instrument for element analysis of planetary surfaces
p 3434 N93-28769
Sources sought for innovative scientific instrumentation for scientific lunar rovers p 3434 N93-28804
Use of particle beams for lunar prospecting
p 3650 N93-28822
The production and evolution of plasma and associated magnetic fields during hypervelocity impacts: Implications for planetary paleomagnetism p 3589 N93-30000

LUNAR SURFACE VEHICLES
The 1990-1991 project summaries
p 3230 N93-29730

LUNGS
The chronic effects of jP-8 jet fuel exposure on the lungs
[AD-A264162] p 3495 N93-30153

M

M STARS
Magnetic activity in low mass stars
[DE93-009073] p 3632 N93-28547
Spectroscopic and photometric studies of main sequence M stars and a search for late-type dwarfs in the solar vicinity p 3629 N93-28608

MACH NUMBER
Effects of flow-path variations on internal reversing flow in a tailpipe offtake configuration for ASTOVL aircraft
[NASA-TM-106149] p 3252 N93-29065
Performance characteristics of two multiaxis thrust-vectoring nozzles at Mach numbers up to 1.28
[NASA-TP-3313] p 3239 N93-29160
Solution of Euler equations for forebody-inlet ensemble of aircraft at high angle of attack
[AD-A263905] p 3240 N93-29862
Measurement of turbulent spots and intermittency modelling at gas-turbine conditions
p 3253 N93-29934

MACHINE LEARNING
Robotics and artificial intelligence for hazardous environments
[DE93-008271] p 3541 N93-29047
Overview of the System of Experts for Intelligent Data Management (SEIDAM) p 3613 N93-29228
A self-learning rule base for command following in dynamical systems p 3512 N93-29531
Learning characteristics of a space-time neural network as a tether skiprope observer p 3512 N93-29534
Fuzzy learning under and about an unfamiliar fuzzy teacher p 3516 N93-29558
Some problems with the design of self-learning management systems p 3516 N93-29559
A conjugate gradients/trust regions algorithms for training multilayer perceptrons for nonlinear mapping
p 3519 N93-29581
An accelerated training method for back propagation networks
[NASA-CASE-MSC-21625-1] p 3498 N93-29610
Analog CMOS circuits for neural networks
p 3355 N93-30223
A motion detector based on a neural network
p 3356 N93-30224
An artificial neural network model for periodic trajectory generation p 3356 N93-30225
Drive-reinforcement learning system applications
[AD-A264514] p 3446 N93-30404
Adaptive networks for sequential decision problems
[AD-A264756] p 3534 N93-30561

MACHINE TOOLS
A virtual environment for manufacturing systems
[AD-A263128] p 3528 N93-29473

MACHINING
A microseismometer for terrestrial and extraterrestrial applications p 3434 N93-28765
A simple model for explosives formulation
[DE93-010703] p 3341 N93-29251
Design and performance evaluation of a gas chromatograph micromachined in a single crystal silicon substrate
[AD-A262594] p 3596 N93-29424

MAGELLANIC CLOUDS
The x ray population in globular clusters and three crab-like SNR in the large Magellanic cloud
[NASA-CR-193172] p 3630 N93-29604

MAGNESIUM ALLOYS
Mechanical properties of several magnesium and aluminum composites
[AD-A262481] p 3299 N93-30137
Constitutive laws for deformation and dynamic recrystallization in cubic metals
[DE93-010740] p 3326 N93-30486

MAGNESIUM OXIDES
Report on the sintering and properties of MgO and MgO-5 percent TiC
[DE93-008676] p 3323 N93-29092
The effect of Bi2 O3 on the electrical properties of Zr O2: 3 percent Mg O ceramic solid electrolytes
[DE93-607029] p 3339 N93-30774

MAGNESIUM TITANATES
Report on the sintering and properties of MgO and MgO-5 percent TiC
[DE93-008676] p 3323 N93-29092

MAGNET COILS
Forces on a magnet moving past figure-eight coils
[DE93-009965] p 3561 N93-29189

MAGNETIC ANOMALIES
Remote sensing survey of Mississippi River-Gulf Outlet, Breton Sound disposal area, Plaquemines Parish, Louisiana
[AD-A263097] p 3459 N93-29146
Spacecraft surface charging handbook
[AD-A262778] p 3279 N93-29305
Heavy ion measurement on LDEF
p 3573 N93-29644

MAGNETIC BEARINGS
Cryogenic magnetic bearing
[AD-A264716] p 3446 N93-30512

MAGNETIC CONTROL
Magnetically operated check valve
[NASA-CASE-MSC-22046-1] p 3442 N93-28501

MAGNETIC CORES
The production and evolution of plasma and associated magnetic fields during hypervelocity impacts: Implications for planetary paleomagnetism p 3589 N93-30000

MAGNETIC DIPOLES
Comparative study of undersea fields produced by various dipoles p 3397 N93-30740
Results of the joint HIPAS/NUWC campaigns to investigate ELF generated by auroral electrojet modulation p 3398 N93-30746

MAGNETIC DISKS
Goddard Conference on Mass Storage Systems and Technologies, Volume 1
[NASA-CP-3198] p 3616 N93-30449
RAID 7 disk array p 3537 N93-30462
Tutorial: Performance and reliability in redundant disk arrays p 3537 N93-30463
Striped tertiary storage arrays p 3620 N93-30464

MAGNETIC EFFECTS
Preliminary investigation of high power microwave plasmas for electrothermal thruster use
[NASA-TM-106207] p 3288 N93-29158
Effect of planar magnetic field on electron transport properties of n-AlGaAs/GaAs heterojunction and photoluminescence measures in GaAs samples
[DE93-608739] p 3601 N93-30776
Regular and chaotic motion of two dimensional electrons in a strong magnetic field
[DE93-604091] p 3607 N93-30933

MAGNETIC FIELD CONFIGURATIONS
Laboratory simulation of field-aligned currents
[NASA-CR-193091] p 3476 N93-28538
Nonlinear coupling of tearing fluctuations in the Madison Symmetric Torus
[DE93-010131] p 3584 N93-28602
Measurements of magnetic fields produced by a 30 kWe class Arcjet Power Conditioning Unit
[AD-A262786] p 3287 N93-28658
Plasma diffusion through multidipole magnetic fields
[DE93-608548] p 3591 N93-31007

MAGNETIC FIELD RECONNECTION
Nonlinear dynamics and plasma transport
[DE93-012238] p 3585 N93-28749
Solar flare MDH
[AD-A262275] p 3652 N93-28756
Poloidal field measurements during transient phenomena on MTX: Sawtooth perturbations and the effect of ECH on disruptions
[DE93-010516] p 3587 N93-29303
Electrodynamics of the dayside cleft region based on ground observations at Svalbard
[AD-A263571] p 3477 N93-29831
Mithras studies of the boundary between open and closed field lines
[AD-A264758] p 3479 N93-30562

MAGNETIC FIELDS
Theory of normal and superconducting properties of fullerene-based solids
[DE93-007722] p 3592 N93-28582
Measurements of magnetic fields produced by a 30 kWe class Arcjet Power Conditioning Unit
[AD-A262786] p 3287 N93-28658
Multifractal analysis of radio lobes
p 3380 N93-28689
Plasma, magnetic, and electromagnetic measurements at nonmagnetic bodies p 3647 N93-28809
Coherent and semi-coherent neutron transfer reactions
[DE93-008336] p 3565 N93-28959
Flux lattice relaxation, noise, and symmetry-breaking in frustrated Josephson junction arrays
[DE93-008713] p 3593 N93-29094
Forces on a magnet moving past figure-eight coils
[DE93-009965] p 3561 N93-29189
Experimental study of location and identification of ferrous spheroids using a smart total field magnetometer
[AD-A263661] p 3324 N93-29391
Reaction mechanism studies of heavy ion induced nuclear reactions
[DE93-010496] p 3569 N93-29807
Magnetic field measurements of the CEBAF (NIST) wiggler using the pulsed wire method
[AD-A263997] p 3439 N93-29867
Pattern measurements of US Navy ELF antennas
p 3399 N93-30752
Measurement of magnetic field penetration depth in niobium polycrystalline films by polarized neutron reflection method
[DE93-606390] p 3600 N93-30771
Effect of planar magnetic field on electron transport properties of n-AlGaAs/GaAs heterojunction and photoluminescence measures in GaAs samples
[DE93-608739] p 3601 N93-30776
Neutrino oscillations and a new Faraday effect
[DE93-606111] p 3571 N93-30789
Orbital motion calculation using Lie method in collider nonlinear magnetic field
[DE93-605733] p 3571 N93-30800
Electric magnetic duality in string theory
[DE93-606061] p 3606 N93-30807
Modification of the S-band phase shifter model 331A-3 of Electromagnetic Sciences Inc.
[DIGEL-1992-5] p 3399 N93-30836
Microwave emission from relativistic electron beams
[AD-A264102] p 3400 N93-30880

MAGNETIC FLUX
Flux lattice relaxation, noise, and symmetry-breaking in frustrated Josephson junction arrays
[DE93-008713] p 3593 N93-29094
Analysis of an MCG/fuse/PFS experiment
[DE93-007355] p 3410 N93-29812
Microsecond ribbon relativistic electron beam in a plane undulator and generation of microwave radiation
[DE93-605693] p 3400 N93-30993

MAGNETIC LEVITATION VEHICLES
Guideway structural design and power/propulsion/braking in relation to guideways, volume 1
[PB93-169902] p 3447 N93-30820

MAGNETIC MATERIALS
Operational results of pilot cell test with cermet inert anodes
[DE93-009338] p 3322 N93-29061

MAGNETIC MEASUREMENT
Measurements of magnetic fields produced by a 30 kWe class Arcjet Power Conditioning Unit
[AD-A262786] p 3287 N93-28658
Remote measurement of planetary magnetic fields by the Hanle effect p 3645 N93-28793
Plasma, magnetic, and electromagnetic measurements at nonmagnetic bodies p 3647 N93-28809
Measurement of magnetic field penetration depth in niobium polycrystalline films by polarized neutron reflection method
[DE93-606390] p 3600 N93-30771

MAGNETIC MIRRORS
Experimental MHD stability limit in the gas-dynamic trap
[DE93-606218] p 3591 N93-30780

MAGNETIC MOMENTS
Magnetic character investigation of higher alcohol synthesis Cu-Co-Cr catalysts
[DE93-009732] p 3316 N93-30653

MAGNETIC PROPERTIES
A detailed technology roadmap for superconductivity
p 3526 N93-29045

MAGNETIC RECORDING
Goddard Conference on Mass Storage Systems and Technologies, Volume 1
[NASA-CP-3198] p 3616 N93-30449
The modern high rate digital cassette recorder
p 3435 N93-30468
Evolution of a high-performance storage system based on magnetic tape instrumentation recorders
p 3435 N93-30470

MAGNETIC RESONANCE
Image segmentation using fuzzy LVQ clustering networks p 3511 N93-29528

MAGNETIC SIGNATURES
Optical system analysis for the ground based EXVM
[NASA-CR-192588] p 3582 N93-31035

MAGNETIC STORMS
Spacecraft surface charging handbook
[AD-A262778] p 3279 N93-29305
SESC products and services user guide
[PB93-178879] p 3653 N93-29679
MAGNETIC SUSPENSION
Forces on a magnet moving past figure-eight coils
[DE93-009965] p 3561 N93-29189
Sensor systems for monitoring Maglev guideway structures
[PB93-154821] p 3444 N93-29205
Cryogenic magnetic bearing
[AD-A264716] p 3446 N93-30512
Guideway structural design and power/propulsion/braking in relation to guideways, volume 1
[PB93-169902] p 3447 N93-30820
MAGNETIC TAPES
Goddard Conference on Mass Storage Systems and Technologies, Volume 1
[NASA-CP-3198] p 3616 N93-30449
GE networked mass storage solutions supporting IEEE network mass storage model p 3618 N93-30458
Striped tertiary storage arrays p 3620 N93-30464
Mass optical storage-tape (MOST)
p 3621 N93-30471
MAGNETIC VARIATIONS
Magnetic activity in low mass stars
[DE93-009073] p 3632 N93-28547
MAGNETIZATION
Enhancements of the critical currents of YBaCuO single crystals by neutron (n) and proton (p) irradiation
[DE93-007892] p 3592 N93-28661
MAGNETOACOUSTIC WAVES
Elemental compositions of high-energy ions produced by magnetosonic waves in quiescent plasmas
[DE93-753241] p 3588 N93-29434
Ion ring distribution produced by a magnetosonic wave
[DE93-754311] p 3590 N93-30533
MAGNETOHYDRODYNAMIC FLOW
Analysis of an MCG/fuse/PFS experiment
[DE93-007355] p 3410 N93-29812
Two-dimensional and three-dimensional time-dependent MHD model of extended corona
p 3653 N93-30496
MAGNETOHYDRODYNAMIC GENERATORS
Magnetohydrodynamic projects at the CDIF
[DE93-012195] p 3584 N93-28649
The design and lifetime calculation of MHD generator walls based on subcritical crack growth in ceramics
[ISBN-90-9004009-9] p 3332 N93-29267
Transient tests on an MHD thruster
[DE93-008656] p 3587 N93-29299
MAGNETOHYDRODYNAMIC STABILITY
JT-60 Upgrade vertical stability experiments and analysis
[DE93-753131] p 3583 N93-28530
Edge plasma control by RF electric field in Compact Helical System (CHS)
[DE93-753242] p 3583 N93-28532
Self-consistent chaos in the beam-plasma instability
[DE93-009581] p 3584 N93-28599
Solar flare MDH
[AD-A262275] p 3652 N93-28756
Self-organized profile relaxation by ion temperature gradient instability in toroidal plasmas
[DE93-009580] p 3585 N93-28910
Collective transport of alpha particles due to Alfven wave instability
[DE93-009578] p 3587 N93-29148
Poloidal field measurements during transient phenomena on MTX: Sawtooth perturbations and the effect of ECH on disruptions
[DE93-010516] p 3587 N93-29303
Ionospheric structure specifications and systems effects
[AD-A263573] p 3476 N93-29343
A novel approach for new radiation sources based on solid state plasma instabilities
[AD-A263699] p 3588 N93-29382
Vertical slot convection: A linear study
[DE93-007643] p 3423 N93-29804
Experimental MHD stability limit in the gas-dynamic trap
[DE93-606218] p 3591 N93-30780
MAGNETOHYDRODYNAMIC WAVES
Collective transport of alpha particles due to Alfven wave instability
[DE93-009578] p 3587 N93-29148
Elemental compositions of high-energy ions produced by magnetosonic waves in quiescent plasmas
[DE93-753241] p 3588 N93-29434
MAGNETOHYDRODYNAMICS
JT-60 Upgrade vertical stability experiments and analysis
[DE93-753131] p 3583 N93-28530
Magnetohydrodynamic projects at the CDIF
[DE93-012195] p 3584 N93-28649
Nonlinear dynamics and plasma transport
[DE93-012238] p 3585 N93-28749
Solar flare MDH
[AD-A262275] p 3652 N93-28756
A study of the physical mechanisms for filament eruption and coronal mass ejection via numerical simulation
[NASA-CR-193180] p 3653 N93-28935
Transient tests on an MHD thruster
[DE93-008656] p 3587 N93-29299
MAGNETOMETERS
Optimism experiment and development of space-qualified seismometers in France
p 3646 N93-28796
Experimental study of location and identification of ferrous spheroids using a smart total field magnetometer
[AD-A263661] p 3324 N93-29391
MAGNETOPLASMADYNAMICS
Engineering consideration for the self-energizing magnetoplasmadynamic (MPD): Type fusion plasma thruster
[AD-A262785] p 3288 N93-29289
MAGNETOSPHERE-IONOSPHERE COUPLING
Laboratory simulation of field-aligned currents
[NASA-CR-193091] p 3476 N93-28538
USU center of excellence in theory and analysis of the geo-plasma environment
[AD-A264750] p 3590 N93-30585
MAGNETOSPHERES
GRO: Red-shifted electron-positron annihilation gamma-rays from radiopulsars
[NASA-CR-193243] p 3635 N93-30053
MAGNETS
New technologies for UV detectors
p 3582 N93-28786
Mechanical behaviour of a closed collar model for an 11.5 T dipole
[NIKHEF-H/92-03] p 3576 N93-30019
MAIN SEQUENCE STARS
Spectroscopic and photometric studies of main sequence M stars and a search for late-type dwarfs in the solar vicinity p 3629 N93-28608
MAINTENANCE
New remote maintenance approach for TPX
[DE93-007857] p 3584 N93-28583
Inservice diagnostic methods for solenoid-operated valves
[DE93-007823] p 3443 N93-28968
An analysis of the correlation between the J52 engine component improvement program and improved maintenance parameters
[AD-A262062] p 3251 N93-28984
Energy efficient drivepower: An overview
[DE93-012435] p 3411 N93-30057
Centralized maintenance evaluation
[AD-A264400] p 3544 N93-30886
MALES
Field trial of caffeine on physical performance at altitude: An attempt to overcome the challenge
[AD-A264260] p 3497 N93-30894
MALFUNCTIONS
Valve malfunction detection apparatus
[NASA-CASE-MFS-29904-1] p 3432 N93-29503
MAN ENVIRONMENT INTERACTIONS
Emission inventories: A global modeling perspective
[DE93-005817] p 3469 N93-28965
Overview of the DOE Atmospheric Chemistry Program's Ozone Project
[DE93-007416] p 3471 N93-29770
MAN MACHINE SYSTEMS
Combat Automation for Airborne Weapon Systems: Man/Machine Interface Trends and Technologies
[AGARD-CP-520] p 3501 N93-28850
Pilot decision aiding for weapon delivery: A novel approach to fire control cueing using parallel computing
p 3501 N93-28853
A new class of mission support for combat air-crew
p 3501 N93-28854
Pilot intent and error recognition as part of a knowledge based cockpit assistant p 3502 N93-28855
The design and development of the new RAF standard HUD format p 3502 N93-28856
Virtual interface applications for airborne weapons systems p 3502 N93-28858
Operator and automation capability analysis: Picking the right team p 3503 N93-28864
System automation and pilot-vehicle-interface for unconstrained low-altitude night attack
p 3503 N93-28867
Computer assisted evaluation for air close combat based on time interval characterization p 3504 N93-28868
Overview of cockpit technology research and development programs for improvement of the man/machine interface: Review of the AGARD AVP Symposium held in Madrid, May 1992
p 3505 N93-28872
Anthropometric data from launch and entry suited test subjects for the design of a recumbent seating system
[NASA-TM-104769] p 3505 N93-29044
Design and implementation of a Global Positioning System (GPS) supported area navigation system with electronic aircraft
[ILR-MITT-275(1992)] p 3246 N93-30671
MAN-COMPUTER INTERFACE
Dynamic object oriented interaction and its implementation in the framework in an interface management system
[ETN-93-93795] p 3523 N93-28526
Natural language generation
[AD-A262578] p 3524 N93-28579
Combat Automation for Airborne Weapon Systems: Man/Machine Interface Trends and Technologies
[AGARD-CP-520] p 3501 N93-28850
A new class of mission support for combat air-crew
p 3501 N93-28854
The design and development of the new RAF standard HUD format p 3502 N93-28856
A distributed system for visualizing and analyzing multivariate and multidisciplinary data
p 3613 N93-29226
A C++ interface for programming on the Connection Machine
[INRIA-RR-1698] p 3538 N93-29487
Intelligent virtual reality in the setting of fuzzy sets
p 3513 N93-29544
Software testing using the IEEE standards
[DE93-009833] p 3532 N93-30050
Intelligent support for human computer interaction and decision-making in distribution planning and scheduling systems
[AD-A263985] p 3610 N93-30124
MANAGEMENT ANALYSIS
Environmental Monitoring and Assessment Program. EMAP: Arid Colorado plateau pilot study
[PB93-181618] p 3474 N93-30823
MANAGEMENT METHODS
Performance measurement systems: A best practices study
[AD-A262180] p 3506 N93-29444
MANAGEMENT PLANNING
The program manager's notebook
[AD-A263074] p 3609 N93-29142
Overview of the DOE Atmospheric Chemistry Program's Ozone Project
[DE93-007416] p 3471 N93-29770
The 1991-1992 aviation system capacity plan
[AD-A263436] p 3261 N93-29788
The 1992 town meetings: Toward a shared vision
[NASA-NP-205] p 3608 N93-30134
The NCAT process p 3626 N93-30697
Technology transfer p 3627 N93-30707
Technology transfer within the government
p 3627 N93-30709
Environmental characteristics of EPA, NRC, and DOE sites contaminated with radioactive substances
[PB93-185551] p 3475 N93-30829
Planning and progress of EPA's pollution prevention research program
[PB93-185767] p 3475 N93-30831
MANAGEMENT SYSTEMS
Some problems with the design of self-learning management systems p 3516 N93-29559
Design of biomass management systems and components for closed loop life support systems
p 3230 N93-29728
Measurements over distributed high performance computing and storage systems p 3622 N93-30476
MANGANESE
Design of a high activity and selectivity alcohol catalyst
[DE93-012277] p 3309 N93-28750
MANGANESE OXIDES
Design of a high activity and selectivity alcohol catalyst
[DE93-012277] p 3309 N93-28750
MANIFOLDS (MATHEMATICS)
Topology of hybrid objects
[ETN-93-93594] p 3546 N93-28466
A covariant form of the Maxwell's equations in four-dimensional spaces with an arbitrary signature
[DE93-606070] p 3605 N93-30783
Abelian gauge theories on homogeneous spaces
[DE92-644730] p 3607 N93-30921
Topology and statistics in zero dimensions
[DE93-604080] p 3607 N93-30932
Equivariant elliptic homology
[DE92-641338] p 3557 N93-30981

The geometry of complex space-times with torsion
[DE92-641343] p 3608 N93-31003

MANIPULATORS

New remote maintenance approach for TPX
[DE93-007857] p 3584 N93-28583

Vision-based control of holonomic robots for 3-dimensional rigid-body positioning using camera-space manipulation p 3578 N93-29178

A manipulator kinematic design for high-vacuum operation
[DE93-010264] p 3444 N93-29247

A portable modular architecture for robotic manipulator control
[DE93-010819] p 3444 N93-29254

An architecture for robotic system integration
[DE93-010829] p 3444 N93-29316

Research on reconfigurable and reliable manipulators
[DE93-010244] p 3444 N93-29330

Advanced design for orbital debris removal in support of solar system exploration p 3229 N93-29724

Planning collision free paths for two cooperating robots using a divide-and-conquer C-space traversal heuristic
[NASA-CR-193252] p 3542 N93-29771

Input relegation control for gross motion of a kinematically redundant manipulator
[DE93-005301] p 3446 N93-30210

A closed-form formula for the manipulator regressor
p 3355 N93-30218

An information theoretic approach to stochastic adaptive control application to manipulators with active inertia
p 3359 N93-30247

Analysis and simulation of a two degrees-of-freedom one-link flexible forearm p 3361 N93-30261

A testbed for autonomous reflexive grasping
[AD-A264557] p 3446 N93-30384

Drive-reinforcement learning system applications
[AD-A264514] p 3446 N93-30404

Micropipet manipulation of lipid membranes: Direct measurement of the material properties of a cohesive structure that is only two molecules thick
p 3291 N93-30953

MANNED MARS MISSIONS

The 1990/1991 project summaries
p 3229 N93-29725

Mars integrated transportation system multistage Mars mission p 3232 N93-29741

Single-stage Mars mission p 3232 N93-29742

Mars habitat p 3233 N93-29747

MANNED REENTRY

Anthropometric data from launch and entry suited test subjects for the design of a recumbent seating system
[NASA-TM-104769] p 3505 N93-29044

MANNED SPACE FLIGHT

Analysis of orbital system logistics in the cis-lunar space with particular consideration of life cycle costs
[ETN-93-93484] p 3268 N93-29063

Technology transfer from the viewpoint of a NASA prime contractor p 3626 N93-30701

MANNED SPACECRAFT

Computerized atmospheric trace contaminant control simulation for manned spacecraft
[NASA-TM-108409] p 3505 N93-28977

Delta Advanced Reusable Transport (DART): An alternative manned spacecraft p 3231 N93-29735

Taurus Lightweight Manned Spacecraft Earth orbiting vehicle p 3231 N93-29736

Spacely's rockets: Personnel launch system/family of heavy lift launch vehicles p 3234 N93-29752

A representative survey of US space systems and methods for estimating their costs
[AD-A264159] p 3272 N93-30881

MANUAL CONTROL

Handedness and motor programming effects of manual control and movement
[AD-A264022] p 3499 N93-30027

MANUALS

Operating manual for single-shot autocorrelator
[AD-A262016] p 3438 N93-29395

Programmer's reference guide to FDMS file formats
[PB93-182038] p 3354 N93-29663

DOE fundamentals handbook: Chemistry
[DE93-012222] p 3314 N93-30198

DOE fundamentals handbook: Material science
[DE93-012224] p 3314 N93-30199

DOE fundamentals handbook: Material science
[DE93-012225] p 3314 N93-30200

MANUFACTURING

Process optimization of Hexoloy SX-SiC towards improved mechanical properties
[DE93-007913] p 3320 N93-28564

Lightweight flexible composite tent materials
[AD-A263021] p 3295 N93-28660

Transient response of embedded thermocouples
[DE93-009889] p 3431 N93-29325

The 17th Annual Electronics Manufacturing Seminar proceedings
[AD-A261963] p 3409 N93-29435

Issues, concepts, and standard techniques in assessing accuracy of coordinate measuring machines
[PB93-184331] p 3354 N93-29666

Lessons learned for composite structures
p 3302 N93-30444

Memory driven feature-based design
[AD-A264697] p 3534 N93-30495

Process and assembly plans for low cost commercial fuselage structure p 3306 N93-30865

Silicon Film(trademark) photovoltaic manufacturing technology
[DE93-010008] p 3466 N93-30891

Application of hardness testing in foundry processing operations: A university and industry partnership
p 3292 N93-30961

Thermoforming from a systems viewpoint
p 3293 N93-30967

MANY BODY PROBLEM

How to write fast and clear parallel programs using algebra
[DE93-000797] p 3524 N93-28640

Numerical simulation of quantum many-body systems
[DE93-008300] p 3603 N93-28958

Implementation of parallel algorithms
[AD-A263126] p 3529 N93-29496

Nonlinear attitude control of planar structures in space using only internal controls p 3280 N93-29991

Extracting infinite system properties from finite size clusters: Phase randomization/boundary condition averaging
[AD-A264712] p 3551 N93-30503

Schroedinger equations of higher (greater than 2) order
[DE92-644677] p 3552 N93-30984

MANY ELECTRON EFFECTS

Excited states in electronic structure calculations
[DE93-007704] p 3592 N93-28642

MAPPING

Near real-time GIS in deep-ocean exploration
[AD-A262073] p 3487 N93-29003

Toward a coordinated spatial data infrastructure for the nation
[B-149] p 3456 N93-30634

MAPS

Estimating the parameters of chaotic maps
[AD-A262574] p 3556 N93-29423

Data quality statements for spatial databases
[AD-A264125] p 3616 N93-30195

MARINE METEOROLOGY

Sensitivity study of cloud/radiation interaction using a second order turbulence radiative-convective model
[DE93-007365] p 3477 N93-29346

Ocean aerosol measurements and models in the straits of Florida (The KEY-90 experiment)
[AD-A264777] p 3487 N93-29659

Oceanographic research towers in european waters
[AD-A264795] p 3489 N93-30612

Marine microbial production of dimethylsulfide from dissolved dimethylsulfoniopropionate
[NASA-CR-193278] p 3492 N93-30665

MARINE RESOURCES

Building alliances to restore coastal environments: A coastal America progress report
[PB93-169464] p 3470 N93-29674

MARINE TECHNOLOGY

Conspicuity of aids to navigation. Part 1: Temporal patterns for flashing lights
[AD-A264626] p 3499 N93-30426

MARKET RESEARCH

Design of a turbofan powered regional transport aircraft p 3228 N93-29721

Helicopter training simulators: Key market factors
p 3237 N93-30683

US space commerce, 1991 p 3625 N93-30695

MARKETING

A fuzzy set preference model for market share analysis p 3514 N93-29548

Evaluation of environmental marketing terms in the United States
[PB93-175784] p 3474 N93-30660

MARKOV CHAINS

Easy-to-apply results for establishing convergence of Markov chains in Bayesian analysis
[AD-A264015] p 3555 N93-29979

MARKOV PROCESSES

Flow control using the theory of zero sum Markov games
[INRIA-RR-1597] p 3553 N93-28507

Asymptotic properties of constrained Markov decision processes
[INRIA-RR-1598] p 3553 N93-28508

Image classification using Markov random fields with two new relaxation methods: Deterministic pseudo annealing and modified metropolis dynamics
[INRIA-RR-1606] p 3553 N93-28510

Optimal control of the M/G/1 queue with repeated vacations of the server
[INRIA-RR-1637] p 3541 N93-28637

Closed-loop control with delayed information
[INRIA-RR-1638] p 3541 N93-28638

Speech recognition by recursive stochastic modelling
[ISBN-90-9005038-8] p 3382 N93-29266

Easy-to-apply results for establishing convergence of Markov chains in Bayesian analysis
[AD-A264015] p 3555 N93-29979

Hidden Markov models for fault detection in dynamic systems
[NASA-CASE-NPO-18982-1-CU] p 3449 N93-30413

MARS (PLANET)

Optimism experiment and development of space-qualified seismometers in France
p 3646 N93-28796

Mass spectrometric measurement of Martian krypton and xenon isotopic abundance p 3646 N93-28798

Prototype backscatter Moessbauer spectrometer for measurement of Martian surface mineralogy
p 3648 N93-28812

MARS ATMOSPHERE

The enhanced-model ladar wind sensor and its application in planetary wind velocity measurements
p 3649 N93-28815

The thermal structure, dust loading, and meridional transport in the Martian atmosphere during late southern summer p 3651 N93-29616

The 1990/1991 project summaries
p 3229 N93-29725

MARS CRATERS

Spacecraft studies of Phobos and Mars
[NASA-CR-193298] p 3651 N93-30635

MARS ENVIRONMENT

An integrated XRF/XRD instrument for Mars exobiology and geology experiments p 3645 N93-28792

The MESUR mission p 3649 N93-28816

Planetary protection issues for the MESUR mission: Probability of growth (Pg)
[NASA-CP-3167] p 3651 N93-30214

MARS LANDING

Mars integrated transportation system multistage Mars mission p 3232 N93-29741

Single-stage Mars mission p 3232 N93-29742

Mars Aquarius Mission and Titan Explorer
p 3235 N93-29756

MARS OBSERVER

DSN support of Mars Observer p 3385 N93-29598

MARS PROBES

The MESUR mission p 3649 N93-28816

MARS SAMPLE RETURN MISSIONS

Benefits of in situ propellant utilization for a Mars sample return mission
[NASA-TM-106243] p 3341 N93-28695

Mars sample return mission: Two alternate scenarios
p 3233 N93-29746

MARS SURFACE

The APX spectrometer for Martian missions
p 3434 N93-28776

Investigation of Mars rotational dynamics using Earth-based radio tracking of Mars landers
p 3642 N93-28777

Optimism experiment and development of space-qualified seismometers in France
p 3646 N93-28796

Mass spectrometric measurement of Martian krypton and xenon isotopic abundance p 3646 N93-28798

A DTA/GC for the in situ identification of the Martian surface material p 3646 N93-28800

Drill/borescope system for the Mars Polar Pathfinder
p 3647 N93-28805

Prototype backscatter Moessbauer spectrometer for measurement of Martian surface mineralogy
p 3648 N93-28812

The MESUR mission p 3649 N93-28816

Mars Aquarius Mission and Titan Explorer
p 3235 N93-29756

Spacecraft studies of Phobos and Mars
[NASA-CR-193298] p 3651 N93-30635

MARS VOLCANOES

Spacecraft studies of Phobos and Mars
[NASA-CR-193298] p 3651 N93-30635

MARTENSITE

International Conference on Martensitic Transformations (ICOMAT 92)
[AD-A262739] p 3321 N93-28591

Transformation toughening
[DE93-011805] p 3321 N93-28631

MARTENSITIC TRANSFORMATION
International Conference on Martensitic Transformations (ICOMAT 92)
[AD-A262739] p 3321 N93-28591
Transformation toughening
[DE93-011805] p 3321 N93-28631
Transformation plasticity in ductile solids
[DE93-008636] p 3321 N93-28902
MASKS
Evaluation and optimization of a flexible filtration system for respiratory protection system 21
[AD-A262467] p 3493 N93-28758
Improved field emitter current densities and stability through the application of a proprietary process
[AD-A263464] p 3411 N93-29833
MASS
QuickStar: System design, capabilities, and tactical applications of a small, smart space system
p 3284 N93-29905
MASS FLOW
Flame or plasma synthesis of diamond under turbulent and transition flow conditions
[AD-D015689] p 3333 N93-29456
Solution of Euler equations for forebody-inlet ensemble of aircraft at high angle of attack
[AD-A263905] p 3240 N93-29862
MASS RATIOS
Design and test of a superconducting RFQ for heavy ions
[DE93-010862] p 3575 N93-29317
MASS SPECTRA
A remote laser-mass spectrometer for determination of elemental composition p 3434 N93-28775
Ion emission during high-energy sputtering of ammonium dinitramide and ammonium nitrate crystals and the determination of ion decomposition pathways using tandem mass spectrometry p 3318 N93-30066
1,2-Dimethyl-1,2-Disila-Closo-Dodecaborane(12), A silicon analog of an ortho-carborane: Synthesis; x ray crystal structure; NMR, vibrational and photoelectron spectra; bonding
[AD-A264709] p 3599 N93-30568
MASS SPECTROMETERS
Clementine 2: A double asteroid flyby and impactor mission p 3268 N93-28770
A remote laser-mass spectrometer for determination of elemental composition p 3434 N93-28775
Mass spectrometric measurement of Martian krypton and xenon isotopic abundance p 3646 N93-28798
A low-cost, lightweight, and miniaturized Time-Of-Flight Mass Spectrometer (TOFMS) p 3434 N93-28817
Scanning ionic microscopy with high spatial resolution: Parallel acquisition of elementary images by high resolution mass spectrometry
[ONERA-NT-1990-7] p 3314 N93-30139
High mass resolution glow discharge mass spectrometry using an external ion source FT-ICR mass spectrometer
[AD-A264347] p 3314 N93-30166
MASS SPECTROSCOPY
Mass spectrometric measurement of Martian krypton and xenon isotopic abundance p 3646 N93-28798
High pressure preignition chemistry of hydrocarbons and hydrocarbon mixtures
[AD-A263611] p 3311 N93-29283
Mass spectrometric investigation of 2-methoxyethanol and 2-ethoxyethanol clusters: Magic numbers and structural implications
[AD-A262822] p 3312 N93-29429
Ion emission during high-energy sputtering of ammonium dinitramide and ammonium nitrate crystals and the determination of ion decomposition pathways using tandem mass spectrometry p 3318 N93-30066
Detonation mass spectrometry p 3319 N93-30076
Flame structure studies of propellant like low pressure flames using optical and mass spectrometric means
p 3319 N93-30081
High mass resolution glow discharge mass spectrometry using an external ion source FT-ICR mass spectrometer
[AD-A264347] p 3314 N93-30166
Detailed studies of soot formation in laminar diffusion flames for application to modeling studies
[AD-A264827] p 3317 N93-30667
MASS TRANSFER
Analysis of mass transport and potential vorticity budget in a simulated tropopause folding
[PB93-156792] p 3476 N93-29197
Velocity measurements of low Reynolds number tube flow using fiber-optic technology
[DE93-009865] p 3422 N93-29335
Scanning probe lithography. Part 1: Scanning tunneling microscope-induced lithography of self-assembled n-alkanethiol monolayer resists
[AD-A263130] p 3432 N93-29476
Vortex structure and mass transfer near the base of a cylinder and a turbine blade p 3253 N93-29929
The swollen polymer technique and its use for heat transfer investigations on film cooled surfaces
p 3255 N93-29944
Complex-compound heat pump: Topical report on phase 1 results
[PB93-185460] p 3466 N93-30814
MASSIVELY PARALLEL PROCESSORS
Parallel computation and the basis system
[DE93-008755] p 3537 N93-28544
BlockSolve v1.1: Scalable library software for the parallel solution of sparse linear systems
[DE93-011391] p 3524 N93-28644
Implementation of a single-material version of PAGOSA on MIMD hypercubes
[SAND-92-0640] p 3526 N93-29127
Computing for magnetic fusion energy research: An updated vision
[DE93-010394] p 3587 N93-29190
The parallel implementation of a backpropagation neural network and its applicability to SPECT image reconstruction
[DE93-010304] p 3567 N93-29416
High performance computing: Advanced Research Projects Agency should do more to foster program goals. Report to the Chairman, Committee on Armed Services, House of Representatives
[GAO/IMTEC-93-24] p 3533 N93-30202
LANL High-Performance Data System (HPDS)
p 3622 N93-30478
Infrared imaging array integrated in three dimensions directly on top of silicon circuits
[AD-A264707] p 3581 N93-30500
Finite element approximation of the shallow water equations on the MASPAR
[AD-A264649] p 3489 N93-30525
Massively parallel spatial light modulation-based optical signal processing
[AD-A264846] p 3581 N93-30905
MATCHED FILTERS
Enhanced convergence adaptive detection
[AD-A264100] p 3399 N93-30879
MATERIAL ABSORPTION
Acid solution absorption of extruded polyethylene foam
[DE93-011701] p 3330 N93-28839
MATERIALS HANDLING
Application of sensors to the control of robotic systems
[DE93-009837] p 3543 N93-30012
Graphical programming: On-line robot simulation for telerobotic control
[DE93-009796] p 3447 N93-30654
Micropipet manipulation of lipid membranes: Direct measurement of the material properties of a cohesive structure that is only two molecules thick
p 3291 N93-30953
MATERIALS RECOVERY
Hydrogen and sulfur production from hydrogen sulfide wastes
[DE93-008658] p 3310 N93-29052
Tool grinding and spark testing p 3291 N93-30954
MATERIALS SCIENCE
Space research in Germany 1990-1991
[ETN-93-93807] p 3654 N93-28477
JPRS report: Science and technology. Central Eurasia: Materials science
[JPRS-UMS-92-008] p 3322 N93-29012
JPRS report: Science and technology. Central Eurasia: Materials science
[JPRS-UMS-92-007] p 3322 N93-29013
JPRS report: Science and technology. Central Eurasia: Materials science
[JPRS-UMS-92-009] p 3322 N93-29015
JPRS report: Science and technology. Central Eurasia: Materials science
[JPRS-UMS-92-012] p 3296 N93-29016
JPRS report: Science and technology. Central Eurasia: Materials science
[JPRS-UMS-92-013] p 3296 N93-29017
JPRS report: Science and technology. Central Eurasia: Materials science
[JPRS-UMS-92-016] p 3296 N93-29018
JPRS report: Science and technology. Central Eurasia: Materials science
[JPRS-UMS-92-014] p 3322 N93-29019
JPRS report: Science and technology. Central Eurasia: Materials science
[JPRS-UMS-92-015] p 3322 N93-29020
JPRS report: Science and technology. Central Eurasia: Materials science
[JPRS-UMS-93-001] p 3296 N93-29021
LDEF materials data bases
[NASA-TM-107757] p 3290 N93-29067
DOE fundamentals handbook: Material science
[DE93-012225] p 3314 N93-30200
JPRS report: Science and technology. Central Eurasia: Materials science
[JPRS-UMS-93-003] p 3327 N93-30623
National Educators' Workshop. Update 92: Standard Experiments in Engineering Materials Science and Technology
[NASA-CP-3201] p 3290 N93-30948
Near net shape processing: A necessity for advanced materials applications p 3290 N93-30949
New materials: Fountainhead for new technologies and new science p 3291 N93-30952
Materials education activities p 3291 N93-30958
Experiments in materials science from household items p 3293 N93-30971
Taguchi method of experimental design in materials education p 3294 N93-30975
Construction and testing of simple airfoils to demonstrate structural design, materials choice, and composite concepts p 3243 N93-30979
MATERIALS TESTS
LDEF materials data bases
[NASA-TM-107757] p 3290 N93-29067
Results of a round robin test program: Complex modulus properties of a polymeric damping material
[AD-A263619] p 3332 N93-29344
Solving a product safety problem using a recycled high density polyethylene container p 3292 N93-30964
The characterization of materials using x ray diffraction p 3293 N93-30968
Construction and testing of simple airfoils to demonstrate structural design, materials choice, and composite concepts p 3243 N93-30979
MATHEMATICAL LOGIC
Crucial role of detailed function, task, timeline, link, and human vulnerability analyses in HRA
[DE93-001923] p 3505 N93-28942
A fuzzy logic optimal control law solution to the CMMCA tracking problem
[AD-A262555] p 3542 N93-29420
Fuzzy knowledge base construction through belief networks based on Lukasiewicz logic
p 3515 N93-29550
Polynomial space polynomial delay algorithms for listing families of graphs
[DE93-010677] p 3530 N93-29808
MATHEMATICAL MODELS
High performance dispersion model PHYSIC
[DE93-753303] p 3467 N93-28536
Magnetic activity in low mass stars
[DE93-009073] p 3632 N93-28547
Deformation mechanisms in Be(sub 12)X compounds
[DE93-009080] p 3320 N93-28548
Finite element analysis of time-independent superconductivity
[NASA-CR-191140] p 3450 N93-28556
A complete set of field equations for the dynamic simulation of a towed cable system
[AD-A262570] p 3442 N93-28578
Influence of optical feedback on the pulse behavior of semiconductor lasers
[ETN-93-93798] p 3436 N93-28614
The dynamics and control of space tethers
p 3274 N93-28629
Closed-loop control with delayed information
[INRIA-RR-1638] p 3541 N93-28638
A one-dimensional continuum model for shape-memory alloys
[AD-A262505] p 3321 N93-28656
Control-structures interaction test of the LACE satellite
p 3263 N93-28706
Liquid Motion in a rotating tank Experiment (LME)
p 3264 N93-28710
Orbital Debris Environment Monitor (ODEM)
p 3267 N93-28735
Numerical simulation of perfect fluid flows around complex 3D configurations by a multidomain solver using the MUSCL approach p 3417 N93-28745
Analysis for thermo-chemical decomposition of composite structures
[NASA-CR-193185] p 3295 N93-28843
Global warming issue and global economic model
[DE93-781334] p 3468 N93-28881
Biophysical model for handwear insulation testing
[AD-A262926] p 3505 N93-28884
A study of the physical mechanisms for filament eruption and coronal mass ejection via numerical simulation
[NASA-CR-193180] p 3653 N93-28935
Composite laminate stiffnesses and their sensitivities
[DLR-FB-92-16] p 3296 N93-29007
Studies in premixed combustion
[DE93-007955] p 3310 N93-29051
The meteorological database
[DE93-007289] p 3481 N93-29054
Atmospheric and Geophysical Sciences Program report, 1990-1991
[DE93-007390] p 3470 N93-29055

A survey of problems in divertor and edge plasma theory
[DE93-007531] p 3586 N93-29056
An experimental study of flow over a 6 to 1 prolate spheroid at incidence p 3239 N93-29124
A four-field approach towards developing a mechanistic model for multiphase flow
[DE93-006572] p 3420 N93-29126
A numerical study of confined turbulent jets
[NASA-TM-106197] p 3420 N93-29161
Resource utilization model for the algorithm to architecture mapping model
[NASA-CR-193122] p 3527 N93-29171
Optical coherent phase diversity systems
[ISBN-90-9004897-9] p 3578 N93-29270
Non-linear wave phenomena in a gas-vapour mixture with phase transition
[ETN-93-93582] p 3422 N93-29319
Integrated approaches to parallelism in optimization and solution of inverse problems
[AD-A262259] p 3452 N93-29349
Modeling the effects of drop drag and breakup on fuel sprays
[AD-A263650] p 3445 N93-29388
Experimental study of location and identification of ferrous spheroids using a smart total field magnetometer
[AD-A263661] p 3324 N93-29391
Two-dimensional model for current and heat transport in solid-armature railguns
[AD-A262014] p 3271 N93-29394
Evaluation of atmospheric wind field and dispersion models for fog-oil smoke dispersion in complex terrain: Field measurement and model evaluation program for assessment of the environmental effects of military smokes
[AD-A262051] p 3482 N93-29399
Advanced thermally-stable, coal-derived, jet fuels program: Experiment system and model development
[AD-A262747] p 3342 N93-29402
Mitigation of shock waves in a cylindrical tunnel by foam
[AD-A262491] p 3423 N93-29419
Mathematical modeling and control law development for the atmospheric monitoring and control system of the Controlled Environment Research Chamber (CERC) at NASA Ames Research Center
[AD-A261978] p 3261 N93-29436
Flight mechanical model for performance calculations and interactions between flight vehicle and ramjet in regard to the flight orbit
[ESA-TT-1267] p 3248 N93-29464
Evaluating the bias of alternative cost progress models: Tests using aerospace industry acquisition programs
[AD-A262870] p 3624 N93-29477
Representation and recognition with invariants and geometric constraint models
[AD-A263235] p 3529 N93-29493
LDEF microenvironments, observed and predicted
p 3283 N93-29623
A generalized approach to the thermal analysis of the Long Duration Exposure Facility's flight experiments
p 3428 N93-29624
Radioactivities induced in some LDEF samples
p 3572 N93-29628
Development and application of a 3-D geometry/mass model for LDEF satellite ionizing radiation assessments
p 3573 N93-29640
Dynamics and photoexcitation in MX and MXX' chain solids
[AD-A264823] p 3561 N93-29711
The XNOVAKTC rheological model
[AD-A263298] p 3342 N93-29762
Modeling the bidirectional reflectance and spectra
[AD-A263570] p 3462 N93-29830
Weakly nonlinear dynamics of near-CJ detonation waves
[DE93-007344] p 3424 N93-29836
The basics of weather models
[AD-A263386] p 3483 N93-29850
Balanced technology initiative on computational mechanics of materials
[AD-A263906] p 3453 N93-29863
Automated modeling of physical systems
[NASA-CR-193256] p 3531 N93-29873
International Journal of Numerical Modeling: Electronic Networks, Devices, and Fields, volume 5, number 3, August 1992
[AD-A263765] p 3387 N93-29877
Some statistical inference problems in linear models and variance components models and their applications
[AD-A264062] p 3555 N93-29923
Measurement of turbulent spots and intermittency modelling at gas-turbine conditions
p 3253 N93-29934
Modelling thermal behaviour of turbomachinery discs and casings p 3256 N93-29949
Evaluation of multi-dimensional flux models for radiative transfer in cylindrical combustion chambers
p 3257 N93-29955
Calculations of reactive turbulent flows in aeronautical chambers p 3257 N93-29956
A Navier-Stokes solver with different turbulence models applied to film-cooled turbine cascades
p 3258 N93-29962
Analysis of a simulation of the seasonal cycle in the tropical Pacific Ocean in an eddy-resolving global ocean model
[AD-A264007] p 3488 N93-29977
Rapidly activated dynamic phase transitions in nonlinear solids
[AD-A263601] p 3299 N93-29982
Nonlinear attitude control of planar structures in space using only internal controls p 3280 N93-29991
Space station attitude disturbance arising from internal motions p 3280 N93-29995
Modeling earthquakes with local and regional broadband data p 3478 N93-30005
Applications of three-dimensional modeling in electromagnetic exploration p 3391 N93-30010
A preliminary review of global CO2 exchange between ocean and atmosphere
[AD-A264019] p 3472 N93-30015
Modelling the dynamics of a large sea area
[DE93-778330] p 3488 N93-30040
Advances in the identification of electrochemical transfer function models using Prony analysis
[DE93-009424] p 3550 N93-30041
A search for radiative neutrino decay from supernovae
[NASA-CR-193118] p 3653 N93-30052
Numerical modeling of multidimensional flames with application to energetic materials p 3319 N93-30079
Damage growth in composite propellants
p 3348 N93-30088
Shock waves and polymorphic phase transitions in energetic materials p 3351 N93-30100
Mathematical model of frost heave and thaw settlement in pavements
[CRREL-REPT-93-2] p 3262 N93-30103
Dynamics and robust control of sampled data systems for large space structures
[AD-A264192] p 3281 N93-30142
Models of star formation in interacting and merging disk galaxies p 3635 N93-30148
Input relegation control for gross motion of a kinematically redundant manipulator
[DE93-005301] p 3446 N93-30210
Containment of explosions in spherical vessels
[DE93-005445] p 3446 N93-30211
Analysis and simulation of a two degrees-of-freedom one-link flexible forearm p 3361 N93-30261
Environmental studies: Mathematical, computational and statistical analyses
[AD-A264223] p 3473 N93-30360
Numerical modeling and parameterization of gravity wave processes and effects in the atmosphere
[AD-A264331] p 3478 N93-30367
Simulation, characterization and control of forced unsteady viscous flows using Navier-Stokes equations
[AD-A264333] p 3425 N93-30369
Detecting residue on a printed circuit board: An application of the Boundary Contour/Feature Contour System
[DE93-006283] p 3412 N93-30370
Young open clusters as probes of the star formation process p 3635 N93-30377
Analytical and experimental study of laminar free convective heat transfer from isothermal convex bodies of arbitrary shape
[ISBN-0-315-72512-5] p 3426 N93-30379
Catastrophic collisions: Laboratory impact experiments, hydrocode simulations, and the scaling problem
p 3635 N93-30411
The calculation of electrostatic interactions and their role in determining the energies and geometries of molecular HE crystals
[DE92-040374] p 3570 N93-30448
Analysis of cache for streaming tape drive
p 3435 N93-30477
Two-dimensional and three-dimensional time-dependent MHD model of extended corona
p 3653 N93-30496
A correlated k-distribution model of the atmospheric heating rates for overlapping spectra of CO2 and H2O
[DE93-007391] p 3474 N93-30504
A ceramic fracture model for high velocity impact
[AD-A264728] p 3454 N93-30545
Procedures for applying Ada quality prediction models
[AD-A264730] p 3534 N93-30546
An approach to software quality prediction from Ada designs
[AD-A264731] p 3534 N93-30547
Topics in inflationary universe medels and cosmic string theories p 3637 N93-30579
Detailed studies of soot formation in laminar diffusion flames for application to modeling studies
[AD-A264827] p 3317 N93-30667
Validation and upgrading of physically based mathematical models p 3237 N93-30688
Numerical modeling of the propagation medium at VLF/LF p 3395 N93-30729
Scaling properties of localized quantum chaos
[DE93-606031] p 3606 N93-30803
Environmental characteristics of EPA, NRC, and DOE sites contaminated with radioactive substances
[PB93-185551] p 3475 N93-30829
Fourth-rank gravity and cosmology
[DE92-644722] p 3637 N93-30918
General scalar-tensor theories for induced gravity inflation
[DE93-602505] p 3479 N93-30940
Fourth-rank cosmology
[DE92-641346] p 3637 N93-30997
Manifold shape: From differential geometry to mathematical morphology
[CS-9204] p 3552 N93-31012
The contact mechanical nonlinearities of a mathematical model of a railway wheel rolling over corrugated rail
[ILR-MITT-266(1991)] p 3454 N93-31015
The steady-state tangential contact problem for a falling drop type of contact area on corrugated rail by simplified theory of rolling contact
[ILR-MITT-267(1991)] p 3455 N93-31016
Theoretical and experimental investigation of slack cable/mass system dynamics p 3455 N93-31028
Structural design using neural networks
p 3545 N93-31029

MATHEMATICAL PROGRAMMING
Research in mathematics and computer science, March 1, 1991 - September 30, 1992
[DE93-011492] p 3509 N93-28573

MATHEMATICS
ICASE
[NASA-CR-193257] p 3520 N93-29864

MATRICES (MATHEMATICS)
A summary of block schemes for reducing a general matrix to Hessenberg form
[DE93-010621] p 3525 N93-28877
A simple parallel prefix algorithm for compact finite-difference schemes
[NASA-CR-191448] p 3525 N93-28976
Index mappings for interactive editing of symbolic matrices
[DE93-009316] p 3549 N93-29060
Exploiting the memory hierarchy in sequential and parallel sparse Cholesky factorization
[AD-A262849] p 3539 N93-29508
Division by polynomial matrix and its application to multivariable linear systems p 3357 N93-30233
A robust model for finding optimal evolutionary trees
[DE93-010682] p 3491 N93-30483
Coupled-channel analysis of low energy nucleon-antinucleon interactions
[DE93-606115] p 3571 N93-30791
Connections between quantized affine algebras and superalgebras
[DE93-606065] p 3551 N93-30810
Manifold shape: From differential geometry to mathematical morphology
[CS-9204] p 3552 N93-31012

MATRIX MATERIALS
Probabilistic simulation of multi-scale composite behavior
[NASA-TM-106196] p 3451 N93-28633
Acousto-Ultrasonic analysis of failure in ceramic matrix composite tensile specimens
[NASA-TM-106219] p 3449 N93-29073
Processing and property evaluation of silver or aluminum matrix YBa2Cu3O(6+x) superconducting materials
[AD-A263382] p 3595 N93-29333
Advanced fiber/matrix material systems
p 3305 N93-30854
Introduction to high performance composites
p 3291 N93-30957

MATTER (PHYSICS)
Research in theoretical nuclear physics
[DE93-008380] p 3565 N93-28960
Borel sum rules for octet baryons in nuclear medium
[DE93-753245] p 3604 N93-29242

MAXIMUM ENTROPY METHOD
Bayesian linear analysis with application to removal of atmospheric influences on optical remote sensing images
[BCRS-92-19] p 3463 N93-31011

MAXIMUM LIKELIHOOD ESTIMATES
A modified Anderson Darling goodness-of-fit test for the gamma distribution with unknown scale and location parameters
[AD-A262486] p 3553 N93-28760
A modified chi-squared goodness-of-fit test for the three-parameter gamma distribution with unknown parameters
[AD-A262553] p 3554 N93-28845
New classification methods p 3459 N93-28932
Parametric likelihood inference for record breaking problems
[AD-A262546] p 3549 N93-29413
MAXWELL EQUATION
Upwind finite element schemes for solving the Maxwell equations
[INRIA-RR-1601] p 3546 N93-28509
Continuation of: Applications of gauge theories to enhance numerical solutions of mixed potential integral equations
[AD-A263763] p 3550 N93-29876
A covariant form of the Maxwell's equations in four-dimensional spaces with an arbitrary signature
[DE93-606070] p 3605 N93-30783
MEAN
Monte Carlo simulation of magnitude-angle error sources
[AD-A263738] p 3555 N93-29857
MEAN SQUARE VALUES
A Monte Carlo study of the raw and normal varimax rotation criterion in factor analysis
[AD-A262516] p 3554 N93-28844
Iterative encoding methods for computer generated holograms
[AD-A263705] p 3431 N93-29297
Estimating the parameters of chaotic maps
[AD-A262574] p 3556 N93-29423
MEASURE AND INTEGRATION
Parametric likelihood inference for record breaking problems
[AD-A262546] p 3549 N93-29413
A remark on the invariant measure for the nonlinear Schroedinger equation
[DE93-609840] p 3552 N93-30946
MEASUREMENT
An algebraic approach to the quantization of constrained systems: Finite dimensional examples
p 3548 N93-28671
MEASURING INSTRUMENTS
Constant frequency pulsed phase-locked loop measuring device
[NASA-CASE-LAR-13823-1] p 3431 N93-29084
Advanced thermally-stable, coal-derived, jet fuels program: Experiment system and model development
[AD-A262747] p 3342 N93-29402
Method of continuously determining crack length
[NASA-CASE-LAR-14480-1-CU] p 3452 N93-29612
Selection and static calibration of the Marsh J1678 pressure gauge p 3249 N93-29779
Advanced coordinate measuring machine at Sandia National Laboratories
[DE93-010618] p 3432 N93-29842
Measurement of electromagnetic properties of composite materials
[AD-A264725] p 3303 N93-30555
VLF propagation measurements in the Canadian Arctic p 3396 N93-30733
Satellite calibration requirements
[AD-A264279] p 3281 N93-30817
MECHANICAL DEVICES
Chaos in mechanical systems with especial reference to rotorcraft and missiles
[AD-A263703] p 3604 N93-29384
Rotational fluid flow experiment p 3235 N93-29761
MECHANICAL DRIVES
The design and modelling of a comb-drive-based microengine for mechanism drive applications
[DE93-009826] p 3443 N93-29185
Joint drive development for the Space Station Remote Manipulator System p 3370 N93-30313
MECHANICAL ENGINEERING
Integrated approaches to parallelism in optimization and solution of inverse problems
[AD-A262259] p 3452 N93-29349
The 1990-1991 project summaries
p 3230 N93-29731
MECHANICAL IMPEDANCE
Trajectory generation for dual-arm robots using artificial impedance approach p 3370 N93-30310
MECHANICAL MEASUREMENT
Cratering in glasses impacted by debris or micrometeorites p 3340 N93-29368
MECHANICAL PROPERTIES
Process optimization of Hexoloy SX-SiC towards improved mechanical properties
[DE93-007913] p 3320 N93-28564
Soft computing in design and manufacturing of advanced materials
[NASA-TM-106032] p 3295 N93-28624
Probabilistic simulation of multi-scale composite behavior
[NASA-TM-106196] p 3451 N93-28633
Thermal and mechanical analysis of flip-chips on a liquid cooled multichip module
[DE93-007609] p 3405 N93-28641
Hydrostatic and uniaxial behavior of a high density polyurethane foam (FR-3720) at various temperatures
[DE93-011486] p 3330 N93-28838
Silicon crystal under bending
[DE93-010522] p 3593 N93-28888
Aligned, short-fiber composites by novel flow processing methods
[DE93-008701] p 3296 N93-28904
Bainitic stabilization of austenite in low alloy steels
[DE93-008275] p 3321 N93-28957
Effects of internal helium on mechanical properties of Nitronic (tm) 40 stainless steel
[DE93-009902] p 3324 N93-29265
Low temperature (LT) GaAs and related materials
[AD-A263607] p 3298 N93-29282
Advanced NDE technology program
[AD-A262008] p 3449 N93-29443
Balanced technology initiative on computational mechanics of materials
[AD-A263906] p 3453 N93-29863
Mechanical behaviour of a closed collar model for an 11.5 T dipole
[NIKHEF-H/92-03] p 3576 N93-30019
Observation of reaction intermediates in crystalline RDX p 3318 N93-30067
Energetic material response to abnormal environments p 3350 N93-30095
Characterization of ceramic composite materials for gas turbine applications
[DE93-009719] p 3259 N93-30168
DOE fundamentals handbook: Material science
[DE93-012224] p 3314 N93-30199
Fundamental studies of the mechanical behavior of microelectronics thin film materials
[AD-A264334] p 3337 N93-30417
The electrodeposition of low contraction chromium using high/low current pulsing
[AD-A264475] p 3327 N93-30538
Wetting and dispersion in ceramic/polymer melt injection molding systems
[DE93-013240] p 3338 N93-30601
JPRS report: Science and technology. Central Eurasia: Materials science
[JPRS-UMS-93-003] p 3327 N93-30623
Mechanical properties of composite materials
p 3290 N93-30951
Micropipet manipulation of lipid membranes: Direct measurement of the material properties of a cohesive structure that is only two molecules thick
p 3291 N93-30953
Direct tension experiments on compacted granular materials p 3292 N93-30960
A 69 cent look at thermoplastic softening
p 3292 N93-30963
MECHANICS (PHYSICS)
Some problems in the mechanics of solids with phase mixtures
[AD-A263652] p 3311 N93-29291
MEDICAL EQUIPMENT
Transcutaneous analyte measuring methods
[AD-A262861] p 3494 N93-29509
MEDICAL SERVICES
Medical aspects of cold weather operations: A handbook for medical officers
[AD-A263559] p 3496 N93-30588
MELTING
Effects of freeze/thaw cycles on hydrostatically conditioned E-glass/J-2 composite
[AD-A262980] p 3298 N93-29425
Interfacial melting in cracked explosives
p 3349 N93-30089
Mathematical model of frost heave and thaw settlement in pavements
[CRREL-REPT-93-2] p 3262 N93-30103
Visualizing weld metal solidification using organic analogs p 3293 N93-30973
MELTS (CRYSTAL GROWTH)
A spectral method determination of the first critical Rayleigh number for a low-Prandtl number crystal melt in a cylindrical container
[NASA-CR-193238] p 3594 N93-29214
MEMBRANE STRUCTURES
Novel polymer compositions for high-temperature membrane applications, phase 1
[PB93-174126] p 3331 N93-29201
MEMBRANES
NASA in-step: Permeable membrane experiment
p 3267 N93-28736
Membrane-based photochemical systems as models for photosynthetic cells
[DE93-009758] p 3310 N93-28911
High pressure studies of hydrated nafion membranes: Dielectric relaxation and deuteron NMR
[AD-A263511] p 3332 N93-29342
Integrated approaches to parallelism in optimization and solution of inverse problems
[AD-A262259] p 3452 N93-29349
The chronic effects of jP-8 jet fuel exposure on the lungs
[AD-A264162] p 3495 N93-30153
Development of an O atom gun
[AD-A264753] p 3570 N93-30558
Decomposition of hydrogen sulfide for small scale gas processing.
[PB93-174704] p 3316 N93-30658
MEMORY
Cognitive and Neural Sciences Division 1992 programs
[AD-A263400] p 3654 N93-29258
Representations of shape in object recognition and long-term visual memory
[AD-A264342] p 3499 N93-30163
MEMORY (COMPUTERS)
Exploiting the memory hierarchy in sequential and parallel sparse Cholesky factorization
[AD-A262849] p 3539 N93-29508
Using synthetic-perturbation techniques for tuning shared memory programs
[PB93-178572] p 3539 N93-29677
An adaptive algorithm for linear associative memory problem p 3360 N93-30255
RAID 7 disk array p 3537 N93-30462
Memory driven feature-based design
[AD-A264697] p 3534 N93-30495
The midway distributed shared memory system
[AD-A264645] p 3534 N93-30523
Massively parallel spatial light modulation-based optical signal processing
[AD-A264846] p 3581 N93-30905
MENTAL PERFORMANCE
Expertise, text coherence, and constraint satisfaction: Effects on harmony and settling rate — mental representations
[AD-A262703] p 3498 N93-28901
Predicting aircrew training performance with psychometric g
[AD-A264021] p 3498 N93-30026
Representations of shape in object recognition and long-term visual memory
[AD-A264342] p 3499 N93-30163
Neural mechanisms of attention
[AD-A264345] p 3544 N93-30165
The air traffic controller's mental model and it's implications for equipment design and trainee selection
p 3372 N93-30322
Independent research and independent exploratory development programs
[AD-A264735] p 3544 N93-30556
MERIDIONAL FLOW
The thermal structure, dust loading, and meridional transport in the Martian atmosphere during late southern summer p 3651 N93-29616
MESOMETEOROLOGY
Leadex data report. Part 1: Weather analysis and satellite images
[AD-A263217] p 3481 N93-28876
MESON-MESON INTERACTIONS
Meson-meson interactions and phi-enhancement in nucleus collisions
[DE93-010725] p 3565 N93-28831
MESONS
Upgrading the LAMPF 201 MHz RF generators
[DE93-010715] p 3406 N93-28830
Research programs from the University of South Carolina on high energy physics
[DE93-007829] p 3574 N93-28969
MESOPAUSE
Activities report of the International Meteorological Institute, Stockholm (Sweden)
[ETN-93-93768] p 3480 N93-28519
MESOSCALE PHENOMENA
Activities report of the International Meteorological Institute, Stockholm (Sweden)
[ETN-93-93768] p 3480 N93-28519
Analysis of mass transport and potential vorticity budget in a simulated tropopause folding
[PB93-156792] p 3476 N93-29197
Convective and stratiform rain: Multichannel microwave sensing over oceans
[NASA-TM-104586] p 3482 N93-29448

MESSAGE PROCESSING
Parcels with TAGS
[PB93-181824] p 3535 N93-30824
METABOLISM
Wound healing and connective tissue metabolism: The role of hyperbaric oxygen therapy
[AD-A262483] p 3493 N93-28759
Regulation of alternative CO2 fixation pathways in procaryotic and eucaryotic photosynthetic organisms
[DE93-012109] p 3491 N93-29181
Evaluation of dried storage of platelets for transfusion: Physiologic integrity and hemostatic functionality
[AD-A263240] p 3494 N93-29620
Beta-adrenergic blockade and lactate metabolism during exercise at high altitude
[AD-A263544] p 3495 N93-29820
METAL AIR BATTERIES
The electrolyte factor in O2 reduction electrocatalysis
[AD-A263565] p 3313 N93-29828
METAL BONDING
Diffusion bonding
[DE93-011480] p 3442 N93-28837
A transient FGM interlayer based approach to joining ceramics
[DE93-010415] p 3331 N93-29248
METAL COATINGS
Effect of metallic-coating properties on the tribology of coated and oil-lubricated ceramics
[DE93-010663] p 3330 N93-28666
Fundamental studies of the morphology, chemistry, and electrical properties of metals on GaAs and other III-V semiconductor compounds
[AD-A264417] p 3597 N93-30120
METAL COMBUSTION
Homogeneous gas phase kinetic model with gradient sensitivity analysis for high temperature particulate boron combustion in fluorine enriched environments
p 3319 N93-30090
METAL CRYSTALS
Anelastic relaxations associated with local disordering in grain boundaries
[AD-A263101] p 3596 N93-29796
METAL FATIGUE
The growth of small corrosion fatigue cracks in alloy 2024
[NASA-TM-107755] p 3451 N93-29069
An experimental/analytical evaluation of biaxial sheet failure
[DE93-010620] p 3453 N93-29843
A miniature fatigue test machine p 3291 N93-30956
METAL FILMS
Diffusion bonding
[DE93-011480] p 3442 N93-28837
Real time self-directed MBE flux control incorporation in situ ellipsometry, phase 1
[AD-A263501] p 3595 N93-29341
Characterization of copper iodide thin films fabricated via laser assisted molecular beam epitaxy
[AD-A262823] p 3596 N93-29430
Structure, adhesion, and stability of metal/oxide and oxide/oxide interfaces
[DE93-012930] p 3325 N93-30060
The electrodeposition of low contraction chromium using high/low current pulsing
[AD-A264475] p 3327 N93-30538
Change of solar cell element properties influenced by adsorbed atoms
[DE93-606694] p 3466 N93-30777
METAL FOILS
The Interstellar Gas Experiment: Analysis in progress
p 3639 N93-29380
Sensitivity of LDEF foil analyses using ultra-low background germanium vs. large NaI(Tl) multidimensional spectrometers p 3318 N93-29627
On the ideality of using a step-function current in a metallic foil to simulate a step-function heat-flux source
[AD-A264627] p 3413 N93-30539
The adhesion of AgI molecules to gaseous metallic silver cluster cations
[AD-A264820] p 3338 N93-30628
METAL GRINDING
Tool grinding and spark testing p 3291 N93-30954
METAL HALIDES
Conjugated polymers from cyclohexadienediol monomers
[AD-A264837] p 3340 N93-30900
METAL HYDRIDES
Development of nickel/metal hydride secondary battery
[DE93-781330] p 3406 N93-28669
METAL IONS
A remote laser-mass spectrometer for determination of elemental composition p 3434 N93-28775
Effect of zinc and iron ions on the electrochemistry of nickel oxide electrode: Slow cyclic voltammetry
[AD-A263098] p 3311 N93-29133
Theoretical hyperfine structure constants for transition metal atoms and ions
[DE93-012325] p 3566 N93-29183
High-dose implantations of Al into Si(111) and Si(100)
[DE93-009552] p 3594 N93-29301
Adsorption of hydrated halide ions on charged electrodes: Molecular dynamics simulation
[AD-A263137] p 3568 N93-29619
METAL JOINTS
Evaluation of polyaryl adhesives in elastomer-stainless steel joints
[DE93-009794] p 3329 N93-28551
METAL MATRIX COMPOSITES
Metal Matrix Laminate Tailoring (MMLT) code: User's manual
[NASA-TM-106052] p 3295 N93-28681
The effect of temperature on the impact behavior of TiB2 reinforced XDTM-TiAl intermetallic matrix composites
[AD-A262924] p 3296 N93-28886
Design of interfaces in metal matrix composites
[AD-A262052] p 3296 N93-29001
Thermoviscoplastic analysis of fibrous periodic composites using triangular subvolumes
[NASA-TM-106076] p 3297 N93-29074
Tailored interfaces for metal-matrix composites-fundamental considerations
[AD-A263048] p 3298 N93-29130
Processing and property evaluation of silver or aluminum matrix YBa2Cu3O(6+x) superconducting materials
[AD-A263382] p 3595 N93-29333
Mechanical properties of several magnesium and aluminum composites
[AD-A262481] p 3299 N93-30137
METAL OXIDE SEMICONDUCTORS
Proposal for a universal particle detector experiment
p 3286 N93-28795
Laboratory experiments in integrated circuit fabrication
p 3292 N93-30962
METAL OXIDES
Structure, adhesion, and stability of metal/oxide and oxide/oxide interfaces
[DE93-012930] p 3325 N93-30060
Colloid and interface chemistry aspects of ceramics
[AD-A264685] p 3337 N93-30552
METAL PARTICLES
Homogeneous gas phase kinetic model with gradient sensitivity analysis for high temperature particulate boron combustion in fluorine enriched environments
p 3319 N93-30090
METAL PLATES
Transient response of embedded thermocouples
[DE93-009889] p 3431 N93-29325
Damage areas on selected LDEF aluminum surfaces
p 3283 N93-29374
METAL POWDER
Aluminium-high strength material by mechanical alloying and reaction milling: Basics of processing and characterisation of material
[ESA-TT-1249] p 3324 N93-29272
Powder metallurgy: Solid and liquid phase sintering of copper p 3294 N93-30976
METAL PROPELLANTS
Propulsion and detonics research in France
p 3344 N93-30070
METAL SHEETS
Diffusion bonding
[DE93-011480] p 3442 N93-28837
An experimental/analytical evaluation of biaxial sheet failure
[DE93-010620] p 3453 N93-29843
METAL SURFACES
Microtextured metals for stray-light suppression in the Clementine startracker p 3286 N93-28785
Electrochemical behavior and surface chemistry of aluminum alloys: Solute-rich interphase model
[AD-A262061] p 3322 N93-29002
Surface diffusion: Atomistics and surface morphology (summary of MRS Symposium B panel discussion)
[DE93-009862] p 3594 N93-29188
In situ Fourier transform infrared spectroscopic study of bisulfate and sulfate adsorption on gold, with and without the underpotential deposition of copper
[AD-A263421] p 3323 N93-29259
Projectile compositions and modal frequencies on the chemistry of micrometeoroids LDEF experiment
p 3638 N93-29370
Damage areas on selected LDEF aluminum surfaces
p 3283 N93-29374
Molecular dynamics modeling of electric double layers with spectroscopic applications
[AD-A263168] p 3568 N93-29489
The mechanical response of gold substrates modified with self-assembling monolayer films
[AD-A262997] p 3452 N93-29515
Interfacial viscosity measurements of adsorbed monolayers on metal surfaces
[AD-A263288] p 3324 N93-29803
Improved heat removal by microscopic surface texturing of capillaries
[AD-A263483] p 3424 N93-29966
Materials studies for preventing corrosion in condensing environments
[PB93-185478] p 3327 N93-30815
METAL WORKING
Examination of formability to seamless tubes on Ni-Cr-W superalloy
[DE93-764156] p 3326 N93-30396
METAL-GAS SYSTEMS
The role of grain boundaries in hydrogen diffusion in metals at 25 C
[NASA-TM-108407] p 3322 N93-29043
METALLIC GLASSES
Thermodynamic and structural properties of metallic glasses and supercooled liquids
[ISBN-0-315-72443-9] p 3605 N93-30359
METALLIZING
Metallization at detonation fronts in solids
p 3319 N93-30087
Unexpected increase in the thermal generation rate of bulk GaAs due to electron-beam metallization
[DE93-009829] p 3598 N93-30511
Adhesion of thick film Au to alumina ceramics
[DE93-009802] p 3339 N93-30656
Laboratory experiments in integrated circuit fabrication
p 3292 N93-30962
METALLOGRAPHY
Improved measurement of thermal effects on microstructure p 3292 N93-30959
METALORGANIC CHEMICAL VAPOR DEPOSITION
Femtosecond carrier processes in compound semiconductors and real time signal processing
[AD-A262966] p 3384 N93-29514
Atomic layer epitaxy of semiconductor heterostructures
[AD-A264755] p 3599 N93-30560
METALS
DOE fundamentals handbook: Material science
[DE93-012224] p 3314 N93-30199
Constitutive laws for deformation and dynamic recrystallization in cubic metals
[DE93-010740] p 3326 N93-30486
Colloid and interface chemistry aspects of ceramics
[AD-A264685] p 3337 N93-30552
Radiation effects in FCC metals and intermetallic compounds: A molecular dynamics computer simulation study
[DE93-009546] p 3600 N93-30668
Tool grinding and spark testing p 3291 N93-30954
Visualizing weld metal solidification using organic analogs p 3293 N93-30973
Temperature-dependent electrical conductivity of soda-lime glass p 3294 N93-30978
METASTABLE STATE
Defect studies in low-temperature-grown GaAs
[DE93-010405] p 3595 N93-29417
Nuclear isomers as ultra-high-energy-density materials
[DE93-009520] p 3568 N93-29784
Thermodynamic and structural properties of metallic glasses and supercooled liquids
[ISBN-0-315-72443-9] p 3605 N93-30359
The adhesion of AgI molecules to gaseous metallic silver cluster cations
[AD-A264820] p 3338 N93-30628
METATHESIS
Synthesis of chiral molybdenum ROMP initiators and all-cis highly tactic Poly-2,3-R2Norbornadiene (R = CF3 or CO2Me)
[AD-A264133] p 3336 N93-30169
METEOR TRAILS
Performance statistics bulletin. High latitude meteor scatter propagation, May, June, July 1989
[AD-A264003] p 3399 N93-30757
METEORITE COLLISIONS
Proposal for a universal particle detector experiment
p 3286 N93-28795
Report of the Meteoroid and Debris Special Investigation Group p 3638 N93-29355
Long Duration Exposure Facility (LDEF) experiment M0003 meteoroid and debris survey
p 3638 N93-29361
Cratering in glasses impacted by debris or micrometeorites p 3340 N93-29368
Asteroidal versus cometary meteoroid impacts on the Long Duration Exposure Facility (LDEF)
p 3638 N93-29371
The production and evolution of plasma and associated magnetic fields during hypervelocity impacts: Implications for planetary paleomagnetism p 3589 N93-30000

Hypervelocity impact testing of the Space Station utility distribution system carrier
[NASA-TM-104771] p 3289 N93-30507

METEORITE CRATERS

Three-D crater analysis of LDEF impact features from stereo imagery p 3283 N93-29359

Further analysis of LDEF FRECOPA micrometeoroid remnants p 3638 N93-29360

Long Duration Exposure Facility (LDEF) experiment M0003 meteoroid and debris survey
p 3638 N93-29361

Derivation of particulate directional information from analysis of elliptical impact craters on LDEF
p 3283 N93-29362

Characteristics of hypervelocity impact craters on LDEF experiment S1003 and implications of small particle impacts on reflective surfaces p 3283 N93-29363

Hypervelocity impact survivability experiments for carbonaceous impactors p 3283 N93-29364

Cratering in glasses impacted by debris or micrometeorites p 3340 N93-29368

Projectile compositions and modal frequencies on the chemistry of micrometeoroids LDEF experiment
p 3638 N93-29370

Asteroidal versus cometary meteoroid impacts on the Long Duration Exposure Facility (LDEF)
p 3638 N93-29371

Interplanetary meteoroid debris in LDEF metal craters
p 3638 N93-29372

Origin of orbital debris impacts on LDEF's trailing surfaces p 3283 N93-29373

Damage areas on selected LDEF aluminum surfaces
p 3283 N93-29374

LDEF data: Comparisons with existing models
p 3283 N93-29375

Elemental analyses of hypervelocity microparticle impact sites on Interplanetary Dust Experiment sensor surfaces
p 3638 N93-29378

METEORITES

Scanning electron microscope/energy dispersive x ray analysis of impact residues in LDEF tray clamps
p 3283 N93-29369

METEORITIC DAMAGE

Long Duration Exposure Facility (LDEF) experiment M0003 meteoroid and debris survey
p 3638 N93-29361

Analysis of LDEF micrometeoroid/debris data and damage to composite materials p 3309 N93-29366

Damage areas on selected LDEF aluminum surfaces
p 3283 N93-29374

Hypervelocity impact testing of the Space Station utility distribution system carrier
[NASA-TM-104771] p 3289 N93-30507

METEORITIC DIAMONDS

Hypervelocity impact survivability experiments for carbonaceous impactors p 3283 N93-29364

METEOROID CONCENTRATION

Predicted and observed directional dependence of meteoroid/debris impacts on LDEF thermal blankets
p 3638 N93-29358

Characteristics of hypervelocity impact craters on LDEF experiment S1003 and implications of small particle impacts on reflective surfaces p 3283 N93-29363

New meteoroid model predictions for directional impacts on LDEF p 3638 N93-29376

METEOROID HAZARDS

Space optical and low-frequency radio searches for Earth-crossing asteroids and comets
[DE93-008716] p 3634 N93-29246

Predicted and observed directional dependence of meteoroid/debris impacts on LDEF thermal blankets
p 3638 N93-29358

METEOROID PROTECTION

Ablative shielding for hypervelocity projectiles
[NASA-CASE-MSC-21884-1] p 3331 N93-29088

Hypervelocity impact testing of the Space Station utility distribution system carrier
[NASA-TM-104771] p 3289 N93-30507

METEOROIDS

Proceedings of the Near-Earth-Object Interception Workshop
[NASA-TM-108236] p 3556 N93-28572

Space optical and low-frequency radio searches for Earth-crossing asteroids and comets
[DE93-008716] p 3634 N93-29246

Report of the Meteoroid and Debris Special Investigation Group p 3638 N93-29355

Continued investigation of LDEF's structural frame and thermal blankets by the Meteoroid and Debris Special Investigation Group p 3282 N93-29357

Three-D crater analysis of LDEF impact features from stereo imagery p 3283 N93-29359

Long Duration Exposure Facility (LDEF) experiment M0003 meteoroid and debris survey
p 3638 N93-29361

Asteroidal versus cometary meteoroid impacts on the Long Duration Exposure Facility (LDEF)
p 3638 N93-29371

Interplanetary meteoroid debris in LDEF metal craters
p 3638 N93-29372

LDEF data: Comparisons with existing models
p 3283 N93-29375

New meteoroid model predictions for directional impacts on LDEF p 3638 N93-29376

Performance statistics bulletin. High latitude meteor scatter propagation, May, June, July 1989
[AD-A264003] p 3399 N93-30757

METEOROLOGICAL CHARTS

Fog studies in the Alpine region with digital NOAA/AVHRR data p 3458 N93-28925

METEOROLOGICAL INSTRUMENTS

The enhanced-model ladar wind sensor and its application in planetary wind velocity measurements
p 3649 N93-28815

The MESUR mission p 3649 N93-28816

METEOROLOGICAL PARAMETERS

Seasonal snowfall statistics for selected stations
[AD-A263173] p 3481 N93-28991

The meteorological database
[DE93-007289] p 3481 N93-29054

Leadex data report. Part 2: Rawinsonde and ice station data
[AD-A263218] p 3483 N93-29491

The basics of weather models
[AD-A263386] p 3483 N93-29850

TACSAT meteorological payloads
p 3391 N93-29913

Meteorological information for aviation: A systems approach p 3367 N93-30298

Air weather service master station catalog USAFETAC climatic database users handbook no. 6
[AD-A264761] p 3484 N93-30608

METEOROLOGICAL RADAR

Contributions to the American Meteorological Society's 26th International Conference on Radar Meteorology
[AD-A263385] p 3481 N93-29257

METEOROLOGICAL SERVICES

Cloudiest year study: An analysis of the 3DNEPH and RTNEPH databases
[AD-A263409] p 3483 N93-29967

Deadliest, costliest, and most intense US hurricanes of this century (and other frequently requested hurricane facts)
[PB93-174993] p 3485 N93-30758

METEOROLOGY

Activities report of the International Meteorological Institute, Stockholm (Sweden)
[ETN-93-93768] p 3480 N93-28519

High performance dispersion model PHYSIC
[DE93-753303] p 3467 N93-28536

Proceedings of the 8th User Seminar of the German Remote Sensing Data Center of the German Aerospace Establishment (DLR)
[DLR-MITT-92-09] p 3456 N93-28915

JPRS report: Science and technology. Central Eurasia: Earth science
[JPRS-UES-93-003] p 3456 N93-29089

Prognostic cloud water in the Los Alamos general circulation model
[DE93-007381] p 3482 N93-29347

Geoscience center research
[AD-A263465] p 3462 N93-29834

Syllabus physical meteorology, part 1
[KNMI-TR-140-PT-1] p 3484 N93-30114

Shuttle landing facility cloud cover study: Climatological analysis and two tenths cloud cover rule evaluation
[NASA-CR-193016] p 3272 N93-31033

METHANATION

Benefits of in situ propellant utilization for a Mars sample return mission
[NASA-TM-106243] p 3341 N93-28695

METHANE

NOx chemistry in natural gas flames
[PB93-175263] p 3317 N93-30760

METHOD OF MOMENTS

An analysis of the Generalized Lambda Distribution
[AD-A262485] p 3555 N93-29447

Scattering through apertures and by three-dimensional structures. Application to the measurement of the surface impedance of conductive materials
[ONERA-P-1990-2] p 3392 N93-30018

Characterizing transient vibrations using band limited temporal moments
[DE93-009639] p 3453 N93-30185

Application of integral and differential equation methods for various EM interaction problems
[AD-A264821] p 3394 N93-30597

Antenna modeling and analysis for ELF/VLF/LF applications p 3398 N93-30751

Optimum design of multiwire cages for high-voltage applications
[AD-A264310] p 3400 N93-30995

METHOXY SYSTEMS

Mass spectrometric investigation of 2-methoxyethanol and 2-ethoxyethanol clusters: Magic numbers and structural implications
[AD-A262822] p 3312 N93-29429

METHYL ALCOHOL

Design of a high activity and selectivity alcohol catalyst
[DE93-012277] p 3309 N93-28750

High octane ethers from synthesis gas-derived alcohols
[DE93-012470] p 3341 N93-28752

A novel process for methanol synthesis
[DE93-013070] p 3314 N93-30188

Magnetic character investigation of higher alcohol synthesis Cu-Co-Cr catalysts
[DE93-009732] p 3316 N93-30653

METRIC SPACE

Fourth-rank gravity and cosmology
[DE92-644722] p 3637 N93-30918

On the energy-momentum tensors for field theories in spaces with affine connection and metric
[DE92-644743] p 3557 N93-30926

Spherically symmetric line element and Killing vectors in five-dimensional space
[DE93-604132] p 3558 N93-30988

A non degenerate semi-classical Lagrangian for dilaton-gravity in two dimensions
[DE92-641339] p 3480 N93-31002

The geometry of complex space-times with torsion
[DE92-641343] p 3608 N93-31003

METROLOGY

Issues, concepts, and standard techniques in assessing accuracy of coordinate measuring machines
[PB93-184331] p 3354 N93-29666

Proceedings of the meeting of the Intergovernmental US-Russian Business Development Committee's Standards Working Group
[PB93-179968] p 3610 N93-30822

Physics laboratory technical activities, 1992
[PB93-178648] p 3561 N93-30888

Thermoforming from a systems viewpoint
p 3293 N93-30967

MICE

Photoreceptors regulating circadian behavior: A mouse model
[AD-A264881] p 3497 N93-30908

MICHELSON INTERFEROMETERS

Measurement of a Michelson interferometer mirror velocity with a time interval analyzer
[AD-A263009] p 3430 N93-28659

MICROBIOLOGY

Planetary protection issues for the MESUR mission: Probability of growth (Pg)
[NASA-CP-3167] p 3651 N93-30214

MICROBURSTS (METEOROLOGY)

Aircraft guidance for wind shear avoidance: Decision-making under uncertainty p 3246 N93-31005

MICROCHANNEL PLATES

New technologies for UV detectors
p 3582 N93-28786

A new multichannel soft x ray framing camera for fusion experiments
[DE93-009302] p 3432 N93-29773

MICROCHANNELS

The microchannel heatsink with liquid nitrogen cooling
[DE93-009258] p 3422 N93-29300

MICROCOMPUTERS

Study on the concurrent calculation with a multitransputer network
[DE93-753191] p 3524 N93-28531

Development of a PC code package for the analysis of research and power reactors
[DE92-638517] p 3536 N93-31001

MICROCRACKS

Preliminary test of liquid metal induced embrittlement in liquid LiPb and stainless-steel systems
[DE93-753130] p 3320 N93-28529

Three-dimensional elastic stress analysis in materials with many inhomogeneities
[AD-A263736] p 3453 N93-29855

Damage growth in composite propellants
p 3348 N93-30088

The initiation, propagation, and effect of matrix microcracks in cross-ply and related laminates
p 3304 N93-30847

MICROELECTRONICS

Field-emitter arrays for RF vacuum microelectronics
[AD-A262677] p 3404 N93-28483

Electronics research report
[AD-A262733] p 3405 N93-28589

Initial graphics exchange specification hybrid microcircuit application protocol
[PB93-175404] p 3407 N93-29203

NSF Tokyo reports: Japanese R and D projects on micro- and nanofabrication and related basic research projects
[PB93-181261] p 3410 N93-29671

New developments in vacuum microelectronics
[AD-A263103] p 3410 N93-29798

Improved field emitter current densities and stability through the application of a proprietary process
[AD-A264048] p 3411 N93-30031

Test structure to microcircuit correlation
[AD-A264157] p 3412 N93-30152

An application protocol for CAD to CAD transfer of electronic information
[AD-A264554] p 3533 N93-30383

RF vacuum microelectronics
[AD-A264528] p 3412 N93-30409

Adhesion of thick film Au to alumina ceramics
[DE93-009802] p 3339 N93-30656

Superconducting flux coupled fast switching device from YBCO films
[AD-A264301] p 3414 N93-30896

MICROGRAVITY APPLICATIONS

Low-frequency vibration environment for five Shuttle missions
[NASA-TM-106059] p 3285 N93-28554

NASA in-step: Permeable membrane experiment
p 3267 N93-28736

A high-temperature furnace for applications in microgravity p 3229 N93-29723

MICROHARDNESS

Comparison of deformation and shock reactivity for single crystals of RDX and ammonium perchlorate
p 3350 N93-30094

MICROMECHANICS

The design and modelling of a comb-drive-based microengine for mechanism drive applications
[DE93-009826] p 3443 N93-29185

An investigation of graphite peek composite under compression with a centrally located circular discontinuity
[AD-A262549] p 3298 N93-29414

Three-dimensional elastic stress analysis in materials with many inhomogeneities
[AD-A263736] p 3453 N93-29855

Long discontinuous fiber composite structure: Forming and structural mechanics p 3301 N93-30437

Micromechanics of fatigue in woven and stitched composites p 3304 N93-30850

MICROMETEORITES

Cratering in glasses impacted by debris or micrometeorites p 3340 N93-29368

MICROMETEOROIDS

Micrometeoroids and debris on LDEF
p 3638 N93-29356

Long Duration Exposure Facility (LDEF) experiment M0003 meteoroid and debris survey
p 3638 N93-29361

Characteristics of hypervelocity impact craters on LDEF experiment S1003 and implications of small particle impacts on reflective surfaces p 3283 N93-29363

Projectile compositions and modal frequencies on the chemistry of micrometeoroids LDEF experiment
p 3638 N93-29370

Damage areas on selected LDEF aluminum surfaces
p 3283 N93-29374

LDEF data: Comparisons with existing models
p 3283 N93-29375

Long-term microparticle flux variability indicated by comparison of Interplanetary Dust Experiment (IDE) timed impacts for LDEF's first year in orbit with impact data for the entire 5.77-year orbital lifetime p 3638 N93-29379

MICROMINIATURIZATION

NSF Tokyo reports: Japanese R and D projects on micro- and nanofabrication and related basic research projects
[PB93-181261] p 3410 N93-29671

MICROMOTORS

The design and modelling of a comb-drive-based microengine for mechanism drive applications
[DE93-009826] p 3443 N93-29185

MICROORGANISMS

Process for selectively recovering algae and protozoa
[NASA-CASE-MFS-26124-1-NPO] p 3491 N93-29174

Marine microbial production of dimethylsulfide from dissolved dimethylsulfoniopropionate
[NASA-CR-193278] p 3492 N93-30665

MICROPARTICLES

Aerosol particle analysis by Raman scattering technique
[DE93-005587] p 3309 N93-28880

Elemental analyses of hypervelocity microparticle impact sites on Interplanetary Dust Experiment sensor surfaces
p 3638 N93-29378

Long-term microparticle flux variability indicated by comparison of Interplanetary Dust Experiment (IDE) timed impacts for LDEF's first year in orbit with impact data for the entire 5.77-year orbital lifetime p 3638 N93-29379

Processing of novel nanoparticle dispersion strengthened ceramics for improved mechanical performance
[AD-A264191] p 3339 N93-30883

MICROPOROSITY

Method for preparation of a microporous structure with layered interstitial surface treatment
[NASA-CASE-MSC-21487-2] p 3296 N93-29023

The synthesis and ab initio structure determination of Zn4O(BO3)2: A microporous zincoborate built up from fused 3-ring and 5-ring sub-units
[AD-A262504] p 3594 N93-29138

Ordered molecular arrays as templates: A new approach to synthesis of mesoporous materials
[AD-A264631] p 3570 N93-30540

Fluids in porous media.
[PB93-175198] p 3428 N93-30759

MICROPROCESSORS

Study on the concurrent calculation with a multitransputer network
[DE93-753191] p 3524 N93-28531

Parallel software tools at Langley Research Center
[NASA-TM-108995] p 3520 N93-29070

Digital hardware architecture implementation
[AD-A263219] p 3521 N93-29492

MICROSCOPES

Ultra-high resolution water window x ray microscope optics design and analysis
[NASA-CR-193225] p 3578 N93-29128

X ray microscopy resource center at the Advanced Light Source
[DE93-010449] p 3261 N93-29869

The x ray microscopy resource center at the advanced light source
[DE93-010443] p 3433 N93-30531

MICROSCOPY

X ray microscopy resource center at the Advanced Light Source
[DE93-010449] p 3261 N93-29869

Atomic force microscopy of ammmonium perchlorate
p 3349 N93-30091

Fundamental studies of friction, lubrication, and wear by atomic force microscopy
[AD-A264647] p 3446 N93-30524

The x ray microscopy resource center at the advanced light source
[DE93-010443] p 3433 N93-30531

MICROSTRIP ANTENNAS

Planar microstrip YAGI antenna array
[NASA-CASE-NPO-17873-2-CU] p 3384 N93-29507

MICROSTRIP TRANSMISSION LINES

Planar active antennas and quasi-optical power combining arrays using FET's and slots
[AD-A263759] p 3387 N93-29875

MICROSTRUCTURE

Process optimization of Hexoloy SX-SiC towards improved mechanical properties
[DE93-007913] p 3320 N93-28564

Microstructural understanding and critical current optimization of advanced high field superconductors
[DE93-011046] p 3592 N93-28643

Microstructural effects on the deformation and fracture of the alloy Ti-25Al-10Nb-3B-1Mo
[AD-A263095] p 3323 N93-29144

Some problems in the mechanics of solids with phase mixtures
[AD-A263652] p 3311 N93-29291

Some effects of composition and microstructure on the B2 in equilibrium to DO3 ordered phase transition in Fe3Al alloys
[DE93-009724] p 3325 N93-29813

Microstructural modeling of electrical breakdown in solid fuel propellants
[AD-A263466] p 3342 N93-29835

Balanced technology initiative on computational mechanics of materials
[AD-A263906] p 3453 N93-29863

Microstructural basis for enhanced shock-induced chemistry in single crystals of ammonium perchlorate
p 3319 N93-30092

Comparison of deformation and shock reactivity for single crystals of RDX and ammonium perchlorate
p 3350 N93-30094

Damage mechanics in 2-D and 3-D microstructures
[AD-A264337] p 3453 N93-30159

The 2-6 semiconductor superlattices
[AD-A264343] p 3597 N93-30164

DOE fundamentals handbook: Material science
[DE93-012224] p 3314 N93-30199

The electrodeposition of low contraction chromium using high/low current pulsing
[AD-A264475] p 3327 N93-30538

Durability of Quick Reaction Satellite Antenna (QRSA) trunnion castings
[AD-A264095] p 3281 N93-30813

Tensile study of single-crystal ternary L1(2) trialuminide Al66Ti25Mn(sub g)
[AD-A264297] p 3601 N93-30819

Micromechanics of fatigue in woven and stitched composites p 3304 N93-30850

Processing of novel nanoparticle dispersion strengthened ceramics for improved mechanical performance
[AD-A264191] p 3339 N93-30883

A miniature fatigue test machine p 3291 N93-30956

Improved measurement of thermal effects on microstructure p 3292 N93-30959

A review of hot cracking in austenitic stainless steel weldments
[DE93-605280] p 3328 N93-31021

MICROWAVE AMPLIFIERS

Field-emitter arrays for RF vacuum microelectronics
[AD-A262677] p 3404 N93-28483

Study of gain in C-band deflection cavities for a frequency-doubling magnicon amplifier
[AD-A263132] p 3409 N93-29478

High-power Ka-band amplifier p 3385 N93-29590

Optimization of HPM device parameters for maximum air transmission
[DE93-007332] p 3386 N93-29765

MICROWAVE ANTENNAS

High-power Ka-band amplifier p 3385 N93-29590

Propagation channel modeling for angle-diversity combining simulation p 3360 N93-30252

MICROWAVE CIRCUITS

Processing, fabrication, and demonstration of HTS integrated microwave circuits
[AD-A263161] p 3406 N93-28940

Optically controlled active impedance element particularly suited for a microwave oscillator
[AD-D015723] p 3408 N93-29281

Planar active antennas and quasi-optical power combining arrays using FET's and slots
[AD-A263759] p 3387 N93-29875

International Journal of Numerical Modeling: Electronic Networks, Devices, and Fields, volume 5, number 3, August 1992
[AD-A263765] p 3387 N93-29877

Design and integration of high bit rate four phase monolithic demodulators and modulators at X band
[LAAS-92354] p 3414 N93-31030

MICROWAVE COUPLING

Coupling gain computation between antennas on circular cylinders at SHF/EHF frequencies p 3369 N93-30309

MICROWAVE EMISSION

A computer simulation of the production of an artificially ionized layer using the Arecibo facility
[DE93-010817] p 3478 N93-30487

Microwave emission from relativistic electron beams
[AD-A264102] p 3400 N93-30880

MICROWAVE EQUIPMENT

Department of defense advisory group on electron devices: Appendix to special technology area review on microwave packaging technology
[AD-A262136] p 3408 N93-29408

MICROWAVE FREQUENCIES

Phase transition studies in barium and strontium titanates at microwave frequencies p 3293 N93-30970

MICROWAVE IMAGERY

Leadex data report. Part 1: Weather analysis and satellite images
[AD-A263217] p 3481 N93-28876

Convective and stratiform rain: Multichannel microwave sensing over oceans
[NASA-TM-104586] p 3482 N93-29448

MICROWAVE LANDING SYSTEMS

Evaluation of category 3 MLS designs
p 3247 N93-30358

MICROWAVE OSCILLATORS

Development of high power microwave source
[DE93-753316] p 3436 N93-28980

Optically controlled active impedance element particularly suited for a microwave oscillator
[AD-D015723] p 3408 N93-29281

Improved design concepts for millimeter wave power sources
[AD-A264060] p 3411 N93-29922

Advanced microwave frequency sources and filters based on superconducting Photonic Band Gap (PBG) structures
[AD-A264404] p 3597 N93-30175

MICROWAVE RADIOMETERS

Miniature modular microwave end-to-end receiver
[NASA-CASE-NPO-18713-1-CU] p 3381 N93-29087

RTE: A UNIX library with on-line documentation and sample programs for microwave radiative transfer calculations
[PB93-180248] p 3386 N93-29680

MICROWAVE RESONANCE
An improved linear ion trap physics package
p 3384 N93-29587
MICROWAVE TRANSMISSION
Development of Si(1-x)Ge(x) technology for microwave sensing applications
[NASA-TM-106157] p 3405 N93-28610
Optimization of HPM device parameters for maximum air transmission
[DE93-007332] p 3386 N93-29765
Propagation channel modeling for angle-diversity combining simulation p 3360 N93-30252
Radiation-hardened microwave communications system
[DE93-007915] p 3394 N93-30631
MICROWAVES
On the meaning of delta T/T
[DE93-008482] p 3653 N93-28962
Report on the sintering and properties of MgO and MgO-5 percent TiC
[DE93-008676] p 3323 N93-29092
Preliminary investigation of high power microwave plasmas for electrothermal thruster use
[NASA-TM-106207] p 3288 N93-29158
Microwave processing of ceramics
[DE93-010708] p 3332 N93-29252
Proceedings of the 25th European Conference on the Application of Polar Dielectrics to celebrate the 25th anniversary of the Dielectric Society, incorporating the 1st International Workshop on Integrated Ferroelectrics
[AD-A263427] p 3332 N93-29337
Department of defense advisory group on electron devices: Appendix to special technology area review on microwave packaging technology
[AD-A262136] p 3408 N93-29408
Microwave processing of silicon nitride for advanced gas turbine applications
[DE93-007910] p 3334 N93-29767
Submillimeter and microwave residual losses in epitaxial films of Y-Ba-Cu-O and Tl-Ca-Ba-Cu-O
[DE93-010430] p 3596 N93-29868
Quantification of thermographic mapping techniques
[AD-A264020] p 3391 N93-30016
A computer simulation of the production of an artificially ionized layer using the Arecibo facility
[DE93-010817] p 3478 N93-30487
Microsecond ribbon relativistic electron beam in a plane undulator and generation of microwave radiation
[DE93-605693] p 3400 N93-30993
MICROYIELD STRENGTH
The effect of oxidation embrittlement on the impact behavior of nicalon reinforced CAS 2 ceramic matrix composites
[AD-A263567] p 3334 N93-29829
MIE SCATTERING
Uplink laser propagation measurements through the sea surface, haze and clouds
[AD-A264687] p 3440 N93-30553
MILITARY AIRCRAFT
Project summary p 3227 N93-29714
MILITARY OPERATIONS
T(lc2)acS(lc3)ats for Surveillance Verification and C3I
[AGARD-CP-522] p 3387 N93-29892
Tactical satellites p 3284 N93-29893
Evolution or revolution: The Catch 22 of TACSATs
p 3269 N93-29894
TACSAT ground control and data collection
p 3388 N93-29895
TACSAT meteorological payloads
p 3391 N93-29913
The environment as an operational center of gravity
[AD-A264170] p 3472 N93-30154
Managing operational intelligence overload: Guidelines for avoiding decision paralysis
[AD-A264184] p 3610 N93-30158
Medical aspects of cold weather operations: A handbook for medical officers
[AD-A263559] p 3496 N93-30588
MILITARY SPACECRAFT
Tactical satellites p 3284 N93-29893
Evolution or revolution: The Catch 22 of TACSATs
p 3269 N93-29894
TACSAT ground control and data collection
p 3388 N93-29895
TACSAT-spacecraft bus concept and design: Application of a multimission bus for TACSAT in LEO
p 3284 N93-29896
Tactical satellites for air command and control
p 3284 N93-29898
Considerations for NATO satellite communications in the post-2000 era p 3388 N93-29899
Advanced technologies for lightweight EHF tactical communications satellites p 3389 N93-29900
Synchronization techniques for medium data rate EHF MILSATCOM systems p 3389 N93-29901
SAR sensors on TACSATS: A feasibility assessment
p 3286 N93-29909
A TACSAT SAR concept p 3286 N93-29910
Cost effective TacSats for military support
p 3285 N93-29912
Canadian EHF MILSATCOM research and development project p 3362 N93-30264
SAW technology for on-board processing in military satellite communications p 3362 N93-30265
FASSET: A development model for a Canadian EHF MILSATCOM system p 3363 N93-30268
MILITARY TECHNOLOGY
Cognitive interface considerations for intelligent cockpits p 3503 N93-28865
System automation and pilot-vehicle-interface for unconstrained low-altitude night attack
p 3503 N93-28867
Computer assisted evaluation for air close combat based on time interval characterization p 3504 N93-28868
A study of the effects of lens focal length on remote driver performance
[AD-A263191] p 3505 N93-28941
Advanced Construction Technology Center research
[AD-A263654] p 3432 N93-29390
Summer Faculty Research Program (SFRP), volume 1
[AD-A261988] p 3608 N93-29440
Defense conversion: Redirecting research and development
[OTA-ITE-552] p 3610 N93-29649
Concept formulation process aid for trade-off determination: Operator's guide
[AD-A263756] p 3531 N93-29874
An overview of DARPA's advanced space technology program p 3269 N93-29908
Low cost TACSAT for NATO surveillance
p 3285 N93-29911
Cost effective TacSats for military support
p 3285 N93-29912
TACSAT meteorological payloads
p 3391 N93-29913
Tethered aerostat VLF/LF transmitter system design considerations p 3399 N93-30753
MILKY WAY GALAXY
Distribution of dark matter in the galaxy and the lower limits for the masses of supersymmetric particles
[BONN-92-31] p 3632 N93-28473
Young open clusters as probes of the star formation process p 3635 N93-30377
MILLIMETER WAVES
Novel low temperature superconducting bolometers
[DE93-010433] p 3430 N93-28664
Superconducting submillimeter and millimeter wave detectors
[DE93-007656] p 3431 N93-29149
Department of defense advisory group on electron devices: Appendix to special technology area review on microwave packaging technology
[AD-A262136] p 3408 N93-29408
Improved design concepts for millimeter wave power sources
[AD-A264060] p 3411 N93-29922
MILLING MACHINES
A virtual environment for manufacturing systems
[AD-A263128] p 3528 N93-29473
MIMD (COMPUTERS)
Implementation of a single-material version of PAGOSA on MIMD hypercubes
[SAND-92-0640] p 3526 N93-29127
Special purpose parallel computer architecture for real-time control and simulation in robotic applications
[NASA-CASE-NPO-17629-1-CU] p 3521 N93-29608
Using synthetic-perturbation techniques for tuning shared memory programs
[PB93-178572] p 3539 N93-29677
Data parallelism
[DE93-009300] p 3539 N93-29782
MIMO (CONTROL SYSTEMS)
An adaptive controller for a class of MIMO non-minimum phase systems with disturbance rejection design
p 3359 N93-30248
MINERAL DEPOSITS
Standard and reference materials for marine science, third edition
[PB93-185684] p 3489 N93-30830
MINERAL EXPLORATION
Prototype backscatter Moessbauer spectrometer for measurement of Martian surface mineralogy
p 3648 N93-28812
MINERALOGY
Laer-induced breakdown spectroscopy instrument for element analysis of planetary surfaces
p 3434 N93-28769
The APX spectrometer for Martian missions
p 3434 N93-28776
A DTA/GC for the in situ identification of the Martian surface material p 3646 N93-28800
Prototype backscatter Moessbauer spectrometer for measurement of Martian surface mineralogy
p 3648 N93-28812
Interplanetary meteoroid debris in LDEF metal craters
p 3638 N93-29372
MINERALS
Frequency dependent electrical properties of minerals and partial-melts
[DE93-009254] p 3410 N93-29793
MINIATURIZATION
Miniature modular microwave end-to-end receiver
[NASA-CASE-NPO-18713-1-CU] p 3381 N93-29087
MINIMAL SURFACES
The global potential energy surfaces of the lowest two 1A-prime states of the ozone molecule: Theoretical determination and analysis
[DE93-007537] p 3313 N93-29837
MINKOWSKI SPACE
Geometrical approach to the dynamics of a relativistic string in the D-dimensional Minkowski space
[DE93-606071] p 3605 N93-30784
The ground state wavefunctions of a conformally invariant scalar field in different spacetime background
[DE93-606063] p 3606 N93-30808
Positive energy representations of the conformal quantum algebra
[DE93-606064] p 3551 N93-30809
A new exact solution to the classical equations of motion of the relativistic string with massive ends
[DE92-644736] p 3557 N93-30922
Invariant structures and static forces in gauge theories
[DE92-644740] p 3607 N93-30925
MINORITIES
Materials education activities p 3291 N93-30958
MIRRORS
Measurement of a Michelson interferometer mirror velocity with a time interval analyzer
[AD-A263009] p 3430 N93-28659
Optical technologies for UV remote sensing instruments p 3582 N93-28788
Effects of vacuum exposure on stress and spectral shift of high reflective coatings
[DE93-009318] p 3437 N93-29207
Problems in the implementation of x ray optics with x ray lasers
[DE93-009297] p 3438 N93-29781
MIS (SEMICONDUCTORS)
Metallization at detonation fronts in solids
p 3319 N93-30087
MISSILE CONFIGURATIONS
Clustered Lance Booster (CLB) feasibility study
[AD-A262746] p 3286 N93-28593
MISSILE CONTROL
Pilot decision aiding for weapon delivery: A novel approach to fire control cueing using parallel computing
p 3501 N93-28853
MISSILE TRACKING
A fuzzy logic optimal control law solution to the CMMCA tracking problem
[AD-A262555] p 3542 N93-29420
MISSILES
Kinetics and energy transfer in nonequilibrium fluid flows
[AD-A263612] p 3240 N93-29284
Chaos in mechanical systems with especial reference to rotorcraft and missiles
[AD-A263703] p 3604 N93-29384
Tactical satellites p 3284 N93-29893
MISSION PLANNING
Planning for air to air combat p 3501 N93-28852
A new class of mission support for combat air-crew
p 3501 N93-28854
Pilot intent and error recognition as part of a knowledge based cockpit assistant p 3502 N93-28855
Mars integrated transportation system multistage Mars mission p 3232 N93-29741
Antares: A low cost modular launch vehicle for the future p 3235 N93-29759
Launch vehicles for lightweight TACSAT deployment
p 3271 N93-29903
The 1992 town meetings: Toward a shared vision
[NASA-NP-205] p 3608 N93-30134
Technology transfer within the NASA Goddard Space Flight Center p 3626 N93-30704
Technology coordination p 3626 N93-30706
Space transfer concepts and analyses for exploration missions, phase 3
[NASA-CR-192584] p 3268 N93-31034
MIST
Systems description of MIVOS (mist forecast system), part 1
[KNMI-TR-141-PT-1] p 3483 N93-30013
MIXERS
Tank Pressure Control Experiment (TPCE)
p 3264 N93-28712

MIXING
Tank Pressure Control Experiment/Thermal Phenomena (TPCE/TP) p 3264 N93-28713
Methods for preparation of mixtures of gases in air at the parts-per-billion to parts-per-million concentration range for calibration of monitors [DE92-642433] p 3317 N93-30982

MIXING LAYERS (FLUIDS)
The development of a mixing layer under the action of weak streamwise vortices [NASA-TM-106089] p 3418 N93-28947
Jet mixer noise suppressor using acoustic feedback [NASA-CASE-LEW-15170-1] p 3561 N93-28953
Compressible turbulence in a high-speed high Reynolds number mixing layer p 3242 N93-30583

MIXING LENGTH FLOW THEORY
Theory of tokamak edge turbulence: Drift-thermal instability-induced turbulence and ionization-driven drift wave turbulence p 3586 N93-29123
Modeling of a turbulent flow in the presence of discrete parietal cooling jets p 3258 N93-29960

MIXTURES
Some problems in the mechanics of solids with phase mixtures [AD-A263652] p 3311 N93-29291

MOBILE COMMUNICATION SYSTEMS
In-step inflatable antenna experiment p 3263 N93-28701
A slotted Aloha satellite channel simulator p 3360 N93-30250
Teleglobe's international Mobile Earth Terminal service p 3371 N93-30317
The evolution of global mobile communications p 3376 N93-30349

MODAL RESPONSE
Dynamical analysis of highly excited molecular spectra [DE93-010771] p 3564 N93-28604
Modal survey of a full-scale F-18 wind tunnel model [AD-A262482] p 3240 N93-29410

MODEL REFERENCE ADAPTIVE CONTROL
Controls for space structures p 3275 N93-29112
Adaptive motion control of mobile robots p 3545 N93-30903
On neural networks in identification and control of dynamic systems [NASA-TM-107702] p 3455 N93-31038

MODELS
The meta model hierarchy: A framework for information systems concepts and techniques [TR-92-17] p 3611 N93-28481
Formal definition of a conceptual language for the description and manipulation of information models [TR-92-16] p 3523 N93-28503
Introduction to cadet center for advanced data evaluation technology p 3614 N93-29240
Mass storage system reference model, Version 4 p 3617 N93-30450

MODEMS
Signal processor based MSAT trellis coded M-DPSK with adaptive Doppler phasor correction p 3373 N93-30332

MODULATION
Modelling of channel thickness modulation effect in SI GaAs MESFET's p 3356 N93-30229
An error control protocol based on trellis coded modulations p 3358 N93-30237

MODULATION TRANSFER FUNCTION
Optical system analysis for the ground based EXVM [NASA-CR-192588] p 3582 N93-31035

MODULATORS
Upgrading the LAMPF 201 MHz RF generators [DE93-010715] p 3406 N93-28830
Constant Average Power Single Sideband (CAPSSB) modulation p 3373 N93-30331
Complex apparatus and results of active experiment Electron-1 with injection of electronic beam in the ionosphere [DE93-605452] p 3480 N93-30991

MODULUS OF ELASTICITY
Aligned, short-fiber composites by novel flow processing methods [DE93-008701] p 3296 N93-28904
Some problems in the mechanics of solids with phase mixtures [AD-A263652] p 3311 N93-29291
Results of a round robin test program: Complex modulus properties of a polymeric damping material [AD-A263619] p 3332 N93-29344

MOIRE INTERFEROMETRY
Two-parameter crack tip field associated with stable crack growth in a thin plate: A hybrid analysis [AD-A264221] p 3453 N93-30147

MOISTURE CONTENT
Sensitivity study of cloud/radiation interaction using a second order turbulence radiative-convective model [DE93-007365] p 3477 N93-29346
Effects of freeze/thaw cycles on hydrostatically conditioned E-glass/J-2 composite [AD-A262980] p 3298 N93-29425

MOLDING MATERIALS
Preliminary properties of a resin from ethynyl terminated materials p 3303 N93-30842

MOLDS
Development of a CFD code for casting simulation [NASA-CR-192577] p 3427 N93-30492
Infiltration/cure modeling of resin transfer molded composite materials using advanced fiber architectures p 3303 N93-30843
Development of stitching reinforcement for transport wing panels p 3304 N93-30852
Development of resins for composites by resin transfer molding p 3305 N93-30853

MOLECULAR BEAM EPITAXY
Luminescence study of ion-implanted and MBE-grown Er-doped GaAs and Al(x)Ga(1-x)As [AD-A262602] p 3591 N93-28471
Infrared rugates by molecular beam epitaxy p 3582 N93-28808
Real time self-directed MBE flux control incorporation in situ ellipsometry, phase 1 [AD-A263501] p 3595 N93-29341
Defect studies in low-temperature-grown GaAs [DE93-010405] p 3595 N93-29417
Characterization of copper iodide thin films fabricated via laser assisted molecular beam epitaxy [AD-A262823] p 3596 N93-29430
The 2-6 semiconductor superlattices [AD-A264343] p 3597 N93-30164
Visible light emitting materials and injection devices [AD-A263499] p 3601 N93-30811

MOLECULAR BEAMS
Low temperature (LT) GaAs and related materials [AD-A263607] p 3298 N93-29282

MOLECULAR BIOLOGY
Proceedings of a Workshop on Molecular Nuclear Medicine [DE93-010828] p 3493 N93-28835
Defining protein electrostatic recognition processes [AD-A264838] p 3571 N93-30901
The Gordon Research Conference on Pineal Cell Biology [AD-A264840] p 3497 N93-30904

MOLECULAR CLOUDS
A characterization of young stellar objects in Bok globules: Infrared imaging, spectral energy distributions, and molecular outflows p 3636 N93-30563
CO lines toward NGC 2024 and other star forming regions: A closer look at the warm gas component [MPE-PREPRINT-223] p 3637 N93-30639

MOLECULAR COLLISIONS
Elastic and reactive collisions of atoms and molecules with neutral alkali clusters [DE93-009313] p 3566 N93-29206
Reaction and reorientation of electronically excited H2(B) [DE93-010435] p 3569 N93-29860

MOLECULAR DIFFUSION
The role of grain boundaries in hydrogen diffusion in metals at 25 C [NASA-TM-108407] p 3322 N93-29043

MOLECULAR EXCITATION
Spectroscopic probes of vibrationally excited molecules at chemically significant energies [DE93-012328] p 3564 N93-28652
The photodissociation and reaction dynamics of vibrationally excited molecules [DE93-010896] p 3565 N93-28879
Quantum lattice fluctuations in a 1-dimensional charge-density-wave material: Luminescence and resonance Raman studies of an MX solid [DE93-007362] p 3593 N93-28966
Magnetic resonance studies of photo-induced electron transfer reactions [DE93-012239] p 3311 N93-29182
Reaction and reorientation of electronically excited H2(B) [DE93-010435] p 3569 N93-29860
Triplet states and optical absorptions in finite polyenes and conjugated polymers [AD-A264552] p 3337 N93-30381

MOLECULAR GASES
Environmental Verification Experiment for the Explorer Platform (EVEEP) p 3266 N93-28726
Return flux experiment p 3266 N93-28727
Radiative interactions in molecular gases under local and nonlocal thermodynamic equilibrium conditions [NASA-CR-193223] p 3604 N93-29168
Vibrational spectroscopy of shock-compressed fluids p 3318 N93-30072
Detonation mass spectrometry p 3319 N93-30076

MOLECULAR INTERACTIONS
NMR studies of molecules in liquid crystals and graphite [DE93-010423] p 3569 N93-29805
The calculation of electrostatic interactions and their role in determining the energies and geometries of molecular HE crystals [DE92-040374] p 3570 N93-30448

MOLECULAR IONS
Mass spectrometric investigation of 2-methoxyethanol and 2-ethoxyethanol clusters: Magic numbers and structural implications [AD-A262822] p 3312 N93-29429

MOLECULAR PHYSICS
Fast multipole method in simulations of aqueous systems [AD-A263422] p 3567 N93-29336
Molecular dynamics modeling of electric double layers with spectroscopic applications [AD-A263168] p 3568 N93-29489
Adsorption of hydrated halide ions on charged electrodes: Molecular dynamics simulation [AD-A263137] p 3568 N93-29619
Dynamics and photoexcitation in MX and MXX' chain solids [AD-A264823] p 3561 N93-29711
Molecular dynamics of detonation in crystals with defects p 3350 N93-30097
Thermodynamic and structural properties of metallic glasses and supercooled liquids [ISBN-0-315-72443-9] p 3605 N93-30359

MOLECULAR RELAXATION
Polar order and relaxation of second order nonlinear optical susceptibility in an electric field polarized amorphous polymer [AD-A262189] p 3329 N93-28489
Quantum dynamics of X2BC van der Waals clusters [DE93-006416] p 3565 N93-28892
Kinetics of nitric oxide formation behind 3 to 4 KM/S shock waves [AD-A263653] p 3312 N93-29389
Dynamics and photoexcitation in MX and MXX' chain solids [AD-A264823] p 3561 N93-29711
Reaction and reorientation of electronically excited H2(B) [DE93-010435] p 3569 N93-29860

MOLECULAR SPECTRA
Dynamical analysis of highly excited molecular spectra [DE93-010771] p 3564 N93-28604
Vibrational spectroscopy of shock-compressed fluids p 3318 N93-30072
Examination of shock induced chemical reactions in liquids using time-resolved optical spectroscopy p 3318 N93-30073

MOLECULAR SPECTROSCOPY
Single-shot femtosecond spectroscopy: A methodology for observation of solid-state chemical reactions p 3319 N93-30075
Detonation mass spectrometry p 3319 N93-30076

MOLECULAR STRUCTURE
Quantum dynamics of X2BC van der Waals clusters [DE93-006416] p 3565 N93-28892
What is underneath? Moving atoms and molecules to find out [AD-A263363] p 3567 N93-29332
Mass spectrometric investigation of 2-methoxyethanol and 2-ethoxyethanol clusters: Magic numbers and structural implications [AD-A262822] p 3312 N93-29429
Molecular dynamics modeling of electric double layers with spectroscopic applications [AD-A263168] p 3568 N93-29489
Observation of phase-separated nanometer scale molecular domains in mixed self-assembled monolayers [AD-A263470] p 3569 N93-29839
Atomic force microscopy of ammmonium perchlorate p 3349 N93-30091
Design of acentric materials: X ray structures of guanidinium p-nitro- and p-hydroxybenzenesulfonate [AD-A264220] p 3597 N93-30146
Organometallic compounds and polymers with second and third order nonlinear optical properties [AD-A264774] p 3338 N93-30610
The adhesion of AgI molecules to gaseous metallic silver cluster cations [AD-A264820] p 3338 N93-30628
Detailed studies of soot formation in laminar diffusion flames for application to modeling studies [AD-A264827] p 3317 N93-30667
Design, synthesis, and chemical processing of hierarchical ceramic structures for aerospace applications [AD-A264227] p 3339 N93-30885

Physical chemical studies on molecular composite compositions
[AD-A264834] p 3339 N93-30898

MOLECULAR THEORY

The 26th International Quantum Chemistry Symposium on Atomic, Molecular, and Condensed Matter Theory and Computational Methods
[AD-A264206] p 3315 N93-30534

MOLECULES

Synthesis of cubane based energetic molecules
[AD-A263271] p 3564 N93-28562

Dynamical analysis of highly excited molecular spectra
[DE93-010771] p 3564 N93-28604

Return flux experiment p 3266 N93-28727

The photodissociation and reaction dynamics of vibrationally excited molecules
[DE93-010896] p 3565 N93-28879

NMR studies of molecules in liquid crystals and graphite
[DE93-010423] p 3569 N93-29805

Observation of phase-separated nanometer scale molecular domains in mixed self-assembled monolayers
[AD-A263470] p 3569 N93-29839

Use of statistics in computational chemistry
[AD-A264307] p 3315 N93-30365

MOLNIYA SATELLITES

Terrain and coverage prediction analyses for non-geostationary orbit EHF satellite communications
p 3389 N93-29902

MOLTEN SALTS

Studies in Lewis acid and superacid ionic liquids
[AD-A264683] p 3316 N93-30551

Gordon Research Conferences, 1991
[AD-A264275] p 3317 N93-30816

MOLYBDENUM ALLOYS

High temperature creep and oxidation resistant chromium silicide matrix alloy containing molybdenum
[NASA-CASE-LEW-15697-1] p 3323 N93-29172

MOLYBDENUM COMPOUNDS

Synthesis of chiral molybdenum ROMP initiators and all-cis highly tactic Poly-2,3-R2Norbornadiene (R = CF3 or CO2Me)
[AD-A264133] p 3336 N93-30169

MOMENTS OF INERTIA

Investigation of Mars rotational dynamics using Earth-based radio tracking of Mars landers
p 3642 N93-28777

Vibration localization in rotating shafts
p 3454 N93-30626

MOMENTUM THEORY

On the energy-momentum tensors for field theories in spaces with affine connection and metric
[DE92-644744] p 3557 N93-30927

MOMENTUM TRANSFER

Electron interactions with non-linear polyatomic molecules and their radicals and ions
[AD-A262279] p 3568 N93-29446

MONATOMIC GASES

The Interstellar Gas Experiment: Analysis in progress
p 3639 N93-29380

FI-STM investigation of atomic hydrogen adsorption on the Si(100)2x1 surface
[AD-A262748] p 3567 N93-29403

MONATOMIC MOLECULES

A simple model for ion solvation with non additive cores
[AD-A263075] p 3566 N93-29143

MONEL (TRADEMARK)

Crack length determination by ultrasonic methods
[DE93-008075] p 3450 N93-28567

MONITORS

Environmental Verification Experiment for the Explorer Platform (EVEEP) p 3266 N93-28726

Sensor systems for monitoring Maglev guideway structures
[PB93-154821] p 3444 N93-29205

Advanced thermally-stable, coal-derived, jet fuels program: Experiment system and model development
[AD-A262747] p 3342 N93-29402

Computer-controlled alignment for a 2000-line color monitor p 3247 N93-30324

MONOCHROMATORS

Measurement of the rotation Raman spectra of nitrogen, oxygen, and water vapor under conditions of a temperature humidity lidar
[GKSS-92/E/32] p 3485 N93-31018

MONOIDS

Antirational transductions and their language families
[ETN-93-93794] p 3611 N93-28525

MONOMERS

Shear sensitive monomer-polymer laminate structure and method of using same
[NASA-CASE-LAR-14654-1-CU] p 3452 N93-29613

Applications of laser light scattering in polymer dilute solution characterization
[AD-A263110] p 3335 N93-30007

Synthesis and characterization of mixed 3-5 and 2-6 semiconductor monomers included in the borate sodalite analogue
[AD-A264523] p 3598 N93-30407

Conjugated polymers from cyclohexadienediol monomers
[AD-A264837] p 3340 N93-30900

MONOMOLECULAR FILMS

The mechanical response of gold substrates modified with self-assembling monolayer films
[AD-A262997] p 3452 N93-29515

Interfacial viscosity measurements of adsorbed monolayers on metal surfaces
[AD-A263288] p 3324 N93-29803

MONOPOLE ANTENNAS

Widebanding techniques for VHF antennas 2
[AD-A263998] p 3387 N93-29882

MONOPOLES

Computation of far-field helicopter rotor tone noise
[ONERA-P-1990-5] p 3562 N93-30110

MONOPULSE RADAR

Evolution of radar data processing in the French air traffic control system p 3247 N93-30325

MONSOONS

A functional implementation of the Jacobi eigen-solver
[DE93-007349] p 3549 N93-29769

MONTE CARLO METHOD

Modified goodness-of-fit tests for the Weibull distribution
[AD-A262552] p 3553 N93-28574

A modified Anderson Darling goodness-of-fit test for the gamma distribution with unknown scale and location parameters
[AD-A262486] p 3553 N93-28760

Information-theoretic performance bounding of Bayesian identifiers
[DE93-010705] p 3554 N93-28763

Meson-meson interactions and phi-enhancement in nucleus collisions
[DE93-010725] p 3565 N93-28831

Comparison of analytical transport and stochastic solutions for neutron slowing down in an infinite medium
[DE93-010799] p 3565 N93-28833

A Monte Carlo study of the raw and normal varimax rotation criterion in factor analysis
[AD-A262516] p 3554 N93-28844

A modified chi-squared goodness-of-fit test for the three-parameter gamma distribution with unknown parameters
[AD-A262553] p 3554 N93-28845

Numerical simulation of quantum many-body systems
[DE93-008300] p 3603 N93-28958

Modern Monte Carlo particle transport simulation for safety and radiation protection applications in accelerometer technology and in space science
[JUEL-2609] p 3574 N93-29062

Reliability assessment of thrust chamber cooling concepts using probabilistic analysis techniques
[NASA-CR-190785] p 3288 N93-29068

Femtosecond carrier processes in compound semiconductors and real time signal processing
[AD-A263076] p 3382 N93-29131

On the value of function evaluation location information in Monte Carlo simulation
[AD-A263662] p 3554 N93-29292

Fast multipole method in simulations of aqueous systems
[AD-A263422] p 3567 N93-29336

Parametric likelihood inference for record breaking problems
[AD-A262546] p 3549 N93-29413

SWAT system performance predictions
[AD-A262857] p 3579 N93-29470

NetStat: A probabilistic network connectivity analysis tool
[AD-A262836] p 3529 N93-29647

Electron transport calculations between 1 MeV and 1 eV
[AD-A263412] p 3568 N93-29787

Monte Carlo simulation of magnitude-angle error sources
[AD-A263738] p 3555 N93-29857

Direct Monte Carlo simulation of the chemical equilibrium composition of detonation products
[DE92-040372] p 3315 N93-30447

Beta/gamma Monte Carlo transport in repetitive structures of satellite systems
[DE93-007610] p 3281 N93-30509

Multidimensional intermittency in hadronic collisions
[DE93-010562] p 3577 N93-30532

Heat generation produced in thin layers of GaAs superconductors under high energy particles irradiation
[DE93-606332] p 3601 N93-30798

MOON

Gamma ray/neutron spectrometers for planetary elemental mapping p 3647 N93-28807

Lunar science: Using the Moon as a testbed
p 3650 N93-28821

MOONQUAKES

Lunar regolith densification p 3276 N93-29115

MORPHOLOGY

Multiscale morphological filtering for analysis of noisy and complex images p 3582 N93-28789

Follow up on the crystal growth experiments of the LDEF p 3602 N93-29381

Atomic layer epitaxy of semiconductor heterostructures
[AD-A264755] p 3599 N93-30560

Eutectic solidification of Al-U at slowly cooling rates (10 C per second)
[DE92-640082] p 3328 N93-30941

Manifold shape: From differential geometry to mathematical morphology
[CS-9204] p 3552 N93-31012

MOSSBAUER EFFECT

Prototype backscatter Moessbauer spectrometer for measurement of Martian surface mineralogy
p 3648 N93-28812

MOTHS

Predicting the response of a temperate forest ecosystem to atmospheric CO2 increase
[DE93-010081] p 3467 N93-28543

MOTION PERCEPTION

A motion detector based on a neural network
p 3356 N93-30224

MOTION SIMULATION

Three-dimensional graphical representation of objects according to movement data in realtime
[ESA-TT-1258] p 3521 N93-30104

Visualization techniques for analyzing control of human movement: Affine mappings between multi-dimensional spaces p 3508 N93-30204

MOUNTAINS

Field trial of caffeine on physical performance at altitude: An attempt to overcome the challenge
[AD-A264260] p 3497 N93-30894

MSM (SEMICONDUCTORS)

Infrared imaging array integrated in three dimensions directly on top of silicon circuits
[AD-A264707] p 3581 N93-30500

MUFFLERS

Investigation of thermoacoustic muffler
[AD-A262009] p 3562 N93-29392

MULLITES

Oxidation behavior in reaction-bonded aluminum-silicon alloy/alumina powder compacts
[DE93-010407] p 3298 N93-29191

MULTIBEAM ANTENNAS

Status of the Canadian military Multibeam Antenna (MBA) development for EHF SATCOM
p 3374 N93-30334

Comparison and design of multiple beam antenna feed networks p 3374 N93-30335

MULTIGRID METHODS

Implementation of a multidomain Navier-Stokes code on the Intel iPSC2 hypercube
[FFA-TN-1992-37] p 3418 N93-28994

A multigrid extension of the FFT for the numerical inversion of Fourier and LaPlace transforms
[TRITA-NA-9204] p 3548 N93-29024

The three-dimensional Multi-Block Advanced Grid Generation System (3DMAGGS)
[NASA-TM-108985] p 3420 N93-29155

The sensitivity of ageostrophic circulations to model resolution: A case study using NGM forecasts of ERICA IOP-4
[AD-A262011] p 3482 N93-29393

A multilevel approach to minimum cost network flows
[AD-A264008] p 3550 N93-29978

MULTIMEDIA

Natural language generation
[AD-A262578] p 3524 N93-28579

A fuzzy measure approach to motion frame analysis for scene detection p 3511 N93-29525

Review of the effectiveness of video media in instruction
[AD-A264228] p 3392 N93-30362

A prototype of a faculty and staff executive information system
[AD-A264852] p 3623 N93-30907

MULTIPATH TRANSMISSION

Propagation channel modeling for angle-diversity combining simulation p 3360 N93-30252

Adaptive airborne radar simulation with equalization filter taps
[AD-A264722] p 3393 N93-30514

MULTIPHASE FLOW

A four-field approach towards developing a mechanistic model for multiphase flow
[DE93-006572] p 3420 N93-29126

Evolution of flow disturbances in cocurrent gas-liquid flows
[DE93-010083] p 3422 N93-29326
MULTIPHOTON ABSORPTION
Discharge of electrically charged clouds
[AD-A263212] p 3480 N93-28518
MULTIPLEXING
A dual polarized broadband multifrequency Earth station feed p 3371 N93-30319
MULTIPLIERS
Measurements of breakaway reaction between beryllium and water vapor for ITER blanket design
[DE93-753270] p 3584 N93-28535
MULTIPOLES
Direct numerical simulations of unsteady separated flows using vortex methods p 3419 N93-29077
Fast multipole method in simulations of aqueous systems
[AD-A263422] p 3567 N93-29336
MULTIPROCESSING (COMPUTERS)
A multiarchitecture parallel-processing development environment
[NASA-TM-106180] p 3538 N93-28628
A modular head/eye platform for real-time reactive vision
[OUEL-1941/92] p 3505 N93-28897
Preemptive scheduling with variable profile, precedence constraints and due dates
[INRIA-RR-1622] p 3538 N93-28937
Distributed Virtual System (DIVIRS) Project
[NASA-CR-193234] p 3526 N93-29169
Multisensor image analysis system
[AD-A263679] p 3528 N93-29294
Using synthetic-perturbation techniques for tuning shared memory programs
[PB93-178572] p 3539 N93-29677
Use of a genetic algorithm to solve two-fluid flow problems on an NCUBE multiprocessor computer
[DE93-009630] p 3425 N93-30184
Task allocation and real-time considerations for the Robot Controller Test Station (RCTS)
p 3364 N93-30278
A multiprocessor architecture for realtime robot control p 3372 N93-30327
Multiprocessing systems: Reliability modelling and analysis using multimode components and dependent failures
[AD-A264230] p 3540 N93-30364
The midway distributed shared memory system
[AD-A264645] p 3534 N93-30523
Promoting high-performance computing and communications
[ISBN-0-16-041828-3] p 3522 N93-30570
Multiprocessing MCNP on an IBM RS/6000 cluster
[DE93-008712] p 3540 N93-30633
Gigabit network communications research
[AD-A264895] p 3536 N93-31026
MULTIPROGRAMMING
Multiprocessing MCNP on an IBM RS/6000 cluster
[DE93-008712] p 3540 N93-30633
MULTISENSOR APPLICATIONS
Multisensor image analysis system
[AD-A263679] p 3528 N93-29294
The fusion of information via fuzzy integration
p 3517 N93-29568
MULTISPECTRAL BAND SCANNERS
Research and development of an airborne multispectral scanner to measure fire, terrestrial and atmospheric characteristics (50 channel)
[NASA-CR-193121] p 3456 N93-28620
The MAESTRO-1 campaign: Analyses of polarimetric SAR data of agricultural fields and forests
[BCRS-92-06] p 3460 N93-29320
MULTISPECTRAL LINEAR ARRAYS
CAESAR development plan 1992-1995
[BCRS-92-17] p 3463 N93-31009
MULTISPECTRAL PHOTOGRAPHY
Systematic processing of Clementine data for scientific analyses p 3624 N93-28803
Remote sensing for water quality monitoring in the Tennessee Valley: Field tests of two systems
[DE93-008997] p 3462 N93-30637
MULTISTATIC RADAR
Application of integral and differential equation methods for various EM interaction problems
[AD-A264821] p 3394 N93-30597
MULTIVARIABLE CONTROL
Multivariable control of the Space Shuttle Remote Manipulator System using linearization by state feedback
[NASA-CR-188248] p 3443 N93-29080
MULTIVARIATE STATISTICAL ANALYSIS
A Monte Carlo study of the raw and normal varimax rotation criterion in factor analysis
[AD-A262516] p 3554 N93-28844
Some statistical inference problems in linear models and variance components models and their applications
[AD-A264062] p 3555 N93-29923
Procedures for applying Ada quality prediction models
[AD-A264730] p 3534 N93-30546
MUON SPIN ROTATION
Spin dependent phenomena in medium energy physics
[DE93-010972] p 3565 N93-28849
MUONS
Exotic atoms
[DE93-010242] p 3564 N93-28611
Spin dependent phenomena in medium energy physics
[DE93-010972] p 3565 N93-28849
MUSCULAR FATIGUE
Sudden loading and fatigue effects on the human spine
[PB93-167526] p 3493 N93-29199
MUSCULAR FUNCTION
Visualization techniques for analyzing control of human movement: Affine mappings between multi-dimensional spaces p 3508 N93-30204
MUSCULOSKELETAL SYSTEM
The physiological limitations of man in the high G environment p 3503 N93-28861
MUTATIONS
Comparative mutagenesis of human cells in vivo and in vitro
[DE93-012269] p 3490 N93-28651
Control and circadian behavior by transplanted suprachiasmatic nuclei
[AD-A264553] p 3496 N93-30382

N

NAP-OF-THE-EARTH NAVIGATION
Flight evaluation of a computer aided low-altitude helicopter flight guidance system p 3260 N93-28869
NAPHTHALENE
Vortex structure and mass transfer near the base of a cylinder and a turbine blade p 3253 N93-29929
NASA PROGRAMS
Proceedings of the Near-Earth-Object Interception Workshop
[NASA-TM-108236] p 3556 N93-28572
RBSE: Product development team research activity deliverables
[NASA-CR-193115] p 3527 N93-29212
NASA SBIR abstracts of 1991 phase 1 projects
[NASA-TM-108240] p 3609 N93-29323
Research and technology objectives and plans: Summary fiscal year 1991
[NASA-TM-103086] p 3660 N93-29452
The 1992 town meetings: Toward a shared vision
[NASA-NP-205] p 3608 N93-30134
Interagency Advanced Power Group (IAPG) Meeting Compendium
[DE93-006189] p 3670 N93-30212
Technology transfer p 3626 N93-30699
Technology transfer needs and experiences: The NASA Research Center perspective p 3626 N93-30703
Technology transfer within the NASA Goddard Space Flight Center p 3626 N93-30704
Technology transfer and space science missions
p 3626 N93-30705
Technology transfer p 3627 N93-30707
Technology transfer within NASA
p 3627 N93-30708
Technology transfer within the government
p 3627 N93-30709
Technology transfer within the government
p 3627 N93-30711
NASP technology transfer p 3627 N93-30713
NASA space research and technology overview (ITP)
p 3628 N93-30722
Space research and technology overview
p 3628 N93-30723
First NASA Advanced Composites Technology Conference, part 2
[NASA-CP-3104-PT-2] p 3303 N93-30841
NASA SPACE PROGRAMS
The MESUR mission p 3649 N93-28816
Pluto fast flyby mission and science overview
p 3649 N93-28818
Venus Interior Structure Mission (VISM): Establishing a seismic network on Venus p 3649 N93-28819
A perspective on acquisition of NASA space systems
[AD-A263246] p 3610 N93-29499
Exploration technology prioritization
p 3629 N93-30726
NASTRAN
NASTRAN analysis for the Airmass Sunburst model 'C' Ultralight Aircraft p 3249 N93-29777
NATIONAL AEROSPACE PLANE PROGRAM
NASP technology transfer p 3627 N93-30713
NATIONAL AIRSPACE SYSTEM
National Airspace System Performance Analysis Capability (NASPAC) simulation model
p 3247 N93-30351
NATURAL GAS
Thermodynamic properties of natural gas mixtures
[PB93-162816] p 3604 N93-29428
Rates and mechanisms of reaction of hydrogen sulfide with iron chelates
[PB93-184299] p 3312 N93-29665
Thermodynamic properties of natural gas mixtures
[PB93-176162] p 3604 N93-29794
Fugitive hydrocarbon emissions from Pacific OCS facilities. Volume 2: Executive summary and user's guide
[PB93-173805-VOL-2] p 3471 N93-29861
Decomposition of hydrogen sulfide for small scale gas processing.
[PB93-174704] p 3316 N93-30658
Diffusion coefficients and heats of mixing in aqueous alkanolamines
[PB93-176212] p 3316 N93-30661
Power generation and transportation systems research department
[PB93-178309] p 3352 N93-30663
NOx chemistry in natural gas flames
[PB93-175263] p 3317 N93-30760
NATURAL LANGUAGE (COMPUTERS)
Natural language generation
[AD-A262578] p 3524 N93-28579
NATURAL SATELLITES
Planetary and satellite x ray spectroscopy: A new window on solid-body composition by remote sensing
p 3641 N93-28773
NAVIER-STOKES EQUATION
Navier-Stokes analysis of radial turbine rotor performance
[NASA-CR-191153] p 3251 N93-28609
A new flux conserving Newton's method scheme for the two-dimensional, steady Navier-Stokes equations
[NASA-TM-106160] p 3416 N93-28626
Implementation of a multidomain Navier-Stokes code on the Intel iPSC2 hypercube
[FFA-TN-1992-37] p 3418 N93-28994
The numerical solution of low Mach number flow in confined regions by Richardson extrapolation
[TRITA-NA-9207] p 3238 N93-29005
An efficient spectral integration method for the solution of the Navier-Stokes equations
[FFA-TN-1992-28] p 3418 N93-29009
High Reynolds number and turbulence effects on aerodynamics and heat transfer in a turbine cascade
[NASA-TM-106187] p 3420 N93-29157
The 3-D viscous flow CFD analysis of the propeller effect on an advanced ducted propeller subsonic inlet
[NASA-TM-106240] p 3252 N93-29162
Nonlinear relaxation algorithms for the compressible Navier-Stokes equations in two and three dimensions
p 3421 N93-29177
Accuracy of least-squares methods for the Navier-Stokes equations
[NASA-TM-106209] p 3421 N93-29208
Development of an unstructured solution adaptive method for the quasi-three-dimensional Euler and Navier-Stokes equations
[NASA-CR-193241] p 3421 N93-29213
An upwind method for the solution of the 3D Euler and Navier-Stokes equations on adaptively refined meshes
[AD-A262863] p 3423 N93-29472
Recent applications of CFD to the aerodynamics of Army projectiles
[AD-A262953] p 3240 N93-29512
The XNOVAKTC rheological model
[AD-A263298] p 3342 N93-29762
Aerothermic calculations of flows in interdisc cavities of turbines p 3256 N93-29947
The aerodynamic effect of coolant ejection in the leading edge region of a film-cooled turbine blade
p 3258 N93-29958
Coupling of 3D-Navier-Stokes external flow calculations and internal 3D-heat conduction calculations for cooled turbine blades p 3258 N93-29961
Navier-Stokes analysis of three-dimensional flow and heat transfer inside turbine blade rows
p 3259 N93-29963
Simulation, characterization and control of forced unsteady viscous flows using Navier-Stokes equations
[AD-A264333] p 3425 N93-30369
Topology and grid adaption for high-speed flow computations
[NASA-CR-4216] p 3426 N93-30375
Computation of a delta-wing roll-and-hold maneuver
[AD-A264704] p 3260 N93-30498

Some implications of a differential turbomachinery equation with viscous correction
[AD-A264693] p 3427 N93-30571
Compressible turbulence in a high-speed high Reynolds number mixing layer p 3242 N93-30583
Strong parallel blade-vortex interaction and noise propagation in helicopter flight p 3563 N93-30980
Godunov-type methods for the equations of compressible fluid mechanics
[KFK-5058] p 3428 N93-31020

NAVIGATION
Advanced Unmanned Search System (AUSS) supervisory command, control and navigation
[AD-A263171] p 3245 N93-28990
Automated satellite image navigation
[AD-A262868] p 3269 N93-29475

NAVIGATION AIDS
A comparison of simulated parallax and single-station range aids to navigation
[AD-A263460] p 3246 N93-29818
Tactical satellites p 3284 N93-29893
High reliability, maintenance-free INS battery development
[AD-A264521] p 3412 N93-30406
Conspicuity of aids to navigation. Part 1: Temporal patterns for flashing lights
[AD-A264626] p 3499 N93-30426
Design and implementation of a Global Positioning System (GPS) supported area navigation system with electronic aircraft
[ILR-MITT-275(1992)] p 3246 N93-30671

NAVIGATION INSTRUMENTS
Design and implementation of a Global Positioning System (GPS) supported area navigation system with electronic aircraft
[ILR-MITT-275(1992)] p 3246 N93-30671

NAVIGATION SATELLITES
Measurements of magnetic fields produced by a 30 kWe class Arcjet Power Conditioning Unit
[AD-A262786] p 3287 N93-28658
System analysis for a kinematic positioning system based on the global positioning system
[AD-A262830] p 3245 N93-29468
System of navigation by satellites with European coverage p 3284 N93-29897
Tactical satellites for air command and control p 3284 N93-29898

NAVY
Independent research and independent exploratory development programs
[AD-A264735] p 3544 N93-30556
Pattern measurements of US Navy ELF antennas p 3399 N93-30752

NEAR FIELDS
Comparative study of undersea fields produced by various dipoles p 3397 N93-30740

NEAR INFRARED RADIATION
Near-infrared line imaging of NGC 6240: Global shock and nuclear starburst
[MPE-PREPRINT-226] p 3631 N93-30641

NEEL TEMPERATURE
Phase separation, antiferromagnetism, and superconductivity in superconducting-superoxygenated La(2-x)Sr(x)CuO(4+(delta))
[DE93-009852] p 3598 N93-30517

NEGATIVE IONS
The production and destruction of negative ions
[DE93-010527] p 3564 N93-28665
Measurement of work function of a plasma grid in a cesium seeded negative ion source
[DE93-764153] p 3589 N93-30190

NEODYMIUM LASERS
Design of the Nova Upgrade laser system for ignition fusion experiments
[DE93-009077] p 3436 N93-29097
Method of emitting on a specific wavelength fraunhofer line using a neodymium doped laser transmitter
[AD-D015710] p 3437 N93-29276
ND laser with co-doped ion(s) pumped by visible laser diodes
[AD-D015711] p 3437 N93-29277
Simulation of transient radiation effects on semiconductor devices using a pulsed Q-switched Nd:YAG laser p 3357 N93-30230

NEON
Measurement of 1s2s(sup 3)S(sub 1)-1s2p(sup 3)P(sub 2,0) intervals in helium-like neon
[DE93-009243] p 3563 N93-28521
Polarization dependence of the ionization of helium and neon by 120 femtosecond pulses at 614 nm
[DE93-010514] p 3564 N93-28762

NEPHANALYSIS
Cloudiest year study: An analysis of the 3DNEPH and RTNEPH databases
[AD-A263409] p 3483 N93-29967

NERVES
Biophysical and biochemical mechanisms in synaptic transmitter release
[AD-A264829] p 3496 N93-30613
An assessment of peripheral nerve damage in the rat following non-freezing cold exposure: An electrophysiological and histopathological examination
[AD-A264293] p 3492 N93-30818
Hydrogen-rated system for in vitro studies at pressure: Operating procedures and emergency procedures
[AD-A264179] p 3497 N93-30882

NERVOUS SYSTEM
Neural mechanisms of attention
[AD-A264345] p 3544 N93-30165
Multiple neuron recording in the hippocampus of freely moving animals
[AD-A264807] p 3492 N93-30594
Biophysical and biochemical mechanisms in synaptic transmitter release
[AD-A264829] p 3496 N93-30613

NETHERLANDS
Remote sensing in Czechoslovakia and Hungary: An analysis of the possible co-operation of The Netherlands with Czechoslovakia and Hungary in the field of remote sensing
[BCRS-92-12] p 3461 N93-29466
Land use database for the Netherlands using LANDSAT Thematic Mapper pictures
[BCRS-91-32] p 3463 N93-30839

NETWORK ANALYSIS
Performance measurement systems: A best practices study
[AD-A262180] p 3506 N93-29444
FDDI installation and performance analysis
[AD-A263263] p 3529 N93-29497
Maximum and minimum return losses from a passive two-port network terminated with a mismatched load p 3385 N93-29594
NetStat: A probabilistic network connectivity analysis tool
[AD-A262838] p 3529 N93-29647
Efficient algorithms for the evaluation of planar network reliability
[AD-A263602] p 3531 N93-29916
A multilevel approach to minimum cost network flows
[AD-A264008] p 3550 N93-29978
Analysis of visual loss from retinal lesions
[AD-A264692] p 3496 N93-30494
Memory driven feature-based design
[AD-A264697] p 3534 N93-30495

NETWORK SYNTHESIS
Memory driven feature-based design
[AD-A264697] p 3534 N93-30495

NEURAL NETS
Artificial intelligence methodologies in flight related differential game, control and optimization problems
[AD-A262405] p 3541 N93-28498
Soft computing in design and manufacturing of advanced materials
[NASA-TM-106032] p 3295 N93-28624
Digital image compression using artificial neural networks p 3624 N93-28811
Using a neural network to estimate solvent consumption
[PB93-173110] p 3467 N93-28873
Neural network simulations on massively parallel computers: Applications in chemical physics
[DE93-006739] p 3538 N93-28894
Neural network technologies
[AD-A262576] p 3541 N93-28987
Spurious symptom reduction in fault monitoring
[NASA-CR-191453] p 3542 N93-29192
Multi-channel holographic birfurcative neural network system for real-time adaptive EOS data analysis p 3614 N93-29231
Cognitive and Neural Sciences Division 1992 programs
[AD-A263400] p 3654 N93-29258
The parallel implementation of a backpropagation neural network and its applicability to SPECT image reconstruction
[DE93-010304] p 3567 N93-29416
A neuro-fuzzy architecture for real-time applications p 3511 N93-29529
Learning characteristics of a space-time neural network as a tether skiprope observer p 3512 N93-29534
Clustering of tethered satellite system simulation data by an adaptive neuro-fuzzy algorithm p 3512 N93-29535
Character recognition using a neural network model with fuzzy representation p 3512 N93-29536
Comparison of crisp and fuzzy character networks in handwritten word recognition p 3514 N93-29545
Fuzzy neural network methodology applied to medical diagnosis p 3498 N93-29546
North American Fuzzy Logic Processing Society (NAFIPS 1992), volume 2
[NASA-CP-10112-VOL-2] p 3515 N93-29556
Adding dynamic rules to self-organizing fuzzy systems p 3515 N93-29557
A neural fuzzy controller learning by fuzzy error propagation p 3516 N93-29560
Incorporation of varying types of temporal data in a neural network p 3518 N93-29575
Fuzzy operators and cyclic behavior in formal neuronal networks p 3519 N93-29576
Neural networks: A simulation technique under uncertainty conditions p 3519 N93-29577
Incomplete fuzzy data processing systems using artificial neural network p 3519 N93-29578
Stochastic architecture for Hopfield neural nets p 3519 N93-29579
Hierarchical model of matching p 3519 N93-29580
A conjugate gradients/trust regions algorithms for training multilayer perceptrons for nonlinear mapping p 3519 N93-29581
An accelerated training method for back propagation networks
[NASA-CASE-MSC-21625-1] p 3498 N93-29610
Neural networks application to divergence-based passive ranging
[NASA-TM-103981] p 3245 N93-29653
Communications neural net processors
[AD-A263330] p 3542 N93-29763
Development of neural network architectures for self-organizing pattern recognition and robotics
[AD-A264831] p 3543 N93-29791
Feature based neural network acoustic transient signal classification
[AD-A263437] p 3562 N93-29816
Computation and generalization in neural networks
[AD-A263752] p 3549 N93-29871
Effect of design selection on response surface performance
[NASA-CR-4520] p 3249 N93-29885
A neural network based approach for machine fault diagnosis
[VTT-TIED-1274] p 3543 N93-29998
Computing with neural maps: Application to perceptual and cognitive function
[AD-A264056] p 3499 N93-30033
Neural mechanisms of attention
[AD-A264345] p 3544 N93-30165
Neural network cloud classification research
[AD-A264628] p 3484 N93-30176
Canadian Conference on Electrical and Computer Engineering, volumes 1 and 2
[ISBN-0-9694170-1-2] p 3354 N93-30215
Improvement of the NRC automatic speech recognition system p 3355 N93-30221
Analog CMOS circuits for neural networks p 3355 N93-30223
A motion detector based on a neural network p 3356 N93-30224
An artificial neural network model for periodic trajectory generation p 3356 N93-30225
Parameter identification of time-varying systems using neural networks p 3356 N93-30226
An architecture for an analog VLSI neural network for early computer vision processing p 3359 N93-30244
An adaptive algorithm for linear associative memory problem p 3360 N93-30255
Cloud classification from satellite imagery using neural computing p 3367 N93-30297
Image enhancement using an analog device neural network p 3376 N93-30346
A testbed for autonomous reflexive grasping
[AD-A264557] p 3446 N93-30384
Drive-reinforcement learning system applications
[AD-A264514] p 3446 N93-30404
Analysis of visual loss from retinal lesions
[AD-A264692] p 3496 N93-30494
Memory driven feature-based design
[AD-A264697] p 3534 N93-30495
Independent research and independent exploratory development programs
[AD-A264735] p 3544 N93-30556
The 1991 neural information processing systems: Natural and synthetic
[AD-A264754] p 3623 N93-30559
Adaptive networks for sequential decision problems
[AD-A264756] p 3534 N93-30561
Evolving neural network architecture
[AD-A264802] p 3544 N93-30592
Principal components of natural images: An analytical solution
[AD-A264800] p 3489 N93-30603
4D interconnect experimental development
[AD-A264298] p 3540 N93-30895

An algorithm for simple and complex feature detection: From retina to primary visual cortex
[AD-A264306] p 3497 N93-30897
Structural design using neural networks
p 3545 N93-31029
On neural networks in identification and control of dynamic systems
[NASA-TM-107702] p 3455 N93-31038

NEURONS
Adding dynamic rules to self-organizing fuzzy systems
p 3515 N93-29557
Parallel processing and learning: Variability and chaos in self-organization of activity in groups of neurons
[AD-A264224] p 3539 N93-30361
Evolving neural network architecture
[AD-A264802] p 3544 N93-30592
Multiple neuron recording in the hippocampus of freely moving animals
[AD-A264807] p 3492 N93-30594

NEUROPHYSIOLOGY
Cognitive and Neural Sciences Division 1992 programs
[AD-A263400] p 3654 N93-29258
Fuzzy operators and cyclic behavior in formal neuronal networks p 3519 N93-29576
The AFOSR Workshop on the Future of EEG and MEG
[AD-A264338] p 3495 N93-30160
Control and circadian behavior by transplanted suprachiasmatic nuclei
[AD-A264553] p 3496 N93-30382
Multiple neuron recording in the hippocampus of freely moving animals
[AD-A264807] p 3492 N93-30594

NEUROTRANSMITTERS
Molecular approach to hypothalamic rhythms
[AD-A264438] p 3496 N93-30421

NEUTRAL BEAMS
NPB cesium space experiment p 3267 N93-28733
Use of particle beams for lunar prospecting
p 3650 N93-28822

NEUTRAL GASES
Effects of neutral gas collisions on the power transmission factor at the divertor sheath
[DE93-009320] p 3588 N93-29334

NEUTRAL PARTICLES
Design of a particle beam satellite system for lunar prospecting p 3434 N93-28768
Effects of neutral gas collisions on the power transmission factor at the divertor sheath
[DE93-009320] p 3588 N93-29334
The Interstellar Gas Experiment: Analysis in progress
p 3639 N93-29380
Electron transport calculations between 1 MeV and 1 eV
[AD-A263412] p 3568 N93-29787

NEUTRINOS
Research in theoretical physics
[DE93-008401] p 3603 N93-28961
Limits on neutrino radiative decay from SN1987A
[NASA-CR-193262] p 3653 N93-29164
Measurement of W-Z interference from neutrino-electron scattering
[DE93-010724] p 3566 N93-29313
Neutrino mass
[DE93-010735] p 3566 N93-29315
A search for radiative neutrino decay from supernovae
[NASA-CR-193118] p 3653 N93-30052
Massive Majorana neutrinos in pre-bounce supernovae
[DE92-642597] p 3572 N93-30931

NEUTRON ACTIVATION ANALYSIS
Instrumental neutron activation analysis developed for silicon integrated circuit technology
[ETN-93-93581] p 3408 N93-29271

NEUTRON COUNTERS
Construction and testing of a neutron and gamma spectrometry system using pulse shape discrimination with an organic scintillator
[AD-A262550] p 3567 N93-29415
Electronics for a neutron detector and a Geiger-Mueller detector for the radiation protection around MEA and AmPS
[DIGEL-1992-6] p 3413 N93-30838

NEUTRON CROSS SECTIONS
Fast neutron cross section measurements
[DE93-009053] p 3563 N93-28546

NEUTRON DIFFRACTION
Neutron scattering studies of the structures and lattice dynamics of the alkali metals
[DE93-008272] p 3593 N93-28956
A possibility to investigate the superconducting gap with the help of neutrons
[DE93-606392] p 3601 N93-30799

NEUTRON FLUX DENSITY
A study on radiation shielding analysis for toroidal field coils of a tokamak-type fusion reactor
[DE93-753398] p 3585 N93-28981

NEUTRON IRRADIATION
Enhancements of the critical currents of YBaCuO single crystals by neutron (n) and proton (p) irradiation
[DE93-007892] p 3592 N93-28661
Irradiation assisted stress corrosion cracking of stainless steel irradiated in FBR
[DE93-764495] p 3326 N93-30191

NEUTRON SCATTERING
Neutron scattering studies of the structures and lattice dynamics of the alkali metals
[DE93-008272] p 3593 N93-28956
A possibility to investigate the superconducting gap with the help of neutrons
[DE93-606392] p 3601 N93-30799

NEUTRON SPECTRA
Construction and testing of a neutron and gamma spectrometry system using pulse shape discrimination with an organic scintillator
[AD-A262550] p 3567 N93-29415

NEUTRON SPECTROMETERS
Gamma ray/neutron spectrometers for planetary elemental mapping p 3647 N93-28807
Construction and testing of a neutron and gamma spectrometry system using pulse shape discrimination with an organic scintillator
[AD-A262550] p 3567 N93-29415

NEUTRON STARS
GRO: Red-shifted electron-positron annihilation gamma-rays from radiopulsars
[NASA-CR-193243] p 3635 N93-30053

NEUTRONS
Measurements of breakaway reaction between beryllium and water vapor for ITER blanket design
[DE93-753270] p 3584 N93-28535
Neutron radiation induced degradation of diode characteristics
[AD-A263277] p 3405 N93-28563
Comparison of analytical transport and stochastic solutions for neutron slowing down in an infinite medium
[DE93-010799] p 3565 N93-28833
Spin dependent phenomena in medium energy physics
[DE93-010972] p 3565 N93-28849
Coherent and semi-coherent neutron transfer reactions
[DE93-008336] p 3565 N93-28959
Construction and testing of a neutron and gamma spectrometry system using pulse shape discrimination with an organic scintillator
[AD-A262550] p 3567 N93-29415
A possibility to investigate the superconducting gap with the help of neutrons
[DE93-606392] p 3601 N93-30799
Development of a PC code package for the analysis of research and power reactors
[DE92-638517] p 3536 N93-31001

NEW ENGLAND (US)
Rhode Island hurricanes and tropical storms: A fifty-six year summary, 1936-1991
[PB93-162006] p 3481 N93-29198

NICKEL ALLOYS
International Conference on Martensitic Transformations (ICOMAT 92)
[AD-A262739] p 3321 N93-28591
Effects of internal helium on mechanical properties of Nitronic (tm) 40 stainless steel
[DE93-009902] p 3324 N93-29265
Platinum-modified diffusion aluminide coatings on nickel-base superalloys
[AD-A263597] p 3325 N93-29981
Order-disorder transformations in Ni-Al alloys
[DE93-009293] p 3326 N93-30389
Examination of formability to seamless tubes on Ni-Cr-W superalloy
[DE93-764158] p 3326 N93-30396
Development of Ni-Cr-W superalloys for high temperature components in high temperature gas-cooled reactors, part 2
[DE93-764469] p 3326 N93-30399
Reactive sintering of Ni3Al intermetallic alloys under compressive stress
[DE93-009729] p 3327 N93-30652
Oxidation and hot corrosion of superalloys Rene 100 and X-40 at temperatures of 1475 F to 2000 F
[AD-A263747] p 3327 N93-30812

NICKEL CADMIUM BATTERIES
Battery testing at Argonne National Laboratory
[DE93-009204] p 3407 N93-29036
High reliability, maintenance-free INS battery development
[AD-A264521] p 3412 N93-30406

NICKEL HYDROGEN BATTERIES
Development of nickel/metal hydride secondary battery
[DE93-781330] p 3406 N93-28669

NICKEL IRON BATTERIES
Battery testing at Argonne National Laboratory
[DE93-009204] p 3407 N93-29036

NICKEL ISOTOPES
Research programs from the University of South Carolina on high energy physics
[DE93-007829] p 3574 N93-28969

NICKEL OXIDES
Effect of zinc and iron ions on the electrochemistry of nickel oxide electrode: Slow cyclic voltammetry
[AD-A263098] p 3311 N93-29133

NICKEL PLATE
Development of nickel/metal hydride secondary battery
[DE93-781330] p 3406 N93-28669

NICKEL ZINC BATTERIES
Battery testing at Argonne National Laboratory
[DE93-009204] p 3407 N93-29036

NIGHT VISION
Evaluation of test methods and requirements for respiratory protection systems 21
[AD-A262466] p 3501 N93-28757
Head-steered sensor flight test results and implications p 3502 N93-28859
System automation and pilot-vehicle-interface for unconstrained low-altitude night attack
p 3503 N93-28867
Design considerations for a night, air-to-surface attack capability on a dual role fighter p 3251 N93-28871
CATS EYES adjustment procedures
[AD-A264069] p 3508 N93-29924
Studies of the effect of image degradation and recombination on visual perception
[AD-A264332] p 3580 N93-30368
The effects of superimposing symbology on a simulated night vision goggle display
[AD-A263458] p 3508 N93-30590

NIOBIUM
Measurement of magnetic field penetration depth in niobium polycrystalline films by polarized neutron reflection method
[DE93-606390] p 3600 N93-30771

NITRAMINE PROPELLANTS
Thermal oxidation of HCN by NO2 in shock waves
p 3318 N93-30064
Thermal decomposition of nitramines
p 3318 N93-30065
Homogeneous gas phase kinetic model with gradient sensitivity analysis for high temperature particulate boron combustion in fluorine enriched environments
p 3319 N93-30090
Condensed phase diagnostics of nitramine propellant combustion p 3320 N93-30102

NITRATION
Selective nitrations. Volume 2: The laser-induced nitration of three cycloalkanes
[AD-A263250] p 3438 N93-29800

NITRIC ACID
Acid solution absorption of extruded polyethylene foam
[DE93-011701] p 3330 N93-28839

NITRIC OXIDE
Analysis of protocol gases: An on-going quality assurance audit
[PB93-168839] p 3311 N93-29204
Kinetics of nitric oxide formation behind 3 to 4 KM/S shock waves
[AD-A263653] p 3312 N93-29389
Rate constant determinations of reactions H + HNO from ab initio reaction path calculations
p 3319 N93-30099

NITRIDES
A study of the chemical mechanism in lubrication
[DE93-012230] p 3330 N93-28650

NITRIDING
Design of interfaces in metal matrix composites
[AD-A262052] p 3296 N93-29001

NITRITES
Technical bases for precipitate hydrolysis process operating parameters, revision 1
[DE93-009894] p 3309 N93-28553

NITROGEN
Preliminary experimental results for a cryogenic brush seal configuration
[NASA-TM-106236] p 3416 N93-28627
Upper ocean model of dissolved atmospheric gases
[DE93-010151] p 3487 N93-29327
Vibrational spectroscopy of shock-compressed fluids
p 3318 N93-30072

NITROGEN COMPOUNDS
Synthesis of cubane based energetic molecules
[AD-A263271] p 3564 N93-28562

Surface chemistry of N2H4 on Si(100)-2x1
[AD-A264819] p 3316 N93-30627
NITROGEN DIOXIDE
NO2 unimolecular decomposition: Step-like variation of k(sub uni)(E) p 3318 N93-30068
NITROGEN OXIDES
Vibrational spectroscopy of shock-compressed fluids
p 3318 N93-30072
NOx chemistry in natural gas flames
[PB93-175263] p 3317 N93-30760
NITROSAMINE
Thermal decomposition of nitramines
p 3318 N93-30065
NOAA SATELLITES
Proceedings of the 8th User Seminar of the German Remote Sensing Data Center of the German Aerospace Establishment (DLR)
[DLR-MITT-92-09] p 3456 N93-28915
Fog studies in the Alpine region with digital NOAA/AVHRR data p 3458 N93-28925
Utilization of NOAA/AVHRR data for energy balance of Lake Constance (Switzerland) p 3458 N93-28926
Derivation of conductive heat transfer in mountains from AVHRR data p 3458 N93-28927
NOAA satellite programs and technology requirements
p 3627 N93-30710
NOISE
Study on decreasing torque noise resulting from feedback noise for the modified bang-bang controller
[AD-A263178] p 3407 N93-29010
Characteristics of high-frequency signals, noise, availability, and duration of bandwidths based on ROTHR Amchitka spectrum measurements
[AD-A264480] p 3393 N93-30423
NOISE (SOUND)
Sound attenuation characteristics of the standard DH-132A and SPH-4 helmets worn in combination with standard issue earplugs
[AD-A263011] p 3506 N93-29406
NOISE GENERATORS
Some aspects of the aeroacoustics of high-speed jets
[NASA-CR-191458] p 3418 N93-28975
NOISE MEASUREMENT
Processing, fabrication, and demonstration of HTS integrated microwave circuits
[AD-A263161] p 3406 N93-28940
External acoustical noise measurements for aviation systems
[AD-A263138] p 3562 N93-29480
Application of non-standard signal processing to ELF noise characterization for the TSS1-OESEE programme
p 3397 N93-30743
ELF/VLF radio noise measurements at high latitudes during solar particle events p 3397 N93-30744
NOISE PREDICTION
A long wave TE/TM noise prediction model
p 3397 N93-30742
NOISE PREDICTION (AIRCRAFT)
Computation of far-field helicopter rotor tone noise
[ONERA-P-1990-5] p 3562 N93-30110
NOISE PROPAGATION
Noise transmission properties and control strategies for composite structures p 3301 N93-30436
Strong parallel blade-vortex interaction and noise propagation in helicopter flight p 3563 N93-30980
NOISE REDUCTION
Jet mixer noise suppressor using acoustic feedback
[NASA-CASE-LEW-15170-1] p 3561 N93-28953
Gyroscope with excess noise subtraction
[AD-D015698] p 3431 N93-29046
Quiet by design: Numerical acousto-elastic analysis of aircraft structures
[ISBN-90-386-0042-9] p 3248 N93-29268
Noise transmission properties and control strategies for composite structures p 3301 N93-30436
VLF propagation measurements in the Canadian Arctic p 3396 N93-30733
NOISE SPECTRA
Strong parallel blade-vortex interaction and noise propagation in helicopter flight p 3563 N93-30980
NOMOGRAPHS
Analysis of LDEF micrometeoroid/debris data and damage to composite materials p 3309 N93-29366
NONDESTRUCTIVE TESTS
Reliability assessment at airline inspection facilities. Volume 2: Protocol for an eddy current inspection reliability experiment
[DOT/FAA/CT-92/12-VOL-2] p 3449 N93-28685
Use of local x ray computerized tomography for high-resolution, region-of-interest inspection of large ceramic components for engines
[DE93-005564] p 3449 N93-28943
Acousto-Ultrasonic analysis of failure in ceramic matrix composite tensile specimens
[NASA-TM-106219] p 3449 N93-29073
Advanced Construction Technology Center research
[AD-A263654] p 3432 N93-29390
Advanced NDE technology program
[AD-A262008] p 3449 N93-29443
Characterization of ceramic composite materials for gas turbine applications
[DE93-009719] p 3259 N93-30168
Logarithmic time scale in thermographic Non Destructive Evaluation (NDE) of materials p 3359 N93-30246
NONEQUILIBRIUM CONDITIONS
Kinetics and energy transfer in nonequilibrium fluid flows
[AD-A263612] p 3240 N93-29284
NONEQUILIBRIUM FLOW
Inviscid quasi one-dimensional nonequilibrium flow
[FFA-TN-1992-35] p 3418 N93-28993
Kinetics and energy transfer in nonequilibrium fluid flows
[AD-A263612] p 3240 N93-29284
NONFERROUS METALS
JPRS report: Science and technology. Central Eurasia: Materials science
[JPRS-UMS-92-008] p 3322 N93-29012
JPRS report: Science and technology. Central Eurasia: Materials science
[JPRS-UMS-92-007] p 3322 N93-29013
JPRS report: Science and technology. Central Eurasia: Materials science
[JPRS-UMS-92-009] p 3322 N93-29015
JPRS report: Science and technology. Central Eurasia: Materials science
[JPRS-UMS-92-012] p 3296 N93-29016
JPRS report: Science and technology. Central Eurasia: Materials science
[JPRS-UMS-92-013] p 3296 N93-29017
JPRS report: Science and technology. Central Eurasia: Materials science
[JPRS-UMS-92-016] p 3296 N93-29018
JPRS report: Science and technology. Central Eurasia: Materials science
[JPRS-UMS-92-014] p 3322 N93-29019
JPRS report: Science and technology. Central Eurasia: Materials science
[JPRS-UMS-92-015] p 3322 N93-29020
JPRS report: Science and technology. Central Eurasia: Materials science
[JPRS-UMS-93-001] p 3296 N93-29021
NONGRAY GAS
Radiative interactions in molecular gases under local and nonlocal thermodynamic equilibrium conditions
[NASA-CR-193223] p 3604 N93-29168
NONLINEAR EQUATIONS
Index mappings for interactive editing of symbolic matrices
[DE93-009316] p 3549 N93-29060
Finite element approximation of the shallow water equations on the MASPAR
[AD-A264649] p 3489 N93-30525
On the method of determining relations
[DE93-606041] p 3551 N93-30765
On the invariant measure for the nonlinear Schroedinger equation
[DE92-644672] p 3551 N93-30912
A numerical solution of the two-center problem
[DE92-644674] p 3551 N93-30913
A remark on the invariant measure for the nonlinear Schroedinger equation
[DE93-609840] p 3552 N93-30946
The contact mechanical nonlinearities of a mathematical model of a railway wheel rolling over corrugated rail
[ILR-MITT-266(1991)] p 3454 N93-31015
NONLINEAR EVOLUTION EQUATIONS
Computer algebra tools for higher symmetry analysis of nonlinear evolution equations
[DE93-606089] p 3535 N93-30787
NONLINEAR FILTERS
Morphological and order statistic filters: A comparative study p 3375 N93-30345
NONLINEAR OPTICS
Polar order and relaxation of second order nonlinear optical susceptibility in an electric field polarized amorphous polymer
[AD-A262189] p 3329 N93-28489
Every good virtue you ever wanted in a Q-switched solid-state laser and more: Monolithic, diode-pumped, self-Q-switched, highly reproducible, diffraction-limited Nd:YAG laser p 3442 N93-28772
Dipolar orientational relaxation in guest/host amorphous polymer probed by second harmonic generation
[AD-A262006] p 3333 N93-29441
Isothermal annealing and relaxation of the second harmonic generation signal from a nonlinear optical polymer
[AD-A262007] p 3333 N93-29442
Polymers with electrical and nonlinear optical properties
[AD-D015691] p 3333 N93-29457
Investigations of self-pumped phase conjugate laser beams and coherence length
[AD-A263438] p 3438 N93-29789
Nonlinear mode coupling in free electron lasers
[AD-A263999] p 3439 N93-29883
Nonlinear spectroscopy of multicomponent droplets and two- and three-dimensional measurements in flames
[AD-A264341] p 3425 N93-30162
Characterization of slow chromophore reorientation in nonlinear optical polymers by two-dimensional MAS NMR
[AD-A264809] p 3338 N93-30596
Organometallic compounds and polymers with second and third order nonlinear optical properties
[AD-A264774] p 3338 N93-30610
NATO Advanced Research Workshop on Frontiers of Optical Phenomena in Semiconductor Structure of Reduced Dimension
[AD-A264813] p 3581 N93-30666
Physical chemical studies on molecular composite compositions
[AD-A264834] p 3339 N93-30898
NONLINEAR PROGRAMMING
Nonsmooth optimization algorithms, system theory, and software tools
[AD-A264679] p 3534 N93-30549
NONLINEAR SYSTEMS
The investigation of nonlinear effects on quasiparticle transport in condensed matter systems
[DE93-009582] p 3565 N93-28914
Uncertainty reasoning in expert systems
[NASA-CR-193120] p 3548 N93-28973
Thermoviscoplastic analysis of fibrous periodic composites using triangular subvolumes
[NASA-TM-106076] p 3297 N93-29074
Multivariable control of the Space Shuttle Remote Manipulator System using linearization by state feedback
[NASA-CR-188248] p 3443 N93-29080
Some problems in the mechanics of solids with phase mixtures
[AD-A263652] p 3311 N93-29291
Proceedings of the 25th European Conference on the Application of Polar Dielectrics to celebrate the 25th anniversary of the Dielectric Society, incorporating the 1st International Workshop on Integrated Ferroelectrics
[AD-A263427] p 3332 N93-29337
Clustering of tethered satellite system simulation data by an adaptive neuro-fuzzy algorithm
p 3512 N93-29535
Fuzzy coordinator in control problems
p 3515 N93-29552
Non-scalar uncertainty: Uncertainty in dynamic systems p 3517 N93-29565
Comparison between the performance of two classes of fuzzy controllers p 3517 N93-29566
Dynamics and photoexcitation in MX and MXX' chain solids
[AD-A264823] p 3561 N93-29711
Weakly nonlinear dynamics of near-CJ detonation waves
[DE93-007344] p 3424 N93-29836
A diffusion approximation for a network of reservoirs with power law release rule
[AD-A263753] p 3550 N93-29872
Control of nonlinear systems with applications to constrained robots and spacecraft attitude stabilization
p 3279 N93-29989
Static and dynamic large deflection flexural response of graphite-epoxy beams
[NASA-CR-4118] p 3454 N93-30374
The middeck 0-gravity dynamics experiment
[NASA-CR-4500] p 3281 N93-30376
Orbital motion calculation using Lie method in collider nonlinear magnetic field
[DE93-605733] p 3571 N93-30800
Control of nonlinear systems with applications to constrained robots and spacecraft attitude stabilization
p 3544 N93-30893
Nonlinear realisations of omega(1 + infinity)
[DE92-644721] p 3557 N93-30917
On neural networks in identification and control of dynamic systems
[NASA-TM-107702] p 3455 N93-31038
NONLINEARITY
Nonlinear coupling of tearing fluctuations in the Madison Symmetric Torus
[DE93-010131] p 3584 N93-28602
Dynamical analysis of highly excited molecular spectra
[DE93-010771] p 3564 N93-28604
Nonlinear dynamics and plasma transport
[DE93-012238] p 3585 N93-28749

Bifurcations phenomena in a nonlinear oscillator: Approximate analytical studies versus computer simulation results p 3407 N93-29037
Nonlinear analyses of composite aerospace structures in sonic fatigue
[NASA-CR-193124] p 3451 N93-29154
Nonlinear relaxation algorithms for the compressible Navier-Stokes equations in two and three dimensions
p 3421 N93-29177
An investigation of graphite peek composite under compression with a centrally located circular discontinuity
[AD-A262549] p 3298 N93-29414
Electron interactions with non-linear polyatomic molecules and their radicals and ions
[AD-A262279] p 3568 N93-29446
A fuzzy measure approach to motion frame analysis for scene detection p 3511 N93-29525
Non-scalar uncertainty: Uncertainty in dynamic systems p 3517 N93-29565
A conjugate gradients/trust regions algorithms for training multilayer perceptrons for nonlinear mapping
p 3519 N93-29581
Measurements of light scattering by small particles at an angle of zero degrees
[AD-A263856] p 3580 N93-29887
Nonlinear realisations of omega(1 + infinity)
[DE92-644721] p 3557 N93-30917
The geometry of complex space-times with torsion
[DE92-641343] p 3608 N93-31003

NONPARAMETRIC STATISTICS
Empirical quantile function nonparametric integrated analyses
[AD-A263704] p 3554 N93-29385

NONUNIFORMITY
The influence of non-uniform spanwise inlet temperature on turbine rotor heat transfer p 3253 N93-29932

NORMAL DENSITY FUNCTIONS
Modified Anderson-Darling and Cramer-Von Mises goodness-of-fit tests for the normal distribution
[AD-A262554] p 3553 N93-28575
Monte Carlo simulation of magnitude-angle error sources
[AD-A263738] p 3555 N93-29857

NORMS
Balanced approximation can be optimal
[OUEL-1950/92] p 3548 N93-28754

NORTH ATLANTIC TREATY ORGANIZATION (NATO)
T(lc2)acS(lc3)ats for Surveillance Verification and C3I
[AGARD-CP-522] p 3387 N93-29892
Considerations for NATO satellite communications in the post-2000 era p 3388 N93-29899
NATO Advanced Research Workshop on Frontiers of Optical Phenomena in Semiconductor Structure of Reduced Dimension
[AD-A264813] p 3581 N93-30666

NOSE TIPS
Ablation problems using a finite control volume technique
[DE93-009861] p 3549 N93-29187
Numerical computation of inviscid flow around nose tip of Space Shuttle with NND scheme
[AD-A264012] p 3421 N93-29260
The equivalent flat nose diameter of hemispherical nose cylindrical projectiles for impact induced detonation of energetic materials
[AD-A263244] p 3342 N93-29494

NOVA LASER SYSTEM
Design of the Nova Upgrade laser system for ignition fusion experiments
[DE93-009077] p 3436 N93-29097

NOZZLE DESIGN
Altitude compensating ablative stiffening band for rocket motor nozzles
[NASA-CASE-MFS-28728-1] p 3288 N93-28950
Heat transfer and aerodynamics of a 3D design nozzle guide vane tested in the Pyestock Isentropic Light Piston Facility p 3252 N93-29928

NOZZLE FLOW
Inviscid quasi one-dimensional nonequilibrium flow
[FFA-TN-1992-35] p 3418 N93-28993
Effects of flow-path variations on internal reversing flow in a tailpipe offtake configuration for ASTOVL aircraft
[NASA-TM-106149] p 3252 N93-29065

NOZZLE GEOMETRY
Altitude compensating ablative stiffening band for rocket motor nozzles
[NASA-CASE-MFS-28728-1] p 3288 N93-28950

NOZZLE INSERTS
Postflight hardware evaluation 360T025 (RSRM-25, STS-46). Appendix A: Insulation PFORs
[NASA-CR-192563] p 3272 N93-30618

NOZZLES
Thermal effects of a coolant film along the suction side of a high pressure turbine nozzle guide vane
p 3253 N93-29930

NUCLEAR BINDING ENERGY
Algorithm for the solution of the Faddeev equation for a system of three identical spinless particles
[DE92-644678] p 3535 N93-30914

NUCLEAR ELECTRIC POWER GENERATION
Excited states in electronic structure calculations
[DE93-007704] p 3592 N93-28642
Design of the Nova Upgrade laser system for ignition fusion experiments
[DE93-009077] p 3436 N93-29097

NUCLEAR ELECTRIC PROPULSION
NEP space test program objective
p 3265 N93-28724

NUCLEAR EMULSIONS
Fluctuations and intermittency in high energy nucleus-nucleus collisions
[DE93-608481] p 3577 N93-30990

NUCLEAR ENERGY
Nuclear isomers as ultra-high-energy-density materials
[DE93-009520] p 3568 N93-29784

NUCLEAR EXPLOSIONS
Energetic material response to abnormal environments p 3350 N93-30095
Radiated fields from an electromagnetic pulse simulator p 3366 N93-30290
Acoustic-gravity waves from low-altitude localized disturbances
[AD-A264804] p 3479 N93-30593
Modeling regional seismic waves
[AD-A264002] p 3479 N93-30756

NUCLEAR FUEL ELEMENTS
Annual progress report on the NSRR experiments, (21)
[DE93-753190] p 3574 N93-29137

NUCLEAR FUELS
Annual progress report on the NSRR experiments, (21)
[DE93-753190] p 3574 N93-29137

NUCLEAR FUSION
Tests of the particle physics-physical cosmology interface
[DE93-008483] p 3634 N93-28963
Computing for magnetic fusion energy research: An updated vision
[DE93-010394] p 3587 N93-29190

NUCLEAR INTERACTIONS
The APX spectrometer for Martian missions
p 3434 N93-28776
Fluctuations and intermittency in high energy nucleus-nucleus collisions
[DE93-608481] p 3577 N93-30990

NUCLEAR MAGNETIC RESONANCE
Be3(AsO4)2 2H2O: A new berylloarsenate phase containing bridged tetrahedral 3-rings
[AD-A262518] p 3592 N93-28584
Synthesis of new high performance lubricants and solid lubricants
[DE93-012237] p 3330 N93-28748
High pressure studies of hydrated nafion membranes: Dielectric relaxation and deuteron NMR
[AD-A263511] p 3332 N93-29342
NMR studies of molecules in liquid crystals and graphite
[DE93-010423] p 3569 N93-29805
Methylhydridopolysilazane and its pyrolytic conversion to Si3N4/SiC ceramics
[AD-A264150] p 3336 N93-30170
1,2-Dimethyl-1,2-Disila-Closo-Dodecaborane(12), A silicon analog of an ortho-carborane: Synthesis; x ray crystal structure; NMR, vibrational and photoelectron spectra; bonding
[AD-A264709] p 3599 N93-30568
Characterization of slow chromophore reorientation in nonlinear optical polymers by two-dimensional MAS NMR
[AD-A264809] p 3338 N93-30596

NUCLEAR MEDICINE
Proceedings of a Workshop on Molecular Nuclear Medicine
[DE93-010828] p 3493 N93-28835

NUCLEAR PHYSICS
Research in theoretical nuclear physics
[DE93-008380] p 3565 N93-28960
Research and education by SF cyclotron facility
[DE93-753135] p 3576 N93-30002
Massive Majorana neutrinos in pre-bounce supernovae
[DE92-642597] p 3572 N93-30931
Fluctuations and intermittency in high energy nucleus-nucleus collisions
[DE93-608481] p 3577 N93-30990

NUCLEAR POWER PLANTS
Analysis of TOPAZ 2 and SPACE-R space nuclear power plants using a modified thermionic model
[AD-A262612] p 3286 N93-28474
Overview of piping issues and trends
[DE93-006628] p 3354 N93-28893
Statement on the United Nations Conference on Environment and Development
[DE93-601878] p 3475 N93-30996

NUCLEAR POWER REACTORS
SIRIUS-P: An inertially confined direct drive laser fusion power reactor
[DE93-012433] p 3439 N93-30186

NUCLEAR RADIATION
Neutron radiation induced degradation of diode characteristics
[AD-A263277] p 3405 N93-28563

NUCLEAR REACTIONS
Fast neutron cross section measurements
[DE93-009053] p 3563 N93-28546
Spin dependent phenomena in medium energy physics
[DE93-010972] p 3565 N93-28849
Coherent and semi-coherent neutron transfer reactions
[DE93-008336] p 3565 N93-28959
Research in theoretical nuclear physics
[DE93-008380] p 3565 N93-28960
Nuclear structure research at the Triangle Universities Nuclear Laboratory
[DE93-009756] p 3566 N93-29184
High-dose implantations of Al into Si(111) and Si(100)
[DE93-009552] p 3594 N93-29301
Charged particle activation studies on the surface of LDEF spacecraft p 3572 N93-29630
Reaction mechanism studies of heavy ion induced nuclear reactions
[DE93-010496] p 3569 N93-29807
Studies of fluctuation processes in nuclear collisions
[DE93-011263] p 3576 N93-30054
Fluctuations and intermittency in high energy nucleus-nucleus collisions
[DE93-608481] p 3577 N93-30990

NUCLEAR REACTORS
Overview of piping issues and trends
[DE93-006628] p 3354 N93-28893
Experiment and analysis on elastic deformation properties of graphite and carbon materials for HTTR core components
[DE93-753271] p 3299 N93-30004

NUCLEAR RESEARCH
The prehistory of ESRO, 1959 - 1960
[ESA-HSR-1] p 3660 N93-29500
Development of a PC code package for the analysis of research and power reactors
[DE92-638517] p 3536 N93-31001

NUCLEAR RESEARCH AND TEST REACTORS
Development of a PC code package for the analysis of research and power reactors
[DE92-638517] p 3536 N93-31001

NUCLEAR STRUCTURE
Nuclear structure research at the Triangle Universities Nuclear Laboratory
[DE93-009756] p 3566 N93-29184
Theoretical studies in nuclear structure
[DE93-012290] p 3570 N93-30505

NUCLEAR WARFARE
Tethered aerostat VLF/LF transmitter system design considerations p 3399 N93-30753

NUCLEAR WEAPONS
Foreign technology assessment: Environmental evaluation of a radiation-hard oscillator/divider
[DE93-011481] p 3412 N93-30127
Effects of device scaling and geometry on MOS radiation hardness assurance
[DE93-009832] p 3413 N93-30516

NUCLEATE BOILING
Tank Pressure Control Experiment/Thermal Phenomena (TPCE/TP) p 3264 N93-28713
Horizontal nucleate flow boiling heat transfer coefficient measurements and visual observations for R12, R134a, and R134a/ester lubricant mixtures
[PB93-178598] p 3475 N93-30887

NUCLEATION
A one-dimensional continuum model for shape-memory alloys
[AD-A262505] p 3321 N93-28656
Pulse mitigation and heat transfer enhancement techniques. Volume 1: Spray cooling
[AD-A263495] p 3423 N93-29352
Diamond nucleation of surfaces using carbon clusters
[AD-A264634] p 3599 N93-30548

NUCLEI (NUCLEAR PHYSICS)
Meson-meson interactions and phi-enhancement in nucleus collisions
[DE93-010725] p 3565 N93-28831
Nuclear structure research at the Triangle Universities Nuclear Laboratory
[DE93-009756] p 3566 N93-29184

NUCLEON-NUCLEON INTERACTIONS
Nuclear structure research at the Triangle Universities Nuclear Laboratory
[DE93-009756] p 3566 N93-29184
NUCLEONS
Towards the results of global analysis of data on nucleon electromagnetic structure
[DE93-606125] p 3571 N93-30792
Fluctuations and intermittency in high energy nucleus-nucleus collisions
[DE93-608481] p 3577 N93-30990
NUMERICAL ANALYSIS
Godunov-type schemes applied to detonation flows
[NASA-CR-191447] p 3509 N93-28841
JPRS report: Science and technology. Central Eurasia: Physics and mathematics
[JPRS-UPM-93-002] p 3560 N93-29022
Quiet by design: Numerical acousto-elastic analysis of aircraft structures
[ISBN-90-386-0042-9] p 3248 N93-29268
ICASE
[NASA-CR-193257] p 3520 N93-29864
Continuation of: Applications of gauge theories to enhance numerical solutions of mixed potential integral equations
[AD-A263763] p 3550 N93-29876
Study of effects of small perturbations on chaotic systems
[DE93-009762] p 3557 N93-30048
Numerical modeling of multidimensional flames with application to energetic materials p 3319 N93-30079
NUMERICAL CONTROL
Computerized atmospheric trace contaminant control simulation for manned spacecraft
[NASA-TM-108409] p 3505 N93-28977
Experimental study of location and identification of ferrous spheroids using a smart total field magnetometer
[AD-A263661] p 3324 N93-29391
Valve malfunction detection apparatus
[NASA-CASE-MFS-29904-1] p 3432 N93-29503
Modification of flux profiles using a faceted concentrator
[DE93-000087] p 3464 N93-29925
A parallel processing system for intensive I/O
p 3362 N93-30262
A transputer based parallel processing architecture for robotics applications p 3362 N93-30263
Laser based 3D volumetric display system
[AD-A264825] p 3441 N93-30599
Computer control of pulsed tunable dye lasers
[DE93-605896] p 3441 N93-30801
NUMERICAL WEATHER FORECASTING
Exploitation of parallelism in climate models
[DE93-011259] p 3470 N93-29318
The sensitivity of ageostrophic circulations to model resolution: A case study using NGM forecasts of ERICA IOP-4
[AD-A262011] p 3482 N93-29393
The basics of weather models
[AD-A263386] p 3483 N93-29850
NUSSELT NUMBER
Transient thermal behaviour of a compressor rotor with axial cooling air flow and co-rotating or contra-rotating shaft p 3255 N93-29946
NUTATION
Investigation of Mars rotational dynamics using Earth-based radio tracking of Mars landers
p 3642 N93-28777
NYLON (TRADEMARK)
Evaluation of personal cooling systems in conjunction with explosive ordnance disposal suits
[AD-A262862] p 3506 N93-29471

O

OBJECT-ORIENTED PROGRAMMING
DOKMA: A document oriented communication model for medical applications as a basis of a role system in the medical field
[ETN-93-93799] p 3492 N93-28469
Dynamic object oriented interaction and its implementation in the framework in an interface management system
[ETN-93-93795] p 3523 N93-28526
Toward reusable graphics components in Ada
[AD-A262568] p 3524 N93-28577
A distributed object-oriented database application design
[AD-A262591] p 3612 N93-28846
Transforming AdaPT to Ada9x
[NASA-CR-193117] p 3526 N93-29026
An architecture for robotic system integration
[DE93-010829] p 3444 N93-29316
OSI transaction processing standard: An introduction and outlines of implementation
[VTT-TIED-1250] p 3532 N93-29997
MLog: A language for prototyping concurrent systems
p 3368 N93-30301
OBSTACLE AVOIDANCE
A study of the effects of lens focal length on remote driver performance
[AD-A263191] p 3505 N93-28941
Research on reconfigurable and reliable manipulators
[DE93-010244] p 3444 N93-29330
OCEAN BOTTOM
Analyses of data from fine structure and circulation studies in the Gulf of California
[AD-A262910] p 3486 N93-28885
Near real-time GIS in deep-ocean exploration
[AD-A262073] p 3487 N93-29003
Ocean waves in SAMSON/SWADE
[AD-A263681] p 3487 N93-29295
ARI: Internal gravity waves at abrupt topography
[AD-A263795] p 3477 N93-29879
OCEAN COLOR SCANNER
SeaWiFS technical report series. Volume 2: Analysis of orbit selection for SeaWiFS: Ascending versus descending node
[NASA-TM-104566-VOL-2] p 3486 N93-28497
SeaWiFS technical report series. Volume 6: SeaWiFS technical report series cumulative index: Volumes 1-5
[NASA-TM-104566-VOL-6] p 3486 N93-28500
OCEAN CURRENTS
Steady-state and transient modeling of tracer and nutrient distributions in the global ocean
[DE93-011043] p 3486 N93-28670
Analyses of data from fine structure and circulation studies in the Gulf of California
[AD-A262910] p 3486 N93-28885
Optical measurements of ripples using a scanning laser slope gauge. Part 1: Instrumentation and preliminary results
[AD-A261939] p 3486 N93-28996
Using C-vector method to derive the three-dimensional circulation pattern near the East Greenland Polar Front
[AD-A261979] p 3487 N93-29437
A water mass analysis of the 1991-1992 El Nino signal in the Farallon Islands region
[AD-A263490] p 3488 N93-29819
Dynamics of small-scale oceanic motions
[AD-A263582] p 3488 N93-29914
Measurements of ocean currents across the continental margin off Point Sur, California, during March 1989
[AD-A264853] p 3489 N93-30178
Hydrographic observations in the western tropical and subtropical north Atlantic Ocean: Atlantic Climate Change Program (ACCP) and Western Tropical Atlantic Experiment (WESTRAX) during 1990
[PB93-184760] p 3489 N93-30827
OCEAN DATA ACQUISITIONS SYSTEMS
Ice-ocean four dimensional structure and dynamics
[AD-A264850] p 3490 N93-30906
ERS-1 directional wave spectra validation with the airborne SAR PHARS
[BCRS-92-18] p 3463 N93-31010
OCEAN DYNAMICS
Dynamics of small-scale oceanic motions
[AD-A263582] p 3488 N93-29914
Analysis of a simulation of the seasonal cycle in the tropical Pacific Ocean in an eddy-resolving global ocean model
[AD-A264007] p 3488 N93-29977
Shear, strain, and thermohaline vertical fine structure in the upper ocean p 3488 N93-30046
Ice-ocean four dimensional structure and dynamics
[AD-A264850] p 3490 N93-30906
OCEAN MODELS
Steady-state and transient modeling of tracer and nutrient distributions in the global ocean
[DE93-011043] p 3486 N93-28670
Upper ocean model of dissolved atmospheric gases
[DE93-010151] p 3487 N93-29327
Dynamics of small-scale oceanic motions
[AD-A263582] p 3488 N93-29914
Analysis of a simulation of the seasonal cycle in the tropical Pacific Ocean in an eddy-resolving global ocean model
[AD-A264007] p 3488 N93-29977
The IUTAM Symposium on Breaking Waves
[AD-A264196] p 3489 N93-30143
Oceanographic data processing program
[AD-A264801] p 3544 N93-30591
OCEAN SURFACE
Processing of altimeter data by the German ERS-1 Processing and Archiving Facility (D-PAF)
p 3457 N93-28917
Optical measurements of ripples using a scanning laser slope gauge. Part 1: Instrumentation and preliminary results
[AD-A261939] p 3486 N93-28996
Ocean waves in SAMSON/SWADE
[AD-A263681] p 3487 N93-29295
Optical slope/height measurements of small scale waves within the SAXON-FPN experiment
[AD-A262572] p 3487 N93-29422
Convective and stratiform rain: Multichannel microwave sensing over oceans
[NASA-TM-104586] p 3482 N93-29448
The IUTAM Symposium on Breaking Waves
[AD-A264196] p 3489 N93-30143
Uplink laser propagation measurements through the sea surface, haze and clouds
[AD-A264687] p 3440 N93-30553
OCEAN TEMPERATURE
Reception at Ascension Island, South Atlantic, of the transmissions from the Heard Island feasibility test
[PB93-176261] p 3394 N93-30662
Hydrographic observations in the western tropical and subtropical north Atlantic Ocean: Atlantic Climate Change Program (ACCP) and Western Tropical Atlantic Experiment (WESTRAX) during 1990
[PB93-184760] p 3489 N93-30827
OCEANOGRAPHIC PARAMETERS
Measurements of ocean currents across the continental margin off Point Sur, California, during March 1989
[AD-A264853] p 3489 N93-30178
A calibration procedure for the SBE 19 Conductivity, Temperature, and Depth (CTD) profiler
[AD-A264435] p 3489 N93-30420
OCEANOGRAPHY
Processing of altimeter data by the German ERS-1 Processing and Archiving Facility (D-PAF)
p 3457 N93-28917
Near real-time GIS in deep-ocean exploration
[AD-A262073] p 3487 N93-29003
JPRS report: Science and technology. Central Eurasia: Earth science
[JPRS-UES-93-003] p 3456 N93-29089
National collaboratories: Applying information technology for scientific research
[LC-93-83795] p 3612 N93-29129
Using C-vector method to derive the three-dimensional circulation pattern near the East Greenland Polar Front
[AD-A261979] p 3487 N93-29437
A water mass analysis of the 1991-1992 El Nino signal in the Farallon Islands region
[AD-A263490] p 3488 N93-29819
Analysis of a simulation of the seasonal cycle in the tropical Pacific Ocean in an eddy-resolving global ocean model
[AD-A264007] p 3488 N93-29977
Oceanographic data processing program
[AD-A264801] p 3544 N93-30591
Oceanographic research towers in european waters
[AD-A264795] p 3489 N93-30612
Standard and reference materials for marine science, third edition
[PB93-185684] p 3489 N93-30830
IOC-UNEP review meeting on oceanographic processes of transport and distribution of pollutants in the sea
[DE93-605070] p 3490 N93-31019
OCEANS
Ocean Margins Program
[DE93-008937] p 3470 N93-29262
Tidal and lunar data for Point Mugu, San Nicolas island, and the Barking Sanda area during 1993
[AD-A262725] p 3477 N93-29401
Clouds and radiation: A primier
[AD-A263136] p 3482 N93-29479
Charting the remote southern oceans with geosat altimetry
[AD-A263452] p 3461 N93-29817
OCTETS
Borel sum rules for octet baryons in nuclear medium
[DE93-753245] p 3604 N93-29242
OFF-ON CONTROL
Study on decreasing torque noise resulting from feedback noise for the modified bang-bang controller
[AD-A263178] p 3407 N93-29010
OFFICE AUTOMATION
High-performance mass storage system for workstations p 3618 N93-30457
OFFSHORE ENERGY SOURCES
Fugitive hydrocarbon emissions from Pacific OCS facilities. Volume 2: Executive summary and user's guide
[PB93-173805-VOL-2] p 3471 N93-29861
OFFSHORE PLATFORMS
Fugitive hydrocarbon emissions from Pacific OCS facilities, volume 1
[PB93-173797] p 3468 N93-28899
Ice-ocean four dimensional structure and dynamics
[AD-A264850] p 3490 N93-30906

OHMIC DISSIPATION
Optimization of HPM device parameters for maximum air transmission
[DE93-007332] p 3386 N93-29765
OIL EXPLORATION
Fugitive hydrocarbon emissions from Pacific OCS facilities. Volume 2: Executive summary and user's guide
[PB93-173805-VOL-2] p 3471 N93-29861
OIL RECOVERY
Study on technology for effective utilization of carbon dioxide in view of global environment
[DE93-781440] p 3468 N93-28883
Fugitive hydrocarbon emissions from Pacific OCS facilities, volume 1
[PB93-173797] p 3468 N93-28899
OIL SLICKS
Atmospheric and Geophysical Sciences Division: G-Division did you know?
[DE93-007412] p 3469 N93-28967
OILS
Atmospheric and Geophysical Sciences Division: G-Division did you know?
[DE93-007412] p 3469 N93-28967
OLIGOMERS
Synthesis of oligoimides and oligoimide anion radicals
[AD-A263129] p 3290 N93-29474
Preliminary properties of a resin from ethynyl terminated materials p 3303 N93-30842
OLIVINE
Frequency dependent electrical properties of minerals and partial-melts
[DE93-009254] p 3410 N93-29793
OMEGA NAVIGATION SYSTEM
Investigations of equatorial ionosphere nighttime mode conversion at VLF p 3396 N93-30735
ON-LINE SYSTEMS
Basic OSF/Motif programming and applications
[DE93-010800] p 3524 N93-28834
NSSDC data listing
[NASA-TM-108264] p 3612 N93-29167
A composite self tuning strategy for fuzzy control of dynamic systems p 3511 N93-29530
Designing a fuzzy scheduler for hard real-time systems p 3512 N93-29537
Some problems with the design of self-learning management systems p 3516 N93-29559
EnviroNET: On-line information for LDEF
p 3624 N93-29625
The planning coordinator: A design architecture for autonomous error recovery and on-line planning of intelligent tasks
[NASA-CR-193250] p 3543 N93-30039
Graphical programming: On-line robot simulation for telerobotic control
[DE93-009796] p 3447 N93-30654
ONBOARD DATA PROCESSING
Onboard signal processing: Wave of the future for planetary radio science? p 3646 N93-28801
Systematic processing of Clementine data for scientific analyses p 3624 N93-28803
On-board B-ISDN fast packet switching architectures. Phase 2: Development. Proof-of-concept architecture definition report
[NASA-CR-191151] p 3273 N93-29884
Synchronization techniques for medium data rate EHF MILSATCOM systems p 3389 N93-29901
SAW technology for on-board processing in military satellite communications p 3362 N93-30265
Airborne data acquisition using a front-end processor architecture p 3373 N93-30329
OPEN CLUSTERS
Young open clusters as probes of the star formation process p 3635 N93-30377
OPENINGS
A Rayleigh-Ritz analysis methodology for cutouts in composite structures p 3307 N93-30869
OPERATING COSTS
STRV1-b flight experiment p 3265 N93-28723
OPERATING SYSTEMS (COMPUTERS)
A temporal proof methodology for reactive systems
[NASA-CR-193145] p 3528 N93-29469
Nonresident and endangered variables: The effects of code generation optimizations on symbolic debugging
[AD-A263149] p 3529 N93-29486
A redesigned Isis and Meta system under Mach
[AD-A263576] p 3531 N93-29976
Using the Mach communication primitives in X11
[AD-A264049] p 3533 N93-30125
OPERATING TEMPERATURE
Ambient-atmosphere compatible superconducting fullerenes
[AD-A262025] p 3595 N93-29397
OPERATIONAL PROBLEMS
Galileo post-Gaspra cruise and Earth-2 encounter
p 3385 N93-29597
OPERATIONS RESEARCH
Assessment of Columbus payload operations capabilities by scheduling with the MARS system
[ESA-STR-235] p 3281 N93-30106
Placement of cells: Theory and solution of a quadratic 0/1 optimization problem
[ETN-93-94182] p 3413 N93-30616
OPERATOR PERFORMANCE
Engineman stress and fatigue: Pilot tests
[PB93-175008] p 3507 N93-29675
The air traffic controller's mental model and it's implications for equipment design and trainee selection
p 3372 N93-30322
OPERATORS (MATHEMATICS)
Topology of hybrid objects
[ETN-93-93594] p 3546 N93-28466
Algorithm for the solution of the Faddeev equation for a system of three identical spinless particles
[DE92-644678] p 3535 N93-30914
Nth roots of normal contractions
[DE92-644725] p 3557 N93-30985
OPTICAL COMMUNICATION
Fundamental study of the signal processing by optics
[DE93-776265] p 3577 N93-28982
Fiber grating-based sensing system with interferometric wavelength-shift detection
[AD-D015697] p 3577 N93-29038
Optical coherent phase diversity systems
[ISBN-90-9004897-9] p 3578 N93-29270
Hybrid data link
[AD-D015714] p 3383 N93-29280
Fiber-optic currents measurements
[DE93-007970] p 3579 N93-29350
Optical antenna beam steering using digital phase shifter control
[AD-D015688] p 3383 N93-29455
Atmospheric transverse coherence length measurement system for laser communications
[AD-A263563] p 3439 N93-29827
Planar active antennas and quasi-optical power combining arrays using FET's and slots
[AD-A263759] p 3387 N93-29875
Electro-optic characterisation of extremely wide bandwidth electrical signals
[AD-A264202] p 3392 N93-30145
Uplink laser propagation measurements through the sea surface, haze and clouds
[AD-A264687] p 3440 N93-30553
Optically powered, optoelectronic spatial light modulators
[AD-A264765] p 3581 N93-30609
OPTICAL COMPUTERS
Accuracy enhancement in optical computing
[AD-A264872] p 3522 N93-30179
Optically powered, optoelectronic spatial light modulators
[AD-A264765] p 3581 N93-30609
4D interconnect experimental development
[AD-A264298] p 3540 N93-30895
OPTICAL CORRELATORS
Spatial Light Modulators (SLMs) surface quality
[AD-A263249] p 3579 N93-29656
OPTICAL DATA PROCESSING
The German satellite ground station in Antarctica: Realization and first results p 3458 N93-28924
Fog studies in the Alpine region with digital NOAA/AVHRR data p 3458 N93-28925
Multi-channel holographic birfurcative neural network system for real-time adaptive EOS data analysis
p 3614 N93-29231
Multisensor image analysis system
[AD-A263679] p 3528 N93-29294
Spatial Light Modulators (SLMs) surface quality
[AD-A263249] p 3579 N93-29656
Photorefractive integrators and correlators
[AD-A264200] p 3597 N93-30144
Acousto-optic time-integrating correlators for processing wideband digital data p 3360 N93-30253
Optically switchable conductive polymers
[AD-A264751] p 3337 N93-30557
Optically powered, optoelectronic spatial light modulators
[AD-A264765] p 3581 N93-30609
4D interconnect experimental development
[AD-A264298] p 3540 N93-30895
Massively parallel spatial light modulation-based optical signal processing
[AD-A264846] p 3581 N93-30905
OPTICAL DATA STORAGE MATERIALS
Holographic data storage crystals for the LDEF
p 3435 N93-29697
ICI optical data storage tape: An archival mass storage media p 3621 N93-30472
Flexible storage medium for write-once optical tape
p 3621 N93-30473
Electron trapping data storage system and applications p 3622 N93-30474
OPTICAL DISKS
Associative memories for supercomputers
[AD-A263142] p 3520 N93-29482
Goddard Conference on Mass Storage Systems and Technologies, Volume 1
[NASA-CP-3198] p 3616 N93-30449
Striped tertiary storage arrays p 3620 N93-30464
OPTICAL EQUIPMENT
JPRS report: Science and technology. Central Eurasia: Engineering and equipment
[JPRS-UEQ-93-001] p 3274 N93-29014
High-efficiency high-reliability optical components for a large, high-average-power visible laser system
[DE93-009225] p 3437 N93-29098
In orbit degradation of EUV optical components in the wavelength range 10-40 nm AO 138-3
p 3582 N93-29691
Degradation of optical components in a space environment p 3582 N93-29692
Studies of effects on optical components and sensors: LDEF experiments AO-147 (ERB components) and S-0014 (APEX) p 3582 N93-29693
LDEF space optics handbook p 3582 N93-29695
OPTICAL FIBERS
Fiber-optic currents measurements
[DE93-007970] p 3579 N93-29350
Fiber-optic polarimetric strain gauge
p 3375 N93-30341
OPTICAL FILTERS
X ray, far, and extreme ultraviolet coatings for space applications p 3340 N93-28829
Laser radiation detection system
[AD-D015724] p 3438 N93-29287
Studies of effects on optical components and sensors: LDEF experiments AO-147 (ERB components) and S-0014 (APEX) p 3582 N93-29693
Applications of the photorefractive effect and damage induced effects in fibers
[AD-A264339] p 3580 N93-30205
Method and apparatus for imaging an object in or through a scattering medium by using multiple-wave mixing
[AD-D015707] p 3581 N93-30410
OPTICAL FLOW (IMAGE ANALYSIS)
Neural networks application to divergence-based passive ranging
[NASA-TM-103981] p 3245 N93-29653
Binocular spherical disparity: A study in representation for a forward translating camera
[PB93-184422] p 3579 N93-29667
OPTICAL MATERIALS
Polar order and relaxation of second order nonlinear optical susceptibility in an electric field polarized amorphous polymer
[AD-A262189] p 3329 N93-28489
Infrared rugates by molecular beam epitaxy
p 3582 N93-28808
Modification of spectral distributions by multilayer structures
[DE93-009308] p 3310 N93-29059
Effects of vacuum exposure on stress and spectral shift of high reflective coatings
[DE93-009318] p 3437 N93-29207
Multichip module high speed testing
[AD-A262989] p 3408 N93-29427
Polymers with electrical and nonlinear optical properties
[AD-D015691] p 3333 N93-29457
Degradation of optical components in a space environment p 3582 N93-29692
Studies of effects on optical components and sensors: LDEF experiments AO-147 (ERB components) and S-0014 (APEX) p 3582 N93-29693
Effects of long term space environment exposure on optical substrates and coatings (S0050-2)
p 3582 N93-29694
Problems in the implementation of x ray optics with x ray lasers
[DE93-009297] p 3438 N93-29781
Characterization of slow chromophore reorientation in nonlinear optical polymers by two-dimensional MAS NMR
[AD-A264809] p 3338 N93-30596
Organometallic compounds and polymers with second and third order nonlinear optical properties
[AD-A264774] p 3338 N93-30610
Visible light emitting materials and injection devices
[AD-A263499] p 3601 N93-30811
OPTICAL MEASUREMENT
Characterization of laboratory generated turbulence by optical phase measurements
[AD-A262596] p 3480 N93-28465
Adsorption of sulfate on metal electrodes
[AD-A263192] p 3309 N93-28540

The enhanced-model ladar wind sensor and its application in planetary wind velocity measurements
p 3649 N93-28815
An automated observing system for passive evaluation of cloud cover and visibility
[AD-A263207] p 3481 N93-28875
Optical measurements of ripples using a scanning laser slope gauge. Part 1: Instrumentation and preliminary results
[AD-A261939] p 3486 N93-28996
Fiber grating-based sensing system with interferometric wavelength-shift detection
[AD-D015697] p 3577 N93-29038
Optical slope/height measurements of small scale waves within the SAXON-FPN experiment
[AD-A262572] p 3487 N93-29422
Design of a high resolution spatial heterodyne interferometer
[AD-A262867] p 3285 N93-29461
Application of Schlieren optical techniques for the measurement of gas temperature and turbulent diffusivity in a diesel engine
[AD-A263810] p 3580 N93-29880
Optical blade vibration measurement
[ETN-93-93454] p 3259 N93-29999

OPTICAL MEASURING INSTRUMENTS
The production and destruction of negative ions
[DE93-010527] p 3564 N93-28665
The enhanced-model ladar wind sensor and its application in planetary wind velocity measurements
p 3649 N93-28815
Environmental monitors in the Midcourse Space Experiments (MSX) p 3286 N93-28826
Precision optical interferometry in space
[NASA-CR-193264] p 3630 N93-29163
Optical slope/height measurements of small scale waves within the SAXON-FPN experiment
[AD-A262572] p 3487 N93-29422

OPTICAL MEMORY (DATA STORAGE)
Associative memories for supercomputers
[AD-A263142] p 3520 N93-29482
Optical media standards for industry
p 3617 N93-30451
The fundamentals and futures of removable mass storage alternatives p 3619 N93-30460
Electron trapping data storage system and applications p 3622 N93-30474

OPTICAL MICROSCOPES
Ultra-high resolution water window x ray microscope optics design and analysis
[NASA-CR-193225] p 3578 N93-29128

OPTICAL POLARIZATION
Rib arrow integrated optic polarizer
p 3357 N93-30231

OPTICAL PROPERTIES
The Optical Properties Monitor (OPM): A multipurpose optical laboratory in space p 3266 N93-28729
Optically controlled active impedance element particularly suited for a microwave oscillator
[AD-D015723] p 3408 N93-29281
Methods for reducing turbulent flow aero-optical distortion
[AD-A263698] p 3423 N93-29353
Quantum devices using Si-based superlattices and structures
[AD-A263700] p 3595 N93-29383
Polymers with electrical and nonlinear optical properties
[AD-D015691] p 3333 N93-29457
Ruled and holographic experiment (AO 138-5)
p 3434 N93-29696
Next generation optical instruments and space experiment based on the LDEF thermal control surfaces experiment (S0069) p 3583 N93-29706
A stochastic formation of radiative transfer in clouds
[DE93-011372] p 3484 N93-30055
Organometallic compounds and polymers with second and third order nonlinear optical properties
[AD-A264774] p 3338 N93-30610
NATO Advanced Research Workshop on Frontiers of Optical Phenomena in Semiconductor Structure of Reduced Dimension
[AD-A264813] p 3581 N93-30666

OPTICAL PUMPING
A high field optical-pumping spin-exchange polarized deuterium source
[DE93-009208] p 3574 N93-28970
Femtosecond laser studies of excited state dynamics
[AD-A263708] p 3439 N93-29918

OPTICAL RADAR
The enhanced-model ladar wind sensor and its application in planetary wind velocity measurements
p 3649 N93-28815
Development of a 9.3 micrometer CW LIDAR for the study of atmospheric aerosol
[NASA-CR-193227] p 3381 N93-29105
Measurement of the rotation Raman spectra of nitrogen, oxygen, and water vapor under conditions of a temperature humidity lidar
[GKSS-92/E/32] p 3485 N93-31018

OPTICAL RANGE FINDERS
A single band processor for the computation of range from optical absorbance p 3363 N93-30272
On the implementation of the BIRIS range sensor for applications in robotic control and autonomous navigation p 3366 N93-30286

OPTICAL REFLECTION
Formulation of Ames 24E2 IR-black coating
[NASA-TM-102864] p 3629 N93-29453

OPTICAL RESONATORS
Method of emitting on a specific wavelength fraunhofer line using a neodymium doped laser transmitter
[AD-D015710] p 3437 N93-29276

OPTICAL SCANNERS
CAESAR development plan 1992-1995
[BCRS-92-17] p 3463 N93-31009

OPTICAL SWITCHING
Ferroelectric liquid crystal optical interconnect switching systems
[AD-A263751] p 3596 N93-29859
Optically switchable conductive polymers
[AD-A264751] p 3337 N93-30557
Ultrafast, passive, broad-band, optical shutter based on novel semiconductor/conducting polymer interfaces
[AD-A264098] p 3601 N93-30878

OPTICAL TRACKING
Subnanoradian, groundbased tracking of spaceborne lasers p 3442 N93-28823
SWAT 2 overview
[AD-A262905] p 3578 N93-29139
SWAT laboratory test results
[AD-A262906] p 3578 N93-29140
Methods for reducing turbulent flow aero-optical distortion
[AD-A263698] p 3423 N93-29353

OPTICAL TRANSFER FUNCTION
Characterization of laboratory generated turbulence by optical phase measurements
[AD-A262596] p 3480 N93-28465

OPTICAL WAVEGUIDES
Nonlinear mode coupling in free electron lasers
[AD-A263999] p 3439 N93-29883
Optoelectronic technology consortium
[AD-A263580] p 3580 N93-29973
Rib arrow integrated optic polarizer
p 3357 N93-30231
Topical meeting of broadband analog and digital optoelectronics
[AD-A264643] p 3581 N93-30522

OPTICS
JPRS report: Science and technology. Central Eurasia: Physics and mathematics
[JPRS-UPM-93-002] p 3560 N93-29022
JPRS report: Science and technology. Central Eurasia: Engineering and equipment
[JPRS-UEQ-93-004] p 3354 N93-29090

OPTIMAL CONTROL
Artificial intelligence methodologies in flight related differential game, control and optimization problems
[AD-A262405] p 3541 N93-28498
Optimal control of the M/G/1 queue with repeated vacations of the server
[INRIA-RR-1637] p 3541 N93-28637
A fuzzy logic optimal control law solution to the CMMCA tracking problem
[AD-A262555] p 3542 N93-29420
An information theoretic approach to stochastic adaptive control application to manipulators with active inertia
p 3359 N93-30247
Nonsmooth optimization algorithms, system theory, and software tools
[AD-A264679] p 3534 N93-30549

OPTIMIZATION
Packing of Steiner trees: Polyhedric studies and application
[ETN-93-93796] p 3547 N93-28527
Optimal control of the M/G/1 queue with repeated vacations of the server
[INRIA-RR-1637] p 3541 N93-28637
Balanced approximation can be optimal
[OUEL-1950/92] p 3548 N93-28754
Preemptive scheduling with variable profile, precedence constraints and due dates
[INRIA-RR-1622] p 3538 N93-28937
Uncertainty reasoning in expert systems
[NASA-CR-193120] p 3548 N93-28973
Design optimization of space structures
p 3278 N93-29122
Enhanced reduction of velocity data obtained during CETA flight experiment
[NASA-TM-4460] p 3431 N93-29209
Some problems in the mechanics of solids with phase mixtures
[AD-A263652] p 3311 N93-29291
Characterization and optimization of a Hot Air Solder-Leveling System
[DE93-010188] p 3332 N93-29328
Integrated approaches to parallelism in optimization and solution of inverse problems
[AD-A262259] p 3452 N93-29349
Nonresident and endangered variables: The effects of code generation optimizations on symbolic debugging
[AD-A263149] p 3529 N93-29486
Fuzzy learning under and about an unfamiliar fuzzy teacher p 3516 N93-29558
A multilevel approach to minimum cost network flows
[AD-A264008] p 3550 N93-29978
Optimal geometric design of robots for environments with obstacles p 3445 N93-30149
Parametric and combinatorial problems in constrained optimization
[AD-A264229] p 3555 N93-30363
Technical examination and simulation of a photovoltaic system: Solar generator, battery, download
[ETN-93-94179] p 3466 N93-30573
Placement of cells: Theory and solution of a quadratic 0/1 optimization problem
[ETN-93-94182] p 3413 N93-30616
Optimum design of multiwire cages for high-voltage applications
[AD-A264310] p 3400 N93-30995

OPTOELECTRONIC DEVICES
Low temperature (LT) GaAs and related materials
[AD-A263607] p 3298 N93-29282

ORBIT CALCULATION
The effect of clock, media, and station location errors on Doppler measurement accuracy
p 3246 N93-29588
Precise tracking of the Magellan and Pioneer Venus orbiters by Same-Beam Interferometry. Part 2: Orbit determination analysis p 3270 N93-29589
Orbital motion calculation using Lie method in collider nonlinear magnetic field
[DE93-605733] p 3571 N93-30800

ORBIT TRANSFER VEHICLES
ELITE program: Electric insertion transfer experiment
p 3264 N93-28709
Advanced engine study program
[NASA-CR-187217] p 3287 N93-28946
Analysis of orbital system logistics in the cis-lunar space with particular consideration of life cycle costs
[ETN-93-93484] p 3268 N93-29063
Project UM-HAUL: A self-unloading reusable lunar lander p 3232 N93-29740
Mars sample return mission: Two alternate scenarios
p 3233 N93-29746
SPECS: Orbital debris removal p 3234 N93-29754
Orbital transfer vehicle oxygen turbopump technology. Volume 3: Hot oxygen testing
[NASA-CR-191036] p 3448 N93-31039

ORBITAL ASSEMBLY
Space Station: Orbiter berthing p 3274 N93-29091
Space construction activities
[NASA-CR-192690] p 3274 N93-29108
Interaction dynamics of on-orbit construction
p 3274 N93-29109
Hybrid CMS methods with model reduction for assembly of structures p 3274 N93-29110
Controls of interaction dynamics of orbital assembly
p 3275 N93-29111
Systems engineering studies of on-orbit assembly operation p 3275 N93-29114

ORBITAL RENDEZVOUS
Reference equations of motion for automatic rendezvous and capture
[NASA-CR-185676] p 3269 N93-29652

ORBITAL SERVICING
Analysis of orbital system logistics in the cis-lunar space with particular consideration of life cycle costs
[ETN-93-93484] p 3268 N93-29063

ORBITAL SPACE TESTS
CSI-Star: A low-cost CSI orbital testbed
p 3263 N93-28707

ORDER-DISORDER TRANSFORMATIONS
Hypervelocity impact survivability experiments for carbonaceous impactors p 3283 N93-29364
Anelastic relaxations associated with local disordering in grain boundaries
[AD-A263101] p 3596 N93-29796
Some effects of composition and microstructure on the B2 in equilibrium to DO3 ordered phase transition in Fe3Al alloys
[DE93-009724] p 3325 N93-29813
Order-disorder transformations in Ni-Al alloys
[DE93-009293] p 3326 N93-30389

ORDNANCE
Ordnance thermal battery
[AD-D015722] p 3412 N93-30201

ORGANIC COMPOUNDS
Marine microbial production of dimethylsulfide from dissolved dimethylsulfoniopropionate
[NASA-CR-193278] p 3492 N93-30665
Standard and reference materials for marine science, third edition
[PB93-185684] p 3489 N93-30830
Visualizing weld metal solidification using organic analogs p 3293 N93-30973

ORGANIC COOLANTS
Thermal and mechanical analysis of flip-chips on a liquid cooled multichip module
[DE93-007609] p 3405 N93-28641

ORGANIC SILICON COMPOUNDS
Applications of transition metal compounds in the preparation of useful silicon-containing ceramics
[AD-A264028] p 3335 N93-30028

ORGANIC SULFUR COMPOUNDS
Process to prepare 1,3-diamino-5-pentafluorosulfanylbenzene
[NASA-CASE-LAR-14773-2-CU] p 3312 N93-29506
Design of acentric materials: X ray structures of guanidinium p-nitro- and p-hydroxybenzenesulfonate
[AD-A264220] p 3597 N93-30146

ORGANISMS
Planetary protection issues for the MESUR mission: Probability of growth (Pg)
[NASA-CP-3167] p 3651 N93-30214

ORGANIZATIONS
Minimum security requirements for multi-user operating systems
[PB93-185999] p 3522 N93-30832

ORGANOMETALLIC COMPOUNDS
Supported organometallic complexes, surface chemistry, spectroscopy, and catalysis
[DE93-011930] p 3309 N93-28688
Quantum lattice fluctuations in a 1-dimensional charge-density-wave material: Luminescence and resonance Raman studies of an MX solid
[DE93-007362] p 3593 N93-28966
Femtosecond carrier processes in compound semiconductors and real time signal processing
[AD-A263076] p 3382 N93-29131
Synthetic lubricating oil greases containing metal chelates of Schiff bases
[AD-D015694] p 3333 N93-29458
Organometallic and surface chemistry of mixed-metal systems
[DE93-012686] p 3325 N93-30059
Methylhydridopolysilazane and its pyrolytic conversion to Si3N4/SiC ceramics
[AD-A264150] p 3336 N93-30170
Organometallic compounds and polymers with second and third order nonlinear optical properties
[AD-A264774] p 3338 N93-30610
Gordon Research Conferences, 1991
[AD-A264275] p 3317 N93-30816

ORGANOMETALLIC POLYMERS
A study of the chemical mechanism in lubrication
[DE93-012230] p 3330 N93-28650
Organometallic compounds and polymers with second and third order nonlinear optical properties
[AD-A264774] p 3338 N93-30610

ORR-SOMMERFELD EQUATIONS
Evolution of flow disturbances in cocurrent gas-liquid flows
[DE93-010083] p 3422 N93-29326

ORTHOGONALITY
Study on various problems in statistical planning and inference
[AD-A262484] p 3554 N93-29411

OSCILLATING CYLINDERS
Stabilized space-time finite element formulations for unsteady incompressible flows involving fluid-body interactions p 3419 N93-29040

OSCILLATIONS
The natural excitation technique (NExT) for modal parameter extraction from operating wind turbines
[DE93-010611] p 3463 N93-28603
Chaos in mechanical systems with especial reference to rotorcraft and missiles
[AD-A263703] p 3604 N93-29384
Theoretical studies in nuclear structure
[DE93-012290] p 3570 N93-30505
Neutrino oscillations and a new Faraday effect
[DE93-606111] p 3571 N93-30789

OSCILLATORS
Every good virtue you ever wanted in a Q-switched solid-state laser and more: Monolithic, diode-pumped, self-Q-switched, highly reproducible, diffraction-limited Nd:YAG laser p 3442 N93-28772
Bifurcations phenomena in a nonlinear oscillator: Approximate analytical studies versus computer simulation results p 3407 N93-29037
Program for an improved hypersonic temperature-sensing probe
[NASA-CR-186025] p 3431 N93-29066
Constant frequency pulsed phase-locked loop measuring device
[NASA-CASE-LAR-13823-1] p 3431 N93-29084
An improved linear ion trap physics package p 3384 N93-29587
The flight performance of the Galileo orbiter USO p 3386 N93-29603
Fusion laser oscillator and pulse-forming system using integrated optics
[DE93-009286] p 3588 N93-29780
Planar active antennas and quasi-optical power combining arrays using FET's and slots
[AD-A263759] p 3387 N93-29875
Foreign technology assessment: Environmental evaluation of a radiation-hard oscillator/divider
[DE93-011481] p 3412 N93-30127

OSCILLOSCOPES
Remote vehicle survey tool
[DE93-010822] p 3460 N93-29255
Electro-optic characterisation of extremely wide bandwidth electrical signals
[AD-A264202] p 3392 N93-30145

OSEEN APPROXIMATION
Hydrodynamic interactions among fibers in high efficiency filters
[DE93-007117] p 3424 N93-30035

OUTGASSING
Return flux experiment p 3266 N93-28727

OVER-THE-HORIZON RADAR
Characteristics of high-frequency signals, noise, availability, and duration of bandwidths based on ROTHR Amchitka spectrum measurements
[AD-A264480] p 3393 N93-30423

OXIDATION
The temperature dependence of the deformation and oxidation behavior of an age-hardenable beta + alpha-two titanium alloy
[AD-A262232] p 3320 N93-28491
Influence of the Cold Buster (tm) sports bar on heat debt, mobilization and oxidation of energy substrates
[AD-A262762] p 3493 N93-28939
Oxidation behavior in reaction-bonded aluminum-silicon alloy/alumina powder compacts
[DE93-010407] p 3298 N93-29191
High pressure preignition chemistry of hydrocarbons and hydrocarbon mixtures
[AD-A263611] p 3311 N93-29283
Super critical water oxidation on energetic materials
[DE93-010704] p 3342 N93-29312
The effect of oxidation embrittlement on the impact behavior of nicalon reinforced CAS 2 ceramic matrix composites
[AD-A263567] p 3334 N93-29829
Air oxidation behavior of fuel for the High Temperature Engineering Test Reactor (HTTR)
[DE93-753349] p 3576 N93-30006
Thermal oxidation of HCN by NO2 in shock waves p 3318 N93-30064
Study of codeposition of aluminum-haffnium and deposition of yttrium by the cementation technique: Elaboration of Ni-Cr-Al and Ni-Cr-Al-Hf felt materials
[ONERA-NT-1990-9] p 3336 N93-30112
Surface chemistry of hydrogen-passivated porous silicon-oxidation of surface Si-H groups by acetone
[AD-A264655] p 3315 N93-30526
Oxidation and hot corrosion of superalloys Rene 100 and X-40 at temperatures of 1475 F to 2000 F
[AD-A263747] p 3327 N93-30812
Laboratory experiments in integrated circuit fabrication p 3292 N93-30962

OXIDATION RESISTANCE
Ultrahigh temperature assessment study: Ceramic matrix composites
[AD-A262740] p 3295 N93-28592
High temperature creep and oxidation resistant chromium silicide matrix alloy containing molybdenum
[NASA-CASE-LEW-15697-1] p 3323 N93-29172
Platinum-modified diffusion aluminide coatings on nickel-base superalloys
[AD-A263597] p 3325 N93-29981
Development of adherent ceramic coatings to reduce contact stress damage of ceramics
[DE93-012518] p 3336 N93-30182
Oxidation and hot corrosion of superalloys Rene 100 and X-40 at temperatures of 1475 F to 2000 F
[AD-A263747] p 3327 N93-30812

OXIDATION-REDUCTION REACTIONS
Scanning probe lithography. Part 1: Scanning tunneling microscope-induced lithography of self-assembled n-alkanethiol monolayer resists
[AD-A263130] p 3432 N93-29476
Hydrogen sulfide decomposition into hydrogen and sulfur by quinone cycles, part 1
[PB93-175297] p 3317 N93-30761

OXIDE FILMS
Structure, adhesion, and stability of metal/oxide and oxide/oxide interfaces
[DE93-012930] p 3325 N93-30060
Polarization modulated ellipsometry
[NASA-CR-4012] p 3580 N93-30372

OXIDES
Solid oxide fuel cells for transportation: A clean, efficient alternative for propulsion
[DE93-010662] p 3464 N93-29844

OXIDIZERS
Super critical water oxidation on energetic materials
[DE93-010704] p 3342 N93-29312

OXYGEN
The electrolyte factor in O2 reduction electrocatalysis
[AD-A263565] p 3313 N93-29828
Vibrational spectroscopy of shock-compressed fluids p 3318 N93-30072
Dioxygen reduction in various acid electrolytes
[AD-A263564] p 3317 N93-30664

OXYGEN ATOMS
Thermal control paints on LDEF: Results of M0003 sub-experiment 18
[AD-A263252] p 3329 N93-28561
Method for preparation of a microporous structure with layered interstitial surface treatment
[NASA-CASE-MSC-21487-2] p 3296 N93-29023
Effects of atomic oxygen and ultraviolet radiation on candidate elastomeric materials for long duration missions. Test series no.1
[NASA-TM-108408] p 3331 N93-29193
Damage areas on selected LDEF aluminum surfaces p 3283 N93-29374
Refinements on the pinhole camera measurements of the LDEF attitude p 3283 N93-29622
LDEF microenvironments, observed and predicted p 3283 N93-29623
Center for surface radiation damage studies
[AD-A264330] p 3570 N93-30366
Development of an O atom gun
[AD-A264753] p 3570 N93-30558

OXYGEN ISOTOPES
Upper ocean model of dissolved atmospheric gases
[DE93-010151] p 3487 N93-29327

OXYGEN MASKS
Evaluation of test methods and requirements for respiratory protection systems 21
[AD-A262466] p 3501 N93-28757

OXYGEN PRODUCTION
Hybrid oxygen system
[AD-A262417] p 3500 N93-28464
Benefits of in situ propellant utilization for a Mars sample return mission
[NASA-TM-106243] p 3341 N93-28695
Alkali metal carbon dioxide electrochemical system for energy storage and/or conversion of carbon dioxide to oxygen
[NASA-CASE-LEW-14973-1] p 3464 N93-28974
Upper ocean model of dissolved atmospheric gases
[DE93-010151] p 3487 N93-29327
Method for producing oxygen from lunar materials
[NASA-CASE-MSC-21759-1] p 3312 N93-29617

OXYGEN SUPPLY EQUIPMENT
Hybrid oxygen system
[AD-A262417] p 3500 N93-28464
Magnetohydrodynamic projects at the CDIF
[DE93-012195] p 3584 N93-28649

OXYGEN-HYDROCARBON ROCKET ENGINES
Advanced Earth-to-orbit propulsion technology information, dissemination and research
[NASA-CR-192561] p 3287 N93-28680

OZONE
Development of ultraviolet absorption photometer for atmospheric ozone measurements and results from mid-latitude investigations p 3468 N93-28949
Emission inventories: A global modeling perspective
[DE93-005817] p 3469 N93-28965
Summer 1990 Atlanta ozone precursor study (January 1993)
[PB93-167203] p 3470 N93-29200
Study to determine the nature and extent of ozone and ozone precursor transport in selected areas of California
[PB93-184828] p 3470 N93-29669
Potential effects of HFC-152a on global ozone and climate
[DE93-008018] p 3471 N93-29792

The global potential energy surfaces of the lowest two 1A-prime states of the ozone molecule: Theoretical determination and analysis [DE93-007537] p 3313 N93-29837

OZONE DEPLETION

Advanced Earth Observing Satellite (ADEOS) p 3279 N93-29648

Overview of the DOE Atmospheric Chemistry Program's Ozone Project [DE93-007416] p 3471 N93-29770

OZONOMETRY

Development of ultraviolet absorption photometer for atmospheric ozone measurements and results from mid-latitude investigations p 3468 N93-28949

Summer 1990 Atlanta ozone precursor study (January 1993) [PB93-167203] p 3470 N93-29200

OZONOSPHERE

Results from the US/Russian Meteor-3/Total Ozone Mapping Spectrometer [NASA-TM-104576] p 3467 N93-28682

Advanced Earth Observing Satellite (ADEOS) p 3279 N93-29648

P

P WAVES

Modern seismic travel time tables and station corrections for P and S waves [AD-A262536] p 3477 N93-29412

P-I-N JUNCTIONS

Widebanding techniques for VHF antennas 2 [AD-A263998] p 3387 N93-29882

Infrared imaging array integrated in three dimensions directly on top of silicon circuits [AD-A264707] p 3581 N93-30500

P-N JUNCTIONS

Laboratory experiments in integrated circuit fabrication p 3292 N93-30962

P-3 AIRCRAFT

Uplink laser propagation measurements through the sea surface, haze and clouds [AD-A264687] p 3440 N93-30553

PACIFIC OCEAN

Upper ocean model of dissolved atmospheric gases [DE93-010151] p 3487 N93-29327

Fugitive hydrocarbon emissions from Pacific OCS facilities. Volume 2: Executive summary and user's guide [PB93-173805-VOL-2] p 3471 N93-29861

Analysis of a simulation of the seasonal cycle in the tropical Pacific Ocean in an eddy-resolving global ocean model [AD-A264007] p 3488 N93-29977

Fiber optic chemical sensors for characterizing the carbon cycle in ocean margin regions [DE93-011442] p 3489 N93-30056

Measurements of ocean currents across the continental margin off Point Sur, California, during March 1989 [AD-A264853] p 3489 N93-30178

PACKAGING

Packing of Steiner trees: Polyhedric studies and application [ETN-93-93796] p 3547 N93-28527

PACKET SWITCHING

On-board B-ISDN fast packet switching architectures. Phase 2: Development. Proof-of-concept architecture definition report [NASA-CR-191151] p 3273 N93-29884

PACKETS (COMMUNICATION)

Flow control using the theory of zero sum Markov games [INRIA-RR-1597] p 3553 N93-28507

On-board B-ISDN fast packet switching architectures. Phase 2: Development. Proof-of-concept architecture definition report [NASA-CR-191151] p 3273 N93-29884

PAINTS

Thermal control paints on LDEF: Results of M0003 sub-experiment 18 [AD-A263252] p 3329 N93-28561

PAIR PRODUCTION

New limits on generation-1 leptoquarks [DE93-008138] p 3567 N93-29351

Pion pair production in photon-photon collisions [DE93-606114] p 3571 N93-30790

Towards the results of global analysis of data on nucleon electromagnetic structure [DE93-606125] p 3571 N93-30792

PALEOCLIMATOLOGY

Drill/borescope system for the Mars Polar Pathfinder p 3647 N93-28805

PALLADIUM

Applications of transition metal compounds in the preparation of useful silicon-containing ceramics [AD-A264028] p 3335 N93-30028

PANELS

Multi-parameter optimization tool for low-cost commercial fuselage crown designs p 3305 N93-30858

Comparison of hand laid-up tape and filament wound composite cylinders and panels with and without impact damage p 3306 N93-30859

Optimization of composite sandwich cover panels subjected to compressive loadings p 3306 N93-30862

Advanced fiber placement of composite fuselage structures p 3306 N93-30864

PARABOLIC BODIES

Three-D crater analysis of LDEF impact features from stereo imagery p 3283 N93-29359

PARABOLIC REFLECTORS

A satellite-tracking millimeter-wave reflector antenna system for mobile satellite-tracking [NASA-CASE-NPO-18772-1-CU] p 3381 N93-28955

Array-fed reflector systems with limited scan p 3371 N93-30318

PARACHUTES

The development of a parachute system for aerial delivery from high speed cargo aircraft [DE93-008339] p 3239 N93-29035

A computational model that couples aerodynamic and structural dynamic behavior of parachutes during the opening process [AD-A264115] p 3241 N93-30119

PARALLAX

A comparison of simulated parallax and single-station range aids to navigation [AD-A263460] p 3246 N93-29818

PARALLEL COMPUTERS

BlockSolve v1.1: Scalable library software for the parallel solution of sparse linear systems [DE93-011391] p 3524 N93-28644

Planning of a West Virginia University Research Center in the basic materials sciences [DE93-011731] p 3592 N93-28647

Parallel software tools at Langley Research Center [NASA-TM-108995] p 3520 N93-29070

Implementation of a single-material version of PAGOSA on MIMD hypercubes [SAND-92-0640] p 3526 N93-29127

Efficient wiring of reconfigurable parallel processors [DE93-009847] p 3538 N93-29186

The parallel implementation of a backpropagation neural network and its applicability to SPECT image reconstruction [DE93-010304] p 3567 N93-29416

Special purpose parallel computer architecture for real-time control and simulation in robotic applications [NASA-CASE-NPO-17629-1-CU] p 3521 N93-29608

High performance computing and communications program p 3627 N93-30715

PARALLEL FLOW

A parallel implicit incompressible flow solver using unstructured meshes [AD-A263395] p 3424 N93-29851

PARALLEL PROCESSING (COMPUTERS)

Design of a hardware discrete event simulation coprocessor [AD-A262614] p 3537 N93-28478

Study on the concurrent calculation with a multitransputer network [DE93-753191] p 3524 N93-28531

Parallel computation and the basis system [DE93-008755] p 3537 N93-28544

A multiarchitecture parallel-processing development environment [NASA-TM-106180] p 3538 N93-28628

How to write fast and clear parallel programs using algebra [DE93-000797] p 3524 N93-28640

BlockSolve v1.1: Scalable library software for the parallel solution of sparse linear systems [DE93-011391] p 3524 N93-28644

Planning of a West Virginia University Research Center in the basic materials sciences [DE93-011731] p 3592 N93-28647

Combat Automation for Airborne Weapon Systems: Man/Machine Interface Trends and Technologies [AGARD-CP-520] p 3501 N93-28850

Pilot decision aiding for weapon delivery: A novel approach to fire control cueing using parallel computing p 3501 N93-28853

Neural network simulations on massively parallel computers: Applications in chemical physics [DE93-006739] p 3538 N93-28894

Preemptive scheduling with variable profile, precedence constraints and due dates [INRIA-RR-1622] p 3538 N93-28937

A simple parallel prefix algorithm for compact finite-difference schemes [NASA-CR-191448] p 3525 N93-28976

Implementation of a multidomain Navier-Stokes code on the Intel iPSC2 hypercube [FFA-TN-1992-37] p 3418 N93-28994

Implementation of a single-material version of PAGOSA on MIMD hypercubes [SAND-92-0640] p 3526 N93-29127

Distributed Virtual System (DIVIRS) Project [NASA-CR-193234] p 3526 N93-29169

Computing for magnetic fusion energy research: An updated vision [DE93-010394] p 3587 N93-29190

Exploitation of parallelism in climate models [DE93-011259] p 3470 N93-29318

The parallel implementation of a backpropagation neural network and its applicability to SPECT image reconstruction [DE93-010304] p 3567 N93-29416

Implementation of parallel algorithms [AD-A263126] p 3529 N93-29496

Exploiting the memory hierarchy in sequential and parallel sparse Cholesky factorization [AD-A262849] p 3539 N93-29508

Special purpose parallel computer architecture for real-time control and simulation in robotic applications [NASA-CASE-NPO-17629-1-CU] p 3521 N93-29608

Using synthetic-perturbation techniques for tuning shared memory programs [PB93-178572] p 3539 N93-29677

Communications neural net processors [AD-A263330] p 3542 N93-29763

Data parallelism [DE93-009300] p 3539 N93-29782

Full abstraction for a shared variable parallel language [AD-A263547] p 3530 N93-29821

NESL: A nested data-parallel language (Version 2.6) [AD-A263548] p 3530 N93-29822

Class notes: Programming parallel algorithms CS 15-840B (Fall 1992) [AD-A263549] p 3530 N93-29823

Tactical satellites p 3284 N93-29893

Use of a genetic algorithm to solve two-fluid flow problems on an NCUBE multiprocessor computer [DE93-009630] p 3425 N93-30184

A parallel processing system for intensive I/O p 3362 N93-30262

A transputer based parallel processing architecture for robotics applications p 3362 N93-30263

Optimized partitioning and balancing for parallel processing p 3365 N93-30280

Parallel processing and learning: Variability and chaos in self-organization of activity in groups of neurons [AD-A264224] p 3539 N93-30361

High-performance mass storage system for workstations p 3618 N93-30457

Infrared imaging array integrated in three dimensions directly on top of silicon circuits [AD-A264707] p 3581 N93-30500

Finite element approximation of the shallow water equations on the MASPAR [AD-A264649] p 3489 N93-30525

Promoting high-performance computing and communications [ISBN-0-16-041828-3] p 3522 N93-30570

Multiprocessing MCNP on an IBM RS/6000 cluster [DE93-008712] p 3540 N93-30633

Transputers, parallel processing in embedded systems for image compression in space applications [NLR-TP-89242-U] p 3522 N93-30840

Massively parallel spatial light modulation-based optical signal processing [AD-A264846] p 3581 N93-30905

PARALLEL PROGRAMMING

A C++ interface for programming on the Connection Machine [INRIA-RR-1698] p 3538 N93-29487

Data parallelism [DE93-009300] p 3539 N93-29782

Full abstraction for a shared variable parallel language [AD-A263547] p 3530 N93-29821

Class notes: Programming parallel algorithms CS 15-840B (Fall 1992) [AD-A263549] p 3530 N93-29823

The midway distributed shared memory system [AD-A264645] p 3534 N93-30523

PARAMETER IDENTIFICATION

Speech recognition by recursive stochastic modelling [ISBN-90-9005038-8] p 3382 N93-29266

Optical coherent phase diversity systems [ISBN-90-9004897-9] p 3578 N93-29270

Estimating the parameters of chaotic maps [AD-A262574] p 3556 N93-29423

Parameter identification of time-varying systems using neural networks p 3356 N93-30226

PARAMETERIZATION

An analysis of the Generalized Lambda Distribution [AD-A262485] p 3555 N93-29447

Beltrami parametrization and gauging of Virasoro and w-infinity algebras
[DE92-644844] p 3557 N93-30928

PARASITIC DISEASES
Project MEDSAT p 3231 N93-29739

PARITY
Tutorial: Performance and reliability in redundant disk arrays p 3537 N93-30463

PARTIAL DIFFERENTIAL EQUATIONS
Index mappings for interactive editing of symbolic matrices
[DE93-009316] p 3549 N93-29060
Difference methods for hyperbolic problems with emphasis on space-centered approximations
[ONERA-NT-1990-4] p 3550 N93-30136

PARTICLE ACCELERATOR TARGETS
Measurements of rare composite objects and high sensitivity searches for novel forms of matter produced in high energy heavy ion collisions
[DE93-009945] p 3574 N93-28569
Studies of relativistic heavy ion collisions at the AGS (E814/E877)
[DE93-008541] p 3564 N93-28678
Design of a particle beam satellite system for lunar prospecting p 3434 N93-28768
Fluctuations and intermittency in high energy nucleus-nucleus collisions
[DE93-608481] p 3577 N93-30990

PARTICLE ACCELERATORS
Modern Monte Carlo particle transport simulation for safety and radiation protection applications in accelerometer technology and in space science
[JUEL-2609] p 3574 N93-29062
Mechanical behaviour of a closed collar model for an 11.5 T dipole
[NIKHEF-H/92-03] p 3576 N93-30019
Orbital motion calculation using Lie method in collider nonlinear magnetic field
[DE93-605733] p 3571 N93-30800
Microwave emission from relativistic electron beams
[AD-A264102] p 3400 N93-30880

PARTICLE BEAMS
Design of a particle beam satellite system for lunar prospecting p 3434 N93-28768
Use of particle beams for lunar prospecting
p 3650 N93-28822
Maximizing the luminosity of hadron, supercolliders at 10-100 TeV
[DE93-009247] p 3574 N93-29103

PARTICLE COLLISIONS
Measurements of rare composite objects and high sensitivity searches for novel forms of matter produced in high energy heavy ion collisions
[DE93-009945] p 3574 N93-28569
Dense inclined flows: Theory and experiments
[DE93-011452] p 3417 N93-28630
Meson-meson interactions and phi-enhancement in nucleus collisions
[DE93-010725] p 3565 N93-28831
Research in theoretical nuclear physics
[DE93-008380] p 3565 N93-28960
Maximizing the luminosity of hadron, supercolliders at 10-100 TeV
[DE93-009247] p 3574 N93-29103
Effects of neutral gas collisions on the power transmission factor at the divertor sheath
[DE93-009320] p 3588 N93-29334
Reaction mechanism studies of heavy ion induced nuclear reactions
[DE93-010496] p 3569 N93-29807
Task A: Theory of elementary particles
[DE93-010561] p 3569 N93-29841
Studies of fluctuation processes in nuclear collisions
[DE93-011263] p 3576 N93-30054
Multidimensional intermittency in hadronic collisions
[DE93-010562] p 3577 N93-30532
Pion pair production in photon-photon collisions
[DE93-606114] p 3571 N93-30790
Orbital motion calculation using Lie method in collider nonlinear magnetic field
[DE93-605733] p 3571 N93-30800
Single t-quark production in high energy (gamma)e collisions
[DE92-644947] p 3572 N93-30930
Fluctuations and intermittency in high energy nucleus-nucleus collisions
[DE93-608481] p 3577 N93-30990
Baryon number violation and particle collider experiments
[NIKHEF-H/92-14] p 3572 N93-31008

PARTICLE DIFFUSION
Theory of tokamak edge turbulence: Drift-thermal instability-induced turbulence and ionization-driven drift wave turbulence p 3586 N93-29123
Detailed studies of soot formation in laminar diffusion flames for application to modeling studies
[AD-A264827] p 3317 N93-30667
Development of a PC code package for the analysis of research and power reactors
[DE92-638517] p 3536 N93-31001

PARTICLE INTERACTIONS
Spin observables in large t elastic N-N scattering
[DE93-009211] p 3564 N93-28549
Macrostatistical hydrodynamics
[DE93-012289] p 3417 N93-28751
Coupled-channel analysis of low energy nucleon-antinucleon interactions
[DE93-606115] p 3571 N93-30791
Quantum-kinetic Green function and macroscopic wave function
[DE93-606040] p 3606 N93-30796
Low-energy behaviour of few-particle scattering amplitudes in two dimensions
[DE93-609834] p 3572 N93-30944

PARTICLE PRECIPITATION
Mithras studies of the boundary between open and closed field lines
[AD-A264758] p 3479 N93-30562

PARTICLE PRODUCTION
Meson-meson interactions and phi-enhancement in nucleus collisions
[DE93-010725] p 3565 N93-28831
Elementary particle interactions
[DE93-005113] p 3568 N93-29764
Task A: Theory of elementary particles
[DE93-010561] p 3569 N93-29841
Parton's picture of the electroweak processes in high energy e(+)e(-)-collisions
[DE93-606107] p 3571 N93-30788
Single t-quark production in high energy (gamma)e collisions
[DE92-644947] p 3572 N93-30930

PARTICLE SIZE DISTRIBUTION
Continued investigation of LDEF's structural frame and thermal blankets by the Meteoroid and Debris Special Investigation Group p 3282 N93-29357

PARTICLE SPIN
Spin observables in large t elastic N-N scattering
[DE93-009211] p 3564 N93-28549

PARTICLE THEORY
A new exact solution to the classical equations of motion of the relativistic string with massive ends
[DE92-644736] p 3557 N93-30922
Invariant structures in gauge theories and confinement
[DE92-644739] p 3607 N93-30924
Invariant structures and static forces in gauge theories
[DE92-644740] p 3607 N93-30925

PARTICLE TRACKS
Interplanetary meteoroid debris in LDEF metal craters
p 3638 N93-29372
High-energy electron-positron interactions
[DE93-011611] p 3576 N93-30488

PARTICLE TRAJECTORIES
Simulation and calculation of diffusive aerosol deposition
[DE93-007518] p 3474 N93-30506

PARTICULATE REINFORCED COMPOSITES
Design of interfaces in metal matrix composites
[AD-A262052] p 3296 N93-29001

PARTICULATES
Environmental Verification Experiment for the Explorer Platform (EVEEP) p 3266 N93-28726
Derivation of particulate directional information from analysis of elliptical impact craters on LDEF
p 3283 N93-29362

PARTITIONS (MATHEMATICS)
Optimized partitioning and balancing for parallel processing p 3365 N93-30280
Direct Monte Carlo simulation of the chemical equilibrium composition of detonation products
[DE92-040372] p 3315 N93-30447

PARTONS
Parton's picture of the electroweak processes in high energy e(+)e(-)-collisions
[DE93-606107] p 3571 N93-30788

PASSIVE SATELLITES
Spaceborne passive radiative cooler
p 3378 N93-28802

PASSIVITY
Fundamental aspects in the design of passive alloys
[DE93-009028] p 3320 N93-28545
Electrochemical behavior and surface chemistry of aluminum alloys: Solute-rich interphase model
[AD-A262061] p 3322 N93-29002

PATHS
Walkway friction: Experiment and analysis
p 3293 N93-30966

PATTERN RECOGNITION
Recognizing parameterized objects from range data
[OUEL-1918/92] p 3523 N93-28486
Information-theoretic performance bounding of Bayesian identifiers
[DE93-010705] p 3554 N93-28763
A corner matching and tracking strategy applied to videophony
[OUEL-1933/92] p 3380 N93-28896
Multi-channel holographic birfurcative neural network system for real-time adaptive EOS data analysis
p 3614 N93-29231
Representation and recognition with invariants and geometric constraint models
[AD-A263235] p 3529 N93-29493
Clustering of tethered satellite system simulation data by an adaptive neuro-fuzzy algorithm
p 3512 N93-29535
The fusion of information via fuzzy integration
p 3517 N93-29568
Neural networks application to divergence-based passive ranging
[NASA-TM-103981] p 3245 N93-29653
Spatial Light Modulators (SLMs) surface quality
[AD-A263249] p 3579 N93-29656
Development of neural network architectures for self-organizing pattern recognition and robotics
[AD-A264831] p 3543 N93-29791
Mixed limit theorems for pattern analysis
[AD-A263735] p 3549 N93-29854
A neural network based approach for machine fault diagnosis
[VTT-TIED-1274] p 3543 N93-29998
Computing with neural maps: Application to perceptual and cognitive function
[AD-A264056] p 3499 N93-30033
Representations of shape in object recognition and long-term visual memory
[AD-A264342] p 3499 N93-30163
Feature segmentation using a multiple-stack based chain coding algorithm p 3359 N93-30243
A robust multi-operator 3-D edge detection approach for range image segmentation p 3366 N93-30288
Recognizing partially overlapping objects
p 3366 N93-30289
Cloud classification from satellite imagery using neural computing p 3367 N93-30297
Classification of radar clutter in an air traffic control environment p 3246 N93-30299
Hidden Markov models for fault detection in dynamic systems
[NASA-CASE-NPO-18982-1-CU] p 3449 N93-30413
Qualitative methods in computer vision
[AD-A264335] p 3533 N93-30418
Multiresolution analysis of SAR data
[AD-A264727] p 3393 N93-30576
An algorithm for simple and complex feature detection: From retina to primary visual cortex
[AD-A264306] p 3497 N93-30897

PATTERN REGISTRATION
Recognizing parameterized objects from range data
[OUEL-1918/92] p 3523 N93-28486

PAVEMENTS
Mathematical model of frost heave and thaw settlement in pavements
[CRREL-REPT-93-2] p 3262 N93-30103

PAYLOAD INTEGRATION
Space transportation analysis and design (Reissue A)
[AD-A262752] p 3271 N93-28487
Project UM-HAUL: A self-unloading reusable lunar lander p 3232 N93-29740

PAYLOAD RETRIEVAL (STS)
Retrievable payload carrier, next generation Long Duration Exposure Facility: Update 1992
p 3283 N93-29705

PAYLOADS
Multipurpose satellite bus (MPS) p 3232 N93-29743
Assessment of Columbus payload operations capabilities by scheduling with the MARS system
[ESA-STR-235] p 3281 N93-30106
Payload flight assignments. NASA mixed fleet
[NASA-TM-108255] p 3268 N93-30133
Aerospace payload design and development
[AD-A264502] p 3289 N93-30402

PEEK
Evaluation of polyaryl adhesives in elastomer-stainless steel joints
[DE93-009794] p 3329 N93-28551
An investigation of graphite peek composite under compression with a centrally located circular discontinuity
[AD-A262549] p 3298 N93-29414
Consolidation of graphite thermoplastic textile preforms for primary aircraft structure p 3302 N93-30439
Delaminations in composite plates under impact loads
p 3304 N93-30849
Advanced fiber/matrix material systems
p 3305 N93-30854

PEGASUS AIR-LAUNCHED BOOSTER

Spacecraft and launch systems for TACSAT applications p 3284 N93-29904

PENETRATION

Lunar regolith penetrators and cutters p 3276 N93-29117

Report of the Meteoroid and Debris Special Investigation Group p 3638 N93-29355

The effect of material strength on segment penetration behavior
[AD-A263262] p 3453 N93-29801

PERCEPTION

Cognitive and Neural Sciences Division 1992 programs
[AD-A263400] p 3654 N93-29258

PERFORMANCE PREDICTION

High performance dispersion model PHYSIC
[DE93-753303] p 3467 N93-28536

The identification of early warning signals prior to contractor default
[AD-A262828] p 3609 N93-29433

Flight mechanical model for performance calculations and interactions between flight vehicle and ramjet in regard to the flight orbit
[ESA-TT-1267] p 3248 N93-29464

SWAT system performance predictions
[AD-A262857] p 3579 N93-29470

Predicting radiation induced performance decrements of AH-1 helicopter crews. Volume 2: Evaluation of modeling and simulation techniques for predicting radiation induced performance decrements
[AD-A262872] p 3506 N93-29484

Predicting aircrew training performance with psychometric g
[AD-A264021] p 3498 N93-30026

A methodology and tool for the prediction of depth of reception in the sea for a VLF/LF communications system p 3397 N93-30741

PERFORMANCE TESTS

Time delay measurements of current primary FAA air/ground transmitters and receivers
[DOT/FAA/CT-TN93/14] p 3379 N93-28555

High octane ethers from synthesis gas-derived alcohols
[DE93-012470] p 3341 N93-28752

Transient tests on an MHD thruster
[DE93-008656] p 3587 N93-29299

Design and performance evaluation of a gas chromatograph micromachined in a single crystal silicon substrate
[AD-A262594] p 3596 N93-29424

Performance measurement systems: A best practices study
[AD-A262180] p 3506 N93-29444

Data Multiplexing Network (DMN) equipment Operational Test and Evaluation (OT&E) integration test report
[AD-A263172] p 3538 N93-29490

FDDI installation and performance analysis
[AD-A263263] p 3529 N93-29497

PERIODIC FUNCTIONS

Extracting infinite system properties from finite size clusters: Phase randomization/boundary condition averaging
[AD-A264712] p 3551 N93-30503

A remark on the invariant measure for the nonlinear Schroedinger equation
[DE93-609840] p 3552 N93-30946

PERIODIC VARIATIONS

Extracting infinite system properties from finite size clusters: Phase randomization/boundary condition averaging
[AD-A264712] p 3551 N93-30503

PERIPHERAL VISION

A simple computational model of center-surround receptive fields in the retina
[AD-A264723] p 3496 N93-30515

PERMAFROST

A field investigation of water and salt movement in permafrost and the active layer
[AD-A263706] p 3487 N93-29298

PERMANENT MAGNETS

Forces on a magnet moving past figure-eight coils
[DE93-009965] p 3561 N93-29189

PERMEABILITY

Gas permeability of E/EP semicrystalline diblock copolymers
[AD-A263241] p 3329 N93-28560

NASA in-step: Permeable membrane experiment p 3267 N93-28736

PERMEATING

Gas permeability of E/EP semicrystalline diblock copolymers
[AD-A263241] p 3329 N93-28560

PERMITTIVITY

Fast multipole method in simulations of aqueous systems
[AD-A263422] p 3567 N93-29336

PERSONAL COMPUTERS

Study on the concurrent calculation with a multitransputer network
[DE93-753191] p 3524 N93-28531

Prototype and short-run printed circuit board creation
[AD-A263245] p 3409 N93-29655

Low cost instrumentation: Parallel port analog to digital converter
[AD-A263468] p 3433 N93-30584

Software conception and structure of automated workstation for an experimental data processing
[DE93-609815] p 3623 N93-30994

PERSONALITY

Accident proneness: A research review
[DOT/FAA/AM-93/9] p 3498 N93-28622

PERSONALITY TESTS

Field test of a computer-driven tool to measure psychological characteristics of aircrew
[AD-A264484] p 3499 N93-30425

PERSONNEL

Technology transfer personnel exchange at the Boeing Company
[DE93-010190] p 3625 N93-29329

PERSONNEL DEVELOPMENT

Profiles of major federal literacy programs
[PB93-163863] p 3608 N93-30657

PERSONNEL MANAGEMENT

Determinants of performance rating accuracy: A field study
[AD-A264726] p 3500 N93-30575

PERTURBATION

Poloidal field measurements during transient phenomena on MTX: Sawtooth perturbations and the effect of ECH on disruptions
[DE93-010516] p 3587 N93-29303

Algorithms for point set congruence
[AD-A264016] p 3532 N93-29980

Study of effects of small perturbations on chaotic systems
[DE93-009762] p 3557 N93-30048

Vibration control of flexible space structures in noisy environment p 3285 N93-30235

Mithras studies of the boundary between open and closed field lines
[AD-A264758] p 3479 N93-30562

Non-perturbative calculation of equilibrium polarization of stored electron beams
[DE93-764500] p 3577 N93-30607

Transient (approximately equals 10 s) VLF amplitude and phase perturbations due to lightning-induced electron precipitation into the ionosphere (the Trimpi effect) p 3396 N93-30736

ELF propagation in deep and shallow sea water p 3397 N93-30739

PERTURBATION THEORY

Electron interactions with non-linear polyatomic molecules and their radicals and ions
[AD-A262279] p 3568 N93-29446

The thermochemistry and reaction pathways of the decomposition and combustion of energetic materials p 3343 N93-30063

Parton's picture of the electroweak processes in high energy e(+)e(-)-collisions
[DE93-606107] p 3571 N93-30788

PETN

A steric hindrance model for the crystal orientation dependence of the shock initiation sensitivity of PETN explosive
[LA-UR-92-1427] p 3345 N93-30074

Computational analysis of slip in PETN
[DE92-040222] p 3598 N93-30445

PETRI NETS

Resource utilization model for the algorithm to architecture mapping model
[NASA-CR-193122] p 3527 N93-29171

Performance analysis of communication protocols using D-timed Petri net p 3356 N93-30227

On analytical performance modelling of software for distributed systems p 3364 N93-30279

PETROLEUM PRODUCTS

Design issues of a reinforcement-based self-learning fuzzy controller for petrochemical process control p 3512 N93-29533

PHARMACOLOGY

Pharmacokinetics and Pharmacodynamics in Space
[NASA-CP-10048] p 3494 N93-29502

Hydrogen-rated system for in vitro studies at pressure: Operating procedures and emergency procedures
[AD-A264179] p 3497 N93-30882

PHASE CHANGE MATERIALS

Thermal energy storage flight experiment in microgravity p 3265 N93-28720

PHASE CONJUGATION

SWAT system performance predictions
[AD-A262857] p 3579 N93-29470

Investigations of self-pumped phase conjugate laser beams and coherence length
[AD-A263438] p 3438 N93-29789

PHASE DEMODULATORS

Design and integration of high bit rate four phase monolithic demodulators and modulators at X band
[LAAS-92354] p 3414 N93-31030

PHASE ERROR

Effects of imbalances and DC offsets on I/Q demodulation
[AD-A264466] p 3393 N93-30537

Study of a VLF distributed antenna array p 3398 N93-30749

PHASE LOCKED SYSTEMS

Constant frequency pulsed phase-locked loop measuring device
[NASA-CASE-LAR-13823-1] p 3431 N93-29084

Theoretical bit error rate performance of the Kalman filter excisor for FM interference
[AD-A263018] p 3383 N93-29407

A fuzzy control design case: The fuzzy PLL p 3515 N93-29555

High-power Ka-band amplifier p 3385 N93-29590

Improved design concepts for millimeter wave power sources
[AD-A264060] p 3411 N93-29922

PHASE MODULATION

Spatial Light Modulators (SLMs) surface quality
[AD-A263249] p 3579 N93-29656

A systolic-array structure for MTCM receivers p 3357 N93-30236

Design and integration of high bit rate four phase monolithic demodulators and modulators at X band
[LAAS-92354] p 3414 N93-31030

PHASE SEPARATION (MATERIALS)

Phase separation, antiferromagnetism, and superconductivity in superconducting-superoxygenated La(2-x)Sr(x)CuO(4+(delta))
[DE93-009852] p 3598 N93-30517

PHASE SHIFT

Constant frequency pulsed phase-locked loop measuring device
[NASA-CASE-LAR-13823-1] p 3431 N93-29084

PHASE SHIFT CIRCUITS

Optical antenna beam steering using digital phase shifter control
[AD-D015688] p 3383 N93-29455

Modification of the S-band phase shifter model 331A-3 of Electromagnetic Sciences Inc.
[DIGEL-1992-5] p 3399 N93-30836

PHASE SHIFT KEYING

Optical coherent phase diversity systems
[ISBN-90-9004897-9] p 3578 N93-29270

Signal-to-noise ratio losses in full spectrum combining of signals with a downconverted subcarrier p 3386 N93-29599

An error control protocol based on trellis coded modulations p 3358 N93-30237

Comparison of diversity combining, interleaving, and decoding techniques of a scintillated channel p 3362 N93-30266

Temporal synchronization of frequency hopped DPSK p 3365 N93-30285

Signal processor based MSAT trellis coded M-DPSK with adaptive Doppler phasor correction p 3373 N93-30332

Two-stage Doppler phasor corrected TCM/DMPSK for shadowed mobile satellite channels p 3373 N93-30333

PHASE TRANSFORMATIONS

Thermodynamics of swelling and collapse of polyelectrolytic gels
[ETN-93-93485] p 3331 N93-29064

A Riemann problem for an elastic bar that changes phase
[AD-A262827] p 3452 N93-29432

Electric field induced phenomena in STM: Tip deformations and Au(111)-surface phase transitions during tunneling spectroscopy experiments
[AD-A262208] p 3596 N93-29445

Diffraction and holography with photoelectrons and Auger electrons: Some new directions
[DE93-007664] p 3313 N93-29766

Some effects of composition and microstructure on the B2 in equilibrium to DO3 ordered phase transition in Fe3Al alloys
[DE93-009724] p 3325 N93-29813

Rapidly activated dynamic phase transitions in nonlinear solids
[AD-A263601] p 3299 N93-29982

Shock waves and polymorphic phase transitions in energetic materials p 3351 N93-30100

Improvement in ductility of the intermetallic compound Ti3Al
[ESA-TT-1276] p 3325 N93-30105
Sensitive detection of new superconductors created at ultra high pressures
[AD-A264340] p 3597 N93-30161
Phase transition studies in barium and strontium titanates at microwave frequencies p 3293 N93-30970
A dynamical model of structural phase transition in La2CuO4
[DE93-605325] p 3602 N93-31025

PHASE VELOCITY
Constant frequency pulsed phase-locked loop measuring device
[NASA-CASE-LAR-13823-1] p 3431 N93-29084

PHASED ARRAYS
Optical antenna beam steering using digital phase shifter control
[AD-D015688] p 3383 N93-29455
Tolerance theory of phased array antennas: A statistical approach p 3369 N93-30307
Adaptive airborne radar simulation with equalization filter taps
[AD-A264722] p 3393 N93-30514

PHENYLS
Physical chemical studies on molecular composite compositions
[AD-A264834] p 3339 N93-30898

PHOBOS
Spacecraft studies of Phobos and Mars
[NASA-CR-193298] p 3651 N93-30635

PHONONS
Theory of normal and superconducting properties of fullerene-based solids
[DE93-007722] p 3592 N93-28582

PHOSPHAZENE
Water-soluble polyphosphazenes and their hydrogels
[AD-A264883] p 3340 N93-30909

PHOSPHORIC ACID
The use of quantum chemistry to estimate the performance and properties of explosives
[DE92-040369] p 3352 N93-30446
Dioxygen reduction in various acid electrolytes
[AD-A263564] p 3317 N93-30664

PHOSPHORUS COMPOUNDS
The use of quantum chemistry to estimate the performance and properties of explosives
[DE92-040369] p 3352 N93-30446

PHOTOACOUSTIC SPECTROSCOPY
The photodissociation and reaction dynamics of vibrationally excited molecules
[DE93-010896] p 3565 N93-28879
Pulsed laser photoacoustic spectrometer for study of solid materials
[DE93-605290] p 3441 N93-31023

PHOTOCATHODES
Gas electron diffraction employing a pulsed electron beam synchronous with photoexcitation
p 3319 N93-30101

PHOTOCHEMICAL REACTIONS
Membrane-based photochemical systems as models for photosynthetic cells
[DE93-009758] p 3310 N93-28911
Magnetic resonance studies of photo-induced electron transfer reactions
[DE93-012239] p 3311 N93-29182
NO2 unimolecular decomposition: Step-like variation of k(sub uni)(E) p 3318 N93-30068
Single-shot femtosecond spectroscopy: A methodology for observation of solid-state chemical reactions
p 3319 N93-30075
Gas electron diffraction employing a pulsed electron beam synchronous with photoexcitation
p 3319 N93-30101
Photo-desorption from copper alloys
[DE93-011872] p 3326 N93-30490

PHOTOCONDUCTORS
Uniaxially stressed Ge:Ga and Ge:Be
[DE93-010426] p 3594 N93-29150

PHOTODETACHMENT
The production and destruction of negative ions
[DE93-010527] p 3564 N93-28665
Partial cross sections in H(-) photodetachment
[DE93-011570] p 3569 N93-30130

PHOTODISSOCIATION
The photodissociation and reaction dynamics of vibrationally excited molecules
[DE93-010896] p 3565 N93-28879
Photodissociation of HBr/LiF(001): A quantum mechanical model
[NASA-CR-193119] p 3603 N93-28933
Femtosecond laser studies of excited state dynamics
[AD-A263708] p 3439 N93-29918
NO2 unimolecular decomposition: Step-like variation of k(sub uni)(E) p 3318 N93-30068
Optically switchable conductive polymers
[AD-A264751] p 3337 N93-30557

PHOTOELASTIC ANALYSIS
Design and implementation of an interactive isochromatic fringe-analysis system using machine-vision techniques p 3369 N93-30305

PHOTOELECTRIC EMISSION
Excited states in electronic structure calculations
[DE93-007704] p 3592 N93-28642

PHOTOELECTRON SPECTROSCOPY
Laser spectroscopy of hydrocarbon radicals
[DE93-012555] p 3436 N93-28653
Energy spectra and photoelectron work function from YBa2Cu3O7 high-T(sub c) superconductor
[DE93-606329] p 3600 N93-30766

PHOTOELECTRONS
Laser spectroscopy of hydrocarbon radicals
[DE93-012555] p 3436 N93-28653
Diffraction and holography with photoelectrons and Auger electrons: Some new directions
[DE93-007664] p 3313 N93-29766
Defect density measurements in a shocked single crystal of ammonium perchlorate p 3319 N93-30093
A quality monitor and monitoring technique employing optically stimulated electron emission
[NASA-CASE-LAR-15063-1] p 3449 N93-30414
1,2-Dimethyl-1,2-Disila-Closo-Dodecaborane(12), A silicon analog of an ortho-carborane: Synthesis; x ray crystal structure; NMR, vibrational and photoelectron spectra; bonding
[AD-A264709] p 3599 N93-30568
Energy spectra and photoelectron work function from YBa2Cu3O7 high-T(sub c) superconductor
[DE93-606329] p 3600 N93-30766

PHOTOEXCITATION
Uniaxially stressed Ge:Ga and Ge:Be
[DE93-010426] p 3594 N93-29150
Dynamics and photoexcitation in MX and MXX' chain solids
[AD-A264823] p 3561 N93-29711
Gas electron diffraction employing a pulsed electron beam synchronous with photoexcitation
p 3319 N93-30101
Photoinduced charge separation in Q1D heterojunction materials: Evidence for electron-hole pair separation in mixed-halide MX solids
[AD-A264711] p 3598 N93-30501

PHOTOGRAPHIC EMULSIONS
The emulsion chamber technology experiment
p 3268 N93-28743

PHOTOGRAPHIC MEASUREMENT
Measurement of 1s2s(sup 3)S(sub 1)-1s2p(sup 3)P(sub 2,0) intervals in helium-like neon
[DE93-009243] p 3563 N93-28521

PHOTOGRAPHS
Digital image processing of descanned terrestrial ground photographs p 3459 N93-28928
Debris/ice/TPS assessment and integrated photographic analysis for Shuttle Mission STS-55
[NASA-TM-107559] p 3271 N93-29136
Image segmentation using fuzzy LVQ clustering networks p 3511 N93-29528
The Visible Human Project of the National Library of Medicine: Remote access and distribution of a multi-gigabyte data set p 3617 N93-30453

PHOTOGRAPHY
Flash x ray system: Techniques and applications
[DE93-011477] p 3430 N93-28645

PHOTOINTERPRETATION
Rejection of archival photographic objects as optical counterparts of gamma ray bursters
[MPE-PREPRINT-228] p 3631 N93-30642

PHOTOIONIZATION
Discharge of electrically charged clouds
[AD-A263212] p 3480 N93-28518
Polarization dependence of the ionization of helium and neon by 120 femtosecond pulses at 614 nm
[DE93-010514] p 3564 N93-28762

PHOTOLITHOGRAPHY
Laboratory experiments in integrated circuit fabrication
p 3292 N93-30962

PHOTOLUMINESCENCE
Luminescence study of ion-implanted and MBE-grown Er-doped GaAs and Al(x)Ga(1-x)As
[AD-A262602] p 3591 N93-28471

PHOTOLYSIS
The photodissociation and reaction dynamics of vibrationally excited molecules
[DE93-010896] p 3565 N93-28879
Observation of reaction intermediates in crystalline RDX p 3318 N93-30067

PHOTON ABSORPTIOMETRY
The production and destruction of negative ions
[DE93-010527] p 3564 N93-28665

PHOTON BEAMS
Research programs from the University of South Carolina on high energy physics
[DE93-007829] p 3574 N93-28969

PHOTON-ELECTRON INTERACTION
Hard photon emission from high energy electrons and positrons in single crystals
[DE93-606328] p 3600 N93-30770
Single t-quark production in high energy (gamma)e collisions
[DE92-644947] p 3572 N93-30930

PHOTONICS
NSF Tokyo reports: Japanese R and D projects on micro- and nanofabrication and related basic research projects
[PB93-181261] p 3410 N93-29671
Ferroelectric liquid crystal optical interconnect switching systems
[AD-A263751] p 3596 N93-29859
Advanced microwave frequency sources and filters based on superconducting Photonic Band Gap (PBG) structures
[AD-A264404] p 3597 N93-30175

PHOTONS
Discharge of electrically charged clouds
[AD-A263212] p 3480 N93-28518
A unique photon bombardment system for space applications p 3286 N93-28790
NO2 unimolecular decomposition: Step-like variation of k(sub uni)(E) p 3318 N93-30068
Applications of the photorefractive effect and damage induced effects in fibers
[AD-A264339] p 3580 N93-30205
On the photonic chiral anomaly in an external gravitational field
[DE93-606082] p 3479 N93-30785
Single t-quark production in high energy (gamma)e collisions
[DE92-644947] p 3572 N93-30930

PHOTOPRODUCTION
Elementary particle interactions
[DE93-005113] p 3568 N93-29764

PHOTORECEPTORS
Photoreceptors regulating circadian behavior: A mouse model
[AD-A264881] p 3497 N93-30908

PHOTOSPHERE
The detection of low-degree solar gravity mode oscillations by differential radius observations, 1986-1987 p 3652 N93-28605
Optical system analysis for the ground based EXVM
[NASA-CR-192588] p 3582 N93-31035

PHOTOSYNTHESIS
Predicting the response of a temperate forest ecosystem to atmospheric CO2 increase
[DE93-010081] p 3467 N93-28543
Membrane-based photochemical systems as models for photosynthetic cells
[DE93-009758] p 3310 N93-28911
Regulation of alternative CO2 fixation pathways in procaryotic and eucaryotic photosynthetic organisms
[DE93-012109] p 3491 N93-29181

PHOTOVOLTAIC CELLS
The Photovoltaic Array Space Power Plus diagnostics (PASP Plus) flight experiment p 3265 N93-28717
STRV1-b flight experiment p 3265 N93-28723
Measurements and Characterization Branch
[DE93-000094] p 3465 N93-30207
Technical examination and simulation of a photovoltaic system: Solar generator, battery, download
[ETN-93-94179] p 3466 N93-30573
Optically powered, optoelectronic spatial light modulators
[AD-A264765] p 3581 N93-30609

PHOTOVOLTAIC CONVERSION
New III-V cell design approaches for very high efficiency
[DE93-000097] p 3464 N93-28971
Measurements and Characterization Branch
[DE93-000094] p 3465 N93-30207
Growth and development of GaInAsP for use in high-efficiency solar cells
[DE93-000098] p 3465 N93-30208

PHYSICAL CHEMISTRY
Use of statistics in computational chemistry
[AD-A264307] p 3315 N93-30365
The use of quantum chemistry to estimate the performance and properties of explosives
[DE92-040369] p 3352 N93-30446

PHYSICAL EXERCISE
Exercise/recreation facility for a lunar or Mars analog
p 3230 N93-29733
Beta-adrenergic blockade and lactate metabolism during exercise at high altitude
[AD-A263544] p 3495 N93-29820

PHYSICAL FACTORS
Factors influencing the interlaminar fracture toughness and its evaluation in composites
[FFA-TN-1991-34] p 3451 N93-29076
PHYSICAL WORK
Field trial of caffeine on physical performance at altitude: An attempt to overcome the challenge
[AD-A264260] p 3497 N93-30894
PHYSICS
JPRS report: Science and technology. Central Eurasia: Physics and mathematics
[JPRS-UPM-93-002] p 3560 N93-29022
PHYSIOLOGICAL EFFECTS
Evaluation of test methods and requirements for respiratory protection systems 21
[AD-A262466] p 3501 N93-28757
Evaluation of personal cooling systems in conjunction with explosive ordnance disposal suits
[AD-A262862] p 3506 N93-29471
Issues on human acceleration tolerance after long-duration space flights
[NASA-TM-104753] p 3495 N93-29651
Sonic boom problem for future highspeed aircraft
[ONERA-NT-1990-3] p 3241 N93-30020
The Environmental Symptoms Questionnaire (ESQ): Development and application
[AD-A264127] p 3495 N93-30196
Acquisition of physiological data during G-induced Loss of Consciousness (G-LOC)
[AD-A264492] p 3496 N93-30400
Hydrogen-rated system for in vitro studies at pressure: Operating procedures and emergency procedures
[AD-A264179] p 3497 N93-30882
PHYSIOLOGICAL FACTORS
Pharmacokinetics and Pharmacodynamics in Space
[NASA-CP-10048] p 3494 N93-29502
PHYSIOLOGICAL RESPONSES
State of the art: Ecological biomarkers
[DE93-006621] p 3469 N93-28992
Pharmacokinetics and Pharmacodynamics in Space
[NASA-CP-10048] p 3494 N93-29502
Beta-adrenergic blockade and lactate metabolism during exercise at high altitude
[AD-A263544] p 3495 N93-29820
PHYSIOLOGICAL TESTS
Pilot Candidate Selection Method (PCSM): What makes it work?
[AD-A262871] p 3498 N93-29481
PHYSIOLOGY
Pharmacokinetics and Pharmacodynamics in Space
[NASA-CP-10048] p 3494 N93-29502
Evaluation of dried storage of platelets for transfusion: Physiologic integrity and hemostatic functionality
[AD-A263240] p 3494 N93-29620
PHYTOTRONS
Growing wheat to maturity in reduced gas pressures
[NASA-CR-193245] p 3491 N93-29216
PICOSECOND PULSES
Response of a Nb/Al2O3/Nb tunnel junction to picosecond electrical pulses
[DE93-010416] p 3594 N93-29249
PICTURE TUBES
Computer-controlled alignment for a 2000-line color monitor p 3247 N93-30324
PIEZOELECTRIC CERAMICS
Materials for adaptive structural acoustic control, volume 1
[AD-A264619] p 3562 N93-30121
Materials for adaptive structural acoustic control, volume 2
[AD-A264620] p 3563 N93-30385
PIEZOELECTRICITY
Structure and switching dynamics in ferroelectric crystal and liquid crystal thin films
[AD-A263664] p 3594 N93-29293
Proceedings of the 25th European Conference on the Application of Polar Dielectrics to celebrate the 25th anniversary of the Dielectric Society, incorporating the 1st International Workshop on Integrated Ferroelectrics
[AD-A263427] p 3332 N93-29337
PILOT ERROR
Pilot intent and error recognition as part of a knowledge based cockpit assistant p 3502 N93-28855
PILOT PERFORMANCE
Combat Automation for Airborne Weapon Systems: Man/Machine Interface Trends and Technologies
[AGARD-CP-520] p 3501 N93-28850
Pilot decision aiding for weapon delivery: A novel approach to fire control cueing using parallel computing
p 3501 N93-28853
A new class of mission support for combat air-crew
p 3501 N93-28854
Pilot intent and error recognition as part of a knowledge based cockpit assistant p 3502 N93-28855
The design and development of the new RAF standard HUD format p 3502 N93-28856
Symbology for head up and head down applications for highly agile fighter aircraft: To improve spatial awareness, trajectory control, and unusual attitude recovery, part 1
p 3502 N93-28857
The quest for an integrated flying helmet
p 3502 N93-28860
The physiological limitations of man in the high G environment p 3503 N93-28861
Oculo-motor responses and virtual image displays
p 3503 N93-28862
Human capabilities and limitations in situation awareness p 3503 N93-28863
Predicting radiation induced performance decrements of AH-1 helicopter crews. Volume 2: Evaluation of modeling and simulation techniques for predicting radiation induced performance decrements
[AD-A262872] p 3506 N93-29484
An evaluation of B-1B pilot performance during simulated instrument approaches with and without status information
[AD-A263874] p 3507 N93-29888
Field test of a computer-driven tool to measure psychological characteristics of aircrew
[AD-A264484] p 3499 N93-30425
The effects of superimposing symbology on a simulated night vision goggle display
[AD-A263458] p 3508 N93-30590
Training effectiveness assessment: Methodological problems and issues p 3237 N93-30684
PILOT SELECTION
Pilot Candidate Selection Method (PCSM): What makes it work?
[AD-A262871] p 3498 N93-29481
PILOT TRAINING
Predicting aircrew training performance with psychometric g
[AD-A264021] p 3498 N93-30026
Part 1: Executive summary p 3236 N93-30674
Helicopter simulator standards p 3236 N93-30675
Helicopter simulation: An aircrew training and qualification perspective p 3236 N93-30676
Simulators for corporate pilot training and evaluation
p 3236 N93-30678
Training effectiveness assessment: Where are we?
p 3236 N93-30679
Current training: Where are we? p 3236 N93-30680
Helicopter simulator qualification
p 3237 N93-30681
Helicopter simulation: Making it work
p 3237 N93-30682
Helicopter training simulators: Key market factors
p 3237 N93-30683
Training effectiveness assessment: Methodological problems and issues p 3237 N93-30684
Determining the transferability of flight simulator data
p 3237 N93-30685
Progress through precedent: Going where no helicopter simulator has gone before p 3237 N93-30686
Transfer of training and simulator qualification or myth and folklore in helicopter simulation
p 3237 N93-30687
PILOTLESS AIRCRAFT
Development and testing of the Perseus proof-of-concept aircraft
[DE93-010121] p 3247 N93-28586
A real-time, hardware-in-the-loop simulation of an unmanned aerial research vehicle
[AD-A262477] p 3248 N93-29409
PILOTS (PERSONNEL)
An analysis of en route controller-pilot voice communications
[AD-A264784] p 3394 N93-30611
PINEAL GLAND
The Gordon Research Conference on Pineal Cell Biology
[AD-A264840] p 3497 N93-30904
PINHOLE CAMERAS
Refinements on the pinhole camera measurements of the LDEF attitude p 3283 N93-29622
PIONEER VENUS SPACECRAFT
Precise tracking of the Magellan and Pioneer Venus orbiters by Same-Beam Interferometry. Part 2: Orbit determination analysis p 3270 N93-29589
PIONS
Pion pair production in photon-photon collisions
[DE93-606114] p 3571 N93-30790
PIPE FLOW
Prediction of gas-liquid two-phase flow regime in microgravity
[NASA-TM-106274] p 3352 N93-30939
PIPELINES
Potential transmission and transients during corrosion: Applications to corrosion monitoring
[DE93-010863] p 3323 N93-29256
Power generation and transportation systems research department
[PB93-178309] p 3352 N93-30663
PIPES (TUBES)
Overview of piping issues and trends
[DE93-006628] p 3354 N93-28893
Potential transmission and transients during corrosion: Applications to corrosion monitoring
[DE93-010863] p 3323 N93-29256
Valve malfunction detection apparatus
[NASA-CASE-MFS-29904-1] p 3432 N93-29503
Examination of formability to seamless tubes on Ni-Cr-W superalloy
[DE93-764158] p 3326 N93-30396
PIPETTES
Micropipet manipulation of lipid membranes: Direct measurement of the material properties of a cohesive structure that is only two molecules thick
p 3291 N93-30953
PISTON ENGINES
Small Stirling dynamic isotope power system for robotic space missions
[NASA-TM-105785] p 3287 N93-28686
PITCH (INCLINATION)
Wind loads on canopy roofs
[RR-CE132] p 3451 N93-29106
PITCHING MOMENTS
Evaluation of four advanced nozzle concepts for short takeoff and landing performance
[NASA-TP-3314] p 3239 N93-29165
Aerodynamic characteristics of a rotorcraft airfoil designed for the tip region of a main rotor blade
[NASA-TM-4264] p 3240 N93-29450
Construction, wind tunnel testing and data analysis for a 1/5 scale ultra-light wing model p 3243 N93-29778
PIXELS
Radiometric calibration system for IR cameras
[DE93-009237] p 3430 N93-28520
Design of a pixel cell optimized for a data push architecture readout
[DE93-011016] p 3616 N93-30122
Feature segmentation using a multiple-stack based chain coding algorithm p 3359 N93-30243
PLANAR STRUCTURES
Planar microstrip YAGI antenna array
[NASA-CASE-NPO-17873-2-CU] p 3384 N93-29507
Nonlinear attitude control of planar structures in space using only internal controls p 3280 N93-29991
PLANCKS CONSTANT
Planck scale effects in neutrino physics
[DE93-606133] p 3571 N93-30793
Formulation of wave mechanics without the Planck constant h/2 pi
[DE93-604083] p 3608 N93-30987
PLANE STRAIN
Bainitic stabilization of austenite in low alloy steels
[DE93-008275] p 3321 N93-28957
PLANE WAVES
The wave, the cylinder, and the plate
[DE93-009458] p 3450 N93-28596
Performance analysis of subspace methods
[AD-A263984] p 3530 N93-29865
Application of integral and differential equation methods for various EM interaction problems
[AD-A264821] p 3394 N93-30597
A tight binding model for the electronic structure of FCC and SC C60
[DE93-606214] p 3601 N93-30794
PLANETARY ATMOSPHERES
Space research in Germany 1990-1991
[ETN-93-93807] p 3654 N93-28477
Rugged, no-moving-parts windspeed and static pressure probe designs for measurements in planetary atmospheres p 3434 N93-28767
Remote measurement of planetary magnetic fields by the Hanle effect p 3645 N93-28793
Mass spectrometric measurement of Martian krypton and xenon isotopic abundance p 3646 N93-28798
PLANETARY BASES
Single-stage Mars mission p 3232 N93-29742
Mars habitat p 3233 N93-29747
PLANETARY COMPOSITION
Thermal Analyzer for Planetary Soil (TAPS): An in situ instrument for mineral and volatile-element measurements p 3643 N93-28782
An integrated XRF/XRD instrument for Mars exobiology and geology experiments p 3645 N93-28792
Visible imaging on the Pluto fast flyby mission
p 3646 N93-28799
A DTA/GC for the in situ identification of the Martian surface material p 3646 N93-28800
Drill/borescope system for the Mars Polar Pathfinder
p 3647 N93-28805
Gamma ray/neutron spectrometers for planetary elemental mapping p 3647 N93-28807

Prototype backscatter Moessbauer spectrometer for measurement of Martian surface mineralogy
p 3648 N93-28812
A team approach to the development of gamma ray and x ray remote sensing and in situ spectroscopy for planetary exploration missions p 3650 N93-28824

PLANETARY CORES
Investigation of Mars rotational dynamics using Earth-based radio tracking of Mars landers
p 3642 N93-28777

PLANETARY ENVIRONMENTS
Thermal Analyzer for Planetary Soil (TAPS): An in situ instrument for mineral and volatile-element measurements p 3643 N93-28782
Lightweight modular instrumentation for planetary applications p 3286 N93-28787

PLANETARY GEOLOGY
An integrated XRF/XRD instrument for Mars exobiology and geology experiments p 3645 N93-28792
Optimism experiment and development of space-qualified seismometers in France
p 3646 N93-28796
Visible imaging on the Pluto fast flyby mission
p 3646 N93-28799
A DTA/GC for the in situ identification of the Martian surface material p 3646 N93-28800
Spacecraft studies of Phobos and Mars
[NASA-CR-193298] p 3651 N93-30635

PLANETARY IONOSPHERES
Space research in Germany 1990-1991
[ETN-93-93807] p 3654 N93-28477
Plasma, magnetic, and electromagnetic measurements at nonmagnetic bodies p 3647 N93-28809

PLANETARY MAGNETIC FIELDS
Remote measurement of planetary magnetic fields by the Hanle effect p 3645 N93-28793
Plasma, magnetic, and electromagnetic measurements at nonmagnetic bodies p 3647 N93-28809

PLANETARY MAGNETOSPHERES
Plasma, magnetic, and electromagnetic measurements at nonmagnetic bodies p 3647 N93-28809

PLANETARY MANTLES
Venus Interior Structure Mission (VISM): Establishing a seismic network on Venus p 3649 N93-28819

PLANETARY MAPPING
Design concept for an IR mapping spectrometer for the Pluto fast flyby mission p 3285 N93-28779
Multibeam laser altimeter for planetary topographic mapping p 3442 N93-28780
Gamma ray/neutron spectrometers for planetary elemental mapping p 3647 N93-28807

PLANETARY RINGS
On symmetric central configurations with application to satellite motion about rings p 3652 N93-31000

PLANETARY STRUCTURE
Drill/borescope system for the Mars Polar Pathfinder
p 3647 N93-28805
Venus Interior Structure Mission (VISM): Establishing a seismic network on Venus p 3649 N93-28819
Design optimization of space structures
p 3278 N93-29122

PLANETARY SURFACES
Laer-induced breakdown spectroscopy instrument for element analysis of planetary surfaces
p 3434 N93-28769
A remote laser-mass spectrometer for determination of elemental composition p 3434 N93-28775
Multibeam laser altimeter for planetary topographic mapping p 3442 N93-28780
Thermal Analyzer for Planetary Soil (TAPS): An in situ instrument for mineral and volatile-element measurements p 3643 N93-28782
Visible imaging on the Pluto fast flyby mission
p 3646 N93-28799
Onboard signal processing: Wave of the future for planetary radio science? p 3646 N93-28801

PLANETARY SYSTEMS
Detection of other planetary systems using photometry p 3632 N93-28791

PLANETOLOGY
Workshop on Advanced Technologies for Planetary Instruments, part 1
[NASA-CR-193015] p 3639 N93-28764

PLANNING
Natural language generation
[AD-A262578] p 3524 N93-28579

PLASMA ACCELERATION
Elemental compositions of high-energy ions produced by magnetosonic waves in quiescent plasmas
[DE93-753241] p 3588 N93-29434
Ion ring distribution produced by a magnetosonic wave
[DE93-754311] p 3590 N93-30533

PLASMA CLOUDS
USU center of excellence in theory and analysis of the geo-plasma environment
[AD-A264750] p 3590 N93-30585

PLASMA CONTROL
JT-60 Upgrade vertical stability experiments and analysis
[DE93-753131] p 3583 N93-28530
Edge plasma control by RF electric field in Compact Helical System (CHS)
[DE93-753242] p 3583 N93-28532
Self-organized profile relaxation by ion temperature gradient instability in toroidal plasmas
[DE93-009580] p 3585 N93-28910
Electron cyclotron heating and current drive in toroidal geometry
[DE93-010400] p 3586 N93-29049
Computing for magnetic fusion energy research: An updated vision
[DE93-010394] p 3587 N93-29190
Poloidal field measurements during transient phenomena on MTX: Sawtooth perturbations and the effect of ECH on disruptions
[DE93-010516] p 3587 N93-29303
Modeling the D3-D plasma boundary with the LEDGE code
[DE93-009301] p 3588 N93-29772
Fundamental studies of fusion plasmas
[DE93-013144] p 3589 N93-30189
Experimental MHD stability limit in the gas-dynamic trap
[DE93-606218] p 3591 N93-30780
Plasma diffusion through multidipole magnetic fields
[DE93-608548] p 3591 N93-31007

PLASMA CURRENTS
Solar flare MDH
[AD-A262275] p 3652 N93-28756
The fluctuation induced Hall effect
[DE93-010130] p 3585 N93-28912
Bootstrap current profiles and scaling in large aspect ratio tokamaks
[DE93-753158] p 3589 N93-30003

PLASMA DENSITY
Start broadened profiles with self-consistent radiation transfer and atomic kinetics in plasmas produced by high intensity lasers
[DE93-008706] p 3586 N93-29093
Effects of neutral gas collisions on the power transmission factor at the divertor sheath
[DE93-009320] p 3588 N93-29334
High density plasma production in a multicusp plasma generator with RF antenna
[DE93-764493] p 3590 N93-30606
Measurements of the energy spectrum of an intense microsecond relativistic electron beam in the beam-plasma experiments using a multi-foil analyzer
[DE93-606271] p 3590 N93-30768

PLASMA DIAGNOSTICS
Plasma diagnostics by antenna impedance measurements p 3400 N93-28820
Start broadened profiles with self-consistent radiation transfer and atomic kinetics in plasmas produced by high intensity lasers
[DE93-008706] p 3586 N93-29093
Modeling the D3-D plasma boundary with the LEDGE code
[DE93-009301] p 3588 N93-29772
A new multichannel soft x ray framing camera for fusion experiments
[DE93-009302] p 3432 N93-29773
Operation of a 20-channel grating polychromator diagnostic system and its application to sawtooth observations in JT-60U
[DE93-764388] p 3590 N93-30398

PLASMA DIFFUSION
Plasma diffusion through multidipole magnetic fields
[DE93-608548] p 3591 N93-31007

PLASMA DYNAMICS
Ion motion effects on charged radiators
[DE93-009257] p 3565 N93-29099

PLASMA ELECTRODES
Engineering consideration for the self-energizing magnetoplasmadynamic (MPD): Type fusion plasma thruster
[AD-A262785] p 3288 N93-29289

PLASMA FOCUS
Engineering consideration for the self-energizing magnetoplasmadynamic (MPD): Type fusion plasma thruster
[AD-A262785] p 3288 N93-29289

PLASMA GENERATORS
High density plasma production in a multicusp plasma generator with RF antenna
[DE93-764493] p 3590 N93-30606

PLASMA HEATING
Observation of a beam energy shift caused by a plasma wakefield
[DE93-753243] p 3583 N93-28533
Development of high power microwave source
[DE93-753316] p 3436 N93-28980
Electron cyclotron heating and current drive in toroidal geometry
[DE93-010400] p 3586 N93-29049
Poloidal field measurements during transient phenomena on MTX: Sawtooth perturbations and the effect of ECH on disruptions
[DE93-010516] p 3587 N93-29303
Fundamental studies of fusion plasmas
[DE93-013144] p 3589 N93-30189
High density plasma production in a multicusp plasma generator with RF antenna
[DE93-764493] p 3590 N93-30606

PLASMA INTERACTION EXPERIMENT
Transfer Orbit Plasma Interaction Experiment (TROPIX) p 3267 N93-28734

PLASMA INTERACTIONS
Transfer Orbit Plasma Interaction Experiment (TROPIX) p 3267 N93-28734
Report on the sintering and properties of MgO and MgO-5 percent TiC
[DE93-008676] p 3323 N93-29092

PLASMA JETS
Preliminary investigation of high power microwave plasmas for electrothermal thruster use
[NASA-TM-106207] p 3288 N93-29158
Plasma/particle interaction in subsonic argon/helium thermal plasma jets
[DE93-010808] p 3589 N93-30181

PLASMA OSCILLATIONS
The fluctuation induced Hall effect
[DE93-010130] p 3585 N93-28912

PLASMA PHYSICS
JT-60 Upgrade vertical stability experiments and analysis
[DE93-753131] p 3583 N93-28530
Edge plasma control by RF electric field in Compact Helical System (CHS)
[DE93-753242] p 3583 N93-28532
Observation of a beam energy shift caused by a plasma wakefield
[DE93-753243] p 3583 N93-28533
New remote maintenance approach for TPX
[DE93-007857] p 3584 N93-28583
JPRS report: Science and technology. Central Eurasia: Physics and mathematics
[JPRS-UPM-93-002] p 3560 N93-29022
A survey of problems in divertor and edge plasma theory
[DE93-007531] p 3586 N93-29056
Novel methods of acceleration
[AD-A264828] p 3590 N93-30600
Plasma Physics Network Newsletter, no. 5
[DE93-606216] p 3591 N93-30795

PLASMA PROPULSION
Engineering consideration for the self-energizing magnetoplasmadynamic (MPD): Type fusion plasma thruster
[AD-A262785] p 3288 N93-29289

PLASMA RADIATION
A remote laser-mass spectrometer for determination of elemental composition p 3434 N93-28775
Ion motion effects on charged radiators
[DE93-009257] p 3565 N93-29099

PLASMA SHEATHS
Effects of neutral gas collisions on the power transmission factor at the divertor sheath
[DE93-009320] p 3588 N93-29334

PLASMA SPRAYING
Plasma/particle interaction in subsonic argon/helium thermal plasma jets
[DE93-010808] p 3589 N93-30181
Method of fabricating a rocket engine combustion chamber
[NASA-CASE-MFS-28569-1] p 3338 N93-30565

PLASMA TEMPERATURE
Self-organized profile relaxation by ion temperature gradient instability in toroidal plasmas
[DE93-009580] p 3585 N93-28910
Start broadened profiles with self-consistent radiation transfer and atomic kinetics in plasmas produced by high intensity lasers
[DE93-008706] p 3586 N93-29093

PLASMA TURBULENCE
Nonlinear dynamics and plasma transport
[DE93-012238] p 3585 N93-28749

PLASMA WAVES
Observation of a beam energy shift caused by a plasma wakefield
[DE93-753243] p 3583 N93-28533
A Fokker-Planck operator for the emission and absorption of electron plasma waves in a magnetized plasma
[DE93-009579] p 3584 N93-28598
A novel approach for new radiation sources based on solid state plasma instabilities
[AD-A263699] p 3588 N93-29382

Elemental compositions of high-energy ions produced by magnetosonic waves in quiescent plasmas
[DE93-753241] p 3588 N93-29434

PLASMA-PARTICLE INTERACTIONS

Plasma/particle interaction in subsonic argon/helium thermal plasma jets
[DE93-010808] p 3589 N93-30181

PLASMAS (PHYSICS)

Moment approach to fast ion neoclassical transport and viscous forces
[DE93-753305] p 3585 N93-28979

Ion motion effects on charged radiators
[DE93-009257] p 3565 N93-29099

Elemental compositions of high-energy ions produced by magnetosonic waves in quiescent plasmas
[DE93-753241] p 3588 N93-29434

Optimization of HPM device parameters for maximum air transmission
[DE93-007332] p 3386 N93-29765

Measurement of work function of a plasma grid in a cesium seeded negative ion source
[DE93-764153] p 3589 N93-30190

High density plasma production in a multicusp plasma generator with RF antenna
[DE93-764493] p 3590 N93-30606

Plasma Physics Network Newsletter, no. 5
[DE93-606216] p 3591 N93-30795

PLASTIC COATINGS

Thermal control paints on LDEF: Results of M0003 sub-experiment 18
[AD-A263252] p 3329 N93-28561

PLASTIC DEFORMATION

Deformation mechanisms in Be(sub 12)X compounds
[DE93-009080] p 3320 N93-28548

Balanced technology initiative on computational mechanics of materials
[AD-A263906] p 3453 N93-29863

Plastic deformation behaviour of oxide dispersion strengthened titanium alloys
[ONERA-NT-1990-6] p 3326 N93-30138

Computational analysis of slip in PETN
[DE92-040222] p 3598 N93-30445

PLASTIC PROPELLANTS

A simple model for explosives formulation
[DE93-010703] p 3341 N93-29251

PLASTIC PROPERTIES

Damage mechanics in 2-D and 3-D microstructures
[AD-A264337] p 3453 N93-30159

A continuum code investigation of stress integration using exact and approximate material rotation
[DE93-001892] p 3454 N93-31013

PLASTICS

Development of a test program to evaluate structural defects in Glass-Reinforced Plastic (GRP), volume 2
[AD-A263814] p 3335 N93-29881

Development of a test program to evaluate structural defects in Glass-Reinforced Plastic (GRP), volume 1
[AD-A263813] p 3335 N93-29886

Mold bolt and means for achieving close tolerances between bolts and bolt holes
[NASA-CASE-MFS-28720-1] p 3447 N93-30567

PLATELETS

Evaluation of dried storage of platelets for transfusion: Physiologic integrity and hemostatic functionality
[AD-A263240] p 3494 N93-29620

PLATES (STRUCTURAL MEMBERS)

Comparison of impact results for several polymeric composites over a wide range of low impact velocities
p 3304 N93-30848

Delaminations in composite plates under impact loads
p 3304 N93-30849

PLATING

Development of nickel/metal hydride secondary battery
[DE93-781330] p 3406 N93-28669

PLATINUM

In-situ x ray studies of the underpotential deposition of copper on platinum (3)
[AD-A263361] p 3595 N93-29331

Platinum-modified diffusion aluminide coatings on nickel-base superalloys
[AD-A263597] p 3325 N93-29981

Applications of transition metal compounds in the preparation of useful silicon-containing ceramics
[AD-A264028] p 3335 N93-30028

Photoinduced charge separation in Q1D heterojunction materials: Evidence for electron-hole pair separation in mixed-halide MX solids
[AD-A264711] p 3598 N93-30501

Dioxygen reduction in various acid electrolytes
[AD-A263564] p 3317 N93-30664

PLOTTING

XRONOS: A timing analysis software package. User's guide, version 3.00
[NASA-TM-109222] p 3532 N93-30023

PLUG NOZZLES

Reliability assessment of thrust chamber cooling concepts using probabilistic analysis techniques
[NASA-CR-190785] p 3288 N93-29068

PLUMES

Return flux experiment p 3266 N93-28727

The Ultraviolet Plume Instrument (UVPI)
p 3285 N93-28784

The +vbar breakout during approach to Space Station Freedom
[NASA-TM-104772] p 3269 N93-30135

PLUTO (PLANET)

Visible imaging on the Pluto fast flyby mission
p 3646 N93-28799

Pluto fast flyby mission and science overview
p 3649 N93-28818

PLUTONIUM

Polymeric materials for use in wet hydrochloric acid environments
[DE93-010881] p 3330 N93-28600

PLY ORIENTATION

Composite laminate stiffnesses and their sensitivities
[DLR-FB-92-16] p 3296 N93-29007

PNEUMATIC EQUIPMENT

Advanced coordinate measuring machine at Sandia National Laboratories
[DE93-010618] p 3432 N93-29842

POINCARE PROBLEM

Positive energy representations of the conformal quantum algebra
[DE93-606064] p 3551 N93-30809

Regular and chaotic motion of two dimensional electrons in a strong magnetic field
[DE93-604091] p 3607 N93-30933

POINT SPREAD FUNCTIONS

Semi-blind restoration of images distorted by random time varying point spread functions
p 3375 N93-30344

POISSON EQUATION

Scaling properties of localized quantum chaos
[DE93-606031] p 3606 N93-30803

POISSON RATIO

Enhanced noncontacting laser extensometer for biaxial strain measurements
[AD-A263170] p 3430 N93-28989

POLAR CAP ABSORPTION

ELF/VLF radio noise measurements at high latitudes during solar particle events p 3397 N93-30744

Performance statistics bulletin. High latitude meteor scatter propagation, May, June, July 1989
[AD-A264003] p 3399 N93-30757

POLAR CAPS

Drill/borescope system for the Mars Polar Pathfinder
p 3647 N93-28805

Electrodynamics of the dayside cleft region based on ground observations at Svalbard
[AD-A263571] p 3477 N93-29831

POLAR CUSPS

The dynamic cusp at low altitudes: A case study combining Viking, DMSP, and Sondrestrom incoherent scatter radar observations
[NASA-CR-193152] p 3476 N93-28842

POLAR REGIONS

NOAA satellite programs and technology requirements
p 3627 N93-30710

ELF/VLF radio noise measurements at high latitudes during solar particle events p 3397 N93-30744

POLARIMETERS

Poloidal field measurements during transient phenomena on MTX: Sawtooth perturbations and the effect of ECH on disruptions
[DE93-010516] p 3587 N93-29303

Polarization experiments with hadronic and electromagnetic probes
[DE93-011375] p 3392 N93-30126

POLARIMETRY

Polarimetric multispectral imaging technology
p 3434 N93-28774

The MAESTRO-1 campaign: Analyses of polarimetric SAR data of agricultural fields and forests
[BCRS-92-06] p 3460 N93-29320

Optical system analysis for the ground based EXVM
[NASA-CR-192588] p 3582 N93-31035

POLARITY

Transient tests on an MHD thruster
[DE93-008656] p 3587 N93-29299

POLARIZATION

Non-perturbative calculation of equilibrium polarization of stored electron beams
[DE93-764500] p 3577 N93-30607

POLARIZATION (CHARGE SEPARATION)

Ultrafast optical studies of surface reaction processes at semiconductor interfaces
[DE93-009049] p 3593 N93-29096

Dynamics and photoexcitation in MX and MXX' chain solids
[AD-A264823] p 3561 N93-29711

Photoinduced charge separation in Q1D heterojunction materials: Evidence for electron-hole pair separation in mixed-halide MX solids
[AD-A264711] p 3598 N93-30501

Photoinduced electron-hole charge separation, intrinsic self-doping and novel device applications of Q1D heterojunction materials: Mixed-halide MX solids
[AD-A264714] p 3600 N93-30569

Charge separation in bipolar transistors
[DE93-009624] p 3413 N93-30650

POLARIZATION (SPIN ALIGNMENT)

A high field optical-pumping spin-exchange polarized deuterium source
[DE93-009208] p 3574 N93-28970

POLARIZATION (WAVES)

Polarization experiments with hadronic and electromagnetic probes
[DE93-011375] p 3392 N93-30126

POLARIZED LIGHT

A compact imaging detector of polarization and spectral content p 3582 N93-28810

Polarization modulated ellipsometry
[NASA-CR-4012] p 3580 N93-30372

POLARIZED RADIATION

Theoretical-experimental study of the non-thermal effects of the polarized laser radiation in living tissues
[DE93-607212] p 3441 N93-30775

POLARIZERS

Rib arrow integrated optic polarizer
p 3357 N93-30231

POLAROGRAPHY

Analytical applications of electrified interfaces between two immiscible solutions
[AD-A263085] p 3311 N93-29132

POLARONS

Photoinduced charge separation in Q1D heterojunction materials: Evidence for electron-hole pair separation in mixed-halide MX solids
[AD-A264711] p 3598 N93-30501

Photoinduced electron-hole charge separation, intrinsic self-doping and novel device applications of Q1D heterojunction materials: Mixed-halide MX solids
[AD-A264714] p 3600 N93-30569

POLICIES

The 9th FLICC Forum on Federal Information Policies
[PB93-184687] p 3624 N93-29668

The 1992 World Administrative Radio Conference: Technology and Policy Implications
[OTA-TCT-549] p 3392 N93-30150

Profiles of major federal literacy programs
[PB93-163863] p 3608 N93-30657

White House/OSTP perspective p 3625 N93-30696

Filling the gaps: An overview of data on education in grades K through 12
[PB93-176550] p 3608 N93-30821

Guide to Federal Water Quality Programs and Information: A Guide with Computer Software Developed by the Interagency Working Group on Water Quality
[PB93-186245] p 3475 N93-30834

POLLUTION

Planning and progress of EPA's pollution prevention research program
[PB93-185767] p 3475 N93-30831

POLLUTION CONTROL

Using a neural network to estimate solvent consumption
[PB93-173110] p 3467 N93-28873

Global warming issue and global economic model
[DE93-781334] p 3468 N93-28881

Fugitive hydrocarbon emissions from Pacific OCS facilities, volume 1
[PB93-173797] p 3468 N93-28899

Building alliances to restore coastal environments: A coastal America progress report
[PB93-169464] p 3470 N93-29674

Multi-Attribute Decision Theory methodology for pollution control measure analysis
[DE93-005444] p 3472 N93-30008

Pollution prevention: A regulatory update
[DE93-009727] p 3472 N93-30180

Planning and progress of EPA's pollution prevention research program
[PB93-185767] p 3475 N93-30831

POLLUTION MONITORING

Summer 1990 Atlanta ozone precursor study (January 1993)
[PB93-167203] p 3470 N93-29200

POLLUTION TRANSPORT
Evaluation of atmospheric wind field and dispersion models for fog-oil smoke dispersion in complex terrain: Field measurement and model evaluation program for assessment of the environmental effects of military smokes
[AD-A262051] p 3482 N93-29399
Study to determine the nature and extent of ozone and ozone precursor transport in selected areas of California
[PB93-184828] p 3470 N93-29669
Annual report on monitoring of the unsaturated zone and recharge areas at INEL to the state of Idaho INLEL oversight committee
[DE93-012947] p 3473 N93-30187
IOC-UNEP review meeting on oceanographic processes of transport and distribution of pollutants in the sea
[DE93-605070] p 3490 N93-31019

POLYAMIDE RESINS
Process to prepare 1,3-diamino-5-pentafluorosulfanylbenzene
[NASA-CASE-LAR-14773-2-CU] p 3312 N93-29506

POLYATOMIC GASES
Radiative interactions in molecular gases under local and nonlocal thermodynamic equilibrium conditions
[NASA-CR-193223] p 3604 N93-29168

POLYATOMIC MOLECULES
Electron interactions with non-linear polyatomic molecules and their radicals and ions
[AD-A262279] p 3568 N93-29446

POLYCARBOSILANES
Catalytic synthesis of silicon carbide preceramic polymers: Polycarbosilanes
[DE93-008634] p 3329 N93-28541

POLYCRYSTALS
Transformation toughening
[DE93-011805] p 3321 N93-28631
Growth, characterization and device development in monocrystalline diamond films
[AD-A263204] p 3593 N93-28874
In situ Fourier transform infrared spectroscopic study of bisulfate and sulfate adsorption on gold, with and without the underpotential deposition of copper
[AD-A263421] p 3323 N93-29259
Balanced technology initiative on computational mechanics of materials
[AD-A263906] p 3453 N93-29863
Damage mechanics in 2-D and 3-D microstructures
[AD-A264337] p 3453 N93-30159
Measurement of magnetic field penetration depth in niobium polycrystalline films by polarized neutron reflection method
[DE93-606390] p 3600 N93-30771
Tensile study of single-crystal ternary L1(2) trialuminide Al66Ti25Mn(sub g)
[AD-A264297] p 3601 N93-30819
Silicon Film(trademark) photovoltaic manufacturing technology
[DE93-010008] p 3466 N93-30891
Tensile creep behavior of polycrystalline alumina fibers
[NASA-TM-106269] p 3340 N93-30938

POLYETHYLENES
Acid solution absorption of extruded polyethylene foam
[DE93-011701] p 3330 N93-28839
Solving a product safety problem using a recycled high density polyethylene container p 3292 N93-30964

POLYGONS
Polygonal approximation overviews and perspectives
[INRIA-RR-1621] p 3547 N93-28513

POLYIMIDES
Polyimides prepared from 3,5-diamino benzo trifluoride
[NASA-CASE-LAR-14206-1] p 3331 N93-29083
Diphenylmethane-containing dianhydride and polyimides prepared therefrom
[NASA-CASE-LAR-14487-1] p 3331 N93-29085
Process to prepare 1,3-diamino-5-pentafluorosulfanylbenzene
[NASA-CASE-LAR-14773-2-CU] p 3312 N93-29506
Advanced fiber/matrix material systems
p 3305 N93-30854

POLYMER CHEMISTRY
Catalytic synthesis of silicon carbide preceramic polymers: Polycarbosilanes
[DE93-008634] p 3329 N93-28541
Diphenylmethane-containing dianhydride and polyimides prepared therefrom
[NASA-CASE-LAR-14487-1] p 3331 N93-29085
Novel polymer compositions for high-temperature membrane applications, phase 1
[PB93-174126] p 3331 N93-29201
Synthesis and polymerization of azaethylenes and aza-1,3-dienes
[AD-A263651] p 3332 N93-29290
Polymers with electrical and nonlinear optical properties
[AD-D015691] p 3333 N93-29457
Chromatographic and solvatochromic measurements on butyl rubbers
[AD-A263088] p 3334 N93-29795
Synthesis and properties of a cation-conducting, high temperature polymer electrolyte
[AD-A263557] p 3334 N93-29825
Synthesis of chiral molybdenum ROMP initiators and all-cis highly tactic Poly-2,3-R2Norbornadiene (R = CF3 or CO2Me)
[AD-A264133] p 3336 N93-30169
Conjugated substituted ionic polyacetylenes
[AD-A264702] p 3337 N93-30497
Characterization of slow chromophore reorientation in nonlinear optical polymers by two-dimensional MAS NMR
[AD-A264809] p 3338 N93-30596

POLYMER MATRIX COMPOSITES
Probabilistic simulation of multi-scale composite behavior
[NASA-TM-106196] p 3451 N93-28633
Aligned, short-fiber composites by novel flow processing methods
[DE93-008701] p 3296 N93-28904
Effects of freeze/thaw cycles on hydrostatically conditioned E-glass/J-2 composite
[AD-A262980] p 3298 N93-29425
SESAME equation of state number 8010: Boron loaded silicone potting material
[DE93-012083] p 3300 N93-30395
Wetting and dispersion in ceramic/polymer melt injection molding systems
[DE93-013240] p 3338 N93-30601
Studies of fiber-matrix adhesion on compression strength p 3304 N93-30846

POLYMERIC FILMS
A simple model for explosives formulation
[DE93-010703] p 3341 N93-29251
Synthesis and properties of a cation-conducting, high temperature polymer electrolyte
[AD-A263557] p 3334 N93-29825
Determination of the space charge distribution within an e-irradiated polymer using the pressure wave propagation method
[ONERA-P-1990-4] p 3335 N93-30024

POLYMERIZATION
Polyimides prepared from 3,5-diamino benzo trifluoride
[NASA-CASE-LAR-14206-1] p 3331 N93-29083
Synthesis and polymerization of azaethylenes and aza-1,3-dienes
[AD-A263651] p 3332 N93-29290
Synthesis of chiral molybdenum ROMP initiators and all-cis highly tactic Poly-2,3-R2Norbornadiene (R = CF3 or CO2Me)
[AD-A264133] p 3336 N93-30169
Conjugated substituted ionic polyacetylenes
[AD-A264702] p 3337 N93-30497
Optically switchable conductive polymers
[AD-A264751] p 3337 N93-30557
Carborane-(siloxane or silane)-unsaturated hydrocarbon based polymers
[AD-D015717] p 3338 N93-30586
Conjugated polymers from cyclohexadienediol monomers
[AD-A264837] p 3340 N93-30900
Water-soluble polyphosphazenes and their hydrogels
[AD-A264883] p 3340 N93-30909

POLYMERS
Polar order and relaxation of second order nonlinear optical susceptibility in an electric field polarized amorphous polymer
[AD-A262189] p 3329 N93-28489
In situ characterization of interfacial and bulk properties of lithium polymer batteries using 4-probe DC techniques
[DE93-007699] p 3405 N93-28581
Polymeric materials for use in wet hydrochloric acid environments
[DE93-010881] p 3330 N93-28600
Novel polymer compositions for high-temperature membrane applications, phase 1
[PB93-174126] p 3331 N93-29201
Results of a round robin test program: Complex modulus properties of a polymeric damping material
[AD-A263619] p 3332 N93-29344
An extension of a kinetic theory of polymer crystallization through the exclusion of negative barriers
[AD-A264810] p 3334 N93-29660
Molecular dynamics of physical aging processes in polymer glasses
[AD-A263737] p 3334 N93-29856
The swollen polymer technique and its use for heat transfer investigations on film cooled surfaces
p 3255 N93-29944
Applications of laser light scattering in polymer dilute solution characterization
[AD-A263110] p 3335 N93-30007
Conjugated substituted ionic polyacetylenes
[AD-A264702] p 3337 N93-30497
A 69 cent look at thermoplastic softening
p 3292 N93-30963
Experiments in materials science from household items p 3293 N93-30971

POLYMETHYL METHACRYLATE
Polar order and relaxation of second order nonlinear optical susceptibility in an electric field polarized amorphous polymer
[AD-A262189] p 3329 N93-28489
Isothermal annealing and relaxation of the second harmonic generation signal from a nonlinear optical polymer
[AD-A262007] p 3333 N93-29442
Characterization of slow chromophore reorientation in nonlinear optical polymers by two-dimensional MAS NMR
[AD-A264809] p 3338 N93-30596

POLYMORPHISM
Shock waves and polymorphic phase transitions in energetic materials p 3351 N93-30100

POLYNOMIALS
Three-D crater analysis of LDEF impact features from stereo imagery p 3283 N93-29359
Polynomial space polynomial delay algorithms for listing families of graphs
[DE93-010677] p 3530 N93-29808
Effect of design selection on response surface performance
[NASA-CR-4520] p 3249 N93-29885
Approximation formulae for functional integrals in P(phi)2-quantum field theory
[DE93-606067] p 3605 N93-30781

POLYPHENYLS
Materials studies for preventing corrosion in condensing environments
[PB93-185478] p 3327 N93-30815

POLYTOPES
Packing odd paths
[CWI-BS-R9207] p 3549 N93-29849

POLYURETHANE FOAM
Hydrostatic and uniaxial behavior of a high density polyurethane foam (FR-3720) at various temperatures
[DE93-011486] p 3330 N93-28838
Generation of carbon monoxide in compartment fires
[PB93-146702] p 3244 N93-29211
Mitigation of shock waves in a cylindrical tunnel by foam
[AD-A262491] p 3423 N93-29419

POLYURETHANE RESINS
Hydrostatic and uniaxial behavior of a high density polyurethane foam (FR-3720) at various temperatures
[DE93-011486] p 3330 N93-28838

PONDEROMOTIVE FORCES
Edge plasma control by RF electric field in Compact Helical System (CHS)
[DE93-753242] p 3583 N93-28532

POPULATION INVERSION
Inner-shell photo-ionized x ray laser schemes
[DE93-009285] p 3438 N93-29309

POPULATIONS
The use of objective prism radial velocities for kinematic studies of galactic populations p 3633 N93-28672
Further analysis of LDEF FRECOPA micrometeoroid remnants p 3638 N93-29360
Origin of orbital debris impacts on LDEF's trailing surfaces p 3283 N93-29373

POROSITY
Healing of lithographically introduced flaws in glass and glass containing ceramics
[DE93-010453] p 3330 N93-28761
Tensile study of single-crystal ternary L1(2) trialuminide Al66Ti25Mn(sub g)
[AD-A264297] p 3601 N93-30819
Ultrasonic detection and identification of fabrication defects in composites p 3305 N93-30856

POROUS MATERIALS
Method for preparation of a microporous structure with layered interstitial surface treatment
[NASA-CASE-MSC-21487-2] p 3296 N93-29023
Velocity measurements of low Reynolds number tube flow using fiber-optic technology
[DE93-009865] p 3422 N93-29335
Hydrodynamic interactions among fibers in high efficiency filters
[DE93-007117] p 3424 N93-30035
Surface chemistry of hydrogen-passivated porous silicon-oxidation of surface Si-H groups by acetone
[AD-A264655] p 3315 N93-30526
Ordered molecular arrays as templates: A new approach to synthesis of mesoporous materials
[AD-A264631] p 3570 N93-30540

PORTABLE EQUIPMENT
A portable modular architecture for robotic manipulator control
[DE93-010819] p 3444 N93-29254
Portable fiber optic coupled Doppler interferometer system for detonation and shock wave diagnostics
[DE93-009827] p 3433 N93-30510
POSITION (LOCATION)
Smart skin structures for identifying and locating laser irradiation
[DE93-005464] p 3436 N93-28887
POSITION ERRORS
Lunar gravitational field estimation and the effects of mismodeling upon lunar satellite orbit prediction
[NASA-CR-188249] p 3634 N93-29042
Adaptive motion control of mobile robots
p 3545 N93-30903
POSITION INDICATORS
Robot arm with positional absolute encoded joints
p 3370 N93-30312
POSITION SENSING
An auto-guiding system for mid-sized telescopes
p 3375 N93-30340
POSITIONING
Lunar crane system p 3277 N93-29118
Lunar rovers and local positioning system
p 3277 N93-29119
Vision-based control of holonomic robots for 3-dimensional rigid-body positioning using camera-space manipulation p 3578 N93-29178
System analysis for a kinematic positioning system based on the global positioning system
[AD-A262830] p 3245 N93-29468
POSITRON ANNIHILATION
Defect studies in low-temperature-grown GaAs
[DE93-010405] p 3595 N93-29417
Task A: Theory of elementary particles
[DE93-010561] p 3569 N93-29841
GRO: Red-shifted electron-positron annihilation gamma-rays from radiopulsars
[NASA-CR-193243] p 3635 N93-30053
Towards the results of global analysis of data on nucleon electromagnetic structure
[DE93-606125] p 3571 N93-30792
POSITRONS
Molecular dynamics of physical aging processes in polymer glasses
[AD-A263737] p 3334 N93-29856
High-energy electron-positron interactions
[DE93-011611] p 3576 N93-30488
Non-perturbative calculation of equilibrium polarization of stored electron beams
[DE93-764500] p 3577 N93-30607
Unitary approximation of Bhabha diffusion by high energies and its implementation in Monte Carlo event generators
[ETN-93-93622] p 3571 N93-30670
POSTFLIGHT ANALYSIS
SPREE Interactive Data Analysis Tool (SIDAT)
[AD-A262782] p 3273 N93-29306
Overview of the Systems Special Investigation Group investigation p 3318 N93-29683
The effect of the low Earth orbit environment on space solar cells: Results of the Advanced Photovoltaic Experiment (S0014) p 3467 N93-29686
New results from FRECOPA analysis
p 3448 N93-29688
LDEF Space Plasma-High Voltage Drainage Experiment post-flight results p 3414 N93-29690
In orbit degradation of EUV optical components in the wavelength range 10-40 nm AO 138-3
p 3582 N93-29691
Ruled and holographic experiment (AO 138-5)
p 3434 N93-29696
Radiation and temperature effects on LDEF fiber optic samples p 3583 N93-29700
Long Duration Exposure Facility (LDEF) low temperature Heat Pipe Experiment Package (HEPP) flight results
p 3429 N93-29701
Next generation optical instruments and space experiment based on the LDEF thermal control surfaces experiment (S0069) p 3583 N93-29706
Postflight hardware evaluation 360T025 (RSRM-25, STS-46)
[NASA-CR-192562] p 3272 N93-30617
Postflight hardware evaluation 360T025 (RSRM-25, STS-46). Appendix A: Insulation PFORs
[NASA-CR-192563] p 3272 N93-30618
Postflight hardware evaluation 360T025 (RSRM-25, STS-46). Appendix B: Case, seals, and joints PFORs
[NASA-CR-192564] p 3272 N93-30619
Postflight hardware evaluation 360T025 (RSRM-25, STS-46). Appendix C: Nozzle PFORs
[NASA-CR-192565] p 3272 N93-30620
Postflight hardware evaluation 360T025 (RSRM-25, STS-46). Appendix E: Insulation postfire data
[NASA-CR-192566] p 3272 N93-30621
Postflight hardware evaluation 360T025 (RSRM-25, STS-46). Appendix D: Nozzle postfire data
[NASA-CR-192580] p 3289 N93-30648
POSTMISSION ANALYSIS (SPACECRAFT)
Debris/ice/TPS assessment and integrated photographic analysis for Shuttle Mission STS-55
[NASA-TM-107559] p 3271 N93-29136
POTENTIAL ENERGY
A field investigation of water and salt movement in permafrost and the active layer
[AD-A263706] p 3487 N93-29298
The global potential energy surfaces of the lowest two 1A-prime states of the ozone molecule: Theoretical determination and analysis
[DE93-007537] p 3313 N93-29837
Molecular dynamics of detonation in crystals with defects p 3350 N93-30097
Shock waves and polymorphic phase transitions in energetic materials p 3351 N93-30100
Biophysical and biochemical mechanisms in synaptic transmitter release
[AD-A264829] p 3496 N93-30613
POTENTIAL FLOW
Unsteady vortex loop/dipole theory applied to the work and acoustics of an ideal low speed propeller
[AD-A264057] p 3241 N93-29891
POTENTIAL THEORY
Finite element analysis of time-independent superconductivity
[NASA-CR-191140] p 3450 N93-28556
POTENTIOMETERS
An automated data collection system for a Charpy impact tester p 3293 N93-30972
POTENTIOMETRIC ANALYSIS
Analytical applications of electrified interfaces between two immiscible solutions
[AD-A263085] p 3311 N93-29132
POWDER (PARTICLES)
Explosive consolidation of combustion synthesized TiC and TiB2: Precursor morphology effects
[AD-A263186] p 3341 N93-28515
Process optimization of Hexoloy SX-SiC towards improved mechanical properties
[DE93-007913] p 3320 N93-28564
Powder x ray diffraction patterns of energetic materials for use as reference standards
[DE93-009903] p 3592 N93-28568
Colloid and interface chemistry aspects of ceramics
[AD-A264685] p 3337 N93-30552
Powder towpreg process development
p 3303 N93-30844
Advanced fiber/matrix material systems
p 3305 N93-30854
Design, synthesis, and chemical processing of hierarchical ceramic structures for aerospace applications
[AD-A264227] p 3339 N93-30885
POWDER METALLURGY
Report on the sintering and properties of MgO and MgO-5 percent TiC
[DE93-008676] p 3323 N93-29092
Near net shape processing: A necessity for advanced materials applications p 3290 N93-30949
Powder metallurgy: Solid and liquid phase sintering of copper p 3294 N93-30976
POWER AMPLIFIERS
Upgrading the LAMPF 201 MHz RF generators
[DE93-010715] p 3406 N93-28830
Design of the Nova Upgrade laser system for ignition fusion experiments
[DE93-009077] p 3436 N93-29097
POWER CONDITIONING
Measurements of magnetic fields produced by a 30 kWe class Arcjet Power Conditioning Unit
[AD-A262786] p 3287 N93-28658
POWER EFFICIENCY
Preliminary investigation of high power microwave plasmas for electrothermal thruster use
[NASA-TM-106207] p 3288 N93-29158
Energy efficient drivepower, volume 2
[DE93-012437] p 3410 N93-29814
POWER LINES
Fundamental study of the signal processing by optics
[DE93-776265] p 3577 N93-28982
POWER REACTORS
Bootstrap current profiles and scaling in large aspect ratio tokamaks
[DE93-753158] p 3589 N93-30003
Development of a PC code package for the analysis of research and power reactors
[DE92-638517] p 3536 N93-31001
POWER SPECTRA
Wavelet transform techniques and signal analysis
[DE93-007919] p 3382 N93-29244
Vortex shedding by blunt/bluff bodies at high Reynolds numbers. Volume 4: Rectangles
[AD-A264154] p 3241 N93-30151
Vortex shedding by blunt/bluff bodies at high reynolds numbers. Volume 1: Data analysis
[AD-A264151] p 3241 N93-30171
Vortex shedding by Blunt/Bluff bodies at high reynolds numbers. Volume 2: Cylinders, octagon, hexagon
[AD-A264152] p 3241 N93-30172
Vortex shedding by blunt/bluff bodies at high reynolds numbers. Volume 3. Cubes
[AD-A264153] p 3242 N93-30173
POWER SUPPLIES
Energy efficient drivepower, volume 2
[DE93-012437] p 3410 N93-29814
High reliability, maintenance-free INS battery development
[AD-A264521] p 3412 N93-30406
POWERED LIFT AIRCRAFT
Effects of flow-path variations on internal reversing flow in a tailpipe offtake configuration for ASTOVL aircraft
[NASA-TM-106149] p 3252 N93-29065
PRECESSION
Investigation of Mars rotational dynamics using Earth-based radio tracking of Mars landers
p 3642 N93-28777
PRECIPITATES
High-dose implantations of Al into Si(111) and Si(100)
[DE93-009552] p 3594 N93-29301
Growth model of Au films on Ru(001)
[DE92-642126] p 3602 N93-30998
PRECIPITATION (METEOROLOGY)
Activities report of the International Meteorological Institute, Stockholm (Sweden)
[ETN-93-93768] p 3480 N93-28519
Case study of Frontal Boundary Study Mission 03
[DE93-007176] p 3473 N93-30183
PRECIPITATION HARDENING
The temperature dependence of the deformation and oxidation behavior of an age-hardenable beta + alpha-two titanium alloy
[AD-A262232] p 3320 N93-28491
PREDICTION ANALYSIS TECHNIQUES
Predicting the response of a temperate forest ecosystem to atmospheric CO2 increase
[DE93-010081] p 3467 N93-28543
Reliability assessment of thrust chamber cooling concepts using probabilistic analysis techniques
[NASA-CR-190785] p 3288 N93-29068
Investigation of a geodesy coexperiment to the Gravity Probe B relativity gyroscope program
[NASA-CR-193263] p 3460 N93-29179
Two-dimensional model for current and heat transport in solid-armature railguns
[AD-A262014] p 3271 N93-29394
Evaluation of atmospheric wind field and dispersion models for fog-oil smoke dispersion in complex terrain: Field measurement and model evaluation program for assessment of the environmental effects of military smokes
[AD-A262051] p 3482 N93-29399
An analysis of possible applications of fuzzy set theory to the actuarial credibility theory p 3510 N93-29517
Optimization of HPM device parameters for maximum air transmission
[DE93-007332] p 3386 N93-29765
Heat Transfer and Cooling in Gas Turbines
[AGARD-CP-527] p 3252 N93-29926
Combustion/explosion chemistry of bulk materials
p 3343 N93-30062
Mathematical model of frost heave and thaw settlement in pavements
[CRREL-REPT-93-2] p 3262 N93-30103
Analytical predictions of the intermodulation noise of semiconductor laser diode p 3361 N93-30256
An approach to software quality prediction from Ada designs
[AD-A264731] p 3534 N93-30547
First NASA Advanced Composites Technology Conference, part 2
[NASA-CP-3104-PT-2] p 3303 N93-30841
PREDICTIONS
Exploitation of parallelism in climate models
[DE93-011259] p 3470 N93-29318
Developments in impact damage modeling for laminated composite structures p 3305 N93-30857
PREFORMS
Environmental effects on stitched RTM composites
[NASA-CR-193221] p 3297 N93-29107
Method and apparatus for weaving a woven angle ply fabric
[NASA-CASE-LAR-14048-1] p 3354 N93-29611

Consolidation of graphite thermoplastic textile preforms for primary aircraft structure p 3302 N93-30439
Infiltration/cure modeling of resin transfer molded composite materials using advanced fiber architectures p 3303 N93-30843
Powder towpreg process development p 3303 N93-30844
Micromechanics of fatigue in woven and stitched composites p 3304 N93-30850

PRELAUNCH TESTS
Debris/ice/TPS assessment and integrated photographic analysis for Shuttle Mission STS-55 [NASA-TM-107559] p 3271 N93-29136

PREMIXED FLAMES
Studies in premixed combustion [DE93-007955] p 3310 N93-29051
Nonlinear spectroscopy of multicomponent droplets and two- and three-dimensional measurements in flames [AD-A264341] p 3425 N93-30162
A novel flame thermometer based on the doppler width of ro-vibrational transitions [AD-A264515] p 3315 N93-30405
Studies of curvature, strain, and unsteady effects on premixed flames p 3316 N93-30646

PREPREGS
Design, analysis, and fabrication of the technology integration box beam p 3300 N93-30433
Comparison of impact results for several polymeric composites over a wide range of low impact velocities p 3304 N93-30848
Development of resins for composites by resin transfer molding p 3305 N93-30853
Advanced fiber placement of composite fuselage structures p 3306 N93-30864

PREPROCESSING
Preprocessing remotely-sensed data for efficient analysis and classification [DE93-007367] p 3611 N93-28580
Pre- and postprocessing techniques for determining goodness of computational meshes [NASA-CR-192553] p 3538 N93-29030

PRESSURE CHAMBERS
Guide for certifying pressure vessels and systems [NASA-TM-107549] p 3449 N93-29220

PRESSURE DEPENDENCE
Pressure dependence of the reaction propagation rate of TATB to 40 GPa p 3319 N93-30082

PRESSURE DISTRIBUTION
Transonic flows on an oscillating airfoil and their effect on the flutter-boundary [DLR-FB-92-08] p 3238 N93-29006
Wind loads on canopy roofs [RR-CE132] p 3451 N93-29106
High Reynolds number and turbulence effects on aerodynamics and heat transfer in a turbine cascade [NASA-TM-106187] p 3420 N93-29157
Performance characteristics of two multiaxis thrust-vectoring nozzles at Mach numbers up to 1.28 [NASA-TP-3313] p 3239 N93-29160
High-Reynolds-number test of a 5-percent-thick low-aspect-ratio semispan wing in the Langley 0.3-meter transonic cryogenic tunnel: Wing pressure distributions [NASA-TM-4227] p 3240 N93-29449
Determination of surface heat transfer and film cooling effectiveness in unsteady wake flow conditions p 3253 N93-29933
The aerodynamic effect of coolant ejection in the leading edge region of a film-cooled turbine blade p 3258 N93-29958
Sound wave scattering from a rigid sphere [AD-A264182] p 3562 N93-30157

PRESSURE EFFECTS
Sensitive detection of new superconductors created at ultra high pressures [AD-A264340] p 3597 N93-30161
Containment of explosions in spherical vessels [DE93-005445] p 3446 N93-30211
Hydrogen-rated system for in vitro studies at pressure: Operating procedures and emergency procedures [AD-A264179] p 3497 N93-30882

PRESSURE GAGES
Selection and static calibration of the Marsh J1678 pressure gauge p 3249 N93-29779

PRESSURE GRADIENTS
Heat transfer with moderate free stream turbulence p 3254 N93-29936

PRESSURE MEASUREMENT
Selection and static calibration of the Marsh J1678 pressure gauge p 3249 N93-29779

PRESSURE OSCILLATIONS
Strong parallel blade-vortex interaction and noise propagation in helicopter flight p 3563 N93-30980

PRESSURE RATIO
Performance characteristics of two multiaxis thrust-vectoring nozzles at Mach numbers up to 1.28 [NASA-TP-3313] p 3239 N93-29160

PRESSURE REGULATORS
Tank Pressure Control Experiment (TPCE) p 3264 N93-28712
Tank Pressure Control Experiment/Thermal Phenomena (TPCE/TP) p 3264 N93-28713

PRESSURE SENSORS
Rugged, no-moving-parts windspeed and static pressure probe designs for measurements in planetary atmospheres p 3434 N93-28767
A calibration procedure for the SBE 19 Conductivity, Temperature, and Depth (CTD) profiler [AD-A264435] p 3489 N93-30420

PRESSURE SWITCHES
Valve malfunction detection apparatus [NASA-CASE-MFS-29904-1] p 3432 N93-29503

PRESSURE VESSEL DESIGN
Guide for certifying pressure vessels and systems [NASA-TM-107549] p 3449 N93-29220

PRESSURE VESSELS
New remote maintenance approach for TPX [DE93-007857] p 3584 N93-28583
Building a generalized distributed system model [NASA-CR-193239] p 3527 N93-29219
Guide for certifying pressure vessels and systems [NASA-TM-107549] p 3449 N93-29220
Stress-intensity-factor influence coefficients for axial and circumferential flaws in reactor pressure vessels [DE93-006206] p 3454 N93-30213
Steps required in the pursuit of quantitative risk management processes for high pressure systems [DE93-007586] p 3378 N93-30508
Structural design, analysis, and code evaluation of an odd-shaped pressure vessel [DE93-008182] p 3447 N93-30632

PRESSURIZED WATER REACTORS
Annual progress report on the NSRR experiments, (21) [DE93-753190] p 3574 N93-29137
Stress-intensity-factor influence coefficients for axial and circumferential flaws in reactor pressure vessels [DE93-006206] p 3454 N93-30213

PREVENTION
Planning and progress of EPA's pollution prevention research program [PB93-185767] p 3475 N93-30831

PRIMITIVE EQUATIONS
High performance dispersion model PHYSIC [DE93-753303] p 3467 N93-28536

PRINTED CIRCUITS
Characterization and optimization of a Hot Air Solder-Leveling System [DE93-010188] p 3332 N93-29328
Prototype and short-run printed circuit board creation [AD-A263245] p 3409 N93-29655
Foreign technology assessment: Environmental evaluation of a radiation-hard oscillator/divider [DE93-011481] p 3412 N93-30127
Detecting residue on a printed circuit board: An application of the Boundary Contour/Feature Contour System [DE93-006283] p 3412 N93-30370
An application protocol for CAD to CAD transfer of electronic information [AD-A264554] p 3533 N93-30383

PRISMS
The use of objective prism radial velocities for kinematic studies of galactic populations p 3633 N93-28672
The HYDICE instrument design and its application to planetary instruments p 3434 N93-28766
An L2F-measurement device with image rotator prism for flow velocity analysis in rotating coolant channels p 3255 N93-29942

PROBABILITY DENSITY FUNCTIONS
An analysis of the Generalized Lambda Distribution [AD-A262485] p 3555 N93-29447

PROBABILITY DISTRIBUTION FUNCTIONS
The use of objective prism radial velocities for kinematic studies of galactic populations p 3633 N93-28672
Monte Carlo simulation of magnitude-angle error sources [AD-A263738] p 3555 N93-29857

PROBABILITY THEORY
Probabilistic simulation of multi-scale composite behavior [NASA-TM-106196] p 3451 N93-28633
Risk-based spacecraft fire safety experiments p 3267 N93-28738
Reliability assessment of thrust chamber cooling concepts using probabilistic analysis techniques [NASA-CR-190785] p 3288 N93-29068
Estimations of expectedness and potential surprise in possibility theory p 3510 N93-29518
Comparison of specificity and information for fuzzy domains p 3510 N93-29519
Decision analysis with approximate probabilities p 3513 N93-29542
Information compression in the context model p 3514 N93-29549
Fuzzy learning under and about an unfamiliar fuzzy teacher p 3516 N93-29558
Quantification of human responses p 3500 N93-29564
Possibilistic measurement and set statistics p 3517 N93-29567
Neural networks: A simulation technique under uncertainty conditions p 3519 N93-29577
On probability-possibility transformations p 3519 N93-29582
NetStat: A probabilistic network connectivity analysis tool [AD-A262838] p 3529 N93-29647
Planetary protection issues for the MESUR mission: Probability of growth (Pg) [NASA-CP-3167] p 3651 N93-30214
Quantum field theory in spaces with closed time-like curves [DE93-010564] p 3605 N93-30481
Steps required in the pursuit of quantitative risk management processes for high pressure systems [DE93-007586] p 3378 N93-30508
On the impossibility of creating the quantum correlations with computers [DE93-606039] p 3606 N93-30806
Probabilistic composite analysis p 3307 N93-30868

PROBLEM SOLVING
Research in mathematics and computer science, March 1, 1991 - September 30, 1992 [DE93-011492] p 3509 N93-28573
Parametric likelihood inference for record breaking problems [AD-A262546] p 3549 N93-29413
Information technology: A force for organizational change [AD-A261986] p 3615 N93-29439
Neural networks: A simulation technique under uncertainty conditions p 3519 N93-29577
Managing operational intelligence overload: Guidelines for avoiding decision paralysis [AD-A264184] p 3610 N93-30158
Nonsmooth optimization algorithms, system theory, and software tools [AD-A264679] p 3534 N93-30549
Intelligent real-time problem solving [AD-A264830] p 3535 N93-30614
Solving a product safety problem using a recycled high density polyethylene container p 3292 N93-30964

PROCEDURES
CATS EYES adjustment procedures [AD-A264069] p 3508 N93-29924

PROCESS CONTROL (INDUSTRY)
Process optimization of Hexoloy SX-SiC towards improved mechanical properties [DE93-007913] p 3320 N93-28564
Design issues of a reinforcement-based self-learning fuzzy controller for petrochemical process control p 3512 N93-29533
Fuzzy simulation in concurrent engineering p 3516 N93-29562
Powder towpreg process development p 3303 N93-30844

PROCUREMENT
Productivity measurement in science and technology contracting [AD-A262077] p 3609 N93-28985
A perspective on acquisition of NASA space systems [AD-A263246] p 3610 N93-29499

PROCUREMENT MANAGEMENT
The program manager's notebook [AD-A263074] p 3609 N93-29142

PRODUCT DEVELOPMENT
RBSE: Product development team research activity deliverables [NASA-CR-193115] p 3527 N93-29212
The NASA SBIR product catalog [NASA-TM-108242] p 3609 N93-29322
North American Fuzzy Logic Processing Society (NAFIPS 1992), volume 2 [NASA-CP-10112-VOL-2] p 3515 N93-29556
Data probe user's guide [PB93-178655] p 3530 N93-29678
The NCAT process p 3626 N93-30697
CAESAR development plan 1992-1995 [BCRS-92-17] p 3463 N93-31009

PRODUCTION COSTS
Silicon Film(trademark) photovoltaic manufacturing technology [DE93-010008] p 3466 N93-30891

PRODUCTION MANAGEMENT
The program manager's notebook [AD-A263074] p 3609 N93-29142

PRODUCTIVITY
Productivity measurement in science and technology contracting
[AD-A262077] p 3609 N93-28985
PRODUCTS
The NASA SBIR product catalog
[NASA-TM-108242] p 3609 N93-29322
SESC products and services user guide
[PB93-178879] p 3653 N93-29679
PROGRAM VERIFICATION (COMPUTERS)
An assessment of space shuttle flight software development processes
[NASA-CR-193179] p 3525 N93-28934
A temporal proof methodology for reactive systems
[NASA-CR-193145] p 3528 N93-29469
Nonresident and endangered variables: The effects of code generation optimizations on symbolic debugging
[AD-A263149] p 3529 N93-29486
Communications systems design for testability: Grey-box testing p 3368 N93-30302
Using Penelope to assess the correctness of NASA Ada software: A demonstration of formal methods as a counterpart to testing
[NASA-CR-4509] p 3533 N93-30380
High-energy electron-positron interactions
[DE93-011611] p 3576 N93-30488
Procedures for applying Ada quality prediction models
[AD-A264730] p 3534 N93-30546
An approach to software quality prediction from Ada designs
[AD-A264731] p 3534 N93-30547
PROGRAMMING (SCHEDULING)
Estimating test range capacity
[AD-A262493] p 3270 N93-28938
PROGRAMMING ENVIRONMENTS
Parallel software tools at Langley Research Center
[NASA-TM-108995] p 3520 N93-29070
An annotated bibliography on integration in software engineering environments
[AD-A264798] p 3535 N93-30602
PROGRAMMING LANGUAGES
Concurrent clean language manual, version 0.8
[TR-92-18] p 3522 N93-28482
The concurrent clean system user's manual and PABCstat user's manual, version 0.8
[TR-92-19] p 3523 N93-28484
Formal definition of a conceptual language for the description and manipulation of information models
[TR-92-16] p 3523 N93-28503
Handshake circuits: An intermediary between communicating processes and VLSI
[ETN-93-93579] p 3408 N93-29269
Implementing error-valued semantics for dataflow languages on imperative machines
[DE93-009319] p 3615 N93-29310
Automated reasoning with function evaluation for COCOLOG
[INRIA-RR-1713] p 3529 N93-29488
Full abstraction for a shared variable parallel language
[AD-A263547] p 3530 N93-29821
Class notes: Programming parallel algorithms CS 15-840B (Fall 1992)
[AD-A263549] p 3530 N93-29823
Turning SOS rules into equations
[CWI-CS-R9218] p 3532 N93-30017
PROJECT MANAGEMENT
Applied research in America
[DE93-011725] p 3625 N93-28646
The program manager's notebook
[AD-A263074] p 3609 N93-29142
The ANL electric vehicle battery R/D program for DOE-EHP
[DE93-010658] p 3408 N93-29311
A perspective on acquisition of NASA space systems
[AD-A263246] p 3610 N93-29499
Air Force CALS business practices
[AD-A264789] p 3610 N93-30177
Interagency Advanced Power Group (IAPG) Meeting Compendium
[DE93-006189] p 3670 N93-30212
The NCAT process p 3626 N93-30697
PROJECT PLANNING
Program plan for an experimenter's laboratory for visualized interactive science p 3613 N93-29224
High performance computing: Advanced Research Projects Agency should do more to foster program goals. Report to the Chairman, Committee on Armed Services, House of Representatives
[GAO/IMTEC-93-24] p 3533 N93-30202
Rotorcraft master plan p 3236 N93-30677
Technology coordination p 3626 N93-30706
PROJECT SETI
Wide-bandwidth high-resolution search for extraterrestrial intelligence
[NASA-CR-193137] p 3509 N93-28895
PROJECTILE CRATERING
Damage areas on selected LDEF aluminum surfaces
p 3283 N93-29374
LDEF data: Comparisons with existing models
p 3283 N93-29375
PROJECTILES
Studies of relativistic heavy ion collisions at the AGS (E814/E877)
[DE93-008541] p 3564 N93-28678
Projectile compositions and modal frequencies on the chemistry of micrometeoroids LDEF experiment
p 3638 N93-29370
The equivalent flat nose diameter of hemispherical nose cylindrical projectiles for impact induced detonation of energetic materials
[AD-A263244] p 3342 N93-29494
Recent applications of CFD to the aerodynamics of Army projectiles
[AD-A262953] p 3240 N93-29512
The effect of material strength on segment penetration behavior
[AD-A263262] p 3453 N93-29801
Measurement of projectile surface temperature by means of its infrared radiation: A preliminary study
[AD-A264053] p 3432 N93-30032
PROKARYOTES
Regulation of alternative CO2 fixation pathways in procaryotic and eucaryotic photosynthetic organisms
[DE93-012109] p 3491 N93-29181
PROLATE SPHEROIDS
An experimental study of flow over a 6 to 1 prolate spheroid at incidence p 3239 N93-29124
PROLOG (PROGRAMMING LANGUAGE)
MLog: A language for prototyping concurrent systems
p 3368 N93-30301
PRONY SERIES
Advances in the identification of electrochemical transfer function models using Prony analysis
[DE93-009424] p 3550 N93-30041
PROPAGATION MODES
Studies of the propagation of Low Frequency (LF) radio waves p 3396 N93-30738
PROPANE
Turbulence characteristics of an axisymmetric reacting flow
[NASA-CR-4110] p 3242 N93-30373
PROPELLANT BINDERS
A simple model for explosives formulation
[DE93-010703] p 3341 N93-29251
PROPELLANT CHEMISTRY
A simple model for explosives formulation
[DE93-010703] p 3341 N93-29251
Strategies for understanding the deflagration-to-detonation transition
p 3319 N93-30077
Applications of density functional theory to calculation of reaction energetics p 3351 N93-30098
PROPELLANT COMBUSTION
The equivalent flat nose diameter of hemispherical nose cylindrical projectiles for impact induced detonation of energetic materials
[AD-A263244] p 3342 N93-29494
The thermochemistry and reaction pathways of the decomposition and combustion of energetic materials
p 3343 N93-30063
Numerical modeling of multidimensional flames with application to energetic materials p 3319 N93-30079
Flame structure studies of propellant like low pressure flames using optical and mass spectrometric means
p 3319 N93-30081
Thermal decomposition pathways of RDX in the condensed phase p 3347 N93-30083
Condensed phase diagnostics of nitramine propellant combustion p 3320 N93-30102
PROPELLANT DECOMPOSITION
Advanced thermally-stable, coal-derived, jet fuels program: Experiment system and model development
[AD-A262747] p 3342 N93-29402
PROPELLANT EXPLOSIONS
Thermal decomposition pathways of RDX in the condensed phase p 3347 N93-30083
PROPELLANT PROPERTIES
Benefits of in situ propellant utilization for a Mars sample return mission
[NASA-TM-106243] p 3341 N93-28695
PROPELLANT SENSITIVITY
A steric hindrance model for the crystal orientation dependence of the shock initiation sensitivity of PETN explosive
[LA-UR-92-1427] p 3345 N93-30074
PROPELLANT TANKS
APU diaphragm testing. Test plan
[NASA-TM-108251] p 3271 N93-29387
PROPELLANT TESTS
Comparison of deformation and shock reactivity for single crystals of RDX and ammonium perchlorate
p 3350 N93-30094
PROPELLANTS
Selective nitrations. Volume 2: The laser-induced nitration of three cycloalkanes
[AD-A263250] p 3438 N93-29800
Examination of shock induced chemical reactions in liquids using time-resolved optical spectroscopy
p 3318 N93-30073
Strategies for understanding the deflagration-to-detonation transition
p 3319 N93-30077
PROPELLER BLADES
An integrated optimum design approach for high speed prop-rotors including acoustic constraints
[NASA-CR-193222] p 3248 N93-29153
Project ARES 2: High-altitude battery-powered aircraft
p 3227 N93-29715
Unsteady vortex loop/dipole theory applied to the work and acoustics of an ideal low speed propeller
[AD-A264057] p 3241 N93-29891
PROPELLERS
Unsteady vortex loop/dipole theory applied to the work and acoustics of an ideal low speed propeller
[AD-A264057] p 3241 N93-29891
PROPORTIONAL CONTROL
Three-parameter tunable Tilt-Integral-Derivative (TID) controller
[NASA-CASE-NPO-18492-1-CU] p 3542 N93-29176
PROPOSALS
NASA SBIR abstracts of 1991 phase 1 projects
[NASA-TM-108240] p 3609 N93-29323
AFOSR Status Report
[AD-A264720] p 3670 N93-30513
PROPULSION
Propulsion and detonics research in France
p 3344 N93-30070
PROPULSION SYSTEM CONFIGURATIONS
Development and testing of the Perseus proof-of-concept aircraft
[DE93-010121] p 3247 N93-28586
Clustered Lance Booster (CLB) feasibility study
[AD-A262746] p 3286 N93-28593
Delta Advanced Reusable Transport (DART): An alternative manned spacecraft p 3231 N93-29735
Solid oxide fuel cells for transportation: A clean, efficient alternative for propulsion
[DE93-010662] p 3464 N93-29844
PROPULSION SYSTEM PERFORMANCE
Development and testing of the Perseus proof-of-concept aircraft
[DE93-010121] p 3247 N93-28586
Additional support for the TDK/MABL computer program
[NASA-CR-193037] p 3526 N93-29028
Solid oxide fuel cells for transportation: A clean, efficient alternative for propulsion
[DE93-010662] p 3464 N93-29844
PROPYLENE
APU diaphragm testing. Test plan
[NASA-TM-108251] p 3271 N93-29387
PROSTHETIC DEVICES
Prosthetic elbow joint
[NASA-CASE-MFS-28707-1] p 3508 N93-30566
PROTECTION
Evaluation of environmental marketing terms in the United States
[PB93-175784] p 3474 N93-30660
PROTECTIVE CLOTHING
Evaluation of test methods and requirements for respiratory protection systems 21
[AD-A262466] p 3501 N93-28757
Evaluation and optimization of a flexible filtration system for respiratory protection system 21
[AD-A262467] p 3493 N93-28758
Biophysical model for handwear insulation testing
[AD-A262926] p 3505 N93-28884
Evaluation of personal cooling systems in conjunction with explosive ordnance disposal suits
[AD-A262862] p 3506 N93-29471
PROTECTIVE COATINGS
Smart skin structures for identifying and locating laser irradiation
[DE93-005464] p 3436 N93-28887
Operational results of pilot cell test with cermet inert anodes
[DE93-009338] p 3322 N93-29061
LDEF: 69 Months in Space. Second Post-Retrieval Symposium, part 2
[NASA-CP-3194-PT-2] p 3654 N93-29354
Characteristics of hypervelocity impact craters on LDEF experiment S1003 and implications of small particle impacts on reflective surfaces p 3283 N93-29363

Post-flight analyses of the crystals from the M0003-14 quartz crystal microbalance experiment
p 3602 N93-29684
Platinum-modified diffusion aluminide coatings on nickel-base superalloys
[AD-A263597] p 3325 N93-29981
Chromate-free corrosion resistant conversion coatings for aluminum
[DE93-009835] p 3336 N93-30051
Laser gas alloying of titanium materials
[ETN-93-93805] p 3325 N93-30115
Development of adherent ceramic coatings to reduce contact stress damage of ceramics
[DE93-012518] p 3336 N93-30182
Flexible storage medium for write-once optical tape
p 3621 N93-30473
Diamond nucleation of surfaces using carbon clusters
[AD-A264634] p 3599 N93-30548
Oxidation and hot corrosion of superalloys Rene 100 and X-40 at temperatures of 1475 F to 2000 F
[AD-A263747] p 3327 N93-30812

PROTEINS
Center of Excellence in Biotechnology (Research)
[AD-A263598] p 3491 N93-29915
Defining protein electrostatic recognition processes
[AD-A264838] p 3571 N93-30901
Computer assisted multiplex sequencing
[DE93-007144] p 3536 N93-30934

PROTOCOL (COMPUTERS)
A survey of network interface designs
[MEMO-INF-92-59] p 3379 N93-28502
Initial graphics exchange specification hybrid microcircuit application protocol
[PB93-175404] p 3407 N93-29203
RBSE: Product development team research activity deliverables
[NASA-CR-193115] p 3527 N93-29212
Building a generalized distributed system model
[NASA-CR-193239] p 3527 N93-29219
Handshake circuits: An intermediary between communicating processes and VLSI
[ETN-93-93579] p 3408 N93-29269
FDDI installation and performance analysis
[AD-A263263] p 3529 N93-29497
Ethernet performance of the Motorola Altair WIN system
[AD-A263877] p 3387 N93-29890
OSI transaction processing standard: An introduction and outlines of implementation
[VTT-TIED-1250] p 3532 N93-29997
Using the Mach communication primitives in X11
[AD-A264049] p 3533 N93-30125
Performance analysis of communication protocols using D-timed Petri net p 3356 N93-30227
Automatic synthesis of protocol specifications
p 3356 N93-30228
An application protocol for CAD to CAD transfer of electronic information
[AD-A264554] p 3533 N93-30383

PROTON BEAMS
Design of a particle beam satellite system for lunar prospecting p 3434 N93-28768

PROTON FLUX DENSITY
Induced activation study of LDEF
p 3572 N93-29632

PROTON IRRADIATION
Enhancements of the critical currents of YBaCuO single crystals by neutron (n) and proton (p) irradiation
[DE93-007892] p 3592 N93-28661

PROTON SCATTERING
Spin observables in large t elastic N-N scattering
[DE93-009211] p 3564 N93-28549

PROTON-PROTON REACTIONS
Multidimensional intermittency in hadronic collisions
[DE93-010562] p 3577 N93-30532

PROTONS
Construction and testing of a neutron and gamma spectrometry system using pulse shape discrimination with an organic scintillator
[AD-A262550] p 3567 N93-29415
Revised prediction of LDEF exposure to trapped protons p 3572 N93-29633

PROTOTYPES
Design and construction of a prototype ACTS propagation terminal
[NASA-CR-193071] p 3404 N93-28539
The lightcraft project p 3233 N93-29749
Concept formulation process aid for trade-off determination: Operator's guide
[AD-A263756] p 3531 N93-29874
Planar active antennas and quasi-optical power combining arrays using FET's and slots
[AD-A263759] p 3387 N93-29875
A prototype of a faculty and staff executive information system
[AD-A264852] p 3623 N93-30907

PROTOZOA
Process for selectively recovering algae and protozoa
[NASA-CASE-MFS-26124-1-NPO] p 3491 N93-29174

PROVING
A temporal proof methodology for reactive systems
[NASA-CR-193145] p 3528 N93-29469
The NCAT process p 3626 N93-30697
ERS-1 directional wave spectra validation with the airborne SAR PHARS
[BCRS-92-18] p 3463 N93-31010

PSEUDORANDOM SEQUENCES
Robot arm with positional absolute encoded joints
p 3370 N93-30312

PSYCHOLOGICAL FACTORS
Evaluation of test methods and requirements for respiratory protection systems 21
[AD-A262466] p 3501 N93-28757
Sound attenuation characteristics of the standard DH-132A and SPH-4 helmets worn in combination with standard issue earplugs
[AD-A263011] p 3506 N93-29406

PSYCHOLOGICAL TESTS
Pilot Candidate Selection Method (PCSM): What makes it work?
[AD-A262871] p 3498 N93-29481
Field test of a computer-driven tool to measure psychological characteristics of aircrew
[AD-A264484] p 3499 N93-30425

PSYCHOLOGY
Geoscience center research
[AD-A263465] p 3462 N93-29834
The dynamics of visual representation, attention, encoding, and retrieval processes
[AD-A264674] p 3500 N93-30543

PSYCHOMETRICS
Predicting aircrew training performance with psychometric g
[AD-A264021] p 3498 N93-30026
Field test of a computer-driven tool to measure psychological characteristics of aircrew
[AD-A264484] p 3499 N93-30425

PULMONARY FUNCTIONS
The chronic effects of jP-8 jet fuel exposure on the lungs
[AD-A264162] p 3495 N93-30153

PULSARS
The x ray population in globular clusters and three crab-like SNR in the large Magellanic cloud
[NASA-CR-193172] p 3630 N93-29604
GRO: Red-shifted electron-positron annihilation gamma-rays from radiopulsars
[NASA-CR-193243] p 3635 N93-30053

PULSE CODE MODULATION
Influence of optical feedback on the pulse behavior of semiconductor lasers
[ETN-93-93798] p 3436 N93-28614

PULSE COMMUNICATION
Advanced HF digital networks p 3375 N93-30343

PULSE COMPRESSION
Accelerator research studies
[DE93-009353] p 3573 N93-28522

PULSE DOPPLER RADAR
The use of data turning in airborne radars
p 3358 N93-30241

PULSE DURATION
Every good virtue you ever wanted in a Q-switched solid-state laser and more: Monolithic, diode-pumped, self-Q-switched, highly reproducible, diffraction-limited Nd:YAG laser p 3442 N93-28772
Multibeam laser altimeter for planetary topographic mapping p 3442 N93-28780
A technique for single-pulse spectrum and pulse width measurements for an IR-FEL
[DE93-007732] p 3436 N93-28847

PULSE GENERATORS
Optically controlled solid state opening switches
[AD-A262404] p 3591 N93-28496
High-voltage pulse generator capable of 2000 J at 10 kV
[AD-A262034] p 3407 N93-28999
Design of the Nova Upgrade laser system for ignition fusion experiments
[DE93-009077] p 3436 N93-29097
Fusion laser oscillator and pulse-forming system using integrated optics
[DE93-009286] p 3588 N93-29780
Analysis of an MCG/fuse/PFS experiment
[DE93-007355] p 3410 N93-29812
Pulse control in an accelerator for heavy-ion fusion
[DE93-009527] p 3576 N93-30390

PULSE REPETITION RATE
All solid-state high power visible laser
[NASA-CR-193163] p 3436 N93-28623
Multibeam laser altimeter for planetary topographic mapping p 3442 N93-28780
High-repetition rate x ray lasers and applications
[DE93-011882] p 3440 N93-30394

PULSED LASERS
Discharge of electrically charged clouds
[AD-A263212] p 3480 N93-28518
All solid-state high power visible laser
[NASA-CR-193163] p 3436 N93-28623
Polarization dependence of the ionization of helium and neon by 120 femtosecond pulses at 614 nm
[DE93-010514] p 3564 N93-28762
Multibeam laser altimeter for planetary topographic mapping p 3442 N93-28780
Low-pump-rate multi-millisecond atomic xenon laser
[DE93-011484] p 3437 N93-29180
Inner-shell photo-ionized x ray laser schemes
[DE93-009285] p 3438 N93-29309
Operating manual for single-shot autocorrelator
[AD-A262016] p 3438 N93-29395
Fusion laser oscillator and pulse-forming system using integrated optics
[DE93-009286] p 3588 N93-29780
High resolution free-electron laser spectroscopy
[AD-A263734] p 3439 N93-29853
Gas electron diffraction employing a pulsed electron beam synchronous with photoexcitation
p 3319 N93-30101
High-repetition rate x ray lasers and applications
[DE93-011882] p 3440 N93-30394
Method and apparatus for imaging an object in or through a scattering medium by using multiple-wave mixing
[AD-D015707] p 3581 N93-30410
Multiparticle imaging technique for two-phase fluid flows using pulsed laser speckle velocimetry
[DE93-011734] p 3427 N93-30489
Computer control of pulsed tunable dye lasers
[DE93-605896] p 3441 N93-30801

PUPILS
A tutorial on exit pupils and eye rotation with virtual image optical displays
[AD-A262399] p 3494 N93-29400

PYRIDINES
Conjugated substituted ionic polyacetylenes
[AD-A264702] p 3337 N93-30497

PYROELECTRICITY
Smart skin structures for identifying and locating laser irradiation
[DE93-005464] p 3436 N93-28887
Proceedings of the 25th European Conference on the Application of Polar Dielectrics to celebrate the 25th anniversary of the Dielectric Society, incorporating the 1st International Workshop on Integrated Ferroelectrics
[AD-A263427] p 3332 N93-29337

PYROLYSIS
Methylhydridopolysilazane and its pyrolytic conversion to Si3N4/SiC ceramics
[AD-A264150] p 3336 N93-30170
Conjugated polymers from cyclohexadienediol monomers
[AD-A264837] p 3340 N93-30900

PYROLYTIC GRAPHITE
Semiconductor cooling apparatus
[NASA-CASE-LEW-14162-3] p 3299 N93-29614

PYROMETERS
A passive infrared ice detection technique for helicopter applications
[NASA-CR-193187] p 3244 N93-29152

Q

Q FACTORS
Design and test of a superconducting RFQ for heavy ions
[DE93-010862] p 3575 N93-29317
Investigation of thermoacoustic muffler
[AD-A262009] p 3562 N93-29392
An approach to software quality prediction from Ada designs
[AD-A264731] p 3534 N93-30547

Q SWITCHED LASERS
Every good virtue you ever wanted in a Q-switched solid-state laser and more: Monolithic, diode-pumped, self-Q-switched, highly reproducible, diffraction-limited Nd:YAG laser p 3442 N93-28772

QUADRUPOLES
An RF driven H(-) source and a low energy beam injection system for RFQ operation
[DE93-010438] p 3575 N93-29302
Design and test of a superconducting RFQ for heavy ions
[DE93-010862] p 3575 N93-29317

QUALITATIVE ANALYSIS
Effect of planar magnetic field on electron transport properties of n-AlGaAs/GaAs heterojunction and photoluminescence measures in GaAs samples
[DE93-608739] p 3601 N93-30776

QUALITY CONTROL

Analysis of protocol gases: An on-going quality assurance audit
[PB93-168839] p 3311 N93-29204

Development of a test program to evaluate structural defects in Glass-Reinforced Plastic (GRP), volume 2
[AD-A263814] p 3335 N93-29881

A guide to total software quality control, volume 1
[AD-A263881] p 3531 N93-29920

A guide to total software quality control, volume 2
[AD-A263891] p 3531 N93-29921

Software testing using the IEEE standards
[DE93-009833] p 3532 N93-30050

Data quality statements for spatial databases
[AD-A264125] p 3616 N93-30195

Procedures for applying Ada quality prediction models
[AD-A264730] p 3534 N93-30546

An approach to software quality prediction from Ada designs
[AD-A264731] p 3534 N93-30547

The quality assurance liaison: Combined technical and quality assurance support
[DE93-008725] p 3450 N93-30636

QUANTILES

Empirical quantile function nonparametric integrated analyses
[AD-A263704] p 3554 N93-29385

QUANTITATIVE ANALYSIS

Quantitative analysis of properties and spatial relations of fuzzy image regions p 3510 N93-29523

Improved measurement of thermal effects on microstructure p 3292 N93-30959

QUANTUM CHEMISTRY

Adsorption of sulfate on metal electrodes
[AD-A263192] p 3309 N93-28540

The use of quantum chemistry to estimate the performance and properties of explosives
[DE92-040369] p 3352 N93-30446

The 26th International Quantum Chemistry Symposium on Atomic, Molecular, and Condensed Matter Theory and Computational Methods
[AD-A264206] p 3315 N93-30534

QUANTUM CHROMODYNAMICS

Studies in theoretical high energy particle physics
[DE93-007990] p 3574 N93-28565

Research in theoretical nuclear physics
[DE93-008380] p 3565 N93-28960

Borel sum rules for octet baryons in nuclear medium
[DE93-753245] p 3604 N93-29242

Task A: Theory of elementary particles
[DE93-010561] p 3569 N93-29841

Unitary approximation of Bhabha diffusion by high energies and its implementation in Monte Carlo event generators
[ETN-93-93622] p 3571 N93-30670

Invariant structures in gauge theories and confinement
[DE92-644739] p 3607 N93-30924

Invariant structures and static forces in gauge theories
[DE92-644740] p 3607 N93-30925

Normal equivariant forms of vector fields
[DE92-644845] p 3551 N93-30929

Spherically symmetric line element and Killing vectors in five-dimensional space
[DE93-604132] p 3558 N93-30988

The geometry of complex space-times with torsion
[DE92-641343] p 3608 N93-31003

QUANTUM EFFICIENCY

High-performance visible/UV CCD focal plane technology for spacebased applications
p 3434 N93-28771

QUANTUM ELECTRODYNAMICS

Topics in gauge theories and the unification of elementary particle interactions
[DE93-009370] p 3563 N93-28542

Invariant structures in gauge theories and confinement
[DE92-644739] p 3607 N93-30924

Regular and chaotic motion of two dimensional electrons in a strong magnetic field
[DE93-604091] p 3607 N93-30933

QUANTUM MECHANICS

Topics in gauge theories and the unification of elementary particle interactions
[DE93-009370] p 3563 N93-28542

Studies in theoretical high energy particle physics
[DE93-007990] p 3574 N93-28565

Photodissociation of HBr/LiF(001): A quantum mechanical model
[NASA-CR-193119] p 3603 N93-28933

Summer research program (1992). High School Apprenticeship Program (HSAP) reports. Volume 16: Arnold Engineering Development Center Civil Engineering Laboratory
[AD-A262024] p 3608 N93-29396

Differential calculus on quantum spaces and quantum groups
[DE93-010425] p 3551 N93-30392

Quantum-kinetic Green function and macroscopic wave function
[DE93-606040] p 3606 N93-30796

Chaotic quantum systems
[DE93-606030] p 3606 N93-30802

Scaling properties of localized quantum chaos
[DE93-606031] p 3606 N93-30803

On two-dimensional quasiclassics
[DE93-606034] p 3606 N93-30805

Positive energy representations of the conformal quantum algebra
[DE93-606064] p 3551 N93-30809

Connections between quantized affine algebras and superalgebras
[DE93-606065] p 3551 N93-30810

Physics laboratory technical activities, 1992
[PB93-178648] p 3561 N93-30888

On the invariant measure for the nonlinear Schroedinger equation
[DE92-644672] p 3551 N93-30912

Algorithm for the solution of the Faddeev equation for a system of three identical spinless particles
[DE92-644678] p 3535 N93-30914

Topology and statistics in zero dimensions
[DE93-604080] p 3607 N93-30932

Regular and chaotic motion of two dimensional electrons in a strong magnetic field
[DE93-604091] p 3607 N93-30933

Low-energy behaviour of few-particle scattering amplitudes in two dimensions
[DE93-609834] p 3572 N93-30944

A squeezed state holomorphic phase space representation of equations of motion
[DE93-609835] p 3607 N93-30945

Formulation of wave mechanics without the Planck constant h/2 pi
[DE93-604083] p 3608 N93-30987

QUANTUM NUMBERS

Integrals of motion on the group of invariance of an interval in three-dimensional spaces
[DE93-606090] p 3606 N93-30797

QUANTUM STATISTICS

On the impossibility of creating the quantum correlations with computers
[DE93-606039] p 3606 N93-30806

Topology and statistics in zero dimensions
[DE93-604080] p 3607 N93-30932

QUANTUM THEORY

The semiclassical stability of de Sitter spacetime
[DESY-92-131] p 3603 N93-28472

Applications of unitarity in the standard model
p 3416 N93-28613

An algebraic approach to the quantization of constrained systems: Finite dimensional examples
p 3548 N93-28671

Quantum devices using Si-based superlattices and structures
[AD-A263700] p 3595 N93-29383

Understanding conformal field theory through parafermions and Chern Simons theory
[DE93-010452] p 3604 N93-29806

Quantum field theory in spaces with closed time-like curves
[DE93-010564] p 3605 N93-30481

NATO Advanced Research Workshop on Frontiers of Optical Phenomena in Semiconductor Structure of Reduced Dimension
[AD-A264813] p 3581 N93-30666

Quantum group and symmetry of the heat equation
[DE93-607560] p 3605 N93-30779

Approximation formulae for functional integrals in P(phi)2-quantum field theory
[DE93-606067] p 3605 N93-30781

Phase structure of three- and four-dimensional phi(exp 4) field theory
[DE93-606069] p 3605 N93-30782

Beyond two dimensions
[DE93-606084] p 3606 N93-30786

Quantum-kinetic Green function and macroscopic wave function
[DE93-606040] p 3606 N93-30796

Physics laboratory technical activities, 1992
[PB93-178648] p 3561 N93-30888

Nonlinear realisations of omega(1 + infinity)
[DE92-644721] p 3557 N93-30917

Compensating fields and anomalies in supergravity
[DE92-644724] p 3637 N93-30919

Quantum group generalization of the heterotic QFT
[DE92-644727] p 3607 N93-30920

Invariant structures and static forces in gauge theories
[DE92-644740] p 3607 N93-30925

On the energy-momentum tensors for field theories in spaces with affine connection and metric
[DE92-644743] p 3557 N93-30926

A squeezed state holomorphic phase space representation of equations of motion
[DE93-609835] p 3607 N93-30945

A non degenerate semi-classical Lagrangian for dilaton-gravity in two dimensions
[DE92-641339] p 3480 N93-31002

QUANTUM WELLS

Low temperature (LT) GaAs and related materials
[AD-A263607] p 3298 N93-29282

Quantum devices using Si-based superlattices and structures
[AD-A263700] p 3595 N93-29383

Nonequilibrium screening and exciton dynamics probed by femtosecond laser pulses
[AD-A263603] p 3439 N93-29983

Development of ultra-low noise, high sensitivity planar metal grating coupled 3-5 multiquantum well infrared detectors for focal plane array staring IR sensor systems
[AD-A264465] p 3599 N93-30536

Electronic states in quantum wells with periodically structured interfaces
[DE93-606295] p 3600 N93-30769

QUARKS

Measurements of rare composite objects and high sensitivity searches for novel forms of matter produced in high energy heavy ion collisions
[DE93-009945] p 3574 N93-28569

New limits on generation-1 leptoquarks
[DE93-008138] p 3567 N93-29351

Single t-quark production in high energy (gamma)e collisions
[DE92-644947] p 3572 N93-30930

Fluctuations and intermittency in high energy nucleus-nucleus collisions
[DE93-608481] p 3577 N93-30990

QUARTZ CRYSTALS

Post-flight analyses of the crystals from the M0003-14 quartz crystal microbalance experiment
p 3602 N93-29684

Radiation sensitivity of quartz crystal oscillators experiment for the Long Duration Exposure Facility (LDEF), part 2 p 3414 N93-29685

QUASARS

Multifractal analysis of radio lobes
p 3380 N93-28689

QUENCHING (ATOMIC PHYSICS)

Reaction and reorientation of electronically excited H2(B)
[DE93-010435] p 3569 N93-29860

QUERY LANGUAGES

Formal definition of a conceptual language for the description and manipulation of information models
[TR-92-16] p 3523 N93-28503

A model for processing the SGML document in version oriented hypertext systems
[ETN-93-93797] p 3611 N93-28528

A distributed object-oriented database application design
[AD-A262591] p 3612 N93-28846

On the evaluation of fuzzy quantified queries in a database management system p 3517 N93-29569

A high performance, ad-hoc, fuzzy query processing system for relational databases p 3518 N93-29571

QUEUEING THEORY

Some qualitative properties in polling systems
[INRIA-RR-1596] p 3552 N93-28506

Flow control using the theory of zero sum Markov games
[INRIA-RR-1597] p 3553 N93-28507

Optimal control of the M/G/1 queue with repeated vacations of the server
[INRIA-RR-1637] p 3541 N93-28637

Closed-loop control with delayed information
[INRIA-RR-1638] p 3541 N93-28638

QUINONES

Hydrogen sulfide decomposition into hydrogen and sulfur by quinone cycles, part 1
[PB93-175297] p 3317 N93-30761

R

RADAR

Modern approach to relativity theory (radar formulation)
[DE93-606032] p 3606 N93-30804

RADAR ANTENNAS

Array-fed reflector systems with limited scan
p 3371 N93-30318

RADAR APPROACH CONTROL

Airspace Design Expert System (ADES), a 2D/3D mapping and modelling tool incorporating an expert system for use in instrument approach design
p 3247 N93-30357

RADAR BEAMS
Radar beam effects for a flight simulator using signal processor based hardware p 3373 N93-30328
RADAR CLUTTER MAPS
Ground clutter measurements for surface-sited radar [AD-A262472] p 3379 N93-28655
RADAR CORNER REFLECTORS
Investigations of self-pumped phase conjugate laser beams and coherence length [AD-A263438] p 3438 N93-29789
RADAR CROSS SECTIONS
Computer-aided modeling for analysis of arbitrary scatterers and feeds p 3367 N93-30293
RCS of fundamental scatterers in the HF band by wire-grid modelling p 3371 N93-30320
Wide frequency polarimetric radar cross section measurements p 3371 N93-30321
Application of integral and differential equation methods for various EM interaction problems [AD-A264821] p 3394 N93-30597
RADAR DATA
Clementine 2: A double asteroid flyby and impactor mission p 3268 N93-28770
Leadex data report. Part 1: Weather analysis and satellite images [AD-A263217] p 3481 N93-28876
Software development and analysis for experimental high frequency surface wave radar data [AD-A261982] p 3383 N93-29438
Classification of radar clutter in an air traffic control environment p 3246 N93-30299
Effects of imbalances and DC offsets on I/Q demodulation [AD-A264466] p 3393 N93-30537
RADAR DETECTION
Modified Acousto-Optic Adaptive Processor (Mod-AOAP) [AD-A261983] p 3381 N93-28997
Project MEDSAT p 3231 N93-29739
A TACSAT SAR concept p 3286 N93-29910
Future directions in aviation security p 3244 N93-30274
Adaptive filtering for clutter suppression in high frequency radar p 3377 N93-30355
Enhanced convergence adaptive detection [AD-A264100] p 3399 N93-30879
RADAR IMAGERY
Multiscale morphological filtering for analysis of noisy and complex images p 3582 N93-28789
Proceedings of the 8th User Seminar of the German Remote Sensing Data Center of the German Aerospace Establishment (DLR) [DLR-MITT-92-09] p 3456 N93-28915
Forest examination with polarimetric radar image data p 3457 N93-28921
Remote sensing of agricultural vegetation: Status and perspectives p 3458 N93-28922
SAR shape-from-shading for a populated alpine area p 3458 N93-28923
The MAESTRO-1 campaign: Analyses of polarimetric SAR data of agricultural fields and forests [BCRS-92-06] p 3460 N93-29320
A TACSAT SAR concept p 3286 N93-29910
Similarities between synthetic aperature radar and ground probing radar imaging p 3376 N93-30347
Segmentation of SAR images p 3376 N93-30348
Multiscale and multigrid information representation, extraction and fusion [AD-A264623] p 3393 N93-30386
RADAR MAPS
Development of an airborne MMW FM-CW radar for mapping river ice [AD-A262655] p 3379 N93-28588
Doppler-radar wind-speed measurements in tornadoes: A comparison of real and simulated spectra [DE93-008734] p 3481 N93-29095
RADAR MEASUREMENT
Ground clutter measurements for surface-sited radar [AD-A262472] p 3379 N93-28655
The enhanced-model ladar wind sensor and its application in planetary wind velocity measurements p 3649 N93-28815
RADAR SCANNING
Array-fed reflector systems with limited scan p 3371 N93-30318
RADAR SCATTERING
The dynamic cusp at low altitudes: A case study combining Viking, DMSP, and Sondrestrom incoherent scatter radar observations [NASA-CR-193152] p 3476 N93-28842
SAR shape-from-shading for a populated alpine area p 3458 N93-28923
RCS of fundamental scatterers in the HF band by wire-grid modelling p 3371 N93-30320
Wide frequency polarimetric radar cross section measurements p 3371 N93-30321
RADAR SIGNATURES
The dynamic cusp at low altitudes: A case study combining Viking, DMSP, and Sondrestrom incoherent scatter radar observations [NASA-CR-193152] p 3476 N93-28842
Forest examination with polarimetric radar image data p 3457 N93-28921
RADAR TARGETS
Wide frequency polarimetric radar cross section measurements p 3371 N93-30321
Adaptive airborne radar simulation with equalization filter taps [AD-A264722] p 3393 N93-30514
RADAR TRACKING
A fuzzy logic optimal control law solution to the CMMCA tracking problem [AD-A262555] p 3542 N93-29420
The effect of clock, media, and station location errors on Doppler measurement accuracy p 3246 N93-29588
Wind measurement accuracy of a loran radiosonde [AD-A263572] p 3483 N93-29832
Evolution of radar data processing in the French air traffic control system p 3247 N93-30325
RADAR TRANSMISSION
Characteristics of high-frequency signals, noise, availability, and duration of bandwidths based on ROTHR Amchitka spectrum measurements [AD-A264480] p 3393 N93-30423
RADIAL FLOW
Two-dimensional and three-dimensional time-dependent MHD model of extended corona p 3653 N93-30496
RADIAL VELOCITY
The use of objective prism radial velocities for kinematic studies of galactic populations p 3633 N93-28672
RADIANCE
Radiometric calibration system for IR cameras [DE93-009237] p 3430 N93-28520
The possible direct use of satellite radiance measurements by the Atmospheric Radiation Measurement Program [DE93-009819] p 3462 N93-30049
RADIANT COOLING
Spaceborne passive radiative cooler p 3378 N93-28802
RADIANT HEATING
The hydraulic analysis of cylindrical Flibe jets in a HYLIFE-2 ICF reactor [DE93-009234] p 3586 N93-29053
Unsteady combustion of energetic materials using laser-recoil p 3319 N93-30085
RADIATION BELTS
Planetary and satellite x ray spectroscopy: A new window on solid-body composition by remote sensing p 3641 N93-28773
Radioactivities induced in some LDEF samples p 3572 N93-29628
Revised prediction of LDEF exposure to trapped protons p 3572 N93-29633
Lightning-induced effects on VLF/LF radio propagation p 3396 N93-30737
RADIATION CHEMISTRY
DOE fundamentals handbook: Chemistry [DE93-012222] p 3314 N93-30198
RADIATION COUNTERS
Proposal for a universal particle detector experiment p 3286 N93-28795
Research programs from the University of South Carolina on high energy physics [DE93-007829] p 3574 N93-28969
Radioactivities induced in some LDEF samples p 3572 N93-29628
Elementary particle interactions [DE93-005113] p 3568 N93-29764
RADIATION DAMAGE
Neutron radiation induced degradation of diode characteristics [AD-A263277] p 3405 N93-28563
Photobiological investigations on spores of streptomyces griseus [ESA-TT-1269] p 3491 N93-29274
Center for surface radiation damage studies [AD-A264330] p 3570 N93-30366
Unexpected increase in the thermal generation rate of bulk GaAs due to electron-beam metallization [DE93-009829] p 3598 N93-30511
Heat generation produced in thin layers of GaAs superconductors under high energy particles irradiation [DE93-606332] p 3601 N93-30798
RADIATION DETECTORS
A compact imaging detector of polarization and spectral content p 3582 N93-28810
Smart skin structures for identifying and locating laser irradiation [DE93-005464] p 3436 N93-28887
Superconducting submillimeter and millimeter wave detectors [DE93-007656] p 3431 N93-29149
New Mexico Center for Particle Physics: Studies of fundamental interactions [DE93-008302] p 3566 N93-29261
Laser radiation detection system [AD-D015724] p 3438 N93-29287
Absorbed dose measurements and predictions on LDEF p 3573 N93-29636
Heavy ion measurement on LDEF p 3573 N93-29644
Progress report on the ultra heavy cosmic ray experiment (AO178) p 3654 N93-29646
Reaction mechanism studies of heavy ion induced nuclear reactions [DE93-010496] p 3569 N93-29807
RADIATION DISTRIBUTION
On the meaning of delta T/T [DE93-008482] p 3653 N93-28962
A study on radiation shielding analysis for toroidal field coils of a tokamak-type fusion reactor [DE93-753398] p 3585 N93-28981
Evaluation of multi-dimensional flux models for radiative transfer in cylindrical combustion chambers p 3257 N93-29955
Radiated fields from an electromagnetic pulse simulator p 3366 N93-30290
Computer-aided modeling for analysis of arbitrary scatterers and feeds p 3367 N93-30293
RADIATION DOSAGE
Radiation monitoring equipment dosimeter experiment p 3266 N93-28730
The meteorological database [DE93-007289] p 3481 N93-29054
Leaky coaxial cable signal transmission for remote facilities [DE93-007916] p 3383 N93-29348
Predicting radiation induced performance decrements of AH-1 helicopter crews. Volume 2: Evaluation of modeling and simulation techniques for predicting radiation induced performance decrements [AD-A262872] p 3506 N93-29484
Revised prediction of LDEF exposure to trapped protons p 3572 N93-29633
A measurement of the radiation dose to LDEF by passive dosimetry p 3572 N93-29634
LDEF: Dosimetric measurement results (AO 138-7 experiment) p 3573 N93-29635
Absorbed dose measurements and predictions on LDEF p 3573 N93-29636
Light-heavy ion measurements in CR-39 located on the Earth side of LDEF p 3573 N93-29638
Development and application of a 3-D geometry/mass model for LDEF satellite ionizing radiation assessments p 3573 N93-29640
Radiation model predictions and validation using LDEF satellite data p 3573 N93-29641
Future directions for LDEF ionizing radiation modeling and assessments p 3573 N93-29642
Progress report on the ultra heavy cosmic ray experiment (AO178) p 3654 N93-29646
Radiation sensitivity of quartz crystal oscillators experiment for the Long Duration Exposure Facility (LDEF), part 2 p 3414 N93-29685
Test structure to microcircuit correlation [AD-A264157] p 3412 N93-30152
Radiation-hardened microwave communications system [DE93-007915] p 3394 N93-30631
Charge separation in bipolar transistors [DE93-009624] p 3413 N93-30650
Hardness assurance and testing issues for bipolar/BiCMOS devices [DE93-009623] p 3570 N93-30669
RADIATION EFFECTS
Neutron radiation induced degradation of diode characteristics [AD-A263277] p 3405 N93-28563
Enhancements of the critical currents of YBaCuO single crystals by neutron (n) and proton (p) irradiation [DE93-007892] p 3592 N93-28661
Transfer Orbit Plasma Interaction Experiment (TROPIX) p 3267 N93-28734
Gene transcription and electromagnetic fields [DE93-010854] p 3490 N93-28848
FNAS CRRES program completion [NASA-CR-192468] p 3476 N93-29032
Photobiological investigations on spores of streptomyces griseus [ESA-TT-1269] p 3491 N93-29274
Response of energetic solids to light, heat and shock pulses [AD-A263702] p 3342 N93-29296

Three-dimensional shielding effects on charged particle fluences measured in the P0006 experiment of LDEF p 3573 N93-29639

Radiation sensitivity of quartz crystal oscillators experiment for the Long Duration Exposure Facility (LDEF), part 2 p 3414 N93-29685

LEO effects on candidate solar cell cover materials p 3467 N93-29687

New results from FRECOPA analysis p 3448 N93-29688

Studies of effects on optical components and sensors: LDEF experiments AO-147 (ERB components) and S-0014 (APEX) p 3582 N93-29693

Effects of long term space environment exposure on optical substrates and coatings (S0050-2) p 3582 N93-29694

Characterization of a space orbited incoherent fiber optic bundle p 3583 N93-29698

Analyses of space environment effects on active fiber optic links orbited aboard the LDEF p 3583 N93-29699

Radiation and temperature effects on LDEF fiber optic samples p 3583 N93-29700

Final results of space exposed experiment developed for students p 3492 N93-29702

Continued results of the seeds in space experiment p 3492 N93-29703

Problems in the implementation of x ray optics with x ray lasers [DE93-009297] p 3438 N93-29781

Total dose tests for the PROMICS-3 instrument [VTT-TIED-1203] p 3411 N93-30108

Test structure to microcircuit correlation [AD-A264157] p 3412 N93-30152

Irradiation assisted stress corrosion cracking of stainless steel irradiated in FBR [DE93-764495] p 3326 N93-30191

Simulation of transient radiation effects on semiconductor devices using a pulsed Q-switched Nd:YAG laser p 3357 N93-30230

Transient field computations within or proximity of complex structures: FD-TD approach p 3366 N93-30292

Effects of device scaling and geometry on MOS radiation hardness assurance [DE93-009832] p 3413 N93-30516

Application of integral and differential equation methods for various EM interaction problems [AD-A264821] p 3394 N93-30597

Radiation effects in FCC metals and intermetallic compounds: A molecular dynamics computer simulation study [DE93-009546] p 3600 N93-30668

Hardness assurance and testing issues for bipolar/BiCMOS devices [DE93-009623] p 3570 N93-30669

Hard photon emission from high energy electrons and positrons in single crystals [DE93-606328] p 3600 N93-30770

Theoretical-experimental study of the non-thermal effects of the polarized laser radiation in living tissues [DE93-607212] p 3441 N93-30775

Mathematical simulation of the induced (gamma)-radiation in structural materials of spaceships. Time dependence [DE93-605312] p 3281 N93-31024

RADIATION HARDENING

Neutron radiation induced degradation of diode characteristics [AD-A263277] p 3405 N93-28563

High-performance visible/UV CCD focal plane technology for spacebased applications p 3434 N93-28771

SEU tolerant computer based on the R3000 [DE93-009294] p 3520 N93-29058

Test structure to microcircuit correlation [AD-A264157] p 3412 N93-30152

Simulation of transient radiation effects on semiconductor devices using a pulsed Q-switched Nd:YAG laser p 3357 N93-30230

Effects of device scaling and geometry on MOS radiation hardness assurance [DE93-009832] p 3413 N93-30516

Hardness assurance and testing issues for bipolar/BiCMOS devices [DE93-009623] p 3570 N93-30669

RADIATION HAZARDS

Radiated fields from an electromagnetic pulse simulator p 3366 N93-30290

RADIATION MEASUREMENT

Proceedings of the Second Atmospheric Radiation Measurement (ARM) Science Team Meeting [DE93-005886] p 3476 N93-28889

Clouds and radiation: A primier [AD-A263136] p 3482 N93-29479

A photon phreak digs the LDEF happening p 3572 N93-29629

A measurement of the radiation dose to LDEF by passive dosimetry p 3572 N93-29634

LDEF: Dosimetric measurement results (AO 138-7 experiment) p 3573 N93-29635

Absorbed dose measurements and predictions on LDEF p 3573 N93-29636

LET spectra measurements of charged particles in the P0006 experiment on LDEF p 3573 N93-29637

Development and application of a 3-D geometry/mass model for LDEF satellite ionizing radiation assessments p 3573 N93-29640

Future radiation measurements in low Earth orbit p 3654 N93-29708

The possible direct use of satellite radiance measurements by the Atmospheric Radiation Measurement Program [DE93-009819] p 3462 N93-30049

RADIATION MEASURING INSTRUMENTS

Lightweight modular instrumentation for planetary applications p 3286 N93-28787

RADIATION PROTECTION

Acid solution absorption of extruded polyethylene foam [DE93-011701] p 3330 N93-28839

Charge to frequency converter for ionization chambers belonging to the radiation protection system of AmPS/MEA [DIGEL-1991-6] p 3577 N93-30837

Electronics for a neutron detector and a Geiger-Mueller detector for the radiation protection around MEA and AmPS [DIGEL-1992-6] p 3413 N93-30838

RADIATION SHIELDING

A study on radiation shielding analysis for toroidal field coils of a tokamak-type fusion reactor [DE93-753398] p 3585 N93-28981

Modern Monte Carlo particle transport simulation for safety and radiation protection applications in accelerometer technology and in space science [JUEL-2609] p 3574 N93-29062

Regolith-structure modeling p 3276 N93-29116

Structural design of cryostat and port penetration of International Thermonuclear Experimental Reactor (ITER) [DE93-753267] p 3587 N93-29243

Absorbed dose measurements and predictions on LDEF p 3573 N93-29636

Light-heavy ion measurements in CR-39 located on the Earth side of LDEF p 3573 N93-29638

Three-dimensional shielding effects on charged particle fluences measured in the P0006 experiment of LDEF p 3573 N93-29639

Beta/gamma Monte Carlo transport in repetitive structures of satellite systems [DE93-007610] p 3281 N93-30509

RADIATION SOURCES

Development of high power microwave source [DE93-753316] p 3436 N93-28980

A novel approach for new radiation sources based on solid state plasma instabilities [AD-A263699] p 3588 N93-29382

ELF propagation in deep and shallow sea water p 3397 N93-30739

RADIATION SPECTRA

Development of a 9.3 micrometer CW LIDAR for the study of atmospheric aerosol [NASA-CR-193227] p 3381 N93-29105

RADIATION TOLERANCE

Spacecraft computer technology at Southwest Research Institute p 3522 N93-28813

Total dose tests for the PROMICS-3 instrument [VTT-TIED-1203] p 3411 N93-30108

Test structure to microcircuit correlation [AD-A264157] p 3412 N93-30152

RADIATION TRANSPORT

Proceedings of the Second Atmospheric Radiation Measurement (ARM) Science Team Meeting [DE93-005886] p 3476 N93-28889

Computational simulations of a soft x ray projection lithography laser plasma source [DE93-009625] p 3437 N93-29264

RADIATION TRAPPING

Radioactivities induced in some LDEF samples p 3572 N93-29628

Future directions for LDEF ionizing radiation modeling and assessments p 3573 N93-29642

RADIATIVE HEAT TRANSFER

Spherically symmetric model atmospheres for late-type giant stars [ISBN-0-315-72632-6] p 3633 N93-28673

Application of ray tracing in radiation heat transfer [NASA-TM-106206] p 3419 N93-29075

Radiative interactions in molecular gases under local and nonlocal thermodynamic equilibrium conditions [NASA-CR-193223] p 3604 N93-29168

Thermal certification tests of Orbiter Thermal Protection System tiles coated with KSC coating slurries [NASA-TM-104766] p 3278 N93-29221

The thermal structure, dust loading, and meridional transport in the Martian atmosphere during late southern summer p 3651 N93-29616

Evaluation of multi-dimensional flux models for radiative transfer in cylindrical combustion chambers p 3257 N93-29955

A stochastic formation of radiative transfer in clouds [DE93-011372] p 3484 N93-30055

RADIATIVE LIFETIME

Limits on neutrino radiative decay from SN1987A [NASA-CR-193262] p 3653 N93-29164

RADIATIVE RECOMBINATION

New III-V cell design approaches for very high efficiency [DE93-000097] p 3464 N93-28971

RADIATIVE TRANSFER

Start broadened profiles with self-consistent radiation transfer and atomic kinetics in plasmas produced by high intensity lasers [DE93-008706] p 3586 N93-29093

Stabilized platform for tethered balloon soundings of broadband long- and short-wave radiation [DE93-007876] p 3383 N93-29308

RTE: A UNIX library with on-line documentation and sample programs for microwave radiative transfer calculations [PB93-180248] p 3386 N93-29680

A stochastic formation of radiative transfer in clouds [DE93-011372] p 3484 N93-30055

A correlated k-distribution model of the atmospheric heating rates for overlapping spectra of CO2 and H2O [DE93-007391] p 3474 N93-30504

RADICALS

Laser spectroscopy of hydrocarbon radicals [DE93-012555] p 3436 N93-28653

Synthesis of oligoimides and oligoimide anion radicals [AD-A263129] p 3290 N93-29474

RADIO ANTENNAS

Widebanding techniques for VHF antennas 2 [AD-A263998] p 3387 N93-29882

Models for performance assessment of HF antennas on the CH-135/Twin Huey helicopter p 3366 N93-30291

VLF/LF transmitting antennas p 3398 N93-30747

Tethered aerostat VLF/LF transmitter system design considerations p 3399 N93-30753

RADIO COMMUNICATION

Activities report of PTT Research [ISBN-9-07-212514-2] p 3392 N93-30025

The 1992 World Administrative Radio Conference: Technology and Policy Implications [OTA-TCT-549] p 3392 N93-30150

Design issues and initial performance of an adaptive air/ground/air HF communication system p 3375 N93-30342

The evolution of global mobile communications p 3376 N93-30349

Introduction p 3395 N93-30728

Numerical modeling of the propagation medium at VLF/LF p 3395 N93-30729

VLF/LF propagation measurements p 3395 N93-30732

Theoretical and experimental coverage analysis of a VLF transmitter p 3396 N93-30734

VLF/LF transmitting antennas p 3398 N93-30747

Study of a VLF distributed antenna array p 3398 N93-30749

Pattern measurements of US Navy ELF antennas p 3399 N93-30752

Viability assessment for reliable long-wave communication links p 3399 N93-30754

RADIO EMISSION

Distribution of dark matter in the galaxy and the lower limits for the masses of supersymmetric particles [BONN-92-31] p 3632 N93-28473

Multifractal analysis of radio lobes p 3380 N93-28689

Space optical and low-frequency radio searches for Earth-crossing asteroids and comets [DE93-008716] p 3634 N93-29246

RADIO EQUIPMENT

Using today's technology to improve mobile C4I for the operational commander [AD-A263613] p 3245 N93-29285

RADIO FREQUENCIES

Large amplitude striations in an RF discharge [DE93-753244] p 3379 N93-28534

Design and construction of a prototype ACTS propagation terminal [NASA-CR-193071] p 3404 N93-28539

Onboard signal processing: Wave of the future for planetary radio science? p 3646 N93-28801
Upgrading the LAMPF 201 MHz RF generators
[DE93-010715] p 3406 N93-28830
Wideband propagation measurements for wireless indoor communication
[PB93-175123] p 3382 N93-29202
An RF driven H(-) source and a low energy beam injection system for RFQ operation
[DE93-010438] p 3575 N93-29302
Design and test of a superconducting RFQ for heavy ions
[DE93-010862] p 3575 N93-29317
The 1992 World Administrative Radio Conference: Technology and Policy Implications
[OTA-TCT-549] p 3392 N93-30150
High-speed, CMOS dual modulus frequency divider for RF frequency synthesis p 3359 N93-30245
High density plasma production in a multicusp plasma generator with RF antenna
[DE93-764493] p 3590 N93-30606

RADIO FREQUENCY DISCHARGE
Large amplitude striations in an RF discharge
[DE93-753244] p 3379 N93-28534

RADIO FREQUENCY HEATING
Microwave processing of ceramics
[DE93-010708] p 3332 N93-29252
Fundamental studies of fusion plasmas
[DE93-013144] p 3589 N93-30189

RADIO FREQUENCY INTERFERENCE
ELF/VLF/LF Radio Propagation and Systems Aspects
[AGARD-CP-529] p 3394 N93-30727

RADIO GALAXIES
Multifractal analysis of radio lobes
p 3380 N93-28689

RADIO METEOROLOGY
Contributions to the American Meteorological Society's 26th International Conference on Radar Meteorology
[AD-A263385] p 3481 N93-29257

RADIO NAVIGATION
The Telecommunications and Data Acquisition Report
[NASA-CR-193144] p 3384 N93-29586

RADIO OBSERVATION
Onboard signal processing: Wave of the future for planetary radio science? p 3646 N93-28801

RADIO RECEIVERS
Design and construction of a prototype ACTS propagation terminal
[NASA-CR-193071] p 3404 N93-28539
Time delay measurements of current primary FAA air/ground transmitters and receivers
[DOT/FAA/CT-TN93/14] p 3379 N93-28555
Miniature modular microwave end-to-end receiver
[NASA-CASE-NPO-18713-1-CU] p 3381 N93-29087
Wideband propagation measurements for wireless indoor communication
[PB93-175123] p 3382 N93-29202
An adaptive maximum likelihood receiver for correlated Rayleigh fading channels p 3371 N93-30316
Embedded GPS: The Canadian Marconi approach
p 3247 N93-30330

RADIO SIGNALS
Upgrading the LAMPF 201 MHz RF generators
[DE93-010715] p 3406 N93-28830
Effects of imbalances and DC offsets on I/Q demodulation
[AD-A264466] p 3393 N93-30537
Numerical modeling of the propagation medium at VLF/LF p 3395 N93-30729

RADIO SPECTRA
Doppler-radar wind-speed measurements in tornadoes: A comparison of real and simulated spectra
[DE93-008734] p 3481 N93-29095

RADIO STARS
GRO: Red-shifted electron-positron annihilation gamma-rays from radiopulsars
[NASA-CR-193243] p 3635 N93-30053

RADIO TRACKING
Investigation of Mars rotational dynamics using Earth-based radio tracking of Mars landers
p 3642 N93-28777

RADIO TRANSMISSION
A comparison of trans-equatorial ionosphere propagation predictions from AMBCOM with measured data
[AD-A264006] p 3391 N93-29987
ELF/VLF/LF Radio Propagation and Systems Aspects
[AGARD-CP-529] p 3394 N93-30727
Introduction p 3395 N93-30728
Theoretical and experimental coverage analysis of a VLF transmitter p 3396 N93-30734
Investigations of equatorial ionosphere nighttime mode conversion at VLF p 3396 N93-30735
Lightning-induced effects on VLF/LF radio propagation p 3396 N93-30737
VLF/LF transmitting antennas p 3398 N93-30747
Study of a VLF distributed antenna array
p 3398 N93-30749
Pattern measurements of US Navy ELF antennas
p 3399 N93-30752
Tethered aerostat VLF/LF transmitter system design considerations p 3399 N93-30753
Orbiting transmitter and antenna for spaceborne communications at ELF/VLF to submerged submarines
p 3399 N93-30755

RADIO TRANSMITTERS
Time delay measurements of current primary FAA air/ground transmitters and receivers
[DOT/FAA/CT-TN93/14] p 3379 N93-28555
Onboard signal processing: Wave of the future for planetary radio science? p 3646 N93-28801
A dynamic bandwidth and phase linearity measurement technique for 4-channel MSK VLF antenna systems
p 3398 N93-30748
Study of a VLF distributed antenna array
p 3398 N93-30749
Tethered aerostat VLF/LF transmitter system design considerations p 3399 N93-30753
Orbiting transmitter and antenna for spaceborne communications at ELF/VLF to submerged submarines
p 3399 N93-30755

RADIO WAVES
A computer simulation of the production of an artificially ionized layer using the Arecibo facility
[DE93-010817] p 3478 N93-30487
Investigations of equatorial ionosphere nighttime mode conversion at VLF p 3396 N93-30735
Lightning-induced effects on VLF/LF radio propagation p 3396 N93-30737
Studies of the propagation of Low Frequency (LF) radio waves p 3396 N93-30738
A methodology and tool for the prediction of depth of reception in the sea for a VLF/LF communications system p 3397 N93-30741

RADIOACTIVE DECAY
Research programs from the University of South Carolina on high energy physics
[DE93-007829] p 3574 N93-28969
Limits on neutrino radiative decay from SN1987A
[NASA-CR-193262] p 3653 N93-29164
Cosmogenic radionuclides on LDEF: An unexpected Be-10 result p 3573 N93-29643
Task A: Theory of elementary particles
[DE93-010561] p 3569 N93-29841
A search for radiative neutrino decay from supernovae
[NASA-CR-193118] p 3653 N93-30052
Study of heavy-flavored particles
[DE93-011535] p 3569 N93-30128
Partial cross sections in H(-) photodetachment
[DE93-011570] p 3569 N93-30130

RADIOACTIVE ISOTOPES
Research programs from the University of South Carolina on high energy physics
[DE93-007829] p 3574 N93-28969
Radioactivities induced in some LDEF samples
p 3572 N93-29628
A photon phreak digs the LDEF happening
p 3572 N93-29629
Charged particle activation studies on the surface of LDEF spacecraft p 3572 N93-29630
Induced activation study of LDEF
p 3572 N93-29632

RADIOACTIVE WASTES
Technical bases for precipitate hydrolysis process operating parameters, revision 1
[DE93-009894] p 3309 N93-28553
Hanford Environmental Information System (HEIS) user's manual, volume 1
[DE93-007465] p 3470 N93-29135
An architecture for robotic system integration
[DE93-010829] p 3444 N93-29316
The quality assurance liaison: Combined technical and quality assurance support
[DE93-008725] p 3450 N93-30636
Environmental characteristics of EPA, NRC, and DOE sites contaminated with radioactive substances
[PB93-185551] p 3475 N93-30829
Statement on the United Nations Conference on Environment and Development
[DE93-601878] p 3475 N93-30996

RADIOACTIVITY
An experimental investigation of radioactivity induced by ions associated with the operation of pulsed-power accelerators
[DE93-011478] p 3575 N93-29151
Status of LDEF ionizing radiation measurements and analysis p 3654 N93-29626
Collection, analysis, and archival of LDEF activation data p 3624 N93-29631
Induced activation study of LDEF
p 3572 N93-29632

RADIOBIOLOGY
Radiation monitoring equipment dosimeter experiment
p 3266 N93-28730

RADIOCHEMISTRY
DOE fundamentals handbook: Chemistry
[DE93-012222] p 3314 N93-30198

RADIOGENIC MATERIALS
Geochemical and fluid dynamic investigations into the nature of chemical heterogeneity in the Earth's mantle
[AD-A262753] p 3477 N93-29405

RADIOGRAPHY
Flash x ray system: Techniques and applications
[DE93-011477] p 3430 N93-28645

RADIOMETERS
Stabilized platform for tethered balloon soundings of broadband long- and short-wave radiation
[DE93-007876] p 3383 N93-29308
Convective and stratiform rain: Multichannel microwave sensing over oceans
[NASA-TM-104586] p 3482 N93-29448
Physics laboratory technical activities, 1992
[PB93-178648] p 3561 N93-30888

RADIOMETRIC CORRECTION
Preprocessing airborne remote sensing PARES calibration maintenance functional design document
[BCRS-92-07] p 3460 N93-29321

RADIOSONDES
Leadex data report. Part 2: Rawinsonde and ice station data
[AD-A263218] p 3483 N93-29491
Wind measurement accuracy of a loran radiosonde
[AD-A263572] p 3483 N93-29832

RAIL TRANSPORTATION
Guideway structural design and power/propulsion/braking in relation to guideways, volume 1
[PB93-169902] p 3447 N93-30820
Determination of low frequency reference slipping for high frequency unstationary motion processes
[ILR-MITT-273(1992)] p 3455 N93-31017

RAILGUN ACCELERATORS
Two-dimensional model for current and heat transport in solid-armature railguns
[AD-A262014] p 3271 N93-29394

RAIN
Convective and stratiform rain: Multichannel microwave sensing over oceans
[NASA-TM-104586] p 3482 N93-29448

RAIN FORESTS
Advanced Earth Observing Satellite (ADEOS)
p 3279 N93-29648

RAMAN SPECTRA
Aerosol particle analysis by Raman scattering technique
[DE93-005587] p 3309 N93-28880
Quantum lattice fluctuations in a 1-dimensional charge-density-wave material: Luminescence and resonance Raman studies of an MX solid
[DE93-007362] p 3593 N93-28966
Method of emitting on a specific wavelength fraunhofer line using a neodymium doped laser transmitter
[AD-D015710] p 3437 N93-29276
In-situ temperature and concentration measurements of organosilicon decomposition in a chemical vapor deposition reactor
[ONERA-P-1990-3] p 3313 N93-30109
Nonlinear spectroscopy of multicomponent droplets and two- and three-dimensional measurements in flames
[AD-A264341] p 3425 N93-30162
Photoinduced charge separation in Q1D heterojunction materials: Evidence for electron-hole pair separation in mixed-halide MX solids
[AD-A264711] p 3598 N93-30501
Measurement of the rotation Raman spectra of nitrogen, oxygen, and water vapor under conditions of a temperature humidity lidar
[GKSS-92/E/32] p 3485 N93-31018

RAMAN SPECTROSCOPY
Aerosol particle analysis by Raman scattering technique
[DE93-005587] p 3309 N93-28880
Characterization of lithium electrode surface in lithium secondary batteries by in situ Raman spectroscopic methods
[AD-A263728] p 3411 N93-29986
Air oxidation behavior of fuel for the High Temperature Engineering Test Reactor (HTTR)
[DE93-753349] p 3576 N93-30006
Vibrational spectroscopy of shock-compressed fluids
p 3318 N93-30072
Photoinduced electron-hole charge separation, intrinsic self-doping and novel device applications of Q1D heterojunction materials: Mixed-halide MX solids
[AD-A264714] p 3600 N93-30569

RAMJET ENGINES
Flight mechanical model for performance calculations and interactions between flight vehicle and ramjet in regard to the flight orbit
[ESA-TT-1267] p 3248 N93-29464
RANDOM ACCESS
NESL: A nested data-parallel language (Version 2.6)
[AD-A263548] p 3530 N93-29822
Comparison of two random access techniques for the North American MSAT system p 3370 N93-30315
RANDOM ACCESS MEMORY
Generation of configurable self-synchronizing synchronous CMOS static RAMs p 3361 N93-30259
RANDOM ERRORS
Tolerance theory of phased array antennas: A statistical approach p 3369 N93-30307
The characterization of materials using x ray diffraction p 3293 N93-30968
RANDOM NOISE
Theory and applications of random fields
[AD-A262829] p 3555 N93-29454
Enhanced convergence adaptive detection
[AD-A264100] p 3399 N93-30879
RANDOM PROCESSES
Selection and transmission of information. Issue 22: Republic interdepartmental collection (selected articles)
[AD-A262825] p 3615 N93-29431
Theory and applications of random fields
[AD-A262829] p 3555 N93-29454
RANDOM SAMPLING
A modified chi-squared goodness-of-fit test for the three-parameter gamma distribution with unknown parameters
[AD-A262553] p 3554 N93-28845
RANDOM VARIABLES
Selection and transmission of information. Issue 22: Republic interdepartmental collection (selected articles)
[AD-A262825] p 3615 N93-29431
Theory and applications of random fields
[AD-A262829] p 3555 N93-29454
RANGE RESOURCES
Estimating test range capacity
[AD-A262493] p 3270 N93-28938
RANGE SAFETY
SeaWiFS technical report series. Volume 2: Analysis of orbit selection for SeaWiFS: Ascending versus descending node
[NASA-TM-104566-VOL-2] p 3486 N93-28497
RANGEFINDING
Neural networks application to divergence-based passive ranging
[NASA-TM-103981] p 3245 N93-29653
Wind measurement accuracy of a loran radiosonde
[AD-A263572] p 3483 N93-29832
A single band processor for the computation of range from optical absorbance p 3363 N93-30272
RANKINE-HUGONIOT RELATION
Nonlinear stability of viscous shock waves
[TRITA-NA-9205] p 3419 N93-29025
RAPID TRANSIT SYSTEMS
Guideway structural design and power/propulsion/braking in relation to guideways, volume 1
[PB93-169902] p 3447 N93-30820
RARE GASES
The Interstellar Gas Experiment: Analysis in progress
p 3639 N93-29380
RATES (PER TIME)
Rate constant determinations of reactions H + HNO from ab initio reaction path calculations
p 3319 N93-30099
RATINGS
Determinants of performance rating accuracy: A field study
[AD-A264726] p 3500 N93-30575
Discomfort glare from high-intensity discharge headlamps: Effects of context and experience
[PB93-174720] p 3496 N93-30659
RATIONAL FUNCTIONS
The generic arithmetic of SISYPHE
[INRIA-RT-0136] p 3524 N93-28755
RATS
The chronic effects of jP-8 jet fuel exposure on the lungs
[AD-A264162] p 3495 N93-30153
An assessment of peripheral nerve damage in the rat following non-freezing cold exposure: An electrophysiological and histopathological examination
[AD-A264293] p 3492 N93-30818
RAWINSONDES
Leadex data report. Part 1: Weather analysis and satellite images
[AD-A263217] p 3481 N93-28876
Leadex data report. Part 2: Rawinsonde and ice station data
[AD-A263218] p 3483 N93-29491
RAY TRACING
Application of ray tracing in radiation heat transfer
[NASA-TM-106206] p 3419 N93-29075
Propagation channel modeling for angle-diversity combining simulation p 3360 N93-30252
USU center of excellence in theory and analysis of the geo-plasma environment
[AD-A264750] p 3590 N93-30585
RAYLEIGH NUMBER
A spectral method determination of the first critical Rayleigh number for a low-Prandtl number crystal melt in a cylindrical container
[NASA-CR-193238] p 3594 N93-29214
RAYLEIGH SCATTERING
SWAT system performance predictions
[AD-A262857] p 3579 N93-29470
Nonlinear spectroscopy of multicomponent droplets and two- and three-dimensional measurements in flames
[AD-A264341] p 3425 N93-30162
RAYLEIGH-BENARD CONVECTION
A spectral method determination of the first critical Rayleigh number for a low-Prandtl number crystal melt in a cylindrical container
[NASA-CR-193238] p 3594 N93-29214
RAYLEIGH-RITZ METHOD
A Rayleigh-Ritz analysis methodology for cutouts in composite structures p 3307 N93-30869
RDX
Thermal decomposition of nitramines
p 3318 N93-30065
Observation of reaction intermediates in crystalline RDX p 3318 N93-30067
Thermal decomposition chemistry and shock sensitivity of thermally aged explosives p 3344 N93-30069
Determination of gas phase species and temperature profiles above solid propellants p 3346 N93-30080
Thermal decomposition pathways of RDX in the condensed phase p 3347 N93-30083
Dislocation roles in energetic crystal responses
p 3348 N93-30086
Comparison of deformation and shock reactivity for single crystals of RDX and ammonium perchlorate
p 3350 N93-30094
Applications of density functional theory to calculation of reaction energetics p 3351 N93-30098
REACTING FLOW
Turbulence characteristics of an axisymmetric reacting flow
[NASA-CR-4110] p 3242 N93-30373
An adaptive Lagrangian method for computing 1-D reacting flows and the theory of Riemann invariant manifolds for the compressible Euler equations
p 3428 N93-30902
REACTION KINETICS
Explosive consolidation of combustion synthesized TiC and TiB2: Precursor morphology effects
[AD-A263186] p 3341 N93-28515
A study of the chemical mechanism in lubrication
[DE93-012230] p 3330 N93-28650
Supported organometallic complexes, surface chemistry, spectroscopy, and catalysis
[DE93-011930] p 3309 N93-28688
Quantum dynamics of X2BC van der Waals clusters
[DE93-006416] p 3565 N93-28892
Membrane-based photochemical systems as models for photosynthetic cells
[DE93-009758] p 3310 N93-28911
Studies of hydrogen-air diffusion flames and of compressibility effects related to high-speed propulsion
p 3310 N93-29125
Generation of carbon monoxide in compartment fires
[PB93-146702] p 3244 N93-29211
Kinetics and energy transfer in nonequilibrium fluid flows
[AD-A263612] p 3240 N93-29284
Kinetics of nitric oxide formation behind 3 to 4 KM/S shock waves
[AD-A263653] p 3312 N93-29389
Rates and mechanisms of reaction of hydrogen sulfide with iron chelates
[PB93-184299] p 3312 N93-29665
Some effects of composition and microstructure on the B2 in equilibrium to DO3 ordered phase transition in Fe3Al alloys
[DE93-009724] p 3325 N93-29813
Calculations of reactive turbulent flows in aeronautical chambers p 3257 N93-29956
Kinetics and dynamics of reacting systems
[AD-A264046] p 3313 N93-30030
ONR/LANL Workshop on the Fundamental Physics and Chemistry of Combustion, Initiation, and Detonation of Energetic Materials
[CPIA-PUBL-589] p 3343 N93-30061
Combustion/explosion chemistry of bulk materials
p 3343 N93-30062
The thermochemistry and reaction pathways of the decomposition and combustion of energetic materials
p 3343 N93-30063
Thermal oxidation of HCN by NO2 in shock waves
p 3318 N93-30064
Chemical dynamics simulations as a probe to the initiation and propagation of condensed phase detonations p 3318 N93-30071
Numerical modeling of multidimensional flames with application to energetic materials p 3319 N93-30079
Pressure dependence of the reaction propagation rate of TATB to 40 GPa p 3319 N93-30082
Thermal decomposition pathways of RDX in the condensed phase p 3347 N93-30083
Kinetic studies on gas-phase reaction mechanisms important to the combustion of energetic materials: The CO/N2O reaction p 3347 N93-30084
Unsteady combustion of energetic materials using laser-recoil p 3319 N93-30085
Detonation shock dynamics of composite energetic materials p 3350 N93-30096
Rate constant determinations of reactions H + HNO from ab initio reaction path calculations
p 3319 N93-30099
Studies of curvature, strain, and unsteady effects on premixed flames p 3316 N93-30646
NOx chemistry in natural gas flames
[PB93-175263] p 3317 N93-30760
REACTION PRODUCTS
A study of the chemical mechanism in lubrication
[DE93-012230] p 3330 N93-28650
High pressure preignition chemistry of hydrocarbons and hydrocarbon mixtures
[AD-A263611] p 3311 N93-29283
Charged particle activation studies on the surface of LDEF spacecraft p 3572 N93-29630
Reaction mechanism studies of heavy ion induced nuclear reactions
[DE93-010496] p 3569 N93-29807
Determination of gas phase species and temperature profiles above solid propellants p 3346 N93-30080
Materials studies for preventing corrosion in condensing environments
[PB93-185478] p 3327 N93-30815
REACTION TIME
Two simulation studies of precision runway monitoring of independent approaches to closely spaced parallel runways
[AD-A263433] p 3261 N93-29815
REACTIVITY
Elastic and reactive collisions of atoms and molecules with neutral alkali clusters
[DE93-009313] p 3566 N93-29206
Applications of transition metal compounds in the preparation of useful silicon-containing ceramics
[AD-A264028] p 3335 N93-30028
Kinetics and dynamics of reacting systems
[AD-A264046] p 3313 N93-30030
Comparison of deformation and shock reactivity for single crystals of RDX and ammonium perchlorate
p 3350 N93-30094
Shock waves and polymorphic phase transitions in energetic materials p 3351 N93-30100
Reactive sintering of Ni3Al intermetallic alloys under compressive stress
[DE93-009729] p 3327 N93-30652
REACTOR DESIGN
Experiment and analysis on elastic deformation properties of graphite and carbon materials for HTTR core components
[DE93-753271] p 3299 N93-30004
SIRIUS-P: An inertially confined direct drive laser fusion power reactor
[DE93-012433] p 3439 N93-30186
Preliminary design study of a steady state tokamak device
[DE93-764162] p 3589 N93-30397
REACTOR MATERIALS
Acid solution absorption of extruded polyethylene foam
[DE93-011701] p 3330 N93-28839
An experimental investigation of radioactivity induced by ions associated with the operation of pulsed-power accelerators
[DE93-011478] p 3575 N93-29151
Experiment and analysis on elastic deformation properties of graphite and carbon materials for HTTR core components
[DE93-753271] p 3299 N93-30004
DOE fundamentals handbook: Material science
[DE93-012224] p 3314 N93-30199
DOE fundamentals handbook: Material science
[DE93-012225] p 3314 N93-30200
Examination of formability to seamless tubes on Ni-Cr-W superalloy
[DE93-764158] p 3326 N93-30396

Development of Ni-Cr-W superalloys for high temperature components in high temperature gas-cooled reactors, part 2
[DE93-764469] p 3326 N93-30399

REACTOR PHYSICS

Wavelet transform techniques and signal analysis
[DE93-007919] p 3382 N93-29244

Development of a PC code package for the analysis of research and power reactors
[DE92-638517] p 3536 N93-31001

REACTOR SAFETY

Measurements of breakaway reaction between beryllium and water vapor for ITER blanket design
[DE93-753270] p 3584 N93-28535

Acid solution absorption of extruded polyethylene foam
[DE93-011701] p 3330 N93-28839

Inservice diagnostic methods for solenoid-operated valves
[DE93-007823] p 3443 N93-28968

Annual progress report on the NSRR experiments, (21)
[DE93-753190] p 3574 N93-29137

TRAB: A transient analysis program for BWR. Part 2: User's manual
[VTT-TIED-1232-PT-2] p 3575 N93-29996

Air oxidation behavior of fuel for the High Temperature Engineering Test Reactor (HTTR)
[DE93-753349] p 3576 N93-30006

Statement on the United Nations Conference on Environment and Development
[DE93-601878] p 3475 N93-30996

REACTOR TECHNOLOGY

Fast neutron cross section measurements
[DE93-009053] p 3563 N93-28546

READING

Expertise, text coherence, and constraint satisfaction: Effects on harmony and settling rate --- mental representations
[AD-A262703] p 3498 N93-28901

Profiles of major federal literacy programs
[PB93-163863] p 3608 N93-30657

READOUT

Associative memories for supercomputers
[AD-A263142] p 3520 N93-29482

Design of a pixel cell optimized for a data push architecture readout
[DE93-011016] p 3616 N93-30122

REAL GASES

Supersonic flow calculation using a Reynolds-stress and an eddy thermal diffusivity turbulence model
[NASA-CR-4515] p 3420 N93-29159

Hypersonic lateral and directional stability characteristics of aeroassist flight experiment configuration in air and CF4
[NASA-TM-4435] p 3239 N93-29166

REAL TIME OPERATION

Radiation monitoring equipment dosimeter experiment
p 3266 N93-28730

Near real-time GIS in deep-ocean exploration
[AD-A262073] p 3487 N93-29003

Improved real-time imaging spectrometer
[NASA-CASE-NPO-18410-1-CU] p 3578 N93-29086

Femtosecond carrier processes in compound semiconductors and real time signal processing
[AD-A263076] p 3382 N93-29131

Resource utilization model for the algorithm to architecture mapping model
[NASA-CR-193122] p 3527 N93-29171

Building a generalized distributed system model
[NASA-CR-193239] p 3527 N93-29219

SPREE Interactive Data Analysis Tool (SIDAT)
[AD-A262782] p 3273 N93-29306

Research on reconfigurable and reliable manipulators
[DE93-010244] p 3444 N93-29330

Real time self-directed MBE flux control incorporation in situ ellipsometry, phase 1
[AD-A263501] p 3595 N93-29341

Operating manual for single-shot autocorrelator
[AD-A262016] p 3438 N93-29395

A real-time, hardware-in-the-loop simulation of an unmanned aerial research vehicle
[AD-A262477] p 3248 N93-29409

Femtosecond carrier processes in compound semiconductors and real time signal processing
[AD-A262966] p 3384 N93-29514

A neuro-fuzzy architecture for real-time applications
p 3511 N93-29529

Designing a fuzzy scheduler for hard real-time systems p 3512 N93-29537

Intelligent fuzzy controller for event-driven real time systems p 3515 N93-29551

Special purpose parallel computer architecture for real-time control and simulation in robotic applications
[NASA-CASE-NPO-17629-1-CU] p 3521 N93-29608

Development of neural network architectures for self-organizing pattern recognition and robotics
[AD-A264831] p 3543 N93-29791

Two simulation studies of precision runway monitoring of independent approaches to closely spaced parallel runways
[AD-A263433] p 3261 N93-29815

Three-dimensional graphical representation of objects according to movement data in realtime
[ESA-TT-1258] p 3521 N93-30104

A parallel processing system for intensive I/O
p 3362 N93-30262

A multiprocessor architecture for realtime robot control p 3372 N93-30327

Issues of ATC conflict resolution under real-time constraints p 3247 N93-30350

A video transmission system for low-bandwidth remote driving
[DE93-010275] p 3544 N93-30529

Intelligent real-time problem solving
[AD-A264830] p 3535 N93-30614

RECEIVERS

Processing, fabrication, and demonstration of HTS integrated microwave circuits
[AD-A263161] p 3406 N93-28940

Optical coherent phase diversity systems
[ISBN-90-9004897-9] p 3578 N93-29270

Acoustic transducer system
[AD-D015713] p 3562 N93-29279

Attitude determination using GPS: Development of an all solid-state guidance, navigation, and control sensor for air and space vehicles based on the global positioning system p 3246 N93-30605

A long wave TE/TM noise prediction model
p 3397 N93-30742

RECEPTORS (PHYSIOLOGY)

Principal components of natural images: An analytical solution
[AD-A264800] p 3489 N93-30603

RECLAMATION

Polymeric materials for use in wet hydrochloric acid environments
[DE93-010881] p 3330 N93-28600

RECOIL IONS

Measurement of 1s2s(sup 3)S(sub 1)-1s2p(sup 3)P(sub 2,0) intervals in helium-like neon
[DE93-009243] p 3563 N93-28521

RECONNAISSANCE AIRCRAFT

High-altitude reconnaissance aircraft
p 3227 N93-29713

RECORDING INSTRUMENTS

The NT digital micro tape recorder
p 3435 N93-30461

RECRYSTALLIZATION

Environmental embrittlement of binary and Zr-doped Ni3Al
[DE93-008575] p 3321 N93-28679

Constitutive laws for deformation and dynamic recrystallization in cubic metals
[DE93-010740] p 3326 N93-30486

RECTANGULAR PANELS

A Rayleigh-Ritz analysis methodology for cutouts in composite structures p 3307 N93-30869

RECTIFICATION

Ultrafast optical studies of surface reaction processes at semiconductor interfaces
[DE93-009049] p 3593 N93-29096

RECURSIVE FUNCTIONS

Iterative encoding methods for computer generated holograms
[AD-A263705] p 3431 N93-29297

RED SHIFT

GRO: Red-shifted electron-positron annihilation gamma-rays from radiopulsars
[NASA-CR-193243] p 3635 N93-30053

REDUCED GRAVITY

Preliminary endurance tests of water vaporizers for resistojet applications
[NASA-TM-106222] p 3287 N93-28694

The MODE family of facility class experiments
p 3263 N93-28705

Vented Tank Resupply Experiment (VTRE) for In-Space Technology Experiment Program (IN-STEP)
p 3264 N93-28711

Tank Pressure Control Experiment/Thermal Phenomena (TPCE/TP) p 3264 N93-28713

Sodium-Sulfur Cell Technology flight experiment (SSCT) p 3264 N93-28715

Thermal energy storage flight experiment in microgravity p 3265 N93-28720

Cryogenic Heat Pipe Experiment (CRYOHP)
p 3265 N93-28721

Heat pipe performance experiment
p 3265 N93-28722

Measurement of the relative and absolute microgravity environment of space platforms, recent flight results, and determination of the spatial microgravity field
p 3266 N93-28725

Effect of microgravity on several visual functions during STS Shuttle missions: Visual Function Tester-Model 1 (VFT-1) p 3268 N93-28740

Effect of microgravity on visual contrast threshold during STS Shuttle missions: Visual Function Tester-Model 2 (VFT-2) p 3268 N93-28741

Effect of microgravity on the visual near point: Visual Function Tester-Model 4 (VFT-4) p 3268 N93-28742

NASA supporting studies for microgravity research on eye movements
[NASA-CR-193233] p 3493 N93-29041

Anthropometric data from launch and entry suited test subjects for the design of a recumbent seating system
[NASA-TM-104769] p 3505 N93-29044

Gravity sensitivity of a resistojet water vaporizer
[NASA-TM-106220] p 3288 N93-29194

Issues on human acceleration tolerance after long-duration space flights
[NASA-TM-104753] p 3495 N93-29651

A high-temperature furnace for applications in microgravity p 3229 N93-29723

Rotational fluid flow experiment p 3235 N93-29761

Planar reorientation of a free-free beam in space using embedded electromechanical actuators
p 3280 N93-29993

Residual acceleration data on IML-1: Development of a data reduction and dissemination plan
[NASA-CR-193224] p 3281 N93-30038

The middeck 0-gravity dynamics experiment
[NASA-CR-4500] p 3281 N93-30376

Prediction of gas-liquid two-phase flow regime in microgravity
[NASA-TM-106274] p 3352 N93-30939

Effects of buoyancy on gas jet diffusion flames
[NASA-CR-191109] p 3352 N93-31031

REDUCTION (CHEMISTRY)

The electrolyte factor in O2 reduction electrocatalysis
[AD-A263565] p 3313 N93-29828

REDUNDANCY

Input relegation control for gross motion of a kinematically redundant manipulator
[DE93-005301] p 3446 N93-30210

REDUNDANCY ENCODING

Compiler-assisted multiple instruction rollback recovery using a read buffer
[NASA-CR-193175] p 3527 N93-29170

REDUNDANT COMPONENTS

Analysis of cache for streaming tape drive
p 3435 N93-30477

REENTRY SHIELDING

Thermal certification tests of Orbiter Thermal Protection System tiles coated with KSC coating slurries
[NASA-TM-104766] p 3278 N93-29221

REENTRY VEHICLES

The infrared measurement for the reentry-body-translation
[AD-A263100] p 3278 N93-29134

Kinetics and energy transfer in nonequilibrium fluid flows
[AD-A263612] p 3240 N93-29284

Taurus Lightweight Manned Spacecraft Earth orbiting vehicle p 3231 N93-29736

REFERENCE ATMOSPHERES

Graphical comparison of U.S. standard atmospheres and military standard climatic extremes
[AD-A264639] p 3484 N93-30521

REFILLING

Vented Tank Resupply Experiment (VTRE) for In-Space Technology Experiment Program (IN-STEP)
p 3264 N93-28711

REFLECTANCE

Texturing of InP surfaces for device applications
[NASA-TM-106061] p 3321 N93-28618

Infrared rugates by molecular beam epitaxy
p 3582 N93-28808

Modification of spectral distributions by multilayer structures
[DE93-009308] p 3310 N93-29059

Maximum and minimum return losses from a passive two-port network terminated with a mismatched load
p 3385 N93-29594

High resolution free-electron laser spectroscopy
[AD-A263734] p 3439 N93-29853

A variable reflectivity output coupler for optically pumped far infrared lasers
[MPE-PREPRINT-225] p 3441 N93-30640

REFLECTOR ANTENNAS

A satellite-tracking millimeter-wave reflector antenna system for mobile satellite-tracking
[NASA-CASE-NPO-18772-1-CU] p 3381 N93-28955

System overview on electromagnetic compensation for reflector antenna surface distortion [NASA-TM-106217] p 3273 N93-29195

Planar microstrip YAGI antenna array [NASA-CASE-NPO-17873-2-CU] p 3384 N93-29507

A note on the computation of antenna-blocking shadows p 3385 N93-29593

Maximum and minimum return losses from a passive two-port network terminated with a mismatched load p 3385 N93-29594

REFLECTORS

Infrared rugates by molecular beam epitaxy p 3582 N93-28808

Maximum and minimum return losses from a passive two-port network terminated with a mismatched load p 3385 N93-29594

REFRACTION

Enhanced photorefractive effects in barium titanate [AD-A264724] p 3599 N93-30554

REFRACTIVITY

Infrared rugates by molecular beam epitaxy p 3582 N93-28808

Investigations of self-pumped phase conjugate laser beams and coherence length [AD-A263438] p 3438 N93-29789

Atmospheric transverse coherence length measurement system for laser communications [AD-A263563] p 3439 N93-29827

Physical chemical studies on molecular composite compositions [AD-A264834] p 3339 N93-30898

REFRACTORIES

A transient FGM interlayer based approach to joining ceramics [DE93-010415] p 3331 N93-29248

Interfacial studies of refractory glass-ceramic matrix/advanced SiC fiber reinforced composites [AD-A263264] p 3299 N93-29802

REFRACTORY MATERIALS

Soft computing in design and manufacturing of advanced materials [NASA-TM-106032] p 3295 N93-28624

Interfacial studies of refractory glass-ceramic matrix/advanced SiC fiber reinforced composites [AD-A263264] p 3299 N93-29802

Carborane-(silane or siloxane)-unsaturated hydrocarbon based thermosetting polymers [AD-D015718] p 3338 N93-30580

Carborane-(siloxane or silane)-unsaturated hydrocarbon based polymers [AD-D015717] p 3338 N93-30586

REFRACTORY METALS

Refractory metal disilicides research [AD-A262416] p 3320 N93-28499

REFRIGERANTS

Complex-compound heat pump: Topical report on phase 1 results [PB93-185460] p 3466 N93-30814

Horizontal nucleate flow boiling heat transfer coefficient measurements and visual observations for R12, R134a, and R134a/ester lubricant mixtures [PB93-178598] p 3475 N93-30887

REFRIGERATING

Hybrid oxygen system [AD-A262417] p 3500 N93-28464

Spaceborne passive radiative cooler p 3378 N93-28802

REFRIGERATORS

Advanced insulations for refrigerator/freezers: The potential for new shell designs incorporating polymer barrier construction [DE93-010600] p 3353 N93-28570

Theoretical and experimental study of thermoacoustic engines [AD-A261934] p 3561 N93-28995

REFUELING

Aircraft and refueler bonding and grounding study [AD-A262027] p 3261 N93-29398

REGOLITH

Clementine 2: A double asteroid flyby and impactor mission p 3268 N93-28770

Lunar regolith densification p 3276 N93-29115

Regolith-structure modeling p 3276 N93-29116

Lunar regolith penetrators and cutters p 3276 N93-29117

Indigenous lunar construction materials p 3277 N93-29120

Systems engineering studies of lunar base construction p 3277 N93-29121

REGRESSION ANALYSIS

A Monte Carlo study of the raw and normal varimax rotation criterion in factor analysis [AD-A262516] p 3554 N93-28844

Pilot Candidate Selection Method (PCSM): What makes it work? [AD-A262871] p 3498 N93-29481

Fuzzy multiple linear regression: A computational approach p 3518 N93-29574

Chromatographic and solvatochromic measurements on butyl rubbers [AD-A263088] p 3334 N93-29795

Easy-to-apply results for establishing convergence of Markov chains in Bayesian analysis [AD-A264015] p 3555 N93-29979

Procedures for applying Ada quality prediction models [AD-A264730] p 3534 N93-30546

REGULATIONS

Evaluation of environmental marketing terms in the United States [PB93-175784] p 3474 N93-30660

REINFORCED PLASTICS

Effect of water immersion on fiber/matrix adhesion in thermoplastic composites [AD-A263646] p 3299 N93-29984

REINFORCEMENT (STRUCTURES)

Development of stitching reinforcement for transport wing panels p 3304 N93-30852

REINFORCING FIBERS

Aligned, short-fiber composites by novel flow processing methods [DE93-008701] p 3296 N93-28904

Interfacial studies of refractory glass-ceramic matrix/advanced SiC fiber reinforced composites [AD-A263264] p 3299 N93-29802

Effect of water immersion on fiber/matrix adhesion in thermoplastic composites [AD-A263646] p 3299 N93-29984

REINFORCING MATERIALS

Lightweight flexible composite tent materials [AD-A263021] p 3295 N93-28660

The effect of oxidation embrittlement on the impact behavior of nicalon reinforced CAS 2 ceramic matrix composites [AD-A263567] p 3334 N93-29829

RELATIVISTIC EFFECTS

Investigation of a geodesy coexperiment to the Gravity Probe B relativity gyroscope program [NASA-CR-193263] p 3460 N93-29179

RELATIVISTIC ELECTRON BEAMS

Measurements of the energy spectrum of an intense microsecond relativistic electron beam in the beam-plasma experiments using a multi-foil analyzer [DE93-606271] p 3590 N93-30768

Microwave emission from relativistic electron beams [AD-A264102] p 3400 N93-30880

Microsecond ribbon relativistic electron beam in a plane undulator and generation of microwave radiation [DE93-605693] p 3400 N93-30993

RELATIVISTIC PARTICLES

Reaction mechanism studies of heavy ion induced nuclear reactions [DE93-010496] p 3569 N93-29807

Invariant structures and static forces in gauge theories [DE92-644740] p 3607 N93-30925

RELATIVISTIC THEORY

An algebraic approach to the quantization of constrained systems: Finite dimensional examples p 3548 N93-28671

Modern approach to relativity theory (radar formulation) [DE93-606032] p 3606 N93-30804

On the energy-momentum tensors for field theories in spaces with affine connection and metric [DE92-644744] p 3557 N93-30927

Fourth-rank cosmology [DE92-641346] p 3637 N93-30997

RELATIVISTIC VELOCITY

A new exact solution to the classical equations of motion of the relativistic string with massive ends [DE92-644736] p 3557 N93-30922

Some problems of relativistic electrodynamics [DE92-644738] p 3400 N93-30923

RELATIVITY

An algebraic approach to the quantization of constrained systems: Finite dimensional examples p 3548 N93-28671

Topics in General Relativity theory: Gravitational-wave measurements of black-hole parameters; gravitational collapse of a cylindrical body; and classical-particle evolution in the presence of closed, timelike curves p 3603 N93-28690

Investigation of a geodesy coexperiment to the Gravity Probe B relativity gyroscope program [NASA-CR-193263] p 3460 N93-29179

A covariant form of the Maxwell's equations in four-dimensional spaces with an arbitrary signature [DE93-606070] p 3605 N93-30783

Geometrical approach to the dynamics of a relativistic string in the D-dimensional Minkowski space [DE93-606071] p 3605 N93-30784

On the photonic chiral anomaly in an external gravitational field [DE93-606082] p 3479 N93-30785

Beyond two dimensions [DE93-606084] p 3606 N93-30786

Modern approach to relativity theory (radar formulation) [DE93-606032] p 3606 N93-30804

A simple formula for reducing Feynman diagrams to scalar integrals [DE92-644717] p 3607 N93-30916

Fourth-rank gravity and cosmology [DE92-644722] p 3637 N93-30918

Some problems of relativistic electrodynamics [DE92-644738] p 3400 N93-30923

On the energy-momentum tensors for field theories in spaces with affine connection and metric [DE92-644744] p 3557 N93-30927

Relativity theory in (2 + 2)-space [DE92-644671] p 3608 N93-30983

Spherically symmetric line element and Killing vectors in five-dimensional space [DE93-604132] p 3558 N93-30988

The geometry of complex space-times with torsion [DE92-641343] p 3608 N93-31003

RELAXATION (MECHANICS)

Flux lattice relaxation, noise, and symmetry-breaking in frustrated Josephson junction arrays [DE93-008713] p 3593 N93-29094

Anelastic relaxations associated with local disordering in grain boundaries [AD-A263101] p 3596 N93-29796

Electrical relaxation in acid-form nafion [AD-A263558] p 3410 N93-29826

Fundamental studies of the mechanical behavior of microelectronics thin film materials [AD-A264334] p 3337 N93-30417

RELAXATION METHOD (MATHEMATICS)

Image classification using Markov random fields with two new relaxation methods: Deterministic pseudo annealing and modified metropolis dynamics [INRIA-RR-1606] p 3553 N93-28510

RELAXATION TIME

Isothermal annealing and relaxation of the second harmonic generation signal from a nonlinear optical polymer [AD-A262007] p 3333 N93-29442

RELIABILITY

Reliability assessment at airline inspection facilities. Volume 2: Protocol for an eddy current inspection reliability experiment [DOT/FAA/CT-92/12-VOL-2] p 3449 N93-28685

Crucial role of detailed function, task, timeline, link, and human vulnerability analyses in HRA [DE93-001923] p 3505 N93-28942

Using today's technology to improve mobile C4I for the operational commander [AD-A263613] p 3245 N93-29285

Tutorial: Performance and reliability in redundant disk arrays p 3537 N93-30463

Striped tertiary storage arrays p 3620 N93-30464

Optimizing digital 8mm drive performance p 3435 N93-30479

RELIABILITY ANALYSIS

Crucial role of detailed function, task, timeline, link, and human vulnerability analyses in HRA [DE93-001923] p 3505 N93-28942

Reliability assessment of thrust chamber cooling concepts using probabilistic analysis techniques [NASA-CR-190785] p 3288 N93-29068

Efficient algorithms for the evaluation of planar network reliability [AD-A263602] p 3531 N93-29916

Multiprocessing systems: Reliability modelling and analysis using multimode components and dependent failures [AD-A264230] p 3540 N93-30364

Using Penelope to assess the correctness of NASA Ada software: A demonstration of formal methods as a counterpart to testing [NASA-CR-4509] p 3533 N93-30380

RELIABILITY ENGINEERING

Development of an updated pinch-welding capability [DE93-009823] p 3442 N93-28552

Using Penelope to assess the correctness of NASA Ada software: A demonstration of formal methods as a counterpart to testing [NASA-CR-4509] p 3533 N93-30380

Steps required in the pursuit of quantitative risk management processes for high pressure systems [DE93-007586] p 3378 N93-30508

REMANENCE

Modification of the S-band phase shifter model 331A-3 of Electromagnetic Sciences Inc. [DIGEL-1992-5] p 3399 N93-30836

REMODULATION
Design and integration of high bit rate four phase monolithic demodulators and modulators at X band
[LAAS-92354] p 3414 N93-31030
REMOTE CONTROL
Development and testing of the Perseus proof-of-concept aircraft
[DE93-010121] p 3247 N93-28586
A study of the effects of lens focal length on remote driver performance
[AD-A263191] p 3505 N93-28941
Remote vehicle survey tool
[DE93-010822] p 3460 N93-29255
Research on reconfigurable and reliable manipulators
[DE93-010244] p 3444 N93-29330
Application of sensors to the control of robotic systems
[DE93-009837] p 3543 N93-30012
Security of the remote control link of Anik E satellites
p 3365 N93-30282
A video transmission system for low-bandwidth remote driving
[DE93-010275] p 3544 N93-30529
Graphical programming: On-line robot simulation for telerobotic control
[DE93-009796] p 3447 N93-30654
REMOTE HANDLING
New remote maintenance approach for TPX
[DE93-007857] p 3584 N93-28583
Robotics and artificial intelligence for hazardous environments
[DE93-008271] p 3541 N93-29047
Structural design of cryostat and port penetration of International Thermonuclear Experimental Reactor (ITER)
[DE93-753267] p 3587 N93-29243
Research on reconfigurable and reliable manipulators
[DE93-010244] p 3444 N93-29330
Leaky coaxial cable signal transmission for remote facilities
[DE93-007916] p 3383 N93-29348
Application of sensors to the control of robotic systems
[DE93-009837] p 3543 N93-30012
Radiation-hardened microwave communications system
[DE93-007915] p 3394 N93-30631
REMOTE MANIPULATOR SYSTEM
Multivariable control of the Space Shuttle Remote Manipulator System using linearization by state feedback
[NASA-CR-188248] p 3443 N93-29080
A functional system architecture for fully autonomous robot p 3370 N93-30311
Joint drive development for the Space Station Remote Manipulator System p 3370 N93-30313
REMOTE SENSING
SeaWiFS technical report series. Volume 6: SeaWiFS technical report series cumulative index: Volumes 1-5
[NASA-TM-104566-VOL-6] p 3486 N93-28500
Preprocessing remotely-sensed data for efficient analysis and classification
[DE93-007367] p 3611 N93-28580
Results from the US/Russian Meteor-3/Total Ozone Mapping Spectrometer
[NASA-TM-104576] p 3467 N93-28682
Polarimetric multispectral imaging technology
p 3434 N93-28774
Imaging spectrometers using concave holographic gratings p 3434 N93-28783
Optical technologies for UV remote sensing instruments p 3582 N93-28788
Remote measurement of planetary magnetic fields by the Hanle effect p 3645 N93-28793
Filtering interpolators for image comparison algorithms
p 3463 N93-28797
Use of particle beams for lunar prospecting
p 3650 N93-28822
A team approach to the development of gamma ray and x ray remote sensing and in situ spectroscopy for planetary exploration missions p 3650 N93-28824
Proceedings of the 8th User Seminar of the German Remote Sensing Data Center of the German Aerospace Establishment (DLR)
[DLR-MITT-92-09] p 3456 N93-28915
The German PAF (Processing and Archiving Facilities) for ERS-1 p 3457 N93-28916
Processing of altimeter data by the German ERS-1 Processing and Archiving Facility (D-PAF)
p 3457 N93-28917
Exact trajectory determinator for ERS-1
p 3457 N93-28918
The interferometric SAR technology and its usability in the framework of ERS-1 p 3457 N93-28919
Recording of forest surface in SAR-images with statistical methods in areas of pronounced relief
p 3457 N93-28920
Forest examination with polarimetric radar image data
p 3457 N93-28921
Remote sensing of agricultural vegetation: Status and perspectives p 3458 N93-28922
SAR shape-from-shading for a populated alpine area
p 3458 N93-28923
Fog studies in the Alpine region with digital NOAA/AVHRR data p 3458 N93-28925
Utilization of NOAA/AVHRR data for energy balance of Lake Constance (Switzerland) p 3458 N93-28926
Model-oriented correction of thematic mapper raw data p 3459 N93-28930
Evidence-based classification of satellite image data
p 3459 N93-28931
Optical measurements of ripples using a scanning laser slope gauge. Part 1: Instrumentation and preliminary results
[AD-A261939] p 3486 N93-28996
Earth observation from space: Competition or cooperation?
[AD-A262044] p 3459 N93-29000
Fiber grating-based sensing system with interferometric wavelength-shift detection
[AD-D015697] p 3577 N93-29038
Remote sensing survey of Mississippi River-Gulf Outlet, Breton Sound disposal area, Plaquemines Parish, Louisiana
[AD-A263097] p 3459 N93-29146
Geographic information system for fusion and analysis of high-resolution remote sensing and ground truth data
p 3614 N93-29234
Spatial Analysis and Modeling Systems (SAMS)
p 3614 N93-29239
Remote vehicle survey tool
[DE93-010822] p 3460 N93-29255
Information system for co-registration of CAESAR sea-images based on two dimensional image matching techniques (SCORE). Part 1: Introduction, user requirements, and feasibility tests
[BCRS-90-40A-PT-1] p 3460 N93-29307
The MAESTRO-1 campaign: Analyses of polarimetric SAR data of agricultural fields and forests
[BCRS-92-06] p 3460 N93-29320
Preprocessing airborne remote sensing PARES calibration maintenance functional design document
[BCRS-92-07] p 3460 N93-29321
Convective and stratiform rain: Multichannel microwave sensing over oceans
[NASA-TM-104586] p 3482 N93-29448
Design of a high resolution spatial heterodyne interferometer
[AD-A262867] p 3285 N93-29461
National remote sensing programme 2 ACMS project. Phase 1: Validation. Part 1: Definition of validation experiment
[BCRS-92-10-PHASE-1-PT-1] p 3461 N93-29465
Remote sensing in Czechoslovakia and Hungary: An analysis of the possible co-operation of The Netherlands with Czechoslovakia and Hungary in the field of remote sensing
[BCRS-92-12] p 3461 N93-29466
Project Copernicus: An Earth observing system
p 3231 N93-29738
Project MEDSAT p 3231 N93-29739
Low cost TACSAT for NATO surveillance
p 3285 N93-29911
Cost effective TacSats for military support
p 3285 N93-29912
What's past is prologue: Supporting global change research with historical data
[DE93-005777] p 3472 N93-30009
Application of sensors to the control of robotic systems
[DE93-009837] p 3543 N93-30012
The estimation and scaling of land-surface fluxes of latent and sensible heat with remotely sensed data over a grassland site p 3462 N93-30045
A stochastic formation of radiative transfer in clouds
[DE93-011372] p 3484 N93-30055
Observing and modelling F-region ionospheric dynamics using the OII 7320A emission p 3479 N93-30564
Remote sensing for water quality monitoring in the Tennessee Valley: Field tests of two systems
[DE93-008997] p 3462 N93-30637
CAESAR development plan 1992-1995
[BCRS-92-17] p 3463 N93-31009
Bayesian linear analysis with application to removal of atmospheric influences on optical remote sensing images
[BCRS-92-19] p 3463 N93-31011
REMOTE SENSORS
Improved real-time imaging spectrometer
[NASA-CASE-NPO-18410-1-CU] p 3578 N93-29086
What's past is prologue: Supporting global change research with historical data
[DE93-005777] p 3472 N93-30009
CAESAR development plan 1992-1995
[BCRS-92-17] p 3463 N93-31009
REMOTELY PILOTED VEHICLES
Advanced Unmanned Search System (AUSS) supervisory command, control and navigation
[AD-A263171] p 3245 N93-28990
A real-time, hardware-in-the-loop simulation of an unmanned aerial research vehicle
[AD-A262477] p 3248 N93-29409
Design study to simulate the development of a commercial transportation system p 3228 N93-29718
Solar powered multipurpose remotely powered aircraft
p 3229 N93-29722
Preliminary development of a VTOL unmanned air vehicle for the close-range mission
[AD-A263514] p 3354 N93-29969
RENDEZVOUS TRAJECTORIES
Galileo post-Gaspra cruise and Earth-2 encounter
p 3385 N93-29597
RENORMALIZATION GROUP METHODS
Topics in gauge theories and the unification of elementary particle interactions
[DE93-009370] p 3563 N93-28542
Phase structure of three- and four-dimensional phi(exp 4) field theory
[DE93-606069] p 3605 N93-30782
REPORTS
NASA/DoD Aerospace Knowledge Diffusion Research Project. Paper 29: The US government technical report and the transfer of federally funded aerospace R and D
[NASA-TM-109221] p 3615 N93-29709
REPRODUCTION (COPYING)
High-speed data duplication/data distribution: An adjunct to the mass storage equation
p 3619 N93-30459
RESEARCH AIRCRAFT
International aviation (Selected articles)
[AD-A262566] p 3227 N93-28576
Development and testing of the Perseus proof-of-concept aircraft
[DE93-010121] p 3247 N93-28586
X-31 demonstration of integrated flight and propulsion control for effective combat at extreme angles of attack
p 3260 N93-28851
RESEARCH AND DEVELOPMENT
JPRS report: Science and technology. Central Eurasia: Engineering and equipment
[JPRS-UEQ-92-007] p 3353 N93-28635
JPRS report: Science and technology. Central Eurasia: Engineering and equipment
[JPRS-UEQ-92-006] p 3353 N93-28636
Applied research in America
[DE93-011725] p 3625 N93-28646
JPRS report: Science and technology. Central Eurasia: Engineering and equipment
[JPRS-UEQ-92-010] p 3353 N93-28674
JPRS report: Science and technology. Central Eurasia: Engineering and equipment
[JPRS-UEQ-92-008] p 3353 N93-28675
Advanced Earth-to-orbit propulsion technology information, dissemination and research
[NASA-CR-192561] p 3287 N93-28680
JPRS report: Science and technology. Central Eurasia: Life sciences
[JPRS-ULS-93-005] p 3490 N93-28683
JPRS report: Science and technology. Central Eurasia: Life sciences
[JPRS-ULS-92-027] p 3490 N93-28684
JPRS report: Science and technology. Central Eurasia: Engineering and equipment
[JPRS-UEQ-93-003] p 3353 N93-28691
Productivity measurement in science and technology contracting
[AD-A262077] p 3609 N93-28985
JPRS report: Science and technology. Central Eurasia: Materials science
[JPRS-UMS-92-008] p 3322 N93-29012
JPRS report: Science and technology. Central Eurasia: Materials science
[JPRS-UMS-92-007] p 3322 N93-29013
JPRS report: Science and technology. Central Eurasia: Engineering and equipment
[JPRS-UEQ-93-001] p 3274 N93-29014
JPRS report: Science and technology. Central Eurasia: Materials science
[JPRS-UMS-92-009] p 3322 N93-29015
JPRS report: Science and technology. Central Eurasia: Materials science
[JPRS-UMS-92-012] p 3296 N93-29016
JPRS report: Science and technology. Central Eurasia: Materials science
[JPRS-UMS-92-013] p 3296 N93-29017
JPRS report: Science and technology. Central Eurasia: Materials science
[JPRS-UMS-92-016] p 3296 N93-29018

JPRS report: Science and technology. Central Eurasia: Materials science [JPRS-UMS-92-014] p 3322 N93-29019

JPRS report: Science and technology. Central Eurasia: Materials science [JPRS-UMS-92-015] p 3322 N93-29020

JPRS report: Science and technology. Central Eurasia: Materials science [JPRS-UMS-93-001] p 3296 N93-29021

JPRS report: Science and technology. Central Eurasia: Physics and mathematics [JPRS-UPM-93-002] p 3560 N93-29022

SIAM Conference on Applications of Dynamical Systems [DE93-007969] p 3548 N93-29057

JPRS report: Science and technology. Central Eurasia: Earth science [JPRS-UES-93-003] p 3456 N93-29089

JPRS report: Science and technology. Central Eurasia: Engineering and equipment [JPRS-UEQ-93-004] p 3354 N93-29090

Applied Information Systems Research Program Workshop [NASA-TM-108773] p 3613 N93-29222

NASA SBIR abstracts of 1991 phase 1 projects [NASA-TM-108240] p 3609 N93-29323

Advanced Construction Technology Center research [AD-A263654] p 3432 N93-29390

Research and technology objectives and plans: Summary fiscal year 1991 [NASA-TM-103086] p 3660 N93-29452

Electronics research at the University of Texas at Austin. Appendix: JSEP sponsored publications [AD-A262993] p 3409 N93-29485

LDEF: 69 Months in Space. Part 1: Second Post-Retrieval Symposium [NASA-CP-3194-PT-1] p 3660 N93-29621

Defense conversion: Redirecting research and development [OTA-ITE-552] p 3610 N93-29649

Computer systems laboratory [PB93-181873] p 3521 N93-29662

NSF Tokyo reports: Japanese R and D projects on micro- and nanofabrication and related basic research projects [PB93-181261] p 3410 N93-29671

LDEF archival system plan p 3624 N93-29704

An overview of DARPA's advanced space technology program p 3269 N93-29908

Center for the Study of Intelligent Control Systems (Fellowships) [AD-A263604] p 3543 N93-29917

Interagency Advanced Power Group (IAPG) Meeting Compendium [DE93-006189] p 3670 N93-30212

Development of an antenna measurement facility operating in the 2 GHz - 100 GHz frequency range p 3369 N93-30308

Independent research and independent exploratory development programs [AD-A264735] p 3544 N93-30556

JPRS report: Science and technology. Central Eurasia: Materials science [JPRS-UMS-93-003] p 3327 N93-30623

JPRS report: Science and technology. Central Eurasia: Earth sciences [JPRS-UES-93-002] p 3456 N93-30624

How to compete for NASA contracts [NASA-TM-109238] p 3610 N93-30644

Rotorcraft master plan p 3236 N93-30677

White House/OSTP perspective p 3625 N93-30696

Technology transfer within the government p 3627 N93-30711

NASP technology transfer p 3627 N93-30713

Robotic technology evolution and transfer p 3627 N93-30714

Strategic directions and mechanisms in technology transfer p 3628 N93-30720

NASA space research and technology overview (ITP) p 3628 N93-30722

Space research and technology overview p 3628 N93-30723

A research experiment on facilitation and formation of joint research and development programs between government, industry, and universities: Overview, preliminary findings, and observations p 3628 N93-30725

Scientific research abstracts in the Republic of China, 1991 (science and technology) p 3670 N93-30911

Research, Development, Test and Evaluation (R, D, T, and E) programs (R-1), Department of Defense budget for fiscal year 1994 [PB93-169878] p 3611 N93-30936

RESEARCH FACILITIES

International aviation (Selected articles) [AD-A262566] p 3227 N93-28576

Ultraviolet free electron laser facility preliminary design report [DE93-009360] p 3435 N93-28594

EnviroNET: On-line information for LDEF p 3624 N93-29625

Oceanographic research towers in european waters [AD-A264795] p 3489 N93-30612

Technology transfer needs and experiences: The NASA Research Center perspective p 3626 N93-30703

RESEARCH MANAGEMENT

Proceedings of a Workshop on Molecular Nuclear Medicine [DE93-010828] p 3493 N93-28835

Summer Faculty Research Program (SFRP), volume 1 [AD-A261988] p 3608 N93-29440

Research and technology objectives and plans: Summary fiscal year 1991 [NASA-TM-103086] p 3660 N93-29452

AFOSR Status Report [AD-A264720] p 3670 N93-30513

Technology transfer within the NASA Goddard Space Flight Center p 3626 N93-30704

Technology transfer within the government p 3627 N93-30709

Exploration technology prioritization p 3629 N93-30726

RESEARCH PROJECTS

Research in theoretical physics [DE93-008401] p 3603 N93-28961

Summer Faculty Research Program (SFRP), volume 1 [AD-A261988] p 3608 N93-29440

Advanced NDE technology program [AD-A262008] p 3449 N93-29443

High-altitude reconnaissance aircraft p 3227 N93-29713

Project summary p 3227 N93-29714

Conceptual design of a two-stage-to-orbit vehicle p 3228 N93-29716

The design of two-stage-to-orbit vehicles p 3228 N93-29719

Design of a turbofan powered regional transport aircraft p 3228 N93-29721

Solar powered multipurpose remotely powered aircraft p 3229 N93-29722

A high-temperature furnace for applications in microgravity p 3229 N93-29723

Advanced design for orbital debris removal in support of solar system exploration p 3229 N93-29724

The 1990/1991 project summaries p 3229 N93-29725

Design, building, and testing of the postlanding systems for the assured crew return vehicle p 3229 N93-29726

Earth to lunar CELSS evolution p 3229 N93-29727

Design of biomass management systems and components for closed loop life support systems p 3230 N93-29728

Lunar lander ground support system p 3230 N93-29729

The 1990-1991 project summaries p 3230 N93-29730

The 1990-1991 project summaries p 3230 N93-29731

Solar energy emplacement developer p 3230 N93-29732

Exercise/recreation facility for a lunar or Mars analog p 3230 N93-29733

Automation of closed environments in space for human comfort and safety p 3230 N93-29734

Delta Advanced Reusable Transport (DART): An alternative manned spacecraft p 3231 N93-29735

Taurus Lightweight Manned Spacecraft Earth orbiting vehicle p 3231 N93-29736

Walking robot: A design project for undergraduate students p 3231 N93-29737

Project Copernicus: An Earth observing system p 3231 N93-29738

Project MEDSAT p 3231 N93-29739

Project UM-HAUL: A self-unloading reusable lunar lander p 3232 N93-29740

Mars integrated transportation system multistage Mars mission p 3232 N93-29741

Single-stage Mars mission p 3232 N93-29742

Multipurpose satellite bus (MPS) p 3232 N93-29743

Project WISH: The Emerald City p 3232 N93-29744

From orbital debris capture systems through internal combustion engines on Mars p 3232 N93-29745

Mars sample return mission: Two alternate scenarios p 3233 N93-29746

Mars habitat p 3233 N93-29747

The lightcraft project p 3233 N93-29749

ASPEC: Solar power satellite p 3233 N93-29750

B and T: Lunar landers p 3234 N93-29751

Spacely's rockets: Personnel launch system/family of heavy lift launch vehicles p 3234 N93-29752

RS Landers: Lunar lander p 3234 N93-29753

SPECS: Orbital debris removal p 3234 N93-29754

The 1990-1991 project summaries p 3234 N93-29755

Mars Aquarius Mission and Titan Explorer p 3235 N93-29756

Thermion: Verification of a thermionic heat pipe in microgravity p 3235 N93-29757

Solar electric propulsion cargo spacecraft for Mars missions p 3235 N93-29758

Antares: A low cost modular launch vehicle for the future p 3235 N93-29759

GENESIS 2: Advanced lunar outpost p 3235 N93-29760

Rotational fluid flow experiment p 3235 N93-29761

Research and education by SF cyclotron facility [DE93-753135] p 3576 N93-30002

AFOSR Status Report [AD-A264720] p 3670 N93-30513

RESEARCH VEHICLES

Advanced Transport Operating System (ATOPS) Flight Management/Flight Controls (FM/FC) software description [NASA-CR-191457] p 3250 N93-28621

STRV1-b flight experiment p 3265 N93-28723

A study of the effects of lens focal length on remote driver performance [AD-A263191] p 3505 N93-28941

A real-time, hardware-in-the-loop simulation of an unmanned aerial research vehicle [AD-A262477] p 3248 N93-29409

Flight control system design factors for applying automated testing techniques [NASA-TM-4242] p 3260 N93-30764

RESERVOIRS

A diffusion approximation for a network of reservoirs with power law release rule [AD-A263753] p 3550 N93-29872

RESIDUAL STRENGTH

Comparison of impact results for several polymeric composites over a wide range of low impact velocities p 3304 N93-30848

Progressive failure methodologies for predicting residual strength and life of laminated composites p 3307 N93-30866

RESIDUAL STRESS

Crack length determination by ultrasonic methods [DE93-008075] p 3450 N93-28567

Development of adherent ceramic coatings to reduce contact stress damage of ceramics [DE93-012518] p 3336 N93-30182

Processing of novel nanoparticle dispersion strengthened ceramics for improved mechanical performance [AD-A264191] p 3339 N93-30883

Fracture of glass p 3293 N93-30969

RESIDUES

Hypervelocity impact survivability experiments for carbonaceous impactors p 3283 N93-29364

SIMS chemical analysis of extended impacts on the leading and trailing edges of LDEF experiment AO187-2 p 3318 N93-29367

Scanning electron microscope/energy dispersive x ray analysis of impact residues in LDEF tray clamps p 3283 N93-29369

Projectile compositions and modal frequencies on the chemistry of micrometeoroids LDEF experiment p 3638 N93-29370

Interplanetary meteoroid debris in LDEF metal craters p 3638 N93-29372

Elemental analyses of hypervelocity microparticle impact sites on Interplanetary Dust Experiment sensor surfaces p 3638 N93-29378

Detecting residue on a printed circuit board: An application of the Boundary Contour/Feature Contour System [DE93-006283] p 3412 N93-30370

RESIN MATRIX COMPOSITES

Environmental effects on stitched RTM composites [NASA-CR-193221] p 3297 N93-29107

Effect of water immersion on fiber/matrix adhesion in thermoplastic composites [AD-A263646] p 3299 N93-29984

Mechanical properties of composite materials p 3290 N93-30951

RESINS

An investigation of stereolithography as a means of prototyping from a cad database [AD-A263410] p 3613 N93-29210

Resin transfer molding for advanced composite primary aircraft structures p 3301 N93-30438

Preliminary properties of a resin from ethynyl terminated materials p 3303 N93-30842

Infiltration/cure modeling of resin transfer molded composite materials using advanced fiber architectures p 3303 N93-30843

Effects of intra- and inter-laminar resin content on the mechanical properties of toughened composite materials p 3303 N93-30845
Micromechanics of fatigue in woven and stitched composites p 3304 N93-30850
Development of stitching reinforcement for transport wing panels p 3304 N93-30852
Development of resins for composites by resin transfer molding p 3305 N93-30853
Advanced fiber/matrix material systems p 3305 N93-30854
Mechanical and analytical screening of braided composites for transport fuselage applications p 3305 N93-30855

RESISTOJET ENGINES
Preliminary endurance tests of water vaporizers for resistojet applications [NASA-TM-106222] p 3287 N93-28694
Gravity sensitivity of a resistojet water vaporizer [NASA-TM-106220] p 3288 N93-29194

RESOLUTION
An investigation of resolution as encountered in various chromatographic operational modes [AD-A262883] p 3312 N93-29510

RESONANCE
Dynamical analysis of highly excited molecular spectra [DE93-010771] p 3564 N93-28604
Aerosol particle analysis by Raman scattering technique [DE93-005587] p 3309 N93-28880

RESONANCE FLUORESCENCE
Remote measurement of planetary magnetic fields by the Hanle effect p 3645 N93-28793

RESONANCE SCATTERING
Quantum lattice fluctuations in a 1-dimensional charge-density-wave material: Luminescence and resonance Raman studies of an MX solid [DE93-007362] p 3593 N93-28966

RESONANT FREQUENCIES
Theoretical and experimental investigation of slack cable/mass system dynamics p 3455 N93-31028

RESONATORS
Investigation of thermoacoustic muffler [AD-A262009] p 3562 N93-29392

RESOURCES MANAGEMENT
Tropical forests and biological diversity: USAID report to Congress 1990-1991 [PB93-180453] p 3471 N93-29681

RESPIRATION
Evaluation of test methods and requirements for respiratory protection systems 21 [AD-A262466] p 3501 N93-28757

RESPIRATORS
Evaluation and optimization of a flexible filtration system for respiratory protection system 21 [AD-A262467] p 3493 N93-28758

RESPIRATORY SYSTEM
Evaluation of test methods and requirements for respiratory protection systems 21 [AD-A262466] p 3501 N93-28757
Evaluation and optimization of a flexible filtration system for respiratory protection system 21 [AD-A262467] p 3493 N93-28758

RESPONSE TIME (COMPUTERS)
Context switch time scalability: Benchmark results [PB93-181832] p 3539 N93-29661

RESTORATION
Strategic Environmental Research and Development Program (SERDP) [AD-A263745] p 3471 N93-29858
Environmental characteristics of EPA, NRC, and DOE sites contaminated with radioactive substances [PB93-185551] p 3475 N93-30829

RETINA
Image enhancement using an analog device neural network p 3376 N93-30346
Analysis of visual loss from retinal lesions [AD-A264692] p 3496 N93-30494
A simple computational model of center-surround receptive fields in the retina [AD-A264723] p 3496 N93-30515
An algorithm for simple and complex feature detection: From retina to primary visual cortex [AD-A264306] p 3497 N93-30897
Photoreceptors regulating circadian behavior: A mouse model [AD-A264881] p 3497 N93-30908

RETINAL IMAGES
Modelling and simulation of human retinal vision processing p 3363 N93-30269

RETURN TO EARTH SPACE FLIGHT
Design, building, and testing of the postlanding systems for the assured crew return vehicle p 3229 N93-29726

REUSABLE HEAT SHIELDING
Debris/ice/TPS assessment and integrated photographic analysis for Shuttle Mission STS-55 [NASA-TM-107559] p 3271 N93-29136

REUSABLE LAUNCH VEHICLES
ASUR p 3228 N93-29720
Spacely's rockets: Personnel launch system/family of heavy lift launch vehicles p 3234 N93-29752

REUSABLE SPACECRAFT
Retrievable payload carrier, next generation Long Duration Exposure Facility: Update 1992 p 3283 N93-29705
Delta Advanced Reusable Transport (DART): An alternative manned spacecraft p 3231 N93-29735
RS Landers: Lunar lander p 3234 N93-29753

REVERSE FIELD PINCH
Nonlinear coupling of tearing fluctuations in the Madison Symmetric Torus [DE93-010131] p 3584 N93-28602
The fluctuation induced Hall effect [DE93-010130] p 3585 N93-28912

REVERSED FLOW
Effects of flow-path variations on internal reversing flow in a tailpipe offtake configuration for ASTOVL aircraft [NASA-TM-106149] p 3252 N93-29065

REVISIONS
CAESAR development plan 1992-1995 [BCRS-92-17] p 3463 N93-31009

REYNOLDS NUMBER
An experimental study of flow over a 6 to 1 prolate spheroid at incidence p 3239 N93-29124
Determination of surface heat transfer and film cooling effectiveness in unsteady wake flow conditions p 3253 N93-29933
Measurement of turbulent spots and intermittency modelling at gas-turbine conditions p 3253 N93-29934
Turbulence characteristics of an axisymmetric reacting flow [NASA-CR-4110] p 3242 N93-30373
Effects of buoyancy on gas jet diffusion flames [NASA-CR-191109] p 3352 N93-31031

REYNOLDS STRESS
Large eddy simulations of shockwave passage through turbulence [DE92-019503] p 3419 N93-29050

RHEOLOGY
Macrostatistical hydrodynamics [DE93-012289] p 3417 N93-28751
The XNOVAKTC rheological model [AD-A263298] p 3342 N93-29762
Wetting and dispersion in ceramic/polymer melt injection molding systems [DE93-013240] p 3338 N93-30601
Physical chemical studies on molecular composite compositions [AD-A264834] p 3339 N93-30898

RHODAMINE
Pulsed laser photoacoustic spectrometer for study of solid materials [DE93-605290] p 3441 N93-31023

RHODE ISLAND
Rhode Island hurricanes and tropical storms: A fifty-six year summary, 1936-1991 [PB93-162006] p 3481 N93-29198

RIBBONS
Microsecond ribbon relativistic electron beam in a plane undulator and generation of microwave radiation [DE93-605693] p 3400 N93-30993

RIBLETS
Turbulent drag reduction: Studies of feedback control and flow over riblets p 3242 N93-30645

RIBONUCLEIC ACIDS
Computer assisted multiplex sequencing [DE93-007144] p 3536 N93-30934

RIDING QUALITY
The Ultra Light Aircraft Testing [NASA-CR-193043] p 3249 N93-29774

RIEMANN MANIFOLD
Integrals of motion on the group of invariance of an interval in three-dimensional spaces [DE93-606090] p 3606 N93-30797
An adaptive Lagrangian method for computing 1-D reacting flows and the theory of Riemann invariant manifolds for the compressible Euler equations p 3428 N93-30902
Fourth-rank gravity and cosmology [DE92-644722] p 3637 N93-30918
Spherically symmetric line element and Killing vectors in five-dimensional space [DE93-604132] p 3558 N93-30988
Superconformal structures and holomorphic 1/2-superdifferentials on N = 1 super Riemann surfaces [DE93-604133] p 3558 N93-30989

RIGID STRUCTURES
Vision-based control of holonomic robots for 3-dimensional rigid-body positioning using camera-space manipulation p 3578 N93-29178
Gravity referenced elevation encoder development p 3385 N93-29592
Attitude stabilization of a rigid spacecraft using gas jet actuators operating in a failure mode p 3280 N93-29992
Planar reorientation of a free-free beam in space using embedded electromechanical actuators p 3280 N93-29993
A continuum code investigation of stress integration using exact and approximate material rotation [DE93-001892] p 3454 N93-31013

RIGIDITY
Development of an experimental method to determine the axial rigidity of a strut-node joint p 3290 N93-30950

RIPPLES
Optical measurements of ripples using a scanning laser slope gauge. Part 1: Instrumentation and preliminary results [AD-A261939] p 3486 N93-28996

RISK
Radiation monitoring equipment dosimeter experiment p 3266 N93-28730
Life insurance risk assessment using a fuzzy logic expert system p 3520 N93-29585
Steps required in the pursuit of quantitative risk management processes for high pressure systems [DE93-007586] p 3378 N93-30508
Uses of risk importance measures [VTT-TIED-1245] p 3378 N93-30581

RIVERS
Development of an airborne MMW FM-CW radar for mapping river ice [AD-A262655] p 3379 N93-28588

ROBOT ARMS
A portable modular architecture for robotic manipulator control [DE93-010819] p 3444 N93-29254
Some results on feedback stabilization of a one-link flexible arm [INRIA-RR-1682] p 3543 N93-30116
Trajectory generation for dual-arm robots using artificial impedance approach p 3370 N93-30310
Robot arm with positional absolute encoded joints p 3370 N93-30312

ROBOT CONTROL
Sources sought for innovative scientific instrumentation for scientific lunar rovers p 3434 N93-28804
Dual arm generalized compliant motion with shared control [NASA-CASE-NPO-18738-1-CU] p 3443 N93-28954
An autonomous vision-based mobile robot p 3443 N93-29082
Vision-based control of holonomic robots for 3-dimensional rigid-body positioning using camera-space manipulation p 3578 N93-29178
A portable modular architecture for robotic manipulator control [DE93-010819] p 3444 N93-29254
An architecture for robotic system integration [DE93-010829] p 3444 N93-29316
Research on reconfigurable and reliable manipulators [DE93-010244] p 3444 N93-29330
Spline screw autochanger [NASA-CASE-GSC-13435-1] p 3445 N93-29505
Special purpose parallel computer architecture for real-time control and simulation in robotic applications [NASA-CASE-NPO-17629-1-CU] p 3521 N93-29608
Application of sensors to the control of robotic systems [DE93-009837] p 3543 N93-30012
The planning coordinator: A design architecture for autonomous error recovery and on-line planning of intelligent tasks [NASA-CR-193250] p 3543 N93-30039
Some results on feedback stabilization of a one-link flexible arm [INRIA-RR-1682] p 3543 N93-30116
Input relegation control for gross motion of a kinematically redundant manipulator [DE93-005301] p 3446 N93-30210
Analysis and simulation of a two degrees-of-freedom one-link flexible forearm p 3361 N93-30261
A parallel processing system for intensive I/O p 3362 N93-30262
Task allocation and real-time considerations for the Robot Controller Test Station (RCTS) p 3364 N93-30278
On the implementation of the BIRIS range sensor for applications in robotic control and autonomous navigation p 3366 N93-30286

Supervised autonomy in telerobotics
p 3372 N93-30326
A multiprocessor architecture for realtime robot control p 3372 N93-30327
Drive-reinforcement learning system applications
[AD-A264514] p 3446 N93-30404
Adaptive networks for sequential decision problems
[AD-A264756] p 3534 N93-30561
Graphical programming: On-line robot simulation for telerobotic control
[DE93-009796] p 3447 N93-30654
Control of nonlinear systems with applications to constrained robots and spacecraft attitude stabilization
p 3544 N93-30893
Adaptive motion control of mobile robots
p 3545 N93-30903

ROBOT DYNAMICS
Dual arm generalized compliant motion with shared control
[NASA-CASE-NPO-18738-1-CU] p 3443 N93-28954
An autonomous vision-based mobile robot
p 3443 N93-29082
Lunar rovers and local positioning system
p 3277 N93-29119
A portable modular architecture for robotic manipulator control
[DE93-010819] p 3444 N93-29254
Spline screw autochanger
[NASA-CASE-GSC-13435-1] p 3445 N93-29505
Walking robot: A design project for undergraduate students p 3231 N93-29737
Optimal geometric design of robots for environments with obstacles p 3445 N93-30149
Input relegation control for gross motion of a kinematically redundant manipulator
[DE93-005301] p 3446 N93-30210
Analysis and simulation of a two degrees-of-freedom one-link flexible forearm p 3361 N93-30261
Trajectory generation for dual-arm robots using artificial impedance approach p 3370 N93-30310
Adaptive networks for sequential decision problems
[AD-A264756] p 3534 N93-30561
Adaptive motion control of mobile robots
p 3545 N93-30903

ROBOT SENSORS
A modular head/eye platform for real-time reactive vision
[OUEL-1941/92] p 3505 N93-28897
Dual arm generalized compliant motion with shared control
[NASA-CASE-NPO-18738-1-CU] p 3443 N93-28954
Application of sensors to the control of robotic systems
[DE93-009837] p 3543 N93-30012
A testbed for autonomous reflexive grasping
[AD-A264557] p 3446 N93-30384

ROBOTICS
Small Stirling dynamic isotope power system for robotic space missions
[NASA-TM-105785] p 3287 N93-28686
Workshop on Advanced Technologies for Planetary Instruments, part 1
[NASA-CR-193015] p 3639 N93-28764
Gamma ray/neutron spectrometers for planetary elemental mapping p 3647 N93-28807
Robotics and artificial intelligence for hazardous environments
[DE93-008271] p 3541 N93-29047
Graphical interface between the CIRSSE testbed and CimStation software with MCS/CTOS
[NASA-CR-193276] p 3527 N93-29218
A manipulator kinematic design for high-vacuum operation
[DE93-010264] p 3444 N93-29247
A portable modular architecture for robotic manipulator control
[DE93-010819] p 3444 N93-29254
An architecture for robotic system integration
[DE93-010829] p 3444 N93-29316
Special purpose parallel computer architecture for real-time control and simulation in robotic applications
[NASA-CASE-NPO-17629-1-CU] p 3521 N93-29608
Advanced design for orbital debris removal in support of solar system exploration p 3229 N93-29724
Walking robot: A design project for undergraduate students p 3231 N93-29737
Development of neural network architectures for self-organizing pattern recognition and robotics
[AD-A264831] p 3543 N93-29791
Application of sensors to the control of robotic systems
[DE93-009837] p 3543 N93-30012
Canadian Conference on Electrical and Computer Engineering, volumes 1 and 2
[ISBN-0-9694170-1-2] p 3354 N93-30215
A closed-form formula for the manipulator regressor
p 3355 N93-30218
An artificial neural network model for periodic trajectory generation p 3356 N93-30225
An expert system for identification of the task status from tactile sensor data p 3368 N93-30300
A functional system architecture for fully autonomous robot p 3370 N93-30311
Drive-reinforcement learning system applications
[AD-A264514] p 3446 N93-30404
Oceanographic data processing program
[AD-A264801] p 3544 N93-30591
Robotic technology evolution and transfer
p 3627 N93-30714

ROBOTS
Graphical interface between the CIRSSE testbed and CimStation software with MCS/CTOS
[NASA-CR-193276] p 3527 N93-29218
A manipulator kinematic design for high-vacuum operation
[DE93-010264] p 3444 N93-29247
An architecture for robotic system integration
[DE93-010829] p 3444 N93-29316
A virtual environment for manufacturing systems
[AD-A263128] p 3528 N93-29473
Planning collision free paths for two cooperating robots using a divide-and-conquer C-space traversal heuristic
[NASA-CR-193252] p 3542 N93-29771
Application of sensors to the control of robotic systems
[DE93-009837] p 3543 N93-30012
Input relegation control for gross motion of a kinematically redundant manipulator
[DE93-005301] p 3446 N93-30210
Analysis and simulation of a two degrees-of-freedom one-link flexible forearm p 3361 N93-30261
Task allocation and real-time considerations for the Robot Controller Test Station (RCTS)
p 3364 N93-30278
Adaptive networks for sequential decision problems
[AD-A264756] p 3534 N93-30561

ROBUSTNESS (MATHEMATICS)
Study on various problems in statistical planning and inference
[AD-A262484] p 3554 N93-29411
Dynamics and robust control of sampled data systems for large space structures
[AD-A264192] p 3281 N93-30142
Robust control via H-infinity optimization
p 3354 N93-30216
A robust model for finding optimal evolutionary trees
[DE93-010682] p 3491 N93-30483

ROCKET ENGINE CASES
Postflight hardware evaluation 360T025 (RSRM-25, STS-46). Appendix B: Case, seals, and joints PFORs
[NASA-CR-192564] p 3272 N93-30619

ROCKET ENGINES
A new facility for advanced rocket propulsion research
[NASA-TM-106193] p 3270 N93-28696
Altitude compensating ablative stiffening band for rocket motor nozzles
[NASA-CASE-MFS-28728-1] p 3288 N93-28950
A fuzzy case based reasoning tool for model based approach to rocket engine health monitoring
p 3289 N93-29570
Conceptual design of a two-stage-to-orbit vehicle
p 3228 N93-29716
Liquid fuel injection elements for rocket engines
[NASA-CASE-MFS-28547-1] p 3289 N93-29847

ROCKET EXHAUST
The Ultraviolet Plume Instrument (UVPI)
p 3285 N93-28784
Kinetics and energy transfer in nonequilibrium fluid flows
[AD-A263612] p 3240 N93-29284

ROCKET LAUNCHING
Wind measurement accuracy of a loran radiosonde
[AD-A263572] p 3483 N93-29832

ROCKET NOZZLES
Altitude compensating ablative stiffening band for rocket motor nozzles
[NASA-CASE-MFS-28728-1] p 3288 N93-28950
Postflight hardware evaluation 360T025 (RSRM-25, STS-46)
[NASA-CR-192562] p 3272 N93-30617
Postflight hardware evaluation 360T025 (RSRM-25, STS-46). Appendix A: Insulation PFORs
[NASA-CR-192563] p 3272 N93-30618
Postflight hardware evaluation 360T025 (RSRM-25, STS-46). Appendix C: Nozzle PFORs
[NASA-CR-192565] p 3272 N93-30620
Postflight hardware evaluation 360T025 (RSRM-25, STS-46). Appendix D: Nozzle postfire data
[NASA-CR-192580] p 3289 N93-30648

ROCKET PROPELLANTS
Benefits of in situ propellant utilization for a Mars sample return mission
[NASA-TM-106243] p 3341 N93-28695

ROCKET-BORNE INSTRUMENTS
Plasma diagnostics by antenna impedance measurements p 3400 N93-28820
Aerospace payload design and development
[AD-A264502] p 3289 N93-30402

RODS
Integrated approaches to parallelism in optimization and solution of inverse problems
[AD-A262259] p 3452 N93-29349

ROLL
Evaluation of four advanced nozzle concepts for short takeoff and landing performance
[NASA-TP-3314] p 3239 N93-29165
Computation of a delta-wing roll-and-hold maneuver
[AD-A264704] p 3260 N93-30498

ROLLER BEARINGS
Cryogenic magnetic bearing
[AD-A264716] p 3446 N93-30512

ROLLING CONTACT LOADS
The contact mechanical nonlinearities of a mathematical model of a railway wheel rolling over corrugated rail
[ILR-MITT-266(1991)] p 3454 N93-31015
The steady-state tangential contact problem for a falling drop type of contact area on corrugated rail by simplified theory of rolling contact
[ILR-MITT-267(1991)] p 3455 N93-31016

ROOFS
Wind loads on canopy roofs
[RR-CE132] p 3451 N93-29106

ROOT-MEAN-SQUARE ERRORS
A Monte Carlo study of the raw and normal varimax rotation criterion in factor analysis
[AD-A262516] p 3554 N93-28844

ROOTS OF EQUATIONS
Zero-crossing rate of some non-Gaussian processes
p 3360 N93-30254

ROSAT MISSION
ROSAT detection of stellar x ray sources in the old open cluster M67
[MPE-PREPRINT-230] p 3631 N93-30578

ROTARY WING AIRCRAFT
Chaos in mechanical systems with especial reference to rotorcraft and missiles
[AD-A263703] p 3604 N93-29384
Rotorcraft master plan p 3236 N93-30677
Determining the transferability of flight simulator data
p 3237 N93-30685
Frequency-response techniques for documentation and improvement of rotorcraft simulators
p 3237 N93-30689
Bandwidth and SIMDUCE as simulator fidelity criteria
p 3238 N93-30690
Methodology development for evaluation of selective-fidelity rotorcraft simulation
p 3238 N93-30691

ROTARY WINGS
A passive infrared ice detection technique for helicopter applications
[NASA-CR-193187] p 3244 N93-29152
Flow visualization on helicopter blades using acenaphthen
[ESA-TT-1255] p 3422 N93-29273
Aerodynamic characteristics of a rotorcraft airfoil designed for the tip region of a main rotor blade
[NASA-TM-4264] p 3240 N93-29450
Computation of far-field helicopter rotor tone noise
[ONERA-P-1990-5] p 3562 N93-30110
Helicopter simulation: An aircrew training and qualification perspective p 3236 N93-30676

ROTATING BODIES
A continuum code investigation of stress integration using exact and approximate material rotation
[DE93-001892] p 3454 N93-31013

ROTATING DISKS
Heat Transfer and Cooling in Gas Turbines
[AGARD-CP-527] p 3252 N93-29926
Study of flow structure in rotating cavities: Numerical predictions of laminar and turbulent, steady, and unsteady flows p 3256 N93-29948
Flow and heat transfer between gas-turbine discs
p 3256 N93-29950
Dioxygen reduction in various acid electrolytes
[AD-A263564] p 3317 N93-30664

ROTATING FLUIDS
Analysis of unsteady wave processes in a rotating channel
[NASA-CR-191154] p 3251 N93-28617
Fluid flow and heat transfer in the entrance region of an annulus between independently rotating tubes with a turbulent axial flow p 3256 N93-29952

ROTATING LIQUIDS

Liquid Motion in a rotating tank Experiment (LME) p 3264 N93-28710

ROTATING SHAFTS

Transient thermal behaviour of a compressor rotor with axial cooling air flow and co-rotating or contra-rotating shaft p 3255 N93-29946

Vibration localization in rotating shafts p 3454 N93-30626

ROTATION

Investigation of Mars rotational dynamics using Earth-based radio tracking of Mars landers p 3642 N93-28777

A Monte Carlo study of the raw and normal varimax rotation criterion in factor analysis [AD-A262516] p 3554 N93-28844

The effect of orthogonal-mode rotation on forced convection in a circular-sectioned tube fitted with full circumferential transverse ribs p 3254 N93-29937

Turbulent flow and heat transfer in idealized blade cooling passages p 3254 N93-29938

An L2F-measurement device with image rotator prism for flow velocity analysis in rotating coolant channels p 3255 N93-29942

Local heat transfer measurement with liquid crystals on rotating surfaces including non-axisymmetric cases p 3255 N93-29943

Heat transfer and leakage in high-speed rotating stepped labyrinth seals p 3256 N93-29951

Theoretical studies in nuclear structure [DE93-012290] p 3570 N93-30505

ROTATIONAL SPECTRA

A novel flame thermometer based on the doppler width of ro-vibrational transitions [AD-A264515] p 3315 N93-30405

ROTOR AERODYNAMICS

Unsteady vortex loop/dipole theory applied to the work and acoustics of an ideal low speed propeller [AD-A264057] p 3241 N93-29891

Three-dimensional fiber-optic LDV measurements in the endwall region of a linear cascade of controlled-diffusion stator blades [AD-A263513] p 3424 N93-29968

ROTOR BLADES

An integrated optimum design approach for high speed prop-rotors including acoustic constraints [NASA-CR-193222] p 3248 N93-29153

ROTOR BLADES (TURBOMACHINERY)

Unsteady vortex loop/dipole theory applied to the work and acoustics of an ideal low speed propeller [AD-A264057] p 3241 N93-29891

ROTOR LIFT

Aerodynamic characteristics of a rotorcraft airfoil designed for the tip region of a main rotor blade [NASA-TM-4264] p 3240 N93-29450

ROTORCRAFT AIRCRAFT

An integrated optimum design approach for high speed prop-rotors including acoustic constraints [NASA-CR-193222] p 3248 N93-29153

ROTORS

Experimental evaluation of a cooled radial-inflow turbine [NASA-TM-106230] p 3251 N93-28697

Use of local x ray computerized tomography for high-resolution, region-of-interest inspection of large ceramic components for engines [DE93-005564] p 3449 N93-28943

Three-dimensional numerical simulation of gradual opening in a wave rotor passage [NASA-CR-191157] p 3252 N93-29072

Robust control of intelligent rotor [AD-A263707] p 3259 N93-29985

Some implications of a differential turbomachinery equation with viscous correction [AD-A264693] p 3427 N93-30571

ROUTES

An analysis of en route controller-pilot voice communications [AD-A264784] p 3394 N93-30611

ROVING VEHICLES

Mars sample return mission: Two alternate scenarios p 3233 N93-29746

RUBBER

APU diaphragm testing. Test plan [NASA-TM-108251] p 3271 N93-29387

Chromatographic and solvatochromic measurements on butyl rubbers [AD-A263088] p 3334 N93-29795

RULES

Automatic rule generation for high-level vision p 3511 N93-29526

A model for amalgamation in group decision making p 3513 N93-29540

Determining rules for closing customer service centers: A public utility company's fuzzy decision p 3516 N93-29561

Comparison between the performance of two classes of fuzzy controllers p 3517 N93-29566

Inference in fuzzy rule bases with conflicting evidence p 3519 N93-29583

Turning SOS rules into equations [CWI-CS-R9218] p 3532 N93-30017

RUN TIME (COMPUTERS)

NESL: A nested data-parallel language (Version 2.6) [AD-A263548] p 3530 N93-29822

RUNGE-KUTTA METHOD

Development of an unstructured solution adaptive method for the quasi-three-dimensional Euler and Navier-Stokes equations [NASA-CR-193241] p 3421 N93-29213

An upwind method for the solution of the 3D Euler and Navier-Stokes equations on adaptively refined meshes [AD-A262863] p 3423 N93-29472

Solution of Euler equations for forebody-inlet ensemble of aircraft at high angle of attack [AD-A263905] p 3240 N93-29862

The application of concentric vortex simulation to calculating the aerodynamic characteristics of bodies of revolution at high angles of attack [AD-A263879] p 3241 N93-29919

RUNWAYS

Two simulation studies of precision runway monitoring of independent approaches to closely spaced parallel runways [AD-A263433] p 3261 N93-29815

RUTHENIUM

Growth model of Au films on Ru(001) [DE92-642126] p 3602 N93-30998

RUTILE

Role of oxygen vacancies in anodic TiO2 thin films [DE92-642137] p 3602 N93-31027

S

S MATRIX THEORY

Errors when shock waves interact due to numerical shock width [DE93-010699] p 3426 N93-30484

Unitary approximation of Bhabha diffusion by high energies and its implementation in Monte Carlo event generators [ETN-93-93622] p 3571 N93-30670

S WAVES

Jet mixer noise suppressor using acoustic feedback [NASA-CASE-LEW-15170-1] p 3561 N93-28953

Modern seismic travel time tables and station corrections for P and S waves [AD-A262536] p 3477 N93-29412

Algorithm of numerical calculations of differential Yakubovsky equations for the (1 + 3) scattering problem [DE92-644679] p 3535 N93-30915

SAFETY

Gene transcription and electromagnetic fields [DE93-010854] p 3490 N93-28848

Weakly nonlinear dynamics of near-CJ detonation waves [DE93-007344] p 3424 N93-29836

Combustion/explosion chemistry of bulk materials p 3343 N93-30062

Using Penelope to assess the correctness of NASA Ada software: A demonstration of formal methods as a counterpart to testing [NASA-CR-4509] p 3533 N93-30380

Uses of risk importance measures [VTT-TIED-1245] p 3378 N93-30581

Vehicle dynamic stability and rollover [PB93-185437] p 3447 N93-30828

Solving a product safety problem using a recycled high density polyethylene container p 3292 N93-30964

SAFETY DEVICES

Inservice diagnostic methods for solenoid-operated valves [DE93-007823] p 3443 N93-28968

SAFETY FACTORS

Energetic material response to abnormal environments p 3350 N93-30095

Solving a product safety problem using a recycled high density polyethylene container p 3292 N93-30964

SAFETY MANAGEMENT

Steps required in the pursuit of quantitative risk management processes for high pressure systems [DE93-007586] p 3378 N93-30508

SALINITY

A water mass analysis of the 1991-1992 El Nino signal in the Farallon Islands region [AD-A263490] p 3488 N93-29819

Hydrographic observations in the western tropical and subtropical north Atlantic Ocean: Atlantic Climate Change Program (ACCP) and Western Tropical Atlantic Experiment (WESTRAX) during 1990 [PB93-184760] p 3489 N93-30827

SALT SPRAY TESTS

Chromate-free corrosion resistant conversion coatings for aluminum [DE93-009835] p 3336 N93-30051

SALTS

A field investigation of water and salt movement in permafrost and the active layer [AD-A263706] p 3487 N93-29298

SAMPLED DATA SYSTEMS

Dynamics and robust control of sampled data systems for large space structures [AD-A264192] p 3281 N93-30142

SAMPLING

Tank issues: Design and placement of floating liquid monitoring wells [PB93-161149] p 3469 N93-29033

Feature based neural network acoustic transient signal classification [AD-A263437] p 3562 N93-29816

Subpicosecond electrooptic sampling [AD-A264635] p 3581 N93-30520

SANDS

Digital image processing of descanned terrestrial ground photographs p 3459 N93-28926

Performance and cost evaluation of bioremediation techniques for fuel spills [PB93-175545] p 3474 N93-30762

SANDWICH STRUCTURES

Optimization of composite sandwich cover panels subjected to compressive loadings p 3306 N93-30862

SAPPHIRE

Healing of lithographically introduced flaws in glass and glass containing ceramics [DE93-010453] p 3330 N93-28761

SATELLITE ALTIMETRY

Processing of altimeter data by the German ERS-1 Processing and Archiving Facility (D-PAF) p 3457 N93-28917

SATELLITE ANTENNAS

Status of the Canadian military Multibeam Antenna (MBA) development for EHF SATCOM p 3374 N93-30334

Durability of Quick Reaction Satellite Antenna (QRSA) trunnion castings [AD-A264095] p 3281 N93-30813

SATELLITE ATTITUDE CONTROL

Control-structures interaction test of the LACE satellite p 3263 N93-28706

Refinements on the pinhole camera measurements of the LDEF attitude p 3283 N93-29622

Attitude- and Orbit Control Subsystem concepts for TACSATS p 3284 N93-29906

Control of nonlinear systems with applications to constrained robots and spacecraft attitude stabilization p 3544 N93-30893

SATELLITE COMMUNICATION

Automating the satellite range scheduling process [AD-A262601] p 3270 N93-28468

Design and construction of a prototype ACTS propagation terminal [NASA-CR-193071] p 3404 N93-28539

T(lc2)acS(lc3)ats for Surveillance Verification and C3I [AGARD-CP-522] p 3387 N93-29892

Tactical satellites p 3284 N93-29893

TACSAT ground control and data collection p 3388 N93-29895

TACSAT-spacecraft bus concept and design: Application of a multimission bus for TACSAT in LEO p 3284 N93-29896

Considerations for NATO satellite communications in the post-2000 era p 3388 N93-29899

Terrain and coverage prediction analyses for non-geostationary orbit EHF satellite communications p 3389 N93-29902

Launch vehicles for lightweight TACSAT deployment p 3271 N93-29903

A slotted Aloha satellite channel simulator p 3360 N93-30250

Canadian EHF MILSATCOM research and development project p 3362 N93-30264

SAW technology for on-board processing in military satellite communications p 3362 N93-30265

A satellite downlink spread spectrum timing beacon p 3362 N93-30267

FASSET: A development model for a Canadian EHF MILSATCOM system p 3363 N93-30268

Coarse synchronization in an EHF frequency-hopped satellite communications system p 3365 N93-30281

Security of the remote control link of Anik E satellites p 3365 N93-30282

Coding for frequency hopped spread spectrum satellite communications p 3365 N93-30283
Adaptive jammer nulling in EHF communications satellites p 3365 N93-30284
Temporal synchronization of frequency hopped DPSK p 3365 N93-30285
Performance of frequency hopped M-ary FSK in Rayleigh fading and partial-band jamming p 3368 N93-30303
Comparison of two random access techniques for the North American MSAT system p 3370 N93-30315
Teleglobe's international Mobile Earth Terminal service p 3371 N93-30317
Constant Average Power Single Sideband (CAPSSB) modulation p 3373 N93-30331
Signal processor based MSAT trellis coded M-DPSK with adaptive Doppler phasor correction p 3373 N93-30332
Two-stage Doppler phasor corrected TCM/DMPSK for shadowed mobile satellite channels p 3373 N93-30333
Engineering management consideration for an integrated aeronautical mobile satellite service p 3374 N93-30337
The evolution of global mobile communications p 3376 N93-30349

SATELLITE CONFIGURATIONS
Multipurpose satellite bus (MPS) p 3232 N93-29743
QuickStar: System design, capabilities, and tactical applications of a small, smart space system p 3284 N93-29905

SATELLITE CONTROL
Upper atmosphere research satellite jitter study p 3264 N93-28708
System of navigation by satellites with European coverage p 3284 N93-29897
Security of the remote control link of Anik E satellites p 3365 N93-30282

SATELLITE DESIGN
International aviation (Selected articles) [AD-A262566] p 3227 N93-28576
Project MEDSAT p 3231 N93-29739
Multipurpose satellite bus (MPS) p 3232 N93-29743
An overview of DARPA's advanced space technology program p 3269 N93-29908
SAR sensors on TACSATS: A feasibility assessment p 3286 N93-29909
A TACSAT SAR concept p 3286 N93-29910

SATELLITE DOPPLER POSITIONING
Precise tracking of the Magellan and Pioneer Venus orbiters by Same-Beam Interferometry. Part 2: Orbit determination analysis p 3270 N93-29589

SATELLITE IMAGERY
Leadex data report. Part 1: Weather analysis and satellite images [AD-A263217] p 3481 N93-28876
Utilization of NOAA/AVHRR data for energy balance of Lake Constance (Switzerland) p 3458 N93-28926
Evidence-based classification of satellite image data p 3459 N93-28931
Earth observation from space: Competition or cooperation? [AD-A262044] p 3459 N93-29000
Convective and stratiform rain: Multichannel microwave sensing over oceans [NASA-TM-104586] p 3482 N93-29448
Automated satellite image navigation [AD-A262868] p 3269 N93-29475
What's past is prologue: Supporting global change research with historical data [DE93-005777] p 3472 N93-30009
Neural network cloud classification research [AD-A264628] p 3484 N93-30176
Interim report on Landsat national archive activities p 3618 N93-30455
Land use database for the Netherlands using LANDSAT Thematic Mapper pictures [BCRS-91-32] p 3463 N93-30839
Bayesian linear analysis with application to removal of atmospheric influences on optical remote sensing images [BCRS-92-19] p 3463 N93-31011

SATELLITE INSTRUMENTS
SeaWiFS technical report series. Volume 2: Analysis of orbit selection for SeaWiFS: Ascending versus descending node [NASA-TM-104566-VOL-2] p 3486 N93-28497
SeaWiFS technical report series. Volume 6: SeaWiFS technical report series cumulative index: Volumes 1-5 [NASA-TM-104566-VOL-6] p 3486 N93-28500
Total dose tests for the PROMICS-3 instrument [VTT-TIED-1203] p 3411 N93-30108
NOAA satellite programs and technology requirements p 3627 N93-30710

SATELLITE NAVIGATION SYSTEMS
T(lc2)acS(lc3)ats for Surveillance Verification and C3I [AGARD-CP-522] p 3387 N93-29892

SATELLITE NETWORKS
On-board B-ISDN fast packet switching architectures. Phase 2: Development. Proof-of-concept architecture definition report [NASA-CR-191151] p 3273 N93-29884
T(lc2)acS(lc3)ats for Surveillance Verification and C3I [AGARD-CP-522] p 3387 N93-29892
TACSAT-spacecraft bus concept and design: Application of a multimission bus for TACSAT in LEO p 3284 N93-29896
System of navigation by satellites with European coverage p 3284 N93-29897

SATELLITE OBSERVATION
SeaWiFS technical report series. Volume 6: SeaWiFS technical report series cumulative index: Volumes 1-5 [NASA-TM-104566-VOL-6] p 3486 N93-28500
IUE observations of cataclysmic variable [NASA-CR-193188] p 3629 N93-28634
Measurements of magnetic fields produced by a 30 kWe class Arcjet Power Conditioning Unit [AD-A262786] p 3287 N93-28658
The dynamic cusp at low altitudes: A case study combining Viking, DMSP, and Sondrestrom incoherent scatter radar observations [NASA-CR-193152] p 3476 N93-28842
Leadex data report. Part 1: Weather analysis and satellite images [AD-A263217] p 3481 N93-28876
Proceedings of the 8th User Seminar of the German Remote Sensing Data Center of the German Aerospace Establishment (DLR) [DLR-MITT-92-09] p 3456 N93-28915
Earth observation from space: Competition or cooperation? [AD-A262044] p 3459 N93-29000
Space optical and low-frequency radio searches for Earth-crossing asteroids and comets [DE93-008716] p 3634 N93-29246
Ionospheric structure specifications and systems effects [AD-A263573] p 3476 N93-29343
A TACSAT SAR concept p 3286 N93-29910
The possible direct use of satellite radiance measurements by the Atmospheric Radiation Measurement Program [DE93-009819] p 3462 N93-30049

SATELLITE ORBITS
Lunar gravitational field estimation and the effects of mismodeling upon lunar satellite orbit prediction [NASA-CR-188249] p 3634 N93-29042
Terrain and coverage prediction analyses for non-geostationary orbit EHF satellite communications p 3389 N93-29902
Attitude- and Orbit Control Subsystem concepts for TACSATS p 3284 N93-29906

SATELLITE POWER TRANSMISSION
ASPEC: Solar power satellite p 3233 N93-29750
Power beaming to communication satellites in GEO [DE93-007608] p 3279 N93-29840

SATELLITE ROTATION
Liquid Motion in a rotating tank Experiment (LME) p 3264 N93-28710

SATELLITE TEMPERATURE
LDEF: 69 Months in Space. Second Post-Retrieval Symposium, part 2 [NASA-CP-3194-PT-2] p 3654 N93-29354

SATELLITE TRACKING
Automating the satellite range scheduling process [AD-A262601] p 3270 N93-28468
A satellite-tracking millimeter-wave reflector antenna system for mobile satellite-tracking [NASA-CASE-NPO-18772-1-CU] p 3381 N93-28955

SATELLITE-BORNE INSTRUMENTS
Miniature long-life space cryocoolers p 3378 N93-28825
Ultraviolet imaging spectrometer p 3582 N93-28827
Development of Miniaturized Optimized Smart Sensors (MOSS) for space plasmas p 3286 N93-28828
Project Copernicus: An Earth observing system p 3231 N93-29738

SATELLITE-BORNE RADAR
SAR shape-from-shading for a populated alpine area p 3458 N93-28923

SATELLITES
Beta/gamma Monte Carlo transport in repetitive structures of satellite systems [DE93-007610] p 3281 N93-30509

SCALARS
Non-scalar uncertainty: Uncertainty in dynamic systems p 3517 N93-29565
The ground state wavefunctions of a conformally invariant scalar field in different spacetime background [DE93-606063] p 3606 N93-30808
A simple formula for reducing Feynman diagrams to scalar integrals [DE92-644717] p 3607 N93-30916
Nonlinear realisations of omega(1 + infinity) [DE92-644721] p 3557 N93-30917
Quantum group generalization of the heterotic QFT [DE92-644727] p 3607 N93-30920
On one-dimensional topological and conformal field theories [DE92-644726] p 3558 N93-30986

SCALE EFFECT
Planck scale effects in neutrino physics [DE93-606133] p 3571 N93-30793
Effects of scale in predicting global structural response p 3306 N93-30860
Evaluation of some scale effects in the response and failure of composite beams p 3308 N93-30874

SCALE HEIGHT
ELF propagation highlights p 3395 N93-30730

SCALE MODELS
Lunar regolith densification p 3276 N93-29115
Lunar crane system p 3277 N93-29118
Analysis of mass transport and potential vorticity budget in a simulated tropopause folding [PB93-156792] p 3476 N93-29197
Exploitation of parallelism in climate models [DE93-011259] p 3470 N93-29318
Design, building, and testing of the postlanding systems for the assured crew return vehicle p 3229 N93-29726
Construction, wind tunnel testing and data analysis for a 1/5 scale ultra-light wing model p 3243 N93-29778
Evaluation of some scale effects in the response and failure of composite beams p 3308 N93-30874

SCALING LAWS
Some aspects of the aeroacoustics of high-speed jets [NASA-CR-191458] p 3418 N93-28975
Optimization of HPM device parameters for maximum air transmission [DE93-007332] p 3386 N93-29765
Catastrophic collisions: Laboratory impact experiments, hydrocode simulations, and the scaling problem p 3635 N93-30411

SCALLOPING
Microwave emission from relativistic electron beams [AD-A264102] p 3400 N93-30880

SCANNERS
Measurement of a Michelson interferometer mirror velocity with a time interval analyzer [AD-A263009] p 3430 N93-28659
Scanning probe lithography. Part 1: Scanning tunneling microscope-induced lithography of self-assembled n-alkanethiol monolayer resists [AD-A263130] p 3432 N93-29476

SCANNING ELECTRON MICROSCOPY
Scanning probe lithography. Part 1: Scanning tunneling microscope-induced lithography of self-assembled n-alkanethiol monolayer resists [AD-A263130] p 3432 N93-29476

SCANNING TUNNELING MICROSCOPY
Surface diffusion: Atomistics and surface morphology (summary of MRS Symposium B panel discussion) [DE93-009862] p 3594 N93-29188
Electric field induced phenomena in STM: Tip deformations and Au(111)-surface phase transitions during tunneling spectroscopy experiments [AD-A262208] p 3596 N93-29445
Scanning probe lithography. Part 1: Scanning tunneling microscope-induced lithography of self-assembled n-alkanethiol monolayer resists [AD-A263130] p 3432 N93-29476
Fundamental studies of friction, lubrication, and wear by atomic force microscopy [AD-A264647] p 3446 N93-30524

SCATHA SATELLITE
Spacecraft surface charging handbook [AD-A262778] p 3279 N93-29305

SCATTER PROPAGATION
Scattering through apertures and by three-dimensional structures. Application to the measurement of the surface impedance of conductive materials [ONERA-P-1990-2] p 3392 N93-30018
Performance statistics bulletin. High latitude meteor scatter propagation, May, June, July 1989 [AD-A264003] p 3399 N93-30757

SCATTERING
Comparison of analytical transport and stochastic solutions for neutron slowing down in an infinite medium [DE93-010799] p 3565 N93-28833
Method and apparatus for imaging an object in or through a scattering medium by using multiple-wave mixing [AD-D015707] p 3581 N93-30410
Algorithm of numerical calculations of differential Yakubovsky equations for the (1 + 3) scattering problem [DE92-644679] p 3535 N93-30915
Low-energy behaviour of few-particle scattering amplitudes in two dimensions [DE93-609834] p 3572 N93-30944

SCATTERING AMPLITUDE
Spin observables in large t elastic N-N scattering
[DE93-009211] p 3564 N93-28549
Coupled-channel analysis of low energy nucleon-antinucleon interactions
[DE93-606115] p 3571 N93-30791
Low-energy behaviour of few-particle scattering amplitudes in two dimensions
[DE93-609834] p 3572 N93-30944

SCATTERING CROSS SECTIONS
Exotic atoms
[DE93-010242] p 3564 N93-28611
Measurement of W-Z interference from neutrino-electron scattering
[DE93-010724] p 3566 N93-29313
Electron interactions with non-linear polyatomic molecules and their radicals and ions
[AD-A262279] p 3568 N93-29446
Unitary approximation of Bhabha diffusion by high energies and its implementation in Monte Carlo event generators
[ETN-93-93622] p 3571 N93-30670
Baryon number violation and particle collider experiments
[NIKHEF-H/92-14] p 3572 N93-31008

SCENE ANALYSIS
Multisensor image analysis system
[AD-A263679] p 3528 N93-29294
Encoding spatial images: A fuzzy set theory approach
p 3511 N93-29527
Binocular spherical disparity: A study in representation for a forward translating camera
[PB93-184422] p 3579 N93-29667

SCHEDULES
A perspective on acquisition of NASA space systems
[AD-A263246] p 3610 N93-29499
Designing a fuzzy scheduler for hard real-time systems p 3512 N93-29537
Payload flight assignments. NASA mixed fleet
[NASA-TM-108255] p 3268 N93-30133
A representative survey of US space systems and methods for estimating their costs
[AD-A264159] p 3272 N93-30881

SCHEDULING
Automating the satellite range scheduling process
[AD-A262601] p 3270 N93-28468
Preemptive scheduling with variable profile, precedence constraints and due dates
[INRIA-RR-1622] p 3538 N93-28937
Designing a fuzzy scheduler for hard real-time systems p 3512 N93-29537
Assessment of Columbus payload operations capabilities by scheduling with the MARS system
[ESA-STR-235] p 3281 N93-30106
Analytical foundations of gain scheduling
[AD-A264682] p 3260 N93-30550

SCHLIEREN PHOTOGRAPHY
Application of Schlieren optical techniques for the measurement of gas temperature and turbulent diffusivity in a diesel engine
[AD-A263810] p 3580 N93-29880

SCHOOLS
Proposal to develop guides for high school teachers on global systems science
[DE93-008759] p 3624 N93-29100
Advanced network technology: Background paper
[OTA-BP-TCT-101] p 3539 N93-29650
Filling the gaps: An overview of data on education in grades K through 12
[PB93-176550] p 3608 N93-30821

SCHROEDINGER EQUATION
The semiclassical stability of de Sitter spacetime
[DESY-92-131] p 3603 N93-28472
On the method of determining relations
[DE93-606041] p 3551 N93-30765
Quantum-kinetic Green function and macroscopic wave function
[DE93-606040] p 3606 N93-30796
On two-dimensional quasiclassics
[DE93-606034] p 3606 N93-30805
The ground state wavefunctions of a conformally invariant scalar field in different spacetime background
[DE93-606063] p 3606 N93-30808
On the invariant measure for the nonlinear Schroedinger equation
[DE92-644672] p 3551 N93-30912
General method for reducing the two-body Dirac equation
[DE93-609833] p 3607 N93-30943
A squeezed state holomorphic phase space representation of equations of motion
[DE93-609835] p 3607 N93-30945
A remark on the invariant measure for the nonlinear Schroedinger equation
[DE93-609840] p 3552 N93-30946
Schroedinger equations of higher (greater than 2) order
[DE92-644677] p 3552 N93-30984
Formulation of wave mechanics without the Planck constant h/2 pi
[DE93-604083] p 3608 N93-30987

SCIENTIFIC SATELLITES
Measurements of magnetic fields produced by a 30 kWe class Arcjet Power Conditioning Unit
[AD-A262786] p 3287 N93-28658
FNAS CRRES program completion
[NASA-CR-192468] p 3476 N93-29032
A program to determine the pointing angle to a specular point
[AD-A262777] p 3630 N93-29460

SCIENTISTS
NASA/DOD Aerospace Knowledge Diffusion Research Project. Paper 28: The technical communication practices of Russian and US aerospace engineers and scientists
[NASA-TM-108249] p 3612 N93-28948
Technology transfer personnel exchange at the Boeing Company
[DE93-010190] p 3625 N93-29329
Advanced network technology: Background paper
[OTA-BP-TCT-101] p 3539 N93-29650

SCINTILLATION
Ionospheric structure specifications and systems effects
[AD-A263573] p 3476 N93-29343
Comparison of diversity combining, interleaving, and decoding techniques of a scintillated channel
p 3362 N93-30266

SCINTILLATION COUNTERS
Construction and testing of a neutron and gamma spectrometry system using pulse shape discrimination with an organic scintillator
[AD-A262550] p 3567 N93-29415
Reaction mechanism studies of heavy ion induced nuclear reactions
[DE93-010496] p 3569 N93-29807
Pion pair production in photon-photon collisions
[DE93-606114] p 3571 N93-30790

SCRAP
Tool grinding and spark testing p 3291 N93-30954

SCREWS
Spline screw autochanger
[NASA-CASE-GSC-13435-1] p 3445 N93-29505

SEA ICE
Leadex data report. Part 2: Rawinsonde and ice station data
[AD-A263218] p 3483 N93-29491
Ice-ocean four dimensional structure and dynamics
[AD-A264850] p 3490 N93-30906

SEA LEVEL
Field trial of caffeine on physical performance at altitude: An attempt to overcome the challenge
[AD-A264260] p 3497 N93-30894

SEA SURFACE TEMPERATURE
Sensitivity study of cloud/radiation interaction using a second order turbulence radiative-convective model
[DE93-007365] p 3477 N93-29346

SEA WATER
Method of emitting on a specific wavelength fraunhofer line using a neodymium doped laser transmitter
[AD-D015710] p 3437 N93-29276
Acoustic transducer system
[AD-D015713] p 3562 N93-29279
A water mass analysis of the 1991-1992 El Nino signal in the Farallon Islands region
[AD-A263490] p 3488 N93-29819
Marine microbial production of dimethylsulfide from dissolved dimethylsulfoniopropionate
[NASA-CR-193278] p 3492 N93-30665
Comparative study of undersea fields produced by various dipoles p 3397 N93-30740

SEALERS
Compatibility studies of AISI type 316 stainless steel with lead-lithium eutectic alloy
[DE93-605281] p 3328 N93-31022

SEALS (STOPPERS)
Postflight hardware evaluation 360T025 (RSRM-25, STS-46). Appendix B: Case, seals, and joints PFORs
[NASA-CR-192564] p 3272 N93-30619

SEAS
Ocean Margins Program
[DE93-008937] p 3470 N93-29262

SEASONS
VLF/LF propagation measurements
p 3395 N93-30732

SECONDARY ION MASS SPECTROMETRY
Scanning ionic microscopy with high spatial resolution: Parallel acquisition of elementary images by high resolution mass spectrometry
[ONERA-NT-1990-7] p 3314 N93-30139

SECURITY
Security classification of information
[DE93-012416] p 3612 N93-28840
Activities report of PTT Research
[ISBN-9-07-212514-2] p 3392 N93-30025
Security of the remote control link of Anik E satellites
p 3365 N93-30282

SEDIMENT TRANSPORT
IOC-UNEP review meeting on oceanographic processes of transport and distribution of pollutants in the sea
[DE93-605070] p 3490 N93-31019

SEEDS
Final results of space exposed experiment developed for students p 3492 N93-29702
Continued results of the seeds in space experiment
p 3492 N93-29703

SEISMIC WAVES
Modern seismic travel time tables and station corrections for P and S waves
[AD-A262536] p 3477 N93-29412
Modeling earthquakes with local and regional broadband data p 3478 N93-30005
Modeling regional seismic waves
[AD-A264002] p 3479 N93-30756

SEISMOGRAPHS
A microseismometer for terrestrial and extraterrestrial applications p 3434 N93-28765
Optimism experiment and development of space-qualified seismometers in France
p 3646 N93-28796
The MESUR mission p 3649 N93-28816
Venus Interior Structure Mission (VISM): Establishing a seismic network on Venus p 3649 N93-28819

SEISMOLOGY
A microseismometer for terrestrial and extraterrestrial applications p 3434 N93-28765
Venus Interior Structure Mission (VISM): Establishing a seismic network on Venus p 3649 N93-28819
Modern seismic travel time tables and station corrections for P and S waves
[AD-A262536] p 3477 N93-29412

SELECTION
An experimental methodology for a fuzzy set preference model p 3514 N93-29547
A fuzzy case based reasoning tool for model based approach to rocket engine health monitoring
p 3289 N93-29570

SELF CONSISTENT FIELDS
Adsorption of sulfate on metal electrodes
[AD-A263192] p 3309 N93-28540
The global potential energy surfaces of the lowest two 1A-prime states of the ozone molecule: Theoretical determination and analysis
[DE93-007537] p 3313 N93-29837
Theoretical studies in nuclear structure
[DE93-012290] p 3570 N93-30505

SELF ERECTING DEVICES
In-step inflatable antenna experiment
p 3263 N93-28701

SELF ORGANIZING SYSTEMS
Adding dynamic rules to self-organizing fuzzy systems
p 3515 N93-29557
A conjugate gradients/trust regions algorithms for training multilayer perceptrons for nonlinear mapping
p 3519 N93-29581
Evolving neural network architecture
[AD-A264802] p 3544 N93-30592

SELF TESTS
Fault tolerance and testing for WSI systems
p 3361 N93-30258

SEMANTICS
Formal definition of a conceptual language for the description and manipulation of information models
[TR-92-16] p 3523 N93-28503
Nets of reactive processes
[INRIA-RR-1588] p 3537 N93-28505
Implementing error-valued semantics for dataflow languages on imperative machines
[DE93-009319] p 3615 N93-29310
Information compression in the context model
p 3514 N93-29549
A functional implementation of the Jacobi eigen-solver
[DE93-007349] p 3549 N93-29769
Full abstraction for a shared variable parallel language
[AD-A263547] p 3530 N93-29821
Turning SOS rules into equations
[CWI-CS-R9218] p 3532 N93-30017

SEMICONDUCTOR DEVICES
Analysis of electrothermal interactions in power semiconductor modules
[ETN-93-93800] p 3591 N93-28470
Optically controlled solid state opening switches
[AD-A262404] p 3591 N93-28496
Excited states in electronic structure calculations
[DE93-007704] p 3592 N93-28642

Semiconductor cooling apparatus [NASA-CASE-LEW-14162-3] p 3299 N93-29614
Simulation of transient radiation effects on semiconductor devices using a pulsed Q-switched Nd:YAG laser p 3357 N93-30230
NATO Advanced Research Workshop on Frontiers of Optical Phenomena in Semiconductor Structure of Reduced Dimension [AD-A264813] p 3581 N93-30666
Heat generation produced in thin layers of GaAs superconductors under high energy particles irradiation [DE93-606332] p 3601 N93-30798
Laboratory experiments in integrated circuit fabrication p 3292 N93-30962

SEMICONDUCTOR DIODES
The 2-6 semiconductor superlattices [AD-A264343] p 3597 N93-30164
Analytical predictions of the intermodulation noise of semiconductor laser diode p 3361 N93-30256

SEMICONDUCTOR JUNCTIONS
Ultrafast optical studies of surface reaction processes at semiconductor interfaces [DE93-009049] p 3593 N93-29096

SEMICONDUCTOR LASERS
Influence of optical feedback on the pulse behavior of semiconductor lasers [ETN-93-93798] p 3436 N93-28614
ND laser with co-doped ion(s) pumped by visible laser diodes [AD-D015711] p 3437 N93-29277
Fiber-optic currents measurements [DE93-007970] p 3579 N93-29350
The 2-6 semiconductor superlattices [AD-A264343] p 3597 N93-30164
Analytical predictions of the intermodulation noise of semiconductor laser diode p 3361 N93-30256

SEMICONDUCTORS (MATERIALS)
Excited states in electronic structure calculations [DE93-007704] p 3592 N93-28642
Planning of a West Virginia University Research Center in the basic materials sciences [DE93-011731] p 3592 N93-28647
Infrared rugates by molecular beam epitaxy p 3582 N93-28808
Subnanosecond high power performance of a bistable optically-controlled GaAs switch [DE93-006285] p 3406 N93-28944
New III-V cell design approaches for very high efficiency [DE93-000097] p 3464 N93-28971
Electrochemical fabrication of cadmium chalcogenide microdiode arrays [AD-A263169] p 3310 N93-28988
Ultrafast optical studies of surface reaction processes at semiconductor interfaces [DE93-009049] p 3593 N93-29096
Femtosecond carrier processes in compound semiconductors and real time signal processing [AD-A263076] p 3382 N93-29131
New Mexico Center for Particle Physics: Studies of fundamental interactions [DE93-008302] p 3566 N93-29261
Low temperature (LT) GaAs and related materials [AD-A263607] p 3298 N93-29282
Femtosecond carrier processes in compound semiconductors and real time signal processing [AD-A262966] p 3384 N93-29514
Proceedings of Symposium F on New Aspects on the Growth, Characterization and Applications of CdTe and related Cd rich alloys 5, 1992 [AD-A263541] p 3597 N93-29974
Nonequilibrium screening and exciton dynamics probed by femtosecond laser pulses [AD-A263603] p 3439 N93-29983
Fundamental studies of the morphology, chemistry, and electrical properties of metals on GaAs and other III-V semiconductor compounds [AD-A264417] p 3597 N93-30120
The 2-6 semiconductor superlattices [AD-A264343] p 3597 N93-30164
Synthesis and characterization of mixed 3-5 and 2-6 semiconductor monomers included in the borate sodalite analogue [AD-A264523] p 3598 N93-30407
Fundamental studies of the mechanical behavior of microelectronics thin film materials [AD-A264334] p 3337 N93-30417
Infrared imaging array integrated in three dimensions directly on top of silicon circuits [AD-A264707] p 3581 N93-30500
Atomic layer epitaxy of semiconductor heterostructures [AD-A264755] p 3599 N93-30560
Study on diamond semiconductor [DE92-531076] p 3413 N93-30622
NATO Advanced Research Workshop on Frontiers of Optical Phenomena in Semiconductor Structure of Reduced Dimension [AD-A264813] p 3581 N93-30666
Ultrafast, passive, broad-band, optical shutter based on novel semiconductor/conducting polymer interfaces [AD-A264098] p 3601 N93-30878

SENSITIVITY
Optimism experiment and development of space-qualified seismometers in France p 3646 N93-28796
Composite laminate stiffnesses and their sensitivities [DLR-FB-92-16] p 3296 N93-29007
Sensitivity study of cloud/radiation interaction using a second order turbulence radiative-convective model [DE93-007365] p 3477 N93-29346
A steric hindrance model for the crystal orientation dependence of the shock initiation sensitivity of PETN explosive [LA-UR-92-1427] p 3345 N93-30074
Sensitive detection of new superconductors created at ultra high pressures [AD-A264340] p 3597 N93-30161

SENSORIMOTOR PERFORMANCE
Human capabilities and limitations in situation awareness p 3503 N93-28863
Cognitive and Neural Sciences Division 1992 programs [AD-A263400] p 3654 N93-29258

SENSORS
The dynamic behavior of constrained adaptive array sensor processors [AD-A262402] p 3541 N93-28494
Development of Miniaturized Optimized Smart Sensors (MOSS) for space plasmas p 3286 N93-28828
Progress in the development of broadband electric-field sensors for transient fields p 3369 N93-30306

SENSORY PERCEPTION
Cognitive and Neural Sciences Division 1992 programs [AD-A263400] p 3654 N93-29258

SEPARATED FLOW
Direct numerical simulations of unsteady separated flows using vortex methods p 3419 N93-29077
An experimental study of flow over a 6 to 1 prolate spheroid at incidence p 3239 N93-29124
The 3-D viscous flow CFD analysis of the propeller effect on an advanced ducted propeller subsonic inlet [NASA-TM-106240] p 3252 N93-29162
A theoretical and computational study on active wake control p 3243 N93-30892

SEPARATION
Process for selectively recovering algae and protozoa [NASA-CASE-MFS-26124-1-NPO] p 3491 N93-29174

SEPARATORS
Combined centrifugal force/gravity gas/liquid separator system [AD-D015726] p 3444 N93-29288

SEQUENCING
Uncorrectable sequences and telecommand p 3385 N93-29596
NESL: A nested data-parallel language (Version 2.6) [AD-A263548] p 3530 N93-29822
Computer assisted multiplex sequencing [DE93-007144] p 3536 N93-30934

SEQUENTIAL COMPUTERS
Neural network simulations on massively parallel computers: Applications in chemical physics [DE93-006739] p 3538 N93-28894

SEROTONIN
Molecular approach to hypothalamic rhythms [AD-A264438] p 3496 N93-30421

SERUMS
Amino acid sequences for the binding regions in serum albumin proteins [NASA-CASE-MFS-28402-1] p 3491 N93-28952

SERVICE LIFE
Sodium sulfur technology program NaSTEC p 3265 N93-28718
Approach to extending the cycle life of lithium secondary battery [DE93-776266] p 3406 N93-28983
Polymer electrolyte fuel cells for transportation applications [DE93-008721] p 3464 N93-29147
APU diaphragm testing [NASA-TM-108254] p 3272 N93-29501
Power beaming to communication satellites in GEO [DE93-007608] p 3279 N93-29840
Direct use geothermal applications for brazed plate heat exchangers [DE93-008559] p 3465 N93-30011

SERVICES
SESC products and services user guide [PB93-178879] p 3653 N93-29679

SERVOMECHANISMS
Measurement of a Michelson interferometer mirror velocity with a time interval analyzer [AD-A263009] p 3430 N93-28659
Leaky coaxial cable signal transmission for remote facilities [DE93-007916] p 3383 N93-29348

SERVOMOTORS
Study on decreasing torque noise resulting from feedback noise for the modified bang-bang controller [AD-A263178] p 3407 N93-29010

SET THEORY
Handshake circuits: An intermediary between communicating processes and VLSI [ETN-93-93579] p 3408 N93-29269
North American Fuzzy Logic Processing Society (NAFIPS 1992), volume 1 [NASA-CP-10112-VOL-1] p 3509 N93-29516
An analysis of possible applications of fuzzy set theory to the actuarial credibility theory p 3510 N93-29517
Estimations of expectedness and potential surprise in possibility theory p 3510 N93-29518
Comparison of specificity and information for fuzzy domains p 3510 N93-29519
Encoding spatial images: A fuzzy set theory approach p 3511 N93-29527
North American Fuzzy Logic Processing Society (NAFIPS 1992), volume 2 [NASA-CP-10112-VOL-2] p 3515 N93-29556
On probability-possibility transformations p 3519 N93-29582
Modeling the bidirectional reflectance and spectra [AD-A263570] p 3462 N93-29830

SETTLING
Macrostatistical hydrodynamics [DE93-012289] p 3417 N93-28751

SEWING
Development of stitching reinforcement for transport wing panels p 3304 N93-30852

SEYFERT GALAXIES
Infrared spectroscopy and imaging of starburst galaxies and AGNs [MPE-PREPRINT-229] p 3632 N93-30643

SHADOWS
A note on the computation of antenna-blocking shadows p 3385 N93-29593

SHAFTS (MACHINE ELEMENTS)
Durability of Quick Reaction Satellite Antenna (QRSA) trunnion castings [AD-A264095] p 3281 N93-30813

SHALLOW WATER
Ocean waves in SAMSON/SWADE [AD-A263681] p 3487 N93-29295
Finite element approximation of the shallow water equations on the MASPAR [AD-A264649] p 3489 N93-30525
ELF propagation in deep and shallow sea water p 3397 N93-30739

SHAPE MEMORY ALLOYS
A one-dimensional continuum model for shape-memory alloys [AD-A262505] p 3321 N93-28656
Nonlinear analyses of composite aerospace structures in sonic fatigue [NASA-CR-193124] p 3451 N93-29154
Articulated fin/wing control system [AD-D015712] p 3259 N93-29278

SHAPES
Three dimensional reconstruction of complex shapes based on the Delaunay triangulation [INRIA-RR-1697] p 3547 N93-28616
Experimental and modal verification of an integral equation solution for a thin-walled dichroic plate with cross-shaped holes p 3385 N93-29591
Methods for characterizing the human head for the design of helmets [AD-A263875] p 3507 N93-29889
Representations of shape in object recognition and long-term visual memory [AD-A264342] p 3499 N93-30163

SHEAR FLOW
Vertical slot convection: A linear study [DE93-007643] p 3423 N93-29804

SHEAR LAYERS
The development of a mixing layer under the action of weak streamwise vortices [NASA-TM-106089] p 3418 N93-28947
Shear, strain, and thermohaline vertical fine structure in the upper ocean p 3488 N93-30046
A theoretical and computational study on active wake control p 3243 N93-30892

SHEAR STRAIN
Enhanced noncontacting laser extensometer for biaxial strain measurements [AD-A263170] p 3430 N93-28989

SHEAR STRESS

Mechanics of elevated temperature fatigue damage in fiber-reinforced ceramics [AD-A262403] p 3329 N93-28495

Influence of ply waviness on stiffness and strength reduction of composite laminates [AD-A263224] p 3294 N93-28559

Shear sensitive monomer-polymer laminate structure and method of using same [NASA-CASE-LAR-14654-1-CU] p 3452 N93-29613

Surface shear stress estimates from geostrophic winds for use in sensible and latent heat flux formulations p 3483 N93-30044

Laboratory studies of gravity wave/mean flow interactions [AD-A264226] p 3478 N93-30174

Compressible turbulence in a high-speed high Reynolds number mixing layer p 3242 N93-30583

Tensile study of single-crystal ternary L1(2) trialuminide Al66Ti25Mn(sub g) [AD-A264297] p 3601 N93-30819

Prediction of stiffener-skin separation in composite panels p 3307 N93-30871

Structural response of bead-stiffened thermoplastic shear webs p 3308 N93-30873

SHEARING

Preliminary experimental results for a cryogenic brush seal configuration [NASA-TM-106236] p 3416 N93-28627

SHIPS

A comparison of simulated parallax and single-station range aids to navigation [AD-A263460] p 3246 N93-29818

SHOCK FRONTS

Large eddy simulations of shockwave passage through turbulence [DE92-019503] p 3419 N93-29050

Detonation shock dynamics of composite energetic materials p 3350 N93-30096

SHOCK LOADS

Examination of shock induced chemical reactions in liquids using time-resolved optical spectroscopy p 3318 N93-30073

A steric hindrance model for the crystal orientation dependence of the shock initiation sensitivity of PETN explosive [LA-UR-92-1427] p 3345 N93-30074

Microstructural basis for enhanced shock-induced chemistry in single crystals of ammonium perchlorate p 3319 N93-30092

Comparison of deformation and shock reactivity for single crystals of RDX and ammonium perchlorate p 3350 N93-30094

Detonation shock dynamics of composite energetic materials p 3350 N93-30096

Isothermal and shock compression of high density ammonium nitrate and ammonium perchlorate [DE93-000682] p 3315 N93-30209

SHOCK RESISTANCE

Testing in combined dynamic environments [DE93-010679] p 3278 N93-29250

SHOCK SIMULATORS

Subjective response to simulated sonic booms with ground reflections [NASA-TM-107764] p 3561 N93-28692

SHOCK SPECTRA

Characterizing transient vibrations using band limited temporal moments [DE93-009639] p 3453 N93-30185

SHOCK TESTS

Errors when shock waves interact due to numerical shock width [DE93-010699] p 3426 N93-30484

Towards a better hydro for dynamic mix calculations [DE93-010702] p 3426 N93-30485

SHOCK TUBES

Experimental study of instability growth patterns of a shock-accelerated, thin fluid layer [DE93-010741] p 3421 N93-29253

Thermal oxidation of HCN by NO2 in shock waves p 3318 N93-30064

Towards a better hydro for dynamic mix calculations [DE93-010702] p 3426 N93-30485

SHOCK TUNNELS

Mitigation of shock waves in a cylindrical tunnel by foam [AD-A262491] p 3423 N93-29419

SHOCK WAVE INTERACTION

Large eddy simulations of shockwave passage through turbulence [DE92-019503] p 3419 N93-29050

Non-linear wave phenomena in a gas-vapour mixture with phase transition [ETN-93-93582] p 3422 N93-29319

Errors when shock waves interact due to numerical shock width [DE93-010699] p 3426 N93-30484

SHOCK WAVE PROPAGATION

Some aspects of the aeroacoustics of high-speed jets [NASA-CR-191458] p 3418 N93-28975

Shock waves and polymorphic phase transitions in energetic materials p 3351 N93-30100

SHOCK WAVES

International aviation (Selected articles) [AD-A262566] p 3227 N93-28576

Analysis of unsteady wave processes in a rotating channel [NASA-CR-191154] p 3251 N93-28617

Nonlinear stability of viscous shock waves [TRITA-NA-9205] p 3419 N93-29025

Implementation of a single-material version of PAGOSA on MIMD hypercubes [SAND-92-0640] p 3526 N93-29127

Experimental study of instability growth patterns of a shock-accelerated, thin fluid layer [DE93-010741] p 3421 N93-29253

Kinetics and energy transfer in nonequilibrium fluid flows [AD-A263612] p 3240 N93-29284

Response of energetic solids to light, heat and shock pulses [AD-A263702] p 3342 N93-29296

Kinetics of nitric oxide formation behind 3 to 4 KM/S shock waves [AD-A263653] p 3312 N93-29389

Mitigation of shock waves in a cylindrical tunnel by foam [AD-A262491] p 3423 N93-29419

Thermal oxidation of HCN by NO2 in shock waves p 3318 N93-30064

Chemical dynamics simulations as a probe to the initiation and propagation of condensed phase detonations p 3318 N93-30071

Shock waves and polymorphic phase transitions in energetic materials p 3351 N93-30100

Contribution to the study of the interaction between acoustic waves and coherent structures induced by a prismatic cylinder in a rectangular cavity [ONERA-NT-1990-10] p 3314 N93-30203

Errors when shock waves interact due to numerical shock width [DE93-010699] p 3426 N93-30484

Towards a better hydro for dynamic mix calculations [DE93-010702] p 3426 N93-30485

Near-infrared line imaging of NGC 6240: Global shock and nuclear starburst [MPE-PREPRINT-226] p 3631 N93-30641

SHORELINES

Building alliances to restore coastal environments: A coastal America progress report [PB93-169464] p 3470 N93-29674

SHORT TAKEOFF AIRCRAFT

Evaluation of four advanced nozzle concepts for short takeoff and landing performance [NASA-TP-3314] p 3239 N93-29165

SHROUDED PROPELLERS

The 3-D viscous flow CFD analysis of the propeller effect on an advanced ducted propeller subsonic inlet [NASA-TM-106240] p 3252 N93-29162

SHUTTERS

Ultrafast, passive, broad-band, optical shutter based on novel semiconductor/conducting polymer interfaces [AD-A264098] p 3601 N93-30878

SHUTTLE DERIVED VEHICLES

Minimum Hamiltonian ascent trajectory evaluation (MASTRE) program (update to automatic flight trajectory design, performance prediction, and vehicle sizing for support of shuttle and shuttle derived vehicles) users manual [NASA-CR-192556] p 3269 N93-28558

SIDEBANDS

Nonlinear mode coupling in free electron lasers [AD-A263999] p 3439 N93-29883

SIGNAL ANALYSIS

A compact imaging detector of polarization and spectral content p 3582 N93-28810

Wavelet transform techniques and signal analysis [DE93-007919] p 3382 N93-29244

The use of data turning in airborne radars p 3358 N93-30241

Classification of radar clutter in an air traffic control environment p 3246 N93-30299

Analysis and computation for vortex dynamics and rarefied gases [AD-A264705] p 3427 N93-30499

Independent research and independent exploratory development programs [AD-A264735] p 3544 N93-30556

SIGNAL ANALYZERS

Digital hardware architecture implementation [AD-A263219] p 3521 N93-29492

Acoustic charge transport technology investigation for advanced development transponder p 3386 N93-29602

SIGNAL DETECTION

Multichannel detection of partially correlated signals in clutter [AD-A261984] p 3381 N93-28998

Improved bounds for synchronization jitter p 3360 N93-30251

SIGNAL DETECTORS

Inservice diagnostic methods for solenoid-operated valves [DE93-007823] p 3443 N93-28968

SIGNAL DISTORTION

Effects of imbalances and DC offsets on I/Q demodulation [AD-A264466] p 3393 N93-30537

SIGNAL ENCODING

Uncorrectable sequences and telecommand p 3385 N93-29596

On subband coding/embedded vector quantization for speech coding p 3355 N93-30220

A systolic-array structure for MTCM receivers p 3357 N93-30236

An error control protocol based on trellis coded modulations p 3358 N93-30237

SIGNAL FADING

Dipolar orientational relaxation in guest/host amorphous polymer probed by second harmonic generation [AD-A262006] p 3333 N93-29441

Propagation channel modeling for angle-diversity combining simulation p 3360 N93-30252

Performance of frequency hopped M-ary FSK in Rayleigh fading and partial-band jamming p 3368 N93-30303

An adaptive maximum likelihood receiver for correlated Rayleigh fading channels p 3371 N93-30316

SIGNAL GENERATORS

Upgrading the LAMPF 201 MHz RF generators [DE93-010715] p 3406 N93-28830

High-resolution signal synthesis for time-frequency distributions [DE93-008735] p 3380 N93-28909

Advanced technologies for lightweight EHF tactical communications satellites p 3389 N93-29900

SIGNAL PROCESSING

Electronics research report [AD-A262733] p 3405 N93-28589

Measurement of a Michelson interferometer mirror velocity with a time interval analyzer [AD-A263009] p 3430 N93-28659

Onboard signal processing: Wave of the future for planetary radio science? p 3646 N93-28801

High-resolution signal synthesis for time-frequency distributions [DE93-008735] p 3380 N93-28909

Fundamental study of the signal processing by optics [DE93-776265] p 3577 N93-28982

Modified Acousto-Optic Adaptive Processor (Mod-AOAP) [AD-A261983] p 3381 N93-28997

Fiber grating-based sensing system with interferometric wavelength-shift detection [AD-D015697] p 3577 N93-29038

Femtosecond carrier processes in compound semiconductors and real time signal processing [AD-A263076] p 3382 N93-29131

Wideband propagation measurements for wireless indoor communication [PB93-175123] p 3382 N93-29202

Acoustic transducer system [AD-D015713] p 3562 N93-29279

Theoretical bit error rate performance of the Kalman filter excisor for FM interference [AD-A263018] p 3383 N93-29407

Programmable interactive system for cochlear implant electrode stimulation [AD-A262558] p 3494 N93-29421

Digital hardware architecture implementation [AD-A263219] p 3521 N93-29492

Femtosecond carrier processes in compound semiconductors and real time signal processing [AD-A262966] p 3384 N93-29514

Performance analysis of subspace methods [AD-A263984] p 3530 N93-29865

Advanced technologies for lightweight EHF tactical communications satellites p 3389 N93-29900

Synchronization techniques for medium data rate EHF MILSATCOM systems p 3389 N93-29901

ARSRP signal processing software [AD-A263543] p 3391 N93-29975

Photorefractive integrators and correlators [AD-A264200] p 3597 N93-30144

Electro-optic characterisation of extremely wide bandwidth electrical signals
[AD-A264202] p 3392 N93-30145
Nonlinear processing of phase vocoded speech
p 3355 N93-30219
A systolic-array structure for MTCM receivers
p 3357 N93-30236
Enhanced resolution and de-aliasing techniques for fast Fourier transforms p 3358 N93-30240
The use of data turning in airborne radars
p 3358 N93-30241
Synchronization of the LAPTV adative filter with input statistics p 3358 N93-30242
Radar beam effects for a flight simulator using signal processor based hardware p 3373 N93-30328
Signal processor based MSAT trellis coded M-DPSK with adaptive Doppler phasor correction
p 3373 N93-30332
Multiscale and multigrid information representation, extraction and fusion
[AD-A264623] p 3393 N93-30386
Analysis and computation for vortex dynamics and rarefied gases
[AD-A264705] p 3427 N93-30499
Adaptive airborne radar simulation with equalization filter taps
[AD-A264722] p 3393 N93-30514
Effects of imbalances and DC offsets on I/Q demodulation
[AD-A264466] p 3393 N93-30537
Enhanced photorefractive effects in barium titanate
[AD-A264724] p 3599 N93-30554
Multiple neuron recording in the hippocampus of freely moving animals
[AD-A264807] p 3492 N93-30594
The use of DFT windows in signal-to-noise ratio and harmonic distortion computations
[DE93-009800] p 3433 N93-30655
Application of non-standard signal processing to ELF noise characterization for the TSS1-OESEE programme
p 3397 N93-30743
Application of the Fourier transform to short antennas
p 3398 N93-30750
Enhanced convergence adaptive detection
[AD-A264100] p 3399 N93-30879
Massively parallel spatial light modulation-based optical signal processing
[AD-A264846] p 3581 N93-30905

SIGNAL RECEPTION
The dynamic behavior of constrained adaptive array sensor processors
[AD-A262402] p 3541 N93-28494

SIGNAL TO NOISE RATIOS
The HYDICE instrument design and its application to planetary instruments p 3434 N93-28766
Development of a 9.3 micrometer CW LIDAR for the study of atmospheric aerosol
[NASA-CR-193227] p 3381 N93-29105
Signal-to-noise ratio losses in full spectrum combining of signals with a downconverted subcarrier
p 3386 N93-29599
The use of DFT windows in signal-to-noise ratio and harmonic distortion computations
[DE93-009800] p 3433 N93-30655
Reception at Ascension Island, South Atlantic, of the transmissions from the Heard Island feasibility test
[PB93-176261] p 3394 N93-30662
Examinations of perturbation reduction by automatic speech dependent recognition of separately spoken single words
[ETN-93-94180] p 3394 N93-30672
Performance statistics bulletin. High latitude meteor scatter propagation, May, June, July 1989
[AD-A264003] p 3399 N93-30757
Investigation of methods for the measurement of small electron bundle currents
[DIGEL-1992-4] p 3413 N93-30763
Evaluation of the scattered pressure due to infinite rigid cylinders, infinite elastic cylindrical shells, and rigid spheres in the presence of an ambient noise field
[AD-A264835] p 3563 N93-30899
Atmospheric studies with SODAR at Kalpakkam
[DE93-605544] p 3480 N93-30992

SIGNAL TRANSMISSION
Wideband propagation measurements for wireless indoor communication
[PB93-175123] p 3382 N93-29202
Leaky coaxial cable signal transmission for remote facilities
[DE93-007916] p 3383 N93-29348
Feature based neural network acoustic transient signal classification
[AD-A263437] p 3562 N93-29816

SIGNATURES
Subjective response to simulated sonic booms with ground reflections
[NASA-TM-107764] p 3561 N93-28692
A covariant form of the Maxwell's equations in four-dimensional spaces with an arbitrary signature
[DE93-606070] p 3605 N93-30783

SIGNS AND SYMPTOMS
Spurious symptom reduction in fault monitoring
[NASA-CR-191453] p 3542 N93-29192
The Environmental Symptoms Questionnaire (ESQ): Development and application
[AD-A264127] p 3495 N93-30196

SILICIDES
High temperature creep and oxidation resistant chromium silicide matrix alloy containing molybdenum
[NASA-CASE-LEW-15697-1] p 3323 N93-29172
Fundamental studies of the mechanical behavior of microelectronics thin film materials
[AD-A264334] p 3337 N93-30417

SILICON
A microseismometer for terrestrial and extraterrestrial applications p 3434 N93-28765
Silicon crystal under bending
[DE93-010522] p 3593 N93-28888
Instrumental neutron activation analysis developed for silicon integrated circuit technology
[ETN-93-93581] p 3408 N93-29271
The microchannel heatsink with liquid nitrogen cooling
[DE93-009258] p 3422 N93-29300
High-dose implantations of Al into Si(111) and Si(100)
[DE93-009552] p 3594 N93-29301
FI-STM investigation of atomic hydrogen adsorption on the Si(100)2x1 surface
[AD-A262748] p 3567 N93-29403
Design and performance evaluation of a gas chromatograph micromachined in a single crystal silicon substrate
[AD-A262594] p 3596 N93-29424
Infrared imaging array integrated in three dimensions directly on top of silicon circuits
[AD-A264707] p 3581 N93-30500
Surface chemistry of hydrogen-passivated porous silicon-oxidation of surface Si-H groups by acetone
[AD-A264655] p 3315 N93-30526
Silicon Film(trademark) photovoltaic manufacturing technology
[DE93-010008] p 3466 N93-30891
Laboratory experiments in integrated circuit fabrication
p 3292 N93-30962

SILICON ALLOYS
Oxidation behavior in reaction-bonded aluminum-silicon alloy/alumina powder compacts
[DE93-010407] p 3298 N93-29191

SILICON CARBIDES
Catalytic synthesis of silicon carbide preceramic polymers: Polycarbosilanes
[DE93-008634] p 3329 N93-28541
Process optimization of Hexoloy SX-SiC towards improved mechanical properties
[DE93-007913] p 3320 N93-28564
Interfacial studies of refractory glass-ceramic matrix/advanced SiC fiber reinforced composites
[AD-A263264] p 3299 N93-29802
The effect of oxidation embrittlement on the impact behavior of nicalon reinforced CAS 2 ceramic matrix composites
[AD-A263567] p 3334 N93-29829
Air oxidation behavior of fuel for the High Temperature Engineering Test Reactor (HTTR)
[DE93-753349] p 3576 N93-30006
Methylhydridopolysilazane and its pyrolytic conversion to Si3N4/SiC ceramics
[AD-A264150] p 3336 N93-30170
Processing of novel nanoparticle dispersion strengthened ceramics for improved mechanical performance
[AD-A264191] p 3339 N93-30883

SILICON COMPOUNDS
Development of Si(1-x)Ge(x) technology for microwave sensing applications
[NASA-TM-106157] p 3405 N93-28610

SILICON DIOXIDE
Electron transport calculations between 1 MeV and 1 eV
[AD-A263412] p 3568 N93-29787
Decomposition of hydrogen sulfide for small scale gas processing.
[PB93-174704] p 3316 N93-30658

SILICON ISOTOPES
1,2-Dimethyl-1,2-Disila-Closo-Dodecaborane(12), A silicon analog of an ortho-carborane: Synthesis; x ray crystal structure; NMR, vibrational and photoelectron spectra; bonding
[AD-A264709] p 3599 N93-30568

SILICON NITRIDES
Improved silicon nitride for advanced heat engines
[NASA-CR-182193] p 3298 N93-29451
Microwave processing of silicon nitride for advanced gas turbine applications
[DE93-007910] p 3334 N93-29767
Methylhydridopolysilazane and its pyrolytic conversion to Si3N4/SiC ceramics
[AD-A264150] p 3336 N93-30170
Colloid and interface chemistry aspects of ceramics
[AD-A264685] p 3337 N93-30552

SILICONES
Effects of atomic oxygen and ultraviolet radiation on candidate elastomeric materials for long duration missions. Test series no.1
[NASA-TM-108408] p 3331 N93-29193
Post-flight analyses of the crystals from the M0003-14 quartz crystal microbalance experiment
p 3602 N93-29684
SESAME equation of state number 8010: Boron loaded silicone potting material
[DE93-012083] p 3300 N93-30395

SILVER
Diffusion bonding
[DE93-011480] p 3442 N93-28837
Processing and property evaluation of silver or aluminum matrix YBa2Cu3O(6+x) superconducting materials
[AD-A263382] p 3595 N93-29333

SILVER IODIDES
The adhesion of AgI molecules to gaseous metallic silver cluster cations
[AD-A264820] p 3338 N93-30628

SIMD (COMPUTERS)
Implementation of a single-material version of PAGOSA on MIMD hypercubes
[SAND-92-0640] p 3526 N93-29127
The parallel implementation of a backpropagation neural network and its applicability to SPECT image reconstruction
[DE93-010304] p 3567 N93-29416
Special purpose parallel computer architecture for real-time control and simulation in robotic applications
[NASA-CASE-NPO-17629-1-CU] p 3521 N93-29608
Data parallelism
[DE93-009300] p 3539 N93-29782

SIMULATED ANNEALING
Structural design using neural networks
p 3545 N93-31029

SIMULATION
Lunar gravitational field estimation and the effects of mismodeling upon lunar satellite orbit prediction
[NASA-CR-188249] p 3634 N93-29042
Adsorption of hydrated halide ions on charged electrodes: Molecular dynamics simulation
[AD-A263137] p 3568 N93-29619
Space station attitude disturbance arising from internal motions p 3280 N93-29995
Radiated fields from an electromagnetic pulse simulator p 3366 N93-30290
Thermodynamic and structural properties of metallic glasses and supercooled liquids
[ISBN-0-315-72443-9] p 3605 N93-30359
Experimental and analytical investigation of finger-follower cam systems p 3446 N93-30378

SIMULATORS
Building a generalized distributed system model
[NASA-CR-193239] p 3527 N93-29219
Programmable interactive system for cochlear implant electrode stimulation
[AD-A262558] p 3494 N93-29421
Exercise/recreation facility for a lunar or Mars analog
p 3230 N93-29733
A functional implementation of the Jacobi eigen-solver
[DE93-007349] p 3549 N93-29769
Development of a concept formulation process aid for analyzing training requirements and developing training devices
[AD-A263579] p 3261 N93-29972

SINE WAVES
Infrared rugates by molecular beam epitaxy
p 3582 N93-28808
The use of DFT windows in signal-to-noise ratio and harmonic distortion computations
[DE93-009800] p 3433 N93-30655

SINGLE CRYSTALS
Be3(AsO4)2 2H2O: A new berylloarsenate phase containing bridged tetrahedral 3-rings
[AD-A262518] p 3592 N93-28584
Enhancements of the critical currents of YBaCuO single crystals by neutron (n) and proton (p) irradiation
[DE93-007892] p 3592 N93-28661
Environmental embrittlement of binary and Zr-doped Ni3Al
[DE93-008575] p 3321 N93-28679
A microseismometer for terrestrial and extraterrestrial applications p 3434 N93-28765

Growth, characterization and device development in monocrystalline diamond films
[AD-A263204] p 3593 N93-28874
Neutron scattering studies of the structures and lattice dynamics of the alkali metals
[DE93-008272] p 3593 N93-28956
Uniaxially stressed Ge:Ga and Ge:Be
[DE93-010426] p 3594 N93-29150
High-dose implantations of Al into Si(111) and Si(100)
[DE93-009552] p 3594 N93-29301
In-situ x ray studies of the underpotential deposition of copper on platinum (3)
[AD-A263361] p 3595 N93-29331
Design and performance evaluation of a gas chromatograph micromachined in a single crystal silicon substrate
[AD-A262594] p 3596 N93-29424
Balanced technology initiative on computational mechanics of materials
[AD-A263906] p 3453 N93-29863
Improved field emitter current densities and stability through the application of a proprietary process
[AD-A264048] p 3411 N93-30031
Structure, adhesion, and stability of metal/oxide and oxide/oxide interfaces
[DE93-012930] p 3325 N93-30060
Observation of reaction intermediates in crystalline RDX p 3318 N93-30067
Microstructural basis for enhanced shock-induced chemistry in single crystals of ammonium perchlorate
p 3319 N93-30092
Defect density measurements in a shocked single crystal of ammonium perchlorate p 3319 N93-30093
Comparison of deformation and shock reactivity for single crystals of RDX and ammonium perchlorate
p 3350 N93-30094
Sensitive detection of new superconductors created at ultra high pressures
[AD-A264340] p 3597 N93-30161
Center for surface radiation damage studies
[AD-A264330] p 3570 N93-30366
The calculation of electrostatic interactions and their role in determining the energies and geometries of molecular HE crystals
[DE92-040374] p 3570 N93-30448
Photoinduced charge separation in Q1D heterojunction materials: Evidence for electron-hole pair separation in mixed-halide MX solids
[AD-A264711] p 3598 N93-30501
Photoinduced electron-hole charge separation, intrinsic self-doping and novel device applications of Q1D heterojunction materials: Mixed-halide MX solids
[AD-A264714] p 3600 N93-30569
Coordination compounds of aluminum as precursors to aluminum nitride
[AD-A264700] p 3327 N93-30574
Hard photon emission from high energy electrons and positrons in single crystals
[DE93-606328] p 3600 N93-30770
Visible light emitting materials and injection devices
[AD-A263499] p 3601 N93-30811
Tensile study of single-crystal ternary L1(2) trialuminide Al66Ti25Mn(sub g)
[AD-A264297] p 3601 N93-30819
Ultrafast, passive, broad-band, optical shutter based on novel semiconductor/conducting polymer interfaces
[AD-A264098] p 3601 N93-30878
Pulsed laser photoacoustic spectrometer for study of solid materials
[DE93-605290] p 3441 N93-31023

SINGLE EVENT UPSETS
SEU tolerant computer based on the R3000
[DE93-009294] p 3520 N93-29058

SINGLE SIDEBAND TRANSMISSION
Constant Average Power Single Sideband (CAPSSB) modulation p 3373 N93-30331

SINGLE STAGE TO ORBIT VEHICLES
Antares: A low cost modular launch vehicle for the future p 3235 N93-29759

SINTERING
Process optimization of Hexoloy SX-SiC towards improved mechanical properties
[DE93-007913] p 3320 N93-28564
Report on the sintering and properties of MgO and MgO-5 percent TiC
[DE93-008676] p 3323 N93-29092
Microwave processing of ceramics
[DE93-010708] p 3332 N93-29252
Properties of superconducting YBa2Cu3O(6+4) ceramic materials: Effect of processing parameters
[AD-A263441] p 3334 N93-29790
Development of adherent ceramic coatings to reduce contact stress damage of ceramics
[DE93-012518] p 3336 N93-30182
Colloid and interface chemistry aspects of ceramics
[AD-A264685] p 3337 N93-30552
Reactive sintering of Ni3Al intermetallic alloys under compressive stress
[DE93-009729] p 3327 N93-30652
Superconducting films of YBaCuO
[DE93-606831] p 3600 N93-30772
Powder metallurgy: Solid and liquid phase sintering of copper p 3294 N93-30976

SIPHONS
Siphon breaker design requirements
[DE93-011799] p 3425 N93-30132

SIS (SEMICONDUCTORS)
Activities report for the Laboratory for Space Research Groningen (Netherlands)
[ETN-93-93688] p 3631 N93-30638

SISO (CONTROL SYSTEMS)
Stabilization using low-gain PI control: SISO case
[OUEL-1947/92] p 3541 N93-28898

SITE SELECTION
Atmospheric studies with SODAR at Kalpakkam
[DE93-605544] p 3480 N93-30992

SIZE DISTRIBUTION
Elastic and reactive collisions of atoms and molecules with neutral alkali clusters
[DE93-009313] p 3566 N93-29206
Micrometeoroids and debris on LDEF
p 3638 N93-29356

SKIN (STRUCTURAL MEMBER)
Fabrication of the V-22 composite AFT fuselage using automated fiber placement p 3302 N93-30443

SKIN FRICTION
The effect of high temperature on wall shear in a two dimensional wall jet
[AD-A262982] p 3423 N93-29426

SKY SURVEYS (ASTRONOMY)
Magnetic activity in low mass stars
[DE93-009073] p 3632 N93-28547
Digital image compression using artificial neural networks p 3624 N93-28811
The multiplicity of T Tauri stars in the star forming regions Taurus-Auriga and Ophiuchus-Scorpius: A 2.2 micron speckle imaging survey p 3634 N93-28945
Bonner Durchmusterung (Southern Durchmusterung)
[NASA-RP-1298-VOL-3] p 3630 N93-29811
Young open clusters as probes of the star formation process p 3635 N93-30377
The faintest stars p 3630 N93-30493
Dense gas in the monoceros OB1 dark cloud and its relationship to star formation p 3636 N93-30502
A characterization of young stellar objects in Bok globules: Infrared imaging, spectral energy distributions, and molecular outflows p 3636 N93-30563

SLIDING
Determination of low frequency reference slipping for high frequency unstationary motion processes
[ILR-MITT-273(1992)] p 3455 N93-31017

SLIDING FRICTION
Interfacial viscosity measurements of adsorbed monolayers on metal surfaces
[AD-A263288] p 3324 N93-29803

SLOT ANTENNAS
Planar active antennas and quasi-optical power combining arrays using FET's and slots
[AD-A263759] p 3387 N93-29875

SLOTS
Additional support for the TDK/MABL computer program
[NASA-CR-193037] p 3526 N93-29028
Vertical slot convection: A linear study
[DE93-007643] p 3423 N93-29804

SLUDGE
An evaluation of factors affecting the solidification/stabilization of heavy metal sludge
[AD-A264128] p 3473 N93-30197

SLURRIES
Method for producing oxygen from lunar materials
[NASA-CASE-MSC-21759-1] p 3312 N93-29617

SMART STRUCTURES
Smart skin structures for identifying and locating laser irradiation
[DE93-005464] p 3436 N93-28887
Robust control of intelligent rotor
[AD-A263707] p 3259 N93-29985

SMOKE
Preliminary design of an intermittent smoke flow visualization system
[NASA-CR-186027] p 3248 N93-28693
Evaluation of atmospheric wind field and dispersion models for fog-oil smoke dispersion in complex terrain: Field measurement and model evaluation program for assessment of the environmental effects of military smokes
[AD-A262051] p 3482 N93-29399

SNOW
Seasonal snowfall statistics for selected stations
[AD-A263173] p 3481 N93-28991

SOCIAL FACTORS
Multi-Attribute Decision Theory methodology for pollution control measure analysis
[DE93-005444] p 3472 N93-30008

SODALITE
Synthesis and characterization of mixed 3-5 and 2-6 semiconductor monomers included in the borate sodalite analogue
[AD-A264523] p 3598 N93-30407

SODAR
Atmospheric studies with SODAR at Kalpakkam
[DE93-605544] p 3480 N93-30992

SODIUM CHLORIDES
The growth of small corrosion fatigue cracks in alloy 2024
[NASA-TM-107755] p 3451 N93-29069

SODIUM SULFUR BATTERIES
Sodium-Sulfur Cell Technology flight experiment (SSCT) p 3264 N93-28715
Sodium sulfur technology program NaSTEC
p 3265 N93-28718
Battery testing at Argonne National Laboratory
[DE93-009204] p 3407 N93-29036

SOFTENING
A 69 cent look at thermoplastic softening
p 3292 N93-30963

SOFTWARE ENGINEERING
Parallel computation and the basis system
[DE93-008755] p 3537 N93-28544
An assessment of space shuttle flight software development processes
[NASA-CR-193179] p 3525 N93-28934
Concept document of the repository-based software engineering program: A constructive appraisal
[NASA-CR-193125] p 3526 N93-29027
Distributed Virtual System (DIVIRS) Project
[NASA-CR-193234] p 3526 N93-29169
RBSE: Product development team research activity deliverables
[NASA-CR-193115] p 3527 N93-29212
National Center for Supercomputer Applications
p 3614 N93-29232
Development of a visual system interface to support a domain-oriented application composition system
[AD-A262489] p 3528 N93-29418
Software development and analysis for experimental high frequency surface wave radar data
[AD-A261982] p 3383 N93-29438
Learning characteristics of a space-time neural network as a tether skiprope observer p 3512 N93-29534
Synthesis techniques and analysis tools for on-chip fault-tolerance
[AD-A263167] p 3409 N93-29654
Capability maturity model for software, version 1.1
[AD-A263403] p 3530 N93-29852
A guide to total software quality control, volume 1
[AD-A263881] p 3531 N93-29920
A guide to total software quality control, volume 2
[AD-A263891] p 3531 N93-29921
Key practices of the capability maturity model, version 1.1
[AD-A263432] p 3610 N93-29970
Accelerating the transfer of technology for implementing domain specific software architectures
[AD-A264017] p 3532 N93-30014
Estimating Ada system size during development
[AD-A263880] p 3532 N93-30022
Software testing using the IEEE standards
[DE93-009833] p 3532 N93-30050
On analytical performance modelling of software for distributed systems p 3364 N93-30279
Communications systems design for testability: Grey-box testing p 3368 N93-30302
Using Penelope to assess the correctness of NASA Ada software: A demonstration of formal methods as a counterpart to testing
[NASA-CR-4509] p 3533 N93-30380
An approach to software quality prediction from Ada designs
[AD-A264731] p 3534 N93-30547
Nonsmooth optimization algorithms, system theory, and software tools
[AD-A264679] p 3534 N93-30549
An annotated bibliography on integration in software engineering environments
[AD-A264798] p 3535 N93-30602
Gigabit network communications research
[AD-A264895] p 3536 N93-31026

SOFTWARE RELIABILITY
An assessment of space shuttle flight software development processes
[NASA-CR-193179] p 3525 N93-28934
Key practices of the capability maturity model, version 1.1
[AD-A263432] p 3610 N93-29970

Using Penelope to assess the correctness of NASA Ada software: A demonstration of formal methods as a counterpart to testing
[NASA-CR-4509] p 3533 N93-30380
Procedures for applying Ada quality prediction models
[AD-A264730] p 3534 N93-30546
An approach to software quality prediction from Ada designs
[AD-A264731] p 3534 N93-30547

SOFTWARE REUSE
Toward reusable graphics components in Ada
[AD-A262568] p 3524 N93-28577

SOFTWARE TOOLS
A proposed approach for developing next-generation computational electromagnetics software
[DE93-007326] p 3380 N93-28900
Parallel software tools at Langley Research Center
[NASA-TM-108995] p 3520 N93-29070
The scientific modeling assistant: An advanced software tool for scientific model building p 3613 N93-29229
Development of a visual system interface to support a domain-oriented application composition system
[AD-A262489] p 3528 N93-29418
SWAT system performance predictions
[AD-A262857] p 3579 N93-29470
Synthesis techniques and analysis tools for on-chip fault-tolerance
[AD-A263167] p 3409 N93-29654
Data probe user's guide
[PB93-178655] p 3530 N93-29678
Nonsmooth optimization algorithms, system theory, and software tools
[AD-A264679] p 3534 N93-30549
Electronics mixed-mode simulation
[AD-A264734] p 3534 N93-30577
Oceanographic data processing program
[AD-A264801] p 3544 N93-30591
Design and implementation of a Global Positioning System (GPS) supported area navigation system with electronic aircraft
[ILR-MITT-275(1992)] p 3246 N93-30671
Multi-parameter optimization tool for low-cost commercial fuselage crown designs
p 3305 N93-30858
The HSCT mission analysis of waverider designs
[NASA-CR-193467] p 3243 N93-31037

SOHO MISSION
Optical technologies for UV remote sensing instruments p 3582 N93-28788

SOIL MECHANICS
Lunar regolith densification p 3276 N93-29115
Regolith-structure modeling p 3276 N93-29116

SOIL MOISTURE
Mathematical model of frost heave and thaw settlement in pavements
[CRREL-REPT-93-2] p 3262 N93-30103

SOIL SCIENCE
Thermal Analyzer for Planetary Soil (TAPS): An in situ instrument for mineral and volatile-element measurements p 3643 N93-28782
Mathematical model of frost heave and thaw settlement in pavements
[CRREL-REPT-93-2] p 3262 N93-30103
Environmental Monitoring and Assessment Program. EMAP: Arid Colorado plateau pilot study
[PB93-181618] p 3474 N93-30823

SOILS
Contamination of soil, soil gas, and ground water by hydrocarbon compounds near Greear, Morgan County, Kentucky
[PB93-182244] p 3474 N93-30825

SOL-GEL PROCESSES
Thermal properties of organic and modified inorganic aerogels
[DE93-009230] p 3311 N93-29263
Structure and switching dynamics in ferroelectric crystal and liquid crystal thin films
[AD-A263664] p 3594 N93-29293
Materials studies for preventing corrosion in condensing environments
[PB93-185478] p 3327 N93-30815

SOLAR ACTIVITY
The Mechanisms of Solar Variability (MSV) program
[AD-A262525] p 3652 N93-28585
SESC products and services user guide
[PB93-178879] p 3653 N93-29679

SOLAR ARRAYS
Developing an inflatable solar array
p 3264 N93-28714
Solar Array Module Plasma Interaction Experiment (SAMPIE) p 3265 N93-28716
The Photovoltaic Array Space Power Plus diagnostics (PASP Plus) flight experiment p 3265 N93-28717
Solar electric propulsion cargo spacecraft for Mars missions p 3235 N93-29758

SOLAR BLANKETS
Developing an inflatable solar array
p 3264 N93-28714

SOLAR CELLS
Texturing of InP surfaces for device applications
[NASA-TM-106061] p 3321 N93-28618
The Photovoltaic Array Space Power Plus diagnostics (PASP Plus) flight experiment p 3265 N93-28717
New III-V cell design approaches for very high efficiency
[DE93-000097] p 3464 N93-28971
The effect of the low Earth orbit environment on space solar cells: Results of the Advanced Photovoltaic Experiment (S0014) p 3467 N93-29686
LEO effects on candidate solar cell cover materials
p 3467 N93-29687
LDEF Space Plasma-High Voltage Drainage Experiment post-flight results p 3414 N93-29690
Low-cost, high-efficiency solar cells utilizing GaAs-on-Si technology
[DE93-000096] p 3464 N93-29965
Measurements and Characterization Branch
[DE93-000094] p 3465 N93-30207
Growth and development of GaInAsP for use in high-efficiency solar cells
[DE93-000098] p 3465 N93-30208
Change of solar cell element properties influenced by adsorbed atoms
[DE93-606694] p 3466 N93-30777
Silicon Film(trademark) photovoltaic manufacturing technology
[DE93-010008] p 3466 N93-30891

SOLAR COLLECTORS
STRV1-b flight experiment p 3265 N93-28723
Solar energy emplacement developer
p 3230 N93-29732
Modification of flux profiles using a faceted concentrator
[DE93-000087] p 3464 N93-29925
Study of parameters affecting the performance of solar desiccant cooling systems
[DE93-000088] p 3465 N93-30206
Thermal effects testing at the National Solar Thermal Test Facility
[DE93-009825] p 3465 N93-30391

SOLAR COOLING
Study of parameters affecting the performance of solar desiccant cooling systems
[DE93-000088] p 3465 N93-30206

SOLAR CORONA
The Mechanisms of Solar Variability (MSV) program
[AD-A262525] p 3652 N93-28585
Solar flare MDH
[AD-A262275] p 3652 N93-28756
Two-dimensional and three-dimensional time-dependent MHD model of extended corona
p 3653 N93-30496

SOLAR CORPUSCULAR RADIATION
ELF/VLF radio noise measurements at high latitudes during solar particle events p 3397 N93-30744

SOLAR DYNAMIC POWER SYSTEMS
Thermal energy storage flight experiment in microgravity p 3265 N93-28720

SOLAR ELECTRIC PROPULSION
ELITE program: Electric insertion transfer experiment
p 3264 N93-28709
Solar electric propulsion cargo spacecraft for Mars missions p 3235 N93-29758

SOLAR ENERGY
Solar energy emplacement developer
p 3230 N93-29732
Solar world congress: Proceedings of the biennial congress of the international solar energy society, volume 1, part 2
[PB93-174779] p 3465 N93-30001
Solar World Congress: Proceedings of the Biennial Congress of the International Solar Energy Society, volume 2, part 2
[PB93-174795] p 3466 N93-30935

SOLAR ENERGY ABSORBERS
Study of parameters affecting the performance of solar desiccant cooling systems
[DE93-000088] p 3465 N93-30206

SOLAR ENERGY CONVERSION
ASPEC: Solar power satellite p 3233 N93-29750
Low-cost, high-efficiency solar cells utilizing GaAs-on-Si technology
[DE93-000096] p 3464 N93-29965
Solar world congress: Proceedings of the biennial congress of the international solar energy society, volume 1, part 2
[PB93-174779] p 3465 N93-30001
Measurements and Characterization Branch
[DE93-000094] p 3465 N93-30207

SOLAR FLARES
The Mechanisms of Solar Variability (MSV) program
[AD-A262525] p 3652 N93-28585
Solar flare MDH
[AD-A262275] p 3652 N93-28756
ELF/VLF radio noise measurements at high latitudes during solar particle events p 3397 N93-30744

SOLAR FLUX
A study of the physical mechanisms for filament eruption and coronal mass ejection via numerical simulation
[NASA-CR-193180] p 3653 N93-28935
Modification of flux profiles using a faceted concentrator
[DE93-000087] p 3464 N93-29925

SOLAR FURNACES
Modification of flux profiles using a faceted concentrator
[DE93-000087] p 3464 N93-29925
Thermal effects testing at the National Solar Thermal Test Facility
[DE93-009825] p 3465 N93-30391

SOLAR GENERATORS
Technical examination and simulation of a photovoltaic system: Solar generator, battery, download
[ETN-93-94179] p 3466 N93-30573

SOLAR GRAVITATION
The detection of low-degree solar gravity mode oscillations by differential radius observations, 1986-1987 p 3652 N93-28605

SOLAR MAGNETIC FIELD
The Mechanisms of Solar Variability (MSV) program
[AD-A262525] p 3652 N93-28585

SOLAR NEUTRINOS
Neutrino oscillations and a new Faraday effect
[DE93-606111] p 3571 N93-30789
Planck scale effects in neutrino physics
[DE93-606133] p 3571 N93-30793

SOLAR OSCILLATIONS
The detection of low-degree solar gravity mode oscillations by differential radius observations, 1986-1987 p 3652 N93-28605

SOLAR PHYSICS
Space research in Germany 1990-1991
[ETN-93-93807] p 3654 N93-28477
Activities report of the Astronomical Society
[MITT-75] p 3629 N93-29008
NSSDC data listing
[NASA-TM-108264] p 3612 N93-29167

SOLAR POWER SATELLITES
ASPEC: Solar power satellite p 3233 N93-29750

SOLAR POWERED AIRCRAFT
Solar powered multipurpose remotely powered aircraft
p 3229 N93-29722

SOLAR RADIATION
The Mechanisms of Solar Variability (MSV) program
[AD-A262525] p 3652 N93-28585
Method of emitting on a specific wavelength fraunhofer line using a neodymium doped laser transmitter
[AD-D015710] p 3437 N93-29276
Clouds and radiation: A primier
[AD-A263136] p 3482 N93-29479
Daily sum of the global radiation: Calculation method and verification of forecast
[KNMI-TR-138] p 3478 N93-30113

SOLAR REFLECTORS
In orbit degradation of EUV optical components in the wavelength range 10-40 nm AO 138-3
p 3582 N93-29691

SOLAR SENSORS
Long Duration Exposure Facility (LDEF) attitude measurements of the Interplanetary Dust Experiment
p 3638 N93-29377

SOLAR SPECTRA
A unique photon bombardment system for space applications p 3286 N93-28790
Method of emitting on a specific wavelength fraunhofer line using a neodymium doped laser transmitter
[AD-D015710] p 3437 N93-29276
The effect of the low Earth orbit environment on space solar cells: Results of the Advanced Photovoltaic Experiment (S0014) p 3467 N93-29686
Modeling the bidirectional reflectance and spectra
[AD-A263570] p 3462 N93-29830
Optical system analysis for the ground based EXVM
[NASA-CR-192588] p 3582 N93-31035

SOLAR STORMS
ELF/VLF radio noise measurements at high latitudes during solar particle events p 3397 N93-30744

SOLAR SYSTEM
Space research in Germany 1990-1991
[ETN-93-93807] p 3654 N93-28477
Workshop on Advanced Technologies for Planetary Instruments, part 1
[NASA-CR-193015] p 3639 N93-28764

SOLAR TERRESTRIAL INTERACTIONS
SESC products and services user guide
[PB93-178879] p 3653 N93-29679
SOLAR WIND
Mithras studies of the boundary between open and closed field lines
[AD-A264758] p 3479 N93-30562
SOLAR X-RAYS
The Mechanisms of Solar Variability (MSV) program
[AD-A262525] p 3652 N93-28585
SOLDERED JOINTS
The 17th Annual Electronics Manufacturing Seminar proceedings
[AD-A261963] p 3409 N93-29435
SOLDERING
Preliminary test of liquid metal induced embrittlement in liquid LiPb and stainless-steel systems
[DE93-753130] p 3320 N93-28529
Characterization and optimization of a Hot Air Solder-Leveling System
[DE93-010188] p 3332 N93-29328
The 17th Annual Electronics Manufacturing Seminar proceedings
[AD-A261963] p 3409 N93-29435
Detecting residue on a printed circuit board: An application of the Boundary Contour/Feature Contour System
[DE93-006283] p 3412 N93-30370
Performance of thermal adhesives in forced convection p 3293 N93-30974
SOLDERS
Characterization and optimization of a Hot Air Solder-Leveling System
[DE93-010188] p 3332 N93-29328
Adhesion of thick film Au to alumina ceramics
[DE93-009802] p 3339 N93-30656
SOLID CRYOGENS
Specific impulse calculations of high energy density solid cryogenic rocket propellants. 1. Atoms in solid H2
[AD-A263208] p 3341 N93-28517
SOLID ELECTROLYTES
In situ characterization of interfacial and bulk properties of lithium polymer batteries using 4-probe DC techniques
[DE93-007699] p 3405 N93-28581
Polymer electrolyte fuel cells for transportation applications
[DE93-008721] p 3464 N93-29147
Synthesis and properties of a cation-conducting, high temperature polymer electrolyte
[AD-A263557] p 3334 N93-29825
Solid oxide fuel cells for transportation: A clean, efficient alternative for propulsion
[DE93-010662] p 3464 N93-29844
The effect of Bi2 O3 on the electrical properties of Zr O2: 3 percent Mg O ceramic solid electrolytes
[DE93-607029] p 3339 N93-30774
SOLID LUBRICANTS
Synthesis of new high performance lubricants and solid lubricants
[DE93-012237] p 3330 N93-28748
SOLID PHASES
The XNOVAKTC rheological model
[AD-A263298] p 3342 N93-29762
Powder metallurgy: Solid and liquid phase sintering of copper p 3294 N93-30976
SOLID PROPELLANT COMBUSTION
Response of energetic solids to light, heat and shock pulses
[AD-A263702] p 3342 N93-29296
The outlook for understanding the combustion of solid propellants and what it will take p 3346 N93-30078
Determination of gas phase species and temperature profiles above solid propellants p 3346 N93-30080
Unsteady combustion of energetic materials using laser-recoil p 3319 N93-30085
SOLID PROPELLANT IGNITION
Response of energetic solids to light, heat and shock pulses
[AD-A263702] p 3342 N93-29296
Interfacial melting in cracked explosives
p 3349 N93-30089
SOLID PROPELLANT ROCKET ENGINES
Microstructural modeling of electrical breakdown in solid fuel propellants
[AD-A263466] p 3342 N93-29835
Postflight hardware evaluation 360T025 (RSRM-25, STS-46)
[NASA-CR-192562] p 3272 N93-30617
Postflight hardware evaluation 360T025 (RSRM-25, STS-46). Appendix A: Insulation PFORs
[NASA-CR-192563] p 3272 N93-30618
Postflight hardware evaluation 360T025 (RSRM-25, STS-46). Appendix B: Case, seals, and joints PFORs
[NASA-CR-192564] p 3272 N93-30619
Postflight hardware evaluation 360T025 (RSRM-25, STS-46). Appendix E: Insulation postfire data
[NASA-CR-192566] p 3272 N93-30621
Postflight hardware evaluation 360T025 (RSRM-25, STS-46). Appendix D: Nozzle postfire data
[NASA-CR-192580] p 3289 N93-30648
SOLID PROPELLANTS
Response of energetic solids to light, heat and shock pulses
[AD-A263702] p 3342 N93-29296
The XNOVAKTC rheological model
[AD-A263298] p 3342 N93-29762
Combustion/explosion chemistry of bulk materials
p 3343 N93-30062
Single-shot femtosecond spectroscopy: A methodology for observation of solid-state chemical reactions
p 3319 N93-30075
SOLID ROCKET PROPELLANTS
Specific impulse calculations of high energy density solid cryogenic rocket propellants. 1. Atoms in solid H2
[AD-A263208] p 3341 N93-28517
Microstructural modeling of electrical breakdown in solid fuel propellants
[AD-A263466] p 3342 N93-29835
The outlook for understanding the combustion of solid propellants and what it will take p 3346 N93-30078
Determination of gas phase species and temperature profiles above solid propellants p 3346 N93-30080
SOLID SOLUTIONS
Synthesis and characterization of mixed 3-5 and 2-6 semiconductor monomers included in the borate sodalite analogue
[AD-A264523] p 3598 N93-30407
SOLID STATE
Structure and switching dynamics in ferroelectric crystal and liquid crystal thin films
[AD-A263664] p 3594 N93-29293
Gordon Research Conferences, 1991
[AD-A264275] p 3317 N93-30816
Ultrafast, passive, broad-band, optical shutter based on novel semiconductor/conducting polymer interfaces
[AD-A264098] p 3601 N93-30878
SOLID STATE DEVICES
In situ characterization of interfacial and bulk properties of lithium polymer batteries using 4-probe DC techniques
[DE93-007699] p 3405 N93-28581
Electronics research report
[AD-A262733] p 3405 N93-28589
Upgrading the LAMPF 201 MHz RF generators
[DE93-010715] p 3406 N93-28830
A novel approach for new radiation sources based on solid state plasma instabilities
[AD-A263699] p 3588 N93-29382
Electronics research at the University of Texas at Austin. Appendix: JSEP sponsored publications
[AD-A262993] p 3409 N93-29485
SOLID STATE LASERS
All solid-state high power visible laser
[NASA-CR-193163] p 3436 N93-28623
Design of the Nova Upgrade laser system for ignition fusion experiments
[DE93-009077] p 3436 N93-29097
Holmium quasi-two level laser
[AD-D015706] p 3440 N93-30427
Portable fiber optic coupled Doppler interferometer system for detonation and shock wave diagnostics
[DE93-009827] p 3433 N93-30510
SOLID SUSPENSIONS
Magnetohydrodynamic projects at the CDIF
[DE93-012195] p 3584 N93-28649
SOLID WASTES
Strategic Environmental Research and Development Program (SERDP)
[AD-A263745] p 3471 N93-29858
Environmental characteristics of EPA, NRC, and DOE sites contaminated with radioactive substances
[PB93-185551] p 3475 N93-30829
SOLIDIFICATION
An evaluation of factors affecting the solidification/stabilization of heavy metal sludge
[AD-A264128] p 3473 N93-30197
Development of a CFD code for casting simulation
[NASA-CR-192577] p 3427 N93-30492
Eutectic solidification of Al-U at slowly cooling rates (10 C per second)
[DE92-640082] p 3328 N93-30941
Visualizing weld metal solidification using organic analogs p 3293 N93-30973
A review of hot cracking in austenitic stainless steel weldments
[DE93-605280] p 3328 N93-31021
SOLIDIFIED GASES
Specific impulse calculations of high energy density solid cryogenic rocket propellants. 1. Atoms in solid H2
[AD-A263208] p 3341 N93-28517
SOLIDS
Theory of normal and superconducting properties of fullerene-based solids
[DE93-007722] p 3592 N93-28582
Some problems in the mechanics of solids with phase mixtures
[AD-A263652] p 3311 N93-29291
Representation and recognition with invariants and geometric constraint models
[AD-A263235] p 3529 N93-29493
Dynamics and photoexcitation in MX and MXX' chain solids
[AD-A264823] p 3561 N93-29711
Rapidly activated dynamic phase transitions in nonlinear solids
[AD-A263601] p 3299 N93-29982
Metallization at detonation fronts in solids
p 3319 N93-30087
Pulsed laser photoacoustic spectrometer for study of solid materials
[DE93-605290] p 3441 N93-31023
SOLIDS FLOW
Dense inclined flows: Theory and experiments
[DE93-011452] p 3417 N93-28630
SOLITARY WAVES
Studies in theoretical high energy particle physics
[DE93-007990] p 3574 N93-28565
Measurements of rare composite objects and high sensitivity searches for novel forms of matter produced in high energy heavy ion collisions
[DE93-009945] p 3574 N93-28569
Dynamics and photoexcitation in MX and MXX' chain solids
[AD-A264823] p 3561 N93-29711
On the invariant measure for the nonlinear Schroedinger equation
[DE92-644672] p 3551 N93-30912
Spherically symmetric line element and Killing vectors in five-dimensional space
[DE93-604132] p 3558 N93-30988
SOLUBILITY
Super critical water oxidation on energetic materials
[DE93-010704] p 3342 N93-29312
Chromatographic and solvatochromic measurements on butyl rubbers
[AD-A263088] p 3334 N93-29795
Water-soluble polyphosphazenes and their hydrogels
[AD-A264883] p 3340 N93-30909
SOLUTES
Studies in Lewis acid and superacid ionic liquids
[AD-A264683] p 3316 N93-30551
SOLUTIONS
Applications of laser light scattering in polymer dilute solution characterization
[AD-A263110] p 3335 N93-30007
SOLVATION
A simple model for ion solvation with non additive cores
[AD-A263075] p 3566 N93-29143
Chromatographic and solvatochromic measurements on butyl rubbers
[AD-A263088] p 3334 N93-29795
SOLVENTS
Acid gas treating by aqueous alkanolamines
[PB93-176188] p 3471 N93-29676
Hydrogen sulfide decomposition into hydrogen and sulfur by quinone cycles, part 1
[PB93-175297] p 3317 N93-30761
SONIC BOOMS
Subjective response to simulated sonic booms with ground reflections
[NASA-TM-107764] p 3561 N93-28692
Sonic boom problem for future highspeed aircraft
[ONERA-NT-1990-3] p 3241 N93-30020
SOOT
Detailed studies of soot formation in laminar diffusion flames for application to modeling studies
[AD-A264827] p 3317 N93-30667
SORET COEFFICIENT
Follow up on the crystal growth experiments of the LDEF p 3602 N93-29381
SOUND DETECTING AND RANGING
Acoustic transducer system
[AD-D015713] p 3562 N93-29279
Oceanographic data processing program
[AD-A264801] p 3544 N93-30591
Atmospheric studies with SODAR at Kalpakkam
[DE93-605544] p 3480 N93-30992
SOUND FIELDS
Investigation of thermoacoustic muffler
[AD-A262009] p 3562 N93-29392
Evaluation of the scattered pressure due to infinite rigid cylinders, infinite elastic cylindrical shells, and rigid spheres in the presence of an ambient noise field
[AD-A264835] p 3563 N93-30899

SOUND GENERATORS
Investigation of thermoacoustic muffler
[AD-A262009] p 3562 N93-29392

SOUND PRESSURE
Acoustic transducer system
[AD-D015713] p 3562 N93-29279

SOUND TRANSDUCERS
Acoustic transducer system
[AD-D015713] p 3562 N93-29279

SOUND TRANSMISSION
Experiments in materials science from household items p 3293 N93-30971

SOUND WAVES
Jet mixer noise suppressor using acoustic feedback
[NASA-CASE-LEW-15170-1] p 3561 N93-28953
Feature based neural network acoustic transient signal classification
[AD-A263437] p 3562 N93-29816
Sound wave scattering from an elastic spherical shell
[AD-A264039] p 3562 N93-30029
Sound wave scattering from a rigid sphere
[AD-A264182] p 3562 N93-30157
Acoustic-gravity waves from low-altitude localized disturbances
[AD-A264804] p 3479 N93-30593

SOUNDS (TOPOGRAPHIC FEATURES)
Remote sensing survey of Mississippi River-Gulf Outlet, Breton Sound disposal area, Plaquemines Parish, Louisiana
[AD-A263097] p 3459 N93-29146

SOUTHERN OSCILLATION
Atmospheric and Geophysical Sciences Division: G-Division did you know?
[DE93-007412] p 3469 N93-28967

SPACE BASED RADAR
Array-fed reflector systems with limited scan
p 3371 N93-30318

SPACE CHARGE
Determination of the space charge distribution within an e-irradiated polymer using the pressure wave propagation method
[ONERA-P-1990-4] p 3335 N93-30024
Some problems of relativistic electrodynamics
[DE92-644738] p 3400 N93-30923

SPACE COMMERCIALIZATION
US space commerce, 1991 p 3625 N93-30695
Sandia National Laboratories p 3626 N93-30702

SPACE COMMUNICATION
System overview on electromagnetic compensation for reflector antenna surface distortion
[NASA-TM-106217] p 3273 N93-29195
The Telecommunications and Data Acquisition Report
[NASA-CR-193144] p 3384 N93-29586

SPACE DEBRIS
Orbital Debris Environment Monitor (ODEM)
p 3267 N93-28735
Proposal for a universal particle detector experiment
p 3286 N93-28795
Report of the Meteoroid and Debris Special Investigation Group p 3638 N93-29355
Micrometeoroids and debris on LDEF
p 3638 N93-29356
Continued investigation of LDEF's structural frame and thermal blankets by the Meteoroid and Debris Special Investigation Group p 3282 N93-29357
Predicted and observed directional dependence of meteoroid/debris impacts on LDEF thermal blankets
p 3638 N93-29358
Long Duration Exposure Facility (LDEF) experiment M0003 meteoroid and debris survey
p 3638 N93-29361
Derivation of particulate directional information from analysis of elliptical impact craters on LDEF
p 3283 N93-29362
Characteristics of hypervelocity impact craters on LDEF experiment S1003 and implications of small particle impacts on reflective surfaces p 3283 N93-29363
Hypervelocity impact facility for simulating materials exposure to impact by space debris
p 3283 N93-29365
Projectile compositions and modal frequencies on the chemistry of micrometeoroids LDEF experiment
p 3638 N93-29370
Interplanetary meteoroid debris in LDEF metal craters
p 3638 N93-29372
Origin of orbital debris impacts on LDEF's trailing surfaces p 3283 N93-29373
Damage areas on selected LDEF aluminum surfaces
p 3283 N93-29374
LDEF data: Comparisons with existing models
p 3283 N93-29375
Long-term microparticle flux variability indicated by comparison of Interplanetary Dust Experiment (IDE) timed impacts for LDEF's first year in orbit with impact data for the entire 5.77-year orbital lifetime p 3638 N93-29379
An LDEF 2 dust instrument for discrimination between orbital debris and natural particles in near-Earth space
p 3286 N93-29707
Advanced design for orbital debris removal in support of solar system exploration p 3229 N93-29724
From orbital debris capture systems through internal combustion engines on Mars p 3232 N93-29745
Hypervelocity impact testing of the Space Station utility distribution system carrier
[NASA-TM-104771] p 3289 N93-30507

SPACE ENVIRONMENT SIMULATION
Laboratory simulation of field-aligned currents
[NASA-CR-193091] p 3476 N93-28538
Lunar regolith penetrators and cutters
p 3276 N93-29117
Radiation model predictions and validation using LDEF satellite data p 3573 N93-29641
Future directions for LDEF ionizing radiation modeling and assessments p 3573 N93-29642
Mathematical simulation of the induced (gamma)-radiation in structural materials of spaceships. Time dependence
[DE93-605312] p 3281 N93-31024

SPACE ERECTABLE STRUCTURES
Vibration control of flexible space structures in noisy environment p 3285 N93-30235

SPACE EXPLORATION
Advanced collapsible tank for liquid containment
[NASA-CR-188247] p 3353 N93-28698
Workshop on Advanced Technologies for Planetary Instruments, part 1
[NASA-CR-193015] p 3639 N93-28764
Plasma, magnetic, and electromagnetic measurements at nonmagnetic bodies p 3647 N93-28809
Advanced design for orbital debris removal in support of solar system exploration p 3229 N93-29724
Project WISH: The Emerald City p 3232 N93-29744
Sandia National Laboratories p 3626 N93-30702
Exploration technology prioritization
p 3629 N93-30726
Space transfer concepts and analyses for exploration missions, phase 3
[NASA-CR-192584] p 3268 N93-31034

SPACE FLIGHT
Armstrong Laboratory space visual function tester program p 3267 N93-28739

SPACE HABITATS
Selenia: A habitability study for the development of a third generation lunar base p 3233 N93-29748

SPACE LOGISTICS
Analysis of orbital system logistics in the cis-lunar space with particular consideration of life cycle costs
[ETN-93-93484] p 3268 N93-29063

SPACE MANUFACTURING
Space construction activities
[NASA-CR-192690] p 3274 N93-29108

SPACE MECHANICS
Quantum-kinetic Green function and macroscopic wave function
[DE93-606040] p 3606 N93-30796
On the invariant measure for the nonlinear Schroedinger equation
[DE92-644672] p 3551 N93-30912

SPACE MISSIONS
Small Stirling dynamic isotope power system for robotic space missions
[NASA-TM-105785] p 3287 N93-28686
The APX spectrometer for Martian missions
p 3434 N93-28776
Detection of other planetary systems using photometry p 3632 N93-28791
The MESUR mission p 3649 N93-28816
Venus Interior Structure Mission (VISM): Establishing a seismic network on Venus p 3649 N93-28819
Pharmacokinetics and Pharmacodynamics in Space
[NASA-CP-10048] p 3494 N93-29502
Technology transfer and space science missions
p 3626 N93-30705
Technology transfer within the government
p 3627 N93-30709
Technology transfer within the government
p 3627 N93-30711

SPACE NAVIGATION
Clementine sensor processing system
p 3285 N93-28778
Reference equations of motion for automatic rendezvous and capture
[NASA-CR-185676] p 3269 N93-29652
Attitude determination using GPS: Development of an all solid-state guidance, navigation, and control sensor for air and space vehicles based on the global positioning system p 3246 N93-30605

SPACE OBSERVATIONS (FROM EARTH)
Advanced research in sky surveillance: A search for low-luminosity objects
[AD-A264832] p 3631 N93-30629

SPACE PERCEPTION
Symbology for head up and head down applications for highly agile fighter aircraft: To improve spatial awareness, trajectory control, and unusual attitude recovery, part 1
p 3502 N93-28857

SPACE PLASMAS
Plasma, magnetic, and electromagnetic measurements at nonmagnetic bodies p 3647 N93-28809
Development of Miniaturized Optimized Smart Sensors (MOSS) for space plasmas p 3286 N93-28828
Ionospheric structure specifications and systems effects
[AD-A263573] p 3476 N93-29343

SPACE PLATFORMS
Measurement of the relative and absolute microgravity environment of space platforms, recent flight results, and determination of the spatial microgravity field
p 3266 N93-28725

SPACE POWER REACTORS
Analysis of TOPAZ 2 and SPACE-R space nuclear power plants using a modified thermionic model
[AD-A262612] p 3286 N93-28474
NEP space test program objective
p 3265 N93-28724
Technology transfer personnel exchange at the Boeing Company
[DE93-010190] p 3625 N93-29329
Thermion: Verification of a thermionic heat pipe in microgravity p 3235 N93-29757

SPACE PROBES
Spaceborne passive radiative cooler
p 3378 N93-28802
Double swingby at Earth-Moon for increase of excess velocity
[ETN-93-94177] p 3270 N93-30582

SPACE PROCESSING
Measurement of the relative and absolute microgravity environment of space platforms, recent flight results, and determination of the spatial microgravity field
p 3266 N93-28725

SPACE PROGRAMS
Decision maker's guide to international space
[ANSER-STDN-93-4] p 3669 N93-29710
Proceedings of the Seventh Annual Summer Conference. NASA/USRA: University Advanced Design Program
[NASA-CR-192962] p 3227 N93-29712
Technology Transfer and the Civil Space Program. Volume 2: Workshop proceedings
[NASA-TM-108250] p 3625 N93-30692
Workshop conclusions: Technology transfer and the civil space program p 3628 N93-30721

SPACE RENDEZVOUS
The +vbar breakout during approach to Space Station Freedom
[NASA-TM-104772] p 3269 N93-30135

SPACE SHUTTLE MAIN ENGINE
Additional support for the TDK/MABL computer program
[NASA-CR-193037] p 3526 N93-29028
High Reynolds number and turbulence effects on aerodynamics and heat transfer in a turbine cascade
[NASA-TM-106187] p 3420 N93-29157

SPACE SHUTTLE MISSIONS
Low-frequency vibration environment for five Shuttle missions
[NASA-TM-106059] p 3285 N93-28554
Description of the Joint Damping Experiment (JDX)
p 3263 N93-28703
Effect of microgravity on several visual functions during STS Shuttle missions: Visual Function Tester-Model 1 (VFT-1) p 3268 N93-28740
Effect of microgravity on visual contrast threshold during STS Shuttle missions: Visual Function Tester-Model 2 (VFT-2) p 3268 N93-28741
Debris/ice/TPS assessment and integrated photographic analysis for Shuttle Mission STS-55
[NASA-TM-107559] p 3271 N93-29136
The middeck 0-gravity dynamics experiment
[NASA-CR-4500] p 3281 N93-30376

SPACE SHUTTLE ORBITERS
Space Station: Orbiter berthing p 3274 N93-29031

SPACE SHUTTLE PAYLOADS
NASA/DOD Flight Experiments Technical Interchange Meeting Proceedings
[NASA-TM-108721] p 3262 N93-28699
The MODE family of facility class experiments
p 3263 N93-28705
Tank Pressure Control Experiment (TPCE)
p 3264 N93-28712
In-STEP Two-Phase Flow (TPF) thermal control experiment p 3265 N93-28719
Payload flight assignments. NASA mixed fleet
[NASA-TM-108255] p 3268 N93-30133
The middeck 0-gravity dynamics experiment
[NASA-CR-4500] p 3281 N93-30376

Aerospace payload design and development [AD-A264502] p 3289 N93-30402

SPACE SHUTTLES

The Orbiter Experiments (OEX) program p 3266 N93-28731

An assessment of space shuttle flight software development processes [NASA-CR-193179] p 3525 N93-28934

Multivariable control of the Space Shuttle Remote Manipulator System using linearization by state feedback [NASA-CR-188248] p 3443 N93-29080

Debris/ice/TPS assessment and integrated photographic analysis for Shuttle Mission STS-55 [NASA-TM-107559] p 3271 N93-29136

Numerical computation of inviscid flow around nose tip of Space Shuttle with NND scheme [AD-A264012] p 3421 N93-29260

Payload flight assignments. NASA mixed fleet [NASA-TM-108255] p 3268 N93-30133

Shuttle landing facility cloud cover study: Climatological analysis and two tenths cloud cover rule evaluation [NASA-CR-193016] p 3272 N93-31033

SPACE STATION FREEDOM

Space Station: Orbiter berthing p 3274 N93-29031

Automation of closed environments in space for human comfort and safety p 3230 N93-29734

From orbital debris capture systems through internal combustion engines on Mars p 3232 N93-29745

The +vbar breakout during approach to Space Station Freedom [NASA-TM-104772] p 3269 N93-30135

Hypervelocity impact testing of the Space Station utility distribution system carrier [NASA-TM-104771] p 3289 N93-30507

Space transfer concepts and analyses for exploration missions, phase 3 [NASA-CR-192584] p 3268 N93-31034

SPACE STATION PAYLOADS

Analysis of orbital system logistics in the cis-lunar space with particular consideration of life cycle costs [ETN-93-93484] p 3268 N93-29063

SPACE STATION STRUCTURES

Space station attitude disturbance arising from internal motions p 3280 N93-29995

SPACE STATIONS

Project WISH: The Emerald City p 3232 N93-29744

SPACE STORAGE

The 1990-1991 project summaries p 3230 N93-29730

SPACE TRANSPORTATION

Space transportation analysis and design (Reissue A) [AD-A262752] p 3271 N93-28487

The Orbiter Experiments (OEX) program p 3266 N93-28731

Antares: A low cost modular launch vehicle for the future p 3235 N93-29759

Space transfer concepts and analyses for exploration missions, phase 3 [NASA-CR-192584] p 3268 N93-31034

SPACE TRANSPORTATION SYSTEM

Analysis of orbital system logistics in the cis-lunar space with particular consideration of life cycle costs [ETN-93-93484] p 3268 N93-29063

Shuttle landing facility cloud cover study: Climatological analysis and two tenths cloud cover rule evaluation [NASA-CR-193016] p 3272 N93-31033

SPACE TRANSPORTATION SYSTEM FLIGHTS

Debris/ice/TPS assessment and integrated photographic analysis for Shuttle Mission STS-55 [NASA-TM-107559] p 3271 N93-29136

Enhanced reduction of velocity data obtained during CETA flight experiment [NASA-TM-4460] p 3431 N93-29209

SPACE-TIME FUNCTIONS

Quantum field theory in spaces with closed time-like curves [DE93-010564] p 3605 N93-30481

Phase structure of three- and four-dimensional phi(exp 4) field theory [DE93-606069] p 3605 N93-30782

Beyond two dimensions [DE93-606084] p 3606 N93-30786

The ground state wavefunctions of a conformally invariant scalar field in different spacetime background [DE93-606063] p 3606 N93-30808

A simple formula for reducing Feynman diagrams to scalar integrals [DE92-644717] p 3607 N93-30916

Fourth-rank gravity and cosmology [DE92-644722] p 3637 N93-30918

Topology and statistics in zero dimensions [DE93-604080] p 3607 N93-30932

Relativity theory in (2 + 2)-space [DE92-644671] p 3608 N93-30983

Spherically symmetric line element and Killing vectors in five-dimensional space [DE93-604132] p 3558 N93-30988

The geometry of complex space-times with torsion [DE92-641343] p 3608 N93-31003

SPACEBORNE ASTRONOMY

Space research in Germany 1990-1991 [ETN-93-93807] p 3654 N93-28477

The Ultraviolet Plume Instrument (UVPI) p 3285 N93-28784

SPACEBORNE EXPERIMENTS

NASA/DOD Flight Experiments Technical Interchange Meeting Proceedings [NASA-TM-108721] p 3262 N93-28699

Low-cost Active Structural Control space experiment (LASC) p 3263 N93-28700

In-step inflatable antenna experiment p 3263 N93-28701

Description of the Joint Damping Experiment (JDX) p 3263 N93-28703

Adaptive structures flight experiments p 3263 N93-28704

The MODE family of facility class experiments p 3263 N93-28705

Control-structures interaction test of the LACE satellite p 3263 N93-28706

CSI-Star: A low-cost CSI orbital testbed p 3263 N93-28707

Vented Tank Resupply Experiment (VTRE) for In-Space Technology Experiment Program (IN-STEP) p 3264 N93-28711

Tank Pressure Control Experiment (TPCE) p 3264 N93-28712

Tank Pressure Control Experiment/Thermal Phenomena (TPCE/TP) p 3264 N93-28713

Solar Array Module Plasma Interaction Experiment (SAMPIE) p 3265 N93-28716

The Photovoltaic Array Space Power Plus diagnostics (PASP Plus) flight experiment p 3265 N93-28717

Sodium sulfur technology program NaSTEC p 3265 N93-28718

In-STEP Two-Phase Flow (TPF) thermal control experiment p 3265 N93-28719

Thermal energy storage flight experiment in microgravity p 3265 N93-28720

Cryogenic Heat Pipe Experiment (CRYOHP) p 3265 N93-28721

STRV1-b flight experiment p 3265 N93-28723

NEP space test program objective p 3265 N93-28724

The Optical Properties Monitor (OPM): A multipurpose optical laboratory in space p 3266 N93-28729

The Orbiter Experiments (OEX) program p 3266 N93-28731

NPB cesium space experiment p 3267 N93-28733

Environmental monitors in the Midcourse Space Experiments (MSX) p 3286 N93-28826

FNAS CRRES program completion [NASA-CR-192468] p 3476 N93-29032

LDEF materials data bases [NASA-TM-107757] p 3290 N93-29067

Enhanced reduction of velocity data obtained during CETA flight experiment [NASA-TM-4460] p 3431 N93-29209

Progress report on the Heavy Ions in Space (HIIS) experiment p 3573 N93-29645

LDEF: 69 Months in Space. Part 4: Second Post-Retrieval Symposium [NASA-CP-3194-PT-4] p 3665 N93-29682

LDEF Space Plasma-High Voltage Drainage Experiment post-flight results p 3414 N93-29690

LDEF space optics handbook p 3582 N93-29695

Retrievable payload carrier, next generation Long Duration Exposure Facility: Update 1992 p 3283 N93-29705

QuickStar: System design, capabilities, and tactical applications of a small, smart space system p 3284 N93-29905

Residual acceleration data on IML-1: Development of a data reduction and dissemination plan [NASA-CR-193224] p 3281 N93-30038

The middeck 0-gravity dynamics experiment [NASA-CR-4500] p 3281 N93-30376

Aerospace payload design and development [AD-A264502] p 3289 N93-30402

SPACEBORNE LASERS

Subnanoradian, groundbased tracking of spaceborne lasers p 3442 N93-28823

SPACEBORNE TELESCOPES

Formulation of Ames 24E2 IR-black coating [NASA-TM-102864] p 3629 N93-29453

SPACECRAFT ANTENNAS

In-step inflatable antenna experiment p 3263 N93-28701

System overview on electromagnetic compensation for reflector antenna surface distortion [NASA-TM-106217] p 3273 N93-29195

Signal-to-noise ratio losses in full spectrum combining of signals with a downconverted subcarrier p 3386 N93-29599

SPACECRAFT CHARGING

Solar Array Module Plasma Interaction Experiment (SAMPIE) p 3265 N93-28716

Spacecraft surface charging handbook [AD-A262778] p 3279 N93-29305

USU center of excellence in theory and analysis of the geo-plasma environment [AD-A264750] p 3590 N93-30585

SPACECRAFT COMPONENTS

Testing in combined dynamic environments [DE93-010679] p 3278 N93-29250

SPACECRAFT CONFIGURATIONS

Adaptive structures flight experiments p 3263 N93-28704

SPACECRAFT CONSTRUCTION MATERIALS

The Optical Properties Monitor (OPM): A multipurpose optical laboratory in space p 3266 N93-28729

Low Earth orbital mission aboard the Space Test Experiments Platform (STEP-3) p 3267 N93-28732

Induced activation study of LDEF p 3572 N93-29632

SPACECRAFT CONTAMINATION

Environmental Verification Experiment for the Explorer Platform (EVEEP) p 3266 N93-28726

Return flux experiment p 3266 N93-28727

Low Earth orbital mission aboard the Space Test Experiments Platform (STEP-3) p 3267 N93-28732

Proposal for a universal particle detector experiment p 3286 N93-28795

New results from FRECOPA analysis p 3448 N93-29688

SPACECRAFT CONTROL

NASA instep/MDMSC jitter suppression experiment (JITTER) p 3263 N93-28702

Adaptive structures flight experiments p 3263 N93-28704

CSI-Star: A low-cost CSI orbital testbed p 3263 N93-28707

Clementine sensor processing system p 3285 N93-28778

Controls for space structures p 3275 N93-29112

Reference equations of motion for automatic rendezvous and capture [NASA-CR-185676] p 3269 N93-29652

Attitude- and Orbit Control Subsystem concepts for TACSATS p 3284 N93-29906

Efficient Reorientation Maneuvers for Spacecraft with Multiple Articulated Payloads [NASA-CR-193142] p 3279 N93-29988

Space station attitude disturbance arising from internal motions p 3280 N93-29995

SPACECRAFT DESIGN

Natural environmental service support to NASA vehicle, technology, and sensor development programs [NASA-CR-192554] p 3469 N93-29029

Conceptual design of a two-stage-to-orbit vehicle p 3228 N93-29716

The design of two-stage-to-orbit vehicles p 3228 N93-29719

ASUR p 3228 N93-29720

Lunar lander ground support system p 3230 N93-29729

Delta Advanced Reusable Transport (DART): An alternative manned spacecraft p 3231 N93-29735

Taurus Lightweight Manned Spacecraft Earth orbiting vehicle p 3231 N93-29736

Project Copernicus: An Earth observing system p 3231 N93-29738

Project WISH: The Emerald City p 3232 N93-29744

The lightcraft project p 3233 N93-29749

B and T: Lunar landers p 3234 N93-29751

RS Landers: Lunar lander p 3234 N93-29753

SPECS: Orbital debris removal p 3234 N93-29754

Mars Aquarius Mission and Titan Explorer p 3235 N93-29756

Solar electric propulsion cargo spacecraft for Mars missions p 3235 N93-29758

Antares: A low cost modular launch vehicle for the future p 3235 N93-29759

Space Generic Open Avionics Architecture (SGOAA) reference model technical guide [NASA-CR-188246] p 3285 N93-31032

Space transfer concepts and analyses for exploration missions, phase 3 [NASA-CR-192584] p 3268 N93-31034

SPACECRAFT DOCKING

Space Station: Orbiter berthing p 3274 N93-29031

Controls of interaction dynamics of orbital assembly p 3275 N93-29111

Controls for space structures p 3275 N93-29112

Reference equations of motion for automatic rendezvous and capture
[NASA-CR-185676] p 3269 N93-29652
The 1990/1991 project summaries
p 3229 N93-29725

SPACECRAFT ELECTRONIC EQUIPMENT
Total dose tests for the PROMICS-3 instrument
[VTT-TIED-1203] p 3411 N93-30108

SPACECRAFT ENVIRONMENTS
Lightweight modular instrumentation for planetary applications p 3286 N93-28787
Proposal for a universal particle detector experiment
p 3286 N93-28795

SPACECRAFT EQUIPMENT
Spaceborne passive radiative cooler
p 3378 N93-28802

SPACECRAFT GLOW
Spacecraft glow and the EISG/skirt experiment
p 3266 N93-28728

SPACECRAFT GUIDANCE
Reference equations of motion for automatic rendezvous and capture
[NASA-CR-185676] p 3269 N93-29652

SPACECRAFT INSTRUMENTS
The Orbiter Experiments (OEX) program
p 3266 N93-28731
Workshop on Advanced Technologies for Planetary Instruments, part 1
[NASA-CR-193015] p 3639 N93-28764
Clementine sensor processing system
p 3285 N93-28778
Pluto fast flyby mission and science overview
p 3649 N93-28818
A team approach to the development of gamma ray and x ray remote sensing and in situ spectroscopy for planetary exploration missions p 3650 N93-28824
Environmental monitors in the Midcourse Space Experiments (MSX) p 3286 N93-28826
Advanced Earth Observing Satellite (ADEOS)
p 3279 N93-29648
Next generation optical instruments and space experiment based on the LDEF thermal control surfaces experiment (S0069) p 3583 N93-29706

SPACECRAFT LANDING
Design, building, and testing of the postlanding systems for the assured crew return vehicle
p 3229 N93-29726
Shuttle landing facility cloud cover study: Climatological analysis and two tenths cloud cover rule evaluation
[NASA-CR-193016] p 3272 N93-31033

SPACECRAFT LAUNCHING
Space transportation analysis and design (Reissue A)
[AD-A262752] p 3271 N93-28487
SeaWiFS technical report series. Volume 2: Analysis of orbit selection for SeaWiFS: Ascending versus descending node
[NASA-TM-104566-VOL-2] p 3486 N93-28497
Benefits of in situ propellant utilization for a Mars sample return mission
[NASA-TM-106243] p 3341 N93-28695
NEP space test program objective
p 3265 N93-28724
DSN support of Mars Observer p 3385 N93-29598
TACSAT ground control and data collection
p 3388 N93-29895
Launch vehicles for lightweight TACSAT deployment
p 3271 N93-29903
Spacecraft and launch systems for TACSAT applications p 3284 N93-29904
QuickStar: System design, capabilities, and tactical applications of a small, smart space system
p 3284 N93-29905
Electric propulsion for lightsats: A review of applications and advantages p 3290 N93-29907
Payload flight assignments. NASA mixed fleet
[NASA-TM-108255] p 3268 N93-30133
A representative survey of US space systems and methods for estimating their costs
[AD-A264159] p 3272 N93-30881

SPACECRAFT MANEUVERS
Efficient Reorientation Maneuvers for Spacecraft with Multiple Articulated Payloads
[NASA-CR-193142] p 3279 N93-29988
Attitude stabilization of a rigid spacecraft using two momentum wheel actuators p 3280 N93-29990
Efficient reorientation of a deformable body in space: A free-free beam example p 3280 N93-29994

SPACECRAFT MOTION
On symmetric central configurations with application to satellite motion about rings p 3652 N93-31000

SPACECRAFT ORBITS
Radiation monitoring equipment dosimeter experiment
p 3266 N93-28730
New meteoroid model predictions for directional impacts on LDEF p 3638 N93-29376

SPACECRAFT POWER SUPPLIES
NASA/DOD Flight Experiments Technical Interchange Meeting Proceedings
[NASA-TM-108721] p 3262 N93-28699
Developing an inflatable solar array
p 3264 N93-28714
Sodium-Sulfur Cell Technology flight experiment (SSCT) p 3264 N93-28715
Solar Array Module Plasma Interaction Experiment (SAMPIE) p 3265 N93-28716
The Photovoltaic Array Space Power Plus diagnostics (PASP Plus) flight experiment p 3265 N93-28717
Sodium sulfur technology program NaSTEC
p 3265 N93-28718
NEP space test program objective
p 3265 N93-28724
Evaluation of actuator energy storage and power sources for spacecraft applications
[NASA-CR-193226] p 3288 N93-29091
LDEF: 69 Months in Space. Second Post-Retrieval Symposium, part 2
[NASA-CP-3194-PT-2] p 3654 N93-29354
The lightcraft project p 3233 N93-29749
Power beaming to communication satellites in GEO
[DE93-007608] p 3279 N93-29840
Change of solar cell element properties influenced by adsorbed atoms
[DE93-606694] p 3466 N93-30777

SPACECRAFT PROPULSION
Advanced Earth-to-orbit propulsion technology information, dissemination and research
[NASA-CR-192561] p 3287 N93-28680
A new facility for advanced rocket propulsion research
[NASA-TM-106193] p 3270 N93-28696
NASA/DOD Flight Experiments Technical Interchange Meeting Proceedings
[NASA-TM-108721] p 3262 N93-28699
ELITE program: Electric insertion transfer experiment
p 3264 N93-28709
Advanced engine study program
[NASA-CR-187217] p 3287 N93-28946
Studies of hydrogen-air diffusion flames and of compressibility effects related to high-speed propulsion
p 3310 N93-29125
LDEF: 69 Months in Space. Second Post-Retrieval Symposium, part 2
[NASA-CP-3194-PT-2] p 3654 N93-29354

SPACECRAFT RADIATORS
Technology transfer personnel exchange at the Boeing Company
[DE93-010190] p 3625 N93-29329

SPACECRAFT SHIELDING
Ablative shielding for hypervelocity projectiles
[NASA-CASE-MSC-21884-1] p 3331 N93-29088
New meteoroid model predictions for directional impacts on LDEF p 3638 N93-29376
Absorbed dose measurements and predictions on LDEF p 3573 N93-29636
Light-heavy ion measurements in CR-39 located on the Earth side of LDEF p 3573 N93-29638
Three-dimensional shielding effects on charged particle fluences measured in the P0006 experiment of LDEF
p 3573 N93-29639
Overview of the Systems Special Investigation Group investigation p 3318 N93-29683
Beta/gamma Monte Carlo transport in repetitive structures of satellite systems
[DE93-007610] p 3281 N93-30509

SPACECRAFT STABILITY
The dynamics and control of space tethers
p 3274 N93-28629
Liquid Motion in a rotating tank Experiment (LME)
p 3264 N93-28710
Controls for space structures p 3275 N93-29112
Control of nonlinear systems with applications to constrained robots and spacecraft attitude stabilization
p 3279 N93-29989

SPACECRAFT STRUCTURES
NASA/DOD Flight Experiments Technical Interchange Meeting Proceedings
[NASA-TM-108721] p 3262 N93-28699
Low-cost Active Structural Control space experiment (LASC) p 3263 N93-28700
NASA instep/MDMSC jitter suppression experiment (JITTER) p 3263 N93-28702
Adaptive structures flight experiments
p 3263 N93-28704
Upper atmosphere research satellite jitter study
p 3264 N93-28708
Space construction activities
[NASA-CR-192690] p 3274 N93-29108
Controls of interaction dynamics of orbital assembly
p 3275 N93-29111
Controls for space structures p 3275 N93-29112
Structural load control during construction
p 3275 N93-29113
Systems engineering studies of on-orbit assembly operation p 3275 N93-29114
Design optimization of space structures
p 3278 N93-29122
Analysis of LDEF micrometeoroid/debris data and damage to composite materials p 3309 N93-29366
Nonlinear attitude control of planar structures in space using only internal controls p 3280 N93-29991
Planar reorientation of a free-free beam in space using embedded electromechanical actuators
p 3280 N93-29993
Mathematical simulation of the induced (gamma)-radiation in structural materials of spaceships. Time dependence
[DE93-605312] p 3281 N93-31024

SPACECRAFT TRACKING
Subnanoradian, groundbased tracking of spaceborne lasers p 3442 N93-28823
The effect of clock, media, and station location errors on Doppler measurement accuracy
p 3246 N93-29588

SPACECRAFT TRAJECTORIES
Double swingby at Earth-Moon for increase of excess velocity
[ETN-93-94177] p 3270 N93-30582

SPACECREWS
Radiation monitoring equipment dosimeter experiment
p 3266 N93-28730

SPACELAB PAYLOADS
Residual acceleration data on IML-1: Development of a data reduction and dissemination plan
[NASA-CR-193224] p 3281 N93-30038

SPACING
Fundamental studies of impingement cooling thermal boundary conditions p 3254 N93-29940

SPALLATION
Cosmogenic radionuclides on LDEF: An unexpected Be-10 result p 3573 N93-29643

SPARKS
Tool grinding and spark testing p 3291 N93-30954

SPATIAL DEPENDENCIES
A neural network based approach for machine fault diagnosis
[VTT-TIED-1274] p 3543 N93-29998

SPATIAL DISTRIBUTION
Ground clutter measurements for surface-sited radar
[AD-A262472] p 3379 N93-28655
Quantitative analysis of properties and spatial relations of fuzzy image regions p 3510 N93-29523
Encoding spatial images: A fuzzy set theory approach
p 3511 N93-29527
Utility of a ghost horizon and climb/dive ladder line tapering on a head-up display
[AD-A264401] p 3508 N93-30167

SPATIAL RESOLUTION
Characterization of laboratory generated turbulence by optical phase measurements
[AD-A262596] p 3480 N93-28465
Acousto-optic infrared spectral imager for Pluto fast flyby p 3285 N93-28781
Resolution-enhanced mapping spectrometer
p 3434 N93-28794
Charting the remote southern oceans with geosat altimetry
[AD-A263452] p 3461 N93-29817

SPECIFIC IMPULSE
Specific impulse calculations of high energy density solid cryogenic rocket propellants. 1. Atoms in solid H2
[AD-A263208] p 3341 N93-28517

SPECIFICATIONS
Concept document of the repository-based software engineering program: A constructive appraisal
[NASA-CR-193125] p 3526 N93-29027
Optical coherent phase diversity systems
[ISBN-90-9004897-9] p 3578 N93-29270
On the evaluation of fuzzy quantified queries in a database management system p 3517 N93-29569
Automatic synthesis of protocol specifications
p 3356 N93-30228

SPECKLE PATTERNS
Applications of mesoscopic physics
[DE93-012104] p 3597 N93-30141
Multiparticle imaging technique for two-phase fluid flows using pulsed laser speckle velocimetry
[DE93-011734] p 3427 N93-30489

SPECTRA
Benchmark eigenvalue spectrum calculations with anisotropic effects
[DE93-006387] p 3548 N93-28891
Precision optical interferometry in space
[NASA-CR-193264] p 3630 N93-29163
4D interconnect experimental development
[AD-A264298] p 3540 N93-30895

SPECTRAL BANDS
Design concept for an IR mapping spectrometer for the Pluto fast flyby mission p 3285 N93-28779

Condensed phase diagnostics of nitramine propellant combustion p 3320 N93-30102

SPECTRAL LINE WIDTH

Every good virtue you ever wanted in a Q-switched solid-state laser and more: Monolithic, diode-pumped, self-Q-switched, highly reproducible, diffraction-limited Nd:YAG laser p 3442 N93-28772

SPECTRAL METHODS

Accelerated motion of rigid spheres in unsteady flows at low to moderate Reynolds numbers
p 3416 N93-28612

A spectral method determination of the first critical Rayleigh number for a low-Prandtl number crystal melt in a cylindrical container
[NASA-CR-193238] p 3594 N93-29214

Study of flow structure in rotating cavities: Numerical predictions of laminar and turbulent, steady, and unsteady flows p 3256 N93-29948

SPECTRAL RECONNAISSANCE

Remote sensing of agricultural vegetation: Status and perspectives p 3458 N93-28922

SPECTRAL REFLECTANCE

Modeling the bidirectional reflectance and spectra
[AD-A263570] p 3462 N93-29830

SPECTRAL RESOLUTION

The HYDICE instrument design and its application to planetary instruments p 3434 N93-28766

Acousto-optic infrared spectral imager for Pluto fast flyby p 3285 N93-28781

Resolution-enhanced mapping spectrometer
p 3434 N93-28794

SPECTRAL THEORY

A spectral method determination of the first critical Rayleigh number for a low-Prandtl number crystal melt in a cylindrical container
[NASA-CR-193238] p 3594 N93-29214

SPECTROGRAPHS

Design concept for an IR mapping spectrometer for the Pluto fast flyby mission p 3285 N93-28779

A technique for single-pulse spectrum and pulse width measurements for an IR-FEL
[DE93-007732] p 3436 N93-28847

SPECTROMETERS

Research and development of an airborne multispectral scanner to measure fire, terrestrial and atmospheric characteristics (50 channel)
[NASA-CR-193121] p 3456 N93-28620

The HYDICE instrument design and its application to planetary instruments p 3434 N93-28766

The APX spectrometer for Martian missions
p 3434 N93-28776

Prototype backscatter Moessbauer spectrometer for measurement of Martian surface mineralogy
p 3648 N93-28812

A technique for single-pulse spectrum and pulse width measurements for an IR-FEL
[DE93-007732] p 3436 N93-28847

Summer research program (1992). High School Apprenticeship Program (HSAP) reports. Volume 16: Arnold Engineering Development Center Civil Engineering Laboratory
[AD-A262024] p 3608 N93-29396

Investigations of self-pumped phase conjugate laser beams and coherence length
[AD-A263438] p 3438 N93-29789

Reaction mechanism studies of heavy ion induced nuclear reactions
[DE93-010496] p 3569 N93-29807

Research and education by SF cyclotron facility
[DE93-753135] p 3576 N93-30002

Polarization experiments with hadronic and electromagnetic probes
[DE93-011375] p 3392 N93-30126

Operation of a 20-channel grating polychromator diagnostic system and its application to sawtooth observations in JT-60U
[DE93-764388] p 3590 N93-30398

SPECTROPHOTOMETERS

Fiber optic chemical sensors for characterizing the carbon cycle in ocean margin regions
[DE93-011442] p 3489 N93-30056

SPECTROSCOPIC ANALYSIS

Spectroscopic probes of vibrationally excited molecules at chemically significant energies
[DE93-012328] p 3564 N93-28652

The production and destruction of negative ions
[DE93-010527] p 3564 N93-28665

The APX spectrometer for Martian missions
p 3434 N93-28776

Ultrafast optical studies of surface reaction processes at semiconductor interfaces
[DE93-009049] p 3593 N93-29096

Elastic and reactive collisions of atoms and molecules with neutral alkali clusters
[DE93-009313] p 3566 N93-29206

Electric field induced phenomena in STM: Tip deformations and Au(111)-surface phase transitions during tunneling spectroscopy experiments
[AD-A262208] p 3596 N93-29445

The 2nd International symposium on electrochemical impedance spectroscopy (extended abstracts)
[AD-A262994] p 3312 N93-29462

Molecular dynamics modeling of electric double layers with spectroscopic applications
[AD-A263168] p 3568 N93-29489

Single-shot femtosecond spectroscopy: A methodology for observation of solid-state chemical reactions
p 3319 N93-30075

SPECTROSCOPY

Excited states in electronic structure calculations
[DE93-007704] p 3592 N93-28642

Thermodynamic properties for polycyclic systems by non-calorimetric methods
[DE93-011373] p 3603 N93-28747

Quantum lattice fluctuations in a 1-dimensional charge-density-wave material: Luminescence and resonance Raman studies of an MX solid
[DE93-007362] p 3593 N93-28966

Molecular dynamics modeling of electric double layers with spectroscopic applications
[AD-A263168] p 3568 N93-29489

Examination of shock induced chemical reactions in liquids using time-resolved optical spectroscopy
p 3318 N93-30073

Nonlinear spectroscopy of multicomponent droplets and two- and three-dimensional measurements in flames
[AD-A264341] p 3425 N93-30162

SPECTRUM ANALYSIS

Tomographic analysis of line-of-sight infrared spectra of low-pressure flames
[AD-A263185] p 3309 N93-28514

Dynamical analysis of highly excited molecular spectra
[DE93-010771] p 3564 N93-28604

Research and development of an airborne multispectral scanner to measure fire, terrestrial and atmospheric characteristics (50 channel)
[NASA-CR-193121] p 3456 N93-28620

Laer-induced breakdown spectroscopy instrument for element analysis of planetary surfaces
p 3434 N93-28769

Planetary and satellite x ray spectroscopy: A new window on solid-body composition by remote sensing
p 3641 N93-28773

Effects of vacuum exposure on stress and spectral shift of high reflective coatings
[DE93-009318] p 3437 N93-29207

Characterization of a space orbited incoherent fiber optic bundle p 3583 N93-29698

Modeling the bidirectional reflectance and spectra
[AD-A263570] p 3462 N93-29830

A search for radiative neutrino decay from supernovae
[NASA-CR-193118] p 3653 N93-30052

Thermal decomposition pathways of RDX in the condensed phase p 3347 N93-30083

Condensed phase diagnostics of nitramine propellant combustion p 3320 N93-30102

Enhanced resolution and de-aliasing techniques for fast Fourier transforms p 3358 N93-30240

The use of data turning in airborne radars
p 3358 N93-30241

ELF/VLF spectrum measurements
p 3398 N93-30745

Computer control of pulsed tunable dye lasers
[DE93-605896] p 3441 N93-30801

ERS-1 directional wave spectra validation with the airborne SAR PHARS
[BCRS-92-18] p 3463 N93-31010

Optical system analysis for the ground based EXVM
[NASA-CR-192588] p 3582 N93-31035

SPECULAR REFLECTION

Formulation of Ames 24E2 IR-black coating
[NASA-TM-102864] p 3629 N93-29453

A program to determine the pointing angle to a specular point
[AD-A262777] p 3630 N93-29460

SPEECH RECOGNITION

Speech recognition by recursive stochastic modelling
[ISBN-90-9005038-8] p 3382 N93-29266

Improvement of the NRC automatic speech recognition system p 3355 N93-30221

The 1991 neural information processing systems: Natural and synthetic
[AD-A264754] p 3623 N93-30559

Examinations of perturbation reduction by automatic speech dependent recognition of separately spoken single words
[ETN-93-94180] p 3394 N93-30672

SPENT FUELS

Compatibility studies of AISI type 316 stainless steel with lead-lithium eutectic alloy
[DE93-605281] p 3328 N93-31022

SPHERES

Sound wave scattering from a rigid sphere
[AD-A264182] p 3562 N93-30157

SPHERICAL ANTENNAS

Progress in the development of broadband electric-field sensors for transient fields p 3369 N93-30306

SPHERICAL HARMONICS

Modern seismic travel time tables and station corrections for P and S waves
[AD-A262536] p 3477 N93-29412

Evaluation of multi-dimensional flux models for radiative transfer in cylindrical combustion chambers
p 3257 N93-29955

SPHERICAL SHELLS

Sound wave scattering from an elastic spherical shell
[AD-A264039] p 3562 N93-30029

Containment of explosions in spherical vessels
[DE93-005445] p 3446 N93-30211

SPIN

Spin observables in large t elastic N-N scattering
[DE93-009211] p 3564 N93-28549

SPIN DYNAMICS

Spin dependent phenomena in medium energy physics
[DE93-010972] p 3565 N93-28849

SPIN EXCHANGE

A high field optical-pumping spin-exchange polarized deuterium source
[DE93-009208] p 3574 N93-28970

SPIN STABILIZATION

Liquid Motion in a rotating tank Experiment (LME)
p 3264 N93-28710

Recent applications of CFD to the aerodynamics of Army projectiles
[AD-A262953] p 3240 N93-29512

SPIN-LATTICE RELAXATION

High pressure studies of hydrated nafion membranes: Dielectric relaxation and deuteron NMR
[AD-A263511] p 3332 N93-29342

SPINE

Sudden loading and fatigue effects on the human spine
[PB93-167526] p 3493 N93-29199

SPLINE FUNCTIONS

A method for intersection line calculation between parametric surfaces
[ETN-93-94178] p 3551 N93-30572

SPLINES

Spline screw autochanger
[NASA-CASE-GSC-13435-1] p 3445 N93-29505

A numerical solution of the two-center problem
[DE92-644674] p 3551 N93-30913

SPORES

Photobiological investigations on spores of streptomyces griseus
[ESA-TT-1269] p 3491 N93-29274

SPRAYERS

Estimation of droplet collision frequency in a spray
[DE93-007991] p 3416 N93-28566

Pulse mitigation and heat transfer enhancement techniques. Volume 1: Spray cooling
[AD-A263495] p 3423 N93-29352

SPREAD F

Ionospheric structure specifications and systems effects
[AD-A263573] p 3476 N93-29343

SPREAD SPECTRUM TRANSMISSION

Theoretical bit error rate performance of the Kalman filter excisor for FM interference
[AD-A263018] p 3383 N93-29407

Electro-optic characterisation of extremely wide bandwidth electrical signals
[AD-A264202] p 3392 N93-30145

A satellite downlink spread spectrum timing beacon
p 3362 N93-30267

Coding for frequency hopped spread spectrum satellite communications p 3365 N93-30283

SPUTTERING

Diffusion bonding
[DE93-011480] p 3442 N93-28837

Electrochemical behavior and surface chemistry of aluminum alloys: Solute-rich interphase model
[AD-A262061] p 3322 N93-29002

Structure and switching dynamics in ferroelectric crystal and liquid crystal thin films
[AD-A263664] p 3594 N93-29293

Improved heat removal by microscopic surface texturing of capillaries
[AD-A263483] p 3424 N93-29966

Ion emission during high-energy sputtering of ammonium dinitramide and ammonium nitrate crystals and the determination of ion decomposition pathways using tandem mass spectrometry p 3318 N93-30066

SQUEEZED STATES (QUANTUM THEORY)
A squeezed state holomorphic phase space representation of equations of motion
[DE93-609835] p 3607 N93-30945
STABILITY
Subnanosecond high power performance of a bistable optically-controlled GaAs switch
[DE93-006285] p 3406 N93-28944
Improved field emitter current densities and stability through the application of a proprietary process
[AD-A263464] p 3411 N93-29833
Structure, adhesion, and stability of metal/oxide and oxide/oxide interfaces
[DE93-012930] p 3325 N93-30060
Two-parameter crack tip field associated with stable crack growth in a thin plate: A hybrid analysis
[AD-A264221] p 3453 N93-30147
STABILITY TESTS
JT-60 Upgrade vertical stability experiments and analysis
[DE93-753131] p 3583 N93-28530
A spectral method determination of the first critical Rayleigh number for a low-Prandtl number crystal melt in a cylindrical container
[NASA-CR-193238] p 3594 N93-29214
Comparison of deformation and shock reactivity for single crystals of RDX and ammonium perchlorate
p 3350 N93-30094
Elastic stability considerations for deep submergence ceramic pressure housing
[AD-A264824] p 3454 N93-30598
STABILIZATION
Stability, bifurcation, and control of Hamiltonian systems
[DE93-012103] p 3547 N93-28648
Bainitic stabilization of austenite in low alloy steels
[DE93-008275] p 3321 N93-28957
Some results on feedback stabilization of a one-link flexible arm
[INRIA-RR-1682] p 3543 N93-30116
STABILIZED PLATFORMS
Stabilized platform for tethered balloon soundings of broadband long- and short-wave radiation
[DE93-007876] p 3383 N93-29308
Derivation of particulate directional information from analysis of elliptical impact craters on LDEF
p 3283 N93-29362
STAINLESS STEELS
Fundamental aspects in the design of passive alloys
[DE93-009028] p 3320 N93-28545
An experimental investigation of radioactivity induced by ions associated with the operation of pulsed-power accelerators
[DE93-011478] p 3575 N93-29151
Effects of internal helium on mechanical properties of Nitronic (tm) 40 stainless steel
[DE93-009902] p 3324 N93-29265
Sensitivity of LDEF foil analyses using ultra-low background germanium vs. large NaI(Tl) multidimensional spectrometers p 3318 N93-29627
High mass resolution glow discharge mass spectrometry using an external ion source FT-ICR mass spectrometer
[AD-A264347] p 3314 N93-30166
Irradiation assisted stress corrosion cracking of stainless steel irradiated in FBR
[DE93-764495] p 3326 N93-30191
Compatibility studies of AISI type 316 stainless steel with lead-lithium eutectic alloy
[DE93-605281] p 3328 N93-31022
STAIRWAYS
Platform stair lift
[NASA-CASE-MFS-28772-1] p 3507 N93-29845
STANDARD DEVIATION
Monte Carlo simulation of magnitude-angle error sources
[AD-A263738] p 3555 N93-29857
Variability of the electric field strength in the earth-ionosphere waveguide due to variations in the electron density profile
[AD-A264808] p 3394 N93-30595
STANDARDIZATION
Standardization of automatic test equipment in the US Air force
[AD-A262076] p 3250 N93-29004
Optical media standards for industry
p 3617 N93-30451
Evaluation of D-1 tape and cassette characteristics: Moisture content of Sony and Ampex D-1 tapes when delivered p 3435 N93-30466
Measurements over distributed high performance computing and storage systems p 3622 N93-30476
Proceedings of the meeting of the Intergovernmental US-Russian Business Development Committee's Standards Working Group
[PB93-179968] p 3610 N93-30822
STANDARDS
OSI transaction processing standard: An introduction and outlines of implementation
[VTT-TIED-1250] p 3532 N93-29997
Consultative Committee for Space Data Systems recommendation for space data system standards: Telecommand. Part 2.1: Command operation procedures
[NASA-TM-108158] p 3393 N93-30371
Grand challenges in mass storage: A systems integrators perspective p 3620 N93-30467
NASA/FAA helicopter simulator workshop
[NASA-CP-3156] p 3236 N93-30673
Part 1: Executive summary p 3236 N93-30674
STANDING WAVES
Three-dimensional simulation analysis of the standing-wave free-electron laser two-beam accelerator
[DE93-010461] p 3575 N93-29870
The IUTAM Symposium on Breaking Waves
[AD-A264196] p 3489 N93-30143
STAR CLUSTERS
ROSAT detection of stellar x ray sources in the old open cluster M67
[MPE-PREPRINT-230] p 3631 N93-30578
STAR DISTRIBUTION
Honeywell's compact, wide-angle UV-visible imaging sensor p 3582 N93-28806
The multiplicity of T Tauri stars in the star forming regions Taurus-Auriga and Ophiuchus-Scorpius: A 2.2 micron speckle imaging survey p 3634 N93-28945
STAR FORMATION
The multiplicity of T Tauri stars in the star forming regions Taurus-Auriga and Ophiuchus-Scorpius: A 2.2 micron speckle imaging survey p 3634 N93-28945
Models of star formation in interacting and merging disk galaxies p 3635 N93-30148
Young open clusters as probes of the star formation process p 3635 N93-30377
The 12 UM contribution of nearby galaxies to the infrared background
[AD-A264336] p 3654 N93-30419
The faintest stars p 3630 N93-30493
Dense gas in the monoceros OB1 dark cloud and its relationship to star formation p 3636 N93-30502
A characterization of young stellar objects in Bok globules: Infrared imaging, spectral energy distributions, and molecular outflows p 3636 N93-30563
CO lines toward NGC 2024 and other star forming regions: A closer look at the warm gas component
[MPE-PREPRINT-223] p 3637 N93-30639
STAR TRACKERS
An auto-guiding system for mid-sized telescopes
p 3375 N93-30340
STARBURST GALAXIES
Models of star formation in interacting and merging disk galaxies p 3635 N93-30148
The 12 UM contribution of nearby galaxies to the infrared background
[AD-A264336] p 3654 N93-30419
Near-infrared line imaging of NGC 6240: Global shock and nuclear starburst
[MPE-PREPRINT-226] p 3631 N93-30641
STARK EFFECT
Start broadened profiles with self-consistent radiation transfer and atomic kinetics in plasmas produced by high intensity lasers
[DE93-008706] p 3586 N93-29093
Ion motion effects on charged radiators
[DE93-009257] p 3565 N93-29099
STARS
Activities report of the Astronomical Society
[MITT-75] p 3629 N93-29008
Bonner Durchmusterung (Southern Durchmusterung)
[NASA-RP-1298-VOL-3] p 3630 N93-29811
STATE VECTORS
Asymptotic properties of constrained Markov decision processes
[INRIA-RR-1598] p 3553 N93-28508
State vector splitting: A numerical scheme for the Euler equations p 3419 N93-29039
STATIC LOADS
Axial impact of composites p 3297 N93-29078
Load test set-up for the Airmass Sunburst Ultra-Light Aircraft p 3249 N93-29776
STATIC PRESSURE
Rugged, no-moving-parts windspeed and static pressure probe designs for measurements in planetary atmospheres p 3434 N93-28767
Performance characteristics of two multiaxis thrust-vectoring nozzles at Mach numbers up to 1.28
[NASA-TP-3313] p 3239 N93-29160
STATIC THRUST
Performance characteristics of two multiaxis thrust-vectoring nozzles at Mach numbers up to 1.28
[NASA-TP-3313] p 3239 N93-29160
STATIONKEEPING
System of navigation by satellites with European coverage p 3284 N93-29897
STATISTICAL ANALYSIS
Information-theoretic performance bounding of Bayesian identifiers
[DE93-010705] p 3554 N93-28763
Recording of forest surface in SAR-images with statistical methods in areas of pronounced relief
p 3457 N93-28920
On the value of function evaluation location information in Monte Carlo simulation
[AD-A263662] p 3554 N93-29292
Characterization and optimization of a Hot Air Solder-Leveling System
[DE93-010188] p 3332 N93-29328
Study on various problems in statistical planning and inference
[AD-A262484] p 3554 N93-29411
Estimating the parameters of chaotic maps
[AD-A262574] p 3556 N93-29423
Character recognition using a neural network model with fuzzy representation p 3512 N93-29536
Inverse problems: Fuzzy representation of uncertainty generates a regularization p 3516 N93-29563
Possibilistic measurement and set statistics
p 3517 N93-29567
Gaussian membership functions are most adequate in representing uncertainty in measurements
p 3520 N93-29584
Some statistical inference problems in linear models and variance components models and their applications
[AD-A264062] p 3555 N93-29923
Propagation channel modeling for angle-diversity combining simulation p 3360 N93-30252
Environmental studies: Mathematical, computational and statistical analyses
[AD-A264223] p 3473 N93-30360
Parametric and combinatorial problems in constrained optimization
[AD-A264229] p 3555 N93-30363
Use of statistics in computational chemistry
[AD-A264307] p 3315 N93-30365
Determinants of performance rating accuracy: A field study
[AD-A264726] p 3500 N93-30575
Oceanographic data processing program
[AD-A264801] p 3544 N93-30591
Chaotic quantum systems
[DE93-606030] p 3606 N93-30802
A miniature fatigue test machine p 3291 N93-30956
STATISTICAL CORRELATION
On the impossibility of creating the quantum correlations with computers
[DE93-606039] p 3606 N93-30806
STATISTICAL DECISION THEORY
Decision analysis with approximate probabilities
p 3513 N93-29542
STATISTICAL DISTRIBUTIONS
Modified goodness-of-fit tests for the Weibull distribution
[AD-A262552] p 3553 N93-28574
A new goodness-of-fit test for the Weibull distribution based on spacings
[AD-A262615] p 3553 N93-28587
Scaling properties of localized quantum chaos
[DE93-606031] p 3606 N93-30803
STATISTICAL MECHANICS
Evaluation of some scale effects in the response and failure of composite beams p 3308 N93-30874
Knot invariants and cellular automata
[AD-A264199] p 3607 N93-30884
STATISTICAL TESTS
Modified goodness-of-fit tests for the Weibull distribution
[AD-A262552] p 3553 N93-28574
Modified Anderson-Darling and Cramer-Von Mises goodness-of-fit tests for the normal distribution
[AD-A262554] p 3553 N93-28575
A new goodness-of-fit test for the Weibull distribution based on spacings
[AD-A262615] p 3553 N93-28587
A modified Anderson Darling goodness-of-fit test for the gamma distribution with unknown scale and location parameters
[AD-A262486] p 3553 N93-28760
A modified chi-squared goodness-of-fit test for the three-parameter gamma distribution with unknown parameters
[AD-A262553] p 3554 N93-28845
STATISTICAL WEATHER FORECASTING
Thunderstorm forecast study for Eglin AFB, Florida
[AD-A263423] p 3483 N93-29810

STATOR BLADES

Three-dimensional fiber-optic LDV measurements in the endwall region of a linear cascade of controlled-diffusion stator blades
[AD-A263513] p 3424 N93-29968

STEADY FLOW

A grid refinement study of two-dimensional transient flow over a backward-facing step using a spectral-element method
[DE92-018262] p 3417 N93-26639

Study of flow structure in rotating cavities: Numerical predictions of laminar and turbulent, steady, and unsteady flows p 3256 N93-29948

STEADY STATE

Steady-state and transient modeling of tracer and nutrient distributions in the global ocean
[DE93-011043] p 3486 N93-28670

Gradient estimation for regenerative processes
[AD-A263766] p 3555 N93-29878

Optimization for steady-state and hybrid operations of ITER by using scaling models of divertor heat load
[DE93-764151] p 3590 N93-30649

Numerical wave propagation and steady-state solutions p 3428 N93-30999

The steady-state tangential contact problem for a falling drop type of contact area on corrugated rail by simplified theory of rolling contact
[ILR-MITT-267(1991)] p 3455 N93-31016

STEEL STRUCTURES

Containment of explosions in spherical vessels
[DE93-005445] p 3446 N93-30211

STEELS

Sound wave scattering from an elastic spherical shell
[AD-A264039] p 3562 N93-30029

STEERABLE ANTENNAS

Optical antenna beam steering using digital phase shifter control
[AD-D015688] p 3383 N93-29455

STEERING

High-current negative-ion beam transport
[DE93-010732] p 3575 N93-29809

STELLAR ACTIVITY

Magnetic activity in low mass stars
[DE93-009073] p 3632 N93-28547

Dense gas in the monoceros OB1 dark cloud and its relationship to star formation p 3636 N93-30502

STELLAR ATMOSPHERES

Spherically symmetric model atmospheres for late-type giant stars
[ISBN-0-315-72632-6] p 3633 N93-28673

STELLAR COLOR

Effects of spiral shocks on disk emission lines
[DE92-641716] p 3637 N93-31004

STELLAR CORES

Why Blue stragglers formed via collisions may not be rapid rotators
[DE93-008708] p 3633 N93-28905

STELLAR ENVELOPES

Why Blue stragglers formed via collisions may not be rapid rotators
[DE93-008708] p 3633 N93-28905

Submillimeter CO observations of warm gas around T-Tauri stars
[MPE-PREPRINT-232] p 3631 N93-30615

STELLAR EVOLUTION

Do the Pop 2 field blue stragglers have a collisional origin?
[DE93-008709] p 3634 N93-28906

Can physical stellar collisions explain the blue stragglers in the dwarf spheroidal galaxies?
[DE93-008711] p 3634 N93-28907

A characterization of young stellar objects in Bok globules: Infrared imaging, spectral energy distributions, and molecular outflows p 3636 N93-30563

STELLAR LUMINOSITY

Effects of spiral shocks on disk emission lines
[DE92-641716] p 3637 N93-31004

STELLAR MAGNITUDE

Bonner Durchmusterung (Southern Durchmusterung)
[NASA-RP-1298-VOL-3] p 3630 N93-29811

STELLAR MASS ACCRETION

The heating and cooling of WZ Sge
[DE93-008720] p 3634 N93-28908

STELLAR MASS EJECTION

A study of the physical mechanisms for filament eruption and coronal mass ejection via numerical simulation
[NASA-CR-193180] p 3653 N93-28935

Submillimeter CO observations of warm gas around T-Tauri stars
[MPE-PREPRINT-232] p 3631 N93-30615

STELLAR MODELS

Spherically symmetric model atmospheres for late-type giant stars
[ISBN-0-315-72632-6] p 3633 N93-28673

Models of star formation in interacting and merging disk galaxies p 3635 N93-30148

Massive Majorana neutrinos in pre-bounce supernovae
[DE92-642597] p 3572 N93-30931

STELLAR PHYSICS

Activities report of the Astronomical Society
[MITT-75] p 3629 N93-29008

STELLAR RADIATION

The x ray population in globular clusters and three crab-like SNR in the large Magellanic cloud
[NASA-CR-193172] p 3630 N93-29604

A search for radiative neutrino decay from supernovae
[NASA-CR-193118] p 3653 N93-30052

STELLAR ROTATION

Why Blue stragglers formed via collisions may not be rapid rotators
[DE93-008708] p 3633 N93-28905

STELLAR SPECTRA

A search for radiative neutrino decay from supernovae
[NASA-CR-193118] p 3653 N93-30052

Rejection of archival photographic objects as optical counterparts of gamma ray bursters
[MPE-PREPRINT-228] p 3631 N93-30642

Infrared spectroscopy and imaging of starburst galaxies and AGNs
[MPE-PREPRINT-229] p 3632 N93-30643

Effects of spiral shocks on disk emission lines
[DE92-641716] p 3637 N93-31004

STELLAR SPECTROPHOTOMETRY

Multiwavelength studies of classical nova shells
p 3636 N93-30412

STELLAR STRUCTURE

Dense gas in the monoceros OB1 dark cloud and its relationship to star formation p 3636 N93-30502

STELLAR SYSTEMS

Stellar encounters in globular clusters
p 3632 N93-28606

STELLAR TEMPERATURE

The heating and cooling of WZ Sge
[DE93-008720] p 3634 N93-28908

STELLARATORS

Edge plasma control by RF electric field in Compact Helical System (CHS)
[DE93-753242] p 3583 N93-28532

STEP FUNCTIONS

Fuzzy operators and cyclic behavior in formal neuronal networks p 3519 N93-29576

On the ideality of using a step-function current in a metallic foil to simulate a step-function heat-flux source
[AD-A264627] p 3413 N93-30539

STEREOSCOPIC VISION

Intermediate levels of visual processing
[AD-A264117] p 3495 N93-30192

Recursive-batch estimation of structure and motion from stereo image sequences p 3363 N93-30271

STEREOSCOPY

Intermediate levels of visual processing
[AD-A264117] p 3495 N93-30192

STIFFENING

Design and analysis of grid stiffened concepts for aircraft composite primary structural applications
p 3306 N93-30861

Prediction of stiffener-skin separation in composite panels p 3307 N93-30871

Experimental behavior of graphite-epoxy Y-stiffened specimens loaded in compression p 3307 N93-30872

Structural response of bead-stiffened thermoplastic shear webs p 3308 N93-30873

STIFFNESS

Influence of ply waviness on stiffness and strength reduction of composite laminates
[AD-A263224] p 3294 N93-28559

Composite laminate stiffnesses and their sensitivities
[DLR-FB-92-16] p 3296 N93-29007

STIMULATED EMISSION

A quality monitor and monitoring technique employing optically stimulated electron emission
[NASA-CASE-LAR-15063-1] p 3449 N93-30414

STIMULATED EMISSION DEVICES

A quality monitor and monitoring technique employing optically stimulated electron emission
[NASA-CASE-LAR-15063-1] p 3449 N93-30414

STIRLING CYCLE

Small Stirling dynamic isotope power system for robotic space missions
[NASA-TM-105785] p 3287 N93-28686

Cryogenic Heat Pipe Experiment (CRYOHP)
p 3265 N93-28721

Miniature long-life space cryocoolers
p 3378 N93-28825

STIRLING ENGINES

Small Stirling dynamic isotope power system for robotic space missions
[NASA-TM-105785] p 3287 N93-28686

STOCHASTIC PROCESSES

Some qualitative properties in polling systems
[INRIA-RR-1596] p 3552 N93-28506

Comparison of analytical transport and stochastic solutions for neutron slowing down in an infinite medium
[DE93-010799] p 3565 N93-28833

Poloidal field measurements during transient phenomena on MTX: Sawtooth perturbations and the effect of ECH on disruptions
[DE93-010516] p 3587 N93-29303

Stochastic architecture for Hopfield neural nets
p 3519 N93-29579

Gradient estimation for regenerative processes
[AD-A263766] p 3555 N93-29878

A stochastic formation of radiative transfer in clouds
[DE93-011372] p 3484 N93-30055

Damage mechanics in 2-D and 3-D microstructures
[AD-A264337] p 3453 N93-30159

An information theoretic approach to stochastic adaptive control application to manipulators with active inertia
p 3359 N93-30247

Zero-crossing rate of some non-Gaussian processes
p 3360 N93-30254

A numerical simulator for testing sliding mode controls in stochastic systems p 3361 N93-30260

Parametric and combinatorial problems in constrained optimization
[AD-A264229] p 3555 N93-30363

Adaptive networks for sequential decision problems
[AD-A264756] p 3534 N93-30561

Evolving neural network architecture
[AD-A264802] p 3544 N93-30592

Chaotic quantum systems
[DE93-606030] p 3606 N93-30802

Determination of low frequency reference slipping for high frequency unstationary motion processes
[ILR-MITT-273(1992)] p 3455 N93-31017

STOICHIOMETRY

Studies in Lewis acid and superacid ionic liquids
[AD-A264683] p 3316 N93-30551

STORAGE BATTERIES

Development of nickel/metal hydride secondary battery
[DE93-781330] p 3406 N93-28669

Research and development of carbon black anodes for lithium secondary cells
[DE93-781331] p 3406 N93-28746

Approach to extending the cycle life of lithium secondary battery
[DE93-776266] p 3406 N93-28983

Effect of zinc and iron ions on the electrochemistry of nickel oxide electrode: Slow cyclic voltammetry
[AD-A263098] p 3311 N93-29133

Research and development of lithium secondary batteries for load conditioner use, volume 2
[DE93-781329] p 3410 N93-29673

Characterization of lithium electrode surface in lithium secondary batteries by in situ Raman spectroscopic methods
[AD-A263728] p 3411 N93-29986

STORAGE RINGS (PARTICLE ACCELERATORS)

A 250 mA toroid monitor for the measurement of the bundle current in the stretcher mode of AmPS
[DIGEL-1992-1] p 3413 N93-30835

Charge to frequency converter for ionization chambers belonging to the radiation protection system of AmPS/MEA
[DIGEL-1991-6] p 3577 N93-30837

Electronics for a neutron detector and a Geiger-Mueller detector for the radiation protection around MEA and AmPS
[DIGEL-1992-6] p 3413 N93-30838

STORAGE STABILITY

ICI optical data storage tape: An archival mass storage media p 3621 N93-30472

STORAGE TANKS

Advanced collapsible tank for liquid containment
[NASA-CR-188247] p 3353 N93-28698

Liquid Motion in a rotating tank Experiment (LME)
p 3264 N93-28710

Vented Tank Resupply Experiment (VTRE) for In-Space Technology Experiment Program (IN-STEP)
p 3264 N93-28711

Tank issues: Design and placement of floating liquid monitoring wells
[PB93-161149] p 3469 N93-29033

STORM DAMAGE

Deadliest, costliest, and most intense US hurricanes of this century (and other frequently requested hurricane facts)
[PB93-174993] p 3485 N93-30758

STRAIN DISTRIBUTION

Thermoviscoplastic analysis of fibrous periodic composites using triangular subvolumes
[NASA-TM-106076] p 3297 N93-29074

Two-parameter crack tip field associated with stable crack growth in a thin plate: A hybrid analysis
[AD-A264221] p 3453 N93-30147

STRAIN GAGES
Tactile sensing for 3-dimensional shape estimation
p 3357 N93-30232
Fiber-optic polarimetric strain gauge
p 3375 N93-30341
STRAIN HARDENING
Constitutive laws for deformation and dynamic recrystallization in cubic metals
[DE93-010740] p 3326 N93-30486
STRAIN MEASUREMENT
The design and testing of a high-temperature graphite dilatometer
[AD-A262185] p 3430 N93-28488
Enhanced noncontacting laser extensometer for biaxial strain measurements
[AD-A263170] p 3430 N93-28989
Results of a round robin test program: Complex modulus properties of a polymeric damping material
[AD-A263619] p 3332 N93-29344
Fiber-optic polarimetric strain gauge
p 3375 N93-30341
STRAIN RATE
Interim fatigue design curves for carbon, low-alloy, and austenitic stainless steels in LWR environments
[DE93-009202] p 3323 N93-29102
Comparison of deformation and shock reactivity for single crystals of RDX and ammonium perchlorate
p 3350 N93-30094
STRANDS
Condensed phase diagnostics of nitramine propellant combustion p 3320 N93-30102
STRATIFIED FLOW
Laboratory studies of gravity wave/mean flow interactions
[AD-A264226] p 3478 N93-30174
STRATIGRAPHY
Drill/borescope system for the Mars Polar Pathfinder
p 3647 N93-28805
STRATOCUMULUS CLOUDS
Sensitivity study of cloud/radiation interaction using a second order turbulence radiative-convective model
[DE93-007365] p 3477 N93-29346
STRATOSPHERE
Analysis of mass transport and potential vorticity budget in a simulated tropopause folding
[PB93-156792] p 3476 N93-29197
STREAK CAMERAS
A new tubeless nanosecond streak camera based on optical deflection and direct CCD imaging
[DE93-011893] p 3433 N93-30491
STREAK PHOTOGRAPHY
Effects of flow-path variations on internal reversing flow in a tailpipe offtake configuration for ASTOVL aircraft
[NASA-TM-106149] p 3252 N93-29065
STREPTOMYCETES
Photobiological investigations on spores of streptomyces griseus
[ESA-TT-1269] p 3491 N93-29274
STRESS (PHYSIOLOGY)
Evaluation of personal cooling systems in conjunction with explosive ordnance disposal suits
[AD-A262862] p 3506 N93-29471
STRESS ANALYSIS
Thermal and mechanical analysis of flip-chips on a liquid cooled multichip module
[DE93-007609] p 3405 N93-28641
Design and evaluation of a uniaxial pull test for lithium hydride/deuteride
[DE93-010760] p 3451 N93-28832
Ceramic matrix composites properties/microstresses with complete and partial interphase bond
[NASA-TM-106136] p 3297 N93-29071
A numerical study of confined turbulent jets
[NASA-TM-106197] p 3420 N93-29161
Effects of vacuum exposure on stress and spectral shift of high reflective coatings
[DE93-009318] p 3437 N93-29207
Structural design of cryostat and port penetration of International Thermonuclear Experimental Reactor (ITER)
[DE93-753267] p 3587 N93-29243
The XNOVAKTC rheological model
[AD-A263298] p 3342 N93-29762
Three-dimensional elastic stress analysis in materials with many inhomogeneities
[AD-A263736] p 3453 N93-29855
Design and implementation of an interactive isochromatic fringe-analysis system using machine-vision techniques p 3369 N93-30305
Elastic stability considerations for deep submergence ceramic pressure housing
[AD-A264824] p 3454 N93-30598
Structural design, analysis, and code evaluation of an odd-shaped pressure vessel
[DE93-008182] p 3447 N93-30632
A Rayleigh-Ritz analysis methodology for cutouts in composite structures p 3307 N93-30869
Direct tension experiments on compacted granular materials p 3292 N93-30960
STRESS CONCENTRATION
Cratering in glasses impacted by debris or micrometeorites p 3340 N93-29368
STRESS CORROSION
Overview of piping issues and trends
[DE93-006628] p 3354 N93-28893
STRESS CORROSION CRACKING
Irradiation assisted stress corrosion cracking of stainless steel irradiated in FBR
[DE93-764495] p 3326 N93-30191
STRESS DISTRIBUTION
Advanced collapsible tank for liquid containment
[NASA-CR-188247] p 3353 N93-28698
Thermoviscoplastic analysis of fibrous periodic composites using triangular subvolumes
[NASA-TM-106076] p 3297 N93-29074
Shear sensitive monomer-polymer laminate structure and method of using same
[NASA-CASE-LAR-14654-1-CU] p 3452 N93-29613
Direct tension experiments on compacted granular materials p 3292 N93-30960
STRESS INTENSITY FACTORS
The growth of small corrosion fatigue cracks in alloy 2024
[NASA-TM-107755] p 3451 N93-29069
Stress-intensity-factor influence coefficients for axial and circumferential flaws in reactor pressure vessels
[DE93-006206] p 3454 N93-30213
STRESS MEASUREMENT
Shear sensitive monomer-polymer laminate structure and method of using same
[NASA-CASE-LAR-14654-1-CU] p 3452 N93-29613
Processing of novel nanoparticle dispersion strengthened ceramics for improved mechanical performance
[AD-A264191] p 3339 N93-30883
STRESS RATIO
Mechanical behaviour of a closed collar model for an 11.5 T dipole
[NIKHEF-H/92-03] p 3576 N93-30019
STRESS TENSORS
Quantum field theory in spaces with closed time-like curves
[DE93-010564] p 3605 N93-30481
STRESS WAVES
Rapidly activated dynamic phase transitions in nonlinear solids
[AD-A263601] p 3299 N93-29982
STRESS-STRAIN RELATIONSHIPS
Thermoviscoplastic analysis of fibrous periodic composites using triangular subvolumes
[NASA-TM-106076] p 3297 N93-29074
An investigation of graphite peek composite under compression with a centrally located circular discontinuity
[AD-A262549] p 3298 N93-29414
The XNOVAKTC rheological model
[AD-A263298] p 3342 N93-29762
Experiment and analysis on elastic deformation properties of graphite and carbon materials for HTTR core components
[DE93-753271] p 3299 N93-30004
Damage growth in composite propellants
p 3348 N93-30088
Damage of multi-directionally reinforced ceramic-matrix composites p 3308 N93-30937
Mechanical properties of composite materials
p 3290 N93-30951
A miniature fatigue test machine p 3291 N93-30956
A continuum code investigation of stress integration using exact and approximate material rotation
[DE93-001892] p 3454 N93-31013
STRIATION
Large amplitude striations in an RF discharge
[DE93-753244] p 3379 N93-28534
STRING THEORY
Topics in gauge theories and the unification of elementary particle interactions
[DE93-009370] p 3563 N93-28542
Studies in theoretical high energy particle physics
[DE93-007990] p 3574 N93-28565
Understanding conformal field theory through parafermions and Chern Simons theory
[DE93-010452] p 3604 N93-29806
Topics in inflationary universe models and cosmic string theories p 3637 N93-30579
Geometrical approach to the dynamics of a relativistic string in the D-dimensional Minkowski space
[DE93-606071] p 3605 N93-30784
Electric magnetic duality in string theory
[DE93-606061] p 3606 N93-30807
A new exact solution to the classical equations of motion of the relativistic string with massive ends
[DE92-644736] p 3557 N93-30922
Invariant structures in gauge theories and confinement
[DE92-644739] p 3607 N93-30924
Invariant structures and static forces in gauge theories
[DE92-644740] p 3607 N93-30925
STRINGS
Geometrical approach to the dynamics of a relativistic string in the D-dimensional Minkowski space
[DE93-606071] p 3605 N93-30784
STRONTIUM TITANATES
Phase transition studies in barium and strontium titanates at microwave frequencies p 3293 N93-30970
STROUHAL NUMBER
Determination of surface heat transfer and film cooling effectiveness in unsteady wake flow conditions
p 3253 N93-29933
Vortex shedding by blunt/bluff bodies at high Reynolds numbers. Volume 4: Rectangles
[AD-A264154] p 3241 N93-30151
STRUCTURAL ANALYSIS
Metal Matrix Laminate Tailoring (MMLT) code: User's manual
[NASA-TM-106052] p 3295 N93-28681
Analysis for thermo-chemical decomposition of composite structures
[NASA-CR-193185] p 3295 N93-28843
TESLA test cell cryostat support post thermal and structural analysis
[DE93-008365] p 3407 N93-29048
Reliability assessment of thrust chamber cooling concepts using probabilistic analysis techniques
[NASA-CR-190785] p 3288 N93-29068
Nonlinear analyses of composite aerospace structures in sonic fatigue
[NASA-CR-193124] p 3451 N93-29154
The Ultra Light Aircraft Testing
[NASA-CR-193043] p 3249 N93-29774
Thermodynamic and structural properties of metallic glasses and supercooled liquids
[ISBN-0-315-72443-9] p 3605 N93-30359
Structural evaluation of curved stiffened composite panels fabricated using a THERM-Xsm process
p 3301 N93-30435
Long discontinuous fiber composite structure: Forming and structural mechanics p 3301 N93-30437
Effects of scale in predicting global structural response p 3306 N93-30860
Multiple methods integration for structural mechanics analysis and design p 3307 N93-30867
Probabilistic composite analysis p 3307 N93-30868
Prediction of stiffener-skin separation in composite panels p 3307 N93-30871
Structural response of bead-stiffened thermoplastic shear webs p 3308 N93-30873
STRUCTURAL DESIGN
Planning of a West Virginia University Research Center in the basic materials sciences
[DE93-011731] p 3592 N93-28647
A demonstration of simple airfoils: Structural design and materials choices
[DE93-007882] p 3238 N93-28662
Indigenous lunar construction materials
p 3277 N93-29120
Structural design of cryostat and port penetration of International Thermonuclear Experimental Reactor (ITER)
[DE93-753267] p 3587 N93-29243
Concept design example, Computer Aided Structural Modeling (CASM). Scheme A
[AD-A264759] p 3529 N93-29657
Concept design example, Computer Aided Structural Modeling (CASM). Scheme B
[AD-A264760] p 3529 N93-29658
From orbital debris capture systems through internal combustion engines on Mars p 3232 N93-29745
B and T: Lunar landers p 3234 N93-29751
Report on the test set-up for the structural testing of the Airmass Sunburst Ultralight Aircraft
p 3249 N93-29775
Effect of design selection on response surface performance
[NASA-CR-4520] p 3249 N93-29885
Structural design, analysis, and code evaluation of an odd-shaped pressure vessel
[DE93-008182] p 3447 N93-30632
Guideway structural design and power/propulsion/braking in relation to guideways, volume 1
[PB93-169902] p 3447 N93-30820
Preliminary properties of a resin from ethynyl terminated materials p 3303 N93-30842
Multi-parameter optimization tool for low-cost commercial fuselage crown designs
p 3305 N93-30858

A comparison of classical mechanics models and finite element simulation of elastically tailored wing boxes
p 3306 N93-30863
Multiple methods integration for structural mechanics analysis and design p 3307 N93-30867
Tailored composite wings with elastically produced chordwise camber p 3308 N93-30876
Design, synthesis, and chemical processing of hierarchical ceramic structures for aerospace applications
[AD-A264227] p 3339 N93-30885
Construction and testing of simple airfoils to demonstrate structural design, materials choice, and composite concepts p 3243 N93-30979
Structural design using neural networks
p 3545 N93-31029

STRUCTURAL ENGINEERING
JPRS report: Science and technology. Central Eurasia: Engineering and equipment
[JPRS-UEQ-93-001] p 3274 N93-29014
Concept design example, Computer Aided Structural Modeling (CASM). Scheme A
[AD-A264759] p 3529 N93-29657
Concept design example, Computer Aided Structural Modeling (CASM). Scheme B
[AD-A264760] p 3529 N93-29658
GENESIS 2: Advanced lunar outpost
p 3235 N93-29760
Geoscience center research
[AD-A263465] p 3462 N93-29834

STRUCTURAL FAILURE
Reliability assessment of thrust chamber cooling concepts using probabilistic analysis techniques
[NASA-CR-190785] p 3288 N93-29068
Sensor systems for monitoring Maglev guideway structures
[PB93-154821] p 3444 N93-29205
Progressive failure methodologies for predicting residual strength and life of laminated composites
p 3307 N93-30866
Probabilistic composite analysis p 3307 N93-30868

STRUCTURAL MEMBERS
Effects of scale in predicting global structural response p 3306 N93-30860

STRUCTURAL PROPERTIES (GEOLOGY)
Venus Interior Structure Mission (VISM): Establishing a seismic network on Venus p 3649 N93-28819

STRUCTURAL STABILITY
Low-cost Active Structural Control space experiment (LASC) p 3263 N93-28700
Bainitic stabilization of austenite in low alloy steels
[DE93-008275] p 3321 N93-28957

STRUCTURAL VIBRATION
The natural excitation technique (NExT) for modal parameter extraction from operating wind turbines
[DE93-010611] p 3463 N93-28603
NASA instep/MDMSC jitter suppression experiment (JITTER) p 3263 N93-28702
Description of the Joint Damping Experiment (JDX)
p 3263 N93-28703
Control-structures interaction test of the LACE satellite
p 3263 N93-28706
Upper atmosphere research satellite jitter study
p 3264 N93-28708
Robust feedforward/feedback control synthesis for uncertain dynamical systems p 3542 N93-29079
Testing in combined dynamic environments
[DE93-010679] p 3278 N93-29250

STRUCTURAL WEIGHT
Construction and testing of simple airfoils to demonstrate structural design, materials choice, and composite concepts p 3243 N93-30979

STRUCTURED PROGRAMMING
Reactive integration for traditional programming languages
[AD-A263986] p 3531 N93-29866

STRUTS
CSI-Star: A low-cost CSI orbital testbed
p 3263 N93-28707
Development of an experimental method to determine the axial rigidity of a strut-node joint
p 3290 N93-30950

STUDENTS
Filling the gaps: An overview of data on education in grades K through 12
[PB93-176550] p 3608 N93-30821
Materials education activities p 3291 N93-30958
Visualizing weld metal solidification using organic analogs p 3293 N93-30973

SUBASSEMBLIES
Hybrid CMS methods with model reduction for assembly of structures p 3274 N93-29110

SUBLIMATION
Vortex structure and mass transfer near the base of a cylinder and a turbine blade p 3253 N93-29929

SUBMARINES
Orbiting transmitter and antenna for spaceborne communications at ELF/VLF to submerged submarines
p 3399 N93-30755

SUBMERGED BODIES
Sound wave scattering from an elastic spherical shell
[AD-A264039] p 3562 N93-30029
Sound wave scattering from a rigid sphere
[AD-A264182] p 3562 N93-30157

SUBMILLIMETER WAVES
Novel low temperature superconducting bolometers
[DE93-010433] p 3430 N93-28664
Superconducting submillimeter and millimeter wave detectors
[DE93-007656] p 3431 N93-29149
Submillimeter and microwave residual losses in epitaxial films of Y-Ba-Cu-O and Tl-Ca-Ba-Cu-O
[DE93-010430] p 3596 N93-29868
Submillimeter CO observations of warm gas around T-Tauri stars
[MPE-PREPRINT-232] p 3631 N93-30615

SUBREFLECTORS
A note on the computation of antenna-blocking shadows p 3385 N93-29593
DSS-14 subreflector actuator dynamics during the Landers earthquake p 3386 N93-29600

SUBROUTINE LIBRARIES (COMPUTERS)
RTE: A UNIX library with on-line documentation and sample programs for microwave radiative transfer calculations
[PB93-180248] p 3386 N93-29680

SUBROUTINES
Development of a PC code package for the analysis of research and power reactors
[DE92-638517] p 3536 N93-31001

SUBSONIC FLOW
The numerical solution of low Mach number flow in confined regions by Richardson extrapolation
[TRITA-NA-9207] p 3238 N93-29005
The 3-D viscous flow CFD analysis of the propeller effect on an advanced ducted propeller subsonic inlet
[NASA-TM-106240] p 3252 N93-29162
Experimental study of heat transfer close to a plane wall heated in the presence of multiple injections (subsonic flow) p 3253 N93-29931
Plasma/particle interaction in subsonic argon/helium thermal plasma jets
[DE93-010808] p 3589 N93-30181
Numerical wave propagation and steady-state solutions p 3428 N93-30999

SUBSTITUTES
Materials characterization of cermet anodes tested in a pilot cell
[DE93-008924] p 3323 N93-29101
Effect of lead addition on the formation of superconducting phases in Bi-Sr-Ca-Cu-O ceramics
[DE93-606893] p 3339 N93-30773

SUBSTRATES
Influence of the Cold Buster (tm) sports bar on heat debt, mobilization and oxidation of energy substrates
[AD-A262762] p 3493 N93-28939
Modification of spectral distributions by multilayer structures
[DE93-009308] p 3310 N93-29059
High-dose implantations of Al into Si(111) and Si(100)
[DE93-009552] p 3594 N93-29301
The mechanical response of gold substrates modified with self-assembling monolayer films
[AD-A262997] p 3452 N93-29515
The 2-6 semiconductor superlattices
[AD-A264343] p 3597 N93-30164
Study on diamond semiconductor
[DE92-531076] p 3413 N93-30622
Superconducting flux coupled fast switching device from YBCO films
[AD-A264301] p 3414 N93-30896

SUBSTRUCTURES
An overview of the crash dynamics failure behavior of metal and composite aircraft structures
p 3308 N93-30875

SUITS
Evaluation of personal cooling systems in conjunction with explosive ordnance disposal suits
[AD-A262862] p 3506 N93-29471

SULFATES
Adsorption of sulfate on metal electrodes
[AD-A263192] p 3309 N93-28540
In situ Fourier transform infrared spectroscopic study of bisulfate and sulfate adsorption on gold, with and without the underpotential deposition of copper
[AD-A263421] p 3323 N93-29259
Marine microbial production of dimethylsulfide from dissolved dimethylsulfoniopropionate
[NASA-CR-193278] p 3492 N93-30665

SULFONATES
Design of acentric materials: X ray structures of guanidinium p-nitro- and p-hydroxybenzenesulfonate
[AD-A264220] p 3597 N93-30146

SULFONIC ACID
Dioxygen reduction in various acid electrolytes
[AD-A263564] p 3317 N93-30664

SULFUR
The thermodynamic properties of thianthrene and phenoxathiin
[DE93-000124] p 3603 N93-28964
Hydrogen and sulfur production from hydrogen sulfide wastes
[DE93-008658] p 3310 N93-29052
Marine microbial production of dimethylsulfide from dissolved dimethylsulfoniopropionate
[NASA-CR-193278] p 3492 N93-30665
Hydrogen sulfide decomposition into hydrogen and sulfur by quinone cycles, part 1
[PB93-175297] p 3317 N93-30761

SULFUR DIOXIDES
Analysis of protocol gases: An on-going quality assurance audit
[PB93-168839] p 3311 N93-29204
Organometallic and surface chemistry of mixed-metal systems
[DE93-012686] p 3325 N93-30059
Decomposition of hydrogen sulfide for small scale gas processing.
[PB93-174704] p 3316 N93-30658

SULFUR FLUORIDES
Global warming potential for SF6
[DE93-007394] p 3469 N93-28972

SULFURIC ACID
In situ Fourier transform infrared spectroscopic study of bisulfate and sulfate adsorption on gold, with and without the underpotential deposition of copper
[AD-A263421] p 3323 N93-29259

SUM RULES
Nonlinear coupling of tearing fluctuations in the Madison Symmetric Torus
[DE93-010131] p 3584 N93-28602
Borel sum rules for octet baryons in nuclear medium
[DE93-753245] p 3604 N93-29242

SUNLIGHT
Optical system analysis for the ground based EXVM
[NASA-CR-192588] p 3582 N93-31035

SUNRISE
Tidal and lunar data for Point Mugu, San Nicolas island, and the Barking Sanda area during 1993
[AD-A262725] p 3477 N93-29401

SUNSET
Tidal and lunar data for Point Mugu, San Nicolas island, and the Barking Sanda area during 1993
[AD-A262725] p 3477 N93-29401

SUPERCHARGERS
Improved silicon nitride for advanced heat engines
[NASA-CR-182193] p 3298 N93-29451

SUPERCOMPUTERS
Installation of a new Fortran compiler and effective programming method on the vector supercomputer
[DE93-753322] p 3524 N93-28537
Computing for magnetic fusion energy research: An updated vision
[DE93-010394] p 3587 N93-29190
National Center for Supercomputer Applications
p 3614 N93-29232
Associative memories for supercomputers
[AD-A263142] p 3520 N93-29482
NESL: A nested data-parallel language (Version 2.6)
[AD-A263548] p 3530 N93-29822
High performance computing: Advanced Research Projects Agency should do more to foster program goals. Report to the Chairman, Committee on Armed Services, House of Representatives
[GAO/IMTEC-93-24] p 3533 N93-30202
Promoting high-performance computing and communications
[ISBN-0-16-041828-3] p 3522 N93-30570
Nonlinear explicit transient finite element analysis on the Intel Delta
[DE93-009561] p 3535 N93-30647
High performance computing and communications program p 3627 N93-30715

SUPERCONDUCTING CAVITY RESONATORS
TESLA test cell cryostat support post thermal and structural analysis
[DE93-008365] p 3407 N93-29048
Design and test of a superconducting RFQ for heavy ions
[DE93-010862] p 3575 N93-29317
Advanced microwave frequency sources and filters based on superconducting Photonic Band Gap (PBG) structures
[AD-A264404] p 3597 N93-30175

SUPERCONDUCTING DEVICES

Novel low temperature superconducting bolometers
[DE93-010433] p 3430 N93-28664

Superconducting submillimeter and millimeter wave detectors
[DE93-007656] p 3431 N93-29149

Quantum devices using Si-based superlattices and structures
[AD-A263700] p 3595 N93-29383

Advanced microwave frequency sources and filters based on superconducting Photonic Band Gap (PBG) structures
[AD-A264404] p 3597 N93-30175

Superconducting flux coupled fast switching device from YBCO films
[AD-A264301] p 3414 N93-30896

SUPERCONDUCTING FILMS

Flux lattice relaxation, noise, and symmetry-breaking in frustrated Josephson junction arrays
[DE93-008713] p 3593 N93-29094

A novel approach for new radiation sources based on solid state plasma instabilities
[AD-A263699] p 3588 N93-29382

Submillimeter and microwave residual losses in epitaxial films of Y-Ba-Cu-O and Tl-Ca-Ba-Cu-O
[DE93-010430] p 3596 N93-29868

Measurement of magnetic field penetration depth in niobium polycrystalline films by polarized neutron reflection method
[DE93-606390] p 3600 N93-30771

Superconducting films of YBaCuO
[DE93-606831] p 3600 N93-30772

Heat generation produced in thin layers of GaAs superconductors under high energy particles irradiation
[DE93-606332] p 3601 N93-30798

Superconducting flux coupled fast switching device from YBCO films
[AD-A264301] p 3414 N93-30896

SUPERCONDUCTING MAGNETS

Microstructural understanding and critical current optimization of advanced high field superconductors
[DE93-011046] p 3592 N93-28643

Flux lattice relaxation, noise, and symmetry-breaking in frustrated Josephson junction arrays
[DE93-008713] p 3593 N93-29094

Preliminary investigation of high power microwave plasmas for electrothermal thruster use
[NASA-TM-106207] p 3288 N93-29158

An RF driven H(-) source and a low energy beam injection system for RFQ operation
[DE93-010438] p 3575 N93-29302

Guideway structural design and power/propulsion/braking in relation to guideways, volume 1
[PB93-169902] p 3447 N93-30820

SUPERCONDUCTING SUPER COLLIDER

Maximizing the luminosity of hadron, supercolliders at 10-100 TeV
[DE93-009247] p 3574 N93-29103

New Mexico Center for Particle Physics: Studies of fundamental interactions
[DE93-008302] p 3566 N93-29261

An RF driven H(-) source and a low energy beam injection system for RFQ operation
[DE93-010438] p 3575 N93-29302

SUPERCONDUCTIVITY

ORNL superconducting technology program for electric energy systems
[DE93-009588] p 3404 N93-28523

Finite element analysis of time-independent superconductivity
[NASA-CR-191140] p 3450 N93-28556

Theory of normal and superconducting properties of fullerene-based solids
[DE93-007722] p 3592 N93-28582

Numerical simulation of quantum many-body systems
[DE93-008300] p 3603 N93-28958

A detailed technology roadmap for superconductivity
p 3526 N93-29045

Design and test of a superconducting RFQ for heavy ions
[DE93-010862] p 3575 N93-29317

Sensitive detection of new superconductors created at ultra high pressures
[AD-A264340] p 3597 N93-30161

Phase separation, antiferromagnetism, and superconductivity in superconducting-superoxygenated La(2-x)Sr(x)CuO(4+(delta))
[DE93-009852] p 3598 N93-30517

The Road to Room Temperature Superconductivity Workshop
[AD-A264633] p 3561 N93-30519

A tight binding model for the electronic structure of FCC and SC C60
[DE93-606214] p 3601 N93-30794

A possibility to investigate the superconducting gap with the help of neutrons
[DE93-606392] p 3601 N93-30799

Superconducting flux coupled fast switching device from YBCO films
[AD-A264301] p 3414 N93-30896

Schroedinger equations of higher (greater than 2) order
[DE92-644677] p 3552 N93-30984

SUPERCONDUCTORS

Theory of normal and superconducting properties of fullerene-based solids
[DE93-007722] p 3592 N93-28582

A detailed technology roadmap for superconductivity
p 3526 N93-29045

Ambient-atmosphere compatible superconducting fullerenes
[AD-A262025] p 3595 N93-29397

Phase separation, antiferromagnetism, and superconductivity in superconducting-superoxygenated La(2-x)Sr(x)CuO(4+(delta))
[DE93-009852] p 3598 N93-30517

A possibility to investigate the superconducting gap with the help of neutrons
[DE93-606392] p 3601 N93-30799

SUPERCOOLING

Thermodynamic and structural properties of metallic glasses and supercooled liquids
[ISBN-0-315-72443-9] p 3605 N93-30359

SUPERGIANT STARS

Spherically symmetric model atmospheres for late-type giant stars
[ISBN-0-315-72632-6] p 3633 N93-28673

SUPERGRAVITY

Topics in gauge theories and the unification of elementary particle interactions
[DE93-009370] p 3563 N93-28542

Compensating fields and anomalies in supergravity
[DE92-644724] p 3637 N93-30919

SUPERHEATING

Tank Pressure Control Experiment/Thermal Phenomena (TPCE/TP) p 3264 N93-28713

SUPERLATTICES

Planning of a West Virginia University Research Center in the basic materials sciences
[DE93-011731] p 3592 N93-28647

Modification of spectral distributions by multilayer structures
[DE93-009308] p 3310 N93-29059

Quantum devices using Si-based superlattices and structures
[AD-A263700] p 3595 N93-29383

The 2-6 semiconductor superlattices
[AD-A264343] p 3597 N93-30164

Electronic states in quantum wells with periodically structured interfaces
[DE93-606295] p 3600 N93-30769

SUPERNOVA REMNANTS

The x ray population in globular clusters and three crab-like SNR in the large Magellanic cloud
[NASA-CR-193172] p 3630 N93-29604

SUPERNOVA 1987A

Limits on neutrino radiative decay from SN1987A
[NASA-CR-193262] p 3653 N93-29164

SUPERNOVAE

A search for radiative neutrino decay from supernovae
[NASA-CR-193118] p 3653 N93-30052

Massive Majorana neutrinos in pre-bounce supernovae
[DE92-642597] p 3572 N93-30931

SUPERSONIC AIRCRAFT

Sonic boom problem for future highspeed aircraft
[ONERA-NT-1990-3] p 3241 N93-30020

SUPERSONIC BOUNDARY LAYERS

Supersonic flow calculation using a Reynolds-stress and an eddy thermal diffusivity turbulence model
[NASA-CR-4515] p 3420 N93-29159

SUPERSONIC COMBUSTION

Studies of hydrogen-air diffusion flames and of compressibility effects related to high-speed propulsion
p 3310 N93-29125

SUPERSONIC COMBUSTION RAMJET ENGINES

Nonlinear relaxation algorithms for the compressible Navier-Stokes equations in two and three dimensions
p 3421 N93-29177

SUPERSONIC FLOW

Development of a 3-D Implicit Euler Code for Hypersonic and High Supersonic Flows
[ONERA-RSF-23/1123-AY-230A] p 3417 N93-28744

Supersonic flow calculation using a Reynolds-stress and an eddy thermal diffusivity turbulence model
[NASA-CR-4515] p 3420 N93-29159

SUPERSONIC JET FLOW

Laser spectroscopy of hydrocarbon radicals
[DE93-012555] p 3436 N93-28653

SUPERSONIC SPEED

Topology and grid adaption for high-speed flow computations
[NASA-CR-4216] p 3426 N93-30375

SUPERSONIC TRANSPORTS

The HSCT mission analysis of waverider designs
[NASA-CR-193467] p 3243 N93-31037

SUPERSONIC TURBINES

The influence of non-uniform spanwise inlet temperature on turbine rotor heat transfer p 3253 N93-29932

SUPERSYMMETRY

Topics in gauge theories and the unification of elementary particle interactions
[DE93-009370] p 3563 N93-28542

Studies in theoretical high energy particle physics
[DE93-007990] p 3574 N93-28565

Dark matter: Theoretical perspectives
[DE93-008484] p 3633 N93-28676

Compensating fields and anomalies in supergravity
[DE92-644724] p 3637 N93-30919

Quantum group generalization of the heterotic QFT
[DE92-644727] p 3607 N93-30920

Superconformal structures and holomorphic 1/2-superdifferentials on N = 1 super Riemann surfaces
[DE93-604133] p 3558 N93-30989

SUPPORT SYSTEMS

A new class of mission support for combat air-crew
p 3501 N93-28854

Natural environmental service support to NASA vehicle, technology, and sensor development programs
[NASA-CR-192554] p 3469 N93-29029

Intelligent support for human computer interaction and decision-making in distribution planning and scheduling systems
[AD-A263985] p 3610 N93-30124

SUPPORTS

Development of an O atom gun
[AD-A264753] p 3570 N93-30558

SURFACE ACOUSTIC WAVE DEVICES

SAW technology for on-board processing in military satellite communications p 3362 N93-30265

SURFACE CRACKS

The growth of small corrosion fatigue cracks in alloy 2024
[NASA-TM-107755] p 3451 N93-29069

SURFACE DEFECTS

Fracture of glass p 3293 N93-30969

SURFACE DIFFUSION

Surface diffusion: Atomistics and surface morphology (summary of MRS Symposium B panel discussion)
[DE93-009862] p 3594 N93-29188

SURFACE DISTORTION

System overview on electromagnetic compensation for reflector antenna surface distortion
[NASA-TM-106217] p 3273 N93-29195

SURFACE ENERGY

A study of the chemical mechanism in lubrication
[DE93-012230] p 3330 N93-28650

SURFACE LAYERS

Acousto-optic infrared spectral imager for Pluto fast flyby p 3285 N93-28781

Elemental analyses of hypervelocity microparticle impact sites on Interplanetary Dust Experiment sensor surfaces
p 3638 N93-29378

Characterization of lithium electrode surface in lithium secondary batteries by in situ Raman spectroscopic methods
[AD-A263728] p 3411 N93-29986

SURFACE NAVIGATION

A comparison of simulated parallax and single-station range aids to navigation
[AD-A263460] p 3246 N93-29818

Conspicuity of aids to navigation. Part 1: Temporal patterns for flashing lights
[AD-A264626] p 3499 N93-30426

SURFACE PROPERTIES

Laer-induced breakdown spectroscopy instrument for element analysis of planetary surfaces
p 3434 N93-28769

Microtextured metals for stray-light suppression in the Clementine startracker p 3286 N93-28785

Visible imaging on the Pluto fast flyby mission
p 3646 N93-28799

Spacecraft surface charging handbook
[AD-A262778] p 3279 N93-29305

Characterization of copper iodide thin films fabricated via laser assisted molecular beam epitaxy
[AD-A262823] p 3596 N93-29430

Improved field emitter current densities and stability through the application of a proprietary process
[AD-A264048] p 3411 N93-30031

Atomic force microscopy of ammmonium perchlorate
p 3349 N93-30091

SURFACE REACTIONS
Measurements of breakaway reaction between beryllium and water vapor for ITER blanket design
[DE93-753270] p 3584 N93-28535
Supported organometallic complexes, surface chemistry, spectroscopy, and catalysis
[DE93-011930] p 3309 N93-28688
Spacecraft glow and the EISG/skirt experiment
p 3266 N93-28728
Electrochemical behavior and surface chemistry of aluminum alloys: Solute-rich interphase model
[AD-A262061] p 3322 N93-29002
Ultrafast optical studies of surface reaction processes at semiconductor interfaces
[DE93-009049] p 3593 N93-29096
A simple model for explosives formulation
[DE93-010703] p 3341 N93-29251
What is underneath? Moving atoms and molecules to find out
[AD-A263363] p 3567 N93-29332
FI-STM investigation of atomic hydrogen adsorption on the Si(100)2x1 surface
[AD-A262748] p 3567 N93-29403
Electric field induced phenomena in STM: Tip deformations and Au(111)-surface phase transitions during tunneling spectroscopy experiments
[AD-A262208] p 3596 N93-29445
The mechanical response of gold substrates modified with self-assembling monolayer films
[AD-A262997] p 3452 N93-29515
Kinetics and dynamics of reacting systems
[AD-A264046] p 3313 N93-30030
Organometallic and surface chemistry of mixed-metal systems
[DE93-012686] p 3325 N93-30059
Unsteady combustion of energetic materials using laser-recoil p 3319 N93-30085
Center for surface radiation damage studies
[AD-A264330] p 3570 N93-30366
Surface chemistry of hydrogen-passivated porous silicon-oxidation of surface Si-H groups by acetone
[AD-A264655] p 3315 N93-30526
Surface chemistry of N2H4 on Si(100)-2x1
[AD-A264819] p 3316 N93-30627
Fluids in porous media.
[PB93-175198] p 3428 N93-30759
Gordon Research Conferences, 1991
[AD-A264275] p 3317 N93-30816

SURFACE ROUGHNESS
Improved heat removal by microscopic surface texturing of capillaries
[AD-A263483] p 3424 N93-29966
Pulse mitigation and heat transfer enhancement techniques. Volume 2: Effect of surface wettability and roughness in evaporative spray cooling
[AD-A264174] p 3425 N93-30155

SURFACE TEMPERATURE
Spacecraft glow and the EISG/skirt experiment
p 3266 N93-28728
Fundamental studies of impingement cooling thermal boundary conditions p 3254 N93-29940
Local heat transfer measurement with liquid crystals on rotating surfaces including non-axisymmetric cases
p 3255 N93-29943
Transient thermal behaviour of a compressor rotor with axial cooling air flow and co-rotating or contra-rotating shaft p 3255 N93-29946
Measurement of projectile surface temperature by means of its infrared radiation: A preliminary study
[AD-A264053] p 3432 N93-30032

SURFACE TREATMENT
Surface modification of tribological components in transportation
[DE93-008647] p 3442 N93-28903
Method for preparation of a microporous structure with layered interstitial surface treatment
[NASA-CASE-MSC-21487-2] p 3296 N93-29023

SURFACE VEHICLES
A video transmission system for low-bandwidth remote driving
[DE93-010275] p 3544 N93-30529

SURFACE WATER
Utilization of NOAA/AVHRR data for energy balance of Lake Constance (Switzerland) p 3458 N93-28926
Molecular dynamics modeling of electric double layers with spectroscopic applications
[AD-A263168] p 3568 N93-29489
Annual report on monitoring of the unsaturated zone and recharge areas at INEL to the state of Idaho INLEL oversight committee
[DE93-012947] p 3473 N93-30187

SURFACE WAVES
Optical slope/height measurements of small scale waves within the SAXON-FPN experiment
[AD-A262572] p 3487 N93-29422
Software development and analysis for experimental high frequency surface wave radar data
[AD-A261982] p 3383 N93-29438
Acoustic charge transport technology investigation for advanced development transponder
p 3386 N93-29602
Modeling regional seismic waves
[AD-A264002] p 3479 N93-30756

SURVEILLANCE
Inservice diagnostic methods for solenoid-operated valves
[DE93-007823] p 3443 N93-28968
T(lc2)acS(lc3)ats for Surveillance Verification and C3I
[AGARD-CP-522] p 3387 N93-29892
TACSAT ground control and data collection
p 3388 N93-29895
Cost effective TacSats for military support
p 3285 N93-29912

SURVEILLANCE RADAR
Low cost TACSAT for NATO surveillance
p 3285 N93-29911

SURVEYS
Remote vehicle survey tool
[DE93-010822] p 3460 N93-29255
Anthropometric survey of the astronaut applicants and astronauts from 1985 to 1991
[NASA-RP-1304] p 3506 N93-29324
Filling the gaps: An overview of data on education in grades K through 12
[PB93-176550] p 3608 N93-30821
A representative survey of US space systems and methods for estimating their costs
[AD-A264159] p 3272 N93-30881

SWELLING
Thermodynamics of swelling and collapse of polyelectrolytic gels
[ETN-93-93485] p 3331 N93-29064

SWEPT FORWARD WINGS
Effect of canard wing positions on aerodynamic characteristics of swept-forward wing
[AD-A262373] p 3238 N93-28493
Flight control system design factors for applying automated testing techniques
[NASA-TM-4242] p 3260 N93-30764

SWEPT WINGS
Computation of a delta-wing roll-and-hold maneuver
[AD-A264704] p 3260 N93-30498

SWINGBY TECHNIQUE
Double swingby at Earth-Moon for increase of excess velocity
[ETN-93-94177] p 3270 N93-30582

SWITCHES
Subnanosecond high power performance of a bistable optically-controlled GaAs switch
[DE93-006285] p 3406 N93-28944
Analysis of an MCG/fuse/PFS experiment
[DE93-007355] p 3410 N93-29812
Ferroelectric liquid crystal optical interconnect switching systems
[AD-A263751] p 3596 N93-29859
Ultrafast, passive, broad-band, optical shutter based on novel semiconductor/conducting polymer interfaces
[AD-A264098] p 3601 N93-30878

SWITCHING
Superconducting flux coupled fast switching device from YBCO films
[AD-A264301] p 3414 N93-30896

SWITCHING CIRCUITS
Optically controlled solid state opening switches
[AD-A262404] p 3591 N93-28496
Widebanding techniques for VHF antennas 2
[AD-A263998] p 3387 N93-29882
Superconducting flux coupled fast switching device from YBCO films
[AD-A264301] p 3414 N93-30896

SYMBOLIC PROGRAMMING
Nonresident and endangered variables: The effects of code generation optimizations on symbolic debugging
[AD-A263149] p 3529 N93-29486

SYMBOLS
Symbology for head up and head down applications for highly agile fighter aircraft: To improve spatial awareness, trajectory control, and unusual attitude recovery, part 1
p 3502 N93-28857

SYMMETRY
Beyond two dimensions
[DE93-606084] p 3606 N93-30786
Computer algebra tools for higher symmetry analysis of nonlinear evolution equations
[DE93-606089] p 3535 N93-30787
Electric magnetic duality in string theory
[DE93-606061] p 3606 N93-30807
Nonlinear realisations of omega(1 + infinity)
[DE92-644721] p 3557 N93-30917
Beltrami parametrization and gauging of Virasoro and w-infinity algebras
[DE92-644844] p 3557 N93-30928
On one-dimensional topological and conformal field theories
[DE92-644726] p 3558 N93-30986
Spherically symmetric line element and Killing vectors in five-dimensional space
[DE93-604132] p 3558 N93-30988

SYNAPSES
Computation and generalization in neural networks
[AD-A263752] p 3549 N93-29871
Analog CMOS circuits for neural networks
p 3355 N93-30223
Evolving neural network architecture
[AD-A264802] p 3544 N93-30592
Biophysical and biochemical mechanisms in synaptic transmitter release
[AD-A264829] p 3496 N93-30613

SYNCHRONISM
Synchronization techniques for medium data rate EHF MILSATCOM systems p 3389 N93-29901
Improved bounds for synchronization jitter
p 3360 N93-30251
Coarse synchronization in an EHF frequency-hopped satellite communications system p 3365 N93-30281
Temporal synchronization of frequency hopped DPSK
p 3365 N93-30285

SYNCHRONOUS PLATFORMS
NOAA satellite programs and technology requirements
p 3627 N93-30710

SYNCHROTRON RADIATION
Multifractal analysis of radio lobes
p 3380 N93-28689
Non-perturbative calculation of equilibrium polarization of stored electron beams
[DE93-764500] p 3577 N93-30607

SYNCHROTRONS
New limits on generation-1 leptoquarks
[DE93-008138] p 3567 N93-29351

SYNCOPE
Acquisition of physiological data during G-induced Loss of Consciousness (G-LOC)
[AD-A264492] p 3496 N93-30400

SYNTAX
Character recognition using a neural network model with fuzzy representation p 3512 N93-29536
Proposal for a numerical array library
[DE93-010678] p 3623 N93-30482

SYNTHESIS (CHEMISTRY)
Synthesis of conducting polymer composite fibers in electrochemical flow cells
[AD-A262233] p 3294 N93-28492
Catalytic synthesis of silicon carbide preceramic polymers: Polycarbosilanes
[DE93-008634] p 3329 N93-28541
Be3(AsO4)2 2H2O: A new berylloarsenate phase containing bridged tetrahedral 3-rings
[AD-A262518] p 3592 N93-28584
Polyimides prepared from 3,5-diamino benzo trifluoride
[NASA-CASE-LAR-14206-1] p 3331 N93-29083
Diphenylmethane-containing dianhydride and polyimides prepared therefrom
[NASA-CASE-LAR-14487-1] p 3331 N93-29085
Synthesis and polymerization of azaethylenes and aza-1,3-dienes
[AD-A263651] p 3332 N93-29290
Flame or plasma synthesis of diamond under turbulent and transition flow conditions
[AD-D015689] p 3333 N93-29456
Polymers with electrical and nonlinear optical properties
[AD-D015691] p 3333 N93-29457
Synthesis of oligoimides and oligoimide anion radicals
[AD-A263129] p 3290 N93-29474
Process to prepare 1,3-diamino-5-pentafluorosulfanylbenzene
[NASA-CASE-LAR-14773-2-CU] p 3312 N93-29506
Synthesis and properties of a cation-conducting, high temperature polymer electrolyte
[AD-A263557] p 3334 N93-29825
A novel process for methanol synthesis
[DE93-013070] p 3314 N93-30188
Ordered molecular arrays as templates: A new approach to synthesis of mesoporous materials
[AD-A264631] p 3570 N93-30540
Design, synthesis, and chemical processing of hierarchical ceramic structures for aerospace applications
[AD-A264227] p 3339 N93-30885

SYNTHETIC APERTURE RADAR
Leadex data report. Part 1: Weather analysis and satellite images
[AD-A263217] p 3481 N93-28876
The interferometric SAR technology and its usability in the framework of ERS-1 p 3457 N93-28919

Recording of forest surface in SAR-images with statistical methods in areas of pronounced relief
p 3457 N93-28920
The German satellite ground station in Antarctica: Realization and first results p 3458 N93-28924
SAR sensors on TACSATS: A feasibility assessment
p 3286 N93-29909
A TACSAT SAR concept p 3286 N93-29910
Low cost TACSAT for NATO surveillance
p 3285 N93-29911
Similarities between synthetic aperature radar and ground probing radar imaging p 3376 N93-30347
Segmentation of SAR images p 3376 N93-30348
Multiresolution analysis of SAR data
[AD-A264727] p 3393 N93-30576
ERS-1 directional wave spectra validation with the airborne SAR PHARS
[BCRS-92-18] p 3463 N93-31010

SYNTHETIC FIBERS
Synthesis of conducting polymer composite fibers in electrochemical flow cells
[AD-A262233] p 3294 N93-28492

SYNTHETIC FUELS
Introductions to the Proceedings of the Fourteenth Symposium on Biotechnology for Fuels and Chemicals
[DE93-006235] p 3490 N93-28890

SYSTEM FAILURES
Multiprocessing systems: Reliability modelling and analysis using multimode components and dependent failures
[AD-A264230] p 3540 N93-30364
Hidden Markov models for fault detection in dynamic systems
[NASA-CASE-NPO-18982-1-CU] p 3449 N93-30413

SYSTEM IDENTIFICATION
Advances in the identification of electrochemical transfer function models using Prony analysis
[DE93-009424] p 3550 N93-30041
On neural networks in identification and control of dynamic systems
[NASA-TM-107702] p 3455 N93-31038

SYSTEMS ANALYSIS
Resource limited reasoning: A study of literature in the context of model-based diagnosis
[MEMO-INF-92-38] p 3540 N93-28480
System analysis for a kinematic positioning system based on the global positioning system
[AD-A262830] p 3245 N93-29468
Overview of the Systems Special Investigation Group investigation p 3318 N93-29683
Advances in the identification of electrochemical transfer function models using Prony analysis
[DE93-009424] p 3550 N93-30041
Nonsmooth optimization algorithms, system theory, and software tools
[AD-A264679] p 3534 N93-30549
Uses of risk importance measures
[VTT-TIED-1245] p 3378 N93-30581
Minimum security requirements for multi-user operating systems
[PB93-185999] p 3522 N93-30832
Optical system analysis for the ground based EXVM
[NASA-CR-192588] p 3582 N93-31035

SYSTEMS ENGINEERING
The meta model hierarchy: A framework for information systems concepts and techniques
[TR-92-17] p 3611 N93-28481
A complete set of field equations for the dynamic simulation of a towed cable system
[AD-A262570] p 3442 N93-28578
Magnetohydrodynamic projects at the CDIF
[DE93-012195] p 3584 N93-28649
Operator and automation capability analysis: Picking the right team p 3503 N93-28864
System automation and pilot-vehicle-interface for unconstrained low-altitude night attack
p 3503 N93-28867
Flight evaluation of a computer aided low-altitude helicopter flight guidance system p 3260 N93-28869
Overview of cockpit technology research and development programs for improvement of the man/machine interface: Review of the AGARD AVP Symposium held in Madrid, May 1992
p 3505 N93-28872
Systems engineering studies of on-orbit assembly operation p 3275 N93-29114
Systems engineering studies of lunar base construction p 3277 N93-29121
Taurus Lightweight Manned Spacecraft Earth orbiting vehicle p 3231 N93-29736
Solid oxide fuel cells for transportation: A clean, efficient alternative for propulsion
[DE93-010662] p 3464 N93-29844
Adapting system engineering principles to the Canadian Airspace System p 3247 N93-30338
Radiation-hardened microwave communications system
[DE93-007915] p 3394 N93-30631
OAST space research and technology applications: Technology transfer successes p 3625 N93-30693
Technology transfer in the NASA Ames Advanced Life Support Division p 3628 N93-30724
Gigabit network communications research
[AD-A264895] p 3536 N93-31026

SYSTEMS INTEGRATION
Combat Automation for Airborne Weapon Systems: Man/Machine Interface Trends and Technologies
[AGARD-CP-520] p 3501 N93-28850
A new class of mission support for combat air-crew
p 3501 N93-28854
Grand challenges in mass storage: A systems integrators perspective p 3620 N93-30467
An annotated bibliography on integration in software engineering environments
[AD-A264798] p 3535 N93-30602

SYSTEMS MANAGEMENT
Distributed Virtual System (DIVIRS) Project
[NASA-CR-193234] p 3526 N93-29169
Changing role of telecommunications management in air traffic control in the FAA p 3247 N93-30354
Office of Water Environmental and Program Information Systems Compendium, FY 1992
[PB93-186203] p 3462 N93-30833

SYSTEMS STABILITY
Stabilization using low-gain PI control: SISO case
[OUEL-1947/92] p 3541 N93-28898

SYSTOLIC ARRAYS
A systolic-array structure for MTCM receivers
p 3357 N93-30236

T

T TAURI STARS
The multiplicity of T Tauri stars in the star forming regions Taurus-Auriga and Ophiuchus-Scorpius: A 2.2 micron speckle imaging survey p 3634 N93-28945
Submillimeter CO observations of warm gas around T-Tauri stars
[MPE-PREPRINT-232] p 3631 N93-30615

TABLES (DATA)
Tables of experimental data used for the correlation of the thermophysical properties of ethane
[PB93-173417] p 3313 N93-29768

TACTILE DISCRIMINATION
Tactile sensing for 3-dimensional shape estimation
p 3357 N93-30232

TACTILE SENSORS (ROBOTICS)
Tactile sensing for 3-dimensional shape estimation
p 3357 N93-30232
An expert system for identification of the task status from tactile sensor data p 3368 N93-30300
A testbed for autonomous reflexive grasping
[AD-A264557] p 3446 N93-30384

TAIWAN
Scientific research abstracts in the Republic of China, 1991 (science and technology) p 3670 N93-30911

TAKEOFF
Effects of flow-path variations on internal reversing flow in a tailpipe offtake configuration for ASTOVL aircraft
[NASA-TM-106149] p 3252 N93-29065

TANTALUM
Gas electron diffraction employing a pulsed electron beam synchronous with photoexcitation
p 3319 N93-30101

TAPE RECORDERS
The NT digital micro tape recorder
p 3435 N93-30461
Towards a 1000 tracks digital tape recorder
p 3435 N93-30469
Evolution of a high-performance storage system based on magnetic tape instrumentation recorders
p 3435 N93-30470

TAPS
Adaptive airborne radar simulation with equalization filter taps
[AD-A264722] p 3393 N93-30514

TARGET ACQUISITION
SWAT 2 overview
[AD-A262905] p 3578 N93-29139
SWAT laboratory test results
[AD-A262906] p 3578 N93-29140
Multisensor image analysis system
[AD-A263679] p 3528 N93-29294
Effects of area-of-interest display characteristics of visual search performance and head movements in simulated low-level flight
[AD-A264661] p 3499 N93-30542
Enhanced convergence adaptive detection
[AD-A264100] p 3399 N93-30879

TARGET RECOGNITION
Information-theoretic performance bounding of Bayesian identifiers
[DE93-010705] p 3554 N93-28763
Multisensor image analysis system
[AD-A263679] p 3528 N93-29294
The fusion of information via fuzzy integration
p 3517 N93-29568
Generalized octrees for constrained object modeling
p 3369 N93-30304
Analysis and computation for vortex dynamics and rarefied gases
[AD-A264705] p 3427 N93-30499
Effects of area-of-interest display characteristics of visual search performance and head movements in simulated low-level flight
[AD-A264661] p 3499 N93-30542

TARGETS
Multisensor image analysis system
[AD-A263679] p 3528 N93-29294
Effects of neutral gas collisions on the power transmission factor at the divertor sheath
[DE93-009320] p 3588 N93-29334

TASK PLANNING (ROBOTICS)
The planning coordinator: A design architecture for autonomous error recovery and on-line planning of intelligent tasks
[NASA-CR-193250] p 3543 N93-30039
Task allocation and real-time considerations for the Robot Controller Test Station (RCTS)
p 3364 N93-30278

TATB
Thermal decomposition chemistry and shock sensitivity of thermally aged explosives p 3344 N93-30069
Pressure dependence of the reaction propagation rate of TATB to 40 GPa p 3319 N93-30082

TDR SATELLITES
Interferometric tracking system for the tracking and data relay satellite
[NASA-CR-193274] p 3382 N93-29217

TEARING MODES (PLASMAS)
Nonlinear coupling of tearing fluctuations in the Madison Symmetric Torus
[DE93-010131] p 3584 N93-28602

TECHNOLOGICAL FORECASTING
JPRS report: Science and technology. Central Eurasia: Engineering and equipment
[JPRS-UEQ-92-006] p 3353 N93-28636
JPRS report: Science and technology. Central Eurasia: Engineering and equipment
[JPRS-UEQ-92-010] p 3353 N93-28674
JPRS report: Science and technology. Central Eurasia: Engineering and equipment
[JPRS-UEQ-92-008] p 3353 N93-28675
JPRS report: Science and technology. Central Eurasia: Engineering and equipment
[JPRS-UEQ-93-003] p 3353 N93-28691

TECHNOLOGIES
JPRS report: Science and technology. Central Eurasia: Materials science
[JPRS-UMS-93-003] p 3327 N93-30623
The NCAT process p 3626 N93-30697

TECHNOLOGY ASSESSMENT
Refractory metal disilicides research
[AD-A262416] p 3320 N93-28499
Reliability assessment at airline inspection facilities. Volume 2: Protocol for an eddy current inspection reliability experiment
[DOT/FAA/CT-92/12-VOL-2] p 3449 N93-28685
Polarimetric multispectral imaging technology
p 3434 N93-28774
New technologies for UV detectors
p 3582 N93-28786
Assessment of energy technologies contributing to environmental conservation
[DE93-781439] p 3468 N93-28882
Sensor systems for monitoring Maglev guideway structures
[PB93-154821] p 3444 N93-29205
The 17th Annual Electronics Manufacturing Seminar proceedings
[AD-A261963] p 3409 N93-29435
Advanced NDE technology program
[AD-A262008] p 3449 N93-29443
Multi-Attribute Decision Theory methodology for pollution control measure analysis
[DE93-005444] p 3472 N93-30008
Foreign technology assessment: Environmental evaluation of a radiation-hard oscillator/divider
[DE93-011481] p 3412 N93-30127
The Visible Human Project of the National Library of Medicine: Remote access and distribution of a multi-gigabyte data set p 3617 N93-30453
The NCAT process p 3626 N93-30697
Technology transfer within NASA
p 3627 N93-30708

TECHNOLOGY TRANSFER
ORNL superconducting technology program for electric energy systems
[DE93-009588] p 3404 N93-28523
Reliability assessment at airline inspection facilities. Volume 2: Protocol for an eddy current inspection reliability experiment
[DOT/FAA/CT-92/12-VOL-2] p 3449 N93-28685
The ANL electric vehicle battery R/D program for DOE-EHP
[DE93-010658] p 3408 N93-29311
Technology transfer personnel exchange at the Boeing Company
[DE93-010190] p 3625 N93-29329
Decision maker's guide to international space
[ANSER-STDN-93-4] p 3669 N93-29710
Accelerating the transfer of technology for implementing domain specific software architectures
[AD-A264017] p 3532 N93-30014
Promoting high-performance computing and communications
[ISBN-0-16-041828-3] p 3522 N93-30570
Technology Transfer and the Civil Space Program. Volume 2: Workshop proceedings
[NASA-TM-108250] p 3625 N93-30692
Departmental technology transfer update p 3625 N93-30694
The role of the University Licensing Office in transferring intellectual property to industry p 3626 N93-30698
Technology transfer p 3626 N93-30699
National Technology Transfer Center p 3626 N93-30700
Technology transfer from the viewpoint of a NASA prime contractor p 3626 N93-30701
Sandia National Laboratories p 3626 N93-30702
Technology transfer needs and experiences: The NASA Research Center perspective p 3626 N93-30703
Technology transfer within the NASA Goddard Space Flight Center p 3626 N93-30704
Technology transfer and space science missions p 3626 N93-30705
Technology coordination p 3626 N93-30706
Technology transfer p 3627 N93-30707
Technology transfer within NASA p 3627 N93-30708
Technology transfer within the government p 3627 N93-30709
Technology transfer within the government p 3627 N93-30711
Technology transfer and Rockwell International p 3627 N93-30712
NASP technology transfer p 3627 N93-30713
Robotic technology evolution and transfer p 3627 N93-30714
High performance computing and communications program p 3627 N93-30715
Technology transfer between the government and the aerospace industry p 3628 N93-30716
National Media Laboratory p 3628 N93-30717

TECHNOLOGY UTILIZATION
Development of Si(1-x)Ge(x) technology for microwave sensing applications
[NASA-TM-106157] p 3405 N93-28610
JPRS report: Science and technology. Central Eurasia: Engineering and equipment
[JPRS-UEQ-92-007] p 3353 N93-28635
JPRS report: Science and technology. Central Eurasia: Life sciences
[JPRS-ULS-93-005] p 3490 N93-28683
JPRS report: Science and technology. Central Eurasia: Life sciences
[JPRS-ULS-92-027] p 3490 N93-28684
JPRS report: Science and technology. Central Eurasia: Engineering and equipment
[JPRS-UEQ-93-003] p 3353 N93-28691
Electrolysis performance improvement and validation experiment p 3267 N93-28737
A unique photon bombardment system for space applications p 3286 N93-28790
Energy efficient drivepower: An overview
[DE93-012435] p 3411 N93-30057
Energy efficient drivepower
[DE93-012436] p 3411 N93-30058
How to compete for NASA contracts
[NASA-TM-109238] p 3610 N93-30644
OAST space research and technology applications: Technology transfer successes p 3625 N93-30693
The NCAT process p 3626 N93-30697
Technology transfer p 3626 N93-30699
Sandia National Laboratories p 3626 N93-30702
Technology transfer p 3627 N93-30707
Technology transfer within the government p 3627 N93-30711
Robotic technology evolution and transfer p 3627 N93-30714

TELECOMMUNICATION
Applying high-level language paradigms to communications software for distributed systems
[AD-A263001] p 3528 N93-29463
The Telecommunications and Data Acquisition Report
[NASA-CR-193144] p 3384 N93-29586
The general theory of convolutional codes p 3385 N93-29595
GE networked mass storage solutions supporting IEEE network mass storage model p 3618 N93-30458

TELECONNECTIONS (METEOROLOGY)
A water mass analysis of the 1991-1992 El Nino signal in the Farallon Islands region
[AD-A263490] p 3488 N93-29819

TELEOPERATORS
Sources sought for innovative scientific instrumentation for scientific lunar rovers p 3434 N93-28804
A study of the effects of lens focal length on remote driver performance
[AD-A263191] p 3505 N93-28941
Graphical interface between the CIRSSE testbed and CimStation software with MCS/CTOS
[NASA-CR-193276] p 3527 N93-29218
Remote vehicle survey tool
[DE93-010822] p 3460 N93-29255
Graphical programming: On-line robot simulation for telerobotic control
[DE93-009796] p 3447 N93-30654

TELEROBOTICS
Sources sought for innovative scientific instrumentation for scientific lunar rovers p 3434 N93-28804
Lunar crane system p 3277 N93-29118
Lunar rovers and local positioning system p 3277 N93-29119
Graphical interface between the CIRSSE testbed and CimStation software with MCS/CTOS
[NASA-CR-193276] p 3527 N93-29218
Supervised autonomy in telerobotics p 3372 N93-30326
A video transmission system for low-bandwidth remote driving
[DE93-010275] p 3544 N93-30529
Graphical programming: On-line robot simulation for telerobotic control
[DE93-009796] p 3447 N93-30654

TELESCOPES
Subnanoradian, groundbased tracking of spaceborne lasers p 3442 N93-28823
A technique for single-pulse spectrum and pulse width measurements for an IR-FEL
[DE93-007732] p 3436 N93-28847
Sodium guide star adaptive optics system for astronomical imaging in the visible and near-infrared
[DE93-009543] p 3630 N93-29785
Advanced research in sky surveillance: A search for low-luminosity objects
[AD-A264832] p 3631 N93-30629

TELEVISION SYSTEMS
Topical meeting of broadband analog and digital optoelectronics
[AD-A264643] p 3581 N93-30522
A video transmission system for low-bandwidth remote driving
[DE93-010275] p 3544 N93-30529

TEMPERATURE COMPENSATION
Temperature compensated lithium battery energy monitor
[AD-D015680] p 3409 N93-29605

TEMPERATURE CONTROL
Thermal control paints on LDEF: Results of M0003 sub-experiment 18
[AD-A263252] p 3329 N93-28561
In-STEP Two-Phase Flow (TPF) thermal control experiment p 3265 N93-28719
LDEF: 69 Months in Space. Second Post-Retrieval Symposium, part 2
[NASA-CP-3194-PT-2] p 3654 N93-29354
Long Duration Exposure Facility (LDEF) low temperature Heat Pipe Experiment Package (HEPP) flight results p 3429 N93-29701
Thermal cycler temperature variation and its effect on the polymerase chain reaction
[AD-A264660] p 3337 N93-30541

TEMPERATURE DEPENDENCE
The temperature dependence of the deformation and oxidation behavior of an age-hardenable beta + alpha-two titanium alloy
[AD-A262232] p 3320 N93-28491
Investigation of ion beam mixing of iron marker layers in aluminum oxide by RBS
[DE93-010727] p 3594 N93-29314
Thermal decomposition chemistry and shock sensitivity of thermally aged explosives p 3344 N93-30069
Thermal cycler temperature variation and its effect on the polymerase chain reaction
[AD-A264660] p 3337 N93-30541
Superconducting films of YBaCuO
[DE93-606831] p 3600 N93-30772
Temperature-dependent electrical conductivity of soda-lime glass p 3294 N93-30978

TEMPERATURE DISTRIBUTION
A thermal stress solution for multilayered composite cylinders
[AD-A262579] p 3295 N93-28657
Supersonic flow calculation using a Reynolds-stress and an eddy thermal diffusivity turbulence model
[NASA-CR-4515] p 3420 N93-29159
The thermal structure, dust loading, and meridional transport in the Martian atmosphere during late southern summer p 3651 N93-29616
A generalized approach to the thermal analysis of the Long Duration Exposure Facility's flight experiments p 3428 N93-29624
Experimental study of heat transfer close to a plane wall heated in the presence of multiple injections (subsonic flow) p 3253 N93-29931
Local heat transfer measurement with liquid crystals on rotating surfaces including non-axisymmetric cases p 3255 N93-29943
Fluid flow and heat transfer in the entrance region of an annulus between independently rotating tubes with a turbulent axial flow p 3256 N93-29952
Cooling predictions in turbofan engine components p 3259 N93-29964

TEMPERATURE EFFECTS
The effect of temperature on the impact behavior of TiB2 reinforced XDTM-TiAl intermetallic matrix composites
[AD-A262924] p 3296 N93-28886
Environmental effects on stitched RTM composites
[NASA-CR-193221] p 3297 N93-29107
System overview on electromagnetic compensation for reflector antenna surface distortion
[NASA-TM-106217] p 3273 N93-29195
Novel polymer compositions for high-temperature membrane applications, phase 1
[PB93-174126] p 3331 N93-29201
Response of energetic solids to light, heat and shock pulses
[AD-A263702] p 3342 N93-29296
The microchannel heatsink with liquid nitrogen cooling
[DE93-009258] p 3422 N93-29300
Pulse mitigation and heat transfer enhancement techniques. Volume 4: Transient behavior of heat pipe with thermal energy storage under pulse heat loads
[AD-A263497] p 3423 N93-29339
Results of a round robin test program: Complex modulus properties of a polymeric damping material
[AD-A263619] p 3332 N93-29344
The effect of high temperature on wall shear in a two dimensional wall jet
[AD-A262982] p 3423 N93-29426
Radiation and temperature effects on LDEF fiber optic samples p 3583 N93-29700
Properties of superconducting YBa2Cu3O(6+4) ceramic materials: Effect of processing parameters
[AD-A263441] p 3334 N93-29790
Thermal effects of a coolant film along the suction side of a high pressure turbine nozzle guide vane p 3253 N93-29930
Study of parameters affecting the performance of solar desiccant cooling systems
[DE93-000088] p 3465 N93-30206
Holmium quasi-two level laser
[AD-D015706] p 3440 N93-30427
Improved measurement of thermal effects on microstructure p 3292 N93-30959

TEMPERATURE GRADIENTS
Analyses of data from fine structure and circulation studies in the Gulf of California
[AD-A262910] p 3486 N93-28885
Self-organized profile relaxation by ion temperature gradient instability in toroidal plasmas
[DE93-009580] p 3585 N93-28910
Investigation of thermoacoustic muffler
[AD-A262009] p 3562 N93-29392

TEMPERATURE MEASUREMENT
Program for an improved hypersonic temperature-sensing probe
[NASA-CR-186025] p 3431 N93-29066
A passive infrared ice detection technique for helicopter applications
[NASA-CR-193187] p 3244 N93-29152
Transient response of embedded thermocouples
[DE93-009889] p 3431 N93-29325
Application of Schlieren optical techniques for the measurement of gas temperature and turbulent diffusivity in a diesel engine
[AD-A263810] p 3580 N93-29880
Cooling predictions in turbofan engine components p 3259 N93-29964

Measurement of projectile surface temperature by means of its infrared radiation: A preliminary study
[AD-A264053] p 3432 N93-30032

In-situ temperature and concentration measurements of organosilicon decomposition in a chemical vapor deposition reactor
[ONERA-P-1990-3] p 3313 N93-30109

A novel flame thermometer based on the doppler width of ro-vibrational transitions
[AD-A264515] p 3315 N93-30405

Studies of curvature, strain, and unsteady effects on premixed flames p 3316 N93-30646

TEMPERATURE PROFILES

Utilization of NOAA/AVHRR data for energy balance of Lake Constance (Switzerland) p 3458 N93-28926

A passive infrared ice detection technique for helicopter applications
[NASA-CR-193187] p 3244 N93-29152

Determination of gas phase species and temperature profiles above solid propellants p 3346 N93-30080

TEMPERATURE SENSORS

Program for an improved hypersonic temperature-sensing probe
[NASA-CR-186025] p 3431 N93-29066

TEMPORAL DISTRIBUTION

Temporal synchronization of frequency hopped DPSK
p 3365 N93-30285

TEMPORAL RESOLUTION

Subnanosecond high power performance of a bistable optically-controlled GaAs switch
[DE93-006285] p 3406 N93-28944

TENNESSEE VALLEY (AL-KY-TN)

Remote sensing for water quality monitoring in the Tennessee Valley: Field tests of two systems
[DE93-008997] p 3462 N93-30637

TENSILE CREEP

Tensile creep behavior of polycrystalline alumina fibers
[NASA-TM-106269] p 3340 N93-30938

TENSILE PROPERTIES

Design and evaluation of a uniaxial pull test for lithium hydride/deuteride
[DE93-010760] p 3451 N93-28832

Microstructural effects on the deformation and fracture of the alloy Ti-25Al-10Nb-3B-1Mo
[AD-A263095] p 3323 N93-29144

APU diaphragm testing
[NASA-TM-108254] p 3272 N93-29501

Development of a test program to evaluate structural defects in Glass-Reinforced Plastic (GRP), volume 2
[AD-A263814] p 3335 N93-29881

Development of a test program to evaluate structural defects in Glass-Reinforced Plastic (GRP), volume 1
[AD-A263813] p 3335 N93-29886

Mechanical properties of several magnesium and aluminum composites
[AD-A262481] p 3299 N93-30137

Tensile study of single-crystal ternary L1(2) trialuminide Al66Ti25Mn(sub g)
[AD-A264297] p 3601 N93-30819

Mechanical properties of composite materials
p 3290 N93-30951

TENSILE STRENGTH

Design and evaluation of a uniaxial pull test for lithium hydride/deuteride
[DE93-010760] p 3451 N93-28832

Aligned, short-fiber composites by novel flow processing methods
[DE93-008701] p 3296 N93-28904

Aluminium-high strength material by mechanical alloying and reaction milling: Basics of processing and characterisation of material
[ESA-TT-1249] p 3324 N93-29272

Studies of fiber-matrix adhesion on compression strength p 3304 N93-30846

Mechanical properties of composite materials
p 3290 N93-30951

Direct tension experiments on compacted granular materials p 3292 N93-30960

Application of hardness testing in foundry processing operations: A university and industry partnership
p 3292 N93-30961

TENSILE STRESS

The design and lifetime calculation of MHD generator walls based on subcritical crack growth in ceramics
[ISBN-90-9004009-9] p 3332 N93-29267

TENSILE TESTS

Design and evaluation of a uniaxial pull test for lithium hydride/deuteride
[DE93-010760] p 3451 N93-28832

Acousto-Ultrasonic analysis of failure in ceramic matrix composite tensile specimens
[NASA-TM-106219] p 3449 N93-29073

TENSOR ANALYSIS

Beyond two dimensions
[DE93-606084] p 3606 N93-30786

TENSORS

Non-scalar uncertainty: Uncertainty in dynamic systems p 3517 N93-29565

Integrals of motion on the group of invariance of an interval in three-dimensional spaces
[DE93-606090] p 3606 N93-30797

A simple formula for reducing Feynman diagrams to scalar integrals
[DE92-644717] p 3607 N93-30916

On the energy-momentum tensors for field theories in spaces with affine connection and metric
[DE92-644743] p 3557 N93-30926

On the energy-momentum tensors for field theories in spaces with affine connection and metric
[DE92-644744] p 3557 N93-30927

The geometry of complex space-times with torsion
[DE92-641343] p 3608 N93-31003

TERMINAL BALLISTICS

The effect of material strength on segment penetration behavior
[AD-A263262] p 3453 N93-29801

Comparison of impact results for several polymeric composites over a wide range of low impact velocities
p 3304 N93-30848

TERMINOLOGY

Application of ray tracing in radiation heat transfer
[NASA-TM-106206] p 3419 N93-29075

TERMS

Handbook of frequently used acronyms and glossary of terms
[DE93-011388] p 3616 N93-30123

TERNARY ALLOYS

Some effects of composition and microstructure on the B2 in equilibrium to DO3 ordered phase transition in Fe3Al alloys
[DE93-009724] p 3325 N93-29813

Improvement in ductility of the intermetallic compound Ti3Al
[ESA-TT-1276] p 3325 N93-30105

Flexible storage medium for write-once optical tape
p 3621 N93-30473

TERRAIN

Evaluation of atmospheric wind field and dispersion models for fog-oil smoke dispersion in complex terrain: Field measurement and model evaluation program for assessment of the environmental effects of military smokes
[AD-A262051] p 3482 N93-29399

Simulation of landscape disturbances and the effect of climatic change
[DE93-011615] p 3472 N93-30131

Spacecraft studies of Phobos and Mars
[NASA-CR-193298] p 3651 N93-30635

TERRAIN ANALYSIS

Terrain and coverage prediction analyses for non-geostationary orbit EHF satellite communications
p 3389 N93-29902

TERRAIN FOLLOWING AIRCRAFT

Optimal trajectories for aircraft terrain following and terrain avoidance: A literature review update
[AD-A264075] p 3260 N93-30604

TEST CHAMBERS

Mathematical modeling and control law development for the atmospheric monitoring and control system of the Controlled Environment Research Chamber (CERC) at NASA Ames Research Center
[AD-A261978] p 3261 N93-29436

TEST EQUIPMENT

Loading and testing a light scattering cell with a binary fluid mixture near its critical composition
[NASA-CR-193147] p 3415 N93-28557

Lunar regolith penetrators and cutters
p 3276 N93-29117

Rotational fluid flow experiment p 3235 N93-29761

The USAF Advanced Turbine Aerothermal Research Rig (ATARR) p 3255 N93-29945

TEST FACILITIES

A new facility for advanced rocket propulsion research
[NASA-TM-106193] p 3270 N93-28696

CSI-Star: A low-cost CSI orbital testbed
p 3263 N93-28707

Testing in combined dynamic environments
[DE93-010679] p 3278 N93-29250

Improved design concepts for millimeter wave power sources
[AD-A264060] p 3411 N93-29922

FASSET: A development model for a Canadian EHF MILSATCOM system p 3363 N93-30268

Task allocation and real-time considerations for the Robot Controller Test Station (RCTS)
p 3364 N93-30278

Development of an antenna measurement facility operating in the 2 GHz - 100 GHz frequency range
p 3369 N93-30308

Thermal effects testing at the National Solar Thermal Test Facility
[DE93-009825] p 3465 N93-30391

TEST RANGES

Estimating test range capacity
[AD-A262493] p 3270 N93-28938

TEST STANDS

CSI-Star: A low-cost CSI orbital testbed
p 3263 N93-28707

Graphical interface between the CIRSSE testbed and CimStation software with MCS/CTOS
[NASA-CR-193276] p 3527 N93-29218

Load test set-up for the Airmass Sunburst Ultra-Light Aircraft p 3249 N93-29776

The USAF Advanced Turbine Aerothermal Research Rig (ATARR) p 3255 N93-29945

TETHERED BALLOONS

Stabilized platform for tethered balloon soundings of broadband long- and short-wave radiation
[DE93-007876] p 3383 N93-29308

TETHERED SATELLITES

SPREE Interactive Data Analysis Tool (SIDAT)
[AD-A262782] p 3273 N93-29306

Learning characteristics of a space-time neural network as a tether skiprope observer p 3512 N93-29534

Clustering of tethered satellite system simulation data by an adaptive neuro-fuzzy algorithm
p 3512 N93-29535

Application of non-standard signal processing to ELF noise characterization for the TSS1-OESEE programme
p 3397 N93-30743

Orbiting transmitter and antenna for spaceborne communications at ELF/VLF to submerged submarines
p 3399 N93-30755

TETHERING

The dynamics and control of space tethers
p 3274 N93-28629

Learning characteristics of a space-time neural network as a tether skiprope observer p 3512 N93-29534

Tethered aerostat VLF/LF transmitter system design considerations p 3399 N93-30753

TETHERLINES

The dynamics and control of space tethers
p 3274 N93-28629

TETRAHEDRONS

Be3(AsO4)2 2H2O: A new berylloarsenate phase containing bridged tetrahedral 3-rings
[AD-A262518] p 3592 N93-28584

TETRAHYDROFURAN

NMR studies of molecules in liquid crystals and graphite
[DE93-010423] p 3569 N93-29805

TETRODES

Upgrading the LAMPF 201 MHz RF generators
[DE93-010715] p 3406 N93-28830

TEXTBOOKS

Syllabus physical meteorology, part 1
[KNMI-TR-140-PT-1] p 3484 N93-30114

TEXTILES

Lightweight flexible composite tent materials
[AD-A263021] p 3295 N93-28660

The 1990-1991 project summaries
p 3230 N93-29731

Infiltration/cure modeling of resin transfer molded composite materials using advanced fiber architectures
p 3303 N93-30843

Advanced fiber/matrix material systems
p 3305 N93-30854

TEXTS

Dynamic object oriented interaction and its implementation in the framework in an interface management system
[ETN-93-93795] p 3523 N93-28526

A model for processing the SGML document in version oriented hypertext systems
[ETN-93-93797] p 3611 N93-28528

Parcels with TAGS
[PB93-181824] p 3535 N93-30824

TEXTURES

Microtextured metals for stray-light suppression in the Clementine startracker p 3286 N93-28785

Improved heat removal by microscopic surface texturing of capillaries
[AD-A263483] p 3424 N93-29966

THEMATIC MAPPERS (LANDSAT)

Model-oriented correction of thematic mapper raw data p 3459 N93-28930

The estimation and scaling of land-surface fluxes of latent and sensible heat with remotely sensed data over a grassland site p 3462 N93-30045

Land use database for the Netherlands using LANDSAT Thematic Mapper pictures
[BCRS-91-32] p 3463 N93-30839

THEMATIC MAPPING
Proceedings of the 8th User Seminar of the German Remote Sensing Data Center of the German Aerospace Establishment (DLR)
[DLR-MITT-92-09] p 3456 N93-28915

THEOREM PROVING
Automated reasoning with function evaluation for COCOLOG
[INRIA-RR-1713] p 3529 N93-29488
Packing odd paths
[CWI-BS-R9207] p 3549 N93-29849

THEOREMS
Lie groups whose set of compact subgroups is inductive
[ETN-93-93791] p 3547 N93-28524
Classification theorem for principal fibre bundles, Berry's phase, and exact cycle evolution
[DE93-011114] p 3556 N93-28601
Closed-loop control with delayed information
[INRIA-RR-1638] p 3541 N93-28638
Mixed limit theorems for pattern analysis
[AD-A263735] p 3549 N93-29854

THEORETICAL PHYSICS
Studies in theoretical high energy particle physics
[DE93-007990] p 3574 N93-28565
Research in theoretical nuclear physics
[DE93-008380] p 3565 N93-28960
Research in theoretical physics
[DE93-008401] p 3603 N93-28961
JPRS report: Science and technology. Central Eurasia: Physics and mathematics
[JPRS-UPM-93-002] p 3560 N93-29022
A survey of problems in divertor and edge plasma theory
[DE93-007531] p 3586 N93-29056
New Mexico Center for Particle Physics: Studies of fundamental interactions
[DE93-008302] p 3566 N93-29261
Task A: Theory of elementary particles
[DE93-010561] p 3569 N93-29841
Continuation of: Applications of gauge theories to enhance numerical solutions of mixed potential integral equations
[AD-A263763] p 3550 N93-29876
Theoretical studies in nuclear structure
[DE93-012290] p 3570 N93-30505
NATO Advanced Research Workshop on Frontiers of Optical Phenomena in Semiconductor Structure of Reduced Dimension
[AD-A264813] p 3581 N93-30666
Plasma Physics Network Newsletter, no. 5
[DE93-606216] p 3591 N93-30795
Connections between quantized affine algebras and superalgebras
[DE93-606065] p 3551 N93-30810
Massive Majorana neutrinos in pre-bounce supernovae
[DE92-642597] p 3572 N93-30931

THERAPY
Wound healing and connective tissue metabolism: The role of hyperbaric oxygen therapy
[AD-A262483] p 3493 N93-28759
Pharmacokinetics and Pharmacodynamics in Space
[NASA-CP-10048] p 3494 N93-29502

THERMAL ANALYSIS
Thermal and mechanical analysis of flip-chips on a liquid cooled multichip module
[DE93-007609] p 3405 N93-28641
Thermal Analyzer for Planetary Soil (TAPS): An in situ instrument for mineral and volatile-element measurements p 3643 N93-28782
A DTA/GC for the in situ identification of the Martian surface material p 3646 N93-28800
TESLA test cell cryostat support post thermal and structural analysis
[DE93-008365] p 3407 N93-29048
Application of ray tracing in radiation heat transfer
[NASA-TM-106206] p 3419 N93-29075
A generalized approach to the thermal analysis of the Long Duration Exposure Facility's flight experiments
p 3428 N93-29624
Progress report on the ultra heavy cosmic ray experiment (AO178) p 3654 N93-29646
Long Duration Exposure Facility (LDEF) low temperature Heat Pipe Experiment Package (HEPP) flight results
p 3429 N93-29701
Aero-thermal design of a cooled transonic NGV and comparison with experimental results
p 3257 N93-29957
Analysis of thermal bar using boundary-layer integral equations gradients
[MATHS-REPT-A-177] p 3462 N93-30107
Thermal cycler temperature variation and its effect on the polymerase chain reaction
[AD-A264660] p 3337 N93-30541

THERMAL BATTERIES
Ordnance thermal battery
[AD-D015722] p 3412 N93-30201

THERMAL CONDUCTIVITY
The microchannel heatsink with liquid nitrogen cooling
[DE93-009258] p 3422 N93-29300
Semiconductor cooling apparatus
[NASA-CASE-LEW-14162-3] p 3299 N93-29614
Diamond nucleation of surfaces using carbon clusters
[AD-A264634] p 3599 N93-30548
High thermal conductivity of diamond
p 3294 N93-30977

THERMAL CONTROL COATINGS
Thermal certification tests of Orbiter Thermal Protection System tiles coated with KSC coating slurries
[NASA-TM-104766] p 3278 N93-29221
LDEF microenvironments, observed and predicted
p 3283 N93-29623
Next generation optical instruments and space experiment based on the LDEF thermal control surfaces experiment (S0069) p 3583 N93-29706

THERMAL CYCLING TESTS
Ruled and holographic experiment (AO 138-5)
p 3434 N93-29696
Analyses of space environment effects on active fiber optic links orbited aboard the LDEF
p 3583 N93-29699
Thermal cycler temperature variation and its effect on the polymerase chain reaction
[AD-A264660] p 3337 N93-30541

THERMAL DECOMPOSITION
Analysis for thermo-chemical decomposition of composite structures
[NASA-CR-193185] p 3295 N93-28843
Thermal decomposition of nitramines
p 3318 N93-30065
Observation of reaction intermediates in crystalline RDX p 3318 N93-30067
Thermal decomposition chemistry and shock sensitivity of thermally aged explosives p 3344 N93-30069
Thermal decomposition pathways of RDX in the condensed phase p 3347 N93-30083
Coordination compounds of aluminum as precursors to aluminum nitride
[AD-A264700] p 3327 N93-30574
Surface chemistry of N2H4 on Si(100)-2x1
[AD-A264819] p 3316 N93-30627

THERMAL DEGRADATION
Energetic material response to abnormal environments p 3350 N93-30095

THERMAL DIFFUSION
Follow up on the crystal growth experiments of the LDEF p 3602 N93-29381
On the ideality of using a step-function current in a metallic foil to simulate a step-function heat-flux source
[AD-A264627] p 3413 N93-30539

THERMAL DIFFUSIVITY
Clementine 2: A double asteroid flyby and impactor mission p 3268 N93-28770
Supersonic flow calculation using a Reynolds-stress and an eddy thermal diffusivity turbulence model
[NASA-CR-4515] p 3420 N93-29159
On the ideality of using a step-function current in a metallic foil to simulate a step-function heat-flux source
[AD-A264627] p 3413 N93-30539
High thermal conductivity of diamond
p 3294 N93-30977

THERMAL EXPANSION
The design and testing of a high-temperature graphite dilatometer
[AD-A262185] p 3430 N93-28488
Influence of ply waviness on stiffness and strength reduction of composite laminates
[AD-A263224] p 3294 N93-28559
The effect of temperature on the impact behavior of TiB2 reinforced XDTM-TiAl intermetallic matrix composites
[AD-A262924] p 3296 N93-28886

THERMAL FATIGUE
Mechanics of elevated temperature fatigue damage in fiber-reinforced ceramics
[AD-A262403] p 3329 N93-28495
Overview of piping issues and trends
[DE93-006628] p 3354 N93-28893

THERMAL INSULATION
Advanced insulations for refrigerator/freezers: The potential for new shell designs incorporating polymer barrier construction
[DE93-010600] p 3353 N93-28570
Thermal properties of organic and modified inorganic aerogels
[DE93-009230] p 3311 N93-29263
Continued investigation of LDEF's structural frame and thermal blankets by the Meteoroid and Debris Special Investigation Group p 3282 N93-29357
Predicted and observed directional dependence of meteoroid/debris impacts on LDEF thermal blankets
p 3638 N93-29358

THERMAL MAPPING
Quantification of thermographic mapping techniques
[AD-A264020] p 3391 N93-30016
Analysis of thermal bar using boundary-layer integral equations gradients
[MATHS-REPT-A-177] p 3462 N93-30107

THERMAL NOISE
A microseismometer for terrestrial and extraterrestrial applications p 3434 N93-28765
Processing, fabrication, and demonstration of HTS integrated microwave circuits
[AD-A263161] p 3406 N93-28940
The flight performance of the Galileo orbiter USO
p 3386 N93-29603

THERMAL PLASMAS
Plasma/particle interaction in subsonic argon/helium thermal plasma jets
[DE93-010808] p 3589 N93-30181

THERMAL PROTECTION
Debris/ice/TPS assessment and integrated photographic analysis for Shuttle Mission STS-55
[NASA-TM-107559] p 3271 N93-29136
Thermal certification tests of Orbiter Thermal Protection System tiles coated with KSC coating slurries
[NASA-TM-104766] p 3278 N93-29221

THERMAL RESISTANCE
Advanced insulations for refrigerator/freezers: The potential for new shell designs incorporating polymer barrier construction
[DE93-010600] p 3353 N93-28570
Biophysical model for handwear insulation testing
[AD-A262926] p 3505 N93-28884
Novel polymer compositions for high-temperature membrane applications, phase 1
[PB93-174126] p 3331 N93-29201
The microchannel heatsink with liquid nitrogen cooling
[DE93-009258] p 3422 N93-29300
Synthesis and properties of a cation-conducting, high temperature polymer electrolyte
[AD-A263557] p 3334 N93-29825

THERMAL SHOCK
DOE fundamentals handbook: Material science
[DE93-012225] p 3314 N93-30200

THERMAL STABILITY
Advanced thermally-stable, coal-derived, jet fuels program: Experiment system and model development
[AD-A262747] p 3342 N93-29402
Synthesis and properties of a cation-conducting, high temperature polymer electrolyte
[AD-A263557] p 3334 N93-29825

THERMAL STRESSES
A thermal stress solution for multilayered composite cylinders
[AD-A262579] p 3295 N93-28657
The design and lifetime calculation of MHD generator walls based on subcritical crack growth in ceramics
[ISBN-90-9004009-9] p 3332 N93-29267
Advanced thermally-stable, coal-derived, jet fuels program: Experiment system and model development
[AD-A262747] p 3342 N93-29402

THERMAL VACUUM TESTS
Long Duration Exposure Facility (LDEF) low temperature Heat Pipe Experiment Package (HEPP) flight results
p 3429 N93-29701

THERMIONIC DIODES
Analysis of TOPAZ 2 and SPACE-R space nuclear power plants using a modified thermionic model
[AD-A262612] p 3286 N93-28474

THERMIONIC POWER GENERATION
Analysis of TOPAZ 2 and SPACE-R space nuclear power plants using a modified thermionic model
[AD-A262612] p 3286 N93-28474
Thermion: Verification of a thermionic heat pipe in microgravity p 3235 N93-29757

THERMOCHEMISTRY
Analysis for thermo-chemical decomposition of composite structures
[NASA-CR-193185] p 3295 N93-28843
Thermodynamics of swelling and collapse of polyelectrolytic gels
[ETN-93-93485] p 3331 N93-29064
The thermochemistry and reaction pathways of the decomposition and combustion of energetic materials
p 3343 N93-30063
Thermal oxidation of HCN by NO2 in shock waves
p 3318 N93-30064
Thermal decomposition of nitramines
p 3318 N93-30065
Thermal decomposition chemistry and shock sensitivity of thermally aged explosives p 3344 N93-30069

Study of codeposition of aluminum-haffnium and deposition of yttrium by the cementation technique: Elaboration of Ni-Cr-Al and Ni-Cr-Al-Hf felt materials
[ONERA-NT-1990-9] p 3336 N93-30112

THERMOCOUPLES
Transient response of embedded thermocouples
[DE93-009889] p 3431 N93-29325
Determination of surface heat transfer and film cooling effectiveness in unsteady wake flow conditions
p 3253 N93-29933

THERMODYNAMIC EQUILIBRIUM
Radiative interactions in molecular gases under local and nonlocal thermodynamic equilibrium conditions
[NASA-CR-193223] p 3604 N93-29168
Decomposition of hydrogen sulfide for small scale gas processing.
[PB93-174704] p 3316 N93-30658

THERMODYNAMIC PROPERTIES
Thermodynamic properties for polycyclic systems by non-calorimetric methods
[DE93-011373] p 3603 N93-28747
The thermodynamic properties of thianthrene and phenoxathiin
[DE93-000124] p 3603 N93-28964
Thermal properties of organic and modified inorganic aerogels
[DE93-009230] p 3311 N93-29263
Geochemical and fluid dynamic investigations into the nature of chemical heterogeneity in the Earth's mantle
[AD-A262753] p 3477 N93-29405
Thermodynamic properties of natural gas mixtures
[PB93-162816] p 3604 N93-29428
Advanced NDE technology program
[AD-A262008] p 3449 N93-29443
Tables of experimental data used for the correlation of the thermophysical properties of ethane
[PB93-173417] p 3313 N93-29768
Thermodynamic properties of natural gas mixtures
[PB93-176162] p 3604 N93-29794
Study of parameters affecting the performance of solar desiccant cooling systems
[DE93-000088] p 3465 N93-30206
Thermodynamic and structural properties of metallic glasses and supercooled liquids
[ISBN-0-315-72443-9] p 3605 N93-30359
Development of an O atom gun
[AD-A264753] p 3570 N93-30558
Effective interactions between concentration fluctuations and charge transfer in chemically ordering liquid alloys
[DE93-606724] p 3327 N93-30778
Knot invariants and cellular automata
[AD-A264199] p 3607 N93-30884
Damage of multi-directionally reinforced ceramic-matrix composites p 3308 N93-30937

THERMODYNAMICS
A one-dimensional continuum model for shape-memory alloys
[AD-A262505] p 3321 N93-28656
Tailored interfaces for metal-matrix composites-fundamental considerations
[AD-A263048] p 3298 N93-29130
Quantum group and symmetry of the heat equation
[DE93-607560] p 3605 N93-30779

THERMOELASTICITY
Influence of ply waviness on stiffness and strength reduction of composite laminates
[AD-A263224] p 3294 N93-28559

THERMOGRAPHY
Quantification of thermographic mapping techniques
[AD-A264020] p 3391 N93-30016
Logarithmic time scale in thermographic Non Destructive Evaluation (NDE) of materials p 3359 N93-30246

THERMOGRAVIMETRY
Measurements of breakaway reaction between beryllium and water vapor for ITER blanket design
[DE93-753270] p 3584 N93-28535

THERMONUCLEAR POWER GENERATION
Structural design of cryostat and port penetration of International Thermonuclear Experimental Reactor (ITER)
[DE93-753267] p 3587 N93-29243

THERMONUCLEAR REACTIONS
Development of high power microwave source
[DE93-753316] p 3436 N93-28980
A study on radiation shielding analysis for toroidal field coils of a tokamak-type fusion reactor
[DE93-753398] p 3585 N93-28981

THERMOPHYSICAL PROPERTIES
Tables of experimental data used for the correlation of the thermophysical properties of ethane
[PB93-173417] p 3313 N93-29768

THERMOPLASTIC RESINS
Effect of water immersion on fiber/matrix adhesion in thermoplastic composites
[AD-A263646] p 3299 N93-29984
Design and manufacturing concepts for thermoplastic structures p 3301 N93-30434
F-15 composite engine access door
p 3302 N93-30442
Structural response of bead-stiffened thermoplastic shear webs p 3308 N93-30873

THERMOPLASTICITY
Influence of ply waviness on stiffness and strength reduction of composite laminates
[AD-A263224] p 3294 N93-28559
Gordon Research Conferences, 1991
[AD-A264275] p 3317 N93-30816
A 69 cent look at thermoplastic softening
p 3292 N93-30963

THERMOSETTING RESINS
Carborane-(silane or siloxane)-unsaturated hydrocarbon based thermosetting polymers
[AD-D015718] p 3338 N93-30580
Carborane-(siloxane or silane)-unsaturated hydrocarbon based polymers
[AD-D015717] p 3338 N93-30586
Performance of thermal adhesives in forced convection p 3293 N93-30974

THERMOSPHERE
Spectral energetics of the lower thermosphere
p 3477 N93-29467

THICK FILMS
Adhesion of thick film Au to alumina ceramics
[DE93-009802] p 3339 N93-30656
Superconducting films of YBaCuO
[DE93-606831] p 3600 N93-30772

THICKNESS
Silicon crystal under bending
[DE93-010522] p 3593 N93-28888
Composite laminate stiffnesses and their sensitivities
[DLR-FB-92-16] p 3296 N93-29007
Superconducting films of YBaCuO
[DE93-606831] p 3600 N93-30772

THIN FILMS
New technologies for UV detectors
p 3582 N93-28786
Growth, characterization and device development in monocrystalline diamond films
[AD-A263204] p 3593 N93-28874
Electrochemical behavior and surface chemistry of aluminum alloys: Solute-rich interphase model
[AD-A262061] p 3322 N93-29002
Modification of spectral distributions by multilayer structures
[DE93-009308] p 3310 N93-29059
Structure and switching dynamics in ferroelectric crystal and liquid crystal thin films
[AD-A263664] p 3594 N93-29293
Investigation of ion beam mixing of iron marker layers in aluminum oxide by RBS
[DE93-010727] p 3594 N93-29314
Proceedings of the 25th European Conference on the Application of Polar Dielectrics to celebrate the 25th anniversary of the Dielectric Society, incorporating the 1st International Workshop on Integrated Ferroelectrics
[AD-A263427] p 3332 N93-29337
Real time self-directed MBE flux control incorporation in situ ellipsometry, phase 1
[AD-A263501] p 3595 N93-29341
Ambient-atmosphere compatible superconducting fullerenes
[AD-A262025] p 3595 N93-29397
Characterization of copper iodide thin films fabricated via laser assisted molecular beam epitaxy
[AD-A262823] p 3596 N93-29430
Flame or plasma synthesis of diamond under turbulent and transition flow conditions
[AD-D015689] p 3333 N93-29456
Shear sensitive monomer-polymer laminate structure and method of using same
[NASA-CASE-LAR-14654-1-CU] p 3452 N93-29613
Interfacial viscosity measurements of adsorbed monolayers on metal surfaces
[AD-A263288] p 3324 N93-29803
Thermal effects of a coolant film along the suction side of a high pressure turbine nozzle guide vane
p 3253 N93-29930
Measurement of turbulent spots and intermittency modelling at gas-turbine conditions
p 3253 N93-29934
Materials for adaptive structural acoustic control, volume 2
[AD-A264620] p 3563 N93-30385
RF vacuum microelectronics
[AD-A264528] p 3412 N93-30409
Fundamental studies of the mechanical behavior of microelectronics thin film materials
[AD-A264334] p 3337 N93-30417
Visible light emitting materials and injection devices
[AD-A263499] p 3601 N93-30811
Silicon Film(trademark) photovoltaic manufacturing technology
[DE93-010008] p 3466 N93-30891
Superconducting flux coupled fast switching device from YBCO films
[AD-A264301] p 3414 N93-30896
Growth model of Au films on Ru(001)
[DE92-642126] p 3602 N93-30998
Role of oxygen vacancies in anodic TiO2 thin films
[DE92-642137] p 3602 N93-31027

THIN WALLS
Experimental and modal verification of an integral equation solution for a thin-walled dichroic plate with cross-shaped holes p 3385 N93-29591

THIOLS
Scanning probe lithography. Part 1: Scanning tunneling microscope-induced lithography of self-assembled n-alkanethiol monolayer resists
[AD-A263130] p 3432 N93-29476
Observation of phase-separated nanometer scale molecular domains in mixed self-assembled monolayers
[AD-A263470] p 3569 N93-29839

THREADS
Development of stitching reinforcement for transport wing panels p 3304 N93-30852

THREE BODY PROBLEM
Double swingby at Earth-Moon for increase of excess velocity
[ETN-93-94177] p 3270 N93-30582
A numerical solution of the two-center problem
[DE92-644674] p 3551 N93-30913
Algorithm for the solution of the Faddeev equation for a system of three identical spinless particles
[DE92-644678] p 3535 N93-30914

THREE DIMENSIONAL BOUNDARY LAYER
The development of a mixing layer under the action of weak streamwise vortices
[NASA-TM-106089] p 3418 N93-28947

THREE DIMENSIONAL FLOW
Development of a 3-D Implicit Euler Code for Hypersonic and High Supersonic Flows
[ONERA-RSF-23/1123-AY-230A] p 3417 N93-28744
Numerical simulation of perfect fluid flows around complex 3D configurations by a multidomain solver using the MUSCL approach p 3417 N93-28745
An experimental study of flow over a 6 to 1 prolate spheroid at incidence p 3239 N93-29124
The 3-D viscous flow CFD analysis of the propeller effect on an advanced ducted propeller subsonic inlet
[NASA-TM-106240] p 3252 N93-29162
Nonlinear relaxation algorithms for the compressible Navier-Stokes equations in two and three dimensions
p 3421 N93-29177
Numerical computation of inviscid flow around nose tip of Space Shuttle with NND scheme
[AD-A264012] p 3421 N93-29260
Navier-Stokes analysis of three-dimensional flow and heat transfer inside turbine blade rows
p 3259 N93-29963
Three-dimensional fiber-optic LDV measurements in the endwall region of a linear cascade of controlled-diffusion stator blades
[AD-A263513] p 3424 N93-29968
Nonlinear spectroscopy of multicomponent droplets and two- and three-dimensional measurements in flames
[AD-A264341] p 3425 N93-30162

THREE DIMENSIONAL MODELS
Recognizing parameterized objects from range data
[OUEL-1918/92] p 3523 N93-28486
High performance dispersion model PHYSIC
[DE93-753303] p 3467 N93-28536
Direct volume visualization of three-dimensional vector fields
[DE93-009233] p 3524 N93-28550
Three dimensional reconstruction of complex shapes based on the Delaunay triangulation
[INRIA-RR-1697] p 3547 N93-28616
Three-dimensional numerical simulation of gradual opening in a wave rotor passage
[NASA-CR-191157] p 3252 N93-29072
NASTRAN analysis for the Airmass Sunburst model 'C' Ultralight Aircraft p 3249 N93-29777
Three-dimensional simulation analysis of the standing-wave free-electron laser two-beam accelerator
[DE93-010461] p 3575 N93-29870
Applications of three-dimensional modeling in electromagnetic exploration p 3391 N93-30010
Three-dimensional graphical representation of objects according to movement data in realtime
[ESA-TT-1258] p 3521 N93-30104
Tactile sensing for 3-dimensional shape estimation
p 3357 N93-30232

THREE DIMENSIONAL MOTION
A corner matching and tracking strategy applied to videophony
[OUEL-1933/92] p 3380 N93-28896

Integrals of motion on the group of invariance of an interval in three-dimensional spaces
[DE93-606090] p 3606 N93-30797

THRESHOLD GATES
Fuzzy operators and cyclic behavior in formal neuronal networks p 3519 N93-29576

THRUST
Thrust augmentation system for low-cost-expendable turbojet engine
[AD-A263727] p 3259 N93-30877

THRUST AUGMENTATION
Thrust augmentation system for low-cost-expendable turbojet engine
[AD-A263727] p 3259 N93-30877

THRUST CHAMBERS
Reliability assessment of thrust chamber cooling concepts using probabilistic analysis techniques
[NASA-CR-190785] p 3288 N93-29068

THRUST VECTOR CONTROL
X-31 demonstration of integrated flight and propulsion control for effective combat at extreme angles of attack
p 3260 N93-28851
Requirements for pilot assistance in a thrust-vectoring combat aircraft p 3504 N93-28870
Performance characteristics of two multiaxis thrust-vectoring nozzles at Mach numbers up to 1.28
[NASA-TP-3313] p 3239 N93-29160

THUNDERSTORMS
Proceedings of the Thunder and Lighting Seminar and the 3D Lightning Warning Workshop
[AD-A262766] p 3482 N93-29304
Thunderstorm forecast study for Eglin AFB, Florida
[AD-A263423] p 3483 N93-29810
Stand alone lightning detection equipment used at Canadian Forces air bases p 3367 N93-30295

TIDES
Spectral energetics of the lower thermosphere
p 3477 N93-29467

TILES
Thermal certification tests of Orbiter Thermal Protection System tiles coated with KSC coating slurries
[NASA-TM-104766] p 3278 N93-29221

TILT ROTOR AIRCRAFT
Rotorcraft master plan p 3236 N93-30677

TIME
Time-interpolation method for digital beamformers
[AD-D015709] p 3383 N93-29275

TIME CONSTANT
Transient response of embedded thermocouples
[DE93-009889] p 3431 N93-29325

TIME DEPENDENCE
Response of a Nb/Al2O3/Nb tunnel junction to picosecond electrical pulses
[DE93-010416] p 3594 N93-29249
Transient response of embedded thermocouples
[DE93-009889] p 3431 N93-29325
Incorporation of varying types of temporal data in a neural network p 3518 N93-29575
Optimization of HPM device parameters for maximum air transmission
[DE93-007332] p 3386 N93-29765

TIME DIVISION MULTIPLE ACCESS
Comparison of two random access techniques for the North American MSAT system p 3370 N93-30315

TIME DIVISION MULTIPLEXING
Fiber grating-based sensing system with interferometric wavelength-shift detection
[AD-D015697] p 3577 N93-29038
Data Multiplexing Network (DMN) equipment Operational Test and Evaluation (OT&E) integration test report
[AD-A263172] p 3538 N93-29490

TIME FUNCTIONS
Selection and transmission of information. Issue 22: Republic interdepartmental collection (selected articles)
[AD-A262825] p 3615 N93-29431

TIME LAG
Time delay measurements of current primary FAA air/ground transmitters and receivers
[DOT/FAA/CT-TN93/14] p 3379 N93-28555
Time-interpolation method for digital beamformers
[AD-D015709] p 3383 N93-29275

TIME MARCHING
The 3-D viscous flow CFD analysis of the propeller effect on an advanced ducted propeller subsonic inlet
[NASA-TM-106240] p 3252 N93-29162
Measurement of turbulent spots and intermittency modelling at gas-turbine conditions
p 3253 N93-29934

TIME MEASUREMENT
Large amplitude striations in an RF discharge
[DE93-753244] p 3379 N93-28534
XRONOS: A timing analysis software package. User's guide, version 3.00
[NASA-TM-109222] p 3532 N93-30023

Foreign technology assessment: Environmental evaluation of a radiation-hard oscillator/divider
[DE93-011481] p 3412 N93-30127

TIME OF FLIGHT SPECTROMETERS
A remote laser-mass spectrometer for determination of elemental composition p 3434 N93-28775
A low-cost, lightweight, and miniaturized Time-Of-Flight Mass Spectrometer (TOFMS) p 3434 N93-28817
Detonation mass spectrometry p 3319 N93-30076

TIME OPTIMAL CONTROL
Robust feedforward/feedback control synthesis for uncertain dynamical systems p 3542 N93-29079

TIME SERIES ANALYSIS
Fundamental study of the signal processing by optics
[DE93-776265] p 3577 N93-28982

TIME SIGNALS
Fundamental study of the signal processing by optics
[DE93-776265] p 3577 N93-28982
Distributed traffic signal control using fuzzy logic
p 3513 N93-29543

TIMOSHENKO BEAMS
Vibration localization in rotating shafts
p 3454 N93-30626

TISSUES (BIOLOGY)
Wound healing and connective tissue metabolism: The role of hyperbaric oxygen therapy
[AD-A262483] p 3493 N93-28759
The chronic effects of jP-8 jet fuel exposure on the lungs
[AD-A264162] p 3495 N93-30153
Theoretical-experimental study of the non-thermal effects of the polarized laser radiation in living tissues
[DE93-607212] p 3441 N93-30775

TITANIUM
Plastic deformation behaviour of oxide dispersion strengthened titanium alloys
[ONERA-NT-1990-6] p 3326 N93-30138

TITANIUM ALLOYS
The temperature dependence of the deformation and oxidation behavior of an age-hardenable beta + alpha-two titanium alloy
[AD-A262232] p 3320 N93-28491
International Conference on Martensitic Transformations (ICOMAT 92)
[AD-A262739] p 3321 N93-28591
Microstructural effects on the deformation and fracture of the alloy Ti-25Al-10Nb-3B-1Mo
[AD-A263095] p 3323 N93-29144
Boron carbide aluminum cermets for external pressure housing applications
[AD-A262749] p 3333 N93-29404
Mechanisms of fracture and creep of structural alloys
[AD-A263108] p 3324 N93-29799
Improvement in ductility of the intermetallic compound Ti3Al
[ESA-TT-1276] p 3325 N93-30105

TITANIUM BORIDES
Explosive consolidation of combustion synthesized TiC and TiB2: Precursor morphology effects
[AD-A263186] p 3341 N93-28515

TITANIUM CARBIDES
Explosive consolidation of combustion synthesized TiC and TiB2: Precursor morphology effects
[AD-A263186] p 3341 N93-28515
Report on the sintering and properties of MgO and MgO-5 percent TiC
[DE93-008676] p 3323 N93-29092
Laser gas alloying of titanium materials
[ETN-93-93805] p 3325 N93-30115

TITANIUM COMPOUNDS
Laser gas alloying of titanium materials
[ETN-93-93805] p 3325 N93-30115
Two new titanium pyroarsenates: Alpha-TiAs2O7 and Beta-TiAs2O7
[AD-A264632] p 3599 N93-30518

TITANIUM NITRIDES
Ion-beam-assisted deposition of wear-resistant coatings
[DE93-011529] p 3330 N93-28687
Design of interfaces in metal matrix composites
[AD-A262052] p 3296 N93-29001
Laser gas alloying of titanium materials
[ETN-93-93805] p 3325 N93-30115

TOKAMAK DEVICES
JT-60 Upgrade vertical stability experiments and analysis
[DE93-753131] p 3583 N93-28530
Measurements of breakaway reaction between beryllium and water vapor for ITER blanket design
[DE93-753270] p 3584 N93-28535
New remote maintenance approach for TPX
[DE93-007857] p 3584 N93-28583
Nonlinear dynamics and plasma transport
[DE93-012238] p 3585 N93-28749

Moment approach to fast ion neoclassical transport and viscous forces
[DE93-753305] p 3585 N93-28979
A study on radiation shielding analysis for toroidal field coils of a tokamak-type fusion reactor
[DE93-753398] p 3585 N93-28981
Theory of tokamak edge turbulence: Drift-thermal instability-induced turbulence and ionization-driven drift wave turbulence p 3586 N93-29123
Effects of neutral gas collisions on the power transmission factor at the divertor sheath
[DE93-009320] p 3588 N93-29334
Modeling the D3-D plasma boundary with the LEDGE code
[DE93-009301] p 3588 N93-29772
Bootstrap current profiles and scaling in large aspect ratio tokamaks
[DE93-753158] p 3589 N93-30003
Fundamental studies of fusion plasmas
[DE93-013144] p 3589 N93-30189
Preliminary design study of a steady state tokamak device
[DE93-764162] p 3589 N93-30397
Operation of a 20-channel grating polychromator diagnostic system and its application to sawtooth observations in JT-60U
[DE93-764388] p 3590 N93-30398
Optimization for steady-state and hybrid operations of ITER by using scaling models of divertor heat load
[DE93-764151] p 3590 N93-30649
Plasma Physics Network Newsletter, no. 5
[DE93-606216] p 3591 N93-30795

TOLERANCES (MECHANICS)
Sensor systems for monitoring Maglev guideway structures
[PB93-154821] p 3444 N93-29205
Mechanical behaviour of a closed collar model for an 11.5 T dipole
[NIKHEF-H/92-03] p 3576 N93-30019
Mold bolt and means for achieving close tolerances between bolts and bolt holes
[NASA-CASE-MFS-28720-1] p 3447 N93-30567
Developments in impact damage modeling for laminated composite structures p 3305 N93-30857
Progressive failure methodologies for predicting residual strength and life of laminated composites
p 3307 N93-30866

TOMATOES
Final results of space exposed experiment developed for students p 3492 N93-29702

TOMOGRAPHY
Tomographic analysis of line-of-sight infrared spectra of low-pressure flames
[AD-A263185] p 3309 N93-28514
Applications of mesoscopic physics
[DE93-012104] p 3597 N93-30141

TOOLING
Development of an updated pinch-welding capability
[DE93-009823] p 3442 N93-28552

TOPOGRAPHY
Multibeam laser altimeter for planetary topographic mapping p 3442 N93-28780
The German PAF (Processing and Archiving Facilities) for ERS-1 p 3457 N93-28916
Charting the remote southern oceans with geosat altimetry
[AD-A263452] p 3461 N93-29817
ARI: Internal gravity waves at abrupt topography
[AD-A263795] p 3477 N93-29879
Simulation of landscape disturbances and the effect of climatic change
[DE93-011615] p 3472 N93-30131

TOPOLOGY
Topology of hybrid objects
[ETN-93-93594] p 3546 N93-28466
NetStat: A probabilistic network connectivity analysis tool
[AD-A262838] p 3529 N93-29647
Ethernet performance of the Motorola Altair WIN system
[AD-A263877] p 3387 N93-29890

TORNADOES
Doppler-radar wind-speed measurements in tornadoes: A comparison of real and simulated spectra
[DE93-008734] p 3481 N93-29095
Case study of the operational usefulness of the sharp workstation in forecasting a mesocyclone-induced cold sector tornado event in California
[PB93-178697] p 3485 N93-30889

TOROIDAL PLASMAS
JT-60 Upgrade vertical stability experiments and analysis
[DE93-753131] p 3583 N93-28530
Nonlinear coupling of tearing fluctuations in the Madison Symmetric Torus
[DE93-010131] p 3584 N93-28602

Self-organized profile relaxation by ion temperature gradient instability in toroidal plasmas
[DE93-009580] p 3585 N93-28910

Electron cyclotron heating and current drive in toroidal geometry
[DE93-010400] p 3586 N93-29049

Poloidal field measurements during transient phenomena on MTX: Sawtooth perturbations and the effect of ECH on disruptions
[DE93-010516] p 3587 N93-29303

Bootstrap current profiles and scaling in large aspect ratio tokamaks
[DE93-753158] p 3589 N93-30003

TOROIDS

A 250 mA toroid monitor for the measurement of the bundle current in the stretcher mode of AmPS
[DIGEL-1992-1] p 3413 N93-30835

TORQUE

Study on decreasing torque noise resulting from feedback noise for the modified bang-bang controller
[AD-A263178] p 3407 N93-29010

TORSION

A complete set of field equations for the dynamic simulation of a towed cable system
[AD-A262570] p 3442 N93-28578

The geometry of complex space-times with torsion
[DE92-641343] p 3608 N93-31003

TORSIONAL VIBRATION

Vibration localization in rotating shafts
p 3454 N93-30626

TORSO

Sudden loading and fatigue effects on the human spine
[PB93-167526] p 3493 N93-29199

TOTAL OZONE MAPPING SPECTROMETER

Results from the US/Russian Meteor-3/Total Ozone Mapping Spectrometer
[NASA-TM-104576] p 3467 N93-28682

TOUGHNESS

The effect of temperature on the impact behavior of TiB2 reinforced XDTM-TiAl intermetallic matrix composites
[AD-A262924] p 3296 N93-28886

Transformation plasticity in ductile solids
[DE93-008636] p 3321 N93-28902

Whisker toughening of ceramic materials: A review
[DE93-011565] p 3336 N93-30129

Effects of intra- and inter-laminar resin content on the mechanical properties of toughened composite materials
p 3303 N93-30845

TOWED BODIES

A complete set of field equations for the dynamic simulation of a towed cable system
[AD-A262570] p 3442 N93-28578

TOWERS

DSS-14 subreflector actuator dynamics during the Landers earthquake p 3386 N93-29600

Oceanographic research towers in european waters
[AD-A264795] p 3489 N93-30612

TOWING

A complete set of field equations for the dynamic simulation of a towed cable system
[AD-A262570] p 3442 N93-28578

TOXIC HAZARDS

Application of sensors to the control of robotic systems
[DE93-009837] p 3543 N93-30012

An evaluation of factors affecting the solidification/stabilization of heavy metal sludge
[AD-A264128] p 3473 N93-30197

TOXICITY

Development of novel models for describing multiple toxicity effects
[AD-A264439] p 3496 N93-30422

TOXINS AND ANTITOXINS

The AFOSR Workshop on the Future of EEG and MEG
[AD-A264338] p 3495 N93-30160

TRACE CONTAMINANTS

Emission inventories: A global modeling perspective
[DE93-005817] p 3469 N93-28965

Global warming potential for SF6
[DE93-007394] p 3469 N93-28972

Computerized atmospheric trace contaminant control simulation for manned spacecraft
[NASA-TM-108409] p 3505 N93-28977

Case study of Frontal Boundary Study Mission 03
[DE93-007176] p 3473 N93-30183

TRACE ELEMENTS

Activities report of the International Meteorological Institute, Stockholm (Sweden)
[ETN-93-93768] p 3480 N93-28519

Emission inventories: A global modeling perspective
[DE93-005817] p 3469 N93-28965

Global warming potential for SF6
[DE93-007394] p 3469 N93-28972

Instrumental neutron activation analysis developed for silicon integrated circuit technology
[ETN-93-93581] p 3408 N93-29271

Geochemical and fluid dynamic investigations into the nature of chemical heterogeneity in the Earth's mantle
[AD-A262753] p 3477 N93-29405

TRACKING (POSITION)

A corner matching and tracking strategy applied to videophony
[OUEL-1933/92] p 3380 N93-28896

An autonomous vision-based mobile robot
p 3443 N93-29082

Interferometric tracking system for the tracking and data relay satellite
[NASA-CR-193274] p 3382 N93-29217

TRACKING PROBLEM

A fuzzy logic optimal control law solution to the CMMCA tracking problem
[AD-A262555] p 3542 N93-29420

Control of nonlinear systems with applications to constrained robots and spacecraft attitude stabilization
p 3279 N93-29989

Synchronization of the LAPTV adative filter with input statistics p 3358 N93-30242

Control of nonlinear systems with applications to constrained robots and spacecraft attitude stabilization
p 3544 N93-30893

TRACKING STATIONS

Investigation of Mars rotational dynamics using Earth-based radio tracking of Mars landers
p 3642 N93-28777

High-power Ka-band amplifier p 3385 N93-29590

TRACKS

Sensor systems for monitoring Maglev guideway structures
[PB93-154821] p 3444 N93-29205

TRADEOFFS

Concept formulation process aid for trade-off determination: Operator's guide
[AD-A263756] p 3531 N93-29874

TRAFFIC

Distributed traffic signal control using fuzzy logic
p 3513 N93-29543

Ethernet performance of the Motorola Altair WIN system
[AD-A263877] p 3387 N93-29890

Vehicle dynamic stability and rollover
[PB93-185437] p 3447 N93-30828

TRAFFIC CONTROL

Distributed traffic signal control using fuzzy logic
p 3513 N93-29543

TRAILING EDGES

Articulated fin/wing control system
[AD-D015712] p 3259 N93-29278

SIMS chemical analysis of extended impacts on the leading and trailing edges of LDEF experiment AO187-2
p 3318 N93-29367

Projectile compositions and modal frequencies on the chemistry of micrometeoroids LDEF experiment
p 3638 N93-29370

Long-term microparticle flux variability indicated by comparison of Interplanetary Dust Experiment (IDE) timed impacts for LDEF's first year in orbit with impact data for the entire 5.77-year orbital lifetime p 3638 N93-29379

Topology and grid adaption for high-speed flow computations
[NASA-CR-4216] p 3426 N93-30375

TRAINING AIRCRAFT

Simulators for corporate pilot training and evaluation
p 3236 N93-30678

TRAINING DEVICES

Concept formulation process aid for trade-off determination: Operator's guide
[AD-A263756] p 3531 N93-29874

Development of a concept formulation process aid for analyzing training requirements and developing training devices
[AD-A263579] p 3261 N93-29972

Review of the effectiveness of video media in instruction
[AD-A264228] p 3392 N93-30362

Virtual reality flight control display with six-degree-of-freedom controller and spherical orientation overlay
[NASA-CASE-NPO-18733-1-CU] p 3251 N93-30416

TRAINING EVALUATION

The air traffic controller's mental model and it's implications for equipment design and trainee selection
p 3372 N93-30322

Helicopter training simulators: Key market factors
p 3237 N93-30683

Training effectiveness assessment: Methodological problems and issues p 3237 N93-30684

Determining the transferability of flight simulator data
p 3237 N93-30685

Progress through precedent: Going where no helicopter simulator has gone before p 3237 N93-30686

Transfer of training and simulator qualification or myth and folklore in helicopter simulation
p 3237 N93-30687

TRAINING SIMULATORS

Radar beam effects for a flight simulator using signal processor based hardware p 3373 N93-30328

NASA/FAA helicopter simulator workshop
[NASA-CP-3156] p 3236 N93-30673

Part 1: Executive summary p 3236 N93-30674

Helicopter simulator standards p 3236 N93-30675

Simulators for corporate pilot training and evaluation
p 3236 N93-30678

TRAJECTORIES

Preliminary design of an intermittent smoke flow visualization system
[NASA-CR-186027] p 3248 N93-28693

An artificial neural network model for periodic trajectory generation p 3356 N93-30225

TRAJECTORY ANALYSIS

Detonation shock dynamics of composite energetic materials p 3350 N93-30096

TRAJECTORY CONTROL

Symbology for head up and head down applications for highly agile fighter aircraft: To improve spatial awareness, trajectory control, and unusual attitude recovery, part 1
p 3502 N93-28857

Exact trajectory determinator for ERS-1
p 3457 N93-28918

A portable modular architecture for robotic manipulator control
[DE93-010819] p 3444 N93-29254

TRAJECTORY MEASUREMENT

Onboard signal processing: Wave of the future for planetary radio science? p 3646 N93-28801

An LDEF 2 dust instrument for discrimination between orbital debris and natural particles in near-Earth space
p 3286 N93-29707

TRAJECTORY OPTIMIZATION

Optimal trajectories for aircraft terrain following and terrain avoidance: A literature review update
[AD-A264075] p 3260 N93-30604

TRAJECTORY PLANNING

An autonomous vision-based mobile robot
p 3443 N93-29082

Planning collision free paths for two cooperating robots using a divide-and-conquer C-space traversal heuristic
[NASA-CR-193252] p 3542 N93-29771

Trajectory generation for dual-arm robots using artificial impedance approach p 3370 N93-30310

Double swingby at Earth-Moon for increase of excess velocity
[ETN-93-94177] p 3270 N93-30582

TRANSCENDENTAL FUNCTIONS

Study on the concurrent calculation with a multitransputer network
[DE93-753191] p 3524 N93-28531

The generic arithmetic of SISYPHE
[INRIA-RT-0136] p 3524 N93-28755

TRANSDUCERS

A microseismometer for terrestrial and extraterrestrial applications p 3434 N93-28765

TRANSFER FUNCTIONS

Advances in the identification of electrochemical transfer function models using Prony analysis
[DE93-009424] p 3550 N93-30041

Control system design and multiparameter variations
p 3355 N93-30217

Realization of high speed adaptive FIR digital filters
p 3355 N93-30222

TRANSFER OF TRAINING

Summer research program (1992). High School Apprenticeship Program (HSAP) reports. Volume 16: Arnold Engineering Development Center Civil Engineering Laboratory
[AD-A262024] p 3608 N93-29396

Transfer of training and simulator qualification or myth and folklore in helicopter simulation
p 3237 N93-30687

TRANSFER ORBITS

Transfer Orbit Plasma Interaction Experiment (TROPIX) p 3267 N93-28734

TRANSFORMATIONS (MATHEMATICS)

The space of spheres, a geometric tool to unify duality results in Voronoi diagrams
[INRIA-RR-1620] p 3547 N93-28512

Polygonal approximation overviews and perspectives
[INRIA-RR-1621] p 3547 N93-28513

Comparison between the performance of two classes of fuzzy controllers p 3517 N93-29566

On probability-possibility transformations
p 3519 N93-29582

Zero-crossing rate of some non-Gaussian processes
p 3360 N93-30254

TRANSFORMERS
Charge to frequency converter for ionization chambers belonging to the radiation protection system of AmPS/MEA
[DIGEL-1991-6] p 3577 N93-30837

TRANSIENT RESPONSE
Transient response of embedded thermocouples
[DE93-009889] p 3431 N93-29325
Pulse mitigation and heat transfer enhancement techniques. Volume 3: Liquid sodium heat transfer facility and transient response of sodium heat pipe to pulse forward and reverse heat load
[AD-A263496] p 3422 N93-29338
Pulse mitigation and heat transfer enhancement techniques. Volume 4: Transient behavior of heat pipe with thermal energy storage under pulse heat loads
[AD-A263497] p 3423 N93-29339
Transient field computations within or proximity of complex structures: FD-TD approach
p 3366 N93-30292

TRANSISTORS
RF vacuum microelectronics
[AD-A264528] p 3412 N93-30409
Effects of device scaling and geometry on MOS radiation hardness assurance
[DE93-009832] p 3413 N93-30516
Superconducting flux coupled fast switching device from YBCO films
[AD-A264301] p 3414 N93-30896

TRANSITION FLOW
A grid refinement study of two-dimensional transient flow over a backward-facing step using a spectral-element method
[DE92-018262] p 3417 N93-28639
Flame or plasma synthesis of diamond under turbulent and transition flow conditions
[AD-D015689] p 3333 N93-29456
Keynote address: Unsteady, multimode transition in gas turbine engines p 3252 N93-29927
Measurement of turbulent spots and intermittency modelling at gas-turbine conditions
p 3253 N93-29934

TRANSITION METALS
Catalytic synthesis of silicon carbide preceramic polymers: Polycarbosilanes
[DE93-008634] p 3329 N93-28541
Supported organometallic complexes, surface chemistry, spectroscopy, and catalysis
[DE93-011930] p 3309 N93-28688
Theoretical hyperfine structure constants for transition metal atoms and ions
[DE93-012325] p 3566 N93-29183
Applications of transition metal compounds in the preparation of useful silicon-containing ceramics
[AD-A264028] p 3335 N93-30028
Organometallic compounds and polymers with second and third order nonlinear optical properties
[AD-A264774] p 3338 N93-30610

TRANSITION POINTS
Materials characterization of cermet anodes tested in a pilot cell
[DE93-008924] p 3323 N93-29101

TRANSITION TEMPERATURE
The Road to Room Temperature Superconductivity Workshop
[AD-A264633] p 3561 N93-30519

TRANSLATING
Transforming AdaPT to Ada9x
[NASA-CR-193117] p 3526 N93-29026

TRANSLATIONAL MOTION
Coarse image motion for saccade control
[OUEL-1916/92] p 3523 N93-28485

TRANSMISSION EFFICIENCY
Theoretical and experimental coverage analysis of a VLF transmitter p 3396 N93-30734

TRANSMISSION LINES
Potential transmission and transients during corrosion: Applications to corrosion monitoring
[DE93-010863] p 3323 N93-29256
Planar active antennas and quasi-optical power combining arrays using FET's and slots
[AD-A263759] p 3387 N93-29875

TRANSMITTANCE
An automated observing system for passive evaluation of cloud cover and visibility
[AD-A263207] p 3481 N93-28875

TRANSMITTER RECEIVERS
Hybrid data link
[AD-D015714] p 3383 N93-29280
High-speed, CMOS dual modulus frequency divider for RF frequency synthesis p 3359 N93-30245
Uplink laser propagation measurements through the sea surface, haze and clouds
[AD-A264687] p 3440 N93-30553
A methodology and tool for the prediction of depth of reception in the sea for a VLF/LF communications system p 3397 N93-30741

TRANSMITTERS
Method of emitting on a specific wavelength fraunhofer line using a neodymium doped laser transmitter
[AD-D015710] p 3437 N93-29276
High-power Ka-band amplifier p 3385 N93-29590
Biophysical and biochemical mechanisms in synaptic transmitter release
[AD-A264829] p 3496 N93-30613
Theoretical and experimental coverage analysis of a VLF transmitter p 3396 N93-30734
A long wave TE/TM noise prediction model
p 3397 N93-30742

TRANSONIC FLOW
Transonic flows on an oscillating airfoil and their effect on the flutter-boundary
[DLR-FB-92-08] p 3238 N93-29006
A Navier-Stokes solver with different turbulence models applied to film-cooled turbine cascades
p 3258 N93-29962
Computational fluid dynamics research on dynamically adaptive mesh methods for transonic flows
[AD-A264833] p 3428 N93-30630

TRANSONIC FLUTTER
Transonic flows on an oscillating airfoil and their effect on the flutter-boundary
[DLR-FB-92-08] p 3238 N93-29006

TRANSONIC WIND TUNNELS
Performance characteristics of two multiaxis thrust-vectoring nozzles at Mach numbers up to 1.28
[NASA-TP-3313] p 3239 N93-29160

TRANSPLANTATION
Incorporation of varying types of temporal data in a neural network p 3518 N93-29575
Control and circadian behavior by transplanted suprachiasmatic nuclei
[AD-A264553] p 3496 N93-30382

TRANSPONDERS
Acoustic charge transport technology investigation for advanced development transponder
p 3386 N93-29602
Satellite calibration requirements
[AD-A264279] p 3281 N93-30817

TRANSPORT AIRCRAFT
The development of a parachute system for aerial delivery from high speed cargo aircraft
[DE93-008339] p 3239 N93-29035
Vortex wake characteristics of B757-200 and B767-200 aircraft using the tower fly-by technique
[PB93-180263] p 3242 N93-30388
Composites technology for transport primary structure
p 3300 N93-30431
Advanced technology commercial fuselage structure
p 3300 N93-30432
Design, analysis, and fabrication of the technology integration box beam p 3300 N93-30433
Mechanical and analytical screening of braided composites for transport fuselage applications
p 3305 N93-30855
Optimization of composite sandwich cover panels subjected to compressive loadings p 3306 N93-30862
Advanced fiber placement of composite fuselage structures p 3306 N93-30864

TRANSPORT PROPERTIES
Ion motion effects on charged radiators
[DE93-009257] p 3565 N93-29099
Analysis of mass transport and potential vorticity budget in a simulated tropopause folding
[PB93-156792] p 3476 N93-29197
High-current negative-ion beam transport
[DE93-010732] p 3575 N93-29809
Studies of fluctuation processes in nuclear collisions
[DE93-011263] p 3576 N93-30054
Effect of planar magnetic field on electron transport properties of n-AlGaAs/GaAs heterojunction and photoluminescence measures in GaAs samples
[DE93-608739] p 3601 N93-30776

TRANSPORT THEORY
Nonlinear dynamics and plasma transport
[DE93-012238] p 3585 N93-28749
The investigation of nonlinear effects on quasiparticle transport in condensed matter systems
[DE93-009582] p 3565 N93-28914
Moment approach to fast ion neoclassical transport and viscous forces
[DE93-753305] p 3585 N93-28979
Modern Monte Carlo particle transport simulation for safety and radiation protection applications in accelerometer technology and in space science
[JUEL-2609] p 3574 N93-29062
Collective transport of alpha particles due to Alfven wave instability
[DE93-009578] p 3587 N93-29148
Modeling the D3-D plasma boundary with the LEDGE code
[DE93-009301] p 3588 N93-29772

TRANSPORTATION
Power generation and transportation systems research department
[PB93-178309] p 3352 N93-30663

TRANSPORTER
Leaky coaxial cable signal transmission for remote facilities
[DE93-007916] p 3383 N93-29348

TRANSPUTERS
Study on the concurrent calculation with a multitranspuler network
[DE93-753191] p 3524 N93-28531
Transputers, parallel processing in embedded systems for image compression in space applications
[NLR-TP-89242-U] p 3522 N93-30840

TRAPPED PARTICLES
The Interstellar Gas Experiment: Analysis in progress
p 3639 N93-29380
LDEF: Dosimetric measurement results (AO 138-7 experiment) p 3573 N93-29635

TRAVELING WAVE TUBES
Novel methods of acceleration
[AD-A264828] p 3590 N93-30600

TRAYS
Scanning electron microscope/energy dispersive x ray analysis of impact residues in LDEF tray clamps
p 3283 N93-29369
Elemental analyses of hypervelocity microparticle impact sites on Interplanetary Dust Experiment sensor surfaces
p 3638 N93-29378

TREES (MATHEMATICS)
Robust and efficient implementation of the Delaunay tree
[INRIA-RR-1619] p 3547 N93-28511
Packing of Steiner trees: Polyhedric studies and application
[ETN-93-93796] p 3547 N93-28527
Generalized octrees for constrained object modeling
p 3369 N93-30304
A robust model for finding optimal evolutionary trees
[DE93-010682] p 3491 N93-30483
Placement of cells: Theory and solution of a quadratic 0/1 optimization problem
[ETN-93-94182] p 3413 N93-30616

TREES (PLANTS)
Predicting the response of a temperate forest ecosystem to atmospheric CO2 increase
[DE93-010081] p 3467 N93-28543

TRELLIS CODING
An error control protocol based on trellis coded modulations p 3358 N93-30237
Signal processor based MSAT trellis coded M-DPSK with adaptive Doppler phasor correction
p 3373 N93-30332
Two-stage Doppler phasor corrected TCM/DMPSK for shadowed mobile satellite channels
p 3373 N93-30333

TREND ANALYSIS
Overview of the DOE Atmospheric Chemistry Program's Ozone Project
[DE93-007416] p 3471 N93-29770

TRENDS
Evaluation of environmental marketing terms in the United States
[PB93-175784] p 3474 N93-30660

TRIANGULATION
Robust and efficient implementation of the Delaunay tree
[INRIA-RR-1619] p 3547 N93-28511
Three dimensional reconstruction of complex shapes based on the Delaunay triangulation
[INRIA-RR-1697] p 3547 N93-28616
Development of a new technique for image reconstruction, enhancement, and visualization
[AD-A263145] p 3528 N93-29483
Multiple image multipoint matching for automatic aerotriangulation p 3461 N93-29615

TRIATOMIC MOLECULES
The global potential energy surfaces of the lowest two 1A-prime states of the ozone molecule: Theoretical determination and analysis
[DE93-007537] p 3313 N93-29837
NO2 unimolecular decomposition: Step-like variation of k(sub uni)(E) p 3318 N93-30068

TRIBOLOGY
Effect of metallic-coating properties on the tribology of coated and oil-lubricated ceramics
[DE93-010663] p 3330 N93-28666
Surface modification of tribological components in transportation
[DE93-008647] p 3442 N93-28903
Polarization modulated ellipsometry
[NASA-CR-4012] p 3580 N93-30372

Fundamental studies of friction, lubrication, and wear by atomic force microscopy
[AD-A264647] p 3446 N93-30524
Tribology: Friction, lubrication, and wear technology
p 3292 N93-30965
Walkway friction: Experiment and analysis
p 3293 N93-30966

TRIGGER CIRCUITS
Improving the jitter of the 150 kJ experiments solid dielectric switches
[DE93-009459] p 3405 N93-28597
High-voltage pulse generator capable of 2000 J at 10 kV
[AD-A262034] p 3407 N93-28999

TRIGONOMETRIC FUNCTIONS
Study on the concurrent calculation with a multitransputer network
[DE93-753191] p 3524 N93-28531

TRINITROTOLUENE
Interfacial melting in cracked explosives
p 3349 N93-30089

TRIODES
Upgrading the LAMPF 201 MHz RF generators
[DE93-010715] p 3406 N93-28830

TRITIUM
Exotic atoms
[DE93-010242] p 3564 N93-28611

TROPICAL METEOROLOGY
Ocean aerosol measurements and models in the straits of Florida (The KEY-90 experiment)
[AD-A264777] p 3487 N93-29659

TROPICAL REGIONS
Advanced Earth Observing Satellite (ADEOS)
p 3279 N93-29648
Tropical forests and biological diversity: USAID report to Congress 1990-1991
[PB93-180453] p 3471 N93-29681
Hydrographic observations in the western tropical and subtropical north Atlantic Ocean: Atlantic Climate Change Program (ACCP) and Western Tropical Atlantic Experiment (WESTRAX) during 1990
[PB93-184760] p 3489 N93-30827
The distribution of the annual and semiannual cycles in the tropics
[DE92-642213] p 3485 N93-31006

TROPICAL STORMS
Rhode Island hurricanes and tropical storms: A fifty-six year summary, 1936-1991
[PB93-162006] p 3481 N93-29198
The sensitivity of ageostrophic circulations to model resolution: A case study using NGM forecasts of ERICA IOP-4
[AD-A262011] p 3482 N93-29393

TROPOPAUSE
Analysis of mass transport and potential vorticity budget in a simulated tropopause folding
[PB93-156792] p 3476 N93-29197

TROPOSPHERE
Distribution of C1-C2 aldehydes in the free troposphere
[JUEL-2650] p 3475 N93-28475
Activities report of the International Meteorological Institute, Stockholm (Sweden)
[ETN-93-93768] p 3480 N93-28519

TRUCKS
Aircraft and refueler bonding and grounding study
[AD-A262027] p 3261 N93-29398

TRUSSES
Description of the Joint Damping Experiment (JDX)
p 3263 N93-28703
CSI-Star: A low-cost CSI orbital testbed
p 3263 N93-28707

TUNABLE LASERS
ND laser with co-doped ion(s) pumped by visible laser diodes
[AD-D015711] p 3437 N93-29277
Tunable CW diode-pumped Tm,Ho:YLiF4 laser operating at or near room temperature
[NASA-CASE-NPO-18611-1-CU] p 3440 N93-30415
Computer control of pulsed tunable dye lasers
[DE93-605896] p 3441 N93-30801

TUNGSTEN ALLOYS
The effect of material strength on segment penetration behavior
[AD-A263262] p 3453 N93-29801
Examination of formability to seamless tubes on Ni-Cr-W superalloy
[DE93-764158] p 3326 N93-30396
Development of Ni-Cr-W superalloys for high temperature components in high temperature gas-cooled reactors, part 2
[DE93-764469] p 3326 N93-30399

TUNING
A composite self tuning strategy for fuzzy control of dynamic systems p 3511 N93-29530
Design issues of a reinforcement-based self-learning fuzzy controller for petrochemical process control
p 3512 N93-29533
Tuning a fuzzy controller using quadratic response surfaces p 3515 N93-29553
A genetic algorithms approach for altering the membership functions in fuzzy logic controllers
p 3518 N93-29573
Widebanding techniques for VHF antennas 2
[AD-A263998] p 3387 N93-29882

TURBIDITY
Loading and testing a light scattering cell with a binary fluid mixture near its critical composition
[NASA-CR-193147] p 3415 N93-28557

TURBINE BLADES
The natural excitation technique (NExT) for modal parameter extraction from operating wind turbines
[DE93-010611] p 3463 N93-28603
Heat Transfer and Cooling in Gas Turbines
[AGARD-CP-527] p 3252 N93-29926
Vortex structure and mass transfer near the base of a cylinder and a turbine blade p 3253 N93-29929
The influence of non-uniform spanwise inlet temperature on turbine rotor heat transfer p 3253 N93-29932
Heat transfer in high turbulence flows: A 2-D planar wall jet p 3254 N93-29935
The effect of orthogonal-mode rotation on forced convection in a circular-sectioned tube fitted with full circumferential transverse ribs p 3254 N93-29937
Cooling geometry optimization using liquid crystal technique p 3254 N93-29939
Prediction of jet impingement cooling scheme characteristics (airfoil leading edge application)
p 3255 N93-29941
An L2F-measurement device with image rotator prism for flow velocity analysis in rotating coolant channels
p 3255 N93-29942
Impingement/effusion cooling p 3257 N93-29954
The aerodynamic effect of coolant ejection in the leading edge region of a film-cooled turbine blade
p 3258 N93-29958
Modeling of a turbulent flow in the presence of discrete parietal cooling jets p 3258 N93-29960
Coupling of 3D-Navier-Stokes external flow calculations and internal 3D-heat conduction calculations for cooled turbine blades p 3258 N93-29961
A Navier-Stokes solver with different turbulence models applied to film-cooled turbine cascades
p 3258 N93-29962
Navier-Stokes analysis of three-dimensional flow and heat transfer inside turbine blade rows
p 3259 N93-29963
Optical blade vibration measurement
[ETN-93-93454] p 3259 N93-29999

TURBINE ENGINES
Navier-Stokes analysis of radial turbine rotor performance
[NASA-CR-191153] p 3251 N93-28609
Aero-thermal design of a cooled transonic NGV and comparison with experimental results
p 3257 N93-29957

TURBINE PUMPS
High Reynolds number and turbulence effects on aerodynamics and heat transfer in a turbine cascade
[NASA-TM-106187] p 3420 N93-29157
Orbital transfer vehicle oxygen turbopump technology. Volume 3: Hot oxygen testing
[NASA-CR-191036] p 3448 N93-31039

TURBINE WHEELS
Improved silicon nitride for advanced heat engines
[NASA-CR-182193] p 3298 N93-29451

TURBINES
Experimental evaluation of a cooled radial-inflow turbine
[NASA-TM-106230] p 3251 N93-28697
Aerothermic calculations of flows in interdisc cavities of turbines p 3256 N93-29947

TURBOCOMPRESSORS
Flow phenomena in turbomachines
[AD-A263049] p 3420 N93-29141
Improved silicon nitride for advanced heat engines
[NASA-CR-182193] p 3298 N93-29451

TURBOFAN AIRCRAFT
Design of a turbofan powered regional transport aircraft p 3228 N93-29721

TURBOFAN ENGINES
Cooling predictions in turbofan engine components
p 3259 N93-29964

TURBOJET ENGINES
Thrust augmentation system for low-cost-expendable turbojet engine
[AD-A263727] p 3259 N93-30877

TURBOMACHINERY
Unsteady vortex loop/dipole theory applied to the work and acoustics of an ideal low speed propeller
[AD-A264057] p 3241 N93-29891
Modelling thermal behaviour of turbomachinery discs and casings p 3256 N93-29949
Some implications of a differential turbomachinery equation with viscous correction
[AD-A264693] p 3427 N93-30571

TURBULENCE
Studies of complexity in fluid systems
[DE93-010776] p 3418 N93-28878
Nonconservative and reverse spectral transfer in Hasegawa-Mima turbulence
[DE93-010132] p 3585 N93-28913
A numerical study of confined turbulent jets
[NASA-TM-106197] p 3420 N93-29161
Chaos in mechanical systems with especial reference to rotorcraft and missiles
[AD-A263703] p 3604 N93-29384
Keynote address: Unsteady, multimode transition in gas turbine engines p 3252 N93-29927
Measurement of turbulent spots and intermittency modelling at gas-turbine conditions
p 3253 N93-29934
Heat transfer in high turbulence flows: A 2-D planar wall jet p 3254 N93-29935
Heat transfer with moderate free stream turbulence
p 3254 N93-29936
Cooling geometry optimization using liquid crystal technique p 3254 N93-29939
An L2F-measurement device with image rotator prism for flow velocity analysis in rotating coolant channels
p 3255 N93-29942
Turbulence characteristics of an axisymmetric reacting flow
[NASA-CR-4110] p 3242 N93-30373
Towards a better hydro for dynamic mix calculations
[DE93-010702] p 3426 N93-30485
Analysis and computation for vortex dynamics and rarefied gases
[AD-A264705] p 3427 N93-30499

TURBULENCE EFFECTS
Large eddy simulations of shockwave passage through turbulence
[DE92-019503] p 3419 N93-29050
Theory of tokamak edge turbulence: Drift-thermal instability-induced turbulence and ionization-driven drift wave turbulence p 3586 N93-29123
High Reynolds number and turbulence effects on aerodynamics and heat transfer in a turbine cascade
[NASA-TM-106187] p 3420 N93-29157

TURBULENCE MODELS
Supersonic flow calculation using a Reynolds-stress and an eddy thermal diffusivity turbulence model
[NASA-CR-4515] p 3420 N93-29159
Development of an unstructured solution adaptive method for the quasi-three-dimensional Euler and Navier-Stokes equations
[NASA-CR-193241] p 3421 N93-29213
Sensitivity study of cloud/radiation interaction using a second order turbulence radiative-convective model
[DE93-007365] p 3477 N93-29346
Methods for reducing turbulent flow aero-optical distortion
[AD-A263698] p 3423 N93-29353
A Navier-Stokes solver with different turbulence models applied to film-cooled turbine cascades
p 3258 N93-29962
Navier-Stokes analysis of three-dimensional flow and heat transfer inside turbine blade rows
p 3259 N93-29963

TURBULENT BOUNDARY LAYER
The effect of high temperature on wall shear in a two dimensional wall jet
[AD-A262982] p 3423 N93-29426
Keynote address: Unsteady, multimode transition in gas turbine engines p 3252 N93-29927
Heat transfer in high turbulence flows: A 2-D planar wall jet p 3254 N93-29935
Heat transfer with moderate free stream turbulence
p 3254 N93-29936
Turbulent drag reduction: Studies of feedback control and flow over riblets p 3242 N93-30645

TURBULENT COMBUSTION
Calculations of reactive turbulent flows in aeronautical chambers p 3257 N93-29956

TURBULENT DIFFUSION
Theory of tokamak edge turbulence: Drift-thermal instability-induced turbulence and ionization-driven drift wave turbulence p 3586 N93-29123
Application of Schlieren optical techniques for the measurement of gas temperature and turbulent diffusivity in a diesel engine
[AD-A263810] p 3580 N93-29880

TURBULENT FLOW
The onset of vortex turbulence
[DE93-010424] p 3417 N93-28663

An efficient spectral integration method for the solution of the Navier-Stokes equations
[FFA-TN-1992-28] p 3418 N93-29009
High Reynolds number and turbulence effects on aerodynamics and heat transfer in a turbine cascade
[NASA-TM-106187] p 3420 N93-29157
A numerical study of confined turbulent jets
[NASA-TM-106197] p 3420 N93-29161
Development of an unstructured solution adaptive method for the quasi-three-dimensional Euler and Navier-Stokes equations
[NASA-CR-193241] p 3421 N93-29213
Experimental study of instability growth patterns of a shock-accelerated, thin fluid layer
[DE93-010741] p 3421 N93-29253
Evolution of flow disturbances in cocurrent gas-liquid flows
[DE93-010083] p 3422 N93-29326
Methods for reducing turbulent flow aero-optical distortion
[AD-A263698] p 3423 N93-29353
The effect of high temperature on wall shear in a two dimensional wall jet
[AD-A262982] p 3423 N93-29426
Flame or plasma synthesis of diamond under turbulent and transition flow conditions
[AD-D015689] p 3333 N93-29456
Heat Transfer and Cooling in Gas Turbines
[AGARD-CP-527] p 3252 N93-29926
Keynote address: Unsteady, multimode transition in gas turbine engines p 3252 N93-29927
Heat transfer in high turbulence flows: A 2-D planar wall jet p 3254 N93-29935
Turbulent flow and heat transfer in idealized blade cooling passages p 3254 N93-29938
Study of flow structure in rotating cavities: Numerical predictions of laminar and turbulent, steady, and unsteady flows p 3256 N93-29948
Fluid flow and heat transfer in the entrance region of an annulus between independently rotating tubes with a turbulent axial flow p 3256 N93-29952
Calculations of reactive turbulent flows in aeronautical chambers p 3257 N93-29956
Modeling of a turbulent flow in the presence of discrete parietal cooling jets p 3258 N93-29960
Laboratory studies of gravity wave/mean flow interactions
[AD-A264226] p 3478 N93-30174
Turbulence characteristics of an axisymmetric reacting flow
[NASA-CR-4110] p 3242 N93-30373
Towards a better hydro for dynamic mix calculations
[DE93-010702] p 3426 N93-30485

TURBULENT HEAT TRANSFER
Turbulent flow and heat transfer in idealized blade cooling passages p 3254 N93-29938
Compressible turbulence in a high-speed high Reynolds number mixing layer p 3242 N93-30583

TURBULENT JETS
A numerical study of confined turbulent jets
[NASA-TM-106197] p 3420 N93-29161

TURBULENT WAKES
Heat Transfer and Cooling in Gas Turbines
[AGARD-CP-527] p 3252 N93-29926
Determination of surface heat transfer and film cooling effectiveness in unsteady wake flow conditions
p 3253 N93-29933

TURING MACHINES
Automated reasoning with function evaluation for COCOLOG
[INRIA-RR-1713] p 3529 N93-29488

TVD SCHEMES
An upwind method for the solution of the 3D Euler and Navier-Stokes equations on adaptively refined meshes
[AD-A262863] p 3423 N93-29472

TWO BODY PROBLEM
A numerical solution of the two-center problem
[DE92-644674] p 3551 N93-30913
General method for reducing the two-body Dirac equation
[DE93-609833] p 3607 N93-30943

TWO DIMENSIONAL FLOW
A grid refinement study of two-dimensional transient flow over a backward-facing step using a spectral-element method
[DE92-018262] p 3417 N93-28639
The onset of vortex turbulence
[DE93-010424] p 3417 N93-28663
Numerical computation of inviscid flow around nose tip of Space Shuttle with NND scheme
[AD-A264012] p 3421 N93-29260
Heat transfer in high turbulence flows: A 2-D planar wall jet p 3254 N93-29935
A theoretical and computational study on active wake control p 3243 N93-30892

TWO DIMENSIONAL MODELS
Coarse image motion for saccade control
[OUEL-1916/92] p 3523 N93-28485
A study of the physical mechanisms for filament eruption and coronal mass ejection via numerical simulation
[NASA-CR-193180] p 3653 N93-28935
Remote vehicle survey tool
[DE93-010822] p 3460 N93-29255
Two-dimensional model for current and heat transport in solid-armature railguns
[AD-A262014] p 3271 N93-29394
Modeling the D3-D plasma boundary with the LEDGE code
[DE93-009301] p 3588 N93-29772
Two-parameter crack tip field associated with stable crack growth in a thin plate: A hybrid analysis
[AD-A264221] p 3453 N93-30147

TWO FLUID MODELS
A four-field approach towards developing a mechanistic model for multiphase flow
[DE93-006572] p 3420 N93-29126
Studies of fluctuation processes in nuclear collisions
[DE93-011263] p 3576 N93-30054

TWO PHASE FLOW
Preliminary endurance tests of water vaporizers for resistojet applications
[NASA-TM-106222] p 3287 N93-28694
In-STEP Two-Phase Flow (TPF) thermal control experiment p 3265 N93-28719
A four-field approach towards developing a mechanistic model for multiphase flow
[DE93-006572] p 3420 N93-29126
Evolution of flow disturbances in cocurrent gas-liquid flows
[DE93-010083] p 3422 N93-29326
Use of a genetic algorithm to solve two-fluid flow problems on an NCUBE multiprocessor computer
[DE93-009630] p 3425 N93-30184
Towards a better hydro for dynamic mix calculations
[DE93-010702] p 3426 N93-30485
Multiparticle imaging technique for two-phase fluid flows using pulsed laser speckle velocimetry
[DE93-011734] p 3427 N93-30489
Prediction of gas-liquid two-phase flow regime in microgravity
[NASA-TM-106274] p 3352 N93-30939

U

UH-60A HELICOPTER
Helicopter approach capability using the differential global positioning system
[NASA-CR-193183] p 3245 N93-28936

ULTRAHIGH VACUUM
Undulator Spectromicroscopy Facility at the Advanced Light Source
[DE93-007964] p 3261 N93-28490
A manipulator kinematic design for high-vacuum operation
[DE93-010264] p 3444 N93-29247
Development of an O atom gun
[AD-A264753] p 3570 N93-30558

ULTRALIGHT AIRCRAFT
The Ultra Light Aircraft Testing
[NASA-CR-193043] p 3249 N93-29774
Report on the test set-up for the structural testing of the Airmass Sunburst Ultralight Aircraft
p 3249 N93-29775
Load test set-up for the Airmass Sunburst Ultra-Light Aircraft p 3249 N93-29776
NASTRAN analysis for the Airmass Sunburst model 'C' Ultralight Aircraft p 3249 N93-29777
Construction, wind tunnel testing and data analysis for a 1/5 scale ultra-light wing model p 3243 N93-29778

ULTRASONIC FLAW DETECTION
Diffusion bonding
[DE93-011480] p 3442 N93-28837
Ultrasonic detection and identification of fabrication defects in composites p 3305 N93-30856

ULTRASONIC RADIATION
Constant frequency pulsed phase-locked loop measuring device
[NASA-CASE-LAR-13823-1] p 3431 N93-29084

ULTRASONIC TESTS
Crack length determination by ultrasonic methods
[DE93-008075] p 3450 N93-28567
Acousto-Ultrasonic analysis of failure in ceramic matrix composite tensile specimens
[NASA-TM-106219] p 3449 N93-29073

ULTRASONIC WELDING
Performance of thermal adhesives in forced convection p 3293 N93-30974

ULTRAVIOLET ABSORPTION
Development of ultraviolet absorption photometer for atmospheric ozone measurements and results from mid-latitude investigations p 3468 N93-28949

ULTRAVIOLET ASTRONOMY
IUE observations of cataclysmic variable
[NASA-CR-193188] p 3629 N93-28634

ULTRAVIOLET DETECTORS
New technologies for UV detectors
p 3582 N93-28786
A quality monitor and monitoring technique employing optically stimulated electron emission
[NASA-CASE-LAR-15063-1] p 3449 N93-30414

ULTRAVIOLET EMISSION
The Mechanisms of Solar Variability (MSV) program
[AD-A262525] p 3652 N93-28585
Kinetics and energy transfer in nonequilibrium fluid flows
[AD-A263612] p 3240 N93-29284

ULTRAVIOLET LASERS
Ultraviolet free electron laser facility preliminary design report
[DE93-009360] p 3435 N93-28594
Femtosecond laser studies of excited state dynamics
[AD-A263708] p 3439 N93-29918
Research studies on short wavelength by selective auger processes
[AD-A264493] p 3440 N93-30401

ULTRAVIOLET PHOTOGRAPHY
The Ultraviolet Plume Instrument (UVPI)
p 3285 N93-28784

ULTRAVIOLET PHOTOMETRY
Development of ultraviolet absorption photometer for atmospheric ozone measurements and results from mid-latitude investigations p 3468 N93-28949

ULTRAVIOLET RADIATION
Thermal control paints on LDEF: Results of M0003 sub-experiment 18
[AD-A263252] p 3329 N93-28561
The Mechanisms of Solar Variability (MSV) program
[AD-A262525] p 3652 N93-28585
New technologies for UV detectors
p 3582 N93-28786
Effects of atomic oxygen and ultraviolet radiation on candidate elastomeric materials for long duration missions. Test series no.1
[NASA-TM-108408] p 3331 N93-29193
An investigation of stereolithography as a means of prototyping from a cad database
[AD-A263410] p 3613 N93-29210
Photobiological investigations on spores of streptomyces griseus
[ESA-TT-1269] p 3491 N93-29274
Kinetics of nitric oxide formation behind 3 to 4 KM/S shock waves
[AD-A263653] p 3312 N93-29389
A quality monitor and monitoring technique employing optically stimulated electron emission
[NASA-CASE-LAR-15063-1] p 3449 N93-30414

ULTRAVIOLET SPECTRA
Optical technologies for UV remote sensing instruments p 3582 N93-28788
Honeywell's compact, wide-angle UV-visible imaging sensor p 3582 N93-28806

ULTRAVIOLET SPECTROMETERS
Optical technologies for UV remote sensing instruments p 3582 N93-28788
Ultraviolet imaging spectrometer p 3582 N93-28827

ULTRAVIOLET SPECTROSCOPY
Measurement of 1s2s(sup 3)S(sub 1)-1s2p(sup 3)P(sub 2,0) intervals in helium-like neon
[DE93-009243] p 3563 N93-28521
Design of a high resolution spatial heterodyne interferometer
[AD-A262867] p 3285 N93-29461

ULTRAVIOLET TELESCOPES
X ray, far, and extreme ultraviolet coatings for space applications p 3340 N93-28829

UNDERGROUND EXPLOSIONS
Modeling regional seismic waves
[AD-A264002] p 3479 N93-30756

UNDERGROUND STORAGE
Tank issues: Design and placement of floating liquid monitoring wells
[PB93-161149] p 3469 N93-29033

UNDERWATER ACOUSTICS
ARSRP signal processing software
[AD-A263543] p 3391 N93-29975
Sound wave scattering from a rigid sphere
[AD-A264182] p 3562 N93-30157

UNDERWATER EXPLOSIONS
Homogeneous gas phase kinetic model with gradient sensitivity analysis for high temperature particulate boron combustion in fluorine enriched environments
p 3319 N93-30090

UNDERWATER VEHICLES

Advanced Unmanned Search System (AUSS) supervisory command, control and navigation [AD-A263171] p 3245 N93-28990

Boron carbide aluminum cermets for external pressure housing applications [AD-A262749] p 3333 N93-29404

The wake software suite: User's guide [AD-A264181] p 3425 N93-30156

Ice-ocean four dimensional structure and dynamics [AD-A264850] p 3490 N93-30906

UNITED STATES

Applied research in America [DE93-011725] p 3625 N93-28646

NASA/DOD Aerospace Knowledge Diffusion Research Project. Paper 28: The technical communication practices of Russian and US aerospace engineers and scientists [NASA-TM-108249] p 3612 N93-28948

Building alliances to restore coastal environments: A coastal America progress report [PB93-169464] p 3470 N93-29674

The 1992 World Administrative Radio Conference: Technology and Policy Implications [OTA-TCT-549] p 3392 N93-30150

Interagency Advanced Power Group (IAPG) Meeting Compendium [DE93-006189] p 3670 N93-30212

US space commerce, 1991 p 3625 N93-30695

White House/OSTP perspective p 3625 N93-30696

Deadliest, costliest, and most intense US hurricanes of this century (and other frequently requested hurricane facts) [PB93-174993] p 3485 N93-30758

UNIVERSE

Dark matter: Theoretical perspectives [DE93-008484] p 3633 N93-28676

Predictions of a non-Gaussian model for large scale structure [DE93-010196] p 3636 N93-30528

Topics in inflationary universe medels and cosmic string theories p 3637 N93-30579

Fourth-rank gravity and cosmology [DE92-644722] p 3637 N93-30918

UNIVERSITIES

ORNL superconducting technology program for electric energy systems [DE93-009588] p 3404 N93-28523

Technology Transfer and the Civil Space Program. Volume 2: Workshop proceedings [NASA-TM-108250] p 3625 N93-30692

The role of the University Licensing Office in transferring intellectual property to industry p 3626 N93-30698

High performance computing and communications program p 3627 N93-30715

A research experiment on facilitation and formation of joint research and development programs between government, industry, and universities: Overview, preliminary findings, and observations p 3628 N93-30725

UNIVERSITY PROGRAM

Natural environmental service support to NASA vehicle, technology, and sensor development programs [NASA-CR-192554] p 3469 N93-29029

Proceedings of the Seventh Annual Summer Conference. NASA/USRA: University Advanced Design Program [NASA-CR-192962] p 3227 N93-29712

High-altitude reconnaissance aircraft p 3227 N93-29713

Project summary p 3227 N93-29714

Project ARES 2: High-altitude battery-powered aircraft p 3227 N93-29715

Conceptual design of a two-stage-to-orbit vehicle p 3228 N93-29716

Preliminary design studies of an advanced general aviation aircraft p 3228 N93-29717

The design of two-stage-to-orbit vehicles p 3228 N93-29719

Design of a turbofan powered regional transport aircraft p 3228 N93-29721

Solar powered multipurpose remotely powered aircraft p 3229 N93-29722

A high-temperature furnace for applications in microgravity p 3229 N93-29723

Advanced design for orbital debris removal in support of solar system exploration p 3229 N93-29724

The 1990/1991 project summaries p 3229 N93-29725

Design, building, and testing of the postlanding systems for the assured crew return vehicle p 3229 N93-29726

Earth to lunar CELSS evolution p 3229 N93-29727

Design of biomass management systems and components for closed loop life support systems p 3230 N93-29728

Lunar lander ground support system p 3230 N93-29729

The 1990-1991 project summaries p 3230 N93-29730

The 1990-1991 project summaries p 3230 N93-29731

Solar energy emplacement developer p 3230 N93-29732

Exercise/recreation facility for a lunar or Mars analog p 3230 N93-29733

Automation of closed environments in space for human comfort and safety p 3230 N93-29734

Delta Advanced Reusable Transport (DART): An alternative manned spacecraft p 3231 N93-29735

Taurus Lightweight Manned Spacecraft Earth orbiting vehicle p 3231 N93-29736

Walking robot: A design project for undergraduate students p 3231 N93-29737

Project Copernicus: An Earth observing system p 3231 N93-29738

Project MEDSAT p 3231 N93-29739

Project UM-HAUL: A self-unloading reusable lunar lander p 3232 N93-29740

Mars integrated transportation system multistage Mars mission p 3232 N93-29741

Single-stage Mars mission p 3232 N93-29742

Multipurpose satellite bus (MPS) p 3232 N93-29743

Project WISH: The Emerald City p 3232 N93-29744

From orbital debris capture systems through internal combustion engines on Mars p 3232 N93-29745

Mars sample return mission: Two alternate scenarios p 3233 N93-29746

Mars habitat p 3233 N93-29747

The lightcraft project p 3233 N93-29749

ASPEC: Solar power satellite p 3233 N93-29750

B and T: Lunar landers p 3234 N93-29751

Spacely's rockets: Personnel launch system/family of heavy lift launch vehicles p 3234 N93-29752

RS Landers: Lunar lander p 3234 N93-29753

SPECS: Orbital debris removal p 3234 N93-29754

The 1990-1991 project summaries p 3234 N93-29755

Mars Aquarius Mission and Titan Explorer p 3235 N93-29756

Thermion: Verification of a thermionic heat pipe in microgravity p 3235 N93-29757

Solar electric propulsion cargo spacecraft for Mars missions p 3235 N93-29758

Antares: A low cost modular launch vehicle for the future p 3235 N93-29759

GENESIS 2: Advanced lunar outpost p 3235 N93-29760

Rotational fluid flow experiment p 3235 N93-29761

Center of Excellence in Biotechnology (Research) [AD-A263598] p 3491 N93-29915

Center for the Study of Intelligent Control Systems (Fellowships) [AD-A263604] p 3543 N93-29917

UNIX (OPERATING SYSTEM)

RTE: A UNIX library with on-line documentation and sample programs for microwave radiative transfer calculations [PB93-180248] p 3386 N93-29680

Measurements over distributed high performance computing and storage systems p 3622 N93-30476

Parcels with TAGS [PB93-181824] p 3535 N93-30824

UNMANNED SPACECRAFT

Project ARES 2: High-altitude battery-powered aircraft p 3227 N93-29715

Project UM-HAUL: A self-unloading reusable lunar lander p 3232 N93-29740

RS Landers: Lunar lander p 3234 N93-29753

UNSTEADY AERODYNAMICS

Transonic flows on an oscillating airfoil and their effect on the flutter-boundary [DLR-FB-92-08] p 3238 N93-29006

Unsteady vortex loop/dipole theory applied to the work and acoustics of an ideal low speed propeller [AD-A264057] p 3241 N93-29891

UNSTEADY FLOW

Accelerated motion of rigid spheres in unsteady flows at low to moderate Reynolds numbers p 3416 N93-28612

Analysis of unsteady wave processes in a rotating channel [NASA-CR-191154] p 3251 N93-28617

A grid refinement study of two-dimensional transient flow over a backward-facing step using a spectral-element method [DE92-018262] p 3417 N93-28639

State vector splitting: A numerical scheme for the Euler equations p 3419 N93-29039

Stabilized space-time finite element formulations for unsteady incompressible flows involving fluid-body interactions p 3419 N93-29040

Direct numerical simulations of unsteady separated flows using vortex methods p 3419 N93-29077

Flow phenomena in turbomachines [AD-A263049] p 3420 N93-29141

Non-linear wave phenomena in a gas-vapour mixture with phase transition [ETN-93-93582] p 3422 N93-29319

Keynote address: Unsteady, multimode transition in gas turbine engines p 3252 N93-29927

Determination of surface heat transfer and film cooling effectiveness in unsteady wake flow conditions p 3253 N93-29933

Study of flow structure in rotating cavities: Numerical predictions of laminar and turbulent, steady, and unsteady flows p 3256 N93-29948

Simulation, characterization and control of forced unsteady viscous flows using Navier-Stokes equations [AD-A264333] p 3425 N93-30369

Computation of a delta-wing roll-and-hold maneuver [AD-A264704] p 3260 N93-30498

Computational fluid dynamics research on dynamically adaptive mesh methods for transonic flows [AD-A264833] p 3428 N93-30630

A theoretical and computational study on active wake control p 3243 N93-30892

An adaptive Lagrangian method for computing 1-D reacting flows and the theory of Riemann invariant manifolds for the compressible Euler equations p 3428 N93-30902

UPLINKING

Experimental and modal verification of an integral equation solution for a thin-walled dichroic plate with cross-shaped holes p 3385 N93-29591

Adaptive jammer nulling in EHF communications satellites p 3365 N93-30284

Uplink laser propagation measurements through the sea surface, haze and clouds [AD-A264687] p 3440 N93-30553

UPPER ATMOSPHERE RESEARCH SATELLITE (UARS)

Upper atmosphere research satellite jitter study p 3264 N93-28708

UPWIND SCHEMES (MATHEMATICS)

Upwind finite element schemes for solving the Maxwell equations [INRIA-RR-1601] p 3546 N93-28509

URANIUM ALLOYS

Eutectic solidification of Al-U at slowly cooling rates (10 C per second) [DE92-640082] p 3328 N93-30941

USER MANUALS (COMPUTER PROGRAMS)

Concurrent clean language manual, version 0.8 [TR-92-18] p 3522 N93-28482

The concurrent clean system user's manual and PABCstat user's manual, version 0.8 [TR-92-19] p 3523 N93-28484

JPDRAW user's manual, version 3.3 [INRIA-RT-0139] p 3523 N93-28504

Minimum Hamiltonian ascent trajectory evaluation (MASTRE) program (update to automatic flight trajectory design, performance prediction, and vehicle sizing for support of shuttle and shuttle derived vehicles) users manual [NASA-CR-192556] p 3269 N93-28558

Predicting radiation characteristics from antenna physical dimensions [AD-A262462] p 3379 N93-28654

Metal Matrix Laminate Tailoring (MMLT) code: User's manual [NASA-TM-106052] p 3295 N93-28681

Users manual for fault tree analysis code: CUT-TD [DE93-753272] p 3525 N93-28978

Hanford Environmental Information System (HEIS) user's manual, volume 1 [DE93-007465] p 3470 N93-29135

The three-dimensional Multi-Block Advanced Grid Generation System (3DMAGGS) [NASA-TM-108985] p 3420 N93-29155

Concept design example, Computer Aided Structural Modeling (CASM). Scheme A [AD-A264759] p 3529 N93-29657

Concept design example, Computer Aided Structural Modeling (CASM). Scheme B [AD-A264760] p 3529 N93-29658

Data probe user's guide [PB93-178655] p 3530 N93-29678

Concept formulation process aid for trade-off determination: Operator's guide [AD-A263756] p 3531 N93-29874

TRAB: A transient analysis program for BWR. Part 2: User's manual [VTT-TIED-1232-PT-2] p 3575 N93-29996

XRONOS: A timing analysis software package. User's guide, version 3.00 [NASA-TM-109222] p 3532 N93-30023

AHP version 5.1 user's manual [DE93-007050] p 3532 N93-30034

Simplified Linear Equation Solvers: User's manual
[DE93-011975] p 3550 N93-30140
The wake software suite: User's guide
[AD-A264181] p 3425 N93-30156

USER REQUIREMENTS
Minimum Hamiltonian ascent trajectory evaluation (MASTRE) program (update to automatic flight trajectory design, performance prediction, and vehicle sizing for support of shuttle and shuttle derived vehicles) users manual
[NASA-CR-192556] p 3269 N93-28558
Information system for co-registration of CAESAR sea-images based on two dimensional image matching techniques (SCORE). Part 1: Introduction, user requirements, and feasibility tests
[BCRS-90-40A-PT-1] p 3460 N93-29307
Satellite calibration requirements
[AD-A264279] p 3281 N93-30817

V

V GROOVES
Texturing of InP surfaces for device applications
[NASA-TM-106061] p 3321 N93-28618

V-22 AIRCRAFT
Fabrication of the V-22 composite AFT fuselage using automated fiber placement p 3302 N93-30443

V/STOL AIRCRAFT
Effects of flow-path variations on internal reversing flow in a tailpipe offtake configuration for ASTOVL aircraft
[NASA-TM-106149] p 3252 N93-29065

VACANCIES (CRYSTAL DEFECTS)
Fundamental aspects in the design of passive alloys
[DE93-009028] p 3320 N93-28545
Role of oxygen vacancies in anodic TiO2 thin films
[DE92-642137] p 3602 N93-31027

VACUUM
Report on the sintering and properties of MgO and MgO-5 percent TiC
[DE93-008676] p 3323 N93-29092
Photobiological investigations on spores of streptomyces griseus
[ESA-TT-1269] p 3491 N93-29274
Phase structure of three- and four-dimensional phi(exp 4) field theory
[DE93-606069] p 3605 N93-30782
Quantum-kinetic Green function and macroscopic wave function
[DE93-606040] p 3606 N93-30796

VACUUM APPARATUS
Advanced coordinate measuring machine at Sandia National Laboratories
[DE93-010618] p 3432 N93-29842

VACUUM CHAMBERS
Growing wheat to maturity in reduced gas pressures
[NASA-CR-193245] p 3491 N93-29216

VACUUM EFFECTS
Effects of vacuum exposure on stress and spectral shift of high reflective coatings
[DE93-009318] p 3437 N93-29207
New results from FRECOPA analysis
p 3448 N93-29688

VACUUM SYSTEMS
A manipulator kinematic design for high-vacuum operation
[DE93-010264] p 3444 N93-29247

VACUUM TUBES
Field-emitter arrays for RF vacuum microelectronics
[AD-A262677] p 3404 N93-28483

VALVES
Preliminary design of an intermittent smoke flow visualization system
[NASA-CR-186027] p 3248 N93-28693
Valve malfunction detection apparatus
[NASA-CASE-MFS-29904-1] p 3432 N93-29503

VAN DER WAALS FORCES
Quantum dynamics of X2BC van der Waals clusters
[DE93-006416] p 3565 N93-28892

VANADIUM OXIDES
Research and development of lithium secondary batteries for load conditioner use, volume 2
[DE93-781329] p 3410 N93-29673

VAPOR DEPOSITION
Surface modification of tribological components in transportation
[DE93-008647] p 3442 N93-28903
Electrochemical behavior and surface chemistry of aluminum alloys: Solute-rich interphase model
[AD-A262061] p 3322 N93-29002
Flame or plasma synthesis of diamond under turbulent and transition flow conditions
[AD-D015689] p 3333 N93-29456
Development of adherent ceramic coatings to reduce contact stress damage of ceramics
[DE93-012518] p 3336 N93-30182
Coordination compounds of aluminum as precursors to aluminum nitride
[AD-A264700] p 3327 N93-30574
Study on diamond semiconductor
[DE92-531076] p 3413 N93-30622
Visible light emitting materials and injection devices
[AD-A263499] p 3601 N93-30811

VAPOR PHASE EPITAXY
Femtosecond carrier processes in compound semiconductors and real time signal processing
[AD-A263076] p 3382 N93-29131
Femtosecond carrier processes in compound semiconductors and real time signal processing
[AD-A262966] p 3384 N93-29514

VAPOR PHASES
Thermodynamic properties for polycyclic systems by non-calorimetric methods
[DE93-011373] p 3603 N93-28747
The thermochemistry and reaction pathways of the decomposition and combustion of energetic materials
p 3343 N93-30063
Thermal decomposition chemistry and shock sensitivity of thermally aged explosives p 3344 N93-30069
Kinetic studies on gas-phase reaction mechanisms important to the combustion of energetic materials: The CO/N2O reaction p 3347 N93-30084

VAPOR PRESSURE
Complex-compound heat pump: Topical report on phase 1 results
[PB93-185460] p 3466 N93-30814

VAPORIZERS
Preliminary endurance tests of water vaporizers for resistojet applications
[NASA-TM-106222] p 3287 N93-28694
Gravity sensitivity of a resistojet water vaporizer
[NASA-TM-106220] p 3288 N93-29194

VAPORS
A four-field approach towards developing a mechanistic model for multiphase flow
[DE93-006572] p 3420 N93-29126
Methods for preparation of mixtures of gases in air at the parts-per-billion to parts-per-million concentration range for calibration of monitors
[DE92-642433] p 3317 N93-30982

VARIABILITY
The Mechanisms of Solar Variability (MSV) program
[AD-A262525] p 3652 N93-28585
Variability of the electric field strength in the earth-ionosphere waveguide due to variations in the electron density profile
[AD-A264808] p 3394 N93-30595

VARIANCE (STATISTICS)
Some statistical inference problems in linear models and variance components models and their applications
[AD-A264062] p 3555 N93-29923

VARIATIONAL PRINCIPLES
Finite element analysis of time-independent superconductivity
[NASA-CR-191140] p 3450 N93-28556

VECTOR ANALYSIS
Using C-vector method to derive the three-dimensional circulation pattern near the East Greenland Polar Front
[AD-A261979] p 3487 N93-29437

VECTOR PROCESSING (COMPUTERS)
Installation of a new Fortran compiler and effective programming method on the vector supercomputer
[DE93-753322] p 3524 N93-28537
NESL: A nested data-parallel language (Version 2.6)
[AD-A263548] p 3530 N93-29822
Multiprocessing MCNP on an IBM RS/6000 cluster
[DE93-008712] p 3540 N93-30633

VECTOR QUANTIZATION
Image segmentation using fuzzy LVQ clustering networks p 3511 N93-29528

VECTOR SPACES
Quantum group generalization of the heterotic QFT
[DE92-644727] p 3607 N93-30920
Normal equivariant forms of vector fields
[DE92-644845] p 3551 N93-30929

VECTORS (MATHEMATICS)
Direct volume visualization of three-dimensional vector fields
[DE93-009233] p 3524 N93-28550
Spherically symmetric line element and Killing vectors in five-dimensional space
[DE93-604132] p 3558 N93-30988

VEGETATION
Modeling the bidirectional reflectance and spectra
[AD-A263570] p 3462 N93-29830
Environmental Monitoring and Assessment Program. EMAP: Arid Colorado plateau pilot study
[PB93-181618] p 3474 N93-30823

VEGETATION GROWTH
Growing wheat to maturity in reduced gas pressures
[NASA-CR-193245] p 3491 N93-29216

VELOCITY
On the meaning of delta T/T
[DE93-008482] p 3653 N93-28962

VELOCITY DISTRIBUTION
The use of objective prism radial velocities for kinematic studies of galactic populations p 3633 N93-28672
Analyses of data from fine structure and circulation studies in the Gulf of California
[AD-A262910] p 3486 N93-28885
Doppler-radar wind-speed measurements in tornadoes: A comparison of real and simulated spectra
[DE93-008734] p 3481 N93-29095
A four-field approach towards developing a mechanistic model for multiphase flow
[DE93-006572] p 3420 N93-29126
Enhanced reduction of velocity data obtained during CETA flight experiment
[NASA-TM-4460] p 3431 N93-29209
Continued investigation of LDEF's structural frame and thermal blankets by the Meteoroid and Debris Special Investigation Group p 3282 N93-29357
Hypervelocity impact facility for simulating materials exposure to impact by space debris
p 3283 N93-29365
Asteroidal versus cometary meteoroid impacts on the Long Duration Exposure Facility (LDEF)
p 3638 N93-29371
Evaluation of atmospheric wind field and dispersion models for fog-oil smoke dispersion in complex terrain: Field measurement and model evaluation program for assessment of the environmental effects of military smokes
[AD-A262051] p 3482 N93-29399
The wake software suite: User's guide
[AD-A264181] p 3425 N93-30156

VELOCITY MEASUREMENT
Velocity measurements of low Reynolds number tube flow using fiber-optic technology
[DE93-009865] p 3422 N93-29335
An LDEF 2 dust instrument for discrimination between orbital debris and natural particles in near-Earth space
p 3286 N93-29707
Modelling the dynamics of a large sea area
[DE93-778330] p 3488 N93-30040
Shear, strain, and thermohaline vertical fine structure in the upper ocean p 3488 N93-30046
Turbulence characteristics of an axisymmetric reacting flow
[NASA-CR-4110] p 3242 N93-30373
Multiparticle imaging technique for two-phase fluid flows using pulsed laser speckle velocimetry
[DE93-011734] p 3427 N93-30489
Portable fiber optic coupled Doppler interferometer system for detonation and shock wave diagnostics
[DE93-009827] p 3433 N93-30510

VENTILATION
Study of parameters affecting the performance of solar desiccant cooling systems
[DE93-000088] p 3465 N93-30206

VENTING
Vented Tank Resupply Experiment (VTRE) for In-Space Technology Experiment Program (IN-STEP)
p 3264 N93-28711

VENUS (PLANET)
Venus Interior Structure Mission (VISM): Establishing a seismic network on Venus p 3649 N93-28819

VERTICAL DISTRIBUTION
Shear, strain, and thermohaline vertical fine structure in the upper ocean p 3488 N93-30046

VERTICAL FLIGHT
Rotorcraft master plan p 3236 N93-30677

VERTICAL LANDING
Effects of flow-path variations on internal reversing flow in a tailpipe offtake configuration for ASTOVL aircraft
[NASA-TM-106149] p 3252 N93-29065

VERTICAL MOTION SIMULATORS
Frequency-response techniques for documentation and improvement of rotorcraft simulators
p 3237 N93-30689

VERTICAL TAKEOFF AIRCRAFT
Preliminary development of a VTOL unmanned air vehicle for the close-range mission
[AD-A263514] p 3354 N93-29969

VERY HIGH FREQUENCIES
Widebanding techniques for VHF antennas 2
[AD-A263998] p 3387 N93-29882

VERY LARGE SCALE INTEGRATION
Femtosecond carrier processes in compound semiconductors and real time signal processing
[AD-A263076] p 3382 N93-29131
Handshake circuits: An intermediary between communicating processes and VLSI
[ETN-93-93579] p 3408 N93-29269
Femtosecond carrier processes in compound semiconductors and real time signal processing
[AD-A262966] p 3384 N93-29514

WARP: Weight Associative Rule Processor. A dedicated VLSI fuzzy logic megacell p 3513 N93-29538
Intelligent fuzzy controller for event-driven real time systems p 3515 N93-29551
An architecture for an analog VLSI neural network for early computer vision processing p 3359 N93-30244
Optically powered, optoelectronic spatial light modulators
[AD-A264765] p 3581 N93-30609
Placement of cells: Theory and solution of a quadratic 0/1 optimization problem
[ETN-93-94182] p 3413 N93-30616

VERY LONG BASE INTERFEROMETRY
The German satellite ground station in Antarctica: Realization and first results p 3458 N93-28924
Interferometric tracking system for the tracking and data relay satellite
[NASA-CR-193274] p 3382 N93-29217

VERY LOW FREQUENCIES
Measurement of the relative and absolute microgravity environment of space platforms, recent flight results, and determination of the spatial microgravity field p 3266 N93-28725
Structural load control during construction p 3275 N93-29113
Introduction p 3395 N93-30728
Numerical modeling of the propagation medium at VLF/LF p 3395 N93-30729
The cone structure and focusing of the electric field of VLF and LF waves at high altitudes of the ionosphere p 3395 N93-30731
VLF propagation measurements in the Canadian Arctic p 3396 N93-30733
Theoretical and experimental coverage analysis of a VLF transmitter p 3396 N93-30734
Investigations of equatorial ionosphere nighttime mode conversion at VLF p 3396 N93-30735
Transient (approximately equals 10 s) VLF amplitude and phase perturbations due to lightning-induced electron precipitation into the ionosphere (the Trimpi effect) p 3396 N93-30736
Lightning-induced effects on VLF/LF radio propagation p 3396 N93-30737
A methodology and tool for the prediction of depth of reception in the sea for a VLF/LF communications system p 3397 N93-30741
ELF/VLF radio noise measurements at high latitudes during solar particle events p 3397 N93-30744
ELF/VLF spectrum measurements p 3398 N93-30745
VLF/LF transmitting antennas p 3398 N93-30747
A dynamic bandwidth and phase linearity measurement technique for 4-channel MSK VLF antenna systems p 3398 N93-30748
Study of a VLF distributed antenna array p 3398 N93-30749
Antenna modeling and analysis for ELF/VLF/LF applications p 3398 N93-30751
Viability assessment for reliable long-wave communication links p 3399 N93-30754
Orbiting transmitter and antenna for spaceborne communications at ELF/VLF to submerged submarines p 3399 N93-30755

VESTS
Evaluation of personal cooling systems in conjunction with explosive ordnance disposal suits
[AD-A262862] p 3506 N93-29471

VETERINARY MEDICINE
Fuzzy neural network methodology applied to medical diagnosis p 3498 N93-29546

VIABILITY
Viability assessment for reliable long-wave communication links p 3399 N93-30754

VIBRATION
Measurement of the relative and absolute microgravity environment of space platforms, recent flight results, and determination of the spatial microgravity field p 3266 N93-28725
The photodissociation and reaction dynamics of vibrationally excited molecules
[DE93-010896] p 3565 N93-28879
Sound wave scattering from an elastic spherical shell
[AD-A264039] p 3562 N93-30029
Characterizing transient vibrations using band limited temporal moments
[DE93-009639] p 3453 N93-30185
Improved bounds for synchronization jitter p 3360 N93-30251
Theoretical studies in nuclear structure
[DE93-012290] p 3570 N93-30505

VIBRATION DAMPING
The natural excitation technique (NExT) for modal parameter extraction from operating wind turbines
[DE93-010611] p 3463 N93-28603
NASA instep/MDMSC jitter suppression experiment (JITTER) p 3263 N93-28702
Description of the Joint Damping Experiment (JDX) p 3263 N93-28703
Control-structures interaction test of the LACE satellite p 3263 N93-28706
Upper atmosphere research satellite jitter study p 3264 N93-28708
Results of a round robin test program: Complex modulus properties of a polymeric damping material
[AD-A263619] p 3332 N93-29344
Modal survey of a full-scale F-18 wind tunnel model
[AD-A262482] p 3240 N93-29410
Vibration control of flexible space structures in noisy environment p 3285 N93-30235
Robust boundary control of flexible structures governed by hybrid dynamics p 3285 N93-30249

VIBRATION EFFECTS
Low-frequency vibration environment for five Shuttle missions
[NASA-TM-106059] p 3285 N93-28554

VIBRATION MEASUREMENT
Low-frequency vibration environment for five Shuttle missions
[NASA-TM-106059] p 3285 N93-28554
Control-structures interaction test of the LACE satellite p 3263 N93-28706
Optical blade vibration measurement
[ETN-93-93454] p 3259 N93-29999

VIBRATION MODE
Modal survey of a full-scale F-18 wind tunnel model
[AD-A262482] p 3240 N93-29410
Theoretical and experimental investigation of slack cable/mass system dynamics p 3455 N93-31028

VIBRATION TESTS
Testing in combined dynamic environments
[DE93-010679] p 3278 N93-29250
Modal survey of a full-scale F-18 wind tunnel model
[AD-A262482] p 3240 N93-29410

VIBRATIONAL SPECTRA
Dynamical analysis of highly excited molecular spectra
[DE93-010771] p 3564 N93-28604
Spectroscopic probes of vibrationally excited molecules at chemically significant energies
[DE93-012328] p 3564 N93-28652
Vibrational spectroscopy of shock-compressed fluids p 3318 N93-30072
A novel flame thermometer based on the doppler width of ro-vibrational transitions
[AD-A264515] p 3315 N93-30405
1,2-Dimethyl-1,2-Disila-Closo-Dodecaborane(12), A silicon analog of an ortho-carborane: Synthesis; x ray crystal structure; NMR, vibrational and photoelectron spectra; bonding
[AD-A264709] p 3599 N93-30568

VIBRATORY LOADS
Vibration control of flexible space structures in noisy environment p 3285 N93-30235

VIDEO COMMUNICATION
A corner matching and tracking strategy applied to videophony
[OUEL-1933/92] p 3380 N93-28896
Review of the effectiveness of video media in instruction
[AD-A264228] p 3392 N93-30362

VIDEO DATA
Systematic processing of Clementine data for scientific analyses p 3624 N93-28803
A fuzzy measure approach to motion frame analysis for scene detection p 3511 N93-29525

VIDEO EQUIPMENT
A passive infrared ice detection technique for helicopter applications
[NASA-CR-193187] p 3244 N93-29152

VIDEO TAPE RECORDERS
Evaluation of D-1 tape and cassette characteristics: Moisture content of Sony and Ampex D-1 tapes when delivered p 3435 N93-30466

VIGNETTING
A tutorial on exit pupils and eye rotation with virtual image optical displays
[AD-A262399] p 3494 N93-29400

VIKING MARS PROGRAM
Mass spectrometric measurement of Martian krypton and xenon isotopic abundance p 3646 N93-28798

VIRTUAL MEMORY SYSTEMS
Distributed Virtual System (DIVIRS) Project
[NASA-CR-193234] p 3526 N93-29169

VIRTUAL REALITY
Virtual interface applications for airborne weapons systems p 3502 N93-28858
Head mounted displays for virtual reality
[AD-A263498] p 3506 N93-29340
Intelligent virtual reality in the setting of fuzzy sets p 3513 N93-29544
Exercise/recreation facility for a lunar or Mars analog p 3230 N93-29733
Virtual reality flight control display with six-degree-of-freedom controller and spherical orientation overlay
[NASA-CASE-NPO-18733-1-CU] p 3251 N93-30416

VISCOPLASTICITY
Thermoviscoplastic analysis of fibrous periodic composites using triangular subvolumes
[NASA-TM-106076] p 3297 N93-29074
Bounds on internal state variables in viscoplasticity
[NASA-TM-106215] p 3451 N93-29196

VISCOSITY
Macrostatistical hydrodynamics
[DE93-012289] p 3417 N93-28751
Interfacial viscosity measurements of adsorbed monolayers on metal surfaces
[AD-A263288] p 3324 N93-29803
Long discontinuous fiber composite structure: Forming and structural mechanics p 3301 N93-30437

VISCOUS DAMPING
Experimental and analytical investigation of finger-follower cam systems p 3446 N93-30378

VISCOUS FLOW
Accelerated motion of rigid spheres in unsteady flows at low to moderate Reynolds numbers p 3416 N93-28612
Moment approach to fast ion neoclassical transport and viscous forces
[DE93-753305] p 3585 N93-28979
Nonlinear stability of viscous shock waves
[TRITA-NA-9205] p 3419 N93-29025
Direct numerical simulations of unsteady separated flows using vortex methods p 3419 N93-29077
The 3-D viscous flow CFD analysis of the propeller effect on an advanced ducted propeller subsonic inlet
[NASA-TM-106240] p 3252 N93-29162
Velocity measurements of low Reynolds number tube flow using fiber-optic technology
[DE93-009865] p 3422 N93-29335
Geochemical and fluid dynamic investigations into the nature of chemical heterogeneity in the Earth's mantle
[AD-A262753] p 3477 N93-29405
Simulation, characterization and control of forced unsteady viscous flows using Navier-Stokes equations
[AD-A264333] p 3425 N93-30369
Some implications of a differential turbomachinery equation with viscous correction
[AD-A264693] p 3427 N93-30571

VISIBILITY
An automated observing system for passive evaluation of cloud cover and visibility
[AD-A263207] p 3481 N93-28875

VISIBLE SPECTRUM
Visible imaging on the Pluto fast flyby mission p 3646 N93-28799
Honeywell's compact, wide-angle UV-visible imaging sensor p 3582 N93-28806

VISION
Armstrong Laboratory space visual function tester program p 3267 N93-28739
Effect of microgravity on several visual functions during STS Shuttle missions: Visual Function Tester-Model 1 (VFT-1) p 3268 N93-28740
Effect of microgravity on visual contrast threshold during STS Shuttle missions: Visual Function Tester-Model 2 (VFT-2) p 3268 N93-28741
Effect of microgravity on the visual near point: Visual Function Tester-Model 4 (VFT-4) p 3268 N93-28742
Analysis of visual loss from retinal lesions
[AD-A264692] p 3496 N93-30494
Photoreceptors regulating circadian behavior: A mouse model
[AD-A264881] p 3497 N93-30908

VISORS
Helmet visor support apparatus
[AD-D015684] p 3507 N93-29606

VISUAL ACUITY
Armstrong Laboratory space visual function tester program p 3267 N93-28739
Effect of microgravity on several visual functions during STS Shuttle missions: Visual Function Tester-Model 1 (VFT-1) p 3268 N93-28740

VISUAL AIDS
Review of the effectiveness of video media in instruction
[AD-A264228] p 3392 N93-30362

VISUAL DISCRIMINATION
Studies of the effect of image degradation and recombination on visual perception
[AD-A264332] p 3580 N93-30368

VISUAL FIELDS
Principal components of natural images: An analytical solution
[AD-A264800] p 3489 N93-30603

VISUAL OBSERVATION

Horizontal nucleate flow boiling heat transfer coefficient measurements and visual observations for R12, R134a, and R134a/ester lubricant mixtures [PB93-178598] p 3475 N93-30887

VISUAL PERCEPTION

Effect of microgravity on the visual near point: Visual Function Tester-Model 4 (VFT-4) p 3268 N93-28742

Vision-based control of holonomic robots for 3-dimensional rigid-body positioning using camera-space manipulation p 3578 N93-29178

Head mounted displays for virtual reality [AD-A263498] p 3506 N93-29340

A tutorial on exit pupils and eye rotation with virtual image optical displays [AD-A262399] p 3494 N93-29400

Quantitative analysis of properties and spatial relations of fuzzy image regions p 3510 N93-29523

A comparison of simulated parallax and single-station range aids to navigation [AD-A263460] p 3246 N93-29818

Computing with neural maps: Application to perceptual and cognitive function [AD-A264056] p 3499 N93-30033

Representations of shape in object recognition and long-term visual memory [AD-A264342] p 3499 N93-30163

Studies of the effect of image degradation and recombination on visual perception [AD-A264332] p 3580 N93-30368

Conspicuity of aids to navigation. Part 1: Temporal patterns for flashing lights [AD-A264626] p 3499 N93-30426

Effects of area-of-interest display characteristics of visual search performance and head movements in simulated low-level flight [AD-A264661] p 3499 N93-30542

The dynamics of visual representation, attention, encoding, and retrieval processes [AD-A264674] p 3500 N93-30543

Discomfort glare from high-intensity discharge headlamps: Effects of context and experience [PB93-174720] p 3496 N93-30659

An algorithm for simple and complex feature detection: From retina to primary visual cortex [AD-A264306] p 3497 N93-30897

VISUAL TASKS

Effect of microgravity on visual contrast threshold during STS Shuttle missions: Visual Function Tester-Model 2 (VFT-2) p 3268 N93-28741

Human capabilities and limitations in situation awareness p 3503 N93-28863

Studies of the effect of image degradation and recombination on visual perception [AD-A264332] p 3580 N93-30368

VITERBI DECODERS

A systolic-array structure for MTCM receivers p 3357 N93-30236

A single chip high-speed CMOS Viterbi decoder p 3358 N93-30238

VITON RUBBER (TRADEMARK)

Effects of atomic oxygen and ultraviolet radiation on candidate elastomeric materials for long duration missions. Test series no.1 [NASA-TM-108408] p 3331 N93-29193

VOCODERS

Nonlinear processing of phase vocoded speech p 3355 N93-30219

On subband coding/embedded vector quantization for speech coding p 3355 N93-30220

VOICE COMMUNICATION

Comparison of multiple access techniques for bandwidth limited land-mobile satellite communications p 3370 N93-30314

Constant Average Power Single Sideband (CAPSSB) modulation p 3373 N93-30331

An analysis of en route controller-pilot voice communications [AD-A264784] p 3394 N93-30611

VOICE DATA PROCESSING

Frequency domain speech compression using the Karhunen-Loeve Transform [AD-A262613] p 3379 N93-28476

Nonlinear processing of phase vocoded speech p 3355 N93-30219

On subband coding/embedded vector quantization for speech coding p 3355 N93-30220

VOIDS

Mechanisms of fracture and creep of structural alloys [AD-A263108] p 3324 N93-29799

VOLT-AMPERE CHARACTERISTICS

Growth, characterization and device development in monocrystalline diamond films [AD-A263204] p 3593 N93-28874

Effect of zinc and iron ions on the electrochemistry of nickel oxide electrode: Slow cyclic voltammetry [AD-A263098] p 3311 N93-29133

VOLUME

Direct volume visualization of three-dimensional vector fields [DE93-009233] p 3524 N93-28550

VORTEX SHEDDING

Vortex shedding by blunt/bluff bodies at high Reynolds numbers. Volume 4: Rectangles [AD-A264154] p 3241 N93-30151

Vortex shedding by blunt/bluff bodies at high reynolds numbers. Volume 1: Data analysis [AD-A264151] p 3241 N93-30171

Vortex shedding by Blunt/Bluff bodies at high reynolds numbers. Volume 2: Cylinders, octagon, hexagon [AD-A264152] p 3241 N93-30172

Vortex shedding by blunt/bluff bodies at high reynolds numbers. Volume 3. Cubes [AD-A264153] p 3242 N93-30173

A theoretical and computational study on active wake control p 3243 N93-30892

VORTEX SHEETS

The development of a mixing layer under the action of weak streamwise vortices [NASA-TM-106089] p 3418 N93-28947

Three-dimensional numerical simulation of gradual opening in a wave rotor passage [NASA-CR-191157] p 3252 N93-29072

The structure and dynamics of the vorticity and passive scalar fields at small scales in homogeneous isotropic turbulence p 3427 N93-30625

VORTEX STREETS

Contribution to the study of the interaction between acoustic waves and coherent structures induced by a prismatic cylinder in a rectangular cavity [ONERA-NT-1990-10] p 3314 N93-30203

VORTICES

The onset of vortex turbulence [DE93-010424] p 3417 N93-28663

Effects of flow-path variations on internal reversing flow in a tailpipe offtake configuration for ASTOVL aircraft [NASA-TM-106149] p 3252 N93-29065

Three-dimensional numerical simulation of gradual opening in a wave rotor passage [NASA-CR-191157] p 3252 N93-29072

Direct numerical simulations of unsteady separated flows using vortex methods p 3419 N93-29077

Supersonic flow calculation using a Reynolds-stress and an eddy thermal diffusivity turbulence model [NASA-CR-4515] p 3420 N93-29159

Experimental study of instability growth patterns of a shock-accelerated, thin fluid layer [DE93-010741] p 3421 N93-29253

Rotational fluid flow experiment p 3235 N93-29761

Unsteady vortex loop/dipole theory applied to the work and acoustics of an ideal low speed propeller [AD-A264057] p 3241 N93-29891

The application of concentric vortex simulation to calculating the aerodynamic characteristics of bodies of revolution at high angles of attack [AD-A263879] p 3241 N93-29919

Vortex structure and mass transfer near the base of a cylinder and a turbine blade p 3253 N93-29929

Three-dimensional fiber-optic LDV measurements in the endwall region of a linear cascade of controlled-diffusion stator blades [AD-A263513] p 3424 N93-29968

Vortex shedding by blunt/bluff bodies at high Reynolds numbers. Volume 4: Rectangles [AD-A264154] p 3241 N93-30151

Numerical modeling and parameterization of gravity wave processes and effects in the atmosphere [AD-A264331] p 3478 N93-30367

Vortex wake characteristics of B757-200 and B767-200 aircraft using the tower fly-by technique [PB93-180255] p 3242 N93-30387

Vortex wake characteristics of B757-200 and B767-200 aircraft using the tower fly-by technique [PB93-180263] p 3242 N93-30388

Analysis and computation for vortex dynamics and rarefied gases [AD-A264705] p 3427 N93-30499

Godunov-type methods for the equations of compressible fluid mechanics [KFK-5058] p 3428 N93-31020

VORTICITY

Analysis of mass transport and potential vorticity budget in a simulated tropopause folding [PB93-156792] p 3476 N93-29197

Using C-vector method to derive the three-dimensional circulation pattern near the East Greenland Polar Front [AD-A261979] p 3487 N93-29437

Hamiltonian dynamics of coupled potential vorticity and internal wave motion: 1. Linear modes [AD-A263469] p 3424 N93-29838

Analysis and computation for vortex dynamics and rarefied gases [AD-A264705] p 3427 N93-30499

Case study of the operational usefulness of the sharp workstation in forecasting a mesocyclone-induced cold sector tornado event in California [PB93-178697] p 3485 N93-30889

VSAT (NETWORK)

Design and construction of a prototype ACTS propagation terminal [NASA-CR-193071] p 3404 N93-28539

System overview on electromagnetic compensation for reflector antenna surface distortion [NASA-TM-106217] p 3273 N93-29195

VULNERABILITY

Crucial role of detailed function, task, timeline, link, and human vulnerability analyses in HRA [DE93-001923] p 3505 N93-28942

W

WAFERS

Infrared rugates by molecular beam epitaxy p 3582 N93-28808

Silicon Film(trademark) photovoltaic manufacturing technology [DE93-010008] p 3466 N93-30891

WAKES

The wake software suite: User's guide [AD-A264181] p 3425 N93-30156

A theoretical and computational study on active wake control p 3243 N93-30892

WALKING

Walking robot: A design project for undergraduate students p 3231 N93-29737

Walkway friction: Experiment and analysis p 3293 N93-30966

WALL FLOW

Supersonic flow calculation using a Reynolds-stress and an eddy thermal diffusivity turbulence model [NASA-CR-4515] p 3420 N93-29159

The effect of high temperature on wall shear in a two dimensional wall jet [AD-A262982] p 3423 N93-29426

Experimental study of heat transfer close to a plane wall heated in the presence of multiple injections (subsonic flow) p 3253 N93-29931

WALL JETS

The effect of high temperature on wall shear in a two dimensional wall jet [AD-A262982] p 3423 N93-29426

Heat transfer in high turbulence flows: A 2-D planar wall jet p 3254 N93-29935

WALL TEMPERATURE

Supersonic flow calculation using a Reynolds-stress and an eddy thermal diffusivity turbulence model [NASA-CR-4515] p 3420 N93-29159

WALLS

Direct numerical simulations of unsteady separated flows using vortex methods p 3419 N93-29077

The design and lifetime calculation of MHD generator walls based on subcritical crack growth in ceramics [ISBN-90-9004009-9] p 3332 N93-29267

Experimental study of heat transfer close to a plane wall heated in the presence of multiple injections (subsonic flow) p 3253 N93-29931

Errors when shock waves interact due to numerical shock width [DE93-010699] p 3426 N93-30484

WARFARE

The environment as an operational center of gravity [AD-A264170] p 3472 N93-30154

WARHEADS

A continuum code investigation of stress integration using exact and approximate material rotation [DE93-001892] p 3454 N93-31013

WARNING SYSTEMS

Results of DATAS investigation of ATCRBS environment at the Los Angeles International Airport [DOT/FAA/CT-93/6] p 3245 N93-28625

Proceedings of the Thunder and Lighting Seminar and the 3D Lightning Warning Workshop [AD-A262766] p 3482 N93-29304

Valve malfunction detection apparatus [NASA-CASE-MFS-29904-1] p 3432 N93-29503

Future directions in aviation security p 3244 N93-30274

Explosives detection systems for airport security gas chromatographic based devices p 3244 N93-30276

Stand alone lightning detection equipment used at Canadian Forces air bases p 3367 N93-30295

Rocket-triggered lightning studies for the protection of critical assets [DE93-009633] p 3484 N93-30651

WASTE DISPOSAL
Super critical water oxidation on energetic materials [DE93-010704] p 3342 N93-29312
An architecture for robotic system integration [DE93-010829] p 3444 N93-29316
Strategic Environmental Research and Development Program (SERDP) [AD-A263745] p 3471 N93-29858
Graphical programming: On-line robot simulation for telerobotic control [DE93-009796] p 3447 N93-30654
WASTE TREATMENT
Technical bases for precipitate hydrolysis process operating parameters, revision 1 [DE93-009894] p 3309 N93-28553
Hydrogen and sulfur production from hydrogen sulfide wastes [DE93-008658] p 3310 N93-29052
Super critical water oxidation on energetic materials [DE93-010704] p 3342 N93-29312
Strategic Environmental Research and Development Program (SERDP) [AD-A263745] p 3471 N93-29858
An evaluation of factors affecting the solidification/stabilization of heavy metal sludge [AD-A264128] p 3473 N93-30197
Environmental characteristics of EPA, NRC, and DOE sites contaminated with radioactive substances [PB93-185551] p 3475 N93-30829
Statement on the United Nations Conference on Environment and Development [DE93-601878] p 3475 N93-30996
WATER
Preliminary endurance tests of water vaporizers for resistojet applications [NASA-TM-106222] p 3287 N93-28694
High octane ethers from synthesis gas-derived alcohols [DE93-012470] p 3341 N93-28752
Ultra-high resolution water window x ray microscope optics design and analysis [NASA-CR-193225] p 3578 N93-29128
Super critical water oxidation on energetic materials [DE93-010704] p 3342 N93-29312
Fast multipole method in simulations of aqueous systems [AD-A263422] p 3567 N93-29336
Electron interactions with non-linear polyatomic molecules and their radicals and ions [AD-A262279] p 3568 N93-29446
Diffusion coefficients and heats of mixing in aqueous alkanolamines [PB93-176212] p 3316 N93-30661
WATER CIRCULATION
IOC-UNEP review meeting on oceanographic processes of transport and distribution of pollutants in the sea [DE93-605070] p 3490 N93-31019
WATER COLOR
SeaWiFS technical report series. Volume 2: Analysis of orbit selection for SeaWiFS: Ascending versus descending node [NASA-TM-104566-VOL-2] p 3486 N93-28497
WATER CONSUMPTION
Growing wheat to maturity in reduced gas pressures [NASA-CR-193245] p 3491 N93-29216
WATER COOLED REACTORS
TRAB: A transient analysis program for BWR. Part 2: User's manual [VTT-TIED-1232-PT-2] p 3575 N93-29996
WATER IMMERSION
Effect of water immersion on fiber/matrix adhesion in thermoplastic composites [AD-A263646] p 3299 N93-29984
WATER LANDING
Design, building, and testing of the postlanding systems for the assured crew return vehicle p 3229 N93-29726
WATER MANAGEMENT
Modelling the dynamics of a large sea area [DE93-778330] p 3488 N93-30040
Guide to Federal Water Quality Programs and Information: A Guide with Computer Software Developed by the Interagency Working Group on Water Quality [PB93-186245] p 3475 N93-30834
WATER POLLUTION
Tank issues: Site characterization for external leak monitoring [PB93-161156] p 3469 N93-29034
Annual report on monitoring of the unsaturated zone and recharge areas at INEL to the state of Idaho INLEL oversight committee [DE93-012947] p 3473 N93-30187
Development of novel models for describing multiple toxicity effects [AD-A264439] p 3496 N93-30422
Performance and cost evaluation of bioremediation techniques for fuel spills [PB93-175545] p 3474 N93-30762
Contamination of soil, soil gas, and ground water by hydrocarbon compounds near Greear, Morgan County, Kentucky [PB93-182244] p 3474 N93-30825
Hydrogeology and ground-water-quality conditions at the Reno County Landfill, South-Central Kansas, 1990-1991 [PB93-183085] p 3474 N93-30826
Guide to Federal Water Quality Programs and Information: A Guide with Computer Software Developed by the Interagency Working Group on Water Quality [PB93-186245] p 3475 N93-30834
IOC-UNEP review meeting on oceanographic processes of transport and distribution of pollutants in the sea [DE93-605070] p 3490 N93-31019
WATER QUALITY
Modelling the dynamics of a large sea area [DE93-778330] p 3488 N93-30040
Remote sensing for water quality monitoring in the Tennessee Valley: Field tests of two systems [DE93-008997] p 3462 N93-30637
Contamination of soil, soil gas, and ground water by hydrocarbon compounds near Greear, Morgan County, Kentucky [PB93-182244] p 3474 N93-30825
Guide to Federal Water Quality Programs and Information: A Guide with Computer Software Developed by the Interagency Working Group on Water Quality [PB93-186245] p 3475 N93-30834
WATER RESOURCES
Office of Water Environmental and Program Information Systems Compendium, FY 1992 [PB93-186203] p 3462 N93-30833
Guide to Federal Water Quality Programs and Information: A Guide with Computer Software Developed by the Interagency Working Group on Water Quality [PB93-186245] p 3475 N93-30834
WATER SPLITTING
Electrolysis performance improvement and validation experiment p 3267 N93-28737
WATER TABLES
Tank issues: Design and placement of floating liquid monitoring wells [PB93-161149] p 3469 N93-29033
Tank issues: Site characterization for external leak monitoring [PB93-161156] p 3469 N93-29034
Performance and cost evaluation of bioremediation techniques for fuel spills [PB93-175545] p 3474 N93-30762
WATER TEMPERATURE
Hydrographic observations in the western tropical and subtropical north Atlantic Ocean: Atlantic Climate Change Program (ACCP) and Western Tropical Atlantic Experiment (WESTRAX) during 1990 [PB93-184760] p 3489 N93-30827
WATER TREATMENT
DOE fundamentals handbook: Chemistry [DE93-012222] p 3314 N93-30198
WATER VAPOR
Measurements of breakaway reaction between beryllium and water vapor for ITER blanket design [DE93-753270] p 3584 N93-28535
Gravity sensitivity of a resistojet water vaporizer [NASA-TM-106220] p 3288 N93-29194
Prognostic cloud water in the Los Alamos general circulation model [DE93-007381] p 3482 N93-29347
WATER WAVES
Optical measurements of ripples using a scanning laser slope gauge. Part 1: Instrumentation and preliminary results [AD-A261939] p 3486 N93-28996
Ocean waves in SAMSON/SWADE [AD-A263681] p 3487 N93-29295
Dynamics of small-scale oceanic motions [AD-A263582] p 3488 N93-29914
The IUTAM Symposium on Breaking Waves [AD-A264196] p 3489 N93-30143
WATERSHEDS
A diffusion approximation for a network of reservoirs with power law release rule [AD-A263753] p 3550 N93-29872
WAVE DISPERSION
Borel sum rules for octet baryons in nuclear medium [DE93-753245] p 3604 N93-29242
WAVE EQUATIONS
Sound wave scattering from an elastic spherical shell [AD-A264039] p 3562 N93-30029
Sound wave scattering from a rigid sphere [AD-A264182] p 3562 N93-30157
WAVE FUNCTIONS
Wavelet transform techniques and signal analysis [DE93-007919] p 3382 N93-29244
The global potential energy surfaces of the lowest two 1A-prime states of the ozone molecule: Theoretical determination and analysis [DE93-007537] p 3313 N93-29837
Quantum-kinetic Green function and macroscopic wave function [DE93-606040] p 3606 N93-30796
A possibility to investigate the superconducting gap with the help of neutrons [DE93-606392] p 3601 N93-30799
The ground state wavefunctions of a conformally invariant scalar field in different spacetime background [DE93-606063] p 3606 N93-30808
Algorithm for the solution of the Faddeev equation for a system of three identical spinless particles [DE92-644678] p 3535 N93-30914
Algorithm of numerical calculations of differential Yakubovsky equations for the (1 + 3) scattering problem [DE92-644679] p 3535 N93-30915
Schroedinger equations of higher (greater than 2) order [DE92-644677] p 3552 N93-30984
WAVE INTERACTION
Laboratory studies of gravity wave/mean flow interactions [AD-A264226] p 3478 N93-30174
An adaptive Lagrangian method for computing 1-D reacting flows and the theory of Riemann invariant manifolds for the compressible Euler equations p 3428 N93-30902
WAVE PACKETS
Quantum dynamics of X2BC van der Waals clusters [DE93-006416] p 3565 N93-28892
WAVE PROPAGATION
Observation of a beam energy shift caused by a plasma wakefield [DE93-753243] p 3583 N93-28533
Three-dimensional numerical simulation of gradual opening in a wave rotor passage [NASA-CR-191157] p 3252 N93-29072
Ocean waves in SAMSON/SWADE [AD-A263681] p 3487 N93-29295
Mitigation of shock waves in a cylindrical tunnel by foam [AD-A262491] p 3423 N93-29419
Optimization of HPM device parameters for maximum air transmission [DE93-007332] p 3386 N93-29765
Determination of the space charge distribution within an e-irradiated polymer using the pressure wave propagation method [ONERA-P-1990-4] p 3335 N93-30024
Applications of mesoscopic physics [DE93-012104] p 3597 N93-30141
Propagation channel modeling for angle-diversity combining simulation p 3360 N93-30252
ELF/VLF/LF Radio Propagation and Systems Aspects [AGARD-CP-529] p 3394 N93-30727
ELF propagation highlights p 3395 N93-30730
VLF/LF propagation measurements p 3395 N93-30732
VLF propagation measurements in the Canadian Arctic p 3396 N93-30733
Investigations of equatorial ionosphere nighttime mode conversion at VLF p 3396 N93-30735
Lightning-induced effects on VLF/LF radio propagation p 3396 N93-30737
Comparative study of undersea fields produced by various dipoles p 3397 N93-30740
A methodology and tool for the prediction of depth of reception in the sea for a VLF/LF communications system p 3397 N93-30741
Numerical wave propagation and steady-state solutions p 3428 N93-30999
WAVE REFLECTION
Errors when shock waves interact due to numerical shock width [DE93-010699] p 3426 N93-30484
WAVE SCATTERING
The wave, the cylinder, and the plate [DE93-009458] p 3450 N93-28596
Sound wave scattering from an elastic spherical shell [AD-A264039] p 3562 N93-30029
Sound wave scattering from a rigid sphere [AD-A264182] p 3562 N93-30157
Errors when shock waves interact due to numerical shock width [DE93-010699] p 3426 N93-30484
WAVEFORMS
Modeling earthquakes with local and regional broadband data p 3478 N93-30005
The use of DFT windows in signal-to-noise ratio and harmonic distortion computations [DE93-009800] p 3433 N93-30655

Modeling regional seismic waves [AD-A264002] p 3479 N93-30756

WAVEGUIDES

A dual polarized broadband multifrequency Earth station feed p 3371 N93-30319

Numerical modeling of the propagation medium at VLF/LF p 3395 N93-30729

Modification of the S-band phase shifter model 331A-3 of Electromagnetic Sciences Inc. [DIGEL-1992-5] p 3399 N93-30836

WAVELENGTH DIVISION MULTIPLEXING

Wavelength-division multiplexed optical integrated circuit with vertical diffraction grating [NASA-CASE-NPO-18357-1-CU] p 3579 N93-29848

WAVERIDERS

The HSCT mission analysis of waverider designs [NASA-CR-193467] p 3243 N93-31037

WEAK INTERACTIONS (FIELD THEORY)

Measurement of W-Z interference from neutrino-electron scattering [DE93-010724] p 3566 N93-29313

Neutrino mass [DE93-010735] p 3566 N93-29315

Unitary approximation of Bhabha diffusion by high energies and its implementation in Monte Carlo event generators [ETN-93-93622] p 3571 N93-30670

Parton's picture of the electroweak processes in high energy e(+)e(-)-collisions [DE93-606107] p 3571 N93-30788

Massive Majorana neutrinos in pre-bounce supernovae [DE92-642597] p 3572 N93-30931

WEAPON SYSTEMS

NPB cesium space experiment p 3267 N93-28733

Combat Automation for Airborne Weapon Systems: Man/Machine Interface Trends and Technologies [AGARD-CP-520] p 3501 N93-28850

Pilot decision aiding for weapon delivery: A novel approach to fire control cueing using parallel computing p 3501 N93-28853

Virtual interface applications for airborne weapons systems p 3502 N93-28858

Magnetic field measurements of the CEBAF (NIST) wiggler using the pulsed wire method [AD-A263997] p 3439 N93-29867

WEAPONS DELIVERY

Pilot decision aiding for weapon delivery: A novel approach to fire control cueing using parallel computing p 3501 N93-28853

WEAR

Preliminary experimental results for a cryogenic brush seal configuration [NASA-TM-106236] p 3416 N93-28627

Fundamental studies of friction, lubrication, and wear by atomic force microscopy [AD-A264647] p 3446 N93-30524

Tribology: Friction, lubrication, and wear technology p 3292 N93-30965

WEAR RESISTANCE

Effect of metallic-coating properties on the tribology of coated and oil-lubricated ceramics [DE93-010663] p 3330 N93-28666

Ion-beam-assisted deposition of wear-resistant coatings [DE93-011529] p 3330 N93-28687

Surface modification of tribological components in transportation [DE93-008647] p 3442 N93-28903

WEAR TESTS

Ion-beam-assisted deposition of wear-resistant coatings [DE93-011529] p 3330 N93-28687

WEATHER

An automated observing system for passive evaluation of cloud cover and visibility [AD-A263207] p 3481 N93-28875

Contributions to the American Meteorological Society's 26th International Conference on Radar Meteorology [AD-A263385] p 3481 N93-29257

Cloudiest year study: An analysis of the 3DNEPH and RTNEPH databases [AD-A263409] p 3483 N93-29967

Air weather service master station catalog USAFETAC climatic database users handbook no. 6 [AD-A264761] p 3484 N93-30608

WEATHER FORECASTING

High performance dispersion model PHYSIC [DE93-753303] p 3467 N93-28536

Leadex data report. Part 1: Weather analysis and satellite images [AD-A263217] p 3481 N93-28876

Proceedings of the Thunder and Lighting Seminar and the 3D Lightning Warning Workshop [AD-A262766] p 3482 N93-29304

Leadex data report. Part 2: Rawinsonde and ice station data [AD-A263218] p 3483 N93-29491

The 17th Annual Climate Diagnostics Workshop [PB93-183895] p 3483 N93-29664

Systems description of MIVOS (mist forecast system), part 1 [KNMI-TR-141-PT-1] p 3483 N93-30013

Daily sum of the global radiation: Calculation method and verification of forecast [KNMI-TR-138] p 3478 N93-30113

Stand alone lightning detection equipment used at Canadian Forces air bases p 3367 N93-30295

STRATUS: A prototype expert advisory system for terminal weather forecasting p 3367 N93-30296

Case study of the operational usefulness of the sharp workstation in forecasting a mesocyclone-induced cold sector tornado event in California [PB93-178697] p 3485 N93-30889

Aircraft guidance for wind shear avoidance: Decision-making under uncertainty p 3246 N93-31005

Shuttle landing facility cloud cover study: Climatological analysis and two tenths cloud cover rule evaluation [NASA-CR-193016] p 3272 N93-31033

WEATHER STATIONS

An automated observing system for passive evaluation of cloud cover and visibility [AD-A263207] p 3481 N93-28875

WEAVING

Method and apparatus for weaving a woven angle ply fabric [NASA-CASE-LAR-14048-1] p 3354 N93-29611

Powder towpreg process development p 3303 N93-30844

Characterization of multiaxial warp knit composites p 3304 N93-30851

Advanced fiber/matrix material systems p 3305 N93-30854

Mechanical and analytical screening of braided composites for transport fuselage applications p 3305 N93-30855

WEBBING

Structural response of bead-stiffened thermoplastic shear webs p 3308 N93-30873

WEBER-FECHNER LAW

Detecting residue on a printed circuit board: An application of the Boundary Contour/Feature Contour System [DE93-006283] p 3412 N93-30370

WEIBULL DENSITY FUNCTIONS

Modified goodness-of-fit tests for the Weibull distribution [AD-A262552] p 3553 N93-28574

A new goodness-of-fit test for the Weibull distribution based on spacings [AD-A262615] p 3553 N93-28587

WEIGHT REDUCTION

Advanced composite structural concepts and material technologies for primary aircraft structures p 3300 N93-30430

Composites technology for transport primary structure p 3300 N93-30431

Advanced technology commercial fuselage structure p 3300 N93-30432

Cost studies for commercial fuselage crown designs p 3302 N93-30440

WEIGHTING FUNCTIONS

Parameter identification of time-varying systems using neural networks p 3356 N93-30226

WEIGHTLESSNESS

Pharmacokinetics and Pharmacodynamics in Space [NASA-CP-10048] p 3494 N93-29502

The middeck 0-gravity dynamics experiment [NASA-CR-4500] p 3281 N93-30376

Effects of buoyancy on gas jet diffusion flames [NASA-CR-191109] p 3352 N93-31031

WELDED JOINTS

Preliminary test of liquid metal induced embrittlement in liquid LiPb and stainless-steel systems [DE93-753130] p 3320 N93-28529

Development of an updated pinch-welding capability [DE93-009823] p 3442 N93-28552

A review of hot cracking in austenitic stainless steel weldments [DE93-605280] p 3328 N93-31021

WELDED STRUCTURES

Visualizing weld metal solidification using organic analogs p 3293 N93-30973

WELDING

Development of an updated pinch-welding capability [DE93-009823] p 3442 N93-28552

JPRS report: Science and technology. Central Eurasia: Materials science [JPRS-UMS-92-015] p 3322 N93-29020

Visualizing weld metal solidification using organic analogs p 3293 N93-30973

WELLS

Tank issues: Design and placement of floating liquid monitoring wells [PB93-161149] p 3469 N93-29033

Tank issues: Site characterization for external leak monitoring [PB93-161156] p 3469 N93-29034

Hydrogeology and ground-water-quality conditions at the Reno County Landfill, South-Central Kansas, 1990-1991 [PB93-183085] p 3474 N93-30826

WETTABILITY

Pulse mitigation and heat transfer enhancement techniques. Volume 2: Effect of surface wettability and roughness in evaporative spray cooling [AD-A264174] p 3425 N93-30155

WETTING

Pulse mitigation and heat transfer enhancement techniques. Volume 2: Effect of surface wettability and roughness in evaporative spray cooling [AD-A264174] p 3425 N93-30155

Wetting and dispersion in ceramic/polymer melt injection molding systems [DE93-013240] p 3338 N93-30601

WHEAT

Growing wheat to maturity in reduced gas pressures [NASA-CR-193245] p 3491 N93-29216

WHEELCHAIRS

Platform stair lift [NASA-CASE-MFS-28772-1] p 3507 N93-29845

WHISKER COMPOSITES

Improved silicon nitride for advanced heat engines [NASA-CR-182193] p 3298 N93-29451

Whisker toughening of ceramic materials: A review [DE93-011565] p 3336 N93-30129

WHITE DWARF STARS

The heating and cooling of WZ Sge [DE93-008720] p 3634 N93-28908

WHITE NOISE

The HYDICE instrument design and its application to planetary instruments p 3434 N93-28766

WICKS

Heat pipe performance experiment p 3265 N93-28722

Pulse mitigation and heat transfer enhancement techniques. Volume 3: Liquid sodium heat transfer facility and transient response of sodium heat pipe to pulse forward and reverse heat load [AD-A263496] p 3422 N93-29338

Pulse mitigation and heat transfer enhancement techniques. Volume 5: Transient liquid movement in heat pipe wicks [AD-A264513] p 3426 N93-30403

WIENER FILTERING

Examinations of perturbation reduction by automatic speech dependent recognition of separately spoken single words [ETN-93-94180] p 3394 N93-30672

WIGGLER MAGNETS

Undulator Spectromicroscopy Facility at the Advanced Light Source [DE93-007964] p 3261 N93-28490

Magnetic field measurements of the CEBAF (NIST) wiggler using the pulsed wire method [AD-A263997] p 3439 N93-29867

WIND (METEOROLOGY)

Evaluation of atmospheric wind field and dispersion models for fog-oil smoke dispersion in complex terrain: Field measurement and model evaluation program for assessment of the environmental effects of military smokes [AD-A262051] p 3482 N93-29399

WIND DIRECTION

Rugged, no-moving-parts windspeed and static pressure probe designs for measurements in planetary atmospheres p 3434 N93-28767

Evaluation of atmospheric wind field and dispersion models for fog-oil smoke dispersion in complex terrain: Field measurement and model evaluation program for assessment of the environmental effects of military smokes [AD-A262051] p 3482 N93-29399

WIND EFFECTS

Digital image processing of descanned terrestrial ground photographs p 3459 N93-28928

WIND MEASUREMENT

Rugged, no-moving-parts windspeed and static pressure probe designs for measurements in planetary atmospheres p 3434 N93-28767

Doppler-radar wind-speed measurements in tornadoes: A comparison of real and simulated spectra [DE93-008734] p 3481 N93-29095

Wind measurement accuracy of a loran radiosonde [AD-A263572] p 3483 N93-29832

Atmospheric studies with SODAR at Kalpakkam [DE93-605544] p 3480 N93-30992

The distribution of the annual and semiannual cycles in the tropics
[DE92-642213] p 3485 N93-31006

WIND PRESSURE

Wind loads on canopy roofs
[RR-CE132] p 3451 N93-29106

WIND PROFILES

Case study of the operational usefulness of the sharp workstation in forecasting a mesocyclone-induced cold sector tornado event in California
[PB93-178697] p 3485 N93-30889

WIND SHEAR

Aircraft guidance for wind shear avoidance: Decision-making under uncertainty p 3246 N93-31005

WIND TUNNEL MODELS

Modal survey of a full-scale F-18 wind tunnel model
[AD-A262482] p 3240 N93-29410

WIND TUNNEL TESTS

International aviation (Selected articles)
[AD-A262566] p 3227 N93-28576

Wind loads on canopy roofs
[RR-CE132] p 3451 N93-29106

Modal survey of a full-scale F-18 wind tunnel model
[AD-A262482] p 3240 N93-29410

High-Reynolds-number test of a 5-percent-thick low-aspect-ratio semispan wing in the Langley 0.3-meter transonic cryogenic tunnel: Wing pressure distributions
[NASA-TM-4227] p 3240 N93-29449

Aerodynamic characteristics of a rotorcraft airfoil designed for the tip region of a main rotor blade
[NASA-TM-4264] p 3240 N93-29450

The Ultra Light Aircraft Testing
[NASA-CR-193043] p 3249 N93-29774

Construction, wind tunnel testing and data analysis for a 1/5 scale ultra-light wing model p 3243 N93-29778

On the development of a film cooling layer
p 3258 N93-29959

Vortex shedding by blunt/bluff bodies at high reynolds numbers. Volume 1: Data analysis
[AD-A264151] p 3241 N93-30171

Vortex shedding by Blunt/Bluff bodies at high reynolds numbers. Volume 2: Cylinders, octagon, hexagon
[AD-A264152] p 3241 N93-30172

Vortex shedding by blunt/bluff bodies at high reynolds numbers. Volume 3. Cubes
[AD-A264153] p 3242 N93-30173

WIND TUNNELS

Summer research program (1992). High School Apprenticeship Program (HSAP) reports. Volume 16: Arnold Engineering Development Center Civil Engineering Laboratory
[AD-A262024] p 3608 N93-29396

WIND TURBINES

The natural excitation technique (NExT) for modal parameter extraction from operating wind turbines
[DE93-010611] p 3463 N93-28603

Solar world congress: Proceedings of the biennial congress of the international solar energy society, volume 1, part 2
[PB93-174779] p 3465 N93-30001

WIND VELOCITY

Rugged, no-moving-parts windspeed and static pressure probe designs for measurements in planetary atmospheres p 3434 N93-28767

Doppler-radar wind-speed measurements in tornadoes: A comparison of real and simulated spectra
[DE93-008734] p 3481 N93-29095

Evaluation of atmospheric wind field and dispersion models for fog-oil smoke dispersion in complex terrain: Field measurement and model evaluation program for assessment of the environmental effects of military smokes
[AD-A262051] p 3482 N93-29399

Surface shear stress estimates from geostrophic winds for use in sensible and latent heat flux formulations
p 3483 N93-30044

Vortex shedding by blunt/bluff bodies at high Reynolds numbers. Volume 4: Rectangles
[AD-A264154] p 3241 N93-30151

WIND VELOCITY MEASUREMENT

The enhanced-model ladar wind sensor and its application in planetary wind velocity measurements
p 3649 N93-28815

WINDOWS (APERTURES)

Ultra-high resolution water window x ray microscope optics design and analysis
[NASA-CR-193225] p 3578 N93-29128

WINDOWS (COMPUTER PROGRAMS)

Using the Mach communication primitives in X11
[AD-A264049] p 3533 N93-30125

WINDPOWER UTILIZATION

Solar world congress: Proceedings of the biennial congress of the international solar energy society, volume 1, part 2
[PB93-174779] p 3465 N93-30001

WING CAMBER

Tailored composite wings with elastically produced chordwise camber p 3308 N93-30876

WING LOADING

High-Reynolds-number test of a 5-percent-thick low-aspect-ratio semispan wing in the Langley 0.3-meter transonic cryogenic tunnel: Wing pressure distributions
[NASA-TM-4227] p 3240 N93-29449

WING PANELS

Design, analysis, and fabrication of the technology integration box beam p 3300 N93-30433

Development of stitching reinforcement for transport wing panels p 3304 N93-30852

WINGS

A demonstration of simple airfoils: Structural design and materials choices
[DE93-007882] p 3238 N93-28662

Articulated fin/wing control system
[AD-D015712] p 3259 N93-29278

Construction, wind tunnel testing and data analysis for a 1/5 scale ultra-light wing model p 3243 N93-29778

Topology and grid adaption for high-speed flow computations
[NASA-CR-4216] p 3426 N93-30375

First NASA Advanced Composites Technology Conference, part 2
[NASA-CP-3104-PT-2] p 3303 N93-30841

Optimization of composite sandwich cover panels subjected to compressive loadings p 3306 N93-30862

A comparison of classical mechanics models and finite element simulation of elastically tailored wing boxes
p 3306 N93-30863

Construction and testing of simple airfoils to demonstrate structural design, materials choice, and composite concepts p 3243 N93-30979

WIRE

ORNL superconducting technology program for electric energy systems
[DE93-009588] p 3404 N93-28523

Welding wire pressure sensor assembly
[NASA-CASE-MFS-26216-1] p 3442 N93-28951

Electromagnetic diffusion and wire coupling
[AD-A263183] p 3381 N93-29011

A miniature fatigue test machine p 3291 N93-30956

WIRELESS COMMUNICATION

Wideband propagation measurements for wireless indoor communication
[PB93-175123] p 3382 N93-29202

Canadian Conference on Electrical and Computer Engineering, volumes 1 and 2
[ISBN-0-9694170-1-2] p 3354 N93-30215

Radiation-hardened microwave communications system
[DE93-007915] p 3394 N93-30631

WIRING

Efficient wiring of reconfigurable parallel processors
[DE93-009847] p 3538 N93-29186

WORD PROCESSING

Dynamic object oriented interaction and its implementation in the framework in an interface management system
[ETN-93-93795] p 3523 N93-28526

WORDS (LANGUAGE)

Comparison of crisp and fuzzy character networks in handwritten word recognition p 3514 N93-29545

WORK FUNCTIONS

Measurement of work function of a plasma grid in a cesium seeded negative ion source
[DE93-764153] p 3589 N93-30190

Energy spectra and photoelectron work function from YBa2Cu3O7 high-T(sub c) superconductor
[DE93-606329] p 3600 N93-30766

WORK-REST CYCLE

Engineman stress and fatigue: Pilot tests
[PB93-175008] p 3507 N93-29675

WORKING FLUIDS

Pulse mitigation and heat transfer enhancement techniques. Volume 3: Liquid sodium heat transfer facility and transient response of sodium heat pipe to pulse forward and reverse heat load
[AD-A263496] p 3422 N93-29338

WORKLOADS (PSYCHOPHYSIOLOGY)

Pilot decision aiding for weapon delivery: A novel approach to fire control cueing using parallel computing
p 3501 N93-28853

A new class of mission support for combat air-crew
p 3501 N93-28854

Human capabilities and limitations in situation awareness p 3503 N93-28863

Engineman stress and fatigue: Pilot tests
[PB93-175008] p 3507 N93-29675

WORKSTATIONS

Using today's technology to improve mobile C4I for the operational commander
[AD-A263613] p 3245 N93-29285

The Canadian Automated Air Traffic System
p 3246 N93-30323

Case study of the operational usefulness of the sharp workstation in forecasting a mesocyclone-induced cold sector tornado event in California
[PB93-178697] p 3485 N93-30889

Software conception and structure of automated workstation for an experimental data processing
[DE93-609815] p 3623 N93-30994

WOUND HEALING

Wound healing and connective tissue metabolism: The role of hyperbaric oxygen therapy
[AD-A262483] p 3493 N93-28759

WOVEN COMPOSITES

Acousto-Ultrasonic analysis of failure in ceramic matrix composite tensile specimens
[NASA-TM-106219] p 3449 N93-29073

Method and apparatus for weaving a woven angle ply fabric
[NASA-CASE-LAR-14048-1] p 3354 N93-29611

Micromechanics of fatigue in woven and stitched composites p 3304 N93-30850

Characterization of multiaxial warp knit composites
p 3304 N93-30851

Mechanical and analytical screening of braided composites for transport fuselage applications
p 3305 N93-30855

Damage of multi-directionally reinforced ceramic-matrix composites p 3308 N93-30937

X

X RAY ABSORPTION

In-situ x ray studies of the underpotential deposition of copper on platinum (3)
[AD-A263361] p 3595 N93-29331

X RAY ANALYSIS

Scanning electron microscope/energy dispersive x ray analysis of impact residues in LDEF tray clamps
p 3283 N93-29369

X ray microscopy resource center at the Advanced Light Source
[DE93-010449] p 3261 N93-29869

Design of acentric materials: X ray structures of guanidinium p-nitro- and p-hydroxybenzenesulfonate
[AD-A264220] p 3597 N93-30146

The x ray microscopy resource center at the advanced light source
[DE93-010443] p 3433 N93-30531

X RAY APPARATUS

Flash x ray system: Techniques and applications
[DE93-011477] p 3430 N93-28645

X RAY ASTRONOMY

The x ray population in globular clusters and three crab-like SNR in the large Magellanic cloud
[NASA-CR-193172] p 3630 N93-29604

XRONOS: A timing analysis software package. User's guide, version 3.00
[NASA-TM-109222] p 3532 N93-30023

ROSAT detection of stellar x ray sources in the old open cluster M67
[MPE-PREPRINT-230] p 3631 N93-30578

X RAY BINARIES

ROSAT detection of stellar x ray sources in the old open cluster M67
[MPE-PREPRINT-230] p 3631 N93-30578

X RAY DIFFRACTION

Powder x ray diffraction patterns of energetic materials for use as reference standards
[DE93-009903] p 3592 N93-28568

An integrated XRF/XRD instrument for Mars exobiology and geology experiments p 3645 N93-28792

1,2-Dimethyl-1,2-Disila-Closo-Dodecaborane(12), A silicon analog of an ortho-carborane: Synthesis; x ray crystal structure; NMR, vibrational and photoelectron spectra; bonding
[AD-A264709] p 3599 N93-30568

Coordination compounds of aluminum as precursors to aluminum nitride
[AD-A264700] p 3327 N93-30574

The characterization of materials using x ray diffraction p 3293 N93-30968

X RAY FLUORESCENCE

Planetary and satellite x ray spectroscopy: A new window on solid-body composition by remote sensing
p 3641 N93-28773

An integrated XRF/XRD instrument for Mars exobiology and geology experiments p 3645 N93-28792

X RAY IMAGERY

Flash x ray system: Techniques and applications
[DE93-011477] p 3430 N93-28645

A new multichannel soft x ray framing camera for fusion experiments
[DE93-009302] p 3432 N93-29773

X ray microscopy resource center at the Advanced Light Source
[DE93-010449] p 3261 N93-29869
Automatic detection of explosives using x ray imaging
p 3244 N93-30275
The x ray microscopy resource center at the advanced light source
[DE93-010443] p 3433 N93-30531

X RAY INSPECTION
Use of local x ray computerized tomography for high-resolution, region-of-interest inspection of large ceramic components for engines
[DE93-005564] p 3449 N93-28943
Automatic detection of explosives using x ray imaging
p 3244 N93-30275
1,2-Dimethyl-1,2-Disila-Closo-Dodecaborane(12), A silicon analog of an ortho-carborane: Synthesis; x ray crystal structure; NMR, vibrational and photoelectron spectra; bonding
[AD-A264709] p 3599 N93-30568

X RAY LASERS
Development of coherent x ray lasers
[DE93-009288] p 3437 N93-29104
Computational simulations of a soft x ray projection lithography laser plasma source
[DE93-009625] p 3437 N93-29264
Inner-shell photo-ionized x ray laser schemes
[DE93-009285] p 3438 N93-29309
Problems in the implementation of x ray optics with x ray lasers
[DE93-009297] p 3438 N93-29781
High-repetition rate x ray lasers and applications
[DE93-011882] p 3440 N93-30394

X RAY SOURCES
Planetary and satellite x ray spectroscopy: A new window on solid-body composition by remote sensing
p 3641 N93-28773
Computational simulations of a soft x ray projection lithography laser plasma source
[DE93-009625] p 3437 N93-29264
The x ray population in globular clusters and three crab-like SNR in the large Magellanic cloud
[NASA-CR-193172] p 3630 N93-29604
X ray microscopy resource center at the Advanced Light Source
[DE93-010449] p 3261 N93-29869

X RAY SPECTRA
Modification of spectral distributions by multilayer structures
[DE93-009308] p 3310 N93-29059
Defect density measurements in a shocked single crystal of ammonium perchlorate p 3319 N93-30093

X RAY SPECTROSCOPY
Undulator Spectromicroscopy Facility at the Advanced Light Source
[DE93-007964] p 3261 N93-28490
Planetary and satellite x ray spectroscopy: A new window on solid-body composition by remote sensing
p 3641 N93-28773
A team approach to the development of gamma ray and x ray remote sensing and in situ spectroscopy for planetary exploration missions p 3650 N93-28824
Modification of spectral distributions by multilayer structures
[DE93-009308] p 3310 N93-29059
In-situ x ray studies of the underpotential deposition of copper on platinum (3)
[AD-A263361] p 3595 N93-29331

X RAY STARS
The x ray population in globular clusters and three crab-like SNR in the large Magellanic cloud
[NASA-CR-193172] p 3630 N93-29604

X RAY TELESCOPES
X ray, far, and extreme ultraviolet coatings for space applications p 3340 N93-28829

X RAYS
Undulator Spectromicroscopy Facility at the Advanced Light Source
[DE93-007964] p 3261 N93-28490
Adsorption of sulfate on metal electrodes
[AD-A263192] p 3309 N93-28540
Flash x ray system: Techniques and applications
[DE93-011477] p 3430 N93-28645
Analysis of an MCG/fuse/PFS experiment
[DE93-007355] p 3410 N93-29812
X ray microscopy resource center at the Advanced Light Source
[DE93-010449] p 3261 N93-29869

X-29 AIRCRAFT
Flight control system design factors for applying automated testing techniques
[NASA-TM-4242] p 3260 N93-30764

XENON
Mass spectrometric measurement of Martian krypton and xenon isotopic abundance p 3646 N93-28798
Low-pump-rate multi-millisecond atomic xenon laser
[DE93-011484] p 3437 N93-29180
What is underneath? Moving atoms and molecules to find out
[AD-A263363] p 3567 N93-29332

XENON ISOTOPES
Mass spectrometric measurement of Martian krypton and xenon isotopic abundance p 3646 N93-28798

XENON 129
Mass spectrometric measurement of Martian krypton and xenon isotopic abundance p 3646 N93-28798

Y

YAG LASERS
Every good virtue you ever wanted in a Q-switched solid-state laser and more: Monolithic, diode-pumped, self-Q-switched, highly reproducible, diffraction-limited Nd:YAG laser p 3442 N93-28772
ND laser with co-doped ion(s) pumped by visible laser diodes
[AD-D015711] p 3437 N93-29277
Simulation of transient radiation effects on semiconductor devices using a pulsed Q-switched Nd:YAG laser p 3357 N93-30230
Intracavity-pumped 2.1 micrometer Ho(3+): YAG laser
[AD-D015728] p 3441 N93-30587

YAGI ANTENNAS
Planar microstrip YAGI antenna array
[NASA-CASE-NPO-17873-2-CU] p 3384 N93-29507

YARNS
Advanced fiber/matrix material systems
p 3305 N93-30854

YAW
Vehicle dynamic stability and rollover
[PB93-185437] p 3447 N93-30828

YBCO SUPERCONDUCTORS
Enhancements of the critical currents of YBaCuO single crystals by neutron (n) and proton (p) irradiation
[DE93-007892] p 3592 N93-28661
Processing and property evaluation of silver or aluminum matrix YBa2Cu3O(6+x) superconducting materials
[AD-A263382] p 3595 N93-29333
Properties of superconducting YBa2Cu3O(6+4) ceramic materials: Effect of processing parameters
[AD-A263441] p 3334 N93-29790
Submillimeter and microwave residual losses in epitaxial films of Y-Ba-Cu-O and Tl-Ca-Ba-Cu-O
[DE93-010430] p 3596 N93-29868
Energy spectra and photoelectron work function from YBa2Cu3O7 high-T(sub c) superconductor
[DE93-606329] p 3600 N93-30766
Superconducting films of YBaCuO
[DE93-606831] p 3600 N93-30772
Superconducting flux coupled fast switching device from YBCO films
[AD-A264301] p 3414 N93-30896

YIELD STRENGTH
Bounds on internal state variables in viscoplasticity
[NASA-TM-106215] p 3451 N93-29196
Tensile study of single-crystal ternary L1(2) trialuminide Al66Ti25Mn(sub g)
[AD-A264297] p 3601 N93-30819

YTTRIUM
Plastic deformation behaviour of oxide dispersion strengthened titanium alloys
[ONERA-NT-1990-6] p 3326 N93-30138

YTTRIUM COMPOUNDS
Process optimization of Hexoloy SX-SiC towards improved mechanical properties
[DE93-007913] p 3320 N93-28564

Z

ZEOLITES
The synthesis and ab initio structure determination of Zn4O(BO3)2: A microporous zincoborate built up from fused 3-ring and 5-ring sub-units
[AD-A262504] p 3594 N93-29138
Synthesis and characterization of mixed 3-5 and 2-6 semiconductor monomers included in the borate sodalite analogue
[AD-A264523] p 3598 N93-30407

ZINC
Effect of zinc and iron ions on the electrochemistry of nickel oxide electrode: Slow cyclic voltammetry
[AD-A263098] p 3311 N93-29133

ZINC COATINGS
The synthesis and ab initio structure determination of Zn4O(BO3)2: A microporous zincoborate built up from fused 3-ring and 5-ring sub-units
[AD-A262504] p 3594 N93-29138

ZINC COMPOUNDS
Conjugated polymers from cyclohexadienediol monomers
[AD-A264837] p 3340 N93-30900

ZINC SELENIDES
Synthesis and characterization of mixed 3-5 and 2-6 semiconductor monomers included in the borate sodalite analogue
[AD-A264523] p 3598 N93-30407

ZIRCONIUM NITRIDES
Design of interfaces in metal matrix composites
[AD-A262052] p 3296 N93-29001

ZIRCONIUM OXIDES
The effect of Bi2 O3 on the electrical properties of Zr O2: 3 percent Mg O ceramic solid electrolytes
[DE93-607029] p 3339 N93-30774

ZODIACAL LIGHT
New meteoroid model predictions for directional impacts on LDEF p 3638 N93-29376

ZONAL FLOW (METEOROLOGY)
The thermal structure, dust loading, and meridional transport in the Martian atmosphere during late southern summer p 3651 N93-29616

PERSONAL AUTHOR INDEX

Typical Personal Author Index Listing

ARMSTRONG, WILLIAM D. .... p 27 N93-10277

PERSONAL AUTHOR | PAGE NUMBER | ACCESSION NUMBER

Listings in this index are arranged alphabetically by personal author. The page number helps you locate the citation in the abstract section. The accession number denotes the number by which the citation is identified.

A

AAMODT, R. E. p 3589 N93-30189
AAZHANG, BEHNAAM p 3519 N93-29581
ABARBANEL, HENRY D. p 3424 N93-29838
ABERLE, JAMES T. p 3400 N93-31036
ABEYARATNE, ROHAN p 3321 N93-28656
ABGRALL, REMI p 3547 N93-28615
ABOLHASSANI, JAMSHID S. p 3426 N93-30375
ABRAHAM, MICHAEL H. p 3334 N93-29795
ABROSE, J. H. p 3426 N93-30403
ABRUNA, HECTOR D. p 3595 N93-29331
ACETO, LUCA p 3532 N93-30017
ACHARYA, ANURAG p 3615 N93-29459
ACHATZ, ROBERT J. p 3382 N93-29202
ACKERMAN, MICHAEL J. p 3617 N93-30453
ACKLER, H. D. p 3330 N93-28761
ACOSTA, R. J. p 3273 N93-29195
ACUNA, MARIO p 3626 N93-30705
ADAMS, JAMES H., JR. p 3573 N93-29645
p 3654 N93-29708
ADAMS, RICHARD J. p 3237 N93-30686
ADHIKARI, S. K. p 3572 N93-30944
ADL-TABATABAI, ALI-REZA p 3529 N93-29486
AFTOSMIS, MICHAEL J. p 3423 N93-29472
AGARWALA, VINOD S. p 3333 N93-29458
AGOSTINHO, RUI JORGE L. S. p 3633 N93-28672
AGOURIS, PANAYOTA p 3461 N93-29615
AGRESTI, D. G. p 3648 N93-28812
AGRESTI, W. W. p 3532 N93-30022
p 3534 N93-30546
p 3534 N93-30547
AGUEERO, RENE C. p 3638 N93-29376
AHEARN, J. S. p 3414 N93-29685
AHMAD, M. OMAIR p 3356 N93-30226
AHMADI, TEMER S. p 3338 N93-30628
AHMADJIAN, MARK p 3266 N93-28728
AHMED, K. p 3571 N93-30789
AHMED, M. JAMIL p 3389 N93-29902
AHMED, N. U. p 3357 N93-30234
p 3285 N93-30235
p 3285 N93-30249
AHN, SEUNGKI p 3239 N93-29124
AINSWORTH, J. C. p 3247 N93-30357
AJAYI, O. O. p 3330 N93-28666
AKDENIZ, Z. p 3327 N93-30778
AKHMEDOV, E. K. p 3571 N93-30793
AKINWANDE, A. I. p 3412 N93-30409
ALASAARELA, E. p 3488 N93-30040
ALBRECHT, A. p 3573 N93-29643
ALBRITTON, J. R. p 3470 N93-29055
ALCORN, T. R. p 3322 N93-29061
p 3323 N93-29101
ALDABAGH, A. M. p 3257 N93-29954
ALEWINE, N. J. p 3527 N93-29170
ALEXANDER, A. G. p 3474 N93-30825
ALEXANDER, J. IWAN D. p 3281 N93-30038
ALLARA, D. L. p 3569 N93-29839
ALLARD, R. p 3364 N93-30278
ALLBROOKS, MARTHA K. p 3283 N93-29374
ALLCOCK, HARRY R. p 3340 N93-30909
ALLEN, DAVID H. p 3307 N93-30866
ALLEN, M. p 3347 N93-30084
p 3581 N93-30500
ALLEN, MARK A. p 3613 N93-29226
ALLEN, R. W. p 3447 N93-30828
ALLEN, T. p 3333 N93-29404
ALLRED, JOHNNY W. p 3443 N93-29175
ALLTON, J. H. p 3643 N93-28782
ALMAGRI, A. F. p 3584 N93-28602
ALOY, A. p 3624 N93-28811
ALPERT, Y. L. p 3395 N93-30731
ALSTAD, JOHN p 3435 N93-30461
ALSTON, JIM A. p 3492 N93-29703
ALTER, STEPHEN J. p 3420 N93-29155
ALTEROVITZ, SAMUEL A. p 3405 N93-28610
ALTMAN, EITAN p 3552 N93-28506
p 3553 N93-28507
p 3553 N93-28508
p 3541 N93-28637
p 3541 N93-28638
ALVERMANN, KLAUS p 3521 N93-30104
ALVES, A. R. p 3601 N93-30776
ALZHEIMER, J. M. p 3383 N93-29308
AMARI, S. p 3318 N93-29367
AMBUR, DAMODAR R. p 3306 N93-30861
AMENDT, P. p 3440 N93-30394
AMERI, ALI p 3420 N93-29157
AMINPOUR, M. A. p 3307 N93-30867
ANDERBERG, JOSEPH p 3597 N93-30175
ANDERSON, DANA Z. p 3580 N93-30205
ANDERSON, G. A. p 3383 N93-29308
ANDERSON, J. D. p 3568 N93-29784
ANDERSON, LOREN A. p 3229 N93-29726
ANDERSON, N. E. p 3631 N93-30615
ANDERSON, NEAL T. p 3284 N93-29905
ANDERSON, ROBERT L. p 3306 N93-30864
ANDERSON, STEVEN PAUL p 3488 N93-30046
ANDERSON, TIM p 3601 N93-30811
ANDERSON, W. R. p 3319 N93-30081
ANDREWS, G. E. p 3257 N93-29954
ANDREWS, M. M. p 3385 N93-29597
ANDRUS, JAMES p 3446 N93-30512
ANEZIRIS, CHARILAOS p 3607 N93-30932
ANGELLI, L. p 3532 N93-30023
ANINI, Y. p 3606 N93-30808
ANNAERT, G. p 3397 N93-30740
ANNIS, MARTIN p 3244 N93-30275
ANTONIAK, Z. I. p 3625 N93-29329
ANTONIO, JOSEPH C. p 3508 N93-29924
ANTONSEN, T. M., JR. p 3585 N93-28749
ANWARMUGHAL, M. p 3571 N93-30789
APOSTOLAKIS, G. p 3267 N93-28738
APPLEBY, JOHN F. p 3639 N93-28764
ARAI, TAKETOSHI p 3299 N93-30004
ARASTEH, D. p 3353 N93-28570
ARATYN, H. p 3574 N93-28565
ARCH, D. K. p 3412 N93-30409
ARDEN, M. E. p 3465 N93-30001
p 3466 N93-30935
ARLANDER, D. W. p 3475 N93-28475
ARMOUR, BERNARD p 3376 N93-30347
ARMSTONG, T. W. p 3573 N93-29640
ARMSTRONG, G. A. p 3460 N93-29255
ARMSTRONG, RONALD W. p 3348 N93-30086
p 3350 N93-30094
ARMSTRONG, T. W. p 3572 N93-29633
p 3573 N93-29636
p 3573 N93-29639
p 3573 N93-29641
p 3573 N93-29642
ARNOLD, JAMES F. p 3544 N93-30591
ARNOTT, W. P. p 3561 N93-28995
ARROTT, MATTHEW p 3614 N93-29232
ARTHUR, A. A. p 3598 N93-30393
ARTHUR, JARVIS J. p 3520 N93-29070
ARTHUR, RICHARD J. p 3318 N93-29627
ARTS, T. p 3253 N93-29930
p 3258 N93-29959
ARZHANNIKOV, A. V. p 3441 N93-30767
p 3400 N93-30993
ASARO, ROBERT J. p 3453 N93-29863
ASAY, BLAINE W. p 3319 N93-30077
ASERE, A. A. p 3257 N93-29954
ASHDOWN, G. A. p 3398 N93-30749
ASHIBE, KUSUO p 3584 N93-28535
ASHLEY, KEVIN p 3323 N93-29259
ASHTON, GARY p 3435 N93-30466
ASMAR, S. W. p 3386 N93-29603
ATCHISON, MICHAEL K. p 3272 N93-31033
ATCHITY, G. J. p 3313 N93-29837
ATHREYA, KRISHNA B. p 3555 N93-29979
ATKINSON, DALE R. p 3638 N93-29355
p 3283 N93-29374
p 3283 N93-29375
p 3582 N93-29695
ATLAS, E. L. p 3616 N93-30122
ATTWOOD, D. p 3261 N93-29869
p 3433 N93-30531
AUBRUN, J. N. p 3434 N93-28794
AUCHAMPAUGH, G. F. p 3647 N93-28807
AURIOL, ANDRE p 3241 N93-30020
AUSTIN, S. p 3634 N93-28908
AUSTON, DAVID H. p 3408 N93-29427
AVERY, JAMES p 3277 N93-29119
AVERY, WILLIAM B. p 3303 N93-30845
p 3305 N93-30857
AYIK, S. p 3576 N93-30054
AZU, CHARLES p 3407 N93-29203
AZU, CHARLES C., JR. p 3533 N93-30383
AZUMI, MASAFUMI p 3585 N93-28979

B

BAAKLINI, GEORGE Y p 3295 N93-28624
BABU, B. N. p 3393 N93-30514
BACHMAN, D. A. p 3575 N93-29302
BACHMANN, MATTHIAS p 3458 N93-28925
BACKES, PAUL G. p 3443 N93-28954
BADA, JEFFREY p 3283 N93-29364
BADEN, A. p 3576 N93-30527
BADER, DOUG E. p 3337 N93-30541
BAER, F. p 3470 N93-29318
BAGRYANSKIJ, P. A. p 3591 N93-30780
BAHADORI, M. YOUSEF p 3352 N93-31031
BAILEY, ALAN D. p 3399 N93-30757
BAILEY, MICHAEL J. p 3613 N93-29226
BAILEY, SHEILA G. p 3321 N93-28618
BAINTER, BILLY D. p 3483 N93-29967
BAINUM, PETER M. p 3281 N93-30142
BAIRD, C. R. p 3359 N93-30248
BAJAJ, CHANDRAJIT L. p 3534 N93-30544
BAJER, V. N. p 3600 N93-30770
BAKER-FULCO, CAROL J. p 3497 N93-30894
BAKER, C. J. p 3286 N93-29910
BAKER, DANIEL R. p 3493 N93-29199
BAKER, K. D. p 3400 N93-28820
BAKER, MARVIN p 3375 N93-30343
BAKER, W. E. p 3446 N93-30211
BAKER, W. L. p 3472 N93-30131
BAKOWSKY, L. p 3325 N93-30115
BAKSHI, P. p 3588 N93-29382
BALAKRISHNAN, GANESHAN p 3310 N93-29125
BALALYKIN, N. I. p 3600 N93-30771
BALANDIN, M. P. p 3606 N93-30805
BALANIS, CONSTANTINE A. p 3400 N93-31036
BALAS, MARK p 3275 N93-29112
BALASUBRAMANIAN, S. p 3375 N93-30340
BALLANTYNE, W. J. p 3370 N93-30313
BAMFORD, DOUGLAS L. p 3247 N93-30353
BANDINELLI, M. p 3398 N93-30751
BANERDT, B. p 3649 N93-28819
BANERDT, W. p 3434 N93-28765
BANFORD, MICHAEL P. p 3240 N93-29410
BANKS, BRUCE A. p 3283 N93-29363
p 3299 N93-29614
BANNER, M. L. p 3489 N93-30143
BANNISTER, P. R. p 3399 N93-30755
BANNISTER, PETER R. p 3395 N93-30730
p 3398 N93-30746
BANNOCHIE, C. J. p 3309 N93-28553
BAR-LEV, ODED p 3607 N93-30933
BARANGER, H. p 3284 N93-29897
BARASHENKOV, V. S. p 3601 N93-30798
p 3281 N93-31024

BARBASHOV, B. M. p 3605 N93-30784
p 3557 N93-30922
BARBEE, T. W., JR. p 3438 N93-29781
BARBER, JUDY A. p 3496 N93-30400
BARCHET, W. R. p 3473 N93-30183
BARCLAY, REBECCA O. p 3612 N93-28948
p 3615 N93-29709
p 3616 N93-30036
p 3616 N93-30037
BARDEEN, J. M. p 3636 N93-30528
BAREL, A. p 3397 N93-30740
BARFKNECHT, A. T. p 3594 N93-29249
BARIBEAU, C. p 3370 N93-30312
BARK, JONG p 3304 N93-30847
BARLETTA, W. A. p 3574 N93-29103
p 3326 N93-30490
BARLOW, LINDA S. p 3506 N93-29406
BARNARD, J. J. p 3576 N93-30390
BARNES, FRANK p 3276 N93-29117
BARNES, LESLIE A. p 3309 N93-28540
BARNETT, A. M. p 3466 N93-30891
BARNETT, JOHN p 3360 N93-30254
BARNIV, YAIR p 3245 N93-29653
BARON, ROBERT V. p 3533 N93-30125
BARONE, JOSEPH M. p 3513 N93-29539
BARRACLOUGH, B. L. p 3647 N93-28807
BARRERAROLDAN, A. S. p 3472 N93-30008
BARRON, CHRIS p 3532 N93-30023
BARSHICK, C. M. p 3314 N93-30166
BARSKI, MARIUSZ p 3369 N93-30306
BARSOTTI, E. p 3382 N93-29245
BARTLETT, RODNEY J. p 3315 N93-30534
BARTO, ANDREW p 3534 N93-30561
BARTOS, R. D. p 3386 N93-29601
BARTS, S. A. p 3319 N93-30081
BARUT, A. O. p 3608 N93-30987
BASCOM, WILLARD D. p 3303 N93-30845
p 3304 N93-30846
BASEDOW, R. p 3434 N93-28766
BASHKANSKY, MARK p 3581 N93-30410
BASRAN, J. p 3372 N93-30326
BASS, HENRY E. p 3561 N93-28995
BASS, J. M. p 3538 N93-29030
BASSETT, ROBERT M. p 3269 N93-29475
BASSI, F. p 3258 N93-29962
BASU, SUNANDA p 3476 N93-29343
BATES, ALBERT M. p 3409 N93-29605
BATTLE, D. S. p 3496 N93-30659
BAUCOM, ROBERT M. p 3303 N93-30844
BAUGHER, GEORGE R. p 3285 N93-28554
BAUMEISTER, JOSEPH F. p 3419 N93-29075
BAUMGARTNER, ERIC THOMAS p 3443 N93-29082
BAYOUMI, M. M. p 3364 N93-30278
BAZDIDI-TEHRANI, F. p 3257 N93-29954
BAZZAZ, F. A. p 3467 N93-28543
BDZIL, J. B. p 3424 N93-29836
BDZIL, JOHN B. p 3350 N93-30096
BEAHM, LORRAINE P. p 3573 N93-29645
BEALE, PAUL D. p 3342 N93-29835
BEARD, B. C. p 3319 N93-30092
p 3319 N93-30093
p 3350 N93-30094
BEAUCHAMP, CHARLES H. p 3259 N93-29278
BEAUJEAN, R. p 3573 N93-29644
BEAULIEU, J.-N. p 3376 N93-30348
BEAULIEU, NORMAN C. p 3360 N93-30251
BEAUSSART, A. J. p 3301 N93-30437
BECK, D. R. p 3566 N93-29183
BECKER, DIETER p 3394 N93-30672
BECKER, JAMES S. p 3415 N93-28557
BECKER, LUANN p 3283 N93-29364
BECKMAN, BRIAN C. p 3251 N93-30416
BEDAIR, SALAH p 3599 N93-30560
BEDARD, A. J., JR. p 3434 N93-28767
BEDINGER, M. S. p 3469 N93-29033
p 3469 N93-29034
BEECK, A. p 3258 N93-29958
BEER, H. p 3256 N93-29952
BEGIN, LOUIS p 3363 N93-30272
BEGUIRISTAIN, R. p 3261 N93-29869
BEHR, V. L. p 3239 N93-29035
BEHRENDT, W. p 3588 N93-29780
BEHRENS, P. p 3570 N93-30540
BEHRENS, RICHARD, JR. p 3347 N93-30083
BEHUNEK, JAN L. p 3462 N93-29834
BEITER, T. A. p 3592 N93-28568
BEJCZY, ANTAL K. p 3521 N93-29608
BEKEFI, GEORGE p 3400 N93-30880
BELCHER, JOHN M. p 3374 N93-30337
BELL, P. M. p 3432 N93-29773
BELL, WAYNE E. p 3538 N93-29490
BELLONI, T. p 3631 N93-30578
BELROSE, JOHN S. p 3395 N93-30728
p 3398 N93-30747
BELYAEV, V. B. p 3535 N93-30914
p 3535 N93-30915
BEN-ZVI, I. p 3435 N93-28594
p 3575 N93-29317
BENDIX, JOERG p 3458 N93-28925
BENEDICT, A. p 3352 N93-30663
BENGISU, M. p 3323 N93-29092
p 3336 N93-30129
BENGOUGH, P. p 3373 N93-30332
BENHABIB, B. p 3369 N93-30305
BENJAMIN, R. F. p 3421 N93-29253
BENNETT, PHILIP DESMOND p 3633 N93-28673
BENNETT, W. S., II p 3503 N93-28867
BENNEY, RICHARD J. p 3241 N93-30119
BENOIT, SANDRA L. p 3499 N93-30426
BENTON, E. R. p 3573 N93-29637
p 3573 N93-29638
BENTON, E. V. p 3573 N93-29636
p 3573 N93-29637
p 3573 N93-29638
p 3573 N93-29639
BENTS, D. J. p 3287 N93-28686
BENTZ, MIKE p 3264 N93-28712
BENZ, E. p 3258 N93-29958
BENZ, M. D. p 3285 N93-29912
BERALDIN, J. A. p 3366 N93-30286
BERDEGUEZ, JAMES p 3482 N93-29393
BERENGUER, M. p 3565 N93-28831
BEREZHIANI, Z. G. p 3571 N93-30793
BEREZINSKY, V. S. p 3632 N93-28473
BERG, L. p 3373 N93-30332
BERG, RICHARD L. p 3262 N93-30103
BERG, S. L. p 3624 N93-28814
BERGEVIN, ROBERT J. p 3555 N93-29447
BERGMAN, L. A. p 3583 N93-29700
BERGMANN, H. W. p 3325 N93-30115
BERK, H. L. p 3587 N93-29148
BERKOFF, T. A. p 3577 N93-29038
BERLINER, R. p 3593 N93-28956
BERNHARD, RONALD P. p 3283 N93-29369
p 3638 N93-29370
BERNHARDT, A. F. p 3422 N93-29300
BERRETTINI, ROBERT p 3291 N93-30958
BERRY, D. H. p 3329 N93-28541
BERRY, GUY C. p 3339 N93-30898
BERRY, J. N. p 3583 N93-29699
BERRY, R. B. p 3430 N93-28645
BERSHAD, BRIAN N. p 3533 N93-30125
p 3534 N93-30523
BERTHOD, MARC p 3553 N93-28510
BERTHOLD, J. W. p 3444 N93-29205
BERTRAND, JEAN M. p 3396 N93-30733
BERWALD, D. H. p 3434 N93-28768
BEST, LEONARD G. p 3501 N93-28479
BEST, S. p 3283 N93-29365
BEUTLER, D. E. p 3598 N93-30511
BEVERSDORFF, M. p 3255 N93-29942
BEYER, P. E. p 3385 N93-29597
BEYER, TODD B. p 3301 N93-30436
BEZDEK, JAMES C. p 3511 N93-29528
BHAGWAN, JAI p 3365 N93-30284
BHARGAVA, VIJAY K. p 3365 N93-30283
BIANCHI, J. C. p 3422 N93-29335
BIBLE, D. W. p 3394 N93-30631
BICKEL, JOHN E. p 3395 N93-30732
BIJVOET, J. A. p 3266 N93-28725
BILARDO, VINCENT p 3628 N93-30724
BILENKAYA, S. I. p 3571 N93-30792
BILLING-ROSS, J. p 3582 N93-28806
BILLINGSLEY, J. B. p 3379 N93-28655
BILLINGSLEY, JAMES P. p 3342 N93-29494
BILTOFT, P. J. p 3310 N93-29059
BINGHAM, C. p 3464 N93-29925
BINQIAN, ZHANG p 3238 N93-28493
BINSTOCK, J. p 3426 N93-30485
BIRENZVIGE, AMNON p 3315 N93-30365
BIRKS, JOHN W. p 3488 N93-29670
BIRMAN, KENNETH P. p 3531 N93-29976
BIRNBACH, RICHARD A. p 3236 N93-30676
BIRNBAUM, L. E. p 3410 N93-29814
p 3411 N93-30057
p 3411 N93-30058
BIRTCHER, CRAIG R. p 3400 N93-31036
BISCHOF, C. H. p 3525 N93-28877
BISHOP, A. R. p 3593 N93-29094
p 3561 N93-29711
p 3598 N93-30501
p 3600 N93-30569
BISHOP, ANN P. p 3616 N93-30036
p 3616 N93-30037
BISWAS, TAPAN p 3361 N93-30256
BITTEN, ROBERT E. p 3504 N93-28870
BITTNER, H. p 3284 N93-29906
BJERKE, TODD W. p 3453 N93-29801
BLAAUBOER, D. p 3483 N93-30013
BLACIC, J. p 3434 N93-28769
BLACK, J. R. p 3287 N93-28946
BLACKBURN, M. R. p 3496 N93-30515
p 3497 N93-30897
BLACKSTEN, H. R. p 3531 N93-29874
BLACKWELL, B. F. p 3549 N93-29187
BLAIS, F. p 3366 N93-30286
BLAIS, NORMAND C. p 3319 N93-30076
BLAKE, IAN F. p 3365 N93-30283
BLAKE, J. B. p 3572 N93-29634
BLAKELY, J. R. p 3266 N93-28725
BLAKKOLB, B. K. p 3414 N93-29690
BLANCHARD, L. A. p 3505 N93-28884
BLANCHARD, ROBERT E. p 3498 N93-28622
BLASING, R. R. p 3374 N93-30336
BLATCHLEY, CHARLES C. p 3424 N93-29966
BLAU, PETER J. p 3292 N93-30965
BLECH, RICHARD p 3538 N93-28628
BLELLOCH, GUY E. p 3530 N93-29822
p 3530 N93-29823
BLERSCH, DONALD p 3669 N93-29710
BLIETZ, M. p 3631 N93-30641
BLINOV, A. E. p 3571 N93-30790
BLINOV, V. E. p 3571 N93-30790
BLISS, D. E. p 3595 N93-29417
BLIX, H. p 3475 N93-30996
BLOM, RONALD G. p 3613 N93-29226
BLOOM, BARD p 3532 N93-30017
BLOOM, DAVID M. p 3581 N93-30520
BLOSWICK, DONALD S. p 3493 N93-29199
BLUE, M. D. p 3582 N93-29689
BLUESTEIN, H. B. p 3481 N93-29095
BLUM, LESSER p 3566 N93-29143
BLUME, LEO p 3613 N93-29226
BLUMSTEIN, ALEXANDRE p 3337 N93-30497
BO, T. p 3254 N93-29938
BOAIN, R. J. p 3268 N93-28770
BOBBITT, S. A. p 3608 N93-30821
BOBERG, PAUL R. p 3573 N93-29645
BOBIAS, S. GEORGE p 3572 N93-29628
BOCHEV, PAVEL B. p 3421 N93-29208
BOCK, ERIK J. p 3486 N93-28996
BOCK, WOJTEK J. p 3375 N93-30341
BODE, ARTHUR P. p 3494 N93-29620
BOEHM, A. P. W. p 3549 N93-29769
BOERCKER, D. B. p 3565 N93-29099
BOERGER, J. p 3463 N93-31009
BOES, J. C. p 3413 N93-30835
p 3577 N93-30837
BOETTGER, J. C. p 3300 N93-30395
BOGDAN, I. p 3515 N93-29555
BOGDZEL, A. A. p 3600 N93-30766
BOGETTI, TRAVIS A. p 3294 N93-28559
BOHLIN, A. K. p 3624 N93-29668
BOHM, A. p 3556 N93-28601
BOHON, HERMAN L. p 3300 N93-30428
p 3303 N93-30841
BOILEAU, JACQUES p 3344 N93-30070
BOISSONNAT, JEAN-DANIEL p 3547 N93-28616
BOITNOTT, RICHARD L. p 3308 N93-30875
BOKHOUR, EDWARD B. p 3281 N93-30376
BOLDMAN, DONALD R. p 3252 N93-29162
BOLIVAR, S. L. p 3450 N93-30636
BOLL, D. J. p 3304 N93-30846
BOLSTAD, CHERYL A. p 3503 N93-28863
BOLTON, P. R. p 3564 N93-28762
BONDAR, A. E. p 3571 N93-30790
BONICAMP, JUDITH M. p 3438 N93-29800
BONITO, N. A. p 3273 N93-29306
BONNEMASON, FRANCIS p 3434 N93-29696
BONNEY, L. A. p 3592 N93-28643
BONTOUX, P. p 3256 N93-29948
BOOTHE, EDWARD M. p 3236 N93-30675
BOOZER, A. p 3586 N93-29056
BORCHERS, WILLIAM R. p 3269 N93-28558
BORDER, J. S. p 3270 N93-29589
BORG, JANET p 3638 N93-29360
BORGMANN, DETLEV p 3396 N93-30734
BORGONOVI, GIANCARLO p 3449 N93-28685
BORREL, M. p 3417 N93-28744
p 3417 N93-28745
BORUCKI, W. p 3632 N93-28791
BOSC, PATRICK p 3517 N93-29569
BOSCH, J. p 3654 N93-29646
BOSCH, WOLFGANG p 3457 N93-28917
BOSSET, M. p 3231 N93-29736
BOSTON, HAROLD G. p 3331 N93-29085
BOTTARO, JEFFREY C. p 3564 N93-28562
BOTTENBERG, W. R. p 3466 N93-30891
BOTTONE, STEVEN p 3479 N93-30593
BOUCARUT, R. A. p 3582 N93-28788
BOUCHARD, J. p 3284 N93-29897
BOUDREAU, G. p 3389 N93-29901
BOUDREAU, GARY p 3363 N93-30268
BOULGUIRA, AZZEDINE p 3361 N93-30257
BOULWARE, D. G. p 3605 N93-30481
BOURASSA, R. J. p 3283 N93-29623
BOURRIEAU, J. p 3573 N93-29635
BOUSGARBIES, J.-L. p 3253 N93-29931
BOUSSINOT, FREDERIC p 3537 N93-28505

BOUST, FABRICE ...... p 3314 N93-30139
BOUTALEBJ, H. ...... p 3479 N93-30940
BOWEN, B. ARCHIE ...... p 3367 N93-30297
BOWEN, BARRY C. ...... p 3271 N93-29136
BOWEN, H. K. ...... p 3339 N93-30885
BOWEN, WILLIAM R. ...... p 3615 N93-29439
BOWER, J. ...... p 3432 N93-29773
BOWER, J. R. ...... p 3444 N93-29205
BOWERSOX, RODNEY DALE WELCH
p 3242 N93-30583
BOWLES, T. J. ...... p 3566 N93-29313
p 3566 N93-29315
BOWMAN, K. J. ...... p 3320 N93-28499
BOWMAN, KEITH J. ...... p 3453 N93-30159
BOWMAN, STEVEN R. ...... p 3440 N93-30427
BOYA, L. J. ...... p 3556 N93-28601
BOYD, JOHN E. ...... p 3618 N93-30455
BOYER, J. H. ...... p 3441 N93-30910
BOZEMAN, RICHARD J., JR. ...... p 3442 N93-28501
BRAAMS, B. ...... p 3586 N93-29056
BRADLEY, J. ...... p 3638 N93-29372
BRADLEY, K. ...... p 3412 N93-30118
BRADY, J. MICHAEL ...... p 3380 N93-28896
BRANDON, S. L. ...... p 3453 N93-29843
BRANDT, M. L. ...... p 3321 N93-28957
BRANSTROM, B. R. ...... p 3287 N93-28946
BRASIC, J. R. ...... p 3376 N93-30349
BRAY, RICHARD S. ...... p 3236 N93-30673
p 3236 N93-30674
BREDEKAMP, JOE ...... p 3613 N93-29223
BREIZMAN, B. N. ...... p 3587 N93-29148
BREKKE, L. ...... p 3574 N93-28565
BRENNAN, J. J. ...... p 3299 N93-29802
BRENNAN, PATRICK J. ...... p 3429 N93-29701
BRENNER, D. W. ...... p 3351 N93-30100
BRENNER, DONALD W. ...... p 3318 N93-30071
BRENNER, H. ...... p 3417 N93-28751
BREWER, DAVID J. ...... p 3369 N93-30304
BREWER, W. V. ...... p 3290 N93-30950
BREWSTER, QUINN ...... p 3319 N93-30085
BRICKA, R. M. ...... p 3473 N93-30197
BRIDEGEMAN, R. C. ...... p 3373 N93-30328
BRIDGES, G. ...... p 3369 N93-30307
BRIDGES, J. S. ...... p 3475 N93-30831
BRILES, S. D. ...... p 3554 N93-28763
BRILL, THOMAS B. ...... p 3343 N93-30062
BRIMHALL, J. L. ...... p 3320 N93-28548
BRINKER, DAVID J. ...... p 3467 N93-29686
p 3582 N93-29693
BRINKKEMPER, S. ...... p 3611 N93-28481
BRINZA, DAVID E. ...... p 3267 N93-28732
BRITTON, BRUCE K. ...... p 3498 N93-28901
BRODSKY, M. T. ...... p 3285 N93-29912
BRODZINSKI, RONALD L. ...... p 3318 N93-29627
BROECKER, W. S. ...... p 3486 N93-28670
BROER, HENK ...... p 3548 N93-28753
BROMAGHIM, DARON ...... p 3287 N93-28658
BRON, C. ...... p 3552 N93-31014
BROOKE, M. ...... p 3581 N93-30500
BROOKES, STEPHEN ...... p 3530 N93-29821
BROOKS, D. ...... p 3524 N93-28834
BROSE, D. J. ...... p 3331 N93-29201
BROST, GEORGE A. ...... p 3597 N93-30144
p 3599 N93-30554
BROUSSEAU, N. ...... p 3360 N93-30253
BROWER, DANIEL ...... p 3622 N93-30474
BROWN, ALAN W. ...... p 3535 N93-30602
BROWN, D. F. ...... p 3482 N93-29399
BROWN, D. M. ...... p 3341 N93-28668
BROWN, GERALD G. ...... p 3528 N93-29345
BROWN, J. LYNN ...... p 3288 N93-28950
BROWN, JAMES M. ...... p 3247 N93-30330
BROWN, L. E. ...... p 3442 N93-28837
BROWN, R. ...... p 3319 N93-30090
BROWN, S. A. ...... p 3601 N93-30819
BROWN, T. G. ...... p 3584 N93-28583
BROWNING, D. F. ...... p 3588 N93-29780
BROWNLEE, D. E. ...... p 3638 N93-29372
p 3638 N93-29378
BRUCKER, G. A. ...... p 3318 N93-30068
BRUEDERLE, E. ...... p 3284 N93-29906
BRUEMMER, S. M. ...... p 3320 N93-28548
BRUENING, HINRICH ...... p 3523 N93-28526
BRUGGINK, D. ...... p 3439 N93-30186
BRUMLIK, CHARLES J. ...... p 3310 N93-28988
BRUNGRABER, ROBERT J. ...... p 3293 N93-30966
BRUNNETT, GUIDO ...... p 3450 N93-28516
BRYANT, PHILLIP G. ...... p 3447 N93-30567
BRYSON, J. W. ...... p 3454 N93-30213
BU, Y. ...... p 3316 N93-30627
BUCHENAUER, D. ...... p 3588 N93-29334
BUCHHEIT, R. G. ...... p 3336 N93-30051
BUCK, O. ...... p 3450 N93-28567
BUCKINGHAM, A. C. ...... p 3419 N93-29050
BUECHNER, KLAUS D. ...... p 3599 N93-30568
BUEHLER, F. ...... p 3639 N93-29380
BUFFETT, A. R. ...... p 3501 N93-28853
BUFTON, J. L. ...... p 3442 N93-28780
BUGG, W. M. ...... p 3568 N93-29764
BUHUSI, CATALIN V. ...... p 3515 N93-29557
BUI, JAMES ...... p 3272 N93-30881
BUKLEY, ANGELIA P. ...... p 3263 N93-28700
BULGADAEV, S. A. ...... p 3558 N93-30986
BULUSU, SURYANARAYANA ...... p 3347 N93-30083
BUNCH, T. E. ...... p 3283 N93-29364
BUNCH, TED E. ...... p 3638 N93-29360
BUNNELL, L. ROY ...... p 3238 N93-28662
p 3291 N93-30958
p 3294 N93-30978
p 3243 N93-30979
BURK, K. W. ...... p 3481 N93-29054
BURK, STEPHEN D. ...... p 3481 N93-28876
BURKE, B. E. ...... p 3434 N93-28771
BURKE, C. P. ...... p 3397 N93-30739
BURKE, W. R. ...... p 3281 N93-30106
BURKHARDT, C. ...... p 3255 N93-29946
BURKS, B. L. ...... p 3460 N93-29255
BURLEY, RICHARD K. ...... p 3432 N93-29503
BURLEY, S. M. A. ...... p 3465 N93-30001
p 3466 N93-30935
BURMAN, R. L. ...... p 3566 N93-29313
BURNS, FOREST ...... p 3572 N93-29630
BURNS, R. B. ...... p 3474 N93-30825
BURNS, WILLIAM K. ...... p 3431 N93-29046
BURPO, STEVEN J. ...... p 3301 N93-30434
BURR, ROBERT E. ...... p 3496 N93-30588
BURSTEIN, ELIAS ...... p 3581 N93-30666
BURT, W. W. ...... p 3647 N93-28807
BURTNYK, N. ...... p 3372 N93-30326
BURTON, REGINA M. ...... p 3399 N93-30757
BUSCH, C. ...... p 3603 N93-28472
BUSH, MARILYN ...... p 3610 N93-29970
BUSH, S. H. ...... p 3354 N93-28893
BUTLER, P. L. ...... p 3444 N93-29254
p 3444 N93-29316
BUTNER, D. B. ...... p 3520 N93-29058
BUTTRAM, J. D. ...... p 3444 N93-29205
BYERS, S. ...... p 3497 N93-30890
BYKOVSKIJ, V. F. ...... p 3480 N93-30991
BYRD, R. C. ...... p 3647 N93-28807

C

CAFLISCH, RUSSEL ...... p 3427 N93-30499
CAGLE, J. A. ...... p 3283 N93-29705
CAILLAU, P. ...... p 3257 N93-29956
CAIN, CLARENCE P. ...... p 3438 N93-29395
CAIN, R. P ...... p 3286 N93-28795
CAINES, PETER E. ...... p 3529 N93-29488
CALAWA, ROBERT ...... p 3298 N93-29282
CALDERON, M. ...... p 3326 N93-30490
CALLEN, J. D. ...... p 3585 N93-28979
CALLEN, W. RUSSELL ...... p 3435 N93-29697
CALLICOTT, WILLIAM M. ...... p 3617 N93-30454
CALMETTA, A. ...... p 3602 N93-30998
CALS, MARIE-PIERRE ...... p 3335 N93-30024
CALVERT, JACK G. ...... p 3488 N93-29670
CALVIGNAC, B. ...... p 3281 N93-30106
CALZONETTI, F. ...... p 3592 N93-28647
CAMERON, C. P. ...... p 3465 N93-30391
CAMERON, M. ...... p 3632 N93-30643
CAMPBELL, D. ...... p 3565 N93-28914
CAMPBELL, D. K. ...... p 3551 N93-30503
CAMPBELL, DAVID K. ...... p 3337 N93-30381
CAMPBELL, E. M. ...... p 3436 N93-29097
CANAVAN, G. H. ...... p 3625 N93-28646
CANAVAN, G. J. ...... p 3556 N93-28572
CANESSA, E. ...... p 3602 N93-30998
CANO, ROBERTO J. ...... p 3297 N93-29107
p 3304 N93-30851
CANTILLO, A. Y. ...... p 3489 N93-30830
CANTRELL, J. S. ...... p 3592 N93-28568
CANTRELL, JOHN H. ...... p 3431 N93-29084
CAPLOT, MICHEL ...... p 3562 N93-30110
CAPONE, FRANCIS J. ...... p 3239 N93-29160
CAPONE, RONALD L. ...... p 3467 N93-28873
CARABETIAN, C. ...... p 3582 N93-29691
CARBONE, D. ...... p 3257 N93-29957
CARCIELLO, N. ...... p 3329 N93-28551
CARD, HOWARD ...... p 3355 N93-30223
CARDEN, HUEY D. ...... p 3308 N93-30875
CARDOSI, KIM M. ...... p 3394 N93-30611
CARLILE, J. A. ...... p 3416 N93-28627
CARLIN, BRADLEY P. ...... p 3549 N93-29413
CARLINI, R. D. ...... p 3566 N93-29313
CARLSON, CURTIS R. ...... p 3628 N93-30718
CARMEL, Y. ...... p 3411 N93-29922
CARNE, THOMAS G. ...... p 3463 N93-28603
CARO, A. ...... p 3600 N93-30668
CARPENTER, GAIL A. ...... p 3543 N93-29791
CARPENTER, WILLIAM C. ...... p 3249 N93-29885
CARR, STEPHEN SCOTT ...... p 3479 N93-30564
CARRENO, LUIS A. ...... p 3520 N93-29585
CARRETTA, THOMAS R. ...... p 3498 N93-29481
CARRICK, PATRICK G. ...... p 3341 N93-28517
CARROLL, D. ...... p 3333 N93-29404
CARROLL, L. W. ...... p 3497 N93-30890
CARROLL, M. A. ...... p 3425 N93-30156
CARTER, DANIEL C. ...... p 3491 N93-28952
CARUTHERS, JERALD W. ...... p 3391 N93-29975
CASSELL, RICK ...... p 3247 N93-30358
CASTERA, J. P. ...... p 3435 N93-30469
CASTLEDINE, C. ...... p 3244 N93-30276
CATHEY, C. T. ...... p 3430 N93-28659
CATTO, P. J. ...... p 3589 N93-30189
CATTON, I. ...... p 3267 N93-28738
CAVANAUGH, KEVIN J. ...... p 3550 N93-29978
CAVIN, O. B. ...... p 3325 N93-29813
CECH, STEVEN D. ...... p 3456 N93-28620
CEKIC, M. ...... p 3584 N93-28602
CERMAK, R. ...... p 3624 N93-29668
CERNANSKY, NICHOLAS P. ...... p 3311 N93-29283
CHACHULA, SANDRA K. ...... p 3506 N93-29444
CHAFFIN, M. H. ...... p 3622 N93-30474
CHAGNOT, D. ...... p 3394 N93-30631
CHAITMAN, B. R. ...... p 3497 N93-30890
CHAKRABARTI, S. K. ...... p 3637 N93-31004
CHALOUPKA, T. ...... p 3283 N93-29365
CHAMIS, C. C. ...... p 3307 N93-30868
CHAMIS, CHRISTOS C. ...... p 3451 N93-28633
p 3297 N93-29071
CHAMMA, W. A. ...... p 3366 N93-30292
CHAMPETIER, ROBERT J. ...... p 3582 N93-29695
CHAN, C. F. ...... p 3575 N93-29302
CHAN, H. C. ...... p 3383 N93-29438
CHAN, HELEN M. ...... p 3339 N93-30883
CHAN, K. K. ...... p 3371 N93-30318
p 3371 N93-30319
p 3374 N93-30334
p 3374 N93-30335
p 3374 N93-30336
CHAN, PAUL ...... p 3614 N93-29239
CHAN, SIU-WAI ...... p 3409 N93-29495
CHANA, K. S. ...... p 3252 N93-29928
CHANCHANI, R. ...... p 3405 N93-28641
CHANDRASEKHAR, P. ...... p 3601 N93-30878
CHANG, CHING-CHUANG ...... p 3516 N93-29563
CHANG, EUGENE JEN-MING ...... p 3416 N93-28612
CHANG, M. J. ...... p 3423 N93-29339
CHANG, R. P. ...... p 3598 N93-30408
p 3599 N93-30548
CHANG, RICHARD K. ...... p 3425 N93-30162
CHANG, S. K. ...... p 3505 N93-28884
CHANG, SIN-CHUNG ...... p 3416 N93-28626
CHANG, STEPHEN ...... p 3306 N93-30863
p 3308 N93-30876
CHAO, T.-H. ...... p 3434 N93-28774
CHAO, TIEN-HSIN ...... p 3578 N93-29086
CHAOUCHE, A. M. ...... p 3256 N93-29948
CHAPMAN, S. P. ...... p 3583 N93-29699
CHAPPELL, P. JEFF ...... p 3467 N93-28873
CHARLOT, L. A. ...... p 3320 N93-28548
CHARLSON, R. J. ...... p 3472 N93-30043
CHARRON, P. ...... p 3371 N93-30321
CHATTERJEE, D. ...... p 3369 N93-30309
CHATTOPADHYAY, ADITI ...... p 3248 N93-29153
CHATTOPADHYAY, S. ...... p 3436 N93-28847
CHE, CHUN-HUA ...... p 3562 N93-29392
CHEIFETZ, MICHAEL G. ...... p 3540 N93-30895
CHEN, L. L. ...... p 3528 N93-29473
CHEN, R. S. ...... p 3332 N93-29342
CHEN, S. R. ...... p 3326 N93-30486
CHEN, S.-K. ...... p 3527 N93-29170
CHEN, VICTOR ...... p 3300 N93-30431
CHEN, WENZONG ...... p 3578 N93-29178
CHEN, X. M. ...... p 3586 N93-29053
CHEN, Y. ...... p 3318 N93-30068
CHEN, Y. C. ...... p 3442 N93-28772
CHENETTE, D. L. ...... p 3641 N93-28773
CHENG, BOLIN ...... p 3596 N93-29796
CHENG, L.-J. ...... p 3434 N93-28774
CHENG, LI-JEN ...... p 3578 N93-29086
CHERNENKO, L. P. ...... p 3600 N93-30771
CHERVYAKOV, A. M. ...... p 3557 N93-30922
CHEW, J. W. ...... p 3256 N93-29949
CHIANG, JUNG-HSIEN ...... p 3514 N93-29545
CHIANG, T. ...... p 3618 N93-30457
CHIDLAW, M. B. ...... p 3331 N93-29201
CHIDUME, C. E. ...... p 3552 N93-30942
CHIKUNOV, V. V. ...... p 3590 N93-30768
CHILDS, ROBERT E. ...... p 3423 N93-29353
CHINNASWAMY, V. ...... p 3435 N93-30477
CHINO, JOHN J. ...... p 3251 N93-28871
CHIPMAN, R. A. ...... p 3582 N93-31035
CHIRICO, R. D. ...... p 3603 N93-28747
p 3603 N93-28964
CHIRIKOV, B. V. ...... p 3606 N93-30802

CHITI, S. p 3398 N93-30751
CHIU, STEPHEN p 3513 N93-29543
CHO, JEONG-HWAN p 3323 N93-29256
CHOI, CHAN K. p 3288 N93-29289
CHOI, HAECHEON p 3242 N93-30645
CHOI, JAI J. p 3542 N93-29192
CHOI, SUHYUN p 3454 N93-30626
CHOPRA, O. K. p 3323 N93-29102
CHOU, JACK C. p 3301 N93-30435
CHOW, L. C. p 3422 N93-29338
p 3423 N93-29339
p 3423 N93-29352
p 3425 N93-30155
p 3426 N93-30403
CHOW, SHUI-NEE p 3548 N93-28753
CHRISSIS, MARY B. p 3610 N93-29970
CHRISSIS, MARY BETH p 3530 N93-29852
CHRISTENSEN, CARISSA BRYCE
p 3627 N93-30709
CHROSTOWSKI, J. p 3357 N93-30231
CHU, JULIO p 3240 N93-29449
CHULYA, ABHISAK p 3449 N93-29073
CHURCH, G. M. p 3536 N93-30934
CHURCH, T. O. p 3503 N93-28867
CIELO, P. p 3359 N93-30246
CIMA, MICHAEL J. p 3339 N93-30885
CINCOTTA, MANUEL, JR. p 3259 N93-29278
CINTRON, NITZA M. p 3494 N93-29502
CIONI, JEAN-PIERRE p 3546 N93-28509
CIONI, R. p 3398 N93-30751
CIOS, KRZYSZTOF J. p 3295 N93-28624
CIPRIANO, ROBERT A. p 3621 N93-30473
CIRRI, GIANFRANCO F. p 3290 N93-29907
CLAPP, JUDITH A. p 3531 N93-29920
p 3531 N93-29921
CLARK, G. L. p 3287 N93-28946
CLARK, J. P. p 3253 N93-29934
CLARK, NOEL A. p 3594 N93-29293
CLARK, RAYMOND p 3260 N93-28869
CLARK, ROBERT p 3628 N93-30717
p 3628 N93-30719
CLARSON, D. R. p 3534 N93-30547
CLAWSON, K. L. p 3242 N93-30387
p 3242 N93-30388
CLEAVER, HARRY E. p 3407 N93-28999
CLELAND, W. E. p 3564 N93-28678
CLEMENT, MAURICE J. p 3633 N93-28905
CLEMOW, MARTIN p 3435 N93-30468
CLINE, D. D. p 3526 N93-29127
p 3425 N93-30184
CLINEDINST, WINSTON C. p 3250 N93-28621
CLONTZ, LESLIE A. p 3288 N93-28950
CLOUSE, PHIL p 3484 N93-30608
CLOUSER, S. p 3253 N93-29933
COAKLEY, P. G. p 3520 N93-29058
COCHRAN, D. R. F. p 3566 N93-29313
COCHRANE, C. G. p 3388 N93-29895
COELHO, A. L. p 3600 N93-30772
COGGI, J. M. p 3638 N93-29361
COGGI, JOHN M. p 3329 N93-28561
COHEN, BERNARD p 3493 N93-29041
COHEN, CLARK EMERSON p 3246 N93-30605
COHEN, M. E. p 3518 N93-29575
COHEN, M. L. p 3592 N93-28582
COHEN, PAUL p 3363 N93-30271
COHEN, R. p 3586 N93-29056
COHEN, R. E. p 3329 N93-28560
COHENOUR, BERNARD C. p 3477 N93-29401
COLANTUONI, S. p 3257 N93-29957
p 3258 N93-29962
COLBORN, B. L. p 3572 N93-29633
p 3573 N93-29636
p 3573 N93-29639
p 3573 N93-29640
p 3573 N93-29641
p 3573 N93-29642
COLE, GARY p 3538 N93-28628
COLELLA, A. p 3257 N93-29957
COLELLA, N. J. p 3520 N93-29058
COLEMAN, M. p 3465 N93-30001
p 3466 N93-30935
COLEMAN, SAM p 3617 N93-30450
COLINEAU, J. p 3435 N93-30469
COLLINS, DONALD J. p 3613 N93-29230
COLLINS, M. WILLIAM p 3622 N93-30478
COLON, JOSE E. p 3591 N93-28471
COLTON, JOEL S. p 3497 N93-30882
COMBS, R. J. p 3430 N93-28659
COMBS, W. E. p 3413 N93-30650
COMELL, DANIEL p 3483 N93-29810
COMLY, J. C. p 3586 N93-29093
CONDO, G. T. p 3568 N93-29764
CONDON, R. J. p 3375 N93-30340
CONNELL, JOHN W. p 3303 N93-30842
CONNELL, KATHLEEN p 3628 N93-30724
CONNOLLY, JAMES J. p 3430 N93-28989
CONROY, PAUL J. p 3342 N93-29762
CONSTANTIN, P. p 3418 N93-28878
CONTE, ALFEO A., JR. p 3333 N93-29458
CONTENT, D. A. p 3582 N93-28788
COOK, DANNY p 3622 N93-30478
COOK, WILLIAM H. p 3454 N93-30545
COOKE, WILLIAM J. p 3638 N93-29377
p 3638 N93-29379
COOLEY, THOMAS W. p 3381 N93-29087
COOMBS, CASSANDRA R. p 3638 N93-29355
p 3283 N93-29374
p 3283 N93-29375
COOPER, B. H. p 3594 N93-29188
COOPER, E. A. p 3594 N93-29314
COOPER, G. W. p 3575 N93-29151
COOPER, J. A., JR. p 3598 N93-30511
COOPER, LEON N. p 3549 N93-29871
COOPER, M. J. p 3434 N93-28771
COOPERMAN, S. p 3618 N93-30457
COPELAND, CARL E. p 3407 N93-29173
COPELAND, CHARLES p 3512 N93-29534
COPENHAVER, A. S. p 3570 N93-30448
COPPA, MARK C. p 3553 N93-28587
CORDS, D. p 3616 N93-30122
CORMACK, G. D. p 3358 N93-30240
CORMIER, R. p 3385 N93-29590
CORNUELLE, CHRISTOPHER STEVEN
p 3652 N93-28605
CORNWELL, L. R. p 3290 N93-30951
CORONAJUAREZ, A. p 3472 N93-30008
CORTELEZZI, LUCA p 3243 N93-30892
CORY, T. S. p 3399 N93-30754
COSENTINO, I. C. p 3339 N93-30774
COSMO, M. L. p 3399 N93-30755
COTLER, C. p 3328 N93-30941
COTTON, P. D. p 3396 N93-30736
COULTER, K. P. p 3574 N93-28970
COULTRIP, ROBERT H. p 3407 N93-29173
COURTRIGHT, E. L. p 3295 N93-28592
COUTELLIER, J. M. p 3435 N93-30469
COUTTS, D. A. p 3431 N93-29325
COWLEY, S. W. p 3317 N93-30761
COX, B. N. p 3304 N93-30850
COX, GEORGE B., JR. p 3289 N93-29847
COYNE, R. A. p 3615 N93-29783
COYNE, ROBERT A. p 3617 N93-30452
CRABB, C. A. p 3247 N93-30350
CRABTREE, G. W. p 3592 N93-28661
CRAGO, RICHARD D. p 3483 N93-30044
CRAIG, DOUGLAS F. p 3290 N93-30948
CRAIG, I. p 3503 N93-28862
CRAWFIS, R. A. p 3524 N93-28550
CRAWFORD, DAVID ALLEN p 3589 N93-30000
CRAWFORD, G. p 3283 N93-29365
CRAWFORD, RICHARD L. p 3399 N93-30753
CRAWLEY, EDWARD F. p 3281 N93-30376
CREE, W. C. p 3367 N93-30298
CREITZER, E. M. p 3420 N93-29141
CREMERS, D. p 3434 N93-28769
CRESPODELARCO, E. p 3256 N93-29948
CREWS, JOHN H., JR. p 3307 N93-30870
CROCHET, M. p 3284 N93-29898
CROOKS, RICHARD M. p 3432 N93-29476
p 3452 N93-29515
CROSLEY, DAVID R. p 3240 N93-29284
CROSS, KENNETH D. p 3237 N93-30684
CROSS, L. E. p 3562 N93-30121
p 3563 N93-30385
CROSS, ROBERT p 3367 N93-30295
CROWDER, KURT VOIGT p 3274 N93-28629
CROZIER, STEWART p 3370 N93-30315
CRUICKSHANK, ALEXANDER p 3317 N93-30816
CRUM, DUANE p 3597 N93-30175
CRUTCHER, R. I. p 3383 N93-29348
p 3394 N93-30631
CRUZ, JUAN R. p 3306 N93-30862
CSIGE, I. p 3573 N93-29637
p 3573 N93-29638
p 3573 N93-29639
CUNNINGHAM, G. S. p 3380 N93-28909
CURRY, DAVID p 3499 N93-30027
CURRY, JOHN D. p 3342 N93-29835
CURTIS, BILL p 3530 N93-29852
CURTIS, CARLTON H. p 3399 N93-30757
CURTIS, HENRY B. p 3265 N93-28717
CUTELLO, VINCENZO p 3513 N93-29540
CYMBALISTA, J. p 3284 N93-29898

D

DABBS, P. p 3608 N93-30821
DABROWSKI, L. p 3551 N93-30809
DADKHAH, M. S. p 3304 N93-30850
DAHIYA, JAI N. p 3293 N93-30970
DAHLKE, WELDON p 3441 N93-30599
DAHLQUIST, GERMUND p 3548 N93-29024
DAHMS, T. E. p 3497 N93-30890
DALEY, R. S. p 3594 N93-29301
DALGLEISH, B. J. p 3331 N93-29248
DALU, G. p 3482 N93-29448
DAM, WAYNE C. p 3371 N93-30316
DAMERJI, TAYEB p 3366 N93-30289
DANA, M. T. p 3473 N93-30183
DANDERWEIDE, T. P. p 3523 N93-28503
DANDO, NEAL R. p 3336 N93-30170
DANE, C. B. p 3440 N93-30394
DANFORD, M. D. p 3322 N93-29043
DANIEL, DAVID W. p 3537 N93-28478
DANIEL, RONALD L. p 3338 N93-30565
DANIEL, TIM p 3247 N93-30339
DARDANO, CLAIRE B. p 3638 N93-29355
DAS, YOGADHISH p 3324 N93-29391
DASARATHY, BELUR V. p 3516 N93-29558
DASILVA, L. B. p 3438 N93-29781
p 3440 N93-30394
DAUBNER, L. p 3320 N93-30277
DAUGHERITY, WALTER C. p 3512 N93-29533
DAUM, C. p 3576 N93-30019
DAVIDSON, KENNETH L. p 3483 N93-29491
DAVIDSON, R. F. p 3454 N93-31013
DAVIDSON, T. N. p 3548 N93-28754
DAVIES, J. p 3320 N93-30277
DAVIES, MELVYN BARRY p 3632 N93-28606
DAVIS, F. C. p 3584 N93-28583
DAVIS, G. D. p 3322 N93-29002
DAVIS, J. BRADLEY p 3271 N93-29136
DAVIS, JOHN G., JR. p 3300 N93-30428
p 3303 N93-30841
DAVIS, JOHN H. p 3634 N93-29042
DAVIS, JOHN M. p 3290 N93-29067
DAVIS, R. p 3472 N93-30015
DAVIS, R. A. p 3471 N93-29676
DAVIS, R. F. p 3593 N93-28874
DAVIS, ROBERT J. p 3408 N93-29427
DAVIS, V. A. p 3279 N93-29305
DAVIS, WILLIAM M. p 3599 N93-30568
DAVYDYCHEV, A. I. p 3607 N93-30916
DAY, C. T. p 3576 N93-30527
DAY, J. L. p 3450 N93-30636
DAYTON, D. C. p 3319 N93-30081
DAYTON, DAVID C. p 3315 N93-30405
DEADWYLER, SAM A. p 3492 N93-30594
DEAN, D. p 3432 N93-29773
DEATON, JERRY W. p 3301 N93-30435
DEBERRY, D. W. p 3312 N93-29665
DECH, STEFAN WERNER p 3458 N93-28924
DEFONTENILLES, H. p 3504 N93-28868
DEGRAFF, DAVID REED p 3380 N93-28689
DEGRANDPRE, M. D. p 3489 N93-30056
DEHAAN, J. F. p 3463 N93-31011
DEHAINAUT, LINDA L. p 3582 N93-29692
DEHEER, D. C. p 3301 N93-30437
DEJONGHE, L. C. p 3405 N93-28581
DEKORVIN, ANDRE p 3516 N93-29561
DEKROM, WILLIBRORDUS HUBERTUS CORNELIS
p 3578 N93-29270
DELABEAUJARDIERE, ODILE p 3476 N93-28842
p 3479 N93-30562
DELABOUDINIERE, J. P. p 3582 N93-29691
DELISI, DONALD P. p 3478 N93-30174
DELISLE, G. Y. p 3366 N93-30290
DELOMBARD, RICHARD p 3285 N93-28554
DELOZANNE, ALEX p 3349 N93-30091
DELUCA, W. H. p 3407 N93-29036
DENG, CONG p 3246 N93-30299
DENHARTOG, D. J. p 3584 N93-28602
DENIBOIRE, P. p 3253 N93-29931
DENMAN, T. F. p 3287 N93-28946
DENOUDEN, A. p 3576 N93-30019
DENSMORE, ARTHUR C. p 3381 N93-28955
DEO, R. B. p 3306 N93-30860
DEO, RAVI B. p 3307 N93-30871
DEPIERO, F. W. p 3544 N93-30529
DERMOTT, WILLIAM p 3271 N93-29215
DERRICKSON, J. H. p 3573 N93-29637
DERSHOWITZ, ADAM L. p 3244 N93-29152
DERVIEUX, ALAIN p 3550 N93-30117
DESHPANDE, N. G. p 3569 N93-29841
DESHPANDE, S. P. p 3283 N93-29362
DESMARAIS, MICHEL C. p 3367 N93-30296
DESMOND, JEMETT L. p 3496 N93-30400
DESPINIC, MILAN p 3360 N93-30252
DEUTSCH-MCLEISH, MARY p 3498 N93-29546
DEVERTEUIL, FANCES p 3367 N93-30296
DEVILLIERS, OLIVIER p 3547 N93-28511
p 3547 N93-28512
DEVLOO, PHILIPPE R. B. p 3538 N93-29487
DEVOTO, J. A. p 3557 N93-30981
DEVRIES, CHRISTOPHER p 3283 N93-29363
DEWALT, STEPHEN A. p 3583 N93-29698
DEWEERTH, S. p 3581 N93-30500

DEWIT, LEO P. H. M. p 3416 N93-28613
DEXTER, H. BENSON p 3297 N93-29107
p 3304 N93-30851
DEYOUNG, R. J. p 3434 N93-28775
DEZFOULY-ARJOMANDY, B. p 3573 N93-29643
DIAZDELARUBIA, T. p 3600 N93-30668
DICICCIO, THOMAS J. p 3554 N93-29292
DICICCO, L. DANIELLE p 3251 N93-28697
DICK, JERRY J. p 3345 N93-30074
DICKIESON, JAN p 3392 N93-30362
DICKINSON, TERRY L. p 3500 N93-30575
DICKSON, RICHARD W. p 3250 N93-28621
DICKSON, T. L. p 3454 N93-30213
DIEDRICH, PAUL p 3235 N93-29756
DIEHL, L. W. p 3367 N93-30298
DIELS, JEAN-CLAUDE p 3480 N93-28518
DIENES, JOHN K. p 3349 N93-30089
DIEP, J. p 3614 N93-29231
DIERBERG, F. p 3462 N93-30637
DIERKING, MATTHEW P. p 3433 N93-30584
DIETRICH, D. D. p 3563 N93-28521
DIETRICH, DANIEL S. p 3379 N93-28654
DIETZ, C. M., JR. p 3594 N93-29214
DIGNON, J. p 3469 N93-28965
DIJKSTRA, E. J. p 3552 N93-31014
DILLON, THOMAS J. p 3507 N93-29607
DING, HEPING p 3358 N93-30242
DINHAM, G. p 3371 N93-30319
DINICOLA, ALBERT J. p 3301 N93-30435
DINOLA, L. p 3257 N93-29957
DION, M. p 3367 N93-30294
DIPLAS, P. p 3594 N93-29214
DIPPO, P. p 3465 N93-30207
DIPPOLITO, D. A. p 3589 N93-30189
DISANTI, M. p 3285 N93-28779
DIVINE, NEIL p 3638 N93-29376
DIXON, ALAN B. C. p 3288 N93-28950
DLOTT, DANA D. p 3342 N93-29296
DOBER, DAVID M. p 3424 N93-29968
DOBIE, D. W. p 3430 N93-28520
DOBREV, V. K. p 3551 N93-30809
DOCKERY, JOHN p 3513 N93-29544
DOCTOR, R. D. p 3310 N93-29052
DODD, J. p 3269 N93-29908
DODGE, F. T. p 3264 N93-28710
DOE, P. J. p 3566 N93-29313
DOHME, JACK p 3237 N93-30687
DOLAN, D. p 3624 N93-29668
DOLEZALEK, HANS p 3489 N93-30612
DOLGOV, A. D. p 3479 N93-30785
DOLINAR, S. p 3385 N93-29596
DOLMAN, V. L. p 3463 N93-31011
DOMBROWSKI, E. G. p 3624 N93-28814
DOMEY, J. p 3366 N93-30286
DOMINGO, C. p 3654 N93-29646
DOMNING, E. E. p 3405 N93-28597
DOMOKOS, G. p 3603 N93-28961
DONATTO, U. A. p 3316 N93-30653
DONGARE, A. S. p 3441 N93-30801
DONNELLY, M. K. p 3550 N93-30041
DOOLEY, W. T. p 3466 N93-30814
DORIGNAC, E. p 3253 N93-29931
DORMIEUX, M. p 3417 N93-28745
DOROSHKIN, A. A. p 3480 N93-30991
DOSS, HANI p 3555 N93-29979
DOST, ERNEST F. p 3305 N93-30857
DOTY, BRIAN E. p 3613 N93-29225
DOW, MARVIN B. p 3304 N93-30852
DOWDY, M. p 3434 N93-28774
DOWELL, EARL H. p 3604 N93-29384
DOYLE, RICHARD J. p 3613 N93-29230
DOYLE, ROBERT J., JR. p 3318 N93-30066
DRAGANESCU, V. p 3438 N93-29797
DRAKE, D. p 3650 N93-28824
DRAKE, D. M. p 3647 N93-28807
DRAKE, J. F. p 3585 N93-28749
DRAPATZ, S. p 3631 N93-30641
DRAPEAU, ANN L. p 3620 N93-30464
DRAPEAU, MICHAEL J. J. p 3365 N93-30282
DREGER, DOUGLAS SCOTT p 3478 N93-30005
DREW, MALCOLM C. p 3491 N93-29216
DROLSHAGEN, GERHARD p 3638 N93-29358
DRYER, FREDERICK L. p 3347 N93-30084
p 3319 N93-30090
DRYLEY, DONALD W. p 3379 N93-28476
DU, CHAU M. p 3334 N93-29795
DUBBELDAM, R. p 3576 N93-30019
DUBNICKA, S. p 3571 N93-30792
DUBNICKOVA, A. Z. p 3571 N93-30792
DUBOIS, PASCALE p 3614 N93-29234
DUBON, O. D., JR. p 3594 N93-29150
DUCHOENY, JOEL p 3371 N93-30317
DUDENHOEFER, J. p 3649 N93-28819
DUFFEY, T. A. p 3446 N93-30211
DUGGAL, B. P. p 3557 N93-30985
DULA, ALEX p 3629 N93-30726
DULLA, BRIAN p 3235 N93-29756
DUMITRAS, D. p 3438 N93-29797
DUNBAR, DENNIS p 3628 N93-30716
DUNCAN, L. M. p 3478 N93-30487
DUNHAM, SCOTT D. p 3269 N93-30135
DUNN, M. G. p 3255 N93-29945
DUNN, STUART S. p 3526 N93-29028
DUNN, W. E. p 3482 N93-29399
DUPOIRIEUX, F. p 3257 N93-29956
DUPONT, T. F. p 3418 N93-28878
DURIN, CHRISTIAN p 3283 N93-29369
p 3448 N93-29688
DURSCH, HARRY p 3318 N93-29683
DUTOYA, D. p 3256 N93-29947
DUVAL, RONALD p 3237 N93-30688
DVORACK, M. A. p 3412 N93-30127
DYER, C. J. p 3399 N93-30755
DYER, GORDON p 3626 N93-30701
p 3628 N93-30719

E

EARMAN, ALLEN p 3622 N93-30474
ECCLES, DAVID A. p 3247 N93-30324
ECHEKKI, TAREK p 3316 N93-30646
ECHEVERRIA, FERNANDO p 3603 N93-28690
ECKART, A. p 3637 N93-30639
ECKERLE, W. A. p 3254 N93-29935
ECKERT, H. p 3598 N93-30407
ECONOMOU, T. p 3434 N93-28776
EDBERG, D. p 3263 N93-28707
EDDINGTON, DONALD K. p 3494 N93-29421
EDELMAN, JOEL p 3318 N93-29683
EDELMAN, RAYMOND B. p 3352 N93-31031
EDER, D. C. p 3438 N93-29309
p 3438 N93-29781
p 3440 N93-30394
EDGAR, G. K. p 3503 N93-28862
EDIGHOFFER, J. A. p 3436 N93-28847
EDWARDS, B. p 3650 N93-28824
EDWARDS, B. C. p 3647 N93-28807
EDWARDS, C. D., JR. p 3642 N93-28777
EDWARDS, C. F. p 3416 N93-28595
EDWARDS, JACK RAY p 3421 N93-29177
EDWARDS, P. A. p 3470 N93-29135
EFFLAND, JOHN E. p 3382 N93-29217
EFIMOV, G. V. p 3605 N93-30782
EFTEKHARI, ABE p 3452 N93-29613
EGELAND, A. p 3477 N93-29831
EGGLESTON, ROBERT G. p 3503 N93-28865
EHHALT, D. H. p 3475 N93-28475
EHJDELMAN, Y. I. p 3571 N93-30800
EHRDEHNEHDEHLGEHR, T. p 3623 N93-30994
EHRHARDT, HARDY M. p 3459 N93-28930
EHRHART, ISABELLE p 3325 N93-30105
EICHENLAUB, CARL T. p 3533 N93-30380
EICKELBERG, W. K. p 3437 N93-29207
EIGLER, D. M. p 3567 N93-29332
EISENHART, F. J. p 3498 N93-28901
EKROOT, LAURA p 3385 N93-29596
EL-SAYED, M. A. p 3338 N93-30628
EL-SHARAWY, EL-BUDAWY p 3400 N93-31036
ELBAN, WAYNE L. p 3348 N93-30086
p 3319 N93-30092
p 3319 N93-30093
p 3350 N93-30094
ELDER, B. L. p 3531 N93-29874
ELENA, L. p 3256 N93-29948
ELERT, MARK L. p 3318 N93-30071
ELGAZZAR, SHADIA p 3372 N93-30327
ELIASSON, PETER p 3418 N93-28994
ELIEZER, ZWY p 3296 N93-29001
ELLINGSON, ROBERT p 3324 N93-29391
ELLINGSON, W. A. p 3449 N93-28943
ELLIOTT, C. J. p 3269 N93-29894
ELLSWORTH, JON p 3499 N93-30425
ELMAHGARY, YEHIA p 3465 N93-30111
ELSON, LEE S. p 3613 N93-29226
ELY, J. F. p 3313 N93-29768
EMERSON, S. p 3487 N93-29327
EMERY, WILLIAM p 3614 N93-29233
ENDSLEY, MICA R. p 3503 N93-28863
ENGE, W. p 3573 N93-29644
ENGEL, JAMES R. p 3430 N93-28989
ENGELMANN, REINHART p 3601 N93-30811
ENGELSTAD, R. L. p 3439 N93-30186
ENGLISH, JEFFREY T. p 3319 N93-30101
ENLOW, EDWARD W. p 3412 N93-30152
ENOEDA, MIKIO p 3320 N93-28529
p 3584 N93-28535
ENOMOTO, A. p 3583 N93-28533
EOM, C. B. p 3596 N93-29868
EPP, L. W. p 3385 N93-29591
EPPLER, D. p 3650 N93-28822
EPSTEIN, A. H. p 3420 N93-29141
p 3253 N93-29932
ERANTI, ESA p 3353 N93-28632
ERCK, R. A. p 3330 N93-28666
ERCOLINE, WILLIAM R. p 3508 N93-30167
ERDEMIR, A. p 3330 N93-28666
ERICKSEN, BRYCE J. p 3501 N93-28479
ERICKSON, KENNETH L. p 3344 N93-30069
ERICSSON, APRILLE J. p 3281 N93-30142
ERIKSEN, FRED p 3342 N93-29835
ERLICHMAN, JOZEF p 3283 N93-29364
ERWIN, L. L. p 3649 N93-28815
ESENER, SADIK C. p 3520 N93-29482
ESFANDIARI, SHAHRAM p 3366 N93-30291
ESKER, BARBARA S. p 3252 N93-29065
ESPOSITO, G. p 3608 N93-31003
ESTEROWITZ, LEON p 3441 N93-30587
ETEMAD, S. p 3596 N93-29868
ETO, MOTOKUNI p 3299 N93-30004
ETTER, BRAD D. p 3491 N93-29216
ETTER, M. C. p 3597 N93-30146
EUGSTER, O. p 3639 N93-29380
EVANCO, W. M. p 3532 N93-30022
p 3534 N93-30546
p 3534 N93-30547
EVANS, L. p 3650 N93-28824
EVERETT, PATRICK N. p 3578 N93-29139
EVERITT, C. W. F. p 3460 N93-29179
EWBANK, JOHN D. p 3319 N93-30101
EYLER, J. R. p 3314 N93-30166

F

FADLEY, C. S. p 3313 N93-29766
FAGERQUIST, CLIFTON K. p 3338 N93-30628
FAHMY, A. A. p 3293 N93-30968
FAHMY, MOUSTAFA M. p 3358 N93-30242
FAIRMAN, F. W. p 3354 N93-30216
FALCO, J. J. p 3327 N93-30812
FALCONE, R. W. p 3438 N93-29309
FALKENBERG, E. D. p 3611 N93-28481
FALKOWSKI, K. M. p 3447 N93-30820
FAMINI, GEORGE R. p 3315 N93-30365
FAN, Z. H. p 3636 N93-30528
FANG, HO T. p 3298 N93-29451
FARACH, M. p 3491 N93-30483
FARAH, JEFFREY J. p 3543 N93-30039
FARHAT, CHARBEL p 3274 N93-29110
FARLEY, GARY L. p 3354 N93-29611
FASANELLA, EDWIN L. p 3308 N93-30875
FATEMI, NAVID S. p 3321 N93-28618
FAUBERT, D. p 3358 N93-30241
p 3374 N93-30335
FAUST, C. M. p 3319 N93-30081
FAUST, WALTER L. p 3319 N93-30101
FAWCETT, W. R. p 3566 N93-29143
FEDOTOV, S. N. p 3281 N93-31024
FEDRO, MARK J. p 3305 N93-30855
FEELEY, O. C. p 3341 N93-28752
FEIBELMAN, P. J. p 3594 N93-29188
FELDMAN, BARRY J. p 3440 N93-30427
FELDMAN, MICHAEL R. p 3431 N93-29297
FELDMAN, W. C. p 3647 N93-28807
FELDSTEIN, A. A. p 3285 N93-28778
FELIPPA, CARLOS p 3278 N93-29122
FELLMAN, LYNNE p 3247 N93-30351
FELSTEAD, E. B. p 3374 N93-30334
FENG, LIQIANG p 3545 N93-30903
FENG, SHECHAO p 3597 N93-30141
FENIMORE, ED p 3653 N93-29164
FENNER, DAVID B. p 3414 N93-30896
FENSKE, G. R. p 3330 N93-28666
p 3442 N93-28903
FERBER, M. K. p 3320 N93-28564
FERGUSON, DALE C. p 3265 N93-28716
FERGUSON, J. A. p 3395 N93-30729
FERIA, Y. p 3386 N93-29599
FERREIRA, J. L. p 3591 N93-31007
FERREIRA, P. L. p 3607 N93-30943
FERRETTA, T. E. p 3430 N93-28520
FERRICK, MICHAEL G. p 3379 N93-28588
FETHEROLF, B. L. p 3346 N93-30080
FETT, ROBERT W. p 3481 N93-28876
FEZOUI, LOULA p 3546 N93-28509
p 3538 N93-29487
p 3550 N93-30117
FIELD, E. C., JR. p 3397 N93-30742
FIERSTEIN, A. R. p 3287 N93-28946
FIFER, ROBERT A. p 3309 N93-28514
FIGAROL, D. p 3247 N93-30325
FIJANY, AMIR p 3521 N93-29608
FIKSEL, G. p 3584 N93-28602
FILEV, DIMITAR P. p 3512 N93-29532
FILGES, DETLEF p 3574 N93-29062
FINCKE, J. R. p 3589 N93-30181
FINCKENOR, M. M. p 3331 N93-29193
FINE, MORRIS E. p 3298 N93-29130

FINK, U. p 3285 N93-28779
FINLEY, TOM D. p 3431 N93-29209
FINN, J. M. p 3585 N93-28749
FINN, SCOTT R. p 3304 N93-30849
FINNIE, J. p 3473 N93-30187
FIRESTONE, ELAINE R. p 3486 N93-28497
p 3486 N93-28500
FISCHER, G. p 3502 N93-28857
FISCHER, SUSAN H. p 3350 N93-30095
FISHER, R. J. p 3484 N93-30651
FISHER, SHALOM p 3263 N93-28706
FISHMAN, G. J. p 3624 N93-29631
p 3572 N93-29632
FISK, CHARLES J. p 3477 N93-29401
FITTINGHOFF, D. N. p 3564 N93-28762
FLACHS, GERALD M. p 3528 N93-29294
FLAMMIA, MADELYN p 3612 N93-28948
FLANAGAN, DAVID T. p 3353 N93-28698
FLANNAGAN, M. J. p 3496 N93-30659
FLECK, VINCENT J. p 3443 N93-29175
FLEETWOOD, C. M. p 3582 N93-28788
FLEETWOOD, D. M. p 3598 N93-30511
p 3413 N93-30516
p 3413 N93-30650
p 3570 N93-30669
FLEISCHMAN, GEORGE p 3265 N93-28722
FLEISCHMAN, ROBERT M. p 3518 N93-29571
FLEMING, J. W. p 3518 N93-29574
FLEMING, K. J. p 3433 N93-30510
FLEMING, R. H. p 3283 N93-29364
FLIKOP, ZINY p 3516 N93-29559
FLOREANINI, R. p 3551 N93-30809
FLOYD, C. L. p 3472 N93-30009
FLOYD, S. p 3650 N93-28824
FLYNN, CHRISTOPHER F. p 3499 N93-30425
FOERESTER, C. p 3326 N93-30490
FOERSTER, BERNHARD p 3457 N93-28921
FOLEY, H. C. p 3309 N93-28750
FOLKMAN, STEVEN L. p 3263 N93-28703
FOLKNER, W. M. p 3642 N93-28777
p 3270 N93-29589
FOLTZ, M. FRANCES p 3319 N93-30082
FONDA, M. L. p 3645 N93-28792
FONDAW, GRANT W. p 3423 N93-29419
FONG, C. VANESSA p 3247 N93-30352
FONTANELLA, J. J. p 3332 N93-29342
p 3334 N93-29825
p 3410 N93-29826
FOOTE, J. p 3318 N93-29367
FORBES, D. A. p 3631 N93-30641
FORMAN, P. R. p 3579 N93-29350
FOROUDI, NAVID p 3359 N93-30245
FOROUHAR, SIAMAK p 3579 N93-29848
FORREST, L. p 3271 N93-28487
FORREST, STEPHEN R. p 3581 N93-30609
FORTIER, PAUL p 3363 N93-30272
FOSDICK, ROGER L. p 3311 N93-29291
FOSTER, RUSSELL G. p 3497 N93-30908
FOTTNER, L. p 3258 N93-29958
FOUCAULT, E. p 3253 N93-29931
FOWLER, EDDIE R. p 3363 N93-30273
FOX, ROBERT D. p 3245 N93-29285
FOX, ROBERT L. p 3407 N93-29173
FRANCIS, MICHAEL S. p 3260 N93-28851
FRANCO, E. D. p 3645 N93-28792
FRANK, A. L. p 3573 N93-29636
p 3573 N93-29637
FRANK, J. S. p 3566 N93-29313
FRANKS, ARCHIE M. p 3616 N93-30193
FRANSON, S. E. p 3474 N93-30823
FRASER-SMITH, A. C. p 3397 N93-30744
FREDERICK, M. S. p 3322 N93-29061
FREED, ALAN D. p 3297 N93-29074
p 3451 N93-29196
FREELAND, R. E. p 3263 N93-28701
FREEMAN, ANTHONY p 3614 N93-29234
FREEMAN, W. TOM p 3302 N93-30441
FRENZEN, C. L. p 3439 N93-29883
FRIEDLANDER, A. p 3650 N93-28822
FRIEDMAN, AVNER p 3473 N93-30360
FRIEND, D. G. p 3313 N93-29768
FRIESEN, D. T. p 3331 N93-29201
FRIGO, L. p 3573 N93-29639
FRIGO, L. A. p 3573 N93-29637
FRIGUI, HICHEM p 3511 N93-29524
FRIM, J. p 3506 N93-29471
FRISCHHERZ, M. C. p 3592 N93-28661
FRISONI, MICHAEL p 3342 N93-29835
FRITTS, DAVID C. p 3478 N93-30367
FRITZ, BERNARD S. p 3592 N93-28590
FRY, EDWARD S. p 3580 N93-29887
FRY, HERBERT A. p 3319 N93-30076
FU, JIANGUO p 3357 N93-30233
FUCHS, W. p 3502 N93-28857
FUCHS, W. K. p 3527 N93-29170
FUJIEDA, HIROBUMI p 3590 N93-30649
FUJISAWA, NOBORU p 3589 N93-30003
FUKUDA, KOUSAKU p 3576 N93-30006
FULCO, CHARLES S. p 3497 N93-30894
FUNG, K. H. p 3309 N93-28880
FUNG, KO p 3613 N93-29228
FUNK, JOAN G. p 3290 N93-29067
FURROW, KEITH W. p 3297 N93-29107
FURUSHO, M. p 3406 N93-28746
FUSS, I. G. p 3392 N93-30145
FUTCH, A. H. p 3588 N93-29334

G

GABERT, G. p 3412 N93-30118
GABRIEL, P. M. p 3484 N93-30055
GADER, PAUL p 3514 N93-29545
GAFF, DOUG p 3404 N93-28539
GAGNON, LUC p 3355 N93-30219
GAIDIS, M. p 3430 N93-28664
GAIER, JAMES R. p 3298 N93-29609
p 3299 N93-29614
GAITAN, V. p 3624 N93-28811
GALEAO, A. P. p 3607 N93-30943
GALETTI, D. p 3607 N93-30945
GALINDO, SAMUAL, JR. p 3496 N93-30400
GALLER, D. E. p 3287 N93-28946
GALVIN, J. E. p 3598 N93-30393
GAMMEL, J. T. p 3561 N93-29711
p 3337 N93-30381
p 3551 N93-30503
p 3600 N93-30569
GAN, X. p 3256 N93-29950
GANAPOL, B. D. p 3565 N93-28833
GANDER, R. E. p 3356 N93-30225
GANESAN, RAMNATH p 3295 N93-28843
GANTNER, T. E. p 3500 N93-29564
GAO, KEQIN p 3356 N93-30226
GARCIA, E. J. p 3443 N93-29185
GARCIA, SHARON K. p 3496 N93-30400
GARCIA, SUZANNE M. p 3610 N93-29970
GARDNER, D. R. p 3526 N93-29127
GARDNER, JAMES E. p 3290 N93-30948
GARDNER, KEITH L. p 3438 N93-29287
GARDNER, M. E. p 3630 N93-29460
GARLAN, DAVID p 3531 N93-29866
GARNEK, MIKE p 3264 N93-28708
GARNESSON, PHILIPPE p 3547 N93-28513
GARNIER, FRANCOIS p 3314 N93-30203
GARODZ, L. J. p 3242 N93-30387
p 3242 N93-30388
GARRIDO, L. p 3624 N93-28811
GARRISON, S. M. p 3596 N93-29868
GARRISON, THOMAS P. p 3284 N93-29905
GARVEY, JAMES F. p 3312 N93-29429
p 3596 N93-29430
GARVIN, J. B. p 3442 N93-28780
GARZON, F. H. p 3464 N93-29147
GATES, RICHARD B. p 3289 N93-30402
GATHMAN, STUART G. p 3487 N93-29659
GAUTHIER, BENOIT G. p 3259 N93-29278
GAUTHIER, P. p 3361 N93-30260
GAUTHIER, S. R. p 3371 N93-30319
GAVEL, D. T. p 3630 N93-29785
GAYDA, CHRISTIAN p 3492 N93-28469
GAYLORD, THOMAS K. p 3435 N93-29697
GE, TINGSUI p 3596 N93-29796
GEBALLE, T. H. p 3596 N93-29868
GEBALLE, THEODORE H. p 3561 N93-30519
GEBHARDT, JOERG p 3514 N93-29549
GEDDES, J. N. p 3367 N93-30298
GEE, T. F. p 3544 N93-30529
GEERINCK, J. p 3576 N93-30019
GEHRELS, TOM p 3631 N93-30629
GEIER, BODO p 3296 N93-29007
GEIER, G. J. p 3245 N93-29468
GEIGER, BERNHARD p 3547 N93-28616
GEISS, J. p 3639 N93-29380
GELDREZ, CECILIA p 3368 N93-30302
GELFAND, ALAN E. p 3549 N93-29413
GELINAS, F. p 3357 N93-30232
GENCO, LOUIS V. p 3268 N93-28740
p 3268 N93-28741
GENZEL, R. p 3637 N93-30639
p 3441 N93-30640
p 3631 N93-30641
p 3632 N93-30643
GEORGE, E. P. p 3321 N93-28679
GEORGES, T. M. p 3394 N93-30662
GERBER, MARGARET K. p 3331 N93-29083
GERDT, V. P. p 3535 N93-30787
GERNAND, JOSEPH p 3627 N93-30712
GERVASIO, D. p 3313 N93-29828
p 3317 N93-30664
GETINO, C. p 3538 N93-28894
GETTMAN, CHANG-CHING LO p 3443 N93-29080
GETZ, P. p 3463 N93-30839
GETZOFF, ELIZABETH D. p 3571 N93-30901
GEVARTER, WILLIAM B. p 3542 N93-29386
GEVINS, ALAN p 3495 N93-30160
GEZARI, DANIEL Y. p 3629 N93-29156
GHAN, L. S. p 3532 N93-30034
GHANBARI, C. M. p 3465 N93-30391
GHEZ, ANDREA p 3634 N93-28945
GHIA, K. N. p 3425 N93-30369
GHIA, U. p 3425 N93-30369
GHOSH, SUBIR p 3554 N93-29411
GIANGREGORIO, ROBERTO P. p 3580 N93-29880
GIBBONS, F. L. p 3643 N93-28782
GIBBONS, STEPHENS p 3261 N93-29972
GIBSON, G. A. p 3522 N93-30480
GIBSON, GARTH A. p 3537 N93-30463
GIBSON, JOHN C. p 3445 N93-29618
GIBSON, W. L. p 3572 N93-30944
GIER, T. E. p 3598 N93-30407
GIER, THURMAN E. p 3592 N93-28584
p 3594 N93-29138
p 3599 N93-30518
GILES, M. B. p 3420 N93-29141
GILES, MICHAEL p 3528 N93-29294
GILL, T. P. S. p 3328 N93-31021
GILLESPIE, JACK W., JR. p 3294 N93-28559
GILLIATT, ROGER W. p 3492 N93-30818
GILLIE, K. R. p 3407 N93-29036
GILLIOM, LAURA R. p 3626 N93-30702
GILLIS, J. R. p 3283 N93-29623
GILMAN, J. A. p 3609 N93-29322
p 3609 N93-29323
GILMAN, JOHN J. p 3319 N93-30087
GILMER, G. H. p 3594 N93-29188
GINGER, J. D. p 3451 N93-29106
GINSBERG, MICHAEL p 3533 N93-30125
GIRAUD, M. p 3645 N93-28793
GIRAUDON, GERARD p 3547 N93-28513
GISH, L. A. p 3334 N93-29829
GISLER, G. R. p 3634 N93-29246
GLAESER, A. M. p 3331 N93-29248
GLANCY, B. C. p 3319 N93-30092
p 3319 N93-30093
p 3350 N93-30094
GLANDT, E. D. p 3428 N93-30759
GLASER, CHRISTINA p 3235 N93-29756
GLASS, J. T. p 3593 N93-28874
GLASSERMAN, PAUL p 3555 N93-29878
GLEASON, GERALD A. p 3267 N93-28739
p 3268 N93-28742
GLENAR, D. A. p 3285 N93-28781
GLOSLI, J. N. p 3568 N93-29489
GLOSLI, JAMES N. p 3567 N93-29336
p 3568 N93-29619
GLOWNIA, J. H. p 3439 N93-29918
GLUMM, MONICA M. p 3505 N93-28941
GLYNN, JOHN E. p 3550 N93-29872
GLYNN, PETER W. p 3554 N93-29292
p 3550 N93-29872
p 3555 N93-29878
GOBIN, VINCENT p 3392 N93-30018
GODBEY, SUSAN E. p 3438 N93-29800
GODDARD, R. E. p 3385 N93-29592
GOELLER, R. M. p 3436 N93-28887
GOLD, S. H. p 3409 N93-29478
GOLDBERG, L. A. p 3530 N93-29808
GOLDEN, GERALD p 3236 N93-30680
GOLDEN, R. p 3624 N93-29100
GOLDFLAM, RUDOLF p 3381 N93-29011
GOLDSACK, STEPHEN J. p 3526 N93-29026
GOLDSBY, J. C. p 3340 N93-30938
GOLDSTEIN, BART p 3381 N93-29011
GOLDSTEIN, JAY S. p 3541 N93-28494
GOLDSTEIN, MARVIN E. p 3418 N93-28947
GOLDSTEIN, R. J. p 3253 N93-29929
GOLDSTONE, J. A. p 3598 N93-30517
GOLIGHTLY, MICHAEL J. p 3266 N93-28730
GONNASON, W. p 3375 N93-30340
GONZALEZ, H. L. p 3382 N93-29245
GONZALEZ, R. R. p 3505 N93-28884
GOODENOUGH, DAVID G. p 3613 N93-29228
GOODING, J. L. p 3643 N93-28782
GOODMAN, B. J. p 3490 N93-28890
GOODMAN, JOSEPH W. p 3596 N93-29859
GOODRICH, CHARLES C. p 3614 N93-29235
GOODSON, T., III p 3333 N93-29441
GOODWIN, MICHAEL J. p 3335 N93-29881
p 3335 N93-29886
GOOLEY, TIMOTHY D. p 3270 N93-28468
GORDA, B. C. p 3539 N93-29782
GORDNIER, RAYMOND E. p 3260 N93-30498
GORDON, L. W. p 3279 N93-29305
GORDON, LAWRENCE J. p 3488 N93-29977
GORDON, LEONARD B. p 3251 N93-28984
GORDON, S. P. p 3438 N93-29309
GORYACHEV, S. B. p 3480 N93-30991

GORZALCZANY, MARIAN B. p 3498 N93-29546
GOSWAMI, S. p 3572 N93-30931
GOTO, D. M. p 3320 N93-28491
GOTTESFELD, S. p 3464 N93-29147
GOTTUK, DANIEL T. p 3244 N93-29211
GOULD, RICHARD D. p 3242 N93-30373
GOURLEY, C. S. p 3444 N93-29316
GOVINDJEE, S. p 3450 N93-28596
GRABOW, M. H. p 3594 N93-29188
GRADIE, J. p 3434 N93-28783
GRAEDEL, T. E. p 3469 N93-28965
GRAESSER, DOUGLAS p 3305 N93-30858
GRAF, U. U. p 3637 N93-30639
p 3441 N93-30640
GRAHAM, A. L. p 3296 N93-28904
GRAHAM, H. C. p 3295 N93-28592
GRAHAM, W. B. p 3370 N93-30310
GRANATSTEIN, V. L. p 3411 N93-29922
GRANDE, DODD H. p 3303 N93-30845
GRANT, CARROLL G. p 3306 N93-30864
GRANT, K. E. p 3474 N93-30504
GRANTHAM, D. D. p 3484 N93-30535
GRANTHAM, WILLIAM p 3264 N93-28708
GRANTNER, JANOS p 3515 N93-29551
GRAY, I. D. p 3501 N93-28852
GRAY, M. G. p 3585 N93-28910
GRAY, P. p 3331 N93-29193
GRAY, S. K. p 3565 N93-28892
GREBOGI, C. p 3557 N93-30048
GREDEL, JOERG p 3457 N93-28916
GREEN, DAVID p 3237 N93-30685
GREEN, J. L. p 3395 N93-30731
GREEN, JAMES M. p 3270 N93-28696
GREEN, JOHN p 3383 N93-29275
GREEN, N. D. C. p 3503 N93-28861
GREEN, S. F. p 3283 N93-29362
GREENBERG, D. S. p 3538 N93-29186
GREENBERG, WILLIAM L. p 3389 N93-29900
GREENE, J. M. p 3446 N93-30211
GREENSPAN, M. p 3357 N93-30232
GREGG, J. S. p 3322 N93-29061
GREGG, M. p 3472 N93-30015
GREGG, WATSON W. p 3486 N93-28497
GREGORY, J. A. p 3434 N93-28771
GREGORY, J. C. p 3573 N93-29643
GREGORY, JOHN C. p 3268 N93-28743
p 3283 N93-29622
GREIDANUS, H. p 3463 N93-31010
GREINER, J. p 3631 N93-30642
GREINER, N. ROY p 3319 N93-30076
GREINER, W. p 3565 N93-28831
GRENANDER, ULF p 3549 N93-29854
GRETH, RICKY L. p 3507 N93-29607
GRIFFIN, C. F. p 3300 N93-30433
GRIFFIN, O. HAYDEN, JR. p 3454 N93-30374
GRIFFIS, D. P. p 3638 N93-29378
GRIFFITH, B. T. p 3353 N93-28570
GRIGSBY, DORIS K. p 3492 N93-29702
GRILO, FRANCISCO C. V. p 3398 N93-30750
GRIMM, JOSE p 3524 N93-28755
GRIMSHAW, R. H. p 3489 N93-30143
GRISHABER, R. p 3330 N93-28838
GRONBECH-JENSEN, N. p 3593 N93-29094
GRONLAND, TOR ARNE p 3418 N93-28993
GROPP, W. p 3550 N93-30140
GROSENBACH, MILTON J. p 3499 N93-30425
GROSS, ANTHONY R. p 3626 N93-30703
GROSSBERG, STEPHEN p 3543 N93-29791
GROSSI, M. D. p 3399 N93-30755
GROSSMAN, A. S. p 3469 N93-28972
p 3474 N93-30504
GROSSMAN, WILLIAM M. p 3436 N93-28623
GROVE, C. M. p 3501 N93-28757
GRUBBS, ROBERT H. p 3340 N93-30900
GRUENER, J. E. p 3643 N93-28782
GU, S. H. p 3329 N93-28489
p 3333 N93-29442
GUAN, H. W. p 3329 N93-28489
p 3333 N93-29442
GUELL, D. C. p 3296 N93-28904
GUENETTE, G. R. p 3253 N93-29932
GUENTHER, R. E. p 3538 N93-28894
GUGGENHEIMER, S. C. p 3441 N93-30910
GUIBORD, ARTHUR F. p 3360 N93-30250
GUIDICE, DONALD A. p 3265 N93-28717
GUILLEN, P. p 3417 N93-28744
GUILLEN, PH. p 3417 N93-28745
GUINAN, M. W. p 3600 N93-30668
GULLIVER, T. AARON p 3365 N93-30283
GUM, J. S. p 3582 N93-28788
GUNSHOR, R. L. p 3597 N93-30164
GUNTHER, CHRISTIAN p 3305 N93-30855
GUNZBURGER, MAX D. p 3421 N93-29208
GUO, H. p 3411 N93-29922
GUPTA, KAMAL KANT p 3363 N93-30270
GUPTA, L. p 3618 N93-30457
GUPTA, S. p 3535 N93-30647
GUPTA, YOGENDRA M. p 3318 N93-30073
GUREVICH, A. V. p 3632 N93-28473
GURSKY, H. p 3624 N93-28814
p 3286 N93-29707
GUSTAVSON, PAUL K. p 3411 N93-30021
p 3352 N93-30424
GUTOWSKI, W. J., JR. p 3476 N93-28677
GUTU, I. p 3438 N93-29797
GUYMON, GARY L. p 3262 N93-30103
GUZDAR, P. N. p 3585 N93-28749
GWINN, DAVID A. p 3553 N93-28575
GYETVAY, S. R. p 3638 N93-29361

H

HAAS, CHARLES N. p 3496 N93-30422
HABEDANK, OTTO D. p 3286 N93-28474
HABETS, G. p 3463 N93-31009
HABETS, G. M. H. J. p 3460 N93-29307
p 3460 N93-29321
HACKEL, L. A. p 3440 N93-30394
HAFIZI, B. p 3409 N93-29478
HAGEDORN, NORMAN H. p 3464 N93-28974
HAGELSTEIN, P. L. p 3565 N93-28959
HAGGARD, D. C. p 3589 N93-30181
HAH, C. p 3259 N93-29963
HAHN, O. J. p 3422 N93-29338
HAKALA, D. B. p 3430 N93-28520
HALAMA, H. p 3326 N93-30490
HALBACH, CARL R. p 3264 N93-28715
HALBLEIB, J. A. p 3281 N93-30509
HALDEMAN, C. W., JR. p 3255 N93-29945
HALE, ROBERT A. p 3251 N93-28871
HALES, J. M. p 3472 N93-30043
HALKA, M. p 3569 N93-30130
HALL, C. D. p 3286 N93-29910
HALL, H. K., JR. p 3332 N93-29290
HALL, J. R. p 3502 N93-28856
HALL, K. R. p 3604 N93-29428
p 3604 N93-29794
HALL, P. M. p 3405 N93-28641
HALL, R. B. p 3466 N93-30891
HALLAM, KENNETH J. p 3617 N93-30451
HALLETT, W. A. p 3563 N93-28521
HALLEY, J. W. p 3602 N93-31027
HALLOY, C. p 3538 N93-28894
HALPERN, M. E. p 3260 N93-30604
HAMEIRI, E. p 3652 N93-28756
HAMEL, H. p 3285 N93-28779
HAMILTON, DAVID B. p 3508 N93-30590
HAMM, M. K. p 3296 N93-28886
p 3298 N93-29425
HAMMAR, GIFFORD A. p 3529 N93-29497
HAMMOND, DANA P. p 3520 N93-29070
HAMPSON, BRIAN p 3237 N93-30681
HAN, ARRIS p 3248 N93-29153
HAN, J. C. p 3253 N93-29933
HANADA, MASAYA p 3589 N93-30190
p 3590 N93-30606
HANDLER, T. p 3568 N93-29764
HANDLEY, THOMAS p 3627 N93-30707
HANDLEY, THOMAS H., JR. p 3613 N93-29230
HANEY, L. N. p 3505 N93-28942
HANISCH, ROBERT J. p 3613 N93-29227
HANKS, R. p 3432 N93-29773
HANNA, C. p 3435 N93-30469
HANNAH, J. H. p 3394 N93-30631
HANSEN, ELAINE R. p 3613 N93-29224
HANSEN, P. M. p 3400 N93-30995
HANSMAN, R. JOHN, JR. p 3244 N93-29152
HARADA, HIROO p 3524 N93-28537
HARDIE, R. W. p 3472 N93-30008
HARDING, D. J. p 3442 N93-28780
HARDWICK, JONATHAN C. p 3530 N93-29823
HARDY, KENNETH A. p 3266 N93-28730
HARGADINE, D. A. p 3474 N93-30826
HARIHARAN, P. C. p 3616 N93-30449
HARJU, JARMO p 3532 N93-29997
HARKNESS, J. B. L. p 3310 N93-29052
HARKRIDER, DAVID G. p 3479 N93-30756
HARMER, MARTIN P. p 3339 N93-30883
HARMON, B. A. p 3624 N93-29631
p 3572 N93-29632
p 3573 N93-29643
HARPER, C. DOUGLAS p 3533 N93-30380
HARPER, ELVIN p 3493 N93-28759
HARPER, TONY R. p 3518 N93-29572
HARRIGAN, R. W. p 3543 N93-30012
HARRINGTON, M. D. p 3398 N93-30748
HARRIS, A. I. p 3631 N93-30615
p 3637 N93-30639
p 3441 N93-30640
HARRIS, CHARLES E. p 3307 N93-30866
HARRIS, H. W. p 3406 N93-28830
HARRIS, JONICE p 3291 N93-30958
HARRIS, S. E. p 3440 N93-30401
HARRIS, STEVEN M. p 3350 N93-30095
HARRISON, J. K. p 3399 N93-30755
HARRISON, W. T. p 3598 N93-30407
HARRISON, WILLIAM T. p 3592 N93-28584
p 3594 N93-29138
p 3599 N93-30518
HART, E. L. p 3568 N93-29764
HART, SEAN M. p 3303 N93-30843
HARTL, PHILIPP p 3457 N93-28919
HARTMAN, STEVEN p 3626 N93-30706
HARTMANN, ROLF p 3458 N93-28923
HARTMAYER, R. p 3583 N93-29700
HARTNESS, J. TIMOTHY p 3305 N93-30854
HARTUNIAN, R. p 3271 N93-28487
HARVEY, KEITH p 3582 N93-29694
HASAN, M. M. p 3264 N93-28713
HASEGAWA, MISAO p 3320 N93-28529
HASHIZUME, T. p 3567 N93-29403
HASKO, GREGORY H. p 3304 N93-30851
HASLETT, J. W. p 3375 N93-30340
HASSAM, A. B. p 3585 N93-28749
HASSAN, T. A. p 3427 N93-30489
HASSON, D. F. p 3296 N93-28886
p 3298 N93-29425
p 3334 N93-29829
HATCHER, DARRIN p 3305 N93-30858
HAUER, J. F. p 3550 N93-30041
HAULE, D. D. p 3359 N93-30244
HAURI, ERIK H. p 3477 N93-29405
HAW, JAMES F. p 3338 N93-30596
HAWLEY, ARTHUR p 3300 N93-30431
HAWLEY, S. L. p 3632 N93-28547
HAWSEY, R. A. p 3404 N93-28523
HAY, N. p 3255 N93-29944
HAYASHI, KIMIO p 3576 N93-30006
HAYES, SCOTT p 3556 N93-29423
HAYKIN, SIMON p 3358 N93-30239
p 3246 N93-30299
HAYS, KEVIN A. p 3488 N93-29819
HE, JIANLIANG p 3561 N93-29189
HE, Y. p 3318 N93-30064
HECK, B. A. p 3474 N93-30826
HECKATHORN, H. M. p 3624 N93-28814
HEFFERNAN, PAUL J. p 3532 N93-29980
HEFNER, BILL BRYAN, JR. p 3449 N93-30414
HEIN, O. p 3255 N93-29942
HEINRICH, PAUL V. p 3459 N93-29146
HELFAND, DAVID J. p 3630 N93-29604
HELMBERGER, DONALD V. p 3479 N93-30756
HENAGER, C. H., JR. p 3323 N93-29101
HENDERSHOTT, MYRL C. p 3486 N93-28885
HENDERSON, A. S. p 3490 N93-28848
HENDERSON, DAVID M. p 3269 N93-29652
HENDERSON, DOUGLAS A. p 3240 N93-29410
HENDERSON, E. DEVERE p 3260 N93-28851
HENDERSON, GEORGE W. p 3430 N93-28488
HENDERSON, LESLIE J. p 3338 N93-30580
p 3338 N93-30586
HENDRICKS, R. C. p 3416 N93-28627
HENKE, R. P. p 3573 N93-29637
HENLINE, P. p 3587 N93-29190
HENNECKE, D. K. p 3257 N93-29953
HENNER, V. K. p 3571 N93-30791
HENNESSY, COREY J. p 3283 N93-29374
HENNINGSON, DAN S. p 3418 N93-29009
HENSHAW, JOHN M. p 3293 N93-30969
HENSHAW, PHILIP D. p 3540 N93-30895
HENSON, TROY F. p 3519 N93-29581
HERBERT, J. M. p 3332 N93-29337
HERBERT, P. J. p 3485 N93-30758
HERCZFELD, R. p 3383 N93-29455
HEREZFELD, PETER R. p 3408 N93-29281
HERGENROTHER, PAUL M. p 3303 N93-30842
HERLIN, NATHALIE p 3313 N93-30109
HERMAN, JAY R. p 3467 N93-28682
HERMAN, R. G. p 3341 N93-28752
HERMANN, M. R. p 3440 N93-30394
HERRICK, ROBERT p 3310 N93-28988
HERRON, WILLIAM J. p 3312 N93-29429
HERTZBACH, S. S. p 3576 N93-30488
HERZOG, DONALD p 3618 N93-30458
HERZOG, G. p 3573 N93-29643
HESELHAUS, A. p 3258 N93-29961
HESEN, P. p 3461 N93-29466
HEURING, VINCENT P. p 3532 N93-30014
HEYOB, JEFFREY J. p 3595 N93-29341
HEZEL, PAUL J. p 3506 N93-29340
HIBBS-BRENNER, MARY p 3580 N93-29973
HIBBS, R. I. p 3416 N93-28627
HICKEY, JOHN R. p 3467 N93-29686
p 3582 N93-29693
HICKMAN, D. p 3391 N93-29913
HICKMAN, MARK p 3267 N93-28734
HIDSON, D. p 3613 N93-29210

HIGHLEY, BOB p 3265 N93-28718
HIGHTOWER, JOHN D. p 3383 N93-29280
HILDEBRAND, VERNE p 3396 N93-30735
HILL, D. N. p 3588 N93-29334
p 3588 N93-29772
HILL, JOHN p 3614 N93-29239
HILLIARD, EDWARD J., JR. p 3562 N93-29279
HILLMAN, J. J. p 3285 N93-28781
HILLMAN, L. W. p 3582 N93-31035
HILLS, J. G. p 3634 N93-29246
HILLSTROEM, LARS p 3259 N93-29999
HINDMAN, RICHARD G. p 3428 N93-30630
HINDS, J. M. p 3478 N93-30487
HINES, AVIS P. p 3311 N93-29204
HIPPENSTEELE, STEVEN A. p 3420 N93-29157
HIRD, GEOFFREY p 3533 N93-30380
HIROMOTO, R. E. p 3549 N93-29769
HIRTH, J. P. p 3320 N93-28548
HLAVA, P. F. p 3339 N93-30656
HO, PAUL p 3358 N93-30237
HO, T. Q. p 3303 N93-30555
HOAGLAND, R. G. p 3320 N93-28548
HOANG, PHILLIP P. p 3538 N93-29490
HOARD, T. L. p 3316 N93-30653
HOCHEDEZ, J. F. p 3582 N93-29691
HOEFER, WOLFGANG p 3387 N93-29877
HOEKMAN, D. H. p 3460 N93-29320
HOELDER, DARRYL p 3409 N93-29655
HOERZ, FRIEDRICH p 3638 N93-29370
p 3638 N93-29372
HOFACRE, K. C. p 3493 N93-28758
HOFF, CHARLES S. p 3285 N93-29911
HOFLUND, GAR B. p 3570 N93-30558
HOGAN, R. E. p 3549 N93-29187
HOKIN, S. A. p 3584 N93-28602
HOLCOMB, LEE p 3627 N93-30715
HOLDEN, A. V. p 3519 N93-29576
HOLECZ, F. p 3457 N93-28920
HOLL, MICHAEL p 3306 N93-30863
HOLL, MICHAEL W. p 3308 N93-30876
HOLLANDER, H. J. p 3413 N93-30763
HOLLICK, H. H. p 3317 N93-30760
HOLLOWAY, D. A. p 3449 N93-28943
HOLLOWAY, PAUL H. p 3601 N93-30811
HOLMBERG, JAN p 3378 N93-30581
HOLMES, JOHN W. p 3329 N93-28495
HOLMES, RICHARD R. p 3338 N93-30565
HOLSTE, J. C. p 3604 N93-29428
p 3604 N93-29794
HOLT, R. J. p 3574 N93-28970
HOLTET, J. A. p 3477 N93-29831
HOLZBACH-VALERO, A. A. p 3526 N93-29026
HOLZHEIMER, T. R. p 3399 N93-30754
HOLZSCHUH, JACK E. p 3383 N93-29280
HONEA, R. B. p 3472 N93-30009
HONEYCUTT, REBECCA L. p 3563 N93-30899
HONG, SUN p 3600 N93-30769
HOO, E. A. p 3465 N93-30206
HOOKER, STANFORD B. p 3486 N93-28497
p 3486 N93-28500
HOOPER, E. B. p 3587 N93-29303
HOOPLE, THOMAS G. p 3382 N93-29202
HOPKINS, ROBERT C. p 3353 N93-28698
HORAN, D. M. p 3285 N93-28784
HORI, MITSUYOSHI p 3379 N93-28534
HORN, D. p 3473 N93-30187
HOROWITZ, PAUL p 3509 N93-28895
HOROWITZ, RICHARD p 3612 N93-29167
HORSTEMEYER, M. F. p 3453 N93-29843
HORTON, W. p 3585 N93-28910
HORZ, FRED p 3638 N93-29355
HOSTERMAN, KENNETH C. p 3229 N93-29726
HOTES, S. A. p 3604 N93-29806
HOUSNER, J. M. p 3307 N93-30867
HOUSTON, J. E. p 3452 N93-29515
HOVENIER, J. W. p 3463 N93-31011
HOVY, EDUARD H. p 3524 N93-28579
HOWARD, EMILY p 3502 N93-28858
p 3504 N93-28870
HOWARD, KEVIN p 3619 N93-30459
HOWARD, S. L. p 3319 N93-30081
HOWLAND, JONATHAN C. p 3487 N93-29003
HROMADKA, THEODORE V. p 3262 N93-30103
HRON, ANNA B. p 3527 N93-29218
HRUBESH, L. W. p 3311 N93-29263
HSIEH, J. H. p 3330 N93-28666
HSU, WENSYANG p 3446 N93-30378
HU, SHOUFENG p 3304 N93-30847
HU, YONG-LIN p 3289 N93-29570
HUANG, CHENHONG p 3550 N93-29876
HUANG, J. C. M. p 3434 N93-28771
HUANG, JOHN p 3384 N93-29507
HUANG, K. p 3614 N93-29231
HUANG, SONG p 3511 N93-29529
HUANG, X. H. p 3518 N93-29574
HUANG, X. Z. p 3600 N93-30569
HUBBARD, B. p 3285 N93-28779
HUBBARD, C. R. p 3325 N93-29813
HUBBARD, DAVID C. p 3499 N93-30542
HUBER, G. p 3417 N93-28663
HUCKETT, S. C. p 3598 N93-30501
HUDSON, CAMILLE T. p 3343 N93-30061
HUDSON, D. L. p 3518 N93-29575
HUDSON, TRACY D. p 3579 N93-29656
HUILI, SHEN p 3240 N93-29862
HUITEMA, HALBE p 3522 N93-28482
p 3523 N93-28484
HULEN, H. p 3615 N93-29783
HULEN, HARRY p 3617 N93-30452
HUMES, KAREN SUE p 3462 N93-30045
HUMMEL, ROBERT p 3393 N93-30576
HUMPHREYS, D. A. p 3583 N93-28530
HUMPHRIES, R. G. p 3367 N93-30298
HUNTER, IAN p 3362 N93-30262
HUNTER, J. L. p 3638 N93-29378
HURLEY, DONNA L. p 3572 N93-29629
HURST, J. K. p 3310 N93-28911
HURTEAU, R. p 3361 N93-30261
HUSAIN, V. p 3551 N93-30809
HUTCHINS, S. p 3474 N93-30762
HUTTON, PATRICIA D. p 3623 N93-30907
HUXHOLD, WENDY L. p 3519 N93-29581
HWA, R. C. p 3577 N93-30532
HWOSCHINSKY, PETER V. p 3236 N93-30677
HWU, W.-M. p 3527 N93-29170
HYLAND, DAVID C. p 3455 N93-31038

I

IBINSON, WILLAM M. p 3554 N93-28844
IBRAHIM, MOUNIR p 3252 N93-29162
ICART, SYLVIE p 3543 N93-30116
IEK, CHANTHY p 3252 N93-29162
IGNATOVICH, V. K. p 3601 N93-30799
IISAKA, JOJI p 3613 N93-29228
IKEYA, T. p 3406 N93-28669
p 3406 N93-28983
ILCEWICZ, L. B. p 3300 N93-30432
ILCEWICZ, LARRY p 3305 N93-30858
ILCEWICZ, LARRY B. p 3248 N93-29498
p 3303 N93-30845
ILINCIC, N. p 3347 N93-30084
IMAMOTO, S. S. p 3572 N93-29634
IMBERT, GUY p 3497 N93-30882
INAL, O. T. p 3323 N93-29092
INAL, T. O. p 3336 N93-30129
INAM, A. p 3596 N93-29868
INAN, U. S. p 3396 N93-30737
INCE, A. NEJAT p 3388 N93-29899
INGHAM, H. p 3313 N93-29768
INGRAM, RAYMOND F. p 3398 N93-30746
INMAN, R. V. p 3304 N93-30850
INMAN, VAUGHAN W. p 3506 N93-29484
INOMATA, SHINJI p 3524 N93-28531
INTERRANTE, LEONARD V. p 3327 N93-30574
IONESCU, DAN p 3359 N93-30243
p 3366 N93-30289
IONOV, S. I. p 3318 N93-30068
IRELAND, P. T. p 3254 N93-29940
IRION, JACK D. p 3459 N93-29146
ISAACS, H. S. p 3323 N93-29256
ISEI, NOBUAKI p 3590 N93-30398
ISHIDA, SHINICHI p 3590 N93-30398
ISHIHARA, K. p 3406 N93-28983
p 3410 N93-29673
ISHINO, R. p 3577 N93-28982
ISOBE, NOBUO p 3524 N93-28537
ISSACCI, F. p 3267 N93-28738
ITAMI, KIYOSHI p 3590 N93-30649
ITOH, TATSUO p 3387 N93-29875
IVANOV, A. A. p 3591 N93-30780
IVANOV, V. G. p 3623 N93-30994
IVKIN, A. V. p 3571 N93-30788
IWAHORI, T. p 3406 N93-28669
p 3406 N93-28746
p 3406 N93-28983
p 3410 N93-29673
IZRAILEV, F. M. p 3606 N93-30803

J

JABBARI, M. Y. p 3253 N93-29929
JACKS, JOHN D. p 3507 N93-29606
JACKSON, ANTHONY p 3300 N93-30430
JACKSON, E. L. p 3466 N93-30891
JACKSON, KAREN E. p 3308 N93-30874
JACKSON, R. p 3320 N93-30277
JACKSON, WADE C. p 3304 N93-30848
JACOB, DENIS p 3367 N93-30296
JACOBS, DONALD T. p 3415 N93-28557
JACOBS, I. p 3493 N93-28939
JACOBS, J. W. p 3421 N93-29253
JACOBS, JAMES A. p 3290 N93-30948
JACOBSON, ALLAN S. p 3613 N93-29226
p 3613 N93-29230
JACQUOTTE, OLIVIER PIERRE p 3417 N93-28744
JADIK, JOHN R. p 3251 N93-28871
JAFARPUR, KHOSROW p 3426 N93-30379
JAFFE, ANDREW H. p 3653 N93-29164
JAGGERS, CHRISTOPHER H. p 3329 N93-28561
JAHNE, B. p 3487 N93-29422
JAHSHAN, S. N. p 3565 N93-28833
JAIN, A. p 3575 N93-29317
JAIN, ASHOK K. p 3568 N93-29446
JAIN, GIAN P. p 3247 N93-30353
JAJA, JOSEPH p 3539 N93-29677
JAMALI, S. H. p 3357 N93-30236
JAMES, GEORGE H., III p 3463 N93-28603
JAMES, MICHAEL D. p 3243 N93-29778
JAMNEJAD, VAHRAZ p 3381 N93-28955
JANABI, T. H. p 3517 N93-29566
JANABI, TALIB p 3515 N93-29554
JANASWAMY, RAMAKRISHNA p 3387 N93-29882
JANI, YASHVANT p 3512 N93-29534
JANKOWSKI, FRANCIS J. p 3264 N93-28714
JANSEN, F. p 3654 N93-29646
JANSSEN, MICHAEL A. p 3381 N93-29087
JARRELL, J. D. p 3485 N93-30758
JARRETT, D. N. p 3502 N93-28860
JASKE, ROBERT p 3614 N93-29239
JASSEMI-ZARGANI, R. p 3370 N93-30310
JAYAKODY, J. P. p 3332 N93-29342
JEGLEY, DAWN C. p 3306 N93-30859
JELINSKI, L. p 3491 N93-29915
JEMISON, WILLIAM D. p 3408 N93-29281
p 3383 N93-29455
JENKINS, D. G. p 3421 N93-29253
JENKINS, M. G. p 3320 N93-28564
JENKINS, PHILIP p 3582 N93-29693
JENKINS, PHILIP N. p 3555 N93-29857
JENKINS, THOMAS J. p 3292 N93-30962
JENNINGS, DON p 3266 N93-28728
JENSEN, M. D. p 3400 N93-28820
JHA, M. K. p 3604 N93-29168
JHA, P. K. p 3605 N93-30779
JI, H. p 3584 N93-28602
JIANG, W. p 3357 N93-30231
JIANG, YI-TSANN p 3421 N93-29213
JIKIA, G. V. p 3572 N93-30930
JOE, EDMOND J. p 3449 N93-30414
JOHANSSON, ARNE V. p 3418 N93-29009
JOHANSSON, B. CHRISTER V. p 3238 N93-29005
JOHANSSON, M. A. p 3341 N93-28752
JOHNS, E. p 3489 N93-30827
JOHNSON, D. R. p 3335 N93-30047
JOHNSON, DANIEL W. p 3446 N93-30404
JOHNSON, E. A. p 3286 N93-28785
JOHNSON, ERIC p 3528 N93-29294
JOHNSON, ERIC R. p 3454 N93-30374
JOHNSON, JAMES D. p 3318 N93-30072
JOHNSON, R. W. p 3481 N93-28875
p 3300 N93-30432
JOHNSON, RICHARD F. p 3495 N93-30196
JOHNSON, SAMUEL D. p 3407 N93-29173
JOHNSON, STEVEN J. p 3563 N93-30899
JOHNSTON, A. R. p 3583 N93-29700
JOHNSTON, DAVID p 3447 N93-30567
JOHNSTON, MARK D. p 3613 N93-29227
JOHNSTON, NORMAN J. p 3291 N93-30957
JOHNSTON, PATRICK H. p 3305 N93-30856
JOKERST, N. p 3581 N93-30500
JONATHAL, D. p 3573 N93-29644
JONES, DAVID I. p 3332 N93-29344
JONES, KEVIN p 3601 N93-30811
JONES, LARRY W. p 3473 N93-30197
JONES, LISA E. p 3308 N93-30875
JONES, LYNN p 3622 N93-30478
JONES, M. T. p 3524 N93-28644
JONES, RAYMOND D. p 3260 N93-28869
JONES, S. p 3267 N93-28738
JONES, T. B. p 3396 N93-30738
JONES, T. V. p 3253 N93-29934
p 3254 N93-29940
JONG, R. A. p 3588 N93-29334
p 3588 N93-29772
JONGEJAN, J. p 3552 N93-31014
JORDAN, D. p 3411 N93-30057
JORDAN, D. L. p 3410 N93-29814
p 3411 N93-30058
JORDAN, ERIC H. p 3297 N93-29074
JORDAN, J. E. p 3373 N93-30329
JORDAN, JAY p 3528 N93-29294
JORDON, KENNETH L. p 3399 N93-30753
JORGENSEN, C. p 3614 N93-29240
JORGENSON, R. E. p 3484 N93-30651
JOSEPH, A. p 3328 N93-31022

JOSEPH, C. L. p 3582 N93-28786
JOSHI, P. B. p 3286 N93-28787
JOSLIN, RONALD D. p 3525 N93-28976
JOSLYN, CLIFF p 3517 N93-29567
JOSWIAK, D. p 3638 N93-29372
JUANG, C. H. p 3518 N93-29574
JUANG, JER-NAN p 3455 N93-31038
JUDGE, ALAN p 3376 N93-30347
JUMARIE, GUY p 3359 N93-30247
JUNG, HYUNG-BAE p 3551 N93-30572
JUSKA, THOMAS p 3299 N93-29984

K

KACHANOV, MARK p 3453 N93-29855
KACHKACHI, H. p 3558 N93-30989
KACHKACHI, M. p 3558 N93-30989
KACKER, RAGHU p 3539 N93-29677
KADANOFF, L. P. p 3418 N93-28878
KAHN, R. D. p 3642 N93-28777
KAIGH, W. D. p 3554 N93-29385
KAISER, W. p 3434 N93-28765
p 3649 N93-28819
KALAYCIOGLU, S. p 3370 N93-30311
KALIAGUINE, N. p 3376 N93-30348
KAMENETZKY, R. R. p 3331 N93-29193
KAMPBELL, D. H. p 3474 N93-30762
KAN, H. P. p 3306 N93-30860
KAN, HAN-PIN p 3307 N93-30871
KANADE, T. p 3444 N93-29330
KANAMORI, NAOKAZU p 3587 N93-29243
KANNAN, S. p 3491 N93-30483
KAO, C. Y. J. p 3477 N93-29346
p 3482 N93-29347
KAPPELSBERGER, E. p 3325 N93-30115
KAR, K. p 3572 N93-30931
KARADI, C. p 3594 N93-29249
KARAM, GERALD M. p 3368 N93-30301
KARAOGLAN, LEVENT p 3297 N93-29078
KARAVIS, A. p 3502 N93-28860
KARCZEWSKI, J. F. p 3646 N93-28796
KAROUI, BADREDDINE p 3366 N93-30289
KARPAS, Z. p 3317 N93-30982
KARPOVSKY, EFIM J. p 3513 N93-29541
KARPUSHOV, A. N. p 3591 N93-30780
KARR, C. LUCAS p 3518 N93-29572
KARR, M. E. p 3481 N93-28875
KARTAVTSEV, O. I. p 3535 N93-30914
KARTAVTSEV, V. I. p 3535 N93-30915
KARTHA, V. B. p 3441 N93-31023
KARUNASIRI, GAMANI p 3595 N93-29383
KARWOWSKI, WALDEMAR p 3510 N93-29517
KASCHMITTER, J. L. p 3520 N93-29058
KASHANI, REZA p 3259 N93-29985
KASHYAP, S. p 3366 N93-30290
p 3367 N93-30294
KASIVISWANATHAN, K. V. p 3328 N93-31022
KASSAPOGLOU, CHRISTOS p 3301 N93-30435
KASSEL, PHILIP C., JR. p 3638 N93-29377
p 3638 N93-29379
KATKOV, V. M. p 3600 N93-30770
KATNIK, GREGORY N. p 3271 N93-29136
KATO, ZOLTAN p 3553 N93-28510
KATTENBORN, GILBERT p 3459 N93-28929
KATZ, A. P. p 3295 N93-28592
KATZ, J. D. p 3332 N93-29252
KAUFFMAN, R. L. p 3432 N93-29773
KAUFMANN, DAVID N. p 3245 N93-28936
KAUL, M. P. p 3475 N93-30887
KAUTZ, HAROLD E. p 3449 N93-29073
KAVANAGH, STEPHEN p 3365 N93-30284
KAVIANY, M. p 3424 N93-30035
KAWASAKI, SHIGEO p 3387 N93-29875
KAY, ANTHONY p 3462 N93-30107
KAYALAR, S. p 3386 N93-29602
KAYE, G. T. p 3440 N93-30553
KEBABIAN, P. L. p 3320 N93-30102
KECSKES, LASZLO J. p 3341 N93-28515
KEDEM, BENJAMIN p 3360 N93-30254
KEDZIERSKI, M. A. p 3475 N93-30887
KEEFER, CHRISTOPHER W. p 3381 N93-28997
KEEGAN, R. p 3654 N93-29646
KEENE, MICHAEL L. p 3612 N93-28948
KEIGHTLEY, R. J. p 3363 N93-30268
KEIGHTLEY, ROBERT J. p 3362 N93-30264
KELLER, BIRGIT p 3491 N93-29274
KELLER, JAMES M. p 3510 N93-29523
p 3517 N93-29568
KELLER, RICHARD M. p 3613 N93-29229
KELLER, TEDDY M. p 3338 N93-30580
p 3338 N93-30586
KELLMAN, M. E. p 3564 N93-28604
KELLY, DOUGLAS MICHAEL p 3632 N93-28607
KELLY, J. M. p 3420 N93-29126
KELLY, P. M. p 3611 N93-28580
KEMME, DAVID A. p 3446 N93-30384
KEMMERLY, GUY T. p 3239 N93-29165
KEMP, WILLIAM T. p 3582 N93-29695
KEMPA, K. p 3588 N93-29382
KEMPSTER, LINDA p 3619 N93-30460
KENDIG, JOHN p 3446 N93-30512
KENEMUTH, JOHN R. p 3582 N93-29692
KENESHEA, T. S. p 3630 N93-29460
KENKRE, V. M. p 3565 N93-28914
KENNEDY, JOHN M. p 3612 N93-28948
p 3615 N93-29709
p 3616 N93-30036
p 3616 N93-30037
KERANS, R. J. p 3295 N93-28592
KERNER, J. A. p 3645 N93-28792
KERR, J. P. p 3567 N93-29416
KERSEY, ALAN D. p 3577 N93-29038
KESKI-KUHA, R. A. M. p 3582 N93-28788
KESSEL, R. A. p 3624 N93-28814
KESSLER, DONALD J. p 3283 N93-29373
KEUNG, WAI-YEE p 3574 N93-28565
KEY, DAVID p 3238 N93-30690
KEY, F. S. p 3447 N93-30820
KEYTE, G. E. p 3286 N93-29910
KHAN, RAFAAT H. p 3377 N93-30355
KHANNA, S. M. p 3405 N93-28563
p 3357 N93-30230
KHATER, H. Y. p 3439 N93-30186
KHER, A. p 3582 N93-28789
KHOSLA, P. K. p 3444 N93-29330
KHRIPLOVICH, I. B. p 3479 N93-30785
KIGGANS, J. O. p 3334 N93-29767
KII, KAZUO p 3247 N93-30324
KIKUCHI, HIRONOBU p 3576 N93-30006
KILBY, M. p 3274 N93-29031
KILCREASE, D. P. p 3586 N93-29093
KILDUFF, PATRICIA W. p 3505 N93-28941
KILIC, M. p 3256 N93-29950
KILKENNY, J. D. p 3432 N93-29773
KILLOUGH, S. M. p 3444 N93-29247
KIM, G. M. p 3325 N93-29981
KIM, GUN-IN p 3305 N93-30858
KIM, J. Y. p 3585 N93-28910
KIM, K. J. p 3436 N93-28847
p 3440 N93-30530
KIM, S. p 3256 N93-29951
KIM, SAN-JOO p 3321 N93-28656
KIM, Y. K. p 3255 N93-29943
KIM, YONG-IN p 3548 N93-28753
KIMURA, C. Y. p 3243 N93-28571
KINARD, WILLIAM H. p 3638 N93-29355
KING, JOSEPH H. p 3612 N93-29167
KING, NANCY p 3497 N93-30894
KING, R. W. P. p 3399 N93-30755
KING, ROBERT N. p 3295 N93-28660
KINNEY, E. R. p 3574 N93-28970
KINSER, DONALD L. p 3340 N93-29368
KINSLEY, PHILIP J. p 3303 N93-30843
KINSNER, W. p 3361 N93-30259
KINTER, JAMES L., III p 3613 N93-29225
KIRK, M. A. p 3592 N93-28661
KIRKPATRICK, JOSEPH DAVY p 3629 N93-28608
KIROL, L. D. p 3466 N93-30814
KISHIMOTO, Y. p 3585 N93-28910
KIYOTA, MIKIO p 3525 N93-28978
KLAMERUS, J. p 3532 N93-30050
KLAVETTER, ELMER p 3342 N93-29402
KLEIJWEG, J. C. M. p 3463 N93-31010
KLEIN, D. L. p 3421 N93-29253
KLEIN, E. J. p 3286 N93-28790
KLEIN, HAROLD P. p 3651 N93-30214
KLEIN, J. p 3573 N93-29643
KLEIN, JONATHAN D. p 3310 N93-28988
KLEIN, L. p 3645 N93-28793
KLEIN, R. p 3424 N93-29836
KLEMETTI, WAYNE I. p 3399 N93-30757
KLEMP, JOSEPH B. p 3613 N93-29224
KLEMP, MARJORIE K. p 3613 N93-29224
KLEUSBERG, ALFRED p 3245 N93-29468
KLEVGARD, P. A. p 3432 N93-29842
KLIER, K. p 3341 N93-28752
KLINGER, H. p 3257 N93-29953
KLINKE, J. p 3487 N93-29422
KLINKHAMER, F. R. p 3572 N93-31008
KLIR, GEORGE J. p 3519 N93-29582
KLOTS, T. D. p 3603 N93-28747
KLOTZSCHE, MAX p 3300 N93-30431
KLUEGEL, LYNN p 3622 N93-30478
KLUTE, GLEN K. p 3505 N93-29044
KLUTE, GLENN K. p 3506 N93-29324
KLYDE, D. H. p 3447 N93-30828
KNAPP, R. B. p 3430 N93-28659
KNIGHT, CURTIS A. p 3382 N93-29217
KNIGHT, G. A. p 3392 N93-30145
KNIPMEYER, S. E. p 3603 N93-28964
KNOLL, G. F. p 3563 N93-28546
KNOLL, R. H. p 3264 N93-28713
KNOWLES, JAMES K. p 3321 N93-28656
KNYAZEV, B. A. p 3590 N93-30768
KO, FRANK K. p 3305 N93-30855
KO, HON-YIM p 3276 N93-29115
p 3276 N93-29116
KOBAYASHI, A. S. p 3453 N93-30147
KOBER, E. M. p 3570 N93-30448
KOBER, N. p 3608 N93-30657
KOBLENTS, B. p 3373 N93-30332
KOBLER, BEN p 3616 N93-30449
KOBRICK, JOHN L. p 3495 N93-30196
KOCH, BARBARA p 3457 N93-28921
KOCH, D. p 3632 N93-28791
KOCH, J. A. p 3438 N93-29781
KOCH, M. W. p 3412 N93-30370
KOCH, S. W. p 3439 N93-29983
KOCHKIN, O. I. p 3535 N93-30914
KOCHKIN, V. I. p 3535 N93-30915
KOCKS, U. F. p 3326 N93-30486
KOCZY, LASZLO T. p 3519 N93-29583
KOERT, DAVID N. p 3311 N93-29283
KOFINAS, P. p 3329 N93-28560
KOFLER, R. R. p 3576 N93-30488
KOHUT, P. p 3548 N93-28891
KOIKE, M. p 3261 N93-29869
p 3433 N93-30531
KOKOTOFF, DAVID p 3400 N93-31036
KOLAROV, KRASIMIR DOBROMIROV
p 3445 N93-30149
KOLB, C. E. p 3319 N93-30090
p 3320 N93-30102
KOLBA, DEAN P. p 3389 N93-29900
KOLESAR, EDWARD S. p 3292 N93-30962
KOLMANOVSKY, ILYA V. p 3280 N93-29993
p 3280 N93-29994
KOMARNENI, SRIDHAR p 3333 N93-29511
KON, ALLAN B. p 3337 N93-30557
KONDO, Y. p 3604 N93-29242
KONNICK, P. J. p 3412 N93-30118
KONSTANTOPOULOS, PANAGIOTIS
p 3552 N93-28506
KOOH, A. p 3318 N93-30065
KOONTZ, STEVEN L. p 3296 N93-29023
KOPONEN, J. p 3488 N93-30040
KOPPEL, L. N. p 3645 N93-28792
KORELLIS, J. S. p 3330 N93-28838
p 3453 N93-29843
KORN, G. p 3326 N93-30490
KORNEEV, D. A. p 3600 N93-30771
KOSHA, M. p 3231 N93-29735
KOSICKI, B. B. p 3434 N93-28771
KOSIER, S. L. p 3413 N93-30650
KOSS, D. A. p 3320 N93-28491
p 3324 N93-29799
KOSTANDARITHES, DANTON p 3459 N93-29146
KOSTYUK, S. V. p 3479 N93-30785
KOTCHETKOV, YOURI p 3547 N93-28667
KOTLAR, ANTHONY J. p 3315 N93-30405
KOTTKE, THOMAS p 3341 N93-28515
KOTZ, TOM p 3484 N93-30608
KOUMOUTSAKOS, PETROS D. p 3419 N93-29077
KOVESI-DOMOKOS, S. p 3603 N93-28961
KOWALCZYK, R. S. p 3574 N93-28970
KOZMINCHUK, BRIAN p 3383 N93-29407
KRABBE, A. p 3631 N93-30641
p 3632 N93-30643
KRAIMER, W. A. p 3399 N93-30752
KRAIN, H. p 3258 N93-29961
KRAKAUER, D. A. p 3566 N93-29313
KRAMER, ROBERT p 3578 N93-29139
KRANBUEHL, DAVID E. p 3303 N93-30843
KRAPEZ, J. C. p 3359 N93-30246
KRASAVIN, S. E. p 3602 N93-31025
KRASLAWSKI, A. p 3516 N93-29562
KREINOVICH, V. p 3516 N93-29563
p 3520 N93-29584
KREINOVICH, VLADIK p 3548 N93-28973
KREJCI, IVAN p 3311 N93-29133
KREMER, FRANS G. J. p 3248 N93-29464
KRESIN, V. V. p 3566 N93-29206
KRESS, GREGORY A. p 3354 N93-29969
KRESS, R. L. p 3460 N93-29255
KRIGE, JOHN p 3660 N93-29500
KRILE, THOMAS F. p 3522 N93-30179
KRIM, JACQUELINE p 3324 N93-29803
KRINER, B. p 3247 N93-30325
KRISHER, T. P. p 3386 N93-29603
KRISHNAMOORTHY, ASHOK p 3520 N93-29482
KRISHNAN, HARIHARAN p 3279 N93-29989
p 3280 N93-29990
p 3280 N93-29992
p 3544 N93-30893
KRISHNAN, P. N. p 3315 N93-30365
KRISHNAPURAM, RAGHU p 3510 N93-29523
p 3511 N93-29524
p 3511 N93-29526

KRISTJANSSON, J. E. p 3482 N93-29347
KRITZ, A. H. p 3586 N93-29049
KROEGER, JOHN p 3446 N93-30512
KROVVIDY, SRINIVAS p 3289 N93-29570
KRUG, DANIEL W. p 3249 N93-29776
KRUGER, R. P. p 3380 N93-28900
KRUIZINGA, S. p 3483 N93-30013
KRUMPELT, M. p 3464 N93-29844
KRUSA, PAUL W. p 3449 N93-29220
KRUSE, RUDOLF p 3514 N93-29549
p 3516 N93-29560
KRUSIUS, J. P. p 3382 N93-29131
p 3384 N93-29514
KRYTER, R. C. p 3443 N93-28968
KUBINA, S. J. p 3369 N93-30309
p 3371 N93-30320
KUBINA, STANLEY J. p 3366 N93-30291
KUEHBAUCH, W. p 3458 N93-28922
KUEHN, G. I. p 3507 N93-29675
KUHN, HOWARD A. p 3290 N93-30949
KUKACKA, L. E. p 3329 N93-28551
p 3327 N93-30815
KULAGA, J. E. p 3407 N93-29036
KULCINSKI, G. L. p 3439 N93-30186
KULISA, P. p 3258 N93-29960
KULLERD, SUSAN M. p 3305 N93-30856
KUMAI, K. p 3406 N93-28669
p 3406 N93-28746
p 3406 N93-28983
KUMAR, A. p 3582 N93-28810
KUMAR, C. K. p 3645 N93-28793
KUMAR, K. S. p 3601 N93-30819
KUMAR, K. VASANTHA p 3495 N93-29651
KUMAR, R. p 3464 N93-29844
KUMAR, V. p 3601 N93-30794
KUMER, J. B. p 3434 N93-28794
KUNDU, NIKHIL p 3293 N93-30967
KUNDU, NIKHIL K. p 3293 N93-30974
KUNG, H. T. p 3542 N93-29763
KUNG, JONG HYUN p 3637 N93-30579
KUNSELMAN, R. p 3564 N93-28611
KUNZ, ERWIN p 3260 N93-28851
KUO, ARTHUR DANIEL p 3508 N93-30204
KUO, STEVE p 3521 N93-29504
KUO, WEN-SHYONG p 3308 N93-30937
KURAEV, E. p 3571 N93-30788
KURIBARA, M. p 3577 N93-28982
KURKCHUBASCHE, RAMON R. p 3454 N93-30598
KUSHNICK, PETER W. p 3431 N93-29084
KUZNETSOV, S. B. p 3447 N93-30820
KWAN, H. C. p 3356 N93-30224
KWAN, H. K. p 3355 N93-30222
KWASNIEWSKI, TAD p 3358 N93-30238
KWASNIEWSKI, TAD A. p 3359 N93-30245
KWEI, G. H. p 3598 N93-30517
KWOK, H. L. p 3356 N93-30229
KYSER, E. A. p 3330 N93-28839

L

LABOS, A. S. p 3519 N93-29576
LABOS, E. p 3519 N93-29576
LACIRE, STEPHAN p 3538 N93-29487
LACKMAN, ROBERT p 3614 N93-29237
LACZKO, J. p 3519 N93-29576
LAD, R. J. p 3325 N93-30060
LADAU, TERRY p 3235 N93-29756
LADELFE, P. C. p 3436 N93-28887
LADUE, J. G. p 3481 N93-29095
LAFLIN, M. G. p 3398 N93-30745
LAFONTAINE, SERGE p 3362 N93-30262
LAGASSA, DAVID p 3235 N93-29756
LAGATTUTA, J. K. p 3586 N93-29093
LAGOW, R. J. p 3330 N93-28748
LAGRAFF, J. E. p 3253 N93-29934
LAI, C. C. p 3433 N93-30491
LAIRD, C. E. p 3624 N93-29631
p 3572 N93-29632
LAKEOTES, CHRISTOPHER D. p 3520 N93-29070
LAM, EDWARD p 3375 N93-30344
LAM, L. p 3247 N93-30357
LAMANNA, THOMAS C. p 3399 N93-30753
LAMARQUE, JEAN-FRANCOIS p 3476 N93-29197
LAMBERT, D. P. p 3309 N93-28553
LAMBERT, JAMES L. p 3578 N93-29086
LAMBERT, ROBERT D. p 3544 N93-30886
LAMBIDONIS, D. p 3359 N93-30244
LAMERS, G. p 3463 N93-31009
LAMERS, P. p 3365 N93-30281
LAMONTIA, MARK A. p 3294 N93-28559
LAMPARD, D. p 3255 N93-29944
LAMPO, S. p 3466 N93-30891
LANCASTER, DALE p 3622 N93-30475
LANDIS, GEOFFREY A. p 3321 N93-28618
LANG, ROBERT J. p 3579 N93-29848
LANGE, G. p 3318 N93-29367
LANGELIERS, J. p 3466 N93-30814
LANGFORD, JOHN S. p 3247 N93-28586
LANGSTON, STEPHEN p 3327 N93-30538
LANOUE, J. C. p 3430 N93-28645
LAPIDUS, I. p 3253 N93-29930
LAPPAS, TASSO p 3428 N93-30902
LARA-ROSANO, FELIPE p 3515 N93-29550
LARBALESTIER, D. C. p 3592 N93-28643
LAROSILIERE, L. M. p 3251 N93-28609
p 3251 N93-28617
LAROSILIERE, LOUIS M. p 3252 N93-29072
LARSEN, E. M. p 3439 N93-30186
LARSEN, WILLIAM E. p 3236 N93-30673
p 3236 N93-30674
LARSON, RONAL W. p 3342 N93-29835
LASATER, SALLY W. p 3613 N93-29224
LASCHKA, B. p 3238 N93-28493
LASH, BRUCE p 3292 N93-30961
LATZ, HANS-WALTER p 3611 N93-28528
LAU, S. K. p 3320 N93-28564
LAUBER, WILFRED R. p 3396 N93-30733
LAUER, JAMES L. p 3580 N93-30372
LAUFFER, JAMES P. p 3463 N93-28603
LAUKIEN, F. H. p 3314 N93-30166
LAULAINEN, N. p 3472 N93-30043
LAUNDER, B. E. p 3254 N93-29938
LAURENDEAU, DENIS p 3363 N93-30272
p 3366 N93-30288
LAURIENTE, MICHAEL p 3624 N93-29625
LAVERMAN, B. p 3552 N93-31014
LAWING, PIERCE L. p 3240 N93-29449
LAWSON, A. C. p 3598 N93-30517
LAXAR, KEVIN p 3246 N93-29818
p 3499 N93-30426
LAZAROFF, SCOTT p 3289 N93-30507
LE-NGOC, THO p 3357 N93-30236
LEA, ROBERT N. p 3512 N93-29534
p 3516 N93-29561
p 3518 N93-29573
LEAKE, WOODROW W. p 3291 N93-30958
LEAL, D. C. p 3368 N93-30303
LEATHERWOOD, J. D. p 3561 N93-28692
LEBERL, FRANZ p 3614 N93-29234
LEBLOND, JULIETTE p 3543 N93-30116
LEBOEUF, F. p 3258 N93-29960
LEBRUN, M. J. p 3585 N93-28910
LECOMTE, CLAUDE p 3241 N93-30020
LEDYARD, KATHLEEN M. p 3492 N93-30665
LEE, CHI H. p 3591 N93-28496
LEE, HON-MUN p 3512 N93-29531
LEE, JAIMIN p 3350 N93-30096
LEE, JIM P. p 3393 N93-30537
LEE, JINHO p 3352 N93-30939
LEE, JONATHAN p 3512 N93-29537
LEE, K. K. p 3442 N93-28772
LEE, K. L. p 3330 N93-28838
p 3453 N93-29843
LEE, RICHARD J. p 3411 N93-30021
p 3352 N93-30424
LEE, RICHARD R. p 3620 N93-30467
LEE, SOOGAB p 3563 N93-30980
LEE, SUNPYO p 3295 N93-28843
LEE, THOMAS F. p 3481 N93-28876
LEE, W. D. p 3500 N93-28464
LEEMANS, W. P. p 3436 N93-28847
p 3440 N93-30530
LEFEBVRE, C. p 3355 N93-30221
LEGRADY, O. p 3244 N93-30276
LEHTINEN, K. p 3488 N93-30040
LEHUREAU, J. C. p 3435 N93-30469
LEIBACHER, JOHN W. p 3652 N93-28585
LEIFER, R. p 3472 N93-30043
LEIGH, ALBERT B. p 3511 N93-29525
LEINENWEVER, ROGER W. p 3501 N93-28479
LEMA, LUIS E. p 3444 N93-29288
LEMMENS, M. J. P. M. p 3460 N93-29307
LEMOINE, G. G. p 3460 N93-29320
LENNON, E. B. p 3521 N93-29662
LEONARD, PETER J. T. p 3633 N93-28905
p 3634 N93-28906
p 3634 N93-28907
LEPRINCE, GUILLAUME p 3336 N93-30112
LERAT, ALAIN p 3550 N93-30136
LEROY, A. p 3394 N93-30631
LESAR, RICHARD p 3318 N93-30072
LESHO, J. C. p 3286 N93-28795
LESSING, PETER A. p 3489 N93-30420
LESTER, HAROLD C. p 3301 N93-30436
LETCHFORD, C. W. p 3451 N93-29106
LEUNG, K. N. p 3575 N93-29302
LEVEQUE, L. p 3284 N93-29898
LEVIN, KERRY M. p 3247 N93-30356
LEVINE, ARLENE S. p 3654 N93-29354
p 3660 N93-29621
p 3665 N93-29682
LEVIT, SHIMON p 3607 N93-30933
LEVITON, D. B. p 3582 N93-28788
LEVRAEA, VINCENT J. p 3240 N93-29410
LEVY, M. p 3327 N93-30812
LEVY, R. p 3385 N93-29593
p 3386 N93-29600
LEWANDOWSKI, A. p 3464 N93-29925
LEWERENZ, T. p 3231 N93-29735
LEWIS, B. B. p 3446 N93-30211
LEWIS, R. G. p 3247 N93-30338
LEWIS, ROGER A. p 3625 N93-30694
LEWIS, WILLIAM D. p 3238 N93-30691
LI, P. p 3285 N93-30249
LI, PENG p 3357 N93-30234
LI, Q. P. p 3355 N93-30222
LI, SHENG S. p 3599 N93-30536
LI, SHULONG p 3294 N93-28492
LI, WEI-SZU p 3487 N93-29437
LI, X. p 3359 N93-30248
LI, YAO p 3581 N93-30905
LIAO, FUJIAN p 3410 N93-29798
LIAO, K. p 3259 N93-30168
LIAW, D. G. p 3451 N93-28633
LIBERA, J. p 3587 N93-29299
LICHTENSTEIN, WENDY L. p 3610 N93-30158
LIFKA, D. p 3576 N93-30527
LIGGETT, PATRICIA p 3615 N93-29241
LIGHTHILL, JAMES p 3418 N93-28975
LIGHTNER, BARRY E. p 3251 N93-28871
LIGHTSTONE, L. p 3358 N93-30241
LIM, P. Y. W. p 3500 N93-29564
LIM, S. S. p 3285 N93-30235
p 3285 N93-30249
LIM, SAM-KYU p 3524 N93-28577
LIMAYE, SANJAY S. p 3614 N93-29236
LIN, C. L. p 3316 N93-30658
LIN, HAI-PING p 3455 N93-31028
LIN, HAI-QING p 3337 N93-30381
LIN, KUEN Y. p 3305 N93-30857
LIN, M. C. p 3318 N93-30064
p 3316 N93-30627
LIN, Y. C. p 3274 N93-29031
LIN, YIER p 3452 N93-29432
LIND, ANN MARIE T. p 3261 N93-29815
LIND, D. L. p 3639 N93-29380
LIND, M. D. p 3602 N93-29381
LINDAU, I. p 3597 N93-30120
LINDBLAD, INGEMAR p 3418 N93-28994
LINDEMUTH, I. R. p 3410 N93-29812
LINDH, J. D. p 3437 N93-29207
LINDSAY, A. C. p 3392 N93-30145
LINTON, R. C. p 3331 N93-29193
LINTON, SAMUEL WITHERSPOON
p 3243 N93-30947
LINTZ, ANDREW T. p 3430 N93-28989
LIOU, J. p 3473 N93-30187
LIPINSKI, R. J. p 3279 N93-29840
LIS, STEVEN A. p 3540 N93-30895
LITTMAN, DAVID p 3513 N93-29544
LITZINGER, THOMAS A. p 3346 N93-30080
LIU, ALEX B. p 3445 N93-29388
LIU, BOWEN p 3309 N93-28540
LIU, C. T. p 3321 N93-28679
p 3324 N93-29786
p 3327 N93-30652
LIU, HUA-KUANG p 3614 N93-29231
LIU, K. C. p 3451 N93-28832
LIU, MEILIN p 3405 N93-28581
LIU, P. K. T. p 3316 N93-30658
LIU, PING p 3292 N93-30964
LIU, QIANG p 3542 N93-29079
LIU, SIULIE p 3304 N93-30847
LIU, YONG p 3489 N93-30603
LIU, ZHEN p 3552 N93-28506
p 3538 N93-28937
LIVSHITS, A. I. p 3466 N93-30777
LLANWYNJONES, D. p 3397 N93-30739
LLINAS, RODOLFO R. p 3496 N93-30613
LO, YEH p 3382 N93-29202
LOBANOV, Y. Y. p 3605 N93-30781
LODGE, J. H. p 3373 N93-30331
LODIGIANI, G. p 3254 N93-29939
LOGAN, J. C. p 3303 N93-30555
LOGNONNE, P. p 3646 N93-28796
LOH, E. Y., JR. p 3337 N93-30381
p 3551 N93-30503
LOHMANN, GABRIELE p 3459 N93-28931
LOHNER, RAINALD p 3424 N93-29851
LOKEN, S. p 3576 N93-30527
LOMDAHL, P. S. p 3593 N93-29094
LONDON, R. A. p 3437 N93-29104
p 3438 N93-29309
p 3440 N93-30394
LONG, EDWARD R., JR. p 3303 N93-30843
p 3305 N93-30856
LONG, F. H. p 3593 N93-28966

LONG, MARSHALL B. p 3425 N93-30162
LONG, WALT p 3497 N93-30882
LONGBOTHAM, HAROLD p 3496 N93-30494
LONGRIDGE, THOMAS M. p 3236 N93-30676
LOOIJEN, W. J. p 3460 N93-29307
p 3460 N93-29321
LOOMIS, PETER V. p 3245 N93-29468
LOONEY, L. D. p 3579 N93-29350
LOOS, ALFRED C. p 3297 N93-29107
p 3303 N93-30843
LOPEZ, JASON p 3235 N93-29756
LOPEZ, OSVALDO F. p 3452 N93-29612
p 3306 N93-30859
LORENTSON, CHRIS p 3266 N93-28726
LORENZINI, E. C. p 3399 N93-30755
LORIOT, FRANCOISE p 3550 N93-30117
LOUBRIEL, G. M. p 3406 N93-28944
LOUIE, A. p 3367 N93-30294
LOUIE, S. G. p 3592 N93-28642
LOVE, S. P. p 3593 N93-28966
LOVELL, E. G. p 3439 N93-30186
LOVERN, MICHAEL p 3440 N93-30553
LOW, F. p 3285 N93-28779
LU, H. p 3567 N93-29403
LU, T. p 3244 N93-30276
LU, W. Y. p 3330 N93-28838
LU, W.-S. p 3355 N93-30218
LUCAS, JEFFREY p 3235 N93-29756
LUCAS, M. G. p 3254 N93-29940
LUCKE, R. L. p 3463 N93-28797
p 3624 N93-28814
LUDWICK, LARRY M. p 3438 N93-29800
LUDWIG, DON E. p 3246 N93-30323
LUHMANN, J. G. p 3647 N93-28809
LUKAC, I. p 3605 N93-30783
p 3606 N93-30797
LUM, BEN T. F. p 3271 N93-29215
LUM, K. K. p 3373 N93-30329
LUMMERZHEIM, DIRK p 3476 N93-28842
LUNDBLADH, ANDERS p 3418 N93-29009
LUNDGREN, P. p 3649 N93-28819
LUNDSTROM, M. S. p 3464 N93-28971
LUNDY, FLOYD p 3449 N93-29220
LUO, JING Y. p 3319 N93-30101
LURIA, S. M. p 3246 N93-29818
LURIE, BORIS J. p 3542 N93-29176
LURMANN, F. W. p 3470 N93-29669
LUSH, G. B. p 3464 N93-28971
LUSHCHIKOV, V. I. p 3606 N93-30796
p 3601 N93-30799
LUSK, E. p 3576 N93-30527
LYDICK, L. N. p 3502 N93-28859
LYKTEY, M. Y. p 3596 N93-29430
LYLES, J. T. M. p 3406 N93-28830
LYON, GORDON p 3539 N93-29677
LYONS, J. T. p 3269 N93-28558
LYONS, R. G. p 3370 N93-30314
LYONS, TIMOTHY p 3497 N93-30894

M

MA, YIBING p 3510 N93-29523
MACARTHUR, C. D. p 3255 N93-29945
MACCRACKEN, M. C. p 3469 N93-28967
p 3470 N93-29055
MACDONALD, D. D. p 3320 N93-28545
MACDONALD, DIGBY D. p 3312 N93-29462
MACFARLANE, J. F. p 3576 N93-30527
MACFARLANE, J. J. p 3439 N93-30186
MACGOWAN, B. J. p 3438 N93-29781
p 3440 N93-30394
MACGREGOR, P. M. p 3470 N93-29055
MACHIDA, MASAHIKO p 3524 N93-28537
MACK, KIMBERLY S. p 3282 N93-29357
MACKAY, N. p 3283 N93-29362
MACKIN, ROBERT p 3628 N93-30720
MACKLIN, JOHN p 3283 N93-29364
MACLEOD, N. p 3255 N93-29944
MACRAE, GREGORY S. p 3287 N93-28694
MADARAS, ERIC I. p 3305 N93-30856
MADEY, JOHN M. p 3439 N93-29853
MADISON, T. J. p 3582 N93-28788
MADYASTHA, RAGHAVENDRA K.
p 3519 N93-29581
MAGARI, P. J. p 3253 N93-29934
MAGAZU, H. p 3231 N93-29735
MAGEE, ERIC P. p 3480 N93-28465
MAHAFFY, P. p 3646 N93-28798
MAHLER, MARY A. p 3307 N93-30871
MAHLER, THOMAS W., JR. p 3609 N93-28985
MAHON, J. p 3302 N93-30439
MAHONEY, C. p 3434 N93-28774
MAIER, M. R. p 3598 N93-30393
MAJUMDAR, S. p 3323 N93-29102
p 3364 N93-30279
MAKI, M. C. p 3244 N93-30274
MAKOSKI, THOMAS p 3407 N93-29203
MALARKY, ALASTAIR p 3362 N93-30265
MALDAGUE, X. p 3359 N93-30246
MALHAME, R. P. p 3361 N93-30260
MALIN, M. C. p 3646 N93-28799
MALL, GERALD H. p 3520 N93-29070
MALONE, PATRICK K. p 3264 N93-28714
MALONEY, D. M. p 3482 N93-29399
MALOWANY, A. S. p 3359 N93-30244
p 3373 N93-30328
MALOWANY, M. E. p 3359 N93-30244
MALOWICKI, JOHN E. p 3381 N93-28997
MAMMERICKX, JACQUELINE p 3461 N93-29817
MANCINELLI, R. L. p 3646 N93-28800
MANDEVILLE, JEAN CLAUDE p 3638 N93-29360
MANDEVILLE, JEAN-CLAUDE p 3638 N93-29356
MANDLER, MARC B. p 3246 N93-29818
MANHEIMER, W. M. p 3409 N93-29478
MANKAMO, TUOMAS p 3378 N93-30581
MANKINS, JOHN C. p 3628 N93-30721
MANKOFSKY, ALAN p 3614 N93-29235
MANN, RICHARD p 3246 N93-30299
MANNA, ZOHAR p 3528 N93-29469
MANNAN, S. L. p 3328 N93-31021
MANNSTEIN, HERMANN p 3458 N93-28927
MANOFF, S. p 3557 N93-30926
p 3557 N93-30927
MANSFIELD, WILLIAM H., JR. p 3518 N93-29571
MANTZ, J. p 3371 N93-30321
MANUELPILLAI, G. p 3309 N93-29366
MAPAR, J. p 3274 N93-29031
MARCHAND, PHILIPPE p 3520 N93-29482
MARCHELLO, JOSEPH M. p 3303 N93-30844
MARCUS, HARRIS L. p 3296 N93-29001
MARK, JON W. p 3355 N93-30220
MARKHAM, R. L. p 3493 N93-28758
MARKIN, KELLY R. p 3247 N93-30358
MARKS, LAURENCE D. p 3570 N93-30366
MARKS, T. J. p 3309 N93-28688
MARKUS, ALAN p 3300 N93-30431
p 3301 N93-30438
MARKWITZ, WINFRIED p 3456 N93-28915
MAROTTA, D. p 3257 N93-29957
MAROUF, E. A. p 3646 N93-28801
MARPET, MARK I. p 3293 N93-30966
MARRA, MARTIN p 3487 N93-29003
MARRAKCHI, A. E. L. p 3637 N93-30997
MARRAKCHI, A. L. p 3637 N93-30918
p 3479 N93-30940
MARSDEN, J. E. p 3547 N93-28648
MARSHALEK, E. R. p 3570 N93-30505
MARSHALL, H. p 3424 N93-30035
MARSHALL, J. R. p 3645 N93-28792
MARSICEK, M. J. p 3451 N93-28832
MARTEL, ADRIAN p 3503 N93-28866
MARTEL, SYLVAIN p 3362 N93-30262
MARTENS, J. S. p 3596 N93-29868
MARTENS, RENEE L. J. p 3375 N93-30345
MARTIN, ALEXANDER p 3547 N93-28527
MARTIN, CHARLES E. p 3244 N93-30194
MARTIN, CHARLES R. p 3310 N93-28988
MARTIN, DONALD H. p 3292 N93-30961
MARTIN, GARY L. p 3285 N93-28554
MARTIN, MAURICE p 3263 N93-28704
MARTIN, MIKE p 3614 N93-29236
MARTIN, R. p 3371 N93-30318
p 3374 N93-30335
MARTIN, R. A. p 3647 N93-28807
MARTIN, STEVE p 3342 N93-29402
MARTINELLI, A. E. p 3339 N93-30773
MARTINEZ, SALVADOR GUTIERREZ
p 3517 N93-29565
MARTINSEN, ROBERT J. p 3486 N93-28996
MARX, K. D. p 3416 N93-28595
MARXER, NORBERT p 3580 N93-30372
MARZOT, G. S. p 3529 N93-29647
MARZULLO, KEITH p 3531 N93-29976
MARZWELL, NEVILLE I. p 3627 N93-30714
MASAPATI, G. H. p 3356 N93-30227
MASARIK, JOZEF p 3572 N93-29628
MASER, J. p 3261 N93-29869
MASI, JAMES V. p 3291 N93-30955
MASLEY, AMY S. p 3505 N93-28941
MASON, JAMES B. p 3318 N93-29683
MASSMANN, FRANZ-HEINRICH p 3457 N93-28918
MASSON, PAUL p 3628 N93-30724
MASTERS, A. I. p 3287 N93-28946
MASTERS, J. E. p 3304 N93-30848
MATESANZ, A. p 3259 N93-29964
MATHER, DANIEL p 3445 N93-29388
MATHERS, BRUCE H. p 3261 N93-29436
MATHEUSVALLE, J. L. p 3607 N93-30920
MATHEW, JOSEPH p 3418 N93-28947
MATHEW, THOMAS p 3555 N93-29923
MATHIAS, S. p 3378 N93-28802
MATIJEVIC, EGON p 3337 N93-30552
MATMOR, A. p 3317 N93-30982
MATORA, I. M. p 3600 N93-30766
MATT, E. E. p 3373 N93-30331
MATTHEWS, D. L. p 3440 N93-30394
MATTHEWS, G. F. p 3588 N93-29334
MATTHEWS, J. A. J. p 3566 N93-29261
MATTICARI, GIOVANNI p 3290 N93-29907
MATTINGLY, J. K. p 3382 N93-29244
MAUBERT, P. p 3256 N93-29948
MAUDLIN, P. J. p 3454 N93-31013
MAUERSBERGER, K. p 3646 N93-28798
MAURICE, F. p 3435 N93-30469
MAURICE, J. M. p 3258 N93-29960
MAUSER, WOLFRAM p 3458 N93-28926
MAWID, M. p 3251 N93-28617
MAX, N. L. p 3524 N93-28550
MAY, E. p 3576 N93-30527
MAY, G. B. p 3453 N93-30147
MAY, L. D. p 3320 N93-30277
MAYER, A. p 3255 N93-29946
MAYER, T. S. p 3598 N93-30511
MAYFIELD, M. p 3485 N93-30758
MAYLE, ROBERT E. p 3252 N93-29927
MAYNARD, JAY W. p 3472 N93-30180
MAYNARD, SHAWN J. p 3305 N93-30853
MAZAHERIBODY, KARIM p 3428 N93-30999
MAZIASZ, P. J. p 3325 N93-29813
MAZUR, B. A. p 3370 N93-30314
MAZZOLA, M. S. p 3406 N93-28944
MCALLISTER, A. p 3423 N93-29804
MCALLISTER, M. LUISA NICOSIA
p 3519 N93-29577
MCANULTY, D. M. p 3508 N93-30590
MCARDLE, JACK G. p 3252 N93-29065
MCBRIDE, J. MICHAEL p 3318 N93-30067
MCCARRICK, MICHAEL J. p 3398 N93-30746
MCCARTHY, THOMAS p 3248 N93-29153
MCCARTY, JOHN E. p 3300 N93-30429
MCCARTY, W. D. p 3260 N93-28467
MCCLAMROCH, HARRIS p 3280 N93-29992
MCCLAMROCH, N. HARRIS p 3279 N93-29988
p 3280 N93-29990
p 3280 N93-29991
p 3280 N93-29993
p 3280 N93-29994
p 3280 N93-29995
MCCLAVE, EDWARD F. p 3335 N93-29881
p 3335 N93-29886
MCCLEELAND, GARY M. p 3446 N93-30524
MCCOLLOUGH, ROGER p 3407 N93-29203
MCCONVILLE, DAVID H. p 3336 N93-30169
MCCRACKEN, H. B. p 3245 N93-28990
MCCRAY, S. B. p 3331 N93-29201
MCCREADY, M. J. p 3422 N93-29326
MCCREIGHT, CRAIG p 3429 N93-29701
MCCUNE, J. E. p 3420 N93-29141
MCDANIEL, PAUL A. p 3270 N93-28938
MCDERMOTT, GENE p 3529 N93-29657
p 3529 N93-29658
MCDONALD, D. S. p 3575 N93-29302
MCDONALD, M. J. p 3447 N93-30654
MCDONNELL, J. A. M. p 3283 N93-29362
MCDONNELL, JOHN R. p 3446 N93-30384
p 3544 N93-30592
MCELIECE, R. p 3385 N93-29596
MCELIECE, R. J. p 3385 N93-29595
MCELROY, DAVID R. p 3389 N93-29900
MCEWEN, A. S. p 3624 N93-28803
MCFEE, JOHN E. p 3324 N93-29391
MCGANN, R. L. p 3649 N93-28815
MCGEE, W. F. p 3355 N93-30219
p 3361 N93-30256
MCGERVEY, J. D. p 3334 N93-29856
MCGONIGAL, GORDON p 3355 N93-30223
MCGOVERN, FRANKLIN M. p 3376 N93-30346
MCGOWAN, GREG p 3236 N93-30679
MCGUCKIN, BRENDAN T. p 3440 N93-30415
MCINTIRE, VAUGHN W., JR. p 3288 N93-28950
MCINTOSH, JOHN p 3237 N93-30683
MCINTOSH, ROY p 3265 N93-28721
p 3429 N93-29701
MCKAMEY, C. G. p 3325 N93-29813
MCKECHNIE, TIMOTHY N. p 3338 N93-30565
MCKIBBEN, R. B. p 3286 N93-29707
MCKINNEY, G. W. p 3540 N93-30633
MCKINSTRY, JOHN W. p 3391 N93-29987
MCKNETT, C. L. p 3520 N93-29058
MCLACHLAN, D. G. p 3375 N93-30342
MCLACHLAN, J. C. p 3392 N93-30362
MCLANE, P. J. p 3373 N93-30332
p 3373 N93-30333
MCLAUCHLAN, PHILIP F. p 3523 N93-28485
p 3505 N93-28897
MCLEOD, R. D. p 3361 N93-30258
MCLIN, M. G. p 3332 N93-29342
p 3334 N93-29825

p 3410 N93-29826
MCMATH, W. S. p 3357 N93-30232
MCMULLIN, J. N. p 3358 N93-30240
MCNALLY, PATRICK J. p 3280 N93-29995
MCNEAL, G. D. p 3393 N93-30423
MCNESBY, KEVIN L. p 3309 N93-28514
MCQUEEN, M. p 3247 N93-30357
MCVEY, S. E. p 3416 N93-28627
MEAD, JAYLEE M. p 3629 N93-29156
MEADE, L. E. p 3300 N93-30433
MEARS, C. A. p 3594 N93-29249
MEGUID, S. A. p 3369 N93-30305
MEI, CHUH p 3451 N93-29154
MEIER, G. H. p 3325 N93-29981
MEILUNAS, R. J. p 3599 N93-30548
MEISER, STEFAN p 3547 N93-28512
MEISS, J. D. p 3584 N93-28599
MELISSOPOULOS, STEPHANOS p 3268 N93-29063
MELIUS, CARL F. p 3343 N93-30063
p 3318 N93-30064
MELLOCH, M. R. p 3464 N93-28971
p 3598 N93-30511
MELLOUL, S. p 3317 N93-30982
MELNIKOV, P. I. p 3590 N93-30768
MELNIKOV, V. K. p 3551 N93-30765
MENA, RAFAEL A. p 3405 N93-28610
MENAKER, MICHAEL p 3496 N93-30382
MENG, Q.-H. p 3355 N93-30218
MENIKOFF, R. p 3426 N93-30484
MENZIES, ROBERT T. p 3440 N93-30415
MERAT, F. L. p 3534 N93-30495
MEREWETHER, K. O. p 3484 N93-30651
MERLET, JEAN-PIERRE p 3523 N93-28504
MERRILL, B. R. p 3241 N93-30151
p 3241 N93-30171
p 3241 N93-30172
p 3242 N93-30173
MERROW, JAMES E. p 3283 N93-29363
MESHCHERYAKOV, V. A. p 3571 N93-30791
MESHISHNEK, M. J. p 3638 N93-29361
MESHJISHNEK, MICHAEL J. p 3329 N93-28561
MESSEH, W. ABDEL p 3255 N93-29941
MESSITT, DON G. p 3233 N93-29749
METSCHAN, S. L. p 3302 N93-30440
METSCHAN, STEPHEN p 3306 N93-30865
METZGER, A. p 3650 N93-28824
METZGER, D. E. p 3255 N93-29943
METZGER, DON p 3391 N93-30016
MEURER, ROBERT H. p 3284 N93-29904
MEYER-ILSE, W. p 3261 N93-29869
p 3433 N93-30531
MEYER, C. p 3434 N93-28804
MEYER, DAVID A. p 3607 N93-30884
MEYER, W. D. p 3483 N93-29850
MICHAL, T. p 3284 N93-29897
MICHALSKE, TERRY A. p 3452 N93-29515
MICHELS, JAMES H. p 3381 N93-28998
MICOL, JOHN R. p 3239 N93-29166
MIDDLETON, R. p 3573 N93-29643
MIGNEREY, A. C. p 3569 N93-29807
MIHOS, JAMES CHRISTOPHER p 3635 N93-30148
MIKULAS, MARTIN M., JR. p 3275 N93-29113
p 3277 N93-29118
MILBURN, GEORGE p 3626 N93-30697
MILHOAN, JAMES D. p 3278 N93-29221
MILIKH, G. M. p 3478 N93-30487
MILLER, D p 3596 N93-29868
MILLER, DAVID L. p 3311 N93-29283
MILLER, DAVID W. p 3263 N93-28705
MILLER, E. K. p 3380 N93-28900
MILLER, GARY A. p 3339 N93-30883
MILLER, GEORGE P. p 3476 N93-29032
MILLER, GLENN E. p 3613 N93-29227
MILLER, J. K. p 3246 N93-29588
MILLER, KAREN p 3497 N93-30882
MILLER, LARRY L. p 3290 N93-29474
MILLER, MARK D. p 3327 N93-30538
MILLER, MARTIN S. p 3413 N93-30539
MILLER, P. J. p 3615 N93-29310
MILLER, R. J. D. p 3593 N93-29096
MILLER, RICHARD S. p 3653 N93-30052
MILLER, STEVE p 3617 N93-30450
MILLER, T. A. p 3595 N93-29397
MILLER, WILLARD, JR. p 3473 N93-30360
MILLS, G. A. p 3309 N93-28750
MILLY, PETER F. p 3442 N93-28951
MINATO, KAZUO p 3299 N93-30004
MING, D. W. p 3643 N93-28782
MINTZ, DANIEL G. p 3620 N93-30467
MIRTICH, MICHAEL J. p 3283 N93-29363
MISHIMA, H. p 3410 N93-29673
MISHRA, S. R. p 3369 N93-30308
p 3371 N93-30321
MISHRA, UMESH p 3298 N93-29282
MISRA, V. p 3638 N93-29378
MITAL, SUBODH K. p 3297 N93-29071
MITCHELL, G. E. p 3566 N93-29184
MITCHELL, M. R. p 3304 N93-30850
MITRA, S. p 3582 N93-28789
MITRA, SUNANDA p 3512 N93-29535
MITTAL, SANJAY p 3419 N93-29040
MITTER, SANJOY K. p 3543 N93-29917
MITU, A. p 3369 N93-30305
MIURA, M. p 3329 N93-28551
MIYA, NAOYUKI p 3589 N93-30397
MIZIOLEK, ANDRZEJ W. p 3319 N93-30081
p 3315 N93-30405
MKPADI, M. C. p 3257 N93-29954
MOBERG, VICTOR L. p 3437 N93-29276
MOELLER, ROBERT P. p 3431 N93-29046
MOGAHED, E. A. p 3439 N93-30186
MOGFORD, RICHARD H. p 3372 N93-30322
MOHAMED, MAGDI p 3514 N93-29545
MOHAMMEDI, N. p 3480 N93-31002
MOHEB, H. p 3367 N93-30293
MOITRA, STUTI p 3520 N93-29070
MOLDOVAN, DAN p 3521 N93-29504
MOLNAR, D. E. p 3501 N93-28757
MOLNAR, JOHN p 3264 N93-28708
MONARSKI, T. W. p 3583 N93-29699
MONICO, R. D. p 3256 N93-29949
MONTAGUE, WILLIAM E. p 3544 N93-30556
MONTEIRO, M. A. R. p 3607 N93-30920
MONTERO, JAVIER p 3513 N93-29540
MONTEVERDI, J. P. p 3485 N93-30889
MONTICONE, LEONE C. p 3247 N93-30353
MOODY, JOHN p 3623 N93-30559
MOORE, DAVID S. p 3318 N93-30072
MOORE, GARY p 3608 N93-29396
p 3608 N93-29440
MOORE, GARY T. p 3235 N93-29760
MOORE, HOMER J. p 3497 N93-30882
MOORE, J. A. p 3394 N93-30631
MORABITO, D. D. p 3386 N93-29603
MORAITES, S. p 3380 N93-28900
MORAN, K. L. p 3598 N93-30407
MOREL, M. R. p 3295 N93-28681
MORENO, HECTOR p 3409 N93-29513
MORGAN, FERRAL p 3272 N93-30617
MORGAN, R. M. p 3279 N93-29840
MORGENTHALER, GEORGE W. p 3275 N93-29114
p 3277 N93-29121
MORIMATSU, O. p 3604 N93-29242
MORIN, G. A. p 3369 N93-30308
p 3374 N93-30334
MORIN, STEPHANE p 3363 N93-30272
MOROSIN, B. p 3598 N93-30517
MORREN, W. EARL p 3287 N93-28694
p 3288 N93-29194
MORRIS, ANDREW p 3506 N93-29471
MORRIS, BRIAN G. p 3442 N93-28501
MORRIS, CHARLES p 3627 N93-30713
MORRIS, D. J. p 3649 N93-28815
MORRIS, J. R. p 3630 N93-29785
MORRIS, M. E. p 3484 N93-30651
MORRIS, R. V. p 3648 N93-28812
MORRIS, TIMOTHY B. p 3442 N93-28951
MORRIS, W. D. p 3254 N93-29937
MORRIS, W. L. p 3304 N93-30850
MORRISON, P. J. p 3584 N93-28599
MORRISON, PETER p 3459 N93-29146
MORRISSEY, JAMES F. p 3483 N93-29832
MORTENSEN, MICHAEL p 3230 N93-29732
MORTON, JOHN p 3308 N93-30874
MOSES, G. A. p 3439 N93-30186
MOSLEY, W. C. p 3324 N93-29265
MOSS, B. p 3271 N93-28487
MOSS, C. p 3650 N93-28824
MOSS, C. E. p 3647 N93-28807
MOSS, CALVIN E. p 3572 N93-29628
MOSTAFAZADEH, A. p 3556 N93-28601
MOTLEY, WILLIAM R., III p 3638 N93-29377
MOULDING, S. M. p 3567 N93-29351
MOUNTAIN, R. W. p 3434 N93-28771
MOYA, M. M. p 3412 N93-30370
MOZO, BEN T. p 3506 N93-29406
MPITSOS, GEORGE J. p 3539 N93-30361
MROWKA, S. p 3438 N93-29781
MUELLER, D. p 3325 N93-30115
MUKKAMALA, R. p 3527 N93-29219
MULARIE, WILLIAM p 3620 N93-30465
MULCAHY, T. H. p 3561 N93-29189
MULFORD, C. p 3624 N93-29668
MULHOLLAND, J. DERRAL p 3638 N93-29377
p 3638 N93-29379
MULLER, PETER p 3477 N93-29879
p 3488 N93-29914
MULLIGAN, W. E. p 3466 N93-30891
MUMMA, M. p 3285 N93-28779
MUNDRA, ANAND D. p 3247 N93-30356
MUNITZ, A. p 3328 N93-30941
MUNZ, C.-D. p 3586 N93-29081
p 3428 N93-31020
MURAKAMI, YOSHIKI p 3590 N93-30649
MURAWSKI, C. G. p 3255 N93-29945
MURPH, JESSE E. p 3427 N93-30492
MURPHY, BARBARA A. p 3506 N93-29406
MURPHY, D. D. p 3534 N93-30546
MURPHY, DANIEL V. p 3578 N93-29140
MURPHY, L. M. p 3286 N93-29910
MURRAY, BRUCE C. p 3651 N93-30635
MURRAY, DAVID W. p 3523 N93-28485
p 3505 N93-28897
MURRAY, H. S. p 3436 N93-28887
MURTHA, J. P. p 3432 N93-29390
MURTHY, P. L. N. p 3295 N93-28681
p 3307 N93-30868
MURTHY, PAPPU L. N. p 3297 N93-29071
MURTHY, S. N. B. p 3254 N93-29936
MURTY, A. N. p 3316 N93-30653
MUSARRA, S. p 3470 N93-29669
MUSKET, R. G. p 3594 N93-29301
MUSTAFA, D. p 3548 N93-28754
MUSTAFA, DENIS p 3541 N93-28898
MUSTICO, ARTHUR p 3582 N93-29694
MUZA, STEPHEN p 3497 N93-30894
MYATT, JAMES H. p 3248 N93-28693
MYERS, A. L. p 3428 N93-30759
MYERS, N. C. p 3474 N93-30826
MYERS, TOM p 3622 N93-30476
MYLES, K. M. p 3464 N93-29844
MYRA, J. R. p 3589 N93-30189
MYRABO, LEIK N. p 3233 N93-29749

N

NACSON, S. p 3244 N93-30276
NAGEL, S. p 3418 N93-28878
NAHUM, M. p 3430 N93-28664
p 3431 N93-29149
NAIK, RAJIV A. p 3307 N93-30870
NAIN, PHILIPPE p 3541 N93-28637
p 3541 N93-28638
NAIR, L. G. p 3441 N93-30801
NAIR, SATISH S. p 3511 N93-29530
NAIRN, JOHN A. p 3304 N93-30846
p 3304 N93-30847
NAKAFUJI, GLEN T. p 3288 N93-29289
NAKAJIMA, HAJIME p 3326 N93-30191
p 3326 N93-30396
NAKAJIMA, K. p 3583 N93-28533
NAKAJIMA, SHINJI p 3589 N93-30397
NAKANISHI, H. p 3583 N93-28533
NAKANO, HIROSHI p 3247 N93-30324
NAKUYAMA, KEN p 3495 N93-30192
NAMKOONG, DAVID p 3265 N93-28720
NANDI, S. p 3270 N93-29589
NARAYANAN, M. A. p 3423 N93-29426
NARAYANAN, R. p 3405 N93-28641
NARUSE, YUJI p 3320 N93-28529
NASRAOUI, OLFA p 3511 N93-29524
NASTASI, M. p 3594 N93-29314
NATARAJAN, SWAMI p 3512 N93-29537
NATION, JOHN A. p 3590 N93-30600
NAUCK, DETLEF p 3514 N93-29549
p 3516 N93-29560
NAYAK, P. P. p 3531 N93-29873
NAZARI, A. p 3257 N93-29954
NAZIROV, M. T. p 3571 N93-30788
NEALY, RANDALL p 3404 N93-28539
NEARY, C. p 3503 N93-28862
NECKER, ERIC p 3522 N93-28482
NECSULESCU, D. S. p 3370 N93-30310
NEDELKO, S. N. p 3605 N93-30782
NEEDHAM, DAVID p 3291 N93-30953
NEER, J. T. p 3285 N93-29912
NEGRON, ANTHONY J. p 3489 N93-30178
NEHAMA, E. p 3328 N93-30941
NEIDIG, DONALD F. p 3652 N93-28585
NEILL, D. T. p 3425 N93-30132
NEILSON, J. E. p 3364 N93-30279
NELSON, G. C. p 3339 N93-30656
NELSON, GERALD p 3342 N93-29402
NELSON, J. R. p 3610 N93-29499
p 3272 N93-30881
NELSON, KEITH A. p 3319 N93-30075
NELSON, L. D. p 3331 N93-29201
NELSON, RANDY E. p 3542 N93-29420
NEMANICH, R. J. p 3593 N93-28874
NEMAWARKAR, S. p 3359 N93-30244
NEMER, E. J. p 3373 N93-30328
NEMOTO, TOSHIYUKI p 3524 N93-28537
NENOFF, TINA M. p 3592 N93-28584
NETA, BENY p 3489 N93-30525
NEUKUM, G. p 3285 N93-28779
NEUMAN, B. CLIFFORD p 3526 N93-29169
NEUMARK, GERTRUDE p 3601 N93-30811
NEVELS, ROBERT D. p 3550 N93-29876

NEWELL, PATRICK T. p 3476 N93-28842
NEWMAN, BRIAN A. p 3334 N93-29660
NEWMAN, D. E. p 3585 N93-28913
NEWMAN, F. H. p 3284 N93-29893
NEWMAN, N. p 3596 N93-29868
NEWMAN, P. J. p 3283 N93-29362
NEWMAN, S. C. p 3283 N93-29705
NGUYEN, A. p 3603 N93-28964
NGUYEN, H. X. p 3422 N93-29338
NGUYEN, T. p 3648 N93-28812
NICASTRI, E. p 3269 N93-29908
NICHOLLS, D. M. p 3397 N93-30741
NICHOLS, ALBERT L., III p 3319 N93-30082
NICHOLS, F. A. p 3330 N93-28666
NICKERSON, G. R. p 3526 N93-29028
NICOL, T. H. p 3407 N93-29048
NIELSEN, K. F. p 3602 N93-29381
NIEMYER, L. LARKIN p 3251 N93-28871
NIERA, H. G. p 3534 N93-30577
NIES, ROGER p 3440 N93-30553
NIETUBICZ, CHARLES J. p 3240 N93-29512
NIILER, ANDRUS p 3341 N93-28515
NIJTMANS, JOANNES JOSEPHUS
p 3382 N93-29266
NIKIFOROV, A. A. p 3590 N93-30768
NISHIDA, Y. p 3583 N93-28533
NISHIYAMA, R. T. p 3434 N93-28767
NIX, WILLIAM D. p 3337 N93-30417
NOBLE, J. p 3624 N93-29668
NOCK, K. p 3649 N93-28819
NODA, N. p 3583 N93-28532
NODARSE, F. F. p 3623 N93-30994
NOE, J. W. p 3575 N93-29317
NOEL, D. PETER p 3360 N93-30250
NOEL, DAVID PETER p 3358 N93-30238
NOELL, T. E. p 3544 N93-30529
NOEVER, DAVID A. p 3491 N93-29174
NOID, D. W. p 3538 N93-28894
NOLAN, ADAM p 3289 N93-29570
NOLAN, M. P. p 3430 N93-28520
NOLET, M. C. p 3478 N93-30113
NOMACHI, M. p 3382 N93-29245
NOMURA, YUKIO p 3587 N93-29243
NOOJIN, GARY D. p 3438 N93-29395
NOONAN, KEVIN W. p 3240 N93-29450
NORDIN, P. p 3434 N93-28768
NORDQUIST, S. E. p 3375 N93-30340
NORFLEET, WILLIAM T. p 3495 N93-29651
NORGARD, JOHN p 3391 N93-30016
NORIKANE, L. p 3614 N93-29234
NORMOYLE, MARIE B. p 3387 N93-29890
NORRIS, BONNIE p 3266 N93-28726
NORTHRUP, V. M. p 3493 N93-28758
NOURRY, G. R. p 3375 N93-30342
NOVAK, B. p 3524 N93-28834
NOVAKOV, T. p 3472 N93-30043
NOWLIN, BRENT C. p 3251 N93-28697
NOWLIN, C. H. p 3394 N93-30631
NOWLIN, R. N. p 3413 N93-30650
p 3570 N93-30669
NOYES, ROBERT W. p 3652 N93-28585
NOZETTE, S. p 3285 N93-28779
NUCCIARONE, J. J. p 3482 N93-29448
NUEESCH, D. p 3457 N93-28920
NUNNALLY, CHARLES p 3404 N93-28539
NUZZO, JAMES G. p 3338 N93-30596
NYSTROM, L. p 3516 N93-29562

O

OAKLEY, WILLIAM S. p 3621 N93-30471
OBERTHALER, DAVID P. p 3459 N93-29000
OBRIEN, T. KEVIN p 3307 N93-30866
ODA, K. p 3573 N93-29637
ODA, O. p 3597 N93-29974
ODEN, J. TINSLEY p 3538 N93-29030
OEI, J. L. H. p 3611 N93-28481
OELSCHLAGER, D. W. p 3471 N93-29676
OGATA, A. p 3583 N93-28533
OGREN, J. p 3472 N93-30043
OHASHI, MASAO p 3326 N93-30396
OHERN, TIM p 3342 N93-29402
OHKAWA, YOSHINAO p 3587 N93-29243
OHL, THORSTEN p 3571 N93-30670
OHSAWA, Y. p 3588 N93-29434
p 3590 N93-30533
OJANPERA, ESKO p 3532 N93-29997
OKAMOTO, Y. p 3334 N93-29825
OKAMOTO, YUKI p 3247 N93-30324
OKES, L. R. p 3444 N93-29205
OKINE, R. K. p 3301 N93-30437
OKSUZOGLU, HAKAN p 3419 N93-29039
OKU, TATSUO p 3299 N93-30004
OKUMURA, YOSHIKAZU p 3589 N93-30190
p 3590 N93-30606
OLAH, ANDRAS p 3379 N93-28502
OLEA, MICHELE M. p 3498 N93-30026
OLEKSUK, L. p 3259 N93-30168
OLINGER, B. p 3315 N93-30209
OLIVER, J. H. p 3528 N93-29473
OLIVER, JAMES M. p 3342 N93-29494
OLIVER, JOHN P. p 3267 N93-28735
p 3638 N93-29377
p 3638 N93-29379
OLMEZ, ILHAN p 3572 N93-29630
OLSON, G. B. p 3321 N93-28902
p 3321 N93-28957
OLSON, G. L. p 3586 N93-29093
OLSON, MICHAEL P. p 3528 N93-29345
OLSON, R. E. p 3437 N93-29264
OLSSON, ROBIN p 3451 N93-29076
OLTHOF, R. p 3463 N93-30839
OLTON, DAVID S. p 3544 N93-30165
ONEAL, MELVIN R. p 3267 N93-28739
p 3268 N93-28740
p 3268 N93-28741
p 3268 N93-28742
ONEIL, D. p 3336 N93-30182
ONG, KOK KIONG p 3270 N93-30582
ONKEN, R. p 3502 N93-28855
ONO, KIYOSHI p 3584 N93-28535
ONO, SHOICHI p 3436 N93-28980
ORCUTT, JOHN A. p 3477 N93-29412
ORENBERG, J. B. p 3646 N93-28800
ORENSTEIN, J. O. p 3594 N93-29249
ORSER, D. J. p 3579 N93-29667
ORSZAG, STEVEN A. p 3528 N93-29483
ORZO, L. p 3519 N93-29576
OSANAI, SEIJI p 3524 N93-28537
OSANTOWSKI, J. F. p 3582 N93-28788
OSCARSON, J. L. p 3316 N93-30661
OSILIKE, M. O. p 3552 N93-30942
OSTASZEWSKI, KRZYSZTOF p 3510 N93-29517
OSTERGAARD, JENS C. p 3399 N93-30757
OSTERKAMP, T. E. p 3487 N93-29298
OSTERYOUNG, ROBERT A. p 3316 N93-30551
OSTOJA-STARZEWSKI, MARTIN p 3453 N93-30159
OSTROM, L. T. p 3505 N93-28942
OSULLIVAN, D. p 3654 N93-29646
OTOOLE, B. J. p 3301 N93-30437
OTOSHI, T. Y. p 3385 N93-29594
OTSUKA, N. p 3597 N93-30164
OVERLAND, JAMES E. p 3483 N93-29491
OVERTON, JAMES MORRIS p 3355 N93-30217
OWEN, J. M. p 3256 N93-29950
OWENS, K. J. p 3447 N93-30828
OXENDINE, CHARLES R. p 3249 N93-29779
OXLEY, JAMES C. p 3318 N93-30065
OZMEN, TAMER p 3553 N93-28760
OZOYA, IBRAHIM OHIOKHOYA p 3513 N93-29541

P

PACE, MICHAEL E. p 3529 N93-29657
p 3529 N93-29658
PACE, SCOTT p 3625 N93-30695
PACI, L. p 3254 N93-29939
PACIA, ARNEL P. p 3240 N93-29410
PADDEN, R. J. p 3583 N93-29699
PAGANO, THOMAS p 3245 N93-28625
PAGE, DANIEL A. p 3578 N93-29139
PAGE, GARY L. p 3531 N93-29874
PAGE, MICHAEL p 3319 N93-30099
PAGNAN, S. p 3397 N93-30743
PAGNI, A. p 3513 N93-29538
PAIGE, D. A. p 3647 N93-28805
PAIGE, J. B. p 3609 N93-29322
p 3609 N93-29323
PAINTER, J. F. p 3549 N93-29060
PAIS, M. R. p 3423 N93-29352
p 3425 N93-30155
PAISLEY, J. A. p 3394 N93-30662
PAK, Y. S. p 3334 N93-29825
PAKNYS, R. p 3369 N93-30309
PAL, NIKHIL R. p 3511 N93-29528
PAL, SANKAR K. p 3511 N93-29525
PALAITH, DAVID p 3595 N93-29341
PALMER, D. R. p 3394 N93-30662
PALMER, DEAN p 3310 N93-28988
PALMER, RAY p 3300 N93-30431
p 3301 N93-30438
PALMER, RAYMOND J. p 3304 N93-30852
PALMQUIST, R. D. p 3447 N93-30654
PAN, J. p 3577 N93-30532
PANKOVE, JACQUES p 3601 N93-30811
PAO, Y. H. p 3534 N93-30495
PAOLELLA, ARTHUR p 3383 N93-29455
PAPATHANASIOU, T. p 3296 N93-28904
PAPAZIAN, PETER B. p 3382 N93-29202
PAPPAS, G. p 3253 N93-29932
PARAMESWAR, AKILESH p 3362 N93-30263
PARENTI, RONALD R. p 3578 N93-29139
p 3578 N93-29140
p 3579 N93-29470
PARIKH, A. N. p 3569 N93-29839
PARK, H. S. p 3430 N93-28520
PARK, K. C. p 3274 N93-29109
PARK, ROBERT p 3601 N93-30811
PARKER, E. L. p 3430 N93-28520
PARKER, ROBERT p 3461 N93-29817
PARKINSON, BRADFORD W. p 3460 N93-29179
PARKS, CURTIS p 3407 N93-29203
PARKS, GARY S. p 3381 N93-29087
PARLETT, B. N. p 3525 N93-28986
PARLOS, ALEXANDER p 3512 N93-29531
PARMAR, DEVENDRA S. p 3452 N93-29613
PARNELL, T. A. p 3624 N93-29631
p 3572 N93-29632
p 3573 N93-29637
p 3573 N93-29639
PARNELL, THOMAS A. p 3654 N93-29626
PARRA, RAMON p 3528 N93-29294
PARRY, DIANE B. p 3323 N93-29259
PARSONS, GEORGE M., III p 3267 N93-28733
PARSONS, W. M. p 3406 N93-28830
PARTRIDGE, C. J. p 3562 N93-30029
p 3562 N93-30157
PARVIZ, BEHZAD p 3519 N93-29582
PASCHEN, K. W. p 3638 N93-29361
PATEL, N. D. p 3441 N93-31023
PATEL, RAKESH R. p 3527 N93-29171
PATKAR, M. P. p 3464 N93-28971
PATTERSON, E. L. p 3437 N93-29180
PATTERSON, R. H. p 3522 N93-30480
PATYRA, MAREK p 3515 N93-29551
PATYRA, MAREK J. p 3519 N93-29578
PAUL, M. p 3267 N93-28738
PAUL, P. p 3575 N93-29317
PAULIUKONIS, R. P. p 3630 N93-2946
PAULK, MARK C. p 3530 N93-29852
p 3610 N93-29970
PAULOS, T. p 3267 N93-28738
PAULSON, JOHN W., JR. p 3239 N93-29165
PAVEL, SANDY p 3519 N93-29579
PAVLOV, D. V. p 3551 N93-30913
PAXTON, K. p 3267 N93-28738
PAYNE, BARRY p 3237 N93-30682
PAYSON, PAUL M. p 3381 N93-28997
PEARCE, J. L. p 3362 N93-30267
PEARCE, W. J. p 3254 N93-29940
PEASE, R. L. p 3570 N93-30669
PECILE, C. A. p 3322 N93-29002
PECKHAM, RICHARD J. p 3288 N93-28950
PEDRYCZ, W. p 3515 N93-29552
PEDRYCZ, WITOLD p 3519 N93-29580
PEGG, D. J. p 3564 N93-28665
PEKALA, R. W. p 3311 N93-29263
PELLERIN, LOUISE DONNA p 3391 N93-30010
PELLETIER, M. p 3366 N93-30290
PELTOLA, ESA p 3465 N93-30111
PEMMARAJU, SURYA p 3512 N93-29535
PENA, F. LOPEZ p 3258 N93-29959
PENARANDA, FRANK E. p 3626 N93-30699
PENCE, THOMAS J. p 3299 N93-29982
PENEDO, MARIA H. p 3535 N93-30602
PENG, JIAN p 3400 N93-31036
PENNER, J. E. p 3472 N93-30043
PENNISTON, R. R., JR. p 3332 N93-29328
PENWELL, PAUL E. p 3564 N93-28562
PEPLIES, R. W. p 3472 N93-30009
PEPPER, G. T. p 3405 N93-28563
p 3357 N93-30230
PERETTIE, DONALD J. p 3621 N93-30473
PEREZ, J. S. p 3382 N93-29244
PEREZ, R. B. p 3382 N93-29244
PEREZ, WILLIAM A. p 3506 N93-29484
PERKINS, STEVEN W. p 3292 N93-30960
PERRIER, CHRISTIAN p 3326 N93-30138
PERROTTA, ANTHONY J. p 3336 N93-30170
PERROTTA, G. p 3290 N93-29907
p 3286 N93-29909
PERRY, A. T. p 3283 N93-29705
PERRY, J. L. p 3505 N93-28977
PERRY, M. R. p 3501 N93-28757
PERSSON, P. A. p 3315 N93-30209
PERSSON, PER-ANDERS p 3350 N93-30096
PESARAN, A. A. p 3465 N93-30206
PETERS, BRUCE p 3435 N93-30470
PETERS, JOSEPH I. p 3506 N93-29484
PETERS, PALMER N. p 3283 N93-29622
PETERSON, P. F. p 3586 N93-29053
PETRENKO, A. V. p 3600 N93-30771
PETRICK, M. p 3587 N93-29299
PETRIU, D. C. p 3364 N93-30279
PETRIU, E. p 3357 N93-30232
p 3370 N93-30312

PETRO, JOHN p 3379 N93-28555
PETRONE, LOUIS p 3334 N93-29660
PETROVIC, J. J. p 3296 N93-28904
PETTIT, D. p 3434 N93-28769
PETTIT, F. p 3327 N93-30812
PETTIT, F. S. p 3325 N93-29981
PEYGHAMBARIAN, N. p 3439 N93-29983
PEZESHKPOUR, G. H. p 3492 N93-30818
PFAHL, C. L. p 3302 N93-30440
PFITZER, H. p 3256 N93-29952
PFLUG, LISA p 3391 N93-29975
PFLUGER, NATHAN p 3512 N93-29537
PHAM, VUONG T. p 3278 N93-29221
PHAN, MINH p 3455 N93-31038
PHARAND, A. p 3370 N93-30312
PHELPS, RANDY LEE p 3635 N93-30377
PHILLIPS, LEE p 3350 N93-30097
PHILLIPS, WILLIAM M., JR. p 3407 N93-29173
PHILPOTT, M. R. p 3568 N93-29489
PHILPOTT, MICHAEL R. p 3309 N93-28540
p 3323 N93-29259
p 3567 N93-29336
p 3568 N93-29619
PHILPOTT, STEPHEN p 3235 N93-29756
PIASCIK, ROBERT S. p 3451 N93-29069
PIBEL, C. D. p 3569 N93-29860
PICKERING, H. W. p 3567 N93-29403
PICKINGS, RICHARD D. p 3306 N93-30863
p 3308 N93-30876
PIEDBOEUF, J. C. p 3361 N93-30261
PIEPER, G. W. p 3509 N93-28573
PIERCE, FREDERICK B. p 3341 N93-28515
PIERSON, E. S. p 3587 N93-29299
PIIPPO, STEVE W. p 3238 N93-28662
PIIPPO, STEVEN W. p 3243 N93-30979
PIJPERS, E. W. p 3505 N93-28872
PILKEY, R. D. p 3432 N93-29842
PINCKNEY, ROBERT L. p 3302 N93-30443
PINELLI, THOMAS E. p 3612 N93-28948
p 3615 N93-29709
p 3616 N93-30036
p 3616 N93-30037
PING, WANG p 3571 N93-30788
PIOTROWSKI, JERZY p 3454 N93-31015
p 3455 N93-31016
PIPE, HARVEY J. p 3501 N93-28854
PIPES, R. B. p 3301 N93-30437
PIPPIN, H. G. p 3283 N93-29623
PIRRELLI, P. p 3254 N93-29939
PISZCZOR, MICHAEL F. p 3265 N93-28717
PITTS, PATRICIA S. p 3629 N93-29156
PIVERT, OLIVIER p 3517 N93-29569
PLAKIDA, N. M. p 3602 N93-31025
PLASKACZ, E. J. p 3535 N93-30647
PLASMEIJER, RINUS p 3522 N93-28482
p 3523 N93-28484
PLASSMANN, P. E. p 3524 N93-28644
PLATT, JONATHAN A. p 3352 N93-30939
PLEDGER, D. p 3582 N93-28806
PLOTKIN, HENRY H. p 3626 N93-30704
PLUMMER, M. A. p 3317 N93-30761
PNUELI, AMIR p 3528 N93-29469
POE, C. C., JR. p 3304 N93-30848
POELKER, M. p 3574 N93-28970
POGLITSCH, A. p 3637 N93-30639
POINSATTE, PHILIP E. p 3420 N93-29157
POL, ELIZABETH E. p 3382 N93-29202
POLAK, ELIJAH p 3534 N93-30549
POLANSKI, A. p 3601 N93-30798
POLICASTRO, A. J. p 3482 N93-29399
POLITZER, PETER p 3351 N93-30098
POLLACK, RANDY B. p 3541 N93-28987
POLLEVOY, Y. p 3317 N93-30982
POLUZZI, R. p 3513 N93-29538
POMMAINVILLE, PIERRE p 3367 N93-30295
PONCELINDERAUCOURT, P. p 3256 N93-29947
POND, CHARLES p 3271 N93-29215
POPE, D. P. p 3321 N93-28679
POPE, J. C. D. p 3503 N93-28862
POPE, ROBERT S. p 3567 N93-29415
POPPE, C. H. p 3568 N93-29784
PORN, KURT p 3378 N93-30581
PORTANOVA, M. A. p 3304 N93-30848
PORTER, G. D. p 3588 N93-29334
p 3588 N93-29772
PORTIER, R. W. p 3354 N93-29663
POSNER, EDWARD C. p 3384 N93-29586
POST, GERHARD p 3547 N93-28667
POTEMRA, THOMAS A. p 3476 N93-28842
POTTER, DANIEL F. p 3487 N93-29003
POTTER, M. E. p 3566 N93-29313
POTTERVELD, D. H. p 3574 N93-28970
POTTS, MARIE K. p 3335 N93-30007
POUND, E. p 3400 N93-28820
POUTIGNAT, P. p 3504 N93-28868
POUWELS, H. p 3463 N93-31009
POWELL, JOHN D. p 3271 N93-29394
POWER, CHRISTOPHER A. p 3338 N93-30565
POWER, JOHN L. p 3288 N93-29158
POWERS, EDWARD J. p 3405 N93-28589
p 3409 N93-29485
POWERS, SID p 3260 N93-28851
PRABHAKARA, C. p 3482 N93-29448
PRABHAKARAN, RAMAMURTHY p 3452 N93-29612
PRABHU, KIKRAM p 3247 N93-30354
PRACCHIA, LOUIS p 3412 N93-30201
PRADE, HENRI p 3510 N93-29518
PRADHAN, DHIRAJ K. p 3409 N93-29654
PRAGER, S. C. p 3584 N93-28602
p 3585 N93-28912
PRASAD, J. V. R. p 3238 N93-30691
PRASD, P. N. p 3596 N93-29430
PRATT, J. RICHARD p 3331 N93-29083
p 3331 N93-29085
PRATT, TIM p 3404 N93-28539
PREDOEHL, ANDREW p 3404 N93-28539
PRESSER, C. p 3416 N93-28566
PRESTAGE, J. D. p 3384 N93-29587
PRESTON, JOHN T. p 3626 N93-30698
PRESTON, R. A. p 3642 N93-28777
PRICE, EDWARD W. p 3346 N93-30078
PRICE, L. E. p 3576 N93-30527
PRIDDY, T. G. p 3378 N93-30508
PRIMEROSE, ANTOINE p 3414 N93-31030
PRINCIPE, E. L. p 3322 N93-29002
PROBER, D. E. p 3430 N93-28664
PROBERT, ROBERT L. p 3368 N93-30302
PROKHOROV, L. V. p 3607 N93-30924
p 3607 N93-30925
PROPER, H. A. p 3523 N93-28503
PRUNIER, A. p 3333 N93-29404
PRYOR, DONALD p 3625 N93-30696
PRYOR, R. J. p 3425 N93-30184
PTAK, ALAN W. p 3361 N93-30258
PUCKETT, PAUL M. p 3305 N93-30853
PUNJABI, V. p 3392 N93-30126
PURDUE, LARRY J. p 3470 N93-29200
PURVIS, BRADLEY D. p 3507 N93-29888
PUTCHA, LAKSHMI p 3494 N93-29502
PUZYNIN, I. V. p 3551 N93-30913
PYZIK, A. p 3333 N93-29404

Q

QI, DEWEI p 3605 N93-30359
QIAO, SANZHENG p 3360 N93-30255
QUAM, WILLIAM p 3266 N93-28730
QUANDT, EARL p 3241 N93-29891
QUANG-QIAN, XING p 3281 N93-30142
QUATTROCCHI, L. S. p 3320 N93-28491
QUINN, P. p 3608 N93-30821
QUINTANA, C. p 3520 N93-29584
QUINTO, P. FRANK p 3239 N93-29165
QUIRK, JAMES J. p 3509 N93-28841
QUIST, A. S. p 3612 N93-28840

R

RABINOWITZ, WILLIAM M. p 3494 N93-29421
RABITZ, H. R. p 3319 N93-30090
RACICOT, RONALD L. p 3407 N93-29010
RADACK, G. M. p 3534 N93-30495
RADACK, S. M. p 3521 N93-29662
RADHAKRISHNAN, G. p 3602 N93-29684
RADICATIDIBROZOLO, FILIPPO p 3638 N93-29360
p 3283 N93-29364
RADKE, L. F. p 3472 N93-30043
RADTKE, PAUL H. p 3392 N93-30362
RAFA, M. J. p 3321 N93-28631
RAFFA, ANTHONY V. p 3259 N93-29278
RAFFERTY, K. p 3465 N93-30011
RAI, SURESH p 3540 N93-30364
RAITANO, PAUL p 3270 N93-28696
RAJ, BALDEV p 3328 N93-31022
RAJ, SAI V. p 3323 N93-29172
RAJAMAEKI, MARKKU p 3575 N93-29996
RAJAN, KRISHNASWAMY S. p 3333 N93-29458
RAJULU, SUDHAKAR L. p 3506 N93-29324
RALPH, M. E. p 3465 N93-30391
RAMAMOORTHY, P. A. p 3511 N93-29529
RAMARAO, B. V. p 3474 N93-30506
RAMER, ARTHUR p 3510 N93-29519
RAMIREZ, M. R. p 3535 N93-30647
RAMIREZ, T. L. p 3501 N93-28757
RAMKUMAR, RAMASWAMY L. p 3302 N93-30442
RAMSAY, M. A. p 3364 N93-30278
RAMSDELL, J. V. p 3481 N93-29054
RAMSEY, CHERYL p 3622 N93-30478
RAMSEY, G. P. p 3564 N93-28549
RANDALL, DONALD P. p 3520 N93-29070
RANDAZZO, PHILIP p 3379 N93-28555
RANDLE, ROBERT J., JR. p 3236 N93-30673
p 3236 N93-30674
RANDORF, J. p 3266 N93-28725
RANDRIAMAMPIANINA, A. p 3256 N93-29948
RANIAMURTI, RAVI p 3424 N93-29851
RAO, A. S. p 3595 N93-29333
p 3334 N93-29790
RAO, BHASKAR D. p 3530 N93-29865
RAO, K. S. p 3374 N93-30334
RAO, LING-FEN p 3315 N93-30526
RAPP, DOUGLAS C. p 3288 N93-29068
RAPPOPORT, W. p 3434 N93-28766
RASKIN, ROBERT GARY p 3477 N93-29467
RASPET, RICHARD p 3561 N93-28995
RASTANI, MANSUR p 3292 N93-30959
RATHER, JOHN D. G. p 3556 N93-28572
RATIU, T. S. p 3547 N93-28648
RATY, HANNA p 3575 N93-29996
RAWICZ, ANDREW H. p 3363 N93-30269
RAY, R. J. p 3331 N93-29201
RAYCHAUDHURI, A. p 3572 N93-30931
RAZAQ, A. p 3313 N93-29828
p 3317 N93-30664
RAZAQ, M. p 3313 N93-29828
p 3317 N93-30664
RCHEULISHVILI, G. p 3558 N93-30988
READ, K. p 3568 N93-29764
READ, MAJORIE S. p 3494 N93-29620
REASENBERG, ROBERT D. p 3630 N93-29163
REBA, R. C. p 3493 N93-28835
REBAY, S. p 3258 N93-29962
REBOLO, R. p 3259 N93-29964
RECK, GREGORY M. p 3625 N93-30693
p 3628 N93-30722
p 3628 N93-30723
RECORDS, ROGER M. p 3542 N93-29192
REDD, FRANK J. p 3263 N93-28703
REDDICK, ROBERT L. p 3494 N93-29620
REDMAN, WAYNE p 3273 N93-29884
REDNER, SIDNEY p 3313 N93-30030
REE, MALCOLM J. p 3498 N93-30026
REED, BRIAN D. p 3286 N93-28619
REED, K. M. p 3501 N93-28757
REEDY, R. p 3650 N93-28824
REEDY, R. C. p 3647 N93-28807
REEDY, ROBERT C. p 3572 N93-29628
REES, B. J. p 3322 N93-29002
REES, WILLIAM S., JR. p 3599 N93-30568
REEVES, JAMES H. p 3318 N93-29627
REEVES, JOHN T. p 3495 N93-29820
REHBEIN, D. K. p 3450 N93-28567
REHFIELD, LAWRENCE W. p 3306 N93-30863
p 3308 N93-30876
REID, IAN D. p 3505 N93-28897
REID, IAN DAVID p 3523 N93-28486
REIF, JOHN H. p 3529 N93-29496
REIFSNIDER, K. p 3259 N93-30168
REILE, E. p 3255 N93-29946
REILLY, RICHARD J. p 3431 N93-29066
REINIGER, KLAUS-DIETER p 3458 N93-28924
REINOVSKY, R. E. p 3410 N93-29812
REINTJES, JOHN F. p 3581 N93-30410
REISTER, D. B. p 3444 N93-29316
REITSEMA, H. p 3632 N93-28791
REITZ, ROLF D. p 3445 N93-29388
p 3580 N93-29880
REMAKLUS, WILL p 3404 N93-28539
RENIERI, MICHAEL P. p 3301 N93-30434
RENLUND, ANITA M. p 3344 N93-30069
p 3350 N93-30095
RENSINK, M. E. p 3588 N93-29772
RESTON, ROCKY R. p 3596 N93-29424
REYES, G. p 3434 N93-28774
REYES, MICHELLE p 3235 N93-29756
REYHANOGLU, MAHMUT p 3280 N93-29990
p 3280 N93-29991
p 3280 N93-29992
REYNOLDS, J. C. p 3386 N93-29680
REZNIK, L. p 3516 N93-29563
p 3520 N93-29584
REZVANI, M. A. p 3447 N93-30632
RHEE, FRANK CHUNG-HOON p 3511 N93-29526
RHEE, M. J. p 3591 N93-28496
RHINE, WENDELL E. p 3339 N93-30885
RIAHI, A. p 3255 N93-29941
RIBEIRO, M. S. p 3441 N93-30775
RICE, B. W. p 3587 N93-29303
RICE, EDWARD J. p 3561 N93-28953
RICE, MALCOLM J. p 3498 N93-29481
RICH, FREDERICK J. p 3476 N93-28842
RICHARD, GEORGES p 3284 N93-29896
RICHARDS, N. E. p 3322 N93-29061
p 3323 N93-29101
RICHARDS, P. L. p 3430 N93-28664
p 3594 N93-29249
p 3596 N93-29868

RICHTER, HELMUT p 3260 N93-28851
RICKEL, D. G. p 3410 N93-29812
RICKS, D. A. p 3638 N93-29378
RIDDLE, R. A. p 3422 N93-29300
RIEKE, G. p 3285 N93-28779
RIEKE, M. p 3285 N93-28779
RIES, HEIDI R. p 3291 N93-30958
RIETVELD, A. J. p 3460 N93-29307
p 3460 N93-29321
RIMRODT, JAMES p 3235 N93-29756
RINKER, E. B. p 3471 N93-29676
RIOUX, M. p 3366 N93-30286
p 3366 N93-30287
RISWICK, R. F. p 3540 N93-28480
RITCHIE, J. P. p 3598 N93-30445
p 3352 N93-30446
p 3570 N93-30448
RIVERA, T. p 3341 N93-29251
RIVERS, LEE W. p 3626 N93-30700
RIVIR, R. B. p 3254 N93-29935
RIVIR, RICHARD B. p 3423 N93-29426
RIZZO, T. R. p 3564 N93-28652
RIZZOTTO, G. G. p 3513 N93-29538
ROACH, DENNIS p 3449 N93-28685
ROACH, R. K. p 3521 N93-29662
ROADIFER, MICHAEL P. p 3382 N93-29202
ROBERTS, J. J. p 3410 N93-29793
ROBERTS, P. T. p 3470 N93-29669
ROBERTS, VICTORIA A. p 3571 N93-30901
ROBERTSON, DANIEL H. p 3318 N93-30071
p 3351 N93-30100
ROBERTSON, J. S. p 3396 N93-30736
ROBERTSON, M. O. p 3444 N93-29205
ROBERTSON, SCOTT D. p 3248 N93-29409
ROBINETT, RUSH p 3263 N93-28700
ROBINETTE, KATHLEEN M. p 3507 N93-29889
ROBINSON, MITCHELL S. p 3272 N93-30881
ROBINSON, N. P. p 3375 N93-30343
ROBINSON, SHARON H. p 3341 N93-28515
ROBINSON, WALDO p 3441 N93-30599
ROCHE, A. E. p 3434 N93-28794
ROCHON, GILBERT p 3614 N93-29239
ROCKENFELLER, U. p 3466 N93-30814
ROCKETT, P. D. p 3437 N93-29264
ROCKWELL, R. p 3434 N93-28766
RODGERS, MARK D. p 3498 N93-28622
RODIE, WARREN W. p 3481 N93-28876
RODIN, ERVIN Y. p 3541 N93-28498
RODRIGUEZ, J. V. p 3396 N93-30737
RODRIGUEZ, M. p 3259 N93-29964
RODRIGUEZ, P. p 3328 N93-31021
ROERDINK, J. B. T. M. p 3552 N93-31012
ROESSLER, N. p 3434 N93-28769
ROGERS, GARY RAY p 3293 N93-30973
ROGERS, J. D. p 3278 N93-29250
ROGERS, MELISSA J. B. p 3281 N93-30038
ROGERS, WAYNE P. p 3277 N93-29120
ROGNLIEN, T. D. p 3588 N93-29772
ROHARDT, CLAAS-HINRIK p 3422 N93-29273
ROMANOVSKIJ, Y. A. p 3466 N93-30777
RONA, M. p 3582 N93-28808
ROONEY, ARTHUR J., JR. p 3250 N93-29004
ROOZEN, NICOLAAS BERNARDUS
p 3248 N93-29268
ROSE, M. F. p 3283 N93-29365
ROSE, TIMOTHY L. p 3337 N93-30557
ROSEMA, A. p 3461 N93-29466
ROSEN, M. D. p 3438 N93-29309
p 3440 N93-30394
ROSEN, M. E. p 3569 N93-29805
ROSENBERG, D. p 3434 N93-28766
ROSENBERG, W. J. p 3434 N93-28794
ROSENFELD, AZRIEL p 3533 N93-30418
ROSENFELD, C. p 3574 N93-28969
ROSENFELD, DAVID p 3405 N93-28610
ROSENGREEN, A. p 3404 N93-28483
ROSENLOF, DARWIN p 3412 N93-30201
ROSENTHAL, T. J. p 3447 N93-30828
ROSS, CLAUDIA B. p 3432 N93-29476
ROSS, WILLIAM L., SR. p 3272 N93-29501
ROSSING, T. D. p 3561 N93-29189
ROSTOKER, NORMAN p 3476 N93-28538
ROTE, D. M. p 3561 N93-29189
ROTH, C. J. p 3273 N93-29306
ROTH, CARL p 3529 N93-29657
p 3529 N93-29658
ROTH, STEVEN F. p 3610 N93-30124
ROTHBERG, EDWARD p 3539 N93-29508
ROTHE, T. p 3256 N93-29952
ROUHI, ALI p 3424 N93-29838
ROUNDY, LANCE M. p 3301 N93-30434
ROUSE, MARSHALL p 3308 N93-30873
ROUSH, R. A. p 3406 N93-28944
ROUSSEL-DUPRE, R. p 3386 N93-29765
ROUSSOPOULOS, NICK p 3614 N93-29238
ROVENTA, EUGENE p 3519 N93-29580
ROWLEY, R. L. p 3316 N93-30661
ROY, RUSTUM p 3333 N93-29511
RUBEY, WAYNE A. p 3312 N93-29510
RUCKER, MICHELLE A. p 3331 N93-29088
RUDDICK, ANDREW J. p 3621 N93-30472
RUDERMAN, MALVIN p 3635 N93-30053
RUDOLPH, G. p 3556 N93-28601
RUDOWSKI, JERZY p 3407 N93-29037
RUEDA, A. p 3515 N93-29552
RUETSCH, GREGORY R. p 3427 N93-30625
RUFFA, A. A. p 3442 N93-28578
RUFFNER, JOHN W. p 3508 N93-30590
RUGH, WILSON J. p 3260 N93-30550
RUITBERG, A. p 3650 N93-28824
RUIZ, C. L. p 3575 N93-29151
RUPP, C. C. p 3399 N93-30755
RUSSELL, A. P. G. p 3631 N93-30615
p 3637 N93-30639
RUSSELL, C. T. p 3647 N93-28809
RUSSELL, D. A. p 3589 N93-30189
RUSSELL, JOHN p 3627 N93-30711
RUSSELL, STEVEN G. p 3307 N93-30869
RUSSELL, V. A. p 3597 N93-30146
RUST, D. M. p 3582 N93-28810
RUSTUM, ROY p 3291 N93-30952
RUTLEDGE, SHARON K. p 3283 N93-29363
RYAN, EILEEN VALERIE CUPTA p 3635 N93-30411
RYAN, L. E. p 3414 N93-29690
RYAN, T. G. p 3505 N93-28942
RYDZEWSKI, ROLAND p 3331 N93-29064
RYE, GILBERT D. p 3284 N93-29904
RYJOV, ALEXANDER P. p 3510 N93-29520
RYKIEL, EDWARD J., JR. p 3491 N93-29216

S

SAABAS, H. J. p 3255 N93-29941
SACKHEIM, ROBERT p 3628 N93-30716
SACKS, M. D. p 3338 N93-30601
SAGALYN, PAUL p 3572 N93-29630
SAGARA, A. p 3583 N93-28532
SAGEEV, R. Z. p 3585 N93-28749
SAHA, T. T. p 3582 N93-28788
SAHRAOUI, M. p 3424 N93-30035
SAHU, JUBARAJ p 3240 N93-29512
SAIZAR, PEDRO p 3636 N93-30412
SAKAWA, YOUICHI p 3379 N93-28534
SAKURAI, T. p 3567 N93-29403
SALAMON, N. J. p 3295 N93-28843
SALEH, KASSEM p 3356 N93-30228
SALEM, KENNETH p 3618 N93-30456
SALEMI, R. p 3254 N93-29937
SALT, J. W. A. p 3360 N93-30253
SAMANT, MAHESH G. p 3323 N93-29259
SAMAYOA, J. A. p 3442 N93-28552
SAMLIN, G. E. p 3437 N93-29180
SAMPAIR, THOMAS R. p 3428 N93-29624
SAMPSON, JAMES B. p 3495 N93-30196
SAMSON, CLAUDE p 3543 N93-30116
SANCHEZ, A. D. p 3583 N93-29699
SANCHEZ, J. A. p 3342 N93-29312
SANCHEZ, ROBERT R. p 3506 N93-29484
SANCHEZBRINGAS, F. p 3551 N93-30929
SANDALL, O. C. p 3471 N93-29676
SANDBERG, V. D. p 3566 N93-29313
SANDHOLT, P. E. p 3477 N93-29831
SANDSTROM, F. W. p 3315 N93-30209
SANDUSKY, H. W. p 3319 N93-30092
p 3319 N93-30093
p 3350 N93-30094
SANDWELL, DAVID T. p 3461 N93-29817
SANKAR, B. V. p 3304 N93-30848
SANLAVILLE, ERIC p 3538 N93-28937
SANTARE, M. H. p 3301 N93-30437
SANTEE, MICHELLE p 3651 N93-29616
SANTEE, W. R. p 3505 N93-28884
SANTORIELLO, G. p 3258 N93-29962
SANTORO, ROBERT J. p 3317 N93-30667
SANTOS, EUGENE, JR. p 3526 N93-29145
SAPER, RON p 3376 N93-30347
SAPP, CLYDE A. p 3283 N93-29359
SARAVANOS, D. A. p 3295 N93-28681
SARFF, J. S. p 3584 N93-28602
SARKISIAN, P. p 3466 N93-30814
SARKKULA, J. p 3488 N93-30040
SARTWELL, B. D. p 3330 N93-28687
SASAKI, O p 3382 N93-29245
SASAKI, TOSHIKAZU p 3435 N93-30461
SASARMAN, MICHAEL A. p 3359 N93-30243
SASIELA, RICHARD J. p 3579 N93-29470
SATO, MASAYASU p 3590 N93-30398
SATO, T. p 3496 N93-30659
SATO, TERUYUKI p 3379 N93-28534
SATYANARAYANA, A. p 3531 N93-29916
SATYANARAYANAN, M. p 3522 N93-30480
SAUDER, D. A. p 3530 N93-29678
SAULS, BOB p 3230 N93-29732
SAUNDERS, R. S. p 3649 N93-28819
p 3614 N93-29236
SAUSA, R. C. p 3319 N93-30081
SAUSA, ROSARIO C. p 3315 N93-30405
SAUTNER, M. p 3253 N93-29933
SAVAGE, LARRY p 3407 N93-29203
SAVARIA, YVON p 3361 N93-30257
SAVELEVA, A. E. p 3606 N93-30796
SAVINI, M. p 3258 N93-29962
SAVOYE, E. D. p 3434 N93-28771
SAWA, MASAFUMI p 3587 N93-29243
SAWDON, WAYNE A. p 3534 N93-30523
SAXELBY, ROBERT M. p 3338 N93-30565
SAXENA, A. p 3561 N93-29711
p 3598 N93-30501
p 3600 N93-30569
SAYEGH, S. p 3359 N93-30244
SAYLES, F. L. p 3489 N93-30056
SCALAPINO, D. J. p 3603 N93-28958
SCHAAF, CRYSTAL B. p 3462 N93-29830
SCHADE, CHRIS p 3284 N93-29904
SCHADEGG, GERRY p 3435 N93-30479
SCHAEFER, JUERGEN p 3611 N93-28525
SCHAFER, DAVID p 3244 N93-30275
SCHAFER, LOTHAR p 3319 N93-30101
SCHAPERY, RICHARD A. p 3348 N93-30088
SCHARRER, J. K. p 3416 N93-28627
SCHEERES, DANIEL JAY p 3652 N93-31000
SCHEFTER, M. p 3389 N93-29901
SCHEIDEMANN, A. p 3566 N93-29206
SCHEIMAN, DAVID A. p 3467 N93-29686
SCHEINBEIM, JERRY I. p 3334 N93-29660
SCHELTENS, PHILIP J. p 3363 N93-30269
SCHEPS, RICHARD p 3437 N93-29277
SCHERER, T. p 3256 N93-29951
SCHIESTEL, R. p 3256 N93-29948
SCHIMPF, M. E. p 3331 N93-29201
SCHIPPER, J. D. p 3399 N93-30836
p 3413 N93-30838
SCHIRBER, J. E. p 3598 N93-30517
SCHLAGER, KENNETH J. p 3494 N93-29509
SCHLATER, NELSON p 3628 N93-30724
SCHLICH, HUGO p 3324 N93-29272
SCHMEGNER, I. F. p 3493 N93-28939
SCHMIDLAPP, F. A. p 3575 N93-29151
SCHMIDT, DANIEL J. p 3507 N93-29606
p 3507 N93-29607
SCHMIDT, STEPHEN C. p 3318 N93-30072
SCHMIDT, U. p 3475 N93-28475
SCHMITT, J. H. M. M. p 3631 N93-30578
SCHMITT, ROBERT J. p 3564 N93-28562
SCHMITZ, MARION p 3629 N93-29156
SCHMOLL, W. J. p 3254 N93-29935
SCHNEIDER, CHRISTIAN p 3355 N93-30223
SCHNEIDER, KARL p 3458 N93-28926
SCHNEIDER, R. p 3586 N93-29081
SCHNEIDER, ROLAND p 3355 N93-30223
SCHNEIDER, STANLEY R. p 3627 N93-30710
SCHNETZER, G. H. p 3484 N93-30651
SCHODL, R. p 3255 N93-29942
SCHOLL, K. p 3464 N93-29925
SCHOOR, B. p 3247 N93-30357
SCHORR, HERBERT p 3526 N93-29169
SCHOTLAND, R. M. p 3381 N93-29105
SCHOTT, BRIAN p 3515 N93-29553
SCHOTT, JOACHIM H. p 3596 N93-29445
SCHRAGE, D. P. p 3238 N93-30691
SCHRAMM, D. N. p 3634 N93-28963
SCHRIJVER, A. p 3549 N93-29849
SCHRIMPF, R. D. p 3413 N93-30650
p 3570 N93-30669
SCHROCK, RICHARD R. p 3336 N93-30169
SCHROCK, V. E. p 3586 N93-29053
SCHROEDER, J. A. p 3386 N93-29680
SCHROEDER, S. p 3304 N93-30850
SCHUBERT, FRANZ H. p 3267 N93-28737
SCHUDLICH, R. p 3487 N93-29327
SCHUKANTZ, J. H. p 3303 N93-30555
SCHULBACH, CATHY p 3614 N93-29240
SCHULER, JAMES J. p 3450 N93-28556
SCHULTZ, S. p 3597 N93-30175
SCHULTZ, SHELDON p 3597 N93-30161
SCHULZ, R. B. p 3335 N93-30047
SCHUMACHER, HELMUT p 3459 N93-28932
SCHUMANN, ROBIN p 3272 N93-31033
SCHUNK, ROBERT W. p 3590 N93-30585
SCHURIG, H. J. p 3414 N93-29690
SCHURMAN, DON p 3449 N93-28685
SCHUSTER, K. F. p 3631 N93-30615
SCHWARTZ, D. E. p 3645 N93-28792
SCHWARTZ, ERIC L. p 3499 N93-30033
SCHWARTZ, S. E. p 3472 N93-30043
SCHWENDE, M. p 3284 N93-29906
SCHWENK, F. CARL p 3609 N93-29322
p 3609 N93-29323

SCHWETTMAN, H. A. p 3436 N93-28847
SCHWOEBEL, P. R. p 3404 N93-28483
SCHWUTTKE, URSULA M. p 3521 N93-29504
SCOTT, CURTIS p 3531 N93-29866
SCOTT, JAMES F. p 3594 N93-29293
SCOTT, JAMES R. p 3416 N93-28626
SEBAK, A. p 3369 N93-30307
SEE, THOMAS H. p 3638 N93-29355
p 3282 N93-29357
p 3283 N93-29359
p 3638 N93-29370
SEED, W. R. p 3362 N93-30267
p 3365 N93-30285
SEEGERS, BRYAN J. p 3259 N93-30877
SEEGMILLER, DAVID W. p 3582 N93-29692
SEHMBEY, M. S. p 3425 N93-30155
SEIDEMAN, TAMAR p 3603 N93-28933
SEKI, H. p 3323 N93-29259
SELCON, S. J. p 3503 N93-28864
SELCUK, NEVIN p 3257 N93-29955
SELESNICK, R. S. p 3641 N93-28773
SELF, HERSCHEL C. p 3494 N93-29400
SELLIS, TIMOLEON p 3614 N93-29238
SELVERIAN, J. H. p 3336 N93-30182
SEMERJIAN, H. G. p 3416 N93-28566
SEMPRUCCI, MARILYN p 3389 N93-29900
SEN, A. p 3606 N93-30807
SEN, BHASWAR p 3468 N93-28949
SEN, PRABIR K. p 3333 N93-29458
SENIW, DAVID p 3512 N93-29536
SENJANOVIC, G. p 3571 N93-30793
SENSHARMA, DILIP K. p 3338 N93-30628
SENSKE, D. p 3649 N93-28819
SENSMEIER, MARK D. p 3454 N93-30374
SERFOSS, GARY L. p 3499 N93-30542
SERGENT, DANIEL G. p 3250 N93-29971
SERRA-RICART, M. p 3624 N93-28811
SESSLER, A. p 3575 N93-29870
SETHURAMAN, JAYARAM p 3549 N93-29854
p 3555 N93-29979
SEVERANCE, PAUL S. p 3265 N93-28717
SEYFERTH, DIETMAR p 3335 N93-30028
p 3599 N93-30568
SEYMOUR, P. D. p 3549 N93-29849
SEZGIN, E. p 3557 N93-30917
SHABANOV, S. V. p 3607 N93-30924
p 3607 N93-30925
SHACK, W. J. p 3323 N93-29102
SHAEFFER, D. L. p 3520 N93-29058
SHAFAI, L. p 3366 N93-30292
p 3367 N93-30293
p 3369 N93-30307
SHAFER, STEVEN A. p 3579 N93-29824
SHAH, M. p 3441 N93-30910
SHALZ, M. L. p 3331 N93-29248
SHAMIR, Y. p 3637 N93-30919
SHANEYFELT, M. R. p 3413 N93-30516
SHANKAR, S. p 3356 N93-30225
SHANKAR, V. p 3328 N93-31021
SHAPIRO, LARRY S. p 3380 N93-28896
SHAPIRO, S. p 3616 N93-30122
SHAPSHAK, MANS p 3476 N93-28842
SHARIQ, SYED Z. p 3628 N93-30725
SHARKEY, PAUL M. p 3505 N93-28897
SHARP, W. M. p 3576 N93-30390
SHARPS, P. R. p 3465 N93-30208
SHAW, B. A. p 3322 N93-29002
SHAW, F. W. p 3303 N93-30555
SHAW, M. S. p 3315 N93-30447
SHAW, MICHAEL p 3362 N93-30265
SHAW, MILTON S. p 3318 N93-30072
SHAW, SCOTT W. p 3544 N93-30591
SHEAFFER, PATRICK M. p 3430 N93-28488
SHEALY, DAVID L. p 3578 N93-29128
SHEHADEH, HANA p 3518 N93-29573
SHELDON, REX p 3294 N93-30976
SHELFER, T. D. p 3648 N93-28812
SHELLEY, RICHARD p 3271 N93-29387
p 3272 N93-29501
SHELLMAN, C. H. p 3394 N93-30595
SHELTON, ROBERT O. p 3498 N93-29610
SHEN, M. H. p 3648 N93-28812
SHEN, W. p 3584 N93-28602
p 3585 N93-28912
SHERBORNE, WILLIAM D. p 3278 N93-29221
SHIAO, M. C. p 3451 N93-28633
SHIBA, KIYOYUKI p 3326 N93-30191
SHIBANUMA, KIYOSHI p 3587 N93-29243
SHIED, R. A. p 3287 N93-28946
SHIEH, C.-Y. p 3511 N93-29530
SHIELDS, J. E. p 3481 N93-28875
SHIGE, TAKASHI p 3320 N93-28529
SHIH, HUI-RU p 3290 N93-30950
SHIH, T.-H. p 3420 N93-29161
SHIMIZU, KATSUHIRO p 3587 N93-29243
SHIPLEY, MARGARET F. p 3516 N93-29561
SHIRLEY, D. J. p 3522 N93-28813
SHMAKOV, S. Y. p 3601 N93-30798
SHOHAM, YOAV p 3535 N93-30614
SHOJI, T. p 3583 N93-28532
p 3583 N93-28533
SHOJI, TATSUO p 3379 N93-28534
SHONTZ, WILLIAM D. p 3542 N93-29192
SHOUVAL, HAREL p 3489 N93-30603
SHREINER, DAVID G. p 3259 N93-30877
SHRIVER, D. F. p 3325 N93-30059
SHU, K. p 3434 N93-28766
SHUART, M. J. p 3307 N93-30872
SHUGART, L. R. p 3469 N93-28992
SHURTLEFF, DAVID p 3492 N93-30818
SHVETZ, N. R. p 3605 N93-30784
SHYY, DONG-JYE p 3273 N93-29884
SIBUM, H. p 3325 N93-30115
SICKAFUS, K. E. p 3594 N93-29314
SIDDIQI, SHAHID p 3302 N93-30441
SIEGEL, ELLEN H. p 3528 N93-29463
SIEJKA-JORMAKKA, HENRYKA p 3532 N93-29997
SIEVERS, ROBERT E. p 3488 N93-29670
SILCOX, RICHARD J. p 3301 N93-30436
SILVER, J. D. p 3563 N93-28521
SILVERGLATE, P. p 3434 N93-28766
SIMBIEROWICZ, P. p 3488 N93-30040
SIMMONS, JOE p 3601 N93-30811
SIMMONS, S. J. p 3365 N93-30281
SIMON, CHARLES G. p 3638 N93-29355
p 3638 N93-29378
p 3638 N93-29379
SIMON, GEORGE W. p 3652 N93-28585
SIMON, WILLIAM E. p 3288 N93-29091
SIMONEN, C. A. p 3481 N93-29054
SIMONS, RAINEE N. p 3405 N93-28610
SIMPSON, J. A. p 3286 N93-29707
SIMS, MICHAEL H. p 3613 N93-29229
SINGER, MICHAEL J. p 3531 N93-29874
p 3261 N93-29972
SINGER, S. FRED p 3638 N93-29377
SINGH, JAG J. p 3452 N93-29613
SINGHAL, S. N. p 3451 N93-28633
SINHA, N. K. p 3357 N93-30233
SINHA, NARESH K. p 3362 N93-30263
SINITSKIJ, S. L. p 3400 N93-30993
SINKOVITS, ROBERT S. p 3350 N93-30097
SION, E. M. p 3634 N93-28908
SIPES, WALTER E. p 3499 N93-30425
SIPILA, KARI p 3465 N93-30111
SITU, W. p 3434 N93-28775
SITZ, JOEL R. p 3260 N93-30764
SIU, T. p 3244 N93-30276
SIVAK, M. p 3496 N93-30659
SIVASHINSKY, G. I. p 3310 N93-29051
SIVERS, E. A. p 3449 N93-28943
SKERRY, BRIAN p 3370 N93-30315
SKRIPNIK, A. V. p 3600 N93-30771
SLATER, RICHARD R. p 3391 N93-29975
SLOAN, J. L. p 3539 N93-29661
p 3535 N93-30824
SLOMINSKI, CHRISTOPHER J. p 3250 N93-28621
SLUITER, M. p 3326 N93-30389
SMAGA, J. A. p 3407 N93-29036
SMALLWOOD, D. O. p 3453 N93-30185
SMETSERS, SJAAK p 3522 N93-28482
SMITH, A. J. p 3396 N93-30736
SMITH, ALAN R. p 3572 N93-29629
SMITH, ALEX E. p 3247 N93-30358
SMITH, B. p 3550 N93-30140
SMITH, DONALD L. p 3304 N93-30852
SMITH, G. R. p 3537 N93-28544
SMITH, H. G. p 3593 N93-28956
SMITH, HOWARD W. p 3249 N93-29774
p 3249 N93-29775
p 3249 N93-29776
p 3249 N93-29777
p 3243 N93-29778
p 3249 N93-29779
SMITH, I. G. p 3247 N93-30350
SMITH, K. C. p 3369 N93-30305
SMITH, M. C. p 3534 N93-30547
SMITH, M. H. p 3582 N93-31035
SMITH, P. J. p 3300 N93-30432
p 3302 N93-30440
SMITH, RON p 3449 N93-28685
SMITH, S. F. p 3383 N93-29348
p 3394 N93-30631
SMITH, SHELDON M. p 3629 N93-29453
SMITH, STEPHEN F. p 3610 N93-30124
SMITH, T. B. p 3470 N93-29669
SMITH, W. S. p 3477 N93-29346
SMITH, WALTER p 3461 N93-29817
SMITHSON, J. p 3371 N93-30321
SMOLDERS, HUBERTUS JOSEPHUS
p 3422 N93-29319
SMOOKE, MITCHELL D. p 3319 N93-30079
SMORENBURG, C. p 3463 N93-31009
SMOTROFF, IRA G. p 3484 N93-30176
SMREKAR, S. p 3649 N93-28819
SMYTH, PADHRAIC J. p 3449 N93-30413
SNAIL, KEITH A. p 3333 N93-29456
SNEGURSKIJ, A. V. p 3466 N93-30777
SNEIDER, C. I. p 3624 N93-29100
SNELICK, ROBERT p 3539 N93-29677
SNIDER, KARL p 3247 N93-30339
SNIEGOWSKI, J. J. p 3443 N93-29185
SNOW, J. W. p 3484 N93-30535
SNYDER, W. A. p 3624 N93-28814
SO, R. M. C. p 3420 N93-29159
SOENCKSEN, KEITH P. p 3432 N93-30032
SOLEM, J. C. p 3556 N93-28572
SOLOMON, O. M., JR. p 3433 N93-30655
SOLOPCHENKO, G. N. p 3516 N93-29563
SOLTAN, PARVIZ p 3441 N93-30599
SOMAYAJI, K. M. p 3480 N93-30992
SOMERVILLE, W. ANDREW p 3265 N93-28718
SOMMER, T. P. p 3420 N93-29159
SON, STEVEN p 3319 N93-30085
SONDHI, S. p 3320 N93-28548
SOONG, M. L. p 3441 N93-30910
SOPER, D. E. p 3569 N93-29841
SOREIDE, D. C. p 3649 N93-28815
SORENSEN, DAVID D. p 3544 N93-30886
SORGE, H. p 3565 N93-28831
SOROKIN, PETER P. p 3439 N93-29918
SORRELL, F. Y. p 3490 N93-30906
SOSNIN, A. N. p 3601 N93-30798
p 3281 N93-31024
SOTO, MARIBEL R. p 3319 N93-30099
SOUCY, MARC p 3366 N93-30288
SOUDER, P. A. p 3565 N93-28849
SOUNDARARAJAN, S. p 3573 N93-29638
SPARKS, W. M. p 3634 N93-28908
SPECK, D. R. p 3588 N93-29780
SPEHEGER, D. p 3481 N93-29095
SPELT, P. F. p 3541 N93-29047
SPENCER, FLOYD p 3449 N93-28685
SPICER, W. E. p 3597 N93-30120
SPIEGEL, F. XAVIER p 3293 N93-30971
p 3293 N93-30972
SPIERING, B. p 3460 N93-29307
SPINDT, C. A. p 3404 N93-28483
SPOLSKY, A. I. p 3376 N93-30349
SPRECHER, A. F., JR. p 3293 N93-30968
SPRINGER, GEORGE S. p 3304 N93-30849
SPRINGER, T. E. p 3464 N93-29147
SQUYRES, S. W. p 3649 N93-28816
SRINIVASAN, G. V. p 3320 N93-28564
SRIVASTAVA, S. K. p 3434 N93-28817
SRIVASTAVA, Y. N. p 3563 N93-28542
SROMOVSKY, L. A. p 3614 N93-29236
ST.CLAIR, ANNE K. p 3331 N93-29083
p 3331 N93-29085
p 3312 N93-29506
ST.CLAIR, TERRY L. p 3331 N93-29083
p 3312 N93-29506
ST.CYR, WILLIAM p 3627 N93-30708
STACHIW, J. D. p 3333 N93-29404
STACHOWICZ, MARIAN S. p 3515 N93-29551
STAGE, S. A. p 3481 N93-29054
STANLEY, ANN E. p 3438 N93-29800
STANLEY, R. P. p 3385 N93-29595
STANTEN, SAUL F. p 3531 N93-29920
p 3531 N93-29921
STANTON, P. H. p 3385 N93-29591
STARK, SHUANE p 3409 N93-29513
STARKEY, NORMAN p 3268 N93-30133
STARKEY, VAL p 3306 N93-30865
STARR, R. p 3650 N93-28824
STARRFIELD, S. G. p 3634 N93-28908
STATMAN, J. p 3386 N93-29599
STATSINGER, J. p 3271 N93-28487
STEBBINS, A. p 3653 N93-28962
STEEL, ROY A. p 3520 N93-29585
STEELE, W. V. p 3603 N93-28747
p 3603 N93-28964
STEENBERGEN, J. DAVID p 3367 N93-30297
STEEVES, EARL C. p 3241 N93-30119
STEHWIEN, WOLFGANG p 3246 N93-30299
STEIN, H. p 3481 N93-29095
STEIN, KEITH R. p 3241 N93-30119
STEINHARDT, ALLAN O. p 3399 N93-30879
STEINLAGE, R. C. p 3500 N93-29564
STEINMAN, D. p 3585 N93-28836
STEINOLFSON, R. p 3423 N93-29804
STELLA, L. p 3532 N93-30023
STELLA, PAUL M. p 3467 N93-29687
STELLE, K. S. p 3557 N93-30917
STENGEL, INGRID p 3459 N93-28928
STENGER-SMITH, JOHN p 3333 N93-29457
STEPHAN, PATRICK M. p 3294 N93-30977
STEPHENS, A. G. p 3425 N93-30132

STEPHENS, B. p 3283 N93-29365
STEPHENS, G. L. p 3484 N93-30055
STEPHENS, J. J. p 3339 N93-30656
STERLE, THOMAS J. p 3554 N93-28845
STERN, A. p 3649 N93-28818
STERN, HERVEY W. p 3392 N93-30362
STERNBERG, SAUL p 3500 N93-30543
STETINA, FRAN p 3614 N93-29239
STEVE, HERVE p 3546 N93-28509
STEVENS, R. R., JR. p 3575 N93-29809
STEVENSON, WARREN H. p 3242 N93-30373
STEWART, J. p 3432 N93-29773
STEWART, REGINA M. p 3336 N93-30170
STEWART, W. K. p 3487 N93-29003
STICHA, PAUL A. p 3261 N93-29972
STICHA, PAUL J. p 3531 N93-29874
STICHEL, SEBASTIAN p 3455 N93-31017
STILLER, L. p 3524 N93-28640
STINCHCOMB, W. p 3259 N93-30168
STINTON, D. p 3259 N93-30168
STOCKDALE, D. A. p 3332 N93-29328
STOCKER, A. D. p 3463 N93-28797
STOCKER, T. F. p 3486 N93-28670
STOECKER, H. p 3565 N93-28831
STOFAN, E. R. p 3649 N93-28819
STOLOFF, N. S. p 3324 N93-29786
STOLZ, C. J. p 3437 N93-29098
p 3437 N93-29207
STOLZE, DETLEF p 3246 N93-30671
STONE, R. E. p 3405 N93-28563
STONEKING, M. R. p 3584 N93-28602
STONEMAN, ROBERT S. p 3441 N93-30587
STONER, G. E. p 3336 N93-30051
STORM, R. S. p 3320 N93-28564
STOUDT, D. C. p 3406 N93-28944
STOUGHTON, JOHN W. p 3527 N93-29171
STOUT, LLOYD p 3537 N93-30462
STOVALL, JOHN R. p 3285 N93-31032
STOYCOS, LARA E. p 3505 N93-29044
STRACHAN, D. M. p 3322 N93-29061
p 3323 N93-29101
STRAHLER, ALAN H. p 3462 N93-29830
STRAIN, D. p 3386 N93-29600
STRAKHOVENKO, V. M. p 3600 N93-30770
STRANDJORD, ANDREW J. G. p 3621 N93-30473
STRANICK, S. J. p 3569 N93-29839
STRATTON, DONALD ALEXANDER
p 3246 N93-31005
STRAUSS, H. p 3652 N93-28756
STRELTSOV, V. N. p 3606 N93-30804
p 3400 N93-30923
p 3608 N93-30983
STRICKLAND, JOHN W. p 3290 N93-29067
STRIZENEC, P. p 3571 N93-30792
STROBEL, G. L. p 3438 N93-29309
STROHMANN, CARSTEN p 3336 N93-30170
STROMBONI, JEAN-PAUL p 3553 N93-28510
STUCHLY, MARIA A. p 3369 N93-30306
STUCHLY, STAN S. p 3369 N93-30306
STUCKEY, W. K. p 3602 N93-29684
STUCKY, G. p 3570 N93-30540
STUCKY, G. D. p 3598 N93-30407
STUCKY, GALEN D. p 3592 N93-28584
p 3594 N93-29138
p 3599 N93-30518
STURDIVAN, LARRY M. p 3315 N93-30365
STURE, STEIN p 3276 N93-29115
p 3276 N93-29116
p 3276 N93-29117
p 3277 N93-29120
STUREK, WALTER B. p 3240 N93-29512
STUTZKI, J. p 3637 N93-30639
p 3441 N93-30640
STUTZMAN, WARREN p 3404 N93-28539
SU, RENJENG p 3275 N93-29111
p 3277 N93-29119
SUAREZ, J. p 3302 N93-30439
SUETSUGU, Y. p 3583 N93-28533
SUGAMA, T. p 3329 N93-28551
p 3327 N93-30815
SUGIHARA, MASAYOSHI p 3590 N93-30649
SUKAMTO, LIN M. p 3381 N93-29087
SUKHATME, U. p 3574 N93-28565
SULLENGER, D. B. p 3592 N93-28568
SULLIVAN, B. M. p 3561 N93-28692
SULLIVAN, C. A. p 3409 N93-29478
SULLIVAN, DANIEL J. p 3288 N93-29158
SULLIVAN, THOMAS A. p 3312 N93-29617
SULTAN, L. H. p 3517 N93-29566
SULTAN, LABIB p 3515 N93-29554
SUMATHIPALA, W. L. p 3485 N93-31006
SUMPTER, B. G. p 3538 N93-28894
SUN, LI p 3432 N93-29476
SUN, WEIMIN p 3400 N93-31036
SUN, XIAN-HE p 3525 N93-28976
SURAUER, M. p 3284 N93-29906
SURD, DAVID J. p 3412 N93-30406
SURI, B. M. p 3441 N93-30801
SUTCLIFFE, J. G. p 3496 N93-30421
SUTTON, GEORGE M. p 3438 N93-29789
SUZUKI, KATSUO p 3524 N93-28531
SUZUKI, KOICHIRO p 3524 N93-28537
SUZUKI, MANABU p 3247 N93-30324
SUZUKI, YASUO p 3589 N93-30190
p 3590 N93-30606
SVEINSSON, J. R. p 3354 N93-30216
SVIATOSLAVSKY, I. N. p 3439 N93-30186
SVOBODA, ROBERT C. p 3653 N93-30052
SWAIM, ROBERT J. p 3407 N93-29173
SWAMY, M. N. S. p 3356 N93-30226
p 3365 N93-30280
SWAN, P. p 3318 N93-29367
SWANK, W. D. p 3589 N93-30181
SWANSON, B. I. p 3593 N93-28966
p 3598 N93-30501
SWANSON, GARY p 3305 N93-30858
SWANSON, GARY D. p 3305 N93-30857
SWANSON, L. p 3385 N93-29596
SWEATT, W. C. p 3437 N93-29264
SWENSON, C. M. p 3400 N93-28820
SWENSON, GARY R. p 3266 N93-28728
SWENSON, HARRY N. p 3260 N93-28869
SWIFT, RICHARD ALAN p 3545 N93-31029
SWITLIK, ROCH A. p 3609 N93-29433
SWYT, D. A. p 3354 N93-29666
SYDOW, P. D. p 3307 N93-30872
SYLVESTER, BILL p 3404 N93-28539
SYMES, WILLIAM p 3452 N93-29349
SYRETT, B. p 3357 N93-30231
SYRZYCKI, MAREK J. p 3363 N93-30269
SZARMES, ERIC B. p 3439 N93-29853
SZCZUR, MARTI p 3613 N93-29224
SZEKERES, R. p 3318 N93-30065
SZEMPLINSKA-STUPNICKA, WANDA
p 3407 N93-29037
SZEPESSY, ANDERS p 3419 N93-29025
SZKODY, PAULA p 3629 N93-28634
SZOSTAK, H. T. p 3447 N93-30828
SZTANDERA, LESZEK M. p 3511 N93-29527
SZUSZCZEWICZ, EDWARD p 3614 N93-29235

T

TABAKA, L. J. p 3579 N93-29350
TABEREAUX, A. T. p 3322 N93-29061
p 3323 N93-29101
TACCONI, G. p 3397 N93-30743
TACHIKAWA, HIROYASU p 3411 N93-29986
TADA, EISUKE p 3587 N93-29243
TAGG, DAVID A. p 3624 N93-29477
TAHANI, HOSSEIN p 3517 N93-29568
TAJIMA, T. p 3585 N93-28910
p 3423 N93-29804
TAKEI, K. p 3406 N93-28746
p 3410 N93-29673
TAKEMURA, MASAHIRO p 3326 N93-30396
TAKEUCHI, K. p 3410 N93-29673
TAKIZUKA, TOMONORI p 3589 N93-30003
TALAGA, R. L. p 3566 N93-29313
TALEGHANI, BARMAC p 3299 N93-30137
TAMBE, MILIND p 3615 N93-29459
TAMIMI, A. p 3471 N93-29676
TAN, C. S. p 3420 N93-29141
TANAKA, MASANOBU p 3589 N93-30190
p 3590 N93-30606
TANAKA, T. p 3410 N93-29673
TANG, I. N. p 3309 N93-28880
TANG, Y. p 3618 N93-30457
TANG, Z. p 3593 N93-28888
TANI, KEIJI p 3585 N93-28979
TAO, L. p 3365 N93-30280
TAO, Y. T. p 3569 N93-29839
TAO, ZHI-JAN p 3571 N93-30793
TAPIA, V. p 3606 N93-30786
p 3637 N93-30918
p 3637 N93-30997
TAPLEY, MARK p 3460 N93-29179
TARANENKO, P. I. p 3281 N93-31024
TARR, MICHAEL J. p 3499 N93-30163
TASK, H. LEE p 3267 N93-28739
p 3268 N93-28740
p 3268 N93-28741
p 3268 N93-28742
TASKER, DOUGLAS G. p 3411 N93-30021
p 3352 N93-30424
TATAR, L. p 3557 N93-30928
TATE, RANJEET SHEKHAR p 3548 N93-28671
TAUB, SUSAN R. p 3405 N93-28610
TAVAKOLI, NASSRIN p 3512 N93-29536
TAYLOR-MYERS, SHARON p 3338 N93-30596
TAYLOR, DESMOND P. p 3360 N93-30252
p 3371 N93-30316
TAYLOR, EDWARD W. p 3583 N93-29698
p 3583 N93-29699
TAYLOR, G. J. p 3650 N93-28821
TAYLOR, GREG p 3272 N93-31033
TAYLOR, J. R. p 3437 N93-29098
p 3437 N93-29207
TAYLOR, LAWRENCE W., JR. p 3263 N93-28706
TAYLOR, R. M. p 3503 N93-28864
TAYLOR, W. W. L. p 3414 N93-29690
TEACHOUT, MARK S. p 3500 N93-30575
TEILLAUD, MONIQUE p 3547 N93-28512
TENKATE, H. H. J. p 3576 N93-30019
TENNILLE, GEOFFREY M. p 3520 N93-29070
TENNYSON, J. L. p 3584 N93-28599
TENNYSON, R. C. p 3309 N93-29366
TEODORESCU, H. N. p 3515 N93-29555
TERADA, N. p 3410 N93-29673
TERAVEST, D. p 3576 N93-30019
TERHOFSTEDE, A. H. M. p 3523 N93-28503
TERP, CHRISTIAN p 3547 N93-28524
TERRY, J. D. p 3273 N93-29195
TERRY, P. W. p 3585 N93-28913
TEWFIK, AHMED p 3393 N93-30386
THANAKIJ, REX p 3489 N93-30525
THANGARAJ, K. p 3441 N93-30910
THANSANDOTE, ART p 3369 N93-30306
THATTEY, S. S. p 3441 N93-30801
THAYER, G. R. p 3472 N93-30008
THAYER, S. M. p 3444 N93-29316
THERY, CHRISTIAN p 3241 N93-30020
THIEM, KEEM B. p 3387 N93-29882
THILLY, W. G. p 3490 N93-28651
THOMA, ARMIN p 3466 N93-30573
THOMAS, JOHN R. p 3492 N93-30818
THOMAS, ROSS C. p 3452 N93-29515
THOMAS, W. M. p 3532 N93-30022
p 3534 N93-30546
THOMPSON, A. p 3654 N93-29646
THOMPSON, D. O. p 3449 N93-29443
THOMPSON, H. DOYLE p 3242 N93-30373
THOMPSON, K. E. p 3582 N93-28810
THOMPSON, MARK E. p 3338 N93-30610
THOMPSON, R. B. p 3450 N93-28567
THOMPSON, T. E. p 3247 N93-30338
THOMPSON, WILLIAM T. p 3481 N93-28876
THORNTON, A. L. p 3549 N93-29187
THORNTON, H. RICHARD p 3290 N93-30951
THORP, J. M. p 3473 N93-30183
THRASHER, JOSEPH S. p 3312 N93-29506
THROCKMORTON, DAVID A. p 3266 N93-28731
THUAN, TRINH X. p 3654 N93-30419
THULASIRAMAN, K. p 3365 N93-30280
THUMANN, MANFRED p 3324 N93-29272
THUNNISSEN, H. p 3463 N93-30839
TIAN, Y. p 3510 N93-29521
TIANO, A. p 3397 N93-30743
TICHY, LORENZ p 3238 N93-29006
TIDLER, CYNTHIA E. p 3582 N93-29692
TIEDEMANN, R. K. p 3247 N93-30330
TIEGS, T. N. p 3334 N93-29767
TIEN, C. p 3474 N93-30506
TIERNEY, J. W. p 3314 N93-30188
TIERNEY, JOSEPH p 3494 N93-29421
TILTON, D. E. p 3423 N93-29352
TINDELL, R. p 3531 N93-29916
TINNEY, CHRISTOPHER GEOFFREY
p 3630 N93-30493
TIPTON, STEVEN M. p 3291 N93-30956
TIRKAS, PANAYIOTIS A. p 3400 N93-31036
TIRRES, LIZET p 3251 N93-28697
TISCHLER, MARK B. p 3237 N93-30689
TIT, N. p 3601 N93-30794
p 3602 N93-31027
TITUS, JENNIFER A. p 3272 N93-30881
TIWARI, S. N. p 3604 N93-29168
TIWARI, SURENDRA N. p 3426 N93-30375
TOEPFER, A. J. p 3650 N93-28822
TOIDA, M. p 3588 N93-29434
p 3590 N93-30533
TOMSIA, A. P. p 3331 N93-29248
TOOMEY, PATRICK p 3407 N93-29203
TOPLOSKY, N. p 3442 N93-28578
TOPORKOV, D. p 3574 N93-28970
TORCZYNSKI, J. R. p 3417 N93-28639
TORR, D. G. p 3340 N93-28829
TORRES, J. A. p 3393 N93-30514
TOSCANO, JOHN P. p 3318 N93-30067
TOSI, M. P. p 3327 N93-30778
TOWNSEND, SCOTT p 3538 N93-28628
TRALLI, D. p 3649 N93-28819
TRAUBE, E. C. p 3496 N93-30659
TRAVIS, L. p 3472 N93-30043
TRAXLER, M. R. p 3385 N93-29598
TREANOR, CHARLES E. p 3312 N93-29389
TREICHEL, CURT p 3236 N93-30678
TREUHAFT, R. N. p 3442 N93-28823

TREW, R. J. p 3593 N93-28874
TRIAS, JOHN p 3441 N93-30599
TRIBBIA, J. J. p 3470 N93-29318
TRIBOULET, R. p 3597 N93-29974
TRIPATHY, K. C. p 3605 N93-30779
TRIPP, JOHN S. p 3431 N93-29209
TRIVISONNO, J. p 3593 N93-28956
TROEDSON, S. C. p 3392 N93-30145
TROFIMENKOFF, F. N. p 3375 N93-30340
TROHA, W. T. p 3254 N93-29935
TROMBKA, J. I. p 3650 N93-28824
TROTT, WAYNE p 3342 N93-29402
TROTT, WAYNE M. p 3344 N93-30069
TROVATI, A. p 3254 N93-29939
TRUDNOWSKI, D. J. p 3550 N93-30041
TRUEMAN, C. W. p 3371 N93-30320
TRUSLOVE, G. p 3302 N93-30440
TRYK, D. p 3313 N93-29828
p 3317 N93-30664
TSAI, WEI K. p 3512 N93-29531
TSANGARAKIS, NIKOS p 3299 N93-30137
TSAO, ERIC CHEN-KUO p 3511 N93-29526
TSOTSOS, J. K. p 3356 N93-30224
TSUJI, HIROKAZU p 3326 N93-30396
TSUKADA, TAKASHI p 3326 N93-30191
TUCK, BRIAN p 3387 N93-29877
TUMMILLO, A. F. p 3407 N93-29036
TUNNELL, T. p 3386 N93-29765
TURCHI, P. E. A. p 3326 N93-30389
TURKO, B. T. p 3598 N93-30393
TURKSEN, I. B. p 3510 N93-29521
p 3514 N93-29547
p 3514 N93-29548
TURNER, M. S. p 3633 N93-28676
TURNER, MICHAEL S. p 3653 N93-29164
TURTLE, J. P. p 3397 N93-30744
TUTTLE, MARK p 3305 N93-30858
TUZZOLINO, A. J. p 3286 N93-29707
TVEEKREM, JUNE L. p 3266 N93-28727
TWARD, E. p 3378 N93-28825
TYBURCZY, J. A. p 3410 N93-29793
TYLKA, ALLAN J. p 3573 N93-29645
TYSON, KAREN W. p 3610 N93-29499

U

UDREA, M. V. p 3438 N93-29797
ULA, S. p 3410 N93-29814
p 3411 N93-30057
p 3411 N93-30058
UNDERWOOD, J. H. p 3438 N93-29781
UNRUH, W. P. p 3481 N93-29095
UNSEREN, M. A. p 3446 N93-30210
UNTHANK, M. D. p 3474 N93-30825
URBACH, HERMAN B. p 3427 N93-30571
URKE, ROBERT L. p 3448 N93-31039
URLI, N. p 3536 N93-31001
URLINGS, P. J. M. p 3505 N93-28872
URQUIDI-MACDONALD, M. p 3320 N93-28545
USAB, WILLIAM J., JR. p 3421 N93-29213
USHER, ROBERT p 3669 N93-29710
USHIGUSA, KENKICHI p 3589 N93-30397
UTECH, DANIEL M. p 3610 N93-29499
UTTAL, WILLIAM R. p 3580 N93-30368
UWAI, T. p 3406 N93-28746
UY, O. M. p 3286 N93-28795
p 3286 N93-28826

V

VAANDRAGER, FRITS W. p 3532 N93-30017
VAATAINEN, ANNE p 3465 N93-30111
VAIDYA, NITIN p 3510 N93-29522
VAIDYANATHAN, C. S. p 3368 N93-30300
VAIDYANATHAN, GOPAL p 3312 N93-29429
VALLEE, DAVID R. p 3481 N93-29198
VALLERAND, A. L. p 3493 N93-28939
VALLIMONT, JOHN p 3582 N93-29694
VALTARI, KIRSI p 3532 N93-29997
VANASUPA, LINDA S. p 3292 N93-30963
VANBERKEL, CORNELIS HERMANUS
p 3408 N93-29269
VANDENHIJLIGENBERG, NICO p 3547 N93-28667
VANDERMOLEN, R. I. p 3394 N93-30631
VANDERPLOEG, M. J. p 3528 N93-29473
VANDERSANDEN, J. J. p 3460 N93-29320
VANDERWERF, P. P. p 3631 N93-30641
VANDIJK, A. p 3461 N93-29466
VANDONGEN, JOHN p 3245 N93-28625
VANEEKELEN, MARKO p 3522 N93-28482
VANEMDEN, W. p 3576 N93-30019
VANES, J. T. p 3413 N93-30835
p 3577 N93-30837
VANFOSSEN, G. JAMES p 3420 N93-29157
VANHEMMEN, L. J. G. T. p 3611 N93-28481
VANHOOK, GORDAN E. p 3472 N93-30154
VANLIEROP, HUBERTUS RENIER MARIA
p 3332 N93-29267
VANLIEROP, J. p 3483 N93-30013
VANMINNEN, P. p 3362 N93-30266
VANPERSIE, M. p 3463 N93-31009
VANSCHOOR, MARTHINUS C. p 3281 N93-30376
VANTERPOOL, LISE p 3355 N93-30220
VANWILLIGEN, H. p 3311 N93-29182
VANWONTERGHEM, B. M. p 3588 N93-29780
VANYSEK, PETR p 3311 N93-29132
p 3311 N93-29133
VANZANDT, T. p 3434 N93-28765
VARNAVAS, KOSTA p 3507 N93-29845
VARY, ALEX p 3295 N93-28624
VASAVADA, A. R. p 3647 N93-28805
VASSILEVICH, D. V. p 3607 N93-30921
VAUGHAN, C. T. p 3526 N93-29127
VAUGHAN, WILLARD S. p 3654 N93-29258
VAUGHN, M. T. p 3563 N93-28542
VEAL, G. p 3263 N93-28701
VEIGA, J. S. p 3607 N93-30945
VELS, L. p 3463 N93-30839
VENABLES, J. D. p 3414 N93-29685
VENDURA, GEORGE J., JR. p 3264 N93-28714
VENETSANOPOULOS, ANASTASIOS N.
p 3375 N93-30345
VENKATESAN, T. p 3596 N93-29868
VENTURINI, E. L. p 3598 N93-30517
VEPSA, HEIMO p 3488 N93-30040
VEPSALAINEN, ARI M. p 3543 N93-29998
VERBESTEL, JOHN p 3249 N93-29777
VERBUNT, F. p 3631 N93-30578
VERGHESE, S. p 3594 N93-29249
VERHEIJKE, MARINUS LEENDERT
p 3408 N93-29271
VERKASALO, RAIMO p 3411 N93-30108
VERMILLION, CHARLES p 3614 N93-29239
VERNON, R. G. p 3630 N93-29785
VERNON, S. M. p 3464 N93-29965
VERNON, TODD H. p 3260 N93-30764
VERON, HARRY p 3506 N93-29340
VERSTEEG, M. H. J. B. p 3522 N93-30840
VERTREES, T. H. p 3294 N93-30978
VETTER, RONALD F. p 3412 N93-30201
VIEDMA, A. p 3259 N93-29964
VILLARREAL, JAMES A. p 3509 N93-29516
p 3512 N93-29534
p 3515 N93-29556
VINDUSKA, M. p 3606 N93-30806
VIRANEN, M. p 3488 N93-30040
VISBAL, MIGUEL p 3260 N93-30498
VISCO, S. J. p 3405 N93-28581
VISENTINE, JIM p 3266 N93-28728
VISHWANATHAN, H. K. p 3592 N93-28661
VLCEK, B. M. p 3592 N93-28661
VOGEL, D. T. p 3258 N93-29961
VOIGT, J. A. p 3598 N93-30517
VOLZ, RICHARD A. p 3526 N93-29026
VONDERHAAR, THOMAS H. p 3462 N93-29834
VONDRA, ROBERT p 3264 N93-28709
VOSBURG, S. K. p 3575 N93-29151
VOSS, H. D. p 3286 N93-29707
VOSTEEN, LOUIS F. p 3302 N93-30441
VRANISH, JOHN M. p 3445 N93-29505
VULLIERME, J.-J. p 3253 N93-29931
VUTETAKIS, DAVID G. p 3412 N93-30406

W

WAAGEN, DON p 3544 N93-30592
WAAS, S. p 3487 N93-29422
WADEL, MARY F. p 3341 N93-28695
WAGNER, D. G. p 3460 N93-29255
WAGNER, G. R. p 3406 N93-28940
WAGNER, JOHN D. p 3283 N93-29374
p 3283 N93-29375
WAGNER, ROBERT p 3529 N93-29496
WAHLUND, PER p 3418 N93-28994
WAITE, WILLIAM M. p 3532 N93-30014
WALBERT, DAVID J. p 3271 N93-29394
WALDROP, D. A. p 3451 N93-28832
WALDROP, RAYMOND S. p 3526 N93-29026
WALKER, KEVIN P. p 3297 N93-29074
WALKER, M. S. p 3584 N93-28583
WALKER, R. M. p 3318 N93-29367
WALKER, T. H. p 3300 N93-30432
p 3302 N93-30440
WALKER, THOMAS H. p 3248 N93-29498
WALKUP, JOHN F. p 3522 N93-30179
WALLACE, D. p 3602 N93-29684
WALLACE, E. W. p 3440 N93-30530
WALLACE, KENNETH M., JR. p 3285 N93-29461
WALLACE, R. p 3432 N93-29773
WALLACE, STEPHEN M. p 3439 N93-29867
WALLACE, W. B. p 3374 N93-30336
WALSH, DANIEL W. p 3293 N93-30973
WALZER, ANN E. p 3472 N93-30180
WANG, AI-HUA p 3653 N93-30496
WANG, C. p 3578 N93-29128
p 3575 N93-29870
WANG, C. H. p 3329 N93-28489
p 3333 N93-29441
p 3333 N93-29442
WANG, CAI Y. p 3480 N93-28518
WANG, F. X. p 3453 N93-30147
WANG, H. p 3575 N93-29317
WANG, HAN p 3380 N93-28896
WANG, HAOJIN p 3512 N93-29533
WANG, JIAN-PING p 3585 N93-28979
WANG, JIANMIN p 3436 N93-28614
WANG, KANG L. p 3595 N93-29383
WANG, QIANG p 3365 N93-30283
WANG, S. p 3434 N93-28783
WANG, SUNING p 3529 N93-29488
WANG, WEGO p 3281 N93-30813
WANG, WEINING p 3319 N93-30075
WANG, XIANGDONG p 3567 N93-29403
WANG, Y. Y. p 3598 N93-30408
WANG, Z. p 3254 N93-29940
WANGEMANN, ROBERT p 3581 N93-30522
WAPELHORST, LEO p 3245 N93-28625
WARBER, C. R. p 3397 N93-30742
WARBURTON, JOHN p 3272 N93-31033
WARD, B. F. L. p 3568 N93-29764
WARD, C. H. p 3474 N93-30762
WARD, C. R. p 3460 N93-29255
WARD, CHARLES H., JR. p 3323 N93-29144
WARD, DONALD T. p 3248 N93-28693
WARD, GEORGE A. p 3503 N93-28866
WARD, M. D. p 3597 N93-30146
WARD, M. J. p 3631 N93-30641
WARD, RABAB K. p 3375 N93-30344
WARE, A. A. p 3584 N93-28598
WARE, ANDREW SIMON p 3586 N93-29123
WARNER, HAROLD D. p 3499 N93-30542
WARNOW, T. p 3491 N93-30483
WARREN, JACK L. p 3282 N93-29357
WARRINGTON, E. M. p 3396 N93-30738
WARSHAW, S. I. p 3610 N93-30822
WARTAK, J. p 3357 N93-30231
WASCHKA, W. p 3256 N93-29951
WASHINGTON, W. p 3412 N93-30118
WASKOM, T. L. p 3292 N93-30964
WATANABE, KENJI p 3524 N93-28537
WATANABE, NORIO p 3525 N93-28978
WATERMANN, JURGEN p 3476 N93-28842
WATKINS, J. C. p 3532 N93-30034
WATSON, C. H. p 3314 N93-30166
WATSON, JAMES C. p 3302 N93-30442
WATSON, R. p 3615 N93-29783
WATSON, RICHARD p 3617 N93-30452
WATTS, ALAN J. p 3638 N93-29355
p 3283 N93-29374
p 3283 N93-29375
WATTS, J. W., JR. p 3573 N93-29637
p 3573 N93-29639
WATTS, JOHN W. p 3572 N93-29633
WAY, JOBEA p 3614 N93-29234
WAYMAN, C. M. p 3321 N93-28591
WAYNE, S. F. p 3336 N93-30182
WDOWIAK, T. J. p 3582 N93-28827
WEAVER, JOHNATHAN M. p 3542 N93-29771
WEBB, STEVEN P. p 3621 N93-30473
WEBBER, JOHN C. p 3382 N93-29217
WEBER, CHARLES V. p 3530 N93-29852
p 3610 N93-29970
WEBER, EICKE p 3298 N93-29282
WEBER, PETER p 3246 N93-30299
WEBSTER, C. E. p 3407 N93-29036
WEDDENDORF, BRUCE p 3507 N93-29845
p 3445 N93-29846
p 3508 N93-30566
WEE, WILLIAM G. p 3289 N93-29570
WEEKS, J. p 3532 N93-30050
WEERTMAN, JULIA R. p 3298 N93-29130
WEIDE, TIMOTHY L. p 3528 N93-29418
WEIDEMAN, MARK H. p 3303 N93-30843
WEIGMAN, BERNARD J. p 3293 N93-30972
WEIJEKOON, W. M. p 3596 N93-29430
WEILMUENSTER, KENNETH J. p 3420 N93-29155
WEINACHT, PAUL p 3240 N93-29512
WEINBERG, JERRY L. p 3638 N93-29377
WEINER, L. D. p 3394 N93-30662
WEINSTEIN, LISA F. p 3508 N93-30167
WEISER, MARTIN W. p 3294 N93-30975
p 3294 N93-30976
WEISMANTEL, ROBERT p 3413 N93-30616
WEISS, M. S. p 3568 N93-29784
WEISS, P. S. p 3567 N93-29332
p 3569 N93-29839

WEITZ, R. p 3650 N93-28822
WEITZNER, H. p 3586 N93-29056
WELCH, CHRISTOPHER S. p 3449 N93-30414
WELCH, R. Q. p 3303 N93-30555
WELLS, MARTIN G. p 3281 N93-30813
WELLS, VALANA p 3248 N93-29153
WELLS, WILLIAM L. p 3239 N93-29166
WELMAN, STEPHEN K. p 3272 N93-30881
WELP, U. p 3592 N93-28661
WEMPLE, C. A. p 3565 N93-28833
WENDER, I. p 3314 N93-30188
WENG, JUYANG p 3363 N93-30271
WENZEL, K.-P. p 3654 N93-29646
WERCHAN, PAUL M. p 3496 N93-30400
WESEMANN, LARS p 3599 N93-30568
WESSEL, FRANK J. p 3476 N93-28538
WESSEL, S. p 3576 N93-30019
WESSELS, H. R. A. p 3483 N93-30013
p 3484 N93-30114
WEST, HARVEY A. p 3293 N93-30968
WEST, J. T. p 3540 N93-30633
WEST, JAMES C. p 3288 N93-28950
WESTERMANN, T. p 3538 N93-29030
WETS, ROGER D. p 3555 N93-30363
WETZEL, C. D. p 3392 N93-30362
WEYRICK, PATRICIA B. p 3379 N93-28588
WHALEN, THOMAS p 3513 N93-29542
p 3515 N93-29553
WHAM, BENJAMIN, II p 3298 N93-29414
WHATMORE, R. W. p 3332 N93-29337
WHEELER, MARK p 3272 N93-31033
WHITE, CARTER T. p 3318 N93-30071
p 3351 N93-30100
WHITE, EDWARD V. p 3263 N93-28702
WHITE, GEORGE M. p 3356 N93-30227
WHITE, HENRY S. p 3294 N93-28492
p 3596 N93-29445
WHITE, J. KEVIN p 3442 N93-28951
WHITE, J. M. p 3611 N93-28580
WHITE, M. R. p 3646 N93-28800
WHITE, STUART C. p 3360 N93-30251
WHITEHAIR, CHESTER L. p 3271 N93-29903
WHITEHEAD, R. S. p 3302 N93-30444
WHITEHOUSE, PAUL N. p 3283 N93-29622
WHITEMAN, C. D. p 3383 N93-29308
WHITESIDE, B. N. p 3381 N93-29105
WHITESTONE, JENNIFER J. p 3507 N93-29889
WHITTLESEY, R. p 3434 N93-28766
WICHERT, TERRY S. p 3562 N93-29816
WICKERSHEIMER, DAVID p 3529 N93-29657
p 3529 N93-29658
WICKMAN, JERRY L. p 3293 N93-30967
WIDENER, EDWARD L. p 3291 N93-30954
WIEDLOCHER, DAVID E. p 3340 N93-29368
WIELWALD, J. p 3432 N93-29773
WIGHT, J. S. p 3362 N93-30267
WIITA, P. J. p 3637 N93-31004
WIKSWO, JOHN, JR. p 3495 N93-30160
WILBURN, A. M. p 3489 N93-30827
WILCOX, R. B. p 3588 N93-29780
WILCOX, W. R. p 3597 N93-29974
WILES, S. p 3320 N93-30277
WILKES, DONALD R. p 3266 N93-28729
p 3583 N93-29706
WILKINS, GARY D. p 3439 N93-29827
WILLARD, SCOTT A. p 3451 N93-29069
WILLDEN, K. S. p 3302 N93-30440
WILLDEN, KURTIS p 3306 N93-30865
WILLIAMS, ELIZABETH p 3622 N93-30476
WILLIAMS, GEOFFERY T. p 3264 N93-28714
WILLIAMS, J. M. p 3330 N93-28600
WILLIAMS, J. W. p 3338 N93-30601
WILLIAMS, MARCIA J. p 3312 N93-29389
WILLIAMS, R. J. p 3616 N93-30195
WILLIAMS, W. J. p 3380 N93-28909
WILLIAMSON, D. L. p 3470 N93-29318
WILLIAMSON, SAMUEL J. p 3495 N93-30160
WILLIS, T. C. p 3592 N93-28643
WILLS, E. L. p 3648 N93-28812
WILLSON, IAN A. p 3514 N93-29547
p 3514 N93-29548
WILLSON, REG G. p 3579 N93-29824
WILSON, BRENDA K. p 3624 N93-29704
WILSON, J. J. p 3394 N93-30662
WILSON, J. T. p 3474 N93-30762
WILSON, JEFF T. p 3368 N93-30301
WILSON, M. S. p 3464 N93-29147
WIMBUSH, R. M. p 3501 N93-28853
WINDISCH, C. F., JR. p 3322 N93-29061
p 3323 N93-29101
WING, DAVID J. p 3239 N93-29160
WINGO, D. R. p 3266 N93-28725
WINIGER, MATTHIAS p 3458 N93-28925
WINOKUR, P. S. p 3413 N93-30516
WINTER, RUDOLF p 3456 N93-28915
WINTERSGILL, M. C. p 3332 N93-29342
p 3410 N93-29826
WISE, GARY L. p 3555 N93-29454
WITHERELL, MARK D. p 3295 N93-28657
WITT, GERALD L. p 3298 N93-29282
WITTEN, MARK L. p 3495 N93-30153
WITTIG, CURT p 3318 N93-30068
WITTIG, S. p 3256 N93-29951
p 3258 N93-29958
WITTIG, T. p 3502 N93-28855
WO, ZUOGUO p 3550 N93-29876
WOCH, JOACHIM p 3476 N93-28842
WOLCOTT, R. W. p 3641 N93-28773
WOLF, GRACE ANNAMARIE p 3636 N93-30502
WOLF, JENNIFER R. p 3336 N93-30169
WOLFE, DANIEL p 3238 N93-30691
WOLFE, DANIEL E. p 3483 N93-29491
WOLFE, M. G. p 3271 N93-28487
WOLFE, MALCOLM G. p 3271 N93-29903
WOLFSON, MARILYN W. p 3481 N93-29257
WOLINSKI, TOMASZ R. p 3375 N93-30341
WOLKOFF, E. A. p 3399 N93-30752
WOLVERTON, DAVID A. p 3250 N93-28621
WONG, ALFRED Y. p 3398 N93-30746
WONG, ANDREW K. C. p 3369 N93-30304
WONG, DOUGLAS T. p 3431 N93-29209
WONG, W. C. p 3414 N93-29690
WOO, EDMUND P. p 3305 N93-30853
WOO, KENNETH E. p 3381 N93-28955
WOOD, H. C. p 3356 N93-30225
p 3368 N93-30300
WOOD, S. E. p 3647 N93-28805
WOODARD, STANLEY p 3264 N93-28708
WOODCOCK, GORDON R. p 3268 N93-31034
WOODSIDE, C. M. p 3364 N93-30279
WOODWARD, J. p 3490 N93-28890
WOODY, B. A. p 3317 N93-30760
WOOLF, STANLEY p 3568 N93-29787
WORL, L. A. p 3598 N93-30501
p 3600 N93-30569
WORMHOUDT, JODA p 3320 N93-30102
WORTMAN, JIM J. p 3638 N93-29377
p 3638 N93-29378
WOSIEK, B. p 3577 N93-30990
WRAY, RICHARD B. p 3285 N93-31032
WRIGHT, G. A. p 3582 N93-28788
WRONKA, J. p 3314 N93-30166
WU, HSIN-FENG p 3612 N93-28846
WU, J. C. S. p 3316 N93-30658
WU, K. H. p 3327 N93-30652
WU, S. T. p 3287 N93-28680
p 3653 N93-28935
WU, SHIN-TING p 3546 N93-28466
WU, YAN p 3358 N93-30237
WUEBBLES, D. J. p 3469 N93-28972
p 3471 N93-29792
WUETHRICH, CHRISTIAN p 3259 N93-29999
WYMAN, C. E. p 3490 N93-28890

X

XIANLIN, BAN p 3241 N93-29919
XIAOQING, ZHENG p 3240 N93-29862
XIE, M. p 3440 N93-30530
XIN, ZHOUPING p 3419 N93-29025
XING, TU p 3241 N93-29919
XIONG, F. p 3598 N93-30408
XU, Z. S. p 3334 N93-29825

Y

YAGER, RONALD R. p 3510 N93-29518
p 3512 N93-29532
YAKIMENKO, V. E. p 3571 N93-30800
YAMAZAWA, HIROMI p 3467 N93-28536
YANG, R. p 3362 N93-30266
YANKIELUM, NORBERT E. p 3379 N93-28588
YATES, JOHN T., JR. p 3315 N93-30526
YAUNG, J. Y. p 3414 N93-29690
YAZDI, RENEE ANNA p 3227 N93-29713
YE, H. p 3587 N93-29148
YEAGER, E. p 3313 N93-29828
YEAGER, E. B. p 3317 N93-30664
YEAP, T. H. p 3356 N93-30224
YEE, HOWELL S. p 3595 N93-29331
YEE, TROY L. p 3363 N93-30270
YEH, CHAO-YUEN p 3480 N93-28518
YEH, FREDERICK C. p 3420 N93-29157
YEH, HARRY C. p 3298 N93-29451
YEN, J. L. p 3365 N93-30284
YEN, JOHN p 3510 N93-29522
p 3512 N93-29533
p 3512 N93-29537
YERSAVICH, ANN p 3272 N93-31033
YETTER, RICHARD A. p 3347 N93-30084
p 3319 N93-30090
YEUNG, S. K. p 3357 N93-30232
p 3370 N93-30312
YODA, SHINICHI p 3299 N93-30004
YOKOKAWA, MITSUO p 3524 N93-28537
YOKOTA, S. H. p 3298 N93-29191
YOKOYA, KAORU p 3577 N93-30607
YONGACOGLU, A. p 3370 N93-30314
YOO, MINSUN p 3349 N93-30091
YORKE, J. A. p 3557 N93-30048
YOSHIDA, HIROSHI p 3320 N93-28529
p 3584 N93-28535
YOSHINO, RYUJI p 3583 N93-28530
YOST, WILLIAM T. p 3431 N93-29084
p 3449 N93-30414
YOUDA, YE p 3421 N93-29260
YOUNG, D. T. p 3286 N93-28828
YOUNG, FRED M. p 3288 N93-29091
YOUNG, L. p 3574 N93-28970
YOUNG, M. P. p 3464 N93-28971
YOUNG, PAUL E. p 3405 N93-28610
YOUNG, ROBERT W. p 3506 N93-29484
YOUNIS, L. T. p 3497 N93-30890
YOUNKER, MIKE p 3435 N93-30461
YU, JEFFREY W. p 3578 N93-29086
YU, S. S. p 3576 N93-30390
YU, YIMING p 3363 N93-30273
YUCEL, EROL p 3553 N93-28574
YUEN, S. p 3357 N93-30231
YUGAMI, N. p 3583 N93-28533
YUN, H. M. p 3340 N93-30938
YUN, JOAO LIN p 3636 N93-30563
YUSHKOV, M. V. p 3400 N93-30993

Z

ZABIELSKI, M. F. p 3317 N93-30760
ZABINSKY, ZELDA p 3305 N93-30858
ZACHARIA, T. p 3325 N93-29813
ZACHARIASEN, F. p 3482 N93-29479
ZAITLIN, MILTON p 3491 N93-29915
ZAKHAREV, B. N. p 3552 N93-30984
ZAKY, S. G. p 3356 N93-30224
ZALEWSKI, E. p 3434 N93-28766
ZAMAN, A. J. p 3273 N93-29195
ZASTAVENKO, L. G. p 3606 N93-30805
ZATZ, MARTIN p 3497 N93-30904
ZAVILOPULO, A. N. p 3466 N93-30777
ZAVOSH, FRANK p 3400 N93-31036
ZAWODZINSKI, T. A. p 3464 N93-29147
ZE, F. p 3432 N93-29773
ZEIDMAN, B. p 3574 N93-28970
ZEJNALOVA, O. V. p 3605 N93-30781
ZEKAUSKAS, MATTHEW J. p 3534 N93-30523
ZENOU, V. Y. p 3328 N93-30941
ZERUBIA, JOSIANE p 3553 N93-28510
ZETTWOCH, D. D. p 3474 N93-30825
ZEYN, J. p 3485 N93-31018
ZHANG, H. S. p 3420 N93-29159
ZHANG, R. B. p 3551 N93-30810
ZHANG, T. X. p 3588 N93-29434
p 3590 N93-30533
ZHANLAV, T. p 3551 N93-30913
ZHAO, CONGZHONG p 3278 N93-29134
ZHAO, XIN M. p 3480 N93-28518
ZHAO, Y. C. p 3365 N93-30280
ZHIDKOV, E. P. p 3605 N93-30781
ZHIDKOV, P. E. p 3552 N93-30946
ZHIDKOV, P. R. p 3551 N93-30912
ZHIQUAN, GUO p 3421 N93-29260
ZHOU, ZIHENG p 3375 N93-30345
ZHU, J. p 3420 N93-29161
ZHU, YUANXIAN p 3580 N93-29880
ZHUKOV, A. I. p 3466 N93-30777
ZHURAVLEV, V. V. p 3600 N93-30766
ZIADA, H. H. p 3447 N93-30632
ZIELINSKI, ALEXANDER E. p 3271 N93-29394
ZIMIN, SERGEI p 3585 N93-28981
ZIMMER, ALFONS MAX p 3458 N93-28924
ZIMMERMAN, WILLIAM p 3249 N93-29775
ZIMMERMANN, S. p 3382 N93-29245
ZINNER, E. p 3318 N93-29367
ZISCHKA, PETER J. p 3308 N93-30876
ZISSMAN, MARC A. p 3494 N93-29421
ZIZKA, G. J. p 3598 N93-30393
ZNOTINAS, NORA M. p 3376 N93-30346
ZOECKLER, JOSEPH G. p 3270 N93-28696
ZOLENSKY, MICHAEL E. p 3638 N93-29355
p 3282 N93-29357
p 3283 N93-29359
p 3283 N93-29369
ZOOK, HERBERT A. p 3638 N93-29355
p 3282 N93-29357
p 3638 N93-29371
ZORY, PETER p 3601 N93-30811
ZUEFLE, ERNST-MICHAEL p 3259 N93-29999

ZUK, JOHN .... p 3236 N93-30673
p 3236 N93-30674
ZUKIC, M. .... p 3340 N93-28829
ZUKOR, K. S. .... p 3270 N93-29589
ZUMINO, B. .... p 3551 N93-30392
ZUPPARDO, JOSEPH C. .... p 3484 N93-30521
ZURLO, J. R. .... p 3416 N93-28566
ZUTAVERN, F. J. .... p 3406 N93-28944
ZWACK, PETER .... p 3367 N93-30296
ZWANZIGER, PETER .... p 3591 N93-28470
ZWIERZYNSKI, DARIUSZ A. .... p 3355 N93-30221
ZYBIN, K. P. .... p 3632 N93-28473

CORPORATE SOURCE INDEX

Typical Corporate Source Index Listing

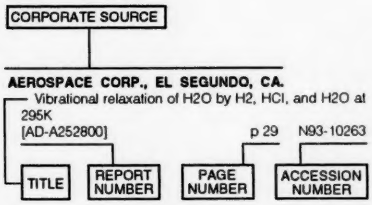
CORPORATE SOURCE
AEROSPACE CORP., EL SEGUNDO, CA.
Vibrational relaxation of H2O by H2, HCl, and H2O at 295K
[AD-A252800] p 29 N93-10263
TITLE
REPORT NUMBER
PAGE NUMBER
ACCESSION NUMBER

Listings in this index are arranged alphabetically by corporate source. The title of the document provides the user with a brief description of the subject matter. The report number helps to indicate the type of document cited (e.g., NASA report, translation, NASA contractor report). The accession number denotes the number by which the citation is identified. The page number helps you locate the citation in the abstract section. The titles are arranged under each corporate source in ascending accession number order.

A

ABB ENVIRONMENTAL SERVICES, INC., PORTLAND, ME.
Fugitive hydrocarbon emissions from Pacific OCS facilities, volume 1
[PB93-173797] p 3468 N93-28899
Fugitive hydrocarbon emissions from Pacific OCS facilities. Volume 2: Executive summary and user's guide
[PB93-173805-VOL-2] p 3471 N93-29861

ABB KRAFTWERKE A.G., MANHEIM (GERMANY).
Optical blade vibration measurement
[ETN-93-93454] p 3259 N93-29999

ABB POWER GENERATION, INC., BADEN (SWITZERLAND).
The aerodynamic effect of coolant ejection in the leading edge region of a film-cooled turbine blade
p 3258 N93-29958

ABT ASSOCIATES, INC., CAMBRIDGE, MA.
Evaluation of environmental marketing terms in the United States
[PB93-175784] p 3474 N93-30660

AC TECHNOLOGY SYSTEMS AND STORAGE TECHNOLOGY, MCLEAN, VA.
RAID 7 disk array p 3537 N93-30462

ACADEMIA R. P. R., BUCHAREST.
Adding dynamic rules to self-organizing fuzzy systems
p 3515 N93-29557

ACADEMY OF SCIENCES OF THE UKRAINE, KIEV.
Change of solar cell element properties influenced by adsorbed atoms
[DE93-606694] p 3466 N93-30777

ACADEMY OF SCIENCES (USSR), NOVOSIBIRSK.
Analysis of possibilities for using laser scattering for MeV electron beam diagnostics
[DE93-606223] p 3441 N93-30767
Measurements of the energy spectrum of an intense microsecond relativistic electron beam in the beam-plasma experiments using a multi-foil analyzer
[DE93-606271] p 3590 N93-30768
Hard photon emission from high energy electrons and positrons in single crystals
[DE93-606328] p 3600 N93-30770
Experimental MHD stability limit in the gas-dynamic trap
[DE93-606218] p 3591 N93-30780
On the photonic chiral anomaly in an external gravitational field
[DE93-606082] p 3479 N93-30785
Parton's picture of the electroweak processes in high energy e(+)e(-)-collisions
[DE93-606107] p 3571 N93-30788
Pion pair production in photon-photon collisions
[DE93-606114] p 3571 N93-30790
Orbital motion calculation using Lie method in collider nonlinear magnetic field
[DE93-605733] p 3571 N93-30800
Chaotic quantum systems
[DE93-606030] p 3606 N93-30802
Scaling properties of localized quantum chaos
[DE93-606031] p 3606 N93-30803
Complex apparatus and results of active experiment Electron-1 with injection of electronic beam in the ionosphere
[DE93-605452] p 3480 N93-30991
Microsecond ribbon relativistic electron beam in a plane undulator and generation of microwave radiation
[DE93-605693] p 3400 N93-30993

ADEPT IC DESIGN, OCEANSIDE, CA.
Design of a pixel cell optimized for a data push architecture readout
[DE93-011016] p 3616 N93-30122

ADVANCED FUEL RESEARCH, INC., EAST HARTFORD, CT.
Superconducting flux coupled fast switching device from YBCO films
[AD-A264301] p 3414 N93-30896

ADVISORY GROUP FOR AEROSPACE RESEARCH AND DEVELOPMENT, NEUILLY-SUR-SEINE (FRANCE).
Combat Automation for Airborne Weapon Systems: Man/Machine Interface Trends and Technologies
[AGARD-CP-520] p 3501 N93-28850
T(Ic2)acS(Ic3)ats for Surveillance Verification and C3I
[AGARD-CP-522] p 3387 N93-29892
Heat Transfer and Cooling in Gas Turbines
[AGARD-CP-527] p 3252 N93-29926
ELF/VLF/LF Radio Propagation and Systems Aspects
[AGARD-CP-529] p 3394 N93-30727

AERODYNE RESEARCH, INC., BILLERICA, MA.
Condensed phase diagnostics of nitramine propellant combustion p 3320 N93-30102

AEROJET-GENERAL CORP., SACRAMENTO, CA.
Orbital transfer vehicle oxygen turbopump technology. Volume 3: Hot oxygen testing
[NASA-CR-191036] p 3448 N93-31039

AERONAUTICAL RESEARCH INST. OF SWEDEN, BROMMA.
Inviscid quasi one-dimensional nonequilibrium flow
[FFA-TN-1992-35] p 3418 N93-28993
Implementation of a multidomain Navier-Stokes code on the Intel iPSC2 hypercube
[FFA-TN-1992-37] p 3418 N93-28994
An efficient spectral integration method for the solution of the Navier-Stokes equations
[FFA-TN-1992-28] p 3418 N93-29009
Factors influencing the interlaminar fracture toughness and its evaluation in composites
[FFA-TN-1991-34] p 3451 N93-29076

AERONAUTICAL RESEARCH LABS., MELBOURNE (AUSTRALIA).
Optimal trajectories for aircraft terrain following and terrain avoidance: A literature review update
[AD-A264075] p 3260 N93-30604

AEROSPACE CORP., EL SEGUNDO, CA.
Space transportation analysis and design (Reissue A)
[AD-A262752] p 3271 N93-28487
The design and testing of a high-temperature graphite dilatometer
[AD-A262185] p 3430 N93-28488
Thermal control paints on LDEF: Results of M0003 sub-experiment 18
[AD-A263252] p 3329 N93-28561
Long Duration Exposure Facility (LDEF) experiment M0003 meteoroid and debris survey
p 3638 N93-29361
Post-flight analyses of the crystals from the M0003-14 quartz crystal microbalance experiment
p 3602 N93-29684

AEROSPACE CORP., LOS ANGELES, CA.
A measurement of the radiation dose to LDEF by passive dosimetry p 3572 N93-29634
Tactical satellites p 3284 N93-29893
Launch vehicles for lightweight TACSAT deployment
p 3271 N93-29903

AEROSPACE INDUSTRIES ASSOCIATION OF AMERICA, INC., WASHINGTON, DC.
A detailed technology roadmap for superconductivity
p 3526 N93-29045

AEROSPACE MEDICAL RESEARCH LABS., BROOKS AFB, TX.
Pilot Candidate Selection Method (PCSM): What makes it work?
[AD-A262871] p 3498 N93-29481
Predicting aircrew training performance with psychometric g
[AD-A264021] p 3498 N93-30026

AEROSPACE MEDICAL RESEARCH LABS., WRIGHT-PATTERSON AFB, OH.
Armstrong Laboratory space visual function tester program p 3267 N93-28739
Effect of microgravity on several visual functions during STS Shuttle missions: Visual Function Tester-Model 1 (VFT-1) p 3268 N93-28740
Effect of microgravity on visual contrast threshold during STS Shuttle missions: Visual Function Tester-Model 2 (VFT-2) p 3268 N93-28741
Effect of microgravity on the visual near point: Visual Function Tester-Model 4 (VFT-4) p 3268 N93-28742
Cognitive interface considerations for intelligent cockpits p 3503 N93-28865
An evaluation of B-1B pilot performance during simulated instrument approaches with and without status information
[AD-A263874] p 3507 N93-29888
Methods for characterizing the human head for the design of helmets
[AD-A263875] p 3507 N93-29889
Handedness and motor programming effects of manual control and movement
[AD-A264022] p 3499 N93-30027

AEROSPATIALE, LES MUREAUX (FRANCE).
Tactical satellites for air command and control
p 3284 N93-29898

AGENCY FOR INTERNATIONAL DEVELOPMENT, WASHINGTON, DC.
Tropical forests and biological diversity: USAID report to Congress 1990-1991
[PB93-180453] p 3471 N93-29681

AIR FORCE ENVIRONMENTAL TECHNICAL APPLICATIONS CENTER, ASHEVILLE, NC.
Air weather service master station catalog USAFETAC climatic database users handbook no. 6
[AD-A264761] p 3484 N93-30608

AIR FORCE ENVIRONMENTAL TECHNICAL APPLICATIONS CENTER, SCOTT AFB, IL.
Seasonal snowfall statistics for selected stations
[AD-A263173] p 3481 N93-28991
Thunderstorm forecast study for Eglin AFB, Florida
[AD-A263423] p 3483 N93-29810

AIR FORCE INST. OF TECH., WRIGHT-PATTERSON AFB, OH.
Characterization of laboratory generated turbulence by optical phase measurements
[AD-A262596] p 3480 N93-28465
Rendering the out-the-window view for the AFIT virtual cockpit
[AD-A262599] p 3260 N93-28467
Automating the satellite range scheduling process
[AD-A262601] p 3270 N93-28468
Luminescence study of ion-implanted and MBE-grown Er-doped GaAs and Al(x)Ga(1-x)As
[AD-A262602] p 3591 N93-28471

Analysis of TOPAZ 2 and SPACE-R space nuclear power plants using a modified thermionic model
[AD-A262612] p 3286 N93-28474
Frequency domain speech compression using the Karhunen-Loeve Transform
[AD-A262613] p 3379 N93-28476
Design of a hardware discrete event simulation coprocessor
[AD-A262614] p 3537 N93-28478
Modified goodness-of-fit tests for the Weibull distribution
[AD-A262552] p 3553 N93-28574
Modified Anderson-Darling and Cramer-Von Mises goodness-of-fit tests for the normal distribution
[AD-A262554] p 3553 N93-28575
Toward reusable graphics components in Ada
[AD-A262568] p 3524 N93-28577
A new goodness-of-fit test for the Weibull distribution based on spacings
[AD-A262615] p 3553 N93-28587
A modified Anderson Darling goodness-of-fit test for the gamma distribution with unknown scale and location parameters
[AD-A262486] p 3553 N93-28760
A Monte Carlo study of the raw and normal varimax rotation criterion in factor analysis
[AD-A262516] p 3554 N93-28844
A modified chi-squared goodness-of-fit test for the three-parameter gamma distribution with unknown parameters
[AD-A262553] p 3554 N93-28845
A distributed object-oriented database application design
[AD-A262591] p 3612 N93-28846
Estimating test range capacity
[AD-A262493] p 3270 N93-28938
The infrared measurement for the reentry-body-translation
[AD-A263100] p 3278 N93-29134
Modelling temporal abductive explanation
[AD-A263096] p 3526 N93-29145
Numerical computation of inviscid flow around nose tip of Space Shuttle with NND scheme
[AD-A264012] p 3421 N93-29260
An investigation of graphite peek composite under compression with a centrally located circular discontinuity
[AD-A262549] p 3298 N93-29414
Construction and testing of a neutron and gamma spectrometry system using pulse shape discrimination with an organic scintillator
[AD-A262550] p 3567 N93-29415
Development of a visual system interface to support a domain-oriented application composition system
[AD-A262489] p 3528 N93-29418
Mitigation of shock waves in a cylindrical tunnel by foam
[AD-A262491] p 3423 N93-29419
A fuzzy logic optimal control law solution to the CMMCA tracking problem
[AD-A262555] p 3542 N93-29420
Design and performance evaluation of a gas chromatograph micromachined in a single crystal silicon substrate
[AD-A262594] p 3596 N93-29424
Selection and transmission of information. Issue 22: Republic interdepartmental collection (selected articles)
[AD-A262825] p 3615 N93-29431
An analysis of the Generalized Lambda Distribution
[AD-A262485] p 3555 N93-29447
Solution of Euler equations for forebody-inlet ensemble of aircraft at high angle of attack
[AD-A263905] p 3240 N93-29862
The application of concentric vortex simulation to calculating the aerodynamic characteristics of bodies of revolution at high angles of attack
[AD-A263879] p 3241 N93-29919
Laboratory experiments in integrated circuit fabrication
p 3292 N93-30962

AIR FORCE OFFICE OF SCIENTIFIC RESEARCH, BOLLING AFB, WASHINGTON, DC.
AFOSR Status Report
[AD-A264720] p 3670 N93-30513

AIR FORCE SYSTEMS COMMAND, BROOKS AFB, TX.
Field test of a computer-driven tool to measure psychological characteristics of aircrew
[AD-A264484] p 3499 N93-30425
Determinants of performance rating accuracy: A field study
[AD-A264726] p 3500 N93-30575

AIR FORCE SYSTEMS COMMAND, WRIGHT-PATTERSON AFB, OH.
Effect of canard wing positions on aerodynamic characteristics of swept-forward wing
[AD-A262373] p 3238 N93-28493
International aviation (Selected articles)
[AD-A262566] p 3227 N93-28576
A tutorial on exit pupils and eye rotation with virtual image optical displays
[AD-A262399] p 3494 N93-29400
Anelastic relaxations associated with local disordering in grain boundaries
[AD-A263101] p 3596 N93-29796
Construction and operation of a gas transport CO2 laser
[AD-A263102] p 3438 N93-29797
New developments in vacuum microelectronics
[AD-A263103] p 3410 N93-29798
Graphical comparison of U.S. standard atmospheres and military standard climatic extremes
[AD-A264639] p 3484 N93-30521

AIR PRODUCTS AND CHEMICALS, INC., ALLENTOWN, PA.
Development of alternative fuels from coal-derived syngas
[DE93-011629] p 3341 N93-28668

AIR WEATHER SERVICE, SCOTT AFB, IL.
The basics of weather models
[AD-A263386] p 3483 N93-29850
Cloudiest year study: An analysis of the 3DNEPH and RTNEPH databases
[AD-A263409] p 3483 N93-29967

ALABAMA UNIV., BIRMINGHAM.
Ultraviolet imaging spectrometer p 3582 N93-28827
Ultra-high resolution water window x ray microscope optics design and analysis
[NASA-CR-193225] p 3578 N93-29128

ALABAMA UNIV., HUNTSVILLE.
Advanced Earth-to-orbit propulsion technology information, dissemination and research
[NASA-CR-192561] p 3287 N93-28680
Measurement of the relative and absolute microgravity environment of space platforms, recent flight results, and determination of the spatial microgravity field
p 3266 N93-28725
The emulsion chamber technology experiment
p 3268 N93-28743
X ray, far, and extreme ultraviolet coatings for space applications p 3340 N93-28829
A study of the physical mechanisms for filament eruption and coronal mass ejection via numerical simulation
[NASA-CR-193180] p 3653 N93-28935
FNAS CRRES program completion
[NASA-CR-192468] p 3476 N93-29032
A high-temperature furnace for applications in microgravity p 3229 N93-29723
Residual acceleration data on IML-1: Development of a data reduction and dissemination plan
[NASA-CR-193224] p 3281 N93-30038
Two-dimensional and three-dimensional time-dependent MHD model of extended corona
p 3653 N93-30496
Optical system analysis for the ground based EXVM
[NASA-CR-192588] p 3582 N93-31035

ALASKA UNIV., FAIRBANKS.
A field investigation of water and salt movement in permafrost and the active layer
[AD-A263706] p 3487 N93-29298

ALBERTA TELECOMMUNICATIONS RESEARCH CENTRE, EDMONTON.
Enhanced resolution and de-aliasing techniques for fast Fourier transforms p 3358 N93-30240

ALENIA SPAZIO S.P.A., ROME (ITALY).
Electric propulsion for lightsats: A review of applications and advantages p 3290 N93-29907
SAR sensors on TACSATS: A feasibility assessment
p 3286 N93-29909

ALFA ROMEO S.P.A., NAPLES (ITALY).
Aero-thermal design of a cooled transonic NGV and comparison with experimental results
p 3257 N93-29957

ALLIED-SIGNAL AEROSPACE CO., KANSAS CITY, MO.
Development of an updated pinch-welding capability
[DE93-009823] p 3442 N93-28552
Characterization and optimization of a Hot Air Solder-Leveling System
[DE93-010188] p 3332 N93-29328

ALLIED-SIGNAL AEROSPACE CO., TORRANCE, CA.
Improved silicon nitride for advanced heat engines
[NASA-CR-182193] p 3298 N93-29451

AMERICAN CHEMICAL SOCIETY, WASHINGTON, DC.
Chemistry of the atmosphere: Its impact on global change. CHEMRAWN 7: Perspectives and recommendations
[PB93-180644] p 3488 N93-29670

AMERICAN SCIENCE AND ENGINEERING, INC., CAMBRIDGE, MA.
Automatic detection of explosives using x ray imaging
p 3244 N93-30275

AMERICAN SOLAR ENERGY SOCIETY, BOULDER, CO.
Solar world congress: Proceedings of the biennial congress of the international solar energy society, volume 1, part 2
[PB93-174779] p 3465 N93-30001
Solar World Congress: Proceedings of the Biennial Congress of the International Solar Energy Society, volume 2, part 2
[PB93-174795] p 3466 N93-30935

AMERICAN SPACE TECHNOLOGY, INC., SANTA MONICA, CA.
Retrievable payload carrier, next generation Long Duration Exposure Facility: Update 1992
p 3283 N93-29705

AMERICAN TECHNOLOGY INITIATIVE FOR AEROSPACE RESEARCH, MENLO PARK, CA.
A research experiment on facilitation and formation of joint research and development programs between government, industry, and universities: Overview, preliminary findings, and observations
p 3628 N93-30725

AMES LAB., IA.
Crack length determination by ultrasonic methods
[DE93-008075] p 3450 N93-28567
Advanced NDE technology program
[AD-A262008] p 3449 N93-29443
The global potential energy surfaces of the lowest two 1A-prime states of the ozone molecule: Theoretical determination and analysis
[DE93-007537] p 3313 N93-29837

ANACAPA SCIENCES, INC., FORT RUCKER, AL.
The effects of superimposing symbology on a simulated night vision goggle display
[AD-A263458] p 3508 N93-30590

ANSER ANALYTIC SERVICES, INC., ARLINGTON, VA.
Decision maker's guide to international space
[ANSER-STDN-93-4] p 3669 N93-29710

ANTHROPOLOGY RESEARCH PROJECT, YELLOW SPRINGS, OH.
Neural network technologies
[AD-A262576] p 3541 N93-28987

APPLIED EXPERTISE, INC., HOUSTON, TX.
Concept document of the repository-based software engineering program: A constructive appraisal
[NASA-CR-193125] p 3526 N93-29027

ARCON CORP., WALTHAM, MA.
Electron transport calculations between 1 MeV and 1 eV
[AD-A263412] p 3568 N93-29787

ARGONNE NATIONAL LAB., IL.
Spin observables in large t elastic N-N scattering
[DE93-009211] p 3564 N93-28549
Research in mathematics and computer science, March 1, 1991 - September 30, 1992
[DE93-011492] p 3509 N93-28573
BlockSolve v1.1: Scalable library software for the parallel solution of sparse linear systems
[DE93-011391] p 3524 N93-28644
Enhancements of the critical currents of YBaCuO single crystals by neutron (n) and proton (p) irradiation
[DE93-007892] p 3592 N93-28661
Effect of metallic-coating properties on the tribology of coated and oil-lubricated ceramics
[DE93-010663] p 3330 N93-28666
A summary of block schemes for reducing a general matrix to Hessenberg form
[DE93-010621] p 3525 N93-28877
Quantum dynamics of X2BC van der Waals clusters
[DE93-006416] p 3565 N93-28892
Surface modification of tribological components in transportation
[DE93-008647] p 3442 N93-28903
Use of local x ray computerized tomography for high-resolution, region-of-interest inspection of large ceramic components for engines
[DE93-005564] p 3449 N93-28943
A high field optical-pumping spin-exchange polarized deuterium source
[DE93-009208] p 3574 N93-28970
Battery testing at Argonne National Laboratory
[DE93-009204] p 3407 N93-29036
Hydrogen and sulfur production from hydrogen sulfide wastes
[DE93-008658] p 3310 N93-29052
Interim fatigue design curves for carbon, low-alloy, and austenitic stainless steels in LWR environments
[DE93-009202] p 3323 N93-29102
Forces on a magnet moving past figure-eight coils
[DE93-009965] p 3561 N93-29189
Transient tests on an MHD thruster
[DE93-008656] p 3587 N93-29299
The ANL electric vehicle battery R/D program for DOE-EHP
[DE93-010658] p 3408 N93-29311

Evaluation of atmospheric wind field and dispersion models for fog-oil smoke dispersion in complex terrain: Field measurement and model evaluation program for assessment of the environmental effects of military smokes
[AD-A262051] p 3482 N93-29399
Solid oxide fuel cells for transportation: A clean, efficient alternative for propulsion
[DE93-010662] p 3464 N93-29844
Simplified Linear Equation Solvers: User's manual
[DE93-011975] p 3550 N93-30140
Requirements for a system to analyze HEP events using database computing
[DE93-009960] p 3576 N93-30527
Nonlinear explicit transient finite element analysis on the Intel Delta
[DE93-009561] p 3535 N93-30647

ARIZONA STATE UNIV., TEMPE.
Robust feedforward/feedback control synthesis for uncertain dynamical systems p 3542 N93-29079
An integrated optimum design approach for high speed prop-rotors including acoustic constraints
[NASA-CR-193222] p 3248 N93-29153
Supersonic flow calculation using a Reynolds-stress and an eddy thermal diffusivity turbulence model
[NASA-CR-4515] p 3420 N93-29159
Local heat transfer measurement with liquid crystals on rotating surfaces including non-axisymmetric cases p 3255 N93-29943
Studies of the effect of image degradation and recombination on visual perception
[AD-A264332] p 3580 N93-30368
Advanced electromagnetic methods for aerospace vehicles
[NASA-CR-193468] p 3400 N93-31036

ARIZONA UNIV., TUCSON.
The detection of low-degree solar gravity mode oscillations by differential radius observations, 1986-1987 p 3652 N93-28605
Near-infrared spectroscopy as an astrophysical tool p 3632 N93-28607
Spectroscopic and photometric studies of main sequence M stars and a search for late-type dwarfs in the solar vicinity p 3629 N93-28608
Design concept for an IR mapping spectrometer for the Pluto fast flyby mission p 3285 N93-28779
Development of a 9.3 micrometer CW LIDAR for the study of atmospheric aerosol
[NASA-CR-193227] p 3381 N93-29105
Synthesis and polymerization of azaethylenes and aza-1,3-dienes
[AD-A263651] p 3332 N93-29290
Advanced design for orbital debris removal in support of solar system exploration p 3229 N93-29724
Nonequilibrium screening and exciton dynamics probed by femtosecond laser pulses
[AD-A263603] p 3439 N93-29983
The estimation and scaling of land-surface fluxes of latent and sensible heat with remotely sensed data over a grassland site p 3462 N93-30045
The chronic effects of jP-8 jet fuel exposure on the lungs
[AD-A264162] p 3495 N93-30153
Catastrophic collisions: Laboratory impact experiments, hydrocode simulations, and the scaling problem p 3635 N93-30411
Dense gas in the monoceros OB1 dark cloud and its relationship to star formation p 3636 N93-30502
Advanced research in sky surveillance: A search for low-luminosity objects
[AD-A264832] p 3631 N93-30629

ARKANSAS UNIV., FAYETTEVILLE.
Gas electron diffraction employing a pulsed electron beam synchronous with photoexcitation p 3319 N93-30101

ARMY AEROSTRUCTURES DIRECTORATE, HAMPTON, VA.
Evaluation of some scale effects in the response and failure of composite beams p 3308 N93-30874

ARMY AIR MOBILITY RESEARCH AND DEVELOPMENT LAB., FORT EUSTIS, VA.
Sound attenuation characteristics of the standard DH-132A and SPH-4 helmets worn in combination with standard issue earplugs
[AD-A263011] p 3506 N93-29406

ARMY ARMAMENT RESEARCH, DEVELOPMENT AND ENGINEERING CENTER, PICATINNY ARSENAL, NJ.
Electronics mixed-mode simulation
[AD-A264734] p 3534 N93-30577

ARMY ARMAMENT RESEARCH, DEVELOPMENT AND ENGINEERING CENTER, WATERVLIET, NY.
A thermal stress solution for multilayered composite cylinders
[AD-A262579] p 3295 N93-28657
Study on decreasing torque noise resulting from feedback noise for the modified bang-bang controller
[AD-A263178] p 3407 N93-29010
The electrodeposition of low contraction chromium using high/low current pulsing
[AD-A264475] p 3327 N93-30538

ARMY COLD REGIONS RESEARCH AND ENGINEERING LAB., HANOVER, NH.
Mathematical model of frost heave and thaw settlement in pavements
[CRREL-REPT-93-2] p 3262 N93-30103

ARMY ENGINEER WATERWAYS EXPERIMENT STATION, VICKSBURG, MS.
An evaluation of factors affecting the solidification/stabilization of heavy metal sludge
[AD-A264128] p 3473 N93-30197

ARMY MISSILE COMMAND, REDSTONE ARSENAL, AL.
The equivalent flat nose diameter of hemispherical nose cylindrical projectiles for impact induced detonation of energetic materials
[AD-A263244] p 3342 N93-29494
Prototype and short-run printed circuit board creation
[AD-A263245] p 3409 N93-29655
Spatial Light Modulators (SLMs) surface quality
[AD-A263249] p 3579 N93-29656
Selective nitrations. Volume 2: The laser-induced nitration of three cycloalkanes
[AD-A263250] p 3438 N93-29800
Monte Carlo simulation of magnitude-angle error sources
[AD-A263738] p 3555 N93-29857

ARMY NATICK LABS., MA.
A computational model that couples aerodynamic and structural dynamic behavior of parachutes during the opening process
[AD-A264115] p 3241 N93-30119

ARMY NATICK RESEARCH AND DEVELOPMENT COMMAND, MA.
The Environmental Symptoms Questionnaire (ESQ): Development and application
[AD-A264127] p 3495 N93-30196

ARMY RESEARCH INST. OF ENVIRONMENTAL MEDICINE, NATICK, MA.
Biophysical model for handwear insulation testing
[AD-A262926] p 3505 N93-28884
Medical aspects of cold weather operations: A handbook for medical officers
[AD-A263559] p 3496 N93-30588
Field trial of caffeine on physical performance at altitude: An attempt to overcome the challenge
[AD-A264260] p 3497 N93-30894

ARMY RESEARCH LAB., ABERDEEN PROVING GROUND, MD.
Tomographic analysis of line-of-sight infrared spectra of low-pressure flames
[AD-A263185] p 3309 N93-28514
Explosive consolidation of combustion synthesized TiC and TiB2: Precursor morphology effects
[AD-A263186] p 3341 N93-28515
Influence of ply waviness on stiffness and strength reduction of composite laminates
[AD-A263224] p 3294 N93-28559
A study of the effects of lens focal length on remote driver performance
[AD-A263191] p 3505 N93-28941
Two-dimensional model for current and heat transport in solid-armature railguns
[AD-A262014] p 3271 N93-29394
Recent applications of CFD to the aerodynamics of Army projectiles
[AD-A262953] p 3240 N93-29512
The XNOVAKTC rheological model
[AD-A263298] p 3342 N93-29762
The effect of material strength on segment penetration behavior
[AD-A263262] p 3453 N93-29801
Measurement of projectile surface temperature by means of its infrared radiation: A preliminary study
[AD-A264053] p 3432 N93-30032
A novel flame thermometer based on the doppler width of ro-vibrational transitions
[AD-A264515] p 3315 N93-30405
On the ideality of using a step-function current in a metallic foil to simulate a step-function heat-flux source
[AD-A264627] p 3413 N93-30539

ARMY RESEARCH LAB., ADELPHI, MD.
Estimating the parameters of chaotic maps
[AD-A262574] p 3556 N93-29423

ARMY RESEARCH LAB., WATERTOWN, MA.
Applications of laser light scattering in polymer dilute solution characterization
[AD-A263110] p 3335 N93-30007
Mechanical properties of several magnesium and aluminum composites
[AD-A262481] p 3299 N93-30137
Oxidation and hot corrosion of superalloys Rene 100 and X-40 at temperatures of 1475 F to 2000 F
[AD-A263747] p 3327 N93-30812
Durability of Quick Reaction Satellite Antenna (QRSA) trunnion castings
[AD-A264095] p 3281 N93-30813

ARMY STRATEGIC DEFENSE COMMAND, HUNTSVILLE, AL.
NPB cesium space experiment p 3267 N93-28733

ARMY TEST AND EVALUATION COMMAND, ABERDEEN PROVING GROUND, MD.
External acoustical noise measurements for aviation systems
[AD-A263138] p 3562 N93-29480

ARMY WAR COLL., CARLISLE BARRACKS, PA.
Using today's technology to improve mobile C4I for the operational commander
[AD-A263613] p 3245 N93-29285
The future role of the Director of Information Management (DOIM) organization within the DOD corporate information management initiative
[AD-A264118] p 3616 N93-30193
Air piracy and terrorism directed against U.S. Air carriers
[AD-A264120] p 3244 N93-30194

ASSISTANT SECRETARY OF DEFENSE (COMPTROLLER), WASHINGTON, DC.
Research, Development, Test and Evaluation (R, D, T, and E) programs (R-1), Department of Defense budget for fiscal year 1994
[PB93-169878] p 3611 N93-30936

ASTRONOMISCHE GESELLSCHAFT, HAMBURG (GERMANY).
Activities report of the Astronomical Society
[MITT-75] p 3629 N93-29008

ATLANTIS SCIENTIFIC SYSTEMS GROUP, INC., OTTAWA (ONTARIO).
The use of data turning in airborne radars p 3358 N93-30241
Similarities between synthetic aperature radar and ground probing radar imaging p 3376 N93-30347

AUBURN UNIV., AL.
Hypervelocity impact facility for simulating materials exposure to impact by space debris p 3283 N93-29365

AURORA FLIGHT SCIENCES CORP., MANASSAS, VA.
Development and testing of the Perseus proof-of-concept aircraft
[DE93-010121] p 3247 N93-28586

AZ TECHNOLOGY, HUNTSVILLE, AL.
The Optical Properties Monitor (OPM): A multipurpose optical laboratory in space p 3266 N93-28729
Next generation optical instruments and space experiment based on the LDEF thermal control surfaces experiment (S0069) p 3583 N93-29706

B

BABCOCK AND WILCOX CO., LYNCHBURG, VA.
Sensor systems for monitoring Maglev guideway structures
[PB93-154821] p 3444 N93-29205
Guideway structural design and power/propulsion/braking in relation to guideways, volume 1
[PB93-169902] p 3447 N93-30820

BALL CORP., BOULDER, CO.
QuickStar: System design, capabilities, and tactical applications of a small, smart space system p 3284 N93-29905

BALL STATE UNIV., MUNCIE, IN.
Thermoforming from a systems viewpoint p 3293 N93-30967

BALLISTIC RESEARCH LABS., ABERDEEN PROVING GROUND, MD.
Flame structure studies of propellant like low pressure flames using optical and mass spectrometric means p 3319 N93-30081

BARRINGER RESEARCH LTD., REXDALE (ONTARIO).
Advanced signal processing requirement in an ion mobility explosives detector p 3320 N93-30277

BASF STRUCTURAL MATERIALS, INC., CHARLOTTE, NC.
Advanced fiber/matrix material systems p 3305 N93-30854

BATH UNIV. (ENGLAND).
Flow and heat transfer between gas-turbine discs p 3256 N93-29950

BATTELLE COLUMBUS LABS., OH.
High reliability, maintenance-free INS battery development
[AD-A264521] p 3412 N93-30406

BATTELLE PACIFIC NORTHWEST LABS., RICHLAND, WA.
Ultrahigh temperature assessment study: Ceramic matrix composites
[AD-A262740] p 3295 N93-28592
The meteorological database
[DE93-007289] p 3481 N93-29054
Temperature-dependent electrical conductivity of soda-lime glass p 3294 N93-30978
Construction and testing of simple airfoils to demonstrate structural design, materials choice, and composite concepts p 3243 N93-30979

BELEIDSCOMMISSIE REMOTE SENSING, DELFT (NETHERLANDS).
Information system for co-registration of CAESAR sea-images based on two dimensional image matching techniques (SCORE). Part 1: Introduction, user requirements, and feasibility tests
[BCRS-90-40A-PT-1] p 3460 N93-29307
The MAESTRO-1 campaign: Analyses of polarimetric SAR data of agricultural fields and forests
[BCRS-92-06] p 3460 N93-29320
Preprocessing airborne remote sensing PARES calibration maintenance functional design document
[BCRS-92-07] p 3460 N93-29321
National remote sensing programme 2 ACMS project. Phase 1: Validation. Part 1: Definition of validation experiment
[BCRS-92-10-PHASE-1-PT-1] p 3461 N93-29465
Remote sensing in Czechoslovakia and Hungary: An analysis of the possible co-operation of The Netherlands with Czechoslovakia and Hungary in the field of remote sensing
[BCRS-92-12] p 3461 N93-29466
Land use database for the Netherlands using LANDSAT Thematic Mapper pictures
[BCRS-91-32] p 3463 N93-30839
CAESAR development plan 1992-1995
[BCRS-92-17] p 3463 N93-31009
ERS-1 directional wave spectra validation with the airborne SAR PHARS
[BCRS-92-18] p 3463 N93-31010
Bayesian linear analysis with application to removal of atmospheric influences on optical remote sensing images
[BCRS-92-19] p 3463 N93-31011

BELL COMMUNICATIONS RESEARCH, INC., LIVINGSTON, NJ.
A high performance, ad-hoc, fuzzy query processing system for relational databases p 3518 N93-29571

BELL-NORTHERN RESEARCH LTD., OTTAWA (ONTARIO).
A numerical simulator for testing sliding mode controls in stochastic systems p 3361 N93-30260
Generalized octrees for constrained object modeling
p 3369 N93-30304
Semi-blind restoration of images distorted by random time varying point spread functions
p 3375 N93-30344

BEND RESEARCH, INC., OR.
Novel polymer compositions for high-temperature membrane applications, phase 1
[PB93-174126] p 3331 N93-29201

BERN UNIV. (SWITZERLAND).
The Interstellar Gas Experiment: Analysis in progress
p 3639 N93-29380

BHABHA ATOMIC RESEARCH CENTRE, BOMBAY (INDIA).
Computer control of pulsed tunable dye lasers
[DE93-605896] p 3441 N93-30801
Pulsed laser photoacoustic spectrometer for study of solid materials
[DE93-605290] p 3441 N93-31023

BIOTRONICS TECHNOLOGIES, INC., WAUKESHA, WI.
Transcutaneous analyte measuring methods
[AD-A262861] p 3494 N93-29509

BOEING CO., SEATTLE, WA.
Developments in impact damage modeling for laminated composite structures p 3305 N93-30857

BOEING COMMERCIAL AIRPLANE CO., SEATTLE, WA.
Spurious symptom reduction in fault monitoring
[NASA-CR-191453] p 3542 N93-29192
Advanced technology composite aircraft structures
[NASA-CR-190420] p 3248 N93-29498
Composites: A viable option p 3300 N93-30429
Advanced technology commercial fuselage structure
p 3300 N93-30432
Cost studies for commercial fuselage crown designs
p 3302 N93-30440
Effects of intra- and inter-laminar resin content on the mechanical properties of toughened composite materials
p 3303 N93-30845
Process and assembly plans for low cost commercial fuselage structure p 3306 N93-30865

BOEING DEFENSE AND SPACE GROUP, HUNTSVILLE, AL.
Space transfer concepts and analyses for exploration missions, phase 3
[NASA-CR-192584] p 3268 N93-31034

BOEING DEFENSE AND SPACE GROUP, KENT, WA.
NASA in-step: Permeable membrane experiment
p 3267 N93-28736

BOEING DEFENSE AND SPACE GROUP, PHILADELPHIA, PA.
Mechanical and analytical screening of braided composites for transport fuselage applications
p 3305 N93-30855

BOEING DEFENSE AND SPACE GROUP, SEATTLE, WA.
Tank Pressure Control Experiment (TPCE)
p 3264 N93-28712
The enhanced-model ladar wind sensor and its application in planetary wind velocity measurements
p 3649 N93-28815
LDEF microenvironments, observed and predicted
p 3283 N93-29623

BOEING HELICOPTER CO., PHILADELPHIA, PA.
Fabrication of the V-22 composite AFT fuselage using automated fiber placement p 3302 N93-30443

BONN UNIV. (GERMANY).
Distribution of dark matter in the galaxy and the lower limits for the masses of supersymmetric particles
[BONN-92-31] p 3632 N93-28473
Remote sensing of agricultural vegetation: Status and perspectives p 3458 N93-28922
Fog studies in the Alpine region with digital NOAA/AVHRR data p 3458 N93-28925

BOSTON COLL., CHESTNUT HILL, MA.
Ionospheric structure specifications and systems effects
[AD-A263573] p 3476 N93-29343
A novel approach for new radiation sources based on solid state plasma instabilities
[AD-A263699] p 3588 N93-29382

BOSTON UNIV., MA.
Development of neural network architectures for self-organizing pattern recognition and robotics
[AD-A264831] p 3543 N93-29791
Kinetics and dynamics of reacting systems
[AD-A264046] p 3313 N93-30030
Young open clusters as probes of the star formation process p 3635 N93-30377
A characterization of young stellar objects in Bok globules: Infrared imaging, spectral energy distributions, and molecular outflows p 3636 N93-30563

BRIGHAM YOUNG UNIV., PROVO, UT.
Diffusion coefficients and heats of mixing in aqueous alkanolamines
[PB93-176212] p 3316 N93-30661

BRITISH AEROSPACE PUBLIC LTD. CO., BRISTOL (ENGLAND).
Oculo-motor responses and virtual image displays
p 3503 N93-28862

BRITISH AEROSPACE PUBLIC LTD. CO., KINGSTON-UPON-THAMES (ENGLAND).
Ergonomic development of digital map displays
p 3503 N93-28866

BRITISH ANTARCTIC SURVEY, CAMBRIDGE (ENGLAND).
Transient (approximately equals 10 s) VLF amplitude and phase perturbations due to lightning-induced electron precipitation into the ionosphere (the Trimpi effect)
p 3396 N93-30736

BRITISH COLUMBIA UNIV., VANCOUVER.
Spherically symmetric model atmospheres for late-type giant stars
[ISBN-0-315-72632-6] p 3633 N93-28673

BROOKHAVEN NATIONAL LAB., UPTON, NY.
Evaluation of polyaryl adhesives in elastomer-stainless steel joints
[DE93-009794] p 3329 N93-28551
Ultraviolet free electron laser facility preliminary design report
[DE93-009360] p 3435 N93-28594
Aerosol particle analysis by Raman scattering technique
[DE93-005587] p 3309 N93-28880
Benchmark eigenvalue spectrum calculations with anisotropic effects
[DE93-006387] p 3548 N93-28891
Potential transmission and transients during corrosion: Applications to corrosion monitoring
[DE93-010863] p 3323 N93-29256
Design and test of a superconducting RFQ for heavy ions
[DE93-010862] p 3575 N93-29317
Materials studies for preventing corrosion in condensing environments
[PB93-185478] p 3327 N93-30815

BROWN UNIV., PROVIDENCE, RI.
Accelerated motion of rigid spheres in unsteady flows at low to moderate Reynolds numbers
p 3416 N93-28612
Computation and generalization in neural networks
[AD-A263752] p 3549 N93-29871
The production and evolution of plasma and associated magnetic fields during hypervelocity impacts: Implications for planetary paleomagnetism p 3589 N93-30000
Topics in inflationary universe medels and cosmic string theories p 3637 N93-30579
Principal components of natural images: An analytical solution
[AD-A264800] p 3489 N93-30603
The structure and dynamics of the vorticity and passive scalar fields at small scales in homogeneous isotropic turbulence p 3427 N93-30625

BUREAU OF MINES, TUSCALOOSA, AL.
Genetic algorithms in adaptive fuzzy control
p 3518 N93-29572

C

CAE ELECTRONICS LTD., SAINT LAURENT (QUEBEC).
Radar beam effects for a flight simulator using signal processor based hardware p 3373 N93-30328

CALGARY UNIV. (ALBERTA).
An auto-guiding system for mid-sized telescopes
p 3375 N93-30340

CALIFORNIA INST. OF TECH., PASADENA.
A one-dimensional continuum model for shape-memory alloys
[AD-A262505] p 3321 N93-28656
Topics in General Relativity theory: Gravitational-wave measurements of black-hole parameters; gravitational collapse of a cylindrical body; and classical-particle evolution in the presence of closed, timelike curves
p 3603 N93-28690
The multiplicity of T Tauri stars in the star forming regions Taurus-Auriga and Ophiuchus-Scorpius: A 2.2 micron speckle imaging survey p 3634 N93-28945
Direct numerical simulations of unsteady separated flows using vortex methods p 3419 N93-29077
The thermal structure, dust loading, and meridional transport in the Martian atmosphere during late southern summer p 3651 N93-29616
Modeling earthquakes with local and regional broadband data p 3478 N93-30005
The faintest stars p 3630 N93-30493
Spacecraft studies of Phobos and Mars
[NASA-CR-193298] p 3651 N93-30635
Modeling regional seismic waves
[AD-A264002] p 3479 N93-30756
A theoretical and computational study on active wake control p 3243 N93-30892
Conjugated polymers from cyclohexadienediol monomers
[AD-A264837] p 3340 N93-30900
An adaptive Lagrangian method for computing 1-D reacting flows and the theory of Riemann invariant manifolds for the compressible Euler equations
p 3428 N93-30902

CALIFORNIA POLYTECHNIC STATE UNIV., SAN LUIS OBISPO.
Helicopter approach capability using the differential global positioning system
[NASA-CR-193183] p 3245 N93-28936
A 69 cent look at thermoplastic softening
p 3292 N93-30963
Visualizing weld metal solidification using organic analogs p 3293 N93-30973

CALIFORNIA STATE POLYTECHNIC COLL., SAN LUIS OBISPO.
Project summary p 3227 N93-29714

CALIFORNIA STATE POLYTECHNIC UNIV., POMONA.
High-altitude reconnaissance aircraft
p 3227 N93-29713

CALIFORNIA STATE UNIV., FRESNO.
Incorporation of varying types of temporal data in a neural network p 3518 N93-29575

CALIFORNIA STATE UNIV., NORTHRIDGE.
Project ARES 2: High-altitude battery-powered aircraft
p 3227 N93-29715

CALIFORNIA UNIV., BERKELEY.
Stability, bifurcation, and control of Hamiltonian systems
[DE93-012103] p 3547 N93-28648
Research in efficient scientific computation
[AD-A262084] p 3525 N93-28986
Proposal to develop guides for high school teachers on global systems science
[DE93-008759] p 3624 N93-29100
A model for amalgamation in group decision making
p 3513 N93-29540

Experimental and analytical investigation of finger-follower cam systems p 3446 N93-30378

Striped tertiary storage arrays p 3620 N93-30464

Nonsmooth optimization algorithms, system theory, and software tools [AD-A264679] p 3534 N93-30549

CALIFORNIA UNIV., BERKELEY. LAWRENCE BERKELEY LAB.

Advanced insulations for refrigerator/freezers: The potential for new shell designs incorporating polymer barrier construction [DE93-010600] p 3353 N93-28570

In situ characterization of interfacial and bulk properties of lithium polymer batteries using 4-probe DC techniques [DE93-007699] p 3405 N93-28581

Theory of normal and superconducting properties of fullerene-based solids [DE93-007722] p 3592 N93-28582

Excited states in electronic structure calculations [DE93-007704] p 3592 N93-28642

The onset of vortex turbulence [DE93-010424] p 3417 N93-28663

Novel low temperature superconducting bolometers [DE93-010433] p 3430 N93-28664

Healing of lithographically introduced flaws in glass and glass containing ceramics [DE93-010453] p 3330 N93-28761

A technique for single-pulse spectrum and pulse width measurements for an IR-FEL [DE93-007732] p 3436 N93-28847

Superconducting submillimeter and millimeter wave detectors [DE93-007656] p 3431 N93-29149

Uniaxially stressed Ge:Ga and Ge:Be [DE93-010426] p 3594 N93-29150

Oxidation behavior in reaction-bonded aluminum-silicon alloy/alumina powder compacts [DE93-010407] p 3298 N93-29191

A transient FGM interlayer based approach to joining ceramics [DE93-010415] p 3331 N93-29248

Response of a Nb/Al2O3/Nb tunnel junction to picosecond electrical pulses [DE93-010416] p 3594 N93-29249

An RF driven H(-) source and a low energy beam injection system for RFQ operation [DE93-010438] p 3575 N93-29302

Defect studies in low-temperature-grown GaAs [DE93-010405] p 3595 N93-29417

A photon phreak digs the LDEF happening p 3572 N93-29629

Diffraction and holography with photoelectrons and Auger electrons: Some new directions [DE93-007664] p 3313 N93-29766

NMR studies of molecules in liquid crystals and graphite [DE93-010423] p 3569 N93-29805

Understanding conformal field theory through parafermions and Chern Simons theory [DE93-010452] p 3604 N93-29806

Reaction and reorientation of electronically excited H2(B) [DE93-010435] p 3569 N93-29860

Submillimeter and microwave residual losses in epitaxial films of Y-Ba-Cu-O and Tl-Ca-Ba-Cu-O [DE93-010430] p 3596 N93-29868

X ray microscopy resource center at the Advanced Light Source [DE93-010449] p 3261 N93-29869

Three-dimensional simulation analysis of the standing-wave free-electron laser two-beam accelerator [DE93-010461] p 3575 N93-29870

Metallization at detonation fronts in solids p 3319 N93-30087

Differential calculus on quantum spaces and quantum groups [DE93-010425] p 3551 N93-30392

A high resolution 14-bit ADC for Gammasphere Project [DE93-010446] p 3598 N93-30393

Experimental test of hole-coupled FEL resonator designs using a CW-HeNe laser [DE93-010439] p 3440 N93-30530

The x ray microscopy resource center at the advanced light source [DE93-010443] p 3433 N93-30531

CALIFORNIA UNIV., DAVIS.

Proposal to develop guides for high school teachers on global systems science [DE93-008759] p 3624 N93-29100

A simple model for ion solvation with non additive cores [AD-A263075] p 3566 N93-29143

Parametric and combinatorial problems in constrained optimization [AD-A264229] p 3555 N93-30363

A comparison of classical mechanics models and finite element simulation of elastically tailored wing boxes p 3306 N93-30863

Tailored composite wings with elastically produced chordwise camber p 3308 N93-30876

CALIFORNIA UNIV., IRVINE.

Laboratory simulation of field-aligned currents [NASA-CR-193091] p 3476 N93-28538

A self-learning rule base for command following in dynamical systems p 3512 N93-29531

CALIFORNIA UNIV., LOS ANGELES.

Risk-based spacecraft fire safety experiments p 3267 N93-28738

Drill/borescope system for the Mars Polar Pathfinder p 3647 N93-28805

Plasma, magnetic, and electromagnetic measurements at nonmagnetic bodies p 3647 N93-28809

Quantum devices using Si-based superlattices and structures [AD-A263700] p 3595 N93-29383

The 1990/1991 project summaries p 3229 N93-29725

Planar active antennas and quasi-optical power combining arrays using FET's and slots [AD-A263759] p 3387 N93-29875

Applications of mesoscopic physics [DE93-012104] p 3597 N93-30141

The adhesion of AgI molecules to gaseous metallic silver cluster cations [AD-A264820] p 3338 N93-30628

CALIFORNIA UNIV., RIVERSIDE.

Study on various problems in statistical planning and inference [AD-A262484] p 3554 N93-29411

CALIFORNIA UNIV., SAN DIEGO.

The dynamics and control of space tethers p 3274 N93-28629

Theory of tokamak edge turbulence: Drift-thermal instability-induced turbulence and ionization-driven drift wave turbulence p 3586 N93-29123

Studies of hydrogen-air diffusion flames and of compressibility effects related to high-speed propulsion p 3310 N93-29125

Shear, strain, and thermohaline vertical fine structure in the upper ocean p 3488 N93-30046

CALIFORNIA UNIV., SAN DIEGO, LA JOLLA.

Wound healing and connective tissue metabolism: The role of hyperbaric oxygen therapy [AD-A262483] p 3493 N93-28759

Associative memories for supercomputers [AD-A263142] p 3520 N93-29482

Hamiltonian dynamics of coupled potential vorticity and internal wave motion: 1. Linear modes [AD-A263469] p 3424 N93-29838

Balanced technology initiative on computational mechanics of materials [AD-A263906] p 3453 N93-29863

Performance analysis of subspace methods [AD-A263984] p 3530 N93-29865

Sensitive detection of new superconductors created at ultra high pressures [AD-A264340] p 3597 N93-30161

Knot invariants and cellular automata [AD-A264199] p 3607 N93-30884

CALIFORNIA UNIV., SANTA BARBARA.

Be3(AsO4)2 2H2O: A new berylloarsenate phase containing bridged tetrahedral 3-rings [AD-A262518] p 3592 N93-28584

Numerical simulation of quantum many-body systems [DE93-008300] p 3603 N93-28958

The synthesis and ab initio structure determination of Zn4O(BO3)2: A microporous zincoborate built up from fused 3-ring and 5-ring sub-units [AD-A262504] p 3594 N93-29138

Acid gas treating by aqueous alkanolamines [PB93-176188] p 3471 N93-29676

Synthesis and characterization of mixed 3-5 and 2-6 semiconductor monomers included in the borate sodalite analogue [AD-A264523] p 3598 N93-30407

Two new titanium pyroarsenates: Alpha-TiAs2O7 and Beta-TiAs2O7 [AD-A264632] p 3599 N93-30518

Ordered molecular arrays as templates: A new approach to synthesis of mesoporous materials [AD-A264631] p 3570 N93-30540

CALSPAN ADVANCED TECHNOLOGY CENTER, BUFFALO, NY.

The USAF Advanced Turbine Aerothermal Research Rig (ATARR) p 3255 N93-29945

CALSPAN-BUFFALO UNIV. RESEARCH CENTER, NY.

Kinetics of nitric oxide formation behind 3 to 4 KM/S shock waves [AD-A263653] p 3312 N93-29389

CAMBRIDGE HYDRODYNAMICS, INC., PRINCETON, NJ.

Development of a new technique for image reconstruction, enhancement, and visualization [AD-A263145] p 3528 N93-29483

CANADA CENTRE FOR REMOTE SENSING, OTTAWA (ONTARIO).

Overview of the System of Experts for Intelligent Data Management (SEIDAM) p 3613 N93-29228

CANADIAN FORCES BASE TRENTON, ASTRA (ONTARIO).

Stand alone lightning detection equipment used at Canadian Forces air bases p 3367 N93-30295

CANADIAN MARCONI CO. LTD., KANATA (ONTARIO).

Embedded GPS: The Canadian Marconi approach p 3247 N93-30330

CANADIAN SPACE AGENCY, OTTAWA (ONTARIO).

Development of an antenna measurement facility operating in the 2 GHz - 100 GHz frequency range p 3369 N93-30308

Robot arm with positional absolute encoded joints p 3370 N93-30312

Wide frequency polarimetric radar cross section measurements p 3371 N93-30321

CAPONE (RONALD L.) AND ASSOCIATES, ARLINGTON, VA.

Using a neural network to estimate solvent consumption [PB93-173110] p 3467 N93-28873

CARLETON UNIV., OTTAWA (ONTARIO).

Rib arrow integrated optic polarizer p 3357 N93-30231

High-speed, CMOS dual modulus frequency divider for RF frequency synthesis p 3359 N93-30245

On analytical performance modelling of software for distributed systems p 3364 N93-30279

MLog: A language for prototyping concurrent systems p 3368 N93-30301

CARNEGIE INST. OF TECH., PITTSBURGH, PA.

Nonresident and endangered variables: The effects of code generation optimizations on symbolic debugging [AD-A263149] p 3529 N93-29486

CARNEGIE-MELLON UNIV., PITTSBURGH, PA.

Research on reconfigurable and reliable manipulators [DE93-010244] p 3444 N93-29330

Collection-oriented match: Scaling up the data in production systems [AD-A262755] p 3615 N93-29459

Applying high-level language paradigms to communications software for distributed systems [AD-A263001] p 3528 N93-29463

Communications neural net processors [AD-A263330] p 3542 N93-29763

Full abstraction for a shared variable parallel language [AD-A263547] p 3530 N93-29821

NESL: A nested data-parallel language (Version 2.6) [AD-A263548] p 3530 N93-29822

Class notes: Programming parallel algorithms CS 15-840B (Fall 1992) [AD-A263549] p 3530 N93-29823

What is the center of the image? [AD-A263550] p 3579 N93-29824

Capability maturity model for software, version 1.1 [AD-A263403] p 3530 N93-29852

Reactive integration for traditional programming languages [AD-A263986] p 3531 N93-29866

Key practices of the capability maturity model, version 1.1 [AD-A263432] p 3610 N93-29970

Intelligent support for human computer interaction and decision-making in distribution planning and scheduling systems [AD-A263985] p 3610 N93-30124

Using the Mach communication primitives in X11 [AD-A264049] p 3533 N93-30125

Tutorial: Performance and reliability in redundant disk arrays p 3537 N93-30463

Using Transparent Informed Prefetching (TIP) to reduce file read latency p 3522 N93-30480

The midway distributed shared memory system [AD-A264645] p 3534 N93-30523

An annotated bibliography on integration in software engineering environments [AD-A264798] p 3535 N93-30602

Physical chemical studies on molecular composite compositions [AD-A264834] p 3339 N93-30898

CASE WESTERN RESERVE UNIV., CLEVELAND, OH.

Conceptual design of a two-stage-to-orbit vehicle p 3228 N93-29716

The electrolyte factor in O2 reduction electrocatalysis [AD-A263565] p 3313 N93-29828

Molecular dynamics of physical aging processes in polymer glasses [AD-A263737] p 3334 N93-29856

Memory driven feature-based design
[AD-A264697] p 3534 N93-30495
Dioxygen reduction in various acid electrolytes
[AD-A263564] p 3317 N93-30664

CENTER FOR MATHEMATICS AND COMPUTER SCIENCE, AMSTERDAM (NETHERLANDS).
Packing odd paths
[CWI-BS-R9207] p 3549 N93-29849
Turning SOS rules into equations
[CWI-CS-R9218] p 3532 N93-30017

CENTRAL RESEARCH INST. OF ELECTRIC POWER INDUSTRY, TOKYO (JAPAN).
Development of nickel/metal hydride secondary battery
[DE93-781330] p 3406 N93-28669
Research and development of carbon black anodes for lithium secondary cells
[DE93-781331] p 3406 N93-28746
Fundamental study of the signal processing by optics
[DE93-776265] p 3577 N93-28982
Approach to extending the cycle life of lithium secondary battery
[DE93-776266] p 3406 N93-28983
Research and development of lithium secondary batteries for load conditioner use, volume 2
[DE93-781329] p 3410 N93-29673

CENTRE D'ETUDES DE LA NAVIGATION AERIENNE, TOULOUSE (FRANCE).
Evolution of radar data processing in the French air traffic control system p 3247 N93-30325

CENTRE NATIONAL D'ETUDES SPATIALES, PARIS (FRANCE).
Consultative Committee for Space Data Systems recommendation for space data system standards: Telecommand. Part 2.1: Command operation procedures
[NASA-TM-108158] p 3393 N93-30371

CENTRE NATIONAL D'ETUDES SPATIALES, TOULOUSE (FRANCE).
New results from FRECOPA analysis
p 3448 N93-29688
Design and integration of high bit rate four phase monolithic demodulators and modulators at X band
[LAAS-92354] p 3414 N93-31030

CENTRE NATIONAL DE LA RECHERCHE SCIENTIFIQUE, ECULLY (FRANCE).
Modeling of a turbulent flow in the presence of discrete parietal cooling jets p 3258 N93-29960

CHAN TECHNOLOGIES, INC., KIRKLAND (QUEBEC).
Array-fed reflector systems with limited scan
p 3371 N93-30318
A dual polarized broadband multifrequency Earth station feed p 3371 N93-30319
Comparison and design of multiple beam antenna feed networks p 3374 N93-30335
Recent advances in bootlace lens design
p 3374 N93-30336

CHEMICAL RESEARCH AND DEVELOPMENT CENTER, ABERDEEN PROVING GROUND, MD.
Measurement of a Michelson interferometer mirror velocity with a time interval analyzer
[AD-A263009] p 3430 N93-28659
Use of statistics in computational chemistry
[AD-A264307] p 3315 N93-30365

CHEMICAL WARFARE/CHEMICAL AND BIOLOGICAL DEFENSE INFORMATION ANALYSIS CENTER, EDGEWOOD, MD.
Evaluation of test methods and requirements for respiratory protection systems 21
[AD-A262466] p 3501 N93-28757
Evaluation and optimization of a flexible filtration system for respiratory protection system 21
[AD-A262467] p 3493 N93-28758

CHICAGO UNIV., IL.
Studies of complexity in fluid systems
[DE93-010776] p 3418 N93-28878
Limits on neutrino radiative decay from SN1987A
[NASA-CR-193262] p 3653 N93-29164
Spatial Analysis and Modeling Systems (SAMS)
p 3614 N93-29239
An LDEF 2 dust instrument for discrimination between orbital debris and natural particles in near-Earth space
p 3286 N93-29707

CINCINNATI UNIV., OH.
A neuro-fuzzy architecture for real-time applications
p 3511 N93-29529
A fuzzy case based reasoning tool for model based approach to rocket engine health monitoring
p 3289 N93-29570
Simulation, characterization and control of forced unsteady viscous flows using Navier-Stokes equations
[AD-A264333] p 3425 N93-30369

CITY COLL. OF THE CITY UNIV. OF NEW YORK, NY.
Studies in premixed combustion
[DE93-007955] p 3310 N93-29051

Massively parallel spatial light modulation-based optical signal processing
[AD-A264846] p 3581 N93-30905

CIVIL AEROMEDICAL INST., OKLAHOMA CITY, OK.
Accident proneness: A research review
[DOT/FAA/AM-93/9] p 3498 N93-28622

CLARKSON UNIV., POTSDAM, NY.
Colloid and interface chemistry aspects of ceramics
[AD-A264685] p 3337 N93-30552

CLEMSON UNIV., SC.
Fuzzy multiple linear regression: A computational approach p 3518 N93-29574

COAST GUARD RESEARCH AND DEVELOPMENT CENTER, GROTON, CT.
A comparison of simulated parallax and single-station range aids to navigation
[AD-A263460] p 3246 N93-29818

COLLEGE OF WESTERN NEW ENGLAND, SPRINGFIELD, MA.
Experiments in corrosion for younger students by and for older students p 3291 N93-30955

COLORADO STATE UNIV., FORT COLLINS.
Electrochemical fabrication of cadmium chalcogenide microdiode arrays
[AD-A263169] p 3310 N93-28988
A stochastic formation of radiative transfer in clouds
[DE93-011372] p 3484 N93-30055

COLORADO UNIV., BOULDER.
Finite element analysis of time-independent superconductivity
[NASA-CR-191140] p 3450 N93-28556
Space construction activities
[NASA-CR-192690] p 3274 N93-29108
Interaction dynamics of on-orbit construction
p 3274 N93-29109
Hybrid CMS methods with model reduction for assembly of structures p 3274 N93-29110
Controls of interaction dynamics of orbital assembly
p 3275 N93-29111
Controls for space structures p 3275 N93-29112
Structural load control during construction
p 3275 N93-29113
Systems engineering studies of on-orbit assembly operation p 3275 N93-29114
Lunar regolith densification p 3276 N93-29115
Regolith-structure modeling p 3276 N93-29116
Lunar regolith penetrators and cutters
p 3276 N93-29117
Lunar crane system p 3277 N93-29118
Lunar rovers and local positioning system
p 3277 N93-29119
Indigenous lunar construction materials
p 3277 N93-29120
Systems engineering studies of lunar base construction p 3277 N93-29121
Design optimization of space structures
p 3278 N93-29122
Program plan for an experimenter's laboratory for visualized interactive science p 3613 N93-29224
Colorado Center for Astrodynamics Research (CCAR)
p 3614 N93-29233
Structure and switching dynamics in ferroelectric crystal and liquid crystal thin films
[AD-A263664] p 3594 N93-29293
Earth to lunar CELSS evolution p 3229 N93-29727
Accelerating the transfer of technology for implementing domain specific software architectures
[AD-A264017] p 3532 N93-30014
Applications of the photorefractive effect and damage induced effects in fibers
[AD-A264339] p 3580 N93-30205
Numerical modeling and parameterization of gravity wave processes and effects in the atmosphere
[AD-A264331] p 3478 N93-30367
The HSCT mission analysis of waverider designs
[NASA-CR-193467] p 3243 N93-31037

COLORADO UNIV., COLORADO SPRINGS.
Quantification of thermographic mapping techniques
[AD-A264020] p 3391 N93-30016

COLORADO UNIV., DENVER.
Beta-adrenergic blockade and lactate metabolism during exercise at high altitude
[AD-A263544] p 3495 N93-29820

COLSA, INC., HUNTSVILLE, AL.
Digital hardware architecture implementation
[AD-A263219] p 3521 N93-29492

COLUMBIA UNIV., NEW YORK, NY.
Multichip module high speed testing
[AD-A262989] p 3408 N93-29427
Symposium on high temperature superconductors: Materials research for emerging technologies
[AD-A263120] p 3409 N93-29495
The x ray population in globular clusters and three crab-like SNR in the large Magellanic cloud
[NASA-CR-193172] p 3630 N93-29604
GRO: Red-shifted electron-positron annihilation gamma-rays from radiopulsars
[NASA-CR-193243] p 3635 N93-30053

COLUMBIA UNIV., PALISADES, NY.
Steady-state and transient modeling of tracer and nutrient distributions in the global ocean
[DE93-011043] p 3486 N93-28670

COM DEV LTD., CAMBRIDGE (ONTARIO).
SAW technology for on-board processing in military satellite communications p 3362 N93-30265
Adaptive jammer nulling in EHF communications satellites p 3365 N93-30284

COMMERCE DEPT., WASHINGTON, DC.
US space commerce, 1991 p 3625 N93-30695

COMMISSION OF THE EUROPEAN COMMUNITIES (LUXEMBOURG).
Proceedings of Symposium F on New Aspects on the Growth, Characterization and Applications of CdTe and related Cd rich alloys 5, 1992
[AD-A263541] p 3597 N93-29974

COMMUNICATIONS RESEARCH CENTRE, OTTAWA (ONTARIO).
A satellite downlink spread spectrum timing beacon
p 3362 N93-30267
Temporal synchronization of frequency hopped DPSK
p 3365 N93-30285
Comparison of two random access techniques for the North American MSAT system p 3370 N93-30315
Constant Average Power Single Sideband (CAPSSB) modulation p 3373 N93-30331
Design issues and initial performance of an adaptive air/ground/air HF communication system
p 3375 N93-30342
Introduction p 3395 N93-30728
VLF propagation measurements in the Canadian Arctic p 3396 N93-30733
VLF/LF transmitting antennas p 3398 N93-30747

COMMUNICATIONS SATELLITE CORP., CLARKSBURG, MD.
On-board B-ISDN fast packet switching architectures. Phase 2: Development. Proof-of-concept architecture definition report
[NASA-CR-191151] p 3273 N93-29884

COMPENGSERV LTD., OTTAWA (ONTARIO).
Cloud classification from satellite imagery using neural computing p 3367 N93-30297
Issues of ATC conflict resolution under real-time constraints p 3247 N93-30350

COMPUTATIONAL MECHANICS CO., AUSTIN, TX.
Pre- and postprocessing techniques for determining goodness of computational meshes
[NASA-CR-192553] p 3538 N93-29030

COMPUTER SCIENCES CORP., HAMPTON, VA.
Advanced Transport Operating System (ATOPS) Flight Management/Flight Controls (FM/FC) software description
[NASA-CR-191457] p 3250 N93-28621

CONCORDIA UNIV., MONTREAL (QUEBEC).
Parameter identification of time-varying systems using neural networks p 3356 N93-30226
A systolic-array structure for MTCM receivers
p 3357 N93-30236
Optimized partitioning and balancing for parallel processing p 3365 N93-30280
Models for performance assessment of HF antennas on the CH-135/Twin Huey helicopter
p 3366 N93-30291
Coupling gain computation between antennas on circular cylinders at SHF/EHF frequencies p 3369 N93-30309
RCS of fundamental scatterers in the HF band by wire-grid modelling p 3371 N93-30320

CONCURRENT TECHNOLOGIES CORP., JOHNSTOWN, PA.
Near net shape processing: A necessity for advanced materials applications p 3290 N93-30949

CONGRESSIONAL BUDGET OFFICE, WASHINGTON, DC.
Promoting high-performance computing and communications
[ISBN-0-16-041828-3] p 3522 N93-30570

CONNECTICUT UNIV., STORRS.
Transformation toughening
[DE93-011805] p 3321 N93-28631

CONSEJO SUPERIOR DE INVESTIGACIONES CIENTIFICAS, TENERIFE (SPAIN).
Digital image compression using artificial neural networks p 3624 N93-28811

CONVEX COMPUTER CORP., RICHARDSON, TX.
The state of the state of the art in mass storage technology p 3622 N93-30475

COOPERATIVE INST. FOR RESEARCH IN THE ATMOSPHERE, FORT COLLINS, CO.
Geoscience center research
[AD-A263465] p 3462 N93-29834

COORDINATING RESEARCH COUNCIL, INC., ATLANTA, GA.
Aircraft and refueler bonding and grounding study [AD-A262027] p 3261 N93-29398

CORNELL UNIV., ITHACA, NY.
Dense inclined flows: Theory and experiments [DE93-011452] p 3417 N93-28630
The MESUR mission p 3649 N93-28816
Femtosecond carrier processes in compound semiconductors and real time signal processing [AD-A263076] p 3382 N93-29131
In-situ x ray studies of the underpotential deposition of copper on platinum (3) [AD-A263361] p 3595 N93-29331
Femtosecond carrier processes in compound semiconductors and real time signal processing [AD-A262966] p 3384 N93-29514
Center of Excellence in Biotechnology (Research) [AD-A263598] p 3491 N93-29915
A redesigned Isis and Meta system under Mach [AD-A263576] p 3531 N93-29976
Surface shear stress estimates from geostrophic winds for use in sensible and latent heat flux formulations p 3483 N93-30044
Novel methods of acceleration [AD-A264828] p 3590 N93-30600
Enhanced convergence adaptive detection [AD-A264100] p 3399 N93-30879

COUNCIL ON ENVIRONMENTAL QUALITY, WASHINGTON, DC.
Building alliances to restore coastal environments: A coastal America progress report [PB93-169464] p 3470 N93-29674

CUYUNA CORP., AUSTIN, TX.
Program for an improved hypersonic temperature-sensing probe [NASA-CR-186025] p 3431 N93-29066

D

DAEDALUS ENTERPRISES, INC., ANN ARBOR, MI.
Research and development of an airborne multispectral scanner to measure fire, terrestrial and atmospheric characteristics (50 channel) [NASA-CR-193121] p 3456 N93-28620

DARTMOUTH COLL., HANOVER, NH.
Development of an airborne MMW FM-CW radar for mapping river ice [AD-A262655] p 3379 N93-28588

DATA STORAGE TECHNOLOGIES, INC., RIDGEWOOD, NJ.
Grand challenges in mass storage: A systems integrators perspective p 3620 N93-30467

DATATAPE, INC., PASADENA, CA.
Evolution of a high-performance storage system based on magnetic tape instrumentation recorders p 3435 N93-30470

DAVID SARNOFF RESEARCH CENTER, PRINCETON, NJ.
Introduction to the National Information Display Laboratory p 3628 N93-30718

DAYTON UNIV., OH.
An investigation of resolution as encountered in various chromatographic operational modes [AD-A262883] p 3312 N93-29510
Quantification of human responses p 3500 N93-29564
Effects of area-of-interest display characteristics of visual search performance and head movements in simulated low-level flight [AD-A264661] p 3499 N93-30542

DAYTON UNIV. RESEARCH INST., EDWARDS AFB, CA.
ELITE program: Electric insertion transfer experiment p 3264 N93-28709

DAYTON UNIV. RESEARCH INST., OH.
CATS EYES adjustment procedures [AD-A264069] p 3508 N93-29924

DEFENCE AND CIVIL INST. OF ENVIRONMENTAL MEDICINE, DOWNSVIEW (ONTARIO).
Influence of the Cold Buster (tm) sports bar on heat debt, mobilization and oxidation of energy substrates [AD-A262762] p 3493 N93-28939
Evaluation of personal cooling systems in conjunction with explosive ordnance disposal suits [AD-A262862] p 3506 N93-29471

DEFENCE RESEARCH AGENCY, BEDFORD (ENGLAND).
The design and development of the new RAF standard HUD format p 3502 N93-28856

DEFENCE RESEARCH AGENCY, FARNBOROUGH (ENGLAND).
The quest for an integrated flying helmet p 3502 N93-28860
Heat transfer and aerodynamics of a 3D design nozzle guide vane tested in the Pyestock Isentropic Light Piston Facility p 3252 N93-29928

DEFENCE RESEARCH AGENCY, LONDON (ENGLAND).
STRV1-b flight experiment p 3265 N93-28723
A methodology and tool for the prediction of depth of reception in the sea for a VLF/LF communications system p 3397 N93-30741
A dynamic bandwidth and phase linearity measurement technique for 4-channel MSK VLF antenna systems p 3398 N93-30748
Study of a VLF distributed antenna array p 3398 N93-30749

DEFENCE RESEARCH ESTABLISHMENT, OTTAWA (ONTARIO).
Neutron radiation induced degradation of diode characteristics [AD-A263277] p 3405 N93-28563
An investigation of stereolithography as a means of prototyping from a cad database [AD-A263410] p 3613 N93-29210
Theoretical bit error rate performance of the Kalman filter excisor for FM interference [AD-A263018] p 3383 N93-29407
Software development and analysis for experimental high frequency surface wave radar data [AD-A261982] p 3383 N93-29438
Simulation of transient radiation effects on semiconductor devices using a pulsed Q-switched Nd:YAG laser p 3357 N93-30230
Acousto-optic time-integrating correlators for processing wideband digital data p 3360 N93-30253
Canadian EHF MILSATCOM research and development project p 3362 N93-30264
An improved model-creation program for EM interaction analysis p 3367 N93-30294
Status of the Canadian military Multibeam Antenna (MBA) development for EHF SATCOM p 3374 N93-30334
Effects of imbalances and DC offsets on I/Q demodulation [AD-A264466] p 3393 N93-30537

DEFENCE RESEARCH ESTABLISHMENT SUFFIELD, RALSTON (ALBERTA).
Experimental study of location and identification of ferrous spheroids using a smart total field magnetometer [AD-A263661] p 3324 N93-29391
Thermal cycler temperature variation and its effect on the polymerase chain reaction [AD-A264660] p 3337 N93-30541

DEFENSE ADVANCED RESEARCH PROJECTS AGENCY, ARLINGTON, VA.
X-31 demonstration of integrated flight and propulsion control for effective combat at extreme angles of attack p 3260 N93-28851
An overview of DARPA's advanced space technology program p 3269 N93-29908

DEFENSE SYSTEMS MANAGEMENT SCHOOL, FORT BELVOIR, VA.
The program manager's notebook [AD-A263074] p 3609 N93-29142

DELAWARE UNIV., NEWARK.
Design of a high activity and selectivity alcohol catalyst [DE93-012277] p 3309 N93-28750
Combustion/explosion chemistry of bulk materials p 3343 N93-30062
Long discontinuous fiber composite structure: Forming and structural mechanics p 3301 N93-30437
Damage of multi-directionally reinforced ceramic-matrix composites p 3308 N93-30937

DEPARTEMENT D'ETUDES ET DE RECHERCHES EN TECHNOLOGIE SPATIALE, TOULOUSE (FRANCE).
Micrometeoroids and debris on LDEF p 3638 N93-29356
LDEF: Dosimetric measurement results (AO 138-7 experiment) p 3573 N93-29635

DEPARTMENT OF EDUCATION, WASHINGTON, DC.
Filling the gaps: An overview of data on education in grades K through 12 [PB93-176550] p 3608 N93-30821

DEPARTMENT OF ENERGY, WASHINGTON, DC.
Proceedings of a Workshop on Molecular Nuclear Medicine [DE93-010828] p 3493 N93-28835
Proceedings of the Second Atmospheric Radiation Measurement (ARM) Science Team Meeting [DE93-005886] p 3476 N93-28889
Computing for magnetic fusion energy research: An updated vision [DE93-010394] p 3587 N93-29190
Ocean Margins Program [DE93-008937] p 3470 N93-29262
Overview of the DOE Atmospheric Chemistry Program's Ozone Project [DE93-007416] p 3471 N93-29770
The possible direct use of satellite radiance measurements by the Atmospheric Radiation Measurement Program [DE93-009819] p 3462 N93-30049
DOE fundamentals handbook: Chemistry [DE93-012222] p 3314 N93-30198
DOE fundamentals handbook: Material science [DE93-012224] p 3314 N93-30199
DOE fundamentals handbook: Material science [DE93-012225] p 3314 N93-30200
Departmental technology transfer update p 3625 N93-30694
Sandia National Laboratories p 3626 N93-30702

DEPARTMENT OF THE NAVY, WASHINGTON, DC.
Fiber grating-based sensing system with interferometric wavelength-shift detection [AD-D015697] p 3577 N93-29038
Gyroscope with excess noise subtraction [AD-D015698] p 3431 N93-29046
Time-interpolation method for digital beamformers [AD-D015709] p 3383 N93-29275
Method of emitting on a specific wavelength fraunhofer line using a neodymium doped laser transmitter [AD-D015710] p 3437 N93-29276
ND laser with co-doped ion(s) pumped by visible laser diodes [AD-D015711] p 3437 N93-29277
Articulated fin/wing control system [AD-D015712] p 3259 N93-29278
Acoustic transducer system [AD-D015713] p 3562 N93-29279
Hybrid data link [AD-D015714] p 3383 N93-29280
Optically controlled active impedance element particularly suited for a microwave oscillator [AD-D015723] p 3408 N93-29281
Laser radiation detection system [AD-D015724] p 3438 N93-29287
Combined centrifugal force/gravity gas/liquid separator system [AD-D015726] p 3444 N93-29288
Optical antenna beam steering using digital phase shifter control [AD-D015688] p 3383 N93-29455
Flame or plasma synthesis of diamond under turbulent and transition flow conditions [AD-D015689] p 3333 N93-29456
Polymers with electrical and nonlinear optical properties [AD-D015691] p 3333 N93-29457
Synthetic lubricating oil greases containing metal chelates of Schiff bases [AD-D015694] p 3333 N93-29458
Temperature compensated lithium battery energy monitor [AD-D015680] p 3409 N93-29605
Helmet visor support apparatus [AD-D015684] p 3507 N93-29606
Goggles emergency release apparatus [AD-D015685] p 3507 N93-29607
Ordnance thermal battery [AD-D015722] p 3412 N93-30201
Method and apparatus for imaging an object in or through a scattering medium by using multiple-wave mixing [AD-D015707] p 3581 N93-30410
Holmium quasi-two level laser [AD-D015706] p 3440 N93-30427
Carborane-(silane or siloxane)-unsaturated hydrocarbon based thermosetting polymers [AD-D015718] p 3338 N93-30580
Carborane-(siloxane or silane)-unsaturated hydrocarbon based polymers [AD-D015717] p 3338 N93-30586
Intracavity-pumped 2.1 micrometer Ho(3+): YAG laser [AD-D015728] p 3441 N93-30587

DESERT RESEARCH INST., RENO, NV.
Environmental Monitoring and Assessment Program. EMAP: Arid Colorado plateau pilot study [PB93-181618] p 3474 N93-30823

DEUTSCHE FORSCHUNGS- UND VERSUCHSANSTALT FUER LUFT- UND RAUMFAHRT, BERLIN (GERMANY).
Consultative Committee for Space Data Systems recommendation for space data system standards: Telecommand. Part 2.1: Command operation procedures [NASA-TM-108158] p 3393 N93-30371

DEUTSCHE FORSCHUNGSANSTALT FUER LUFT- UND RAUMFAHRT, BRUNSWICK (GERMANY).
Composite laminate stiffnesses and their sensitivities [DLR-FB-92-16] p 3296 N93-29007

DEUTSCHE FORSCHUNGSANSTALT FUER LUFT- UND RAUMFAHRT, COLOGNE (GERMANY).
An L2F-measurement device with image rotator prism for flow velocity analysis in rotating coolant channels p 3255 N93-29942

Coupling of 3D-Navier-Stokes external flow calculations and internal 3D-heat conduction calculations for cooled turbine blades p 3258 N93-29961

DEUTSCHE FORSCHUNGSANSTALT FUER LUFT- UND RAUMFAHRT, GOETTINGEN (GERMANY).
Transonic flows on an oscillating airfoil and their effect on the flutter-boundary
[DLR-FB-92-08] p 3238 N93-29006

DEUTSCHE FORSCHUNGSANSTALT FUER LUFT- UND RAUMFAHRT, OBERPFAFFENHOFEN (GERMANY).
Proceedings of the 8th User Seminar of the German Remote Sensing Data Center of the German Aerospace Establishment (DLR)
[DLR-MITT-92-09] p 3456 N93-28915
The German PAF (Processing and Archiving Facilities) for ERS-1 p 3457 N93-28916
The German satellite ground station in Antarctica: Realization and first results p 3458 N93-28924
Derivation of conductive heat transfer in mountains from AVHRR data p 3458 N93-28927
Evidence-based classification of satellite image data
p 3459 N93-28931

DEUTSCHE FORSCHUNGSGEMEINSCHAFT, BONN (GERMANY).
Space research in Germany 1990-1991
[ETN-93-93807] p 3654 N93-28477

DEUTSCHES ELEKTRONEN-SYNCHROTRON, HAMBURG (GERMANY).
The semiclassical stability of de Sitter spacetime
[DESY-92-131] p 3603 N93-28472

DEUTSCHES GEODAETISCHES FORSCHUNGSINST., MUNICH (GERMANY).
Processing of altimeter data by the German ERS-1 Processing and Archiving Facility (D-PAF)
p 3457 N93-28917
Exact trajectory determinator for ERS-1
p 3457 N93-28918

DIGITAL EQUIPMENT CORP., MAYNARD, MA.
Analysis of cache for streaming tape drive
p 3435 N93-30477

DORNIER LUFTFAHRT G.M.B.H., FRIEDRICHSHAFEN (GERMANY).
Symbology for head up and head down applications for highly agile fighter aircraft: To improve spatial awareness, trajectory control, and unusual attitude recovery, part 1
p 3502 N93-28857

DOUGLAS AIRCRAFT CO., INC., LONG BEACH, CA.
Composites technology for transport primary structure
p 3300 N93-30431
Resin transfer molding for advanced composite primary aircraft structures p 3301 N93-30438

DOW CHEMICAL CO., MIDLAND, MI.
Flexible storage medium for write-once optical tape
p 3621 N93-30473
Development of resins for composites by resin transfer molding p 3305 N93-30853

DRAPER (CHARLES STARK) LAB., INC., CAMBRIDGE, MA.
Lunar gravitational field estimation and the effects of mismodeling upon lunar satellite orbit prediction
[NASA-CR-188249] p 3634 N93-29042
Multivariable control of the Space Shuttle Remote Manipulator System using linearization by state feedback
[NASA-CR-188248] p 3443 N93-29080

DREXEL UNIV., PHILADELPHIA, PA.
High pressure preignition chemistry of hydrocarbons and hydrocarbon mixtures
[AD-A263611] p 3311 N93-29283
Development of novel models for describing multiple toxicity effects
[AD-A264439] p 3496 N93-30422

DUBLIN INST. FOR ADVANCED STUDIES (IRELAND).
Progress report on the ultra heavy cosmic ray experiment (AO178) p 3654 N93-29646

DUKE UNIV., DURHAM, NC.
Chaos in mechanical systems with especial reference to rotorcraft and missiles
[AD-A263703] p 3604 N93-29384
Implementation of parallel algorithms
[AD-A263126] p 3529 N93-29496
High resolution free-electron laser spectroscopy
[AD-A263734] p 3439 N93-29853
Micropipet manipulation of lipid membranes: Direct measurement of the material properties of a cohesive structure that is only two molecules thick
p 3291 N93-30953

DYNACS ENGINEERING CO., INC., HOUSTON, TX.
Space Station: Orbiter berthing p 3274 N93-29031

DYNETICS, INC., HUNTSVILLE, AL.
Minimum Hamiltonian ascent trajectory evaluation (MASTRE) program (update to automatic flight trajectory design, performance prediction, and vehicle sizing for support of shuttle and shuttle derived vehicles) users manual
[NASA-CR-192556] p 3269 N93-28558

Fuzzy learning under and about an unfamiliar fuzzy teacher p 3516 N93-29558

E

E-SYSTEMS, INC., GREENVILLE, TX.
Viability assessment for reliable long-wave communication links p 3399 N93-30754

EAST CAROLINA UNIV., GREENVILLE, NC.
Evaluation of dried storage of platelets for transfusion: Physiologic integrity and hemostatic functionality
[AD-A263240] p 3494 N93-29620

EASTMAN KODAK CO., ROCHESTER, NY.
Effects of long term space environment exposure on optical substrates and coatings (S0050-2)
p 3582 N93-29694

ECOLE POLYTECHNIQUE, MONTREAL (QUEBEC).
Performance enhancement of dynamic CMOS logic circuits p 3361 N93-30257
Recursive-batch estimation of structure and motion from stereo image sequences p 3363 N93-30271

ECOLE POLYTECHNIQUE FEMININE, SCEAUX (FRANCE).
ASUR p 3228 N93-29720

EDGERTON, GERMESHAUSEN AND GRIER, INC., IDAHO FALLS, ID.
Comparison of analytical transport and stochastic solutions for neutron slowing down in an infinite medium
[DE93-010799] p 3565 N93-28833
Basic OSF/Motif programming and applications
[DE93-010800] p 3524 N93-28834
Crucial role of detailed function, task, timeline, link, and human vulnerability analyses in HRA
[DE93-001923] p 3505 N93-28942
AHP version 5.1 user's manual
[DE93-007050] p 3532 N93-30034
Plasma/particle interaction in subsonic argon/helium thermal plasma jets
[DE93-010808] p 3589 N93-30181

EG AND G MOUND APPLIED TECHNOLOGIES, MIAMISBURG, OH.
Powder x ray diffraction patterns of energetic materials for use as reference standards
[DE93-009903] p 3592 N93-28568

EIC, INC., NORWOOD, MA.
Optically switchable conductive polymers
[AD-A264751] p 3337 N93-30557

ELECTRO MAGNETIC APPLICATIONS, INC., DENVER, CO.
Microstructural modeling of electrical breakdown in solid fuel propellants
[AD-A263466] p 3342 N93-29835

ELECTRONICS RESEARCH LAB., ADELAIDE (AUSTRALIA).
Electro-optic characterisation of extremely wide bandwidth electrical signals
[AD-A264202] p 3392 N93-30145
Data quality statements for spatial databases
[AD-A264125] p 3616 N93-30195

ELLIOTT-AUTOMATION SPACE AND ADVANCED MILITARY SYSTEMS LTD., CAMBERLEY (ENGLAND).
Pilot decision aiding for weapon delivery: A novel approach to fire control cueing using parallel computing
p 3501 N93-28853

ELORET CORP., PALO ALTO, CA.
Photodissociation of HBr/LiF(001): A quantum mechanical model
[NASA-CR-193119] p 3603 N93-28933

EMORY UNIV., ATLANTA, GA.
Thermal oxidation of HCN by NO2 in shock waves
p 3318 N93-30064
Surface chemistry of N2H4 on Si(100)-2x1
[AD-A264819] p 3316 N93-30627

ENDL ASSOCIATES, SAN JUAN CAPISTRANO, CA.
Optical media standards for industry
p 3617 N93-30451

ENGINEERING INST. OF CANADA, MONTREAL (QUEBEC).
Canadian Conference on Electrical and Computer Engineering, volumes 1 and 2
[ISBN-0-9694170-1-2] p 3354 N93-30215

ENGINEERING RESEARCH AND CONSULTING, INC., HUNTSVILLE, AL.
Development of a CFD code for casting simulation
[NASA-CR-192577] p 3427 N93-30492

ENSCO, INC., MELBOURNE, FL.
Shuttle landing facility cloud cover study: Climatological analysis and two tenths cloud cover rule evaluation
[NASA-CR-193016] p 3272 N93-31033

ENVIRONMENTAL ANALYSIS AND REMOTE SENSING, DELFT (NETHERLANDS).
National remote sensing programme 2 ACMS project. Phase 1: Validation. Part 1: Definition of validation experiment
[BCRS-92-10-PHASE-1-PT-1] p 3461 N93-29465

ENVIRONMENTAL PROTECTION AGENCY, CINCINNATI, OH.
Planning and progress of EPA's pollution prevention research program
[PB93-185767] p 3475 N93-30831

ENVIRONMENTAL PROTECTION AGENCY, RESEARCH TRIANGLE PARK, NC.
Summer 1990 Atlanta ozone precursor study (January 1993)
[PB93-167203] p 3470 N93-29200
Analysis of protocol gases: An on-going quality assurance audit
[PB93-168839] p 3311 N93-29204

ENVIRONMENTAL PROTECTION AGENCY, WASHINGTON, DC.
Environmental characteristics of EPA, NRC, and DOE sites contaminated with radioactive substances
[PB93-185551] p 3475 N93-30829
Office of Water Environmental and Program Information Systems Compendium, FY 1992
[PB93-186203] p 3462 N93-30833
Guide to Federal Water Quality Programs and Information: A Guide with Computer Software Developed by the Interagency Working Group on Water Quality
[PB93-186245] p 3475 N93-30834

ERIL RESEARCH, INC., SAN RAFAEL, CA.
Absorbed dose measurements and predictions on LDEF p 3573 N93-29636
Light-heavy ion measurements in CR-39 located on the Earth side of LDEF p 3573 N93-29638

EUROPEAN SPACE AGENCY, PARIS (FRANCE).
Aluminium-high strength material by mechanical alloying and reaction milling: Basics of processing and characterisation of material
[ESA-TT-1249] p 3324 N93-29272
Flow visualization on helicopter blades using acenaphthen
[ESA-TT-1255] p 3422 N93-29273
Photobiological investigations on spores of streptomyces griseus
[ESA-TT-1269] p 3491 N93-29274
Flight mechanical model for performance calculations and interactions between flight vehicle and ramjet in regard to the flight orbit
[ESA-TT-1267] p 3248 N93-29464
The prehistory of ESRO, 1959 - 1960
[ESA-HSR-1] p 3660 N93-29500
Three-dimensional graphical representation of objects according to movement data in realtime
[ESA-TT-1258] p 3521 N93-30104
Improvement in ductility of the intermetallic compound Ti3Al
[ESA-TT-1276] p 3325 N93-30105
Assessment of Columbus payload operations capabilities by scheduling with the MARS system
[ESA-STR-235] p 3281 N93-30106
Consultative Committee for Space Data Systems recommendation for space data system standards: Telecommand. Part 2.1: Command operation procedures
[NASA-TM-108158] p 3393 N93-30371

EUROPEAN SPACE AGENCY. EUROPEAN SPACE RESEARCH AND TECHNOLOGY CENTER, ESTEC, NOORDWIJK (NETHERLANDS).
Predicted and observed directional dependence of meteoroid/debris impacts on LDEF thermal blankets
p 3638 N93-29358

EXABYTE CORP., BOULDER, CO.
High-speed data duplication/data distribution: An adjunct to the mass storage equation
p 3619 N93-30459
Optimizing digital 8mm drive performance
p 3435 N93-30479

F

FEDERAL AVIATION ADMINISTRATION, ATLANTIC CITY, NJ.
Time delay measurements of current primary FAA air/ground transmitters and receivers
[DOT/FAA/CT-TN93/14] p 3379 N93-28555
Results of DATAS investigation of ATCRBS environment at the Los Angeles International Airport
[DOT/FAA/CT-93/6] p 3245 N93-28625
Data Multiplexing Network (DMN) equipment Operational Test and Evaluation (OT&E) integration test report
[AD-A263172] p 3538 N93-29490

FEDERAL AVIATION ADMINISTRATION, CAMBRIDGE, MA.
An analysis of en route controller-pilot voice communications
[AD-A264784] p 3394 N93-30611

FEDERAL AVIATION ADMINISTRATION, WASHINGTON, DC.
FAA international conference on airplane ground deicing
[AD-A263617] p 3244 N93-29286
FEDERAL LIBRARY AND INFORMATION CENTER COMMITTEE, WASHINGTON, DC.
The 9th FLICC Forum on Federal Information Policies
[PB93-184687] p 3624 N93-29668
FERMI NATIONAL ACCELERATOR LAB., BATAVIA, IL.
Dark matter: Theoretical perspectives
[DE93-008484] p 3633 N93-28676
Silicon crystal under bending
[DE93-010522] p 3593 N93-28888
On the meaning of delta T/T
[DE93-008482] p 3653 N93-28962
Tests of the particle physics-physical cosmology interface
[DE93-008483] p 3634 N93-28963
TESLA test cell cryostat support post thermal and structural analysis
[DE93-008365] p 3407 N93-29048
A comparison of high-speed links, their commercial support and ongoing R/D activities
[DE93-008134] p 3382 N93-29245
New limits on generation-1 leptoquarks
[DE93-008138] p 3567 N93-29351
FIAT AVIAZIONE S.P.A., TURIN (ITALY).
Cooling geometry optimization using liquid crystal technique p 3254 N93-29939
FLORIDA AGRICULTURAL AND MECHANICAL UNIV., TALLAHASSEE.
Electron interactions with non-linear polyatomic molecules and their radicals and ions
[AD-A262279] p 3568 N93-29446
Lunar lander ground support system
p 3230 N93-29729
FLORIDA STATE UNIV., TALLAHASSEE.
Mixed limit theorems for pattern analysis
[AD-A263735] p 3549 N93-29854
Easy-to-apply results for establishing convergence of Markov chains in Bayesian analysis
[AD-A264015] p 3555 N93-29979
FLORIDA UNIV., GAINESVILLE.
Design of biomass management systems and components for closed loop life support systems
p 3230 N93-29728
High mass resolution glow discharge mass spectrometry using an external ion source FT-ICR mass spectrometer
[AD-A264347] p 3314 N93-30166
The 26th International Quantum Chemistry Symposium on Atomic, Molecular, and Condensed Matter Theory and Computational Methods
[AD-A264206] p 3315 N93-30534
Development of ultra-low noise, high sensitivity planar metal grating coupled 3-5 multiquantum well infrared detectors for focal plane array staring IR sensor systems
[AD-A264465] p 3599 N93-30536
Development of an O atom gun
[AD-A264753] p 3570 N93-30558
Wetting and dispersion in ceramic/polymer melt injection molding systems
[DE93-013240] p 3338 N93-30601
Visible light emitting materials and injection devices
[AD-A263499] p 3601 N93-30811
FORSCHUNGSZENTRUM JUELICH G.M.B.H. (GERMANY).
Distribution of C1-C2 aldehydes in the free troposphere
[JUEL-2650] p 3475 N93-28475
Modern Monte Carlo particle transport simulation for safety and radiation protection applications in accelerometer technology and in space science
[JUEL-2609] p 3574 N93-29062
FREIBURG UNIV. (GERMANY).
Utilization of NOAA/AVHRR data for energy balance of Lake Constance (Switzerland) p 3458 N93-28926
Atmospheric correction of LANDSAT-TM-data for forest inventory p 3459 N93-28929

G

GANDALF TECHNOLOGIES, INC., NEPEAN (ONTARIO).
A single chip high-speed CMOS Viterbi decoder
p 3358 N93-30238
A slotted Aloha satellite channel simulator
p 3360 N93-30250
GANDHI (INDIRA) CENTRE FOR ATOMIC RESEARCH, KALPAKKAM (INDIA).
Atmospheric studies with SODAR at Kalpakkam
[DE93-605544] p 3480 N93-30992
A review of hot cracking in austenitic stainless steel weldments
[DE93-605280] p 3328 N93-31021
Compatibility studies of AISI type 316 stainless steel with lead-lithium eutectic alloy
[DE93-605281] p 3328 N93-31022
GAS RESEARCH INST., CHICAGO, IL.
Decomposition of hydrogen sulfide for small scale gas processing.
[PB93-174704] p 3316 N93-30658
Power generation and transportation systems research department
[PB93-178309] p 3352 N93-30663
GEC FERRANTI, EDINBURGH (SCOTLAND).
Planning for air to air combat p 3501 N93-28852
GEC SENSORS LTD., BASILDON (ENGLAND).
A new class of mission support for combat air-crew
p 3501 N93-28854
GENERAL ACCOUNTING OFFICE, WASHINGTON, DC.
High performance computing: Advanced Research Projects Agency should do more to foster program goals. Report to the Chairman, Committee on Armed Services, House of Representatives
[GAO/IMTEC-93-24] p 3533 N93-30202
GENERAL ATOMIC CO., SAN DIEGO, CA.
Inertial confinement fusion target component fabrication and technology development support
[DE93-010836] p 3585 N93-28836
GENERAL DYNAMICS CORP., FORT WORTH, TX.
Head-steered sensor flight test results and implications p 3502 N93-28859
GENERAL DYNAMICS CORP., SAN DIEGO, CA.
Technology transfer between the government and the aerospace industry p 3628 N93-30716
GENERAL ELECTRIC CO., CAMDEN, NJ.
GE networked mass storage solutions supporting IEEE network mass storage model p 3618 N93-30458
GENERAL ELECTRIC CO., GILBERT, AZ.
Low-cost helmet-mounted displays
[AD-A262616] p 3501 N93-28479
GENERAL ELECTRIC CO., SCHENECTADY, NY.
Representation and recognition with invariants and geometric constraint models
[AD-A263235] p 3529 N93-29493
GENOA UNIV. (ITALY).
Application of non-standard signal processing to ELF noise characterization for the TSS1-OESEE programme
p 3397 N93-30743
GEOLOGICAL SURVEY, FLAGSTAFF, AZ.
Systematic processing of Clementine data for scientific analyses p 3624 N93-28803
GEOLOGICAL SURVEY, LAWRENCE, KS.
Hydrogeology and ground-water-quality conditions at the Reno County Landfill, South-Central Kansas, 1990-1991
[PB93-183085] p 3474 N93-30826
GEOLOGICAL SURVEY, LOUISVILLE, KY.
Contamination of soil, soil gas, and ground water by hydrocarbon compounds near Greear, Morgan County, Kentucky
[PB93-182244] p 3474 N93-30825
GEOLOGICAL SURVEY, SIOUX FALLS, SD.
Interim report on Landsat national archive activities
p 3618 N93-30455
GEORGE MASON UNIV., FAIRFAX, VA.
Intelligent virtual reality in the setting of fuzzy sets
p 3513 N93-29544
GEORGIA INST. FOR RESEARCH, ATLANTA.
The 1990-1991 project summaries
p 3230 N93-29730
The 1990-1991 project summaries
p 3230 N93-29731
GEORGIA INST. OF TECH., ATLANTA.
Holographic data storage crystals for the LDEF
p 3435 N93-29697
The outlook for understanding the combustion of solid propellants and what it will take p 3346 N93-30078
Infrared imaging array integrated in three dimensions directly on top of silicon circuits
[AD-A264707] p 3581 N93-30500
GEORGIA STATE UNIV., ATLANTA.
Decision analysis with approximate probabilities
p 3513 N93-29542
Tuning a fuzzy controller using quadratic response surfaces p 3515 N93-29553
GEORGIA TECH RESEARCH INST., ATLANTA.
Degradation of electro-optic components aboard LDEF p 3582 N93-29689
GEORGIA UNIV., ATHENS.
Expertise, text coherence, and constraint satisfaction: Effects on harmony and settling rate
[AD-A262703] p 3498 N93-28901
GEOSYSTEMS G.M.B.H., GERMERING (GERMANY).
Model-oriented correction of thematic mapper raw data p 3459 N93-28930
GHG CORP., HOUSTON, TX.
RBSE: Product development team research activity deliverables
[NASA-CR-193115] p 3527 N93-29212
GKSS-FORSCHUNGSZENTRUM GEESTHACHT (GERMANY).
Measurement of the rotation Raman spectra of nitrogen, oxygen, and water vapor under conditions of a temperature humidity lidar
[GKSS-92/E/32] p 3485 N93-31018
GOODWIN (R. CHRISTOPHER) AND ASSOCIATES, INC., NEW ORLEANS, LA.
Remote sensing survey of Mississippi River-Gulf Outlet, Breton Sound disposal area, Plaquemines Parish, Louisiana
[AD-A263097] p 3459 N93-29146
GORDON RESEARCH CONFERENCES, INC., KINGSTON, RI.
Gordon Research Conferences, 1991
[AD-A264275] p 3317 N93-30816
The Gordon Research Conference on Pineal Cell Biology
[AD-A264840] p 3497 N93-30904
GOSUDARSTVENNYI KOMITET PO ISPOLZOVANIYU ATOMNOI ENERGII, SERPUKHOV (USSR).
Single t-quark production in high energy (gamma)e collisions
[DE92-644947] p 3572 N93-30930
GRAMBLING STATE UNIV., LA.
Magnetic character investigation of higher alcohol synthesis Cu-Co-Cr catalysts
[DE93-009732] p 3316 N93-30653
GRONINGEN RIJKSUNIV. (NETHERLANDS).
A normally elliptic Hamiltonian bifurcation
[W-9201] p 3548 N93-28753
Manifold shape: From differential geometry to mathematical morphology
[CS-9204] p 3552 N93-31012
Short-circuit evaluation of Boolean expressions
[CS-9205] p 3552 N93-31014
GRUMMAN AEROSPACE CORP., BETHPAGE, NY.
Design of a particle beam satellite system for lunar prospecting p 3434 N93-28768
Use of particle beams for lunar prospecting
p 3650 N93-28822
Consolidation of graphite thermoplastic textile preforms for primary aircraft structure p 3302 N93-30439
GTE LABS., INC., WALTHAM, MA.
Development of adherent ceramic coatings to reduce contact stress damage of ceramics
[DE93-012518] p 3336 N93-30182
GUELPH UNIV. (ONTARIO).
Fuzzy neural network methodology applied to medical diagnosis p 3498 N93-29546
GUMBS (R.) ASSOCIATES, EAST BRUNSWICK, NJ.
Ultrafast, passive, broad-band, optical shutter based on novel semiconductor/conducting polymer interfaces
[AD-A264098] p 3601 N93-30878

H

HARRIS CORP., ROCHESTER, NY.
Advanced HF digital networks p 3375 N93-30343
HARVARD UNIV., BOSTON, MA.
Laser spectroscopy of hydrocarbon radicals
[DE93-012555] p 3436 N93-28653
Computer assisted multiplex sequencing
[DE93-007144] p 3536 N93-30934
HARVARD UNIV., CAMBRIDGE, MA.
Predicting the response of a temperate forest ecosystem to atmospheric CO2 increase
[DE93-010081] p 3467 N93-28543
Stellar encounters in globular clusters
p 3632 N93-28606
Wide-bandwidth high-resolution search for extraterrestrial intelligence
[NASA-CR-193137] p 3509 N93-28895
Intermediate levels of visual processing
[AD-A264117] p 3495 N93-30192
HAWAII UNIV., HONOLULU.
Lunar science: Using the Moon as a testbed
p 3650 N93-28821
ARI: Internal gravity waves at abrupt topography
[AD-A263795] p 3477 N93-29879
Dynamics of small-scale oceanic motions
[AD-A263582] p 3488 N93-29914
HERCULES AEROSPACE CO., MAGNA, UT.
Advanced fiber placement of composite fuselage structures p 3306 N93-30864
HICKLING (JAMES F.) MANAGEMENT CONSULTANTS LTD., OTTAWA (ONTARIO).
The air traffic controller's mental model and it's implications for equipment design and trainee selection
p 3372 N93-30322
HONEYWELL, INC., BLOOMINGTON, MN.
Optically tiled flat panel displays. A feasibility study
[AD-A262737] p 3592 N93-28590
RF vacuum microelectronics
[AD-A264528] p 3412 N93-30409

HONEYWELL, INC., GLENDALE, AZ.
Cryogenic magnetic bearing
[AD-A264716] p 3446 N93-30512
HONEYWELL, INC., MINNEAPOLIS, MN.
Optoelectronic technology consortium
[AD-A263580] p 3580 N93-29973
HONEYWELL CORPORATE RESEARCH CENTER, BLOOMINGTON, MN.
Honeywell's compact, wide-angle UV-visible imaging sensor p 3582 N93-28806
HORIZON DATA CORP., RESTON, VA.
Interagency Advanced Power Group (IAPG) Meeting Compendium
[DE93-006189] p 3670 N93-30212
HOUSTON UNIV., TX.
Development of ultraviolet absorption photometer for atmospheric ozone measurements and results from mid-latitude investigations p 3468 N93-28949
Solar energy emplacement developer
p 3230 N93-29732
HOWARD UNIV., WASHINGTON, DC.
Remote measurement of planetary magnetic fields by the Hanle effect p 3645 N93-28793
Dynamics and robust control of sampled data systems for large space structures
[AD-A264192] p 3281 N93-30142
HUGHES AIRCRAFT CO., GOLETA, CA.
The Canadian Automated Air Traffic System
p 3246 N93-30323
HUGHES AIRCRAFT CO., LOS ANGELES, CA.
Low cost TACSAT for NATO surveillance
p 3285 N93-29911
HUGHES AIRCRAFT CO., TORRANCE, CA.
Heat pipe performance experiment
p 3265 N93-28722
HUGHES DANBURY OPTICAL SYSTEMS, INC., CT.
The HYDICE instrument design and its application to planetary instruments p 3434 N93-28766
HUMAN RESOURCES RESEARCH ORGANIZATION, ALEXANDRIA, VA.
Concept formulation process aid for trade-off determination: Operator's guide
[AD-A263756] p 3531 N93-29874
Development of a concept formulation process aid for analyzing training requirements and developing training devices
[AD-A263579] p 3261 N93-29972
HUNGARIAN ACADEMY OF SCIENCES, BUDAPEST.
Fuzzy operators and cyclic behavior in formal neuronal networks p 3519 N93-29576
HUNTER COLL., NEW YORK, NY.
Every good virtue you ever wanted in a Q-switched solid-state laser and more: Monolithic, diode-pumped, self-Q-switched, highly reproducible, diffraction-limited Nd:YAG laser p 3442 N93-28772
Gene transcription and electromagnetic fields
[DE93-010854] p 3490 N93-28848

I

IBM FEDERAL SYSTEMS DIV., HOUSTON, TX.
Technology for national asset storage systems
p 3617 N93-30452
IBM FEDERAL SYSTEMS DIV., YORKTOWN HEIGHTS, NY.
Femtosecond laser studies of excited state dynamics
[AD-A263708] p 3439 N93-29918
IBM RESEARCH LAB., SAN JOSE, CA.
Adsorption of sulfate on metal electrodes
[AD-A263192] p 3309 N93-28540
Molecular dynamics modeling of electric double layers with spectroscopic applications
[AD-A263168] p 3568 N93-29489
Adsorption of hydrated halide ions on charged electrodes: Molecular dynamics simulation
[AD-A263137] p 3568 N93-29619
Fundamental studies of friction, lubrication, and wear by atomic force microscopy
[AD-A264647] p 3446 N93-30524
IDAHO STATE UNIV., POCATELLO.
Siphon breaker design requirements
[DE93-011799] p 3425 N93-30132
IDAHO UNIV., MOSCOW.
Exercise/recreation facility for a lunar or Mars analog
p 3230 N93-29733
Annual report on monitoring of the unsaturated zone and recharge areas at INEL to the state of Idaho INLEL oversight committee
[DE93-012947] p 3473 N93-30187
IDS INGEGNERIA DEI SISTEMI S.P.A., PISA (ITALY).
Antenna modeling and analysis for ELF/VLF/LF applications p 3398 N93-30751
IIT RESEARCH INST., BARTLESVILLE, OK.
Thermodynamic properties for polycyclic systems by non-calorimetric methods
[DE93-011373] p 3603 N93-28747
The thermodynamic properties of thianthrene and phenoxathiin
[DE93-000124] p 3603 N93-28964
IIT RESEARCH INST., CHICAGO, IL.
Engineman stress and fatigue: Pilot tests
[PB93-175008] p 3507 N93-29675
ILLINOIS UNIV., CHICAGO.
Studies in theoretical high energy particle physics
[DE93-007990] p 3574 N93-28565
ILLINOIS UNIV., URBANA.
International Conference on Martensitic Transformations (ICOMAT 92)
[AD-A262739] p 3321 N93-28591
National Center for Supercomputer Applications
p 3614 N93-29232
Response of energetic solids to light, heat and shock pulses
[AD-A263702] p 3342 N93-29296
ILLINOIS UNIV., URBANA-CHAMPAIGN.
Compiler-assisted multiple instruction rollback recovery using a read buffer
[NASA-CR-193175] p 3527 N93-29170
Unsteady combustion of energetic materials using laser-recoil p 3319 N93-30085
ILLINOIS UNIV. AT URBANA-CHAMPAIGN, SAVOY.
Advanced Construction Technology Center research
[AD-A263654] p 3432 N93-29390
IMPERIAL CHEMICAL INDUSTRIES LTD., BRANTHAM (ENGLAND).
ICI optical data storage tape: An archival mass storage media p 3621 N93-30472
INDIAN SPACE RESEARCH ORGANIZATION, BANGALORE.
Consultative Committee for Space Data Systems recommendation for space data system standards: Telecommand. Part 2.1: Command operation procedures
[NASA-TM-108158] p 3393 N93-30371
INDUSTRIAL COLL. OF THE ARMED FORCES, WASHINGTON, DC.
Productivity measurement in science and technology contracting
[AD-A262077] p 3609 N93-28985
Earth observation from space: Competition or cooperation?
[AD-A262044] p 3459 N93-29000
Standardization of automatic test equipment in the US Air force
[AD-A262076] p 3250 N93-29004
Information technology: A force for organizational change
[AD-A261986] p 3615 N93-29439
INNOVATIVE CONCEPTS CO., MCLEAN, VA.
Clementine sensor processing system
p 3285 N93-28778
INSTITUT DE MECANIQUE DES FLUIDES DE MARSEILLE (FRANCE).
Study of flow structure in rotating cavities: Numerical predictions of laminar and turbulent, steady, and unsteady flows p 3256 N93-29948
INSTITUT DE RECHERCHE EN INFORMATIQUE ET SYSTEMES ALEATOIRES, LANNION (FRANCE).
On the evaluation of fuzzy quantified queries in a database management system p 3517 N93-29569
INSTITUT NATIONAL DE RECHERCHE D'INFORMATIQUE ET D'AUTOMATIQUE, VALBONNE (FRANCE).
JPDRAW user's manual, version 3.3
[INRIA-RT-0139] p 3523 N93-28504
Nets of reactive processes
[INRIA-RR-1588] p 3537 N93-28505
Some qualitative properties in polling systems
[INRIA-RR-1596] p 3552 N93-28506
Flow control using the theory of zero sum Markov games
[INRIA-RR-1597] p 3553 N93-28507
Asymptotic properties of constrained Markov decision processes
[INRIA-RR-1598] p 3553 N93-28508
Upwind finite element schemes for solving the Maxwell equations
[INRIA-RR-1601] p 3546 N93-28509
Image classification using Markov random fields with two new relaxation methods: Deterministic pseudo annealing and modified metropolis dynamics
[INRIA-RR-1606] p 3553 N93-28510
Robust and efficient implementation of the Delaunay tree
[INRIA-RR-1619] p 3547 N93-28511
The space of spheres, a geometric tool to unify duality results in Voronoi diagrams
[INRIA-RR-1620] p 3547 N93-28512
Polygonal approximation overviews and perspectives
[INRIA-RR-1621] p 3547 N93-28513
Design of an essentially non-oscillatory reconstruction procedure in finite-element type meshes
[INRIA-RR-1584] p 3547 N93-28615
Three dimensional reconstruction of complex shapes based on the Delaunay triangulation
[INRIA-RR-1697] p 3547 N93-28616
Optimal control of the M/G/1 queue with repeated vacations of the server
[INRIA-RR-1637] p 3541 N93-28637
Closed-loop control with delayed information
[INRIA-RR-1638] p 3541 N93-28638
The generic arithmetic of SISYPHE
[INRIA-RT-0136] p 3524 N93-28755
Preemptive scheduling with variable profile, precedence constraints and due dates
[INRIA-RR-1622] p 3538 N93-28937
A C++ interface for programming on the Connection Machine
[INRIA-RR-1698] p 3538 N93-29487
Automated reasoning with function evaluation for COCOLOG
[INRIA-RR-1713] p 3529 N93-29488
Some results on feedback stabilization of a one-link flexible arm
[INRIA-RR-1682] p 3543 N93-30116
On high resolution extensions of Lagrange-Galerkin finite-element schemes
[INRIA-RR-1703] p 3550 N93-30117
INSTITUTE FOR COMPUTER APPLICATIONS IN SCIENCE AND ENGINEERING, HAMPTON, VA.
Godunov-type schemes applied to detonation flows
[NASA-CR-191447] p 3509 N93-28841
Some aspects of the aeroacoustics of high-speed jets
[NASA-CR-191458] p 3418 N93-28975
A simple parallel prefix algorithm for compact finite-difference schemes
[NASA-CR-191448] p 3525 N93-28976
ICASE
[NASA-CR-193257] p 3520 N93-29864
INSTITUTE FOR DEFENSE ANALYSES, ALEXANDRIA, VA.
A perspective on acquisition of NASA space systems
[AD-A263246] p 3610 N93-29499
A representative survey of US space systems and methods for estimating their costs
[AD-A264159] p 3272 N93-30881
INSTITUTE FOR SPACE SCIENCE AND TECHNOLOGY, INC., GAINESVILLE, FL.
Orbital Debris Environment Monitor (ODEM)
p 3267 N93-28735
Elemental analyses of hypervelocity microparticle impact sites on Interplanetary Dust Experiment sensor surfaces
p 3638 N93-29378
INSTITUTE FOR TELECOMMUNICATION SCIENCES, BOULDER, CO.
ELF/VLF spectrum measurements
p 3398 N93-30745
INSTITUTE OF ELECTRICAL AND ELECTRONICS ENGINEERS, PISCATAWAY, NJ.
Topical meeting of broadband analog and digital optoelectronics
[AD-A264643] p 3581 N93-30522
INSTITUTE OF ENERGY ECONOMICS OF JAPAN.
Global warming issue and global economic model
[DE93-781334] p 3468 N93-28881
INSTITUTE OF NUCLEAR PHYSICS, KRAKOW (POLAND).
Fluctuations and intermittency in high energy nucleus-nucleus collisions
[DE93-608481] p 3577 N93-30990
INSTITUTO DE FISICA TEORICA, SAO PAULO (BRAZIL).
General method for reducing the two-body Dirac equation
[DE93-609833] p 3607 N93-30943
Low-energy behaviour of few-particle scattering amplitudes in two dimensions
[DE93-609834] p 3572 N93-30944
A squeezed state holomorphic phase space representation of equations of motion
[DE93-609835] p 3607 N93-30945
INSTITUTO DE PESQUISAS ENERGETICAS E NUCLEARES, SAO PAULO (BRAZIL).
Superconducting films of YBaCuO
[DE93-606831] p 3600 N93-30772
Effect of lead addition on the formation of superconducting phases in Bi-Sr-Ca-Cu-O ceramics
[DE93-606893] p 3339 N93-30773
The effect of Bi2 O3 on the electrical properties of Zr O2: 3 percent Mg O ceramic solid electrolytes
[DE93-607029] p 3339 N93-30774
Theoretical-experimental study of the non-thermal effects of the polarized laser radiation in living tissues
[DE93-607212] p 3441 N93-30775

INSTITUTO DE PESQUISAS ESPACIAIS, SAO JOSE DOS CAMPOS (BRAZIL).

Consultative Committee for Space Data Systems recommendation for space data system standards: Telecommand. Part 2.1: Command operation procedures
[NASA-TM-108158] p 3393 N93-30371

Plasma diffusion through multidipole magnetic fields
[DE93-608548] p 3591 N93-31007

INSTITUTO TECNOLOGICO DE MORELIA (MEXICO).

Non-scalar uncertainty: Uncertainty in dynamic systems p 3517 N93-29565

INSTITUTUL POLITEHNIC DIN IASI (ROMANIA).

A fuzzy control design case: The fuzzy PLL
p 3515 N93-29555

Stochastic architecture for Hopfield neural nets
p 3519 N93-29579

INTERFEROMETRICS, INC., VIENNA, VA.

Interferometric tracking system for the tracking and data relay satellite
[NASA-CR-193274] p 3382 N93-29217

INTERNATIONAL ATOMIC ENERGY AGENCY, VIENNA (AUSTRIA).

Plasma Physics Network Newsletter, no. 5
[DE93-606216] p 3591 N93-30795

Statement on the United Nations Conference on Environment and Development
[DE93-601878] p 3475 N93-30996

Development of a PC code package for the analysis of research and power reactors
[DE92-638517] p 3536 N93-31001

INTERNATIONAL BUSINESS MACHINES CORP., SAN JOSE, CA.

In situ Fourier transform infrared spectroscopic study of bisulfate and sulfate adsorption on gold, with and without the underpotential deposition of copper
[AD-A263421] p 3323 N93-29259

Fast multipole method in simulations of aqueous systems
[AD-A263422] p 3567 N93-29336

INTERNATIONAL CENTRE FOR THEORETICAL PHYSICS, TRIESTE (ITALY).

Electronic states in quantum wells with periodically structured interfaces
[DE93-606295] p 3600 N93-30769

Effective interactions between concentration fluctuations and charge transfer in chemically ordering liquid alloys
[DE93-606724] p 3327 N93-30778

Quantum group and symmetry of the heat equation
[DE93-607560] p 3605 N93-30779

Neutrino oscillations and a new Faraday effect
[DE93-606111] p 3571 N93-30789

Planck scale effects in neutrino physics
[DE93-606133] p 3571 N93-30793

A tight binding model for the electronic structure of FCC and SC C60
[DE93-606214] p 3601 N93-30794

Electric magnetic duality in string theory
[DE93-606061] p 3606 N93-30807

The ground state wavefunctions of a conformally invariant scalar field in different spacetime background
[DE93-606063] p 3606 N93-30808

Positive energy representations of the conformal quantum algebra
[DE93-606064] p 3551 N93-30809

Connections between quantized affine algebras and superalgebras
[DE93-606065] p 3551 N93-30810

Nonlinear realisations of omega(1 + infinity)
[DE92-644721] p 3557 N93-30917

Fourth-rank gravity and cosmology
[DE92-644722] p 3637 N93-30918

Compensating fields and anomalies in supergravity
[DE92-644724] p 3637 N93-30919

Quantum group generalization of the heterotic QFT
[DE92-644727] p 3607 N93-30920

Abelian gauge theories on homogeneous spaces
[DE92-644730] p 3607 N93-30921

Beltrami parametrization and gauging of Virasoro and w-infinity algebras
[DE92-644844] p 3557 N93-30928

Normal equivariant forms of vector fields
[DE92-644845] p 3551 N93-30929

Massive Majorana neutrinos in pre-bounce supernovae
[DE92-642597] p 3572 N93-30931

General scalar-tensor theories for induced gravity inflation
[DE93-602505] p 3479 N93-30940

Fixed point iterations for quasi-contractive maps in uniformly smooth Banach spaces
[DE92-641348] p 3552 N93-30942

Equivariant elliptic homology
[DE92-641338] p 3557 N93-30981

Nth roots of normal contractions
[DE92-644725] p 3557 N93-30985

On one-dimensional topological and conformal field theories
[DE92-644726] p 3558 N93-30986

Formulation of wave mechanics without the Planck constant h/2 pi
[DE93-604083] p 3608 N93-30987

Spherically symmetric line element and Killing vectors in five-dimensional space
[DE93-604132] p 3558 N93-30988

Superconformal structures and holomorphic 1/2-superdifferentials on N = 1 super Riemann surfaces
[DE93-604133] p 3558 N93-30989

Fourth-rank cosmology
[DE92-641346] p 3637 N93-30997

Growth model of Au films on Ru(001)
[DE92-642126] p 3602 N93-30998

A non degenerate semi-classical Lagrangian for dilaton-gravity in two dimensions
[DE92-641339] p 3480 N93-31002

The geometry of complex space-times with torsion
[DE92-641343] p 3608 N93-31003

Effects of spiral shocks on disk emission lines
[DE92-641716] p 3637 N93-31004

The distribution of the annual and semiannual cycles in the tropics
[DE92-642213] p 3485 N93-31006

Role of oxygen vacancies in anodic TiO2 thin films
[DE92-642137] p 3602 N93-31027

INTERNATIONAL METEOROLOGICAL INST., STOCKHOLM (SWEDEN).

Activities report of the International Meteorological Institute, Stockholm (Sweden)
[ETN-93-93768] p 3480 N93-28519

IONA COLL., NEW ROCHELLE, NY.

Adaptive defuzzification for fuzzy systems modeling
p 3512 N93-29532

IOWA STATE UNIV. OF SCIENCE AND TECHNOLOGY, AMES.

Modeling land-surface/atmosphere dynamics for CHAMMP
[DE93-008520] p 3476 N93-28677

The parallel implementation of a backpropagation neural network and its applicability to SPECT image reconstruction
[DE93-010304] p 3567 N93-29416

A virtual environment for manufacturing systems
[AD-A263128] p 3528 N93-29473

Computational fluid dynamics research on dynamically adaptive mesh methods for transonic flows
[AD-A264833] p 3428 N93-30630

ISRAEL ATOMIC ENERGY COMMISSION, NEGEV.

Eutectic solidification of Al-U at slowly cooling rates (10 C per second)
[DE92-640082] p 3328 N93-30941

Methods for preparation of mixtures of gases in air at the parts-per-billion to parts-per-million concentration range for calibration of monitors
[DE92-642433] p 3317 N93-30982

IWG CORP., SAN DIEGO, CA.

Investigations of equatorial ionosphere nighttime mode conversion at VLF p 3396 N93-30735

J

JACKSON STATE UNIV., MS.

Characterization of lithium electrode surface in lithium secondary batteries by in situ Raman spectroscopic methods
[AD-A263728] p 3411 N93-29986

Development of an experimental method to determine the axial rigidity of a strut-node joint
p 3290 N93-30950

JAPAN ATOMIC ENERGY RESEARCH INST., IBARAKI.

Measurement of work function of a plasma grid in a cesium seeded negative ion source
[DE93-764153] p 3589 N93-30190

JAPAN ATOMIC ENERGY RESEARCH INST., NAKA.

Preliminary design study of a steady state tokamak device
[DE93-764162] p 3589 N93-30397

Operation of a 20-channel grating polychromator diagnostic system and its application to sawtooth observations in JT-60U
[DE93-764388] p 3590 N93-30398

Optimization for steady-state and hybrid operations of ITER by using scaling models of divertor heat load
[DE93-764151] p 3590 N93-30649

JAPAN ATOMIC ENERGY RESEARCH INST., TOKAI.

Air oxidation behavior of fuel for the High Temperature Engineering Test Reactor (HTTR)
[DE93-753349] p 3576 N93-30006

Irradiation assisted stress corrosion cracking of stainless steel irradiated in FBR
[DE93-764495] p 3326 N93-30191

Examination of formability to seamless tubes on Ni-Cr-W superalloy
[DE93-764158] p 3326 N93-30396

JAPAN ATOMIC ENERGY RESEARCH INST., TOKYO.

Preliminary test of liquid metal induced embrittlement in liquid LiPb and stainless-steel systems
[DE93-753130] p 3320 N93-28529

JT-60 Upgrade vertical stability experiments and analysis
[DE93-753131] p 3583 N93-28530

Study on the concurrent calculation with a multitransputer network
[DE93-753191] p 3524 N93-28531

Measurements of breakaway reaction between beryllium and water vapor for ITER blanket design
[DE93-753270] p 3584 N93-28535

High performance dispersion model PHYSIC
[DE93-753303] p 3467 N93-28536

Installation of a new Fortran compiler and effective programming method on the vector supercomputer
[DE93-753322] p 3524 N93-28537

Users manual for fault tree analysis code: CUT-TD
[DE93-753272] p 3525 N93-28978

Moment approach to fast ion neoclassical transport and viscous forces
[DE93-753305] p 3585 N93-28979

A study on radiation shielding analysis for toroidal field coils of a tokamak-type fusion reactor
[DE93-753398] p 3585 N93-28981

Annual progress report on the NSRR experiments, (21)
[DE93-753190] p 3574 N93-29137

Structural design of cryostat and port penetration of International Thermonuclear Experimental Reactor (ITER)
[DE93-753267] p 3587 N93-29243

Bootstrap current profiles and scaling in large aspect ratio tokamaks
[DE93-753158] p 3589 N93-30003

Experiment and analysis on elastic deformation properties of graphite and carbon materials for HTTR core components
[DE93-753271] p 3299 N93-30004

Development of Ni-Cr-W superalloys for high temperature components in high temperature gas-cooled reactors, part 2
[DE93-764469] p 3326 N93-30399

High density plasma production in a multicusp plasma generator with RF antenna
[DE93-764493] p 3590 N93-30606

JET PROPULSION LAB., CALIFORNIA INST. OF TECH., PASADENA.

Low Earth orbital mission aboard the Space Test Experiments Platform (STEP-3) p 3267 N93-28732

A microseismometer for terrestrial and extraterrestrial applications p 3434 N93-28765

Clementine 2: A double asteroid flyby and impactor mission p 3268 N93-28770

Polarimetric multispectral imaging technology
p 3434 N93-28774

Investigation of Mars rotational dynamics using Earth-based radio tracking of Mars landers
p 3642 N93-28777

A low-cost, lightweight, and miniaturized Time-Of-Flight Mass Spectrometer (TOFMS) p 3434 N93-28817

Subnanoradian, groundbased tracking of spaceborne lasers p 3442 N93-28823

Dual arm generalized compliant motion with shared control
[NASA-CASE-NPO-18738-1-CU] p 3443 N93-28954

A satellite-tracking millimeter-wave reflector antenna system for mobile satellite-tracking
[NASA-CASE-NPO-18772-1-CU] p 3381 N93-28955

Improved real-time imaging spectrometer
[NASA-CASE-NPO-18410-1-CU] p 3578 N93-29086

Miniature modular microwave end-to-end receiver
[NASA-CASE-NPO-18713-1-CU] p 3381 N93-29087

Three-parameter tunable Tilt-Integral-Derivative (TID) controller
[NASA-CASE-NPO-18492-1-CU] p 3542 N93-29176

A distributed system for visualizing and analyzing multivariate and multidisciplinary data
p 3613 N93-29226

DataHub knowledge based assistance for science visualization and analysis using large distributed databases p 3613 N93-29230

Multi-channel holographic birfurcative neural network system for real-time adaptive EOS data analysis
p 3614 N93-29231

Geographic information system for fusion and analysis of high-resolution remote sensing and ground truth data
p 3614 N93-29234

Flight Projects Office Information Systems Testbed (FIST) p 3615 N93-29241

New meteoroid model predictions for directional impacts on LDEF p 3638 N93-29376

The Telecommunications and Data Acquisition Report [NASA-CR-193144] p 3384 N93-29586

An improved linear ion trap physics package p 3384 N93-29587

The effect of clock, media, and station location errors on Doppler measurement accuracy p 3246 N93-29588

Precise tracking of the Magellan and Pioneer Venus orbiters by Same-Beam Interferometry. Part 2: Orbit determination analysis p 3270 N93-29589

High-power Ka-band amplifier p 3385 N93-29590

Experimental and modal verification of an integral equation solution for a thin-walled dichroic plate with cross-shaped holes p 3385 N93-29591

Gravity referenced elevation encoder development p 3385 N93-29592

A note on the computation of antenna-blocking shadows p 3385 N93-29593

Maximum and minimum return losses from a passive two-port network terminated with a mismatched load p 3385 N93-29594

The general theory of convolutional codes p 3385 N93-29595

Uncorrectable sequences and telecommand p 3385 N93-29596

Galileo post-Gaspra cruise and Earth-2 encounter p 3385 N93-29597

DSN support of Mars Observer p 3385 N93-29598

Signal-to-noise ratio losses in full spectrum combining of signals with a downconverted subcarrier p 3386 N93-29599

DSS-14 subreflector actuator dynamics during the Landers earthquake p 3386 N93-29600

An analysis of the 70-meter antenna hydrostatic bearing by means of computer simulation p 3386 N93-29601

Acoustic charge transport technology investigation for advanced development transponder p 3386 N93-29602

The flight performance of the Galileo orbiter USO p 3386 N93-29603

Special purpose parallel computer architecture for real-time control and simulation in robotic applications [NASA-CASE-NPO-17629-1-CU] p 3521 N93-29608

LEO effects on candidate solar cell cover materials p 3467 N93-29687

Radiation and temperature effects on LDEF fiber optic samples p 3583 N93-29700

Wavelength-division multiplexed optical integrated circuit with vertical diffraction grating [NASA-CASE-NPO-18357-1-CU] p 3579 N93-29848

Hidden Markov models for fault detection in dynamic systems [NASA-CASE-NPO-18982-1-CU] p 3449 N93-30413

Tunable CW diode-pumped Tm,Ho:YLiF4 laser operating at or near room temperature [NASA-CASE-NPO-18611-1-CU] p 3440 N93-30415

Virtual reality flight control display with six-degree-of-freedom controller and spherical orientation overlay [NASA-CASE-NPO-18733-1-CU] p 3251 N93-30416

Technology transfer p 3627 N93-30707

Robotic technology evolution and transfer p 3627 N93-30714

Strategic directions and mechanisms in technology transfer p 3628 N93-30720

JOBIN ET YVON S.A., LONGJUMEAU (FRANCE).

Ruled and holographic experiment (AO 138-5) p 3434 N93-29696

JOHNS HOPKINS UNIV., BALTIMORE, MD.

Research in theoretical physics [DE93-008401] p 3603 N93-28961

Neural mechanisms of attention [AD-A264345] p 3544 N93-30165

Analytical foundations of gain scheduling [AD-A264682] p 3260 N93-30550

JOHNS HOPKINS UNIV., COLUMBIA, MD.

ONR/LANL Workshop on the Fundamental Physics and Chemistry of Combustion, Initiation, and Detonation of Energetic Materials [CPIA-PUBL-589] p 3343 N93-30061

JOHNS HOPKINS UNIV., LAUREL, MD.

Proposal for a universal particle detector experiment p 3286 N93-28795

A compact imaging detector of polarization and spectral content p 3582 N93-28810

Environmental monitors in the Midcourse Space Experiments (MSX) p 3286 N93-28826

JOINT INST. FOR NUCLEAR RESEARCH, DUBNA (USSR).

On the method of determining relations [DE93-606041] p 3551 N93-30765

Energy spectra and photoelectron work function from YBa2Cu3O7 high-T(sub c) superconductor [DE93-606329] p 3600 N93-30766

Measurement of magnetic field penetration depth in niobium polycrystalline films by polarized neutron reflection method [DE93-606390] p 3600 N93-30771

Approximation formulae for functional integrals in P(phi)2-quantum field theory [DE93-606067] p 3605 N93-30781

Phase structure of three- and four-dimensional phi(exp 4) field theory [DE93-606069] p 3605 N93-30782

A covariant form of the Maxwell's equations in four-dimensional spaces with an arbitrary signature [DE93-606070] p 3605 N93-30783

Geometrical approach to the dynamics of a relativistic string in the D-dimensional Minkowski space [DE93-606071] p 3605 N93-30784

Beyond two dimensions [DE93-606084] p 3606 N93-30786

Computer algebra tools for higher symmetry analysis of nonlinear evolution equations [DE93-606089] p 3535 N93-30787

Coupled-channel analysis of low energy nucleon-antinucleon interactions [DE93-606115] p 3571 N93-30791

Towards the results of global analysis of data on nucleon electromagnetic structure [DE93-606125] p 3571 N93-30792

Quantum-kinetic Green function and macroscopic wave function [DE93-606040] p 3606 N93-30796

Integrals of motion on the group of invariance of an interval in three-dimensional spaces [DE93-606090] p 3606 N93-30797

Heat generation produced in thin layers of GaAs superconductors under high energy particles irradiation [DE93-606332] p 3601 N93-30798

A possibility to investigate the superconducting gap with the help of neutrons [DE93-606392] p 3601 N93-30799

Modern approach to relativity theory (radar formulation) [DE93-606032] p 3606 N93-30804

On two-dimensional quasiclassics [DE93-606034] p 3606 N93-30805

On the impossibility of creating the quantum correlations with computers [DE93-606039] p 3606 N93-30806

On the invariant measure for the nonlinear Schroedinger equation [DE92-644672] p 3551 N93-30912

A numerical solution of the two-center problem [DE92-644674] p 3551 N93-30913

Algorithm for the solution of the Faddeev equation for a system of three identical spinless particles [DE92-644678] p 3535 N93-30914

Algorithm of numerical calculations of differential Yakubovsky equations for the (1 + 3) scattering problem [DE92-644679] p 3535 N93-30915

A new exact solution to the classical equations of motion of the relativistic string with massive ends [DE92-644736] p 3557 N93-30922

Some problems of relativistic electrodynamics [DE92-644738] p 3400 N93-30923

Invariant structures in gauge theories and confinement [DE92-644739] p 3607 N93-30924

Invariant structures and static forces in gauge theories [DE92-644740] p 3607 N93-30925

On the energy-momentum tensors for field theories in spaces with affine connection and metric [DE92-644743] p 3557 N93-30926

On the energy-momentum tensors for field theories in spaces with affine connection and metric [DE92-644744] p 3557 N93-30927

A remark on the invariant measure for the nonlinear Schroedinger equation [DE93-609840] p 3552 N93-30946

Relativity theory in (2 + 2)-space [DE92-644671] p 3608 N93-30983

Schroedinger equations of higher (greater than 2) order [DE92-644677] p 3552 N93-30984

Software conception and structure of automated workstation for an experimental data processing [DE93-609815] p 3623 N93-30994

Mathematical simulation of the induced (gamma)-radiation in structural materials of spaceships. Time dependence [DE93-605312] p 3281 N93-31024

A dynamical model of structural phase transition in La2CuO4 [DE93-605325] p 3602 N93-31025

JOINT PUBLICATIONS RESEARCH SERVICE, ARLINGTON, VA.

JPRS report: Science and technology. Central Eurasia: Engineering and equipment [JPRS-UEQ-92-007] p 3353 N93-28635

JPRS report: Science and technology. Central Eurasia: Engineering and equipment [JPRS-UEQ-92-006] p 3353 N93-28636

JPRS report: Science and technology. Central Eurasia: Engineering and equipment [JPRS-UEQ-92-010] p 3353 N93-28674

JPRS report: Science and technology. Central Eurasia: Engineering and equipment [JPRS-UEQ-92-008] p 3353 N93-28675

JPRS report: Science and technology. Central Eurasia: Life sciences [JPRS-ULS-93-005] p 3490 N93-28683

JPRS report: Science and technology. Central Eurasia: Life sciences [JPRS-ULS-92-027] p 3490 N93-28684

JPRS report: Science and technology. Central Eurasia: Engineering and equipment [JPRS-UEQ-93-003] p 3353 N93-28691

JPRS report: Science and technology. Central Eurasia: Materials science [JPRS-UMS-92-008] p 3322 N93-29012

JPRS report: Science and technology. Central Eurasia: Materials science [JPRS-UMS-92-007] p 3322 N93-29013

JPRS report: Science and technology. Central Eurasia: Engineering and equipment [JPRS-UEQ-93-001] p 3274 N93-29014

JPRS report: Science and technology. Central Eurasia: Materials science [JPRS-UMS-92-009] p 3322 N93-29015

JPRS report: Science and technology. Central Eurasia: Materials science [JPRS-UMS-92-012] p 3296 N93-29016

JPRS report: Science and technology. Central Eurasia: Materials science [JPRS-UMS-92-013] p 3296 N93-29017

JPRS report: Science and technology. Central Eurasia: Materials science [JPRS-UMS-92-016] p 3296 N93-29018

JPRS report: Science and technology. Central Eurasia: Materials science [JPRS-UMS-92-014] p 3322 N93-29019

JPRS report: Science and technology. Central Eurasia: Materials science [JPRS-UMS-92-015] p 3322 N93-29020

JPRS report: Science and technology. Central Eurasia: Materials science [JPRS-UMS-93-001] p 3296 N93-29021

JPRS report: Science and technology. Central Eurasia: Physics and mathematics [JPRS-UPM-93-002] p 3560 N93-29022

JPRS report: Science and technology. Central Eurasia: Earth science [JPRS-UES-93-003] p 3456 N93-29089

JPRS report: Science and technology. Central Eurasia: Engineering and equipment [JPRS-UEQ-93-004] p 3354 N93-29090

JPRS report: Science and technology. Central Eurasia: Materials science [JPRS-UMS-93-003] p 3327 N93-30623

JPRS report: Science and technology. Central Eurasia: Earth sciences [JPRS-UES-93-002] p 3456 N93-30624

K

KANSAS STATE UNIV., MANHATTAN.

Automation of closed environments in space for human comfort and safety p 3230 N93-29734

A new way to use fuzzy sets in image sharpening p 3363 N93-30273

KANSAS UNIV., LAWRENCE.

Preliminary design studies of an advanced general aviation aircraft p 3228 N93-29717

Simulation of landscape disturbances and the effect of climatic change [DE93-011615] p 3472 N93-30131

KANSAS UNIV. CENTER FOR RESEARCH, INC., LAWRENCE.

The Ultra Light Aircraft Testing [NASA-CR-193043] p 3249 N93-29774

Report on the test set-up for the structural testing of the Airmass Sunburst Ultralight Aircraft p 3249 N93-29775

Load test set-up for the Airmass Sunburst Ultra-Light Aircraft p 3249 N93-29776

NASTRAN analysis for the Airmass Sunburst model 'C' Ultralight Aircraft p 3249 N93-29777

Construction, wind tunnel testing and data analysis for a 1/5 scale ultra-light wing model p 3243 N93-29778

Selection and static calibration of the Marsh J1678 pressure gauge p 3249 N93-29779

KARLSRUHE UNIV. (GERMANY).

Heat transfer and leakage in high-speed rotating stepped labyrinth seals p 3256 N93-29951

KENT UNIV., CANTERBURY (ENGLAND).

Derivation of particulate directional information from analysis of elliptical impact craters on LDEF p 3283 N93-29362

KENTUCKY UNIV., LEXINGTON.

Pulse mitigation and heat transfer enhancement techniques. Volume 3: Liquid sodium heat transfer facility and transient response of sodium heat pipe to pulse forward and reverse heat load [AD-A263496] p 3422 N93-29338

Pulse mitigation and heat transfer enhancement techniques. Volume 4: Transient behavior of heat pipe with thermal energy storage under pulse heat loads [AD-A263497] p 3423 N93-29339

Pulse mitigation and heat transfer enhancement techniques. Volume 1: Spray cooling [AD-A263495] p 3423 N93-29352

Pulse mitigation and heat transfer enhancement techniques. Volume 2: Effect of surface wettability and roughness in evaporative spray cooling [AD-A264174] p 3425 N93-30155

Pulse mitigation and heat transfer enhancement techniques. Volume 5: Transient liquid movement in heat pipe wicks [AD-A264513] p 3426 N93-30403

KERNFORSCHUNGSZENTRUM G.M.B.H., KARLSRUHE (GERMANY).

Numerical modelling of the cold plasma with time-dependent, magnetohydrodynamic methods [KFK-5053] p 3586 N93-29081

Godunov-type methods for the equations of compressible fluid mechanics [KFK-5058] p 3428 N93-31020

KERR (ROBERT S.) WATER RESEARCH CENTER, ADA, OK.

Performance and cost evaluation of bioremediation techniques for fuel spills [PB93-175545] p 3474 N93-30762

KET CANADA, INC., WINNIPEG (MANITOBA).

A unique photon bombardment system for space applications p 3286 N93-28790

KIEL UNIV. (GERMANY).

Heavy ion measurement on LDEF p 3573 N93-29644

KINGS COLL., LONDON (ENGLAND).

ELF propagation in deep and shallow sea water p 3397 N93-30739

KLEIN UND STEKL G.M.B.H., STUTTGART (GERMANY).

New classification methods p 3459 N93-28932

KRUG LIFE SCIENCES, INC., HOUSTON, TX.

Advanced collapsible tank for liquid containment [NASA-CR-188247] p 3353 N93-28698

KRUG LIFE SCIENCES, INC., SAN ANTONIO, TX.

Operating manual for single-shot autocorrelator [AD-A262016] p 3438 N93-29395

Utility of a ghost horizon and climb/dive ladder line tapering on a head-up display [AD-A264401] p 3508 N93-30167

Acquisition of physiological data during G-induced Loss of Consciousness (G-LOC) [AD-A264492] p 3496 N93-30400

L

L'GARDE, INC., TUSTIN, CA.

In-step inflatable antenna experiment p 3263 N93-28701

Developing an inflatable solar array p 3264 N93-28714

LABORATOIRE CENTRAL DE RECHERCHES THOMSON-CSF, ORSAY (FRANCE).

Towards a 1000 tracks digital tape recorder p 3435 N93-30469

LABORATOIRE D'AUTOMATIQUE ET D'ANALYSE DES SYSTEMES, TOULOUSE (FRANCE).

Design and integration of high bit rate four phase monolithic demodulators and modulators at X band [LAAS-92354] p 3414 N93-31030

LABORATORIUM VOOR RUIMTEONDERZOEK, UTRECHT (NETHERLANDS).

Activities report for the Laboratory for Space Research Groningen (Netherlands) [ETN-93-93688] p 3631 N93-30638

LABORATORY FOR ASTROPHYSICS AND SPACE RESEARCH, CHICAGO, IL.

The APX spectrometer for Martian missions p 3434 N93-28776

LAMAR UNIV., BEAUMONT, TX.

Evaluation of actuator energy storage and power sources for spacecraft applications [NASA-CR-193226] p 3288 N93-29091

LAPPEENRANTA UNIV. OF TECHNOLOGY (FINLAND).

Fuzzy simulation in concurrent engineering p 3516 N93-29562

LASERTAPE SYSTEMS, INC., SAN JOSE, CA.

Mass optical storage-tape (MOST) p 3621 N93-30471

LAVAL UNIV. (QUEBEC).

Logarithmic time scale in thermographic Non Destructive Evaluation (NDE) of materials p 3359 N93-30246

A single band processor for the computation of range from optical absorbance p 3363 N93-30272

A robust multi-operator 3-D edge detection approach for range image segmentation p 3366 N93-30288

Radiated fields from an electromagnetic pulse simulator p 3366 N93-30290

Segmentation of SAR images p 3376 N93-30348

LAWRENCE LIVERMORE NATIONAL LAB., CA.

Radiometric calibration system for IR cameras [DE93-009237] p 3430 N93-28520

Measurement of 1s2s(sup 3)S(sub 1)-1s2p(sup 3)P(sub 2,0) intervals in helium-like neon [DE93-009243] p 3563 N93-28521

Parallel computation and the basis system [DE93-008755] p 3537 N93-28544

Magnetic activity in low mass stars [DE93-009073] p 3632 N93-28547

Direct volume visualization of three-dimensional vector fields [DE93-009233] p 3524 N93-28550

World commercial aircraft accidents [DE93-010892] p 3243 N93-28571

The wave, the cylinder, and the plate [DE93-009458] p 3450 N93-28596

Improving the jitter of the 150 kJ experiments solid dielectric switches [DE93-009459] p 3405 N93-28597

Polarization dependence of the ionization of helium and neon by 120 femtosecond pulses at 614 nm [DE93-010514] p 3564 N93-28762

Emission inventories: A global modeling perspective [DE93-005817] p 3469 N93-28965

Atmospheric and Geophysical Sciences Division: G-Division did you know? [DE93-007412] p 3469 N93-28967

Global warming potential for SF6 [DE93-007394] p 3469 N93-28972

Large eddy simulations of shockwave passage through turbulence [DE92-019503] p 3419 N93-29050

The hydraulic analysis of cylindrical Flibe jets in a HYLIFE-2 ICF reactor [DE93-009234] p 3586 N93-29053

Atmospheric and Geophysical Sciences Program report, 1990-1991 [DE93-007390] p 3470 N93-29055

SEU tolerant computer based on the R3000 [DE93-009294] p 3520 N93-29058

Modification of spectral distributions by multilayer structures [DE93-009308] p 3310 N93-29059

Index mappings for interactive editing of symbolic matrices [DE93-009316] p 3549 N93-29060

Design of the Nova Upgrade laser system for ignition fusion experiments [DE93-009077] p 3436 N93-29097

High-efficiency high-reliability optical components for a large, high-average-power visible laser system [DE93-009225] p 3437 N93-29098

Ion motion effects on charged radiators [DE93-009257] p 3565 N93-29099

Maximizing the luminosity of hadron, supercolliders at 10-100 TeV [DE93-009247] p 3574 N93-29103

Development of coherent x ray lasers [DE93-009288] p 3437 N93-29104

Elastic and reactive collisions of atoms and molecules with neutral alkali clusters [DE93-009313] p 3566 N93-29206

Effects of vacuum exposure on stress and spectral shift of high reflective coatings [DE93-009318] p 3437 N93-29207

Thermal properties of organic and modified inorganic aerogels [DE93-009230] p 3311 N93-29263

The microchannel heatsink with liquid nitrogen cooling [DE93-009258] p 3422 N93-29300

High-dose implantations of Al into Si(111) and Si(100) [DE93-009552] p 3594 N93-29301

Poloidal field measurements during transient phenomena on MTX: Sawtooth perturbations and the effect of ECH on disruptions [DE93-010516] p 3587 N93-29303

Inner-shell photo-ionized x ray laser schemes [DE93-009285] p 3438 N93-29309

Implementing error-valued semantics for dataflow languages on imperative machines [DE93-009319] p 3615 N93-29310

Effects of neutral gas collisions on the power transmission factor at the divertor sheath [DE93-009320] p 3588 N93-29334

Modeling the D3-D plasma boundary with the LEDGE code [DE93-009301] p 3588 N93-29772

A new multichannel soft x ray framing camera for fusion experiments [DE93-009302] p 3432 N93-29773

Fusion laser oscillator and pulse-forming system using integrated optics [DE93-009286] p 3588 N93-29780

Problems in the implementation of x ray optics with x ray lasers [DE93-009297] p 3438 N93-29781

Data parallelism [DE93-009300] p 3539 N93-29782

Storage systems for national information assets [DE93-009303] p 3615 N93-29783

Nuclear isomers as ultra-high-energy-density materials [DE93-009520] p 3568 N93-29784

Sodium guide star adaptive optics system for astronomical imaging in the visible and near-infrared [DE93-009543] p 3630 N93-29785

Potential effects of HFC-152a on global ozone and climate [DE93-008018] p 3471 N93-29792

Frequency dependent electrical properties of minerals and partial-melts [DE93-009254] p 3410 N93-29793

Hydrodynamic interactions among fibers in high efficiency filters [DE93-007117] p 3424 N93-30035

Pressure dependence of the reaction propagation rate of TATB to 40 GPa p 3319 N93-30082

Order-disorder transformations in Ni-Al alloys [DE93-009293] p 3326 N93-30389

Pulse control in an accelerator for heavy-ion fusion [DE93-009527] p 3576 N93-30390

High-repetition rate x ray lasers and applications [DE93-011882] p 3440 N93-30394

Mass storage system reference model, Version 4 p 3617 N93-30450

Photo-desorption from copper alloys [DE93-011872] p 3326 N93-30490

A new tubeless nanosecond streak camera based on optical deflection and direct CCD imaging [DE93-011893] p 3433 N93-30491

A correlated k-distribution model of the atmospheric heating rates for overlapping spectra of CO2 and H2O [DE93-007391] p 3474 N93-30504

Simulation and calculation of diffusive aerosol deposition [DE93-007518] p 3474 N93-30506

Radiation effects in FCC metals and intermetallic compounds: A molecular dynamics computer simulation study [DE93-009546] p 3600 N93-30668

LEEDS UNIV. (ENGLAND).

Impingement/effusion cooling p 3257 N93-29954

LEHIGH UNIV., BETHLEHEM, PA.

High octane ethers from synthesis gas-derived alcohols [DE93-012470] p 3341 N93-28752

Electron cyclotron heating and current drive in toroidal geometry [DE93-010400] p 3586 N93-29049

Processing of novel nanoparticle dispersion strengthened ceramics for improved mechanical performance [AD-A264191] p 3339 N93-30883

LEICESTER UNIV. (ENGLAND).

Studies of the propagation of Low Frequency (LF) radio waves p 3396 N93-30738

LIFE SYSTEMS, INC., CLEVELAND, OH.

Electrolysis performance improvement and validation experiment p 3267 N93-28737

LIGHTWAVE ELECTRONICS CORP., MOUNTAIN VIEW, CA.

All solid-state high power visible laser [NASA-CR-193163] p 3436 N93-28623

LITTLE (ARTHUR D.), INC., CAMBRIDGE, MA.

Hybrid oxygen system [AD-A262417] p 3500 N93-28464

Spaceborne passive radiative cooler p 3378 N93-28802

Infrared rugates by molecular beam epitaxy
p 3582 N93-28808

LOCKHEED AERONAUTICAL SYSTEMS CO., BURBANK, CA.
Advanced composite structural concepts and material technologies for primary aircraft structures
p 3300 N93-30430
Design, analysis, and fabrication of the technology integration box beam p 3300 N93-30433

LOCKHEED AIRCRAFT CORP., PALO ALTO, CA.
Planetary and satellite x ray spectroscopy: A new window on solid-body composition by remote sensing
p 3641 N93-28773

LOCKHEED ENGINEERING AND SCIENCES CO., HAMPTON, VA.
A generalized approach to the thermal analysis of the Long Duration Exposure Facility's flight experiments
p 3428 N93-29624

LOCKHEED ENGINEERING AND SCIENCES CO., HOUSTON, TX.
LDEF data: Comparisons with existing models
p 3283 N93-29375
Space Generic Open Avionics Architecture (SGOAA) reference model technical guide
[NASA-CR-188246] p 3285 N93-31032

LOCKHEED MISSILES AND SPACE CO., PALO ALTO, CA.
Resolution-enhanced mapping spectrometer
p 3434 N93-28794

LOCKHEED MISSILES AND SPACE CO., SUNNYVALE, CA.
Cost effective TacSats for military support
p 3285 N93-29912

LODESTAR RESEARCH CORP., BOULDER, CO.
Fundamental studies of fusion plasmas
[DE93-013144] p 3589 N93-30189

LOKI SOFTWARE, INC., LIBERTY CORNER, NJ.
Evaluation of fuzzy inference systems using fuzzy least squares p 3513 N93-29539

LORAL AEROSYS, SEABROOK, MD.
High-performance mass storage system for workstations p 3618 N93-30457

LOS ALAMOS NATIONAL LAB., NM.
Preprocessing remotely-sensed data for efficient analysis and classification
[DE93-007367] p 3611 N93-28580
Polymeric materials for use in wet hydrochloric acid environments
[DE93-010881] p 3330 N93-28600
How to write fast and clear parallel programs using algebra
[DE93-000797] p 3524 N93-28640
Applied research in America
[DE93-011725] p 3625 N93-28646
Information-theoretic performance bounding of Bayesian identifiers
[DE93-010705] p 3554 N93-28763
Laer-induced breakdown spectroscopy instrument for element analysis of planetary surfaces
p 3434 N93-28769
Gamma ray/neutron spectrometers for planetary elemental mapping p 3647 N93-28807
Upgrading the LAMPF 201 MHz RF generators
[DE93-010715] p 3406 N93-28830
Meson-meson interactions and phi-enhancement in nucleus collisions
[DE93-010725] p 3565 N93-28831
Smart skin structures for identifying and locating laser irradiation
[DE93-005464] p 3436 N93-28887
A proposed approach for developing next-generation computational electromagnetics software
[DE93-007326] p 3380 N93-28900
Aligned, short-fiber composites by novel flow processing methods
[DE93-008701] p 3296 N93-28904
Why Blue stragglers formed via collisions may not be rapid rotators
[DE93-008708] p 3633 N93-28905
Do the Pop 2 field blue stragglers have a collisional origin?
[DE93-008709] p 3634 N93-28906
Can physical stellar collisions explain the blue stragglers in the dwarf spheroidal galaxies?
[DE93-008711] p 3634 N93-28907
The heating and cooling of WZ Sge
[DE93-008720] p 3634 N93-28908
High-resolution signal synthesis for time-frequency distributions
[DE93-008735] p 3380 N93-28909
The investigation of nonlinear effects on quasiparticle transport in condensed matter systems
[DE93-009582] p 3565 N93-28914
Quantum lattice fluctuations in a 1-dimensional charge-density-wave material: Luminescence and resonance Raman studies of an MX solid
[DE93-007362] p 3593 N93-28966
Report on the sintering and properties of MgO and MgO-5 percent TiC
[DE93-008676] p 3323 N93-29092
Start broadened profiles with self-consistent radiation transfer and atomic kinetics in plasmas produced by high intensity lasers
[DE93-008706] p 3586 N93-29093
Flux lattice relaxation, noise, and symmetry-breaking in frustrated Josephson junction arrays
[DE93-008713] p 3593 N93-29094
Doppler-radar wind-speed measurements in tornadoes: A comparison of real and simulated spectra
[DE93-008734] p 3481 N93-29095
Polymer electrolyte fuel cells for transportation applications
[DE93-008721] p 3464 N93-29147
Space optical and low-frequency radio searches for Earth-crossing asteroids and comets
[DE93-008716] p 3634 N93-29246
A simple model for explosives formulation
[DE93-010703] p 3341 N93-29251
Microwave processing of ceramics
[DE93-010708] p 3332 N93-29252
Experimental study of instability growth patterns of a shock-accelerated, thin fluid layer
[DE93-010741] p 3421 N93-29253
Super critical water oxidation on energetic materials
[DE93-010704] p 3342 N93-29312
Measurement of W-Z interference from neutrino-electron scattering
[DE93-010724] p 3566 N93-29313
Investigation of ion beam mixing of iron marker layers in aluminum oxide by RBS
[DE93-010727] p 3594 N93-29314
Neutrino mass
[DE93-010735] p 3566 N93-29315
Sensitivity study of cloud/radiation interaction using a second order turbulence radiative-convective model
[DE93-007365] p 3477 N93-29346
Prognostic cloud water in the Los Alamos general circulation model
[DE93-007381] p 3482 N93-29347
Fiber-optic currents measurements
[DE93-007970] p 3579 N93-29350
Radioactivities induced in some LDEF samples
p 3572 N93-29628
Optimization of HPM device parameters for maximum air transmission
[DE93-007332] p 3386 N93-29765
A functional implementation of the Jacobi eigen-solver
[DE93-007349] p 3549 N93-29769
High-current negative-ion beam transport
[DE93-010732] p 3575 N93-29809
Analysis of an MCG/fuse/PFS experiment
[DE93-007355] p 3410 N93-29812
Weakly nonlinear dynamics of near-CJ detonation waves
[DE93-007344] p 3424 N93-29836
Multi-Attribute Decision Theory methodology for pollution control measure analysis
[DE93-005444] p 3472 N93-30008
Vibrational spectroscopy of shock-compressed fluids
p 3318 N93-30072
A steric hindrance model for the crystal orientation dependence of the shock initiation sensitivity of PETN explosive
[LA-UR-92-1427] p 3345 N93-30074
Detonation mass spectrometry p 3319 N93-30076
Strategies for understanding the deflagration-to-detonation transition
p 3319 N93-30077
Interfacial melting in cracked explosives
p 3349 N93-30089
Whisker toughening of ceramic materials: A review
[DE93-011565] p 3336 N93-30129
Partial cross sections in H(-) photodetachment
[DE93-011570] p 3569 N93-30130
Isothermal and shock compression of high density ammonium nitrate and ammonium perchlorate
[DE93-000682] p 3315 N93-30209
Containment of explosions in spherical vessels
[DE93-005445] p 3446 N93-30211
SESAME equation of state number 8010: Boron loaded silicone potting material
[DE93-012083] p 3300 N93-30395
Computational analysis of slip in PETN
[DE92-040222] p 3598 N93-30445
The use of quantum chemistry to estimate the performance and properties of explosives
[DE92-040369] p 3352 N93-30446
Direct Monte Carlo simulation of the chemical equilibrium composition of detonation products
[DE92-040372] p 3315 N93-30447
The calculation of electrostatic interactions and their role in determining the energies and geometries of molecular HE crystals
[DE92-040374] p 3570 N93-30448
LANL High-Performance Data System (HPDS)
p 3622 N93-30478
Errors when shock waves interact due to numerical shock width
[DE93-010699] p 3426 N93-30484
Towards a better hydro for dynamic mix calculations
[DE93-010702] p 3426 N93-30485
Constitutive laws for deformation and dynamic recrystallization in cubic metals
[DE93-010740] p 3326 N93-30486
A computer simulation of the production of an artificially ionized layer using the Arecibo facility
[DE93-010817] p 3478 N93-30487
Multiprocessing MCNP on an IBM RS/6000 cluster
[DE93-008712] p 3540 N93-30633
The quality assurance liaison: Combined technical and quality assurance support
[DE93-008725] p 3450 N93-30636
A continuum code investigation of stress integration using exact and approximate material rotation
[DE93-001892] p 3454 N93-31013

LOUGHBOROUGH UNIV. OF TECHNOLOGY (ENGLAND).
Analysis of thermal bar using boundary-layer integral equations gradients
[MATHS-REPT-A-177] p 3462 N93-30107

LOUISIANA STATE UNIV., BATON ROUGE.
Multiprocessing systems: Reliability modelling and analysis using multimode components and dependent failures
[AD-A264230] p 3540 N93-30364

LOUISVILLE UNIV., KY.
An analysis of possible applications of fuzzy set theory to the actuarial credibility theory p 3510 N93-29517

LOYOLA COLL., BALTIMORE, MD.
Microstructural basis for enhanced shock-induced chemistry in single crystals of ammonium perchlorate
p 3319 N93-30092
Experiments in materials science from household items p 3293 N93-30971
An automated data collection system for a Charpy impact tester p 3293 N93-30972

LUDWIG-MAXIMILIANS-UNIV., MUNICH (GERMANY).
Forest examination with polarimetric radar image data
p 3457 N93-28921
International Journal of Numerical Modeling: Electronic Networks, Devices, and Fields, volume 5, number 3, August 1992
[AD-A263765] p 3387 N93-29877

LUNAR AND PLANETARY INST., HOUSTON, TX.
Workshop on Advanced Technologies for Planetary Instruments, part 1
[NASA-CR-193015] p 3639 N93-28764

M

M-DOT, INC., PHOENIX, AZ.
Thrust augmentation system for low-cost-expendable turbojet engine
[AD-A263727] p 3259 N93-30877

MACDONALD, DETTWILER AND ASSOCIATES LTD., OTTAWA (ONTARIO).
Application and integration of diverse technology in an aviation system: The National Aeronautical Information Processing System p 3247 N93-30339

MACDONALD, DETTWILER AND ASSOCIATES LTD., RICHMOND (BRITISH COLUMBIA).
Meteorological information for aviation: A systems approach p 3367 N93-30298

MACDONALD, DETTWILER PROPRIETARY LTD., NEW SOUTH WALES (AUSTRALIA).
Application and integration of diverse technology in an aviation system: The National Aeronautical Information Processing System p 3247 N93-30339

MAINE UNIV., ORONO.
Structure, adhesion, and stability of metal/oxide and oxide/oxide interfaces
[DE93-012930] p 3325 N93-30060

MALIN SPACE SCIENCE SYSTEMS, SAN DIEGO, CA.
Visible imaging on the Pluto fast flyby mission
p 3646 N93-28799

MANCHESTER COLL. OF SCIENCE AND TECHNOLOGY (ENGLAND).
Turbulent flow and heat transfer in idealized blade cooling passages p 3254 N93-29938

MANITOBA UNIV., WINNIPEG.
Fuzzy coordinator in control problems
p 3515 N93-29552

Hierarchical model of matching p 3519 N93-29580
Analog CMOS circuits for neural networks p 3355 N93-30223
Generation of configurable self-synchronizing synchronous CMOS static RAMs p 3361 N93-30259
Transient field computations within or proximity of complex structures: FD-TD approach p 3366 N93-30292
Computer-aided modeling for analysis of arbitrary scatterers and feeds p 3367 N93-30293
Tolerance theory of phased array antennas: A statistical approach p 3369 N93-30307

MAR, INC., ROCKVILLE, MD.
Development of a test program to evaluate structural defects in Glass-Reinforced Plastic (GRP), volume 2 [AD-A263814] p 3335 N93-29881
Development of a test program to evaluate structural defects in Glass-Reinforced Plastic (GRP), volume 1 [AD-A263813] p 3335 N93-29886

MARATHON OIL CO., LITTLETON, CO.
Hydrogen sulfide decomposition into hydrogen and sulfur by quinone cycles, part 1 [PB93-175297] p 3317 N93-30761

MARMARA RESEARCH INST., GEBZE (TURKEY).
Considerations for NATO satellite communications in the post-2000 era p 3388 N93-29899

MARTIN MARIETTA CORP., BALTIMORE, MD.
Drive-reinforcement learning system applications [AD-A264514] p 3446 N93-30404

MARTIN MARIETTA CORP., DENVER, CO.
Vented Tank Resupply Experiment (VTRE) for In-Space Technology Experiment Program (IN-STEP) p 3264 N93-28711

MARTIN MARIETTA CORP., NEW ORLEANS, LA.
Technology transfer from the viewpoint of a NASA prime contractor p 3626 N93-30701
Technology transfer to the broader economy p 3628 N93-30719

MARTIN MARIETTA ENERGY SYSTEMS, INC., OAK RIDGE, TN.
Tribology: Friction, lubrication, and wear technology p 3292 N93-30965

MARTIN MARIETTA LABS., BALTIMORE, MD.
Electrochemical behavior and surface chemistry of aluminum alloys: Solute-rich interphase model [AD-A262061] p 3322 N93-29002
Radiation sensitivity of quartz crystal oscillators experiment for the Long Duration Exposure Facility (LDEF), part 2 p 3414 N93-29685
Tensile study of single-crystal ternary L1(2) trialuminide Al66Ti25Mn(sub g) [AD-A264297] p 3601 N93-30819

MARYLAND UNIV., BALTIMORE.
Exploitation of parallelism in climate models [DE93-011259] p 3470 N93-29318
Some statistical inference problems in linear models and variance components models and their applications [AD-A264062] p 3555 N93-29923

MARYLAND UNIV., COLLEGE PARK.
Optically controlled solid state opening switches [AD-A262404] p 3591 N93-28496
Accelerator research studies [DE93-009353] p 3573 N93-28522
Nonlinear dynamics and plasma transport [DE93-012238] p 3585 N93-28749
Grid Analysis and Display System (GrADS): A practical tool for earth science visualization p 3613 N93-29225
VIEWCACHE: An incremental database access method for autonomous interoperable databases p 3614 N93-29238
Delta Advanced Reusable Transport (DART): An alternative manned spacecraft p 3231 N93-29735
Taurus Lightweight Manned Spacecraft Earth orbiting vehicle p 3231 N93-29736
Walking robot: A design project for undergraduate students p 3231 N93-29737
Reaction mechanism studies of heavy ion induced nuclear reactions [DE93-010496] p 3569 N93-29807
Improved design concepts for millimeter wave power sources [AD-A264060] p 3411 N93-29922
Study of effects of small perturbations on chaotic systems [DE93-009762] p 3557 N93-30048
Dislocation roles in energetic crystal responses p 3348 N93-30086
Qualitative methods in computer vision [AD-A264335] p 3533 N93-30418

MASSACHUSETTS INST. OF TECH., CAMBRIDGE.
Gas permeability of E/EP semicrystalline diblock copolymers [AD-A263241] p 3329 N93-28560
Comparative mutagenesis of human cells in vivo and in vitro [DE93-012269] p 3490 N93-28651
Ground clutter measurements for surface-sited radar [AD-A262472] p 3379 N93-28655
The MODE family of facility class experiments p 3263 N93-28705
Macrostatistical hydrodynamics [DE93-012289] p 3417 N93-28751
Coherent and semi-coherent neutron transfer reactions [DE93-008336] p 3565 N93-28959
Flow phenomena in turbomachines [AD-A263049] p 3420 N93-29141
A passive infrared ice detection technique for helicopter applications [NASA-CR-193187] p 3244 N93-29152
Programmable interactive system for cochlear implant electrode stimulation [AD-A262558] p 3494 N93-29421
A Riemann problem for an elastic bar that changes phase [AD-A262827] p 3452 N93-29432
Charged particle activation studies on the surface of LDEF spacecraft p 3572 N93-29630
Project Copernicus: An Earth observing system p 3231 N93-29738
Center for the Study of Intelligent Control Systems (Fellowships) [AD-A263604] p 3543 N93-29917
The influence of non-uniform spanwise inlet temperature on turbine rotor heat transfer p 3253 N93-29932
Applications of transition metal compounds in the preparation of useful silicon-containing ceramics [AD-A264028] p 3335 N93-30028
Single-shot femtosecond spectroscopy: A methodology for observation of solid-state chemical reactions p 3319 N93-30075
Synthesis of chiral molybdenum ROMP initiators and all-cis highly tactic Poly-2,3-R2Norbornadiene (R = CF3 or CO2Me) [AD-A264133] p 3336 N93-30169
Methylhydridopolysilazane and its pyrolytic conversion to Si3N4/SiC ceramics [AD-A264150] p 3336 N93-30170
The middeck 0-gravity dynamics experiment [NASA-CR-4500] p 3281 N93-30376
1,2-Dimethyl-1,2-Disila-Closo-Dodecaborane(12), A silicon analog of an ortho-carborane: Synthesis; x ray crystal structure; NMR, vibrational and photoelectron spectra; bonding [AD-A264709] p 3599 N93-30568
The role of the University Licensing Office in transferring intellectual property to industry p 3626 N93-30698
Microwave emission from relativistic electron beams [AD-A264102] p 3400 N93-30880
Design, synthesis, and chemical processing of hierarchical ceramic structures for aerospace applications [AD-A264227] p 3339 N93-30885

MASSACHUSETTS INST. OF TECH., LEXINGTON.
High-performance visible/UV CCD focal plane technology for spacebased applications p 3434 N93-28771
SWAT 2 overview [AD-A262905] p 3578 N93-29139
SWAT laboratory test results [AD-A262906] p 3578 N93-29140
Contributions to the American Meteorological Society's 26th International Conference on Radar Meteorology [AD-A263385] p 3481 N93-29257
SWAT system performance predictions [AD-A262857] p 3579 N93-29470
Two simulation studies of precision runway monitoring of independent approaches to closely spaced parallel runways [AD-A263433] p 3261 N93-29815
Advanced technologies for lightweight EHF tactical communications satellites p 3389 N93-29900

MASSACHUSETTS UNIV., AMHERST.
High-energy electron-positron interactions [DE93-011611] p 3576 N93-30488
Adaptive networks for sequential decision problems [AD-A264756] p 3534 N93-30561

MASSACHUSETTS UNIV., BOSTON.
Magnetic resonance studies of photo-induced electron transfer reactions [DE93-012239] p 3311 N93-29182

MASSACHUSETTS UNIV., LOWELL.
Conjugated substituted ionic polyacetylenes [AD-A264702] p 3337 N93-30497

MATERIALS AND ELECTROCHEMICAL RESEARCH CORP., TUCSON, AZ.
Ambient-atmosphere compatible superconducting fullerenes [AD-A262025] p 3595 N93-29397

MATERIALS RESEARCH LABS., ASCOT VALE (AUSTRALIA).
Sound wave scattering from an elastic spherical shell [AD-A264039] p 3562 N93-30029
The wake software suite: User's guide [AD-A264181] p 3425 N93-30156
Sound wave scattering from a rigid sphere [AD-A264182] p 3562 N93-30157

MATERIALS RESEARCH SOCIETY, PITTSBURG, PA.
Low temperature (LT) GaAs and related materials [AD-A263607] p 3298 N93-29282

MATRA MARCONI SPACE (ENGLAND).
TACSAT ground control and data collection p 3388 N93-29895
A TACSAT SAR concept p 3286 N93-29910
TACSAT meteorological payloads p 3391 N93-29913

MATRA MARCONI SPACE, TOULOUSE (FRANCE).
TACSAT-spacecraft bus concept and design: Application of a multimission bus for TACSAT in LEO p 3284 N93-29896

MAX-PLANCK-INST. FUER EXTRATERRESTRISCHE PHYSIK, GARCHING (GERMANY).
ROSAT detection of stellar x ray sources in the old open cluster M67 [MPE-PREPRINT-230] p 3631 N93-30578
Submillimeter CO observations of warm gas around T-Tauri stars [MPE-PREPRINT-232] p 3631 N93-30615
CO lines toward NGC 2024 and other star forming regions: A closer look at the warm gas component [MPE-PREPRINT-223] p 3637 N93-30639
A variable reflectivity output coupler for optically pumped far infrared lasers [MPE-PREPRINT-225] p 3441 N93-30640
Near-infrared line imaging of NGC 6240: Global shock and nuclear starburst [MPE-PREPRINT-226] p 3631 N93-30641
Rejection of archival photographic objects as optical counterparts of gamma ray bursters [MPE-PREPRINT-228] p 3631 N93-30642
Infrared spectroscopy and imaging of starburst galaxies and AGNs [MPE-PREPRINT-229] p 3632 N93-30643

MAXWELL LABS., INC., LA JOLLA, CA.
Spacecraft surface charging handbook [AD-A262778] p 3279 N93-29305

MCDONNELL AIRCRAFT CO., SAINT LOUIS, MO.
Design and manufacturing concepts for thermoplastic structures p 3301 N93-30434

MCDONNELL-DOUGLAS MISSILE SYSTEMS CO., SAINT LOUIS, MO.
NASA instep/MDMSC jitter suppression experiment (JITTER) p 3263 N93-28702

MCDONNELL-DOUGLAS SPACE SYSTEMS CO., HUNTINGTON BEACH, CA.
CSI-Star: A low-cost CSI orbital testbed p 3263 N93-28707

MCGILL UNIV., MONTREAL (QUEBEC).
An architecture for an analog VLSI neural network for early computer vision processing p 3359 N93-30244
A parallel processing system for intensive I/O p 3362 N93-30262

MCMASTER UNIV., HAMILTON (ONTARIO).
Division by polynomial matrix and its application to multivariable linear systems p 3357 N93-30233
QR decomposition based least squares lattice algorithm p 3358 N93-30239
Propagation channel modeling for angle-diversity combining simulation p 3360 N93-30252
An adaptive algorithm for linear associative memory problem p 3360 N93-30255
A transputer based parallel processing architecture for robotics applications p 3362 N93-30263
Classification of radar clutter in an air traffic control environment p 3246 N93-30299
An adaptive maximum likelihood receiver for correlated Rayleigh fading channels p 3371 N93-30316

MEMORIAL UNIV. OF NEWFOUNDLAND, SAINT JOHNS.
Adaptive filtering for clutter suppression in high frequency radar p 3377 N93-30355

MEMPHIS STATE UNIV., TN.
Algorithms for point set congruence [AD-A264016] p 3532 N93-29980

MENTALOGIC SYSTEMS, INC., MARKHAM (ONTARIO).
The cognitive bases for the design of a new class of fuzzy logic controllers: The clearness transformation fuzzy logic controller p 3515 N93-29554
Comparison between the performance of two classes of fuzzy controllers p 3517 N93-29566

MESSER GRIESHEIM G.M.B.H., FRANKFURT AM MAIN (GERMANY).
Laser gas alloying of titanium materials [ETN-93-93805] p 3325 N93-30115

MESSERSCHMITT-BOELKOW-BLOHM G.M.B.H., MUNICH (GERMANY).
Attitude- and Orbit Control Subsystem concepts for TACSATS p 3284 N93-29906

MICHIGAN STATE UNIV., EAST LANSING.
Rapidly activated dynamic phase transitions in nonlinear solids
[AD-A263601] p 3299 N93-29982

MICHIGAN TECHNOLOGICAL UNIV., HOUGHTON.
Theoretical hyperfine structure constants for transition metal atoms and ions
[DE93-012325] p 3566 N93-29183
Robust control of intelligent rotor
[AD-A263707] p 3259 N93-29985

MICHIGAN UNIV., ANN ARBOR.
Mechanics of elevated temperature fatigue damage in fiber-reinforced ceramics
[AD-A262403] p 3329 N93-28495
Fast neutron cross section measurements
[DE93-009053] p 3563 N93-28546
Applications of unitarity in the standard model
p 3416 N93-28613
Spectral energetics of the lower thermosphere
p 3477 N93-29467
Project MEDSAT p 3231 N93-29739
Project UM-HAUL: A self-unloading reusable lunar lander p 3232 N93-29740
Efficient Reorientation Maneuvers for Spacecraft with Multiple Articulated Payloads
[NASA-CR-193142] p 3279 N93-29988
Control of nonlinear systems with applications to constrained robots and spacecraft attitude stabilization
p 3279 N93-29989
Attitude stabilization of a rigid spacecraft using two momentum wheel actuators p 3280 N93-29990
Attitude stabilization of a rigid spacecraft using gas jet actuators operating in a failure mode
p 3280 N93-29992
Planar reorientation of a free-free beam in space using embedded electromechanical actuators
p 3280 N93-29993
Efficient reorientation of a deformable body in space: A free-free beam example p 3280 N93-29994
Space station attitude disturbance arising from internal motions p 3280 N93-29995
Hydrodynamic interactions among fibers in high efficiency filters
[DE93-007117] p 3424 N93-30035
Models of star formation in interacting and merging disk galaxies p 3635 N93-30148
Observing and modelling F-region ionospheric dynamics using the OII 7320A emission p 3479 N93-30564
Vibration localization in rotating shafts
p 3454 N93-30626
Discomfort glare from high-intensity discharge headlamps: Effects of context and experience
[PB93-174720] p 3496 N93-30659
Control of nonlinear systems with applications to constrained robots and spacecraft attitude stabilization
p 3544 N93-30893
Adaptive motion control of mobile robots
p 3545 N93-30903
Numerical wave propagation and steady-state solutions p 3428 N93-30999
On symmetric central configurations with application to satellite motion about rings p 3652 N93-31000
Theoretical and experimental investigation of slack cable/mass system dynamics p 3455 N93-31028

MICROELECTRONICS AND COMPUTER TECHNOLOGY CORP., AUSTIN, TX.
An MCM/chip concurrent engineering validation
[AD-A262959] p 3409 N93-29513

MICROTEL PACIFIC RESEARCH LTD., BURNABY (BRITISH COLUMBIA).
Terrain and coverage prediction analyses for non-geostationary orbit EHF satellite communications
p 3389 N93-29902

MIDDLE EAST TECHNICAL UNIV., ANKARA (TURKEY).
Evaluation of multi-dimensional flux models for radiative transfer in cylindrical combustion chambers
p 3257 N93-29955

MIDWEST RESEARCH INST., GOLDEN, CO.
New III-V cell design approaches for very high efficiency
[DE93-000097] p 3464 N93-28971
Modification of flux profiles using a faceted concentrator
[DE93-000087] p 3464 N93-29925
Low-cost, high-efficiency solar cells utilizing GaAs-on-Si technology
[DE93-000096] p 3464 N93-29965
Study of parameters affecting the performance of solar desiccant cooling systems
[DE93-000088] p 3465 N93-30206
Measurements and Characterization Branch
[DE93-000094] p 3465 N93-30207
Growth and development of GaInAsP for use in high-efficiency solar cells
[DE93-000098] p 3465 N93-30208
Silicon Film(trademark) photovoltaic manufacturing technology
[DE93-010008] p 3466 N93-30891

MINAS GERAIS UNIV., BELO HORIZONTE (BRAZIL).
Effect of planar magnetic field on electron transport properties of n-AlGaAs/GaAs heterojunction and photoluminescence measures in GaAs samples
[DE93-608739] p 3601 N93-30776

MINNESOTA UNIV., DULUTH.
Incomplete fuzzy data processing systems using artificial neural network p 3519 N93-29578

MINNESOTA UNIV., MINNEAPOLIS.
Synthesis of conducting polymer composite fibers in electrochemical flow cells
[AD-A262233] p 3294 N93-28492
Research in theoretical nuclear physics
[DE93-008380] p 3565 N93-28960
Stabilized space-time finite element formulations for unsteady incompressible flows involving fluid-body interactions p 3419 N93-29040
Some problems in the mechanics of solids with phase mixtures
[AD-A263652] p 3311 N93-29291
Electric field induced phenomena in STM: Tip deformations and Au(111)-surface phase transitions during tunneling spectroscopy experiments
[AD-A262208] p 3596 N93-29445
Synthesis of oligoimides and oligoimide anion radicals
[AD-A263129] p 3290 N93-29474
Intelligent fuzzy controller for event-driven real time systems p 3515 N93-29551
Mars integrated transportation system multistage Mars mission p 3232 N93-29741
Single-stage Mars mission p 3232 N93-29742
Vortex structure and mass transfer near the base of a cylinder and a turbine blade p 3253 N93-29929
Design of acentric materials: X ray structures of guanidinium p-nitro- and p-hydroxybenzenesulfonate
[AD-A264220] p 3597 N93-30146
Environmental studies: Mathematical, computational and statistical analyses
[AD-A264223] p 3473 N93-30360
Multiscale and multigrid information representation, extraction and fusion
[AD-A264623] p 3393 N93-30386

MISSION RESEARCH CORP., ALBUQUERQUE, NM.
Test structure to microcircuit correlation
[AD-A264157] p 3412 N93-30152

MISSION RESEARCH CORP., NEWINGTON, VA.
Acoustic-gravity waves from low-altitude localized disturbances
[AD-A264804] p 3479 N93-30593

MISSION RESEARCH CORP., SANTA BARBARA, CA.
Electromagnetic diffusion and wire coupling
[AD-A263183] p 3381 N93-29011

MISSISSIPPI UNIV., UNIVERSITY.
Theoretical and experimental study of thermoacoustic engines
[AD-A261934] p 3561 N93-28995

MISSOURI UNIV., COLUMBIA.
Quantitative analysis of properties and spatial relations of fuzzy image regions p 3510 N93-29523
A fuzzy clustering algorithm to detect planar and quadric shapes p 3511 N93-29524
Automatic rule generation for high-level vision
p 3511 N93-29526
Encoding spatial images: A fuzzy set theory approach
p 3511 N93-29527
A composite self tuning strategy for fuzzy control of dynamic systems p 3511 N93-29530
Comparison of crisp and fuzzy character networks in handwritten word recognition p 3514 N93-29545
The fusion of information via fuzzy integration
p 3517 N93-29568

MITECH, INC., WASHINGTON, DC.
Evaluation of category 3 MLS designs
p 3247 N93-30358

MITRE CORP., BEDFORD, MA.
Head mounted displays for virtual reality
[AD-A263498] p 3506 N93-29340
NetStat: A probabilistic network connectivity analysis tool
[AD-A262838] p 3529 N93-29647
Ethernet performance of the Motorola Altair WIN system
[AD-A263877] p 3387 N93-29890
A guide to total software quality control, volume 1
[AD-A263881] p 3531 N93-29920
A guide to total software quality control, volume 2
[AD-A263891] p 3531 N93-29921
Neural network cloud classification research
[AD-A264628] p 3484 N93-30176
Adaptive airborne radar simulation with equalization filter taps
[AD-A264722] p 3393 N93-30514

MITRE CORP., MCLEAN, VA.
Clouds and radiation: A primier
[AD-A263136] p 3482 N93-29479
The 1991-1992 aviation system capacity plan
[AD-A263436] p 3261 N93-29788
A preliminary review of global CO2 exchange between ocean and atmosphere
[AD-A264019] p 3472 N93-30015
Estimating Ada system size during development
[AD-A263880] p 3532 N93-30022
National Airspace System Performance Analysis Capability (NASPAC) simulation model
p 3247 N93-30351
Procedural development prototype in Automated En Route Air Traffic Control p 3247 N93-30352
Enhancing availability, performance, and flexibility of air traffic control air-ground services p 3247 N93-30353
Changing role of telecommunications management in air traffic control in the FAA p 3247 N93-30354
Developing automation for terminal air traffic control: Case study of the imaging aid p 3247 N93-30356
Procedures for applying Ada quality prediction models
[AD-A264730] p 3534 N93-30546
An approach to software quality prediction from Ada designs
[AD-A264731] p 3534 N93-30547

MONTANA STATE UNIV., BOZEMAN.
Direct tension experiments on compacted granular materials p 3292 N93-30960

MORAVIAN COLL., BETHLEHEM, PA.
Neural networks: A simulation technique under uncertainty conditions p 3519 N93-29577

MOSCOW STATE UNIV. (RUSSIA).
A simple formula for reducing Feynman diagrams to scalar integrals
[DE92-644717] p 3607 N93-30916

MOTOREN- UND TURBINEN-UNION MUENCHEN G.M.B.H. (GERMANY).
Transient thermal behaviour of a compressor rotor with axial cooling air flow and co-rotating or contra-rotating shaft p 3255 N93-29946

MOUNT SINAI SCHOOL OF MEDICINE, NEW YORK, NY.
NASA supporting studies for microgravity research on eye movements
[NASA-CR-193233] p 3493 N93-29041

MPR TELTECH LTD., BURNABY (BRITISH COLUMBIA).
The evolution of global mobile communications
p 3376 N93-30349

MPR TELTECH LTD., OTTAWA (ONTARIO).
Synchronization techniques for medium data rate EHF MILSATCOM systems p 3389 N93-29901
FASSET: A development model for a Canadian EHF MILSATCOM system p 3363 N93-30268

MSE, INC., BUTTE, MT.
Magnetohydrodynamic projects at the CDIF
[DE93-012195] p 3584 N93-28649

N

NAGOYA UNIV. (JAPAN).
Edge plasma control by RF electric field in Compact Helical System (CHS)
[DE93-753242] p 3583 N93-28532
Observation of a beam energy shift caused by a plasma wakefield
[DE93-753243] p 3583 N93-28533
Large amplitude striations in an RF discharge
[DE93-753244] p 3379 N93-28534
Elemental compositions of high-energy ions produced by magnetosonic waves in quiescent plasmas
[DE93-753241] p 3588 N93-29434
Ion ring distribution produced by a magnetosonic wave
[DE93-754311] p 3590 N93-30533

NATIONAAL INST. VOOR KERNFYSICA EN HOGE ENERGIEFYSICA, AMSTERDAM (NETHERLANDS).
Mechanical behaviour of a closed collar model for an 11.5 T dipole
[NIKHEF-H/92-03] p 3576 N93-30019
Investigation of methods for the measurement of small electron bundle currents
[DIGEL-1992-4] p 3413 N93-30763
A 250 mA toroid monitor for the measurement of the bundle current in the stretcher mode of AmPS
[DIGEL-1992-1] p 3413 N93-30835
Modification of the S-band phase shifter model 331A-3 of Electromagnetic Sciences Inc.
[DIGEL-1992-5] p 3399 N93-30836
Charge to frequency converter for ionization chambers belonging to the radiation protection system of AmPS/MEA
[DIGEL-1991-6] p 3577 N93-30837

Electronics for a neutron detector and a Geiger-Mueller detector for the radiation protection around MEA and AmPS
[DIGEL-1992-6] p 3413 N93-30838
Baryon number violation and particle collider experiments
[NIKHEF-H/92-14] p 3572 N93-31008

NATIONAL ACADEMY OF SCIENCES - NATIONAL RESEARCH COUNCIL, WASHINGTON, DC.
An assessment of space shuttle flight software development processes
[NASA-CR-193179] p 3525 N93-28934
National collaboratories: Applying information technology for scientific research
[LC-93-83795] p 3612 N93-29129
Toward a coordinated spatial data infrastructure for the nation
[B-149] p 3456 N93-30634

NATIONAL AERONAUTICS AND SPACE ADMINISTRATION, WASHINGTON, DC.
Proceedings of the Near-Earth-Object Interception Workshop
[NASA-TM-108236] p 3556 N93-28572
NASA/DOD Flight Experiments Technical Interchange Meeting Proceedings
[NASA-TM-108721] p 3262 N93-28699
Applied Information Systems Research Program Workshop
[NASA-TM-108773] p 3613 N93-29222
Applied Information Systems Research Program Workshop p 3613 N93-29223
The NASA SBIR product catalog
[NASA-TM-108242] p 3609 N93-29322
NASA SBIR abstracts of 1991 phase 1 projects
[NASA-TM-108240] p 3609 N93-29323
Research and technology objectives and plans: Summary fiscal year 1991
[NASA-TM-103086] p 3660 N93-29452
Payload flight assignments. NASA mixed fleet
[NASA-TM-108255] p 3268 N93-30133
The 1992 town meetings: Toward a shared vision
[NASA-NP-205] p 3608 N93-30134
Consultative Committee for Space Data Systems recommendation for space data system standards: Telecommand. Part 2.1: Command operation procedures
[NASA-TM-108158] p 3393 N93-30371
How to compete for NASA contracts
[NASA-TM-109238] p 3610 N93-30644
Technology Transfer and the Civil Space Program. Volume 2: Workshop proceedings
[NASA-TM-108250] p 3625 N93-30692
OAST space research and technology applications: Technology transfer successes p 3625 N93-30693
Technology transfer p 3626 N93-30699
Technology coordination p 3626 N93-30706
NASP technology transfer p 3627 N93-30713
High performance computing and communications program p 3627 N93-30715
Workshop conclusions: Technology transfer and the civil space program p 3628 N93-30721
NASA space research and technology overview (ITP) p 3628 N93-30722
Space research and technology overview p 3628 N93-30723

NATIONAL AERONAUTICS AND SPACE ADMINISTRATION. AMES RESEARCH CENTER, MOFFETT FIELD, CA.
Detection of other planetary systems using photometry p 3632 N93-28791
An integrated XRF/XRD instrument for Mars exobiology and geology experiments p 3645 N93-28792
A DTA/GC for the in situ identification of the Martian surface material p 3646 N93-28800
Flight evaluation of a computer aided low-altitude helicopter flight guidance system p 3260 N93-28869
The scientific modeling assistant: An advanced software tool for scientific model building p 3613 N93-29229
Introduction to cadet center for advanced data evaluation technology p 3614 N93-29240
Further analysis of LDEF FRECOPA micrometeoroid remnants p 3638 N93-29360
Hypervelocity impact survivability experiments for carbonaceous impactors p 3283 N93-29364
MoCog1: A computer simulation of recognition-primed human decision making
[NASA-TM-103868] p 3542 N93-29386
Formulation of Ames 24E2 IR-black coating
[NASA-TM-102864] p 3629 N93-29453
Neural networks application to divergence-based passive ranging
[NASA-TM-103981] p 3245 N93-29653
Planetary protection issues for the MESUR mission: Probability of growth (Pg)
[NASA-CP-3167] p 3651 N93-30214
NASA/FAA helicopter simulator workshop
[NASA-CP-3156] p 3236 N93-30673
Part 1: Executive summary p 3236 N93-30674
Helicopter simulator standards p 3236 N93-30675
Helicopter simulation: An aircrew training and qualification perspective p 3236 N93-30676
Rotorcraft master plan p 3236 N93-30677
Simulators for corporate pilot training and evaluation p 3236 N93-30678
Training effectiveness assessment: Where are we? p 3236 N93-30679
Current training: Where are we? p 3236 N93-30680
Helicopter simulator qualification p 3237 N93-30681
Helicopter simulation: Making it work p 3237 N93-30682
Helicopter training simulators: Key market factors p 3237 N93-30683
Training effectiveness assessment: Methodological problems and issues p 3237 N93-30684
Determining the transferability of flight simulator data p 3237 N93-30685
Progress through precedent: Going where no helicopter simulator has gone before p 3237 N93-30686
Transfer of training and simulator qualification or myth and folklore in helicopter simulation p 3237 N93-30687
Validation and upgrading of physically based mathematical models p 3237 N93-30688
Frequency-response techniques for documentation and improvement of rotorcraft simulators p 3237 N93-30689
Bandwidth and SIMDUCE as simulator fidelity criteria p 3238 N93-30690
Methodology development for evaluation of selective-fidelity rotorcraft simulation p 3238 N93-30691
Technology transfer needs and experiences: The NASA Research Center perspective p 3626 N93-30703
Technology transfer in the NASA Ames Advanced Life Support Division p 3628 N93-30724

NATIONAL AERONAUTICS AND SPACE ADMINISTRATION. GODDARD SPACE FLIGHT CENTER, GREENBELT, MD.
SeaWiFS technical report series. Volume 2: Analysis of orbit selection for SeaWiFS: Ascending versus descending node
[NASA-TM-104566-VOL-2] p 3486 N93-28497
SeaWiFS technical report series. Volume 6: SeaWiFS technical report series cumulative index: Volumes 1-5
[NASA-TM-104566-VOL-6] p 3486 N93-28500
Results from the US/Russian Meteor-3/Total Ozone Mapping Spectrometer
[NASA-TM-104576] p 3467 N93-28682
Cryogenic Heat Pipe Experiment (CRYOHP) p 3265 N93-28721
Environmental Verification Experiment for the Explorer Platform (EVEEP) p 3266 N93-28726
Return flux experiment p 3266 N93-28727
Spacecraft glow and the EISG/skirt experiment p 3266 N93-28728
Multibeam laser altimeter for planetary topographic mapping p 3442 N93-28780
Acousto-optic infrared spectral imager for Pluto fast flyby p 3285 N93-28781
Optical technologies for UV remote sensing instruments p 3582 N93-28788
Mass spectrometric measurement of Martian krypton and xenon isotopic abundance p 3646 N93-28798
A team approach to the development of gamma ray and x ray remote sensing and in situ spectroscopy for planetary exploration missions p 3650 N93-28824
Far infrared supplement. Third edition: Catalog of infrared observations (lambda greater than or equal to 4.6 micrometers)
[NASA-RP-1295] p 3629 N93-29156
NSSDC data listing
[NASA-TM-108264] p 3612 N93-29167
Convective and stratiform rain: Multichannel microwave sensing over oceans
[NASA-TM-104586] p 3482 N93-29448
Spline screw autochanger
[NASA-CASE-GSC-13435-1] p 3445 N93-29505
EnviroNET: On-line information for LDEF p 3624 N93-29625
Overview of the Systems Special Investigation Group investigation p 3318 N93-29683
Long Duration Exposure Facility (LDEF) low temperature Heat Pipe Experiment Package (HEPP) flight results p 3429 N93-29701
Bonner Durchmusterung (Southern Durchmusterung)
[NASA-RP-1298-VOL-3] p 3630 N93-29811
XRONOS: A timing analysis software package. User's guide, version 3.00
[NASA-TM-109222] p 3532 N93-30023
Quantifying and minimizing uncertainty of climate forcing by anthropogenic aerosols
[NASA-TM-108259] p 3472 N93-30043
Goddard Conference on Mass Storage Systems and Technologies, Volume 1
[NASA-CP-3198] p 3616 N93-30449
MR-CDF: Managing multi-resolution scientific data p 3618 N93-30456
Technology transfer within the NASA Goddard Space Flight Center p 3626 N93-30704
Technology transfer and space science missions p 3626 N93-30705
The cone structure and focusing of the electric field of VLF and LF waves at high altitudes of the ionosphere p 3395 N93-30731

NATIONAL AERONAUTICS AND SPACE ADMINISTRATION. HUGH L. DRYDEN FLIGHT RESEARCH FACILITY, EDWARDS, CA.
Flight control system design factors for applying automated testing techniques
[NASA-TM-4242] p 3260 N93-30764

NATIONAL AERONAUTICS AND SPACE ADMINISTRATION. JOHN C. STENNIS SPACE CENTER, BAY SAINT LOUIS, MS.
Technology transfer within NASA p 3627 N93-30708

NATIONAL AERONAUTICS AND SPACE ADMINISTRATION. JOHN F. KENNEDY SPACE CENTER, COCOA BEACH, FL.
Debris/ice/TPS assessment and integrated photographic analysis for Shuttle Mission STS-55
[NASA-TM-107559] p 3271 N93-29136
Guide for certifying pressure vessels and systems
[NASA-TM-107549] p 3449 N93-29220

NATIONAL AERONAUTICS AND SPACE ADMINISTRATION. LYNDON B. JOHNSON SPACE CENTER, HOUSTON, TX.
Magnetically operated check valve
[NASA-CASE-MSC-22046-1] p 3442 N93-28501
Radiation monitoring equipment dosimeter experiment p 3266 N93-28730
Thermal Analyzer for Planetary Soil (TAPS): An in situ instrument for mineral and volatile-element measurements p 3643 N93-28782
Sources sought for innovative scientific instrumentation for scientific lunar rovers p 3434 N93-28804
Prototype backscatter Moessbauer spectrometer for measurement of Martian surface mineralogy p 3648 N93-28812
Method for preparation of a microporous structure with layered interstitial surface treatment
[NASA-CASE-MSC-21487-2] p 3296 N93-29023
Anthropometric data from launch and entry suited test subjects for the design of a recumbent seating system
[NASA-TM-104769] p 3505 N93-29044
Ablative shielding for hypervelocity projectiles
[NASA-CASE-MSC-21884-1] p 3331 N93-29088
Thermal certification tests of Orbiter Thermal Protection System tiles coated with KSC coating slurries
[NASA-TM-104766] p 3278 N93-29221
Anthropometric survey of the astronaut applicants and astronauts from 1985 to 1991
[NASA-RP-1304] p 3506 N93-29324
Report of the Meteoroid and Debris Special Investigation Group p 3638 N93-29355
Continued investigation of LDEF's structural frame and thermal blankets by the Meteoroid and Debris Special Investigation Group p 3282 N93-29357
Three-D crater analysis of LDEF impact features from stereo imagery p 3283 N93-29359
Scanning electron microscope/energy dispersive x ray analysis of impact residues in LDEF tray clamps p 3283 N93-29369
Projectile compositions and modal frequencies on the chemistry of micrometeoroids LDEF experiment p 3638 N93-29370
Asteroidal versus cometary meteoroid impacts on the Long Duration Exposure Facility (LDEF) p 3638 N93-29371
Interplanetary meteoroid debris in LDEF metal craters p 3638 N93-29372
Origin of orbital debris impacts on LDEF's trailing surfaces p 3283 N93-29373
APU diaphragm testing
[NASA-TM-108254] p 3272 N93-29501
Pharmacokinetics and Pharmacodynamics in Space
[NASA-CP-10048] p 3494 N93-29502
North American Fuzzy Logic Processing Society (NAFIPS 1992), volume 1
[NASA-CP-10112-VOL-1] p 3509 N93-29516
A fuzzy measure approach to motion frame analysis for scene detection p 3511 N93-29525
Learning characteristics of a space-time neural network as a tether skiprope observer p 3512 N93-29534
North American Fuzzy Logic Processing Society (NAFIPS 1992), volume 2
[NASA-CP-10112-VOL-2] p 3515 N93-29556

Determining rules for closing customer service centers: A public utility company's fuzzy decision
p 3516 N93-29561

A genetic algorithms approach for altering the membership functions in fuzzy logic controllers
p 3518 N93-29573

An accelerated training method for back propagation networks
[NASA-CASE-MSC-21625-1] p 3498 N93-29610

Method for producing oxygen from lunar materials
[NASA-CASE-MSC-21759-1] p 3312 N93-29617

Issues on human acceleration tolerance after long-duration space flights
[NASA-TM-104753] p 3495 N93-29651

The +vbar breakout during approach to Space Station Freedom
[NASA-TM-104772] p 3269 N93-30135

Hypervelocity impact testing of the Space Station utility distribution system carrier
[NASA-TM-104771] p 3289 N93-30507

Exploration technology prioritization
p 3629 N93-30726

NATIONAL AERONAUTICS AND SPACE ADMINISTRATION. LANGLEY RESEARCH CENTER, HAMPTON, VA.

Subjective response to simulated sonic booms with ground reflections
[NASA-TM-107764] p 3561 N93-28692

Control-structures interaction test of the LACE satellite
p 3263 N93-28706

Upper atmosphere research satellite jitter study
p 3264 N93-28708

The Orbiter Experiments (OEX) program
p 3266 N93-28731

A remote laser-mass spectrometer for determination of elemental composition p 3434 N93-28775

NASA/DOD Aerospace Knowledge Diffusion Research Project. Paper 28: The technical communication practices of Russian and US aerospace engineers and scientists
[NASA-TM-108249] p 3612 N93-28948

LDEF materials data bases
[NASA-TM-107757] p 3290 N93-29067

The growth of small corrosion fatigue cracks in alloy 2024
[NASA-TM-107755] p 3451 N93-29069

Parallel software tools at Langley Research Center
[NASA-TM-108995] p 3520 N93-29070

Polyimides prepared from 3,5-diamino benzo trifluoride
[NASA-CASE-LAR-14206-1] p 3331 N93-29083

Constant frequency pulsed phase-locked loop measuring device
[NASA-CASE-LAR-13823-1] p 3431 N93-29084

Diphenylmethane-containing dianhydride and polyimides prepared therefrom
[NASA-CASE-LAR-14487-1] p 3331 N93-29085

The three-dimensional Multi-Block Advanced Grid Generation System (3DMAGGS)
[NASA-TM-108985] p 3420 N93-29155

Performance characteristics of two multiaxis thrust-vectoring nozzles at Mach numbers up to 1.28
[NASA-TP-3313] p 3239 N93-29160

Evaluation of four advanced nozzle concepts for short takeoff and landing performance
[NASA-TP-3314] p 3239 N93-29165

Hypersonic lateral and directional stability characteristics of aeroassist flight experiment configuration in air and CF4
[NASA-TM-4435] p 3239 N93-29166

Heating head for induction heating apparatus
[NASA-CASE-LAR-14429-1] p 3407 N93-29173

Single acting translation/rotational brake
[NASA-CASE-LAR-14738-1] p 3443 N93-29175

Enhanced reduction of velocity data obtained during CETA flight experiment
[NASA-TM-4460] p 3431 N93-29209

LDEF: 69 Months in Space. Second Post-Retrieval Symposium, part 2
[NASA-CP-3194-PT-2] p 3654 N93-29354

Long Duration Exposure Facility (LDEF) attitude measurements of the Interplanetary Dust Experiment
p 3638 N93-29377

Long-term microparticle flux variability indicated by comparison of Interplanetary Dust Experiment (IDE) timed impacts for LDEF's first year in orbit with impact data for the entire 5.77-year orbital lifetime p 3638 N93-29379

High-Reynolds-number test of a 5-percent-thick low-aspect-ratio semispan wing in the Langley 0.3-meter transonic cryogenic tunnel: Wing pressure distributions
[NASA-TM-4227] p 3240 N93-29449

Aerodynamic characteristics of a rotorcraft airfoil designed for the tip region of a main rotor blade
[NASA-TM-4264] p 3240 N93-29450

Process to prepare 1,3-diamino-5-pentafluorosulfanylbenzene
[NASA-CASE-LAR-14773-2-CU] p 3312 N93-29506

Method and apparatus for weaving a woven angle ply fabric
[NASA-CASE-LAR-14048-1] p 3354 N93-29611

Method of continuously determining crack length
[NASA-CASE-LAR-14480-1-CU] p 3452 N93-29612

Shear sensitive monomer-polymer laminate structure and method of using same
[NASA-CASE-LAR-14654-1-CU] p 3452 N93-29613

LDEF: 69 Months in Space. Part 1: Second Post-Retrieval Symposium
[NASA-CP-3194-PT-1] p 3660 N93-29621

LDEF: 69 Months in Space. Part 4: Second Post-Retrieval Symposium
[NASA-CP-3194-PT-4] p 3665 N93-29682

NASA/DoD Aerospace Knowledge Diffusion Research Project. Paper 29: The US government technical report and the transfer of federally funded aerospace R and D
[NASA-TM-109221] p 3615 N93-29709

NASA/DoD Aerospace Knowledge Diffusion Research Project. Paper 30: The electronic transfer of information and aerospace knowledge diffusion
[NASA-TM-109223] p 3616 N93-30036

NASA/DoD Aerospace Knowledge Diffusion Research Project. Paper 31: The information-seeking behavior of engineers
[NASA-TM-109224] p 3616 N93-30037

A quality monitor and monitoring technique employing optically stimulated electron emission
[NASA-CASE-LAR-15063-1] p 3449 N93-30414

The First NASA Advanced Composites Technology Conference, part 1
[NASA-CP-3104-PT-1] p 3300 N93-30428

Structural evaluation of curved stiffened composite panels fabricated using a THERM-Xsm process
p 3301 N93-30435

Noise transmission properties and control strategies for composite structures p 3301 N93-30436

A unified approach for composite cost reporting and prediction in the ACT program p 3302 N93-30441

First NASA Advanced Composites Technology Conference, part 2
[NASA-CP-3104-PT-2] p 3303 N93-30841

Preliminary properties of a resin from ethynyl terminated materials p 3303 N93-30842

Infiltration/cure modeling of resin transfer molded composite materials using advanced fiber architectures
p 3303 N93-30843

Powder towpreg process development
p 3303 N93-30844

Comparison of impact results for several polymeric composites over a wide range of low impact velocities
p 3304 N93-30848

Characterization of multiaxial warp knit composites
p 3304 N93-30851

Development of stitching reinforcement for transport wing panels p 3304 N93-30852

Ultrasonic detection and identification of fabrication defects in composites p 3305 N93-30856

Comparison of hand laid-up tape and filament wound composite cylinders and panels with and without impact damage p 3306 N93-30859

Design and analysis of grid stiffened concepts for aircraft composite primary structural applications
p 3306 N93-30861

Optimization of composite sandwich cover panels subjected to compressive loadings p 3306 N93-30862

Progressive failure methodologies for predicting residual strength and life of laminated composites
p 3307 N93-30866

Multiple methods integration for structural mechanics analysis and design p 3307 N93-30867

Effects of bolt-hole contact on bearing-bypass damage-onset strength p 3307 N93-30870

Experimental behavior of graphite-epoxy Y-stiffened specimens loaded in compression p 3307 N93-30872

Structural response of bead-stiffened thermoplastic shear webs p 3308 N93-30873

An overview of the crash dynamics failure behavior of metal and composite aircraft structures
p 3308 N93-30875

National Educators' Workshop. Update 92: Standard Experiments in Engineering Materials Science and Technology
[NASA-CP-3201] p 3290 N93-30948

Introduction to high performance composites
p 3291 N93-30957

On neural networks in identification and control of dynamic systems
[NASA-TM-107702] p 3455 N93-31038

NATIONAL AERONAUTICS AND SPACE ADMINISTRATION. LEWIS RESEARCH CENTER, CLEVELAND, OH.

Low-frequency vibration environment for five Shuttle missions
[NASA-TM-106059] p 3285 N93-28554

Development of Si(1-x)Ge(x) technology for microwave sensing applications
[NASA-TM-106157] p 3405 N93-28610

Texturing of InP surfaces for device applications
[NASA-TM-106061] p 3321 N93-28618

Small hydrogen/oxygen rocket flowfield behavior from heat flux measurements
[NASA-TM-106233] p 3286 N93-28619

Soft computing in design and manufacturing of advanced materials
[NASA-TM-106032] p 3295 N93-28624

A new flux conserving Newton's method scheme for the two-dimensional, steady Navier-Stokes equations
[NASA-TM-106160] p 3416 N93-28626

Preliminary experimental results for a cryogenic brush seal configuration
[NASA-TM-106236] p 3416 N93-28627

A multiarchitecture parallel-processing development environment
[NASA-TM-106180] p 3538 N93-28628

Probabilistic simulation of multi-scale composite behavior
[NASA-TM-106196] p 3451 N93-28633

Metal Matrix Laminate Tailoring (MMLT) code: User's manual
[NASA-TM-106052] p 3295 N93-28681

Small Stirling dynamic isotope power system for robotic space missions
[NASA-TM-105785] p 3287 N93-28686

Preliminary endurance tests of water vaporizers for resistojet applications
[NASA-TM-106222] p 3287 N93-28694

Benefits of in situ propellant utilization for a Mars sample return mission
[NASA-TM-106243] p 3341 N93-28695

A new facility for advanced rocket propulsion research
[NASA-TM-106193] p 3270 N93-28696

Experimental evaluation of a cooled radial-inflow turbine
[NASA-TM-106230] p 3251 N93-28697

Tank Pressure Control Experiment/Thermal Phenomena (TPCE/TP) p 3264 N93-28713

Solar Array Module Plasma Interaction Experiment (SAMPIE) p 3265 N93-28716

The Photovoltaic Array Space Power Plus diagnostics (PASP Plus) flight experiment p 3265 N93-28717

Thermal energy storage flight experiment in microgravity p 3265 N93-28720

Transfer Orbit Plasma Interaction Experiment (TROPIX) p 3267 N93-28734

Venus Interior Structure Mission (VISM): Establishing a seismic network on Venus p 3649 N93-28819

The development of a mixing layer under the action of weak streamwise vortices
[NASA-TM-106089] p 3418 N93-28947

Jet mixer noise suppressor using acoustic feedback
[NASA-CASE-LEW-15170-1] p 3561 N93-28953

Alkali metal carbon dioxide electrochemical system for energy storage and/or conversion of carbon dioxide to oxygen
[NASA-CASE-LEW-14973-1] p 3464 N93-28974

Effects of flow-path variations on internal reversing flow in a tailpipe offtake configuration for ASTOVL aircraft
[NASA-TM-106149] p 3252 N93-29065

Ceramic matrix composites properties/microstresses with complete and partial interphase bond
[NASA-TM-106136] p 3297 N93-29071

Acousto-Ultrasonic analysis of failure in ceramic matrix composite tensile specimens
[NASA-TM-106219] p 3449 N93-29073

Thermoviscoplastic analysis of fibrous periodic composites using triangular subvolumes
[NASA-TM-106076] p 3297 N93-29074

Application of ray tracing in radiation heat transfer
[NASA-TM-106206] p 3419 N93-29075

High Reynolds number and turbulence effects on aerodynamics and heat transfer in a turbine cascade
[NASA-TM-106187] p 3420 N93-29157

Preliminary investigation of high power microwave plasmas for electrothermal thruster use
[NASA-TM-106207] p 3288 N93-29158

A numerical study of confined turbulent jets
[NASA-TM-106197] p 3420 N93-29161

The 3-D viscous flow CFD analysis of the propeller effect on an advanced ducted propeller subsonic inlet
[NASA-TM-106240] p 3252 N93-29162

High temperature creep and oxidation resistant chromium silicide matrix alloy containing molybdenum
[NASA-CASE-LEW-15697-1] p 3323 N93-29172

Gravity sensitivity of a resistojet water vaporizer
[NASA-TM-106220] p 3288 N93-29194

System overview on electromagnetic compensation for reflector antenna surface distortion
[NASA-TM-106217] p 3273 N93-29195

Bounds on internal state variables in viscoplasticity
[NASA-TM-106215] p 3451 N93-29196

Accuracy of least-squares methods for the Navier-Stokes equations
[NASA-TM-106209] p 3421 N93-29208
Characteristics of hypervelocity impact craters on LDEF experiment S1003 and implications of small particle impacts on reflective surfaces p 3283 N93-29363
Apparatus for intercalating large quantities of fibrous structures
[NASA-CASE-LEW-15077-2] p 3298 N93-29609
Semiconductor cooling apparatus
[NASA-CASE-LEW-14162-3] p 3299 N93-29614
The effect of the low Earth orbit environment on space solar cells: Results of the Advanced Photovoltaic Experiment (S0014) p 3467 N93-29686
Studies of effects on optical components and sensors: LDEF experiments AO-147 (ERB components) and S-0014 (APEX) p 3582 N93-29693
Navier-Stokes analysis of three-dimensional flow and heat transfer inside turbine blade rows
p 3259 N93-29963
Probabilistic composite analysis p 3307 N93-30868
Tensile creep behavior of polycrystalline alumina fibers
[NASA-TM-106269] p 3340 N93-30938
Prediction of gas-liquid two-phase flow regime in microgravity
[NASA-TM-106274] p 3352 N93-30939

NATIONAL AERONAUTICS AND SPACE ADMINISTRATION. MARSHALL SPACE FLIGHT CENTER, HUNTSVILLE, AL.
Low-cost Active Structural Control space experiment (LASC) p 3263 N93-28700
Altitude compensating ablative stiffening band for rocket motor nozzles
[NASA-CASE-MFS-28728-1] p 3288 N93-28950
Welding wire pressure sensor assembly
[NASA-CASE-MFS-26216-1] p 3442 N93-28951
Amino acid sequences for the binding regions in serum albumin proteins
[NASA-CASE-MFS-28402-1] p 3491 N93-28952
Computerized atmospheric trace contaminant control simulation for manned spacecraft
[NASA-TM-108409] p 3505 N93-28977
The role of grain boundaries in hydrogen diffusion in metals at 25 C
[NASA-TM-108407] p 3322 N93-29043
Process for selectively recovering algae and protozoa
[NASA-CASE-MFS-26124-1-NPO] p 3491 N93-29174
Effects of atomic oxygen and ultraviolet radiation on candidate elastomeric materials for long duration missions. Test series no.1
[NASA-TM-108408] p 3331 N93-29193
Valve malfunction detection apparatus
[NASA-CASE-MFS-29904-1] p 3432 N93-29503
System for testing bearings
[NASA-CASE-MFS-28589-1] p 3445 N93-29618
Refinements on the pinhole camera measurements of the LDEF attitude p 3283 N93-29622
Status of LDEF ionizing radiation measurements and analysis p 3654 N93-29626
Collection, analysis, and archival of LDEF activation data p 3624 N93-29631
Induced activation study of LDEF
p 3572 N93-29632
Revised prediction of LDEF exposure to trapped protons p 3572 N93-29633
LET spectra measurements of charged particles in the P0006 experiment on LDEF p 3573 N93-29637
Three-dimensional shielding effects on charged particle fluences measured in the P0006 experiment of LDEF
p 3573 N93-29639
Cosmogenic radionuclides on LDEF: An unexpected Be-10 result p 3573 N93-29643
Platform stair lift
[NASA-CASE-MFS-28772-1] p 3507 N93-29845
Quick connect fastener
[NASA-CASE-MFS-28833-1] p 3445 N93-29846
Liquid fuel injection elements for rocket engines
[NASA-CASE-MFS-28547-1] p 3289 N93-29847
Method of fabricating a rocket engine combustion chamber
[NASA-CASE-MFS-28569-1] p 3338 N93-30565
Prosthetic elbow joint
[NASA-CASE-MFS-28707-1] p 3508 N93-30566
Mold bolt and means for achieving close tolerances between bolts and bolt holes
[NASA-CASE-MFS-28720-1] p 3447 N93-30567
Orbiting transmitter and antenna for spaceborne communications at ELF/VLF to submerged submarines
p 3399 N93-30755

NATIONAL AERONAUTICS AND SPACE ADMINISTRATION. PASADENA OFFICE, CA.
Dual arm generalized compliant motion with shared control
[NASA-CASE-NPO-18738-1-CU] p 3443 N93-28954
A satellite-tracking millimeter-wave reflector antenna system for mobile satellite-tracking
[NASA-CASE-NPO-18772-1-CU] p 3381 N93-28955
Improved real-time imaging spectrometer
[NASA-CASE-NPO-18410-1-CU] p 3578 N93-29086
Miniature modular microwave end-to-end receiver
[NASA-CASE-NPO-18713-1-CU] p 3381 N93-29087
Three-parameter tunable Tilt-Integral-Derivative (TID) controller
[NASA-CASE-NPO-18492-1-CU] p 3542 N93-29176
Parallel inferencing method and apparatus for rule-based expert systems
[NASA-CASE-NPO-18004-1-CU] p 3521 N93-29504
Planar microstrip YAGI antenna array
[NASA-CASE-NPO-17873-2-CU] p 3384 N93-29507
Special purpose parallel computer architecture for real-time control and simulation in robotic applications
[NASA-CASE-NPO-17629-1-CU] p 3521 N93-29608
Wavelength-division multiplexed optical integrated circuit with vertical diffraction grating
[NASA-CASE-NPO-18357-1-CU] p 3579 N93-29848
Hidden Markov models for fault detection in dynamic systems
[NASA-CASE-NPO-18982-1-CU] p 3449 N93-30413
Tunable CW diode-pumped Tm,Ho:YLiF4 laser operating at or near room temperature
[NASA-CASE-NPO-18611-1-CU] p 3440 N93-30415
Virtual reality flight control display with six-degree-of-freedom controller and spherical orientation overlay
[NASA-CASE-NPO-18733-1-CU] p 3251 N93-30416

NATIONAL AEROSPACE LAB., AMSTERDAM (NETHERLANDS).
Overview of cockpit technology research and development programs for improvement of the man/machine interface: Review of the AGARD AVP Symposium held in Madrid, May 1992
p 3505 N93-28872
Transputers, parallel processing in embedded systems for image compression in space applications
[NLR-TP-89242-U] p 3522 N93-30840

NATIONAL BOARD OF WATERS AND THE ENVIRONMENT, HELSINKI (FINLAND).
Modelling the dynamics of a large sea area
[DE93-778330] p 3488 N93-30040

NATIONAL CENTER FOR ADVANCED TECHNOLOGIES, WASHINGTON, DC.
The NCAT process p 3626 N93-30697

NATIONAL CENTER FOR ATMOSPHERIC RESEARCH, BOULDER, CO.
Analysis of mass transport and potential vorticity budget in a simulated tropopausa folding
[PB93-156792] p 3476 N93-29197
Interactive interface to NCAR graphics
p 3614 N93-29237
Parcels with TAGS
[PB93-181824] p 3535 N93-30824

NATIONAL DEFENCE HEADQUARTERS, OTTAWA (ONTARIO).
Security of the remote control link of Anik E satellites
p 3365 N93-30282
Performance of frequency hopped M-ary FSK in Rayleigh fading and partial-band jamming p 3368 N93-30303

NATIONAL ENVIRONMENTAL SATELLITE SERVICE, SUITLAND, MD.
Data management in NOAA p 3617 N93-30454

NATIONAL ENVIRONMENTAL SATELLITE SERVICE, WASHINGTON, DC.
NOAA satellite programs and technology requirements
p 3627 N93-30710

NATIONAL HURRICANE CENTER, CORAL GABLES, FL.
Deadliest, costliest, and most intense US hurricanes of this century (and other frequently requested hurricane facts)
[PB93-174993] p 3485 N93-30758

NATIONAL INST. FOR FUSION SCIENCE, NAGOYA (JAPAN).
Development of high power microwave source
[DE93-753316] p 3436 N93-28980

NATIONAL INST. FOR RESEARCH IN INORGANIC MATERIALS, IBARAKI (JAPAN).
Study on diamond semiconductor
[DE92-531076] p 3413 N93-30622

NATIONAL INST. OF STANDARDS AND TECHNOLOGY, BOULDER, CO.
Tables of experimental data used for the correlation of the thermophysical properties of ethane
[PB93-173417] p 3313 N93-29768

NATIONAL INST. OF STANDARDS AND TECHNOLOGY, GAITHERSBURG, MD.
Estimation of droplet collision frequency in a spray
[DE93-007991] p 3416 N93-28566
A study of the chemical mechanism in lubrication
[DE93-012230] p 3330 N93-28650
Initial graphics exchange specification hybrid microcircuit application protocol
[PB93-175404] p 3407 N93-29203
Computer systems laboratory
[PB93-181873] p 3521 N93-29662
Programmer's reference guide to FDMS file formats
[PB93-182038] p 3354 N93-29663
Issues, concepts, and standard techniques in assessing accuracy of coordinate measuring machines
[PB93-184331] p 3354 N93-29666
Binocular spherical disparity: A study in representation for a forward translating camera
[PB93-184422] p 3579 N93-29667
Using synthetic-perturbation techniques for tuning shared memory programs
[PB93-178572] p 3539 N93-29677
Data probe user's guide
[PB93-178655] p 3530 N93-29678
Proceedings of the meeting of the Intergovernmental US-Russian Business Development Committee's Standards Working Group
[PB93-179968] p 3610 N93-30822
Minimum security requirements for multi-user operating systems
[PB93-185999] p 3522 N93-30832
Horizontal nucleate flow boiling heat transfer coefficient measurements and visual observations for R12, R134a, and R134a/ester lubricant mixtures
[PB93-178598] p 3475 N93-30887
Physics laboratory technical activities, 1992
[PB93-178648] p 3561 N93-30888

NATIONAL LAB. FOR HIGH ENERGY PHYSICS, TSUKUBA (JAPAN).
Non-perturbative calculation of equilibrium polarization of stored electron beams
[DE93-764500] p 3577 N93-30607

NATIONAL LIBRARY OF MEDICINE, BETHESDA, MD.
The Visible Human Project of the National Library of Medicine: Remote access and distribution of a multi-gigabyte data set p 3617 N93-30453

NATIONAL MEDIA LAB., SAINT PAUL, MN.
National Media Laboratory media testing results
p 3620 N93-30465
Evaluation of D-1 tape and cassette characteristics: Moisture content of Sony and Ampex D-1 tapes when delivered p 3435 N93-30466
National Media Laboratory p 3628 N93-30717
Technology transfer to the broader economy
p 3628 N93-30719

NATIONAL OCEAN SERVICE, ROCKVILLE, MD.
Standard and reference materials for marine science, third edition
[PB93-185684] p 3489 N93-30830

NATIONAL OCEANIC AND ATMOSPHERIC ADMINISTRATION, BOULDER, CO.
Rugged, no-moving-parts windspeed and static pressure probe designs for measurements in planetary atmospheres p 3434 N93-28767
Context switch time scalability: Benchmark results
[PB93-181832] p 3539 N93-29661
RTE: A UNIX library with on-line documentation and sample programs for microwave radiative transfer calculations
[PB93-180248] p 3386 N93-29680

NATIONAL OCEANIC AND ATMOSPHERIC ADMINISTRATION, MIAMI, FL.
Reception at Ascension Island, South Atlantic, of the transmissions from the Heard Island feasibility test
[PB93-176261] p 3394 N93-30662
Hydrographic observations in the western tropical and subtropical north Atlantic Ocean: Atlantic Climate Change Program (ACCP) and Western Tropical Atlantic Experiment (WESTRAX) during 1990
[PB93-184760] p 3489 N93-30827

NATIONAL OCEANIC AND ATMOSPHERIC ADMINISTRATION, SILVER SPRING, MD.
Vortex wake characteristics of B757-200 and B767-200 aircraft using the tower fly-by technique
[PB93-180255] p 3242 N93-30387
Vortex wake characteristics of B757-200 and B767-200 aircraft using the tower fly-by technique
[PB93-180263] p 3242 N93-30388

NATIONAL RESEARCH COUNCIL OF CANADA, OTTAWA (ONTARIO).
Improvement of the NRC automatic speech recognition system p 3355 N93-30221
On the implementation of the BIRIS range sensor for applications in robotic control and autonomous navigation p 3366 N93-30286
Applications of digital 3-D imaging
p 3366 N93-30287
Supervised autonomy in telerobotics
p 3372 N93-30326
A multiprocessor architecture for realtime robot control p 3372 N93-30327

Airborne data acquisition using a front-end processor architecture p 3373 N93-30329

NATIONAL SCIENCE COUNCIL, TAIPEI (TAIWAN).

Scientific research abstracts in the Republic of China, 1991 (science and technology) p 3670 N93-30911

NATIONAL SCIENCE FOUNDATION OF US, TOKYO (JAPAN).

NSF Tokyo reports: Japanese R and D projects on micro- and nanofabrication and related basic research projects
[PB93-181261] p 3410 N93-29671

NATIONAL SPACE DEVELOPMENT AGENCY, TOKYO (JAPAN).

Advanced Earth Observing Satellite (ADEOS) p 3279 N93-29648

Consultative Committee for Space Data Systems recommendation for space data system standards: Telecommand. Part 2.1: Command operation procedures
[NASA-TM-108158] p 3393 N93-30371

NATIONAL TELECOMMUNICATIONS AND INFORMATION ADMINISTRATION, BOULDER, CO.

Wideband propagation measurements for wireless indoor communication
[PB93-175123] p 3382 N93-29202

NATIONAL WEATHER SERVICE, BOHEMIA, NY.

Rhode Island hurricanes and tropical storms: A fifty-six year summary, 1936-1991
[PB93-162006] p 3481 N93-29198

NATIONAL WEATHER SERVICE, WASHINGTON, DC.

The 17th Annual Climate Diagnostics Workshop
[PB93-183895] p 3483 N93-29664

NAVAL ACADEMY, ANNAPOLIS, MD.

The effect of temperature on the impact behavior of TiB2 reinforced XDTM-TiAl intermetallic matrix composites
[AD-A262924] p 3296 N93-28886

High pressure studies of hydrated nafion membranes: Dielectric relaxation and deuteron NMR
[AD-A263511] p 3332 N93-29342

Effects of freeze/thaw cycles on hydrostatically conditioned E-glass/J-2 composite
[AD-A262980] p 3298 N93-29425

Mars Aquarius Mission and Titan Explorer p 3235 N93-29756

Synthesis and properties of a cation-conducting, high temperature polymer electrolyte
[AD-A263557] p 3334 N93-29825

Electrical relaxation in acid-form nafion
[AD-A263558] p 3410 N93-29826

The effect of oxidation embrittlement on the impact behavior of nicalon reinforced CAS 2 ceramic matrix composites
[AD-A263567] p 3334 N93-29829

NAVAL AIR SYSTEMS COMMAND, POINT MUGU, CA.

Tidal and lunar data for Point Mugu, San Nicolas island, and the Barking Sanda area during 1993
[AD-A262725] p 3477 N93-29401

NAVAL AIR WARFARE CENTER, CHINA LAKE, CA.

The 17th Annual Electronics Manufacturing Seminar proceedings
[AD-A261963] p 3409 N93-29435

NAVAL AIR WARFARE CENTER, TRENTON, NJ.

Determination of surface heat transfer and film cooling effectiveness in unsteady wake flow conditions p 3253 N93-29933

NAVAL COMMAND, CONTROL AND OCEAN SURVEILLANCE CENTER, SAN DIEGO, CA.

Advanced Unmanned Search System (AUSS) supervisory command, control and navigation
[AD-A263171] p 3245 N93-28990

Boron carbide aluminum cermets for external pressure housing applications
[AD-A262749] p 3333 N93-29404

Ocean aerosol measurements and models in the straits of Florida (The KEY-90 experiment)
[AD-A264777] p 3487 N93-29659

Dynamics and photoexcitation in MX and MXX' chain solids
[AD-A264823] p 3561 N93-29711

Triplet states and optical absorptions in finite polyenes and conjugated polymers
[AD-A264552] p 3337 N93-30381

An application protocol for CAD to CAD transfer of electronic information
[AD-A264554] p 3533 N93-30383

A testbed for autonomous reflexive grasping
[AD-A264557] p 3446 N93-30384

Photoinduced charge separation in Q1D heterojunction materials: Evidence for electron-hole pair separation in mixed-halide MX solids
[AD-A264711] p 3598 N93-30501

Extracting infinite system properties from finite size clusters: Phase randomization/boundary condition averaging
[AD-A264712] p 3551 N93-30503

A simple computational model of center-surround receptive fields in the retina
[AD-A264723] p 3496 N93-30515

Uplink laser propagation measurements through the sea surface, haze and clouds
[AD-A264687] p 3440 N93-30553

Measurement of electromagnetic properties of composite materials
[AD-A264725] p 3303 N93-30555

Photoinduced electron-hole charge separation, intrinsic self-doping and novel device applications of Q1D heterojunction materials: Mixed-halide MX solids
[AD-A264714] p 3600 N93-30569

Evolving neural network architecture
[AD-A264802] p 3544 N93-30592

Variability of the electric field strength in the earth-ionosphere waveguide due to variations in the electron density profile
[AD-A264808] p 3394 N93-30595

Elastic stability considerations for deep submergence ceramic pressure housing
[AD-A264824] p 3454 N93-30598

Laser based 3D volumetric display system
[AD-A264825] p 3441 N93-30599

Numerical modeling of the propagation medium at VLF/LF p 3395 N93-30729

VLF/LF propagation measurements p 3395 N93-30732

An algorithm for simple and complex feature detection: From retina to primary visual cortex
[AD-A264306] p 3497 N93-30897

Efficient laser action from two CW laser pumped pyrromethene-BF2 complexes
[AD-A264887] p 3441 N93-30910

Optimum design of multiwire cages for high-voltage applications
[AD-A264310] p 3400 N93-30995

NAVAL MEDICAL RESEARCH INST., BETHESDA, MD.

An assessment of peripheral nerve damage in the rat following non-freezing cold exposure: An electrophysiological and histopathological examination
[AD-A264293] p 3492 N93-30818

Hydrogen-rated system for in vitro studies at pressure: Operating procedures and emergency procedures
[AD-A264179] p 3497 N93-30882

NAVAL OCEANOGRAPHIC OFFICE, BAY SAINT LOUIS, MS.

A calibration procedure for the SBE 19 Conductivity, Temperature, and Depth (CTD) profiler
[AD-A264435] p 3489 N93-30420

NAVAL POSTGRADUATE SCHOOL, MONTEREY, CA.

The curvature of plane elastic curves
[AD-A263198] p 3450 N93-28516

Predicting radiation characteristics from antenna physical dimensions
[AD-A262462] p 3379 N93-28654

An analysis of the correlation between the J52 engine component improvement program and improved maintenance parameters
[AD-A262062] p 3251 N93-28984

Dynamic factorization in large-scale optimization
[AD-A263993] p 3528 N93-29345

Investigation of thermoacoustic muffler
[AD-A262009] p 3562 N93-29392

The sensitivity of ageostrophic circulations to model resolution: A case study using NGM forecasts of ERICA IOP-4
[AD-A262011] p 3482 N93-29393

The identification of early warning signals prior to contractor default
[AD-A262828] p 3609 N93-29433

Mathematical modeling and control law development for the atmospheric monitoring and control system of the Controlled Environment Research Chamber (CERC) at NASA Ames Research Center
[AD-A261978] p 3261 N93-29436

Using C-vector method to derive the three-dimensional circulation pattern near the East Greenland Polar Front
[AD-A261979] p 3487 N93-29437

Performance measurement systems: A best practices study
[AD-A262180] p 3506 N93-29444

Design of a high resolution spatial heterodyne interferometer
[AD-A262867] p 3285 N93-29461

Automated satellite image navigation
[AD-A262868] p 3269 N93-29475

Evaluating the bias of alternative cost progress models: Tests using aerospace industry acquisition programs
[AD-A262870] p 3624 N93-29477

FDDI installation and performance analysis
[AD-A263263] p 3529 N93-29497

Multipurpose satellite bus (MPS) p 3232 N93-29743

Investigations of self-pumped phase conjugate laser beams and coherence length
[AD-A263438] p 3438 N93-29789

Feature based neural network acoustic transient signal classification
[AD-A263437] p 3562 N93-29816

A water mass analysis of the 1991-1992 El Nino signal in the Farallon Islands region
[AD-A263490] p 3488 N93-29819

Magnetic field measurements of the CEBAF (NIST) wiggler using the pulsed wire method
[AD-A263997] p 3439 N93-29867

Widebanding techniques for VHF antennas 2
[AD-A263998] p 3387 N93-29882

Nonlinear mode coupling in free electron lasers
[AD-A263999] p 3439 N93-29883

Three-dimensional fiber-optic LDV measurements in the endwall region of a linear cascade of controlled-diffusion stator blades
[AD-A263513] p 3424 N93-29968

Preliminary development of a VTOL unmanned air vehicle for the close-range mission
[AD-A263514] p 3354 N93-29969

A concluding study of the altitude determination deficiencies of the Service Aircraft Instrumentation Package (SAIP)
[AD-A263515] p 3250 N93-29971

Analysis of a simulation of the seasonal cycle in the tropical Pacific Ocean in an eddy-resolving global ocean model
[AD-A264007] p 3488 N93-29977

A multilevel approach to minimum cost network flows
[AD-A264008] p 3550 N93-29978

A comparison of trans-equatorial ionosphere propagation predictions from AMBCOM with measured data
[AD-A264006] p 3391 N93-29987

Measurements of ocean currents across the continental margin off Point Sur, California, during March 1989
[AD-A264853] p 3489 N93-30178

Finite element approximation of the shallow water equations on the MASPAR
[AD-A264649] p 3489 N93-30525

A prototype of a faculty and staff executive information system
[AD-A264852] p 3623 N93-30907

NAVAL RESEARCH LAB., BAY SAINT LOUIS, MS.

ARSRP signal processing software
[AD-A263543] p 3391 N93-29975

NAVAL RESEARCH LAB., MONTEREY, CA.

Leadex data report. Part 1: Weather analysis and satellite images
[AD-A263217] p 3481 N93-28876

Leadex data report. Part 2: Rawinsonde and ice station data
[AD-A263218] p 3483 N93-29491

NAVAL RESEARCH LAB., WASHINGTON, DC.

Ion-beam-assisted deposition of wear-resistant coatings
[DE93-011529] p 3330 N93-28687

The Ultraviolet Plume Instrument (UVPI) p 3285 N93-28784

Filtering interpolators for image comparison algorithms p 3463 N93-28797

The Backgrounds Data Center p 3624 N93-28814

Study of gain in C-band deflection cavities for a frequency-doubling magnicon amplifier
[AD-A263132] p 3409 N93-29478

Progress report on the Heavy Ions in Space (HIIS) experiment p 3573 N93-29645

Future radiation measurements in low Earth orbit p 3654 N93-29708

A parallel implicit incompressible flow solver using unstructured meshes
[AD-A263395] p 3424 N93-29851

Ion emission during high-energy sputtering of ammonium dinitramide and ammonium nitrate crystals and the determination of ion decomposition pathways using tandem mass spectrometry p 3318 N93-30066

Chemical dynamics simulations as a probe to the initiation and propagation of condensed phase detonations p 3318 N93-30071

Molecular dynamics of detonation in crystals with defects p 3350 N93-30097

Rate constant determinations of reactions H + HNO from ab initio reaction path calculations p 3319 N93-30099

Shock waves and polymorphic phase transitions in energetic materials p 3351 N93-30100

Characteristics of high-frequency signals, noise, availability, and duration of bandwidths based on ROTHR Amchitka spectrum measurements
[AD-A264480] p 3393 N93-30423

NAVAL SUBMARINE MEDICAL RESEARCH LAB., GROTON, CT.

Conspicuity of aids to navigation. Part 1: Temporal patterns for flashing lights
[AD-A264626] p 3499 N93-30426

NAVAL SURFACE WARFARE CENTER, BETHESDA, MD.

Processing and property evaluation of silver or aluminum matrix YBa2Cu3O(6+x) superconducting materials
[AD-A263382] p 3595 N93-29333

Properties of superconducting YBa2Cu3O(6+4) ceramic materials: Effect of processing parameters
[AD-A263441] p 3334 N93-29790

Unsteady vortex loop/dipole theory applied to the work and acoustics of an ideal low speed propeller
[AD-A264057] p 3241 N93-29891

Effect of water immersion on fiber/matrix adhesion in thermoplastic composites
[AD-A263646] p 3299 N93-29984

Some implications of a differential turbomachinery equation with viscous correction
[AD-A264693] p 3427 N93-30571

Evaluation of the scattered pressure due to infinite rigid cylinders, infinite elastic cylindrical shells, and rigid spheres in the presence of an ambient noise field
[AD-A264835] p 3563 N93-30899

NAVAL SURFACE WARFARE CENTER, DAHLGREN, VA.

High-voltage pulse generator capable of 2000 J at 10 kV
[AD-A262034] p 3407 N93-28999

An explosively actuated electrical switch using Kapton insulation
[AD-A263835] p 3411 N93-30021

The measurement of electrical conductivity in detonating condensed explosives
[AD-A264482] p 3352 N93-30424

NAVAL SURFACE WARFARE CENTER, SILVER SPRING, MD.

Zero-crossing rate of some non-Gaussian processes
p 3360 N93-30254

NAVAL SURFACE WEAPONS CENTER, SILVER SPRING, MD.

Defect density measurements in a shocked single crystal of ammonium perchlorate p 3319 N93-30093

Comparison of deformation and shock reactivity for single crystals of RDX and ammonium perchlorate
p 3350 N93-30094

NAVAL UNDERSEA WARFARE CENTER, NEW LONDON, CT.

A complete set of field equations for the dynamic simulation of a towed cable system
[AD-A262570] p 3442 N93-28578

ELF propagation highlights p 3395 N93-30730

Pattern measurements of US Navy ELF antennas
p 3399 N93-30752

NAVAL UNDERWATER SYSTEMS CENTER, NEW LONDON, CT.

Results of the joint HIPAS/NUWC campaigns to investigate ELF generated by auroral electrojet modulation p 3398 N93-30746

NAVAL WAR COLL., NEWPORT, RI.

The environment as an operational center of gravity
[AD-A264170] p 3472 N93-30154

Managing operational intelligence overload: Guidelines for avoiding decision paralysis
[AD-A264184] p 3610 N93-30158

NAVY PERSONNEL RESEARCH AND DEVELOPMENT CENTER, SAN DIEGO, CA.

Review of the effectiveness of video media in instruction
[AD-A264228] p 3392 N93-30362

Independent research and independent exploratory development programs
[AD-A264735] p 3544 N93-30556

NEBRASKA UNIV., LINCOLN.

Polar order and relaxation of second order nonlinear optical susceptibility in an electric field polarized amorphous polymer
[AD-A262189] p 3329 N93-28489

Dipolar orientational relaxation in guest/host amorphous polymer probed by second harmonic generation
[AD-A262006] p 3333 N93-29441

Isothermal annealing and relaxation of the second harmonic generation signal from a nonlinear optical polymer
[AD-A262007] p 3333 N93-29442

NESTE OY, HELSINKI (FINLAND).

New hydrogen technologies
[DE93-778353] p 3343 N93-30042

NEVADA UNIV., LAS VEGAS.

Tank issues: Design and placement of floating liquid monitoring wells
[PB93-161149] p 3469 N93-29033

Tank issues: Site characterization for external leak monitoring
[PB93-161156] p 3469 N93-29034

NEW ENERGY AND INDUSTRIAL TECHNOLOGY DEVELOPMENT ORGANIZATION, TOKYO (JAPAN).

Assessment of energy technologies contributing to environmental conservation
[DE93-781439] p 3468 N93-28882

Study on technology for effective utilization of carbon dioxide in view of global environment
[DE93-781440] p 3468 N93-28883

Trend survey on the elucidation of the global warming mechanism by the governments of major industrialized nations
[DE93-776427] p 3470 N93-29672

NEW HAMPSHIRE UNIV., DURHAM.

A search for radiative neutrino decay from supernovae
[NASA-CR-193118] p 3653 N93-30052

NEW MEXICO INST. OF MINING AND TECHNOLOGY, SOCORRO.

Report on the sintering and properties of MgO and MgO-5 percent TiC
[DE93-008676] p 3323 N93-29092

Thermal decomposition of nitramines
p 3318 N93-30065

Detonation shock dynamics of composite energetic materials p 3350 N93-30096

Whisker toughening of ceramic materials: A review
[DE93-011565] p 3336 N93-30129

NEW MEXICO STATE UNIV., LAS CRUCES.

Multisensor image analysis system
[AD-A263679] p 3528 N93-29294

NEW MEXICO UNIV., ALBUQUERQUE.

Discharge of electrically charged clouds
[AD-A263212] p 3480 N93-28518

The investigation of nonlinear effects on quasiparticle transport in condensed matter systems
[DE93-009582] p 3565 N93-28914

New Mexico Center for Particle Physics: Studies of fundamental interactions
[DE93-008302] p 3566 N93-29261

Scanning probe lithography. Part 1: Scanning tunneling microscope-induced lithography of self-assembled n-alkanethiol monolayer resists
[AD-A263130] p 3432 N93-29476

The mechanical response of gold substrates modified with self-assembling monolayer films
[AD-A262997] p 3452 N93-29515

Taguchi method of experimental design in materials education p 3294 N93-30975

Powder metallurgy: Solid and liquid phase sintering of copper p 3294 N93-30976

NEW ORLEANS UNIV., LA.

Applications of density functional theory to calculation of reaction energetics p 3351 N93-30098

NEW SOUTH WALES UNIV., KENSINGTON (AUSTRALIA).

Comparison of specificity and information for fuzzy domains p 3510 N93-29519

The IUTAM Symposium on Breaking Waves
[AD-A264196] p 3489 N93-30143

NEW YORK MEDICAL COLL., NY.

Biophysical and biochemical mechanisms in synaptic transmitter release
[AD-A264829] p 3496 N93-30613

NEW YORK UNIV., NEW YORK.

Solar flare MDH
[AD-A262275] p 3652 N93-28756

A survey of problems in divertor and edge plasma theory
[DE93-007531] p 3586 N93-29056

Multiresolution analysis of SAR data
[AD-A264727] p 3393 N93-30576

NEW YORK UNIV. MEDICAL CENTER.

Computing with neural maps: Application to perceptual and cognitive function
[AD-A264056] p 3499 N93-30033

NIELSEN ENGINEERING AND RESEARCH, INC., MOUNTAIN VIEW, CA.

Methods for reducing turbulent flow aero-optical distortion
[AD-A263698] p 3423 N93-29353

NIJMEGEN UNIV. (NETHERLANDS).

The meta model hierarchy: A framework for information systems concepts and techniques
[TR-92-17] p 3611 N93-28481

Concurrent clean language manual, version 0.8
[TR-92-18] p 3522 N93-28482

The concurrent clean system user's manual and PABCstat user's manual, version 0.8
[TR-92-19] p 3523 N93-28484

Formal definition of a conceptual language for the description and manipulation of information models
[TR-92-16] p 3523 N93-28503

NORFOLK STATE UNIV., VA.

Polarization experiments with hadronic and electromagnetic probes
[DE93-011375] p 3392 N93-30126

Materials education activities p 3291 N93-30958

NORTH CAROLINA AGRICULTURAL AND TECHNICAL STATE UNIV., GREENSBORO.

Improved measurement of thermal effects on microstructure p 3292 N93-30959

NORTH CAROLINA STATE UNIV., RALEIGH.

Growth, characterization and device development in monocrystalline diamond films
[AD-A263204] p 3593 N93-28874

Nonlinear relaxation algorithms for the compressible Navier-Stokes equations in two and three dimensions
p 3421 N93-29177

Nuclear structure research at the Triangle Universities Nuclear Laboratory
[DE93-009756] p 3566 N93-29184

Atomic layer epitaxy of semiconductor heterostructures
[AD-A264755] p 3599 N93-30560

Ice-ocean four dimensional structure and dynamics
[AD-A264850] p 3490 N93-30906

The characterization of materials using x ray diffraction p 3293 N93-30968

NORTH CAROLINA UNIV., CHAPEL HILL.

The use of objective prism radial velocities for kinematic studies of galactic populations p 3633 N93-28672

Multifractal analysis of radio lobes
p 3380 N93-28689

NORTH CAROLINA UNIV., CHARLOTTE.

Iterative encoding methods for computer generated holograms
[AD-A263705] p 3431 N93-29297

Character recognition using a neural network model with fuzzy representation p 3512 N93-29536

NORTHEASTERN UNIV., BOSTON, MA.

Topics in gauge theories and the unification of elementary particle interactions
[DE93-009370] p 3563 N93-28542

Interfacial viscosity measurements of adsorbed monolayers on metal surfaces
[AD-A263288] p 3324 N93-29803

NORTHROP CORP., HAWTHORNE, CA.

F-15 composite engine access door
p 3302 N93-30442

Lessons learned for composite structures
p 3302 N93-30444

Effects of scale in predicting global structural response p 3306 N93-30860

A Rayleigh-Ritz analysis methodology for cutouts in composite structures p 3307 N93-30869

Prediction of stiffener-skin separation in composite panels p 3307 N93-30871

NORTHWEST RESEARCH ASSOCIATES, INC., BELLEVUE, WA.

Laboratory studies of gravity wave/mean flow interactions
[AD-A264226] p 3478 N93-30174

NORTHWESTERN UNIV., EVANSTON, IL.

Supported organometallic complexes, surface chemistry, spectroscopy, and catalysis
[DE93-011930] p 3309 N93-28688

Transformation plasticity in ductile solids
[DE93-008636] p 3321 N93-28902

Bainitic stabilization of austenite in low alloy steels
[DE93-008275] p 3321 N93-28957

Tailored interfaces for metal-matrix composites-fundamental considerations
[AD-A263048] p 3298 N93-29130

Organometallic and surface chemistry of mixed-metal systems
[DE93-012686] p 3325 N93-30059

Center for surface radiation damage studies
[AD-A264330] p 3570 N93-30366

Complex dielectric function of amorphous diamond films deposited by pulsed excimer (ArF) laser ablation of graphite
[AD-A264527] p 3598 N93-30408

Diamond nucleation of surfaces using carbon clusters
[AD-A264634] p 3599 N93-30548

NORTON CO., NORTHBORO, MA.

High thermal conductivity of diamond
p 3294 N93-30977

NOTRE DAME UNIV., IN.

An autonomous vision-based mobile robot
p 3443 N93-29082

Vision-based control of holonomic robots for 3-dimensional rigid-body positioning using camera-space manipulation p 3578 N93-29178

Evolution of flow disturbances in cocurrent gas-liquid flows
[DE93-010083] p 3422 N93-29326

Design study to simulate the development of a commercial transportation system p 3228 N93-29718

Theoretical studies in nuclear structure
[DE93-012290] p 3570 N93-30505

Structural design using neural networks
p 3545 N93-31029

NOTTINGHAM UNIV. (ENGLAND).

The swollen polymer technique and its use for heat transfer investigations on film cooled surfaces p 3255 N93-29944

NOVA SCOTIA TECHNICAL COLL., HALIFAX.

An adaptive controller for a class of MIMO non-minimum phase systems with disturbance rejection design p 3359 N93-30248

NYNEX SCIENCE AND TECHNOLOGY, INC., WHITE PLAINS, NY.

Some problems with the design of self-learning management systems p 3516 N93-29559

O

OAK RIDGE K-25 SITE, TN.

Security classification of information [DE93-012416] p 3612 N93-28840

OAK RIDGE NATIONAL LAB., TN.

ORNL superconducting technology program for electric energy systems [DE93-009588] p 3404 N93-28523

Process optimization of Hexoloy SX-SiC towards improved mechanical properties [DE93-007913] p 3320 N93-28564

New remote maintenance approach for TPX [DE93-007857] p 3584 N93-28583

Environmental embrittlement of binary and Zr-doped Ni3Al [DE93-008575] p 3321 N93-28679

Introductions to the Proceedings of the Fourteenth Symposium on Biotechnology for Fuels and Chemicals [DE93-006235] p 3490 N93-28890

Neural network simulations on massively parallel computers: Applications in chemical physics [DE93-006739] p 3538 N93-28894

Neutron scattering studies of the structures and lattice dynamics of the alkali metals [DE93-008272] p 3593 N93-28956

Inservice diagnostic methods for solenoid-operated valves [DE93-007823] p 3443 N93-28968

State of the art: Ecological biomarkers [DE93-006621] p 3469 N93-28992

Robotics and artificial intelligence for hazardous environments [DE93-008271] p 3541 N93-29047

Wavelet transform techniques and signal analysis [DE93-007919] p 3382 N93-29244

A manipulator kinematic design for high-vacuum operation [DE93-010264] p 3444 N93-29247

A portable modular architecture for robotic manipulator control [DE93-010819] p 3444 N93-29254

Remote vehicle survey tool [DE93-010822] p 3460 N93-29255

An architecture for robotic system integration [DE93-010829] p 3444 N93-29316

Leaky coaxial cable signal transmission for remote facilities [DE93-007916] p 3383 N93-29348

Microwave processing of silicon nitride for advanced gas turbine applications [DE93-007910] p 3334 N93-29767

Low temperature environmental embrittlement in ordered intermetallics [DE93-009711] p 3324 N93-29786

Some effects of composition and microstructure on the B2 in equilibrium to DO3 ordered phase transition in Fe3Al alloys [DE93-009724] p 3325 N93-29813

What's past is prologue: Supporting global change research with historical data [DE93-005777] p 3472 N93-30009

The drive to cost-effective structural ceramics [DE93-009722] p 3335 N93-30047

Characterization of ceramic composite materials for gas turbine applications [DE93-009719] p 3259 N93-30168

Pollution prevention: A regulatory update [DE93-009727] p 3472 N93-30180

Development of adherent ceramic coatings to reduce contact stress damage of ceramics [DE93-012518] p 3336 N93-30182

Input relegation control for gross motion of a kinematically redundant manipulator [DE93-005301] p 3446 N93-30210

Stress-intensity-factor influence coefficients for axial and circumferential flaws in reactor pressure vessels [DE93-006206] p 3454 N93-30213

A video transmission system for low-bandwidth remote driving [DE93-010275] p 3544 N93-30529

Radiation-hardened microwave communications system [DE93-007915] p 3394 N93-30631

Reactive sintering of Ni3Al intermetallic alloys under compressive stress [DE93-009729] p 3327 N93-30652

OAK RIDGE Y-12 PLANT, TN.

Design and evaluation of a uniaxial pull test for lithium hydride/deuteride [DE93-010760] p 3451 N93-28832

ODESSA INST. OF NATIONAL ECONOMY (UKRAINE).

Fuzzy forecasting and decision making in short dynamic time series p 3513 N93-29541

OFFICE NATIONAL D'ETUDES ET DE RECHERCHES AEROSPATIALES, BAGNEUX (FRANCE).

Aerothermic calculations of flows in interdisc cavities of turbines p 3256 N93-29947

OFFICE NATIONAL D'ETUDES ET DE RECHERCHES AEROSPATIALES, PARIS (FRANCE).

Development of a 3-D Implicit Euler Code for Hypersonic and High Supersonic Flows [ONERA-RSF-23/1123-AY-230A] p 3417 N93-28744

Numerical simulation of perfect fluid flows around complex 3D configurations by a multidomain solver using the MUSCL approach p 3417 N93-28745

System of navigation by satellites with European coverage p 3284 N93-29897

Calculations of reactive turbulent flows in aeronautical chambers p 3257 N93-29956

Scattering through apertures and by three-dimensional structures. Application to the measurement of the surface impedance of conductive materials [ONERA-P-1990-2] p 3392 N93-30018

Sonic boom problem for future highspeed aircraft [ONERA-NT-1990-3] p 3241 N93-30020

Determination of the space charge distribution within an e-irradiated polymer using the pressure wave propagation method [ONERA-P-1990-4] p 3335 N93-30024

In-situ temperature and concentration measurements of organosilicon decomposition in a chemical vapor deposition reactor [ONERA-P-1990-3] p 3313 N93-30109

Computation of far-field helicopter rotor tone noise [ONERA-P-1990-5] p 3562 N93-30110

Study of codeposition of aluminum-haffnium and deposition of yttrium by the cementation technique: Elaboration of Ni-Cr-Al and Ni-Cr-Al-Hf felt materials [ONERA-NT-1990-9] p 3336 N93-30112

Difference methods for hyperbolic problems with emphasis on space-centered approximations [ONERA-NT-1990-4] p 3550 N93-30136

Plastic deformation behaviour of oxide dispersion strengthened titanium alloys [ONERA-NT-1990-6] p 3326 N93-30138

Scanning ionic microscopy with high spatial resolution: Parallel acquisition of elementary images by high resolution mass spectrometry [ONERA-NT-1990-7] p 3314 N93-30139

Contribution to the study of the interaction between acoustic waves and coherent structures induced by a prismatic cylinder in a rectangular cavity [ONERA-NT-1990-10] p 3314 N93-30203

OFFICE OF NAVAL RESEARCH, ARLINGTON, VA.

Cognitive and Neural Sciences Division 1992 programs [AD-A263400] p 3654 N93-29258

Ocean waves in SAMSON/SWADE [AD-A263681] p 3487 N93-29295

Oceanographic research towers in european waters [AD-A264795] p 3489 N93-30612

OFFICE OF SCIENCE AND TECHNOLOGY, WASHINGTON, DC.

White House/OSTP perspective p 3625 N93-30696

OFFICE OF TECHNOLOGY ASSESSMENT, WASHINGTON, DC.

Defense conversion: Redirecting research and development [OTA-ITE-552] p 3610 N93-29649

Advanced network technology: Background paper [OTA-BP-TCT-101] p 3539 N93-29650

The 1992 World Administrative Radio Conference: Technology and Policy Implications [OTA-TCT-549] p 3392 N93-30150

Profiles of major federal literacy programs [PB93-163863] p 3608 N93-30657

OFFICE OF THE SECRETARY OF DEFENSE, WASHINGTON, DC.

Strategic Environmental Research and Development Program (SERDP) [AD-A263745] p 3471 N93-29858

OFFICE OF THE UNDER SECRETARY OF DEFENSE (ACQUISITIONS), WASHINGTON, DC.

Department of defense advisory group on electron devices: Appendix to special technology area review on microwave packaging technology [AD-A262136] p 3408 N93-29408

OHIO AEROSPACE INST., BROOK PARK.

Navier-Stokes analysis of radial turbine rotor performance [NASA-CR-191153] p 3251 N93-28609

Analysis of unsteady wave processes in a rotating channel [NASA-CR-191154] p 3251 N93-28617

Three-dimensional numerical simulation of gradual opening in a wave rotor passage [NASA-CR-191157] p 3252 N93-29072

OHIO STATE UNIV., COLUMBUS.

Regulation of alternative CO2 fixation pathways in procaryotic and eucaryotic photosynthetic organisms [DE93-012109] p 3491 N93-29181

Multiple image multipoint matching for automatic aerotriangulation p 3461 N93-29615

The design of two-stage-to-orbit vehicles p 3228 N93-29719

Project WISH: The Emerald City p 3232 N93-29744

Multiwavelength studies of classical nova shells p 3636 N93-30412

OKLAHOMA STATE UNIV., STILLWATER.

Final results of space exposed experiment developed for students p 3492 N93-29702

OLD DOMINION UNIV., NORFOLK, VA.

Nonlinear analyses of composite aerospace structures in sonic fatigue [NASA-CR-193124] p 3451 N93-29154

Radiative interactions in molecular gases under local and nonlocal thermodynamic equilibrium conditions [NASA-CR-193223] p 3604 N93-29168

Resource utilization model for the algorithm to architecture mapping model [NASA-CR-193122] p 3527 N93-29171

Building a generalized distributed system model [NASA-CR-193239] p 3527 N93-29219

From orbital debris capture systems through internal combustion engines on Mars p 3232 N93-29745

Topology and grid adaption for high-speed flow computations [NASA-CR-4216] p 3426 N93-30375

OPTEX, INC., ROCKVILLE, MD.

Electron trapping data storage system and applications p 3622 N93-30474

OPTRA, INC., BEVERLY, MA.

Enhanced noncontacting laser extensometer for biaxial strain measurements [AD-A263170] p 3430 N93-28989

ORA CORP., ITHACA, NY.

Using Penelope to assess the correctness of NASA Ada software: A demonstration of formal methods as a counterpart to testing [NASA-CR-4509] p 3533 N93-30380

ORBITAL SCIENCES CORP., CHANTILLY, VA.

Spacecraft and launch systems for TACSAT applications p 3284 N93-29904

ORCON CORP., UNION CITY, CA.

Lightweight flexible composite tent materials [AD-A263021] p 3295 N93-28660

OREGON GRADUATE CENTER FOR STUDY AND RESEARCH, BEAVERTON.

Membrane-based photochemical systems as models for photosynthetic cells [DE93-009758] p 3310 N93-28911

OREGON INST. OF TECH., KLAMATH FALLS.

Direct use geothermal applications for brazed plate heat exchangers [DE93-008559] p 3465 N93-30011

OREGON STATE UNIV., NEWPORT.

Parallel processing and learning: Variability and chaos in self-organization of activity in groups of neurons [AD-A264224] p 3539 N93-30361

OREGON UNIV., EUGENE.

Dynamical analysis of highly excited molecular spectra [DE93-010771] p 3564 N93-28604

Task A: Theory of elementary particles [DE93-010561] p 3569 N93-29841

Multidimensional intermittency in hadronic collisions [DE93-010562] p 3577 N93-30532

OSLO UNIV. (NORWAY).

Electrodynamics of the dayside cleft region based on ground observations at Svalbard [AD-A263571] p 3477 N93-29831

OTTAWA UNIV. (ONTARIO).

Nonlinear processing of phase vocoded speech p 3355 N93-30219

A motion detector based on a neural network p 3356 N93-30224

Performance analysis of communication protocols using D-timed Petri net p 3356 N93-30227

Automatic synthesis of protocol specifications
p 3356 N93-30228

Tactile sensing for 3-dimensional shape estimation
p 3357 N93-30232

Optimal filtering and LQR theory with constraints on system and control matrices p 3357 N93-30234

Vibration control of flexible space structures in noisy environment p 3285 N93-30235

Feature segmentation using a multiple-stack based chain coding algorithm p 3359 N93-30243

Robust boundary control of flexible structures governed by hybrid dynamics p 3285 N93-30249

Analytical predictions of the intermodulation noise of semiconductor laser diode p 3361 N93-30256

Recognizing partially overlapping objects
p 3366 N93-30289

Communications systems design for testability: Grey-box testing p 3368 N93-30302

Progress in the development of broadband electric-field sensors for transient fields p 3369 N93-30306

Trajectory generation for dual-arm robots using artificial impedance approach p 3370 N93-30310

Comparison of multiple access techniques for bandwidth limited land-mobile satellite communications
p 3370 N93-30314

OXFORD UNIV. (ENGLAND).

Coarse image motion for saccade control
[OUEL-1916/92] p 3523 N93-28485

Recognizing parameterized objects from range data
[OUEL-1918/92] p 3523 N93-28486

Balanced approximation can be optimal
[OUEL-1950/92] p 3548 N93-28754

A corner matching and tracking strategy applied to videophony
[OUEL-1933/92] p 3380 N93-28896

A modular head/eye platform for real-time reactive vision
[OUEL-1941/92] p 3505 N93-28897

Stabilization using low-gain PI control: SISO case
[OUEL-1947/92] p 3541 N93-28898

Measurement of turbulent spots and intermittency modelling at gas-turbine conditions
p 3253 N93-29934

Fundamental studies of impingement cooling thermal boundary conditions p 3254 N93-29940

P

PACIFIC NORTHWEST LAB., RICHLAND, WA.

Deformation mechanisms in Be(sub 12)X compounds
[DE93-009080] p 3320 N93-28548

A demonstration of simple airfoils: Structural design and materials choices
[DE93-007882] p 3238 N93-28662

Overview of piping issues and trends
[DE93-006628] p 3354 N93-28893

Operational results of pilot cell test with cermet inert anodes
[DE93-009338] p 3322 N93-29061

Materials characterization of cermet anodes tested in a pilot cell
[DE93-008924] p 3323 N93-29101

A four-field approach towards developing a mechanistic model for multiphase flow
[DE93-006572] p 3420 N93-29126

Stabilized platform for tethered balloon soundings of broadband long- and short-wave radiation
[DE93-007876] p 3383 N93-29308

Technology transfer personnel exchange at the Boeing Company
[DE93-010190] p 3625 N93-29329

Sensitivity of LDEF foil analyses using ultra-low background germanium vs. large NaI(Tl) multidimensional spectrometers p 3318 N93-29627

Advances in the identification of electrochemical transfer function models using Prony analysis
[DE93-009424] p 3550 N93-30041

Case study of Frontal Boundary Study Mission 03
[DE93-007176] p 3473 N93-30183

PACIFIC-SIERRA RESEARCH CORP., SANTA MONICA, CA.

A long wave TE/TM noise prediction model
p 3397 N93-30742

PARIS VI UNIV. (FRANCE).

Optimism experiment and development of space-qualified seismometers in France
p 3646 N93-28796

PARIS XI UNIV., ORSAY (FRANCE).

In orbit degradation of EUV optical components in the wavelength range 10-40 nm AO 138-3
p 3582 N93-29691

PARK SEED CO., INC., GREENWOOD, SC.

Continued results of the seeds in space experiment
p 3492 N93-29703

PENNSYLVANIA STATE UNIV., UNIVERSITY PARK.

The temperature dependence of the deformation and oxidation behavior of an age-hardenable beta + alpha-two titanium alloy
[AD-A262232] p 3320 N93-28491

Fundamental aspects in the design of passive alloys
[DE93-009028] p 3320 N93-28545

Analysis for thermo-chemical decomposition of composite structures
[NASA-CR-193185] p 3295 N93-28843

What is underneath? Moving atoms and molecules to find out
[AD-A263363] p 3567 N93-29332

Proceedings of the 25th European Conference on the Application of Polar Dielectrics to celebrate the 25th anniversary of the Dielectric Society, incorporating the 1st International Workshop on Integrated Ferroelectrics
[AD-A263427] p 3332 N93-29337

FI-STM investigation of atomic hydrogen adsorption on the Si(100)2x1 surface
[AD-A262748] p 3567 N93-29403

The 2nd International symposium on electrochemical impedance spectroscopy (extended abstracts)
[AD-A262994] p 3312 N93-29462

Crystallization of nanocomposite glasses made by the SSG process
[AD-A262892] p 3333 N93-29511

Mars sample return mission: Two alternate scenarios
p 3233 N93-29746

Mechanisms of fracture and creep of structural alloys
[AD-A263108] p 3324 N93-29799

Observation of phase-separated nanometer scale molecular domains in mixed self-assembled monolayers
[AD-A263470] p 3569 N93-29839

Determination of gas phase species and temperature profiles above solid propellants p 3346 N93-30080

Materials for adaptive structural acoustic control, volume 1
[AD-A264619] p 3562 N93-30121

Materials for adaptive structural acoustic control, volume 2
[AD-A264620] p 3563 N93-30385

Detailed studies of soot formation in laminar diffusion flames for application to modeling studies
[AD-A264827] p 3317 N93-30667

Water-soluble polyphosphazenes and their hydrogels
[AD-A264883] p 3340 N93-30909

New materials: Fountainhead for new technologies and new science p 3291 N93-30952

PENNSYLVANIA UNIV., PHILADELPHIA.

Catalytic synthesis of silicon carbide preceramic polymers: Polycarbosilanes
[DE93-008634] p 3329 N93-28541

The dynamics of visual representation, attention, encoding, and retrieval processes
[AD-A264674] p 3500 N93-30543

NATO Advanced Research Workshop on Frontiers of Optical Phenomena in Semiconductor Structure of Reduced Dimension
[AD-A264813] p 3581 N93-30666

Fluids in porous media.
[PB93-175198] p 3428 N93-30759

PENNY AND GILES DATA RECORDERS LTD. (ENGLAND).

The modern high rate digital cassette recorder
p 3435 N93-30468

PHILLIPS LAB., EDWARDS AFB, CA.

Specific impulse calculations of high energy density solid cryogenic rocket propellants. 1. Atoms in solid H2
[AD-A263208] p 3341 N93-28517

ELITE program: Electric insertion transfer experiment
p 3264 N93-28709

PHILLIPS LAB., HANSCOM AFB, MA.

The Mechanisms of Solar Variability (MSV) program
[AD-A262525] p 3652 N93-28585

Adaptive structures flight experiments
p 3263 N93-28704

Sodium sulfur technology program NaSTEC
p 3265 N93-28718

STRV1-b flight experiment p 3265 N93-28723

NEP space test program objective
p 3265 N93-28724

Modeling the bidirectional reflectance and spectra
[AD-A263570] p 3462 N93-29830

Wind measurement accuracy of a loran radiosonde
[AD-A263572] p 3483 N93-29832

Cloud Impacts on DOD Operations and Systems Conference (CIDOS-91)
[AD-A264463] p 3484 N93-30535

Performance statistics bulletin. High latitude meteor scatter propagation, May, June, July 1989
[AD-A264003] p 3399 N93-30757

PHILLIPS LAB., KIRTLAND AFB, NM.

Degradation of optical components in a space environment p 3582 N93-29692

Characterization of a space orbited incoherent fiber optic bundle p 3583 N93-29698

Analyses of space environment effects on active fiber optic links orbited aboard the LDEF
p 3583 N93-29699

Vortex shedding by blunt/bluff bodies at high Reynolds numbers. Volume 4: Rectangles
[AD-A264154] p 3241 N93-30151

Vortex shedding by blunt/bluff bodies at high reynolds numbers. Volume 1: Data analysis
[AD-A264151] p 3241 N93-30171

Vortex shedding by Blunt/Bluff bodies at high reynolds numbers. Volume 2: Cylinders, octagon, hexagon
[AD-A264152] p 3241 N93-30172

Vortex shedding by blunt/bluff bodies at high reynolds numbers. Volume 3. Cubes
[AD-A264153] p 3242 N93-30173

Technology transfer within the government
p 3627 N93-30711

PHYSICAL SCIENCES, INC., ANDOVER, MA.

Low Earth orbital mission aboard the Space Test Experiments Platform (STEP-3) p 3267 N93-28732

Lightweight modular instrumentation for planetary applications p 3286 N93-28787

PITTSBURGH UNIV., PA.

Studies of relativistic heavy ion collisions at the AGS (E814/E877)
[DE93-008541] p 3564 N93-28678

Platinum-modified diffusion aluminide coatings on nickel-base superalloys
[AD-A263597] p 3325 N93-29981

A novel process for methanol synthesis
[DE93-013070] p 3314 N93-30188

Surface chemistry of hydrogen-passivated porous silicon-oxidation of surface Si-H groups by acetone
[AD-A264655] p 3315 N93-30526

POD ASSOCIATES, INC., ALBUQUERQUE, NM.

Damage areas on selected LDEF aluminum surfaces
p 3283 N93-29374

LDEF data: Comparisons with existing models
p 3283 N93-29375

POHANG INST. OF SCIENCE AND TECHNOLOGY (REPUBLIC OF KOREA).

Inference in fuzzy rule bases with conflicting evidence
p 3519 N93-29583

POITIERS UNIV. (FRANCE).

Experimental study of heat transfer close to a plane wall heated in the presence of multiple injections (subsonic flow) p 3253 N93-29931

POLISH ACADEMY OF SCIENCES, WARSAW.

Bifurcations phenomena in a nonlinear oscillator: Approximate analytical studies versus computer simulation results p 3407 N93-29037

Experimental and theoretical aspects of excited state electron transfer and related phenomena
[AD-A263457] p 3570 N93-30589

POLITECNICO DI MILANO (ITALY).

A Navier-Stokes solver with different turbulence models applied to film-cooled turbine cascades
p 3258 N93-29962

PORTO UNIV. (PORTUGAL).

Application of the Fourier transform to short antennas
p 3398 N93-30750

PRAIRIE VIEW AGRICULTURAL AND MECHANICAL COLL., TX.

Mars habitat p 3233 N93-29747

PRATT AND WHITNEY AIRCRAFT, WEST PALM BEACH, FL.

Advanced engine study program
[NASA-CR-187217] p 3287 N93-28946

PRATT AND WHITNEY AIRCRAFT OF CANADA LTD., LONGUEUIL (QUEBEC).

Prediction of jet impingement cooling scheme characteristics (airfoil leading edge application)
p 3255 N93-29941

PRINCETON SYNERGETICS, INC., NJ.

Technology transfer within the government
p 3627 N93-30709

PRINCETON UNIV., NJ.

Kinetic studies on gas-phase reaction mechanisms important to the combustion of energetic materials: The CO/N2O reaction p 3347 N93-30084

Homogeneous gas phase kinetic model with gradient sensitivity analysis for high temperature particulate boron combustion in fluorine enriched environments
p 3319 N93-30090

Optically powered, optoelectronic spatial light modulators
[AD-A264765] p 3581 N93-30609

Organometallic compounds and polymers with second and third order nonlinear optical properties
[AD-A264774] p 3338 N93-30610

Aircraft guidance for wind shear avoidance: Decision-making under uncertainty p 3246 N93-31005

PROFESSIONAL ANALYSIS, INC., LAS VEGAS, NV.
Handbook of frequently used acronyms and glossary of terms
[DE93-011388] p 3616 N93-30123
PTT RESEARCH, LEIDSCHENDAM (NETHERLANDS).
Activities report of PTT Research
[ISBN-9-07-212514-2] p 3392 N93-30025
PUERTO RICO UNIV., RIO PIEDRAS.
Selenia: A habitability study for the development of a third generation lunar base p 3233 N93-29748
PURDUE UNIV., ELKHART, IN.
Performance of thermal adhesives in forced convection p 3293 N93-30974
PURDUE UNIV., WEST LAFAYETTE, IN.
Refractory metal disilicides research
[AD-A262416] p 3320 N93-28499
New III-V cell design approaches for very high efficiency
[DE93-000097] p 3464 N93-28971
Development of an unstructured solution adaptive method for the quasi-three-dimensional Euler and Navier-Stokes equations
[NASA-CR-193241] p 3421 N93-29213
Engineering consideration for the self-energizing magnetoplasmadynamic (MPD): Type fusion plasma thruster
[AD-A262785] p 3288 N93-29289
Design of a turbofan powered regional transport aircraft p 3228 N93-29721
Heat transfer with moderate free stream turbulence p 3254 N93-29936
Damage mechanics in 2-D and 3-D microstructures
[AD-A264337] p 3453 N93-30159
The 2-6 semiconductor superlattices
[AD-A264343] p 3597 N93-30164
Turbulence characteristics of an axisymmetric reacting flow
[NASA-CR-4110] p 3242 N93-30373
Tool grinding and spark testing p 3291 N93-30954

Q

QUALITY MANAGEMENT CONTROL, INC., OTTAWA (ONTARIO).
Control system design and multiparameter variations p 3355 N93-30217
QUEBEC UNIV., HULL.
Fiber-optic polarimetric strain gauge p 3375 N93-30341
QUEBEC UNIV., MONTREAL.
An information theoretic approach to stochastic adaptive control application to manipulators with active inertia p 3359 N93-30247
STRATUS: A prototype expert advisory system for terminal weather forecasting p 3367 N93-30296
QUEENS UNIV., KINGSTON (ONTARIO).
Robust control via H-infinity optimization p 3354 N93-30216
Synchronization of the LAPTV adative filter with input statistics p 3358 N93-30242
Task allocation and real-time considerations for the Robot Controller Test Station (RCTS) p 3364 N93-30278
Coarse synchronization in an EHF frequency-hopped satellite communications system p 3365 N93-30281
Signal processor based MSAT trellis coded M-DPSK with adaptive Doppler phasor correction p 3373 N93-30332
Two-stage Doppler phasor corrected TCM/DMPSK for shadowed mobile satellite channels p 3373 N93-30333
QUEENSLAND UNIV., BRISBANE (AUSTRALIA).
Wind loads on canopy roofs
[RR-CE132] p 3451 N93-29106

R

RADEX, INC., BEDFORD, MA.
SPREE Interactive Data Analysis Tool (SIDAT)
[AD-A262782] p 3273 N93-29306
RADIAN CORP., AUSTIN, TX.
Rates and mechanisms of reaction of hydrogen sulfide with iron chelates
[PB93-184299] p 3312 N93-29665
RANGE COMMANDERS COUNCIL, WHITE SANDS MISSILE RANGE, NM.
Proceedings of the Thunder and Lighting Seminar and the 3D Lightning Warning Workshop
[AD-A262766] p 3482 N93-29304
Satellite calibration requirements
[AD-A264279] p 3281 N93-30817
RAYTHEON CANADA LTD., WATERLOO (ONTARIO).
Improved bounds for synchronization jitter p 3360 N93-30251
Comparison of diversity combining, interleaving, and decoding techniques of a scintillated channel p 3362 N93-30266
RENSSELAER POLYTECHNIC INST., TROY, NY.
Graphical interface between the CIRSSE testbed and CimStation software with MCS/CTOS
[NASA-CR-193276] p 3527 N93-29218
The lightcraft project p 3233 N93-29749
Planning collision free paths for two cooperating robots using a divide-and-conquer C-space traversal heuristic
[NASA-CR-193252] p 3542 N93-29771
Keynote address: Unsteady, multimode transition in gas turbine engines p 3252 N93-29927
The planning coordinator: A design architecture for autonomous error recovery and on-line planning of intelligent tasks
[NASA-CR-193250] p 3543 N93-30039
Polarization modulated ellipsometry
[NASA-CR-4012] p 3580 N93-30372
Coordination compounds of aluminum as precursors to aluminum nitride
[AD-A264700] p 3327 N93-30574
RESEARCH AND DEVELOPMENT LABS., CULVER CITY, CA.
Summer research program (1992). High School Apprenticeship Program (HSAP) reports. Volume 16: Arnold Engineering Development Center Civil Engineering Laboratory
[AD-A262024] p 3608 N93-29396
Summer Faculty Research Program (SFRP), volume 1
[AD-A261988] p 3608 N93-29440
RESEARCH INST. FOR COMPUTING AND INFORMATION SYSTEMS, HOUSTON, TX.
Transforming AdaPT to Ada9x
[NASA-CR-193117] p 3526 N93-29026
Concept document of the repository-based software engineering program: A constructive appraisal
[NASA-CR-193125] p 3526 N93-29027
RBSE: Product development team research activity deliverables
[NASA-CR-193115] p 3527 N93-29212
RESEARCH TRIANGLE INST., RESEARCH TRIANGLE PARK, NC.
Growth and development of GaInAsP for use in high-efficiency solar cells
[DE93-000098] p 3465 N93-30208
RICE UNIV., HOUSTON, TX.
Integrated approaches to parallelism in optimization and solution of inverse problems
[AD-A262259] p 3452 N93-29349
A conjugate gradients/trust regions algorithms for training multilayer perceptrons for nonlinear mapping p 3519 N93-29581
RJO ENTERPRISES, INC., DAYTON, OH.
Air Force CALS business practices
[AD-A264789] p 3610 N93-30177
ROCHESTER UNIV., NY.
Spectroscopic probes of vibrationally excited molecules at chemically significant energies
[DE93-012328] p 3564 N93-28652
Ultrafast optical studies of surface reaction processes at semiconductor interfaces
[DE93-009049] p 3593 N93-29096
ROCKWELL INTERNATIONAL CORP., DOWNEY, CA.
Strategic avionics technology definition studies. Subtask 3-1A: Electrical Actuation (ELA) systems
[NASA-CR-193237] p 3271 N93-29215
Technology transfer and Rockwell International p 3627 N93-30712
ROCKWELL INTERNATIONAL CORP., LOS ANGELES, CA.
Virtual interface applications for airborne weapons systems p 3502 N93-28858
Requirements for pilot assistance in a thrust-vectoring combat aircraft p 3504 N93-28870
ROCKWELL INTERNATIONAL SCIENCE CENTER, THOUSAND OAKS, CA.
Distributed traffic signal control using fuzzy logic p 3513 N93-29543
Micromechanics of fatigue in woven and stitched composites p 3304 N93-30850
ROCKY RESEARCH CORP., BOULDER CITY, NV.
Complex-compound heat pump: Topical report on phase 1 results
[PB93-185460] p 3466 N93-30814
ROLLS-ROYCE LTD., DERBY (ENGLAND).
Modelling thermal behaviour of turbomachinery discs and casings p 3256 N93-29949
ROME LAB., GRIFFISS AFB, NY.
The dynamic behavior of constrained adaptive array sensor processors
[AD-A262402] p 3541 N93-28494
Modified Acousto-Optic Adaptive Processor (Mod-AOAP)
[AD-A261983] p 3381 N93-28997
Multichannel detection of partially correlated signals in clutter
[AD-A261984] p 3381 N93-28998
Photorefractive integrators and correlators
[AD-A264200] p 3597 N93-30144
Enhanced photorefractive effects in barium titanate
[AD-A264724] p 3599 N93-30554
ROYAL AIR FORCE INST. OF AVIATION MEDICINE, FARNBOROUGH (ENGLAND).
The physiological limitations of man in the high G environment p 3503 N93-28861
Operator and automation capability analysis: Picking the right team p 3503 N93-28864
ROYAL INST. OF TECH., STOCKHOLM (SWEDEN).
The numerical solution of low Mach number flow in confined regions by Richardson extrapolation
[TRITA-NA-9207] p 3238 N93-29005
A multigrid extension of the FFT for the numerical inversion of Fourier and LaPlace transforms
[TRITA-NA-9204] p 3548 N93-29024
Nonlinear stability of viscous shock waves
[TRITA-NA-9205] p 3419 N93-29025
ROYAL MILITARY COLL. OF CANADA, KINGSTON (ONTARIO).
Analysis and simulation of a two degrees-of-freedom one-link flexible forearm p 3361 N93-30261
ROYAL NETHERLANDS METEOROLOGICAL INST., DE BILT.
Systems description of MIVOS (mist forecast system), part 1
[KNMI-TR-141-PT-1] p 3483 N93-30013
Daily sum of the global radiation: Calculation method and verification of forecast
[KNMI-TR-138] p 3478 N93-30113
Syllabus physical meteorology, part 1
[KNMI-TR-140-PT-1] p 3484 N93-30114
RUTGERS - THE STATE UNIV., PISCATAWAY, NJ.
An extension of a kinetic theory of polymer crystallization through the exclusion of negative barriers
[AD-A264810] p 3334 N93-29660

S

SAINT JOHN'S UNIV., JAMAICA, NY.
Walkway friction: Experiment and analysis p 3293 N93-30966
SAINT LOUIS UNIV., MO.
Carbon monoxide exposure of subjects with documented cardiac arrhythmias
[PB93-179943] p 3497 N93-30890
SAN FRANCISCO STATE UNIV., CA.
Case study of the operational usefulness of the sharp workstation in forecasting a mesocyclone-induced cold sector tornado event in California
[PB93-178697] p 3485 N93-30889
SAN JOSE STATE UNIV., CA.
Onboard signal processing: Wave of the future for planetary radio science? p 3646 N93-28801
SANDIA NATIONAL LABS., ALBUQUERQUE, NM.
The natural excitation technique (NExT) for modal parameter extraction from operating wind turbines
[DE93-010611] p 3463 N93-28603
A grid refinement study of two-dimensional transient flow over a backward-facing step using a spectral-element method
[DE92-018262] p 3417 N93-28639
Thermal and mechanical analysis of flip-chips on a liquid cooled multichip module
[DE93-007609] p 3405 N93-28641
Flash x ray system: Techniques and applications
[DE93-011477] p 3430 N93-28645
Reliability assessment at airline inspection facilities. Volume 2: Protocol for an eddy current inspection reliability experiment
[DOT/FAA/CT-92/12-VOL-2] p 3449 N93-28685
Diffusion bonding
[DE93-011480] p 3442 N93-28837
Subnanosecond high power performance of a bistable optically-controlled GaAs switch
[DE93-006285] p 3406 N93-28944
The development of a parachute system for aerial delivery from high speed cargo aircraft
[DE93-008339] p 3239 N93-29035
Implementation of a single-material version of PAGOSA on MIMD hypercubes
[SAND-92-0640] p 3526 N93-29127
An experimental investigation of radioactivity induced by ions associated with the operation of pulsed-power accelerators
[DE93-011478] p 3575 N93-29151
Low-pump-rate multi-millisecond atomic xenon laser
[DE93-011484] p 3437 N93-29180
The design and modelling of a comb-drive-based microengine for mechanism drive applications
[DE93-009826] p 3443 N93-29185

Efficient wiring of reconfigurable parallel processors
[DE93-009847] p 3538 N93-29186
Ablation problems using a finite control volume technique
[DE93-009861] p 3549 N93-29187
Surface diffusion: Atomistics and surface morphology (summary of MRS Symposium B panel discussion)
[DE93-009862] p 3594 N93-29188
Testing in combined dynamic environments
[DE93-010679] p 3278 N93-29250
Computational simulations of a soft x ray projection lithography laser plasma source
[DE93-009625] p 3437 N93-29264
Polynomial space polynomial delay algorithms for listing families of graphs
[DE93-010677] p 3530 N93-29808
Power beaming to communication satellites in GEO
[DE93-007608] p 3279 N93-29840
Application of sensors to the control of robotic systems
[DE93-009837] p 3543 N93-30012
Software testing using the IEEE standards
[DE93-009833] p 3532 N93-30050
Chromate-free corrosion resistant conversion coatings for aluminum
[DE93-009835] p 3336 N93-30051
Thermal decomposition chemistry and shock sensitivity of thermally aged explosives p 3344 N93-30069
Energetic material response to abnormal environments p 3350 N93-30095
Characteristic and development report SA3581/MC4196 Lightning Arrestor Connector (LAC)
[DE93-010610] p 3412 N93-30118
Foreign technology assessment: Environmental evaluation of a radiation-hard oscillator/divider
[DE93-011481] p 3412 N93-30127
Use of a genetic algorithm to solve two-fluid flow problems on an NCUBE multiprocessor computer
[DE93-009630] p 3425 N93-30184
Characterizing transient vibrations using band limited temporal moments
[DE93-009639] p 3453 N93-30185
Detecting residue on a printed circuit board: An application of the Boundary Contour/Feature Contour System
[DE93-006283] p 3412 N93-30370
Thermal effects testing at the National Solar Thermal Test Facility
[DE93-009825] p 3465 N93-30391
Proposal for a numerical array library
[DE93-010678] p 3623 N93-30482
A robust model for finding optimal evolutionary trees
[DE93-010682] p 3491 N93-30483
Steps required in the pursuit of quantitative risk management processes for high pressure systems
[DE93-007586] p 3378 N93-30508
Beta/gamma Monte Carlo transport in repetitive structures of satellite systems
[DE93-007610] p 3281 N93-30509
Portable fiber optic coupled Doppler interferometer system for detonation and shock wave diagnostics
[DE93-009827] p 3433 N93-30510
Unexpected increase in the thermal generation rate of bulk GaAs due to electron-beam metallization
[DE93-009829] p 3598 N93-30511
Effects of device scaling and geometry on MOS radiation hardness assurance
[DE93-009832] p 3413 N93-30516
Phase separation, antiferromagnetism, and superconductivity in superconducting-superoxygenated La(2-x)Sr(x)CuO(4+(delta))
[DE93-009852] p 3598 N93-30517
Charge separation in bipolar transistors
[DE93-009624] p 3413 N93-30650
Rocket-triggered lightning studies for the protection of critical assets
[DE93-009633] p 3484 N93-30651
Graphical programming: On-line robot simulation for telerobotic control
[DE93-009796] p 3447 N93-30654
The use of DFT windows in signal-to-noise ratio and harmonic distortion computations
[DE93-009800] p 3433 N93-30655
Adhesion of thick film Au to alumina ceramics
[DE93-009802] p 3339 N93-30656
Hardness assurance and testing issues for bipolar/BiCMOS devices
[DE93-009623] p 3570 N93-30669

SANDIA NATIONAL LABS., LIVERMORE, CA.
Limitations of the ideal phase-Doppler system: Extension to spatially and temporally inhomogeneous particle flows with an application to diesel sprays
[DE93-009447] p 3416 N93-28595
Hydrostatic and uniaxial behavior of a high density polyurethane foam (FR-3720) at various temperatures
[DE93-011486] p 3330 N93-28838
Implementation of a single-material version of PAGOSA on MIMD hypercubes
[SAND-92-0640] p 3526 N93-29127
Advanced coordinate measuring machine at Sandia National Laboratories
[DE93-010618] p 3432 N93-29842
An experimental/analytical evaluation of biaxial sheet failure
[DE93-010620] p 3453 N93-29843
The thermochemistry and reaction pathways of the decomposition and combustion of energetic materials p 3343 N93-30063
Thermal decomposition pathways of RDX in the condensed phase p 3347 N93-30083

SASKATCHEWAN UNIV., SASKATOON.
An artificial neural network model for periodic trajectory generation p 3356 N93-30225
An expert system for identification of the task status from tactile sensor data p 3368 N93-30300

SCHAFER (W. J.) ASSOCIATES, INC., ARLINGTON, VA.
Damage areas on selected LDEF aluminum surfaces p 3283 N93-29374

SCHAFER (W. J.) ASSOCIATES, INC., HAMPTON, VA.
LDEF archival system plan p 3624 N93-29704

SCIENCE APPLICATIONS INTERNATIONAL CORP., ALBUQUERQUE, NM.
Use of particle beams for lunar prospecting p 3650 N93-28822

SCIENCE APPLICATIONS INTERNATIONAL CORP., FALLS CHURCH, VA.
Centralized maintenance evaluation
[AD-A264400] p 3544 N93-30886

SCIENCE APPLICATIONS INTERNATIONAL CORP., MCLEAN, VA.
SAVS: A Space Data Analysis and Visualization System p 3614 N93-29235
Predicting radiation induced performance decrements of AH-1 helicopter crews. Volume 2: Evaluation of modeling and simulation techniques for predicting radiation induced performance decrements
[AD-A262872] p 3506 N93-29484

SCIENCE APPLICATIONS INTERNATIONAL CORP., PROSPECT, TN.
Development and application of a 3-D geometry/mass model for LDEF satellite ionizing radiation assessments p 3573 N93-29640
Radiation model predictions and validation using LDEF satellite data p 3573 N93-29641
Future directions for LDEF ionizing radiation modeling and assessments p 3573 N93-29642

SCIENCE APPLICATIONS INTERNATIONAL CORP., SANTA MONICA, CA.
LDEF space optics handbook p 3582 N93-29695

SCIENCE APPLICATIONS INTERNATIONAL CORP., TORRANCE, CA.
Effects of buoyancy on gas jet diffusion flames
[NASA-CR-191109] p 3352 N93-31031

SCINTREX LTD., CONCORD (ONTARIO).
Explosives detection systems for airport security gas chromatographic based devices p 3244 N93-30276

SCRIPPS CLINIC AND RESEARCH FOUNDATION, LA JOLLA, CA.
Molecular approach to hypothalamic rhythms
[AD-A264438] p 3496 N93-30421
Defining protein electrostatic recognition processes
[AD-A264838] p 3571 N93-30901

SCRIPPS INSTITUTION OF OCEANOGRAPHY, LA JOLLA, CA.
An automated observing system for passive evaluation of cloud cover and visibility
[AD-A263207] p 3481 N93-28875
Analyses of data from fine structure and circulation studies in the Gulf of California
[AD-A262910] p 3486 N93-28885
Modern seismic travel time tables and station corrections for P and S waves
[AD-A262536] p 3477 N93-29412
Optical slope/height measurements of small scale waves within the SAXON-FPN experiment
[AD-A262572] p 3487 N93-29422
Charting the remote southern oceans with geosat altimetry
[AD-A263452] p 3461 N93-29817

SENER INGENIERIA Y SISTEMAS S.A., MADRID (SPAIN).
Cooling predictions in turbofan engine components p 3259 N93-29964

SENSTAR CORP., KANATA (ONTARIO).
Future directions in aviation security p 3244 N93-30274

SGS-THOMSON MICROELECTRONICS, INC., AGRATE BRIANZA (ITALY).
WARP: Weight Associative Rule Processor. A dedicated VLSI fuzzy logic megacell p 3513 N93-29538

SIMON FRASER UNIV., BURNABY (BRITISH COLUMBIA).
An error control protocol based on trellis coded modulations p 3358 N93-30237
Modelling and simulation of human retinal vision processing p 3363 N93-30269
Quantization effects in segmentation of range images p 3363 N93-30270

SMITH ASSOCIATES LTD., GUILDFORD (ENGLAND).
Evolution or revolution: The Catch 22 of TACSATs p 3269 N93-29894

SMITH SYSTEM ENGINEERING LTD., GUILDFORD (ENGLAND).
Evolution or revolution: The Catch 22 of TACSATs p 3269 N93-29894

SMITHSONIAN ASTROPHYSICAL OBSERVATORY, CAMBRIDGE, MA.
Precision optical interferometry in space
[NASA-CR-193264] p 3630 N93-29163

SOCIETE NATIONALE DES POUDRES ET EXPLOSIFS, PARIS (FRANCE).
Propulsion and detonics research in France p 3344 N93-30070

SOCIETY FOR INDUSTRIAL AND APPLIED MATHEMATICS, PHILADELPHIA, PA.
SIAM Conference on Applications of Dynamical Systems
[DE93-007969] p 3548 N93-29057

SOFTWARE AND ENGINEERING ASSOCIATES, INC., CARSON CITY, NV.
Additional support for the TDK/MABL computer program
[NASA-CR-193037] p 3526 N93-29028

SOL-RF ENERGY SYSTEMS, INC., WINNIPEG (MANITOBA).
A unique photon bombardment system for space applications p 3286 N93-28790

SONOMA TECHNOLOGY, INC., SANTA ROSA, CA.
Study to determine the nature and extent of ozone and ozone precursor transport in selected areas of California
[PB93-184828] p 3470 N93-29669

SONY CORP. OF AMERICA, SAN DIEGO, CA.
Computer-controlled alignment for a 2000-line color monitor p 3247 N93-30324

SONY MAGNETIC PRODUCTS, INC., CYPRESS, CA.
The NT digital micro tape recorder p 3435 N93-30461

SOUTH CAROLINA UNIV., COLUMBIA.
Research programs from the University of South Carolina on high energy physics
[DE93-007829] p 3574 N93-28969
Application of integral and differential equation methods for various EM interaction problems
[AD-A264821] p 3394 N93-30597

SOUTHWEST RESEARCH INST., SAN ANTONIO, TX.
Liquid Motion in a rotating tank Experiment (LME) p 3264 N93-28710
Spacecraft computer technology at Southwest Research Institute p 3522 N93-28813
Pluto fast flyby mission and science overview p 3649 N93-28818
Development of Miniaturized Optimized Smart Sensors (MOSS) for space plasmas p 3286 N93-28828

SOVIET ASSOCIATION OF FUZZY SYSTEMS, MOSCOW (RUSSIA).
The axiomatic definition of a linguistic scale fuzziness degree, its major properties, and applications p 3510 N93-29520

SPACE ENVIRONMENT SERVICES CENTER, BOULDER, CO.
SESC products and services user guide
[PB93-178879] p 3653 N93-29679

SPACE SYSTEMS/LORAL, PALO ALTO, CA.
Sodium-Sulfur Cell Technology flight experiment (SSCT) p 3264 N93-28715

SPACE TELESCOPE SCIENCE INST., BALTIMORE, MD.
Data reduction expert assistant p 3613 N93-29227

SPAR AEROSPACE LTD., WESTON (ONTARIO).
Joint drive development for the Space Station Remote Manipulator System p 3370 N93-30313

SPARTA, INC., EDWARDS AFB, CA.
Measurements of magnetic fields produced by a 30 kWe class Arcjet Power Conditioning Unit
[AD-A262786] p 3287 N93-28658

SPARTA, INC., LEXINGTON, MA.
4D interconnect experimental development
[AD-A264298] p 3540 N93-30895

SPIRE CORP., BEDFORD, MA.
Microtextured metals for stray-light suppression in the Clementine startracker p 3286 N93-28785
Low-cost, high-efficiency solar cells utilizing GaAs-on-Si technology
[DE93-000096] p 3464 N93-29965
Improved heat removal by microscopic surface texturing of capillaries
[AD-A263483] p 3424 N93-29966

SRI INTERNATIONAL CORP., ARLINGTON, VA.

Tethered aerostat VLF/LF transmitter system design considerations p 3399 N93-30753

SRI INTERNATIONAL CORP., MENLO PARK, CA.

Field-emitter arrays for RF vacuum microelectronics [AD-A262677] p 3404 N93-28483

Synthesis of cubane based energetic molecules [AD-A263271] p 3564 N93-28562

The dynamic cusp at low altitudes: A case study combining Viking, DMSP, and Sondrestrom incoherent scatter radar observations [NASA-CR-193152] p 3476 N93-28842

Kinetics and energy transfer in nonequilibrium fluid flows [AD-A263612] p 3240 N93-29284

Mithras studies of the boundary between open and closed field lines [AD-A264758] p 3479 N93-30562

Oceanographic data processing program [AD-A264801] p 3544 N93-30591

STANFORD UNIV., CA.

State vector splitting: A numerical scheme for the Euler equations p 3419 N93-29039

Axial impact of composites p 3297 N93-29078

Investigation of a geodesy coexperiment to the Gravity Probe B relativity gyroscope program [NASA-CR-193263] p 3460 N93-29179

On the value of function evaluation location information in Monte Carlo simulation [AD-A263662] p 3554 N93-29292

Parametric likelihood inference for record breaking problems [AD-A262546] p 3549 N93-29413

A temporal proof methodology for reactive systems [NASA-CR-193145] p 3528 N93-29469

Exploiting the memory hierarchy in sequential and parallel sparse Cholesky factorization [AD-A262849] p 3539 N93-29508

Ferroelectric liquid crystal optical interconnect switching systems [AD-A263751] p 3596 N93-29859

A diffusion approximation for a network of reservoirs with power law release rule [AD-A263753] p 3550 N93-29872

Automated modeling of physical systems [NASA-CR-193256] p 3531 N93-29873

Gradient estimation for regenerative processes [AD-A263766] p 3555 N93-29878

Fundamental studies of the morphology, chemistry, and electrical properties of metals on GaAs and other III-V semiconductor compounds [AD-A264417] p 3597 N93-30120

Optimal geometric design of robots for environments with obstacles p 3445 N93-30149

Visualization techniques for analyzing control of human movement: Affine mappings between multi-dimensional spaces p 3508 N93-30204

Research studies on short wavelength by selective auger processes [AD-A264493] p 3440 N93-30401

Fundamental studies of the mechanical behavior of microelectronics thin film materials [AD-A264334] p 3337 N93-30417

The Road to Room Temperature Superconductivity Workshop [AD-A264633] p 3561 N93-30519

Subpicosecond electrooptic sampling [AD-A264635] p 3581 N93-30520

Attitude determination using GPS: Development of an all solid-state guidance, navigation, and control sensor for air and space vehicles based on the global positioning system p 3246 N93-30605

Intelligent real-time problem solving [AD-A264830] p 3535 N93-30614

Turbulent drag reduction: Studies of feedback control and flow over riblets p 3242 N93-30645

Studies of curvature, strain, and unsteady effects on premixed flames p 3316 N93-30646

Lightning-induced effects on VLF/LF radio propagation p 3396 N93-30737

ELF/VLF radio noise measurements at high latitudes during solar particle events p 3397 N93-30744

Delaminations in composite plates under impact loads p 3304 N93-30849

The numerical simulation of circulation controlled airfoil flowfields p 3243 N93-30947

Strong parallel blade-vortex interaction and noise propagation in helicopter flight p 3563 N93-30980

STATE UNIV. OF NEW YORK, ALBANY.

Study of heavy-flavored particles [DE93-011535] p 3569 N93-30128

STATE UNIV. OF NEW YORK, BINGHAMTON.

Possibilistic measurement and set statistics p 3517 N93-29567

On probability-possibility transformations p 3519 N93-29582

STATE UNIV. OF NEW YORK, BUFFALO.

Mass spectrometric investigation of 2-methoxyethanol and 2-ethoxyethanol clusters: Magic numbers and structural implications [AD-A262822] p 3312 N93-29429

Characterization of copper iodide thin films fabricated via laser assisted molecular beam epitaxy [AD-A262823] p 3596 N93-29430

STATE UNIV. OF NEW YORK AT BUFFALO, AMHERST.

Studies in Lewis acid and superacid ionic liquids [AD-A264683] p 3316 N93-30551

STATE UNIV. OF SOUTHEAST MISSOURI, CAPE GIRARDEAU.

Phase transition studies in barium and strontium titanates at microwave frequencies p 3293 N93-30970

STEVENS INST. OF TECH., HOBOKEN, NJ.

Efficient algorithms for the evaluation of planar network reliability [AD-A263602] p 3531 N93-29916

STRATEGIC DEFENSE INITIATIVE ORGANIZATION, WASHINGTON, DC.

STRV1-b flight experiment p 3265 N93-28723

STRATEGIC MANAGEMENT RESOURCES LTD., BOWIE, MD.

The fundamentals and futures of removable mass storage alternatives p 3619 N93-30460

STUTTGART UNIV. (GERMANY).

The interferometric SAR technology and its usability in the framework of ERS-1 p 3457 N93-28919

SUPERCOMPUTER RESEARCH CENTER, BOWIE, MD.

Measurements over distributed high performance computing and storage systems p 3622 N93-30476

SVERDRUP TECHNOLOGY, INC., BROOK PARK, OH.

Reliability assessment of thrust chamber cooling concepts using probabilistic analysis techniques [NASA-CR-190785] p 3288 N93-29068

SYRACUSE UNIV., NY.

An algebraic approach to the quantization of constrained systems: Finite dimensional examples p 3548 N93-28671

Spin dependent phenomena in medium energy physics [DE93-010972] p 3565 N93-28849

Simulation and calculation of diffusive aerosol deposition [DE93-007518] p 3474 N93-30506

SYSTEMS TECHNOLOGY, INC., HAWTHORNE, CA.

Vehicle dynamic stability and rollover [PB93-185437] p 3447 N93-30828

T

TECHNICAL RESEARCH CENTRE OF FINLAND, ESPOO.

Dynamic ice structure interaction: Theory and applications [VTT-PUBS-90] p 3353 N93-28632

TRAB: A transient analysis program for BWR. Part 2: User's manual [VTT-TIED-1232-PT-2] p 3575 N93-29996

OSI transaction processing standard: An introduction and outlines of implementation [VTT-TIED-1250] p 3532 N93-29997

A neural network based approach for machine fault diagnosis [VTT-TIED-1274] p 3543 N93-29998

Total dose tests for the PROMICS-3 instrument [VTT-TIED-1203] p 3411 N93-30108

Prefeasibility study on compressed air energy storage systems [VTT-TIED-1267] p 3465 N93-30111

Uses of risk importance measures [VTT-TIED-1245] p 3378 N93-30581

TECHNICAL UNIV. OF DENMARK, LYNGBY.

Follow up on the crystal growth experiments of the LDEF p 3602 N93-29381

TECHNISCHE HOCHSCHULE, DARMSTADT (GERMANY).

Topology of hybrid objects [ETN-93-93594] p 3546 N93-28466

Lie groups whose set of compact subgroups is inductive [ETN-93-93791] p 3547 N93-28524

Antirational transductions and their language families [ETN-93-93794] p 3611 N93-28525

Dynamic object oriented interaction and its implementation in the framework in an interface management system [ETN-93-93795] p 3523 N93-28526

Unitary approximation of Bhabha diffusion by high energies and its implementation in Monte Carlo event generators [ETN-93-93622] p 3571 N93-30670

TECHNISCHE UNIV., BERLIN (GERMANY).

DOKMA: A document oriented communication model for medical applications as a basis of a role system in the medical field [ETN-93-93799] p 3492 N93-28469

Analysis of electrothermal interactions in power semiconductor modules [ETN-93-93800] p 3591 N93-28470

Packing of Steiner trees: Polyhedric studies and application [ETN-93-93796] p 3547 N93-28527

A model for processing the SGML document in version oriented hypertext systems [ETN-93-93797] p 3611 N93-28528

Influence of optical feedback on the pulse behavior of semiconductor lasers [ETN-93-93798] p 3436 N93-28614

Analysis of orbital system logistics in the cis-lunar space with particular consideration of life cycle costs [ETN-93-93484] p 3268 N93-29063

Thermodynamics of swelling and collapse of polyelectrolytic gels [ETN-93-93485] p 3331 N93-29064

A method for intersection line calculation between parametric surfaces [ETN-93-94178] p 3551 N93-30572

Technical examination and simulation of a photovoltaic system: Solar generator, battery, download [ETN-93-94179] p 3466 N93-30573

Double swingby at Earth-Moon for increase of excess velocity [ETN-93-94177] p 3270 N93-30582

Placement of cells: Theory and solution of a quadratic 0/1 optimization problem [ETN-93-94182] p 3413 N93-30616

Design and implementation of a Global Positioning System (GPS) supported area navigation system with electronic aircraft [ILR-MITT-275(1992)] p 3246 N93-30671

Examinations of perturbation reduction by automatic speech dependent recognition of separately spoken single words [ETN-93-94180] p 3394 N93-30672

The contact mechanical nonlinearities of a mathematical model of a railway wheel rolling over corrugated rail [ILR-MITT-266(1991)] p 3454 N93-31015

The steady-state tangential contact problem for a falling drop type of contact area on corrugated rail by simplified theory of rolling contact [ILR-MITT-267(1991)] p 3455 N93-31016

Determination of low frequency reference slipping for high frequency unstationary motion processes [ILR-MITT-273(1992)] p 3455 N93-31017

TECHNISCHE UNIV., BRUNSWICK (GERMANY).

Information compression in the context model p 3514 N93-29549

A neural fuzzy controller learning by fuzzy error propagation p 3516 N93-29560

TECHNISCHE UNIV., DARMSTADT (GERMANY).

Fluid flow and heat transfer in the entrance region of an annulus between independently rotating tubes with a turbulent axial flow p 3256 N93-29952

The effect of main stream flow angle on flame tube film cooling p 3257 N93-29953

TECHNISCHE UNIV., EINDHOVEN (NETHERLANDS).

Speech recognition by recursive stochastic modelling [ISBN-90-9005038-8] p 3382 N93-29266

The design and lifetime calculation of MHD generator walls based on subcritical crack growth in ceramics [ISBN-90-9004009-9] p 3332 N93-29267

Quiet by design: Numerical acousto-elastic analysis of aircraft structures [ISBN-90-386-0042-9] p 3248 N93-29268

Handshake circuits: An intermediary between communicating processes and VLSI [ETN-93-93579] p 3408 N93-29269

Optical coherent phase diversity systems [ISBN-90-9004897-9] p 3578 N93-29270

Instrumental neutron activation analysis developed for silicon integrated circuit technology [ETN-93-93581] p 3408 N93-29271

Non-linear wave phenomena in a gas-vapour mixture with phase transition [ETN-93-93582] p 3422 N93-29319

TECHNOLOGY ASSESSMENT AND TRANSFER, INC., ANNAPOLIS, MD.

Real time self-directed MBE flux control incorporation in situ ellipsometry, phase 1 [AD-A263501] p 3595 N93-29341

TELEFUNKEN SYSTEM TECHNIK G.M.B.H., ULM (GERMANY).

Theoretical and experimental coverage analysis of a VLF transmitter p 3396 N93-30734

TELEGLOBE CANADA, MONTREAL (QUEBEC).

Teleglobe's international Mobile Earth Terminal service p 3371 N93-30317

TENNESSEE TECHNOLOGICAL UNIV., COOKEVILLE.
Studies of fluctuation processes in nuclear collisions [DE93-011263] p 3576 N93-30054

TENNESSEE UNIV., KNOXVILLE.
The production and destruction of negative ions [DE93-010527] p 3564 N93-28665
Elementary particle interactions [DE93-005113] p 3568 N93-29764
Efficient algorithms and data structures in geometric design [AD-A264678] p 3534 N93-30544

TENNESSEE VALLEY AUTHORITY, CHATTANOOGA.
Remote sensing for water quality monitoring in the Tennessee Valley: Field tests of two systems [DE93-008997] p 3462 N93-30637

TERRA SYSTEMS, INC., KAILUA, HI.
Imaging spectrometers using concave holographic gratings p 3434 N93-28783

TEXAS A&M UNIV., COLLEGE STATION.
Preliminary design of an intermittent smoke flow visualization system [NASA-CR-186027] p 3248 N93-28693
Growing wheat to maturity in reduced gas pressures [NASA-CR-193245] p 3491 N93-29216
Thermodynamic properties of natural gas mixtures [PB93-162816] p 3604 N93-29428
Approximate reasoning using terminological models p 3510 N93-29522
Design issues of a reinforcement-based self-learning fuzzy controller for petrochemical process control p 3512 N93-29533
Designing a fuzzy scheduler for hard real-time systems p 3512 N93-29537
Synthesis techniques and analysis tools for on-chip fault-tolerance [AD-A263167] p 3409 N93-29654
Thermodynamic properties of natural gas mixtures [PB93-176162] p 3604 N93-29794
Continuation of: Applications of gauge theories to enhance numerical solutions of mixed potential integral equations [AD-A263763] p 3550 N93-29876
Measurements of light scattering by small particles at an angle of zero degrees [AD-A263856] p 3580 N93-29887
Multiparticle imaging technique for two-phase fluid flows using pulsed laser speckle velocimetry [DE93-011734] p 3427 N93-30489
Characterization of slow chromophore reorientation in nonlinear optical polymers by two-dimensional MAS NMR [AD-A264809] p 3338 N93-30596
Mechanical properties of composite materials p 3290 N93-30951

TEXAS TECHNOLOGICAL UNIV., LUBBOCK.
Multiscale morphological filtering for analysis of noisy and complex images p 3582 N93-28789
Human capabilities and limitations in situation awareness p 3503 N93-28863
Clustering of tethered satellite system simulation data by an adaptive neuro-fuzzy algorithm p 3512 N93-29535
Accuracy enhancement in optical computing [AD-A264872] p 3522 N93-30179

TEXAS UNIV., AUSTIN.
Electronics research report [AD-A262733] p 3405 N93-28589
A Fokker-Planck operator for the emission and absorption of electron plasma waves in a magnetized plasma [DE93-009579] p 3584 N93-28598
Self-consistent chaos in the beam-plasma instability [DE93-009581] p 3584 N93-28599
Classification theorem for principal fibre bundles, Berry's phase, and exact cycle evolution [DE93-011114] p 3556 N93-28601
Synthesis of new high performance lubricants and solid lubricants [DE93-012237] p 3330 N93-28748
Self-organized profile relaxation by ion temperature gradient instability in toroidal plasmas [DE93-009580] p 3585 N93-28910
Design of interfaces in metal matrix composites [AD-A262052] p 3296 N93-29001
Collective transport of alpha particles due to Alfven wave instability [DE93-009578] p 3587 N93-29148
Theory and applications of random fields [AD-A262829] p 3555 N93-29454
Electronics research at the University of Texas at Austin. Appendix: JSEP sponsored publications [AD-A262993] p 3409 N93-29485
ASPEC: Solar power satellite p 3233 N93-29750
B and T: Lunar landers p 3234 N93-29751
Spacely's rockets: Personnel launch system/family of heavy lift launch vehicles p 3234 N93-29752
RS Landers: Lunar lander p 3234 N93-29753
SPECS: Orbital debris removal p 3234 N93-29754
The 1990-1991 project summaries p 3234 N93-29755
Vertical slot convection: A linear study [DE93-007643] p 3423 N93-29804
Damage growth in composite propellants p 3348 N93-30088
Atomic force microscopy of ammmonium perchlorate p 3349 N93-30091

TEXAS UNIV., EL PASO.
Uncertainty reasoning in expert systems [NASA-CR-193120] p 3548 N93-28973
Empirical quantile function nonparametric integrated analyses [AD-A263704] p 3554 N93-29385
Inverse problems: Fuzzy representation of uncertainty generates a regularization p 3516 N93-29563
Gaussian membership functions are most adequate in representing uncertainty in measurements p 3520 N93-29584

TEXAS UNIV., SAN ANTONIO.
Analysis of visual loss from retinal lesions [AD-A264692] p 3496 N93-30494

THIOKOL CORP., BRIGHAM CITY, UT.
Postflight hardware evaluation 360T025 (RSRM-25, STS-46) [NASA-CR-192562] p 3272 N93-30617
Postflight hardware evaluation 360T025 (RSRM-25, STS-46). Appendix A: Insulation PFORs [NASA-CR-192563] p 3272 N93-30618
Postflight hardware evaluation 360T025 (RSRM-25, STS-46). Appendix B: Case, seals, and joints PFORs [NASA-CR-192564] p 3272 N93-30619
Postflight hardware evaluation 360T025 (RSRM-25, STS-46). Appendix C: Nozzle PFORs [NASA-CR-192565] p 3272 N93-30620
Postflight hardware evaluation 360T025 (RSRM-25, STS-46). Appendix E: Insulation postfire data [NASA-CR-192566] p 3272 N93-30621
Postflight hardware evaluation 360T025 (RSRM-25, STS-46). Appendix D: Nozzle postfire data [NASA-CR-192580] p 3289 N93-30648

THOMPSON-HICKLING AVIATION, INC., OTTAWA (ONTARIO).
Engineering management consideration for an integrated aeronautical mobile satellite service p 3374 N93-30337

THOMSON-CSF, TRAPPES (FRANCE).
Computer assisted evaluation for air close combat based on time interval characterization p 3504 N93-28868

THOMSON-CSF SYSTEMS CANADA, INC., NEPEAN (ONTARIO).
A functional system architecture for fully autonomous robot p 3370 N93-30311

TOGAI INFRALOGIC, INC., HOUSTON, TX.
Life insurance risk assessment using a fuzzy logic expert system p 3520 N93-29585

TOKYO UNIV., TANASHI (JAPAN).
Borel sum rules for octet baryons in nuclear medium [DE93-753245] p 3604 N93-29242
Research and education by SF cyclotron facility [DE93-753135] p 3576 N93-30002

TOLEDO UNIV., OH.
Encoding spatial images: A fuzzy set theory approach p 3511 N93-29527

TORONTO UNIV., NORTH YORK (ONTARIO).
Analysis of LDEF micrometeoroid/debris data and damage to composite materials p 3309 N93-29366

TORONTO UNIV. (ONTARIO).
How to select combination operators for fuzzy expert systems using CRI p 3510 N93-29521
An experimental methodology for a fuzzy set preference model p 3514 N93-29547
A fuzzy set preference model for market share analysis p 3514 N93-29548
Design and implementation of an interactive isochromatic fringe-analysis system using machine-vision techniques p 3369 N93-30305
Morphological and order statistic filters: A comparative study p 3375 N93-30345

TOULOUSE UNIV. (FRANCE).
Estimations of expectedness and potential surprise in possibility theory p 3510 N93-29518

TRANSPORT CANADA, OTTAWA (ONTARIO).
Adapting system engineering principles to the Canadian Airspace System p 3247 N93-30338
Airspace Design Expert System (ADES), a 2D/3D mapping and modelling tool incorporating an expert system for use in instrument approach design p 3247 N93-30357

TRANSPORT CANADA, WINNIPEG (MANITOBA).
Fault tolerance and testing for WSI systems p 3361 N93-30258

TRI-STATE UNIV., ANGOLA, IN.
Application of hardness testing in foundry processing operations: A university and industry partnership p 3292 N93-30961

TRIMBLE NAVIGATION, SUNNYVALE, CA.
System analysis for a kinematic positioning system based on the global positioning system [AD-A262830] p 3245 N93-29468

TRISTAN TECHNOLOGIES, INC., SAN DIEGO, CA.
Advanced microwave frequency sources and filters based on superconducting Photonic Band Gap (PBG) structures [AD-A264404] p 3597 N93-30175

TRW, INC., HOUSTON, TX.
Reference equations of motion for automatic rendezvous and capture [NASA-CR-185676] p 3269 N93-29652

TRW, INC., REDONDO BEACH, CA.
Miniature long-life space cryocoolers p 3378 N93-28825
Technology transfer between the government and the aerospace industry p 3628 N93-30716

TRW SPACE AND DEFENSE SECTOR, REDONDO BEACH, CA.
In-STEP Two-Phase Flow (TPF) thermal control experiment p 3265 N93-28719

TRW SPACE TECHNOLOGY LABS., REDONDO BEACH, CA.
LDEF Space Plasma-High Voltage Drainage Experiment post-flight results p 3414 N93-29690

TUFTS UNIV., MEDFORD, MA.
Three-dimensional elastic stress analysis in materials with many inhomogeneities [AD-A263736] p 3453 N93-29855

TULSA UNIV., OK.
A miniature fatigue test machine p 3291 N93-30956
Fracture of glass p 3293 N93-30969

U

UNITED NATIONS EDUCATIONAL, SCIENTIFIC AND CULTURAL ORGANIZATION, PARIS (FRANCE).
IOC-UNEP review meeting on oceanographic processes of transport and distribution of pollutants in the sea [DE93-605070] p 3490 N93-31019

UNITED TECHNOLOGIES CORP., EAST HARTFORD, CT.
NOx chemistry in natural gas flames [PB93-175263] p 3317 N93-30760

UNITED TECHNOLOGIES RESEARCH CENTER, EAST HARTFORD, CT.
Interfacial studies of refractory glass-ceramic matrix/advanced SiC fiber reinforced composites [AD-A263264] p 3299 N93-29802

UNIVERSIDAD NACIONAL AUTONOMA DE MEXICO, COYOACAN.
Fuzzy knowledge base construction through belief networks based on Lukasiewicz logic p 3515 N93-29550

UNIVERSITAET DER BUNDESWEHR MUENCHEN, NEUBIBERG (GERMANY).
Pilot intent and error recognition as part of a knowledge based cockpit assistant p 3502 N93-28855

UNIVERSITEIT TWENTE, ENSCHEDE (NETHERLANDS).
Resource limited reasoning: A study of literature in the context of model-based diagnosis [MEMO-INF-92-38] p 3540 N93-28480
A survey of network interface designs [MEMO-INF-92-59] p 3379 N93-28502
Deformations of the Lie algebras L1(H(2)) and L1(W(2)) [MEMO-1056] p 3547 N93-28667

UNIVERSITIES SPACE RESEARCH ASSOCIATION, HOUSTON, TX.
Proceedings of the Seventh Annual Summer Conference. NASA/USRA: University Advanced Design Program [NASA-CR-192962] p 3227 N93-29712

UNIVERSITIES SPACE RESEARCH ASSOCIATION, HUNTSVILLE, AL.
Natural environmental service support to NASA vehicle, technology, and sensor development programs [NASA-CR-192554] p 3469 N93-29029

UNIVERSITY COLL., LONDON (ENGLAND).
Chromatographic and solvatochromic measurements on butyl rubbers [AD-A263088] p 3334 N93-29795

UNIVERSITY COLL. OF SWANSEA (WALES).
The effect of orthogonal-mode rotation on forced convection in a circular-sectioned tube fitted with full circumferential transverse ribs p 3254 N93-29937

UNIVERSITY OF CENTRAL FLORIDA, ORLANDO.
Design, building, and testing of the postlanding systems for the assured crew return vehicle p 3229 N93-29726

UNIVERSITY OF EASTERN ILLINOIS, CHARLESTON.
Solving a product safety problem using a recycled high density polyethylene container p 3292 N93-30964
UNIVERSITY OF NORTHERN ILLINOIS, DE KALB.
Analytical applications of electrified interfaces between two immiscible solutions
[AD-A263085] p 3311 N93-29132
Effect of zinc and iron ions on the electrochemistry of nickel oxide electrode: Slow cyclic voltammetry
[AD-A263098] p 3311 N93-29133
UNIVERSITY OF PETROLEUM AND MINERALS, DHAHRAN (SAUDI ARABIA).
Nonlinear attitude control of planar structures in space using only internal controls p 3280 N93-29991
UNIVERSITY OF SOUTH FLORIDA, TAMPA.
Effect of design selection on response surface performance
[NASA-CR-4520] p 3249 N93-29885
UNIVERSITY OF SOUTHERN CALIFORNIA, LOS ANGELES.
Distributed Virtual System (DIVIRS) Project
[NASA-CR-193234] p 3526 N93-29169
NO2 unimolecular decomposition: Step-like variation of k(sub uni)(E) p 3318 N93-30068
UNIVERSITY OF SOUTHERN CALIFORNIA, MARINA DEL REY.
Natural language generation
[AD-A262578] p 3524 N93-28579
Gigabit network communications research
[AD-A264895] p 3536 N93-31026
UNIVERSITY OF WEST FLORIDA, PENSACOLA.
Image segmentation using fuzzy LVQ clustering networks p 3511 N93-29528
UTAH STATE UNIV., LOGAN.
Description of the Joint Damping Experiment (JDX)
p 3263 N93-28703
Plasma diagnostics by antenna impedance measurements p 3400 N93-28820
Thermion: Verification of a thermionic heat pipe in microgravity p 3235 N93-29757
USU center of excellence in theory and analysis of the geo-plasma environment
[AD-A264750] p 3590 N93-30585
UTAH UNIV., SALT LAKE CITY.
Sudden loading and fatigue effects on the human spine
[PB93-167526] p 3493 N93-29199
Applications of three-dimensional modeling in electromagnetic exploration p 3391 N93-30010
Studies of fiber-matrix adhesion on compression strength p 3304 N93-30846
The initiation, propagation, and effect of matrix microcracks in cross-ply and related laminates
p 3304 N93-30847

V

VANDERBILT UNIV., NASHVILLE, TN.
Cratering in glasses impacted by debris or micrometeorites p 3340 N93-29368
The AFOSR Workshop on the Future of EEG and MEG
[AD-A264338] p 3495 N93-30160
VARIAN ASSOCIATES, PALO ALTO, CA.
Improved field emitter current densities and stability through the application of a proprietary process
[AD-A263464] p 3411 N93-29833
Improved field emitter current densities and stability through the application of a proprietary process
[AD-A264048] p 3411 N93-30031
VERMONT UNIV., BURLINGTON.
Velocity measurements of low Reynolds number tube flow using fiber-optic technology
[DE93-009865] p 3422 N93-29335
VICTORIA UNIV. (BRITISH COLUMBIA).
A closed-form formula for the manipulator regressor
p 3355 N93-30218
Modelling of channel thickness modulation effect in SI GaAs MESFET's p 3356 N93-30229
Coding for frequency hopped spread spectrum satellite communications p 3365 N93-30283
VIRGINIA POLYTECHNIC INST. AND STATE UNIV., BLACKSBURG.
Design and construction of a prototype ACTS propagation terminal
[NASA-CR-193071] p 3404 N93-28539
Environmental effects on stitched RTM composites
[NASA-CR-193221] p 3297 N93-29107
An experimental study of flow over a 6 to 1 prolate spheroid at incidence p 3239 N93-29124
Generation of carbon monoxide in compartment fires
[PB93-146702] p 3244 N93-29211
A spectral method determination of the first critical Rayleigh number for a low-Prandtl number crystal melt in a cylindrical container
[NASA-CR-193238] p 3594 N93-29214
Solar electric propulsion cargo spacecraft for Mars missions p 3235 N93-29758
Static and dynamic large deflection flexural response of graphite-epoxy beams
[NASA-CR-4118] p 3454 N93-30374
Compressible turbulence in a high-speed high Reynolds number mixing layer p 3242 N93-30583
VIRGINIA UNIV., CHARLOTTESVILLE.
Control and circadian behavior by transplanted suprachiasmatic nuclei
[AD-A264553] p 3496 N93-30382
The 12 UM contribution of nearby galaxies to the infrared background
[AD-A264336] p 3654 N93-30419
Photoreceptors regulating circadian behavior: A mouse model
[AD-A264881] p 3497 N93-30908
VISIDYNE, INC., BURLINGTON, MA.
A program to determine the pointing angle to a specular point
[AD-A262777] p 3630 N93-29460
VON KARMAN INST. FOR FLUID DYNAMICS, RHODE-SAINT-GENESE (BELGIUM).
Thermal effects of a coolant film along the suction side of a high pressure turbine nozzle guide vane
p 3253 N93-29930
On the development of a film cooling layer
p 3258 N93-29959
VOUGHT SYSTEMS DIV., DALLAS, TX.
Clustered Lance Booster (CLB) feasibility study
[AD-A262746] p 3286 N93-28593
VRIJE UNIV., BRUSSELS (BELGIUM).
Comparative study of undersea fields produced by various dipoles p 3397 N93-30740

W

WAKE FOREST UNIV., WINSTON-SALEM, NC.
Multiple neuron recording in the hippocampus of freely moving animals
[AD-A264807] p 3492 N93-30594
WASHINGTON STATE UNIV., PULLMAN.
Examination of shock induced chemical reactions in liquids using time-resolved optical spectroscopy
p 3318 N93-30073
WASHINGTON UNIV., SAINT LOUIS, MO.
Artificial intelligence methodologies in flight related differential game, control and optimization problems
[AD-A262405] p 3541 N93-28498
SIMS chemical analysis of extended impacts on the leading and trailing edges of LDEF experiment AO187-2
p 3318 N93-29367
WASHINGTON UNIV., SEATTLE.
IUE observations of cataclysmic variable
[NASA-CR-193188] p 3629 N93-28634
Upper ocean model of dissolved atmospheric gases
[DE93-010151] p 3487 N93-29327
Antares: A low cost modular launch vehicle for the future p 3235 N93-29759
Two-parameter crack tip field associated with stable crack growth in a thin plate: A hybrid analysis
[AD-A264221] p 3453 N93-30147
Quantum field theory in spaces with closed time-like curves
[DE93-010564] p 3605 N93-30481
Predictions of a non-Gaussian model for large scale structure
[DE93-010196] p 3636 N93-30528
Multi-parameter optimization tool for low-cost commercial fuselage crown designs
p 3305 N93-30858
WATERLOO UNIV. (ONTARIO).
On subband coding/embedded vector quantization for speech coding p 3355 N93-30220
Thermodynamic and structural properties of metallic glasses and supercooled liquids
[ISBN-0-315-72443-9] p 3605 N93-30359
Analytical and experimental study of laminar free convective heat transfer from isothermal convex bodies of arbitrary shape
[ISBN-0-315-72512-5] p 3426 N93-30379
WEIZMANN INST. OF SCIENCE, REHOVOTH (ISRAEL).
Topology and statistics in zero dimensions
[DE93-604080] p 3607 N93-30932
Regular and chaotic motion of two dimensional electrons in a strong magnetic field
[DE93-604091] p 3607 N93-30933
WENTWORTH INST., BOSTON, MA.
Aerospace payload design and development
[AD-A264502] p 3289 N93-30402
WEST VIRGINIA UNIV., MORGANTOWN.
Planning of a West Virginia University Research Center in the basic materials sciences
[DE93-011731] p 3592 N93-28647
WESTINGHOUSE ELECTRIC CORP., BALTIMORE, MD.
Design considerations for a night, air-to-surface attack capability on a dual role fighter p 3251 N93-28871
WESTINGHOUSE ELECTRIC CORP., ORLANDO, FL.
Design considerations for a night, air-to-surface attack capability on a dual role fighter p 3251 N93-28871
WESTINGHOUSE ELECTRIC CORP., PITTSBURGH, PA.
Processing, fabrication, and demonstration of HTS integrated microwave circuits
[AD-A263161] p 3406 N93-28940
WESTINGHOUSE HANFORD CO., RICHLAND, WA.
Hanford Environmental Information System (HEIS) user's manual, volume 1
[DE93-007465] p 3470 N93-29135
Structural design, analysis, and code evaluation of an odd-shaped pressure vessel
[DE93-008182] p 3447 N93-30632
WESTINGHOUSE SAVANNAH RIVER CO., AIKEN, SC.
Technical bases for precipitate hydrolysis process operating parameters, revision 1
[DE93-009894] p 3309 N93-28553
Acid solution absorption of extruded polyethylene foam
[DE93-011701] p 3330 N93-28839
Effects of internal helium on mechanical properties of Nitronic (tm) 40 stainless steel
[DE93-009902] p 3324 N93-29265
Transient response of embedded thermocouples
[DE93-009889] p 3431 N93-29325
WHEELING COLL., WV.
National Technology Transfer Center
p 3626 N93-30700
WHITE SANDS TEST FACILITY, LAS CRUCES, NM.
APU diaphragm testing. Test plan
[NASA-TM-108251] p 3271 N93-29387
WICKERSHEIMER ENGINEERS, INC., CHAMPAIGN, IL.
Concept design example, Computer Aided Structural Modeling (CASM). Scheme A
[AD-A264759] p 3529 N93-29657
Concept design example, Computer Aided Structural Modeling (CASM). Scheme B
[AD-A264760] p 3529 N93-29658
WILFRID LAURIER UNIV., WATERLOO (ONTARIO).
Image enhancement using an analog device neural network p 3376 N93-30346
WINDSOR UNIV. (ONTARIO).
Realization of high speed adaptive FIR digital filters
p 3355 N93-30222
WISCONSIN UNIV., MADISON.
Undulator Spectromicroscopy Facility at the Advanced Light Source
[DE93-007964] p 3261 N93-28490
Nonlinear coupling of tearing fluctuations in the Madison Symmetric Torus
[DE93-010131] p 3584 N93-28602
Microstructural understanding and critical current optimization of advanced high field superconductors
[DE93-011046] p 3592 N93-28643
New technologies for UV detectors
p 3582 N93-28786
The photodissociation and reaction dynamics of vibrationally excited molecules
[DE93-010896] p 3565 N93-28879
The fluctuation induced Hall effect
[DE93-010130] p 3585 N93-28912
Nonconservative and reverse spectral transfer in Hasegawa-Mima turbulence
[DE93-010132] p 3585 N93-28913
A planetary version of PC-McIDAS
p 3614 N93-29236
Application of Schlieren optical techniques for the measurement of gas temperature and turbulent diffusivity in a diesel engine
[AD-A263810] p 3580 N93-29880
SIRIUS-P: An inertially confined direct drive laser fusion power reactor
[DE93-012433] p 3439 N93-30186
WISCONSIN UNIV., MILWAUKEE.
GENESIS 2: Advanced lunar outpost
p 3235 N93-29760
WISCONSIN UNIV. HOSPITAL, MADISON.
Modeling the effects of drop drag and breakup on fuel sprays
[AD-A263650] p 3445 N93-29388
WOODS HOLE OCEANOGRAPHIC INST., MA.
Optical measurements of ripples using a scanning laser slope gauge. Part 1: Instrumentation and preliminary results
[AD-A261939] p 3486 N93-28996
Near real-time GIS in deep-ocean exploration
[AD-A262073] p 3487 N93-29003

Geochemical and fluid dynamic investigations into the nature of chemical heterogeneity in the Earth's mantle
[AD-A262753] p 3477 N93-29405

Fiber optic chemical sensors for characterizing the carbon cycle in ocean margin regions
[DE93-011442] p 3489 N93-30056

Marine microbial production of dimethylsulfide from dissolved dimethylsulfoniopropionate
[NASA-CR-193278] p 3492 N93-30665

WOOSTER COLL., OH.

Loading and testing a light scattering cell with a binary fluid mixture near its critical composition
[NASA-CR-193147] p 3415 N93-28557

WORCESTER POLYTECHNIC INST., MA.

Solar powered multipurpose remotely powered aircraft
p 3229 N93-29722

Rotational fluid flow experiment p 3235 N93-29761

WRIGHT LAB., EGLIN AFB, FL.

A ceramic fracture model for high velocity impact
[AD-A264728] p 3454 N93-30545

WRIGHT LAB., WRIGHT-PATTERSON AFB, OH.

System automation and pilot-vehicle-interface for unconstrained low-altitude night attack
p 3503 N93-28867

Microstructural effects on the deformation and fracture of the alloy Ti-25Al-10Nb-3B-1Mo
[AD-A263095] p 3323 N93-29144

Results of a round robin test program: Complex modulus properties of a polymeric damping material
[AD-A263619] p 3332 N93-29344

Advanced thermally-stable, coal-derived, jet fuels program: Experiment system and model development
[AD-A262747] p 3342 N93-29402

A real-time, hardware-in-the-loop simulation of an unmanned aerial research vehicle
[AD-A262477] p 3248 N93-29409

Modal survey of a full-scale F-18 wind tunnel model
[AD-A262482] p 3240 N93-29410

The effect of high temperature on wall shear in a two dimensional wall jet
[AD-A262982] p 3423 N93-29426

An upwind method for the solution of the 3D Euler and Navier-Stokes equations on adaptively refined meshes
[AD-A262863] p 3423 N93-29472

Atmospheric transverse coherence length measurement system for laser communications
[AD-A263563] p 3439 N93-29827

Heat transfer in high turbulence flows: A 2-D planar wall jet p 3254 N93-29935

Computation of a delta-wing roll-and-hold maneuver
[AD-A264704] p 3260 N93-30498

Low cost instrumentation: Parallel port analog to digital converter
[AD-A263468] p 3433 N93-30584

WUERZBURG UNIV. (GERMANY).

Digital image processing of descanned terrestrial ground photographs p 3459 N93-28928

WYOMING UNIV., LARAMIE.

Exotic atoms
[DE93-010242] p 3564 N93-28611

Energy efficient drivepower, volume 2
[DE93-012437] p 3410 N93-29814

Energy efficient drivepower: An overview
[DE93-012435] p 3411 N93-30057

Energy efficient drivepower
[DE93-012436] p 3411 N93-30058

Y

YALE UNIV., NEW HAVEN, CT.

Measurements of rare composite objects and high sensitivity searches for novel forms of matter produced in high energy heavy ion collisions
[DE93-009945] p 3574 N93-28569

Observation of reaction intermediates in crystalline RDX p 3318 N93-30067

Numerical modeling of multidimensional flames with application to energetic materials p 3319 N93-30079

Nonlinear spectroscopy of multicomponent droplets and two- and three-dimensional measurements in flames
[AD-A264341] p 3425 N93-30162

Representations of shape in object recognition and long-term visual memory
[AD-A264342] p 3499 N93-30163

Analysis and computation for vortex dynamics and rarefied gases
[AD-A264705] p 3427 N93-30499

The 1991 neural information processing systems: Natural and synthetic
[AD-A264754] p 3623 N93-30559

Z

ZEISS (CARL), JENA (GERMANY).

SAR shape-from-shading for a populated alpine area
p 3458 N93-28923

ZURICH UNIV. (SWITZERLAND).

Recording of forest surface in SAR-images with statistical methods in areas of pronounced relief
p 3457 N93-28920

CONTRACT NUMBER INDEX

SCIENTIFIC AND TECHNICAL AEROSPACE REPORTS VOLUME 31 NUMBER 11

Typical Contract Number Index Listing

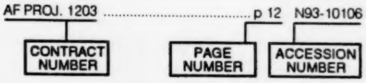
AF PROJ. 1203 .... p 12 N93-10106
CONTRACT NUMBER
PAGE NUMBER
ACCESSION NUMBER

Listings in this index are arranged alphanumerically by contract number. Under each contract number the accession numbers denoting documents that have been produced as a result of research done under that contract are arranged in ascending order. The page number helps to locate the citation in the abstract section. The accession number denotes the number by which the citation is identified.

AF PROJ. ILI-R p 3439 N93-29827
AF PROJ. 1121 p 3498 N93-30026
AF PROJ. 2302 p 3454 N93-30545
AF PROJ. 2306 p 3323 N93-29144
AF PROJ. 2311 p 3652 N93-28585
AF PROJ. 2401 p 3332 N93-29344
AF PROJ. 2403 p 3248 N93-29409
AF PROJ. 2420 p 3295 N93-28592
AF PROJ. 3048 p 3342 N93-29402
p 3312 N93-29510
AF PROJ. 4643 p 3399 N93-30757
AF PROJ. 6670 p 3484 N93-30535
AF PROJ. 7184 p 3507 N93-29888
p 3507 N93-29889
AF PROJ. 7719 p 3498 N93-29481
AF-AFOSR-0013-90 p 3427 N93-30499
AF-AFOSR-0025-91 p 3540 N93-30364
AF-AFOSR-0026-90 p 3590 N93-30585
AF-AFOSR-0034-90 p 3428 N93-30630
AF-AFOSR-0035-90 p 3420 N93-29141
AF-AFOSR-0043-89 p 3298 N93-29130
AF-AFOSR-0044-91 p 3652 N93-28756
AF-AFOSR-0045-90 p 3570 N93-30366
AF-AFOSR-0050-91 p 3555 N93-30363
AF-AFOSR-0068-90 p 3534 N93-30549
AF-AFOSR-0082-89 p 3400 N93-30880
AF-AFOSR-0082-90 p 3477 N93-29831
AF-AFOSR-0083-90 p 3543 N93-29791
AF-AFOSR-0092-90 p 3492 N93-30594
AF-AFOSR-0094-88 p 3340 N93-30900
AF-AFOSR-0098-90 p 3496 N93-30382
AF-AFOSR-0099-90 p 3316 N93-30551
AF-AFOSR-0106-91 p 3329 N93-28495
AF-AFOSR-0115-91 p 3554 N93-29411
AF-AFOSR-0122-90 p 3338 N93-30610
AF-AFOSR-0138-90 p 3260 N93-30550
AF-AFOSR-0142-90 p 3411 N93-29922
AF-AFOSR-0149-91 p 3399 N93-30879
AF-AFOSR-0150-91 p 3425 N93-30162
AF-AFOSR-0185-89 p 3337 N93-30417
AF-AFOSR-0192-91 p 3522 N93-30179
AF-AFOSR-0198-90 p 3580 N93-30205
AF-AFOSR-0199-91 p 3495 N93-30153
AF-AFOSR-0202-90 p 3555 N93-29979
AF-AFOSR-0205-91 p 3535 N93-30614
AF-AFOSR-0206-89 p 3339 N93-30898
AF-AFOSR-0237-89 p 3555 N93-29923
AF-AFOSR-0239-91 p 3533 N93-30418
AF-AFOSR-0246-88 p 3591 N93-28496
AF-AFOSR-0249-90 p 3425 N93-30369
AF-AFOSR-0260-88 p 3581 N93-30905
AF-AFOSR-0268-91 p 3317 N93-30816
AF-AFOSR-0275-88 p 3499 N93-30033
AF-AFOSR-0276-91 p 3534 N93-30544
AF-AFOSR-0279-91 p 3497 N93-30904
AF-AFOSR-0285-90 p 3317 N93-30667
AF-AFOSR-0363-89 p 3452 N93-29349
AF-AFOSR-0365-90 p 3597 N93-30161
AF-AFOSR-0380-91 p 3321 N93-28591
AF-AFOSR-0399-91 p 3298 N93-29282
AF-AFOSR-0413-91 p 3493 N93-28759
AF-AFOSR-0422-91 p 3599 N93-30560
AF-AFOSR-0423-89 p 3453 N93-30159
AF-AFOSR-0427-89 p 3253 N93-29934
AF-AFOSR-0428-91 p 3496 N93-30422
AF-AFOSR-0438-89 p 3597 N93-30164
AF-AFOSR-0438-91 p 3623 N93-30559
AF-AFOSR-0441-89 p 3337 N93-30552
AF-AFOSR-0446-89 p 3333 N93-29511
AF-AFOSR-0467-89 p 3654 N93-30419
AF-AFOSR-0481-89 p 3544 N93-30165
AF-AFOSR-0490-89 p 3496 N93-30494
AF-AFOSR-0518-89 p 3541 N93-28498
AF-AFOSR-0526-89 p 3534 N93-30561
AFOSR-MIPR-0007-92 p 3528 N93-29345
ARB-A932-129 p 3470 N93-29669
ARPA ORDER 6822 p 3531 N93-29873
ARPA ORDER 7330 p 3533 N93-30125
p 3534 N93-30523
ARPA ORDER 7597 p 3615 N93-29459
p 3530 N93-29821
p 3530 N93-29822
p 3530 N93-29823
p 3579 N93-29824
ARPA ORDER 7932 p 3406 N93-28940
ARPA ORDER 8162 p 3404 N93-28483
p 3412 N93-30409
ARPA ORDER 8228 p 3529 N93-29493
ARPA ORDER 8351 p 3580 N93-29973
ARPA ORDER 8363 p 3409 N93-29513
BCRS PROJ. AO-2.24 p 3460 N93-29320
BCRS PROJ. TE-2.10 p 3460 N93-29321
BCRS PROJ. TE-2.11 p 3460 N93-29307
BCRS PROJ. 3.2/CO-01 p 3461 N93-29465
BCRS PROJ. 6.5/IS-08 p 3461 N93-29466
BMFT-0326800D p 3259 N93-29999
BMFT-13-N-5439/6 p 3325 N93-30115
CONACYT-60558 p 3515 N93-29552
DA PROJ. IL1-61102-AH-43 p 3315 N93-30405
DA PROJ. LDF-P p 3597 N93-30144
DA PROJ. 1L1-61102-AH-43 p 3309 N93-28514
p 3341 N93-28515
p 3342 N93-29762
p 3432 N93-30032
p 3413 N93-30539
DA PROJ. 1L1-62211-A-47-AA p 3240 N93-29450
DA PROJ. 1L1-62618-AH-80 p 3294 N93-28559
p 3453 N93-29801
DA PROJ. 1L1-62716-AH-70 p 3505 N93-28941
DA PROJ. 1L1-62786-AH-98 p 3495 N93-30196
DA PROJ. 2Q2-63007-A-795 p 3261 N93-29972
DA PROJ. 2930 p 3508 N93-30167
DA PROJ. 3E1-62720-A-835 p 3482 N93-29399
DA PROJ. 3M1-61102-BS-15 p 3495 N93-29820
DA PROJ. 3058 p 3287 N93-28658
DA PROJ. 3103 p 3481 N93-28876
DA PROJ. 4A7-62784-AT-42 p 3379 N93-28588
DA PROJ. 4135 p 3597 N93-30146
DAAG46-85-K-0008 p 3325 N93-29981
DAAH01-92-C-R359 p 3259 N93-30877
DAAH04-93-G-0068 p 3387 N93-29875
DAAK60-91-C-0028 p 3295 N93-28660
DAAL02-87-C-0113 p 3381 N93-29011
DAAL03-86-G-0208 p 3543 N93-29917
DAAL03-86-K-0174 p 3445 N93-29388
p 3580 N93-29880
DAAL03-86-K-0175 p 3462 N93-29834
DAAL03-87-C-0021 p 3342 N93-29835
DAAL03-87-K-0004 p 3491 N93-29915
DAAL03-87-K-0006 p 3432 N93-29390
DAAL03-87-K-0023 p 3604 N93-29384
DAAL03-87-K-0106 p 3528 N93-29294
DAAL03-88-K-0027 p 3453 N93-29855
DAAL03-88-K-0109 p 3439 N93-29853
DAAL03-88-K-0116 p 3549 N93-29871
DAAL03-89-G-0089 p 3299 N93-29982
DAAL03-89-G-0098 p 3554 N93-29385
DAAL03-89-G-0105 p 3411 N93-29986
DAAL03-89-K-0025 p 3313 N93-30030
DAAL03-89-K-0100 p 3439 N93-29983
DAAL03-89-K-0102 p 3596 N93-29859
DAAL03-89-K-0106 p 3487 N93-29298
DAAL03-89-K-0167 p 3595 N93-29383
DAAL03-90-C-0006 p 3439 N93-29918
DAAL03-90-G-0002 p 3594 N93-29293
DAAL03-90-G-0015 p 3588 N93-29382
DAAL03-90-G-0023 p 3334 N93-29856
DAAL03-90-G-0024 p 3311 N93-29283
DAAL03-90-G-0030 p 3342 N93-29296
DAAL03-90-G-0078 p 3531 N93-29916
DAAL03-90-G-0095 p 3530 N93-29865
DAAL03-90-G-0103 p 3549 N93-29854
p 3555 N93-29979
DAAL03-90-G-0328 p 3610 N93-30124
DAAL03-90-K-0001 p 3240 N93-29284
DAAL03-91-C-0008 p 3320 N93-30102
DAAL03-91-G-0032 p 3332 N93-29290
DAAL03-91-G-0091 p 3431 N93-29297
DAAL03-91-G-0101 p 3554 N93-29292
p 3550 N93-29872
p 3555 N93-29878
DAAL03-91-G-0184 p 3311 N93-29291
DAAL03-91-G-0203 p 3532 N93-30014
DAAL03-92-C-0015 p 3423 N93-29353
DAAL03-92-G-0214 p 3315 N93-30534
DAAL03-92-G-0296 p 3580 N93-29887
DAAL03-92-G-0303 p 3259 N93-29985
DAAL03-92-G-0378 p 3532 N93-29980
DAAL03-92-K-0003 p 3312 N93-29389
DAAL04-92-C-0005 p 3430 N93-28989
DABT63-91-C-0001 p 3536 N93-31026
DACA39-86-C-0024 p 3529 N93-29657
p 3529 N93-29658
DACA89-90-K-0003 p 3379 N93-28588
DACW29-90-D-0018 p 3459 N93-29146
DACW72-89-C-0025 p 3245 N93-29468
DAHC35-89-D-0046 p 3531 N93-29874
p 3261 N93-29972
DAJA-91-M-0311 p 3387 N93-29877
DAJA45-91-C-0022 p 3334 N93-29795
DAJA45-92-M-0260 p 3597 N93-29974
DAMD17-91-C-1112 p 3495 N93-29820
DARPA ORDER 56743 p 3597 N93-30120
DASG60-90-C-0103 p 3434 N93-28768
p 3650 N93-28822
DASG60-91-C-0006 p 3521 N93-29492
DASG60-92-C-0087 p 3595 N93-29397
DASG60-92-C-0120 p 3286 N93-28593
DE-AC01-90CE-90053 p 3670 N93-30212
DE-AC02-76CH-00016 p 3329 N93-28551
p 3435 N93-28594
p 3309 N93-28880
p 3548 N93-28891
p 3323 N93-29256
p 3575 N93-29317
DE-AC02-76CH-03000 p 3633 N93-28676
p 3593 N93-28888
p 3653 N93-28962
p 3634 N93-28963
p 3407 N93-29048
p 3382 N93-29245
p 3567 N93-29351
DE-AC02-83CH-10093 p 3490 N93-28890
p 3464 N93-28971
p 3464 N93-29925
p 3464 N93-29965
p 3465 N93-30206
p 3465 N93-30207
p 3465 N93-30208
p 3466 N93-30891
DE-AC02-85ER-40194 p 3576 N93-30488
DE-AC03-76SF-00098 p 3353 N93-28570
p 3405 N93-28581
p 3592 N93-28582
p 3592 N93-28642
p 3417 N93-28663
p 3430 N93-28664
p 3330 N93-28761
p 3436 N93-28847
p 3431 N93-29149
p 3594 N93-29150
p 3298 N93-29191
p 3331 N93-29248
p 3594 N93-29249
p 3575 N93-29302
p 3595 N93-29417
p 3572 N93-29629

p 3313 N93-29766
p 3569 N93-29805
p 3604 N93-29806
p 3569 N93-29860
p 3596 N93-29868
p 3261 N93-29869
p 3575 N93-29870
p 3551 N93-30392
p 3598 N93-30393
p 3440 N93-30530
p 3433 N93-30531
DE-AC03-76SF-00515 .... p 3616 N93-30122
DE-AC03-89ER-51114 .... p 3588 N93-29334
DE-AC03-91SF-18601 .... p 3585 N93-28836
DE-AC04-76DP-00613 .... p 3442 N93-28552
p 3332 N93-29328
DE-AC04-76DP-00789 .... p 3463 N93-28603
p 3417 N93-28639
p 3405 N93-28641
p 3430 N93-28645
p 3442 N93-28837
p 3406 N93-28944
p 3239 N93-29035
p 3526 N93-29127
p 3575 N93-29151
p 3437 N93-29180
p 3443 N93-29185
p 3538 N93-29186
p 3549 N93-29187
p 3594 N93-29188
p 3278 N93-29250
p 3437 N93-29264
p 3588 N93-29334
p 3530 N93-29808
p 3279 N93-29840
p 3543 N93-30012
p 3532 N93-30050
p 3336 N93-30051
p 3344 N93-30069
p 3412 N93-30118
p 3412 N93-30127
p 3425 N93-30184
p 3453 N93-30185
p 3412 N93-30370
p 3465 N93-30391
p 3623 N93-30482
p 3491 N93-30483
p 3378 N93-30508
p 3281 N93-30509
p 3433 N93-30510
p 3598 N93-30511
p 3413 N93-30516
p 3598 N93-30517
p 3413 N93-30650
p 3484 N93-30651
p 3447 N93-30654
p 3433 N93-30655
p 3339 N93-30656
p 3570 N93-30669
DE-AC04-76DR-00789 .... p 3416 N93-28595
p 3330 N93-28838
p 3432 N93-29842
p 3453 N93-29843
DE-AC04-88DP-43495 .... p 3592 N93-28568
DE-AC05-76ER-01067 .... p 3566 N93-29184
DE-AC05-76ER-02504 .... p 3566 N93-29313
DE-AC05-76OR-00001 .... p 3472 N93-30180
DE-AC05-84OR-21400 .... p 3404 N93-28523
p 3320 N93-28564
p 3584 N93-28583
p 3321 N93-28679
p 3490 N93-28890
p 3538 N93-28894
p 3593 N93-28956
p 3443 N93-28968
p 3469 N93-28992
p 3541 N93-29047
p 3382 N93-29244
p 3444 N93-29247
p 3444 N93-29254
p 3460 N93-29255
p 3444 N93-29316
p 3383 N93-29348
p 3334 N93-29767
p 3324 N93-29786
p 3325 N93-29813
p 3472 N93-30009
p 3335 N93-30047
p 3259 N93-30168
p 3472 N93-30180
p 3336 N93-30182
p 3446 N93-30210
p 3454 N93-30213
p 3544 N93-30529
p 3394 N93-30631
p 3327 N93-30652
DE-AC05-84OS-21400 .... p 3451 N93-28832
DE-AC05-84OT-21400 .... p 3612 N93-28840
DE-AC06-76RL-01830 .... p 3320 N93-28548
p 3238 N93-28662
p 3354 N93-28893
p 3481 N93-29054
p 3322 N93-29061
p 3323 N93-29101
p 3383 N93-29308
p 3625 N93-29329
p 3318 N93-29627
p 3550 N93-30041
p 3473 N93-30183
DE-AC06-87RL-10930 .... p 3470 N93-29135
p 3447 N93-30632
DE-AC07-76ID-01570 .... p 3565 N93-28833
p 3524 N93-28834
p 3505 N93-28942
p 3532 N93-30034
p 3589 N93-30181
DE-AC09-89SR-18035 .... p 3309 N93-28553
p 3330 N93-28839
p 3324 N93-29265
p 3431 N93-29325
DE-AC22-88ID-12735 .... p 3584 N93-28649
DE-AC22-90PC-90044 .... p 3341 N93-28752
DE-AC22-91PC-90018 .... p 3341 N93-28668
DE-AC22-91PC-90183 .... p 3417 N93-28630
DE-AI01-86CE-90213 .... p 3416 N93-28566
DE-AI02-88CE-90024 .... p 3330 N93-28687
DE-AI05-84ER-13230 .... p 3330 N93-28650
DE-AI79-90BP-08212 .... p 3410 N93-29814
p 3411 N93-30057
p 3411 N93-30058
DE-AS03-88DP-10754 .... p 3439 N93-30186
DE-FC03-90ER-61010 .... p 3247 N93-28586
p 3624 N93-29100
DE-FC22-83FE-60149 .... p 3603 N93-28964
DE-FG01-89CE-34023 .... p 3490 N93-28848
DE-FG02-84ER-13242 .... p 3311 N93-29182
DE-FG02-84ER-40146 .... p 3565 N93-28849
DE-FG02-84ER-40173 .... p 3574 N93-28565
DE-FG02-84ER-60257 .... p 3467 N93-28543
DE-FG02-85ER-40211 .... p 3603 N93-28961
DE-FG02-85ER-40233 .... p 3563 N93-28542
DE-FG02-85ER-53198 .... p 3584 N93-28602
p 3585 N93-28912
DE-FG02-86ER-13500 .... p 3565 N93-28879
DE-FG02-86ER-13511 .... p 3309 N93-28688
DE-FG02-86ER-13640 .... p 3325 N93-30059
DE-FG02-86ER-52131 .... p 3592 N93-28643
DE-FG02-86ER-53223 .... p 3586 N93-29056
DE-FG02-86ER-60448 .... p 3490 N93-28651
DE-FG02-87ER-40328 .... p 3565 N93-28960
DE-FG02-87ER-40333 .... p 3564 N93-28611
DE-FG02-87ER-40339 .... p 3563 N93-28546
DE-FG02-87ER-40363 .... p 3564 N93-28678
DE-FG02-87ER-45318 .... p 3321 N93-28631
DE-FG02-87ER-60565 .... p 3536 N93-30934
DE-FG02-88ER-12813 .... p 3427 N93-30489
DE-FG02-88ER-13822 .... p 3310 N93-29051
DE-FG02-88ER-13896 .... p 3417 N93-28751
DE-FG02-88ER-13913 .... p 3422 N93-29326
DE-FG02-88ER-13965 .... p 3564 N93-28652
DE-FG02-88ER-25053 .... p 3419 N93-29025
DE-FG02-88ER-45365 .... p 3321 N93-28902
p 3321 N93-28957
DE-FG02-88ER-53263 .... p 3589 N93-30189
DE-FG02-89ER-14012 .... p 3565 N93-28959
DE-FG02-89ER-14042 .... p 3444 N93-29330
DE-FG02-89ER-53291 .... p 3585 N93-28913
DE-FG02-89ER-60883 .... p 3472 N93-30131
DE-FG02-90ER-14132 .... p 3436 N93-28653
DE-FG02-90ER-40562 .... p 3574 N93-28569
DE-FG02-90ER-45417 .... p 3325 N93-30060
DE-FG02-90ER-61067 .... p 3484 N93-30055
DE-FG02-91CH-10482 .... p 3592 N93-28647
DE-FG02-91ER-14173 .... p 3329 N93-28541
DE-FG02-91ER-14185 .... p 3593 N93-29096
DE-FG02-91ER-20033 .... p 3491 N93-29181
DE-FG02-91ER-40631 .... p 3569 N93-30128
DE-FG02-91ER-40640 .... p 3570 N93-30505
DE-FG02-91ER-45461 .... p 3320 N93-28545
DE-FG02-91ER-61173 .... p 3422 N93-29335
DE-FG02-91ER-61202 .... p 3486 N93-28670
DE-FG02-92ER-14282 .... p 3566 N93-29183
DE-FG02-92ER-14288 .... p 3603 N93-28747
DE-FG02-92ER-25119 .... p 3418 N93-28878
DE-FG02-92ER-25146 .... p 3548 N93-29057
DE-FG02-92ER-40719 .... p 3574 N93-28969
DE-FG02-92ER-45468 .... p 3261 N93-28490
DE-FG02-92ER-54141 .... p 3586 N93-29049
DE-FG02-92ER-61437 .... p 3489 N93-30056
DE-FG02-92ER-61473 .... p 3476 N93-28677
DE-FG02-92ER-75700 .... p 3567 N93-29416
DE-FG03-85ER-45197 .... p 3603 N93-28958
DE-FG03-88ER-45378 .... p 3597 N93-30141
DE-FG03-92ER-25129 .... p 3547 N93-28648
DE-FG03-92ER-40732 .... p 3566 N93-29261
DE-FG03-93ER-40757 .... p 3556 N93-28601
DE-FG05-80ET-53088 .... p 3584 N93-28598
p 3584 N93-28599
p 3585 N93-28910
p 3587 N93-29148
p 3423 N93-29804
DE-FG05-85ER-13456 .... p 3564 N93-28665
DE-FG05-85ER-45202 .... p 3338 N93-30601
DE-FG05-87ER-25036 .... p 3557 N93-30048
DE-FG05-87ER-40321 .... p 3569 N93-29807
DE-FG05-88ER-40441 .... p 3566 N93-29184
DE-FG05-88ER-40442 .... p 3566 N93-29184
DE-FG05-89ER-40525 .... p 3392 N93-30126
DE-FG05-89ER-40530 .... p 3576 N93-30054
DE-FG05-89ER-53301 .... p 3585 N93-28749
DE-FG05-91ER-12119 .... p 3330 N93-28748
DE-FG05-91ER-40627 .... p 3568 N93-29764
DE-FG05-91ER-40642 .... p 3573 N93-28522
DE-FG05-91ER-61219 .... p 3470 N93-29318
DE-FG06-85ER-40224 .... p 3569 N93-29841
p 3577 N93-30532
DE-FG06-87ER-13664 .... p 3310 N93-28911
DE-FG06-90ER-61037 .... p 3487 N93-29327
DE-FG06-91ER-40614 .... p 3605 N93-30481
p 3636 N93-30528
DE-FG06-91ER-40637 .... p 3577 N93-30532
DE-FG06-92ER-14236 .... p 3564 N93-28604
DE-FG07-88ER-12820 .... p 3425 N93-30132
DE-FG07-89ER-12893 .... p 3512 N93-29531
DE-FG07-90ID-13040 .... p 3465 N93-30011
DE-FG07-91ID-13042 .... p 3473 N93-30187
DE-FG22-89PC-89762 .... p 3316 N93-30653
DE-FG22-89PC-89786 .... p 3314 N93-30188
DE-FG22-90PC-90291 .... p 3309 N93-28750
DI-14-35-0001-30428 .... p 3468 N93-28899
p 3471 N93-29861
DLA900-86-C-2045 .... p 3501 N93-28757
p 3493 N93-28758
DLA900-90-D-0305 .... p 3320 N93-28499
DNA001-86-C-0308 .... p 3506 N93-29484
DNA001-88-C-0223 .... p 3479 N93-30593
DRET-88-34-001 .... p 3417 N93-28744
DTCG39-91-D-E33A21 .... p 3335 N93-29881
p 3335 N93-29886
DTFA-01-91-Z-02036 .... p 3481 N93-29257
DTFA01-84-Z-02038 .... p 3262 N93-30103
DTFA01-88-Z-02015 .... p 3236 N93-30673
DTFA01-89-Z-02033 .... p 3261 N93-29815
DTFR53-82-C-00254 .... p 3507 N93-29675
DTFR53-91-C-00064 .... p 3444 N93-29205
DTFR53-91-C-00065 .... p 3447 N93-30820
DTNH22-88-C-07384 .... p 3447 N93-30828
EPA-R-814701 .... p 3469 N93-29033
p 3469 N93-29034
EPA-68-D9-0169 .... p 3474 N93-30660
FAA-T1101-F .... p 3245 N93-28625
FISCCSE-3321190 .... p 3541 N93-28637
p 3541 N93-28638
FY1457-91-N-5014 .... p 3449 N93-29443
F04611-90-K-0054 .... p 3288 N93-29289
F04701-85-C-0086 .... p 3430 N93-28488
F04701-88-C-0089 .... p 3271 N93-28487
p 3329 N93-28561
p 3572 N93-29634
F19628-88-C-0031 .... p 3289 N93-30402
F19628-88-C-0154 .... p 3481 N93-28875
F19628-89-C-0001 .... p 3506 N93-29340
p 3387 N93-29890
p 3531 N93-29920
p 3531 N93-29921
p 3532 N93-30022
p 3534 N93-30546
p 3534 N93-30547
F19628-89-C-0189 .... p 3568 N93-29787
F19628-89-C-0209 .... p 3279 N93-29305
F19628-89-K-0015 .... p 3397 N93-30744
F19628-90-C-0002 .... p 3379 N93-28655
p 3578 N93-29139
p 3578 N93-29140
p 3481 N93-29257
p 3494 N93-29421
p 3579 N93-29470
p 3261 N93-29815
p 3389 N93-29900
F19628-90-C-0003 .... p 3610 N93-29970
p 3535 N93-30602
F19628-90-C-0187 .... p 3630 N93-29460
F19628-90-K-0007 .... p 3476 N93-29343
F19628-90-K-0049 .... p 3479 N93-30756
F19628-90-K-0053 .... p 3477 N93-29412
F19628-90-K-0056 .... p 3480 N93-28518
F19628-91-C-0128 .... p 3528 N93-29463
F29601-89-C-0014 .... p 3412 N93-30152

F30602-88-D-0028 p 3542 N93-29763
F30602-89-C-0041 p 3524 N93-28579
F30602-89-C-0145 p 3520 N93-29482
F30602-91-C-0113 p 3391 N93-30016
F30602-91-D-0007 p 3544 N93-30886
F33615-86-C-4505 p 3500 N93-28464
F33615-86-C-5015 p 3446 N93-30512
F33615-87-C-2777 p 3422 N93-29338
p 3423 N93-29339
p 3423 N93-29352
p 3425 N93-30155
p 3426 N93-30403
F33615-87-C-5242 p 3302 N93-30442
F33615-87-C-5250 p 3534 N93-30495
F33615-88-C-0014 p 3501 N93-28479
F33615-88-C-0631 p 3438 N93-29395
F33615-89-C-0572 p 3541 N93-28987
F33615-89-C-0603 p 3496 N93-30400
F33615-89-C-1023 p 3446 N93-30404
F33615-89-C-1087 p 3393 N93-30576
F33615-89-C-3225 p 3281 N93-30142
F33615-90-C-0005 p 3508 N93-29924
p 3499 N93-30542
F33615-90-C-1465 p 3615 N93-29459
p 3530 N93-29821
p 3530 N93-29822
p 3530 N93-29823
p 3579 N93-29824
F33615-90-C-2032 p 3568 N93-29446
F33615-92-C-2252 p 3424 N93-29966
F33615-92-C-5942 p 3595 N93-29341
F33657-90-D-2190 p 3412 N93-30406
F33657-92-D-2171 p 3610 N93-30177
F49620-87-K-0008 p 3254 N93-29936
F49620-89-C-0068 p 3446 N93-30524
F49620-89-C-0102 p 3339 N93-30885
F49620-90-C-0028 p 3528 N93-29483
F49620-90-C-0039 p 3382 N93-29131
p 3384 N93-29514
F49620-90-C-0076 p 3608 N93-29396
p 3608 N93-29440
F49620-91-C-0002 p 3540 N93-30895
F49620-91-C-0067 p 3414 N93-30896
F49620-91-C-0087 p 3570 N93-30558
F49620-91-C-0099 p 3601 N93-30819
F49620-92-C-0005 p 3478 N93-30174
F49620-92-C-0011 p 3479 N93-30562
F49620-92-C-0027 p 3405 N93-28589
p 3409 N93-29485
F49620-92-C-0040 p 3601 N93-30878
F49620-92-C-0041 p 3337 N93-30557
F49620-92-C-0045 p 3597 N93-30175
F49620-92-J-0016 p 3495 N93-30192
F49620-92-J-0051 p 3631 N93-30629
F49620-92-J-0079 p 3253 N93-29934
F49620-92-J-0099 p 3581 N93-30520
F49620-92-J-0134 p 3393 N93-30386
F49620-92-J-0138 p 3478 N93-30367
F49620-92-J-0140 p 3539 N93-30361
F49620-92-J-0153 p 3590 N93-30600
F49620-92-J-0169 p 3499 N93-30163
F49620-92-J-0176 p 3580 N93-30368
F49620-92-J-0188 p 3496 N93-30421
F49620-92-J-0199 p 3581 N93-30522
F49620-92-J-0205 p 3497 N93-30908
F49620-92-J-0214 p 3495 N93-30160
F49620-92-J-0363 p 3496 N93-30613
F49620-92-J-0410 p 3473 N93-30360
F49620-92-J-0432 p 3581 N93-30609
F49620-93-1-0038 p 3561 N93-30519
GRI-5086-260-1228 p 3317 N93-30760
GRI-5086-260-1252 p 3428 N93-30759
GRI-5087-260-1449 p 3604 N93-29428
p 3604 N93-29794
GRI-5089-243-1903 p 3466 N93-30814
GRI-5089-260-1779 p 3317 N93-30761
GRI-5089-260-1875 p 3312 N93-29665
GRI-5089-260-1982 p 3316 N93-30658
GRI-5090-260-1948 p 3327 N93-30815
GRI-5092-260-2345 p 3471 N93-29676
GRI-5092-260-2356 p 3316 N93-30661
MDA903-92-D-0025 p 3508 N93-30590
MDA972-90-C-0035 p 3529 N93-29486
p 3533 N93-30125
p 3534 N93-30523
MDA972-91-C-0029 p 3404 N93-28483
MDA972-91-C-0030 p 3412 N93-30409
MDA972-91-C-0053 p 3529 N93-29493
MDA972-92-C-0022 p 3409 N93-29513
MDA972-92-C-0033 p 3411 N93-29833
p 3411 N93-30031
MDA972-92-C-0071 p 3580 N93-29973
MDA972-92-J-1002 p 3531 N93-29866
MDA972-92-M-0007 p 3592 N93-28590
MIPR-FY1455-91N-0638 p 3342 N93-29402
MIPR-FY1457-88-N-5052 p 3295 N93-28592
MIPR-Z51100-1-E27A57 p 3499 N93-30426
MIPR-Z51100-9-0002 p 3246 N93-29818
NAGW-1333 p 3527 N93-29218
p 3542 N93-29771
p 3543 N93-30039
NAGW-1388 p 3274 N93-29108
NAGW-1426 p 3651 N93-30635
NAGW-1647 p 3630 N93-29163
NAGW-1682 p 3615 N93-29709
p 3616 N93-30036
NAGW-1998 p 3493 N93-29041
NAGW-2335 p 3404 N93-28539
NAGW-2655 p 3476 N93-28538
NAGW-2872 p 3509 N93-28895
NAGW-3037 p 3476 N93-28842
NAGW-3078 p 3286 N93-29707
NAGW-606 p 3492 N93-30665
NAGW-9 p 3653 N93-28935
NAG1-1080 p 3420 N93-29159
NAG1-1082 p 3400 N93-31036
NAG1-1084 p 3594 N93-29214
NAG1-1114 p 3527 N93-29219
NAG1-1218 p 3638 N93-29379
NAG1-1295 p 3243 N93-31037
NAG1-1358 p 3451 N93-29154
NAG1-1378 p 3249 N93-29885
NAG1-1419 p 3279 N93-29988
NAG1-237 p 3303 N93-30843
NAG1-343 p 3297 N93-29107
p 3454 N93-30374
p 3303 N93-30843
NAG1-345 p 3249 N93-29774
p 3249 N93-29775
p 3249 N93-29776
p 3249 N93-29777
p 3243 N93-29778
p 3249 N93-29779
NAG1-423 p 3604 N93-29168
NAG1-613 p 3527 N93-29170
NAG2-581 p 3531 N93-29873
NAG2-651 p 3248 N93-28693
NAG2-703 p 3528 N93-29469
NAG2-765 p 3653 N93-29164
NAG3-1127 p 3421 N93-29213
NAG3-1354 p 3415 N93-28557
NAG3-222 p 3580 N93-30372
NAG3-502 p 3242 N93-30373
NAG3-927 p 3244 N93-29152
NAG3-934 p 3450 N93-28556
NAG5-1155 p 3460 N93-29179
NAG5-1557 p 3630 N93-29604
NAG5-2016 p 3635 N93-30053
NAG5-2062 p 3653 N93-30052
NAG8-168 p 3573 N93-29637
p 3573 N93-29639
NAG8-759 p 3281 N93-30038
NAG8-766 p 3381 N93-29105
NAG8-879 p 3295 N93-28843
NAG9-482 p 3548 N93-28973
p 3516 N93-29563
p 3520 N93-29584
NAG9-509 p 3512 N93-29535
NAG9-561 p 3288 N93-29091
NAG9-582 p 3491 N93-29216
NANB-1-D1176 p 3244 N93-29211
NASA ORDER H-06815-D p 3572 N93-29629
NASA ORDER H-08071-D p 3624 N93-29631
NASA ORDER H-13006-D p 3578 N93-29128
NASA ORDER H-13029-D p 3624 N93-29631
NASA ORDER L-17761-D p 3340 N93-29368
NASW-4003 p 3525 N93-28934
NASW-4435 p 3227 N93-29712
p 3235 N93-29760
NASW-4574 p 3639 N93-28764
NASW-4603 p 3476 N93-28842
NASW-4711 p 3273 N93-29884
NAS1-14101 p 3509 N93-28841
NAS1-14472 p 3509 N93-28841
NAS1-15350 p 3582 N93-29693
NAS1-15370 p 3435 N93-29697
NAS1-15830 p 3509 N93-28841
NAS1-16394 p 3509 N93-28841
NAS1-17070 p 3509 N93-28841
NAS1-17130 p 3509 N93-28841
NAS1-17699 p 3300 N93-30433
NAS1-18027 p 3542 N93-29192
NAS1-18107 p 3509 N93-28841
NAS1-18605 p 3509 N93-28841
p 3520 N93-29864
NAS1-18690 p 3281 N93-30376
NAS1-18754 p 3308 N93-30876
NAS1-18758 p 3301 N93-30437
NAS1-18778 p 3304 N93-30849
NAS1-18799 p 3301 N93-30435
NAS1-18833 p 3304 N93-30847
NAS1-18834 p 3305 N93-30854
NAS1-18840 p 3304 N93-30850
NAS1-18841 p 3305 N93-30853
NAS1-18842 p 3306 N93-30860
p 3307 N93-30869
p 3307 N93-30871
NAS1-18883 p 3304 N93-30846
NAS1-18888 p 3300 N93-30433
NAS1-18889 p 3248 N93-29498
p 3300 N93-30432
p 3302 N93-30440
p 3303 N93-30845
p 3305 N93-30855
p 3305 N93-30857
NAS1-18972 p 3533 N93-30380
NAS1-19038 p 3250 N93-28621
NAS1-19245 p 3263 N93-28702
NAS1-19247 p 3283 N93-29623
NAS1-19480 p 3509 N93-28841
p 3418 N93-28975
p 3525 N93-28976
p 3520 N93-29864
NAS1-8605 p 3547 N93-28615
NAS10-11844 p 3272 N93-31033
NAS2-13036 p 3456 N93-28620
NAS2-13178 p 3638 N93-29360
p 3283 N93-29364
NAS2-13457 p 3431 N93-29066
NAS3-22822 p 3352 N93-31031
NAS3-23772 p 3448 N93-31039
NAS3-23858 p 3287 N93-28946
NAS3-24385 p 3298 N93-29451
NAS3-25266 p 3538 N93-28628
p 3288 N93-29068
NAS3-25958 p 3582 N93-29693
NAS3-25977 p 3264 N93-28711
NAS5-30313 p 3382 N93-29217
NAS5-30960 p 3630 N93-29811
NAS7-1145 p 3436 N93-28623
NAS7-918 p 3443 N93-28954
p 3381 N93-28955
p 3578 N93-29086
p 3381 N93-29087
p 3542 N93-29176
p 3579 N93-29848
p 3449 N93-30413
p 3440 N93-30415
p 3251 N93-30416
NAS8-156 p 3340 N93-29368
NAS8-32695 p 3340 N93-29368
NAS8-36639 p 3469 N93-29029
NAS8-36955 p 3287 N93-28680
NAS8-37857 p 3268 N93-31034
NAS8-38100 p 3272 N93-30617
p 3272 N93-30618
p 3272 N93-30619
p 3272 N93-30620
p 3272 N93-30621
p 3289 N93-30648
NAS8-38121 p 3573 N93-29640
NAS8-38478 p 3538 N93-29030
NAS8-38609 p 3476 N93-29032
p 3582 N93-31035
NAS8-38610 p 3573 N93-29636
p 3573 N93-29638
NAS8-38770 p 3573 N93-29641
NAS8-38981 p 3269 N93-28558
NAS8-39048 p 3526 N93-29028
NAS8-39241 p 3427 N93-30492
NAS8-39386 p 3573 N93-29640
p 3573 N93-29641
p 3573 N93-29642
NAS9-17900 p 3505 N93-29044
p 3506 N93-29324
p 3269 N93-29652
p 3285 N93-31032
NAS9-18426 p 3443 N93-29080
NAS9-18436 p 3634 N93-29042
NAS9-18492 p 3353 N93-28698
p 3495 N93-29651
NAS9-18880 p 3271 N93-29215
NCC1-136 p 3527 N93-29171
NCC1-68 p 3426 N93-30375
NCC2-537 p 3531 N93-29873
NCC2-539 p 3526 N93-29169
NCC2-737 p 3603 N93-28933
NCC2-775 p 3245 N93-28936
NCC2-795 p 3248 N93-29153
NCC3-208 p 3251 N93-28609
p 3251 N93-28617
p 3252 N93-29072
NCC3-233 p 3418 N93-28947
p 3421 N93-29208
NCC9-16 p 3526 N93-29026
p 3526 N93-29027
p 3527 N93-29212
NGT-50757 p 3517 N93-29567

NR PROJ. MR0-4101 .... p 3497 N93-30882
NR PROJ. S03-97 .... p 3245 N93-28990
NR PROJ. 3103 .... p 3483 N93-29491
NSERC-A1329 .... p 3529 N93-29488
NSF ATM-88-22560 .... p 3476 N93-28842
p 3397 N93-30744
NSF ATM-90-22197 .... p 3476 N93-28842
NSF ATM-91-08193 .... p 3476 N93-28842
NSF ATM-91-12680 .... p 3476 N93-28842
NSF ATM-91-13012 .... p 3396 N93-30737
NSF ATM-92-02795 .... p 3476 N93-28842
NSF CCR-90-03441 .... p 3532 N93-30017
NSF CDA-90-15006 .... p 3516 N93-29563
p 3520 N93-29584
NSF CDA-90-21110 .... p 3612 N93-29129
NSF DMR-91-12993 .... p 3329 N93-28489
p 3333 N93-29441
p 3333 N93-29442
NSF DMR-92-08511 .... p 3594 N93-29138
NSF DMS-90-02286 .... p 3419 N93-29025
NSF DMS-92-04938 .... p 3555 N93-29979
NSF DPP-87-20167 .... p 3397 N93-30744
NSF DPP-90-20687 .... p 3396 N93-30737
NSF DPP-91-19552 .... p 3397 N93-30744
NSF EAR-87-08372 .... p 3477 N93-29405
NSF IRI-90-03252 .... p 3511 N93-29528
NSF IRI-90-15675 .... p 3519 N93-29582
NSF ISI-88-60947 .... p 3331 N93-29201
NSF MIP-91-13268 .... p 3549 N93-29769
NSF MSS-90-20252 .... p 3518 N93-29574
NSF MSS-91-14630 .... p 3280 N93-29990
p 3280 N93-29991
p 3280 N93-29992
p 3280 N93-29993
p 3280 N93-29994
p 3280 N93-29995
NSF OCE-90-2532 .... p 3492 N93-30665
NSF USE-91-52078 .... p 3292 N93-30963
NSG-5395 .... p 3629 N93-28634
NUTEK-5622-92-04537 .... p 3418 N93-29009
NUTEK-726-91-01071 .... p 3238 N93-29005
NUTEK-90-02278P .... p 3418 N93-28994
NWO-PGS-78-277 .... p 3631 N93-30578
N00012-90-J-1334 .... p 3550 N93-29876
N00014-81-K-0382 .... p 3397 N93-30744
N00014-82-K-0489 .... p 3396 N93-30737
N00014-82-K-0612 .... p 3310 N93-28988
N00014-82-0280 .... p 3315 N93-30526
N00014-83-K-0422 .... p 3238 N93-29005
N00014-85-C-0638 .... p 3322 N93-29002
N00014-86-C-0699 .... p 3564 N93-28562
N00014-87-C-0699 .... p 3299 N93-29802
N00014-87-J-1248 .... p 3314 N93-30166
N00014-87-K-0828 .... p 3539 N93-29508
N00014-87-K-2016 .... p 3440 N93-30401
N00014-88-K-0483 .... p 3312 N93-29429
p 3596 N93-29430
N00014-89-J-1083 .... p 3597 N93-30120
N00014-89-J-11745 .... p 3571 N93-30901
N00014-89-J-1235 .... p 3316 N93-30627
N00014-89-J-1276 .... p 3453 N93-30147
N00014-89-J-1301 .... p 3597 N93-30146
N00014-89-J-1315 .... p 3477 N93-29879
N00014-89-J-1350 .... p 3338 N93-30628
N00014-89-J-1848 .... p 3598 N93-30408
p 3599 N93-30548
N00014-89-J-1853 .... p 3324 N93-29803
N00014-89-J-1912 .... p 3424 N93-29838
N00014-89-J-1949 .... p 3318 N93-30064
N00014-89-J-3087 .... p 3561 N93-28995
N00014-89-J-3222 .... p 3487 N93-29422
N00014-89-J-3235 .... p 3453 N93-29863
N00014-90-F-0078 .... p 3343 N93-30063
p 3318 N93-30064
N00014-90-J-1080 .... p 3397 N93-30744
N00014-90-J-1159 .... p 3592 N93-28584
p 3594 N93-29138
p 3598 N93-30407
p 3599 N93-30518
p 3570 N93-30540
N00014-90-J-1164 .... p 3296 N93-29001
N00014-90-J-1212 .... p 3313 N93-29828
p 3317 N93-30664
N00014-90-J-1255 .... p 3487 N93-29295
N00014-90-J-1372 .... p 3525 N93-28986
N00014-90-J-1419 .... p 3488 N93-29914
N00014-90-J-1569 .... p 3290 N93-29474
N00014-90-J-1590 .... p 3599 N93-30568
N00014-90-J-1604 .... p 3593 N93-28874
N00014-90-J-1712 .... p 3555 N93-29454
N00014-90-J-1717 .... p 3486 N93-28996
N00014-90-J-1848 .... p 3487 N93-29003
N00014-90-J-1858 .... p 3349 N93-30091
N00014-90-J-1871 .... p 3321 N93-28656
p 3452 N93-29432
N00014-90-J-1912 .... p 3487 N93-29003
N00014-90-J-4015 .... p 3318 N93-30067
N00014-90-J-4128 .... p 3490 N93-30906
N00014-91-C-0001 .... p 3343 N93-30061
N00014-91-C-0112 .... p 3406 N93-28940
N00014-91-C-0190 .... p 3494 N93-29509
N00014-91-J-1045 .... p 3329 N93-28560
N00014-91-J-1058 .... p 3311 N93-29132
p 3311 N93-29133
N00014-91-J-1078 .... p 3334 N93-29660
N00014-91-J-1189 .... p 3567 N93-29403
N00014-91-J-1194 .... p 3340 N93-30909
N00014-91-J-1316 .... p 3489 N93-30603
N00014-91-J-1404 .... p 3409 N93-29654
N00014-91-J-1414 .... p 3320 N93-28491
p 3324 N93-29799
N00014-91-J-1512 .... p 3607 N93-30884
N00014-91-J-1538 .... p 3489 N93-30143
N00014-91-J-1590 .... p 3335 N93-30028
p 3336 N93-30170
N00014-91-J-1630 .... p 3567 N93-29332
p 3569 N93-29839
N00014-91-J-1642 .... p 3461 N93-29817
N00014-91-J-1716 .... p 3286 N93-29707
N00014-91-J-1738 .... p 3348 N93-30088
N00014-91-J-1791 .... p 3486 N93-28885
N00014-91-J-1917 .... p 3327 N93-30574
N00014-91-J-1920 .... p 3337 N93-30497
N00014-91-J-1927 .... p 3294 N93-28492
p 3596 N93-29445
N00014-91-J-1976 .... p 3599 N93-30536
N00014-91-J-1985 .... p 3529 N93-29496
N00014-91-J-1991 .... p 3432 N93-29476
p 3452 N93-29515
N00014-91-J-1997 .... p 3409 N93-29495
N00014-91-J-4045 .... p 3408 N93-29427
N00014-92-C-0015 .... p 3544 N93-30591
N00014-92-C-0173 .... p 3309 N93-28540
p 3323 N93-29259
p 3567 N93-29336
p 3568 N93-29489
p 3568 N93-29619
N00014-92-J-1244 .... p 3494 N93-29620
N00014-92-J-1264 .... p 3549 N93-29413
N00014-92-J-1433 .... p 3336 N93-30169
N00014-92-J-1497 .... p 3332 N93-29337
N00014-92-J-1510 .... p 3562 N93-30121
p 3563 N93-30385
N00014-92-J-1557 .... p 3581 N93-30666
N00014-92-J-1576 .... p 3397 N93-30744
N00014-92-J-1579 .... p 3396 N93-30737
N00014-92-J-1635 .... p 3339 N93-30883
N00014-92-J-1705 .... p 3312 N93-29462
N00014-92-J-1866 .... p 3531 N93-29976
N00014-92-J-1895 .... p 3601 N93-30811
N00014-92-J-4092 .... p 3528 N93-29473
N00014-93-WR-24016 .... p 3332 N93-29342
p 3334 N93-29825
p 3410 N93-29826
N00014-93-WR-24019 .... p 3334 N93-29829
N00014-93-1-0351 .... p 3566 N93-29143
N00019-88-C-0288 .... p 3504 N93-28870
N00039-91-C-0138 .... p 3539 N93-29508
OTKA-2621 .... p 3519 N93-29576
PHS-R03-OH0-2821-01 .... p 3493 N93-29199
POD PROJ. 019201 .... p 3283 N93-29375
POD PROJ. 019202 .... p 3283 N93-29374
PROJ. AE-4051 .... p 3418 N93-28993
PROJ. AU-4093 .... p 3418 N93-28994
PROJ. AU-4109 .... p 3418 N93-29009
RF PROJ. 5696 .... p 3604 N93-29428
RICIS PROJ. RB-04 .... p 3526 N93-29027
RICIS PROJ. RB-05 .... p 3527 N93-29212
RICIS PROJ. SE-35 .... p 3526 N93-29026
RTOP 186-58-01 .... p 3651 N93-30214
RTOP 188-78-44 .... p 3629 N93-29453
RTOP 199-52-12 .... p 3638 N93-29360
p 3283 N93-29364
RTOP 310-10-62-15 .... p 3384 N93-29587
RTOP 310-10-63-84-02 .... p 3246 N93-29588
RTOP 310-10-63-88-01 .... p 3270 N93-29589
RTOP 310-20-64-22 .... p 3385 N93-29590
RTOP 310-20-64-86-02 .... p 3385 N93-29591
RTOP 310-20-65-67 .... p 3385 N93-29592
RTOP 310-20-65-86-04 .... p 3385 N93-29593
RTOP 310-20-65-86-08 .... p 3385 N93-29594
RTOP 310-30-71-83-04 .... p 3385 N93-29595
p 3385 N93-29596
RTOP 314-30-42-10-87 .... p 3386 N93-29601
RTOP 314-30-45-10-21 .... p 3386 N93-29600
RTOP 314-30-61-02-10 .... p 3386 N93-29599
RTOP 314-40-22-30-01 .... p 3385 N93-29598
RTOP 314-40-22-37-01 .... p 3385 N93-29597
RTOP 314-40-31-30-26 .... p 3386 N93-29603
RTOP 315-91-10-13-12 .... p 3386 N93-29602
RTOP 472-47-12-50 .... p 3431 N93-29209
RTOP 50-90-52-01 .... p 3418 N93-28975
RTOP 505-03-10 .... p 3252 N93-29162
RTOP 505-44-2C .... p 3405 N93-28610
RTOP 505-59-30-02 .... p 3239 N93-29165
RTOP 505-61-01-01 .... p 3240 N93-29449
RTOP 505-61-59-76 .... p 3240 N93-29450
RTOP 505-62-10 .... p 3251 N93-28609
p 3251 N93-28617
p 3252 N93-29072
RTOP 505-62-21 .... p 3418 N93-28947
RTOP 505-62-30-01 .... p 3239 N93-29160
RTOP 505-62-52 .... p 3416 N93-28626
p 3538 N93-28628
p 3420 N93-29157
RTOP 505-63-01-11 .... p 3454 N93-30374
RTOP 505-63-01 .... p 3580 N93-30372
RTOP 505-63-5A .... p 3297 N93-29074
p 3451 N93-29196
RTOP 505-63-50-01 .... p 3290 N93-30948
RTOP 505-63-50 .... p 3249 N93-29885
RTOP 505-64-10-05 .... p 3533 N93-30380
RTOP 505-64-13-22 .... p 3542 N93-29192
RTOP 505-64-13 .... p 3250 N93-28621
RTOP 505-64-52 .... p 3245 N93-29653
RTOP 505-68-32 .... p 3252 N93-29065
RTOP 505-68-50 .... p 3431 N93-29066
RTOP 505-70-59-08 .... p 3420 N93-29159
RTOP 505-90-11 .... p 3242 N93-30373
RTOP 505-90-21-02 .... p 3426 N93-30375
RTOP 505-90-5K .... p 3420 N93-29161
p 3421 N93-29208
RTOP 505-90-52-01 .... p 3509 N93-28841
p 3525 N93-28976
p 3520 N93-29864
RTOP 505-90-53-02 .... p 3520 N93-29070
RTOP 506-40-41-01 .... p 3239 N93-29166
RTOP 506-40-91-02 .... p 3420 N93-29155
RTOP 506-41-11 .... p 3321 N93-28618
RTOP 506-42-31 .... p 3286 N93-28619
p 3287 N93-28694
p 3288 N93-29158
p 3288 N93-29194
RTOP 506-42-72 .... p 3341 N93-28695
p 3270 N93-28696
RTOP 506-43-61 .... p 3290 N93-29067
RTOP 506-48-00 .... p 3638 N93-29360
p 3283 N93-29364
RTOP 506-48-91-11 .... p 3654 N93-29354
p 3660 N93-29621
p 3665 N93-29682
RTOP 506-72-21 .... p 3273 N93-29884
RTOP 509-10-11 .... p 3450 N93-28556
RTOP 510-01-50 .... p 3295 N93-28624
p 3295 N93-28681
p 3297 N93-29071
p 3449 N93-29073
RTOP 510-02-11 .... p 3300 N93-30428
p 3303 N93-30841
RTOP 510-02-12 .... p 3451 N93-28633
RTOP 533-02-35 .... p 3248 N93-28693
RTOP 533-02-51 .... p 3260 N93-30764
RTOP 533-05-01 .... p 3298 N93-29451
RTOP 535-05-10 .... p 3251 N93-28697
RTOP 537-03-21-03 .... p 3561 N93-28692
RTOP 537-04-21 .... p 3340 N93-30938
RTOP 538-02-10-01 .... p 3451 N93-29069
RTOP 579-50-00 .... p 3273 N93-29195
RTOP 584-03-11 .... p 3416 N93-28627
RTOP 584-04-11 .... p 3288 N93-29068
RTOP 585-03-11-09 .... p 3455 N93-31038
RTOP 589-01-21-01 .... p 3281 N93-30376
RTOP 590-12-42 .... p 3542 N93-29386
RTOP 593-12-11 .... p 3287 N93-28946
RTOP 596-13-11 .... p 3287 N93-28686
RTOP 694-03-OH .... p 3285 N93-28554
RTOP 694-03-0A .... p 3352 N93-30939
p 3352 N93-31031
RTOP 889-54-62-01 .... p 3386 N93-29603
SBIR-08.29-5649 .... p 3456 N93-28620
SDIO-SC-02N0165768 .... p 3283 N93-29375
SDIO-SC-89W-26-11 .... p 3283 N93-29374
SDIO-89-C-0034 .... p 3283 N93-29374
SRC-GR/D/53029 .... p 3257 N93-29954
TFR-91-402 .... p 3238 N93-29005
W-31-109-ENG-38 .... p 3564 N93-28549
p 3509 N93-28573
p 3524 N93-28644
p 3592 N93-28661
p 3330 N93-28666
p 3525 N93-28877
p 3565 N93-28892
p 3442 N93-28903
p 3449 N93-28943
p 3574 N93-28970
p 3407 N93-29036
p 3310 N93-29052
p 3323 N93-29102

	p 3561	N93-29189
	p 3587	N93-29299
	p 3408	N93-29311
	p 3566	N93-29313
	p 3464	N93-29844
	p 3550	N93-30140
	p 3576	N93-30527
	p 3535	N93-30647
W-7405-ENG-36	p 3556	N93-28572
	p 3611	N93-28580
	p 3330	N93-28600
	p 3524	N93-28640
	p 3625	N93-28646
	p 3554	N93-28763
	p 3406	N93-28830
	p 3565	N93-28831
	p 3436	N93-28887
	p 3380	N93-28900
	p 3296	N93-28904
	p 3633	N93-28905
	p 3634	N93-28906
	p 3634	N93-28907
	p 3634	N93-28908
	p 3380	N93-28909
	p 3565	N93-28914
	p 3593	N93-28966
	p 3323	N93-29092
	p 3586	N93-29093
	p 3593	N93-29094
	p 3481	N93-29095
	p 3464	N93-29147
	p 3634	N93-29246
	p 3341	N93-29251
	p 3332	N93-29252
	p 3421	N93-29253
	p 3342	N93-29312
	p 3566	N93-29313
	p 3594	N93-29314
	p 3566	N93-29315
	p 3477	N93-29346
	p 3482	N93-29347
	p 3579	N93-29350
	p 3386	N93-29765
	p 3549	N93-29769
	p 3575	N93-29809
	p 3410	N93-29812
	p 3424	N93-29836
	p 3472	N93-30008
	p 3345	N93-30074
	p 3336	N93-30129
	p 3569	N93-30130
	p 3315	N93-30209
	p 3446	N93-30211
	p 3300	N93-30395
	p 3598	N93-30445
	p 3352	N93-30446
	p 3315	N93-30447
	p 3570	N93-30448
	p 3426	N93-30484
	p 3426	N93-30485
	p 3326	N93-30486
	p 3478	N93-30487
	p 3598	N93-30517
	p 3540	N93-30633
	p 3450	N93-30636
	p 3454	N93-31013
W-7405-ENG-48	p 3430	N93-28520
	p 3563	N93-28521
	p 3537	N93-28544
	p 3632	N93-28547
	p 3524	N93-28550
	p 3243	N93-28571
	p 3450	N93-28596
	p 3405	N93-28597
	p 3564	N93-28762
	p 3469	N93-28965
	p 3469	N93-28967
	p 3469	N93-28972
	p 3419	N93-29050
	p 3586	N93-29053
	p 3470	N93-29055
	p 3520	N93-29058
	p 3310	N93-29059
	p 3549	N93-29060
	p 3436	N93-29097
	p 3437	N93-29098
	p 3565	N93-29099
	p 3574	N93-29103
	p 3437	N93-29104
	p 3566	N93-29206
	p 3437	N93-29207
	p 3311	N93-29263
	p 3422	N93-29300
	p 3594	N93-29301
	p 3587	N93-29303
	p 3438	N93-29309
	p 3615	N93-29310
	p 3588	N93-29334
	p 3588	N93-29772
	p 3432	N93-29773
	p 3588	N93-29780
	p 3438	N93-29781
	p 3539	N93-29782
	p 3615	N93-29783
	p 3568	N93-29784
	p 3630	N93-29785
	p 3471	N93-29792
	p 3410	N93-29793
	p 3424	N93-30035
	p 3472	N93-30043
	p 3319	N93-30082
	p 3326	N93-30389
	p 3576	N93-30390
	p 3440	N93-30394
	p 3326	N93-30490
	p 3433	N93-30491
	p 3474	N93-30504
	p 3474	N93-30506
	p 3600	N93-30668
W-7405-ENG-82	p 3450	N93-28567
	p 3313	N93-29837

REPORT NUMBER INDEX

SCIENTIFIC AND TECHNICAL AEROSPACE REPORTS VOLUME 31 NUMBER 11

Typical Report Number Index Listing

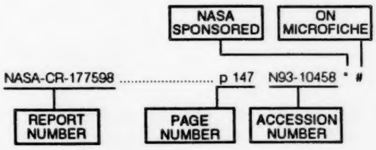

Listings in this index are arranged alphanumerically by report number. The accession number denotes the number by which the citation is identified. The page number helps to locate the citation in the abstract section. An asterisk (*) indicates that the item is a NASA report. A pound sign (#) indicates that the item is available on microfiche.

A-90280 .... p 3629 N93-29453 * #
A-91160 .... p 3542 N93-29386 * #
A-92020 .... p 3236 N93-30673 * #
A-92078 .... p 3651 N93-30214 * #
A-92198 .... p 3245 N93-29653 * #

AD-A261934 .... p 3561 N93-28995 #
AD-A261939 .... p 3486 N93-28996 #
AD-A261963 .... p 3409 N93-29435
AD-A261978 .... p 3261 N93-29436 #
AD-A261979 .... p 3487 N93-29437 #
AD-A261982 .... p 3383 N93-29438 #
AD-A261983 .... p 3381 N93-28997 #
AD-A261984 .... p 3381 N93-28998 #
AD-A261986 .... p 3615 N93-29439 #
AD-A261988 .... p 3608 N93-29440 #
AD-A262006 .... p 3333 N93-29441 #
AD-A262007 .... p 3333 N93-29442 #
AD-A262008 .... p 3449 N93-29443 #
AD-A262009 .... p 3562 N93-29392 #
AD-A262011 .... p 3482 N93-29393 #
AD-A262014 .... p 3271 N93-29394 #
AD-A262016 .... p 3438 N93-29395 #
AD-A262024 .... p 3608 N93-29396 #
AD-A262025 .... p 3595 N93-29397 #
AD-A262027 .... p 3261 N93-29398 #
AD-A262034 .... p 3407 N93-28999 #
AD-A262044 .... p 3459 N93-29000 #
AD-A262051 .... p 3482 N93-29399 #
AD-A262052 .... p 3296 N93-29001 #
AD-A262061 .... p 3322 N93-29002 #
AD-A262062 .... p 3251 N93-28984 #
AD-A262073 .... p 3487 N93-29003 #
AD-A262076 .... p 3250 N93-29004 #
AD-A262077 .... p 3609 N93-28985 #
AD-A262084 .... p 3525 N93-28986 #
AD-A262136 .... p 3408 N93-29408 #
AD-A262180 .... p 3506 N93-29444
AD-A262185 .... p 3430 N93-28488 #
AD-A262189 .... p 3329 N93-28489 #
AD-A262208 .... p 3596 N93-29445
AD-A262232 .... p 3320 N93-28491 #
AD-A262233 .... p 3294 N93-28492 #
AD-A262259 .... p 3452 N93-29349
AD-A262275 .... p 3652 N93-28756
AD-A262279 .... p 3568 N93-29446 #
AD-A262373 .... p 3238 N93-28493 #
AD-A262399 .... p 3494 N93-29400 #
AD-A262402 .... p 3541 N93-28494 #
AD-A262403 .... p 3329 N93-28495 #
AD-A262404 .... p 3591 N93-28496 #
AD-A262405 .... p 3541 N93-28498 #
AD-A262416 .... p 3320 N93-28499 #
AD-A262417 .... p 3500 N93-28464 #
AD-A262462 .... p 3379 N93-28654 #
AD-A262466 .... p 3501 N93-28757 #
AD-A262467 .... p 3493 N93-28758 #
AD-A262472 .... p 3379 N93-28655 #
AD-A262477 .... p 3248 N93-29409 #
AD-A262481 .... p 3299 N93-30137 #
AD-A262482 .... p 3240 N93-29410
AD-A262483 .... p 3493 N93-28759 #
AD-A262484 .... p 3554 N93-29411
AD-A262485 .... p 3555 N93-29447 #
AD-A262486 .... p 3553 N93-28760 #
AD-A262489 .... p 3528 N93-29418 #
AD-A262491 .... p 3423 N93-29419 #
AD-A262493 .... p 3270 N93-28938 #
AD-A262504 .... p 3594 N93-29138 #
AD-A262505 .... p 3321 N93-28656 #
AD-A262516 .... p 3554 N93-28844 #
AD-A262518 .... p 3592 N93-28584 #
AD-A262525 .... p 3652 N93-28585 #
AD-A262536 .... p 3477 N93-29412 #
AD-A262546 .... p 3549 N93-29413 #
AD-A262549 .... p 3298 N93-29414 #
AD-A262550 .... p 3567 N93-29415 #
AD-A262552 .... p 3553 N93-28574 #
AD-A262553 .... p 3554 N93-28845 #
AD-A262554 .... p 3553 N93-28575 #
AD-A262555 .... p 3542 N93-29420 #
AD-A262558 .... p 3494 N93-29421 #
AD-A262566 .... p 3227 N93-28576 #
AD-A262568 .... p 3524 N93-28577 #
AD-A262570 .... p 3442 N93-28578 #
AD-A262572 .... p 3487 N93-29422 #
AD-A262574 .... p 3556 N93-29423 #
AD-A262576 .... p 3541 N93-28987 #
AD-A262578 .... p 3524 N93-28579 #
AD-A262579 .... p 3295 N93-28657 #
AD-A262591 .... p 3612 N93-28846 #
AD-A262594 .... p 3596 N93-29424
AD-A262596 .... p 3480 N93-28465 #
AD-A262599 .... p 3260 N93-28467 #
AD-A262601 .... p 3270 N93-28468 #
AD-A262602 .... p 3591 N93-28471 #
AD-A262612 .... p 3286 N93-28474 #
AD-A262613 .... p 3379 N93-28476 #
AD-A262614 .... p 3537 N93-28478 #
AD-A262615 .... p 3553 N93-28587 #
AD-A262616 .... p 3501 N93-28479 #
AD-A262655 .... p 3379 N93-28588 #
AD-A262677 .... p 3404 N93-28483 #
AD-A262703 .... p 3498 N93-28901 #
AD-A262725 .... p 3477 N93-29401 #
AD-A262733 .... p 3405 N93-28589 #
AD-A262737 .... p 3592 N93-28590 #
AD-A262739 .... p 3321 N93-28591 #
AD-A262740 .... p 3295 N93-28592 #
AD-A262746 .... p 3286 N93-28593 #
AD-A262747 .... p 3342 N93-29402 #
AD-A262748 .... p 3567 N93-29403 #
AD-A262749 .... p 3333 N93-29404 #
AD-A262752 .... p 3271 N93-28487 #
AD-A262753 .... p 3477 N93-29405 #
AD-A262755 .... p 3615 N93-29459 #
AD-A262762 .... p 3493 N93-28939 #
AD-A262766 .... p 3482 N93-29304 #
AD-A262777 .... p 3630 N93-29460 #
AD-A262778 .... p 3279 N93-29305 #
AD-A262782 .... p 3273 N93-29306 #
AD-A262785 .... p 3288 N93-29289 #
AD-A262786 .... p 3287 N93-28658 #
AD-A262822 .... p 3312 N93-29429 #
AD-A262823 .... p 3596 N93-29430 #
AD-A262825 .... p 3615 N93-29431 #
AD-A262827 .... p 3452 N93-29432 #
AD-A262828 .... p 3609 N93-29433 #
AD-A262829 .... p 3555 N93-29454 #
AD-A262830 .... p 3245 N93-29468 #
AD-A262838 .... p 3529 N93-29647 #
AD-A262848 .... p 3528 N93-29469 * #
AD-A262849 .... p 3539 N93-29508 #
AD-A262857 .... p 3579 N93-29470 #
AD-A262861 .... p 3494 N93-29509 #
AD-A262862 .... p 3506 N93-29471 #
AD-A262863 .... p 3423 N93-29472 #
AD-A262867 .... p 3285 N93-29461 #
AD-A262868 .... p 3269 N93-29475 #
AD-A262870 .... p 3624 N93-29477 #
AD-A262871 .... p 3498 N93-29481 #
AD-A262872 .... p 3506 N93-29484 #
AD-A262883 .... p 3312 N93-29510 #
AD-A262892 .... p 3333 N93-29511 #
AD-A262905 .... p 3578 N93-29139 #
AD-A262906 .... p 3578 N93-29140 #
AD-A262910 .... p 3486 N93-28885 #
AD-A262924 .... p 3296 N93-28886 #
AD-A262926 .... p 3505 N93-28884 #
AD-A262953 .... p 3240 N93-29512 #
AD-A262959 .... p 3409 N93-29513 #
AD-A262966 .... p 3384 N93-29514 #
AD-A262980 .... p 3298 N93-29425 #
AD-A262982 .... p 3423 N93-29426 #
AD-A262989 .... p 3408 N93-29427 #
AD-A262993 .... p 3409 N93-29485 #
AD-A262994 .... p 3312 N93-29462 #
AD-A262997 .... p 3452 N93-29515 #
AD-A263001 .... p 3528 N93-29463 #
AD-A263009 .... p 3430 N93-28659 #
AD-A263011 .... p 3506 N93-29406 #
AD-A263018 .... p 3383 N93-29407 #
AD-A263021 .... p 3295 N93-28660 #
AD-A263048 .... p 3298 N93-29130 #
AD-A263049 .... p 3420 N93-29141 #
AD-A263074 .... p 3609 N93-29142 #
AD-A263075 .... p 3566 N93-29143 #
AD-A263076 .... p 3382 N93-29131 #
AD-A263085 .... p 3311 N93-29132 #
AD-A263088 .... p 3334 N93-29795
AD-A263095 .... p 3323 N93-29144 #
AD-A263096 .... p 3526 N93-29145 #
AD-A263097 .... p 3459 N93-29146 #
AD-A263098 .... p 3311 N93-29133 #
AD-A263100 .... p 3278 N93-29134 #
AD-A263101 .... p 3596 N93-29796 #
AD-A263102 .... p 3438 N93-29797 #
AD-A263103 .... p 3410 N93-29798 #
AD-A263108 .... p 3324 N93-29799 #
AD-A263110 .... p 3335 N93-30007 #
AD-A263120 .... p 3409 N93-29495 #
AD-A263126 .... p 3529 N93-29496 #
AD-A263128 .... p 3528 N93-29473 #
AD-A263129 .... p 3290 N93-29474 #
AD-A263130 .... p 3432 N93-29476 #
AD-A263132 .... p 3409 N93-29478 #
AD-A263136 .... p 3482 N93-29479 #
AD-A263137 .... p 3568 N93-29619 #
AD-A263138 .... p 3562 N93-29480 #
AD-A263142 .... p 3520 N93-29482 #
AD-A263145 .... p 3528 N93-29483 #
AD-A263149 .... p 3529 N93-29486 #
AD-A263161 .... p 3406 N93-28940 #
AD-A263167 .... p 3409 N93-29654 #
AD-A263168 .... p 3568 N93-29489 #
AD-A263169 .... p 3310 N93-28988 #
AD-A263170 .... p 3430 N93-28989 #
AD-A263171 .... p 3245 N93-28990 #
AD-A263172 .... p 3538 N93-29490 #
AD-A263173 .... p 3481 N93-28991 #
AD-A263178 .... p 3407 N93-29010 #
AD-A263183 .... p 3381 N93-29011 #
AD-A263185 .... p 3309 N93-28514 #
AD-A263186 .... p 3341 N93-28515 #
AD-A263191 .... p 3505 N93-28941 #
AD-A263192 .... p 3309 N93-28540 #
AD-A263198 .... p 3450 N93-28516 #
AD-A263204 .... p 3593 N93-28874 #
AD-A263207 .... p 3481 N93-28875 #
AD-A263208 .... p 3341 N93-28517 #
AD-A263212 .... p 3480 N93-28518 #
AD-A263217 .... p 3481 N93-28876 #
AD-A263218 .... p 3483 N93-29491 #
AD-A263219 .... p 3521 N93-29492 #
AD-A263224 .... p 3294 N93-28559 #
AD-A263235 .... p 3529 N93-29493 #
AD-A263240 .... p 3494 N93-29620 #
AD-A263241 .... p 3329 N93-28560 #
AD-A263244 .... p 3342 N93-29494 #
AD-A263245 .... p 3409 N93-29655 #
AD-A263246 .... p 3610 N93-29499 #

AD-A263249 .... p 3579 N93-29656 #
AD-A263250 .... p 3438 N93-29800 #
AD-A263252 .... p 3329 N93-28561 #
AD-A263262 .... p 3453 N93-29801 #
AD-A263263 .... p 3529 N93-29497 #
AD-A263264 .... p 3299 N93-29802 #
AD-A263271 .... p 3564 N93-28562 #
AD-A263277 .... p 3405 N93-28563 #
AD-A263288 .... p 3324 N93-29803 #
AD-A263298 .... p 3342 N93-29762 #
AD-A263330 .... p 3542 N93-29763
AD-A263361 .... p 3595 N93-29331 #
AD-A263363 .... p 3567 N93-29332 #
AD-A263382 .... p 3595 N93-29333 #
AD-A263385 .... p 3481 N93-29257 #
AD-A263386 .... p 3483 N93-29850 #
AD-A263395 .... p 3424 N93-29851 #
AD-A263400 .... p 3654 N93-29258 #
AD-A263403 .... p 3530 N93-29852 #
AD-A263409 .... p 3483 N93-29967 #
AD-A263410 .... p 3613 N93-29210 #
AD-A263412 .... p 3568 N93-29787 #
AD-A263421 .... p 3323 N93-29259 #
AD-A263422 .... p 3567 N93-29336 #
AD-A263423 .... p 3483 N93-29810 #
AD-A263427 .... p 3332 N93-29337 #
AD-A263432 .... p 3610 N93-29970 #
AD-A263433 .... p 3261 N93-29815 #
AD-A263436 .... p 3261 N93-29788 #
AD-A263437 .... p 3562 N93-29816 #
AD-A263438 .... p 3438 N93-29789 #
AD-A263441 .... p 3334 N93-29790 #
AD-A263452 .... p 3461 N93-29817 #
AD-A263457 .... p 3570 N93-30589
AD-A263458 .... p 3508 N93-30590
AD-A263460 .... p 3246 N93-29818 #
AD-A263464 .... p 3411 N93-29833 #
AD-A263465 .... p 3462 N93-29834 #
AD-A263466 .... p 3342 N93-29835 #
AD-A263468 .... p 3433 N93-30584
AD-A263469 .... p 3424 N93-29838 #
AD-A263470 .... p 3569 N93-29839 #
AD-A263483 .... p 3424 N93-29966 #
AD-A263490 .... p 3488 N93-29819 #
AD-A263495 .... p 3423 N93-29352 #
AD-A263496 .... p 3422 N93-29338 #
AD-A263497 .... p 3423 N93-29339 #
AD-A263498 .... p 3506 N93-29340 #
AD-A263499 .... p 3601 N93-30811
AD-A263501 .... p 3595 N93-29341 #
AD-A263511 .... p 3332 N93-29342 #
AD-A263513 .... p 3424 N93-29968 #
AD-A263514 .... p 3354 N93-29969 #
AD-A263515 .... p 3250 N93-29971 #
AD-A263541 .... p 3597 N93-29974 #
AD-A263543 .... p 3391 N93-29975 #
AD-A263544 .... p 3495 N93-29820 #
AD-A263547 .... p 3530 N93-29821 #
AD-A263548 .... p 3530 N93-29822 #
AD-A263549 .... p 3530 N93-29823 #
AD-A263550 .... p 3579 N93-29824 #
AD-A263557 .... p 3334 N93-29825 #
AD-A263558 .... p 3410 N93-29826 #
AD-A263559 .... p 3496 N93-30588 #
AD-A263563 .... p 3439 N93-29827 #
AD-A263564 .... p 3317 N93-30664
AD-A263565 .... p 3313 N93-29828 #
AD-A263567 .... p 3334 N93-29829 #
AD-A263570 .... p 3462 N93-29830 #
AD-A263571 .... p 3477 N93-29831 #
AD-A263572 .... p 3483 N93-29832 #
AD-A263573 .... p 3476 N93-29343 #
AD-A263576 .... p 3531 N93-29976 #
AD-A263579 .... p 3261 N93-29972 #
AD-A263580 .... p 3580 N93-29973 #
AD-A263582 .... p 3488 N93-29914 #
AD-A263597 .... p 3325 N93-29981 #
AD-A263598 .... p 3491 N93-29915 #
AD-A263601 .... p 3299 N93-29982 #
AD-A263602 .... p 3531 N93-29916 #
AD-A263603 .... p 3439 N93-29983 #
AD-A263604 .... p 3543 N93-29917 #
AD-A263607 .... p 3298 N93-29282 #
AD-A263611 .... p 3311 N93-29283 #
AD-A263612 .... p 3240 N93-29284 #
AD-A263613 .... p 3245 N93-29285 #
AD-A263617 .... p 3244 N93-29286 #
AD-A263619 .... p 3332 N93-29344 #
AD-A263646 .... p 3299 N93-29984 #
AD-A263650 .... p 3445 N93-29388 #
AD-A263651 .... p 3332 N93-29290 #
AD-A263652 .... p 3311 N93-29291 #
AD-A263653 .... p 3312 N93-29389 #
AD-A263654 .... p 3432 N93-29390 #
AD-A263661 .... p 3324 N93-29391 #
AD-A263662 .... p 3554 N93-29292 #
AD-A263664 .... p 3594 N93-29293 #
AD-A263679 .... p 3528 N93-29294 #
AD-A263681 .... p 3487 N93-29295 #
AD-A263698 .... p 3423 N93-29353 #
AD-A263699 .... p 3588 N93-29382 #
AD-A263700 .... p 3595 N93-29383 #
AD-A263702 .... p 3342 N93-29296 #
AD-A263703 .... p 3604 N93-29384 #
AD-A263704 .... p 3554 N93-29385 #
AD-A263705 .... p 3431 N93-29297 #
AD-A263706 .... p 3487 N93-29298 #
AD-A263707 .... p 3259 N93-29985 #
AD-A263708 .... p 3439 N93-29918 #
AD-A263727 .... p 3259 N93-30877 #
AD-A263728 .... p 3411 N93-29986 #
AD-A263734 .... p 3439 N93-29853 #
AD-A263735 .... p 3549 N93-29854 #
AD-A263736 .... p 3453 N93-29855 #
AD-A263737 .... p 3334 N93-29856 #
AD-A263738 .... p 3555 N93-29857 #
AD-A263745 .... p 3471 N93-29858 #
AD-A263747 .... p 3327 N93-30812 #
AD-A263751 .... p 3596 N93-29859 #
AD-A263752 .... p 3549 N93-29871 #
AD-A263753 .... p 3550 N93-29872 #
AD-A263755 .... p 3531 N93-29873 * #
AD-A263756 .... p 3531 N93-29874 #
AD-A263759 .... p 3387 N93-29875 #
AD-A263763 .... p 3550 N93-29876 #
AD-A263765 .... p 3387 N93-29877
AD-A263766 .... p 3555 N93-29878 #
AD-A263795 .... p 3477 N93-29879 #
AD-A263810 .... p 3580 N93-29880 #
AD-A263813 .... p 3335 N93-29886 #
AD-A263814 .... p 3335 N93-29881 #
AD-A263835 .... p 3411 N93-30021 #
AD-A263856 .... p 3580 N93-29887 #
AD-A263874 .... p 3507 N93-29888 #
AD-A263875 .... p 3507 N93-29889 #
AD-A263877 .... p 3387 N93-29890 #
AD-A263879 .... p 3241 N93-29919 #
AD-A263880 .... p 3532 N93-30022 #
AD-A263881 .... p 3531 N93-29920 #
AD-A263891 .... p 3531 N93-29921 #
AD-A263905 .... p 3240 N93-29862 #
AD-A263906 .... p 3453 N93-29863 #
AD-A263983 .... p 3520 N93-29864 * #
AD-A263984 .... p 3530 N93-29865 #
AD-A263985 .... p 3610 N93-30124 #
AD-A263986 .... p 3531 N93-29866 #
AD-A263993 .... p 3528 N93-29345 #
AD-A263997 .... p 3439 N93-29867 #
AD-A263998 .... p 3387 N93-29882 #
AD-A263999 .... p 3439 N93-29883 #
AD-A264002 .... p 3479 N93-30756 #
AD-A264003 .... p 3399 N93-30757 #
AD-A264006 .... p 3391 N93-29987 #
AD-A264007 .... p 3488 N93-29977 #
AD-A264008 .... p 3550 N93-29978 #
AD-A264012 .... p 3421 N93-29260 #
AD-A264015 .... p 3555 N93-29979 #
AD-A264016 .... p 3532 N93-29980 #
AD-A264017 .... p 3532 N93-30014 #
AD-A264019 .... p 3472 N93-30015 #
AD-A264020 .... p 3391 N93-30016 #
AD-A264021 .... p 3498 N93-30026 #
AD-A264022 .... p 3499 N93-30027 #
AD-A264028 .... p 3335 N93-30028 #
AD-A264039 .... p 3562 N93-30029 #
AD-A264046 .... p 3313 N93-30030 #
AD-A264048 .... p 3411 N93-30031 #
AD-A264049 .... p 3533 N93-30125 #
AD-A264053 .... p 3432 N93-30032 #
AD-A264056 .... p 3499 N93-30033 #
AD-A264057 .... p 3241 N93-29891 #
AD-A264060 .... p 3411 N93-29922 #
AD-A264062 .... p 3555 N93-29923 #
AD-A264069 .... p 3508 N93-29924 #
AD-A264075 .... p 3260 N93-30604
AD-A264095 .... p 3281 N93-30813 #
AD-A264098 .... p 3601 N93-30878 #
AD-A264100 .... p 3399 N93-30879 #
AD-A264102 .... p 3400 N93-30880 #
AD-A264115 .... p 3241 N93-30119 #
AD-A264117 .... p 3495 N93-30192 #
AD-A264118 .... p 3616 N93-30193 #
AD-A264120 .... p 3244 N93-30194 #
AD-A264125 .... p 3616 N93-30195 #
AD-A264127 .... p 3495 N93-30196 #
AD-A264128 .... p 3473 N93-30197 #
AD-A264133 .... p 3336 N93-30169 #
AD-A264150 .... p 3336 N93-30170 #
AD-A264151 .... p 3241 N93-30171 #
AD-A264152 .... p 3241 N93-30172 #
AD-A264153 .... p 3242 N93-30173 #
AD-A264154 .... p 3241 N93-30151 #
AD-A264157 .... p 3412 N93-30152 #
AD-A264159 .... p 3272 N93-30881 #
AD-A264162 .... p 3495 N93-30153 #
AD-A264170 .... p 3472 N93-30154 #
AD-A264174 .... p 3425 N93-30155 #
AD-A264179 .... p 3497 N93-30882 #
AD-A264181 .... p 3425 N93-30156 #
AD-A264182 .... p 3562 N93-30157 #
AD-A264184 .... p 3610 N93-30158 #
AD-A264191 .... p 3339 N93-30883 #
AD-A264192 .... p 3281 N93-30142 #
AD-A264196 .... p 3489 N93-30143 #
AD-A264199 .... p 3607 N93-30884 #
AD-A264200 .... p 3597 N93-30144 #
AD-A264202 .... p 3392 N93-30145 #
AD-A264206 .... p 3315 N93-30534 #
AD-A264220 .... p 3597 N93-30146 #
AD-A264221 .... p 3453 N93-30147 #
AD-A264223 .... p 3473 N93-30360 #
AD-A264224 .... p 3539 N93-30361 #
AD-A264226 .... p 3478 N93-30174 #
AD-A264227 .... p 3339 N93-30885 #
AD-A264228 .... p 3392 N93-30362 #
AD-A264229 .... p 3555 N93-30363 #
AD-A264230 .... p 3540 N93-30364 #
AD-A264260 .... p 3497 N93-30894 #
AD-A264275 .... p 3317 N93-30816 #
AD-A264279 .... p 3281 N93-30817 #
AD-A264293 .... p 3492 N93-30818 #
AD-A264297 .... p 3601 N93-30819 #
AD-A264298 .... p 3540 N93-30895 #
AD-A264301 .... p 3414 N93-30896 #
AD-A264306 .... p 3497 N93-30897 #
AD-A264307 .... p 3315 N93-30365 #
AD-A264310 .... p 3400 N93-30995 #
AD-A264330 .... p 3570 N93-30366 #
AD-A264331 .... p 3478 N93-30367 #
AD-A264332 .... p 3580 N93-30368 #
AD-A264333 .... p 3425 N93-30369 #
AD-A264334 .... p 3337 N93-30417 #
AD-A264335 .... p 3533 N93-30418 #
AD-A264336 .... p 3654 N93-30419 #
AD-A264337 .... p 3453 N93-30159 #
AD-A264338 .... p 3495 N93-30160 #
AD-A264339 .... p 3580 N93-30205 #
AD-A264340 .... p 3597 N93-30161 #
AD-A264341 .... p 3425 N93-30162 #
AD-A264342 .... p 3499 N93-30163 #
AD-A264343 .... p 3597 N93-30164 #
AD-A264345 .... p 3544 N93-30165 #
AD-A264347 .... p 3314 N93-30166 #
AD-A264371 .... p 3387 N93-29892 #
AD-A264400 .... p 3544 N93-30886 #
AD-A264401 .... p 3508 N93-30167 #
AD-A264404 .... p 3597 N93-30175 #
AD-A264417 .... p 3597 N93-30120
AD-A264435 .... p 3489 N93-30420 #
AD-A264438 .... p 3496 N93-30421 #
AD-A264439 .... p 3496 N93-30422 #
AD-A264463 .... p 3484 N93-30535 #
AD-A264465 .... p 3599 N93-30536 #
AD-A264466 .... p 3393 N93-30537 #
AD-A264475 .... p 3327 N93-30538 #
AD-A264480 .... p 3393 N93-30423 #
AD-A264482 .... p 3352 N93-30424 #
AD-A264484 .... p 3499 N93-30425 #
AD-A264492 .... p 3496 N93-30400 #
AD-A264493 .... p 3440 N93-30401 #
AD-A264502 .... p 3289 N93-30402 #
AD-A264513 .... p 3426 N93-30403 #
AD-A264514 .... p 3446 N93-30404 #
AD-A264515 .... p 3315 N93-30405 #
AD-A264521 .... p 3412 N93-30406 #
AD-A264523 .... p 3598 N93-30407 #
AD-A264527 .... p 3598 N93-30408 #
AD-A264528 .... p 3412 N93-30409 #
AD-A264552 .... p 3337 N93-30381 #
AD-A264553 .... p 3496 N93-30382 #
AD-A264554 .... p 3533 N93-30383 #
AD-A264557 .... p 3446 N93-30384 #
AD-A264619 .... p 3562 N93-30121
AD-A264620 .... p 3563 N93-30385 #
AD-A264623 .... p 3393 N93-30386 #
AD-A264626 .... p 3499 N93-30426 #
AD-A264627 .... p 3413 N93-30539 #
AD-A264628 .... p 3484 N93-30176
AD-A264631 .... p 3570 N93-30540 #
AD-A264632 .... p 3599 N93-30518 #
AD-A264633 .... p 3561 N93-30519 #
AD-A264634 .... p 3599 N93-30548 #
AD-A264635 .... p 3581 N93-30520 #
AD-A264639 .... p 3484 N93-30521 #
AD-A264643 .... p 3581 N93-30522 #
AD-A264645 .... p 3534 N93-30523 #
AD-A264647 .... p 3446 N93-30524 #
AD-A264649 .... p 3489 N93-30525 #

AD-A264655 .... p 3315 N93-30526 #
AD-A264660 .... p 3337 N93-30541 #
AD-A264661 .... p 3499 N93-30542 #
AD-A264674 .... p 3500 N93-30543 #
AD-A264678 .... p 3534 N93-30544 #
AD-A264679 .... p 3534 N93-30549 #
AD-A264682 .... p 3260 N93-30550 #
AD-A264683 .... p 3316 N93-30551 #
AD-A264685 .... p 3337 N93-30552 #
AD-A264687 .... p 3440 N93-30553 #
AD-A264692 .... p 3496 N93-30494 #
AD-A264693 .... p 3427 N93-30571 #
AD-A264697 .... p 3534 N93-30495 #
AD-A264700 .... p 3327 N93-30574 #
AD-A264702 .... p 3337 N93-30497 #
AD-A264704 .... p 3260 N93-30498 #
AD-A264705 .... p 3427 N93-30499 #
AD-A264707 .... p 3581 N93-30500 #
AD-A264709 .... p 3599 N93-30568 #
AD-A264711 .... p 3598 N93-30501 #
AD-A264712 .... p 3551 N93-30503 #
AD-A264714 .... p 3600 N93-30569 #
AD-A264716 .... p 3446 N93-30512 #
AD-A264720 .... p 3670 N93-30513 #
AD-A264722 .... p 3393 N93-30514 #
AD-A264723 .... p 3496 N93-30515 #
AD-A264724 .... p 3599 N93-30554 #
AD-A264725 .... p 3303 N93-30555 #
AD-A264726 .... p 3500 N93-30575 #
AD-A264727 .... p 3393 N93-30576 #
AD-A264728 .... p 3454 N93-30545 #
AD-A264730 .... p 3534 N93-30546 #
AD-A264731 .... p 3534 N93-30547 #
AD-A264734 .... p 3534 N93-30577 #
AD-A264735 .... p 3544 N93-30556 #
AD-A264750 .... p 3590 N93-30585 #
AD-A264751 .... p 3337 N93-30557 #
AD-A264753 .... p 3570 N93-30558 #
AD-A264754 .... p 3623 N93-30559 #
AD-A264755 .... p 3599 N93-30560 #
AD-A264756 .... p 3534 N93-30561 #
AD-A264758 .... p 3479 N93-30562 #
AD-A264759 .... p 3529 N93-29657 #
AD-A264760 .... p 3529 N93-29658 #
AD-A264761 .... p 3484 N93-30608 #
AD-A264765 .... p 3581 N93-30609 #
AD-A264774 .... p 3338 N93-30610 #
AD-A264777 .... p 3487 N93-29659 #
AD-A264784 .... p 3394 N93-30611 #
AD-A264789 .... p 3610 N93-30177 #
AD-A264794 .... p 3492 N93-30665 * #
AD-A264795 .... p 3489 N93-30612 #
AD-A264798 .... p 3535 N93-30602 #
AD-A264800 .... p 3489 N93-30603 #
AD-A264801 .... p 3544 N93-30591 #
AD-A264802 .... p 3544 N93-30592 #
AD-A264804 .... p 3479 N93-30593 #
AD-A264807 .... p 3492 N93-30594 #
AD-A264808 .... p 3394 N93-30595 #
AD-A264809 .... p 3338 N93-30596 #
AD-A264810 .... p 3334 N93-29660 #
AD-A264813 .... p 3581 N93-30666 #
AD-A264819 .... p 3316 N93-30627 #
AD-A264820 .... p 3338 N93-30628 #
AD-A264821 .... p 3394 N93-30597 #
AD-A264823 .... p 3561 N93-29711 #
AD-A264824 .... p 3454 N93-30598 #
AD-A264825 .... p 3441 N93-30599 #
AD-A264827 .... p 3317 N93-30667 #
AD-A264828 .... p 3590 N93-30600 #
AD-A264829 .... p 3496 N93-30613 #
AD-A264830 .... p 3535 N93-30614 #
AD-A264831 .... p 3543 N93-29791 #
AD-A264832 .... p 3631 N93-30629 #
AD-A264833 .... p 3428 N93-30630 #
AD-A264834 .... p 3339 N93-30898 #
AD-A264835 .... p 3563 N93-30899 #
AD-A264837 .... p 3340 N93-30900 #
AD-A264838 .... p 3571 N93-30901 #
AD-A264840 .... p 3497 N93-30904 #
AD-A264846 .... p 3581 N93-30905 #
AD-A264850 .... p 3490 N93-30906 #
AD-A264852 .... p 3623 N93-30907 #
AD-A264853 .... p 3489 N93-30178
AD-A264872 .... p 3522 N93-30179
AD-A264881 .... p 3497 N93-30908 #
AD-A264883 .... p 3340 N93-30909 #
AD-A264887 .... p 3441 N93-30910 #
AD-A264895 .... p 3536 N93-31026 #

AD-B156202L .... p 3240 N93-29450 * #

AD-D015680 .... p 3409 N93-29605
AD-D015684 .... p 3507 N93-29606
AD-D015685 .... p 3507 N93-29607
AD-D015688 .... p 3383 N93-29455
AD-D015689 .... p 3333 N93-29456
AD-D015691 .... p 3333 N93-29457
AD-D015694 .... p 3333 N93-29458
AD-D015697 .... p 3577 N93-29038 #
AD-D015698 .... p 3431 N93-29046 #
AD-D015706 .... p 3440 N93-30427 #
AD-D015707 .... p 3581 N93-30410 #
AD-D015709 .... p 3383 N93-29275
AD-D015710 .... p 3437 N93-29276
AD-D015711 .... p 3437 N93-29277
AD-D015712 .... p 3259 N93-29278
AD-D015713 .... p 3562 N93-29279
AD-D015714 .... p 3383 N93-29280
AD-D015717 .... p 3338 N93-30586 #
AD-D015718 .... p 3338 N93-30580 #
AD-D015722 .... p 3412 N93-30201
AD-D015723 .... p 3408 N93-29281
AD-D015724 .... p 3438 N93-29287
AD-D015726 .... p 3444 N93-29288
AD-D015728 .... p 3441 N93-30587 #

AD-E201426 .... p 3630 N93-29460 #
AD-E201429 .... p 3287 N93-28658 #
AD-E201436 .... p 3279 N93-29305 #
AD-E201447 .... p 3288 N93-29289 #
AD-E501645 .... p 3272 N93-30881 #
AD-E951985 .... p 3555 N93-29857 #
AD-E951998 .... p 3342 N93-29494 #
AD-E952001 .... p 3438 N93-29800 #
AD-E952002 .... p 3409 N93-29655 #
AD-E952004 .... p 3579 N93-29656 #

AFIT/DS/ENG/93M-01 .... p 3596 N93-29424

AFIT/DS/ENP/93-01 .... p 3591 N93-28471 #

AFIT/EN/TR-93-01 .... p 3526 N93-29145 #

AFIT/GA/93M-01 .... p 3298 N93-29414 #

AFIT/GCE/ENG/93M-01 .... p 3537 N93-28478 #

AFIT/GCS/ENG/93M-03 .... p 3524 N93-28577 #
AFIT/GCS/ENG/93M-04 .... p 3260 N93-28467 #
AFIT/GCS/ENG/93M-05 .... p 3528 N93-29418 #
AFIT/GCS/ENG/93M-06 .... p 3612 N93-28846 #

AFIT/GEO/ENG/93M-02 .... p 3379 N93-28476 #
AFIT/GEO/ENG/93M-03 .... p 3480 N93-28465 #

AFIT/GNE/ENP/93M-03 .... p 3286 N93-28474 #
AFIT/GNE/ENP/93M-2 .... p 3423 N93-29419 #
AFIT/GNE/ENP/93M-6 .... p 3567 N93-29415 #

AFIT/GOR/ENS/93M-06 .... p 3270 N93-28468 #
AFIT/GOR/ENS/93M-07 .... p 3553 N93-28575 #
AFIT/GOR/ENS/93M-21 .... p 3554 N93-28845 #
AFIT/GOR/ENS/93M-24 .... p 3553 N93-28760 #
AFIT/GOR/ENS/93M-25 .... p 3553 N93-28574 #
AFIT/GOR/ENS/93M-27 .... p 3554 N93-28844 #

AFIT/GST/ENS/93M-01 .... p 3555 N93-29447 #
AFIT/GST/ENS/93M-02 .... p 3553 N93-28587 #
AFIT/GST/ENS/93M-08 .... p 3270 N93-28938 #
AFIT/GST/ENS/93M-10 .... p 3542 N93-29420 #

AFL-RN-92-11-78 .... p 3425 N93-30369 #

AFOSR-03-0245TR .... p 3597 N93-30164 #
AFOSR-91-0015 .... p 3500 N93-30543 #
AFOSR-93-0110TR-VOL-1 .... p 3608 N93-29440 #
AFOSR-93-0126TR-VOL-16 .... p 3608 N93-29396 #
AFOSR-93-0162TR .... p 3652 N93-28756
AFOSR-93-0172TR .... p 3329 N93-28495 #
AFOSR-93-0177TR .... p 3333 N93-29511 #
AFOSR-93-0181TR .... p 3298 N93-29282 #
AFOSR-93-0187TR .... p 3541 N93-28498 #
AFOSR-93-0190TR .... p 3298 N93-29130 #
AFOSR-93-0194TR .... p 3420 N93-29141 #
AFOSR-93-0196TR .... p 3452 N93-29349
AFOSR-93-0197TR .... p 3591 N93-28496 #
AFOSR-93-0199TR .... p 3321 N93-28591 #
AFOSR-93-0200TR .... p 3554 N93-29411
AFOSR-93-0202TR .... p 3493 N93-28759 #
AFOSR-93-0204TR .... p 3590 N93-30585 #
AFOSR-93-0205TR .... p 3428 N93-30630 #
AFOSR-93-0206TR .... p 3339 N93-30898 #
AFOSR-93-0207TR .... p 3425 N93-30369 #
AFOSR-93-0208TR .... p 3534 N93-30561 #
AFOSR-93-0213TR .... p 3453 N93-30159 #
AFOSR-93-0214TR .... p 3533 N93-30418 #
AFOSR-93-0216TR .... p 3340 N93-30900 #
AFOSR-93-0217TR .... p 3497 N93-30904 #
AFOSR-93-0219TR .... p 3570 N93-30558 #
AFOSR-93-0237TR .... p 3499 N93-30163 #
AFOSR-93-0238TR .... p 3539 N93-30361 #
AFOSR-93-0240TR .... p 3425 N93-30162 #
AFOSR-93-0241TR .... p 3654 N93-30419 #
AFOSR-93-0242TR .... p 3496 N93-30422 #
AFOSR-93-0243TR .... p 3479 N93-30562 #
AFOSR-93-0244TR .... p 3599 N93-30560 #
AFOSR-93-0246TR .... p 3597 N93-30161 #
AFOSR-93-0247TR .... p 3580 N93-30205 #
AFOSR-93-0248TR .... p 3317 N93-30816 #
AFOSR-93-0251TR .... p 3540 N93-30364 #
AFOSR-93-0254TR .... p 3544 N93-30165 #
AFOSR-93-0255TR .... p 3528 N93-29483 #
AFOSR-93-0256TR .... p 3495 N93-30160 #
AFOSR-93-0257TR .... p 3561 N93-30519 #
AFOSR-93-0258TR .... p 3581 N93-30520 #
AFOSR-93-0262TR .... p 3478 N93-30367 #
AFOSR-93-0263TR .... p 3580 N93-30368 #
AFOSR-93-0265TR .... p 3478 N93-30174 #
AFOSR-93-0268TR .... p 3535 N93-30614 #
AFOSR-93-0270TR .... p 3496 N93-30494 #
AFOSR-93-0271TR .... p 3623 N93-30559 #
AFOSR-93-0272TR .... p 3337 N93-30417 #
AFOSR-93-0273TR .... p 3570 N93-30366 #
AFOSR-93-0274TR .... p 3543 N93-29791 #
AFOSR-93-0276TR .... p 3590 N93-30600 #
AFOSR-93-0280TR .... p 3496 N93-30421 #
AFOSR-93-0281TR .... p 3496 N93-30613 #
AFOSR-93-0284TR .... p 3631 N93-30629 #
AFOSR-93-0285TR .... p 3492 N93-30594 #
AFOSR-93-0285TR .... p 3317 N93-30667 #
AFOSR-93-0287TR .... p 3601 N93-30819 #
AFOSR-93-0288TR .... p 3337 N93-30557 #
AFOSR-93-0289TR .... p 3540 N93-30895 #
AFOSR-93-0291TR .... p 3597 N93-30175 #
AFOSR-93-0292TR .... p 3414 N93-30896 #
AFOSR-93-0294TR .... p 3339 N93-30885 #
AFOSR-93-0296TR .... p 3555 N93-30363 #
AFOSR-93-0301TR .... p 3601 N93-30878 #
AFOSR-93-0302TR .... p 3495 N93-30153 #
AFOSR-93-0308TR .... p 3495 N93-30192 #
AFOSR-93-0309TR .... p 3400 N93-30880 #
AFOSR-93-0311TR .... p 3411 N93-29922 #
AFOSR-93-0312TR .... p 3555 N93-29923 #
AFOSR-93-0313TR .... p 3399 N93-30879 #
AFOSR-93-0314TR .... p 3499 N93-30033 #
AFOSR-93-0317TR .... p 3473 N93-30360 #
AFOSR-93-0318TR .... p 3581 N93-30522 #
AFOSR-93-0322TR .... p 3393 N93-30386 #
AFOSR-93-0324TR .... p 3427 N93-30499 #
AFOSR-93-0325TR .... p 3260 N93-30550 #
AFOSR-93-0327TR .... p 3534 N93-30549 #
AFOSR-93-0328TR .... p 3534 N93-30544 #
AFOSR-93-0329TR .... p 3337 N93-30552 #
AFOSR-93-0333TR .... p 3446 N93-30524 #
AFOSR-93-0337TR .... p 3496 N93-30382 #
AFOSR-93-0338TR .... p 3316 N93-30551 #
AFOSR-93-0339TR .... p 3500 N93-30543 #
AFOSR-93-0340TR .... p 3670 N93-30513 #
AFOSR-93-0343TR .... p 3338 N93-30610 #
AFOSR-93-0350TR .... p 3581 N93-30905 #
AFOSR-93-0351TR .... p 3581 N93-30609 #
AFOSR-93-0352TR .... p 3497 N93-30908 #
AFOSR-93-0354TR .... p 3522 N93-30179

AGARD-CP-520 .... p 3501 N93-28850 #
AGARD-CP-522 .... p 3387 N93-29892 #
AGARD-CP-527 .... p 3252 N93-29926 #
AGARD-CP-529 .... p 3394 N93-30727 #

AIAA PAPER 93-1795 .... p 3251 N93-28697 * #
AIAA PAPER 93-1847 .... p 3252 N93-29162 * #
AIAA PAPER 93-1859 .... p 3270 N93-28696 * #
AIAA PAPER 93-2106 .... p 3288 N93-29158 * #
AIAA PAPER 93-2162 .... p 3286 N93-28619 * #
AIAA PAPER 93-2163 .... p 3288 N93-29068 * #
AIAA PAPER 93-2244 .... p 3341 N93-28695 * #
AIAA PAPER 93-2252 .... p 3420 N93-29157 * #
AIAA PAPER 93-2402 .... p 3288 N93-29194 * #
AIAA PAPER 93-2403 .... p 3287 N93-28694 * #
AIAA PAPER 93-2438 .... p 3252 N93-29065 * #
AIAA PAPER 93-2526 .... p 3252 N93-29072 * #
AIAA PAPER 93-2527 .... p 3251 N93-28617 * #
AIAA PAPER 93-2535 .... p 3416 N93-28627 * #
AIAA PAPER 93-2555 .... p 3251 N93-28609 * #

AID-PN-ABL-711 .... p 3471 N93-29681 #

AID-PN-ABM-278 .... p 3488 N93-29670

AL-SR-1993-0002 .... p 3541 N93-28987 #

AL-TP-1992-0053 .... p 3496 N93-30400 #
AL-TP-1992-0063 .... p 3498 N93-29481 #
AL-TP-1993-0010 .... p 3500 N93-30575 #
AL-TP-1993-0011 .... p 3498 N93-30026 #

AL-TR-1992-0014 .... p 3500 N93-28464 #

AL-TR-1992-0061 .... p 3507 N93-29889 #
AL-TR-1992-0088 .... p 3507 N93-29888 #
AL-TR-1992-0113 .... p 3438 N93-29395 #
AL-TR-1992-0127 .... p 3499 N93-30027 #
AL-TR-1992-0168 .... p 3508 N93-30167 #
AL-TR-1992-0171 .... p 3499 N93-30425 #
AL-TR-1993-0008 .... p 3501 N93-28479 #
AL-TR-1993-0010 .... p 3494 N93-29400 #
AL-TR-1993-0023 .... p 3499 N93-30542 #
AL-TR-1993-0025 .... p 3508 N93-29924 #

AMSMI/TR-RD-GC-93-4 .... p 3555 N93-29857 #

AMSMI/TR-RD-SS-92-11 .... p 3342 N93-29494 #

AMSMI/TR-RD-WS-92-13 .... p 3409 N93-29655 #
AMSMI/TR-RD-WS-93-1 .... p 3438 N93-29800 #
AMSMI/TR-RD-WS-93-3 .... p 3579 N93-29656 #

ANL-HEP-CP-92-101 .... p 3576 N93-30527 #
ANL-HEP-CP-93-02 .... p 3564 N93-28549 #

ANL-92/37 .... p 3509 N93-28573 #
ANL-92/46 .... p 3524 N93-28644 #
ANL-93/8 .... p 3550 N93-30140 #

ANL/CHM/CP-78499 .... p 3565 N93-28892 #

ANL/CMT/CP-77168 .... p 3407 N93-29036 #
ANL/CMT/CP-77865 .... p 3464 N93-29844 #

ANL/CMT/RP-79188 .... p 3408 N93-29311 #

ANL/CTD/CP-78758 .... p 3535 N93-30647 #

ANL/ES/CP-78832 .... p 3310 N93-29052 #
ANL/ES/CP-78904 .... p 3587 N93-29299 #

ANL/MCS-TM-175 .... p 3525 N93-28877 #

ANL/MCT/CP-77166 .... p 3442 N93-28903 #
ANL/MCT/CP-77501 .... p 3449 N93-28943 #
ANL/MCT/CP-77794 .... p 3330 N93-28666 #
ANL/MCT/CP-77846 .... p 3561 N93-29189 #
ANL/MCT/CP-78588 .... p 3323 N93-29102 #

ANL/MSD/CP-78800 .... p 3592 N93-28661 #

ANL/PHY/CP-79003 .... p 3574 N93-28970 #

ANL/VU-77166 .... p 3442 N93-28903 #

ANSER-STDN-93-4 .... p 3669 N93-29710 #

APL-UW-TR-9212 .... p 3595 N93-29341 #

AR-9301 .... p 3247 N93-28586 #

ARCCB-TR-93005 .... p 3295 N93-28657 #
ARCCB-TR-93008 .... p 3407 N93-29010 #
ARCCB-TR-93012 .... p 3327 N93-30538 #

ARFSD-TR-93003 .... p 3534 N93-30577 #

ARI-RR-1636 .... p 3508 N93-30590
ARI-RR-1637 .... p 3261 N93-29972 #

ARI-93-07 .... p 3531 N93-29874 #

ARL-CR-50 .... p 3325 N93-29981 #
ARL-CR-54 .... p 3381 N93-29011 #

ARL-MR-47 .... p 3342 N93-29762 #
ARL-MR-51 .... p 3453 N93-29801 #
ARL-MR-62 .... p 3432 N93-30032 #
ARL-MR-65 .... p 3413 N93-30539 #

ARL-TR-107 .... p 3341 N93-28515 #
ARL-TR-108 .... p 3309 N93-28514 #
ARL-TR-110 .... p 3294 N93-28559 #
ARL-TR-129 .... p 3315 N93-30405 #
ARL-TR-22 .... p 3240 N93-29512 #
ARL-TR-25 .... p 3505 N93-28941 #
ARL-TR-34 .... p 3299 N93-30137 #
ARL-TR-5 .... p 3260 N93-30604
ARL-TR-74 .... p 3271 N93-29394 #
ARL-TR-85 .... p 3335 N93-30007 #
ARL-TR-87 .... p 3327 N93-30812 #
ARL-TR-89 .... p 3281 N93-30813 #
ARL-TR-95 .... p 3556 N93-29423 #

ARO-23555.12-EG .... p 3604 N93-29384 #
ARO-24605.164-EG-UIR .... p 3432 N93-29390 #
ARO-24608.15-GS-UIR .... p 3462 N93-29834 #
ARO-24623.125-EG-UIR .... p 3580 N93-29880 #
ARO-24623.126-EG-UIR .... p 3445 N93-29388 #
ARO-24629.68-LS-UIR .... p 3491 N93-29915 #
ARO-24637.Z-MA-UIF .... p 3543 N93-29917 #
ARO-24927.4-EGS .... p 3342 N93-29835 #
ARO-25173.44-EL-SAH .... p 3528 N93-29294 #
ARO-25345.13-EG .... p 3453 N93-29855 #
ARO-25349.1-PH .... p 3439 N93-29853 #
ARO-25515.3-LS .... p 3549 N93-29871 #
ARO-25706.10-MA .... p 3531 N93-29916 #
ARO-26256.21-CH .... p 3313 N93-30030 #
ARO-26281.5-GS .... p 3487 N93-29298 #
ARO-26682.12-PH .... p 3588 N93-29382 #
ARO-26695.7-PH .... p 3596 N93-29859 #
ARO-26802.20-MA-SDI .... p 3530 N93-29865 #
ARO-26896.11-EL .... p 3595 N93-29383 #
ARO-26974.15-PH .... p 3439 N93-29983 #
ARO-27025.16-CH .... p 3342 N93-29296 #
ARO-27037.6-MS .... p 3334 N93-29856 #
ARO-27077.7-MA-SM .... p 3299 N93-29982 #
ARO-27159.9-MA-SAH .... p 3554 N93-29385 #
ARO-27241.1-CH-SAH .... p 3411 N93-29986 #
ARO-27417.6-EG .... p 3311 N93-29283 #
ARO-27440.6-CH .... p 3332 N93-29290 #
ARO-27508.9-PH .... p 3439 N93-29918 #
ARO-27864.3-EG-SDI .... p 3240 N93-29284 #
ARO-27868.25-MA .... p 3549 N93-29854 #
ARO-27868.26-MA .... p 3555 N93-29979 #
ARO-28416.2-PH .... p 3431 N93-29297 #
ARO-28809.10-MA-SDI .... p 3550 N93-29872 #
ARO-28809.11-MA-SDI .... p 3554 N93-29292 #
ARO-28809.8-MA-SDI .... p 3555 N93-29878 #
ARO-28950.1-MA .... p 3532 N93-30014 #
ARO-28986.1-MA .... p 3311 N93-29291 #
ARO-29354.3-MA .... p 3411 N93-30021 #
ARO-29354.3-MA .... p 3610 N93-30124 #
ARO-29669.2-PH-CF .... p 3315 N93-30534 #
ARO-30299-1-EG-II .... p 3259 N93-29985 #
ARO-30404.1-EG-SDI .... p 3312 N93-29389 #
ARO-30431.1-EG-SBI .... p 3423 N93-29353 #
ARO-30495.3-GS .... p 3580 N93-29887 #
ARO-30778.3-MA .... p 3532 N93-29980 #
ARO-30921.1-EL .... p 3387 N93-29875 #

ASC-TR-93-5002 .... p 3484 N93-30521 #

ASL-91-4 .... p 3244 N93-29152 * #

ATC-190 .... p 3261 N93-29815 #
ATC-199 .... p 3481 N93-29257 #

AVSCOM-TR-91-B-003 .... p 3240 N93-29450 * #

AWS/FM-93/001 .... p 3483 N93-29850 #

AWS/PR-93/004 .... p 3483 N93-29967 #

B-149 .... p 3456 N93-30634 #
B-160439 .... p 3474 N93-30506 #
B-252539 .... p 3533 N93-30202 #

BARC-1991/E/017 .... p 3441 N93-31023 #
BARC-1992/E/005 .... p 3441 N93-30801 #

BCRS-90-40A-PT-1 .... p 3460 N93-29307 #
BCRS-91-32 .... p 3463 N93-30839 #
BCRS-92-06 .... p 3460 N93-29320 #
BCRS-92-07 .... p 3460 N93-29321 #
BCRS-92-10-PHASE-1-PT-1 .... p 3461 N93-29465 #
BCRS-92-12 .... p 3461 N93-29466 #
BCRS-92-17 .... p 3463 N93-31009 #
BCRS-92-18 .... p 3463 N93-31010 #
BCRS-92-19 .... p 3463 N93-31011 #

BGSM-PP-92-001 .... p 3492 N93-30594 #

BNL-48089 .... p 3329 N93-28551 #
BNL-48146 .... p 3309 N93-28880 #
BNL-48228 .... p 3548 N93-28891 #
BNL-48565 .... p 3435 N93-28594 #
BNL-48571 .... p 3575 N93-29317 #
BNL-48601 .... p 3323 N93-29256 #

BONN-92-31 .... p 3632 N93-28473 #

CAL-2115 .... p 3630 N93-29604 * #
CAL-2118 .... p 3635 N93-30053 * #

CARDEROCKDIV-SSM-61-93/04 p 3334 N93-29790 #
CARDEROCKDIV-SSM-61-93/05 p 3595 N93-29333 #

CBIAC-SS-335 .... p 3501 N93-28757 #
CBIAC-SS-373 .... p 3493 N93-28758 #

CCMS-93-07 .... p 3297 N93-29107 * #

CCSDS-202.1-R-4 .... p 3393 N93-30371 * #

CDNSWC-MRD-80-93-10 .... p 3427 N93-30571 #

CDNSWC-SIG-93/108-745 .... p 3563 N93-30899 #

CDNSWC/PAS-92/52 .... p 3241 N93-29891 #

CDNSWC/SSM-64-93/02 .... p 3299 N93-29984 #

CI-2071-93-0008 .... p 3521 N93-29492 #

CIRSSE-131 .... p 3527 N93-29218 * #
CIRSSE-134 .... p 3543 N93-30039 * #
CIRSSE-136 .... p 3542 N93-29771 * #

CMOTT-93-07 .... p 3420 N93-29161 * #

CMU-CS-92-217 .... p 3531 N93-29866 #
CMU-CS-92-221 .... p 3529 N93-29486 #
CMU-CS-93-115 .... p 3530 N93-29823 #
CMU-CS-93-119 .... p 3534 N93-30523 #
CMU-CS-93-11 .... p 3528 N93-29463 #
CMU-CS-93-121 .... p 3533 N93-30125 #
CMU-CS-93-122 .... p 3579 N93-29824 #
CMU-CS-93-129 .... p 3530 N93-29822 #
CMU-CS-93-141 .... p 3530 N93-29821 #

CMU/CS-92-218 .... p 3615 N93-29459 #

CMU/SEI-93-TR-24 .... p 3530 N93-29852 #
CMU/SEI-93-TR-25 .... p 3610 N93-29970 #

COELMN/PD-93/05 .... p 3459 N93-29146 #

CONF-9103123-4 .... p 3380 N93-28900 #
CONF-9105381 .... p 3490 N93-31019 #
CONF-911033-6 .... p 3476 N93-28889 #
CONF-9111208-4 .... p 3574 N93-29103 #
CONF-920113-7 .... p 3493 N93-28835 #
CONF-920180 .... p 3556 N93-28572 * #
CONF-9202103-6 .... p 3563 N93-28521 #
CONF-9202154-1 .... p 3436 N93-28887 #
CONF-920311-27 .... p 3588 N93-29334 #
CONF-9203139-4 .... p 3630 N93-29785 #
CONF-9203232-1 .... p 3633 N93-28676 #
CONF-920362-43 .... p 3432 N93-29773 #
CONF-920384-SUMM .... p 3670 N93-30212 #
CONF-9204235-1 .... p 3568 N93-29784 #
CONF-920471-6 .... p 3430 N93-28520 #
CONF-920508-6 .... p 3490 N93-28890 #
CONF-920523-8 .... p 3438 N93-29781 #
CONF-9205307-1 .... p 3416 N93-28566 #
CONF-9205310-1 .... p 3593 N93-29094 #
CONF-9205319-1 .... p 3310 N93-29059 #
CONF-920607-20 .... p 3586 N93-29053 #
CONF-920610-15 .... p 3588 N93-29772 #
CONF-9206138-2 .... p 3437 N93-29207 #
CONF-9206148 .... p 3475 N93-30996 #
CONF-9206185-11 .... p 3549 N93-29060 #
CONF-9206234-2 .... p 3323 N93-29256 #
CONF-9206255-2 .... p 3565 N93-29099 #
CONF-9206332-2 .... p 3313 N93-29766 #
CONF-9206339-1 .... p 3469 N93-28992 #
CONF-920656-5 .... p 3575 N93-29317 #
CONF-920706-50 .... p 3575 N93-29302 #
CONF-920706-51 .... p 3326 N93-30490 #
CONF-9207151-1 .... p 3416 N93-28595 #
CONF-9207187-1 .... p 3520 N93-29058 #
CONF-920722-5 .... p 3593 N93-28956 #
CONF-920735-5 .... p 3592 N93-28642 #
CONF-920792-49 .... p 3422 N93-29300 #
CONF-920792-51 .... p 3261 N93-29869 #
CONF-920799-6 .... p 3450 N93-28567 #
CONF-920802-51 .... p 3592 N93-28661 #
CONF-9208109-78 .... p 3576 N93-30390 #
CONF-9208142-20 .... p 3436 N93-28847 #
CONF-9208146-2 .... p 3600 N93-30668 #
CONF-920821-3 .... p 3433 N93-30531 #
CONF-9208215-1 .... p 3410 N93-29793 #
CONF-9209166-2 .... p 3524 N93-28834 #
CONF-9209188-10 .... p 3433 N93-30491 #
CONF-9209200-8 .... p 3594 N93-29301 #
CONF-920921-9 .... p 3566 N93-29206 #
CONF-920927-3 .... p 3326 N93-30389 #
CONF-9209328-1 .... p 3324 N93-29786 #
CONF-9209330-1 .... p 3316 N93-30653 #
CONF-921005-28 .... p 3382 N93-29245 #
CONF-921005-32 .... p 3598 N93-30393 #
CONF-921007-23 .... p 3323 N93-29102 #
CONF-9210261-2 .... p 3309 N93-28880 #
CONF-9210280-1 .... p 3469 N93-28965 #
CONF-9210298-1 .... p 3424 N93-29836 #
CONF-9210315-2 .... p 3436 N93-29097 #
CONF-9210316-1 .... p 3634 N93-28963 #
CONF-9210317-ABSTS .... p 3548 N93-29057 #
CONF-9210321-1 .... p 3565 N93-28959 #
CONF-9210322-1 .... p 3321 N93-28957 #

CONF-9210324-1 .... p 3634 N93-28907 #
CONF-9210324-2 .... p 3634 N93-28906 #
CONF-9210324-3 .... p 3633 N93-28905 #
CONF-9210332-1 .... p 3311 N93-29263 #
CONF-921079-4 .... p 3524 N93-28550 #
CONF-921101-102 .... p 3325 N93-29813 #
CONF-921101-107 .... p 3594 N93-29314 #
CONF-921101-109 .... p 3327 N93-30652 #
CONF-921101-90 .... p 3405 N93-28581 #
CONF-921101-98 .... p 3321 N93-28679 #
CONF-921103-8 .... p 3437 N93-29104 #
CONF-921103-9 .... p 3584 N93-28602 #
CONF-9211101-4 .... p 3442 N93-28903 #
CONF-9211101-5 .... p 3407 N93-29036 #
CONF-9211101-6 .... p 3335 N93-30047 #
CONF-9211178-3 .... p 3238 N93-28662 #
CONF-9211205-1 .... p 3320 N93-28548 #
CONF-9211209-1 .... p 3632 N93-28547 #
CONF-9211211-1 .... p 3586 N93-29093 #
CONF-9211218-1 .... p 3331 N93-29248 #
CONF-9211219-1 .... p 3551 N93-30392 #
CONF-921122-44 .... p 3567 N93-29351 #
CONF-921125-7 .... p 3615 N93-29783 #
CONF-921131-8 .... p 3564 N93-28549 #
CONF-921131-9 .... p 3574 N93-28970 #
CONF-921133-17 .... p 3410 N93-29812 #
CONF-921145-6 .... p 3575 N93-29809 #
CONF-921206-12 .... p 3594 N93-29188 #
CONF-921217-5 .... p 3430 N93-28664 #
CONF-921217-6 .... p 3596 N93-29868 #
CONF-921256-3 .... p 3440 N93-30394 #
CONF-921261-3 .... p 3653 N93-28962 #
CONF-921262-1 .... p 3354 N93-28893 #
CONF-921266-1 .... p 3566 N93-29315 #
CONF-930111-1 .... p 3634 N93-28908 #
CONF-930117-6 .... p 3539 N93-29782 #
CONF-930129-2 .... p 3615 N93-29310 #
CONF-930133-8 .... p 3383 N93-29308 #
CONF-930135-1 .... p 3588 N93-29780 #
CONF-930135-2 .... p 3437 N93-29098 #
CONF-930140-2 .... p 3477 N93-29346 #
CONF-930140-3 .... p 3482 N93-29347 #
CONF-930150-REV .... p 3594 N93-29249 #
CONF-930159-10 .... p 3593 N93-28966 #
CONF-930159-17 .... p 3386 N93-29765 #
CONF-930159-19 .... p 3438 N93-29309 #
CONF-930159-20 .... p 3440 N93-30530 #
CONF-930159-26 .... p 3575 N93-29870 #
CONF-930159-4 .... p 3565 N93-28892 #
CONF-930178-1 .... p 3471 N93-29792 #
CONF-930185-1 .... p 3634 N93-29246 #
CONF-930194-2 .... p 3538 N93-29186 #
CONF-930197-1 .... p 3565 N93-28831 #
CONF-930198-1 .... p 3587 N93-29303 #
CONF-930202-4 .... p 3322 N93-29061 #
CONF-930202-5 .... p 3323 N93-29101 #
CONF-930205-54 .... p 3472 N93-30180 #
CONF-930208-2 .... p 3472 N93-30008 #
CONF-930216-1 .... p 3587 N93-29299 #
CONF-930244-2 .... p 3472 N93-30009 #
CONF-930258-2 .... p 3279 N93-29840 #
CONF-930264-1 .... p 3541 N93-29047 #
CONF-930271-1 .... p 3320 N93-28545 #
CONF-930279-2 .... p 3550 N93-30041 #
CONF-930286-1 .... p 3535 N93-30647 #
CONF-930292-1 .... p 3406 N93-28830 #
CONF-930293-1 .... p 3566 N93-29313 #
CONF-930296-1 .... p 3332 N93-29252 #
CONF-9303100-2 .... p 3623 N93-30482 #
CONF-9303108-1 .... p 3310 N93-29052 #
CONF-9303110-1 .... p 3296 N93-28904 #
CONF-9303119-1 .... p 3564 N93-28762 #
CONF-9303126-1 .... p 3426 N93-30485 #
CONF-9303126-2 .... p 3421 N93-29253 #
CONF-9303128-1 .... p 3433 N93-30510 #
CONF-930367-2 .... p 3598 N93-30517 #
CONF-930391-2 .... p 3278 N93-29250 #
CONF-930401-1 .... p 3443 N93-28968 #
CONF-930403-20 .... p 3383 N93-29348 #
CONF-930403-21 .... p 3394 N93-30631 #
CONF-930403-23 .... p 3584 N93-28583 #
CONF-930403-34 .... p 3444 N93-29316 #
CONF-930403-35 .... p 3444 N93-29254 #
CONF-930403-36 .... p 3444 N93-29247 #
CONF-930403-40 .... p 3544 N93-30529 #
CONF-930403-41 .... p 3460 N93-29255 #
CONF-930404-8 .... p 3565 N93-28833 #
CONF-930404-9 .... p 3425 N93-30184 #
CONF-9304103-1 .... p 3336 N93-30051 #
CONF-9304103-2 .... p 3324 N93-29265 #
CONF-9304103-3 .... p 3339 N93-30656 #
CONF-9304105-1 .... p 3426 N93-30484 #
CONF-9304110-1 .... p 3341 N93-29251 #
CONF-9304110-2 .... p 3342 N93-29312 #
CONF-930416-1 .... p 3561 N93-29189 #
CONF-930435-6 .... p 3465 N93-30206 #
CONF-930435-7 .... p 3464 N93-29925 #
CONF-930445-2 .... p 3611 N93-28580 #
CONF-930445-4 .... p 3554 N93-28763 #
CONF-930461-3 .... p 3576 N93-30527 #
CONF-930489-2 .... p 3380 N93-28909 #
CONF-930491-2 .... p 3447 N93-30654 #
CONF-930502-2 .... p 3449 N93-28943 #
CONF-930502-3 .... p 3320 N93-28564 #
CONF-930502-4 .... p 3334 N93-29767 #
CONF-930502-6 .... p 3259 N93-30168 #
CONF-930513-1 .... p 3330 N93-28666 #
CONF-9305133-1 .... p 3579 N93-29350 #
CONF-9305139-1 .... p 3481 N93-29095 #
CONF-930514-1 .... p 3484 N93-30651 #
CONF-9305150-1 .... p 3464 N93-29147 #
CONF-9305153-1 .... p 3530 N93-29808 #
CONF-9305153-2 .... p 3491 N93-30483 #
CONF-9305159-1 .... p 3437 N93-29264 #
CONF-9305160-1 .... p 3532 N93-30050 #
CONF-9305161-1 .... p 3532 N93-30050 #
CONF-930529-2 .... p 3453 N93-30185 #
CONF-930561-3 .... p 3465 N93-30391 #
CONF-930571-8 .... p 3464 N93-29844 #
CONF-930577-1 .... p 3433 N93-30655 #
CONF-930580-2 .... p 3239 N93-29035 #
CONF-930601-4 .... p 3382 N93-29244 #
CONF-930601-8 .... p 3540 N93-30633 #
CONF-9306101-1 .... p 3538 N93-28894 #
CONF-9306102-1 .... p 3549 N93-29769 #
CONF-9306104-3 .... p 3405 N93-28641 #
CONF-9306114-1 .... p 3450 N93-30636 #
CONF-9306118-1 .... p 3443 N93-29185 #
CONF-9306127-1 .... p 3543 N93-30012 #
CONF-9306128-1 .... p 3549 N93-29187 #
CONF-9306130-1 .... p 3589 N93-30181 #
CONF-930616-1 .... p 3406 N93-28944 #
CONF-930621-1 .... p 3417 N93-28639 #
CONF-930621 .... p 3419 N93-29050 #
CONF-930649-1 .... p 3524 N93-28640 #
CONF-930651-1 .... p 3548 N93-28891 #
CONF-930661-1 .... p 3505 N93-28942 #
CONF-930702-11 .... p 3378 N93-30508 #
CONF-930702-2 .... p 3446 N93-30211 #
CONF-930702-4 .... p 3454 N93-30213 #
CONF-930702-8 .... p 3447 N93-30632 #
CONF-930704-1 .... p 3281 N93-30509 #
CONF-930704-3 .... p 3570 N93-30669 #
CONF-930704-4 .... p 3413 N93-30650 #
CONF-930704-5 .... p 3598 N93-30511 #
CONF-930704-6 .... p 3413 N93-30516 #
CONF-930713-1 .... p 3598 N93-30445 #
CONF-930713-2 .... p 3352 N93-30446 #
CONF-930713-3 .... p 3315 N93-30447 #
CONF-930713-4 .... p 3570 N93-30448 #
CONF-930713-5 .... p 3315 N93-30209 #
CONF-930729-1 .... p 3326 N93-30486 #
CONF-930736-1 .... p 3446 N93-30210 #
CONF-930741-2 .... p 3412 N93-30370 #

COO-2197-133 .... p 3564 N93-28611 #

CPIA-PUBL-589 .... p 3343 N93-30061

CRC-583 .... p 3261 N93-29398 #

CRDEC-TR-356 .... p 3430 N93-28659 #
CRDEC-TR-420 .... p 3315 N93-30365 #

CRHC-93-11 .... p 3527 N93-29170 * #

CRIE-T-91044 .... p 3577 N93-28982 #
CRIE-T-91052 .... p 3406 N93-28983 #
CRIE-T-91054 .... p 3406 N93-28746 #
CRIE-T-91078 .... p 3410 N93-29673 #
CRIE-T-91084 .... p 3406 N93-28669 #

CRREL-REPT-93-2 .... p 3262 N93-30103 #

CRREL-93-1 .... p 3379 N93-28588 #

CS-9204 .... p 3552 N93-31012 #
CS-9205 .... p 3552 N93-31014 #

CSDL-T-1176 .... p 3443 N93-29080 * #
CSDL-T-1180 .... p 3634 N93-29042 * #

CSL-TR-92-555 .... p 3539 N93-29508 #

CTN-93-60717 .... p 3354 N93-30215

CTP-TAMU-26/91 .... p 3557 N93-30917 #

CUPP-92/3 .... p 3572 N93-30931 #

CWI-BS-R9207 .... p 3549 N93-29849 #
CWI-CS-R9218 .... p 3532 N93-30017 #

DCIEM-92-31 .... p 3506 N93-29471 #
DCIEM-92-60 .... p 3493 N93-28939 #

DESY-92-131 .... p 3603 N93-28472 #

DE92-018262 .... p 3417 N93-28639 #
DE92-019503 .... p 3419 N93-29050 #
DE92-040222 .... p 3598 N93-30445 #
DE92-040369 .... p 3352 N93-30446 #
DE92-040372 .... p 3315 N93-30447 #
DE92-040374 .... p 3570 N93-30448 #
DE92-531076 .... p 3413 N93-30622 #
DE92-638517 .... p 3536 N93-31001 #
DE92-640082 .... p 3328 N93-30941 #
DE92-641338 .... p 3557 N93-30981 #
DE92-641339 .... p 3480 N93-31002 #
DE92-641343 .... p 3608 N93-31003 #
DE92-641346 .... p 3637 N93-30997 #
DE92-641348 .... p 3552 N93-30942 #
DE92-641716 .... p 3637 N93-31004 #
DE92-642126 .... p 3602 N93-30998 #
DE92-642137 .... p 3602 N93-31027 #
DE92-642213 .... p 3485 N93-31006 #
DE92-642433 .... p 3317 N93-30982 #
DE92-642597 .... p 3572 N93-30931 #
DE92-644671 .... p 3608 N93-30983 #
DE92-644672 .... p 3551 N93-30912 #
DE92-644674 .... p 3551 N93-30913 #
DE92-644677 .... p 3552 N93-30984 #
DE92-644678 .... p 3535 N93-30914 #
DE92-644679 .... p 3535 N93-30915 #
DE92-644717 .... p 3607 N93-30916 #
DE92-644721 .... p 3557 N93-30917 #
DE92-644722 .... p 3637 N93-30918 #
DE92-644724 .... p 3637 N93-30919 #
DE92-644725 .... p 3557 N93-30985 #
DE92-644726 .... p 3558 N93-30986 #
DE92-644727 .... p 3607 N93-30920 #
DE92-644730 .... p 3607 N93-30921 #
DE92-644736 .... p 3557 N93-30922 #
DE92-644738 .... p 3400 N93-30923 #
DE92-644739 .... p 3607 N93-30924 #
DE92-644740 .... p 3607 N93-30925 #
DE92-644743 .... p 3557 N93-30926 #
DE92-644744 .... p 3557 N93-30927 #
DE92-644844 .... p 3557 N93-30928 #
DE92-644845 .... p 3551 N93-30929 #
DE92-644947 .... p 3572 N93-30930 #
DE93-000087 .... p 3464 N93-29925 #
DE93-000088 .... p 3465 N93-30206 #
DE93-000094 .... p 3465 N93-30207 #
DE93-000096 .... p 3464 N93-29965 #
DE93-000097 .... p 3464 N93-28971 #
DE93-000098 .... p 3465 N93-30208 #
DE93-000124 .... p 3603 N93-28964 #
DE93-000682 .... p 3315 N93-30209 #
DE93-000797 .... p 3524 N93-28640 #
DE93-001892 .... p 3454 N93-31013 #
DE93-001923 .... p 3505 N93-28942 #
DE93-005113 .... p 3568 N93-29764 #
DE93-005301 .... p 3446 N93-30210 #
DE93-005444 .... p 3472 N93-30008 #
DE93-005445 .... p 3446 N93-30211 #
DE93-005464 .... p 3436 N93-28887 #
DE93-005564 .... p 3449 N93-28943 #
DE93-005587 .... p 3309 N93-28880 #
DE93-005777 .... p 3472 N93-30009 #
DE93-005817 .... p 3469 N93-28965 #
DE93-005886 .... p 3476 N93-28889 #
DE93-006189 .... p 3670 N93-30212 #
DE93-006206 .... p 3454 N93-30213 #
DE93-006235 .... p 3490 N93-28890 #
DE93-006283 .... p 3412 N93-30370 #
DE93-006285 .... p 3406 N93-28944 #
DE93-006387 .... p 3548 N93-28891 #
DE93-006416 .... p 3565 N93-28892 #
DE93-006572 .... p 3420 N93-29126 #
DE93-006621 .... p 3469 N93-28992 #
DE93-006628 .... p 3354 N93-28893 #
DE93-006739 .... p 3538 N93-28894 #
DE93-007050 .... p 3532 N93-30034 #
DE93-007117 .... p 3424 N93-30035 #
DE93-007144 .... p 3536 N93-30934 #
DE93-007176 .... p 3473 N93-30183 #
DE93-007289 .... p 3481 N93-29054 #
DE93-007326 .... p 3380 N93-28900 #
DE93-007332 .... p 3386 N93-29765 #
DE93-007344 .... p 3424 N93-29836 #
DE93-007349 .... p 3549 N93-29769 #
DE93-007355 .... p 3410 N93-29812 #
DE93-007362 .... p 3593 N93-28966 #
DE93-007365 .... p 3477 N93-29346 #
DE93-007367 .... p 3611 N93-28580 #
DE93-007381 .... p 3482 N93-29347 #

DE93-007390 p 3470 N93-29055 #
DE93-007391 p 3474 N93-30504 #
DE93-007394 p 3469 N93-28972 #
DE93-007412 p 3469 N93-28967 #
DE93-007416 p 3471 N93-29770 #
DE93-007465 p 3470 N93-29135 #
DE93-007518 p 3474 N93-30506 #
DE93-007531 p 3586 N93-29056 #
DE93-007537 p 3313 N93-29837 #
DE93-007586 p 3378 N93-30508 #
DE93-007608 p 3279 N93-29840 #
DE93-007609 p 3405 N93-28641 #
DE93-007610 p 3281 N93-30509 #
DE93-007643 p 3423 N93-29804 #
DE93-007656 p 3431 N93-29149 #
DE93-007664 p 3313 N93-29766 #
DE93-007699 p 3405 N93-28581 #
DE93-007704 p 3592 N93-28642 #
DE93-007722 p 3592 N93-28582 #
DE93-007732 p 3436 N93-28847 #
DE93-007823 p 3443 N93-28968 #
DE93-007829 p 3574 N93-28969 #
DE93-007857 p 3584 N93-28583 #
DE93-007876 p 3383 N93-29308 #
DE93-007882 p 3238 N93-28662 #
DE93-007892 p 3592 N93-28661 #
DE93-007910 p 3334 N93-29767 #
DE93-007913 p 3320 N93-28564 #
DE93-007915 p 3394 N93-30631 #
DE93-007916 p 3383 N93-29348 #
DE93-007919 p 3382 N93-29244 #
DE93-007955 p 3310 N93-29051 #
DE93-007964 p 3261 N93-28490 #
DE93-007969 p 3548 N93-29057 #
DE93-007970 p 3579 N93-29350 #
DE93-007990 p 3574 N93-28565 #
DE93-007991 p 3416 N93-28566 #
DE93-008018 p 3471 N93-29792 #
DE93-008075 p 3450 N93-28567 #
DE93-008134 p 3382 N93-29245 #
DE93-008138 p 3567 N93-29351 #
DE93-008182 p 3447 N93-30632 #
DE93-008271 p 3541 N93-29047 #
DE93-008272 p 3593 N93-28956 #
DE93-008275 p 3321 N93-28957 #
DE93-008300 p 3603 N93-28958 #
DE93-008302 p 3566 N93-29261 #
DE93-008336 p 3565 N93-28959 #
DE93-008339 p 3239 N93-29035 #
DE93-008365 p 3407 N93-29048 #
DE93-008380 p 3565 N93-28960 #
DE93-008401 p 3603 N93-28961 #
DE93-008482 p 3653 N93-28962 #
DE93-008483 p 3634 N93-28963 #
DE93-008484 p 3633 N93-28676 #
DE93-008520 p 3476 N93-28677 #
DE93-008541 p 3564 N93-28678 #
DE93-008559 p 3465 N93-30011 #
DE93-008575 p 3321 N93-28679 #
DE93-008634 p 3329 N93-28541 #
DE93-008636 p 3321 N93-28902 #
DE93-008647 p 3442 N93-28903 #
DE93-008656 p 3587 N93-29299 #
DE93-008658 p 3310 N93-29052 #
DE93-008676 p 3323 N93-29092 #
DE93-008701 p 3296 N93-28904 #
DE93-008706 p 3586 N93-29093 #
DE93-008708 p 3633 N93-28905 #
DE93-008709 p 3634 N93-28906 #
DE93-008711 p 3634 N93-28907 #
DE93-008712 p 3540 N93-30633 #
DE93-008713 p 3593 N93-29094 #
DE93-008716 p 3634 N93-29246 #
DE93-008720 p 3634 N93-28908 #
DE93-008721 p 3464 N93-29147 #
DE93-008725 p 3450 N93-30636 #
DE93-008734 p 3481 N93-29095 #
DE93-008735 p 3380 N93-28909 #
DE93-008755 p 3537 N93-28544 #
DE93-008759 p 3624 N93-29100 #
DE93-008924 p 3323 N93-29101 #
DE93-008937 p 3470 N93-29262 #
DE93-008997 p 3462 N93-30637 #
DE93-009028 p 3320 N93-28545 #
DE93-009049 p 3593 N93-29096 #
DE93-009053 p 3563 N93-28546 #
DE93-009073 p 3632 N93-28547 #
DE93-009077 p 3436 N93-29097 #
DE93-009080 p 3320 N93-28548 #
DE93-009202 p 3323 N93-29102 #
DE93-009204 p 3407 N93-29036 #
DE93-009208 p 3574 N93-28970 #
DE93-009211 p 3564 N93-28549 #
DE93-009225 p 3437 N93-29098 #
DE93-009230 p 3311 N93-29263 #
DE93-009233 p 3524 N93-28550 #
DE93-009234 p 3586 N93-29053 #
DE93-009237 p 3430 N93-28520 #
DE93-009243 p 3563 N93-28521 #
DE93-009247 p 3574 N93-29103 #
DE93-009254 p 3410 N93-29793 #
DE93-009257 p 3565 N93-29099 #
DE93-009258 p 3422 N93-29300 #
DE93-009285 p 3438 N93-29309 #
DE93-009286 p 3588 N93-29780 #
DE93-009288 p 3437 N93-29104 #
DE93-009293 p 3326 N93-30389 #
DE93-009294 p 3520 N93-29058 #
DE93-009297 p 3438 N93-29781 #
DE93-009300 p 3539 N93-29782 #
DE93-009301 p 3588 N93-29772 #
DE93-009302 p 3432 N93-29773 #
DE93-009303 p 3615 N93-29783 #
DE93-009308 p 3310 N93-29059 #
DE93-009313 p 3566 N93-29206 #
DE93-009316 p 3549 N93-29060 #
DE93-009318 p 3437 N93-29207 #
DE93-009319 p 3615 N93-29310 #
DE93-009320 p 3588 N93-29334 #
DE93-009338 p 3322 N93-29061 #
DE93-009353 p 3573 N93-28522 #
DE93-009360 p 3435 N93-28594 #
DE93-009370 p 3563 N93-28542 #
DE93-009424 p 3550 N93-30041 #
DE93-009447 p 3416 N93-28595 #
DE93-009458 p 3450 N93-28596 #
DE93-009459 p 3405 N93-28597 #
DE93-009520 p 3568 N93-29784 #
DE93-009527 p 3576 N93-30390 #
DE93-009543 p 3630 N93-29785 #
DE93-009546 p 3600 N93-30668 #
DE93-009552 p 3594 N93-29301 #
DE93-009561 p 3535 N93-30647 #
DE93-009578 p 3587 N93-29148 #
DE93-009579 p 3584 N93-28598 #
DE93-009580 p 3585 N93-28910 #
DE93-009581 p 3584 N93-28599 #
DE93-009582 p 3565 N93-28914 #
DE93-009588 p 3404 N93-28523 #
DE93-009623 p 3570 N93-30669 #
DE93-009624 p 3413 N93-30650 #
DE93-009625 p 3437 N93-29264 #
DE93-009630 p 3425 N93-30184 #
DE93-009633 p 3484 N93-30651 #
DE93-009639 p 3453 N93-30185 #
DE93-009711 p 3324 N93-29786 #
DE93-009719 p 3259 N93-30168 #
DE93-009722 p 3335 N93-30047 #
DE93-009724 p 3325 N93-29813 #
DE93-009727 p 3472 N93-30180 #
DE93-009729 p 3327 N93-30652 #
DE93-009732 p 3316 N93-30653 #
DE93-009756 p 3566 N93-29184 #
DE93-009758 p 3310 N93-28911 #
DE93-009762 p 3557 N93-30048 #
DE93-009794 p 3329 N93-28551 #
DE93-009796 p 3447 N93-30654 #
DE93-009800 p 3433 N93-30655 #
DE93-009802 p 3339 N93-30656 #
DE93-009819 p 3462 N93-30049 #
DE93-009820 p 3472 N93-30043 * #
DE93-009823 p 3442 N93-28552 #
DE93-009825 p 3465 N93-30391 #
DE93-009826 p 3443 N93-29185 #
DE93-009827 p 3433 N93-30510 #
DE93-009829 p 3598 N93-30511 #
DE93-009832 p 3413 N93-30516 #
DE93-009833 p 3532 N93-30050 #
DE93-009835 p 3336 N93-30051 #
DE93-009837 p 3543 N93-30012 #
DE93-009847 p 3538 N93-29186 #
DE93-009852 p 3598 N93-30517 #
DE93-009861 p 3549 N93-29187 #
DE93-009862 p 3594 N93-29188 #
DE93-009865 p 3422 N93-29335 #
DE93-009889 p 3431 N93-29325 #
DE93-009894 p 3309 N93-28553 #
DE93-009902 p 3324 N93-29265 #
DE93-009903 p 3592 N93-28568 #
DE93-009945 p 3574 N93-28569 #
DE93-009960 p 3576 N93-30527 #
DE93-009965 p 3561 N93-29189 #
DE93-010008 p 3466 N93-30891 #
DE93-010081 p 3467 N93-28543 #
DE93-010083 p 3422 N93-29326 #
DE93-010121 p 3247 N93-28586 #
DE93-010130 p 3585 N93-28912 #
DE93-010131 p 3584 N93-28602 #
DE93-010132 p 3585 N93-28913 #
DE93-010151 p 3487 N93-29327 #
DE93-010188 p 3332 N93-29328 #
DE93-010190 p 3625 N93-29329 #
DE93-010196 p 3636 N93-30528 #
DE93-010242 p 3564 N93-28611 #
DE93-010244 p 3444 N93-29330 #
DE93-010264 p 3444 N93-29247 #
DE93-010275 p 3544 N93-30529 #
DE93-010304 p 3567 N93-29416 #
DE93-010394 p 3587 N93-29190 #
DE93-010400 p 3586 N93-29049 #
DE93-010405 p 3595 N93-29417 #
DE93-010407 p 3298 N93-29191 #
DE93-010415 p 3331 N93-29248 #
DE93-010416 p 3594 N93-29249 #
DE93-010423 p 3569 N93-29805 #
DE93-010424 p 3417 N93-28663 #
DE93-010425 p 3551 N93-30392 #
DE93-010426 p 3594 N93-29150 #
DE93-010430 p 3596 N93-29868 #
DE93-010433 p 3430 N93-28664 #
DE93-010435 p 3569 N93-29860 #
DE93-010438 p 3575 N93-29302 #
DE93-010439 p 3440 N93-30530 #
DE93-010443 p 3433 N93-30531 #
DE93-010446 p 3598 N93-30393 #
DE93-010449 p 3261 N93-29869 #
DE93-010452 p 3604 N93-29806 #
DE93-010453 p 3330 N93-28761 #
DE93-010461 p 3575 N93-29870 #
DE93-010496 p 3569 N93-29807 #
DE93-010514 p 3564 N93-28762 #
DE93-010516 p 3587 N93-29303 #
DE93-010522 p 3593 N93-28888 #
DE93-010527 p 3564 N93-28665 #
DE93-010561 p 3569 N93-29841 #
DE93-010562 p 3577 N93-30532 #
DE93-010564 p 3605 N93-30481 #
DE93-010600 p 3353 N93-28570 #
DE93-010610 p 3412 N93-30118 #
DE93-010611 p 3463 N93-28603 #
DE93-010618 p 3432 N93-29842 #
DE93-010620 p 3453 N93-29843 #
DE93-010621 p 3525 N93-28877 #
DE93-010658 p 3408 N93-29311 #
DE93-010662 p 3464 N93-29844 #
DE93-010663 p 3330 N93-28666 #
DE93-010677 p 3530 N93-29808 #
DE93-010678 p 3623 N93-30482 #
DE93-010679 p 3278 N93-29250 #
DE93-010682 p 3491 N93-30483 #
DE93-010699 p 3426 N93-30484 #
DE93-010702 p 3426 N93-30485 #
DE93-010703 p 3341 N93-29251 #
DE93-010704 p 3342 N93-29312 #
DE93-010705 p 3554 N93-28763 #
DE93-010708 p 3332 N93-29252 #
DE93-010715 p 3406 N93-28830 #
DE93-010724 p 3566 N93-29313 #
DE93-010725 p 3565 N93-28831 #
DE93-010727 p 3594 N93-29314 #
DE93-010732 p 3575 N93-29809 #
DE93-010735 p 3566 N93-29315 #
DE93-010740 p 3326 N93-30486 #
DE93-010741 p 3421 N93-29253 #
DE93-010760 p 3451 N93-28832 #
DE93-010771 p 3564 N93-28604 #
DE93-010776 p 3418 N93-28878 #
DE93-010799 p 3565 N93-28833 #
DE93-010800 p 3524 N93-28834 #
DE93-010808 p 3589 N93-30181 #
DE93-010817 p 3478 N93-30487 #
DE93-010819 p 3444 N93-29254 #
DE93-010822 p 3460 N93-29255 #
DE93-010828 p 3493 N93-28835 #
DE93-010829 p 3444 N93-29316 #
DE93-010836 p 3585 N93-28836 #
DE93-010854 p 3490 N93-28848 #
DE93-010862 p 3575 N93-29317 #
DE93-010863 p 3323 N93-29256 #
DE93-010881 p 3330 N93-28600 #
DE93-010892 p 3243 N93-28571 #
DE93-010896 p 3565 N93-28879 #
DE93-010972 p 3565 N93-28849 #
DE93-011016 p 3616 N93-30122 #
DE93-011040 p 3556 N93-28572 * #
DE93-011043 p 3486 N93-28670 #
DE93-011046 p 3592 N93-28643 #
DE93-011114 p 3556 N93-28601 #
DE93-011259 p 3470 N93-29318 #
DE93-011263 p 3576 N93-30054 #
DE93-011372 p 3484 N93-30055 #
DE93-011373 p 3603 N93-28747 #
DE93-011375 p 3392 N93-30126 #
DE93-011388 p 3616 N93-30123 #
DE93-011391 p 3524 N93-28644 #
DE93-011442 p 3489 N93-30056 #
DE93-011452 p 3417 N93-28630 #
DE93-011477 p 3430 N93-28645 #

DE93-011478 p 3575 N93-29151 #
DE93-011480 p 3442 N93-28837 #
DE93-011481 p 3412 N93-30127 #
DE93-011484 p 3437 N93-29180 #
DE93-011486 p 3330 N93-28838 #
DE93-011492 p 3509 N93-28573 #
DE93-011529 p 3330 N93-28687 #
DE93-011535 p 3569 N93-30128 #
DE93-011565 p 3336 N93-30129 #
DE93-011570 p 3569 N93-30130 #
DE93-011611 p 3576 N93-30488 #
DE93-011615 p 3472 N93-30131 #
DE93-011629 p 3341 N93-28668 #
DE93-011701 p 3330 N93-28839 #
DE93-011725 p 3625 N93-28646 #
DE93-011731 p 3592 N93-28647 #
DE93-011734 p 3427 N93-30489 #
DE93-011799 p 3425 N93-30132 #
DE93-011805 p 3321 N93-28631 #
DE93-011872 p 3326 N93-30490 #
DE93-011882 p 3440 N93-30394 #
DE93-011893 p 3433 N93-30491 #
DE93-011930 p 3309 N93-28688 #
DE93-011975 p 3550 N93-30140 #
DE93-012083 p 3300 N93-30395 #
DE93-012103 p 3547 N93-28648 #
DE93-012104 p 3597 N93-30141 #
DE93-012109 p 3491 N93-29181 #
DE93-012195 p 3584 N93-28649 #
DE93-012222 p 3314 N93-30198 #
DE93-012224 p 3314 N93-30199 #
DE93-012225 p 3314 N93-30200 #
DE93-012230 p 3330 N93-28650 #
DE93-012237 p 3330 N93-28748 #
DE93-012238 p 3585 N93-28749 #
DE93-012239 p 3311 N93-29182 #
DE93-012269 p 3490 N93-28651 #
DE93-012277 p 3309 N93-28750 #
DE93-012289 p 3417 N93-28751 #
DE93-012290 p 3570 N93-30505 #
DE93-012325 p 3566 N93-29183 #
DE93-012328 p 3564 N93-28652 #
DE93-012416 p 3612 N93-28840 #
DE93-012433 p 3439 N93-30186 #
DE93-012435 p 3411 N93-30057 #
DE93-012436 p 3411 N93-30058 #
DE93-012437 p 3410 N93-29814 #
DE93-012470 p 3341 N93-28752 #
DE93-012518 p 3336 N93-30182 #
DE93-012555 p 3436 N93-28653 #
DE93-012686 p 3325 N93-30059 #
DE93-012930 p 3325 N93-30060 #
DE93-012947 p 3473 N93-30187 #
DE93-013070 p 3314 N93-30188 #
DE93-013144 p 3589 N93-30189 #
DE93-013240 p 3338 N93-30601 #
DE93-601878 p 3475 N93-30996 #
DE93-602505 p 3479 N93-30940 #
DE93-604080 p 3607 N93-30932 #
DE93-604083 p 3608 N93-30987 #
DE93-604091 p 3607 N93-30933 #
DE93-604132 p 3558 N93-30988 #
DE93-604133 p 3558 N93-30989 #
DE93-605070 p 3490 N93-31019 #
DE93-605280 p 3328 N93-31021 #
DE93-605281 p 3328 N93-31022 #
DE93-605290 p 3441 N93-31023 #
DE93-605312 p 3281 N93-31024 #
DE93-605325 p 3602 N93-31025 #
DE93-605452 p 3480 N93-30991 #
DE93-605544 p 3480 N93-30992 #
DE93-605693 p 3400 N93-30993 #
DE93-605733 p 3571 N93-30800 #
DE93-605896 p 3441 N93-30801 #
DE93-606030 p 3606 N93-30802 #
DE93-606031 p 3606 N93-30803 #
DE93-606032 p 3606 N93-30804 #
DE93-606034 p 3606 N93-30805 #
DE93-606039 p 3606 N93-30806 #
DE93-606040 p 3606 N93-30796 #
DE93-606041 p 3551 N93-30765 #
DE93-606061 p 3606 N93-30807 #
DE93-606063 p 3606 N93-30808 #
DE93-606064 p 3551 N93-30809 #
DE93-606065 p 3551 N93-30810 #
DE93-606067 p 3605 N93-30781 #
DE93-606069 p 3605 N93-30782 #
DE93-606070 p 3605 N93-30783 #
DE93-606071 p 3605 N93-30784 #
DE93-606082 p 3479 N93-30785 #
DE93-606084 p 3606 N93-30786 #
DE93-606089 p 3535 N93-30787 #
DE93-606090 p 3606 N93-30797 #
DE93-606107 p 3571 N93-30788 #
DE93-606111 p 3571 N93-30789 #
DE93-606114 p 3571 N93-30790 #
DE93-606115 p 3571 N93-30791 #
DE93-606125 p 3571 N93-30792 #
DE93-606133 p 3571 N93-30793 #
DE93-606214 p 3601 N93-30794 #
DE93-606216 p 3591 N93-30795 #
DE93-606218 p 3591 N93-30780 #
DE93-606223 p 3441 N93-30767 #
DE93-606271 p 3590 N93-30768 #
DE93-606295 p 3600 N93-30769 #
DE93-606328 p 3600 N93-30770 #
DE93-606329 p 3600 N93-30766 #
DE93-606332 p 3601 N93-30798 #
DE93-606390 p 3600 N93-30771 #
DE93-606392 p 3601 N93-30799 #
DE93-606694 p 3466 N93-30777 #
DE93-606724 p 3327 N93-30778 #
DE93-606831 p 3600 N93-30772 #
DE93-606893 p 3339 N93-30773 #
DE93-607029 p 3339 N93-30774 #
DE93-607212 p 3441 N93-30775 #
DE93-607560 p 3605 N93-30779 #
DE93-608481 p 3577 N93-30990 #
DE93-608548 p 3591 N93-31007 #
DE93-608739 p 3601 N93-30776 #
DE93-609815 p 3623 N93-30994 #
DE93-609833 p 3607 N93-30943 #
DE93-609834 p 3572 N93-30944 #
DE93-609835 p 3607 N93-30945 #
DE93-609840 p 3552 N93-30946 #
DE93-753130 p 3320 N93-28529 #
DE93-753131 p 3583 N93-28530 #
DE93-753135 p 3576 N93-30002
DE93-753158 p 3589 N93-30003
DE93-753190 p 3574 N93-29137 #
DE93-753191 p 3524 N93-28531 #
DE93-753241 p 3588 N93-29434 #
DE93-753242 p 3583 N93-28532 #
DE93-753243 p 3583 N93-28533 #
DE93-753244 p 3379 N93-28534 #
DE93-753245 p 3604 N93-29242 #
DE93-753267 p 3587 N93-29243 #
DE93-753270 p 3584 N93-28535 #
DE93-753271 p 3299 N93-30004
DE93-753272 p 3525 N93-28978 #
DE93-753303 p 3467 N93-28536 #
DE93-753305 p 3585 N93-28979 #
DE93-753316 p 3436 N93-28980 #
DE93-753322 p 3524 N93-28537 #
DE93-753349 p 3576 N93-30006
DE93-753398 p 3585 N93-28981 #
DE93-754311 p 3590 N93-30533 #
DE93-764151 p 3590 N93-30649
DE93-764153 p 3589 N93-30190 #
DE93-764158 p 3326 N93-30396
DE93-764162 p 3589 N93-30397
DE93-764388 p 3590 N93-30398
DE93-764469 p 3326 N93-30399
DE93-764493 p 3590 N93-30606
DE93-764495 p 3326 N93-30191 #
DE93-764500 p 3577 N93-30607
DE93-776265 p 3577 N93-28982 #
DE93-776266 p 3406 N93-28983 #
DE93-776427 p 3470 N93-29672 #
DE93-778330 p 3488 N93-30040 #
DE93-778353 p 3343 N93-30042 #
DE93-781329 p 3410 N93-29673 #
DE93-781330 p 3406 N93-28669 #
DE93-781331 p 3406 N93-28746 #
DE93-781334 p 3468 N93-28881 #
DE93-781439 p 3468 N93-28882 #
DE93-781440 p 3468 N93-28883 #

DIGEL-1991-6 p 3577 N93-30837 #
DIGEL-1992-1 p 3413 N93-30835 #
DIGEL-1992-4 p 3413 N93-30763 #
DIGEL-1992-5 p 3399 N93-30836 #
DIGEL-1992-6 p 3413 N93-30838 #

DLO-168 p 3463 N93-30839 #

DLR-FB-90-29 p 3324 N93-29272 #
DLR-FB-90-37 p 3422 N93-29273 #
DLR-FB-90-51 p 3521 N93-30104 #
DLR-FB-91-03 p 3248 N93-29464 #
DLR-FB-91-14 p 3491 N93-29274 #
DLR-FB-92-08 p 3238 N93-29006 #
DLR-FB-92-16 p 3296 N93-29007 #

DLR-MITT-92-09 p 3456 N93-28915 #

DNA-TR-92-140 p 3479 N93-30593 #
DNA-TR-92-54-V2-VOL-2 p 3506 N93-29484 #

DODA-AR-006-357 p 3562 N93-30029 #
DODA-AR-006-630 p 3260 N93-30604
DODA-AR-006-971 p 3616 N93-30195 #
DODA-AR-008-114 p 3392 N93-30145 #
DODA-AR-008-249 p 3425 N93-30156 #

DODA-R-006-356 p 3562 N93-30157 #

DOE-HDBK-1015/2-93 p 3314 N93-30198 #
DOE-HDBK-1017/1-93 p 3314 N93-30199 #
DOE-HDBK-1017/2-93 p 3314 N93-30200 #

DOE/BP-08212/T2 p 3411 N93-30057 #
DOE/BP-08212/T3-VOL-1 p 3411 N93-30058 #
DOE/BP-08212/T3-VOL-2 p 3410 N93-29814 #

DOE/CE-34023/T1 p 3490 N93-28848 #
DOE/CE-90024/11 p 3330 N93-28687 #

DOE/CH-10482/1 p 3592 N93-28647 #

DOE/DP-10754/1 p 3439 N93-30186 #

DOE/ER-0575T p 3471 N93-29770 #
DOE/ER-0579T p 3470 N93-29262 #
DOE/ER-0583T p 3587 N93-29190 #
DOE/ER-0585T p 3462 N93-30049 #
DOE/ER-12119/2 p 3330 N93-28748 #
DOE/ER-12813/1 p 3427 N93-30489 #
DOE/ER-12820/T1 p 3425 N93-30132 #
DOE/ER-13230/T2 p 3330 N93-28650 #
DOE/ER-13242/9 p 3311 N93-29182 #
DOE/ER-13456/47 p 3564 N93-28665 #
DOE/ER-13500/T3 p 3565 N93-28879 #
DOE/ER-13511/7 p 3309 N93-28688 #
DOE/ER-13640/6 p 3325 N93-30059 #
DOE/ER-13664/6 p 3310 N93-28911 #
DOE/ER-13822/6 p 3310 N93-29051 #
DOE/ER-13896/5 p 3417 N93-28751 #
DOE/ER-13913/5 p 3422 N93-29326 #
DOE/ER-13965/5 p 3564 N93-28652 #
DOE/ER-14042/4 p 3444 N93-29330 #
DOE/ER-14132/3 p 3436 N93-28653 #
DOE/ER-14173/T1 p 3329 N93-28541 #
DOE/ER-14185/2 p 3593 N93-29096 #
DOE/ER-14236/1 p 3564 N93-28604 #
DOE/ER-14282/1 p 3566 N93-29183 #
DOE/ER-14288/1 p 3603 N93-28747 #
DOE/ER-20033/1 p 3491 N93-29181 #
DOE/ER-25036/6 p 3557 N93-30048 #
DOE/ER-25119/1 p 3418 N93-28878 #
DOE/ER-25129/T1 p 3547 N93-28648 #
DOE/ER-25146/1 p 3548 N93-29057 #
DOE/ER-40146/4 p 3565 N93-28849 #
DOE/ER-40173/8 p 3574 N93-28565 #
DOE/ER-40194/6 p 3576 N93-30488 #
DOE/ER-40211/8 p 3603 N93-28961 #
DOE/ER-40224/228 p 3569 N93-29841 #
DOE/ER-40224/243 p 3577 N93-30532 #
DOE/ER-40233/8 p 3563 N93-28542 #
DOE/ER-40321/12 p 3569 N93-29807 #
DOE/ER-40328/1 p 3565 N93-28960 #
DOE/ER-40333/133 p 3564 N93-28611 #
DOE/ER-40339/6 p 3563 N93-28546 #
DOE/ER-40363/6 p 3564 N93-28678 #
DOE/ER-40441/5 p 3566 N93-29184 #
DOE/ER-40525/6 p 3392 N93-30126 #
DOE/ER-40530/4 p 3576 N93-30054 #
DOE/ER-40562/T1 p 3574 N93-28569 #
DOE/ER-40614/19 p 3605 N93-30481 #
DOE/ER-40614/26 p 3636 N93-30528 #
DOE/ER-40627/2 p 3568 N93-29764 #
DOE/ER-40631/2 p 3569 N93-30128 #
DOE/ER-40640/2 p 3570 N93-30505 #
DOE/ER-40642/2 p 3573 N93-28522 #
DOE/ER-40719/1 p 3574 N93-28969 #
DOE/ER-40732/T1 p 3566 N93-29261 #
DOE/ER-40757/005 p 3556 N93-28601 #
DOE/ER-45197/T1 p 3603 N93-28958 #
DOE/ER-45202/T1 p 3338 N93-30601 #
DOE/ER-45318/6 p 3321 N93-28631 #
DOE/ER-45365/5 p 3321 N93-28902 #
DOE/ER-45378/T4 p 3597 N93-30141 #
DOE/ER-45417/4 p 3325 N93-30060 #
DOE/ER-45461/3 p 3320 N93-28545 #
DOE/ER-45468/1 p 3261 N93-28490 #
DOE/ER-52131/13 p 3592 N93-28643 #
DOE/ER-53198/211 p 3584 N93-28602 #
DOE/ER-53198/216 p 3585 N93-28912 #
DOE/ER-53223/196 p 3586 N93-29056 #
DOE/ER-53263/28 p 3589 N93-30189 #
DOE/ER-53291/215 p 3585 N93-28913 #
DOE/ER-53301/2 p 3585 N93-28749 #
DOE/ER-54141/1 p 3586 N93-29049 #
DOE/ER-60257/7 p 3467 N93-28543 #
DOE/ER-60448/T6 p 3490 N93-28651 #
DOE/ER-60565 p 3536 N93-30934 #
DOE/ER-60883/3 p 3472 N93-30131 #
DOE/ER-61010/T6 p 3624 N93-29100 #

DOE/ER-61010/002 .... p 3247 N93-28586 #
DOE/ER-61037/1 .... p 3487 N93-29327 #
DOE/ER-61067/2 .... p 3484 N93-30055 #
DOE/ER-61173/T1 .... p 3422 N93-29335 #
DOE/ER-61202/2 .... p 3486 N93-28670 #
DOE/ER-61219/2 .... p 3470 N93-29318 #
DOE/ER-61437/1 .... p 3489 N93-30056 #
DOE/ER-61473/1 .... p 3476 N93-28677 #
DOE/ER-75700/T3 .... p 3567 N93-29416 #

DOE/ET-53088/584 .... p 3423 N93-29804 #
DOE/ET-53088/587 .... p 3584 N93-28599 #
DOE/ET-53088/589 .... p 3585 N93-28910 #
DOE/ET-53088/590 .... p 3584 N93-28598 #
DOE/ET-53088/591 .... p 3587 N93-29148 #

DOE/ID-12735/T25 .... p 3584 N93-28649 #
DOE/ID-13040/18 .... p 3465 N93-30011 #
DOE/ID-13042/22 .... p 3473 N93-30187 #

DOE/NBB-0092T .... p 3472 N93-30043 * #

DOE/NV-360 .... p 3616 N93-30123 #

DOE/PC-89786/T15 .... p 3314 N93-30188 #
DOE/PC-90018/T6 .... p 3341 N93-28668 #
DOE/PC-90044/9 .... p 3341 N93-28752 #
DOE/PC-90183/T6 .... p 3417 N93-28630 #
DOE/PC-90291/T11 .... p 3309 N93-28750 #

DOT-HS-807 956 .... p 3447 N93-30828 #

DOT-VNTSC-FAA-93-2 .... p 3394 N93-30611 #

DOT/FAA/ACS-91-1 .... p 3261 N93-29788 #

DOT/FAA/AM-93/9 .... p 3498 N93-28622 #

DOT/FAA/CT-TN93/14 .... p 3379 N93-28555 #
DOT/FAA/CT-TN9 .... p 3538 N93-29490 #

DOT/FAA/CT-92/12-VOL-2 .... p 3449 N93-28685 #
DOT/FAA/CT-93/6 .... p 3245 N93-28625 #

DOT/FAA/NR-92/9 .... p 3261 N93-29815 #

DOT/FAA/RD-92-2 .... p 3236 N93-30673 * #
DOT/FAA/RD-93/11 .... p 3394 N93-30611 #
DOT/FAA/RD-93/14 .... p 3481 N93-29257 #
DOT/FAA/RD-93/15 .... p 3262 N93-30103 #

DOT/FRA/NMI-92/12 .... p 3444 N93-29205 #
DOT/FRA/NMI-92/25-VOL-1 .... p 3447 N93-30820 #

DREO-TN-92-25 .... p 3613 N93-29210 #

DREO-1148 .... p 3393 N93-30537 #
DREO-1153 .... p 3383 N93-29438 #
DREO-1155 .... p 3405 N93-28563 #
DREO-1163 .... p 3383 N93-29407 #

DRES-SR-582 .... p 3324 N93-29391 #
DRES-SR-583 .... p 3337 N93-30541 #

D615-10062-2 .... p 3268 N93-31034 * #

E-3173 .... p 3580 N93-30372 * #
E-3813 .... p 3242 N93-30373 * #
E-7079 .... p 3352 N93-30939 * #
E-7215 .... p 3287 N93-28686 * #
E-7597 .... p 3295 N93-28624 * #
E-7643 .... p 3252 N93-29065 * #
E-7644 .... p 3295 N93-28681 * #
E-7661 .... p 3285 N93-28554 * #
E-7664 .... p 3321 N93-28618 * #
E-7686 .... p 3297 N93-29074 * #
E-7720 .... p 3352 N93-31031 * #
E-7724 .... p 3418 N93-28947 * #
E-7744 .... p 3538 N93-28628 * #
E-7791 .... p 3420 N93-29157 * #
E-7816 .... p 3297 N93-29071 * #
E-7843 .... p 3405 N93-28610 * #
E-7852 .... p 3450 N93-28556 * #
E-7870 .... p 3288 N93-29194 * #
E-7871 .... p 3287 N93-28694 * #
E-7895 .... p 3416 N93-28626 * #
E-7899 .... p 3270 N93-28696 * #
E-7904 .... p 3451 N93-28633 * #
E-7906 .... p 3420 N93-29161 * #
E-7909 .... p 3287 N93-28946 * #
E-7915 .... p 3419 N93-29075 * #
E-7917 .... p 3288 N93-29158 * #
E-7919 .... p 3421 N93-29208 * #
E-7924 .... p 3451 N93-29196 * #
E-7926 .... p 3341 N93-28695 * #
E-7928 .... p 3273 N93-29195 * #
E-7930 .... p 3449 N93-29073 * #
E-7931 .... p 3273 N93-29884 * #
E-7932 .... p 3288 N93-29068 * #
E-7937 .... p 3251 N93-28609 * #
E-7939 .... p 3251 N93-28617 * #
E-7948 .... p 3251 N93-28697 * #
E-7952 .... p 3416 N93-28627 * #
E-7953 .... p 3286 N93-28619 * #
E-7957 .... p 3252 N93-29072 * #
E-7958 .... p 3252 N93-29162 * #
E-7995 .... p 3340 N93-30938 * #

EGG-ERTP-10585 .... p 3532 N93-30034 #

EGG-M-92402 .... p 3505 N93-28942 #
EGG-M-92454 .... p 3589 N93-30181 #
EGG-M-92468 .... p 3565 N93-28833 #
EGG-M-92535 .... p 3524 N93-28834 #

EMA-90-R-51 .... p 3342 N93-29835 #

EPA/230/B-93/001 .... p 3475 N93-30834 #
EPA/402/R-93/011 .... p 3475 N93-30829 #
EPA/600/A-93/044 .... p 3470 N93-29200 #
EPA/600/A-93/055 .... p 3311 N93-29204 #
EPA/600/A-93/063 .... p 3467 N93-28873 #
EPA/600/A-93/073 .... p 3474 N93-30762 #
EPA/600/A-93/093 .... p 3475 N93-30831 #
EPA/600/R-93/058B .... p 3465 N93-30001
EPA/600/R-93/058D .... p 3466 N93-30935
EPA/600/9-90/045 .... p 3469 N93-29033 #
EPA/600/9-90/046 .... p 3469 N93-29034 #
EPA/620/R-93/001 .... p 3474 N93-30823 #
EPA/741/R-92/003 .... p 3474 N93-30660 #
EPA/800/B-92/001 .... p 3462 N93-30833 #

ERC/HSV-TR93-01 .... p 3427 N93-30492 * #

ERL-0632-RN .... p 3616 N93-30195 #
ERL-0673-RR .... p 3392 N93-30145 #

ERP-1107 .... p 3399 N93-30757 #
ERP-1110 .... p 3483 N93-29832 #
ERP-1116 .... p 3484 N93-30535 #

ESA-HSR-1 .... p 3660 N93-29500 #

ESA-STR-235 .... p 3281 N93-30106 #

ESA-TM-165 .... p 3532 N93-30023 * #

ESA-TT-1249 .... p 3324 N93-29272 #
ESA-TT-1255 .... p 3422 N93-29273 #
ESA-TT-1258 .... p 3521 N93-30104 #
ESA-TT-1267 .... p 3248 N93-29464 #
ESA-TT-1269 .... p 3491 N93-29274 #
ESA-TT-1276 .... p 3325 N93-30105 #

ESC-TR-92-135 .... p 3379 N93-28655 #
ESC-TR-92-139 .... p 3494 N93-29421 #
ESC-TR-92-143-REV-1 .... p 3578 N93-29140 #
ESC-TR-92-144-REV-1 .... p 3579 N93-29470 #
ESC-TR-92-145-REV-1 .... p 3578 N93-29139 #
ESC-TR-92-276 .... p 3387 N93-29890 #
ESC-TR-93-177 .... p 3530 N93-29852 #
ESC-TR-93-178 .... p 3610 N93-29970 #

ESD-PUBL-4018 .... p 3469 N93-28992 #

ESG-188 .... p 3436 N93-28847 #
ESG-199 .... p 3575 N93-29870 #
ESG-246 .... p 3440 N93-30530 #

ETDE/JP-MF-92531076 .... p 3413 N93-30622 #

ETN-91-90083 .... p 3417 N93-28744 #
ETN-93-03891 .... p 3547 N93-28511 #
ETN-93-92721 .... p 3335 N93-30024 #
ETN-93-93231 .... p 3532 N93-30017 #
ETN-93-93247 .... p 3549 N93-29849 #
ETN-93-93298 .... p 3576 N93-30019 #
ETN-93-93305 .... p 3413 N93-30835 #
ETN-93-93307 .... p 3413 N93-30763 #
ETN-93-93308 .... p 3399 N93-30836 #
ETN-93-93309 .... p 3577 N93-30837 #
ETN-93-93310 .... p 3413 N93-30838 #
ETN-93-93315 .... p 3463 N93-30839 #
ETN-93-93317 .... p 3522 N93-30840 #
ETN-93-93330 .... p 3548 N93-28753 #
ETN-93-93341 .... p 3392 N93-30025 #
ETN-93-93454 .... p 3259 N93-29999 #
ETN-93-9345758 .... p 3629 N93-29008 #
ETN-93-93463 .... p 3586 N93-29081 #
ETN-93-93464 .... p 3574 N93-29062 #
ETN-93-93484 .... p 3268 N93-29063 #
ETN-93-93485 .... p 3331 N93-29064 #
ETN-93-93575 .... p 3456 N93-28915 #
ETN-93-93576 .... p 3382 N93-29266 #
ETN-93-93577 .... p 3332 N93-29267 #
ETN-93-93578 .... p 3248 N93-29268 #
ETN-93-93579 .... p 3408 N93-29269 #
ETN-93-93580 .... p 3578 N93-29270 #
ETN-93-93581 .... p 3408 N93-29271 #
ETN-93-93582 .... p 3422 N93-29319 #
ETN-93-93588 .... p 3478 N93-30113
ETN-93-93590 .... p 3484 N93-30114
ETN-93-93591 .... p 3483 N93-30013
ETN-93-93594 .... p 3546 N93-28466 #
ETN-93-93622 .... p 3571 N93-30670 #
ETN-93-93688 .... p 3631 N93-30638 #
ETN-93-93711 .... p 3324 N93-29272 #
ETN-93-93712 .... p 3422 N93-29273 #
ETN-93-93713 .... p 3521 N93-30104 #
ETN-93-93714 .... p 3248 N93-29464 #
ETN-93-93715 .... p 3491 N93-29274 #
ETN-93-93716 .... p 3325 N93-30105 #
ETN-93-93717 .... p 3532 N93-30023 * #
ETN-93-93718 .... p 3281 N93-30106 #
ETN-93-93719 .... p 3392 N93-30018 #
ETN-93-93720 .... p 3313 N93-30109 #
ETN-93-93722 .... p 3562 N93-30110 #
ETN-93-93723 .... p 3241 N93-30020 #
ETN-93-93724 .... p 3550 N93-30136 #
ETN-93-93725 .... p 3326 N93-30138 #
ETN-93-93726 .... p 3314 N93-30139 #
ETN-93-93727 .... p 3336 N93-30112 #
ETN-93-93728 .... p 3314 N93-30203 #
ETN-93-93733 .... p 3238 N93-29006 #
ETN-93-93734 .... p 3296 N93-29007 #
ETN-93-93741 .... p 3462 N93-30107 #
ETN-93-93750 .... p 3460 N93-29307 #
ETN-93-93751 .... p 3460 N93-29320 #
ETN-93-93752 .... p 3460 N93-29321 #
ETN-93-93753 .... p 3461 N93-29465 #
ETN-93-93754 .... p 3461 N93-29466 #
ETN-93-93768 .... p 3480 N93-28519 #
ETN-93-93770 .... p 3411 N93-30108 #
ETN-93-93771 .... p 3575 N93-29996 #
ETN-93-93772 .... p 3378 N93-30581 #
ETN-93-93773 .... p 3532 N93-29997 #
ETN-93-93774 .... p 3465 N93-30111 #
ETN-93-93775 .... p 3543 N93-29998 #
ETN-93-93777 .... p 3353 N93-28632 #
ETN-93-93791 .... p 3547 N93-28524 #
ETN-93-93794 .... p 3611 N93-28525 #
ETN-93-93795 .... p 3523 N93-28526 #
ETN-93-93796 .... p 3547 N93-28527 #
ETN-93-93797 .... p 3611 N93-28528 #
ETN-93-93798 .... p 3436 N93-28614 #
ETN-93-93799 .... p 3492 N93-28469 #
ETN-93-93800 .... p 3591 N93-28470 #
ETN-93-93801 .... p 3603 N93-28472 #
ETN-93-93804 .... p 3632 N93-28473 #
ETN-93-93805 .... p 3325 N93-30115 #
ETN-93-93806 .... p 3475 N93-28475 #
ETN-93-93807 .... p 3654 N93-28477 #
ETN-93-93836 .... p 3540 N93-28480 #
ETN-93-93837 .... p 3379 N93-28502 #
ETN-93-93841 .... p 3547 N93-28667 #
ETN-93-93844 .... p 3547 N93-28615 * #
ETN-93-93870 .... p 3523 N93-28503 #
ETN-93-93871 .... p 3611 N93-28481 #
ETN-93-93872 .... p 3522 N93-28482 #
ETN-93-93873 .... p 3523 N93-28484 #
ETN-93-93874 .... p 3523 N93-28485 #
ETN-93-93875 .... p 3523 N93-28486 #
ETN-93-93876 .... p 3380 N93-28896 #
ETN-93-93877 .... p 3505 N93-28897 #
ETN-93-93878 .... p 3541 N93-28898 #
ETN-93-93879 .... p 3548 N93-28754 #
ETN-93-93882 .... p 3524 N93-28755 #
ETN-93-93883 .... p 3523 N93-28504 #
ETN-93-93885 .... p 3537 N93-28505 #
ETN-93-93886 .... p 3552 N93-28506 #
ETN-93-93887 .... p 3553 N93-28507 #
ETN-93-93888 .... p 3553 N93-28508 #
ETN-93-93889 .... p 3546 N93-28509 #
ETN-93-93890 .... p 3553 N93-28510 #
ETN-93-93892 .... p 3547 N93-28512 #
ETN-93-93893 .... p 3547 N93-28513 #
ETN-93-93894 .... p 3538 N93-28937 #
ETN-93-93896 .... p 3541 N93-28637 #
ETN-93-93897 .... p 3541 N93-28638 #
ETN-93-93903 .... p 3543 N93-30116 #
ETN-93-93909 .... p 3547 N93-28616 #
ETN-93-93910 .... p 3538 N93-29487 #
ETN-93-93911 .... p 3550 N93-30117 #
ETN-93-93912 .... p 3529 N93-29488 #
ETN-93-93935 .... p 3637 N93-30639
ETN-93-93937 .... p 3441 N93-30640
ETN-93-93938 .... p 3631 N93-30641
ETN-93-93939 .... p 3631 N93-30642

ETN-93-93940 p 3632 N93-30643
ETN-93-93941 p 3631 N93-30578
ETN-93-93942 p 3631 N93-30615
ETN-93-94085 p 3572 N93-31008 #
ETN-93-94089 p 3463 N93-31009 #
ETN-93-94090 p 3463 N93-31010 #
ETN-93-94091 p 3463 N93-31011 #
ETN-93-94094 p 3552 N93-31012 #
ETN-93-94095 p 3552 N93-31014 #
ETN-93-94171 p 3454 N93-31015 #
ETN-93-94172 p 3455 N93-31016 #
ETN-93-94173 p 3455 N93-31017 #
ETN-93-94175 p 3246 N93-30671 #
ETN-93-94177 p 3270 N93-30582 #
ETN-93-94178 p 3551 N93-30572 #
ETN-93-94179 p 3466 N93-30573 #
ETN-93-94180 p 3394 N93-30672 #
ETN-93-94182 p 3413 N93-30616 #
ETN-93-94188 p 3485 N93-31018 #
ETN-93-94190 p 3428 N93-31020 #
ETN-93-94235 p 3414 N93-31030 #

FASTC-ID(RS)T-0307-92 p 3438 N93-29797 #
FASTC-ID(RS)T-0308-92 p 3596 N93-29796 #
FASTC-ID(RS)T-0311-92 p 3278 N93-29134 #
FASTC-ID(RS)T-0314-92 p 3410 N93-29798 #
FASTC-ID(RS)T-0625-92 p 3227 N93-28576 #
FASTC-ID(RS)T-0825-92 p 3238 N93-28493 #
FASTC-ID(RS)T-0867-92 p 3421 N93-29260 #
FASTC-ID(RS)T-0869-92 p 3241 N93-29919 #
FASTC-ID(RS)T-0870-92 p 3240 N93-29862 #
FASTC-ID(RS)T-0962-92 p 3615 N93-29431 #

FEL-92-C282 p 3463 N93-31010 #

FFA-TN-1991-34 p 3451 N93-29076 #
FFA-TN-1992-28 p 3418 N93-29009 #
FFA-TN-1992-35 p 3418 N93-28993 #
FFA-TN-1992-37 p 3418 N93-28994 #

FNAL-TM-1794 p 3407 N93-29048 #
FNAL-TM-1827 p 3593 N93-28888 #

FNAL/C-92/288 p 3382 N93-29245 #
FNAL/C-92/341-E p 3567 N93-29351 #
FNAL/C-92/382-A p 3633 N93-28676 #
FNAL/C-93/014-A p 3653 N93-28962 #
FNAL/C-93/022-A p 3634 N93-28963 #

FRA/ORD-92/17 p 3507 N93-29675

FSU-R-885 p 3549 N93-29854 #

FSU-TR-884 p 3555 N93-29979 #

GA-A-21203 p 3585 N93-28836 #

GAO/IMTEC-93-24 p 3533 N93-30202 #

GKSS-92/E/32 p 3485 N93-31018 #

GRI-92/0317 p 3352 N93-30663 #
GRI-92/0400.1 p 3317 N93-30761 #
GRI-92/0511 p 3327 N93-30815 #
GRI-92/0528 p 3471 N93-29676
GRI-93/0006 p 3604 N93-29794
GRI-93/0019 p 3312 N93-29665
GRI-93/0040 p 3316 N93-30658
GRI-93/0043 p 3317 N93-30760 #
GRI-93/0082 p 3316 N93-30661 #
GRI-93/0088 p 3428 N93-30759 #
GRI-93/0113 p 3466 N93-30814 #

H-1631 p 3260 N93-30764 * #
H-1893 p 3431 N93-29066 * #
H-1917 p 3248 N93-28693 * #

HEI/RR-92/52 p 3497 N93-30890 #

HVE-042-93 p 3409 N93-29513 #

IAEA-R-5132-F p 3536 N93-31001 #

IC-92/108 p 3558 N93-30988 #
IC-92/111 p 3485 N93-31006 #
IC-92/122 p 3557 N93-30917 #
IC-92/123 p 3602 N93-30998 #
IC-92/124 p 3637 N93-30918 #
IC-92/126 p 3557 N93-30928 #
IC-92/131 p 3637 N93-30919 #
IC-92/132 p 3479 N93-30940 #
IC-92/133 p 3557 N93-30985 #
IC-92/135 p 3558 N93-30986 #
IC-92/138 p 3607 N93-30920 #
IC-92/140 p 3551 N93-30929 #
IC-92/146 p 3558 N93-30989 #
IC-92/149 p 3607 N93-30921 #
IC-92/163 p 3605 N93-30779 #
IC-92/168 p 3601 N93-30794 #
IC-92/169 p 3608 N93-30987 #
IC-92/171 p 3606 N93-30807 #
IC-92/184 p 3606 N93-30808 #
IC-92/185 p 3571 N93-30789 #
IC-92/187 p 3551 N93-30809 #
IC-92/190 p 3551 N93-30810 #
IC-92/191 p 3600 N93-30769 #
IC-92/196 p 3571 N93-30793 #
IC-92/204 p 3327 N93-30778 #
IC-92/72 p 3557 N93-30981 #
IC-92/73 p 3480 N93-31002 #
IC-92/80 p 3608 N93-31003 #
IC-92/82 p 3637 N93-31004 #
IC-92/86 p 3637 N93-30997 #
IC-92/88 p 3602 N93-31027 #
IC-92/92 p 3572 N93-30931 #
IC-92/93 p 3552 N93-30942 #

ICASE-93-15 p 3509 N93-28841 * #
ICASE-93-16 p 3525 N93-28976 * #
ICASE-93-20 p 3418 N93-28975 * #

ICOMP-93-18 p 3420 N93-29161 * #
ICOMP-93-19 p 3421 N93-29208 * #
ICOMP-93-9 p 3418 N93-28947 * #

IDA-D-1182 p 3272 N93-30881 #
IDA-D-1224 p 3610 N93-29499 #

IDA/HQ-92-41994 p 3272 N93-30881 #
IDA/HQ-92-42612 p 3610 N93-29499 #

IEE-SR-237 p 3468 N93-28881 #

IFSR-584 p 3423 N93-29804 #
IFSR-587 p 3584 N93-28599 #
IFSR-589 p 3585 N93-28910 #
IFSR-590 p 3584 N93-28598 #
IFSR-591 p 3587 N93-29148 #

IFT-P-004/92 p 3607 N93-30943 #
IFT-P-024/92 p 3572 N93-30944 #
IFT-P-031/92 p 3607 N93-30945 #

IGC-119 p 3328 N93-31021 #
IGC-122 p 3328 N93-31022 #
IGC-125 p 3480 N93-30992 #

IHEP-OTF-91-33 p 3572 N93-30930 #

IITRI-E06641 p 3507 N93-29675

ILR-MITT-266(1991) p 3454 N93-31015 #
ILR-MITT-267(1991) p 3455 N93-31016 #
ILR-MITT-273(1992) p 3455 N93-31017 #
ILR-MITT-275(1992) p 3246 N93-30671 #

IMPERIAL/TP-90-91/21 p 3557 N93-30917 #

INIS-BR-2958 p 3441 N93-30775 #
INIS-BR-2987 p 3600 N93-30772 #
INIS-BR-2988 p 3339 N93-30773 #
INIS-BR-2989 p 3339 N93-30774 #
INIS-BR-2992 p 3601 N93-30776 #

INIS-MF-13356 p 3475 N93-30996 #
INIS-MF-13361 p 3591 N93-30795 #
INIS-MF-13371 p 3490 N93-31019 #

INP-MSU-91-10-214 p 3607 N93-30916 #

INP-1533/PH p 3577 N93-30990 #

INPE-5384 p 3591 N93-31007 #

INRIA-RR-1584 p 3547 N93-28615 * #
INRIA-RR-1588 p 3537 N93-28505 #
INRIA-RR-1596 p 3552 N93-28506 #
INRIA-RR-1597 p 3553 N93-28507 #
INRIA-RR-1598 p 3553 N93-28508 #
INRIA-RR-1601 p 3546 N93-28509 #
INRIA-RR-1606 p 3553 N93-28510 #
INRIA-RR-1619 p 3547 N93-28511 #
INRIA-RR-1620 p 3547 N93-28512 #
INRIA-RR-1621 p 3547 N93-28513 #
INRIA-RR-1622 p 3538 N93-28937 #
INRIA-RR-1637 p 3541 N93-28637 #
INRIA-RR-1638 p 3541 N93-28638 #
INRIA-RR-1682 p 3543 N93-30116 #
INRIA-RR-1697 p 3547 N93-28616 #
INRIA-RR-1698 p 3538 N93-29487 #
INRIA-RR-1703 p 3550 N93-30117 #
INRIA-RR-1713 p 3529 N93-29488 #
INRIA-RT-0136 p 3524 N93-28755 #
INRIA-RT-0139 p 3523 N93-28504 #

INS-T-507 p 3576 N93-30002

INS-933 p 3604 N93-29242 #

INT-PATENT-CLASS-B01J-19/28 p 3298 N93-29609 *
INT-PATENT-CLASS-B23Q-3/155 p 3445 N93-29505 *
INT-PATENT-CLASS-B25J-15/04 p 3445 N93-29505 *
INT-PATENT-CLASS-B64D-7/00 . p 3331 N93-29088 *

INT-PATENT-CLASS-C07C-323/09 p 3312 N93-29506 *
INT-PATENT-CLASS-C25B-1/02 . p 3312 N93-29617 *
INT-PATENT-CLASS-C25B-1/22 . p 3312 N93-29617 *
INT-PATENT-CLASS-C25C-1/06 . p 3312 N93-29617 *

INT-PATENT-CLASS-D03C-13/00 p 3354 N93-29611 *
INT-PATENT-CLASS-D03D-13/00 p 3354 N93-29611 *
INT-PATENT-CLASS-D03D-41/00 p 3354 N93-29611 *

INT-PATENT-CLASS-F16K-37/00 p 3432 N93-29503 *

INT-PATENT-CLASS-G01J-3/12 . p 3578 N93-29086 *
INT-PATENT-CLASS-G01N-19/02 p 3445 N93-29618 *
INT-PATENT-CLASS-G01N-19/08 p 3452 N93-29612 *
INT-PATENT-CLASS-G01R-27/02 p 3452 N93-29612 *
INT-PATENT-CLASS-G01S-3/02 . p 3381 N93-29087 *
INT-PATENT-CLASS-G06F-15/16 p 3521 N93-29608 *
INT-PATENT-CLASS-G06F-15/18 p 3521 N93-29504 *
INT-PATENT-CLASS-G06F-15/18 p 3498 N93-29610 *
INT-PATENT-CLASS-G06F-9/00 . p 3521 N93-29608 *

INT-PATENT-CLASS-H01L-23/02 p 3381 N93-29087 *
INT-PATENT-CLASS-H01M-8/14 p 3464 N93-28974 *
INT-PATENT-CLASS-H01Q-1/380 p 3384 N93-29507 *
INT-PATENT-CLASS-H01Q-19/300 p 3384 N93-29507 *
INT-PATENT-CLASS-H05K-5/00 . p 3381 N93-29087 *
INT-PATENT-CLASS-H05K-7/20 . p 3299 N93-29614 *

IS-M-739 p 3450 N93-28567 #

IS-T-1217 p 3313 N93-29837 #

ISBN-0-16-041766-X p 3392 N93-30150 #
ISBN-0-16-041779-1 p 3610 N93-29649 #
ISBN-0-16-041805-4 p 3539 N93-29650 #
ISBN-0-16-041828-3 p 3522 N93-30570 #
ISBN-0-309-04848-6 p 3612 N93-29129
ISBN-0-309-04880-X p 3525 N93-28934 * #
ISBN-0-309-04899-0 p 3456 N93-30634 #
ISBN-0-315-72443-9 p 3605 N93-30359
ISBN-0-315-72512-5 p 3426 N93-30379
ISBN-0-315-72632-6 p 3633 N93-28673
ISBN-0-86776-462-7 p 3451 N93-29106 #
ISBN-0-9694170-1-2 p 3354 N93-30215
ISBN-9-03-692007-8 p 3478 N93-30113
ISBN-9-03-692010-8 p 3484 N93-30114
ISBN-9-03-692012-4 p 3483 N93-30013
ISBN-9-05-411053-8 p 3463 N93-30839 #
ISBN-9-05-411059-7 p 3463 N93-31009 #
ISBN-9-05-411060-0 p 3463 N93-31011 #
ISBN-9-05-411061-9 p 3463 N93-31010 #
ISBN-9-07-212514-2 p 3392 N93-30025 #
ISBN-9-29-092168-4 p 3281 N93-30106 #
ISBN-9-51-383899-4 p 3465 N93-30111 #
ISBN-9-51-383929-X p 3411 N93-30108 #
ISBN-9-51-384068-9 p 3353 N93-28632 #
ISBN-90-386-0042-9 p 3248 N93-29268 #
ISBN-90-5411-037-6 p 3460 N93-29320 #
ISBN-90-5411-040-6 p 3460 N93-29321 #
ISBN-90-5411-044-9 p 3460 N93-29307 #
ISBN-90-5411-048-1 p 3461 N93-29465 #
ISBN-90-5411-050-3 p 3461 N93-29466 #
ISBN-90-9004009-9 p 3332 N93-29267 #
ISBN-90-9004897-9 p 3578 N93-29270 #
ISBN-90-9005038-8 p 3382 N93-29266 #
ISBN-92-835-0700-2 p 3387 N93-29892 #
ISBN-92-835-0701-0 p 3252 N93-29926 #
ISBN-92-835-0706-1 p 3501 N93-28850 #
ISBN-92-835-0712-6 p 3394 N93-30727 #
ISBN-92-9092-221-4 p 3532 N93-30023 * #
ISBN-951-38-3875-7 p 3575 N93-29996 #
ISBN-951-38-3877-3 p 3378 N93-30581 #
ISBN-951-38-3882-X p 3532 N93-29997 #
ISBN-951-38-4007-7 p 3543 N93-29998 #
ISBN-951-47-4284-2 p 3488 N93-30040 #

ITP-UH-9/92 p 3603 N93-28472 #

IYAF-90-136 p 3571 N93-30788 #
IYAF-91-102 p 3441 N93-30767 #
IYAF-91-111 p 3600 N93-30770 #
IYAF-91-31 p 3479 N93-30785 #
IYAF-91-62 p 3480 N93-30991 #
IYAF-91-66 p 3590 N93-30768 #

IYAF-91-68 p 3591 N93-30780 #
IYAF-91-6 p 3571 N93-30800 #
IYAF-91-71 p 3571 N93-30790 #
IYAF-91-83 p 3606 N93-30802 #
IYAF-91-85 p 3400 N93-30993 #
IYAF-91-97 p 3606 N93-30803 #

JAERI-M-92-064 p 3589 N93-30003
JAERI-M-92-066 p 3320 N93-28529 #
JAERI-M-92-069 p 3583 N93-28530 #
JAERI-M-92-072 p 3574 N93-29137 #
JAERI-M-92-083 p 3584 N93-28535 #
JAERI-M-92-084 p 3524 N93-28531 #
JAERI-M-92-085 p 3299 N93-30004
JAERI-M-92-089 p 3525 N93-28978 #
JAERI-M-92-094 p 3587 N93-29243 #
JAERI-M-92-102 p 3467 N93-28536 #
JAERI-M-92-105 p 3524 N93-28537 #
JAERI-M-92-107 p 3585 N93-28979 #
JAERI-M-92-111 p 3590 N93-30398
JAERI-M-92-114 p 3576 N93-30006
JAERI-M-92-120 p 3585 N93-28981 #
JAERI-M-92-137 p 3326 N93-30399
JAERI-M-92-140 p 3589 N93-30397
JAERI-M-92-145 p 3590 N93-30649
JAERI-M-92-148 p 3326 N93-30396
JAERI-M-92-156 p 3590 N93-30606
JAERI-M-92-165 p 3326 N93-30191 #
JAERI-M-92-168 p 3589 N93-30190 #

JINR-D-2-91-436 p 3606 N93-30804 #

JINR-E-11-91-352 p 3605 N93-30781 #
JINR-E-17-91-159 p 3602 N93-31025 #
JINR-E-2-91-118 p 3557 N93-30922 #
JINR-E-2-91-133 p 3606 N93-30805 #
JINR-E-2-91-184 p 3400 N93-30923 #
JINR-E-2-91-195 p 3607 N93-30924 #
JINR-E-2-91-266 p 3607 N93-30925 #
JINR-E-2-91-316 p 3606 N93-30786 #
JINR-E-2-91-360 p 3571 N93-30791 #
JINR-E-2-91-445 p 3605 N93-30782 #
JINR-E-2-91-448 p 3605 N93-30783 #
JINR-E-2-91-475 p 3571 N93-30792 #
JINR-E-2-91-77 p 3557 N93-30926 #
JINR-E-2-91-78 p 3557 N93-30927 #
JINR-E-2-91-7 p 3605 N93-30784 #
JINR-E-2-91-97 p 3608 N93-30983 #
JINR-E-3-91-330 p 3600 N93-30771 #
JINR-E-5-91-174 p 3551 N93-30912 #
JINR-E-5-91-402 p 3535 N93-30787 #
JINR-E-5-91-485 p 3606 N93-30806 #
JINR-E-5-92-23 p 3552 N93-30946 #

JINR-R-10-91-105 p 3623 N93-30994 #
JINR-R-11-91-138 p 3551 N93-30913 #
JINR-R-13-91-158 p 3600 N93-30766 #
JINR-R-17-91-446 p 3606 N93-30796 #
JINR-R-2-91-242 p 3281 N93-31024 #
JINR-R-2-91-315 p 3606 N93-30797 #
JINR-R-2-91-333 p 3601 N93-30798 #
JINR-R-2-91-403 p 3551 N93-30765 #
JINR-R-4-91-127 p 3552 N93-30984 #
JINR-R-4-91-142 p 3601 N93-30799 #
JINR-R-4-91-254 p 3535 N93-30914 #
JINR-R-4-91-261 p 3535 N93-30915 #

JPRS-UEQ-92-006 p 3353 N93-28636 #
JPRS-UEQ-92-007 p 3353 N93-28635 #
JPRS-UEQ-92-008 p 3353 N93-28675 #
JPRS-UEQ-92-010 p 3353 N93-28674 #
JPRS-UEQ-93-001 p 3274 N93-29014 #
JPRS-UEQ-93-003 p 3353 N93-28691 #
JPRS-UEQ-93-004 p 3354 N93-29090 #

JPRS-UES-93-002 p 3456 N93-30624 #
JPRS-UES-93-003 p 3456 N93-29089 #

JPRS-ULS-92-027 p 3490 N93-28684 #
JPRS-ULS-93-005 p 3490 N93-28683 #

JPRS-UMS-92-007 p 3322 N93-29013 #
JPRS-UMS-92-008 p 3322 N93-29012 #
JPRS-UMS-92-009 p 3322 N93-29015 #
JPRS-UMS-92-012 p 3296 N93-29016 #
JPRS-UMS-92-013 p 3296 N93-29017 #
JPRS-UMS-92-014 p 3322 N93-29019 #
JPRS-UMS-92-015 p 3322 N93-29020 #
JPRS-UMS-92-016 p 3296 N93-29018 #
JPRS-UMS-93-001 p 3296 N93-29021 #
JPRS-UMS-93-003 p 3327 N93-30623 #

JPRS-UPM-93-002 p 3560 N93-29022 #

JSC-26067 p 3278 N93-29221 * #

JSR-90-302 p 3472 N93-30015 #
JSR-90-307 p 3482 N93-29479 #

JUEL-2609 p 3574 N93-29062 #
JUEL-2650 p 3475 N93-28475 #

K/CG-1077/V2 p 3612 N93-28840 #

KCP-613-4863 p 3442 N93-28552 #
KCP-613-5164 p 3332 N93-29328 #

KEK-92-6 p 3577 N93-30607

KFK-5053 p 3586 N93-29081 #
KFK-5058 p 3428 N93-31020 #

KIYAI-91-8 p 3466 N93-30777 #

KNMI-TR-138 p 3478 N93-30113
KNMI-TR-140-PT-1 p 3484 N93-30114
KNMI-TR-141-PT-1 p 3483 N93-30013

L-16704 p 3240 N93-29449 * #
L-16855 p 3240 N93-29450 * #
L-16889-PT-2 p 3303 N93-30841 * #
L-16889 p 3300 N93-30428 * #
L-16998 p 3239 N93-29165 * #
L-17151 p 3239 N93-29160 * #
L-17154 p 3239 N93-29166 * #
L-17168 p 3431 N93-29209 * #
L-17196-PT-1 p 3660 N93-29621 * #
L-17196-PT-2 p 3654 N93-29354 * #
L-17196-PT-4 p 3665 N93-29682 * #
L-17236 p 3290 N93-30948 * #

LA-SUB-93-11/1 p 3323 N93-29092 #
LA-SUB-93-11/2 p 3336 N93-30129 #
LA-SUB-93-127 p 3565 N93-28914 #
LA-SUB-93-152 p 3478 N93-30487 #

LA-UR-92-1427 p 3345 N93-30074
LA-UR-92-2773 p 3598 N93-30445 #
LA-UR-92-2793 p 3315 N93-30447 #
LA-UR-92-2794 p 3570 N93-30448 #
LA-UR-92-2824 p 3352 N93-30446 #
LA-UR-92-2924 p 3524 N93-28640 #
LA-UR-92-3008 p 3315 N93-30209 #
LA-UR-92-4061 p 3446 N93-30211 #
LA-UR-92-4063 p 3472 N93-30008 #
LA-UR-92-4353 p 3436 N93-28887 #
LA-UR-93-0003 p 3593 N93-28966 #
LA-UR-93-0044 p 3410 N93-29812 #
LA-UR-93-1003 p 3565 N93-28831 #
LA-UR-93-1004 p 3566 N93-29313 #
LA-UR-93-1009 p 3566 N93-29315 #
LA-UR-93-1038 p 3575 N93-29809 #
LA-UR-93-1059 p 3421 N93-29253 #
LA-UR-93-1065 p 3326 N93-30486 #
LA-UR-93-165 p 3424 N93-29836 #
LA-UR-93-201 p 3482 N93-29347 #
LA-UR-93-298 p 3549 N93-29769 #
LA-UR-93-301 p 3611 N93-28580 #
LA-UR-93-315 p 3477 N93-29346 #
LA-UR-93-361 p 3386 N93-29765 #
LA-UR-93-418 p 3579 N93-29350 #
LA-UR-93-428 p 3380 N93-28900 #
LA-UR-93-460 p 3593 N93-29094 #
LA-UR-93-463 p 3540 N93-30633 #
LA-UR-93-467 p 3634 N93-28907 #
LA-UR-93-471 p 3634 N93-28906 #
LA-UR-93-472 p 3633 N93-28905 #
LA-UR-93-478 p 3586 N93-29093 #
LA-UR-93-569 p 3296 N93-28904 #
LA-UR-93-599 p 3634 N93-29246 #
LA-UR-93-638 p 3380 N93-28909 #
LA-UR-93-639 p 3481 N93-29095 #
LA-UR-93-690 p 3450 N93-30636 #
LA-UR-93-728 p 3464 N93-29147 #
LA-UR-93-731 p 3634 N93-28908 #
LA-UR-93-823 p 3406 N93-28830 #
LA-UR-93-903 p 3332 N93-29252 #
LA-UR-93-919 p 3554 N93-28763 #
LA-UR-93-921 p 3342 N93-29312 #
LA-UR-93-922 p 3341 N93-29251 #
LA-UR-93-923 p 3426 N93-30485 #
LA-UR-93-958 p 3426 N93-30484 #
LA-UR-93-985 p 3594 N93-29314 #

LA-12314-MS p 3330 N93-28600 #
LA-12389-MS p 3454 N93-31013 #
LA-12448-MS p 3625 N93-28646 #
LA-12476-C p 3556 N93-28572 * #
LA-12533-T p 3569 N93-30130 #
LA-12541-MS p 3300 N93-30395 #

LAAS-92354 p 3414 N93-31030 #

LBL-32246 p 3598 N93-30393 #
LBL-32284 p 3436 N93-28847 #
LBL-32323 p 3261 N93-29869 #
LBL-32367 p 3433 N93-30531 #
LBL-32481 p 3575 N93-29870 #
LBL-32593 p 3575 N93-29302 #
LBL-32901-REV p 3594 N93-29249 #
LBL-32955 p 3592 N93-28582 #
LBL-33039 p 3431 N93-29149 #
LBL-33186 p 3604 N93-29806 #
LBL-33249 p 3551 N93-30392 #
LBL-33306 p 3313 N93-29766 #
LBL-33349 p 3430 N93-28664 #
LBL-33356 p 3592 N93-28642 #
LBL-33367 p 3405 N93-28581 #
LBL-33376 p 3353 N93-28570 #
LBL-33378 p 3595 N93-29417 #
LBL-33405 p 3298 N93-29191 #
LBL-33407 p 3331 N93-29248 #
LBL-33454 p 3594 N93-29150 #
LBL-33473 p 3569 N93-29860 #
LBL-33488 p 3330 N93-28761 #
LBL-33517 p 3417 N93-28663 #
LBL-33520 p 3569 N93-29805 #
LBL-33557 p 3596 N93-29868 #
LBL-33603 p 3440 N93-30530 #

LC-93-83795 p 3612 N93-29129
LC-93-84335 p 3456 N93-30634 #
LC-93-84549 p 3525 N93-28934 * #

LESC-30347-A p 3285 N93-31032 * #

LHC-NOTE-181 p 3576 N93-30019 #

LMU-09/92 p 3571 N93-30793 #

LNGS-92/40 p 3632 N93-28473 #

LPI-TR-93-02-PT-1 p 3639 N93-28764 * #

LRC-93-41 p 3589 N93-30189 #

LSU-HEPA-93-7 p 3653 N93-30052 * #

LTR93-003 p 3540 N93-30895 #

M-93B0000034 p 3529 N93-29647 #
M-93B0000041 p 3393 N93-30514 #

MATHS-REPT-A-177 p 3462 N93-30107 #

MEMO-INF-92-38 p 3540 N93-28480 #
MEMO-INF-92-59 p 3379 N93-28502 #

MEMO-1056 p 3547 N93-28667 #

MF-125 p 3586 N93-29056 #

MIAC-2 p 3320 N93-28499 #

MIT-TR-786-REV-1 p 3379 N93-28655 #

MITT-75 p 3629 N93-29008 #

MLM-3774 p 3592 N93-28568 #

MML-TR-93-01 p 3601 N93-30819 #
MML-TR-93-04 p 3322 N93-29002 #

MPE-PREPRINT-223 p 3637 N93-30639
MPE-PREPRINT-225 p 3441 N93-30640
MPE-PREPRINT-226 p 3631 N93-30641
MPE-PREPRINT-228 p 3631 N93-30642
MPE-PREPRINT-229 p 3632 N93-30643
MPE-PREPRINT-230 p 3631 N93-30578
MPE-PREPRINT-232 p 3631 N93-30615

MPL-U-65/92 p 3481 N93-28875 #

MRC-R-1156 p 3381 N93-29011 #

MRC/ABQ-R-1467 p 3412 N93-30152 #

MRC/WDC-R-296 p 3479 N93-30593 #

MRL-GD-0050 p 3425 N93-30156 #

MRL-TR-91-10 p 3562 N93-30029 #
MRL-TR-91-9 p 3562 N93-30157 #

MTL-TR-92-60 p 3430 N93-28989 #

MTR-11284-VOL-2 p 3531 N93-29921 #
MTR-90-W0000165 p 3534 N93-30546 #
MTR-90-W00135 p 3534 N93-30547 #

MTR-91W00132 .... p 3532 N93-30022 #
MTR-92B0000122 .... p 3387 N93-29890 #
MTR-93B0000015 .... p 3506 N93-29340 #
MTR-93B0000039 .... p 3484 N93-30176

MTR11284-VOL-1 .... p 3531 N93-29920 #

NAS 1.15:102864 .... p 3629 N93-29453 * #
NAS 1.15:103086 .... p 3660 N93-29452 * #
NAS 1.15:103868 .... p 3542 N93-29386 * #
NAS 1.15:103981 .... p 3245 N93-29653 * #
NAS 1.15:104566-VOL-2 .... p 3486 N93-28497 * #
NAS 1.15:104566-VOL-6 .... p 3486 N93-28500 * #
NAS 1.15:104576 .... p 3467 N93-28682 * #
NAS 1.15:104586 .... p 3482 N93-29448 * #
NAS 1.15:104753 .... p 3495 N93-29651 * #
NAS 1.15:104766 .... p 3278 N93-29221 * #
NAS 1.15:104769 .... p 3505 N93-29044 * #
NAS 1.15:104771 .... p 3289 N93-30507 * #
NAS 1.15:104772 .... p 3269 N93-30135 * #
NAS 1.15:105785 .... p 3287 N93-28686 * #
NAS 1.15:106032 .... p 3295 N93-28624 * #
NAS 1.15:106052 .... p 3295 N93-28681 * #
NAS 1.15:106059 .... p 3285 N93-28554 * #
NAS 1.15:106061 .... p 3321 N93-28618 * #
NAS 1.15:106076 .... p 3297 N93-29074 * #
NAS 1.15:106089 .... p 3418 N93-28947 * #
NAS 1.15:106136 .... p 3297 N93-29071 * #
NAS 1.15:106149 .... p 3252 N93-29065 * #
NAS 1.15:106157 .... p 3405 N93-28610 * #
NAS 1.15:106160 .... p 3416 N93-28626 * #
NAS 1.15:106180 .... p 3538 N93-28628 * #
NAS 1.15:106187 .... p 3420 N93-29157 * #
NAS 1.15:106193 .... p 3270 N93-28696 * #
NAS 1.15:106196 .... p 3451 N93-28633 * #
NAS 1.15:106206 .... p 3419 N93-29075 * #
NAS 1.15:106207 .... p 3288 N93-29158 * #
NAS 1.15:106209 .... p 3421 N93-29208 * #
NAS 1.15:106215 .... p 3451 N93-29196 * #
NAS 1.15:106217 .... p 3273 N93-29195 * #
NAS 1.15:106219 .... p 3449 N93-29073 * #
NAS 1.15:106220 .... p 3288 N93-29194 * #
NAS 1.15:106222 .... p 3287 N93-28694 * #
NAS 1.15:106230 .... p 3251 N93-28697 * #
NAS 1.15:106233 .... p 3286 N93-28619 * #
NAS 1.15:106236 .... p 3416 N93-28627 * #
NAS 1.15:106240 .... p 3252 N93-29162 * #
NAS 1.15:106243 .... p 3341 N93-28695 * #
NAS 1.15:106269 .... p 3340 N93-30938 * #
NAS 1.15:106274 .... p 3352 N93-30939 * #
NAS 1.15:107549 .... p 3449 N93-29220 * #
NAS 1.15:107559 .... p 3271 N93-29136 * #
NAS 1.15:107702 .... p 3455 N93-31038 * #
NAS 1.15:107755 .... p 3451 N93-29069 * #
NAS 1.15:107757 .... p 3290 N93-29067 * #
NAS 1.15:107764 .... p 3561 N93-28692 * #
NAS 1.15:108158 .... p 3393 N93-30371 * #
NAS 1.15:108236 .... p 3556 N93-28572 * #
NAS 1.15:108240 .... p 3609 N93-29323 * #
NAS 1.15:108242 .... p 3609 N93-29322 * #
NAS 1.15:108249 .... p 3612 N93-28948 * #
NAS 1.15:108250 .... p 3625 N93-30692 * #
NAS 1.15:108251 .... p 3271 N93-29387 * #
NAS 1.15:108254 .... p 3272 N93-29501 * #
NAS 1.15:108255 .... p 3268 N93-30133 * #
NAS 1.15:108259 .... p 3472 N93-30043 * #
NAS 1.15:108264 .... p 3612 N93-29167 * #
NAS 1.15:108407 .... p 3322 N93-29043 * #
NAS 1.15:108408 .... p 3331 N93-29193 * #
NAS 1.15:108409 .... p 3505 N93-28977 * #
NAS 1.15:108721 .... p 3262 N93-28699 * #
NAS 1.15:108773 .... p 3613 N93-29222 *
NAS 1.15:108985 .... p 3420 N93-29155 * #
NAS 1.15:108995 .... p 3520 N93-29070 * #
NAS 1.15:109221 .... p 3615 N93-29709 * #
NAS 1.15:109222 .... p 3532 N93-30023 * #
NAS 1.15:109223 .... p 3616 N93-30036 * #
NAS 1.15:109224 .... p 3616 N93-30037 * #
NAS 1.15:109238 .... p 3610 N93-30644 * #
NAS 1.15:4227 .... p 3240 N93-29449 * #
NAS 1.15:4242 .... p 3260 N93-30764 * #
NAS 1.15:4264 .... p 3240 N93-29450 * #
NAS 1.15:4435 .... p 3239 N93-29166 * #
NAS 1.15:4460 .... p 3431 N93-29209 * #
NAS 1.26:106197 .... p 3420 N93-29161 * #
NAS 1.26:182193 .... p 3298 N93-29451 * #
NAS 1.26:185676 .... p 3269 N93-29652 * #
NAS 1.26:186025 .... p 3431 N93-29066 * #
NAS 1.26:186027 .... p 3248 N93-28693 * #
NAS 1.26:187217 .... p 3287 N93-28946 * #
NAS 1.26:188246 .... p 3285 N93-31032 * #
NAS 1.26:188247 .... p 3353 N93-28698 * #
NAS 1.26:188248 .... p 3443 N93-29080 * #
NAS 1.26:188249 .... p 3634 N93-29042 * #
NAS 1.26:190420 .... p 3248 N93-29498 * #
NAS 1.26:190785 .... p 3288 N93-29068 * #
NAS 1.26:191036 .... p 3448 N93-31039 * #
NAS 1.26:191109 .... p 3352 N93-31031 * #
NAS 1.26:191140 .... p 3450 N93-28556 * #
NAS 1.26:191151 .... p 3273 N93-29884 * #
NAS 1.26:191153 .... p 3251 N93-28609 * #
NAS 1.26:191154 .... p 3251 N93-28617 * #
NAS 1.26:191157 .... p 3252 N93-29072 * #
NAS 1.26:191447 .... p 3509 N93-28841 * #
NAS 1.26:191448 .... p 3525 N93-28976 * #
NAS 1.26:191453 .... p 3542 N93-29192 * #
NAS 1.26:191457 .... p 3250 N93-28621 * #
NAS 1.26:191458 .... p 3418 N93-28975 * #
NAS 1.26:192468 .... p 3476 N93-29032 * #
NAS 1.26:192553 .... p 3538 N93-29030 * #
NAS 1.26:192554 .... p 3469 N93-29029 * #
NAS 1.26:192556 .... p 3269 N93-28558 * #
NAS 1.26:192561 .... p 3287 N93-28680 * #
NAS 1.26:192562 .... p 3272 N93-30617 * #
NAS 1.26:192563 .... p 3272 N93-30618 * #
NAS 1.26:192564 .... p 3272 N93-30619 * #
NAS 1.26:192565 .... p 3272 N93-30620 * #
NAS 1.26:192566 .... p 3272 N93-30621 * #
NAS 1.26:192577 .... p 3427 N93-30492 * #
NAS 1.26:192580 .... p 3289 N93-30648 * #
NAS 1.26:192584 .... p 3268 N93-31034 * #
NAS 1.26:192588 .... p 3582 N93-31035 * #
NAS 1.26:192690 .... p 3274 N93-29108 * #
NAS 1.26:192962 .... p 3227 N93-29712 * #
NAS 1.26:193015 .... p 3639 N93-28764 * #
NAS 1.26:193016 .... p 3272 N93-31033 * #
NAS 1.26:193037 .... p 3526 N93-29028 * #
NAS 1.26:193043 .... p 3249 N93-29774 * #
NAS 1.26:193071 .... p 3404 N93-28539 * #
NAS 1.26:193091 .... p 3476 N93-28538 * #
NAS 1.26:193115 .... p 3527 N93-29212 * #
NAS 1.26:193117 .... p 3526 N93-29026 * #
NAS 1.26:193118 .... p 3653 N93-30052 * #
NAS 1.26:193119 .... p 3603 N93-28933 * #
NAS 1.26:193120 .... p 3548 N93-28973 * #
NAS 1.26:193121 .... p 3456 N93-28620 * #
NAS 1.26:193122 .... p 3527 N93-29171 * #
NAS 1.26:193124 .... p 3451 N93-29154 * #
NAS 1.26:193125 .... p 3526 N93-29027 * #
NAS 1.26:193137 .... p 3509 N93-28895 * #
NAS 1.26:193142 .... p 3279 N93-29988 * #
NAS 1.26:193144 .... p 3384 N93-29586 * #
NAS 1.26:193145 .... p 3528 N93-29469 * #
NAS 1.26:193147 .... p 3415 N93-28557 * #
NAS 1.26:193152 .... p 3476 N93-28842 * #
NAS 1.26:193163 .... p 3436 N93-28623 * #
NAS 1.26:193172 .... p 3630 N93-29604 * #
NAS 1.26:193175 .... p 3527 N93-29170 * #
NAS 1.26:193179 .... p 3525 N93-28934 * #
NAS 1.26:193180 .... p 3653 N93-28935 * #
NAS 1.26:193183 .... p 3245 N93-28936 * #
NAS 1.26:193185 .... p 3295 N93-28843 * #
NAS 1.26:193187 .... p 3244 N93-29152 * #
NAS 1.26:193188 .... p 3629 N93-28634 * #
NAS 1.26:193221 .... p 3297 N93-29107 * #
NAS 1.26:193222 .... p 3248 N93-29153 * #
NAS 1.26:193223 .... p 3604 N93-29168 * #
NAS 1.26:193224 .... p 3281 N93-30038 * #
NAS 1.26:193225 .... p 3578 N93-29128 * #
NAS 1.26:193226 .... p 3288 N93-29091 * #
NAS 1.26:193227 .... p 3381 N93-29105 * #
NAS 1.26:193233 .... p 3493 N93-29041 * #
NAS 1.26:193234 .... p 3526 N93-29169 * #
NAS 1.26:193237 .... p 3271 N93-29215 * #
NAS 1.26:193238 .... p 3594 N93-29214 * #
NAS 1.26:193239 .... p 3527 N93-29219 * #
NAS 1.26:193241 .... p 3421 N93-29213 * #
NAS 1.26:193243 .... p 3635 N93-30053 * #
NAS 1.26:193245 .... p 3491 N93-29216 * #
NAS 1.26:193250 .... p 3543 N93-30039 * #
NAS 1.26:193252 .... p 3542 N93-29771 * #
NAS 1.26:193256 .... p 3531 N93-29873 * #
NAS 1.26:193257 .... p 3520 N93-29864 * #
NAS 1.26:193262 .... p 3653 N93-29164 * #
NAS 1.26:193263 .... p 3460 N93-29179 * #
NAS 1.26:193264 .... p 3630 N93-29163 * #
NAS 1.26:193274 .... p 3382 N93-29217 * #
NAS 1.26:193276 .... p 3527 N93-29218 * #
NAS 1.26:193278 .... p 3492 N93-30665 * #
NAS 1.26:193298 .... p 3651 N93-30635 * #
NAS 1.26:193467 .... p 3243 N93-31037 * #
NAS 1.26:193468 .... p 3400 N93-31036 * #
NAS 1.26:4012 .... p 3580 N93-30372 * #
NAS 1.26:4110 .... p 3242 N93-30373 * #
NAS 1.26:4118 .... p 3454 N93-30374 * #
NAS 1.26:4216 .... p 3426 N93-30375 * #
NAS 1.26:4500 .... p 3281 N93-30376 * #
NAS 1.26:4509 .... p 3533 N93-30380 * #
NAS 1.26:4515 .... p 3420 N93-29159 * #
NAS 1.26:4520 .... p 3249 N93-29885 * #
NAS 1.55:10048 .... p 3494 N93-29502 * #
NAS 1.55:10112-VOL-1 .... p 3509 N93-29516 * #
NAS 1.55:10112-VOL-2 .... p 3515 N93-29556 * #
NAS 1.55:3104-PT-1 .... p 3300 N93-30428 * #
NAS 1.55:3104-PT-2 .... p 3303 N93-30841 * #
NAS 1.55:3156 .... p 3236 N93-30673 * #
NAS 1.55:3167 .... p 3651 N93-30214 * #
NAS 1.55:3194-PT-1 .... p 3660 N93-29621 * #
NAS 1.55:3194-PT-2 .... p 3654 N93-29354 * #
NAS 1.55:3194-PT-4 .... p 3665 N93-29682 * #
NAS 1.55:3198 .... p 3616 N93-30449 * #
NAS 1.55:3201 .... p 3290 N93-30948 * #
NAS 1.60:3313 .... p 3239 N93-29160 * #
NAS 1.60:3314 .... p 3239 N93-29165 * #
NAS 1.61:1295 .... p 3629 N93-29156 * #
NAS 1.61:1298-VOL-3 .... p 3630 N93-29811 * #
NAS 1.61:1304 .... p 3506 N93-29324 * #
NAS 1.71:LAR-14429-1 .... p 3407 N93-29173 * #
NAS 1.71:LAR-14738-1 .... p 3443 N93-29175 * #
NAS 1.71:LAR-15063-1 .... p 3449 N93-30414 * #
NAS 1.71:LEW-15170-1 .... p 3561 N93-28953 * #
NAS 1.71:LEW-15697-1 .... p 3323 N93-29172 * #
NAS 1.71:MFS-26124-1-NPO .... p 3491 N93-29174 * #
NAS 1.71:MFS-26216-1 .... p 3442 N93-28951 * #
NAS 1.71:MFS-28402-1 .... p 3491 N93-28952 * #
NAS 1.71:MFS-28547-1 .... p 3289 N93-29847 * #
NAS 1.71:MFS-28569-1 .... p 3338 N93-30565 * #
NAS 1.71:MFS-28707-1 .... p 3508 N93-30566 * #
NAS 1.71:MFS-28720-1 .... p 3447 N93-30567 * #
NAS 1.71:MFS-28728-1 .... p 3288 N93-28950 * #
NAS 1.71:MFS-28772-1 .... p 3507 N93-29845 * #
NAS 1.71:MFS-28833-1 .... p 3445 N93-29846 * #
NAS 1.71:MSC-22046-1 .... p 3442 N93-28501 * #
NAS 1.71:NPO-18357-1-CU .... p 3579 N93-29848 * #
NAS 1.71:NPO-18492-1-CU .... p 3542 N93-29176 * #
NAS 1.71:NPO-18611-1-CU .... p 3440 N93-30415 * #
NAS 1.71:NPO-18733-1-CU .... p 3251 N93-30416 * #
NAS 1.71:NPO-18738-1-CU .... p 3443 N93-28954 * #
NAS 1.71:NPO-18772-1-CU .... p 3381 N93-28955 * #
NAS 1.71:NPO-18982-1-CU .... p 3449 N93-30413 * #
NAS 1.83:205 .... p 3608 N93-30134 * #

NASA-CASE-GSC-13435-1 .... p 3445 N93-29505 *

NASA-CASE-LAR-13823-1 .... p 3431 N93-29084 *
NASA-CASE-LAR-14048-1 .... p 3354 N93-29611 *
NASA-CASE-LAR-14206-1 .... p 3331 N93-29083 *
NASA-CASE-LAR-14429-1 .... p 3407 N93-29173 * #
NASA-CASE-LAR-14480-1-CU .... p 3452 N93-29612 *
NASA-CASE-LAR-14487-1 .... p 3331 N93-29085 *
NASA-CASE-LAR-14654-1-CU .... p 3452 N93-29613 *
NASA-CASE-LAR-14738-1 .... p 3443 N93-29175 * #
NASA-CASE-LAR-14773-2-CU .... p 3312 N93-29506 *
NASA-CASE-LAR-15063-1 .... p 3449 N93-30414 * #

NASA-CASE-LEW-14162-3 .... p 3299 N93-29614 *
NASA-CASE-LEW-14973-1 .... p 3464 N93-28974 *
NASA-CASE-LEW-15077-2 .... p 3298 N93-29609 *
NASA-CASE-LEW-15170-1 .... p 3561 N93-28953 * #
NASA-CASE-LEW-15697-1 .... p 3323 N93-29172 * #

NASA-CASE-MFS-26124-1-NPO . p 3491 N93-29174 * #
NASA-CASE-MFS-26216-1 .... p 3442 N93-28951 * #
NASA-CASE-MFS-28402-1 .... p 3491 N93-28952 * #
NASA-CASE-MFS-28547-1 .... p 3289 N93-29847 * #
NASA-CASE-MFS-28569-1 .... p 3338 N93-30565 * #
NASA-CASE-MFS-28589-1 .... p 3445 N93-29618 *
NASA-CASE-MFS-28707-1 .... p 3508 N93-30566 * #
NASA-CASE-MFS-28720-1 .... p 3447 N93-30567 * #
NASA-CASE-MFS-28728-1 .... p 3288 N93-28950 * #
NASA-CASE-MFS-28772-1 .... p 3507 N93-29845 * #
NASA-CASE-MFS-28833-1 .... p 3445 N93-29846 * #
NASA-CASE-MFS-29904-1 .... p 3432 N93-29503 *

NASA-CASE-MSC-21487-2 .... p 3296 N93-29023 *
NASA-CASE-MSC-21625-1 .... p 3498 N93-29610 *
NASA-CASE-MSC-21759-1 .... p 3312 N93-29617 *
NASA-CASE-MSC-21884-1 .... p 3331 N93-29088 *
NASA-CASE-MSC-22046-1 .... p 3442 N93-28501 * #

NASA-CASE-NPO-17629-1-CU .... p 3521 N93-29608 *
NASA-CASE-NPO-17873-2-CU .... p 3384 N93-29507 *
NASA-CASE-NPO-18004-1-CU .... p 3521 N93-29504 *
NASA-CASE-NPO-18357-1-CU .... p 3579 N93-29848 * #
NASA-CASE-NPO-18410-1-CU .... p 3578 N93-29086 *
NASA-CASE-NPO-18492-1-CU .... p 3542 N93-29176 * #
NASA-CASE-NPO-18611-1-CU .... p 3440 N93-30415 * #
NASA-CASE-NPO-18713-1-CU .... p 3381 N93-29087 *
NASA-CASE-NPO-18733-1-CU .... p 3251 N93-30416 * #
NASA-CASE-NPO-18738-1-CU .... p 3443 N93-28954 * #
NASA-CASE-NPO-18772-1-CU .... p 3381 N93-28955 * #
NASA-CASE-NPO-18982-1-CU .... p 3449 N93-30413 * #

NASA-CP-10048 .... p 3494 N93-29502 * #
NASA-CP-10112-VOL-1 .... p 3509 N93-29516 * #
NASA-CP-10112-VOL-2 .... p 3515 N93-29556 * #
NASA-CP-3104-PT-1 .... p 3300 N93-30428 * #
NASA-CP-3104-PT-2 .... p 3303 N93-30841 * #

NASA-CP-3156 .... p 3236 N93-30673 * #
NASA-CP-3167 .... p 3651 N93-30214 * #
NASA-CP-3194-PT-1 .... p 3660 N93-29621 * #
NASA-CP-3194-PT-2 .... p 3654 N93-29354 * #
NASA-CP-3194-PT-4 .... p 3665 N93-29682 * #
NASA-CP-3198 .... p 3616 N93-30449 * #
NASA-CP-3201 .... p 3290 N93-30948 * #

NASA-CR-182193 .... p 3298 N93-29451 * #
NASA-CR-185676 .... p 3269 N93-29652 * #
NASA-CR-186025 .... p 3431 N93-29066 * #
NASA-CR-186027 .... p 3248 N93-28693 * #
NASA-CR-187217 .... p 3287 N93-28946 * #
NASA-CR-188246 .... p 3285 N93-31032 * #
NASA-CR-188247 .... p 3353 N93-28698 * #
NASA-CR-188248 .... p 3443 N93-29080 * #
NASA-CR-188249 .... p 3634 N93-29042 * #
NASA-CR-190420 .... p 3248 N93-29498 * #
NASA-CR-190785 .... p 3288 N93-29068 * #
NASA-CR-191036 .... p 3448 N93-31039 * #
NASA-CR-191109 .... p 3352 N93-31031 * #
NASA-CR-191140 .... p 3450 N93-28556 * #
NASA-CR-191151 .... p 3273 N93-29884 * #
NASA-CR-191153 .... p 3251 N93-28609 * #
NASA-CR-191154 .... p 3251 N93-28617 * #
NASA-CR-191157 .... p 3252 N93-29072 * #
NASA-CR-191447 .... p 3509 N93-28841 * #
NASA-CR-191448 .... p 3525 N93-28976 * #
NASA-CR-191453 .... p 3542 N93-29192 * #
NASA-CR-191457 .... p 3250 N93-28621 * #
NASA-CR-191458 .... p 3418 N93-28975 * #
NASA-CR-192468 .... p 3476 N93-29032 * #
NASA-CR-192553 .... p 3538 N93-29030 * #
NASA-CR-192554 .... p 3469 N93-29029 * #
NASA-CR-192556 .... p 3269 N93-28558 * #
NASA-CR-192561 .... p 3287 N93-28680 * #
NASA-CR-192562 .... p 3272 N93-30617 * #
NASA-CR-192563 .... p 3272 N93-30618 * #
NASA-CR-192564 .... p 3272 N93-30619 * #
NASA-CR-192565 .... p 3272 N93-30620 * #
NASA-CR-192566 .... p 3272 N93-30621 * #
NASA-CR-192577 .... p 3427 N93-30492 * #
NASA-CR-192580 .... p 3289 N93-30648 * #
NASA-CR-192584 .... p 3268 N93-31034 * #
NASA-CR-192588 .... p 3582 N93-31035 * #
NASA-CR-192690 .... p 3274 N93-29108 * #
NASA-CR-192962 .... p 3227 N93-29712 * #
NASA-CR-193015 .... p 3639 N93-28764 * #
NASA-CR-193016 .... p 3272 N93-31033 * #
NASA-CR-193037 .... p 3526 N93-29028 * #
NASA-CR-193043 .... p 3249 N93-29774 * #
NASA-CR-193071 .... p 3404 N93-28539 * #
NASA-CR-193091 .... p 3476 N93-28538 * #
NASA-CR-193115 .... p 3527 N93-29212 * #
NASA-CR-193117 .... p 3526 N93-29026 * #
NASA-CR-193118 .... p 3653 N93-30052 * #
NASA-CR-193119 .... p 3603 N93-28933 * #
NASA-CR-193120 .... p 3548 N93-28973 * #
NASA-CR-193121 .... p 3456 N93-28620 * #
NASA-CR-193122 .... p 3527 N93-29171 * #
NASA-CR-193124 .... p 3451 N93-29154 * #
NASA-CR-193125 .... p 3526 N93-29027 * #
NASA-CR-193137 .... p 3509 N93-28895 * #
NASA-CR-193142 .... p 3279 N93-29988 * #
NASA-CR-193144 .... p 3384 N93-29586 * #
NASA-CR-193145 .... p 3528 N93-29469 * #
NASA-CR-193147 .... p 3415 N93-28557 * #
NASA-CR-193152 .... p 3476 N93-28842 * #
NASA-CR-193163 .... p 3436 N93-28623 * #
NASA-CR-193172 .... p 3630 N93-29604 * #
NASA-CR-193175 .... p 3527 N93-29170 * #
NASA-CR-193179 .... p 3525 N93-28934 * #
NASA-CR-193180 .... p 3653 N93-28935 * #
NASA-CR-193183 .... p 3245 N93-28936 * #
NASA-CR-193185 .... p 3295 N93-28843 * #
NASA-CR-193187 .... p 3244 N93-29152 * #
NASA-CR-193188 .... p 3629 N93-28634 * #
NASA-CR-193221 .... p 3297 N93-29107 * #
NASA-CR-193222 .... p 3248 N93-29153 * #
NASA-CR-193223 .... p 3604 N93-29168 * #
NASA-CR-193224 .... p 3281 N93-30038 * #
NASA-CR-193225 .... p 3578 N93-29128 * #
NASA-CR-193226 .... p 3288 N93-29091 * #
NASA-CR-193227 .... p 3381 N93-29105 * #
NASA-CR-193233 .... p 3493 N93-29041 * #
NASA-CR-193234 .... p 3526 N93-29169 * #
NASA-CR-193237 .... p 3271 N93-29215 * #
NASA-CR-193238 .... p 3594 N93-29214 * #
NASA-CR-193239 .... p 3527 N93-29219 * #
NASA-CR-193241 .... p 3421 N93-29213 * #
NASA-CR-193243 .... p 3635 N93-30053 * #
NASA-CR-193245 .... p 3491 N93-29216 * #
NASA-CR-193250 .... p 3543 N93-30039 * #
NASA-CR-193252 .... p 3542 N93-29771 * #
NASA-CR-193256 .... p 3531 N93-29873 * #
NASA-CR-193257 .... p 3520 N93-29864 * #
NASA-CR-193262 .... p 3653 N93-29164 * #
NASA-CR-193263 .... p 3460 N93-29179 * #
NASA-CR-193264 .... p 3630 N93-29163 * #
NASA-CR-193274 .... p 3382 N93-29217 * #
NASA-CR-193276 .... p 3527 N93-29218 * #
NASA-CR-193278 .... p 3492 N93-30665 * #
NASA-CR-193298 .... p 3651 N93-30635 * #
NASA-CR-193467 .... p 3243 N93-31037 * #
NASA-CR-193468 .... p 3400 N93-31036 * #
NASA-CR-4012 .... p 3580 N93-30372 * #
NASA-CR-4110 .... p 3242 N93-30373 * #
NASA-CR-4118 .... p 3454 N93-30374 * #
NASA-CR-4216 .... p 3426 N93-30375 * #
NASA-CR-4500 .... p 3281 N93-30376 * #
NASA-CR-4509 .... p 3533 N93-30380 * #
NASA-CR-4515 .... p 3420 N93-29159 * #
NASA-CR-4520 .... p 3249 N93-29885 * #

NASA-NP-205 .... p 3608 N93-30134 * #

NASA-RP-1295 .... p 3629 N93-29156 * #
NASA-RP-1298-VOL-3 .... p 3630 N93-29811 * #
NASA-RP-1304 .... p 3506 N93-29324 * #

NASA-TM-102864 .... p 3629 N93-29453 * #
NASA-TM-103086 .... p 3660 N93-29452 * #
NASA-TM-103868 .... p 3542 N93-29386 * #
NASA-TM-103981 .... p 3245 N93-29653 * #
NASA-TM-104566-VOL-2 .... p 3486 N93-28497 * #
NASA-TM-104566-VOL-6 .... p 3486 N93-28500 * #
NASA-TM-104576 .... p 3467 N93-28682 * #
NASA-TM-104586 .... p 3482 N93-29448 * #
NASA-TM-104753 .... p 3495 N93-29651 * #
NASA-TM-104766 .... p 3278 N93-29221 * #
NASA-TM-104769 .... p 3505 N93-29044 * #
NASA-TM-104771 .... p 3289 N93-30507 * #
NASA-TM-104772 .... p 3269 N93-30135 * #
NASA-TM-105785 .... p 3287 N93-28686 * #
NASA-TM-106032 .... p 3295 N93-28624 * #
NASA-TM-106052 .... p 3295 N93-28681 * #
NASA-TM-106059 .... p 3285 N93-28554 * #
NASA-TM-106061 .... p 3321 N93-28618 * #
NASA-TM-106076 .... p 3297 N93-29074 * #
NASA-TM-106089 .... p 3418 N93-28947 * #
NASA-TM-106136 .... p 3297 N93-29071 * #
NASA-TM-106149 .... p 3252 N93-29065 * #
NASA-TM-106157 .... p 3405 N93-28610 * #
NASA-TM-106160 .... p 3416 N93-28626 * #
NASA-TM-106180 .... p 3538 N93-28628 * #
NASA-TM-106187 .... p 3420 N93-29157 * #
NASA-TM-106193 .... p 3270 N93-28696 * #
NASA-TM-106196 .... p 3451 N93-28633 * #
NASA-TM-106197 .... p 3420 N93-29161 * #
NASA-TM-106206 .... p 3419 N93-29075 * #
NASA-TM-106207 .... p 3288 N93-29158 * #
NASA-TM-106209 .... p 3421 N93-29208 * #
NASA-TM-106215 .... p 3451 N93-29196 * #
NASA-TM-106217 .... p 3273 N93-29195 * #
NASA-TM-106219 .... p 3449 N93-29073 * #
NASA-TM-106220 .... p 3288 N93-29194 * #
NASA-TM-106222 .... p 3287 N93-28694 * #
NASA-TM-106230 .... p 3251 N93-28697 * #
NASA-TM-106233 .... p 3286 N93-28619 * #
NASA-TM-106236 .... p 3416 N93-28627 * #
NASA-TM-106240 .... p 3252 N93-29162 * #
NASA-TM-106243 .... p 3341 N93-28695 * #
NASA-TM-106269 .... p 3340 N93-30938 * #
NASA-TM-106274 .... p 3352 N93-30939 * #
NASA-TM-107549 .... p 3449 N93-29220 * #
NASA-TM-107559 .... p 3271 N93-29136 * #
NASA-TM-107702 .... p 3455 N93-31038 * #
NASA-TM-107755 .... p 3451 N93-29069 * #
NASA-TM-107757 .... p 3290 N93-29067 * #
NASA-TM-107764 .... p 3561 N93-28692 * #
NASA-TM-108158 .... p 3393 N93-30371 * #
NASA-TM-108236 .... p 3556 N93-28572 * #
NASA-TM-108240 .... p 3609 N93-29323 * #
NASA-TM-108242 .... p 3609 N93-29322 * #
NASA-TM-108249 .... p 3612 N93-28948 * #
NASA-TM-108250 .... p 3625 N93-30692 * #
NASA-TM-108251 .... p 3271 N93-29387 * #
NASA-TM-108254 .... p 3272 N93-29501 * #
NASA-TM-108255 .... p 3268 N93-30133 * #
NASA-TM-108259 .... p 3472 N93-30043 * #
NASA-TM-108264 .... p 3612 N93-29167 * #
NASA-TM-108407 .... p 3322 N93-29043 * #
NASA-TM-108408 .... p 3331 N93-29193 * #
NASA-TM-108409 .... p 3505 N93-28977 * #
NASA-TM-108721 .... p 3262 N93-28699 * #
NASA-TM-108773 .... p 3613 N93-29222 *
NASA-TM-108985 .... p 3420 N93-29155 * #
NASA-TM-108995 .... p 3520 N93-29070 * #
NASA-TM-109221 .... p 3615 N93-29709 * #
NASA-TM-109222 .... p 3532 N93-30023 * #
NASA-TM-109223 .... p 3616 N93-30036 * #
NASA-TM-109224 .... p 3616 N93-30037 * #
NASA-TM-109238 .... p 3610 N93-30644 * #
NASA-TM-4227 .... p 3240 N93-29449 * #
NASA-TM-4242 .... p 3260 N93-30764 * #
NASA-TM-4264 .... p 3240 N93-29450 * #
NASA-TM-4435 .... p 3239 N93-29166 * #
NASA-TM-4460 .... p 3431 N93-29209 * #

NASA-TP-3313 .... p 3239 N93-29160 * #
NASA-TP-3314 .... p 3239 N93-29165 * #

NATICK/TR-93/026 .... p 3495 N93-30196 #
NATICK/TR-93/029 .... p 3241 N93-30119 #

NAVY-CASE-73910 .... p 3431 N93-29046 #
NAVY-CASE-74075 .... p 3441 N93-30587 #
NAVY-CASE-74106 .... p 3577 N93-29038 #
NAVY-CASE-74205 .... p 3440 N93-30427 #
NAVY-CASE-74287 .... p 3581 N93-30410 #
NAVY-CASE-74945 .... p 3338 N93-30586 #
NAVY-CASE-74948 .... p 3338 N93-30580 #

NAWCWPNS-TM-7469 .... p 3477 N93-29401 #

NAWCWPNS-TP-8096 .... p 3409 N93-29435

NCAR/CT-142 .... p 3476 N93-29197 #

NCAR/TN-377+IA .... p 3535 N93-30824 #
NCAR/TN-378+STR .... p 3539 N93-29661

NCCOSC/RDT/E-TR-26 .... p 3441 N93-30910 #

NCCOSC/RDT/E/TR-1574 .... p 3333 N93-29404 #

NCES-92-132 .... p 3608 N93-30821 #

NDU-ICAF-92-A208 .... p 3459 N93-29000 #
NDU-ICAF-92-S10 .... p 3615 N93-29439 #
NDU-ICAF-92-S60 .... p 3609 N93-28985 #
NDU-ICAF-92-S79 .... p 3250 N93-29004 #

NEAR-TR-460 .... p 3423 N93-29353 #

NEDO-ITE-9105 .... p 3468 N93-28882 #
NEDO-ITE-9106 .... p 3468 N93-28883 #
NEDO-ITE-9108 .... p 3470 N93-29672 #

NEI-FI-184 .... p 3343 N93-30042 #

NIFS-MEMO-6 .... p 3436 N93-28980 #

NIIYAF-MGU-91-10-214 .... p 3607 N93-30916 #

NIKHEF-H/92-03 .... p 3576 N93-30019 #
NIKHEF-H/92-14 .... p 3572 N93-31008 #

NIPER-659 .... p 3603 N93-28964 #

NIST/GCR-92/619 .... p 3244 N93-29211

NIST/TN-1295 .... p 3407 N93-29203 #
NIST/TN-1400 .... p 3354 N93-29666 #

NISTIR-3953 .... p 3313 N93-29768 #
NISTIR-4865 .... p 3579 N93-29667 #
NISTIR-5127 .... p 3521 N93-29662
NISTIR-5133 .... p 3561 N93-30888 #
NISTIR-5139 .... p 3539 N93-29677
NISTIR-5141 .... p 3530 N93-29678
NISTIR-5144 .... p 3475 N93-30887
NISTIR-5153 .... p 3522 N93-30832 #
NISTIR-5162 .... p 3354 N93-29663
NISTIR-5166 .... p 3610 N93-30822 #

NLR-CR-92043-L .... p 3460 N93-29321 #
NLR-CR-92045-L-PT-1 .... p 3460 N93-29307 #

NLR-TP-89242-U .... p 3522 N93-30840 #

NMRI-93-14 .... p 3497 N93-30882 #
NMRI-93-1 .... p 3492 N93-30818 #

NOAA-DR-ERL-AOML-22 .... p 3489 N93-30827 #

NOAA-TM-ERL-AOML-73 .... p 3394 N93-30662 #

NOAA-TM-ERL-ARL-199-VOL-1 .. p 3242 N93-30387 #
NOAA-TM-ERL-ARL-199-VOL-2 .. p 3242 N93-30388 #

NOAA-TM-ERL-WPL-229 .... p 3386 N93-29680

NOAA-TM-NOS-ORCA-68 .... p 3489 N93-30830 #

NOAA-TM-NWS-ER-86 .... p 3481 N93-29198 #

NOAA-TM-NWS-NHC-31 .... p 3485 N93-30758 #

NOAA-TM-NWS-WR-219 .... p 3485 N93-30889 #

NOO-TN-02-93 .... p 3489 N93-30420 #

NPRDC-AP-93-4 .... p 3544 N93-30556 #

NPRDC-TR-93-4 .... p 3392 N93-30362 #

NPS-MA-93-012 .... p 3439 N93-29883 #
NPS-MA-93-013 .... p 3450 N93-28516 #
NPS-MA-93-014 .... p 3489 N93-30525 #

NPSEC-93-007 .... p 3387 N93-29882 #

NPSOR-93-008 .... p 3528 N93-29345 #

NRAD-TD-2410 .... p 3394 N93-30595 #
NRAD-TD-2453 .... p 3394 N93-30597 #
NRAD-TD-2454 .... p 3496 N93-30515 #
NRAD-TD-2456 .... p 3497 N93-30897 #
NRAD-TD-2457 .... p 3303 N93-30555 #

NRAD-TR-1495 .... p 3400 N93-30995 #
NRAD-TR-1533 .... p 3245 N93-28990 #

NRCN(TN)-131 .... p 3317 N93-30982 #

NRCN-612 .... p 3328 N93-30941 #

NREL/TP-411-5455 .... p 3466 N93-30891 #
NREL/TP-412-5422 .... p 3465 N93-30207 #
NREL/TP-451-5353 .... p 3464 N93-29965 #
NREL/TP-451-5355 .... p 3464 N93-28971 #
NREL/TP-451-5414 .... p 3465 N93-30208 #
NREL/TP-471-5352 .... p 3464 N93-29925 #
NREL/TP-471-5375 .... p 3465 N93-30206 #

NRL/FR/5324-93-9536 .... p 3393 N93-30423 #

NRL/MR/6410-93-7178 .... p 3424 N93-29851 #
NRL/MR/6793-93-7197 .... p 3409 N93-29478 #
NRL/MR/7173-92-7004 .... p 3391 N93-29975 #

NRL/PU/7531-92-0003 .... p 3481 N93-28876 #
NRL/PU/7541-92-0004 .... p 3483 N93-29491 #

NSF/ISI-89035-PHASE-1 .... p 3331 N93-29201 #

NSMRL-1168 .... p 3246 N93-29818 #
NSMRL-1187 .... p 3499 N93-30426 #

NSSDC/WDC-A-R/S-93-18 .... p 3612 N93-29167 * #

NSWCDD/MP-92/222 .... p 3407 N93-28999 #

NSWCDD/TR-92/124 .... p 3411 N93-30021 #
NSWCDD/TR-92/218 .... p 3352 N93-30424 #

NTIA-93-292 .... p 3382 N93-29202 #

NUWC-NL-TR-10231 .... p 3442 N93-28578 #

NWRA-CR-92-R095 .... p 3478 N93-30174 #

OCNR-11492-17 .... p 3654 N93-29258 #

OCS/MMS-92/0043-VOL-1 .... p 3468 N93-28899 #
OCS/MMS-92/0044-VOL-2 .... p 3471 N93-29861

OITS-494 .... p 3577 N93-30532 #

ONERA-NT-1990-10 .... p 3314 N93-30203 #
ONERA-NT-1990-3 .... p 3241 N93-30020 #
ONERA-NT-1990-4 .... p 3550 N93-30136 #
ONERA-NT-1990-6 .... p 3326 N93-30138 #
ONERA-NT-1990-7 .... p 3314 N93-30139 #
ONERA-NT-1990-9 .... p 3336 N93-30112 #
ONERA-NT-1991-6 .... p 3325 N93-30105 #

ONERA-P-1990-2 .... p 3392 N93-30018 #
ONERA-P-1990-3 .... p 3313 N93-30109 #
ONERA-P-1990-4 .... p 3335 N93-30024 #
ONERA-P-1990-5 .... p 3562 N93-30110 #

ONERA-RSF-23/1123-AY-230A .. p 3417 N93-28744 #
ONERA-RSF-23/1123-AY-232A .. p 3417 N93-28744 #

ONREUR-92-7-R .... p 3489 N93-30612 #

ORNL/HTSPC-4 .... p 3404 N93-28523 #

ORNL/SUB-89-95915/2 .... p 3336 N93-30182 #

OTA-BP-TCT-101 .... p 3539 N93-29650 #

OTA-ITE-552 .... p 3610 N93-29649 #

OTA-TCT-549 .... p 3392 N93-30150 #

OUEL-1916/92 .... p 3523 N93-28485 #
OUEL-1918/92 .... p 3523 N93-28486 #
OUEL-1933/92 .... p 3380 N93-28896 #
OUEL-1941/92 .... p 3505 N93-28897 #
OUEL-1947/92 .... p 3541 N93-28898 #
OUEL-1950/92 .... p 3548 N93-28754 #

PARGUM-92-03 .... p 3561 N93-28995 #

PB93-146702 .... p 3244 N93-29211
PB93-154821 .... p 3444 N93-29205 #
PB93-156792 .... p 3476 N93-29197 #
PB93-161149 .... p 3469 N93-29033 #
PB93-161156 .... p 3469 N93-29034 #
PB93-162006 .... p 3481 N93-29198 #
PB93-162816 .... p 3604 N93-29428 #
PB93-163863 .... p 3608 N93-30657 #
PB93-167203 .... p 3470 N93-29200 #
PB93-167526 .... p 3493 N93-29199 #
PB93-168839 .... p 3311 N93-29204 #
PB93-169464 .... p 3470 N93-29674
PB93-169878 .... p 3611 N93-30936 #
PB93-169902 .... p 3447 N93-30820 #
PB93-173110 .... p 3467 N93-28873 #
PB93-173417 .... p 3313 N93-29768 #
PB93-173797 .... p 3468 N93-28899 #
PB93-173805-VOL-2 .... p 3471 N93-29861
PB93-174126 .... p 3331 N93-29201 #
PB93-174704 .... p 3316 N93-30658
PB93-174720 .... p 3496 N93-30659 #
PB93-174779 .... p 3465 N93-30001
PB93-174795 .... p 3466 N93-30935
PB93-174993 .... p 3485 N93-30758 #
PB93-175008 .... p 3507 N93-29675
PB93-175123 .... p 3382 N93-29202 #
PB93-175198 .... p 3428 N93-30759 #
PB93-175263 .... p 3317 N93-30760 #
PB93-175297 .... p 3317 N93-30761 #
PB93-175404 .... p 3407 N93-29203 #
PB93-175545 .... p 3474 N93-30762 #
PB93-175784 .... p 3474 N93-30660 #
PB93-176162 .... p 3604 N93-29794
PB93-176188 .... p 3471 N93-29676
PB93-176212 .... p 3316 N93-30661 #
PB93-176261 .... p 3394 N93-30662 #
PB93-176550 .... p 3608 N93-30821 #
PB93-178309 .... p 3352 N93-30663 #
PB93-178572 .... p 3539 N93-29677
PB93-178598 .... p 3475 N93-30887
PB93-178648 .... p 3561 N93-30888 #
PB93-178655 .... p 3530 N93-29678
PB93-178697 .... p 3485 N93-30889 #
PB93-178879 .... p 3653 N93-29679
PB93-179943 .... p 3497 N93-30890 #
PB93-179968 .... p 3610 N93-30822 #
PB93-180248 .... p 3386 N93-29680
PB93-180255 .... p 3242 N93-30387 #
PB93-180263 .... p 3242 N93-30388 #
PB93-180453 .... p 3471 N93-29681 #
PB93-180644 .... p 3488 N93-29670
PB93-181261 .... p 3410 N93-29671 #
PB93-181618 .... p 3474 N93-30823 #
PB93-181824 .... p 3535 N93-30824 #
PB93-181832 .... p 3539 N93-29661
PB93-181873 .... p 3521 N93-29662
PB93-182038 .... p 3354 N93-29663
PB93-182244 .... p 3474 N93-30825 #
PB93-183085 .... p 3474 N93-30826 #
PB93-183895 .... p 3483 N93-29664
PB93-184299 .... p 3312 N93-29665
PB93-184331 .... p 3354 N93-29666 #
PB93-184422 .... p 3579 N93-29667 #
PB93-184687 .... p 3624 N93-29668
PB93-184760 .... p 3489 N93-30827 #
PB93-184828 .... p 3470 N93-29669
PB93-185437 .... p 3447 N93-30828 #
PB93-185460 .... p 3466 N93-30814 #
PB93-185478 .... p 3327 N93-30815 #
PB93-185551 .... p 3475 N93-30829 #
PB93-185684 .... p 3489 N93-30830 #
PB93-185767 .... p 3475 N93-30831 #
PB93-185999 .... p 3522 N93-30832 #
PB93-186203 .... p 3462 N93-30833 #
PB93-186245 .... p 3475 N93-30834 #

PERLAB-1 .... p 3580 N93-30368 #

PL-PU/92003 .... p 3288 N93-29289 #

PL-TR-92-1013 .... p 3412 N93-30152 #
PL-TR-92-1053-VOL-1 .... p 3241 N93-30171 #
PL-TR-92-1053-VOL-2 .... p 3241 N93-30172 #
PL-TR-92-1053-VOL-3 .... p 3242 N93-30173 #
PL-TR-92-1053-VOL-4 .... p 3241 N93-30151 #
PL-TR-92-2186 .... p 3479 N93-30756 #
PL-TR-92-2202 .... p 3481 N93-28875 #
PL-TR-92-2222 .... p 3399 N93-30757 #
PL-TR-92-2232 .... p 3279 N93-29305 #
PL-TR-92-2262 .... p 3483 N93-29832 #
PL-TR-92-2266 .... p 3480 N93-28518 #
PL-TR-92-2292 .... p 3289 N93-30402 #
PL-TR-92-2331 .... p 3273 N93-29306 #
PL-TR-92-2332 .... p 3630 N93-29460 #
PL-TR-92-2336 .... p 3484 N93-30535 #
PL-TR-92-3043 .... p 3288 N93-29289 #
PL-TR-92-3049 .... p 3287 N93-28658 #
PL-TR-93-2001 .... p 3477 N93-29412 #
PL-TR-93-2018 .... p 3476 N93-29343 #
PL-TR-93-2022 .... p 3477 N93-29831 #
PL-TR-93-2054 .... p 3652 N93-28585 #
PL-TR-93-2096 .... p 3462 N93-29830 #
PL-TR-93-3014 .... p 3341 N93-28517 #

PNL-SA-18878 .... p 3420 N93-29126 #
PNL-SA-21085 .... p 3323 N93-29101 #
PNL-SA-21089 .... p 3383 N93-29308 #
PNL-SA-21117 .... p 3322 N93-29061 #
PNL-SA-21260 .... p 3354 N93-28893 #
PNL-SA-21265 .... p 3550 N93-30041 #
PNL-SA-21288 .... p 3320 N93-28548 #
PNL-SA-21578 .... p 3238 N93-28662 #

PNL-8384 .... p 3473 N93-30183 #
PNL-8549 .... p 3625 N93-29329 #

PNWD-2090-HEDR .... p 3481 N93-29054 #

PR-SWP-3-REV-1 .... p 3578 N93-29139 #
PR-SWP-6-REV-1 .... p 3578 N93-29140 #
PR-SWP-8-REV-1 .... p 3579 N93-29470 #

PRE-1750 .... p 3591 N93-31007 #

PSC-17 .... p 3588 N93-29434 #
PSC-18 .... p 3583 N93-28532 #
PSC-19 .... p 3379 N93-28534 #
PSC-20 .... p 3583 N93-28533 #
PSC-23 .... p 3590 N93-30533 #

R-95-7376-10 .... p 3317 N93-30760 #

R/D-6882-EE-02 .... p 3597 N93-29974 #

R/DC-16A/92-VOL-1 .... p 3335 N93-29886 #
R/DC-16B/92-VOL-2 .... p 3335 N93-29881 #

RCC-751-93 .... p 3281 N93-30817 #

RCN-296-009-04-01 .... p 3312 N93-29665

RED-BOOK-ISSUE-4 .... p 3393 N93-30371 * #

REPT-TR-1 .... p 3332 N93-29342 #
REPT-TR-3 .... p 3410 N93-29826 #
REPT-TR-8 .... p 3569 N93-29839 #

REPT-0650-350-W410 .... p 3570 N93-30366 #
REPT-46 .... p 3405 N93-28589 #
REPT-47 .... p 3409 N93-29485 #
REPT-56913-10 .... p 3500 N93-28464 #
REPT-88-61608 .... p 3298 N93-29451 * #
REPT-92B00122 .... p 3486 N93-28497 * #
REPT-92SBIRPBGFINAL .... p 3597 N93-30175 #
REPT-93-001 .... p 3272 N93-31033 * #
REPT-93A00689 .... p 3629 N93-29156 * #
REPT-93B00016 .... p 3486 N93-28500 * #
REPT-93B00029 .... p 3467 N93-28682 * #
REPT-93B00049 .... p 3630 N93-29811 * #
REPT-93B00084 .... p 3482 N93-29448 * #

RJO-93-7091-ILS .... p 3610 N93-30177 #

RL-TR-92-273 .... p 3524 N93-28579 #
RL-TR-92-295 .... p 3520 N93-29482 #
RL-TR-92-306 .... p 3542 N93-29763
RL-TR-92-310 .... p 3381 N93-28997 #
RL-TR-92-311 .... p 3568 N93-29787 #
RL-TR-92-314 .... p 3599 N93-30554 #
RL-TR-92-315 .... p 3534 N93-30547 #
RL-TR-92-316-VOL-1 .... p 3531 N93-29920 #
RL-TR-92-316-VOL-2 .... p 3531 N93-29921 #
RL-TR-92-317 .... p 3534 N93-30546 #
RL-TR-92-318 .... p 3532 N93-30022 #
RL-TR-92-320 .... p 3391 N93-30016 #
RL-TR-92-327 .... p 3541 N93-28494 #
RL-TR-92-329 .... p 3544 N93-30886 #
RL-TR-92-332 .... p 3381 N93-28998 #
RL-TR-92-340 .... p 3597 N93-30144 #

RR-CE132 .... p 3451 N93-29106 #

RXR-92101 .... p 3273 N93-29306 #

R93-918246-6 .... p 3299 N93-29802 #

S-686 .... p 3495 N93-29651 * #
S-702-VOL-1 .... p 3509 N93-29516 * #
S-702-VOL-2 .... p 3515 N93-29556 * #
S-716 .... p 3278 N93-29221 * #
S-718 .... p 3506 N93-29324 * #
S-720 .... p 3505 N93-29044 * #
S-723 .... p 3289 N93-30507 * #
S-724 .... p 3269 N93-30135 * #

SAND-92-0406 .... p 3412 N93-30118 #
SAND-92-0640 .... p 3526 N93-29127 #
SAND-92-1561C .... p 3417 N93-28639 #
SAND-92-1666 .... p 3463 N93-28603 #
SAND-92-1889C .... p 3239 N93-29035 #
SAND-92-1941 .... p 3442 N93-28837 #
SAND-92-1974C .... p 3279 N93-29840 #
SAND-92-2011C .... p 3538 N93-29186 #
SAND-92-2075 .... p 3575 N93-29151 #
SAND-92-2167C .... p 3465 N93-30391 #
SAND-92-2442 .... p 3430 N93-28645 #
SAND-92-2473 .... p 3412 N93-30127 #
SAND-92-2483C .... p 3530 N93-29808 #
SAND-92-2497C .... p 3443 N93-29185 #
SAND-92-2521C .... p 3532 N93-30050 #
SAND-92-2554C .... p 3405 N93-28641 #
SAND-92-2847C .... p 3425 N93-30184 #
SAND-92-2874C .... p 3406 N93-28944 #
SAND-92-2901C .... p 3412 N93-30370 #
SAND-92-8540 .... p 3416 N93-28595 #
SAND-93-0003C .... p 3447 N93-30654 #
SAND-93-0057 .... p 3437 N93-29180 #
SAND-93-0090C .... p 3278 N93-29250 #
SAND-93-0147C .... p 3281 N93-30509 #
SAND-93-0170C .... p 3378 N93-30508 #
SAND-93-0211C .... p 3437 N93-29264 #
SAND-93-0284C .... p 3549 N93-29187 #
SAND-93-0335C .... p 3339 N93-30656 #
SAND-93-0341C .... p 3594 N93-29188 #
SAND-93-0361C .... p 3491 N93-30483 #
SAND-93-0366C .... p 3598 N93-30517 #
SAND-93-0380C .... p 3570 N93-30669 #
SAND-93-0381C .... p 3413 N93-30650 #
SAND-93-0382C .... p 3598 N93-30511 #
SAND-93-0416C .... p 3453 N93-30185 #
SAND-93-0518C .... p 3433 N93-30655 #
SAND-93-0530C .... p 3484 N93-30651 #
SAND-93-0531C .... p 3413 N93-30516 #
SAND-93-0589C .... p 3543 N93-30012 #
SAND-93-0591C .... p 3336 N93-30051 #
SAND-93-0670C .... p 3623 N93-30482 #
SAND-93-0712C .... p 3433 N93-30510 #
SAND-93-8208 .... p 3432 N93-29842 #
SAND-93-8226 .... p 3453 N93-29843 #
SAND-93-8227 .... p 3330 N93-28838 #

SATCOM-93-5 .... p 3404 N93-28539 * #

SBIR-07.03-8500 .... p 3382 N93-29217 * #
SBIR-91-2 .... p 3609 N93-29323 * #

SERC-16-92-R .... p 3281 N93-30376 * #

SIO-REF-92-22 .... p 3481 N93-28875 #

SISSA-137/92/FM .... p 3551 N93-30809 #
SISSA-140/92/EP .... p 3571 N93-30793 #

SKBS-A1/92-19 .... p 3540 N93-28480 #

SLAC-TN-92-2 .... p 3616 N93-30122 #

SMC-TR-93-16 .... p 3329 N93-28561 #

SN-130 .... p 3526 N93-29028 * #

SR-1 .... p 3479 N93-30756 #
SR-2 .... p 3476 N93-29343 #
SR-2 .... p 3630 N93-29460 #
SR-6 .... p 3273 N93-29306 #

SRI-2743 .... p 3404 N93-28483 #
SRI-3047 .... p 3544 N93-30591 #

SSD-TR-92-25 .... p 3430 N93-28488 #

SSD93D0354 .... p 3271 N93-29215 * #

SSS-DPR-91-12305 .... p 3279 N93-29305 #

STI-TR-1268-1 .... p 3447 N93-30828 #

SU-STAN-CS-92-1443 .... p 3531 N93-29873 * #
SU-STAN-CS-92-1459 .... p 3539 N93-29508 #
SU-STAN-CS-92-1463 .... p 3528 N93-29469 * #

SU-TR-92-20 .... p 3550 N93-29872 #
SU-TR-92-8 .... p 3555 N93-29878 #

S71-1180-1.0-1 .... p 3446 N93-30512 #

T-6 .... p 3594 N93-29138 #

TD-92-2791-PT-1 .... p 3460 N93-29307 #
TD-92-2904 .... p 3460 N93-29320 #
TD-92-2906 .... p 3460 N93-29321 #
TD-92-2907 .... p 3461 N93-29466 #
TD-92-9548-PHASE-1-PT-1 .... p 3461 N93-29465 #

TDA-PR-42-113 .... p 3384 N93-29586 * #

TEC-DRP-92-8 .... p 3245 N93-29468 #

TEES-AERO-TR-91-1 .... p 3248 N93-28693 * #

TIFR-TH-92-41 .... p 3606 N93-30807 #

TIOS-92-26 .... p 3379 N93-28502 #

TN-93-4 .... p 3496 N93-30588 #

TOP-7-3-526 .... p 3562 N93-29480 #

TOR-92(2464)-1-A .... p 3271 N93-28487 #

TP-WSTF-682 .... p 3271 N93-29387 * #

TP-930072 .... p 3445 N93-29388 #

TR-0088(3935-06)-2 .... p 3430 N93-28488 #
TR-02 .... p 3309 N93-28540 #
TR-03 .... p 3567 N93-29336 #
TR-049 .... p 3311 N93-29133 #
TR-051 .... p 3311 N93-29132 #
TR-05 .... p 3323 N93-29259 #
TR-06 .... p 3568 N93-29489 #
TR-10 .... p 3596 N93-29445
TR-11 .... p 3321 N93-28656 #
TR-11 .... p 3340 N93-30909 #
TR-12 .... p 3599 N93-30548 #
TR-13-ONR .... p 3598 N93-30408 #
TR-19-ONR .... p 3336 N93-30169 #
TR-20 .... p 3333 N93-29441 #
TR-21 .... p 3294 N93-28492 #
TR-21 .... p 3333 N93-29442 #
TR-22 .... p 3329 N93-28489 #
TR-24 .... p 3597 N93-30146 #
TR-2 .... p 3334 N93-29825 #
TR-40-ONR .... p 3599 N93-30568 #
TR-41 .... p 3312 N93-29429 #
TR-41 .... p 3335 N93-30028 #
TR-42 .... p 3596 N93-29430 #
TR-465 .... p 3549 N93-29413 #
TR-4 .... p 3452 N93-29515 #
TR-5 .... p 3320 N93-28491 #
TR-5 .... p 3567 N93-29332 #
TR-5 .... p 3432 N93-29476 #
TR-682-001 .... p 3272 N93-29501 * #
TR-6 .... p 3324 N93-29799 #
TR-8 .... p 3329 N93-28560 #
TR-91-ONR .... p 3317 N93-30664
TR-92-ONR .... p 3313 N93-29828 #
TR-92-16 .... p 3523 N93-28503 #
TR-92-17 .... p 3611 N93-28481 #
TR-92-17 .... p 3554 N93-29292 #
TR-92-18 .... p 3522 N93-28482 #
TR-92-19 .... p 3523 N93-28484 #
TR-93(3935)-3 .... p 3329 N93-28561 #
TR-93-042 .... p 3269 N93-28558 * #
TR-93-06 .... p 3538 N93-29030 * #
TR-9302 .... p 3531 N93-29916 #
TR-970 .... p 3494 N93-29421 #

TRC-EM-CAB-9306 .... p 3400 N93-31036 * #

TRITA-NA-9204 .... p 3548 N93-29024 #
TRITA-NA-9205 .... p 3419 N93-29025 #
TRITA-NA-9207 .... p 3238 N93-29005 #

TRW-91:J431.1-182 .... p 3269 N93-29652 * #

TVA/WR-92/17 .... p 3462 N93-30637 #

TWR-60699-APP-A .... p 3272 N93-30618 * #
TWR-60699-APP-B .... p 3272 N93-30619 * #
TWR-60699-APP-C .... p 3272 N93-30620 * #
TWR-60699-APP-D .... p 3289 N93-30648 * #
TWR-60699-APP-E .... p 3272 N93-30621 * #
TWR-60699 .... p 3272 N93-30617 * #

T93-0345 .... p 3526 N93-29028 * #

UAH-5-32210FNL .... p 3287 N93-28680 * #

UC-705 .... p 3526 N93-29127 #

UCLA-ENG-93-22 .... p 3387 N93-29875 #

UCRL-CR-109547 .... p 3586 N93-29053 #
UCRL-CR-111779 .... p 3474 N93-30506 #
UCRL-CR-111783 .... p 3424 N93-30035 #

UCRL-ID-111489 .... p 3450 N93-28596 #
UCRL-ID-112018 .... p 3469 N93-28967 #
UCRL-ID-112497 .... p 3405 N93-28597 #
UCRL-ID-112628 .... p 3474 N93-30504 #
UCRL-ID-112738 .... p 3537 N93-28544 #
UCRL-ID-112905 .... p 3243 N93-28571 #
UCRL-ID-112944 .... p 3469 N93-28972 #

UCRL-JC-105899 .... p 3437 N93-29104 #
UCRL-JC-108444 .... p 3430 N93-28520 #
UCRL-JC-109267 .... p 3422 N93-29300 #
UCRL-JC-109480 .... p 3437 N93-29207 #
UCRL-JC-109538 .... p 3588 N93-29772 #
UCRL-JC-109575 .... p 3520 N93-29058 #
UCRL-JC-109606 .... p 3630 N93-29785 #
UCRL-JC-109615 .... p 3433 N93-30491 #
UCRL-JC-109741 .... p 3326 N93-30490 #
UCRL-JC-109786 .... p 3310 N93-29059 #
UCRL-JC-109885 .... p 3524 N93-28550 #
UCRL-JC-109893 .... p 3436 N93-29097 #
UCRL-JC-109928 .... p 3568 N93-29784 #
UCRL-JC-109944 .... p 3326 N93-30389 #
UCRL-JC-109999 .... p 3588 N93-29334 #
UCRL-JC-110094 .... p 3432 N93-29773 #
UCRL-JC-110220 .... p 3563 N93-28521 #
UCRL-JC-110221 .... p 3576 N93-30390 #
UCRL-JC-110338 .... p 3594 N93-29301 #
UCRL-JC-110372 .... p 3469 N93-28965 #
UCRL-JC-110700 .... p 3549 N93-29060 #
UCRL-JC-110768 .... p 3574 N93-29103 #
UCRL-JC-110878 .... p 3440 N93-30394 #
UCRL-JC-110949 .... p 3565 N93-29099 #
UCRL-JC-110956 .... p 3438 N93-29309 #
UCRL-JC-111080 .... p 3419 N93-29050 #
UCRL-JC-111333 .... p 3311 N93-29263 #
UCRL-JC-111340 .... p 3410 N93-29793 #
UCRL-JC-111376 .... p 3438 N93-29781 #
UCRL-JC-111393 .... p 3588 N93-29780 #
UCRL-JC-111550 .... p 3615 N93-29310 #
UCRL-JC-111558 .... p 3615 N93-29783 #
UCRL-JC-111650 .... p 3566 N93-29206 #
UCRL-JC-111827 .... p 3539 N93-29782 #
UCRL-JC-112059 .... p 3600 N93-30668 #
UCRL-JC-112499 .... p 3437 N93-29098 #
UCRL-JC-112640 .... p 3632 N93-28547 #
UCRL-JC-112718 .... p 3587 N93-29303 #
UCRL-JC-112945 .... p 3471 N93-29792 #
UCRL-JC-113259 .... p 3564 N93-28762 #

UCRL-51444-90/91 .... p 3470 N93-29055 #

UDR-TR-92-53 .... p 3312 N93-29510 #

UILU-ENG-93-2220 .... p 3527 N93-29170 * #

UK-ME-92-01 .... p 3426 N93-30403 #
UK-ME-92-02 .... p 3423 N93-29352 #
UK-ME-92-03 .... p 3422 N93-29338 #
UK-ME-92-04 .... p 3423 N93-29339 #
UK-ME-92-05 .... p 3425 N93-30155 #

UMTRI-93-10 .... p 3496 N93-30659 #

US-PATENT-APPL-SN-009908 ..... p 3338 N93-30565 * #
US-PATENT-APPL-SN-009909 ..... p 3447 N93-30567 * #
US-PATENT-APPL-SN-010037 ..... p 3289 N93-29847 * #
US-PATENT-APPL-SN-023253 ..... p 3542 N93-29176 * #
US-PATENT-APPL-SN-024547 ..... p 3491 N93-28952 * #
US-PATENT-APPL-SN-030894 ..... p 3407 N93-29173 * #
US-PATENT-APPL-SN-033512 ..... p 3579 N93-29848 * #
US-PATENT-APPL-SN-034452 ..... p 3288 N93-28950 * #
US-PATENT-APPL-SN-034608 ..... p 3443 N93-28954 * #
US-PATENT-APPL-SN-035345 ..... p 3507 N93-29845 * #
US-PATENT-APPL-SN-038748 ..... p 3442 N93-28501 * #
US-PATENT-APPL-SN-044668 ..... p 3440 N93-30415 * #
US-PATENT-APPL-SN-045142 ..... p 3491 N93-29174 * #
US-PATENT-APPL-SN-046256 ..... p 3561 N93-28953 * #
US-PATENT-APPL-SN-047135 ..... p 3449 N93-30413 * #
US-PATENT-APPL-SN-056503 ..... p 3251 N93-30416 * #
US-PATENT-APPL-SN-060617 ..... p 3449 N93-30414 * #
US-PATENT-APPL-SN-064324 ..... p 3443 N93-29175 * #
US-PATENT-APPL-SN-067184 ..... p 3323 N93-29172 * #
US-PATENT-APPL-SN-069481 ..... p 3445 N93-29846 * #
US-PATENT-APPL-SN-070132 ..... p 3442 N93-28951 * #

US-PATENT-APPL-SN-429574 ..... p 3331 N93-29083 *
US-PATENT-APPL-SN-429739 ..... p 3296 N93-29023 *
US-PATENT-APPL-SN-458280 ..... p 3521 N93-29608 *
US-PATENT-APPL-SN-501892 ..... p 3384 N93-29507 *
US-PATENT-APPL-SN-501893 ..... p 3299 N93-29614 *
US-PATENT-APPL-SN-587328 ..... p 3333 N93-29456
US-PATENT-APPL-SN-608493 ..... p 3298 N93-29609 *
US-PATENT-APPL-SN-643257 ..... p 3383 N93-29275
US-PATENT-APPL-SN-657238 ..... p 3299 N93-29614 *
US-PATENT-APPL-SN-664445 ..... p 3384 N93-29507 *
US-PATENT-APPL-SN-677059 ..... p 3521 N93-29504 *
US-PATENT-APPL-SN-682159 ..... p 3409 N93-29605
US-PATENT-APPL-SN-682169 ..... p 3333 N93-29457
US-PATENT-APPL-SN-700373 ..... p 3333 N93-29458
US-PATENT-APPL-SN-705474 ..... p 3452 N93-29612 *
US-PATENT-APPL-SN-716182 ..... p 3498 N93-29610 *
US-PATENT-APPL-SN-718316 ..... p 3437 N93-29277
US-PATENT-APPL-SN-735471 ..... p 3438 N93-29287
US-PATENT-APPL-SN-735548 ..... p 3298 N93-29609 *
US-PATENT-APPL-SN-749737 ..... p 3431 N93-29084 *
US-PATENT-APPL-SN-750158 ..... p 3331 N93-29085 *
US-PATENT-APPL-SN-755207 ..... p 3312 N93-29506 *
US-PATENT-APPL-SN-764581 ..... p 3312 N93-29617 *
US-PATENT-APPL-SN-766593 ..... p 3464 N93-28974 *
US-PATENT-APPL-SN-766609 ..... p 3354 N93-29611 *
US-PATENT-APPL-SN-790607 ..... p 3259 N93-29278
US-PATENT-APPL-SN-802078 ..... p 3381 N93-29087 *
US-PATENT-APPL-SN-805281 ..... p 3507 N93-29606
US-PATENT-APPL-SN-805341 ..... p 3578 N93-29086 *
US-PATENT-APPL-SN-813628 ..... p 3445 N93-29618 *
US-PATENT-APPL-SN-815294 ..... p 3507 N93-29607
US-PATENT-APPL-SN-816514 ..... p 3437 N93-29276
US-PATENT-APPL-SN-843677 ..... p 3408 N93-29281
US-PATENT-APPL-SN-849612 ..... p 3452 N93-29613 *
US-PATENT-APPL-SN-853229 ..... p 3383 N93-29455
US-PATENT-APPL-SN-862689 ..... p 3444 N93-29288
US-PATENT-APPL-SN-871255 ..... p 3383 N93-29280
US-PATENT-APPL-SN-880851 ..... p 3299 N93-29614 *
US-PATENT-APPL-SN-887674 ..... p 3331 N93-29088 *
US-PATENT-APPL-SN-892063 ..... p 3562 N93-29279
US-PATENT-APPL-SN-894505 ..... p 3296 N93-29023 *
US-PATENT-APPL-SN-912953 ..... p 3508 N93-30566 * #
US-PATENT-APPL-SN-918746 ..... p 3445 N93-29505 *
US-PATENT-APPL-SN-957127 ..... p 3432 N93-29503 *
US-PATENT-APPL-SN-971117 ..... p 3577 N93-29038 #
US-PATENT-APPL-SN-983194 ..... p 3338 N93-30586 #
US-PATENT-APPL-SN-983334 ..... p 3581 N93-30410 #
US-PATENT-APPL-SN-983335 ..... p 3431 N93-29046 #
US-PATENT-APPL-SN-991940 ..... p 3338 N93-30580 #
US-PATENT-APPL-SN-998347 ..... p 3440 N93-30427 #
US-PATENT-APPL-SN-998348 ..... p 3441 N93-30587 #
US-PATENT-APPL-SN-999794 ..... p 3381 N93-28955 * #

US-PATENT-CLASS-102-207 .... p 3412 N93-30201
US-PATENT-CLASS-116-70 .... p 3432 N93-29503 *
US-PATENT-CLASS-137-554 .... p 3432 N93-29503 *
US-PATENT-CLASS-137-557 .... p 3432 N93-29503 *
US-PATENT-CLASS-139-DIG.1 .... p 3354 N93-29611 *
US-PATENT-CLASS-139-11 .... p 3354 N93-29611 *
US-PATENT-CLASS-165-185 .... p 3299 N93-29614 *
US-PATENT-CLASS-174-16.3 ...... p 3299 N93-29614 *
US-PATENT-CLASS-2-424 .... p 3507 N93-29606
US-PATENT-CLASS-204-104 .... p 3312 N93-29617 *
US-PATENT-CLASS-204-105R .... p 3312 N93-29617 *
US-PATENT-CLASS-204-112 .... p 3312 N93-29617 *
US-PATENT-CLASS-204-129 .... p 3312 N93-29617 *
US-PATENT-CLASS-210-512.1 .... p 3444 N93-29288
US-PATENT-CLASS-244-121 .... p 3331 N93-29088 *
US-PATENT-CLASS-244-122 .... p 3507 N93-29607
US-PATENT-CLASS-244-158R .... p 3331 N93-29088 *
US-PATENT-CLASS-244-219 .... p 3259 N93-29278
US-PATENT-CLASS-244-3.12 ...... p 3383 N93-29280
US-PATENT-CLASS-250-226 .... p 3438 N93-29287
US-PATENT-CLASS-250-339 .... p 3578 N93-29086 *
US-PATENT-CLASS-252-42.7 ...... p 3333 N93-29458
US-PATENT-CLASS-257-712 .... p 3381 N93-29087 *
US-PATENT-CLASS-324-431 .... p 3409 N93-29605
US-PATENT-CLASS-324-699 .... p 3452 N93-29612 *
US-PATENT-CLASS-324-718 .... p 3452 N93-29612 *
US-PATENT-CLASS-331-66 .... p 3408 N93-29281
US-PATENT-CLASS-340-611 .... p 3432 N93-29503 *
US-PATENT-CLASS-342-351 .... p 3381 N93-29087 *
US-PATENT-CLASS-342-368 .... p 3383 N93-29455
US-PATENT-CLASS-343-700MS . p 3384 N93-29507 *
US-PATENT-CLASS-343-700 .... p 3381 N93-29087 *
US-PATENT-CLASS-343-819 .... p 3384 N93-29507 *
US-PATENT-CLASS-343-833 .... p 3384 N93-29507 *
US-PATENT-CLASS-343-834 .... p 3384 N93-29507 *
US-PATENT-CLASS-356-326 .... p 3578 N93-29086 *
US-PATENT-CLASS-356-51 .... p 3578 N93-29086 *
US-PATENT-CLASS-359-308 .... p 3578 N93-29086 *
US-PATENT-CLASS-359-67 .... p 3452 N93-29613 *
US-PATENT-CLASS-359-74 .... p 3452 N93-29613 *
US-PATENT-CLASS-359-82 .... p 3452 N93-29613 *
US-PATENT-CLASS-361-386 .... p 3299 N93-29614 *
US-PATENT-CLASS-361-394 .... p 3381 N93-29087 *
US-PATENT-CLASS-364-DIG.1 .... p 3521 N93-29608 *
US-PATENT-CLASS-364-231.9 .... p 3521 N93-29608 *
US-PATENT-CLASS-364-723 .... p 3383 N93-29275
US-PATENT-CLASS-367-131 .... p 3562 N93-29279
US-PATENT-CLASS-372-22 .... p 3437 N93-29276
US-PATENT-CLASS-372-69 .... p 3437 N93-29277
US-PATENT-CLASS-374-119 .... p 3431 N93-29084 *
US-PATENT-CLASS-395-11 .... p 3521 N93-29504 *
US-PATENT-CLASS-395-23 .... p 3498 N93-29610 *
US-PATENT-CLASS-395-51 .... p 3521 N93-29504 *
US-PATENT-CLASS-395-800 .... p 3521 N93-29608 *
US-PATENT-CLASS-414-729 .... p 3445 N93-29505 *
US-PATENT-CLASS-422-136 .... p 3298 N93-29609 *
US-PATENT-CLASS-422-209 .... p 3298 N93-29609 *
US-PATENT-CLASS-423-446 .... p 3333 N93-29456
US-PATENT-CLASS-427-244 .... p 3296 N93-29023 *
US-PATENT-CLASS-427-269 .... p 3296 N93-29023 *
US-PATENT-CLASS-427-270 .... p 3296 N93-29023 *
US-PATENT-CLASS-427-287 .... p 3296 N93-29023 *
US-PATENT-CLASS-427-377 .... p 3296 N93-29023 *
US-PATENT-CLASS-427-535 .... p 3296 N93-29023 *
US-PATENT-CLASS-428-1 .... p 3452 N93-29613 *
US-PATENT-CLASS-428-225 .... p 3354 N93-29611 *
US-PATENT-CLASS-428-409 .... p 3452 N93-29613 *
US-PATENT-CLASS-428-480 .... p 3452 N93-29613 *
US-PATENT-CLASS-428-614 .... p 3299 N93-29614 *
US-PATENT-CLASS-428-913 .... p 3452 N93-29613 *
US-PATENT-CLASS-429-103 .... p 3464 N93-28974 *
US-PATENT-CLASS-429-16 .... p 3464 N93-28974 *
US-PATENT-CLASS-429-27 .... p 3464 N93-28974 *
US-PATENT-CLASS-429-29 .... p 3464 N93-28974 *
US-PATENT-CLASS-429-30 .... p 3464 N93-28974 *
US-PATENT-CLASS-429-46 .... p 3464 N93-28974 *
US-PATENT-CLASS-483-16 .... p 3445 N93-29505 *
US-PATENT-CLASS-483-901 .... p 3445 N93-29505 *
US-PATENT-CLASS-526-256 .... p 3333 N93-29457
US-PATENT-CLASS-528-125 .... p 3331 N93-29083 *
US-PATENT-CLASS-528-125 .... p 3331 N93-29085 *
US-PATENT-CLASS-528-126 .... p 3331 N93-29085 *
US-PATENT-CLASS-528-128 .... p 3331 N93-29083 *
US-PATENT-CLASS-528-128 .... p 3331 N93-29085 *
US-PATENT-CLASS-528-170 .... p 3331 N93-29083 *
US-PATENT-CLASS-528-172 .... p 3331 N93-29083 *
US-PATENT-CLASS-528-172 .... p 3331 N93-29085 *
US-PATENT-CLASS-528-173 .... p 3331 N93-29085 *
US-PATENT-CLASS-528-179 .... p 3331 N93-29085 *
US-PATENT-CLASS-528-188 .... p 3331 N93-29085 *
US-PATENT-CLASS-528-26 .... p 3331 N93-29083 *
US-PATENT-CLASS-528-28 .... p 3331 N93-29083 *
US-PATENT-CLASS-528-353 .... p 3331 N93-29083 *
US-PATENT-CLASS-562-827 .... p 3312 N93-29506 *
US-PATENT-CLASS-564-417 .... p 3312 N93-29506 *
US-PATENT-CLASS-564-440 .... p 3312 N93-29506 *
US-PATENT-CLASS-73-24.05 ...... p 3431 N93-29084 *
US-PATENT-CLASS-73-32A .... p 3431 N93-29084 *
US-PATENT-CLASS-73-5.97 .... p 3431 N93-29084 *
US-PATENT-CLASS-73-61.75 ...... p 3431 N93-29084 *
US-PATENT-CLASS-73-61.79 ...... p 3431 N93-29084 *
US-PATENT-CLASS-73-64.53 ...... p 3431 N93-29084 *
US-PATENT-CLASS-73-799 .... p 3452 N93-29612 *
US-PATENT-CLASS-73-9 .... p 3445 N93-29618 *
US-PATENT-CLASS-89-36.02 ...... p 3331 N93-29088 *
US-PATENT-CLASS-901-30 .... p 3445 N93-29505 *
US-PATENT-CLASS-901-41 .... p 3445 N93-29505 *

US-PATENT-5,147,567 .... p 3333 N93-29458
US-PATENT-5,162,470 .... p 3333 N93-29457
US-PATENT-5,162,741 .... p 3409 N93-29605
US-PATENT-5,164,736 .... p 3383 N93-29455
US-PATENT-5,174,983 .... p 3333 N93-29456
US-PATENT-5,176,342 .... p 3507 N93-29607
US-PATENT-5,177,816 .... p 3507 N93-29606
US-PATENT-5,181,212 .... p 3437 N93-29276
US-PATENT-5,186,414 .... p 3383 N93-29280
US-PATENT-5,186,420 .... p 3259 N93-29278
US-PATENT-5,187,690 .... p 3562 N93-29279
US-PATENT-5,191,546 .... p 3383 N93-29275
US-PATENT-5,198,783 .... p 3408 N93-29281
US-PATENT-5,200,972 .... p 3437 N93-29277
US-PATENT-5,202,026 .... p 3444 N93-29288
US-PATENT-5,206,502 .... p 3438 N93-29287
US-PATENT-5,213,908 .... p 3464 N93-28974 *
US-PATENT-5,214,955 .... p 3431 N93-29084 *
US-PATENT-5,215,790 .... p 3296 N93-29023 *
US-PATENT-5,216,484 .... p 3578 N93-29086 *
US-PATENT-5,217,185 .... p 3331 N93-29088 *
US-PATENT-5,218,077 .... p 3331 N93-29085 *
US-PATENT-5,218,083 .... p 3331 N93-29083 *
US-PATENT-5,218,357 .... p 3381 N93-29087 *
US-PATENT-5,218,709 .... p 3521 N93-29608 *
US-PATENT-5,219,318 .... p 3445 N93-29505 *
US-PATENT-5,220,070 .... p 3312 N93-29506 *
US-PATENT-5,220,335 .... p 3384 N93-29507 *
US-PATENT-5,223,310 .... p 3452 N93-29613 *
US-PATENT-5,224,030 .... p 3299 N93-29614 *
US-PATENT-5,224,519 .... p 3354 N93-29611 *
US-PATENT-5,225,171 .... p 3298 N93-29609 *
US-PATENT-5,226,110 .... p 3521 N93-29504 *
US-PATENT-5,226,308 .... p 3445 N93-29618 *
US-PATENT-5,226,447 .... p 3432 N93-29503 *
US-PATENT-5,227,032 .... p 3312 N93-29617 *
US-PATENT-5,227,731 .... p 3452 N93-29612 *
US-PATENT-5,228,113 .... p 3498 N93-29610 *

USAARL-93-10 .... p 3506 N93-29406 #

USAFETAC/PR-93/001 .... p 3483 N93-29810 #

USAFETAC/TN-88/005-REV .... p 3481 N93-28991 #

USAFETAC/UH-93/001 .... p 3484 N93-30608 #

USARIEMT7-93 .... p 3505 N93-28884 #

USCG-D-02A-93-VOL-1 .... p 3335 N93-29886 #
USCG-D-02B-93-VOL-2 .... p 3335 N93-29881 #
USCG-D-03-93 .... p 3246 N93-29818 #

USGS/WRI-92-4138 .... p 3474 N93-30825 #
USGS/WRI-92-4169 .... p 3474 N93-30826 #

USNA-EW-05-93 .... p 3334 N93-29829 #
USNA-EW-23-92 .... p 3296 N93-28886 #

UT-KBS-92-40 .... p 3540 N93-28480 #

UTS-DFT-22-92 .... p 3551 N93-30809 #

UWA/DME/TR-93-71 .... p 3453 N93-30147 #

VI-1982 .... p 3630 N93-29460 #

VPI-E-87-7 .... p 3454 N93-30374 * #
VPI-E-93-06 .... p 3297 N93-29107 * #

VTT-PUBS-90 .... p 3353 N93-28632 #

VTT-TIED-1203 .... p 3411 N93-30108 #
VTT-TIED-1232-PT-2 .... p 3575 N93-29996 #
VTT-TIED-1245 .... p 3378 N93-30581 #
VTT-TIED-1250 .... p 3532 N93-29997 #
VTT-TIED-1267 .... p 3465 N93-30111 #
VTT-TIED-1274 .... p 3543 N93-29998 #

VYH-PUB-7 .... p 3488 N93-30040 #

W-9201 .... p 3548 N93-28753 #

WES/IR/ITL-92-3 .... p 3529 N93-29657 #
WES/IR/ITL-92-3 .... p 3529 N93-29658 #

WES/TR/EL-93-4 .... p 3473 N93-30197 #

WHC-EP-0372-VOL-1-REV-1 .... p 3470 N93-29135 #

WHC-SA-1684 .... p 3447 N93-30632 #

WHOI-CONTRIB-8046 .... p 3487 N93-29003 #
WHOI-CONTRIB-8701 .... p 3486 N93-28996 #

WHOI-92-32 .... p 3477 N93-29405 #
WHOI-93-07 .... p 3492 N93-30665 * #

WIS-PH-92-38 .... p 3607 N93-30932 #
WIS-PH-92-45 .... p 3607 N93-30933 #

WL-TM-92-350-FIBG .... p 3240 N93-29410
WL-TM-93-102 .... p 3433 N93-30584

WL-TR-91-4061 .... p 3295 N93-28592 #
WL-TR-91-4150 .... p 3446 N93-30512 #
WL-TR-92-1122 .... p 3446 N93-30404 #
WL-TR-92-2053 .... p 3312 N93-29510 #
WL-TR-92-2079 .... p 3568 N93-29446 #
WL-TR-92-2082 .... p 3412 N93-30406 #
WL-TR-92-2086 .... p 3423 N93-29352 #
WL-TR-92-2091 .... p 3423 N93-29426 #
WL-TR-92-2096 .... p 3425 N93-30155 #
WL-TR-92-2097 .... p 3422 N93-29338 #
WL-TR-92-2098 .... p 3423 N93-29339 #
WL-TR-92-2099 .... p 3426 N93-30403 #
WL-TR-92-2105 .... p 3342 N93-29402 #
WL-TR-92-3088 .... p 3281 N93-30142 #
WL-TR-92-3104 .... p 3332 N93-29344 #
WL-TR-92-3107 .... p 3423 N93-29472 #
WL-TR-92-4068 .... p 3449 N93-29443 #
WL-TR-92-4104 .... p 3323 N93-29144 #
WL-TR-93-1011 .... p 3393 N93-30576 #
WL-TR-93-1023 .... p 3439 N93-29827 #
WL-TR-93-1060 .... p 3424 N93-29966 #
WL-TR-93-3005 .... p 3248 N93-29409 #
WL-TR-93-3016 .... p 3260 N93-30498 #

WL-TR-93-4021 .... p 3534 N93-30495 #
WL-TR-93-4039 .... p 3595 N93-29341 #
WL-TR-93-7023 .... p 3454 N93-30545 #

WSRC-MS-93-134 .... p 3324 N93-29265 #

WSRC-TR-92-458-REV-1 .... p 3309 N93-28553 #
WSRC-TR-92-73-REV-1 .... p 3431 N93-29325 #
WSRC-TR-93-011 .... p 3330 N93-28839 #

XC-PL/HANSCOM .... p 3481 N93-28875 #

XC-SMC .... p 3271 N93-28487 #

Y-2447 .... p 3451 N93-28832 #

APPENDIX

NASA SCIENTIFIC AND TECHNICAL INFORMATION PROGRAM PRODUCTS AND SERVICES

The NASA Scientific and Technical Information (STI) Program provides for the collection and announcement of aerospace-related reports and literature obtained worldwide through agreements and exchanges. The result of the collection is the comprehensive NASA STI Database that covers aeronautics, space, and supporting disciplines.

The STI Database, documents generated or obtained by NASA, and products and services derived from or supporting the database are made available to the NASA research community and to the public. Descriptions and sources of these items are presented in the following pages.

Scientific and Technical Aerospace Reports (STAR) is an abstract journal, listing citations with abstracts for aerospace-related reports obtained from worldwide sources. *STAR* is issued on the first of each month, and announces current documents that have been entered into the NASA STI Database during the previous month. The reports are of the following types:

- NASA, NASA contractor, and NASA grantee reports;
- Reports issued by other U.S. Government agencies, domestic and foreign institutions, universities, and private firms;
- Translations in report form;
- NASA-owned patents and patent applications
- Other U.S. Government agency and foreign patents and patent applications
- Domestic and foreign dissertations and theses.

Journal, book, and conference literature, journal translations, and certain foreign dissertations having the same subject scope as *STAR* are announced in a companion journal, *International Aerospace Abstracts (IAA). IAA* is issued on the 1st and 15th of each month and is available from the American Institute of Aeronautics and Astronautics, Technical Information Service, 555 West 57th Street, 12th Floor, New York, NY 10019.

ELIGIBILITY AND REGISTRATION FOR NASA STI PRODUCTS AND SERVICES

Organizations of the type listed below that have registered with NASA can receive products and services.

- NASA offices and installations, contractors, subcontractors, grantees, and consultants;
- Other U.S. Government agencies and their contractors;
- Libraries in the United States that have arrangements with NASA to maintain collections of NASA documents for public reference;
- Other organizations in the United States having a need for NASA documents in work related to aeronautics and space research;
- Organizations abroad that have established reciprocal documents exchange arrangements with NASA.

The central service points—central points of document acquisition and control within qualified organizations—or individuals are eligible to register for NASA STI products and services. Domestic organizations or individuals may be eligible to receive various classes of NASA publications and services and should address their requests for registration or further information to:

ATTN: Registration Services
NASA Center for AeroSpace Information
800 Elkridge Landing Road
Linthicum Heights, MD 21090-2934
301-621-0390

Organizations abroad should direct requests to:

National Aeronautics and Space Administration
Scientific and Technical Information Program (JTT)
International STI Program
Washington, DC 20546-0001
USA
703-271-5640

SUBJECT SCOPE

The subject scope of *STAR* and *IAA* includes all aspects of aeronautics and space research and development, supporting basic and applied research, and applications. Aerospace aspects of Earth resources, energy development, conservation, oceanography, environmental protection, urban transportation, and other topics of high national priority are also covered.

HOW TO USE *STAR* SUBJECT CATEGORIES

Abstracts in *STAR* are categorized by 10 major subject divisions that are divided further into 76 specific subject categories. The subject divisions and categories are listed in the Table of Contents together with a note for each that defines its scope and provides any cross-references. For example:

> **16 SPACE TRANSPORTATION**
>
> Includes passenger and cargo space transportation, e.g., shuttle operations; and space rescue techniques. For related information see also *03 Air Transportation and Safety* and *18 Spacecraft Design, Testing and Performance*. For space suits see *54 Man/System Technology and Life Support.*

CROSS-REFERENCES

Individual *STAR* abstracts are not ordinarily cross-referenced, except for certain conference reports or book translations that have had separate abstracts written for their component papers or chapters. Citations and abstracts of the components follow immediately after those of the parent document. When the subject content of a component differs sufficiently from the general content of the parent, a cross-reference citation also is printed at the end of the category to which it normally would have been assigned if it were independent.

DOCUMENTS ON MICROFICHE

Documents available on microfiche are designated by a pound sign (#) following the accession number.

LIMITED REPRODUCIBILITY

A note of limited reproducibility appears in the citation, if there are factors affecting the reproducibility of more than 20% of the document. These factors include faint or broken type, color photographs, black and white photographs, foldouts, dot matrix print, or some other factor that limits the reproducibility of the document. This notation also appears on the microfiche header.

COLOR COPIES

An increasing number of NASA scientific and technical reports are being produced with color graphs, charts, illustrations, and photographs. An indication that a document has color pages follows the source and pricing (SAP) information in the *STAR* citation.

Registered users of the NASA Scientific and Technical Information Program will receive ordered documents with color at no additional cost, as long as stock copies of the document are available. Otherwise, an additional fee of $2.00 per color page will be charged. The NASA Center for AeroSpace Information staff will contact registered users to determine individual user's needs.

NASA PATENTS AND PATENT APPLICATIONS

Patents and patent applications owned by NASA are announced in *STAR* under appropriate subject categories and are referenced in the *STAR* indexes. In the Report Number Index, patents are indexed by the NASA Case Number, and the U.S. Patent Class. Patent applications are indexed by the NASA Case Number and the U.S. Patent Application Serial Number.

Printed copies of patents (which are not microfiched) are available for purchase from the U.S. Patent and Trademark Office.

When ordering patents, the U.S. Patent Number should be used, and payment must be remitted in advance, by money order or check payable to the Commissioner of Patents and Trademarks. Prepaid purchase coupons for ordering are also available from the U.S. Patent and Trademark Office.

NASA patent application specifications are sold in both paper copy and microfiche by the NASA Center for AeroSpace Information (CASI). The N accession number should be used in ordering either paper copy or microfiche from CASI.

The patents and patent applications announced in *STAR* are owned by NASA and are available for royalty-free licensing. Requests for licensing terms and further information should be addressed to:

National Aeronautics and Space Administration
Associate General Counsel for Intellectual Property
Code GP
Washington, DC 20546-0001

SOURCES FOR DOCUMENTS

One or more sources from which a document announced in *STAR* is available to the public is ordinarily given on the last line of the citation. The most commonly indicated sources and their acronyms or abbreviations are listed below, and their addresses are listed on page A-6. If the publication is available from a source other than those listed, the publisher and his address will be displayed on the availability line or in combination with the corporate source line.

Avail: CASI. Sold by the NASA Center for AeroSpace Information. Prices for hard copy (HC) and microfiche (MF) are indicated by a price code following the letters HC or MF in the *STAR* citation. Current values for the price codes are given in the tables on page A-7.

NOTE ON ORDERING DOCUMENTS: When ordering publications from CASI, use the N accession number or other report number. It is also advisable to cite the title and other bibliographic identification.

Avail: SOD (or GPO). Sold by the Superintendent of Documents, U.S. Government Printing Office, in hard copy.

Avail: BLL (formerly NLL): British Library Lending Division, Boston Spa, Wetherby, Yorkshire, England. Photocopies available from this organization at the price shown. (If none is given, inquiry should be addressed to the BLL.)

Avail: DOE Depository Libraries. Organizations in U.S. cities and abroad that maintain collections of Department of Energy reports, usually in microfiche form, are listed in *Energy Research Abstracts.* Services available from the DOE and its depositories are described in a booklet, *DOE Technical Information Center - Its Functions and Services* (TID-4660), which may be obtained without charge from the DOE Technical Information Center.

Avail: ESDU. Pricing information on specific data, computer programs, and details on Engineering Sciences Data Unit (ESDU) topic categories can be obtained from ESDU International Ltd. Requesters in North America should use the Virginia address while all other requesters should use the London address, both of which are on page A-6.

Avail: Fachinformationszentrum, Karlsruhe. Gesellschaft für wissenschaftlich-technische Information mbH 7514 Eggenstein-Leopoldshafen 2, Germany.

Avail: HMSO. Publications of Her Majesty's Stationery Office are sold in the U.S. by Pendragon House, Inc. (PHI), Redwood City, CA. The U.S. price (including a service and mailing charge) is given, or a conversion table may be obtained from PHI.

Avail: Issuing Activity, or Corporate Author, or no indication of availability. Inquiries as to the availability of these documents should be addressed to the organization shown in the citation as the corporate author of the document.

Avail: NASA Public Document Rooms. Documents so indicated may be examined at or purchased from the National Aeronautics and Space Administration (JBD-4), Public Documents Room (Room 1H23), Washington, DC 20546-0001, or public document rooms located at NASA installations, and the NASA Pasadena Office at the Jet Propulsion Laboratory.

Avail: NTIS. Sold by the National Technical Information Service. Initially distributed microfiche under the NTIS SRIM (Selected Research in Microfiche) are available. For information concerning this service, consult the NTIS Subscription Section, Springfield, VA 22161.

Avail: Univ. Microfilms. Documents so indicated are dissertations selected from *Dissertation Abstracts* and are sold by University Microfilms as xerographic copy (HC) and microfilm. All requests should cite the author and the Order Number as they appear in the citation.

Avail: US Patent and Trademark Office. Sold by Commissioner of Patents and Trademarks, U.S. Patent and Trademark Office, at the standard price of $1.50 each, postage free. (See discussion of NASA patents and patent applications on page A-3.)

Avail: (US Sales Only). These foreign documents are available to users within the United States from the National Technical Information Service (NTIS). They are available to users outside the United States through the International Nuclear Information Service (INIS) representative in their country, or by applying directly to the issuing organization.

Avail: USGS. Originals of many reports from the U.S. Geological Survey, which may contain color illustrations, or otherwise may not have the quality of illustrations preserved in the microfiche or facsimile reproduction, may be examined by the public at the libraries of the USGS field offices whose addresses are listed on page A-6. The libraries may be queried concerning the availability of specific documents and the possible utilization of local copying services, such as color reproduction.

FEDERAL DEPOSITORY LIBRARY PROGRAM

In order to provide the general public with greater access to U.S. Government publications, Congress established the Federal Depository Library Program under the Government Printing Office (GPO), with 53 regional depositories responsible for permanent retention of material, inter-library loan, and reference services. At least one copy of nearly every NASA and NASA-sponsored publication, either in printed or microfiche format, is received and retained by the 53 regional depositories. A list of the regional GPO libraries, arranged alphabetically by state, appears on page A-8. These libraries are *not* sales outlets. A local library can contact a regional depository to help locate specific reports, or direct contact may be made by an individual.

PUBLIC COLLECTION OF NASA DOCUMENTS

An extensive collection of NASA and NASA-sponsored publications is maintained by the British Library Lending Division, Boston Spa, Wetherby, Yorkshire, England for public access. The British Library Lending Division also has available many of the non-NASA publications cited in *STAR*. European requesters may purchase facsimile copy or microfiche of NASA and NASA-sponsored documents, those identified by both the symbols # and * from ESA — Information Retrieval Service European Space Agency, 8-10 rue Mario-Nikis, 75738 CEDEX 15, France.

SUBMITTING DOCUMENTS

All users of this abstract service are urged to forward reports to be considered for announcement in *STAR*. This will aid NASA in its efforts to provide the fullest possible coverage of all scientific and technical publications that might support aeronautics and space research and development. If you have prepared relevant reports (other than those you will transmit to NASA, DOD, or DOE through the usual contract- or grant-reporting channels), please send them for consideration to the NASA Center for AeroSpace Information, 800 Elkridge Landing Road, Linthicum Heights, MD 21090-2934.

Reprints of journal articles, book chapters, and conference papers are also welcome. These will be considered for announcement in *STAR's* companion journal, *IAA*.

You may specify a particular source to be included in a report announcement if you wish; otherwise the report will be placed on a public sale at the NASA Center for AeroSpace Information. Copyrighted publications will be announced but not distributed or sold.

PURCHASE OF *STAR*

STAR is publicly available on annual subscription from the NASA Center for AeroSpace Information (CASI) at $94.00/domestic, $117.00/foreign. Single copy prices: $33.00/domestic, $41.00/foreign.

An annual, cumulative *STAR Index* is also available at $54.00/domestic, $65.00/foreign.

STAR is available to registered users on annual subscription from the NASA Center for AeroSpace Information, ATTN: Registration Services, 800 Elkridge Landing Road, Linthicum Heights, MD 21090-2934.

ADDRESSES OF ORGANIZATIONS

American Institute of Aeonautics
and Astronautics
Technical Information Service
555 West 57th Street, 12th Floor
New York, NY 10019

British Library Lending Division
Boston Spa, Wetherby, Yorkshire
England

Commissioner of Patents and Trademarks
U.S. Patent and Trademark Office
Washington, DC 20231

Department of Energy
Technical Information Center
P.O. Box 62
Oak Ridge, TN 37830

European Space Agency-
Information Retrieval Service ESRIN
Via Galileo Galilei
00044 Frascati (Rome) Italy

Engineering Sciences Data Unit International
P.O. Box 1633
Manassas, VA 22110

Engineering Sciences Data Unit
International, Ltd.
251-259 Regent Street
London, W1R 7AD, England

Fachinformationszentrum Karlsruhe
Gesellschaft für wissenschaftlich-technische
Information mbH
7514 Eggenstein-Leopoldshafen 2, Germany

Her Majesty's Stationery Office
P.O. Box 569, S.E. 1
London, England

NASA Center for AeroSpace Information
800 Elkridge Landing Road
Linthicum Heights, MD 21090-2934

National Aeronautics and Space Administration
Scientific and Technical Information Program
(JTT)
Washington, DC 20546-0001

National Technical Information Service
5285 Port Royal Road
Springfield, VA 22161

Pendragon House, Inc.
899 Broadway Avenue
Redwood City, CA 94063

Superintendent of Documents
U.S. Government Printing Office
Washington, DC 20402

University Microfilms
A Xerox Company
300 North Zeeb Road
Ann Arbor, MI 48106

University Microfilms, Ltd.
Tylers Green
London, England

U.S. Geological Survey Library National Center
MS 950
12201 Sunrise Valley Drive
Reston, VA 22092

U.S. Geological Survey Library
2255 North Gemini Drive
Flagstaff, AZ 86001

U.S. Geological Survey
345 Middlefield Road
Menlo Park, CA 94025

U.S. Geological Survey Library
Box 25046
Denver Federal Center, MS914
Denver, CO 80225

CASI PRICE TABLES

(Effective August 1, 1993)

STANDARD PRICE DOCUMENTS

PRICE CODE	NORTH AMERICAN PRICE	FOREIGN PRICE
A01	$ 9.00	$ 18.00
A02	12.50	25.00
A03	17.50	35.00
A04-A05	19.50	39.00
A06-A09	27.00	54.00
A10-A13	36.50	73.00
A14-A17	44.50	89.00
A18-A21	52.00	104.00
A22-A25	61.00	122.00
A99	Call For Price	Call For Price

MICROFICHE

PRICE CODE	NORTH AMERICAN PRICE	FOREIGN PRICE
A01	$ 9.00	$ 18.00
A02	12.50	25.00
A03	17.50	35.00
A04	19.50	39.00
A06	27.00	54.00
A10	36.50	73.00

IMPORTANT NOTICE

CASI Shipping and Handling Charges
U.S.—ADD $3.00 per TOTAL ORDER
Canada and Mexico—ADD $3.50 per TOTAL ORDER
All Other Countries—ADD $7.50 per TOTAL ORDER
Does NOT apply to orders
requesting CASI RUSH HANDLING.
CASI accepts charges to American Express, Diners Club, MasterCard and VISA.

FEDERAL REGIONAL DEPOSITORY LIBRARIES

ALABAMA

AUBURN UNIV. AT MONTGOMERY LIBRARY
Documents Dept.
7300 University Dr.
Montgomery, AL 36117-3596
(205) 244-3650 Fax: (205) 244-0678

UNIV. OF ALABAMA
Amelia Gayle Gorgas Library
Govt. Documents
Box 870266
Tuscaloosa, AL 35487-0266
(205) 348-6046 Fax: (205) 348-8833

ARIZONA

DEPT. OF LIBRARY, ARCHIVES, AND PUBLIC RECORDS
Federal Documents
Third Floor State Capitol
1700 West Washington
Phoenix, AZ 85007
(602) 542-4121 Fax: (602) 542-4400, 542-4500

ARKANSAS

ARKANSAS STATE LIBRARY
State Library Services
One Capitol Mall
Little Rock, AR 72201
(501) 682-2869

CALIFORNIA

CALIFORNIA STATE LIBRARY
Govt. Publications Section
914 Capitol Mall - P.O. Box 942837
Sacramento, CA 94237-0001
(916) 322-4572 Fax: (916) 324-8120

COLORADO

UNIV. OF COLORADO - BOULDER
Norlin Library
Govt. Publications
Campus Box 184
Boulder, CO 83309-0184
(303) 492-8834 Fax: (303) 492-2185

DENVER PUBLIC LIBRARY
Govt. Publications Dept. BS/GPD
1357 Broadway
Denver, CO 80203
(303) 571-2135

CONNECTICUT

CONNECTICUT STATE LIBRARY
231 Capitol Avenue
Hartford, CT 06106
(203) 566-4971 Fax: (203) 566-3322

FLORIDA

UNIV. OF FLORIDA LIBRARIES
Documents Dept.
Library West
Gainesville, FL 32611-2048
(904) 392-0366 Fax: (904) 392-7251

GEORGIA

UNIV. OF GEORGIA LIBRARIES
Govt. Documents Dept.
Jackson Street
Athens, GA 30602
(404) 542-8949 Fax: (404) 542-6522

HAWAII

UNIV. OF HAWAII
Hamilton Library
Govt. Documents Collection
2550 The Mall
Honolulu, HI 96822
(808) 948-8230 Fax: (808) 956-5968

IDAHO

UNIV. OF IDAHO LIBRARY
Documents Section
Moscow, ID 83843
(208) 885-6344 Fax: (208) 885-6817

ILLINOIS

ILLINOIS STATE LIBRARY
Reference Dept.
300 South Second
Springfield, IL 62701-1796
(217) 782-7596 Fax: (217) 524-0041

INDIANA

INDIANA STATE LIBRARY
Serials/Documents Section
140 North Senate Avenue
Indianapolis, IN 46204
(317) 232-3678 Fax: (317) 232-3728

IOWA

UNIV. OF IOWA LIBRARIES
Govt. Publications Dept.
Washington & Madison Streets
Iowa City, IA 52242
(319) 335-5926 Fax: (319) 335-5830

KANSAS

UNIV. OF KANSAS
Govt. Documents & Map Library
6001 Malatt Hall
Lawrence, KS 66045-2800
(913) 864-4660 Fax: (913) 864-5380

KENTUCKY

UNIV. OF KENTUCKY LIBRARIES
Govt. Publications/Maps Dept.
Lexington, KY 40506-0039
(606) 257-3139 Fax: (606) 257-1563, 257-8379

LOUISIANA

LOUISIANA STATE UNIV.
Middleton Library
Govt. Documents Dept.
Baton Rouge, LA 70803
(504) 388-2570 Fax: (504) 388-6992

LOUISIANA TECHNICAL UNIV.
Prescott Memorial Library
Govt. Documents Dept.
305 Wisteria Street
Ruston, LA 71270-9985
(318) 257-4962 Fax: (318) 257-2447

MAINE

TRI-STATE DOCUMENTS DEPOS.
Raymond H. Fogler Library
Govt. Documents & Microforms Dept.
Univ. of Maine
Orono, ME 04469
(207) 581-1680

MARYLAND

UNIV. OF MARYLAND
Hornbake Library
Govt. Documents/Maps Unit
College Park, MD 20742
(301) 454-3034 Fax: (301) 454-4985

MASSACHUSETTS

BOSTON PUBLIC LIBRARY
Govt. Documents Dept.
666 Boylston Street
Boston, MA 02117
(617) 536-5400 ext. 226
Fax: (617) 267-8273, 267-8248

MICHIGAN

DETROIT PUBLIC LIBRARY
5201 Woodward Avenue
Detroit, MI 48202-4093
(313) 833-1440, 833-1409
Fax: (313) 833-5039

LIBRARY OF MICHIGAN
Govt. Documents Unit
P.O. Box 30007
Lansing, MI 48909
(517) 373-0640 Fax: (517) 373-3381

MINNESOTA

UNIV. OF MINNESOTA
Wilson Library
Govt. Publications Library
309 19th Avenue South
Minneapolis, MN 55455
(612) 624-5073 Fax: (612) 626-9353

MISSISSIPPI

UNIV. OF MISSISSIPPI
J.D. Williams Library
Federal Documents Dept.
106 Old Gym Bldg.
University, MS 38677
(601) 232-5857 Fax: (601) 232-5453

MISSOURI

UNIV. OF MISSOURI - COLUMBIA
Ellis Library
Govt. Documents
Columbia, MO 65201
(314) 882-6733 Fax: (314) 882-8044

MONTANA

UNIV. OF MONTANA
Maureen & Mike Mansfield Library
Documents Div.
Missoula, MT 59812-1195
(406)243-6700 Fax: (406) 243-2060

NEBRASKA

UNIV. OF NEBRASKA - LINCOLN
D.L. Love Memorial Library
Documents Dept.
Lincoln, NE 68588
(402) 472-2562

NEVADA

UNIV. OF NEVADA
Reno Library
Govt. Publications Dept.
Reno, NV 89557
(702) 784-6579 Fax: (702) 784-1751

NEW JERSEY

NEWARK PUBLIC LIBRARY
U.S. Documents Div.
5 Washington Street - P.O. Box 630
Newark, NJ 07101-0630
(201) 733-7812 Fax: (201) 733-5648

NEW MEXICO

UNIV. OF NEW MEXICO
General Library
Govt. Publications Dept.
Albuquerque, NM 87131-1466
(505) 277-5441 Fax: (505) 277-6019

NEW MEXICO STATE LIBRARY
325 Don Gaspar Avenue
Santa Fe, NM 87503
(505) 827-3826 Fax: (505) 827-3820

NEW YORK

NEW YORK STATE LIBRARY
Documents/Gift & Exchange Section
Federal Depository Program
Cultural Education Center
Albany, NY 12230
(518) 474-5563 Fax: (518) 474-5786

NORTH CAROLINA

UNIV. OF NORTH CAROLINA - CHAPEL HILL
CB#3912, Davis Library
BA/SS Dept. - Documents
Chapel Hill, NC 27599
(919) 962-1151 Fax: (919) 962-0484

NORTH DAKOTA

NORTH DAKOTA STATE UNIV. LIB.
Documents Office
Fargo, ND 58105
(701) 237-8886 Fax: (701) 237-7138
In cooperation with Univ. of North Dakota, Chester Fritz Library Grand Forks

OHIO

STATE LIBRARY OF OHIO
Documents Dept.
65 South Front Street
Columbus, OH 43266
(614) 644-7051 Fax: (614) 752-9178

OKLAHOMA

OKLAHOMA DEPT. OF LIBRARIES
U.S. Govt. Information Div.
200 NE 18th Street
Oklahoma City, OK 73105-3298
(405) 521-2502, ext. 252, 253
Fax: (405) 525-7804

OKLAHOMA STATE UNIV.
Edmon Low Library
Documents Dept.
Stillwater, OK 74078
(405) 744-6546 Fax: (405) 744-5183

OREGON

PORTLAND STATE UNIV.
Millar Library
934 SW Harrison - P.O. Box 1151
Portland, OR 97207
(503) 725-3673 Fax: (503) 725-4527

PENNSYLVANIA

STATE LIBRARY OF PENN.
Govt. Publications Section
Walnut St. & Commonwealth Ave. - P.O. Box 1601
Harrisburg, PA 17105
(717) 787-3752

SOUTH CAROLINA

CLEMSON UNIV.
Cooper Library
Public Documents Unit
Clemson, SC 29634-3001
(803) 656-5174 Fax: (803) 656-3025
In cooperation with Univ. of South Carolina, Thomas Cooper Library, Columbia

TENNESSEE

MEMPHIS STATE UNIV. LIBRARIES
Govt. Documents
Memphis, TN 38152
(901) 678-2586 Fax: (901) 678-2511

TEXAS

TEXAS STATE LIBRARY
United States Documents
P.O. Box 12927 - 1201 Brazos
Austin, TX 78711
(512) 463-5455 Fax: (512) 463-5436

TEXAS TECH. UNIV. LIBRARY
Documents Dept.
Lubbock, TX 79409
(806) 742-2268 Fax: (806) 742-1920

UTAH

UTAH STATE UNIV.
Merrill Library & Learning Resources Center, UMC-3000
Documents Dept.
Logan, UT 84322-3000
(801) 750-2684 Fax: (801) 750-2677

VIRGINIA

UNIV. OF VIRGINIA
Aldermman Library
Govt. Documents
Charlottesville, VA 22903-2498
(804) 824-3133 Fax: (804) 924-4337

WASHINGTON

WASHINGTON STATE LIBRARY
Document Section
MS AJ-11
Olympia, WA 98504-0111
(206) 753-4027 Fax: (206) 753-3546

WEST VIRGINIA

WEST VIRGINIA UNIV. LIBRARY
Govt. Documents Section
P.O. Box 6069
Morgantown, WV 26506
(304) 293-3640

WISCONSIN

ST. HIST. SOC. OF WISCONSIN LIBRARY
Govt. Publications Section
816 State Street
Madison, WI 53706
(608) 262-2781 Fax: (608) 262-4711
In cooperation with Univ. of Wisconsin - Madison, Memorial Library

MILWAUKEE PUBLIC LIBRARY
Documents Div.
814 West Wisconsin Avenue
Milwaukee, WI 53233
(414) 278-2167 Fax: (414) 278-2137

National Aeronautics and
Space Administration
Code JTT
Washington, DC
20546-0001

Official Business
Penalty for Private Use, $300

SPECIAL FOURTH-CLASS RATE
POSTAGE & FEES PAID
NASA
PERMIT No. G27

NASA

POSTMASTER: If Undeliverable (Section 158
Postal Manual) Do Not Return

Please circulate this publication to other colleagues within your organization.

______________________________ ______________________________

______________________________ ______________________________

______________________________ ______________________________

______________________________ ______________________________

______________________________ ______________________________

______________________________ ______________________________

NASA
STI PROGRAM
SCIENTIFIC &
TECHNICAL
INFORMATION